UCOR
an Amentum-led partnership with Jacobs

UCOR-5094/R2

Performance Assessment for the Environmental Management Disposal Facility at the Y-12 National Security Complex, Oak Ridge, Tennessee

This document is approved for public release per review by:

Peter Kortman (signature on file)	04-23-2020
UCOR Classification & Information Control Office	Date

UCOR-5094/R2

Performance Assessment for the Environmental Management Disposal Facility at the Y-12 National Security Complex, Oak Ridge, Tennessee

Date Issued—April 2020

Prepared for the
U.S. Department of Energy
Office of Environmental Management

URS | CH2M Oak Ridge LLC
Safely Delivering the Department of Energy's Vision
for the East Tennessee Technology Park Mission
under contract DE-SC-0004645

This page intentionally left blank.

APPROVALS

Performance Assessment for the Environmental Management Disposal Facility at the Y-12 National Security Complex, Oak Ridge, Tennessee	UCOR-5094/R2
	April 2020

USQD Review Determination	☐ USQD ☐ UCD ☐ CAT X ☐ Exempt (Select Criteria 1–3 below.) USQD/UCD/CAT X No.:
Exemption Criteria	☐ (1) Non-Intent Change ☐ (2) DOE-Approved Safety Basis Document ☐ (3) Chief Accounting Officer, Internal Audit, Labor Relations, General Counsel, Outreach & Public Affairs, or Project Controls Services OR ☒ (4) Document identified in USQD-MS-CX-REPORTS-1074
USQD Preparer:	KAREN BALO (Affiliate) Digitally signed by KAREN BALO (Affiliate) Date: 2020.04.27 12:28:18 -04'00' Name / Date
Exhibit L Mandatory Contractor Document	☒ No (No PCCB Reviewer Signature Required.) ☐ Yes (Requires review by the Proforma Change Control Board.)
PCCB Reviewer:	Name / Date

Prepared by: Stephen Kenworthy Digitally signed by Stephen Kenworthy Date: 2020.04.27 14:30:13 -04'00'
Steve Kenworthy, Senior Hydrogeologist
UCOR
Date

Concurred by: JULIE PFEFFER (Affiliate) Digitally signed by JULIE PFEFFER (Affiliate) Date: 2020.04.27 18:54:20 -04'00'
Julie Pfeffer, EMDF Project Manager
UCOR
Date

Approved by: *John Wrapp (signature on file)*
John Wrapp, Waste Program and Disposition Manager
UCOR
04-28-2020
Date

This page intentionally left blank.

REVISION LOG		
Revision Number	Description of Changes	Pages Affected
0	Initial issue of document.	All
1	Addressed OREM comments.	All
2	Addressed LFRG comments	All

This page intentionally left blank.

CONTENTS

This page intentionally left blank.

FIGURES

This page intentionally left blank.

TABLES

ACRONYMS

ALARA	as low as reasonably achievable
ANA	aquatic natural area
ARAR	applicable or relevant and appropriate requirement
ASTM	American Society for Testing and Materials
BCBG	Bear Creek Burial Ground
BCK	Bear Creek kilometer
BCV	Bear Creek Valley
BG	burial ground
bgs	below ground surface
BJC	Bechtel Jacobs Company LLC
C2DF	Class L-II Disposal Facility
CA	Composite Analysis
CBCV	Central Bear Creek Valley
CERCLA	Comprehensive Environmental Response, Compensation, and Liability Act of 1980
CFR	*Code of Federal Regulations*
D	dimensional
DAS	Disposal Authorization Statement
DCS	Derived Concentration Standard
D&D	deactivation and decommissioning
DMC	Document Management Center
DOE	U.S. Department of Energy
DOE O	DOE Order
DOE M	DOE Manual
EBCV	East Bear Creek Valley
Eh	oxidation-reduction potential
EMDF	Environmental Management Disposal Facility
EMWMF	Environmental Management Waste Management Facility
EOW	edge of waste
EPA	U.S. Environmental Protection Agency
EPM	equivalent porous medium
ETSZ	East Tennessee Seismic Zone
ETTP	East Tennessee Technology Park
FLUTe™	Flexible Liner Underground Technologies, LLC
FFA	Federal Facility Agreement
Golder	Golder Associates, Inc.
HA	habitat area
HDPE	high-density polyethylene
HELP	Hydrologic Evaluation of Landfill Performance
IAEA	International Atomic Energy Agency
IHI	inadvertent human intrusion
K_d	partition coefficient
LDR	Land Disposal Restriction
LLW	low-level (radioactive) waste
MCL	maximum contaminant level
MEI	maximally exposed individual
MSL	mean sea level
NA	natural area
NQA	Nuclear Quality Assurance

NRC	U.S. Nuclear Regulatory Commission
NT	North Tributary
NWS	National Weather Service
Ogden	Ogden Environmental and Energy Services Co., Inc.
OM	organic matter
OREM	Oak Ridge Office of Environmental Management
ORERP	Oak Ridge Environmental Research Park
ORNL	Oak Ridge National Laboratory
ORR	Oak Ridge Reservation
PA	Performance Assessment
PNNL	Pacific Northwest National Laboratory
POA	point of assessment
QA	quality assurance
RCRA	Resource Conservation and Recovery Act of 1976
RER	Remediation Effectiveness Report
RESRAD	RESidual RADioactivity
RI/FS	Remedial Investigation/Feasibility Study
ROD	Record of Decision
SR	State Route
SRS	Savannah River Site
SRSG	Single Radionuclide Soil Guideline
STOMP	Subsurface Transport Over Multiple Phases
SWSA	Solid Waste Storage Area
TDEC	Tennessee Department of Environment and Conservation
TVA	Tennessee Valley Authority
UCL	upper confidence limit
USDA	U.S. Department of Agriculture
USGS	U.S. Geological Survey
VMC	volumetric moisture content
WAC	waste acceptance criteria
WAG	Waste Area Grouping
WBCV	West Bear Creek Valley
WMFS	Waste Management Federal Services, Inc.
Y-12	Y-12 National Security Complex

EXECUTIVE SUMMARY

This report documents the Performance Assessment (PA) for the Environmental Management Disposal Facility (EMDF). The EMDF is a proposed, new low-level (radioactive) waste (LLW) disposal facility on the U.S. Department of Energy (DOE) Oak Ridge Reservation (ORR). This executive summary includes an overview of the following:

- Need for EMDF and basis for the PA
- Features and safety functions of the EMDF disposal system, including a summary of the estimated radionuclide inventory
- Key assumptions
- Conceptual models and model codes implemented for analysis of performance and quality assurance (QA) processes
- Summary of results, including sensitivity and uncertainty analysis
- Evaluation of EMDF performance relative to the requirements of DOE Manual (M) 435.1-1 (DOE 2011a).

NEED FOR THE EMDF AND BASIS FOR THE PA

A detailed description of the basis for the PA is provided in Sect. 1.1.

Mission Need and PA Development

DOE is responsible for sitewide waste management and environmental restoration activities on the ORR under its Office of Environmental Management Program at the national level and locally under the Oak Ridge Office of Environmental Management (OREM). OREM is responsible for minimizing potential hazards to human health and the environment associated with contamination from past DOE practices and addressing the waste management and disposal needs of the ORR. Under the requirements of the Federal Facility Agreement (FFA) for the ORR (DOE 1992a) established by DOE, the U.S. Environmental Protection Agency, and the Tennessee Department of Environment and Conservation, environmental restoration activities on the ORR are performed in accordance with the Comprehensive Environmental Response, Compensation, and Liability Act of 1980 (CERCLA).

Timely and effective ORR cleanup is essential to facilitate reindustrialization of the East Tennessee Technology Park, and to ensure worker safety and the success of DOE missions at the Y-12 National Security Complex (Y-12) and Oak Ridge National Laboratory (ORNL). The Environmental Management Waste Management Facility (EMWMF), constructed in Bear Creek Valley (BCV) near Y-12 (Fig. ES.1), is accepting CERCLA cleanup wastes. The authorized disposal capacity of EMWMF is 2.3 million cy (DOE 1999a, DOE 2010a). The scope of the OREM cleanup effort has expanded since EMWMF began operations in 2002. Approximately 1.6 million cy of additional CERCLA waste is expected to be generated and require disposal after EMWMF has reached maximum capacity in the late-2020s.

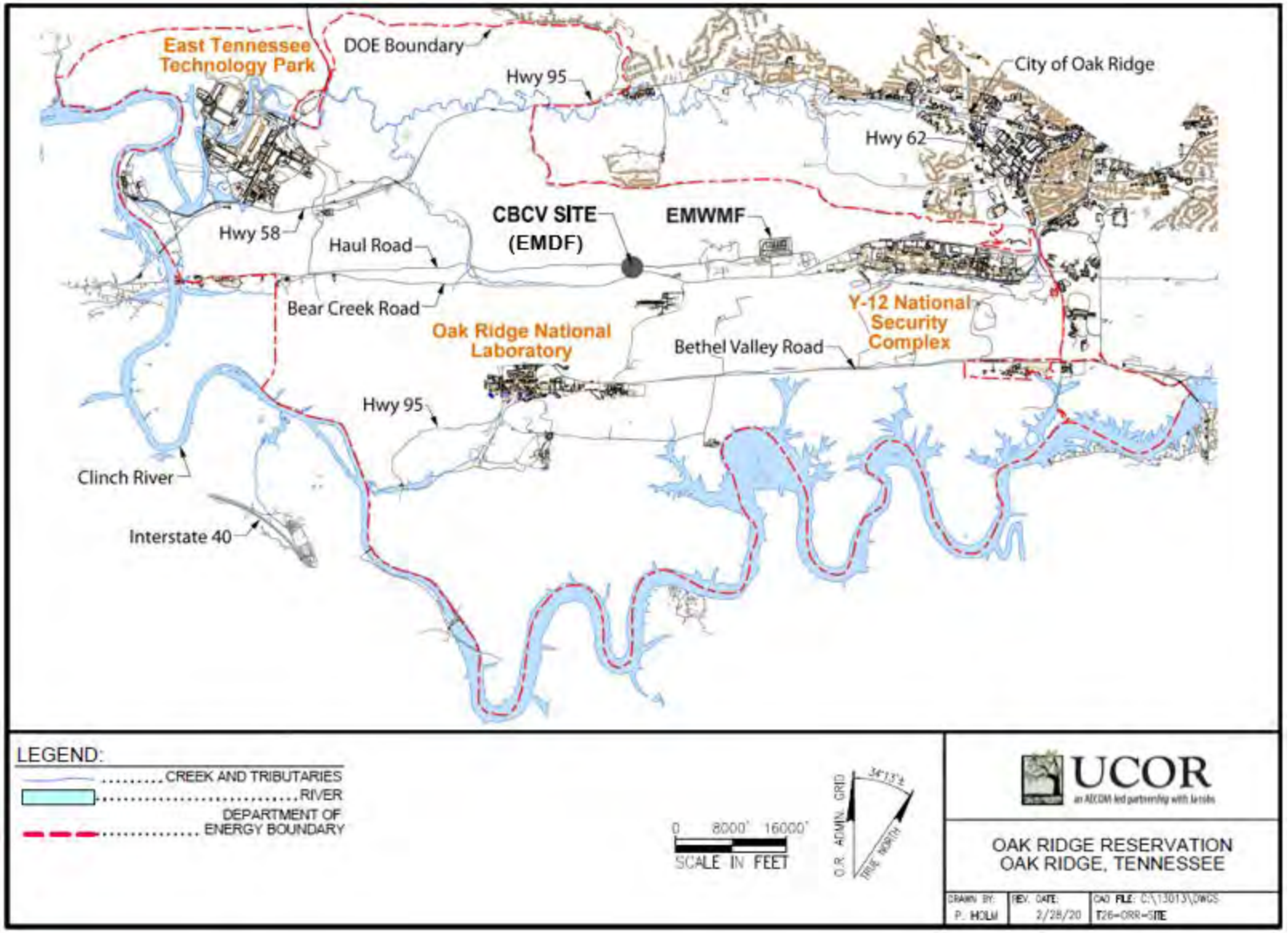

Fig. ES.1. ORR map with locations of DOE facilities, including EMWMF and EMDF sites

A new facility is required to ensure sufficient future LLW disposal capacity for CERCLA environmental cleanup activities on the ORR. The FFA parties issued a Proposed Plan (DOE 2018a) for the disposal of future ORR CERCLA waste for public comment in 2018. Since the Proposed Plan was issued, the design of the EMDF has been advanced to a preliminary design (60 percent) stage and is the basis for technical analyses in this PA. The total airspace capacity of the EMDF preliminary design is 2.2 million cy.

This EMDF PA has been developed to support DOE approval of a Disposal Authorization Statement (DAS) for construction of EMDF. Development of the EMDF PA and facility design activities are being conducted in parallel with activities required for approval of EMDF for onsite LLW disposal under the FFA. Documentation to support a final Disposal Authorization Statement for operations of the landfill will occur in parallel with the final design of the facility. A Composite Analysis (CA) (UCOR, an Amentum-led partnership with Jacobs, 2020a) has been prepared to evaluate the cumulative impacts of potential releases from historical waste disposal sites, the existing EMWMF, and the future EMDF in BCV.

The EMDF PA includes site-specific model simulations for release of radionuclides from the facility and dose analyses for post-closure exposure to releases, as well as analysis of inadvertent human intrusion (IHI) scenarios. The primary purpose of the EMDF PA is to provide a reasonable expectation that DOE M 435.1-1 performance objectives will be met.

Performance Objectives

EMDF performance objectives for the PA analysis are summarized in Table ES.1. Additional detail is provided in Sect. 1.5.1. The performance objectives are taken directly from DOE M 435.1-1 and do not reflect any site-specific regulatory requirements other than the application of drinking water maximum contaminant levels for water resources protection objectives.

Table ES.1. Exposure scenarios, performance objectives and measures, and points of assessment for the EMDF PA

Exposure scenario	Performance objective or measure	Point of assessment
All pathways	25 mrem/year	Groundwater: 100 m from waste margin at the point of maximum concentration (plume centerline) Surface water: Bear Creek downstream of NT-11
Air pathway[a]	10 mrem/year[b]	100 m from waste margin
Radon flux	20 pCi/m^2/sec	EMDF cover surface
Water resources (groundwater) • Ra-226 + Ra-228 • Gross alpha activity[c] • Beta/photon activity • H-3 • Sr-90 • Uranium (total)	 5 pCi/L 15 pCi/L 4 mrem/year 20,000 pCi/L 8 pCi/L 30 µg/L	Groundwater at 100 m
Water resources (surface water)	DOE *Derived Concentration Technical Standard*[d]	Bear Creek at NT-11 tributary junction

Table ES.1. Exposure scenarios, performance objectives and measures, and points of assessment for the EMDF PA (cont.)

Exposure scenario	Performance objective or measure	Point of assessment
Inadvertent human intrusion		
• Chronic exposure	100 mrem/year	At EMDF
• Acute exposure	500 mrem	At EMDF

[a]Air pathway is screened from the EMDF PA.
[b]Excluding radon in air.
[c]Including Ra-226, but excluding radon and uranium.
[d]DOE 2011b.

DOE = U.S. Department of Energy
EMDF = Environmental Management Disposal Facility
NT = North Tributary
PA = Performance Assessment

Point of Assessment, Institutional Control, and Timing Assumptions

A point of assessment (POA) is provided for each exposure scenario listed in Table ES.1. For the EMDF PA, the POAs are identical to DOE M 435.1-1 requirements and consistent with the Disposal Authorization Statement and Tank Closure Documentation standard (DOE 2017a). The assumed POAs do not vary with the post-closure time period, even though expected future land use and institutional controls would preclude public exposure at the 100-m buffer zone boundary for as long as waste remains above unrestricted use criteria in the area (as required under CERCLA). Institutional controls limiting site access are assumed to be effective for 100 years following closure. For analysis of IHI, intrusion is assumed to occur no earlier than 100 years post-closure as a result of a temporary loss of institutional control of the Central Bear Creek Valley (CBCV) site. These assumptions are pessimistic given that DOE is required to maintain control over land containing radionuclide sources until the land can be safely released pursuant to DOE Order (O) 458.1, *Radiation Protection of the Public and the Environment* (DOE 2013a), and CERCLA. Additional consideration of land use and institutional controls is provided in Sect. 1.6.

EMDF performance with respect to the performance objectives or performance measures is based on deterministic model results for specific pathways and environmental media. Compliance with performance objectives and measures is based on PA results for the compliance period from EMDF closure to 1000 years post-closure, with the exception of the IHI analysis for which compliance is assessed beginning at the assumed end of institutional control (100 years). Quantitative dose estimates are presented for a period of 10,000 years post-closure to provide perspective on the potential impacts beyond the compliance period. For long-lived, relatively immobile radionuclides that are significant components of the estimated EMDF inventory (e.g., radionuclides of uranium), PA model saturated zone concentration results beyond 10,000 years also are provided. These model predictions for the period beyond 10,000 years are highly uncertain and are presented only to indicate very long-term trends, rather than for comparison to regulatory standards.

AS LOW AS REASONABLY ACHIEVALBE ANALYSIS

The As Low As Reasonably Achievable (ALARA) process (DOE 2013a) is used to optimize EMDF performance and maintain doses to members of the public (both individual and collective) and releases to the environment ALARA. DOE M 435.1-1 includes a requirement for an ALARA analysis as part of the PA. The ALARA handbook (DOE 2014) describes a graded approach to implementing the ALARA process, including the use of reference doses for determining the level of analysis required for a given project. The reference dose for a maximally exposed individual and the reference collective dose below which only qualitative ALARA analysis is sufficient are 1 mrem/year and 10 person-rem/year, respectively.

For a LLW disposal project, the timeframe of consideration for an ALARA analysis of any level should be no greater than 1000 years (DOE 2014, pages 5–8), so the peak total dose within the compliance period and the estimated EMDF dose at 1000 years are compared to the reference values.

The EMDF PA modeling predicts a base case all-pathways maximum individual dose within the 1000-year compliance period of 1.03 mrem/year (Sect. 4.5.1). The results of the probabilistic uncertainty analysis (Sect. 5.4 and Appendix G, Sect. G.6.3.3) suggest a median peak individual dose of 1.0 mrem/year and a mean all pathways dose of 1.0 mrem/year at 1000 years. These results for individual exposure indicate that a semi-quantitative ALARA analysis could be considered; however, the ALARA guidance also states that "it is the collective dose that is utilized in the ALARA analysis to select a radiation protection alternative". Given the likelihood that BCV and the CBCV site will remain under DOE control indefinitely, there are a limited range of collective exposure scenarios that are credible, and the collective dose from EMDF release is expected to remain far below the reference collective dose of 10 person-rem/year (refer to Sect. 1.5.4 for additional detail). Based on the 10 person-rem/year reference value for collective dose, these model-based quantitative estimates indicate that a qualitative ALARA analysis for EMDF design and operations is sufficient.

The EMDF Remedial Investigation/Feasibility Study (RI/FS) (DOE 2017b) includes an analysis of alternatives for disposition of LLW from CERCLA actions on the ORR. The RI/FS includes identification and screening of disposal technologies and process options (DOE 2017b, Sect. 5) and considers broader social, economic, and public policy aspects in the analysis of remedial alternatives (DOE 2017b, Sect. 7). The disposal technology screening and conceptual facility design for the CBCV site (DOE 2017b, Sect. 6) served as the foundation for preliminary engineering design of the Resource Conservation and Recovery Act of 1976-type disposal facility at the CBCV site.

The EMDF Proposed Plan (DOE 2018a) describes the remedial action objectives for CERCLA waste disposal and presents onsite disposal at the CBCV site as the preferred (optimal) alternative based on the range of considerations required under CERCLA and the FFA. CERCLA alternative evaluation threshold criteria for remedial actions include overall protection of human health and the environment and compliance with applicable or relevant and appropriate requirements (ARARs). Balancing criteria include long-term effectiveness and permanence; reduction of toxicity, mobility, or volume through treatment; short-term effectiveness; implementability; and cost. Considerations of state and community acceptance are incorporated following public review of the Proposed Plan. Thus, the FFA remedy selection process has addressed key considerations for an ALARA analysis and the disposal options considered and conclusions presented in the EMDF RI/FS and Proposed Plan are considered to meet the intent of the DOE ALARA requirements for the EMDF PA.

EMDF DISPOSAL SYSTEM

The proposed site for EMDF in BCV is southwest of the city of Oak Ridge, Tennessee, and Y-12 (Fig. ES.1). The LLW disposal concept and preliminary design are similar to EMWMF (i.e., an engineered multicell, near-surface disposal unit for solid LLW derived from CERCLA response actions on ORR). The EMDF disposal system encompasses the natural features of the CBCV site, design features of the engineered disposal unit, waste characteristics, and the operating limits (e.g., waste acceptance criteria [WAC]) and other waste and safety management practices that ensure worker protection and post-closure facility performance.

Site Characteristics

The ORR lies in the western portion of the Valley and Ridge physiographic province, which is characterized by long, parallel ridges and valleys that follow a northeast-to-southwest trend. EMDF will be located on DOE property approximately 3 miles southwest of Y-12 (Fig. ES.1). BCV lies between Pine Ridge to the northwest and Chestnut Ridge to the southeast. The upper portion of the Bear Creek watershed between Y-12 and the EMDF site contains several closed disposal facilities, contaminant source areas, and groundwater contaminant plumes, in addition to the currently operating EMWMF.

The EMDF PA analysis incorporates an extensive body of environmental information drawn from over two decades of RIs and monitoring in BCV. CBCV site characterization efforts have been completed to support FFA approval of the proposed site and to support engineering design (DOE 2018b, DOE 2019). Proposed activities, new regulatory requirements, or other new information that could challenge key assumptions for the EMDF performance analysis (Sect. 1.7) will be evaluated in accordance with the EMDF change control process to assess the potential for such changes to require a Special Analysis or revisions to the PA.

An extensive review of the ORR, BCV, and CBCV site characteristics, including demographics, climate, geology, ecology and natural resources, hydrology and hydrogeology, and subsurface geochemistry is provided in Sect. 2.1. The geologic and hydrogeologic setting are briefly summarized in the following paragraphs.

The Valley and Ridge physiographic province developed on thick, folded and thrust-faulted beds of sedimentary rock (Figs. ES.2 and ES.3). The interbedded clastic and carbonate sedimentary rocks are variably fractured and weathered, resulting in significant vertical and horizontal subsurface heterogeneity. The sequence of geologic formations underlying BCV from Pine Ridge southward to Bear Creek includes the Rome Formation of lower Cambrian age and formations of the Middle Cambrian Conasauga Group (Fig. ES.3). The EMDF footprint is underlain by the moderately to steeply dipping beds of the Maryville Formation on the northern end and by the Nolichucky Formation on the southern end of the site (Sect. 2.1.3).

The hydrogeologic system in BCV reflects the geologic complexity of the location and the abundant precipitation associated with a humid subtropical climate. The depth to the water table (unsaturated zone thickness) varies from greater than 30 ft below the crest of Pine Ridge and other upland areas to near zero in seasonal wetland belts along the margins of some Bear Creek tributaries. Shallow groundwater also occurs at springs in narrow headwater ravines of Pine Ridge and across broader seepage areas along tributary valleys. In most of the lower elevation areas, the water table is at depths of less than 20 ft below the surface. Groundwater flow in the saturated zone is strongly influenced by the orientation of bedding surfaces and the distribution of fracture systems in the rock units. Shallow groundwater within the saturated zone converges and discharges into stream channels along the tributary valley floors, supporting dry-weather base flow, primarily during the wetter portions of the year. Deeper groundwater that does not discharge to the tributaries moves southward from Pine Ridge toward Bear Creek along pathways that reflect the bedding geometry and fracture characteristics of the sedimentary strata. Additional detail on BCV hydrogeology is provided in Sect. 2.1.5.

Selection of the CBCV site for construction of EMDF is based on the objective of hydrologically isolating the waste from natural drainage systems. Natural topographic and hydrologic boundaries and the properties of geologic materials that influence groundwater flow and subsurface geochemistry are fundamentally important to the isolation of EMDF waste from potential receptors. Natural surface and subsurface boundaries limit the potential for short and long-term contaminant migration via surface water and groundwater pathways to the nearest populations in the city of Oak Ridge located north of the EMDF site.

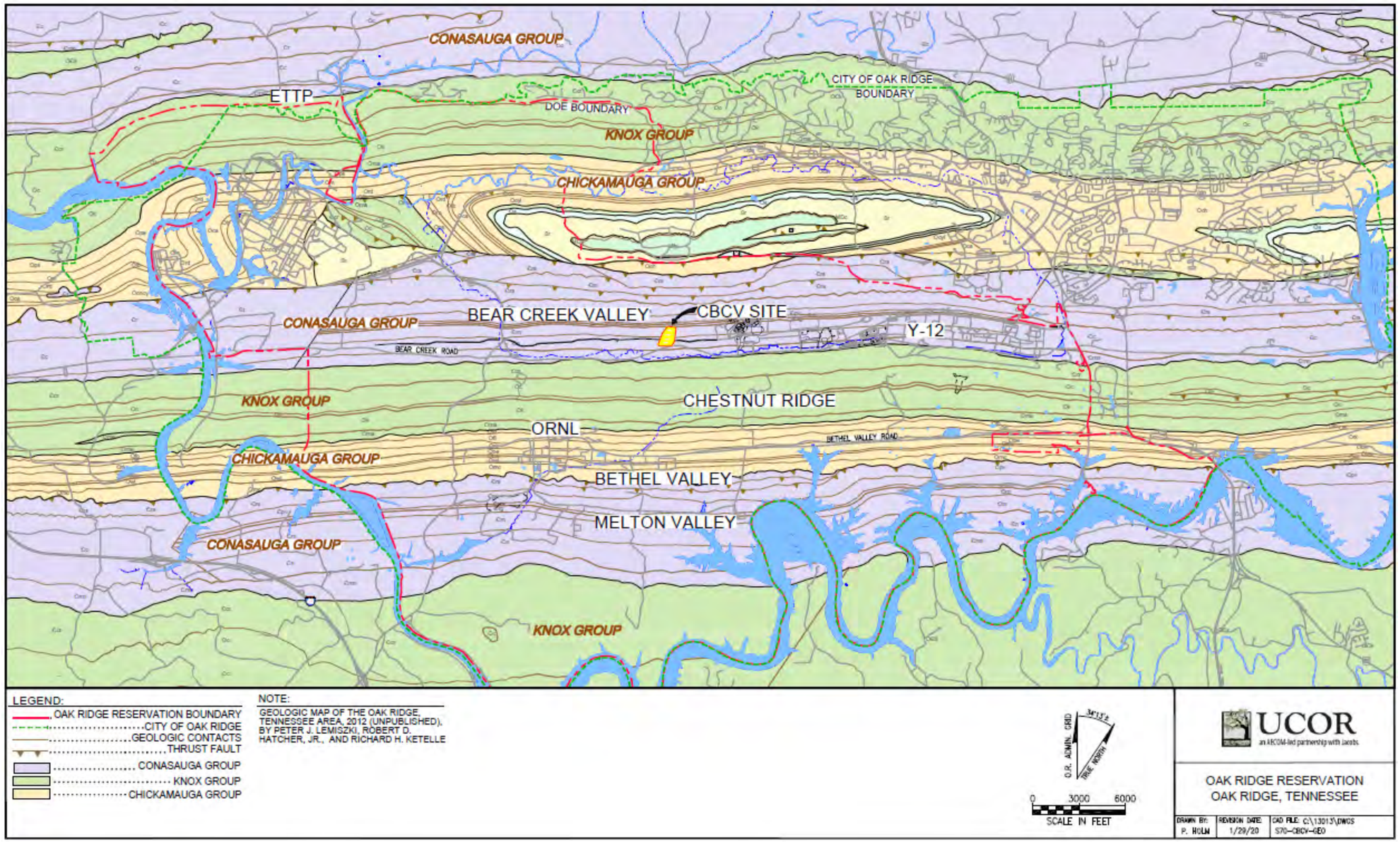

Fig. ES.2. Geologic map of the ORR

This page intentionally left blank.

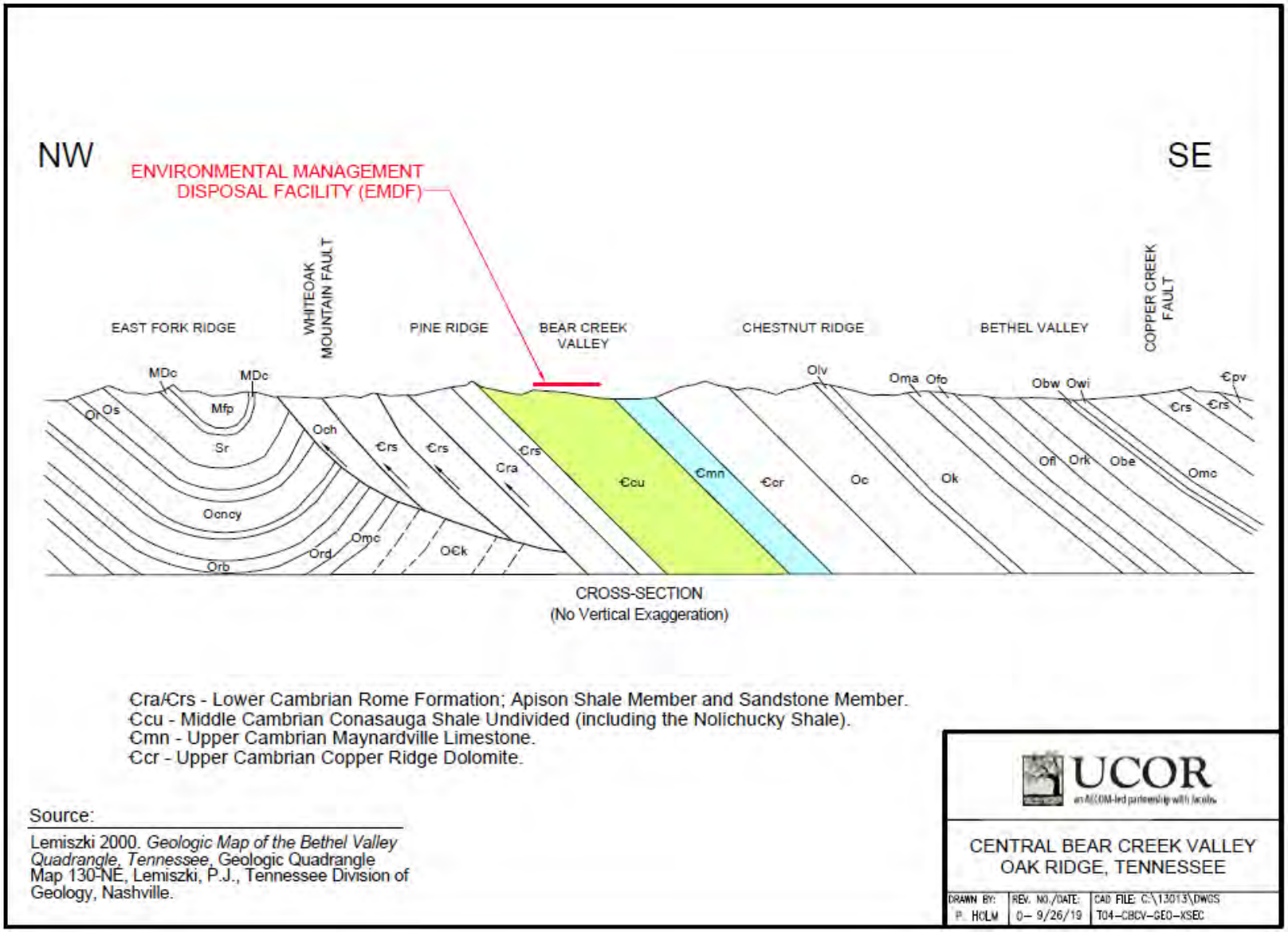

Fig. ES.3. Northwest-southeast geologic cross-section across the ORR

Under a long-term performance scenario, contaminant retardation in the vadose zone beneath EMDF and within the saturated matrix of the fractured rock at the CBCV site serve disposal system safety functions by delaying and attenuating impacts of radionuclide release at potential groundwater and surface water exposure points.

EMDF Design Features and Safety Functions

In accordance with CERCLA, the EMDF preliminary design will satisfy ARARs for hazardous and toxic waste disposal units (Sect. 1.5.5). The engineered disposal unit consists of a multilayer liner, leachate collection and treatment systems, lined embankments for lateral containment and stability, and a multilayer final cover (cap) to completely encapsulate the waste in the post-closure period. A CBCV site map showing key EMDF disposal system features and safety functions is provided as Fig. ES.4. A typical EMDF cross-section, based on the preliminary design (UCOR 2020b), is shown on Fig. ES.5 and a schematic profile of EMDF disposal system components and associated safety functions is shown on Fig. ES.6.

The engineered barriers of the cover and liner systems are designed to impede the percolation of water into the waste and to retard the (post-closure) release of radionuclides through the bottom liner and into the surrounding environmental media. Perimeter berms and the cover system also serve to deter biointrusion and/or IHI that could lead to direct exposure to the waste. Engineered surface and subsurface drainage systems outside of the liner footprint serve to maintain groundwater drainage and to limit increases in water table elevation below the liner in the event of cover and/or liner system failure. The facility is designed to maintain vertical separation of the waste from groundwater in the saturated zone beneath the disposal facility and includes a 10-ft-thick layer of geologic buffer material between the waste and the water table (Fig. ES.6). Detailed descriptions of the EMDF design features and safety functions are provided in Sects. 1.3, 2.2, and Appendix C. The natural characteristics of the EMDF site, as well as the fact that DOE is required to maintain control of the site as long as there is a potential risk from the waste, also represent important safety functions that are factored into site selection.

The EMDF will begin accepting waste after the first phase of construction is completed, projected for the late-2020s. The current scope of ORR cleanup work is projected to be completed in the 2050s timeframe; therefore, the approximate duration of EMDF operations is 25 years. EMDF operations will include waste receipt and placement, water management, and environmental monitoring of facility performance. EMDF waste certification practices are expected to be carried over from current EMWMF WAC attainment and tracking systems (DOE 2001a). EMDF waste receipt operations will include unloading and placing waste into the landfill and spreading and compacting bulk waste using heavy equipment while placing fill materials, as required, to fill voids. As portions of the landfill are filled to design capacity, an interim cover will be put in place to limit infiltration and leachate generation from that portion of the disposal facility. The EMDF interim cover design is assumed to be similar to that implemented for the EMWMF, which consists of a geotextile separator layer and an approximately 1-ft-thick contouring soil layer on top of the waste, overlain by a temporary flexible geomembrane to minimize infiltration into the waste zone.

EMDF closure activities will involve construction of the final cover system and removal of any unneeded infrastructure. Post-closure activities will involve cap maintenance, continued leachate collection and management, and site environmental monitoring. Final closure plans will be detailed in approved documents required under DOE orders and manuals and by the FFA. Post-closure performance monitoring will include CERCLA 5-year reviews of remedial effectiveness.

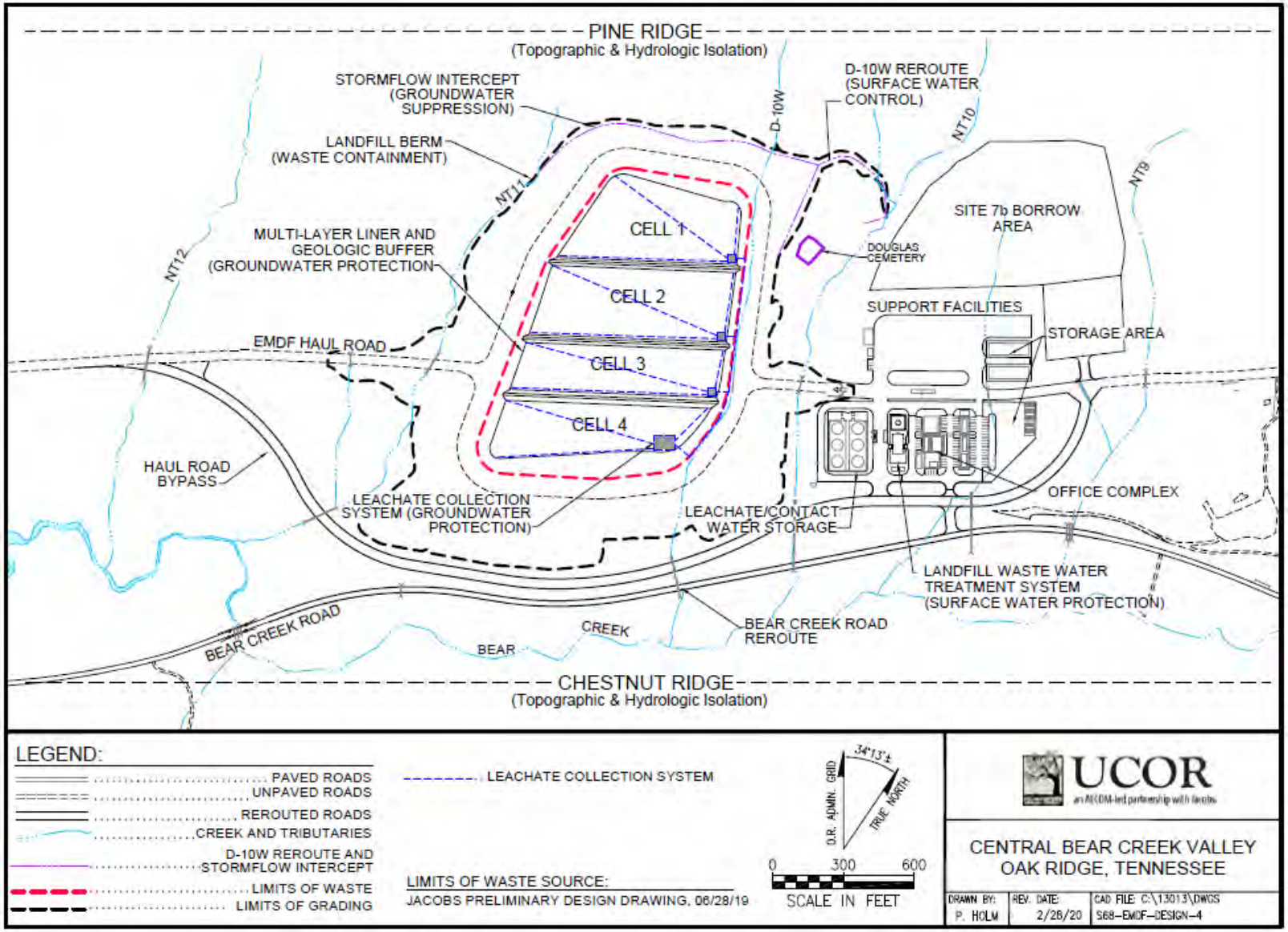

Fig. ES.4. EMDF site and design features and safety functions

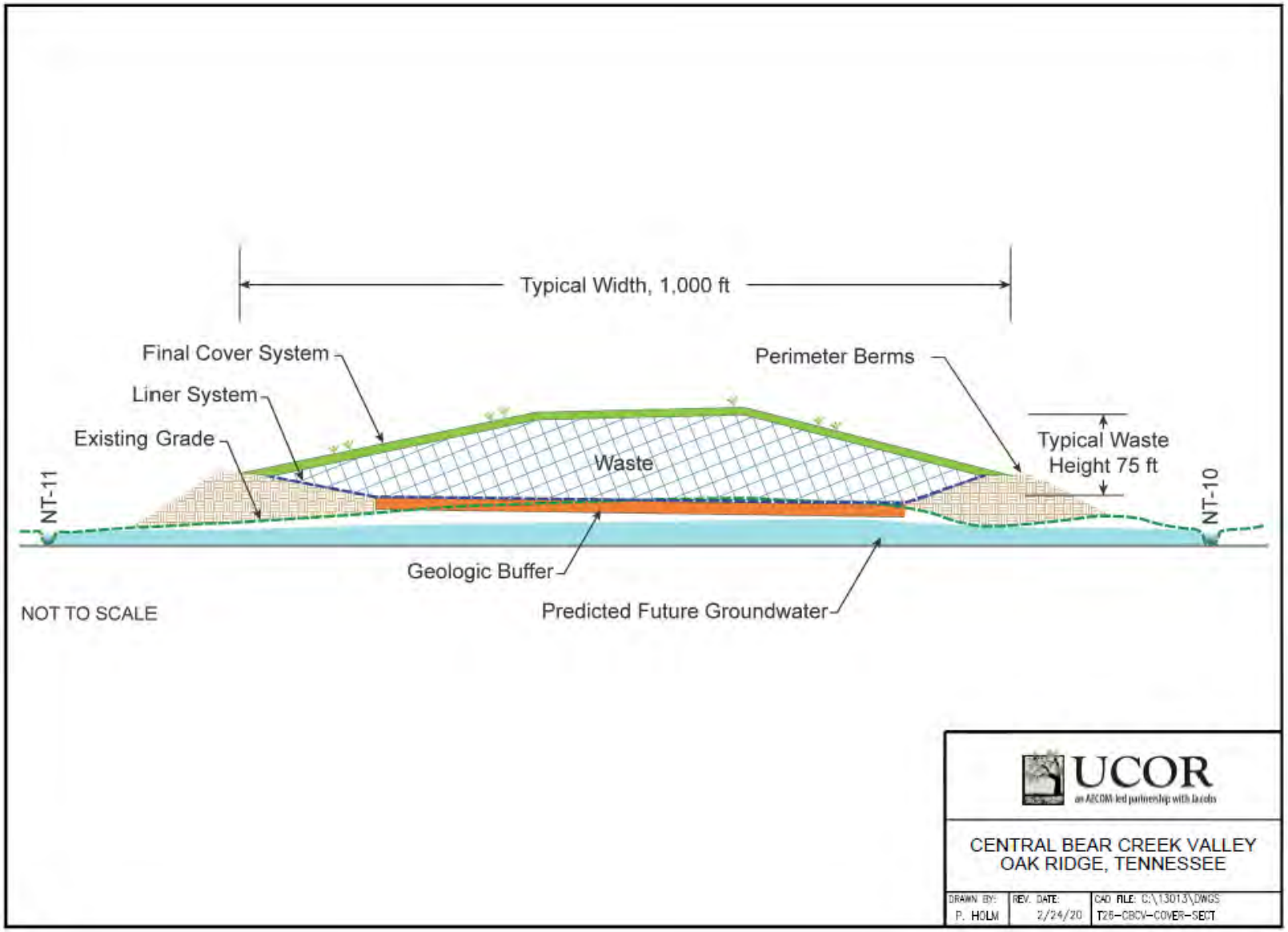

Fig. ES.5. Typical cross-section of EMDF

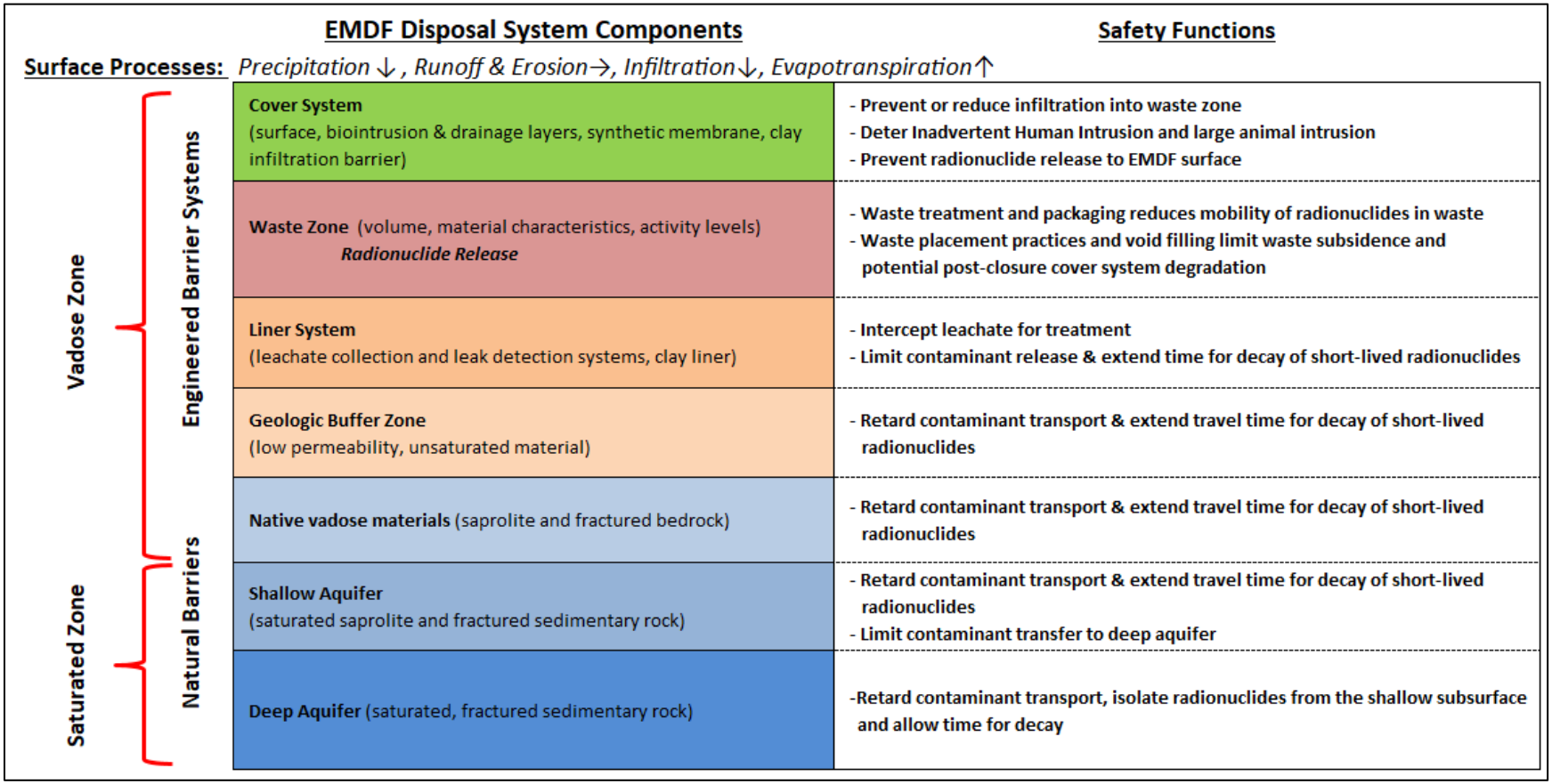

Fig. ES.6. EMDF disposal system schematic profile and safety functions

Waste Stream Characteristics and Estimated Radionuclide Inventory

LLW disposed at EMDF will originate primarily from facility deactivation and decommissioning (D&D) or environmental remediation projects at Y-12 and ORNL. The waste will include facility demolition debris (including structural steel and concrete), contaminated equipment and soil, and other soil-like wastes. EMDF will accept both containerized LLW and bulk (uncontainerized) waste for disposal. Waste quantities are based on the estimates provided in the OREM Waste Generation Forecast. Waste stream characteristics are estimated from a variety of information sources and are described in more detail in Sect. 2.3 and Appendix B. More detailed characterization of waste streams for disposal at EMDF will be the responsibility of the waste generator(s) once EMDF is operational.

Wastes derived from CERCLA cleanup at Y-12 and ORNL will contain a wide range of radionuclides. The primary radioactive contaminants in Y-12 waste streams are uranium isotopes, whereas ORNL waste streams will contain a greater variety of radionuclides, including relatively large quantities of some fission products (e.g., Cs-137 and Sr-90), lower quantities of other fission products (e.g., Tc-99 and I-129), and trace quantities of transuranic radionuclides (e.g., plutonium and americium). This difference is important for estimation of the EMDF radionuclide inventory because Y-12 waste accounts for approximately 70 percent of the forecast waste volume and ORNL waste accounts for the remaining 30 percent. Due to these differences in waste volume and radiological characteristics, Y-12 waste accounts for the majority of uranium activity in the estimated EMDF inventory, whereas ORNL waste accounts for the majority of the total radionuclide inventory.

The method for estimating radionuclide profiles for specific EMDF LLW streams is to apply the available data to capture the differences between ORNL and Y-12 wastes and between remedial action wastes (primarily soils) and facility D&D wastes (primarily debris). Average, decay-corrected radionuclide activity concentrations for each waste stream are estimated from a combination of data sources, including EMWMF waste characterization data for previously generated and disposed (historical) Y-12 and ORNL waste lots, data from detailed facility and environmental characterization studies, and data from the OREM SORTIE 2.0 facility inventory database, which includes radionuclide activity quantities derived from various types of facility safety analyses and other data sources.

Uncertainty in the EMDF estimated inventory includes uncertainty in the underlying characterization data, as well as uncertainty associated with the assumption that the radionuclides and activity concentrations in the selected data source are representative of all future EMDF waste. In general the approach to managing the uncertainty in the estimated EMDF radionuclide inventory is to bias the inventory estimates toward higher values. For example, the use of the SORTIE data should lead to overestimation of average waste activity concentrations because the facility inventories developed for safety analysis tend to be bounding (maximum likely) estimates.

For each EMDF waste stream identified, the estimated average radionuclide activity concentrations are applied to the projected total waste quantity (mass) to derive the total estimated inventory at EMDF closure. For use in model calculations, the estimated EMDF average as-generated waste activity concentrations are adjusted (Sect. 3.2.2.5) to account for the addition of clean fill during disposal operations (to fill voids and increase stability). In addition, operational period losses of highly mobile radionuclides (H-3, C-14, Tc-99, and I-129) are estimated and used to adjust (decrease) the assumed post-closure inventory for those nuclides. The assumptions and modeling applied to estimate these operational losses and reductions in mobility resulting from treatment of collected leachate are described in Sect. 3.2.2.5.

Radionuclide Screening

There are 70 radionuclides included in the screening-level inventory (Sect. 2.3.2 and Appendix B). For the EMDF PA, a two-step approach was used for screening out radionuclides that do not contribute significantly to the total dose. The first step involved screening based on radionuclide half-life. Any parent isotope in the EMDF inventory with a half-life of less than 5 years was screened out from further analysis because during the first 100 years of post-closure institutional control, the engineered barrier systems (cover and liner, including the leachate collection system) will prevent cover infiltration and leachate release. During this 100-year time period, over 20 half-lives will have elapsed, resulting in decay of short-lived radionuclides to very low concentrations.

Additional justification for using the 5-year half-life as a cutoff is related to the anticipated travel time from the waste to the underlying groundwater. Vadose zone Subsurface Transport Over Multiple Phases (STOMP) model simulations (Appendix E) indicate that for a highly mobile radionuclide such as C-14, the average travel time from waste to the water table is greater than 200 years (approximately 40 or more half-lives for the short-lived radionuclides screened in the first step). Screening of inventory based on half-life was not performed for any isotopes that are also progeny of other parent isotopes included in the inventory. In summary, for Phase 1 screening, a total of 61 radionuclides passed and a total of nine radionuclides were screened from further consideration. Seven radionuclides were screened out based on their half-life, and two radionuclides were screened out for other reasons.

The second screening step involved implementation of a computer model (RESidual RADioactivity [RESRAD]-OFFSITE, refer to Sect. 3.3.4 and Appendix G) used to screen individual radionuclides based on a peak dose criterion of 0.4 mrem/year, which is 10 percent of the 4 mrem/year national primary drinking water standard for beta-gamma emitters (40 *Code of Federal Regulations 141*). The 0.4 mrem/year screening criterion is applied to all radionuclides, including alpha emitters, for the all-pathways dose analysis (refer to Sect. 2.3.2). The screening model implemented for the EMDF site assumes exposure via groundwater ingestion only and incorporates pessimistically biased assumptions regarding inventory levels (screening level estimates), disposal conditions (no engineered barriers to limit water infiltration), and mobility of radionuclides (distribution coefficients decreased by a factor of 10 or 100 from base-case values [see Sect. 3.2.2.6; and Appendix G, Sects. G.4.3.6 and G.4.4.1]). Out of the 70 radionuclides in the waste inventory, a total of 42 were retained for analysis (Table ES.2). For analysis of IHI, only radionuclides with half-lives less than 5 years were screened from consideration.

Based on the EMDF estimated inventory, anticipated operational conditions, and design features of the EMDF cover system, post-closure release of radionuclides in the vapor-phase is expected to be negligible. The estimated inventory of potentially volatile radionuclides is limited to H-3, C-14, Kr-85, and I-129. Small quantities of Cl-36 could be present in future EMDF LLW, associated with irradiated graphite or metals from ORNL research reactor facilities; however, Cl-36 has not been a radionuclide of concern for LLW disposed at the EMWMF, and identification of Cl-36 in environmental samples from the ORR is extremely rare. Additional discussion of the limited potential for radionuclide release through the EMDF final cover, including results of a quantitative screening model, is provided in Sect. 3.2.2.2.

Table ES.2. Screening source concentrations and radionuclide screening results

Radionuclide	Half-life (years)	Screening source concentration (pCi/g)	Phase 1: Half-life > 5 years?	Phase 2: Peak Groundwater Dose > 0.4 mrem/year for 10,000-year simulation?	Retain for dose analysis?
Ac-227	2.18E+01	4.89E+04	Yes	Yes	Yes
Am-241	4.32E+02	2.30E+03	Yes	Yes	Yes
Am-243	7.38E+03	2.29E+01	Yes	Yes	Yes
Ba-133	1.07E+01	2.71E+01	Yes	No	Intruder
Be-10	1.50E+06	7.16E+05	Yes	Yes	Yes
C-14	5.73E+03	6.27E+05	Yes	Yes	Yes
Ca-41	1.00E+05	4.11E+06	Yes	Yes	Yes
Cd-113m	1.36E+01	1.11E+05	Yes	No	No[a]
Cf-249	3.51E+02	3.92E-04	Yes	No	Intruder
Cf-250	1.31E+01	1.70E-02	Yes	No	Intruder
Cf-251	8.98E+02	7.36E-05	Yes	No	Intruder
Cf-252	2.60E+00	1.25E+03	No	NS[b]	No
Cl-36[e]	3.01E+05	1.00E+00	Yes	Yes	No[a]
Cm-243	2.85E+01	4.37E+01	Yes	Yes	Yes
Cm-244	1.81E+01	5.26E+05	Yes	Yes	Yes
Cm-245	8.50E+03	9.80E+01	Yes	Yes	Yes
Cm-246	4.73E+03	1.97E+00	Yes	Yes	Yes
Cm-247	1.56E+07	2.35E+01	Yes	Yes	Yes
Cm-248	3.39E+05	2.29E+01	Yes	Yes	Yes
Co-60	5.27E+00	1.93E+06	Yes	No	Intruder
Cs-134	2.10E+00	1.39E+05	No	NS[b]	No
Cs-135	2.30E+06	2.46E+06	Yes	Yes	No[a]
Cs-137	3.00E+01	3.82E+08	Yes	No	Intruder
Eu-152	1.33E+01	5.84E+05	Yes	No	Intruder
Eu-154	8.80E+00	7.85E+05	Yes	No	Intruder
Eu-155	4.80E+00	9.98E+05	No	NS[b]	No
Fe-55	2.70E+00	4.71E+07	No	NS[b]	No
H-3	1.24E+01	4.84E+06	Yes	Yes	Yes
I-129	1.57E+07	4.86E+05	Yes	Yes	Yes
K-40	1.28E+09	5.65E+01	Yes	Yes	Yes
Kr-85	1.10E+01	1.16E+08	Yes	NS[c]	No
Mo-93	3.50E+03	4.99E+03	Yes	Yes	Yes
Mo-100	8.50E+18	2.55E-03	Yes	NS[c]	No
Na-22	2.60E+00	5.96E-01	No	NS[b]	No
Nb-93m	1.36E+01	3.00E+03	Yes	No	Yes[d]
Nb-94	2.03E+04	1.90E+05	Yes	Yes	Yes
Ni-59	7.50E+04	1.55E+06	Yes	Yes	Yes
Ni-63	9.60E+01	1.03E+07	Yes	No	Intruder
Np-237	2.14E+06	5.63E+01	Yes	Yes	Yes

Table ES.2. Screening source concentrations and radionuclide screening results (cont.)

Radionuclide	Half-Life (years)	Screening source concentration (pCi/g)	Phase 1: Half-life > 5 years?	Phase 2: Peak Groundwater Dose > 0.4 mrem/year for 10,000-year simulation?	Retain for Dose Analysis?
Pa-231	3.28E+04	3.17E+00	Yes	Yes	Yes
Pb-210	2.23E+01	4.48E+02	Yes	No	Yes[d]
Pd-107	6.50E+06	3.34E+06	Yes	Yes	No[a]
Pm-146	5.50E+00	1.24E-01	Yes	No	Intruder
Pm-147	2.60E+00	2.67E+06	No	NS[b]	No
Pu-238	8.77E+01	7.15E+03	Yes	Yes	Yes
Pu-239	2.41E+04	1.85E+05	Yes	Yes	Yes
Pu-240	6.54E+03	8.44E+03	Yes	Yes	Yes
Pu-241	1.44E+01	2.83E+05	Yes	Yes	Yes
Pu-242	3.76E+05	4.98E+01	Yes	Yes	Yes
Pu-244	8.26E+07	1.11E+01	Yes	Yes	Yes
Ra-226	1.60E+03	1.35E+01	Yes	Yes	Yes
Ra-228	5.75E+00	3.46E+00	Yes	No	Yes[d]
Re-187	4.12E+10	1.94E-03	Yes	No	Intruder
Sb-125	2.80E+00	1.37E+06	No	NS[b]	No
Se-79	6.50E+04	2.47E+06	Yes	Yes	No[a]
Sm-151	9.00E+01	5.75E+06	Yes	No	No[a]
Sn-121m	5.50E+01	6.41E+01	Yes	No	No[a]
Sn-126	1.00E+05	1.89E+06	Yes	Yes	No[a]
Sr-90	2.91E+01	3.93E+08	Yes	Yes	Yes
Tc-99	2.13E+05	1.35E+06	Yes	Yes	Yes
Th-228	1.90E+00	1.14E+05	No	No	Yes[d]
Th-229	7.34E+03	3.48E+03	Yes	No	Yes[d]
Th-230	7.70E+04	1.48E+02	Yes	Yes	Yes
Th-232	1.41E+10	2.67E+06	Yes	Yes	Yes
U-232	7.20E+01	8.43E+05	Yes	Yes	Yes
U-233	1.59E+05	5.49E+05	Yes	Yes	Yes
U-234	2.45E+05	1.67E+03	Yes	Yes	Yes
U-235	7.04E+08	2.57E+03	Yes	Yes	Yes
U-236	2.34E+07	4.87E+02	Yes	Yes	Yes
U-238	4.47E+09	2.07E+09	Yes	Yes	Yes
Zr-93	1.53E+06	5.56E+05	Yes	Yes	No[a]

[a]Radionuclide not simulated because insufficient inventory data were available
[b]Radionuclide not simulated due to screening in Phase 1
[c]Radionuclide not simulated due to other reasons
[d]Isotope has half-life less than 5 years or screening dose less than 0.4 mrem/year, but was retained for further analysis because it is progeny of another isotope in the inventory. Intruder identifies isotopes simulated for IHI models, but not retained for further analysis.
[e]Cl-36 is not included in the inventory but was simulated in the screening model provide information for future waste management decisions.

IHI = inadvertent human intrusion
NS = not simulated

KEY ASSUMPTIONS

Key technical assumptions for the EMDF performance analyses are listed below. Proposed activities, new regulatory requirements, or other new information that could challenge key assumptions for the EMDF performance analysis will be evaluated in accordance with the EMDF change control process to assess the potential for such changes to require a Special Analysis or revisions to the PA.

Key parameter assumptions for EMDF compliance include:

1) Iodine-129 partition coefficient (K_d) values for the engineered barriers and geologic materials below the EMDF liner are greater than 1 cm^3/g.
2) IF the I-129 K_d value is less than 1.5 cm^3/g, THEN the values for the input parameters that determine cover infiltration, vadose zone thickness, and saturated zone flux (Darcy velocity) satisfy one or more of the following conditions:
   a) Average annual cover infiltration is less than or equal to 0.88 in./year.
   b) The average thickness of the unsaturated zone below the waste is greater than or equal to 31 ft.
   c) The Darcy velocity characterizing long-term average conditions within the saturated zone along the flow path from the waste to the well is greater than or equal to 4.75 ft/year.
3) The estimated post-closure EMDF average I-129 activity concentration is less than 0.41 pCi/g.

Uncertainty in these three key model input parameter assumptions will be addressed with laboratory measurements of iodine K_d for CBCV site materials and by future refinements in the estimated I-129 inventory.

Conceptual models of the evolution of engineered barrier performance and radionuclide release are important for understanding the implications of selecting one conceptualization versus another, and for integrating model codes that apply different conceptual models or levels of detail. Key assumptions related to conceptual models adopted for the PA analysis include:

1) **Failure of engineered barriers.** Post-closure degradation of the EMDF cover and liner systems occurs gradually and results in increasing cover infiltration and leachate release.
2) **Cover system performance.** The EMDF final cover will prevent significant release of radionuclides to the cover surface. Infiltration barriers in the cover fail completely within 1000 years and cover infiltration increases gradually to a maximum average annual long-term value of 0.88 in./year at 1000 years post-closure.
3) **Liner system performance.** The liner system will release leachate at a rate sufficient to prevent waste saturation and overtopping of the liner (bathtub conditions).
4) **Radionuclide release.** EMDF waste is conceptualized as homogeneous, soil-like material in which the estimated radionuclide inventory is uniformly distributed. Radionuclide release from the waste is modeled as equilibrium desorption from a soil-like material.
5) **Uniform release to groundwater.** Radionuclide release from the waste and liner system to the vadose and saturated zones is spatially uniform. Non-uniform release does not result in earlier or larger peak concentrations at the POA locations.

Model sensitivity and uncertainty analyses in the PA (Sect. 5) are completed to assess and manage uncertainty in key parameter and conceptual model assumptions. Several important pessimistic assumptions regarding the exposure scenario, radionuclide inventories, long-term cover performance, and waste

characteristics are incorporated in the PA to account for uncertainty in future human behavior, waste volumes, and waste management practices (e.g., waste treatment and containerization). These pessimistic assumptions bias the analysis toward larger estimated all-pathways dose (refer to Sect. 1.7.3).

CONCEPTUAL MODELS, MODEL CODES, AND QUALITY ASSURANCE

The EMDF site characteristics and facility features described in the preceding paragraphs are incorporated into the conceptual models and performance analyses of the PA. It is assumed in the PA modeling that the effectiveness of engineered barriers decreases over time, leading to the release of radionuclides through the liner system. A detailed description of the natural processes that degrade design features and limit safety functions over time and a generalized conceptual model of EMDF performance evolution is provided in Sect. 3.2.1 and Appendix C.

Conceptualization of the EMDF disposal system for performance analysis and modeling is organized around four related components as shown in Table ES.3.

Table ES.3. EMDF disposal system components, conceptual model elements, and model codes

Disposal system component	Conceptual model elements	Model codes
Water Balance and Performance of Engineered Barriers (Sect. 3.2.1)	• Facility water balance • Performance of engineered systems • Degradation of synthetic and earthen barriers • Assumed evolution of EMDF cover infiltration and leachate release	HELP RESRAD-OFFSITE
Radionuclide Release and Vadose Zone Transport (Sect. 3.2.2)	• EMDF radionuclide inventory • Disposal practices and waste forms • Facility design geometry • EMDF cover performance evolution • Vapor phase release and radon flux • Aqueous phase release from waste • Transport through waste and liner system, including chemical retardation • Vadose zone transport below liner	STOMP RESRAD-OFFSITE
Saturated Zone Flow and Radionuclide Transport (Sect. 3.2.3)	• Vadose zone flux to saturated zone • CBCV site geology and topography • CBCV site geology and topography • CBCV hydrogeology • CBCV surface water features • CBCV saturated zone flow and transport, including chemical retardation	MODFLOW MT3D RESRAD-OFFSITE
Exposure Pathways and Scenarios (Sect. 3.2.4) (analysis of the inadvertent human intrusion scenario is presented in Sect. 6)	• Resident farmer exposure scenario • Groundwater POA (well location) • Surface water POA • Exposure pathways, abiotic and biotic • Dose analysis	RESRAD-OFFSITE

CBCV = Central Bear Creek Valley
EMDF = Environmental Management Disposal Facility
HELP = Hydrologic Evaluation of Landfill Performance
POA = point of assessment
RESRAD = RESidual RADioactivity
STOMP = Subsurface Transport Over Multiple Phases

Conceptual models of post-closure and long-term performance of engineered barriers are incorporated in the assumed evolution of the EMDF water balance as controlled by the safety functions of engineered cover and liner system features. These conceptual models include pessimistic biases intended to lead to increased infiltration versus what is expected as a means to address uncertainty in cover performance and are described in Sect. 3.2.1 and in the cover system analysis presented in Appendix C.

The base case EMDF performance scenario assumes full design performance (zero infiltration through the cover and into the waste) for a period of 200 years post-closure. A period of increasing cover infiltration and leachate release due to degradation of engineered barriers is assumed to occur between 200 and 1000 years post-closure, followed by a long-term performance period of indefinite duration. A generalized conceptual model of changes in cover infiltration and leachate release assumed to result from natural processes and events that can impact cover and liner performance over time is presented in Sect. 3.2.1. The purpose of the model is to integrate and generalize the impact of multiple events and processes on safety functions and EMDF performance over time, incorporating uncertainty in timing and degree of degradation and the occurrence of severe events. Implementation of this general model of increasing cover infiltration over time for each of the PA models is described in Sect. 3.3. Uncertainty in the timing and degree of performance degradation (relative to the base case performance evolution scenario) is addressed in the probabilistic RESRAD-OFFSITE analysis presented in Sect. 5.4.

Conceptual models of post-closure radionuclide release from the EMDF disposal system include analysis and screening of radionuclide release through the cover to the atmosphere or biosphere, diffusive transport and release of radon through the cover (refer to Appendix H), and radionuclide release and transport in the aqueous phase (Sect. 3.2.2). Conceptual models for aqueous release incorporate the assumed changes in cover infiltration over time (Sect. 3.2.1) and include waste zone radionuclide release and unsaturated vertical flow and radionuclide transport through the waste, liner system, and underlying vadose zone. These conceptual models are based on the estimated EMDF radionuclide inventory (Appendix B), assumed waste disposal practices and waste forms (Sect. 3.2.2.5), sorptive properties of EMDF materials (Sect. 3.2.2.6), the vertical sequence of vadose zone materials (Sect. 3.2.2.4), and the analysis of cover performance presented in Sect. 3.2.1 and Appendix C.

Conceptual models of saturated zone flow and radionuclide transport are based on the hydrogeologic conceptual model for BCV (Sect. 2.1.5.1), including the lithology and stratigraphy of the EMDF site, major topographic and structural controls on groundwater movement, surface water features, and chemical retardation properties of the saprolite and bedrock. Conceptualization of the saturated zone for purposes of EMDF performance analysis is described in Sect. 3.2.3.

Conceptual models of post-closure public exposure to radionuclides include the general resident farmer scenario considered for the analysis, as well as detailed assumptions for abiotic (e.g., water ingestion, inhalation) and biotic (e.g., ingestion of contaminated fish and produce) exposure pathways. The exposure pathways assumed for the all-pathways dose analysis are shown on Fig. ES.7. The exposure scenario and pathway assumptions which form the basis for the dose analysis are described in Sect. 3.2.4.

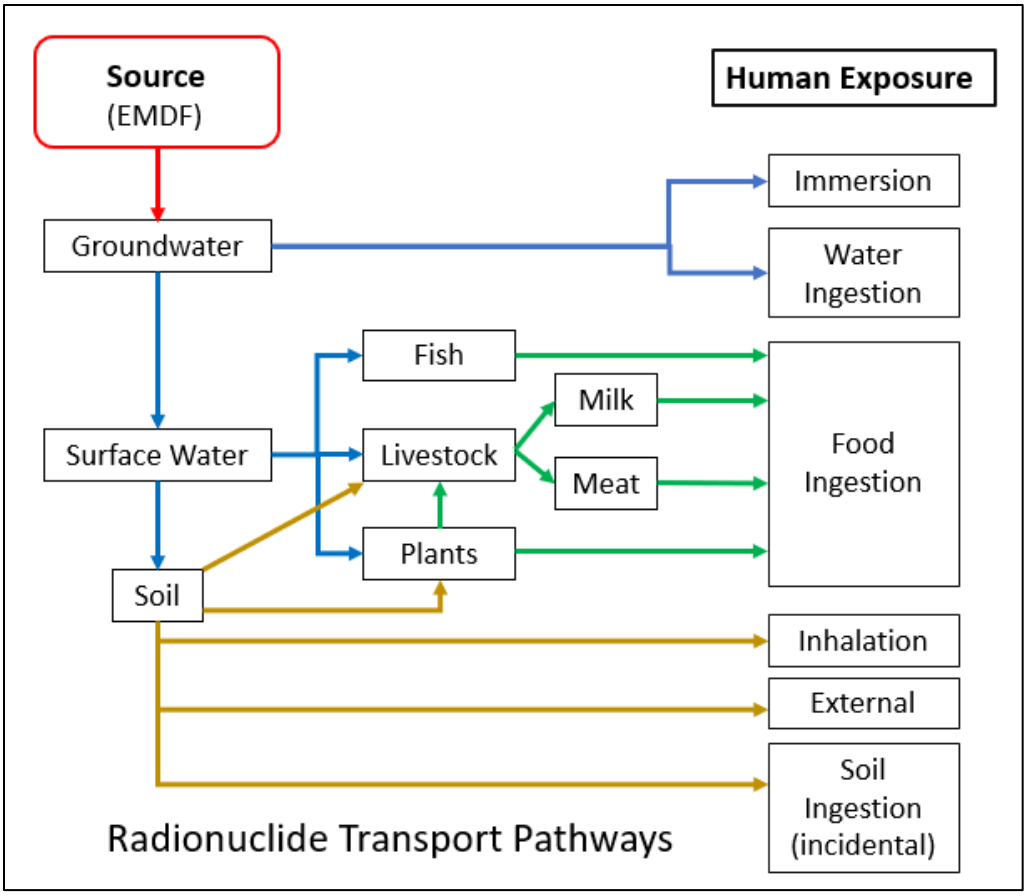

Fig. ES.7. Flow chart of environmental transport and exposure pathways for the all-pathways analysis

PA Model Implementation and Integration

Implementation of EMDF system conceptual models with computer modeling codes is structured around the four conceptual components (Table ES.3 and Fig. ES.8) and includes detailed process model codes for the components that encompass engineered facility performance and abiotic transport elements. Also included is a total system model code that encompasses all four conceptual components, including the exposure scenario and biotic pathways for radionuclide transfer. The PA model codes include: the Hydrologic Evaluation of Landfill Performance model for simulating the EMDF water balance; the STOMP model for simulating radionuclide release and vadose zone transport; MODFLOW, MODPATH, and MT3D model codes for saturated zone groundwater flow and radionuclide transport simulation; and RESRAD-OFFSITE for holistic simulation of radionuclide release and transport, as well as exposure scenarios and dose analysis. Table ES.4 identifies the PA appendices that fully describe the implementation of each of the models.

The more detailed process models (STOMP, MT3D) were used for modeling the complexities of primarily abiotic environmental transport pathways to predict concentrations of key radionuclides at the POA, while the total system model (RESRAD-OFFSITE) uses simplified representations of transport pathways along with biotic transformations and scenario-specific exposure factors to identify which radionuclides are likely key dose contributors and to quantify total dose for comparison to performance objectives.

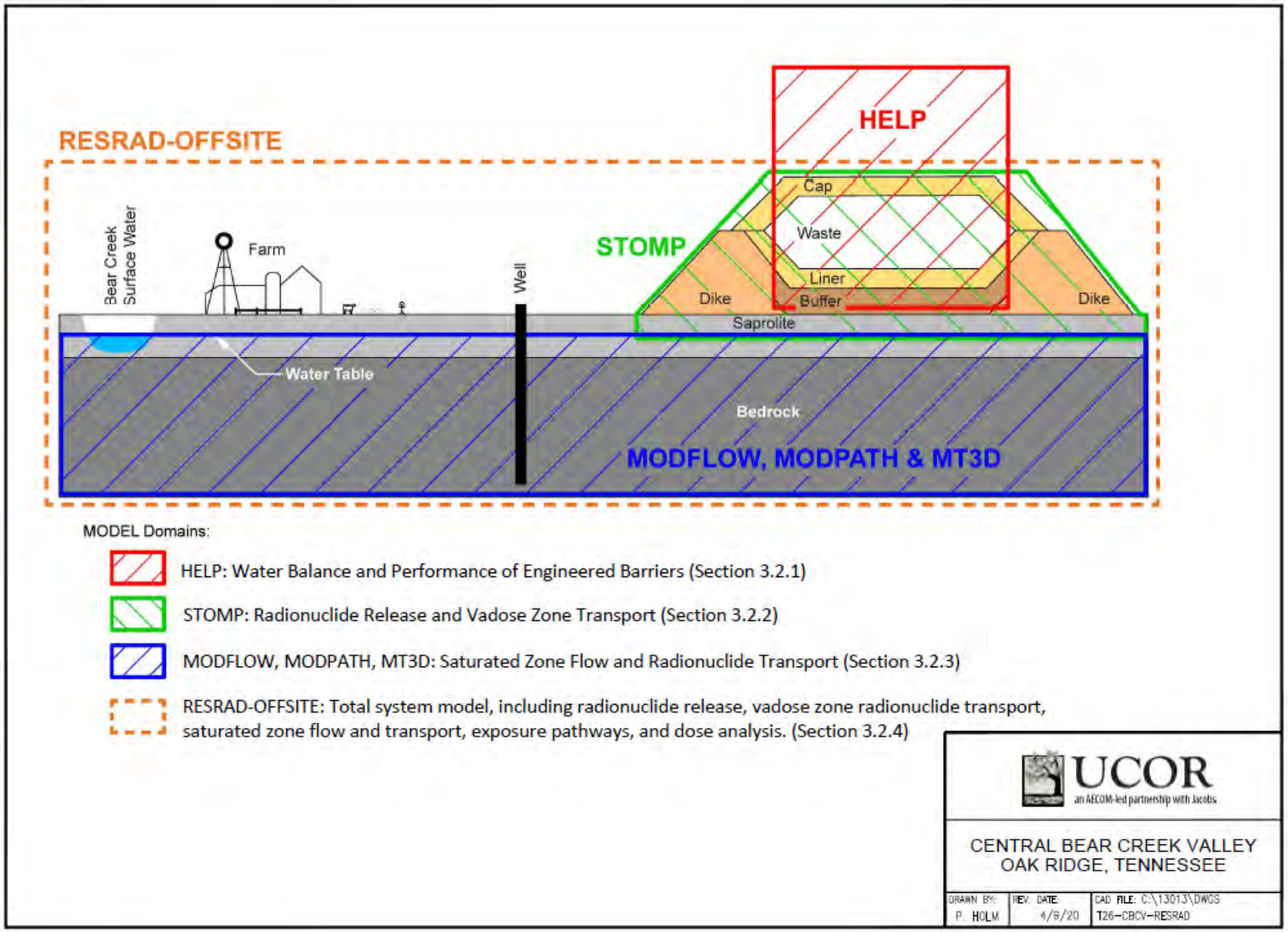

Fig. ES.8. Schematic illustration of EMDF disposal system conceptual models and modeling tools used for implementation

Implementation of the more detailed component-level EDMF PA models and the total system model proceeded concurrently, with iterative development and refinement of model assumptions, cover performance and source release approaches, and parameter value selections for each of the model tools. Some model outputs serve as inputs for other modeling tools. The primary model output-to-input linkages and the key comparisons of model outputs (presented in Sect. 3.3.5) are shown on Fig. ES.9 and Table ES.4. Inputs common to all model codes include radionuclide inventories, EMDF design specifications, and CBCV site characteristics. Selection, implementation, and integration of these model codes for EMDF performance analysis is explained in Sect. 3.3.

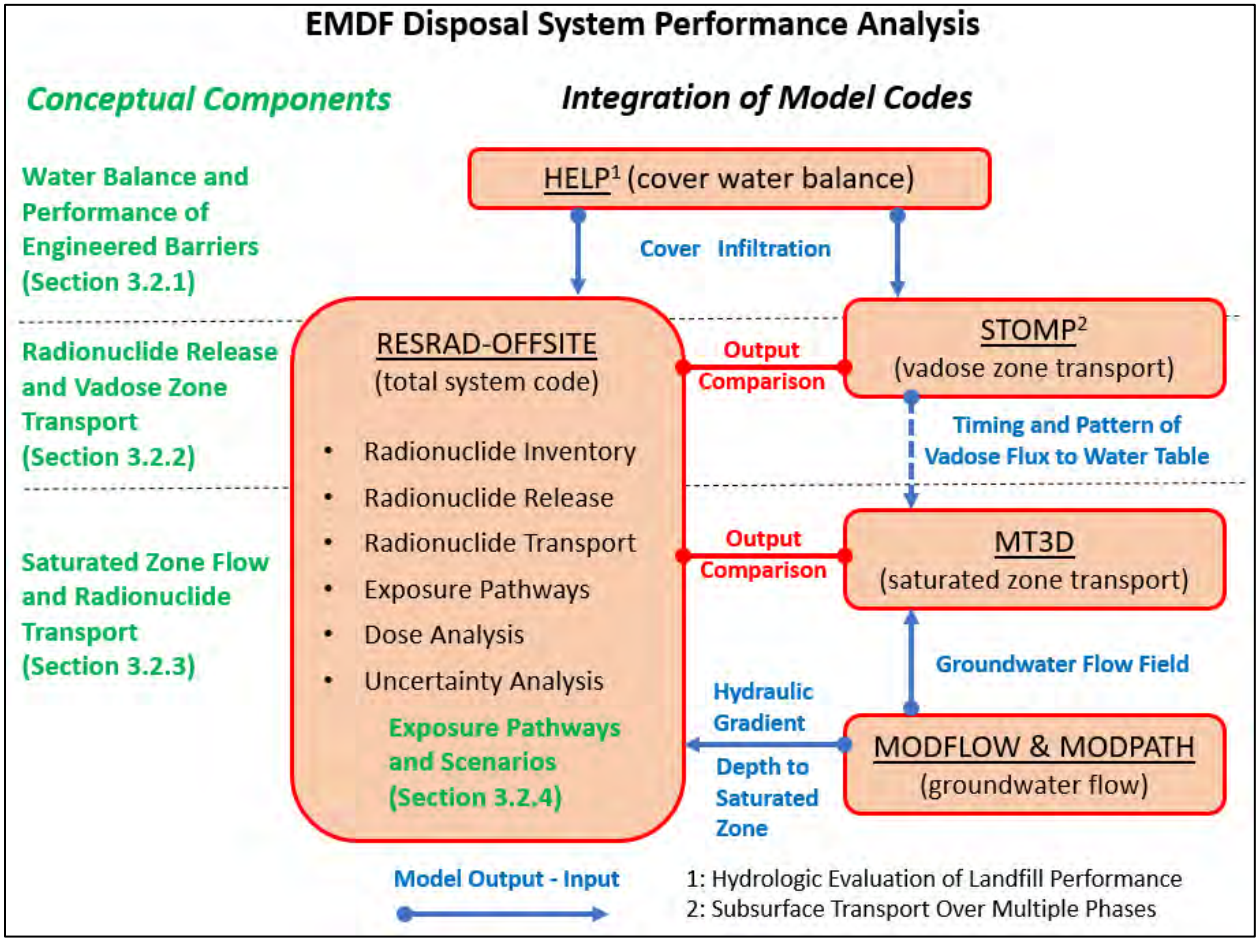

Fig. ES.9. EMDF disposal system conceptual components and integration of model codes for performance analysis

Table ES.4. EMDF PA model input parameters and linkages among models

Model and purpose	Primary model inputs	Primary model output (used as input to or compared with other PA models)
HELP Water balance and engineered barrier performance (Appendix C)	• Local climate data • EMDF preliminary design (geometry and material specifications)	• Cover infiltration rates
MODFLOW Saturated zone flow (Appendix D)	• EMDF preliminary design • Bear Creek Valley topography, geology, and surface water features • Conasauga group hydraulic conductivities • EMDF cover infiltration • Estimated natural recharge rates	• Flow directions • Hydraulic gradients • 3-D groundwater flow field • Depth to groundwater
STOMP Unsaturated flow and transport (Appendix E)	• EMDF radionuclide inventory • EMDF preliminary design • Estimated natural recharge rates • EMDF cover infiltration • Conasauga group hydraulic conductivities and porosity • Solid-aqueous partition coefficients	• Radionuclide release • Vadose zone flux • Water table flux • Water table time of arrival (vadose delay times)
MT3D Saturated zone transport model (Appendix F)	• EMDF radionuclide inventory • EMDF preliminary design • EMDF cover infiltration • Effective porosities • 3-D groundwater flow field • Solid-aqueous partition coefficients • Radionuclide flux from vadose zone	• Plume location, evolution and maximum extent • Peak groundwater concentration and time of peak at well • Contaminant discharge to Bear Creek surface waters
RESRAD-OFFSITE Radionuclide release and transport; exposure and dose analysis (Appendix G)	• EMDF radionuclide inventory • EMDF preliminary design (material specifications) • EMDF cover infiltration • Hydraulic gradients • Effective porosities • Solid-aqueous partition coefficients • Biotic transfer factors • Dose conversion factors • Exposure scenario and exposure factors (ingestions rates, etc.)	Outputs for evaluating compliance with performance objectives: • Peak total dose during compliance period • Dose contributions by exposure pathway • Key radionuclide contributions to total dose • Well water and surface water concentrations

D = dimensional
EMDF = Environmental Management Disposal Facility
HELP = Hydrologic Evaluation of Landfill Performance
PA = Performance Assessment
RESRAD = RESidual RADioactivity
STOMP = Subsurface Transport Over Multiple Phases

Quality Assurance

The *Quality Assurance Report for Modeling of the Bear Creek Valley Low-level Radioactive Waste Disposal Facilities, Oak Ridge, Tennessee* (QA Report) (UCOR 2020b) was prepared to document the QA activities for this Revision 2 PA and the companion Revision 2 CA (UCOR 2020a).

The salient components of the QA program that were implemented during the preparation of this PA include the following:

- Software QA procedures for code verification and documentation for each model code per *Software Quality Assurance Program* (PPD-IT-6007).
- Formal independent checking and review of calculation and data packages that document input parameter values and other model assumptions, model implementation, model output data, and post-processing activities for each PA model.
- Documentation of PA model development, implementation, sensitivity-uncertainty analyses, and PA model integration contained in the EMDF PA report and report appendices.
- Configuration management for PA documents and calculation packages per UCOR procedures for document control.
- Maintenance of the digital modeling information archive of PA documents, model codes, model input and output files, formal QA documentation, and reference materials in compliance with requirements of the UCOR QA Program (UCOR 2019), DOE QA Program (DOE 2012, Attachments G and H), and DOE O 414.1D (DOE 2013b).

The QA procedures and documentation for the EMDF PA are described in Sect. 9.

RESULTS OF BASE CASE ALL-PATHWAYS DOSE AND UNCERTAINTY ANALYSES

This section summarizes the results of the base case dose analysis using the total system model code RESRAD-OFFSITE. A summary of the sensitivity and uncertainty evaluations performed for the PA modeling and a brief presentation the probabilistic uncertainty analysis are also included in this executive summary. Detailed presentations of PA model results are included in Sect. 4 and Appendices C, D, E, F, and G. Results of the radon flux analysis and RESRAD-OFFSITE results used to demonstrate water resources protection are presented in the Evaluation of Performance section of this executive summary.

All-pathways dose analysis

Total system simulations were run for a post-closure period of 10,000 years to provide dose estimates for comparison with EMDF performance objectives, with a focus on predicted peak total dose within the 1000-year compliance period. Potential future release of less mobile radionuclides with significant estimated inventories (e.g., radionuclides of uranium) was evaluated with a separate 100,000-year RESRAD-OFFSITE simulation to saturated zone concentrations at the 100-m POA. These model predictions for the period beyond 10,000 years are highly uncertain and are presented only to indicate very long-term trends, rather than for comparison to regulatory standards. Results for the 100,000-year simulation are presented in Sect. 4.8.

Predicted total dose over time for the base case model is presented in Fig. ES.10. The peak total dose (i.e., all-pathways dose from all simulated radionuclides summed) within the 1000-year compliance period occurs at 490 years post-closure and is 1.03 mrem/year. The peak compliance period dose is associated with C-14. Total dose then decreases through 750 years and remains less than 0.2 mrem/year from that time to the end of the compliance period. After the compliance period, the total dose increases to a peak of 0.95 mrem/year associated with Tc-99 at approximately 1700 years. After the Tc-99 peak, the total dose increases to a maximum of 9.13 mrem/year at approximately 5084 years and then gradually decreases through 10,000 years to a predicted total dose at 10,000 years of 0.114 mrem/year. The primary isotopic contributors to the total dose are C-14, Tc-99, and I-129 (Fig. ES.11).

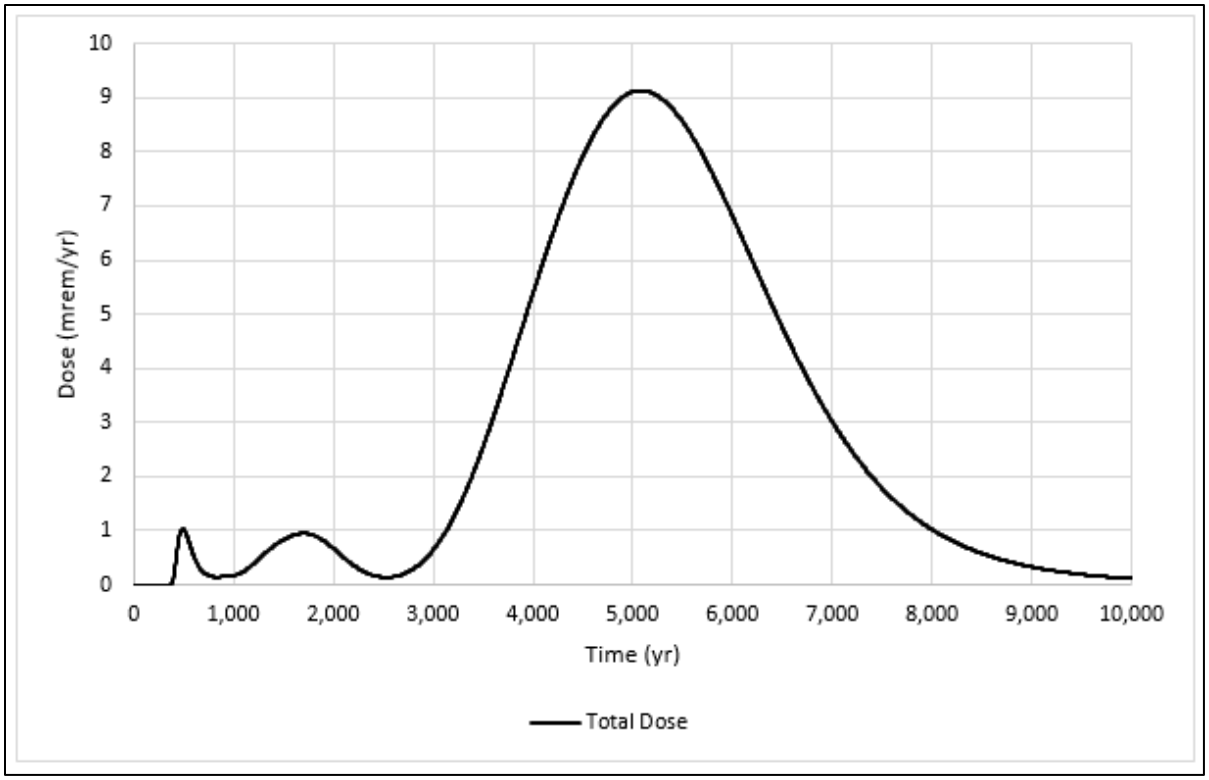

Fig. ES.10. Base case predicted total dose (all pathways, 0 to 10,000 years)

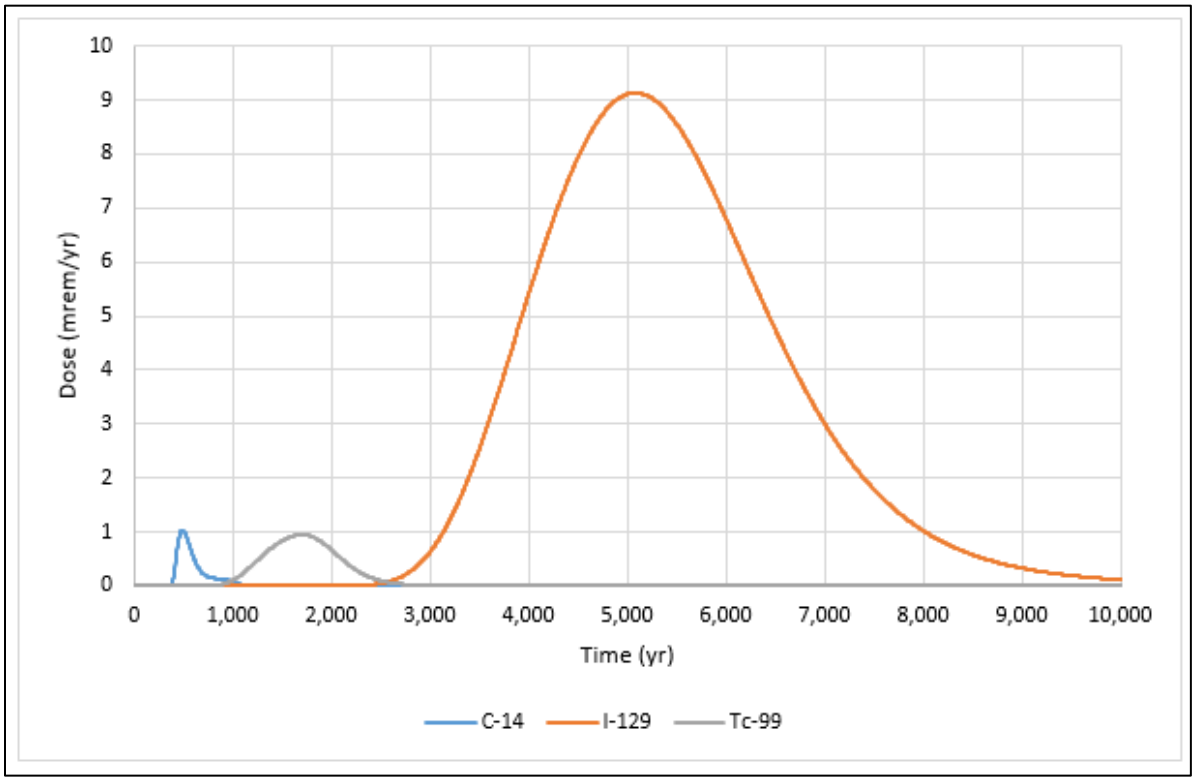

Fig. ES.11. Base case predicted total dose by isotope (0 to 10,000 years)

The three distinct peaks in total dose are each associated with one of these three radionuclides. Overall, the predicted maximum total dose during the compliance period of 1.03 mrem/year is less than 5 percent of the performance objective (25 mrem/year).

The groundwater ingestion pathway (ingestion of well water) is the dominant contributor to total dose (Fig. ES.12). Note that the dose axis on Fig. ES.12 is logarithmic to facilitate comparison of pathway dose contributions. In addition to the drinking water exposure pathway, the pathways contributing most of the remaining dose are ingestion of fish (during the compliance period) and, after about 1200 years, meat ingestion, which includes beef, poultry, and eggs (refer to Sect. 3.4.3 for additional detail).

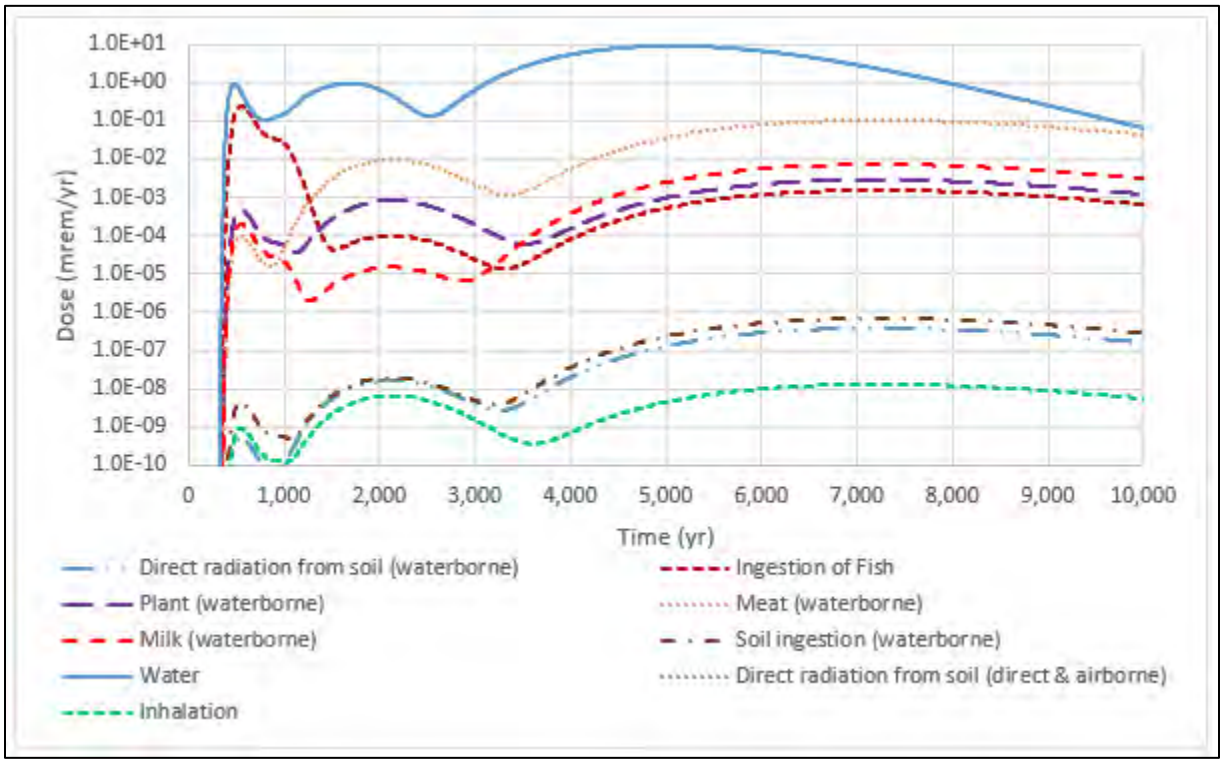

Fig. ES.12. Predicted base case dose by exposure pathway (0 to 10,000 years)

Sensitivity and Uncertainty Analysis

The goal of sensitivity-uncertainty analysis for the EMDF PA is understanding sensitivity of model predictions to uncertainty in input parameter values for those radionuclides and transport pathways that are the primary contributors to the all-pathways dose during the 1000-year compliance period. The focus is on uncertainty in long-term cover performance, partition coefficient values for dose-significant radionuclides, and hydrogeologic parameters that affect environmental transport pathways. Detailed presentation of sensitivity-uncertainty analyses is provided in Sect. 5.

The analysis includes selected sensitivity cases (what-if scenarios) for the detailed vadose and saturated zone transport models, single factor (increasing and decreasing one parameter at a time from the assumed base case value) sensitivity evaluations of the total system model predictions, and an uncertainty analysis to address the importance of key uncertainties relative to evaluation of compliance with the all-pathways dose performance objective. The uncertainty analysis involves assigning probability distributions to selected input parameters and running multiple simulations with different sets of input values, and statistical analysis of the results. The sensitivity and uncertainty evaluations undertaken for the EMDF PA are

summarized in Table ES.5. Results from model sensitivity cases and single-factor evaluations (Sect. 5 and Appendices C, D, E, F, and G) were used to inform the selection of input parameters and parameter distributions for the probabilistic analysis.

Table ES.5. Summary of sensitivity-uncertainty analyses for the EMDF PA

Type of sensitivity-uncertainty analysis	Subsystems and models evaluated	Parameters selected for analysis (related uncertainty)
Model sensitivity cases (what-if analysis)	Saturated Zone Flow – MODFLOW	• Increased recharge (climate)
	Vadose Zone Transport – STOMP	• Increased cover infiltration (climate, cover performance) • Increased waste K_d (materials and geochemistry) • Decreased non-waste K_d (materials and geochemistry)
	Saturated Zone Transport – MT3D	• Increased layer 2 hydraulic conductivity value (materials) • Non-uniform source release (uniform source release assumption)
Single factor sensitivity	Total System – RESRAD-OFFSITE	• Refer to Table 5.2
Probabilistic input parameter uncertainty analysis	Total System – RESRAD-OFFSITE	• Refer to Appendix G, Attachment G.3

EMDF = Environmental Management Disposal Facility
PA = Performance Assessment
RESRAD = RESidual RADioactivity
STOMP = Subsurface Transport Over Multiple Phases

The sensitivity cases evaluated for the STOMP and MT3D models are detailed in Sect. 5.1 and 5.2, respectively. The RESRAD-OFFSITE model single factor sensitivity evaluations are presented in Sect. 5.3. The results of the more detailed process models and model sensitivity to input assumptions were compared to RESRAD-OFFSITE model predictions to guide the RESRAD-OFFSITE model saturated zone parameter inputs and to ensure that the simplified total system model results were broadly consistent with the more detailed models. This model integration process is described in Sect. 3.3.5.

The RESRAD-OFFSITE model uncertainty analysis is summarized in Sect. 5.4 and described in detail in Appendix G, Sect. G.6.3. The probabilistic analysis addresses input parameter uncertainty by assigning probability distributions to key input variables, randomly sampling sets of input parameters values, and running multiple simulations to obtain the predicted peak dose for each realization of the EMDF disposal system. Distributions of predicted dose are used to understand the range and likelihood of peak dose related to uncertainty in input parameters. Multiple regression analysis of peak dose as a function of the probabilistic input variables is used to determine which input parameters have the greatest impact on model results. Separate RESRAD-OFFSITE uncertainty analyses were completed for the 1000-year compliance period and for the longer 10,000-year period.

To simplify the analysis, only C-14, Tc-99, and I-129 were included in the compliance period probabilistic evaluation. Selection of input parameters for probabilistic analysis focused on uncertainty in future precipitation and cover performance, K_d values for EMDF materials, and other properties of the vadose and saturated zone media that influence radionuclide transport. Assigned probability distribution parameters and assumed correlations between input parameters are summarized in Appendix G, Attachment G.3.

Figure ES.13 shows the variation of median, mean, and 95th percentile dose during the compliance period for each of 10 repetitions of 300 simulations. The deterministic base case model all-pathways dose curve

for the compliance period is also shown on Fig. ES.13 for comparison to the probabilistic results. The peak of the mean probabilistic dose (i.e., the maximum value of the mean dose over time for each repetition) occurred at 1030 years for all 10 repetitions, ranging from 0.92 to 1.2 mrem/year, which is a range that includes the deterministic base case compliance period peak dose of approximately 1 mrem/year (Fig. ES.10). The 95th percentiles of the probabilistic total dose also reached maximum values at 1030 years, with a range from 1.7 to 2.1 mrem/year among the 10 repetitions.

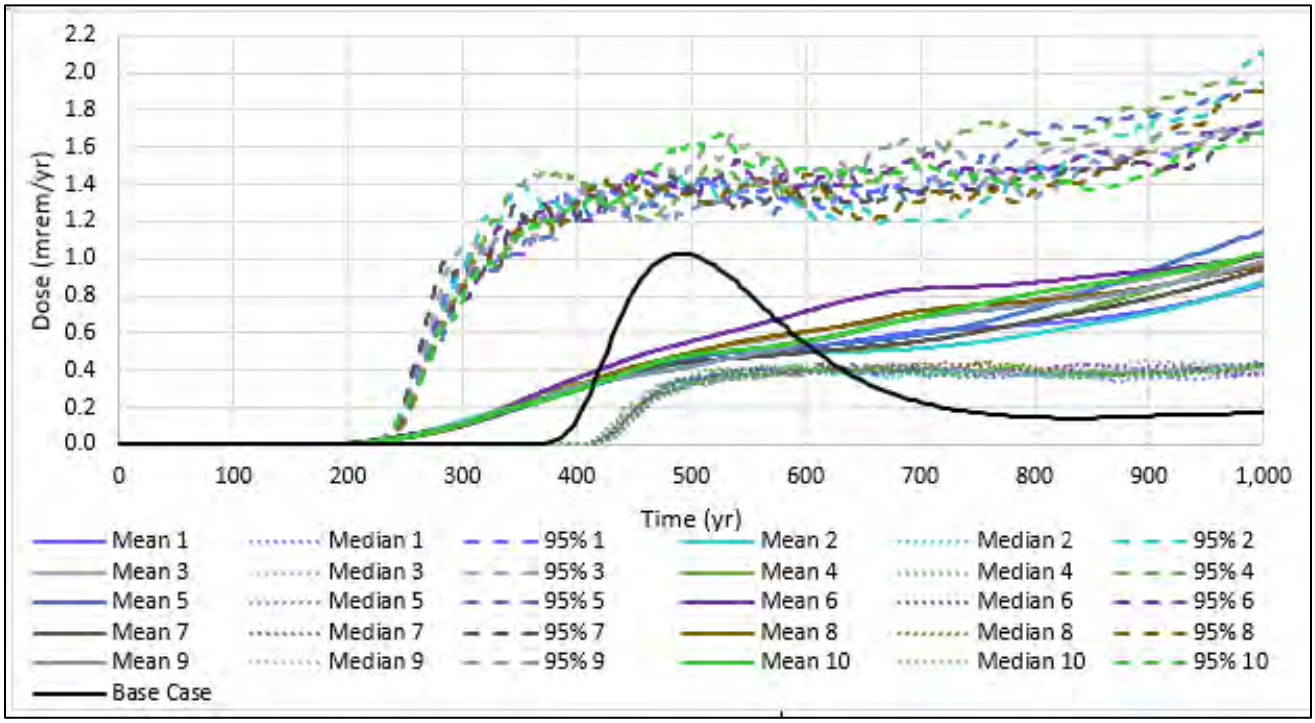

Fig. ES.13. Probabilistic all pathways dose summary for RESRAD-OFFSITE probabilistic uncertainty analysis

The difference between the deterministic base case dose curve and the probabilistic results (percentiles of the total dose distribution as a function of time) occurs because the time of peak total dose for any single probabilistic simulation varies widely (230 to 1030 years) due to variable sampling of input parameters that control release timing (particularly K_d values) among the 3000 realizations. The differences between the deterministic and probabilistic results also reflect the likelihood of much larger dose contributions from Tc-99 and I-129 toward the end of the compliance period probabilistic simulations. Carbon-14 is the primary dose contributor for times prior to about 800 years. After 800 years, I-129 and Tc-99 have mean dose contributions equal to or greater than mean C-14 contributions. Additional detail on variation of radionuclide dose over the compliance period is provided in Sect. G.6.3.3 of Appendix G. For I-129 and Tc-99, compliance period peak doses that occur at the end of the simulation period are cases in which higher long-term radionuclide peaks will occur well after 1000 years in the longer simulations. The uncertainty analysis results for the 10,000 year simulation period are presented in Sect. 5.4.2.

Regression analysis of the compliance period probabilistic peak dose output suggests that among the 33 input parameters for which probability distributions were assigned, the five most influential variables are:

- Runoff coefficient (cover infiltration rate)
- Release duration (affects release rate)
- Hydraulic conductivity of the saturated zone (saturated zone mixing)
- Mean residence time in the surface water body (C-14 fish ingestion dose)
- Depth of aquifer contributing to well (exposure factor, affects well water concentrations).

These results are consistent with results from the single parameter sensitivity analysis presented in Sect. 5.3, which show that total dose and timing of peaks are sensitive to changes in these parameters. The results of the uncertainty analysis suggest that the uncertainty in key input parameter values does not affect the conclusion that the all-pathways dose performance objective will be met during the 1000-year compliance period, and that the 25mrem/year limit is unlikely to be exceeded within timeframes of several thousand years post-closure.

INADVERTENT HUMAN INTRUSION

This section presents a brief summary of the results of the analysis of IHI for EMDF; the IHI analysis is described in more detail in Sect. 6 of the PA. Selection of IHI scenarios was guided by consideration of EMDF site characteristics and facility design as well as review of IHI analyses performed for other historical and proposed LLW disposal facilities on the ORR. Additional details on this IHI analysis, the scenarios evaluated, and the other PAs that were reviewed are provided in Appendix I. The IHI analysis for EMDF considers an acute discovery scenario that involves attempted excavation into the final cover and an acute drilling and chronic post-drilling (agricultural) scenario that involve direct contact with the waste. A summary of the three IHI scenarios analyzed for EMDF is provided in Table ES.6.

Table ES.6. Summary of IHI scenarios analyzed for EMDF and corresponding DOE performance measures

Scenario type/name	DOE Order 435.1 performance measure	Exposure scenario description
Acute exposure –discovery (excavation)	500 mrem	Intruder initiates excavation into EMDF cover, but stops digging before exposing waste; exposure to external radiation
Acute exposure – drilling (water well)	500 mrem	Intruder drills irrigation well through waste and is exposed to waste in exhumed drill cuttings; exposure to external radiation, inhalation and incidental ingestion of contaminated soil
Chronic exposure – post-drilling (subsistence garden)	100 mrem/year	Intruder uses contaminated drill cuttings to amend soil in a vegetable garden; exposure to external radiation, inhalation, and ingestion of contaminated food and soil

DOE = U.S. Department of Energy
EMDF = Environmental Management Disposal Facility
IHI = inadvertent human intrusion

The IHI analysis assumes that intrusion is an accidental occurrence resulting from a temporary loss of institutional control. The occurrence of accidental intrusion also presumes a loss of societal memory of the ORR and radioactive waste disposal facilities in the area, despite existing long-term stewardship commitments of the DOE and the likelihood of legal controls such as property record restrictions and notices. For each IHI scenario, active institutional controls are assumed to preclude intrusion for the first 100 years following closure of the disposal facility.

Several key assumptions for the intruder analyses (e.g., cover and waste thickness) are based on the specifics of the EMDF design that are described in Sects. 1.3 and 2.2 and in Appendix C. The estimated EMDF radionuclide inventory (Appendix B) was used with the RESRAD-OFFSITE code to model doses resulting from these unlikely future intrusion scenarios. The results are used to establish compliance with DOE O 435.1 dose performance measures for IHI (Table ES.6).

The results of the IHI analyses are summarized in Table ES.7. The model results for the three IHI scenarios suggest the chronic post-drilling scenario is the bounding scenario (largest predicted dose). Predicted dose over time for the chronic post-drilling scenario is presented in Fig. ES.14. The total dose (all radionuclides and pathways summed) at 100 years post-closure is 3.56 mrem/year. Total dose decreases to a minimum of 2.95 mrem/year at approximately 340 years, and then gradually increases through the compliance period. After 1000 years, the dose increases more rapidly as concentrations of radioactive progeny (uranium decay products) increase. Total dose at 10,000 years is 8.24 mrem/year. The maximum predicted dose is a factor of 10 times lower than the chronic IHI performance measure of 100 mrem/year.

Table ES.7. Summary of IHI analysis results for the EMDF

EMDF IHI scenario	DOE O 435.1 IHI performance measure	Maximum dose during the 1000-year compliance period
Acute exposure – discovery (excavation)	500 mrem	1.3E-04 mrem
Acute exposure – drilling (water well)	500 mrem	0.38 mrem
Chronic exposure – post-drilling (subsistence garden)	100 mrem/year	3.56 mrem/year

DOE O = U.S. Department of Energy Order
EMDF = Environmental Management Disposal Facility
IHI = inadvertent human intrusion

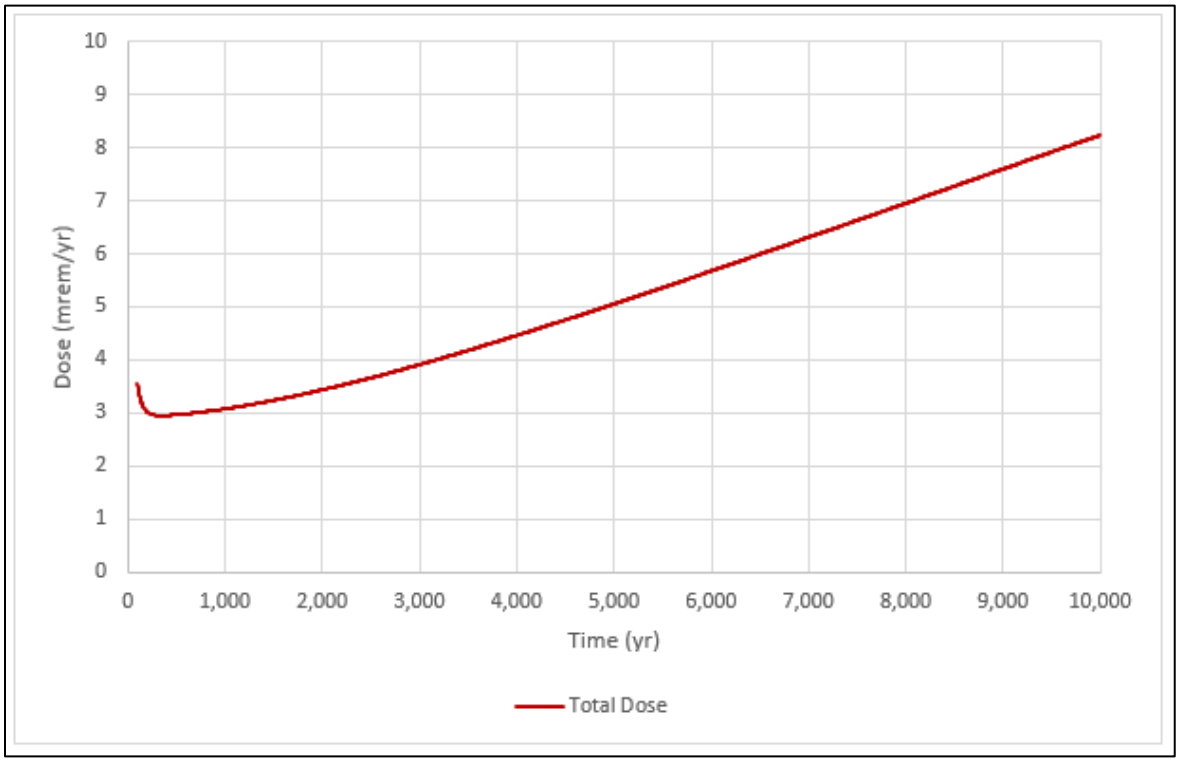

Fig. ES.14. Chronic post-drilling scenario total dose (all radionuclides and pathways summed)

EVALUATION OF PERFORMANCE

The base case analysis and sensitivity-uncertainty analysis performed for the EMDF PA demonstrate that there is a reasonable expectation that the facility will meet the established all-pathways dose performance objective during the 1000-year compliance period and within the first several thousand years post-closure. Analytical results are summarized in Table ES.8.

Table ES.8. Exposure scenarios, performance objectives and measures, and base case results for the EMDF PA

Exposure scenario	Performance objective or measure	EMDF PA results
All pathways	25 mrem/year	Base case maximum dose during compliance period: 1.03 mrem/year Base case peak dose through 10,000 years: 9.13 mrem/year (at 5100 years)
Air pathway[a]	10 mrem/year[b]	Pathway screened from analysis (Sect. 3.2.2)
Radon flux	20 pCi/m^2/sec	EMDF cover surface: 5.0E-08 pCi/m^2/sec EMDF waste surface (no cover): 0.80 pCi/m^2/sec
Water resources (groundwater) • Ra-226 + Ra-228 • Gross alpha activity[c] • Beta/photon activity • H-3 • Sr-90 • Uranium (total)	 5 pCi/L 15 pCi/L 4 mrem/year 20,000 pCi/L 8 pCi/L 30 µg/L	Groundwater during compliance period: • Ra-226 + Ra-228: 0.0 pCi/L (negligible) • Gross alpha activity: 0.0 pCi/L (negligible) • Beta/photon activity: 1.03 mrem/year • H-3: 0.0 pCi/L (negligible) • Sr-90: 0.0 pCi/L (negligible) • Uranium (total): 0.0 µg/L (negligible).
Water resources (surface water)	DOE DCS[d]	Bear Creek peak concentration less than DCS standard for all radionuclides in EMDF inventory (Sect. 4.7.2)
Inadvertent human intrusion • Chronic exposure • Acute exposure	 100 mrem/year 500 mrem	IHI dose at 100 years (compliance period maximum): Chronic post-drilling: 3.56 mrem/year Acute discovery: 1.30E-04 mrem Acute drilling: 0.38 mrem

[a]Air pathway is screened from the EMDF PA.
[b]Excluding radon in air.
[c]Including Ra-226, but excluding radon and uranium.
[d]DOE 2011b.

DCS = Derived Concentration Standard
DOE = U.S. Department of Energy
EMDF = Environmental Management Disposal Facility
IHI = inadvertent human intrusion
PA = Performance Assessment

Results of the radon flux analysis are shown in Table ES.8, discussed in Sect. 4.4, and presented in detail in Appendix H. The results suggest that EMDF can meet the 20 pCi/m^2/sec radon flux performance objective even if the cover is severely eroded. Also included in Table ES.8 is a summary of the results of RESRAD-OFFSITE modeling to demonstrate protection of water resources during the 1000-year compliance period. Modeled well water and surface water concentrations are compared to maximum contaminant levels for drinking water systems and to the DOE *Derived Concentration Technical Standard* (DOE 2011b), respectively. The results suggest there is a reasonable expectation that the EMDF disposal system will be protective of water resources during the compliance period.

With respect to performance measures for IHI, the EMDF analysis suggests that, based on the current estimated EMDF radionuclide inventory, there is a reasonable expectation that the engineering design for EMDF will protect a future inadvertent human intruder for the specific IHI scenarios considered.

USE OF PERFORMANCE ASSESSMENT RESULTS

The primary uses of this EMDF PA are to support issuance of a DAS by demonstrating the likelihood of meeting performance objectives based on the expected EMDF waste forms, estimated radionuclide inventory, preliminary facility design, and site characteristics, and to identify key site, waste, and facility uncertainties that can be prioritized for further work prior to the start of operations.

FURTHER WORK

Near-term priorities for research and development activities to support PA maintenance include the following:

- Perform laboratory evaluations of EMDF materials to reduce uncertainty in the assumed K_d values for Tc-99 and I-129
- Monitor EMDF design evolution through final design and assess changes through the EMDF change control process.

In parallel with these near-term PA maintenance activities, the FFA parties will approve operating limits, including WAC, and will issue a WAC compliance document prior to EMDF operations. Review of proposed activities, new regulatory requirements, or other new information that could challenge key assumptions for the EMDF performance analysis will be evaluated in accordance with the EMDF change control process to assess the potential for such changes to require a Special Analysis or revisions to the PA.

This page intentionally left blank.

1. INTRODUCTION

This report documents the Performance Assessment (PA) for a proposed solid low-level (radioactive) waste (LLW) disposal facility at the U.S. Department of Energy (DOE) Oak Ridge Reservation (ORR). A new facility is required to ensure sufficient future LLW disposal capacity for environmental cleanup activities on the ORR performed under the ORR Federal Facility Agreement (FFA) (DOE 1992a).

This section of the Environmental Management Disposal Facility (EMDF) PA report provides general background information, including a facility description, a summary of the EMDF regulatory framework and need for the PA, and a summary of key assumptions. Information provided in subsequent sections of the report includes the following:

- Sect. 2 – detailed information on EMDF site characteristics and design features and the estimated radionuclide inventory used in the PA modeling analysis
- Sect. 3 – EMDF analysis of performance, including conceptual models, modeling tools, model implementation, and dose analysis
- Sect. 4 – results of the performance analysis
- Sect. 5 – sensitivity of the results to uncertainty in model inputs
- Sect. 6 – results of the analysis of (hypothetical) inadvertent human intrusion (IHI)
- Sect. 7 – integration and interpretation of results
- Sect. 8 – overall evaluation of EMDF performance
- Sect. 9 – quality assurance (QA) procedures
- Sects. 10 and 11 – information on the preparers of the PA and references
- Appendix A – PA review criteria
- Appendix B – radionuclide inventory for wastes disposed in EMDF
- Appendix C – analysis of EMDF cover system
- Appendix D – groundwater flow modeling (MODFLOW)
- Appendix E – Subsurface Transport Over Multiple Phases (STOMP) modeling
- Appendix F – MT3D modeling
- Appendix G – RESidual RADioactivity (RESRAD)-OFFSITE modeling
- Appendix H – radon flux analysis
- Appendix I – IHI analysis.

The remainder of Sect. 1 reviews the basis and programmatic context for the EMDF PA, including related analyses (Sect. 1.1), and provides general facility information and design features (Sects. 1.2 and 1.3); facility life-cycle assumptions, including closure planning (Sect. 1.4); regulatory context for the EMDF PA (Sect. 1.5); expectations regarding future land use and institutional controls (Sect. 1.6); and a summary of key assumptions that underlie the conclusions of the PA (Sect. 1.7).

1.1 BASIS FOR PERFORMANCE ASSSESSMENT

This EMDF PA has been developed to support DOE approval of a Disposal Authorization Statement (DAS) to support design and construction of EMDF. Development of the EMDF PA and early facility design activities are being conducted in parallel with activities required for approval of the EMDF for onsite LLW disposal under the FFA. Remaining documentation to support a final Disposal Authorization Statement to support operations of the landfill will occur in parallel with the final design of the facility.

1.1.1 Programmatic Background

DOE is responsible for sitewide waste management and environmental restoration activities on the ORR under its Office of Environmental Management Program at the national level and locally under the Oak Ridge Office of Environmental Management (OREM). OREM is responsible for minimizing potential hazards to human health and the environment associated with contamination from past DOE practices and addressing the waste management and disposal needs of the ORR. Under the requirements of the FFA established by DOE, the U.S. Environmental Protection Agency (EPA), and the Tennessee Department of Environment and Conservation (TDEC), environmental restoration activities on the ORR are performed in accordance with the Comprehensive Environmental Response, Compensation, and Liability Act of 1980 (CERCLA).

The major focus of the OREM Program has been remediation of facilities within the installations that are contaminated by historical Manhattan Project and Cold War activities. This cleanup mission is projected to take approximately three decades to complete and will result in large volumes of radioactive, hazardous, and mixed waste requiring disposal. The focus of CERCLA cleanup since the early 1990s has been the remediation of existing waste disposal sites and deactivation and decommissioning (D&D) of excess facilities at the East Tennessee Technology Park (ETTP), the Y-12 National Security Complex (Y-12), and the Oak Ridge National Laboratory (ORNL). Timely and effective ORR cleanup is essential to facilitate reindustrialization of the ETTP site and to ensure worker safety and the success of DOE missions at Y-12 and ORNL.

A 1999 Record of Decision (ROD) (DOE 1999a) authorized construction of a facility located in Bear Creek Valley (BCV) on the ORR to provide permanent disposal for radioactive, hazardous, and mixed wastes resulting from cleanup of facilities and media that present unacceptable risks to human health and the environment in their current setting at ORR and associated sites. This facility, the Environmental Management Waste Management Facility (EMWMF), has been constructed and is accepting CERCLA cleanup wastes. The capacity of EMWMF is 2.3 million cy as authorized by the ROD and a subsequent Explanation of Significant Difference (DOE 2010a).

The scope of the OREM cleanup effort has expanded since EMWMF began operations in 2002. Approximately 1.6 million cy of additional CERCLA waste is expected to be generated and require disposal after EMWMF has reached maximum capacity in the mid-2020s.

1.1.2 EMDF Performance Assessment Development and Related Analyses

The anticipated need for additional LLW disposal capacity is the basis for a second ORR CERCLA waste disposal facility. The associated Remedial Investigation/Feasibility Study (RI/FS) analyzed the feasibility of siting a new disposal facility at several alternative sites in BCV (DOE 2017b). The FFA parties issued a Proposed Plan (DOE 2018a) for disposal of future ORR CERCLA waste for public comment in 2018. A conceptual design for the Central Bear Creek Valley (CBCV) site contained in the EMDF RI/FS is the basis for the EMDF Proposed Plan. Since the proposed plan was issued, the design of the EMDF has been advanced to a preliminary design (60 percent) stage and is the basis for technical analyses in this PA.

The EMDF PA analysis incorporates an extensive body of environmental data drawn from over two decades of RI and monitoring in BCV. In addition, CBCV site characterization activities, including surface water and groundwater monitoring, have been completed to support FFA approval of the proposed site and development of the preliminary engineering design. Information from the CBCV site characterization was used in revising the PA models used in this revision of the document. Following the issue of a DAS for EMDF, proposed activities, new regulatory requirements, or other new information that could challenge key assumptions for the PA will be reviewed and evaluated with the EMDF change control process to assess the potential for such changes to require a Special Analysis or revisions to the PA.

Two other ORR LLW disposal facility PAs that may be of interest for comparison to the EMDF PA include the analyses performed for Solid Waste Storage Area (SWSA) 6 in Melton Valley near ORNL (ORNL 1997a) and for EMWMF (DOE 1998a) in BCV near the west end of the Y-12 site. The SWSA 6 and EMWMF PAs differ from the EMDF PA primarily in terms of facility design, conceptual models, and selection of computer codes for analysis. Table 1.1 provides a summary of the differences in facility design, release pathway and exposure assumptions, model codes, and partition coefficient (K_d) values. The EMDF and EMWMF facilities and performance analyses are very similar, whereas the SWSA 6 PA encompassed a number of different LLW disposal units within a common area (Melton Valley) on the ORR, and applied several model codes developed at ORNL. For assumed partition coefficients, the EMDF PA draws upon the currently available data for Conasauga Group materials (Sect. 2.1.6.3), whereas the SWSA 6 and EMWMF analyses used a combination of semi-empirical derivation of partition coefficients for waste forms and assumed higher mobility for technetium and iodine in the natural environment (K_d=0 in the vadose and saturated zone) than does the EMDF analysis.

Both the SWSA 6 and EMWMF analyses included derivation of performance-based radioactivity concentration limits. The EMWMF analysis applied a unit concentration approach to developing activity concentration limits (analytical waste acceptance criteria [WAC]). The EMDF RI/FS identified a preliminary range of concentration limits for radionuclides and included a discussion of the WAC development and compliance process that will be developed under the FFA (DOE 2018a, Sect. 6.2.3, pages 6-85 to 6-91, Table 6.5). The EMDF PA includes calculated site-specific Single Radionuclide Soil Guidelines (SRSGs) that can be used to evaluate proposed limits on radionuclide inventories or concentrations.

A Composite Analysis (CA) has been prepared to evaluate cumulative impacts of potential releases from historical waste disposal sites, the existing EMWMF, and the future EMDF in BCV (UCOR, an Amentum-led partnership with Jacobs, 2020a). The CA for EMWMF and EMDF summarizes modeling activities to estimate peak radiological dose at a downgradient point of assessment (POA) on Bear Creek. The resident farmer exposure scenario assumed for the EMWMF/EMDF CA differs from the EMDF PA in that surface water rather than groundwater is assumed as the source for drinking and domestic use. The CA concludes that cumulative dose will not exceed DOE Manual (M) 435.1-1 (DOE 2011a) performance objectives.

This page intentionally left blank.

Table 1.1. Comparison of EMDF, EMWMF, and SWSA 6 performance assessments

Site, disposal facility, and waste characteristics; Exposure scenarios				
PA Characteristic	**EMDF**	**EMWMF**	**SWSA 6**	**Comments**
Location and conceptual site model	BCV	BCV	Melton Valley	Identical geological sequence (Cambrian Conasauga Group sedimentary formations), very similar conceptual site model for Melton Valley and BCV
Type of facility	Above-grade Subtitle C Landfill	Above-grade Subtitle C Landfill	Various disposal units: tumulus facility – waste in B-25 containers	SWSA 6 PA encompassed a variety of adjacent disposal units (including trenches and wells) in Melton Valley
Cover system	11-ft-thick multicomponent	11-ft-thick multicomponent	Tumulus: 4-ft-thick multicomponent	
Liner system	RCRA-compliant	RCRA-compliant	Above-grade concrete pads with gravel drainage	RCRA-compliant liners contain HDPE flexible membranes and 3-ft-thick clay layer
Facility failure – degradation assumptions	HDPE and clay degrades from 200 to 1000 years post-closure	HDPE non-functional, clay degrades at end of institutional control	Complete cover and pad failure at end of institutional control	Recent research on geosynthetics supports longer cover performance for EMDF and EMWMF; refer to Appendix C, Sect. C.1.
Cover infiltration rate(s)	Linear increase from zero at 200 years to 0.88 in./year at 1000 years	0.43 in./year at closure	Natural recharge	
Waste types	LLW, mixed, TSCA	LLW, mixed, TSCA	LLW – CH and RH	
Waste form	Soil and demolition debris from CERCLA response actions	Soil and demolition debris from CERCLA response actions	Various- from ORNL operations and legacy wastes	EMWMF and projected EMDF waste is a combination of compacted bulk waste, containerized waste, and various types of treated or stabilized waste forms (e.g., equipment grouted in place)
Radionuclide inventory	Estimated (Appendix B of this PA)	Unit concentrations approach to develop analytical WAC	Estimated	The EMWMF dose analysis for the BCV CA uses a current radionuclide inventory estimate
Exposure scenario	Resident farmer- drinking water well, surface water agricultural use	Resident farmer- drinking water well, surface water agricultural use	Resident farmer groundwater- drinking, milk, and meat; surface water- drinking, milk, meat, and fish	
Hypothetical receptor location	100 m from waste edge @ plume centerline	Bear Creek at NT-5 confluence (about 300 m from edge of facility)	100 m from edge of cover	EMWMF receptor well location selected onsite with TDEC and EPA representatives
Assumed K_d values (cm^3/g)				
Element	**Waste K_d, vadose zone K_d, saturated zone K_d**	**Waste K_d, vadose zone K_d, saturated zone K_d**	**Waste K_d, soil and environmental transport K_d**	**Comments**
Carbon	0, 0, 0	1.09, 0, 0	1.09, 0	
Hydrogen	0, 0, 0	0.199, 0, 0	0.199, 0	
Iodine	2, 4, 4	0.199, 0.199, 0	0.551, 0	
Technetium	0.36, 0.72, 0.72	1.29, 0, 0	3.18, 0	
Uranium	25, 50, 50	40, 20, 7	3820, 40	
Model codes applied to release, transport, and dose analysis				
Medium or Transport Pathway	**EMDF**	**EMWMF**	**SWSA 6**	**Comments**
Groundwater flow	MODFLOW	MODFLOW	USGS MOC	
Surface water flow	No model	No model	UTM	
Radionuclide release	STOMP, MT3D, RESRAD-OFFSITE	PATHRAE-RAD	SOURCE1, SOURCE2	
Radionuclide transport	MT3D, RESRAD-OFFSITE	PATHRAE-RAD	PADSIM, HOLSIM	
Air pathway	RESRAD-OFFSITE (atmospheric loading for irrigated areas and cover release pathway screening model)	No model; atmospheric pathway eliminated from consideration	ISCLT3	
Dose analysis	RESRAD-OFFSITE	PATHRAE-RAD	No model code identified, dose analysis is detailed in Appendix G of ORNL 1997a	For EMWMF, performance objectives were based on risk metrics rather than dose
Reference documents	This document	DOE 1998a, DOE 1998b	ORNL 1997a	

BCV = Bear Creek Valley
CA = Composite Analysis
CERCLA = Comprehensive Environmental Response, Compensation, and Liability Act of 1980
CH = contact handled
DOE = U.S. Department of Energy
EMDF = Environmental Management Disposal Facility
EMWMF = Environmental Management Waste Management Facility
EPA = U.S. Environmental Protection Agency
HDPE = high-density polyethylene
LLW = low-level (radioactive) waste
NT = North Tributary
ORNL = Oak Ridge National Laboratory
PA = Performance Assessment
RCRA = Resource Conservation and Recovery Act of 1976
RESRAD = RESidual RADioactivity
RH = remote handled
STOMP = Subsurface Transport Over Multiple Phases
SWSA = Solid Waste Storage Area
TDEC = Tennessee Department of Environment and Conservation
TSCA = Toxic Substances Control Act of 1976
WAC = waste acceptance criteria

This page intentionally left blank.

1.2 GENERAL FACILITY DESCRIPTION

The proposed site for the EMDF in BCV is southwest of the city of Oak Ridge, Tennessee, and Y-12 (Fig. 1.1). The LLW disposal concept and preliminary design are similar to EMWMF (i.e., an engineered near-surface disposal facility for solid LLW derived from CERCLA response actions on the ORR). Given the humid-temperate climate and shallow groundwater conditions prevailing in East Tennessee, long-term performance of engineered barriers, including the composite final cover and liner systems, is critical to the overall performance of the EMDF disposal system. Sections 1.3 and 2.2 provide additional details on EMDF preliminary design features.

The proposed CBCV site for EMDF lies in an area currently designated in the Phase I BCV ROD (DOE 2000) to require cleanup levels that would be protective for future public recreational use in the near term and unrestricted use in the future. The Y-12 facility is located approximately 3 miles to the northeast. The currently operating onsite waste disposal facility (EMWMF), as well as other former waste disposal and waste management facilities, are located between Y-12 and the CBCV site, within the area with cleanup levels for DOE-controlled industrial use (i.e., Zone 3). Section 1.6 provides additional discussion of future land-use assumptions for BCV.

LLW disposed at EMDF will originate primarily from facility D&D or environmental remediation projects at Y-12 and ORNL. The waste will include facility demolition debris (including structural steel and concrete), contaminated equipment and soil, and other soil-like wastes. EMDF will accept both containerized LLW and bulk (uncontainerized) waste for disposal. Some in situ waste stabilization (grouting) may occur. Waste quantities are based on the OREM Waste Generation Forecast. Waste stream characteristics are estimated from a variety of sources and are described in detail in Sect. 2.3 and Appendix B. Detailed characterization of waste destined for EMDF will occur at the cleanup project level and is the responsibility of the waste generator(s).

EMDF operations will include waste receipt and placement, water management, and environmental monitoring of facility performance. EMDF waste certification practices are expected to be carried over from current EMWMF WAC attainment and tracking systems (DOE 2001a). Each waste lot/stream will be certified and approved for disposal at EMDF by the WAC Attainment Team before shipments of waste to EMDF are scheduled. A WAC Compliance Plan, similar to that used at EMWMF, will specify the processes to be used for certification of waste streams for disposal at EMDF. Additional discussion of the FFA process for developing EMDF WAC and waste acceptance practices is provided in Sect. 1.5.5.

EMDF waste receipt operations will include unloading and placing waste into the landfill, spreading and compacting bulk waste using heavy equipment, and placing fill materials and filling void spaces, as required. Void filling and compaction are performed to reduce the potential for post-closure waste settlement that could affect the long-term performance of the cover system. Current EMWMF waste receipt, staging, and placement practices are detailed in UCOR procedure *Waste Placement* (PROC-EMWMF-OP-003); similar procedures will be developed and approved for EMDF prior to operations.

Water management operations and performance monitoring protocols for EMDF also will be similar to those in effect for EMWMF. The potential significance of these operational activities for long-term EMDF performance is addressed in Sect. 1.3.

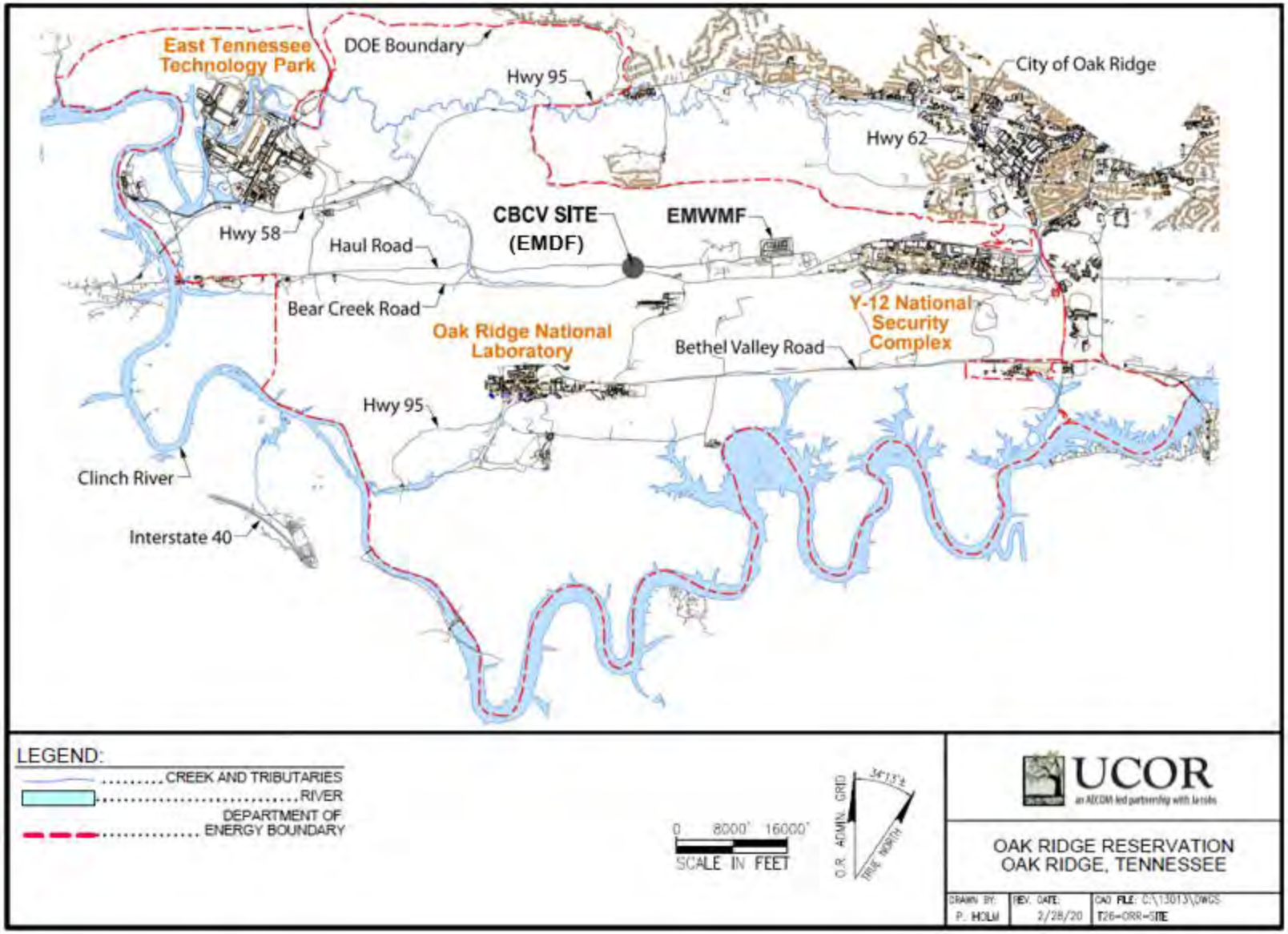

Fig. 1.1. Location map for EMDF on the ORR.

1.3 DESIGN FEATURES AND DISPOSAL SYSTEM SAFETY FUNCTIONS

The EMDF disposal system encompasses the natural features of the CBCV site, design features of the engineered disposal unit, and the operating limits (e.g., WAC) and other waste and safety management practices that ensure worker protection and post-closure facility performance. A CBCV site map showing key EMDF disposal system features and safety function is provided on Fig. 1.2. A simplified profile schematic of EMDF design and natural features and associated safety functions is provided on Fig. 1.3.

Natural features of the CBCV site important for disposal system function include the topography and geologic materials that influence groundwater flow and subsurface geochemistry. Natural topographic and hydrologic boundaries are fundamentally important to the isolation of EMDF waste from potential receptors outside of the Bear Creek watershed. These natural surface and subsurface boundaries limit the potential for short- and long-term contaminant migration via surface and groundwater pathways to the nearest populations in the city of Oak Ridge, located north of the EMDF site. The natural characteristics of the EMDF site, as well as the fact that DOE is required to maintain control of the site as long as there is a potential risk from the waste, represent important safety functions that are factored into site selection.

Selection of the small knob at the foot of Pine Ridge (Fig. 1.2) for construction of EMDF is based on the objective of hydrologically isolating the waste from natural drainage systems. The facility has been designed to maintain vertical separation of the waste from groundwater in the saturated zone beneath the disposal facility and will include a low-permeability multilayer liner and a 10-ft-thick layer of geologic buffer material between the waste and the water table. Under a long-term performance scenario, contaminant retardation in the vadose zone beneath EMDF and within the saturated matrix of the fractured rock at the CBCV site serve safety functions by delaying and attenuating impacts of radionuclide release at potential groundwater and surface water exposure points.

The EMDF preliminary design satisfies Resource Conservation and Recovery Act of 1976 (RCRA) and Toxic Substances Control Act of 1976 design requirements for hazardous and toxic waste disposal units. The engineered disposal unit consists of a multilayer liner, leachate collection and treatment systems, lined embankments for lateral containment and stability, and a multilayer final cover that completely encapsulates the waste in the post-closure period. The engineered barriers of the cover and liner systems are designed to impede the percolation of water into the waste and to retard (post-closure) the release of radionuclides through the bottom liner and into the surrounding environmental media. Perimeter berms and the cover system also serve to deter biointrusion and/or IHI that could lead to direct exposure to the waste. Engineered surface drainage systems outside of the liner footprint serve to maintain groundwater drainage and to limit increases in water-table elevation below the liner in the event of cover and/or liner system failure. A detailed description of the EMDF design features and safety functions is provided in Sect. 2.2 and Appendix C.

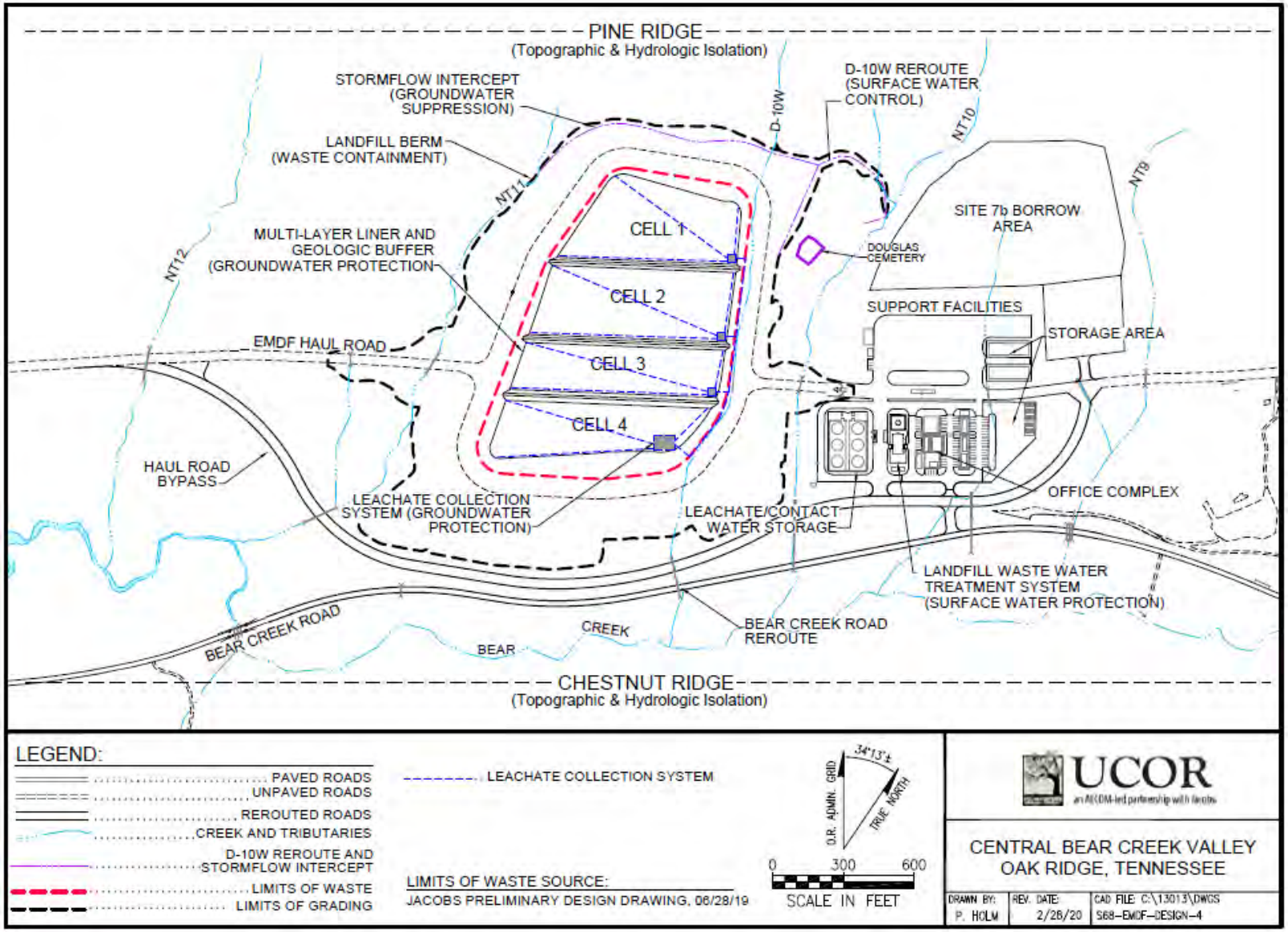

Fig. 1.2. EMDF site and design features and safety functions.

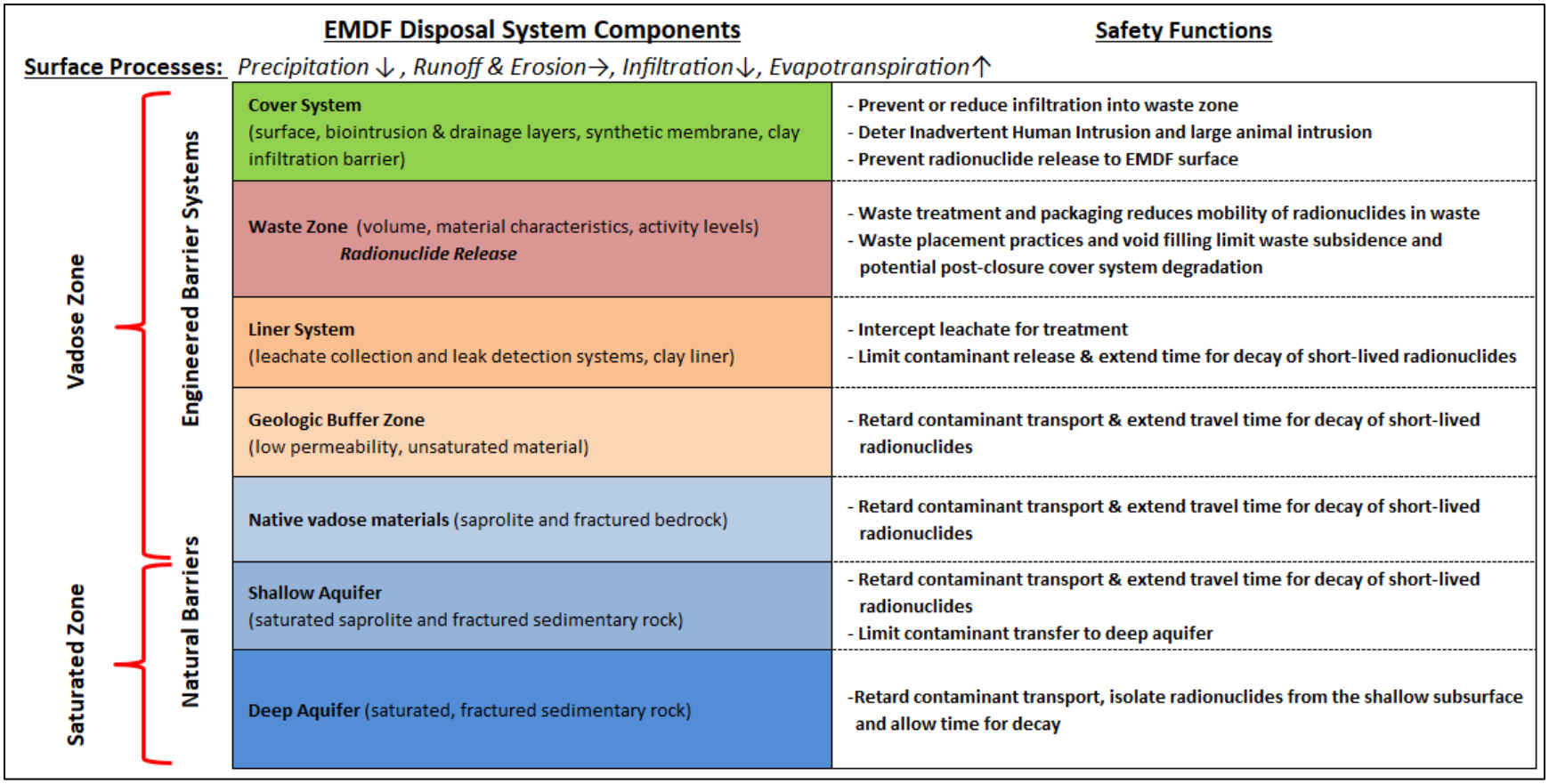

Fig. 1.3. EMDF disposal system schematic profile and safety functions.

The EMDF site and facility features are incorporated into the conceptual models and performance analyses of the PA. In general, it is assumed in the PA modeling that the effectiveness of engineered barriers decreases over time, leading to release of radionuclides through the liner system. A detailed description of natural processes that degrade design features and limit safety functions over time, and a generalized conceptual model of EMDF performance evolution, is provided in Sect. 3.2.1 and Appendix C.

EMWMF operations monitoring, including monitoring of the leachate collection and leak detection systems, provides a basis for understanding disposal system behavior during the operational period. The collection and treatment of contaminated landfill wastewater (leachate and contact water) are important safety functions of the EMDF design which can reduce the inventory of more mobile radionuclides (e.g., H-3) prior to closure, when the flux of water in contact with waste is high. For radionuclides that are assumed to be highly mobile in the PA modeling (H-3, C-14, Tc-99, and I-129), the estimated EMDF radionuclide inventory at closure (Sect. 2.3) is reduced to account for operational period losses and/or reduced mobility of contaminants in leachate treatment residuals that could be disposed in the facility. (Sect. 3.2.2.5).

Remedial investigation of historical waste disposal sites in BCV and elsewhere on the ORR and ongoing CERCLA remedial effectiveness monitoring (DOE 2017c) have provided extensive insight into the likely behavior of the EMDF system in the decades following closure, once the performance of engineered systems begins to degrade. Detailed discussion of BCV hydrology, geology, and studies of contaminant transport phenomena on the ORR is provided in Sect. 2.1.

For purposes of modeling radionuclide release, waste disposal practices that are not credited explicitly in the PA analysis include the use of waste containers (e.g., metal drums and boxes) and waste treatment prior to disposal (e.g., grouting of waste containers, macroencapsulation, etc.). Enforcement of EMDF inventory limits, activity concentration limits, and other WAC (to be developed) will provide defense-in-depth to facility performance.

Another aspect of the EMDF disposal system not credited in the PA analysis is long-term commitments of OREM and the other FFA parties to maintaining land use controls, post-closure monitoring, and facility maintenance to ensure future performance and mitigate the risk of public exposure to radionuclides. The conceptual model of EMDF performance evolution and the exposure scenarios assumed for the PA modeling do not incorporate the likelihood that DOE and successor agencies will retain control of the CBCV site well into the future. Under DOE Order (O) 458.1, requirements for public protection and CERCLA requirements for monitoring remedial performance essentially in perpetuity, loss of institutional control and/or societal memory of the disposal facility are unlikely to occur, and future release of radionuclides or other public exposure risks are likely to be identified and addressed.

1.4 LLW DISPOSAL FACILITY LIFE CYCLE AND CLOSURE PLAN

EMDF will begin accepting waste after the first phase of construction is completed, projected for the late-2020s timeframe. The current scope of ORR cleanup work is projected to be completed by approximately 2050; therefore, the expected period of EMDF operations is approximately 25 years. Construction of the EMDF is planned in three phases, proceeding from the upper (northern) to lower (southern) disposal cell. As each of the four individual disposal cells is filled to design capacity, an interim cover will be put in place to limit infiltration and leachate generation from that portion of the disposal facility. The EMDF interim cover design is assumed to be similar to that implemented for the EMWMF, which consists of a geotextile separator layer and an approximately 1-ft-thick contouring soil layer on top of the waste, overlain by a temporary flexible geomembrane to minimize infiltration into the waste zone.

EMDF closure activities will involve construction of the final cover system and removal of any unneeded infrastructure. Post-closure activities will involve cap maintenance, continued leachate collection and management, and site environmental monitoring. Final closure plans will be detailed in approved documents required under DOE orders and manuals and by the FFA (DOE 1992a). Post-closure performance monitoring will include CERCLA 5-year reviews of remedial effectiveness.

1.5 REGULATORY CONTEXT

The regulatory context for the EMDF PA is primarily set by DOE M 435.1-1 performance requirements. Additional regulatory requirements that could influence the EMDF PA analyses may be included in future documents required for authorization of EMDF operations under the FFA, including, but not limited to, the EMDF ROD, remedial design documentation, and WAC development and compliance documentation. The EMDF RI/FS includes remedial action objectives (DOE 2017b, Sect. 4) and a preliminary set of applicable or relevant and appropriate requirements (ARARs) for the disposal facility (DOE 2017b, Appendix G). Final FFA determination of the remedial action objectives, ARARs for EMDF, and a general framework for WAC development will not be available until the EMDF ROD is approved.

1.5.1 Performance Objectives

EMDF performance objectives for the PA analysis are summarized in Table 1.1. The performance objectives are taken directly from DOE M 435.1-1 and do not reflect any site-specific regulatory requirements other than the application of drinking water maximum contaminant levels (MCLs) for water resources protection objectives. EMDF performance with respect to the performance objectives or performance measures is based on PA model results for specific environmental media, transport pathways, and exposure scenarios. The period during which compliance with performance objectives must be demonstrated is 1000 years post-closure.

All Pathway: Meeting this performance objective provides a reasonable expectation that representative members of the public will not receive more than 25 percent of the primary dose limit of 100 mrem in a year from the disposal of LLW. The requirement addresses the annual total effective dose, inclusive of all potential exposure pathways except for dose from radon and its decay products in air. For the EMDF PA, the all-pathways dose considers exposures resulting from releases to groundwater and surface water only.

Air Pathway: Meeting this performance objective provides a reasonable expectation that representative members of the public will not receive, from the disposed waste, via the air pathway alone, more than 10 mrem in a year, excluding the dose from radon and its progeny. For the EMDF PA, the engineered cover system is credited for eliminating exposure via the air pathway. Justification for this assumption is provided in Sect. 3.2.2.2.

Radon Release: Meeting this performance objective provides a reasonable expectation that radon, either as a constituent of waste at the time of disposal or produced by radioactive decay following disposal, is not released from the disposal facility at a rate that would exceed the limit established in 40 *Code of Federal Regulations* (*CFR*) Part 61, Subpart Q, *National Emission Standards for Radon Emissions from Department of Energy Facilities*. The limit on ground emanation of radon (radon flux per area) is applied to the EMDF cover surface.

Water Resources Protection: Site-specific application of regulatory standards for groundwater resources is limited to assessment of compliance with MCLs for drinking water specified by EPA in the Radionuclides Final Rule (EPA 2000), promulgated in 40 *CFR* 141.66, for which the State of Tennessee has primary enforcement responsibility. Limits are specified for combined Ra-226 and Ra-228 activity concentration,

gross alpha activity concentration, total annual dose from beta decay and photon emission, and total uranium (Table 1.2). The EMDF PA demonstrates that groundwater at 100 m from the waste boundary meets these limits.

Table 1.2. Exposure scenarios, performance objectives and measures, and POAs for the EMDF PA

Exposure scenario	Performance objective or measure	POA
All pathways	25 mrem/year	Groundwater: 100 m from waste margin at the point of maximum concentration (plume centerline) Surface water: Bear Creek downstream of NT-11
Air pathway[a]	10 mrem/year[b]	100 m from waste margin
Radon flux	20 pCi/m^2/sec	EMDF cover surface
Water resources (groundwater) • Ra-226 + Ra-228 • Gross alpha activity[c] • Beta/photon activity • H-3 • Sr-90 • Uranium (total)	 5 pCi/L 15 pCi/L 4 mrem/year 20,000 pCi/L 8 pCi/L 30 µg/L	Groundwater at 100 m
Water resources (surface water)	DOE *Derived Concentration Technical Standard*[d]	Bear Creek at NT-11 tributary junction
Inadvertent human intrusion • Chronic exposure • Acute exposure	 100 mrem/year 500 mrem	 At EMDF At EMDF

[a]Air pathway is screened from the EMDF PA.
[b]Excluding radon in air.
[c]Including Ra-226, but excluding radon and uranium.
[d]DOE 2011b.

DOE = U.S. Department of Energy
EMDF = Environmental Management Disposal Facility
NT = North Tributary
PA = Performance Assessment
POA = point of assessment

In the absence of local radiological standards for surface water protection, *Derived Concentration Standards* (DCS) (DOE 2011b) are adopted for purposes of evaluating impacts to surface water resources. The impact of any future regulatory agreements regarding surface water protection standards will be evaluated.

1.5.2 POA and Timeframes for Analysis

POAs are provided for each exposure scenario shown in Table 1.2. For the EMDF PA, the POAs are identical to DOE M 435.1-1 requirements and consistent with the Disposal Authorization Statement and Tank Closure Documentation standard (DOE 2017a). The POAs do not vary with the post-closure time period, even though expected future land use and institutional controls (refer to Sect. 1.6) would preclude public exposure at the 100-m buffer zone boundary for as long as waste remains above unrestricted use criteria in the area (as required under CERCLA). Institutional controls limiting site access are assumed to be effective for 100 years following closure. These assumptions are pessimistic given that DOE is required to maintain control over land containing radionuclide sources until the land can be safely released pursuant

to DOE O 458.1, *Radiation Protection of the Public and the Environment*, and CERCLA. Additional consideration of land use and institutional controls is provided in Sect. 1.6 of this report.

Compliance with performance objectives and measures is based on PA results for the period from EMDF closure to 1000 years post-closure, with the exception of the IHI analysis for which compliance is assessed beginning at the assumed end of institutional control (100 years). Quantitative dose estimates are presented for a period of 10,000 years post-closure to provide perspective on the potential impacts beyond the 1000-year compliance period. For long-lived, relatively immobile species (e.g., radionuclides of uranium) that are significant components of the estimated EMDF inventory, PA model saturated zone concentration results beyond 10,000 years are also provided. These model predictions for the period beyond 10,000 years are highly uncertain and are presented only to indicate very long-term trends, rather than for comparison to regulatory standards.

1.5.3 Inadvertent Intrusion

Analysis of performance relative to hypothetical future IHI at EMDF is based on the performance measures for acute and chronic exposures specified in DOE M 435.1-1 and listed in Table 1.2. The EMDF PA considers two acute exposure scenarios (excavation and discovery, and well drilling) and one chronic scenario (post-drilling agricultural) consistent with the guidance in *Disposal Authorization Statement and Tank Closure Documentation* (DOE 2017a). IHI is assumed to occur after 100 years post-closure as a result of a temporary loss of institutional control of the CBCV site. IHI at EMDF is highly unlikely given that DOE is required to maintain control over land containing radionuclide sources until the land can be safely released pursuant to DOE O 458.1 and that CERCLA requires remediated sites be monitored until shown to be acceptable for unrestricted use. The extremely pessimistic biases in the IHI analysis assumptions are discussed in Sect. 6 and Appendix I.

A compliance period of 1000 years post-closure is considered for purposes of assessing EMDF performance relative to IHI performance measures. To provide perspective on potential impacts to human intruders beyond 1000 years, IHI model results are presented for a period of 10,000 years post-closure.

1.5.4 As Low As Reasonably Achievable Analysis

The as low as reasonably achievable (ALARA) process (DOE 2013a) is used to optimize EMDF performance and maintain doses to members of the public (both individual and collective) and releases to the environment as low as reasonably achievable. DOE M 435.1-1 includes a requirement for an ALARA analysis as part of the PA. The scope of ALARA considerations for the EMDF includes design optimization, disposal protocols for worker and public protection during operations, and the development of WAC by the FFA parties. These three aspects are not included in this ALARA analysis for the EMDF PA, although insights gained from the PA modeling may be relevant to design optimization or to worker protection in the post-closure period. The scope of this ALARA analysis is restricted to: (1) presenting evidence to support the finding that only a qualitative ALARA analysis is required; and (2) describing the CERCLA process for identifying LLW disposal options for the ORR CERCLA cleanup, the basis for the EMDF preliminary design and selection of the CBCV site for EMDF.

The ALARA handbook (DOE 2014) describes a graded approach to implementing the ALARA process, including the use of reference doses for determining the level of analysis required for a given project. The reference dose for a maximally exposed individual (MEI) and the reference collective dose below which only qualitative ALARA analysis is sufficient are 1 mrem/year and 10 person-rem/year, respectively. For a LLW disposal project, the timeframe of consideration for an ALARA analysis of any level should be no greater than 1000 years (DOE 2014, pages 5–8), so estimated EMDF peak dose within 1000 years is compared to the reference values. The EMDF PA modeling predicts a base case all-pathways maximum

individual dose within the 1000-year compliance period of 1.0 mrem/year (Sect. 4.5.1). The results of the probabilistic uncertainty analysis (Sect. 5.4 and Appendix G, Sect. G.6.3.3) suggest a median peak all-pathways dose of 1.0 mrem/year and a mean all pathways dose of 1.0 mrem/year at 1000 years. Based on the guidance in the ALARA handbook, these results for individual exposure indicate that a semi-quantitative ALARA analysis could be considered. However, the ALARA guidance also states that "it is the collective dose that is utilized in the ALARA analysis to select a radiation protection alternative".

Collective exposure was not modeled for the EMDF all-pathways analysis, but, given the likelihood that BCV and the CBCV site will remain under DOE control indefinitely, there are a limited range of collective exposure scenarios that are credible. Based on the assumed resident farmer scenario for the EMDF all-pathways dose analysis, a resident family of four would receive a collective dose of four persons times 1.0 mrem/year, or 4.0E-3 person-rem/year, which is far below the 10 person-rem/year reference value. Assuming a wider area of exposure would increase the potential number of exposed individuals but would decrease the number of significant exposure pathways and the maximum individual dose. The most likely scenario leading to significant collective dose would be a number of recreational fishers eating contaminated fish from Bear Creek. The EMDF PA modeling predicts a peak individual fish ingestion dose (based on a recreational rate of catch and consumption) of 0.25 mrem/year (Sect. 4.5.3). Based on this estimate, 100 recreational fish consumers would receive a collective dose of 2.5E-02 person-rem/year.

Based on the 10 person-rem/year reference value for collective dose, these model-based quantitative estimates indicate that a qualitative ALARA analysis for EMDF design and operations is sufficient. The remainder of the analysis focuses on the process for identifying LLW disposal options for the ORR CERCLA cleanup, the basis for the EMDF preliminary design, and selection of the CBCV site for EMDF.

The EMDF RI/FS includes an analysis of alternatives for disposition of LLW from CERCLA actions on the ORR. The RI/FS includes identification and screening of disposal technologies and process options (DOE 2017b, Sect. 5) and considers broader social, economic, and public policy aspects in the analysis of remedial alternatives (DOE 2017b, Sect. 7). The disposal technology screening and conceptual facility design for the CBCV site (DOE 2017b, Sect. 6) served as the foundation for preliminary engineering design (UCOR 2020b) of the RCRA-type disposal facility at the CBCV site.

The EMDF Proposed Plan (DOE 2018a) describes the remedial action objectives for CERCLA waste disposal and presents onsite disposal at the CBCV site as the preferred (optimal) alternative based on the range of considerations required under CERCLA and the FFA. CERCLA alternative evaluation threshold criteria for remedial actions include overall protection of human health and the environment and compliance with ARARs. Balancing criteria include long-term effectiveness and permanence; reduction of toxicity, mobility, or volume through treatment; short-term effectiveness; implementability, and cost. Considerations of state and community acceptance are incorporated following public review of the Proposed Plan. Thus, the FFA remedy selection process has addressed key considerations for an ALARA analysis and the disposal options considered and conclusions presented in the EMDF RI/FS and Proposed Plan are considered to meet the intent of the DOE ALARA requirements for the EMDF PA.

1.5.5 Other Requirements

1.5.5.1 DOE safety basis requirements for EMDF design

DOE expects safety to be fully integrated into the design process for new facilities. DOE O 413.3B, Chg4 (DOE 2010b) identifies the safety design basis documentation that must be developed to support each stage of a facility design effort. The safety design basis documentation provides a preliminary identification of the required engineered safety design features early in the design process. Hazard categorization and classification is performed in accordance with the methodology described in *Hazard Categorization and*

Accident Analysis Techniques for Compliance with DOE Order 5480.23, Nuclear Safety Analysis Reports (DOE 1997a). The current safety design basis documentation for EMDF includes the *Safety Design Strategy for the Environmental Management Disposal Facility, Y-12 National Security Complex, Oak Ridge, Tennessee* (UCOR 2018a) and a Conceptual Safety Design Report (UCOR 2018b) that provides the initial hazard analysis. Progressively more detailed hazard analysis documents will be developed as the EMDF design process proceeds.

1.5.5.2 Non-DOE requirements

Non-DOE regulatory requirements for design, construction, operation, and closure of EMDF derive from the FFA and CERCLA. Landfill water radiological discharge limits for EMWMF and EMDF are being determined in consultation with the FFA parties and are currently in dispute. Once finalized, the discharge limits could be applied as surface water resources protection objectives for the EMDF.

The EMDF RI/FS contains a listing of potential ARARs (DOE 2017b, Appendix G) for EMDF and analysis of potential compliance with ARARs. The final set of ARARs will be included in the EMDF ROD. Land Disposal Restrictions (LDRs) per 40 *CFR* 268 will be an ARAR for EMDF disposal of waste containing hazardous constituents above regulatory limits (e.g., for mercury). Requirements for treatment to reduce the concentration or mobility of hazardous constituents to meet LDRs will apply to some EMDF waste.

Post-ROD FFA documents will establish additional design and operational requirements for the EMDF based on collaborative discussions among the FFA parties. Future EMDF annual summary reports will include external regulatory requirements that are relevant to PA assumptions and/or the modeling approach. As part of the development of annual summary reports for the EMDF, proposed activities, new ARARs, or other new information that could challenge key assumptions for the EMDF performance analysis will be evaluated in accordance with the EMDF change control process to assess the potential for such changes to require a Special Analysis or revisions to the PA.

1.6 LAND USE AND INSTITUTIONAL CONTROLS

The EMDF site is near existing DOE waste disposal facilities and mission-critical operational facilities at Y-12 and ORNL. BCV will remain under DOE control and within DOE ORR boundaries for the foreseeable future.

Post-closure land use designations and other institutional controls are included in RODs for cleanup actions on the ORR. These controls include property record restrictions, property record notices, and access controls to limit physical access to the EMDF site (Table 1.3). A modification to the Phase I BCV ROD or some other decision document will be needed to extend the area of DOE-controlled restricted industrial use to include the CBCV site. The future land use designations in the ROD are defined solely for the purpose of setting target cleanup levels (acceptable risk criteria) and do not reflect DOE's future land use plans. The EMDF Proposed Plan (DOE 2018a) includes discussion of land use controls for BCV that would apply to the EMDF.

Assumed POAs for the EMDF PA do not take credit for the existence of land use or other institutional controls beyond 100 years post-closure. As such, the likelihood that DOE or successor federal agencies will maintain control of closed waste management facilities in BCV is considered as an aspect of defense-in-depth for the EMDF disposal system.

Table 1.3. Land use controls for EMDF

Type of control	Purposes of control	Implementation	Affected areas[a]
1. Property record restrictions[b]	Restrict use of certain property by restricting soil and groundwater use in perpetuity	Drafted and implemented by DOE upon closure of EMDF and/or transfer	EMDF landfill and site
2. Property record notices[c]	Provide information to the public about the existence and location of waste disposal areas and applicable restrictions in perpetuity	General notice of Land Use Restrictions recorded in Roane County Register of Deeds office upon completion of the remedial activity	EMDF landfill and site
3. Access controls (e.g., signs, fences, gates, portals, etc.)	Control and restrict access to the public in perpetuity	Maintained by federal government and its contractors	EMDF landfill and site

[a]Affected areas – Specific locations will be identified in the completion documents where hazardous waste has been left in place.
[b]Property record restrictions – Includes conditions and/or covenants that restrict or prohibit certain uses of real property and are recorded along with original property acquisition records of DOE and its predecessor agencies.
[c]Property record notices – Refers to any informational document recorded that alerts anyone searching property records to important information about residual contamination/waste disposal areas on the property (TCA requirement).

DOE = U.S. Department of Energy
EMDF = Environmental Management Disposal Facility
TCA = Tennessee Code Annotated

1.7 KEY ASSUMPTIONS AND MANAGING UNCERTAINTY

This section presents eight key assumptions underlying the results of the PA analyses and the compliance conclusions drawn from those results, and addresses the need to manage uncertainty in those assumptions. Section 1.7.1 presents key assumptions concerning model input parameters that could alter the conclusions of the PA concerning EMDF compliance with performance objectives. Section 1.7.2 is a description of key assumptions associated with the conceptual models that underlie the PA analyses. Section 1.7.3 presents a summary of pessimistic biases built into the PA to make the analysis conservative by over-predicting public exposure and dose. Section 1.7.4 summarizes the eight key assumptions in the context of managing uncertainties in the PA analysis.

The key assumptions presented in Sects. 1.7.1 and 1.7.2 comprise the set of critical assumptions against which new information must be reviewed to assess the need for a Special Analysis or revision of the PA. Examples of new information requiring screening or evaluation under the EMDF change control process include proposed design changes, new data relevant to key parameter uncertainties, changes in disposal practices, new regulatory requirements, new waste streams or updated inventory estimates. This summary of assumptions does not encompass specific preliminary design specifications for the EMDF. Any new information that could challenge key assumptions for the EMDF performance analysis will be evaluated in accordance with the EMDF change control process.

1.7.1 Key Parameter Assumptions

Based on the particular conceptual models (Sect. 3.2) and model codes (Sect. 3.3) adopted for the EMDF performance modeling, the assumed range of values for a few key input parameters determines the likelihood of peak all-pathways dose exceeding the 25 mrem/year performance objective during the 1000-year compliance period. Results from the probabilistic uncertainty analysis for the compliance period (Sect. 5.4.1) show peak total doses that exceed 25 mrem/year are associated with I-129 contributions that

occur at the end of the simulation period. Those extreme peaks are rare (< 1 percent of 3000 simulated peaks) and result from lower than average sampled K_d values for I-129 in combination with other factors that favor earlier release and rapid radionuclide transport. Uncertainty in the estimated inventory of dose-significant, mobile radionuclides (C-14, Tc-99, and I-129) is also important to consider in judging the likelihood of EMDF compliance from the results of the compliance period performance modeling. The key parameter assumptions are listed below, and the remainder of Sect. 1.7.1 provides additional detail and context:

1) Iodine-129 partition coefficient (K_d) values for the engineered barriers and geologic materials below the EMDF liner are greater than 1 cm^3/g.
2) IF the I-129 K_d value is less than 1.5 cm^3/g, THEN: the values for the input parameters (refer to following paragraph) that determine cover infiltration, vadose zone thickness, and saturated zone flux (Darcy velocity) satisfy one or more of the following conditions:
    a) Average annual cover infiltration is less than or equal to 0.88 in./year.
    b) The average thickness of the unsaturated zone below the waste is greater than or equal to 31 ft.
    c) The Darcy velocity characterizing long-term average conditions within the saturated zone along the flow path from the waste to the well is greater than or equal to 4.75 ft/year.
3) The estimated post-closure EMDF average I-129 activity concentration is less than 0.41 pCi/g.

K_d for I-129 > 1 cm^3/g. Compliance period peak total doses greater than 25 mrem/year were associated exclusively with sampled I-129 K_d values ≤ 1 cm^3/g, whereas the assumed value for the base case deterministic model run is 2 cm^3/g for the waste and 4 cm^3/g for all other materials. However, not all simulations with sampled I-129 K_d values ≤ 1 cm^3/g are associated with very large peaks because other input parameter also affect the timing and rate of I-129 release or how quickly radionuclides arrive at the groundwater POA. The RESRAD-OFFSITE model input parameter values that favor very large peak doses (for I-129, K_d ≤ 1 cm^3/g) include waste zone properties (large b-parameter and small dispersivity), high cover infiltration (> 0.88 in./year) small (< 800 year) release duration, small (< 16 ft) thickness of unsaturated zone 5, and a combination of small (< 4.75 ft/year) saturated zone Darcy velocity and shallow (< 131 ft) well depth. Uncertainty in most of these input parameters is difficult to quantify or reduce, whereas the uncertainty in I-129 K_d values is essentially a data gap in the PA analysis. Laboratory measurements of Tc-99 and I-129 sorption on Conasauga Group samples have been planned to eliminate this data gap (Sect. 8.3). For the present EMDF performance modeling, adopting an I-129 K_d value > 1 cm^3/g is a key parameter assumption that supports a reasonable expectation of compliance with the 25 mrem/year performance objective during the 1000-year compliance period.

Estimated inventories for mobile radionuclides. There is considerable uncertainty in the estimated activity inventories of C-14, Tc-99, and I-129, which are the three more mobile dose drivers for the performance analysis. The estimated radionuclide inventory for EMDF waste (Appendix B) is biased high (overestimated activity concentrations) to manage uncertainty in future waste characteristics. Carbon-14 and I-129 inventories in particular may be overestimated due to inclusion of some non-representative, high activity data in the analysis. However, operational period losses of mobile radionuclides are estimated (Sect. 2.3) and used to adjust (reduce) the modeled inventories of H-3, C-14, Tc-99, and I-129, which introduces additional uncertainty in the post-closure average concentrations assumed for the highly mobile dose-drivers. For C-14 and Tc-99 the estimated operational losses are high (81 percent and 44 percent respectively), but model sensitivity analysis (Sect. 5.3) and the compliance period distribution of peak total dose (Sect. 5.4.1) suggests that this uncertainty is unlikely to challenge the conclusion that C-14 and Tc-99 dose contributions combined will not exceed the all-pathways performance objective. For I-129, estimated operational losses are small (< 13 percent) due to the assumed K_d value for the waste (2 cm^3/g), so the assumed I-129 activity inventory is still biased high relative to more realistic expectations. The likelihood

that I-129 inventory is overestimated also decreases the probability that a lower than assumed I-129 K_d value will result in the peak compliance period dose exceeding 25 mrem/year. The conclusion is that although post-operational inventory uncertainties for C-14, Tc-99, and I-129 are high, only the assumed EMDF average I-129 activity concentration value applied in the PA models constitutes a key parameter assumption that supports determination of EMDF compliance with the all-pathways performance objective.

1.7.2 Key Conceptual Model Assumptions

Conceptual models for the evolution of EMDF hydrologic performance (Sect. 3.2.1), radionuclide release as engineered barriers degrade (Sect. 3.2.2), and transport of radionuclides upon release to the natural environment (Sects. 3.2.2 and 3.2.3) are the basis for the selection and implementation of computer software (model codes) to simulate EMDF performance. Simplifying assumptions associated with particular conceptual models and codes can constrain the range of PA model results produced to support compliance conclusions. There are a few simplifying assumptions that apply to the EMDF performance analyses for which alternative conceptualizations (different assumptions) could affect the PA results, if not the conclusions concerning EMDF compliance. The PA model sensitivity and uncertainty evaluations (Sect. 5) are performed to address uncertainty in conceptual models.

1) **Failure of Engineered Barriers**. The PA modeling assumes that post-closure degradation of the EMDF cover and liner systems occurs gradually due to the cumulative effect of environmental processes (e.g., cover erosion, waste settlement, oxidation and stresses on the high-density polyethylene [HDPE] layer) on the properties of engineered materials (Sect. 3.3.1). Progressive failure of engineered barriers results in increasing cover infiltration and leachate release. The assumed rate of degradation (see item #2 below) is highly pessimistic based on reasonable expectations for the performance of HDPE membranes and clay infiltration barriers. The EMDF preliminary engineering design (including seismic stability evaluations) is assumed to prevent sudden EMDF failure due to extreme (very low probability) seismic or weather events.

2) **Cover System Performance.** The EMDF final cover design is assumed to effectively prevent significant release of radionuclides through the cover to the atmosphere and biosphere (Sect. 3.2.2). Failure of the cover (increasing infiltration) due to HDPE and clay barrier degradation begins at 200 years post-closure. Cover infiltration increases gradually to a maximum average annual long-term value of 0.88 in./year at 1000 years post-closure. Sensitivity to uncertainty in the potential impacts of release through the cover was evaluated to support screening of that release pathway from the PA analysis (Sect. 3.2.2.3). Sensitivity to uncertainty in the timing and duration of cover performance degradation and the magnitude of long-term cover infiltration was evaluated for the PA models (Sect. 5).

3) **Liner System Performance.** The base case EMDF performance scenario assumes that during the post-closure period after leachate collection ends, the liner system will release leachate at a rate sufficient to prevent waste saturation and overtopping of the liner (bathtub conditions). The potential impact of a persistent bathtub condition leading to leachate release at the cover surface is analyzed in Appendix C, Sect. C.3.

4) **Radionuclide Release.** In the PA models, the EMDF waste volume is conceptualized as a homogeneous, soil-like material in which the estimated radionuclide inventory is uniformly distributed. This conceptual model includes an assumption about the mass of clean fill material that is required to minimize void space and limit post-closure waste settlement. Estimated waste average activity concentrations are adjusted (reduced) to account for this mass of clean fill (Sect. 3.2.2.5). Radionuclide release from the waste is based on equilibrium partition between the solid and aqueous phases and assumes that a concentration-independent K_d adequately captures the desorption process (Sect. 3.2.2.6). To account for uncertainty in waste geochemistry and release kinetics, the waste K_d values are reduced

by a factor of two from the assumed base case values; this is a pessimistic approach because it is likely that sorption by the clean fill emplaced with the waste will be substantial. This conceptual model does not account for the variety of different waste forms (e.g., contaminated demolition debris and equipment) or the effect of waste containers, waste stabilization (grouting), or treatment to reduce the mobility of radionuclide in EMDF waste (Sect. 1.7.3, item #5). The sensitivity of RESRAD-OFFSITE model results to assuming alternative release models (Sect. 5.3) was evaluated to account for the possibility that these waste forms would tend to delay and/or retard the release of radionuclides.

5) **Uniform Release to Groundwater**. The sloping geometry of the EMDF liner system, heterogeneity in activity concentrations, and the possibility of spatially variable failure (leakage) of the cover and liner systems over time could cause non-uniform radionuclide release from the waste to the underlying vadose zone. The STOMP model (Sect. 3.3.2) is used to capture the impact of the sloping liner and variable waste thickness on the release pattern, but assumes homogenous activity concentrations in waste and uniform cover infiltration. The MT3D saturated zone radionuclide transport model (Sect. 3.3.3.2) is used to evaluate the difference between a uniform release conceptual model and a simplified non-uniform release conceptualization. Those results (Sect. 5.2.2) and the STOMP model release simulations are compared to total system model (RESRAD-OFFSITE) results that assume uniform radionuclide release and incorporate less detailed, semi-analytical models of transport through the vadose and unsaturated zones. The comparison of model results (Sect. 3.3.5) is the basis for ensuring that the RESRAD-OFFSITE uniform release model and simplified representation of the transport pathways do not under predict peak radionuclide concentrations at the groundwater POA. This model integration process served to manage uncertainty about the uniformity of release by demonstrating that the uniform release assumption would lead to earlier and higher peak concentrations at the POA.

1.7.3 Pessimistic Biases Intended to Make the Analysis Conservative

There are a number of important assumptions made that are intended to bias the analysis to predict higher potential exposure and dose. These assumptions are adopted to manage the uncertainty in future waste characteristics and public exposure scenarios.

1) **Institutional control of the EMDF**. The PA analyses assume loss of institutional control by DOE or successor agencies at 100 years post-closure. DOE O 458.1 requires that DOE maintain control over sites until they can be released, and public knowledge of the activities at the Oak Ridge site would be expected to persist well into the future. Thus, it is more likely that institutional and societal knowledge of the facility and radiation risks would persist over multiple centuries and that efforts to maintain facility performance to protect the public will continue.

2) **Early cover system failure.** The PA base case modeling pessimistically assumes that significant degradation of the EMDF cover system begins 100 years after the loss of institutional control (i.e., 200 years post-closure). The conceptual model also assumes that complete degradation (maximum long-term cover infiltration) occurs by 1000 years post-closure. These assumptions result in relatively early peak concentrations at the POA locations. Based on the potential for long-term institutional control (refer to item #1 above) and extended performance of cover components (> 1000 years; Appendix C, Section C.1.2), it is likely that the cover system performance will be much better over the 1000-year compliance period than is assumed for the PA. Radionuclide release over a period longer than 800 years could also reduce peak environmental concentrations and dose impacts compared to the base case assumption.

3) **Exposure scenario**. The exposure scenario for the all-pathways dose analysis assumes an MEI rather than a more representative future member of the public. The receptor is assumed to be a farming household member (residential farmer) that drinks contaminated groundwater from a well at 100 m

from the waste at the location of maximum radionuclide concentration. The receptor also consumes plant and animal foods grown onsite using contaminated Bear Creek water for irrigation and watering livestock. The assumed proximity of the groundwater POA (100 m) and surface water POA (approximately 300 m) to the facility is extremely pessimistic, even in the absence of institutional controls on site access (refer to item # 1 above). These MEI and POA assumptions result in higher dose predictions than would similar public exposure scenarios with equally likely assumptions regarding human behaviors and exposure locations.

4) **Estimated radionuclide inventory.** Modeled radionuclide inventories are based on the full EMDF waste volume capacity (2.2 million cy), and average activity concentrations for EMDF waste streams are likely over-estimated. The EMDF design capacity incorporates an added 25 percent to the projected CERCLA waste volume (DOE 2017b, Appendix A) to account for volume uncertainty. The approach to estimating activity concentrations in waste is intended to overestimate concentrations to account for uncertainty in the characteristics of future remediation waste (Appendix B). As a result, the activity inventories used in the PA models are higher than inventories likely to be present at EMDF closure.

5) **Waste containers and stabilization.** The conceptual model of radionuclide release from waste disposed in EMDF (Sect. 1.7.2, item #4) incorporates no assumptions to account for (credit) the use of waste packaging (containers), waste stabilization (e.g., grouting in the disposal facility), or treatment to reduce the mobility of contaminants. It is likely that these waste disposal practices would delay and/or retard the release of radionuclides, and possible that peak concentrations at the POA locations would be delayed and/or decreased relative to the results of the PA modeling.

1.7.4 Summary of Key Assumptions in the PA

Key parameter assumptions for EMDF compliance include:

1) Iodine-129 partition coefficient (K_d) values for the engineered barriers and geologic materials below the EMDF liner are greater than 1 cm^3/g.
2) IF the I-129 K_d value is less than 1.5 cm^3/g, THEN: the values for the input parameters (refer to following paragraph) that determine cover infiltration, vadose zone thickness, and saturated zone flux (Darcy velocity) satisfy one or more of the following conditions:
   a) Average annual cover infiltration is less than or equal to 0.88 in./year.
   b) The average thickness of the unsaturated zone below the waste is greater than or equal to 31 ft.
   c) The Darcy velocity characterizing long-term average conditions within the saturated zone along the flow path from the waste to the well is greater than or equal to 4.75 ft/year.
3) The estimated post-closure EMDF average I-129 activity concentration is less than 0.41 pCi/g.

Uncertainty in these three key assumptions will be addressed with laboratory measurements of iodine K_d for CBCV site materials and by future refinements in the estimated I-129 inventory.

Conceptual models of the evolution of engineered barrier performance and radionuclide release are important for understanding the implications of selecting once conceptualization versus another, and for integrating model codes that apply different conceptual models or levels of detail. Key assumptions related to conceptual models adopted for the PA analysis include:

1) **Failure of engineered barriers.** Post-closure degradation of the EMDF cover and liner systems occurs gradually and results in increasing cover infiltration and leachate release.

2) **Cover system performance.** The EMDF final cover will prevent significant release of radionuclides to the cover surface. Infiltration barriers in the cover fail completely within 1000 years and cover infiltration increases gradually to a maximum average annual long-term value of 0.88 in./year at 1000 years post-closure.

3) **Liner system performance.** The liner system will release leachate at a rate sufficient to prevent waste saturation and overtopping of the liner (bathtub conditions).

4) **Radionuclide release.** EMDF waste is conceptualized as homogeneous, soil-like material in which the estimated radionuclide inventory is uniformly distributed. Radionuclide release from the waste is modeled as equilibrium desorption from a soil-like material.

5) **Uniform release to groundwater.** Radionuclide release from the waste and liner system to the vadose and saturated zones is spatially uniform. Non-uniform release does not result in earlier or larger peak concentrations at the POA locations.

Model sensitivity and uncertainty analyses in the PA (Sect. 5) are completed to assess and manage uncertainty in key parameter and conceptual model assumptions. The potential for new information to challenge PA key assumptions will be evaluated in accordance with the EMDF change control process. Several important pessimistic assumptions regarding the exposure scenario, radionuclide inventories, long-term cover performance, and waste characteristics are incorporated in the PA to account for uncertainty in future human behavior and waste management practices (e.g., waste treatment and containerization). These pessimistic assumptions bias the analysis toward larger estimated all-pathways dose.

This page intentionally left blank.

2. SITE AND FACILITY CHARACTERISTICS

This section provides detailed descriptive information and data for the EMDF site, the local environment, and the disposal facility to provide the basis for the conceptual model(s) of the disposal system. A total systems perspective is provided, recognizing the interrelationship of site characteristics and the conceptual facility design, including reasonably foreseeable natural processes (e.g., climate impacts) that might disrupt natural and engineered barriers**.**

2.1 SITE CHARACTERISTICS

2.1.1 Geography, Demographics, and Land Use

2.1.1.1 Site description

The proposed EMDF site is located on the 33,542-acre ORR within the city limits of Oak Ridge, Tennessee, approximately 12.5 miles west-northwest of Knoxville, Tennessee, in Roane and Anderson counties. The regional setting is shown on Fig. 2.1, including the Lower Clinch and Tennessee Rivers and the locations of the three DOE sites (ETTP, ORNL, and Y-12) within the ORR. The proposed EMDF will be located on DOE property approximately 3 miles southwest of Y-12. BCV between Y-12 and the CBCV site (Fig. 2.2) is a historical waste management area that contains several closed disposal facilities, contaminant source areas, and groundwater contaminant plumes, in addition to the currently operating EMWMF.

The ORR is located in the western portion of the Valley and Ridge physiographic province, which is characterized by long, parallel ridges and valleys that follow a northeast-to-southwest trend. The ground elevations within the ORR range from a low of 750 ft above mean sea level (MSL) along the Clinch River to a high of over 1300 ft above MSL on Copper Ridge. The Valley and Ridge physiographic province developed on thick, folded, and thrust-faulted beds of sedimentary rock deposited during the Paleozoic era. Thrust fault patterns and the strike and dip of the beds control the locations, shapes, and orientations of the ridges and intervening valleys. The topography of the BCV watershed and surrounding areas along with underlying geologic units is illustrated in Fig. 2.2. Additional detail on the local topography in relation to geologic features is provided in Sect. 2.1.3.1.

BCV is approximately 10 miles long and extends from the topographical divide near the west end of the Y-12 industrial area to the Clinch River. The valley is bounded by Pine Ridge on the northwest and Chestnut Ridge on the southeast. Bear Creek drains to the southwest along the lower elevation southeast margin of the valley. Elevations range from highs near 1260 ft along the crest of Pine Ridge to around 800 ft where Bear Creek exits BCV through the water gap in Pine Ridge at State Route (SR) 95. The topographic relief between valley floors and ridge crests is generally on the order of 300 to 350 ft. Several smaller tributaries, designated as the North Tributaries (NTs) (numbered sequentially as NT-1, -2, etc. from northeast to southwest) drain southward into Bear Creek from Pine Ridge across the geologic strike of the valley. The proposed EMDF site is located between Bear Creek tributaries NT-10 and NT-11 on the discontinuous ridge that lies between Pine Ridge and Bear Creek (Fig. 1.2).

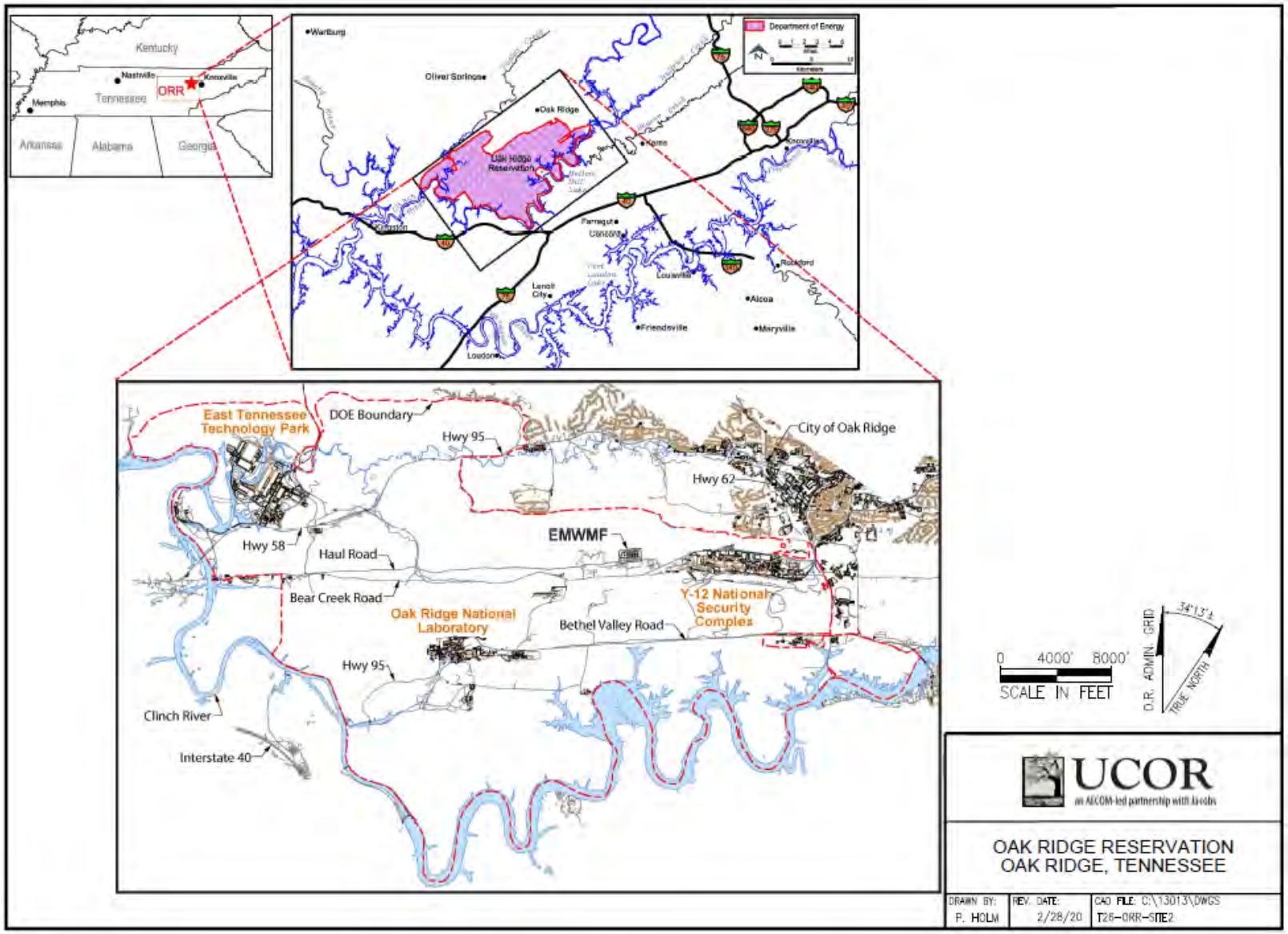

Fig. 2.1. ORR, EMWMF and nearby population centers

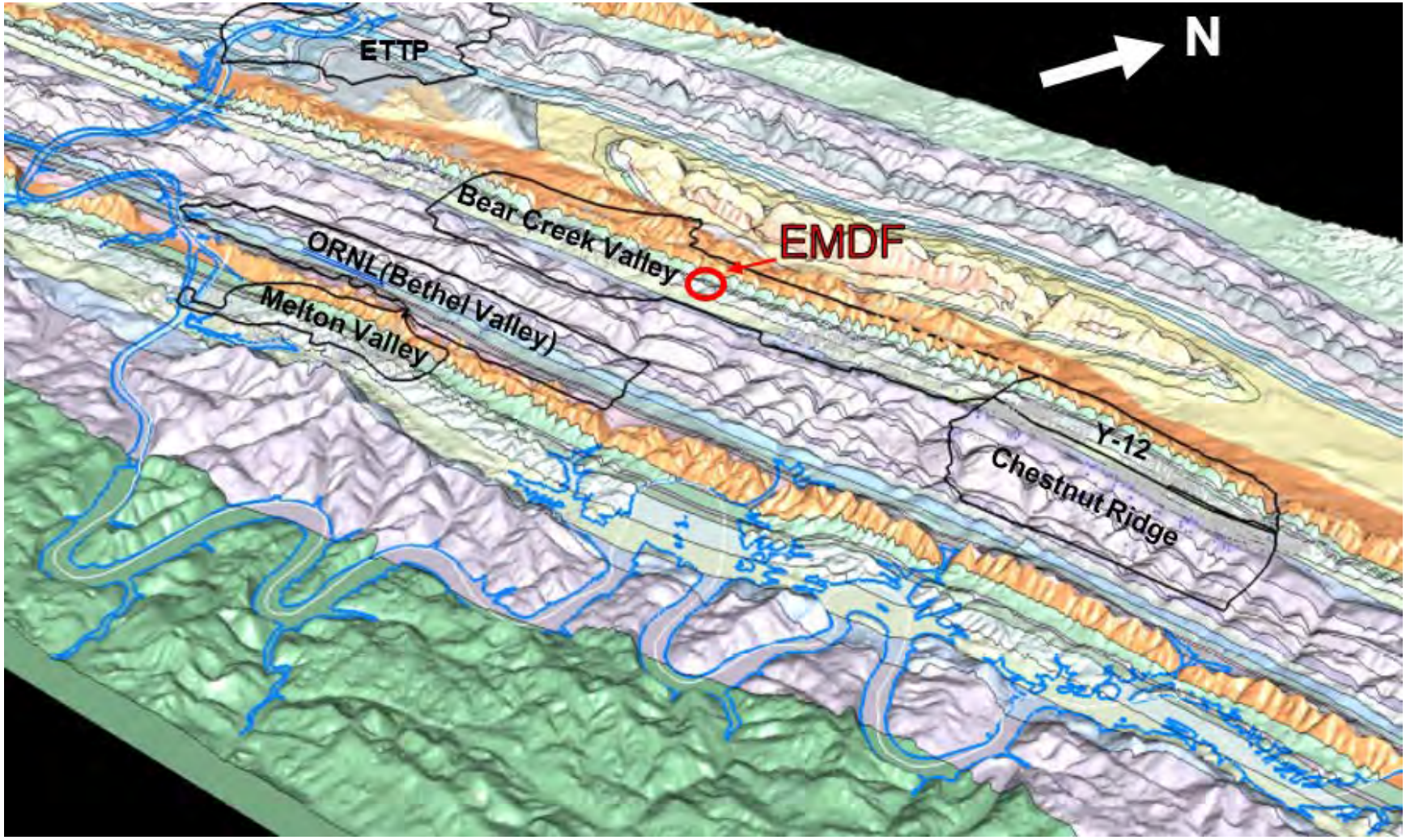

Fig. 2.2. Perspective view of topography and geologic units underlying the ORR, with CERCLA administrative watershed boundaries and EMDF location

2.1.1.2 Population distribution

The five Tennessee counties surrounding the proposed EMDF site (Anderson, Knox, Loudon, Morgan, and Roane) have a total 2010 census population of 632,079 and over 286,000 housing units. The basic demographic data for the five-county area is summarized in Table 2.1.

Table 2.1. Total 2010 population in five nearest counties

County	Population	Housing units
Anderson	75,129	34,717
Knox	432,226	194,949
Loudon	48,556	21,725
Morgan	21,987	8,920
Roane	54,181	25,716
TOTALS	**632,079**	**286,027**

Source: U.S. Census Bureau, 2010 Census.

Oak Ridge, the nearest city, has a population of 29,330 (2010 census), of which 3059 reside in Roane County and the remaining 26,271 reside in Anderson County (Fig. 2.3). The proposed EMDF site lies in Roane County census tract 9801, which has no residential population. Populations of adjoining census tracts are provided in Tables 2.1 and 2.2. Roane County census tract 301 is closest to the proposed EMDF site and had a 2010 population of 3224. This tract includes the entire west end of Oak Ridge east of the Clinch River. Tract 301 had a population density of 459 persons/sq mile in 2010. Anderson County census Tract 201 is closer to the EMWMF site and had a population of 3111 in 2010. The 2010 population density for tract 201, which includes much of the center of Oak Ridge, is 585 persons/sq mile. Tract 9801 includes the DOE property in Anderson and Roane counties and has a residential population of zero. The U.S. Census Bureau projected that Anderson County population would grow by 19 percent from 2010 (75,129) to 2064 (89,814), and that Roane County population (54,181) would decline by about 10 percent over the same period (53,373).

The age distribution for Oak Ridge is skewed towards an older population than for the state of Tennessee as a whole, with slightly lower percentages in the age groups from birth to age 44 and slightly greater population in the age groups from age 45 to over age 85. The gender distribution for Oak Ridge is similar to that of the rest of Tennessee. The estimated 2017 racial composition of Oak Ridge is 78.2 percent white, 7.0 percent Hispanic, 6.8 percent black, 3.5 percent Asian, and 0.4 percent other races. About 4.4 percent of the population identifies as mixed race (City Data 2020).

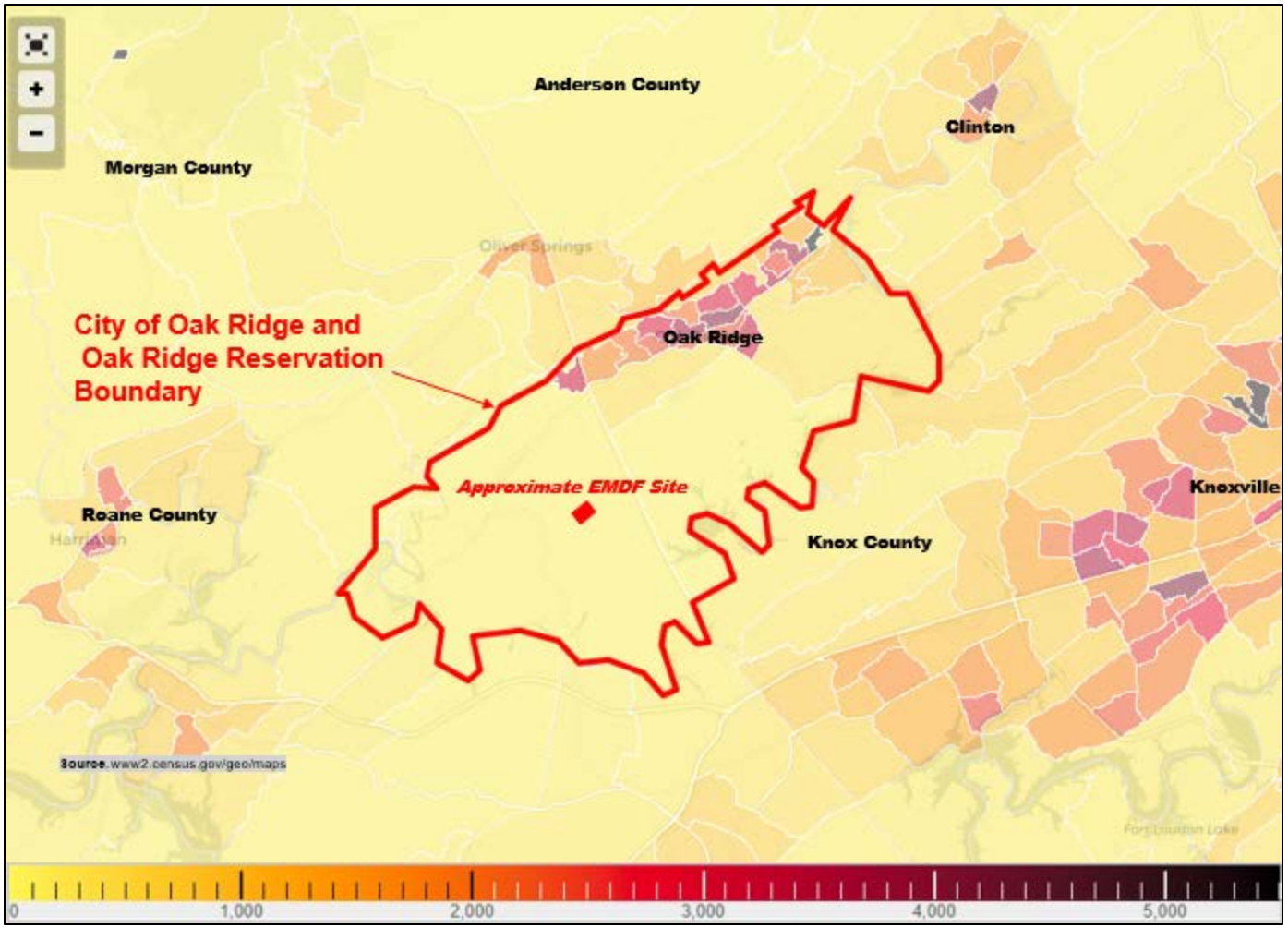

Fig. 2.3. Population density by census block group in the vicinity of the ORR

Table 2.2. Population data for adjacent census tracts in the 2010 census

County	Tract	2010 population
Anderson	201	3111
	202.01	3670
	202.02	4507
	9801	0
Roane	9801	0
	301	3224
Knox	59.06	1671
	59.07	2970

Source: U.S. Census Bureau, 2010 Census.

DOE and DOE contractors employ a large proportion of the local work force. The number of employees involved in DOE OREM work during 2009 was 13,621. This total includes both federal and contractor employees. Employees reside in over 20 counties (Fig. 2.4). Knox, Anderson, and Roane counties together are home to about 82 percent of these employees. The top five counties account for 89 percent of employees and 92 percent of the 2009 DOE payroll. Payroll data for the top five counties in 2012 are provided in Table 2.3.

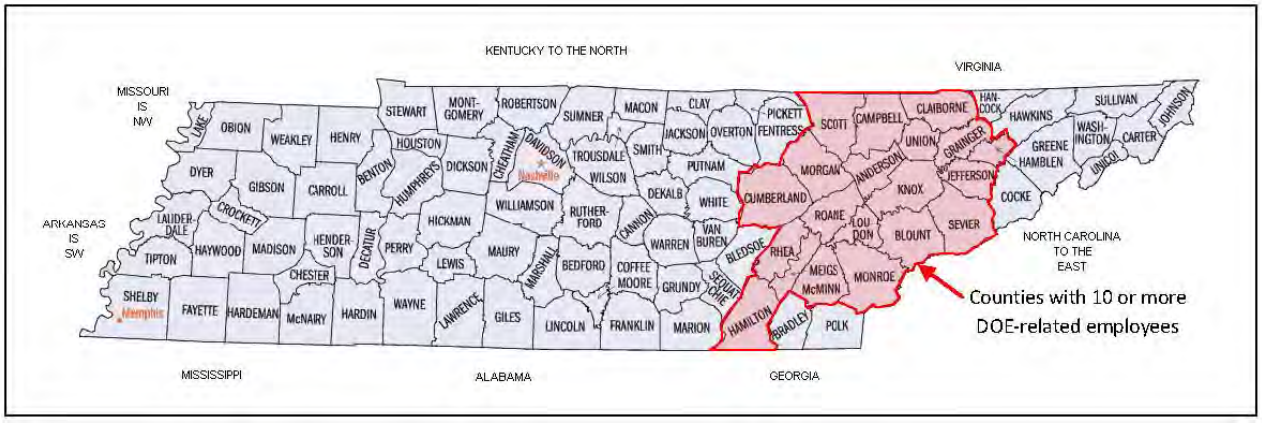

Fig. 2.4. Tennessee counties in which 10 or more OREM employees lived during 2012

Table 2.3. DOE OREM employees and payroll for the top five counties in 2012

County	2012 employees	2012 payroll
Knox	5721	$511,329,075
Anderson	3065	$246,469,051
Roane	1978	$157,088,580
Loudon	669	$56,489,413
Blount	405	$31,332,173

Source: http://www.oakridge.doe.gov/external/portals/0/hr/12-31-12%20payearoll%20&%20residence.pdf.

DOE = U.S. Department of Energy
OREM = Oak Ridge Office of Environmental Management

2.1.1.3 Use of adjacent lands

DOE Land Use Near the EMDF Site. The land on the ORR is used for multiple purposes to meet the mission goals and objectives of DOE, and approximately one-third of the land (11,300 acres) is thoroughly developed for research and operations (ORNL 2002) as ETTP, ORNL, and Y-12. Uses of the land area surrounding the developed DOE facilities include national security activities, site safety and security operations, and emergency planning; research and education; environmental cleanup and remediation; environmental monitoring; wildlife management; biosolids land application; protection of cultural and historic resources; wildland fire prevention; land-stewardship activities; use and maintenance of reservation infrastructure; and activities in public areas (DOE 2008). Biological and ecological research also occurs within in the large-scale Oak Ridge Environmental Research Park (ORERP), which encompasses the majority of the ORR's 20,000 acres (DOE 2011c). The ORERP, established in 1980, is used by the nation's scientific community as an outdoor laboratory for environmental science research on the impact of human activities on the eastern deciduous forest ecosystem.

The EMDF site is near existing waste disposal facilities, the operational area of Y-12, and the Spallation Neutron Source at ORNL (SNS on Fig. 2.5), and will remain under DOE control and within DOE ORR boundaries for the foreseeable future. The Phase I BCV I ROD (DOE 2000) divides the BCV watershed into three zones to set cleanup goals and define residual risks following remediation. The proposed EMDF site is located in Zone 2, which requires cleanup levels that meet future recreational use in the near-term and unrestricted use in the future. The EMDF ROD will modify the land use to extend Zone 3 (designated future cleanup to a land use of "Controlled Industrial Use" in the Phase I BCV ROD) to encompass the EMDF site.

Existing source areas and groundwater contaminant plumes from the S-3 Ponds and former Boneyard/Burnyard, Oil Landfarm, and Bear Creek Burial Grounds (BCBG) disposal sites are all hydraulically upgradient of the proposed EMDF site. Implications of this historical contamination into the protectiveness assessment are presented in the CA and will be considered when designing future EMDF performance monitoring.

Non-DOE Land Use Near the EMDF. Land uses nearby, but outside of ORR, are predominantly rural, with agricultural and forest land dominating, and urban development within adjacent portions of the city of Oak Ridge. The residential areas of the city of Oak Ridge that abut the ORR are primarily along the northern and eastern boundaries of the reservation (Fig. 2.3). Some Roane County residents have homes adjacent to the western boundary of the ORR.

The EMDF site in relation to the nearest residential areas bordering the DOE property boundary to the north (areas to the south of BCV include non-residential DOE controlled land) is shown in Fig. 2.5. The nearest Oak Ridge communities include Country Club Estates (0.8 mile away on the north side of Pine Ridge) and the historic Scarboro community (3.5 miles away), as well as isolated homes located across the more rural intervening area. Pine Ridge separates these residential areas from Y-12 and BCV. Groundwater and surface water flow directions and prevailing wind patterns would move any EMWMF or EMDF releases away from these residential areas. Future development in these areas may increase populations near the EMDF site, but residential use of the adjacent property will not be impacted by EMDF operations.

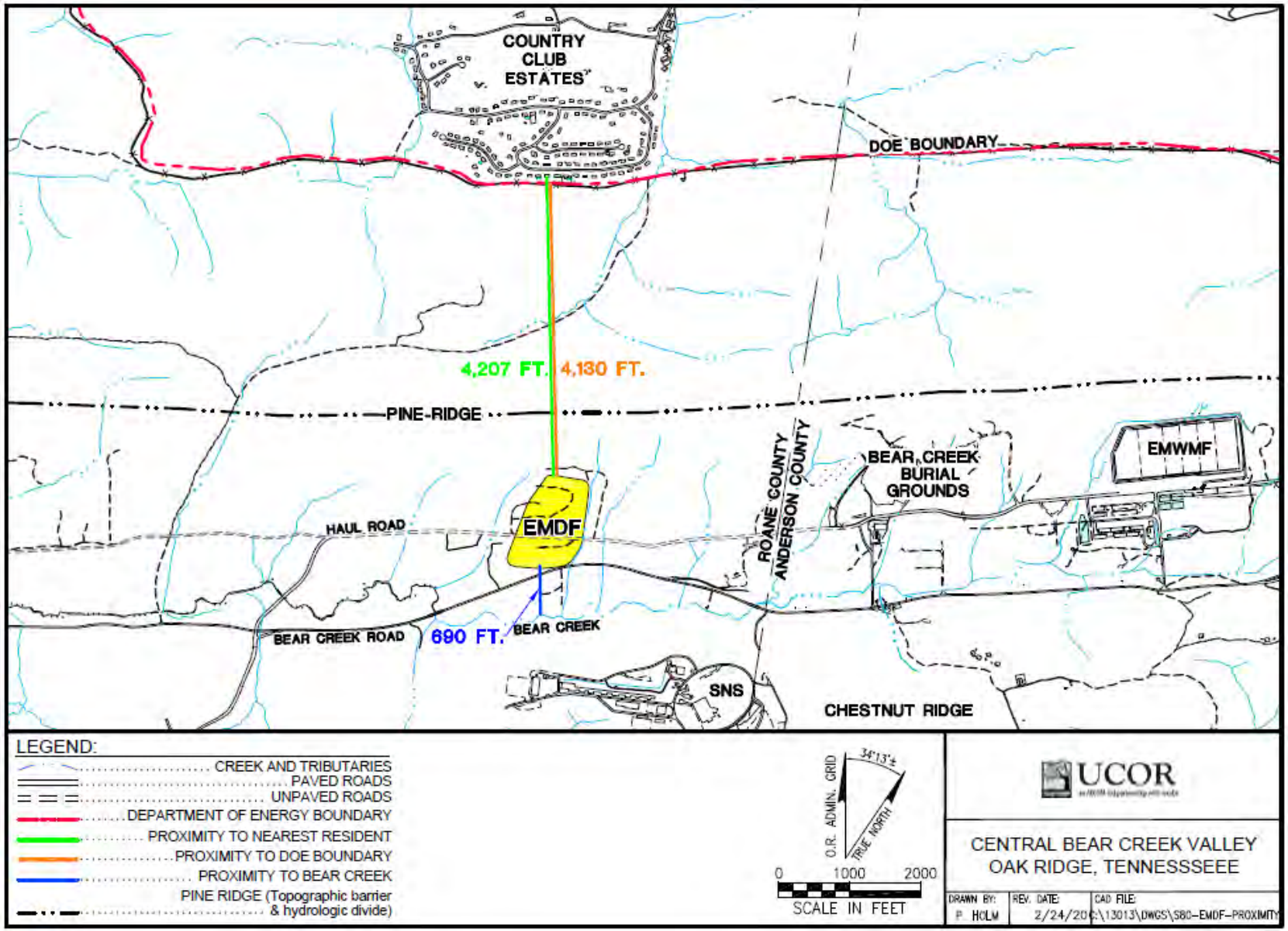

Fig. 2.5. DOE boundary and residential land use near the EMDF site in Bear Creek Valley

2.1.2 Meteorology and Climatology

The Oak Ridge area climate may be broadly classified as humid subtropical (Parr and Hughes 2006). The region experiences warm to hot summers and cool winters. Abundant climate data are available from the National Oceanic and Atmospheric Administration stations in Oak Ridge and ORNL, which operates seven meteorological towers scattered over the ORR. The summary of climate information provided in this section is limited to precipitation records to support hydrologic model inputs for the EMDF PA.

Current climate normal values (1981 to 2010) from the National Weather Service (NWS) for the Oak Ridge area are 50.91 in. for annual precipitation and 58.8°F for mean annual temperature. Precipitation is distributed uniformly through most of the year, with normal monthly precipitation for August through October averaging about 1 in. lower than during other months (Fig. 2.6). These 3 months of lower precipitation and high temperatures tend to comprise a seasonal dry period in which evapotranspiration losses are large relative to inputs of rainfall.

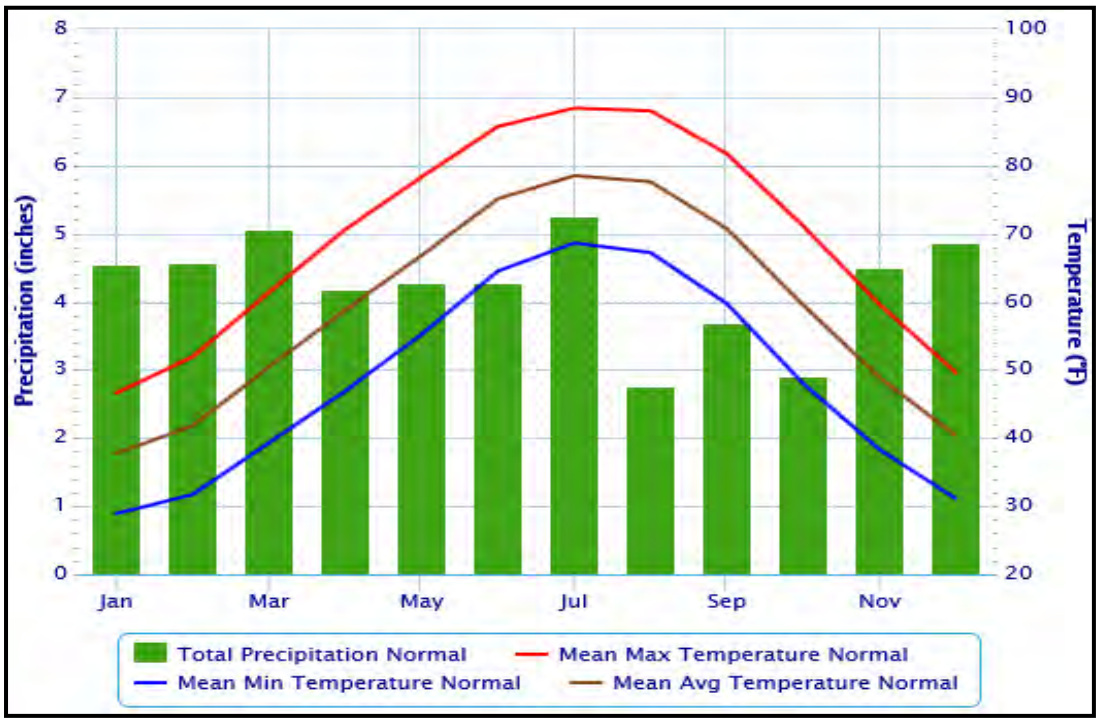

(Source: National Atmospheric and Oceanic Administration – NWS)

Fig. 2.6. Monthly climate normals (1981 to 2010), Oak Ridge area, Tennessee

Local inter-annual variability in precipitation is significant. For the NWS meteorological station in Oak Ridge (KOQT), precipitation records from 1999 through 2013 show a range in annual totals from 34.9 in. (2007) to 71.1 in. (2011), with the average annual total of 54.7 in. (Fig. 2.7). Precipitation records assembled from Oak Ridge and nearby stations for the 68-year period from 1948 to 2015 indicate minimum, average, and maximum annual precipitation totals of 35.9, 52.64, and 76.3 in., respectively (ORNL 2014). These data do not suggest any trend or cyclic variation in annual total precipitation on the time scale of the period of record (Fig. 2.8). Longer term records (1895 to 2013) assembled for the East Tennessee region indicate a similar average and range in annual total precipitation.

Rainfall intensity varies widely on seasonal, monthly, and shorter timescales (Fig. 2.9). Oak Ridge monthly total precipitation for the period 1990 to 2014 ranged from less than 0.1 in./month to over 14 in./month, with an average monthly total of 4.6 in. Monthly values of 24-hour maximum precipitation for the same period range from less than 0.1 in./24 hours to over 6.5 in./24 hours, with an average of 1.7 in./24 hours.

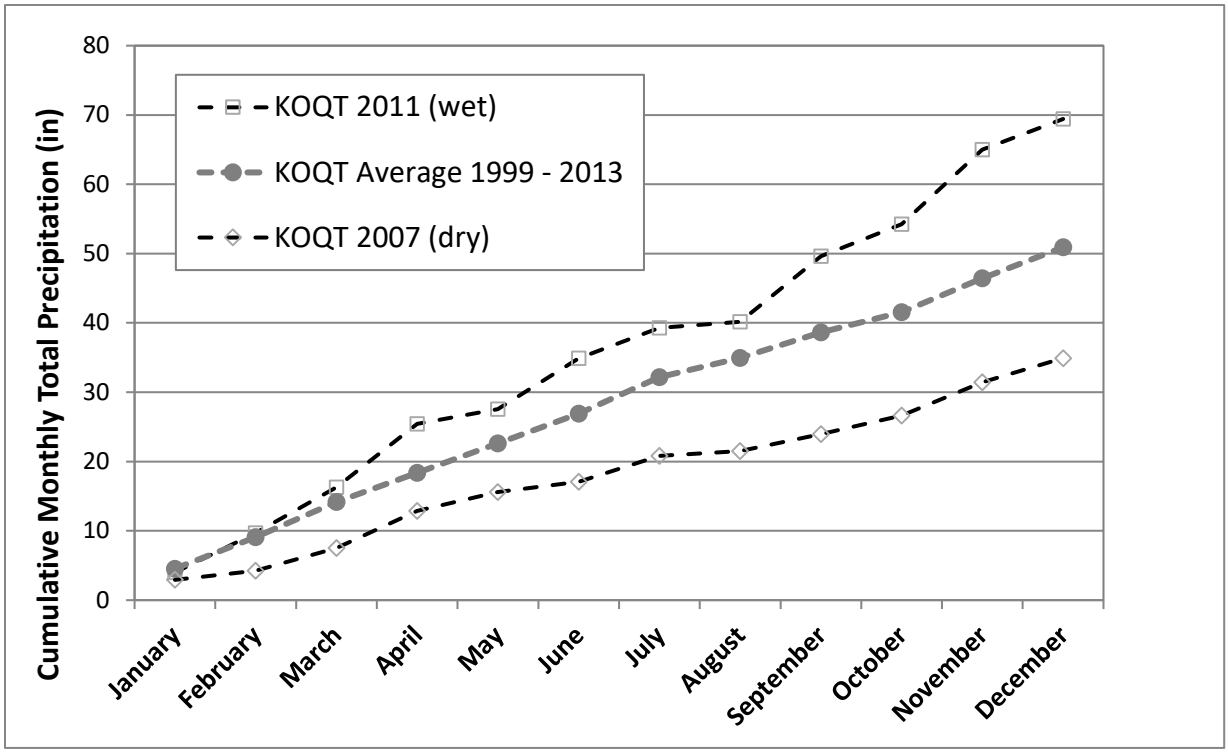

Fig. 2.7. Cumulative monthly precipitation for the NWS meteorological station (KOQT) in Oak Ridge

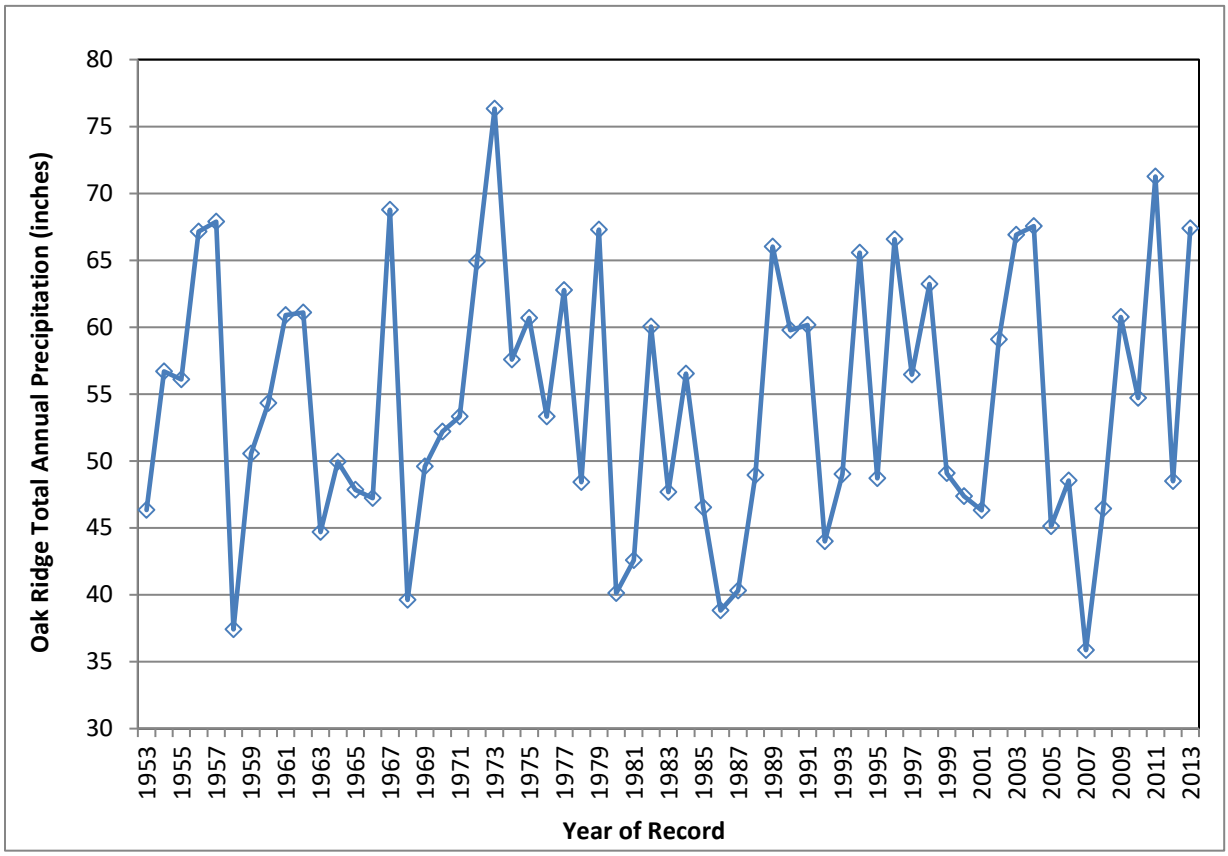

Fig. 2.8. Annual total precipitation for Oak Ridge (1953 to 2013)

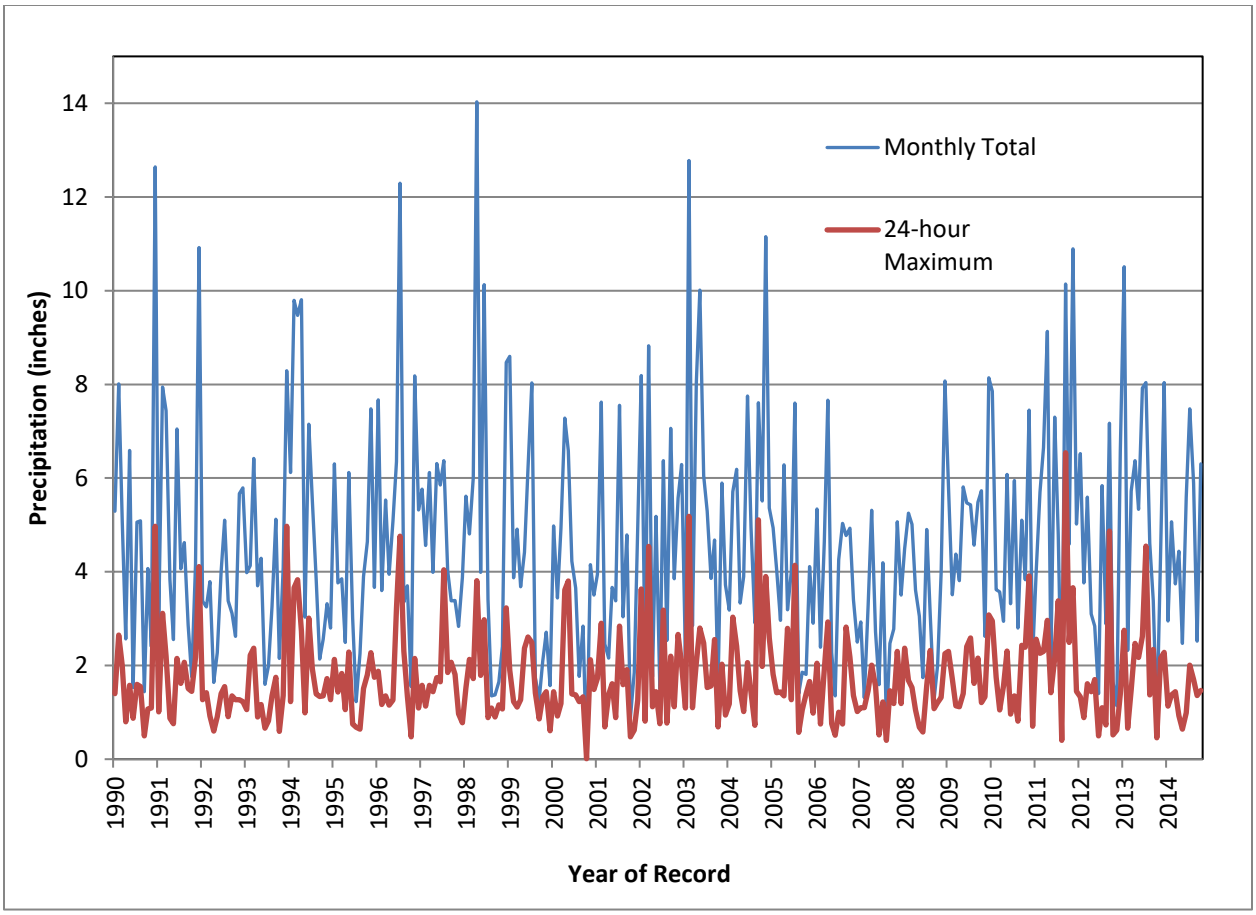

Fig. 2.9. Monthly total and 24-hour maximum precipitation and for Oak Ridge (1990 to 2014)

Precipitation intensity at hourly timescales is much larger than intensities averaged over longer periods. At the National Oceanic and Atmospheric Administration Atmospheric Turbulence and Diffusion Division station (near the Y-12 site), the point precipitation frequency estimate for hourly rainfall intensity (annual maximum series) at a 1-year average recurrence interval is 1.14 in./hour. This meteorological statistic indicates that precipitation in excess of 1 in./hour is likely to occur at least once each year.

Climate data and related assumptions about variability in annual precipitation used in hydrologic modeling for the EMDF PA are drawn from these local records and are described in Sect. 3.3. The possible impact of extreme precipitation events on EMDF performance is addressed in Sect. 3.2.1 and Appendix C. Consideration of potential future increases in average annual precipitation (climate uncertainty) is provided as part of the sensitivity-uncertainty analysis in Sect. 5.

2.1.3 Geology, Seismology, and Volcanology

The following sections address the regional geology, local geology in and around BCV, and the site-specific geology as inferred from investigations to date at similar locations in BCV. Recent characterization of the CBCV site to support EMDF site selection and preliminary design has provided additional information on groundwater and surface water hydrology, including field estimates of hydraulic conductivity (Sect. 2.1.5.4).

2.1.3.1 Regional geology

Following is a summary description of the regional geological setting for EMDF. A comprehensive and detailed report on the geology of the ORR, including a review of the regional and local structural geology,

was prepared by a panel of researchers from the ORNL Environmental Sciences Division. The *Status Report on the Geology of the Oak Ridge Reservation* (ORNL 1992a) contains detailed descriptions of soils, bedrock lithologies and stratigraphy, and geological structures within BCV at and near EMDF.

The ORR is located in the southwestern portion of the Valley and Ridge physiographic province (Fig. 2.10), which is characterized by a series of long, parallel ridges and valleys that follow a northeast-to-southwest trend. The Valley and Ridge physiographic province developed on thick, folded, and thrust-faulted beds of sedimentary rock deposited during the Paleozoic era. Thrust fault patterns and the strike and dip of the beds control the shapes and orientations of a series of the ridges and intervening valleys. The topographically high ridges are underlain by more resistant geologic formations with broad intervening valleys underlain by less resistant formations (Fig. 2.11).

The ORR lies within a classic foreland fold-thrust belt, characterized by a number of northeast/southwest striking, southeast dipping imbricate thrust sheets (ORNL 1992a). Ten major imbricate thrust faults, in which thrust sheets overlap somewhat like roof shingles, have been mapped in East Tennessee. Two of these thrust sheets, defined by the Copper Ridge and Whiteoak Mountain thrust faults, cross the ORR (Lemiszki 2000, ORNL 1992a). The cross-section in shown in Fig. 2.12 illustrates the Whiteoak Mountain thrust fault outcropping north of Pine Ridge and passing below BCV in the very deep subsurface. The Whiteoak Mountain thrust fault, along with other similar thrust faults in the Valley and Ridge province, are ancient faults inactive since the close of the Alleghanian orogeny at the end of the Paleozoic era around 250 M years ago.

The ORR and BCV are underlain by thick sequences of early Paleozoic sedimentary rocks that are stacked within adjacent thrust sheets and that generally strike northeast-southwest around N50°E. Bedding planes mostly dip to the southeast, with dip angles averaging around 45° (Fig. 2.12), but dips may vary widely on a local scale. Strike and dip measurements within BCV taken along the north tributary stream paths near EMDF (Lemiszki 2000) vary from 23° to 80° southeast to vertical.

Bedrock on the ORR consists of a variety of interbedded clastic and carbonate sedimentary rocks. The rocks are variably fractured and weathered, resulting in significant vertical and horizontal subsurface heterogeneity. The differing degrees of resistance to erosion of the shales, sandstones, and carbonate rocks that comprise the regional bedrock influence local relief. Carbonate units (limestone/dolostone) are commonly extensively weathered with massive clay overburden with dispersed residual chert nodules and pinnacled bedrock surfaces. The more resistant clastic rocks (sandstone, siltstone, mudstone/shale) generally weather to an extensively fractured residuum (saprolite) with highly interconnected fracture networks overlying less weathered to unweathered more intermittently fractured bedrock.

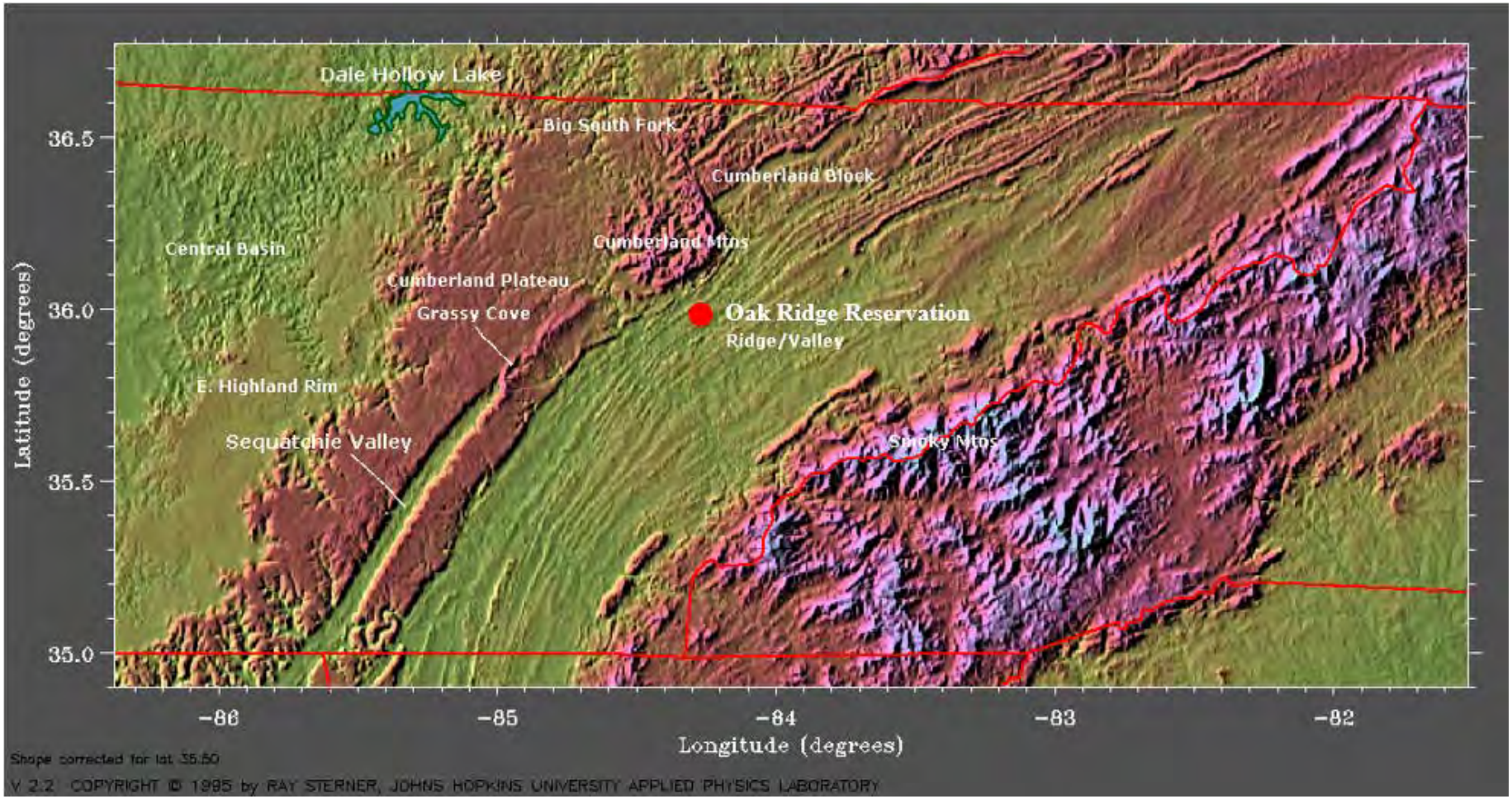

Fig. 2.10. Regional topography of Central and East Tennessee, including the southern portion of the Valley and Ridge physiographic province

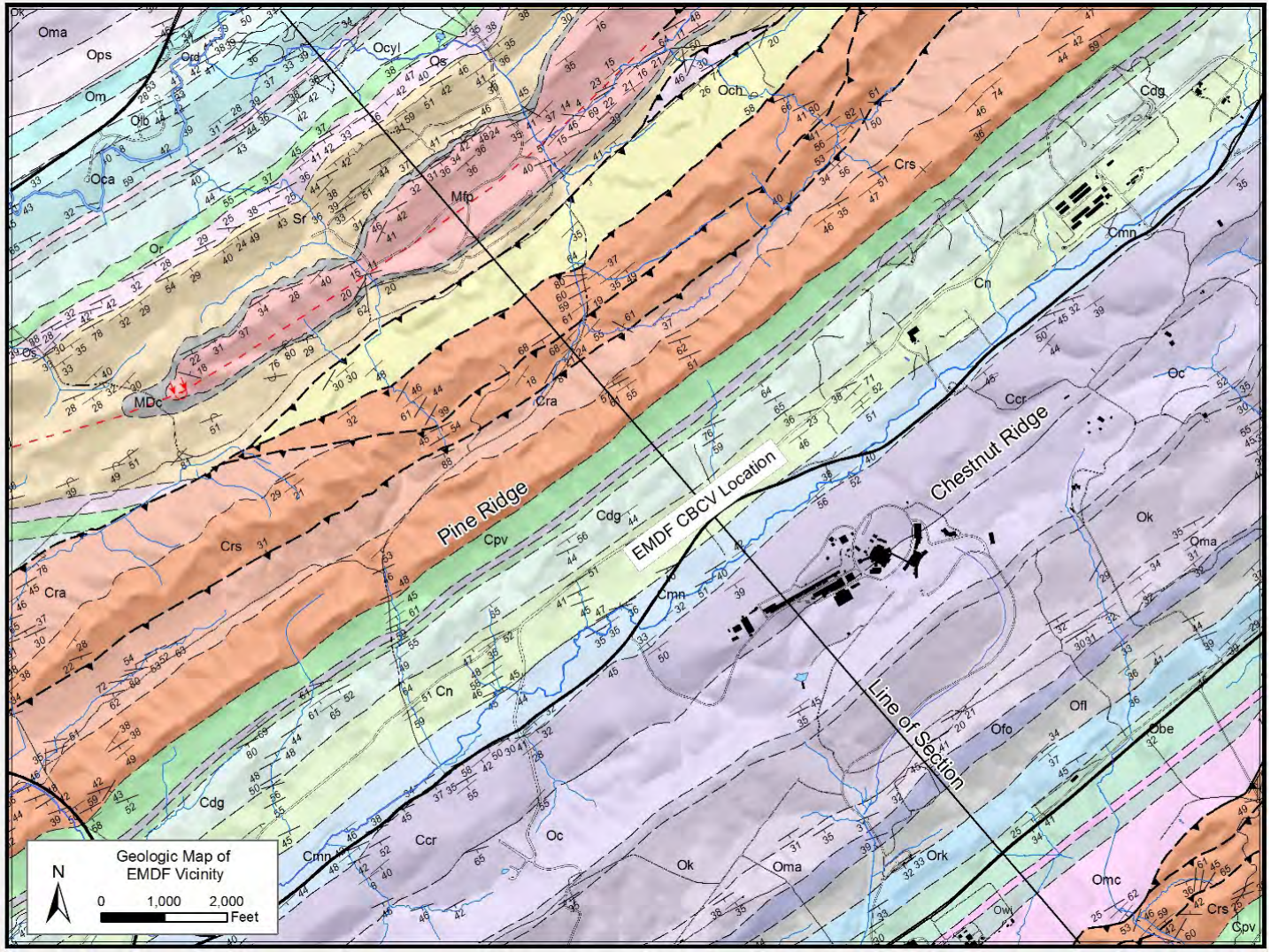

Source: Lemiszki 2000.

Note: Map shows geologic formations at and near BCV, the outcrop trace of the Whiteoak Mountain thrust fault, strike and dip measurements along BCV, and the approximate location of the proposed EMDF site.

Fig. 2.11. Geologic map of the Bethel Valley Quadrangle

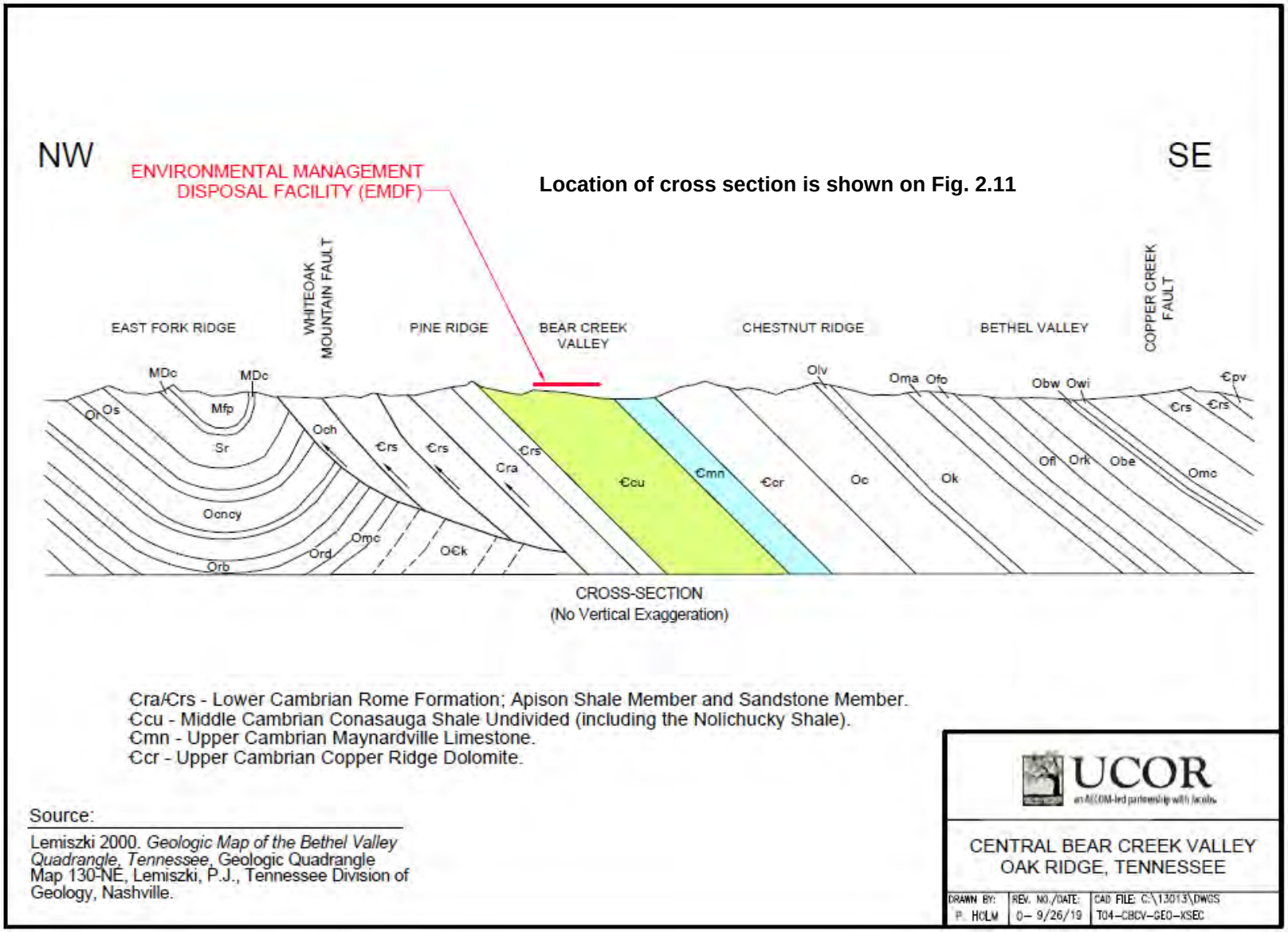

Fig. 2.12. Northwest-southeast cross-section across the ORR

2.1.3.2 Stratigraphy of Bear Creek Valley

The sequence of geologic formations underlying BCV from Pine Ridge southward to Bear Creek includes the Rome Formation of lower Cambrian age and formations of the Middle Cambrian Conasauga Group (Figs. 2.11, 2.12, and 2.13). Resistant sandstone beds of the upper Rome Formation form the crest of Pine Ridge. The Conasauga Group is overlain by the Knox Group formations that outcrop along the southern border of BCV. Cherty dolomite beds of the Knox Group form the crest of Chestnut Ridge along the south side of the valley. Within the Conasauga Group, only the Maynardville Formation consists predominantly of carbonate rocks. The remaining formations of the Conasauga Group are predominantly clastic rocks composed mostly of fine-grained shales, mudstones, and siltstones. Limestones are interbedded with fine-grained rocks in portions of the Rutledge Formation and the Maryville Formation, but the only well-documented karst dissolution features in BCV are primarily associated with the Maynardville Limestone and the Copper Ridge Dolomite (Knox Group).

The stratigraphic sequence of formations in the Conasauga Group in BCV (Table 2.4) consists from bottom to top of the Pumpkin Valley Formation, the Rutledge Formation, the Rogersville Formation, the Maryville Formation, the Nolichucky Formation, and Maynardville Limestone (Lemiszki 2000, ORNL 1992a). The Rutledge and Maryville Formations consist mostly of insoluble clastic on the ORR relative to the original type sections designated at locations outside the ORR, where limestone beds are more predominant. Among the Conasauga Group formations, only the Maynardville Limestone has been recognized as containing significant conduit flow and karst features associated with limestone dissolution along the strike path of the Maynardville subcrop. That subcrop belt runs roughly parallel with the axis of Bear Creek draining toward the southwest along the margin of Chestnut Ridge.

The stratigraphic column for BCV is presented in Table 2.4 and more detailed lithologic descriptions for the geologic formations underlying BCV are provided in Table 2.5. The tables and descriptions are adapted from *Geology of the West Bear Creek Site* (Lee and Ketelle 1989). Detailed descriptions of the geologic formations for the entire ORR also are described in the *Status Report on the Geology of the Oak Ridge Reservation* (ORNL 1992a), but the descriptions and thicknesses from the Lee and Ketelle report are specific to BCV and the Whiteoak Mountain thrust sheet. The descriptions, thickness determinations, and other geologic characteristics described by Lee and Ketelle are based on hundreds of feet of bedrock cores at the West Bear Creek site used to thoroughly define the entire stratigraphic sequence across BCV. An additional report, *Subsurface-Controlled Geological Maps for the Y-12 Plant and Adjacent Areas of Bear Creek Valley* (King and Haase 1987), presents geologic maps and cross-sections for BCV that identify the contacts between and thicknesses for each of the individual Conasauga Group formations. This report addresses bedrock geology based on several additional valley-wide transects with deep boreholes and extensive bedrock cores located at the east end of BCV near Y-12, near the center of BCV at the BCBG site (Fig. 2.13), and at the West Bear Creek site. Each of these three reports, along with many others referenced in those reports, provide additional details on bedrock geology and geological structures underlying BCV.

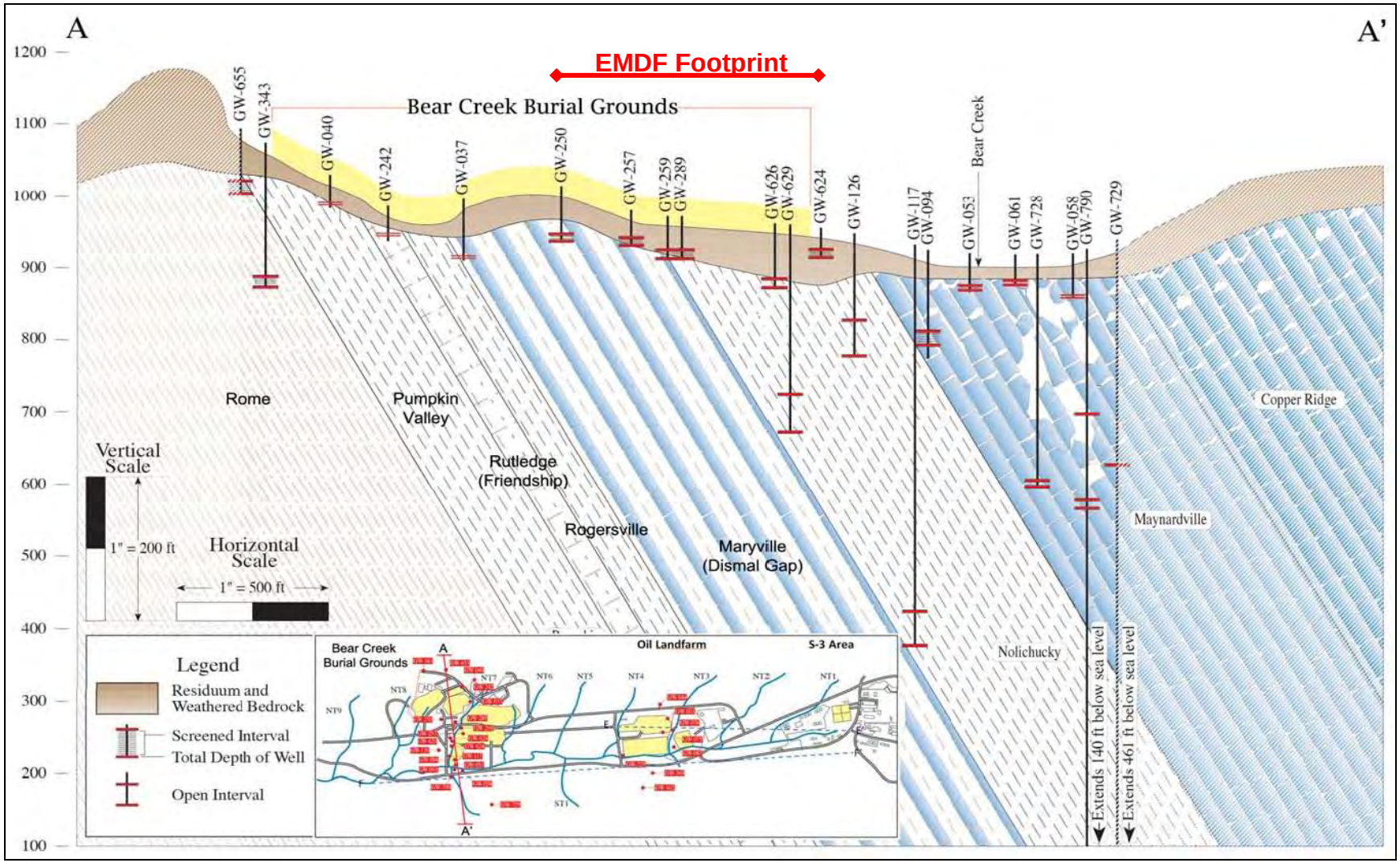

Source: ORR groundwater strategy (DOE 2013c).

Fig. 2.13. Stratigraphic cross-section for Bear Creek Valley near the Bear Creek Burial Grounds

Table 2.4. Stratigraphic column for bedrock formations in BCV

Age	Group	Formation/Unit	Description	Thickness (ft)
MIDDLE CAMBRIAN	CONASAUGA (Cc)	MAYNARDVILLE Fm.	Upper (Chances Branch Mbr.) – limestone and dolomitic limestone in thick massive beds. Lower (Low Hollow Mbr.) – dolomitic limestone in thick massive beds. Light gray to buff.	140 200
		NOLICHUCKY Fm.	Upper – shale and limestone in thin to thick beds. Shale dark gray or maroon. Limestone light gray, oolitic, wavy-bedded, or massive. Lower – shale and limestone in medium to thick beds. Shale dark gray, olive gray or maroon. Limestone light gray, oolitic, glauconitic, wavy-bedded, and intraclastic.	60–140 430–450
		MARYVILLE Fm.	Limestone and shale or siltstone in medium beds. Limestone light gray, intraclastic, or wavy-bedded. Shale or siltstone dark gray.	320–410
		ROGERSVILLE Fm.	Shale and argillaceous limestone. Laminated to thin bedded, maroon, dark gray, and light gray.	80–110
		RUTLEDGE Fm.	Limestone and shale in thin beds. Limestone light to olive gray. Shale gray or maroon.	100–120
		PUMPKIN VALLEY Fm.	Upper – shale and calcareous siltstone. Laminated to very thin-bedded. Shale reddish brown, reddish-gray, or gray. Calcareous siltstone light gray or glauconitic. Lower – shale and siltstone or silty sandstone. Thin-bedded. Shale reddish-brown or gray to greenish gray. Siltstone and silty sandstone light gray.	130–150 175
LOWER CAMBRIAN		ROME Fm. (Cr)	Sandstone with thin shale interbeds. Sandstone fine-grained, light gray or pale maroon. Shale maroon or olive gray.	Unknown

Source: Lee and Ketelle 1989.

Table 2.5. Lithologic descriptions and thicknesses of geologic formations in BCV

Geologic formations	Downhole thickness (ft)	Equivalent true thickness assuming 45° dip to SE (ft)	Lithologic and contact descriptions[a] (based on extensive rock cores collected at the proposed low level waste disposal demonstration and development site in WBCV)
Maynardville Formation - Cmn	Not reported	Not Reported	The Maynardville is divided into lower and upper members (Low Hollow and Chances Branch members). The Low Hollow member is generally a ribbon-bedded or mottled, fine-to-medium-grained dolomitic calcarenite with stylolites and irregularly spaced beds of oolitic calcarenite. Thin beds and shaley partings occur commonly within the ribbon-banded lithology. Basal portions include several laterally continuous dark gray shale beds roughly 0.5 to 2 ft thick. The Chances Branch member consists of bioturbated and thin-laminated, fine-to-medium-grained dolomicrite and dolomitic calcarenite in massive beds.
Cn/Cmn Contact			Abrupt Contact: The contact was located at the base of massive ribbon-bedded or mottled limestone of the Maynardville and uppermost thick (> 2 ft) shale in the Nolichucky.
Nolichucky Formation - Cn	Not reported	Not Reported	The lower Nolichucky is generally medium-bedded shale and limestone or calcareous siltstone resembling the underlying Maryville. The upper part of the lower Nolichucky is thick-to-very-thick-bedded maroon or olive gray shale and oolitic, coarse grained, or intraclastic limestone. The upper Nolichucky is lithologically diverse, consisting dominantly of dark gray shale with planar and wavy-laminate or ribbon-bedded micrite in thin beds (< 1 to > 2 in. thick).
Cmr/Cn Contact			Gradational Contact: The contact was placed above a 6-in.- to 2-ft-thick intraclastic limestone bed in the upper Maryville and at the base of the first clean dark gray or maroon shale bed > 2 ft thick.
Maryville Formation - Cmr	430	304	The Maryville consists of oolitic, intraclastic (flat pebble conglomerate), and thin-bedded limestone interbedded with dark gray shale that typically contains thin, planar, and wavy-laminated, coalesced lenses of light gray limestone and calcareous siltstone. Fine-grained glauconite often occurs at the tops of the thin-laminated limestone lithology. Several isolated dark maroon shale beds typically occur in both the upper and lower Maryville. Although considerable mixing of limestone lithologies is noted, the upper Maryville generally contains greater amounts of intraclastic limestone, while thin-laminated and oolitic limestone is more prevalent in the lower portion. The contact separating these two upper and lower portions is gradational over tens of feet of section. Limestone intraclasts are randomly oriented and roughly 2 to 10 cm in length. In roughly the lower 40 ft of the Maryville, a variable number of prominent, coarse-grained, pinkish limestone beds occur, which contain coarser and more abundant glauconite pellets than those higher in the section.
Crg/Cmr Contact			Abrupt Contact: The Rogersville is terminated abruptly by the occurrence of the comparatively thick limestone beds of the overlying Maryville, with the contact placed at the bottom of the first such limestone.
Rogersville Formation - Crg	90 and 150	64 and 106	The lower Rogersville consists dominantly of dark gray shale containing thin- laminated and bioturbated argillaceous limestone lenses less than 1 in thick. When maroon shales occur in the lower portion, they are thinner and more chocolate brown than the maroon shales in the upper portion. Glauconite partings are commonly interlaminated with the limestones but also occur as bioturbated beds several inches thick. The Craig Member, recognized elsewhere in East Tennessee, is not present at the WBCV site. In the approximate position of the member are a few thin limestone beds which may represent the Craig Member at the site. The beds are 4 to 6 in. thick and composed of interlaminated, light gray, silty limestone and dark gray shale. These beds differ from those in the lower Rogersville principally in thickness and may be more appropriately considered the uppermost portion of the lower Rogersville at the site. The upper Rogersville consists dominantly of maroon shale containing thin (less than 1 in. thick), wavy, light gray, calcareous siltstone or argillaceous limestone lenses in varying amounts. Thin glauconitic partings are liberally incorporated within the siltstone and limestone lenses. The interlamination of these variably colored lithologies gives the upper Rogersville an overall thinly laminated appearance. Thicker beds (more than 1 ft thick) of clean, maroon-to-brownish-maroon shale are occasionally interspersed within the thin-laminated lithology.
Crt/Crg Contact			Abrupt Contact: The contact with the Rogersville is abrupt and recognized by the absence of 1-ft-thick limestone beds and the introduction of maroon shale. The contact is placed at the top of the uppermost such limestone bed.
Rutledge Formation - Crt	124 and 126	88 and 89	The Rutledge consists of light gray, bedded limestone, often containing shaley partings interbedded with dark gray or maroon thin-bedded or internally clean shale in beds from 2 to 5 ft thick. Limestones are generally evenly divided between wavy laminated and bioturbated. Horizontal burrows are frequently observed. Maroon shale is more common in the lower Rutledge, and two distinctive beds on the order of 3 ft thick occur at the bottom of the formation and are separated by three limestone beds of similar thickness. These limestones are referred to as the “three limestones” of the lower Rutledge, but their lithologic similarity with limestones in the bulk of the Rutledge makes them less distinctive than the two maroon shales. The relatively clean, dark maroon shales in the lower Rutledge give way to dark gray shale with thin calcareous siltstone interbeds. Upper Rutledge interbeds are generally thinner than those below and more coalescing of lithologies is recognized. Limestone beds are often ribbon or wavy bedded and some are heavily bioturbated with abundant glauconite pellets. Glauconite stringers also occur commonly within the calcareous siltstone interbeds.
Cpv/Crt Contact			Abrupt Contact: The contact with the overlying Rutledge is abrupt and placed at the top of generally uninterrupted, thin-bedded, reddish-brown shale and below the interbedded limestone and dark maroon shale of the Rutledge.
Pumpkin Valley Formation - Cpv	376 and 398	266 and 281	The Pumpkin Valley Formation is readily divisible into upper and lower units of nearly equal thickness. The lower Pumpkin Valley consists of reddish brown and gray-to-greenish-gray shale with thin interbeds of siltstone and silty, fine-grained sandstone. Shales typically contain thin, wavy laminated siltstone drapes and discrete laminate of fine-grained glauconite. Silty sandstone interbeds are typically wavy laminated to thin bedded, but are often heavily bioturbated. High concentrations of large glauconitic pellets occur in the bioturbated lithology. Decreasing silty sandstone content upward within the lower Pumpkin Valley attests to its transitional nature above the Rome. The upper Pumpkin Valley is laminated to thin-bedded, dominantly reddish-brown, reddish-gray, and gray shale with thin, wavy, and planar-laminated siltstone lenses. Shales are generally fissile and may be massive or thin laminated. Thin partings of fine-grained glauconite pellets are ubiquitously interlaminated within the siltstone lenses.
Cr/Cpv Contact			Gradational Contact: The contact with the overlying Pumpkin Valley Formation is gradational and placed at the top of the uppermost thick, clean, planar laminated, 8- to 12-in.-thick, sandstone bed of the Rome.
Rome Formation - Cr	>>195	>>138	The Upper Rome consists of thick beds of gray or pale maroon, fine-grained arkosic to subarkosic sandstone with occasional interbeds of maroon shale that often contain thin siltstone bands. Sandstones are typically planar to wavy-laminated or current-rippled. Vertical burrows are in great abundance in the interbedded lithology, but are also recognized in the sandstone-dominated lithology. Burrows diminish in abundance down section. Upper Rome sandstone/shale interbeds occur non-uniformly at the two site locations from which the core was acquired. The common occurrence of such interbeds on the western portion of the site is almost entirely replaced in the center of the site by gray or pale maroon sandstone couplets with a total absence of shale. Such lateral facies changes within roughly 1000 ft suggest the Upper Rome was subject to locally variable clastic influx in a low-relief paleodepositional setting.

[a]Lee and Ketelle 1989.

BCV = Bear Creek Valley
SE = southeast

WBCV = West Bear Creek Valley

This page intentionally left blank.

2.1.3.3 Conasauga Group bedrock fractures in Bear Creek Valley

Descriptions and data on bedrock fractures applicable to the EMDF site are available from site investigations and research reported from Conasauga Group sites in BCV and elsewhere on the ORR. The RI completed for BCV (BCV RI) (DOE 1997b) addresses bedrock fractures in BCV (DOE 1997b, Appendix C, Sect. C.3.3). The report notes that because of the large-scale faulting and folding characteristic of ORR geology, all bedrock lithologic units in BCV are highly fractured, consisting of extensional, hybrid, and shear fractures. Core hole studies of fractures in bedrock along a transect across BCV near the head of Bear Creek (Dreier et al. 1987, Dreier and Davidson 1994) demonstrate the existence of several major fracture sets that are dominated by a strike-parallel set. Most fractures in ORR bedrock constitute a single cubic system (three orthogonal sets) of extension fractures (Dreier et al. 1987, Sledz and Huff 1981). One fracture set is formed by bedding planes dipping to the southeast. Two other fracture sets generally parallel strike and dip. At shallow depths, these sets are commonly angled 50˚ to 60˚ below the horizon. These three fracture sets may occur in any locality and other extensions and shear fractures may also be present (DOE 1997b).

In general, fracture spacing is a function of lithology and bed thickness. Fractures in more massively bedded formations tend to have longer trace lengths and are more widely spaced. An average fracture density of approximately 60/ft was measured in saprolite of the Maryville Formation and Nolichucky Formation (Dreier et al. 1987). At the other extreme, a minimum of five fractures per meter (1.5/ft) in fresh rock was documented in the Sledz and Huff (1981). Fewer open fractures occur at deeper levels. As described in Haase et al. (1985), fracture frequency is variable, but most fractures observed in cores occur within limestone or sandstone layers > 1.6 ft thick and many are filled or partly filled with secondary minerals.

Most fractures are short, a few centimeters to approximately 3.3 ft in length (longest dimension). Fracture length at outcrops is relatively uniform (approximately 5 in.) in shale, but increases with bed thickness in siltstone (Sledz and Huff 1981). There are numerous fractures approximately 0.3 to 5 ft long in limestone and sandstone units of the Conasauga Group and Rome Formation (Haase et al. 1985). In limestone, typical fracture spacings range from < 2 in. for very thin beds to > 10 ft for very thick to massive beds.

Detailed logging of core material from wells at the BCBG site (located southwest of the EMWMF and along strike with the EMDF) has provided information on the relative changes in densities of open (hydraulically active) fractures in the Nolichucky Formation compared to depth and lithology (Dreier and Davidson 1994). This information was supported by estimates of spacings for hydraulically active fractures from resistivity, temperature, and flow meter logs of the same borings. The resulting estimates ranged from approximately 3 ft in the shallow intervals to more than 20 ft in the deep intervals.

2.1.3.4 Geologic units at the EMDF site

The CBCV site is underlain by the moderately to steeply dipping beds of the Maryville Formation on the northern end and by Nolichucky Formation on the southern end of the site (Fig. 2.13). The Maryville Formation includes limestone interbedded with fine-grained clastic rocks. Based on the inferred location of the contact between the Nolichucky Formation and the Maynardville Limestone at the EMDF site, the distance from the southernmost margin of the facility to the karstic Maynardville unit is approximately 350 ft. Field mapping of the surficial geologic unit contacts is included as part of the initial CBCV site characterization effort.

2.1.3.5 Surficial geology

In the humid subtropical climate of the southeast, the rocks have weathered over time to create a surficial regolith that includes topsoil, clayey residual soil, and highly weathered rock (saprolite) covering the

unweathered (competent) bedrock below. Unconsolidated mixtures of mud, sand, and gravel deposits (alluvium) occur along stream valleys, and relatively thin surficial deposits of colluvium may occur, generally along the lower portions of steeper slopes.

A simplified conceptual model of surficial geology in BCV is adopted for describing the natural components of the disposal system (Fig. 2.14). The saprolite zone includes all materials that overlay unweathered (competent) bedrock, corresponding to the overburden in engineering terminology. Depending on the site topography and local conditions, the saprolite zone at the EMDF site may include surficial soils (organic-rich topsoil and clayey residual subsoils), colluvium and alluvium along flanks and floors of the NT valleys, and the underlying saprolite, which is bedrock that has been completely chemically weathered but remains otherwise undisturbed. Saprolite can generally be drilled using a hollow-stem auger rig to the depth of auger refusal where the transition to less weathered or unweathered bedrock occurs. For practical purposes, the depth of the saprolite zone may be considered as auger refusal drilling depth, which typically ranges from 10 to 30 ft, but can exceed 50 ft in some locations. Saprolite retains the fabric and structure of the parent sedimentary rocks, including fracture sets (Sect. 2.1.3.3). Beneath the saprolite zone lies a bedrock zone that comprises less weathered and fractured bedrock. In general, the degree of weathering, average aperture and density of fractures, porosity, and permeability decrease with increasing depth below the surface. Materials near the saprolite-bedrock boundary are transitional and can include less weathered rock fragments (mostly shale and siltstone) in a fine-grained saprolite matrix.

The thin topsoil layer of organic rich soil varies from a few inches to < 1 ft thick. The zone of fine-grained residual soil varies from < 2 ft to 10 ft in thickness. The thickness of these intervals and the underlying saprolite varies and downward transition from one to the next may be rapid or gradual depending on the topographic position and history of profile development. Pore structure within the clayey residuum reflects surface soil formation processes, including macropore structures related to root growth and bioturbation (e.g., earthworm activity). Structural features of the underlying saprolite reflect the bedding and fracture geometry of the parent sedimentary rocks. As documented in Driese et al. (2001), there is extensive filling in saprolite fractures at the base of the residual soil due to translocation of clays. These clays and associated iron and manganese deposits contribute to the decrease in permeability with depth within the regolith.

Along the valley floors of Bear Creek tributaries, the soil-and saprolite upper portion of the subsurface profile may be replaced with alluvial sediment deposits that vary in width and thickness (Fig. 2.15). Colluvial deposits may occur along the lower slopes of these valleys. A thicker belt of alluvial deposits occurs within the floodplain of BCV. Colluvial or alluvial deposits also may occur in places outside of the current stream valleys as demonstrated by detailed site soil surveys completed for a waste disposal demonstration project in West Bear Creek Valley (WBCV) (Lietzke et al. 1988).

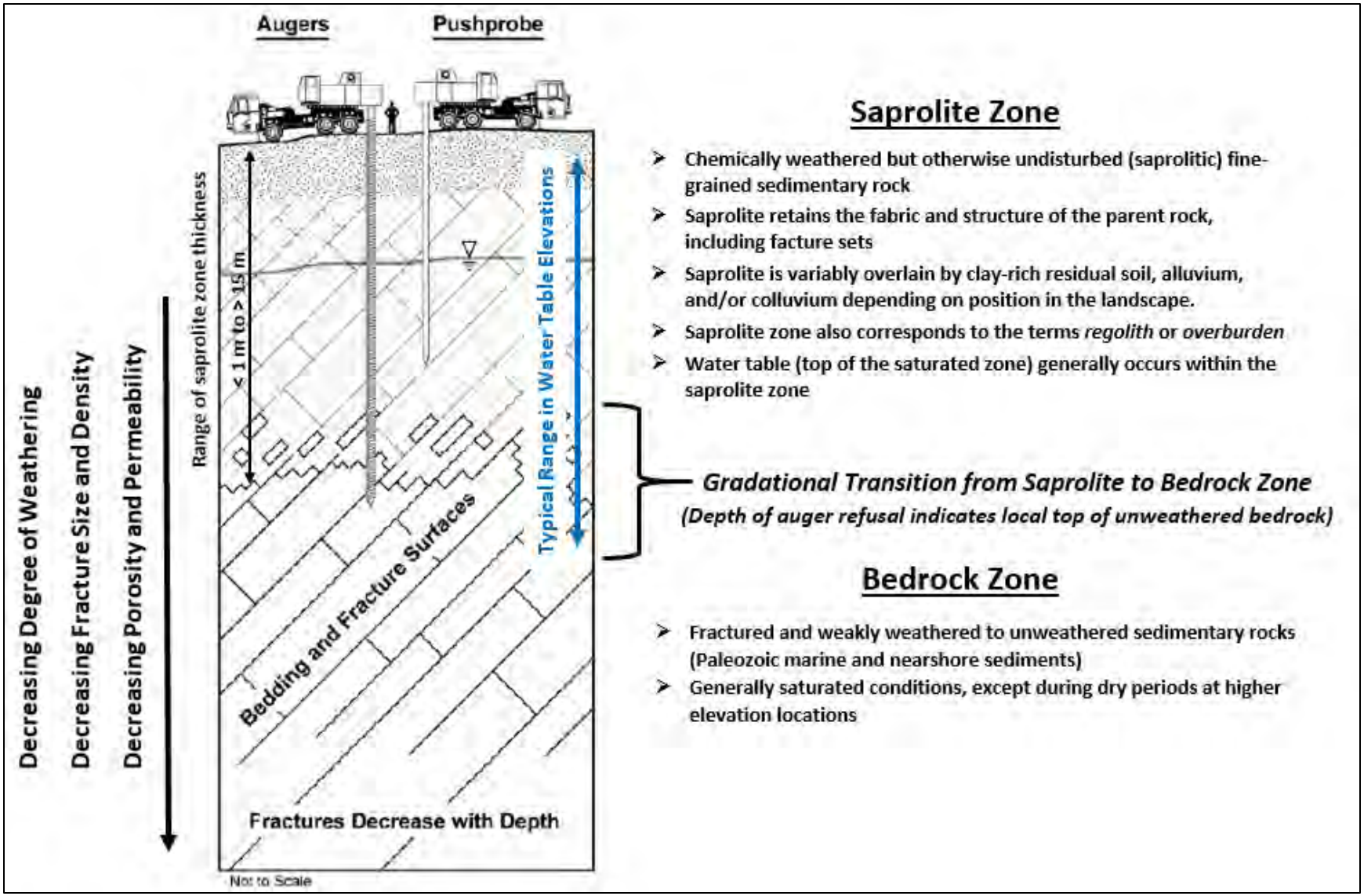

Fig. 2.14. Simplified conceptual model of geologic material types in Bear Creek Valley

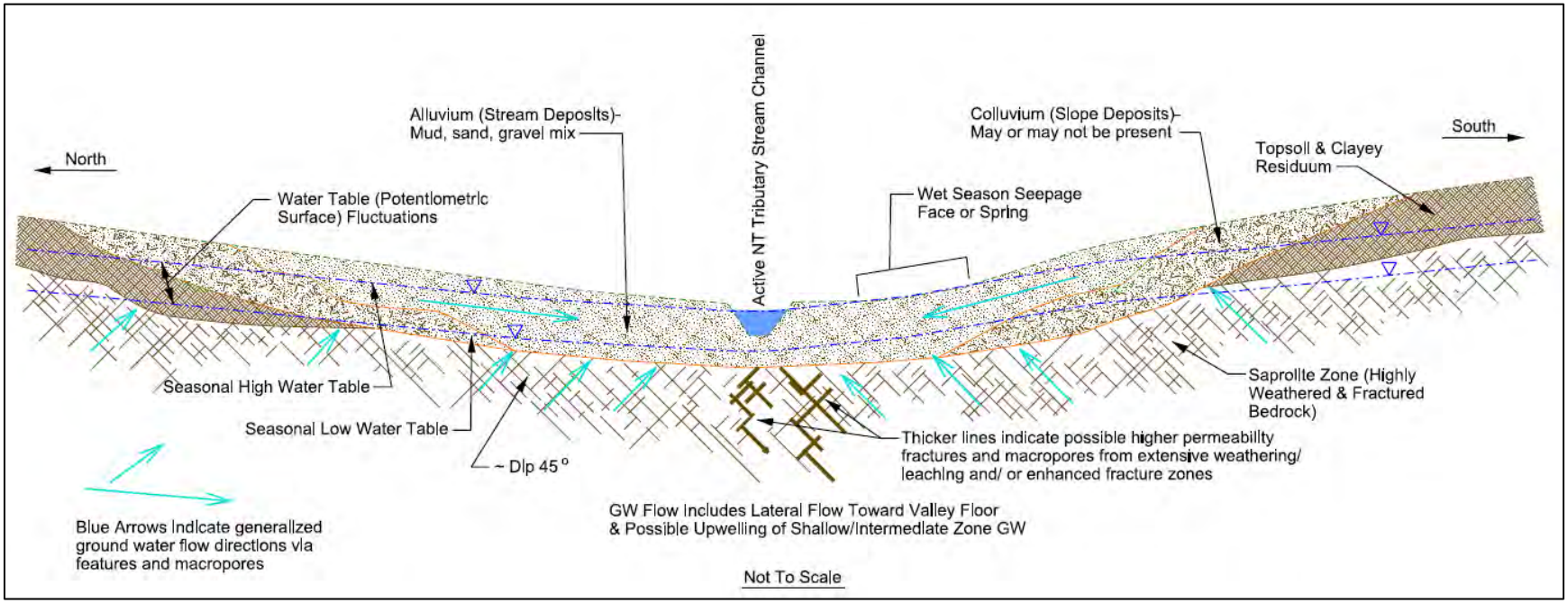

Fig. 2.15. Typical subsurface profile expected across Bear Creek tributary valleys

2.1.3.6 Seismology

Oak Ridge and the EMDF site are located within a broad zone of elevated activity of historically low-magnitude seismicity known as the East Tennessee Seismic Zone (ETSZ), a narrow zone of seismicity east of the New York-Alabama magnetic lineament (Fig. 2.16). Although there is a higher rate of seismic activity in the ETSZ, the largest documented historical earthquake in the region was approximately magnitude 4.6 (Tennessee Valley Authority [TVA] 2016).

Studies at Douglas Reservoir (Hatcher et al. 2012) concluded that at least two moment magnitude 6.5 or greater earthquakes could be associated with the ETSZ within the last approximately 73,000 to 112,000 years. However, these results are preliminary, and timing of proposed earthquake events and recurrence intervals are not established. Therefore, a reoccurring large magnitude event source zone is not defined based on the Douglas Reservoir features (TVA 2016).

There is no evidence of active, seismically capable faults in the ORR area (DOE 2011c). The Oak Ridge area lies in Uniform Building Code seismic zones 1 and 2, indicating that minor to moderate damage could typically be expected from an earthquake. Although there are a number of inactive faults passing through the ORR, there are no known or suspected seismically capable faults. As defined in 10 *CFR* 100, Appendix A, a seismically capable fault is one that has had movement at or near the ground surface at least once within the past 35,000 years, or recurrent movement within the past 500,000 years. The nearest capable faults are approximately 300 miles west-northwest of the ORR in the New Madrid (Reelfoot Rift) Seismic Zone (DOE 2011c). Historical earthquakes occurring in the ETSZ are not attributable to fault structures in underlying sedimentary rocks, but rather occur at depth in basement rock (Powell et al. 1994).

Historic earthquakes in the ETSZ typically are of small magnitude and mostly go unfelt by people. However, a number of historic earthquakes have had magnitudes greater than 4.0 and were, therefore, capable of producing at least some surface damage. Between 1844 and 1989, East Tennessee experienced 26 earthquakes that were widely felt, seven causing at least minor damage (Stover and Coffman 1993). An earthquake that shook Knoxville in 1913 was estimated to have a moment magnitude of about 5.0. Another earthquake that occurred in 1930, with an epicenter approximately 5 miles from Oak Ridge, had a Mercalli intensity of V to VII. Table 2.6 presents a description of scales. The largest recent seismic event was a moment magnitude 4.7 earthquake that had an epicenter near Alcoa, Tennessee, 21.6 miles southeast of Oak Ridge, in 1973. The intensity of this earthquake felt in Oak Ridge was estimated to be in the range of V to VI (light).

The Oak Ridge region continues to be seismically active, with 50 earthquakes recorded within a radius of 62 miles of the ORR since 1973. Approximately 60 percent of the 50 earthquakes within this radius occurred at depths greater than 6 miles. The closest of those events occurred on June 17, 1998, with an epicenter within ORR near ETTP, registering a magnitude 3.3 (U.S. Geological Survey [USGS] 2013). Two other earthquakes with epicenters beneath the ORR have been recorded since 1973. These occurred on May 2, 1975 (magnitude of approximately 2.6) and April 11, 2013 (magnitude of approximately 2.2).

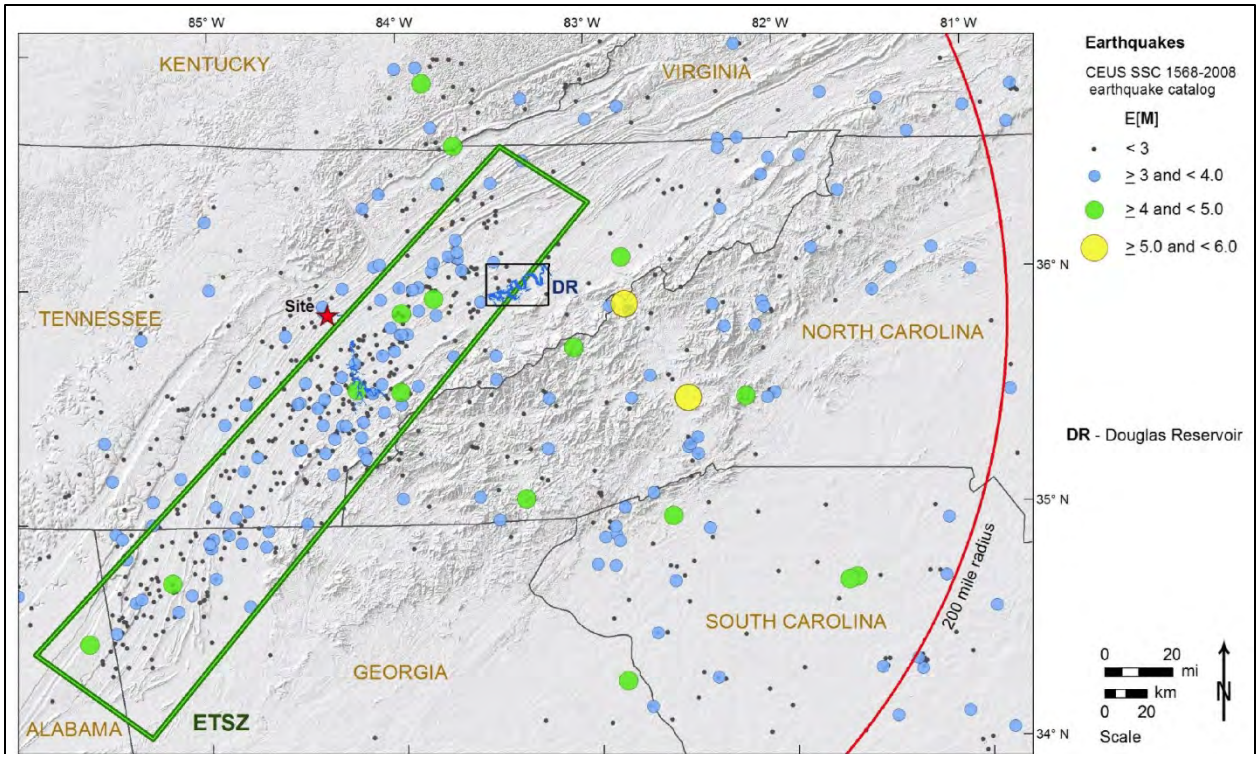

Source: TVA 2016.

Fig. 2.16. Eastern Tennessee Seismic Zone Location - U.S. Geological Survey

Table 2.6. Earthquake magnitude and intensity scales

Moment magnitude scale	Modified Mercalli scale	Intensity descriptor	Peak ground acceleration (g)
< 2.0	I	Minor	< 0.0017 to 0.039
2.0 – 2.9	I - II		
3.0 – 3.9	II – IV		
4.0 – 4.9	IV - VI	Light	0.039 to 0.092
5.0 – 5.9	VI - VII	Moderate	0.092 to– 0.18
6.0 – 6.9	VII - IX	Strong	0.18 to 0.34
7.0 and up	VIII - XII	Major to catastrophic	0.34 to > 1.24

Source: USGS 2020.

USGS = U.S. Geogolical Survey

2.1.3.7 Volcanology

Active volcanoes, lava flows, and other features of geologically recent volcanic activity do not occur in the southeastern United States anywhere near the EMDF site. Based on tectonic plate boundaries and the great distance of the site from any hot spots or plate subduction zones, volcanic activity would not be expected to occur within any future timeframes of concern relevant to the EMDF site.

2.1.4 Ecology and Natural Areas of Bear Creek Valley

The following subsections review the general ecological conditions and natural resource areas of BCV. Implications of potential impacts of biological processes on long-term changes in EMDF performance are considered in Sects. 3.2.1 and 3.2.2.1. Section 2.8.1 describes the results of ecological surveys recently completed at the CBCV site to satisfy applicable regulatory requirements for the protection of natural resources.

Ecological conditions in BCV were described in Southworth et al. (1992). This report presented results of biological monitoring for the 1984 to 1988 monitoring period, including habitat evaluation, toxicity monitoring, and surveys of fish and benthic macroinvertebrates, within the context of impacts from historical waste sites located in the central and upper parts of BCV. Extensive biological monitoring of Bear Creek for the 1989 to 1994 period was presented in the ORNL 1996. This report presented detailed descriptions of the Bear Creek watershed and results and analyses of toxicity monitoring, bioaccumulation studies, and instream ecological monitoring of fish and benthic macroinvertebrates. The BCV RI (DOE 1997b) subsequently presented results of ecological characterization and a baseline ecological risk assessment for BCV in a comprehensive assessment of risks to fish, benthic invertebrates, soil invertebrates, plants, wildlife from chemicals, and terrestrial biota from exposure to radionuclides.

Several more recent reports document ecological monitoring in BCV, including the Annual Site Environmental Report for the ORR (DOE 2015a), the annual Remediation Effectiveness Report (RER) for the ORR (DOE 2018c), and the Y-12 Biological Monitoring and Abatement Program reports (Peterson et al. 2009). The ecological monitoring includes surface water and biota sampling and analysis at stations along Bear Creek and several north tributaries in BCV. The RER aquatic biomonitoring of streams in BCV includes bioaccumulation (contaminant accumulation in fish) monitoring, fish community surveys, and benthic macroinvertebrate community surveys.

2.1.4.1 Terrestrial and aquatic natural areas in Bear Creek Valley

Outside of the Y-12 area, BCV is designated as part of the ORERP and the Oak Ridge Biosphere Reserve (Parr and Hughes 2006). In two separate but related reports, an ORR-wide analysis, evaluation, and ranking of terrestrial natural areas (NAs) (Baranski 2009) and aquatic natural areas (ANAs) (Baranski 2011) were presented. These reports compiled information from several previous reports into a comprehensive review of NAs and sensitive habitats for the ORR. The purpose of these studies "*was to evaluate and rank those specially designated areas on the Reservation that contain sensitive species, special habitats, and natural area value. Natural areas receive special protections through established statutes, regulations, and policies.*" As shown in Fig. 2.17, a swath along almost the entire length of Bear Creek and some tributaries within BCV are designated as ANA2. In the vicinity of the proposed EMDF, terrestrial NA13 and habitat area (HA) 2 are recognized. The NA13 and HA2 areas are confirmed habitats for rare plant and animal species (state and/or federal candidate and/or listed) and include terrestrially and aquatically sensitive habitats (Parr and Hughes 2006, Fig. 13). The ANA2 area (Bear Creek), NA13, and HA2 areas coincide with areas given a highest biological significance ranking of BSR-2 (very high significance) in a Nature Conservancy Report of biodiversity on the ORR (Parr and Hughes 2006).

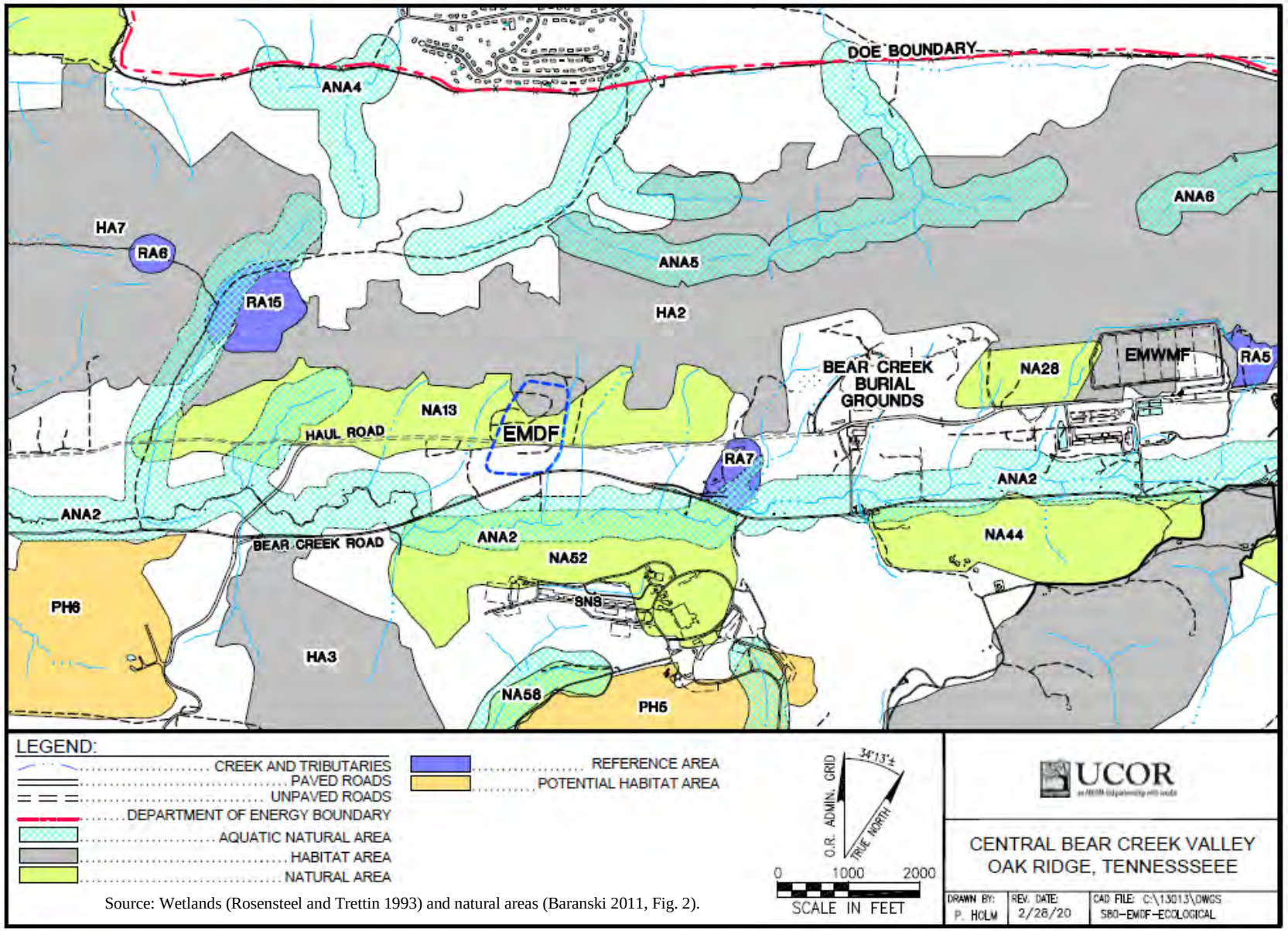

Source: Wetlands (Rosensteel and Trettin 1993) and natural areas (Baranski 2011, Fig. 2).

Fig. 2.17. Officially recognized special and sensitive areas near BCV

2.1.4.2 Wetlands and sensitive species surveys in Bear Creek Valley

Results of wetland surveys for the entire BCV watershed were presented in Rosensteel and Trettin (1993). Wetlands were delineated along the valley floors of local tributaries. The wetland locations suggest the influence of strike-parallel shallow groundwater flow from the uplands toward the adjacent tributary valley floors.

An environmental survey was conducted in 2004 and 2005 to assess sensitive natural resources that would be impacted by the Haul Road corridor between ETTP and EMWMF. The Haul Road generally follows the strike of BCV along the power line right of way north of and roughly parallel with Bear Creek Road. The survey evaluated rare plants and vegetation assemblages, rare wildlife and their habitat, rare aquatic species, and wetland/floodplain areas along BCV. The survey concluded that "*the most significant natural resource disturbance associated with the Haul Road's construction is undoubtedly the potential aquatic and wetland impacts near Bear Creek and its major tributaries. Bear Creek and its major tributaries contain the rare Tennessee dace, and forested wetlands adjacent to these streams were generally found to be of high natural quality. Fragmentation of interior forest was also a concern as road construction was deemed a potential impact on forest-interior neotropical migrant birds. However, a thorough review of past records as well as the present surveys found no evidence of rare, T&E wildlife species or plants present within the Haul Road corridor*" (Peterson et al. 2005).

An ORR-wide survey of bat species was conducted and reported on in late 2015 (McCracken et al. 2015). That survey confirmed Indiana and gray bats (endangered species) and the northern long-eared bat (threatened) make their home on the ORR. Additional endangered species were identified acoustically by the study, but their presence was not confirmed through capture.

2.1.4.3 Biological monitoring in Bear Creek

Virtually all of Bear Creek within BCV is designated as ANA2 within the ORERP (Baranski 2011, and Fig. 2.17). The stream habitats of upper Bear Creek and its tributaries have been impacted from headwater contamination originating from Y-12 waste disposal sites in East Bear Creek Valley (EBCV) (Southworth et al. 1992) and support small populations of benthic macroinvertebrates that are relatively intolerant to pollution. Although segments of the upper Bear Creek stream channel are periodically dry from karst stream flow capture in the summer/fall dry season, portions of the stream support a rather healthy community of benthic macroinvertebrates. During dry periods, much of the benthic fauna may migrate to the hyporheic zone of the stream.

In general, the diversity and abundance of aquatic fauna were found to increase with distance from the contaminated headwaters (Southworth et al. 1992). This also may be due, in part, to increases in stream depth and continuity of flow. A total of 126 benthic invertebrate taxa were recorded in Bear Creek, including crustaceans, aquatic worms, snails, mussels, and insects. Representatives of 11 orders of insects were collected. Mayflies, highly sensitive to heavy metal pollution, were almost totally absent in all but the lower reaches of Bear Creek. Upstream areas were numerically dominated by midge larvae, which is typical of polluted streams.

Nineteen species of fish were recorded in Bear Creek during surveys in 1984 and 1987, and data provide evidence of ecological recovery in Bear Creek since 1984 (Southworth et al. 1992, Ryon 1998). Studies concluded that much of Bear Creek contains a limited number of fish species that appear to have robust populations (high densities and biomass). Fish surveys reported over two decades ago near the headwaters demonstrated a stressed condition without a stable, resident fish population (Southworth et al. 1992). However, headwater streams often do not support very diverse fish fauna. Four fish species were found to

predominate in the upper reaches of Bear Creek (above Bear Creek kilometer [BCK] 11); by comparison, 14 fish species occur downstream from SR 95.

Biological monitoring of stream sites in BCV watershed has been conducted since 2004 to measure the effectiveness of watershed-scale remedial actions (DOE 2015b). Biological monitoring includes contaminant accumulation in fish, fish community surveys, and benthic macroinvertebrate community surveys. Fish communities in Bear Creek have generally been stable or slightly variable in terms of species richness.

The Tennessee dace, a major constituent of the fish population above the weir at BCK 4.55, is a Tennessee-listed in-need-of-management species and its habitat is protected by the state of Tennessee. No federal- or state-listed threatened and endangered aquatic species have been observed in Bear Creek or its tributaries (Southworth et al. 1992).

2.1.4.4 Terrestrial habitats in Bear Creek Valley

The CBCV site and surrounding areas are largely forested. Regional plant communities within BCV typify those found in Appalachia from southern Pennsylvania to northern Alabama.

Terrestrial flora. Much of the natural upland forest on the ORR, including much of BCV, is a mixed mesophytic forest dominated by oaks, hickories, and yellow poplar, with co- or subdominant beech and maples. Evergreens such as shortleaf pine, Virginia pine, and loblolly pine are intermixed in deciduous-dominated forests and are found in more or less pure stands, especially on recovering disturbed land and in plantations. Other trees that may be present as secondary or understory species include black cherry and dogwood (Kitchings and Mann 1976). Much of the forest is open, with little herbaceous undergrowth. Some areas may have moderate to dense undergrowth composed of rhododendron or laurel, but these are confined to relatively small niche areas. The herbaceous layer includes ferns, plantains, groundsel, and vines.

Bottomland and wetland sites are characterized by sweet gum, sycamore, and black willow, with red maple, black walnut, and boxelder. The herbaceous layer may contain sedges, rushes, cattails, and bulrushes.

Terrestrial fauna. Predators, including the coyote, red and gray fox, bobcat, and weasel, are widespread throughout the ORR. Black bears have occasionally been reported on the ORR, but these appear to be animals in transit, not permanent residents. White-tail deer, the only ungulate currently known to frequent the area, inhabit upland and bottomland forests throughout the ORR. Elk also are occasionally sighted on the ORR.

Striped skunk, opossum, raccoon, eastern cottontail rabbit, and groundhogs are small omnivores and herbivores common to both forest and field. Numerous members of the order Rodentia are present, including chipmunks, eastern grey squirrel, and flying squirrel, as well as several species of mice. Shrews and voles also are common throughout the ORR.

Streams and lake banks offer suitable habitat for muskrats and beaver. Marsh rice rats may live in wet areas along open waters that have a dense herbaceous growth of grasses and sedges.

Avifauna. The upland forest provides habitat for a large number of resident and migratory bird species. Resident woodpecker species common to mature deciduous forests include yellow-shafted flickers, redbellied woodpeckers, hairy woodpecker, downy woodpeckers, and pileated woodpeckers. The common crow and blue jay also are present in the deciduous forest.

Songbirds found in ORR forests are represented by the Kentucky warbler, pine warbler, and yellow-breasted chat; however, the ovenbird, Carolina chickadee, scarlet tanager, mourning dove and tufted titmouse are considerably less selective. Game birds include turkey and ruffed grouse.

Red-tailed hawk and sharp-shinned hawk are raptors common year-round on the ORR. Turkey vultures and black vultures also are common on the ORR. The Northern harrier and broad-winged hawk are migratory visitors.

2.1.5 Hydrogeology

Due to the abundant precipitation and shallow water tables in BCV, surface and groundwater hydrology are closely related. The information below is tailored toward the most relevant to modeling the long-term performance of the disposal facility.

2.1.5.1 Bear Creek Valley hydrogeologic framework

The BCV RI (DOE 1997b) provided the first comprehensive assessment of the environmental setting and hydrogeological conceptual model encompassing the entire length of BCV. The report incorporates the hydrologic framework for the ORR developed by ORNL researchers (ORNL 1992a, ORNL 1992b, Moore and Toran 1992), includes a comprehensive assessment of historical waste sites and groundwater contaminant plumes, and presents human health and ecological risk assessments for BCV. Section 2 of the BCV RI presents a summary presentation of the BCV conceptual model, but a more detailed presentation of the model is presented in Appendix C of that report and draws upon data from over three decades of investigations and reporting.

Most relevant to the PA and CA for the EMDF site, the BCV RI addresses details of the surface water hydrology and hydrogeology across the entire length and width of BCV, covering the broader area surrounding the EMDF site. The site-specific hydrogeologic conceptual model for EMDF (Sect. 3.2.3) is largely based on the synthesis of the large body of information on BCV surface hydrology and hydrogeology that is contained in the BCV RI.

The BCV hydrogeologic conceptual model differentiates between the surface water and groundwater flow within and across the predominantly clastic lithology underlying most of the valley floor and the flow along Bear Creek, including groundwater flow within the karstic carbonate rocks along the southern margin of BCV. This configuration of the clastic and carbonate rocks is illustrated conceptually in Fig. 2.13. Across the clastic outcrop belts, groundwater at shallow to intermediate depth tends to flow south to southwest, whereas flow within the Maynardville and along Bear Creek tends to more closely parallel the geologic strike toward the southwest. Hydraulic gradients mirror the topography and are much higher within the clastic rocks north of Bear Creek than gradients along the valley floor and Maynardville Formation outcrop. The cross-section shown on Fig. 2.13 is located near the center of the BCV watershed across the BCBG (as shown on the inset map). The proposed EMDF footprint at the CBCV site is centered across outcrop belts of the Maryville Formation and the lower portion of the Nolichucky Formation, corresponding to the lower half of the BCBG footprint shown in yellow on Fig. 2.13.

Hydrologic subsystems for areas underlain by predominantly clastic (non-carbonate) rocks (sometimes referred to on the ORR as aquitards) were defined in ORNL status report (ORNL 1992b); likewise, the technical basis for these subsystems are described in detail in the status report and in Moore and Toran (1992). The subsystems include a shallow subsurface stormflow zone, the vadose zone, three intervals within the saturated zone (water table, intermediate, and deep intervals), and an aquiclude at great depth where minimal water flux is presumed to occur. The stormflow and vadose zones and the uppermost saturated zone (water table interval) generally occur within materials of the saprolite zone presented in

Fig. 2.14. A majority of the estimated subsurface water flux occurs within these uppermost parts of the subsurface hydrogeologic profile (ORNL 1992b). In general, the seasonal range of water table elevations tends to span the transition between the saprolite zone and the underlying bedrock, suggesting that the weathering profile reflects the complexity of variably-saturated flow dynamics in space and time.

Subsurface flow within the saprolite zone is directed downward and laterally from higher elevations toward stream valleys where shallow groundwater discharge occurs. Water flux through the lower part of the vadose zone is primarily vertically downward. The vertical component of flow below the water table varies according to topographic position (recharge versus discharge areas). Shallow subsurface flux in the uppermost saprolite zone and lateral flux near the saprolite-bedrock interface respond rapidly to heavier precipitation events and contribute much of the quickflow component of storm-period runoff. At increasing depths (on the order of 100 ft or more), flow within the saturated zone contributes proportionally less to the overall subsurface flux, reflecting the decrease in porosity and permeability with increasing depth. A complete description of research methods, locations, interpretations, and findings completed in the headwaters areas of Melton Branch underlain by the same Conasauga Group formations present in BCV is documented in an ORNL status report (ORNL 1992b, pages 3-5 through 3-28). Subsequent watershed studies (Clapp 1998) indicated the proportion of flux via the uppermost saprolite zone may be less than reported by ORNL (1992b), but generally confirmed that most of the active groundwater flux occurs in the saprolite zone.

Another important aspect of the conceptual model relates to groundwater flow paths and rates that are dominant along fractures that trend parallel to geologic strike. Tracer tests and investigations of groundwater contaminant plumes on the ORR and in BCV demonstrate that groundwater tends to move more rapidly along fracture flow paths that are parallel to geologic strike versus flow paths that are perpendicular to strike. This is particularly true for the shallower portions of the saturated zone where most groundwater flux occurs.

The distinction between the shallower parts of the saturated zone and deeper levels is based on variation in groundwater chemical composition with depth thought to be related to water residence time. The approximate boundary between mixed-cation-bicarbonate (HCO_3) water and Na-HCO_3 water was defined at depths ranging from 30 to 50 m (approximately 100 to 165 ft) for the predominantly clastic rocks on the ORR such as those at the EMDF site. The deep "aquiclude," composed of saline water having total dissolved solids ranging from 2000 to 275,000 mg/L lies beneath the deep interval at depths in portions of BCV believed to be greater than 300 m (approximately 1000 ft) (ORNL 1992b). Additional information on groundwater geochemical zones is presented in Sect. 2.1.6.1.

2.1.5.2 Groundwater hydrology overview

The depth to the water table or unsaturated zone thickness varies across a relatively wide range from upland to lowland areas. Vadose zone thickness is greatest below upland areas such as those along Pine Ridge and along the subsidiary ridges underlying the Maryville outcrop belt. In these topographic positions, the water table can lie within the bedrock zone (Fig. 2.14), at depths exceeding 30 ft below the surface. Away from these upland areas of groundwater recharge, the vadose zone thins along the transition to groundwater discharge areas in valley floors where the water table is at or near the ground surface. In most lower elevation areas, the water table lies within the saprolite zone materials at depths less than 20 ft below the surface.

Groundwater within the saturated zone converges and discharges into stream channels along the tributary valley floors, supporting dry-weather base flow, primarily during the wetter portions of the year. During drier periods, groundwater may support little or no stream base flow, but may continue to slowly migrate southward toward Bear Creek along the tributary valley floor areas within alluvium, saprolite, and bedrock

fractures below the active stream channels. Deeper groundwater that does not discharge to the tributaries moves southward toward Bear Creek along pathways through the bedrock zone. Most of the groundwater flux within the saturated zone has been demonstrated to occur via the saprolite zone with progressively less flux occurring at greater depth. The flux decreases in proportion to a general decrease in saturated hydraulic conductivity (K_{sat}) with depth that is associated with smaller fracture apertures and an overall decrease in the number and density of interconnected fractures capable of transmitting groundwater.

Shallow groundwater also discharges to springs in narrow headwater ravines of Pine Ridge and across broader seepage faces along portions of the tributary valleys. Groundwater from these discharge locations contributes to stream channel base flow, particularly during the wet season. Water level hydrographs indicate that recharge to the water table occurs rapidly in response to significant rainfall events in most areas, but the response may be subdued and delayed in wells below upland areas where the water table is at greater depth and recharge rates are slower (DOE 2019). In general, water table elevations are several feet higher, on average, during the wet season (approximately December through March or April) compared to the remainder of the year.

The following subsections address hydraulic characteristics of materials and flow systems within the unsaturated (vadose) and saturated zone.

2.1.5.3 Unsaturated zone hydraulic characteristics

Unsaturated flow in undisturbed areas will migrate to the water table through the typical sequence of topsoil, silty/clayey residuum, and saprolite as described in Sect. 2.1.3.5, which may also include veneers of alluvial and colluvial materials along the flanks and floors of the tributary valleys. According to research (ORNL 1992b, Moore and Toran 1992), most of the water infiltrating the surface during and immediately after storm events travels laterally and relatively quickly through the uppermost part of the soil profile to discharge along stream channels.

Research on the ORR (ORNL 1992b, Moore and Toran 1992, Clapp 1998) has demonstrated that recharge through the unsaturated zone in undisturbed natural settings is episodic and occurs along discrete permeable features that may become saturated during storm events, even though surrounding macro and micropores remain unsaturated and contain trapped air. During recharge events, flow paths in the unsaturated zone are complex, controlled to a large degree by the nature and orientation of structures such as relict fractures in saprolite (ORNL 1992b). It is important to note that much of the surficial material of the saprolite zone at the CBCV site will be removed during site preparation for EMDF construction, and that highly permeable vadose pathways will be less prevalent in the remaining saprolite, geologic buffer, and structural fill materials below the disposal unit.

Virtually all efforts to determine hydraulic conductivity (i.e., slug tests, packer tests, borehole flow meter tests, and pumping tests) reported from sites in BCV have been conducted in the saturated zone or using laboratory tests on soil samples designed to determine K values under saturated conditions. Saturated K measurements have been made in the vadose zone using infiltration tests and packer tests (ORNL 1992b, page 3-13) and the data are lognormally distributed with a geometric mean K_{sat} of 1.9E-03 m/day (2.2E-06 cm/sec) and a range (± one standard deviation) of 1.74E-07 cm/sec to 1E-04 cm/sec.

Previous investigations of waste sites and proposed waste management/disposal sites in BCV provide considerable engineering and hydrogeological data on saprolite zone materials in the EMWMF footprint and at an adjacent site east of the EMWMF footprint (Golder Associates, Inc. [Golder] 1988a; Ogden Environmental and Energy Services Co., Inc. [Ogden] 1993a, Ogden 1993b; Bechtel Jacobs Company LLC [BJC] 1999; Waste Management Federal Services, Inc. [WMFS] 2000; CH2M-Hill 2000). With regard to K_{sat} measurements in the vadose zone, bulk soil samples from two test pits (TP12 and TP16)

excavated in the unsaturated zone at the EMWMF site were submitted for laboratory analysis of permeability (per American Society for Testing and Materials [ASTM] Method D5084) from depths of 4 ft and 8 ft below surface, respectively. TP12 was located within the outcrop belt of the Rutledge Formation and the sample was classified as silt. TP16 was located in the outcrop belt of the upper Maryville Formation and the sample classified as clay. Permeabilities ranged between 1E-06 and 1E-08 cm/sec for four tests conducted on remolded and compacted samples (two tests per sample were conducted at 5 and 30 psi confining pressures with lower permeabilities associated with the 30-psi tests). Characterization of a previous EMDF candidate site just east of EMWMF included collecting five Shelby tube samples for laboratory analysis (ASTM Method D5084) of K_{sat} (DOE 2017c). Two samples were collected from the unsaturated zone at depths of 2 to 4 ft and 10 to 11 ft below the surface. Hydraulic conductivity values were 3.5E-06 cm/sec and 5.0E-06 cm/sec, respectively, and both samples were described as silty clay (decomposed shale). These results, based on a small sample size and remolding of bulk soil materials, are not representative of bulk K_{sat} values for natural in situ soils and saprolite, but they may be applicable to overburden material (soil and saprolite) that is selected for engineered fill/geobuffer materials.

Information on vadose material characteristic curves for moisture retention or relative permeability relationships for variably saturated flow conditions is limited. Laboratory measurements of moisture characteristic curves were obtained for vadose zone soils samples at seven locations at a site in Melton Valley underlain by formations of the Conasauga Group (Rothschild et al. 1984). The samples were collected from the upper 2 m of the soil profile. The K_{sat} values were estimated in the field using a constant head technique, and hydraulic conductivity relationships were derived based on the K_{sat} estimates and the measured characteristic curves (Rothschild et al. 1984, pages 18–30 and Appendix C). The applicability of these measurements to vadose zone materials at the EMDF site is difficult to assess, but the estimates of K_{sat} obtained are generally on the upper end of the range of other laboratory estimates of K_{sat} described in the preceding paragraphs. Although geotechnical data collection to support EMDF design and construction is being conducted, unsaturated material characteristic curves are not typically measured in such investigations. Section 2.1.11 summarizes the results of recently completed characterization activities at the CBCV site.

2.1.5.4 Saturated zone hydraulic characteristics

Hydraulic characteristics of the saturated zone in BCV have been determined by numerous investigations at sites in BCV. The following subsections review the findings from site investigations and research in BCV most relevant to the hydraulic characteristics of saturated subsurface materials at the proposed EMDF site.

Porosity, effective porosity, and matrix diffusion in the saturated zone. Estimates of porosity and effective porosity reported for subsurface materials in BCV vary along the vertical subsurface profile (Fig. 2.14) and among geologic units. This variation is closely correlated with variability in hydraulic conductivity measurements that are available.

While total porosity can be high (> 0.4) in fine-grained (silty clay), porous materials of the upper saprolite zone in BCV, the drainable porosity is typically lower because the small pore size and high capillarity of the fine-grained materials prevent water from freely draining from the bulk of the material. Effective porosity (the fraction of total porosity associated with fluid advection) under hydraulic gradient conditions other than gravity-driven drainage can be higher than the drainable fraction of the total porosity.

Below the clay-rich upper portion of the saprolite zone, the highly weathered and fractured saprolite and the upper bedrock zone materials are associated with higher total and effective porosities than the deeper, less weathered and fractured bedrock at depth. Within the saprolite, porosity also varies between fragments of less-weathered rock that are embedded in the highly weathered matrix material. These general features

and downward transitions are evident in tube samples and test pits of soils and saprolite, and in bedrock cores. Local variations in porosity also reflect variability in the density and size of fractures in both saprolite and less weathered bedrock.

Total porosity values have been rarely presented in the ORR literature. A mean porosity of 0.50 for shaley saprolite in trench walls at ORNL Waste Area Grouping (WAG) 6 has been reported based on bulk density calculations (Moore and Toran 1992, page 15). The majority of porosity estimates from the ORR are presented as effective porosities or closely related quantities, such as storativity. The effective porosity and related data from various reports and research conducted on the ORR and in BCV is summarized in Table 2.7. The values for effective porosity range over several orders of magnitude depending on the methods, assumptions, and calculations applied for their determination.

Table 2.7. Effective porosity estimates (percent) from various ORR sources

Paper/report source	Mean effective porosity (%)	Range - effective porosity (%)	Notes
Dorsch et al. 1996	9.9	4.58-13.00	Bedrock cores - GW-132, 133, 134 EBCV transect shales from various Conasauga Group Formations in BCV, cores from 40 to 1156 ft bgs
Dorsch and Katsube 1996, GW-821, -822, -833 WBCV transect; Mudrock saprolite from Nolichucky Formation	39.0		Saprolite groundmass
	16.1		Less weathered saprolite mudrock fragments
		26.2-51.3	Calculated effective porosities, larger volumes of saprolite and mudrock fragments
Moore as reported in ORNL 1992b	3.2	3.2-3.6	Stormflow zone (topsoil/near surface)
	0.23		Groundwater zone (shallow water table interval)
ORNL 1992b, ORR Hydro Framework	4.0		Stormflow zone
	0.42		Vadose zone
		0.25-0.33	Groundwater zone (shallow water table interval)
		0.1-0.001	Groundwater zone appears to include entire saturated zone from shallow water table interval through intermediate to deep intervals
	Mean storativity (%)	**Range - effective porosity (%)**	
	0.084	0.58-0.0048	Storativity from field tests (10^{-3} to 10^{-5})
Moore and Toran 1992, Supplement to Hydrologic Framework for the ORR (see descriptions and Table 1, page 38-39)	**Mean effective porosity (%)**		
	3.5		Stormflow zone
	0.23		Groundwater zone
	Effective fracture porosity (%)		
	0.035		Groundwater zone
	Total matrix porosity (%)		
	0.96		Groundwater zone
	Fracture porosity (%)		
	0.05		Groundwater zone
	Storativity (%)		
	0.076		Groundwater zone
	Mean effective porosity (%)	**Range - effective porosity (%)**	
Lee et al. 1992, Tracer test/modeling at WBCV site	3	1-10	Wells screened in regolith (saprolite) and unweathered bedrock of Maryville Formation

Table 2.7. Effective porosity estimates (percent) from various ORR sources (cont.)

Paper/report source	Calculated effective porosity (%)	Estimated matrix porosity (%)	Notes
McKay et al. 1997, EPM Modeling/Tritium Tracer Test	9	8-40	ORNL Burial Ground 4 in saturated fractured weathered shale saprolite of Pumpkin Valley Formation similar to EMDF/BCV, but in different fault block
	Mean Effective Porosity (%)		
ORNL 1997b, Performance Assessment for WBCV Site	5		Values based on field tests at Engineering Test Facility in similar geology at ORNL/Melton Valley
Law Engineering 1983	0.3		OLF/BCBG pumping test
Lozier et al. 1987	0.06		OLF/BCBG pumping test
Geraghty and Miller 1986	0.01-0.04		S-3 Ponds site pumping test
Golder Associates 1988a	0.01		WBCV site (near EMDF Site 14)

BCBG = Bear Creek Burial Grounds
BCV = Bear Creek Valley
bgs = below ground surface
EBCV = East Bear Creek Valley
EMDF = Environmental Management Disposal Facility
EPM = equivalent porous medium
OLF = Oil Landfarm
ORNL = Oak Ridge National Laboratory
ORR = Oak Ridge Reservation
WBCV = West Bear Creek Valley

The values reported in Dorsch et al. 1996 and Dorsch and Katsube 1996 are based on laboratory analysis of cores from saturated portions of bedrock and saprolite, respectively. Values of effective porosity were obtained using petrophysical methods on bedrock core samples of mudrock specimens from Conasauga Group formations (Dorsch et al. 1996). Two hundred specimens were analyzed from among the Nolichucky, Maryville, Rogersville, Rutledge, and Pumpkin Valley Formations. A mean value of $0.099 \pm 0.0261$was obtained using the immersion-saturation method (judged as the most reliable of the three methods used) based on a total of 56 measurements. The authors noted that the values were significantly higher than those previously reported to range between 0.001 and 0.034.

In a separate study (Dorsch and Katsube 1996), effective porosities of saprolite were determined using Rotasonic core samples collected in the saprolite zone of the Nolichucky Formation at the WBCV site. Calculated (averaged) effective porosities for larger volumes including both saprolite matrix and mudrock fragments were determined to range from 0.51 to 0.26. These results suggest considerably higher effective porosity values for saprolite versus fractured bedrock (determined by the same author using similar methodologies) and much higher values than those noted above (ORNL 1992b) for materials within the range of water table fluctuations, typically within the saprolite zone. The calculated effective porosity data for larger volumes displayed a smooth decrease with depth, mirroring the saprolite weathering profile. The calculated effective porosities were noted as probably best suited for the task of modeling and evaluating matrix diffusion as a transport mechanism within the saprolite mantle.

The values reported by Dorsch et al. (1996) and Dorsch and Katsube (1996) are at least one to two (or more) orders of magnitude higher than those reported by ORNL (1992b) and Moore and Toran (1992) for the saturated zone, which were partly derived from analysis of groundwater level recession curves. In general, estimates based on laboratory measurements of porosity or based on other bulk sample characteristics range from a few percent to around 30 percent. Estimates of effective porosity based on pumping tests or other hydraulic analyses are generally less than 1 percent. This dependence on analytical

methods highlights the difference between the porosity associated with hydraulically efficient fracture networks and the larger porosity associated with the geologic matrix materials, which may be effective, but have much lower permeability than the factures. The values shown on Table 2.7 and used in Lee et al. 1992, McKay et al. 1997, and in the ORNL PA for the proposed Class L-II Disposal Facility (C2DF) disposal facility in WBCV (ORNL 1997b) are values assumed for the purposes of groundwater and contaminant transport modeling.

The uncertainty and analytical variability in estimating effective porosity highlights the potential importance of contaminant mass transfer between highly conductive hydraulic pathways and less permeable zones. Contaminant mass transfer between highly mobile and less mobile domains is commonly referred to as matrix diffusion, though both advective and diffusive transport may occur between flow in more permeable and less permeable material zones. A summary of relationships between matrix diffusion and effective porosity in relation to the clastic "mudrock" saprolite and bedrock of BCV that dominates the subsurface environment in BCV is provided in Dorsch et al. (1996). Figure 2.18 conceptually illustrates the partitioning of contaminants by matrix diffusion to or from groundwater fracture flow paths into the adjacent pores and micropores of the surrounding host rock "matrix". The availability and permeability of highly weathered matrix materials decreases with depth below the water table in the clastic rocks of BCV. As discussed in the review of tracer tests below, matrix diffusion is thought to play a critical role in attenuating the migration rates and concentrations of contaminants from source areas to downgradient locations. Depending on the rate of contaminant decay or degradation processes, diffusion of dissolved contaminants from more transmissive zones into less mobile micropores and microfractures can result in enhanced attenuation along flow paths.

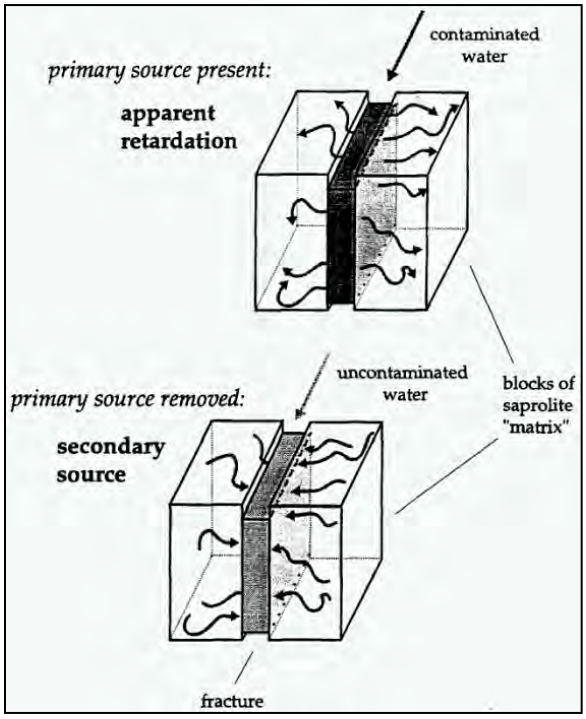

Source: Dorsch et al. 1996, Fig. 3

Fig. 2.18. Schematic diagram illustrating matrix diffusion in a fractured saprolite

Hydraulic conductivity of the saturated zone. The most recent compilation of K_{sat} values reported for BCV (UCOR 2014, Appendix C, page C-36) span seven orders of magnitude ranging from a minimum of 5E-05 ft/day (Nolichucky Formation) to a maximum of 164 ft/day (Maynardville Limestone). The values range from low K values determined from packer tests in deep core holes to relatively high values measured in wells completed in karst conduits in the Maynardville Limestone. The K_{sat} varies by lithology, degree of weathering and fracturing, and depth. The K_{sat} values are influenced by the test method, borehole or well completion interval tested, number and vertical spacing among permeable fractures/fracture intervals and intervening relatively impermeable rock matrix intervals, and other factors.

One of the earliest compilations and statistical analyses of K_{sat} data was reported in Connell and Bailey (1989). Pre-1985 K_{sat} data was evaluated from 10 investigation reports with 338 single-well aquifer tests from BCV and Melton Valley at ORNL. Results were segregated and evaluated by regolith and bedrock tests and by geologic formations. In BCV, 232 tests were selected from 153 wells for statistical analysis; 63 in regolith (saprolite zone), 164 in bedrock, and five in deep bedrock. Within BCV, the tested wells were located at the BCBG, Oil Landfarm, and S-3 Ponds waste sites near EMWMF, and from the proposed Exxon Nuclear site between SR 95 and the Clinch River. These results include wells completed in the same geologic formations underlying and downgradient of the CBCV site and are, therefore, representative of the range of K_{sat} values that may be expected at and near EMDF. The BCV data is summarized in terms of the distributions of K_{sat} values within and among the geologic formations spanning the width of BCV in Fig. 2.19. The median K_{sat} values for the clastic rock formations underlying the EMDF site (i.e., Maryville Formation and Nolichucky Formation) are roughly an order of magnitude lower than the median K value of the Maynardville Limestone.

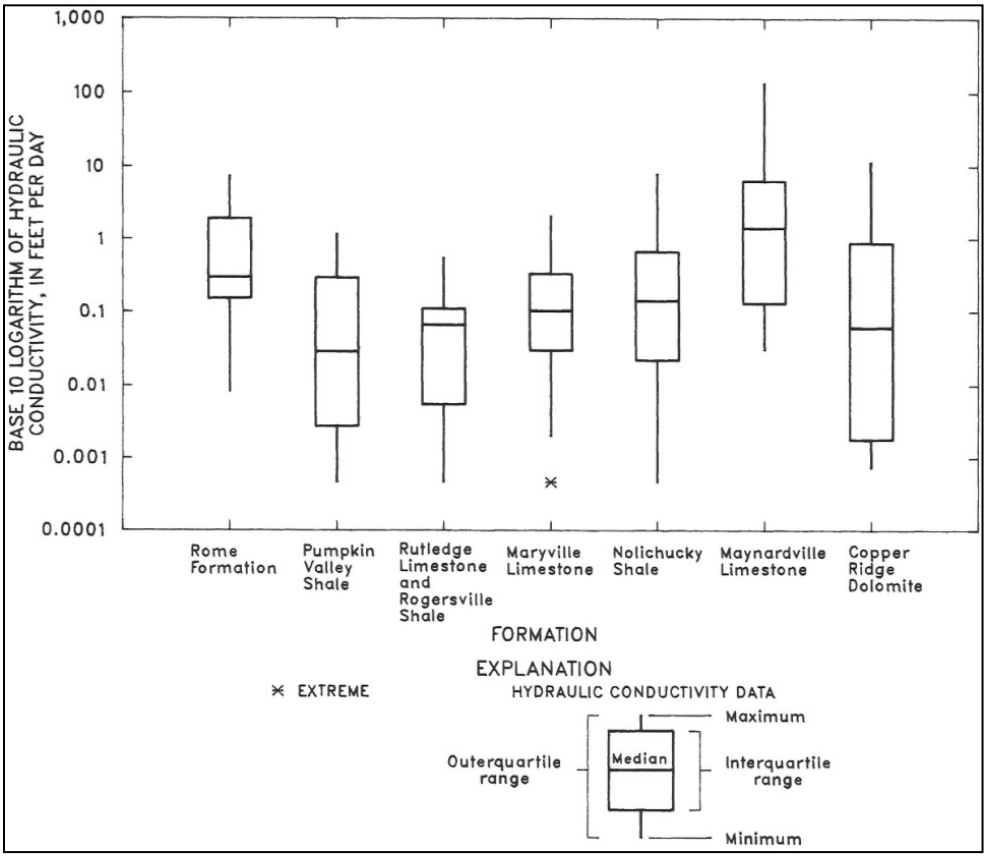

Source: Connell and Bailey 1989, based on pre-1985 wells.

Fig. 2.19. Results of statistical analysis of hydraulic conductivity of 232 tests in BCV wells

In addition, BCV specific information included K_{sat} data from a total of 120 packer tests, 66 slug tests, and four pumping tests across a broad area of WBCV in support of the planning for the proposed C2DF (Golder 1988b). In this report, the K_{sat} results were plotted and analyzed by test method, geologic formation, and depth. The K_{sat} data was subdivided into three depth horizons (0 to 50 ft, 50 to 300 ft, and > 300 ft) and was provided frequency distribution plots of log K data according to these three depth levels. It was concluded that "*there does not appear to be a strong relationship between K and geologic formation. However, K is clearly depth dependent*." The 0- to 50-ft interval was considered the most permeable and most representative of saprolite or shallow bedrock, with progressive decreases in K with depth for the lower horizons. From shallow to deep, geometric mean K_{sat} values were assigned for the three horizons of 1E-04 cm/sec, 1E-05 cm/sec, and 1E-07 cm/sec.

A linear regression analysis performed of the K_{sat} data with depth as the independent variable is shown in Fig. 2.20, with a correlation coefficient of 0.46. This data set was considered too limited to conduct multivariate analysis to assess the effects of test type, test scale, and geologic formations. It was also noted that a "significant emphasis" was placed on testing the Nolichucky Formation and Maryville Formation.

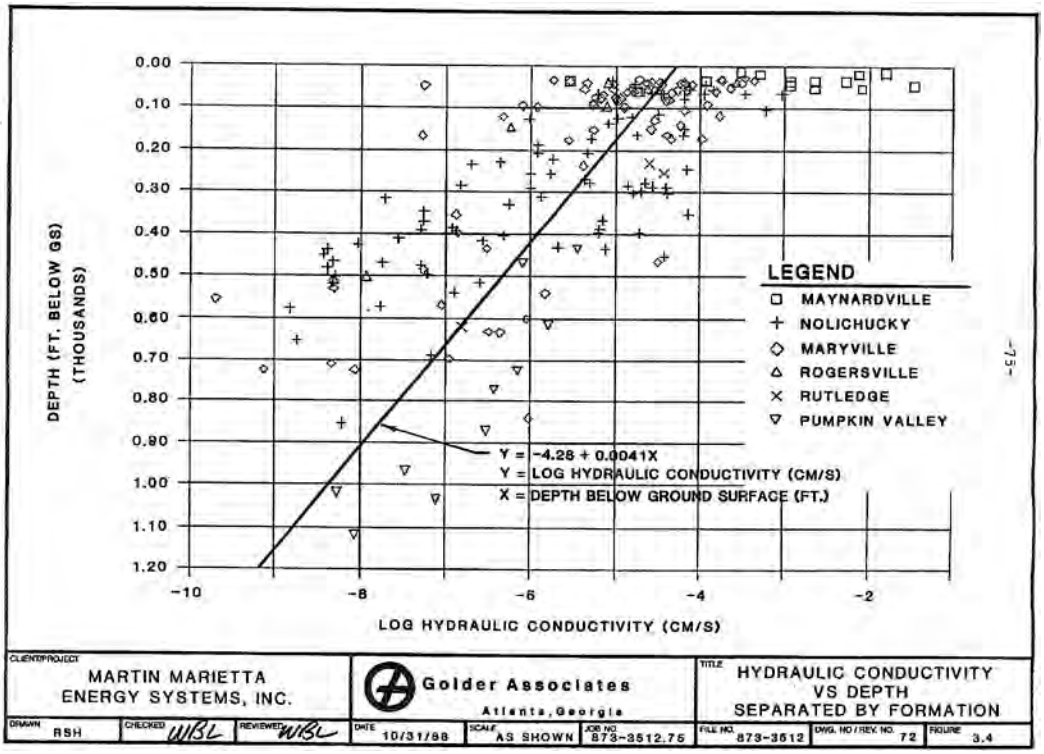

Source: Golder 1989

Fig. 2.20. Linear regression plot of hydraulic conductivity at depth at WBCV (Site 14)

A more recent comprehensive compilation, summary, and analysis of K_{sat} data from multiple sites in BCV (including other groundwater hydraulic characteristics) were presented in the BCV FS (DOE 1997c). More than 200 test results from wells completed in BCV up through 1997 are included in Appendix F of the BCV FS, Sect. 3.5. The data were derived from slug tests/bailer recovery tests, packer tests, and pumping tests, including packer test intervals conducted in deep core holes between depths of approximately 250 to 950 ft. The results were used in support of the construction and calibration of the original 3-dimensional (3-D) regional groundwater flow model for BCV used for evaluating remedial actions at the hazardous waste sites and contaminant plumes in EBCV.

The results of the K_{sat} tests presented in the BCV FS are summarized in Table 2.8 and Figs. 2.21 and 2.22. The relationship between log K_{sat} values and depths for the predominantly clastic (shaley) formations in BCV from the Rome through the Nolichucky Formation is illustrated in Fig. 2.21, while results for the carbonate formations of the Maynardville and Knox Group along the south side of BCV are illustrated in Fig. 2.21. The plots illustrate the larger number of wells and test results available for relatively shallow wells (< approximately 100 ft) versus results available for intermediate and deep levels of the saturated zone (> approximately 100 ft). The plots and regression lines also illustrate that while there is considerable scatter in the range of K_{sat} values by depth, the data suggest an overall general tendency toward reduced K_{sat} values with depth that is consistent with less weathering and fracturing evident in subsurface samples/rock cores, and a general reduction in transmissive fractures with depth.

Table 2.8. Summary statistics compiled by for K data in BCV

Hydrogeologic unit	K (min) (ft/day)	K (max) (ft/day)	K (avg) (ft/day)	Count
Knox	0.0002	3.67	0.511	27
Maynardville Limestone	0.000027	99.0	8.132	41
Nolichucky Formation	0.000009	7.1	0.723	109
Maryville Formation/Rutledge Formation/Rogersville	0.00003	2.08	0.192	33
Pumpkin Valley/Roane	0.00086	1.156	0.223	18

Source: DOE 1997c.

BCV = Bear Creek Valley
DOE = U.S. Department of Energy
K = hydraulic conductivity

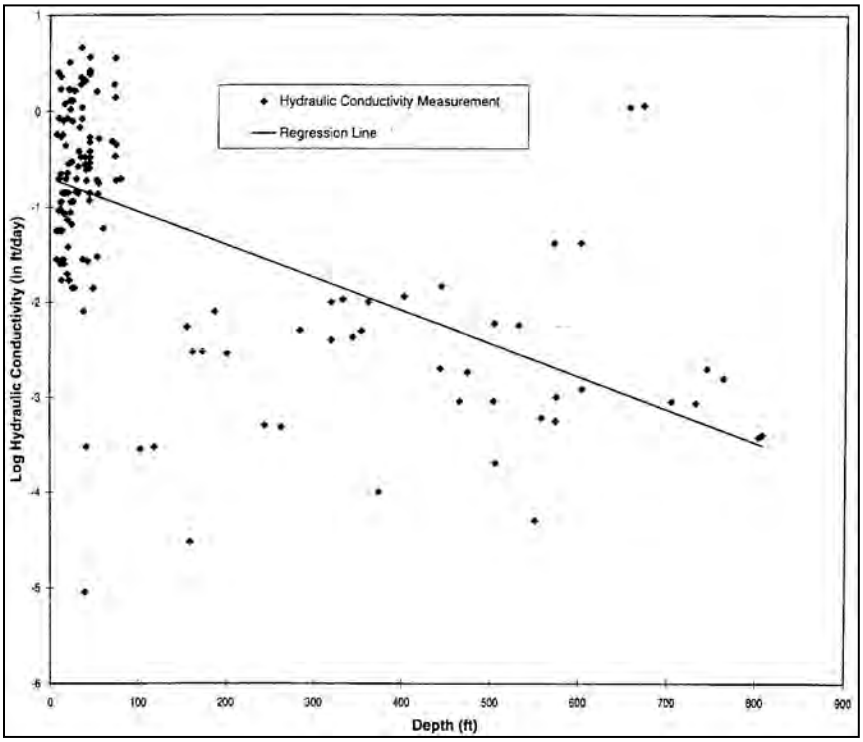

Source: DOE 1997c, Fig. F.20.

Fig. 2.21. Relationship between Log K_{sat} and depth in the clastic formations underlying BCV

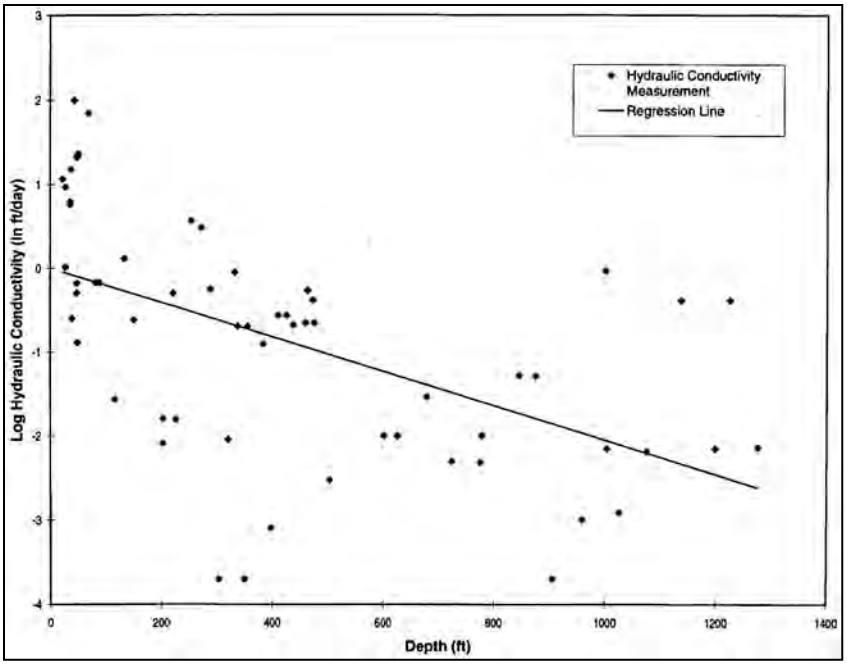

Source: DOE 1997c, Fig. F.19.

Fig. 2.22. Relationship between log K_{sat} and depth in predominantly carbonate formations, BCV

In addition to these earlier efforts, UCOR completed an effort to summarize and statistically evaluate hydraulic properties of BCV units by geologic formation (UCOR 2014, Appendix C). This effort was developed for a Y-12 centered test case of a larger-scale regional groundwater flow model for the entire ORR (UCOR 2015, DOE 2016a).

Field and laboratory measurement of hydraulic conductivity at the CBCV site. Recent characterization of the CBCV site to support EMDF site selection and preliminary design has provided additional information on groundwater and surface water hydrology, including field estimates of hydraulic conductivity. The K_{sat} data are summarized in the following paragraphs, and the surface water flow measurements are summarized in Sect. 2.1.7.2. Section 2.1.11 provides a general summary of the CBCV characterization activities and references to reports that summarize the results.

Hydrologic tests, including Flexible Liner Underground Technologies, LLC (FLUTe™) tests in the deeper bedrock intervals (open boreholes) and slug tests in shallow piezometers, were conducted to provide information of the in situ hydraulic properties.

FLUTe™ testing was performed within the open, uncased boreholes at the CBCV site (GW-978, GW-980R, GW-982, GW-986, GW-988, GW-992R, GW-994, and GW-998) to determine transmissivity (and/or hydraulic conductivity) values within the bedrock (DOE 2019). The results from the FLUTe™ testing and interpretation of the borehole logs, relative to identifying target intervals of permeable water-bearing bedrock, were used to determine screen and sand-pack intervals for both the intermediate and shallow piezometers at each location. During FLUTe™ testing, a flexible borehole liner made of a water-tight, urethane-coated, nylon fabric is lowered into the borehole. The rate at which water is added to the liner is governed mostly by the rate at which the water can escape into the permeable features in the open hole below the descending liner as it forces the water out into the permeable zones in the formation. The liner descent-rate or velocity is a measure of transmissivity of the entire borehole. As the liner continues

down the borehole and seals each permeable feature, changes in the liner velocity indicate the position of each feature and an estimate of transmissivity is provided.

As seen in Table 2.9, total borehole transmissivity ranged from 0.052 sq cm/sec at GW-982, located on the knoll in the Maryville, to 0.198 sq cm/sec at GW-998, located in the Nolichucky south of the proposed disposal facility. The average total borehole transmissivity for the tested boreholes was 0.118 sq cm/sec. Also of importance in Table 2.9 is the "length of the borehole remaining" column. The FLUTe™ liner is inserted into the borehole as water is added inside the liner, driving it downward. If the borehole has a very low transmissivity, the liner will not reach the bottom (water within the borehole below the liner cannot be pushed out into the geologic formation). GW-982 was nearly impermeable below 54 ft below ground surface (bgs) with 71.5 ft of borehole remaining and GW-980R had a permeability too low to conduct profiling. The results generally indicated a decreasing hydraulic conductivity with depth.

Table 2.9. FLUTe™ measurements in Phase 1 piezometers

Well ID	Depth of FLUTe™ profile (ft bgs)	Total borehole transmissivity (cm^2/sec)	Length of borehole remaining (ft)	Transmissivity of remaining borehole (cm^2/sec)	Average hydraulic conductivity for remaining borehole (cm/sec)	Geologic formation
GW-978	76.85	0.16164	5.24	0.02705	1.30E-04	Rutledge
GW-980R	--	--	--	--	--	Maryville
GW-982	53.74	0.05181	71.56	0.0045	2.06E-06	Maryville
GW-986	49.17	0.09862	10.25	0.01538	1.02E-04	Maryville
GW-988	75.37	0.10648	3.64	0.056714	5.12E-04	Maryville
GW-992R	51.12	0.10757	3.71	0.04239	3.75E-04	Nolichucky
GW-994	52.02	0.09845	2.73	0.06932	8.34E-04	Nolichucky
GW-998	39.92	0.19806	5.16	0.05684	3.62E-04	Nolichucky

-- = not available/applicable

bgs = below ground surface.
FLUTe™ = Flexible Liner Underground Technologies, LLC

Hydraulic conductivity (horizontal) was measured by performing slug tests for piezometers completed in the upper bedrock and residuum (DOE 2019). Slug tests were performed in shallow piezometers GW-979, GW-981, GW-983, GW-987, GW-989, GW-993, GW-995, and GW-999. Slug-test data were analyzed using the Bouwer-Rice method (Bouwer and Rice 1976, Bouwer 1989) with the AQTESOLV™ software. The results indicate that hydraulic conductivity ranged from 4.6E-05 to 5.0E-03 cm/sec in the shallow piezometers. The average/mean hydraulic conductivity determined for the two individual tests for each piezometer ranged from 5.5E-05 to 5.0E-03 cm/sec.

Anisotropy of hydraulic conductivity. Hydraulic conductivity tends to be anisotropic in BCV, with higher K_{sat} associated with bedding planes and joints in the strike-parallel direction relative to joint sets oriented at right angles to geologic strike. Expressed in general terms of the relationship of strike-parallel, dip-parallel, and cross-strata fracture flow pathways, $K_{strike} >> K_{dip} > K_{cross\text{-}strata}$ on a whole-rock basis. Anisotropy has been observed and estimated in BCV and elsewhere on the ORR by the tendency of tracers and contaminant plumes to elongate in the direction of strike, and by elongations in the cone of depression during pumping tests. Some estimates of the degree of anisotropy in BCV, presented in Table 2.10, range from 1:1 to 38:1, but most fall between 2:1 and 10:1.

Table 2.10. Permeability anisotropy ratios determined for predominantly clastic formations of the Conasauga Group

Ratio of strike-parallel versus dip-parallel hydraulic conductivity	Test method	Analytic method	Reference
1:1	Groundwater flow model calibrated to actual conditions in portions of EBCV	Finite-difference model	Bailey and Lee 1991
2:1	Pumping tests at depths of 3 m and 33 m in Maryville Formation, BCV	Gringarten & Witherspoon Fractured Aquifer Solution	Lee et al. 1992
38:1		Papadopulos Infinite Aquifer Solution	
4:1	Pump test in Conasauga Group, Melton and BCV	Gringarten & Witherspoon Fractured Aquifer Solution	ORNL 1984
8:1	Pump test	Various analytical methods developed for use with pumping tests	Golder Associates 1989
10:1	Groundwater flow model calibrated to actual conditions in EBCV	MODFLOW	Evans et al. 1996
5:1	Pump test in Conasauga Group	Gringarten & Witherspoon Fractured Aquifer Solution	Smith and Vaughn 1985
3:1	Model Calibration; Conasauga Group, UEFPC	Numerical model	Geraghty and Miller 1990
30:1	NaCl tracer test in BCV	Papadopulos Infinite Aquifer Solution	Lozier et al. 1987
5:1	Nitrate plume and head modeling, Conasauga Group, BCV	Numerical model	Tang et al. 2010

BCV = Bear Creek Valley
EBCV = East Bear Creek Valley
ORNL = Oak Ridge National Laboratory
UEFPC = Upper East Fork Poplar Creek

A sensitivity analysis of anisotropy was conducted in Bailey and Lee (1991) by varying K_{sat} values for strike and dip flow and comparing the actual groundwater head at numerous wells with that predicted by their model. The analysis found that anisotropy of 1.1 to 1.25:1 provided the best matches between modeled and actual groundwater head and that preferential flow along strike is not indicated in BCV, except in the Maynardville Limestone. However, results of tracer tests conducted in the predominantly clastic formations of the Conasauga Group also exhibit anisotropy. A particle tracking model was used to investigate anisotropy in BCV in "Application of particle tracking and inverse modeling to reduce flow model calibration uncertainty in an anisotropic aquifer system" (Evans et al. 1996). They found empirically that particle tracks best mimic the S-3 Ponds contaminant plume at an anisotropy ratio of 10:1. Sensitivity analysis indicated that anisotropy ratios lower than 10:1 provided better fits to the contaminant plume than did ratios higher than 10:1.

Hydraulic gradients. Potentiometric surface contour maps (Fig. 2.23) developed prior to the construction of EMWMF show horizontal hydraulic gradients and generalized groundwater flow paths across the upper part of BCV. Similar patterns are present farther down valley, closer to the EMDF site. The upper half of Fig. 2.23 illustrates the shallow water table interval in saprolite zone materials, and the lower half illustrates the shallow to intermediate depths of the bedrock zone. Hydraulic head patterns show convergent flow to the Maynardville Limestone in the valley floor aligned with the southwesterly flow along Bear Creek and indicating that it serves as the hydraulic drain for BCV. The anisotropy associated with strike-parallel fracture pathways tends to modify local flow directions from the more general pattern of flow directions indicated on the maps in Fig. 2.23.

Horizontal gradients tend to vary in proportion to the local topography so that steeper gradients occur along the steeper south flanks of Pine Ridge and adjacent to the subsidiary ridges underlain by the Maryville Formation. An average horizontal gradient of 0.05 for the ORR aquitards (i.e., predominantly clastic rock formations of the Conasauga Group) was reported in Moore and Toran (1992). Measured and model-simulated hydraulic heads and cross-valley/vertical hydraulic gradients in BCV are shown in Figs. 2.24 and 2.25. Hydraulic head data obtained from discrete multiport well intervals in a series of deep core holes along a north-south transect near the S-3 ponds at the west end of the Y-12 site is presented in Fig. 2.24 (Dreier et al. 1993). The multiport depths where head data were obtained are shown as black squares down the length of each borehole in Fig. 2.24. The figure illustrates horizontal gradients from north to south (left to right on Fig. 2.24), with an upward vertical component extending across the Conasauga Group formations toward the Maynardville Limestone. The figure also illustrates mostly downward and lateral gradients below Chestnut Ridge from south to north converging toward the Maynardville. An isolated high pressure zone in the Nolichucky Formation appears to be a relic of higher density fluids flowing down dip from the S-3 Ponds. The lowest hydraulic heads around 990 ft converge within the Maynardville Limestone from higher heads below Chestnut Ridge and southward from Pine Ridge, supporting the concept that the Maynardville, along with Bear Creek, serves as the principal hydrologic exit pathway for BCV as a whole (Dreier et al. 1993). Flow in BCV was modeled and found to have a similar head distribution as shown in Fig. 2.25 (Bailey and Lee 1991).

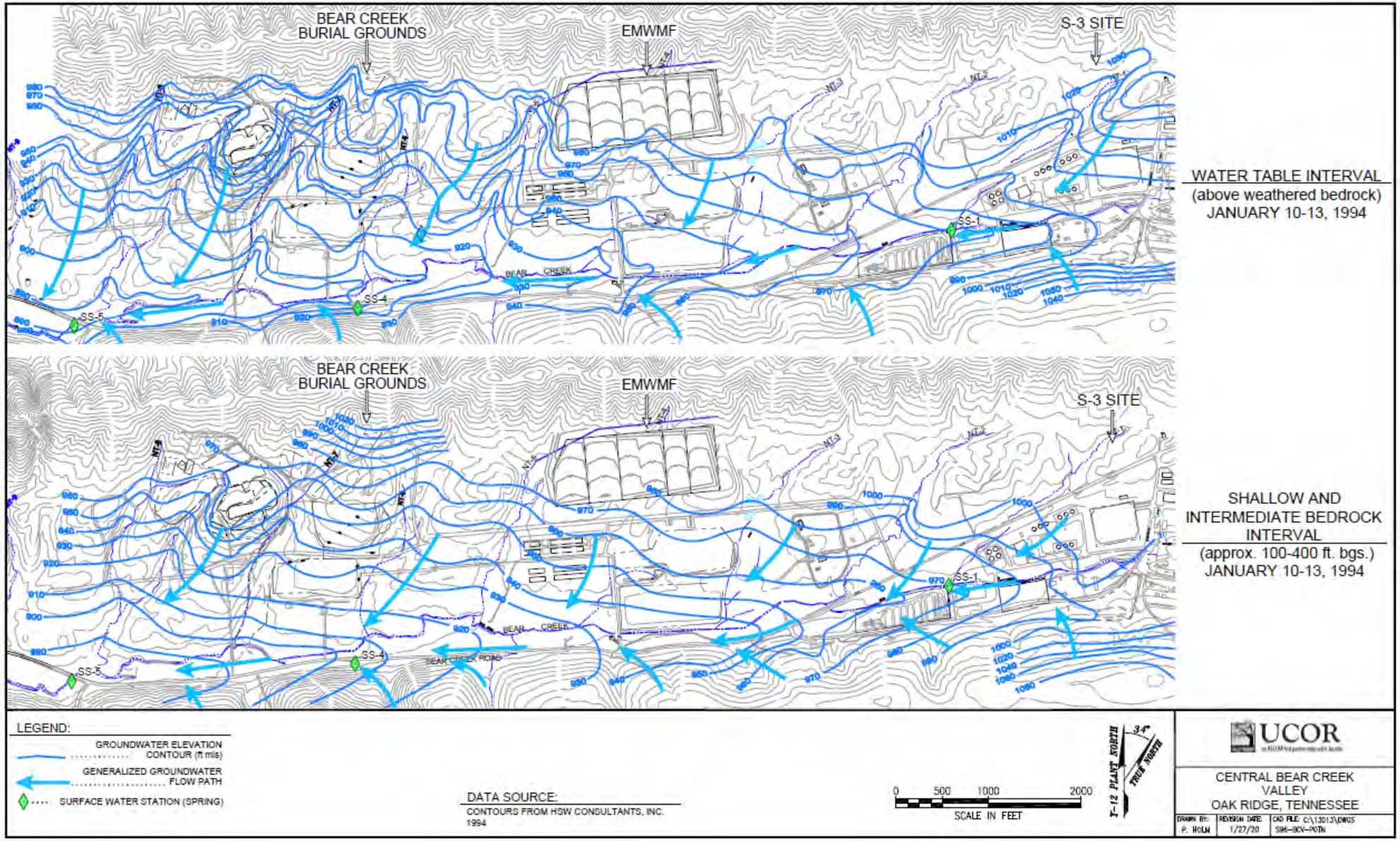

Fig. 2.23. Potentiometric surface contour maps and generalized groundwater flow directions for Upper BCV

This page intentionally left blank.

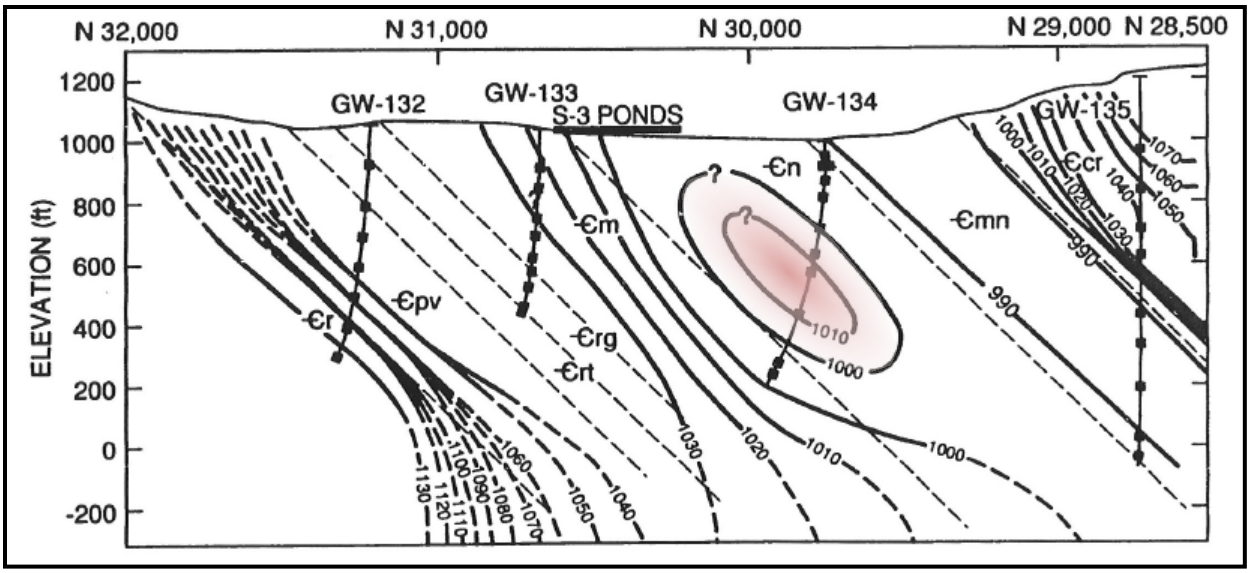

Fig. 2.24. Hydraulic head distribution across Bear Creek Valley along a deep transect near the S-3 Ponds

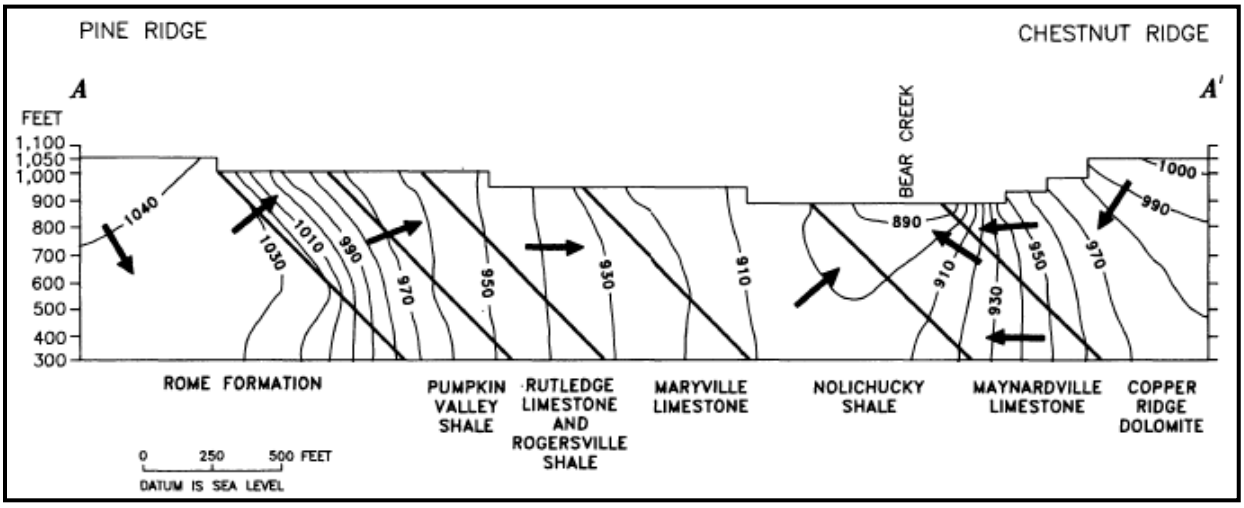

Source: Bailey and Lee 1991.

Fig. 2.25. Cross sectional representation from a computer model of groundwater hydraulic head and flow patterns in EBCV

2.1.6 Groundwater Geochemistry and Radionuclide Transport Processes

2.1.6.1 Groundwater geochemical zones and deep groundwater circulation

The boundaries between the shallow, intermediate, and deep groundwater zones defined in the hydrologic framework for the ORR and BCV (ORNL 1992b) are transitional and not precisely defined. The boundaries vary with changes in local topography, vadose zone thickness, degree and depth of saprolite zone and bedrock zone weathering, and bedrock stratigraphy. The zones occur at different levels in different parts of the ORR (Moore and Toran 1992) and field identification is commonly based on vertical changes in groundwater chemistry. Hydrogeochemical processes involving exchange of cations on clays and other minerals result in a change from calcium bicarbonate to sodium bicarbonate (Na-HCO_3) and ultimately to

a sodium chloride (Na-Cl) type water at depth. These geochemical zones reflect groundwater residence times and reduction of water flux with depth.

The top of the intermediate groundwater zone is marked by a change in the dominant cations from calcium, magnesium, and Na-HCO_3 to predominantly Na-HCO_3, and extends from approximately 100 ft to over 275 ft, where the transition to the deep zone is marked by a gradual increase in Na-Cl (Haase et al. 1987, Bailey and Lee 1991). The intermediate and deep groundwater zones are distinguished from the shallow (water table) zone by a change from a calcium-magnesium-bicarbonate (Ca-Mg-HCO_3) chemistry to a chemistry dominated by Na-HCO_3 (Moore and Toran 1992). The transition from Ca-Mg-HCO_3 to Na-HCO_3-dominant water is abrupt, occurring between depths of 80 to 200 ft in the Nolichucky Formation underlying BCV, which suggests a well-defined flow boundary (Haase 1991).

This groundwater type is common to all Conasauga Group formations (Dreier et al. 1987) at intermediate and deep depths except in the Maynardville Limestone, and appears to be unrelated to stratigraphic changes. The Maynardville Limestone and adjacent Copper Ridge Dolomite both exhibit a Na-HCO_3 water type with distinct zones of Ca-Mg-Na-sulfate (SO_4) water. These sulfate-rich water zones appear to be related to the presence of gypsum beds in the carbonate units. Table 2.11 summarizes this geochemistry information for the Conasauga Group.

Table 2.11. Geochemical groundwater zones in predominantly clastic rock formations of the Conasauga

	Bear Creek Valley[a]			**Bear Creek Valley[b]**		**Melton Valley[c,d]**		
Interval or zone	**Depth (ft)**	**Type**	**pH**	**Depth (ft)**	**Type**	**Depth (ft)**	**Type**	**pH**
Shallow	75	Ca, Mg-HCO_3	NA	< 50	Ca, Mg-HCO_3 or SO_4	< 75	Ca, Mg-HCO_3 or SO_4	6.5 – 7.5
Intermediate	NA	NA	NA	50–500	Na-HCO_3 (with some Na-Cl and Na-SO_4)	75-275	Na-HCO_3	6.0 – 8.5
Deep	NA	NA	NA			75-530	Na-HCO_3 to Na-Cl	8.0 – 10.0
Brine (aquiclude)	> 530	Na-Cl	NA	NA	NA	590 (GW-121)	Ca-Na-Mg-Cl + SO_4	11.6

[a]Haase 1991.
[b]Bailey and Lee 1991.
[c]Haase et al. 1985.
[d]Nativ et al. 1997a.

NA = not applicable

The change in groundwater chemistry with depth is interpreted to be the result of rock-water interactions and diagenesis of minerals. The rate at which the groundwater reaches chemical equilibrium with source minerals is important in the diagenetic evolution of Na-HCO_3, indicating that the groundwater is reaching equilibrium with the host rock. If clay alteration is an important control on groundwater geochemistry, then Na-HCO_3 type water may mark the transition between the actively circulating shallow zone and stagnating groundwater in deeper zones (ORNL 1992b).

Studies of deep boreholes in the Conasauga Group and the Copper Creek Dolomite of the Knox Group in EBCV indicate that deep groundwater chemistry trends from Na-HCO_3-dominated water to increasing Na-Cl content between 550 ft below grade near Pine Ridge to over 1150 ft below grade in the Maynardville Limestone on the south side of BCV (Dreier et al. 1993). This trend is associated with an

increase in total dissolved solids and pH that appears to be related to long-term rock-water reactions. These deep transitional waters are saturated with calcite and dolomite as stated in Haase (1991).

The aquiclude zone is so named because the extremely high salinity of this water indicates that little or no groundwater movement occurs. The aquiclude is well defined in the Conasauga Group of Melton Valley, but is less well documented in BCV. Detailed water chemistry data has been provided for four wells positioned across strike in EBCV and drilled to depths between 557 ft and 1196 ft below grade (Dreier et al. 1993, Haase 1991). Both reports noted an abrupt increase in total dissolved solids to about 28,000 ppm, increase in pH to the 8.5 to 10.0 range, and change from Na-HCO_3 as the dominant ion pair to dominance of Na-Cl below 1150 ft. This increase occurred just below a major fracture zone. The deep Na-Cl groundwater in four deep wells sampled for this study was saturated with respect to calcium and magnesium, and contained barium at near-saturation concentrations, which is indicative of long residence time and little or no recharge by fresher water (Haase 1991).

The presence of tritium[1] and modern C-14 in some deep brine samples from the Conasauga of Melton Valley suggests that some meteoric water commingles with the brine at depths (Nativ et al. 1997a). Groundwater flow has been measured by down-hole flow meter in various deep boreholes below 750 ft. Based on these considerations, it is postulated that flow occurs in the deep brine, and that at least some meteoritic water is transported to depth (Nativ et al. 1997b). This interpretation is refuted in Moline et al. (1998) noting that the persistence of brine over geologic time provides a strong indication that deep groundwater circulation is minimal and that deep rocks exhibit very low K_{sat} values, on the order of 1E-07 to 1E-09 cm/sec, which suggests either an absence of or minimal number of permeable fractures.

The presence of shallow water signatures (comparatively low total dissolved solids, tritium, and relatively high percentages of modern carbon) may be induced by drilling, well installation and development, open borehole circulation, or purging prior to sampling. Development and purging of deep wells is hampered by extremely low flow rates and long recovery times (Moline et al. 1998).

While some groundwater exchange may occur between the halocline and shallower groundwater zones, it is volumetrically very minor and does not appear to play a significant role in regional flow patterns. As noted above, there is a significant difference in density between the shallow groundwater and the brine. The density of uncontaminated water, or water contaminated at low concentrations by dissolved constituents, is around 1.01 g/cm^3; in comparison, the density of sea water is 1.022 g/cm^3, and brine is over 1.20 g/cm^3. A great deal of hydraulic head would be required to drive fresh water into the brine zone. The S-3 Ponds nitrate plume, which extends to depths of more than 400 ft is acknowledged as a density-driven plume, with a density range between 1.06 and 1.12 g/cm^3 (DOE 1997b). This density difference is sufficient to drive the plume below the uppermost fresh water zone, but not into the brine zone. Thus, density differences also prevent deeper downward penetration of shallow groundwater. This is analogous to the fresh water – sea water boundary that develops in coastal aquifers.

2.1.6.2 Tracer tests in Conasauga Group formations

Tracer tests are conducted by introducing a locally distinct tracer (dye, chemical, radionuclide, or particulates) into groundwater and monitoring along possible flow paths or discharge points to determine if and when the tracer first arrives, when the peak concentration occurs, and how long it takes the tracer to recede. Tracer tests are commonly used in fractured and karst systems because they are often strongly anisotropic, heterogeneous, and have complex flow paths and travel times that may be difficult to

1 Although some tritium is produced in the atmosphere by cosmic rays, it is mostly the result of atomic testing, and its presence in deep groundwater suggests that there have been recent additions of shallow water. Tritium has a half-life of 12.3 years and it would, therefore, be expected to have decayed to undetectable concentrations if groundwater migration times were very long.

determine. Tracer tests conducted in the saturated zone in Conasauga Group formations in BCV and/or in similar geologic formations elsewhere on the ORR are reviewed below along with key findings from the tests most relevant to saturated zone contaminant transport at the EMDF site.

Tracer tests have been conducted at field sites in WBCV and at field sites in Melton Valley at ORNL near burial ground (BG) Sites BG4 and BG6 and WAG 5. The tests were all conducted under natural gradients in shallow groundwater in areas underlain by predominantly clastic formations of the Conasauga Group. The tracers were all introduced at or near the water table in highly weathered and fractured shaley saprolite. The monitored plume areas were all relatively small in areal extent (less than approximately 20 ft to 100 to 200 ft in any direction) and involved a variety of tracers: (1) fluorescent dyes, (2) tritiated water, (3) noble gases (helium, neon) and bromide, and (4) colloids. Among all the tracer tests conducted on the ORR, the WBCV field site is the most intensively studied with the largest network of downgradient monitoring wells. The longest duration tests were those conducted at the BG4 and BG6 sites in Melton Valley. The other tests vary in terms of monitoring duration and/or the configuration of the network of wells used for monitoring.

Tracing studies also have been conducted in the karstic carbonate rocks on the south side of BCV and Chestnut Ridge. In general, those studies are less relevant to the release of radionuclides to the near-field environment at the EMDF site, which is situated on Conasauga Group formations north of Bear Creek.

Tests at the WBCV tracer site. The most intensively tested tracer site within predominantly clastic rock formations on the ORR is located in WBCV southwest of the proposed EMDF site. The test site is located along the contact between the Maryville Formation and the Nolichucky Formation with subsurface conditions similar to those of the EMDF site. The WBCV tracer study area is approximately 150 ft long by 70 ft wide. The first tracer tests were conducted there in 1998 by Golder. Seventy-two monitoring wells (single and nested) were installed at 45 locations along several transects roughly perpendicular to topographic and hydraulic gradients. General shallow groundwater flow direction is toward the southwest and the nearby valley of NT-15.

The Golder scope of work also included drilling and logging of regolith materials and rock cores, packer tests, slug tests, pumping tests, and groundwater solute transport modeling. The collective data were used to calibrate and refine model results. The results of the initial tracer tests, in situ hydraulic tests, and preliminary modeling were presented by Golder in a Task 5 report for the WBCV site (Golder 1988b). The results of subsequent tracer work and modeling at the same site were published in an ORNL report (Lee and Ketelle 1989) and journal article (Lee et al. 1992) authored by an ORNL and university research team.

Findings from the 1992 summary article are summarized below. The results provide insight into the complexities associated with characterization, monitoring, and modeling contaminant releases in areas of BCV underlain by predominantly clastic rock formations (i.e., Conasauga Group formations north of the Maynardville).

The tracer plume configuration at the 3- and 12-month time periods after the initial dye injection (10 L of 40 percent rhodamine-WT dye solution) on April 20, 1988, are illustrated on Figs. 2.26 and 2.27. The dye was introduced at the water table in GW-484. Tracer analysis at 1 ppb resolution was performed using fluorimetric techniques. A longitudinal cross-section through the tracer test site (Fig. 2.28) illustrating some of the main subsurface conditions (water table within saprolite; southeasterly dipping bedrock of interbedded shale, siltstone, and limestone of the Maryville Formation; and upward vertical gradients across the site measured among nested monitoring wells).

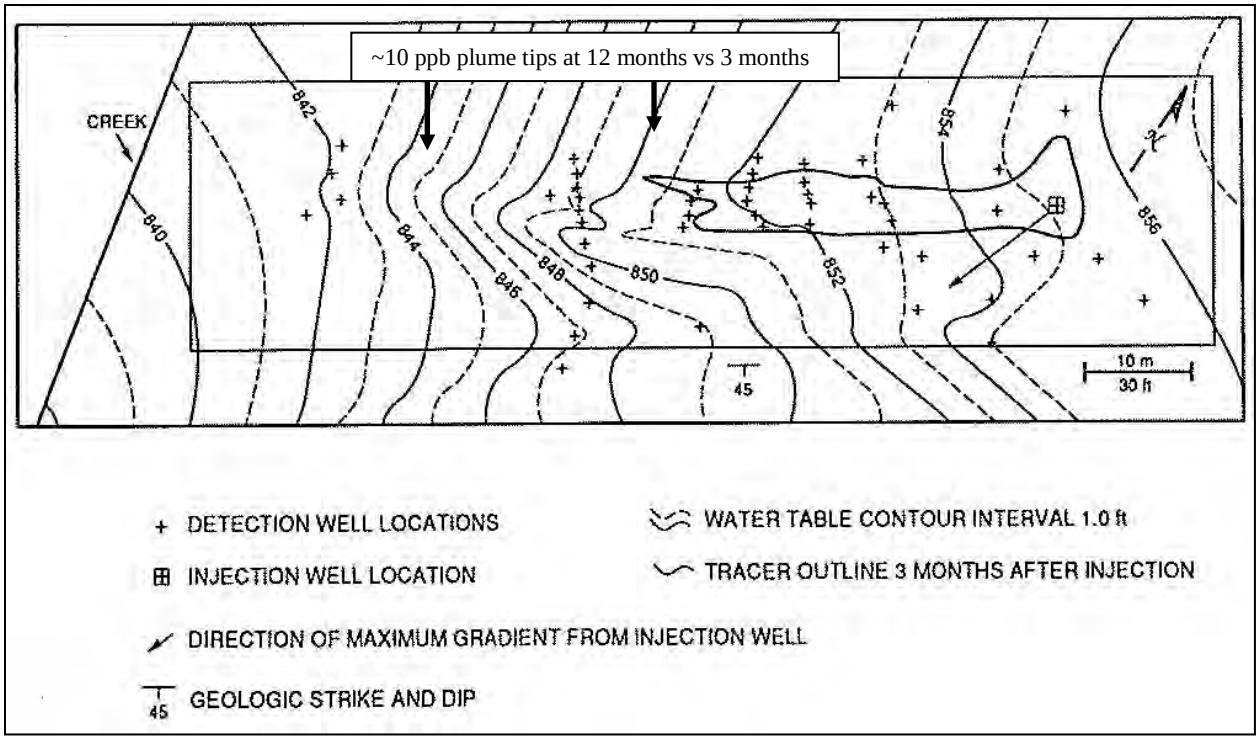

Source: adapted from Lee et al. 1992.

Fig. 2.26. WBCV tracer test site plume map (10 ppb concentration contour [~40 m or 131 ft long] 3 months after injection).

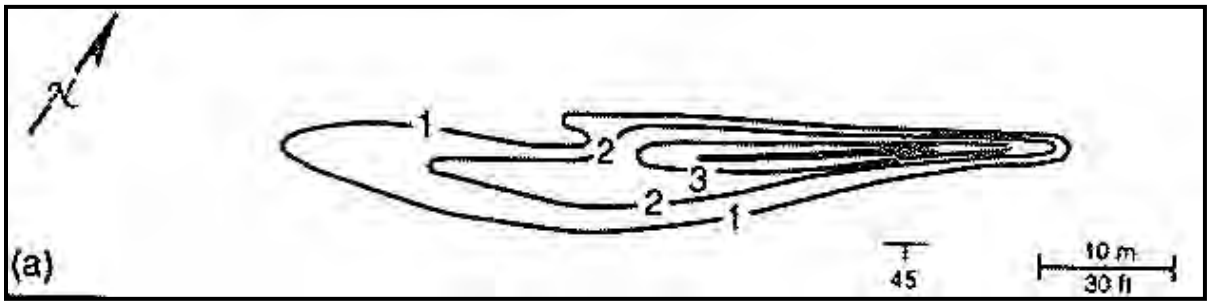

Source: adapted from Lee et al. 1992.

Fig. 2.27. WBCV tracer test site plume map (log concentration contours [10 ppb extent ~60 m or 197 ft long] 12 months after injection).

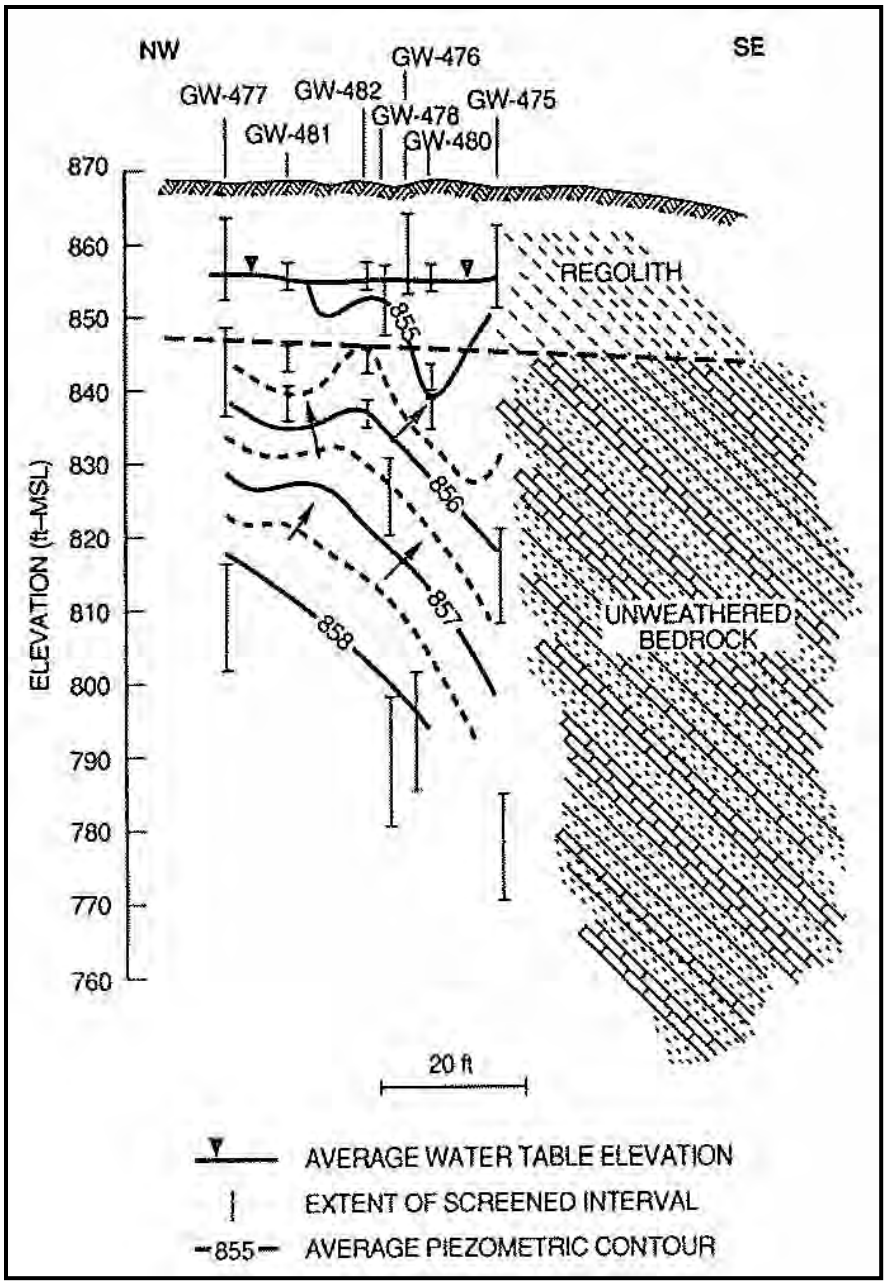

Fig. 2.28. Potentiometric contours for a northwest-southeast cross-section through the WBCV tracer test site.

Water table contours indicate horizontal groundwater flow directions toward the southwest to the local discharge zone along the valley floor of NT-15, parallel to subparallel with the geologic strike. Tracer movement at the WBCV site was found to be predominantly strike-parallel; however, at local scales on the order of inter-well distances (i.e., 10 to 30 m), plume migration was not always consistent with the local direction of maximum horizontal hydraulic gradients measured in the test wells (Fig. 2.26). The tracer plume was monitored for a period of more than 1 year and was found to remain within the water table interval throughout its length. Upward vertical gradients measured at the site were identified as the most probable factor preventing the tracer plume from deeper migration along its downgradient flow path (Fig. 2.28). The authors describe the evolution of the plume configuration over time (Lee et al. 1992):

> "In the first two weeks, a high concentration plume migrated as rapidly as 1.0 m/day for about 14m in the near-field, but another 9m of migration in the mid-field required an additional 230 days (0.04 m/day). Total migration distance of 33 m (the far-field) for the 100 ppb front required 370 days (0.09 m/day average).
>
> Data analysis could not attribute the erratic rate of migration to the presence of a concentration gradient induced by the slug dye injection, and no consistent correlation could be found with changes in the water table gradient profile or with precipitation. Rather, the migration rate, narrow overall plume shape, and slightly meandering and fingering plume all suggested the presence of lithologic and/or fracture-related pathways of preferred flow.
>
> The general upward vertical gradient observed at the site explains the observation of tracer only in the water table zone of the aquifer. Tracer was never detected at depth despite long-term monitoring at various depths in bedrock within the tracer pathway and in stratigraphically correlative core holes downdip and downslope of the tracer injection zone. Tracer detection and observed vertical gradients at the site demonstrate that neutral density solutes introduced at the water table mix in a thin zone below the water table and migrate through the bedding plane dominated fracture system. This thin mixing zone which is recharged by local precipitation infiltration from above and by upward leakage from below approximates a two-dimensional solute mixing domain."

Analysis of "broad" and "narrow" tracer test plumes at BG4 and the WBCV site. In conjunction with simulations of fractured-rock flow using a dual permeability model (Stafford et al. 1998) and a 2-D equivalent porous medium (EPM) model (McKay et al. 1997), researchers at ORNL and the University of Tennessee contrasted the broad plume from a tracer test at the BG4 site at ORNL with the narrow tracer test plume at the WBCV site described above. The analyses noted that the orientation of shallow horizontal groundwater gradients with respect to geologic strike strongly influences the rate and direction of groundwater flow and contaminant transport. Broad plumes develop where the average water table gradient is perpendicular to the geologic strike (in the direction of lower permeability) (Fig. 2.29). Narrow, elongated groundwater contaminant plumes in the water table interval develop where the average water table gradient is roughly parallel with the geologic strike (in the direction of greater permeability) (Fig. 2.30).

As described in the article "Influence of fracture truncation on dispersion: A dual permeability model" (Stafford et al. 1998), the BG4 plume:

> "…exhibited an unusually large transverse spreading, with the width of the plume approximately equal to its length. The experiment is unique due to the high levels of tritium injected (50 curies) and the long monitoring period (16 years to date). The water table gradient from the injection well to monitoring well 7 (directly downslope) averages 0.15. The migration of the plume is characterized by a fast moving, low concentration front (10's of cm/day), a slower moving center of mass (< 1 cm/day), a very long (up to 16 years) low concentration tail, and an unusually large degree of transverse spreading."

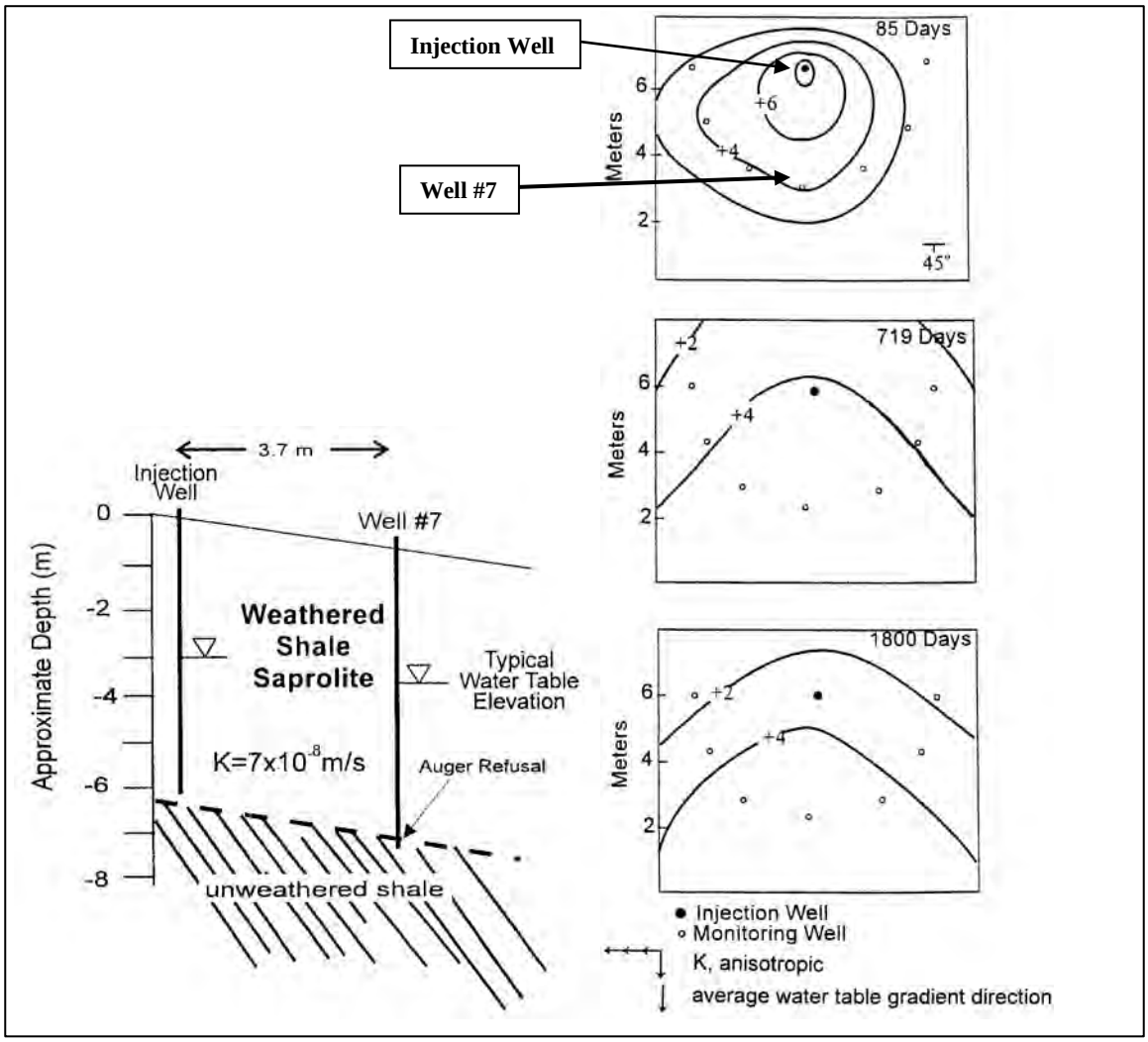

Sources: Stafford et al. 1998, McKay et al. 1997.

Fig. 2.29. Schematic cross-section and contours of tritium concentration (log [pCi/mL]) over time for the "broad" plume at the BG4 tracer test site.

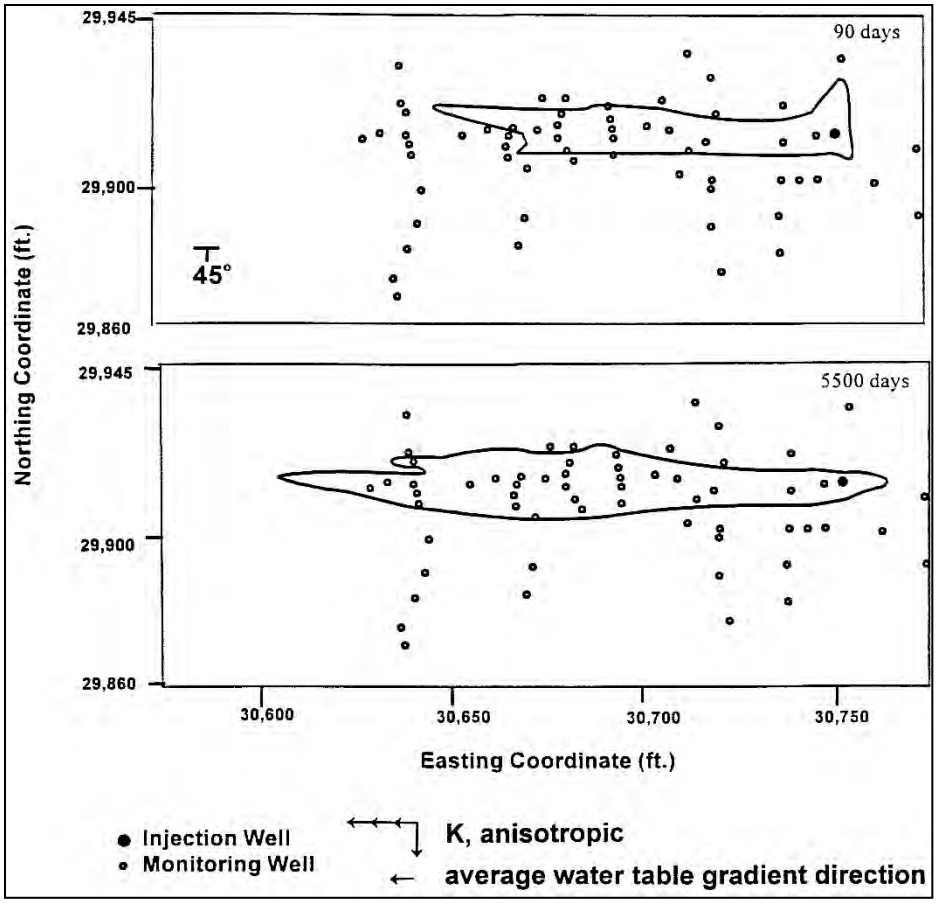

Source: Stafford et al. 1998.

Note: For the 5500-day (15-year) test period shown in the lower map, the scale indicates a total plume length of ~160 ft, less than the ~197 ft illustrated in Fig. 2.26 at 12 months (Lee et al. 1992). Dye breakdown is one possible explanation for this difference.

Fig. 2.30. Contours of 10 ppb dye concentration for the "narrow" plume at the WBCV tracer test site

At the WBCV site, the article continues:

> "The geologic material at this site is similar to that at the BG4 site in terms of porosity, hydraulic conductivity, and fracture spacing and orientation. However, the shape of the plume was very narrow (Figure 3-31) as compared to the wide shape of the BG4 plume (Figure 3-30). The major difference between the two sites is that the average water table gradient direction at the WBCV site is approximately parallel to strike of the bedding plane, and at the BG4 site it is nearly perpendicular to strike. The orientation of the water table gradient with respect to the fracture planes likely contributed to the difference in plume shapes. The hydraulic conductivity is expected to be higher in the direction of strike at both locations due to bedding plane partings or fractures (Solomon et al. 1992). With this in mind, transverse spreading at the WBCV site, where there is a strike-parallel gradient, would not be strongly influenced by fluctuating water table direction and secondary fractures perpendicular to strike because of the lower hydraulic conductivity in the transverse direction. Conversely, at the BG4 site, where the average hydraulic gradient is in the direction of the lower hydraulic conductivity (perpendicular to strike) fluctuating water table direction and fractures perpendicular to bedding are expected to have more of

an influence on transverse spreading. It is likely that at other locations, where water table slope is neither parallel nor perpendicular to bedding strike, the shape of the plumes would be intermediate between these two extremes."

In the dual permeability model developed in Stafford et al. (1998), the discrete fracture approach was combined with an EPM approach to investigate the influence of a few widely spaced, larger-aperture fractures in a highly fractured matrix (e.g., that found in saprolite and shallow bedrock in the clastic rock formations of BCV). The simulations demonstrated that a limited number of truncated fractures within a permeable matrix can create nearly circular plumes, with about the same degree of spreading in the direction transverse to the average hydraulic gradient as in the longitudinal direction. By comparison, continuous fractures in the direction of flow tend to produce elongated plumes, similar to those typically seen in granular materials. The following conclusions were also noted (Stafford et al. 1998):

> "The combined discrete-fracture/equivalent porous media (DF-EPM) approach is useful for looking at possible causes of features such as the observed transverse spreading, but in the absence of detailed data on the fracture network, it is likely that it would be no more effective than the EPM approach in predicting future behavior of the plume."

The main conclusions from the 2-D EPM modeling of the BG4 site (McKay et al. 1997) that are relevant in the context of EMDF modeling include the following:

> "1) This study shows that a relatively simple EPM modeling approach can be successfully applied to a complex, highly fractured system, for describing general plume behavior and future concentration trends, **provided that** [bold added] there is sufficient monitoring data available for calibration of the model. This indicates that, at least for this type of fractured clay-rich material, the time span over which monitoring data are collected is a critical factor in model calibration and may even be more important than the number of monitoring wells or the frequency of sampling.
>
> 2) The study also illustrates the importance of using tracers that are measurable over a wide concentration range…. where the regulatory limit for the contaminant of interest is many orders of magnitude below the source concentration.
>
> 3) The model calibration may be very site- or direction-specific, as indicated by the large difference in transverse dispersivity values or ratios of longitudinal and transverse dispersivity, observed between the BG4 site and another experiment in similar materials in WBCV. This could strongly influence application of models calibrated to small-scale tracer experiments for simulating behavior at a larger scale, or at different sites.
>
> 4) Finally, the results of the tracer experiments and the modeling indicate that in cases where extensive contamination has occurred in fractured, porous materials such as shale saprolite, it may take many tens if not hundreds of years of natural flushing to remove dissolved contaminants. Because of the influence of matrix diffusion, attempts to remove dissolved contaminants by pumping would also take a very long time."

Tracer plume evolution at the BG4 site. D. A. Webster of the USGS presented the original detailed documentation of the BG4 and BG6 tracer tests (Webster 1996). The tests were conducted using tritiated water injected at the water table in shaley saprolite of the regolith in July 1977. Monitoring results were reported for the 5-year period from 1977 through 1982, but continued after 1982 (Stafford et al. 1998, McKay et al. 1997). The BG4 test site is located in the Pumpkin Valley Formation and the BG6 site is located in the Nolichucky Formation. The BG tracer tests were designed to examine the hypothesis that groundwater in regolith can flow transverse to the bedding. The layout of the injection well and downgradient monitoring wells was, thus, established so that the horizontal gradients and flow directions

of the water table interval would be perpendicular to the geologic strike (i.e., water table/potentiometric contours are parallel with the strike of the beds, in contrast to the WBCV site where the opposite occurs). At the BG4 site, seven monitoring wells were installed along a 12-ft radius downgradient of the injection well (with a 30-ft radius at the BG6 site, where plume configurations over time were similar to those at BG4). The wells at site BG4 were numbered clockwise from right to left as 4-4 through 4-10, with similar numbering at the BG6 site.

The wells with the highest tritium concentrations were located directly downgradient and strike-normal relative to the injection well. Plots of concentrations over time for several of the BG4 wells show variations in the rate of change over the first two years (Fig. 2.31) and three additional single-point observations over the longer 5-year time frame (Fig. 2.32). Note the concentration scale changes from log to arithmetic.

The BG4 plume maps show that, over time, the initial elongated plume expands laterally and downgradient into a more circular plume that widens and decreases in concentration as the center of mass moves slowly downgradient away from the injection well (Fig. 2.33). Similar plume maps and plots are illustrated for the BG6 tracer test site in Webster 1996. The annual point concentrations in 1980, 1981, and 1982 illustrate the long-term progressive decline in concentrations in downgradient wells (Fig. 2.32).

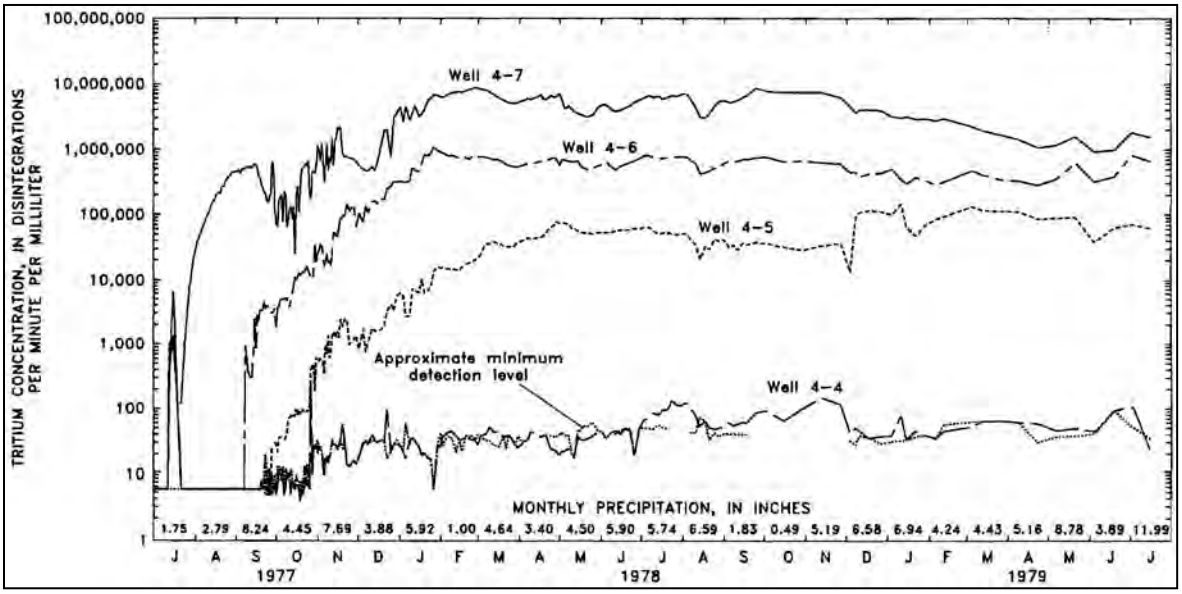

Note: From observation wells at BG4 tracer test site, 1997 to 1979 (Webster 1996).

Fig. 2.31. Tritium concentrations in groundwater over 2 years, BG4 tracer tests

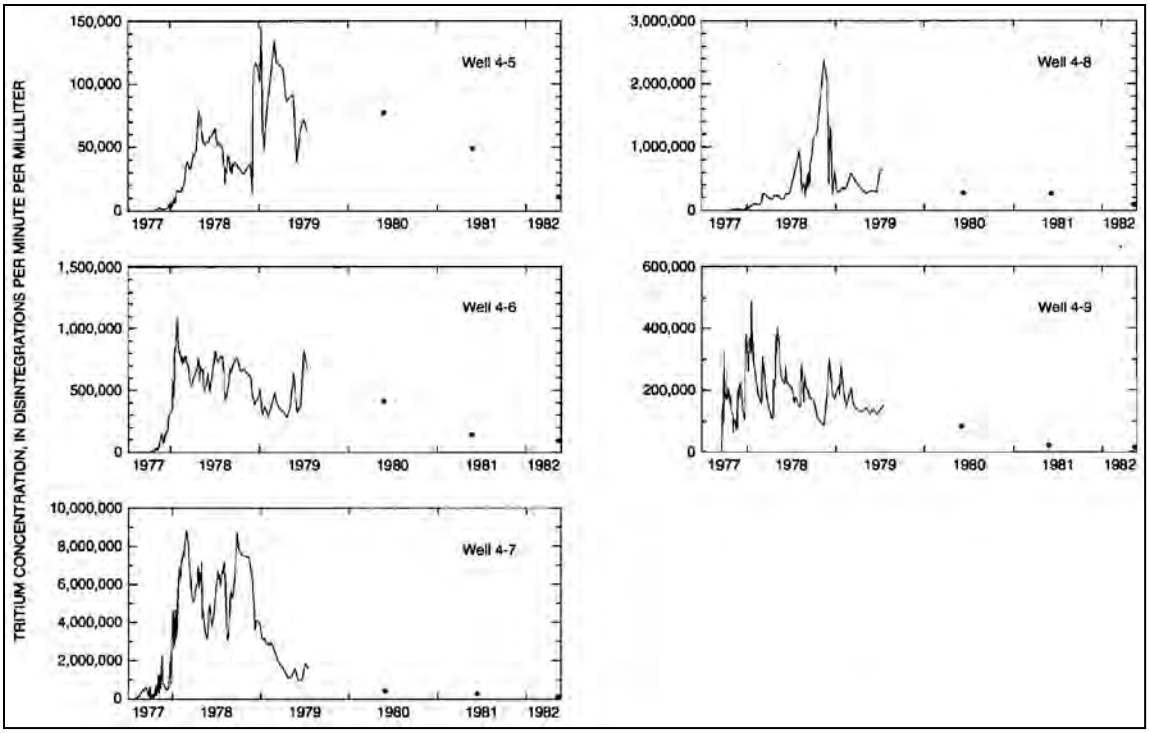

Note: From observation wells at BG4 tracer test site, 1997 to 1979 (Webster 1996).

Fig. 2.32. Tritium concentrations in groundwater over 5 years, BG4 tracer tests

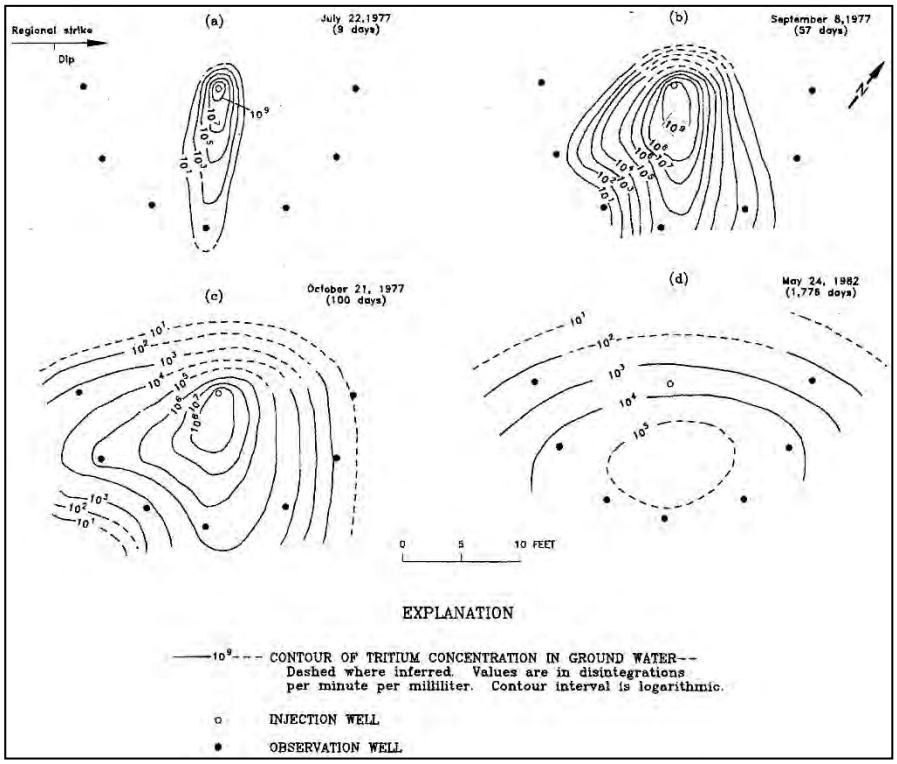

Data from the BG4 tracer site at 9 days, 57 days, 100 days, and 1776 days (4.9 years) after tracer injection on July 13, 1977 (Webster 1996).

Fig. 2.33. Contours of tritium groundwater concentrations in tracer tests

For the BG4 site, Webster states:

> "…although the leading edge of the plume arrived within 9 days, 5 to 6 months elapsed before concentrations began their rapid increase to maximum values, signaling arrival of the main part of the plume."

For the BG4 test, the travel rate for first arrival equates to 1.3 ft/day (12 ft in 9 days). The peak concentration in well 4-7 occurred 229 days after the test began. Therefore, the average travel rate to reach peak concentration would be 0.05 ft/day.

For the BG6 site, the fastest first arrival time of 112 days was significantly slower than that at the BG4 site. This equates to a first arrival travel rate of 0.27 ft/day (30 ft/112 days). At the BG6 site, the peak concentration in well 6-7, where the highest concentrations occurred, was reached during the 16th month of the test (around 465 days). Therefore, the average travel rate to reach peak concentration would be 0.06 ft/day.

Matrix diffusion may have played an important role in these tests by acting as a mechanism for retarding transport (Webster 1996). Evidence for matrix diffusion includes the following:

- Length of time that large tracer concentrations were detected at many observation wells
- Persistence of residual concentrations at the injection wells and observation wells
- Relatively rapid movement of the leading edge of the plumes, but very slow movement of the centers of mass
- Reoccurrence of large concentrations of tritium in water of the BG4 injection well shortly after each of several flushings.

At injection well 4-11, the observed loss in tritium activity during the 5 years was seven orders of magnitude. To examine the possibility of matrix diffusion effects, the concentration data for well 4-11 were incorporated into a simple model simulating matrix diffusion. The observed concentrations were generally found to conform with the model simulations. Webster also noted the implications of matrix diffusion on limiting groundwater cleanup. Pumping would quickly remove contaminated water from joints and fractures, but only slowly remove contaminated water from the interstices or pores of the fine-grained saprolite material.

Colloidal tracer tests at the WBCV site. The results of tracer tests at the WBCV tracer site using colloidal tracers (latex microspheres and three bacteriophage strains) were presented in "Field-Scale Migration of Colloidal Tracers in a Fractured Shale Saprolite" (McKay et al. 2000). Colloidal tracers were introduced in well GW-484 and samples were collected from the downgradient well field. All tracers were detected at distances of at least 44 ft, and two of the tracers were found in all downgradient wells. The authors summarize the test results as follows.

> "In most wells the colloidal tracers appeared as a "pulse", with rapid first arrival [corresponding to 5 to 200 m/d transport velocity], one to six days of high concentrations, and then a rapid decline to below the detection limit. The colloids were transported at velocities of up to 500 times faster than solute tracers (He, Ne, and rhodamine-WT) from previous tests at the site. This is believed to be largely due to greater diffusion of the solutes into the relatively immobile pore water of the fine-grained matrix between fractures.

> Peak colloid tracer concentrations in the monitoring wells varied substantially, with the microspheres exhibiting the highest relative concentrations and hence the least retention. Rates of concentration decline with distance also varied, indicating that retention is not a uniform process in this heterogeneous material."

The reported trace test results (McKay et al. 2000) summarizes key findings from the rhodamine dye tests reported above (Lee and Ketelle 1989, Lee et al. 1992) and similar tests using dissolved helium and neon (Sanford and Solomon 1998, Sanford et al. 1996).

> "Important findings from these two tracer tests include: (1) solute tracer plumes tend to develop that are elongated along strike, with little transverse dispersion; and (2) solute transport rates are strongly influenced by matrix diffusion. In both tracer tests, transport rates (for a given relative concentration contour) decreased with time and distance from the injection well, and the low concentration "front" of the plumes tended to migrate at rates hundreds of times faster than the high concentration region. Both of these types of behavior indicate a high degree of longitudinal dispersion, which is typical of systems in which matrix diffusion is dominant."

These reports note that although this difference in transport rates may be "*partly attributable to physical heterogeneity, it is also consistent with greater losses of the tracer pulse with increasing time due to diffusion into the matrix.*"

Dissolved gas tracer tests at WAG 5 (ORNL). Results of dissolved noble gas (helium, neon) and bromide tracer tests initiated in October 1994 at WAG 5 in Melton Valley, south of the main ORNL campus, are presented in "Dissolved gas tracers in groundwater: Simplified injection, sampling, and analysis" (Sanford et al. 1996). The site is described as the shallow aquifer in fractured weathered shale, similar to conditions at the EMDF site. Water table contour maps were not included in the paper, but surface topographic slopes are roughly parallel with the geologic strike (similar to the configuration at the WBCV tracer site), so shallow groundwater flow directions would be anticipated to follow the geologic strike. Unlike the "slug" injections of tracers such as fluorescent dyes, the gases in these tests are injected into the well bore over a sustained period of time at a relatively constant source concentration. Breakthrough curves for the first 155 days of the test show initial breakthrough occurring at about 15 days at a well located along strike 75 ft downgradient of the injection well. This would indicate a groundwater flow rate for first arrival of 5 ft/day. The relatively low concentrations of the tracers in the breakthrough curves were explained by "*diffusion of the tracers into the less mobile matrix*".

Bromide/helium tracer tests at GW-462 site in WBCV. Tracer tests using helium and bromide were conducted at a WBCV location approximately 1500 ft southwest of the intensively studied tracer test site described above (Schreiber 1995, Moline and Schreiber 1996, Schreiber et al. 1999). This test site is hydraulically separated from the other WBCV tracer test site by the valley of NT-15 and is located near the center of the outcrop belt of the Nolichucky Formation. The Schreiber helium/bromide test site covered a small area (approximately 50 × 50 ft) and included only three shallow/deep observation well clusters with various locations relative to the maximum water table gradient toward the southwest. The relationships between the injection well (GW-462), three shallow/deep observation well clusters (GW-456 through GW-461), and average water table contours are shown on Fig. 2.34. The three shallow/deep cluster wells were originally placed at right angles up-dip, down-dip, and along strike from GW-462 for pumping tests (Schreiber et al. 1999). One of the well clusters is located over 30 ft upgradient to the injection well, while the remaining two clusters are located at angles cross gradient to the average maximum water table gradients (the three multilevel discrete interval monitoring wells, GW-821, -822, and -823, were not part of the tracer testing). Hydraulic gradients were at oblique angles with respect to geologic strike/dip directions (Fig. 2.34). Detailed topographical maps of the site area show an entrenched ravine located about 300 ft

southwest of the test site that apparently influenced shallow flow directions and local discharge toward the southwest.

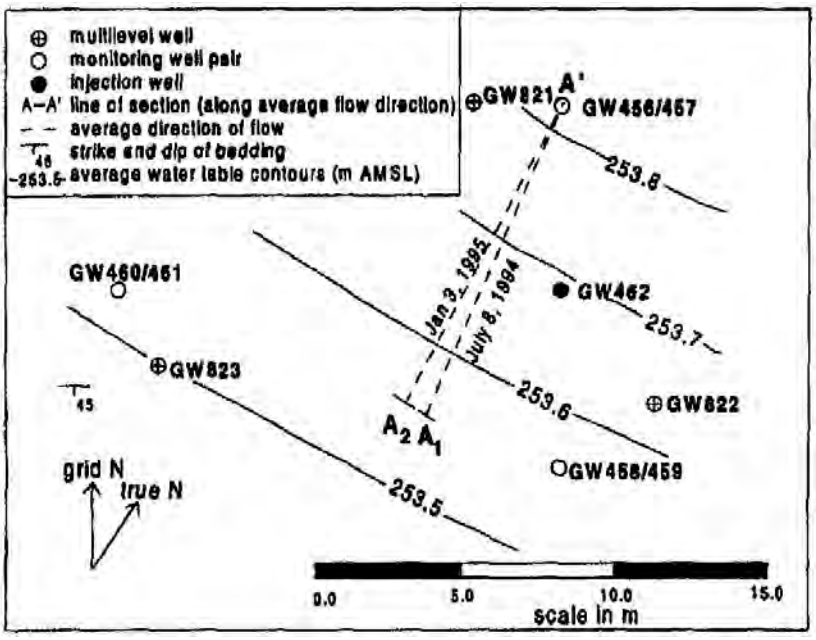

Note: Multilevel wells GW-821, -822, and -823 were not used in tracer monitoring.

Fig. 2.34. Well locations and water table contours for the helium/bromide tracer test site in WBCV (approximately 1500 ft west of NT-15)

Due to limitations in the numbers and placement of the tracer test monitoring wells, test results were presented with qualified interpretations. Both tests indicated the highest concentration ratios of helium and bromide in the shallow GW-461 well located southwest and along geologic strike of the injection well (GW-462). A slug of bromide was introduced in GW-462 on April 11, 1994, and was monitored for approximately 6 months in the well pairs. Bromide breakthrough was only consistently detected in the water table well (GW-461) located along strike from the injection well. First arrival of low concentrations occurred on June 15, 1994, indicating a first arrival velocity of 0.75 ft/day.

The helium test involved a helium injection and sampling method (Sanford et al. 1996) and was used in the WAG 5 tracer test. The method involved sustained diffusion of helium to saturation levels through injection tubing over a period of several months from March 25 through December 12, 1994. As with the bromide test, the highest concentration ratios were detected in GW-461 along geologic strike. But concentration ratios several orders of magnitude below those in GW-461 were detected in shallow and deep wells up and downgradient of the injection well. The occurrences in upgradient wells were attributed to storm-related changes in flow conditions. Fracture pathways across the strike-parallel bedding were cited to explain helium transport to GW-458 in the downgradient (normal to strike) direction (Schreiber et al. 1999). First arrivals in the along-strike GW-460(deep)/GW-461(shallow) cluster occurred on May 15, 1994, corresponding to a first arrival velocity of 0.9 ft/day, similar to that for bromide.

Summary of key findings from tracer tests in Conasauga Group formations

- The orientation of tracer plumes and average velocities of tracers vary according to the orientation of the strike and dip of the beds with respect to the maximum hydraulic gradient:
  - — Relatively narrow elongated plumes develop where shallow groundwater flow gradients are parallel to geologic strike (e.g., WBCV tracer test field)
  - — Broader more diffuse plumes develop more slowly where shallow groundwater flow gradients are perpendicular to geologic strike (e.g., BG4/BG6 sites)
  - — Plumes intermediate between these extremes appear likely to develop in areas with intermediate flow gradients relative to geologic strike.
- Tracer concentration contour maps and breakthrough curves for the WBCV and BG4/BG6 sites illustrate that most of the injected tracer mass lags far behind the advancing low concentration front, indicating significant longitudinal dispersion and attenuation of peak concentrations.
- Tracer transport velocities, based on first arrival times and distances for very low concentration fronts, vary and can be much higher than velocities based on arrival times of higher or peak concentration levels.
- Groundwater tracer velocities based on first arrival times vary significantly with distance from the injection well and orientation of water table gradients with respect to geologic strike:
  - — Dye tracer velocities based on first arrival times at the WBCV site ranged from 3.3 ft/day in the near field (46 ft in about 14 days) to 0.3 ft/day to reach the far field (108 ft in 370 days) where flow paths and gradients were parallel to geologic strike.
  - — Tritiated water velocities based on first arrival were 1.3 ft/day (12 ft in about 9 days) at BG4 and 0.27 ft/day (30 ft in about 112 days) where flow paths and gradients were perpendicular to geologic strike.
- Groundwater tracer velocities based on time-to-peak concentration are much less than velocities based on first arrival times. At BG4 and BG6, velocities based on time to peak concentrations were as follows:
  - — 0.05 ft/day (12 ft in about 229 days) at BG4 versus a first arrival rate of 1.3 ft/day
  - — 0.06 ft/day (30 ft in about 465 days) at BG6 versus a first arrival rate of 0.27 ft/day.
- Tracer plumes introduced at the water table in saprolite at the WBCV site remained within the shallow water table interval and did not migrate vertically to greater depths (i.e., intermediate/deep intervals).
- Matrix diffusion into the pores and microfractures of the fine-grained matrix between fractures transmitting groundwater flow (and contaminants) appears to play a major role in groundwater tracer movement and variation in concentration over time.

2.1.6.3 Laboratory measurements of solid-aqueous partition coefficients for Bear Creek Valley geologic materials

Results of laboratory evaluations of solid-aqueous K_d values for clay-rich soils, saprolite, and less weathered rock from the geologic units that underlie the EMDF site are available in several reports (Table 2.12). These references are summarized in this section along with references where potential liner and geologic buffer materials at the EMWMF site and other nearby areas were tested to determine K_d results. Several of these studies were based on samples from existing and potential waste management areas in Melton Valley (south of ORNL), which are located on the same Conasauga Group units as the EMDF site, specifically the Maryville Formation and the Nolichucky Formation. Two geotechnical investigations

were completed in support of final EMWMF design and construction (CH2M-Hill 2000, WMFS 2000). Both investigations involved test pit sampling and laboratory testing of low-permeability soils as potential liner and/or cover material for EMWMF.

Table 2.12. Sources of laboratory data on K_d values for Conasauga Group samples and local clay-rich soils

Data source	Radionuclides or elements evaluated	Geologic units and source of materials tested
Rothschild et al. 1984. *Characterization of Soils at Proposed Solid Waste Storage Area (SWSA) 7*	Am-241, Co-58, Cs-134, I-125, Sr-85	Melton Valley soils, proposed SWSA 7 site on Conasauga Group units (Maryville Formation or Nolichucky Formation)
Davis et al. 1984. *Site Characterization Techniques Used at a Low-Level Waste Shallow Land Burial Field Demonstration Facility*	Am-241, Co-58, Cr-51,Cs-134, Fe-59, I-125, Sr-85, Ca+Mg	Melton Valley SWSA 6 site near surface soils (0 to 2 m), Maryville Formation boring, depth 2 to 35 m (saprolite and rock)
ORNL 1987. *Geochemical Behavior of Cs, Sr, Tc, Np, and U in Saline Groundwaters: Sorption Experiments on Shales and Their Clay Mineral Components*	Cs-137, Np-235, Sr-85, Tc-95m, U-233	Nolichucky and Pumpkin Valley Formations, Joy-2 well (location unknown) Nolichucky 181- to 128-m depth Pumpkin Valley 604- to 605-m depth
Friedman et al. 1990. *Laboratory Measurement of Radionuclide Sorption in Solid Waste Storage Area 6 Soil/Groundwater Systems*	Co-60, Cs-137, Eu-55, Sr-89, U-233	Melton Valley SWSA 6 saturated zone saprolite, (Maryville Formation or Nolichucky Formation), coarse materials screened
DOE 1992b. *Site Characterization Summary Report for Waste Area Grouping 1 at Oak Ridge National Laboratory, Oak Ridge, TN*, Appendix A	Co-60, Cs-137, Ra-226, Sr-90, Tc-99	Bethel Valley clay-rich soils developed on Chickamauga Group units, three locations, boring intervals range from 5 to 30 ft below ground, sampled intervals at or near water table
CH2M Hill 2000. *Phase IV Final Site Investigation Report*	U, Pb	Near surface, low-permeability soils from the EMWMF site and nearby sites on Chestnut Ridge and in Union Valley (Rogers Quarry)
BJC 2000. *Final Site Investigation Report*	U, Pb	Near surface, low-permeability soils from the EMWMF site and nearby sites on Chestnut Ridge and in Union Valley (Rogers Quarry)

BJC = Bechtel Jacobs Company LLC
DOE = U.S. Department of Energy
EMWMF = Environmental Management Waste Management Facility
ORNL = Oak Ridge National Laboratory
SWSA = Solid Waste Storage Area

All laboratory studies utilized a batch-contact method to estimate the fraction of solute partitioned to the solid phase. These K_d data for local materials were utilized in combination with data from other sources in the selection of assumed K_d values and ranges for the base-case release to groundwater scenario (Sect. 4.5) and for selecting K_d probability distributions used in the uncertainty analysis (Sect. 5.4). Detailed explanation of assumed base-case K_d values is provided in Sect. 3.3.2.4.

2.1.7 Surface Water Hydrology

The surface water hydrology for BCV is well documented based on both valley-wide and smaller-scale investigations. The results indicate the close interrelationships among precipitation, runoff, and surface water/groundwater flux. The following sections review the results of previous surface water investigations in BCV, surface water features of the watershed, important relationships between streamflow and groundwater, and results of water budget analyses conducted for BCV.

2.1.7.1 Previous surface water investigations

USGS prepared an inventory of spring and seep locations and single measurements of flow at spring, seep, and selected stream locations across the entire length of BCV in 1994 that included all of the north Bear Creek tributaries (NTs) in BCV (Robinson and Johnson 1995, Robinson and Mitchell 1996). The single event measurements were made during March 1994 to represent wet season base flow conditions and again in September 1994 to represent dry season base flow conditions. The measurements were made during periods at least 72 hours after rainfall events when base flow runoff was relatively low and stable. The lowest USGS measureable flow rates were 0.005 ft^3/sec or 2.2 gpm. Flow rates below that level were designated as zero (or dry) on their report drawings.

Additional stream flow and contaminant monitoring has been completed at several flume/weir locations in BCV associated with site-specific investigations and valley-wide assessments of contaminant migration and flux. Stream flow and contaminant monitoring has been conducted for a decade or more and continues at many locations along various NTs and along the main channel of Bear Creek as part of ORR-wide CERCLA monitoring of surface and groundwater contamination. Many of the locations are equipped with weirs/flumes and data loggers to provide continuous data on flow rates and water quality parameters.

2.1.7.2 North Tributaries of Bear Creek

The lengths and watershed areas of the NTs tend to be roughly similar along the length of BCV, with a few exceptions such as NT-14, which cuts all the way through Pine Ridge and drains a larger tributary watershed. While stream flow along Bear Creek increases incrementally with flow from each of the NTs, the stream flow conditions along each of the NTs tend to be similar due to their similarity in length and size. The many springs, seeps, and wetland areas within the NT watersheds reflect the relatively shallow water table that intersects with the surface in the ravines and valleys of the tributary channel networks (Fig. 2.35).

Springs, seeps, and wetland areas. The USGS inventory identified hundreds of springs and seeps along the NT tributaries and sub tributaries throughout the BCV watershed. These springs and seeps represent the point locations of shallow groundwater discharge that supports base flow for the NT stream channels. The locations occur where the water table or potentiometric surface intersects the ground surface. Flows at these locations increase during the wet season when evapotranspiration is lowest and groundwater recharge and flux are highest, and decrease during the hotter drier summer and fall seasons when evapotranspiration is highest and recharge and rainfall are typically lowest. Headwater springs with low flows (< 1 gpm) are common near the base of some of the narrow incised valleys heading into the south flank of Pine Ridge. Other springs and seeps commonly occur along or adjacent to lower flatter areas of valley floors farther downstream along the NT tributary paths. Many of the seep/spring areas fall within wetland boundaries that have been delineated and mapped during assessments of BCV and during specific projects where wetlands have been disturbed. The locations of many springs and seeps in the vicinity of the CBCV site are shown on Fig. 2.35.

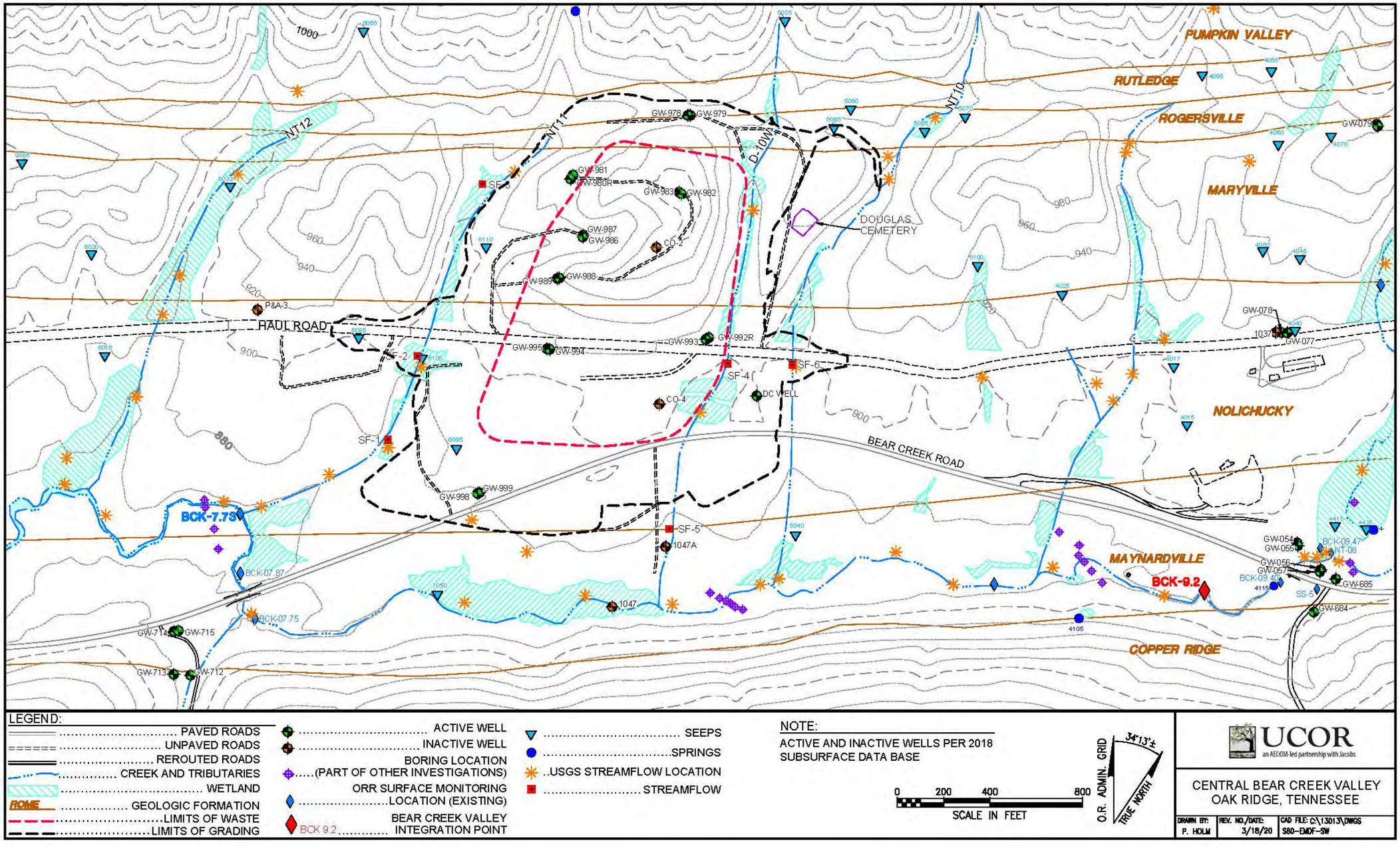

Fig. 2.35. Surface water features near the EMDF site in Central Bear Creek Valley

This page intentionally left blank.

Tributary stream flow. Stream flow along the relatively small channels of the NTs varies seasonally and in response to precipitation events. Hydrographs from continuous monitoring of NT stream flows and rainfall demonstrate that runoff occurs relatively quickly in peak episodes of a few hours or more during and immediately after storm events. The regression phases of the hydrographs show that the rapid peak runoff tapers into a stage of soil drainage and base flow conditions spanning one to several days depending on location within the watershed, antecedent conditions, and other environmental factors.

The USGS inventory data were used to map reaches of the NTs and Bear Creek that were subject intermittent periods of low to zero flow under wet and dry season base flow conditions represented by the March and September 1994 data, respectively. The results of the USGS analysis for the upper half of the BCV watershed between NT-1 and NT-8 is summarized on Fig. 2.36. These results are based on data from Robinson and Mitchell (1996) as reported by UCOR (2013). The bottom portion of the figure illustrates representative dry conditions that commonly prevail across much of the NT stream channels during the warm season, particularly during the late summer and fall seasons. In contrast, winter/early spring base flow in the upper NTs is continuous during the wet season when evapotranspiration is low, soil moisture conditions are high, and steady rainfall more common.

Period flow measurements and continuous stream flow monitoring of the NTs have been conducted in BCV in relation to site-specific investigations and for overall monitoring within BCV as a whole. The locations of ongoing stream flow monitoring across the BCV watershed are shown on Fig. 2.37. Stream flow (and water quality) is measured at weir/flume locations at stations along the lowermost sections of NT-1, NT-2, NT-3, NT-7, and NT-8, and at several locations along Bear Creek from BCK 4.55 near SR 95 upstream to the integration point at BCK 9.2, and farther upstream to BCK 12.47 near NT-1. Some of these stations provide longer-term multiyear historical stream flow data.

Flow data collection was conducted for 1 year at NT-10 and NT-11, adjacent to the EMDF site. A total of six surface water flow measurement stations (flumes) were installed at the CBCV site at locations identified during a surface water walkdown survey (Fig. 2.35). The flumes were located in the Nolichucky Formation and Maryville Formation outcrop areas in NT-10, D-10W, and NT-11. Surface water flow data collected from April 2018 to April 2019 at the flow measurement stations at the CBCV site are documented in a pair of technical memoranda (DOE 2018b, DOE 2019). Table 2.13 provides a summary of the flow rates recorded during this time at the CBCV flumes. As expected, flow rates increase downstream, from north to south, and increase quickly in response to rainfall.

The stream channels crossing the site are small and site reconnaissance indicates that there are no upstream dams or ponded structures that would release flood waters across the site. The NT-10 and NT-11 watersheds are relatively small, so extreme precipitation events could cause significant flooding near the disposal unit boundary. However, flooding under this circumstance would be limited to the tributary valleys along the perimeter of the site and would not be likely to cause significant erosional damage to the EMDF perimeter berms. Another potential cause of tributary flooding over geologic time is the occurrence of landslide deposits that dam narrow valleys and alter drainage patterns or create impounded water bodies susceptible to catastrophic release. Field observations in the Bear Creek tributary valleys have yielded no evidence of significant landslide deposits.

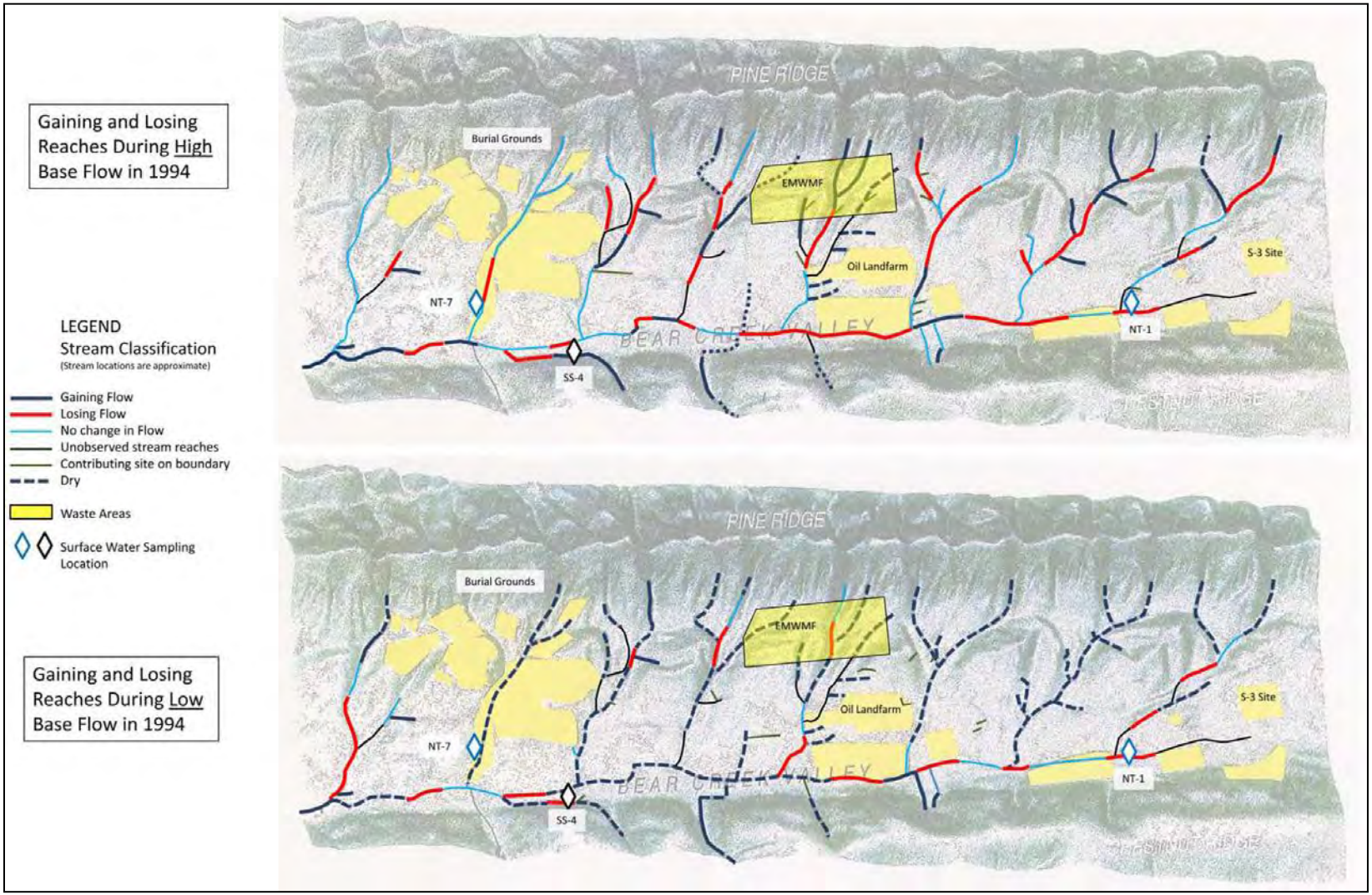

Source: UCOR 2013, Robinson and Mitchell 1996.

Note: Dry indicates flows were at immeasurable rates < 0.005 ft^3/sec (2.2 gpm), not necessarily completely dry.

Fig. 2.36. Measured base flow conditions for NT streams and Bear Creek

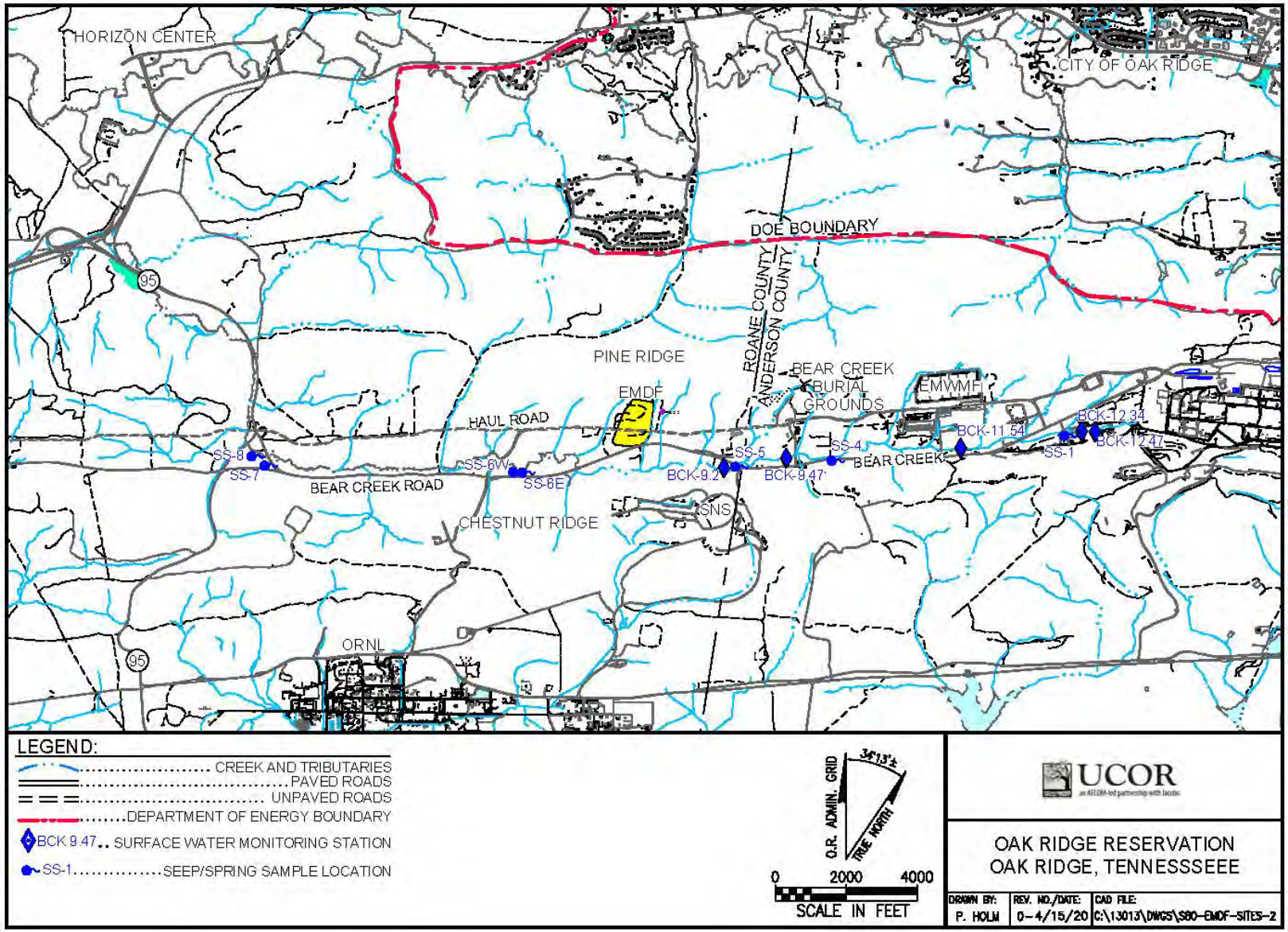

Fig. 2.37. Surface water monitoring locations in Bear Creek Valley

Table 2.13. Minimum and maximum flow rates for the CBCV site flumes, April 2018 to April 2019

Tributary measured	Flume	Minimum flow rate (gpm)	Date of minimum flow rate	Maximum flow rate (gpm)	Date of maximum flow rate
NT-11	SF-1	0.3	9/18–19/2018	5612	2/23/2019
NT-11	SF-2	0.7	9/05/2018 9/09/2018 9/12/2018	6810	2/23/2019
NT-11	SF-3	0.1[a]	9/01/2018 9/03/2018 9/05–09/2018 9/12–16/2018 9/18–19/2018 9/22–23/2018	2678	2/23/2019
D-10W	SF-4	0.1[a]	9/01–10/2018 9/13–24/2018	3042	2/23/2019
D-10W	SF-5	0.1[a]	9/10/2018 9/13/2018 9/24–25/2018	5273	2/23/2019
NT-10	SF-6	0.1[a]	9/01/2018 9/10/2018 9/14/2018 9/17/2018 9/24/2018 9/28/2018	4426	2/23/2019

[a]Essentially no flow periods.

CBCV = Central Bear Creek Valley
D = Drainage
NT = North Tributary

2.1.7.3 Bear Creek

Bear Creek provides the main surface water drainage pathway for the entire BCV watershed, following the axis of the valley toward the southwest from its head waters near the S-3 Ponds to the point near SR 95 where the channel turns north, exiting BCV through a water gap in Pine Ridge. Bear Creek follows the outcrop belt of the Maynardville Limestone along the entire length of the valley and is intimately linked with karst conduit groundwater flow in the Maynardville. Several relatively large springs (SS-1 through SS-8, Fig. 2.37) also occur at several locations along the lower slopes of Chestnut Ridge south of Bear Creek that drain groundwater from the carbonate rock formations and regolith mantle of the Knox Group. These springs interact hydraulically with groundwater and surface water flow in Bear Creek and the karst conduits of the Maynardville. Groundwater from these springs drains mostly fromuncontaminated areas along Chestnut Ridge, although dye tracing and contaminants in some of these springs demonstrate connections with surface/subsurface flow along Bear Creek and groundwater in the Maynardville Limestone.

Except for its uppermost sections near NT-1/NT-2, stream flow along Bear Creek is perennial. However, because of the karst conduit system in bedrock underlying Bear Creek, stream flow disappears along stretches of the channel between NT-3 and NT-8 during low flow periods. The lower half of Fig. 2.36 illustrates the two main portions of Bear Creek where stream flow is diverted underground into karst conduits. The primary section is approximately 3800 ft long and extends from about 600 ft west of the NT-3 confluence downstream to near SS-4. The second smaller dry section extends for approximately 1500 ft upstream from NT-8. Downstream from NT-8 and BCK 9.47, Bear Creek flow is perennial. Conduit flow

continues in bedrock below that point, but the subsurface conduits remain saturated preventing complete capture of stream flow from the surface channel. The BCV RI (DOE 1997b), Appendices C and D, includes a much more detailed presentation and analysis of the surface and subsurface flow system along Bear Creek, including supporting data, figures, and references that substantiate the karst flow system and the existing contaminant plumes along Bear Creek.

Stream flow data for the continuous monitoring stations along Bear Creek are available from the DOE web-based Oak Ridge Environmental Information System. The station nearest to the EMDF site is at BCK 9.2 (Fig. 2.37). The flow record at BCK 9.2 shows winter season average daily flows over 10,000 gpm in wetter years and typical dry season flows less than 10 gpm over the 13-year period from 2001 to early 2014 (Fig. 2.38). Given the important role played by the Maynardville Formation in transmitting the subsurface component of runoff in the watershed, large magnitude floods on Bear Creek are probably rare. The EMDF RI/FS (DOE 2017b) shows that the EMDF does not lie within the estimated limits of the 100-year floodplain.

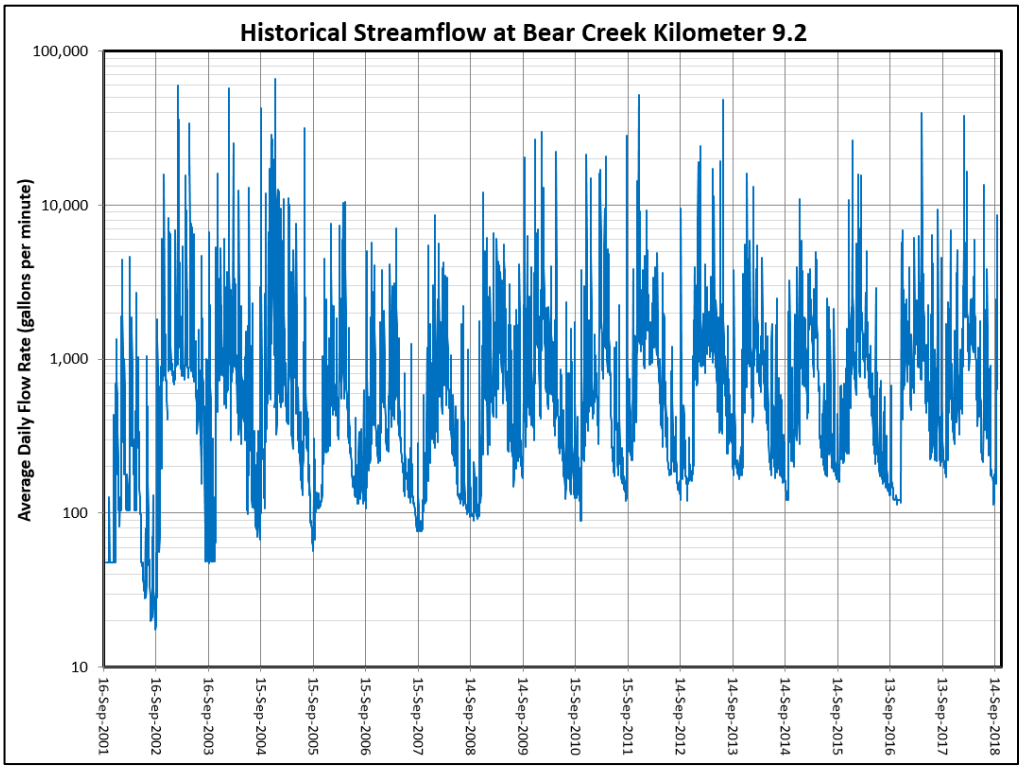

Fig. 2.38. Average daily stream flow at BCK 9.2 (2001 to 2013)

2.1.7.4 Bear Creek water quality

Table 2.14 summarizes basic water quality parameters measured at several stations along Bear Creek in the eastern part of BCV between the BCBG and S-3 ponds sites. The pH of water in the upper reaches of Bear Creek averages close to 8 standard units based on 135 measurements at six stations (BCK 9.47, BCK 11.54, BCK 11.84, BCK 12.34, BCK 12.38, and BCK 12.47; refer to Fig. 2.37 for monitoring locations) at various times between 1998 and 2009. Specific conductivity, a measure of total dissolved solids, is highly variable, ranging from < 1 μS/cm to 2738 μS/cm in samples taken at the same locations and times. In general, the average specific conductivity by measurement station decreases downstream, and the exception, BCK 12.34, is near the former S-3 Ponds possibly affected by S-3 site contaminants.

Table 2.14. Summary of Bear Creek water quality parameters

Station[a]	N	Period	pH	Specific conductivity (µS/cm)	Temperature (°C)	Dissolved oxygen (ppm)	Redox potential (mV)
BCK 9.47	21	2/98 – 8/06	8.06	395	15.7	10.2	132.1
BCK 11.54	10	3/02 – 8/06	7.96	552	17.5	8.2	109.1
BCK 11.84	9	3/02 – 8/06	7.98	675	16.2	8.9	106.7
BCK 12.34	66	10/01 – 9/09	7.47	994	16.7	8.4	134.6
BCK 12.47	26	3/98 – 9/03	7.6	653	16.5	8.1	102.7
Upper BCV	21	2/98 – 9/09	7.65	801	16.5	8.6	125.8
Uncontaminated river water[b]			6.5 – 8.5	50 – 50,000	NA		

[a]Station 12.38 had only two measurements and was not included in the summary table.
[b]USGS 1989.

BCK = Bear Creek kilometer
BCV = Bear Creek Valley
N = number of measurements
USGS = U.S. Geological Survey

2.1.8 Ecology and Natural Resources of the CBCV site

Ecological surveys have been completed at the CBCV site to satisfy applicable regulatory requirements for the protection of natural resources. This field work included stream surveys to define conditions (hydrologic classification), wetland delineation surveys, and aquatic and terrestrial surveys to identify threatened and endangered species. Results of these surveys are presented in a Natural Resource Assessment for the proposed EMDF(ORNL 2018). The following summarizes results of that assessment:

- Wetland surveys in the area of the proposed EMDF found extensive acreage of jurisdictional wetland. Seventeen separate wetlands are located within or partially within the EMDF study area, comprising 11.81 acres of wetland, some of which may be near or outside of the actual area used for the EMDF. The wetlands are largely found in conjunction with Bear Creek and its tributary streams, including NT-9, NT-10, NT-11, D-10W, and an unnamed tributary stream located between NT-10 and NT-9.
- Stream surveys identified five separate tributary stream sections within the EMDF study area covering 3303 m of stream. Fish communities within the five tributaries to Bear Creek that lie within the proposed area for the EMDF are typical of other first and second order streams in this watershed. No Tennessee dace, a species listed in need of management by the state of Tennessee, were observed in these surveys; however, they do occur throughout the watershed and are known to migrate in small streams annually.
- The timber assessment documented 36 species of trees within the EMDF study area. Tulip poplar is the single most common species of mature tree by quantity and volume. There is ample merchantable timber on the site. Merchantable trees are real estate assets and DOE has a mechanism in place for their disposal. EMDF access, egress and terrain are favorable for safe logging.
- Rare species surveys found rare plant and animals using the EMDF site. Four rare plant species identified within the EMDF study area include: tubercled rein orchid (*Platanthera flava var. herbiola*), American ginseng (*Panax quinquefolius*), pink lady's-slipper (*Cypripedium acaule*), and Canada lily (*Lilium canadense*). Of these, tubercled rein orchid is the rarest species. This species was found in every tributary and along Bear Creek, but the largest populations were found along NT-9 and drainage channel D10-W. These populations are the largest on the ORR and are considered large for the state.
- The bat acoustic monitoring was performed at 12 locations on the EMDF site in both 2017 and 2018. Analysis of recorded bat calls at all sites indicate that the open forested portions of the proposed EMDF

site are used as summer habitat by state and federally-listed bat species. Large numbers of calls from one state and federally listed endangered species, gray bat (*Myotis grisescens*), indicate usage across the forested areas of the proposed EMDF site. Foraging habitat and/or travel corridors to foraging grounds exist within the proposed EMDF site. Calls from the little brown bat (*Myotis lucifugus)* and tri-colored bat (*Perimyotis subflavus*) were also recorded in large numbers across the EMDF site. Both species are state-listed threatened, and both species likely roost and forage within the site. Other state or federally listed endangered bat species were recorded in small numbers, indicating minimal presence on the site.

- Drainages and wetlands on the site support relatively diverse amphibian populations. During informal site reconnaissance in 2019, biologists observed four-toed salamanders (*Hemidactylium scutatum*) on the site, a species listed as "In Need of Management" by the state.
- The area is on the southern edge of the largest area of contiguous interior forest on the ORR. Several forest bird species that can be impacted by forest fragmentation were recorded on the site, including the wood thrush (*Hylochichla mustelina*), listed by the state as "in need of management", and the American woodcock (*Scolopax minor*), blue-winged warbler (*Vermivora cyanoptera*), chuck-will's widow (*Antrostomus carolinensis*), and Kentucky warbler (*Geothlypis formosa*), which are listed federally as being of "management concern". Other bird species were observed that are in decline on the ORR.

2.1.9 Geologic Resources

No geological resources (e.g., ores, fossil fuel sources, industrial mineral deposits, geothermal resources, etc.) are known to be present at or near the EMDF site that would affect the performance of the proposed disposal facility. The Maynardville Limestone is a source of limestone aggregate in the local area and is mined from an open face quarry located about 5 miles northeast of and along geologic strike with the EMDF. However, DOE property controls preclude any use of the Maynardville near EMDF in the foreseeable future, and other local outcrop areas ensure the availability of ample source locations elsewhere over the long term.

2.1.10 Water Resources

2.1.10.1 Surface water resources and use

The city of Oak Ridge relies on surface water for its municipal water supply, but the intakes on Melton Hill Lake are miles above the surface water exiting Bear Creek, which ultimately drains into East Fork Poplar Creek and the Clinch River several miles downstream of Melton Hill Dam.

TDEC is responsible for management and protection of surface waters in Tennessee as a natural resource for human recreation and for fish and aquatic life. According to TDEC regulations (TDEC Rule 1200-40-04-.09, *Clinch River Basin – Use Classification for Surface Water*), Bear Creek, as well as East Fork Poplar Creek, Poplar Creek, and the Clinch River downstream, is classified for fish and aquatic life, recreational use, livestock watering and wildlife, and irrigation.

The EMDF site and surrounding areas are located within the DOE property boundaries. Future land use, including use of water resources, would be restricted to industrial use by DOE. Surface water use at and near the EMDF site in BCV and within the DOE property boundary as a whole is prohibited, although public access is possible in limited areas where public roads pass through the DOE property. These areas are actively patrolled.

The intermittent surface water flow and small stream channels within east BCV and along the NTs at and near EMDF will not support populations of large fish, so that fishing and fish consumption are only likely

several miles below the site where the Bear Creek contributing area is larger. The future exposure scenario adopted for the EMDF PA includes use of Bear Creek surface water to support agriculture (for irrigation and livestock water needs) and fish ingestion consistent with recreational fishing in Bear Creek; both surface water uses are highly unlikely given the anticipated actual land use and hydrologic characteristics of the watershed.

2.1.10.2 Groundwater use

The location of EMDF on DOE property and DOE property ownership and controls for areas downgradient of EMDF preclude any domestic use of groundwater in the foreseeable future. However, no water supply wells are located in BCV anywhere near the current downgradient margins of contaminant plumes originating from sources in BCV. Groundwater flow at and downgradient of the EMDF site is constrained within the groundwater divides below Pine Ridge and Chestnut Ridge. Based on the predominance of relatively shallow groundwater discharge pathways in BCV (Sect. 2.1.5.1), BCV water wells for domestic supply would have to be in relatively close proximity (i.e., within < 0.5 to 1 mile) to EMDF for release from the site to pose a measurable risk to a future hypothetical user.

TDEC well construction standards and typical well construction. TDEC is responsible for management and protection of groundwater in Tennessee. The TDEC Water Resources Division has established requirements for water well construction in Tennessee (TDEC Rule 0400-45-09, *Water Well Licensing Regulations and Well Construction Standards*). The primary requirement relevant to the PA for EMDF states that the source of water for any well shall be at least 19 ft bgs. Exceptions can be made for shallower water sources provided that other minimum requirements are met (e.g., casing and sealing off of the upper 10 ft of the subsurface). Water wells may be completed in unconsolidated materials (e.g., sand/gravel), in overburden materials above bedrock, or in bedrock, but the minimum depth of watertight casing is established at least 19 ft bgs, unless an exception is granted. Bedrock wells must be cased at least 5 ft into the top of bedrock, and the top of well slots or screens placed in overburden wells at or above bedrock must be at least 20 ft bgs. The overriding depth standard for surface isolation casing is therefore normally set at a minimum depth of 19 ft bgs.

2.1.11 Recently Completed CBCV Site Characterization

Characterization of the EMDF site began in February 2018 and was conducted in two major phases. Phase 1 characterization was intended to demonstrate the suitability of the site for onsite CERCLA waste disposal. The primary goal of the Phase 1 site characterization was to provide initial data on groundwater elevations and surface water flows to support site selection and the overall waste disposal decision. Secondary Phase 1 goals were to obtain geotechnical data to support preliminary design activities. The Phase 2 characterization effort was conducted to develop additional hydrogeologic and geotechnical information to support EMDF preliminary design.

The Phase 1 and Phase 2 subsurface hydrogeologic investigations (DOE 2018b, DOE 2019) included borehole drilling to obtain representative lithologic data, collect subsurface geotechnical samples, conduct geophysical logging, estimate hydraulic conductivities, and to support groundwater monitoring and seismic investigations. Phase 2 characterization also included digging test pits for additional geotechnical sampling. The results for Phase 2 efforts have not yet been documented. A total of 32 piezometers were installed (26 paired shallow and intermediate depth, and six single piezometers) for monitoring groundwater levels within the disposal facility boundary and on the periphery of the site. In addition, six surface water flow measurement stations (flumes) were established to document streamflow in Bear Creek tributaries.

Figure 2.39 shows the current site topography, hydrogeologic investigation locations, and key groundwater and surface water features in the proposed EMDF area. In addition to hydrogeologic characterization and monitoring, there was additional field work to delineate wetland areas and locate geologic contacts as well

as civil surveying to refine topographic data for design and to document the locations of flumes, piezometers, soil borings, and test pits.

The general observations and conclusions based on the Phase 1 characterization effort were:

- Geology is typical of BCV with steeply dipping, fractured bedrock, and there are no major karstic features in the Maryville, Nolichucky, or Rogersville Formations underlying the CBCV site.
- The contact with the Maynardville Limestone is located south of the proposed CBCV footprint. The observed locations in the field were approximately 50 ft further south than represented on geologic maps prior to the field mapping effort (DOE 2018b).
- Precipitation primarily runs off as surface water and shallow groundwater in the stormflow zone. This is consistent with the BCV conceptual site model.
- Potentiometric surface elevations are typical of other BCV wells in similar topographic and geologic settings.

Information from the Phase 1 field activities (DOE 2018b, DOE 2019), including surface water records and groundwater data that had been collected from the 16 Phase 1 piezometers over the first year of monitoring (March 2018 through early March 2019), was used in the development and calibration of the CBCV groundwater flow model (refer to Sect. 3.3.3.1 and Appendix D for details).

The Phase 1 (DOE 2018b, DOE 2019) and 2 piezometer monitoring results show that the average potentiometric surfaces are primarily influenced by topography and local recharge. There is subdued mounding of the potentiometric surface under the knoll. Generally, piezometer levels respond quickly during precipitation events then decrease rapidly to average conditions within days. Groundwater levels vary seasonally, with maximum elevations generally occurring in the interval between December and April or May, and annual low elevations occurring in drier parts of the year (which can include months from May to November).

Comparison of the piezometer pairs monitoring the shallow and intermediate groundwater zones demonstrates that in most cases, a downward-to-zero vertical gradient exists in the knoll area and slight upward vertical gradients exist away from the knoll nearer to the surface water drainages. Most of the recharge to the groundwater moves quickly to adjacent surface water bodies with limited replenishment of the deeper underlying groundwater. In general, groundwater moves from the ridges toward Bear Creek and its tributaries. The results of EMDF site characterization efforts are consistent with the general BCV hydrogeologic framework presented in Sect. 2.1.5.

This page intentionally left blank.

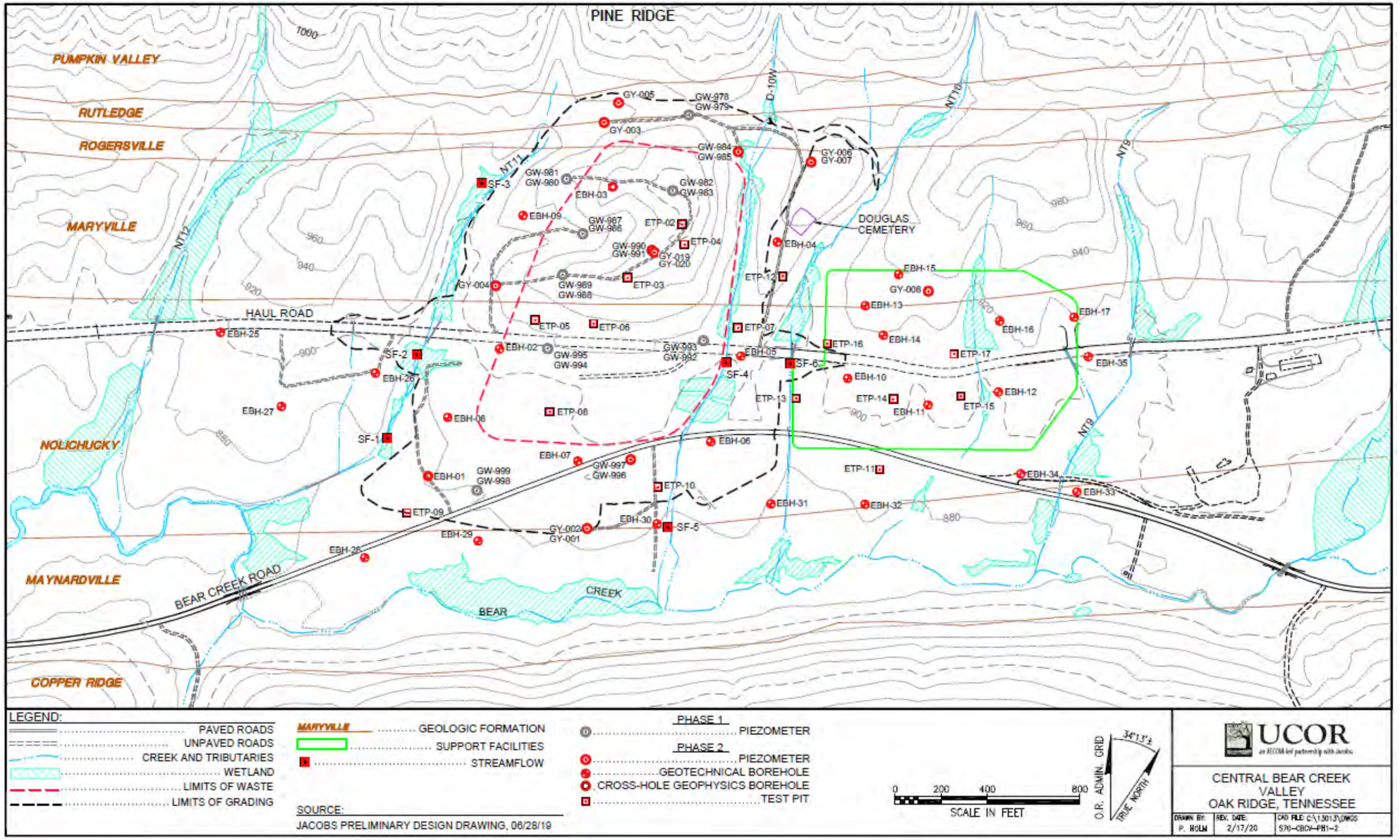

Fig. 2.39. EMDF site characterization map

This page intentionally left blank.

2.2 PRINCIPAL FACILITY DESIGN FEATURES

The EMDF Preliminary Design consists of four individual disposal cells covering a footprint of approximately 50 acres situated between the southern flank of Pine Ridge and Bear Creek and between tributaries NT-10 and NT-11. The upper portion of another surface drainage channel (D-10W) will be rerouted to accommodate the eastern section of the landfill. A site plan for EMDF is provided in Fig. 2.40 that shows the location of the disposal facility and potential areas for the required infrastructure, including operations/support trailers, material staging/laydown areas, a stockpile area, and parking areas; wastewater storage tanks, a wastewater treatment facility, and a truck loading station; storm water basins; a haul road; electrical, water, and communications utilities; a truck weigh scale; and guard stations.

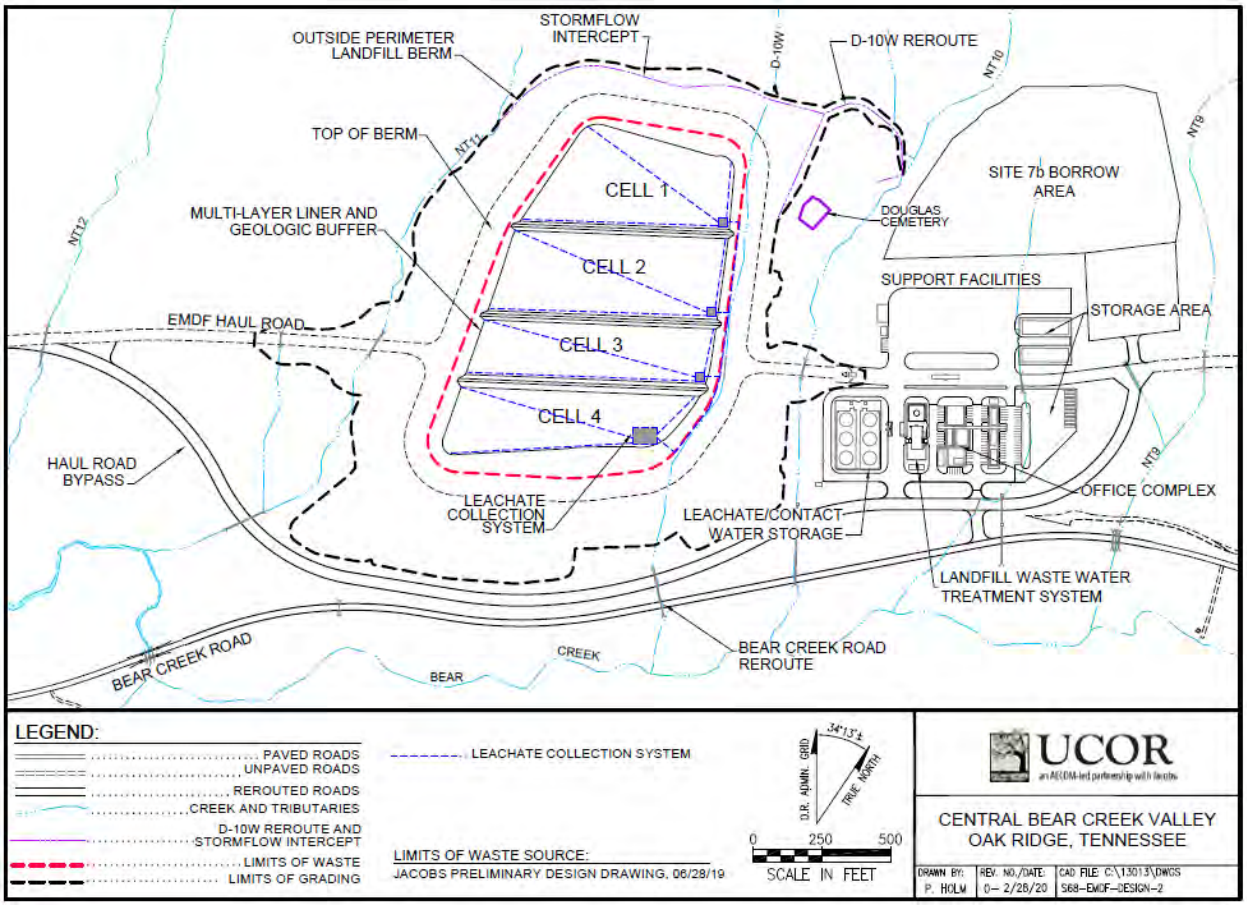

Fig. 2.40. EMDF site plan

Key engineered features of the disposal facility design include a perimeter berm to laterally contain the waste, a multilayer basal liner system along the floor of the facility with a double leachate collection/leak detection system to limit release of leachate, a 10-ft-thick geologic buffer to isolate the waste from groundwater, and the multilayer cover to reduce infiltration and isolate the waste from human and environmental receptors. Appendix C provides a detailed description of EMDF design features, associated safety functions, and natural events and processes that can limit safety functions over time. The remainder of Sect. 2.2 provides summary information on EMDF cover design features and structural stability of the disposal unit.

2.2.1 EMDF Final Cover Design

The primary waste containment feature that provides for long-term performance of EMDF is the multilayer cap. The final cover system, which is to function with little maintenance, would be designed and constructed to provide the following:

- Minimize migration of liquids through the closed landfill over the long term
- Promote efficient drainage while minimizing erosion or abrasion of the cover
- Control migration of gas generated by decomposition of organic materials and other chemical reactions occurring within the waste, if found to be necessary
- Accommodate settling and subsidence to maintain the cover integrity
- Provide resistance to rill erosion and gullying
- Provide a permeability less than or equal to the permeability of any bottom-liner system or natural subsoil present
- Resist inadvertent intrusion of humans, plants, and animals.

The final cover would be sloped to facilitate runoff and would be placed over the waste and tie into the top of the perimeter berm. It is anticipated the surface of the final cover system over the waste would be sloped at a grade of 2 to 5 percent and the sides would be sloped at a maximum grade of 25 percent. The cover is assumed to include 20-ft-wide horizontal benches spaced at maximum vertical intervals of 50 ft to reduce slope lengths, increase erosion resistance, and enhance slope stability. Actual slopes may vary and would depend on slope stability and erosion analyses performed during final design. The layers of the final cover system are depicted in Fig. 2.41. The approximately 11-ft-thick multilayer final cover system presented in the EMDF RI/FS is comprised of the following layers, starting from the top downward:

1) Erosion Control Layer: 4-ft-thick vegetated soil/rock matrix comprised of a mixture of crushed rock and native soil and constructed over the disposal facility to protect the underlying cover layers from the effects of frost penetration and wind and water erosion. This layer would also provide a medium for growth of plant root systems and would include a surficial grass cover or other appropriate vegetation with seed mix specially designed for this application.
2) Granular Filter Layer: 12-in.-thick layer of granular material graded to act as a filter layer to prevent clogging of the biointrusion layer with soil from the overlying erosion control layer. The required gradation would depend on the particle size distributions of both the erosion control layer and biointrusion layer and would be calculated using standard soil filter design criteria once these properties have been established.
3) Geotextile Separator Layer: nonwoven, needle-punched geotextile used as a separator between the granular filter layer and biointrusion layer.
4) Biointrusion Layer: 2-ft-thick layer of free-draining, siliceous coarse granular material sized to prevent burrowing animals and plant root systems from penetrating the cover system and reduce the likelihood of inadvertent intrusion by humans by increasing the difficulty of digging or drilling into the landfill.
5) Lateral Drainage Layer: 1-ft-thick layer of hard, durable, free-draining granular material with sufficient transmissivity to drain the cover system and satisfy the requirements of the infiltration analysis.
6) Geotextile Cushion Layer: nonwoven, needle-punched geotextile used as a cushion over the underlying geomembrane.

7) Geomembrane Layer: 60-mil-thick HDPE geomembrane textured on both sides to enhance sliding resistance that provides an impermeable layer to enhance water removal by the lateral drainage layer (layer 5).

8) Amended Clay Layer: 1-ft-thick (minimum) layer of native soil amended with bentonite and compacted to produce an in-place hydraulic conductivity less than or equal to 1E-07 cm/sec. It is necessary to amend native soil with bentonite for this layer to achieve the very low design hydraulic conductivity.

9) Compacted Clay Layer: 1-ft-thick (minimum) layer of native clay soil or amended soil compacted to produce an in-place hydraulic conductivity less than or equal to 1E-07 cm/sec. This layer, in conjunction with the overlying amended clay layer and geomembrane layer, would function as a composite hydraulic barrier to infiltration. Similar to the compacted clay liner for the liner system, compacted clay layer material would be selected on the basis of a borrow source assessment that would include performing a suite of geotechnical laboratory tests.

10) Contouring Layer: typically consists of a 1-ft-thick (minimum) layer of stone to serve the dual function of contour fill layer and gas vent layer (if necessary). This layer would provide a smooth, firm foundation for construction of the overlying cover layers.

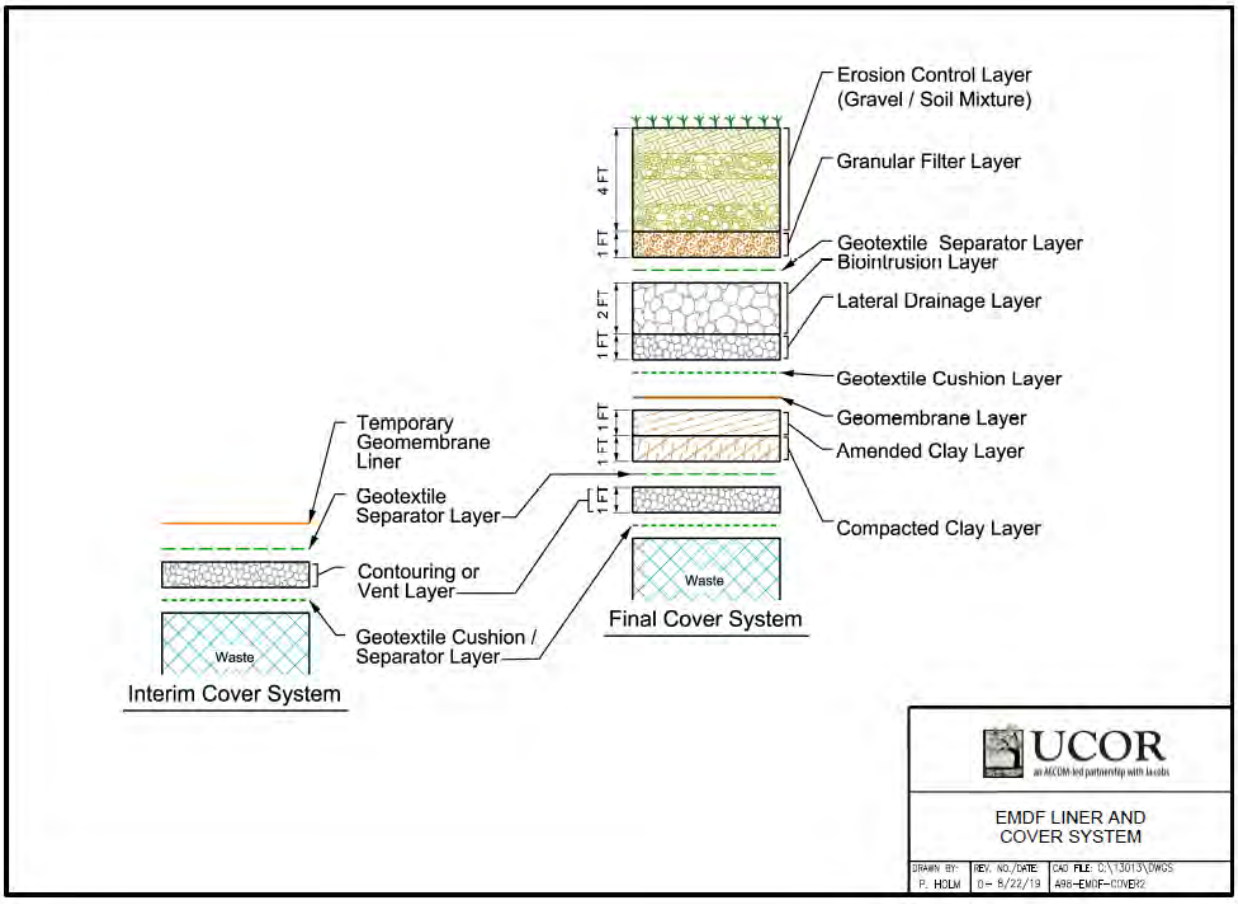

Fig. 2.41. EMDF final cover system components.

2.2.2 Biointrusion Barrier

The biointrusion layer would inhibit deep penetration by burrowing animals that could transfer radionuclides to the surface. The granular filter, biointrusion, and drainage layers will be constructed of siliceous rock that is not easily degraded by natural processes. The biointrusion layer also will limit the potential impact of cover erosion if the surface vegetation is disturbed by severe storm events. The total cap thickness in the preliminary design is 11 ft, which provides for sufficient depth-to-waste to make exposure of the waste under certain excavation scenarios (e.g., installation of a basement for a house) unlikely. However, other IHI scenarios such as well drilling may be envisioned. Section 6 and Appendix I present the IHI analysis for the EMDF.

2.2.3 Disposal Unit Cover Integrity

The overall effectiveness of the final cover system in reducing infiltration is a key long-term performance objective of the landfill. Clay layers in the final cover system are below 8 ft of engineered materials. The clay layers retain their hydraulic conductivity parameters based on their depth bgs, which ensures there is no direct exposure to freeze-thaw conditions; no cracking/tunneling due to roots or burrowing animals/insects; and limited temperature or moisture variation. High overburden pressure will maintain low permeability characteristics of the clay barrier in the cover (Boynton and Daniel 1985, Albrecht and Benson 2001). The biointrusion layer serves multiple safety functions, including preventing severe erosion that could expose the underlying clay barriers, preventing biointrusion, and serving as a redundant lateral drainage pathway. These characteristics of the cover design provide resistance to degradation mechanisms affecting the compacted clay layer. Appendix C, Sect. C.1, provides a more detailed analysis of natural events and processes that can limit the function of EMDF design features.

Long-term monitoring and maintenance actions would be conducted to control erosion, repair cap settlement/subsidence and slope erosion, repair run-on and run-off control systems, prevent rodent infestation, and prevent tree and other deep-rooted plant growth on the final cover and side slopes.

With the robust design of the cap, it is reasonable to expect that the EMDF cap will remain largely intact for many decades or centuries with little or no maintenance. The requirement for long-term cover integrity will be included in the preliminary and final design of the EMDF final cover system. For the PA analysis, the cover system is assumed to completely degrade much earlier and more rapidly (between 200 and 1000 years post-closure) than is likely given the robust engineering design.

2.2.4 Structural Stability

Detailed analysis of the structural stability, including slope stability and seismic hazard analysis, is being performed as part of the preliminary and final design. Details of the final design and associated structural stability evaluations will be evaluated with respect to their relevance to the performance analysis. Based either on applicable laws or regulations pertaining to landfills or on lessons learned from existing landfills, the final design will evaluate the following stability conditions:

- Perimeter berm stability – Site characterization data will be incorporated into design parameters to establish size and elevation of the perimeter berm necessary to ensure lateral confinement. Calculations to determine the maximum allowable slopes to ensure berm stability and requirements for compaction and lift placement parameters and appropriate slope armoring to achieve long-term stability will be part of the engineering design process.
- Waste mass stability – Operational procedures for waste placement and requirements for waste compaction and filling voids to prevent differential settlement, and best management practices to ensure proper drainage of water within disposal cells will be developed prior to EMDF operations.

- Liner stability and integrity – Calculations for maximum allowable slopes, selection of appropriate geosynthetics for predicted site conditions, and effective anchor systems at the landfill perimeter will ensure stability of the bottom liner and continued long-term performance.
- Landfill seismic stability – Using site characterization data, evaluations will be performed to determine that the landfill liner, leachate collection system, and landfill appurtenances remain functional when subjected to earthquake-induced forces. Leachate collection systems and waste cells will be designed to function with embankments that are predicted to undergo less than 6 in. of deformation.

2.3 DEVELOPMENT OF PA WASTE INVENTORY

This section summarizes the estimated radionuclide inventory for EMDF and the process for screening radionuclides for inclusion in PA analysis. Development of the estimated radionuclide inventory is documented in Appendix B. Development and application of the radionuclide screening model is documented in Appendix G, Sect. G.4.2. Discussion of waste characteristics relevant to radionuclide release modeling are presented in Sect. 3.2.2.5.

The estimated radionuclide inventory for the EMDF PA is based in part on the analysis of expected waste stream characteristics and volumes presented in the EMDF RI/FS (DOE 2017b, Sect. 2 and Appendix A). The EMDF RI/FS established the required EMDF volume capacity of 2.2 million cy based on a best estimate for the total as-generated volume of waste in the EMDF at closure of approximately 1,949,000 cy (DOE 2017b, Table 2-5). This volume was based on the OREM Waste Generation Forecast and includes a 25 percent increase from base volume estimates to allow for uncertainty in the volume of CERCLA waste generated by currently planned remedial action and facility D&D projects. The total capacity requirement reflects adjustments to the as-generated volume to account for in-cell waste compaction and addition of clean fill material (soil) to meet facility operational requirements (DOE 2017b, pages 2-8 to 2-11 and Appendix A, pages A-4 to A-5).

The approach for estimating the EMDF radionuclide inventory is based on using as-generated waste volumes without the added 25 percent uncertainty allowance to derive average activity concentrations for each waste stream (refer to Appendix B for additional detail on waste stream characteristics and waste stream inventories). The +25 percent volume uncertainty factor and added clean fill mass are incorporated into the PA analysis by adjusting the estimated average waste activity concentrations to account for clean fill (Sect. 3.2.2.5) and applying these as-disposed concentrations to the EMDF design disposal capacity of 2.2 million cy. Figure 2.42 is a flow chart depicting sources of information and the process for development of the required EMDF disposal capacity, the estimated radionuclide inventory, and the application of assumed clean fill additions to derive the as-disposed concentrations utilized in the PA modeling. For radionuclide screening, bounding activity concentration estimates (screening source concentrations) that include all maximum and upper confidence limit (UCL) data values are used as inputs to the screening model without corrections for radioactive decay or adjustments for addition of clean fill.

The procedure for adjusting the estimated as-generated activity concentrations to account for the mass of clean fill added during disposal is presented in Sect. 3.2.2.5.

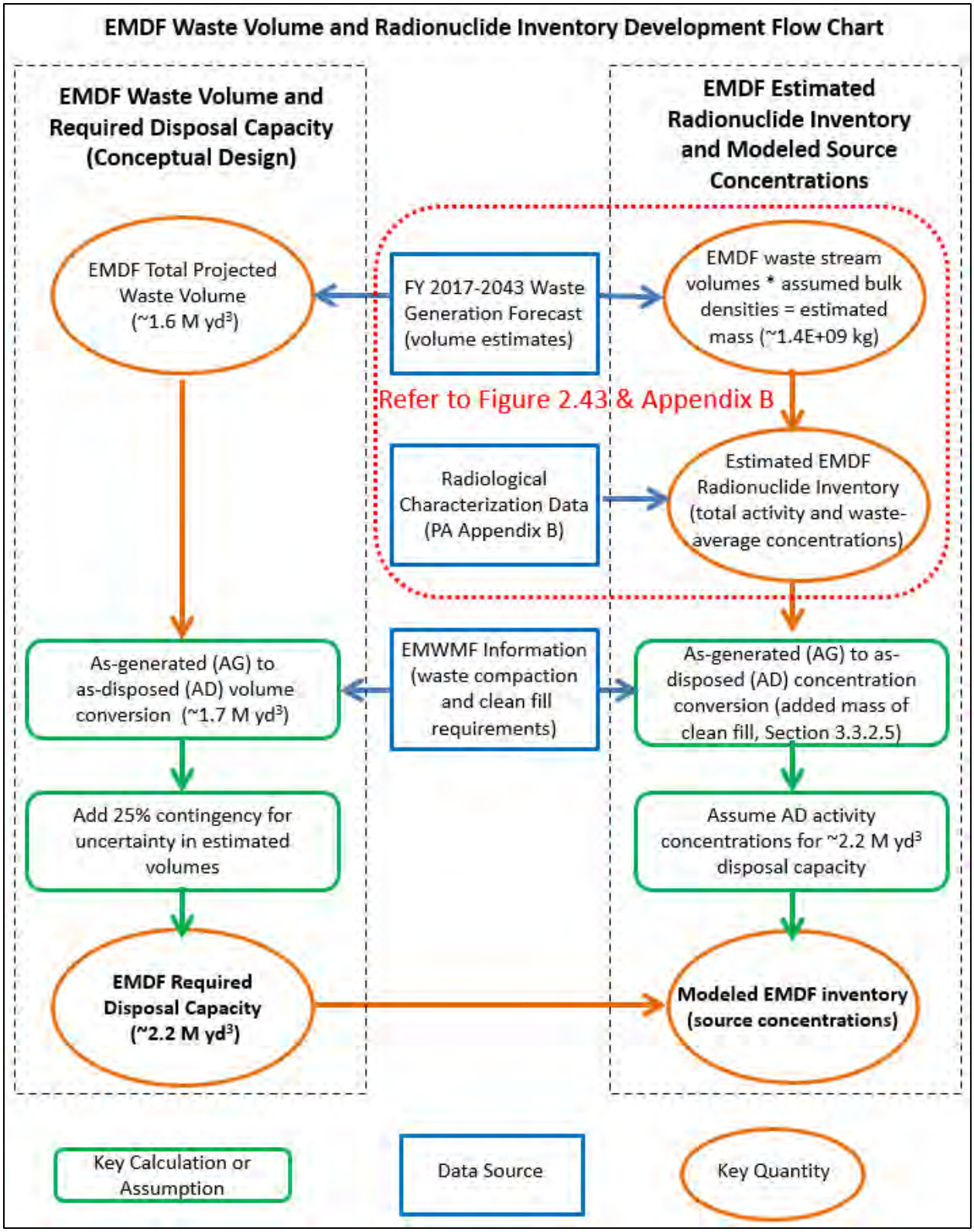

Fig. 2.42. Sources of information for development of the required EMDF disposal capacity, the estimated radionuclide inventory, and the as-disposed activity concentrations utilized in the PA modeling

2.3.1 Waste Characteristics for Screening and Inventory Estimation

Wastes derived from CERCLA cleanup at Y-12 and ORNL will contain a wide range of radionuclides that reflects the extensive duration and scope of weapons production and nuclear science activities at these two sites. The expected differences in radiological contamination reflect the different operational histories of the two DOE sites (i.e., weapons production at Y-12 versus research and development related to reactor design and the nuclear fuel cycle, radioisotope production, radioactive waste management, and biological and environmental sciences at ORNL). The primary radioactive contaminants in Y-12 waste streams are uranium isotopes, whereas ORNL waste streams will contain a greater variety of radioisotopes, including large quantities of some fission products (e.g., Cs-137 and Sr-90), lower quantities of other fission products (e.g., Tc-99 and I-129), and trace quantities of transuranic radioisotopes (e.g., plutonium and americium). This difference is important for estimation of the EMDF inventory because Y-12 waste accounts for approximately 70 percent of the forecast waste volume and ORNL waste the remaining 30 percent. Due to these differences in waste volume and radiological characteristics, Y-12 waste accounts for the majority of uranium activity in the estimated EMDF inventory, whereas ORNL waste accounts for the majority of total inventory.

For estimating EMDF radionuclide inventory, projected waste volumes for individual cleanup projects are aggregated into waste streams based on the site of origin (Y-12 or ORNL) and project type (facility D&D or remedial action). Additional differentiation of Y-12 facility D&D waste streams is based on the availability of detailed characterization data for certain Y-12 facilities. Bounding EMDF source concentrations for screening and average radionuclide activity concentrations for each waste stream were estimated from a combination of data sources, including: (1) EMWMF waste characterization data for previously generated and disposed Y-12 and ORNL waste lots, (2) data from detailed facility and environmental characterization studies, and (3) data from the OREM SORTIE 2.0 facility inventory database, which include radionuclide activity quantities derived from various types of facility safety analyses and other sources. Figure 2.43 provides a schematic overview of data sources, radiological profiles and waste quantities used to estimate EMDF radionuclide inventories.

For input to the screening model, all data including maximum and UCL-95 values were averaged without disaggregating the data by waste stream, and the resulting screening source concentrations were applied to the entire EMDF disposal volume capacity, without adjustment for addition of clean fill or radioactive decay.

To develop estimated radiological profiles the available data for specific EMDF waste streams are applied to the as-generated waste quantities (volumes and average bulk densities). Six waste streams are defined to capture the differences between ORNL and Y-12 wastes and between remedial action wastes (primarily soils) and facility D&D wastes (primarily debris). Radioisotopes having half-lives less than 1 year were not included in the EMDF estimated inventory calculations. The combination of radiological information sources provided data on 70 radionuclides having half-lives greater than 1 year. However, due to data limitations (generally the availability of only a single record for a radionuclide and/or inability to independently confirm some data from original sources), estimated waste-stream average activity concentrations (including only expected, average, and limiting value types) were developed for only 56 radionuclides. Data for nine less commonly reported fission products (Cd-113m, Cs-135, Kr-85, Pd-107, Se-79, Sm-151, Sn-121m, Sn-126, and Zr-93) could not be verified against the original data sources; therefore, these nine radionuclides are not included in the estimated EMDF inventory. EMDF waste average concentrations for five other radionuclides (Ba-133, Be-10, Ca-41, Mo-93, and Nb-93m) were estimated by applying additional assumptions to the EMDF waste quantity and radionuclide data. The assumptions made to estimate the as-generated EMDF waste average concentration values used in the EMDF PA models for these five radionuclides are presented in Attachment B.3.

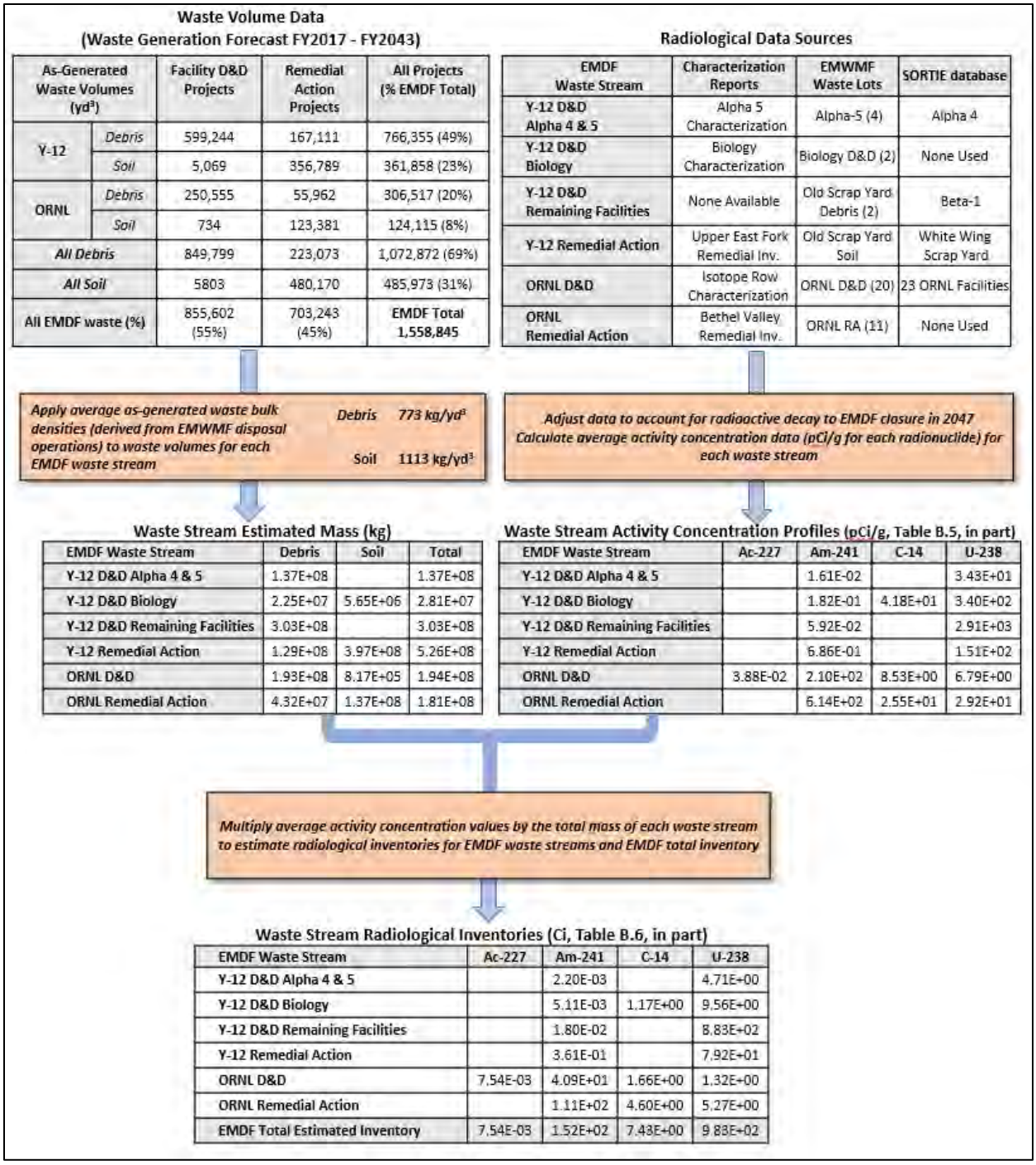

Fig. 2.43. Schematic overview of data sources, radiological profiles and waste stream masses used to estimate EMDF radionuclide inventories

Profile activity concentrations are calculated as the arithmetic averages of all the mean, expected, or limiting values assigned to a waste stream. Applying an arithmetic average rather than a geometric mean to radioactivity concentration data that typically span many orders of magnitude results in an intentional bias toward higher estimated concentrations. Activity concentrations for each data source are adjusted for radiological decay to the assumed year of EMDF closure (2047) based on radioisotope half-life and the year of data collection. To estimate the radionuclide inventory for each EMDF waste stream, the estimated average radionuclide activity concentrations are multiplied by the estimated waste stream mass. An average soil density of 1113 kg/cy was assumed for the soil waste volumes. An average debris density of 773 kg/cy was determined based on the bulk densities compiled for EMWMF in the Capacity Assurance Remedial Action Report (DOE 2004). Total estimated EMDF waste inventory for each radionuclide (Table 2.15) is the sum of the six waste stream inventory estimates.

Table 2.15. Total EMDF waste radionuclide inventory (Ci decayed to 2047)

	ORNL D&D	ORNL RA	Y-12 D&D Alpha-4 and Alpha-5	Y-12 D&D Biology	Y-12 D&D Remaining Facilities	Y-12 RA	EMDF Waste Total Inventory (Ci)	EMDF waste average activity concentration (pCi/g)
Waste mass (g)	1.94E+11	1.81E+11	1.37E+11	2.81E+10	3.03E+11	5.26E+11	1.37E+12	
Radio-isotope	**EMDF activity by waste stream (Ci)**							
Ac-227	7.54E-03						7.54E-03	5.50E-03
Am-241	4.09E+01	1.11E+02	2.20E-03	5.11E-03	1.80E-02	3.61E-01	1.52E+02	1.11E+02
Am-243	5.30E-01	7.12E+00					7.65E+00	5.59E+00
Ba-133	Refer to Attachment B.3 for basis of inventory estimate						4.14E+00	3.02E+00
Be-10	Refer to Attachment B.3 for basis of inventory estimate						6.52E-05	4.76E-05
C-14	1.66E+00	4.60E+00		1.17E+00			7.43E+00	5.43E+00
Ca-41	Refer to Attachment B.3 for basis of inventory estimate						1.09E-01	7.92E-02
Cf-249	2.80E-06						2.80E-06	2.05E-06
Cf-250	1.91E-05						1.91E-05	1.39E-05
Cf-251	5.42E-07						5.42E-07	3.96E-07
Cf-252	3.37E-07						3.37E-07	2.46E-07
Cm-243	1.01E+00	1.02E-01					1.11E+00	8.10E-01
Cm-244	3.23E+02	2.53E+00	5.39E-04				3.26E+02	2.38E+02
Cm-245	9.87E-02						9.87E-02	7.21E-02
Cm-246	4.10E-01						4.10E-01	2.99E-01
Cm-247	2.68E-02						2.68E-02	1.96E-02
Cm-248	1.44E-03						1.44E-03	1.05E-03
Co-60	4.23E-02	7.90E-03	8.87E-04			4.20E-04	5.15E-02	3.76E-02
Cs-134	5.41E-09	2.19E-08					2.73E-08	1.99E-08
Cs-137	4.11E+02	2.63E+03	2.73E-02	3.71E-03	1.42E-02	2.84E+00	3.04E+03	2.22E+03
Eu-152	7.25E+01	1.46E+00					7.40E+01	5.40E+01
Eu-154	1.65E+01	2.52E-01					1.67E+01	1.22E+01
Eu-155	1.72E-02	1.44E-04					1.74E-02	1.27E-02
Fe-55		2.31E-06					2.31E-06	1.68E-06
H-3	2.52E+01	3.56E+00		6.25E-02			2.88E+01	2.10E+01
I-129	9.56E-01	9.35E-02					1.05E+00	7.66E-01
K-40	1.07E+00	3.43E+00		6.27E-01		3.33E+00	8.46E+00	6.18E+00
Mo-100	1.08E-05						1.08E-05	7.92E-06
Mo-93	Refer to Attachment B.3 for basis of inventory estimate						1.00E+00	7.30E-01
Na-22	2.09E-06	2.63E-08					2.12E-06	1.55E-06
Nb-93m	Refer to Attachment B.3 for basis of inventory estimate						6.01E-01	4.39E-01
Nb-94	4.20E-02						4.20E-02	3.07E-02
Ni-59	7.84E+00						7.84E+00	5.73E+00

Table 2.15. Total EMDF waste radionuclide inventory (Ci decayed to 2047) (cont.)

	ORNL D&D	ORNL RA	Y-12 D&D Alpha-4 and Alpha-5	Y-12 D&D Biology	Y-12 D&D Remaining Facilities	Y-12 RA	EMDF Waste Total Inventory (Ci)	EMDF waste average activity concentration (pCi/g)
Waste mass (g)	1.94E+11	1.81E+11	1.37E+11	2.81E+10	3.03E+11	5.26E+11	1.37E+12	
Radio-isotope	**EMDF activity by waste stream (Ci)**							
Ni-63	1.17E+02	1.62E+03		4.84E-02			1.74E+03	1.27E+03
Np-237	8.92E-02	5.08E-01	6.72E-03	6.04E-03		2.27E-01	8.37E-01	6.12E-01
Pa-231	6.15E-01						6.15E-01	4.49E-01
Pb-210	9.09E+00	4.08E-01					9.50E+00	6.93E+00
Pm-146	2.28E-04						2.28E-04	1.66E-04
Pm-147	5.49E-04	1.69E-05					5.66E-04	4.13E-04
Pu-238	1.43E+02	9.86E+01	2.52E-02		1.20E-01	4.62E-03	2.42E+02	1.77E+02
Pu-239	4.61E+01	1.04E+02			2.31E-02	3.12E-01	1.50E+02	1.10E+02
Pu-240	6.81E+01	9.18E+01	9.29E-03	5.07E-03			1.60E+02	1.17E+02
Pu-241	1.33E+01	5.12E+02					5.25E+02	3.83E+02
Pu-242	3.55E-02	4.10E-01					4.45E-01	3.25E-01
Pu-244	9.49E-03						9.49E-03	6.93E-03
Ra-226	5.68E-01	7.08E-01		2.80E-02		7.63E-01	2.07E+00	1.51E+00
Ra-228	1.27E-03	2.52E-03			5.17E-02	1.41E-03	5.69E-02	4.15E-02
Re-187	4.40E-06						4.40E-06	3.21E-06
Sb-125	7.82E-08						7.82E-08	5.71E-08
Sr-90	4.21E+02	7.50E+01		4.93E-02	5.02E-02		4.96E+02	3.62E+02
Tc-99	2.57E+00	7.11E-01	1.48E-01	1.14E+00	2.36E-01	2.43E+00	7.23E+00	5.28E+00
Th-228	2.25E-07	3.40E-10	8.14E-08	3.58E-07	4.78E-06		5.45E-06	3.98E-06
Th-229	3.36E-01	1.44E+01			1.43E-02		1.47E+01	1.08E+01
Th-230	3.30E-01	3.81E+00	5.92E-02		2.38E-02	7.20E-01	4.94E+00	3.61E+00
Th-232	2.32E-01	1.69E+00	5.14E-02	2.24E-02	1.98E-01	6.87E+00	9.07E+00	6.62E+00
U-232	1.62E-01	2.61E+01					2.63E+01	1.92E+01
U-233	5.15E+01	5.27E+01		2.71E+00	3.33E-01		1.07E+02	7.83E+01
U-234	2.15E+00	2.72E+01	1.25E+00	2.34E+00	1.58E+03	8.24E+00	1.62E+03	1.19E+03
U-235	8.15E-02	4.23E-01	1.02E-01	2.02E-01	9.57E+01	5.84E+00	1.02E+02	7.47E+01
U-236	5.14E-02	1.95E-01	5.22E-02	1.19E-01	2.26E+01	1.19E-01	2.32E+01	1.69E+01
U-238	1.32E+00	5.27E+00	4.71E+00	9.56E+00	8.83E+02	7.92E+01	9.83E+02	7.18E+02

D&D = deactivation and decommissioning
EMDF = Environmental Management Disposal Facility
ORNL = Oak Ridge National Laboratory
RA = remedial action
Y-12 = Y-12 National Security Complex

2.3.2 Radionuclide Screening

There are 70 radionuclides included in the data sources assembled for the EMDF waste inventory (Appendix B). To provide computational efficiency and enable extensive single parameter sensitivity analysis simulation and probabilistic simulations, a methodology was employed to screen (i.e., remove from further analysis) radionuclides that do not contribute significantly to the total dose. For the EMDF PA, a two-phase approach was used for screening radionuclides for further simulations (Fig. 2.44). Phase 1 involved screening based on radionuclide half-life. Any parent radionuclide in the EMDF inventory with a half-life of less than 5 years was screened out from further analysis because during the first 100 years of post-closure institutional control, the engineered barrier systems (cover and liner, including the leachate collection system) will prevent cover infiltration and leachate release, and DOE control of all property immediately surrounding the EMDF site will prevent inadvertent intrusion. During this 100-year time

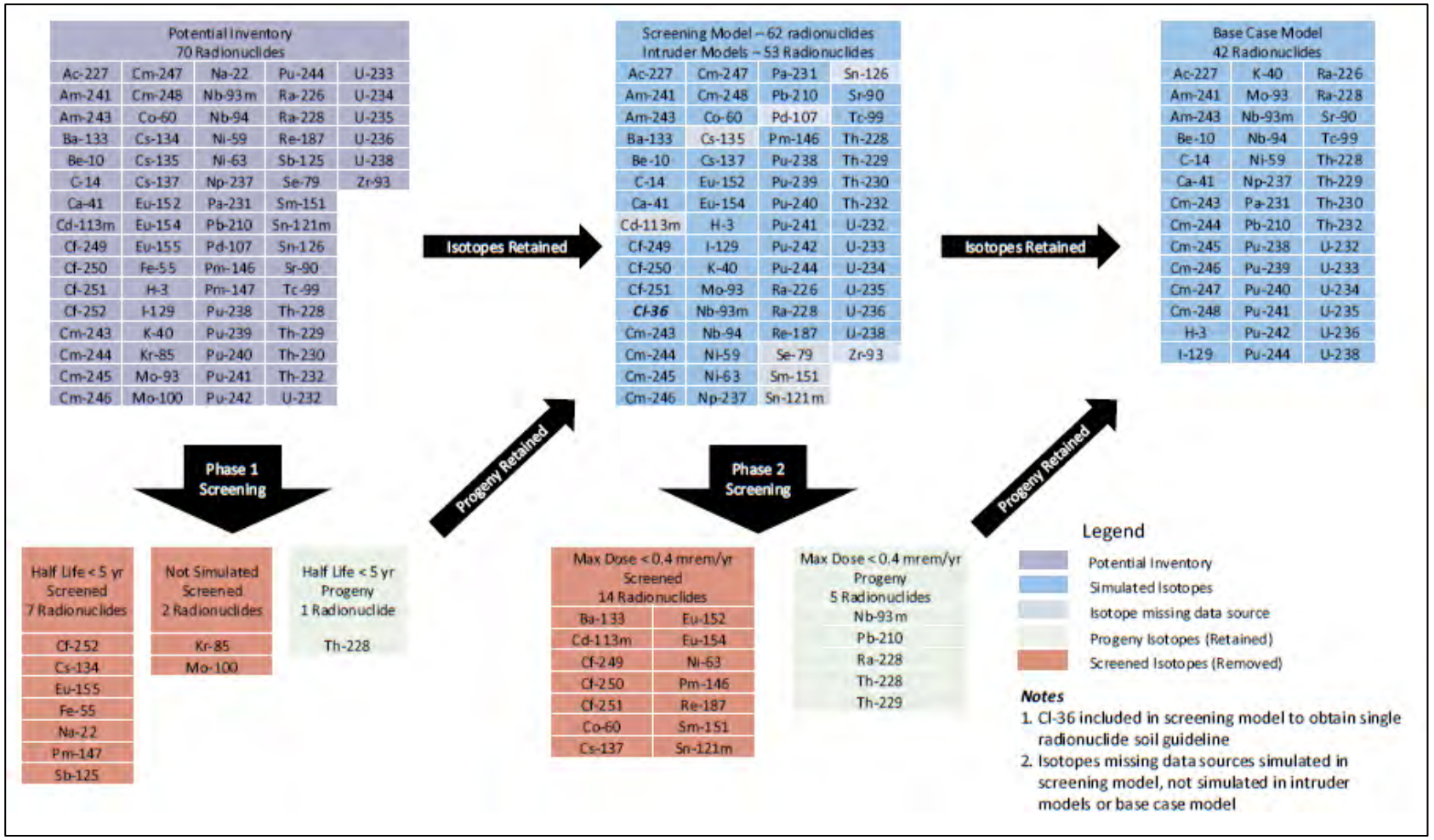

Fig. 2.44. Radionuclide screening for EMDF PA dose analysis

period, over 20 half-lives will have elapsed, resulting in decay of short-lived radionuclides to very low concentrations. Screening of radionuclides based on half-life was not performed for any nuclides that also are progeny of other parent nuclides included in the inventory. This approach avoids potential delay in progeny generation and ensures inventory progeny are accounted for in model simulations.

Additional justification for using the 5-year half-life as a cutoff for the analysis of leachate release to groundwater is the anticipated travel time from the waste to the underlying water table. STOMP model simulations (Appendix E) indicate that the average travel time from waste to the water table is greater than 200 years for a highly mobile radionuclide such as C-14 (approximately 40 or more half-lives for the screened short-lived radionuclides). Seven radionuclides were screened out in Phase 1, including: Cf-252, Cs-134, Eu-155, Fe-55, Na-22, Pm-147, and Sb-125. Thorium-228 has a half-life less than 5 years, but it was retained for the groundwater screening model because it is a progeny of several radionuclides in the inventory.

Based on the EMDF estimated inventory, anticipated operational conditions, and design features of the EMDF cover system, post-closure release of radionuclides in the vapor-phase is expected to be negligible. The estimated inventory of radioactive nuclides of noble gases and halogens is limited to Kr-85 and I-129. Other radionuclides that could be released from the EMDF waste as vapor include H-3 and C-14. Additional discussion of the potential for atmospheric release through the cover is provided in Sect. 3.2.2.2. Krypton-85 was eliminated prior to Phase 2 screening due to the expectation that significant amounts of krypton gas will not be present after waste generation, transport, placement, and in-cell compaction are complete. Molybdenum-100 is a very stable radionuclide (half-life 8.5E+18 years) that does not have a dose conversion factor in the RESRAD-OFFSITE database. The very low projected Mo-100 inventory (approximately 1.08E-05 Ci) is not expected to be a significant contributor to dose; therefore, Mo-100 was also excluded from further analysis.

In summary, for Phase 1 screening, a total of 61 radionuclides passed and a total of 9 radionuclides were screened from further consideration. Seven radionuclides were screened out based on their half-life and two radionuclides were screened out for other reasons (Fig. 2.44). For the IHI scenario, only the Phase 1 screening was applied (Sect. 6.2).

Phase 2 of the screening analysis applied a groundwater pathway screening model, which consists of a modified version of the base case model using isotope-specific distribution coefficients decreased by a factor of 10 or 100 (see Appendix G, Sects. G.4.3.6 and G.4.4.1) and other pessimistically biased assumptions that result in greater model-predicted doses regarding inventory (elevated screening source concentrations) and disposal conditions (no engineered barriers). A more detailed description of screening model simulations is provided in Sect. G.4.4.

The screening model dose is based exclusively on groundwater ingestion and applied a screening dose criterion of 0.4 mrem/year, which is 10 percent of the 4 mrem/year national primary drinking water standard for beta-gamma emitters (40 *CFR* 141). The 0.4 mrem/year screening criterion is applied to all radionuclides, including alpha emitters, for the all-pathways dose analysis. Compliance with drinking water MCLs for radionuclides, including alpha emitters, is evaluated separately from the all-pathways dose analysis (Sect. 4.7.1). Among the alpha emitting radionuclides in the estimated inventory, only Cf-249, Cf-250, and Cf-251 were eliminated from further consideration based on the Phase 2 screening criterion (Fig. 2.44). The estimated inventories of those three radionuclides are very small relative to the other alpha-emitting nuclides (Table 2.15), therefore neglecting their contributions to the estimated gross alpha activity concentration in groundwater (Sect. 4.7.1) is justified.

A total of 62 radionuclides were simulated in the groundwater screening model, which included the 61 radionuclides that passed Phase 1 of the screening process, as well as Cl-36.

Small quantities of Cl-36 could be present in future EMDF LLW associated with irradiated graphite or metals from ORNL research reactor facilities. However, Cl-36 has not been a radionuclide of concern for LLW disposed at the EMWMF, and identification of Cl-36 in environmental samples from the ORR is extremely rare. The compilation of facility inventory data, EMWMF waste profiles, and environmental characterization data used to estimate the EMDF radionuclide inventory at closure (refer to Appendix B) includes no data on Cl-36 activity. Due to this lack of information, and the likelihood that any Cl-36 will be limited to small volumes of waste, Cl-36 was included only in the Phase 2 screening model using a unit source concentration of 1 pCi/g to provide information for future waste management decisions.

Of the 62 simulated radionuclides, 43 radionuclides (42 plus Cl-36) produced a peak dose greater than 0.4 mrem/year and 19 produced a peak dose of less than 0.4 mrem/year. Out of the 19 radionuclides that produced a peak dose of less than 0.4 mrem/year, five radionuclides (Nb-93m, Pb-210, Ra-228, Th-228, and Th-229) are progeny of one of the 43 that exceeded the dose criteria. These five are retained as source concentrations for the base case groundwater pathway analysis (Fig. 2.44). The remaining 14 radionuclides removed because their individual predicted doses were less than 0.4 mrem/year were subsequently simulated together to confirm that the sum of the peak doses from the screened nuclides was less than 0.4 mrem/year. Although Cl-36 would have passed Phase 2 of the screening process, it is not simulated in the inadvertent human intruder or base case scenario simulations because there are no data available to estimate an EMDF Cl-36 inventory. A total of 47 radionuclides (42 with peak dose greater than 0.4 mrem/year plus five progeny) passed Phase 2 of the screening analysis (Table 2.16).

Table 2.16. Screening source concentrations and radionuclide screening results

Radionuclide	Half-life (years)	Screening source concentration (pCi/g)	Phase 1: Half-life > 5 years?	Phase 2: Peak Groundwater Dose > 0.4 mrem/year for 10,000-year simulation?	Retain for dose analysis?
Ac-227	2.18E+01	4.89E+04	Yes	Yes	Yes
Am-241	4.32E+02	2.30E+03	Yes	Yes	Yes
Am-243	7.38E+03	2.29E+01	Yes	Yes	Yes
Ba-133	1.07E+01	2.71E+01	Yes	No	Intruder
Be-10	1.50E+06	7.16E+05	Yes	Yes	Yes
C-14	5.73E+03	6.27E+05	Yes	Yes	Yes
Ca-41	1.00E+05	4.11E+06	Yes	Yes	Yes
Cd-113m	1.36E+01	1.11E+05	Yes	No	No[a]
Cf-249	3.51E+02	3.92E-04	Yes	No	Intruder
Cf-250	1.31E+01	1.70E-02	Yes	No	Intruder
Cf-251	8.98E+02	7.36E-05	Yes	No	Intruder
Cf-252	2.60E+00	1.25E+03	No	NS[b]	No
Cl-36[e]	3.01E+05	1.00E+00	Yes	Yes	No[a]
Cm-243	2.85E+01	4.37E+01	Yes	Yes	Yes
Cm-244	1.81E+01	5.26E+05	Yes	Yes	Yes
Cm-245	8.50E+03	9.80E+01	Yes	Yes	Yes
Cm-246	4.73E+03	1.97E+00	Yes	Yes	Yes
Cm-247	1.56E+07	2.35E+01	Yes	Yes	Yes
Cm-248	3.39E+05	2.29E+01	Yes	Yes	Yes
Co-60	5.27E+00	1.93E+06	Yes	No	Intruder
Cs-134	2.10E+00	1.39E+05	No	NS[b]	No

Table 2.16. Screening source concentrations and radionuclide screening results (cont.)

Radionuclide	Half-Life (years)	Screening source concentration (pCi/g)	Phase 1: Half-life > 5 years?	Phase 2: Peak Groundwater Dose > 0.4 mrem/year for 10,000-year simulation?	Retain for Dose Analysis?
Cs-135	2.30E+06	2.46E+06	Yes	Yes	No[a]
Cs-137	3.00E+01	3.82E+08	Yes	No	Intruder
Eu-152	1.33E+01	5.84E+05	Yes	No	Intruder
Eu-154	8.80E+00	7.85E+05	Yes	No	Intruder
Eu-155	4.80E+00	9.98E+05	No	NS[b]	No
Fe-55	2.70E+00	4.71E+07	No	NS[b]	No
H-3	1.24E+01	4.84E+06	Yes	Yes	Yes
I-129	1.57E+07	4.86E+05	Yes	Yes	Yes
K-40	1.28E+09	5.65E+01	Yes	Yes	Yes
Kr-85	1.10E+01	1.16E+08	Yes	NS[c]	No
Mo-93	3.50E+03	4.99E+03	Yes	Yes	Yes
Mo-100	8.50E+18	2.55E-03	Yes	NS[c]	No
Na-22	2.60E+00	5.96E-01	No	NS[b]	No
Nb-93m	1.36E+01	3.00E+03	Yes	No	Yes[d]
Nb-94	2.03E+04	1.90E+05	Yes	Yes	Yes
Ni-59	7.50E+04	1.55E+06	Yes	Yes	Yes
Ni-63	9.60E+01	1.03E+07	Yes	No	Intruder
Np-237	2.14E+06	5.63E+01	Yes	Yes	Yes
Pa-231	3.28E+04	3.17E+00	Yes	Yes	Yes
Pb-210	2.23E+01	4.48E+02	Yes	No	Yes[d]
Pd-107	6.50E+06	3.34E+06	Yes	Yes	No[a]
Pm-146	5.50E+00	1.24E-01	Yes	No	Intruder
Pm-147	2.60E+00	2.67E+06	No	NS[b]	No
Pu-238	8.77E+01	7.15E+03	Yes	Yes	Yes
Pu-239	2.41E+04	1.85E+05	Yes	Yes	Yes
Pu-240	6.54E+03	8.44E+03	Yes	Yes	Yes
Pu-241	1.44E+01	2.83E+05	Yes	Yes	Yes
Pu-242	3.76E+05	4.98E+01	Yes	Yes	Yes
Pu-244	8.26E+07	1.11E+01	Yes	Yes	Yes
Ra-226	1.60E+03	1.35E+01	Yes	Yes	Yes
Ra-228	5.75E+00	3.46E+00	Yes	No	Yes[d]
Re-187	4.12E+10	1.94E-03	Yes	No	Intruder
Sb-125	2.80E+00	1.37E+06	No	NS[b]	No
Se-79	6.50E+04	2.47E+06	Yes	Yes	No[a]
Sm-151	9.00E+01	5.75E+06	Yes	No	No[a]
Sn-121m	5.50E+01	6.41E+01	Yes	No	No[a]
Sn-126	1.00E+05	1.89E+06	Yes	Yes	No[a]
Sr-90	2.91E+01	3.93E+08	Yes	Yes	Yes
Tc-99	2.13E+05	1.35E+06	Yes	Yes	Yes
Th-228	1.90E+00	1.14E+05	No	No	Yes[d]

Table 2.16. Screening source concentrations and radionuclide screening results (cont.)

Radionuclide	Half-Life (years)	Screening source concentration (pCi/g)	Phase 1: Half-life > 5 years?	Phase 2: Peak Groundwater Dose > 0.4 mrem/year for 10,000-year simulation?	Retain for Dose Analysis?
Th-229	7.34E+03	3.48E+03	Yes	No	Yes[d]
Th-230	7.70E+04	1.48E+02	Yes	Yes	Yes
Th-232	1.41E+10	2.67E+06	Yes	Yes	Yes
U-232	7.20E+01	8.43E+05	Yes	Yes	Yes
U-233	1.59E+05	5.49E+05	Yes	Yes	Yes
U-234	2.45E+05	1.67E+03	Yes	Yes	Yes
U-235	7.04E+08	2.57E+03	Yes	Yes	Yes
U-236	2.34E+07	4.87E+02	Yes	Yes	Yes
U-238	4.47E+09	2.07E+09	Yes	Yes	Yes
Zr-93	1.53E+06	5.56E+05	Yes	Yes	No[a]

[a]Radionuclide not simulated because insufficient inventory data were available.
[b]Radionuclide not simulated due to screening in Phase 1.
[c]Radionuclide not simulated due to other reasons.
[d]Isotope has half-life less than 5 years or screening dose less than 0.4 mrem/year, but was retained for further analysis because it is progeny of another isotope in the inventory. Intruder identifies isotopes simulated for IHI models, but not retained for further analysis.
[e]Cl-36 is not included in the inventory but was simulated in the screening model provide information for future waste management decisions.

IHI = inadvertent human intrusion
NS = not simulated

2.3.3 Radionuclide Inventories for Further Analysis

Nine radionuclides (less commonly reported fission products) had inventory data that could not be verified from the original sources and were not included in the IHI analysis or base case models. These nine radionuclides are: Cd-113m, Cs-135, Kr-85, Pd-107, Se-79, Sm-151, Sn-121m, Sn-126, and Zr-93. Five of these nine passed the Phase 2 groundwater pathway screening; one was screened out at a noble gas. Including the removal of Mo-100, out of the 70 total isotopes considered in the EMDF waste inventory (see Appendix B), 53 isotopes were simulated in the IHI analysis models and 42 radionuclides were simulated in the base case (release to groundwater) model (Table 2.16).

As a final step in developing the estimated radionuclide inventory for the PA analysis, operational period losses of highly mobile radionuclides (H-3, C-14, Tc-99, and I-129) are estimated and used to adjust (decrease) the assumed post-closure inventory for those nuclides. The assumptions and modeling applied to estimate these operational losses and reductions in mobility resulting from treatment of collected leachate are described in Sect. 3.2.2.5.

This page intentionally left blank.

3. ANALYSIS OF PERFORMANCE

This section of the report provides detailed descriptions of the conceptual models, modeling tools, and exposure scenario used to analyze EMDF performance. The following section provides an overview of the analysis and provides summary information on the conceptual models, modeling tools, and exposure pathways in the context of the total EMDF disposal system described in Sect. 1.3 and Appendix C.

3.1 OVERVIEW OF ANALYSIS

The approach to selecting the range of potential future conditions analyzed for this PA is a top-down, total system analysis of the EMDF disposal system that is structured around the safety functions served by the engineered and natural elements of the system. An overview of safety functions for the EMDF disposal system is provided in Sect. 1.3. Appendix C provides additional detail on EMDF design features and safety functions and includes analysis of natural events and processes that can impact the safety functions of key features. Uncertainties in future environmental conditions and the long-term performance of engineered barriers are integrated and generalized in a conceptual model of EMDF performance evolution that is expressed in terms of changes in cover infiltration and leachate release over time (refer to Sect. 3.2.1 and Appendix C, Sect. C.1.3). To address these uncertainties, the PA incorporates a range of potential future conditions defined by selection of input parameter values for model sensitivity evaluations and the uncertainty analysis presented in Sect. 5. In addition, a separate analysis of the potential impact of an alternative conceptual model of EMDF failure in which cover infiltration greater than liner system release leads to waste saturation and overtopping of the liner (bathtub condition) is provided in Appendix C, Sect. C.3.

3.1.1 Conceptual Models of the EMDF Disposal System

Conceptualization of the EMDF disposal system for performance analysis and modeling is organized around four related components, as described in Table 3.1.

Table 3.1. EMDF disposal system components, conceptual model elements, and model codes

Disposal system component	Conceptual model elements	Model codes
Water Balance and Performance of Engineered Barriers (Sect. 3.2.1)	• Facility water balance • Performance of engineered systems • Degradation of synthetic and earthen barriers • Assumed evolution of EMDF cover infiltration and leachate release	HELP RESRAD-OFFSITE
Radionuclide Release and Vadose Zone Transport (Sect. 3.2.2)	• EMDF radionuclide inventory • Disposal practices and waste forms • Facility design geometry • EMDF cover performance evolution • Vapor phase release and radon flux • Aqueous phase release from waste • Transport through waste and liner system, including chemical retardation • Vadose zone transport below liner	STOMP RESRAD-OFFSITE

Table 3.1. EMDF disposal system components, conceptual model elements, and model codes (cont.)

Disposal system component	Conceptual model elements	Model codes
Saturated Zone Flow and Radionuclide Transport (Sect. 3.2.3)	• Vadose zone flux to saturated zone • CBCV site geology and topography • CBCV hydrogeology • CBCV surface water features • CBCV saturated zone flow and transport, including chemical retardation	MODFLOW MT3D RESRAD-OFFSITE
Exposure Pathways and Scenarios[a] (Sect. 3.2.4)	• Resident farmer exposure scenario • Groundwater POA (well location) • Surface water POA • Exposure pathways, abiotic and biotic • Dose analysis	RESRAD-OFFSITE

[a]Analysis of the inadvertent human intrusion scenario is presented in Sect. 6

CBCV = Central Bear Creek Valley
EMDF = Environmental Management Disposal Facility
HELP = Hydrologic Evaluation of Landfill Performance
POA = point of assessment
RESRAD = RESidual RADioactivity
STOMP = Subsurface Transport over Multiple Phases

Conceptual models of post-closure and long-term performance of engineered barriers are incorporated in the assumed evolution of the EMDF water balance as the safety functions of engineered cover and liner system features become limited by natural processes of degradation. These conceptual models include pessimistic biases intended to lead to increased infiltration versus what is expected as a means to address uncertainty in cover performance (Sect. 3.2.1 and Appendix C, Sect. C.1).

Conceptual models of post-closure radionuclide release from the EMDF disposal system (Sect. 3.2.2) include analysis and screening of radionuclide release through the cover to the atmosphere or biosphere, diffusive transport and release of radon through the cover (Appendix H), and radionuclide release and transport in the aqueous phase. Conceptual models for aqueous release incorporate the assumed changes in cover infiltration over time and include waste zone radionuclide release and unsaturated vertical flow and radionuclide transport through the waste, liner system, and underlying vadose zone. These conceptual models are based on the estimated EMDF radionuclide inventory (Appendix B), assumed waste disposal practices and waste forms (Sect. 3.2.2.5), sorptive properties of EMDF materials (Sect. 3.2.2.8), the vertical sequence of vadose zone materials, and the analysis of cover performance presented in Sect. 3.2.1 and Appendix C.

Conceptual models of saturated zone flow and radionuclide transport are based on the hydrogeologic conceptual model for BCV (Sect. 2.1.5.1), including the lithology and stratigraphy of the EMDF site, major topographic and structural controls on groundwater movement, surface water features, and chemical retardation properties of the saprolite and bedrock. Conceptualization of the saturated zone for purposes of EMDF performance analysis is described in detail in Sect. 3.2.3.

Conceptual models of post-closure public exposure to radionuclides include the general resident farmer scenario considered for the analysis (Sect. 3.2.4) as well as detailed assumptions for abiotic (e.g., water ingestion, inhalation) and biotic (e.g., ingestion of contaminated fish and produce) exposure pathways. Section 3.2.4 presents the exposure scenario and pathway assumptions in detail and describes the basis for the inputs and assumptions incorporated into the dose analysis.

3.1.2 PA Model Implementation and Integration

Implementation of the EMDF system conceptual models with computer modeling codes is structured around the four conceptual components (Table 3.1 and Fig. 3.1). This implementation includes detailed process model codes for the components that encompass engineered facility performance and abiotic transport elements, as well as a total system model code that encompasses all four conceptual components including the exposure scenario and biotic pathways for radionuclide transfer. The more detailed models were used for modeling the complexities of primarily abiotic environmental transport pathways to predict concentrations of key radionuclides at the POA. The total system model uses simplified representations of transport pathways, along with biotic transformations and scenario-specific exposure factors, to identify radionuclides that are likely key dose contributors and quantify total dose for comparison to performance objectives.

Implementation of the more detailed component-level EDMF PA models and the total system model proceeded concurrently, along with iterative development and refinement of model assumptions, cover performance and source release approaches, and parameter value selections for each of the model tools. Some model outputs serve as inputs for other modeling tools. The primary model output-to-input linkages are shown in Fig. 3.2 and are described along with comparisons of model outputs in Sect. 3.3. Inputs common to all model codes include radionuclide inventories, EMDF design specifications, and CBCV site characteristics. Selection, implementation, and integration of these model codes for EMDF performance analysis is explained in Sect. 3.3. QA activities for model implementation are described in Sect. 9.

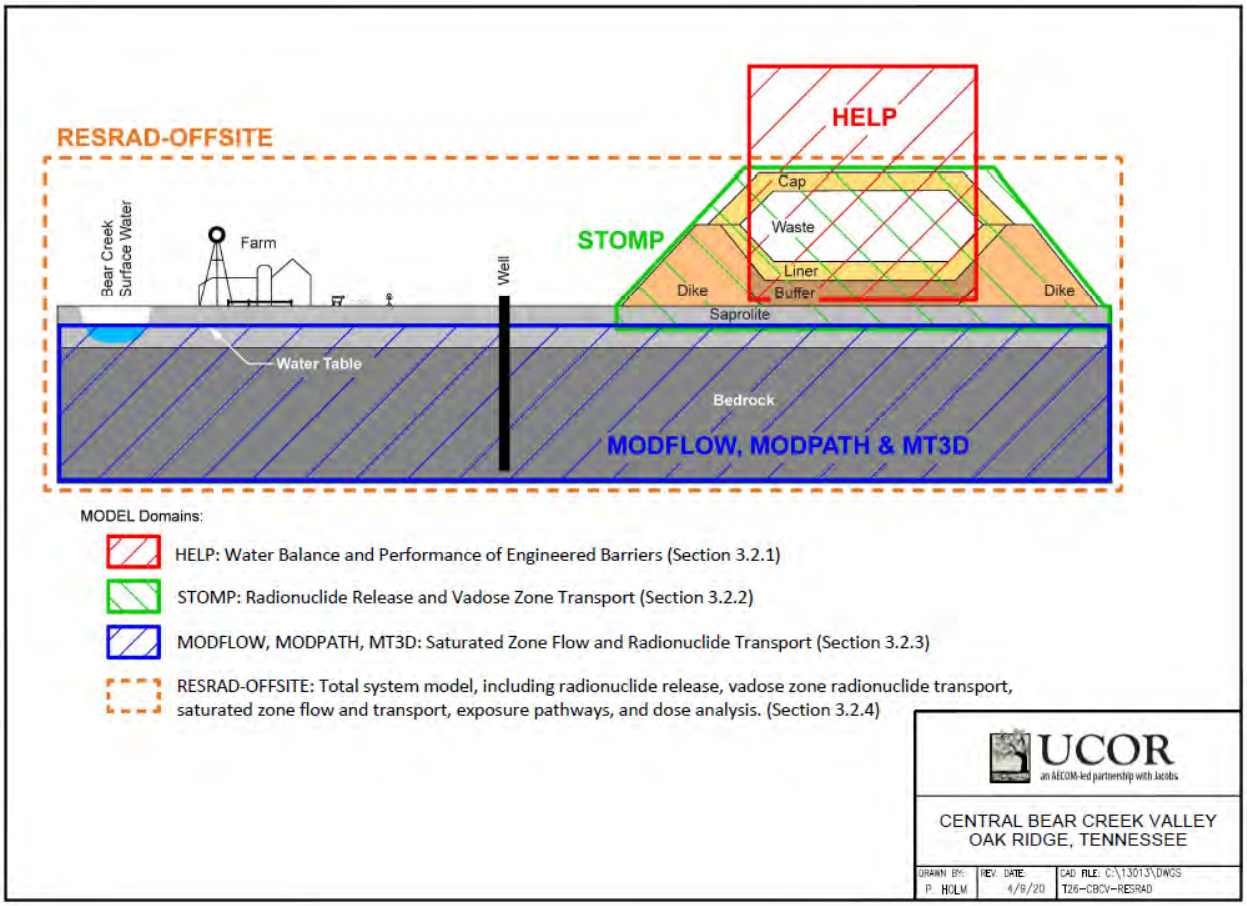

Fig. 3.1. Schematic illustration of EMDF disposal system conceptual models and modeling tools used for implementation

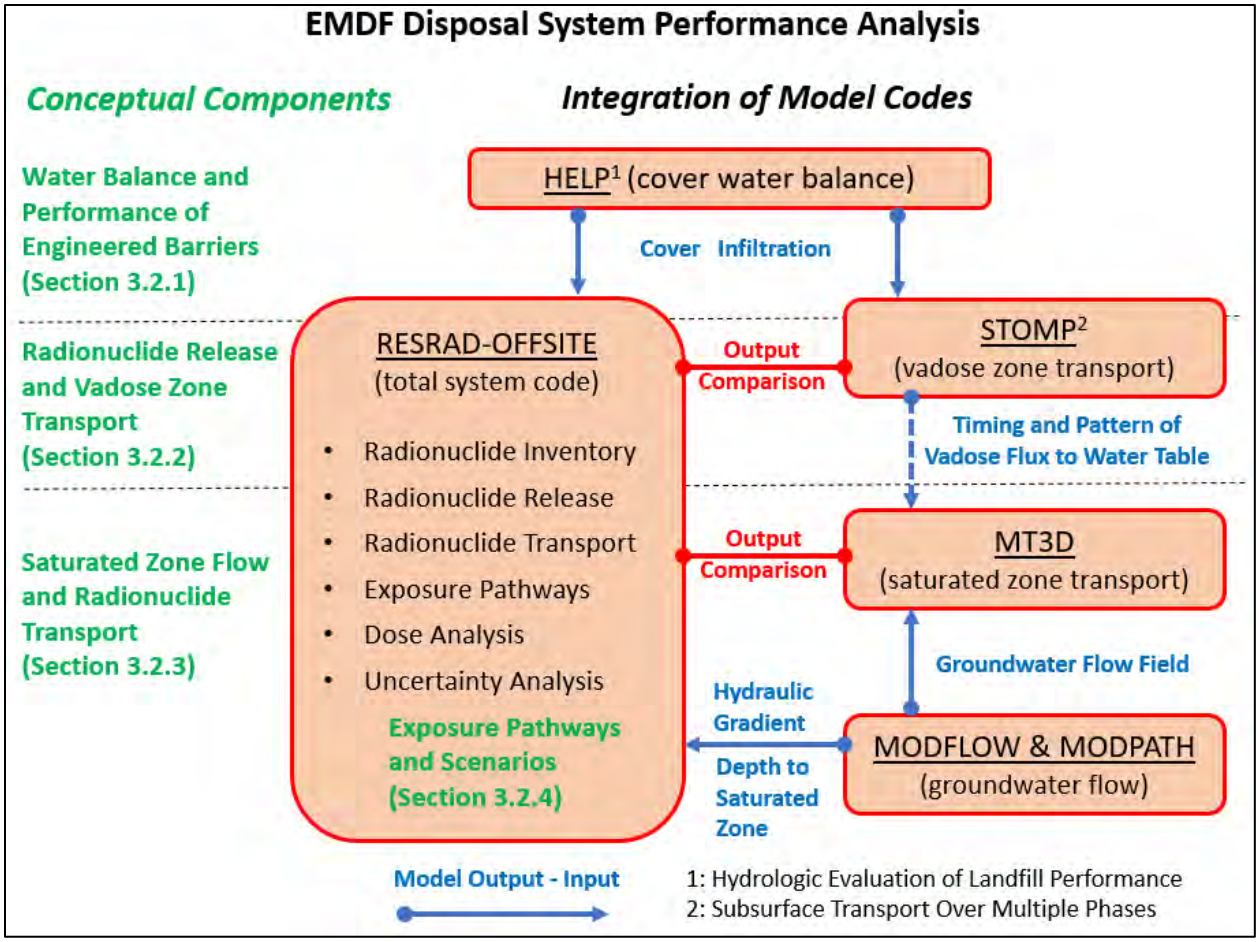

Fig. 3.2. EMDF disposal system conceptual components and integration of model codes for performance analysis

3.2 CONCEPTUAL MODELS

The following sections present more detailed descriptions of conceptual models for EMDF system features and processes, including the facility water balance and degradation of engineered components (Sect. 3.2.1), source release and vadose zone transport (Sect. 3.2.2), and radionuclide transport in the saturated zone and discharge to surface water (Sect. 3.2.3). The assumptions regarding exposure pathways and scenarios considered for each disposal facility performance objective are described in Sect. 3.2.4.

3.2.1 Water Balance and Performance of Engineered Barriers

The basic conceptual model for the water balance of the EMDF system includes the natural environmental drivers of land surface hydrology and the engineered drainage features and barrier systems of the landfill design (Fig. 3.3). Infiltration of water through the surface layer and into the cover lateral drainage system is a function of climatic and meteorological dynamics and characteristics of the surface soil and vegetation that control local surface water and energy budgets. Subsurface percolation of water is conceptualized as predominantly vertical within the waste zone and earthen barriers of the cover and liner systems, whereas both vertical and lateral drainage are assumed to occur within the engineered drainage layers while they

remain functional. Water movement through the unsaturated zone beneath the liner is also conceptualized as vertically downward to the water table.

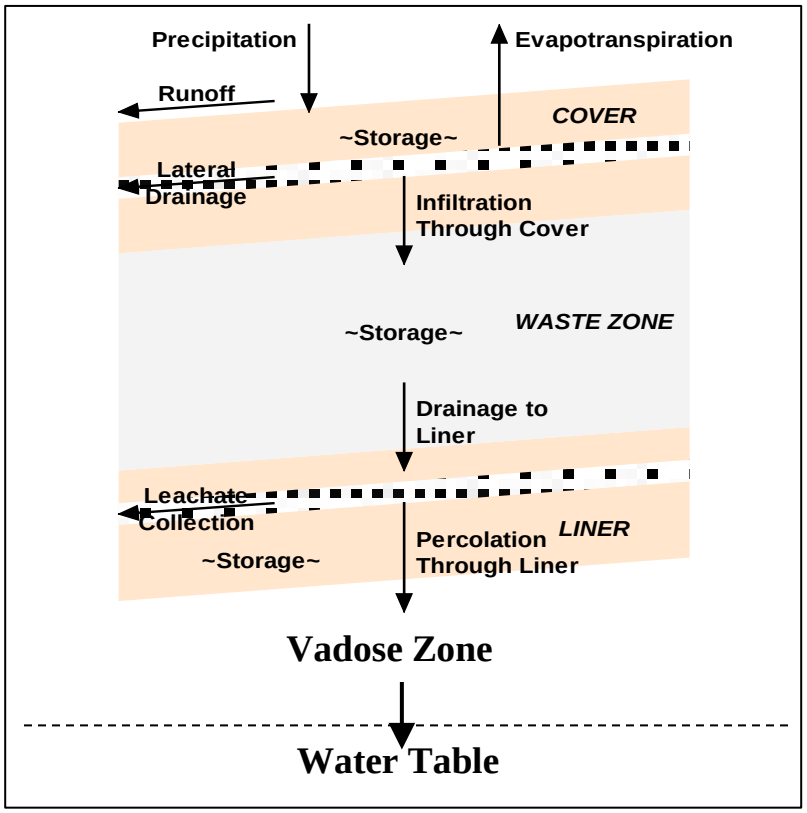

Fig. 3.3. Schematic conceptual model of EMDF water balance

EMDF design features are described in Sect. 2.2 and additional detail on the water balance model is provided in Appendix C, along with the analysis of features, events, and processes that influence system performance. The remainder of this section summarizes the information and uncertainties that are incorporated into the generalized conceptual model of EMDF system performance.

Engineered barriers of primary concern for long-term facility performance include the synthetic (HDPE) membranes and clay barrier layers of the cover and liner systems. Synthetic membrane service life and the long-term performance of engineered earthen barriers are key uncertainties. A simplified profile of the EMDF, with safety functions and events and processes important for long-term performance, is provided in Fig. 3.4. The safety functions of the various cover and liner system layers are interdependent so that the function of one layer may be limited by impaired function of one or more other layers in the system. The synthetic membranes serve as the primary short-term (decades to centuries) infiltration and leachate barriers that support the function of lateral drainage layers in the cover and liner. Thermal oxidative degradation is a primary breakdown mechanism for HDPE membranes and is highly sensitive to temperature, so that the thermal buffer provided by the overlying materials is a factor regulating the potential rate of degradation.

This page intentionally left blank.

	EMDF Engineered Features	Safety Functions	Limiting Events and Processes
Cover System Components	**Vegetated erosion control layer (4 ft)**	- Provides growth medium for cover vegetation - Protects underlying cover components from erosion and variability in temperature and moisture	- Surface water balance, infiltration and runoff - Vegetation and soil development, biointrusion - Surface erosion and gullying - Severe storms/flood events, landslides
	Granular filter layer (1 ft)	- Prevents filling of the biointrusion layer pore space	- Biointrusion
	Biointrusion layer (2 ft)	- Deters inadvertent human intrusion - Limits damage to hydrologic barriers by roots and burrowing animals - Secondary erosion control (defense-in-depth)	- Weathering and physical breakdown of cobbles/boulders - Pore space infilling and root penetration
	Lateral drainage layer (1 ft)	- Provides subsurface drainage to reduce deep cover infiltration through the less permeable underlying layers	- Infilling of pore spaces with fine particulates and/or by chemical precipitation - Waste subsidence (differential settlement)
	Synthetic (HDPE) membrane (60 mil)	- Primary cover infiltration barrier (initial post closure period) - Protects underlying clay barrier from desiccation and cracking	- Installation-related defects/damage - HDPE thermal oxidative degradation processes - Severe seismic event and/or rapid waste subsidence causing early membrane failure
	Amended/compacted clay barriers (2 ft)	- Primary long-term infiltration barrier - Limits vapor phase release to the cover surface (radon barrier)	- Improper clay compaction - Root penetration, thermal and moisture cycles (increasing permeability) - Waste subsidence (differential settlement) - Severe seismic or storm event causing damage to cover
	Contour soil layer (1ft)	- Provides a level foundation for construction of the compacted clay infiltration barrier(s)	-Improper construction impacts performance of overlying clay barrier
Waste Forms	**Waste containers**	- Containers isolate waste from water and reduce radionuclide mobility	- Corrosion of metal containers - Insufficient filling of void space in waste containers
	Treated and stabilized waste forms	- Provides chemical and physical stability to reduce radionuclide mobility	- Degradation of stabilized waste forms
	Void filling and bulk waste compaction protocols	- Limits long-term subsidence of bulk waste and maintains cover system function	- Waste consolidation and subsidence
Liner System Components	**Protective material layer (1 ft)**	- Protects underlying liner system components from damage during disposal operations.	- Improper installation - Unintentional disturbance during waste placement
	Leachate collection (drainage) layer (1 ft)	- Ensures protection of human health and the environment (operations & early post-closure) - Waste mass dewatering (early post-closure)	- Damage to overlying geotextile during installation - Clogging, chemical precipitation
	Primary synthetic (HDPE) membrane (60 mil)	- Ensures leachate drainage for treatment (operations) - Serves as primary leachate barrier (early post-closure period)	- Installation-related defects/damage - Chemical degradation of HDPE by leachate - HDPE thermal oxidative degradation processes
	Geosynthetic clay Layer (0.02 ft)	- Reduces leachate flux through HDPE membrane holes and defects	- Installation-related defects/damage - Geochemical alteration of sodium bentonite clay (divalent cations)
	Leak detection layer (0.03 ft)	- Provides performance monitoring for overlying composite leachate barrier - Provides secondary leachate removal function	- Degradation of synthetic drainage material
	Secondary synthetic (HDPE) membrane (60 mil)	- Supports performance monitoring for overlying composite leachate barrier - Serves as secondary leachate barrier	- Chemical degradation of HDPE by leachate - HDPE thermal oxidative degradation processes
	Compacted clay layer (3 ft)	- Serves as primary long-term leachate barrier - Provides chemical retardation of radionuclide migration	- Improper clay compaction - Physical and geochemical alteration of clay - Severe seismic event or slope failure damage to perimeter berms and clay barriers
	Geologic buffer zone (unsaturated, low permeability, 10 ft)	- Isolates radionuclides from saturated zone - Provides chemical retardation of radionuclide migration	- Physical and geochemical alteration of geologic buffer material - Water table incursion into geologic buffer

Fig. 3.4. Simplified EMDF design profile, safety functions, and processes relevant to long-term performance

This page intentionally left blank.

Differential settlement (subsidence) of waste during the post-closure period can limit the safety functions of cover system components. Physical stress due to subsidence can damage the HDPE membrane and clay barrier in the cover, increasing water infiltration. Lateral drainage efficiency also can be impaired by subsidence, which will also increase infiltration. Due to the variety of expected EMDF waste forms, this degradation mechanism is an important uncertainty in the conceptual model of EMDF performance evolution. EMDF waste placement and compaction practices are developed to limit future subsidence and final cover design may incorporate features that impart resilience of the cover components to limited subsidence. In addition, post-closure monitoring and maintenance will permit timely repair of damaged cover areas that may develop due to subsidence.

For long-term (centuries to millennia) EMDF performance, function of the clay barrier layer in the cover system is essential. The cover system for EMDF has a robust configuration to protect the compacted clay layers from degrading processes in the surface environment. The vegetated surface layer serves to protect the underlying hydraulic barrier system from erosion and environmental fluctuations that can accelerate degradation of materials and impair safety functions. Site characteristics and processes that will determine the evolution of the surface layer after the cover vegetation is no longer maintained include long-term interactions among climate, soil development, vegetation, and associated successional changes in vegetation over time. These changes will affect the surface water balance, erosion of the cover surface, and infiltration of water. Eventually, severe weather events and progressive climate and vegetation changes could lead to erosion of the protective cover components and cause localized degradation of the clay barrier in the cover, increasing the potential for increased water infiltration over time. Detailed consideration of these processes and events is presented in Appendix C.

The progression of degradation of clay barrier(s) and the overlying components of the cover is contingent on the intensity and timing of multiple processes and events in the post-closure period. Although a general progression from full design performance to some long-term degraded performance condition will occur, the timing and magnitude of degradation is highly uncertain, particularly given the potential interactions among the various disposal system elements, safety functions, and degradation processes described above. One important aspect of this uncertainty is the timing of cover performance degradation (increasing cover infiltration) relative to evolution in the function of liner system components, which may be different due to the differing environments that develop in the cover and liner systems over time. There is a possibility that the cover components will degrade more rapidly than the liner components and that, after leachate collection ceases, the water (im)balance will cause accumulation of water on the liner over time (bathtub scenario). The performance implications of such a bathtub scenario for EMDF are developed in Appendix C, Sect. C.3. Uncertainty in the longevity of the engineered barriers that limit cover infiltration is addressed in the sensitivity and uncertainty analysis applied to the total system model (Sect. 5.4).

A generalized conceptual model of changes in cover infiltration and leachate release assumed as a result of natural processes and events that can impact cover and liner performance over time is shown in Fig. 3.5. The goal of the model is to integrate and generalize the impact of multiple events and processes on safety functions and EMDF performance over time, incorporating uncertainty in timing and degree of degradation and the occurrence of severe events. EMDF performance is expressed in terms of changes in cover infiltration and leachate release, beginning at the time of final cap completion and facility closure. A post-closure performance timeline (bottom of Fig. 3.5) can be divided into a 100-year institutional control period (during which facility maintenance and active institutional controls are assumed), a period during which full (or near) design performance is maintained after the end of institutional control, a period of degrading performance (increasing cover infiltration and leachate release), and a final period during which water flux into and out of the disposal unit reaches some long-term, relatively stable limit. Implementation of this general model of increasing cover infiltration over time for each of the PA models is described in Sect. 3.3.

This page intentionally left blank.

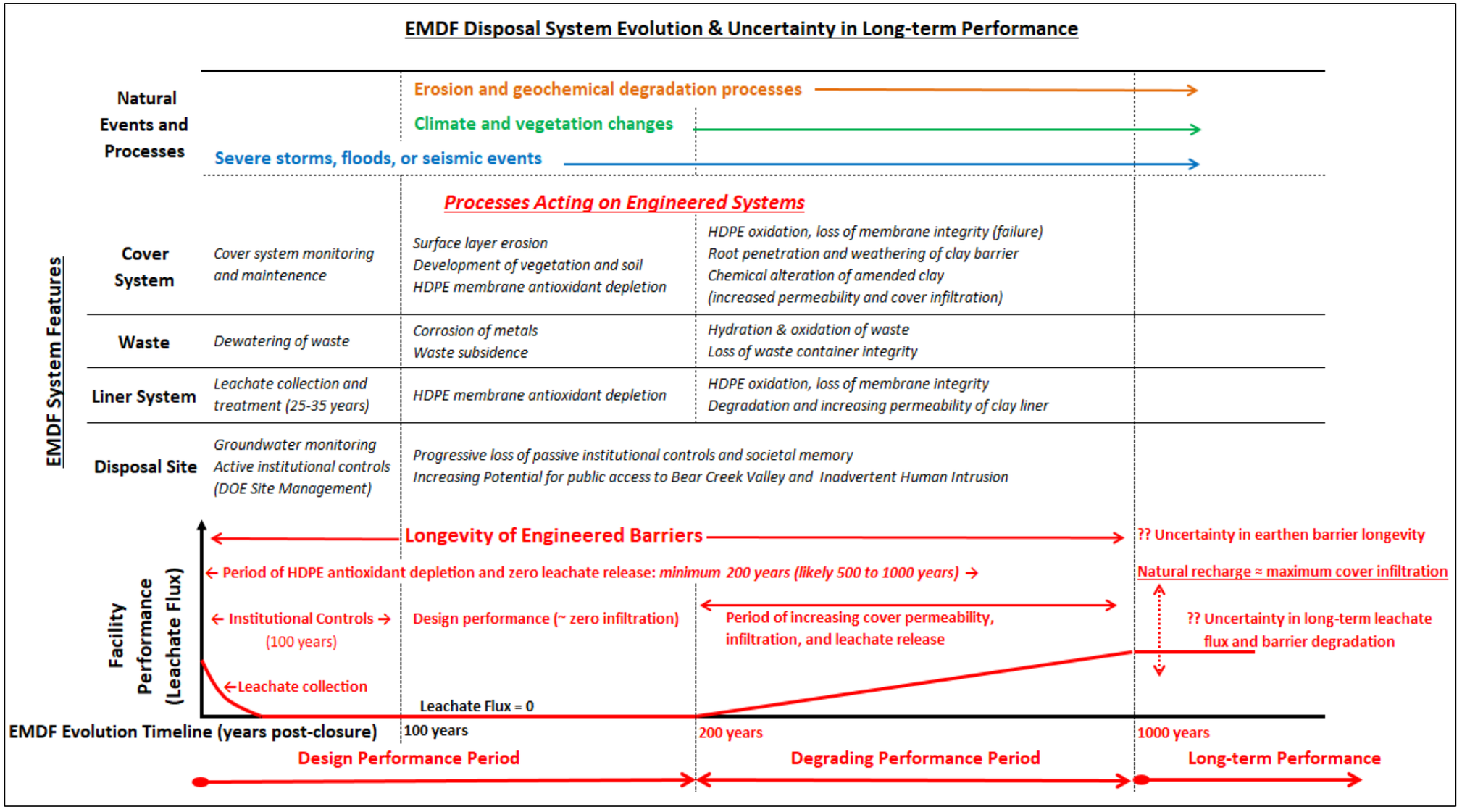

Fig. 3.5. Generalized conceptual model of EMDF performance evolution showing changes in cover infiltration and leachate release over time

This page intentionally left blank.

3.2.2 Radionuclide Release and Vadose Zone Transport

Conceptual models of post-closure EMDF radionuclide release include (1) upward transport through the EMDF cover system via diffusive or biologically driven transport processes that allow release to the atmosphere and biosphere, and (2) downward transport of radionuclides in solution through the variably saturated waste and liner system components and release to the vadose zone materials and groundwater underlying the disposal facility. In the humid environment of East Tennessee, the impact of upward aqueous phase diffusive transport is limited by the predominance of downward advective transport, but vapor-phase or biologically-driven upward transport of radionuclides is possible. Sections 3.2.2.1, 3.2.2.2, and 3.2.2.3 address the limited potential for significant radionuclide release through the EMDF cover system and provide the basis for screening such releases to the atmosphere or biosphere from the all pathways dose analysis of the PA. Appendix H presents model analysis of diffusive transport and release of radon gas from the EMDF cover. Sections 3.2.2.4 through 3.2.2.8. focus on the conceptual model of aqueous phase transport through to the vadose zone and release to the saturated zone, including waste forms and sorptive characteristics.

3.2.2.1 Biointrusion and biologically driven radionuclide release

Biointrusion of the EMDF cover by root systems or ground-dwelling animals is considered as a possible mechanism for release of radionuclides to the surface. Following the end of post-closure care and active institutional control, development of natural vegetation and unimpeded inhabitation of the cover system by various animals is likely. Biological intrusion by root systems, insects, and vertebrate animals will contribute to the natural evolution of the cover system components. In the absence of significant cover erosion, the five-foot thickness of the materials overlying the biointrusion layer (Fig. 3.4) is sufficient to prevent biointrusion into the waste by all but the deepest roots (Canadell et al. 1996, Jackson et al. 1996). In addition, the capillary break creased at the top of the biointrusion layer will also inhibit deeper root penetration. The potential for erosion of the cover surface is considered in detail in Appendix C, Sect. C.1.2 and the magnitude of long-term cover erosion is estimated in Appendix C, Sect. C.4.

The coarse material of the biointrusion layer is expected to be resistant to even severe erosive events and, therefore, will prevent large burrowing animals from bringing waste to the surface. Much smaller species that inhabit the subsurface (e.g., ants) would not be effectively excluded by the biointrusion layer and could potentially penetrate the cover system clay barriers in areas where erosion reduces the thickness of the material above the biointrusion barrier. Transfer of radionuclides to the cover surface by ants or other small soil-dwelling organisms would be limited to relatively small areas and is thus unlikely to produce significant airborne activity concentrations near the EMDF. Similarly, deep tree roots could penetrate the biointrusion layer and clay barrier, but typically more than 75 percent of temperate deciduous forest root systems are limited to the upper 50 cm of the soil profile (Jackson et al. 1996). Uptake of radionuclides by root systems could make radionuclides available in plant tissues at the surface, but human exposure routes originating from this transport mechanism (e.g., consumption of wild plants or animals) would make negligible dose contributions relative to the ingestion of contaminated water and farm-raised foods assumed for the resident farmer dose analysis.

Given the expectation of a relatively stable vegetated cover surface and that the coarse materials of the biointrusion barrier will prevent deep burrowing by large animals, the potential for biologically driven release of radionuclides from EMDF is small in comparison to abiotic release processes. Based on these considerations limiting human exposure to biologically-driven release of radionuclides to the cover surface, this release mechanism was eliminated from the all-pathways dose analysis.

3.2.2.2 Vapor-phase release through the EMDF cover

Previous risk analyses for BCV (DOE 1997b) and the original CA completed for the EMWMF (DOE 1999b, Appendix A) have identified radionuclide release to groundwater and surface water as the primary environmental transport pathways from waste disposal sites on the ORR. In 1996, a multidisciplinary technical steering committee for composite analyses was formed to develop a coherent composite analysis strategy for the EMWMF and another LLW disposal facility in Melton Valley. The steering committee analyzed site-specific conditions on the ORR and concluded that airborne contamination is not a significant public exposure pathway for waste disposal units in BCV and elsewhere on the reservation (DOE 1999b, pages A-15 to A-16). Similarly, the risk assessment and WAC development procedure for the EMWMF (DOE 1998a, Appendix E) excluded the atmospheric release pathway from consideration on the basis that the nearest public receptors were outside the DOE boundary at a significant distance from each of the sites considered.

Based on the EMDF estimated radionuclide inventory, anticipated losses of volatile chemical species during disposal operations, and design features of the EMDF cover system, post-closure release of radionuclides in the vapor-phase is not expected to result in a significant dose to nearby receptors. The remainder of this section explains the characteristics of the estimated inventory and EMDF design features that will limit vapor-phase release from the EMDF. Radon release through the cover is estimated in a separate radon analysis in Appendix H.

The estimated inventory of radionuclides that have the potential to exist in gaseous forms is limited to H-3, C-14, and I-129 (Table 3.2). Small quantities of Cl-36 could be present in future EMDF LLW associated with irradiated graphite or metals from ORNL research reactor facilities; however, these forms of Cl-36 would not be easily volatilized. Furthermore, Cl-36 has not been a radionuclide of concern for LLW disposed at the EMWMF and identification of Cl-36 in environmental samples from the ORR is extremely rare. Some ORNL facility safety documents include Kr-85 estimates in facility inventory estimates, but the utility of these data for estimating activity concentrations in demolition waste is limited. Based on the gaseous form and short half-life (11 years) of Kr-85, quantities of Kr-85 present in EMDF waste at closure are likely to be negligible; therefore, Kr-85 was screened from the PA analyses (refer to Sect. 2.3.2).

Table 3.2. EMDF waste activity concentrations and estimated radionuclide dose for RESRAD-OFFSITE cover release screening models.

Isotope	Half-life (years)	EMDF waste average activity concentration (pCi/g)	Maximum EMDF waste stream average concentration used for cover release screening (pCi/g)	Maximum estimated dose (mrem/year)
H-3	1.24E+01	2.10E+01	1.30E+02	0.023
C-14	5.73E+03	5.43E+00	4.18E+01	0.044
I-129	1.57E+07	7.66E-01	4.92E-00	4.8E-06
Total potential (bounding) dose due to release through the EMDF cover				**0.067**

EMDF = Environmental Management Disposal Facility
RESRAD = RESidual RADioactivity

For elements and compounds that commonly occur in gaseous forms, including krypton, carbon, and hydrogen, loss of more volatile chemical species during the generation, transport, and disposal of uncontainerized waste will reduce the inventory that is potentially available for vapor-phase release following closure. Similarly, exposure of soluble chemical forms of these radionuclides (e.g., as CO_2, HCO_2^-) and iodine (as I^-) to precipitation and infiltration (prior to placement of less permeable interim cover

materials) can further diminish the post-closure inventory through leaching and treatment of collected leachate. For the PA analysis, the estimated post-closure inventories of radionuclides that are highly mobile in the aqueous phase, including H-3, C-14, Tc-99, and I-129, are adjusted (reduced) based on modeling of operational period leaching (results are presented in Sect. 3.2.2.5 and in Appendix G, Sect. G.4.3.4). EMDF leachate treatment wastes (e.g., isotope exchange resins) that could be returned to the EMDF for disposal would be less likely to release these radionuclides in either the vapor or aqueous phase.

The screening analysis for radionuclide release through the EMDF cover does not, however, take credit for operational period losses of mobile species. To ensure an additional pessimistic bias for the screening analysis, the quantitative cover release screening model presented in the following section applies activity concentrations corresponding to the EMDF waste stream with the highest average concentration for each radionuclide (refer to Appendix B, Table B.5) rather than the overall as-generated EMDF waste average concentrations (Table 3.2).

Volatile forms of radionuclides remaining after final cover construction can migrate by diffusion (and potentially, biological disturbance of the cover material) toward the EMDF surface and could be available for inhalation as vapor or in suspended particulate form. The expected longevity of the cover system (provided by design features that protect the flexible geomembrane and clay barriers from degradation) will limit diffusive transport to the EMDF surface for many decades, and likely for centuries. Appendix C provides additional detail on engineered features and degradation processes for the cover system.

Transport of volatile forms to the surface will become more likely over the long-term, as cover performance declines and the hydraulic barriers of the EMDF cover become more permeable. Corrosion of waste containers and degradation of stabilized waste forms also may release previously unavailable portions of the radionuclide inventory. Vapor- or aqueous-phase diffusion can transport radionuclides toward the surface under these conditions, but other processes may be dominant. Given the abundant, year-round rainfall in the East Tennessee region, the persistent downward flux of water through the cover and underlying waste will continue to limit diffusive transport of radionuclides to the EMDF surface.

Some of the preceding arguments for limitation of vapor-phase release also apply to radon transport to the EMDF cover surface. A quantitative radon release analysis is necessary to demonstrate compliance with the DOE radon flux (or dose) performance objective (Sect. 1.5.1). Appendix H presents model analysis of diffusive transport and release of radon gas from the EMDF cover. The conceptual model of radon release incorporates the differing material layers of the cover system (Fig. 3.4; see also Appendix H, Fig. H.2). The approach does not take credit for the presence of the HDPE membrane in the cover. The method for radon flux estimation is derived from techniques for design of uranium tailings cover systems (U.S. Nuclear Regulatory Commission [NRC] 1984) and is described in detail in Appendix H. The results of the analysis suggest that radon flux at the top of the cover clay barrier is negligible as long as the clay retains a sufficient moisture content.

The limited initial quantities of potentially volatile radionuclides (Table 3.2) and likely mobility of those radionuclides in both the vapor and aqueous-phase during EMDF operations will result in very small amounts available for release as vapor after facility closure. Based on the range of operational, facility design, and environmental considerations limiting vapor-phase transport and release of radionuclides at the cover surface, this release mechanism was eliminated from the EMDF all-pathways dose analysis. To support this release pathway screening, the following section presents the results of a screening model application intended to bound the potential dose associated with the release of C-14 (as CO_2), H-3 (as water vapor), and I-129 at the EMDF cover surface.

3.2.2.3 Quantitative Cover Release Screening Model

Based on the limited inventory of potentially volatile radionuclides, the humid climate in East Tennessee, and EMDF design features that will mitigate vapor-phase diffusion, the potential dose contribution associated with release through the cover is unlikely to exceed the 10 mrem/year performance objective for the air pathway (DOE 2011a). To support the decision to eliminate cover release mechanisms from further consideration in the PA, the RESRAD-OFFSITE code was used to develop screening scenarios to bound the potential dose resulting from radionuclide release at the cover surface.

Release of volatile phases of H-3, C-14, and radon are simulated in the RESRAD-OFFSITE code with nuclide-specific submodels (Yu et al. 2001, Appendices C and L). The RESRAD-OFFSITE code also incorporates a surface mixing model that represents processes (e.g., plowing) acting to transport radionuclides from the waste zone into the overlying cover material (Yu et al. 2007). The cover is represented as a homogeneous layer above the waste that has time-varying thickness (due to erosion) and radionuclide concentrations (due to surface mixing processes). For these submodels of vapor release and upward mixing from the waste into the cover, the thickness of the cover relative to other fixed or user-specified quantities (e.g., soil mixing depth) controls the predicted radionuclide concentration in soil and air at the cover surface.

For the cover release screening model implementation, the cover thickness was assumed to be 6 ft or less, representing an extreme degraded condition in which the upper 5 ft of material (or more) has been eroded. In addition to the severely eroded cover assumption, additional pessimistic assumptions are incorporated into the screening analysis, including higher than estimated average radionuclide concentrations in the waste (waste stream maxima without adjustment for operational period loss or addition of clean fill), and assignment of zero leach rates for all radionuclides, eliminating loss to the environment below the EMDF. The exposure scenario is a human receptor that spends 50 percent of the time (e.g., 12 out of every 24 hours) on the EMDF cover. No other release mechanisms or exposure paths are included, so the modeled dose represents only inhalation of radionuclides released to the cover surface. Appendix G, Sect. G.4.4.2, provides additional detail on implementation of the RESRAD-OFFSITE code for screening of release through the EMDF cover.

Tritium and Carbon-14

For the H-3 and C-14 RESRAD-OFFSITE conceptual models, the radionuclides are released from the cover surface as water vapor and CO_2, respectively. The release of tritiated water vapor is driven by the estimated rate of evapotranspiration and occurs only when the cover thickness is less than 30 cm, whereas the evasion of CO_2 from the cover takes place over a user-specified C-14 evasion thickness. For the cover release screening model, the C-14 evasion thickness is set at 2.0 m, with the result that CO_2 loss to the surface occurs from the upper 0.18 m of the waste (cover thickness minus evasion thickness = 2.0 m – 1.82 m = 0.18 m). Loss of C-14 from the evasion thickness is based on a proportional evasion rate (22 $year^{-1}$); that is the highest value among the field-based measurements cited in the RESRAD-OFFSITE documentation (Yu et al. 2001, Table L.2). To provide a bounding estimate of the potential H-3 dose due to water vapor release from the cover, an extreme sensitivity case was evaluated in which the RESRAD-OFFSITE cover thickness value was reduced to approximately 0.27 m, which represents evaporative loss of tritiated water from the upper 0.03 m of the waste.

The results of the cover release screening model (Table 3.2) indicate that loss of C-14 as CO_2 from the upper 0.18 m of the waste would occur rapidly, based on the underlying assumptions of the conceptual model. The predicted C-14 dose decreases rapidly from an initial value of 0.044 mrem/year to zero dose by 25 years after closure. The rapid release of C-14 from the upper part of the waste is not representative of what is expected, even in the case of a severely eroded cover system, but the associated maximum C-14 dose

is useful as a bounding estimate for screening vapor phase release through the cover. Sensitivity analysis assuming a C-14 evasion thickness of 2.18 m, representing CO_2 loss from the uppermost 0.36 m of the waste, results in approximately twice the dose at time zero, but the value is still less than 0.1 mrem/year.

The magnitude of cover erosion represented by the sensitivity case evaluated for H-3 dose is totally unrealistic, but the result provides an appropriate bounding estimate for release pathway screening. The maximum H-3 dose is 0.023 mrem/year and occurs at time zero. During the institutional control period (100 years post-closure) the potential dose to a member of the public due to release of H-3 through the EMDF cover will never approach this bounding value. The short half-life of H-3 ensures that by the end of the 100 year institutional control period, the dose to a member of the public will be insignificant.

Iodine -129

Volatilization of iodine from soil depends on several factors including pH, total iodine concentration, and the presence of organic matter and iron oxides in the soil. Even if conditions in the EMDF waste favored production of iodine gas and diffusive transport toward the surface, the soil at the cover surface will likely be high in organic matter and at circumneutral pH, which would not favor vapor-phase release of iodine for inhalation or external exposure. Similarly, vegetation on the cover surface will limit wind-driven suspension of I-129 in particulate form.

To account for the potential vapor phase loss of I-129 that is not captured by the RESRAD-OFFSITE code, the surface mixing model was employed by setting the soil mixing depth to the maximum allowable value (1 m) and evaluating a scenario where the cover thickness is reduced to 0.97 m. In this case the soil mixing model represents uniform mixing of the upper 0.03 m of waste with the overlying cover material, which results in a cover radionuclide concentration equal to approximately 5 percent of the underlying waste concentration. This level of cover surface contamination, as an average over the whole EMDF cover surface, represents an extreme condition of cover degradation that would allow upward diffusive or biologically driven transport of all radionuclides to the surface. Exposure to surface contamination in the screening model reflects inhalation of airborne particulates suspended from the cover surface. The RESRAD-OFFSITE default value for the concentration of contaminated airborne particulates (based on a mass loading model representative of agricultural settings) is considered to be conservative (i.e., higher than expected) (Yu et al. 2001, Appendix B page B-6), so the default value (1E-04 g/m^3) is used in the screening model.

The scenario in which the cover thickness is reduced to 0.97 m (0.03 m less than the soil mixing depth) results in a constant I-129 dose of 4.8E-06 mrem/year. The invariance of the I-129 dose reflects the nature of the RESRAD-OFFSITE soil mixing model which predicts a nearly constant surface soil concentration due to the very long half-life of I-129 and the specification of zero leach rates.

The maximum annual doses for H-3, C-14, and I-129 estimated with the cover release screening model are given in Table 3.2. These doses are considered bounding as potential cover release pathway contributions to a total inhalation dose or total all-pathways dose for the resident farmer scenario, or for the total atmospheric (air) pathway dose for a receptor at 100 m from the edge of waste. The set of unrealistically pessimistic assumptions underlying the cover release screening model, including severe cover erosion, higher than estimated (base case) radionuclide inventories, and an extreme exposure scenario ensure that the predicted dose contributions, are bounding and represent unrealistically high exposures.

3.2.2.4 Aqueous-phase release and vadose transport

The conceptual model of radionuclide release and transport within the vadose zone is based on EMDF design geometry and a simplified representation of the waste as uniform and soil-like in terms of its

hydraulic and chemical retardation properties. Infiltration through the cover is assumed to occur uniformly over the area above the waste and liner system and to follow the generalized model of EMDF performance evolution over time (Fig. 3.5). Flow and radionuclide transport are assumed to be vertically downward through the waste zone, with horizontal flow components arising along the sloping surfaces of the basal liner system. The sloping geometry of EMDF liner system, heterogeneity in activity concentrations, and the possibility of spatially variable failure (leakage) of the cover and liner systems over time could cause non-uniform radionuclide release from the waste to the underlying vadose zone. The saturated zone radionuclide transport model (Sect. 3.3.3.2) is used to evaluate the difference between a uniform release conceptual model and a simplified non-uniform release conceptualization. The total system model analysis (Sect. 3.3.4) assumes homogeneous waste properties and uniform release to the vadose and saturated zones.

Radionuclide release and transport are conceptualized in terms of linear, equilibrium solid-aqueous phase partitioning via surface complexation and other sorption processes within the waste, liner, and underlying vadose zone. Equilibrium (de)sorption is assumed to govern release from the solid phase. Potential solubility limits are not incorporated into the source release representation. Flow and transport through the waste, clay barriers, and geologic buffer materials is primarily downward though vadose material zones (Fig. 3.4) that differ in moisture retention and permeability characteristics. Assumed hydraulic and physical parameters for the waste and liner system materials are presented in Sect. 3.3.2. The conceptual model of waste characteristics and the approach to calculating EMDF average activity concentrations, which accounts for the addition of clean fill and operational period losses, are described in Sect. 3.2.2.5. The basis for assumed K_d values for various hydrologic and material zones are described in Sects. 3.2.2.6, 3.2.2.7, and 3.2.2.8. Section 3.2.2.9 provides a summary of radionuclide release and vadose zone conceptual model assumptions.

3.2.2.5 Waste characteristics and modeled radionuclide concentrations

EMDF waste forms will include contaminated soil, sediment and other soil-like waste, and contaminated demolition debris, including equipment. The majority of debris generated from facility demolition activities will be concrete and masonry (walls, floors, ceilings, and building structure), steel (building structural members, piping, ductwork, and some equipment), and contaminated process equipment (gloveboxes, machining equipment, pumps, and other). Ventilation ducting, process equipment and piping, and hot-cell debris (internal surfaces, manipulators, and equipment) are expected to compose a smaller volume of more highly contaminated debris that may require decontamination or stabilization prior to waste acceptance and disposal at EMDF. Radionuclide contamination will include fixed surface contamination as well as contamination distributed within the matrix of more porous materials such as concrete and masonry. Activated metals from demolition of some facilities may be present, but the proportion of radionuclides in activated metal form is likely to be small. Waste that does not meet EMDF WAC (e.g., maximum allowable activity concentrations) will be disposed at one or more offsite disposal facilities.

The majority of EMDF waste is expected to be disposed in bulk (uncontainerized) form and transported by dump trucks to the landfill. Other volumes of waste, including mercury-contaminated debris or soil that requires treatment to meet CERCLA ARARs, may be grouted in containers or otherwise treated or stabilized prior to disposal, but no explicit assumptions regarding physical or chemical waste forms for specific waste streams are incorporated in this analysis. Additional information on particular ONRL and Y-12 waste stream characteristics are provided in Appendix B.

Due to uncertainty in the sequencing of future cleanup efforts and placement of waste streams within EMDF, the preliminary state of waste characterization (i.e., uncertainty in the physical and chemical characteristics of future EMDF LLW), and practical limitations in representing waste heterogeneity in some model codes, simplifying assumptions are adopted for representing the waste. The EMDF waste mass is conceptualized as a homogeneous, soil-like material in which the radionuclide inventory (Sect. 2.3 and

Appendix B) is uniformly distributed. Waste placement practices consistent with current EMWMF operations are assumed for future EMDF waste, including compaction of waste using heavy equipment and the use of clean fill material (generally clay-rich soil) to fill voids in bulk debris waste. Although soil and soil-like wastes comprise only approximately 30 percent of the estimated EMDF waste inventory, the volume of uncompacted clean soil added during placement of bulk debris is larger than the debris volume (DOE 2004). The requirement for additional clean fill material is the basis for adjusting estimated EMDF average waste activity concentrations (Table 2.15) to derive the source concentrations (average as-disposed EMDF waste concentrations, Table 3.3) used in the PA models. Figure 2.42 provides a schematic overview of the process.

Activity concentration adjustment to account for clean fill

The adjustment to estimated waste activity concentrations to account for the mass of clean fill is derived by taking the estimated total EMDF waste mass (refer to Fig. 2.42) and dividing that quantity by the combined mass of waste and clean fill:

$$\text{Source concentration/estimated waste concentration} = \text{waste mass} / (\text{waste mass} + \text{clean fill mass})$$

$$= 1 - [\text{clean fill mass} / (\text{waste mass} + \text{clean fill mass})]$$

The mass of clean fill required for disposal is based on the clean soil requirements algorithm described in DOE 2004. For purposes of estimating the average source concentrations for EMDF PA modeling, it is assumed that all the contaminated waste soil is used as fill, so the amount of clean fill required is minimized. The required clean fill volume is calculated as:

$$\text{Total fill required} = 2.26 \times \text{debris volume (as-disposed)}$$

$$\text{Clean fill required} = \text{total fill required} - \text{waste soil volume (as-disposed)}$$

Based on the total volumes of debris and soil waste types (Appendix B, Table B.1), the total as-disposed volume of clean fill required is 832,488 cy. The mass of added clean fill is calculated based on the EMWMF average as-disposed soil bulk density (DOE 2004), which is a factor of 1.3 higher than the average asgenerated bulk density assumed for soil (1113 kg/cy, refer to Sect. 2.3.1). The total clean fill mass is estimated as:

$$832{,}488 \text{ cy} \times 1113 \text{ kg/cy} \times 1.3 = 1.21\text{E+}09 \text{ kg}$$

The total waste mass is calculated based on the assumed average as-generated bulk densities for debris and soil as described in Sect. 2.3.1. Based on the estimated total waste mass of 1.37E+09 kg (Fig. 2.42 and Appendix B, Sect. B.4), the adjusted waste activity concentrations (source concentrations) are calculated as:

$$\text{Source concentration (pCi/g)} = \text{waste concentration (pCi/g)} \times 1.37\text{E+}09 \text{ kg} / (1.37\text{E+}09 \text{ kg} + 1.21\text{E+}09 \text{ kg})$$

$$= \text{waste concentration (pCi/g)} \times 0.531$$

$$= \text{waste concentration (pCi/g)} / 1.88$$

This derivation of the source concentrations is based on EMDF total waste volume estimates that do not include the added 25 percent volume estimate uncertainty that was assumed for calculating the total disposal

capacity requirement (design capacity) for the EMDF (refer to Sect. 2.3). The +25 percent waste volume uncertainty factor is incorporated into the PA analysis by applying the calculated source concentrations (accounting for clean fill mass) to the total mass of waste and clean fill that corresponds to the EMDF design disposal capacity of 2.2 million cy. The total mass of material emplaced in the EMDF is based on an estimated average as-disposed bulk density (approximately 1480 kg/cy) that incorporates the clean fill and compaction factors (ratios of as-disposed to as-generated volumes for debris and soil). The same clean fill assumptions were used to derive both the capacity requirement and the adjusted activity concentrations.

Activity concentration adjustment to account for operational period losses

In addition to the activity concentration adjustment for clean fill, the estimated post-closure inventories of radionuclides that are highly mobile in the aqueous phase, including H-3, C-14, Tc-99, and I-129, are adjusted (reduced) based on modeling of operational period leaching. Taking credit for operational period losses is conceptually consistent with the equilibrium desorption model for radionuclide release adopted for the PA models (Sect. 3.2.2.4). The modeling approach to estimating operational period inventory reduction for mobile radionuclides is presented in Sect. G.4.3.4 of Appendix G. Removal of mobile radionuclides by the leachate collection system is assumed to effectively reduce the total inventories (and average concentrations) of H-3, C-14, Tc-99, and I-129. This is justified even for leachate treatment residuals that could be returned to the EMDF for disposal because such wastes (e.g., isotope exchange resins) would, by design, retain the target radionuclides resulting in much lower release rates than assumed for a generic waste form. The adjusted average activity concentrations for H-3, C-14, Tc-99, and I-129 are referred to as post-operational concentrations.

The activity losses due to leaching during the 25-year operational period were quantified using four RESRAD-OFFSITE models, one for each disposal cell. The four cells are assumed to be filled sequentially, with the filling duration (simulation period as a fraction of 25 years) for each cell proportional to the corresponding fraction of the total EMDF volume capacity. For each cell, leaching losses were estimated from the onset of filling until the following cell is filled to capacity, at which time enhanced operational cover is applied and leaching ceases. Estimates of the volume of leachate collected by the liner system and of contact water that moves through waste but exits as surface runoff were based on EMDF preliminary design analyses (for leachate) and EMWMF operational records (for contact water).

Activity losses estimated for each disposal cell were added to obtain the total loss during the operational period. The proportional inventory losses for the four radionuclides simulated were used to adjust the (as-disposed) source concentrations to obtain the post-operational concentrations. Estimated waste inventory values, as-generated waste average concentrations, as-disposed waste average concentrations, and post-operational waste average concentrations for the 42 radionuclides simulated in the base case model are provided in Table 3.3. For all radionuclides other than H-3, C-14, Tc-99, and I-129 the post-operational average activity concentrations are the same as the as-disposed concentrations.

Table 3.3. Waste activity concentrations used for the EMDF PA models

Isotope	Half-life (year)	Estimated waste inventory (Ci)	EMDF as-generated waste average concentration (pCi/g)	EMDF as-disposed waste average concentration (pCi/g)	EMDF post-operational waste average concentration (pCi/g)
Ac-227	2.18E+01	7.54E-03	5.50E-03	2.92E-03	2.92E-03
Am-241	4.32E+02	1.52E+02	1.11E+02	5.90E+01	5.90E+01
Am-243	7.38E+03	7.65E+00	5.59E+00	2.97E+00	2.97E+00
Be-10	1.50E+06	6.52E-05[a]	4.76E-05[a]	2.53E-05	2.53E-05

Table 3.3. Waste activity concentrations used for the EMDF PA models (cont.)

Isotope	Half-life (year)	Estimated waste inventory (Ci)	EMDF as-generated waste average concentration (pCi/g)	EMDF as-disposed waste average concentration (pCi/g)	EMDF post-operational waste average concentration (pCi/g)
C-14	5.73E+03	7.43E+00	5.43E+00	2.88E+00	5.40E-01[b]
Ca-41	1.00E+05	1.09E-01[a]	7.92E-02[a]	4.21E-02	4.21E-02
Cm-243	2.85E+01	1.11E+00	8.10E-01	4.30E-01	4.30E-01
Cm-244	1.81E+01	3.26E+02	2.38E+02	1.26E+02	1.26E+02
Cm-245	8.50E+03	9.87E-02	7.21E-02	3.83E-02	3.83E-02
Cm-246	4.73E+03	4.10E-01	2.99E-01	1.59E-01	1.59E-01
Cm-247	1.56E+07	2.68E-02	1.96E-02	1.04E-02	1.04E-02
Cm-248	3.39E+05	1.44E-03	1.05E-03	5.59E-04	5.59E-04
H-3	1.24E+01	2.88E+01	2.10E+01	1.12E+01	4.64E+00[b]
I-129	1.57E+07	1.05E+00	7.66E-01	4.07E-01	3.50E-01[b]
K-40	1.28E+09	8.46E+00	6.18E+00	3.28E+00	3.28E+00
Mo-93	3.50E+03	1.00E+00[a]	7.30E-01[a]	3.88E-01	3.88E-01
Nb-93m	1.36E+01	6.01E-01[a]	4.39E-01[a]	2.33E-01	2.33E-01
Nb-94	2.03E+04	4.20E-02	3.07E-02	1.63E-02	1.63E-02
Ni-59	7.50E+04	7.84E+00	5.73E+00	3.04E+00	3.04E+00
Np-237	2.14E+06	8.37E-01	6.12E-01	3.25E-01	3.25E-01
Pa-231	3.28E+04	6.15E-01	4.49E-01	2.39E-01	2.39E-01
Pb-210	2.23E+01	9.50E+00	6.93E+00	3.68E+00	3.68E+00
Pu-238	8.77E+01	2.42E+02	1.77E+02	9.38E+01	9.38E+01
Pu-239	2.41E+04	1.50E+02	1.10E+02	5.83E+01	5.83E+01
Pu-240	6.54E+03	1.60E+02	1.17E+02	6.20E+01	6.20E+01
Pu-241	1.44E+01	5.25E+02	3.83E+02	2.04E+02	2.04E+02
Pu-242	3.76E+05	4.45E-01	3.25E-01	1.73E-01	1.73E-01
Pu-244	8.26E+07	9.49E-03	6.93E-03	3.68E-03	3.68E-03
Ra-226	1.60E+03	2.07E+00	1.51E+00	8.01E-01	8.01E-01
Ra-228	5.75E+00	5.69E-02	4.15E-02	2.21E-02	2.21E-02
Sr-90	2.91E+01	4.96E+02	3.62E+02	1.92E+02	1.92E+02
Tc-99	2.13E+05	7.23E+00	5.28E+00	2.80E+00	1.56E+00[b]
Th-228	1.90E+00	5.45E-06	3.98E-06	2.11E-06	2.11E-06
Th-229	7.34E+03	1.47E+01	1.08E+01	5.71E+00	5.71E+00
Th-230	7.70E+04	4.94E+00	3.61E+00	1.92E+00	1.92E+00
Th-232	1.41E+10	9.07E+00	6.62E+00	3.52E+00	3.52E+00
U-232	7.20E+01	2.63E+01	1.92E+01	1.02E+01	1.02E+01
U-233	1.59E+05	1.07E+02	7.83E+01	4.16E+01	4.16E+01
U-234	2.45E+05	1.62E+03	1.19E+03	6.30E+02	6.30E+02
U-235	7.04E+08	1.02E+02	7.47E+01	3.97E+01	3.97E+01
U-236	2.34E+07	2.32E+01	1.69E+01	8.98E+00	8.98E+00
U-238	4.47E+09	9.83E+02	7.18E+02	3.81E+02	3.81E+02

[a]Data limited radionuclide with non-standard basis of estimate, refer to Appendix B.
[b]Post-operational waste concentration adjusted for operational period activity loss.

EMDF = Environmental Management Disposal Facility
PA = Performance Assessment

3.2.2.6 Assumed partition coefficient (K_d) values

Solid-aqueous partition coefficients are key parameters that represent sorption and chemical retardation phenomena in the conceptual models of radionuclide release and transport. For modeling source release and chemical retardation of radionuclide transport, equilibrium, linear isotherm sorption is assumed and a single parameter, K_d, defines the partition between radionuclide concentrations in the aqueous phase and the concentration of the sorbed phase within the porous matrix. The validity of the equilibrium sorption assumption depends on a variety of material, geochemical and hydrodynamic factors that can vary in space and time in the subsurface (Valocchi 1985). Although laboratory determinations of K_d values for some radionuclides using samples of clay-rich soils, saprolite, and rock cores collected in the Maryville Formation and the Nolichucky Formation are available in several reports (refer to Sect. 2.1.6.3 and Table 2.12), the assignment of representative K_d values to represent sorption processes integrated over long time periods is an important uncertainty in the EMDF performance analysis. The following paragraphs outline the general approach to selecting K_d values and ranges of values for the EMDF disposal system analysis, including the waste, saprolite, and bedrock zone materials.

For the EMDF PA, a graded approach to selection of K_d values was adopted in which use of the available laboratory data for Conasauga Group materials was combined with information from previous modeling in related, comparable assessments along with other published reports and compilations of K_d data for materials similar to those of the EMDF system. Different radionuclides of a given element are assumed to have the same K_d value because sorption is a chemical phenomenon that is primarily dependent on oxidation state rather than isotopic mass. For elements that had been evaluated in sorption studies using local materials, those data sources were verified by experts and given precedence, followed by comparable ORR performance modeling K_d value assumptions. Specific experimental conditions (e.g., ionic strength, pH) in each local study were also considered in the selection of K_d value for these elements, and data from other sources were used as supporting information. On this basis, base case K_d values for the clay rich saprolitic and bedrock materials were assigned. Section 3.2.2.8 provides additional detail on the rationale for assigning K_d values to different engineered and natural materials. The waste materials will include debris, equipment, soil waste, and clean fill (Sect. 3.2.2.5). The clean fill accounts for almost half of the estimated mass in the disposal facility. Clean fill will be sourced from saprolite zone material in local borrow areas, and soil remediation waste will have similar characteristics. Given that approximately one-half of the waste mass is thus similar to saprolite zone material, the K_d values in the waste zone are assumed for the base case to be one-half the K_d values assumed for the saprolite and bedrock zone materials.

Table 3.4 summarizes the assumed base case K_d values and provides the primary and supporting references used as the basis for each value, including the material type associated with the K_d value in the primary reference. In general, for elements without data derived from local laboratory studies, values were adopted from existing performance analyses of SWSA 6 (ORNL 1997a) and the EMWMF (DOE 1998a, BJC 2010a), with a material type listed as generic soil in Table 3.4. Generic references (e.g., Sheppard and Thibault 1990) were used as primary references for those elements that were not included in the previous ORR performance analyses.

Table 3.4. Solid-aqueous K_d values assumed for the EMDF PA analyses

Element	K_d, EMDF base case model (cm^3/g)		K_d, EMDF screening model (cm^3/g)	Primary reference	Material/soil texture in primary reference associated with base case value	Supporting references
	Waste zone	Saprolite and Bedrock zones				
Ac	20	40	2	ORNL 1997a (Table 2.3, p.2-18)	Generic soil	
Am	2000	4100[a]	20[b]	Rothschild et al. 1984b (Table 6, p. 38), Davis et al. 1984 (Table 7, p.40)	Silty clay (Maryville Formation)	Sheppard and Thibault 1990
Ba	28	55	3	DOE 1998a (Appendix E, p. E 71-73)	Generic soil	Baes et al. 1984
Be	400	800	40	DOE 1998a (Appendix E, p. E 71-73)	Generic soil	Sheppard and Thibault 1990
C	0	0	0	ORNL 1997a (Table 2.3, p.2-18)	Generic soil	
Ca	15	30	2	ORNL 1997a (Table 2.3, p.2-18)	Generic soil	Sheppard and Thibault 1990
Cd	100	200	10	ORNL 1997a (Table 2.3, p.2-18)	Generic soil	
Cf	20	40	2	ORNL 1997a (Table 2.3, p.2-18)	Generic soil	
Cl	N/A[c]	N/A[c]	0	ORNL 1997a (Table 2.3, p.2-18)	Generic soil	
Cm	20	40	2	ORNL 1997a (Table 2.3, p.2-18)	Generic soil	
Co	400	800	40	ORNL 1997a (Table 2.3, p.2-18)	Generic soil	Rothschild et al. 1984
Cs	1500	3000	150	Friedman et al. 1990 (Table 3.1, p.7)	Silty clay (Maryville Formation)	Davis et al. 1984
Eu	20	40	2	ORNL 1997a (Table 2.3, p.2-18)	Generic soil	Friedman et al. 1990
Fe	450	890	45	Yu et al. 2015 (Table 2.13.2, p. 67)	Loam	Davis et al. 1984
Gd	410	820	40	Yu et al. 2007 (Appendix B, Attachment A Table 2-4, p. AttA-60)	N/A	
H	0	0	0	ORNL 1997a (Table 2.3, p.2-18)	Generic soil	DOE 1998a, IAEA 2010
I	2	4	0.2	Davis et al. 1984 (Figure 14)	Silty clay (Maryville Formation)	Rothschild et al. 1984
K	15	30	2	ORNL 1997a (Table 2.3, p.2-18)	Generic soil	DOE 1998a
Mo	45	90	5	Sheppard and Thibault 1990	Clay	
Na	5	10	1	Yu et al. 2007 (Appendix B, Attachment A Table 2-4, p. AttA-60)	N/A	IAEA 2010
Nb	50	100	5	ORNL 1997a (Table 2.3, p.2-18)	Generic soil	DOE 1998a
Ni	1000	2000	100	ORNL 1997a (Table 2.3, p.2-18)	Generic soil	DOE 1998a

Table 3.4. Solid-aqueous K_d values assumed for the EMDF PA analyses (cont.)

Element	K_d, EMDF base case model (cm^3/g)		K_d, EMDF screening model (cm^3/g)	Primary reference	Material/soil texture in primary reference associated with base case value	Supporting references
	Waste zone	Saprolite and Bedrock zones				
Np	20	40	2	ORNL 1997a (Table 2.3, p.2-18)	Generic soil	ORNL 1987
Pa	200	400	20	ORNL 1997a (Table 2.3, p.2-18)	Generic soil	DOE 1998a
Pb	50	100	5	ORNL 1997a (Table 2.3, p.2-18)	Generic soil	
Pd	1000	2000	100	ORNL 1997a (Table 2.3, p.2-18)	Generic soil	
Pm	410	820	40	Yu et al. 2007 (Appendix B, Attachment A Table 2-4, p. AttA-60)	NA	IAEA 2010
Pu	20	40	2	ORNL 1997a (Table 2.3, p.2-18)	Generic soil	Gil-Garcia et al. 2008
Ra	1500	3000	150	ORNL 1997a (Table 2.3, p.2-18)	Generic soil	DOE 1998a
Re	20	40	2	Sheppard and Thibault 1990	Loam	
Sb	75	150	8	Sheppard and Thibault 1990	Loam	
Se	250	500	25	Sheppard and Thibault 1990	Loam	
Sm	500	1000	50	ORNL 1997a (Table 2.3, p.2-18)	Generic soil	
Sn	50	100	5	ORNL 1997a (Table 2.3, p.2-18)	Generic soil	Sheppard and Thibault 1990
Sr	15	30	2	Friedman et al. 1990 (Table 4.1, p.21)	Generic soil	ORNL 1997a, DOE 1998a
Tc	0.36	0.72	0.04	DOE 1992b (Appendix A, Table A.4.1.8, p. 86)	Silty clay	ORNL 1987
Th	1500	3000	150	ORNL 1997a (Table 2.3, p.2-18)	Generic soil	Sheppard and Thibault 1990
U	25	50	3	Friedman et al. 1990 (Table 3.8, p.12)	Clay	ORNL 1987, ORNL 1997a, CH2M-Hill 2000
Zr	25	50	3	ORNL 1997a (Table 2.3, p.2-18)	Generic soil	Sheppard and Thibault 1990

Table 3.4. Solid-aqueous K_d values assumed for the EMDF PA analyses (cont.)

[a] Weighted average of 14 samples from Rothschild et al. 1984 (Table 6, samples #4 and 16-18 omitted as non-representative), and 24 samples from Davis et al. 1984 (Table 7)
[b] Screening model K_d value decrease by a factor of 100 from base case value based on range of data in primary and supporting references.
[c] Chlorine (Cl-36) is not included in the EMDF estimated radionuclide inventory. Cl-36 is included in the EMDF radionuclide screening model

DOE = U.S. Department of Energy
EMDF = Environmental Management Disposal Facility
EPA = U.S. Environmental Protection Agency
IAEA = International Atomic Energy Agency
N/A = not applicable
ORNL = Oak Ridge National Laboratory
PA = Performance Assessment
RESRAD = RESidual RADioactivity
SWSA = Solid Waste Storage Area

For uranium and transuranic elements, site-specific laboratory K_d measurements are used for uranium and americium, but the values for plutonium, neptunium, curium, and californium are taken from the SWSA 6 PA, which applied a value of 40 cm^3/g to uranium and all transuranics in the saturated zone (ORNL 1997a). Although the K_d of uranium species can vary over a very wide range depending on the geochemistry of the system, the uranium base case value of 50 cm^3/g is likely to be lower and of the expected range for Conasauga Group materials. Uranium sorption experiments on local clay rich soils were performed during the design phase for the EMWMF (WMFS 2000) and the results indicated that the sorptive capacity of those materials was very high, implying $K_d > 1000$ cm^3/g. Similarly, the uranium K_d sources and data compiled by EPA (EPA 1999, page 5.75) suggests that for pH in the 6 to 7 range, minimum uranium K_d values are > 50 cm^3/g. This evidence supports the adoption of uranium $K_d = 50$ cm^3/g as a pessimistic assumption for the PA modeling.

Data from supporting references were used to assess possible ranges of values for similar material types and to support selection of K_d values used for the radionuclide screening model (refer to Sect. 2.3.2 and Appendix G for description of the model used for radionuclide screening). Following an initial selection of K_d values generally chosen to be representative for medium to fine textured soils, the waste zone values were decreased by a factor of 10 or 100 to provide a pessimistic (lower than likely) assumed value for use in the screening model (Table 3.4). The K_d values were reduced by a factor of 100 in cases where a factor of 10 reduction was judged insufficiently pessimistic for use in the screening model, on the basis of the ranges of values reported in the primary and/or supporting references. Application of the screening process reduced the number of radionuclides carried forward in the all-pathways scenario from 70 to 42, representing 21 different elements. Preliminary dose modeling results (refer to Sects. 3.3.4 and 3.4) identified key radionuclides for EMDF performance (including C-14, Tc-99, and I-129) for which uncertainty in the assumed K_d value could significantly impact the magnitude or timing of the peak all-pathways dose, and additional scrutiny of the available data for these highly mobile radionuclides provided a basis for the assumed K_d values for the base case all-pathways dose analysis. Details are provided in Sect. 3.2.2.7.

3.2.2.7 Partition coefficients for I-129 and Tc-99

As two of the key radionuclides in terms of dose, I-129 and Tc-99 K_d values as determined in previous ORR studies were reviewed in detail. These studies and conclusions supporting the K_d values adopted for the PA are summarized below.

Iodine-129 partition coefficient (K_d)

Partitioning of iodine in a soil/water matrix is dependent on the iodine speciation as well as the soil and water properties. Organic content of the soil is a key soil parameter influencing iodine sorption (EPA 2004, Serne 2007, Kaplan et al. 2000). Iodine can form very strong (covalent) bonds with soil organic matter (OM) and slight increases in OM, even at trace concentrations (0.1 to 0.4 wt percent), can result in corresponding increases in iodine K_d values (Xu et al. 2015, Kaplan et al. 2014). Soil and saprolite OM concentrations are generally quite high for ORR soils. Rothschild et al. (1984) reported an average of 3.31 wt percent OM in 15 soils collected from SWSA 7 in Melton Valley, where Conasauga soils are dominant. Davis et al. (1984) reported value values of 0.37 wt percent organic matter from 3 cores and 24 samples, also from Conasauga soils in Melton Valley.

Iodine sorption by geological materials is influenced by pH and iron- and manganese-oxide content. As a general rule, lower pH and greater iron- and manganese-oxide contents result in greater iodine sorption (EPA 2004). At low pH values, mineral surfaces become protonated and have a net positive charge, whereas at higher pH values, the surfaces become deprotonated and have a net negative charge. The surface charge of iron- and manganese-oxides is comprised almost entirely of this pH-dependent charge, which promotes

greater anion exchange capacity at lower pH levels. The iron- and manganese-oxide contents in Conasauga soils, saprolite, and shale bedrock are considered high; for example, Rothschild et al. (1984) reported soil manganese concentrations of 412 ± 322 mg/kg and soil iron concentrations of 139 ± 69 mg/kg. Following the conceptual geochemical model put forth by Watson et al. (2004) for the Oak Ridge Field Research Center located in Bear Creek, the pH in the soil/saprolite above the water table is likely to be acidic, pH 4.5 to 6, while the pH in the saturated zone will be near neutral, 7 to 8. If similar pH conditions occur in the unsaturated materials below the EMDF clay liner, the vadose interval may be especially well suited for binding iodine.

Mineralogy can also play an important role in binding iodine (Kaplan et al. 2014, Kaplan et al. 2000). In an evaluation of various minerals, illite, a common mineral at the ORR and within the Conasauga soil profiles, had the greatest iodine K_d value, 15.14 cm^3/g (Kaplan et al. 2000), of the wide suite of investigated minerals. Mineralogical characterization of soils (Davis et al. 1984, page 58, Table 17) and bedrock (Davis et al. 1984, page 22, Table 3) of the Maryville Formation indicates illite to be the predominant clay mineral. Rothschild et al. (1984b, pages 53-60) also found illite to be abundant in the clay size fraction of Conasauga group soils at ORNL. Similarly, mineralogical analysis of the Nolichucky formation (ORNL 1987, page 4, Table 3.1) identified illite to be the most abundant of all minerals including quartz and feldspars. Significant iodine sorption to illite over a very wide range of pH values has been demonstrated (Kaplan et al. 2000, Table 5), reproduced below as Fig. 3.6), with K_d values > 20 cm^3/g at pH > 9.0. Laboratory K_d measurements on samples of cuttings from a 35 m deep borehole in the Maryville Formation also show significant iodine sorption (K_d > 7 cm^3/g) at pH > 7.0 for increments deeper than 5 m below the surface (Davis et al. 1984, Sect. 4.1.2.3, Fig. 14 and Table 4, pages 23 to 29), which is consistent with the predominance of illite identified in the Maryville Formation.

Iodide K_d Values on Illite as a Function of pH[a]

pH	electrical conductivity (mS/cm)	K_d (mL/g)
3.6	2.52 ± 0.03	46 ± 3.9
5.0	2.31 ± 0.03	59 ± 2.2
7.9	2.35 ± 0.04	24 ± 1.2
9.4	2.41 ± 0.04	22 ± 0.2

[a] Background electrolyte was 0.01 M $CaCl_2$; pH adjustment with NaOH and HCl, three replicates; pH equilibration period was 5 weeks; $^{125}I^-$ contact time with the pH equilibrated sediments was 1 week.

Source: Kaplan et al. 2000.

Fig. 3.6. Laboratory measurement of iodide sorption on illite

Together the combination of pH (circumneutral to weakly acidic), OM, iron- and manganese-oxide, and mineralogical (presence of illites) conditions that are likely to exist at the EMDF site in BCV would be expected to promote the sorption of iodine. Conversely, conditions known to resist iodine binding are less likely to exist at the site, including sandy texture, low OM (< 0.1 wt percent), low iron- and manganese-oxide content, with high pH groundwater (pH > approximately 8).

Iodine K_d values measured for soils and saprolite of the Maryville Formation were reported by Rothschild et al. (1984) and Davis et al. (1984). The quality of these measurements is high because (1) the experimental conditions correspond reasonably well with those likely to exist at the EMDF; (2) they used ASTM methods; (3) they conducted replicates; (4) important attributes of the solid and aqueous phases were characterized, permitting variation in data to be assessed within a geochemical context (e.g., through regression on principles of radiochemistry and geochemistry); and (5) iodine K_d values were measured on

a large number of samples (15). Rothschild et al. (1984) collected soil samples from the SWSA 7 site and combined them with stream water spiked with I-125. The resulting K_d values and associated geochemical parameters are presented in Table 3.5, where the average iodine K_d value in is 17.1 ± 13.4 cm^3/g and the data had a range of 3.6 to 54.4 cm^3/g for 15 values (excluding results from the "stream sediment" samples because they differ from materials at the EMDF). The equilibrium pH values for these soil samples taken from the upper 2 to 3 m of the saprolite zone ranged from 4.6 to 6.2, whereas the three samples of stream sediment from the SWSA 7 site resulted in equilibrium pH of 7.2 to 7.3 (Table 3.5, samples 16-18). The K_d values estimated for the three stream sediment samples were relatively high (> 10 cm^3/g), especially given the neutral pH conditions.

Table 3.5. Laboratory iodine K_d values from geological samples collected from SWSA 7

Iodine K_d (cm^3/g)	Description	pH	Organic Matter (%)	Manganese (mg/kg)	Iron (mg/kg)	Comment
9.4	Sample 1	5	3.06	360	118	Soil
4.7	Sample 2	6.2	4.15	715	151	Soil
3.6	Sample 3	6	4.99	1160	250	Soil
54.4	Sample 4	4.7	0.4	170.5	118	Soil
12.3	Sample 5	4.5	2.06	169	120	Soil
19.9	Sample 6	5.4	3.48	390	119	Soil
14.8	Sample 7	4.7	3.43	655	245.5	Soil
11.2	Sample 8	4.9	3.8	645	209	Soil
20.1	Sample 9	4.9	2.01	153.5	78.5	Soil
16.3	Sample 10	4.6	3.4	277.5	88.5	Soil
17	Sample 11	5	2.84	367.5	112.5	Soil
10.9	Sample 12	4.6	4.61	148.5	96.5	Soil
37.7	Sample 13	4.9	3.25	28.5	41	Drainage side slopes
19.5	Sample 14	4.9	4.73	825	257	Drainage side slopes
4.4	Sample 15	4.6	3.48	109.5	83.5	Drainage side slopes
11.1	Sample 16	7.2	0.883	1910	237	Stream sediment
11	Sample 17	7.2	0.847	1575	192	Stream sediment
17	Sample 18	7.3	0.515	4950	317	Stream sediment
17.1	**Ave. #1-#15**	**5.0**	**3.31**	**412**	**139**	**Ave., excluding stream sediments**
13.4	**Stdev #1-#15**	**0.5**	**1.2**	**321.9**	**68.5**	**Stdev., excluding stream sediments**

Data taken from Tables 6 and 7 in Rothschild et al. 1984.

SWSA = Solid Waste Storage Area

Davis et al. (1984) also reported iodine K_d values for soil and saprolite that correspond with those at the EMDF. Again, the data is of high quality for similar reasons as used to describe the data from Rothschild et al. (1984). They collected Conasauga group soils from SWSA 6, and the results were intended to be relevant to the LLW disposal site, shallow land burial. They collected three profiles from three trenches. The results from these iodine K_d values are summarized in Table 3.6. The average iodine K_d value was 11.7 ± 9.0 cm^3/g and had a range of 1 to 21.4 cm^3/g. All but one of the pH values for these samples

were less than 5, and the highest pH was 5.8. The results from Davis et al. (1984) and Rothschild et al. (1984) are consistent in that they report similar average iodine K_d values for Conasauga Group soils recovered from the ORR. Both sources attributed the appreciable iodine attenuation to the low pH conditions and the presence of iron/manganese oxides and natural OM.

Table 3.6. Iodine K_d values of 24 soils collected from three cores recovered from SWSA 6

Iodine K_d (cm^3/g)	Description (core ID/core depth-cm)	pH	Organic matter (wt%)
21.4	334/20	4.3	1.4
18.5	334/40	4	1.4
22.8	334/60	4.2	0.26
2.2	334/100	4.4	0.15
1.1	334/130	4.4	0.14
4.2	334/150	4.3	0.11
10.5	334/180	4.3	0.11
11.3	334/200	4.3	0.11
4.1	338/20	4.4	1.24
11.1	338/40	4.4	0.83
1	338/60	4.3	0.3
18.6	338/100	4.4	0.16
0.3	338/130	4.4	0.11
3.8	338/150	4.6	0.27
2.6	338/180	4.7	0.09
0.1	338/200	5.8	0.11
10.1	342/20	4.4	0.41
14.8	342/40	4.3	0.45
13.8	342/60	4.6	0.21
23	342/100	4.3	0.29
14	342/130	4.2	0.28
31.7	342/150	4.3	0.12
24	342/180	4.3	0.2
16	342/200	4.2	0.07
11.7	**Ave of 24 samples**	**4.4**	**0.37**
9.0	**Stdev of 24 samples**	**0.3**	**0.41**

Data taken from Table 7 in Davis et al. 1984.

ID = identification
SWSA = Solid Waste Storage Area

Importantly, the K_d values most likely to be representative are those based on experimental conditions and materials similar to those at the EMDF. The Davis et al. (1984) and Rothschild et al. (1984b) data are of high quality and used methods that approximate a geochemical environment (low pH, oxidizing) which is within the range observed at the EMWMF. For this reason, it is more reasonable to rely on these site-specific values than to include iodine K_d measurements using off site samples. Most of the available ORR data for iodine sorption reflect low pH (< 6.0) conditions, whereas the likely range of geochemical

environments within the EMDF system (waste, vadose zone, saturated zone) are likely to have higher pH (> 6).

Recent studies of iodine sorption on sediments from the Savannah River Site (SRS) provide a useful point of reference for evaluating the Oak Ridge data because the SRS has similar climate and deeply weathered soils, although the soils have developed from different parent materials at the two sites. Kaplan et al. (2013) evaluated radioiodine geochemistry and sorption on three different SRS sediment types. This study evaluated variation in iodine sorption related to oxidation state (iodide vs iodate) and pH conditions to support SRS performance assessments. The SRS results for the clay soil type (most similar to EMDF soils) under aerobic conditions indicate that K_d values for iodide and iodate decrease toward zero as pH approaches 6.5 (Fig. 3.7). The data for Oak Ridge Conasauga soil and saprolite samples are similar, with the highest measured iodine K_d values associated with pH < 5.0 (Fig. 3.8). Oak Ridge K_d values higher than 20 cm^3/g at pH< 5.0 are similar to SRS data for iodate sorption to clay soil, which may indicate that a portion of iodine in the Oak Ridge studies was present as iodate.

There is limited but significant evidence in the two Oak Ridge studies that iodine sorption can occur at pH > 6.0. (Fig. 3.8). The two SWSA 7 soil samples analyzed by Rothschild et al. (1984) having pH ≥ 6.0 have K_d values > 3 cm^3/g, and the three stream sediment samples analyzed had pH > 7.0 and iodine K_d > 10 cm^3/g. Similarly, the deeper (> 5m) Maryville Formation samples analyzed by Davis et al. (1984) had pH values that range from 7.3 to 8.0 and geometric mean K_d value of 8.4 cm^3/g (range 4.8 to 13.2 cm^3/g). It is possible that these nonzero K_d values at higher pH result in part from the abundance of illite present in the soils, saprolite and bedrock of the Maryville Formation.

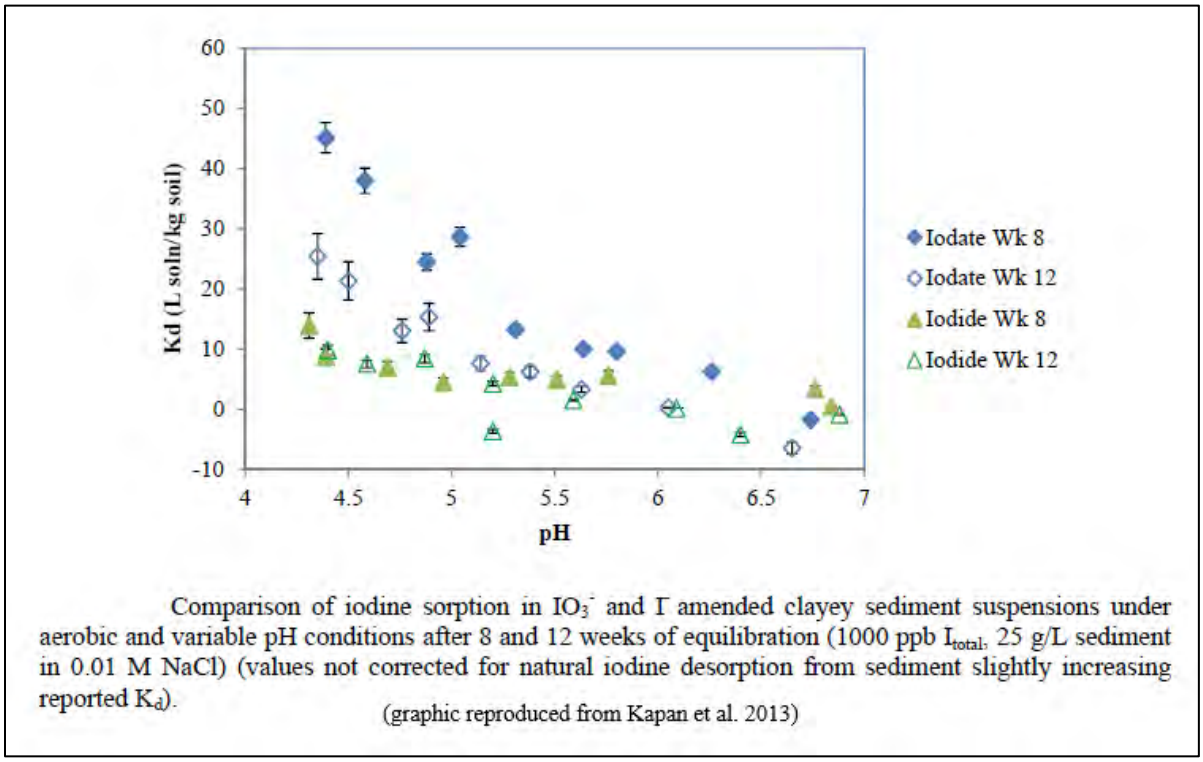

Comparison of iodine sorption in IO_3^- and I^- amended clayey sediment suspensions under aerobic and variable pH conditions after 8 and 12 weeks of equilibration (1000 ppb I_{total}, 25 g/L sediment in 0.01 M NaCl) (values not corrected for natural iodine desorption from sediment slightly increasing reported K_d).

(graphic reproduced from Kapan et al. 2013)

Fig. 3.7. Experimental results for iodine sorption on SRS clay sediments showing effects of pH and oxidation state

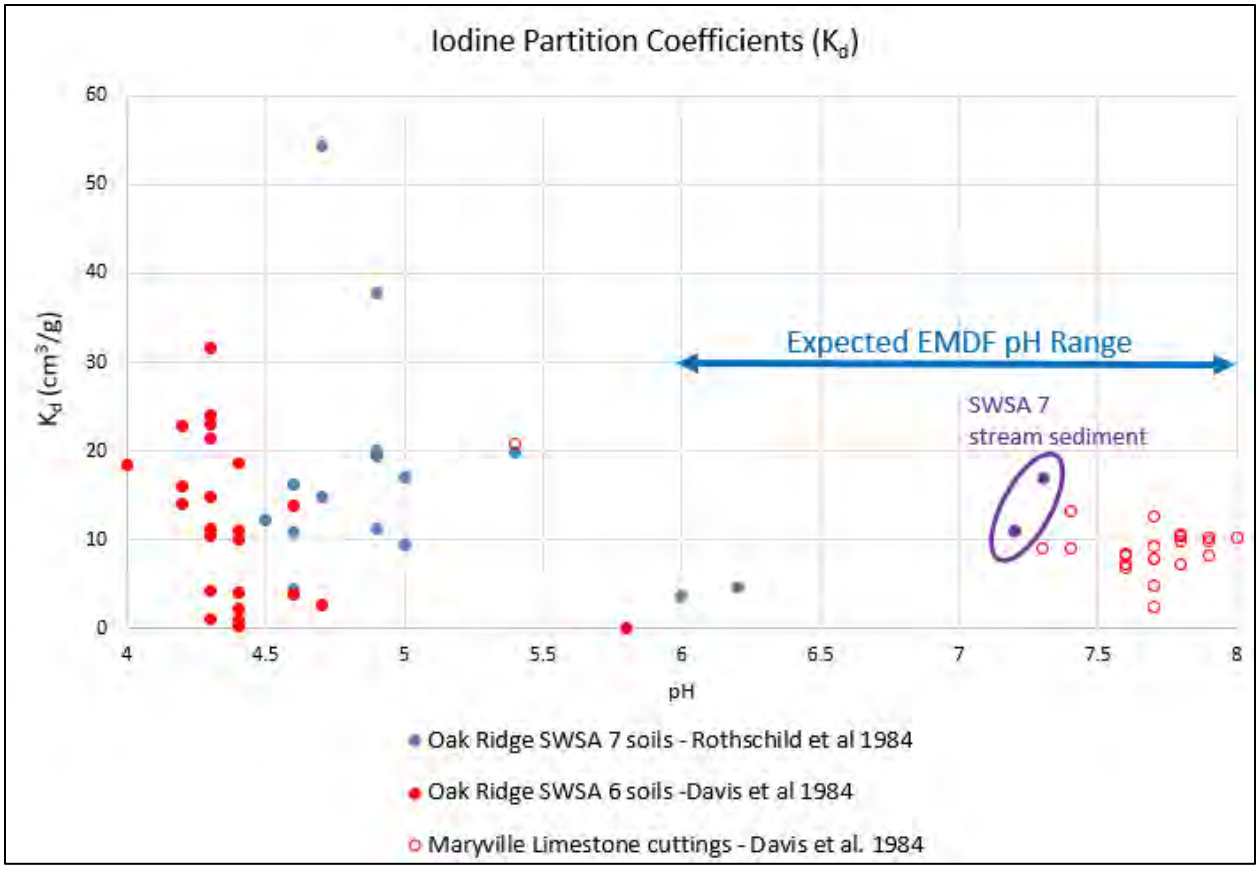

Fig. 3.8. Experimentally determined iodine partition coefficients for samples of Oak Ridge Conasauga Group soils, sediment, and bedrock

Given that the likely geochemical conditions in the EMDF disposal system are oxidizing and slightly acidic to circumneutral, adopting relatively high iodine K_d values (> 10 cm^3/g) is not justified by the available data. However, the likely abundance of the mineral illite in the soils and bedrock of the EMDF system and the possibility that the iodate oxidation state will be sustained by the expected pH and redox conditions suggest that a nonzero K_d value for iodine is reasonable and defensible. Based on the potential for iodine sorption at pH > 6.0 in material derived from the Maryville Formation (Fig. 3.8), a K_d value of 4 cm^3/g is proposed for iodine in the natural soils, saprolite, and bedrock of the EMDF system. This K_d value represents the lower end of the range of measured values for the range of pH values anticipated to exist at the EMDF site (Fig. 3.8). Additional support for the proposed K_d value for EMDF is found in a recent recommended iodine K_d value of 3.0 cm^3/g for clayey sediments at SRS (Kaplan et al. 2013), which was increased from a previous estimate of 0.9 cm^3/g. The proposed iodine K_d value for SRS PAs is relevant because it is derived over pH and oxidizing geochemical conditions that are similar to what is likely at the EMDF, and because the EMDF saprolites contain an abundance of illite (Kim et al. 2009), more so than do the clayey SRS sediments tested by Kaplan et al. (2013). The K_d value adopted for iodine in the EMDF waste zone is 2.0 cm^3/g. Adopting this lower iodine K_d value for the waste zone reflects significance of this parameter assumption for the maximum total dose that could occur during the 1000-year compliance period.

The lack of iodine K_d measurements on materials derived from the Nolichucky Formation is a source of uncertainty in the selection of a single representative K_d value for the bedrock and saprolite below the EMDF. However, field evidence of the similarity between the Maryville and Nolichucky units of the Conasauga Group in the vicinity of the ORR (ORNL 1992a, Sect. 3.3, pages 18–40) provides a reasonable

level of confidence that the iodine sorption properties of the Nolichucky Formation are similar to those of the Maryville Formation. On the ORR and at the EMDF site, the Maryville Formation is dominated (> 50 percent relative abundance) by mudstone lithologies (claystone, siltstone, and shale) rather than limestone lithologies (ORNL 1992a, Fig. 3-3). General descriptions of these two geological units in the vicinity of the EMDF site (Lee and Ketelle 1989, Sect. 4.2.5 and 4.2.6, pages 15–18) suggest that these Conasauga units comprise similarly interbedded mudstone and limestone lithologies in comparable proportions. Borehole logs obtained during recent EMDF site characterization (DOE 2018b, DOE 2019) also support this characterization of the lithology of the Maryville Formation and Nolichucky Formation at the disposal site. In addition, the two Conasauga Group units are mineralogically similar, with illite and chlorite predominant among the clay minerals (Davis et al. 1984, Table 3; ORNL 1987, Table 3.1), and have similar bulk density, grain density, and porosity characteristics (Dorsch et al. 1996, Table 3 and Fig. 23).

Previous Oak Ridge PA documents and modeling (ORNL 1997a, DOE 1998a, DOE 1998b) used lower values for the iodine K_d (0.0 and 0.199 cm^3/g, refer to Table 1.1). However, the data presented in the preceding paragraphs strongly suggests that the assumed base case value of 4 cm^3/g, is reasonable given that it is on the low end of the range of values for pH > 6 (Fig. 3.8). To increase confidence in the iodine K_d values applied in the EMDF PA, controls on the partitioning of iodine will be experimentally determined for local site materials (clayey soils and saprolite) derived from the Maryville and Nolichucky Formations. These data will evaluated through the EMDF change control process.

Technetium-99 partition coefficient (K_d)

Technetium exists in nature either as the highly mobile oxidized species, TcO_4^-, or the appreciably less mobile, less soluble Tc^{+4} species. Technetium at the EMDF is likely to exist primarily as dissolved TcO_4^-, with relatively small amounts of bound TcO_4^- or Tc^{4+} species. However, the small amounts of soil-bound technetium are very important for evaluating the efficacy of the EMDF and are the focus of this discussion. The primary conditions influencing technetium geochemistry are pH, Eh (the oxidation reduction potential, or redox), and the presence or absence of iron/manganese oxides and natural OM (EPA 2004).

The primary factor controlling technetium sorption to geological media is the redox status. Under high redox conditions, the poorly sorbing species, TcO_4^-, exists. This oxyanion sorbs very weakly to soils, however sorption increases when groundwater pH decreases in the presences of OM and iron- and manganese-oxides. As the pH decreases, these surfaces become protonated, thereby creating more positive surface charge sites for the anionic TcO_4^- species to bind. Above a critical pH value, referred to the point-of-zero-charge, the net charge becomes negative, thereby diminishing the extent of anion sorption. The point-of-zero-charge for iron oxides is about pH 7.8 and manganese oxides is pH 2.8. The point-of-zero-charge of OM varies greatly depending on its source, age, and how it is measured, but is commonly measured between pH 6 and 8 (Stumm and Morgan 1996). Especially as it applies to the EMDF, an important impact of OM on technetium mobility is not the tendency to sorb (more specifically, to complex) TcO_4^-, but instead the tendency for OM to convert TcO_4^- into the less mobile Tc^{4+} form by chemical reduction. This was demonstrated using geological media collected from the Field Research Center on the ORR (Gu et al. 2011).

Following the conceptual geochemical model put forth by Watson et al. (2004) for the Oak Ridge Field Research Center located in BCV, the pH in the soil/saprolite above the water table can be acidic, pH 4.5 to 6.0, while the pH in the saturated zone will be near neutral, 7 to 8. Furthermore, they describe the oxidation-reduction state of the system as primarily oxidizing, but with microenvironments of reducing conditions. This acknowledgement of the presence of reducing microenvironments is especially important for technetium because the pH/Eh conditions separating TcO_4^- from Tc^{4+} exists within the common domain of natural subsurface ORR conditions (Fig. 3.9). Moderately high concentrations of OM and high

concentrations of iron- and manganese-oxides likely exist at the EMDF (see data presented above from Rothschild et al. 1984 and Davis et al. 1984, and similar information in ORNL 1987; DOE 1992b). While together these geochemical conditions appear to support conditions conducive for technetium sorption, there is a great deal of uncertainty, especially regarding the redox conditions that may exist at the EMDF. Consequently, this analysis emphasizes ORR-specific measurements of technetium K_d values.

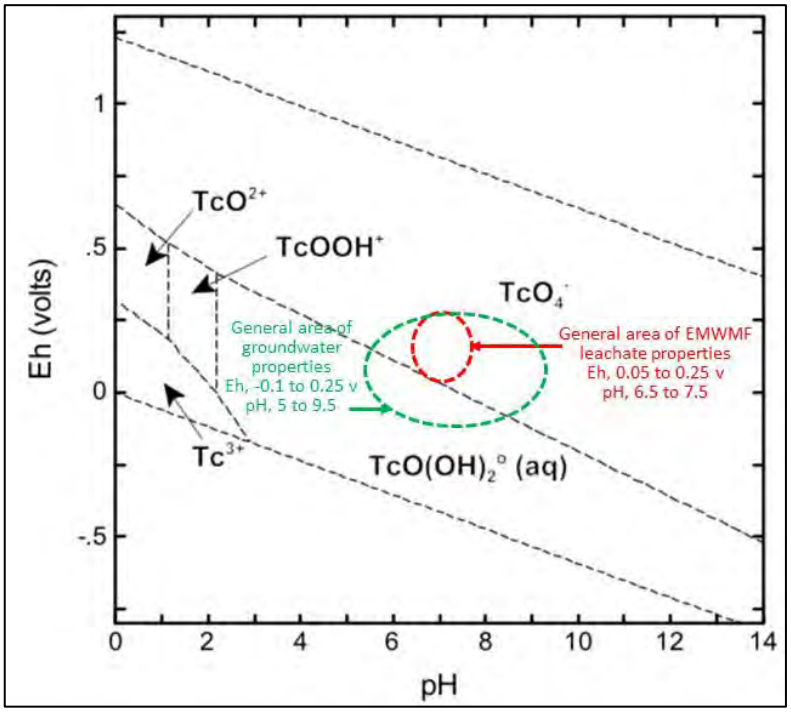

Diagram based on a total concentration of 10^{-8} mol/L dissolved technetium (from EPA 2004 VIII, Fig. 5.9).

Fig. 3.9. Eh-pH stability diagram for the dominant technetium aqueous species at 25°C

Two studies were identified that measure technetium K_d values under conditions that approximate those of the EMDF subsurface (DOE 1992b, ORNL 1987). DOE (1992b) reported K_d measurements of technetium (along with cesium, strontium, neptunium, and uranium) using soil sampled from Bethel Valley near the WAG 1. The studies followed an acceptable ASTM method and obtained an average technetium K_d value of 0.72 ± 0.16 cm^3/g, with a range of 0.53 to 1.04 cm^3/g (see Table 3.7). Also noteworthy, little time dependency of sorption with contact time was observed, suggesting that steady state conditions with respect to technetium were achieved in less than or equal to 1 day. This has important implications because flow through fractured media in the EMDF subsurface may be faster than through unfractured porous media. This data indicates that the full extent of technetium sorption, albeit quite small, is completed in a short period of time.

The data from DOE (1992b) is of high quality and the experimental conditions are largely appropriate for estimating technetium K_d values at the EMDF. The WAG 1 data (Table 3.7) provides a reasonable and defensible K_d value of 0.72 cm^3/g for technetium in the EMDF soils, saprolite, and bedrock for modeling purposes. ORNL (1987) found higher technetium K_d values in test on samples of the Nolichucky Formation (K_d=1.2 cm^3/g for dilute brine groundwater). Sensitivity analyses conducted in this PA will consider both lower and higher K_d values for Tc-99.

Table 3.7. Technetium K_d values measured from shales samples recovered from near the Waste Area Group 1 in Bethel Valley

Technetium K_d (cm^3/g)	Sample ID	Contact Time (day)	Sample description[a]
1.04	01.SB103	1	#1
0.84	01.SB103	3	#1
0.79	01.SB103	14	#1
0.76	01.SB135	1	#2
0.67	01.SB135	3	#2
0.68	01.SB135	14	#2
0.53	01.SB184B	1	#3
0.59	01.SB184B	3	#3
0.61	01.SB184B	14	#3
0.72 ± 0.16	**Ave. ± Stdev.**		
0.53 to 1.04	**Range**		

Data taken from Table A4.1.8 and geological media descriptions from page 10 of DOE 1992b,

[a] #1 - clay texture sediment, 8 to 9 ft interval from boring 01.SB103 adjacent to Impoundment 3513

#2 - predominant clay texture sediment, red/yellow & brown color; 24 to 25.8 ft interval from boring 01.SB135 located just south of Building 3019; "Explosion 3019"
#3 - clay texture sediment; yellow-brown; 6 to 8 ft interval from boring 01.SB184B located at the southeast corner of Building 3525; "Leak 3525"

DOE = U.S. Department of Energy
ID = identification
K_d = partition coefficient

Previous PA documents and modeling (ORNL 1997a, DOE 1998a, DOE 1998b) used zero values for the technetium K_d cm^3/g in the vadose and saturated zones, but higher values (> 1 cm^3/g) for waste forms (refer to Table 1.1 for a comparison). To increase confidence in the iodine K_d values applied in the EMDF PA, controls on the partitioning of technetium will be experimentally determined for local site materials (clayey soils and saprolite) derived from the Maryville Formation and Nolichucky Formation units. These data will be incorporated in future performance analyses as determined to necessary through the EMDF change control process.

3.2.2.8 Variations in K_d due to material characteristics and geochemical conditions

The K_d values are typically assigned to specific waste forms and earthen material components of a modeled system, and compilations of K_d values (e.g., International Atomic Energy Agency [IAEA 2010], Sheppard and Thibault 1990) include average values and ranges of values for different soil types, reflecting the significance of mineralogy and organic matter content to sorption phenomena. For different components of the EMDF system (e.g., waste materials and clean fill in the disposal unit, engineered basal liner and geobuffer clays, and native clay rich saprolite and sedimentary rocks underneath the disposal unit), the approach to representing variation in K_d values is based on several factors, including: (1) the limited availability of K_d data for EMDF waste materials, (2) the common local geologic source(s) and similar mineralogical characteristics of the materials expected to be used as clean fill and for liner and geologic buffer construction (UCOR 2018a), and (3) the variability and uncertainty in geochemical conditions present in different components of the disposal system during the post-closure period.

Previous radionuclide release and transport modeling for LLW disposal units on the ORR have applied different K_d values to different materials including waste, vadose zone materials (generally corresponding to soil and saprolite), and saturated zone materials (generally corresponding to saprolite and bedrock) (ORNL 1997a, DOE 1998b, BJC 2010b). For the EMDF waste zone material, the assumption is to assign a K_d value equal to one-half the K_d assigned to the saprolite zone material (Sect. 3.2.2.6), based on incorporating large volumes of clean fill (refer to Sect. 3.2.2.5) with textural and mineralogical characteristics similar to those of geologic materials at the EMDF site. This assumption conservatively reduces the K_d in the waste zone, based on the lack of information regarding soil waste also occupying the waste zone, and also conservatively assumes all contaminants sorbed or embedded in debris are immediately released to the surrounding soil. The locally sourced, clay-rich materials used as clean fill and the onsite materials that meet geotechnical requirements for use as EMDF liner and geologic buffer materials are derived from the underlying bedrock of the Maryville Formation and Nolichucky Formation. These materials are rich in clay minerals (e.g., illite) demonstrated to have high sorptive capacity in tests on samples from those geologic units (ORNL 1987, Friedman et al. 1990, Watson et al. 2004). Most of the available K_d measurements for Conasauga Group materials have been performed on saprolite or clayey soils, rather than bedrock samples (refer to Table 2.12). In the absence of data on differences in sorptive capacity between local saprolite and bedrock materials, K_d values for the bedrock zone are assumed to be the same as the saprolite zone values.

This simplifying assumption that all model material zones have similar K_d values (based on similarity in material characteristics) does not account for potential differences in geochemical environment (e.g., oxidation-reduction potential [Eh] and pH) within the waste zone, unsaturated zone, and saturated materials at the EMDF site, or the possibility for evolution in the geochemical conditions that control sorption and radionuclide mobility over time as the cover system degrades, cover infiltration increases, and leachate release begins. Leachate and groundwater monitoring at the EMWMF site provide a limited basis for anticipating the range of future geochemical conditions that may affect radionuclide release and transport mechanisms. Periodic field measurements of the EMWMF leachate collection system, underdrain outflow, and groundwater in monitoring wells along the facility perimeter indicate a wide range of pH and Eh conditions (Fig. 3.10).

The EMWMF leachate samples (black symbols in Fig. 3.10) span a range of pH values from 5.3 to 9.1 and a range of Eh values from -85 mV to 392 mV. Most of the leachate data fall within a pH range of 6.6 to 7.5 and an Eh value range of 50 to 250 mV (oxidizing conditions). Groundwater measurements from the EMWMF underdrain tend to have pH values and Eh values similar to leachate observations. Data from EMWMF groundwater monitoring wells span a wide range, with pH ranging from 5 to 10 and Eh values as low as -150 mV (reducing conditions).

In general, the groundwater data are most relevant to geochemical conditions in the saturated zone (Sect. 3.2.3), whereas the EMWMF leachate observations may be more representative of waste and vadose zone conditions. The data represent pre-closure, operational conditions at EMWMF and may or may not be representative of future EMDF conditions. Given that the general composition and range of EMWMF waste material types (concrete, steel, soil, etc.) is similar to the expected EMDF waste, the data are taken as the best available indication of future geochemical conditions in the EMDF waste and underlying vadose zone. The central tendency and range of pH and Eh observations for EMWMF leachate and underdrain samples (i.e., circumneutral to weakly acidic, oxidizing conditions) suggest that the K_d values within the EMDF waste zone and unsaturated zone may be similar to each other, and that adopting K_d values representing circumneutral, oxidizing conditions is appropriate. The assumption of near neutral, oxidizing conditions for the EMDF waste zone is reasonable considering the large volume of clean fill used in disposal operations that will provide buffering capacity for waste types (e.g., concrete) associated with higher pH values.

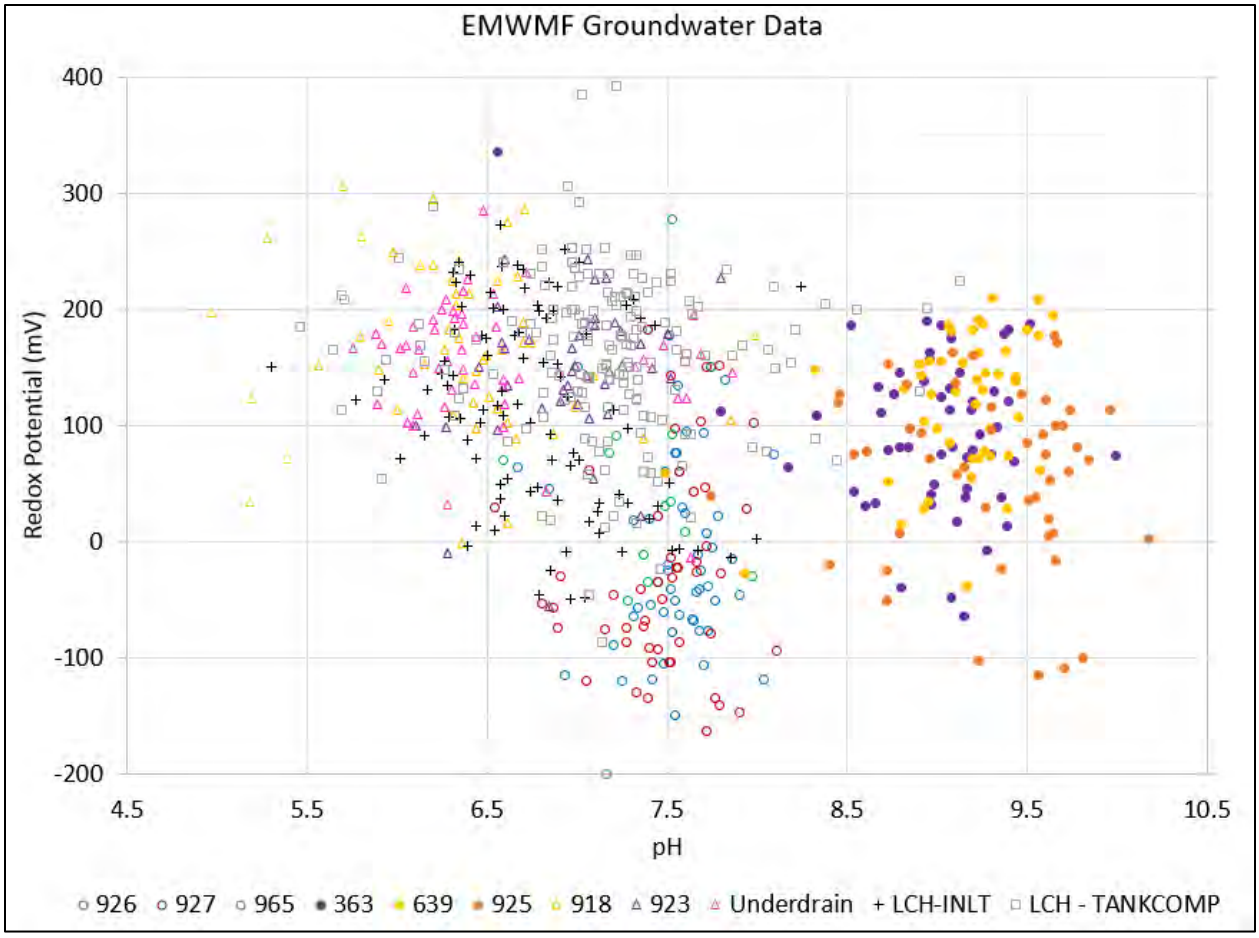

Fig. 3.10. Paired pH and redox potential observations from samples of EMWMF leachate, underdrain groundwater, and groundwater monitoring wells near the facility

While the EMWMF groundwater monitoring well data suggest that a wider range of pH and redox conditions is possible in the saturated zone, the clusters in the well data do not coincide with similarities in well location relative to the disposal unit, and so do not provide a strong basis for concluding that the geochemical environment in the saturated zone will be less acidic or less oxidizing, in general, than the overlying unsaturated and waste zones. Thus, the EMWMF leachate and groundwater data do not suggest systematic differences in pore water chemistry among the waste, vadose zone, and saturated zone.

The EMWMF field data show temporal variability in leachate chemistry that probably reflects changes in waste composition and environmental fluctuations such as seasonal cycles. However, these data from the operational period do not show any persistent trend in pH or redox conditions. Geochemical evolution of the EMDF waste and vadose zone may occur in the post-closure period as waste-dewatering and long-term changes in cover and liner system performance cause variations in the flux and chemistry of infiltrating water. However, no general model of geochemical evolution of the EMDF system that would result in progressive changes in K_d values has been assumed for the PA, in part due to limitations in specifying time-variable input parameter values.

For purposes of modeling source release and radionuclide transport, the geochemical environment is assumed to remain stable throughout the post-closure period, and the uncertainty in K_d values associated with differences in materials or geochemical conditions is addressed as part of the sensitivity and

uncertainty analysis for the each of the models (refer to Sect. 5). Assuming a single, constant K_d value for the engineered materials, saprolite, and bedrock below the waste does not capture the potential geochemical complexity of the disposal system. However, given the anticipated similarity in material characteristics and uncertainty in the variation of geochemical conditions over time, the simplified assumption is adopted for the base case model implementation and combined with a focus on model sensitivity to uncertainty in K_d values applied to different material and model zones (i.e., waste versus saprolite and bedrock, vadose versus saturated zone). In general, the all-pathways dose analysis is most sensitive to the K_d value assigned to the waste material, which governs the rate of radionuclide release from the disposal unit. From that perspective, a significant conservative step is taken in assuming these K_d values are one-half the values of the other zones. Sensitivity of PA model results to uncertainty in K_d values is addressed in Sect. 5.

3.2.2.9 Summary of radionuclide release and vadose zone conceptual model assumptions

Key assumptions for the conceptual models of radionuclide release and vadose zone transport include the following:

- Based on the EMDF estimated inventory, anticipated operational conditions, and design features of the EMDF cover system, post-closure release of radionuclides through the cover is assumed to be negligible (Sect. 3.2.2.1, 3.2.2.2, and 3.2.2.3).
- Infiltration through the cover is assumed to occur uniformly over the area above the waste and liner system (Sect. 3.2.2.4), and to follow the generalized model of EMDF performance evolution over time (Fig. 3.5).
- Equilibrium desorption is assumed to govern release from the solid phase (refer to Table 3.4 for assumed K_d values).
- Potential solubility limits are not incorporated in the source release representation.
- The EMDF waste mass is conceptualized as a homogeneous, soil-like material in which the estimated radionuclide inventory is uniformly distributed.
- Estimated post-closure inventories of radionuclides that are highly mobile in the aqueous phase (H-3, C-14, Tc-99, and I-129) are adjusted (reduced) based on modeling of operational period leaching (Sect. 3.2.2.5).
- The assumed mass of clean fill disposed with EMDF waste is based on average clean fill-to-waste ratios documented for the EMWMF. Average waste inventory concentrations are adjusted downward to account for this added mass (Sect. 3.2.2.5).
- Assumptions regarding the geochemical environment in the disposed wastes and pore water and the potential for changes over time are limited to assumed ranges in pH and Eh (Sect. 3.2.2.8).
- Geochemical conditions in the waste and vadose zone are assumed to be circumneutral and oxidizing.
- For purposes of modeling source release and radionuclide transport, the geochemical environment is assumed to remain stable throughout the post-closure period, and saturated and unsaturated material zones are assumed to have identical (invariant among zones) radionuclide-specific K_d values, while the waste zone radionuclide-specific K_d values are assumed to be equal to one-half these K_d values based on clean fill accounting for approximately one-half the mass in the waste zone (Sect. 3.2.2.6).

3.2.3 Saturated Zone Flow and Radionuclide Transport

Based on the BCV hydrogeologic conceptual model (Sect. 2.1.5) and the evidence from BCV tracer studies presented in Sect. 2.1.6.2, flow within the saturated zone near EMDF is expected to be 3-D, with

groundwater close to the water table (generally within the saprolite zone) diverging toward lower surface elevations (e.g., Bear Creek tributary channels) around the periphery of the disposal unit. With increasing depth, groundwater flow direction becomes predominantly along-strike toward the south-southwest and the vertical component of flow decreases with increasing depth into the bedrock zone. This flow pattern reflects the pronounced horizontal anisotropy associated with strike-parallel fracture pathways as well as decreasing porosity and permeability with depth. Based on evidence from several BCV saturated zone tracer studies, radionuclides reaching the saturated zone will be transported laterally toward shallow groundwater discharge areas with limited downward transport into the deeper portions of the bedrock zone. Deeper groundwater and radionuclide transport pathways will be directed down valley and toward Bear Creek, with surface discharge occurring at more distant locations relative to shallower transport pathways (Fig. 3.11).

Saturated zone groundwater flux is conceptualized as a traditional Darcian porous media system. Neither statistical nor more detailed, discrete representation of fracture networks is adopted due to limitations in the types and quantity of field data available to support parameterization of such conceptual models of flow in fractured media. The large amount of existing permeability data compiled for Conasauga Formations and applied in previous BCV modeling efforts (Sect. 2.1.5.4) is the basis for an EPM representation of the heterogeneous, anisotropic nature of the geologic media at the CBCV site. Specifically, stratigraphic variation in hydraulic conductivity and vertical variation in porosity and horizontal anisotropy in conductivity is the basis for parameterization of the 3-D complexity of the saturated zone. More detailed information on this parameterization scheme is presented in Sect. 3.3.3.

Saturated zone radionuclide transport is conceptualized as advective, chemically retarded aqueous-phase transport within the porous medium (saprolite and bedrock), with a simple equilibrium, linear isotherm sorption model assumed for retardation. This conceptual model is represented with a standard formulation (Bouwer 1991) for retarded aqueous-phase transport in porous media. The influence of discrete fracture networks and matrix diffusion on radionuclide transport are not explicitly incorporated because the site-specific data required to parameterize more detailed representations of subsurface transport are not available. Without detailed field measurements of the spatial variability in fracture size and frequency at the scale of the disposal site, even finer-resolution EPM representation of simple retarded transport in a fractured rock system is not possible. EMDF site characterization (DOE 2018b, DOE 2019) has provided a general confirmation of the hydrogeologic conceptual model adopted for the PA modeling.

The conceptual model of radionuclide flux from the vadose zone to the water table incorporates the possibility of non-uniform concentration and flux below the facility footprint. Simplified representations of both non-uniform and uniform fluxes to the water table are applied to the site-specific saturated zone transport model described in Sect. 3.3.3. A uniform flux to the saturated zone is assumed for purposes of total-system modeling (described in Sect. 3.3.4).

The conceptual model of saturated zone flow and radionuclide transport is a simplification of the geochemistry and hydrogeology of the EMDF saturated zone. However, the practical limitations on implementation of fracture-matrix type conceptual and mathematical models (i.e., lack of data for parameterization and calibration of more complex approaches) are significant constraints on the utility of such alternative conceptual models for this performance analysis. Efforts to further evaluate the data collection requirements and calibration approaches that might be applicable to fractured-rock modeling of the EMDF saturated zone may have value in the context of PA maintenance.

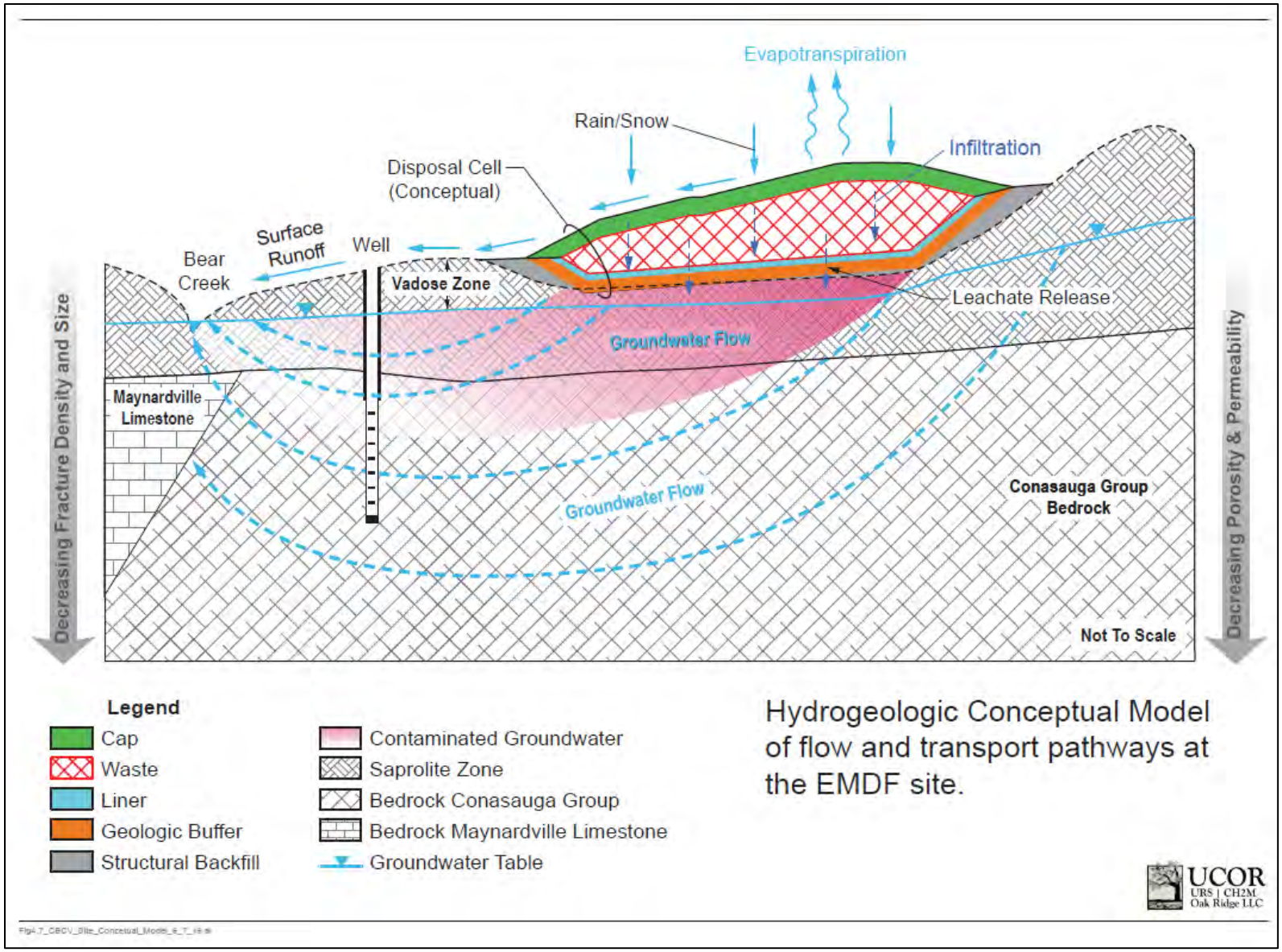

Fig. 3.11. Simplified conceptual model of flow and transport pathways at and downgradient of the EMDF site

3.2.4 Exposure Pathways and Scenarios

This section includes the descriptions of the exposure pathways and scenario(s) considered for each of the DOE M 435.1-1 performance objectives and measures, including atmospheric and all-pathways release and radon flux from the EMDF cover. Detail on key input parameters and assumptions is provided in Sect. 3.4. Exposure pathways and scenarios for IHI are presented in Sect. 6.

3.2.4.1 Atmospheric pathway and radon flux

Release of radionuclides through the EMDF cover is assumed to be negligible (Sect. 3.2.2). One of the exposure pathways included in the all-pathways analysis is inhalation of and immersion in air contaminated with radionuclides (external exposure) that are mobilized in particulate form from soil in food production plots (Fig. 3.12 and Appendix G). The performance measure for radon flux is assessed at the EMDF cover surface and does not explicitly incorporate specific exposure pathway or scenario assumptions (Appendix H).

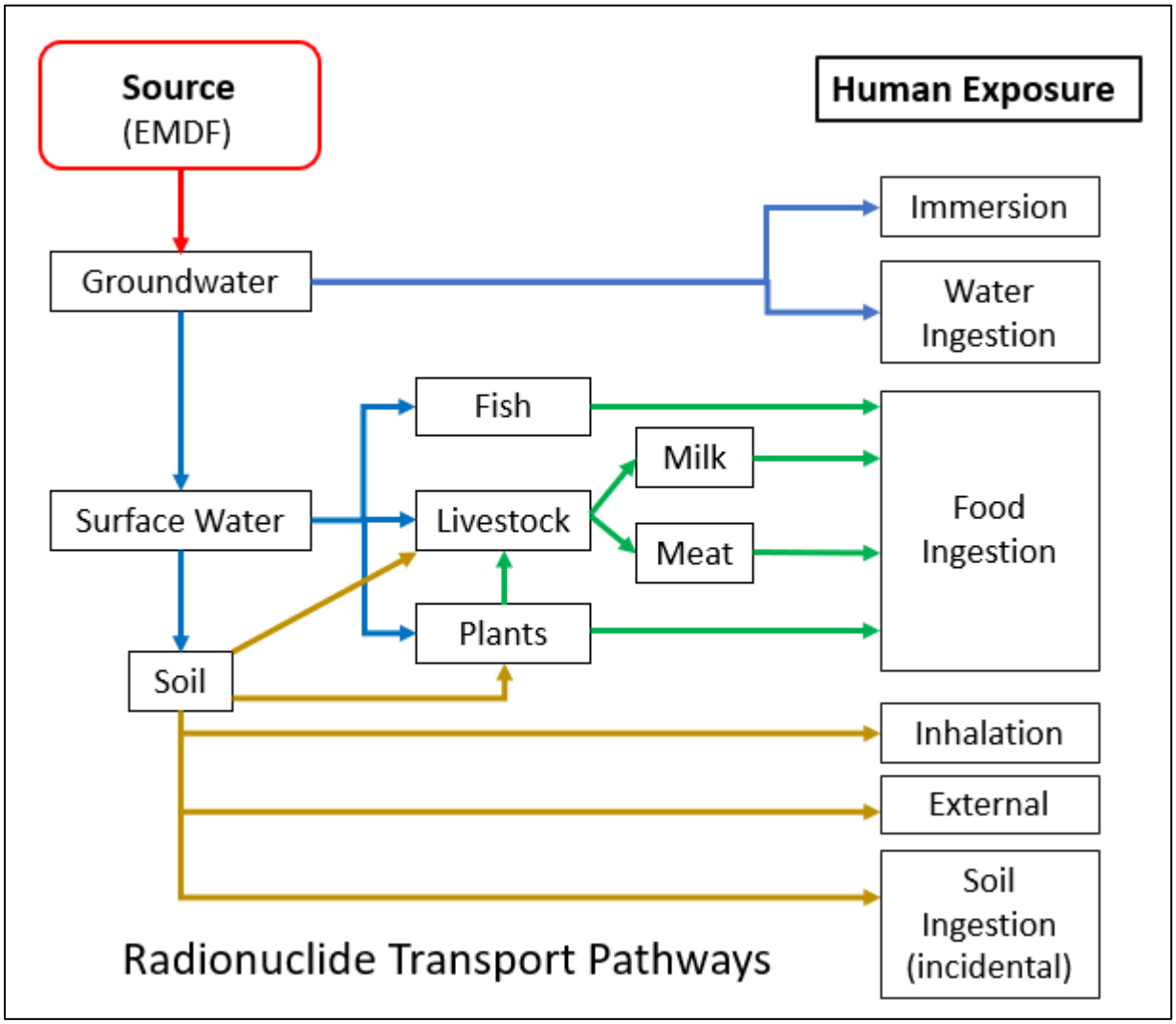

Fig. 3.12. Flow chart of environmental transport and exposure pathways for the all-pathways analysis

3.2.4.2 All-pathways exposure scenario

For the all-pathways exposure scenario (Fig. 3.12), radionuclide release through the EMDF cover is not included based on the screening analysis presented in Sect. 3.2.2. Release of radionuclides to groundwater and discharge of contaminated groundwater to surface streams are the environmental transport pathways modeled to estimate groundwater and surface water concentrations at the time and place of maximum concentration. The all-pathways scenario assumes that a resident farmer sets up a homestead somewhere near the disposal facility and pumps groundwater for drinking and household use from a well at the location of highest radionuclide concentration that is 100 m from the waste limit (Fig. 3.11). In addition, the farmer is assumed to draw contaminated surface water for crop irrigation and to support livestock from Bear Creek at the point where most of the contaminated groundwater is predicted to discharge. The basis for assuming use of surface water for agricultural activity is presented below.

In addition to consumption of contaminated groundwater from the well, the all-pathways scenario considers exposure due to immersion and inhalation during showering with contaminated groundwater. Contaminated surface water used to irrigate food production areas is the transport pathway that drives exposure from ingestion of contaminated agricultural products, including plant foods, meat, eggs, and milk. Working in contaminated food production areas is assumed to cause direct external exposure to radiation from contaminated soil as well as internal exposure by incidental soil ingestion and inhalation of particulates entrained from the ground surface.

Use of Water Resources

In East Tennessee, abundant rainfall and numerous surface water reservoirs support extensive use of surface water resources. Based on a recent TVA water use report, in Anderson and Roane Counties (the counties in which the Oak Ridge Reservation is located), surface water withdrawals for public water supply and crop irrigation are much greater than groundwater withdrawals for those two uses (TVA 2012). The proportion of total public water supplies withdrawn from groundwater sources in 2010 was 1.6 percent and 16 percent for Anderson and Roane Counties, respectively (Table 3.8). The residential exposure scenario adopted for the EMDF PA all-pathways analysis assumes the use of local groundwater for drinking and household use, even though facilities in BCV draw from surface water sources. The assumptions regarding the use of groundwater and surface water resources by the resident farmer are consistent with the exposure scenarios used in the evaluation of EMWMF performance and the development of the EMWMF WAC (DOE 1998b).

Table 3.8. Groundwater and surface water withdrawals in Anderson and Roane Counties for 2010

Tennessee county and water use		Surface water withdrawal (2010) in million gal/day (% of total)	Groundwater withdrawal (2010) in in million gal/ (% of total)
Anderson	Public Supply	13.2 (98%)	0.22 (1.6%)
Roane	Public Supply	6.65 (84%)	1.28 (16%)
Anderson + Roane	Public Supply	19.85 (93%)	1.5 (7%)
Anderson	Irrigation	0.45 (98%)	< 0.01 (< 2.2%)
Roane	Irrigation	0.04 (> 80%)	< 0.01 (< 20%)
Anderson + Roane	Irrigation	0.49 (96%)	< 0.02 (3.9%)

Data Source: TVA 2012, Table 2-21 (public supply) and Table 2-24 (irrigation)

TVA = Tennessee Valley Authority

In Anderson and Roane Counties, relatively little groundwater withdrawal for agriculture is required to supplement natural precipitation and surface water. For irrigation of crops, the proportions of water

withdrawals from groundwater and surface water in 2010 for Anderson and Roane Counties were similar to proportions withdrawn for public supply (Table 3.8). The predominant use of surface water for irrigation reflects its accessibility. When a source is available, reliable, and convenient, such as Bear Creek, surface water is used for irrigation rather than groundwater.

County level water use data available from USGS indicates that withdrawals of surface water to support livestock exceed groundwater withdrawals for that purpose by a factor of 2 or more (http://waterdata.usgs.gov/tn/nwis/water_use/). In the USGS database for 2010, Anderson and Roane Counties together used 0.27 million gal/day for livestock, which is less than the irrigation total for that year based on the TVA water use report (Table 3.8). However the USGS data for years 2000, 2005, 2010, and 2015 all indicate that surface water withdrawals for livestock are two to 10 times larger than total crop irrigation withdrawals, which is consistent with the abundant rainfall and ready availability of surface water sources to support agriculture in Anderson and Roane Counties. The predominant use of surface water for irrigation and livestock in the vicinity of the ORR supports the PA exposure scenario assumption that water from Bear Creek is used for agriculture.

Ingestion of Plant and Animal Foods

Selection of the types of contaminated products included in the food ingestion pathway is based on review of performance analyses for the EMWMF and other similar facilities (e.g., Portsmouth onsite waste disposal facility [DOE 2015c]). The agricultural products consumed include leafy vegetables and produce (non-leafy vegetables), as well as meat and milk from animals that drink contaminated surface water and are fed with contaminated feed grown in plots irrigated with surface water. The types of farm-raised meats could include beef, pork, and poultry. Farm-raised eggs could also be included in the range of locally grown foods. Locally obtained game (e.g., deer, turkey, geese) could also be consumed, but wild animals would not feed exclusively on contaminated agricultural products or drink only contaminated surface water; therefore, they would have lower radionuclide concentrations in muscle tissue than livestock.

For the EMDF PA, the assumed ingestion of animal foods is limited to meat and milk from cows, poultry, eggs, and fish from Bear Creek. This range of foods accounts for the most likely ingestion-based dose contributions to a resident farmer. Ingestion of fish from Bear Creek is based on an assumption for recreational catch rates because of the limited populations of large fish in the areas near the EMDF site. It is assumed there is no consumption of crustacea or mollusks, which is reasonable given the EMDF location in eastern Tennessee.

In summary the exposure pathways incorporated in the all-pathways dose analysis (Fig. 3.12) include the following:

- Ingestion of contaminated groundwater
- Immersion and inhalation during showering with contaminated groundwater
- Direct exposure to radiation from contaminated garden soil
- Inhalation of contaminated soil particles entrained from contaminated garden soil
- Incidental ingestion of contaminated garden soil
- Ingestion of plant foods irrigated with contaminated surface water
- Ingestion of meat and milk from cows that eat plants irrigated with contaminated surface water and drink contaminated surface water

- Ingestion of meat and eggs from poultry that ingestion contaminated feed and water
- Ingestion of fish caught from Bear Creek (based on recreational fishing).

While not unrealistic, the all-pathways exposure scenario is based on a local agricultural subsistence lifestyle that is uncommon in present day East Tennessee, which provides bias toward more highly exposed individuals. A subsistence farmer is specified as the receptor to incorporate a diverse set of exposure pathways. For purposes of EMDF performance analysis, the exposure at the time of peak dose is evaluated relative to the performance objective of 25 mrem/year.

3.2.4.3 Water resources protection

The performance criteria identified for protection of groundwater resources are the MCLs for drinking water specified by EPA in the Radionuclides Final Rule (EPA 2000), promulgated in 40 *CFR* 141.66, for which the State of Tennessee has primary enforcement responsibility. These radiological limits on public drinking water sources are based on drinking water ingestion only. The POA is the groundwater well at 100 m from the waste limit.

The performance criteria identified for protection of surface water resources are based on the DCS for water ingestion (DOE 2011b). The DCSs are based on total water ingestion including water as a beverage and water used in preparation of other beverages and food. The POA is Bear Creek immediately downstream of the NT-11 tributary confluence. Most of the radionuclide flux from the EMDF is predicted to discharge to surface water at or upstream of NT-11 (Sect. 3.3.3).

3.3 MODELING TOOLS AND IMPLEMENTATION

Selection of modeling tools to simulate the EMDF cover system water balance and radionuclide transport is based on the conceptual models presented above. The PA model codes include: the Hydrologic Evaluation of Landfill Performance (HELP) model for simulating the EMDF water balance; the STOMP model for simulating radionuclide release and vadose zone transport; MODFLOW, MODPATH, and MT3D model codes for saturated zone groundwater flow and radionuclide transport simulation; and RESRAD-OFFSITE for holistic simulation of radionuclide release and transport as well as exposure scenarios and dose analysis.

Simulation of transient hydrologic phenomena (i.e., variability in precipitation, runoff and evapotranspiration) is necessary for prediction of long-term cover system performance. Short-term dynamics of flow and contaminant transport within the unsaturated zone below the cover and in the saturated zone are considered less important to capture for simulation of long-term facility performance. Rather, the evolution of cover system performance and release of radionuclides over hundreds to thousands of years is the transient aspect of most significance for simulating disposal facility performance.

For cover system water balance modeling that incorporates daily and seasonal fluctuations in weather, the HELP computer code (Schroeder et al. 1994) is used to estimate post-closure rates of vertical percolation into the waste zone under different cover performance scenarios. Flow and contaminant transport in the vadose zone below the cover are modeled using the STOMP code (White and Oostrom 2000, White and Oostrom and 2006). The STOMP model is used to analyze the impact of disposal cell geometry on the timing and location of release from the engineered barriers of the liner system. STOMP results are used to guide the development of input flux boundary conditions (radionuclide release) for the saturated zone transport model, and are then compared to the simplified vadose zone representation in the total-system model.

Saturated zone groundwater flow and radionuclide transport are modeled using the MODFLOW and MT3D model codes, respectively. These 3-D flow and contaminant transport codes represent the hydrogeologic complexity of the EMDF site explicitly, incorporating a simplified EPM representation of fractured-rock characteristics that influence radionuclide transport. As with the STOMP modeling of the vadose zone, the 3-D saturated zone models provide a basis for assessment of the less complex model of saturated zone transport in the total-system model code, RESRAD-OFFSITE, which is used to integrate conceptual models of the EMDF system, including exposure pathways and scenarios. Simplified representation of environmental transport processes in the total-system model permits holistic simulation of release, transport, and exposure pathways, and facilitates a probabilistic analysis of the impact of input parameter uncertainty on dose predictions. Model sensitivity evaluations and the total system uncertainty analysis is presented in Sect. 5.

Table 3.9 presents a summary of how specific components of each model code represent the EMDF engineered materials, waste and natural geologic materials of the disposal system. The HELP model represents only the unsaturated, engineered materials and waste materials. The materials above the liner system are not included in the 3D MODFLOW and MT3D models, which simulate flow and radionuclide transport in the saturated parts of the saprolite and bedrock zones. The STOMP and RESRAD-OFFSITE models include the engineered barriers, waste, and natural material components, which are represented as variably saturated in the STOMP model. The RESRAD-OFFSITE model represents the engineered and waste materials and uppermost saprolite zone as unsaturated. The saturated zone component (aquifer) of the RESRAD-OFFSITE model is assigned porosity and permeability characteristics intermediate between the saprolite zone and the bedrock zone. Linkages among models are illustrated in Figs. 3.1 and 3.2 (Sect. 3.1.2) and summarized in Table 3.10. The remainder of this section provides summary information on each of the model codes utilized and the selection of parameter values for the EMDF system. Model results that support parameterization of other PA models are presented as necessary. More detailed information on model setup and implementation is provided in separate appendices for each model (first column of Table 3.10).

Table 3.9. Representation of material zones of the EMDF system within different PA model codes

PA Model Codes → / Material Zones ↓	HELP	MODFLOW & MT3D	STOMP	RESRAD-OFFSITE
Engineered Materials and Waste	Cover, waste, liner, and geologic buffer layers	Model layer 1 (EMDF liner & geobuffer)	Material zones 1-9, 18	Cover, waste, and unsaturated zone layers UZ1 –UZ4
Saprolite Zone	Not represented	Model layer 1	Material zones 10-13	UZ5 saturated zone (aquifer)
Bedrock Zone	Not represented	Model layers 2-9	Material zones 14-17	Saturated zone (aquifer)

EMDF = Environmental Management Disposal Facility
HELP = Hydrologic Evaluation of Landfill Performance
PA = Performance Assessment
RESRAD = RESidual RADioactivity
STOMP = Subsurface Transport Over Multiple Phases
UZ = unsaturated zone

Table 3.10. EMDF PA model input parameters and linkages among models

Model and purpose	Primary model inputs	Primary model output (used as input to or compared with other PA models)
HELP Water balance and engineered barrier performance (Appendix C)	• Local climate data • EMDF Preliminary Design (geometry and material specifications)	• Cover infiltration rates
MODFLOW Saturated zone flow (Appendix D)	• EMDF Preliminary Design • Bear Creek Valley topography, geology, and surface water features • Conasauga Group hydraulic conductivities • EMDF cover infiltration • Estimated natural recharge rates	• Flow directions • Hydraulic gradients • 3-D groundwater flow field • Depth to groundwater
STOMP Unsaturated flow and transport (Appendix E)	• EMDF radionuclide inventory • EMDF Preliminary Design • Estimated natural recharge rates • EMDF cover infiltration • Conasauga Group hydraulic conductivities and porosity • Solid-aqueous partition coefficients	• Radionuclide release • Vadose zone flux • Water table flux • Water table time of arrival (vadose delay times)
MT3D Saturated zone transport model (Appendix F)	• EMDF radionuclide inventory • EMDF Preliminary Design • EMDF cover infiltration • Effective porosities • 3-D groundwater flow field • solid-aqueous partition coefficients • Radionuclide flux from vadose zone	• Plume location, evolution and maximum extent • Peak groundwater concentration and time of peak at well • Contaminant discharge to Bear Creek surface waters
RESRAD-OFFSITE Radionuclide release and transport; exposure and dose analysis (Appendix G)	• EMDF radionuclide inventory • EMDF Preliminary Design (material specifications) • EMDF cover infiltration • Hydraulic gradients • Effective porosities • Solid-aqueous partition coefficients • Biotic transfer factors • Dose conversion factors • Exposure scenario and exposure factors (ingestions rates, etc.)	OUTPUTS for evaluating compliance with performance objectives: • Peak total dose during compliance period • Dose contributions by exposure pathway • Key radionuclide contributions to total dose • Well water and surface water concentrations

D = dimensional
EMDF = Environmental Management Disposal Facility
HELP = Hydrologic Evaluation of Landfill Performance
PA = Performance Assessment
RESRAD = RESidual RADioactivity
STOMP = Subsurface Transport Over Multiple Phases

Due to limitations in representing the sequence of material layers in the cover system for radon flux modeling, the RESRAD-OFFSITE code was not utilized for the radon analysis. The tool for modeling radon flux from the EMDF cover is the 1984 NRC technique for design of uranium tailings cover systems (NRC 1984) and is described in detail in Appendix H.

QA activities that support model implementation include software QA, input data validation and checking, documentation and independent review of model outputs and post-processing procedures, and archival and configuration management of model files and supporting QA documentation. Additional detail on the QA activities for the PA is provided in Sect. 9 and model QA activities are documented in *Quality Assurance Report for the Performance Modeling of the Bear Creek Valley Low-level Radioactive Waste Disposal Facilities, Oak Ridge, Tennessee* (QA Report) (UCOR 2020b).

3.3.1 Engineered Barrier Performance Model Code (HELP)

The HELP model was selected for hydrologic modeling of EMDF performance based onsite characteristics (weather and climate) and the EMDF Preliminary Design. The HELP model helps to identify a reasonable range of cover infiltration and leachate release rates applicable to short-term and long-term post-closure performance periods, with a focus performance within the 1000-year, post-closure compliance period. Sections 1.3, 2.2, and 3.2.1 review EMDF design features and safety functions that HELP modeling integrates to represent facility hydrologic performance. Appendix C provides additional detail on EMDF system features, events, and processes relevant to performance and more detailed presentation of HELP model input parameter selection.

The HELP model was developed at the U.S. Army Corps of Engineer Waterways Experiment Station under a cooperative agreement with EPA to support RCRA and Superfund programs (Schroeder et al. 1994). The HELP model is recommended by EPA and required by most states for evaluation of closure designs of hazardous and nonhazardous waste management facilities. The HELP code has been widely used for landfill design and performance evaluation over more than two decades.

HELP is a quasi 2-D hydrologic model of water movement into and through landfill systems. The model accepts climate, soil, and design data, and uses estimation techniques that account for the effects of surface storage, snowmelt, runoff, infiltration, evapotranspiration, vegetative growth, soil moisture storage, lateral subsurface drainage, and unsaturated vertical drainage as well as leakage through soil, geomembrane, or composite liners. Landfill systems including various combinations of vegetation, cover soils, waste cells, lateral drain layers, low permeability barrier soils, and synthetic geomembrane liners may be modeled. The HELP model has been used for design and performance modeling of EMWMF and EMDF.

The HELP model uses an extensive set of submodels to represent the water and energy balance at the surface; the U.S. Department of Agriculture (USDA)-Standardized Partial Regression Coefficient Standard Curve Number method for estimating surface runoff (USDA 1986); a Dupuit-Forcheimer approximation for saturated flow in lateral drainage layers; and simplified algorithms for vertical flow and routing of water through a user-defined profile of landfill layers that may include lateral drainage layers, vertical percolation layers, soil barrier layers, and synthetic geomembranes (Schroeder et al. 1994).

The HELP model includes approximations that can affect the predicted surface water balance and vertical fluxes below the surface. Parameterization of surface soil and vegetation characteristics in particular will affect the estimated net infiltration through the surface layer (precipitation–runoff–evapotranspiration), which sets an upper bound on percolation through the cover system as a whole. HELP utilizes a soil moisture characteristic model for unsaturated flow based on moisture content at soil field capacity and at wilting point and employs a unit hydraulic gradient assumption (Darcy velocity equal to (un)saturated hydraulic conductivity) for each vertical percolation layer. Soil barrier layers are assumed to remain saturated, with flow driven by the estimated head on the top of the barrier. Depending on the predicted net infiltration, lateral drainage flux, and specified soil hydraulic characteristics, these simplifying vertical flow assumptions will tend to over predict downward vertical water movement through the modeled profile. In particular, these unsaturated flow approximations omit more complex surface tension physics such as the effect of capillary barriers designed to inhibit downward subsurface flow. Detailed presentation of the

mathematical expressions for various HELP submodels, methods of solution, and model limitations can be found in Schroeder et al. (1994). Additional discussion of HELP model limitations, reviews of previous applications of HELP, and evaluations of model results relative to other models and field data are included in Appendix C, Sect. C.2.2.2.

3.3.1.1 HELP input data requirements

HELP model inputs include climatic data, design specifications for the thickness and hydrologic characteristics of each soil layer or synthetic membrane, and parameter selections concerning the condition of vegetation on the surface layer and the quality of synthetic membrane placement.

Climatic Data. HELP requires inputs of precipitation, air temperature, and solar radiation data as well as data for estimating evapotranspiration, which includes latitude, growing season dates, wind speed, quarterly average relative humidity, evaporative zone depth, and maximum leaf area index. Daily precipitation and temperature data for Oak Ridge, Tennessee from 1961 to 1990 are input for the EMDF model runs, whereas the solar radiation and evapotranspiration data are supplied by HELP based on user specification of Knoxville, Tennessee as the landfill location. Both earlier and more recent climate data are similar to the 1961 to 1990 data set and do not justify updating the HELP model files. The average annual total precipitation based on this data set is 54.39 in. The evaporative zone depth specified for all EMDF base case model runs is the HELP-suggested value (21 in.) for the Knoxville, Tennessee area. Maximum leaf area index was set to the HELP-suggested value 3.50. Model sensitivity to climate parameter values is presented in Appendix C.

Soil and Design Data. Soil and design data inputs define the profile(s) of landfill layers simulated by HELP. In addition to total landfill area and the percent of the area that generates surface runoff (assumed 100 percent), the thickness and soil properties of each layer are the essential data inputs. There are eight discrete layers incorporated into the cover design and eight layers incorporated into the liner design below the waste (Sect. 2.2). Additional geotextile layers incorporated into the design to protect the geomembrane layers were not considered in the HELP model as they do not significantly alter or retard the movement of infiltrating water.

Necessary data on the soil material include total porosity, volumetric moisture content (VMC) at field capacity (defined as VMC at 0.33 bars capillary pressure), VMC at wilting point (defined as VMC at 15 bars capillary pressure), and saturated hydraulic conductivity. The porosity, field capacity, wilting point, and saturated hydraulic conductivity are used to estimate the soil-water evaporation coefficients and Brooks-Corey soil moisture characteristic function parameters. The HELP model code contains default soil characteristics for 42 soil texture types (Schroeder et al. 1994, pages 30-31). The selected soil texture type and corresponding default characteristics for each EMDF layer are given in Table 3.11. The HELP profile of EMDF layer thickness, layer type designations, and soil characteristics is based on the preliminary design information referenced in the QA Report (UCOR 2020b). As engineering design for the EMDF proceeds, the HELP parameter assignments for future PA evaluations will be reviewed for consistency with updated design specifications.

The HELP model input data also includes the length and slope of lateral drainage layers, and assumptions regarding synthetic membrane quality, including pinhole density, installation defect density, and membrane placement quality. Values for these parameters based on the EMDF Preliminary Design are given in Table 3.12.

Table 3.11. HELP layer soil characteristics for EMDF design

EMDF profile	Layer #	Material description	Layer type[a]	Layer thickness (in.)	Soil texture type[b]	Total porosity (vol/vol)	Wilting point (vol/vol)	Field capacity (vol/vol)	Saturated hydraulic conductivity (cm/sec)
Final cover	1	Top soil/rock mix (vegetative/erosion control layer)	1	48	11	0.464	0.310	0.187	6.40E-05
	2	Sand/gravel (granular filter/drainage layer)	1	12	3	0.457	0.083	0.033	3.10E-03
	3	Large rock/riprap (biointrusion layer)	1	24	21	0.397	0.032	0.013	3.00E-01
	4	Gravel (lateral drainage layer)	2	12	21	0.397	0.032	0.013	3.00E-01
	5	HDPE-FML (geomembrane layer)	4	0.06	35				2.00E-13
	6	Amended compacted clay (low permeability)	3	12	0	0.427	0.418	0.367	2.50E-08
	7	Cover compacted clay (low permeability)	1	12	16	0.427	0.418	0.367	1.00E-07
	8	Contour gravel (waste surface layer)	1	12	24	0.365	0.305	0.202	2.70E-06
Waste	9	Waste	1	690.45	22	0.419	0.307	0.180	1.90E-05
Liner	10	Protective soil (layer protects liner)	1	12	8	0.463	0.232	0.116	3.70E-04
	11	Drainage (leachate collection system)	2	12	21	0.397	0.032	0.013	3.00E-01
	12	HDPE-FML (geomembrane layer)	4	0.06	35				2.00E-13
	13	GCL (low permeability)	3	0.24	17	0.750	0.747	0.400	3.00E-09
	14	Geonet leak detection layer (leak detection)	2	0.3	20	0.850	0.010	0.005	1.00E+01
	15	HDPE-FML (geomembrane layer)	4	0.06	35				2.00E-13
	16	Compacted clay layer (low permeability)	3	36	16	0.427	0.418	0.367	1.00E-07
	17	Soil geobuffer (barrier layer)	1	120	0	0.419	0.307	0.180	1.00E-05

[a]1 = vertical percolation, 2 = lateral drainage, 3 = barrier soil, 4 = geomembrane

[b]Soil texture types as defined in Schroeder et al. 1994, Table 4, pages 30–31.

EMDF = Environmental Management Disposal Facility
FML = flexible membrane liner
GCL = geosynthetic clay liner
HDPE = high-density polyethylene
HELP = Hydrologic Evaluation of Landfill Performance

Table 3.12. HELP model parameters for EMDF Preliminary Design lateral drainage and geomembrane layers

Drainage layer parameters			HDPE geomembrane quality characteristics (HELP layers 5, 12, 15)
HELP layer number	Drainage length (ft)	Drainage slope (%)	• Pinhole density: 1 hole/acre • Installation defect density: 1 hole/acre • Membrane placement quality: good
4	476.9	21.52	
11, 14	258.8	4.22	

EMDF = Environmental Management Disposal Facility
HDPE = high-density polyethylene
HELP = Hydrologic Evaluation of Landfill Performance

3.3.1.2 Engineered barrier performance assumptions

To account for long-term degradation of engineered barrier materials, consistent with the conceptual model of EMDF performance evolution (Fig. 3.5), the following three performance conditions are considered for disposal facility performance:

- Full design performance (design performance period, EMDF closure through 200 years post-closure): All layers are functional and included in the simulated HELP profile (Appendix C, Table C.2). This period includes the 100-year, post-closure period of institutional control and the first 100 years following the assumed loss of institutional control by DOE. Every component of the cover system is assumed to perform as designed, including the HDPE membrane and engineered drainage layer.
- Partial design performance (representative of the degrading performance period from 200 to 1000 years post-closure): Geomembrane liner layers and geosynthetic clay layers are assumed to be totally ineffective (i.e., no longer function as impermeable layers in the cover and liner systems) after 200 years post-closure. Assuming 200 years for the service life of the HDPE membrane is pessimistic given that recent studies have estimated much longer periods of full HDPE membrane performance in mixed LLW facilities (Tian et al. 2017). These layers (Appendix C, Table C.2, layers 5, 12, 13, and 15) are eliminated from the simulated EMDF profile for this performance period. In addition, the lateral drainage layers in the liner system are designated as vertical percolation layers, consistent with the expectation that active leachate collection will not continue for more than a few decades. The amended clay layer (Appendix C, Table C.2, layer 6) is also assumed to be degraded from 2.5E-08 to 3.5E-08 cm/sec due to the failure of the geomembrane liner above. In the context of the generalized conceptual model of EMDF performance evolution (Appendix C, Fig. C.4), this modeled performance condition provides a reference performance level (cover infiltration rate) for the period of degrading EMDF performance. Modeling EMDF performance without the HDPE membranes and assuming slightly degraded performance of the clay barriers is consistent with the expectation that while the membranes are intact, degradation of the clay layers by natural processes is limited. Full design performance is assumed for the lateral drainage layer in the cover system due to the expectation that the cover system remains largely intact, clogging of the drainage layer is unlikely (refer to Appendix C, Sect. C.1.2.2.1), and the overlying biointrusion layer will provide effective lateral drainage capacity in the event that the drainage layer capacity is reduced.
- Long-term performance (long-term performance period, > 1000 years post-closure): Degradation of the cover system due to some combination of erosion, root penetration, soil development, damage by storms, floods, or other natural hazards or differential settlement of the underlying waste causes an increase in the permeability of the clay barriers in the cover and a decrease in the efficiency of the engineered lateral drainage layer of the cover. The degraded condition for this performance period is represented by changes in the hydraulic conductivity of the lateral drainage layer (factor of 3 decrease) and amended clay layer (factor of 2.8 increase from design specification) in the HELP model profile.

HELP model parameter values chosen to represent degraded performance conditions are summarized in Table 3.13 for the full design, partial design and long-term performance conditions.

Table 3.13. Summary of HELP model input parameter assumptions and model output representing design and degraded EMDF hydrologic performance conditions

HELP model input parameter or predicted output flux		Full design performance (0–200 years)	Partial design performance (201–1000 years)	Long-term performance (> 1000 years)
HELP inputs (cover)	Lateral drainage layer hydraulic conductivity (cm/sec)	3.0E-01	3.0E-01	1.0E-01
	HDPE geomembrane function[a]	Functional	Degraded	
	Amended clay hydraulic conductivity (cm/sec)	2.5E-08	3.5E-08	7.0E-08
HELP output flux (in./year)	Lateral drainage collected	18.50	18.07	17.62
	Infiltration through cover clay barrier and into waste zone	0.00	0.43	0.88
HELP inputs (liner)	Leachate collection drainage layer function[a]	Functional	Not functional	
	HDPE geomembrane function[a]	Functional	Degraded	
	Geosynthetic clay layer function[a]	Functional	Degraded	
	Leak detection drainage layer function[a]	Functional	Not functional	
	HDPE geomembrane function[a]	Functional	Degraded	
HELP output flux (in./year)	Leachate collection layer drainage	0.00	Degraded	
	Leak detection layer drainage	0	Degraded	
	Infiltration through liner clay barrier	0	0.43	0.88

[a]Model layer function "Degraded" indicates the layer has been removed from the HELP profile for that performance stage. For lateral drainage layers in the liner system, "Not Functional" indicates that the layer type has been changed from lateral drainage to vertical percolation in the HELP profile.

EMDF = Environmental Management Disposal Facility
HELP = Hydrologic Evaluation of Landfill Performance
HDPE = high-density polyethylene

3.3.1.3 HELP model results and sensitivity to parameter assumptions

HELP model results and sensitivity to key input parameters are presented to provide the basis for quantitative cover infiltration inputs to the PA models described in subsequent sections. Additional information on the evaluation of HELP model sensitivity is provided in Sect. 5 and Appendix C.

HELP model runs were performed for each of the three disposal facility performance conditions described above. HELP model outputs (Table 3.13) provide estimated water fluxes through the EMDF cover system into the waste and out of the EMDF liner system. The HELP-predicted values are used to guide inputs (cover infiltration rates) to the more complex models of flow and contaminant transport used for the EMDF PA. Because the HELP model is primarily intended as a design tool rather than for predictions of long-term landfill hydraulic performance, the model outputs for the two degraded performance conditions are utilized as a general indication of the magnitude of increases in cover infiltration and leachate release that could be realized. Sensitivity of the HELP model results to input parameter uncertainty also is used to define the range of cover infiltration applied to evaluate uncertainty in long-term EMDF performance evolution.

Uncertainty in using the HELP model to predict long-term hydrologic performance of the EMDF cover system is related to the difficulty of specifying representative degraded-condition hydraulic conductivity (K_{sat}) values based on very limited understanding of the long-term performance evolution of earthen barriers and engineered drainage systems. The degree of degradation of clay barrier performance that could occur (due to natural processes over hundreds of years under stable climate conditions) is plausibly bounded by the upper end of the estimated range of rates of natural annual average recharge to groundwater in BCV, estimated at 7 to 12 in./year (DOE 1997b, Volume 2, Appendix F, pages F-36 and F-40). Additional HELP

model runs were performed to evaluate the sensitivity of estimated infiltration to the degree of degradation (change in saturated hydraulic conductivity, K_{sat}, value) assumed for the lateral drainage layer and the clay barrier of the cover, and to possible increases in future precipitation. The results of the sensitivity runs are summarized in the following paragraphs.

HELP model predicted cover infiltration values associated with different values of K_{sat} for the clay barriers of the cover system are shown in Fig. 3.13. For the partial design performance and long-term performance conditions, the amended clay and compacted clay units are modeled as separate layers (layers 6 and 7 in Table 3.11). For the sensitivity cases that represent more severe cover degradation, the clay barriers are modeled as a single uniform 2-ft-thick barrier layer in the HELP model. The value of K_{sat} given on the horizontal axis of Fig. 3.13 represents the hydraulic conductivity of the amended clay layer for the partial design and long-term performance conditions.

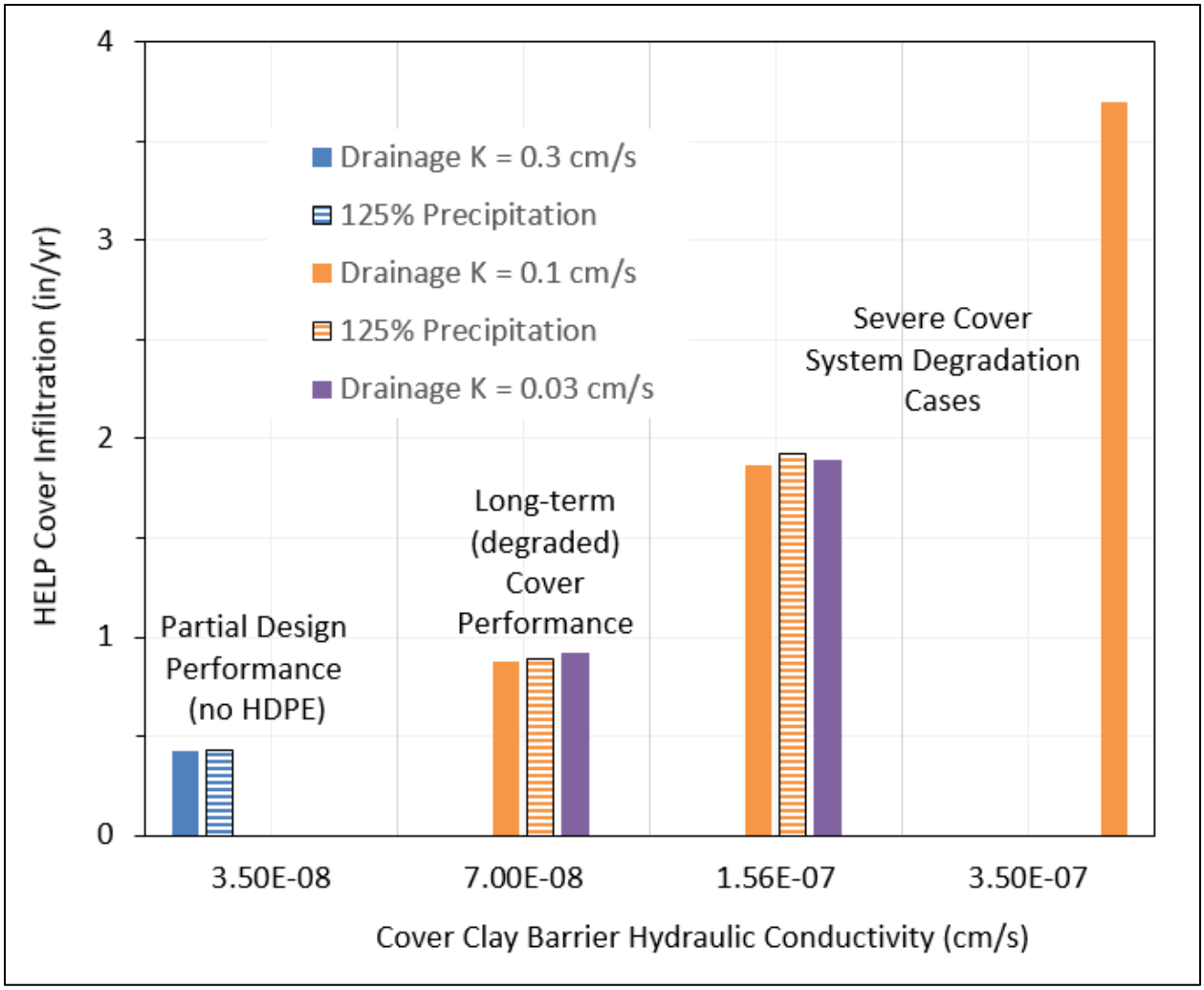

Fig. 3.13. HELP model sensitivity to cover layer parameter assumptions and precipitation inputs

The left-hand pair of bars in Fig. 3.13 represents infiltration predictions for the partial-design performance condition (without HDPE membranes) under the current average annual precipitation (approximately 54 in./year) and for a 25 percent increase in total annual precipitation. HELP-predicted infiltration sensitivity to the increased precipitation is minimal (1 percent increase) for the partial design performance

condition. For the long-term performance condition and the degraded cover sensitivity case with clay K_{sat} = 1.56E-07 cm/sec, a 25 percent increase in precipitation results in increases in cover infiltration of 2 percent and 3 percent, respectively (compare solid orange and striped orange bars on Fig. 3.13).

Results of HELP model sensitivity evaluation for anticipated future changes (Appendix C, Table C.4) in the clay barrier K_{sat} (increase from full design performance) and the lateral drainage layer K_{sat} (decrease from full design performance) show that sensitivity to cover drainage K_{sat} is much lower than for cover clay K_{sat} (Fig. 3.13) and that sensitivity to these two parameters is interdependent. Increases in infiltration are roughly proportional to the modeled increases in clay barrier K_{sat} (orange bars on Fig. 3.13) whereas decreases in lateral drainage K_{sat} result in much smaller increases (< 5 percent) in cover infiltration (compare the solid orange and purple bars on Fig. 3.13).

The sensitivity of the HELP model predictions to these parameter values, particularly the K_{sat} of the amended clay barrier in the cover system, indicates the importance of uncertainty in selecting parameter values to represent long-term performance conditions. HELP model parameter values selected for the EMDF long-term performance condition (Table 3.13, Fig. 3.13) result in predicted infiltration of 0.88 in./year, whereas the highest values of cover infiltration from the HELP sensitivity evaluation (3 to 4 in./year) are equivalent to approximately 50 percent of natural recharge rates estimated for geologic units at the EMDF site. The predicted fluxes are consistent with the expectation that the EMDF cover system, even in a degraded condition, will promote lateral drainage above the clay barrier and limit vertical percolation through the barrier, relative to natural conditions, for hundreds of years.

The HELP model tendency to over predict cover infiltration at humid sites (Appendix C, Sect. C.2.2.2) may mitigate some of the uncertainty in specifying degraded-condition parameter values for the HELP-modeled, long-term performance condition. In the context of EMDF performance modeling over thousands of years, using HELP to estimate EMDF performance degradation resulting from the full range of climatic and geologic processes and events is not justified, given the uncertainties at such extended time scales. For the EMDF PA, STOMP model sensitivity evaluation (Sect. 5.1) and sensitivity-uncertainty analysis for the EMDF total system model (Sects. 5.3 and 5.4) incorporates uncertainty in future precipitation and the degree of EMDF cover performance degradation consistent with the range of HELP modeled infiltration values.

3.3.2 Radionuclide Release and Vadose Zone Model Codes

Models of radionuclide release from the EMDF waste mass and vadose zone transport between the bottom of the waste and the water table are included in EMDF PA models at different levels of detail and complexity. A relatively complex numerical model, STOMP (White and Oostrom 2000, White and Oostrom 2006) has been implemented to simulate release of radionuclides from EMDF waste in the aqueous phase and to provide information on variations in the location, magnitude, and timing of radionuclide release beneath the disposal unit under different cover performance conditions and radionuclide mobility assumptions. The STOMP output provides the basis for developing a simplified representation of the pattern of release to the water table that is applied in the 3-D saturated zone transport model (Sect. 3.3.3). The STOMP model provides radionuclide flux exiting the liner and entering groundwater in the saturated zone below the facility that is compared to similar outputs from the total-system model (used for dose analysis and described in Sects. 3.3.4 and 3.4). This provides a basis for assessing the simplified radionuclide release and vadose zone representations in the total-system model.

The STOMP model was developed by Pacific Northwest National Laboratory (PNNL) for modeling variably saturated subsurface flow and transport systems. The STOMP code meets Nuclear Quality Assurance (NQA)-1-2000 software requirements and DOE O 414.1D (DOE 2013b) requirements for safety software. PNNL maintains the STOMP code in accordance with DOE contractor requirements.

Documentation of all verification and validation testing is publicly available (White and Oostrom 2000, White and Oostrom 2006, and Nichols et al. 1997).

A summary description of STOMP model inputs and implementation for the EMDF system is provided in the following subsections. Additional detail on the STOMP model architecture, governing equations, and solution schemes is provided in White and Oostrom (2000 and 2006). Detailed information on STOMP model setup and parameterization for the EMDF is provided in Appendix E of this PA.

3.3.2.1 STOMP model domain setup for EMDF

EMDF preliminary design data and existing information on stratigraphic geometry and hydrogeologic properties of rock and saprolite units in BCV (Sects. 2.1.3 and 2.1.5) were used to create two 2-D cross-section STOMP models for the EMDF site (Figs. 3.14 through 3.18). The 2-D approach to STOMP implementation is based on how the geometry of the liner system is expected to control spatial patterns and timing of leachate release. It is also based on the practical consideration of the computing resources required to develop a fully 3-D model grid with sufficiently fine resolution to capture liner design details at the scale of the facility. Because flow and radionuclide transport in the vadose zone is likely to be predominantly vertical (downward), the 2-D representation is appropriate. The results of the 2-D implementation are judged to adequately capture the effects of the sloping cell bottoms and sides (berms), variable waste thickness, and modeled variation in vadose zone thickness (water table depth below the liner bottom, refer to Sect. 4.1). A primary purpose of the STOMP simulations is to guide development of simplified uniform and non-uniform models of release to the saturated zone, for which the 2-D results are sufficient.

The Section A-A′ (Section A) STOMP model is a northwest to southeast (NW-SE) section oriented parallel to the predominant disposal facility floor slope (Fig. 3.14). Section A crosses cells 1, 2, 3, and 4 obliquely and captures the horizontal drainage impact of the liner system geometry. The northwest end of the model (A) starts at the crest of Pine Ridge while the southeast ends (A′) at Bear Creek. The Section B-B′ (Section B) STOMP model is a northeast to southwest (northeast to southwest) oriented section through the crest of the final cover surface that captures the maximum waste thickness across all four waste disposal cells.

The material type boundaries defined at each cross-section are shown on Figs. 3.15 and 3.16, based on the preliminary design and configuration of geologic materials at the site. For the STOMP modeling, the HDPE and other synthetic components of the liner system are assumed to be fully degraded. Each figure also shows the current (pre-construction) topography, estimated top of bedrock and approximate location of the post-closure water table based on the long-term performance condition groundwater flow model results (refer to Sect. 3.3.3.1 for detail on implementation of the EMDF groundwater flow model).

Model Discretization. A uniform grid spacing of 10 ft is used in the X (horizontal) direction. Each grid is assumed to have a 1 ft thickness in the Y (normal to section) direction for easy mass calculation. A refined and uniform 1-ft grid space is used to represent the lithologic and design component variation in the vertical (Z) direction in most of the section, except in the deeper bedrock zone where it transitions to 5 ft and 10 ft in thickness. The finer grid spacing in the vertical direction represents the disposal facility features and lithologic variation more precisely for predicting movement of the contaminants in the unsaturated zone beneath the facility. The same model grid design is used for both southwest to northeast and west to east cross-sections. Additional detail on STOMP model discretization is presented in Appendix E, Sect. E.2.2.

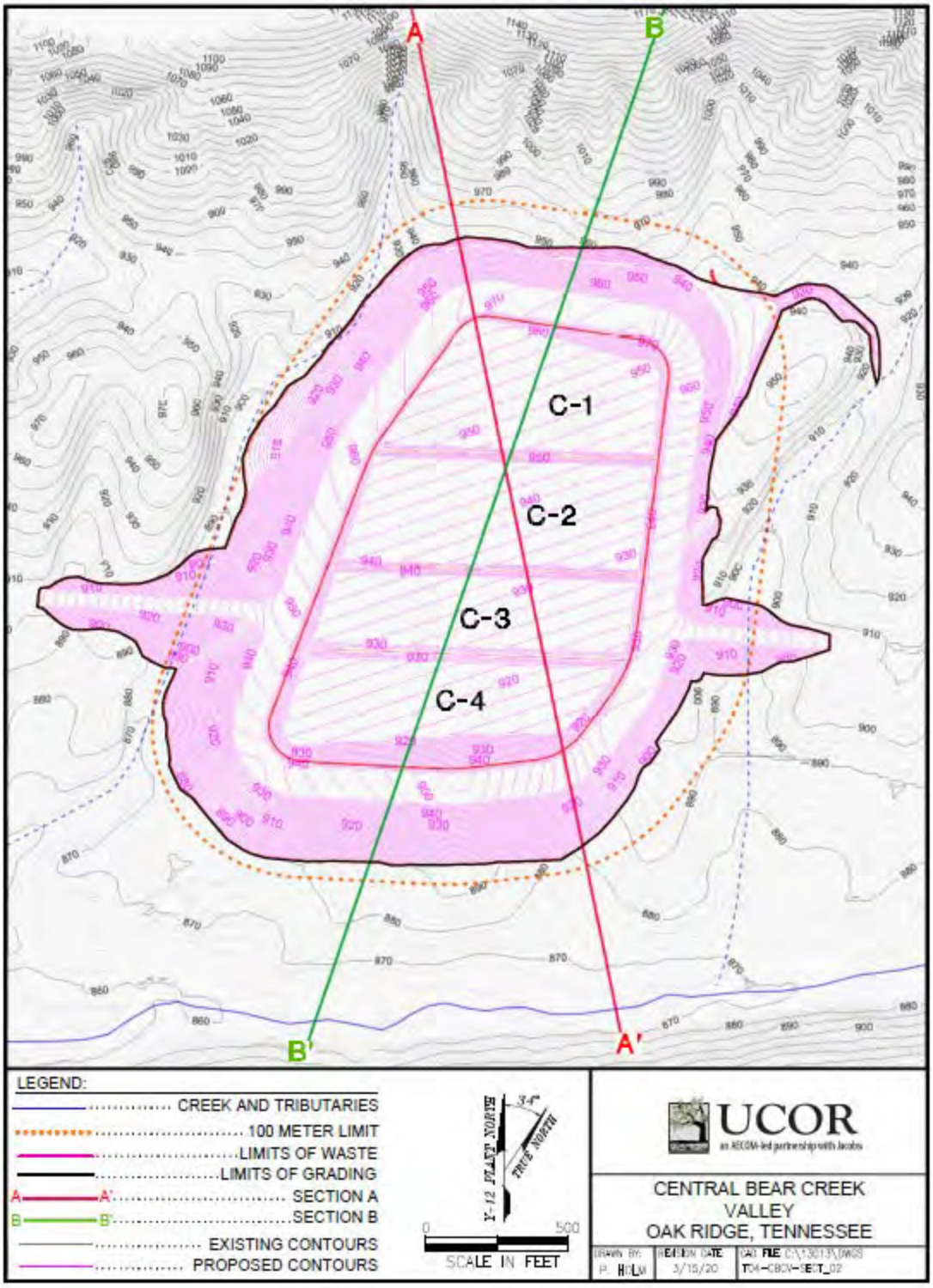

Fig. 3.14. Location of STOMP model cross-sections for EMDF

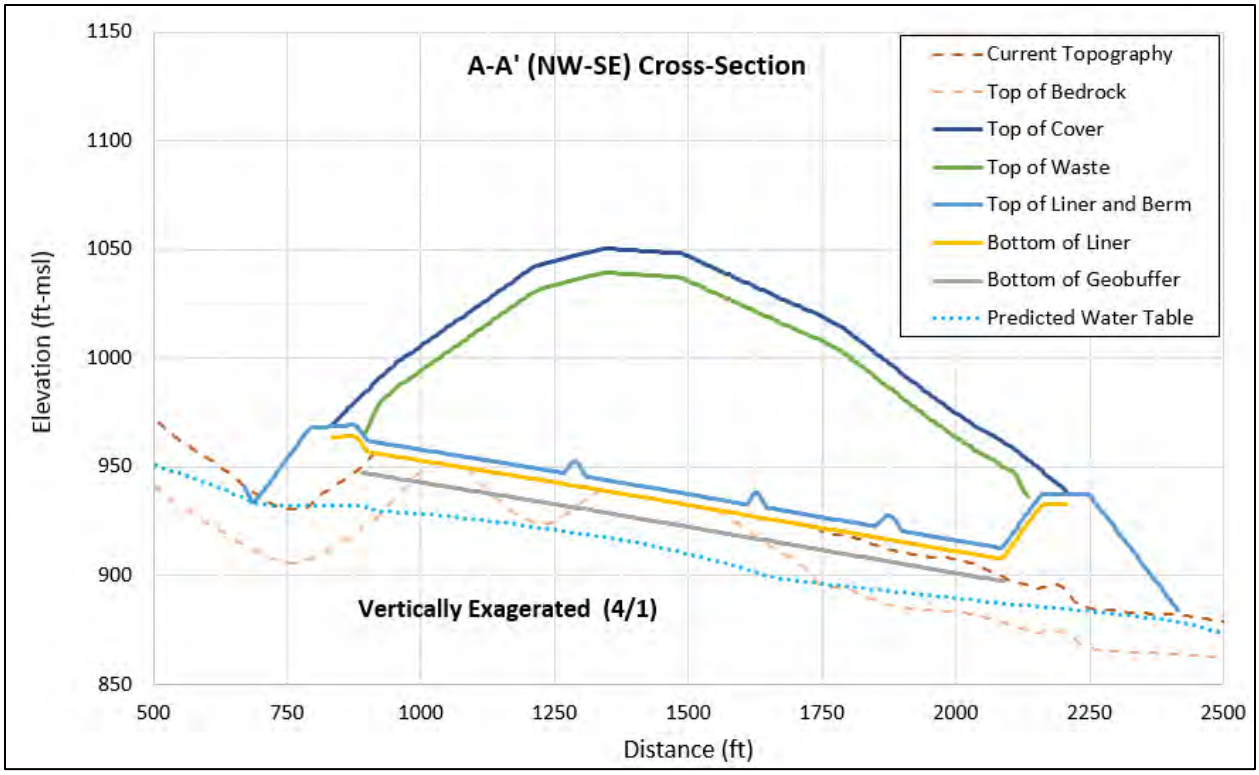

Fig. 3.15. Cross-section A-A′ material boundaries for STOMP model discretization

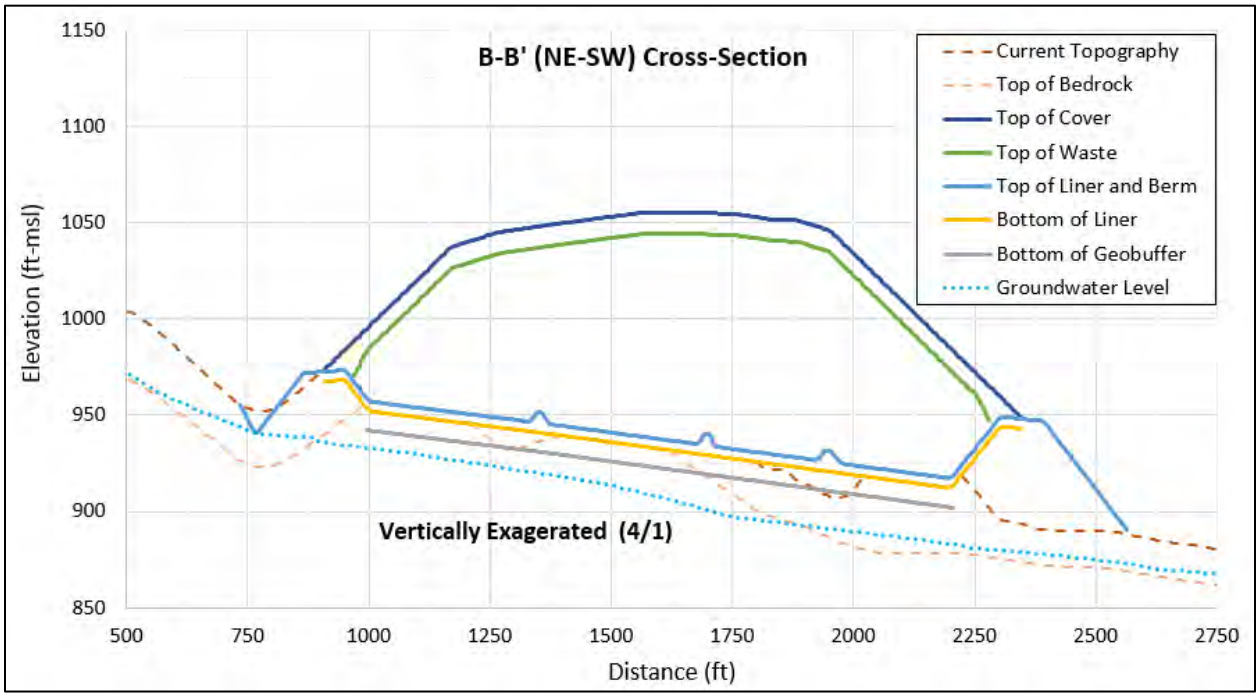

Fig. 3.16. Cross-section B-B′ material boundaries for STOMP model discretization

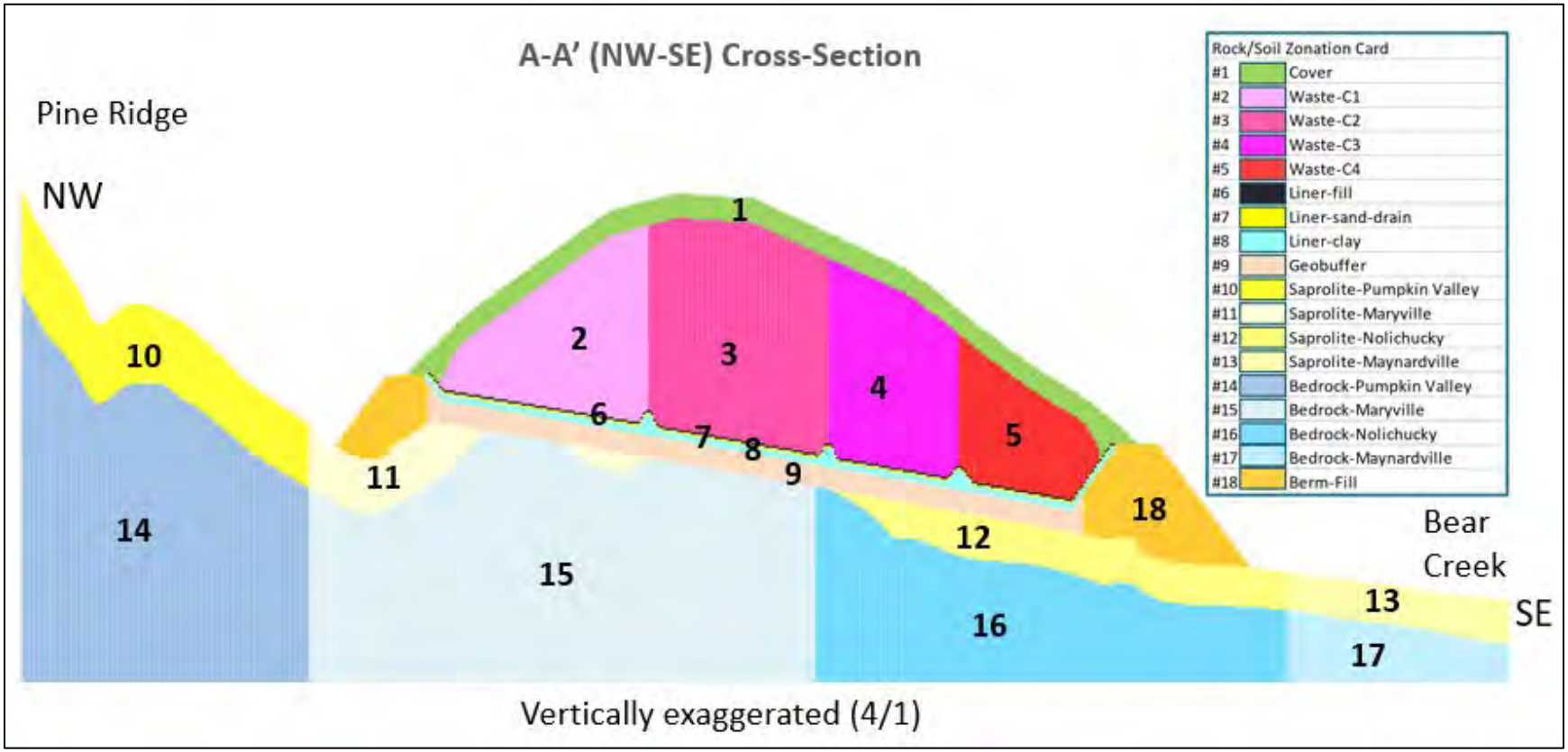

Fig. 3.17. Cross-section A-A′ material property zones

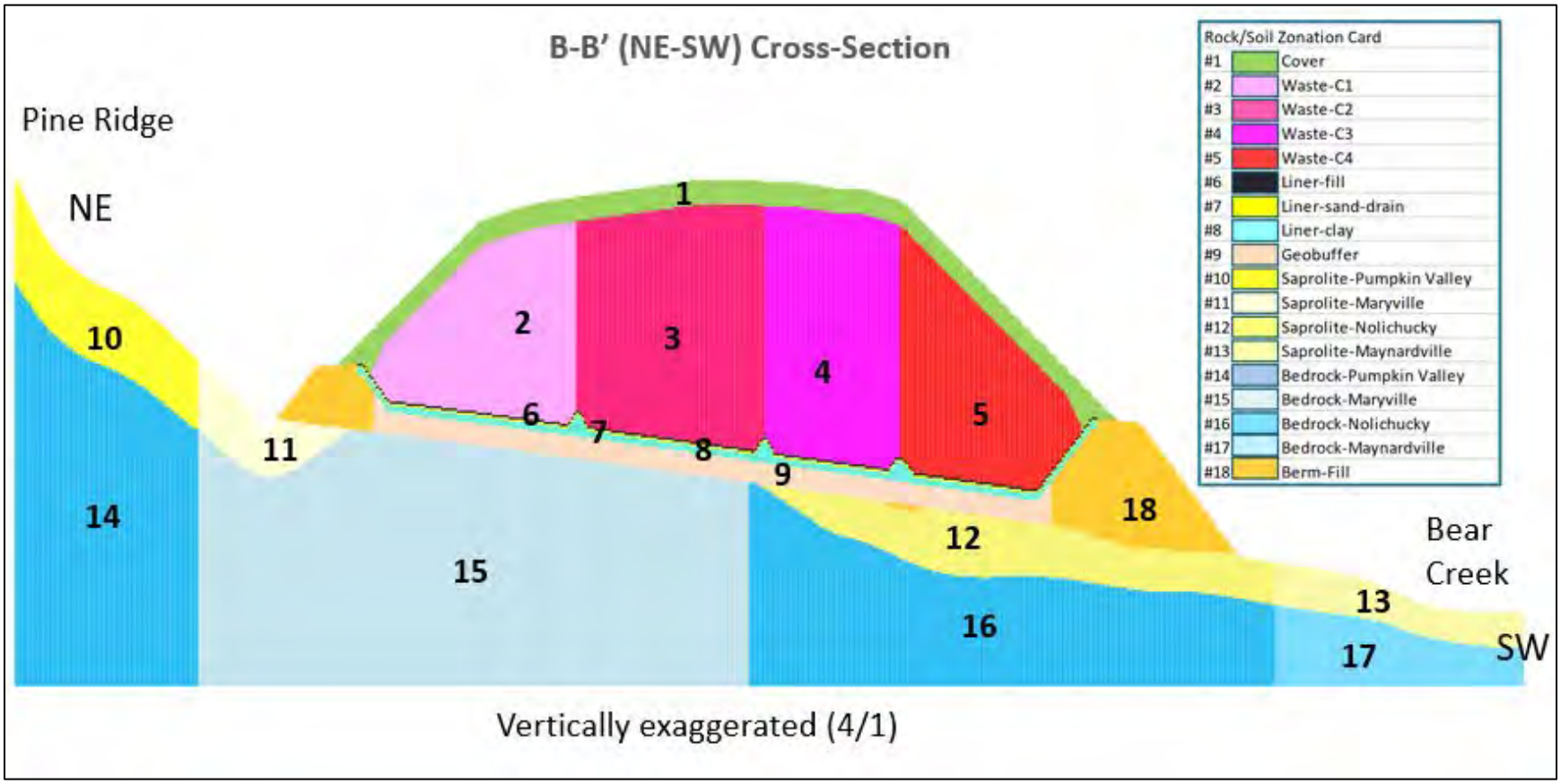

Fig. 3.18. Cross-section B-B' material property zones

Material Types. Properties of the materials in each 2-D zone of each cross-section (Figs. 3.17 and 3.18) are assigned for the following material types:

1) EMDF cover (single material type with properties derived from multilayer cover system design)
2) Waste-cell 1
3) Waste-cell 2
4) Waste-cell 3
5) Waste-cell 4
6) Liner-fill (protective material at the top of the liner system)
7) Liner-sand-drain (leachate drainage layer)
8) Liner-clay (infiltration barrier)
9) Geobuffer (geologic buffer zone)
10) Saprolite-Pumpkin Valley
11) Saprolite-Maryville (includes Rogersville and Rutledge units)
12) Saprolite-Nolichucky
13) Saprolite-Maynardville
14) Bedrock-Pumpkin Valley
15) Bedrock-Maryville (includes Rogersville and Rutledge units)
16) Bedrock-Nolichucky
17) Bedrock-Maynardville
18) Berm-fill (perimeter berms and structural fill).

The four waste material zones (2 through 5) are assigned a common set of properties, including initial radionuclide mass concentrations.

3.3.2.2 Model boundary conditions

The topographic surface for the EMDF (top of cover and berm) and the area outside of the footprint is the set of uppermost active model cells (nodes) where a free-air model boundary condition is assigned. All other boundary nodes where an unsaturated condition is present also have free-air boundary conditions that permit water discharge if the water pressure is greater than the atmospheric pressure. The bottom model boundary is assumed to be a no flow boundary. For the vertical boundaries at either end (southwest/northeast or west/east) of the model cross-sections, a hydraulic head gradient boundary condition (constant flux) is assigned for the saturated model nodes, allowing groundwater to flow in and out of the model domain at either end of the cross-section. The lower limit of the model domain was set well below the predicted long-term post-closure water table elevation (within the saturated zone) so that applied surface recharge rates and lateral flux boundary conditions do not lead to saturated conditions within the model domain above that elevation. For these 2-D model cross-sections, there is no flux into or out of the model domain in the Y direction.

Cover infiltration or (outside the cover limits) recharge boundary conditions are assigned along the top of the active model domain for each modeled cross-section. Spatial variation in the infiltration/recharge rate is assigned as shown in Fig. 3.19 for the Section A model. The same general recharge pattern is applied for

Section B. The infiltration/recharge rates applied in different areas include the natural recharge zones (6.1, 6.6, 9.6, and 13.1 in./year, depending on geologic unit), the berm side slopes (1 in./year), and the central cover/liner zone (increasing from 0 to 0.88 in./year between 200 and 1000 years post-closure). The maximum cover infiltration rate (0.88 in./year) is based on hydrologic performance model results for the long-term cover performance condition (Table 3.13), and the timing of the increase in infiltration is based on the assumed evolution of EMDF cover performance over time (Fig. 3.5). Sensitivity to the long-term cover performance assumption is addressed with a simulation assuming long-term cover infiltration increases to 1.76 in./year at 1000 years post-closure (Sect. 5.1).

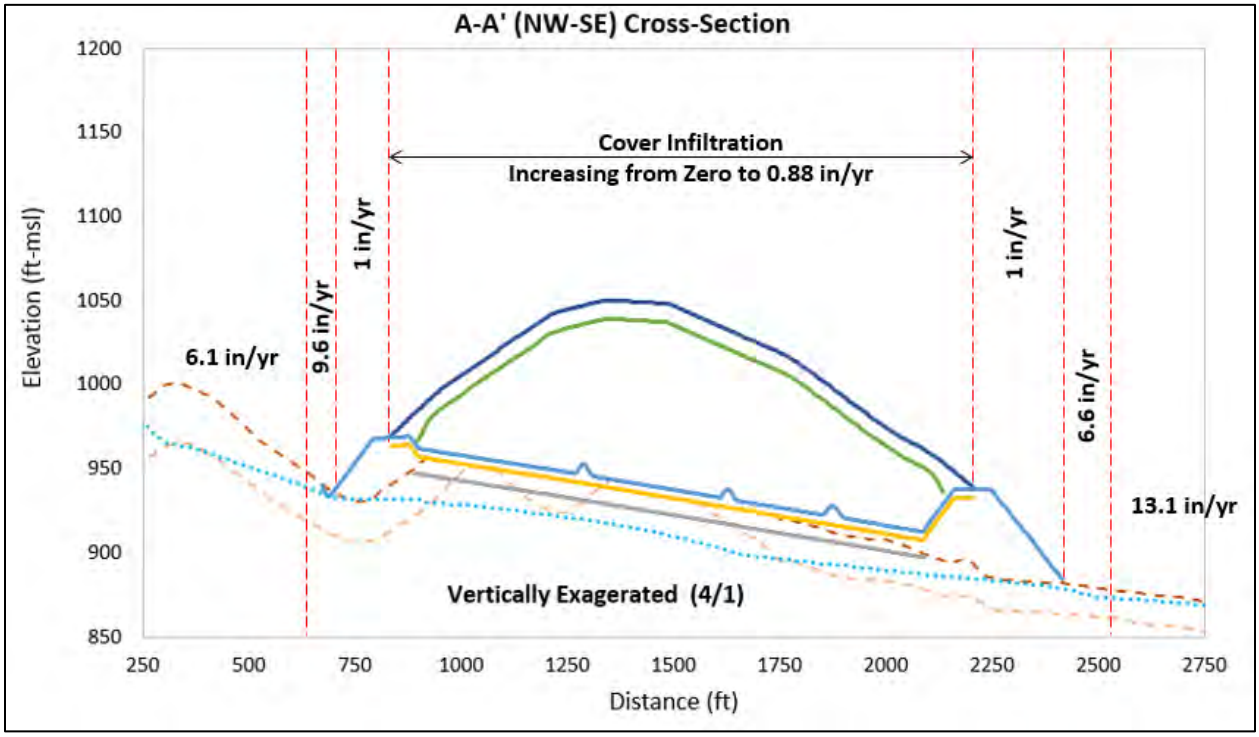

Fig. 3.19. Recharge zones applied to the STOMP Section A model

3.3.2.3 Material property inputs

The input parameter categories required to conduct a STOMP simulation include media mechanical and hydraulic properties; saturation function parameters; aqueous relative permeability relationship parameters for unsaturated flow; solute-fluid interaction; and solute-porous media interaction. These specific properties include the following:

- Mechanical properties include a particle density, porosity (total and diffusive), specific storativity, compressibility, and tortuosity function for each defined rock/soil type
- Hydraulic properties include an intrinsic permeability or hydraulic conductivities in each coordinate direction for each defined rock/soil type
- Saturation function parameters define a saturation-capillary pressure function for each defined rock/soil type
- Aqueous relative permeability parameters defines a relative permeability-saturation function for the aqueous phase for each defined rock/soil type

- Solute-fluid interactions define solutes, solutes, solubilities, diffusion coefficients, and solute radioactive decay path parameters (half-life)
- Solute-porous media interactions define solid-aqueous phase K_d and porous-media-dependent hydraulic dispersivities; solute-porous parameters are dependent on both the solute and rock/soil type.

Tables of STOMP input parameter values are provided in Appendix E, Sect. E.2.5. In general, the waste properties are assumed to be the same for all disposal cells, and material properties vary among the waste, cover, and liner system components as well as the geobuffer material, saprolite, and bedrock zones. The engineered materials and waste are assumed to be hydraulically isotropic, whereas the natural materials have anisotropic hydraulic conductivity values identical to those applied in the EMDF groundwater flow model (refer to Appendix D). Saturation and relative permeability functions are assumed to be similar across vadose material types except for minimum relative saturation values, which vary according to assumed material texture/pore size distribution (refer to Appendix E).

Values for all material property input parameters used in the EMDF STOMP models are based on available BCV data, design assumptions, or literature values. Values for material parameters (e.g., bulk density, porosity, saturated hydraulic conductivity, etc.) that are used in multiple EMDF models are consistent (equal values) in all cases where material zones or engineered layers were defined similarly across models. In some cases, (weighted) average values for some parameters are utilized for models with less detailed representation of system components such as cover system layers (STOMP) or saturated zone stratigraphy (RESRAD-OFFSITE). Detailed descriptions of input parameter values, data sources, and approaches for deriving average quantities are provided in the model-specific appendices (Appendix E for the STOMP model) and QA documentation (UCOR 2020b). An additional description of the QA procedures for ensuring and documenting consistency in assumptions and parameter values across models is provided in Sect. 9.

3.3.2.4 Initial radionuclide concentrations and solid-aqueous partition coefficients

Initial Radionuclide Concentrations in Waste. Based on initial simulations with the total system model (Sect. 3.3.4), a limited number of highly mobile or long-lived radionuclides were selected from the EMDF estimated inventory (Sect. 2.3 and Appendix B). These radionuclides have estimated inventories and other characteristics that result in large predicted dose contributions (relative to other radionuclides), either in the first few thousand years post-closure (C-14, Tc-99, I-129) or much later due to greater chemical retardation of transport (U-234, U-238, Pu-239). Tritium was also included in the STOMP simulations.

It is assumed that the waste has a uniform average initial radionuclide mass concentration throughout the four disposal cells. Estimated inventory concentrations are expressed in terms of activity concentrations (pCi/g) and must be converted to radionuclide mass per waste volume units (mg/L) as initial waste concentrations in the STOMP model. Table 3.14 summarizes the estimated waste average (as-generated) activity concentrations, adjusted concentrations to account for addition of clean fill (soil) and operational period losses of mobile radionuclides, and equivalent mass concentrations based on radionuclide specific activities and an assumed waste dry bulk density of 1900 kg/m^3.

Table 3.14. Initial activity and mass concentrations for the waste in STOMP model simulations

Radionuclide	As-generated waste average activity concentration (pCi/g)	As-disposed[a] waste average activity concentration (pCi/g, corrected for added clean soil mass)	Initial mass concentration (g/g)	Initial Volumetric concentration (mg/L)
H-3	2.10E+01	4.64E+00	4.73E-16	9.00E-10
C-14	5.43E+00	5.40E-01	1.20E-13	2.28E-07
Tc-99	5.28E+00	1.56E+00	9.18E-11	1.74E-04
I-129	7.66E-01	3.50E-01	1.94E-09	3.69E-03
U-234	1.19E+03	6.30E+02	1.02E-07	1.93E-01
U-238	7.18E+02	3.81E+02	1.12E-03	2.13E+03
Pu-239	1.10E+02	5.83E+01	9.25E-10	1.76E-03

[a] H-3, C-14, Tc-99, and I-129 concentrations are decreased to account for operational period losses.

STOMP = Subsurface Transport Over Multiple Phases

Solid-Aqueous Partition Coefficients. The assumed solid-aqueous partition coefficient values (K_d values, Table 3.15) for each of the radionuclides included in the STOMP model is based on available data for ORR materials and review of other data sources. Base case K_d values and data sources for all radionuclides included in the estimated EMDF radionuclide inventory are provided in Sect. 3.2.2.6. The base case K_d values in the waste zone are assumed to be one-half the base case K_d values assigned to the non-waste materials.

Table 3.15. Solid-aqueous partition coefficients for radionuclides included in STOMP modeling

Radionuclide	K_d (Waste) (cm^3/g)	K_d (Other Materials) (cm^3/g)	Half-life (year)	Specific Activity (Ci/g)
H-3	0	0	1.23E+01	9.80E+03
C-14	0	0	5.70E+03	4.50E+00
Tc-99	0.36	0.72	2.11E+05	1.70E-02
I-129	2	4	1.57E+07	1.80E-04
U-234	25	50	2.46E+05	6.20E-03
U-238	25	50	4.47E+09	3.40E-07
Pu-239	20	40	2.41E+04	6.30E-02

K_d = partition coefficient
STOMP = Subsurface Transport Over Multiple Phases

Model sensitivity to uncertainty in K_d values was evaluated with sensitivity runs utilizing either lower values for all non-waste media or higher values for the waste zone. For K_d value sensitivity runs, both the waste and non-waste media were assigned either the (lower) waste K_d value or the (higher) non-waste value. Results of STOMP model sensitivity runs are presented in Sect. 5.1 and Appendix E, Sect. E.3.3.

The STOMP model results are used to estimate an average vadose delay time for each radionuclide. This delay is due to the cover/liner system preventing infiltration and leachate release during the design performance period (assumed as 200 years for the PA analysis) and also results from chemical retardation of radionuclides migrating vertically through the unsaturated zone above the water table. The vadose delay time was assigned as the year at which the STOMP model total radionuclide flux reached 50 percent of the

peak simulated flux at the water table elevation. Additional detail is provided in Appendix E, Sect. E.3.4.2. The STOMP-based delay times were used in developing radionuclide-specific release models for calculating radionuclide flux to the water table in the MT3D saturated zone transport model (refer to Sect. 3.3.3.2 and Appendix F).

In addition to providing the basis for the vadose delay time estimates, the STOMP model results were used to quantify non-uniformity in volumetric leachate flux and radionuclide flux at the water table beneath the EMDF liner and geologic buffer. These STOMP results were applied develop non-uniform waste area leachate flux and recharge concentrations for the MT3D model analysis of the impact of non-uniform release on saturated zone model results at the groundwater POA. Additional details on the use of STOMP model results to support the saturated zone radionuclide transport modeling are provided in Sect. 3.3.3.2 and Appendix F.

3.3.3 Saturated Zone Flow and Transport Model Codes

Model tools utilized for the EMDF saturated zone are 3-D models of groundwater flow (MODFLOW) and radionuclide transport (MT3D). This pair of models is used to simulate the effect of the local reduction in groundwater recharge below EMDF following facility closure and to provide a fully 3-D simulation of radionuclide transport in the heterogeneous, anisotropic, fractured-rock system at the CBCV site. A separate radionuclide release approximation (release model) was developed to provide the time-varying radionuclide flux to the water table below the disposal unit.

3.3.3.1 Groundwater flow model

The groundwater model was developed based on the BCV regional groundwater flow model (DOE 1997b). This regional model forms the foundation for all the sub-regional and site-specific models developed for the Bear Creek, Y-12, and the EMWMF sites (DOE 1998a, BJC 2003, BJC 2010a). The BCV model and site-specific models were developed using MODFLOW code, a finite-difference groundwater flow code developed by USGS (USGS 1988a). MODFLOW is a modular, block-centered finite-difference groundwater flow code capable of simulating both transient and steady-state saturated groundwater flow in one, two, or three dimensions.

MODFLOW implicitly considers that the system can be characterized as a porous medium. The application of a porous media code to a fractured bedrock system such as BCV is, therefore, an EPM approach. This approach assumes the rock is fractured to the extent that it behaves hydraulically as a porous medium. Three-D representation of hydraulic properties within MODLFOW also provides flexibility to represent fracture orientations in terms of anisotropy and fracture distribution in terms of heterogeneity. This approach is applicable to BCV given the high degree of weathering near the surface, numerous bedding planes and fractures in the sedimentary rock units, presence of a very active groundwater flow system, and extensive groundwater-surface water interaction. Previous model applications in BCV show consistency with field groundwater and surface flow measurements through mass balance analyses and with contaminant plume extent and movement through particle tracking (USGS 1988b, DOE 1997b, BJC 2010a).

Groundwater flow models were developed to represent current, pre-construction conditions (CBCV model) and future, post-closure conditions (EMDF model). The CBCV model incorporates recently completed site characterization data (Sect. 2.1.11) and was calibrated against a year of groundwater and surface water monitoring data (Appendix D, Sect. D.3.3). The EMDF model incorporates preliminary design features and incorporates the assumptions regarding long-term changes in cover infiltration in the post-closure period. Setup of the model domain, vertical discretization (model layering), and parameterization are reviewed

briefly in the following subsections. Additional detail on model development, including calibration, is provided in Appendix D.

MODFLOW code setup and parameterization. The extent of the model domain for the CBCV and EMDF flow models was selected based on the EMDF location, calibration data availability, and consideration of the effects of imposed boundary conditions on model predictions close to the disposal site. The model domain (Fig. 3.20) and finite difference grid are based on a telescopic mesh refinement applied to the calibrated regional flow model originally constructed for the BCV FS (DOE 1997c). The models have a 10 ft × 10 ft horizontal grid spacing with nine vertical layers (Fig. 3.21).

Material parameters for the nine model layers are selected to reflect vertical variation in the hydraulic properties (porosity, hydraulic conductivity, anisotropy) of the geologic media and engineered materials. Model layer 1 represents the saprolite zone and engineered features (e.g., berms and liner system in the EMDF model). Model layers 2, 3, and 4 represent highly fractured bedrock, and layers 5 through 9 represent less fractured bedrock. The EMDF flow model includes modifications to the upper two model layers to represent the EMDF liner and geobuffer configuration. The top two model layers have variable thicknesses ranging from 4 to 88 ft, reflecting variation in the thickness of the saprolite zone (Fig. 3.21) and the engineered features in the EMDF model.

Six distinct hydraulic conductivity zones for each model layer (shown for model layer 1 in Fig. 3.22) were used in the flow models to represent the eight geologic units that exist in BCV (Knox, Maynardville, Nolichucky, Maryville-Rogersville-Rutledge [combined], Pumpkin Valley, and Rome Formations) based on existing field measurements (Sect. 2.1.5.4) of hydrological properties. The selection of these geologic units as distinct hydraulic units is based on the thickness of the units, the availability of hydraulic data, and lithologic and hydraulic similarity among units. For the EMDF model, additional zones for layer 1 were incorporated to represent liner/geobuffer materials and areas of structural fill (Fig. 3.22). The CBCV site is modeled as a single unconfined system, with decreasing hydraulic conductivity with depth, and the 45-degree dip in the geological strata represented by staggering hydrogeologic units (conductivity zones) with depth (Fig. 3.23, Table 3.16).

Previous BCV field observations and modeling efforts (Sect. 2.1.5.4) have established that the groundwater system is strongly anisotropic and flows preferentially along the geologic strike (model y-coordinate direction). The K_y value represents the conductivity parallel to strike, K_x is the horizontal conductivity perpendicular to strike, and K_z represents the vertical hydraulic conductivity. Anisotropy ratios [K_y vs. K_x or K_z] of 5:1 (for model layer 1) and 10:1 (for layers 2-9) were used to represent the preferred fracture/bedding orientation of the geologic units (Table 3.17). Both field data and previous modeling sensitivity analyses support the anisotropy ratios used in the model (Appendix D, Sect. D.3.2.1).

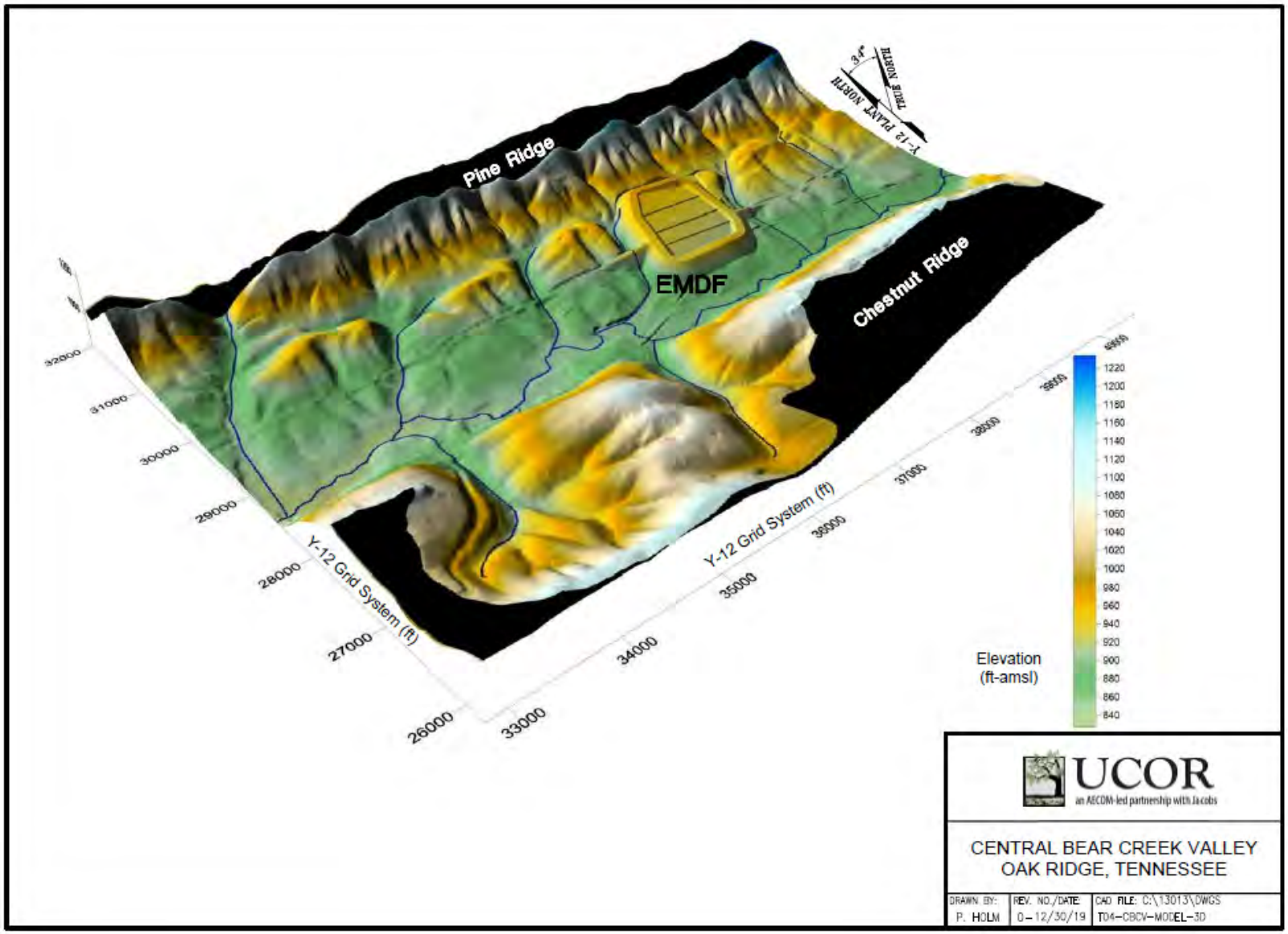

Fig. 3.20. EMDF groundwater flow model domain and topography

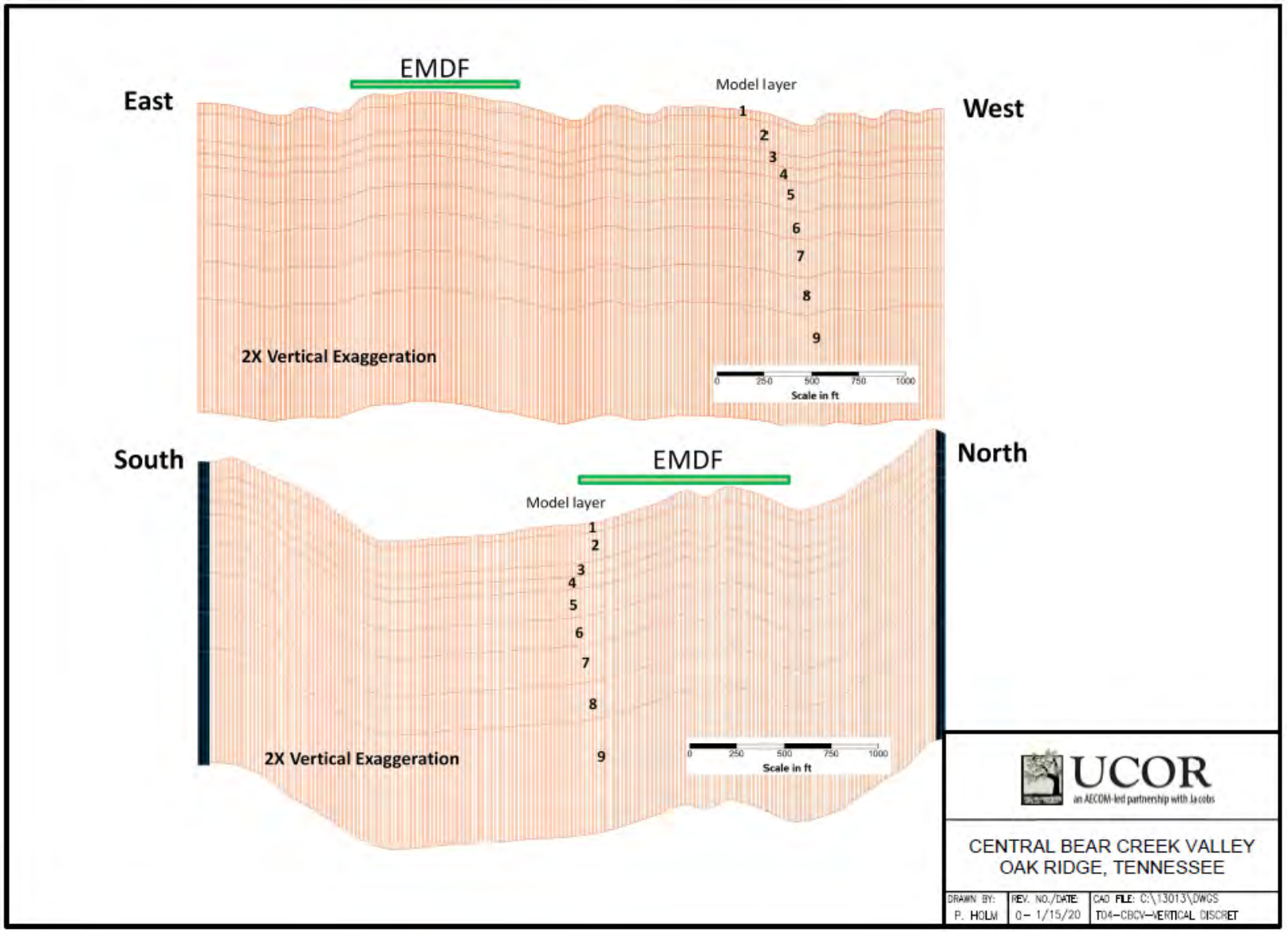

Fig. 3.21. CBCV model vertical cross-sections showing horizontal and vertical discretization

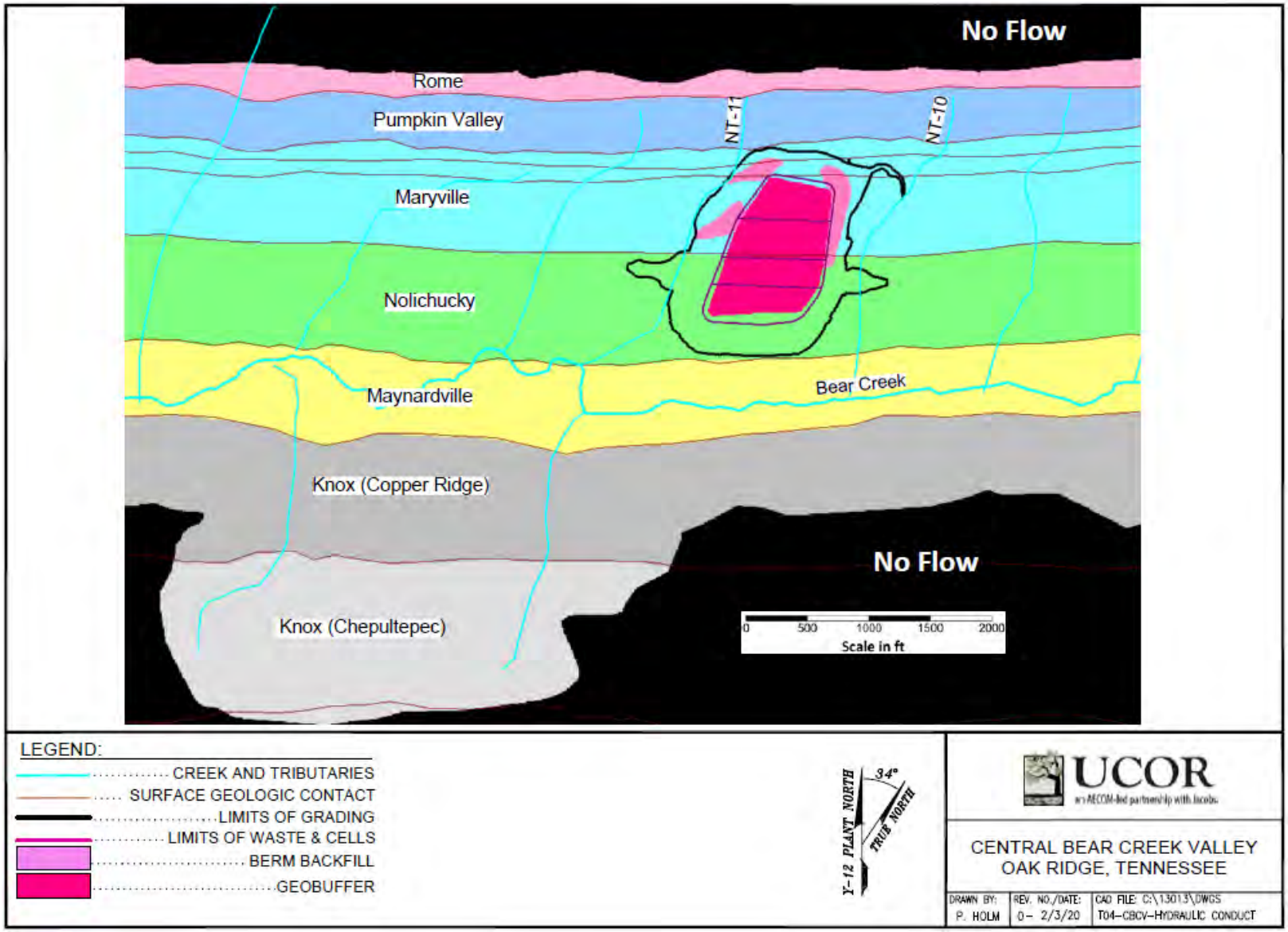

Fig. 3.22. Hydraulic conductivity zones corresponding to geological units in EMDF model layer 1

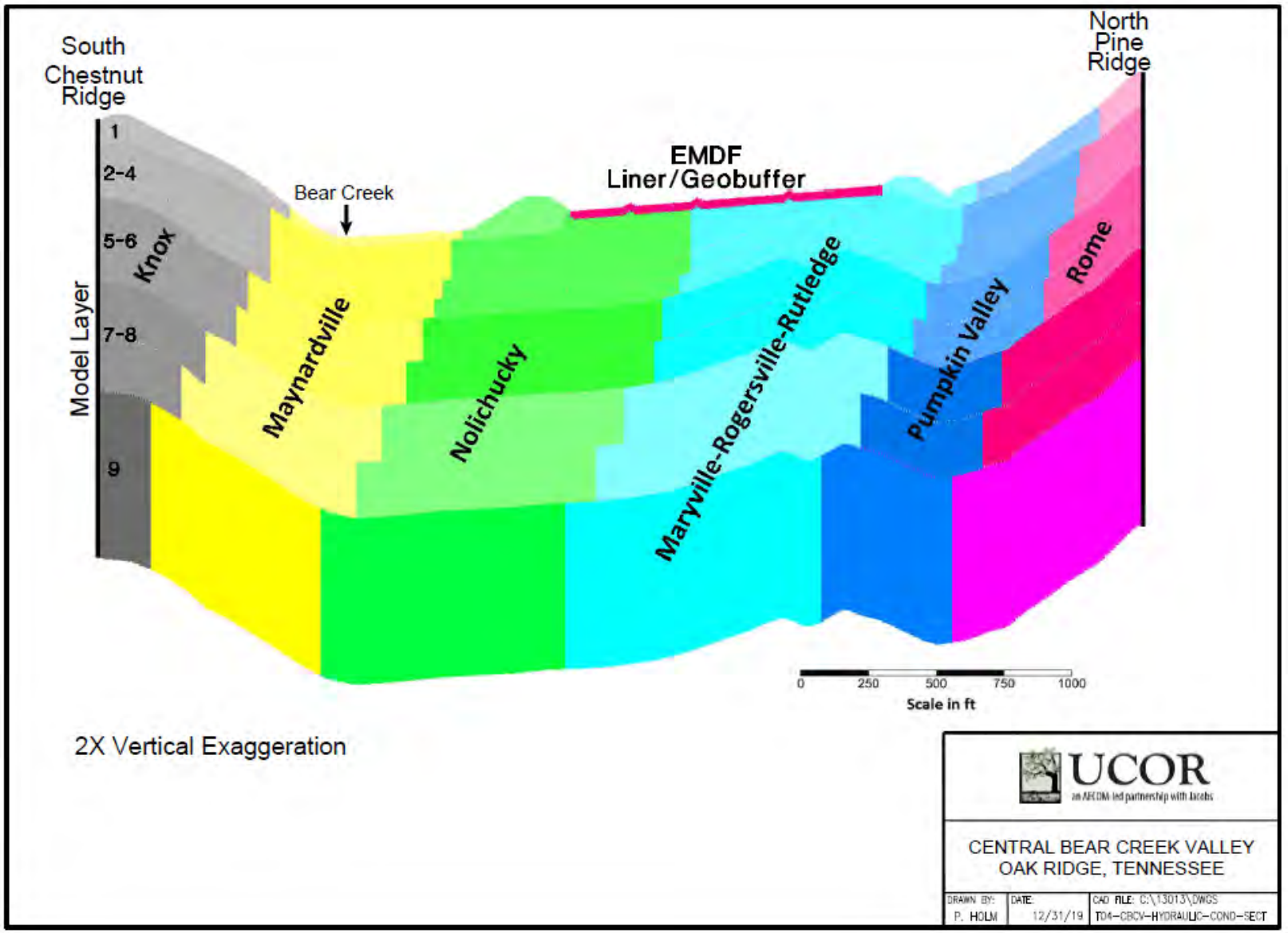

Fig. 3.23. Hydraulic conductivity field representing BCV stratigraphy and engineered features in the EMDF flow model

Table 3.16. Hydraulic conductivity values for geologic formations and model layers of the CBCV and EMDF flow models

Geologic Formation	Model Layer	Kx (ft/day)	Ky (ft/day)	Kz (ft/day)	Ky/Kx Ky/Kz	Kx (cm/sec)	Ky (cm/sec)	Kz (cm/sec)
Knox	1	1.56E+00	7.80E+00	1.56E+00	5	5.5E-04	2.7E-03	5.5E-04
	2--4	9.18E-03	9.18E-02	9.18E-03	10	3.2E-06	3.2E-05	3.2E-06
	5--6	2.54E-03	2.54E-02	2.54E-03	10	8.9E-07	8.9E-06	8.9E-07
	7--8	1.16E-03	1.16E-02	1.16E-03	10	4.1E-07	4.1E-06	4.1E-07
	9	5.00E-04	5.00E-03	5.00E-04	10	1.8E-07	1.8E-06	1.8E-07
Maynardville	1	2.13E+00	1.07E+01	2.13E+00	5	7.5E-04	3.8E-03	7.5E-04
	2--4	5.00E-02	5.00E-01	5.00E-02	10	1.8E-05	1.8E-04	1.8E-05
	5--6	3.34E-03	3.34E-02	3.34E-03	10	1.2E-06	1.2E-05	1.2E-06
	7--8	1.52E-03	1.52E-02	1.52E-03	10	5.4E-07	5.4E-06	5.4E-07
	9	4.80E-04	4.80E-03	4.80E-04	10	1.7E-07	1.7E-06	1.7E-07
Nolichucky	1	1.50E-01	7.50E-01	1.50E-01	5	5.3E-05	2.6E-04	5.3E-05
	2--4	9.50E-03	9.50E-02	9.50E-03	10	3.4E-06	3.4E-05	3.4E-06
	5--6	2.52E-03	2.52E-02	2.52E-03	10	8.9E-07	8.9E-06	8.9E-07
	7--8	6.10E-04	6.10E-03	6.10E-04	10	2.2E-07	2.2E-06	2.2E-07
	9	5.00E-05	5.00E-04	5.00E-05	10	1.8E-08	1.8E-07	1.8E-08
Maryville-Rogersville-Rutledge	1	1.00E-01	5.00E-01	1.00E-01	5	3.5E-05	1.8E-04	3.5E-05
	2--4	3.60E-03	3.60E-02	3.60E-03	10	1.3E-06	1.3E-05	1.3E-06
	5--6	1.35E-03	1.35E-02	1.35E-03	10	4.8E-07	4.8E-06	4.8E-07
	7--8	3.20E-04	3.20E-03	3.20E-04	10	1.1E-07	1.1E-06	1.1E-07
	9	4.50E-05	4.50E-04	4.50E-05	10	1.6E-08	1.6E-07	1.6E-08
Pumpkin Valley	1	1.00E-01	5.00E-01	1.00E-01	5	3.5E-05	1.8E-04	3.5E-05
	2--4	4.72E-03	4.72E-02	4.72E-03	10	1.7E-06	1.7E-05	1.7E-06
	5--6	1.75E-03	1.75E-02	1.75E-03	10	6.2E-07	6.2E-06	6.2E-07
	7--8	4.20E-04	4.20E-03	4.20E-04	10	1.5E-07	1.5E-06	1.5E-07
	9	5.60E-05	5.60E-04	5.60E-05	10	2.0E-08	2.0E-07	2.0E-08
Rome	1	4.00E-01	2.00E+00	4.00E-01	5	1.4E-04	7.1E-04	1.4E-04
	2--4	4.00E-02	4.00E-01	4.00E-02	10	1.4E-05	1.4E-04	1.4E-05
	5--6	5.00E-03	5.00E-02	5.00E-03	10	1.8E-06	1.8E-05	1.8E-06
	7--8	1.00E-03	1.00E-02	1.00E-03	10	3.5E-07	3.5E-06	3.5E-07
	9	5.00E-04	5.00E-03	5.00E-04	10	1.8E-07	1.8E-06	1.8E-07

CBCV = Central Bear Creek Valley
EMDF = Environmental Management Disposal Facility

Table 3.17. Recharge rates for the EMDF flow model

Recharge areas	Recharge rate	
	ft/day	in./year
Rome	2.20E-03	9.6E+00
Pumpkin Valley	1.40E-03	6.1E+00
Maryville-Rogersville-Rutledge	2.20E-03	9.6E+00
Nolichucky	1.50E-03	6.6E+00
Maynardville	3.00E-03	1.3E+01
Knox (Copper Ridge)	1.00E-03	4.4E+00
Knox (Chepultepec)	5.00E-04	2.2E+00
EMDF berm slope	2.28E-04	1.0E+00
EMDF lined area	2.00E-04	8.8E-01

EMDF = Environmental Management Disposal Facility

Groundwater Flow Model Boundary Conditions. The groundwater system in BCV is bounded by Pine Ridge to the north and Chestnut Ridge to the south; the two ridge crests coincide with the northern and southern no-flow boundaries of the groundwater model domain (Fig. 3.24). The vertical base (bottom) of the model also is assumed to be a no-flow boundary because minimal exchange of meteoric water with mineralized groundwater occurs below this depth (about 800 ft bgs [Sect. 2.1.6.1]). Constant head boundary conditions were assumed along the west (outflow) and east (inflow) ends of the model, based on a steady-state simulation of the calibrated regional BCV groundwater flow model (Appendix D).

Recharge from precipitation is the primary source of inflow to groundwater for the model because the domain is bounded on two sides by no-flow boundaries and two sides by the constant head boundaries. Varying recharge rates were assigned in the model for different zones corresponding to surface exposure of different geological units, hydrologic properties of soils, and assumed values for the perimeter berms (1 in./year) and the EMDF liner footprint (Table 3.17). For the EMDF flow model, cover infiltration rates representing three different performance conditions (Sect. 3.3.1.2) were applied as the recharge rate to the lined area (Fig. 3.22). Model sensitivity to higher and lower recharge rates was evaluated for both the CBCV model and the EMDF model.

The EMDF flow model results supported the development of the preliminary design and the long-term performance analysis, providing estimated water table elevations and groundwater flow fields beneath the disposal unit. For the saturated zone radionuclide transport modeling described in the following section, the EMDF model with the recharge rate that represents the long-term performance condition (0.88 in./year applied to the lined area of the disposal unit) is used to provide the flow field for the MT3D transport model. This approach over estimates EMDF recharge for the period of degrading cover performance (between 200 and 1000 years) assumed for the base case scenario, and results in quicker saturated zone transport toward the 100 m buffer during that period. This simplification in applying the recharge boundary condition to the EMDF footprint thus provides a measure of pessimistic bias to the modeling.

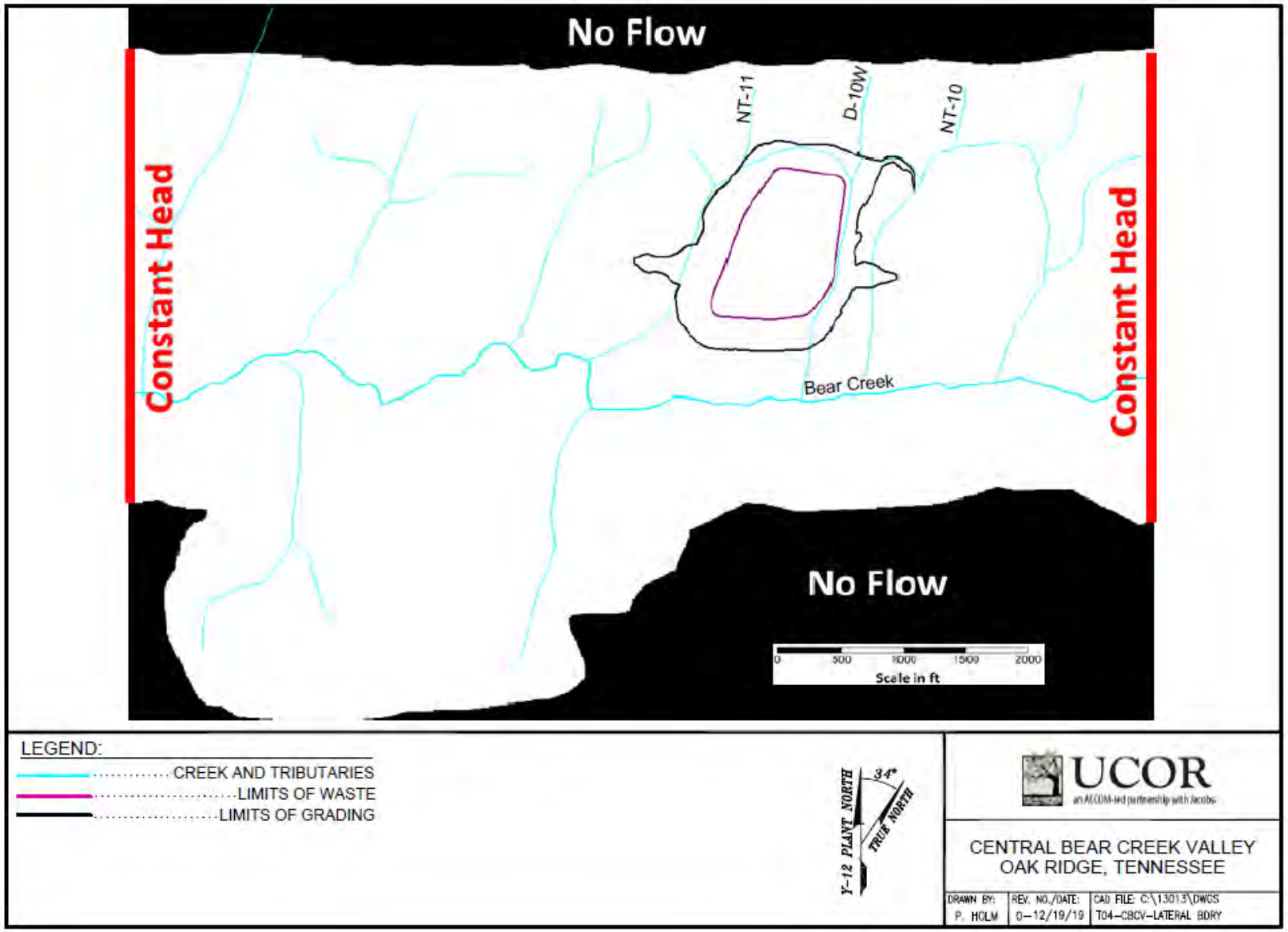

Fig. 3.24. Hydraulic boundary conditions for the EMDF flow model

Model domain interior boundary conditions represent the surface water-groundwater connections. The surface drainage features are represented in the model as either drain cells (for Bear Creek tributaries) or river cells. Both drain cells and river cells are head-dependent flux boundary conditions. Drain cells only allow groundwater to discharge at a surface water feature, whereas river cells allow both influx (gaining) and outflux (loosing) interaction with the groundwater. Section 2.1.7 presents a discussion of spatial and seasonal variations in surface water flows that reflect variability in groundwater discharge.

Appendix D provides a detailed description of the development and calibration of the CBCV model and the application of the EMDF model to the PA analyses. The primary uses of the EMDF flow model results are to provide an estimate of the average vertical interval between the bottom of waste and the water table (vadose zone thickness) for the long-term performance condition, and as the groundwater flow field for the MT3D saturated zone radionuclide transport model. These flow model results support the parameterization of the vadose zone (thickness) in the total system model (RESRAD-OFFSITE) and identifying the location of the groundwater and surface water POAs, as described in the following section. The EMDF model results are presented in Sect. 4.1.

3.3.3.2 Saturated Zone Radionuclide Transport Model

The MT3D model uses the EMDF flow model results for the long-term performance condition as the flow field for simulation of saturated zone radionuclide transport. The purposes of the MT3D modeling include the following:

1) Delimit the maximum extent of the contaminant plume
2) Determine the location of maximum concentration along the 100-m buffer zone boundary (groundwater POA)
3) Quantify the pattern of radionuclide discharge to streams and identify the surface water POA
4) Predict the peak concentrations and timing of peak for selected radionuclides at the 100-m groundwater well location
5) Evaluate the potential impact of non-uniform radionuclide release from the EMDF.

MT3D (Zheng 1990) is a comprehensive 3-D numerical simulation code that incorporates physical and geochemical processes that influence radionuclide fate and transport including advection, hydrodynamic dispersion, chemical retardation, and radioactive decay. Necessary input parameters include solute dispersivity in the three model coordinate directions, solid-aqueous phase K_d values, and radionuclide half-life. Bulk density and effective porosities of the saprolite and bedrock are also needed for parameterizing chemical retardation. The boundary condition for radionuclide flux from the vadose zone to the water table below the disposal unit, including the area and timing of release, is estimated with a simplified release model developed for each radionuclide of interest.

Based on the radionuclide release and vadose zone transport modeling results (STOMP model, Appendix E), only three of the radionuclides in the EMDF estimated inventory (Tc-99, C-14, and I-129) will be released to the saturated zone within the EMDF post-closure period before 10,000 years. The others will either decay before release (H-3) or arrive at the groundwater table after 50,000 years (uranium and plutonium isotopes). Therefore, the MT3D fate-transport modeling of saturated zone is conducted only for Tc-99, C-14, and I-129.

The MT3D model domain and discretization scheme are identical to the EMDF flow model, which provides the saturated zone flow field for the radionuclide transport simulation. Parameterization of the MT3D model and application for the five purposes listed above are reviewed briefly in the following subsections.

Additional detail on model development and parameterization, including use of STOMP model results to determine the timing of release for each radionuclide, is provided in Appendix F.

Material properties, dispersivity, and retardation parameters. Total and effective porosity values for different layers in the transport model are listed in Table 3.18. For the saturated zone, a single porosity conceptualization is adopted and only the effective porosity is used in the MT3D model (total and effective porosity were assumed to be equal). Decreased effective porosity values in deeper model layers reflect the fact that the bedrock at depth is less fractured and less weathered. Based on the total porosity, the dry bulk density values are calculated assuming average solid particle densities of 2.65 g/cm^3 for model layer 1 and 2.78 g/cm^3 for all other layers (Table 3.18). The same material properties were applied in all the PA models to the extent possible given differing levels of model detail.

Table 3.18. Porosity and bulk density values assigned in the MT3D model

Model layer	Total porosity	Effective porosity	Bulk Density (g/cm^3)
1	0.27	0.27	1.93
2	0.20	0.20	2.22
3	0.15	0.15	2.36
4	0.10	0.10	2.50
5	0.05	0.05	2.64
6	0.04	0.04	2.67
7	0.03	0.03	2.70
8	0.02	0.02	2.72
9	0.01	0.01	2.75

The transport model assumes a longitudinal (Y-direction) dispersivity of 10 m, based on the 100-m distance to the groundwater well and a 10 percent rule-of-thumb (Gelhar et al. 1992) for estimating longitudinal dispersivity as a fraction of travel distance. In the absence of site specific data, horizontal (X-direction) transverse dispersivity is assumed to be one order of magnitude smaller than longitudinal dispersivity while vertical transverse (Z-direction) dispersivity is assumed to be two orders of magnitude smaller than longitudinal dispersivity (Zheng and Bennett 1995).

For chemical retardation of radionuclide transport, linear isotherm equilibrium sorption is assumed and a single distribution coefficient, K_d, defines the relationship between radionuclide concentrations in the aqueous phase and the concentration of sorbed material in the porous matrix. The assignment of an appropriate, constant K_d value to represent the retardation effect of sorption processes integrated over long time periods is an important uncertainty in the PA analysis. This key uncertainty is addressed with a probabilistic analysis (described in Sect. 5.4) using the total system model presented in Sect. 3.3.4. For the MT3D saturated zone transport simulations, a single K_d is assumed to apply to all the solid media (rock) types in the model for each radionuclide.

The base-case K_d values used for the three radionuclides evaluated in the MT3D simulations are listed in Table 3.19, along with corresponding half-lives and specific activity values. These three radionuclides were selected on the basis of predicted dose contributions in preliminary runs using the total system model. Detailed discussion of the basis for selection of base case K_d values for all radionuclides in the EMDF radionuclide inventory is provided in Sect. 3.2.2.6.

Table 3.19. Radionuclide parameter values for MT3D saturated zone transport modeling

Radionuclide	K_d (cm^3/g)	Half-life (year)	Specific activity (Ci/g)
C-14	0	5.70E+03	4.50E+00
Tc-99	0.72	2.13E+05	1.70E-02
I-129	4.0	1.57E+07	1.80E-04

Initial and boundary conditions. For the PA analyses, only EMDF contributions to groundwater contamination are considered. The initial concentration within the model domain for all radionuclides is assumed to be zero. There has been no existing radiological contamination of groundwater at the CBCV site, although there is the potential for BCV groundwater contaminants from sites higher in the watershed to extend as far as CBCV near the main channel of Bear Creek. The CA for EMDF and EMWMF (UCOR 2020a) considers the contributions of other BCV waste sites to potential future total doses assessed downstream of EMDF.

In addition to boundary conditions identified for the groundwater flow model (Sect. 3.3.3.1), boundary conditions for the transport model include recharge concentrations for each radionuclide that represent leachate emanating from the EMDF (radionuclide flux to the water table). This radionuclide flux is a function of the recharge concentration for each nuclide and the estimated volumetric recharge rate from the disposal unit to the saturated zone. For purposes of saturated zone flow and transport modeling, the volume flux of leachate from the vadose zone to the water table beneath the disposal facility (recharge) is based on the modeled EMDF cover infiltration for the long-term performance condition (0.88 in./year, Sect. 3.3.1). The recharge areas defined for the saturated zone transport model are shown in Fig. 3.25. The leachate recharge area is defined by the waste limits. The outer lined area and berm/side slope area are assigned low recharge rates (0.88 in./year and 1.0 in./year, respectively) but have zero recharge concentration and do not contribute radionuclide flux to the saturated zone.

A general application of the MT3D model (advective transport only with no retardation or decay) was used to determine the general plume extent, location of maximum concentration at 100 m (groundwater POA location), and to locate the surface water POA. For the general application a uniform, non-depleting source is modeled by assigning a constant unit recharge concentration to the waste area shown on Fig. 3.25. For modeling transport of C-14, Tc-99, and I-129 to determine peak POA concentrations and the timing of peaks, a simple model of radionuclide release is used to specify time-varying recharge concentrations for each radionuclide. The mass-balance calculation of time-varying leachate concentration is explained in the following subsection that describes the MT3D modeling to estimate peak radionuclide concentrations at the groundwater POA.

Plume extent and groundwater well (POA) location. A simplified general application of the transport model was first used to delineate the plume extent, determine the location of maximum groundwater concentration along the 100-m buffer zone boundary (groundwater POA), and estimate the pattern of mass flux to streams to locate the surface water POA. For these purposes, hydrodynamic dispersion, chemical retardation, and radioactive decay were neglected and only advective transport is simulated in the MT3D model. In addition, an infinite (non-depleting) contaminant source is assumed, and a constant recharge (leachate) concentration of 1 unit (units are arbitrary for the general application) is assigned for the waste area. These simplifying assumptions will result in the largest (relative) concentrations at the assessment locations.

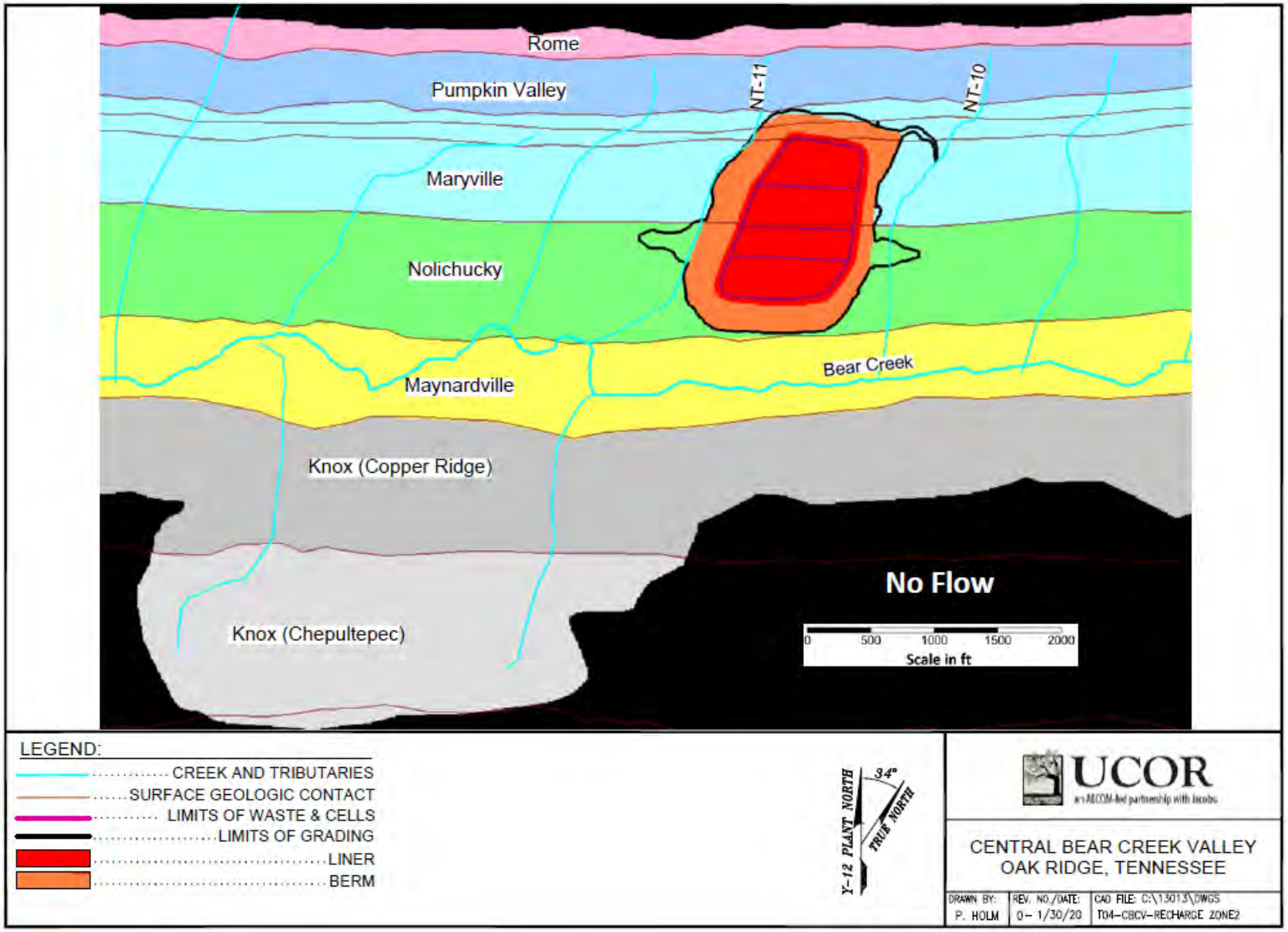

Fig. 3.25. EMDF disposal facility recharge zones for the saturated zone transport model

The model was run to a near steady-state plume configuration which was achieved after 2000 years of simulation. The steady-state plume configuration (maximum concentration of all model layers) is shown in Fig. 3.26. The simulation indicates that most groundwater contamination will discharge into Bear Creek and its tributaries near the EMDF site. The (minor) remaining contaminant mass will move downstream along the more permeable formations (Maynardville Limestone) below Bear Creek and discharge to the surface farther downstream. The transport model predicts that essentially all of release from the disposal facility discharges into Bear Creek surface water upstream of the Gum Branch tributary (NT-14). This pattern of predominantly shallow groundwater flow and contaminant transport is consistent with the BCV hydrogeologic conceptual model presented in Sect. 2.1.5 and with observations of plume migration from other sources in BCV.

Based on the steady-state advective transport model results representing the long-term performance condition, the maximum concentration 100-m buffer zone limit is located southwest of the disposal facility (Fig. 3.26). This location is the POA for groundwater concentrations (hypothetical drinking water well location). For the simplified transport model based on the constant, uniform source release, the location of maximum concentration does not vary appreciably over time. The steady-state vertical distribution of relative concentration at the groundwater POA (Fig. 3.27) indicates the highest concentrations in the model layers 2, 3, and 4 at the well location.

Radionuclide discharge to surface water. The general application MT3D transport model result was used to quantify groundwater and contaminant discharge to the model river cells and drain cells that represent surface water features near the EMDF. The simulated contaminant mass discharge to NT-10, NT-11, and the Bear Creek main channel segment between those tributaries was determined for corresponding areas of the model domain. The model calculates contaminant mass flux as groundwater discharge times the concentration at each model drain or river cell. Polygons identifying the areas for each of the stream channel segments and the simulated concentrations for model layer 1 (where contaminant discharge to river and drain cells occurs) are shown on Fig. 3.28.

Table 3.20 summarizes the distribution of contaminant mass discharge to the three stream channel segments. The discharge is expressed as a percentage of the total (steady-state) contaminant mass discharge from the entire model domain. Most of the contaminant mass discharge (> 87 percent) is received by NT-11, whereas NT-10 and the Bear Creek main channel segment receive only 8.2 and 2.8 percent, respectively. Together the three model channel segments account for over 98 percent of the release from the model domain. These results are the basis for selection of Bear Creek at the junction with NT-11 as the surface water POA (i.e., water for agricultural use is drawn from a single location that integrates most of the simulated release from the EMDF). It also validates that use the junction of Bear Creek and NT-11 as the point of compliance for evaluating protection of surface water resources.

Table 3.20. Contaminant mass discharge to surface water features in the MT3D model (simulation year 2000)

NT-10	Bear Creek between NT-10 and NT-11	NT-11	Total of three surface water model segments
8.17	2.80	87.12	98.09

Values in table are percent of total contaminant discharge within the entire model domain

NT = North Tributary

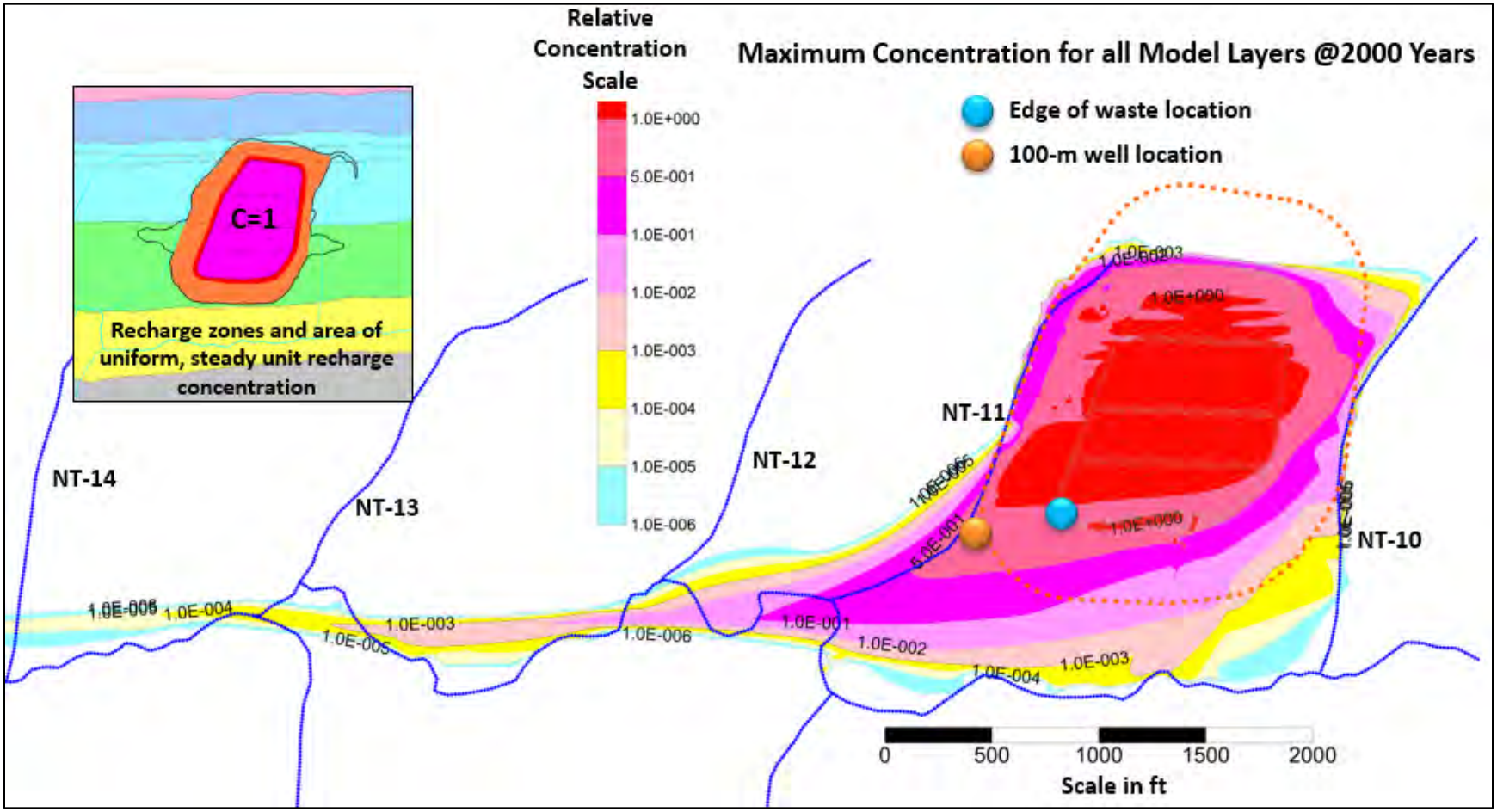

Fig. 3.26. Plume distribution (maximum concentrations) for non-depleting release from EMDF

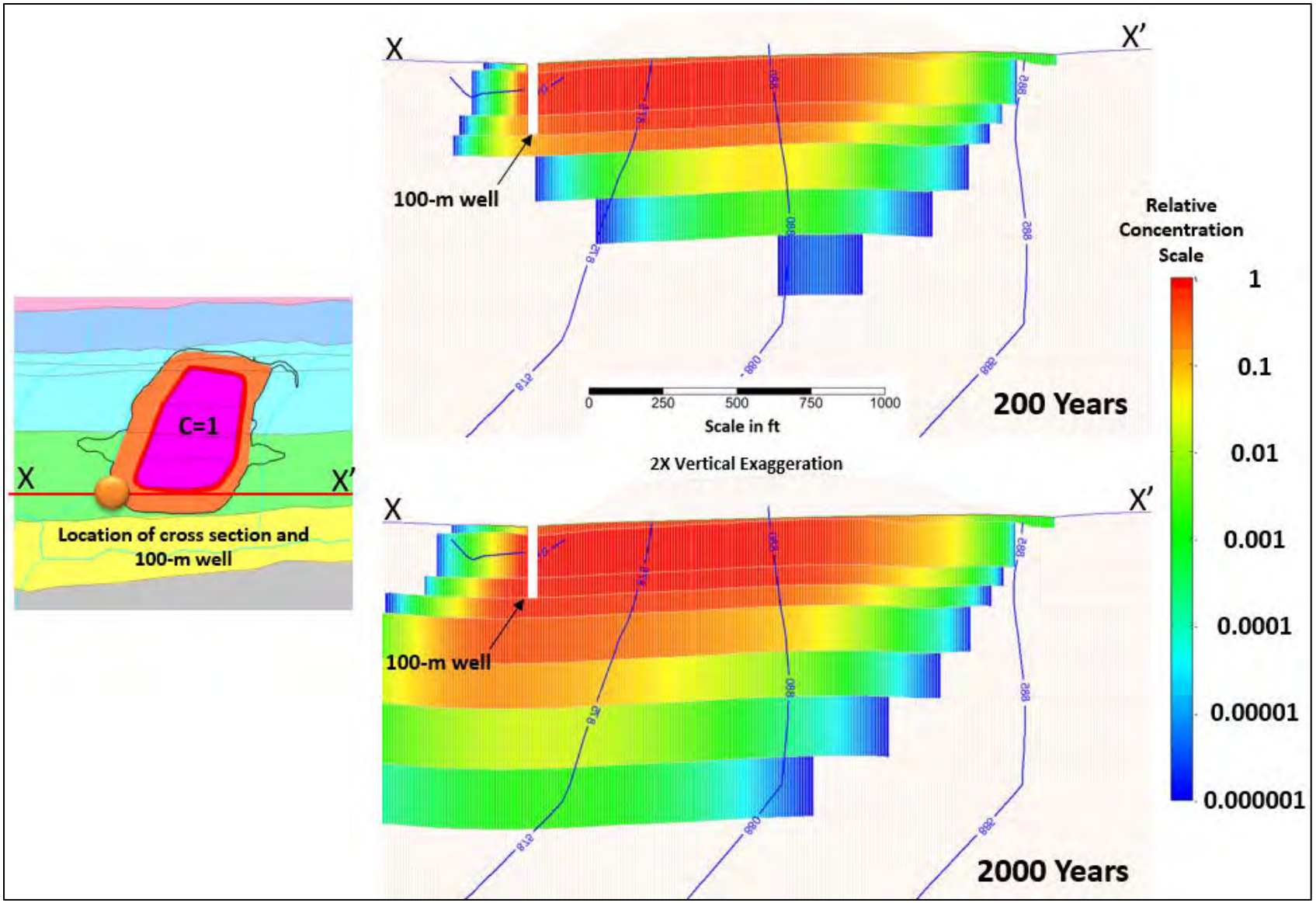

Fig. 3.27. Subsurface distribution of concentration for the general application of the MT3D transport model

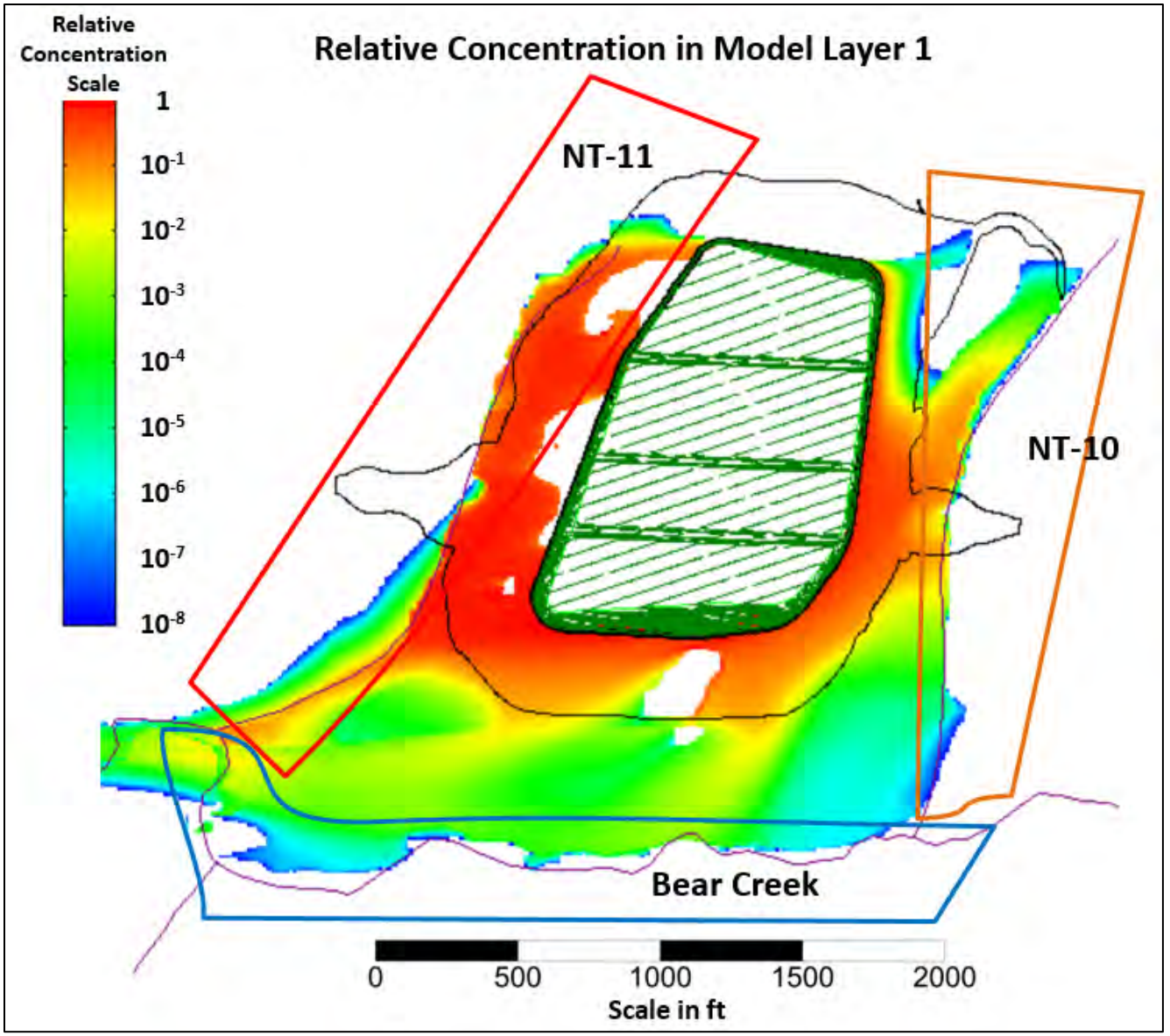

Fig. 3.28. Segments of surface water features defined for quantifying groundwater and contaminant discharge from the transport model domain

Saturated zone radionuclide transport to the groundwater POA. For simulating peak concentrations of C-14, Tc-99, and I-129 at the groundwater POA, the full implementation of the MT3D model incorporates radioactive decay, chemical retardation, and hydrodynamic dispersion in addition to advective transport. To model depletion of a finite radionuclide source, a simple radionuclide release model was developed. Based on the estimated initial radionuclide concentrations in the waste and assumed K_d values for radionuclides, initial moisture (pore water) concentrations are calculated for the waste. This approach assumes equilibrium solid-aqueous partitioning for a linear isotherm. The pore water concentration and volumetric leachate release rate based on the assumed increase in cover infiltration are used in a mass balance framework to calculate the decrease in radionuclide inventory, pore water (leachate) concentration, and radionuclide flux to the water table over time. This mass balance approach also incorporates post-closure radioactive decay and the vadose delay times derived from the STOMP model results (Table 3.21).

Table 3.21. Estimated vadose delay time for radionuclides released from the EMDF

Radionuclide	Delay time (years)
C-14	530
Tc-99	850
I-129	1750

EMDF = Environmental Management Disposal Facility

The calculated leachate concentration is applied during successive model stress periods to approximate the effect of source depletion on radionuclide flux to the water table. The recharge concentration from the release model is adjusted (decreased) as necessary for times prior to 1000 years (when the assumed leachate release is less than the constant 0.88 in./year applied to the waste area in the MT3D model) to ensure the correct mass flux to the saturated zone. The radionuclide flux to the water table applied to the MT3D model is compared to the STOMP model results and to the RESRAD-OFFSITE release model results in Sect. 3.3.5.

Estimated radionuclide flux to the water table is restricted to the waste area based on the assumption of primarily vertical transport through the vadose zone, which is generally supported by the STOMP simulations (STOMP results are presented in Sect. 4.2). For the base case simulations, the release of radionuclides was assumed to enter the saturated zone uniformly below the waste area. Because release from the disposal unit could be non-uniform, a sensitivity case simulation of non-uniform, time-varying Tc-99 recharge based on a modified release model also was performed. This sensitivity evaluation is performed to assess the significance of the simplified geometric representation of the waste and vadose zone that is assumed in the total system model.

The non-uniform release model for Tc-99 incorporates the funneling effects of the liner side slopes and sloping floors by restricting leachate recharge to the area directly below the cell floors (i.e., no leachate recharge beneath side slopes) and by assuming a higher release from the lower elevation (southeast) half of each of the four disposal cells (Fig. 3.29). The non-uniform release model also accounts for variation in waste volume between disposal cells. Additional detail on the radionuclide release model for MT3D simulations is provided in Appendix F, Sect. F.4.1.3. Development of the non-uniform sensitivity case is described in Sect. F.4.2.

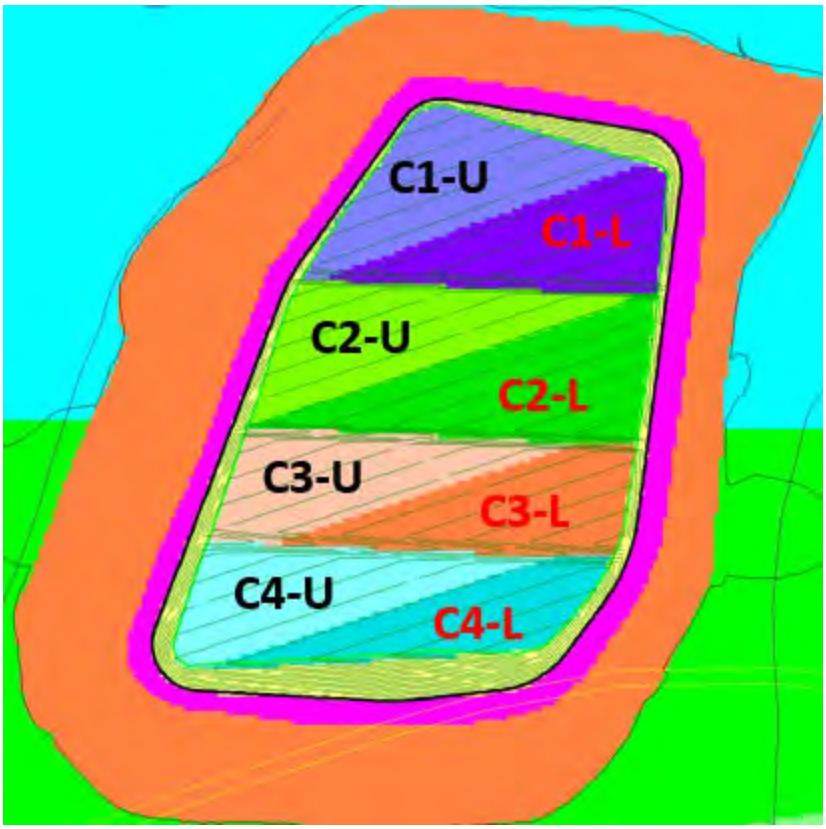

Fig. 3.29. Disposal cell floor areas defined for the non-uniform source release simulation with MT3D

MT3D model results (peak concentration and timing of peaks) for the upper four model layers at the groundwater POA location were compared to saturated zone results from the RESRAD-OFFSITE model that are used for the dose analysis. This model integration step is presented in Sect. 3.3.5.

3.3.4 Total System Model Code (RESRAD-OFFSITE)

For purposes of modeling the total EMDF disposal system, including radionuclide release, environmental transport, exposure pathways, and dose analysis, the computational code RESRAD-OFFSITE version 3.2 was selected (Yu et al. 2007, Gnanapragasam and Yu 2015). In general the detailed representations of the vadose and saturated zones that are described in the preceding sections have simplified conceptualizations and parameterizations in the RESRAD-OFFSITE model (Fig. 3.30). The advantage of the total system model is that it provides a holistic, integrated representation of the EMDF disposal system. As the total system model and detailed models were developed in parallel, predicted concentrations and fluxes in EMDF subsystems can be compared to provide confidence that simplified total system sub-model results are consistent with the more complex models of the system. The RESRAD-OFFSITE code was also used as an initial radionuclide screening tool (refer to Sect. 2.3.2) and for IHI dose analysis, which is described in Sect. 6.

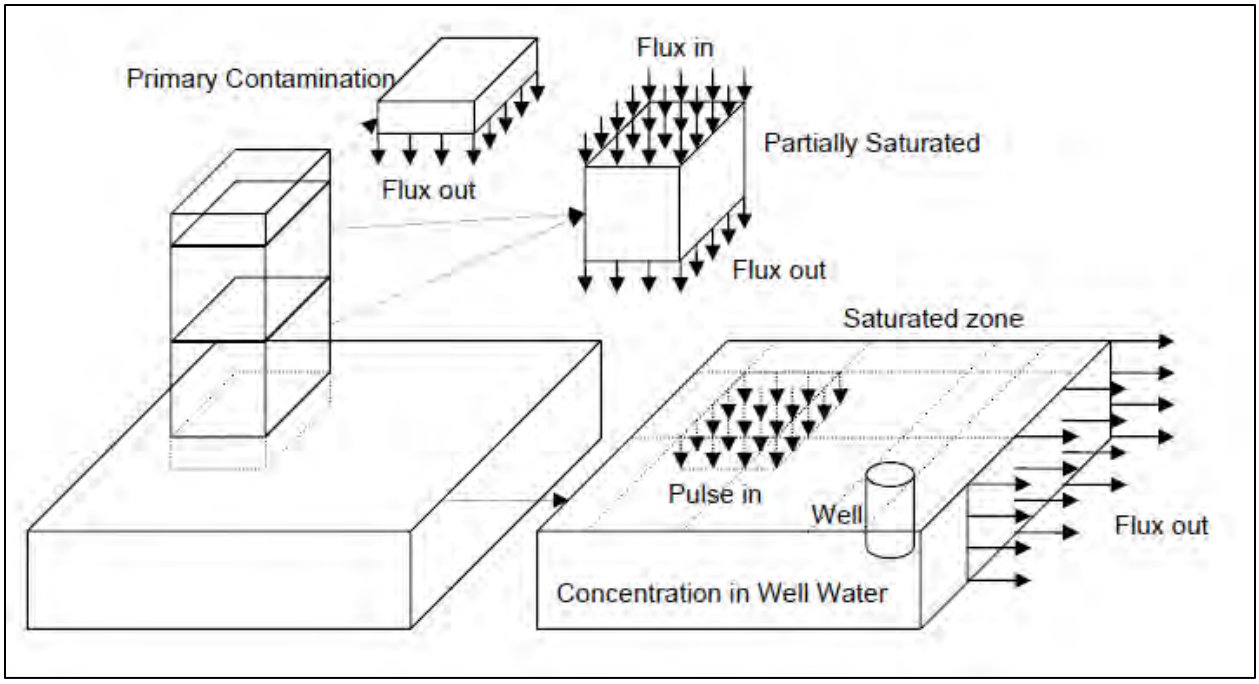

Fig. 3.30. Schematic of RESRAD-OFFSITE conceptual model of the primary contamination, vadose ("partially saturated") zone and saturated zone (Yu et al. 2007, Fig. 3.1)

Total system simulations were run for a post-closure period of 10,000 years to provide dose estimates for comparison with EMDF performance objectives, with a focus on predicted peak total dose within the 1000-year compliance period. Potential future release of relatively immobile radionuclides with significant estimated inventories (e.g., radionuclides of uranium) was evaluated with a 100,000-year RESRAD-OFFSITE simulation to estimate peak groundwater concentrations at the 100-m POA.

This section summarizes the RESRAD-OFFSITE simplified representation of the EMDF system and describes parameterization of the abiotic radionuclide transport pathways, including radionuclide release and the vadose and saturated zones. The RESRAD-OFFSITE model exposure scenario, biotic pathways, and dose analysis for the EMDF PA is described in Sect. 3.4. There are hundreds of input parameters for the RESRAD-OFFSITE model and only the most significant parameters are presented in this section of the EMDF PA report. Detailed explanation of all RESRAD-OFFSITE model input parameters and tabulation of all base case parameter values are provided in Appendix G.

The RESRAD-OFFSITE model identifies subsystems (Fig. 3.30), including the primary contamination (EMDF waste) and cover soil layer, a layered vadose zone below the waste, the aquifer (saturated zone), and dwelling and agricultural areas that can be affected by release of radionuclides from the primary contamination.

3.3.4.1 Climate parameters

Climate parameters specified in the RESRAD-OFFSITE model include annual precipitation and an evapotranspiration coefficient. Average precipitation is assumed to be 54.4 in./year and the evapotranspiration coefficient was assigned based on the average annual evapotranspiration estimated by the HELP model base case simulations, approximately 60 percent of precipitation.

3.3.4.2 Cover performance, primary contamination and radionuclide release

Thickness of the soil cover layer (11 ft) and average waste thickness (57.5 ft) are based on the EMDF Preliminary Design (Sect. 2.2). Other physical and hydraulic parameters values for the cover soil and primary contamination are provided in Table 3.22. Cover infiltration (for a given precipitation and evapotranspiration coefficient) is determined by the value of the runoff coefficient for the primary contamination, which is back-calculated to obtain the base-case long-term infiltration rate of 0.88 in./year. Evolution of EMDF cover performance is also represented in the source release parameterization described below. Erosion of the cover and upward transport of radionuclides into the clean cover by biological soil mixing or vapor phase transport are assumed to be negligible (refer to Sect. 3.2.2 and Appendix C), so erosion parameters for the cover soil are set to zero.

For modeling purposes, the 2.2 million cy of emplaced waste in EMDF was assumed to be of uniform thickness, homogenous both horizontally and vertically, and soil like (uncontainerized). The simplified representation of the primary contamination in RESRAD-OFFSITE (Fig. 3.30) as a homogeneous rectangular prism is consistent with the conceptual model of radionuclide release described in Sect. 3.2.2.4. Radionuclide concentrations in the primary contamination are based on the EMDF estimated radionuclide inventory (Sect. 2.3 and Appendix B) and adjusted to account for the addition of clean fill during waste placement and compaction (Sect. 3.2.2.5). In addition, operational period losses of highly mobile radionuclides (H-3, C-14, Tc-99, and I-129) are estimated to derive post-operational source concentrations for those for nuclides.

The RESRAD-OFFSITE code offers three options to simulate source release (Yu et al. 2013): First-Order Rate Controlled Release with Transport, Version 2 Release, and Instantaneous Equilibrium Desorption Release. All three release options were evaluated in the EMDF PA (Instantaneous Equilibrium Desorption Release in the base case and First Order Rate Controlled Release with Transport and Version 2 Release as part of the sensitivity analysis described in Sect. 5.3). An important limitation of RESRAD-OFFSITE is that the code does not account for solubility limits, which can allow for unrealistically high aqueous concentrations and predicted dose.

Instantaneous Equilibrium Desorption release assumes that equilibrium radionuclide concentrations in the solid and aqueous phases are achieved as soon as water contacts the waste and these equilibrium concentrations are governed by both the nuclide-specific K_d values in the contaminated zone and the soil/waste concentration. Additionally, the K_d determines the rate at which the radionuclides are transported by infiltration down through the primary contamination (Yu et al. 2013). In addition to the suitability of the Instantaneous Equilibrium Desorption release option for the expected waste forms and conceptual model of radionuclide release (Sect. 3.2.2.4), selection of this release option yields more rapid release of radionuclides compared to both the First Order Rate Controlled Release with Transport and Version 2 release options. Selecting this RESRAD-OFFSITE release model option is one important source of pessimistic bias toward higher release (and dose impacts) incorporated in the PA analysis.

First Order Rate Controlled Release with Transport assumes that radionuclide transfer from waste to pore water at any time is proportional to the radionuclide inventory at that time and occurs uniformly over the thickness of the primary contamination (i.e., the horizontal area does not change). The proportionality constant is the time varying leach rate. Version 2 release is a first-order exponential leaching model that accounts for radiological transformations (decay and ingrowth), but not for radionuclide transport in the waste. When Version 2 release is used, leached material is assumed to leave the contaminated zone as soon as it is leached. A time delay cannot be added when this release option is used, so all material is available for leaching at the beginning of the simulation period.

Table 3.22. Summary of material zone parameter values for RESRAD-OFFSITE modeling

RESRAD-OFFSITE zone	Layer (zone) thickness		Bulk density (g/cm^3)	Total porosity (vol/vol)	Effective porosity (vol/vol)	Field capacity (vol/vol)	Saturated hydraulic conductivity	
	in.	m					cm/sec	m/year
Clean cover	132	3.35	1.5	0.400	[a]	[a]	[a]	[a]
Primary contamination (waste)	690	17.5	1.9	0.419	0.234	0.307	1.90E-05	5.99E+00
UZ1 (protective soil)	12	0.305	1.4	0.463	0.294	0.232	3.70E-04	1.17E+02
UZ2 (leachate drainage)	12	0.305	1.6	0.397	0.389	0.032	3.00E-01	9.46E+04
UZ3 (clay liner)	36	0.914	1.5	0.427	0.195	0.418	1.00E-06	3.15E-01
UZ4 (geologic buffer)	120	3.05	1.5	0.419	0.234	0.307	1.00E-05	3.15E-00
UZ5 (saprolite or bedrock)	120	4.85	1.8	0.353	0.270	0.247	5.30E-05	1.67E+01
Aquifer (saturated zone)	2400	61	2.1	0.240	0.200	NA	8.49E-05	2.68E+01

[a]Parameter not required for RESRSAD-OFFSITE.

RESRAD = RESidual RADioactivity
UZ = unsaturated zone

The Instantaneous Equilibrium Desorption release model is applied consistent with the assumed evolution of EMDF cover performance and leachate release (Sect. 3.2.1). One of the limitations of the RESRAD-OFFSITE code is that the infiltration rate cannot be varied over time, so a constant infiltration rate must be applied for the entire simulation period. The RESRAD-OFFSITE model runoff coefficient input parameter was assigned a value to produce the HELP-calculated long-term performance infiltration rate (0.88 in./year), based on the base case values for the evapotranspiration coefficient and average annual precipitation (refer to Appendix G, Sect. G.4.3.5.2).

The release model incorporates the assumed evolution in EMDF performance by assigning a release time (initially set at 200 years) and a release duration set at 800 years. As a surrogate representation of the assumed increase in cover infiltration over the release duration, and to account for the higher than assumed infiltration rate from years 200 to 1000, the release model applies a releasable fraction parameter which is increased from zero to one over the 800 year release. The model requires an initial value of the releasable fraction (set to zero at the release time, 200 years) and a final value (set to one at 1000 years) for each radionuclide.

Based on comparison of the RESRAD-OFFSITE model results to the STOMP and MT3D model results for C-14 and Tc-99, the initial release time was adjusted upwards to 300 years for all radionuclides. To adequately capture the high mobility of radionuclides with K_d = zero, increasing the initial releasable fraction from zero to 0.75 for C-14 was found necessary. This adjustment produced peak C-14 release concentrations consistent with the STOMP and MT3D model results for C-14. Initial releasable fraction was also changed to 0.75 for H-3, (also K_d = zero) for consistency. Similarly, the release duration was decreased to 500 years for C-14 and H-3 to better match MT3D model output. Comparison and integration of RESRAD-OFFSITE model results with STOMP and MT3D model results is presented in Sect. 3.3.5.

3.3.4.3 Solid-aqueous partition coefficients

The K_d values used in the RESRAD-OFFSITE modeling were based on ORR-specific values where such data are available or used generic values based on soil type (Sect. 3.2.2.6). Base case K_d values for each element in the EMDF radionuclide inventory are listed in Table 3.4. These base case values are identical to those listed for radionuclides considered in the vadose (STOMP) and saturated zone (MT3D) models. Also shown in Table 3.4 are K_d values used for the radionuclide screening model described in Sect. 2.3.2, along with references used to guide selection of the base case values. Detailed discussion of the available ORR-specific data on distribution coefficient values is provided in Sect. 2.1.6.3. Where ranges reported in general compilations of values were utilized, lower values (generally pessimistic in term of dose predictions) were selected as base case values for the EMDF PA. A more detailed presentation of the approach to selection of base case K_d values is provided in Sect. 3.2.2.6.

In the RESRAD-OFFSITE model, distribution coefficients are assigned to various disposal system components, including the waste, vadose zone layers, aquifer (saturated zone), and surface water feature sediments. The K_d values are also assigned for soils in agricultural fields and the dwelling site (Sect. 3.4). The distribution coefficient for sediment in the surface waterbody was specified as zero for all radionuclides as a pessimistic assumption in the context of bioaccumulation in fish and the fish ingestion exposure pathway.

Sensitivity of dose estimates to variation in K_d values for particular model material zones (primary contamination, vadose zone, saturated zone) is evaluated in Appendix G, Sect. G.6.2. Sensitivity of total dose to variation in the I-129 K_d values for different material zones is shown in Fig. 5.7. The sensitivity of peak dose estimates to uncertainties in K_d values for key dose-contributing radionuclides is a primary focus of the probabilistic analysis presented in Sect. 5.4 and in Appendix G, Sect. G.6.3.

3.3.4.4 Vadose zone parameterization

In addition to the clean soil cover layer and the primary contamination (EMDF waste), the RESRAD-OFFSITE model identifies the following five layers in the unsaturated zone between the waste and the water table:

- UZ1 – Protective soil (layer protects liner)
- UZ2 – Drainage layer (leachate collection system)
- UZ3 – Compacted clay liner
- UZ4 – Low-permeability geobuffer
- UZ5 – Native vadose saprolite or bedrock.

A summary of key input parameters by zone is provided in Table 3.22. The model layer thicknesses for the cover through the geobuffer (UZ4) are based on the EMDF preliminary design. The thickness of UZ5 (16 ft) is based on predicted water table elevation from the EMDF flow model (Sect. 3.3.3.1), assuming long-term performance (0.88 in./year) cover infiltration. The uncertainty in the thickness of UZ5 primarily reflects uncertainty in long-term site hydrogeologic conditions that, in combination with the effectiveness of the cover, will determine the long-term average water table elevation below the disposal unit.

Values for porosity, field capacity, and hydraulic conductivity for the waste and non-native (engineered) materials were specified to align with HELP default values for each specific material type. Waste bulk density is based on estimated average bulk densities and proportions of waste soil, clean fill, and demolition debris expected for the EMDF (Appendix B). Bulk density and porosity values for native materials in UZ5 and the saturated zone are from based on analysis of Nolichucky Formation samples (Dorsch and Katsube 1996). The EMDF preliminary design specified a K value of 1.0E-07 cm/sec, but the RESRAD-OFFSITE code would not accommodate such a low value for the imposed infiltration rate (0.88 in./year) through the vadose zone. For the RESRAD-OFFSITE model the K value for UZ3 was increased by a factor of 10 to 1.0E-06 cm/sec, to accommodate the limitation in executing the code. Hydraulic conductivity for UZ5 is based on estimates for the Nolichucky Formation vertical conductivity (refer to Sect. 2.1.5.4).

For the primary contamination, the longitudinal (vertical) dispersivity is set as 10 percent of the average waste thickness, or 1.8 m, based on the scale and likely heterogeneity of the waste zone. Each unsaturated zone unit is assigned a longitudinal dispersivity of 0.1 m.

3.3.4.5 Saturated zone parameterization

The saturated zone representation in RESRAD-OFFSITE is a simplified homogeneous, isotropic unconfined groundwater flow system (Fig. 3.30). The term aquifer is used to refer to the saturated zone submodel in RESRAD-OFFSITE. Saturated zone parameter values given in Table 3.22 are based on laboratory and field measurements, with the exception of aquifer thickness set at 200 ft. The active BCV saturated zone is much thicker than 200 ft, but the BCV hydrogeologic conceptual model and results of tracer studies in BCV and from the 3-D groundwater flow and radionuclide transport models for the EMDF site suggest that the depth to which contamination introduced at the surface penetrates the saturated zone is limited. Given the RESRAD-OFFSITE model structure, radionuclide concentrations at the receptor well can depend on the depth of the well relative to the depth of the aquifer. Preliminary sensitivity analysis suggested that given the well depth assumed for the analysis (131 ft, which is based on comparison of the RESRAD-OFFSITE and MT3D model results), the well concentration and predicted peak dose would not be sensitive to assuming a more realistic (larger) value for aquifer depth. Parameterization of the

groundwater well (well depth and location) is presented in the context of the all-pathways exposure scenario (Sect. 3.4.2).

The average horizontal hydraulic gradient (slope of the potentiometric surface) along the flow path to the groundwater well is approximately 0.036 ft/ft, based on the EMDF model results for the long-term performance condition. The hydraulic gradient to the surface water body is also assumed as 0.036 ft/ft. Due to the sensitivity of the RESRAD-OFFSITE predicted well concentrations to hydraulic gradient to the well, the value for the gradient was increased to 0.054 ft/ft. This adjustment was made to account for less saturated zone dilution in the RESRAD-OFFSITE model compared to the MT3D model (Sect. 3.3.5).

The RESRAD-OFFSITE model requires both longitudinal (horizontal) and lateral (horizontal and vertical) dispersivities for the aquifer. A longitudinal dispersivity of 10 m was initially assigned based on the 100-m distance to the groundwater well (10 percent rule-of-thumb) and for consistency with the MT3D saturated zone transport model parameterization. As assumed for the MT3D radionuclide transport model, horizontal lateral and vertical lateral dispersivities are set at 10 percent and 1 percent of the longitudinal value.

3.3.4.6 Surface waterbody

The surface water point of exposure is assumed to occur at a location that would provide flow during drier parts of the year. A surface water exposure location on Bear Creek near the junction of NT-11 was selected because year-round flow is more typically encountered there than in surface water tributaries closer to the landfill.

The dimensions of the section of Bear Creek assumed to be impacted by radionuclides are 100 m in length, 5 m in width, and 0.5 m in depth with a simulated surface area of 500 m^2 and volume of 250 m^3. A representative mean residence time in the surface waterbody of 0.0001 year was specified based on an estimated average flow rate in Bear Creek at NT-11 of approximately 1570 gpm (UCOR 2020a, Sect. 4.2).

3.3.4.7 Other applications of the RESRAD-OFFSITE model for the EMDF PA

In addition to the base case holistic system simulation for the all-pathways dose analysis, the RESRAD-OFFSITE code was used for several other applications to the EMDF analysis, including the following:

1) Operational period inventory depletion estimates – Four simulations were performed to quantify activity loss from the waste due to leaching during the 25-year operational period for the four mobile radionuclides (C-14, H-3, I-129, and Tc-99). A summary of this application is provided in Sect. 3.2.2.5.
2) Screening models for radionuclide release through the EMDF cover– Two models were developed to support screening of the cover release pathway from the all-pathways analysis and to provide bounding estimates for demonstrating compliance for the air pathway. Results of these applications are presented in Sect. 3.2.2.3.
3) IHI scenarios – Three IHI scenarios were evaluated: acute discovery, acute drilling, and chronic post-drilling. IHI development and results are summarized in Sect. 6 and presented in detail in Appendix I.
4) Long-term simulations – These extended duration simulations were performed similar to the 10,000-year base case simulation, with the simulation duration extended to 100,000 years to evaluate radionuclides, such as uranium isotopes, with peak predicted concentrations occurring after tens of thousands of years (Sect. 4.8).
5) Sensitivity and uncertainty analysis –RESRAD-OFFSITE was used to perform a comprehensive set of single-factor model sensitivity evaluations for the base case scenario and a more limited set for the long-term simulation (Sect. 5.3). Based on initial sensitivity evaluations, a probabilistic uncertainty

analysis was performed to evaluate the sensitivity of RESRAD-OFFSITE model results to uncertainty in important input parameters (Sect.5.4). The sensitivity and uncertainty analysis provides perspective on the potential range of uncertainty in modeled dose predictions and insight into which input parameter value assumptions are most important in supporting the conclusions of the PA.

3.3.5 Radionuclide Transport Model Integration

Prior to final implementation of the exposure and dose analysis using the total system model (described in Sect. 3.4), the results obtained from the more complex transport model codes (STOMP and MT3D) were compared to radionuclide release and transport output from the total system model (RESRAD-OFFSITE). This model integration step was performed to ensure that the simplified representations of the vadose and saturated zones in the RESRAD-OFFSITE model were producing results consistent with the more detailed models. Based on preliminary dose predictions from the total system model, the model output comparison was focused on C-14, Tc-99, and I-129, three radionuclides that make primary contributions to the predicted total dose at various times during the post-closure period. The model output examples in the following subsections are for Tc-99, because the examples incorporate output from sensitivity runs (e.g., MT3D non-uniform release scenario) that were only performed for Tc-99.

3.3.5.1 Vadose zone model comparison

STOMP results from the Section A model show complex non-uniform patterns of radionuclide release over time (Sect. 4.2). To compare results of radionuclide release to the vadose zone across models having different dimensionality and complexity, the total activity flux from the waste and from the vadose zone, including variation over time, was selected as the quantity of interest. The STOMP model predicted total vertical activity flux across the output surface for the waste-liner interface and the water table output surface were calculated by summing the vertical flux for all model nodes along each output surface. Because the STOMP model is a 2-D representation, the activity flux results were scaled up for comparison to the MT3D release model and the RESRAD-OFFSITE model based on the ratio of the STOMP model total initial activity to the total EMDF inventory represented in the other two models.

For the initial RESRAD-OFFSITE input parameter value selections for the release model (release time = 200 years and release duration = 800 years), the RESRAD-OFFSITE model predicted earlier Tc-99 release from the waste than the STOMP model. Based on this difference, the RESRAD-OFFSITE model release time was increased to 300 years for all radionuclides. This adjustment resulted in a better match in release timing for both flux from the waste (Fig. 3.31 solid curves) and from the vadose zone (flux to water table, Fig. 3.31 dashed curves). Technetium-99 flux from the waste shows similar peak values and timing of peak flux for the two models, with the RESRAD-OFFSITE predicted release occurring from 300 to approximately 2000 years post-closure. The (scaled) STOMP model flux from the waste occurs slightly later and extends over slightly longer (200 to 300 years) period. This difference reflects the STOMP model 2-D representation of a complex combination of faster and slower transport pathways (refer to Sect. 4.2), compared to the simpler 1-D release model. In general the results from the two models are quite consistent in terms of the timing and peak flux from the waste, providing confidence in the results.

The STOMP and RESRAD-OFFSITE model Tc-99 flux curves representing transport from the vadose zone to the saturated zone (flux to water table) are very closely aligned over the period of increasing flux from 600 to 1000 years post-closure (Fig. 3.31). The STOMP predicted flux peaks soon after 1000 years, but the RESRAD-OFFSITE model predicted flux continues to increase between 1000 and 1500 years post-closure, and peaks higher than the STOMP model output. The disparity in the predicted vadose zone Tc-99 transport reflects the difference between the more detailed 2-D STOMP model representation and the simpler RESRAD-OFFSITE 1-D vadose zone model, and suggests that RESRAD-OFFSITE under-predicts vadose zone performance (over-predicts peak flux at the water table) relative to the STOMP model.

The vadose zone flux results from the STOMP and RESRAD-OFFSITE models are compared to Tc-99 fluxes calculated from the radionuclide release model applied to the MT3D saturated zone transport model in Figs. 3.32 and 3.33. The timing of the MT3D release model (vadose delay time, Sect. 3.3.2) is based on the STOMP water table flux output. The MT3D Tc-99 release model is a simplified approximation of flux to the saturated zone beginning at 850 years post-closure, corresponding to the time when the STOMP modeled flux reaches 50 percent of its peak value (Fig. 3.32). The onset of Tc-99 release applied to the MT3D model is about 200 years later than the predicted beginning of release based on the STOMP and RESRAD-OFFSITE models. The peak Tc-99 flux applied to the MT3D model is earlier than predicted by the other two models, and the MT3D model peak flux is very close to the RESRAD-OFFSITE model peak Tc-99 flux.

Comparison of the STOMP and RESRAD-OFFSITE Tc-99 output with the MT3D Tc-99 release model input in terms of cumulative flux (Fig. 3.33) shows that in general, there is very good consistency between the model representations of Tc-99 release prior to 1500 years post-closure. After 1500 years, the rate of release for the RESRAD-OFFSITE model is unchanged and over 90 percent of the total activity release is complete by 2000 years post-closure. For the STOMP model Tc-99 output and the Tc-99 release model input to the saturated zone MT3D model, the rate of release becomes more gradual after 1500 year and the duration of release is extended compared to the RESRAD-OFFSITE results. These model similarities and differences suggest that the EMDF total system model of radionuclide release to the saturated zone is consistent with the STOMP vadose zone model results and the MT3D saturated zone model implementation for Tc-99.

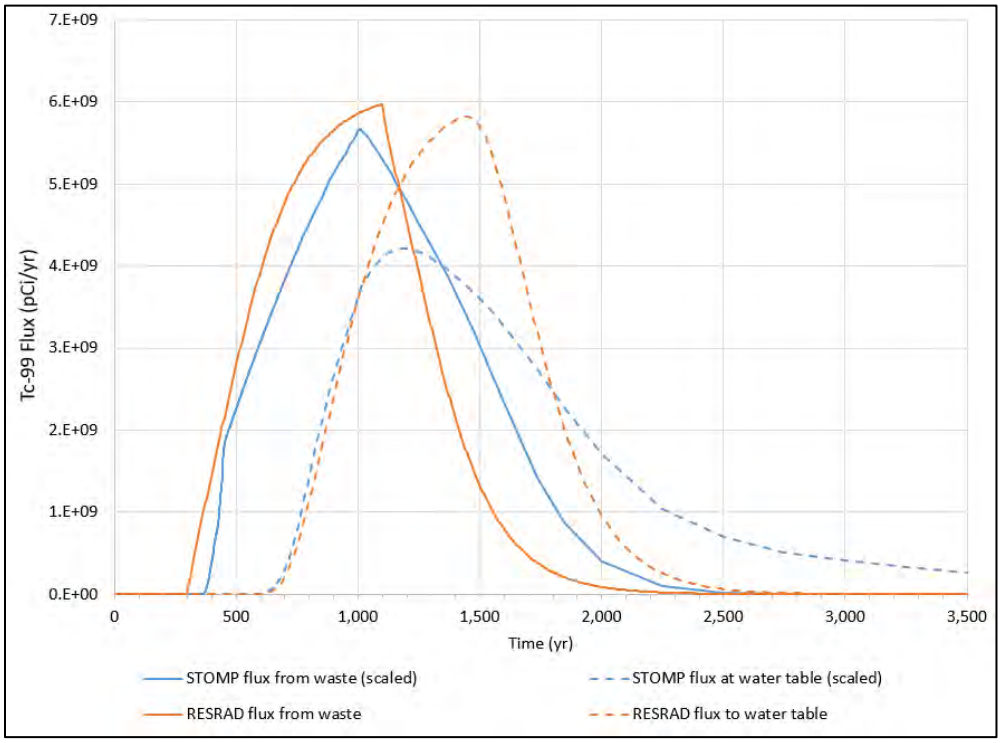

Fig. 3.31. Comparison of Tc-99 flux from the waste and from the vadose zone for the STOMP and RESRAD-OFFSITE models of the EMDF

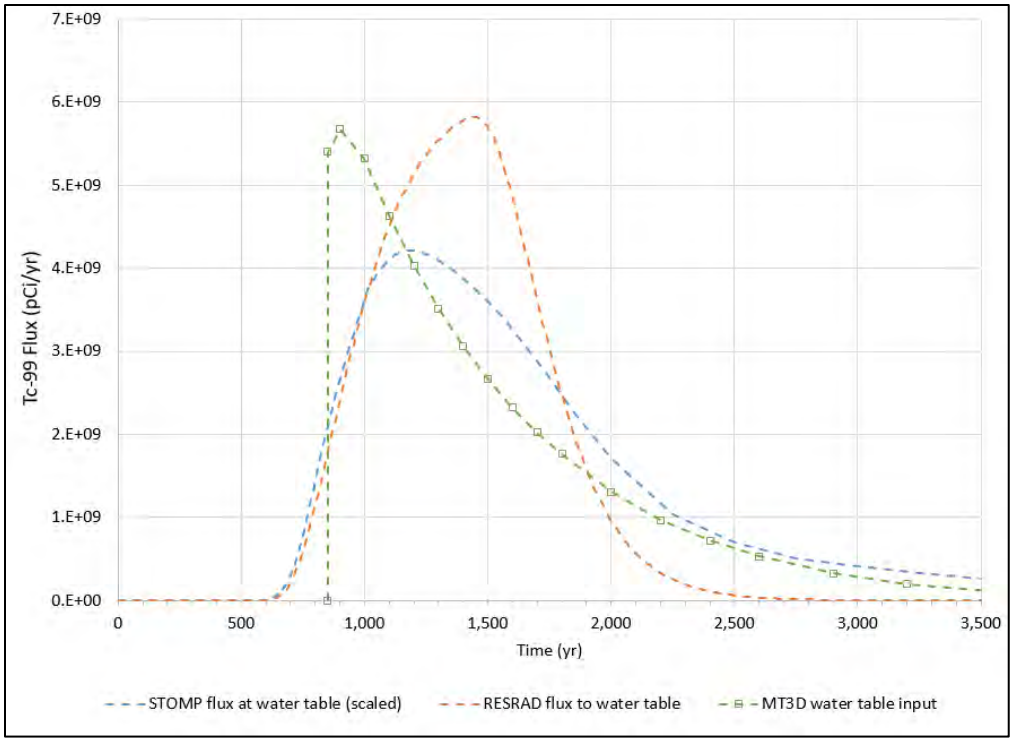

Fig. 3.32. Comparison of STOMP and RESRAD-OFFSITE predicted Tc-99 flux from vadose zone with Tc-99 release applied to the MT3D saturated zone model

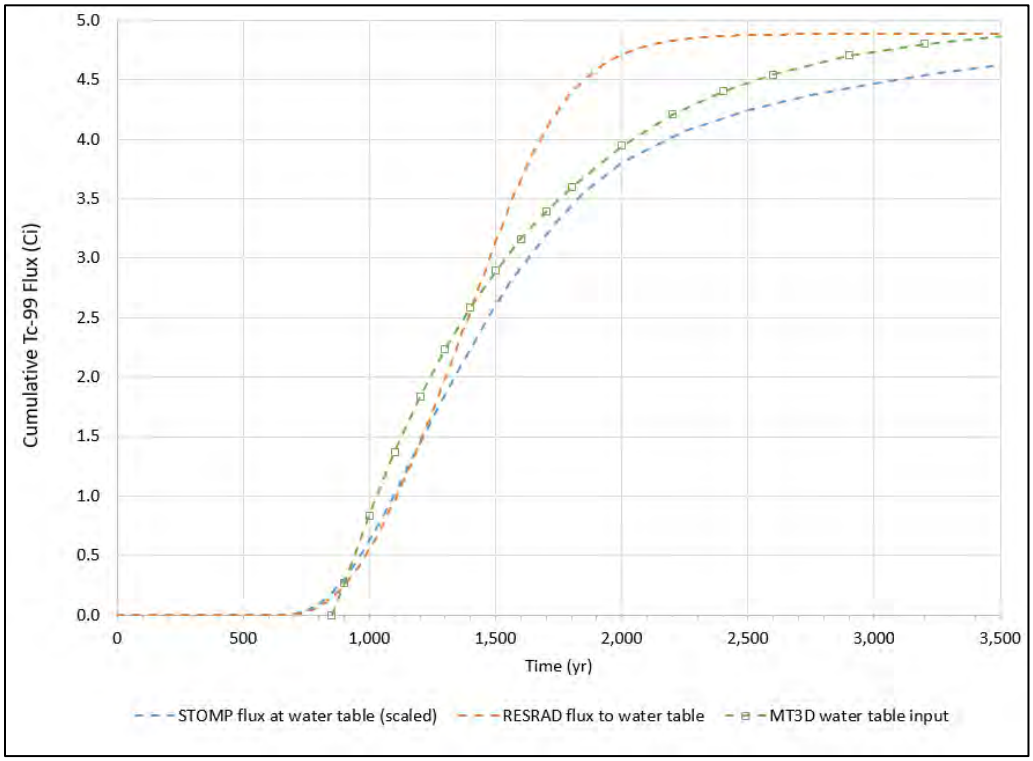

Fig. 3.33. Comparison of STOMP and RESRAD-OFFSITE predicted cumulative Tc-99 flux from vadose zone with cumulative Tc-99 release applied to the MT3D saturated zone model

Predicted release of I-129 and U-234 to the vadose zone and flux into the saturated zone for the STOMP and RESRAD-OFFSITE models are compared in Figs. 3.34 and 3.35. For these two radionuclides that have assumed base case K_d values greater than 1 cm^3/g (i.e., 4 and 50 cm^3/g for iodine and uranium, respectively), the instantaneous equilibrium desorption release model in the RESRAD-OFFSITE code over-predicts peak activity flux rates significantly relative to the scaled STOMP model simulations. Consistent with the model comparison for Tc-99 (Fig. 3.32) the RESRAD-OFFSITE model-predicted peak flux to the water table occurs somewhat later than the corresponding STOMP model-predicted peak, but for I-129 and U-234 the RESRAD-OFFSITE model peak flux rates are approximately 2.5 times larger than the STOMP model peaks.

The differences between the STOMP model and the RESRAD OFFSITE model predictions for the flux of Tc-99, I-129, and U-234 entering the saturated zone suggest that for K_d values greater than 1 cm^3/g, the instantaneous equilibrium desorption release model and vadose zone representation in the RESRAD OFFSITE code do not capture extent to which the EMDF design and the vadose zone below the disposal facility contribute to long-term performance of the disposal system. This limitation of the RESRAD-OFFSITE model is consistent with the simplified radionuclide release and vadose zone conceptualizations of the total system model. Use of the RESRAD-OFFSITE model predictions for the dose analysis is therefore a pessimistic approach for the less mobile radionuclides because the peak dose will be over-estimated relative to dose estimates based on the more detailed radionuclide transport models (STOMP and MT3D).

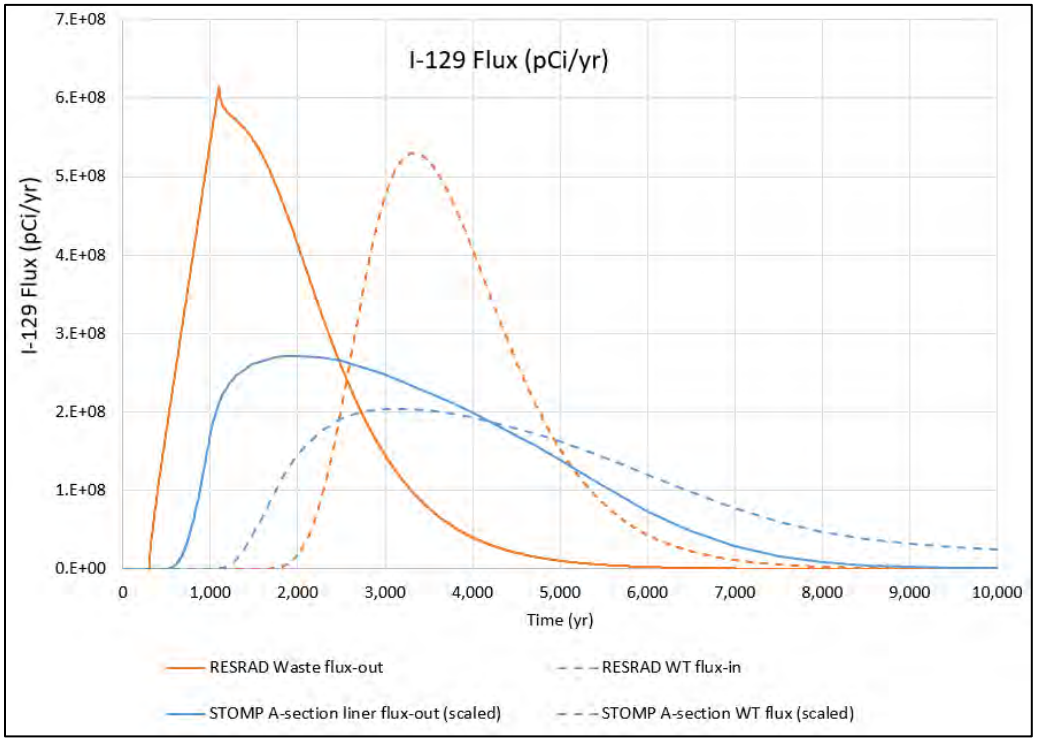

Fig. 3.34. Comparison of Tc-99 flux from the waste and from the vadose zone for the STOMP and RESRAD-OFFSITE models of the EMDF

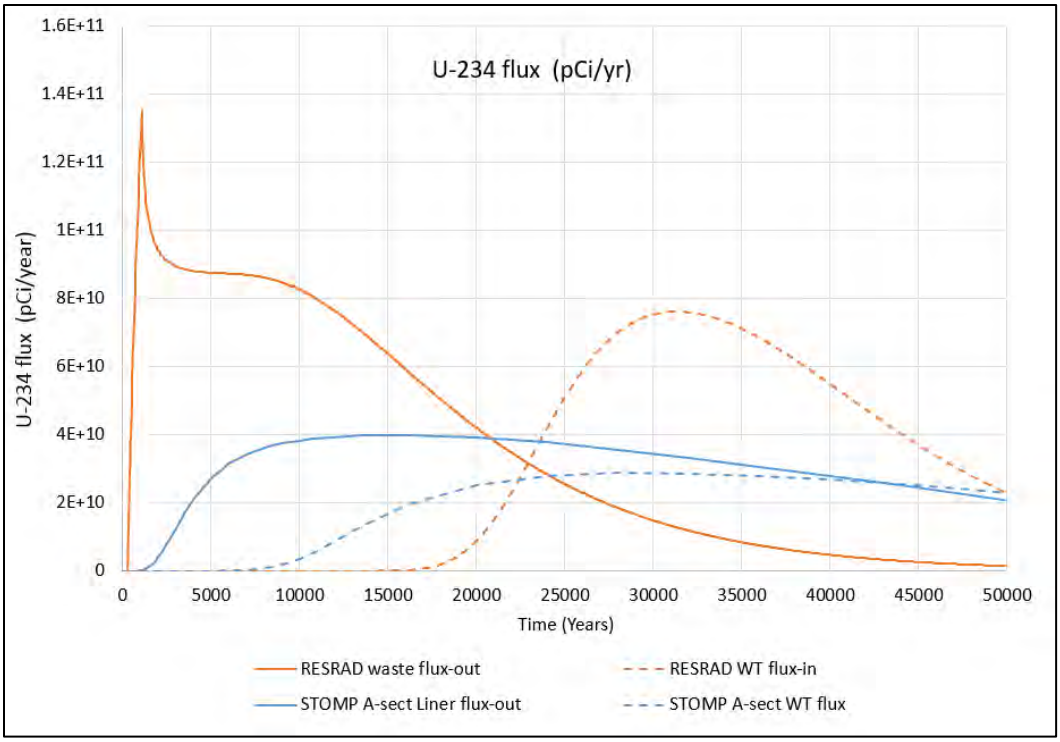

Fig. 3.35. Comparison of Tc-99 flux from the waste and from the vadose zone for the STOMP and RESRAD-OFFSITE models of the EMDF

3.3.5.2 Saturated zone model comparison

Aqueous activity concentrations are the basis for comparison of the MT3D and RESRAD-OFFSITE saturated zone model results. To provide linkage between the vadose zone results reviewed in Sect. 3.3.5.1 and the saturated zone model results, the Tc-99 recharge concentrations are compared to RESRAD-OFFSITE model vadose zone concentrations at the water table, and to saturated zone concentrations at downgradient edge of waste (EOW) location along the flow path to the groundwater POA (Fig. 3.34). The RESRAD-OFFSITE model vadose Tc-99 concentrations are calculated as the model predicted flux (activity/time) divided by the assumed leachate flux (volume/time) corresponding to the (constant) 0.88 in./year infiltration rate for the long-term performance condition. The two vadose Tc-99 concentration time series shown in Fig. 3.32 (dashed curves) correspond to the MT3D and RESRAD-OFFSITE flux curves plotted in Figs. 3.36 and 3.37.

The Tc-99 saturated zone concentrations at the EOW for MT3D model layer 2 (model layer 1 is above the water table at the EOW) and for a RESRAD-OFFSITE model well at zero distance from the EOW are also shown in Fig. 3.36 (dotted curves). The RESRAD-OFFSITE model EOW well depth is 65.6 ft (specified as 20 m in model units), which is approximately the same as the thickness of MT3D model layer 2 at the EOW (70 ft). The Tc-99 saturated zone concentration curves are closely aligned during the period of increasing concentration from approximately 700 to 1100 years post-closure. After 1100 years, the RESRAD-OFFSITE model saturated zone concentrations increase faster than the MT3D model layer 2 Tc-99 concentration and reach a peak at approximately 1600 years post-closure. The MT3D model saturated zone concentration at the EOW reaches a somewhat lower peak (20 percent less than the RESRAD-OFFSITE model maximum) approximately 500 years later (around 2100 years). The difference between peak vadose zone Tc-99 concentration and peak saturated zone concentration is similar for the two models; peak saturated zone concentrations are about a factor of 4 less than peak vadose concentrations, suggesting

a similar degree of predicted saturated zone dilution. The difference in the peak Tc-99 saturated zone concentration (MT3D Tc-99 peak is smaller and occurs later) is related to the difference in release models (Figs. 3.36 and 3.37) and to the difference between the simplified analytical saturated zone model in the RESRAD-OFFSITE code and the more detailed MT3D numerical model. The RESRAD-OFFSITE model predicted well concentration is highly sensitive to the specified well depth (Sect. 5.3), but for a similar thickness of saturated zone at the EOW, the two models predict similar peak Tc-99 concentrations.

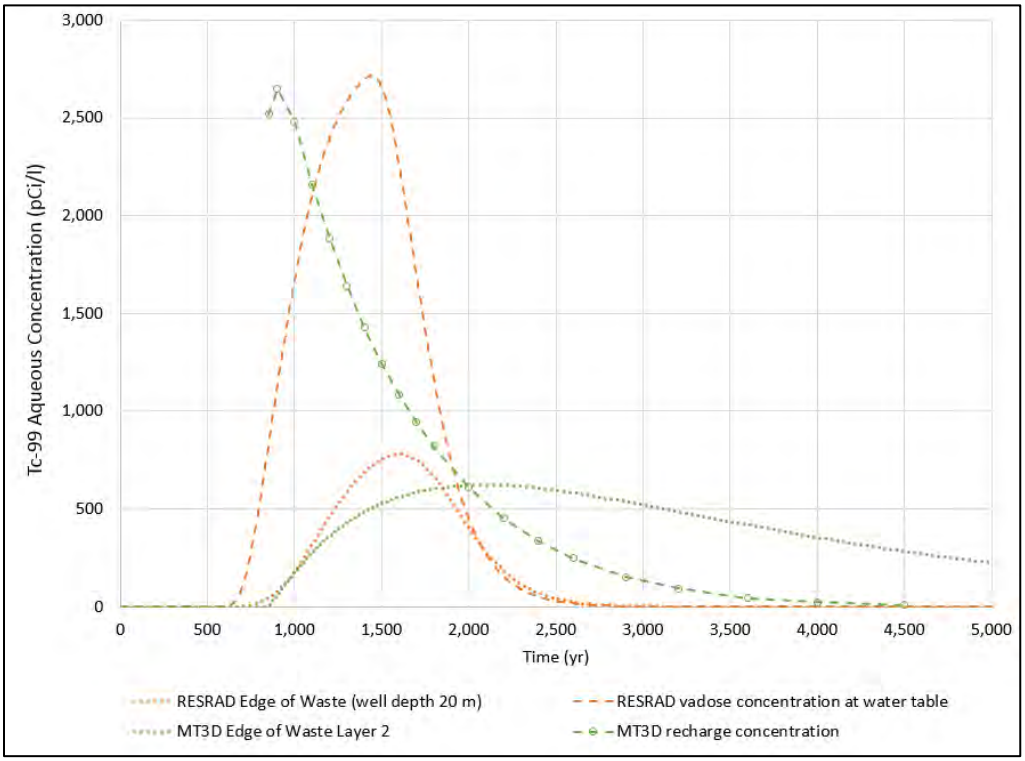

Fig. 3.36. Comparison of vadose zone (at water table) and saturated zone (at edge of waste) Tc-99 concentrations for the MT3D and RESRAD-OFFSITE models.

Predicted saturated zone Tc-99 concentrations at the EOW and at the groundwater POA located 100 m from the EOW (100-m well) for the MT3D and RESRAD-OFFSITE models are plotted in Fig. 3.37. The well depth for the RESRAD-OFFSITE model 100-m well is 131 ft (specified as 40 m in model units), which is approximately equal to the total thickness of MT3D model layers 1 to 3 at the groundwater POA. MT3D model layers 1 to 3 typically have the highest peak activity concentrations at the 100-m well location (Sect. 4.3). For the RESRAD-OFFSITE model, the saturated zone Tc-99 concentration curves for the EOW and 100-m well are similar, with the peak concentration at the 100-m well about half the peak concentration at the EOW due to the difference in the specified well depth (131 ft versus 65.6 ft for the EOW). The RESRAD-OFFSITE model Tc-99 peak at the 100-m well occurs only 100 years later than the EOW peak (1700 versus 1600 years), whereas the peak Tc-99 concentrations for the MT3D model occur later (after 2500 years) and the delay between the EOW Tc-99 concentration peak and the peak at the 100-m well is much larger for the MT3D model (Fig. 3.37). The differences in timing of the saturated zone Tc-99 concentration peaks is the result of the difference in release models (Sect. 3.3.5.1) and to the difference between the simplified analytical saturated zone model in the RESRAD-OFFSITE code and the more detailed MT3D numerical model representation.

The MT3D model results for the 100-m well show a complex pattern of saturated zone Tc-99 concentrations over time, with model layer 1 concentration increasing quickly in parallel with the RESRAD-OFFSITE

model results and then increasing more gradually after about 1100 years to reach a peak at approximately 3000 years post-closure. MT3D model layer 2 Tc-99 concentrations at the 100-m well increase gradually between 1500 and 3500 years post-closure, exceeding model layer 1 Tc-99 concentrations after about 2500 years and reaching a peak at approximately 4000 years. The MT3D model layer 1 and layer 2 Tc-99 peaks at the 100-m well are lower than the RESRAD-OFFSITE model peak by about 50 percent and 30 percent, respectively (Fig. 3.37).

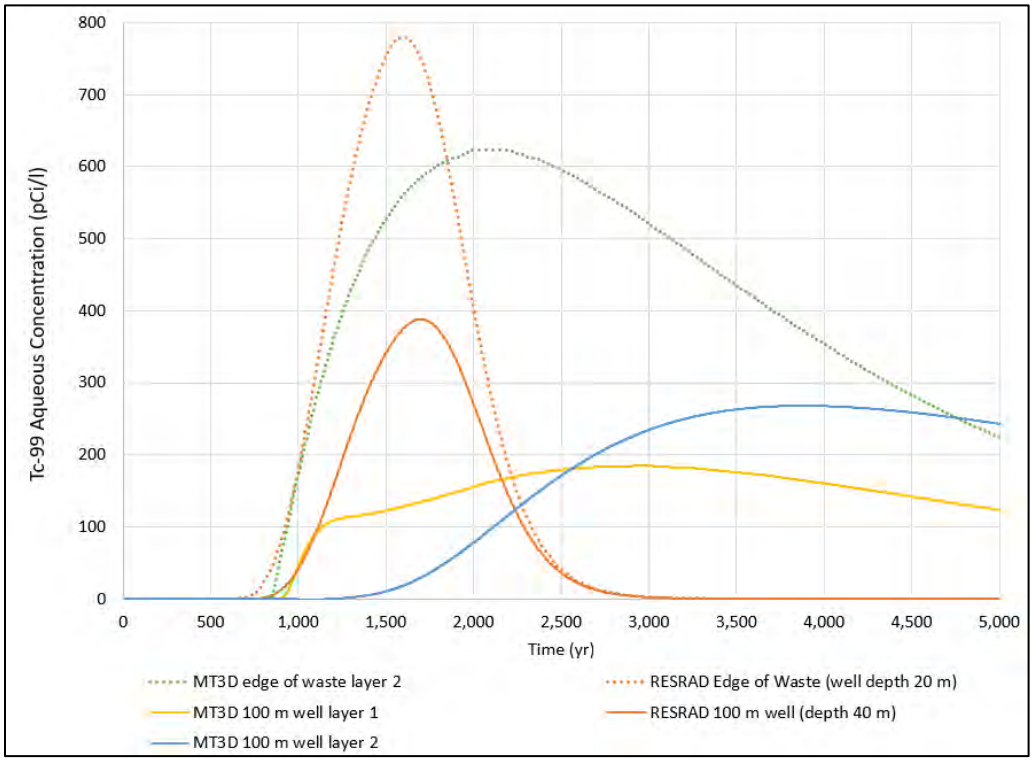

Fig. 3.37. Comparison of predicted saturated zone Tc-99 concentrations for the MT3D and RESRAD-OFFSITE models

The RESRAD-OFFSITE model tends to predict larger and earlier peak saturated zone activity concentrations than does the MT3D model due to the differences in model structure and complexity. The saturated zone concentrations from the RESRAD-OFFSITE model are sensitive to a number of saturated zone input parameters in addition to the well depth specification. The saturated zone hydraulic gradient in particular has a large impact on the predicted 100-m well concentration, as does the assumed value of saturated zone hydraulic conductivity. The product of these two input parameters is the saturated zone Darcy velocity, which determines the predicted dilution of leachate as it arrives at the water table. The hydraulic conductivity of the saturated zone assigned to the RESRAD-OFFSITE model was a transmissivity-weighted average of the K values assigned to MT3D model layers 1 and 2 for the Nolichucky Formation (Sect. 3.3.3.1). The final RESRAD-OFFSITE model input parameter values for the hydraulic gradient to the well and the well depth were selected to ensure general consistency in predicted saturated zone concentrations with the MT3D model results. The well depth of 131 ft was considered reasonable given that MT3D model layers 1 to 3 typically showed the largest peak concentrations and the total thickness of the saturated zone represented was similar. This interval is also consistent with the range of local water well depths (Sect. 3.4.2). The base case value for hydraulic gradient was specified as 0.054, which is higher than the estimated average gradient (0.036) of the water table along the flow path toward the groundwater POA derived from the EMDF flow model results for the long-term performance condition (Sect. 4.1). Applying the higher base case value of hydraulic gradient in the RESRAD-OFFSITE model

resulted in predicted peak saturated zone concentrations at the 100-m well that are broadly consistent (but higher than) the peak concentrations for MT3D model layers 1 and 2, although predicted MT3D model peaks occur later. The sensitivity of RESRAD-OFFSITE model dose predictions to these and other saturated zone input parameter assumptions is presented in Sect. 5.3.

Conceptual model uncertainty. The RESRAD-OFFSITE model saturated zone Tc-99 concentration results are also compared to the results of MT3D model sensitivity evaluations for the hydraulic conductivity of model layer 2 and the non-uniform radionuclide release scenario. These comparisons were made to address potential conceptual model uncertainties related to the characteristics of saprolite and bedrock along the flow path to the groundwater POA and to the assumption of uniform radionuclide release to the saturated zone.

The relatively large thickness (70 ft) of model layer 2 in the EMDF model compared to the thickness of layers 1 and 3 at the 100-m well location suggested that the hydrogeologic properties assigned to layer 2 along the flow path from the EOW to well location could have a large effect on predicted saturated zone activity concentrations. A sensitivity case was evaluated for the EMDF groundwater flow model and the MT3D model Tc-99 transport simulation in which the hydraulic conductivity of model layer 2 was increased to the value assigned to model layer 1, constituting an 8-fold increase. Applying the larger K value to model layer 2 is not an accurate representation of site conditions, based on the CBCV site characterization results (DOE 2018b, DOE 2019), but the sensitivity case does illustrate how a different configuration of material properties affects the results of the MT3D saturated zone radionuclide transport model (Fig. 3.38). Peak saturated zone Tc-99 concentrations at the 100-m well location are higher with the increase in the K values for MT3D model layer 2, reflecting the impact of reduced saturated thickness (decreased water table elevation) within model layer 2 beneath the EMDF waste footprint, and the increased transport velocity associated with the increased conductivity. The MT3D model Tc-99 concentration peaks for the increased K sensitivity case are also much earlier than the base case MT3D model Tc-99 peaks, coinciding with the earlier Tc-99 saturated zone concentrations predicted by the RESRAD-OFFSITE model (Fig. 3.36). The RESRAD-OFFSITE model Tc-99 peak concentration falls between the Tc-99 peaks for MT3D model layers 1 and 2 predicted for the increased layer 2 hydraulic conductivity. This result, for which the MT3D model sensitivity case predictions are closer to the RESRAD-OFFSITE model Tc-99 results, is expected because the increase in K for model MT3D layer 2 creates a groundwater flow system closer to the simplified RESRAD-OFFSITE analytical model of the saturated zone. The MT3D model sensitivity case results are consistent with expectations based on the differences in conceptualization and parameterization of the saturated zone between models.

The sensitivity of MT3D model Tc-99 concentration results to the assumption of uniform radionuclide release to the saturated zone was evaluated with a non-uniform release scenario (Sects. 3.3.3.2 and 5.1). The details of implementing the non-uniform Tc-99 release model for the MT3D sensitivity evaluation are presented in Appendix F, Sect. F.4.2. The non-uniform Tc-99 release scenario results indicate that the impact is greatest on early (prior to 2500 years post-closure) Tc-99 concentrations for MT3D model layer 1, which do not show the rapid increase at around 1000 years, increasing more gradually from 1200 to 3500 years to a peak Tc-99 concentration that is slightly less than the base case result for MT3D model layer 1 (Fig. 3.39). The increase in MT3D model layer 2 Tc-99 concentrations is also delayed relative to the base case result, but the layer 2 peak Tc-99 concentrations are nearly the same as the base case peak concentrations in model layer 2. These results were the basis for concluding that assuming a uniform release of leachate to the saturated zone (as applied to the MT3D model base case simulations and as the conceptual basis for the RESRAD-OFFSITE model code) does not lead to underestimating the impacts of release at the groundwater and surface water POAs because the RESRAD-OFFSITE model used for the total system simulation and dose analysis predicts earlier and larger peak concentrations.

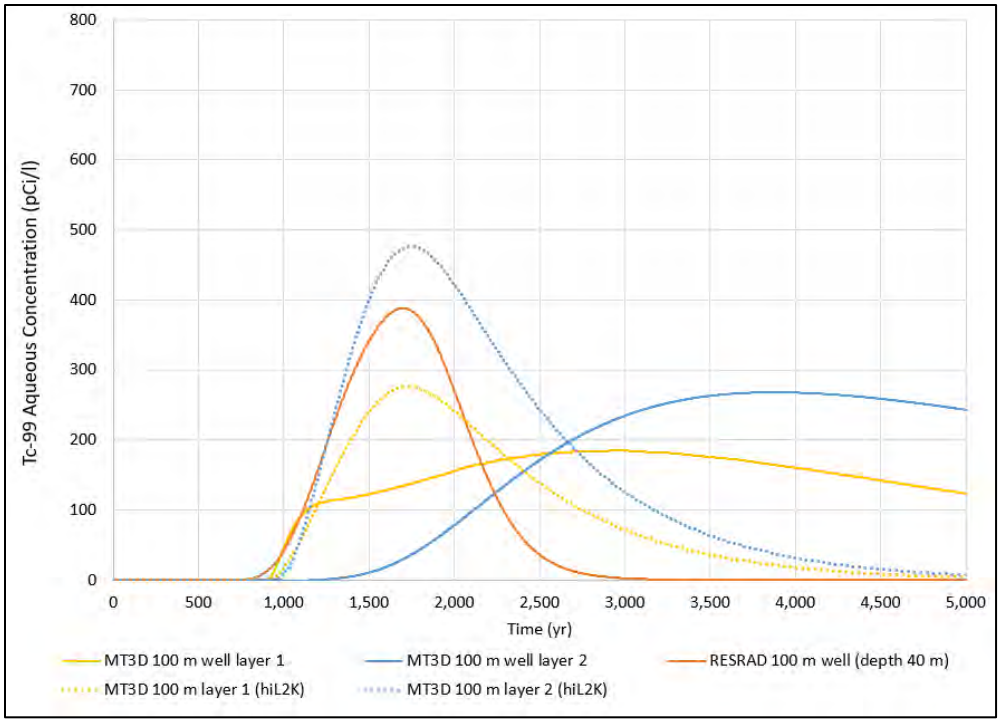

Fig. 3.38. Sensitivity of MT3D model predicted Tc-99 concentrations (groundwater POA) to increased hydraulic conductivity of MT3D model layer 2

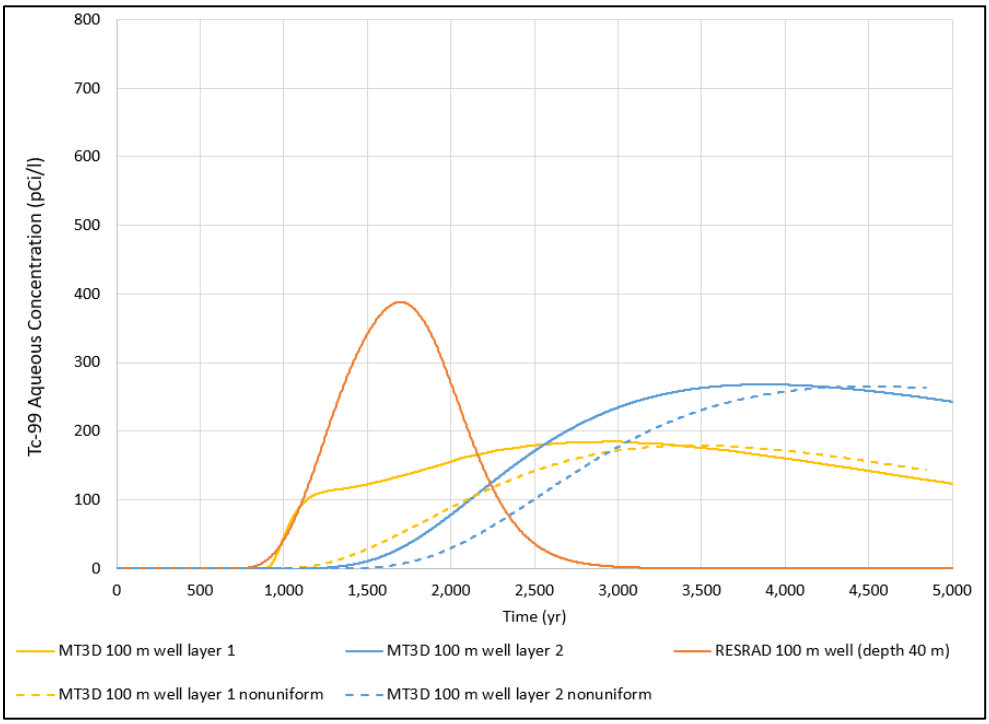

Fig. 3.39. Sensitivity of MT3D model predicted Tc-99 concentrations (groundwater POA) for the non-uniform radionuclide release scenario

3.3.5.3 Transport model integration – summary and conclusion

Based on the comparison of PA model results for Tc-99 flux from the waste and vadose zone (Sect. 3.3.5.1), saturated zone Tc-99 concentration results from the MT3D and RESRAD-OFFSITE models, and MT3D model sensitivity evaluations related to conceptual model uncertainties (Sect. 3.3.5.2), RESRAD-OFFSITE model base case predictions of peak concentrations at the groundwater POA are larger and earlier than corresponding predictions from the more detailed MT3D transport model. Final base case values for critical RESRAD-OFFSITE model input parameters that impact the simulated saturated zone concentrations, including the well depth and hydraulic gradient to the well, were adopted on this basis. For radionuclides with assumed base case K_d values greater than 1 cm^3/g, the instantaneous equilibrium desorption release model and vadose zone representation in the RESRAD-OFFSITE code do not capture the extent to which the EMDF design and the vadose zone below the disposal facility contribute to long-term performance of the disposal system. The conclusion is that the RESRAD-OFFSITE model saturated zone concentration estimates are pessimistically biased high relative to predictions from the more detailed models, and this bias provides a measure of conservatism to the PA dose analysis.

3.4 EXPOSURE AND DOSE ANALYSIS

This section describes implementation of the exposure pathways and scenario described in Sect. 3.2.4 using the total system simulation code RESRAD-OFFSITE.

3.4.1 Site Layout

The EMDF site layout implemented in the RESRAD-OFFSITE model (Fig. 3.40) is based on the assumed resident farmer exposure scenario and site-specific conditions including topography and surface water locations. One limitation of the RESRAD-OFFSITE model is that the primary contamination must be specified as a rectangle, which only approximates the layout of the facility as designed. The EMDF dimensions in the model were specified such that the shorter dimension (822 ft) is equal to the average east-west dimension of the EMDF preliminary design, and the longer dimension (1255 ft) is input as the value that maintains the total design waste volume of 2.2 million cy, based on the average waste thickness (57.5 ft). Sizes and locations of the dwelling site and agricultural fields shown on Fig. 3.40 are assumptions based on topography and proximity to the groundwater well and Bear Creek water supply. The receptor well is located 100 m from the southwest corner of the EMDF rectangle in the direction of groundwater flow as indicated by the EMDF flow model (Sect. 4.1). The well is assumed to be located along the centerline of the modeled plume. The distance to the surface water body in the RESRAD-OFFSITE model layout is 1035 ft, based on the distance from the edge of waste to Bear Creek downstream of NT-11.

3.4.2 Well Construction and Water Use Assumptions

The subsurface vertical interval from which groundwater is withdrawn for human consumption and domestic use is parameterized in the RESRAD-OFFSITE model as “depth of aquifer contributing to well”, defined as the depth from the water table (top of the model domain for the aquifer) to the bottom of the well. This depth is set to 131 ft, consistent with the combined thickness of the MT3D model layers having the highest predicted concentrations at the groundwater POA (Sect. 3.3.3.2). Selection of the final base case value for the well depth was also influenced by the fact that the predicted concentration is highly sensitive to this input parameter and values much smaller than 131 ft produced peak concentrations much higher than saturated zone peak concentrations predicted the MT3D model. The final value selected was therefore an outcome of the comparison and integration of results obtained from different PA models (Sect. 3.3.5.2).

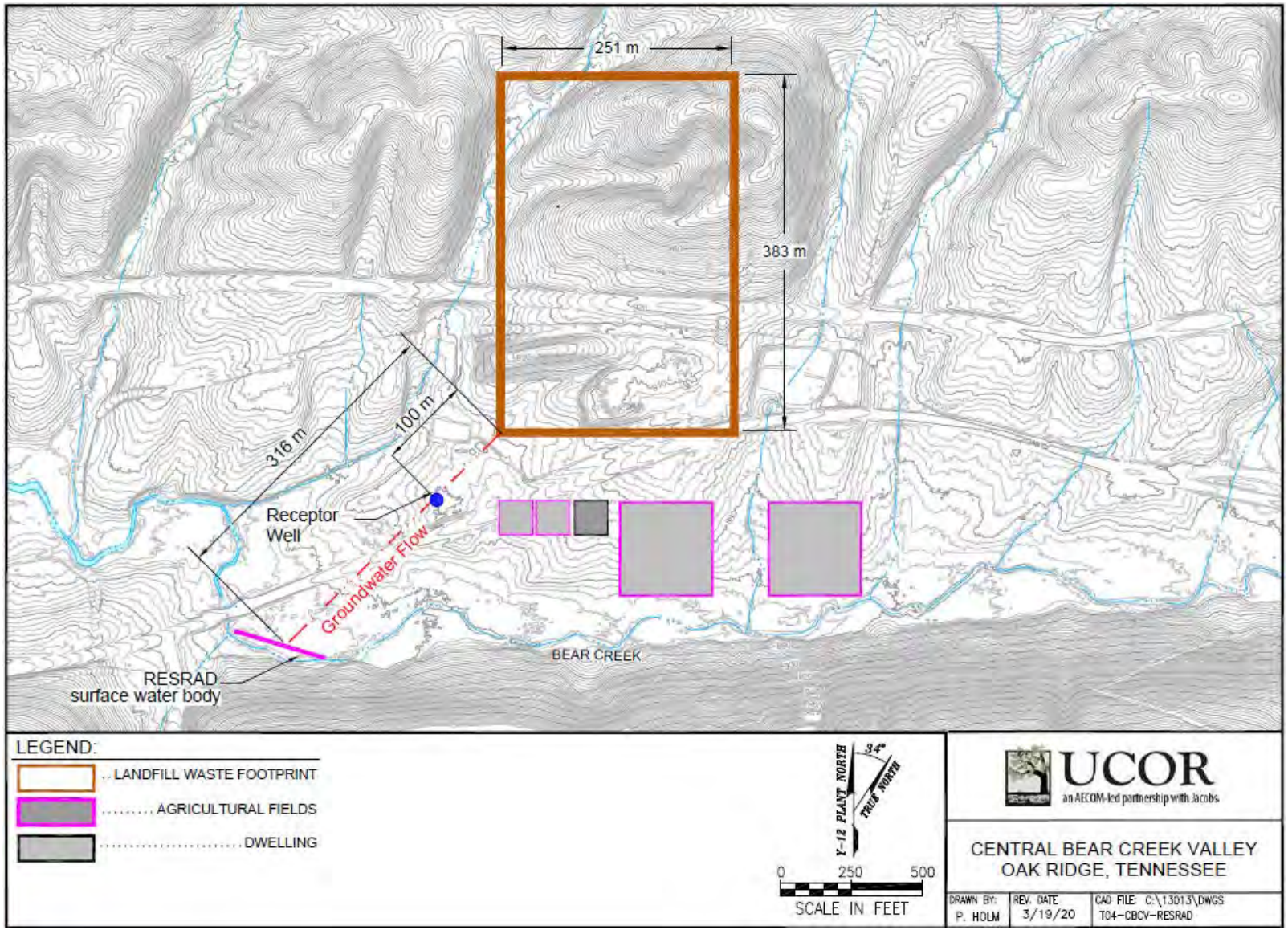

Fig. 3.40. Site map showing conceptual layout of EMDF footprint, dwelling and agricultural fields, groundwater well, and surface water body (Bear Creek)

The assumed well depth is consistent with the documented range of local water well depths in the area, which vary from less than 100 ft to more than 300 ft deep. The RESRAD-OFFSITE analytical model of the saturated zone predicts the highest concentrations at or very near the water table at the 100-m location, so that the 131-ft-deep cylindrical zone over which groundwater concentration is averaged includes the most contaminated upper part of the saturated zone, consistent with the results from the MT3D model (Sect. 3.3.3.2).

The water source assumption is that 100 percent of water that is used for drinking and to cook food and for cleaning and showering inside the dwelling is obtained from the well located 100 m from the EOW. Water ingestion for an individual was assumed to be 2 L/day. The livestock (assumed to include two beef cattle and two dairy cows) derive 100 percent of their drinking water from Bear Creek surface water that is impacted by contaminated groundwater emanating from the disposal facility. Irrigation water use for the various crop fields was assumed to be 0.15 m/year, with 100 percent of the irrigation water coming from contaminated portions of Bear Creek. The use of surface water for irrigation of crops is consistent with the predominance of surface water withdrawals for agricultural purposes in Anderson and Roane Counties (Sect. 3.2.4.2) due to the reliable nature of precipitation and surface water availability. The assumed values for key water use parameters are provided in Table 3.23.

Table 3.23. Key water use parameter values assumed for RESRAD-OFFSITE

Water use or ingestion parameter	Value	Units
Human consumption	730	L/year
Indoor dwelling use	225	L/day
Beef cattle	50	L/day
Dairy cows	160	L/day
Well pumping rate	332	m^3/year

RESRAD = RESidual RADioactivity

3.4.3 Food and Soil Ingestion Rates

Assumed values for ingestion of foods and soil are presented in Table 3.24. Ingestion rates of food consumed by the receptor are based on EPA guidance (EPA 2011) for plant foods and Putnam et al. (1999) for beef, poultry, and eggs. The fish ingestion rate reflects limited recreational fishing in Bear Creek. It is assumed there is no consumption of crustacea or mollusks, which is reasonable given the EMDF location in eastern Tennessee.

Table 3.24. Simulated ingestion rate values

Parameter	Value	Units	Fraction from affected area
Fish	2.43	kg/year	1.0
Fruit, grain, non-leafy vegetables	176	kg/year	0.5
Leafy vegetables	17	kg/year	0.5
Meat	92	kg/year	0.25
Milk	110	L/year	0.5
Soil (incidental)	36.53	g/year	[a]

[a]The fraction of this intake from each contaminated area is proportional to the occupancy in that area.

Total fluid milk ingestion is given as the equivalent of 84 L/year on Table 11-12 of EPA 2011; however, the base case milk ingestion value for EMDF is set at 110 L/year. The higher milk ingestion value serves to increase the total food ingestion dose and thereby bias the dose estimate toward higher values. Values for ingestion of non-leafy produce and leafy vegetables are consistent with the data listed in Tables 9-1, 9-6, and 12-1 of EPA 2011.

The RESRAD-OFFSITE model exposure pathways do not include poultry or egg consumption explicitly. The animal food ingestion pathways represented in the model are limited to meat and milk from cows. To account for possible dose contributions from consumption of poultry and eggs, an effective meat ingestion rate (91.9 kg/year) is applied, representing the sum of beef (55.4 kg/year), poultry (21.3 kg/year), and eggs (15.2 kg/year) given in Putnam et al. (1999). Adjusted meat transfer factors are also calculated and applied in the RESRAD –OFFSITE model dose analysis (Sect. 3.4.5).

The Oak Ridge area is assumed to remain populated and urbanized in the future, with many commercial food sources (e.g., restaurants, grocery stores, farmer's markets) available in close proximity to the hypothetical BCV farm adjacent to EMDF. Food consumption is assumed to include some uncontaminated food as well as locally grown agricultural products contaminated with radionuclides released from the EMDF. For plant foods and milk, 50 percent of the food ingested is assumed to come from the contaminated agricultural areas. For meat ingestion, 25 percent is assumed to come from farm raised animals that ingest contaminated water and feed. The RESRAD-OFFSITE model sensitivity analyses include evaluating uncertainty in the fraction of food products obtained from contaminated areas (Appendix G, Sect. G.6.3).

Fish ingestion is based an EPA recommendation of 54 g/day for recreational fishing in areas with large bodies of water (EPA 1990), combined with an exposure frequency of 45 days/year, which is the value used as recreational surface water exposure frequency for the human health risk assessment in the BCV RI (DOE 1997b). Because of the limited populations of larger fish in BCV, and because the proportion of fish caught locally is set at 1.0, the fish ingestion rate of 2.43 kg/year overestimates the likely fish ingestion dose.

The incidental soil ingestion rate is based on the EPA recommended value (100 mg/day) and the fractional occupancy time in the agricultural areas (Sect. 3.4.4). The annual inhalation rate required for the inhalation pathway dose calculation (Sect. 3.2.4) was set at the RESRAD-OFFSITE default value of 8400 m^3/year.

3.4.4 Occupancy

Specified occupancy fractions represent the assumed fractional annual time period (fractional years) that the receptor spends inside or outside the specified exposure areas. For example, occupancy factors are specified for the EMDF area and for farmed areas or pasture land contaminated by irrigation. Those occupancy factors are used to compute exposure from direct external radiation from contaminated soil in irrigated fields, and internal exposure due to incidental ingestion of soil and inhalation of dust resuspended from contaminated soil. The RESRAD-OFFSITE base case model assumes that the receptor spends approximately 2.6 weeks outdoors on the primary contamination (5 percent of time), half the time inside the offsite dwelling (50 percent of time), 2.6 weeks outdoors at the offsite dwelling (5 percent of time), and 10 percent of the time at each of the four agricultural areas (40 percent of the time total). Overall, the representative receptor is assumed to spend 100 percent of the time at EMDF, thereby inducing a bias toward a greater dose from the external, inhalation, and soil ingestion pathways.

3.4.5 Biotic Transfer Factors and Dose Conversion Parameters

3.4.5.1 Biotic transfer factors

The RESRAD-OFFSITE model uses transfer factors to convert soil and/or water concentrations to concentrations in plant and animal tissues. Below are brief descriptions of the transfer factor types included in the default library:

- Soil to plant transfer factors: Represents the nuclide concentration in vegetables, fruits, and in livestock feed products at the time of harvest (fresh weight basis) due to root uptake from soil containing a unit concentration (dry weight basis) of the nuclide
- Intake to animal product transfer factors: Represents the nuclide concentration in the animal meat and milk at the time of slaughter or milking, respectively, due to a uniform intake of unit activity of radionuclide per day
- Water to aquatic food transfer factors: Represents the nuclide concentration in aquatic food products such as fish and crustacea at the time of harvest from the simulated surface waterbody containing a unit concentration of radionuclide in the aqueous phase.

The RESRAD-OFFSITE model exposure pathways do not include poultry or egg consumption explicitly. The animal food ingestion pathways represented in the model are limited to meat and milk from cows, fish, and crustaceans. To account for possible dose contributions from consumption of poultry and eggs, an effective (total) meat ingestion rate is applied (Sect. 3.4.3) and adjusted feed consumption to meat transfer factors are calculated and applied in the RESRAD–OFFSITE model dose analysis.

With the exception of transfer factors for H-3, C-14, I-129, all values are from PNNL 2003, which are reproduced in Yu et al. (2015). RESRAD default values are applied for the H-3 freshwater fish transfer factor and the I-129 soil to plant transfer factor. Transfer factors for H-3 (except fish) and C-14 (except fish) are calculated within specialized RESRAD-OFFSITE submodels for these two radionuclides. The adjusted radionuclide-specific transfer factors represent consumption rate weighted average transfer factors for beef, poultry, and eggs as follows:

$$\text{Consumption Weighted TF} = (CR_{beef}TF_{beef} + CR_{poultry}TF_{poultry} + CR_{eggs}TF_{eggs}) / (CR_{beef} + CR_{poultry} + CR_{eggs})$$

where:

CR = Consumption Rate of Specified Animal Product (kg/year)
TF = Intake-to-Animal Transfer Factor for Specified Meat Type (pCi/kg)/(pCi/day).

3.4.5.2 Dose conversion factors

The RESRAD-OFFSITE model libraries (Table 3.25) contain the dose conversion factor databases for external exposure and internal exposure as inhalation and ingestion that are applied in the dose analysis (Gnanapragasam and Yu 2015). The library of default transfer factors is used to supplement the values given in PNNL (2003).

Table 3.25. Key radiological and dose conversion factor data sources

Parameter/library	Basis
Basis for radiological transformations	ICRP 2008
External exposure library	DCFPAK3.02 database, https://www.dcfpak.org, DOE 2017a
Internal exposure dose library	DOE 2011b (reference person)
Slope factor (risk) library	DCFPAK3.02 morbidity, https://www.dcfpak.org, DOE 2017a
Transfer factor library	RESRAD default transfer factors
Calculation time points	2048

DCFPAK = Dose Coefficient File Package (database)
ICRP = International Commission on Radiological Protection
RESRAD = RESidual RADioactivity

This page intentionally left blank.

4. RESULTS OF ANALYSES

This section presents the environmental transport modeling results and the dose analysis performed for the EMDF disposal system. HELP model results for evaluating cover design performance and potential degraded performance conditions are summarized in Sect. 3.3.1 and detailed in Appendix C, Sect. C.2. Those results are the basis for the assumed evolution of cover performance and cover infiltration rates applied in the radionuclide transport models.

4.1 PREDICTED GROUNDWATER CONDITIONS

This section provides a succinct summary of the groundwater flow model results used directly or indirectly as inputs to the environmental transport modeling. Additional detail on the groundwater flow model results including particle tracking analysis and model sensitivity evaluations is provided in Appendix D.

The steady-state flow model results for the CBCV model (current conditions) and the EMDF model (long-term performance condition) are shown in Figs. 4.1 and 4.2. The EMDF model provides the flow field (Fig. 4.2) for the 3-D saturated zone radionuclide transport model. The general flow pattern for the long-term performance condition is downward flow below the disposal unit directed horizontally toward Bear Creek and the NT-10 and NT-11 tributaries. Flow farther south between disposal cell 3 and Bear Creek is directed predominantly down valley toward NT-11 and Bear Creek. The estimated water table elevation below the EMDF and average hydraulic gradient from the EMDF model are used for parameterizing the total system model (RESRAD-OFFSITE) simulation (Appendix G).

The effect of long-term cover system degradation leading to increased cover infiltration and recharge to the saturated zone below the facility is illustrated in Fig. 4.3, which shows EMDF model results for both the full design performance condition (zero cover infiltration/recharge) and the long-term performance condition (0.88 in./year cover infiltration/recharge). The predicted impact of cover degradation and leachate release on the water table is significant, with elevation differences of up to 8 ft near the center of disposal cell 2 (Fig.4.4). However, the predicted groundwater levels for the long-term performance condition are still below the base of the geobuffer zone.

For the EMDF model long-term performance condition, simulated depth to the water table below the waste ranges between 20 and 50 ft (Fig. 4.5). The average vertical interval between the bottom of waste and the water table is approximately 31 ft. This average total vadose zone thickness below the waste is used to set the base case thickness for unsaturated zone 5 in the RESRAD-OFFSITE model (Sect. 3.3.4, Table 3.22).

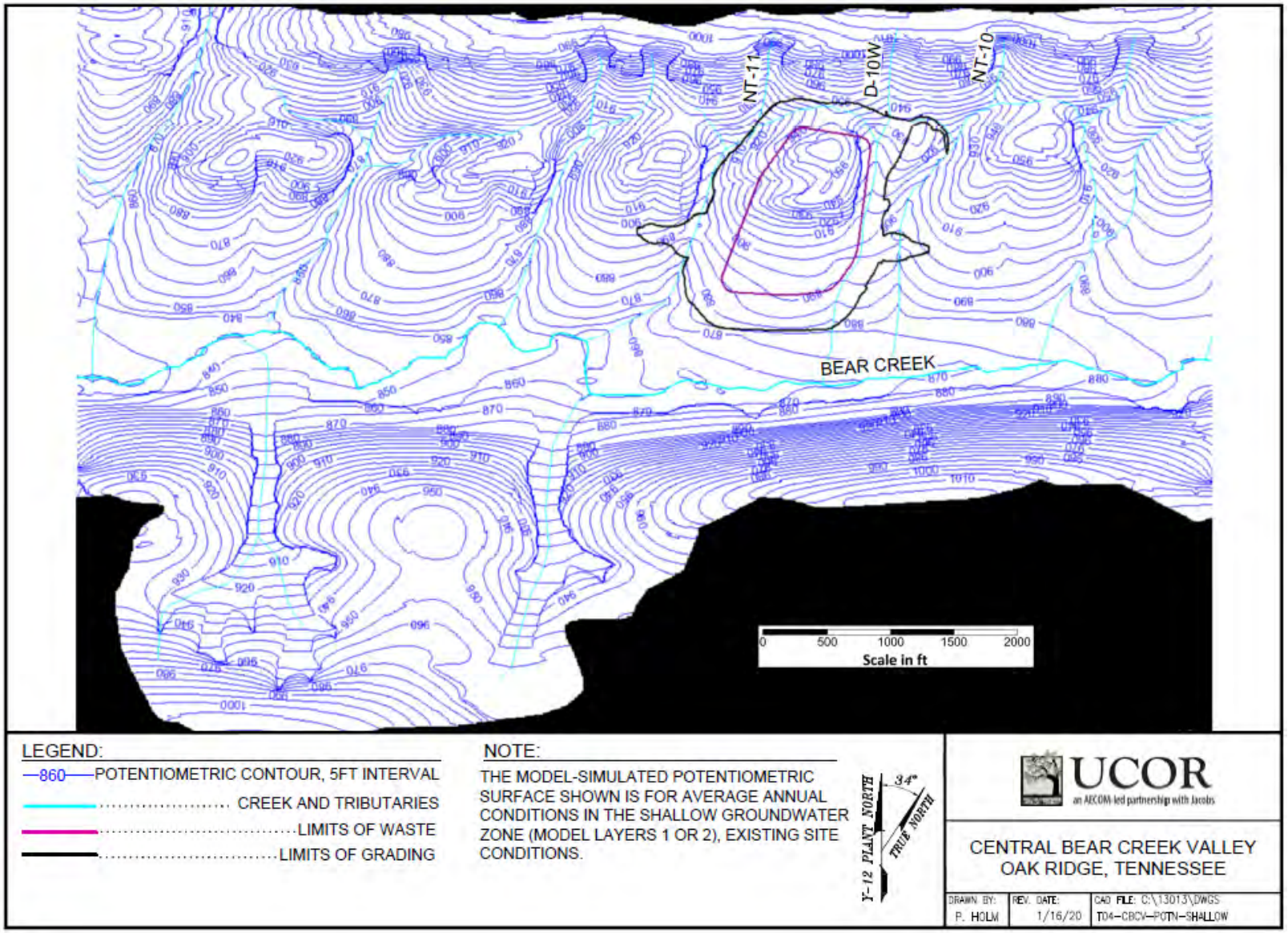

Fig. 4.1. CBCV model predicted water table elevation

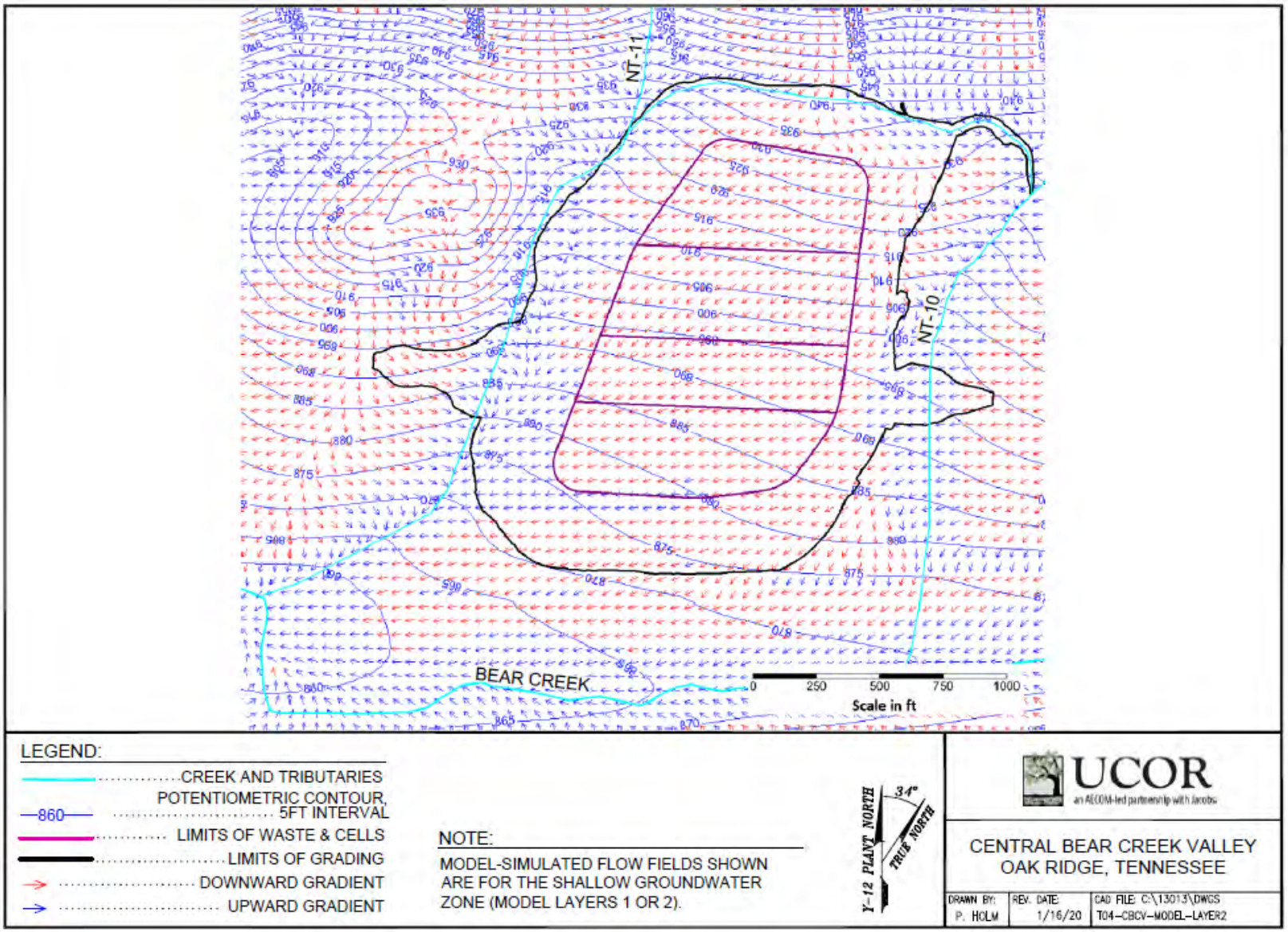

Fig. 4.2. EMDF model long-term performance condition predicted potentiometric surface and flow field for model layer 2

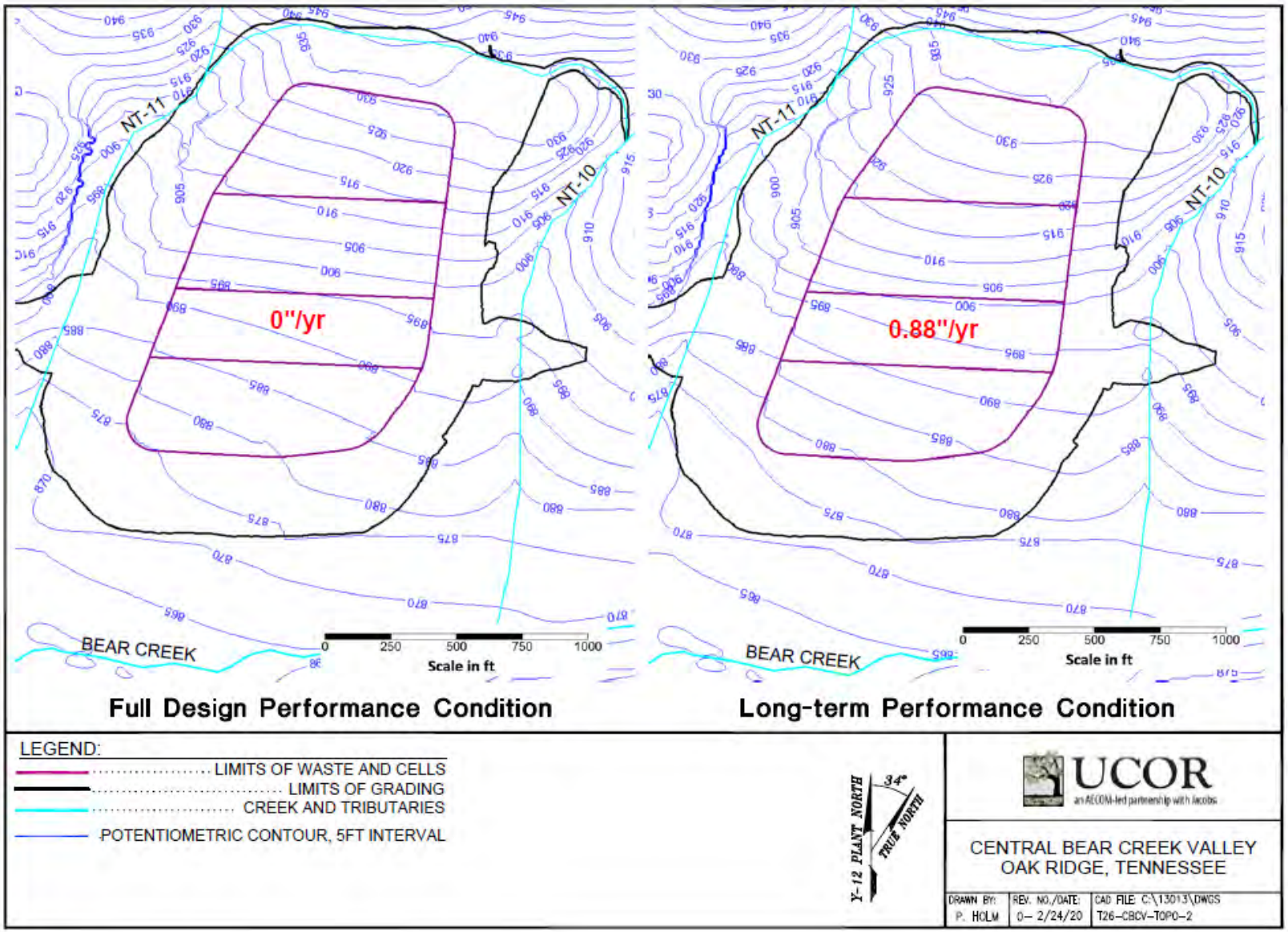

Fig. 4.3. EMDF model predicted groundwater levels for full design performance condition and long-term performance condition

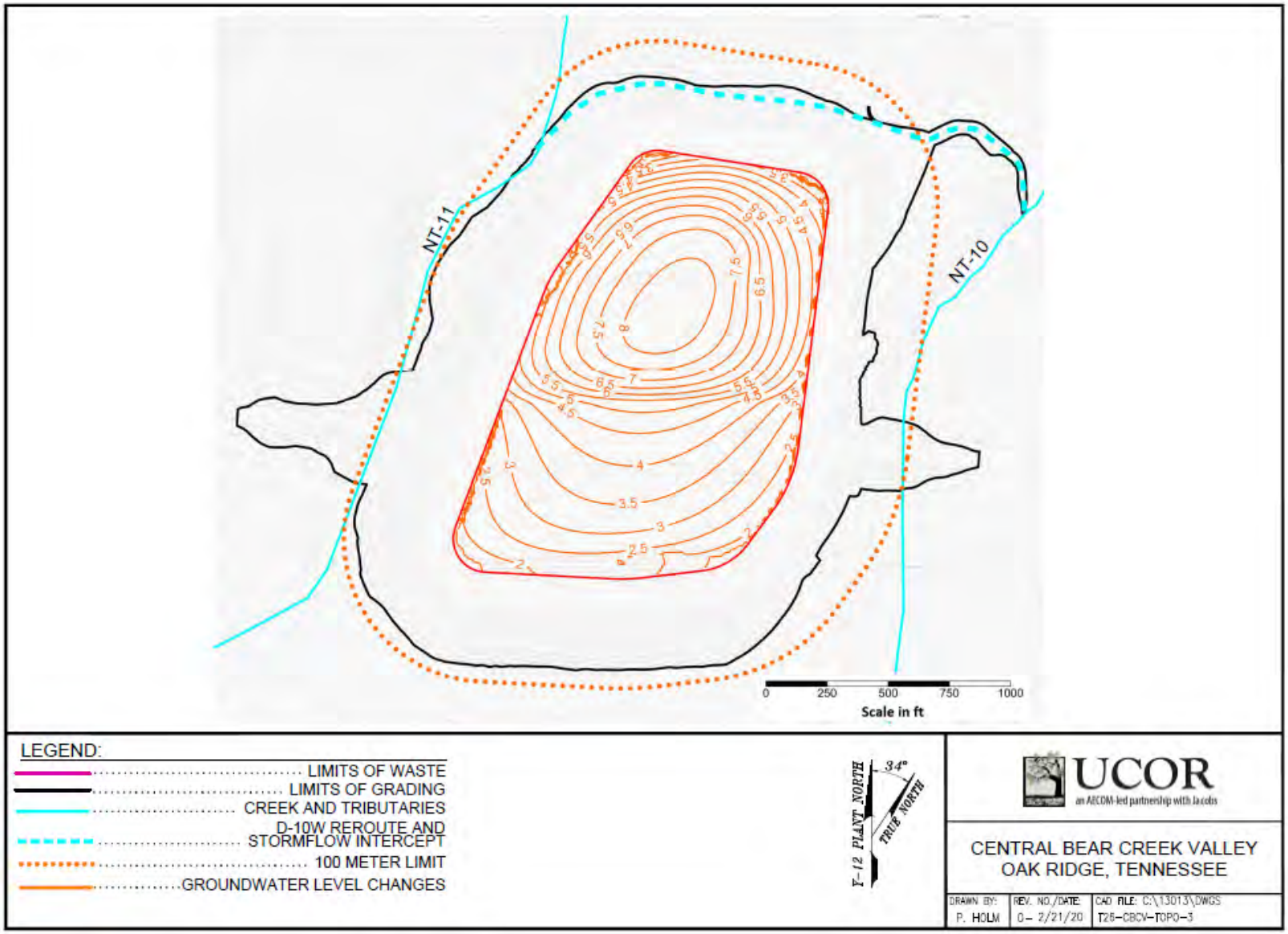

Fig. 4.4. Groundwater level changes from full design performance to long-term performance condition

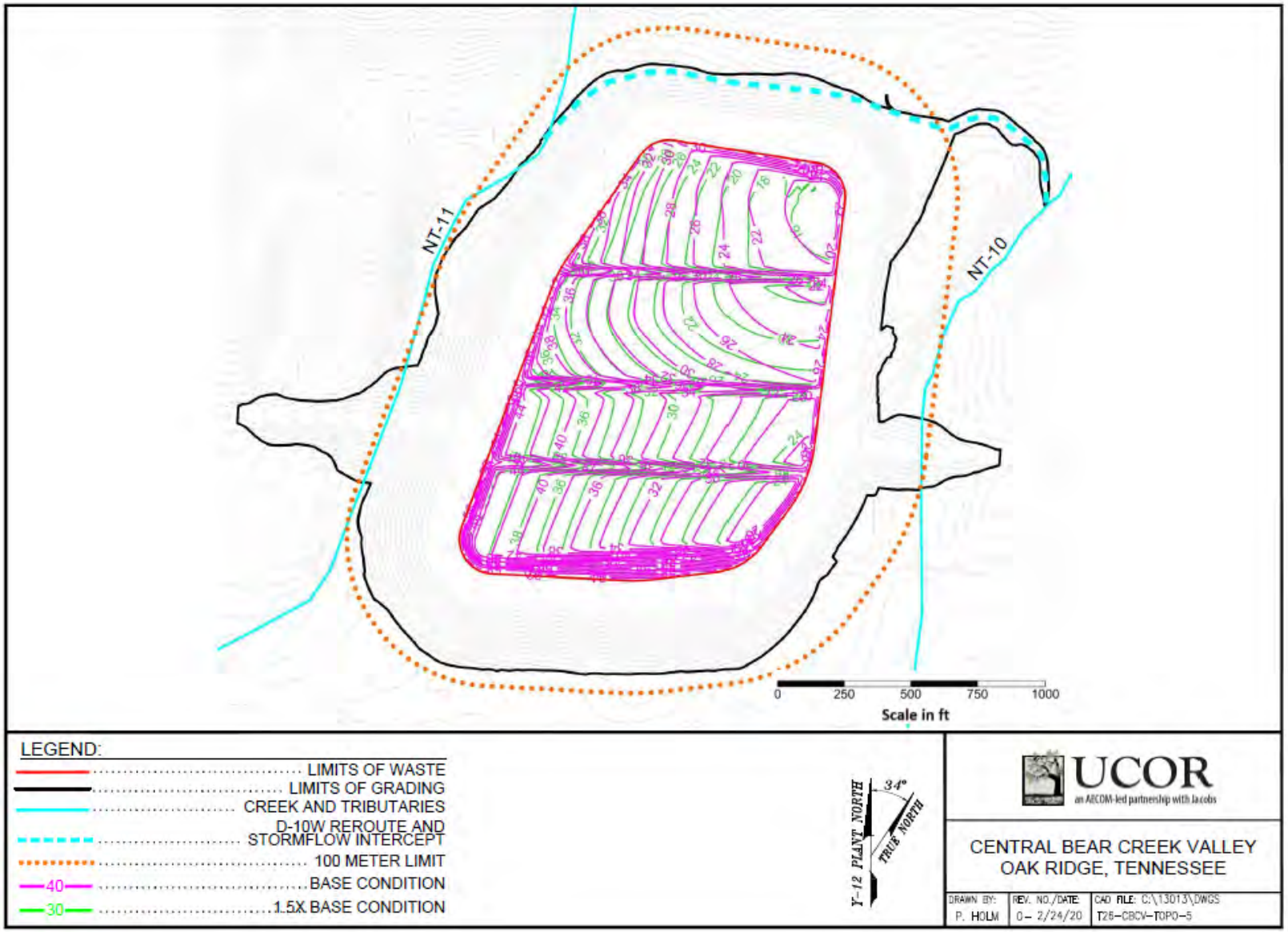

Fig. 4.5. Depth to groundwater contours for 1.5 times base recharge and the base recharge case

4.2 RADIONUCLIDE RELEASE AND VADOSE ZONE TRANSPORT

4.2.1 STOMP Model Simulations

The STOMP model simulations provided a detailed representation of patterns of radionuclide release beneath the EMDF, and were used to quantify average vadose travel times, total activity flux at particular locations, and the non-uniformity of release for seven radionuclides (H-3, C-14, Tc-99, I-129, U-234, U-238, and Pu-239). Six of these radionuclides were selected on the basis of potential dose contributions within the general 10,000-year timeframe for the PA analysis (C-14, Tc-99, and I-129), or dose impacts over much longer timespans (U-234, U-238, and Pu-239). STOMP model runs were extended to 1,000,000 years to simulate release of less mobile radionuclides such as U-234. Section 3.3.2 provides a summary of the STOMP model implementation. Detailed description of STOMP model input parameters including mechanical and hydraulic properties of materials, initial radionuclide concentrations, assumed K_d values, as well as model domain setup and assignment of boundary conditions is provided in Appendix E.

Two 2-D cross-section STOMP models were developed for the EMDF site (Section A and Section B, refer to Fig. 3.14). Due to the large number of model nodes and the extended period of simulation, and in order to streamline output data post-processing, a limited number of model outputs were specified. The STOMP output included data for selected model nodes at several vertical output profiles and along three output surfaces (Fig. 4.6), and data for all model nodes at selected model time steps. The three output surfaces comprised all model nodes along the top of the liner (bottom of waste), bottom of the liner, and along the estimated water table elevation beneath the EMDF (based on the EMDF flow model long-term performance condition output shown in Fig. 4.2). The data output surfaces were used to calculate the total vertical activity flux across the surface as a function of time. These activity flux time series were then used to estimate the average vadose delay times and to support development of the non-uniform Tc-99 release scenario for the MT3D model (Sect. 4.3). The STOMP model output was also compared to the radionuclide release model developed for the MT3D saturated zone model and the predicted release to the vadose and saturated zones from the RESRAD-OFFSITE model code (refer to Sect. 3.3.5 for description of PA model integration).

Appendix E presents detailed model output for individual STOMP model nodes, as well as total activity flux estimates and cross-sectional graphics for specific model time steps. The remainder of Sect. 4.2 provides a limited range of STOMP model output examples, including saturation and activity concentration fields, and activity flux time series used to estimate the vadose delay times applied to the MT3D model inputs and outputs.

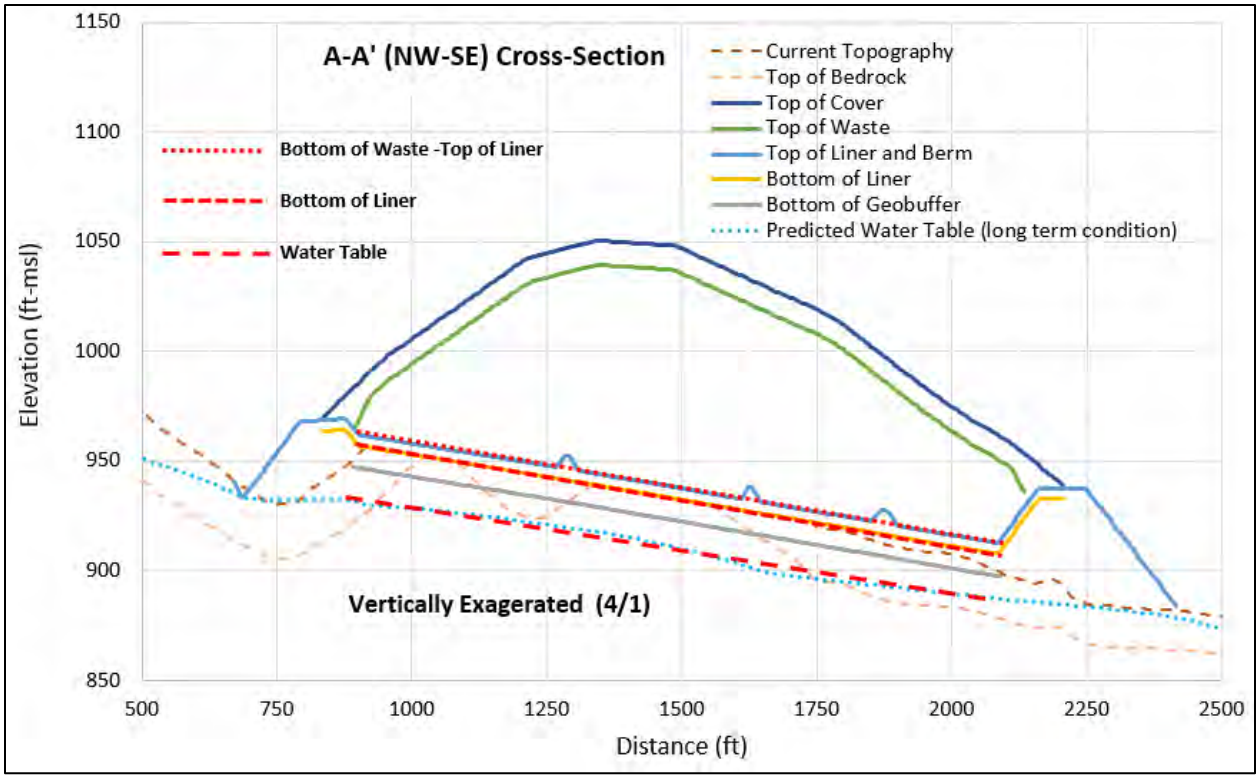

Fig. 4.6. Data output surfaces defined in the STOMP Section A model

4.2.2 Water Movement and Saturation

Water input along the top of the STOMP model domain represents the estimated natural rates of groundwater recharge (from 6 to 13 in./year depending on geologic unit) outside the perimeter berms, lower rates applied to the berm areas outside of the cover (1 in./year) and time varying cover infiltration along the central area (final cover system) of the disposal unit (refer to Fig. 3.19). The evolution of relative saturation (water content as a fraction of total available porosity) for the Section A model is shown in Fig. 4.7. Increasing cover infiltration begins at 200 years post-closure, but significant increases in saturation for most model nodes do not occur until the interval between 350 and 450 years. As early as 500 years, a strongly non-uniform pattern of saturation develops along the base of the liner system within the geologic buffer and underlying natural materials. Wetter areas develop beneath the downslope (lower) end of each disposal cell, reflecting the strong impact of the liner system geometry (sloping drainage layer above the clay barrier) in controlling the pattern of water flow. Equilibrium (steady state) saturation levels are achieved by approximately 1200 years for all materials. The progressive increase in relative saturation varies with material type and location in the cross section, reflecting the systematic pattern of leachate drainage along the liner and into the underlying materials. The liner system geometry causes non-uniformity in water flux and saturation that drive similar non-uniformity in patterns of radionuclide flux below the disposal unit.

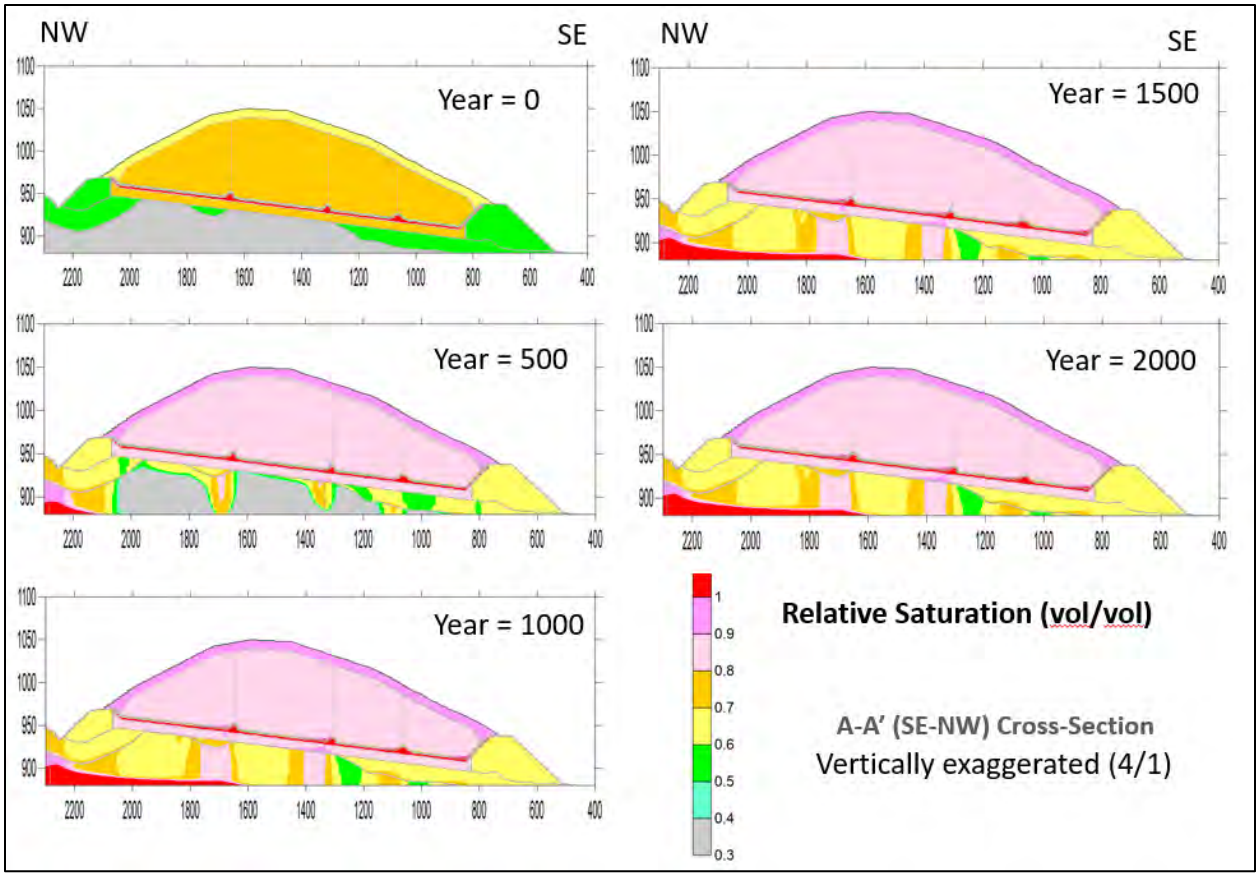

Fig. 4.7. Saturation change with time in the STOMP Section A model

4.2.3 Source Depletion and Vertical Migration of Radionuclides

STOMP model activity concentrations fields presented in this section are limited to results for C-14, Tc-99, and I-129. Results for the other radionuclides included in the STOMP modeling are presented in Appendix E. Section A modeled activity concentration fields for C-14, Tc-99, and I-129 at successive simulation times are presented in Figs. 4.8, 4.9, and 4.10. The successive radionuclide concentration fields illustrate both downward and lateral transport and highlight the strongly non-uniform pattern of release below the disposal unit. The time increments between panels in Figs. 4.8, 4.9, and 4.10 vary among radionuclides because of differences in mobility (K_d). Differences in the patterns of radionuclide depletion from the waste and migration into the vadose zone below the liner are controlled by differences in half-life and sorption (K_d value), and also reflect variation in waste thickness, disposal cell dimensions and liner system geometry.

The biggest control on the duration of radionuclide release and eventual depletion is the K_d value. Carbon-14 (K_d = zero) is completely depleted from the waste by 1500 years post-closure (Fig. 4.8), whereas depletion of I-129 (waste K_d = 2 ml/g) requires more than 5000 years (Fig. 4.10). There are different durations of radionuclide release for different disposal cells due to variable waste thickness. Disposal cells 1 and 4 have lower average waste thickness and therefore less radionuclide inventory and are depleted more quickly than the middle two cells (cells 2 and 3). The width of each cell and resulting differences in total water influx also influences this pattern. Cell 4 is relatively narrow and has a relatively small waste thickness and so is depleted most quickly (e.g., for Tc-99, cell 4 is nearly depleted by 2000 years, Fig. 4.9).

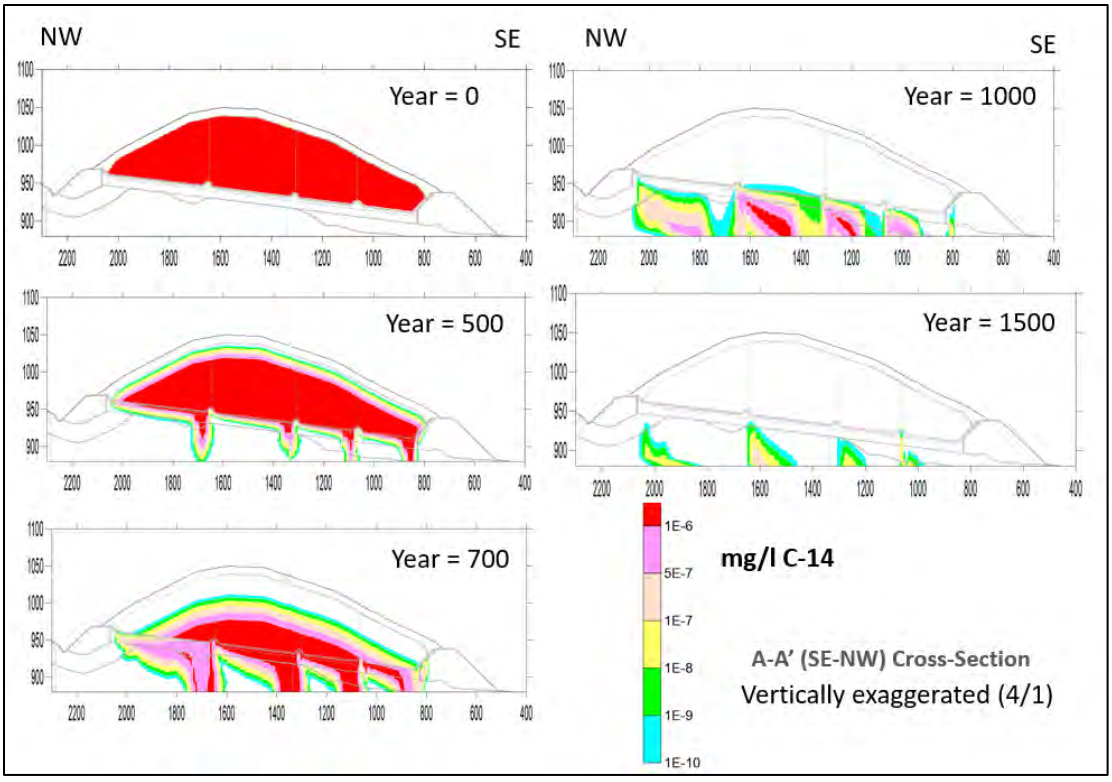

Fig. 4.8. C-14 concentration fields for the STOMP A-section model at successive simulation times

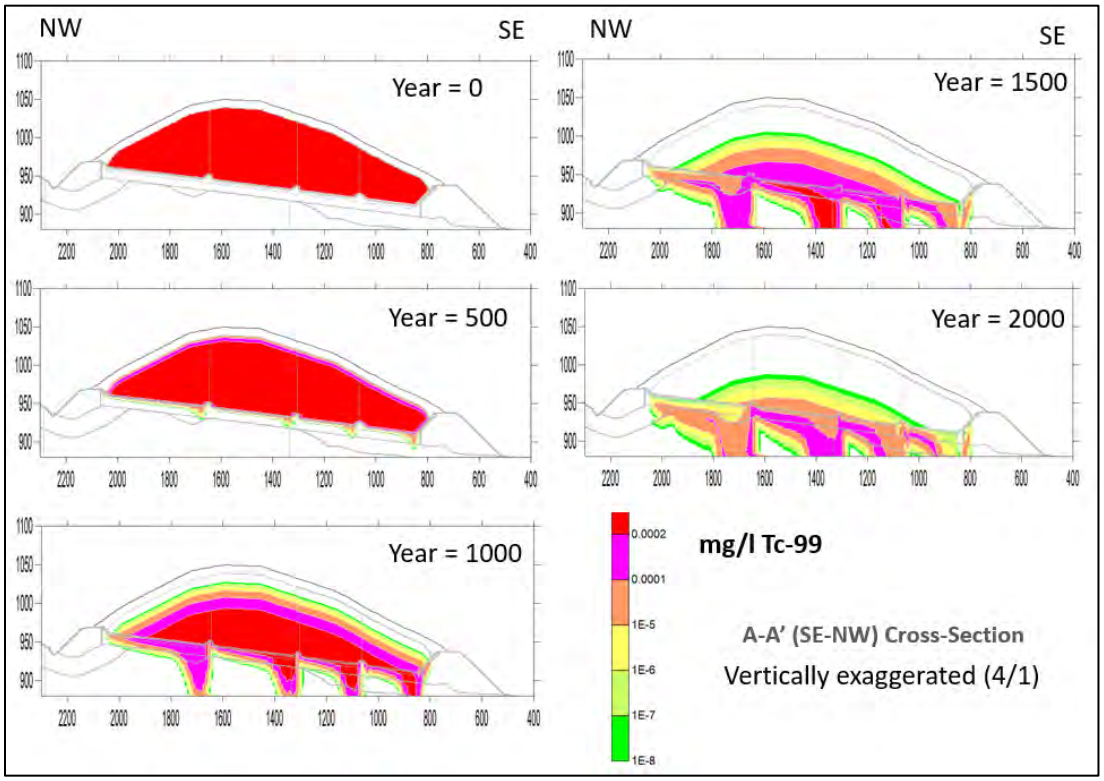

Fig. 4.9. Tc-99 concentration fields for the STOMP A-section model at successive simulation times

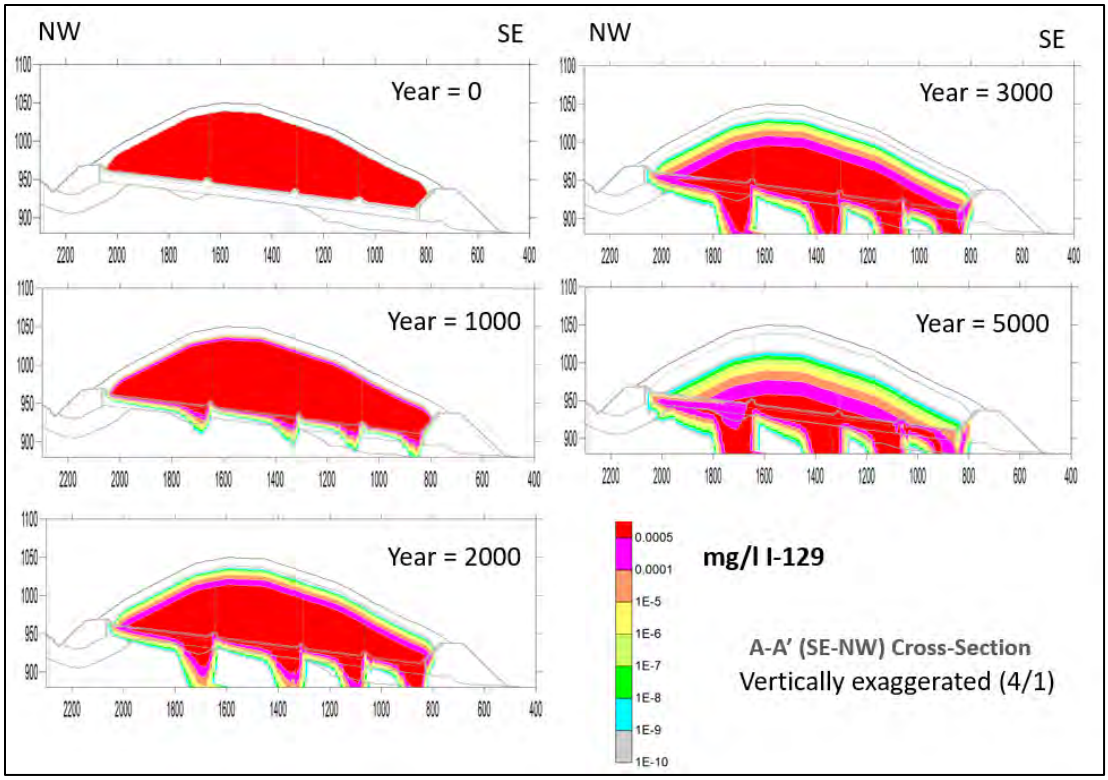

Fig. 4.10. I-129 concentration fields for the STOMP A-section model at successive simulation times

The non-uniform pattern of release beneath each disposal cell corresponds to variations in saturation and leachate concentration that results from downslope leachate movement along the liner system. The magnitude, duration, and timing of peak concentrations varies strongly along the base of each disposal cell and also varies among the four disposal cells (particularly the timing and duration of maximum concentrations; refer to Appendix E for illustrative graphics). The non-uniform release through the vadose zone to the saturated zone represented in the STOMP model simulations is summarized in terms of separate radionuclide flux curves developed for each disposal cell and presented in the following section.

These detailed modeling results show the potential complexity of contaminant movement in variably saturated and transient conditions and provide a good illustration of the value of the STOMP model in representing a complex system. The complexity of the radionuclide transport field within the vadose zone is greatly simplified for the 3-D saturated zone model (MT3D) and total system model (RESRAD-OFFSITE). An evaluation of the significance of non-uniform release to the predicted radionuclide concentrations at the groundwater well POA is presented in Sect. 5.2.

4.2.4 Radionuclide Flux at Output Surfaces

The radionuclide flux into the vadose zone below the liner and into the saturated zone were quantified based on the STOMP model results at the data output surfaces described in Sect. 4.2.1. The total flux calculations are a useful summary of STOMP model release predictions for comparison to the other release models (MT3D radionuclide input and RESRAD-OFFSITE output, refer to Sect. 3.3.5).

Figures 4.11, 4.12, and 4.13 show the activity flux rate across the three output surfaces for C-14, Tc-99, and I-129, respectively, and illustrate the progressive migration of radionuclides from waste through the liner and through the vadose zone. (Note the different time scales on the horizontal axes in these three

figures.) The increase in cover infiltration between 200 and 1000 years post-closure is also plotted on each figure. Carbon-14 has a much earlier release and shorter depletion time (Fig. 4.11) than either Tc-99 or I-129 due to the zero K_d value. The C-14 migrates quickly with water and the peak flux rate out of the waste occurs at 650 years, well before the water infiltration rate reaches its maximum rate at 1000 years. The peak flux rate at the water table for C-14 occurs at about 775 years.

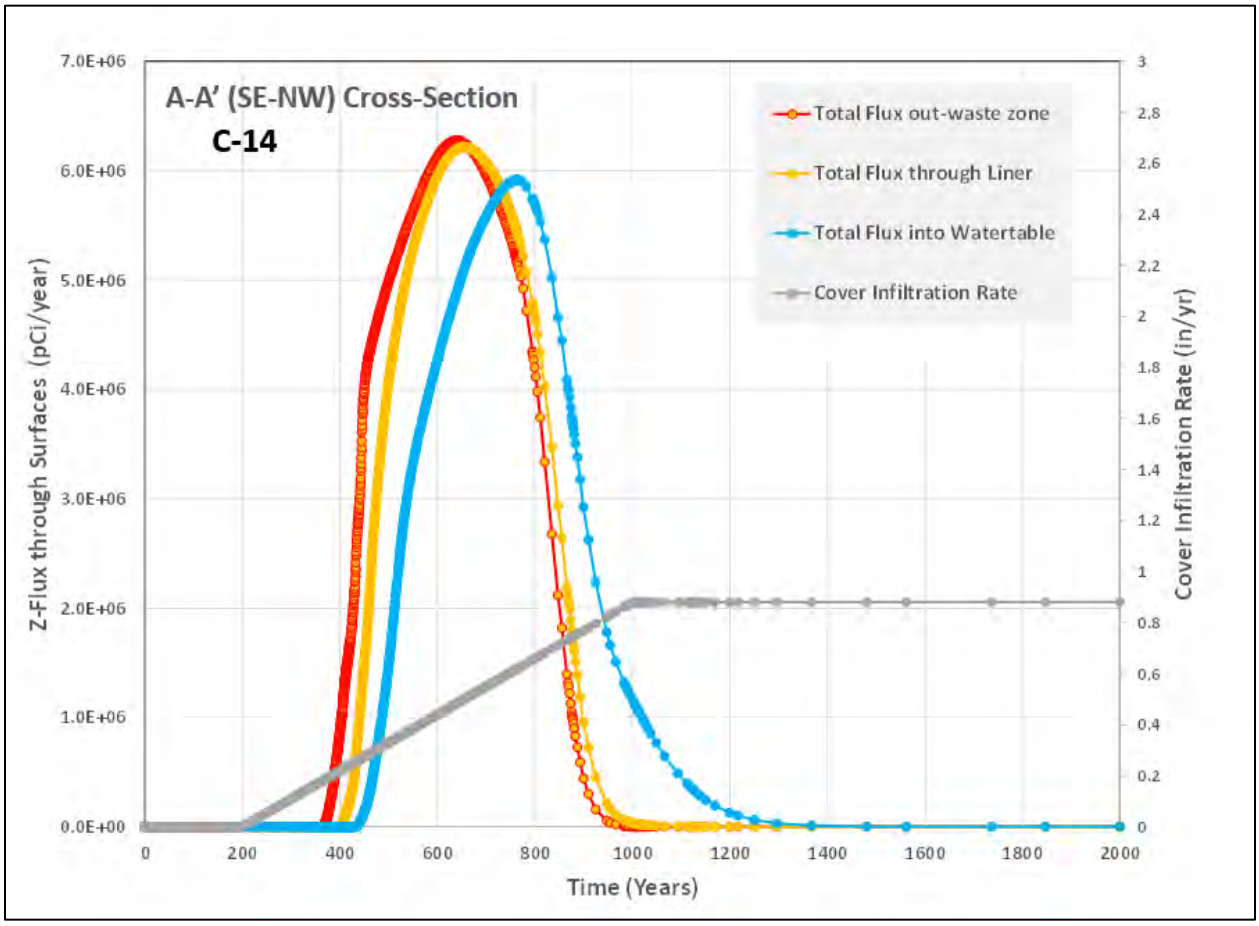

Fig. 4.11. C-14 flux in the STOMP Section A model over time

Technetium-99 starts to migrate from the waste zone into the liner system at year 400 when the infiltration of water from the cover reaches the bottom of the waste zone (Fig. 4.12). The mass flux rate increases with increased water infiltration rate until year 1000 when the water infiltration rate reaches the long-term EMDF performance condition (0.88 in./year). The mass flux rate then starts to decrease due to source depletion. The mass flux rate at the bottom of the liner system begins to increase slightly later (450 to 500 years) due to sorption in the liner and peaks at year 1000. The decline in mass flux from the waste and liner output surfaces is rapid between 1000 and 1600 years, after which the rate of decline decreases due to radionuclide depletion (refer to Fig. 4.9). The Tc-99 mass flux rate at the water table output surface increases later (600 to 1000 years) and peaks lower and later (1200 years) due to sorption and mass retention in the vadose zone. The decline in flux to the saturated zone decreases more gradually than the flux from the liner, reflecting mass depletion along faster transport paths combined with continued migration of residual contamination along slower paths in the vadose zone. This residual mass is concentrated beneath the upslope end of each disposal cell (refer to the C-14 concentrations at years 1000 and 1500 in Fig. 4.8).

Iodine-129 also starts to release from the waste zone to the liner system at year 400 (Fig. 4.13). However, due to its higher K_d, the peak flux rates at the base of the liner and the water table output surface occur 1000 to 2000 years later than for the Tc-99 simulation. Also in contrast to the Tc-99 example, the I-129 peak from the liner output surface is much later than the peak flux from the waste output surface, reflecting greater sorption and mass retention in the clay liner material. The peak flux rate at the water table for I-129 occurs at about 3225 years.

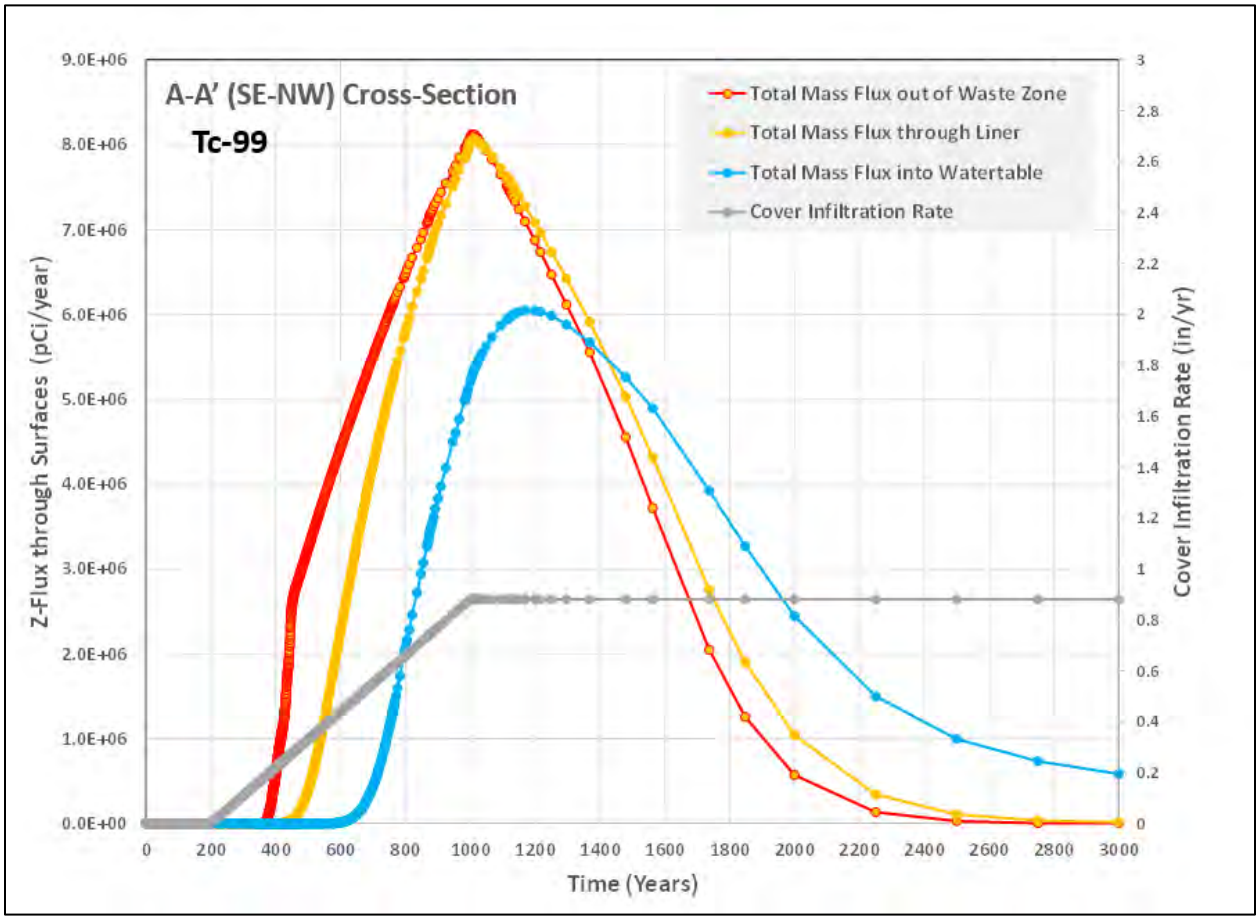

Fig. 4.12. Tc-99 flux in the STOMP Section A model over time

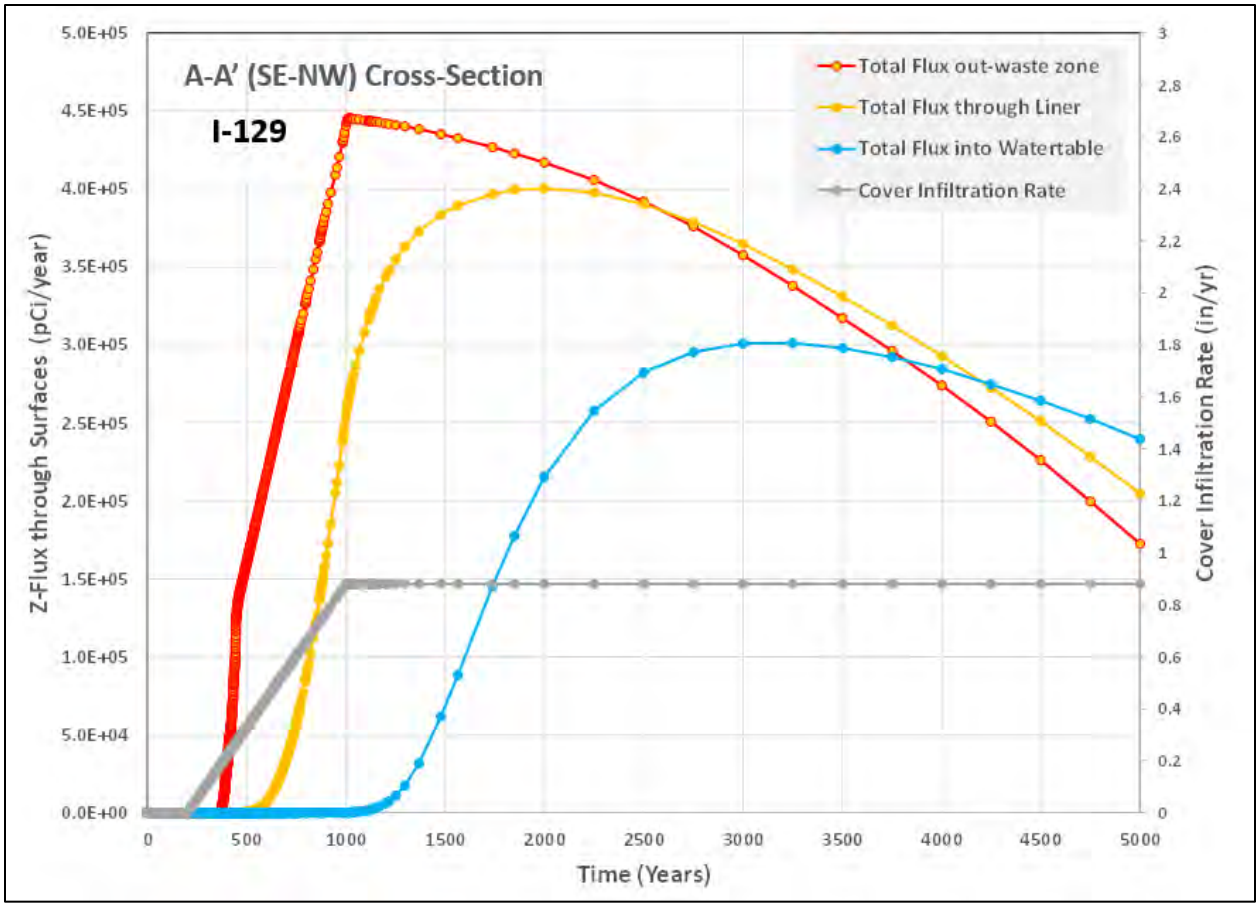

Fig. 4.13. I-129 flux in the STOMP Section A model over time

4.2.5 Estimated Vadose Zone Delay Times

As discussed above, STOMP modeling provides a detailed understanding of source depletion and the impact of liner system design on release to and transport in the vadose zone. Two key output products provided by the STOMP modeling are used to implement the other PA models. These outputs relate to the non-uniform pattern of release and the vadose zone transport time (arrival time at the water table elevation below the disposal unit). These outputs were calculated and applied to the saturated zone radionuclide transport analysis conducted using the MT3D model (see Sect. 3.3.3 and Appendix F). Use of the STOMP model output to develop the non-uniform Tc-99 release scenario for the MT3D model is summarized in Sect. 5.2.

The STOMP model results clearly show the impact of the vadose zone on the movement of the radionuclides. The vadose zone both retards transport and reduces the radionuclide aqueous concentration between the waste and saturated zone beneath the EMDF due to the sorption and desorption process. To provide an estimated average vadose delay time for the MT3D saturated zone transport model the total radionuclide flux rate at the water table output surface in the STOMP Section A model is utilized. The Section A results were selected rather than the Section B model results because the former yielded smaller delay times and earlier saturated zone arrival times.

The Tc-99 total mass flux rate at the water table surface in the Section A model is shown on Fig. 4.14. The plot illustrates the initial arrival time of approximately 600 years and peak flux time of 1180 years. The

time when the flux reaches 50 percent of the peak rate is approximately 850 years. (The time to 50 percent peak water table Tc-99 flux rate based on the Section B model output is approximately 910 years due to greater average thickness of the vadose zone.) Since the saturated zone transport model applies a simplified depleting source approximation for radionuclide release at the water table (Appendix F, Sect. F.4.1), using the STOMP model-based 50 percent peak mass flux time to represent the saturated zone arrival time is a reasonable approach. This STOMP model-based arrival time incorporates the assumed (base case) progression of cover degradation and maximum cover infiltration rate, as well as the simulated vadose transport time in representing the release to the saturated zone. The average arrival times were calculated for the three radionuclides that make the primary dose contributions in the performance analysis (see Table 3.21).

In addition to overall average vadose delay, the complexity of the EMDF design (multiple disposal cells with variable liner floor elevations) and the effect of non-uniform vadose zone thickness results in variable initial arrival times and peak concentrations for radionuclides entering the saturated zone. To support the non-uniform release scenario applied to the MT3D model, radionuclide-specific arrival times (refer to Appendix E, Table E.8) for each disposal cell were also calculated based on the flux output from the corresponding water table surface segments (Fig. 4.14, cell-by-cell flux curves).

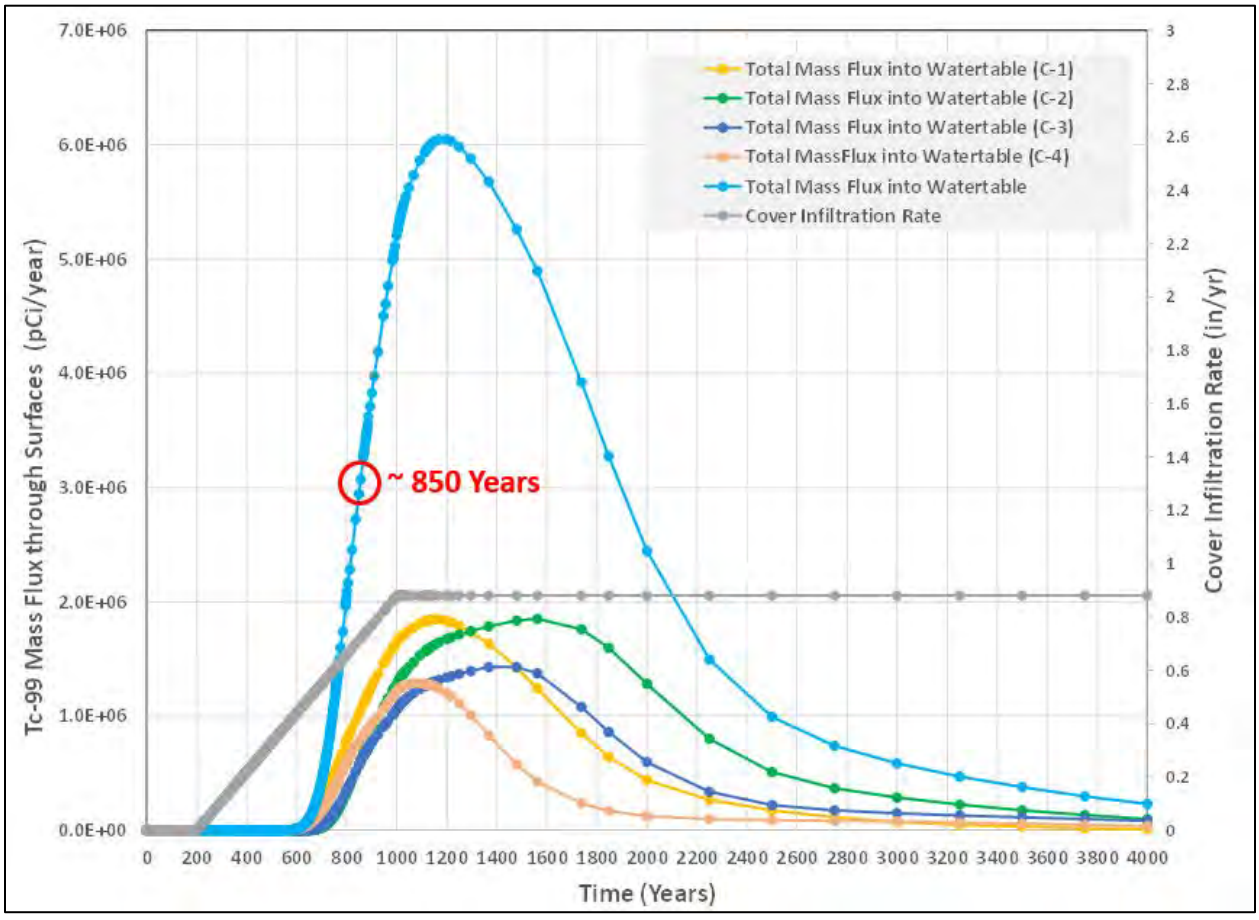

Fig. 4.14. Time to 50 percent peak Tc-99 flux at water table surface in the STOMP Section A Model

4.3 SATURATED ZONE RADIONUCLIDE TRANSPORT

This section presents the results of the 3-D saturated zone radionuclide transport modeling, focusing on results for Tc-99. Evidence from the STOMP modeling that contaminant release from the EMDF liner system may be non-uniform (even under the assumption of uniform cover infiltration) motivated the development of a simplified non-uniform representation of leachate flux to the water table to compare to model results using the uniform leachate flux boundary condition. The results of the non-uniform release MT3D model simulations are compared to the base case uniform release results in Sect. 5.2.

Model results for the base case (uniform release and leachate flux) Tc-99 simulation show the effect of the depleting source approximation (release model) used for the leachate flux boundary condition at the water table below the disposal unit. The Tc-99 plume evolution for the base case release is shown on Fig. 4.15. Technetium-99 concentration time series for individual MT3D model layers at the downgradient EOW location and the 100-m well are shown on Fig. 4.16. The modeled concentrations for each model layer at the EOW and POA locations reflect the relatively complex spatial and temporal evolution of the plume. Model layer 2 at the EOW (Fig. 4.16 upper plot) has the highest peak concentration due to proximity to the upgradient source area. At the EOW location, most of the contamination is restricted to the shallow groundwater zone (model layers 2, 3 and 4). The peak time for the model layer 2 at the EOW is 2100 years, where peak concentrations for model layers 3 and 4 occur after 4000 years. Peak concentrations at the 100-m well are lower than peaks at the EOW, and occur much later for model layer 2 (peak at 3750 years), layer 3 (> 5000 years), and layer 4 (> 5000 years) compared to the EOW location (Fig. 4.16 lower plot). Model layer 1 concentrations at the 100-m well increase quickly between 850 and 1200 years and then more gradually to a peak around 2700 years, whereas model layer 2 concentrations increase significantly at the 100-m well only after 1500 years. Transmissivity-weighted average concentrations at the POA for model layers 1+2 and layers 1+2+3 are calculated to provide a vertically integrated estimate of well concentrations over potential well screen intervals (Fig. 4.16 lower plot). The transmissivity-weighted concentrations peak around 2750 years at approximately 200 pCi/L.

MT3D transport model results for C-14 and I-129 show similar variations in concentration and peak timing between output locations and among model layers to the Tc-99 results, but the range of concentrations and timing reflect the difference in assumed K_d values. The model-predicted C-14 concentrations at the EOW and 100-m well locations reflect rapid release (delay time is 530 years) and transport due to the zero K_d of C-14 applied in the release model and saturated zone media (Fig. 4.17). The highest C-14 concentration for model layer 2 at the 100-m well is just over 600 pCi/L between 1100 and 1200 years post-closure, and the peak transmissivity-weighted concentrations are approximately 450 pCi/L at nearly the same time as the layer 2 peak (Fig. 4.17 lower plot). Deeper model layers 4 and 5 reach C-14 concentrations that are closer to shallow layer concentrations than for either Tc-99 or I-129, due to the higher mobility of C-14. Similarly, the difference in the timing of peak concentrations between output locations and among model layers is much less for C-14 (Fig. 4.17) than for Tc-99 (Fig. 4.16) or I-129 (Fig. 4.18), which have non-zero K_d values.

The MT3D predicted I-129 concentrations at the EOW and 100-m well locations are lower than Tc-99 and C-14 as a result of the smaller initial source inventory and higher K_d for I-129 (Fig. 4.18). The initial release (delay time 1750 years) and peak concentrations occur much later than for C-14 and Tc-99, due to the higher assumed K_d value for I-129. The I-129 concentrations in model layer 1 at the 100-m well increase rapidly between 2000 and 3000 years to about 6 pCi/L, and increase gradually to 8 pCi/L by approximately 10,000 years. Model layer 2 I-129 concentrations begin increasing just after 4000 years and reach a peak of 12 pCi/L at approximately 16,000 years post-closure.

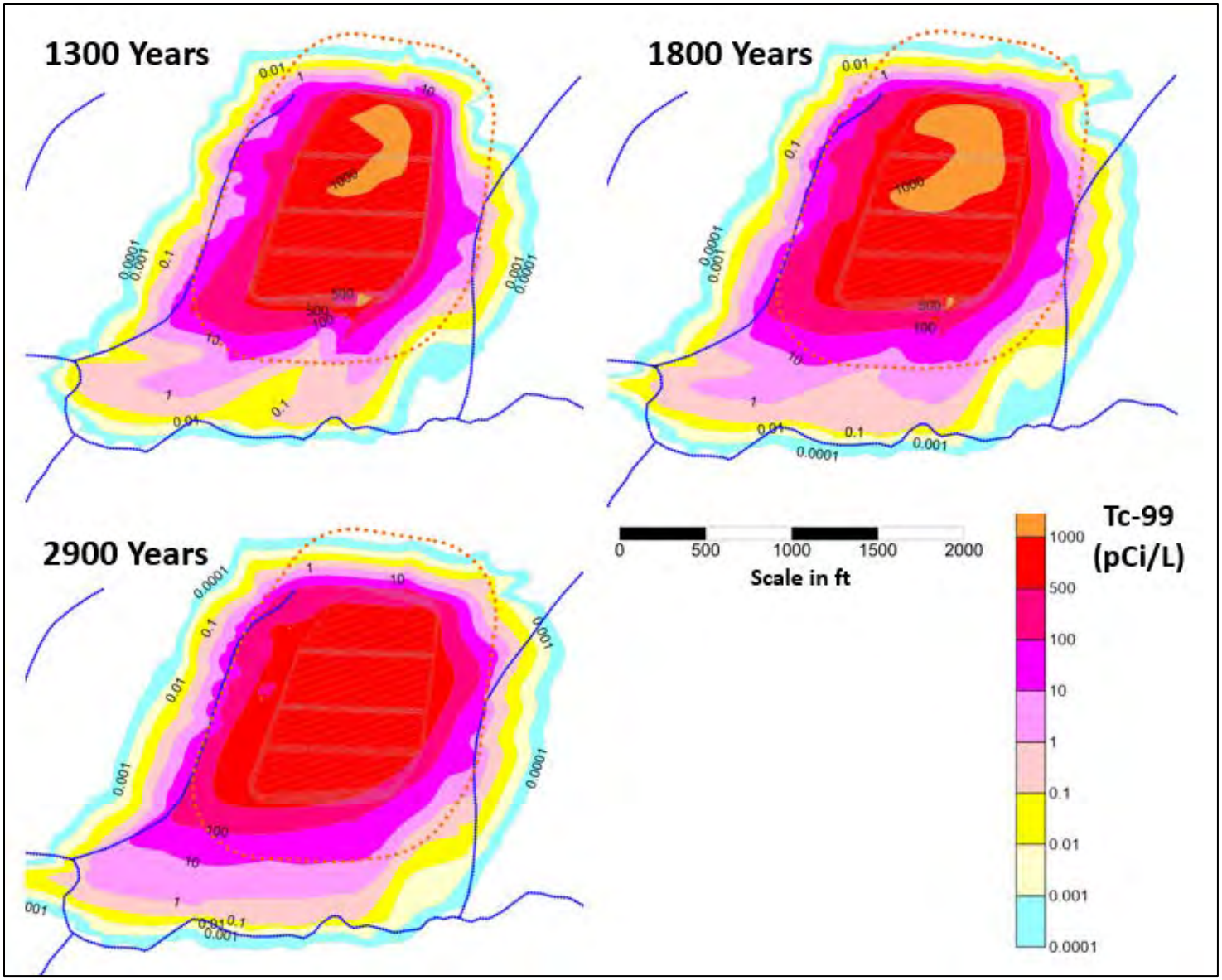

Fig. 4.15. Modeled Tc-99 plume evolution for model layer 2 of the MT3D transport model

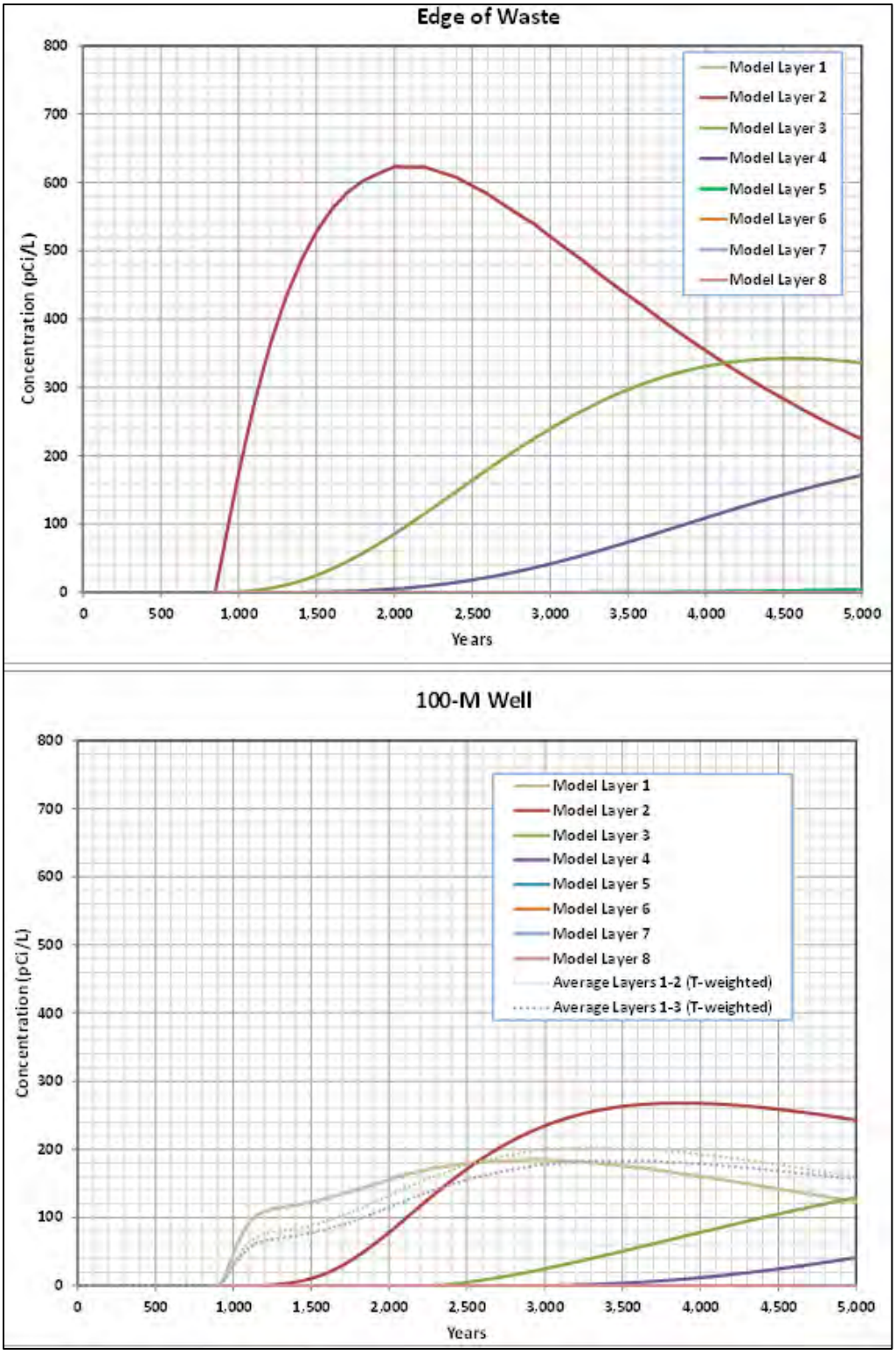

Fig. 4.16. MT3D Tc-99 concentration time series for the waste edge location and at the 100-m well

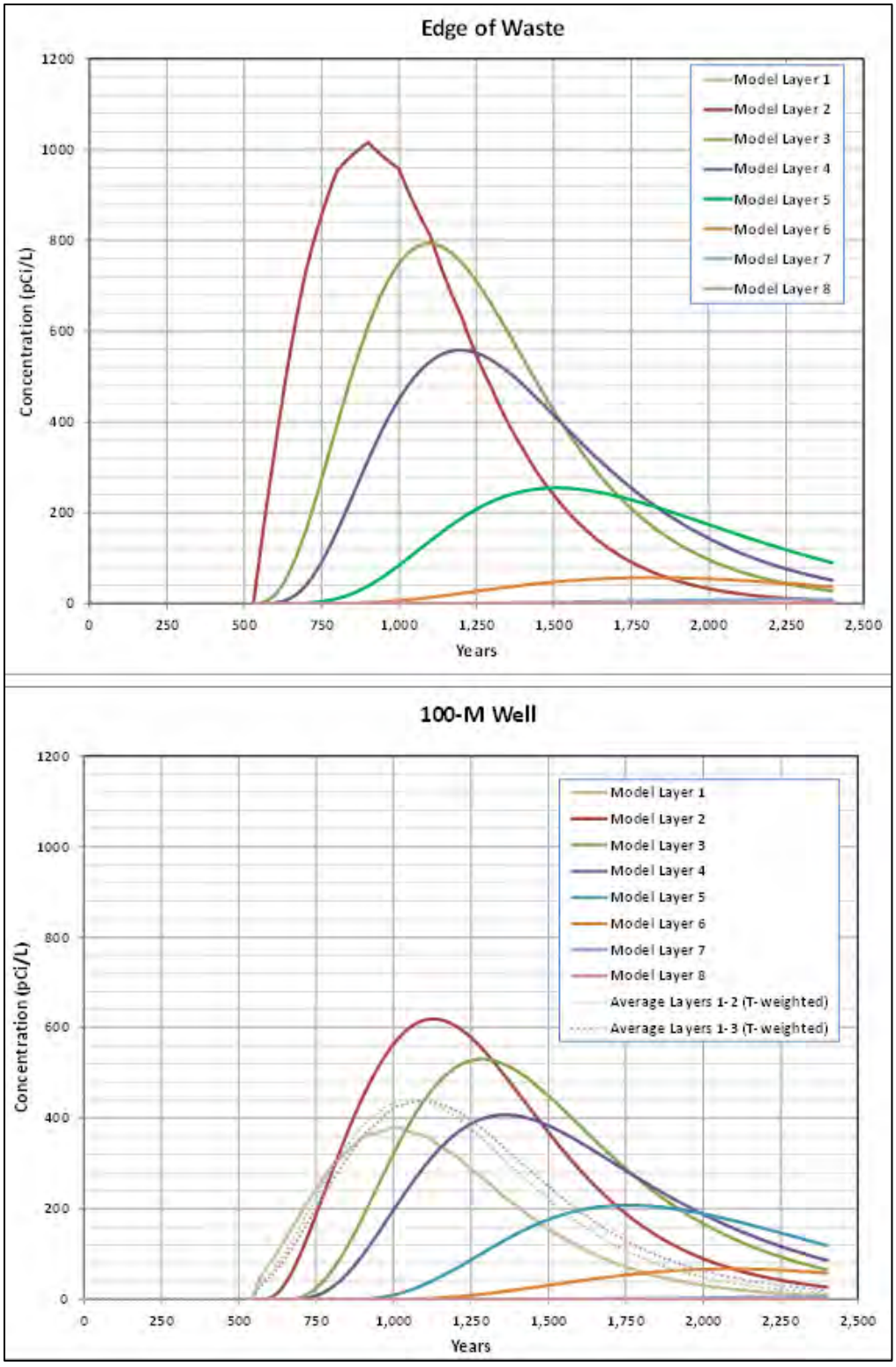

Fig. 4.17. MT3D C-14 concentration time series for the waste edge location and at the 100-m well

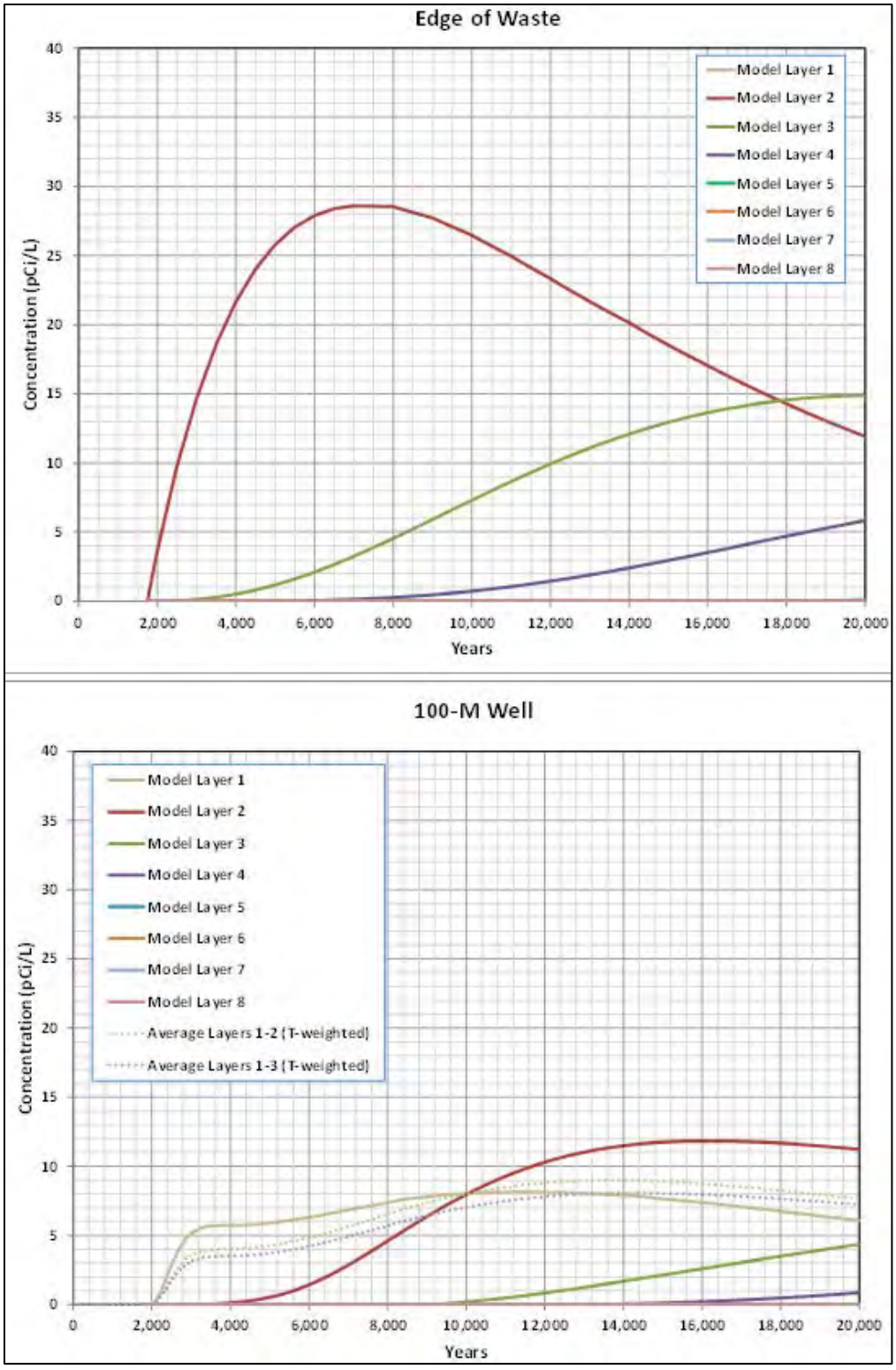

Fig. 4.18. MT3D I-129 concentration time series for the waste edge location and at the 100-m well

RESRAD-OFFSITE saturated zone model outputs were evaluated against the MT3D model results to provide confidence in the saturated zone parameterization for the total system model. Those model comparisons were presented in Sect. 3.3.5. Figure 3.37 shows the comparison of MT3D and RESRAD-OFFSITE model saturated zone results for Tc-99.

4.4 RADON FLUX ANALYSIS

This section summarizes the radon flux analysis, which is presented in detail in Appendix H. Based on the EMDF cover system characteristics and estimated Ra-226 activity, the radon flux was estimated for the design condition of the final cover and for three degraded cover scenarios: fully exposed waste, a severely eroded residual 2-ft-thick clay cover, and cover eroded to the biointrusion layer. A radon emanation coefficient of 0.25 for Rn-222, the default value in the RESRAD model (Gnanapragasam and Yu 2015) was assumed. The value is on the higher end of the reported radon emanation coefficients for Rn-222 in various soils (Yu et al. 2015, Sect. 4.2.2, page 122), which typically range from less than 0.01 to 0.30.

The radon flux is primarily controlled by clay layers that lie below the biointrusion layer. Even with some expected erosion of the cover system, the integrity of the clay layers will likely be preserved within the first 1000 years. Uncertainty in the radon release performance of the EMDF cover is minimal. The predicted radon flux at the EMDF cover surface is 5.0E-08 pCi/m^2/sec. The predicted radon flux for fully exposed waste at year 1000 is 0.80 pCi/m^2/sec. The radon fluxes for the residual clay cover and the erosion to biointrusion layer scenarios are 6.6E-06 and 5.4E-06 pCi/m^2/sec, respectively. Sensitivity evaluations for higher concentrations of radon parents and for potential release of Rn-222 indicate that EMDF compliance with the 20 pCi/m^2/sec performance objective is not affected (Appendix H, Sect. H.7).

The radon calculation indicates that, based on the estimated radionuclide inventory and assuming a uniform distribution of contamination within the waste mass, there will be minimal post-closure radon flux from the proposed EMDF within the 1000-year compliance period, even with significant erosion of the 4-ft-thick cover surface layer (refer to Appendix C for discussion and analysis of potential cover erosion).

4.5 ALL-PATHWAYS DOSE ANALYSIS

This section includes the results of simulations using the total system model, RESRAD-OFFSITE.

4.5.1 All-Pathways Dose Analysis - Base Case Model Results

Predicted total dose over time for the base case model is presented in Fig. 4.19 for the 1000-year compliance period and Fig. 4.20 for the 10,000-year time period including the compliance period and the subsequent 9000 years. The peak total dose (i.e., dose from all simulated radionuclides summed) for the 1000-year compliance period is 1.03 mrem/year and occurs at 490 years. The peak compliance period dose is associated with C-14. Total dose then decreases through 750 years and remains less than 0.2 mrem/year from that time to the end of the compliance period. After the compliance period, the total dose increases to a peak of 0.95 mrem/year associated with Tc-99 at approximately 1700 years. After the Tc-99 peak, the total dose increases to a maximum of 9.13 mrem/year at approximately 5084 years and then gradually decreases through 10,000 years to a predicted total dose at 10,000 years of 0.114 mrem/year. The three distinct peaks in total dose are each associated with a single radionuclide, as presented in the following subsection. Overall, the predicted maximum total dose during the compliance period of 1.03 mrem/year is less than 5 percent of the performance objective (25 mrem/year).

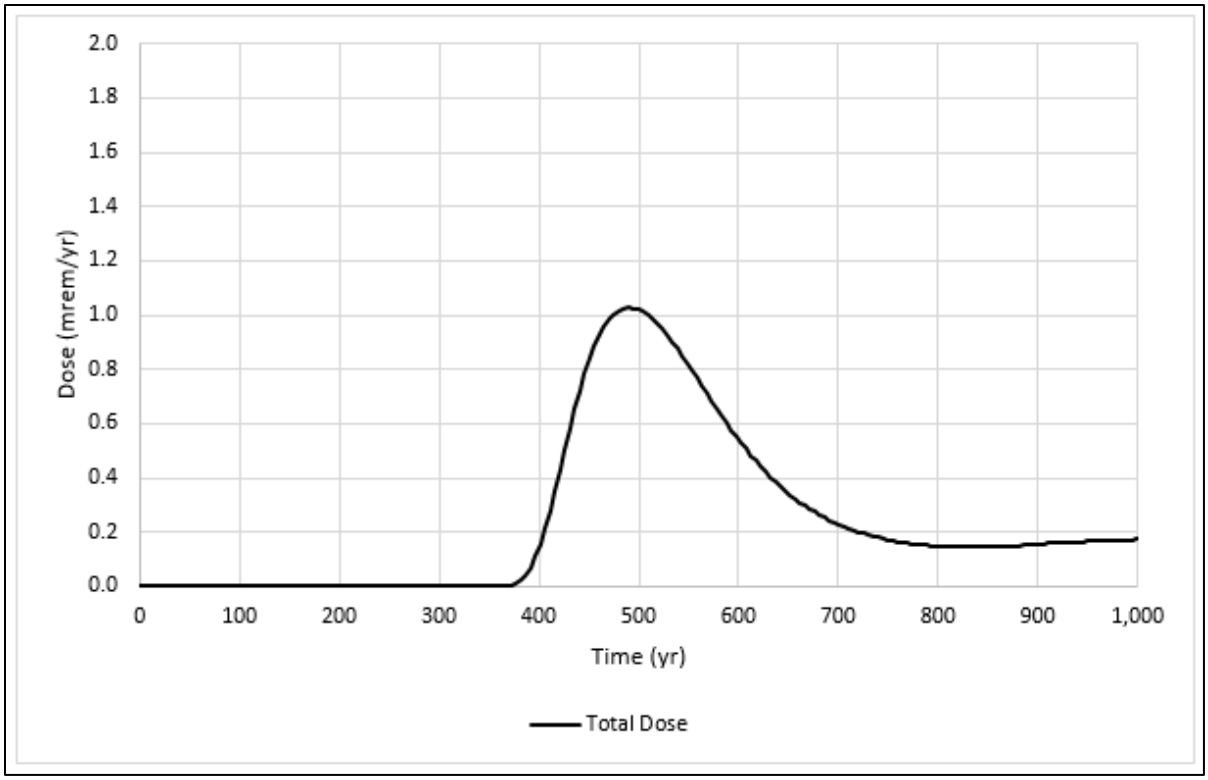

Fig. 4.19. Base case predicted total dose (all pathways; compliance period)

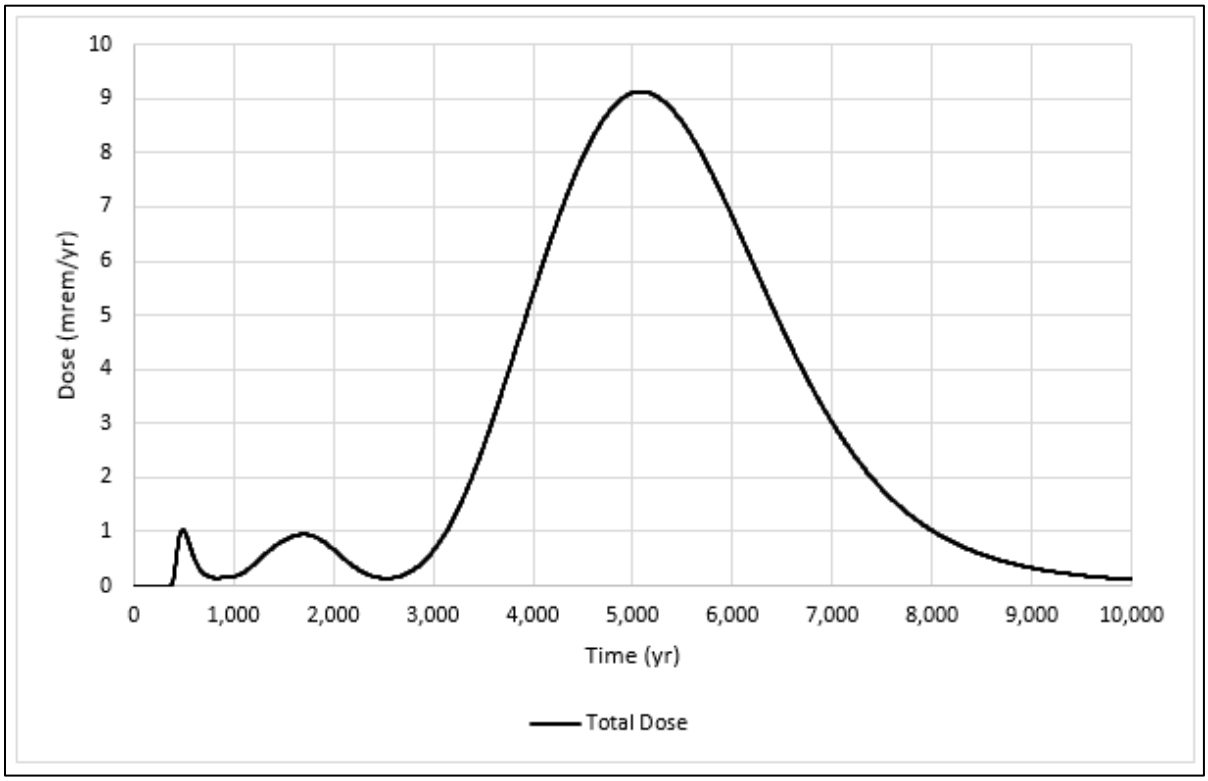

Fig. 4.20. Base case predicted total dose (all pathways; 0 to 10,000 years)

4.5.2 Base Case-Peak Dose for Each Radionuclide

The primary contributors to total dose consist of C-14, I-129, and Tc-99. Source concentrations input for C-14, I-129, and Tc-99 are based on the post-operational waste concentrations (Table 3.3).

For the compliance period, the greatest predicted dose is 1.03 mrem/year from C-14 contributions at 490 years (Fig. 4.21). Peak dose contributions from Tc-99 and I-129 occur after 1000 years. After the compliance period through 10,000 years, I-129 is the largest dose contributor, with a maximum predicted dose of 9.13 mrem/year at 5084 years (Fig. 4.22). The peak Tc-99 dose is 0.95 mrem/year at 1700 years.

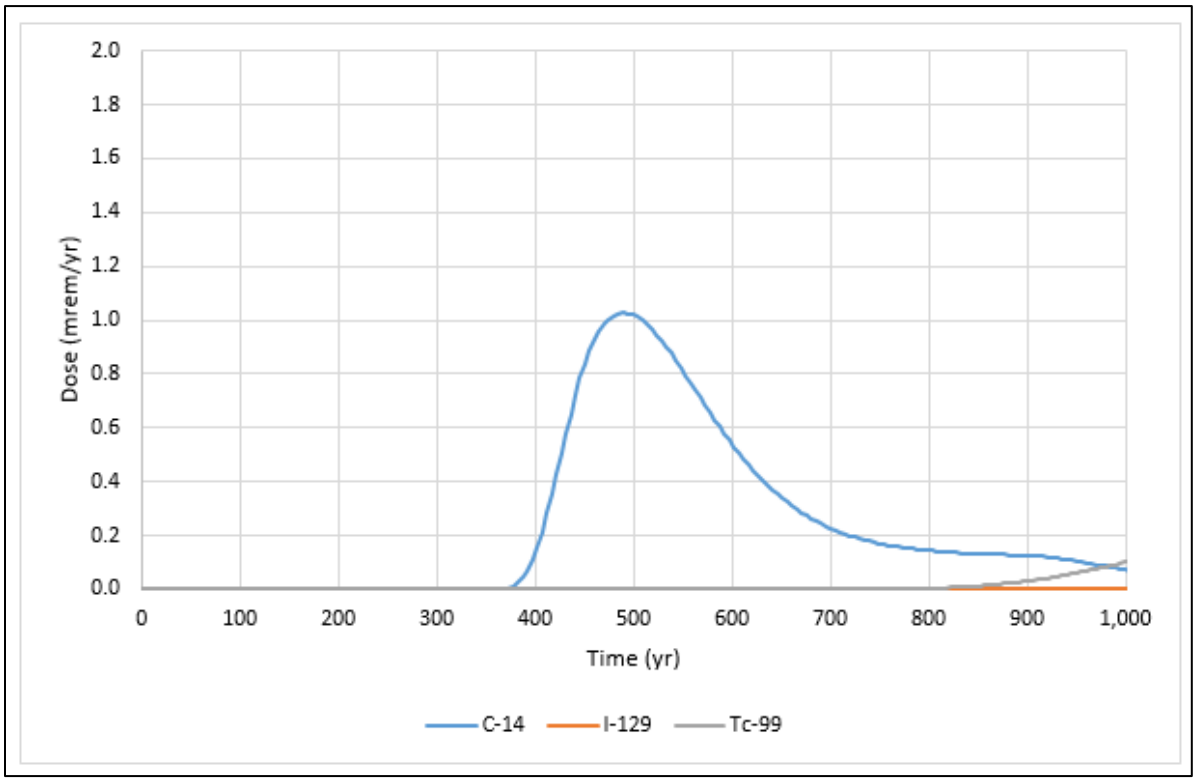

Fig. 4.21. Base case predicted dose by isotope for the compliance period

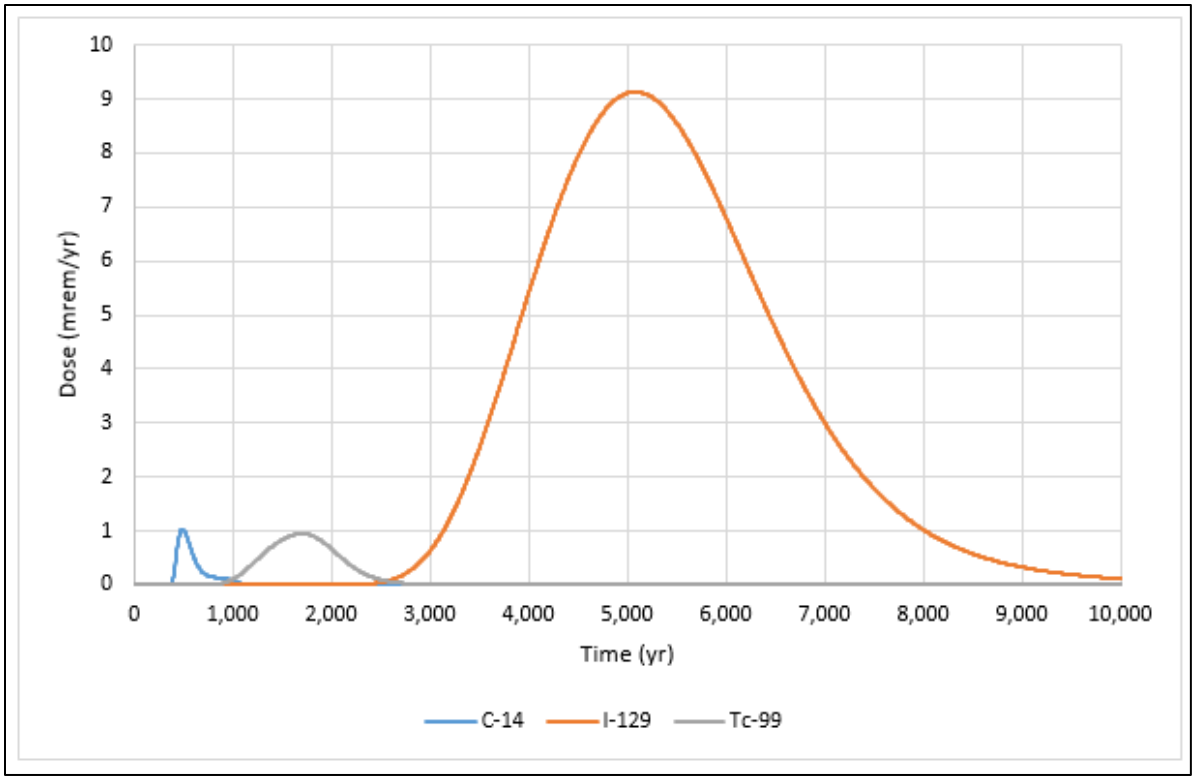

Fig. 4.22. Base case predicted total dose by isotope (0 to 10,000 years)

4.5.3 Base Case-Dose by Exposure Pathway

The groundwater ingestion pathway (ingestion of well water) is the dominant contributor to total dose. In addition to the drinking water exposure pathway, the four pathways contributing most of the remaining dose during the compliance period in order of descending dose contribution are ingestion of fish, plants (waterborne), milk (waterborne), and meat (waterborne) (Fig. 4.23). During the 10,000-year simulation period, the water pathway remains dominant with ingestion of meat (waterborne), milk (waterborne), plant (waterborne), and fish also contributing to the total dose. Because the cover system is assumed to maintain integrity and prevent waste from leaving the facility, there are no predicted dose contributions from any of the airborne (atmospheric) pathways. Doses from individual exposure pathways for the post-closure period from 0 to 10,000 years are shown in Fig. 4.24. The same output data on an altered (logarithmic) scale to highlight the very small (negligible relative to total dose) base case contributions of exposure pathways other than water and fish ingestion is shown on Fig. 4.25. Note that pathways with no calculated dose contribution, which include the direct and airborne pathway components of plant, meat, milk, and soil ingestion and the radon pathway, are not included in the plots in Figs. 4.23 to 4.25.

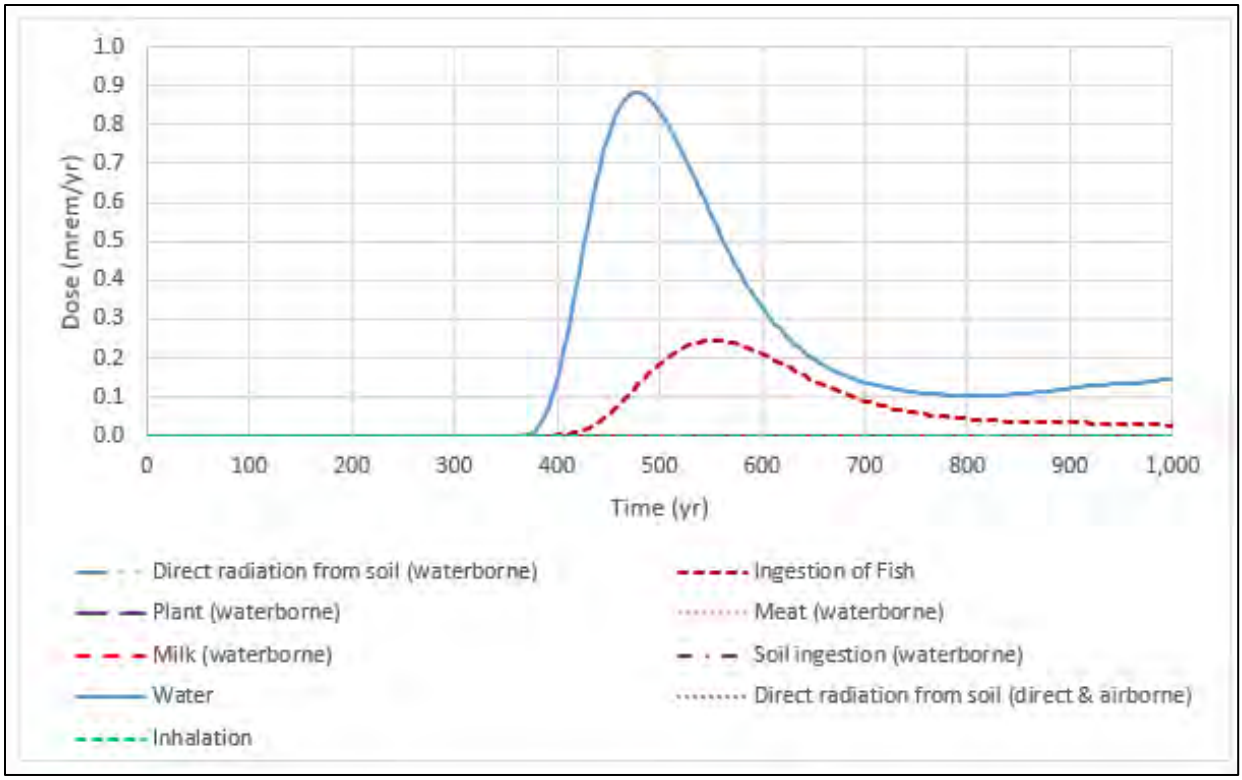

Fig. 4.23. Predicted base case dose by pathway during the compliance period

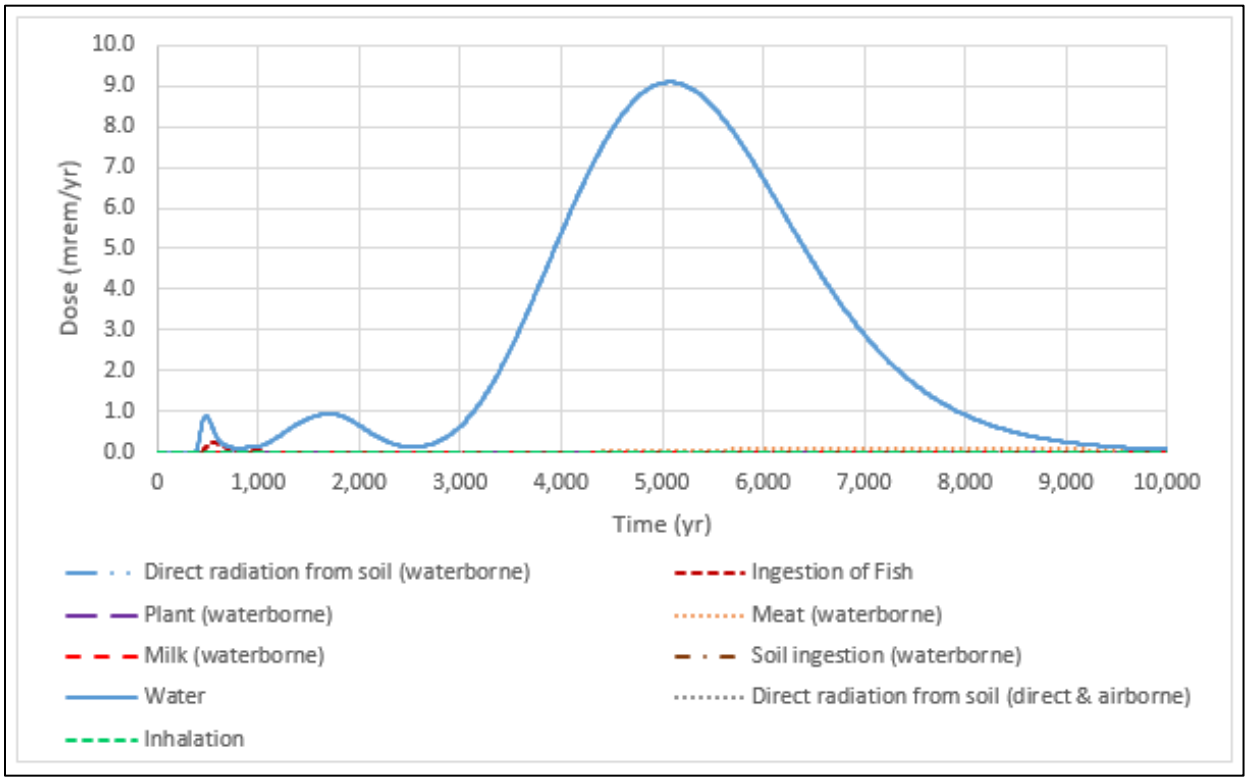

Fig. 4.24. Predicted base case dose by exposure pathway (0 to 10,000 years)

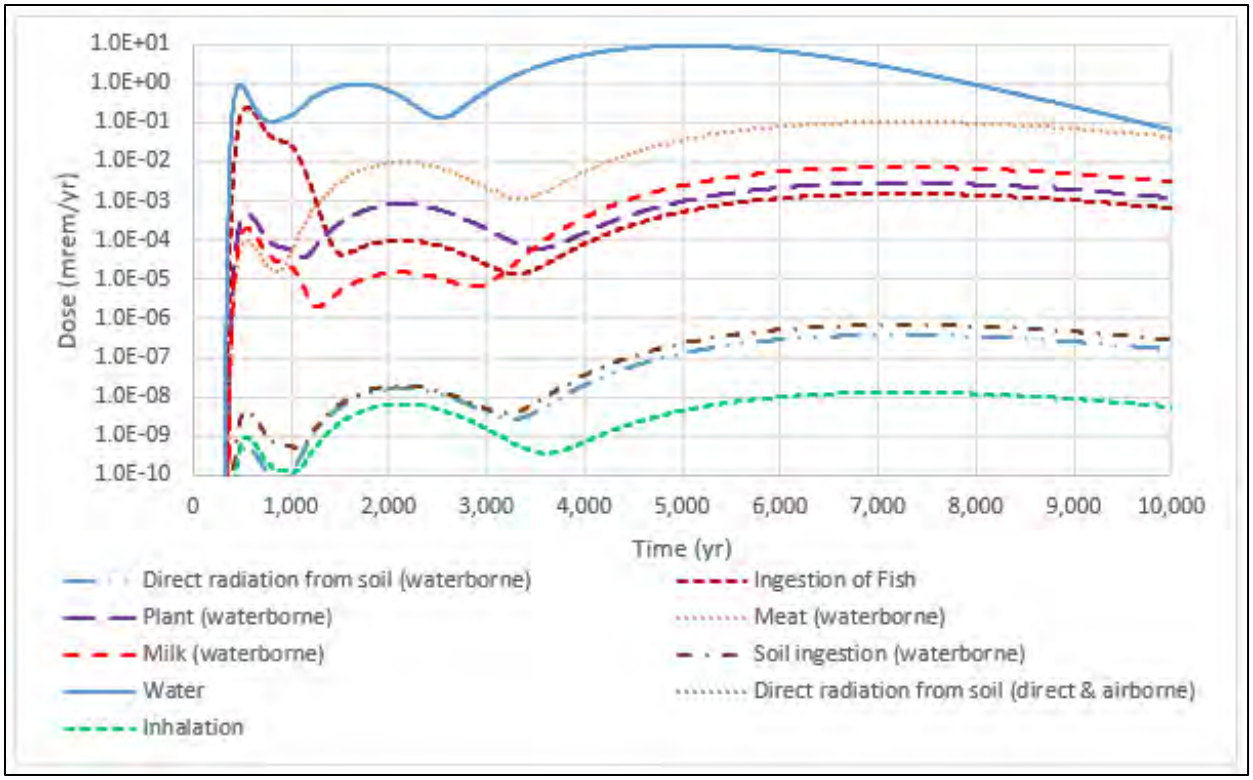

Fig. 4.25. Predicted base case dose by exposure pathway (0 to 10,000 years)

4.6 RESRAD-OFFSITE SINGLE RADIONUCLIDE SOIL GUIDELINES

Dose-based performance criteria are one basis for setting radionuclide concentration limits for LLW to ensure protection of members of the public. RESRAD-OFFSITE SRSGs are calculated waste activity concentrations that will meet a specific dose target for a single radionuclide at a specific time, based on the modeled scenario. The SRSGs do not depend on the assumed radionuclide concentrations or the corresponding modeled doses, but only on the target dose value and the specific exposure scenario considered. Thus, the SRSGs are dose-based radionuclide source concentration limits for the particular system and scenario simulated.

The RESRAD-OFFSITE SRSG values represent the source concentrations corresponding to the 25 mrem/year dose target, calculated for the base case (all pathways dose) model scenario. For most radionuclides, the minimum SRSG within the 1000-year compliance period occurs at or near 1000 years post-closure.

Table 4.1 presents the compliance period minimum SRSG values for the base case scenario, and the corresponding estimated EMDF average (post-operational) concentrations used in the dose analysis for comparison. For the suite of simulated isotopes, the modeled EMDF source concentrations are less than the model-predicted minimum SRSG values.

Table 4.1. RESRAD-OFFSITE SRSGs for the all pathways scenario (compliance period minimum values)

Radionuclide	SRSG (25 mrem/year) (pCi/g)	EMDF post-operational source concentration (pCi/g)
Ac-227[a]	7.23E+13	2.92E-03
Am-241[a]	3.43E+12	5.90E+01
Am-243[a]	2.00E+11	2.97E+00
Be-10[a]	2.36E+10	2.53E-05
C-14	1.32E+01	5.40E-01
Ca-41[a]	8.35E+10	4.21E-02
Cm-243[a]	5.05E+13	4.30E-01
Cm-244[a]	8.09E+13	1.26E+02
Cm-245[a]	1.72E+11	3.83E-02
Cm-246[a]	3.05E+11	1.59E-01
Cm-247[a]	9.28E+07	1.04E-02
Cm-248[a]	4.14E+09	5.59E-04
H-3	8.52E+12	4.64E+00
I-129[a]	1.75E+08	3.50E-01
K-40[a]	6.98E+06	3.28E+00
Mo-93[a]	9.52E+11	3.88E-01
Nb-93m[a]	2.39E+14	2.33E-01
Nb-94[a]	1.86E+11	1.63E-02
Ni-59[a]	5.91E+10	3.04E+00
Np-237[a]	7.03E+08	3.25E-01
Pa-231[a]	4.72E+10	2.39E-01
Pb-210[a]	7.63E+13	3.68E+00
Pu-238[a]	1.71E+13	9.38E+01
Pu-239[a]	6.20E+10	5.83E+01
Pu-240[a]	2.27E+11	6.20E+01
Pu-241[a]	1.03E+14	2.04E+02
Pu-242[a]	3.94E+09	1.73E-01
Pu-244[a]	1.83E+07	3.68E-03
Ra-226[a]	9.89E+11	8.01E-01
Ra-228[a]	2.73E+14	2.21E-02
Sr-90[a]	1.37E+14	1.92E+02
Tc-99	3.80E+02	1.56E+00
Th-228[a]	8.20E+14	2.11E-06
Th-229[a]	2.13E+11	5.71E+00
Th-230[a]	2.06E+10	1.92E+00
Th-232[a]	1.10E+05	3.52E+00

Table 4.1. RESRAD-OFFSITE SRSGs for the all pathways scenario (compliance period minimum values) (cont.)

Radionuclide	SRSG (25 mrem/year) (pCi/g)	EMDF post-operational source concentration (pCi/g)
U-232[a]	2.24E+13	1.02E+01
U-233[a]	9.64E+09	4.16E+01
U-234[a]	6.22E+09	6.30E+02
U-235[a]	2.16E+06	3.97E+01
U-236[a]	6.47E+07	8.98E+00
U-238[a]	3.36E+05	3.81E+02

[a]Indicates SRSG at specific activity limit

EMDF = Environmental Management Disposal Facility SRSG = Single Radionuclide Soil Guideline
RESRAD = RESidual RADioactivity

4.7 WATER RESOURCES PROTECTION ASSESSMENT

This section presents estimated radionuclide doses and concentrations during the compliance period for comparison to regulatory standards for water resources protection.

4.7.1 Groundwater Protection Assessment

Protection of groundwater is demonstrated by comparing well water radionuclide concentrations under the base case scenario to MCLs for drinking water specified by EPA in the Radionuclides Final Rule (EPA 2000), promulgated in 40 *CFR* 141.66, for which the State of Tennessee has primary enforcement responsibility. Radionuclide MCLs are as follows:

- Radium-226/228 combined standard is 5 pCi/L.
- Gross alpha standard for all alpha emitters is 15 pCi/L (not including radon and uranium).
- Beta/photon emitters combined standard is 4 mrem/year dose.
- Strontium-90 standard is 8 pCi/L.
- Hydrogen-3 standard is 20,000 pCi/L.
- Uranium (all isotopes combined) is 30 µg/L.

The following subsections compare modeled radionuclide concentrations in well water for the base case to the MCLs given above.

4.7.1.1 Radium-226 and radium-228

The maximum activity concentration of Ra-226 + Ra-228 in well water during the compliance period is 0.0 pCi/L (negligible) compared to the MCL of 5 pCi/L for these combined isotopes.

4.7.1.2 Gross alpha activity

The radionuclides included in the gross alpha activity analysis are shown on Table 4.2. Radionuclides not simulated because they were screened from analysis include Cf-249, Cf-250, and Cf-251 (Sect. 2.3.2). The

maximum summed gross alpha activity concentration in well water during the compliance period is 0.0 pCi/L (negligible) compared to the MCL of 15 pCi/L for all alpha emitters (not including radon and uranium).

Table 4.2. Radionuclides for water resources protection assessment - gross alpha activity

Am-241	Cm-246	Pu-242
Am-243	Cm-247	Pu-244
Cf-249[a]	Cm-248	Th-228
Cf-250[a]	Np-237	Th-229
Cf-251[a]	Pa-231	Th-230
Cm-243	Pu-238	Th-232
Cm-244	Pu-239	
Cm-245	Pu-240	

[a]Indicates isotope not simulated.

4.7.1.3 Beta/photon activity

The 13 radionuclides simulated for the beta/photon MCL compliance analysis are listed in Table 4.3. Sixteen radionuclides were not simulated because they either did not have a verified inventory data source, or because they were screened from the all pathways dose analysis (see Appendix G, Sect. G.4.2). The 15 radionuclides not included are: Cd-113m, Co-60, Cs-135, Cs-137, Eu-152, Eu-154, Ni-63, Pd-107, Pm-146, Re-187, Se-79, Sm-151, Sn-121m, Sn-126, and Zr-93 (see Table 2.16). The MCL for total beta/photon emitters is expressed as a water ingestion dose of 4 mrem/year (Table 4.3). RESRAD-OFFSITE simulations indicate that only C-14 and Tc-99 contribute substantially to the total beta/photon dose during the compliance period. The maximum dose over 1000 years is 1.03 mrem/year at 475 years (Fig. 4.26), which is less than the corresponding MCL for each radionuclide, yielding a dose of 4 mrem/year (Table 4.3).

Table 4.3. Water resources protection assessment –beta/photon activity

Radionuclide	Decay	MCL (pCi/L) yielding a dose of 4 mrem/year (EPA 2002a)
Ac-227	beta	15
Be-10	beta	1000
C-14	beta	2000
H-3	beta	20,000
I-129	beta	1
K-40[a]	beta	192
Nb-93m	gamma	1000
Nb-94[a]	beta	720
Ni-59	beta	300
Pb-210[a]	beta	1.6
Pu-241	beta	300
Sr-90	beta	8
Tc-99	beta	900

[a]The MCL for given isotope was not included in EPA 2002a, therefore the Derived Concentration Standard (DOE 2011b) was used to calculate the MCL at 4 mrem/year.

EPA = U.S. Environmental Protection Agency
MCL = maximum contaminant level

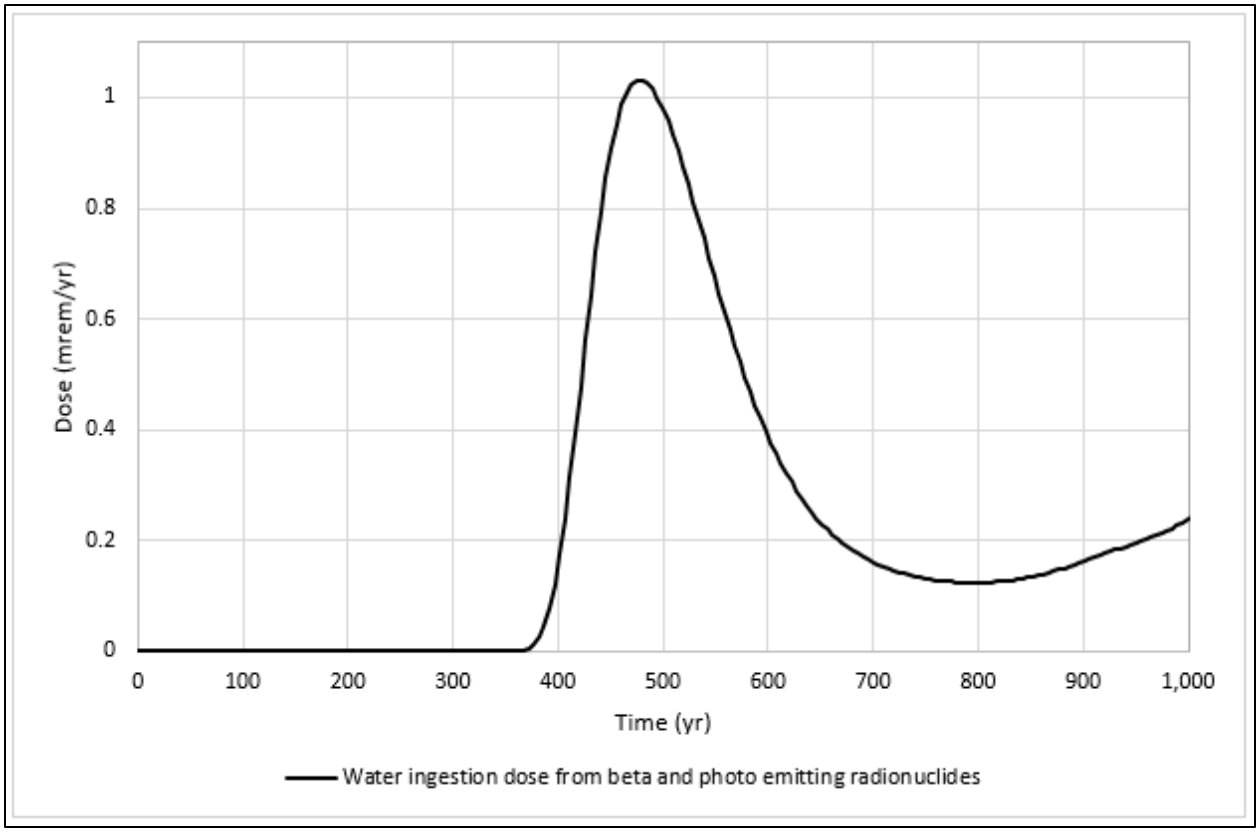

Fig. 4.26. Predicted water ingestion dose from beta/photon emitters (0 to 1000 years)

4.7.1.4 Hydrogen-3 and strontium-90

The maximum predicted groundwater well H-3 concentration during the compliance period is 0.0 pCi/L (negligible). The regulatory standard (MCL) for H-3 concentration is 20,000 pCi/L.

The maximum predicted Sr-90 groundwater well water concentration during the compliance period is 0.0 pCi/L (negligible). The regulatory standard (MCL) for Sr-90 concentration is 8 pCi/L.

4.7.1.5 Uranium (total)

The total uranium MCL is 30 µg/L. The predicted total mass concentration in well water was calculated by summing the activity concentrations for the uranium isotopes (U-232, U-233, U-234, U-235, U-236, and U-238) that RESRAD-OFFSITE predicts in the groundwater well, then converting from the total uranium activity concentration to the mass concentration using the conversion factor 1.49 µg/pCi (EPA 2002b). The maximum predicted total uranium mass concentration for the compliance period is 0.0 µg/L.

4.7.2 Surface Water Protection Assessment

Of the 42 radionuclides included in the base case (i.e., those not screened under the screening model scenario [see Sect. 2.3]), only three have predicted peak surface water concentrations greater than 1.0E-06 pCi/L within the 10,000 year simulation period. Within the 1000-year compliance period, only C-14 and Tc-99 have substantial (greater than 1.0E-06 pCi/L) predicted concentrations in the surface water body (Bear Creek). None of the predicted non-zero peak surface water concentrations for the 10,0000-year simulation period exceeds the corresponding DCS value (DOE 2011b), which serve as the regulatory basis

for discharge limits applied to the existing EMWMF landfill for discharge to surface waters in BCV (DOE 2016b). Table 4.4 summarizes the peak surface water concentrations for the three dose significant radionuclides within the 1000-year compliance period and the 10,000-year post-closure period and for uranium isotopes predicted to reach peak concentrations after 10,000 years. Model results for nuclides of uranium at times greater than 10,000 years post-closure are presented in Sect. 4.8.

Table 4.4. Predicted non-zero peak surface water concentrations for radionuclides compared to the DOE-STD-1196 DCS limits

Radionuclide	Peak surface water concentration, compliance period (pCi/L)	Peak surface water concentration, 10,0000-year simulation	DOE-STD-1196 DCS (pCi/L)	Time of simulated peak (year)
Tc-99	2.34E-03	6.24E-01	4.40E+04	2,130
C-14	8.61E-01	8.61E-01	6.20E+04	553
I-129	< 1.0E-06	3.53E-02	3.30E+02	7,219
U-233	< 1.0E-06	< 1.0E-06	6.60E+02	~50,000
U-234	< 1.0E-06	< 1.0E-06	6.80E+02	~50,000
U-235	< 1.0E-06	< 1.0E-06	7.20E+02	~50,000
U-236	< 1.0E-06	< 1.0E-06	7.20E+02	~50,000
U-238	< 1.0E-06	< 1.0E-06	7.50E+02	~50,000

DCS = Derived Concentration Standard

4.8 PREDICTIONS FOR TIMES GREATER THAN 10,000 YEARS

Results from simulations of tens of thousands of years are highly speculative and have limited, if any, quantitative value. However, results from very long-term simulations can be informative on a qualitative basis for long-lived, less mobile radionuclides. To assess the potential release of such radionuclides, simulations were performed for a post-closure duration of 100,000 years.

The RESRAD-OFFSITE long-term simulations indicate that peak well water concentrations of U-233, U-235, and U-236 do not exceed the DCS limits (DOE 2011b, Table G.21), but that peak concentrations of U-234 and U-238 occurring after 30,000 years are larger than the DCS limits (Fig. 4.27). The predicted peak groundwater concentrations of U-234 and U-238 are very high (> 1000 pCi/L), but the RESRAD-OFFSITE source release model does not incorporate solubility limits on the release of uranium in solution, so the model may overestimate the peak concentrations. In addition, the comparison of STOMP model simulations of U-234 release to the RESRAD-OFFSITE release predictions (refer to Sect. 3.3.5, Fig. 3.35) shows that the equilibrium desorption release model over-predicts peak U-234 release significantly relative to the scaled STOMP model simulations. The model output comparison also shows that the simplified RESRAD-OFFSITE vadose zone representation appears to match the timing of the STOMP model peak U-234 flux to the water table, but that the predicted peak RESRAD-OFFSITE U-234 flux is over twice as large as the peak STOMP U-234 flux to the water table beneath the EMDF. This difference in U-234 release model predictions suggests that the RESRAD-OFFSITE peak well water concentrations are too uncertain (probably over-estimated) to draw conclusions about the very-long-term performance of the EMDF with respect to less mobile radionuclides (K_d > 1.0 cm^3/g) including nuclides of uranium and possibly also I-129 (refer to Sects. 3.3.5, 5.3 and 5.4).

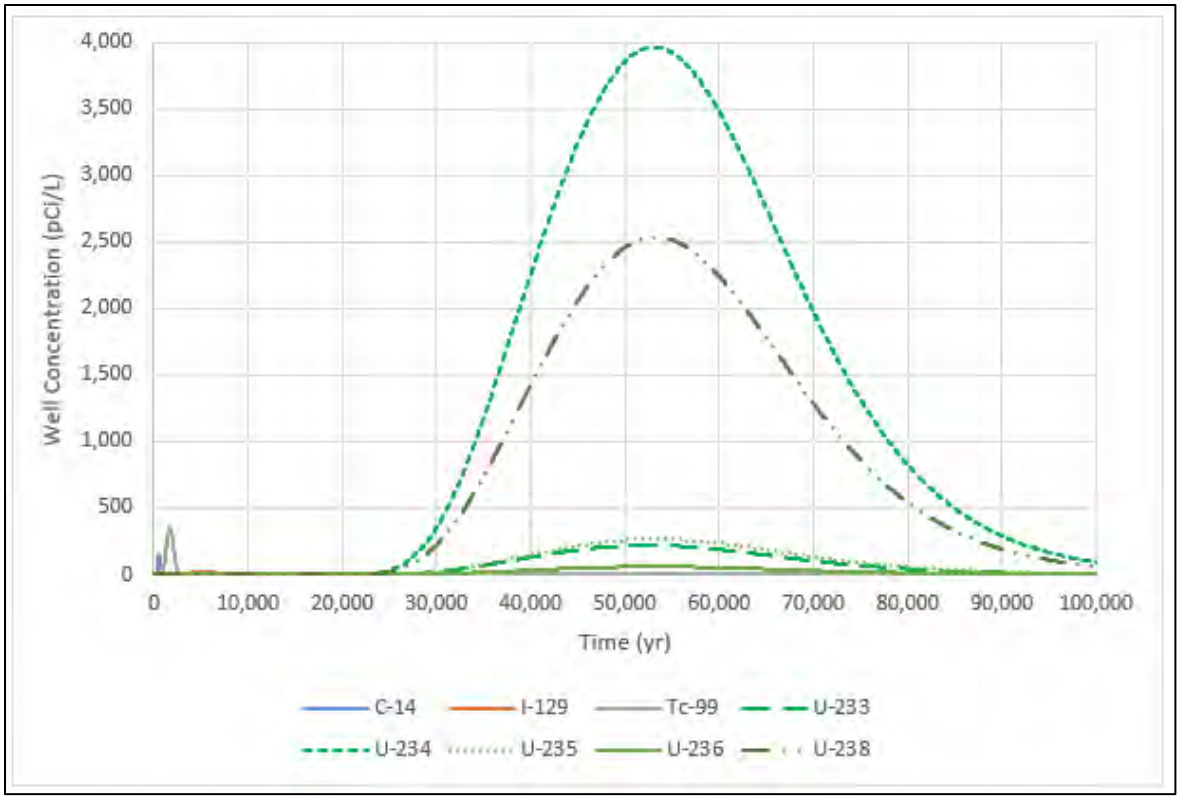

Fig. 4.27. RESRAD-OFFSITE predicted radionuclide concentrations in well water, 100,000-year simulation

5. SENSITIVITY AND UNCERTAINTY ANALYSIS

The goal of sensitivity-uncertainty analysis for the EMDF PA is understanding sensitivity of model predictions to uncertainty in input parameter values for those radionuclides and transport pathways that are the primary contributors to the all-pathways dose within the 1000-year compliance period. The base case all-pathways maximum dose during the compliance period is approximately 1 mrem/year, and the peak dose within 10,000 years is less than half of the 25 mrem/year performance objective. The focus of the analysis is on importance of uncertainty in long-term cover performance, partition coefficient values for key radionuclides, and hydrogeologic parameters for meeting DOE performance objectives. Given the pessimistic exposure assumptions incorporated in the base case all pathways scenario (Sect. 1.7), consideration of uncertainty in exposure factor assumptions (e.g., ingestion rates) was limited to the ingestion rates of fish and meat, and the depth of aquifer contributing to well (well depth).

The analysis includes selected sensitivity cases (what-if scenarios) for the detailed vadose and saturated zone transport models. For the RESRAD-OFFSITE model that analysis includes single factor sensitivity evaluations (increasing and decreasing one parameter at a time from the assumed base case value) and an uncertainty analysis to address the importance of key uncertainties relative to compliance with the 25 mrem/year performance objective. The uncertainty analysis involves assigning probability distributions to selected input parameters and running multiple simulations with different sets of input values, and statistical analysis of the results. The sensitivity and uncertainty evaluations undertaken for the EMDF PA are summarized in Table 5.1.

Table 5.1. Summary of sensitivity-uncertainty analyses for the EMDF PA

Type of sensitivity-uncertainty analysis	Subsystems and models evaluated	Parameters selected for analysis (related uncertainty)
Model sensitivity cases (what-if analysis)	Saturated Zone Flow – MODFLOW	• Increased recharge (climate)
	Vadose Zone Transport – STOMP	• Increased cover infiltration (climate, cover performance) • Increased waste K_d (materials and geochemistry) • Decreased non-waste K_d (materials and geochemistry)
	Saturated Zone Transport – MT3D	• Increased layer 2 hydraulic conductivity value (materials) • Non-uniform source release (uniform source release assumption)
Single factor sensitivity	Total System – RESRAD-OFFSITE	• Refer to Table 5.2
Probabilistic input parameter uncertainty analysis	Total System – RESRAD-OFFSITE	• Refer to Appendix G, Attachment G.3

EMDF = Environmental Management Disposal Facility
K_d = partition coefficient
PA = Performance Assessment
RESRAD = RESidual RADioactivity
STOMP = Subsurface Transport Over Multiple Phases

HELP model sensitivity evaluation is presented in Sect. 3.3.1.3 and Appendix C, Sect. C.2.5. The range of cover infiltration considered in the probabilistic uncertainty analysis is consistent with the uncertainty in HELP model predictions of cover performance. Sensitivity of the groundwater flow model results to increased recharge (future wet condition) is presented in Sect. 5.1 and Appendix D, Sect. D.5.6.

5.1 STOMP MODEL SENSITIVITY

Presentation of STOMP model sensitivity evaluations is limited to Tc-99 results, which are representative of the sensitivity of predicted concentrations of other radionuclides with nonzero K_d values (e.g., I-129) to the uncertainties in K_d values. STOMP model sensitivity to increased long-term maximum cover infiltration was also evaluated. The base case assumption for all radionuclides with nonzero K_d, for all PA models, is that the waste K_d value is one-half of the value assumed for all non-waste materials (refer to Sect. 3.2.2 and Table 3.4). The STOMP model sensitivity evaluations for (nonzero) K_d values included increasing the waste K_d value to the value assumed for non-waste materials (i.e., doubling the waste K_d), and decreasing the non-waste K_d value to the waste value (i.e., reducing the non-waste K_d value by half). For Tc-99, the waste K_d value was increased to 0.72 cm^3/g and the non-waste value was reduced to 0.35 cm^3/g. Sensitivity to increased maximum cover infiltration (twice the base case value), representing uncertainty in long-term cover performance was evaluated for all seven radionuclides included in the STOMP modeling. The potential for long-term cover performance to be better than assumed (lower maximum cover infiltration) is evaluated with the total system model in Sects. 5.3 and 5.4.

The sensitivity of STOMP predicted Tc-99 flux over time to the alternative K_d values and maximum cover infiltration are shown in Figs. 5.1 and 5.2. In each figure the upper plot is the base case STOMP model result and the lower plot is the sensitivity case. The K_d value controls the initial aqueous concentrations in waste materials and governs the release rate for a given inventory and cover infiltration. For the higher Tc-99 waste K_d the following differences from the base case are observed (Fig. 5.1):

- Lower peak mass flux rates at the base of the liner and the water table output surface due to lower initial aqueous concentrations
- Delayed peak flux at the water table surface (1400 years versus 1200 years for the base case)
- Longer duration of Tc-99 release from waste and flux into the saturated zone.

The results for lower K_d in the non-waste materials are shown on Fig. 5.2. Compared to the base case result the following differences are observed:

- Essentially the same Tc-99 mass flux at the liner output surface due to the same waste zone K_d value and initial aqueous concentration as the base case
- More rapid increase in mass flux at the water table output surface due to the lower K_d values in the vadose zone
- Higher and earlier peak mass flux at the water table surface (1100 years versus 1200 years for the base case).

These results are expected based on the K_d relationships to radionuclide release and transport. An increased waste K_d has a larger impact on release to the saturated zone than does a decreased vadose zone K_d.

For cover performance uncertainty, a maximum cover infiltration rate two times the base case long-term performance condition value was simulated. The linear increase between 200 and 1000 years changed from 0 to 0.88 in./year to 0 to 1.76 in./year and stayed at 1.76 in./year beyond 1000 years. Changing the maximum infiltration rate but not the assumed timing of cover degradation represents more rapid increase in cover infiltration than the base case scenario. Due to the increased amount of the water flux, there is also earlier Tc-99 mass release from the waste and a higher (nearly double) peak mass flux rate at the water table output surface (Fig. 5.3). The higher maximum infiltration also results in much faster waste zone depletion and faster migration to the saturated zone (peak flux occurs 200 years earlier) due to the larger water flux.

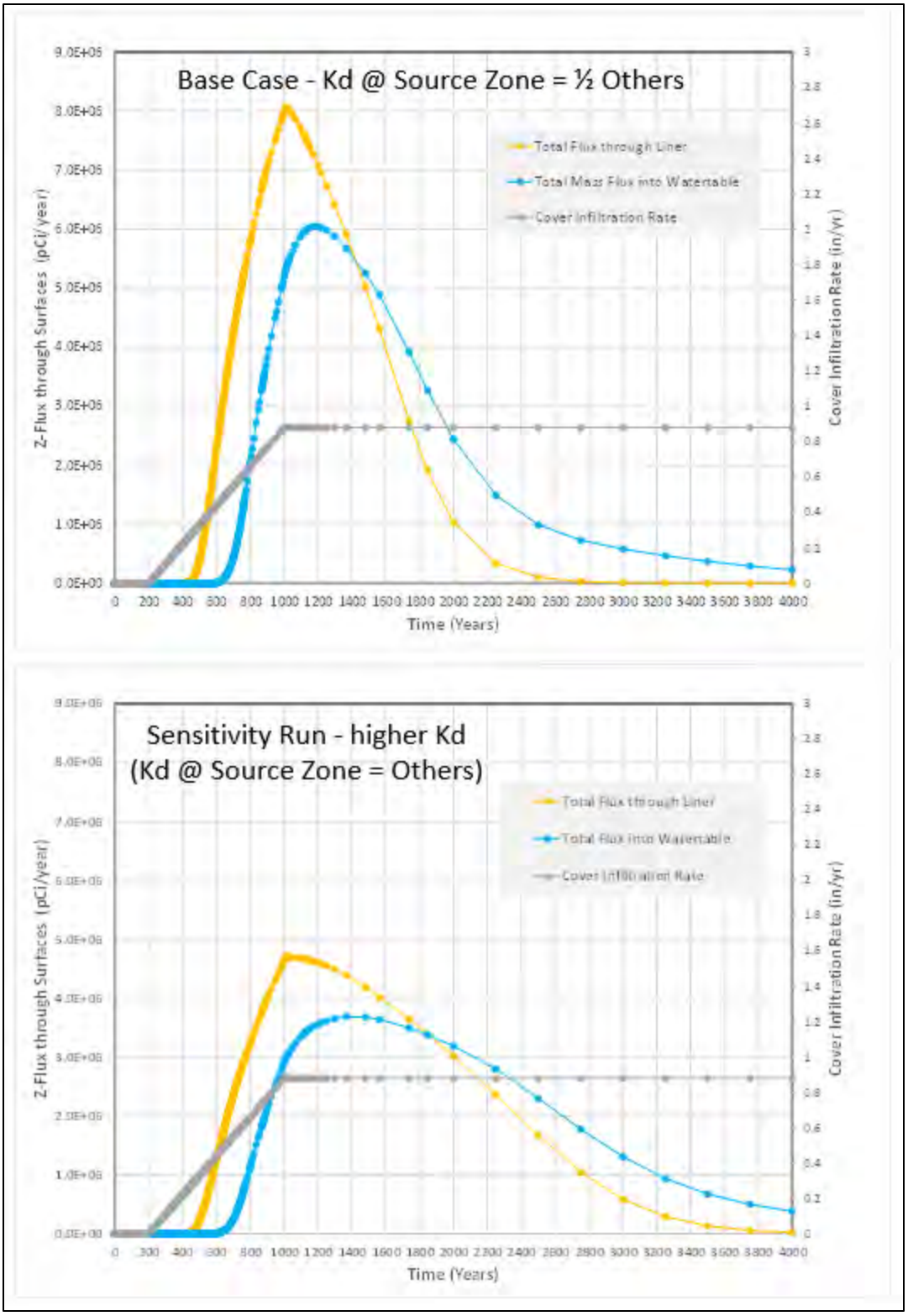

Fig. 5.1. Waste zone K_d impact on STOMP model Tc-99 flux

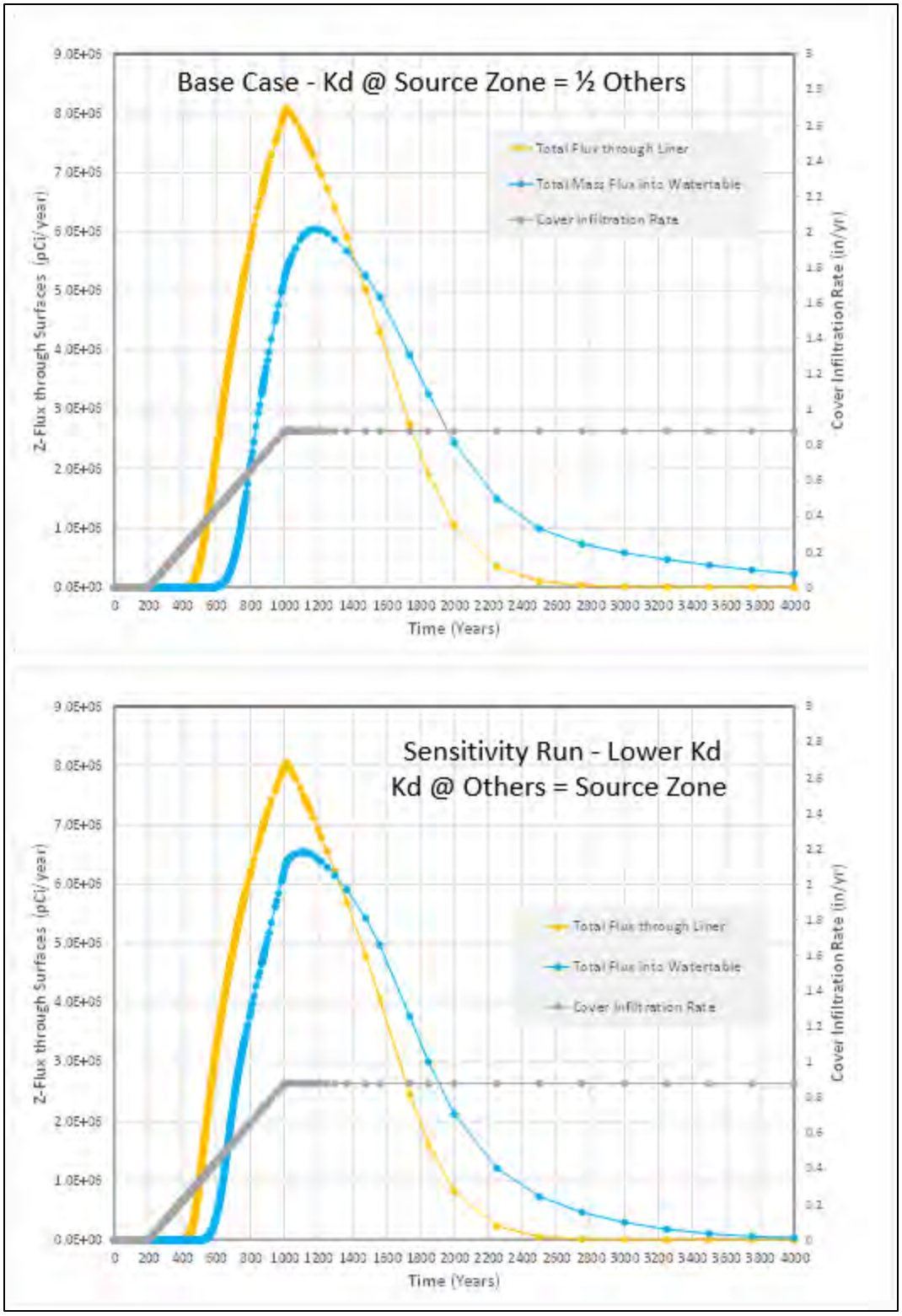

Fig. 5.2. Vadose zone K_d impact on STOMP model Tc-99 flux

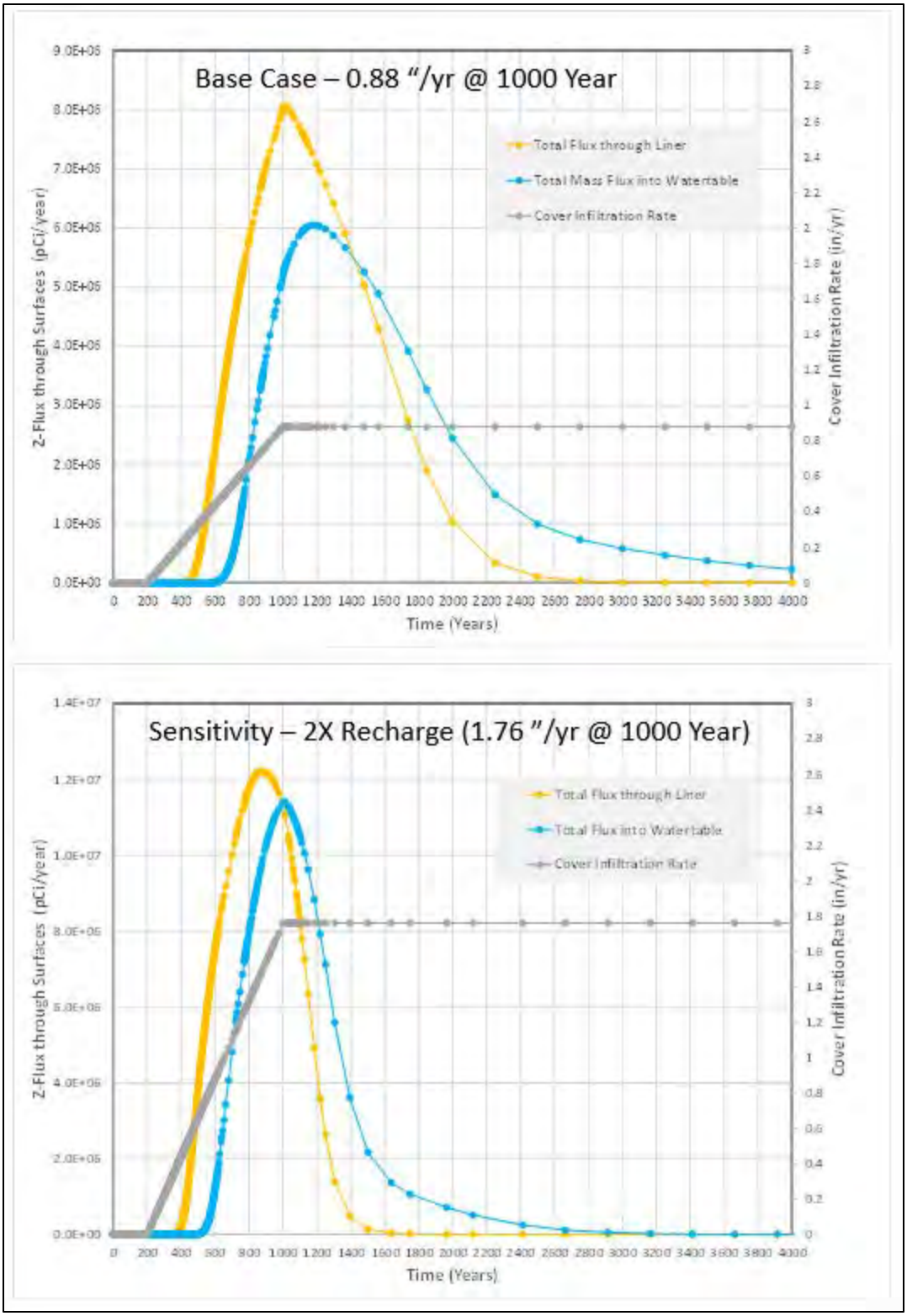

Fig. 5.3. Higher cover infiltration impact on STOMP model Tc-99 flux

The maximum aqueous concentrations in the waste zone and vadose zone are the same as for the base condition since K_d controls the mass partition between solid and aqueous phases. However, the resulting saturated zone concentrations underneath the EMDF would be higher than for the base case since there is more mass flux into the groundwater system from the vadose zone.

5.2 MT3D MODEL SENSITIVITY

MT3D results for two sensitivity cases are presented in this section. The sensitivity evaluations for the MT3D model included a scenario in which the hydraulic conductivity of model layer 2 was increased, and the non-uniform radionuclide release scenario. These two sensitivity cases address potential conceptual model uncertainties related to the characteristics of saprolite and bedrock along the flow path to the groundwater POA and to the assumption of uniform radionuclide release to the saturated zone. Results for these two sensitivity cases are also presented in Sect. 3.3.5 in the context of integrating the results from the different PA models.

5.2.1 Sensitivity to Hydraulic Conductivity of the Shallow Aquifer

To evaluate the impact of shallow aquifer hydraulic conductivity uncertainty and possible variation from the base case flow model assumptions, a sensitivity analysis was performed by applying higher hydraulic conductivity values in model layer 2. The relatively large thickness (70 ft) of model layer 2 in the EMDF model compared to the thickness of layers 1 and 3 at the 100-m well location suggested that the hydrogeologic properties assigned to layer 2 along the flow path from the EOW to well location could have a large effect on predicted saturated zone activity concentrations. The hydraulic conductivity of model layer 2 was increased to the value assigned to model layer 1, constituting an 8-fold increase. Applying the larger K value to model layer 2 is not an accurate representation of site conditions, based on the CBCV site characterization results (DOE 2018b, DOE 2019), but the sensitivity case does illustrate how a different configuration of material properties affects the results of the MT3D saturated zone radionuclide transport model. After the flow simulation was conducted with the higher hydraulic conductivity, impact on Tc-99 transport simulation with the MT3D model was evaluated. Additional detail is provided in Appendix F, Sect. F.4.3.

The Tc-99 concentration time series for all MT3D model layers at the 100-m well location for both base case and the layer 2 high K scenario are plotted in Fig. 5.4. Compared with base case scenario, the peak Tc-99 concentrations in different model layers are either higher or lower and occur earlier for the layer 2, high K sensitivity run. This difference is associated with the lower water table elevation and more rapid flow due to higher conductivity in model layer 2 beneath the waste and along the transport path to the 100-m well. Most of the Tc-99 movement occurs within model layer 2 due to its higher hydraulic conductivity, resulting in a very low concentration in the deeper model layers. At the 100-m well location, the model layer 1 and 2 peak Tc-99 concentrations are significantly higher and much earlier for the high K sensitivity run, peaking around 1750 years post-closure (vs peak concentrations occurring after 2500 years for the base case). The peak transmissivity-weighted average Tc-99 concentrations are approximately 50 percent higher than the base case peaks (300 pCi/L vs 200 pCi/L for the base case). The peak model layer 2 Tc-99 concentration is over 70 percent higher than for the base case.

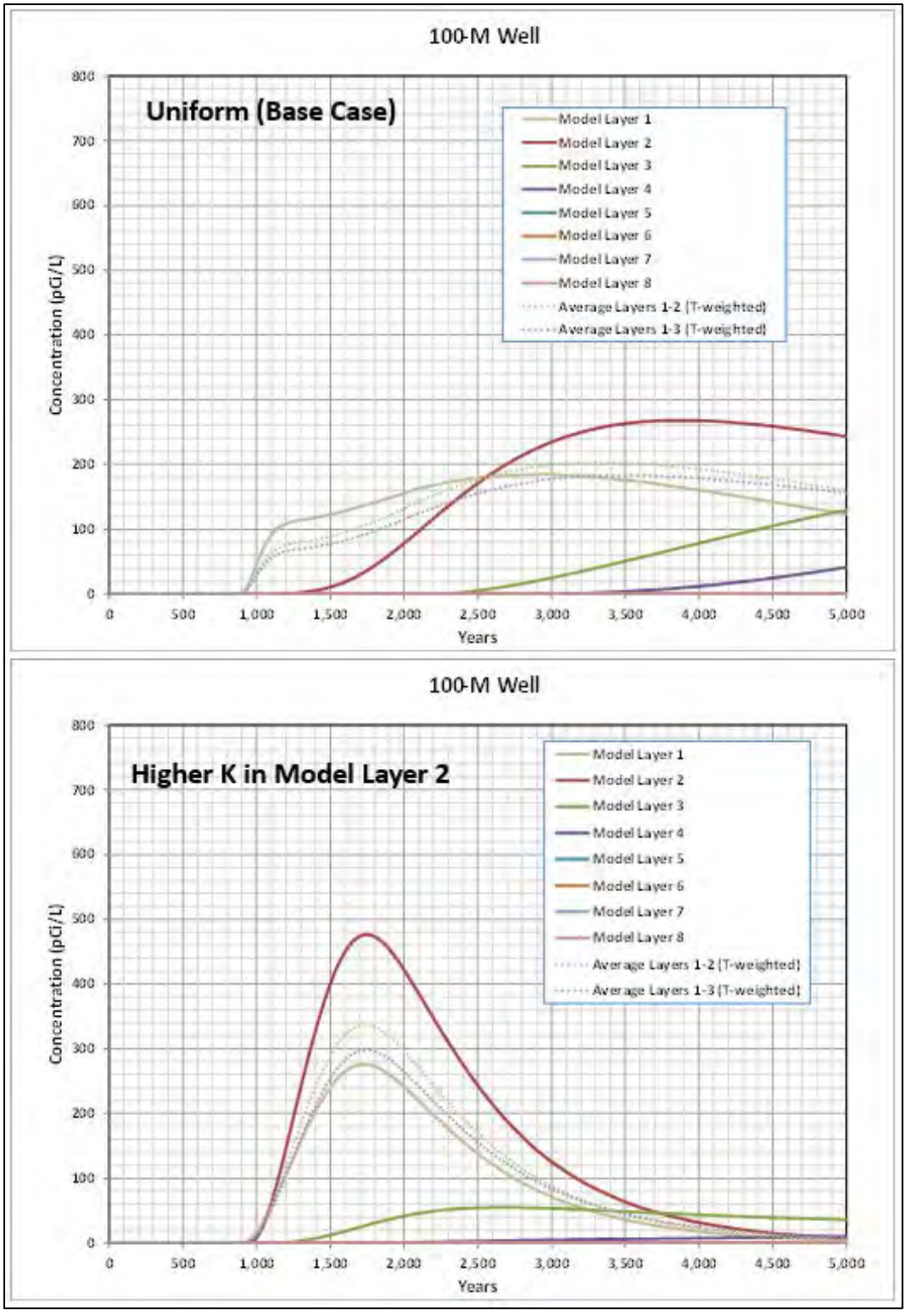

Fig. 5.4. MT3D predicted Tc-99 groundwater concentrations at the 100-m well (sensitivity to high K in layer 2)

Although the simulated Tc-99 concentrations at the 100-m well are very sensitive to the nearly 10-fold increase in the hydraulic conductivity of model layer 2, applying the higher K values representative of the saprolite zone to the deeper parts of the model domain is not an accurate representation of EMDF site conditions. The sensitivity run results suggest that uncertainty in hydrogeologic characteristics of the shallow subsurface materials in the vicinity of the disposal unit may be important for evaluating uncertainty in peak concentrations at the POA, but the uncertainty in field conditions is not as large as the applied increase in layer 2 conductivity. Due to the potential sensitivity of results to saturated zone hydraulic conductivity, the probabilistic uncertainty analysis for the PA total disposal system model (RESRAD-OFFSITE) includes a range of possible K values based on the available field data.

5.2.2 Non-uniform Release Scenario

The base condition saturated zone transport model assumes that the leachate flux from the waste area is uniform, implying that the waste volume has both a uniform radionuclide concentration and uniform thickness. The STOMP model simulation for EMDF (see Appendix E) demonstrates that there can be spatially variable (non-uniform) release rates within the facility footprint due to variation in waste thickness and liner system control of leachate drainage patterns. Variable leachate release rates will result in different radionuclide mass flux rates into the saturated zone that could have an impact on radionuclide concentrations at the 100-m well location. To evaluate this possibility, a non-uniform release scenario for the flow and transport model was developed using STOMP model results to estimate the variation in leachate flux and radionuclide concentration within the waste area. This sensitivity analysis was performed for Tc-99 transport only since it has a relatively small non-zero K_d value and the initial arrival time at the POA for the base condition falls within the 1000 year post-closure compliance period for the PA.

The non-uniform pattern of leachate flux beneath the EMDF predicted by the STOMP model was used to develop a non-uniform Tc-99 release model for MT3D based on the radionuclide release model (Sect. 3.3.3.2) developed for the uniform release scenario. The Section A STOMP model results were used to calculate the cumulative total volumetric leachate flux (volume/time) and cumulative total Tc-99 activity flux (activity/time) at the water table elevation directly below the upper half (upslope portion with lower flux) and the lower half (downslope portion with higher flux) of each disposal cell. The lower half to upper half ratios of leachate flux and Tc-99 flux represent a time-integrated measure of the non-uniformity of release from each disposal cell, derived from the STOMP Section A model results. An average Tc-99 concentration ratio is obtained by dividing the Tc-99 flux ratio by the leachate flux ratio for each cell.

The calculated leachate flux ratios were used to assign water recharge rates to each of eight cell floor sub-areas (upper and lower halves) of the floor of each cell (refer to Appendix F, Fig. F.17), accounting for the funneling effect of the outer sideslopes of each disposal cell and the pattern of water flux driven by the sloping cell floors. The individual water recharge (leachate flux) rates were applied in the MODFLOW model code to generate the flow field for the non-uniform Tc-99 release scenario MT3D transport model.

The Tc-99 mass in each disposal cell was calculated based on the cell volume and EMDF average initial (post-operational) Tc-99 concentration. Applying these initial Tc-99 masses, and utilizing STOMP model results to estimate Tc-99 vadose delay times for each disposal cell (Appendix E, Table E.8), a Tc-99 release model for each cell was created (refer to Appendix F, Sect. F.4.2.3). The Tc-99 recharge concentrations for each disposal cell were then partitioned into concentrations applied to the upper and lower half of each disposal cell on the basis of the calculated Tc-99 concentration ratio value. The resulting non-uniform Tc-99 release model accounts for variation in waste volume, water infiltration, and liner geometry among the four disposal cells. Additional detail on implementation of the non-uniform Tc-99 release model is provided in Appendix F.

The Tc-99 concentration time series for all model layers at the 100-m well location for both uniform and non-uniform release scenarios are plotted in Fig. 5.5. At the 100-m well, the model layer 1 and 2 peak Tc-99 concentrations are nearly the same for the uniform and non-uniform release scenarios, but the initial increase in layer 1 concentrations is much more gradual in the non-uniform release scenario. This difference in layer 1 concentrations directly reflects the non-uniform release to model layer 2 within the upgradient waste area, where model layer 1 remains unsaturated (i.e., recharge concentrations are applied to model layer 2). The peak transmissivity-weighted average Tc-99 concentrations occur slightly later for the non-uniform release, but are essentially the same (190 to 200 pCi/L) as the peak concentrations for the uniform release scenario.

This model sensitivity evaluation of uniformity of leachate release suggests that the base case uniform release scenario, although incorporating simplified release assumptions, does not underestimate peak concentrations relative to a more complex conceptualization and model implementation of non-uniform release. Using a more complex source representation could provide more information on variability in saturated zone concentrations in space and time, but will also introduce more uncertainty to the dose analysis associated with uncertainty in waste inventory and recharge distributions. Assuming non-uniform release would also increase the uncertainty in the selection of a groundwater POA location that will capture peak saturated zone impacts under differing sets of model input assumptions.

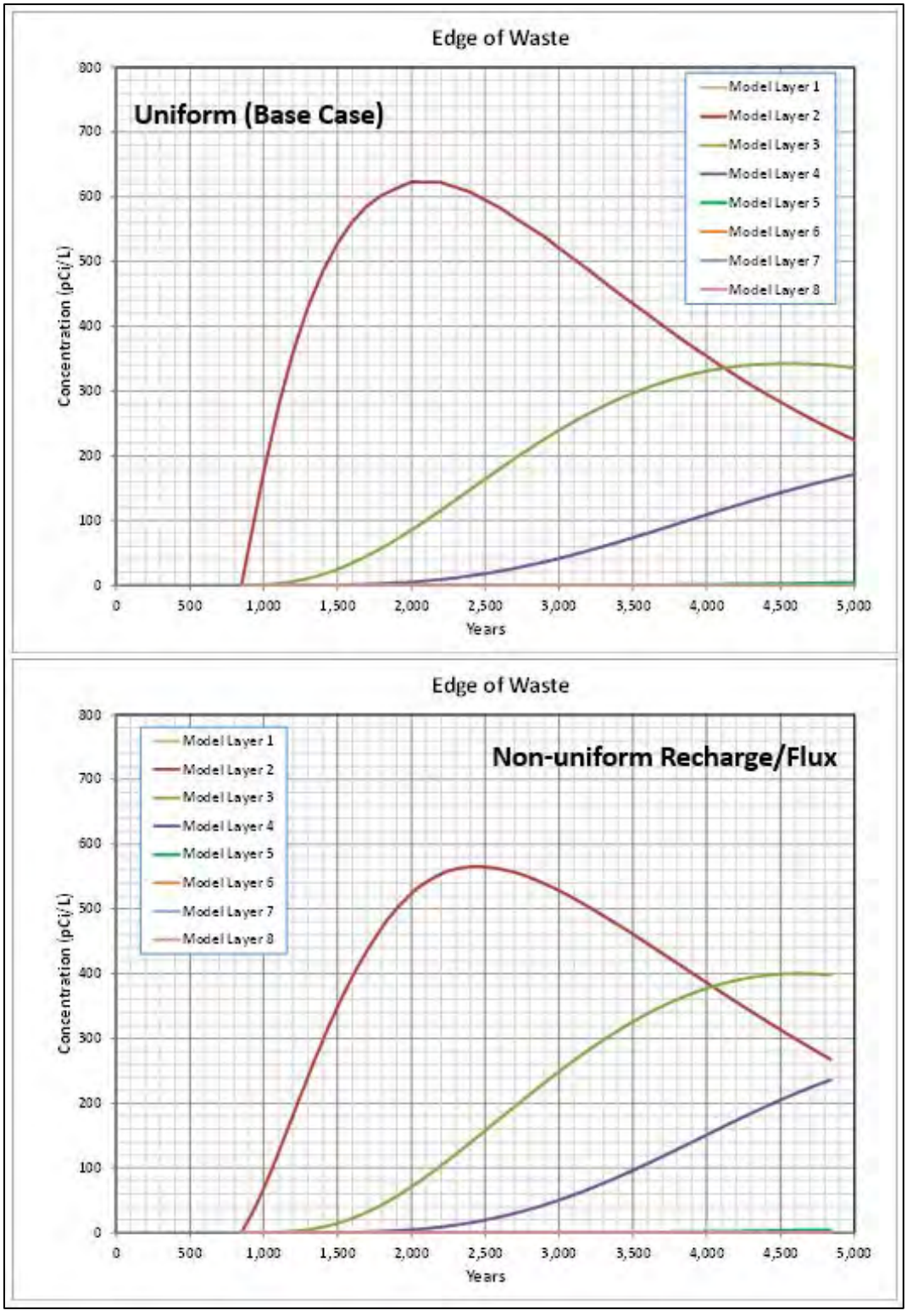

Fig. 5.5. Comparison of MT3D base case Tc-99 concentrations with results for the non-uniform source release simulation

5.3 RESRAD-OFFSITE SINGLE-FACTOR SENSITIVITY

The RESRAD-OFFSITE model was used to perform a large number of sensitivity evaluations for individual model input parameters (Appendix G, Sect. G.6.2). The utility of single factor analysis is limited because potential sensitivity of modeled dose to changing multiple parameter values is not captured. The qualitative evaluation of relative dose sensitivity to input values presented in Appendix G is also influenced by the selection of the range over which individual parameters are varied. The selected range is usually based on likely ranges of natural parameter variability or judgements about the degree of uncertainty associated with the assumed base case value. The single factor analyses are used to guide the selection of input parameters for which probability distributions are assigned in the probabilistic uncertainty analysis presented in Sect. 5.4.

The RESRAD-OFFSITE code package provides convenient evaluation of sensitivity for single input parameters. Input parameters can be increased and decreased by a user-selected factor. Table 5.2 contains the input parameters for which single factor sensitivity was evaluated and presented in Appendix G, and identifies the corresponding plots from this section and from Appendix G, Sect. G.6.2. The selection of input parameters was based on preliminary evaluations performed during development of the total system model. To focus the sensitivity analysis, parameters were varied for sitewide parameters (e.g., precipitation, runoff coefficient, residence time in lake) as well as for select radionuclides. The selected radionuclides are the top three contributors to total dose: C-14, Tc-99, and I-129. Sensitivity analysis results are for total dose and include contributions from all isotopes simulated during base case modeling. Graphical output for all of the parameter sensitivities evaluated are provided in Appendix G. Five of those graphics are included in this section to highlight a few of the more sensitive parameters.

Table 5.2. RESRAD-OFFSITE sensitivity analysis parameters, base case scenario

Parameter Description	RESRAD parameter identifier	Factor applied to base case value	Total dose plot figure
C-14 K_d in contaminated zone	DCACTC(C-14)	N/A	G.18
C-14 K_d (UZ1-UZ5)	DCACTU1-5(C-14)	N/A	G.18
C-14 K_d in saturated zone	DCACTS(C-14)	N/A	G.19
I-129 K_d contaminated zone	DCACTC(I-129)	5	G.19
I-129 K_d (UZ1-UZ5)	DCACTU1-5(I-129)	5	G.19
I-129 K_d saturated zone	DCACTS(I-129)	5	G.19
Tc-99 K_d contaminated zone	DCACTC(Tc-99)	5	G.20
Tc-99 K_d (UZ1-UZ5)	DCACTU1-5(Tc-99)	5	G.20
Tc-99 K_d saturated zone	DCACTS(Tc-99)	5	G.20
Precipitation	PRECIP	1.25	5.9, G.21
Initial releasable fraction	RELFRACINIT	(C-14) = 0.998, 0.564 (I-129, Tc-99) = 0.5, 0	G.22
Time at which C-14 first becomes releasable (delay time)	RELTIMEINIT(C-14)	2	G.23
Time at which I-129 first becomes releasable (delay time)	RELTIMEINIT(I-129)	2	G.23
Time at which Tc-99 first becomes releasable (delay time)	RELTIMEINIT(Tc-99)	2	G.23
Time over which transformation to releasable form occurs (C-14)	RELDUR(C-14)	2	G.24

Table 5.2. RESRAD-OFFSITE sensitivity analysis parameters, base case scenario (cont.)

Parameter Description	RESRAD parameter identifier	Factor applied to base case value	Total dose plot figure
Time over which transformation to releasable form occurs (I-129)	RELDUR(I-129)	2	G.24
Time over which transformation to releasable form occurs (Tc-99)	RELDUR(Tc-99)	2	G.24
Runoff coefficient	RUNOFF	N/A	5.10, G.25
Source release	--	N/A	5.6, G.17
Source concentrations	--	N/A	5.8, G.26
C-14 K_d in contaminated zone	DCACTC(C-14)	N/A	G.18
I-129 K_d contaminated zone	DCACTC(I-129)	5	5.7, G.19
Tc-99 K_d contaminated zone	DCACTC(I-129)	5	G.20
Longitudinal dispersivity of contaminated zone	ALPHLCZ	5	G.27
Contaminated zone b parameter	BCZ	1.4	G.27
Hydraulic conductivity of contaminated zone	HCCZ	5	G.27
Total porosity of contaminated zone	TPCZ	1.1	G.27
Effective porosity of contaminated zone	EPCZ	1.5	G.27
C-14 K_d (UZ1-UZ5)	DCACTU1-5(C-14)	N/A	G.18
I-129 K_d (UZ1-UZ5)	DCACTU1-5(I-129)	5	5.7, G.19
Tc-99 K_d (UZ1-UZ5)	DCACTU1-5(Tc-99)	5	G.20
Bulk density of UZ3	DENSUZ(3)	1.05	G.28
Total porosity of UZ3	TPUZ(3)	1.1	G.28
Effective porosity of UZ3	EPUZ(3)	1.1	G.28
Bulk density of UZ4	DENSUZ(4)	1.05	G.29
Total porosity of UZ4	TPUZ(4)	1.1	G.29
Effective porosity of UZ4	EPUZ(4)	1.1	G.29
Bulk density of UZ5	DENSUZ(5)	1.05	G.30
Total porosity of UZ5	TPUZ(5)	1.1	G.30
Effective porosity in native vadose zone (UZ5)	EPUZ(5)	1.5	G.30
Longitudinal dispersivity of native vadose zone (UZ5)	ALPHALU(5)	2	G.30
Thickness of native vadose zone (UZ5)	H(5)	2	G.31
Thickness of native vadose zone (UZ5)	H(5)	H(5) = 0.01 m	G.31
C-14 K_d in saturated zone	DCACTS(C-14)	N/A	G.18
I-129 K_d saturated zone	DCACTS(I-129)	5	5.7, G.19
Tc-99 K_d saturated zone	DCACTS(Tc-99)	5	G.20
Dry bulk density of saturated zone	DENSAQ	1.15	G.32
Total porosity of saturated zone	TPSZ	1.5	G.32

Table 5.2. RESRAD-OFFSITE sensitivity analysis parameters, base case scenario (cont.)

Parameter Description	RESRAD parameter identifier	Factor applied to base case value	Total dose plot figure
Effective porosity of saturated zone	EPSZ	1.5	G.32
Thickness of saturated zone	DPTHAQ	1.5	G.32
Hydraulic conductivity of saturated zone	HCSZ	2	G.32
Hydraulic gradient of aquifer to well	HGW	2	5.11, G.33
Longitudinal dispersivity of aquifer to well	ALPHALOW	2	5.11, G.33
Hydraulic gradient of aquifer to surface water body	HGSW	2	G.34
Longitudinal dispersivity of aquifer to surface waterbody	ALPHALOSW	2	G.34
Depth of aquifer contributing to surface waterbody	DPTHAQSW	2	G.34
Mean residence time of water in surface waterbody	TLAKE	10	G.34
Meat ingestion	DMI(1)	1.19	G.35
Fish ingestion	DFI(1)	2	G.35
Fraction of meat from affected area	FMEMI(1)	2	G.35
Depth of aquifer contributing to well	DWIBWT	1.5	G.36

N/A = not applicable
RESRAD = RESidual RADioactivity
UZ = unsaturated zone

The conceptual model of radionuclide release from the waste is an important uncertainty in the PA. Figure 5.6 shows predicted dose sensitivity to the selection of the RESRAD-OFFSITE release model option. RESRAD-OFFSITE offers three options to simulate source release (Sect. 3.3.4.2): First-Order Rate Controlled Release with Transport, Version 2 Release, and Instantaneous Equilibrium Desorption Release. The Version 2 release model does not allow for a time delay like the other two release models, so for comparison of predicted dose from the three release models, results from the sensitivity simulation with this release option were shifted by 300 years. Dose peaks are lower for the first two release model options, which may be more representative of a release limited by containerization or treatment of some portion of the total waste, or the impact of non-uniform cover failure and infiltration that leads to preferential release and transport paths through the waste zone.

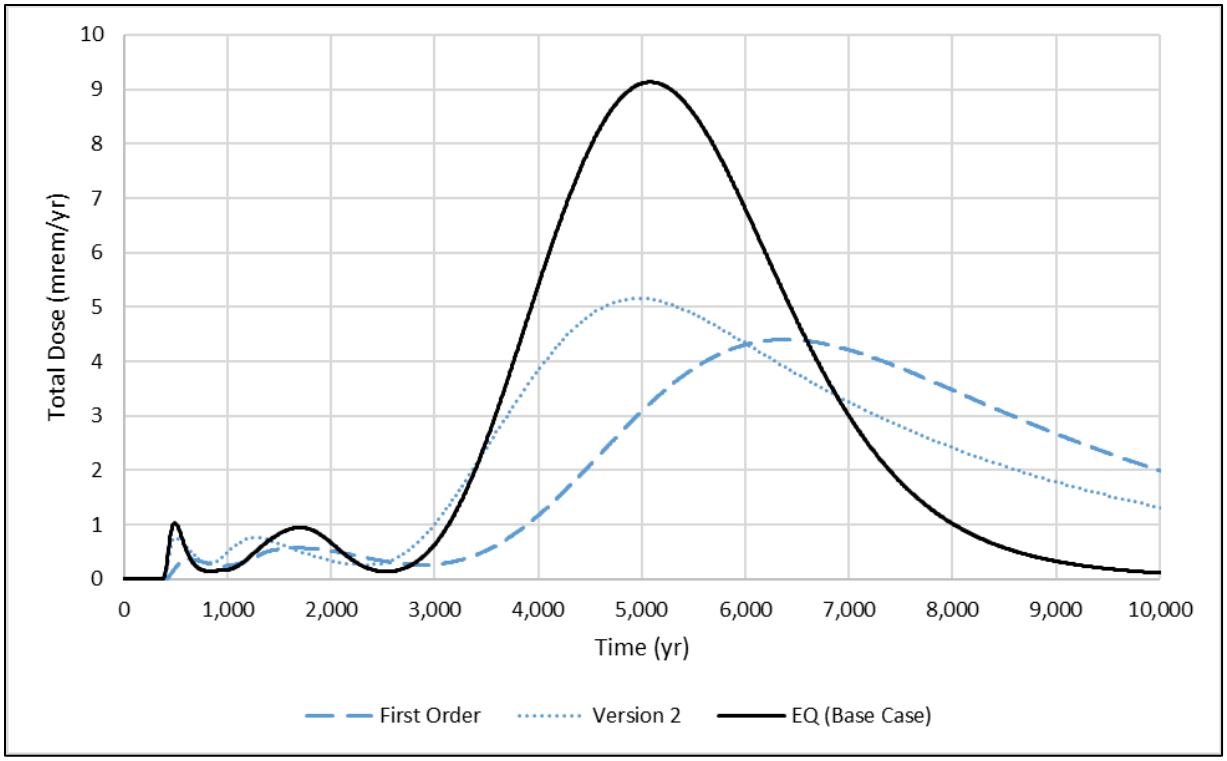

Fig. 5.6. Sensitivity analysis on RESRAD-OFFSITE release option

The factor of 5 sensitivity analysis on the specified distribution coefficient of I-129 in the contaminated zone, saturated zone, and unsaturated zones indicates that the predicted total dose is sensitive after the compliance period to variation of K_d for I-129. Increasing the K_d in each of the zones causes lower peak doses that occur later, while decreasing the K_d causes higher peak doses that occur earlier. Predicted total dose for the 10,000-year simulation period is most sensitive to the K_d of I-129 in the contaminated zone and the saturated zone and least sensitive to K_d of I-129 in the unsaturated zone. Results from the factor of 5 sensitivity analyses on the K_d of I-129 are shown in Fig. 5.7.

To evaluate the impact of radionuclide source concentrations in the waste on deterministic dose, the base case model was simulated with source concentrations higher than and lower than base case values for C-14, I-129, and Tc-99. Soil concentrations were not changed for any other simulated radionuclide, as dose contributions from all other radionuclides besides C-14, I-129, and Tc-99 are negligible. High-source concentrations evaluated are equal to as-disposed source concentrations, which do not account for operational period losses. Low-source concentrations are equal to 10 percent of the base as-disposed value (for C-14) or based on excluding the high outliers from the available radionuclide inventory data for I-129 and Tc-99.

Results from the sensitivity analysis on source concentrations are shown in Fig. 5.8. Predicted total dose for the compliance period is sensitive to varying the C-14 concentrations. Higher C-14 source concentrations cause a higher peak dose while lower source concentrations cause a lower peak dose. The high C-14 source concentrations are probably not realistic given that the estimated inventory (unadjusted for operational losses) is likely biased high. The timing of the peak dose for the compliance period is not sensitive to the C-14 source concentrations. Predicted total dose for the 10,000-year simulation period is also sensitive to varying the source concentrations. The lower I-129 source concentrations are probably a more realistic estimate of EMDF average as-disposed waste concentrations because of one particularly large I-129 data point included in the estimate used for the base case.

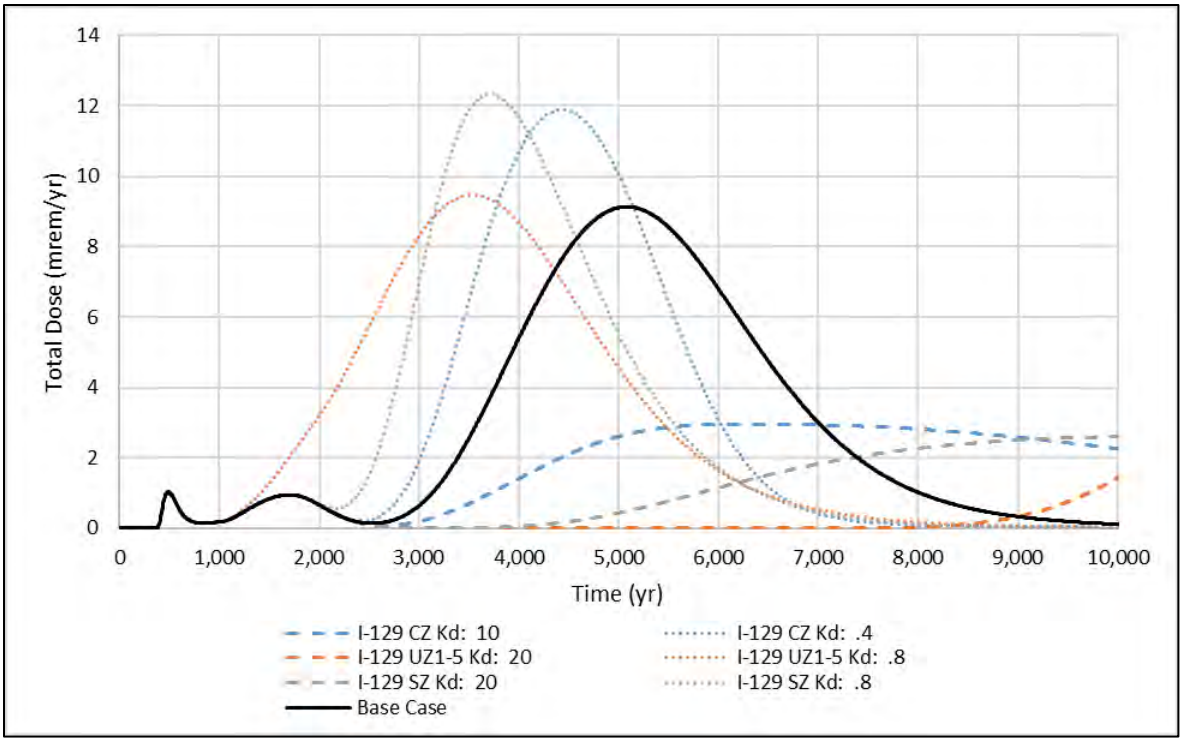

Fig. 5.7. Sensitivity analysis on I-129 distribution coefficient in the contaminated zone (CZ), saturated zone (SZ), and unsaturated zones (UZ1 - UZ5) with adjustment factor of 5

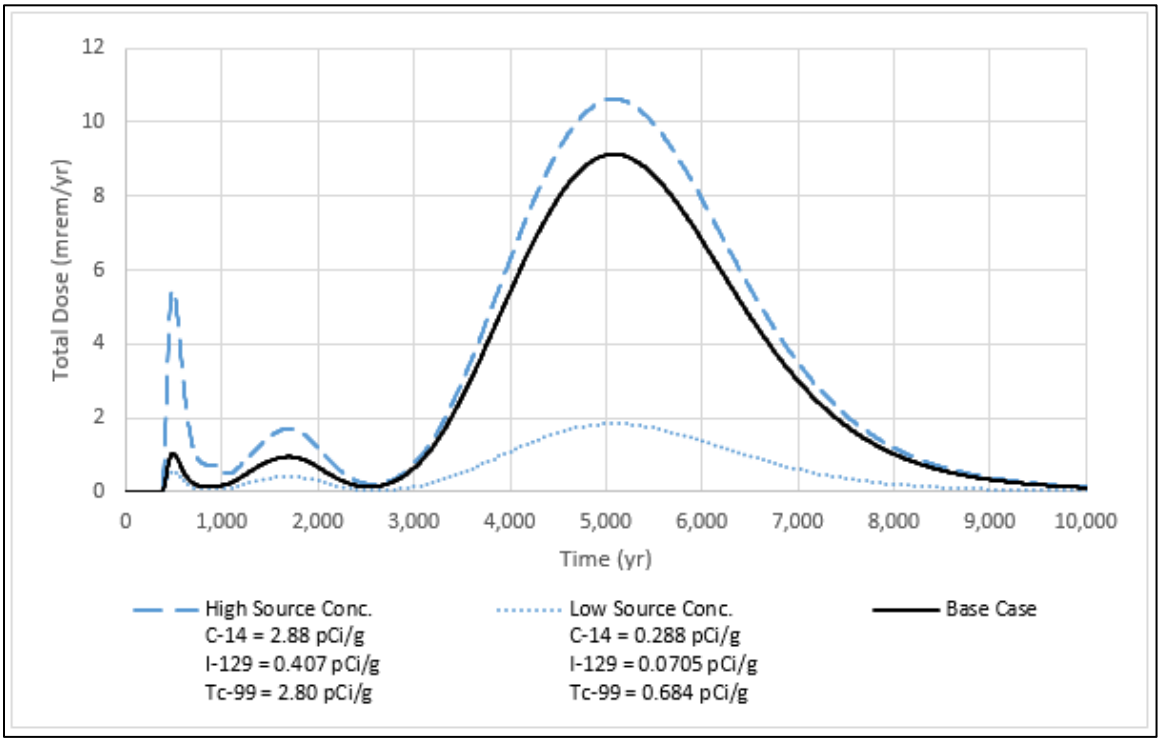

Fig. 5.8. Sensitivity analysis on radionuclide source concentrations for key radionuclides (C-14, I-129, and Tc-99)

Total dose sensitivity to variation in assumed values of average annual precipitation (representing climate uncertainty) and the runoff coefficient (representing uncertainty in long-term cover performance) confirms that uncertainty in future climatic conditions and cover system degradation are important for EMDF performance analysis (Figs. 5.9 and 5.10). The range in assumed precipitation evaluated corresponds to a range in modeled cover infiltration of 0.70 to 1.1 in./year (Fig. 5.9), while the range in the assumed value of the runoff coefficient corresponds to a 10-fold range in cover infiltration from 0.43 to 4.0 in./year (Fig. 5.10). The upper end of this range of modeled cover infiltration rates is much larger than rates reasonably expected for long-term EMDF cover performance.

Total dose peaks and the timing of peaks are sensitivity to varying the precipitation rate (Fig. 5.9). The factor of 1.25 is an extreme range of variation for a long-term annual average, at least on the upper end of the range (68 in./year). However the increases in total dose at the peak times are proportionally limited (about 15 percent or less). Proportional total dose increases in response to increased cover infiltration (decreased runoff coefficient) are more dramatic (Fig. 5.10). Compliance period impacts of increase cover infiltration on the C-14 dose peak are limited, but the I-129 peak is increased by 30 percent and occurs over 2000 years earlier than the based case scenario. The RESRAD-OFFSITE release model (instantaneous equilibrium release option) and one-dimensional vadose zone representation appear to over-predict the activity flux from EMDF for radionuclides having K_d values > 1 cm^3/g, including I-129 and U-234 (refer to Sect. 3.3.5 and Appendix G, Sect. G.5.6). The sensitivity evaluation on the lower runoff coefficient value (0.83) corresponding to 4 in./year cover infiltration produced extremely large doses after 5000 years that are associated with actinides (e.g., U-234 and Pu-239) in the EMDF estimated inventory. These extreme dose levels are not likely representative of future releases of uranium and plutonium for EMDF, and so the results of the sensitivity evaluation for the runoff coefficient are presented only for the total dose associated with C-14, Tc-99 and I-129 in Fig. 5.10.

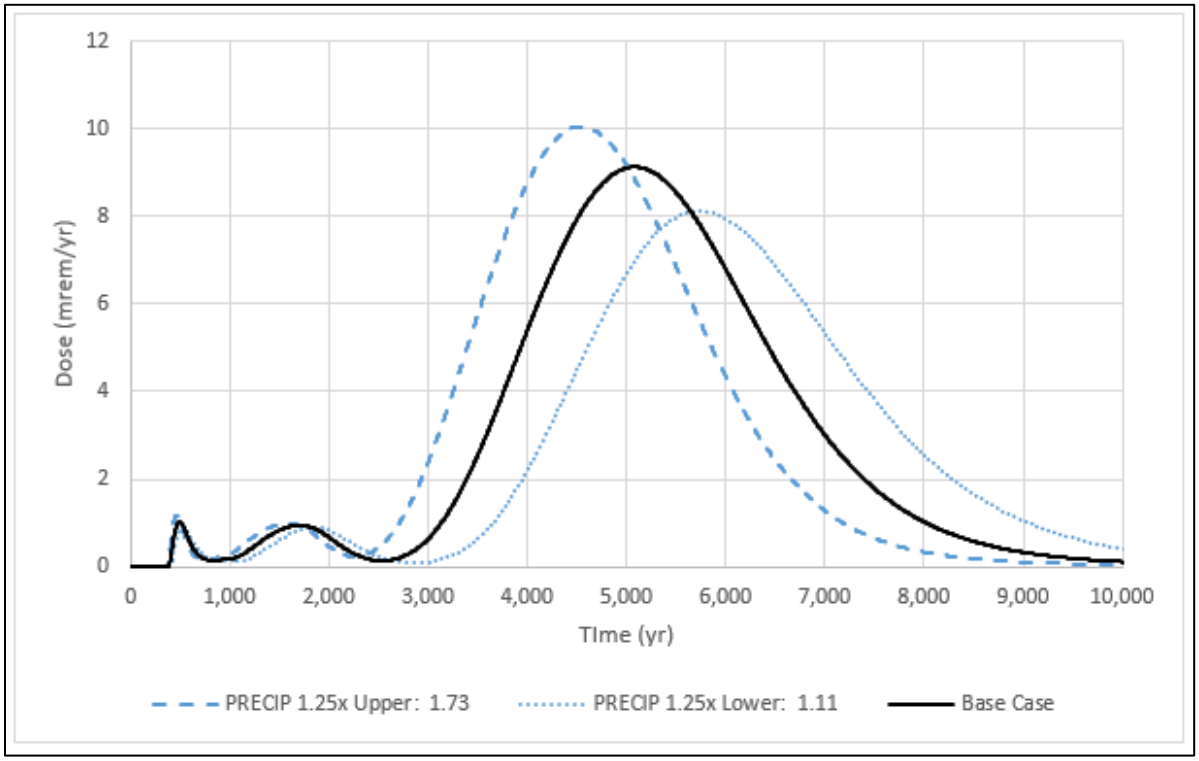

Fig. 5.9. Sensitivity analysis on precipitation rate (PRECIP) with adjustment factor of 1.25

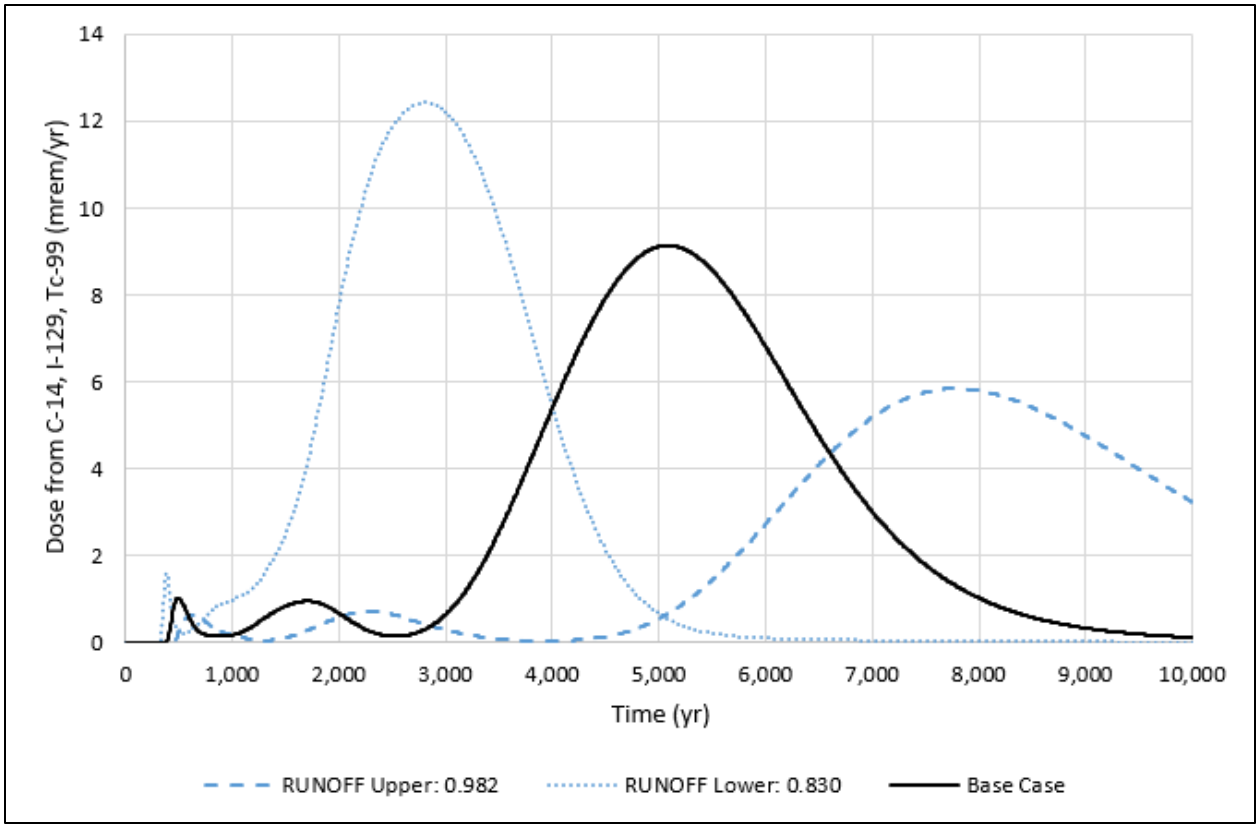

Fig. 5.10. Sensitivity analysis on runoff coefficient of the waste (RUNOFF)

Total dose sensitivity to variation in parameters that represent hydrologic controls on saturated zone radionuclide concentrations is significant for the range of parameter values evaluated (Fig. 5.11). Hydraulic gradient to the well location has relatively large impacts on total dose for the factor of 2 range of input values considered. The sensitivity appears to represent a source dilution effect that scales directly with the flux of groundwater through the aquifer. Dose sensitivity to the hydraulic conductivity of the saturated zone (Appendix G, Fig. G.32) is essentially the same as sensitivity to the hydraulic gradient because the product of those two parameters sets the Darcy velocity for the saturated zone and the magnitude of leachate dilution.

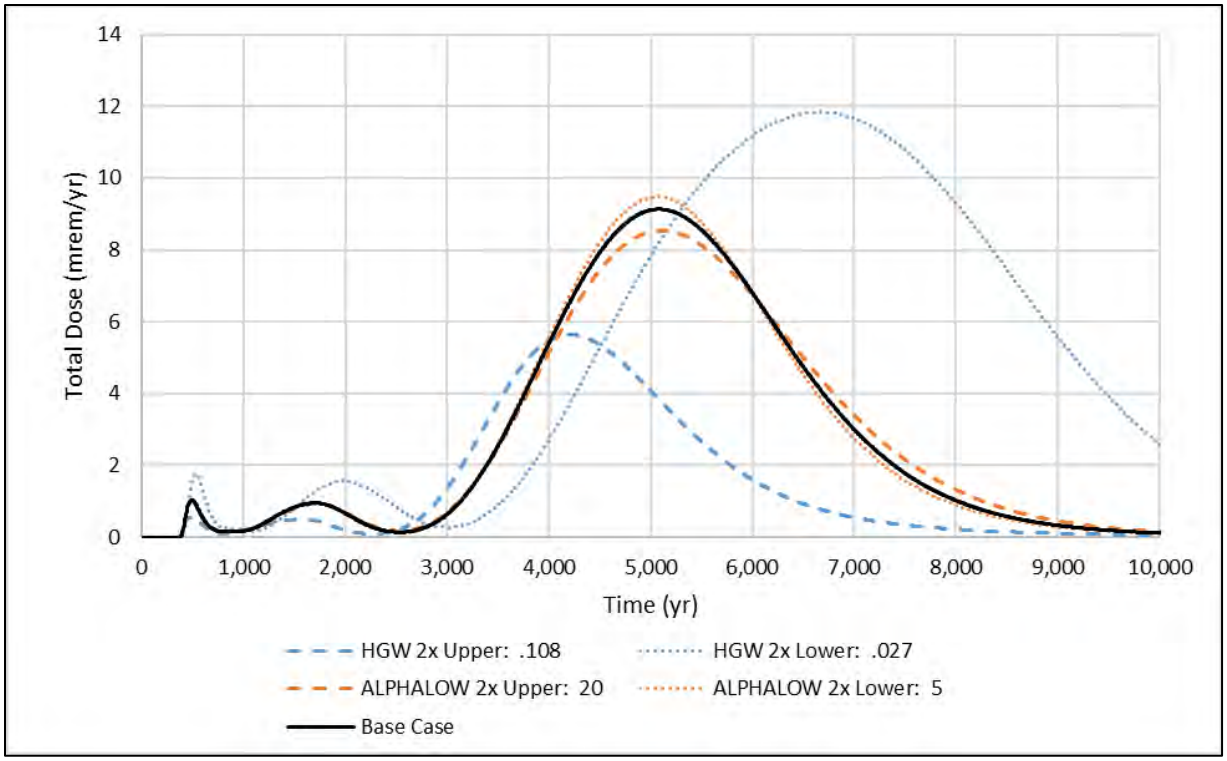

Fig. 5.11. Sensitivity analysis on hydraulic gradient of aquifer to well (HGW) and longitudinal dispersivity of aquifer to well with (ALPHALOW) and adjustment factor of 2

5.4 PROBABILISTIC UNCERTAINTY ANALYSIS

The RESRAD-OFFSITE probabilistic uncertainty analysis is described in detail in Appendix G and the results are briefly summarized in this section the EMDF PA report. The probabilistic analysis addresses input parameter uncertainty by assigning probability distributions to key input variables, randomly sampling sets of input parameters values and running multiple simulations to obtain the predicted peak dose for each of 3000 realizations of the disposal system. Distributions of predicted dose can be used to understand the range and likelihood of peak dose related to uncertainty in input parameters. Multiple regression analysis of peak dose as a function of the probabilistic input variables is used to determine which input parameters have the greatest impact on model results. Separate RESRAD-OFFSITE uncertainty analyses were completed for the 1000-year compliance period and for the longer 10,000-year period. The assignment of probability distributions for input parameters, relationships among parameters (including assigned correlations), and the sampling approach used to select input values for each simulation are described in detail in Appendix G, Sect. G.6.3. Appendix G also includes an evaluation of parameter value combinations that result in rare cases for which the simulated peak total dose exceeds 25 mrem/year.

Initially, using insights gained from preliminary model runs and sensitivity analysis simulations, key RESRAD-OFFSITE parameters for which uncertainty could have significant dose impacts were identified. C-14, I-129, and Tc-99 were identified as the radionuclides which had the most influence on total dose predictions during the compliance period; therefore, the compliance period probabilistic analysis includes only these three radionuclides. Preliminary model runs and sensitivity analysis simulations showed that Pu-239, U-234, U-235, and U-238 could potentially have dose contributions during the 10,000-year simulation period; accordingly, these radionuclides along with C-14, I-129 and Tc-99 were included in the 10,000-year probabilistic and uncertainty analysis. Both the compliance period and 10,000-year uncertainty

and probabilistic analyses focused on parameters with significant uncertainty in the assignment of deterministic base case values, which include radionuclide release parameters (initial releasable fraction, initial release time, release duration), isotope-specific K_d values, the surface runoff coefficient (cover performance uncertainty), precipitation (climate uncertainty), and parameters controlling flow in the waste, unsaturated, and saturated zones.

5.4.1 Probabilistic Results – Compliance Period

To simplify the analysis and to make total run time shorter, only C-14, Tc-99, and I-129 were included in the probabilistic evaluation for the compliance period. For the compliance period probabilistic simulations presented in this section, total dose refers to the dose resulting from C-14, Tc-99, and I-129.

The RESRAD-OFFSITE uncertainty analysis calculates statistics of the total dose distribution for each repetition at each simulation time step. Figure 5.12 shows the variation of median, mean, and 95th percentile dose over time for each of the 10 repetitions of 300 compliance period simulations. The deterministic base case model all-pathways dose curve is also shown on Fig. 5.12 for comparison to the probabilistic results. By 250 years, the mean of the simulated dose distribution begins a steady, gradual increase through 1000 years. The 95th percentile values increase rapidly between 250 and 400 years and then increase more gradually through 1000 years in parallel with the mean. In contrast, the median of the simulated dose distribution increases between 400 and 550 years and then becomes steady at approximately 0.4 mrem/year through the end of the compliance period. The difference between the deterministic base case dose curve and the probabilistic results (percentiles of the total dose distribution as a function of time) occurs because the time of peak total dose for any single probabilistic simulation varies widely (230 to 1030 years) due to variable sampling of input parameters that control release timing (particularly K_d values) among the 3000 realizations. The differences between the deterministic and probabilistic results also reflect the likelihood of much larger dose contributions from Tc-99 and I-129 toward the end of the compliance period probabilistic simulations.

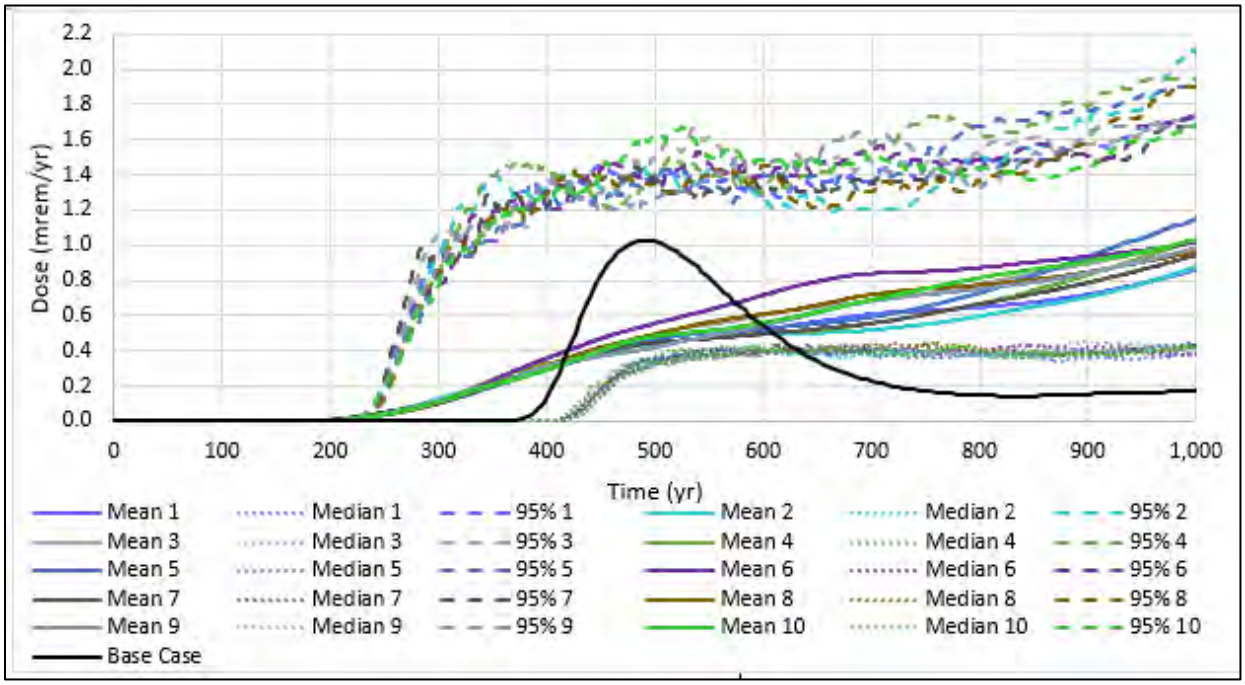

Fig. 5.12. Probabilistic total dose summary for 10 sets of 300 RESRAD-OFFSITE compliance period simulations, all pathways, all calculation points

The peak mean probabilistic dose (i.e., the maximum value of the mean dose for each repetition) occurred at 1030 years for all 10 repetitions, ranging from 0.92 to 1.2 mrem/year, which is a range that includes the deterministic base case compliance period peak dose of approximately 1 mrem/year. The 95th percentiles of the probabilistic total dose also reached maximum values at 1030 years, with a range from 1.7 to 2.1 mrem/year among the 10 repetitions.

Carbon-14 is the primary dose contributor for times prior to about 800 years. After 800 years, Tc-99 and I-129 have mean dose contributions equal to or greater than mean C-14 contributions. Additional detail on variation of radionuclide dose over the compliance period is provided in Appendix G, Sect. G.6.3.3.

The timing of peak radionuclide doses varies among simulations and radionuclides. For C-14, roughly 95 percent of the radionuclide peaks occur between 300 and 900 years, with an average peak dose of 1.03 mrem/year and average time of peak dose at 560 years. Most of the Tc-99 and I-129 peaks occur at the end of the simulation period (1030 years) as a result of the probability distributions of K_d values assigned to Tc-99 and I-129 (the C-14 K_d value was zero for all probabilistic simulations). For Tc-99, only the earliest 8 percent of radionuclide peak doses occur prior to 1030 years and the other 92 percent of peaks occur at the end of the simulation period. For I-129, only seven out of 3000 peaks (0.23 percent) occur prior to 1030 years. For Tc-99 and I-129, compliance period peak doses that occur at the end of the simulation period are cases in which higher long-term radionuclide peaks will occur well after 1000 years in the longer simulations.

Table 5.3 provides peak radionuclide dose statistics for the compliance period uncertainty analysis. For I-129, the average peak dose is larger than the 95th percentile because there are is a very large proportion of zero peak values for I-129 in the compliance period uncertainty analysis. The compliance period distributions of peak total dose for each of the ten repetitions of 300 simulations are shown in Fig. 5.13. The median (average median value of the 10 repetitions) peak total dose (all pathways) is 1.0 mrem/year and the 95th percentile value of peak dose (average of the 10 repetitions) is approximately 2.5 mrem/year. Extreme values (> 25 mrem/year) of peak total dose are associated with rare (< 1 percent) large I-129 contributions at the end of the simulation period. The extreme high end (> 25 mrem/year) of the distribution of compliance period peak dose and the factors that contribute to extreme dose peaks are considered in Appendix G, Sect. G.6.3.3.5.

Table 5.3. Compliance period peak radionuclide dose statistics

Radionuclide	Average peak dose (mrem/year)	95th percentile peak dose (mrem/year)
C-14	1.03	1.96
I-129	0.48	0.26
Tc-99	0.40	1.34

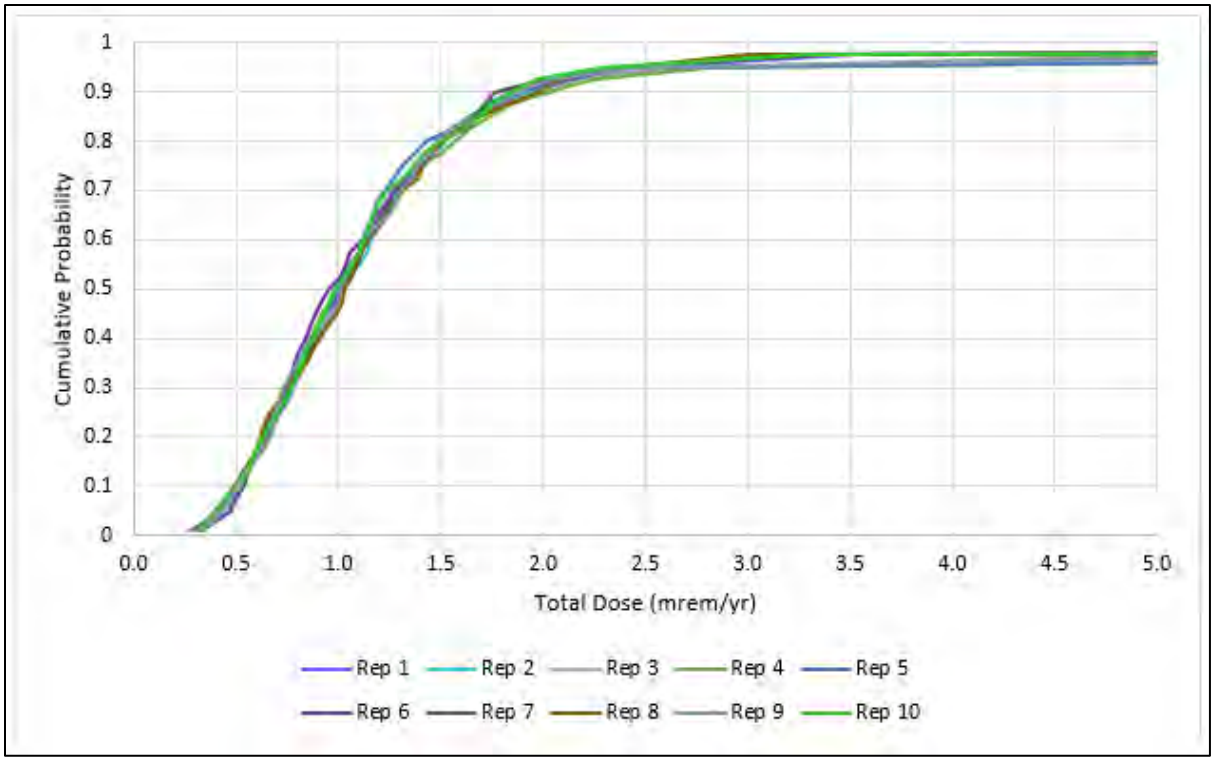

Fig. 5.13. Cumulative distribution function curves, peak all-pathways dose over 10,000 years

Regression analysis of the compliance period probabilistic peak dose output suggests that among the 33 input parameters for which probability distributions were assigned, the most influential variables fall into four categories: (1) contaminated zone parameters, (2) unsaturated zone parameters, (3) saturated zone parameters, and (4) human exposure parameters. Table G.26 of Appendix G provides a complete list of the probabilistic input parameters and the standardized rank regression coefficients calculated for each repetition of 300 simulations. For the entire range of compliance period peak doses, the five most influential parameters are:

- Runoff coefficient (cover infiltration rate)
- Release duration (affects release rate)
- Hydraulic conductivity of the saturated zone (saturated zone mixing)
- Mean residence time in the surface water body (C-14 fish ingestion dose)
- Depth of aquifer contributing to well (exposure factor, affects well water concentrations).

These results are consistent with results from the single parameter sensitivity analysis presented in Sect. 5.3, which show that total dose and timing of peaks are sensitive to changes in these parameters. Appendix G, Sect. G.6.3.3.4 provides more detailed discussion of the results of the regression analysis for the compliance period. Figure 5.14 is a summary graphic for the compliance period probabilistic results. Additional interpretation of the results of the uncertainty analysis is included in Sect. 7.4.

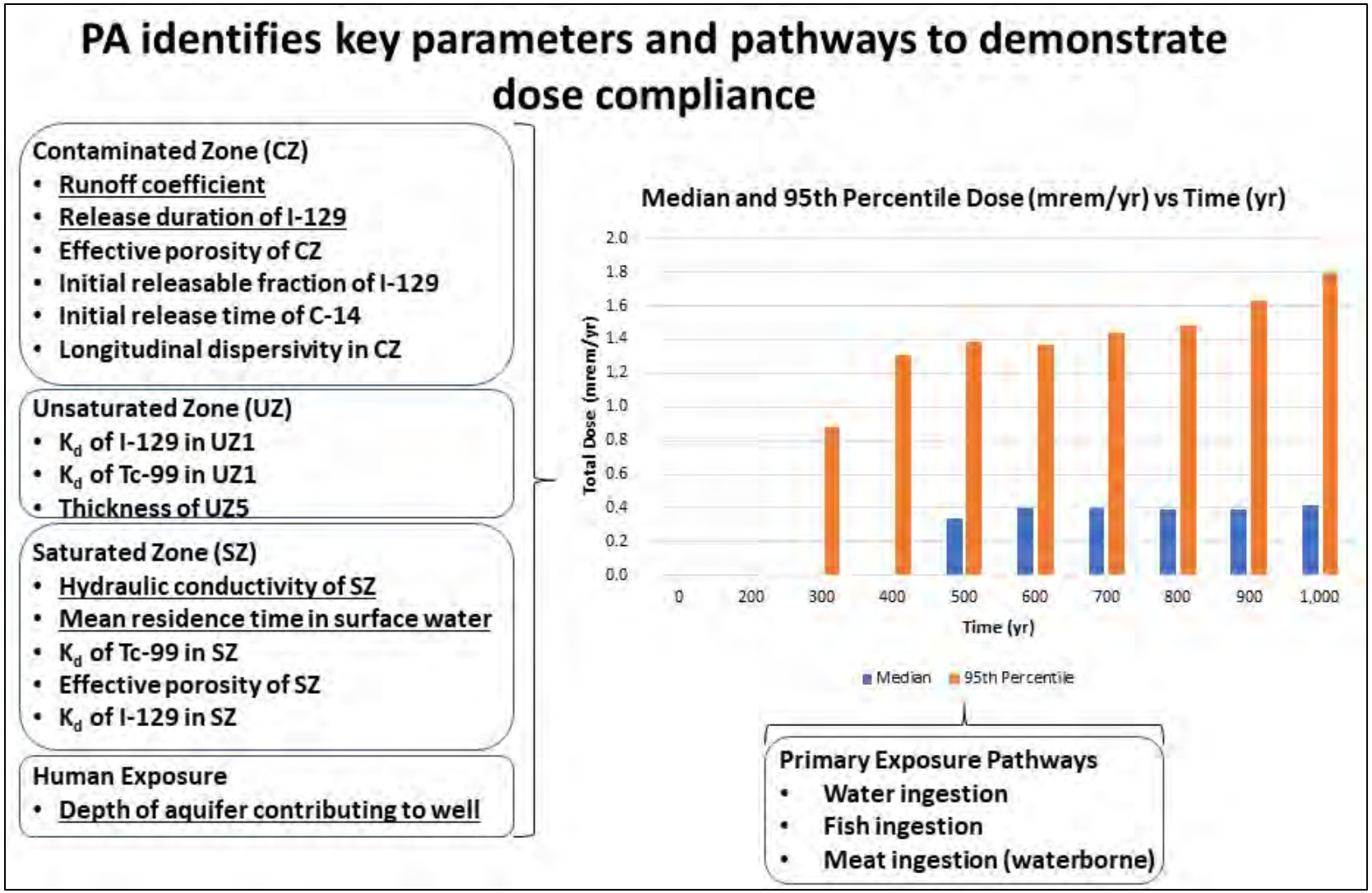

Note: Underlined parameters are the top five factors controlling peak total compliance period dose.

Fig. 5.14. Summary of influential variables, primary exposure pathways, and total dose at select reporting times for the 1000-year compliance period

5.4.2 Probabilistic Results – 10,000-year Simulation Period

This section presents the results of the 10,000-year simulation period probabilistic uncertainty analysis with a focus on results beyond the compliance period. The variation of median, mean, and 95th percentile dose over time for each of the 10 repetitions of 300 simulations is shown on Fig. 5.15. The deterministic base case model all-pathways dose curve is also shown on Fig. 5.15 for comparison to the probabilistic results. Results for the period prior to 1000 years were described in Sect. 5.4.1. The remainder of the simulated period can be divided into an early portion between 1000 and approximately 6000 years, and a later portion extending to 10,000 years. The early portion of the results are dominated by the fission products Tc-99 and I-129 dose contributions, whereas the later (> 6000 years) results reflect the potential impacts of the actinides included in the 10,000-year analysis (Pu-239, U-234, U-235, and U-238).

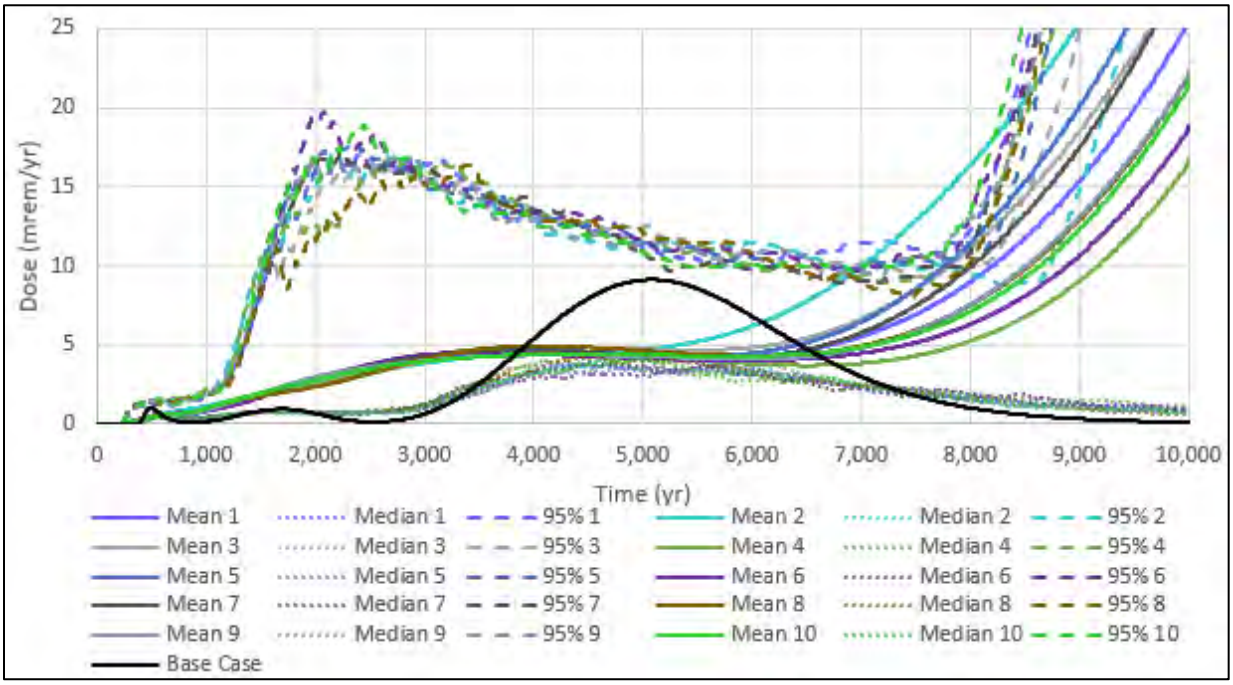

Fig. 5.15. Probabilistic total dose summary for 10 sets of 300 RESRAD-OFFSITE 10,000-year simulations, all pathways, all calculation points

The changing distribution of total dose over time reflects the varying contributions by the fission products and the actinides. The mean total dose increases gradually between 1000 years and approximately 4000 years and then remains nearly steady at just under 5 mrem/year (solid curves on Fig. 5.15). Then the mean total dose increases rapidly beginning at about 6500 years, reaching values that exceed 25 mrem/year by 10,000 years for 5 of the 10 repetitions of 300 simulations. The median simulated total dose approaches the mean total dose around 4500 years and remains below 5 mrem/year throughout the simulation period (dotted curves on Fig. 5.15). The 95th percentile of total dose increases quickly between 1000 and 2000 years to values around 15 mrem/year (fission product dose contributions) and then decreases more gradually through 8000 years. At 8000 years there is a second sharp increase in the 95th percentiles as actinide dose contributions begin to rise and simulated total doses > 25 mrem/year become more frequent. Significant dose contributions from the actinides can occur much earlier than in the deterministic base case, primarily because of lower actinide K_d values, shorter release durations, and greater cover infiltration rates. The divergence of the mean probabilistic dose from the median value (which decreases after 5000 years) reflects the strong negative skew that develops in the distribution of total dose after 5000 years, due to a large proportion of very small total doses and a small proportion of very high doses. Additional discussion

of the factors associated with the occurrence of peak total doses greater than 25 mrem/year for the 10,000-year uncertainty analysis, and the potential for these actinide peaks to be over-estimated by the RESRAD-OFFSITE model is included in Appendix G, Sect. G.6.3.4.

The largest radionuclide dose contributions for Tc-99 occur between 1000 and 2000 years post-closure, whereas for I-129 the largest doses occur between 2000 and 4000 years (refer to Appendix G, Sect. G.6.3.4.2). These fission product contributions combine to produce the period between roughly 2000 and 3000 years during which the 95th percentile of total dose exceeds 15 mrem/year (Fig. 5.15). Peak radionuclide dose statistics for I-129 and Tc-99 are provided in Table 5.4. The average values of peak dose for Tc-99 and I-129 are consistent with the deterministic base case peak values; the median peak probabilistic dose values for Tc-99 and I-129 are essentially the same as the average peak values (refer to Appendix G, Figs. G.56 and G.57). Approximately 90 percent of the peak I-129 doses occur between 2000 and 9700 years, with a mean I-129 peak time of approximately 5200 years. For Tc-99, 90 percent of the 3000 simulated peak doses occur between 900 and 2700 years, with a mean Tc-99 peak time of 1700 years. Approximately 4 percent of the simulated I-129 peak doses exceed 25 mrem/year, whereas Tc-99 peak doses are all less than 2.5 mrem/year. Peak doses greater than 25 mrem/year associated with I-129 are discussed in Appendix G, Sect. G.6.3.4.5.

Table 5.4. Peak radionuclide dose statistics

Radionuclide	Average peak dose (mrem/year)	95th percentile peak dose (mrem/year)
I-129	10.6	23.1
Tc-99	0.94	1.62

Over the 10,000-year simulation period, the median peak total dose (average of the 10 repetitions) is approximately 10 mrem/year. Seventy percent of the peak total doses were distributed evenly between about 2000 and 8000 years, and about 15 percent of the peaks occurred at the end of the simulation period. A total of 379 out of 3000 realizations (approximately 13 percent) produced a peak total dose above 25 mrem/year. Seventy-two percent of the peak total doses that exceeded 25 mrem/year occurred at the end of the simulation period (approximately 10,000 years) suggesting that these peaks were associated with combined contributions of Pu-239 and uranium nuclides. The remaining 28 percent of peak doses greater than 25 mrem/year occur prior to 3800 years. These earlier extreme peaks correspond to dose contributions from (primarily) I-129 and Tc-99. The earlier subset of peak doses (I-129 peaks greater than 25 mrem/year) are generally associated with smaller than average sampled I-129 K_d values (< 3.5 cm^3/g) and with smaller than average sampled release duration. The earlier peaks greater than 25 mrem/year also tend to be associated with larger than average modeled cover infiltration (> 0.88 in./year) and smaller than average values of the saturated zone Darcy velocity (calculated as hydraulic conductivity multiplied by hydraulic gradient, refer to Appendix G, Fig. G.60). This correlation suggests that saturated zone mixing is particularly important in determining the likelihood of peak I-129 dose exceeding 25 mrem/year. This dependence of higher I-129 dose on saturated zone mixing is consistent with the high dose conversion factor for I-129, which reflects potentially large exposures associated with small environmental concentrations. The extreme I-129 dose peaks are probably over-estimated and not likely to be realized given the combination of unrealistically large I-129 source inventory (Appendix B) and the RESRAD-OFFSITE over-estimate of peak I-129 flux to the water table relative to the more detailed STOMP model of release from the vadose zone (refer to Sect. 3.3.5).

These extreme peak total dose values should be viewed with caution given the inherent limitations and uncertainty of the RESRAD-OFFSITE release model. These limitations include the modeled cover

infiltration remaining constant rather than increasing over time, the lack of solubility limits that may lead to overestimated leachate concentrations for uranium species, and the relatively rapid release for radionuclides having $K_d > 1$ cm^3/g produced by the constant cover infiltration rate applied to the instantaneous equilibrium desorption release model. Comparison of STOMP model simulations of U-234 release to the RESRAD-OFFSITE release predictions shows that the predicted peak RESRAD-OFFSITE U-234 flux is over twice as large as the peak STOMP U-234 flux to the water table beneath the EMDF. This difference in U-234 release model predictions suggests that the RESRAD-OFFSITE peak well water concentrations are too uncertain (probably over-estimated) to draw conclusions about the very-long-term performance of the EMDF with respect to less mobile radionuclides ($K_d > 1.0$ cm^3/g) including nuclides of uranium and possibly also I-129.

This page intentionally left blank.

6. INADVERTENT INTRUDER ANALYSIS

6.1 INADVERTENT HUMAN INTRUSION SCENARIOS

Selection of IHI scenarios was guided by consideration of EMDF site characteristics and facility design, as well as review of IHI analyses performed for other historical and proposed LLW disposal facilities on the ORR. Additional details on this IHI analysis and the other PAs that were reviewed are provided in Appendix I. The IHI analysis for the EMDF considers an acute discovery scenario that involves attempted excavation into the final cover for construction of a residence, and acute drilling and chronic post-drilling (agricultural) scenarios that involve direct contact with the waste. A summary of the three IHI scenarios analyzed for the EMDF is provided in Table 6.1.

Table 6.1. Summary of IHI scenarios analyzed for the EMDF

Scenario type/name	DOE O 435.1 performance measure	Exposure scenario description
Acute exposure –discovery (basement excavation)	500 mrem	Intruder initiates excavation into EMDF cover, but stops digging before exposing waste. Exposure to external radiation.
Acute exposure – drilling (water well)	500 mrem	Intruder drills irrigation well through waste and is exposed to waste in exhumed drill cuttings. Exposure to external radiation, inhalation and incidental ingestion of contaminated soil.
Chronic exposure – post-drilling (subsistence garden)	100 mrem/year	Intruder uses contaminated drill cuttings to amend soil in a vegetable garden. Exposure to external radiation, inhalation, and ingestion of contaminated food and soil.

DOE O = U.S. Department of Energy Order
EMDF = Environmental Management Disposal Facility
IHI = inadvertent human intrusion

The IHI analysis assumes that intrusion is an accidental occurrence resulting from a temporary loss of institutional control. The occurrence of accidental intrusion also presumes a loss of societal memory of the ORR and radioactive waste disposal facilities in the area, despite existing long-term stewardship commitments of the DOE and the likelihood of legal controls such as property record restrictions and notices. For each of the IHI scenarios, active institutional controls are assumed to preclude intrusion for the first 100 years following closure of the disposal facility.

Several important assumptions for the intruder analyses are based on the specifics of the EMDF Preliminary Design that are described in Sects. 1.3, 2.2, and Appendix C. The estimated EMDF radionuclide inventory (Appendix B) was used with the RESRAD-OFFSITE code to model doses resulting from these unlikely future intrusion scenarios. The results are used to establish compliance with DOE O 435.1 dose performance measures for IHI (DOE 2001b). The model results can also be used to evaluate the protectiveness of proposed concentration limits for radionuclides, prior to the beginning of EMDF operations.

6.2 INVENTORY SCREENING FOR IHI

The radionuclide inventory screening for the IHI analysis differs from the screening for the radionuclide release scenarios in that the sole screening criterion is a 5-year minimum half-life for radionuclides that are not radioactive progeny. Refer to Fig. 2.44 for an overview of the radionuclide screening process. Additional description of the screening and estimated source concentrations is included in Appendix I, Sect. I.2.2 and Table I.1.

6.3 ACUTE IHI SCENARIOS AND EXPOSURE PATHWAYS

Two acute exposure scenarios were evaluated. The acute discovery scenario assumes that an intruder attempts to excavate a basement for a home on the disposal site, but stops prior to excavating into the waste and moves elsewhere because of the unusual nature of the engineered material layers encountered. The acute drilling scenario assumes that an irrigation well is drilled through the waste, bringing contaminated material to the surface as drill cuttings and causing an acute exposure to the well drillers.

6.3.1 Acute Discovery Scenario (Cover Excavation)

The acute discovery analysis assumes that the intruder begins excavating but stops digging upon reaching the geotextile and HDPE geomembrane layer overlying the amended clay barrier (Fig. 6.1). The discovery and decision to cease digging occurs after excavating through 8 ft of engineered cover materials including the vegetated surface layer, filter layer, biointrusion layer, and lateral drainage layer. It is assumed that 3 ft of undisturbed barrier material remains between the bottom of the excavation and the underlying waste.

For this scenario, only the external radiation exposure pathway (for photon emissions) is considered for the hypothetical intruder. The inhalation and ingestion pathways are not considered because it is assumed that the clay barrier materials in the cover remain undisturbed and saturated and excavation does not penetrate into the waste. Shielding by the clay barrier eliminates alpha and beta-particle exposure.

6.3.2 Acute Drilling Scenario (Irrigation Well)

For the acute drilling scenario (Fig. 6.2), intruders are assumed to drill a well for irrigation on the EMDF. This scenario is highly unlikely given that drilling in more accessible areas at lower elevations would be much more cost effective due to the shallower depth to groundwater. This exposure scenario also assumes that the drilling crew is not deterred by encountering the large rocks in the biointrusion layer, structural steel, concrete, or rebar in the waste zone, or by the exhumation of any of these or other unusual materials in the drill cuttings.

The following exposure pathways were considered for the acute drilling scenario:

- External exposure to radiation from the unshielded drill cuttings that contain waste
- Inhalation of radionuclides suspended in air from the uncovered cuttings containing waste
- Incidental ingestion of soil containing radionuclides from the uncovered cuttings containing waste.

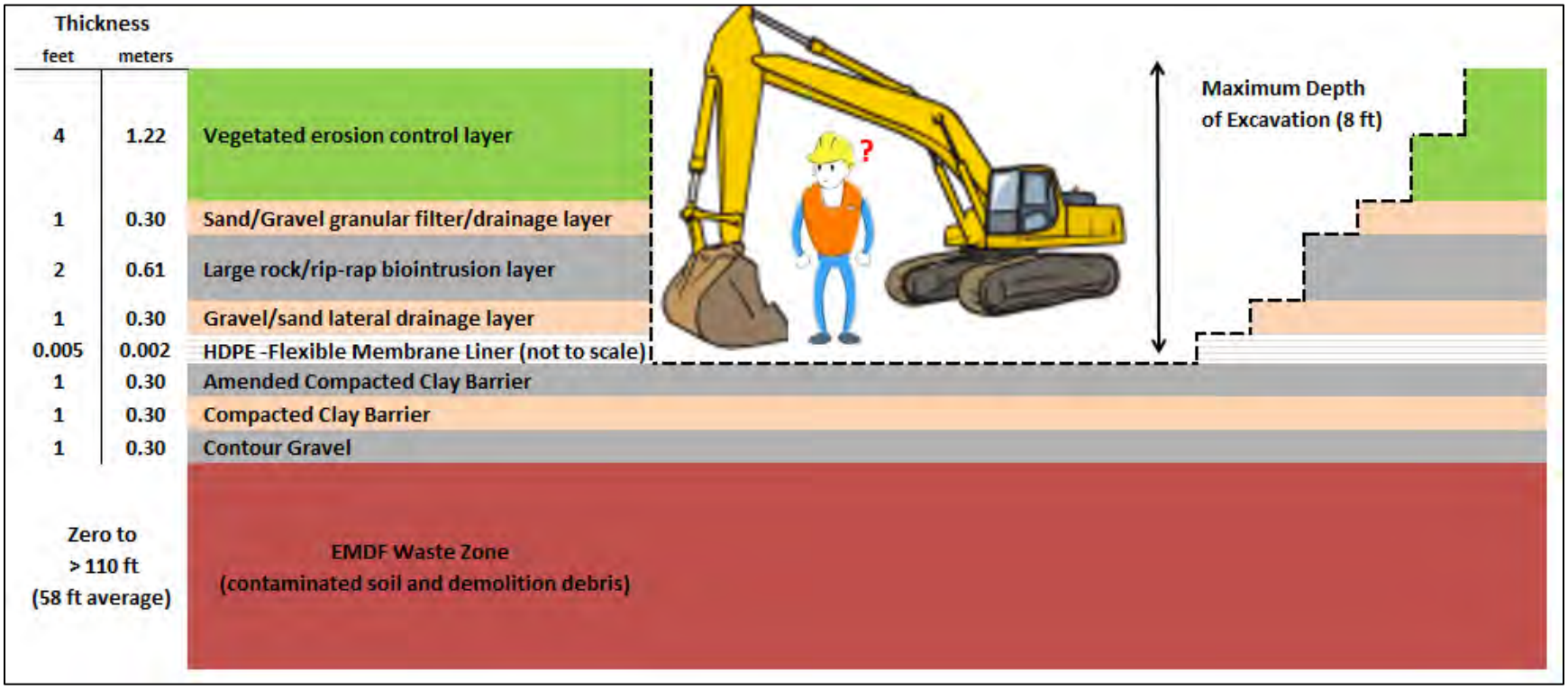

Fig. 6.1. EMDF cover system schematic and acute discovery IHI scenario

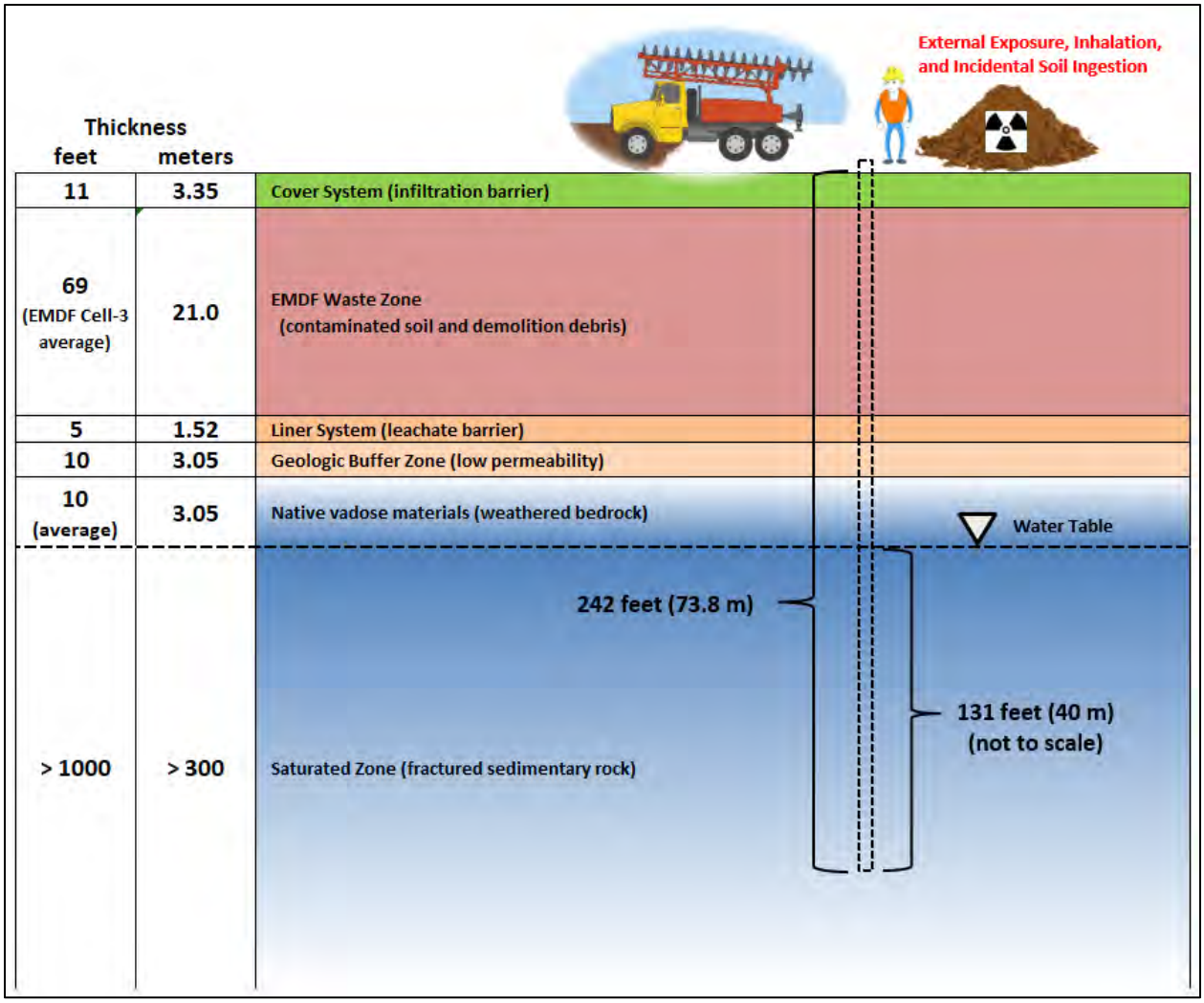

Fig. 6.2. EMDF schematic profile and acute drilling IHI scenario

6.4 CHRONIC IHI SCENARIO AND EXPOSURE PATHWAYS

The chronic IHI scenario selected for the EMDF is a post-drilling exposure to contaminated garden soil and contaminated produce grown in that soil. Intruders are assumed to drill a residential well on the EMDF and to mix the drill cuttings into the garden soil to grow food for human consumption and feed for livestock (Fig. 6.3). This scenario is highly unlikely in terms of the location selected for the well (as for the acute drilling scenario) and in the required assumption that the contaminated cuttings are indistinguishable from native soil and used to amend the garden soil. It is more likely that drill cuttings would be used to build up the area around the well to direct runoff away from the borehole.

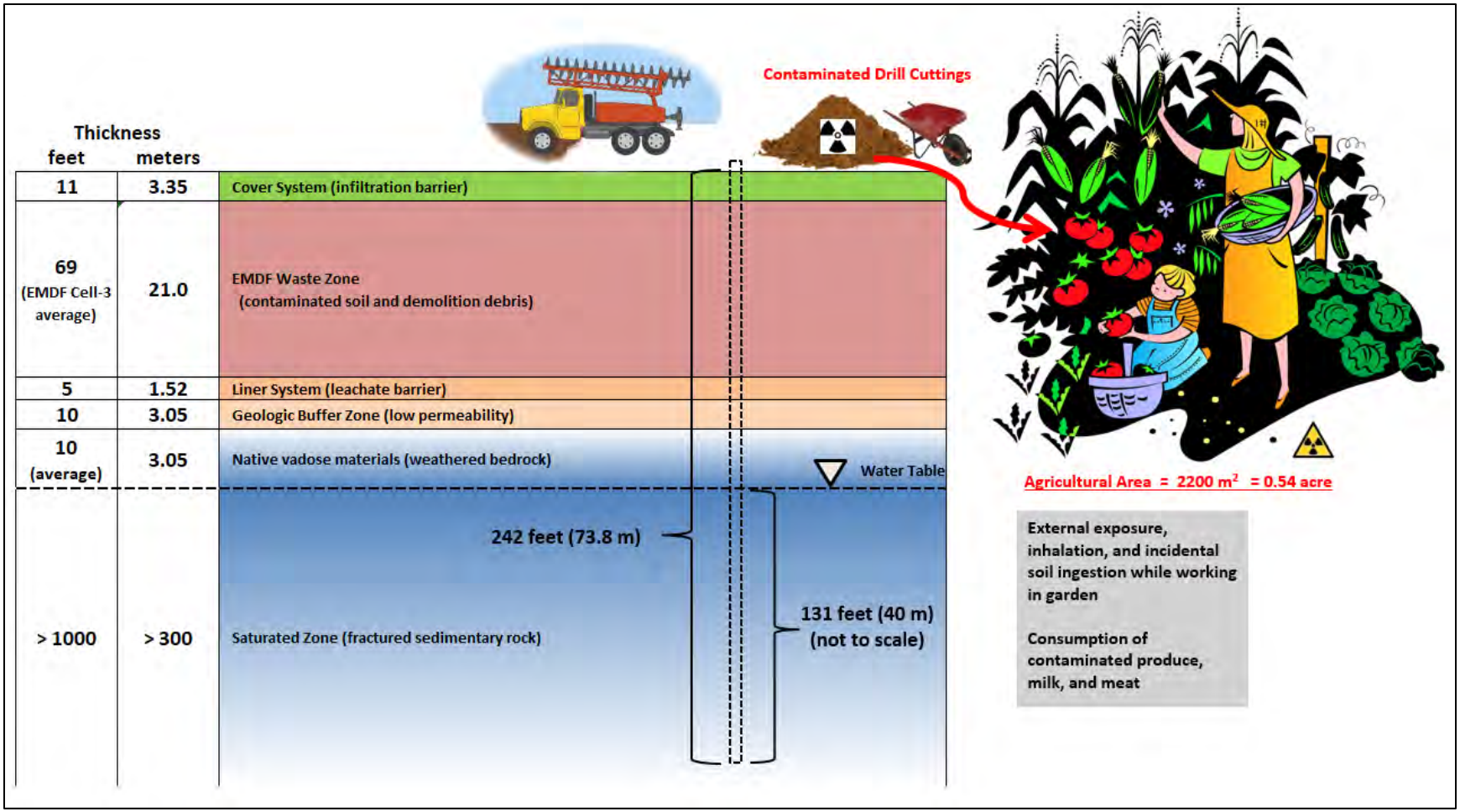

Fig. 6.3. EMDF schematic and chronic post-drilling IHI scenario

The chronic post-drilling scenario only considers exposures after drilling and construction of the residential well. The following exposure pathways were considered:

- Ingestion of vegetables grown in contaminated garden soil
- Ingestion of contaminated garden soil
- External exposure while working in the garden
- Inhalation exposure while working in the garden.

To add conservatism, other exposure pathways that are less likely to occur were also simulated, including:

- Ingestion of contaminated milk from animals eating feed from the garden
- Ingestion of contaminated meat from animals eating feed from the garden.

Groundwater transport pathways are not included in the IHI scenarios and are not modeled, consistent with *Disposal Authorization Statement and Tank Closure Documentation* (DOE 2017a) guidance. Radionuclide release associated with groundwater and surface water pathways is considered in the all pathways dose analysis of this PA (Sect. 4.5) and is evaluated relative to the 25 mrem/year performance objective for public protection. Similarly, the water resource protection analysis (Sect. 4.7) evaluates potential impacts to groundwater and surface water relative to applicable water quality standards.

6.5 IHI SCENARIO MODELING

The RESRAD-OFFSITE Version 3.2 model (Gnanapragasam and Yu 2015) was used for estimating doses to a hypothetical inadvertent intruder under each of the three exposure scenarios. For the modeling of IHI dose, it is assumed that the waste disposal in the EMDF is completed at time zero, the site is under active institutional control for the next 100 years, and that inadvertent intrusion can occur at any time after loss of active control of the site. RESRAD-OFFSITE simulations were completed to 10,000 years to provide information on long-term increases in predicted dose that occur following the 1000-year compliance period.

In general, simulation of IHI exposure using the RESRAD-OFFSITE model involves assumptions required for the calculation of average radionuclide concentrations in exhumed drill cuttings or garden soil and selection of the relevant exposure pathways for each exposure scenario. For all of the IHI scenario modeling, the RESRAD-OFFSITE release rate (leach rate for the first-order release model option) was set to zero to effectively eliminate leaching of contamination from the waste and to provide a conservative bias toward higher estimated dose. Similarly, precipitation input was set to the near-zero value of 1E-06 m/year and irrigation of the garden area was assumed to be zero for the chronic well drilling scenario. Loss of contaminated materials (cuttings or garden soil) due to erosion was not included in the analysis.

RESRAD-OFFSITE model setup and key parameter assumptions for each scenario are summarized in the following sections and described in detail in Appendix I, Sect. I.4. Additional detail on model parameterization and supporting calculations are provided in the QA documentation for the IHI analyses (UCOR 2020b).

6.5.1 Acute Discovery Scenario

The acute discovery scenario assumes that an intruder attempts to excavate a basement for a home on the disposal site. The key assumption is that the intruder stops excavation activities upon reaching the geotextile

cushion and HDPE geomembrane below the drainage layer, leaving 3 ft of earthen materials between the bottom of the excavation and the underlying waste.

For the EMDF analysis, only the dose resulting from external exposure to radiation that penetrates the residual materials (lower 3 ft of 11-ft EMDF total cover thickness) overlying the waste is modeled (Fig. 6.1). Formulation of the expression for calculating dose due to external radiation is given in the RESRAD-OFFSITE User's Manual (Yu et al. 2007, pages 6-1 to 6-2). Mathematical expressions for the conceptual model of the zone of primary contamination including a clean cover layer on top of the waste are described in detail in the user's manual for RESRAD-OFFSITE Version 2 (Yu et al. 2007, pages 2-1 to 2-3). The materials of the EMDF cover layer are assumed to remain uncontaminated because processes that could lead to contamination of the cover material such as bioturbation by burrowing animals are inhibited by the overall thickness of the cover design and robust biointrusion barrier.

Important assumptions and calculated parameter values for the EMDF acute discovery scenario modeling include the thickness of clean cover material overlying the waste (3 ft) and the assumption that excavation ceases after encountering the HDPE membrane at the interface between the lateral drainage layer and the amended clay barrier. Excavation for the acute discovery scenario is assumed to take place over 10 8-hour days for a total of 80 hours. To provide additional bias toward higher dose estimates, it is also assumed that the maximum depth of excavation is completed over the full basement area immediately, after which exposure to external radiation occurs over the assumed duration of excavation.

6.5.2 Acute Well Drilling Scenario

The acute well drilling scenario assumes that an intruder drills an irrigation well directly through a disposal unit (Fig. 6.2). The acute well drilling scenario only considers exposures during the short period of time for drilling and construction of the well, during which the hypothetical intruder could be exposed to unshielded cuttings for an extended period. Exposure to external radiation, inhalation of contaminated particulates, and (incidental) soil ingestion by a member of the drill crew is assumed to occur during the period of drilling and distribution of the drill cuttings (both clean and contaminated).

The RESRAD-OFFSITE model simulation of external exposure, inhalation, and (incidental) soil ingestion requires specifying the thickness and radionuclide concentrations of the drill cuttings to which a driller would be exposed as well as the duration of (acute) exposure. Mathematical expressions for the conceptual model of the zone of primary contamination are described in detail in the User's Manual for RESRAD-OFFSITE, Version 2 (Yu et al. 2007, pages 2-1 to 2-3). The thickness of the clean cover is assumed to be zero. Assumed values for atmospheric particulate loading and soil ingestion during drilling are also required. Formulation of the expressions for calculating dose due to external radiation and inhalation of contaminated dust are also given in the RESRAD-OFFSITE User's Manual (Yu et al. 2007, pages 6-1 to 6-3). Similarly, formulation of the expressions for calculating dose due to incidental ingestion of contaminated soil is given on pages 6-4 and 6-5 of the User's Manual.

Important assumptions and calculated parameter values for the EMDF acute well drilling scenario include the waste thickness at the well location (68.7 ft), and the average waste thickness in EMDF disposal cell #3 based on the EMDF Preliminary Design (UCOR 2020b). The average EMDF waste thickness is approximately 57.5 ft, and the maximum thickness is approximately 113 ft. The assumed thickness of waste at the well location is used to adjust the as-disposed waste concentrations to account for co-mingling of clean drill cuttings with waste as materials are brought to the surface. The borehole is assumed to be completed at a depth equivalent to 131 ft below the estimated water table elevation, or 242 ft below the surface of the disposal facility. The calculated dilution factor applied to the post-operational activity concentrations is thus equal to 68.7 ft/242 ft, or 0.284.

The borehole diameter is assumed to be 18 in., which is representative of a well designed for irrigation in East Tennessee. Use of the 18-in. diameter for the acute drilling scenario provided a degree of pessimistic bias to offset some of the uncertainty associated with simplification of the complex external exposure to drill cuttings applied in the acute scenario. The total combined volume of waste and clean drill cuttings based on the assumed borehole length and diameter is 427 ft^3. The mixed clean cuttings and exhumed waste from the borehole are assumed to be distributed over an area centered on the bore hole of 2150 sq ft, resulting in an average thickness of 0.20 ft (2.4 in.). This value is input as the thickness of the primary contamination for the RESRAD-OFFSITE dose analysis. Sensitivity of the modeled dose to assumptions that affect the calculated average thickness of cuttings is addressed in Sect. 6.6.2.

For the acute drilling scenario, the duration of exposure is assumed to be 30 hours, the equivalent of three 10-hour working days. A more realistic assumption for the time required to drill an approximately 250-ft-deep well using typical drilling equipment would be less than 30 hours. The calculated occupancy factor for the RESRAD-OFFSITE model (outdoor annual time fraction on primary contamination) is 0.0034 = (30 hours/year)/ [(365.25 days/year) × (24 hours/day)].

For both the acute drilling and chronic post-drilling scenarios, the incidental soil ingestion rate is assumed to be 100 mg/day, consistent with the RESRAD-OFFSITE default value and the EPA recommended value for outdoor workers. The average mass loading of airborne particulates for estimating inhalation exposure for both the acute drilling and chronic post-drilling scenarios was assumed to be 0.001 g/m^3, a value representative of construction activities (Maheras et al. 1997). The annual inhalation rate for both scenarios was set at the RESRAD-OFFSITE default value of 8400 m^3/year.

6.5.3 Chronic Post-drilling Scenario

The chronic post-drilling scenario assumes that a hypothetical intruder drills a residential well directly through the disposal unit and then mixes contaminated drill cuttings into the soil in a garden used to grow food for people and livestock (Fig. 6.3). The chronic IHI scenario only considers exposure that follows drilling and construction of the well. Exposure to contaminated soil (external radiation, inhalation and soil ingestion) occurs during the portion of time that the intruder works in the garden.

The RESRAD-OFFSITE model simulation of exposure to contaminated soil and ingestion of contaminated food requires specifying the thickness and radionuclide concentrations of the garden soil, as well as the duration of exposure. Mathematical expressions for the conceptual model of the zone of primary contamination are described in detail in the User's Manual for RESRAD-OFFSITE Version 2 (Yu et al. 2007, pages 2-1 to 2-3). The thickness of the clean cover is assumed to be zero. Assumed values for atmospheric particulate loading and soil ingestion during gardening are also required. Formulation of the expressions for calculating dose due to external radiation and inhalation of contaminated dust are also given in the RESRAD-OFFSITE User's Manual (Yu et al. 2007, pages 6-1 to 6-3). Similarly, formulation of the expressions for calculating dose due to of contaminated soil and food is given on pages 6-4 and 6-5 of the User's Manual.

Key assumptions and calculated parameter values for the chronic well drilling scenario include waste thickness at the well location (68.7 ft), borehole depth (242 ft), and incidental soil ingestion rate (100 mg/day), which are identical to those made for the acute drilling scenario. Inhalation parameter values are also identical to the acute drilling scenario. Values for agricultural and animal product (beef, poultry, eggs, milk) transfer factors are set to values published by PNNL (2003), which are identical to the values used in the base case model.

The borehole diameter is assumed to be 12 in., which is representative of a well designed for residential use in the region. The resulting volume of exhumed waste is 54 ft^3. The 12-in. residential water well

diameter is reasonable for the chronic IHI analysis given that the hilltop location assumed for the well construction is more appropriate for a residential supply well than an irrigation well with a larger diameter.

The total volume of contaminated drill cuttings is assumed to be completely and uniformly tilled into uncontaminated surface soil to a depth of 1 ft over an area of approximately one-half acre (2200 m^2). Average radionuclide concentrations in the amended garden soil are calculated by applying a dilution factor equal to the ratio of the volume of waste contained in drill cuttings to the total volume of uncontaminated garden soil: 54 ft^3 / (1 ft × 23,668 sq ft) = 0.00228 or approximately 0.2 percent. Calculate post-operational radionuclide concentrations (Sect. 4.2) are multiplied by the tilling dilution factor to give the input soil concentrations for the RESRAD-OFFSITE dose analysis. This approximation assumes that the volume of cuttings is negligible compared to the total soil volume, and neglects any difference in the average dry bulk densities of the waste and the garden soil. The implications of using this simplified calculation of the tilling dilution factor for the intruder dose analysis are addressed in Sect. 6.6 in the context of uncertainty and overall pessimistic bias in dose calculations.

The fraction of feed for livestock obtained from the contaminated garden is conservatively assumed to be 0.5 (50 percent). The fraction of milk consumed from the dairy cows raised on the contaminated area is assumed to be 0.5 (50 percent) and the fraction of meat (beef, poultry, eggs) from the contaminated area is assumed to be 0.25 (25 percent). The fractional duration of exposure for the external radiation, inhalation, and soil ingestion pathways is assumed to be 1/6, equivalent to 4 out of every 24 hours. This value is consistent with the (pessimistic) assumption that 50 percent of food consumed by the intruder is grown in the contaminated garden soil.

6.6 INTRUDER ANALYSIS RESULTS

6.6.1 Acute Discovery Scenario Results

Predicted dose as a function of time of intrusion for the acute discovery scenario is presented in Fig. 6.4. The total dose (i.e., dose from all simulated radionuclides summed) at 100 years post-closure is 1.3E-04 mrem. Total dose decreases to a minimum of 6.7E-05 mrem at approximately 540 years, and then gradually increases through 10,000 years as concentrations of radioactive progeny increase. Total dose at 10,000 years is 2.5E-04 mrem. The predicted dose is extremely sensitive to the assumed thickness of the uncontaminated material (clean cover) overlying the waste. Decreasing the assumed thickness from 3 ft to 1 ft increases the dose by three orders of magnitude (dashed curve in Fig. 6.4). This sensitivity case represents the assumption that a 10-ft-deep basement excavation is completed in the EMDF cover, which results in estimated dose that is three to four orders of magnitude smaller than the acute intrusion performance measure of 500 mrem.

Primary contributors to the acute discovery IHI dose prior to 1000 years post-closure include Th-232, and initially (at 100 years) Cs-137 and U-232 (Fig. 6.5). After 1000 years, other isotopes of uranium, particularly U-234 and progeny, become proportionally significant and eventually predominant dose contributors.

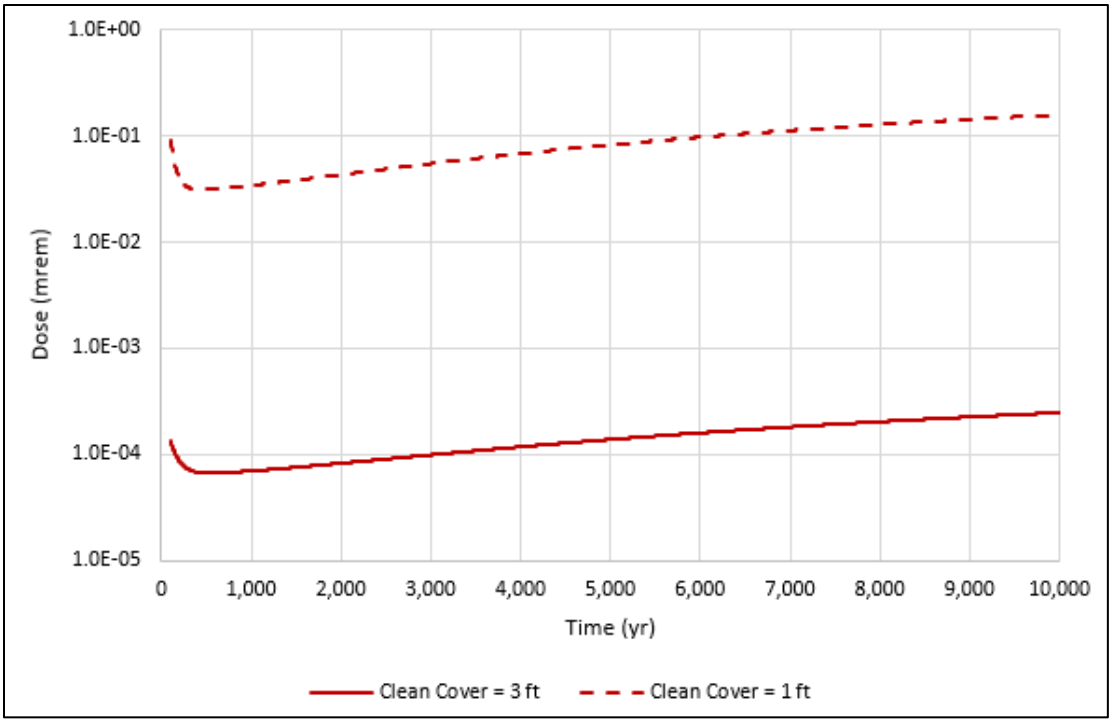

Note: Vertical axis is logarithmic for clarity.

Fig. 6.4. Acute discovery scenario total dose (all radionuclides summed)

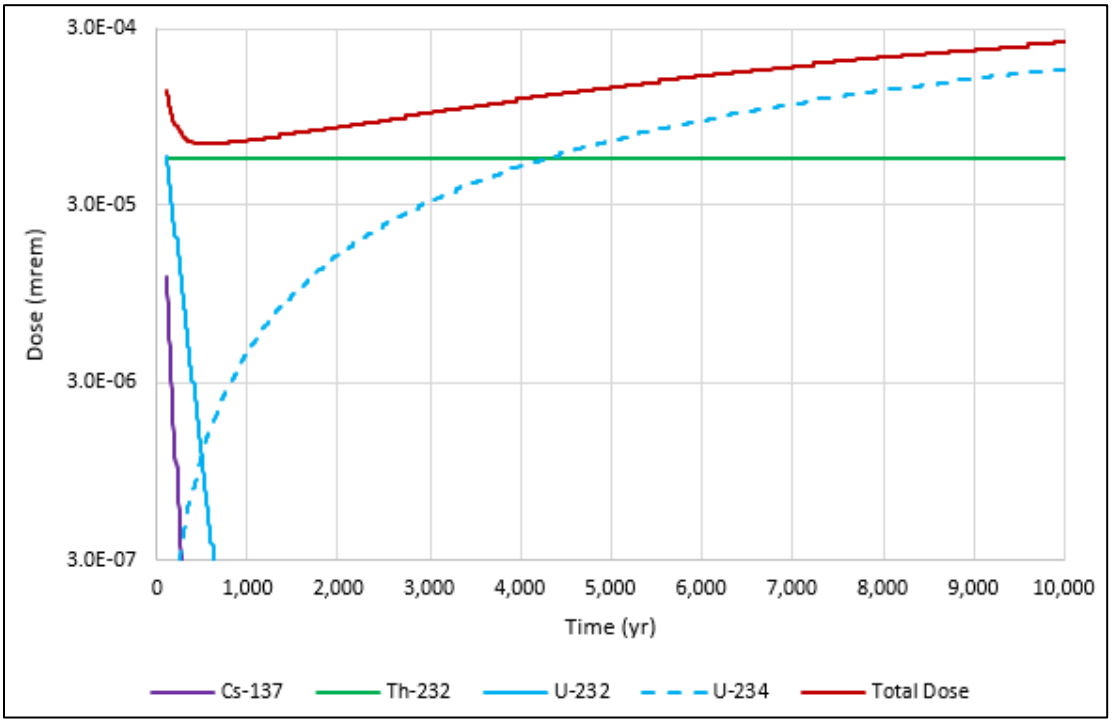

Note: Vertical axis is logarithmic for clarity.

Fig. 6.5. Acute discovery scenario dose contributions by radionuclide

6.6.2 Acute Well Drilling Scenario Results

Predicted dose as a function of time of intrusion for the acute drilling scenario is presented in Fig. 6.6. The total dose (all radionuclides and pathways summed) at 100 years post-closure is 0.38 mrem. Total dose decreases to a minimum of 0.17 mrem at approximately 600 years and then gradually increases through 10,000 years as concentrations of radioactive progeny increase. Total dose at 10,000 years is 0.42 mrem.

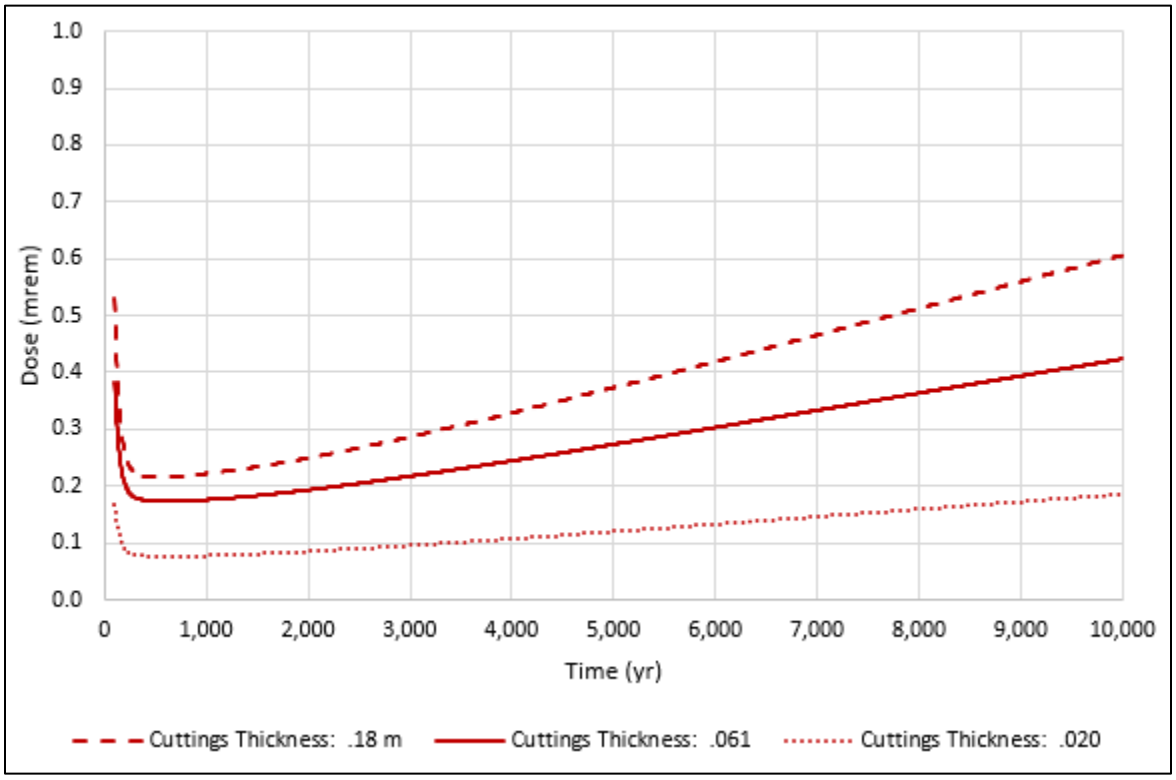

Fig. 6.6. Acute well drilling scenario total dose (all radionuclides and pathways summed)

The dotted and dashed curves shown on Fig. 6.6 represent model sensitivity to the calculated value for the thickness of mixed drill cuttings and indicate dose associated with the thickness increased by a factor of 3 (dashed) and decreased by a factor of 3 (dotted). For the increased thickness of cuttings (0.18 m), the acute dose remains less than 1 mrem between 100 and 10,000 years, a value much less than the acute intrusion performance measure of 500 mrem. Parameter values that affect the calculated average thickness of cuttings include borehole depth and diameter and the area over which cuttings are spread.

Figure 6.7 presents the dose contributions for each of the simulated exposure pathways for the acute drilling scenario: external (direct) radiation, inhalation, and incidental soil ingestion. The direct external dose (solid red curve) is the largest contributor to the total dose during the simulation period, whereas soil ingestion contributes least to the total acute drilling intruder dose.

Primary contributors to the acute drilling IHI dose prior to 1000-year post-closure include U-235, U-238, Th-232, and Cs-137 (Fig. 6.8). The increase in dose after 500 years is driven by U-234, U-235, and their progeny. Radionuclides of thorium and plutonium contribute proportionally significant, but much smaller doses through 10,000 years.

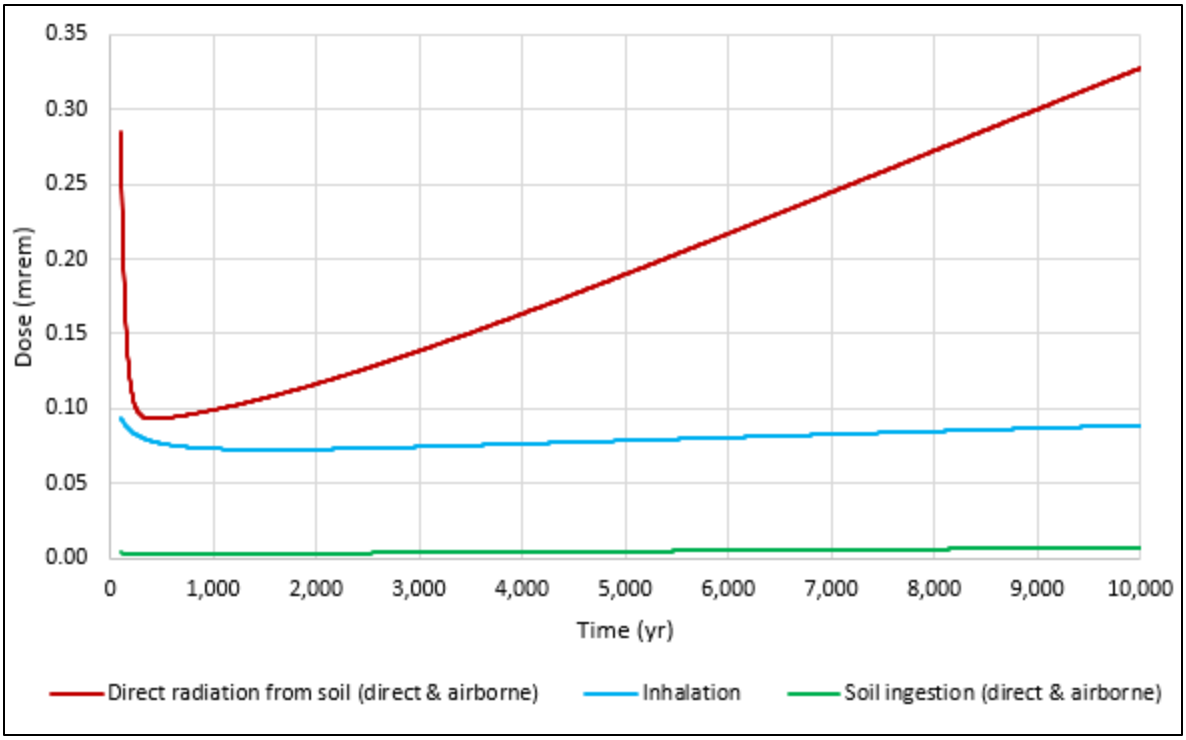

Fig. 6.7. Acute well drilling scenario radiological dose by exposure pathway for all radionuclides summed

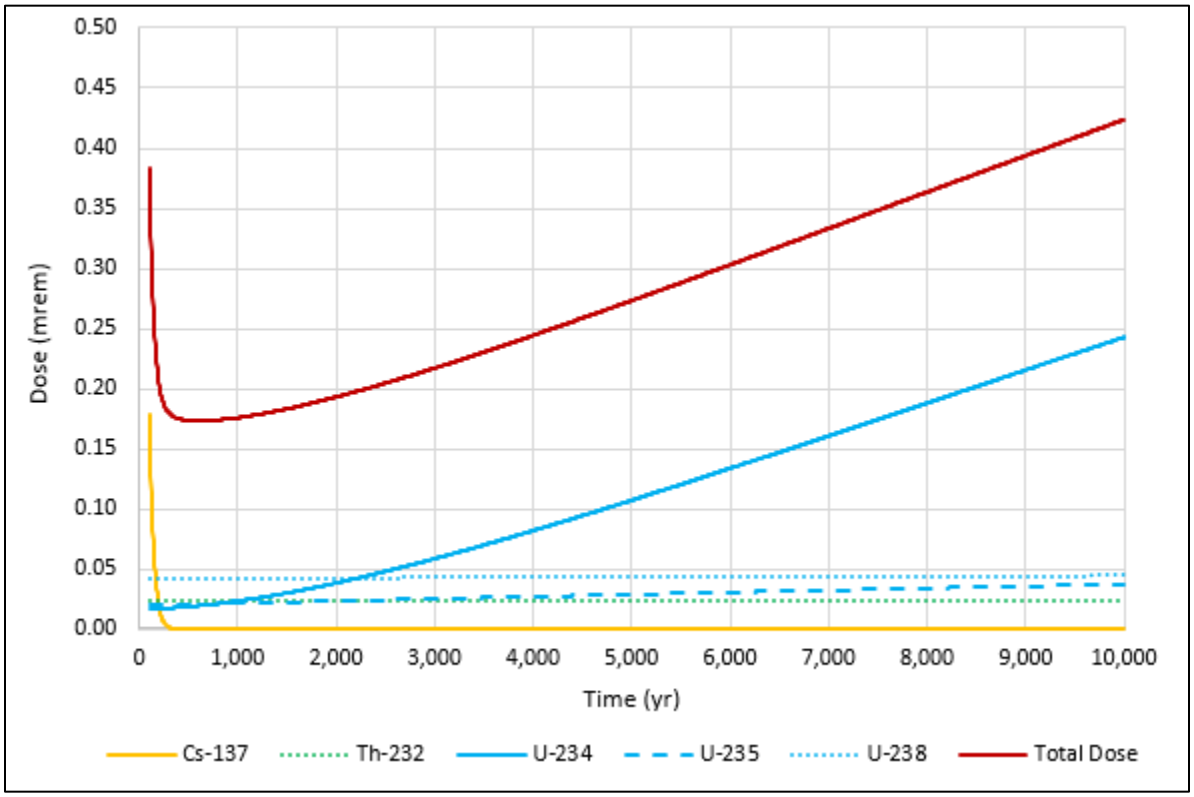

Fig. 6.8. Acute well drilling scenario dose contributions by radionuclide

6.6.3 Chronic Post-drilling Scenario Results

Predicted dose as a function of time of intrusion for the chronic drilling scenario is presented in Fig. 6.9. The total dose (all radionuclides and pathways summed) at 100 years post-closure is 3.56 mrem/year. Total dose decreases to a minimum of 2.95 mrem/year at approximately 340 years and gradually increases through 10,000 years as concentrations of radioactive progeny increase. Total dose at 10,000 years is 8.24 mrem/year. The maximum predicted dose is a factor of 10 lower than the chronic IHI performance measure of 100 mrem/year.

Figure 6.10 presents the dose contributions for each of the simulated exposure pathways for the chronic drilling scenario: direct radiation from garden soil, ingestion of plants, meat, and milk, inhalation, and incidental soil ingestion. The direct external and meat ingestion dose contributions comprise 90 percent or more of the total dose (dashed black curve). Plant ingestion, milk ingestion, and inhalation together comprise 2 to 7 percent. The contribution of soil ingestion (< 1 percent of the total dose) is negligible relative to the chronic IHI performance measure of 100 mrem/year.

Primary contributors to the chronic post-drilling IHI dose prior to 1000-year post-closure include U-234, U-238, Cs-137, and U-235 (Fig. 6.11). After 500 years total dose is driven by U-234, U-238, and their associated progeny.

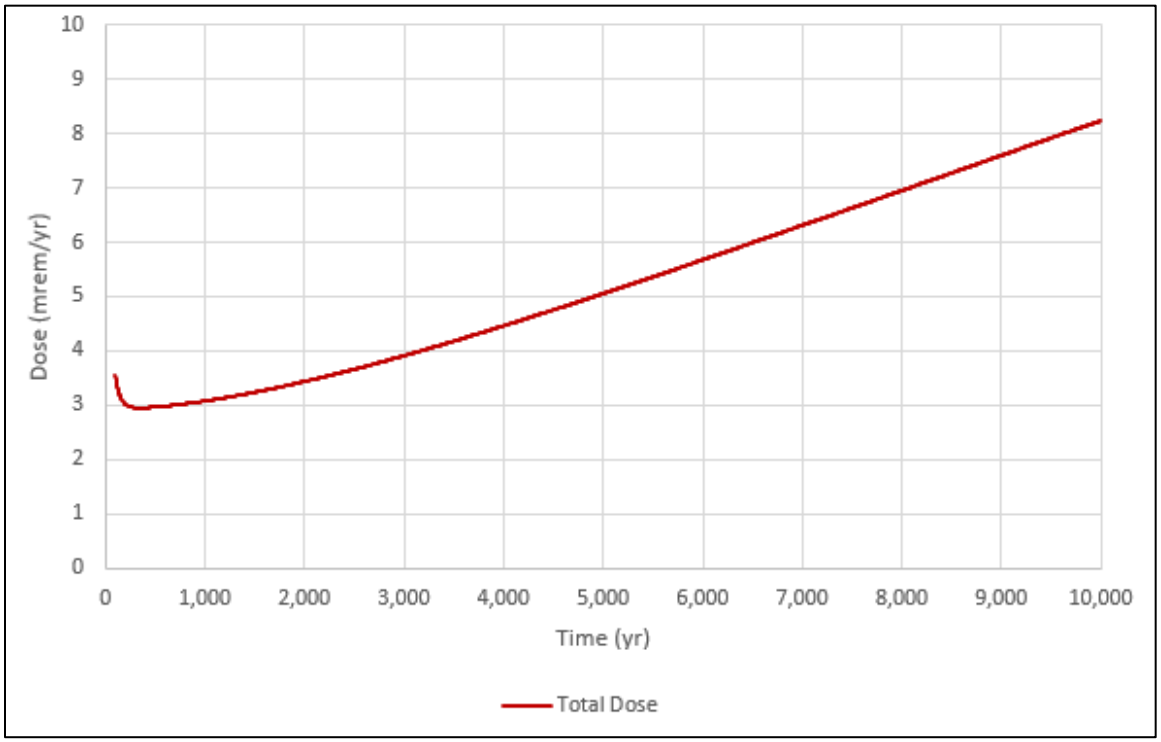

Fig. 6.9. Chronic post-drilling scenario total dose (all radionuclides and pathways summed)

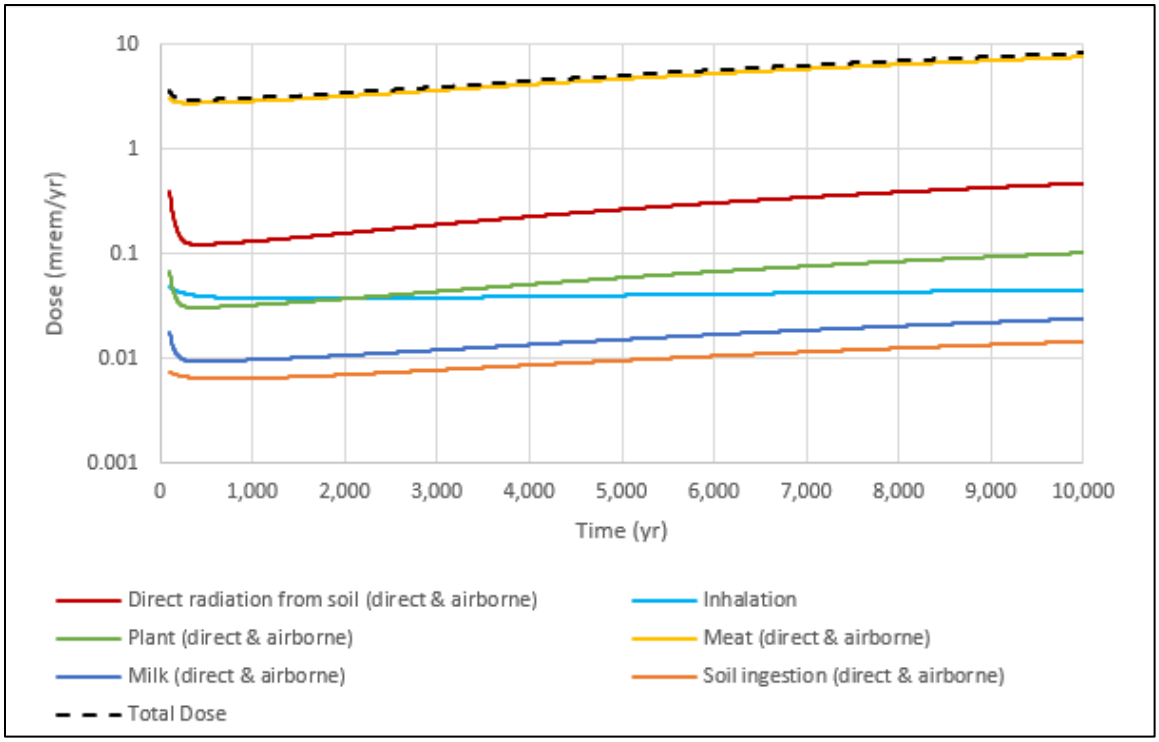

Note: Vertical axis is logarithmic for clarity.

Fig. 6.10. Chronic post-drilling scenario total dose and dose contributions by pathway

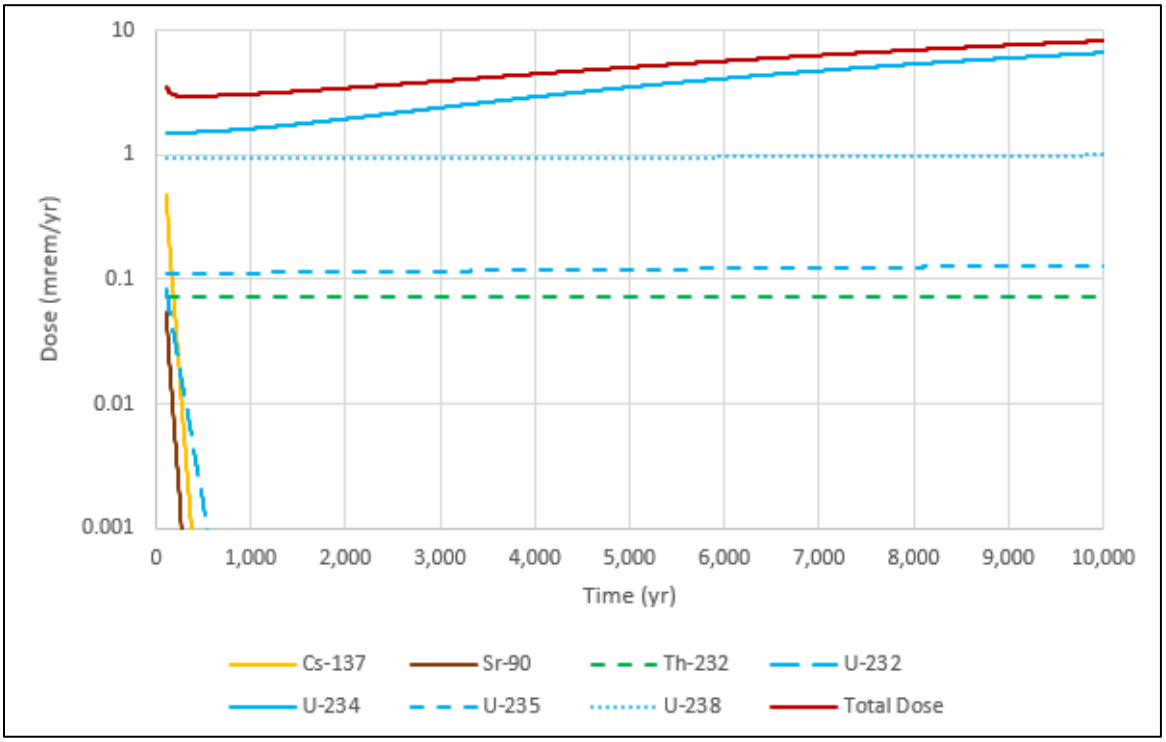

Note: Vertical axis is logarithmic for clarity.

Fig. 6.11. Chronic post-drilling scenario dose contributions by radionuclide

6.7 SUMMARY OF RESULTS AND RESRAD-OFFSITE SINGLE RADIONUCLIDE SOIL GUIDELINES

With respect to performance measures for IHI, the EMDF analysis suggests that, based on the current estimated EMDF radionuclide inventory, there is a reasonable expectation that the facility design will protect a future inadvertent human intruder for the specific IHI scenarios considered. The analysis is pessimistic in that DOE is expected to maintain control of the EMDF site indefinitely into the future.

The dose analysis suggests that, based on the estimated EMDF inventory, IHI-based radionuclide concentration limits (WAC) are not required to meet the DOE M 435.1-1 performance measures for exposure from IHI.

A summary of the results of the IHI modeling results for the period from 100 to 10,000 years post-closure is shown in Table 6.2.

Table 6.2. Summary of modeled doses for acute and chronic EMDF IHI scenarios

EMDF IHI scenario	DOE O 435.1 IHI performance measure	Modeled EMDF dose range (100-10,000 years post-closure)
Acute exposure – discovery (excavation)	500 mrem	6.7E-05 to 2.5E-04 mrem
Acute exposure – drilling (water well)	500 mrem	1.7E-01 to 4.2E-01 mrem
Chronic exposure – post-drilling (subsistence garden)	100 mrem/year	3.0E+00 to 8.2E+00 mrem/year

DOE O = U.S. Department of Energy Order
EMDF = Environmental Management Disposal Facility
IHI = inadvertent human intrusion

IHI analyses provide one basis for setting radionuclide concentration limits to ensure protection of members of the public. RESRAD-OFFSITE SRSGs are calculated activity concentrations that meet a specific dose target for a single radionuclide at a specific time, based on the modeled scenario. The SRSGs do not depend on the assumed radionuclide concentrations or the corresponding modeled doses, but only on the target dose value and the specific exposure scenario considered. Thus, the SRSGs are dose-based radionuclide concentration limits for the particular system and scenario simulated.

For the IHI scenarios presented here, the most restrictive (lowest) SRSG values are based on the 100 mrem/year dose measure associated with the chronic drilling exposure scenario. For most radionuclides, the minimum SRSG within this period occurs at either 100 or 1000 years post-closure. This approach was taken for all radionuclides except for C-14. Carbon-14 is a highly mobile radionuclide that easily transitions to the gaseous or dissolved form. In the acute and chronic drilling scenarios, the dispersed drill cuttings are exposed to the atmosphere, which causes the C-14 to volatilize from the soil completely within the first five years of the simulation. Due to the volatility of C-14, the minimum SRSG between 100 and 1000 years was calculated by adjusting the SRSG at year 0 for 100 years of radioactive decay. A detailed description of how the C-14 SRSG was calculated is provided in the QA documentation for the IHI analysis (UCOR 2020b).

The correct application of the predicted SRSG to set or evaluate waste concentration limits based on the IHI dose must account for the assumed dilution of radionuclides when mixed with the uncontaminated materials when being placed in the facility and when they are exhumed and mixed with clean drill cuttings or garden soil. The source SRSG values output by the RESRAD-OFFSITE model are divided by the dilution factor(s) applied to the waste concentrations in the IHI analysis to derive corresponding SRSG values for comparison to as-disposed (including clean fill) or as-generated activity concentrations. SRSGs calculated

for C-14, H-3, I-129, and Tc-99 are not back-adjusted to account for potential activity loss during operations as a conservative measure biased towards lower SRSGs. Table 6.3 presents the SRSG values for both the acute drilling and chronic post-drilling scenarios. The minimum SRSG values occur at 100 years post-closure unless indicated otherwise in Table 6.3. After accounting for the assumed dilution, as-disposed and as-generated SRSG values for the chronic post-drilling scenario are less than the as-disposed and as-generated SRSG values for the acute drilling scenario for all radionuclides.

Table 6.3. RESRAD-OFFSITE SRSG for acute drilling and chronic post-drilling IHI scenarios

Radionuclide	Acute drilling source SRSG (pCi/g)	Acute drilling as-disposed SRSG (pCi/g)	Acute drilling as-generated SRSG (pCi/g)	Chronic post-drilling source SRSG (pCi/g)	Chronic post-drilling as-disposed SRSG (pCi/g)	Chronic post-drilling as-generated SRSG (pCi/g)
Ac-227	2.08E+06	7.31E+06	1.38E+07	2.96E+03	1.30E+06	2.45E+06
Am-241	6.05E+05	2.13E+06	4.01E+06	1.27E+03	5.55E+05	1.05E+06
Am-243	1.78E+05	6.26E+05	1.18E+06	2.90E+02	1.27E+05	2.39E+05
Ba-133	1.00E+08	3.52E+08	6.64E+08	1.24E+05	5.45E+07	1.03E+08
Be-10	1.74E+08	6.13E+08	1.15E+09	1.36E+04	5.98E+06	1.13E+07
C-14[a]	2.79E+09[b]	9.83E+09[b]	1.85E+10[b]	7.07E+01[b]	3.10E+04[b]	5.84E+04[b]
Ca-41	1.72E+10	6.04E+10	1.14E+11	5.13E+03	2.25E+06	4.24E+06
Cf-249	1.24E+05	4.36E+05	8.22E+05	1.80E+02	7.92E+04	1.49E+05
Cf-250	7.69E+07	2.71E+08	5.10E+08	1.47E+05	6.45E+07	1.21E+08
Cf-251	2.02E+05	7.11E+05	1.34E+06	3.65E+02	1.60E+05	3.01E+05
Cm-243	2.98E+06	1.05E+07	1.98E+07	4.76E+03	2.09E+06	3.93E+06
Cm-244	3.58E+07	1.26E+08	2.37E+08	7.72E+04	3.39E+07	6.38E+07
Cm-245	2.13E+05[c]	7.48E+05[c]	1.41E+06[c]	4.00E+02[c]	1.75E+05[c]	3.30E+05[c]
Cm-246	5.55E+05	1.95E+06	3.68E+06	1.13E+03	4.97E+05	9.35E+05
Cm-247	1.12E+05[c]	3.93E+05[c]	7.40E+05[c]	1.55E+02[c]	6.81E+04[c]	1.28E+05[c]
Cm-248	3.14E+04	1.11E+05	2.08E+05	3.58E+01	1.57E+04	2.96E+04
Co-60	1.05E+10	3.69E+10	6.94E+10	1.06E+07	4.65E+09	8.76E+09
Cs-137	8.82E+05	3.10E+06	5.84E+06	5.30E+02	2.32E+05	4.38E+05
Eu-152	7.42E+06	2.61E+07	4.92E+07	8.21E+03	3.60E+06	6.78E+06
Eu-154	1.31E+08	4.62E+08	8.71E+08	1.44E+05	6.33E+07	1.19E+08
H-3[a]	3.35E+13	1.18E+14	2.22E+14	1.30E+06	5.72E+08	1.08E+09
I-129[a]	1.23E+07	4.31E+07	8.12E+07	1.38E+01	6.06E+03	1.14E+04
K-40	3.22E+05	1.13E+06	2.13E+06	4.10E+01	1.80E+04	3.39E+04
Mo-93	2.67E+08	9.39E+08	1.77E+09	1.26E+02	5.52E+04	1.04E+05
Nb-93m	1.34E+11	4.70E+11	8.85E+11	3.57E+07	1.57E+10	2.95E+10
Nb-94	3.19E+04	1.12E+05	2.11E+05	3.61E+01	1.59E+04	2.99E+04
Ni-59	2.57E+09	9.04E+09	1.70E+10	1.72E+05	7.56E+07	1.42E+08
Ni-63	2.69E+10	9.45E+10	1.78E+11	1.46E+05	6.39E+07	1.20E+08
Np-237	1.82E+05[d]	6.42E+05[d]	1.21E+06[d]	2.35E+02[c]	1.03E+05[c]	1.94E+05[c]
Pa-231	6.06E+04[d]	2.13E+05[d]	4.01E+05[d]	9.40E+01[d]	4.12E+04[d]	7.77E+04[d]
Pb-210	3.12E+07	1.10E+08	2.07E+08	4.72E+01	2.07E+04	3.90E+04

Table 6.3. RESRAD-OFFSITE SRSG for acute drilling and chronic post-drilling IHI scenarios (cont.)

Radionuclide	Acute drilling source SRSG (pCi/g)	Acute drilling as-disposed SRSG (pCi/g)	Acute drilling as-generated SRSG (pCi/g)	Chronic post-drilling source SRSG (pCi/g)	Chronic post-drilling as-disposed SRSG (pCi/g)	Chronic post-drilling as-generated SRSG (pCi/g)
Pm-146	1.86E+10	6.53E+10	1.23E+11	2.19E+07	9.61E+09	1.81E+10
Pu-238	1.14E+06	4.02E+06	7.58E+06	2.87E+03	1.26E+06	2.37E+06
Pu-239	4.71E+05	1.66E+06	3.12E+06	1.19E+03	5.22E+05	9.83E+05
Pu-240	4.75E+05	1.67E+06	3.15E+06	1.20E+03	5.27E+05	9.92E+05
Pu-241	1.77E+07	6.22E+07	1.17E+08	3.70E+04	1.62E+07	3.06E+07
Pu-242	4.94E+05	1.74E+06	3.27E+06	1.25E+03	5.47E+05	1.03E+06
Pu-244	1.09E+05[c]	3.84E+05[c]	7.24E+05[c]	1.44E+02[c]	6.31E+04[c]	1.19E+05[c]
Ra-226	2.97E+04	1.05E+05	1.97E+05	2.00E+00[d]	8.77E+02[d]	1.65E+03[d]
Ra-228	2.82E+09	9.93E+09	1.87E+10	1.64E+06	7.21E+08	1.36E+09
Re-187	SA[e]	SA[e]	SA[e]	SA[e]	SA[e]	SA[e]
Sr-90	5.75E+07	2.02E+08	3.81E+08	7.44E+02	3.26E+05	6.15E+05
Tc-99[a]	1.02E+09	3.58E+09	6.73E+09	1.09E+02	4.80E+04	9.03E+04
Th-228	SA[e]	SA[e]	SA[e]	SA[e]	SA[e]	SA[e]
Th-229	9.58E+04	3.37E+05	6.35E+05	1.44E+02	6.32E+04	1.19E+05
Th-230	7.08E+04[c]	2.49E+05[c]	4.69E+05[c]	5.48E+00[c]	2.40E+03[c]	4.53E+03[c]
Th-232	2.05E+04[d]	7.21E+04[d]	1.36E+05[d]	1.09E+01[d]	4.79E+03[d]	9.02E+03[d]
U-232	8.99E+04	3.16E+05	5.96E+05	2.69E+01	1.18E+04	2.22E+04
U-233	8.78E+05[c]	3.09E+06[c]	5.82E+06[c]	8.79E+01[c]	3.86E+04[c]	7.26E+04[c]
U-234	3.80E+06[c]	1.34E+07[c]	2.52E+07[c]	8.87E+01[c]	3.89E+04[c]	7.33E+04[c]
U-235	2.62E+05[c]	9.22E+05[c]	1.74E+06[c]	8.03E+01[c]	3.52E+04[c]	6.64E+04
U-236	5.82E+06	2.05E+07	3.86E+07	1.02E+02	4.47E+04	8.42E+04
U-238	SA[e]	SA[e]	SA[e]	9.29E+01[c]	4.08E+04[c]	7.68E+04[c]

[a]SRSG was not back-adjusted to account for activity loss during operations.
[b]SRSG equal to SRSG at 0 year adjusted for 100 years of radioactive decay.
[c]Minimum SRSG occurs at 1000 years.
[d]Minimum SRSG occurs after 100 years and before 1000 years.
[e]The SRSG is equal to or greater than the SA for the radionuclide.

IHI = inadvertent human intrusion
RESRAD = RESidual RADioactivity
SA = specific activity
SRSG = Single Radionuclide Soil Guideline

This page intentionally left blank.

7. INTEGRATION AND INTERPRETATION OF RESULTS

This section provides a summary of key elements of the analyses that support compliance decisions for the EMDF system with respect to DOE M 435.1-1 performance objectives and measures.

7.1 RADIONUCLIDE INVENTORY

The PA analyses of the EMDF system are based on an estimated radionuclide inventory and Preliminary Design parameters. Both the facility design and the estimated inventory will be refined as the EMDF design development process proceeds and additional waste stream characterization data become available.

Base case all-pathway peak doses for each radionuclide that was not screened from further analysis (Sect. 2.3.3) indicate that for the period from EMDF closure to 10,000 years post-closure, the primary contributors to total dose are C-14, Tc-99, and I-129 (Figs. 4.8 through 4.10). The inventory component that has the greatest impact on maximum dose during the compliance period is C-14; contributions from Tc-99 and I-129 occur after 1000 years. Uncertainty in EMDF inventory of the three dose-significant radionuclides is important for understanding the likely impacts of potential future releases. There is uncertainty in the estimated waste average activity concentrations used to derive the modeled source concentrations, and uncertainty in the magnitude of operational period losses credited for reducing the post-closure inventory of C-14, Tc-99, and I-129 (Fig. 5.8).

7.2 COVER SYSTEM PERFORMANCE

7.2.1 Cover Infiltration

The EMDF cover design and assumed long-term cover performance are key elements of the performance analysis. The assumed post-closure cover infiltration rate is a primary driver of predicted dose, affecting the rate of radionuclide release from the disposal unit and peak concentrations in groundwater and surface water. Based on the RESRAD-OFFSITE sensitivity analysis, the maximum all-pathways dose during the compliance period (i.e., at 1000 years post-closure) is very sensitive to parameters that determine the rate of cover infiltration (Fig. 5.8).

Uncertainty in future annual average precipitation and the degree of cover system degradation (two fundamental controls on cover infiltration) are two of the key parameter uncertainties identified in the RESRAD-OFFSITE probabilistic uncertainty analysis (refer to Appendix G, Sect. G.6.3.3.3). The upper limit of cover infiltration evaluated for the probabilistic analysis (approximately 3.7 in./year) is much larger than is reasonably expected during the 1000-year compliance period, given the likely service life of the HDPE membrane in the cover. The assumptions applied to the HELP modeling of cover infiltration (Appendix C, Sect. C.2) regarding degradation of the lateral drainage function of the cover system are very pessimistic, particularly because the coarse materials of the biointrusion layer above the lateral drainage layer in the cover (Fig. 2.41) will provide drainage even in the event of clogging of the underlying engineered drainage layer.

Degradation of the clay infiltration barrier of the EMDF cover (increased hydraulic conductivity) should be significantly delayed relative to the base case assumptions applied to the timing of cover failure (progressive failure from 200 to 1000 years post-closure), because of the likelihood that overlying HDPE membrane will function effectively for much more than 200 years. Extended HDPE membrane longevity is expected based on existing research (Appendix C, Sect. C.1.2.2.2) and the protection from the surface

environment provided by 11 ft of overlying material (the lateral drainage layer, biointrusion barrier, and cover surface layers).

Erosion of the cover system over very long periods of time is inevitable, and long-term degradation of waste containers and stabilized waste forms may contribute to differential settlement that can impair the efficiency of the engineered lateral drainage system. However, water-driven cover erosion should facilitate effective lateral drainage even in the case of relatively severe dissection (gullying) of the cover surface, and the biointrusion layer should limit the depth of gully formation so that direct exposure of the underlying infiltration barriers is unlikely even over very long periods of time. Natural vegetation dynamics in the warm humid climate of the southeast United States should also promote cover longevity and limit the potential for severe erosion, although a forested EMDF cover would be subject to natural processes of tree-throw and weather-related forest disturbance that could also cause localized erosion. In general, the earthen cover components overlying the HDPE and clay infiltration barriers should be relatively stable under the natural range of environmental conditions, even considering natural climate fluctuations or the potential for progressive climate change.

The distributions selected for the timing and duration of cover degradation, and for the cover infiltration rate (runoff coefficient) in the RESRAD-OFFSITE probabilistic uncertainty analysis (Appendix G, Sect. G.6.3.2.1 and Table G.23) provide a robust assessment of the base case assumptions for cover performance. For the probabilistic dose analysis, the mean (average mean value for ten repetitions of 300 system realizations) of the all-pathways dose at 1000 years is approximately 1 mrem/year (Fig. 5.12), and the average 95^{th} percentile at 1000 years is less than 2 mrem/year (20 percent of the 25 mrem/year performance objective). Higher peak doses associated with fission products (Tc-99 and I-129) and actinides occur after 1000 years. However, comparison of release predictions from the STOMP and RESRAD-OFFSITE models suggest that the post-1000 year peaks may be over-estimated by the relatively simple release and vadose zone conceptualizations implemented in RESRAD-OFFSITE.

7.2.2 Atmospheric (Vapor Phase) and Biological Release

EMDF cover performance is also a key assumption in the screening of atmospheric (vapor-phase) release from detailed analysis. The estimated inventories of H-3, C-14, and I-129 have the greatest potential for vapor-phase release, but vapor-phase release and aqueous-phase leaching of these relatively mobile radionuclides from the waste during disposal and prior to EMDF closure will reduce the amounts available for post-closure release to the atmosphere or to porewater. Post-closure release of volatile hydrocarbons incorporating H-3 or C-14 (above background levels) and release of vapor-phase radioiodine will be limited by the synthetic and clay barriers of the EMDF cover system, which are expected to remain fully functional for several centuries, and at least partially functional for the duration of the compliance period.

Following the end of post-closure care and active institutional control, development of natural vegetation and inhabitation of the cover system by various animals is likely. Biological intrusion by root systems, insects, and larger animals will contribute to the natural evolution of the cover system components. Based on the expectation of a relatively stable cover surface, and the prevention of deep burrowing by large animals or severe gully erosion by the coarse materials of the biointrusion barrier, the potential for significant biologically-driven release of radionuclides is limited, and biological release was eliminated from consideration in the PA analysis.

7.2.3 Inadvertent Human Intrusion

The analysis of IHI for the EMDF includes acute and chronic exposure scenarios that are based on the EMDF Preliminary Design for the CBCV site. The continuing presence of the HDPE liner and general stability of the cover system over the 1000-year compliance period is significant for the IHI analysis acute

discovery scenario, which is based on a hypothetical excavation of the cover that does not expose the waste. The discovery scenario credits the engineered barriers of the EMDF cover with deterring completion of an excavation into the waste that could lead to direct exposure to radionuclides in EMDF waste. Erosion of the cover system that could reduce the thickness of the cover components would not significantly impact the deterrent to excavation provided by the engineered biointrusion barrier and underlying cover system components.

7.3 RADIONUCLIDE RELEASE AND TRANSPORT MODELS

7.3.1 Release Conceptualization

Similar approaches to representation of radionuclide release from the EMDF were implemented in the more detailed models of the vadose and saturated zone and in the total system transport model. The PA models incorporate no assumptions related to the use of waste containers or stabilized waste forms that can limit or delay release of radionuclides. The relatively simple equilibrium sorption model for radionuclide release applied in the STOMP model (Appendix E) and in developing the source release boundary condition (leachate flux to the water table) for the MT3D model (Appendix F) is pessimistic given the likelihood of non-uniform cover infiltration that limits water intrusion to particular locations and flow pathways through the waste. Waste heterogeneity will also focus infiltrating water along preferred transport paths. The simplified source release representation in these two models assumes that the entire radionuclide inventory is available for aqueous release and transport as soon as cover infiltration becomes non-zero, whereas it is likely that heterogeneity in water intrusion and radionuclide transfer to the aqueous phase will limit release rates. Figures 3.31, 3.32 and 3.33 show a comparison of vadose zone flux predicted by STOMP and RESRAD-OFFSITE and the release model applied to the MT3D saturated zone transport model for Tc-99. The consistency among the model outputs and MT3D model input is good.

The potential impact of non-uniform release to the saturated zone that is possible due to sloping liner surfaces and variability in waste thickness was evaluated by applying a simple non-uniform leachate flux boundary condition to the MT3D model (Sect. 3.3.3.2). The non-uniform release was found to decrease the predicted peak Tc-99 concentration at the groundwater well (Fig. 5.5). Source release to the saturated zone in the total system model is assumed to occur uniformly over a simplified rectangular footprint area based on the EMDF preliminary design. However, sensitivity evaluation with the MT3D model suggests that the uniform source release assumption for the total system model simulations is not critical to the assessment of EMDF compliance with the 25 mrem/year performance objective. The model intercomparison for the saturated zone activity concentration results also suggests that uncertainties related to conceptual models of radionuclide release and materials in the shallow aquifer are not significant in terms of the range of predicted peak saturated zone concentrations, at least for highly mobile radionuclides like C-14 and Tc-99.

7.3.2 Assumed K_d Values for Dose-Significant Radionuclides

The PA model results are sensitive to the assumed values for partition coefficients for Tc-99 and, particularly, I-129. To account for uncertainty in waste geochemistry and release kinetics, the waste K_d values for all radionuclides are reduced by a factor of two from the assumed base case values; this is a fairly pessimistic approach because it is likely that sorption by the clean fill emplaced with the waste will be substantial. Uncertainty in assigning K_d values is significant, but the base case values for Tc-99 and I-129 are reasonably pessimistic (lower than is likely) given the available information regarding the sorptive capacity of Conasauga Group materials, and the likely range of geochemical conditions. Similarly, the assumed K_d value for uranium is probably on the lower end of the range of likely values for the materials of the EMDF system, based on the available information. Uranium sorption experiments on local clay rich soils were performed during the design phase for the EMWMF (WMFS 2000) and the results indicated that

the sorptive capacity of those materials was very high, implying K_d > 1000 cm^3/g. Lower than expected K_d values may result for particular chemical species and geochemical environments, but the uncertainty analysis (Sect. 5.4) evaluated K_d values as low as zero for both Tc-99 and I-129, the two radionuclides for which the uncertainty in assigning an appropriate long-term value is most significant for the results of the PA. New laboratory studies of the sorptive capacity of Conasauga Group materials for Tc-99 and I-129 are planned to reduce the uncertainty in these important model input parameters.

7.3.3 Transport Model Uncertainty

The PA applied 2-D and 3-D radionuclide transport models to the vadose and saturated zone, respectively. These models capture much of the complexity in the configuration of waste, engineered barriers, and natural geologic materials for the EMDF system. The results obtained from the more complex transport model codes (STOMP and MT3D) were compared to radionuclide release and transport output from the total system model (RESRAD-OFFSITE). This model integration step was performed to ensure that the simplified representations of the vadose and saturated zones in the RESRAD-OFFSITE model were producing results consistent with the more detailed models, and to address uncertainty associated with applying a simplified conceptualization of radionuclide release and transport to a fairly complex LLW disposal system like the EMDF.

In general, the RESRAD-OFFSITE model base case predictions of peak concentrations at the groundwater POA are larger and earlier than corresponding predictions from the more detailed MT3D transport model. Final base case values for critical RESRAD-OFFSITE input parameters that impact the simulated saturated zone concentrations, including the well depth and hydraulic gradient to the well, were adopted on this basis. This approach to managing transport model uncertainty imparts a pessimistic bias to the transport modeling because the RESRAD-OFFSITE concentration estimates are biased high relative to predictions from the more detailed models, and provide a measure of conservatism to the PA dose analysis.

7.4 ALL-PATHWAYS DOSE UNCERTAINTY

The RESRAD-OFFSITE compliance period probabilistic uncertainty analysis includes only estimated inventories of C-14, Tc-99, and I-129. These three radionuclides are the primary dose contributors for the base case EMDF performance scenario. Sensitivity of the predicted total dose to uncertainties in selected model parameters representing climate (precipitation), long-term cover performance, radionuclide mobility (K_d values), subsurface material properties, and groundwater conditions was evaluated by probabilistic sampling of input parameter values and multiple regression analysis of predicted peak total dose (Sect. 5.4).

For the probabilistic analysis, K_d values for Tc-99 and I-129 were permitted to vary independently between maximum (twice the base case values) and zero minimum values, with the result that earlier, higher additive doses can occur in the probabilistic than for the deterministic base case scenario. For the compliance period analysis, the mean probabilistic dose at 1000 years was similar to the deterministic base case peak dose, approximately 1 mrem/year (Fig. 5.12), and the 95^{th} percentile of the probabilistic peak total dose was less than 3 mrem/year.

Although approximately 5 percent of post compliance period probabilistic peak doses between 2000 and 3000 years exceed 15 mrem/year, the mean of the probabilistic dose remains less than 5 mrem/year for simulations times before about 6000 years. Higher probabilistic uranium and plutonium dose predictions beyond about 6000 years appear to be over-estimated by the RESRAD-OFFSITE code using the instantaneous equilibrium desorption model, which appears to predict much higher peak activity flux to the saturated zone than do the STOMP model simulations for radionuclide with assigned K_d > 1 cm^3/g, such as I-129 and U-234 (Sect. 3.3.5). In addition, uranium solubility limits and the effect of waste containers,

waste stabilization (grouting), or treatment to reduce the mobility of some of the estimated actinide inventory are not considered in the model predictions.

These results suggest that the uncertainty in key input parameter values does not affect the conclusion that the all-pathways dose performance objective will be met during the 1000-year compliance period, and that the 25 mrem/year limit is unlikely to be exceeded within timeframes of several thousand years post-closure.

This page intentionally left blank.

8. PERFORMANCE EVALUATION

8.1 COMPARISON OF RESULTS TO PERFORMANCE OBJECTIVES

The base case analysis and sensitivity-uncertainty analysis performed for the EMDF PA demonstrate that there is a reasonable expectation that the facility will meet the established all-pathways dose performance objective during the 1000-year compliance period and within the first several thousand years post-closure. Analytical results of the EMDF performance modeling are summarized in Table 8.1.

Table 8.1. Exposure scenarios, performance objectives and measures, and base case results for the EMDF PA

Exposure scenario	Performance objective or measure	EMDF PA results
All pathways	25 mrem/year	Base case maximum dose during compliance period: 1.03 mrem/year Base case peak dose through 10,000 years: 9.13 mrem/year (at 5100 years)
Air pathway[a]	10 mrem/year[b]	Pathway screened from analysis (Sect. 3.2.2)
Radon flux	20 pCi/m^2/sec	EMDF cover surface: 5.0E-08 pCi/m^2/sec EMDF waste surface (no cover): 0.80 pCi/m^2/sec
Water resources (groundwater) • Ra-226 + Ra-228 • Gross alpha activity[c] • Beta/photon activity • H-3 • Sr-90 • Uranium (total)	 5 pCi/L 15 pCi/L 4 mrem/year 20,000 pCi/L 8 pCi/L 30 µg/L	Groundwater during compliance period: • Ra-226 + Ra-228: 0.0 pCi/L (negligible) • Gross alpha activity: 0.0 pCi/L (negligible) • Beta/photon activity: 1.03 mrem/year • H-3: 0.0 pCi/L (negligible) • Sr-90: 0.0 pCi/L (negligible) • Uranium (total): 0.0 µg/L (negligible).
Water resources (surface water)	DOE DCS[d]	Bear Creek peak concentration less than DCS standard for all radionuclides in EMDF inventory (Sect. 4.7.2)
Inadvertent human intrusion • Chronic exposure • Acute exposure	 100 mrem/year 500 mrem	IHI dose at 100 years (compliance period maximum): Chronic post-drilling: 3.56 mrem/year Acute discovery: 1.30E-04 mrem Acute drilling: 0.38 mrem

[a]Air pathway is screened from the EMDF PA.
[b]Excluding radon in air.
[c]Including Ra-226, but excluding radon and uranium.
[d]DOE 2011b.

DCS = Derived Concentration Standard
DOE = U.S. Department of Energy
EMDF = Environmental Management Disposal Facility
IHI = inadvertent human intrusion
PA = Performance Assessment

Results of the radon flux analysis, which are provided in Sect. 4.4 and presented in detail in Appendix H, are included in Table 8.1. The results suggest that the EMDF can meet the 20 pCi/m^2/sec radon flux performance objective even if the cover is severely eroded. Also included in Table 8.1 is a summary of the results of RESRAD-OFFSITE modeling to demonstrate protection of water resources during the 1000-year compliance period. Modeled well water and surface water concentrations are compared to maximum contaminant levels for drinking water systems and to DCSs (DOE 2011b), respectively. The results suggest

that there is a reasonable expectation that the EMDF disposal system will be protective of water resources during the compliance period.

With respect to performance measures for IHI, the EMDF analysis suggests that, based on the current estimated EMDF radionuclide inventory, there is a reasonable expectation that the facility design will protect a future inadvertent human intruder for the specific IHI scenarios considered.

8.2 USE OF PERFORMANCE ASSESSMENT RESULTS

The primary uses of this EMDF PA are to support issuance of a DAS by demonstrating the likelihood of meeting performance objectives based on the expected EMDF waste forms, estimated radionuclide inventory, preliminary facility design, and site characteristics and to identify key site, waste, and facility uncertainties that can be prioritized for further work prior to start of operations.

8.3 FURTHER WORK

Near-term priorities for research and development activities to support PA maintenance include the following:

- Perform laboratory evaluations of EMDF materials to reduce uncertainty in the assumed K_d values for Tc-99 and I-129
- Monitor EMDF design evolution through final design and assess changes through the EMDF change control process.

In parallel with these near-term PA maintenance activities, the FFA parties will approve operating limits, including WAC, and will issue a WAC compliance document prior to EMDF operations. Review of proposed activities, new regulatory requirements, or other new information that could challenge key assumptions for the EMDF performance analysis will be evaluated in accordance with the EMDF change control process to assess the potential for such changes to require a Special Analysis or revisions to the PA.

9. QUALITY ASSURANCE

The QA Report (UCOR 2020b) was prepared to comprehensively document the QA record for this Revision 2 PA (and the companion Revision 2 CA [UCOR 2020a]). This QA Report accompanies this PA and details the QA protocol applied during the preparation of this PA. It identifies the electronic files created during the modeling and their location; it identifies the modeling input parameters and documents their technical assessment; and it documents the technical review of the draft PA before it was finalized. An assessment of the QA associated with the development of this PA must include a review of the QA Report.

UCOR, in accordance with DOE O 414.1C, 10 *CFR* 830, Subpart A, federal regulations, and contractual requirements, maintains an NQA-1-compliant QA program. Drummond Carpenter, PLLC (Drummond Carpenter) and Jacobs provided groundwater and contaminant fate and transport modeling support to this PA under a UCOR Professional Services Agreement and a Request for Offsite Services, respectively. UCOR flows its QA requirements to companies providing support via the Professional Services Agreements and Requests for Offsite Services.

The salient components of the QA program that were implemented during the preparation of this PA include the following:

- Software QA procedures for code verification and documentation for each model code per *Software Quality Assurance Program* (PPD-IT-6007)
- Formal independent checking and review of calculation and data packages that document input parameter values and other model assumptions, model implementation, model output data, and post-processing activities for each PA model
- Documentation of PA model development, implementation, sensitivity-uncertainty analyses, and PA model integration contained in the EMDF PA report and report appendices
- Configuration management for PA documents and calculation packages per UCOR procedures for document control
- Maintenance of the digital modeling information archive of PA documents, model codes, model input and output files, formal QA documentation, and reference materials in compliance with requirements of the UCOR QA Program (UCOR 2019), DOE QA Program (DOE 2012, Attachments G and H), and DOE O 414.1D (DOE 2013b).

9.1 SOFTWARE QUALITY ASSURANCE

Documentation of software QA, including code validation on computers used for PA modeling follows the requirements of UCOR Software QA procedure (PPD-IT-6007). All PA model codes have been categorized as UCOR category C (Business Impacting Software). Documentation of code validation, including model input and output files for validation runs are available for each PA model code in the UCOR Software QA database system. In addition, all software QA documentation is included in the EMDF PA Library.

A management assessment of the compliance of the EMDF Project Software with the requirements in the current revision of UCOR procedure PROC-IT-6008 was conducted in March 2019. There were no observations of findings identified during this assessment. A copy of this assessment is in the QA Report.

9.2 INPUT DATA QUALITY ASSURANCE

Development and independent checking of one or more calculation packages for each EMDF PA model code is the basis for ensuring the accuracy and consistency of model input data. Data and calculation packages for each model code document input parameter values and other model assumptions, information sources, model implementation, model outputs, and post-processing activities. The calculation package for the EMDF estimated radionuclide inventory that documents the data structure and data sources used to estimate the estimated inventory is a supporting QA document for all of the radionuclide transport models.

A list of all EMDF PA calculation packages and the model(s) supported by each is shown on Table 9.1. All calculation packages, including model input and output files, data for supporting calculations, and copies of all supporting references will be maintained in electronic format (pdf) and available on digital media or in controlled hard copy form as required.

Table 9.1. Data and calculation packages for the EMDF PA

Calculation Package Title	Author	UCOR Calculation Number	Document Reference(s)
Data and Calculation Package-EMDF Radiological Inventory	UCOR	CAW-90EMDF-F898	Sect. 2.3, Appendix B
Calculation and Data Package for the HELP Model	Jacobs	CAW-90EMDF-G118	Sect. 3.3.1, Appendix C
Calculation and Data Package for the Parameter Development based on EMDF Design	Jacobs	CAW-90EMDF-G119	Sect. 2.2, Appendix C
Calculation and Data Package for the STOMP Model	Jacobs	CAW-90EMDF-G120	Sect. 3.3.2, Appendix E
Calculation and Data Package for the MODFLOW Model	Jacobs	CAW-90EMDF-G121	Sect. 3.3.3, Appendix D
Calculation and Date Package for the MT3D Model	Jacobs	CAW-90EMDF-G122	Sect. 3.3.3, Appendix F
EMDF RESRAD-OFFSITE Operational Period Inventory Depletion Calculation Package	Drummond Carpenter	CAW-90EMDF-G182	Sect. 3.2.2.5, Appendix G
EMDF RESRAD-OFFSITE Performance Assessment and Composite Analysis Calculations Package	Drummond Carpenter	CAW-90EMDF-G183	Sects. 3.3.4, 3.4, Appendix G
EMDF IHI RESRAD-OFFSITE Modeling Calculations Package	Drummond Carpenter	CAW-90EMDF-G184	Sect. 6, Appendix I
EMDF Cover Erosion Calculation (RUSLE2)	UCOR	CAW-90EMDF-G123	Sect. 3.2.1, Appendix C
EMDF Radon Flux Calculation	UCOR	CAW-90EMDF-G124	Sect. 3.2.2.2, Appendix H
EMDF Bathtub Scenario Analysis	UCOR	CAW-90EMDF-G048	Sect. 3.2.1, Appendix C
Data and Calculation Package – Average Properties of EMDF Waste	UCOR	CAW-90EMDF-G496	Sect. 3.3, Appendices C, D, E, F, G (all models except HELP)
Data and Calculation Package – EMDF Engineered Material Properties	UCOR	CAW-90EMDF-G497	Sect. 3.3, Appendices C, D, E, F, G (all models except HELP)

EMDF = Environmental Management Disposal Facility
HELP = Hydrologic Evaluation of Landfill Performance
IHI = inadvertent human intrusion
PA = Performance Assessment
RESRAD = RESidual RADioactivity

9.3 DOCUMENTATION OF MODEL DEVELOPMENT AND OUTPUT DATA

Model development and output data for each of the EMDF PA model codes is documented in the appendices to the PA report document, and additional detail is provided in model-specific calculation packages (Table 9.1). Model output files and separate electronic tabulations of model output used for plotting or post-processing are included for archival purposes as digital attachments to calculation packages.

9.4 INDEPENDENT TECHNICAL REVIEW OF THE REVISED PERFORMANCE ASSESSMENT

UCOR performed an independent technical review of the final draft of the Revision 2 EMDF PA prior to its transmittal to DOE for distribution. This review was conducted using the UCOR Form-141, "Document Review Request." These forms document the names of those reviewing the document, the scope (purpose) of the reviews, how comments on the documents were transmitted from the reviewers to the preparer, and that comments were resolved.

The scope of this review process included the following (at a minimum):

- An OREM (DOE) review (two reviewers, a technical review by a subcontractor)
- A review by the UCOR EMDF Project Manager
- A technical consistency review by the primary author of the Revision 2 PA (UCOR)
- Technical reviews by various subject matter experts (primarily geologists)
- Verification that values in the document that originated in calculation packages, modeling, etc. have been correctly transcribed to the document from those sources.

More details, as well as the competed Forms-141, are included in the QA Report.

9.5 CONFIGURATION MANAGEMENT AND MAINTENANCE OF PA MODELING INFORMATION ARCHIVE

Calculation packages have been developed according to the calculation procedures and quality management protocols of the specific company responsible for model development (UCOR, Jacobs, or Drummond Carpenter). All calculation packages have been reviewed and approved under either the existing UCOR procedure PROC-DE-0704, *Project Calculations*, or PROC-WM-2031, *Waste Management Calculations*. Configuration control of calculation packages will be governed by contractor-specific protocols for change control of calculations as well as UCOR protocol. Both of these procedures require submittal of approved calculation packages to the Document Management Center (DMC) in accordance with UCOR procedure PROC-OS-1001, *Records Management, Including Document Control*. Both of the calculation procedures also require a hardcopy submittal and an electronic copy in native format (such as Word or Excel) to the DMC when possible. This requirement is being interpreted as including digital files (such as input and output files) created during the performance modeling simulations.

Configuration control and archival of digital files for the PA, supporting data, and calculation packages have been performed in accordance with UCOR procedure PROC-OS-1001, *Records Management, Including Document Control*. This procedure allows for the submittal and defines the requirements for submitting records on media other than paper (such as input and output files from performance modeling

simulations). This PA, as well as the QA Report, were entered into the DMC upon transmittal to DOE for distribution. At that time, all associated “records” were submitted to the DMC.

10. PREPARERS

Chad Drummond, PE, D.WRE, BCEE

Chad Drummond is a Principal Engineer/Modeler with Drummond Carpenter and has over 20 years of experience conceptualizing, developing, and applying environmental numerical models for sites across the United States and in Australia. His role on the EMDF PA included RESRAD-OFFSITE model conceptualization, model parameterization, and model simulation. Documentation of the RESRAD-OFFSITE modeling is included in Appendix G, the main PA report text, and associated calculations packages.

Over his career, his technical focus has been on unsaturated flow, groundwater hydrogeology, environmental assessment and remediation/restoration, and the fate and transport of various contaminants, including emerging contaminants and radionuclides. He has nearly 12 years of project experience performing environmental modeling at several DOE sites, including the Paducah Gaseous Diffusion Plant; ORR; and the Shiprock, Rocky Flats, and Tuba City DOE Legacy Management sites.

Modeling performed at Paducah Gaseous Diffusion Plant was primarily performed as part of the RI/FS and included sitewide groundwater flow and contaminant transport simulations, volatile organic compound and radionuclide leaching simulations, radon emanation modeling, and WAC modeling. WAC modeling was performed to assess disposal criteria for nearly 100 potential contaminants of interest. His experience at ORR includes the PA documented herein, modeling to specify contaminant Authorized Limits, and reviewing the ORR sitewide model to facilitate development of the site-specific RESRAD-OFFSITE model. His tasks at the various DOE Legacy Management sites include source and plume remediation, site modeling, and configuring and assessing pump tests to provide parameters for the site groundwater models.

In addition to DOE projects, he has worked on projects for other federal entities including National Air and Space Agency, Air National Guard, U.S. Army Corps of Engineers, and the U.S. Air Force. He also has experience in private sector projects and has been accepted as an expert witness and has deposition and court testimony experience.

Mr. Drummond is a licensed Professional Engineer and his credentials include BCEE (Board Certified Environmental Engineer) by the American Academy of Environmental Engineers and Scientists (AAEES) and D.WRE (Diplomate, Water Resources Engineer) by the American Academy of Water Resources Engineers. He has taught environmental modeling and environmental engineering courses to undergraduate and graduate students.

Ryan Hupfer, MS

Ryan Hupfer is a Senior Staff Geologist with Drummond Carpenter and has 4 years of experience performing environmental assessment and remediation and aquifer characterization activities. He has developed, calibrated, and applied environmental numerical models at sites in the eastern United States. Mr. Hupfer provided RESRAD-OFFSITE modeling support to the development of the EMDF source term dose at the CA POA. Prior to that, he provided modeling support on this PA. His role on the EMDF PA included parameterizing the RESRAD-OFFSITE model, conducting inadvertent human intruder and base case model simulations, and performing the sensitivity analysis and probabilistic model simulations. Mr. Hupfer provided documentation support of the completed RESRAD-OFFSITE modeling included in Appendix G, the main PA text, and associated calculations packages.

His technical focus is on hydrogeology, geochemistry, and the predictive migration and attenuation of various contaminants, including chlorinated solvents, inorganics, and radionuclides. Mr. Hupfer's project experience includes working in a variety of geologic settings, including unconsolidated sediment, fractured bedrock, and karst environments. He has applied geographic information system platforms, computer-aided design, and Python scripting to facilitate pre- and post-processing model data. In addition to his RESRAD-OFFSITE modeling experience, he has developed and used MATLAB, Surfer, AQTESOLV, and MODFLOW to assess environmental condition. He holds a bachelor's degree and a master's degree (Rutgers) in geology and is credentialed as a Professional Geologist in Tennessee and a Geologist-in-Training in Florida.

Stephen Kenworthy, Ph.D.

Steve Kenworthy is a hydrologist and environmental scientist with StrataG in Oak Ridge, TN. Dr. Kenworthy has 7 years of experience as a postdoctoral research associate and university professor focused on field and laboratory studies of fluvial hydrology and hydraulics and earth surface processes. His research experience includes field measurements and analysis of stream flow dynamics and sediment transport in agricultural settings in Illinois, field studies of slope stability in southeast Alaska, laboratory analysis and modeling of fluvial sediment transport mechanics, field studies of topographic controls on soil moisture, field monitoring and analysis of the hydrology and suspended sediment dynamics of the Green River system in Kentucky, and field monitoring of flow, sediment transport and contaminant dynamics in karst conduits of the Mammoth Cave system.

Dr. Kenworthy has over 8 years of experience providing technical support to the OREM program, including contributions to the Mercury Technology Development project, development of the EMDF RI/FS, and was the document lead for this EMDF PA. He recently participated in an international expert review of the performance analysis prepared for licensing a LLW disposal facility near Ottawa, Ontario, Canada.

Dr. Kenworthy's contributions to preparing the EMDF PA included primary responsibility for coordination and integration of the modeling team and development of the main text of the report. He also was responsible for developing the radionuclide inventory (Appendix B) and contributed to the analysis of EMDF cover performance (HELP model and Appendix C) and the analysis of IHI (Appendix I).

Changsheng Lu, Ph.D., PG

Changsheng Lu is a Professional Geologist and senior hydrogeologist with Jacobs Engineering in Oak Ridge, Tennessee. He has over 30 years of environmental modeling application experience, including 25 years of groundwater and contaminant fate and transport modeling in BCV, including support for EMWMF and the proposed EMDF. Dr. Lu has provided technical and modeling support for the EMWMF RI/FS and CA, and for the RI/FS and PA for the onsite disposal facility at the Portsmouth Gaseous Diffusion Plant as well as many other DOE, Department of Defense, EPA, and industrial clients.

Dr. Lu's contributions to development of the EMDF PA included vadose zone flow and transport analysis (STOMP model implementation, Appendix E), 3-D saturated zone flow and radionuclide transport analysis (MODFLOW and MT3D model implementation, Appendices D and F), cover and liner performance modeling (RUSLE2 model implementation and EMDF bathtub analysis in Appendix C) and the analysis of radon flux (Appendix H).

11. REFERENCES

Albrecht and Bensen 2001. "Effect of Desiccation on Compacted Natural Clays," *Journal of Geotechnical Engineering*, Vol. 127, No. 1, Paper No. 16291, B. A. Albrecht and C. H. Benson, January.

Baes et al. 1984. *A Review and Analysis of Parameters for Assessing Transport of Environmentally Released Radionuclides through Agriculture*, ORNL-5786, Oak Ridge National Laboratory, Oak Ridge, TN, September.

Bailey and Lee 1991. *Hydrogeology and Geochemistry in Bear Creek and Union Valleys, Near Oak Ridge, Tennessee*, USGS Water Resources Investigation 90-4008, Z. C. Bailey and R. W. Lee, U.S. Geological Survey, Reston, VA.

Baranski 2009. *Natural Areas Analysis and Evaluation: Oak Ridge Reservation*, ORNL/TM-2009/201, Oak Ridge National Laboratory, Oak Ridge, TN, November.

Baranski 2011. *Aquatic Natural Areas Analysis and Evaluation: Oak Ridge Reservation*, ORNL/TM-2011/13, Oak Ridge National Laboratory, Oak Ridge, TN, April.

BJC 1999. *Predesign Site Characterization Summary Report for the Environmental Management Waste Management Facility, Oak Ridge, Tennessee*, BJC/OR-255, Bechtel Jacobs Company LLC, Oak Ridge, TN, May.

BJC 2000. *Final Site Investigation Report,* SSRS Item No. 3.5, Rev. 1, Bechtel Jacobs Company LLC, Oak Ridge, TN, August.

BJC 2003. *Engineering Feasibility Plan for Groundwater Suppression of the Environmental Management Waste Facility, Oak Ridge, Tennessee*, BJC/OR-1478, Bechtel Jacobs Company LLC, Oak Ridge, TN.

BJC 2010a. *Summary Report on the 2010 on the Environmental Management Waste Management Facility Groundwater Model and Fate-Transport Analyses, Oak Ridge, Tennessee,* BJC/OR-3434, Bechtel Jacobs Company LLC, Oak Ridge, TN, May.

BJC 2010b. *Calculation Package for the Analysis of Performance of Cells 1-6, with Underdrain, of the Environmental Management Waste Management Facility Oak Ridge, Tennessee,* I-60442-0001, Bechtel Jacobs Company LLC, Oak Ridge, TN, March.

Bouwer 1989. The Bouwer and Rice Slug Test – An Update, *Groundwater*, Vol. 27, Issue 3, pages 304−309.

Bouwer 1991. "Simple Derivation of the Retardation Equation and Application to Preferential Flow and Macrodispersion," *Ground Water*, Vol 29, No. 1, H. Bouwer, January-February.

Bouwer and Rice 1976. *A Slug Test for Determining Hydraulic Conductivity of Unconfined Aquifers with Completely or Partially Penetrating Wells*, Water Resources Research, Vol. 12, No. 3, pages 423−428.

Boynton and Daniel 1985. "Hydraulic Conductivity Tests on Compacted Clays", *Journal of Geotechnical Engineering*, ASCE, 111(4), 465–478. Boynton, S. S., and Daniel, D. E.

Canadell et al. 1996. *Maximum rooting depth of vegetation types at the global scale*, J. Canadell, R.B. Jackson, J.R. Ehleringer, H.A. Mooney, O.E. Sala- E.-D. Schulze. Oecologia 108:583-595.

CH2M-Hill 2000. *Phase IV Final Site Investigation Report, SSRS Item No.3.3, Rev. 1,* CH2MHill Constructors, Inc., under contract to Waste Management Federal Services, Inc., for Bechtel Jacobs Company LLC, Oak Ridge, TN, March.

City Data 2020. "Races in Oak Ridge, Tennessee (TN) Detailed Stats", https://www.city-data.com/races/races-Oak-Ridge-Tennessee.html., accessed March 12.

Clapp 1998. *Environmental Sciences Division Groundwater Program Office Report of Fiscal Years 1995- 1997*, "Water Balance Modeling," Sect. 5.1, D. Huff (ed.), Environmental Sciences Division Publication No. 4751, ORNL/GWPO-027 (ESD Publ. No, 4751), pages 13-14, R. B. Clapp, Oak Ridge National Laboratory, Oak Ridge, TN.

Connell and Bailey 1989. *Statistical and Simulation Analysis of Hydraulic Conductivity Data for Bear Creek and Melton Valleys, Oak Ridge Reservation, Tennessee,* USGS Water-Resources Investigations Report 89-4062, U.S. Geological Survey, Reston, VA.

Davis et al. 1984. *Site Characterization Techniques Used at a Low-Level Waste Shallow Land Burial Field Demonstration Facility*, ORNL-9146, E. C. Davis, W. J. Boegly, Jr., E. R. Rothschild, B. P. Spalding, N. D. Yaughan C. S. Haase, D. D. Huff, S. Y. Lee, E. C. Walls, J. D. Newbold: and E. D. Smith, Oak Ridge National Laboratory, Oak Ridge, TN, July.

DOE 1992a. *Federal Facility Agreement for the Oak Ridge Reservation,* DOE/OR-1014, U.S. Environmental Protection Agency Region 4, Atlanta, GA; U.S. Department of Energy, Oak Ridge, TN; and Tennessee Department of Environment and Conservation, Nashville, TN, January.

DOE 1992b. *Site Characterization Summary Report for Waste Area Grouping 1 at Oak Ridge National Laboratory, Oak Ridge, Tennessee Vol. 3*, DOE/OR/01-1043/V3&D1, U.S. Department of Energy, Oak Ridge, TN, September.

DOE 1997a. *Hazard Categorization and Accident Analysis Techniques for Compliance with DOE Order 5480.23, Nuclear Safety Analysis Reports*, DOE-STD-1027-92, U.S. Department of Energy, Washington, D.C., December.

DOE 1997b. *Report on the Remedial Investigation of Bear Creek Valley at the Oak Ridge Y-12 Plant, Oak Ridge, Tennessee,* DOE/OR/01-1455/V1-V6&D2, U.S. Department of Energy, Oak Ridge, TN, May.

DOE 1997c. *Feasibility Study for Bear Creek at the Oak Ridge Y-12 Plant, Oak Ridge, Tennessee*, DOE/OR/02-1525/V2&D2, U.S. Department of Energy, Oak Ridge, TN, November.

DOE 1998a. *Remedial Investigation/Feasibility Study for the Disposal of Oak Ridge Reservation Comprehensive Environmental Response, Compensation, and Liability Act of 1980 Waste*, DOE/OR/02-1637&D2, U.S. Department of Energy, Oak Ridge, TN, January.

DOE 1998b. *Addendum to Remedial Investigation/Feasibility Study for the Disposal of Oak Ridge Reservation Comprehensive Environmental Response, Compensation, and Liability Act of 1980 Waste*, DOE/OR/02-1637&D2/A1, U.S. Department of Energy, Oak Ridge, TN, September.

DOE 1999a. *Record of Decision for the Disposal of Oak Ridge Reservation Comprehensive Environmental Response, Compensation, and Liability Act of 1980 Waste*, DOE/OR/01-1791&D3, U.S. Department of Energy, Oak Ridge, TN, November.

DOE 1999b. *Proposed Plan for the Disposal of Oak Ridge Reservation Comprehensive Environmental Response, Compensation, and Liability Act of 1980 Waste*, DOE/OR/01-1761&D3, U.S. Department of Energy, Oak Ridge, TN, January.

DOE 2000. *Record of Decision for the Phase I Activities in Bear Creek Valley at the Oak Ridge Y-12 Plant, Oak Ridge, Tennessee*, DOE/OR/01-1750&D4, U.S. Department of Energy, Oak Ridge, TN, May.

DOE 2001a. *Attainment Plan for Risk/Toxicity-Based Waste Acceptance Criteria at the Oak Ridge Reservation, Oak Ridge, Tennessee*, DOE/OR/01-1909&D3, U.S. Department of Energy, Oak Ridge, TN, October.

DOE 2001b. *Radioactive Waste Management*, DOE Order 435.1 Chg 1 (PgChg), U.S. Department of Energy, Washington, D.C., August.

DOE 2004. *Environmental Management Waste Management Facility Capacity Assurance Remedial Action Report*, DOE/OR/01-2145&D2, U.S. Department of Energy, Oak Ridge, TN, September.

DOE 2008. *Oak Ridge Reservation Planning: Integrating Multiple Land Use Needs*, DOE/ORO/01-2264, U.S. Department of Energy, Oak Ridge, TN, May.

DOE 2010a. *Explanation of Significant Differences for the Record of Decision for the Disposal of Oak Ridge Reservation Comprehensive Environmental Response, Compensation, and Liability Act of 1980 Waste, Oak Ridge, Tennessee*, DOE/OR/01-2426&D2, U.S. Department of Energy, Oak Ridge, TN, May.

DOE 2010b. *Program and Project Management for the Acquisition of Capital Assets*, DOE Order 413.3B Chg5 (MinChg), U.S. Department of Energy, Washington, D.C., April.

DOE 2011a. *Radioactive Waste Management Manual*, DOE Manual 435.1-1 Chg 2, U.S. Department of Energy, Washington, D.C., June.

DOE 2011b. *Derived Concentration Technical Standard*, DOE-STD-1196-2011, U.S. Department of Energy, Washington, D.C., April.

DOE 2011c. *Final Site-Wide Environmental Impact Statement for the Y-12 National Security Complex*, DOE/EIS-0387, U.S. Department of Energy, Oak Ridge, TN, February.

DOE 2012. *EM Quality Assurance Program*, EM-QA-001 Rev. 1, U.S. Department of Energy, Washington, D.C., June 11.

DOE 2013a. *Radiation Protection of the Public and the Environment*, DOE Order 458.1, U.S. Department of Energy, Office of Health, Safety, and Security, Washington, D.C.

DOE 2013b. *Quality Assurance*, DOE Order 414.1D, Admin Chg 1, U.S. Department of Energy, Washington, D.C., May 8.

DOE 2013c. *Groundwater Strategy for the U.S. Department of Energy, Oak Ridge Reservation, Oak Ridge, Tennessee*, DOE/OR/01-2628/V2&D1, U.S. Department of Energy, Oak Ridge, TN, September.

DOE 2014. *Optimizing Radiation Protection of the Public and the Environment for use with DOE O 458.1, ALARA Requirements*, DOE-HDBK-1215-2014, U.S. Department of Energy, Washington, D.C., October.

DOE 2015a. *Oak Ridge Reservation Annual Site Environmental Report for 2014*, DOE/ORO/2502, U.S. Department of Energy, Oak Ridge, TN, September.

DOE 2015b. *2015 Remediation Effectiveness Report for the U.S. Department of Energy Oak Ridge Reservation Oak Ridge, Tennessee*, DOE/OR/01-2675&D1, U.S. Department of Energy, Oak Ridge, TN, March.

DOE 2015c. *Performance Assessment Report for the Proposed Disposal Facility at the Portsmouth Gaseous Diffusion Plant, Piketon, Ohio*, DOE/PPPO/03-0607&D2, U.S. Department of Energy, Lexington, KY.

DOE 2016a. *Oak Ridge Reservation Regional Groundwater Flow Model Development – Fiscal Year 2016 Progress Report, 2016*, DOE/OR/01-2743&D1, U.S. Department of Energy, Oak Ridge, TN.

DOE 2016b. *Sampling and Analysis Plan/Quality Assurance Project Plan for Environmental Monitoring at the Environmental Management Waste Management Facility, Oak Ridge, Tennessee*, DOE/OR/01-2734&D1, U.S. Department of Energy, Oak Ridge, TN, November.

DOE 2017a. *2017 Disposal Authorization Statement and Tank Closure Documentation*, DOE-STD-5002-2017, U.S. Department of Energy, Washington, D.C, July.

DOE 2017b. *Remedial Investigation/Feasibility Study for Comprehensive Environmental Response, Compensation, and Liability Act Oak Ridge Reservation Waste Disposal, Oak Ridge, Tennessee*, DOE/OR/01-2535&D5, U.S. Department of Energy, Oak Ridge, TN, February.

DOE 2017c. *Remediation Effectiveness Report for the U.S. Department of Energy Oak Ridge Reservation, Oak Ridge, Tennessee*, DOE/OR/01-2731&D2, U.S. Department of Energy, Oak Ridge, TN.

DOE 2018a. *Proposed Plan for the Disposal of Oak Ridge Reservation Comprehensive Environmental Response, Compensation, and Liability Act (CERCLA) Waste*, DOE/OR/01-2695&D2/R1 U.S. Department of Energy, Oak Ridge, TN, September.

DOE 2018b. *Technical Memorandum #1, Environmental Management Disposal Facility Phase 1 Field Sampling Results Oak Ridge, Tennessee*, DOE/OR/01-2785&D1, U.S. Department of Energy, Oak Ridge, TN, July.

DOE 2018c. *2018 Remediation Effectiveness Report for the U.S. Department of Energy Oak Ridge Site, Oak Ridge, Tennessee*, DOE/OR/01-2757&D2, U.S. Department of Energy, Oak Ridge, TN, September.

DOE 2019. *Technical Memorandum #2, Environmental Management Disposal Facility, Phase 1 Monitoring*, DOE/OR/01-2819&D1, U.S. Department of Energy, Oak Ridge, TN, May.

Dorsch and Katsube 1996. *Effective Porosity and Pore-Throat Sizes of Mudrock Saprolite from the Nolichucky Shale within Bear Creek Valley on the Oak Ridge Reservation: Implications for Contaminant Transport and Retardation Through Matrix Diffusion*, ORNL/GWPO-025, J. Dorsch and T. J. Katsube, Oak Ridge National Laboratory, Oak Ridge, TN, May.

Dorsch et al. 1996. *Effective Porosity and Pore-Throat Sizes of Conasauga Group Mudrock: Application, Test and Evaluation of Petrophysical Techniques*, ORNL/GWPO-021, J. Dorsch, T. J. Katsube, W. E. Sanford, B. E. Dugan, and L. M. Tourkow, Oak Ridge National Laboratory, Oak Ridge, TN.

Dreier et al. 1987. "Vol. 42, Flow and Transport Through Unsaturated Fractured Rock," *American Geophysical Union Monograph*, R. B. Dreier, D. K. Solomon, and C. M. Beaudoin, pages 51-59.

Dreier et al. 1993. *Results and Interpretation of Groundwater Data Obtained from Multiport-Instrumented Coreholes (GW-131 through GW-135), Fiscal Years 1990 and 1991*, Y/TS-803, R.B. Dreier, T.O. Early, and H.L. King, Oak Ridge National Laboratory, Oak Ridge, TN, January.

Dreier and Davidson 1994. "Fracture Spacing and Connectivity Observed in Multiport Instrumented Wells," *Geological Society of America Abstracts with Programs*, v. 25, no. 7, p. A412, R. B. Dreier and G.L. Davidson.

Driese et al. 2001. "Lithologic and pedogenic influences on porosity distribution and groundwater flow in fractured sedimentary saprolite: a new application of environmental sedimentology", S. G. Dreise, L. D. McKay, and C. P. Penfield, *Journal of Sedimentary Research*, Vol.71, No. 5, September, p.843-857.

EPA 1990. *Exposure Factors Handbook*, EPA/600/8-89/043, U.S. Environmental Protection Agency, Office of Health and Environmental Assessment, Washington, D.C.

EPA 1999. *Understanding Variation In Partition Coefficient, K_d, Values. Volume II: Review of Geochemistry and Available K_d Values for Cadmium, Cesium, Chromium, Lead, Plutonium, Radon, Strontium, Thorium, Tritium (^3H), and Uranium*, EPA 402-R-99-004B, U.S. Environmental Protection Agency, Office of Air and Radiation, Washington, D.C., August.

EPA 2000. Final Radionuclides Rule, 66 Federal Register 76708, Vol. 65, No. 236, U.S. Environmental Protection Agency, December 7.

EPA 2002a. *Radionuclides in Drinking water: A Small Entity Compliance Guide*, U.S. Environmental Protection Agency, Office of Ground Water and Drinking Water, Washington, D.C., February.

EPA 2002b. *U.S. Implementation Guidance for Radionuclides*, EPA 816-F-00-002, U.S. Environmental Protection Agency, Office of Ground Water and Drinking Water, Washington, D.C., March.

EPA 2004. *Understanding Variation in Partition Coefficient, K_d, Values*, EPA 402-R-04-002C, U.S. Environmental Protection Agency, Office of Air and Radiation, Washington, D.C., July.

EPA 2011. *Exposure Factors Handbook: 2011 Edition*, EPA/600/R-090/052F, U.S. Environmental Protection Agency, Washington, D.C., September.

Evans et al. 1996. "Application of particle tracking and inverse modeling to reduce flow model calibration uncertainty in an anisotropic aquifer system," *Proceedings of the ModelCARE 96 Conference: Calibration and Reliability in Groundwater Modelling*, E. K. Evans, C. Lu, S. Ahmed, and J. Archer, Golden, CO.

Friedman et al. 1990. *Laboratory Measurement of Radionuclides Sorption in Solid Waste Storage Area 6 Soil/Groundwater Systems*, ORNL/TM-10561, Oak Ridge National Laboratory, Oak Ridge, TN, June.

Gelhar et al. 1992. "A Critical Review of Data on Field-Scale Dispersion in Aquifer," L. W. Gelhar, C. Welty, and K. R. Rehfeldt, *Water Resources Research*, v. 28, no. 7, pages 1955-1974.

Geraghty and Miller 1986. *Aquifer Test Data and Design of Recovery Wells, S-3 Ponds*, Y/SUB/86-O0206C/3, Geraghty and Miller, Oak Ridge, TN.

Geraghty and Miller 1990. *Development of Ground-Water Flow Models for the S-3 Waste Management Area, Y-12 Facility, Oak Ridge, Tennessee*, Y/SUB/89-00206C/3, Geraghty and Miller, Oak Ridge, TN.

Gil-Garcia et al. 2008. "New best estimates for radionuclide solid–liquid distribution coefficients in soils. Part 3: miscellany of radionuclides (Cd, Co, Ni, Zn, I, Se, Sb, Pu, Am, and others)", *Journal of Environmental Radioactivity*, 100, 704–715.

Gnanapragasam and Yu 2015. *User's Guide for RESRAD-OFFSITE*, NUREG/CR-7189, ANL/EVS/TM-14/2, E. K. Gnanapragasam and C. Yu, Argonne National Laboratory, Argonne, IL, U.S. Nuclear Regulatory Commission, Rockville, MD, April.

Golder 1988a. *Task 2 – Well Logging and Geohydrologic Testing, Site Characterization, and Groundwater Flow Computer Model Application*, Vol. 1, Martin Marietta Energy Systems, Inc. (MMES) Contract No. 30X-SA706C; Golder Associates, Inc., May (copy unavailable).

Golder 1988b. *Task 5 – Contaminant Transport Model Validation, Geohydrologic Site Characterization, and Groundwater Flow Computer Model Application*, Vol. 1, MMES Contract No. 30X-SA706C; ORNL/Sub/88-SA706/5/V1, Golder Associates, Inc., September.

Golder 1989. *Task 7 – Groundwater Flow Computer Model*, MMES Contract No. 30X-SA706C, Golder Associates, Inc., September.

Gu et al. 2011. "Dissolution of technetium (IV) oxide by natural and synthetic organic ligands under both reducing and oxidizing conditions", B. Gu, Wenming Dong, Liyuan Liang, and N. A. Wall, *Environmental Science & Technology* 45, 4771-4777.

Haase 1991. *Geochemical Identification of Groundwater Flow Systems in Fractured Bedrock Near Oak Ridge, Tennessee*, C. S. Haase, Oak Ridge National Laboratory, Oak Ridge, TN. Source: info.ngwa.org/gwol/pdf/910155202.pdf.

Haase et al. 1985. *Geology of the Host Formation for the New Hydrofracture Facility at the Oak Ridge National Laboratory*, C. S. Haase, S. H. Stow, and C. L. Zucker, Waste Man agement Symposium 1985, v. 2, pages 473-480.

Haase et al. 1987. *Geochemistry of Formation Waters in the Lower Conasauga Group at the New Hydrofracture Facility: Preliminary Data from the Deep Monitoring (DM) wells*, ORNL/RAP-6, C. S. Haase, J. Switek, and S. H. Stow, Oak Ridge National Laboratory, Oak Ridge, TN.

Hatcher et al. 2012. *Large earthquake paleoseismology in the East Tennessee seismic zone: Results of an 18-month pilot study*, Special Paper 493, R. D. Hatcher, Jr., J. D. Vaughn, and S. F. Obermeier, The Geological Society of America, Boulder, CO.

IAEA 2010. *Handbook of Parameter Values for the Prediction of Radionuclide Transfer in Terrestrial and Freshwater Environments*, Technical Reports Series No. 472, International Atomic Energy Agency, Vienna, Austria.

ICRP (International Commission on Radiological Protection) 2008. *Nuclear Decay Data for Dosimetric Calculations*, Publication 107, International Commission on Radiological Protection, Ottawa, Ontario K1P 5S9, Canada.

Jackson et al. 1996. *A global analysis of root distributions for terrestrial biomes.* R.B. Jackson, J. Canadell, J.R. Ehleringer, H.A. Mooney, O.E. Sala- E.-D. Schulze. Oecologia 108:389-411.

Kaplan et al. 2000. "Iodide Sorption to Subsurface Sediments and Illitic Minerals", D. I. Kaplan, R.J. Serne, K.E. Parker, and I.V Kutnyakov, *Environmental Science and Technology*, 34 (3) pages 399-405, December.

Kaplan et al. 2013. *Radioiodine Geochemistry in the SRS Subsurface Environment*, SRNL-STI-2012-00518, D. I. Kaplan, H. P. Emerson, B. A.Powell, K. A. Roberts, S. Zhang, C. Xu, K. A. Schwehr, H. P. Li, Y. F. Ho, M. E. Denham, C. Yeager, and P. H. Santschi, Savannah River National Laboratory, Aiken, SC, May.

Kaplan et al. 2014. "Radioiodine biogeochemistry and prevalence in groundwater", D. I. Kaplan, M. E. Denham, S. Zhang, C. Yeager, C. Xu, K. A. Schwehr, H. P. Li, Y. F. Ho, D. Wellman, and P. H. Santschi, *Critical Reviews of Environmental Science and Technology*, 44, 2287-2337.

Kim et al. 2009. "Mineralogical characterization of saprolite ast the FRC background site in Oak Ridge, Tennessee", Y-J.Kim, J-W. Moon, Y. Roh, and S.C. Brooks, *Environmental Geology* 58: 1301-1307.

King and Haase 1987. *Subsurface-Controlled Geological Maps for the Y-12 Plant and Adjacent Areas of Bear Creek Valley*, ORNL/TM-10112, H. L. King and C. S. Haase, Oak Ridge National Laboratory, Oak Ridge, TN.

Kitchings and Mann 1976. *A Description of the Terrestrial Ecology of the Oak Ridge Environmental Research Park*, ORNL/TM-5073, T. Kitchings and L. K. Mann, Oak Ridge National Laboratory, Oak Ridge, TN.

Law Engineering 1983. *Results of Ground-Water Monitoring Studies at Y-12 Plant*, Y/SUB/83-47936/1, Law Engineering, Oak Ridge, TN.

Lee and Ketelle 1989. *Geology of the West Bear Creek Site*, ORNL/TM-10887 R. R. Lee and R. H. Ketelle, Oak Ridge National Laboratory, Oak Ridge, TN.

Lee et al. 1992. “Aquifer Analysis and Modeling in a Fractured Heterogeneous Medium,” R. R. Lee, R. H. Ketelle, J. M. Bownds, and T. A. Rizk, *Groundwater*, vol. 30, no. 4, pages 589-597.

Lemiszki, P. J. 2000. *Geologic Map of the Bethel Valley Quadrangle, Tennessee*, Geologic Quadrangle Map 130-NE, Tennessee Division of Geology, Nashville, TN.

Lietzke et al. 1988. *Soils, Surficial Geology, and Geomorphology of the Bear Creek Valley Low-Level Waste Disposal Development and Demonstration Program Site*, ORNL/TM-10573, D. A. Lietzke, S. Y. Lee, and R. E. Lambert, Oak Ridge National Laboratory, Oak Ridge, TN.

Lozier et al. 1987. Aquifer Pump Test with Tracers, ORNL/SUB/86-32136, Golder and Associates, Inc., October.

Maheras et al. 1997. *Addendum to Radioactive Waste Management Complex Low-Level Waste Radiological Performance Assessment*, INEEL/EXT-97-00462 (formerly EGG-WM-8773), S. J. Maheras, A. S. Rood, S. O. Magnuson, M. E. Sussman, and R. N. Bhatt, Idaho National Engineering and Environmental Laboratory, Idaho Falls, ID, April.

McCracken et al. 2015. *Bat Species Distribution on the Oak Ridge Reservation*, ORNL/TM-2015/248, M. K. McCracken, N. R. Giffen, A. M. Haines, B. J. Guge, and J. W. Evans, Oak Ridge National Laboratory, Oak Ridge, TN, October.

McKay et al. 1997. “EPM Modeling of a Field-Scale Tritium Tracer Experiment in Fractured, Weathered Shale,” *Groundwater*, vol. 35, no.6, pages 997–1007, L. D. McKay, P. L. Stafford, and L. E. Toran.

McKay et al. 2000. “Field-Scale Migration of Colloidal Tracers in a Fractured Shale Saprolite,” *Groundwater*, vol. 38, no.1, pages 139–147, L. D. McKay, W. E. Sanford, and J. M. Strong.

Moline and Schreiber 1996. *FY94 Site Characterization and Multilevel Well Installation at a West Bear Creek Valley Research Site on the Oak Ridge Reservation*, ORNL/TM-13029, G.R. Moline and M. E. Schreiber, Oak Ridge National Laboratory, Oak Ridge, TN, March.

Moline et al. 1998. “Discussion of Nativ, et al. 1997,” *Groundwater*, Vol. 36, No. 5, pages 711-712, G. R. Moline, C. T. Rightmire, R. H. Ketelle, and D. D. Huff.

Moore and Toran 1992. *Supplement to a Hydrogeologic Framework for the Oak Ridge Reservation*, ORNL/TM-12191, G. K. Moore and L. E. Toran, Oak Ridge National Laboratory, Oak Ridge, TN, November.

Nativ et al. 1997a. *The Deep Hydrologic Flow System Underlying the Oak Ridge Reservation – Assessing the Potential for Active Groundwater Flow and Origin of the Brine*, ORNL/GWPO-018, R. Nativ, A. Halleran, and A. Hunley, Oak Ridge National Laboratory, Oak Ridge, TN.

Nativ et al. 1997b. “Evidence for Groundwater Circulation in the Brine-Filled Aquitard,” R. Nativ, A. Halleran, and A. Hunley, Oak Ridge, Tennessee, *Groundwater*, Vol. 35, No. 4, July-August.

Nichols et al. 1997. *STOMP – Subsurface Transport Over Multiple Phases Application Guide*, PNNL-11216 (UC-2010), W. E. Nichols, N. J. Aimo, M. Oostrom, M. D. White, Pacific Northwest National Laboratory, Richland, WA.

NRC 1984. *Radon Attenuation Handbook for Uranium Mill Tailings Cover Design*, NUREG/CR-3533, U.S. Nuclear Regulatory Commission, Washington, D.C., April.

Ogden 1993a. *Geotechnical Study, ORR Storage Facility, Site "B", Y-12 Plant, Oak Ridge, Tennessee,* Contract No. 88B-99977V, Release C-53, Ogden Environmental and Energy Services, Knoxville, TN, May.

Ogden 1993b. *Geotechnical Study, ORR Storage Facility, Site "C", Y-12 Plant, Oak Ridge, Tennessee,* Contract No. 88B-99977V, Release C-53, Ogden Environmental and Energy Services, Knoxville, TN, May.

ORNL 1984. *Site Characterization Techniques Used at a Low-Level Waste Shallow Land Burial Field Demonstration Facility*, ORNL-9146, Oak Ridge National Laboratory, Oak Ridge, TN, July.

ORNL 1987. *Geochemical Behavior of Cs, Sr, Tc, Np, and U in Saline Groundwaters: Sorption Experiments on Shales and Their Clay Mineral Components*, ORNL/TM-10364, Oak Ridge National Laboratory, Oak Ridge, TN, November.

ORNL 1992a. *Status Report on the Geology of the Oak Ridge Reservation*, ORNL/TM 12074, Environmental Sciences Division Publication No. 3860, Oak Ridge National Laboratory, Oak Ridge, TN, October.

ORNL 1992b. *Status Report: A Hydrologic Framework for the Oak Ridge Reservation*, ORNL/TM-12026, Oak Ridge National Laboratory, Oak Ridge, TN, May.

ORNL 1996. *Report on the Biological Monitoring Program for Bear Creek at the Oak Ridge Y-12 Plant, Oak Ridge, Tennessee (1989-1994)*, ORNL/TM-12884, ESD Publication No. 4357, R. L. Hinzman (ed.), Oak Ridge National Laboratory, Oak Ridge, TN, April.

ORNL 1997a. *Performance Assessment for Continuing and Future Operations at Solid Waste Disposal Area 6*, ORNL-6783/R1, Volume 1, Oak Ridge National Laboratory, Oak Ridge, TN, September.

ORNL 1997b. *Performance Assessment for the Class L-II Disposal Facility*, ORNL/TM-13401, Oak Ridge National Laboratory, Oak Ridge, TN, March.

ORNL 2002. *Oak Ridge National Laboratory Land and Facilities Plan*, ORNL/TM-2002/1, Oak Ridge National Laboratory, Oak Ridge, TN.

ORNL 2014. *Climate Normals (1981-2010) and Extremes (1948-2015) for Oak Ridge, Tennessee (Town Site) with 2015 Comparisons*, Oak Ridge National Laboratory, Oak Ridge, TN. https://web.ornl.gov/~birdwellkr/web/Normals/30YEARNorm.pdf, last accessed March 12, 2018.

ORNL 2018. *Natural Resource Assessment for the Proposed Environmental Management Disposal Facility (EMDF), Oak Ridge, Tennessee*, ORNL/TM-2018/515, Oak Ridge National Laboratory, Oak Ridge, TN, June.

Parr and Hughes 2006. *Oak Ridge Reservation Physical Characteristics and Natural Resources*, ORNL/TM-2006/110, P. D. Parr and J.F. Hughes, Oak Ridge National Laboratory, Oak Ridge, TN.

Peterson et al. 2005. *Environmental Survey Report for the ETTP: Environmental Management Waste Management Facility (EMWMF) Haul Road Corridor, Oak Ridge, Tennessee*, ORNL/TM-2005/215, M. J. Peterson, N. R. Giffen, M. G. Ryon, L. R. Pounds, and E. L. Fyan, Jr., Oak Ridge National Laboratory, Oak Ridge, TN, September.

Peterson et al. 2009. *Performance Monitoring Report for the Restored North Tributary 3 (NT-3), Bear Creek Valley, Oak Ridge, Tennessee*, ORNL/TM-2009/53, M. J. Peterson, J. G. Smith, M. G. Ryon, W. K. Roy, and J. A. Darby, Oak Ridge National Laboratory, Oak Ridge, TN.

PNNL 2003. *A Compendium of Transfer Factors for Agricultural and Animal Products*, PNNL-13421, L. H. Staven, B. A. Napier, K. Rhoads, and D. L. Strenge, Pacific Northwest National Laboratory, Richland, WA, June.

Powell et al. 1994. *A Seismotectonic Model for the 300-Kilometer-Long Eastern Tennessee Seismic Zone*, *Science*, v. 264, 29, C. A. Powell, G. A. Bollinger, M. C. Chapman, M. S. Sibol, A. C. Johnston, and R. L. Wheeler, April, pages 686–688.

Putnam et al. 1999. *Food Consumption, Prices, and Expenditure, 1970–1997*, J. J. Putnam, J. E. Allshouse, U.S. Department of Agriculture, Statistical Bulletin No. 965, Washington, D.C., April.

Robinson and Johnson 1995. *Results of a Seepage Investigation at Bear Creek Valley, Oak Ridge, Tennessee January – September 1994*, USGS Open-File Report 95-459, J. A. Robinson and G. C. Johnson, U.S. Geological Survey, Reston, VA.

Robinson and Mitchell 1996. *Gaining, Losing, and Dry Stream Reaches at Bear Creek Valley, Oak Ridge, Tennessee March and September 1994*, USGS Open-File Report 96-557, J. A. Robinson and R. L. Mitchell III, U.S. Geological Survey, Reston, VA.

Rosensteel and Trettin 1993. *Identification and Characterization of Wetlands in the Bear Creek Watershed*, Y/TS-1016, B. A. Rosensteel and C. C. Trettin, Environmental Sciences Division, Oak Ridge National Laboratory, Oak Ridge, TN, October.

Rothschild et al. 1984. *Characterization of Soils at Proposed Solid Waste Storage Area (SWSA) 7*, ORNL/TM-9326, E. R. Rothschild, D. D. Huff, B. P. Spalding, S. Y. Lee, R.B. Clapp, D. A. Lietzke, R. G. Stansfield, N. D. Farrow, C. D. Farmer, I. L. Munro, Oak Ridge National Laboratory, Oak Ridge, TN, December.

Ryon 1998. *Evaluation of Protected, Threatened, and Endangered Fish Species in Upper Bear Creek Watershed*, ORNL/M-6567, M. G. Ryon, Oak Ridge National Laboratory, Oak Ridge, TN.

Sanford and Solomon 1998. "Site characterization and containment assessment with dissolved gases", *J. Environmental Engineering*, vol. 124, no. 6, pages 572-574, W. E. Sanford and D. K. Solomon.

Sanford et al. 1996. "Dissolved gas tracers in groundwater: Simplified injection, sampling, and analysis," *Water Resources Research*, vol. 32, no. 6, pages 1635-642, W. E. Sanford, R. G. Shropshire, and D. K. Solomon.

Schreiber 1995. *Spatial Variation in Groundwater Chemistry in Fractured Rock: Nolichucky Shale, Oak Ridge, TN*, M. E. Schrieber, Master Thesis: University of Wisconsin-Madison, Madison, WI.

Schreiber et al. 1999. "Using Hydrochemical Facies to Delineate Groundwater Flowpaths in Fractured Shale," *Groundwater Monitoring Review – Winter 1999*, p. 95-109, M. E. Schreiber, G. R. Moline, and J. M. Bahr.

Schroeder et al. 1994. *The Hydrologic Evaluation of Landfill Performance (HELP) Model: Engineering Documentation for Version 3*, EPA/600/R-94/168b, P. R. Schroeder, T. S. Dozier, P. A. Zappi, B. M. McEnroe, J. W. Sjostrom, and R. L. Peyton, U.S. Environmental Protection Agency, Office of Research and Development, Washington, D.C., September.

Serne R., 2007. *Kd Values for Agricultural and Surface Soils for Use in Hanford Site Farm, Residential, and River Shoreline Scenarios*, PNNL-16531, Pacific Northwest National Laboratory, Richland, WA, August.

Sheppard and Thibault 1990. "Default Soil Solid/Liquid Partition Coefficients, K_ds, for Four Major Soil Types: A Compendium," *Health Physics*, M. Sheppard and D. H. Thibault, Vol. 59, No. 4, pages 471-481, October.

Sledz and Huff 1981. *Computer Model for Determining Fracture Porosity and Permeability in the Conasauga Group, Oak Ridge National Laboratory, Tennessee*, ORNL/TM-7695, J. J. Sledz and D. D. Huff, Oak Ridge National Laboratory, Oak Ridge, TN.

Smith and Vaughn 1985. "Aquifer test analysis in nonradial flow regimes: A case study," *Ground Water*, Vol. 23, no. 2, pages 167-175, E. D. Smith and N. D. Vaughn.

Southworth et al. 1992. *Ecological Effects of Contaminants and Remedial Actions in Bear Creek*, ORNL/TM-11977, G. R. Southworth, J. M. Loar, M. G. Ryon, J. S. Smith, A. J. Stewart, and J. A. Burris, Oak Ridge National Laboratory, Oak Ridge, TN.

Stafford et al. 1998. "Influence of fracture truncation on dispersion: A dual permeability model," *Journal of Contaminant Hydrology*, 30, p. 79-100, P. Stafford, L. Toran, and L. McKay.

Stover and Coffman 1993. *Seismicity of the United States 1568 – 1989 (Revised)*, USGS Prof. Paper 1527, C. W. Stover and J. L. Coffman, U.S. Geological Survey, Reston, VA.

Stumm, W, and J Morgan 1996. "Aquatic Chemistry, Chemical Equilibria and Rates in Natural Waters," John Wiley & Sons, Inc., New York.

Tang et al. 2010. "Long-Term Nitrate Migration and Attenuation in a Saprolite/Shale Pathway from a Former Waste Disposal Site," abstract published in *Geochinica et Cosmochimica Acta*, vol. 27, no. 12, Supplement 1 A1118 for Goldschmidt 2010 Conference, G. Tang, D. B. Watson, J. C. Parker, P. M. Jardine, and S. C. Brooks, S.C.

Tian et al. 2017. "Antioxidant Depletion and Service Life Prediction for HDPE Geomembranes Exposed to Low-Level Radioactive Waste Leachate", *Geotechnical & Geoenvironmental Engineering*, K. Tian, C. H. Benson, J. M. Tinjum, Vol. 143 Issue 6, June.

TVA 2012. *Water Use in the Tennessee Valley for 2010 and the Projected Use in 2035*, Tennessee Valley Authority, Knoxville, TN, July.

TVA 2016. Clinch River Nuclear Site License-Application for Early Site Permit (ESP), Site Safety Analysis Report (SSAR), Revision 0, May 25.

UCOR 2013. *Engineering Feasibility Plan for the Elevated Groundwater Levels in the Vicinity of PP-01, EMWMF, Oak Ridge, Tennessee*, UCOR-4517, UCOR, Oak Ridge, TN.

UCOR 2014. *Oak Ridge Reservation Regional Groundwater Flow Model Development – Fiscal Year 2014 Progress Report, U.S. Department of Energy Oak Ridge Reservation Oak Ridge, Tennessee*, UCOR-4634/R0, UCOR, Oak Ridge, TN, November.

UCOR 2015. *Regional Groundwater Flow Model Development – Fiscal Year 2015 Progress Report, U.S. Department of Energy Oak Ridge Reservation Oak Ridge, Tennessee*, UCOR-4753/R0, UCOR, Oak Ridge, TN, December.

UCOR 2018a. *Safety Design Strategy for the Environmental Management Disposal Facility, Y-12 National Security Complex, Oak Ridge, Tennessee*, SDS-YT-EMDF-0001/R1, UCOR, Oak Ridge, TN, September.

UCOR 2018b. *Conceptual Safety Design Report for the Environmental Management Disposal Facility, Y-12 National Security Complex, Oak Ridge, Tennessee*, CSDR-YT-EMDF-0001, UCOR, Oak Ridge, TN, February.

UCOR 2019. *URS | CH2M Oak Ridge LLC Quality Assurance Program Plan Oak Ridge, Tennessee*, UCOR-4141/R6, UCOR, Oak Ridge, TN, June.

UCOR 2020a. *Composite Analysis for the Environmental Management Waste Management Facility and the Environmental Management Disposal Facility, Oak Ridge, Tennessee*, UCOR-5095/R2 UCOR, Oak Ridge, TN, April.

UCOR 2020b. *Quality Assurance Report for Modeling of the Bear Creek Valley Low-level Radioactive Waste Disposal Facilities, Oak Ridge, Tennessee*, UCOR-5234/R0, UCOR, Oak Ridge, TN, April.

USDA 1986. *Urban Hydrology for Small Watersheds (TR-55)*, U.S. Department of Agriculture Natural Resources Conservation Service, Conservation Engineering Division Technical Release 55, June.

USGS 1988a. *A Modular Three-Dimensional Finite Difference Groundwater Flow Model*, Book 6, Modeling Techniques, Chapter A1, M. G. McDonald and A. W. Harbaugh, U.S. Geological Survey, Reston, VA.

USGS 1988b. *Preliminary Evaluation of Groundwater Flow in Bear Creek Valley, Oak Ridge Reservation, Tennessee*, WRIR 88-4010, U.S. Geological Survey, Reston, VA.

USGS 1989. *Study and Interpretation of the Chemical Characteristics of Natural Water*, U.S. Geological Survey Water-Supply Paper 2254, J. D. Hem, U.S. Geological Survey, Reston, VA.

USGS 2013. Earthquake Probability Map for Magnitude 5 and 7 within 1000 years for Oak Ridge, Tennessee, map developed at http://geohazards.usgs.gov/eqprob/2009/index.php on October 18.

USGS 2020. Earthquake Magnitude, Energy Release, and Shaking Intensity, U.S. Geological Survey, https://www.usgs.gov/natural-hazards/earthquake-hazards/science/earthquake-magnitude-energy-release-and-shaking-intensity.

Valocchi 1985. "Validity of the Local Equilibrium Assumption for Modeling Sorbing Solute Transport Through Homogeneous Soils," *Water Resources Research*, Vol 21, No. 6, pages 808-820, A. J. Valocchi, June.

Watson et al. 2004. *The Oak Ridge Field Research Center Conceptual Model*, Environmental Sciences Division, Oak Ridge National Laboratory, August.

Webster 1996. *Results of Ground-Water Tracer Tests Using Tritiated Water at Oak Ridge National Laboratory, Tennessee*, Water-Resources Investigations Report 95-4182, D. A. Webster, U.S. Geological Survey, Reston, VA.

White and Oostrom 2000. *STOMP Subsurface Transport over Multiple Phases: Theory Guide*, PNNL-12030 (UC-2010), M. D. White and M. Oostrom, Pacific Northwest National Laboratory, Richland, WA.

White and Oostrom 2006. *STOMP Subsurface Transport over Multiple Phases, Version 4.0, User's Guide*, PNNL-15782, M. D. White and M. Oostrom, Pacific Northwest National Laboratory, Richland, WA.

WMFS 2000. *Final Site Investigation Report, SSRS Item No. 3.5, Rev. 1*, August 2000, prepared for Bechtel Jacobs Company LLC, Oak Ridge, TN, August.

Xu et al. 2015. "Radioiodine Sorption/desorption and Speciation Transformation by Subsurface Sediments from the Hanford Site", *Journal of Environmental Radioactivity*, 139, pg. 43-55.

Yu et al. 2001. *User's Manual for RESRAD Version 6*, ANL/EAD-4 C. Yu, A.J. Zielen, J.-J. Cheng, D.J. LePoire, E. Gnanapragasam, S. Kamboj, J. Arnish, A. Wallo III, W.A. Williams, and H. Peterson Environmental Assessment Division Argonne National Laboratory, Argonne, IL, July.

Yu et al. 2007. *User's Manual for RESRAD-OFFSITE Version 2* ANL/EVS/TM/07-1, C. Yu, E. K. Gnanapragasam, B. M. Biwer, S. Kamboj, J.-J. Cheng, T. Klett, D. LePoire, A. J. Zielen, S. Y. Chen and W. A. Williams, Argonne National Laboratory, Argonne, IL, June.

Yu et al. 2013. *New Source Term Model for the RESRAD-OFFSITE Code Version 3*. NUREG/CR-7127, ANL/EVS/TM/11-5, C. Yu, E. Gnanapragasam, J.-J. Cheng, S. Kamboj, and S.Y. Chen, U.S. Nuclear Regulatory Commission, Office of Nuclear Regulatory Research, Washington, D.C.

Yu et al. 2015. *Data Collection Handbook to Support Modeling Impacts of Radioactive Material in Soil and Building Structures*, ANL/EVS/TM-14/4, C. Yu, J.-J. Cheng, L. Jones, Y. Wang, Y. Chia, and E. Faillace, Argonne National Laboratory for U.S. Department of Energy, Office of Science, Oak Ridge, TN, September.

Zheng 1990. *A Modular Three-Dimensional Transport Model for Simulation of Advection, Dispersion and Chemical Reactions of Contaminants in Groundwater Systems; Documentation and Users Guide*, report to the U.S. Environmental Protection Agency, C. Zheng, S.S. Papadopulos & Associates, Inc., Bethesda, MD.

Zheng and Bennett 1995. *Applied Contaminant Transport Modeling: Theory and Practice***,** John Wiley & Sons, New York, page 440.

This page intentionally left blank.

APPENDIX A.
PERFORMANCE ASSESSMENT REVIEW CRITERIA

This page intentionally left blank.

Performance Assessment Review Criteria

ID	Review criteria	Preparer guidance for reviewers
PA-1	The PA provides an adequate description of other relevant statutes, regulations and/or agreements that have an influence on the assumptions for the PA or criteria that are applied.	FFA requirements are briefly described in Sect. 1.1.1 and the introductory paragraph of Sect. 1.5 of the EMDF PA. Sect. 1.5.5 provides a general description of DOE safety design basis requirements and FFA/CERCLA requirements that may be relevant to the EMDF PA.
PA-2	The PA adequately identifies and describes other modeling efforts for the facility and other programs at the site in the context of consistency with assumptions made in the PA. Any existing secondary issues from previous PAs are identified and potential inconsistencies with other modeling efforts are identified and addressed.	Sect. 1.1.2 identifies PAs for SWSA 6 in Melton Valley and for the EMWMF in BCV for comparison to the EMDF PA. Table 1.1 summarizes key attributes and assumptions of the EMDF, EMWMF, and SWSA 6 analyses to facilitate reviewer comparison. The IHI scenarios analyzed for the SWSA 6 are compared to the EMDF IHI scenarios in Appendix I, Sect. I.3. The CA for EMWMF and EMDF also is identified in Sect. 1.1.2 and the difference in the exposure scenario assumptions between the EMDF CA and PA is explained. Following an LFRG review of Revision 1 of the EMDF PA, extensive modifications to the analysis were completed to resolve all of the primary and many of the secondary issues identified in the LFRG review report. One of the secondary issues was providing adequate information on other relevant modeling efforts. Table 1.1 was prepared to resolve that issue.
PA-3	The PA adequately describes the total disposal system, including roles of key features, and assumptions regarding operations, design and closure that are critical to the conclusions and meeting the performance objectives and must be protected in procedures, closure documentation and/or other regulatory agreements.	Sect. 1.2 provides a general description of EMDF, including operations. Sections 1.3 and 2.2 and Appendix C of the EMDF PA describe the design features and safety functions of the disposal system, including the roles of engineered barriers and site characteristics. Site characteristics are described in detail in Sect. 2.1, including a summary of the results of recently completed characterization of the EMDF site. EMDF waste characteristics and the estimated radiological inventory are described in Sect. 2.3. Section 3.2.2 and Appendix B also address waste characteristics relevant to the PA. Section 1.7 presents a list of key model input parameter assumptions and key conceptual model assumptions that are critical to the PA conclusions. These key assumptions are referenced in the UCOR, an Amentum-led partnership with Jacobs, procedure PROC-EMDF-0001, *EMDF Design DOE Order 435.1 Changed Condition*, for screening and evaluation of design changes or other new information that has the potential to change the DOE O 435.1 compliance conclusions of PA.
PA-4	The PA adequately describes the context for the performance assessment and compliance with requirements in DOE O 435.1A: *The context includes the performance objectives from DOE O 435.1A and any alternative indicators that may be used, the basis for the selection of specific radon and water resources protection objectives, the basis for the time periods considered and receptor locations (points of assessment), approach used to determine compliance during the compliance period (probabilistic or deterministic) and to assess impacts after the compliance period (e.g., alternative indicators), general approach*	Section 1.1 describes the context and need for the PA. Section 1.5 describes the regulatory context for the PA, including DOE M 435.1-1 performance objectives (Sects. 1.5.1 and 1.5.3), assumed points of assessment and time periods for analysis (Sect. 1.5.2), ALARA requirements (Sect. 1.5.4), and DOE safety design and FFA requirements (Sect. 1.5.5).

Performance Assessment Review Criteria (cont.)

ID	Review criteria	Preparer guidance for reviewers
	adopted to address inadvertent intrusion (e.g., timing and extent), and considerations related to ALARA. *The PA time of compliance is a 1,000 year period after the assumed end of facility operations. If a longer compliance period is used (e.g., required by other DOE programs and plans; or other applicable Federal, state, or local statutes, regulations, or agreements), documentation is provided to support the longer time frame. The location of the point of assessment is clearly identified and justified based on land use and institutional control assumptions.*	
PA-5	The PA adequately describes the Site Characteristics and their significance to support the site evaluation process and to support the assumptions made for the conceptual models and site evolution that were adopted. *The site characteristics include a broad collection of information, including but not limited to geography and demographics, land uses, meteorology, hydrology, geochemistry, natural resources, and background radiation levels. Uncertainties and reasonably foreseeable natural processes that could affect the evolution of the system are also addressed. The basis for ranges or distributions of parameters used for uncertainty quantification are adequately justified.*	Detailed description of the characteristics of BCV and the CBCV site is contained in Sect. 2.1 of the EMDF PA report. The information presented encompasses the geography, demographics, climate, geology, hydrology, geochemistry, biology, and natural resources of BCV. A summary of recently completed characterization of the CBCV site and references to full documentation are also included in Sect. 2.1. This information supports the conceptual models of the disposal system that are presented in Sect. 3.2. The conceptual model incorporating uncertainties in site characteristics and reasonably foreseeable natural processes that could affect evolution of the EMDF disposal system is presented in Sect. 3.2.1. Appendix C, Sect. C.1, contains a review of features, events, and processes that can potentially affect the long-term performance of the EMDF disposal system. The empirical basis for assumed values of hydraulic conductivity (K) is presented in Sects. 2.1.5.3 and 2.1.5.4 and Appendix D. The empirical basis for ranges of solid-aqueous partition coefficient (K_d) values is described in Sect. 2.1.6.3 and Sects. 3.2.2.6 through 3.2.2.8. The basis for ranges and distributions of parameters used for uncertainty quantification is presented in Appendix G, Sect. G.6.3.2.1 and Attachment G.3.
PA-6	The PA adequately describes the facility design and operational approach and the significance of different features to support the conceptual models and evolution of parameters over time. *The facility design includes a detailed description of any engineered barriers and a description of their functional roles in terms of controlling releases from the facility, specifics about waste placement plans, and the expected waste inventory. Waste forms and containers are also generally discussed in the context of the placement plans. Uncertainties, data gaps and the expected evolution of the design features are also addressed.*	A general facility description, overview of EMDF design features and safety functions, and facility life cycle are presented in Sects. 1.2, 1.3, and 1.4, respectively. Principal facility design features are discussed in Sect. 2.2. The conceptual model incorporating EMDF design features, safety functions, and events and process that could affect evolution of the EMDF disposal system is presented in Sect. 3.2.1. Appendix C, Sect. C.1, contains a detailed review of design features, safety functions, and events and processes most likely to limit safety functions of each design feature. Characteristics of EMDF waste streams, including physical forms and estimated radiological inventories are summarized in Sect. 2.3 and presented in detail in Appendix B. Waste characteristics and disposal practices relevant to radionuclide release, including assumptions about waste forms and containers are discussed in Sect. 3.2.2.5.

Performance Assessment Review Criteria (cont.)

ID	Review criteria	Preparer guidance for reviewers
		Specifics concerning EMDF waste placement plans will be captured in operating documents.
PA-7	Radionuclide inventories and their basis, including uncertainty, are adequately documented and defensible. *Inventory estimates are quantified and supported by a thorough analysis of disposal records, data, studies and evaluations to ensure that all of the radionuclides disposed and anticipated to be present in forecast wastes are evaluated. The technical bases for estimates of the radionuclide concentrations, including assumptions for distributions or ranges for any uncertainties, for past and future waste disposal is sufficiently described and documented.*	Projected EMDF waste streams and waste characteristics and development of the estimated EMDF radionuclide inventory are summarized in Sect. 2.3. Detailed description of waste volume projections, anticipated waste characteristics, radiological data sources and procedures for developing estimated radiological profiles for each waste stream is provided in Appendix B. Management of EMDF inventory uncertainty is considered in Sect. B.6 of Appendix B.
PA-8	The radionuclides and pathways screened and included for the PA are clearly identified, and the bases for inclusion or screening and exclusion are adequately documented and defensible. *The screening method provides a logical basis for including or excluding radionuclides and pathways based on the expected contribution to the impacts and the influence on the conclusions of the assessment. Radionuclides and pathways that do not contribute significantly to the project dose and influence the decision are documented. A method to track changes in assumptions (e.g., unexpected increase in inventories, changes in conceptual models) that could change the results of screening and, for example, cause a radionuclide or pathway that had been screened to be included in the full PA is described.*	Release pathways are considered and screened based on expected contributions to public exposure in Sect. 3.2.2. Screening of biological and diffusive release pathways through the EMDF cover is justified in Sects. 3.2.2.1 through 3.2.2.3. Detailed description of implementation of the RESRAD-OFFSITE screening model release through the EMDF cover is provided in Appendix G, Sect. G.4.4.2 Exposure routes for all-pathways dose analysis are considered and selected in Sect. 3.2.4. Exposure due to IHI is addressed in Sects. 6.3 and 6.4. The results of radionuclide screening based on expected contributions to total dose for IHI scenarios and for the water pathway is described in Sects. 2.3.2 and 2.3.3. Figure 2.44 summarizes the radionuclide screening process. Detailed description of implementation of the RESRAD-OFFSITE screening model for the water pathway is provided in Appendix G, Sect. G.4.4.1. The UCOR procedure PROC-EMDF-0001, *EMDF Design DOE Order 435.1 Changed Condition*, is used to track changes in assumptions and is described in the introduction to Sect. 1.7.
PA-9	The characteristics of the waste are adequately described and provide a defensible basis for the conceptual model for the source term. *The physical and chemical characteristics of the waste that may affect the release of radionuclides including the potential interactions of chemical or hazardous constituents are adequately described. The physical and chemical characteristics of the waste form, including any waste treatments that affect contaminant release, are fully documented, and supported by laboratory or field studies. The expected effects of waste form and container degradation are incorporated in the analysis as necessary to support the intended use of the PA. Characteristics that are not credited in the analysis are identified to provide perspective on conservatisms. The basis for the assumptions is clearly described.*	Characteristics of the waste are described in Sect. 2.3.1 and Appendix B. Waste characteristics most relevant for source term conceptualization and modeling are considered in Sect. 3.2.2.5. Section 3.2.2.9 provides a summary of radionuclide release and vadose zone conceptual model assumptions relevant to the source term representation.
PA-10	The conceptual models for the source term, disposal facility and engineered features, and the natural system are adequately described and defensible. The description is sufficient to support selection of the mathematical models and development of the overall modeling approach. The interfaces between the source term, facility features, natural system and exposure pathways are clearly described.	An overview of conceptual models for specific features of the EMDF disposal system, including processes contributing to the evolution of facility performance, is provided in Sect. 3.1 which also provides an overview of the integration of conceptual models and model codes for the PA. Section 3.2 provides detailed descriptions of conceptual models for EMDF water balance and performance of

Performance Assessment Review Criteria (cont.)

ID	Review criteria	Preparer guidance for reviewers
	The PA provides a clear description of the conceptual model of the disposal facility and site, and constitutes a reasonable interpretation of the existing geochemical, geologic, meteorologic, hydrologic, and ecologic data for the site and disposal facility. The conceptual model accounts for all relevant processes for the release of radionuclides from the waste materials and these processes are justified by reference to relevant studies, available data, or supporting analyses in the PA in a manner sufficient for the intended use of the PA. The conceptual model incorporates alternative interpretations of the composite processes that control the release and transport of radionuclides at the disposal site as applicable. *The conceptual model constitutes a reasonable interpretation of the source term and releases, the design features of the disposal facility, the operational procedures used in disposing of waste, and the interim and final closure configurations identified in the closure plan that is sufficient for the intended use of the PA. Credit taken for the performance of engineered features is based on data derived from laboratory and field studies or documented sources of information that are relevant to the disposal site and facility, and takes into account the degradation of the engineered features incorporates the design and engineered features of the facility, including closure plans or reasonable assumptions for facility closure.* *The conceptual model includes assessment of natural processes that could affect the long-term stability of a disposal facility (e.g., flooding, mass wasting, erosion, and weathering) over the time period considered in the analysis. The conceptual models are justified based on referenced data, investigations and supporting analysis.*	engineered barriers (Sect. 3.2.1), radionuclide release and vadose zone transport (Sect. 3.2.2), and natural system including flow and radionuclide transport in the saturated zone (Sect. 3.2.3). Section 3.2.4 summarizes exposure pathways and scenarios. Appendix C, Sect. C.1, develops the generalized conceptual model of EMDF performance evolution, expressed as increasing cover infiltration, that is implemented in each of the PA model codes. Appendix G, Sect. G.2 presents a summary of the EMDF conceptual site model, exposure scenarios, and major assumptions for implementation of the total system model.
PA-11	The conceptual models and mathematical approach for the exposure pathways, scenarios and dose analysis are adequately described and defensible. *The PA provides a complete description of, and justification for, the selected exposure pathways and scenarios used to evaluate potential doses to receptors (members of the public). The dose analysis is conducted for reasonable and/or accepted scenarios for the setting of the facility and are consistent with site-specific environmental conditions and local and regional practices. If there is a link to a risk assessment, the relationship assumed between dose and risk is adequately described.* *All assumptions regarding exposure (e.g., rates of ingestion, inhalation) and any representations of groundwater well performance (e.g., construction, diameter, yield, depth of penetration, screen length) are reasonable reflections of regional practices or bounding and are justified.* *If radiation dose is used as a measure of groundwater resource protection, the exposure scenarios consider the ingestion of water (at 2 liters per day or an alternative rate, if a justification is included) at the point of assessment, which represents the location of maximum*	Conceptual models for human exposure scenarios and pathways are described in Sect. 3.2.4. Assumptions for implementation of exposure scenarios and pathways and dose analysis using RESRAD-OFFSITE are described in Sect. 3.4 of the PA and detailed in Appendix G, Sects. G.2, G.3, and G.4. The exposure scenario for the all-pathways analysis assumes a resident agricultural receptor that represents a maximally exposed individual member of the public. Modeling assumptions regarding groundwater well construction (depth of withdrawal relative to the vertical distribution of radionuclides) are pessimistic but reasonable reflections of local practices for water supply wells. These assumptions are addressed in Sect. 3.4.2 of the PA and in Sect. G.4.3 of Appendix G. Groundwater resource protection is based on maximum contaminant levels for radionuclides in public water systems (Sect. 4.7). The dose from beta/photon decay is based on groundwater ingestion of 2 L/day from the well at the location of maximum exposure (groundwater POA).

Performance Assessment Review Criteria (cont.)

ID	Review criteria	Preparer guidance for reviewers
	exposure and a well developed using current practices typical for the local area.	
PA-12	The analytical and numerical models for source term, disposal facility and the natural environment are adequately described and are reasonable and defensible representations of the conceptual model(s). *There is sufficient documentation and verification of the appropriateness of the analytical and numerical models used to provide reasonable confidence in the model results. The complexity of the mathematical models selected for the determination of compliance is commensurate with available site data and sufficient for the intended use of the PA.* *The input data used in the analytical and numerical models are described and are traceable to sources derived from field data from the site, laboratory data interpreted for field applications, and referenced literature sources which are applicable to the site. Assumptions which are used to formulate input data are justified and have a defensible technical basis. The basis for distributions developed to support an uncertainty analysis is adequate and defensible to support the use of the uncertainty analysis results.* *The computational steps in the implementation of analytical and numerical models are clearly described and traceable. Linkages between the different models are clearly described.* *The analytical and numerical models are tested, by comparison to benchmarked analytical calculations or results of other well-established models, and demonstrate that the results are consistent with the conceptual model, available site data or referenced documentation or literature.* *The initial conditions, the boundary conditions, and the up scaling (i.e., normalization to field scale) of parameter data are applicable to the disposal facility and the expected ranges in the physical and hydrologic properties of the site over 1,000 years for the purpose of compliance. The PA includes a discussion of the methods used for the sensitivity and uncertainty analysis and identify the parameters and assumptions that when changed can influence the conclusions of the analysis.*	An overview of the selection of model codes and integration of model codes for the PA analysis is provided in the introduction to Sect. 3.3. Detailed description of model codes used to implement conceptual models of cover system performance, source release and vadose transport, saturated zone flow and radionuclide transport, and the total system model is presented in Sects. 3.3.1, 3.3.2, 3.3.3, and 3.3.4. These sections describe the implementation of each model and the linkages between different models. Results for individual model codes representing different EMDF disposal subsystems (Sect. 4) are consistent with the conceptual models and referenced documentation for BCV contaminant transport. Section 3.3.5 details the comparison of model outputs and the integration of results applied to predict groundwater and surface water radionuclide concentrations at the selected POAs. Additional detail concerning model parameterization and input data for specific model codes is provided in Appendices C, D, E, F, and G (refer to Table 3.10). A complete listing of RESRAD-OFFSITE input parameter values and the basis or data source for the assumed base case values is provided as Attachment G.1 to Appendix G. The basis for ranges and distributions of parameters used for uncertainty quantification is presented in Appendix G, Sect. G.6.3.2 and Attachment G.3. Methods for sensitivity and uncertainty analysis are described in Sect. 5 of the PA. Section G.6.3 of Appendix G describes the setup and results of the uncertainty analysis in detail, including identification of those input parameters for which uncertainty is critical to the conclusions of the analysis. The key parameter assumptions identified in the uncertainty analysis are listed in Sect. 1.7.1. Quality assurance activities and records that document input data traceability are summarized in a separate QA Report for modeling in the EMDF PA and CA. Section 9 provides an overview of the QA activities and documentation.
PA-13	Intermediate results for the source term, facility and environmental transport are described to highlight key features in the disposal system and to build confidence in the overall consistency of the results for the total system used to demonstrate compliance with the performance objectives. *The assessment includes intermediate results illustrating releases from the source term, effects of any barriers in the disposal facility, and the role of the natural system. These results can be in the form of concentrations or fluxes at key locations in the disposal system as a function of time. The magnitude and trends in intermediate results are discussed in the context of magnitudes and trends in subsequent steps (e.g., source term to disposal facility to natural system) to confirm that behavior is consistent and explainable for the total system. The results are also used*	Section 3.3.5 presents intermediate results from the STOMP, MT3D, and RESRAD-OFFSITE models. Vadose zone fluxes are compared in Sect. 3.3.5.1 and Saturated zone concentrations are compared in Sect. 3.3.5.2. The comparison in Sect. 3.3.5.2 illustrates differences between the 3-dimensional numerical model formulation and the analytical formulation in the total system model of the saturated zone. The model integration discussion in Sect. 3.3.5 also addresses the significance of uncertainties in conceptual models of radionuclide release and the vertical distribution of saturated zone material properties such as hydraulic conductivity. These uncertainties are relevant to confidence in the overall consistency of the results for the total system.

Performance Assessment Review Criteria (cont.)

ID	Review criteria	Preparer guidance for reviewers
	to identify key aspects of the disposal system that have significant influence on the demonstration of compliance and as a quality assurance check on the linking of different conceptual and mathematical models.	
PA-14	The assumptions for the dose assessment are documented and defensible. The dose assessment results identify key radionuclides, pathways and scenarios and are sufficient to support a determination of reasonable expectation that the performance objectives will be met. *DOE-approved dose coefficients and defensible data for transfer factors, external exposure rates, inhalation and other inputs are used. All radionuclides and pathways that were identified in the screening are addressed in the analysis. The dose analysis considers the exposure pathways and transfer factors between media and calculates the maximum dose using acceptable methodologies and parameters. The radionuclides, pathways and exposure scenarios resulting in the peak doses are identified.* *For probabilistic analyses used for compliance, the mean and median doses as a function of time are provided and peaks for both are identified. The maximum projected dose, flux, or radionuclide concentration and time of occurrence during the compliance period is presented in the PA. Potential peaks impacts after the compliance period are also identified.*	The exposure pathways and scenarios included in the dose assessment are presented in Sect. 3.2.4. The screening analysis to justify eliminating radionuclide release through the EMDF cover is explained in Sect. 3.2.2. Assumptions and input parameter data sources for the dose assessment are documented and defensible as described in Sect. 3.4. DOE-approved dose coefficients and standard radiological data were used for the RESRAD-OFFSITE dose calculations (Table 3.25). A complete listing of RESRAD-OFFSITE input parameter values and the basis or data source for the assumed base case values is provided as Attachment G.1 to Appendix G. Results for the all-pathways dose analysis including radionuclides and pathways resulting in the peak dose rates, the time of occurrence of peak dose during the compliance period, and dose peaks occurring after 1000 years are presented in Sect. 4.5. Additional evidence supporting the determination of reasonable expectation of EMDF compliance with performance objectives is provided by the sensitivity evaluations and the uncertainty analysis presented in Sect. 5. Discussion of the uncertainty associated with the all-pathways dose analysis for the compliance period is presented in Sect. 7.4.
PA-15	Sensitivity and uncertainty analyses are documented and conducted at a sufficient level of detail to increase confidence in model results and identify critical aspects of the assessment in the context of the demonstration of reasonable expectation of compliance. *Acceptable methods (deterministic and/or probabilistic) of sensitivity analysis are used to identify important assumptions and parameters based on their influence on the conclusions of the analysis at a sufficient level of detail to use the results to prioritize future data or model refinements or to confirm the sufficiency of existing information. Efforts are made to apply sensitivity and uncertainty analysis across key components of complex models to address expected variability and sufficiently identify the assumptions and processes that are most significant in the context of demonstrating compliance. Assumptions and parameters that lead to results in the uncertainty analysis that are important to the conclusions are justified as reasonable for the site and facility using data or related laboratory/field investigations and are sufficient for the intended use of the PA.* *The results of the sensitivity and uncertainty analyses are sufficient to support the discussion of the effects of uncertainty on interpretations of model results. The results of the analysis are used to test and build confidence in the assumptions and conclusions of the PA.* *Estimates of the uncertainty in disposed and forecast waste inventory are adequately described along with the methods used to quantify uncertainty, including decay corrections.*	The introduction to Sect. 5 of the EMDF PA report provides an overview of the sensitivity and uncertainty evaluations performed. Results of sensitivity runs with the vadose zone (STOMP) and saturated zone (MT3D models) are presented in Sects. 5.1 and 5.2, respectively. Additional detail on STOMP model sensitivity is given in Appendix E, Sect. E.3.3. Single parameter sensitivity evaluations of RESRAD-OFFSITE dose predictions are summarized in Sect. 5.3. Section 5.4 presents a summary of the results of the uncertainty analysis performed with the probabilistic module of the RESRAD-OFFSITE model. Appendix G, Sect. G.6, provides additional detail on the sensitivity-uncertainty analysis of the total system model (RESRAD-OFFSITE) results. Section 7 presents integration and interpretation of the PA results, including consideration of uncertainty in the estimated radionuclide inventory (Sect. 7.1). Section 7.2 addresses uncertainties in cover performance in the context of assumed infiltration rates, release pathways, and intrusion scenarios. Section 7.3 provides an overview of uncertainties related to models of radionuclide release and transport, including K_d values for dose-significant radionuclides. Uncertainty in the all-pathways dose assessment that was evaluated with the RESRAD-OFFSITE probabilistic module is summarized in Sect. 7.4.

Performance Assessment Review Criteria (cont.)

ID	Review criteria	Preparer guidance for reviewers
PA-16	The analysis of potential inadvertent intrusion is adequate and defensible. The results are provided in a manner to support identification of potential operational, design, or closure features to reduce the potential for or consequences of intrusion. *Acute and chronic exposure scenarios for hypothetical inadvertent intrusion are reasonable, justified and consider direct intrusion into the disposal site and exhumation of accessible waste material.* *The hypothetical inadvertent intruder analysis considers the natural and man-made processes that impact the possible exposure to an intruder and calculates the dose using acceptable methodologies and parameters. Exposure pathways from inadvertent intrusion into the waste disposal units identify the chronic (no more than one year) and acute exposure pathways for each of the exposure scenarios considered. The exposure pathways include all relevant ingestion, external exposure, and inhalation pathways for each exposure scenario. The hypothetical inadvertent intruder analysis accounts for naturally occurring processes (e.g., erosion, precipitation, flooding) and the degradation of engineered barriers in the calculation of results.* *The hypothetical inadvertent intruder analysis specifies the reductions in concentrations of radioactive material from mixing with uncontaminated material or the transport of radionuclides from the disposed waste mass, and justifies the parameters used in the analysis with site data, supporting analysis or referenced information.* *The hypothetical inadvertent intruder analysis calculates the maximum dose from disposed waste during the period from the end of active institutional controls to 1,000 years after site closure using DOE-approved dose coefficients from recognized published sources. In the hypothetical intruder assessment, institutional controls are assumed to be ineffective in preventing temporary intrusion after 100 years following disposal facility closure; longer periods may be assumed with justification (e.g. land use planning, passive controls*	The analysis of EMDF performance with respect to IHI is presented in Sect. 6. Acute and chronic IHI scenarios and assumptions, including exposure pathways that are implemented in RESRAD-OFFSITE are described in Sects. 6.3 and 6.4, respectively. Model parameter assignments for IHI scenarios are discussed in Sect. 6.5. The final cover design features that reduce the potential for and consequences of intrusion are discussed in Sect. 1.3 of the PA, Sect. C.1 of Appendix C, and Sects. I.2.1 and I.6.2 of Appendix I. IHI results are presented in Sect. 6.6 and summarized in Sect. 6.7 of the PA. Appendix I provides a more comprehensive description of IHI scenarios, model implementation details (parameter assumptions and data sources), and dose results, including sensitivities to critical assumptions. Discussion of uncertainties, sensitivity to assumptions, and conservative bias in the IHI analysis, including sensitivities to the assumptions adopted to calculate source concentrations, are provided in Appendix I, Sect. I.6.
PA-17	The body of evidence in the PA provides a sufficient understanding of the behavior of the disposal system and the radionuclides, pathways and features of the engineered and natural system that have the greatest influence on the determination of compliance. *The results presented in the PA are consistent with the site characteristics, the waste characteristics, and the conceptual model of the facility. The demonstration of consistency is supported by available site monitoring data and supporting laboratory/field investigations. The results of the analyses for transport of radionuclides and the hypothetical inadvertent intrusion into the disposal facility, and the sensitivity and uncertainty of the calculated results are sufficiently comprehensive representations of the existing knowledge of the site and the disposal facility design and operations for the intended use of the PA.* *Inventory limits are developed from reasonable projections of waste to be disposed and analyses that*	The body of evidence provided in Sects. 3.3.5, 4, 5, 6, and 7 suggests that exposures to C-14 and long-lived fission products (Tc-99 and I-129) via the water and fish ingestion paths are the primary dose-significant results of the PA. Peak doses are sensitive to cover performance (long-term infiltration) assumptions and other factors that affect radionuclide release, including K_d values for the waste, as documented in Sect. 5 and discussed in Sect. 7. Field monitoring of groundwater levels and surface flow rates suggest that the saturated zone flow model results (the EMDF model is described in Sect. 3.3.3.1 and Appendix D) are consistent with the hydrogeologic conceptual model of the CBCV site. Reasonable projections of waste to be disposed were developed. Inventory limits for radionuclides are not developed in the EMDF PA. Inventory limits and other Waste Acceptance Criteria will be developed in consultation with the FFA parties prior to EMDF operations.

Performance Assessment Review Criteria (cont.)

ID	Review criteria	Preparer guidance for reviewers
	consider the physical and chemical characteristics of the wastes if those characteristics affect the release and transport of the radionuclides as necessary to support the intended use of the PA. *The conclusions of the PA address and incorporate any constraints included in any Federal, state, and local statutes or regulations or agreements that impact the site design, facility design, or facility operations. The conclusions also address any procedural or site documentation changes or constraints due to the results of the facility PA. Reasonable assurance exists that these constraints and impacts are appropriately addressed in the PA.* *The PA integrates the results of the analysis, key assumptions made in the analysis, the sensitivity and uncertainty analysis, the comparisons with the performance objectives, WAC, operating procedures, and applicable regulations/policies to formulate conclusions.* *The PA conclusions incorporate the findings of the calculated results for the all pathways analysis, air pathway analysis, groundwater resource protection analysis, hypothetical inadvertent intruder analysis, protection of individuals during operations, and sensitivity and uncertainty analysis. The results are interpreted and integrated to formulate conclusions which are supported by the results and the uncertainties in the results. The conclusions are consistent with the uncertainty of the results.* *The analysis, results, and conclusions of the PA provide both a reasonable representation of the disposal facility's long-term performance and a reasonable expectation that the disposal facility will remain in compliance with applicable performance objectives of DOE O 435.1A during the compliance period.* *If peak impacts calculated by the performance assessment occur beyond 1,000 years, then those results are interpreted in an increasingly qualitative manner recognizing the increasing speculation and uncertainty at later times. The intent is to identify trends that suggest the potential for catastrophic effects and to support decision-making regarding recommendations for design or operational improvements.*	Section 1.7 summarizes key parameter assumptions and key conceptual model assumptions that are critical to the conclusions of the PA. Section 7 provides integration and interpretation of PA model results in the context of uncertainties in inventory, long-term facility hydrologic performance, and uncertainties in conceptual models of radionuclide release and transport. PA conclusions are presented in Sect. 8; these conclusions address compliance period performance as well as impacts beyond 1000 years. PA results relative to performance objectives are summarized in Table 8.1 and uses of PA results are explained in Sect. 8.2. The EMDF design and the conclusions of the PA analyses based on the design incorporate relevant federal and state requirements, including water resource protection criteria. The regulatory requirements are considered in Sect. 1.5. FFA requirements developed in future decision documents or operational documents that could impact the conclusions of the EMDF PA will be evaluated according to the UCOR procedure PROC-EMDF-0001, *EMDF Design DOE Order 435.1 Changed Condition*, for considering proposed activities, design or operational changes, or new information that could alter the assumptions of the PA analyses.
PA-18	The body of evidence in the PA is sufficient to provide a reasonable expectation of compliance with the performance objectives in DOE O 435.1 and other regulatory constraints/objectives specific to the facility. The PA provides a defensible approach for the application of the results to develop WAC or operational limits for the facility and includes a discussion of how ALARA principles have been addressed. *The performance objectives used in the PA are identified and are consistent with those found in DOE O 435.1A. Compliance with all of the objectives for the 1,000 year compliance period is confirmed in a summary table (other time frames are also addressed as applicable). The PA identifies and justifies any site-specific determinations/assumptions related to the specific objectives for groundwater resource protection. For*	The base case all-pathways analysis (Sect. 4.5) and sensitivity and uncertainty analyses (Sect. 5) provide understanding of the key radionuclides, exposure paths, design features, and model assumptions that control the predicted maximum compliance period and peak dose levels. Based on these analyses, there is a defensible and reasonable expectation of EMDF compliance with the performance objectives Uncertainty in input parameter values does not preclude a reasonable expectation of compliance with performance objectives (Sect. 5.4). Perspective on uncertainties of radionuclide inventories, cover performance assumptions, and model differences are provided in Sect. 7. These uncertainties do not

Performance Assessment Review Criteria (cont.)

ID	Review criteria	Preparer guidance for reviewers
	example, a PA for tank closure, as appropriate, includes a determination of reasonable assurance that exposures to humans are within the limits established in the performance objectives of 10 CFR 61 (Sections 61.41 through 61.44). *The hypothetical inadvertent intruder results demonstrate reasonable expectation that doses will be less than 100 mrem/year total effective dose for chronic exposure and 500 mrem total effective dose for acute exposure are met within the disposal facility over the assessment period after the end of active institutional controls. Potential for doses in excess of those values is discussed from the perspective of optimization of the disposal system.* *The PA adequately addresses ALARA requirements.*	preclude a reasonable expectation of compliance with performance objectives. The analysis of potential IHI is presented in Sect. 6. The results of the analysis suggest that the estimated EMDF radionuclide inventory and facility design will not exceed dose performance measures for IHI. Discussion of ALARA requirements is addressed in Sect. 1.5.4.
PA-19	Appropriate QA associated with the PA has been implemented for consistent with the requirements of DOE O 414.1D, DOE G 414.1-4 and EM-QA-001. *The input data used in the analytical and numerical models are described and are traceable to sources derived from field data from the site, laboratory data interpreted for field applications, and referenced literature sources which are applicable to the site. Assumptions which are used to formulate input data are justified and have a defensible technical basis.* *The computational steps in the implementation of analytical and numerical models are clearly described and traceable.* *Intermediate calculations are performed and results are presented that demonstrate, by comparison to site data or related investigations, the calculations used in the PA are representative of disposal site and facility behavior for important mechanisms represented in the mathematical models.* *The analytical and numerical models are tested, by comparison to benchmarked analytical calculations or results of other well-established models, and demonstrate that the results are consistent with the conceptual model, available site data or referenced documentation or literature.*	Appropriate QA was implemented consistent with DOE O 414.1D, DOE G 414.1-4 and EM-QA-001 as summarized in Sect. 9 and described in detail in the *Quality Assurance Report for the Performance Modeling of the Bear Creek Valley Low-level Radioactive Waste Disposal Facilities, Oak Ridge, Tennessee* (QA Report, UCOR 2020). The QA Report contains the description of the input data traceable to sources, and documentation for software, models, and records.

ALARA = as low as reasonably achievable
BCV = Bear Creek Valley
CA = Composite Analysis
CBCV = Central Bear Creek Valley
CERCLA = Comprehensive Environmental Response, Compensation, and Liability Act of 1980
CFR = Code of Federal Regulations
DOE = U.S. Department of Energy
DOE G = DOE Guide
DOE M = DOE Manual
DOE O = DOE Order
EMDF = Environmental Management Disposal Facility
EMWMF = Environmental Management Waste Management Facility
FFA = Federal Facility Agreement
IHI = Inadvertent Human Intrusion
LFRG = Low-level Waste Disposal Facility Federal Review Group
PA = Performance Assessment
POA = point of assessment
QA = quality assurance
RESRAD = RESidual RADioactivity
STOMP = Subsurface Transport Over Multiple Phases
SWSA = Solid Waste Storage Area
WAC = waste acceptance criteria

REFERENCE

UCOR 2020. *Quality Assurance Report for Modeling of the Bear Creek Valley Low-level Radioactive Waste Disposal Facilities, Oak Ridge, Tennessee*, UCOR-5234/R0, UCOR, Oak Ridge, TN, April.

APPENDIX B.
RADIONUCLIDE INVENTORY ESTIMATE FOR THE ENVIRONMENTAL MANAGEMENT DISPOSAL FACILITY

This page intentionally left blank.

CONTENTS

This page intentionally left blank.

FIGURES

TABLES

This page intentionally left blank.

ACRONYMS

BV	Bethel Valley
CARAR	Capacity Assurance Remedial Action Report
CERCLA	Comprehensive Environmental Response, Compensation and Liability Act of 1980
D&D	deactivation and decommissioning
DOE	U.S. Department of Energy
DOE O	DOE Order
EMDF	Environmental Management Disposal Facility
EMWMF	Environmental Management Waste Management Facility
LLW	low-level (radioactive) waste
LWTS	Landfill Wastewater Treatment System
ORAU	Oak Ridge Associated Universities
OREM	Oak Ridge Office of Environmental Management
ORNL	Oak Ridge National Laboratory
ORR	Oak Ridge Reservation
PA	Performance Assessment
RA	remedial action
R&D	research and development
RI/FS	Remedial Investigation/Feasibility Study
ROD	Record of Decision
SC	Office of Science
TRU	transuranic
UCL	upper confidence limit
UEFPC	Upper East Fort Poplar Creek
WAC	waste acceptance criteria
WGF	Waste Generation Forecast
WL	waste lot
Y-12	Y-12 National Security Complex

This page intentionally left blank.

B.1 INTRODUCTION

B.1.1 PURPOSE

This appendix describes the development of the radioactive contaminant inventory for wastes disposed in the proposed Environmental Management Disposal Facility (EMDF) on the U.S. Department of Energy (DOE) Oak Ridge Reservation (ORR). The purpose of radionuclide inventory development is two-fold: (1) to support the EMDF Performance Assessment (PA) required under DOE Order (O) 435.1, *Radioactive Waste Management*, and (2) to support design of the EMDF Landfill Wastewater Treatment System (LWTS). The inventory also can be used to identify radionuclides to consider for development of EMDF waste acceptance criteria (WAC).

This data analysis provides estimates of radionuclide concentrations for waste streams disposed in EMDF, which in turn are applied to the forecast waste volume estimates to estimate the radionuclide inventory for EMDF at closure. The radionuclide inventory provides the source term for modeling the release of radionuclides to the environment. In addition, the EMDF radionuclide inventory is used in conjunction with existing wastewater concentration data from the Environmental Management Waste Management Facility (EMWMF) to estimate the potential influent concentrations to the EMDF LWTS for selection of treatment process options for radiological contaminants.

B.1.2 BACKGROUND

The DOE Oak Ridge Office of Environmental Management (OREM) has proposed the construction of a new mixed, low-level (radioactive) waste (LLW) disposal facility, EMDF, on the ORR. EMDF will be constructed to dispose of future-generated Comprehensive Environmental Response, Compensation, and Liability Act of 1980 (CERCLA) waste that will exceed the capacity of the existing LLW landfill, EMWMF. EMDF is designed as an above-grade, engineered waste disposal facility (i.e., landfill) located in Central Bear Creek Valley on the ORR. The current preliminary design is a multi-cell facility supported by the LWTS. The total capacity required to support future cleanup projects is currently projected at approximately 2.2 M cy (DOE 2017).

Candidate wastes for onsite disposal include LLW and mixed LLW that contains Resource Conservation and Recovery Act of 1976 and/or Toxic Substances Control Act of 1976 contaminants. These waste streams result from the deactivation and decommissioning (D&D) of facilities at the ORR Y-12 National Security Complex (Y-12) and Oak Ridge National Laboratory (ORNL) as well as remedial action (RA) waste from cleanup of those sites that will be completed over the next two or three decades. For this radionuclide inventory estimate, it was assumed that all waste from the East Tennessee Technology Park will be disposed in EMWMF. This analysis is concerned only with the radioactive contaminants of potential concern in those wastes, not the hazardous contaminants. Liquid wastes, transuranic (TRU) wastes[1], and spent nuclear fuel are excluded from onsite disposal and are not considered as candidate waste streams for EMDF. Uncontaminated materials or wastes containing extremely low levels of residual radioactivity generated during CERCLA actions that can meet the WAC of existing ORR industrial or construction/demolition

[1] TRU waste is defined by the Waste Isolation Pilot Plant Land Withdrawal Act as "waste containing more than 100 nanocuries of alpha-emitting transuranic isotopes per gram of waste with half-lives greater than 20 years." EMDF LLW may contain such transuranic isotopes at less than this activity concentration level.

landfills also are not considered to be candidate waste streams for EMDF. Wastes not meeting (exceeding) the EMDF WAC would be transported to offsite treatment/disposal facilities or treated for onsite disposal.

B.1.3 METHODOLOGY

The primary objective of this radionuclide inventory estimate is to develop a defensible radionuclide inventory (total activity for each radionuclide and each waste stream) and corresponding average EMDF waste activity concentrations (average radioactivity per waste mass prior to disposal, for each radionuclide) for use in the PA modeling.

The approach to developing waste volume estimates and associated waste characterization takes into account substantial historical and forecast information available for future ORR CERCLA cleanup projects. However, volumes and characteristics of waste that will be generated from the implementation of future CERCLA actions can only be estimated at this time. Development of EMDF waste volume estimates, reported in the Remedial Investigation/Feasibility Study (RI/FS) for future CERCLA waste disposal (DOE 2017) and used in this document, relies on reasonable assumptions for proposed future cleanup actions. Volume estimates in the RI/FS are delineated into soil (including soils, sediment, and sludge) and debris waste forms only.

For estimating EMDF radionuclide inventory, projected waste volumes for individual cleanup projects are aggregated into waste streams based on site of origin (Y-12 or ORNL) and project type (facility D&D or RA). Additional differentiation of Y-12 facility D&D waste streams is based on the availability of detailed characterization data for certain Y-12 facilities. Average radionuclide activity concentrations for each waste stream are estimated from a combination of data sources as presented in Sect. B.3. The radiological data sources include (1) EMWMF waste characterization data for previously generated and disposed (historical) Y-12 and ORNL waste lots (WLs); (2) data from detailed facility and environmental characterization studies; and (3) data from the OREM SORTIE 2.0 facility inventory database (Redus 2014), which include radionuclide quantities derived from various types of facility safety analyses and other sources. The estimated average concentrations are biased toward high values to manage uncertainty regarding inventory upper bounds; this approach is discussed in Sects. B.3 through B.5. For each EMDF waste stream, the estimated average radionuclide activity concentrations (activity per waste mass) are applied to the projected total waste quantity (mass) to derive the total estimated inventory (total activity for each radionuclide). In addition, the overall average activity concentrations for all EMDF waste included in the analysis are calculated for use in the PA modeling.

The method for developing radiological profiles (average radionuclide activity concentrations, pCi/g) for specific EMDF LLW streams is to apply the available data most representative of ORNL and Y-12 wastes and to distinguish between RA wastes (primarily soils) and facility D&D wastes (primarily debris). The expected differences in radiological contamination reflect the different operational histories of the two DOE sites (i.e., weapons production at Y-12 verses research and development [R&D] related to reactor design and the nuclear fuel cycle, radioisotope production, radioactive waste management, and biological and environmental sciences at ORNL). The primary radioactive contaminants in Y-12 waste streams are uranium isotopes, whereas ORNL waste streams contain a greater variety of radioisotopes, including large quantities of some fission products (e.g., Cs-137 and Sr-90), lower quantities of other fission products (e.g., Tc-99 and I-129), and trace quantities of transuranic radioisotopes (e.g., plutonium and americium). This difference is important for estimating the EMDF inventory because Y-12 waste accounts for approximately 70 percent of the forecast waste volume and ORNL waste accounts for the remaining 30 percent. Due to these differences in waste volume and radiological characteristics, Y-12 waste accounts for the majority of uranium activity in the estimated EMDF inventory, whereas ORNL waste accounts for the majority of the total radioactive inventory.

Section B.2 presents the project-level waste volumes. Section B.3 provides a review of the sources of data used to identify the radionuclides associated with each EMDF waste stream and presents the radiological profiles. Section B.4 completes the analysis by calculating the inventory of the anticipated EMDF waste for all radionuclides. Section B.5 explains the use of the estimated waste inventory for the PA modeling. A discussion of the uncertainties in this analysis is provided in Sect. B.6, with a focus on key radioisotopes of concern for meeting DOE O 435.1 performance objectives.

Section 9 of the PA Report details the quality assurance activities and documentation that apply to the estimated radionuclide inventory.

B.2 WASTE VOLUMES AND WASTE STREAMS

B.2.1 WASTE FORMS

EMDF waste forms will include contaminated soil (including contaminated sediment and other soil-like waste) and debris. The bulk of the debris expected from demolition activities will be concrete and masonry (walls, floors, ceilings, and building structure), steel (building structural members, rebar, piping, and some equipment), and process equipment (gloveboxes, machining equipment, pumps, and other). Generally, this lightly contaminated debris has a high potential for meeting the WAC. Ventilation ducting, specific equipment and piping, and hot-cell-associated debris (internal surfaces, manipulators, and equipment) are expected to compose a smaller volume of more contaminated debris with a high potential for offsite disposal.

The majority of waste debris and soil is expected to be disposed in bulk (uncontainerized) form and transported by dump trucks to the landfill. Mercury is a contaminant of concern in a portion of Y-12 waste. Approximately 150,000 cy of debris and 67,000 cy of soil (as estimated in the RI/FS, DOE 2017) may require packaging and treatment to meet land disposal restrictions for mercury. Similarly, other small volumes of waste may be containerized and/or stabilized prior to disposal. However, the mercury-contaminated LLW is not defined as a separate waste stream for purposes of estimating the EMDF radionuclide inventory and no assumption regarding packaging or treatment of waste for disposal is necessary for this analysis because packaging or stabilization materials would increase the waste mass, but not the radionuclide inventory.

B.2.2 WASTE VOLUME FORECAST DATA

Development of the estimated EMDF inventory is organized based on future cleanup information from DOE OREM, Office of Science (SC), Office of Nuclear Energy, and the National Nuclear Security Administration as provided in the OREM Baseline Critical Decision-1-level baseline packages. These are referred to as the OREM Baseline Books. The Fiscal Year 2014, or more recent (if available), OREM Baseline Books document the strategy for (1) preparation for and completion of demolition of facilities or complexes resulting in debris waste, and (2) preparation for and completion of RA activities involving the remediation of media (soils, sludge, sediment, and subsurface structures) resulting in soil waste (and some debris). The majority of these cleanup strategies are approved CERCLA actions (i.e., decision documents [Records of Decision (RODs) or Action Memoranda]). However, in a few instances, strategies have been assumed, but do not have existing decision documents.

The OREM baseline assumes a sequenced execution of Y-12 and ORNL facility demolition and remediation projects that was incorporated into the estimate for required additional LLW disposal capacity

(DOE 2017, Appendix A). Waste volume uncertainty associated with future decision documents, as well as other possible waste volume variations, were evaluated in the RI/FS (DOE 2017, pages 2-10 to 2-12) and translated into a range of landfill volume capacity of 1.2 to 2.4 M cy. Thus, the current onsite disposal capacity required, 2.2 M cy, which includes a +25 percent allowance for uncertainty and incorporates debris compaction and addition of clean fill, is considered a reasonable and bounding estimate.

OREM Baseline Books and supporting information provide project-specific waste volumes that are incorporated into the Waste Generation Forecast (WGF) for OREM. The WGF volumes tagged for onsite disposal (in an existing or future LLW landfill) served as the source of waste volumes for the RI/FS (DOE 2017) and for this radionuclide inventory estimate. Confidence in project-level WGF waste volumes is estimated as -50 percent to +100 percent, a range encompassing the +25 percent volume uncertainty allowance applied in the RI/FS. RA waste volumes were estimated based on limited knowledge of extent of contamination and decisions documented in RODs for cleanup levels. D&D waste volumes were estimated for demolition of each building using either a detailed methodology (building drawings were used to calculate debris volumes, typically for larger facilities) or using a parametric estimation technique (typically used for smaller facilities). In addition, development of the waste debris volumes relies on data taken from the Facility Information Management System as well as completed CERCLA documents, available characterization reports, and information from representative WLs previously disposed in EMWMF. Uncertainty associated with these volume estimates results from several factors, including the use of parametric assumptions for waste volume estimates, lack of detailed characterization data and uncertainty in offsite disposal volumes, assumptions regarding actions where cleanup decision documents are not available, and unknown/undefined packaging needs/treatment methods (e.g., for mercury-contaminated waste) that may affect volumes.

The radionuclide inventory estimation approach adopted for the EMDF PA uses the project-level, as-generated LLW volumes designated for onsite disposal in the WGF, without the +25 percent uncertainty adjustment used in the RI/FS (DOE 2017). The EMDF waste volumes shown by D&D facility complex (group of facilities) or RA project in Table B.1 are broken down as debris or soil volumes and no differentiation is made regarding classified or mixed waste components. The volumes given are limited to the portion that has been identified in the WGF for disposal in an onsite LLW facility. In addition, volumes are given only for waste expected to be disposed in EMDF based on the execution schedule for cleanup projects that was assumed in the RI/FS. Waste expected to be generated as a result of Y-12 and ORNL cleanup, but disposed offsite (due to high activity levels [i.e., above assumed EMDF WAC limits]), in the existing EMWMF, or at other ORR landfills are not included.

Table B.1. Waste volumes projected for disposal in EMDF

Project	Site	Debris volume (cy)	Soil volume (cy)	Total EMDF (cy)
Y-12 D&D Projects				
9206 Complex	Y-12	15,490		15,490
9212 Complex	Y-12	113,571		113,571
9213 and 9401-2 Demolition	Y-12	8,000		8000
Alpha-2 Complex[a]	Y-12	72,990		72,990
Alpha-3 Complex	Y-12	37,108		37,108
Alpha-4 Complex[a]	Y-12	55,085		55,085
Alpha-5 Complex[a]	Y-12	122,623		122,623
Beta-1 Complex	Y-12	46,920		46,920
Beta-3 Deactivation Only	Y-12	19,502		19,502
Beta-4 Complex[a]	Y-12	75,787		75,787

Table B.1. Waste volumes projected for disposal in EMDF (cont.)

Project	Site	Debris volume (cy)	Soil volume (cy)	Total EMDF (cy)
Biology Complex	Y-12	29,088	5069	34,157
Steam Plant Complex Legacy Material Disposition	Y-12	80		80
Tank Facilities Demolition	Y-12	3000		3000
Y-12 Remedial Action Projects				
BCV S-3 Ponds	Y-12		1094	1094
BCV White Wing Scrap Yard Remedial Action	Y-12	10,017	62,506	72,523
UEFPC Remaining Slabs and Soils[a]	Y-12	156,814	276,532	433,346
UEFPC Sediments - Streambed and Lake Reality[a]	Y-12		11,966	11,966
UEFPC Soils[a]	Y-12		3,154	3,154
UEFPC Soils 81-10 Area[a]	Y-12	280	1,537	1,817
ORNL D&D Projects				
2026 Complex	ORNL	10,012		10,012
2528 Complex	ORNL	484		484
3019A and Ancillary Facilities	ORNL	62,263		62,263
3525 Complex	ORNL	7659		7659
3544 Complex	ORNL	295		295
3608 Complex	ORNL	4466		4466
4501/4505 Complex	ORNL	22,814		22,814
5505 Building	ORNL	3689		3689
6010 and East BV Complex	ORNL	44,916		44,916
BV Chemical Development Laboratory Facilities	ORNL	1189		1189
BV Reactor Area Facilities	ORNL	7220	552	7772
BV Isotope Area Facilities (3038)	ORNL	1825		1825
BV Isotope Area Facilities	ORNL	6102		6102
BV Tank Area Facilities	ORNL	3433	182	3615
Central Stack East Hot Cell Complex	ORNL	5647		5647
Central Stack West Hot Cell Complex	ORNL	4356		4356
EGCR Complex	ORNL	45,811		45,811
Fire Station Complex	ORNL	815		815
Hot Storage Garden	ORNL	190		190
HPRR Complex	ORNL	2553		2553
Liquid Low Level Waste Complex	ORNL	1773		1773
MV HRE Facility	ORNL	725		725
MV LGWO Complex	ORNL	7859		7859
MV Waste Storage Facilities	ORNL	1129		1129
Southeast Services Group Complex	ORNL	112		112
Sewage Treatment Plant Complex	ORNL	73		73
Southeast Laboratory Support Complex	ORNL	39		39
TWPC Complex	ORNL	3106		3106

Table B.1. Waste volumes projected for disposal in EMDF (cont.)

Project	Site	Debris volume (cy)	Soil volume (cy)	Total EMDF (cy)
ORNL Remedial Action Projects				
BV Inactive Tanks and Pipelines	ORNL	405	158	563
BV Remaining Inactive Tanks and Pipeline	ORNL	23,446		23,446
BV Remaining Slabs and Soils	ORNL	30,024	46,660	76,684
ORNL Non-Hydrofracture Well P&A	ORNL	20		20
ORNL Remaining Non-Hydrofracture Well P&A	ORNL	14		14
ORNL Soils and Sediments	ORNL	2053	76,563	78,616
TOTAL VOLUME		**1,072,872**	**485,973**	**1,558,845**

[a]A portion of waste (debris and soil) from these projects will be associated with mercury contamination.

BCV = Bear Creek Valley
BV = Bethel Valley
D&D = deactivation and decommissioning
EGCR = Experimental Gas Cooled Reactor
EMDF = Environmental Management Disposal Facility
HPRR = Health Physics Research Reactor
HRE = Homogeneous Reactor Experiment
LGWO = Liquid and Gaseous Waste Operations
MV = Melton Valley
ORNL = Oak Ridge National Laboratory
P&A = plugging and abandonment
TWPC = Transuranic Waste Processing Center
UEFPC = Upper East Fork Poplar Creek
Y-12 = Y-12 National Security Complex

B.2.3 WASTE STREAMS FOR EMDF RADIONUCLIDE INVENTORY ESTIMATE

Six EMDF waste streams are identified to account for differences in site of origin (Y-12 or ORNL) and project type (facility D&D versus RA). These include three Y-12 D&D waste streams, one ORNL D&D waste stream, and two RA waste streams (Y-12 RA and ORNL RA). Total forecast debris and soil volumes for these six EMDF waste streams are given in Table B.2. The basis for defining two of the three Y-12 D&D waste streams is the availability of detailed radiological facility characterization data for the Alpha-5 building (DOE 2012) and the remaining Biology Complex facilities (UCOR, an Amentum-led partnership with Jacobs, 2017). Data of similar quality exist for ORNL Isotope Row facilities (Oak Ridge Associated Universities [ORAU] 2013), but the small waste volume associated with these facilities (3000 cy) does not justify defining a separate waste stream for estimating the total radionuclide inventory.

Table B.2. Debris and soil volumes for EMDF waste streams

EMDF waste stream	Debris volume (cy)	Soil volume (cy)	Total volume (cy)
Y-12 D&D Alpha-4 and Alpha-5	177,708	0	177,708
Y-12 D&D Biology Complex	29,088	5069	34,157
Y-12 D&D Remaining Facilities	392,448	0	392,448
Y-12 Remedial Action	167,111	356,789	523,900
ORNL D&D	250,555	734	251,289
ORNL Remedial Action	55,962	123,381	179,343
TOTAL EMDF	**1,072,872**	**485,973**	**1,558,845**

D&D = deactivation and decommissioning
EMDF = Environmental Management Disposal Facility
ORNL = Oak Ridge National Laboratory
Y-12 = Y-12 National Security Complex

B.2.3.1 Y-12 D&D Waste Stream Volumes

The total forecast volume of Y-12 D&D waste (approximately 600,000 cy) is composed of Y-12 D&D Alpha-4 and Alpha-5, Y-12 D&D Biology, and Y-12 D&D Remaining Facilities. The Alpha-4 and Alpha-5 facility complexes include very large former uranium and lithium isotope separation process buildings and smaller ancillary facilities. The Biology Complex facilities include former uranium process buildings that also were used for DOE SC R&D in later years. The Y-12 D&D Remaining Facilities waste stream includes all other complexes, including currently active uranium processing facilities and mercury-contaminated facilities (Alpha-2 and Beta-4) that have less detailed characterization information than is available for Alpha-4 and Alpha-5. Attachment B.1 includes more detailed descriptions and historical information on these Y-12 facility complexes.

B.2.3.2 ORNL D&D Waste Stream Volume

The ORNL D&D waste stream includes 28 facility complexes that comprise a total volume of approximately 250,000 cy. These excess ORNL facilities include inactive research reactors, hot cell facilities, and waste treatment facilities. Attachment B.1 includes more detailed descriptions and historical information on these ORNL facility complexes.

B.2.3.3 Y-12 and ORNL RA Waste Stream Volumes

The Y-12 and ORNL RA waste streams include estimated waste volumes (primarily soil) for six RA projects at each site (Table B.2), comprising approximately 524,000 cy (Y-12) and 180,000 cy (ORNL). These waste streams consist of contaminated soils and subsurface debris (building foundations and buried tanks and pipelines) and are described in more detail in Attachment B.2.

B.3 RADIOLOGICAL PROFILES FOR EMDF WASTE STREAMS

Identification of radiological contaminants and estimation of their activities for EMDF waste is based on the review of several sources of data, consideration of appropriate data sources for each waste stream, and understanding of the data quantity and quality limitations. The six waste streams defined in Sect. B.2.3 reflect differences in the likely types and levels of contamination based on careful review of the available characterization data. Figure B.1 provides a schematic overview of the data processing used to derive estimated EMDF inventory values, including data sources and the development of radiological profiles and waste stream masses used to estimate radionuclide inventories.

B.3.1 SOURCES OF CONTAMINANT CHARACTERIZATION INFORMATION

Facility- and site-specific characterization data for estimating waste radioactivity levels are not available for much of the forecast waste volume, although several sources exist that provide data for contaminated soils and specific excess facilities identified for cleanup at Y-12 and ORNL (Table B.3).

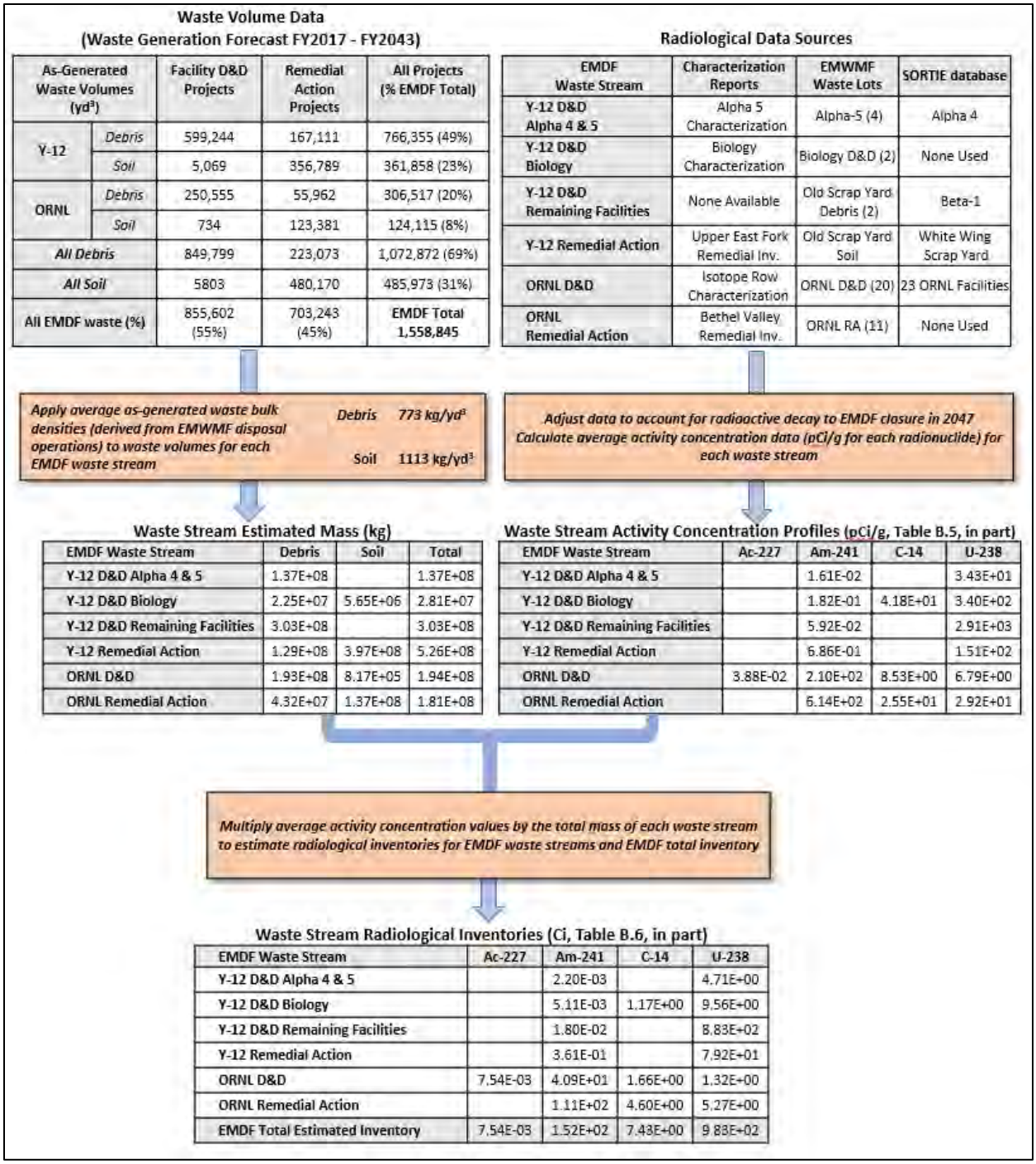

Fig. B.1. Schematic overview of data sources and the development of radiological profiles and waste stream masses used to estimate EMDF radionuclide inventories.

Table B.3. Characterization data reports applicable to future EMDF waste streams

Source of characterization data	Corresponding project	Reference
UEFPC Remedial Investigation	Y-12 soils and subgrade debris (subsurface pipes and building foundations)	DOE 1998
Bethel Valley Watershed Remedial Investigation	ORNL soils and subgrade debris (subsurface tanks, pipelines, and building foundations)	DOE 1999
Isotope Row Facilities Characterization Report	ORNL excess facility demolition debris	ORAU 2013
Alpha-5 Characterization Report	Y-12 Alpha-5 demolition debris	DOE 2012
Biology Complex Characterization Report	Y-12 Biology Complex demolition debris and soils	UCOR 2017

DCN = Document Control Number
DOE = U.S. Department of Energy
EMDF = Environmental Management Disposal Facility
ORAU = Oak Ridge Associated Universities
ORNL = Oak Ridge National Laboratory
UEFPC = Upper East Fork Poplar Creek
Y-12 = Y-12 National Security Complex

A large amount of facility- and site-specific data is available from various types of DOE nuclear safety analyses (e.g., Preliminary Hazards Screening documents). The OREM SORTIE 2.0 database (Redus 2014) has been developed to aggregate and structure these safety analyses and other data sources to produce a comprehensive assembly of facility- and site-specific radionuclide inventory data. The SORTIE database includes many high radioactivity values that may not be representative of future LLW suitable for onsite disposal. The most extreme values among those data were identified and filtered out for this analysis. However, given that the SORTIE data tend to represent bounding facility inventories developed for nuclear facility safety categorization rather than likely D&D waste concentrations, the inclusion of the SORTIE data tends to bias the activity concentration estimates toward high values.

Representative waste characterization data from Y-12 and ORNL WLs disposed in EMWMF are a third data source that can be used to approximate the radioactivity levels in future CERCLA waste designated for EMDF. The methods and procedures for characterizing wastes for acceptance at EMWMF were followed in the development of these historical WL profiles, which include statistical evaluations to determine the central tendency and range of contaminant concentrations (i.e., minimum, arithmetic mean, median, and maximum) and fitted probability distribution functions, expected values and upper confidence limits (UCLs) based on 90^{th} and 95^{th} percentile concentrations (DOE 2001). The expected values from these WL profiles incorporate the full range and relative frequency of measured values and are used as surrogate data for estimating the average radioactivity concentrations for EMDF waste streams.

Each of the data sources (site/facility characterization reports, SORTIE data, and EMWMF WL data) is useful for estimating future EMDF waste radioactivity concentrations, but each also has certain limitations. The RIs for ORNL (Bethel Valley [BV]) and Y-12 (Upper East Fork Poplar Creek [UEFPC]) provide a good basis for estimating RA waste characteristics. On the other hand, detailed facility characterization data suitable for estimating radioactivity levels of future demolition debris are limited to a few small facilities at ORNL (Isotope Row) and a few large inactive process facilities at Y-12 (Alpha-4 and Alpha-5 Complexes and Biology Complex [Table B.1]). These data sources should provide representative radioactivity concentrations for the applicable waste streams. The majority of the SORTIE data are probably more representative of facility radionuclide inventories than future waste characteristics, but provide the most comprehensive survey of potential radioisotopes and the range of concentrations that may be present in the hundreds of facilities to be demolished at ORNL and Y-12. EMWMF WL profiles for ORNL and Y-12 waste streams are based on rigorous sampling and analysis protocols for waste characterization. These WL profiles are likely to be representative of some future EMDF waste streams similar to those that have been

accepted for disposal at EMWMF, but are limited to those radionuclides that have established WAC. The limitations associated with each of the three data sources introduce uncertainty in the estimated EMDF radionuclide inventory, but the data sources are complementary, so when used in combination, the impact of these limitations is mitigated.

B.3.2 SELECTION OF RADIOLOGICAL DATA FOR EMDF WASTE STREAMS

Estimated radiological profiles for the six EMDF waste streams are based on data from the three sources described in Sect. B.3.1. For each waste stream, the selected data includes expected activity concentration values (typically in picocuries per gram) taken from selected EMWMF WL analyses, facility characterization reports (for the Y-12 D&D Alpha-4 and Alpha-5 and Y-12 D&D Biology Complex waste streams), and RIs (for RA waste streams). Some data sources provide mean and maximum values instead of expected and UCL-95 values. Radioactivity data derived from SORTIE facility inventory estimates (derived from safety analyses) are generally identified as "limiting values" to denote that these data are based on facility total activity inventories applied to the corresponding estimated mass of facility D&D waste. Some of the SORTIE limiting values represent contaminated process systems that could be easily removed prior to facility demolition, which suggests the use of the SORTIE data may tend to overestimate radionuclide activity concentrations in demolition debris.

The following subsections summarize the basis for data selections for each waste stream. The specific data sources used to estimate the radiological characteristics of each EMDF waste stream are summarized in Table B.4.

Table B.4. Data sources for EMDF waste stream characterization

EMDF waste stream	Sources of waste characterization data
Y-12 D&D Alpha-4 and Alpha-5	Alpha-5 Building Characterization Report, four EMWMF WLs, SORTIE Alpha-4
Y-12 D&D Biology Complex	Biology Complex Characterization Report, two EMWMF WLs
Y-12 D&D Remaining Facilities	SORTIE: Beta-1 Complex, two EMWMF WLs
Y-12 Remedial Action	UEFPC RI, one EMWMF WL, SORTIE White Wing Scrapyard
ORNL D&D	Isotope Row Characterization Report, SORTIE 23 ORNL facilities, 20 EMWMF WLs, one Bldg. 3019 WL
ORNL Remedial Action	Bethel Valley RI, 11 EMWMF WLs

D&D = deactivation and decommissioning
EMDF = Environmental Management Disposal Facility
EMWMF = Environmental Management Waste Management Facility
ORNL = Oak Ridge National Laboratory
RI = remedial investigation
UEFPC = Upper East Fork Poplar Creek
WL = waste lot
Y-12 = Y-12 National Security Complex

B.3.2.1 Y-12 D&D Waste Stream Data

The radiological profile for the Y-12 D&D Alpha-4 and Alpha-5 waste stream is based on recent characterization of the Alpha-5 facility (DOE 2012, Appendix G), four EMWMF WLs from Alpha-5 and SORTIE data for Alpha-4. Similarly, characterization data from the Biology Complex (UCOR 2017, Appendix G) was combined with analytical data from two EMWMF WLs to derive the profile for the Y-12 D&D Biology Complex waste stream. The radiological profile for the Y-12 D&D Remaining Facilities waste stream is based on SORTIE data for the Beta-1 Complex, combined with two EMWMF WL profiles that comprise Old Scrap Yard Debris wastes. One additional EMWMF WL, WL 114.01 Jack Case Center

Contaminated Force Main, was reviewed and judged unrepresentative of the Y-12 D&D Remaining Facilities waste due to high levels of Tc-99.

B.3.2.2 ORNL D&D Waste Stream Data

The estimated radiological profile for the ORNL D&D waste stream is based on data from the Isotope Row Facilities characterization report (ORAU 2013), SORTIE data for 23 ORNL facilities, 20 EMWMF WL profiles from ORNL cleanup projects, and one additional waste profile for ORNL Bldg. 3019 waste disposed at the DOE Nevada National Security Site.

B.3.2.3 Y-12 and ORNL RA Waste Stream Data

The estimated radiological composition of Y-12 and ORNL RA waste soils and debris are based on soils data for the UEFPC Characterization Area (UEFPC RI [DOE 1998]) and the BV area at ORNL (BV RI [DOE 1999]). The UEFPC data are combined with EMWMF WL 303.1 (Old Scrap Yard Soils) and SORTIE data for the White Wing Scrapyard for the Y-12 RA profile. EMWMF WL 1.0 (Boneyard/ Burnyard) was reviewed and judged unrepresentative of the entirety of Y-12 RA waste due to high levels of Tc-99. The BV data are combined with analytical data for 11 EMWMF WLs from ORNL RA projects for the ORNL RA waste stream. Two available ORNL WLs were reviewed and judged unrepresentative of the entire ORNL RA waste. EMWMF WLs 87.01 (Surface Impoundments Operable Unit Bricks) and 149.07 (New Hydrofracture Facility Process Equipment and Debris) were not used due to high levels of C-14 and Tc-99.

B.3.3 ESTIMATED RADIOLOGICAL WASTE PROFILES

Radioisotopes having half-lives less than 1 year were not included in the EMDF estimated inventory calculations. The combination of radiological information sources provided data on 70 radionuclides with half-lives greater than 1 year. To provide bounding activity concentration estimates for purposes of radioisotope screening (refer to Sect. 2.3.2 of the PA), overall arithmetic averages of all values (including maximum and UCL-95 values) for all waste streams, without corrections for radioactive decay, were calculated. These screening level concentrations were developed for all 70 radionuclides in the source data (refer to Table 2.16 in Sect. 2.3.2 of the PA).

The radiological profiles for the EMWF waste streams are estimated average activity concentrations (calculated from only the expected, average, and limiting values) for each radionuclide. However, due to data limitations (generally the availability of only a single record for a radionuclide and/or inability to independently confirm some data from original sources), estimated waste stream average activity concentrations were developed for only 56 radionuclides. Data for nine less commonly reported fission products (Cd-113m, Cs-135, Kr-85, Pd-107, Se-79, Sm-151, Sn-121m, Sn-126, and Zr-93) could not be verified against the original data sources; therefore, these nine radionuclides are not included in the estimated EMDF inventory. EMDF waste average concentrations for five other radionuclides (Ba-133, Be-10, Ca-41, Mo-93, and Nb-93m) were estimated by applying additional assumptions to the EMDF waste quantity and radionuclide data. The assumptions made to estimate the as-generated EMDF waste average concentration values used in the EMDF PA models for these five radionuclides are presented in Attachment B.3. This remainder of this subsection presents the waste stream average activity concentrations for the 56 radionuclides for which data were available and confirmed against original source documents.

Profile activity concentrations are calculated as the arithmetic averages of all the average (mean), expected, or limiting values assigned to a waste stream. Applying an arithmetic average rather than a geometric mean to radioactivity concentration data that typically span many orders of magnitude results in an intentional

bias toward higher estimated concentrations. Activity concentrations are adjusted for radiological decay to the assumed year of EMDF closure (2047) based on radioisotope half-life and the year of data collection.

The estimated average activity concentrations for all EMDF waste streams are shown in Table B.5.

Table B.5. Arithmetic average activity concentrations for EMDF waste streams

	EMDF waste stream average activity concentration (pCi/g)					
Radioisotope	**ORNL D&D**	**ORNL RA**	**Y-12 D&D Alpha-4 and Alpha-5**	**Y-12 D&D Biology**	**Y-12 D&D Remaining Facilities**	**Y-12 RA**
Ac-227	3.88E-02					
Am-241	2.10E+02	6.14E+02	1.61E-02	1.82E-01	5.96E-02	6.86E-01
Am-243	2.73E+00	3.95E+01				
C-14	8.53E+00	2.55E+01		4.18E+01		
Cf-249	1.44E-05					
Cf-250	9.82E-05					
Cf-251	2.79E-06					
Cf-252	1.74E-06					
Cm-243	5.18E+00	5.65E-01				
Cm-244	1.67E+03	1.40E+01	3.93E-03			
Cm-245	5.08E-01					
Cm-246	2.11E+00					
Cm-247	1.38E-01					
Cm-248	7.43E-03					
Co-60	2.18E-01	4.38E-02	6.47E-03			7.98E-04
Cs-134	2.79E-08	1.21E-07				
Cs-137	2.11E+03	1.46E+04	1.99E-01	1.32E-01	4.68E-02	5.40E+00
Eu-152	3.73E+02	8.08E+00				
Eu-154	8.49E+01	1.39E+00				
Eu-155	8.87E-02	7.95E-04				
Fe-55		1.28E-05				
H-3	1.30E+02	1.97E+01		2.23E+00		
I-129	4.92E+00	5.18E-01				
K-40	5.53E+00	1.90E+01		2.23E+01		6.33E+00
Mo-100	5.58E-05					
Na-22	1.08E-05	1.45E-07				
Nb-94	2.16E-01					
Ni-59	4.04E+01					
Ni-63	6.02E+02	8.97E+03		1.72E+00		
Np-237	4.59E-01	2.81E+00	4.90E-02	2.15E-01		4.32E-01
Pa-231	3.17E+00					
Pb-210	4.68E+01	2.26E+00				
Pm-146	1.17E-03					
Pm-147	2.83E-03	9.38E-05				
Pu-238	7.37E+02	5.46E+02	1.84E-01		3.95E-01	8.77E-03
Pu-239	2.37E+02	5.76E+02			7.62E-02	5.93E-01
Pu-240	3.51E+02	5.08E+02	6.77E-02	1.80E-01		
Pu-241	6.87E+01	2.83E+03				
Pu-242	1.83E-01	2.27E+00				
Pu-244	4.89E-02					
Ra-226	2.92E+00	3.92E+00		9.97E-01		1.45E+00

Table B.5. Arithmetic average activity concentrations for EMDF waste streams (cont.)

	EMDF waste stream average activity concentration (pCi/g)					
Radioisotope	**ORNL D&D**	**ORNL RA**	**Y-12 D&D Alpha-4 and Alpha-5**	**Y-12 D&D Biology**	**Y-12 D&D Remaining Facilities**	**Y-12 RA**
Ra-228	6.54E-03	1.39E-02			1.71E-01	2.68E-03
Re-187	2.27E-05					
Sb-125	4.02E-07					
Sr-90	2.16E+03	4.15E+02		1.75E+00	1.66E-01	
Tc-99	1.32E+01	3.94E+00	1.08E+00	4.06E+01	7.78E-01	4.61E+00
Th-228	1.16E-06	1.88E-09	5.93E-07	1.27E-05	1.58E-05	
Th-229	1.73E+00	7.96E+01			4.71E-02	
Th-230	1.70E+00	2.11E+01	4.32E-01		7.85E-02	1.37E+00
Th-232	1.19E+00	9.36E+00	3.74E-01	7.96E-01	6.54E-01	1.31E+01
U-232	8.34E-01	1.45E+02				
U-233	2.65E+02	2.92E+02		9.65E+01	1.10E+00	
U-234	1.11E+01	1.51E+02	9.10E+00	8.33E+01	5.23E+03	1.56E+01
U-235	4.20E-01	2.34E+00	7.47E-01	7.18E+00	3.16E+02	1.11E+01
U-236	2.65E-01	1.08E+00	3.80E-01	4.23E+00	7.47E+01	2.26E-01
U-238	6.79E+00	2.92E+01	3.43E+01	3.40E+02	2.91E+03	1.51E+02

D&D = deactivation and decommissioning
EMDF = Environmental Management Disposal Facility
ORNL = Oak Ridge National Laboratory
RA = remedial action
Y-12 = Y-12 National Security Complex

B.4 DEVELOPMENT OF ESTIMATED EMDF RADIONUCLIDE INVENTORY

A projected total radioactivity inventory for EMDF waste was developed by applying the activity concentrations (units of pCi/g) from each EMDF radiological profile to the mass of the corresponding waste stream, and summing the activities for the six EMDF waste streams (see Fig. B.1) The waste mass was estimated based on the forecast waste volume for each waste stream and an assumed bulk density for the debris and soil waste forms.

An average soil density of 2450 lb/cy (1113 kg/cy) was assumed for the soil waste volumes. A debris density of 1700 lb/cy (773 kg/cy) was determined based on the bulk densities compiled for EMWMF in the Capacity Assurance Remedial Action Report (CARAR) (DOE 2004). An analysis described in the RI/FS (DOE 2017) resulted in a distribution of various debris types for EMDF as follows:

- Equipment, 19 percent (density = 680 lb/cy)
- Heavy steel, 25 percent (density = 1040 lb/cy)
- Concrete and masonry, 42 percent (density = 2600 lb/cy)
- General demolition, 7 percent (density = 1620 lb/cy)
- Light gauge metals and siding, 3 percent (density = 1040 lb/cy)
- Roofing materials, 4 percent (density = 1520 lb/cy).

Applying the distribution as shown to the bulk densities reported in the CARAR results in an estimated average debris density of 1700 lb/cy.

The radionuclide inventory derived from the forecast waste volumes, average bulk densities, and radiological profiles for each EMDF waste stream is given in Table B.6 for each of the 56 radionuclides in Table B.5, and for 5 other radionuclides. The total estimated EMDF inventory at closure (in curies) is shown in column 8 and the equivalent waste-average activity concentration (in pCi/g) is shown in column 9. For the five radionuclides that have concentrations estimated with additional assumptions (refer to Attachment B.3), only EMDF total activity inventory and EMDF waste average activity concentration are given in Table B.6. In general, the total estimated radionuclide inventory at closure is dominated by ORNL wastes, which constitute less than 30 percent of the total forecast waste volume. ORNL waste is projected to account for approximately 65 percent of the radioactivity and Y-12 debris and soil is projected to contribute the remaining approximately 35 percent. In terms of total activity, the estimated EMDF radionuclide inventory is dominated by Cs-137, Ni-63, U-234, U-238, and Pu-241, which account for approximately 80 percent of the estimated total.

Table B.6. Total EMDF waste radionuclide inventory (Ci decayed to 2047)

Waste mass (g)	ORNL D&D	ORNL RA	Y-12 D&D Alpha-4 and Alpha-5	Y-12 D&D Biology	Y-12 D&D Remaining Facilities	Y-12 RA	EMDF Waste Total Inventory (Ci)	EMDF waste average activity concentration (pCi/g)
	1.94E+11	1.81E+11	1.37E+11	2.81E+10	3.03E+11	5.26E+11	1.37E+12	
Radio-isotope	**EMDF activity by waste stream (Ci)**							
Ac-227	7.54E-03						7.54E-03	5.50E-03
Am-241	4.09E+01	1.11E+02	2.20E-03	5.11E-03	1.80E-02	3.61E-01	1.52E+02	1.11E+02
Am-243	5.30E-01	7.12E+00					7.65E+00	5.59E+00
Ba-133	Refer to Attachment B.3 for basis of inventory estimate						4.14E+00	3.02E+00
Be-10	Refer to Attachment B.3 for basis of inventory estimate						6.52E-05	4.76E-05
C-14	1.66E+00	4.60E+00		1.17E+00			7.43E+00	5.43E+00
Ca-41	Refer to Attachment B.3 for basis of inventory estimate						1.09E-01	7.92E-02
Cf-249	2.80E-06						2.80E-06	2.05E-06
Cf-250	1.91E-05						1.91E-05	1.39E-05
Cf-251	5.42E-07						5.42E-07	3.96E-07
Cf-252	3.37E-07						3.37E-07	2.46E-07
Cm-243	1.01E+00	1.02E-01					1.11E+00	8.10E-01
Cm-244	3.23E+02	2.53E+00	5.39E-04				3.26E+02	2.38E+02
Cm-245	9.87E-02						9.87E-02	7.21E-02
Cm-246	4.10E-01						4.10E-01	2.99E-01
Cm-247	2.68E-02						2.68E-02	1.96E-02
Cm-248	1.44E-03						1.44E-03	1.05E-03
Co-60	4.23E-02	7.90E-03	8.87E-04			4.20E-04	5.15E-02	3.76E-02
Cs-134	5.41E-09	2.19E-08					2.73E-08	1.99E-08
Cs-137	4.11E+02	2.63E+03	2.73E-02	3.71E-03	1.42E-02	2.84E+00	3.04E+03	2.22E+03
Eu-152	7.25E+01	1.46E+00					7.40E+01	5.40E+01
Eu-154	1.65E+01	2.52E-01					1.67E+01	1.22E+01
Eu-155	1.72E-02	1.44E-04					1.74E-02	1.27E-02
Fe-55		2.31E-06					2.31E-06	1.68E-06
H-3	2.52E+01	3.56E+00		6.25E-02			2.88E+01	2.10E+01
I-129	9.56E-01	9.35E-02					1.05E+00	7.66E-01
K-40	1.07E+00	3.43E+00		6.27E-01		3.33E+00	8.46E+00	6.18E+00
Mo-100	1.08E-05						1.08E-05	7.92E-06
Mo-93	Refer to Attachment B.3 for basis of inventory estimate						1.00E+00	7.30E-01

Table B.6. Total EMDF radionuclide inventory (Ci decayed to 2047) (cont.)

Waste mass (g)	ORNL D&D 1.94E+11	ORNL RA 1.81E+11	Y-12 D&D Alpha-4 and Alpha-5 1.37E+11	Y-12 D&D Biology 2.81E+10	Y-12 D&D Remaining Facilities 3.03E+11	Y-12 RA 5.26E+11	EMDF Waste Total Inventory (Ci) 1.37E+12	EMDF waste average activity concentration (pCi/g)
Radio-isotope	**EMDF activity by waste stream (Ci)**							
Na-22	2.09E-06	2.63E-08					2.12E-06	1.55E-06
Nb-93m	Refer to Attachment B.3 for basis of inventory estimate						6.01E-01	4.39E-01
Nb-94	4.20E-02						4.20E-02	3.07E-02
Ni-59	7.84E+00						7.84E+00	5.73E+00
Ni-63	1.17E+02	1.62E+03		4.84E-02			1.74E+03	1.27E+03
Np-237	8.92E-02	5.08E-01	6.72E-03	6.04E-03		2.27E-01	8.37E-01	6.12E-01
Pa-231	6.15E-01						6.15E-01	4.49E-01
Pb-210	9.09E+00	4.08E-01					9.50E+00	6.93E+00
Pm-146	2.28E-04						2.28E-04	1.66E-04
Pm-147	5.49E-04	1.69E-05					5.66E-04	4.13E-04
Pu-238	1.43E+02	9.86E+01	2.52E-02		1.20E-01	4.62E-03	2.42E+02	1.77E+02
Pu-239	4.61E+01	1.04E+02			2.31E-02	3.12E-01	1.50E+02	1.10E+02
Pu-240	6.81E+01	9.18E+01	9.29E-03	5.07E-03			1.60E+02	1.17E+02
Pu-241	1.33E+01	5.12E+02					5.25E+02	3.83E+02
Pu-242	3.55E-02	4.10E-01					4.45E-01	3.25E-01
Pu-244	9.49E-03						9.49E-03	6.93E-03
Ra-226	5.68E-01	7.08E-01		2.80E-02		7.63E-01	2.07E+00	1.51E+00
Ra-228	1.27E-03	2.52E-03			5.17E-02	1.41E-03	5.69E-02	4.15E-02
Re-187	4.40E-06						4.40E-06	3.21E-06
Sb-125	7.82E-08						7.82E-08	5.71E-08
Sr-90	4.21E+02	7.50E+01		4.93E-02	5.02E-02		4.96E+02	3.62E+02
Tc-99	2.57E+00	7.11E-01	1.48E-01	1.14E+00	2.36E-01	2.43E+00	7.23E+00	5.28E+00
Th-228	2.25E-07	3.40E-10	8.14E-08	3.58E-07	4.78E-06		5.45E-06	3.98E-06
Th-229	3.36E-01	1.44E+01			1.43E-02		1.47E+01	1.08E+01
Th-230	3.30E-01	3.81E+00	5.92E-02		2.38E-02	7.20E-01	4.94E+00	3.61E+00
Th-232	2.32E-01	1.69E+00	5.14E-02	2.24E-02	1.98E-01	6.87E+00	9.07E+00	6.62E+00
U-232	1.62E-01	2.61E+01					2.63E+01	1.92E+01
U-233	5.15E+01	5.27E+01		2.71E+00	3.33E-01		1.07E+02	7.83E+01
U-234	2.15E+00	2.72E+01	1.25E+00	2.34E+00	1.58E+03	8.24E+00	1.62E+03	1.19E+03
U-235	8.15E-02	4.23E-01	1.02E-01	2.02E-01	9.57E+01	5.84E+00	1.02E+02	7.47E+01
U-236	5.14E-02	1.95E-01	5.22E-02	1.19E-01	2.26E+01	1.19E-01	2.32E+01	1.69E+01
U-238	1.32E+00	5.27E+00	4.71E+00	9.56E+00	8.83E+02	7.92E+01	9.83E+02	7.18E+02

D&D = deactivation and decommissioning
EMDF = Environmental Management Disposal Facility
ORNL = Oak Ridge National Laboratory
RA = remedial action
Y-12 = Y-12 National Security Complex

B.5 USE OF THE ESTIMATED WASTE INVENTORY IN THE PA MODELING

Development of the estimated radionuclide inventory and utilization of the inventory data in the EMDF performance modeling is summarized in Sect. 2.3 of the PA. The estimated total waste activity (EMDF total waste inventory given in curies in Table B.6) is not used directly in the PA modeling. The estimated

waste inventory applies only to the total waste volume (approximately 1.6 M cy) projected for EMDF disposal. An added 25 percent waste volume uncertainty adjustment (and the estimated volume of clean fill required) was applied in deriving the EMDF disposal capacity requirement of 2.2 M cy. The PA modeling is based on the assumption that the EMDF is filled to design capacity at closure.

The calculated EMDF waste average concentrations (Table B.6, rightmost column) represent as-generated waste and do not account for the addition of clean soil required to fill voids in debris during disposal. The PA models employ source activity concentrations adjusted from the estimated EMDF waste average concentrations to account for the added soil mass. The +25 percent waste volume factor and added clean fill mass are incorporated into the PA analysis by applying these adjusted (as-disposed) concentrations to the total mass of waste and clean fill that corresponds to the EMDF design disposal capacity of 2.2 M cy. Thus, the inventory estimate presented in this appendix is based on the forecast as-generated waste volumes, but the PA modeling explicitly considers the assumed 25 percent waste volume contingency as well as the added mass of clean soil that would be required for disposal.

The use of data and assumptions in developing the EMDF disposal capacity, estimating the EMDF waste average activity concentrations, and calculating the modeled source concentrations that account for added clean fill mass is summarized in Fig. 2.41 and the introductory text of Sect. 2.3 of the PA. The procedure for adjusting the estimated waste average activity concentrations to account for the mass of clean fill added during disposal is presented in Sect. 3.2.2 of the PA.

B.6 INVENTORY UNCERTAINTY AND KEY RADIOISOTOPES OF CONCERN

Uncertainty in the EMDF estimated inventory includes uncertainty in the underlying characterization data and uncertainty associated with the assumption that the radioisotopes and activity concentrations in the selected historical WLs disposed at EMWMF are representative of future Y-12 and ORNL CERCLA wastes. There is also uncertainty associated with use of the SORTIE facility inventory data to estimate waste characteristics, but the use of the SORTIE data should lead to overestimation of average waste concentrations because the facility inventories developed for safety analysis tend to be bounding (maximum likely) estimates. In general, the approach to managing uncertainty in the estimated EMDF radionuclide inventory is to bias the inventory estimates toward higher values. This approach incorporates the following:

1) Inclusion of expected values based on estimated frequency distributions from EMWMF WLs and facility characterization reports (Alpha-5 and Biology facilities). In most cases, the expected values are higher than the average values based on sampling data.
2) Inclusion of SORTIE facility inventory-based concentrations, which are likely to be higher than facility demolition waste concentrations due to the bounding facility inventories utilized and because some high activity systems and components may be disposed offsite prior to facility demolition for onsite disposal.
3) Use of arithmetic rather than geometric averaging to estimate representative average concentrations for EMDF wastes, which also should tend to bias the inventory estimates toward higher values.

There are some radioisotopes that do not represent a large proportion of the estimated inventory, but are of concern for contributions to total doses that can challenge performance standards under certain assumptions. These include radioisotopes of relatively mobile, long-lived radioisotopes, including C-14, I-129, and Tc-99. The C-14 and I-129 are associated primarily with ORNL remediation activities, whereas Tc-99 is expected from both ORNL and Y-12 remediation activities. Also of potential concern are Rn-222

parents, including U-234, U-238, Ra-226, and Th-230. In the context of an inadvertent intruder exposure scenario, key radioisotopes of concern include some that comprise large proportions of the estimated inventory such as Cs-137, U-234, and U-238.

Uncertainty in the estimated inventory could be reduced with further review of currently available characterization data for ORNL hot cell and reactor facilities and additional information on Y-12 uranium processing facilities, and by incorporating the results of future waste characterization efforts. Based on the dose analysis presented in the PA, the primary radionuclides of concern are C-14, I-129, and Tc-99. The estimated waste average concentrations for I-129 are probably much higher than is reasonably expected, due to the inclusion of one small volume and high activity waste lot (WL-149.10) that was characterized for EMWMF disposal. Similarly, estimated average concentrations of C-14 and Tc-99 may overestimate EMDF total inventory at closure, due to the disproportional impact of a few higher concentration values included in the data set. The likelihood of significant inventories of less commonly reported fission products (e.g., Cd-113m, Cs-135, Pd-107, Se-79, Sm-151, Sn-121m, Sn-126, and Zr-93) is another uncertainty that will be reduced with additional future collection of ORNL process knowledge and/or characterization data for waste management decisions.

Although no local data are available for estimating future EMDF Cl-36 inventory, small quantities of Cl-36 could be present in future EMDF LLW, particularly from ORNL research reactor facilities. Uncertainty related to potential Cl-36 contamination in some EMDF waste streams is addressed in the PA in the context of radionuclide screening and PA change control procedures.

B.7 REFERENCES

DOE 1998. *Report on the Remedial Investigation of the Upper East Fork Poplar Creek Characterization Area at the Oak Ridge Y-12 Plant, Oak Ridge, Tennessee*, DOE/OR/01-1641/V1&D2, U.S. Department of Energy, Oak Ridge, TN, August.

DOE 1999. *Remedial Investigation/Feasibility Study for the Bethel Valley Watershed at Oak Ridge National Laboratory, Oak Ridge, Tennessee*, DOE/OR/01-1748/V1&D2, U.S. Department of Energy, Oak Ridge, TN, May.

DOE 2001. *Attainment Plan for Risk/Toxicity-Based Waste Acceptance Criteria at the Oak Ridge Reservation, Oak Ridge, Tennessee*, DOE/OR/01-1909&D3, U.S. Department of Energy, Oak Ridge, TN, October.

DOE 2004. *Environmental Management Waste Management Facility Capacity Assurance Remedial Action Report*, DOE/OR/01-2145&D2, U.S. Department of Energy, Oak Ridge, TN, September.

DOE 2012. *Characterization Report for Alpha 5 Building 9201-5 at the Y-12 National Security Complex, Oak Ridge, Tennessee*, DOE/OR/01-2540&D2, U.S. Department of Energy, Oak Ridge, TN, March.

DOE 2017. *Remedial Investigation/Feasibility Study for Comprehensive Environmental Response, Compensation and Liability Act Oak Ridge Reservation Waste Disposal, Oak Ridge, Tennessee*, DOE/OR/01-2535&D5, U.S. Department of Energy, Oak Ridge, TN, February.

ORAU 2013. *Data Sharing Report Characterization of Isotope Row Facilities Oak Ridge National Laboratory, Oak Ridge, Tennessee*, DCN: 5118-SR-04-0, Oak Ridge Associated Universities, Oak Ridge, TN.

Redus 2014. *Project Execution Plan for Source Term for Input to the Environmental Management Waste Management Facility, Oak Ridge, Tennessee Performance Assessment*, Redus and Associates, LLC, Oak Ridge, TN.

UCOR 2017. *Characterization Report for the Biology Complex Facilities, Y-12 National Security Complex, Oak Ridge, Tennessee*, UCOR-4992/R0, UCOR, Oak Ridge, TN.

ATTACHMENT B.1.
Y-12 NATIONAL SECURITY COMPLEX AND OAK RIDGE NATIONAL LABORATORY DEACTIVATION AND DECOMMISIONING WASTE STREAM FACILITY DESCRIPTIONS

This page intentionally left blank.

ACRONYMS

ACM	asbestos-containing material
ARRA	American Recovery and Reinvestment Act of 2009
BV	Bethel Valley
CERCLA	Comprehensive Environmental Response, Compensation and Liability Act of 1980
COPC	contaminant of concern
D&D	deactivation and decommissioning
DOE	U.S. Department of Energy
EGCR	Experimental Gas-cooled Reactor
EMDF	Environmental Management Disposal Facility
FY	fiscal year
HEU	highly enriched uranium
HPRR	Health Physics Research Reactor
HRE	Homogeneous Reactor Experiment
HSG	Hot Storage Garden
IPDP	Isotopes Production and Distribution Program
LLLW	liquid low-level (radioactive) waste
MV	Melton Valley
OGR	Oak Ridge Graphite Reactor
OREM	Oak Ridge Office of Environmental Management
ORNL	Oak Ridge National Laboratory
ORRR	Oak Ridge Research Reactor
PCB	polychlorinated biphenyl
R&D	research and development
RCRA	Resource Conservation and Recovery Act of 1976
S&M	surveillance and maintenance
SWSA	Solid Waste Storage Area
TWPC	Transuranic Waste Processing Center
Y-12	Y-12 National Security Complex

This page intentionally left blank.

Y-12 D&D WASTE – FACILITY DESCRIPTIONS

In the following sections, Y-12 National Security Complex (Y-12) deactivation and decommissioning (D&D) projects (buildings grouped into complexes) are described based on facility characteristics and process knowledge for individual building complexes at each site. Table B.1.1 is a listing of Y-12 facility complexes to be demolished. Following the table, summaries of each facility complex document historical activities that took place in those complexes/associated facilities and discuss contaminants of potential concern (COPCs) associated with those facilities (U.S. Department of Energy [DOE] 2010).

Table B.1.1. Y-12 D&D facility complexes and contaminants of potential concern

Y-12 D&D Project	Total waste volume (cy)	Contaminants of potential concern
9206 Complex	15,490	• Uranium isotopes are a primary concern at all facilities. Thorium isotopes are also present in some facilities. • Some facilities also have transuranic radionuclides that may include Np-237 and Pu 239/240. • Biology Complex facilities characterization indicates the presence of C-14, H-3, Np-237, Pu 239/240, and Tc-99 in addition to uranium isotopes.
9212 Complex	113,571	
9213 and 9401-2 Demolition	8000	
Alpha-2 Complex[a]	72,990	
Alpha-3 Complex	37,108	
Alpha-4 Complex[a]	55,085	
Alpha-5 Complex[a]	122,623	
Beta-1 Complex	46,920	
Beta-3 Deactivation Only	19,502	
Beta-4 Complex[a]	75,787	
Biology Complex	34,157	
Steam Plant Complex Legacy Material Disposition	80	
Tank Facilities Demolition	3000	

[a]A portion of waste (debris and soil) from these projects will be associated with mercury contamination.

D&D = deactivation and decommissioning
Y-12 = Y-12 National Security Complex

9206 COMPLEX

Building 9206 was constructed in 1945 with an original mission to recover highly enriched uranium (HEU) and process salvaged uranium from the electromagnetic separation process. From 1947 until 1994, Bldg. 9206 operated as a uranium product recovery and salvage facility. In addition, operations consisted of uranium chemical processing and metal production operations between 1951 and 1994. From 1994 until the present, the facility has undergone deactivation of systems, has had minimal surveillance and maintenance activities, and has served as a storage facility for in-process materials. However, all systems/components have not been cleaned and some HEU may remain in the equipment and processes. In 2006, the southwestern corner of the facility was decontaminated and demolished. In 2011, the Filter House and Room 25 (incinerator) was demolished under the American Recovery and Reinvestment Act of 2009 (ARRA). The facility contains large areas posted as contamination, high contamination, and fixed contamination areas (DOE 2008).

The facilities included in the 9206 Complex are Bldg. 9206, Production; Bldg. 9720-17, Warehouse/ Industrial; Bldgs. 9744 and 9768, Utilities; and the 9206 Tank Farm.

9212 COMPLEX

The 9212 Complex consists of 26 facilities that total 548,709 sq ft. Building 9212 is a two-story reinforced concrete, concrete block, and steel building that was constructed in 1949. This building is used for the recovery, purification, and processing of enriched uranium into usable products. The building is comprised of multiple wings that contain different manufacturing and production functions. The first and second floors are primarily concrete and the third and fourth floors are primarily metal grating. There are miles of stainless steel process piping and equipment throughout the facility as well as an extensive heating, ventilation, and air conditioning system that runs throughout the facility. There are numerous radiological hazards present in the facility, including fixed contamination and removable surface contamination. Fissile material is present in the facility and holdup material in process equipment is likely to be encountered during D&D activities. Asbestos, polychlorinated biphenyls (PCBs), lead, and other chemical hazards, including nitric acid, ammonium hydroxide, hydrogen peroxide, and hydrofluoric acid, are present in the facility. There are also beryllium-contaminated material storage areas in the facility.

The facility has a basement averaging 9 ft deep. All the subsurface structures within the basement areas will be managed as part of the remedial actions associated with the Upper East Fork Poplar Creek Remaining Slabs and Soils Project.

BUILDINGS 9213 AND 9401-2

The Bldgs. 9213 and 9401-2 project consists of two facilities that total 37,308 sq ft. Building 9213 (23,635 sq ft), Critical Experiment Facility, was built in 1950 in a forested valley on Chestnut Ridge south of Y-12. The facility housed activities to collect data from assemblies of solid and liquid fissile materials in both subcritical and critical configurations. Over the years, work on basic research of reactor physics and critical geometries, testing of reactor fuel elements, reactor design, and development of fissionable material transport has been completed in the facility. From 1965 to 1987, the west test cell was used by Oak Ridge National Laboratory (ORNL) for initial testing of fresh fuel for the High Flux Isotope Reactor. Regular operations ceased in 1987 and the facility was approved for shutdown and transfer to the Oak Ridge Office of Environmental Management (OREM) in 1992. All utilities have been deactivated and the facility is cold and dark. Current activities are restricted to surveillance and maintenance (S&M) and limited use by the U.S. Army as a Nuclear/Radiological Field Training Center. There is fixed and removable contamination present in the test cells and small amounts of residual radioactive material (enriched uranium solutions) in tanks and process equipment, particularly in the west test cell area that was used for critical experiments with aqueous solutions.

Building 9401-2 (13,673 sq ft) was built in the early 1940s to house steam plant operations until a replacement facility was constructed in the mid-1950s. Building 9401-2 was reconfigured in 1955 as the General Plating Facility (plating shop) for the Y-12 Metal Preparation Division. This non-radiological workshop housed various metal plating/coating processes, metal cleaning, and finishing operations. These operations involved a variety of metals and hazardous chemicals, including copper, zinc, chromium, nickel, acidic and caustic solutions, and cyanide. Cyanide plating operations ceased in the 1980s. In the late 1990s, deactivation activities included draining and cleaning of plating tanks; removal of process materials, debris, and hazardous waste; and deactivation of process equipment and unneeded utility services. Steam, building ventilation, lighting, and sprinkler system services remain active to support routine S&M activities.

Final decommissioning of Bldg. 9401-2 will require the removal of legacy materials and process equipment prior to demolition. There is fixed radiological contamination on equipment in one area inside the building. It is likely that the plating process equipment (piping and pumps) contains holdup of hazardous materials. All stored hazardous materials were removed during the initial deactivation. Process ventilation equipment (fans, ductwork, and exhaust stacks) is likely to be contaminated. Abatement of asbestos-containing material (ACM) and other hazardous substances in preparation for demolition will require a significant

effort. Fixation of contaminated surfaces also may be required. There are two empty 5000-gal Resource Conservation and Recovery Act of 1976 (RCRA) tanks (closed) and an approximate 1000-gal condensate tank outside of the building that will be removed as part of the demolition.

ALPHA-2 COMPLEX

The Alpha-2 Complex consists of four facilities that total 332,595 sq ft. The Complex was constructed in the 1940s for uranium enrichment and lithium isotope separations and is currently a contaminated mercury-use facility, which is excess to Y-12 mission needs.

The Alpha-2 Facility (Bldg. 9201-2) is the largest facility in the Alpha-2 Complex at 324,448 sq ft. It is a two-floor facility with a partially concreted basement with varying depths of 7.5-15 ft deep. The footprint occupies 107,619 sq ft. Alpha-2 was constructed in 1943 to house two alpha-stage calutrons for uranium enrichment and was operated until 1951. Demolition of the calutrons occurred between 1951 and 1952 when most of the associated operations were removed and reconfiguration efforts began for the ELEX and COLEX lithium/mercury enrichment operations. Alpha-2 was used as a pilot plant for these operations. These processes used substantial quantities of mercury as a solvent agent to separate the lithium-6 isotope from lithium-7 (in the form of lithium hydroxide). During operations as a pilot plant, large amounts of mercury were lost and the building structures, particularly the basement, were contaminated. The lithium separation and enrichment operations continued until 1963 when the equipment was drained of the majority of process materials, including mercury. However, not all systems/components were cleaned and some recoverable quantities of mercury and lithium hydroxide may remain in the equipment and lines. As a result, airborne mercury is a continual hazard for workers in the facility and is a minor contributor to ambient air mercury concentrations at the Y-12 site. The COPCs include, but are not limited to, mercury, asbestos, PCBs, beryllium, and radiological contamination.

The facility was transferred from Y-12 operations control to ORNL for research and development (R&D) operations in 1963. The facility is still operated by ORNL, with minimal research activities being conducted. Currently, the Alpha-2 facility houses office space, maintenance operations, and occasional small-scale experiments.

ALPHA-3 COMPLEX

The Alpha-3 Complex consists of three facilities that total 196,870 sq ft. The Alpha-3 facility (97 percent of the complex square footage) was constructed in 1943 to house 96 calutrons, known as racetracks, for uranium enrichment. Uranium enrichment operations ended in 1951, at which time uranium salvage operations began. Salvage operations ended in 1964. The building was transferred to ORNL and R&D operations continued until 1995. ORNL operations included management and development offices; maintenance and machine shops; laboratories for multidisciplinary R&D relevant to energy conservation and utilization; mechanical, structural, and thermal sciences; and manufacturing technologies. Many areas of the facility have been emptied of everything except basic furniture. Currently, the building houses offices. The building was turned over to Y-12 in October 2001.

Most of the calutron equipment, components, and systems have been removed and drained. However, the smaller self-contained experimental systems still have hazardous chemical holdup present. The facility is considered to have up to 60-65 percent radiologically contaminated floors and walls. Beryllium contamination characterization surveys have been completed for the floors, lower walls, and some equipment within the facility. The beryllium survey has shown levels of beryllium in excess of the guidelines in some areas. The facility also contains quantities of ACM, PCBs, lead, and universal waste.

ALPHA-4 COMPLEX

Alpha-4 was constructed in 1944 to house the alpha-stage electromagnetic uranium enrichment process. The facility was used until 1946, at which time the process was abandoned in favor of the gaseous diffusion process being performed at the K-25 plant. From 1947 until 1953, the facility was placed on standby while process equipment was removed. Installation of the column exchange process began in 1953 and was operational until 1963. The process used mercury as a solvent to separate lithium-6 from natural lithium. After shutdown in 1963, the equipment was drained of most of the process materials, but was not cleaned. This system remained in standby until 1983. From 1974 to 1984, electrochemical machining operations were conducted in areas of the building separated from the process area. The facility was transferred to the DOE Office of Environmental Management in 1993. Removal of large portions of elemental mercury was accomplished in the 1990s, along with some equipment removal and treatment and disposal of large volumes of lithium hydroxide. Since that time, Alpha-4 has been maintained through S&M activities.

The four facilities included in the Alpha-4 Complex are Bldg. 9201-4 (Alpha-4) and other minor facilities, Transfer Station #699 and #674 (9501-5); Bldg. 9720-46, Storage; and Bldg. 9804, Utilities. Radiological surface contamination is expected to be present in most of these facilities.

ALPHA-5 COMPLEX

The Alpha-5 Complex consists of 15 facilities that total 662,540 sq ft and is located within the Y-12 Protected Area.

The Alpha-5 facility is the largest in the Complex at 613,642 sq ft (representing over 90 percent of the gross square footage and total footprint for the entire Alpha-5 Complex). Alpha-5 was constructed in 1944 to house alpha-stage calutrons for uranium enrichment. The facility was used until 1946 for uranium enrichment operations. From 1953 until 1963, the facility was used for COLEX lithium/mercury enrichment operations, and from the 1950s until 1995 the facility was used for various complex metallurgical and machining processes and involving uranium, thorium, and beryllium. Contaminants of concern and hazardous materials include, but are not limited to, mercury, asbestos, PCBs, beryllium, and radiological contamination (uranium and thorium).

BETA-1 COMPLEX

Beta-1 (Bldg. 9204-1) occupies 210,491 sq ft of the 213,162 sq ft total for the Complex. Beta-1 was constructed in the 1943 to 1944 time frame to house beta calutrons “racetracks,” track 1 and 2, which operated only until 1945. The facility was placed in operational standby for a short period and was decommissioned by 1947. Over the next 3 years it served as a location for various R&D and uranium recovery operations. In 1950, the facility was transitioned to ORNL and R&D work continued until 1995. During that period, stable isotopes such as depleted uranium and thorium were used in some research. The facility is currently home to shutdown experiments, office space, maintenance operations, and possible small-scale research projects. In 1947, most of the calutron equipment, components, and systems were removed and drained. However, radiological scoping surveys show that piping and other components have residual radiological holdup. The smaller, self-contained experimental systems typically did not involve radiation in their processes, but still have hazardous chemical holdup present. The facility is considered a “fixed contamination area” as noted on entryways to the building. Transuranic limits may apply. The facility also contains large quantities of ACM and universal wastes.

Other small facilities included in the Beta-1 Complex are Bldg. 9422, Helium Compressor Building, and Bldg. 9501-4, Primary Substation #824.

BETA-3 COMPLEX (DEACTIVATION ONLY)

Beta-3 (Bldg. 9204-3) was constructed in 1943 for the second pass separation of uranium-235 through the beta tracks 5 and 6. The calutrons operated until 1951 in this capacity, at which time they were converted to produce stable isotopes for medical, business, and agricultural uses. The facility operated in this capacity until 1985, when the east beta track was taken out of service. The west calutron was used until July 1998. The west calutron has been maintained periodically and brought to 85 percent power as late as 2005. Presently, this facility is considered to be in operational standby and represents what the calutron operation of the past resembled. The eastern track is still radiologically contaminated with the actinide series of nuclides and no decontamination or dismantlement has been performed. Holdup within the process lines has not been drained or characterized. The western beta track was cleaned with minimal D&D performed in preparation of being placed on the National Historic Preservation List. The remaining equipment in the basement and above floors still remains intact and requires decontamination, but not dismantlement. Labs contain much of the equipment that was used during operations, including hoods, ventilation, building surfaces, and equipment being contaminated. Currently, this facility has a very well-defined inventory list of hazards, stored equipment, and product inventories within the facility. Pounds of stable isotope bulk powders are stored in this facility. ACM is present throughout the facility in varying degrees of degradation, beryllium has been identified in several rooms, and other universal waste remains in the facility.

BETA-4 COMPLEX

The Beta-4 Complex consists of 10 facilities that total 347,132 sq ft. The largest building in the Complex, Beta-4, consists of a basement, first and second floors, and mezzanines. This building was constructed in 1944-1945 to house calutrons for uranium enrichment. The process was discontinued in 1946 and the equipment was removed. Other operations in the facility have included production of lithium-6 using the electro-exchange separation process; weapon fabrication support operations, including quality evaluation; general storage; and maintenance operations. The facility underwent partial excess material removal (second floor and mezzanine) as part of an ARRA project.

Depleted uranium, HEU, and thorium are considered the main radiological contaminants. Transuranic contamination is expected in the vicinity of the old “racetrack.” Chemical hazards include beryllium, mercury, lead, PCBs, freon, oils, and asbestos.

BIOLOGY COMPLEX

The Biology Complex consists of eight facilities that total 346,278 sq ft. Building 9207, Biology (approximately 75 percent of square footage of the Complex), was constructed in 1943 and originally was used for uranium salvage and recovery operations. In 1964-1995, the facility was used for ORNL Biology Division research operations. With the exception of Bldg. 9401-1, the buildings of the Biology Complex are “cold and dark” (i.e., all service utilities are deactivated in shutdown status pending demolition).

STEAM PLANT COMPLEX

The Steam Plant Complex consists of six facilities that total 68,951 sq ft and is located along the south side of the western Main Plant Area of Y-12. The majority of resulting waste debris is not expected to be contaminated with radiological contaminants, however, a small volume has been estimated.

TANK FACILITIES COMPLEX

The Tank Facilities include a RCRA storage tank facility and oil/solvent storage tank facility that account for 80 percent of the square footage (tanks and associated piping and equipment), with expected fixed and removable radioactive contamination present as well as some minor buildings and tanks. Two large

subsurface concrete vaults that measure 20 ft × 80 ft × 20 ft deep are part of this project. One vault was not used and the other was used for the storage of uranium oxide solution.

ORNL D&D WASTE – FACILITY DESCRIPTIONS

In the following sections, ORNL facility D&D projects (buildings grouped into complexes) are described based on facility characteristics and process knowledge for individual building complexes at each site. Table B.1.2 shows a listing of ORNL facility complexes to be demolished. Following the table, summaries of each facility complex document historical activities along with the COPCs associated with those facilities (ORNL 2008).

Table B.1.2. ORNL D&D facility complexes and contaminants of potential concern

ORNL D&D Project	Total waste volume (cy)	Contaminants of potential concern
2026 Complex	10,012	Th, U, Np, Pu, Am, Cm, Cf, Co, Sr, Cs, I, Eu
2528 Complex	484	Sr, Cs, others
3019A and Ancillary Facilities	62,263	Pu, U, Th, Am, others
3525 Complex	7659	U, Pu, others
3544 Complex	295	Sr, Cs
3608 Complex	4466	Sr, Cs
4501/4505 Complex	22,814	Sr, Cs, U, Pu, others
5505 Building	3689	Transuranics
6010 and East BV Complex	44,916	H-3, activated metals
BV Chemical Development Laboratory Facilities	1189	Alpha emitters, H-3
BV Reactor Area Facilities	7772	Sr, Cs, C-14, activated metals
BV Isotope Area Facilities (3038)	1825	Sr, Cs, Pu, Am, Eu, Tc, U, Pm, Y, Co
BV Isotope Area Facilities (2 projects)	6102	C-14, H-3, I-129, Cm, others
BV Tank Area Facilities	3615	Sr, Cs, others
Central Stack East Hot Cell Complex	5647	Sr, Cs, alpha emitters
Central Stack West Hot Cell Complex	4356	Sr, Cs, alpha emitters
EGCR Complex	45,811	Sr, Cs, others
Fire Station Complex	815	Sr, Cs, others
Hot Storage Garden	190	Sr, Cs, others
HPRR Complex	2553	Sr, Cs, others
LLLW Complex	1773	Sr, Cs, others
MV HRE Facility	725	Sr, Cs
MV LGWO Complex	7859	Sr, Cs, others
MV Waste Storage Facilities	1129	Sr, Cs, others
Southeast Services Group Complex	112	Sr, Cs, others
Sewage Treatment Plant Complex	73	Sr, Cs, others
Southeast Laboratory Support Complex	39	Sr, Cs, others
TWPC Complex	3106	Transuranics, others

BV = Bethel Valley
D&D = deactivation and decommissioning
EGCR = Experimental Gas-cooled Reactor
HPRR = Health Physics Research Reactor
HRE = Homogeneous Reactor Experiment
LGWO = Liquid and Gaseous Waste Operations
LLLW = liquid low-level waste
MV = Melton Valley
ORNL = Oak Ridge National Laboratory
TWPC=Transuranic Waste Processing Center

2026 COMPLEX

The 2026 Complex consists of seven facilities that total 42,654 sq ft and is located within the ORNL Central Campus. Only Bldg. 2026 is significant in terms of size and radioactive contamination.

Constructed in 1964, Building 2026, Radioactive Materials Analytical Laboratory (Category-3 nuclear facility) is considered to be in good condition. It is a two-story structure with a total area of approximately 26,640 sq ft and historically was used for general analytical chemistry of radioactive materials. The facility is equipped with special containment and ventilation systems to handle high levels of radioactivity in hot cells (high gamma dose) and in glovebox systems (high alpha radiation levels are present).

Radiological contamination that exists in Bldg. 2026 is relatively well characterized and controlled. Current survey data exists for most equipment, including gloveboxes, fume hoods, and other ancillary equipment. As a radiochemical laboratory, all isotopes may be expected in waste resulting from the demolition of this facility.

2528 COMPLEX

Building 2528, Coal Research Lab, was built in 1959. It is a single-level, metal-sided building originally used as a coal research laboratory, but recently used to store Research Reactors Division and High Flux Isotope Reactor material. The Bldg. 2528 steam line insulation and some of the flooring tile contain asbestos and some radioactive contamination exists in the building.

Facilities located in the 2528 Complex include Bldg. 2528, Coal Research Laboratory (4105 sq ft), and Bldg. 2528A, Melton Valley (MV) Storage Tanks Demonstration Facility (1887 sq ft).

3019A COMPLEX

The 3019A Complex consists of 15 facilities that total 84,925 sq ft and is located within the ORNL Central Campus. Building 3019A accounts for the majority of the square footage and radioactive contamination in the complex.

Building 3019A was built in 1944 to support the ORNL Graphite Reactor, the second operating reactor in the world. It was used for a wide range of research activities from very small-scale development to pilot plant operations (all radioactive). A deep canal that runs underground from Bldg. 3019A to the Graphite Reactor was used for storing and transferring highly radioactive materials from the reactor to the test facilities. Because of the extended history of operations, there are a number of legacy issues in the Bldg. 3019 Complex, which include the following:

- In 1959, a chemical explosion in a Bldg. 3019A cell distributed plutonium contamination throughout the interior and exterior of the building. Although extensive decontamination was performed, most interior and exterior surfaces of the building used paint bonding to prevent spread of the residual alpha contamination.
- Most areas of the facility contain out-of-service, contaminated equipment remaining from extensive pilot operations and special campaigns with spent nuclear fuel, plutonium, U-233, thorium, and other radionuclides.
- Tank P-24, which is enclosed in an underground ventilated bunker, contains approximately 4000 gal of thorium nitrate solution contaminated with U-233.

- The out-of-service sample conveyor, which crosses the roof from Bldg. 3019A to Bldg. 3019B, has been a recurring source of contamination to areas of the exterior roof.
- The older exterior ventilation ducting requires periodic sealing to prevent leakage of radioactive contaminants.

The current principal function of Bldg. 3019A is to provide safe and secure storage of fissile materials, principally U-233. The removal and disposition of these materials will be completed prior to demolition. Building 3019A also contains operational laboratories with gloveboxes and hoods, and several areas with out-of-service gloveboxes. The walls of the hot cells are radioactively contaminated and the cells contain contaminated equipment and piping. The building will require the removal of asbestos pipe insulation, floor tiles, and transite wall board; an estimated 50 tons of lead shielding bricks; and electrical transformers containing PCBs.

3028 FACILITY (BETHEL VALLEY ISOTOPE AREA FACILITIES)

Building 3028 was constructed in 1950 and originally housed the I-131 processing facility and the separation facility for Pm-147. The facility was operated for the Isotopes Production and Distribution Program (IPDP). Only one facility, Bldg. 3028, Radioisotope Production Lab-A (7000 sq ft), is included in this project.

The facility was operated for the IPDP from the early 1950s until it was shut down in the mid-1980s. This facility was deactivated in 1997. The deactivation included removal of loose radioactive materials and waste from the hot cells; replacement of all manipulator boots to ensure containment in the cells; and removal of office furniture, files, and other miscellaneous combustibles and chemicals from the facility.

The significant issues associated with Bldg. 3028 include high levels of curium contamination in Hot Cells 1 through 5 and their associated ductwork and the lack of process knowledge regarding the conditions in Hot Cell 6 and the three cubicles behind Hot Cell 7. Cell 6, known to contain vacuum off-gas equipment and filters that were connected to the curium cells, is likely to be contaminated with curium and other alpha-emitting isotopes. Many of the short-lived isotopes such as Pm-147 or I-131 have decayed through 10-plus half-lives since shutdown of facility operations and would typically be present as low levels of contamination. Peeling paint on the upper floors is known to be covering curium and plutonium contamination.

BUILDING 3038 (BETHEL VALLEY ISOTOPE AREA FACILITIES)

Building 3038 was constructed in 1949. Operations in the facility reflected the changing missions of ORNL, but the original mission was dedicated to radioisotope shipping. The western portion of the building became the Alpha Handling Facility, which was used for fabrication of actinide targets. The east portion of the building was converted into a R&D facility and an isotope production facility. The hot cell and counting room facilities were converted into a development laboratory.

Building 3038 underwent preparations for demolition under an ARRA Project during fiscal year (FY) 2011 through FY 2013. The majority of legacy materials were removed and disposed and the building has been transitioned to S&M pending final disposition.

3525 COMPLEX

The 3525 Complex is located within the ORNL Central Campus and consists of one major and three very minor facilities that total 27,624 sq ft. The Irradiated Fuels Examination Laboratory, Bldg. 3525, was initially designed and constructed to be used for metallurgical and metallographic studies to support the development of more economic fuels and blankets for power and high flux test reactors. The facility has

been used for similar examinations of test loops and other reactor components, which were sufficiently radioactive to require handling under shielded conditions and in radiological hot cells (six cells in facility). The facility was built to study the various phase and microstructural changes induced by thermal effects in a reactor environment, including changes in and the composition of materials associated with the production of plutonium.

Current activities in the facility include examining/testing irradiated materials, transferring materials, packaging and shipping materials, maintaining remote equipment, and decontaminating the facility and equipment. This facility is actively ventilated by the ORNL Central Gaseous System.

3544 COMPLEX

The 3544 Complex is located within the Central Campus area of ORNL and consists of five facilities that total 5117 sq ft. The facilities are part of the ORNL Process Waste Treatment Complex.

Building 3544 was constructed in 1975 and has undergone several changes over its life to improve the capability and efficiency for removing Sr-90 and Cs-137 from process wastewater and groundwater. This building contains large amounts of equipment with areas of fixed radiologic contamination, mainly Sr-90 and Cs-137.

3608 COMPLEX

Building 3608 treats wastewater generated at ORNL before it is discharged into White Oak Creek. Building 3608 is a wastewater treatment facility that incorporates various unit operations, including filtration, carbon columns, and an air stripper to remove organics, particulates, and heavy metals, and to provide pH adjustment. Additional processing systems were constructed in 1989 at Bldg. 3608 to address hazardous organic and heavy metal contaminant in the wastewater. In a later upgrade, the building reactor clarifier system was modified to enhance the removal of Sr-90 and Cs-137. Building 3608 is being retrofitted with a zeolite system for removal of radioactive Sr-90 and Cs-137 to improve the efficiency and reduce the cost of process wastewater treatment at ORNL.

4501/4505 COMPLEX

The 4501/4505 Complex consists of two facilities that total 117,207 sq ft and include the legacy material removal project from two additional facilities. Buildings 4501 and 4505 were constructed in 1951 as radiochemical R&D facilities. Extensive research operations have been performed in the facilities. The 4501 laboratories contain various radioactive contaminants (Co-60, Cs-137, Sr-90, Kr-85, U-235, Pu-239, Am-241, and Th-232) and fixed radioactive contamination within hot cells and laboratory hoods in the facilities.

5505 FACILITY

The 5505 Facility consists of 23,191 sq ft and construction was completed in 1967. This building contains a radiochemical glovebox and laboratory hood facility that has been used to support research work with transuranic isotopes and the chemistry, physics, and material science of actinides and their compounds. At present, no radioactive liquid waste is generated in the facility, but provisions are in place for a radioactive bottling station if needed. The facility maintains negative pressure through the interaction of the laboratory and office air supply system, the laboratory exhaust system, and the glovebox exhaust system. Research in the facility involves the chemistry, physics, and material science of actinides and their compounds to provide fundamental and technological information as well as a platform for the development of analytical instrumentation. Americium-241 is of particular concern in the facility due to a past accident (DOE 2008).

6010 AND EAST BETHEL VALLEY COMPLEX

The largest facility included in the 6010 and East Bethel Valley (BV) Complex is Bldg. 6010, Oak Ridge Electron Linear Accelerator Facility, which was constructed during 1966-1968. This facility is a powerful electron accelerator-based neutron source that was historically used in applied research. Subgrade structures are extensive, but are not included for demolition.

Legacy materials include activated metals (Fe-55, Ni-63, and Co-60), sources, contaminated safes, accelerator components, and a tantalum target. The target room/magnet room/igloo is a high contamination, high radiological area. There is potential H-3 and beryllium contamination in this area. In addition to Bldg. 6010, facilities included in the Complex are Bldg. 7019, Hazardous Materials Storage, and Bldg. 7048, 7025 Local Air Monitoring Station.

BETHEL VALLEY CHEMICAL DEVELOPMENT LABORATORY FACILITIES

The BV Chemical Development Laboratory facilities consist of 6240 sq ft that were constructed for use in various R&D studies, including fuel studies, at ORNL. The major facility, Bldg. 4507 (High Level Chemical Development Laboratory), includes four hot cells with 3.5-4.5-ft-thick concrete walls/ceilings with lead-covered pit areas that contain tanks. Significant alpha contamination exists in the facility. The facility is not active, but is structurally sound. An underground filter pit, Bldg. 4556, is associated with the facility.

Building 7025, Tritium Target Preparation Facility, was previously used for fabricating titanium tritide targets, for preparing metallurgical samples for embrittlement studies, and for preparing thin films of thorium oxide and uranium oxide by vacuum evaporation. Following approximately 22 years of operations and processing, Bldg. 7025 was designated a surplus facility and currently has no future mission. All thorium/uranium equipment associated with film production has been removed from the building. Equipment remaining in the hood has residual H-3 contamination. Slight contamination from traces of natural thorium and uranium also remains.

BETHEL VALLEY REACTOR AREA FACILITIES

The BV Reactor Area Facilities project consists of 16 structures that total 85,416 sq ft to be demolished and one facility, Bldg. 3001 with 31,138 sq ft, to be stabilized only. The project facilities are located within the ORNL Central Campus.

Building 3001, Oak Ridge Graphite Reactor (OGR), has been designated a National Historic Landmark and will be preserved for public visitation and education. The OGR, an air-cooled graphite reactor, was once fueled with natural uranium and successfully operated for 20 years (1943 to 1963). Other major facilities in the complex include the Oak Ridge Research Reactor (ORRR), Bulk Shielding Reactor, Low-Intensity Test Reactor, and several research facilities (Bldg. 3019B, High Level Radiation Analytical Lab; Bldg. 3003, Solid State Accelerator Facility; and the West Complex Maintenance Shop). Ten other small structures/buildings remain and account for 10 percent of the area to be demolished.

All fuels have been removed from the facilities. Contamination is expected to be associated with the reactor facilities. Hot cell facilities (contained in Bldg. 3019B and ORRR) will likely have more significant contamination, some of which may require offsite disposal.

BV ISOTOPE AREA FACILITIES

The BV Isotope Facilities project is located within the ORNL Central Campus and includes 16 facilities that total 20,658 sq ft. (Note: The OREM baseline has Bldg. 3028 is a separate demolition project, leaving

the Isotope Facilities project with 15 facilities and 13,658 sq ft.) Facilities within the BV Isotope Area Facilities were primarily used during the Isotopes Program at ORNL and most have undergone deactivation activities for a safe and stable configuration. Many of the facilities in this group were connected to the central ORNL ventilation systems, although several facilities had local ventilation systems. Some radiological contamination is present, which is comprised of a variety of isotopes based on the nature of past activities conducted within the facilities. Ventilation services remain active for containment.

Building 3029, Radioisotope Production Lab-B, consists of 3122 sq ft and is the second most significant building in this grouping. It contains four manipulator-type hot cells and two hoods that were modified for use as gloveboxes. Much of the interior painted surfaces are peeling badly and are assumed to contain lead-based paint. The paint in the east wing also is very likely to be contaminated with Cs-137. Much of the asbestos floor tile in the operating area is loose and broken. Cell 4 was used for the fabrication of Ir-192 and the handling of small Co-60 sources. As the need for larger Co-60 sources increased, a more heavily shielded hot cell (Cell 1) was built in 1955 to handle these sources. The cell currently designated Cell 3 was built in the early 1960s for fabrication of Cs-137 sources. Soon after the addition of Cell 3, the building footprint was extended to include a subterranean Co-60 irradiation facility (Cobalt Garden) located outside near the facility and to provide an airlock on the east end. Originally, the area between Cell 1 and Cell 3 was used for decontamination, but later was enclosed and became Cell 2, which was primarily used as a waste handling cell and a pass through between Cells 1 and 3. Major radiological contaminants include Co-60, Cs-137, Sr-90, I-129, C-14, and Tc-99.

The remaining 14 facilities are smaller and some contain significant radioactive contamination throughout the ventilation systems and in hoods and hot cells, with some walls, floors, and ceilings containing residual contamination. Many of these facilities were used for storage and isotope production activities. Most notably, Bldgs. 3033 and 3033A were used in the production of C-14, Kr-85, and H-3.

BETHEL VALLEY TANK AREA FACILITIES

The BV Tank Area Facilities project is located within the ORNL Central Campus and consists of seven facilities that total 20,203 sq ft. Buildings 3515 and 3517 were used to recover radioisotopes from generated waste. Building 3515 was constructed in 1948, while Bldg. 3517 was constructed in 1958 to take over future operations from Bldg. 3515. In the late 1960s, operations were redirected to processing megacurie quantities of non-fissionable radioactive elements separated in other DOE facilities (mainly cesium and strontium); handling large quantities of reactor-produced isotopes such as Co-60 and Ir-192; equipment decontamination; and the storage of Cm-244, H-3, and Am-241. The facility is currently shutdown, but contains numerous hot cells with extensive contamination in some cases, as is also the case with Bldg. 3515.

CENTRAL STACK EAST HOT CELL COMPLEX

The Central Stack East Hot Cell Complex is located within the ORNL Central Campus and consists of 12 facilities that total 38,257 sq ft. The major facility, Bldg. 3047, accounts for 24,215 sq ft and is comprised of 3047A and 3047B. The area designated 3047B was designed and built in 1962 as a glovebox, laboratory, and hot cell facility (five hot cells that consist of four beta/gamma cells and one alpha cell) and designated as the principal facility at ORNL for all facets of research, development, and production of radioisotopes for medical, industrial, and research applications. A significant amount of radioactive contamination is present in Bldg. 3047B. Process systems include an inactive liquid low-level (radioactive) waste (LLLW) drain system, four independent systems that form the primary confinement exhaust ventilation system, and a process drain system that connects to the ORNL Process Waste Treatment Complex.

CENTRAL STACK WEST HOT CELL COMPLEX

The Central Stack West Hot Cell Complex is located within the ORNL Central Campus and consists of 10 facilities that total 68,014 sq ft. One major facility, Bldg. 3025E, was constructed in 1950 and has historically been used to perform physical properties testing of gamma-emitting materials. The tests and examinations of irradiated samples or materials are primarily conducted within the hot cells. Facility challenges are expected to include hot cell decontamination, storage well relocation and/or waste disposal, contaminated ductwork, and a pit in the unloading area with an unknown use. Contaminants of concern for some of the buildings in the complex include low amounts of radioactive contamination. The facility has off-gas ventilation and inactive LLLW lines.

Other facilities in the complex include the 3039 Stack (central off-gas stack for ORNL) and associated facilities, including the 3092 scrubber facility for the stack. Building 3025M is the largest facility in the complex, contains laboratories and office space, and is expected to have quite low levels of radiological contamination. The other significant facility, Bldg. 3150, Solid State Research Facility, is a non-nuclear research facility with laboratories and offices. Non-nuclear facilities account for the major area (70 percent) of this project and are not included in the waste volume estimate.

EXPERIMENTAL GAS-COOLED REACTOR COMPLEX

Construction of the Experimental Gas-cooled Reactor (EGCR) was completed during 1959-1965. Shakedown of reactor systems and loading of the fuel were planned for 1966. At the same time, the similar Peach Bottom gas-cooled reactor was nearing initial criticality. The technology demonstration objective for EGCR was deemed redundant and the project was terminated on January 7, 1966. Following minimal shutdown activities, the entire EGCR site was abandoned in place in that year.

Aside from minor salvage, maintenance, and research activities, including one activity that left minor levels of radiological contamination in the lowest floor of the building, the facility is largely in the same condition as it was when abandoned in 1966. There are no primary chemical COPCs and no significant quantities of legacy waste. There may be asbestos in the pipe and tank insulation and the lube oil system may contain PCBs.

The EGCR facilities include the Reactor Containment Building (Bldg. 7600) and three ancillary facilities (Bldgs. 7609, 7610, and 7614).

FIRE STATION COMPLEX

The 2500 Guard and Fire Headquarters Building is headquarters to the ORNL Fire Department. Construction of Bldg. 2500 was completed in 1943. The building is used to house emergency response apparatus, the ORNL Fire Alarm Receiving Station, administrative offices, fire department, and fire protection systems inspecting, testing, and maintenance operations. The 2500 building flooring, ceiling, roof, and pipe insulation contain asbestos.

The Fire Station Complex is located within ORNL and consists of 10 facilities that total 43,728 sq ft. Other COPCs in this complex include minor radiological surface contamination (mostly associated with Bldg. 2523, Decontamination Laundry Facility), lead, and asbestos.

HOT STORAGE GARDEN

Building 3597, Hot Storage Garden (HSG), is included in the HSG project and totals 2500 sq ft. The HSG was used to store radioactive material, including spent fuel rods, in below-grade wells and in a canal. In 1980, all the spent reactor fuel from the storage wells and canal were removed. The remaining contents of

the wells were subsequently removed, although some contamination remains. Very little demolition debris is projected to require disposal in the onsite radioactive disposal facility.

HEALTH PHYSICS RESEARCH REACTOR COMPLEX

The Health Physics Research Reactor (HPRR) Complex is located within the MV area of ORNL and consists of five facilities that total 16,780 sq ft. The HPRR was constructed in 1962 for the operation of a fast-burst reactor assembly. Building 7709 served as an unshielded reactor building located 800 ft over a ridge from the 7710 DOSAR building, which contained the reactor controls. Radiological materials remaining in the 7710 building include sealed radiological sources (americium, californium, copper, cobalt, cesium, tritium, nickel, promethium, plutonium, radium, thorium, uranium, and others), other stored or purchased radiological material (U-234, U-235, U-238, and Ac-227), contamination (Am-241 and U-238), and waste (Cs-137 and U-238). The HPRR operated from the mid-1960s until its shutdown in 1987. At that time, the reactor assembly was removed to safe storage at Y-12.

LIQUID LOW-LEVEL WASTE COMPLEX

The LLLW Complex project is located within the western portion of the ORNL Central Campus and consists of 10 facilities that total 17,290 sq ft.

The LLLW system consists of support facilities, liquid and gaseous processing equipment, and storage tanks, including five 50,000-gal below-grade tanks in vaults that manage and collect aqueous radioactive waste solutions from various programmatic sources for onsite neutralization, concentration, and storage. Demolition includes only above-grade structures, therefore, projected waste volumes are limited.

MELTON VALLEY HOMOGENEOUS REACTOR EXPERIMENT FACILITY

The MV Homogeneous Reactor Experiment (HRE) building is located in the MV watershed region of ORNL and is comprised of one facility, Bldg. 7500. The HRE Research Reactor supported research on aqueous uranium fuel reactor technologies and breeding of plutonium (with a depleted uranium blanket solution) and U-233 (using a thorium slurry blanket). The HRE building contains a series of below-grade cells and access areas classified as radiation and contamination areas. Planning for demolition involves in situ grouting/entombment, so very little waste is identified to be disposed in an onsite radioactive disposal facility.

MELTON VALLEY LIQUID AND GASEOUS WASTE OPERATIONS COMPLEX

The MV Liquid and Gaseous Waste Operations Complex is located within the MV area of ORNL and consists of six facilities that total 37,876 sq ft. The complex is composed of storage facilities, waste transfer equipment, and tanks.

The 7830 building consists of eight 50,000-gal storage tanks in two stainless-steel-lined, concrete underground vaults; associated liquid and ventilation piping and equipment; and associated control room. This building was constructed in 1980 to provide collection and storage for all liquid radioactive wastes generated by past and ongoing ORNL activities. Each tank contains sludge and supernate with an extensive variety of isotopes. Contents will be removed and treated for offsite disposal. The 7856 building contains a control room, equipment room, and six 100,000-gal tanks that are each contained in individual stainless-steel-lined concrete vaults (above grade). Contents of the tanks are not included in the inventory for disposal at the Environmental Management Disposal Facility (EMDF).

The third significant facility is Bldg. 7961, which is part of the ORNL Process Waste Collection System. This building consists of an above-ground, concrete-diked area with four 100,000-gal storage tanks and

associated piping and equipment. Other facilities are minor in size and operation. Demolition scope for the project as a whole assumes all subgrade facilities will be stabilized in place.

MELTON VALLEY WASTE STORAGE FACILITIES

The MV Waste Storage Facilities project is located across the MV area of ORNL and consists of 35 facilities that total 115,643 sq ft. Eighteen facilities are located in Solid Waste Storage Area (SWSA) 5, SWSA 6, and the New Hydrofracture Area. These include mostly storage facilities as well as the TRIAD facilities, a tank, an equipment tent, and an office building and trailer. Three buildings (all storage buildings) are located near the High Flux Isotope Reactor, directly south of the ORNL Main Campus. The Hazardous Waste Management Area is where 13 of the remaining 14 facilities (mostly storage facilities) are located. The last facility, Bldg. 2660, is located in BV. A limited number of these facilities contain radioactive contamination and would require disposal in EMDF.

SOUTHEAST SERVICES GROUP COMPLEX

The Southeast Services Group Complex is located within the ORNL Central Campus and consists of nine facilities that total 21,571 sq ft. The facilities include Bldg. 3501, Sewage Pumping Station; Bldg. 3502, East Research Service Center; Bldg. 3502B, Data Concentrator 4 Waste Operations Control Center 3502; Bldg. 3532, Container Paint Storage; Bldg. 3587, Mail Services Building; Bldg. 3610, Storage Building; Bldg. 3614, Manhole 190 Monitoring Station 4; Bldg. 3618, WC-10 Tank Farm Pumping Station; and Bldg. 3621, Spill Response Vehicle Shelter Tent. Only a very limited amount of waste projected by the demolition of this Complex requires disposal in an onsite Comprehensive Environmental Response, Compensation, and Liability Act of 1980 (CERCLA) radioactive/mixed waste disposal facility.

SEWAGE TREATMENT COMPLEX

The Sewage Treatment Plant Complex is located within the southwest portion of the ORNL Central Campus and consists of 13 facilities that total 12,248 sq ft.

The facilities in this project support the ORNL sewage treatment systems and will not be demolished until replacement facilities are in place. Only a very limited amount of waste projected by the demolition of this complex requires disposal in an onsite CERCLA radioactive/mixed waste disposal facility.

SOUTHEAST LABORATORY SUPPORT COMPLEX

The Southeast Laboratory Support Complex consists of six facilities that include Bldg. 3523, Electronic Fabrication Shop; Bldg. 3606, Instrumentation Development Facility; Bldg. 3613, Diversion Box Monitoring Station 3; Bldg. 3615, Manhole 235 Monitoring Station 5; Bldg. 3616, Manhole 149 Monitoring Station 6; and Bldg. 3617, Manhole 229 Monitoring Station 7. Only a very limited amount of waste projected by the demolition of this complex requires disposal in an onsite CERCLA radioactive/mixed waste disposal facility.

TRANSURANIC WASTE PROCESSING CENTER COMPLEX

The Transuranic Waste Processing Center (TWPC) Complex is located within the MV area of ORNL and consists of 35 facilities that total 100,376 sq ft.

In 2003, DOE designed and completed construction of the TWPC, a special facility equipped to handle a number of different types and classifications of waste, including liquid and solid waste streams or waste forms. TWPC serves as a center for management, treatment, packaging, and shipment of DOE transuranic legacy inventory. A large majority of structures will not require disposal as radioactive waste, however, the facility has a hot cell structure and associated equipment that will require disposal as radioactive waste.

REFERENCES

DOE 2008. *Assessments of the IFDP at ORNL and Y-12 for Transfer of Facilities and Materials to DOE-EM*, Andrew Szilagyi, EM-23, U.S. Department of Energy, Washington, D.C.

DOE 2010. *Engineering Evaluation/Cost Analysis for the Y-12 Facilities Deactivation/Demolition Project Oak Ridge, Tennessee*, DOE/OR/01-2424&D2, U.S. Department of Energy, Oak Ridge, TN, February.

ORNL 2008. *Oak Ridge National Laboratory Legacy Material Inventory Estimate in Support of the Integrated Facilities Disposition Project*, ORNL/TM-2007/209-R0 (OUO), Oak Ridge National Laboratory, Oak Ridge, TN.

This page intentionally left blank.

ATTACHMENT B.2.
Y-12 NATIONAL SECURITY COMPLEX AND OAK RIDGE NATIONAL LABORATORY REMEDIAL ACTION WASTE STREAM DESCRIPTIONS

This page intentionally left blank.

ACRONYMS

BCV	Bear Creek Valley
BV	Bethel Valley
CERCLA	Comprehensive Environmental Response, Compensation and Liability Act of 1980
LLLW	liquid low-level (radioactive) waste
ORNL	Oak Ridge National Laboratory
RA	remedial action
RCRA	Resource Conservation and Recovery Act of 1976
ROD	Record of Decision
UEFPC	Upper East Fort Poplar Creek
WWSY	White Wing Scrap Yard
Y-12	Y-12 National Security Complex

This page intentionally left blank.

Y-12 NATIONAL SECURITY COMPLEX REMEDIAL ACTION WASTE STREAM DESCRIPTIONS

Soil and debris waste is expected to result from Comprehensive Environmental Response, Compensation, and Liability Act of 1980 (CERCLA) remediation projects to be conducted at both sites. Weapons production activities and multidisciplinary research conducted at the Y-12 National Security Complex (Y-12) over the years has resulted in contamination of environmental media. Plans are underway to remediate contamination throughout the Y-12 site to reduce risks to human health and the environment. Remediation scope includes removal of contaminated soils in the Upper East Fork Poplar Creek (UEFPC) watershed (Main Plant Area) and subsurface structures (e.g., basements) and groundwater treatment and soil and debris removal in the Bear Creek Valley (BCV) watershed. Table B.2.1 summarizes the volumes of soil and debris waste associated with each Y-12 remedial action (RA) project. More detailed information for each RA project is provided in the following paragraphs.

Table B.2.1. Y-12 RA Projects

Y-12 RA Project	Debris material type (cy)	Soil material type (cy)	Total EMDF (cy)
BCV S-3 Ponds Pathway 3		1094	1094
BCV White Wing Scrap Yard Remedial Action	10,017	62,506	72,523
UEFPC Remaining Slabs and Soils[a]	156,814	276,532	433,346
UEFPC Sediments - Streambed and Lake Reality[a]		11,966	11,966
UEFPC Soils[a]		3154	3154
UEFPC Soils 81-10 Area[a]	280	1537	1817

[a]A portion of waste (debris and soil) from these projects will be associated with mercury contamination.

BCV = Bear Creek Valley
EMDF = Environmental Management Disposal Facility
RA = remedial action
UEFPC = Upper East Fork Poplar Creek
Y-12 = Y-12 National Security Complex

BEAR CREEK VALLEY S-3 PONDS PATHWAY 3

The S-3 Ponds site is located adjacent to the west end of the Y-12 Main Plant Area and consists of four unlined ponds formerly used for managing liquid waste.

The S-3 Ponds site has undergone closure under the Resource Conservation and Recovery Act of 1976 (RCRA) and has been converted to a parking lot; however, the site remains a source of groundwater contamination. The aim of the BCV S-3 Ponds Pathway 3 project is to intercept and treat shallow groundwater contamination at the S-3 Ponds site. This project is expected to generate a minor volume of soil waste.

BEAR CREEK VALLEY WHITE WING SCRAP YARD

The BCV White Wing Scrap Yard (WWSY), also known as Waste Area Grouping 11, covers an area approximately 30 acres in size near the intersection of Highway 95 and the Oak Ridge Turnpike.

The WWSY was a storage area for radioactively contaminated scrap and debris from the three DOE Oak Ridge Reservation sites (East Tennessee Technology Park, Oak Ridge National Laboratory [ORNL], and Y-12). Material (steel tanks, metal, glass, concrete, and miscellaneous trash) with alpha, beta, and gamma

contamination was first stored at WWSY in the early 1950s; however, precise dates of operation are unknown. Although a Record of Decision (ROD) on actions to be taken has not been submitted, RAs at the site are assumed to generate a significant amount of debris and soil.

UPPER EAST FORK POPLAR CREEK REMAINING SLABS AND SOILS

The UEFPC Remaining Slabs and Soils Project objective is to remediate contaminated media throughout the Y-12 industrial area that pose an unacceptable current or future risk to workers, the public, and the environment.

UEFPC Remaining Slabs and Soils RAs will be sequenced with facility demolition activities. Contaminated soils, building slabs, and debris will be excavated and disposed. Other selected at- or below-grade substructure removal actions such as tanks, basins, vaults, pits/sumps, equipment housings, and basements will be included in this scope.

UPPER EAST FORK POPLAR CREEK SEDIMENTS - STREAMBED AND LAKE REALITY

The UEFPC Sediments - Streambed and Lake Reality Project includes removal of contaminated sediments at Y-12. The objective of this project is to design and implement the excavation of contaminated sediments located in the UEFPC streambed channel and in Lake Reality, a lined retention basin located near the point where UEFPC leaves the Y-12 site.

UPPER EAST FORK POPLAR CREEK SOILS

The UEFPC Soils Project will provide design and implementation of selected remedies pursuant to the CERCLA ROD for Phase II interim RA for contaminated soils and scrapyard in UEFPC. Leaks and spills from pipelines and storage tanks, and spills in RCRA and hazardous waste storage areas, have resulted in soil contamination from radionuclides, beryllium, mercury, chlorinated organics, chlorinated organic solvents, and non-chlorinated flammable solvents, coolant oils, transformer oils, machine oils, polychlorinated biphenyls, RCRA metals, and RCRA materials. Remediation will involve the excavation of contaminated soils and debris.

UPPER EAST FORK POPLAR CREEK SOILS 81-10 AREA

The Building 81-10 Area was a mercury-recovery facility/mercury-contaminated soil storage area located at the intersection of G Road and Third Street in the south-central portion of Y-12.

The objective of this project is to design and implement the excavation of contaminated soils at the UEFPC Building 81-10 Area. The area now consists of a concrete slab. The contaminant signature is defined by mercury and radiological isotopes, but also contains volatile organic compounds, metals, and other inorganics associated with upgradient sources. Primary sources of mercury include spills and leaks during recovery and storage operations conducted at Building 81-10.

OAK RIDGE NATIONAL LABORATORY REMEDIAL ACTION WASTE STREAM DESCRIPTIONS

As a result of the multidisciplinary research activities performed at ORNL, environmental media became contaminated. Several projects to remediate contamination throughout the laboratory are planned to reduce risks to human health and the environment. The current list of ORNL cleanup projects expected to generate

waste and the projected soil and debris volumes are given in Table B.2.2. More detailed information for the four largest (in terms of waste forecast) ORNL RA projects is provided in the following paragraphs.

Table B.2.2. ORNL remedial action projects

ORNL RA Project	Debris material type (cy)	Soil material type (cy)	Total EMDF (cy)
BV Inactive Tanks and Pipelines	405	158	563
BV Remaining Inactive Tanks and Pipeline	23,446		23,446
BV Remaining Slabs and Soils	30,024	46,660	76,684
ORNL Non-HF Well P&A	20		20
ORNL Remaining Non-HF Well P&A	14		14
ORNL Soils and Sediments	2053	76,563	78,616

BV = Bethel Valley
EMDF = Environmental Management Disposal Facility
HF = hydrogen fluoride
ORNL = Oak Ridge National Laboratory
P&A = plug and abandon
RA = remedial action

BETHEL VALLEY INACTIVE TANKS AND PIPELINES/REMAINING INACTIVE TANKS AND PIPELINES

The inactive tanks and pipelines included in this project are located in Bethel Valley (BV), ORNL Main Campus. The objective of this project is to limit any potential future migration of contaminants through inactive liquid low-level (radioactive) waste (LLLW) pipelines and bedding materials by blocking the conduits for contaminant transport to the neighboring media and by stabilizing the pipelines. This effort includes grouting approximately 50,000 linear ft of inactive LLLW pipeline and installing 5000 ft of grout walls to block the migration of contamination through pipe bedding in central BV. A small volume of waste soil is expected to be generated through this effort as well as some debris.

BETHEL VALLEY REMAINING SLABS AND SOILS

The objective of this BV Remaining Slabs and Soils Project is to remediate contaminated media throughout BV in the ORNL Main Plant Area that pose an unacceptable current or future risk to workers, the public, or the environment. This project includes remediation of contaminated soils, sediments, slabs, and other below-grade structures (tanks, basins, vaults, pits/sumps, equipment housings) remaining from previous demolition activities. Debris and soil wastes are expected to be generated in significant quantities.

ORNL SOILS AND SEDIMENTS

The ORNL Soils and Sediments Project scope encompasses the remediation of multiple contaminated soil sites and sediment/floodplain soils at ORNL. As such, a significant volume of soil and sediment is projected for excavation and disposal.

This page intentionally left blank.

ATTACHMENT B.3.
ASSUMED SOURCE CONCENTRATIONS FOR SELECTED EMDF RADIONUCLIDES

This page intentionally left blank.

ACRONYMS

BV	Bethel Valley
D&D	deactivation and decommissioning
EMDF	Environmental Management Disposal Facility
MSRE	Molten Salt Reactor Experiment
NRC	U.S. Nuclear Regulatory Commission
OREM	Oak Ridge Office of Environmental Management
ORNL	Oak Ridge National Laboratory
PA	Performance Assessment

This page intentionally left blank.

ASSUMED SOURCE CONCENTRATIONS FOR SELECTED EMDF RADIONUCLIDES

There are 70 radionuclides included in the data sources assembled for the Environmental Management Disposal Facility (EMDF) waste inventory (Appendix B, Sect. B.3.3). However, due to data limitations (generally the availability of only a single record for a radionuclide), estimated average activity concentrations were developed for only 56 radionuclides. Most or all of the data for nine less commonly reported fission products (Cd-113m, Cs-135, Pd-107, Se-79, Kr-85, Sm-151, Sn-121m, Sn-126, and Zr-93) could not be confirmed against the original data sources. Eight of these nine radionuclides are not included in the estimated EMDF inventory because none of the data selected for inclusion in the analysis could be verified.

Six radionuclides without sufficient local data to apply the methodology described in Sect. B.3 with confidence are Ba-133, Be-10, Ca-41, Kr-85 (a single maximum value), Mo-93, and Nb-93m. This Attachment documents the basis for developing the assumed concentration values used in the EMDF Performance Assessment (PA) models for five of these six radionuclides. Kr-85 was eliminated from consideration because krypton is a noble gas and unlikely to be present in EMDF waste following placement in EMDF. The assumed average EMDF waste concentrations for the remaining five radionuclides are based on different approaches to utilizing the waste quantities and radiological characterization data used for the other 56 radionuclides, and in some cases incorporate additional information from non-Oak Ridge Reservation waste materials. Table B.3.1 summarizes the approach taken for each radionuclide and the paragraphs following Table B.3.1 describe the data and calculations for each radionuclide. Waste masses used in the calculations appear in Table B.6 of this Appendix. Table B.3.2 summarizes the assumed EMDF waste average values and source concentrations used as PA model inputs.

Table B.3.1. Summary of approach to develop assumed EMDF waste concentrations for selected radionuclides

Radionuclide	Screening source concentration[a] (pCi/g)	Basis for assumed EMDF waste average concentration
Ba-133	2.71E+01	Use decayed screening value for intruder scenario[b], short half-life 10.7 years
Be-10	7.16E+05	Be-10/Co-60 scaling factor (NRC 2000) applied to ORNL D&D waste Co-60 concentration to estimate the average Be-10 concentration of all ORNL D&D waste and convert to EMDF waste average concentration
Ca-41	4.11E+06	Apply assumed average Ca-41 concentration (1 Bq/g based on measurements of research reactor shielding concrete samples [Hou 2005]) to 10% of debris mass from ORNL Linear Accelerator and Reactor Facility Complexes and convert to EMDF waste average concentration
Kr-85	6.41E+01	Eliminated from further consideration
Mo-93	4.99E+03	Assume MSRE inventory of Mo-93 is EMDF waste inventory
Nb-93m	3.00E+03	Assume MSRE inventory of Nb-93m is EMDF waste inventory

[a]Screening source concentrations based on arithmetic averages of all available Oak Ridge data, including maximum and upper confidence limit values, without correction for decay prior to EMDF closure.
[b]Ba-133 is screened from the groundwater impact analysis in the PA (Sect. 2.3.2).

D&D = deactivation and decommissioning
EMDF = Environmental Management Disposal Facility
MSRE = Molten Salt Reactor Experiment
NRC = U.S. Nuclear Regulatory Commission
ORNL = Oak Ridge National Laboratory
PA = Performance Assessment

Ba-133

Ba-133 is screened from the groundwater impact analysis based on the calculated screening source concentrations see (PA Sect. 2.3.2), but an average concentration was estimated for use in the inadvertent human intrusion analysis. The approach for the assumed EMDF concentration values of Ba-133, which has a relatively short half-life of 10.7 years, is to correct the screening source concentration (Table B.3.1) for decay to 2047 and use the resulting value as the average waste concentrations for the inadvertent intrusion scenario modeling. The decay calculations are based on the year of the data source report for Ba-133, which is dated 2013:

- Assumed Ba-133 Concentration = 2.71E+01 pCi/g × $(½)^{\{(2047-2013)/10.7\}}$ = 3.00E+00 pCi/g.

Be-10

The approach for estimating a Be-10 average waste concentration is to utilize a published Be-10/Co-60 scaling factor value of 2.4 E-03 measured in commercial reactor control rod waste (U.S. Nuclear Regulatory Commission [NRC] 2000, Table 8.1) to estimate an average Be-10 concentration for the Oak Ridge National Laboratory (ORNL) deactivation and decommissioning (D&D) waste stream. The scaling factor is applied to the estimated average ORNL D&D Co-60 concentration of 2.18E-01 pCi/g. This approach should provide a bounding estimate for the Be-10 inventory because only 20 percent of the ORNL D&D waste mass is associated with research reactor facilities that are likely to have irradiated boron or beryllium components that contain Be-10:

- Assumed Be-10 concentration = 2.4E-03 × 2.18E-01 pCi/g = 5.23 E-04 pCi/g
- Oak Ridge Office of Environmental Management (OREM) D&D waste stream Be-10 inventory = 5.23E-04 pCi/g × 1.94E+11 g = 1.02E+08 pCi
- EMDF waste average Be-10 concentration = 1.02E+08 pCi/1.37E+12 g = 7.41E-05 pCi/g.

Ca-41

The approach for estimating a Ca-41 average waste concentration is to assume an average Ca-41 concentration for 10 percent for the debris waste mass associated with the ORNL 6010 and East Bethel Valley (BV) Complex and BV Reactor Area Facilities Complex (10 percent of 4.02E+10 g, or about 2 percent of total ORNL D&D debris mass). ORNL Bldg. 6010 is an accelerator facility with a large quantity of concrete. Demolition of the ORNL research reactors also will produce concrete debris that could contain Ca-41. The basis for the assumed average Ca-41 concentration (1 Bq/g or 27 pCi/g) is a study of laboratory measurement techniques applied to samples of concrete shielding from a European research reactor (Hou 2005). The Ca-41 inventory estimated for the ORNL D&D debris is assumed to constitute the entire EMDF waste inventory:

- Assumed OREM D&D waste stream Ca-41 inventory = 27 pCi/g ×4.02E+09 g = 1.09E+11 pCi
- EMDF waste average Ca-41 concentration = 1.09E+11 pCi/1.37E+12 g = 7.92E-02 pCi/g.

Mo-93 and Nb-93m

The approach for the assumed values of Mo-93 and Nb-93m is to use the Molten Salt Reactor Experiment Facility (MSRE) inventory values expressed as an EMDF waste average concentration. Although MSRE waste is not included in the assumed EMDF waste inventory, the MSRE data are the only source of

information on these two radionuclides. These inventory values come from the OREM SORTIE 2.0 facility inventory database (Redus 2014):

- Assumed Mo-93 inventory = 1.0 Ci = 1.0E+12 pCi
- EMDF waste average Mo-93 concentration = 1.0E+12 pCi/1.37E+12 g = 7.30E-01 pCi/g
- Assumed Nb-93m inventory =0.601 Ci = 6.01E+11 pCi
- EMDF waste average Nb-93m concentration = 6.01E+11 pCi/1.37E+12 g = 4.39E-01 pCi/g.

Table B.3.2 summarizes the assumed EMDF waste average concentrations as well as the values of the corresponding source concentrations that account for the addition of clean fill during disposal. The basis for the clean fill adjustment is multiplication by a factor of 0.531 (PA Sect. 3.2.2.4).

Table B.3.2. Summary of assumed EMDF waste concentrations for selected radionuclides

Radionuclide	Assumed waste average concentration (pCi/g)	Source concentration (pCi/g)
Ba-133	3.00E+00	1.59E+00
Be-10	7.41E-05	3.93E-05
Ca-41	7.92E-02	4.21E-02
Mo-93	7.30E-01	3.88E-01
Nb-93m	4.39E-01	2.33E-01

EMDF = Environmental Management Disposal Facility

REFERENCES

Hou 2005. "Radiochemical determination of 41Ca in nuclear reactor concrete," Xiolin Hou, *Radiochimica Acta*, 93, 611-617, January 2005.

NRC 2000. *Low-Level Radioactive Waste Classification, Characterization, and Assessment: Waste Streams and Neutron-Activated Metals*, NUREG/CR-6567, D. E. Robertson, C. W. Thomas, S. L. Pratt, E. A. Lepel, and V. W. Thomas, Pacific Northwest Laboratory, Richland, WA, August.

Redus 2014. *Project Execution Plan for Source Term for Input to the Environmental Management Waste Management Facility, Oak Ridge, Tennessee Performance Assessment*, Redus and Associates, LLC, Oak Ridge, TN.

This page intentionally left blank.

APPENDIX C.
COVER SYSTEM ANALYSES FOR THE ENVIRONMENTAL MANAGEMENT DISPOSAL FACILITY

This page intentionally left blank.

CONTENTS

FIGURES

TABLES

This page intentionally left blank.

ACRONYMS

BCK	Bear Creek kilometer
BCV	Bear Creek Valley
CBCV	Central Bear Creek Valley
DOE	U.S. Department of Energy
EPA	U.S. Environmental Protection Agency
EMDF	Environmental Management Disposal Facility
ET	evapotranspiration
GCL	geosynthetic clay liner
HDPE	high-density polyethylene
HELP	Hydrologic Evaluation of Landfill Performance
LAI	leaf area index
LCRS	Leachate Collection and Removal System
LDRS	Leak Detection and Removal System
LLW	low-level (radioactive) waste
NRCS	Natural Resources Conservation Service
PA	Performance Assessment
QA	quality assurance
RUSLE2	Revised Universal Soil Loss Equation model
TDEC	Tennessee Department of Environment and Conservation
USDA	U.S. Department of Agriculture
VMC	volumetric moisture content

This page intentionally left blank.

C.1 EMDF SAFETY FUNCTIONS AND HYDROLOGIC PERFORMANCE

The purpose of this appendix is to establish the basis for assumptions concerning hydrologic performance of the Environmental Management Disposal Facility (EMDF) in the post-closure period. The analysis is focused primarily on the cover system water balance and resulting net infiltration into the waste as the system evolves from as-built performance (zero net infiltration) to progressively degraded future performance during the period after EMDF closure and loss of institutional control of the facility. This section includes a review of EMDF design features and their safety functions and considers the range of future events and natural processes that can potentially degrade the hydrologic performance of the cover system components over time. The safety functions analysis is the basis for development of a generalized conceptual model of EMDF performance evolution. Section C.2 presents the application of the Hydrologic Evaluation of Landfill Performance (HELP) model to estimate infiltration rates. Results of the water balance modeling are used to identify a reasonable range of infiltration rates to represent future degraded performance conditions. Section C.3 considers the potential impact of a hypothetical bathtub scenario on EMDF performance. Section C.4 presents application of the Revised Universal Soil Loss Equation Version 2 (RUSLE2) model to the EMDF cover slope profile to estimate erosion rates based on soil loss predictions. Section C.5 provides a summary of the cover and liner system features and processes that interact over time to determine the performance evolution of the EMDF disposal system.

Key assumptions for the analyses presented in this appendix include the following:

- Site selection and facility design: The EMDF preliminary design, including overall facility geometry and the specific set of engineered cover and liner system components, serves as the basis for the analyses presented in this appendix. The design for the final cover system is at the conceptual stage of development.
- Post-closure EMDF performance monitoring and facility maintenance (institutional control) for 100 years, through approximately year 2140, will maintain facility performance.
- Degradation of EMDF engineered barriers occurs gradually as a result of natural processes during the post-closure period rather than by low-probability events that lead to catastrophic failure of the disposal unit.

C.1.1 EMDF DESIGN FEATURES

Key EMDF preliminary design features and disposal system elements are summarized in Fig. C.1. Individual system elements and design features provide specific safety functions for the total disposal system. The following subsections provide details on EMDF design features evaluated in the Performance Assessment (PA) and associated safety functions, and summarize natural processes and events that can potentially degrade design features and impair EMDF safety functions. The focus is on features and safety functions that can be impacted by events and processes in the post-closure period rather than waste management and safety practices implemented during the operational period.

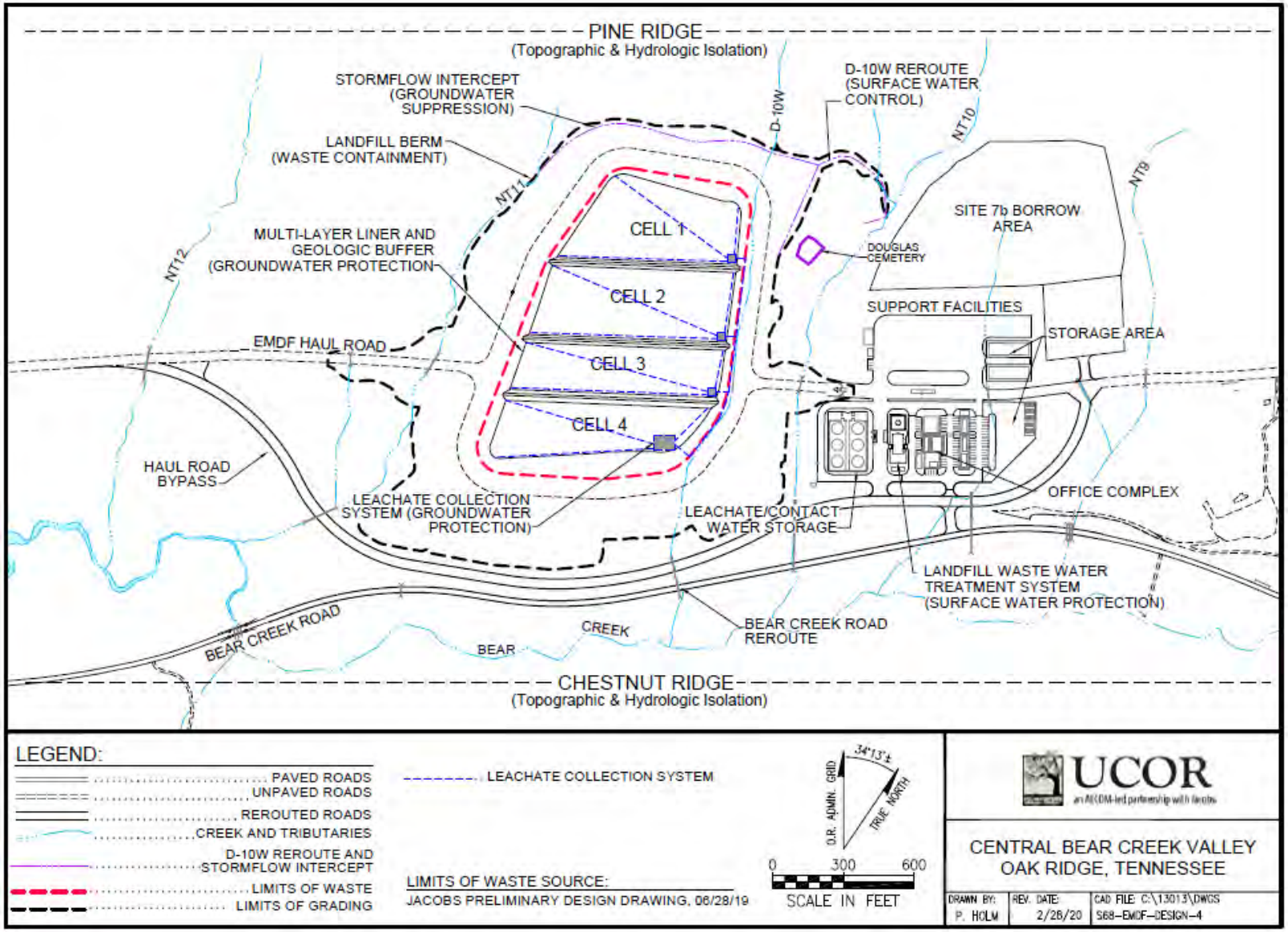

Fig. C.1. EMDF disposal system with key features and safety functions

The key design features of EMDF include:

1) A perimeter berm to laterally contain the waste
2) A multilayer liner system with a double leachate collection/detection system to prevent contamination of groundwater
3) A geologic buffer zone to maintain a minimum vertical separation between the liner system and the seasonal high water table
4) A final multilayer cover to shed precipitation, reduce infiltration, and isolate the waste from the surface environment and human receptors.

The preliminary design also incorporates upgradient diversion systems to divert and reroute shallow groundwater and surface water. EMDF preliminary design components are described in the following sections. Note that final specifications (e.g., thicknesses of geomembranes) will be determined in the final design.

C.1.1.1 Perimeter Berm

An engineered berm is constructed around the perimeter of the landfill to provide lateral containment and stability to the waste (Fig. C.2). The perimeter berm also will protect against erosion, biointrusion, and inadvertent intrusion by humans. The perimeter berm will be constructed of structural fill to create a stable supporting base along the edge of the liner and cover systems. Native soil excavated from the site may be deemed suitable for use as structural fill if it is free from large rocks and exhibits the appropriate compressibility and shear strength. The inner slope of the berm will be covered by the liner system. The top of the berm will anchor the liner components, tie into the cover system, and provide for drainage ditches and a perimeter access road. It is anticipated the perimeter berm will have a typical grade of 33 percent or lower (3H:1V or flatter) that will be determined by slope stability and erosion analyses in the final design phase.

C.1.1.2 Upgradient Drainage Control

A stormflow intercept channel will be constructed along the upper (i.e., northern) side of the landfill to intercept and divert upgradient storm water and shallow groundwater (stormflow) away from the landfill. By diverting water that moves through the upper few feet of soil during storm events, this system will reduce recharge to the groundwater table in the vicinity of the topographic saddle at the northern perimeter of EMDF. The drainage feature will be a passive system requiring little maintenance.

C.1.1.3 Liner System

A multilayer liner system will be installed to prevent leachate from migrating out of the disposal unit and impacting groundwater. The composite liner system will include an upper leachate collection system, an underlying leak detection and collection system, and a compacted clay leachate barrier (Fig. C.3). The lower (leak detection) component of the composite bottom liner will be designed and constructed of material to minimize the migration of hazardous constituents if a breach in the primary liner component were to occur. As detailed below, the liner system will be comprised of multiple layers of synthetic and

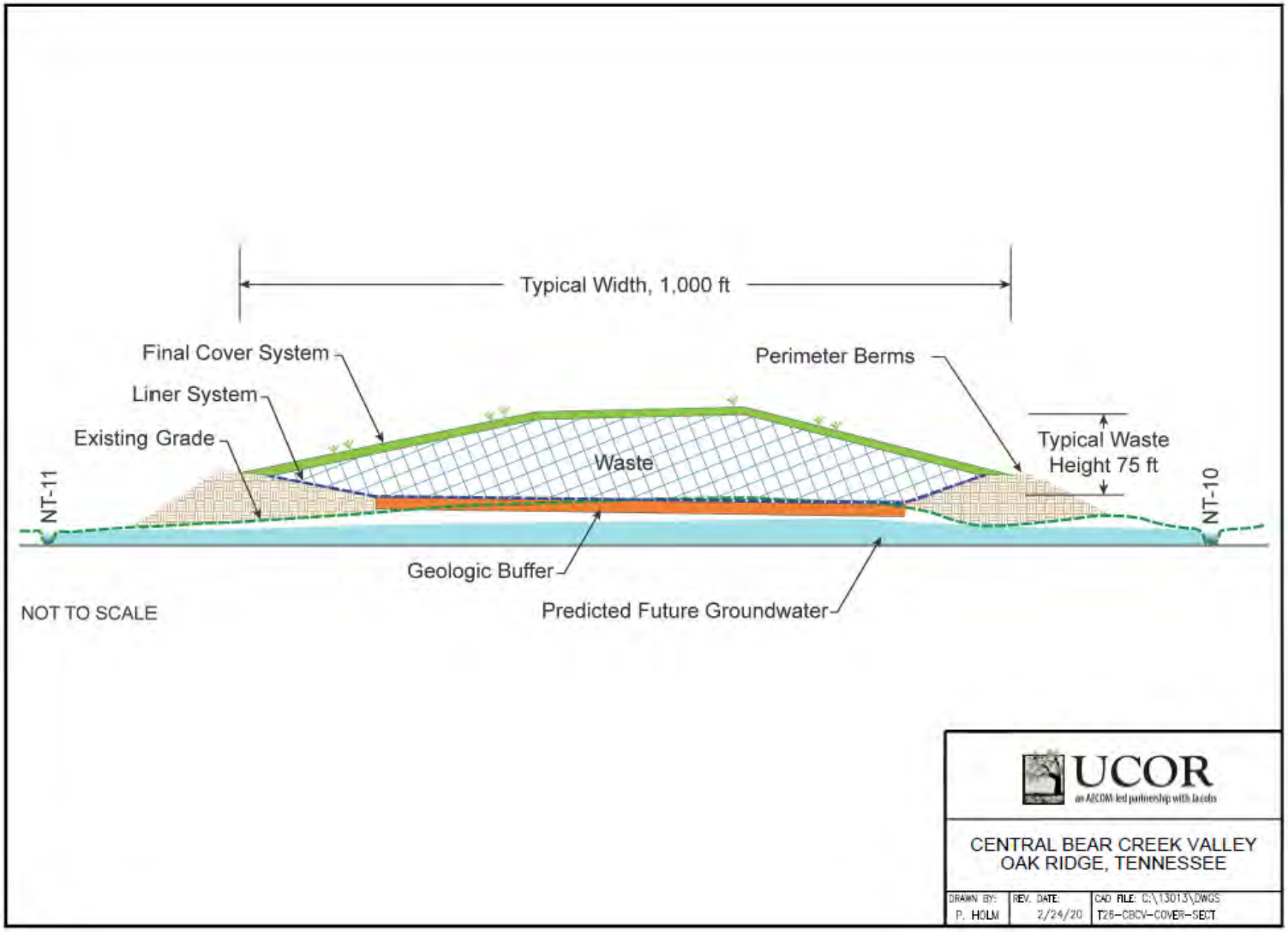

Fig. C.2. Typical cross-section of EMDF

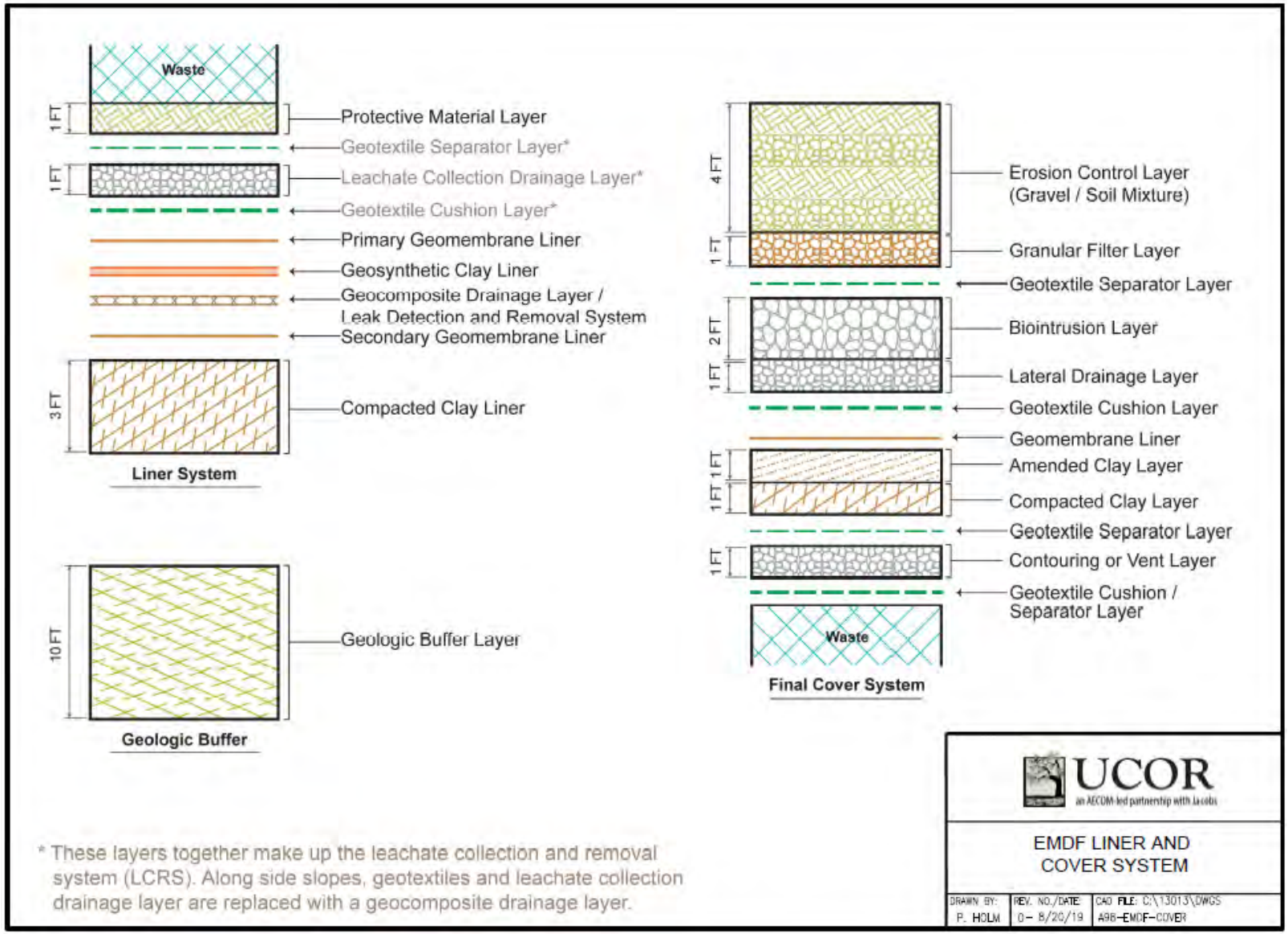

Fig. C.3. EMDF liner and cover layers

natural materials that are compatible with the waste and resistant to degradation by chemical constituents expected to be present in the leachate (UCOR, an Amentum-led partnership with Jacobs, 2018, Appendix F). The 5-ft-thick liner system will extend up the sides of the perimeter berms and over the internal berms constructed between disposal cells. The liner system is comprised of the following components from the bottom of waste downward:

- Protective Material Layer – A 12-in.-thick (minimum) layer of native soil will be used to support truck and equipment traffic during initial waste placement operations. The primary purpose of this layer is to protect the underlying components of the liner system from damage during waste placement during the operational life of the landfill. The thickness and composition of this layer may be variable and will consider the physical nature of the waste to be placed immediately above it, waste placement procedures, and water management operations within the disposal cell (e.g., a thicker and harder protective soil layer may be required for bulky structural steel debris than for soil-like waste materials).
- Leachate Collection and Removal System (LCRS) – To enhance slope stability and constructability, design components of the LCRS may be somewhat different on the floor of the landfill than on the sideslopes.
    - Geotextile separator layer – A non-woven, needle-punched geotextile will be used to separate the protective soil layer and leachate collection drainage stone. The purpose of the geotextile separator layer is to provide a filter that restricts finer particles of a material on one side of the textile from traveling through to the other side to reduce the potential for clogging of the underlying drainage layer.
    - Leachate collection drainage layer – A 12-in.-thick (minimum) layer of hard, durable, inert (siliceous) granular material, will serve as the primary leachate collection and removal layer. Perforated high-density polyethylene (HDPE) pipe (i.e., leachate collection piping) will be installed in this layer to collect and direct the leachate to low points (sumps) in each cell. Leachate will be pumped to the wastewater storage and treatment system (Fig. C.1).
    - Geotextile cushion layer – A non-woven, needle-punched layer will be used as a cushion over the underlying geomembrane. The purpose of the geotextile cushion layer is to provide protection of the underlying geomembrane by acting as a cushion to absorb impacts and potential sharp edges of overlying materials.
    - Sideslopes – A geocomposite drainage layer consisting of an HDPE geonet core with non-woven, needle-punched geotextiles thermally bonded to both sides will be used on the side slopes in place of the leachate collection drainage layer. This steeply sloped geocomposite drainage layer will drain to the leachate collection drainage layer on the floor of each cell.
- Primary Geomembrane Liner – A 60-mil (1.5-mm)-thick HDPE geomembrane will be used to retard leachate migration out of the LCRS and promote drainage of leachate via the primary leachate collection layer.
- Geosynthetic Clay Liner (GCL) – A GCL layer will be used to provide additional leakage protection under the primary geomembrane liner and thereby reduce the leakage rate into the leak detection system. The GCL will plug or mitigate any pinholes or other defects that may be present in the primary geomembrane liner. The GCL layer will be used only on the floor of each cell, where a maximum hydraulic head of 12 in. may develop on top of the primary geomembrane liner.
- Leak Detection and Removal System (LDRS) – This layer will be used to detect and remove any leachate that may leak through the primary geomembrane liner. A geocomposite drainage layer consisting of an HDPE geonet core with non-woven, needle-punched geotextiles thermally bonded to both sides will serve as the leak detection layer. The geocomposite drainage layer will be sloped to drain to perforated HDPE pipe (i.e., leak detection piping).

- Secondary Geomembrane Liner – A 60-mil (1.5-mm)-thick HDPE geomembrane will be used to retard leachate migration out of the LDRS and promote drainage of leachate via the leak detection layer.
- Compacted Clay Liner – A 3-ft-thick (minimum) layer of compacted clay will be used to further reduce the potential for leachate migrating out of the landfill. The compacted clay liner will consist of unamended, native clay soil or bentonite-amended soil, compacted to produce an in-place hydraulic conductivity less than or equal to 1E-07 cm/sec.

C.1.1.4 Geologic Buffer Layer

The EMDF preliminary design includes a 10-ft-thick geologic buffer beneath the liner system to maintain separation between the landfill liner and groundwater table per Tennessee Department of Environment and Conservation (TDEC) Rule 0400-11-01-.04(4)(a)(2). The material will have a saturated hydraulic conductivity ≤ 1E-05 cm/sec. The geologic buffer layer will not extend laterally beneath the sideslopes of the liner system (Fig. C.2). The thickness of the geologic buffer is measured from the bottom of the landfill liner to the top of the seasonal high water table of the uppermost unconfined aquifer (or to the top of the formation of a confined aquifer).

The actual hydraulic conductivity of the geologic buffer will depend on the subsurface conditions determined during the hydrogeological and geotechnical investigations for EMDF. The geologic buffer could be comprised of compacted native soil or in situ fine-grained native soil, saprolite, or a combination of these geologic materials depending on measured in situ hydraulic conductivity and layer thickness.

C.1.1.5 Final Cover System

After waste disposal is complete for final facility closure, an approximately 11-ft-thick multilayer cover system (or cap) will be installed to prevent infiltration of precipitation into the waste. Note that some of the final cover layers may be installed as an interim cover system to reduce the volume of leachate generated during active operations. The cover system conceptual design (Fig. C.3) is described in detail below.

In accordance with regulatory requirements, the final cover system will be designed and constructed to accomplish the following:

- Minimize migration of liquids through the closed landfill over the long term
- Promote efficient lateral drainage while minimizing erosion or abrasion of the cover
- Control migration of gas generated by decomposition of organic materials and other chemical reactions occurring within the waste, if found to be necessary
- Accommodate settling and subsidence to maintain the cover integrity
- Provide a permeability less than or equal to the permeability of any bottom-liner system or natural subsoil present
- Resist inadvertent intrusion of humans, plants, and animals
- Function with little maintenance

The final cover over the waste will be sloped to facilitate runoff and will tie into the top of the perimeter berm. It is anticipated that the uppermost surface of the final cover system will be sloped at a grade of 2 to 5 percent and the sides will be sloped at a maximum grade of 25 percent. Actual slopes may vary and would depend on slope stability and erosion analyses performed during remedial design. The approximately

11-ft-thick multilayer final cover system will be comprised of the following layers, starting from the top of the waste and proceeding upward:

- Contouring Layer – This layer on top of the waste provides a working and contouring surface. Suitable structural fill will be contoured and compacted to provide a stable base for the landfill cover system.
- Compacted Clay Layer – A 1-ft-thick (minimum) layer of native clay soil will be placed and compacted to produce an in-place hydraulic conductivity less than or equal to 1E-07 cm/sec. This layer, in conjunction with the overlying amended clay layer and geomembrane layer, will function as a composite hydraulic barrier to infiltration.
- Amended Clay Layer – A 1-ft-thick (minimum) layer of native soil will be amended with bentonite and compacted to produce an in-place hydraulic conductivity less than or equal to 3.5E-08 cm/sec. It will be necessary to amend native soil with bentonite for this layer to achieve the very low design hydraulic conductivity value.
- Geomembrane Layer – A 60-mil (1.5-mm)-thick HDPE geomembrane will be placed on top of the amended clay layer.
- Geotextile Cushion Layer – A non-woven, needle-punched geotextile will be used as a cushion over the underlying geomembrane.
- Lateral Drainage Layer – A 1-ft-thick layer of hard, durable, free-draining granular material with sufficient transmissivity will be used to drain the cover system. The drainage and overlying layers will discharge water into perimeter ditches that carry the runoff away from the landfill.
- Biointrusion Layer – A 2-ft-thick layer of free-draining, siliceous coarse granular material (e.g., 4- to 12-in.-diameter riprap) will be used to prevent burrowing animals and plant root systems from penetrating the cover system, and reduce the likelihood of inadvertent intrusion by humans by increasing the difficulty of digging or drilling into the landfill.
- Geotextile Separator Layer – A non-woven, needle-punched geotextile will be used as a separator between the granular filter layer and biointrusion layer.
- Granular Filter Layer – A 12-in.-thick layer of granular material will be used as a filter layer to prevent clogging of the biointrusion layer with soil from the overlying erosion control layer.
- Erosion Control Layer – A 4-ft-thick mixture of crushed rock and native soil will be constructed over the disposal facility to protect the underlying cover layers from the effects of frost penetration and wind and water erosion. This layer will also provide a medium for growth of plant root systems and will include a surficial grass cover or other appropriate vegetation.

The long-term effectiveness of the final cover system in promoting lateral drainage and reducing infiltration is a key performance objective for the design. Cover technology is evolving and additional methods for reducing infiltration may be available at the time of final design. The overall goal is to reduce leachate generation through the reduction of infiltration into the waste beneath the cap.

Table C.1 summarizes the key EMDF design features and associated safety functions and identifies events and natural processes that can impact EMDF post-closure performance.

Table C.1. Summary of EMDF system features and safety functions

Features		Safety functions (S) and limiting processes (P)	Events impacting performance evolution
Site Characteristics			
Climate, soil, and EMDF cover vegetation	S	Vegetation promotes stable soils, limits hillslope erosion by wind and water, and limits atmospheric release through cover	• Severe vegetation disturbance (weather events, pests) • Severe climate anomaly (transient) • Rapid climate shift to altered conditions (persistent)
	P	Climate variability and climate change impacts on vegetation	
	P	Ecological succession (e.g., cover vegetation transition to forest)	
	P	Bioturbation (burrowing fauna) and soil profile development	
Topography and hydrology	S	Upland location isolates waste from groundwater, favors runoff to lower elevations	• Severe storms/flood events • Landslides
	S	Ridge and valley topography isolates EMDF from public and reduces probability of exposure	
	P	Erosion and mass movement	
Geology/hydrogeology, seismicity	S	Site lithology and structure and related hydraulic and geochemical characteristics of the groundwater system control radionuclide travel time, dilution, and chemical retardation	• Earthquakes, landslides
	S	Limited seismicity favors slope stability	
	P	Groundwater flow and contaminant transport, geochemical retardation (e.g., sorption)	
Cover Design Features			
Vegetated erosion control layer (cover)	S	Protection of underlying cover system components from erosion and variability in temperature and moisture conditions	• Severe storms/flood events • Surface erosion and gullying • Landslides
	P	Surface water balance, infiltration and runoff, surface erosion	
	P	Vegetation and soil development (hydraulic properties)	
Granular filter layer (cover)	S	Prevent filling of the biointrusion layer pore space with soil from the overlying erosion control layer	
	P	Biointrusion (impaired filtration)	
Biointrusion layer (cover)	S	Deters inadvertent human intrusion	
	S	Limits damage to hydrologic barriers by roots and burrowing animals	
	S	Secondary erosion control (defense-in-depth)	
	P	Weathering and physical breakdown of cobbles/boulders	
	P	Pore space infilling and root penetration	
Lateral drainage layer (cover)	S	Provides subsurface drainage to reduce deep cover infiltration through the less permeable underlying layers	• Failure of underlying HDPE membrane
	P	Clogging of pore spaces by infilling with fine particulates and chemical precipitation	
	P	Waste subsidence (differential settlement)	

Table C.1. Summary of EMDF system features and safety functions (cont.)

Features	Safety functions (S) and limiting processes (P)	Events impacting performance evolution
Synthetic (HDPE) membrane (cover)	P Primary cover infiltration barrier (initial post closure period) P Protects underlying clay barrier from desiccation and cracking P HDPE thermal oxidative degradation processes (antioxidant depletion, oxidation, macromolecule scission)	• Installation-related defects/damage • Severe seismic event and/or rapid waste subsidence causing early membrane failure
Amended/compacted clay barriers (cover)	S Primary long-term infiltration barrier and radon barrier P Root penetration P Thermal and moisture cycles (increasing permeability) P Waste subsidence (differential settlement)	• Improper clay compaction • Severe seismic event and/or rapid waste subsidence causing damage to cover
Contour gravel layer (cover)	S Provides a level foundation for construction of the compacted clay infiltration barrier(s)	• Poor construction impacts performance of overlying clay barrier
Waste Placement, Containerization, Waste Treatment and Stabilization Processes		
Waste containers	S Isolates waste from water and reduces radionuclide mobility P Corrosion of metal containers	• Insufficient filling of void space in waste containers
Waste treatment and stabilization	S Provides chemical and physical stability to reduce radionuclide mobility P Degradation of stabilized waste forms	
Void filling and bulk waste compaction	S Limits long-term subsidence of bulk waste and maintains cover safety functions P Waste consolidation and subsidence	
Liner Design Features		
Protective material layer (liner)	S Protects underlying components of the liner system from damage during waste disposal operations.	• Improper installation • Unintentional disturbance during waste placement
Leachate collection (drainage) layer (liner)	S Leachate collection and treatment systems ensure protection of human health and the environment during operational/post-closure period S Waste mass dewatering during early post-closure period P Clogging, chemical precipitation, declining drainage efficiency	• Damage to overlying geotextile during installation causes early clogging and reduced drainage efficiency
Primary synthetic (HDPE) membrane (liner)	S Ensures leachate drainage for treatment S Primary leachate barrier (early post-closure period) P HDPE thermal oxidative degradation processes (antioxidant depletion, oxidation, macromolecule scission) P Chemical degradation of HDPE by leachate	• Installation-related defects/damage

Table C.1. Summary of EMDF system features and safety functions (cont.)

Features		Safety functions (S) and limiting processes (P)	Events impacting performance evolution
Geosynthetic clay layer (liner)	P	Supports primary infiltration barrier (initial post-closure period)	• Installation-related defects/damage
	S	Reduces infiltration through HDPE membrane holes and defects	
	P	Geochemical alteration of sodium bentonite clay (divalent cations)	
Leak detection layer (synthetic, liner)	S	Provides performance monitoring for overlying composite leachate barrier	• Installation-related defects/failures
	S	Provides secondary leachate removal function	
	P	Degradation of synthetic drainage material (impaired drainage)	
Secondary synthetic (HDPE) membrane (liner)	S	Supports performance monitoring for overlying composite leachate barrier	• Installation-related defects/failures
	S	Serves as secondary leachate barrier	
	P	HDPE thermal oxidative degradation processes (antioxidant depletion, oxidation, macromolecule scission)	
	P	Chemical degradation of HDPE by leachate	
Compacted clay layer (liner)	S	Serves as primary long-term leachate barrier	• Improper clay compaction • Severe seismic event or slope failure causing damage to perimeter berms and clay barriers
	S	Provides chemical retardation of radionuclide migration	
	P	Physical and geochemical alteration of clay	
Low permeability geologic buffer layer	S	Isolates radionuclides from saturated zone	• Water table incursion into geologic buffer
	S	Provides chemical retardation of radionuclide migration	
	P	Physical and geochemical alteration of geobuffer material	
	P	Increasing water table elevations (decreasing geobuffer thickness)	
Other Design Features			
Perimeter berms	S	Provide waste mass stability and physical isolation of waste	• Severe storms/flood events • Severe seismic event
	P	Erosion	
	P	Engineered slope failure (increased pore pressure and/or seismic acceleration)	
Slope protection (riprap on steeper segments)	S	Limits hillslope erosion	
	P	Engineered slope failure (increased pore pressure and/or seismic acceleration)	
Surface and shallow subsurface runoff controls (ditches, drains, etc.)	S	Limits recharge near margins of disposal cell	• Severe storms/flood events
	S	Mitigates stormwater impacts	
	P	Erosion and sedimentation of surface features	
	P	Physical/chemical/biological clogging of subsurface drains	
Engineered dewatering features (perimeter underdrains)	S	Limits groundwater elevation beneath cell footprint during construction, operations, and post-closure period	• Landslide blocking drainage feature outlet
	P	Physical/chemical/biological clogging of subsurface drains	

Table C.1. Summary of EMDF system features and safety functions (cont.)

Features	Safety functions (S) and limiting processes (P)	Events impacting performance evolution
Leachate management systems	S Ensure protection of human health and water resources during operational and/or early post-closure period P Physical/chemical/biological processes reduce effectiveness of post-closure passive treatment system over time	• Severe weather causes exceedance of treatment system flow capacity or damage to critical components • Weather-related or other natural disturbance causes early failure of passive treatment system

EMDF = Environmental Management Disposal Facility
HDPE = high-density polyethylene

C.1.2 EMDF SAFETY FUNCTIONS AND LIMITING PROCESSES

This section identifies events and natural processes that can impact the safety functions provided by EMDF site characteristics and design features. The features, events, and processes identified provide the basis for a conceptual model of EMDF performance evolution that generalizes performance in terms of cover infiltration and leachate production. Accordingly, the focus of the discussion is on events and processes that can affect EMDF cover system performance (infiltration) and the timing and volume of leachate release to groundwater. Post-closure EMDF leachate management, performance monitoring, facility maintenance practices, and institutional controls that mitigate the short-term risk of impaired safety functions also are considered in the generalized conceptual model. The discussion that follows is structured to align with Table C.1, which summarizes the information. Rare events that could cause catastrophic failure of EMDF safety functions are acknowledged but are not incorporated into the general conceptual model of EMDF performance evolution.

C.1.2.1 Site Characteristics and Safety Functions

Natural characteristics of the EMDF site that influence the performance of the facility include the vegetation and soils associated with the humid temperate climate and Paleozoic sedimentary rocks that underlie Bear Creek Valley (BCV). Although the final cover surface layer is an engineered feature that will be monitored and maintained, long-term evolution of the cover surface soil will be constrained by the local climate and ecological processes that govern the succession of biological communities over time. In particular, it is likely that once the site is no longer actively maintained, it will eventually become forested. In both the short- and long-term, the vegetation and soil characteristics of the cover surface are dominant controls on the hydrology and stability of the cover system. Surface runoff and infiltration are strongly linked to soil texture and vegetation cover, and these surface processes dictate the patterns of soil erosion that take place on the cover surface.

The general topography of the site and disposal cell geometry also are important for cover surface hydrology, hillslope stability, and water table elevations. The relatively steep slopes and significant topographic relief in the area tend to promote runoff and limit infiltration in upland areas such as the disposal cell footprint. In this sense the topography of the site and disposal unit serve a safety function in promoting efficient drainage. However, runoff generation also favors soil erosion, and steep slopes are often less stable than more gentle slopes of similar height and material characteristics, so that slope stability is an important consideration both in site selection and facility design.

The topographic saddle lying between Pine Ridge and the knoll upon which the upper portion of the EMDF will lie serves a safety function by limiting the elevation of the water table south of the saddle. This hydraulic control on the saturated zone, in combination with EMDF design geometry, will provide an unsaturated geologic buffer zone between the waste and the water table that is a key design requirement. Extreme geological events such as landslides that would fill Bear Creek tributaries with debris and/or block surface drainages could affect the safety functions provided by the topography and surface drainage network in limiting water table elevations near the perimeter of the disposal unit.

Topography serves another safety function in the EMDF disposal system by geographically isolating the site from the nearest public areas, thus facilitating institutional control of site access in the earlier portion of the post-closure period.

Natural events that can impact EMDF performance include transient or persistent shifts in climate conditions that would significantly disrupt or alter surface vegetation and hydrology, possibly leading to increased surface erosion or greater infiltration of water through the cover system barriers and into the waste. Sudden disturbance of vegetation cover by large storms or foreign pest infestations also could lead

to abrupt changes in surface erosion and cover infiltration and, possibly, decreases in slope stability. Changes in cover surface vegetation caused by severe events can be persistent depending on the extent of loss of the upper portion (soil) of the cover that overlies the biointrusion barrier. Possible impacts of surface process on the safety functions of specific cover system components are discussed in Sect. C.1.2.2.

Site geology, including lithology, stratigraphy, structural features, and seismic characteristics, can influence the nature and stability of surficial materials, as well as play a dominant role in the configuration of groundwater flow systems and geochemical conditions in the subsurface. In terms of safety functions of the disposal system, geologic formations at the Central Bear Creek Valley (CBCV) site, including the Maryville and Nolichucky units have developed relatively thick, clay-rich weathered profiles that may serve as a source of low-permeability material for construction of the disposal unit. The abundant clay minerals in these rocks (e.g., illite) also serve to enhance surface complexation and other sorption mechanisms that can retard the transport of radionuclides in the subsurface (ORNL 1987).

East Tennessee is an active seismic zone, but earthquakes of sufficient magnitude to severely impact site stability are rare in East Tennessee. Although there is a higher rate of seismic activity in this zone, the largest documented historical earthquake in the region was approximately magnitude 4.6 (Tennessee Valley Authority 2016). Historical data on East Tennessee seismic activity are presented in Sect. 2.1.3.6 of the EMDF PA Report. EMDF site characterization included geophysical surveys to estimate bedrock peak ground accelerations for use in slope stability and liquefaction assessments required for facility design.

Slope failures can evolve relatively slowly or be triggered rapidly by severe weather events or seismic events, both of which are possible in the 1000 to 10,000-year post-closure time frame considered for the EMDF PA. Large-magnitude, low-probability events have the potential to cause severe impairment of EMDF performance in the long-term, but these extreme events are not explicitly included in the conceptual model of EMDF system evolution. For example, a large hillslope failure on Pine Ridge upgradient from EMDF, or on the disposal unit itself, or severe flooding that undermined the perimeter berms could cause catastrophic damage to the structure of cover and/or liner systems. A much more likely evolutionary scenario would involve progressive, cumulative impacts of more gradual processes that can degrade safety functions, combined with severe events of intermediate magnitude that can cause relatively rapid damage to EMDF design features. The following subsection details processes and events relevant to the performance of specific design features and the safety functions those features serve in the EMDF disposal system.

C.1.2.2 Design Features and Safety Functions

The primary focus of the conceptual model of EMDF performance evolution presented in Sect. C.1.3 is the safety functions served by the cover system (primarily limiting infiltration), and the processes and events that can limit those functions over time. Individual components of the cover and liner systems and the safety function(s) they serve are presented along with potentially limiting natural processes and events in Table C.1. The following subsections discuss the range of events and processes that are expected to be significant for EMDF performance evolution over time.

C.1.2.2.1 Cover system components and processes

Vegetated erosion control layer

The vegetated surface layer serves to protect the underlying cover system components from erosion and environmental fluctuations in temperature and moisture that can accelerate degradation of materials and lead to impaired safety functions. The cover surface soil and vegetation are designed to limit surface runoff and erosion, thereby preserving the thickness and protective functions of the surface layer. Final design work for the cover surface will utilize applicable engineering tools (hydrologic models and design storm

events) to ensure resistance to rill and interrill erosion. In addition, the results of applying an agricultural soil erosion model to the EMDF cover profile to evaluate the potential cumulative impact of erosion over time is presented in Sect. C.4.

Site characteristics and processes that will determine the evolution of the surface layer after the cover vegetation is no longer maintained include interactions among climate, soil development and vegetation, and resulting changes in vegetation over time (ecological succession). These changes will affect the surface water balance, including atmospheric exchange, runoff generation processes, and infiltration of water to deeper portions of the cover profile. Surface erosion processes also will be affected, possibly leading to greater spatial variation and the potential for gully formation. The occurrence of severe erosion that could remove major portions of the cover surface layers is contingent upon a large number of factors, including climate variability, development of soil profiles and vegetation, and frequency and timing of extreme weather events.

Biointrusion and lateral drainage layers

The primary safety functions of the biointrusion barrier are to prevent burrowing animals and root penetration from damaging or accelerating the degradation of hydraulic barriers and to deter inadvertent human intrusion. Natural processes acting on the biointrusion barrier that will eventually limit these safety functions include mineral weathering and particle disintegration as well as downward transport of fine material into interstitial spaces. The safety function of the overlying granular filter layer (and geotextile) is to limit intrusion of fine materials into the biointrusion layer. The low moisture retention of the very coarse material will limit root growth into the biointrusion layer until sufficient fine materials have accumulated or other changes in the material favor root incursion. Extreme weather events or disposal unit slope failure could damage the granular filter biointrusion barrier, but these impacts would probably be localized.

The lateral drainage layer in the cover system (overlying the HDPE membrane) plays an essential role in transmitting water away from the disposal unit, thereby limiting infiltration into the waste. The drainage layer is subject to natural geologic processes that can decrease hydraulic conductivity of the material and impede lateral drainage. Relevant processes include dissolution and mineral weathering (various geochemical transformations), particle disintegration, chemical precipitation, and downward transport of clay particles. The impact of lateral drainage layer clogging is limited as long as the underlying HDPE membrane in the cover maintains very low permeability, so that expected membrane service life is an important consideration. Root penetration also may affect drainage layer characteristics, but the 7 ft of cover material overlying the drainage layer, including the surface layer, granular filter layer, and biointrusion layer, serve to reduce the likelihood of root penetration and the influx of fine materials that could lead to clogging and decreased drainage efficiency. As a measure of defense-in-depth, the biointrusion layer also can serve a lateral drainage function in the event that the underlying drainage layer is degraded and no longer functions as designed.

Benson and Benavides (2018) provided several examples of the durability of distinct layers of different natural materials to address concerns about infilling and loss of functionality of a drainage layer. A short-term example was provided from a cover system that was excavated after 8 years. The cover included a uniform sand layer directly overlain by a fine soil used as the water storage layer in a capillary barrier (no geotextile filter layer). No evidence of fines migration was observed. Longer-term performance of layers in a cover system was explored by considering covers over tombs that were excavated in Japan and China. The tomb in Japan included alternating layers of clay and loam. After 2000 years, distinct layers were observed with no significant mixing. The tomb in China involved alternating layers of clay and fine sand. After roughly 3000 years, there were still distinct layers visible in the cover. A natural analog was also identified at the Hanford Reservation (Bjornstad and Teel 1993) that illustrated the persistence of stratification within natural sediments having a layer of fines directly over coarse material over time frames

on the order of 30,000 years. The conclusion was that such texturally stratified systems, especially with a geotextile filter layer and substantial cover, would be expected to continue to function for long times.

Synthetic membrane

Geomembrane liners of the EMDF cover and liner systems are expected to be effective in limiting infiltration and controlling releases of leachate for their estimated service life, reported to range from a few hundred years to 1000 years or more (Koerner et al. 2011, Rowe et al. 2009, Benson 2014, EPA 1993). As described in *Geomembrane-Leachate Compatibility for U.S. Department of Energy CERCLA Waste Disposal Facilities* (Bonaparte et al. 2016), it appears that HDPE geomembranes of the type being used in some mixed low-level (radioactive) waste (LLW) disposal facilities are relatively unaffected at total alpha doses of 5 Mrad or more. These geomembranes also are reportedly unaffected by radiation from gamma and/or beta sources until total doses reach on the order of 1-10 Mrad, which is much higher than what would be expected for waste disposed in EMDF. Chemical degradation of synthetic components also is possible depending on the contaminants present in EMDF LLW and related characteristics of the leachate. Leachate and geosynthetic material compatibility studies have been completed as part of early EMDF engineering design (UCOR 2018, Appendix F). For HDPE membranes, thermal oxidative degradation is most often cited as the key degradation process.

The proposed three stages of HDPE geomembrane service life described *in Assessment and Recommendations for Improving the Performance of Waste Containment Systems* (Bonaparte et al. 2002) include (1) depletion of antioxidants, (2) induction, and (3) degradation of material properties. Despite the depletion of antioxidants in Stage 1 and oxidation induced-scission of polyethylene chains in Stage 2, there is no loss of performance during these stages. Stage 3, or degradation, occurs when the effect of oxidation induced-scission of polyethylene chains becomes measurable. The approximate durations for each stage for a 1.5-mm HDPE geomembrane include antioxidant depletion (200 years), induction (20 years), and degradation (750 years), expressed as the half-life (50 percent degradation) of an engineering property (Bonaparte et al. 2002). This implies a service lifetime of 800 to 1000 years for an HDPE geomembrane of the thickness specified in the EMDF preliminary design (1.5 mm). Subsequent research (Rowe and Islam 2009) found similar durations and concluded that HDPE liners may perform as designed for upwards of 500 to 1000 years. Similarly, research results (Phifer 2012) estimates that the HDPE liners in the Portsmouth Comprehensive Environmental Response, Compensation, and Liability Act of 1980 cell design may function for 600 to 1400 years. A service life of about 500 years would ensure enough containment time to allow for decay of short-lived radionuclide contaminants (e.g., less than 100-year half-life) to innocuous levels (U.S. Nuclear Regulatory Commission [NRC] 1981).

More recently, Benson and Benavides (2018) suggest that lifetimes for substantial HDPE membranes on the order of 1900 years or more are likely, although it is assumed that some pinholes or other defects that permit limited moisture movement will be present at the time of installation. Benson and Benavides (2018) also place emphasis on the synergistic roles of an HDPE membrane over a clay layer (composite barrier) that contribute to an expectation for long functionality of a cover system. It is reasonable to expect that an HDPE membrane will continue to serve a functional role as a substantial barrier to water flow and to protect the clay layer well beyond the 1000-year compliance period for the U.S. Department of Energy (DOE) LLW disposal facilities.

Amended/compacted clay barriers

Prior to substantial membrane degradation, a clay layer or GCL beneath an HDPE membrane serves to limit flow that may occur through inevitable imperfections or flaws in the HDPE membrane. Performance of the clay barrier depends on proper installation and how its properties change over time. To ensure the compacted clay layers meet the design-specified hydraulic conductivities at the time of installation, strict

construction quality assurance (QA) and control measures will be implemented. Test pad construction is utilized to verify materials and methods of installation.

Once the synthetic membrane in the cover (or liner) system has become ineffective in limiting infiltration, the underlying amended and/or compacted clay layer(s) are the primary hydraulic barriers to downward water movement. Environmental conditions that have been shown to alter the effectiveness (i.e., hydraulic conductivity) of the compacted clay layers in cover systems include freeze-thaw cycles, penetration by plant roots and/or burrowing animals and insects, and desiccation and rewetting of the clay (Benson and Othman 1993, Daniel 1993, Albrecht and Benson 2001, Bonaparte et al. 2002). All of these factors can lead to cracks and loosening of the clay layer that create preferential flow paths that allow for more water to pass through the material (Albright et al. 2006).

The potential for degradation of a clay layer due to cation exchange was discussed in Benson and Benavides (2018). Recent studies have shown that hydrated clays are resistant to changes in hydraulic conductivity due to cation exchange (Scalia and Benson 2011). Two recent examples were provided where the hydraulic conductivity of hydrated clays were not adversely impacted by cation exchange. In one of the examples, the clay retained low hydraulic conductivity in the presence of some differential settlement.

The cover system for EMDF has a robust configuration to protect the amended and compacted clay layers from degrading processes. The cover system layers above the clay barriers, including the membrane, provide a buffer from environmental variations in moisture and temperature that could cause freeze-thaw cycles, desiccation, cracking, and loss of clay barrier performance. Further, the high rock content in the layers above the compacted clay have unit weights greater than typical soils, which will provide higher overburden stresses and help protect the installed material properties of the clay. These conditions differ greatly from those described in Albright et al. (2006) where the cover systems typically consisted of only a protective surface layer atop a compacted clay barrier layer and were on average 4 ft thick.

Severe cover erosion and waste subsidence

Should there be severe erosion of the cover surface, it could reduce evapotranspiration and lead to larger water fluxes to the drainage layer. If extensive gully erosion were to occur, localized exposure of the biointrusion layer could facilitate deeper root penetration and larger fluctuations in moisture and temperature below the base of the erosion control layer (Fig. C.3). Those changes may affect lateral drainage efficiency and enhance degradation of the HDPE membrane and clay infiltration barriers of the cover. Gully erosion could enhance localized infilling of the biointrusion and lateral drainage layers with fine sediment, but will also facilitate rapid cover system drainage during storm events, so that the net impact of severe erosion on lateral drainage efficiency and cover infiltration is uncertain. The coarse material of the biointrusion layer should limit the depth of gully development in the long term, providing a stable residual thickness of earthen materials over the HDPE membrane in areas of deeper erosion, which would be limited in total extent. As an additional measure of defense-in-depth, the size of the riprap in the biointrusion layer required for stability under a low-probability, high-magnitude design storm could be determined using industry standard models and methods.

Another process that can compromise the function of cover components is post-closure differential settlement (subsidence) of the waste. Waste subsidence can lead to stress on overlying barrier layers (HDPE membrane and amended/compacted clay) that causes tearing and cracking in these materials. In addition to providing pathways for infiltration through the hydraulic barriers, changes in the slope of the drainage layer and overlying cover surface resulting from significant differential settlement can impact surface runoff and infiltration and subsurface drainage efficiency, contributing to increased waste infiltration. Due to the variety and heterogeneous nature of expected EMDF waste forms and the resulting potential for subsidence that could impair cover system functions, this degradation mechanism is an important uncertainty in the conceptual model of EMDF performance evolution. Factors that mitigate the potential impact of

post-closure waste subsidence include careful placement and compaction of waste (operational requirements that provide a long-term safety function), active cover system monitoring, maintenance, and implementation of corrective remedies in the initial post-closure period.

Evolution of EMDF cover performance

In the post-closure period, differential settlement of the waste can impair performance of the overlying cover components in the absence of corrective maintenance. Eventually, naturally occurring soil and vegetation changes, severe weather events, or other natural disturbances can contribute to erosion of the cover above the biointrusion layer, enhanced HDPE and clay barrier degradation, and increasing water infiltration into the waste. The progress of cover degradation is contingent upon the intensity and timing of multiple processes and events in the post-closure period. Although a general progression from full design performance to some long-term degraded performance condition will occur, the timing and magnitude of degradation is quite uncertain, particularly given the potential interactions among the various disposal system elements, safety functions, and degradation processes described above. The generalized conceptual model of EMDF cover performance evolution is presented in Sect. C.1.3.

One important aspect of EMDF performance uncertainty is the timing of cover degradation (increasing cover infiltration) relative to evolution in the function of liner system components, which may be different as a result of the differing environments expected in the cover and liner systems over time. In the following subsection, a summary discussion of liner system safety functions and limiting processes is provided in the context of interaction with the progression of cover system performance. A more detailed listing of liner features, functions, and limiting processes and events is included in Table C.1.

C.1.2.2.2 Liner system components and processes

The primary initial function of the liner system is to intercept and remove leachate for treatment, if needed, during the operational and initial post-closure periods. The leachate collection and removal system and the underlying leak detection system are designed to be effective through an initial period that includes final cover construction and many years (decades, if necessary) of active leachate collection and management, performance monitoring, and facility maintenance. The assumed duration of EMDF post-closure institutional control, including groundwater monitoring and facility maintenance, is 100 years. During this period, the performance of the leachate collection system will be closely tracked and groundwater monitoring downgradient of the disposal unit can identify leaks in the clay barrier at the base of the liner system. Degrading processes such as HDPE oxidation will occur but should have negligible impacts on liner system performance during the initial post-closure period. The clay barrier should be protected from processes that could increase its permeability while the overlying membrane and GCL retain physical integrity. With completion of the final engineered cover system, infiltration reaching the waste should be effectively eliminated and leachate collection will decrease over time as the waste mass dewaters. It is assumed that at some time after leachate production decreases sufficiently, active leachate collection will be discontinued and the leachate collection system will be decommissioned. Facility performance monitoring will continue as long as active institutional controls are maintained, assumed for the EMDF PA to be 100 years post-closure.

Over the long-term (centuries to millennia after EMDF closure), degradation of the cover system and increasing infiltration into the waste will increase leachate delivery to the liner system, and the impacts of potentially limiting processes on liner safety functions will become important. Degradation of liner system HDPE membranes and the GCL will eventually limit the effectiveness of these components in preventing release of leachate from the waste, and the clay barrier layer will serve as the primary leachate barrier. Once leachate begins penetrating the compacted clay liner, this barrier will serve the safety function of impeding contaminant transport via low permeability and chemical retardation (sorption) properties of the clay. Degradation of the hydraulic properties of the clay barrier (increasing permeability) can result from the

same process that affects clay barriers in landfill cover systems (e.g., thermal and moisture cycles), but because liner system clays are more isolated from environmental fluctuations than cover system clay barriers, the liner barriers may retain their safety functions for a longer period.

Retardation of short-lived radionuclides (half-lives of 1000 years or less) by the liner clay barrier and underlying geologic buffer layer can provide additional time for radioactive decay to reduce activity concentrations prior to reaching the saturated zone. For longer-lived radionuclides, retardation can delay release to groundwater. Environmental factors that affect retardation include the chemical form and oxidation state of the radioisotope, mineral composition and organic content of the geologic medium, and pore water geochemistry (particularly ionic strength, pH, and oxidation-reduction potential). Environmental variability in the factors controlling sorption can limit this important safety function.

The final cover system is designed to have a lower minimum permeability than the liner system and geologic buffer material. In principle this difference could offset the possibility that the cover components will degrade more rapidly than the liner components and, after leachate collection ceases, lead to accumulation of water on the liner over time (bathtub scenario). Monitoring and maintenance of the cover system should limit the probability of bathtubbing during the initial post-closure period of active institutional control. The implications of a bathtub scenario for the EMDF are developed in Sect. C.3. A generalized scenario for changes in cover infiltration and leachate release in relation to the natural processes and events affecting cover and liner degradation over time is developed in Sect. C.1.3.

C.1.2.2.3 Surface water and shallow subsurface drainage systems

Engineered surface and shallow subsurface drainage systems are included in the EMDF preliminary design to facilitate construction and to promote surface runoff and thereby limit the potential for groundwater recharge and erosion near the disposal unit. The stormflow intercept feature between Pine Ridge and EMDF will provide diversion of upgradient surface and shallow subsurface flow away from the disposal unit, reduce local recharge and protect against erosion at the toe of the upslope perimeter berm. Over the long term, slope failures could reduce the effectiveness of the stormflow intercept by filling the drainage path, but erosional process would likely serve to re-establish effective drainage over time. Any subsurface drainage systems would be designed with graded filtration and non-weathering materials to provide extended post-closure performance.

C.1.2.2.4 Perimeter berms and surface armoring

Perimeter berms of EMDF serve to provide lateral confinement and structural stability to the disposal facility and contribute to physical isolation of the waste from potential receptors. Composed of structural fill, these features are subject to erosion under normal conditions. Steeper sections of the berm final design may incorporate features (e.g., riprap armor) to protect slopes from erosion. Over time, berms could be subject to slope failure (mass movement) under extreme conditions of pore pressure or as a result of seismic destabilization. Design specifications for berm geometry and geotechnical specifications will consider the likely range of ground acceleration for the EMDF site. Catastrophic berm failure is not considered as part of the normal evolution of EMDF performance.

C.1.3 CONCEPTUAL MODEL OF EMDF PERFORMANCE EVOLUTION

The preceding discussion of EMDF site characteristics and design features, safety functions, and potentially limiting events and processes provides a framework for developing a general conceptual model of EMDF performance evolution (Fig. C.4). The goal of the conceptual model is to integrate and generalize the impact of multiple events and processes on safety functions and EMDF performance over time, acknowledging

uncertainty in timing and degree of degradation and the occurrence of severe events. EMDF performance is expressed in terms of changes in cover infiltration and leachate release, beginning at the time of final cap completion and facility closure. A post-closure performance timeline (bottom of Fig. C.4) is divided into:

1) Full Design Performance (design performance period): a 100-year institutional control period (during which facility maintenance and active institutional controls are assumed) followed by a period during which full (or near) design performance is maintained after the end of institutional control
2) Partial Design Performance (degrading performance period): a period of degrading performance (increasing cover infiltration and leachate release)
3) Long-term Performance (long-term performance period): a final period during which water flux into and out of the disposal unit reaches some long-term, relatively stable limit.

The end of design performance and the beginning of degrading performance is associated with the onset of significant deterioration of the synthetic membrane in the cover and increasing infiltration through the underlying clay barriers. The base case assumption for this onset is 200 years post-closure, which is highly pessimistic based on the evidence for the longevity of HDPE flexible membranes reviewed in Sect. C.1.2.2.1. Progressive degradation of EMDF cover performance (increasing infiltration) is assumed to occur over the following 800 years (i.e., from 200 to 1000 years post-closure). This duration is consistent with the expected service life of the HDPE membrane, but pessimistic in terms of the early onset and the maximum level of clay barrier degradation and estimated cover infiltration associated with the long-term degraded performance condition (Fig. C.4). A long-term maximum cover infiltration rate of 0.88 in./year is adopted as the base case assumption for the PA, based on the HELP water balance model results presented in Sect. C.2.

The assumed long-term condition of degraded cover system performance would likely not fully be realized until after the compliance period, but the conceptual model pessimistically incorporates these potential effects by assuming the synthetic layers in the cover begin to fail at 200 years. Accelerated loss of functionality of natural materials is also captured by assuming infiltration continuously increases between 200 and 1000 years after closure. Recent studies and historical evidence (e.g., Benson and Benavides 2018) suggest that engineered and natural features of a cover are likely to maintain some integrity for time frames beyond 1000 years, potentially well beyond 1000 years. Benson and Benavides (2018) also projected very good long-term performance for a similar cover design at the Savannah River Site. For a composite barrier consisting of a flexible geomembrane over a GCL, modeled percolation rates were less than 1 mm/year for conditions reasonably expected to extend for up to 2000 years, and less than 10 mm/year for cases encompassing more severe degradation of the drainage medium and wetter than expected conditions within 2000 years. These values are provided for perspective about the levels of performance that may actually be achieved as a comparison to the assumptions in the EMDF PA modeling. It is notable that the cover infiltration value (0.88 in./year) assumed beyond 1000 years in the EMDF PA is similar to the upper bound of 19.7 mm/year (0.78 in./year) associated with a degraded GCL in the Benson and Benavides analysis.

The conceptual model of EMDF performance evolution assumes that the liner system degrades at a rate similar to the cover system such that a persistent bathtub condition does not occur in the base case evolution scenario. A bathtub scenario in which leachate accumulates on the liner system and is released to the surface at a cover margin seep is analyzed in Sect. C.3. The long-term severity of cover system degradation assumed for the base case represents the possible net impact of a variety of naturally occurring processes (Table C.1, Sect. C.1.2) acting over an extended period (800 years), expressed as a maximum long-term cover infiltration rate. Uncertainty in this measure of long-term hydrologic performance is a primary focus of model sensitivity and performance uncertainty analyses described in Sect. 5 of the PA main text. Details of the HELP model analysis of the EMDF water balance are described in the following section.

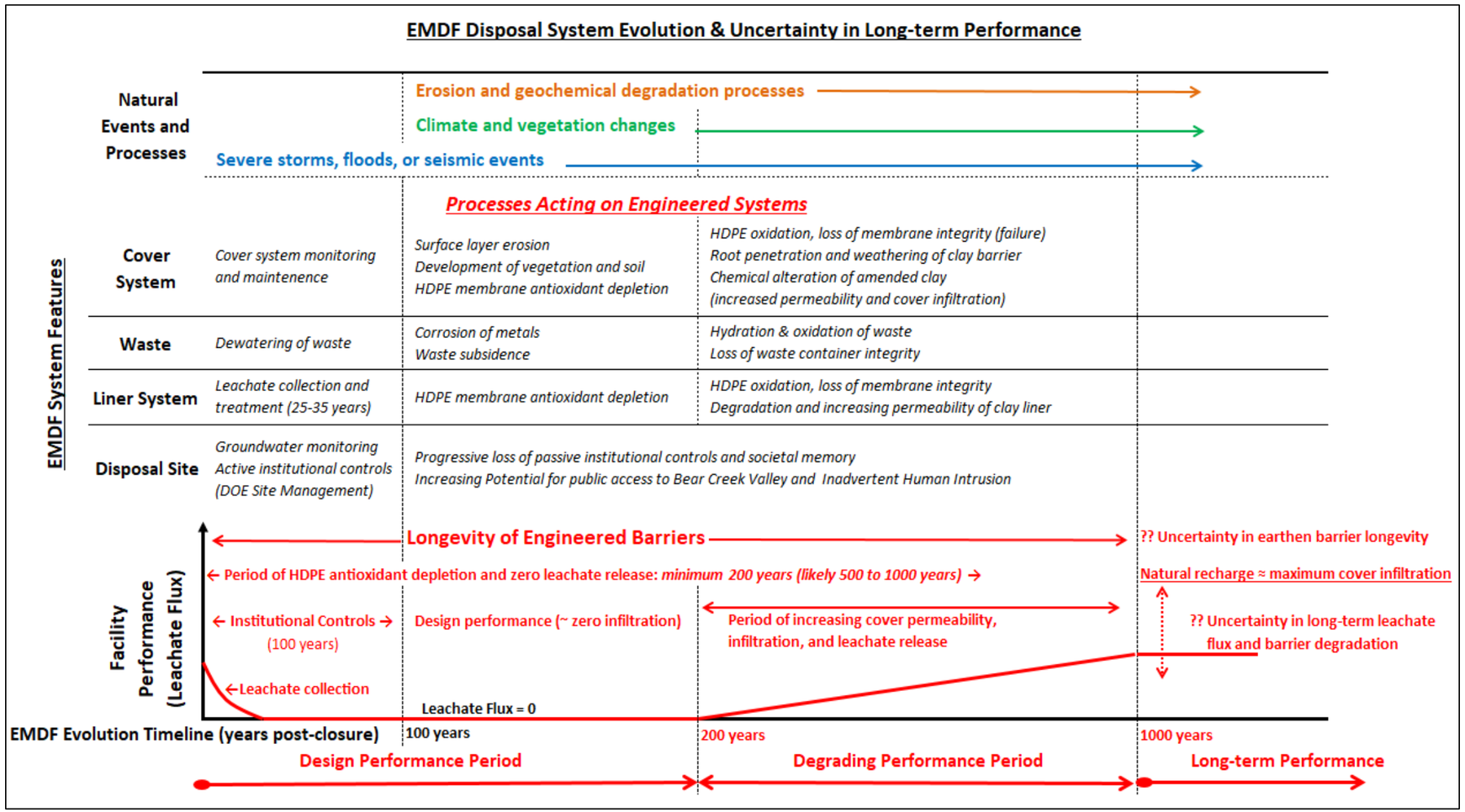

Fig. C.4. Generalized conceptual model of EMDF performance evolution

This page intentionally left blank.

C.2 HELP MODEL EVALUATION OF EMDF WATER BALANCE

C.2.1 CONCEPTUAL MODEL OF EMDF WATER BALANCE

A basic conceptual model for the water balance of the EMDF system includes the natural land surface hydrology and the engineered drainage features and barrier systems of the landfill design (Fig. C.5). Net infiltration of water through the surface layer and into the cover lateral drainage system is a function of climatic and meteorological dynamics and characteristics of the surface soil and vegetation that control local surface water and energy budgets. Subsurface percolation of water is conceptualized as predominantly vertical within the waste zone and earthen barriers of the cover and liner systems, whereas both vertical and lateral drainage are assumed to occur within the engineered drainage layers. Water movement through the unsaturated zone beneath the liner also is conceptualized as vertically downward to the water table.

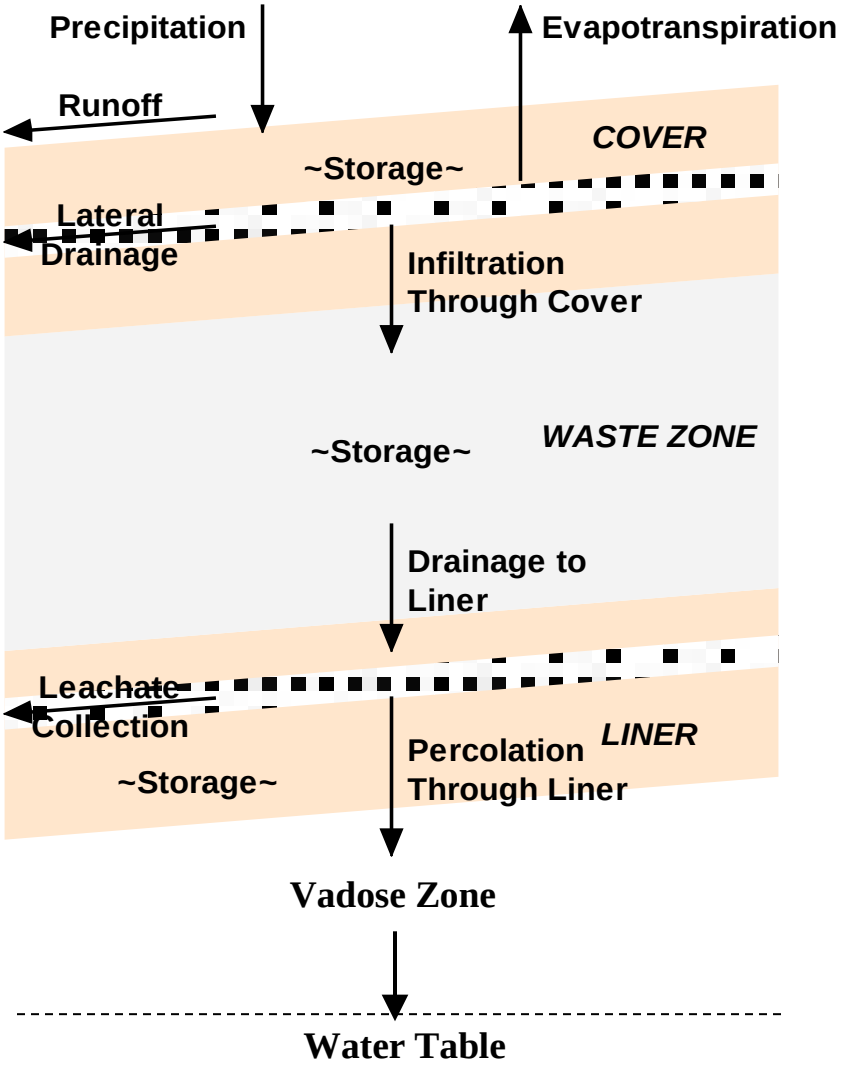

Fig. C.5. Schematic diagram of EMDF water balance

C.2.2 HELP MODEL CODE

Selection of the modeling tool to simulate EMDF cover system hydrologic dynamics and variably saturated zone flow through the landfill is based on the conceptual model presented above. Simulation of transient hydrologic phenomena (i.e., variability in precipitation, runoff, and evapotranspiration) is necessary for adequate prediction of long-term cover system performance. For cover system water balance modeling that incorporates daily and seasonal fluctuations in weather, the HELP computer code (Schroeder et al. 1994a, 1994b) is utilized to estimate post-closure rates of vertical percolation from the cover into the waste zone and out of the liner system under different environmental scenarios.

The HELP model was developed at the U.S. Army Corps of Engineer Waterways Experiment Station under a cooperative agreement with the U.S. Environmental Protection Agency (EPA) to support Resource Conservation and Recovery Act of 1976 and Superfund programs. Use of the HELP model is recommended by EPA and required by most states for the evaluation of closure designs for hazardous and non-hazardous waste management facilities. Numerous private engineering firms and federal, state, and municipal governmental agencies use the model for design evaluation and regulatory permitting actions. The model also is used for training and continuing research at many universities. The HELP code (Version 3.07) reflects the most recent modifications and corrections suggested by independent source code verification, sensitivity analysis, and related activities.

Section 9 of the PA Report details the QA activities and documentation that apply to the HELP model analysis.

C.2.2.1 HELP Model Description

HELP is a quasi-two-dimensional hydrologic model of water movement into and through landfill systems. The model accepts climate, soil, and design data, and uses estimation techniques that account for the effects of surface storage, snowmelt, runoff, infiltration, evapotranspiration, vegetative growth, soil moisture storage, lateral subsurface drainage, leachate recirculation, and unsaturated vertical drainage as well as leakage through soil, geomembrane, or composite liners. Landfill systems, including various combinations of vegetation, cover soils, waste cells, lateral drain layers, low permeability barrier soils, and synthetic geomembrane liners, may be modeled. The HELP model was developed to assist hazardous waste landfill designers and regulators in evaluating the hydrologic performance of proposed landfill designs. The program was developed to conduct water balance analyses of landfills, cover systems, and solid waste disposal and containment facilities. The model facilitates rapid estimation of the amounts of runoff, evapotranspiration, drainage, leachate collection, and liner leakage that may be expected to result from the operation of a wide variety of landfill designs. The HELP model has been used for design and performance modeling of the Environmental Management Waste Management Facility in BCV and has been selected for use in the EMDF design.

The HELP code has been widely used for landfill design and performance evaluation over more than two decades. The HELP model employs an extensive set of submodels to represent the water and energy balance at the surface, the U.S. Department of Agriculture (USDA) Natural Resources Conservation Service (NRCS) Curve Number method for estimating surface runoff (USDA 1986), a Dupuit-Forcheimer approximation for saturated flow in lateral drainage layers, and simplified algorithms for vertical flow and routing of water through a user-defined profile of landfill layers that may include lateral drainage layers, vertical percolation layers, soil barrier layers, and synthetic geomembranes (Schroeder et al. 1994a, 1994b).

The HELP model includes approximations that can affect the predicted surface water balance and vertical fluxes below the surface. Parameterization of surface soil and vegetation characteristics, in particular, will affect the estimated net infiltration through the surface layer (precipitation–runoff–evapotranspiration),

which sets an upper bound on percolation through the cover system as a whole. HELP utilizes a soil moisture characteristic model for unsaturated flow based on moisture content at soil field capacity and wilting point and employs a unit hydraulic gradient assumption (Darcy velocity equal to [un]saturated hydraulic conductivity) for each vertical percolation layer. Soil barrier layers are assumed to remain saturated, with flow driven by the estimated head on the top of the barrier. Depending on the predicted net infiltration, lateral drainage flux, and specified soil hydraulic characteristics, these simplifying vertical flow assumptions will tend to over predict downward vertical water movement through the modeled profile. In particular, these HELP flow approximations omit more complex surface tension physics such as the effect of capillary barriers designed to inhibit downward subsurface flow.

C.2.2.2 Previous Applications of HELP to Landfill Water Balance Modeling

Evaluations of HELP results relative to predictions of more complex, mechanistic models of subsurface flow and to field measurements of landfill hydrologic fluxes have yielded variable conclusions. As discussed in "Water Balance Modeling of Earthen Final Covers" in the *Journal of Geotechnical and Geoenvironmental Engineering* (Khire et al. 1997), HELP and UNSAT-H model predictions were compared to field measurements at an arid site and it was found that HELP grossly under predicted surface runoff using the curve-number approach and that percolation from the evaporative zone was over predicted due to the simplified flow and routing procedures employed. Another comparison of HELP and UNSAT-H models applied to a hypothetical humid site suggested that UNSAT-H predictions of vertical percolation based on daily rainfall data were higher than HELP-predicted rates (NRC 1996). A comprehensive study of multiple landfills in a variety of climatic settings (Albright et al. 2013) that compared HELP predictions to field data found that, for the two humid sites included, HELP tended to over predict both runoff and percolation from the cover barriers. In general, the available studies indicate that HELP tends to over predict vertical percolation at humid sites, suggesting that use of HELP for modeling humid site conditions may be conservative (pessimistic) in terms of estimating cover system performance.

In consideration of these particular model-structure uncertainties in use of HELP for design and performance modeling, it is essential to develop a detailed understanding of model sensitivity to parameter choices so that the most important parameter uncertainties may be identified. HELP simulations for the EMDF cover/liner design, estimated long-term performance conditions, and model sensitivity and uncertainty analysis are described in Sects. C.2.4 and C.2.5. HELP model estimates representing long-term performance conditions are only very general indications of the actual long-term average cover infiltration that could result from an uncertain combination of changes in engineered barrier properties and should not be considered as precise estimates of cover infiltration that will occur during the centuries following EMDF closure.

C.2.3 DATA REQUIREMENTS AND DATA SOURCES

HELP model inputs include climatic data, design specifications for the thickness and hydrologic characteristics of each soil layer or synthetic membrane, and parameter selections concerning the condition of vegetation on the surface layer and the quality of synthetic membrane placement.

C.2.3.1 Climatic Data

HELP requires input of precipitation, air temperature, and solar radiation data as well as data for estimating evapotranspiration (ET), which includes latitude, growing season dates, wind speed, quarterly average relative humidity, evaporative zone depth, and maximum leaf area index (LAI). These data can be user-supplied or imported from a variety of data sources and formats. Daily precipitation and temperature data for Oak Ridge, Tennessee for a period of 30 years from 1961 to 1990 are the basis for the EMDF model

runs, whereas the solar radiation and ET data are supplied by HELP based on user specification of Knoxville, Tennessee as the landfill location. Both earlier and more recent climate data are similar to the 1961 to 1990 data set and do not justify updating the HELP model files. The average annual total precipitation based on this data set is 54.4 in. The evaporative zone depth (21 in.) specified for all EMDF base case model runs is the HELP-suggested value for the Knoxville, Tennessee area. Based on sensitivity runs with the HELP model (Sect. C.2.5), the net infiltration at the surface layer is more sensitive to the value of this parameter than to most other characteristics of the surface layer. A summary of the climate data from a HELP model output file is provided as Fig. C.6.

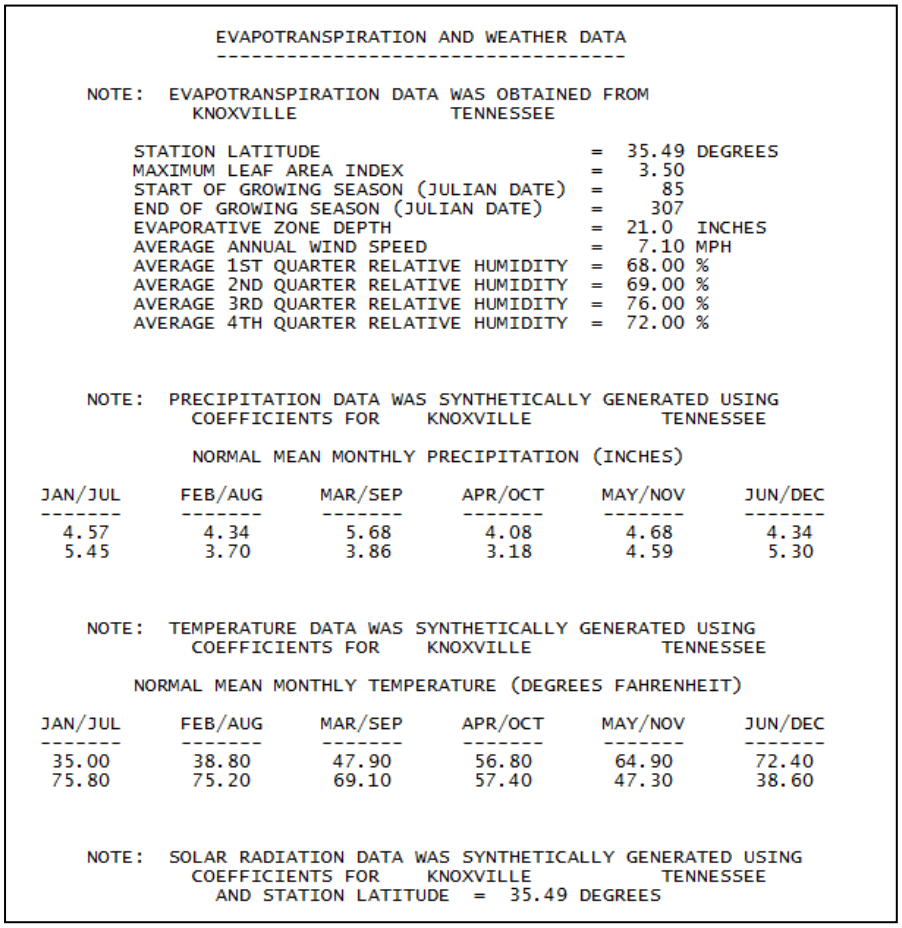

EVAPOTRANSPIRATION AND WEATHER DATA

NOTE: EVAPOTRANSPIRATION DATA WAS OBTAINED FROM
KNOXVILLE TENNESSEE

STATION LATITUDE	=	35.49 DEGREES
MAXIMUM LEAF AREA INDEX	=	3.50
START OF GROWING SEASON (JULIAN DATE)	=	85
END OF GROWING SEASON (JULIAN DATE)	=	307
EVAPORATIVE ZONE DEPTH	=	21.0 INCHES
AVERAGE ANNUAL WIND SPEED	=	7.10 MPH
AVERAGE 1ST QUARTER RELATIVE HUMIDITY	=	68.00 %
AVERAGE 2ND QUARTER RELATIVE HUMIDITY	=	69.00 %
AVERAGE 3RD QUARTER RELATIVE HUMIDITY	=	76.00 %
AVERAGE 4TH QUARTER RELATIVE HUMIDITY	=	72.00 %

NOTE: PRECIPITATION DATA WAS SYNTHETICALLY GENERATED USING
COEFFICIENTS FOR KNOXVILLE TENNESSEE

NORMAL MEAN MONTHLY PRECIPITATION (INCHES)

JAN/JUL	FEB/AUG	MAR/SEP	APR/OCT	MAY/NOV	JUN/DEC
4.57	4.34	5.68	4.08	4.68	4.34
5.45	3.70	3.86	3.18	4.59	5.30

NOTE: TEMPERATURE DATA WAS SYNTHETICALLY GENERATED USING
COEFFICIENTS FOR KNOXVILLE TENNESSEE

NORMAL MEAN MONTHLY TEMPERATURE (DEGREES FAHRENHEIT)

JAN/JUL	FEB/AUG	MAR/SEP	APR/OCT	MAY/NOV	JUN/DEC
35.00	38.80	47.90	56.80	64.90	72.40
75.80	75.20	69.10	57.40	47.30	38.60

NOTE: SOLAR RADIATION DATA WAS SYNTHETICALLY GENERATED USING
COEFFICIENTS FOR KNOXVILLE TENNESSEE
AND STATION LATITUDE = 35.49 DEGREES

Fig. C.6. Example of HELP output file summary of Oak Ridge climate data used for EMDF model simulations

C.2.3.2 Soil and Design Data

Soil and design data inputs define the profile(s) of landfill layers simulated by HELP. In addition to total landfill area and the percent of the area that generates surface runoff (assumed 100 percent), the thickness and soil properties of each layer are the essential data inputs. The cover design of the proposed EMDF includes multiple layers designed to reduce water infiltration, minimize erosion, and prevent intrusion into the wastes. There are eight discrete layers incorporated into the cover design and eight layers incorporated into the liner design below the waste (refer to Sect. C.1). Additional geotextile layers incorporated into the design to protect the geomembrane layers were not considered in the HELP model because they do not significantly alter or retard the movement of infiltrating water.

Necessary data on the soil material include total porosity, volumetric moisture content (VMC) at field capacity (defined as VMC at 0.33 bars capillary pressure), VMC at wilting point (defined as VMC at 15 bars capillary pressure), and saturated hydraulic conductivity (K_{sat}). The porosity, field capacity, wilting point, and saturated hydraulic conductivity are used to estimate the soil-water evaporation coefficients and Brooks-Corey soil moisture characteristic function parameters. The HELP model code contains default soil characteristics for 42 soil texture types (Schroeder et al. 1994a, Table 4, pages 30–31), and the selected soil texture type and corresponding default characteristics for each EMDF layer are given in Table C.2. The HELP profile of EMDF layer thickness, layer type designations, and soil characteristics is based on the preliminary design as documented in the EMDF QA Report for Modeling (UCOR 2020). As engineering design for the EMDF proceeds, these parameter assignments will be reviewed for consistency with current design specifications.

Table C.2. HELP layer soil characteristics for EMDF preliminary design

EMDF profile	Layer #	Material description	Layer type[a]	Layer thickness (in.)	Soil texture type[b]	Total porosity (vol/vol)	Wilting point (vol/vol)	Field capacity (vol/vol)	Saturated hydraulic conductivity (cm/sec)
Final cover	1	Top soil/rock mix (vegetative/erosion control layer)	1	48	11	0.464	0.310	0.187	6.40E-05
	2	Sand/gravel (granular filter/drainage layer)	1	12	3	0.457	0.083	0.033	3.10E-03
	3	Large rock/riprap (biointrusion layer)	1	24	21	0.397	0.032	0.013	3.00E-01
	4	Gravel (lateral drainage layer)	2	12	21	0.397	0.032	0.013	3.00E-01
	5	HDPE-FML (geomembrane layer)	4	0.06	35				2.00E-13
	6	Amended compacted clay (low permeability)	3	12	0	0.427	0.418	0.367	2.50E-08
	7	Cover compacted clay (low permeability)	1	12	16	0.427	0.418	0.367	1.00E-07
	8	Contour gravel (waste surface layer)	1	12	24	0.365	0.305	0.202	2.70E-06
Waste	9	Waste	1	690.45	22	0.419	0.307	0.180	1.90E-05
Liner	10	Protective soil (layer protects liner)	1	12	8	0.463	0.232	0.116	3.70E-04
	11	Drainage (leachate collection system)	2	12	21	0.397	0.032	0.013	3.00E-01
	12	HDPE-FML (geomembrane layer)	4	0.06	35				2.00E-13
	13	GCL (low permeability)	3	0.24	17	0.750	0.747	0.400	3.00E-09
	14	Geonet leak detection layer (leak detection)	2	0.3	20	0.850	0.010	0.005	1.00E+01
	15	HDPE-FML (geomembrane layer)	4	0.06	35				2.00E-13
	16	Compacted clay layer (low permeability)	3	36	16	0.427	0.418	0.367	1.00E-07
	17	Soil geobuffer (barrier layer)	1	120	0	0.419	0.307	0.180	1.00E-05

[a]1 = vertical percolation, 2 = lateral drainage, 3 = barrier soil, 4 = geomembrane

[b]Soil texture types as defined in Table 4, pages 30–31, *The Hydrologic Evaluation of Landfill Performance (HELP) Model: User's Guide for Version 3*, EPA/600/R-94/168a, P. R. Schroeder, C. M. Lloyd, P. A. Zappi, and N. M. Aziz, U.S. Environmental Protection Agency, Office of Research and Development, Washington, D.C., September 1994.

EMDF = Environmental Management Disposal Facility
FML = flexible membrane liner
GCL = geosynthetic clay liner
HDPE = high-density polyethylene
HELP = Hydrologic Evaluation of Landfill Performance

The HELP model input data also includes the length and slope of lateral drainage layers and the assumptions regarding synthetic membrane quality, including pinhole density, installation defect density, and membrane placement quality. Values for these parameters based on the EMDF conceptual cover design are given in Table C.3.

Table C.3. HELP model parameters for EMDF cover conceptual design lateral drainage and geomembrane layers

Drainage layer parameters			HDPE geomembrane quality characteristics (HELP layers 5, 12, 15)
HELP layer number	**Drainage length (ft)**	**Drainage slope (%)**	• Pinhole density: 1 hole/acre • Installation defect density: 1 hole/acre • Membrane placement quality: good
4	476.9	21.52	
11, 14	258.8	4.22	

EMDF = Environmental Management Disposal Facility
HDPE = high-density polyethylene
HELP = Hydrologic Evaluation of Landfill Performance

C.2.4 EMDF PERFORMANCE CONDITIONS

Because of the long period considered for the PA analysis, the EMDF cover and liner systems performance will change over time. Consistent with the conceptual model of cover performance evolution presented in Fig. C.4, the following three performance conditions are developed for HELP modeling:

- Full design performance (design performance period – EMDF closure through 200 years post-closure) – All layers are functional and included in the simulated HELP profile (Table C.2). This period includes the 100-year, post-closure period of institutional control and the first 100 years following the assumed loss of institutional control by DOE. Every component of the cover system is assumed to perform as designed, including the HDPE membrane and engineered drainage layer. Assuming 200 years for the service life of the HDPE membrane is pessimistic given that recent studies have estimated much longer periods of full HDPE membrane performance in mixed LLW facilities (Tian et al. 2017).
- Partial design performance (representative of the degrading performance period from 200 to 1000 years post-closure) – Geomembrane liner layers and geosynthetic clay layers are assumed to be totally ineffective (i.e., no longer function as impermeable layers in the cover and liner systems) after 200 years post-closure. These layers (Table C.2, layers 5, 12, 13, and 15) are eliminated from the simulated EMDF profile for this performance period. In addition, the lateral drainage layers in the liner system are designated as vertical percolation layers, consistent with the expectation that active leachate collection will not continue for more than a few decades. The amended clay layer (Table C.2, layer 6) is also assumed to be degraded from 2.5E-08 to 3.5E-08 cm/sec due to the failure of the geomembrane liner above. In the context of the generalized conceptual model of EMDF performance evolution (Fig. C.4), this modeled performance condition provides a reference performance level (cover infiltration rate) for the period of degrading EMDF performance. Modeling EMDF performance without the HDPE membranes and assuming slightly degraded performance of the clay barriers is consistent with the expectation that while the membranes are intact, degradation of the clay layers by natural processes is limited. Full design performance is assumed for the lateral drainage layer in the cover system due to the expectation that the cover system remains largely intact, clogging of the drainage layer is unlikely (refer to Sect. C.1.2.2.1), and the overlying biointrusion layer will provide effective lateral drainage capacity in the event that the drainage layer capacity is reduced.
- Long-term performance (long-term degraded performance period, > 1000 years post-closure) – Degradation of the cover system due to some combination of erosion, root penetration, soil development, damage by storms, floods, or other natural hazards or differential settlement of the underlying waste causes an increase in the permeability of the clay barriers in the cover and a decrease in the efficiency of the engineered lateral drainage layer of the cover. The degraded condition for this performance period is represented by changes in the hydraulic conductivity of the lateral drainage layer

(factor of 3 decrease) and amended clay layer (factor of 2.8 increase from design specification) in the HELP model profile.

HELP model parameter values chosen to represent degraded performance conditions are summarized in Table C.4 for the full design, partial design, and long-term performance conditions.

Table C.4. Summary of HELP model input parameter assumptions and model output representing design and degraded EMDF hydrologic performance conditions

HELP model input parameter or predicted output flux		Full design performance (0–200 years)	Partial design performance (201–1000 years)	Long-term performance (> 1000 years)
HELP inputs (cover)	Lateral drainage layer hydraulic conductivity (cm/sec)	3.0E-01	3.0E-01	1.0E-01
	HDPE geomembrane function[a]	Functional	Degraded	
	Amended clay hydraulic conductivity (cm/sec)	2.5E-08	3.5E-08	7.0E-08
HELP output flux (in./year)	Lateral drainage collected	18.50	18.07	17.62
	Infiltration through cover clay barrier and into waste zone	0.00	0.43	0.88
HELP inputs (liner)	Leachate collection drainage layer function[a]	Functional	Not functional	
	HDPE geomembrane function[a]	Functional	Degraded	
	Geosynthetic clay layer function[a]	Functional	Degraded	
	Leak detection drainage layer function[a]	Functional	Not functional	
	HDPE geomembrane function[a]	Functional	Degraded	
HELP output flux (in./year)	Leachate collection layer drainage	0.00	Degraded	
	Leak detection layer drainage	0	Degraded	
	Infiltration through liner clay barrier	0	0.43	0.88

[a]Model layer function "Degraded" indicates the layer has been removed from the HELP profile for that performance stage. For lateral drainage layers in the liner system, "Not Functional" indicates that the layer type has been changed from lateral drainage to vertical percolation in the HELP profile.

EMDF = Environmental Management Disposal Facility
HDPE = high-density polyethylene
HELP = Hydrologic Evaluation of Landfill Performance

C.2.5 HELP MODEL RESULTS AND SENSTIVITY TO PARAMETER ASSUMPTIONS

HELP model runs were performed for each of the three disposal cell performance conditions described above. HELP model outputs (Table C.4) provide estimated water fluxes through the EMDF cover system into the waste and out of the EMDF liner system. Because the HELP model is primarily intended as a design tool rather than for predictions of long-term landfill hydraulic performance, the model outputs for the three performance scenarios are utilized as a general indication of the magnitude of increases in cover infiltration and leachate release that could be realized under degraded performance conditions.

Uncertainty in using the HELP model to predict long-term hydrologic performance of the EMDF cover system is due in part to the difficulty of specifying representative degraded-condition hydraulic conductivity (K) values based on very limited understanding of the long-term performance evolution of earthen barriers and engineered drainage systems. The degree of degradation of clay barrier performance and increased cover infiltration that could occur due to natural processes over hundreds of years (assuming stable climate conditions) is plausibly bounded by the estimated range of natural annual average rates of recharge to groundwater in BCV, estimated at 7 to 12 in./year (DOE 1997, Volume 2, Appendix F, pages F-36 and

F-40). Additional HELP model runs were performed to evaluate the sensitivity of estimated infiltration to the degree of degradation assumed for the lateral drainage layer (changes in K_{sat}, slope, and drainage length), degradation (increased K_{sat}) of the amended clay and compacted clay barriers of the cover, and to increases in precipitation. The results of the sensitivity runs are summarized in the following paragraphs and the detailed information on HELP model implementation, model results, and quality assurance are provided in the EMDF QA Report for Modeling (UCOR 2020).

HELP model predicted cover infiltration values associated with different values of K_{sat} for the clay barriers of the cover system are shown in Fig. C.7. For the partial design performance and long-term degraded performance conditions, the amended clay and compacted clay units are modeled as separate layers (layers #6 and #7 in Table C.2). For the sensitivity cases that represent more severe cover degradation, the clay barriers are modeled as a single uniform 2-ft-thick barrier layer in the HELP model. The value of K_{sat} given on the horizontal axis of Fig. C.7 represents the hydraulic conductivity of the amended clay layer for the partial design and long-term degraded performance conditions.

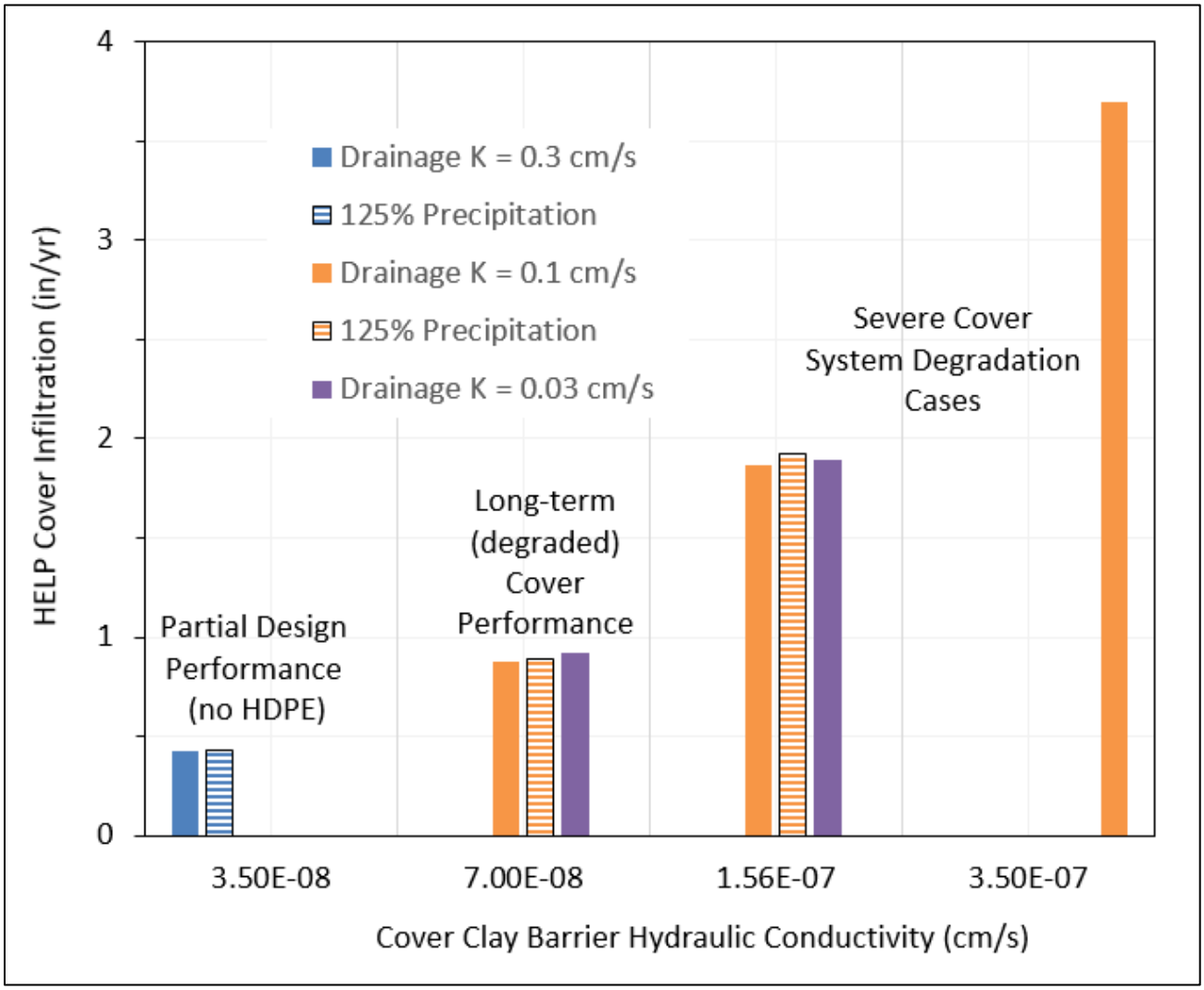

Fig. C.7. HELP model sensitivity to cover layer parameter assumptions and precipitation inputs

The left-hand pair of bars in Fig. C.7 represents infiltration predictions for the partial-design performance condition (without HDPE membranes) under the current average annual precipitation (~54 in./year) and for a 25 percent increase in total annual precipitation. HELP-predicted infiltration sensitivity to the increased precipitation is minimal (1 percent increase) for the partial design performance condition. For the long-term performance condition and the degraded cover condition with clay K_{sat} = 1.56E-07 cm/sec, a 25 percent increase in precipitation results in increases in cover infiltration of 2 percent and 3 percent, respectively (compare solid orange and striped orange bars on Fig. C.7)

Results of HELP model sensitivity evaluation for anticipated future changes (Table C.4) in the clay barrier K_{sat} (increase from full design performance) and the lateral drainage layer K_{sat} (decrease from full design performance) show that sensitivity to cover drainage K_{sat} is much lower than for cover clay K_{sat} (Fig. C.7) and that sensitivity to these two parameters is interdependent. Increases in infiltration are roughly proportional to the modeled increases in clay barrier K_{sat} (orange bars on Fig. C.7) whereas decreases in lateral drainage K_{sat} result in much smaller increases (< 5 percent) in cover infiltration (compare the solid orange and purple bars on Fig. C.7).

The results of HELP model simulations and sensitivity evaluation are summarized as follows:

- Cover infiltration for the partial design performance condition is 0.43 in./year.
- Cover infiltration for the long-term performance condition is 0.88 in./year.
- HELP cover infiltration predictions for the EMDF preliminary design are highly sensitive to the assumed value of K_{sat} for the amended clay barrier of the cover; increase in infiltration is roughly proportional to the increase in clay K_{sat} (Fig. C.7).
- HELP cover infiltration predictions are less sensitive to the decreasing K_{sat} for the cover lateral drainage layer or to increased precipitation than to the assumed value for clay K_{sat}.
- Predicted fluxes are consistent with the expectation that the EMDF cover system, even in a degraded condition, will promote lateral drainage above the clay barrier and limit vertical percolation through the barrier, relative to natural conditions, for hundreds of years.

C.2.6 USE OF HELP MODEL RESULTS IN THE EMDF PERFORMANCE ASSESSMENT

The range of HELP-predicted values is used to guide inputs (cover infiltration rates) to the more complex models of EMDF flow and contaminant transport used for the EMDF PA (Fig. C.8). For the base case EMDF performance scenario, cover infiltration is assumed to increase linearly from the full design performance condition (zero infiltration) at 200 years to the long-term degraded performance condition (0.88 in./year) at 1000 years. The sensitivity of the HELP model predictions to the K_{sat} of the amended clay barrier in the cover system indicates the importance of uncertainty in selecting parameter values to represent the long-term performance condition. The highest value of cover infiltration from the HELP sensitivity evaluation (3.7 in./year [Fig. C.7]) is equivalent to approximately 50 percent of natural groundwater recharge rates estimated for geologic units at the EMDF site.

In the context of EMDF performance modeling over thousands of years, extensive use of the HELP model to estimate EMDF performance degradation resulting from the full range of climatic and geologic processes and events (Fig. C.4) is not justified due to the uncertainties at such extended time scales. For the EMDF PA, sensitivity runs with the STOMP model and the sensitivity and uncertainty analysis for the EMDF total system model (Sects. 5.3 and 5.4 of the PA Report) evaluates uncertainty in future precipitation and the degree of EMDF cover performance degradation consistent with the range of HELP-modeled cover infiltration values.

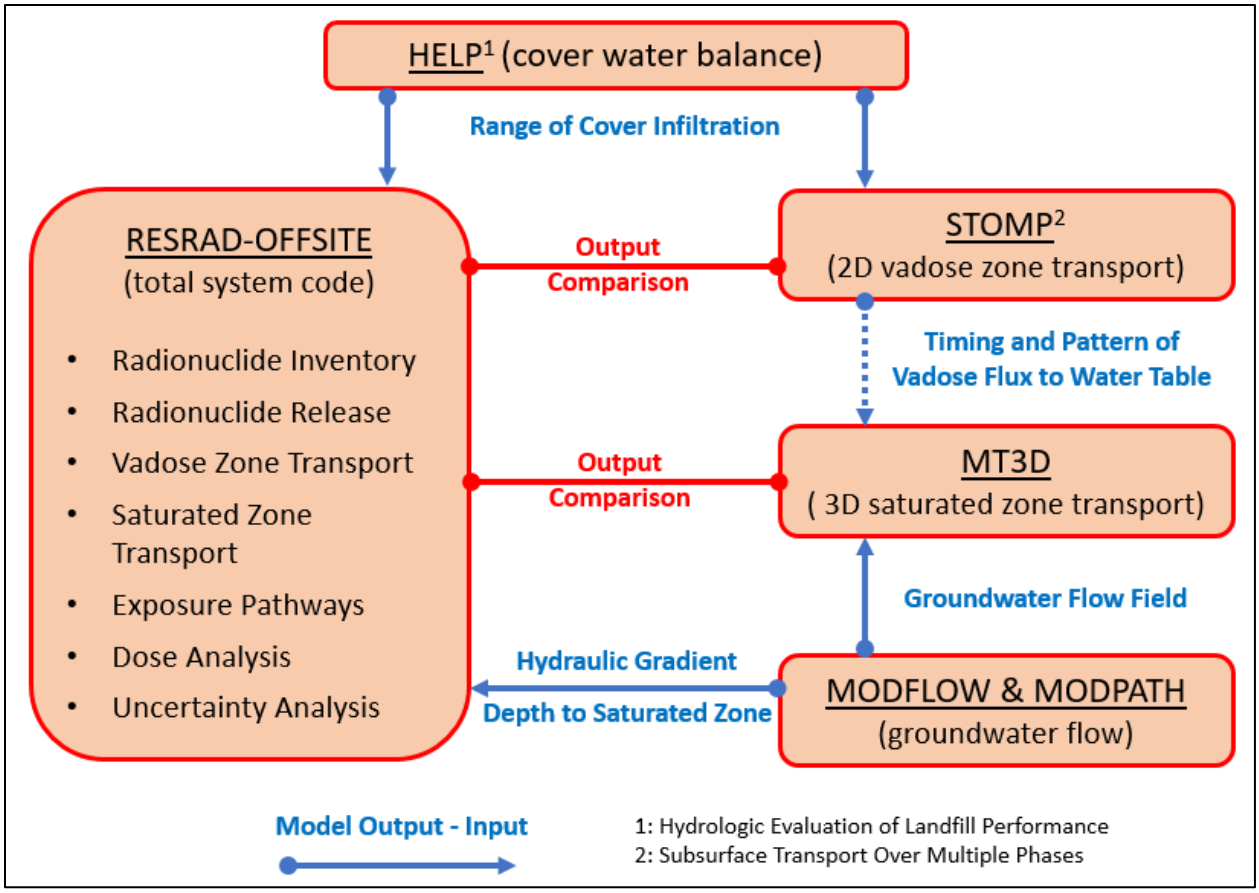

Fig. C.8. Integration of HELP model output with other flow and radionuclide transport models used in the EMDF Performance Assessment

C.3 BATHTUB SCENARIO ANALYSIS

C.3.1 INTRODUCTION

DOE Manual 435.1-1 (DOE 2011a) requires assessment of LLW disposal facility performance over an extended time period under various future condition scenarios. This section presents an analysis of a hypothetical bathtub scenario to assess the possibility of water accumulating in the facility during the post-closure period.

This type of scenario could occur if the cover system and/or any post-closure leachate management systems were to fail or degrade, but the liner system continues to prevent leaching from the base of the disposal unit. Under this scenario, the waste cells would start to accumulate water and portions of the waste may become saturated, potentially impacting facility performance.

The bathtub analysis for EMDF assumes that the liner system remains impermeable but without the leachate collection and drainage functions layers after the HDPE liner and synthetic components of the cover have completely degraded. This condition is assumed to occur after DOE institutional control ceases (100 years post-facility closure) and to begin no earlier than 200 years post-closure based on the conceptual model of cover system degradation (refer to Sect. C.1.3). Progressive saturation of the waste cells is assumed to

proceed at a rate limited by the assumed increase in cover infiltration rate between 200 and 1000 years post closure. Due to the imbalance of the water entering and leaving the system, waste could become saturated and static water pressure in the waste zone is assumed to cause leachate seepage along the perimeter of the liner at the lowest point of intersection with the cover. The analysis assumes that human exposure to radionuclide releases via leachate seepage occurs through use of local surface water and groundwater impacted by the release of contamination.

Section 9 of the PA Report details the QA activities and documentation that apply to the analysis of the bathtub scenario.

C.3.2 CONCEPTUAL MODEL OF BATHTUB CONDITION

EMDF preliminary design features are presented in Sect. C.1. Based on the EMDF preliminary design and site characteristics, the lowest permeability layers between the waste and groundwater will be the liner clay and geologic buffer material. The clay liner is assumed to have a hydraulic conductivity of 1E-07 cm/sec and the geologic buffer layer is assumed to have a maximum hydraulic conductivity on the order of 1E-05 to 1E-06 cm/sec. The cover amended clay barrier is assumed to have a lower hydraulic conductivity, on the order of 1E-08 cm/sec (Fig. C.3 and Table C.2).

If the cover system experiences more degradation than the liner, the decrease in performance of the cover could result in higher infiltration than the liner system leakage rate, especially after active management of the leachate and leak detection systems has ceased. In this scenario, the imbalance between water influx and leachate release could cause water saturation in the lower portions of waste within each disposal cell. This scenario is unlikely to occur for centuries because the HDPE membrane and amended clay layer in the cover are overlain by an 8-ft-thick section of sand, gravel, rock, soil, and suitable vegetation, which will protect the cover system from degrading for a long time. Recent research has shown that the HDPE will perform at least for hundreds of years under typical LLW disposal design conditions (Tian et al. 2017).

The proposed EMDF preliminary design has four disposal cells with progressively lower cell floor elevations from north to south (Fig. C.9). The floor of each disposal cell is sloped toward the southeast to facilitate leachate drainage and collection. Under the hypothetical bathtub scenario, the liner geometry controls the accumulation of infiltrating water and the waste at the lower end of each cell becomes saturated. Within the upper three disposal cells (Cells 1 to 3), if the elevation of waste saturation exceeds the upper elevation of the liner above the interior berms that separate adjacent cells, flow over the berm into an adjacent cell may occur. Eventually, saturation and resulting hydrostatic pressure in the waste zone might exceed the confining pressure along a zone of potential weakness (e.g., the seam along the cover/liner interface) and a leachate seep would develop to relieve the pressure. Due to the release of the pressure, catastrophic failure and loss of waste confinement for EMDF would not likely occur. The lowest portion of the cover/liner interface would be subject to the highest hydrostatic pressure, which is the most likely leachate seep location. For the EMDF preliminary design, this location is on the southeastern edge of Cell 4, which has an elevation of 930 ft above mean sea level. Based on the CBCV site topography (Fig. C.9), the seepage would flow toward NT-10 and Bear Creek, where it would impact the surface water quality. The leachate will be diluted by creek baseflow (groundwater discharge) and storm runoff from the facility cover and other contributing areas.

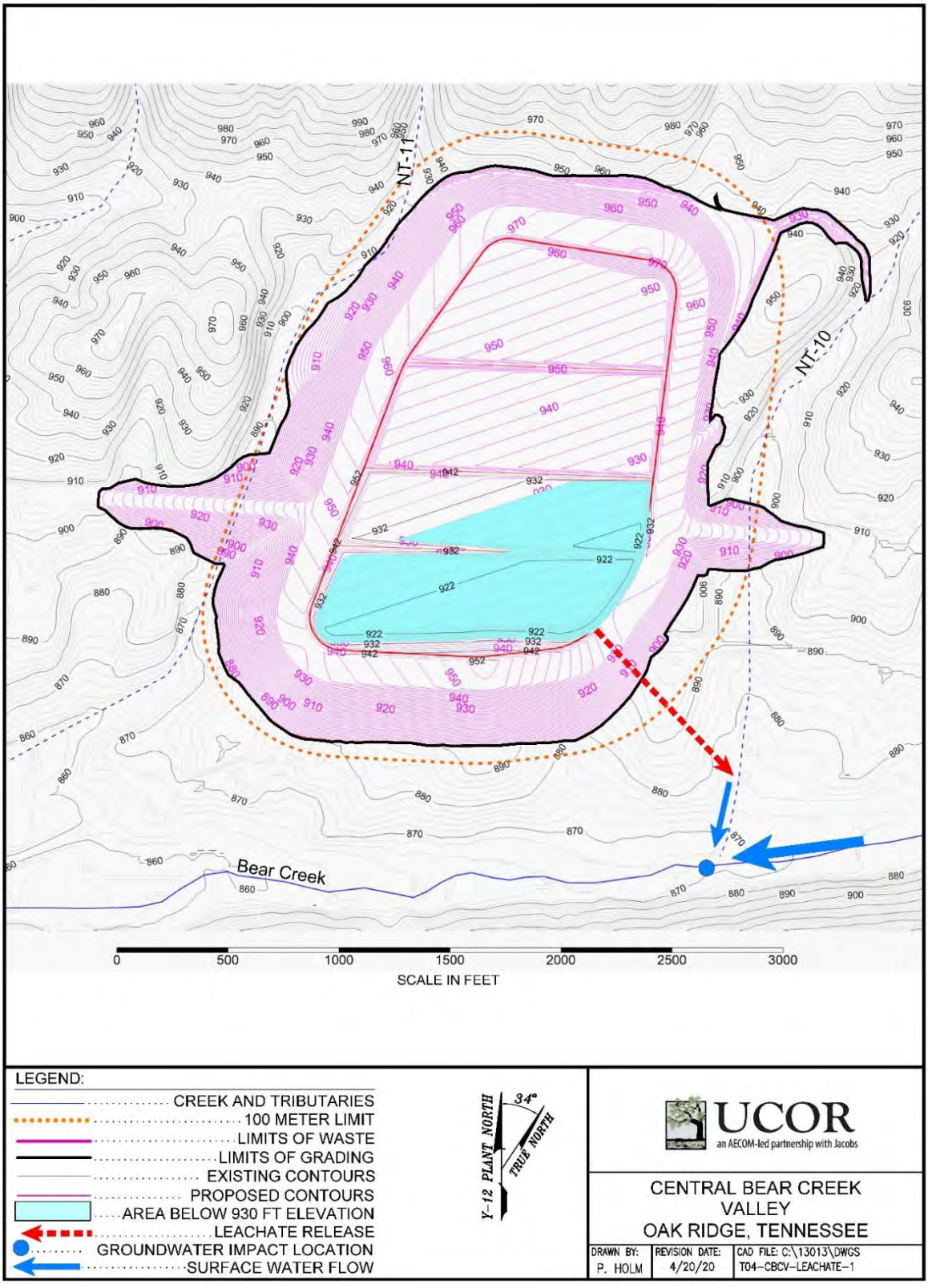

Fig. C.9. EMDF cell floor (liner) topography and assumed bathtub scenario surface water impact location

The EMDF bathtub condition scenario is simplified in the conceptualization of the factors that control water accumulation in the waste. Degradation of the cover and performance of the liner will be non-uniform, and increasing hydraulic head on the liner may increase vertical transmission of leachate sufficiently to balance the influx through the cover in a particular area, limiting the impact of waste saturation. The spatial distribution of cover infiltration and local liner leakage will influence the development of saturated regions of waste in different disposal cells, so that the magnitude and timing of seepage at the landfill surface is highly uncertain. The EMDF bathtub scenario provides a simplified case for evaluating the potential magnitude of seepage and activity concentrations associated with this mode of facility failure.

C.3.3 COVER INFILTRATION AND LEACHATE RELEASE ASSUMPTIONS

The time required to reach saturation and leachate release under a hypothetical bathtub scenario is based on the conceptual model of cover system degradation, assumed to begin starting at 200 years post closure (see Fig. C.4). From 200-1000 years, the cover infiltration is assumed to increase linearly, representing a gradual degradation of cover system performance. A basic assumption for the calculation is that the cover performance is uniformly degraded (i.e., leakage occurs over the entire cover area).

Based on the conceptual model of EMDF performance evolution (Sect. C.1.3) and the HELP model results (Sect. C.2.4) the cover infiltration is estimated as:

- 0 to 200 years – no water influx into the disposal cells
- 200 to 1000 years – linear increase from 0.00 to 0.88 in./year
- > 1,000 years – 0.88 in./year.

Using yearly water influx rates based on the waste planar area and the assumed infiltration rates given above, the time required for the waste to become saturated up to the lowest liner/cover perimeter seam elevation (930 ft) and the time required to saturate the entire waste volume are calculated. The volume of pore space that must be filled is based on assuming 0.419 total porosity and initial moisture content of 0.307 for the waste (values obtained from the HELP model inputs and results presented in Sect. C.2.5). These two saturation volumes effectively bound the possible timing of the onset of leachate release under the assumed progression of cover degradation. The areal extent of the portion of the waste in Cells 3 and 4 that lies below the 930 ft elevation is shown in Fig. C.9.

The maximum hydraulic stress under the bathtub scenario occurs when the entire volume of waste is saturated prior to seep development. For the assumed rates of cover infiltration, it would take 575 years after cell closure for the whole waste zone volume to become saturated. Leachate seepage would likely occur well before this extent of saturation was reached. It would take 310 years to reach saturation for the portion of waste in Cells 3 and 4 lying below 930 ft elevation. (Note that to simplify the analysis, only the contribution of water infiltration through the cover above the lower two cells [Cells 3 and 4] is assumed to contribute to saturation of the waste below 930 ft elevation. Accounting for the contribution of infiltration into Cell 2 would decrease the required duration only slightly.) However, the onset of leachate seepage could be delayed beyond 310 years if the hydrostatic pressure was insufficient to initiate the seepage at the cover-liner interface on the southeast margin of disposal Cell 4. Once seepage begins the leachate release rate is assumed to be the same as the influx rate into the waste. Based on the total waste cell planar area of 1,032,375 sq ft, the total influx rate through the EMDF cover corresponding to the long-term degraded performance condition (0.88 in./year) is calculated as 1.08 gpm.

C.3.4 LEACHATE MIXING WITH SURFACE WATER

The leachate seepage developed under the bathtub condition would flow down the side of the disposal unit to a surface water drainage channel leading to NT-10. The likely final discharge location would be the Bear Creek channel south of the EMDF. Note that the average water seepage rate of only 1.08 gpm may not be sufficient to sustain surface flow in a natural drainage feature, but higher flux rates would occur over the course of an average year. For purposes of this analysis, all the leachate flux is assumed to be discharged to the receiving stream (Bear Creek) at the confluence with NT-10.

The seepage will be diluted by surface water runoff from the nearby area and the flow in Bear Creek from the upper watershed area. Bear Creek stream flow has been continuously monitored at Bear Creek kilometer (BCK) 9.2, just west of the confluence of Bear Creek and NT-8. Daily measurements have been conducted since 2001. Shorter interval (15-minute) monitoring at BCK 9.2 was initiated in October 2013. The average flow rate at BCK 9.2 is 1100 gpm based on daily measurement data from October 1, 2001 to October 31, 2018.

Since BCK 9.2 is upgradient of the surface water impact point, there are additional surface water contributions below BCK 9.2 but above the surface impact area. The BCK 9.2 location, the assumed seepage impact location on Bear Creek, and the area that will contribute to the surface flow between those two points is shown on Fig. C.10.

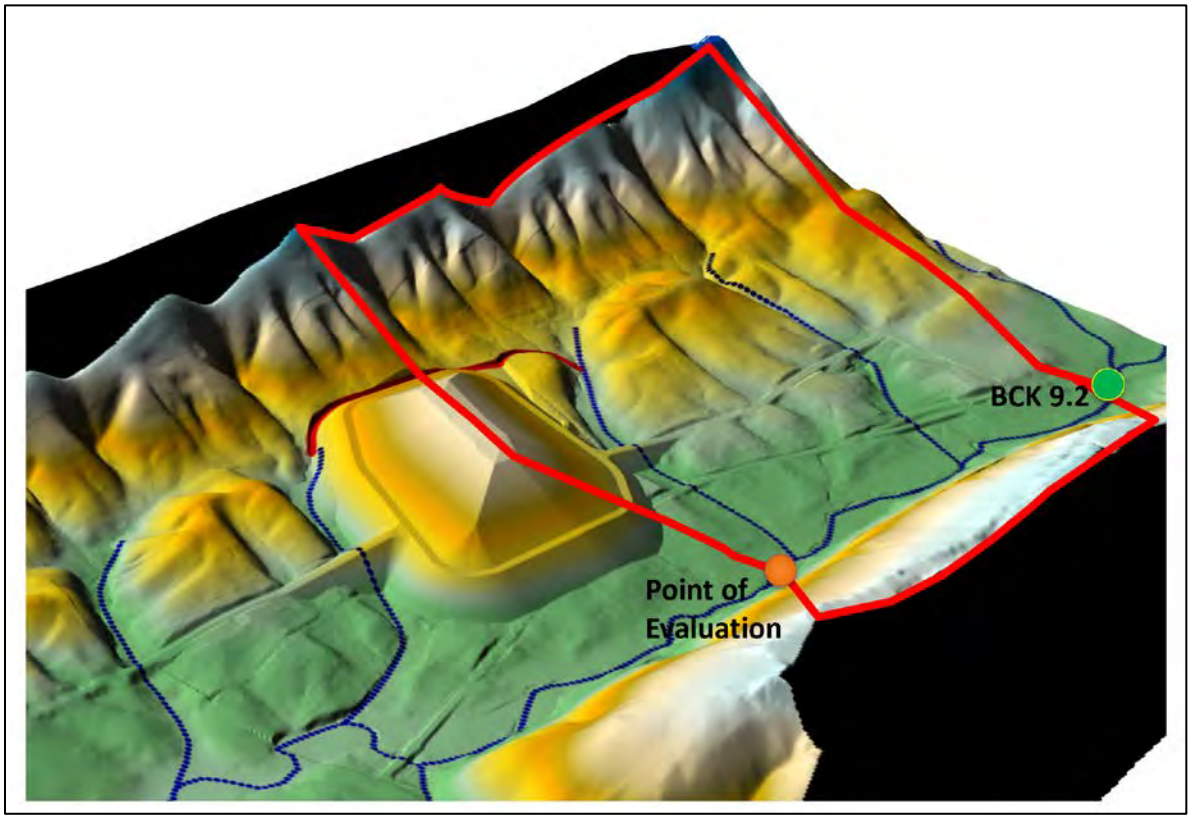

Fig. C.10. Area contributing to Bear Creek between BCK 9.2 and the point of surface water impact.

Because there is no long-term surface water monitoring station on Bear Creek near the point of leachate seepage impact, the surface water flow resulting from storm runoff and groundwater discharge for the additional contributing area is calculated from estimates of precipitation and evapotranspiration (i.e., water

balance approach). The additional contributing area is 1.08E+07 sq ft. The annual precipitation for the EMDF area is approximately 54 in./year. Based on the estimation of evapotranspiration as a function of climate and land cover for the conterminous United States (Sanford and Selnick 2013), the estimated fraction of precipitation lost to evapotranspiration for the EMDF area is approximately 0.50 (Fig. C.11). For the grass-covered landfill area, the HELP model (Sect. C.2) predicted a long-term 0.56 ratio of evapotranspiration to precipitation. Therefore, 50 percent of the annual precipitation volume from the contributing area was assumed to add to the flow measurement at BCK 9.2. The additional surface water from the precipitation is calculated to be 346 gpm. Thus, the total flow rate at the Bear Creek impact point is estimated as 1447 gpm.

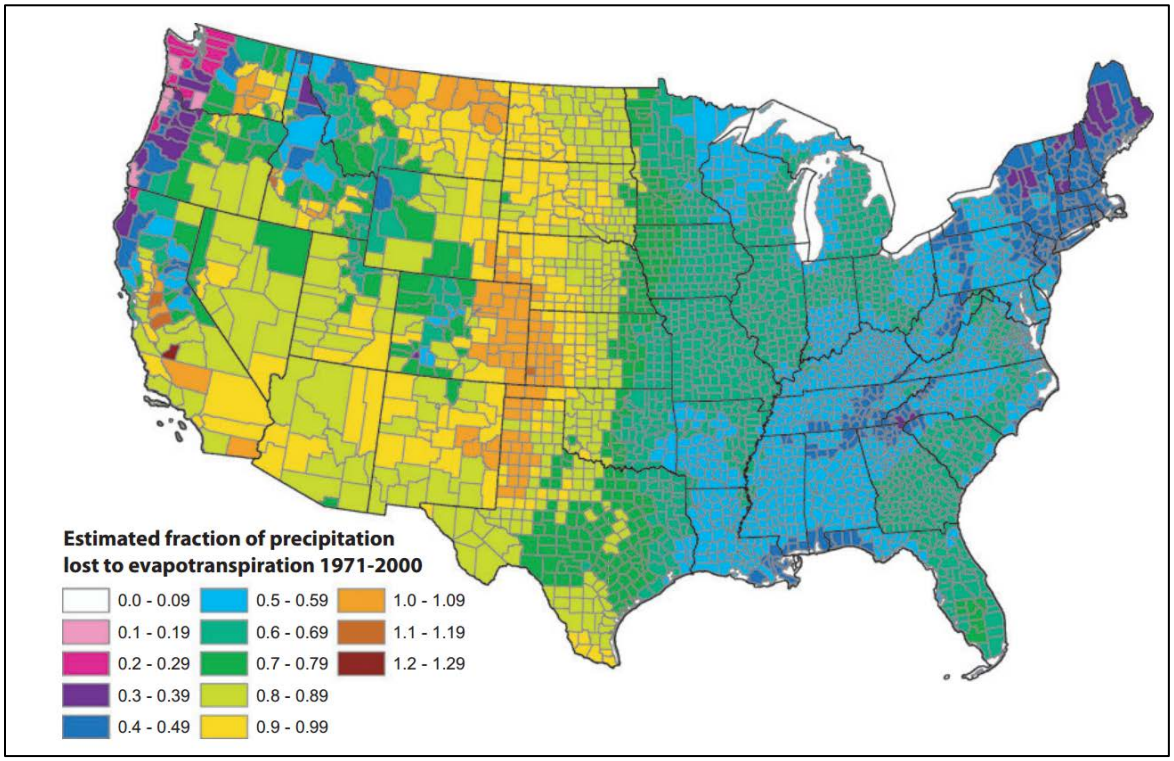

Source: Sanford and Selnick 2013.

Fig. C.11. Evapotranspiration-precipitation relationship

The resulting mixing ratio (Bear Creek flow divided by leachate seepage flux) at the surface water impact location is 9767 for the cover infiltration rate at the earliest time (310 years) for the onset of seepage. As cover infiltration (and leachate seepage) increases toward the long-term performance condition (0.88 in./year or 1.08 gpm after 1000 years), the mixing ratio drops to 1343 (Fig. C.12).

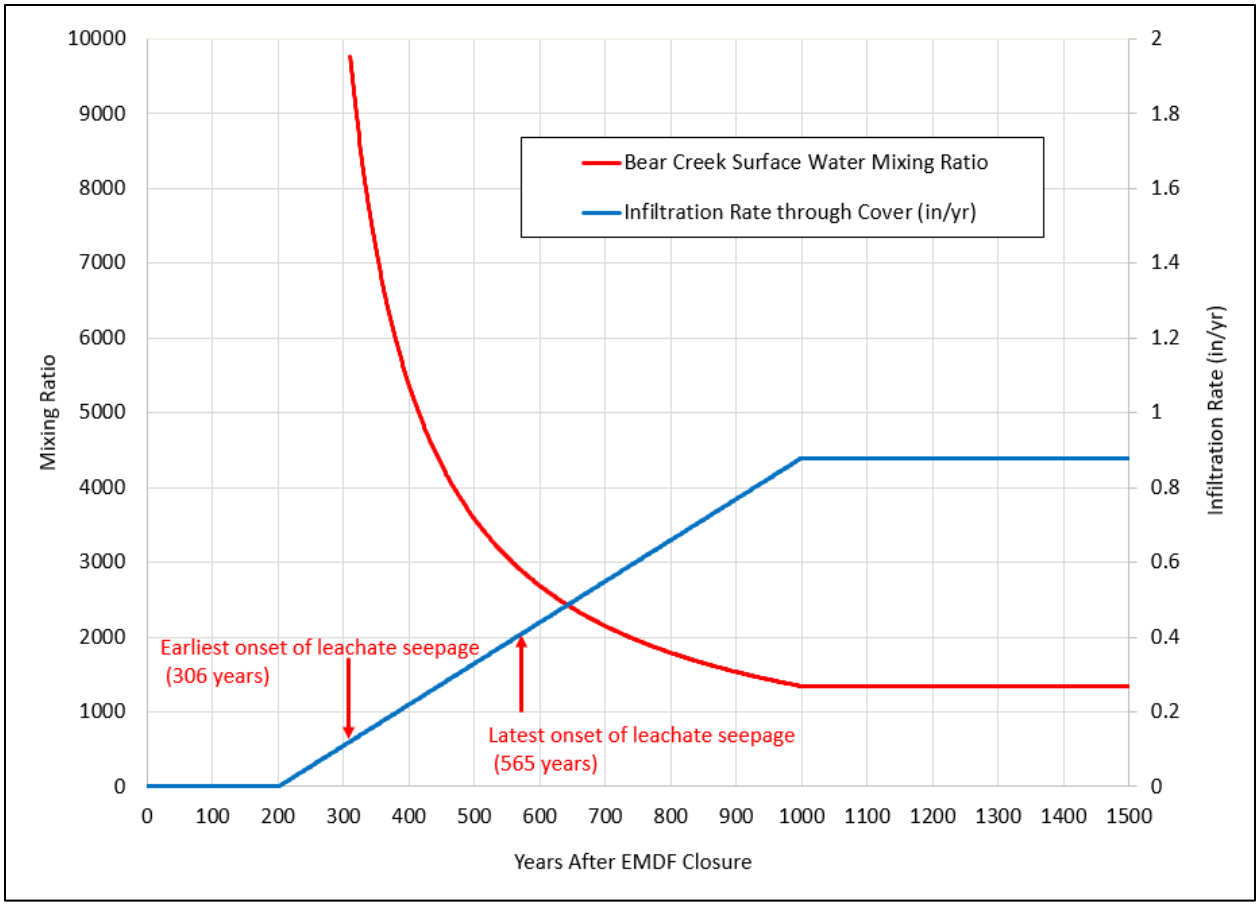

Fig. C.12. Surface water mixing ratio

C.3.5 BATHTUB IMPACTS ON SURFACE WATER CONCENTRATIONS

The leachate concentrations for each radionuclide in the estimated inventory are calculated for the waste zone. The total source concentration (C) is a combined solute mass absorbed on soil (C_S) and dissolved in the aqueous phase (C_L) based on linear partitioning of solutes between the porous media and aqueous phase:

$$C = C_L \times \text{porosity} \times \text{aqueous initial saturation} + C_S \times (1 - \text{porosity})$$

where:

C_L = C_S / (K_d × particle density)

K_d = solid-aqueous phase partition coefficient for each radionuclide.

Therefore, the initial source aqueous concentration of each solute at the source in the model simulation is dependent on the source K_d values.

It should be noted that the mass of radionuclides in waste placed in EMDF would be subjected to processes that may result in reduction over time, including the following:

- Mass reduction due to decay
- Mass removed during cell operations by collection and removal of contact water and by the leachate collection system
- Mass removed by leachate collection system during the active cell maintenance period (assumed to be 100 years) after EMDF closure.

Based on the initial radionuclide inventory presented in Sect. 2.3 and Appendix B of the EMDF PA, the initial leachate concentrations within the source zone were calculated. A particle density of 3.27 g/cm^3, 0.419 porosity, and radionuclide-specific K_d values for the waste zone (refer to Sect. 3.2.2.6 of the PA) were used for the calculation. An initial relative saturation of 1.0 also was assumed for the waste zone since the waste will be saturated at the point of seepage. Applying the radionuclide half-life, the leachate concentration at the earliest (310 years post-closure) and latest (575 years) times for the onset of seepage was calculated based on radionuclide half-life. Leachate concentration was also calculated for the end of the DOE Order 435.1 compliance period (i.e., 1000 years post-closure). No credit is taken for removal of highly mobile radionuclides (e.g., C-14) by leachate collection and treatment operations during the 100 years of post-closure institutional control. The resulting surface water concentrations at Bear Creek for the radionuclides then were calculated based on estimated mixing ratios (Fig. C.12) for 310, 575, and 1000 years post-closure.

Table C.5 provides a summary of the calculation results. Several very short-lived (half-life < 10 years) radionuclides with small source concentrations (e.g., Cf-252) will decay significantly before the leachate seepage is likely to occur. Most of the remaining radionuclides will have very low estimated leachate concentrations. The estimated surface water concentrations for the bathtub scenario may be compared to applicable water quality criteria (such as DOE Derived Concentration Standards [DOE 2011b]) or to predicted surface water concentrations for the EMDF base case performance scenario (i.e., leachate release through the liner system to groundwater). Those surface water concentrations are presented in Sect. 4.7.2 of the EMDF PA Report.

C.3.6 BATHTUB IMPACTS ON GROUNDWATER CONCENTRATIONS

An alternative exposure scenario was evaluated in which the leachate seepage would infiltrate into the groundwater along its flow path before discharge into the surface water body and a future resident would consume the groundwater from a well constructed outside of the berm. Rather than assuming that the entire flux of leachate seepage is transmitted along near surface pathways to surface water, this scenario assumes that a portion of the leachate flux enters the groundwater downslope of the seepage location at the edge of the EMDF cover. The groundwater flow direction for the site is mostly southwestward which is oblique to the leachate drainage path.

For groundwater impact under a bathtub scenario, it is assumed that the leachate is released along a 200-ft-wide section of the edge of the EMDF cover (Fig. C.13) centered on the likely seepage point identified for the surface water impact described in Sect. C.3.5 (refer to Fig. C.9). This assumption is reasonable in that the seepage failure would probably occur over an extended portion of the EMDF cover-liner system interface rather than at a single point of lowest elevation. The elevation of the liner edge along the assumed seepage release zone is close to the 930 ft elevation minimum over the 200 ft width.

Table C.5. Bathtub scenario calculated leachate and surface water concentrations

Nuclide	Source (As-Disposed) Concentration (pCi/g)	Waste K_d (cm^3/g)	Half-Life (year)	Source Leachate Concentration (pCi/L) at T=0	Source Leachate Concentration (pCi/L) at T=310 year	Source Leachate Concentration (pCi/L) at T=575 year	Source Leachate Concentration (pCi/L) at T=1000 year	BC SW Concentration (pCi/L) at T=310 year	BC SW Concentration (pCi/L) at T=575 year	BC SW Concentration (pCi/L) at T=1000 year
Ac-227	2.92E-03	20	2.18E+01	1.44E-01	7.47E-06	< 1.0E-06[a]	< 1.0E-06[a]	< 1.0E-06[a]	< 1.0E-06[a]	< 1.0E-06[a]
Am-241	5.90E+01	2000	4.32E+02	2.95E+01	1.79E+01	1.17E+01	5.93E+00	1.85E-03	4.16E-03	4.42E-03
Am-243	2.97E+00	2000	7.38E+03	1.48E+00	1.44E+00	1.41E+00	1.35E+00	1.48E-04	4.91E-04	1.01E-03
Ba-133	1.60E+00	28	1.05E+01	5.67E+01	< 1.0E-06[a]	< 1.0E-06[a]	< 1.0E-06[a]	< 1.0E-06[a]	< 1.0E-06[a]	< 1.0E-06[a]
Be-10	2.53E-05	400	1.51E+06	6.32E-05	6.32E-05	6.32E-05	6.32E-05	< 1.0E-06[a]	< 1.0E-06[a]	< 1.0E-06[a]
C-14	5.40E-01	0	5.73E+03	2.45E+03	2.36E+03	2.28E+03	2.17E+03	2.42E-01	7.98E-01	1.62E+00
Ca-41	4.21E-02	15	1.02E+05	2.77E+00	2.76E+00	2.76E+00	2.75E+00	2.83E-04	9.62E-04	2.05E-03
Cf-249	1.09E-06	20	3.51E+02	5.39E-05	2.92E-05	1.73E-05	7.46E-06	< 1.0E-06[a]	< 1.0E-06[a]	< 1.0E-06[a]
Cf-250	7.40E-06	20	1.31E+01	3.66E-04	< 1.0E-06[a]	< 1.0E-06[a]	< 1.0E-06[a]	< 1.0E-06[a]	< 1.0E-06[a]	< 1.0E-06[a]
Cf-251	2.10E-07	20	8.98E+02	1.04E-05	8.18E-06	6.66E-06	4.80E-06	< 1.0E-06[a]	< 1.0E-06[a]	< 1.0E-06[a]
Cf-252	1.31E-07	20	2.60E+00	6.48E-06	< 1.0E-06[a]	< 1.0E-06[a]	< 1.0E-06[a]	< 1.0E-06[a]	< 1.0E-06[a]	< 1.0E-06[a]
Cm-243	4.30E-01	20	2.85E+01	2.13E+01	1.13E-02	1.80E-05	< 1.0E-06[a]	1.28E-06	< 1.0E-06[a]	< 1.0E-06[a]
Cm-244	1.26E+02	20	1.81E+01	6.23E+03	4.38E-02	1.72E-06	< 1.0E-06[a]	5.23E-06	< 1.0E-06[a]	< 1.0E-06[a]
Cm-245	3.83E-02	20	8.50E+03	1.89E+00	1.85E+00	1.81E+00	1.75E+00	1.89E-04	6.31E-04	1.30E-03
Cm-246	1.59E-01	20	4.73E+03	7.86E+00	7.51E+00	7.23E+00	6.79E+00	7.70E-04	2.53E-03	5.06E-03
Cm-247	1.04E-02	20	1.56E+07	5.14E-01	5.14E-01	5.14E-01	5.14E-01	5.27E-05	1.80E-04	3.83E-04
Cm-248	5.59E-04	20	3.39E+05	2.76E-02	2.76E-02	2.76E-02	2.76E-02	2.83E-06	9.64E-06	2.05E-05
Co-60	2.00E-02	400	5.27E+00	5.00E-02	< 1.0E-06[a]	< 1.0E-06[a]	< 1.0E-06[a]	< 1.0E-06[a]	< 1.0E-06[a]	< 1.0E-06[a]
Cs-134	1.06E-08	1500	2.10E+00	< 1.0E-06[a]	< 1.0E-06[a]	< 1.0E-06[a]	< 1.0E-06[a]	< 1.0E-06[a]	< 1.0E-06[a]	< 1.0E-06[a]
Cs-137	1.18E+03	1500	3.00E+01	7.87E+02	6.10E-01	1.34E-03	< 1.0E-06[a]	6.85E-05	< 1.0E-06[a]	< 1.0E-06[a]
Eu-152	2.87E+01	20	1.33E+01	1.42E+03	1.42E-04	< 1.0E-06[a]	< 1.0E-06[a]	< 1.0E-06[a]	< 1.0E-06[a]	< 1.0E-06[a]
Eu-154	6.49E+00	20	8.80E+00	3.21E+02	< 1.0E-06[a]	< 1.0E-06[a]	< 1.0E-06[a]	< 1.0E-06[a]	< 1.0E-06[a]	< 1.0E-06[a]
Eu-155	6.74E-03	20	4.80E+00	3.33E-01	< 1.0E-06[a]	< 1.0E-06[a]	< 1.0E-06[a]	< 1.0E-06[a]	< 1.0E-06[a]	< 1.0E-06[a]
Fe-55	8.95E-07	450	2.70E+00	1.99E-06	< 1.0E-06[a]	< 1.0E-06[a]	< 1.0E-06[a]	< 1.0E-06[a]	< 1.0E-06[a]	< 1.0E-06[a]
H-3	4.64E+00	0	1.24E+01	2.10E+04	5.85E-04	< 1.0E-06[a]	< 1.0E-06[a]	< 1.0E-06[a]	< 1.0E-06[a]	< 1.0E-06[a]
I-129	3.50E-01	2	1.57E+07	1.58E+02	1.58E+02	1.58E+02	1.58E+02	1.61E-02	5.50E-02	1.17E-01
K-40	3.28E+00	15	1.28E+09	2.15E+02	2.15E+02	2.15E+02	2.15E+02	2.21E-02	7.52E-02	1.60E-01
Mo-100	4.20E-06	45	8.50E+18	9.29E-05	9.29E-05	9.29E-05	9.29E-05	< 1.0E-06[a]	< 1.0E-06[a]	< 1.0E-06[a]
Mo-93	3.88E-01	45	4.00E+03	8.58E+00	8.13E+00	7.77E+00	7.22E+00	8.33E-04	2.72E-03	5.37E-03
Na-22	8.22E-07	5	2.60E+00	1.57E-04	< 1.0E-06[a]	< 1.0E-06[a]	< 1.0E-06[a]	< 1.0E-06[a]	< 1.0E-06[a]	< 1.0E-06[a]
Nb-93m	2.33E-01	50	1.61E+01	4.64E+00	7.60E-06	< 1.0E-06[a]	< 1.0E-06[a]	< 1.0E-06[a]	< 1.0E-06[a]	< 1.0E-06[a]
Nb-94	1.63E-02	50	2.03E+04	3.25E-01	3.21E-01	3.18E-01	3.14E-01	3.29E-05	1.11E-04	2.34E-04

Table C.5. Bathtub scenario calculated leachate and surface water concentrations (cont.)

Nuclide	Source (As-Disposed) Concentration (pCi/g)	Waste K_d (cm^3/g)	Half-Life (year)	Source Leachate Concentration (pCi/L) at T=0	Source Leachate Concentration (pCi/L) at T=310 year	Source Leachate Concentration (pCi/L) at T=575 year	Source Leachate Concentration (pCi/L) at T=1000 year	BC SW Concentration (pCi/L) at T=310 year	BC SW Concentration (pCi/L) at T=575 year	BC SW Concentration (pCi/L) at T=1000 year
Ni-59	3.04E+00	1000	7.50E+04	3.04E+00	3.03E+00	3.02E+00	3.01E+00	3.10E-04	1.06E-03	2.24E-03
Ni-63	6.73E+02	1000	9.60E+01	6.73E+02	7.18E+01	1.06E+01	4.92E-01	7.56E-03	3.97E-03	3.67E-04
Np-237	3.25E-01	20	2.14E+06	1.61E+01	1.61E+01	1.61E+01	1.61E+01	1.65E-03	5.61E-03	1.20E-02
Pa-231	2.39E-01	200	3.28E+04	1.19E+00	1.19E+00	1.18E+00	1.17E+00	1.21E-04	4.12E-04	8.70E-04
Pb-210	3.68E+00	50	2.23E+01	7.33E+01	4.79E-03	1.27E-06	< 1.0E-06[a]	< 1.0E-06[a]	< 1.0E-06[a]	< 1.0E-06[a]
Pm-146	8.84E-05	410	5.50E+00	2.15E-04	< 1.0E-06[a]	< 1.0E-06[a]	< 1.0E-06[a]	< 1.0E-06[a]	< 1.0E-06[a]	< 1.0E-06[a]
Pm-147	2.20E-04	410	2.60E+00	5.36E-04	< 1.0E-06[a]	< 1.0E-06[a]	< 1.0E-06[a]	< 1.0E-06[a]	< 1.0E-06[a]	< 1.0E-06[a]
Pu-238	9.38E+01	20	8.77E+01	4.64E+03	4.01E+02	4.94E+01	1.72E+00	4.23E-02	1.87E-02	1.28E-03
Pu-239	5.83E+01	20	2.41E+04	2.88E+03	2.86E+03	2.84E+03	2.80E+03	2.93E-01	9.90E-01	2.09E+00
Pu-240	6.20E+01	20	6.54E+03	3.07E+03	2.97E+03	2.88E+03	2.76E+03	3.04E-01	1.01E+00	2.05E+00
Pu-241	2.04E+02	20	1.44E+01	1.01E+04	3.34E-03	< 1.0E-06[a]	< 1.0E-06[a]	< 1.0E-06[a]	< 1.0E-06[a]	< 1.0E-06[a]
Pu-242	1.73E-01	20	3.76E+05	8.56E+00	8.55E+00	8.55E+00	8.54E+00	8.75E-04	2.98E-03	6.36E-03
Pu-244	3.68E-03	20	8.26E+07	1.82E-01	1.82E-01	1.82E-01	1.82E-01	1.86E-05	6.35E-05	1.36E-04
Ra-226	8.01E-01	1500	1.60E+03	5.34E-01	4.67E-01	4.16E-01	3.46E-01	4.79E-05	1.46E-04	2.58E-04
Ra-228	2.21E-02	1500	5.75E+00	1.47E-02	< 1.0E-06[a]	< 1.0E-06[a]	< 1.0E-06[a]	< 1.0E-06[a]	< 1.0E-06[a]	< 1.0E-06[a]
Re-187	1.71E-06	20	4.12E+10	8.46E-05	8.46E-05	8.46E-05	8.46E-05	< 1.0E-06[a]	< 1.0E-06[a]	< 1.0E-06[a]
Sb-125	3.03E-08	75	2.80E+00	< 1.0E-06[a]	< 1.0E-06[a]	< 1.0E-06[a]	< 1.0E-06[a]	< 1.0E-06[a]	< 1.0E-06[a]	< 1.0E-06[a]
Sr-90	1.92E+02	15	2.91E+01	1.26E+04	7.87E+00	1.43E-02	< 1.0E-06[a]	8.87E-04	6.35E-06	< 1.0E-06[a]
Tc-99	1.56E+00	0.36	2.13E+05	2.69E+03	2.68E+03	2.68E+03	2.68E+03	2.75E-01	9.36E-01	1.99E+00
Th-228	2.11E-06	1500	1.90E+00	1.41E-06	< 1.0E-06[a]	< 1.0E-06[a]	< 1.0E-06[a]	< 1.0E-06[a]	< 1.0E-06[a]	< 1.0E-06[a]
Th-229	5.71E+00	1500	7.34E+03	3.81E+00	3.70E+00	3.60E+00	3.46E+00	3.79E-04	1.26E-03	2.58E-03
Th-230	1.92E+00	1500	7.70E+04	1.28E+00	1.28E+00	1.27E+00	1.27E+00	1.31E-04	4.44E-04	9.44E-04
Th-232	3.52E+00	1500	1.41E+10	2.35E+00	2.35E+00	2.35E+00	2.35E+00	2.40E-04	8.19E-04	1.75E-03
U-232	1.02E+01	25	7.20E+01	4.04E+02	2.05E+01	1.60E+00	2.67E-02	2.18E-03	6.13E-04	1.99E-05
U-233	4.16E+01	25	1.59E+05	1.65E+03	1.65E+03	1.65E+03	1.64E+03	1.69E-01	5.74E-01	1.22E+00
U-234	6.30E+02	25	2.45E+05	2.50E+04	2.50E+04	2.49E+04	2.49E+04	2.56E+00	8.70E+00	1.85E+01
U-235	3.97E+01	25	7.04E+08	1.57E+03	1.57E+03	1.57E+03	1.57E+03	1.61E-01	5.49E-01	1.17E+00
U-236	8.98E+00	25	2.34E+07	3.56E+02	3.56E+02	3.56E+02	3.56E+02	3.65E-02	1.24E-01	2.65E-01
U-238	3.81E+02	25	4.47E+09	1.51E+04	1.51E+04	1.51E+04	1.51E+04	1.55E+00	5.27E+00	1.12E+01

[a]Calculated activity concentrations are less than 1.0E-06 pCi/

BC = Bear Creek SW = surface water

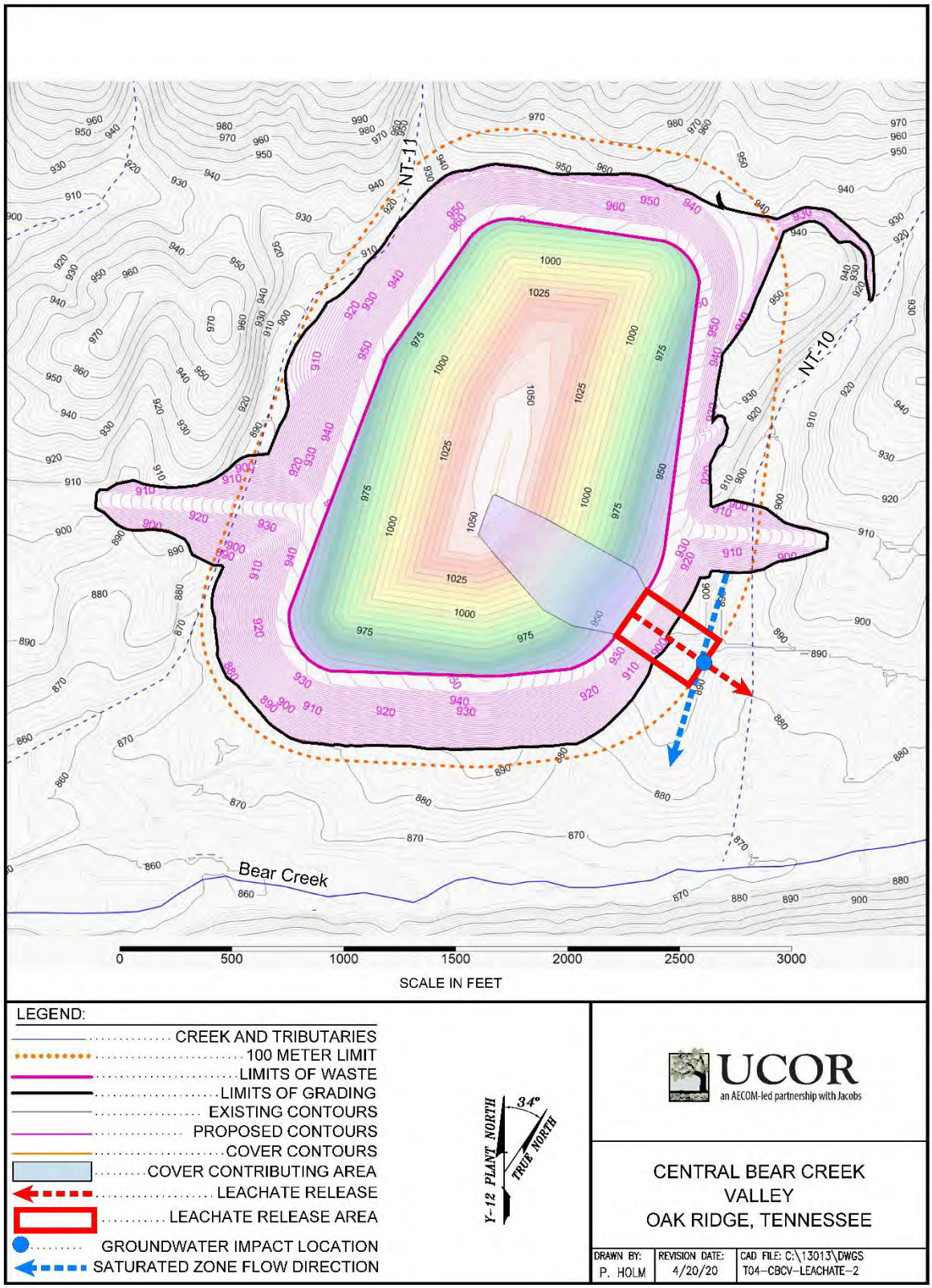

Fig. C.13. EMDF cover topography and assumed groundwater impact area associated with a bathtub scenario

For estimating impact to groundwater, it is assumed that a portion of the leachate released is mixed with storm runoff from the cover surface upslope of the release zone and transported quickly via surface and shallow subsurface flow down the berm and across the ground to the 100-m buffer zone limit (i.e., 100 m from the edge of waste). The remainder of the leachate and storm runoff that percolates to the saturated zone along the release pathway is uniformly mixed with groundwater that flows to the southwest toward Bear Creek (Fig. C.13). The direction of groundwater flow is oblique to the assumed direction of mixed leachate and storm runoff.

To simplify the analysis, the net impact of the leachate mixing with surface runoff, transport of leachate along rapid stormflow pathways to surface water features, and leachate percolation and mixing with groundwater is represented approximately with a generalized mixing model. This conceptual mixing model accounts for the relative volumes of leachate flux, stormwater runoff, and groundwater flux in determining radionuclides in groundwater along the release pathway.

The leachate flux will increase over time to a steady state rate as described in Sect. C.3.3. Leachate will be mixed with storm runoff from the cover and precipitation falling on the berm and the ground surface along the 200 ft wide release pathway, which extends 328 ft (100 m) beyond the edge of the waste. Rather than estimate the fraction of radionuclide mass flux that bypasses the deeper saturated zone and is discharged to surface water, the average concentration of mixed leachate and stormflow that enters the saturated zone is approximated with a mixing ratio based on annual precipitation, the contributing area of the cover and release pathway area, and the leachate volume flux rate. The precipitation rate applied over the total cover and release area is the volume flux of uncontaminated water in the numerator of the mixing ratio, approximating the net impact of radionuclide loss to surface water and dilution by precipitation and runoff.

The contributing area of the cover upslope of the seepage zone was estimated from the EMDF conceptual design for the final cover surface (Fig. C.13). This area (121,800 sq ft) is added to the area of the perimeter berm and ground surface within the release pathway (200 ft × 328 ft = 65,600 sq ft) and multiplied by the average annual total precipitation (54.3 in.) assumed for the cover system analysis (refer to Sect. C.2.3). The resulting total input rate of uncontaminated water is 12.1 gpm.

To approximate mixing of percolating leachate groundwater, the groundwater flux is estimated across a vertical plane extending from the toe of the perimeter berm to the 100 m buffer limit, a distance of about 150 ft near the leachate release area. The mixed leachate and uncontaminated surface water entering the saturated zone is assumed to be uniformly mixed with the estimated groundwater flux across this vertical plane extending 131 ft below the water table. This vertical depth corresponds to the assumed groundwater well intake interval (40 m) assumed for the EMDF performance analysis for release through the liner system. The total groundwater flux (Q) through the plane can be calculated with groundwater flow equation below:

$$Q = \text{width} \times \text{depth} \times K \times HG$$

where:

width = saturated zone width, equal to the length of the leachate release pathway along which infiltration occurs (150 ft)

depth = saturated zone depth (131 ft), equal to the groundwater withdrawal interval (40 m)

K = aquifer hydraulic conductivity (2.65E-04 cm/sec), representative of the saprolite zone

HG = hydraulic gradient (0.036 ft/ft), based on the EMDF saturated zone flow model for the long-term performance condition (Appendix D, Sect. D.5.2).

Using the values above, the groundwater flux beneath the leachate release area would be 2.76 gpm.

The estimated average groundwater radionuclide concentration at 100 m resulting from the bathtub scenario is based on a mixing ratio that combines the mixing of leachate with storm runoff and groundwater. The numerator of the mixing ratio is the sum of the precipitation and surface runoff (12.1 gpm) and the groundwater flux (2.76 gpm), or 14.86 gpm. The denominator of the mixing ratio is the leachate seepage rate, which is a function of time during the period over which cover infiltration and waste saturation are increasing. The change in the groundwater mixing ratio with time parallels the decrease in the surface water impact mixing ratio in Fig. C.12, decreasing from 99 at 310 years to 14 at 1000 years post-closure.

The estimated precipitation/storm runoff and groundwater mixing rate at 1000 years would result in radionuclide concentrations in the well approximately 96 times higher than the surface water concentrations associated with the bathtub scenario at that time.

C.4 RUSLE2 MODEL EVALUATION OF COVER SURFACE EROSION

C.4.1 INTRODUCTION

A cover erosion calculation was performed for the proposed EMDF using the RUSLE2 program. The RUSLE2 application was developed cooperatively by the USDA Agricultural Research Service, the USDA-NRCS, and the Biosystems Engineering and Environmental Science Department of the University of Tennessee (USDA 2013).

RUSLE2 is a mathematical model that uses a system of equations implemented in a computer program to estimate erosion rates. The other major component of RUSLE2 is a database containing an extensive array of values that are used by the RUSLE2 user to describe a site-specific condition so that RUSLE2 can compute erosion values that directly reflect conditions at a particular site. The RUSLE2 program is in the public domain and can be downloaded from the USDA website.

The RUSLE2 estimates soil loss, sediment yield, and sediment characteristics from rill and interrill (sheet) erosion caused by rainfall and its associated overland flow. RUSLE2 uses factors that represent the effects of climate (erosivity, precipitation, and temperature), soil erodibility, topography, cover management, and support practices to compute erosion.

RUSLE2 is used to evaluate potential erosion rates at a specific site, guide conservation and erosion control planning, inventory erosion rates over large geographic areas, and estimate sediment production on upland areas that might become sediment yield in watersheds. RUSLE2 is land use independent; therefore, it can be used on cropland, pastureland, rangeland, disturbed forestland, construction sites, mined land, reclaimed land, landfills, military lands, and other areas where mineral soil is exposed to raindrop impact and surface overland flow produced by rainfall intensity exceeding infiltration rate (i.e., Hortonian overland flow).

The surface layer characteristics and geometry of the cover design of the proposed EMDF and area-specific meteorological parameters were used. During the model application, various sensitivity runs were conducted to estimate the impact of uncertainty in assigning input parameter values.

Section 9 of the PA Report details the QA activities and documentation that apply to the RUSLE2 erosion modeling.

C.4.2 RUSLE2 MODEL CODE AND PARAMETERS

The RUSLE2 program and supporting documents were downloaded from the http://fargo.nserl.purdue.edu/rusle2_dataweb/RUSLE2_Index.htm website. The software version used for this analysis is the official NRCS RUSLE2 version 2.5.2.11 with a build date of August 18, 2014. The soil, climate, and cover management databases were downloaded and installed.

The program was verified by conducting a program run following the example problem as documented in the RUSLE2 user's guide (USDA 2004). Details of this verification and application testing are provided in the EMDF data and calculation package for RUSLE2 erosion modeling (refer to Sect. 8 of the EMDF QA Report for Modeling [UCOR 2020]).

Section 9 of the PA Report details the QA activities and documentation for the RUSLE2 model.

The key model parameters for the RUSLE2 modeling analysis include the listed categories that are either location-specific or design based:

- Climate – The most important climatic variable used by RUSLE2 is rainfall erosivity, which is related to rainfall amount (how much it rains) and intensity (how hard it rains). Another important climatic variable is temperature because temperature and precipitation together determine the longevity of biological materials like crop residue and applied mulch used to control erosion. Climate varies by location and choosing a location in RUSLE2 chooses the erosivity, precipitation, and temperature values needed to apply RUSLE2 at a particular site.
- Soils – Soils vary in their inherent erodibility. RUSLE2 includes a procedure for estimating soil erodibility for highly disturbed soils at construction sites and reclaimed mined land.
- Topography – Slope length, steepness, and shape are the topographic characteristics that most affect rill and interrill erosion. Site-specific values are entered for these variables.
- Land Use – Land use is the single most important factor affecting rill and interrill erosion because type of land use and land use condition are features that can be most easily changed to reduce excessive erosion.
- Cover management practices affect both the forces applied to the soil by erosive agents and the susceptibility of the soil to detachment.
- Support practices include ridging (e.g., contouring), vegetative strips and barriers (e.g., buffer strips, strip cropping, fabric fence, gravel bags), runoff interceptors (e.g., terraces, diversions), and small impoundments (e.g., sediment basins, impoundment terraces). These practices reduce erosion primarily by reducing the erosivity of surface runoff and by causing deposition. Site-specific information, such as the location of a diversion on the hillslope, is entered as required for each practice.

The proposed EMDF surface layer properties were used to define the soil and design geometry used to set the slope in the RUSLE2 model analysis.

The erosion control layer at the top of the cover was the only EMDF cover layer modeled in the RUSLE2 application. Based on the conceptual design, the cover surface layer is a 4-ft-thick vegetated soil/rock matrix comprised of a mixture of crushed rock and native soil that protects the underlying cover layers and provides a stable soil for growth of cover vegetation. This type of material specification is most similar to the gravelly loam material types as defined in the RUSLE2 model. The most appropriate RUSLE2 soil type was determined to be a gravelly silt-clay loam with coarse material between 15 and 60 percent. Based on this

soil-type designation and the site-specific (Anderson County) soil and climate data from the RUSLE2 database, the code package selects appropriate soil erosion model parameter values.

The plan view of the proposed EMDF cover conceptual design is shown on Fig. C.14 along with the locations of two cross-sections of the conceptual design that are shown on Fig. C.15. The cover has a flatter top with a 2 to 5 percent grade and is surrounded by sideslopes with maximum slope ratio of 4 to 1 (25 percent). The sideslope horizontal length ranges from 250 to 460 ft, not including the flatter top portion. The calculated weighted-average slope for the entire cover is 21.52 percent, with a mean slope length (including the flatter top) of 476.9 ft.

The largest values for slope (25 percent uniform slope with no slope breaks) and slope length (476.9 ft) were adopted for the cover erosion evaluation as the base case. Sensitivity runs were conducted for various alternative (lower) values of slope and slope length, as well as for alternative assumptions for soil type and ground cover (vegetation).

Other applicable parameters, including soil, climate, and cover management databases also were downloaded from the RUSLE2 website. The complete soil data, location-specific climate, and predicted cover management information for Anderson County, Tennessee were applied in this modeling analysis.

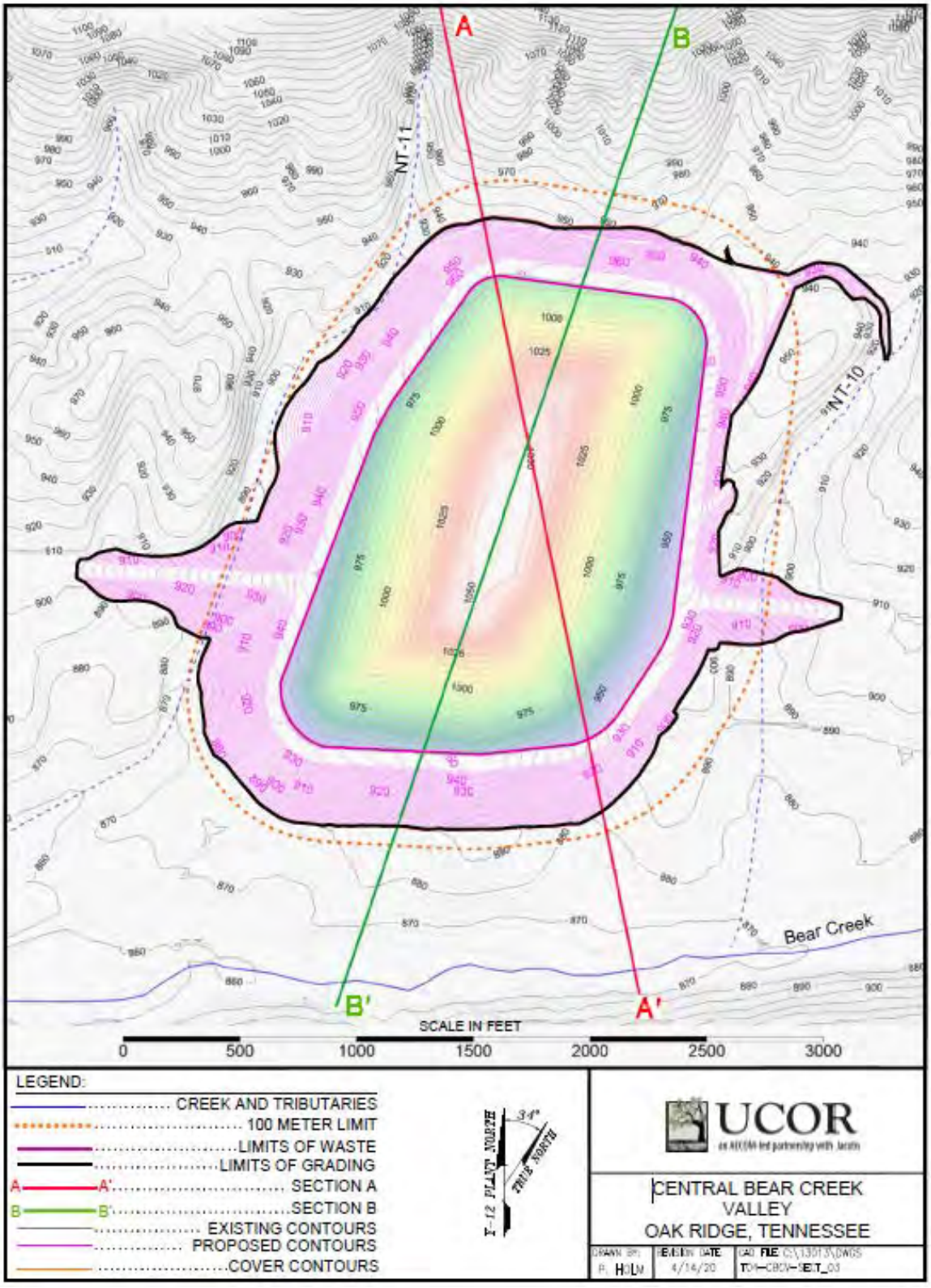

Fig. C.14. EMDF surface contours (ft above mean sea level)

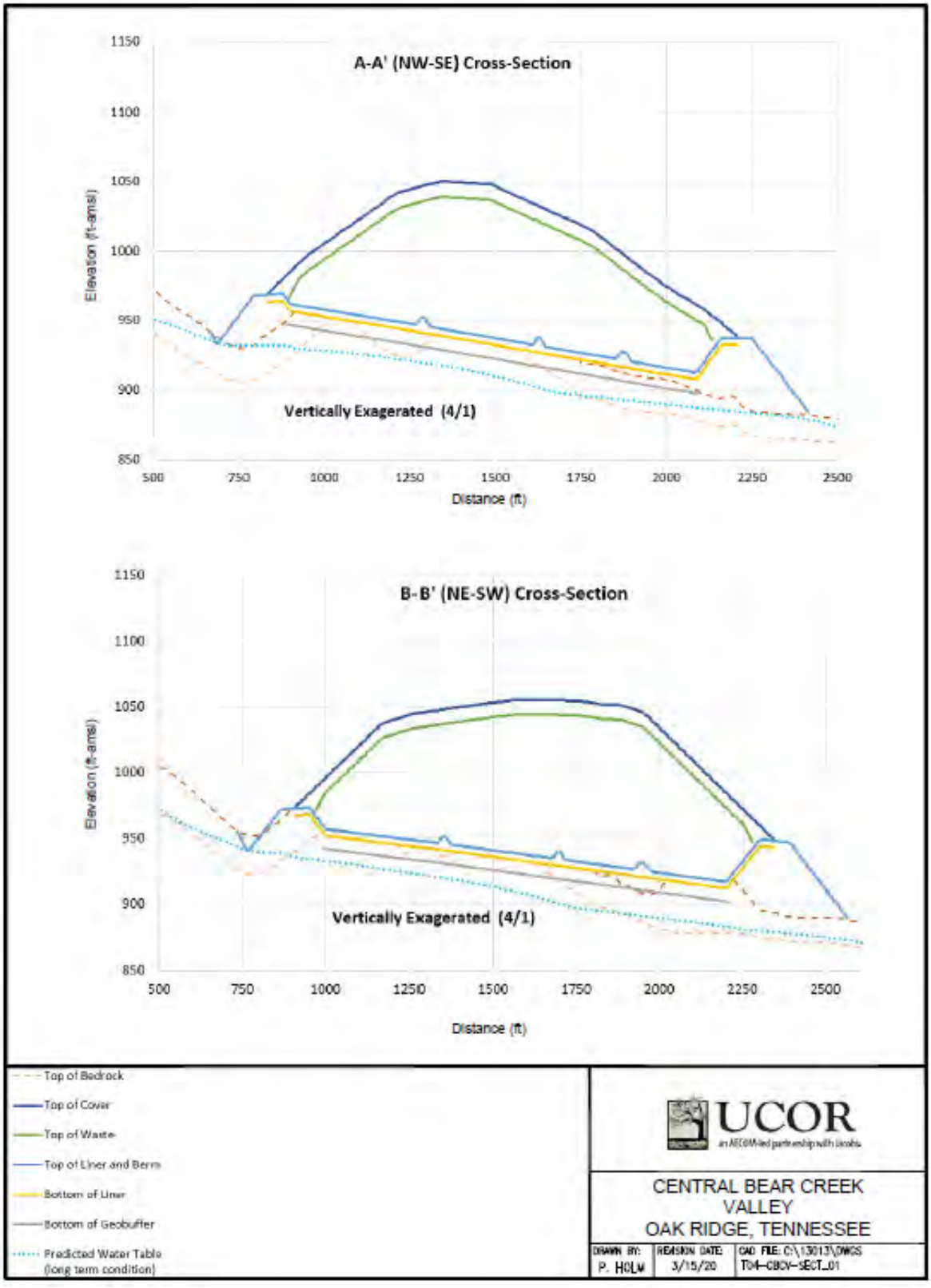

Fig. C.15. EMDF cross-sections with typical cover sideslopes

C.4.3 EMDF COVER EROSION MODELING CALCULATION

The RUSLE2 potential erodibility profile module was used to conduct the erosion calculation for the proposed EMDF. The module uses soil, topography, and cover management databases to calculate the soil loss under applicable local specific climate conditions.

As described in Sect. C.4.2, the following parameter selections were applied for the base case model application:

- Climate – Anderson County, Tennessee
- Soil – gravelly silt clay loam with coarse fragment content between 15 to 60 percent
- Cover management – Bermuda grass cover
- Topography – 25 percent slope with slope horizontal length of 480 ft (10 ft precision limit of RUSLE2 model to represent site-specific 476.9 ft)

Using these parameters, a soil loss of 0.42 tons/acre/year was predicted by the RUSLE2 model. The screen capture of the model key input parameters and result is shown on Fig. C.16.

To calculate a surface erosion rate based on predicted soil loss, an assumption for the soil bulk density is needed. Bulk density is dependent on soil texture and the densities of soil mineral (sand, silt, and clay) and organic matter particles as well as their packing arrangement. The RUSLE2 model uses a particle density of 2.65 g/cm^3 for the sand and silt and 2.60 for g/cm^3 for the clay in its erosion mass calculation (USDA 2013). Using the porosity of 0.464 for the cover erosion control layer in the HELP model, a soil bulk density of 1.42 g/cm^3 is calculated for the cover erosion control layer using a particle density of 2.65 g/cm^3.

The bulk density value was used to calculate the erosion rate. Based on the 0.42 tons/acre/year soil loss, a corresponding average erosion rate of 2.2E-04 ft/year was calculated. Assuming the soil loss is uniformly distributed over the slope surface, this erosion rate will result in an average decrease of 2.6 in. in the thickness of the cover soil over the first 1000 years after facility closure. Non-uniform application of the model predicted soil loss to only half of the total slope surface would result in an average erosion depth of $2 \times 2.6 = 5.2$ in. over a period of 1000 years.

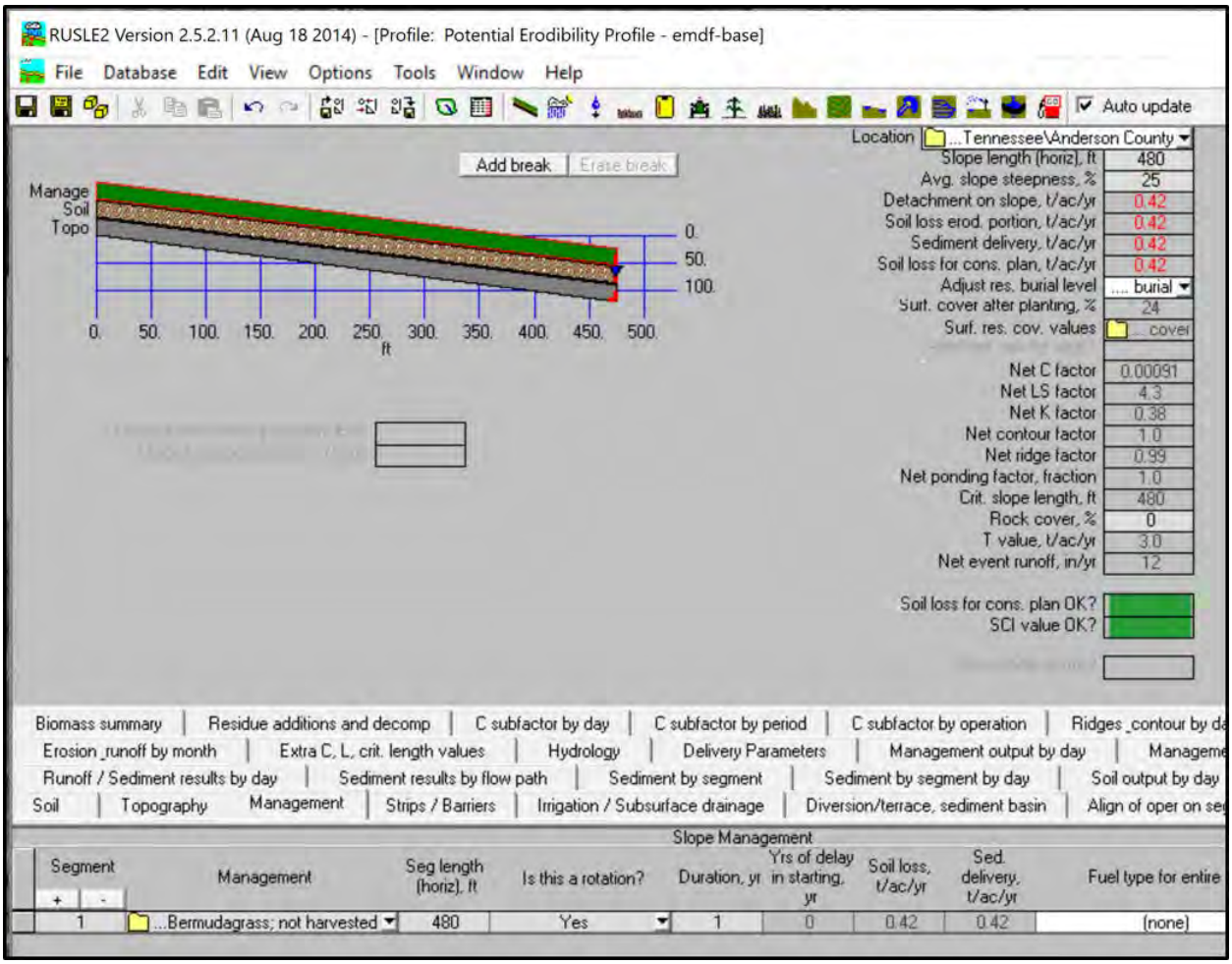

Fig. C.16. RUSLE2 model input parameters and result

C.4.4 SENSITIVITY ANALYSIS

Sensitivity of RUSLE2 soil loss predictions to uncertainty in input parameters was evaluated. The sensitivity runs included all the input parameters as described below:

- Soil type – gravelly sandy loam and gravelly clay loam
- Slope steepness – 21.5 percent (weighted average for the cover)
- Slope length – 250 ft (shorter sideslope portion only)
- Top portion of the cell – flatter top (3.5 percent)
- Ground cover – bluegrass, Bahia grass (not harvested), and harvested hay field.

A summary of the sensitivity runs are presented in Table C.6. The results indicate that the base case erosion evaluation provides a more pessimistic erosion scenario (i.e., higher erosion rate) for the proposed EMDF cover than most of the other sensitivity cases. With even less protective ground cover assumptions (hay field with regular harvests), the predicted erosion rate (2.4 ft per 1000 years) is only one order of magnitude higher than the base case.

Table C.6. Summary of RUSLE2 sensitivity analysis

Data category	Parameters	Units	Base case	Model sensitivity run scenarios							
				Soil type (sides lope)	Soil type (side slope)	Slope steepness (side slope)	Slope length (side slope)	Cover vegetation (side slope)	Cover vegetation (side slope)	Cover vegetation (side slope)	Top slope
Climatic	Weather		Anderson County	Anderson County	Anderson County	Anderson County	Anderson County	Anderson County	Anderson County	Anderson County	Anderson County
Soil/profile	Profile		Side slope	Side slope	Side slope	Side slope	Side slope	Side slope	Side slope	Side slope	top
	Soil bulk density	g/cm^3	1.42	1.42	1.42	1.42	1.42	1.42	1.42	1.42	1.42
	Slope length	ft	480	480	480	480	250	480	480	480	100
	Slope steepness	%	25	25	25	22	25	25	25	25	3.5
	Soil type		Gravelly silt clay loam	Gravelly sandy loam	Gravelly clay loam	Gravelly silt clay loam	Gravelly silt clay loam	Gravelly silt clay loam	Gravelly silt clay loam	Gravelly silt clay loam	Gravelly silt clay loam
Cover management	Grass type		Bermuda grass	Bermuda grass	Bermuda grass	Bermuda grass	Bermuda grass	KY Bluegrass	Bahia grass (not harvested)	Alfalfa hay (with harvest)	Bermuda grass
Results	Model result	ton/acre /year	0.42	0.26	0.43	0.37	0.39	0.32	0.95	4.60	0.07
	Erosion rate	ft/year	2.18E-04	1.35E-04	2.23E-04	1.92E-04	2.02E-04	1.66E-04	4.92E-04	2.38E-03	3.63E-05
	Erosion for 1000 years	ft	2.18E-01	1.35E-01	2.23E-01	1.92E-01	2.02E-01	1.66E-01	4.92E-01	2.38E+00	3.63E-02
	Time to reach 5 ft (biointrusion layer)	years	22,985	37,130	22,451	26,091	24,753	30,168	10,162	2,099	137,910

RUSLE2 = Revised Universal Soil Loss Equation Version 2 model

Given that the RUSLE2 model is based on observations of erosion in agricultural settings, the predictions for the more heavily managed/harvested cover types should be larger than what might be expected following the loss of institutional control (cover system monitoring and maintenance) assuming that the site remains undisturbed by sustained human activity. Due to the large number of factors that can affect site-specific erosion processes, predictions of the magnitude of cover erosion based on long-term average estimates are of limited utility for understanding cover performance. The resilience of the cover design to episodes of severe erosion is a more important consideration for understanding the likelihood of cover system damage that would expose the biointrusion barrier, which will limit the depth of erosion associated with gullying. Sensitivity of EMDF performance model results to reduced cover thickness assumptions is presented as part of the radon flux analysis (Sect. 4.4 of the PA and Appendix H) and incorporated into the discussion of radionuclide release through the cover in Sects. 3.2.2.1 through 3.2.2.3 of the PA.

C.4.5 USES OF THE RESULTS OF THE COVER EROSION CALCULATION

The results of the cover erosion calculation were not directly or indirectly incorporated into any other models used to assess the performance of the EMDF. The results were incorporated into the generalized conceptual model of EMDF system performance (Sect. C.1.3). The results support the cover performance assumptions in the HELP modeling and the inadvertent human intrusion evaluations. Since the erosion of the cover was insignificant during the 1000-year compliance period, it was decided that the total system modeling performed by RESRAD-OFFSITE would not include erosion.

C.5 SUMMARY OF PERFORMANCE OF ENGINEERED BARRIERS

This section summarizes the information and uncertainties that are incorporated into the generalized conceptual model of EMDF system performance (Sect. C.1.3).

Engineered barriers of primary concern for long-term facility performance include the synthetic (HDPE) membranes and clay barrier layers of the cover and liner systems (SRNL 2014). Synthetic membrane service life and the long-term performance of engineered earthen barriers are key uncertainties. A simplified profile of the EMDF facility, along with safety functions and events and processes important for long-term performance, is provided in Fig. C.17. The safety functions of the various cover and liner system layers are interdependent, so that the function of one layer may be limited by impaired function of one or more other layers in the system. The synthetic membranes serve as the primary short-term (decades to centuries) infiltration and leachate barriers that support the function of lateral drainage layers in the cover and liner. Thermal oxidative degradation is a primary breakdown mechanism for HDPE membranes and is highly sensitive to temperature, so that the thermal buffer provided by the overlying materials is a factor regulating the potential rate of degradation.

Differential settlement (subsidence) of the waste during the post-closure period can limit the safety functions of cover system components. Physical stress due to subsidence can damage the HDPE membrane and clay barrier in the cover, increasing water infiltration. Lateral drainage efficiency also can be impaired by subsidence, which will also increase infiltration. Due to the variety of expected EMDF waste forms, this degradation mechanism is an important uncertainty in the conceptual model of EMDF performance evolution. EMDF waste placement and compaction practices are developed to limit future subsidence and final cover design may incorporate features that impart resilience of the cover components to limited subsidence. In addition, post-closure monitoring and maintenance will permit timely repair of damaged cover areas that may develop due to subsidence.

	EMDF Engineered Features	Safety Functions	Limiting Events and Processes
Cover System Components	**Vegetated erosion control layer (4 ft)**	- Provides growth medium for cover vegetation - Protects underlying cover components from erosion and variability in temperature and moisture	- Surface water balance, infiltration and runoff - Vegetation and soil development, biointrusion - Surface erosion and gullying - Severe storms/flood events, landslides
	Granular filter layer (1 ft)	- Prevents filling of the biointrusion layer pore space	- Biointrusion
	Biointrusion layer (2 ft)	- Deters inadvertent human intrusion - Limits damage to hydrologic barriers by roots and burrowing animals - Secondary erosion control (defense-in-depth)	- Weathering and physical breakdown of cobbles/boulders - Pore space infilling and root penetration
	Lateral drainage layer (1 ft)	- Provides subsurface drainage to reduce deep cover infiltration through the less permeable underlying layers	- Infilling of pore spaces with fine particulates and/or by chemical precipitation - Waste subsidence (differential settlement)
	Synthetic (HDPE) membrane (60 mil)	- Primary cover infiltration barrier (initial post closure period) - Protects underlying clay barrier from desiccation and cracking	- Installation-related defects/damage - HDPE thermal oxidative degradation processes - Severe seismic event and/or rapid waste subsidence causing early membrane failure
	Amended/compacted clay barriers (2 ft)	- Primary long-term infiltration barrier - Limits vapor phase release to the cover surface (radon barrier)	- Improper clay compaction - Root penetration, thermal and moisture cycles (increasing permeability) - Waste subsidence (differential settlement) - Severe seismic or storm event causing damage to cover
	Contour soil layer (1ft)	- Provides a level foundation for construction of the compacted clay infiltration barrier(s)	-Improper construction impacts performance of overlying clay barrier
Waste Forms	**Waste containers**	- Containers isolate waste from water and reduce radionuclide mobility	- Corrosion of metal containers - Insufficient filling of void space in waste containers
	Treated and stabilized waste forms	- Provides chemical and physical stability to reduce radionuclide mobility	- Degradation of stabilized waste forms
	Void filling and bulk waste compaction protocols	- Limits long-term subsidence of bulk waste and maintains cover system function	- Waste consolidation and subsidence
Liner System Components	**Protective material layer (1 ft)**	- Protects underlying liner system components from damage during disposal operations.	- Improper installation - Unintentional disturbance during waste placement
	Leachate collection (drainage) layer (1 ft)	- Ensures protection of human health and the environment (operations & early post-closure) - Waste mass dewatering (early post-closure)	- Damage to overlying geotextile during installation - Clogging, chemical precipitation
	Primary synthetic (HDPE) membrane (60 mil)	- Ensures leachate drainage for treatment (operations) - Serves as primary leachate barrier (early post-closure period)	- Installation-related defects/damage - Chemical degradation of HDPE by leachate - HDPE thermal oxidative degradation processes
	Geosynthetic clay Layer (0.02 ft)	- Reduces leachate flux through HDPE membrane holes and defects	- Installation-related defects/damage - Geochemical alteration of sodium bentonite clay (divalent cations)
	Leak detection layer (0.03 ft)	- Provides performance monitoring for overlying composite leachate barrier - Provides secondary leachate removal function	- Degradation of synthetic drainage material
	Secondary synthetic (HDPE) membrane (60 mil)	- Supports performance monitoring for overlying composite leachate barrier - Serves as secondary leachate barrier	- Chemical degradation of HDPE by leachate - HDPE thermal oxidative degradation processes
	Compacted clay layer (3 ft)	- Serves as primary long-term leachate barrier - Provides chemical retardation of radionuclide migration	- Improper clay compaction - Physical and geochemical alteration of clay - Severe seismic event or slope failure damage to perimeter berms and clay barriers
	Geologic buffer zone (unsaturated, low permeability, 10 ft)	- Isolates radionuclides from saturated zone - Provides chemical retardation of radionuclide migration	- Physical and geochemical alteration of geologic buffer material - Water table incursion into geologic buffer

Fig. C.17. Simplified EMDF design profile, safety functions, and processes relevant to long-term performance

This page intentionally left blank.

For long-term (centuries to millennia) EMDF performance, function of the clay barrier layer in the cover system is essential. The cover system for EMDF has a robust configuration to protect the compacted clay layers from degrading processes in the surface environment. The vegetated surface layer serves to protect the underlying hydraulic barrier system from erosion and environmental fluctuations that can accelerate degradation of materials and impair safety functions. Site characteristics and processes that will determine the evolution of the surface layer after the cover vegetation is no longer maintained include long-term interactions among climate, soil development and vegetation, and associated successional changes in vegetation over time. These changes will affect the surface water balance, erosion of the cover surface, and infiltration of water. Eventually, severe weather events and progressive climate and vegetation changes could lead to erosion of the protective cover components and accelerate degradation of the clay barrier in the cover, increasing the likelihood of increased water infiltration over time. Detailed consideration of these processes and events was presented in Sect. C.1.2. Based on HELP water balance modeling (Sect. C.2), the estimated long-term (degraded condition) cover infiltration rate assumed for the PA analyses is 0.88 in./year.

The progression of degradation of clay barrier(s) and the overlying components of the cover is contingent upon the intensity and timing of multiple processes and events in the post-closure period. Although a general progression from full design performance to some long-term degraded performance condition will occur, the timing and magnitude of degradation is highly uncertain, particularly given the potential interactions among the various disposal system elements, safety functions, and degradation processes described above. One important aspect of this uncertainty is the timing of cover performance degradation (increasing cover infiltration) relative to evolution in the function of liner system components, which may be different due to the differing environments expected in the cover and liner systems over time. There is a possibility that the cover components will degrade more rapidly than the liner components and that, after leachate collection ceases, the water imbalance will cause accumulation of water on the liner over time (bathtub scenario). The performance implications of such a bathtub scenario for EMDF are developed in Sect. C.3.

C.6 REFERENCES

Albrecht and Bensen 2001. "Effect of Desiccation on Compacted Natural Clays," *Journal of Geotechnical Engineering*, Vol. 127, No. 1, Paper No. 16291, B. A. Albrecht and C. H. Benson, January.

Albright et al. 2006. "Field Performance of Three Compacted Clay Landfill Covers," *Vadose Zone Journal* 5:1157-1171, W. H. Albright, C. H. Benson, G. W. Gee, T. Abichou, S. W. Tyler, and S. A. Rock, Soil Science Society of America, Madison, WI.

Albright et al. 2013. "Field Hydrology of Landfill Final Covers with Composite Barrier Layers," *Journal of Geotechnical and Geoenvironmental Engineering*, 139, No. 1, W. H. Albright, C. H. Benson, and P. Apiwantragooon, American Society of Civil Engineers, Reston, VA, January 1.

Benson 2014. *Performance of Engineered Barriers: Lessons Learned*, Performance and Risk Assessment Community of Practice Webinar, February 20.

Benson and Benavides 2018. "Predicting Long-Term Percolation from the SDF Closure Cap," Report No. GENV-18-05, School of Engineering, University of Virginia, Charlottesville, VA, April 23.

Benson and Othman 1993. "Hydraulic Conductivity of Compacted Clay Frozen and Thawed In Situ," *Journal of Geotechnical Engineering*, Vol. 119, No.2, Paper No. 3071, C. H. Benson and M. A. Othman, February.

Bjornstad and Teel 1993. *Natural Analog Study of Engineered Protective Barriers at the Hanford Site*, PNL-8840, Pacific Northwest National Laboratory, Richland, WA.

Bonaparte et al. 2002. *Assessment and Recommendations for Improving the Performance of Waste Containment Systems*, EPA/600/R-02-099, R. Bonaparte, R. M. Koerner, and D. E. Daniel, U.S. Environmental Protection Agency, National Risk Management Research Laboratory, Washington, D.C.

Bonaparte et al. 2016. *Geomembrane-Leachate Compatibility for U.S. Department of Energy CERCLA Waste Disposal Facilities*, R. Bonaparte, M. Z. Islam, V. Damasenco, S. A. Fountain, M. A. Othman, and J. F. Beech, ASCE GEO Sustainability & Geoenvironmental Conference, Chicago, IL, Aug 14-18.

Daniel 1993. *Case Histories Compacted Clay Liners and Covers for Waste Disposal Facilities, International Conference on Case Histories in Geotechnical Engineering*, Paper 2, D. E. Daniel, http://scholarsmine.mst.edu/icchge/3icchge/3icchge-session15/2, June.

DOE 1997. *Feasibility Study for Bear Creek Valley at the Oak Ridge Y-12 Plant, Oak Ridge, Tennessee*, DOE/OR/02-1525/V2&D2, U.S. Department of Energy, Oak Ridge, TN, November.

DOE 2011a. *Radioactive Waste Management Manual*, DOE Manual 435.1-1 Chg. 2, U.S. Department of Energy, Washington, D.C., June.

DOE 2011b. *Derived Concentration Technical Standard*. DOE-STD-1196-2011, U.S. Department of Energy, Washington, D.C., April.

EPA 1993. *Technical Guidance Document: Quality Assurance and Quality Control for Waste Containment Facilities*, EPA/600/R-93/182, U.S. Environmental Protection Agency, Risk Reduction Engineering Laboratory Office of Research and Development, Cincinnati, OH, September.

Khire et al. 1997. "Water Balance Modeling of Earthen Final Covers," *Journal of Geotechnical and Geoenvironmental Engineering*, 123, No. 8, M. V. Khire, C. H. Benson, and P. J. Bosscher, American Society of Civil Engineers, Reston, VA, August.

Koerner et al. 2011. *Geomembrane Lifetime Prediction: Unexposed and Exposed Conditions*, Geosynthetic Institute GRI White Paper #6, R. M. Koerner, Y. G. Hsuan, and G. R. Koerner, Folsom, PA, February.

NRC 1981. Draft Environmental Impact Statement on 10 *Code of Federal Regulations* Part 61, "Licensing Requirements for Land Disposal of Radioactive Waste," NUREG-0782, Volumes 1-4, U.S. Nuclear Regulatory Commission, Washington, D.C., September.

NRC 1996. *Hydrologic Evaluation Methodology for Estimating Water Movement Through the Unsaturated Zone at Commercial Low-Level Radioactive Waste Disposal Sites*, NUREG/CR-6346, U.S. Nuclear Regulatory Commission, Washington, D.C., January.

ORNL 1987. *Geochemical Behavior of Cs, Sr, Tc, Np, and U in Saline Groundwaters: Sortion Experiments on Shales and Their Clay Mineral Components,* ORNL/TM-10364, Oak Ridge National Laboratory, Oak Ridge, TN, November.

Phifer, Mark A 2012. *Portsmouth On-Site Disposal Cell (OSDC) High Density Polyethylene (HDPE) Geomembrane Longevity*, SRNL-STI-2012-00061, Savannah River National Laboratory, Jackson, SC, January.

Rowe, R. K. and M. Z. Islam 2009. "Impact of Landfill Liner Time-Temperature History on the Service Life of HDPE Geomembranes", *Waste Management*, Vol. 29, No. 10, pages 2689–2699.

Rowe et al. 2009. "Ageing of HDPE geomembrane exposed to air, water and leachate at different temperatures," *Geotextiles and Geomembranes*, Vol. 27, No. 2, pages 137–151, R. K. Rowe, S. Rimal, and H. P. Sangam, International Geosynthetics Society, Jupiter, FL.

Sanford and Selnick 2013. "Estimation of Evapotranspiration Across the Conterminous United States Using a Regression with Climate and Land-Cover Data," *Journal of the American Water Resources Association*, Vol. 49, No 1, pages 217–230, Ward E. Sanford and David L. Selnick, American Water Resources Association.

Scalia and Benson 2011. "Hydraulic Conductivity of Geosynthetic Clay Liners Exhumed from Landfill Final Covers with Composite Barriers, *J. Geotech. Geoenvironmental Eng.*, 137(1), pages 1-13.

Schroeder et al. 1994a. *The Hydrologic Evaluation of Landfill Performance (HELP) Model: User's Guide for Version 3*, EPA/600/R-94/168a, P. R. Schroeder, C. M. Lloyd, P. A. Zappi, and N. M. Aziz, U.S. Environmental Protection Agency, Office of Research and Development, Washington, D.C., September.

Schroeder et al. 1994b. *The Hydrologic Evaluation of Landfill Performance (HELP) Model: Engineering Documentation for Version 3*, EPA/600/R-94/168b, P. R. Schroeder, T. S. Dozier, P. A. Zappi, B. M. McEnroe, J. W. Sjostrom, and R. L. Peyton, U.S. Environmental Protection Agency, Office of Research and Development, Washington, D.C., September.

SRNL 2014. *Consideration of Liners and Covers in Performance Assessments*, SRNL-STI-2014-00409, Rev. 0, Savannah River National Laboratory, Jackson, SC, September.

Tennessee Valley Authority 2016. Clinch River Nuclear Site License-Application for Early Site Permit (ESP), Site Safety Analysis Report (SSAR), Revision 0, Knoxville, TN, May 25.

Tian et al. 2017. "Antioxidant Depletion and Service Life Prediction for HDPE Geomembranes Exposed to Low-Level Radioactive Waste Leachate", Kuo Tian, Craig H. Benson, James M. Tinjum, and Tuncer B. Edil J., *Geotechnical & Geoenvironmental Engineering*, Vol. 143 Issue 6, June.

UCOR 2018. *Conceptual Design Report for the Environmental Management Disposal Facility, Oak Ridge, Tennessee*, UCOR-4841/R1, UCOR, Oak Ridge, TN, January.

UCOR 2020 *Quality Assurance Report for Modeling of the Bear Creek Valley Low-level Radioactive Waste Disposal Facilities, Oak Ridge, Tennessee"*, UCOR-5234/R0, UCOR, Oak Ridge, TN, April.

USDA 1986. *Urban Hydrology for Small Watersheds (TR-55)*, U.S. Department of Agriculture-Natural Resources Conservation Service, Conservation Engineering Division Technical Release 55, June.

USDA 2004. *RUSLE2 – Instructions and User Guide*, U.S. Department of Agriculture-Natural Resources Conservation Service, Washington, D.C., May.

USDA 2013. *Science Documentation, Revised Universal Soil Loss Equation Version 2 (RUSLE2)*, U.S. Department of Agriculture-Agricultural Research Service, Washington, D.C.

APPENDIX D.
GROUNDWATER FLOW MODELING FOR THE ENVIRONMENTAL MANAGEMENT DISPOSAL FACILITY

This page intentionally left blank.

CONTENTS

FIGURES

TABLES

ACRONYMS

BCV	Bear Creek Valley
BJC	Bechtel Jacobs Company LLC
CBCV	Central Bear Creek Valley
CERCLA	Comprehensive Environmental Response, Compensation, and Liability Act of 1980
D	Drainage
DOE	U.S. Department of Energy
EMDF	Environmental Management Disposal Facility
EMWMF	Environmental Management Waste Management Facility
EPM	equivalent porous media
ESI	Environmental Simulations, Inc.
FS	feasibility study
HDPE	high-density polyethylene
HELP	Hydrologic Evaluation of Landfill Performance
NT	North Tributary
ORNL	Oak Ridge National Laboratory
ORR	Oak Ridge Reservation
PA	Performance Assessment
QA	quality assurance
RI	remedial investigation
TMR	telescopic mesh refinement
USGS	U.S. Geological Survey
W	west
Y-12	Y-12 National Security Complex

This page intentionally left blank.

D.1 INTRODUCTION

A series of three-dimensional groundwater flow models were developed for the proposed Environmental Management Disposal Facility (EMDF) at the Central Bear Creek Valley (CBCV) site on the U.S. Department of Energy (DOE) Oak Ridge Reservation (ORR) in Oak Ridge, Tennessee. The site-specific models were used to predict the groundwater levels under current conditions and groundwater levels after construction of a new disposal facility. The predictive results of the groundwater flow models are being used to guide the design process of the new disposal facility. In addition, the future condition (degraded cover and liner performance) of the design model provides required key input parameters to support the Performance Assessment (PA) of the EMDF.

These site-specific groundwater flow models were developed for the proposed EMDF area based on the Bear Creek Valley (BCV) regional groundwater flow model. During the BCV feasibility study (FS) (DOE 1997a), a BCV regional model was developed based on data collected during comprehensive remedial investigation (RI) activities (DOE 1997b) and recently developed conceptual frameworks for geology and hydrology of the ORR (Oak Ridge National Laboratory [ORNL] 1992a, ORNL 1992b, ORNL 1988). The BCV regional groundwater flow model was used to refine and quantify components of the hydrogeologic conceptual model for BCV, and quantitatively evaluate alternatives for remediation as discussed in the BCV FS.

The groundwater flow models for the EMDF site in CBCV were developed in two stages. The site-specific flow model for the CBCV (CBCV model) representing current (pre-construction) site conditions was the first stage. The CBCV model incorporates all the recently available site characterization data collected at the EMDF site, including well tests, groundwater levels, and stream flow rates. The CBCV model results were compared to the field data and model parameters were refined (calibrated) to better represent site specific groundwater conditions. Sensitivity analyses were conducted to establish the key hydrogeologic parameters influencing predicted conditions as part of the model refinement.

The design condition model (EMDF model) was the second stage of the model development. The EMDF model started from the calibrated CBCV model and incorporated the EMDF preliminary design features into the model grid. The EMDF model was used to predict post-construction disposal facility groundwater conditions, assuming zero recharge to the saturated zone.

For the EMDF PA, the EMDF model was run assuming long-term cover and liner hydrologic performance (non-zero recharge directly beneath the disposal unit) to provide the following information:

- Groundwater levels for various performance conditions
- Depth to groundwater beneath the disposal cells
- Groundwater flow field and discharge locations
- Delineation of the likely maximum impact location for groundwater
- Sensitivity analysis for key model parameters
- Flow linking files to conduct contaminant fate-transport modeling in the saturated zone.

The BCV regional, CBCV, and EMDF groundwater models all use the MODFLOW code—a finite-difference groundwater flow code developed by the U.S. Geological Survey (USGS) (McDonald and Harbaugh 1988). MODFLOW is a modular, block-centered finite-difference groundwater flow code capable of simulating both transient and steady-state saturated groundwater flow in one, two, or three

dimensions. MODFLOW calculates potentiometric head distribution, groundwater flow rates, velocities, and water balances throughout an aquifer system. It also includes modules simulating recharge, flow toward wells, and groundwater flowing into drains and rivers. A number of different boundary conditions are available, including specified head, areal recharge, injection or extraction wells, evapotranspiration, drains, and streams or rivers. Aquifers can be simulated as unconfined, confined, or a combination of unconfined and confined. The finite-difference equations may be solved using a strongly implicit procedure, slice-successive over-relaxation, or preconditioned conjugate gradient method.

MODFLOW assumes that the aquifer can be characterized as a porous medium. The application of a porous media code (i.e., MODFLOW) to a fractured bedrock system, such as BCV, is termed the equivalent porous media (EPM) approach. This approach assumes that the media is fractured to the extent that it behaves hydraulically as a porous media. Three-dimensional representation of hydraulic properties within MODLFOW also provides flexibility to present fracture orientation and distribution. This approach is applicable to BCV given the high degree of weathering near the surface, numerous bedding planes and fractures in the sedimentary rock units, presence of a very active groundwater flow system, and extensive groundwater-surface water interaction. Given the large scale of the model domain (kilometers) compared to the fractured nature of the underlying geologic units (on the order of centimeters to meters), and the degree of precision required to support the PA, the MODFLOW model can accurately predict the nature of the groundwater flow system for the area. In addition, the EPM approach is the most practicable modeling approach for the BCV area. Previous model applications have shown its predictability and consistency with field groundwater and surface flow measurements through mass balance analyses and contaminant plume extent and movement through particle tracking (USGS 1988, DOE 1997a, Bechtel Jacobs Company LLC]BJC] 2010).

MODFLOW was selected for the BCV site because it is in public domain and is widely used by the industrial, scientific, and governmental communities in the United States and around the world. The code has been rigorously tested and verified, and a variety of software tools are available for graphical pre- and post-processing. MODFLOW models also were developed for the BCV RI and FS as well as the Environmental Management Waste Management Facility (EMWMF) design and performance evaluations. These models received tri-party approval under the Comprehensive Environmental Response, Compensation, and Liability Act of 1980 (CERCLA) process (DOE 1997a, DOE 1998a). All groundwater flow model simulations were conducted using MODFLOW-2005 code (Harbaugh 2005).

Section 9 of the PA Report details the quality assurance (QA) activities and documentation that apply to the groundwater flow model development and application.

D.2 EMDF SITE CHARACTERIZATION SUMMARY

D.2.1 EMDF SITE DESCRIPTION

The proposed EMDF site is located in the CBCV of the DOE ORR, approximately 1.5 miles southwest of the existing EMWMF (Fig. D.1). BCV between the Y-12 National Security Complex (Y-12) (3 miles northeast) and the CBCV site is a historical waste management area containing several closed disposal facilities, contaminant source areas, and ground water contaminant plumes. The ORR is located in the western portion of the Valley and Ridge physiographic province, which is characterized by long, parallel ridges and valleys that follow a northeast-to-southwest trend (ORNL 1992a). The Valley and Ridge physiographic province developed on thick, folded and thrust-faulted beds of sedimentary rock deposited during the Paleozoic era. Thrust fault patterns and the strike and dip of the beds control the location, shapes and orientations of the ridges and intervening valleys.

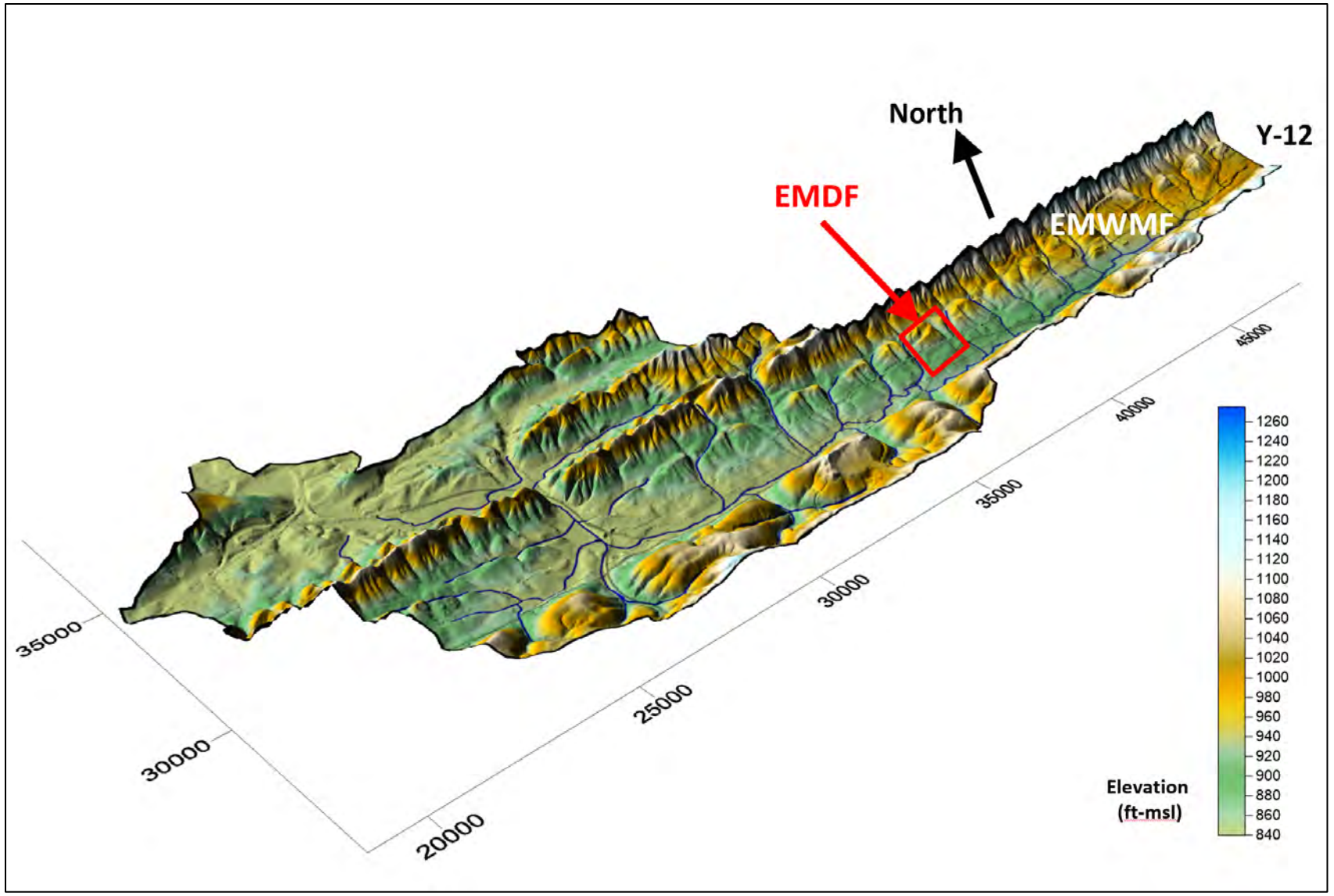

Fig. D.1. Proposed EMDF location in Bear Creek watershed

BCV is approximately 10 miles long and extends from the topographical divide near the west end of the Y-12 industrial area to the Clinch River. The valley is bounded by Pine Ridge on the northwest and Chestnut Ridge on the southeast. Bear Creek drains to the southwest along the lower elevation southeast margin of the valley. Elevations range from highs near 1260 ft along the crest of Pine Ridge to around 800 ft where Bear Creek exits BCV through the water gap in Pine Ridge at State Road 95. The topographic relief between valley floors and ridge crests is generally on the order of 300 to 350 ft. Majority of the surface water are contributed from a series of small tributaries that drain southward into Bear Creek from Pine Ridge across the geologic strike of the valley. Due to the landform topography, Bear Creek is the solo pathway for the groundwater discharge and surface water outflow for the BCV.

The EMDF will be constructed on a knoll on the southern slope of Pine Ridge between two streams, North Tributary (NT)-10 and NT-11. A smaller stream at the site, Drainage (D)-10 West (W), is located just west of NT-10. The area is mostly forested, except for a cleared area with a large soil pile and two constructed wetlands for Y-12.

The proposed disposal cells would overlie steeply angled bedrock unit consisting of shales, siltstones, and mudstones with some limestone layers. Recent stream deposits are present on the valley floors, particularly along D-10W at the eastern side of the site. Karst features, such as sinkholes, sinking streams, and resurgent springs, are not present beneath the proposed footprint of the CBCV site, but are present along Bear Creek south of the site. Precipitation primarily runs off as surface water and shallow groundwater in the stormflow zone. During the summer/fall growing season, the streams within the CBCV site may dry up. The main channel of the Bear Creek located south of the site has continuous surface water flow throughout the year.

D.2.2 HYDROGEOLOGIC CHARACTERIZATION

Characterization of the EMDF site began in February 2018 and was conducted in two major phases. Phase 1 characterization was intended to demonstrate the suitability of the site for onsite CERCLA waste disposal. The primary goal of the Phase I site characterization was to provide initial data on groundwater elevations and surface water flows to support site selection and the overall waste disposal decision. Secondary Phase 1 goals were to obtain geotechnical data to support preliminary design activities. The Phase 2 characterization effort was conducted to develop additional hydrogeologic and geotechnical information to support EMDF preliminary design.

The Phase 1 (DOE 2018, DOE 2019) and Phase 2 subsurface hydrogeologic investigations included borehole drilling to obtain representative lithologic data, collect subsurface geotechnical samples, conduct geophysical logging, estimate hydraulic conductivities, and to support groundwater monitoring and seismic investigations. Phase 2 characterization also included digging test pits for additional geotechnical sampling. The documentation of Phase 2 results is not complete. A total of 32 piezometers were installed (26 paired shallow and intermediate depth, and six single piezometers) for monitoring groundwater levels within the disposal cell boundary and on the periphery of the site. In addition, six surface water flow measurement stations (flumes) were established to document streamflow in Bear Creek tributaries. Figure D.2 shows the current site topography, hydrogeologic investigation locations, and key groundwater and surface water features in the proposed EMDF area. In addition to hydrogeologic characterization and monitoring, there was additional field work to delineate wetland areas and locate geologic contacts as well as civil surveying to refine topographic data for design and to document the locations of flumes, piezometers, soil borings, and test pits.

Documentation of the Phase 1 field activities (DOE 2018, DOE 2019), including surface water records and groundwater data that had been collected from the 16 Phase 1 piezometers over the first year of monitoring (March 2018 through early March 2019), were used in the development and calibration of the CBCV model (refer to Sect. D.3.3 for details).

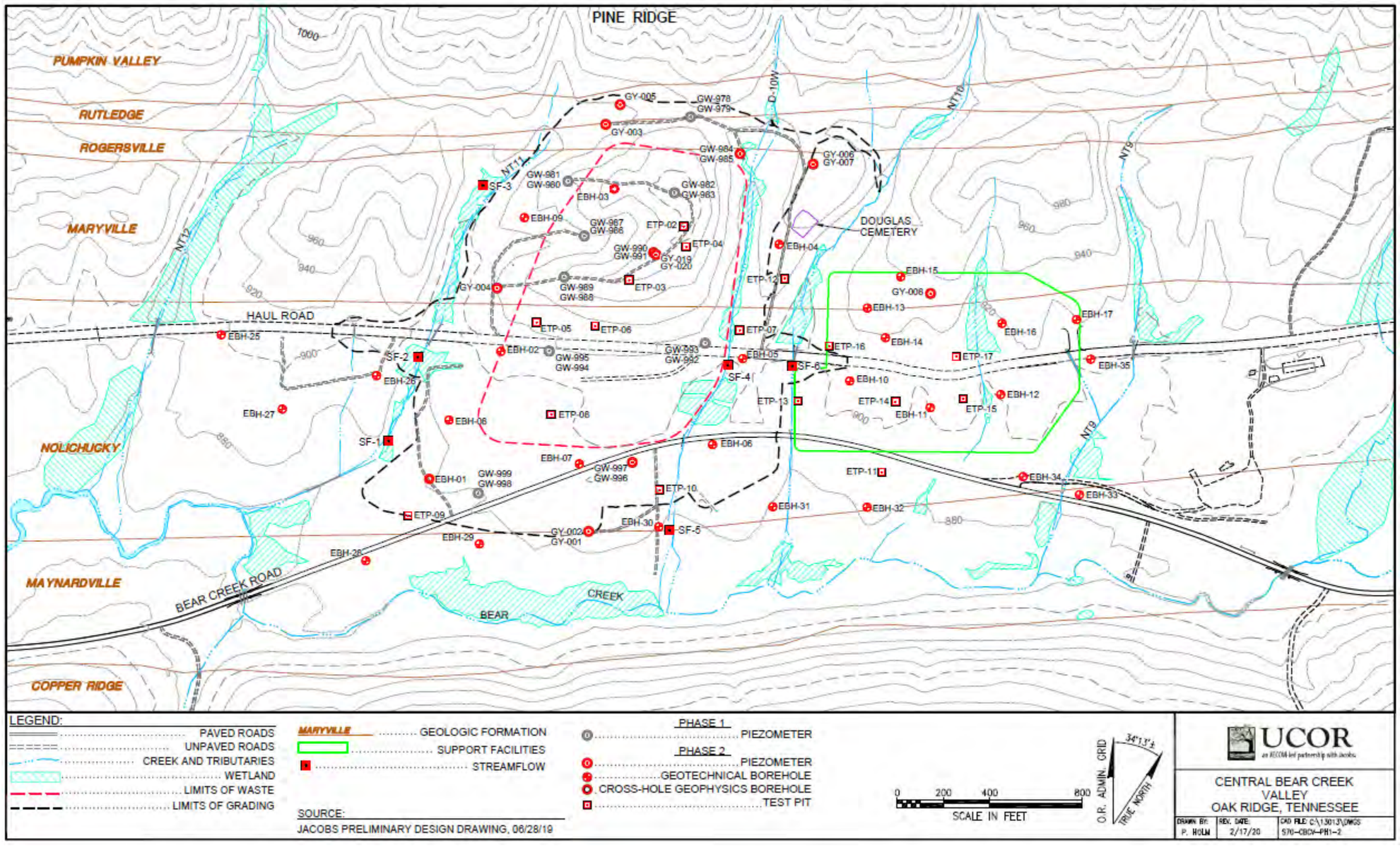

Fig. D.2. EMDF site characterization map

This page intentionally left blank.

The Phase 1 (DOE 2019) and 2 piezometer monitoring results show that the average potentiometric surfaces are primarily influenced by topography and local recharge. There is subdued mounding of the potentiometric surface under the knoll. Generally, piezometer levels respond quickly during precipitation events then decrease rapidly to average conditions within days. Groundwater levels vary seasonally, with maximum elevations generally occurring in the interval between December and April or May, and annual low elevations occurring in drier parts of the year (which can include months from May to November).

Comparison of the piezometer pairs monitoring the shallow and intermediate groundwater zones demonstrates that in most cases, a downward-to-zero vertical gradient exists in the knoll area and slight upward vertical gradients exist away from the knoll nearer to the surface water drainages. Most of the recharge to the groundwater moves quickly to adjacent surface water bodies with limited replenishment of the deeper underlying groundwater. In general, groundwater moves from the ridges toward Bear Creek and its tributaries. The results of EMDF site characterization efforts are consistent with the general BCV hydrogeologic framework presented in Sect. 2.1.5 of the PA.

D.2.3 INFORMATION USED FOR GROUNDWATER MODEL DEVELOPMENT

Groundwater model development occurred concurrently with the site characterization process. All site characterization data (DOE 2018, DOE 2019) available at the time of CBCV model development and calibration were considered (refer to Sect. D.3.2) Additional model verification to support engineering design was based on longer periods of groundwater level monitoring and additional analysis of streamflow data (the documentation of groundwater analysis is not complete). For development of the CBCV and EMDF models, the following information was used:

- Soil and bedrock lithologic boring data were used to define vertical variation of the geologic units (for model layer elevation assignments).
- Hydraulic test data (slug test and FLUTe test) were used to bound hydraulic conductivity values for specific geologic units and model layers.
- Aerial topographic mapping (Light Detection and Ranging method, referred to as LIDAR) and field survey data were used for establishing model topographic controls (e.g., stream channel elevations), piezometer and flume locations, and wetland boundaries. The topographic data can be found in the Oak Ridge Environmental Information System.

In addition, Phase 1 monitoring data for the groundwater levels and surface water flows were used during the calibration of the CBCV model:

- Observed surface water flow rates were used to guide assignment of recharge rates based on comparison to simulated surface water flows.
- Groundwater elevation measurements from March 2018 to March 2019 (Phase 1 piezometers) and the inferred flow fields were used to assess CBCV model performance for calibration.

For the EMDF model, disposal cell design and other site modifications that would have an impact on the post-construction groundwater flow conditions were incorporated. Design information used to develop the EMDF model included the geometry and material properties of engineered features and estimated cover infiltration rates (refer to Appendix C of the PA). The design information used for the EMDF model came from the final preliminary design package for the EMDF, dated July 2019, as described in Sect. 2.1 of *Quality Assurance Report for Modeling of the Bear Creek Valley Low-level Radioactive Waste Disposal Facilities, Oak Ridge, Tennessee* (QA Report) (UCOR, an Amentum-led partnership with Jacobs, 2020).

Detailed application of the site characterization data and EMDF preliminary design information in groundwater model development are presented in Sects. D.3, D.4, and D.5.

D.3 CBCV FLOW MODEL DEVELOPMENT AND CALIBRATION

Development of the CBCV flow model representing current site conditions (2019 topography) prior to EMDF construction was the first stage of modeling process. It includes the use of site characterization data, for model setup and comparison to Phase 1 monitoring data (such as groundwater levels and stream flow) for calibration. The model output was verified as accurate using both Phase 1 and 2 data. The CBCV flow model forms the foundation of the EMDF flow model.

D.3.1 CBCV FLOW MODEL CONSTRUCTION

A telescopic mesh refinement (TMR) modeling approach was used to develop the CBCV model from the calibrated BCV regional flow model originally constructed by the Jacobs Environmental Management Team for the BCV FS (DOE 1997a). The TMR approach enables the user to develop a site-specific model using existing regional information and allows focus on areas of interest with increased model grid resolution and more accurate representation of site-specific features. The TMR approach utilizes the results from the calibrated regional flow model to assign preliminary boundary conditions and model parameters in the TMR model, which reduces the degree of detailed model recalibration. Further refinements were made to the TMR model framework after extraction and incorporated to better represent the location of streams, hydrogeological units, and existing topography in the CBCV model, as described below.

Groundwater Vistas (Environmental Simulations, Inc. 2017), a graphic user interface program to aid in model development, simulation, and pre- and post-modeling processes, was used to perform the TMR model approach. Refinement of the CBCV model was also conducted using the Groundwater Vistas software. The use of a graphic interface allows both simpler refinement and quality control in model development.

Construction of the CBCV model consisted of the following steps:

1. Establish CBCV model domain and dimension.
   The TMR approach was used to develop the CBCV model from the calibrated regional BCV flow model (DOE 1997a) by extracting boundary conditions, model layers, and model properties. A refined horizontal grid cell size (10 ft × 10 ft) was used for the new model domain to better represent detailed current condition and disposal cell design feature.

2. Refine CBCV model.
   To represent the detailed current site-specific features, the following refinements were made after the CBCV flow model domain was constructed:

   - Refinement in the vertical direction was achieved by dividing the original five regional model layers into nine vertical layers to represent the current site conditions, allowing for future EMDF engineering features and supporting better resolution of the vertical distribution of radionuclides.
   - Site-specific lithologic data from borings were used to define the lateral and vertical distribution of the strata and corresponding model layer elevations in the model.

- The refined model parameters used in the calibrated EMWMF models and other site-specific models in the BCV (DOE 1998b, BJC 2003, BJC 2010) were incorporated into the model.
- Adjustments were made to model boundaries and hydraulic parameter zones to smooth transitions and to represent field conditions more precisely using the refined discretization. Hydraulic conductivity zone values and boundaries were adjusted based on field conditions and geological maps.
- Field surveys of surface water features in BCV were incorporated into the CBCV model, including Bear Creek and its tributaries and associated wetlands. The surface drainage features were represented in the model as drain cells or, for Bear Creek, as river cells. Actual stream and wetland elevations were used to assign drain/river cell parameters in the model.
- The most recent topographic data were used to define the upper-most layer surface elevations in the model.

D.3.2 CBCV MODEL DOMAIN AND DISCRETIZATION

The CBCV model covers a portion of the watershed extending from NT-8 to NT-14 (Gum Branch) and from the top of Chestnut Ridge to the top of Pine Ridge (south-north). It is 8700 ft from east to west (Y-12 administrative grid directions) and 6200 ft from south to north, covering a planar area of 5.39E+07 sq ft (1.93 sq mile). The existing topography within the model domain is shown on Fig. D.3.

Discretization is the process of transferring continuous functions, models, variables, and equations into discrete units in a numerical representation. Model discretization refers to the assignment and alignment of the numerical cells in the model and establishes its relationship of those cells to actual natural and engineered conditions. A uniform horizontal grid size of 10 ft × 10 ft was used for the model domain. There are 870 rows and 620 columns in the model horizontal grid. To better represent the hydrogeologic property orientation and anisotropy in the model, the model grid was rotated from true north to align with the southwest to northeast valley-ridge direction, consistent with previous, parent models.

The CBCV model uses nine model layers to reflect the vertical variation in the hydraulic properties at the site, with the deeper model layers representing decreasing degrees of fracturing and permeability with depth. The hydraulic conductivity zones within each layer are used to represent the different geologic formations. Using multiple layers, even with same hydraulic properties among these layers, allows the model to predict refined potentiometric head and hydraulic gradient in the vertical direction. It also allows refined contaminant fate-transport simulation based on the flow model results.

- Layer 1. The top of model layer 1 reflects the current (2019) topography for the CBCV model. The top model layer represents the saprolite zone (saprolite and the upper weathered bedrock). Site-specific boring data were used to develop the relationship between surface elevation and saprolite zone depth. The relationship was applied to derive the applicable saprolite zone depth (layer 1 thickness) across the site based on surface elevation. The bottom of layer 1 corresponds approximately to the top of unweathered but fractured bedrock resulting in variable thickness in layer 1 ranging from 20 to 45 ft.
- Layers 2, 3, and 4. Layers 2 through 4 represent highly fractured bedrock. Layer 2 has a variable thickness between 4 and 88 ft with a mean of 63 ft for all the model domain. Near the EMDF area, layer 2 has a variable thickness between 39 and 82 ft. Layers 3 and 4 are uniformly 33 ft thick each.
- Layers 5 and 6. Layers 5 and 6 represent less fractured bedrock, each uniformly 75 ft thick.
- Layers 7, 8, and 9. Layers 7 through 9 represent even less fractured and less permeable deeper bedrock and are 100, 100, and 300 ft thick, respectively.

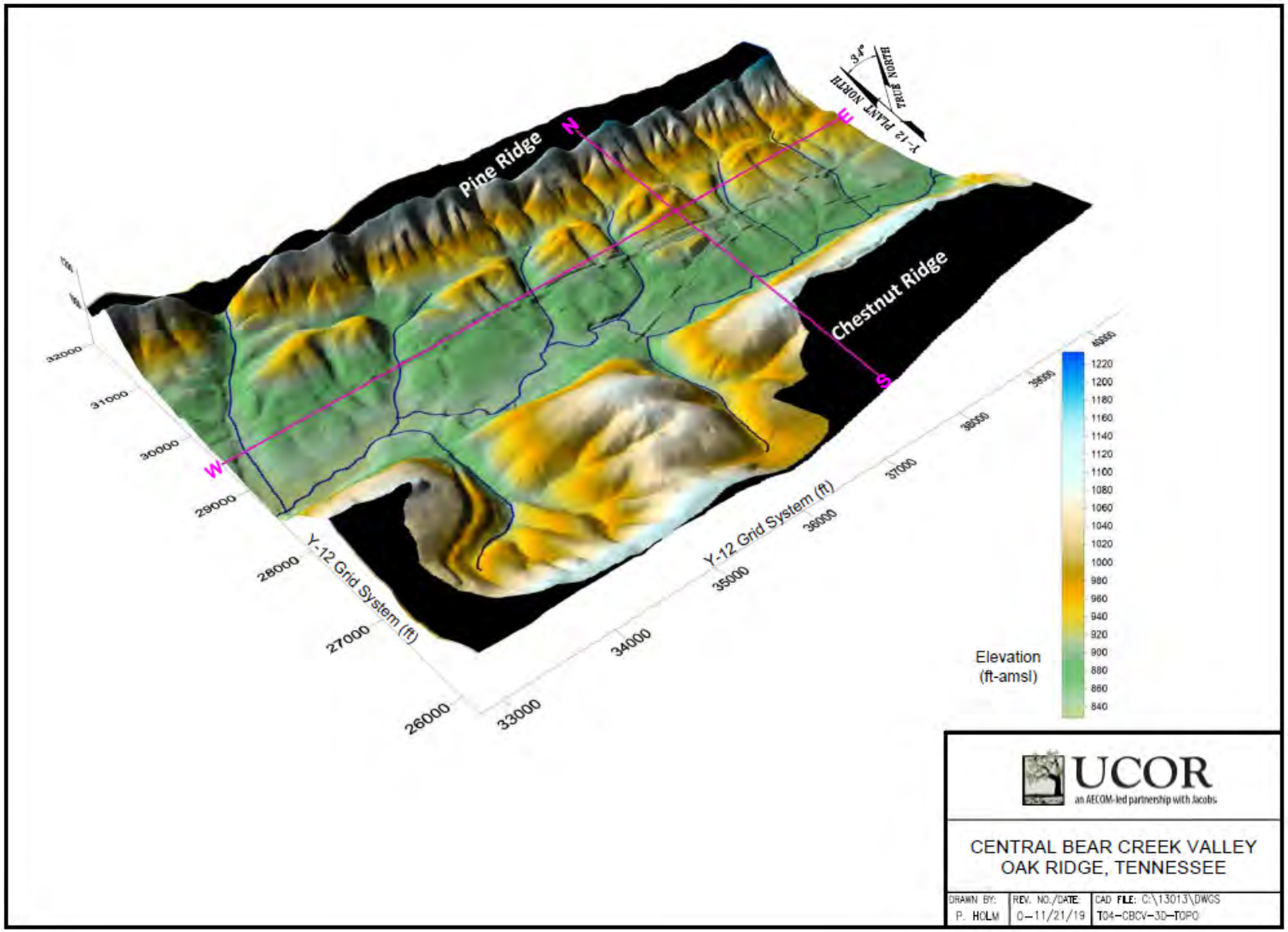

Fig. D.3. CBCV model domain and topography

Fig. D.4 shows the vertical discretization for the CBCV model along the east-west and south-north cross-sections that are shown in Fig. D.3. There are 4,854,600 cells with 3,537,604 being active in groundwater flow simulation.

The construction and discretization of the CBCV model is summarized in Table D.1. The model coordinate system relation to the Y-12 administrative coordinate system (coordinate transformation) is also provided. As previously noted, the model coordinate system was rotated to align with BCV and the associated geologic and hydrogeologic features. The model y-direction is oriented perpendicular to the valley axis, and the x-direction is parallel to the valley and the geologic strike.

Table D.1. CBCV model domain and discretization summary

Grid Information	
Number of rows	870
Number of columns	620
Number of layers	9
Total cells	4,854,600
Total active cells	3,537,604
Grid Dimensions (ft)	
Horizontal row spacing	10
Horizontal column spacing	10
Vertical spacing	
Layer 1	Variable (20-45)
Layer 2	Variable (3-86)
Layers 3-4	33
Layers 5-6	75
Layers 7-8	100
Layer 9	300
Coordinate Transformation	
X offset (to Y-12 coordinate system)	41,530.016 ft
Y offset (to Y-12 coordinate system)	25,825.516 ft
Rotation	90.23 degree

CBCV = Central Bear Creek Valley
Y-12 = Y-12 National Security Complex

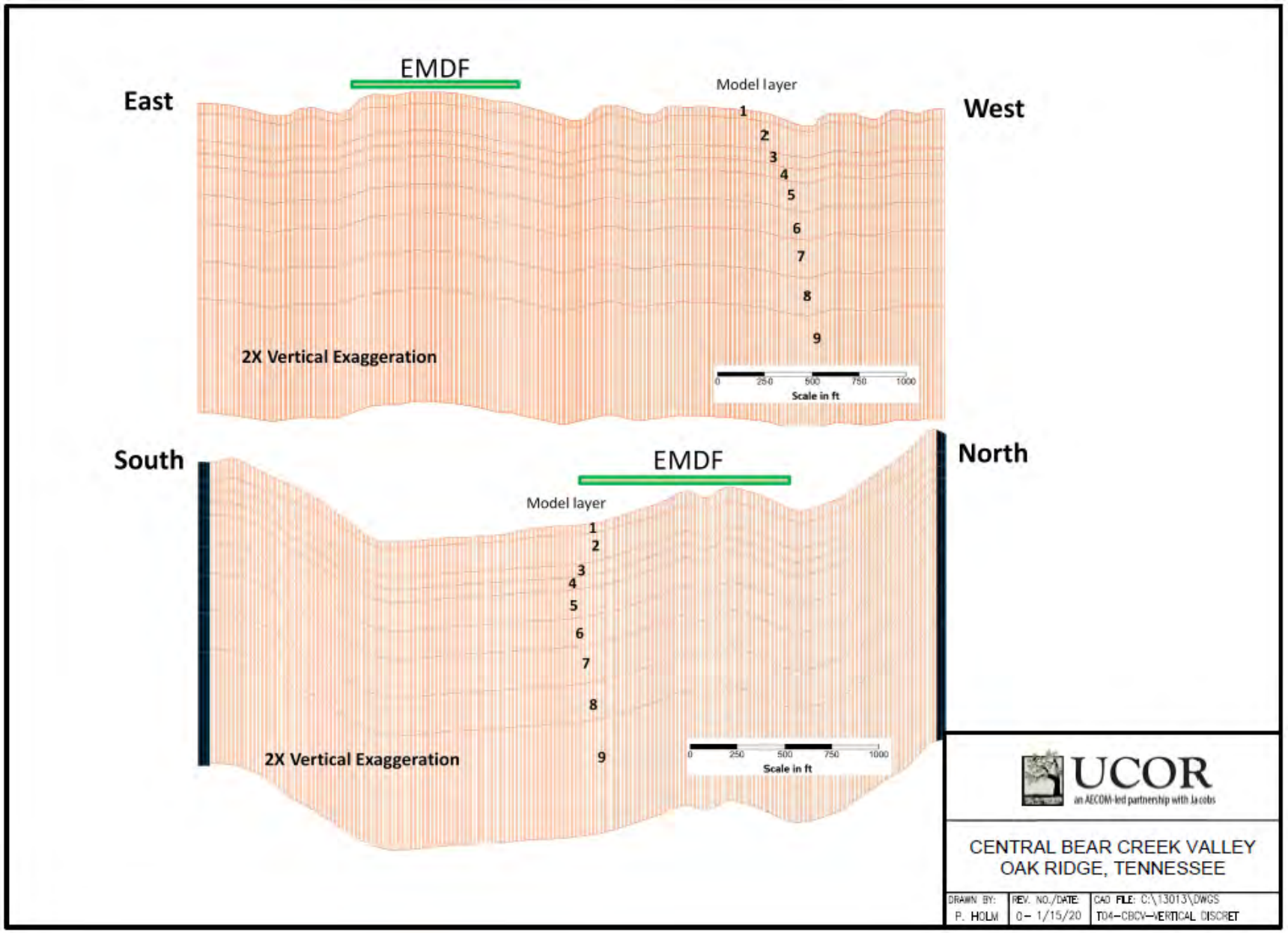

Fig. D.4. CBCV model vertical discretization

D.3.2.1 Hydraulic Properties

Six distinct hydraulic conductivity zones were used in the CBCV model to represent the nine geologic units (ORNL 1992a) that exist in BCV based on existing field measurements of hydrological properties (DOE 1997a). Figure D.5 shows the six hydraulic units and are listed below:

- Knox Group (Chepultepec Dolomite and Copper Ridge Dolomite)
- Maynardville Limestone
- Nolichucky Shale
- Maryville-Rogersville-Rutledge Formations (Shale)
- Pumpkin Valley Shale
- Rome Formation (Shale/Sandstone).

The selection of these geologic units as explicit hydraulic units is based on the thickness of the units, the availability of hydraulic data, their lithologic similarity, and their observed hydrogeologic influence elsewhere in the BCV. The formation boundaries were obtained from the geologic mapping of the ORR (ORNL 1992a). A summary of BCV field estimates of hydraulic conductivity and it variation with depth is provided in Appendix C of UCOR 2014.

Previous BCV field observations and modeling efforts suggest that groundwater flows preferentially along the geologic strike (model y-coordinate direction). Anisotropic ratios (K_y versus K_x [K_z]) of 5:1 (saprolite zone, layer 1) and 10:1 (fractured bedrock zone, layers 2 through 9) were used to represent the fracture/bedding orientation of the geologic units. In this case, K_y represents the conductivity parallel to strike, K_x represents the horizontal conductivity perpendicular to strike, and K_z represents the vertical hydraulic conductivity. Both field data and previous modeling sensitivity analyses support the anisotropic ratios used in the model. Extensive modeling sensitivity analyses were conducted during development of the Bear Creek regional model and were reported in the BCV FS. Field hydraulic conductivity data and anisotropy information is derived from aquifer tests and observed plume distributions within BCV. A detailed summary of the aquifer test data is provided in the BCV FS (DOE 1997a, Appendix F). These data support an anisotropic nature within the BCV hydrogeologic units. In addition, calibration of the BCV test case model for the Oak Ridge regional groundwater flow modeling effort also concluded that horizontal anisotropy of 10:1 was optimal for matching field observations (UCOR 2015, Sect. 4.4) The regional flow model is a larger scale model that covers the entire ORR (DOE 2016).

For variation in the vertical dimension, the site is modeled as a single, unconfined aquifer with nine layers to simulate the changes in hydraulic conductivity with depth. All model layers are represented as unconfined since the modeled hydraulic conductivity decreases with depth.

The approximately 45-degree dip in the geological strata is represented by staggering the hydraulic conductivity (representing the different hydrogeologic units) with depth. The zones of hydraulic conductivities used to represent hydrogeologic units in layer 1 of the CBCV model are shown on Fig. D.5. The hydraulic conductivity zonation in a vertical south-north cross section is shown on Fig. D.6, which illustrates the offset of the hydrogeologic units with depth to simulate the dipping hydrogeologic units in the model.

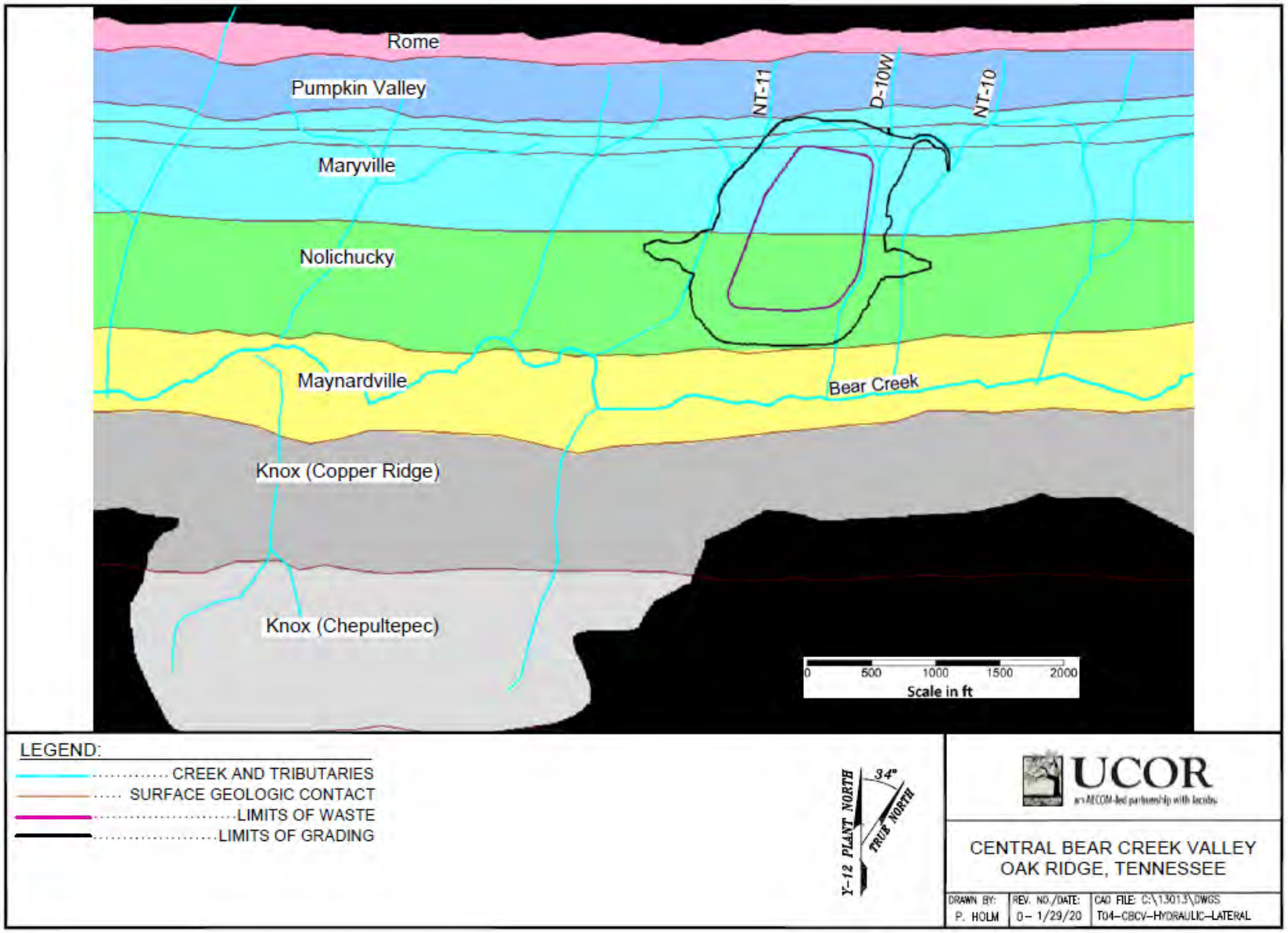

Fig. D.5. Hydraulic conductivity zones in CBCV model layer 1

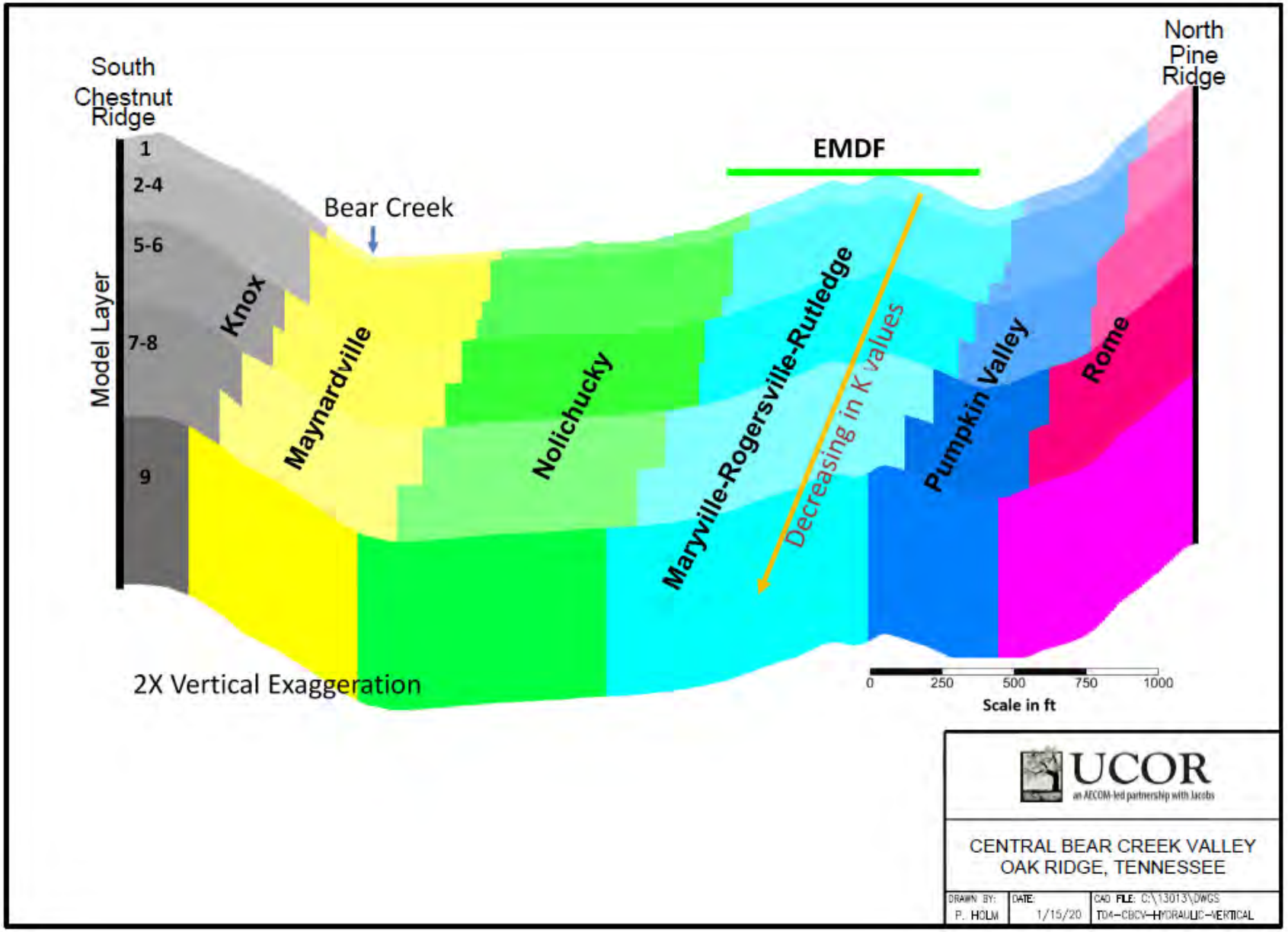

Fig. D.6. Hydraulic conductivity zones in the CBCV model (vertical section)

Both the previously available hydraulic conductivity data from BCV and site-specific hydraulic tests performed at the EMDF area were used to refine the hydraulic conductivity values during the model calibration. The site-specific tests included slug tests and FLUTe tests across the site. FLUTe is a new test method for transmissivity profiling in a borehole (Keller 2012). The hydraulic conductivity values from the slug tests range from 1E-03 to 1E-06 cm/sec. The inferred hydraulic conductivity values from the FLUTe tests range from 1E-04 to 1E-06 cm/sec.

Hydraulic conductivities for each hydraulic unit by model layer for the final calibrated CBCV model are provided in Table D.2. These values are similar to the BCV regional model with only small changes (less than 50 percent) in some zones.

Because the CBCV model is applied as a long-term steady-state groundwater flow condition, other hydraulic properties and parameters, such as storage and transport terms, were not quantified or applied in the flow model application.

Table D.2. CBCV model hydraulic conductivity summary

Material or Geologic Formation	Model Layer	K_x	K_y	K_z	Unit
Knox	1	1.56E+00	7.80E+00	1.56E+00	ft/day
	2--4	9.18E-03	9.18E-02	9.18E-03	ft/day
	5--6	2.54E-03	2.54E-02	2.54E-03	ft/day
	7--8	1.16E-03	1.16E-02	1.16E-03	ft/day
	9	5.00E-04	5.00E-03	5.00E-04	ft/day
Maynardville	1	2.13E+00	1.07E+01	2.13E+00	ft/day
	2--4	5.00E-02	5.00E-01	5.00E-02	ft/day
	5--6	3.34E-03	3.34E-02	3.34E-03	ft/day
	7--8	1.52E-03	1.52E-02	1.52E-03	ft/day
	9	4.80E-04	4.80E-03	4.80E-04	ft/day
Nolichucky	1	1.50E-01	7.50E-01	1.50E-01	ft/day
	2--4	9.50E-03	9.50E-02	9.50E-03	ft/day
	5--6	2.52E-03	2.52E-02	2.52E-03	ft/day
	7--8	6.10E-04	6.10E-03	6.10E-04	ft/day
	9	5.00E-05	5.00E-04	5.00E-05	ft/day
Maryville-Rogersville-Rutledge	1	1.00E-01	5.00E-01	1.00E-01	ft/day
	2--4	3.60E-03	3.60E-02	3.60E-03	ft/day
	5--6	1.35E-03	1.35E-02	1.35E-03	ft/day
	7--8	3.20E-04	3.20E-03	3.20E-04	ft/day
	9	4.50E-05	4.50E-04	4.50E-05	ft/day
Pumpkin Valley	1	1.00E-01	5.00E-01	1.00E-01	ft/day
	2--4	4.72E-03	4.72E-02	4.72E-03	ft/day
	5--6	1.75E-03	1.75E-02	1.75E-03	ft/day
	7--8	4.20E-04	4.20E-03	4.20E-04	ft/day
	9	5.60E-05	5.60E-04	5.60E-05	ft/day
Rome	1	4.00E-01	2.00E+00	4.00E-01	ft/day
	2--4	4.00E-02	4.00E-01	4.00E-02	ft/day
	5--6	5.00E-03	5.00E-02	5.00E-03	ft/day
	7--8	1.00E-03	1.00E-02	1.00E-03	ft/day
	9	5.00E-04	5.00E-03	5.00E-04	ft/day

CBCV = Central Bear Creek Valley

D.3.2.2 Model Boundary Conditions

D.3.2.2.1 No-flow boundary conditions

The BCV groundwater system is bounded by Pine Ridge to the north and Chestnut Ridge to the south; the two ridge crests form the northern and southern boundaries of the modeled domain (Fig. D.1). These ridges are straight, sub-parallel in a northeast-southwest direction, and have relatively high topographic relief. Pine Ridge is narrow and steep, while Chestnut Ridge has a broader crest, yet still has a well-defined surface water divide. The groundwater divide mirrors the surface water divide. The planes extending vertically downward from the crests of the ridges are specified to be no-flow boundaries for the groundwater flow system, and there is no groundwater import or export across the ridge crests (Fig. D.7). The vertical base of the model is assumed to be a no-flow boundary because of the minimal exchange of meteoric source groundwater with the highly mineralized groundwater at greater depth (about 800 ft below ground surface) (ORNL 1992b).

D.3.2.2.2 Constant head boundary conditions

Constant head boundary conditions were assumed along the west and east side of the model domain based on a steady-state simulation of the calibrated regional BCV groundwater flow model (Fig. D.7). Constant head boundary condition allows the groundwater to flow into and out of the CBCV model area. These model boundaries were located at a sufficient distance from the proposed EMDF site and assessment locations, so the constant head boundary condition would not greatly influence the groundwater flow in the EMDF footprint and adjacent areas.

D.3.2.2.3 Surface water drainage boundary conditions

Surface water drainage features are represented in the CBCV model as either drain cells or river cells (Fig. D.8). Both are head-dependent flux boundary conditions.

Drain cells allow groundwater to discharge at a surface water location and then out of the model domain when the groundwater level is above the stream bottom elevation. River cells allow both discharge (gaining surface flow) and recharge (losing surface flow) surface water interaction with the groundwater based on head difference. River cells are used for the main channel of Bear Creek because although much of the stream has flow throughout the year, losing reaches have been documented seasonally (Robinson and Mitchell 1996) can be represented in the model. The tributaries to Bear Creek are generally seasonally dry (Robinson and Johnson 1995, DOE 2019) and gaining reaches; therefore, they are represented as drains in the model. The current site-specific investigation of the surface flow at the tributaries also suggest a great variation in flow rate and gaining nature of the stream toward the lower reach so the drain representation is appropriate.

Actual stream bottom elevations based on detailed topographic data were assigned in the model for the elevations of the river and drain cells. The Bear Creek main channel and its tributaries are directly above the weathered bedrock. Therefore, the streambed conductance for these river and drain cells were set to arbitrarily high values (10,000 sq ft/day) to allow instant groundwater-surface water interaction in the model simulation.

Table D.3 provides a summary of the CBCV model boundary conditions applied in the final calibrated model.

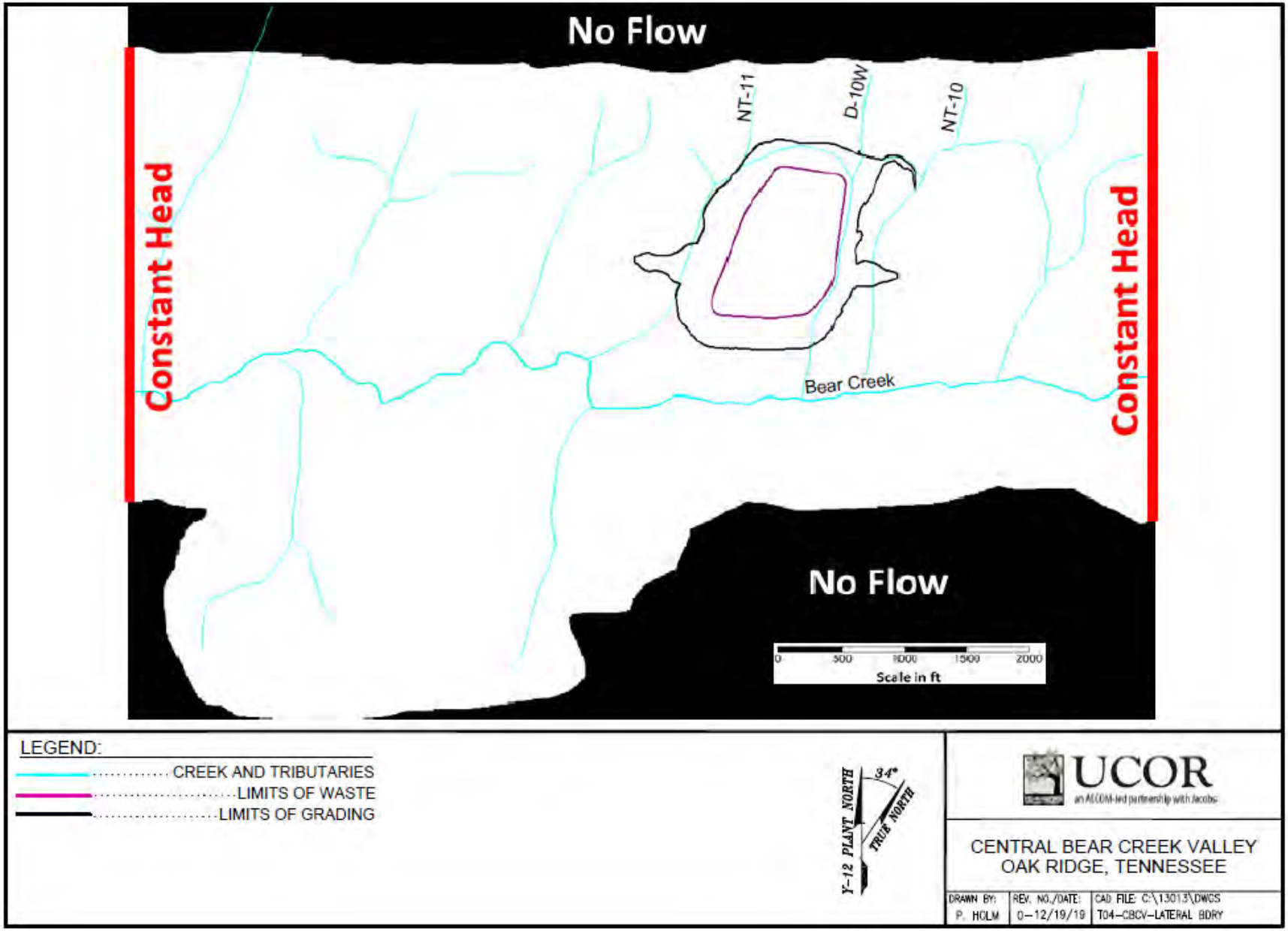

Fig. D.7. Lateral boundary conditions in the CBCV model

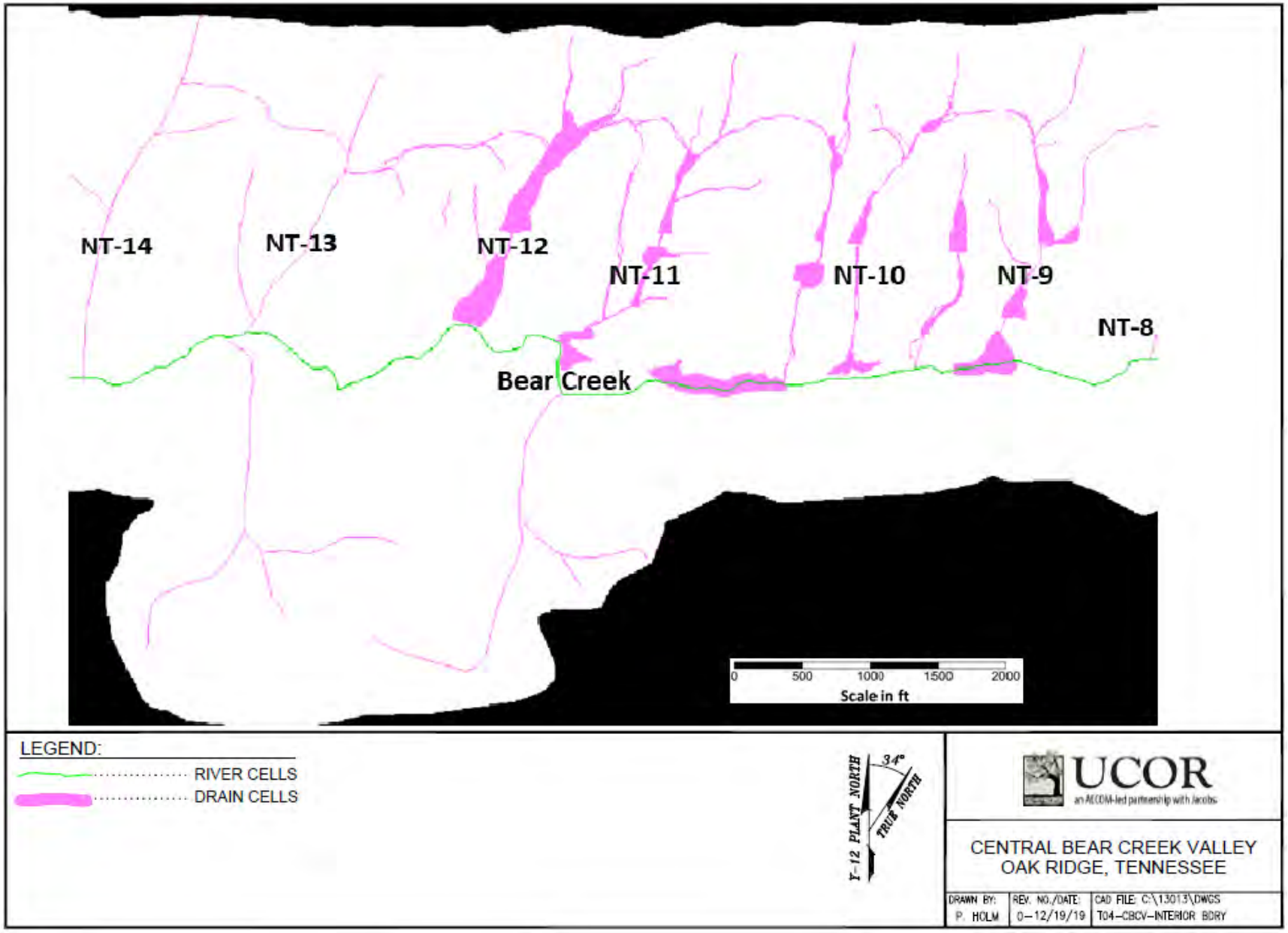

Fig. D.8. CBCV model interior boundary conditions representing surface water features

Table D.3. CBCV model boundary conditions summary

Number of CBCV Model Cells by Boundary Condition Type	
Constant head	6,427
Rivers	1,386
Drains	16,425
No flow	1,316,996

CBCV = Central Bear Creek Valley

D.3.2.3 Sources and Sinks

Groundwater sources simulated in the model are the following:

- Recharge from precipitation
- Inflow from the losing reaches of Bear Creek
- Lateral inflow through constant head boundary conditions.

Groundwater sinks simulated in the model are the following:

- Outflow to the drain cells representing surface water drainage features
- Outflow to Bear Creek
- Lateral outflow through constant head boundary conditions.

Groundwater recharge from precipitation is assumed to be the only source of inflow to the CBCV model outside of the boundary conditions. Groundwater recharge is precipitation minus runoff and evapotranspiration, and the recharge rate is a function of geologic media, surface slope, and vegetation. Several recharge rates were assigned in the model corresponding to surface expression of different geological units (see Fig. D.9) and corresponding topographic features and hydrologic properties of soils.

Similar to hydraulic conductivity values in the model, the recharge rates for the units were initially adapted from the BCV regional groundwater model (DOE 1997a). These values were adjusted during the CBCV model calibration based on site-specific data. These site-specific data included surface water flow measurements, and groundwater levels. Final values of the recharge rates based on calibration of the base steady-state model are listed in Table D.4.

Table D.4. CBCV Model Recharge Rate Summary

Recharge Areas	Recharge Rate	
	(ft/day)	(in./year)
Rome	2.2E-03	9.6E+00
Pumpkin Valley	1.4E-03	6.1E+00
Maryville-Rogersville-Rutledge	2.2E-03	9.6E+00
Nolichucky	1.5E-03	6.6E+00
Maynardville	3.0E-03	1.3E+01
Knox (Copper Ridge)	1.0E-03	4.4E+00
Knox (Chepultepec)	5.0E-04	2.2E+00
Soil Spoils Pile	5.0E-04	2.2E+00

CBCV = Central Bear Creek Valley

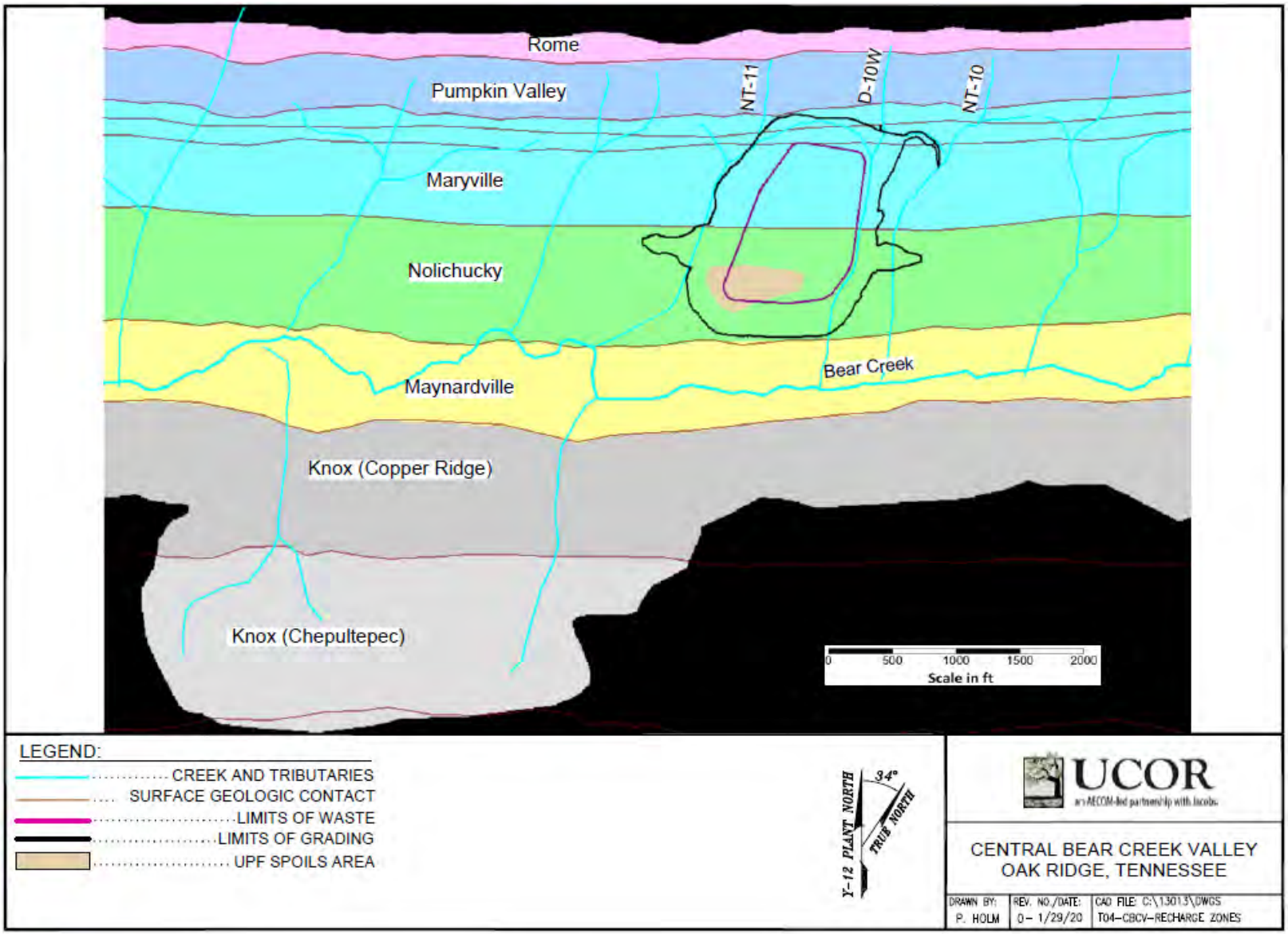

Fig. D.9. Groundwater recharge zones in the CBCV model

D.3.3 MODEL CALIBRATION

Calibration is a process wherein certain parameters of the model, such as recharge and hydraulic conductivity, are altered in a systematic fashion, and the model is repeatedly run until the computed solution matches field-observed values within an acceptable level of accuracy. Modelers use different quantitative measures to demonstrate the accuracy of a groundwater flow model. Common model performance measures include the mean error, the mean absolute error, and the root mean squared error. The areal distribution of residuals (differences between measured and simulated values) also is important to determine whether some areas of the model are biased either too high or too low.

However, the appropriateness of the conceptualization of the groundwater system and processes should always be evaluated during calibration. Thus, the method of calibration, the closeness of fit between the simulated and observed conditions, and the extent to which important aspects of the simulation were considered during the calibration process are important in evaluating the appropriateness of the model to address the objectives. For the CBCV and EMDF models, the objective is to develop a high-resolution (small-scale) site-specific model that retains the regional flow characteristics expected from previous efforts.

The CBCV model was constructed based on the BCV regional groundwater flow model (DOE 1997a). The BCV regional model was extensively calibrated based on a larger quantity of available data collected and summarized during the BCV RI/FS study. The CBCV model also incorporates extensive knowledge derived from development of several different sub-regional and site-specific models for Bear Creek, Y-12, and EMWMF and an early site proposed for EMDF All these previous modeling applications ensure that the groundwater flow models are representative of the groundwater system in BCV (DOE 1998b, BJC 2003, and BJC 2010).

Phase 1 field characterization data were used during the CBCV model development, application, and calibration. Inclusion of site-specific field data enables targeted calibration of the CBCV model to ensure model accuracy in the immediate vicinity of the disposal facility. Lithologic logs and hydraulic test data (DOE 2018, DOE 2019) were used to refine model layer geometry and hydraulic conductivity assignments. The potential range in recharge rates was bounded by local precipitation data and water balance considerations. Calibration of recharge rates applied to different geologic units guided by comparison of observed streamflow to model-predicted discharge at the locations of the six flow measurement stations. Final assignment of hydraulic conductivity values was guided by comparison of observed median groundwater levels to model-predicted hydraulic heads at locations corresponding to the piezometer screen intervals.

D.3.3.1 Quantitative Calibration Targets

Central to the model calibration considerations described above, groundwater and surface water data were used quantitatively as model calibration targets. Groundwater elevations in Phase 1 piezometers were logged continuously with 30-minute intervals beginning in March 2018. Groundwater elevations in Phase 2 piezometers were logged continuously beginning in December 2018. Table D.5 shows a statistical summary of the groundwater level data for Phase 1 (upper block of rows) and Phase 2 (lower block of rows) from March 2018 through early March 2019. This approximately year-long period of monitoring data from the Phase 1 piezometers was used during the final CBCV model calibration process. Phase 2 piezometer observations through March 2019 represent only the wet season and, therefore, were not suitable for calibrating the CBCV model simulation of average annual conditions.

Table D.5. EMDF site groundwater well and water level data summary

PZ ID	Boring/Piezometer Construction Information												Groundwater Measurement Data Summary For Model Application							
	Y-12 easting (ft)	Y-12 northing (ft)	Well development completion date	Phase	Boring depth (ft)	Shallow/ deep	Ground surface elevation (ft-msl)	Top of casing elevation (ft-msl)	Top of screen elevation (ft-msl)	Bottom of screen elevation (ft-msl)	Screen length (ft)	Mid-point screen elevation (ft-msl)	Starting date used	Ending date used	Minimum (ft-msl)	Maximum (ft-msl)	Varying range (ft)	Average (ft-msl)	Median[a] (ft-msl)	No. of data points
GW-978	38643.59	30656.68	2/27/2018	1	80.0	D	953.86	955.97	894.36	884.26	10.1	889.31	3/2/2018	3/6/2019	934.78	948.72	13.94	938.44	**937.65**	17,698
GW-979	38653.90	30656.61	2/27/2018	1	37.8	S	953.99	955.99	927.69	917.69	10.0	922.69	3/8/2018	3/6/2019	934.78	948.86	14.09	938.51	**937.81**	15,774
GW-980R	38138.34	30379.90	3/5/2018	1	74.4	D	963.38	965.63	903.48	893.38	10.1	898.43	3/6/2018	3/6/2019	935.60	940.81	5.21	937.06	**937.02**	17,524
GW-981	38148.33	30396.70	3/6/2018	1	34.0	S	963.52	965.74	941.42	931.42	10.0	936.42	3/8/2018	3/6/2019	942.78	951.04	8.26	944.24	**944.04**	17,424
GW-982	38617.04	30317.82	3/5/2018	1	126.5	D	1015.91	1018.02	913.81	903.81	10.0	908.81	3/6/2018	3/6/2019	943.41	955.90	12.49	948.16	**947.76**	17,523
GW-983	38606.49	30325.62	3/6/2018	1	92.2	S	1015.76	1018.07	936.66	926.56	10.1	931.61	3/8/2018	3/6/2019	943.35	956.23	12.89	948.29	**948.34**	16,281
GW-986	38191.80	30130.30	3/1/2018	1	59.6	D	930.51	932.37	889.51	884.51	5.0	887.01	3/2/2018	3/6/2019	918.75	929.76	11.01	922.17	**921.72**	17,523
GW-987	38194.40	30138.34	3/3/2018	1	27.9	S	930.89	932.94	914.79	904.79	10.0	909.79	3/8/2018	3/6/2019	918.43	929.17	10.75	922.38	**922.21**	14,264
GW-988	38091.14	29952.47	3/1/2018	1	78.5	D	956.75	958.95	894.85	884.85	10.0	889.85	3/2/2018	3/6/2019	928.78	949.16	20.38	937.59	**937.88**	17,523
GW-989	38082.67	29950.44	3/6/2018	1	45.0	S	955.57	957.86	921.97	911.97	10.0	916.97	3/8/2018	3/6/2019	929.26	951.30	22.04	938.95	**939.28**	16,519
GW-992R	38737.35	29698.29	3/3/2018	1	55.5	D	909.30	911.40	870.00	864.90	5.1	867.45	3/3/2018	3/6/2019	902.12	909.16	7.03	904.17	**903.87**	15,308
GW-993	38724.90	29690.50	3/3/2018	1	35.5	S	909.70	911.76	886.70	876.70	10.0	881.70	3/8/2018	3/6/2019	901.06	908.24	7.17	903.53	**903.32**	17,432
GW-994	38051.04	29644.99	3/1/2018	1	55.0	D	917.01	918.89	875.01	865.01	10.0	870.01	3/2/2018	3/6/2019	901.69	913.47	11.79	905.92	**905.50**	17,523
GW-995	38039.32	29646.82	3/3/2018	1	34.0	S	916.75	918.76	894.65	884.65	10.0	889.65	3/8/2018	3/6/2019	901.60	912.71	11.11	905.25	**904.80**	17,431
GW-998	37742.36	29021.82	2/27/2018	1	45.0	D	877.75	880.18	851.15	841.15	10.0	846.15	3/2/2018	3/6/2019	865.42	878.76	13.34	872.52	**873.37**	17,523
GW-999	37750.58	29025.01	3/5/2018	1	22.0	S	877.79	880.11	867.49	857.49	10.0	862.49	3/8/2018	3/6/2019	868.28	878.27	9.99	874.06	**874.44**	11,763
GW-984	38868.33	30499.01	12/6/2018	2	35.0	D	926.83	929.28	902.83	892.83	10.0	897.83	12/7/2018	3/5/2019	924.19	926.15	1.96	924.85	924.87	4233
GW-985	38865.91	30487.01	12/6/2018	2	10.3	S	926.31	928.96	921.31	916.31	5.0	918.81	12/7/2018	3/5/2019	923.87	925.84	1.96	924.54	924.55	4233
GW-990	38511.81	30081.29	12/6/2018	2	107.8	D	993.95	996.22	893.95	888.95	5.0	891.45	12/7/2018	3/5/2019	944.30	950.15	5.85	946.63	946.43	4228
GW-991	38503.75	30076.06	12/6/2018	2	19.5	S	992.91	995.55	983.66	973.66	10.0	978.66	Dry well							
GW-996	38409.68	29154.25	12/6/2018	2	50.0	D	898.47	900.84	860.47	850.47	10.0	855.47	12/7/2018	3/5/2019	879.31	890.90	11.59	884.28	884.06	4239
GW-997	38408.15	29164.13	12/6/2018	2	29.05	S	898.13	900.70	879.33	869.33	10.0	874.33	12/7/2018	3/5/2019	879.31	890.85	11.54	884.27	884.04	4238
GY-001	38221.50	28857.20	12/6/2018	2	41.8	D	888.73	891.09	852.18	847.18	5.0	849.68	12/7/2018	3/5/2019	869.49	883.82	14.33	875.61	874.78	4241
GY-002	38220.50	28865.23	12/6/2018	2	22.5	S	888.84	891.16	876.59	866.59	10.0	871.59	12/7/2018	3/5/2019	869.68	887.07	17.39	876.15	875.11	4240
GY-003	38306.54	30626.13	12/6/2018	2	19.4	S	930.84	933.44	917.94	912.94	5.0	915.44	12/7/2018	3/5/2019	922.40	927.65	5.25	925.39	925.79	4233
GY-004	37820.51	29914.13	12/6/2018	2	25.3	S	920.96	923.55	906.46	896.46	10.0	901.46	12/7/2018	3/5/2019	905.27	916.91	11.65	907.19	906.13	4230
GY-005	38316.38	30686.53	12/6/2018	2	37.0	S	933.43	935.88	913.43	908.43	5.0	910.93	12/7/2018	3/5/2019	928.52	935.91	7.40	931.98	932.31	4234
GY-006	39184.09	30455.04	12/6/2018	2	37.0	D	943.38	945.92	917.38	912.38	5.0	914.88	12/7/2018	3/5/2019	926.85	936.24	9.39	929.69	929.59	4232
GY-007	39180.83	30461.69	12/6/2018	2	20.0	S	943.01	945.50	933.26	923.26	10.0	928.26	12/7/2018	3/5/2019	927.50	939.95	12.46	930.27	929.74	4231
GY-008	39693.48	29898.41	12/6/2018	2	26.0	S	932.65	935.27	917.15	907.15	10.0	912.15	12/7/2018	3/5/2019	907.14	926.81	19.67	919.55	920.66	3946
GY-019	38495.78	30070.16	1/18/2019	2	86.0	D	992.29	994.60	917.49	907.49	10.0	912.49	No data collected for the data application period							
GY-020	38501.06	30064.06	1/18/2019	2	64.0	D	992.36	994.52	939.56	929.56	10.0	934.56	1/24/2019	3/5/2019	948.64	952.75	4.11	950.48	950.03	1921

[a]Calculated median elevations for Phase 1 piezometers were used as calibration targets for the CBCV model.

CBCV = Central Bear Creek Valley
EMDF = Environmental Management Disposal Facility
ID = identification
PZ = piezometer

This page intentionally left blank.

Calculated median groundwater elevations for Phase 1 piezometers represent a full year and were used as model calibration targets (Table D.5). (The last column of Table D.5 provides the number of observations used to compute the average and median values for each Phase 1 piezometer. Missing data and slightly different periods of record account for the variation in the number of observations.) These median observed elevations are appropriate calibration targets for a steady-state model intended to represent long-term average hydrologic conditions. However, precipitation at the EMDF area from March 1, 2018 through February 28, 2019 was 73.15 in. (ORNL 2019), which is approximately 33 percent higher than the Oak Ridge local long-term yearly average (~55 in./year). The total recorded precipitation in February 2019 was 15.16 in., making it the wettest month since 2001 recorded at the Y-12-W meteorological tower station, the nearest ORR weather station. The February 2019 total precipitation also exceeds the 1948-2015 Oak Ridge area record maximum monthly total for any month except July (ORNL 2015). In addition, February 2018, the month before the beginning of Phase 1 data collection, was also very wet month with 11.3 in. of precipitation, more than two times higher than the February average (5.4 in.), which can have an influence on the March groundwater measurements in 2018. Therefore, the 2018-2019 median water levels represent higher groundwater elevations than would be expected in an average year. Using these target median values for the CBCV model calibration should produce higher simulated groundwater elevations in the vicinity of the EMDF than would be expected in an average year. This intentional bias provides a measure of confidence in the facility design for which EMDF model results are used to demonstrate attainment of a minimum 15 ft depth to water performance criterion.

Surface water flow measurements were collected continuously at six stream locations along NT-10, NT-11, and D-10W for 1 year (see Fig. D.2). Table D.6 provides a summary of the surface water flow data for April 2018 to April 2019. Measured stream flow includes storm flow/surface water runoff and groundwater discharge (base flow). A majority of the higher flows are directly associated with storm events, with storm runoff the primary contributor. Because the groundwater model only simulates the groundwater discharge component (base flow), the calculated average flow rates from May 1 to June 16, 2018 at these locations were used as the surface water calibration targets since there were relatively few storm events during this period.

Table D.6. EMDF site surface water flow data summary

Streamflow Measurement Location	Minimum[a] Rate (gpm)	Maximum[a] Rate (gpm)	Count	Calibration Target Rate (Average Flow May 1-June 16, 2018) (gpm)
SF-1	0	5612.4	15,864	23.1
SF-2	0	6810.0	16,080	18.4
SF-3	0	2678.3	30,720	12.1
SF-4	0	3042.2	16,079	8.2
SF-5	0	5273.2	34,230	9.2
SF-6	0	4426.4	34,110	15.1

[a]Minimum and maximum flows during the period from April 2018 through April 2019.

EMDF = Environmental Management Disposal Facility

D.3.3.2 Model Calibration Processes

Because many groundwater flow models have been developed and applied within the BCV, the major parameters impacting model results are well understood. Hydraulic conductivity and recharge are the key model parameters. Therefore, the model-specific calibration for the CBCV model involved adjusting hydraulic conductivity values and recharge rates for defined hydrogeologic units. Comparison was then made between simulated groundwater elevations and surface water flow rates and groundwater elevation

targets from the site piezometers and surface water flow rates measured in flumes installed in the primary tributaries (NT-10, D-10W, and NT-11). The adjustment ranges for the parameters were bounded by the site-specific data (hydraulic conductivity values from field tests). These parameters were varied systematically across the model calibration runs while maintaining a reasonable overall representation of site conditions and relative relationships of the hydraulic properties among geologic units.

The goal of the calibration was a base case simulation matching observed (median) groundwater elevations, gradients, and flow directions. Agreement between simulated and observed groundwater elevations was considered the primary model calibration metric because groundwater elevations are one of the important design parameters. A good match (less than 20 percent difference) between model-predicted groundwater discharge rates and the surface water flow calibration target values was also an important calibration goal for providing realistic constraints on the site-specific hydraulic conductivities and recharge rates applied in the model. Comparing model results to the calibration targets based on observed surface water flow rates provided additional validation of simulated groundwater flow patterns.

D.3.3.3 Model Calibration Result

Fig. D.10 shows a scatter plot of simulated versus observed (median) groundwater head targets (median of Phase 1 groundwater elevations) for the final calibrated CBCV model. In a perfectly calibrated model, where simulated groundwater elevations equal observed groundwater elevations, plotted values would fall along a straight line (shown on Fig. D.10 as a red line). The residual mean, which is an average of the simulation errors (simulated minus observed values), is -0.91 ft, indicating a very reasonable calibration with a slight overall tendency for the model to underpredict (less than 1 ft) groundwater elevations at the calibration target locations.

About half of groundwater targets have model-simulated groundwater elevations within 5 ft of observed values (absolute residual mean of 4.13 ft for all targets). In addition, the model-predicted groundwater heads in the paired wells all have vertical gradients consistent with vertical gradients inferred from the field observations. The EMDF site has a groundwater elevation variation of approximately 100 ft near the facility and approximately 300 ft within the model domain, and the simulated absolute deviation of less than 5 percent (4.13/100) near the facility and less than 2 percent (4.13/300) within the model domain is considered acceptable.

The largest residuals are associated with piezometers GW-989/988 and GW-981, which are underestimated by the CBCV model, and GW-986/987, which is overestimated by the model. These piezometers are located west of the horseshoe-shaped crest of the knoll, an area with large elevation differences. These errors are likely an artifact of grid spacing and the large surface elevation differences in that part of the model domain. The CBCV model also overestimates levels for GW-978/979 in the saddle upgradient of the knoll, and at the top of the knoll for the shallow depth piezometer GW-983.

The Phase 2 piezometer data available at the time of model calibration, only represent seasonal high groundwater elevations. Therefore, they were not used for the base condition (long-term average) CBCV model calibration. The Phase 2 piezometer groundwater elevation data were applied to evaluating the model results as part of the sensitivity analysis presented in Sect. D.3.5.

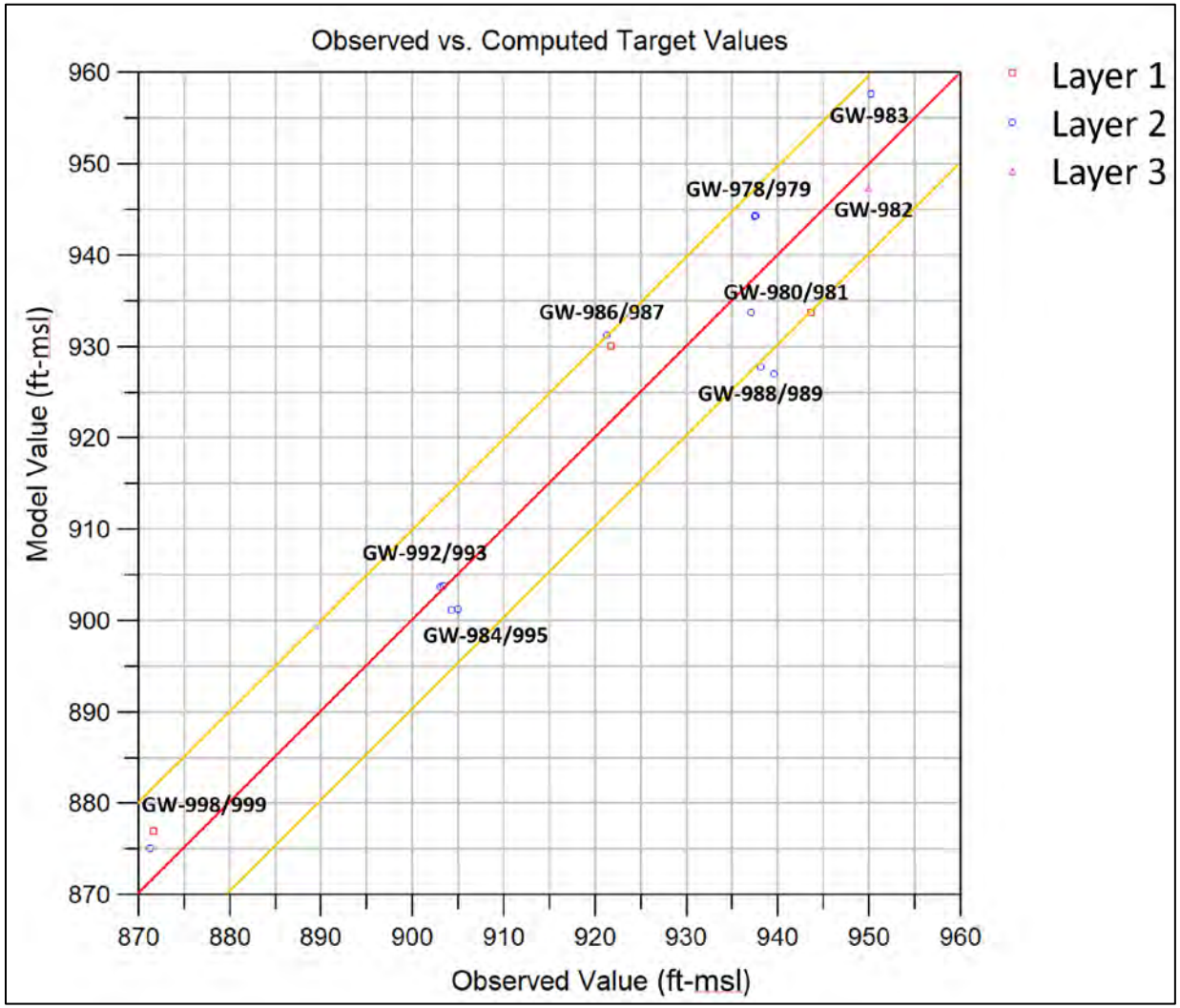

Fig. D.10. CBCV model-simulated and observed groundwater levels (Phase 1 median values)

Observed surface water flows in Bear Creek and associated tributaries (NT-10, D-10W, and NT-11) were also compared to model-simulated values to evaluate calibration (Fig. D.11). The CBCV model simulates flow rates within 15 percent of the May 1 through June 16, 2018 measured flume flow rate targets and similar trends in terms of flow rates along each tributary segment. These results help validate the groundwater model parameters and that the model represents site-specific conditions.

The model-predicted water balance for the final calibrated site-specific base conditions model is shown on Fig. D.12. Model water balance is the measure of water inflow versus outflow. The simulated water budget identifies inflow to and outflow from the aquifer system for simulated features that add or remove water (in terms of cubic ft per day). The simulated water balance is consistent with the hydrologic conceptual model for the area.

The inflow of groundwater (in red) into the model domain is mostly from precipitation recharge, followed by surface water recharge to groundwater from the Bear Creek main channel, and lateral groundwater inflow from the eastern (upgradient) constant head boundary. The outflow of groundwater (in green) out of the model domain is through drainage to surface water features (Bear Creek and its tributaries) and lateral groundwater outflow from the western (downgradient) constant head boundary condition. The model predicted more lateral outflow through the downgradient boundary condition than inflow from the upgradient boundary condition. The model also predicted that a majority of the groundwater discharge (outflow) is to the Bear Creek tributaries (drain cells). The water balance for the Bear Creek main channel (river cells) suggests that it acts as both a sink (outflow) and source (inflow) since the Bear Creek channel is located above the highly conductive Maynardville Limestone, where extensive groundwater-surface water interaction is expected. All these results are in line with the conceptual site model for the area and Bear Creek.

The overall water balance error for the CBCV site-specific base conditions model is 0.11 percent and is well within the typically accepted limit of simulation error. This result shows that water has been mathematically accounted for in the model, and the MODFLOW simulation has correctly solved the governing flow equations.

Based on the base conditions model calibration results, the CBCV model predicts groundwater elevations and groundwater-surface water interaction acceptably. Therefore, the model is able to represent site-specific conditions and can be used as the foundation to develop the EMDF design condition model.

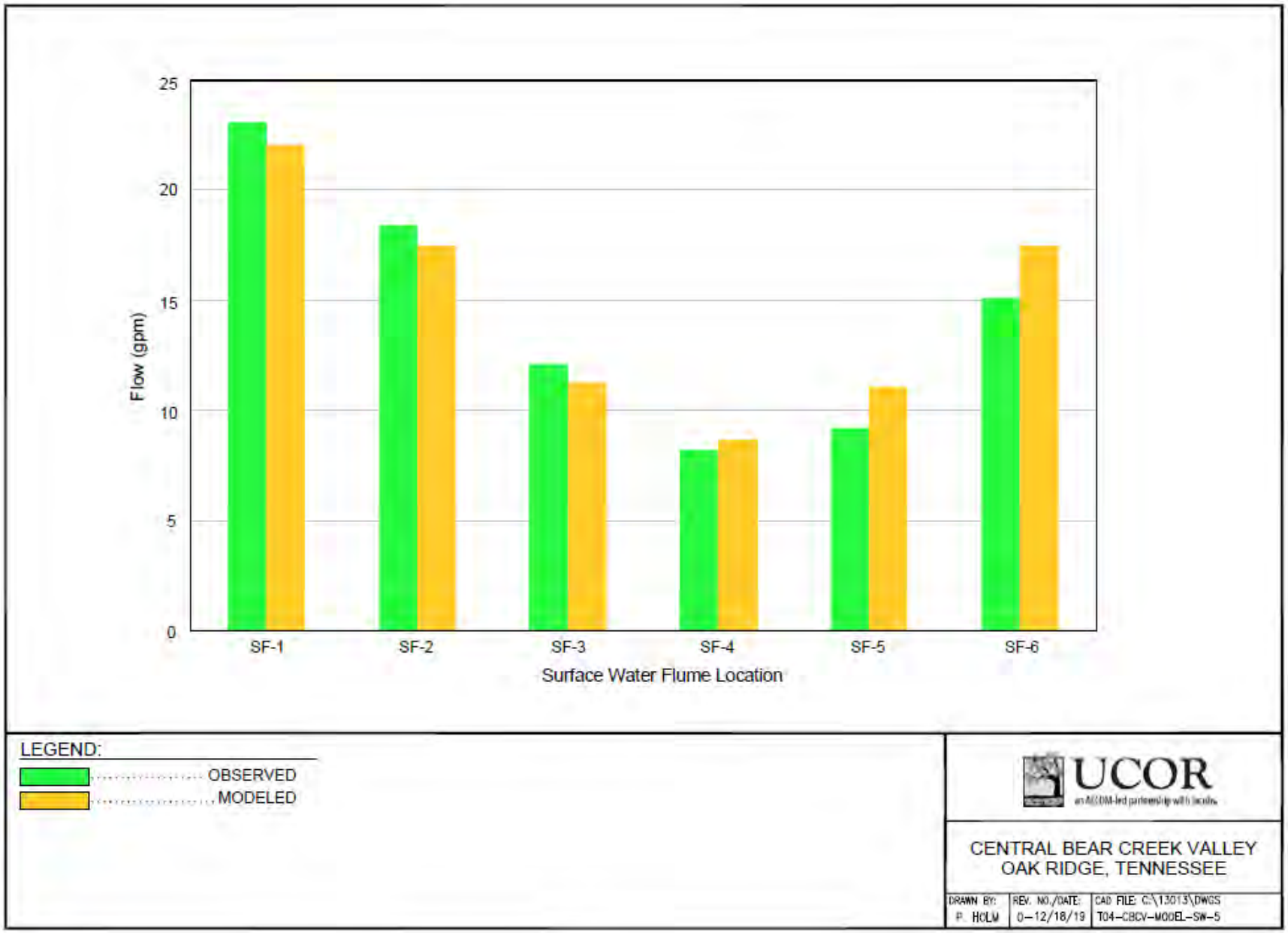

Fig. D.11. CBCV model-simulated and observed surface water flows

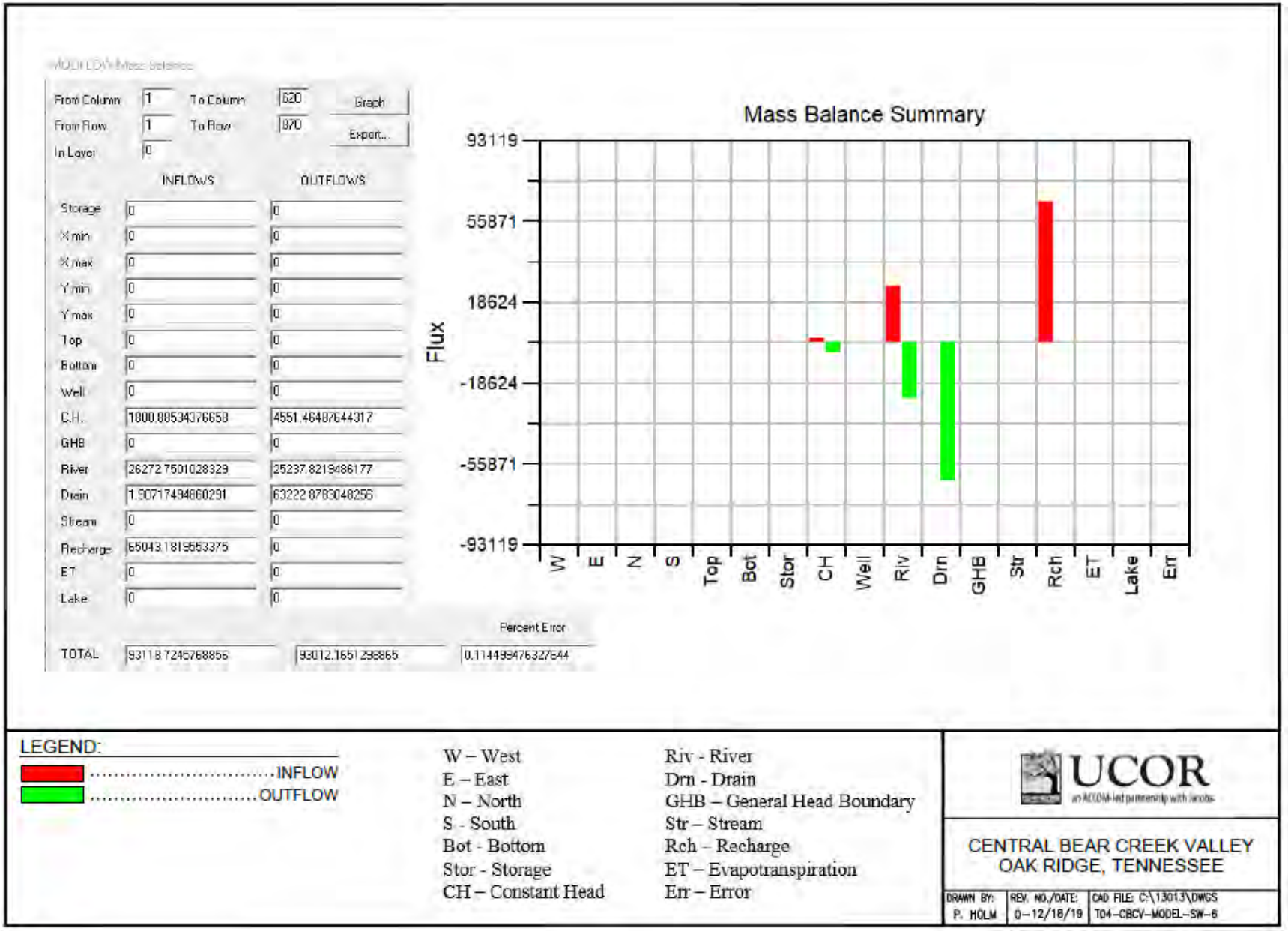

Fig. D.12. CBCV model average annual water balance summary

D.3.4 CBCV FLOW MODEL RESULTS

All groundwater flow model simulations were conducted using MODFLOW-2005 code (Harbaugh 2005). For the model runs, the following model conditions and solver were applied:

- Unconfined model layers
- Steady-state condition
- Re-wetting function
- Preconditioned conjugate-gradient package (PCG 2 Solver).

Based on the flow model results, particle tracking was performed using the MODPATH model developed by USGS (Pollock 1989) for selected flow model runs. Particle tracking is a technique that uses the velocity field produced by the model to delineate the path that a molecule of water, or contaminant, would take from its origin to a discharge point. This information is especially important because of the high anisotropy associated with the aquifer units underlying the BCV watershed. MODPATH Version 5 was used for the simulation and was used to help illustrate the groundwater flow paths, including the high anisotropy of the different geologic layers and with depth.

D.3.4.1 Base Condition Flow Model Results

The model-simulated water table under steady-state conditions for the base recharge condition is shown on Fig. D.13. The steady-state simulation represents the long-term annual average condition. The water table surface generally mirrors the site topography and shows a strong influence by the surface drainage features. Particle tracking results used for the starting locations at the water table are shown on Fig. D.14. Particle tracking indicates that shallow groundwater is strongly influenced by the surface drainage features and discharges into Bear Creek and its tributaries. Almost all the particle tracks originating in the upper tributary watersheds discharge into NT-10 and NT-11. The particle tracking shows the hydraulic influence of the saddle below the steep slope of Pine Ridge above the proposed EMDF site, with flow discharging from the Pine Ridge slope and from the knoll area into the surface drainages. Based on the particle tracking, only groundwater in the lower portion of the watersheds would discharge into Bear Creek.

The simulated shallow groundwater flow field is consistent with the site conceptual model, measured groundwater surface maps constructed based on monitoring data, and the general understanding of groundwater flow at the site.

Fig. D.15 shows the groundwater potentiometric surface in the deeper part of the aquifer (the deeper fractured bedrock represented by model layer 4). While the influence of the anisotropy and lateral discharge to the drainages and Bear Creek is still apparent, the strong influence of Bear Creek as a valley-wide groundwater discharge boundary along the south side of the site is more evident.

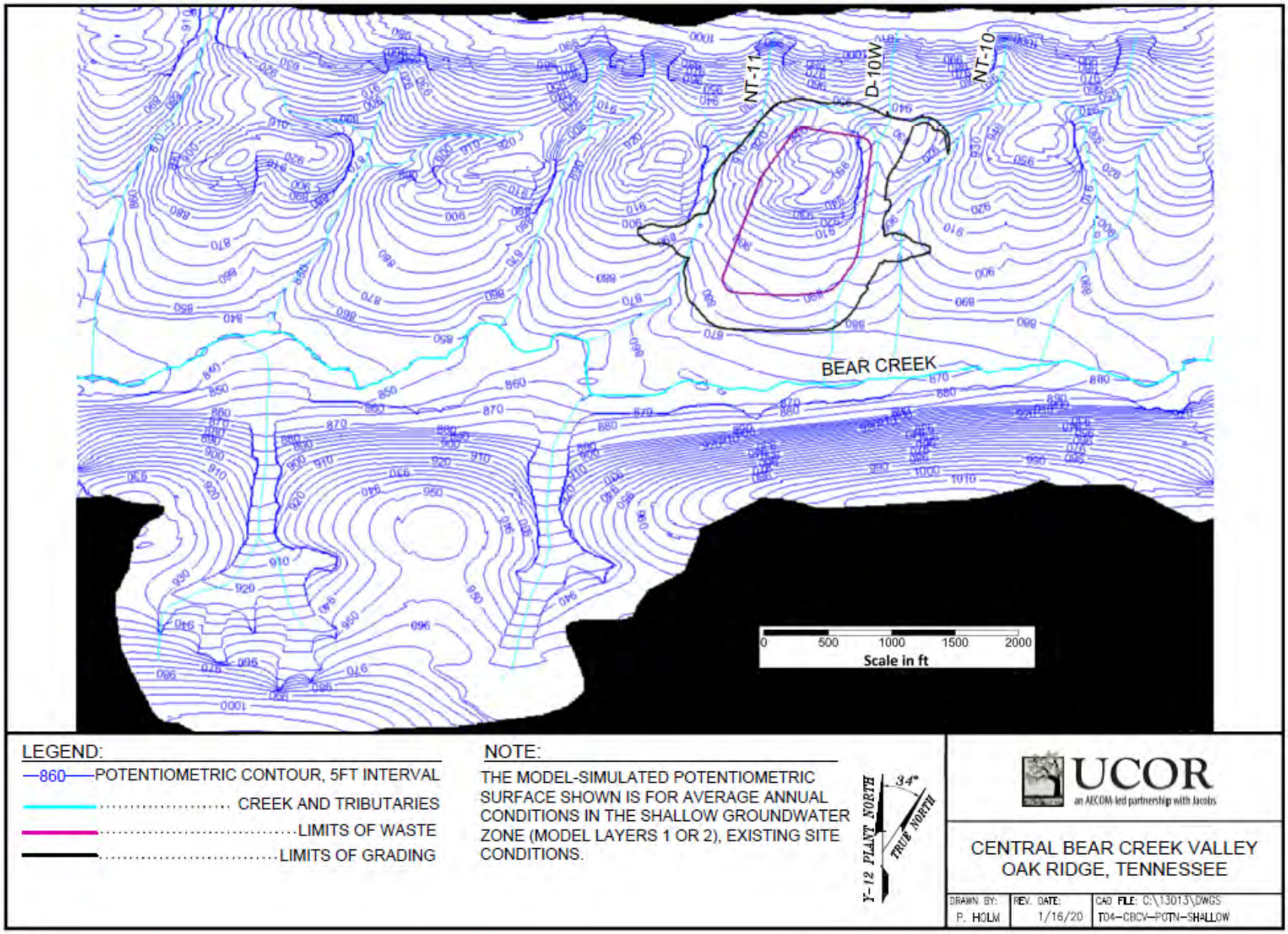

Fig. D.13. CBCV model predicted water table elevation

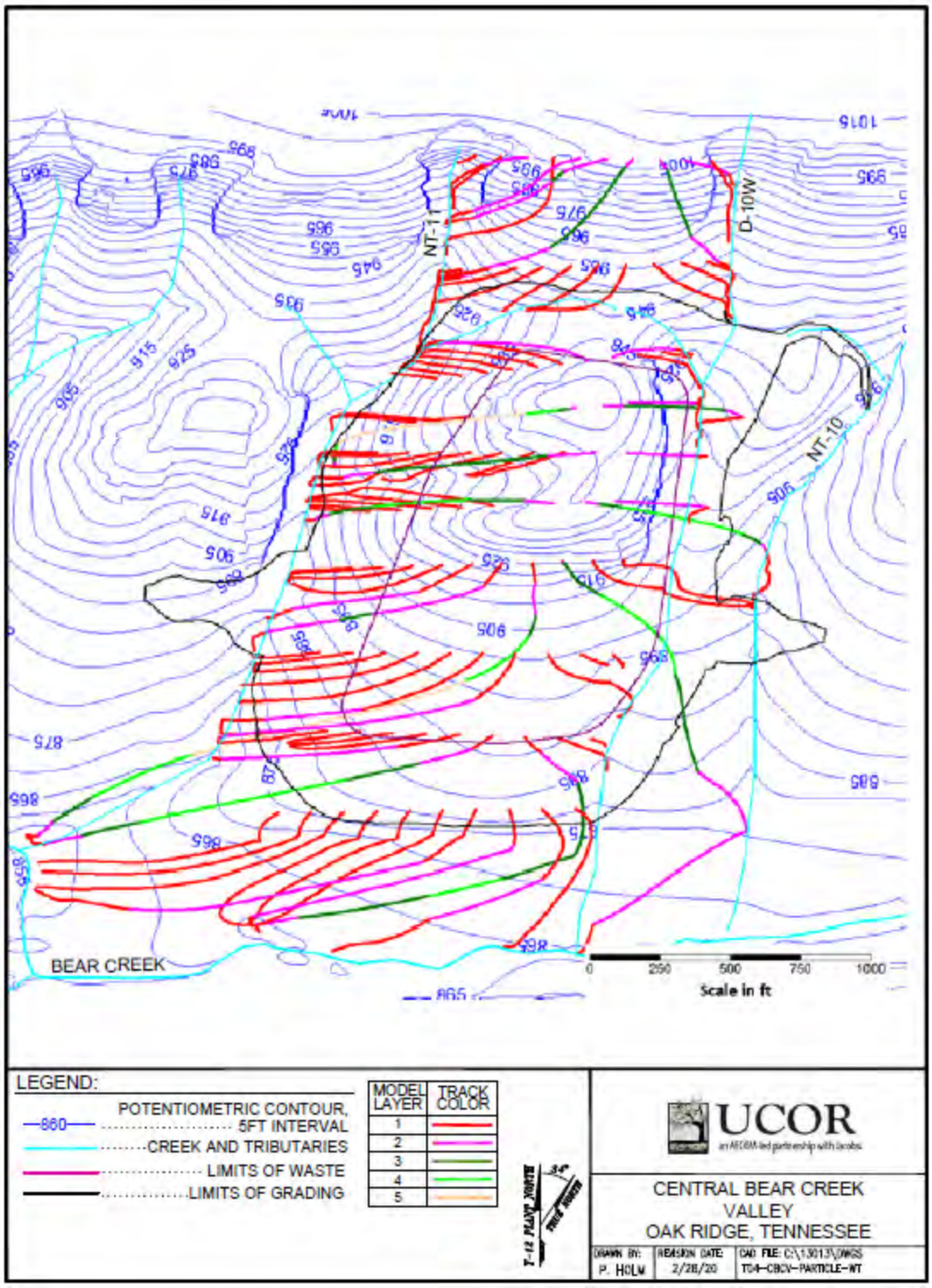

Fig. D.14. CBCV model particle tracks from water table location

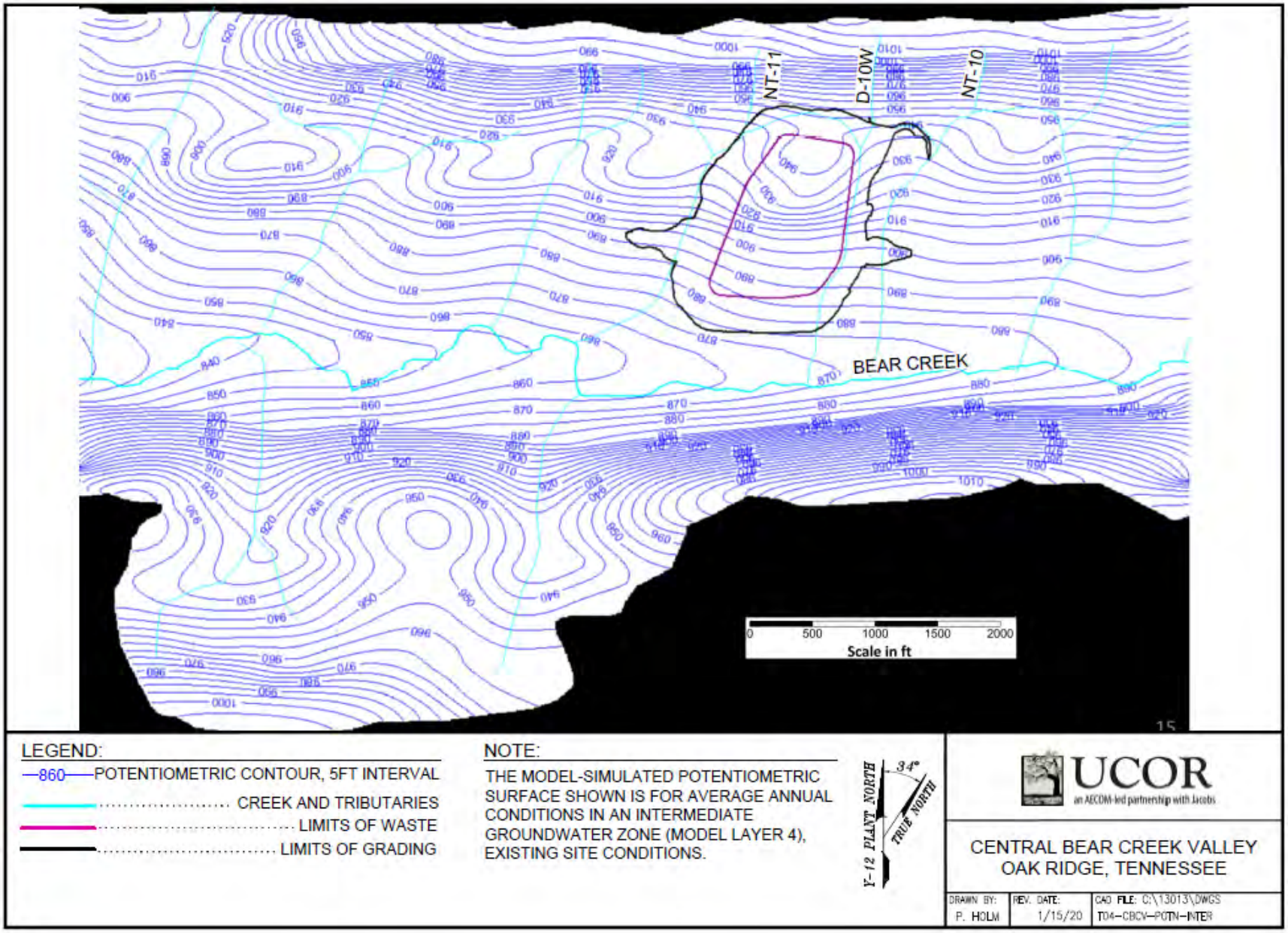

Fig. D.15. CBCV model-predicted potentiometric surface in the fractured bedrock zone

A flow vector analysis was performed to further interpret the simulated groundwater flow field in the model. The flow vectors for model layer 1 (water table) and model layer 4 (fractured bedrock/intermediate groundwater zone) near the proposed disposal cell location are shown on Fig. D.16. Model layers 1 and 2 receives recharge and groundwater flows from the ridge and knobs toward the surface drainages and vertically downward. In the shallow fractured bedrock zone (model layers 3 through 5), the groundwater maintains downward flow, except near the discharge zones along the surface drainages and along the steep slope of the Pine Ridge where the vertical gradient is upward. The simulated flow field displays the same behaviors observed in the piezometer measurements and is consistent with the conceptual model of the groundwater flow field for BCV.

Flow vectors are shown in cross sections on Fig. D.17. Both sections show strong influence of the surface recharge and surface drainage features on the groundwater flow. The proposed disposal cell location is marked on the cross sections for reference, but these sections show existing (pre-construction) groundwater flow conditions.

D.3.4.2 Wet and Dry Condition Results

The CBCV model base condition represents the long-term annual average hydrologic conditions consistent with site characterization and hydrogeologic monitoring data. Groundwater elevations fluctuate across the site due to seasonal changes in surface recharge. To support model sensitivity analysis for the PA, a range of recharge rates was simulated with the calibrated CBCV model. Based on comparing those model results to field data, a 50 percent higher than the base condition recharge (1.5x) was selected to represent groundwater elevations for wet (average seasonal high water levels) conditions, and a 50 percent lower than base recharge value (0.5x) was selected to represent dry (average seasonal low water levels) conditions at the EMDF site.

Fig. D.18 shows the CBCV model-predicted wet condition groundwater levels using recharge rates which were 50 percent higher than the base condition rates for all hydrogeologic formations. The predicted groundwater levels are higher than the base condition and compare well to the observed monthly average elevations for February 2019, the period with the highest piezometer measurements during the initial 12 months of monitoring. While groundwater elevations are higher within the knoll area, the general groundwater flow field does not change significantly from the base condition (Fig. D.13), suggesting the same general flow pattern.

Fig. D.19 shows the CBCV model-predicted groundwater elevations using 50 percent of the base recharge rate, representing dry conditions. The groundwater elevations are lower, and the model has more dry cells in model layer 1. Again, the general flow field is similar to the base condition flow with lower groundwater elevations and hydraulic gradients.

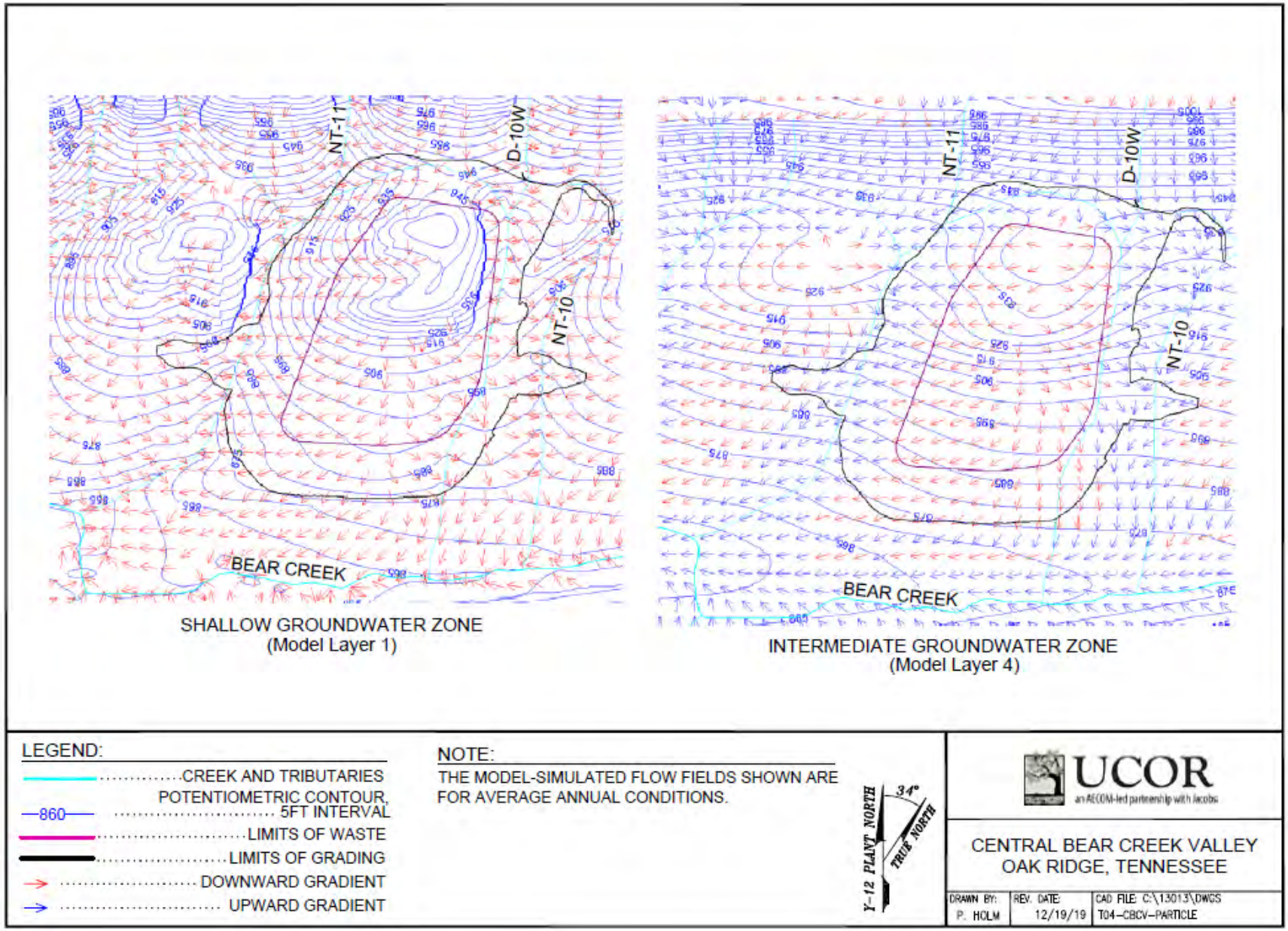

Fig. D.16. CBCV model-predicted flow vectors

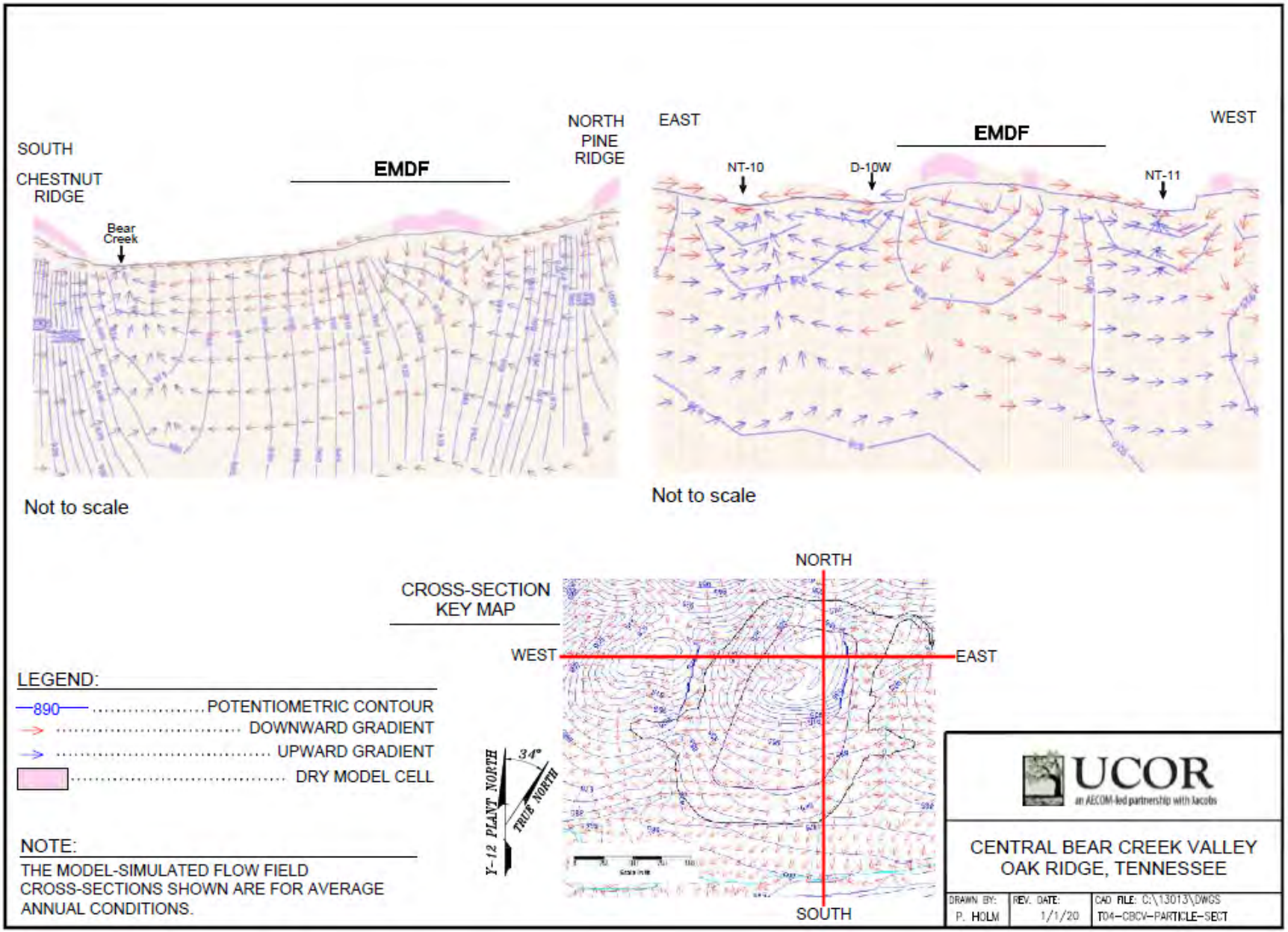

Fig. D.17. CBCV model-predicted flow vectors in cross section

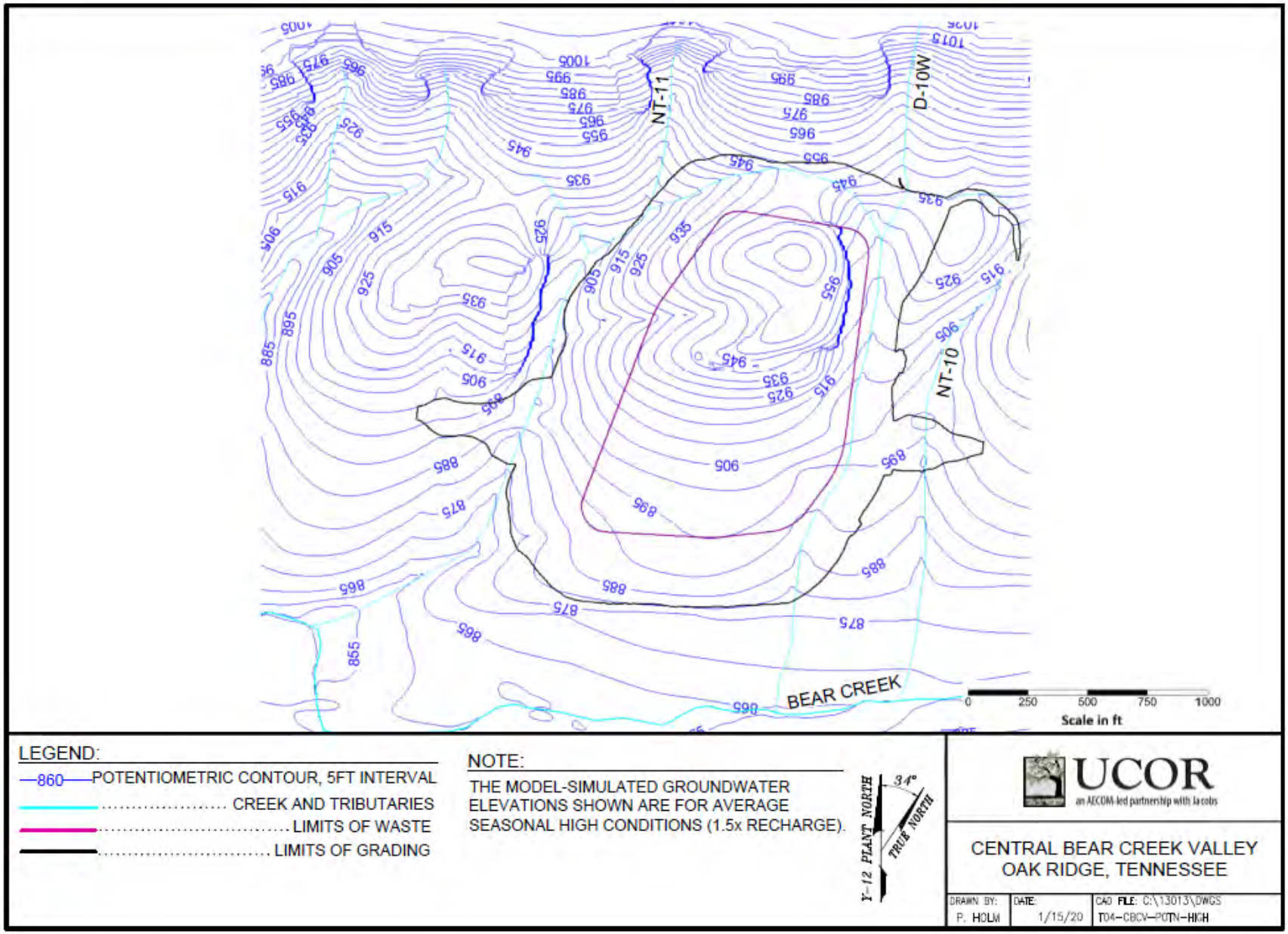

Fig. D.18. CBCV model-predicted groundwater levels for wet conditions (150 percent base recharge)

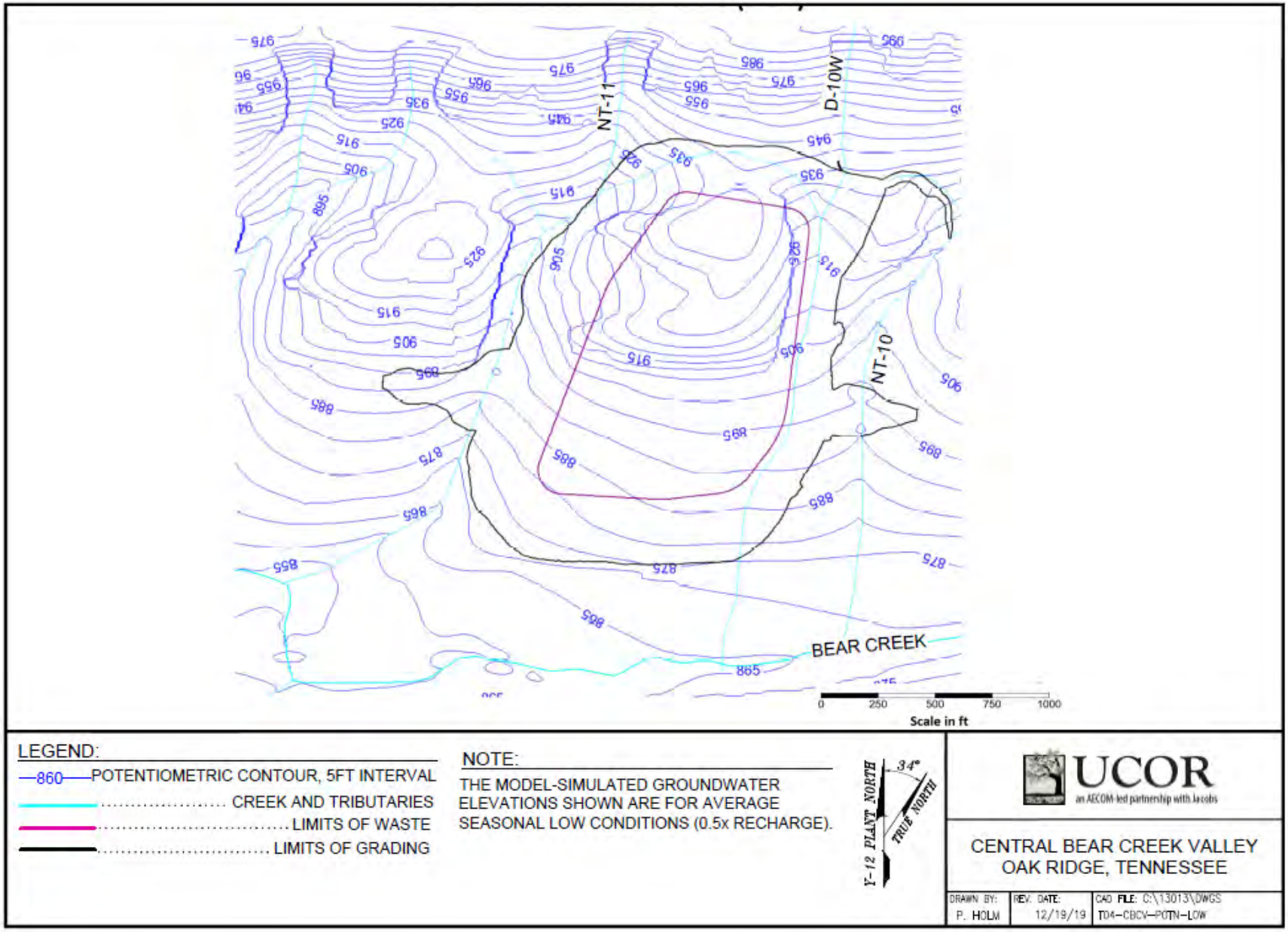

Fig. D.19. CBCV model-predicted groundwater levels for dry conditions (50 percent of base recharge)

D.3.5 CBCV MODEL SENSITIVITY ANALYSES

A sensitivity analysis is the process of varying one or more model parameters to determine the sensitivity of the model results to changes in the parameter value. For the CBCV model, a detailed sensitivity analysis was conducted on the recharge parameter since it has been identified from past models as a key parameter with the greatest impact on the results of the model. The recharge rates are also varied to more accurately reflect seasonal variation in the balance between precipitation and evapotranspiration that increases recharge rate, groundwater elevations, and stream base flow in the wet (winter-spring) period (refer to Sect. D.3.4.2). Average, post-construction seasonal high groundwater elevations are an important EMDF design performance metric.

Recharge was initially calibrated using site-specific median annual groundwater elevation data, hydrogeologic unit properties, and surface flow measurements. Two types of sensitivity evaluations were conducted for recharge: model-wide and hydrogeologic/topographic unit-specific.

The first type of sensitivity evaluation varied recharge rates model-wide (all hydrogeologic/topographic recharge areas, Fig. D.9) to represent wetter and drier conditions. The sensitivity analysis varied recharge in the CBCV model by 0.5, 0.75, 1.25, 1.5, 1.75, and 2 times the calibrated CBCV model rates for each recharge area. The sensitivity of the model to these varying values is presented in terms of changes in simulated stream base flow (discharge from model drain cells). Figure D.20 shows the base condition observed streamflow (May 1 to June 16, 2018 average as approximation of annual average base flow, Table D.6) for the six flow measurement stations on Bear Creek tributaries near the EMDF (refer to Sect. D.3.3.1 and Fig. D.2), along with model-simulated values for varying recharge rate multipliers.

Varying model recharge for model calibration and sensitivity analysis confirmed the recharge rates that provide model-simulated groundwater elevations corresponding to observed seasonal wet/dry conditions (Sect. D.3.4.2). The maximum observed groundwater elevations in Phase 1 and Phase 2 piezometers within the February 2019 were compared to model-simulated values from the recharge sensitivity runs. The wet condition (1.5 times base recharge) model-calculated groundwater elevations correlate very well to observed maximum elevations (Fig. D.21).

The comparison of these model-wide recharge sensitivity results (Figs. D.20 and D.21) and the calibrated (base recharge) CBCV model output (Figs. D.10 and D.11) with field observations demonstrates that the CBCV model accurately represents both average annual and extreme seasonal (Phases 1 and 2 February 2018 peaks) wet conditions.

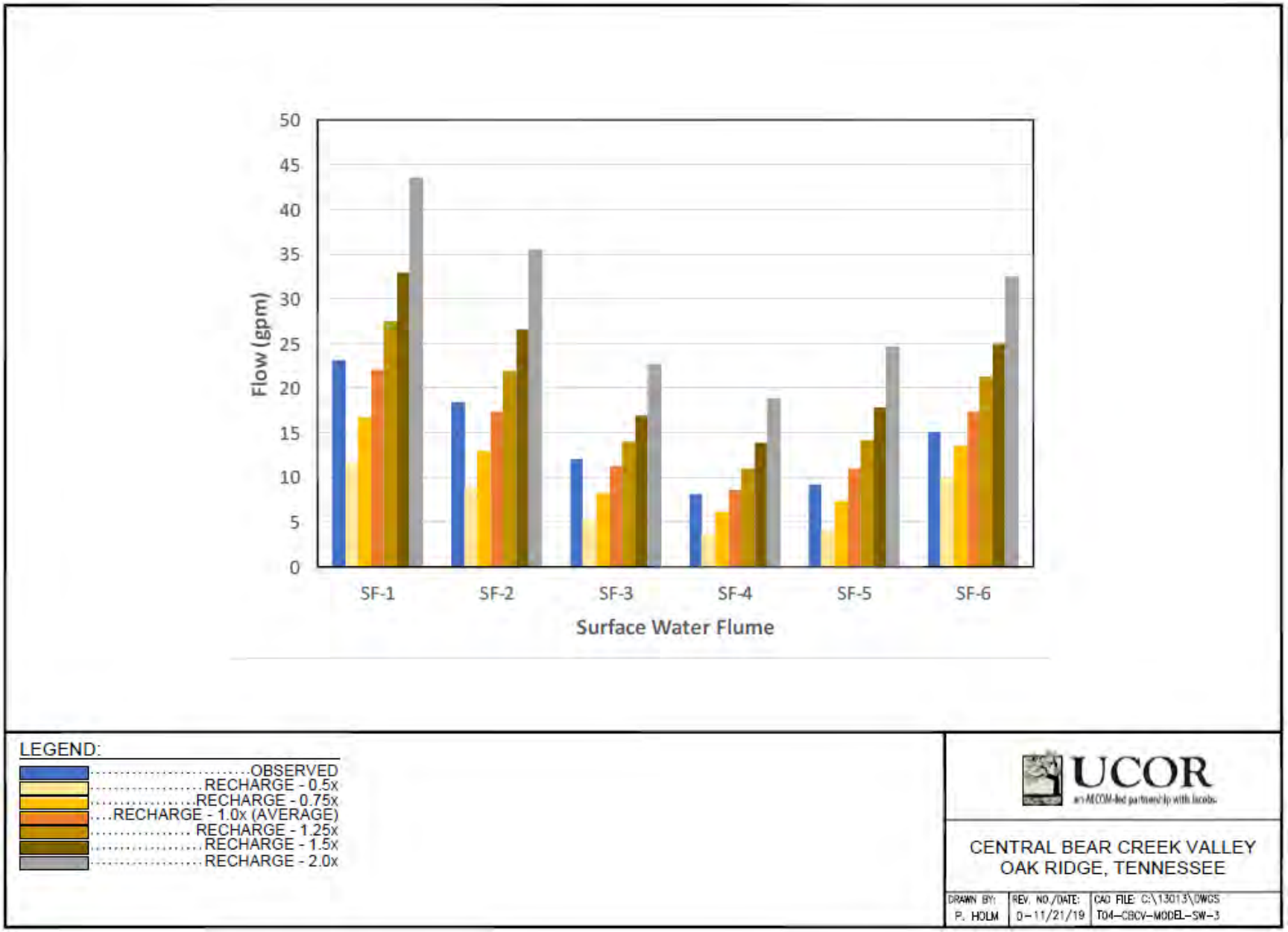

Fig. D.20. Observed and CBCV model-simulated stream discharges for varying recharge conditions

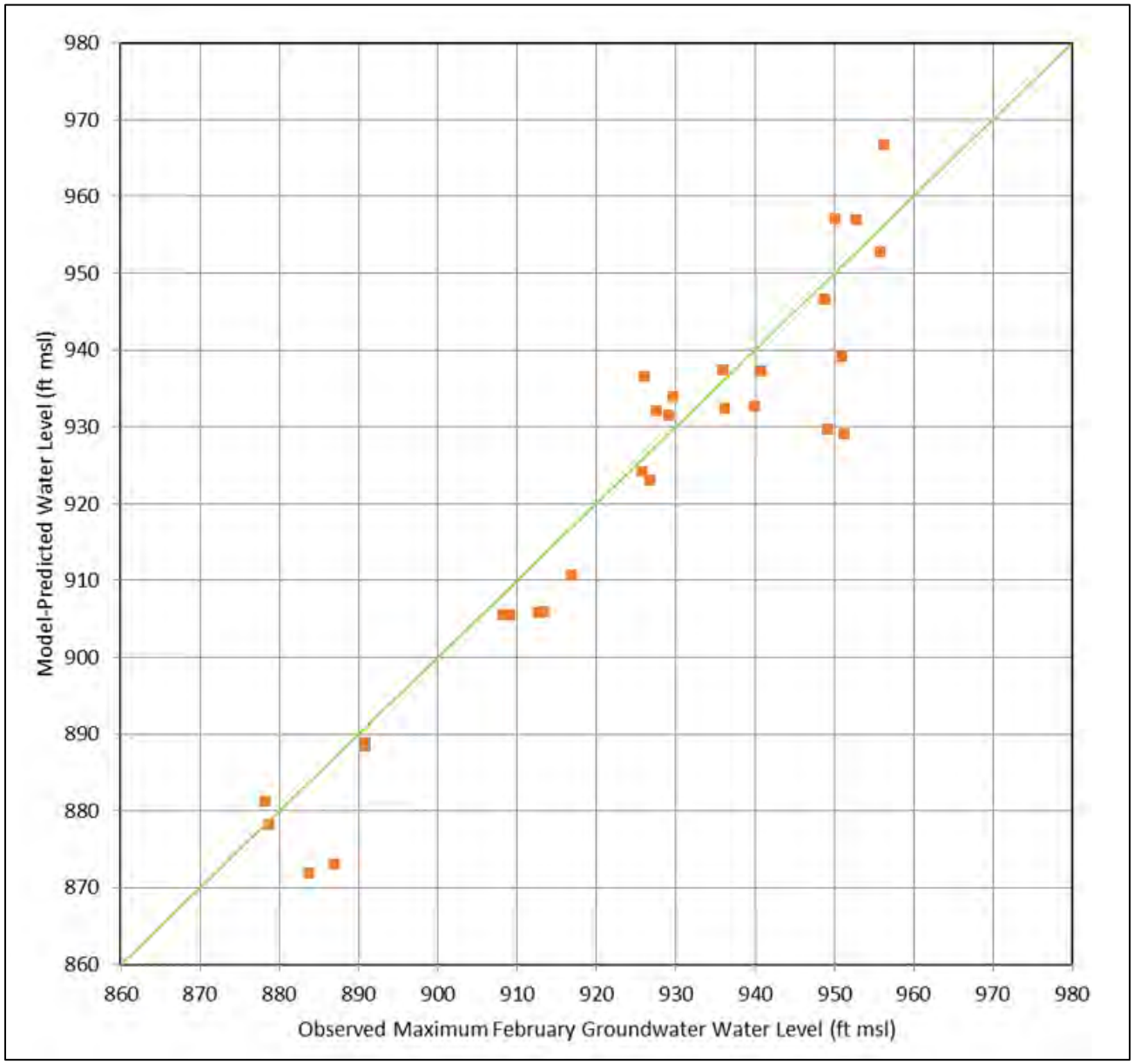

Fig. D.21. Observed February 2018 maximum water levels and CBCV model-predicted groundwater levels for wet conditions (1.5x recharge)

The second type of sensitivity evaluation varied recharge rates for specific hydrogeologic and topographic zones at the crest of Pine Ridge (refer to recharge areas in Fig. D.9). These sensitivity runs evaluated the potential groundwater elevation impact at the EMDF site due to higher recharge rates along parts of Pine Ridge upgradient of the proposed disposal area. For this set of sensitivity runs, three scenarios were considered:

- Recharge rates 50 percent higher (multiplier of 1.5) than the base rates for the upper part of Pine Ridge (topographically defined area), including both the Pumpkin Valley Shale (the steep south-facing slope) and the Rome Sandstone (ridge top area).
- Recharge rates 100 percent higher (multiplier of 2) than the base rates for the upper part of Pine Ridge (as defined for the 1.5 Pine Ridge recharge multiplier scenario).
- Recharge rates 100 percent higher (multiplier of 2) than the base rate for only the Rome Sandstone (geologically defined ridge top area), a hydrogeological consideration related to higher permeability of the sandstone and relatively gentle topography.

These recharge sensitivity simulation results were compared to the CBCV model-simulated base condition and evaluated for the following:

- Changes in simulated groundwater elevations
- Changes in groundwater discharges to surface water features
- Changes in groundwater flow field and flow directions.

Fig. D.22 shows the simulated increase in groundwater elevations (color shaded areas) associated with the simulated higher recharge rates. Higher recharge rates applied to Pine Ridge will result in higher groundwater elevations along the ridge but will have minimal impact on the groundwater elevations beneath the footprint area of the EMDF under all three scenarios. Light blue shaded areas on Fig. D.22 show where groundwater elevations increased from the base case by 0.5 to 1 ft. Minimal changes to the predicted groundwater flow field and groundwater flow directions occurred beneath the EMDF footprint area in response to higher recharge and groundwater elevations in the Pine Ridge Formations

Higher recharge rates for the Pine Ridge resulted in higher simulated groundwater discharges to surface waters, an increase of almost 50 percent over observed average surface water flow rates (Sect. D.3.3.1). That the calculated surface water flows are so much greater than observed provides additional validation for the calibrated recharge rates used for the CBCV model.

The recharge sensitivity results are consistent with the conceptual site model, with patterns of groundwater elevation influenced by existing topography and drainage features, including the “saddle” between Pine Ridge and the EMDF site.

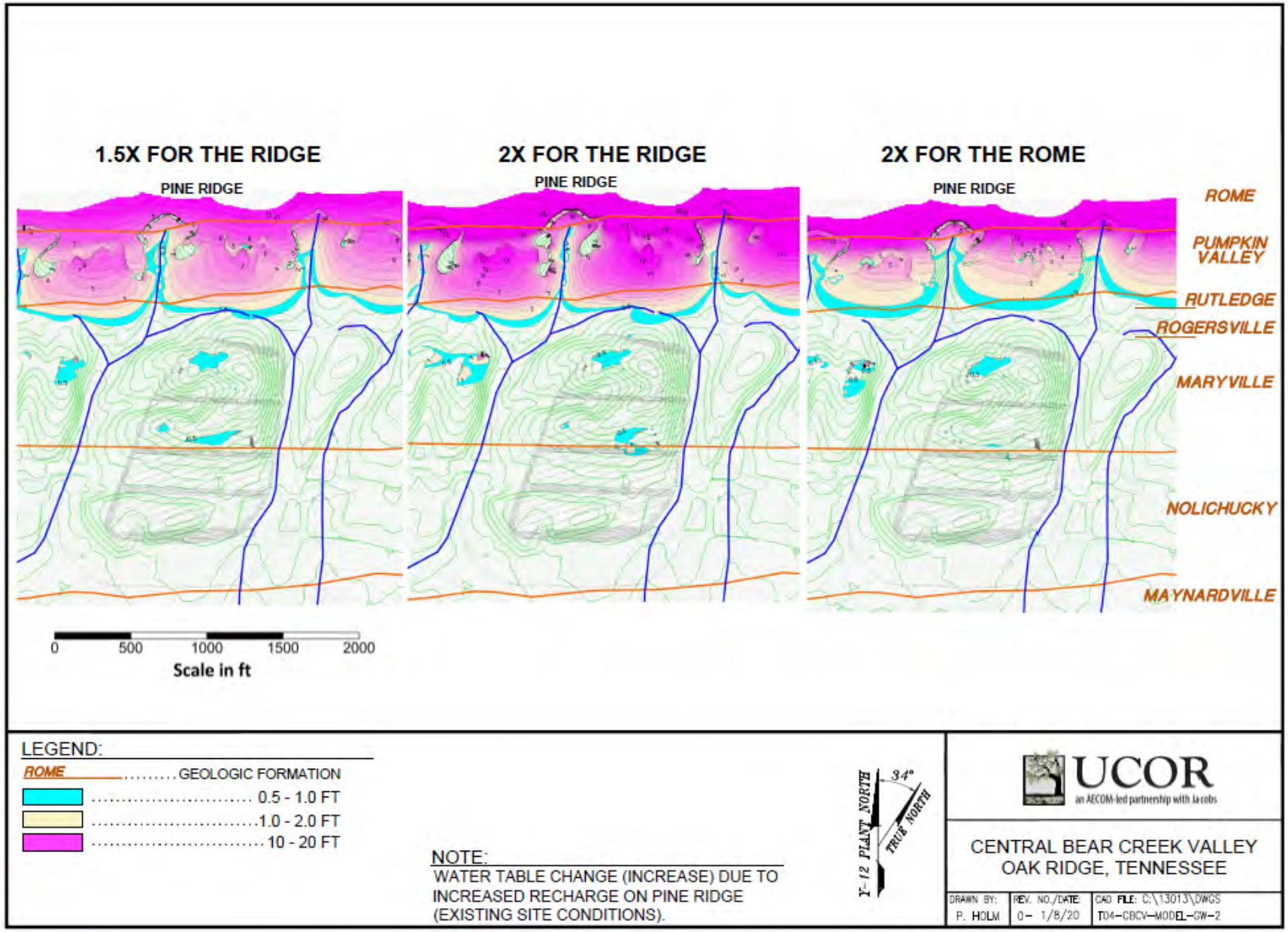

Fig. D.22. CBCV model-predicted groundwater level increases for higher recharge on Pine Ridge

D.4 EMDF FLOW MODEL DEVELOPMENT AND APPLICATION

The calibrated CBCV model, which represents current site conditions and the groundwater conceptual site model, was revised to develop the design condition model (EMDF model). Disposal cell design and other site variations that would have an impact on the groundwater flow conditions after construction were incorporated. The following parameters in the model were revised to represent the design and used in the EMDF model:

- EMDF preliminary design geometry and post-construction topography
- Parameters representing material properties of engineered features of the EMDF preliminary design
- Estimated EMDF performance parameters, such as water infiltration rates through the lined waste zone that were predicted using the Hydrologic Evaluation of Landfill Performance (HELP) model (Schroeder et al. 1994; refer to Appendix C, Sect. C.2 of the PA) and recharge rates for the outer perimeter berm zone calculated based on as permeability-recharge relationship.

The EMDF model was developed iteratively during the EMDF design process. Topographic and design parameter changes (liner/geobuffer elevations and extent, berm limits, etc.) required different model discretization in terms of model layer elevations and material zones for recharge and hydraulic conductivity. Therefore, many working versions of the EMDF model were developed over the course of the design progression. The design information used for the EMDF model came from the final preliminary design package for the EMDF, dated July 2019, as described in Sect. 4.1 of the QA Report (UCOR 2020).

D.4.1 EMDF GROUNDWATER FLOW MODEL DEVELOPMENT

D.4.1.1 Model Discretization

The model domain in the calibrated CBCV model was also used for the EMDF model. The EMDF preliminary design features were incorporated into the EMDF model, implemented as revisions to model layer 1. Within the EMDF footprint, the top of model layer 1 was revised to represent the final grade of the berms, side slopes, and the bottom of the waste (top of the liner system). The thickness of model layer 1 was modified in the area of the disposal cells to represent the newly placed liner system (15 ft thick) and the geologic buffer. The EMDF model layer 1 surface is shown on Fig. D.23.

The EMDF design will result in some significant topographic changes in the disposal cell footprint area. Figure D.24 shows the topographic changes between the existing topography and the finished grade (bottom of waste, top of berms). The light blue indicates areas of fill, while the bright pink indicates areas of cut. The amount of cut and fill is shown using 5-ft intervals, indicating the change from the existing elevation.

To maintain the horizontal continuity of the model layer as required by the model mathematics, the model layer 2 top surface (layer 1 bottom) also was modified for the cut areas.

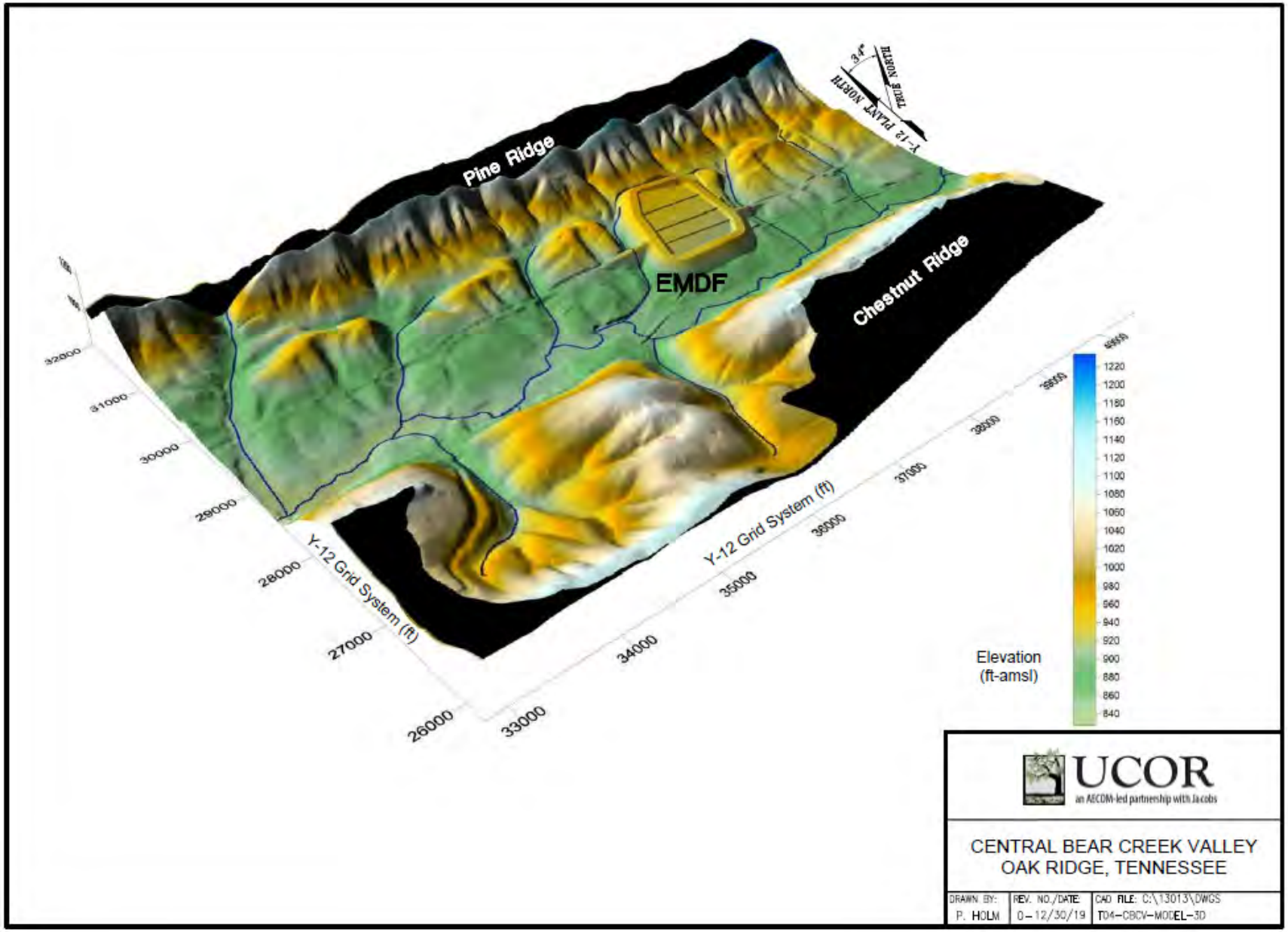

Fig. D.23. EMDF model domain and topography

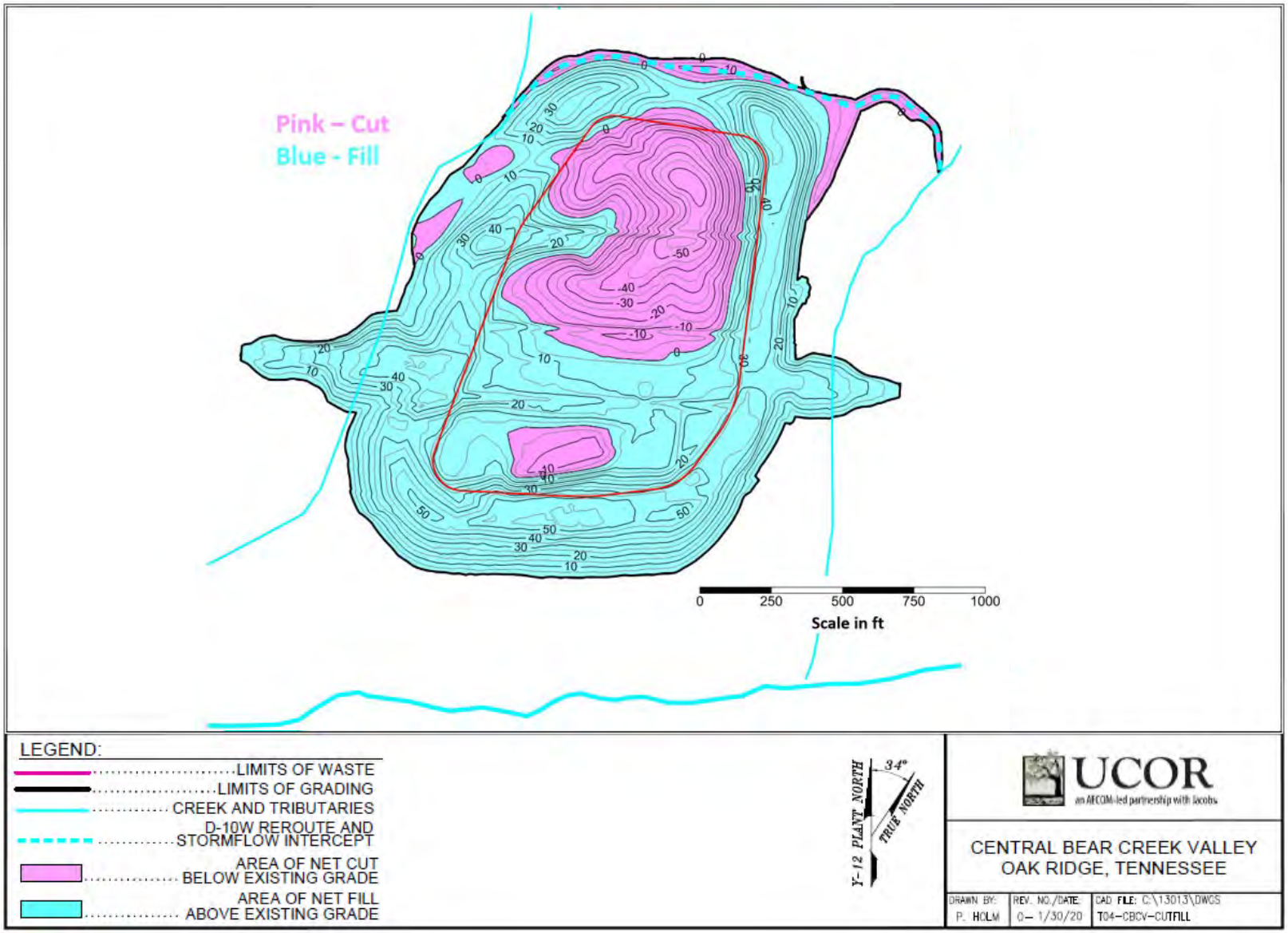

Fig. D.24. Topographic change (cut and fill) within the EMDF footprint area

D.4.1.2 Hydraulic Properties

The liner and geologic buffer areas are assigned a hydraulic conductivity of 1.0E-05 cm/sec in model layer 1 as shown on Fig. D.25 (dark pink within disposal cell limits). This value corresponds to an EMDF design requirement for maximum hydraulic conductivity of the geologic buffer material. Areas of fill outside the disposal cell limits are represented by a hydraulic conductivity in model layer 1 of 2.0E-05 cm/sec. These fill areas are underneath the perimeter berms. The fill was assumed to be low permeability material similar to the berm material. That assumption may result in higher predicted groundwater elevations in these areas. The vertical distribution of the hydraulic conductivity for the EMDF model layers is shown on Fig. D.26. Because the cut and fill required for the proposed design only affects model layer 1 and the shallow portion of model layer 2, the hydraulic conductivity values for EMDF model layer 2 and deeper are the same as the CBCV model.

D.4.1.3 Surface Drainage Boundary Conditions

Surface drainage features around the disposal area were revised to represent the topography changes associated with the proposed disposal cell design, including the following (Fig. D.27):

- A stormwater interception channel will be constructed upgradient from the disposal cell footprint along the existing saddle area.
- A diversion channel will intercept and divert flow from the upper part of D-10W to NT-10.
- Fill will extend into some areas across the D-10W channel due to berm construction.
- Existing surface drainage features will be backfilled during construction.

These surface feature changes were represented in the EMDF model as changes in the distribution of drain cells, as shown on Fig. D.27 and Table D.7. The river cells representing the Bear Creek reach were not changed from the CBCV model. Drain cell elevations were adjusted to represent the engineered surface drainage features, such as the D-10W diversion channel and stormwater channels within the berm areas.

Table D.7. Summary of EMDF boundary conditions

Number of EMDF model cells by boundary condition type	
Constant head	6427
Rivers	1386
Drains	15,629
No flow	1,316,996

EMDF = Environmental Management Disposal Facility

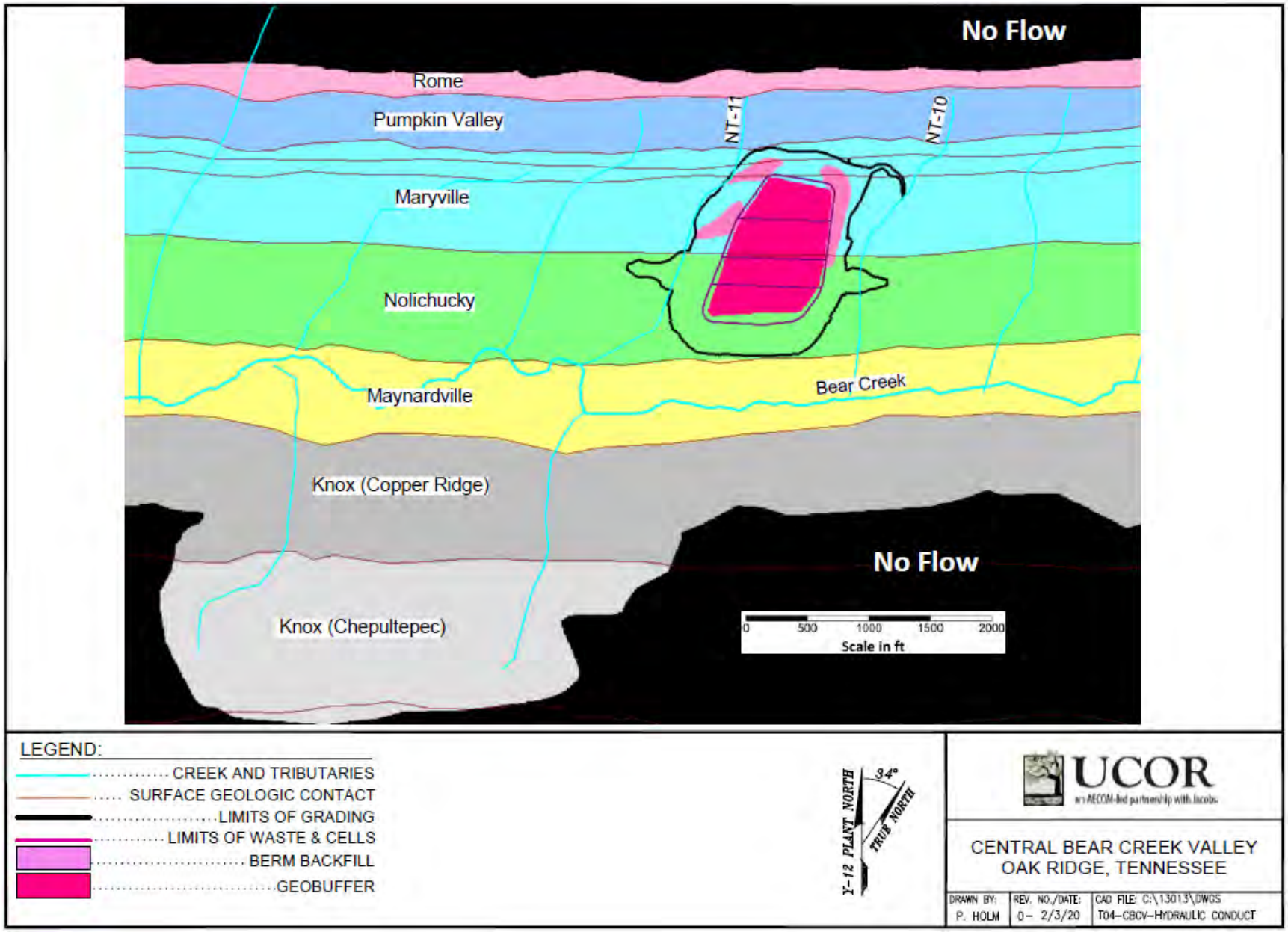

Fig. D.25. EMDF model hydraulic conductivity zones

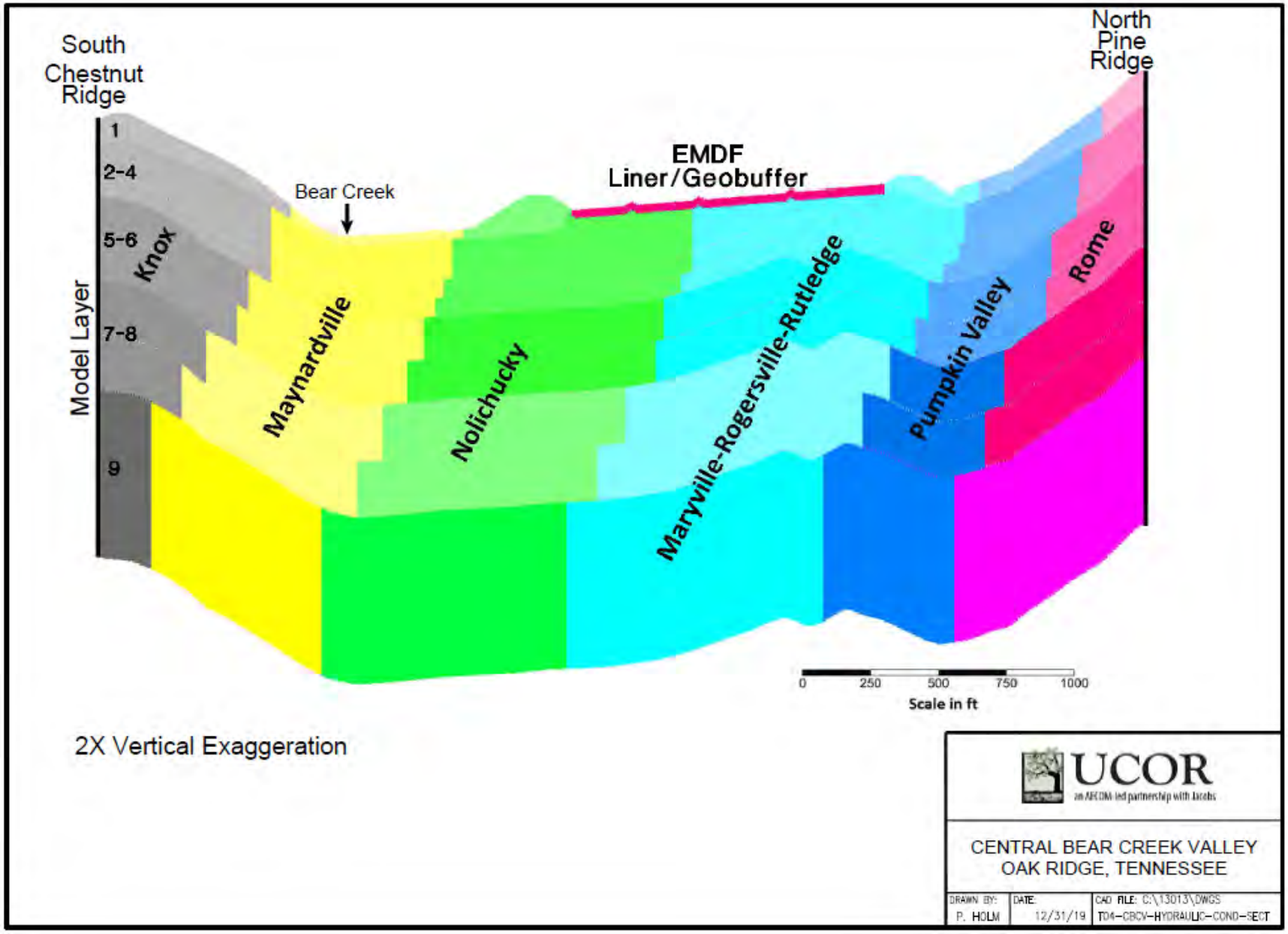

Fig. D.26. EMDF model hydraulic conductivity zones in cross section

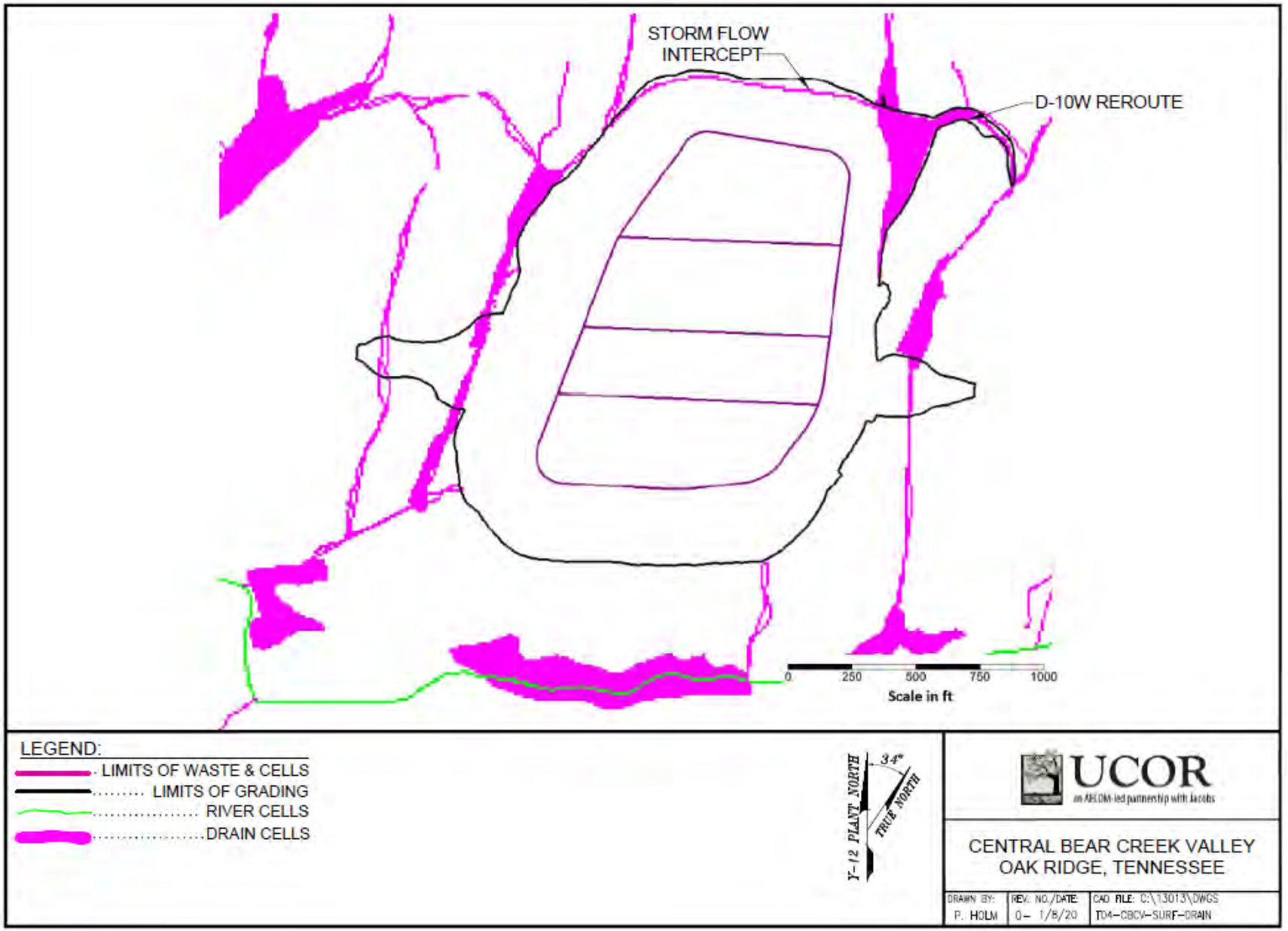

Fig. D.27. Surface drainage features in the EMDF model

D.4.1.4 Recharge

The assigned recharge rates for the disposal cell area are based on HELP modeling of the proposed EMDF cover and liner system. For the design performance condition simulation, there is no leakage from the liner system because of the presence of multiple high-density polyethylene (HDPE) liners. Therefore, the recharge rate of 0.0 in./year was used to represent the leakage rate from a lined cell area.

The HELP model used to evaluate cell area infiltration rates is not suitable for the berm area. Instead, a recharge rate-hydraulic conductivity (permeability) relationship was applied to estimate the mostly likely groundwater recharge rate for the berm zone. Groundwater recharge rate is primarily governed by the hydraulic conductivity values of near-surface material under similar precipitation, surface slope, and surface vegetation conditions.

The majority of the EMDF preliminary design lies upon the Maryville-Rogersville-Rutledge and Nolichucky Formations. Based on site-specific slug tests, the average hydraulic conductivity value of these formations is 8.77E-04 cm/sec, and the CBCV model used hydraulic conductivity values of 2.6E-04 to 3.8E-03 cm/sec for the shallow zone of these formations (Table D.2). The CBCV model used recharge rates ranging from 6.6 to 9.6 in./year for these formations (Table D.4). The berm materials will be similar to materials used for the geologic buffer with a hydraulic conductivity in the 1E-05 cm/sec range. Compared to the slug test data (1E-04 cm/sec range), the berm material permeability will be one order of magnitude lower. Applying the recharge rate-K relationship for the geologic formations, the applicable recharge rate for the berm would be approximately one-tenth of the 6.6 to 9.6 in./year applied to Nolichucky and Maryville-Rogersville-Rutledge Formations. A conservative estimate of 1 in./year recharge rate was therefore applied to the berm in the EMDF model (Table D.8). The distribution of the recharge rates for the EMDF model are shown on Fig. D.28.

Table D.8. EMDF model recharge summary

Recharge areas	CBCV model	EMDF model	
	ft/day	ft/day	in./year
Rome	2.20E-03	2.20E-03	9.6E+00
Pumpkin Valley	1.40E-03	1.40E-03	6.1E+00
Maryville-Rogersville-Rutledge	2.20E-03	2.20E-03	9.6E+00
Nolichucky	1.50E-03	1.50E-03	6.6E+00
Maynardville	3.00E-03	3.00E-03	1.3E+01
Knox (Copper Ridge)	1.00E-03	1.00E-03	4.4E+00
Knox (Chepultepec)	5.00E-04	5.00E-04	2.2E+00
Soil Storage Pile near proposed site	5.00E-04	NA	NA
EMDF berm slope	NA	2.28E-04	1.0E+00
EMDF lined area	NA	0	0

CBCV = Central Bear Creek Valley
EMDF = Environmental Management Disposal Facility
NA = not applicable

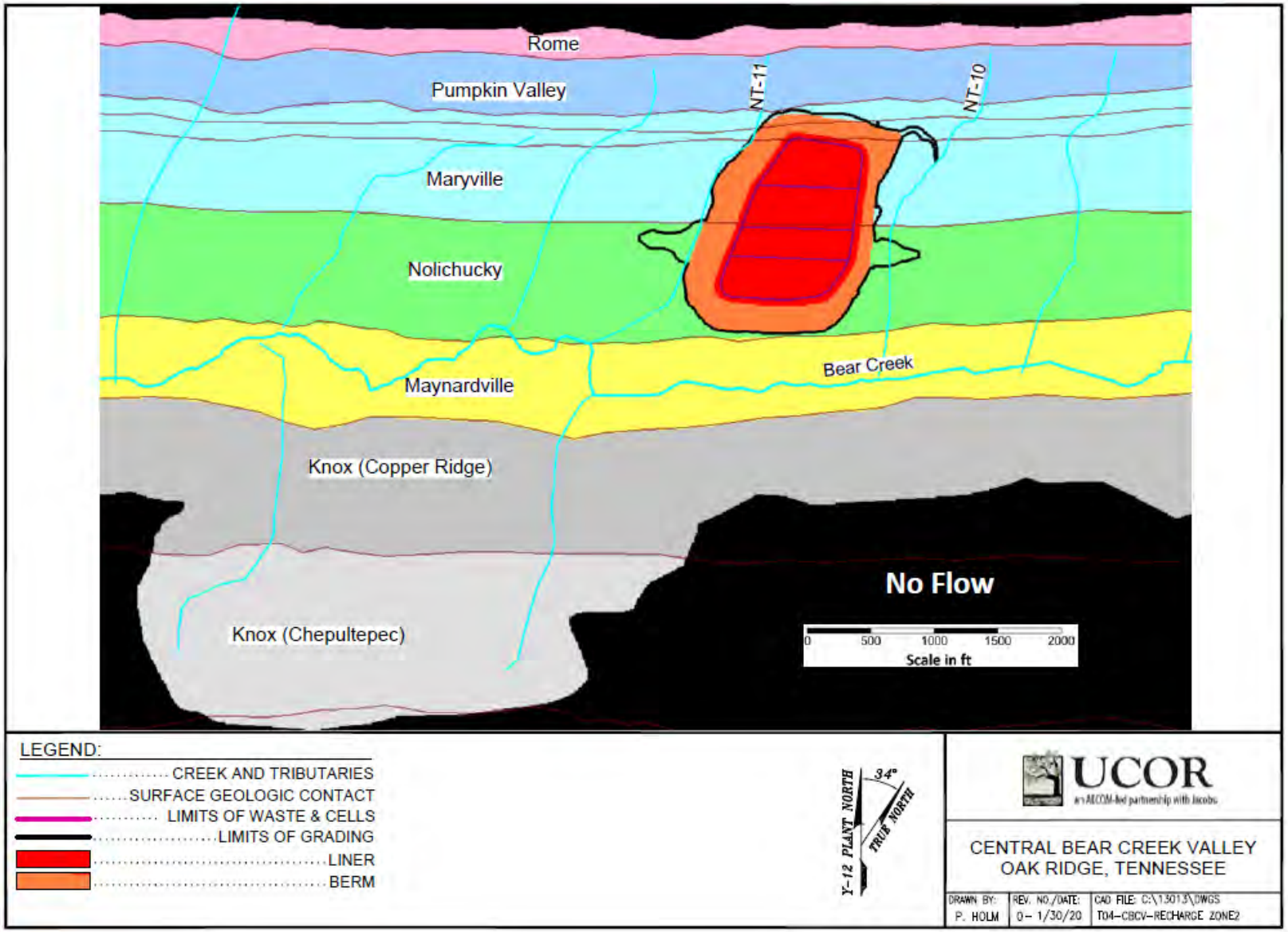

Fig. D.28. EMDF model recharge zones

D.4.2 EMDF MODEL RESULTS FOR DESIGN PERFORMANCE CONDITIONS

After the EMDF model was developed based on the initial design assumptions, it was used to conduct various simulations to support progression of the EMDF preliminary design. These simulations were primarily focused on design performance objectives for minimum vertical separation from the bottom of the waste to the water table. Predictive simulations were conducted under steady-state conditions, representing the long-term annual average, high (wet season), and low (dry season) groundwater conditions using the recharge rates developed for the CBCV model as described in Sect. D.3.5. The remainder of this section includes EMDF model results for the design performance condition in which there is no recharge to groundwater beneath the lined area of the disposal unit.

D.4.2.1 Design Condition Groundwater Elevations

The EMDF model-calculated groundwater elevations for the final preliminary design are shown on Fig. D.29. The groundwater elevations changed significantly from the CBCV model (see Fig. D.13). The EMDF model groundwater elevations are lower beneath the lined areas and higher than the CBCV model elevations in the area of the berm fill in D-10W. The groundwater elevations show a smooth gradient from Pine Ridge to Bear Creek within the EMDF footprint, with much less complexity than the pre-construction simulation

D.4.2.2 Groundwater Flow Field and Discharge Locations

The EMDF model predicted flow field for model layer 2 (shallow groundwater) is shown on Fig. D.30. Model layer 2 was used because the area of model layer 1 representing the liner and geologic buffer was dry. The flow field is more uniform than the pre-construction CBCV model results (Fig. D.16), with flow to the southwest direction under the disposal cell area due to reduced recharge and the reconfiguration of surface water features, such as the stormflow intercept and D-10 diversion channel. The groundwater discharges to Bear Creek and its tributaries (NT-10 and NT-11).

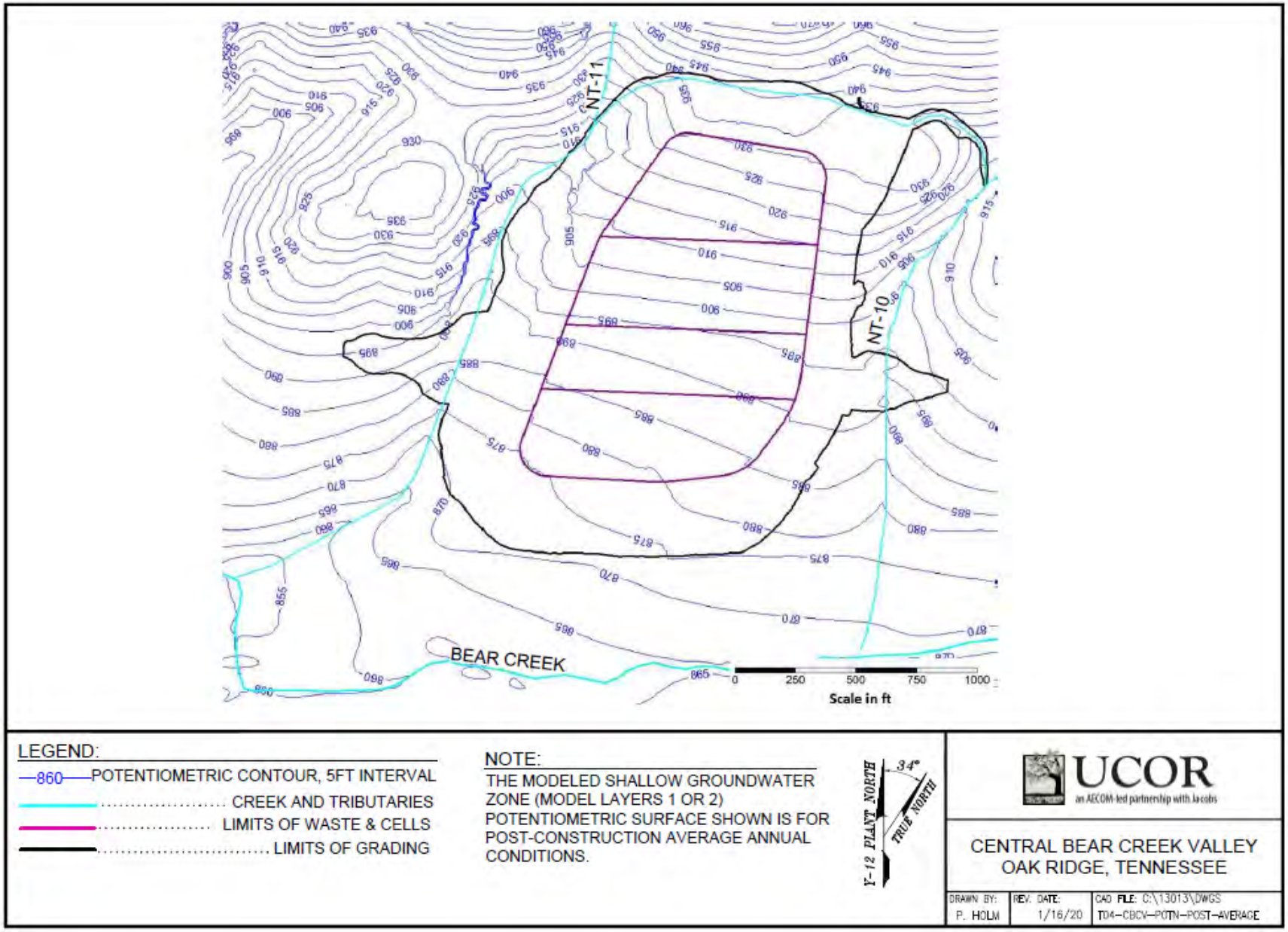

Fig. D.29. Simulated groundwater elevations for the EMDF model design condition

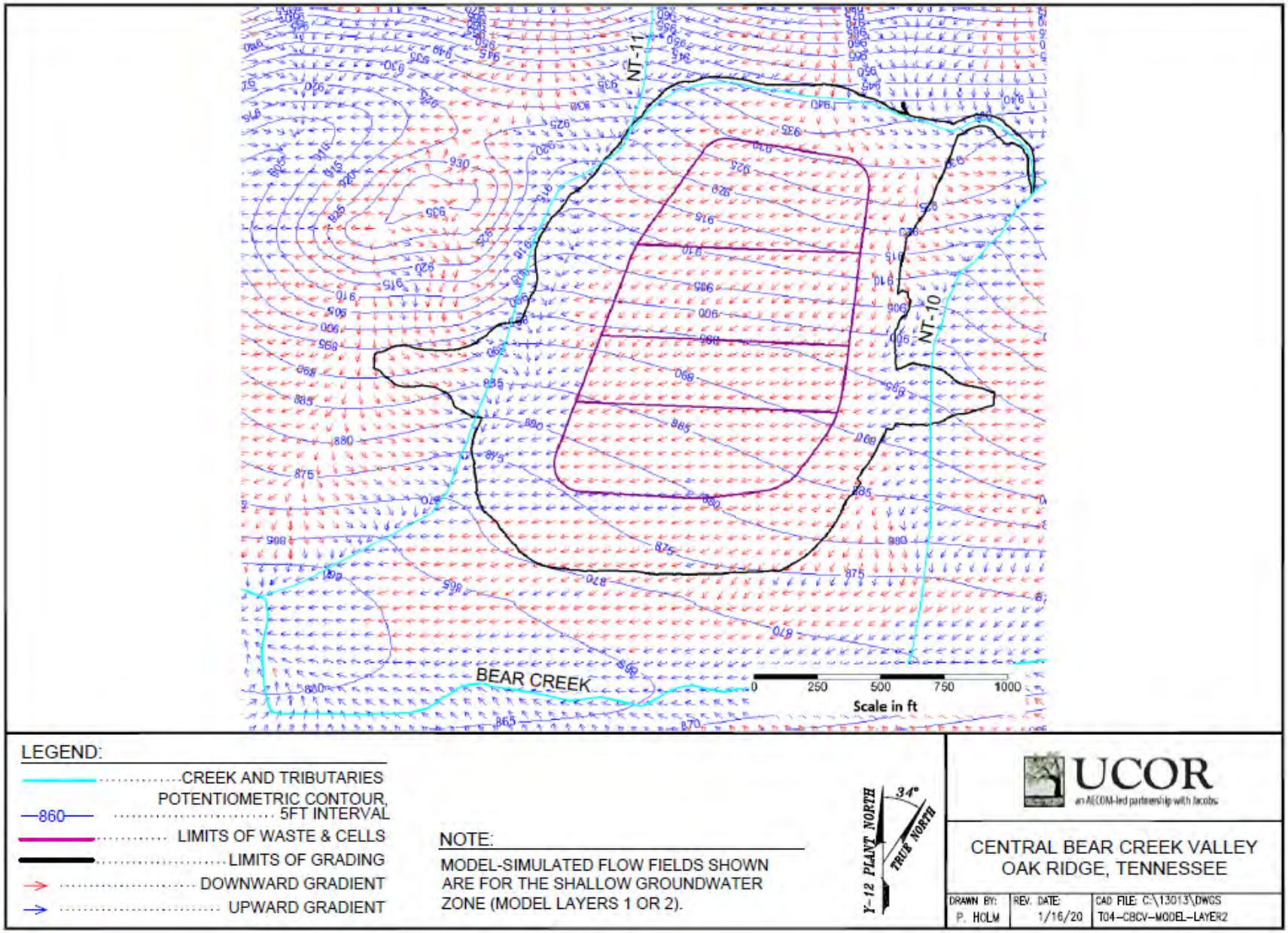

Fig. D.30. Simulated shallow groundwater flow field in the EMDF model (model layer 2)

D.5 EMDF MODEL PA APPLICATION

The EMDF flow model was used to conduct various simulations to provide required parameters used in other models for the performance assessment of EMDF. The groundwater flow model was used to support the following performance assessment applications:

- Groundwater levels for various performance conditions
- Depth to groundwater beneath the disposal cells
- Groundwater flow field and discharge locations
- Delineation of the likely maximum impact location for groundwater
- Sensitivity analysis for key model parameters
- Flow linking files to conduct contaminant fate-transport modeling in the saturated zone.

All groundwater flow model simulations were conducted using MODFLOW-2005 code (Harbaugh 2005). Groundwater Vistas software (ESI 2011) was used during the pre- and post-processing stage to help processing and visualizing modeling results.

D.5.1 FLOW MODEL APPLICATION TO REPRESENT EMDF PERFORMANCE IN THE FUTURE

Because of the long time period considered and the lack of maintenance of the cover after 100 years of institutional controls assumed for the PA analysis, the EMDF cover and liner systems performance will change (degrade) over time. To account for changes to material characteristics, the following three scenarios (performance conditions) are considered for EMDF performance based on use of the HELP model to estimate average annual cover infiltration and leachate release (Appendix C of the PA):

- **Full design performance** (design performance period – EMDF closure through 200 years post-closure): All layers are functional and included in the simulated HELP profile. This period includes the 100-year post-closure period of institutional control and the first 100 years following the assumed loss of institutional control by DOE. Every component of the cover system is assumed to perform as designed, including the HDPE membranes and engineered drainage layers.
- **Partial design performance** (representative of the degrading performance period between 200 and 1000 years post-closure): Geomembrane layers and the geosynthetic clay liner are assumed to be totally ineffective (i.e., no longer function as impermeable layers in the cover and liner systems). Without the overlying protective geomembrane, the amended clay layer of the cover is also degraded (higher conductivity) but still functional and limited cover infiltration and leachate release occurs. The leachate collection system is no longer operational and leachate release occurs via percolation through the clay barrier of the liner system.
- **Long-term performance** (long-term performance period, >1000 years post-closure): Degradation of the cover and liner systems due to some combination of natural processes (e.g., erosion, differential waste settlement) and events (e.g., damage by severe storms, or seismic everts) causes leachate release and recharge to the saturated zone beneath the EMDF to increase to long-term average rates.

For these three performance conditions, the respective groundwater recharge rates (as predicted by the HELP model) applied to the disposal cell footprint are:

- Full design performance – 0.0 in./year (design condition EMDF model)
- Partial design performance – 0.43 in./year
- Long-term performance – 0.88 in./year.

Using the two non-zero recharge rates, the EMDF model predicted the steady-state groundwater levels and flow field associated with the partial design and fully degraded future performance conditions.

D.5.2 GROUNDWATER LEVELS FOR LONG-TERM PERFORMANCE

The steady-state future condition model simulations represent long-term average groundwater elevations and flows under degraded EMDF performance scenarios. For each of the future performance conditions, the HELP model-estimated recharge rate was applied to the disposal cell footprint (liner-geobuffer area in Figs. D.25 and D.26) in the EMDF model. Recharge for other areas was the same as for the design condition model, representing average annual hydrologic conditions (Table D.8). The long-term degraded performance condition represents the most pessimistic scenario for risk evaluation. Thus, the modeled water table elevations and flow field for the long-term degraded scenario was used to derive several groundwater system parameters used for the EMDF performance analysis. The model-predicted water levels in the disposal cell area for the long-term degraded condition are shown on Fig. D.31.

Compared to the full design performance condition when there is no water leakage from the lined cell area, the predicted water levels would increase around the EMDF as shown in Fig. D.32. The water level changes within the lined area are shown in Fig. D.33. The estimated water level increases by up to 8 ft; however, the predicted groundwater levels for the long-term performance condition are still below the base of the geobuffer zone.

D.5.3 DEPTH TO GROUNDWATER FOR THE CELL LOCATIONS

Based on the EMDF model-predicted water levels for the long-term degraded condition, the depth to water table is calculated from the bottom of the waste. The depth to water contours within the cell area are shown on Fig. D.34. The vertical interval from the bottom of waste to the top of the saturated zone ranges from 18.4 to 49.9 ft within the interior cell floor area (lined area excluding the perimeter side slopes). The arithmetic mean (average) depth to water is 30.9 ft. The simulated water table elevations and the average depth to water value are applied to other flow and transport models in the PA.

D.5.4 GROUNDWATER FLOW FIELD AND GW DISCHARGE LOCATIONS

The flow field for the EMDF model long-term degraded performance condition is shown in Fig. D.35. The flow vectors plotted in Fig. D.35 are for model layer 2, because model layer 1 remains dry within the liner and geobuffer area. The flow field changes from the topography-controlled flow pattern in the current-condition CBCV model (radial flow field toward the surrounding tributaries as shown in Fig. D.16) to a mostly south and west flow pattern under the disposal cell footprint. The groundwater from the EMDF footprint discharges predominately to Bear Creek tributary NT-11.

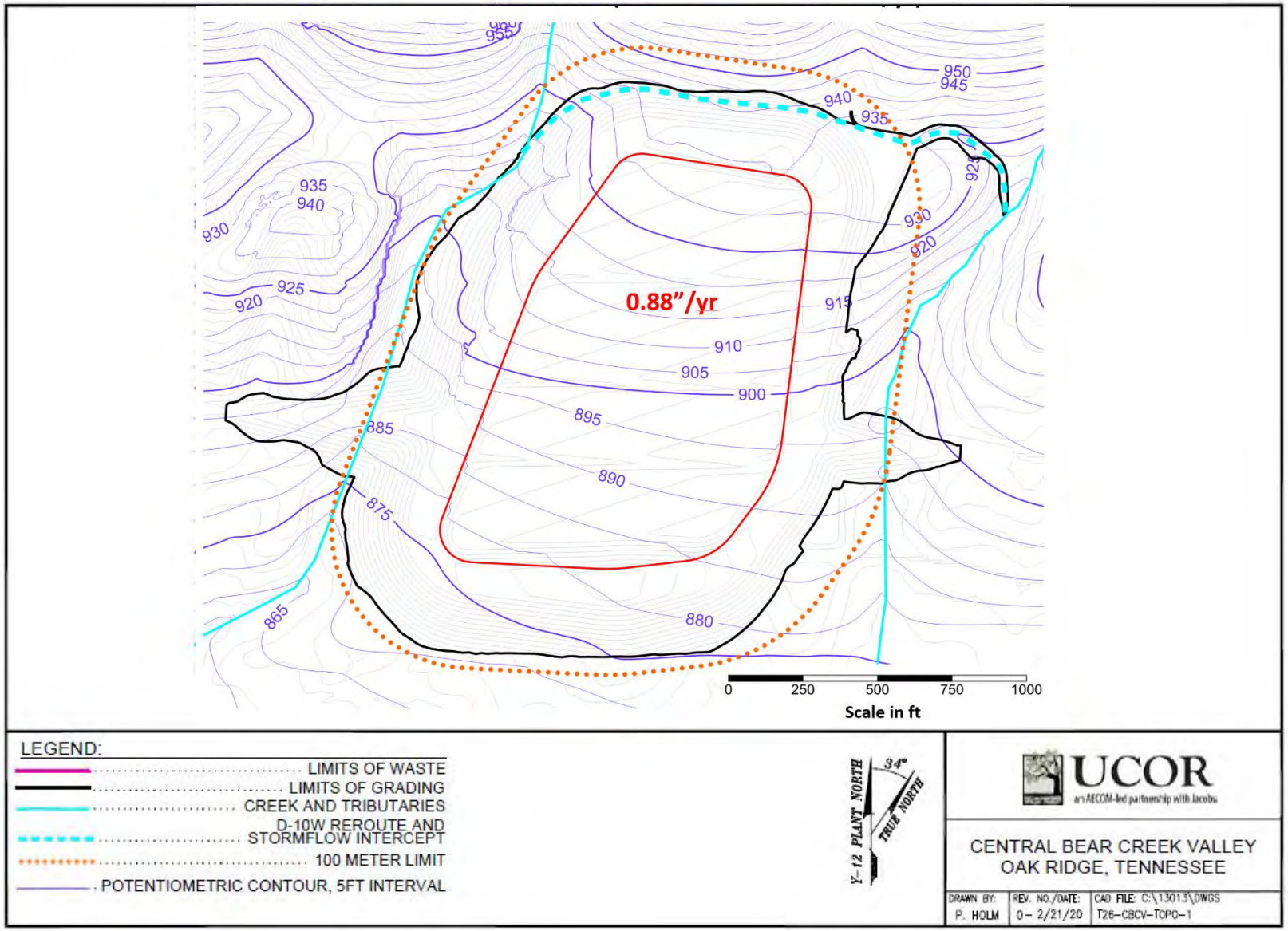

Fig. D.31. EMDF model predicted long-term performance condition water levels

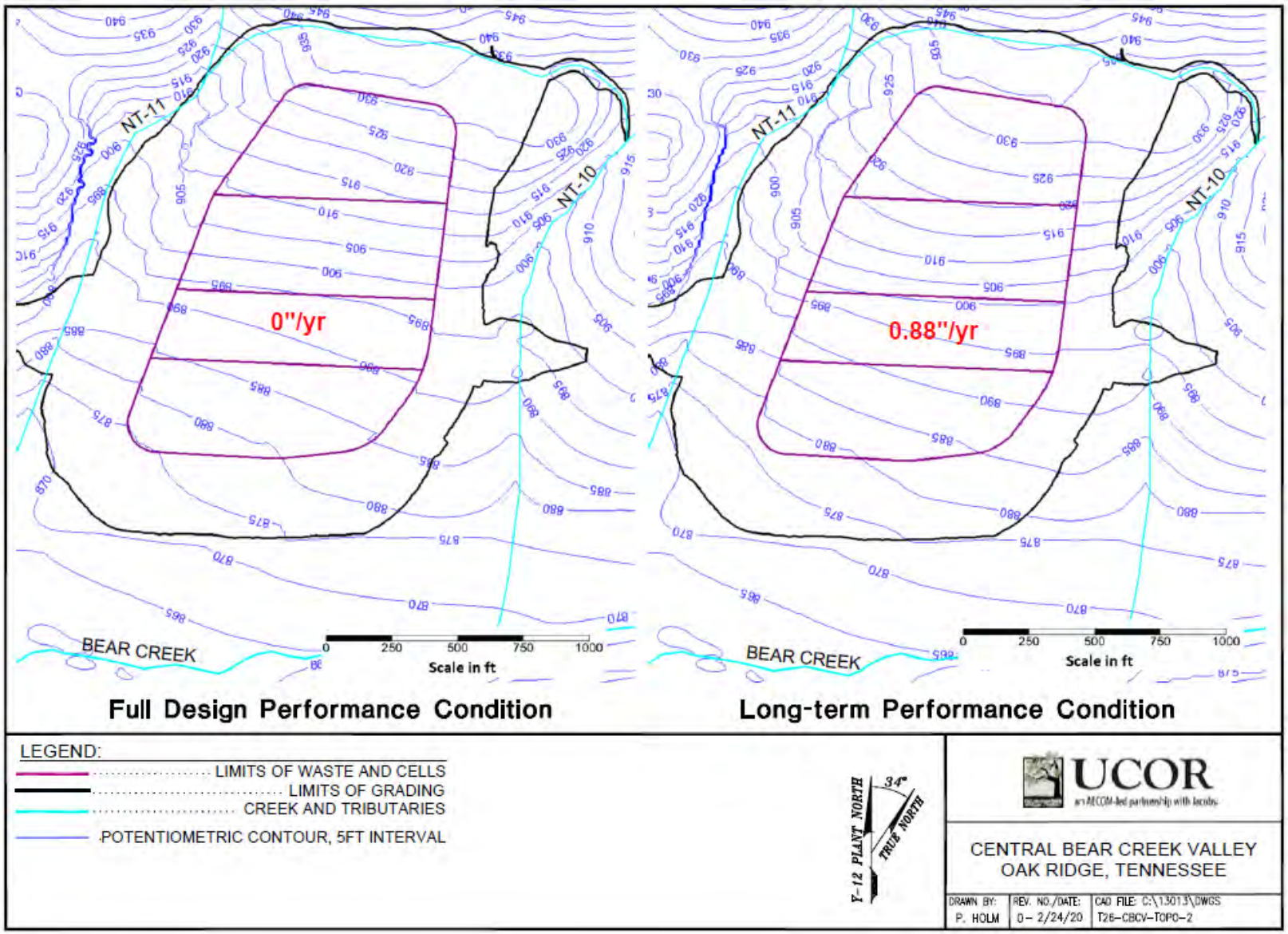

Fig. D.32. EMDF model predicted groundwater levels for full design performance condition and long-term performance condition

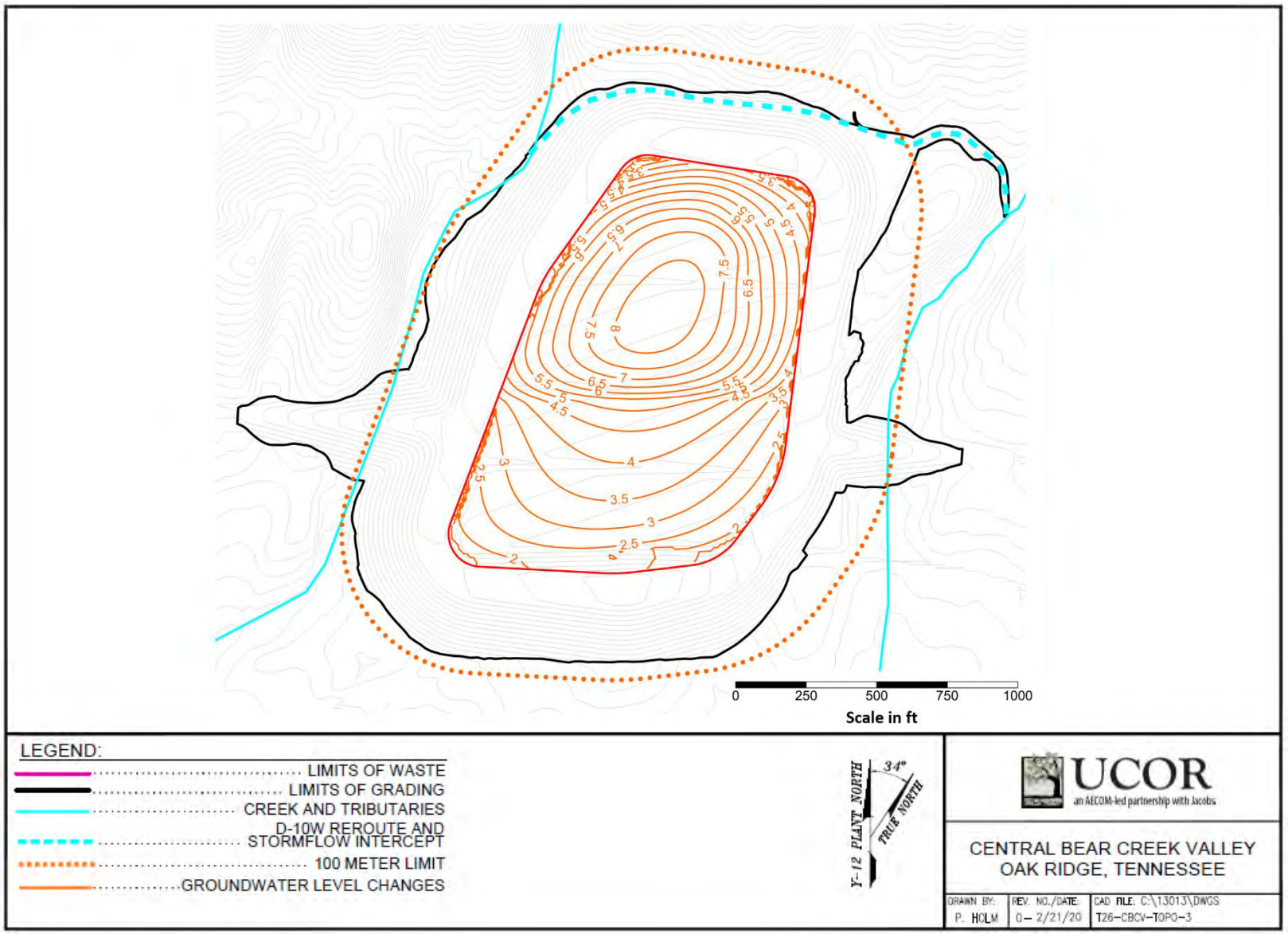

Fig. D.33. Groundwater level changes from full design performance to long-term performance condition

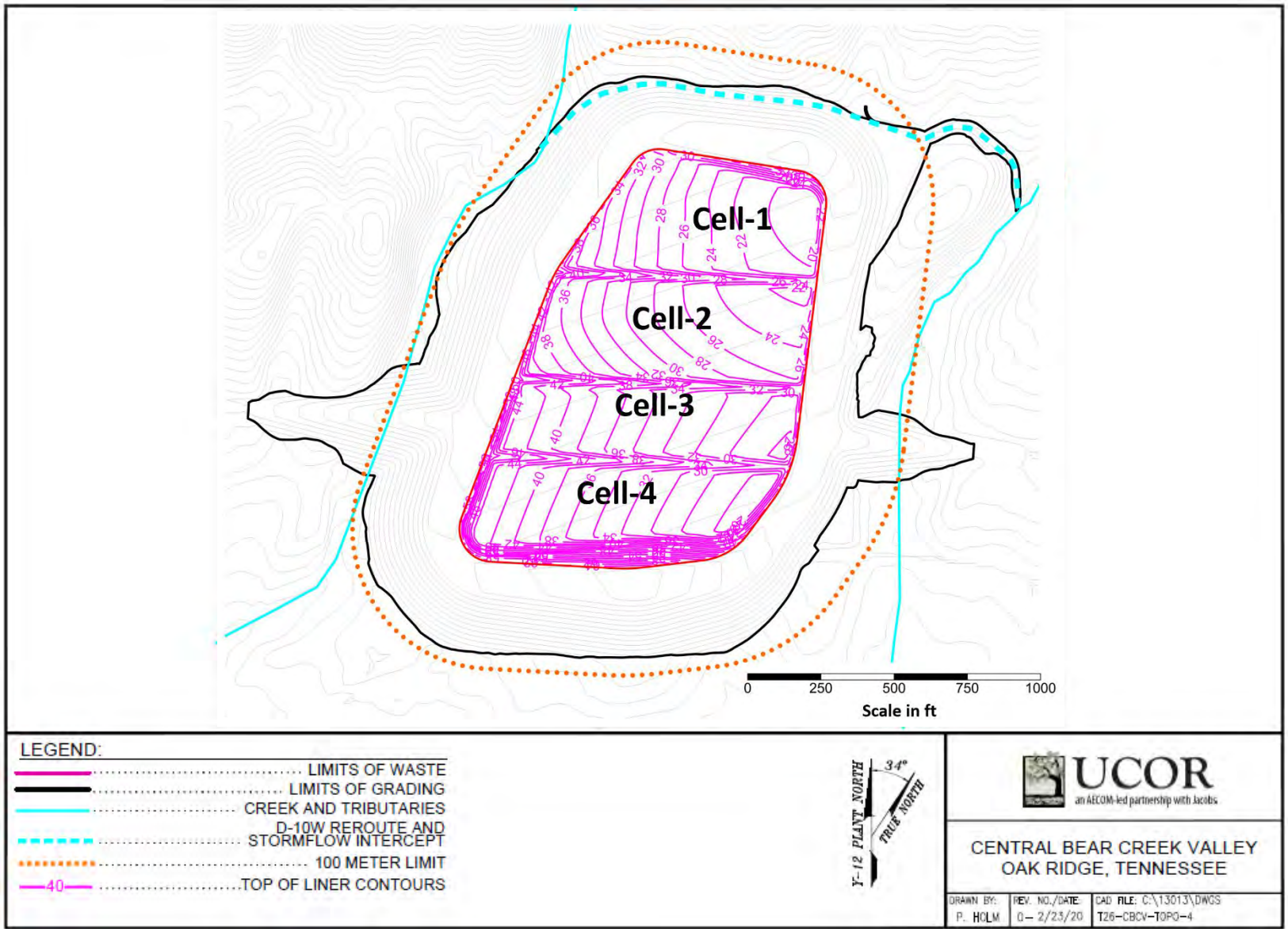

Fig. D. 34. Depth to the water table for the long-term performance condition

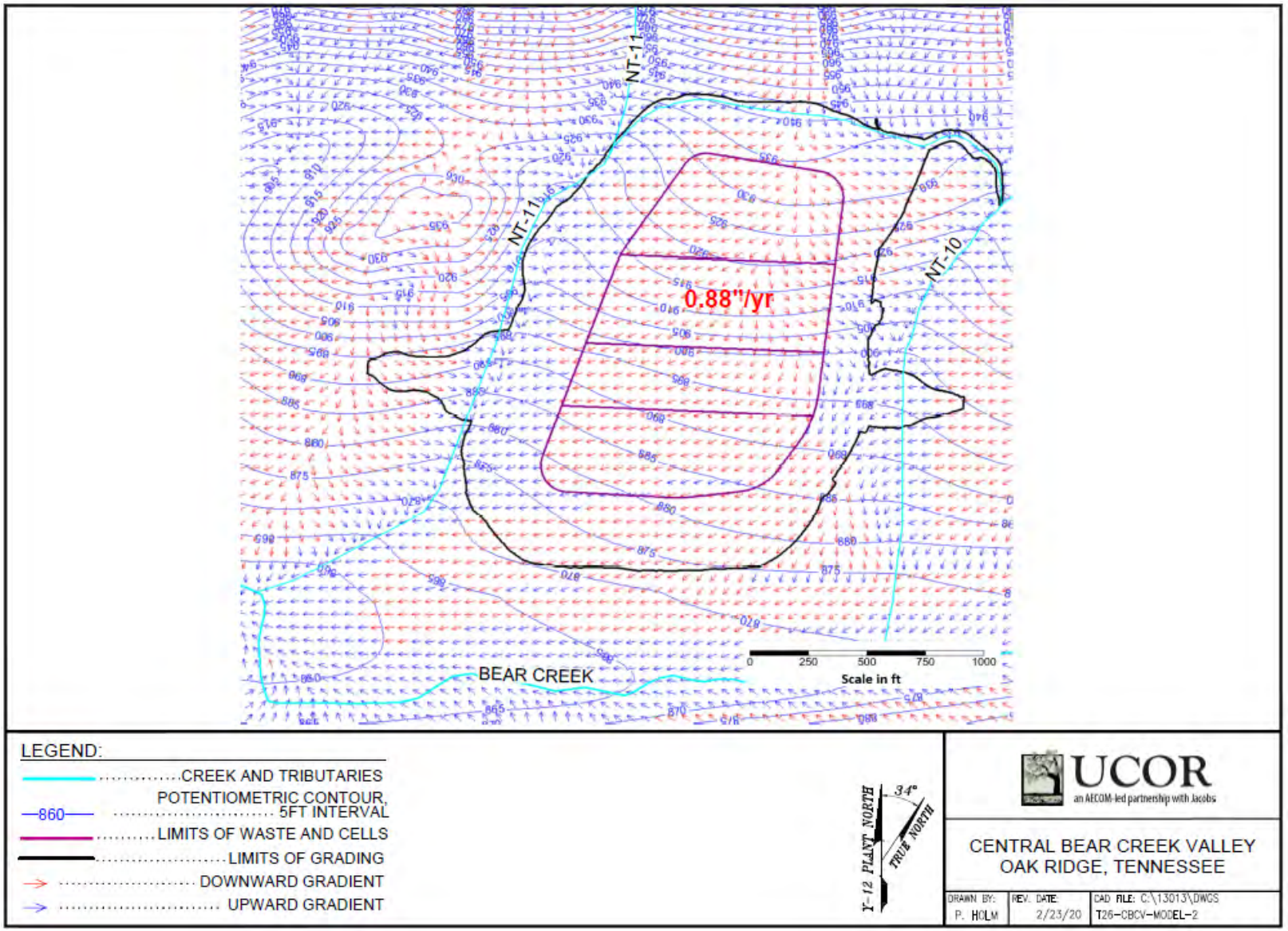

Fig. D.35. Groundwater flow (model layer 2) for the long-term performance condition

D.5.5 MAXIMUM GROUNDWATER IMPACT LOCATION FOR LEACHATE RELEASE

Particle tracking using the MODPATH model was used to identify the potential maximum impact location(s) for leachate release from the disposal cell. The EMDF model particle tracking result for the long-term degraded performance condition is shown on Fig. D.36. This scenario has the particles starting at top of the water table in selected locations within the cell footprint area. The location of likely maximum groundwater impact (highest occurrence of contaminant particle tracks) at 100 m from the waste is at NT-11 on the southwest perimeter of the disposal unit.

Final determination of the 100-m maximum impact location (groundwater point of assessment) was based on contaminant fate-transport model results utilizing the long-term performance condition groundwater flow field. The fate-transport modeling was conducted using MT3D code (Zheng 1990; Zheng and Wang 1999). Detailed discussion of the MT3D model for this application is presented in Appendix F of the PA.

D.5.6 SENSITIVITY ANALYSIS FOR KEY MODEL INPUT PARAMETERS

Sensitivity runs were conducted for the uncertain model input parameters for the EMDF future condition model. Based on the previous model study results (DOE 1998a, BJC 2010), the groundwater recharge rates for the cell area applied in the model have the most impact on the performance of the disposal facility. This is due to the recharge rate affecting the water flux and water levels below the cell footprint and impacting the contaminant mass release due to source leaching from infiltration. Therefore, the recharge rate impact was evaluated in this analysis. The recharge rate changes could result from both EMDF performance uncertainty and climatic changes such as an extremely long wet period or increased long-term average precipitation. A global 1.5 times base recharge rate for the whole model domain (including the EMDF footprint) was applied. Specifically, under this scenario the recharge rate for the lined cell area is 1.32 in./year (1.5 times 0.88).

The model-predicted water levels and particle tracks for the EMDF model long-term degraded performance condition and for the sensitivity run with 1.5 times base recharge rate are shown on Fig. D.37.

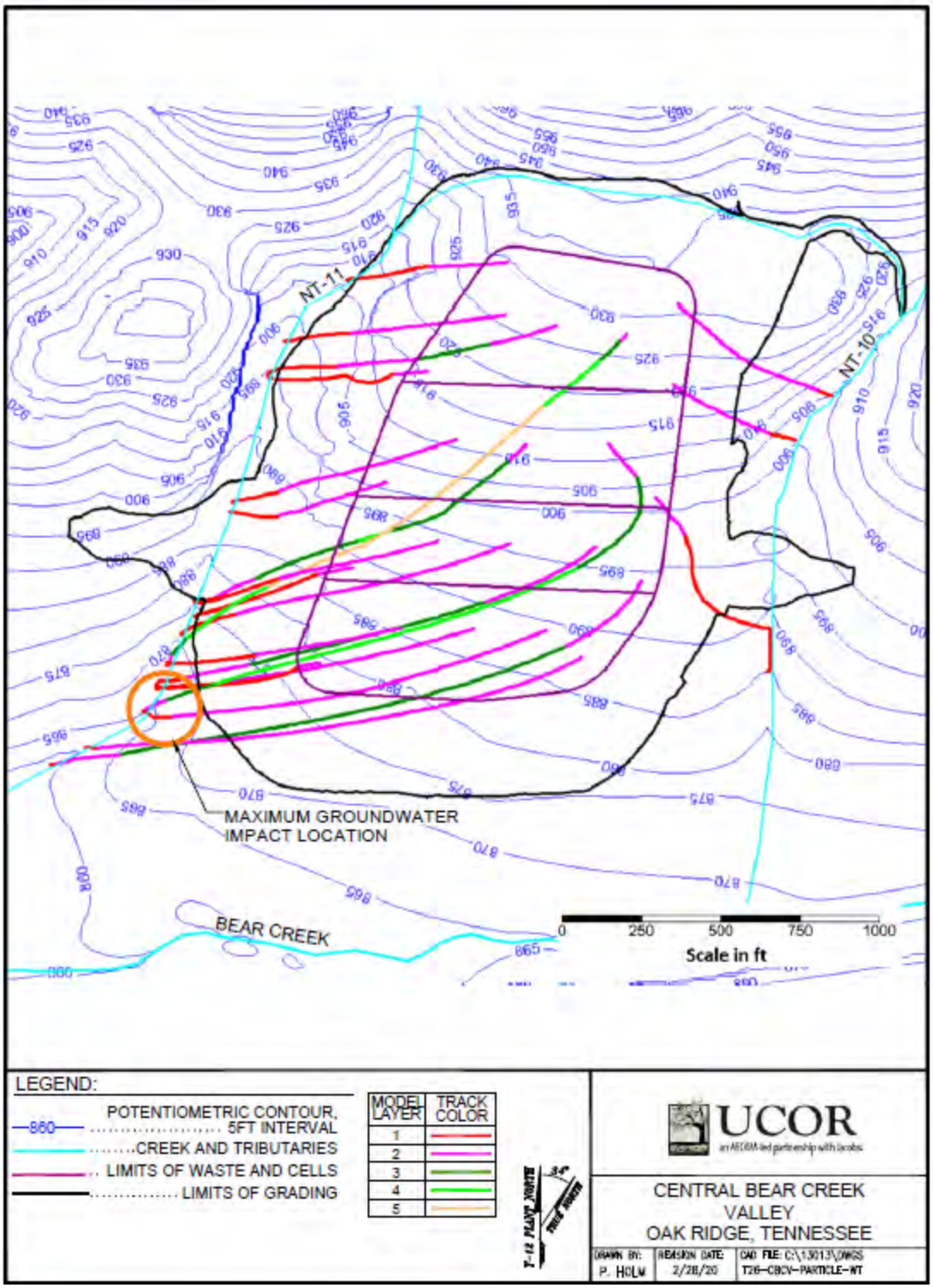

Fig. D.36. EMDF model particle tracks for the long-term performance condition

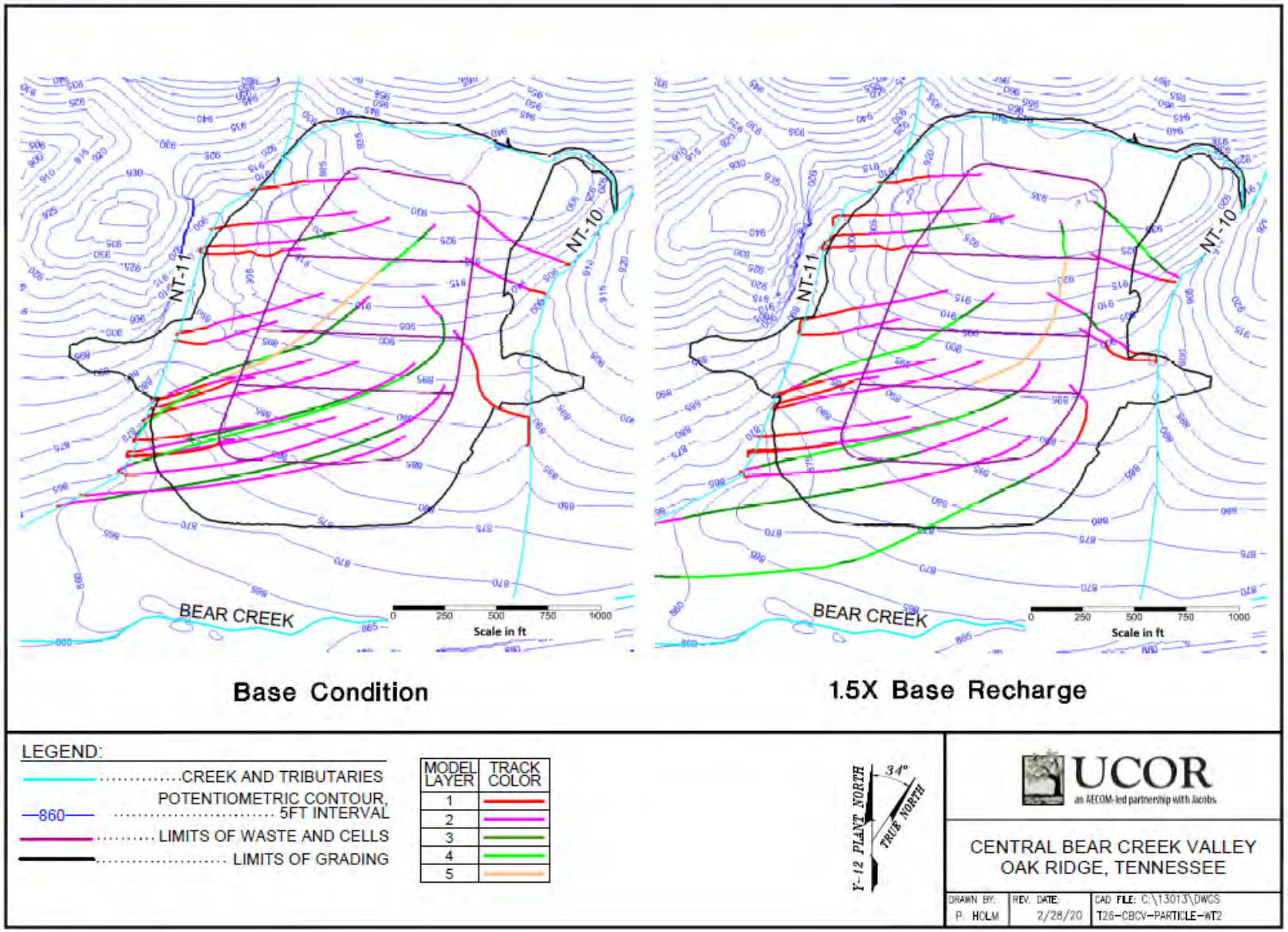

Fig. D.37. EMDF model predicted water levels and particle tracks for the higher recharge sensitivity case

The groundwater levels beneath the disposal cells only increased slightly compared with the base (long-term degraded performance) condition and the resulting particle tracks did not change significantly from the base condition. The resulting depth-to-water contours for the higher recharge rate simulation and the base condition EMDF model is shown on Fig. D.38. The vertical interval from the bottom of waste to the top of the saturated zone is reduced by about 2 to 4 ft for the higher recharge scenario. This is a minor change considering the water table elevation range under the cell is 60 ft.

Other model parameters that may affect the groundwater flow field are the hydraulic conductivities in the three directions and associated anisotropy ratios. Two scenarios were evaluated:

- Lower anisotropy – 3/5 times the anisotropy ratio in the base model; the base model anisotropy ranges from 5/1 for model layer 1 to 10/1 for other model layers
- Higher anisotropy – 2 times the anisotropy ratio in the base model.

The sensitivity analyses were performed applied the same K_y values (along strike east-west direction) while changing the K_x (along dipping north-south) and K_z (vertical) values. The changes were applied for the whole model domain.

The model-predicted water levels and particle tracks for the sensitivity run with lower anisotropy are shown on Fig. D.39, along with the base condition EMDF model results. The predicted water levels are similar to the base condition, but the particle tracks show a more southward flow pattern. The results are expected based on the reduced anisotropy. However, the maximum groundwater impact is still located near the southwest corner of the EMDF footprint.

The model-predicted water levels and particle tracks for the sensitivity run with higher anisotropy are shown on Fig. D.40, along with the base condition EMDF model results. The predicted water levels are only slightly higher than the base condition, but the particle tracks show a more strike-parallel (east-west) flow pattern. Most of the particle tracks still discharge into the NT-11. However, the maximum groundwater impact is still located near the southwest corner of the EMDF footprint.

The EMDF model sensitivity run results suggest that these uncertainties (recharge and anisotropy) will not result in significant variations from the base condition (long-term degraded performance) simulation that provides groundwater system parameter values for the EMDF PA.

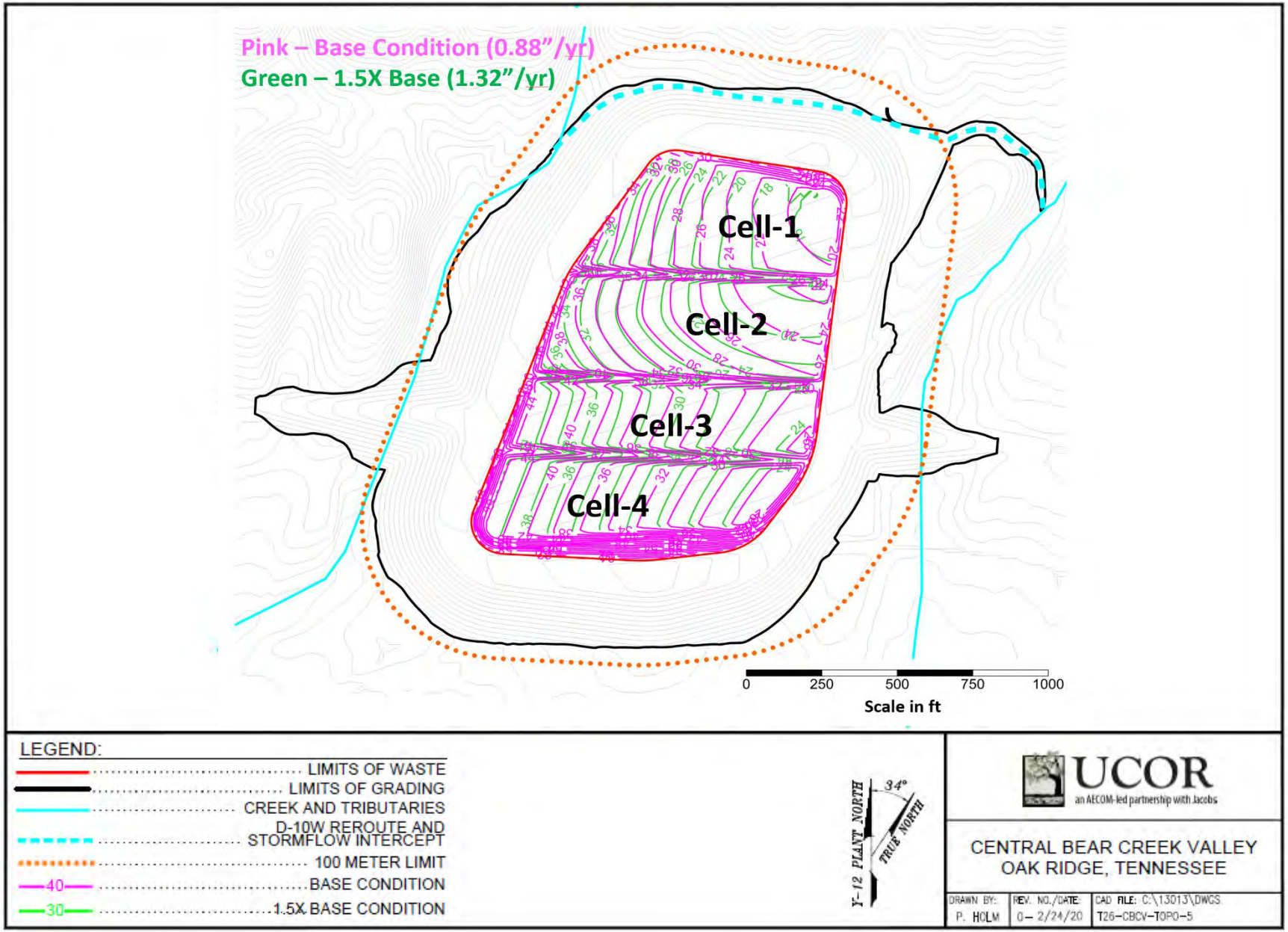

Fig. D.38. Depth to groundwater contours for 1.5X recharge and the base recharge case

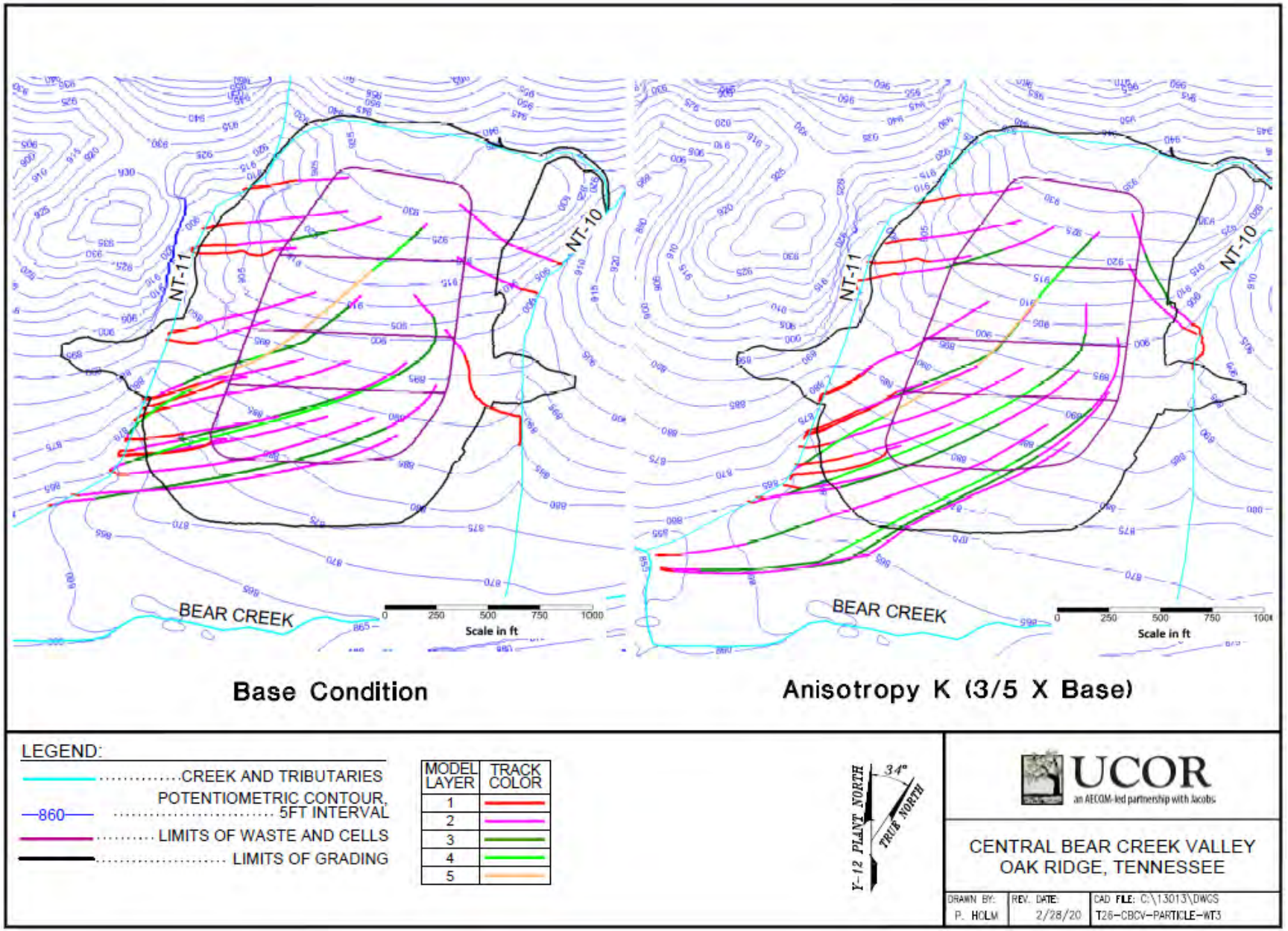

Fig. D.39. EMDF model-predicted groundwater levels and particle tracks for lower anisotropy sensitivity case

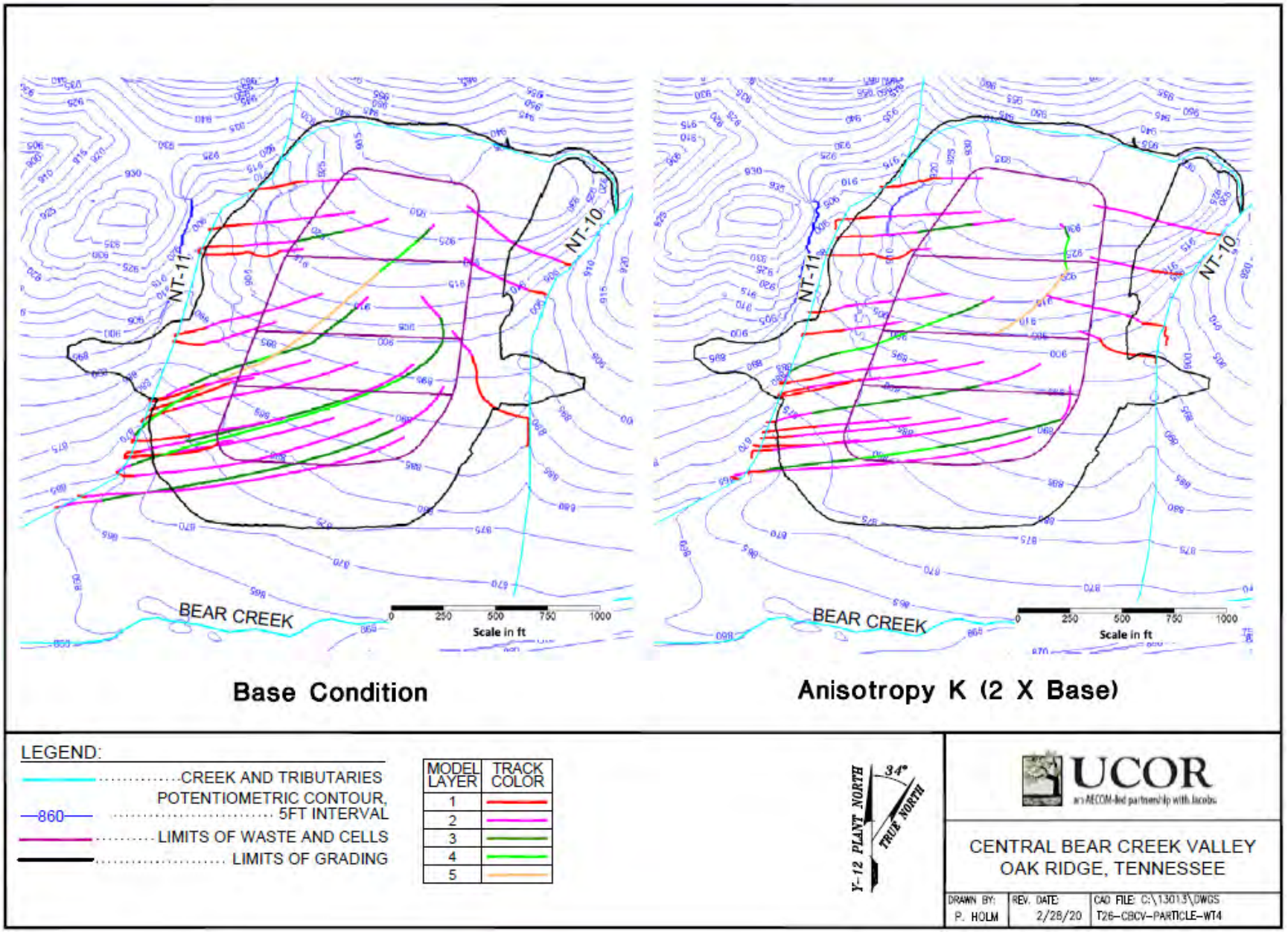

Fig. D.40. EMDF model-predicted groundwater levels and particle tracks for higher anisotropy sensitivity case

D.6 REFERENCES

BJC 2003. *Engineering Feasibility Plan for Groundwater Suppression of the Environmental Management Waste Facility, Oak Ridge, Tennessee*, BJC/OR-1478, Bechtel Jacobs Company LLC, Oak Ridge, TN.

BJC 2010. *Summary Report on the 2010 Environmental Management Waste Management Facility Groundwater Model and Flow/Fate-Transport Analyses, Oak Ridge, Tennessee*, BJC/OR-3434, Bechtel Jacobs Company LLC, Oak Ridge, TN, May.

DOE 1997a. *Feasibility Study for Bear Creek at the Oak Ridge Y-12 Plant, Oak Ridge, Tennessee*, DOE/OR/02-1525/V2&D2, U.S. Department of Energy, Oak Ridge, TN, November.

DOE 1997b. *Report on the Remedial Investigation of Bear Creek Valley at the Oak Ridge Y-12 Plant, Oak Ridge, Tennessee*, DOE/OR/01-1455/V1-V6&D2, U.S. Department of Energy, Oak Ridge, TN, May.

DOE 1998a. *Addendum to Remedial Investigation/Feasibility Study for the Disposal of Oak Ridge Reservation Comprehensive Environmental Response, Compensation, and Liability Act of 1980 Waste*, DOE/OR/02-1637&D2/A1, U.S. Department of Energy, Oak Ridge, TN, September.

DOE 1998b. *Remedial Investigation/Feasibility Study for the Disposal of Oak Ridge Reservation Comprehensive Environmental Response, Compensation, and Liability Act of 1980 Waste*, DOE/OR/02-1637&D2, U.S. Department of Energy, Oak Ridge, TN, January.

DOE 2016. *Oak Ridge Reservation Regional Groundwater Flow Model Development – Fiscal Year 2016 Progress Report, 2016*, DOE/OR/01-2743&D1, U.S. Department of Energy, Oak Ridge, TN.

DOE 2018. *Technical Memorandum #1, Environmental Management Disposal Facility Phase 1 Field Sampling Results Oak Ridge, Tennessee*, DOE/OR/01-2785&D1, U.S. Department of Energy, Oak Ridge, TN, July.

DOE 2019. *Technical Memorandum #2, Environmental Management Disposal Facility, Phase 1 Monitoring*, DOE/OR/01-2819&D1, U.S. Department of Energy, Oak Ridge, TN, May.

Environmental Simulations, Inc. 2017. Groundwater Vistas, Version 7.20, Environmental Solutions, Inc., Leesport, PA.

Harbaugh, A.W. 2005. *MODFLOW-2005, the U.S. Geological Survey Modular Ground-Water Model -- the Ground Water Flow Process*, Techniques and Methods 6-A16, U.S. Geological Survey, Reston, VA.

Keller, C. 2012. "Hydro-geologic Spatial Resolution using Flexible Liners." *TPG*. Vol. 51. pages 45-51, May/June.

McDonald, M.G., and A.W. Harbaugh 1988. "A Modular Three-dimensional Finite-difference Ground-water Flow Model", *Geological Survey Techniques of Water-Resources Investigations*, Book 6, Chap. A1.

ORNL 1988. *Concepts of Groundwater Occurrence and Flow Near Oak Ridge National Laboratory, Tennessee*, ORNL/TM-10969, Oak Ridge National Laboratory, Environmental Sciences Division, Oak Ridge, TN, November.

ORNL 1992a. *Status Report on the Geology of the Oak Ridge Reservation*, ORNL/TM 12074, Environmental Sciences Division Publication No. 3860, Oak Ridge National Laboratory, Oak Ridge, TN, October.

ORNL 1992b. *Status Report: A Hydrologic Framework for the Oak Ridge Reservation*, ORNL/TM-12026, Environmental Sciences Division Publication No. 3815, Oak Ridge National Laboratory, Oak Ridge, TN, May.

ORNL 2015. Climate Normals (1981-2010) and Extremes (1948-2015) for Oak Ridge, Tennessee (Town Site) with 2015 Comparisons, https://web.ornl.gov/~birdwellkr/web/Normals/30YRNorm.pdf.

ORNL 2019. Y-12 Tower "W" Precipitation data, https://metweb.ornl.gov/page5.htm.

Pollock, D.W. 1989. *Documentation of Computer Programs to Compute and Display Pathlines Using Results from the U.S. Geological Survey Modular Three-Dimensional Finite-Difference Groundwater Flow Model*, Open-file Report 89-381, U.S. Geological Survey, Reston, VA.

Robinson, J., and G.C. Johnson 1995. *Results of a Seepage Investigation at Bear Creek Valley, Oak Ridge, Tennessee January – September 1994*, USGS Open-File Report 95-459, J. A. Robinson and G. C. Johnson, U.S. Geological Survey, Reston, VA.

Robinson and Mitchell 1996. *Gaining, Losing, and Dry Stream Reaches at Bear Creek Valley, Oak Ridge, Tennessee March and September 1994*, USGS Open-File Report 96-557, J. A. Robinson and R. L. Mitchell III, U.S. Geological Survey, Reston, VA.

Schroeder et al.1994. *The Hydrologic Evaluation of Landfill Performance (HELP) Model: Engineering Documentation for Version 3*, EPA/600/R-94/168b, P. R. Schroeder, T. S. Dozier, P. A. Zappi, B. M. McEnroe, J. W. Sjostrom, and R. L. Peyton, U.S. Environmental Protection, Agency Office of Research and Development, Washington, D.C., September.

UCOR 2014. *Oak Ridge Reservation Regional Groundwater Flow Model Development – Fiscal Year 2014 Progress Report, U.S. Department of Energy Oak Ridge Reservation Oak Ridge, Tennessee*, UCOR-4634/R0, UCOR, Oak Ridge, TN, November.

UCOR 2015. *Regional Groundwater Flow Model Development – Fiscal Year 2015 Progress Report, U.S. Department of Energy Oak Ridge Reservation Oak Ridge, Tennessee*, UCOR-4753/R0, UCOR, Oak Ridge, TN, December.

UCOR 2020. *Quality Assurance Report for Modeling of the Bear Creek Valley Low-level Radioactive Waste Disposal Facilities, Oak Ridge, Tennessee*, UCOR-5234/R0, UCOR, Oak Ridge, TN, April.

USGS 1988. *Preliminary Evaluation of Groundwater Flow in Bear Creek Valley, Oak Ridge Reservation, Tennessee*, WRIR 88-4010. U.S. Geological Survey, Reston, VA.

Zheng 1990. *A Modular Three-Dimensional Transport Model for Simulation of Advection, Dispersion and Chemical Reactions of Contaminants in Groundwater Systems; Documentation and Users Guide*, report to the U.S. Environmental Protection Agency, C. Zheng, S.S. Papadopulos & Associates, Inc., Bethesda, MD.

Zheng and Wang 1999. *MT3DMS: A Modular Three-dimensional Multispecies Model for Simulation of Advection, Dispersion and Chemical Reactions of Contaminants in Groundwater Systems; Documentation and User's Guide*, C. Zheng, P. P. Wang Contract Report SERDP-99-1, U.S. Army Engineer Research and Development Center, Vicksburg, MS.

This page intentionally left blank.

APPENDIX E.
STOMP UNSATURATED ZONE TRANSPORT MODEL FOR THE ENVIRONMENTAL MANAGEMENT DISPOSAL FACILITY

This page intentionally left blank.

CONTENT

This page intentionally left blank.

FIGURES

TABLES

ACRONYMS

D	dimensional
DOE	U.S. Department of Energy
EMDF	Environmental Management Disposal Facility
PA	Performance Assessment
PNNL	Pacific Northwest National Laboratory
QA	quality assurance
RESRAD	RESidual RADioactivity
STOMP	Subsurface Transport Over Multiple Phases

This page intentionally left blank.

E.1 INTRODUCTION

The Environmental Management Disposal Facility (EMDF) at the Central Bear Creek Valley site will be built in an elevated area between drainages to provide sufficient separation between the waste and groundwater to meet a key design requirement. In addition to the disposal cell liner system, there will be a minimum of a 10-ft engineered geologic buffer zone plus any unsaturated in situ soil/bedrock interval above the groundwater table. Therefore, the vadose (unsaturated) zone above the groundwater table is expected to have a significant impact on the fate and transport of radionuclides that may be released from the disposal cell.

The Subsurface Transport Over Multiple Phases (STOMP) model (White and Oostrom 2000, White and Oostrom 2006) is used to simulate radionuclide release and vadose zone transport for the EMDF. The other models applied in the Performance Assessment (PA) analysis do not explicitly represent vadose zone contaminant transport or incorporate simplified waste geometry and vadose transport representations (refer to the description of the RESidual RADioactivity [RESRAD]-OFFSITE model in Sect. 3.3.4 and Appendix G of the PA). The STOMP model provides information on the spatial distribution and timing of radionuclide flux through the vadose zone to the water table, and explicitly represents the geometry of the EMDF preliminary design (waste and liner system) and materials below the liner (geologic buffer zone, saprolite, and fractured bedrock).

The STOMP model was developed by Pacific Northwest National Laboratory (PNNL) for modeling subsurface flow and transport systems. The fundamental purpose of the STOMP simulator is to produce numerical predictions of thermal and hydrogeologic flow and transport phenomena in variably saturated and fractured subsurface environments that are contaminated with radionuclides and organic compounds. The STOMP model is selected due to its ability to simulate transient flow and radionuclide transport phenomena in complex, variably saturated subsurface environments. Although the STOMP model is capable of simulating contaminant transport in saturated media, the EMDF application of the model is limited to transport in the waste and unsaturated zone above the water table. The STOMP model also has been applied at the U.S. Department of Energy (DOE) Hanford and Portsmouth facilities for PAs.

Quantitative predictions from the STOMP simulator are generated from the numerical solution of partial differential equations that describe subsurface environmental transport phenomena. Representation of the contaminated subsurface environment is based on governing conservative equations and constitutive functions. Governing coupled flow equations are partial differential equations for the conservation of water mass, air mass, carbon dioxide mass, methane mass, volatile organic compound mass, salt mass, and thermal energy. Constitutive functions relate primary variables to secondary variables. The solution of the governing partial differential equations occurs by using the integral volume finite difference method. The governing equations that describe thermal and hydrogeological flow processes are solved simultaneously using the Newton-Raphson iteration to resolve the nonlinearities in the governing equations. Governing transport equations are partial differential equations for the conservation of solute mass. The governing equations for solute mass conservation are solved sequentially following the solution of the coupled flow equations.

The STOMP model software meets Nuclear Quality Assurance-1-2000 software requirements and the safety software requirements specified under DOE Order 414.1C, Quality Assurance. Specifically, STOMP follows the PNNL standards based management system safety software subject area that has been written to meet those quality assurance (QA) requirements. STOMP development is managed under a configuration management plan in conjunction with a software test plan that details the procedures used to test, document, and archive modifications to the source code. Formal procedures for software problem reporting and corrective actions for software errors and updates are maintained and rigorously implemented. The model

simulations of various scenarios have compared to existing analytical and numerical models. Documentation of all verification and validation testing is publicly available (White and Oostrom 2000, White and Oostrom 2006, and Nichols et al. 1997).

The STOMP model code may be obtained from the model author at DOE PNNL (http://stomp.pnnl.gov/) and the user manual may be downloaded (in portable document format) from http://stomp.pnnl.gov/training/trainingdoc.stm.

E.2 STOMP MODEL DEVELOPMENT

Construction of the EMDF model to represent actual site and design conditions requires a detailed 3-dimensional (D) representation of the various engineered features and material zones and definition of the boundary conditions. The 3-D site topography and EMDF design features are shown in Fig. E.1, including the liner system surface (lower panel), post-closure cover surface (upper panel), and Bear Creek and its tributaries. The following site-specific data were used to construct the 3-D STOMP model:

- Existing topography (found in the Oak Ridge Environmental Information System)
- Lithology and material property values (Oak Ridge National Laboratory 1992, and sources cited for groundwater flow model in Appendix D of the PA)
- EMDF preliminary design parameters and topography (UCOR, an Amentum-led partnership with Jacobs, 2020, Sect. 4.1)
- Boundary conditions (Oak Ridge Environmental Information System).

Two 2-D STOMP cross-section models were constructed for the EMDF analysis. Selection of a 2-D rather than a 3-D modeling approach reduced the complexity of and time required for model development. While a 3-D model could provide more detailed 3-D flow and transport outputs, the simpler, 2-D vertical cross-sections capture the essential impact of site-specific conditions and design features on patterns of radionuclide release and vadose transport. Landfill design features, including liner system slopes and elevations, and variation in waste thickness, engineered material properties, and natural hydrogeologic properties cause non-uniform patterns of release and transport to the water table. However, because the dominant direction of vadose flow is vertical, the 2-D sections are sufficient to approximate the non-uniformity in the timing and magnitude of flux to the water table. The application of these approximate STOMP results to the 3-D saturated zone radionuclide transport model is described in Sect. E.3.4 and in Appendix F of the PA. The STOMP model domain location, orientation, and extent were selected based on EMDF preliminary design details (specifically cell floor and leachate drainage system slopes) and lithological unit configurations in order to capture the key parameters controlling the pattern of radionuclide release and vadose zone transport.

Section 9 of the PA details the QA activities and documentation that apply to the STOMP model analysis.

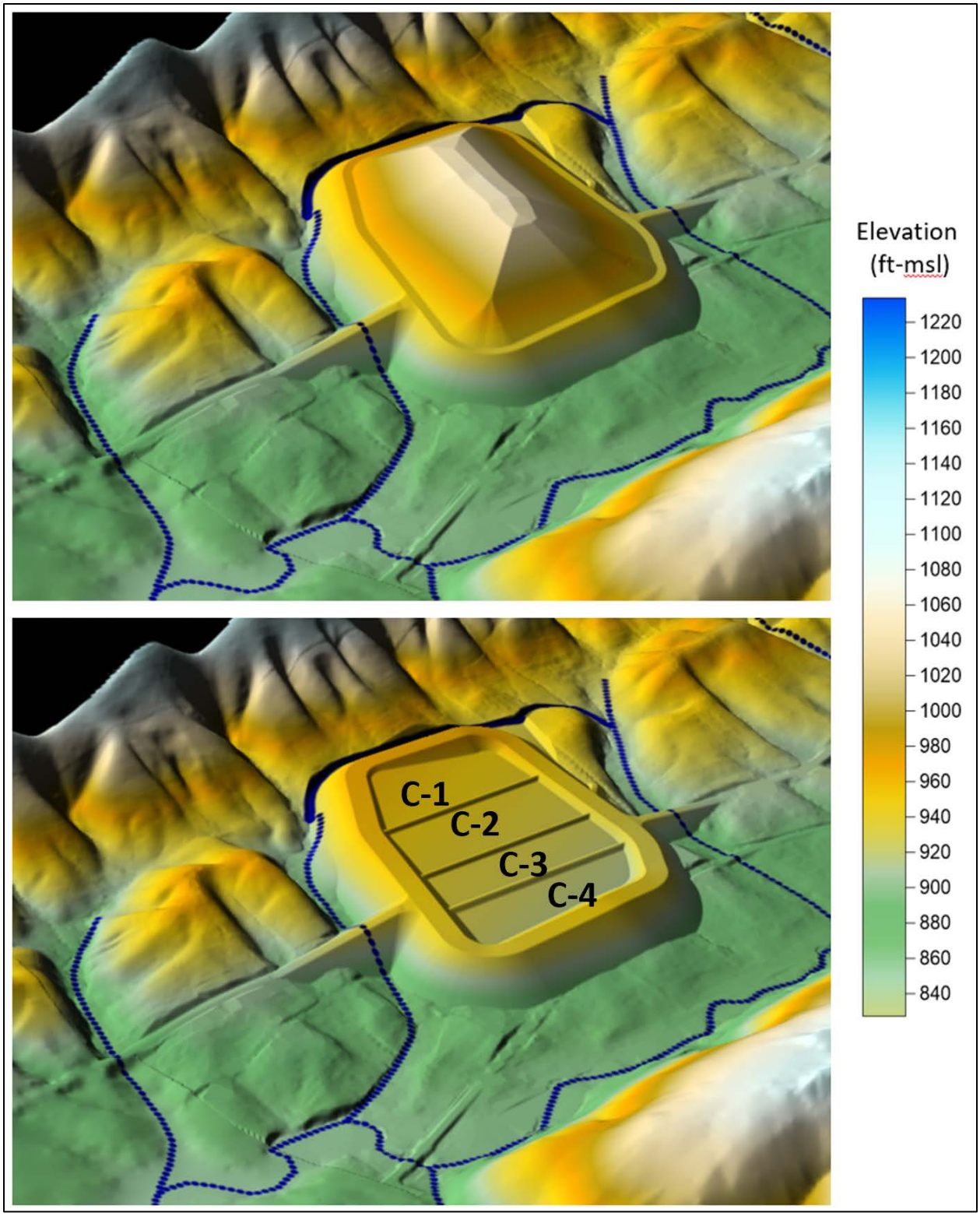

Fig. E.1. EMDF design and relationship to nearby features

E.2.1 CONSTRUCTION OF MODEL DOMAIN

Two 2-D cross-section STOMP models were developed for the EMDF site (see Fig. E.2). Section A-A′ (Section A) is a northwest to southeast section oriented parallel to the predominant cell floor slope. Section A crosses Cells 1, 2, 3, and 4 obliquely and captures the horizontal drainage impact of the liner system geometry. The northwest end of the model (A) starts at the crest of Pine Ridge while the southeast ends (A′) at Bear Creek. Section B-B′ (Section B) is a northeast to southwest oriented section through the crest of the final cover surface that captures the maximum waste thickness across all four waste disposal cells.

Key features and boundaries of the EMDF preliminary design that were used to guide construction of the model cross-sections are shown on Fig. E.2.

E.2.1.1 Material Zone Boundaries

The current surface topography and estimated top of the fractured bedrock were obtained from the 3-D groundwater model as described in Appendix D, Sect. D.3. Based on detailed EMDF preliminary design information (UCOR 2020, Sect. 4.1), the following 3-D surfaces for the design components were generated using Surfer (Golden 2016), a graphic mapping software package that uses a data extraction and mosaic method:

- Future topo surface outside of the cover (perimeter berms)
- Top of final cover
- Top of waste
- Top of liner system (bottom of waste)
- Top of drainage layer in liner
- Top of clay liner
- Top of geobuffer zone (bottom of liner system)
- Top of remaining saprolite/weathered bedrock
- Top of fractured bedrock (bottom of saprolite zone).

To create the STOMP model grids, the boundaries between material zones were extracted from the 3-D surface datasets for each component along the two cross sections. The boundaries for these material components within Section A are shown on Fig. E.3 and Section B is shown on Fig. E.4. The current topography is shown in the cross-sections to illustrate the estimated cut and fill requirements. The estimated long-term groundwater elevation (top of the saturated zone for the post-closure degraded cover and liner performance condition) based on the EMDF groundwater flow model simulation (refer to subsection E.2.1.2 and Appendix D of the PA) is also plotted on Figs. E.3 and E.4 to indicate the likely position and total thickness of the vadose zone beneath the geobuffer.

E.2.1.2 Predicted Post-Closure Groundwater Levels Beneath the EMDF

EMDF groundwater flow model (Appendix D) predicted future groundwater levels (top of the saturated zone) for the long-term degraded performance condition assuming 0.88 in./year recharge rate through the liner system (Fig. E.5). The predicted shallow saturated zone (groundwater model layer 2) flow vectors and equipotential contours are shown in the lower panel of Fig. E.5. Due to the anisotropic nature of the aquifer system, the overall groundwater flow direction under the EMDF is predominantly west-southwestward.

The STOMP cross-sections are not aligned with the general flow direction in the saturated zone; therefore, the 2-D STOMP simulations are not representative of the saturated zone flow predicted by the 3-D EMDF groundwater model. The STOMP model results are only representative of radionuclide release and vadose zone transport above the water table. The predicted post-closure groundwater levels are used to identify the likely vertical extent (thickness) of the vadose zone and variation in vadose thickness below the geobuffer, which provides the basis for estimating the timing of radionuclide flux to the water table, as described in Sect. E.3.4 and Appendix D.

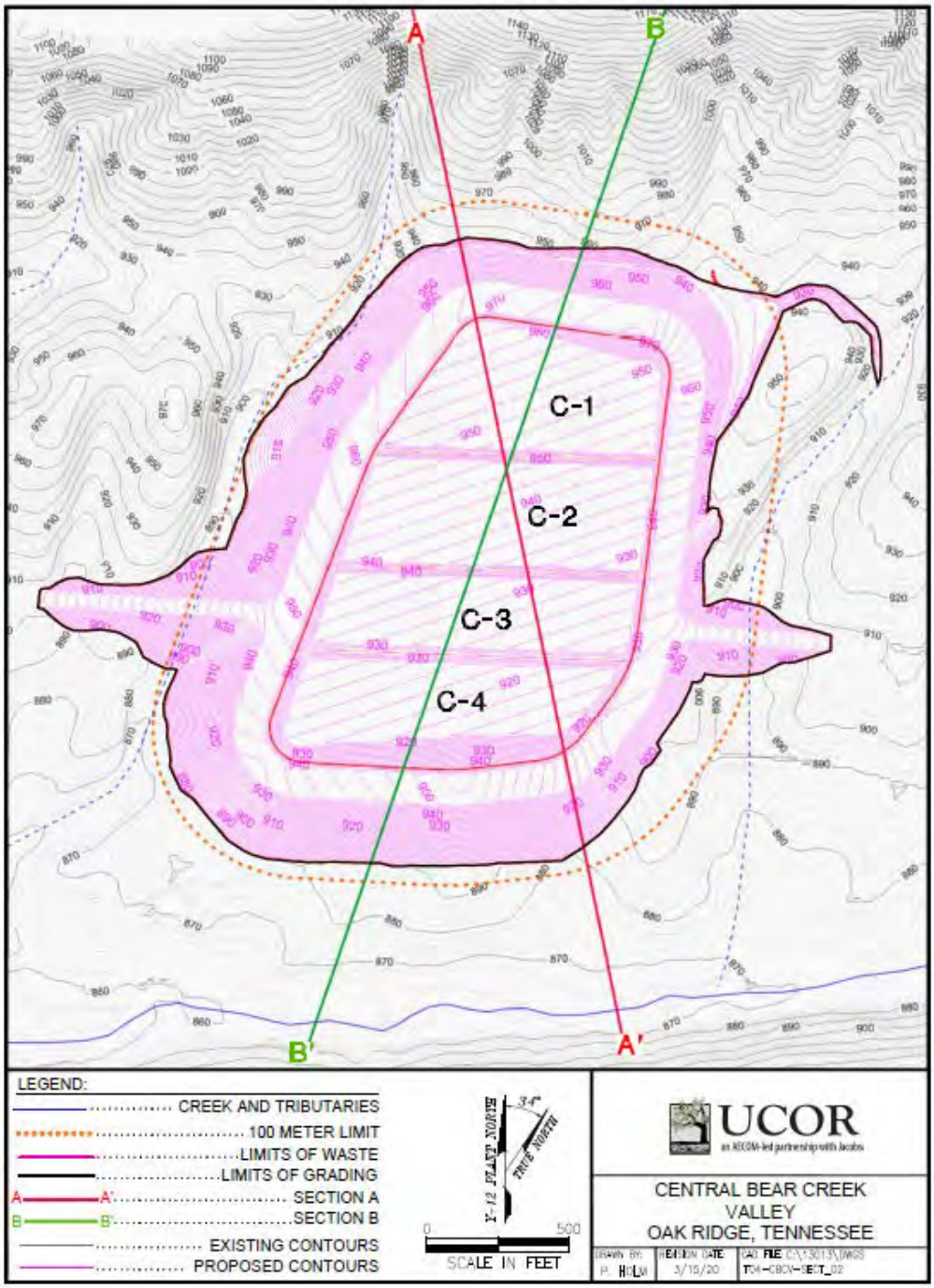

Fig. E.2. EMDF site map with cross-sections

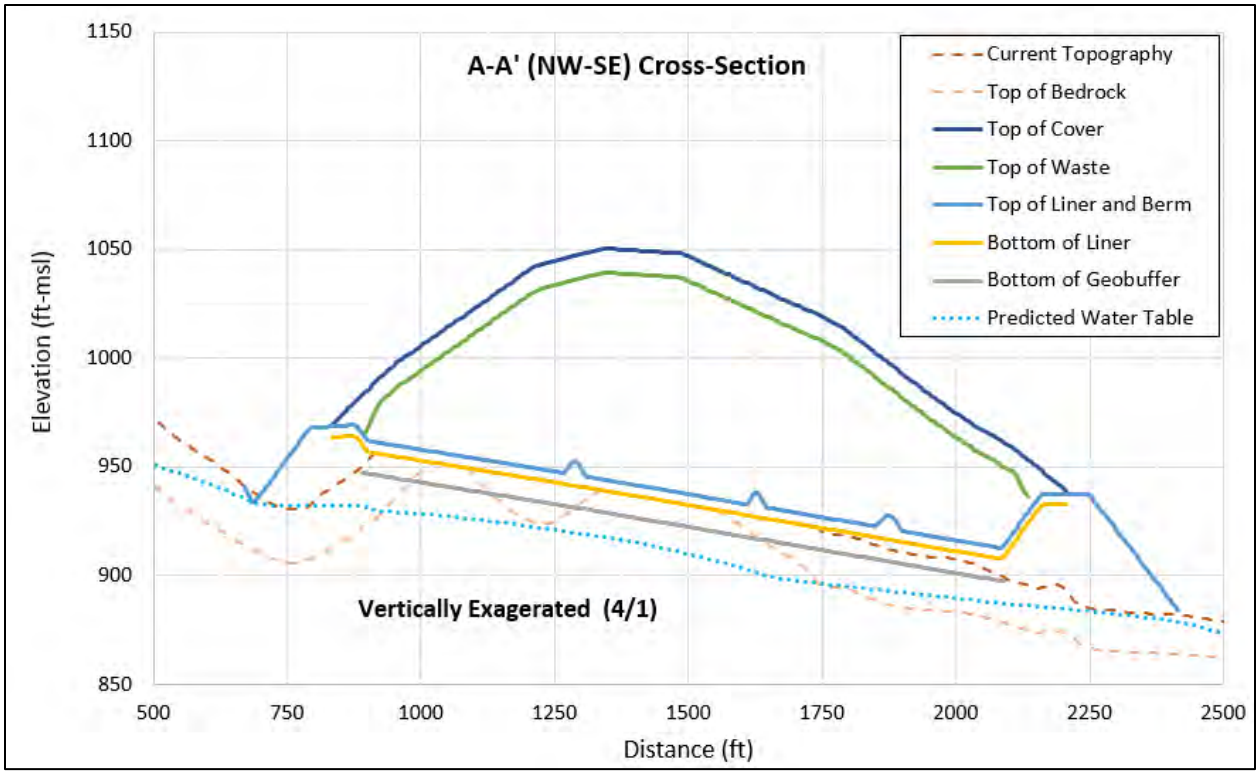

Fig. E.3. Cross-section A-A′ material boundaries for STOMP model discretization

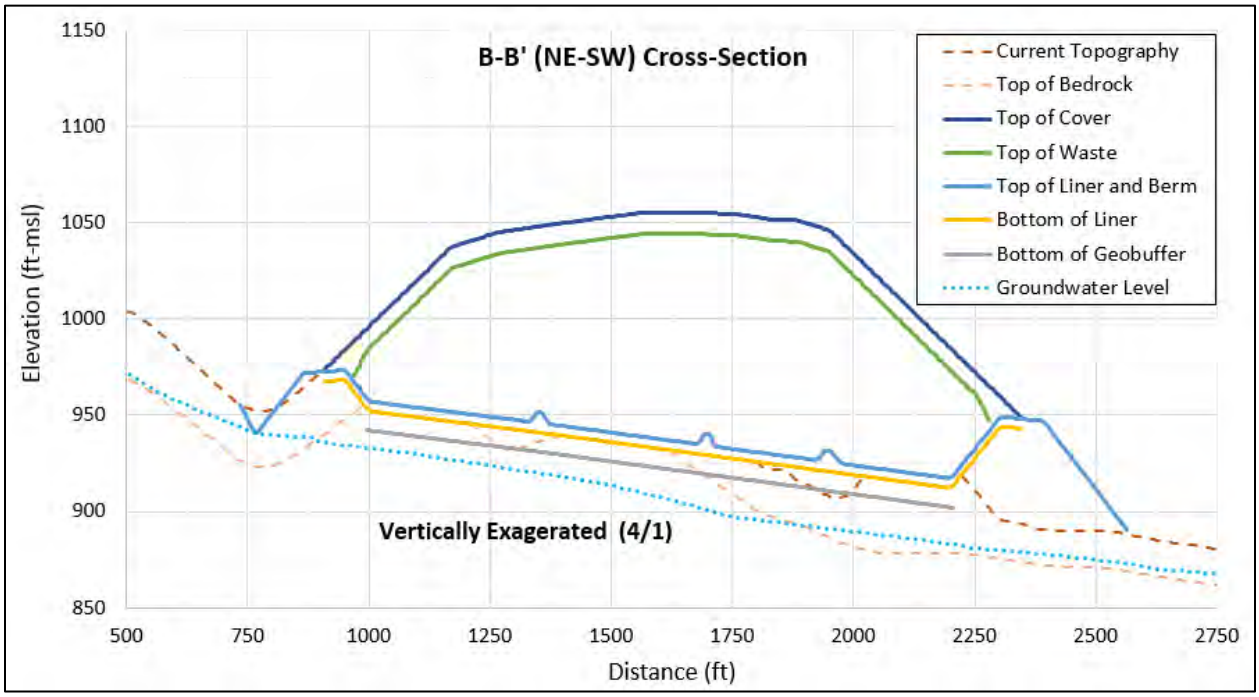

Fig. E.4. Cross-section B-B′ material boundaries for STOMP model discretization

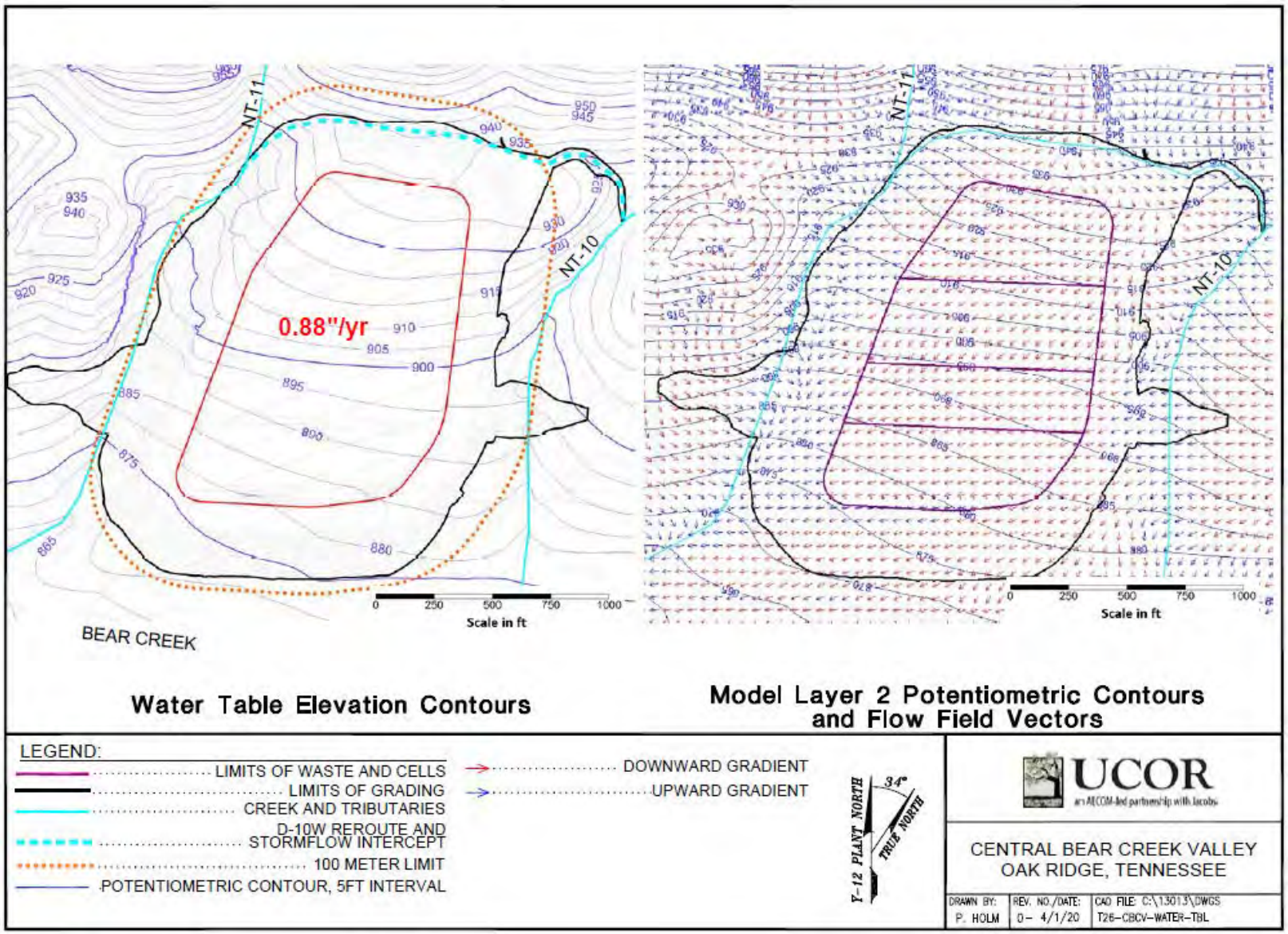

Fig. E.5. Groundwater levels and shallow flow field predicted by the EMDF saturated zone model

E.2.2 MODEL DISCRETIZATION

Discretization is the process of transferring continuous functions, models, variables, and equations into discrete units in a numerical representation. Model discretization refers to the assignment and alignment of the numerical cells in the model and establishes its relationship of those cells to actual natural and engineered conditions. A uniform grid space of 5 ft is used in the X direction (horizontal in the plane of the cross section). Each model grid is assumed to have a 1-ft width in the Y direction (orthogonal to the cross section plane) for easy mass calculation. The model grid and domain parameters in the Section A and B models are summarized in Table E.1.

Table E.1. STOMP model domain and discretization summary

	A-A′ section			B-B′ section		
Model discretization	**# of nodes**		**Grid size (ft)**	**# of nodes**		**Grid size (ft)**
I-indexed nodes (X)	565		5	559		5
J-indexed nodes (Y)	1		1	1		1
K-indexed nodes (Z)	222	214	1	227	219	1
		5	5		5	5
		3	10		3	10
Total number of nodes	120,910			122,421		
Number of active nodes	65,005			56,556		
Number of inactive nodes	71,479			43,746		
Extent of model domain	**Distance (ft)**			**Distance (ft)**		
X direction	2825			2725		
Y direction	1			1		
Z direction	269			274		

STOMP = Subsurface Transport Over Multiple Phases

A uniform 1-ft vertical grid spacing is used to represent the lithologic and design component material variations within each cross section, except in the deeper bedrock zone where vertical grid intervals transition to 5 ft and 10 ft. The smaller grid spacing in vertical direction allows the model to represent the disposal cell features (e.g., sloping liner drainage layer) and lithologic variations more precisely for predicting movement of radionuclides in the waste, liner system, and unsaturated zone beneath the liner. The same model grid design is used for both Section A and B models.

E.2.3 MODEL PROPERTY REPRESENTATION

The 2-D distribution of the rock/soil/design component types is represented in the STOMP model cross-sections by assigning nodes to one of the following material types:

1) EMDF cover (single material type with properties derived from multilayer cover system design)
2) Waste-Cell 1
3) Waste-Cell 2
4) Waste-Cell 3
5) Waste-Cell 4
6) Liner-fill (protective material at the top of the liner system)

7) Liner-sand-drain (leachate drainage layer)

8) Liner-clay (infiltration barrier)

9) Geobuffer (geologic buffer zone)

10) Saprolite-Pumpkin Valley

11) Saprolite-Maryville (includes Rogersville and Rutledge units)

12) Saprolite-Nolichucky

13) Saprolite-Maynardville

14) Bedrock-Pumpkin Valley

15) Bedrock-Maryville (includes Rogersville and Rutledge units)

16) Bedrock-Nolichucky

17) Bedrock-Maynardville

18) Berm-fill (perimeter berms and structural fill).

The material property assignments in the A and B sections are shown on Figs. E.6 and E.7. The material zone boundaries (Figs. E.3 and E.4) described in Sect. E.2.1.1 are the basis for these assignments.

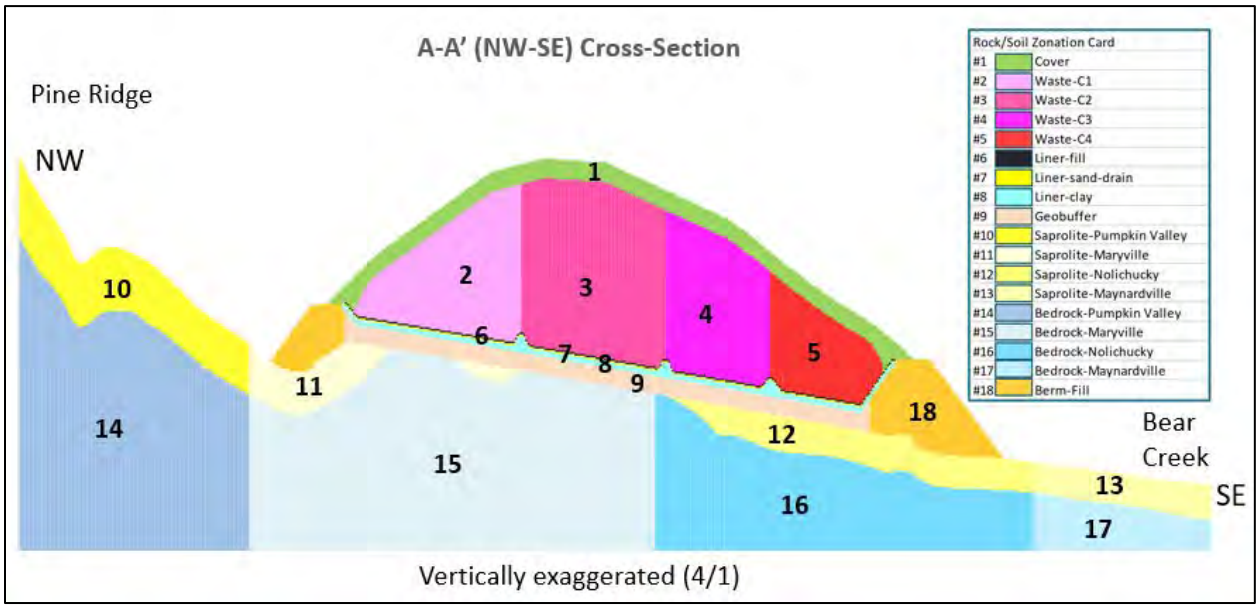

Fig. E.6. Cross-section A-A′ material property zones

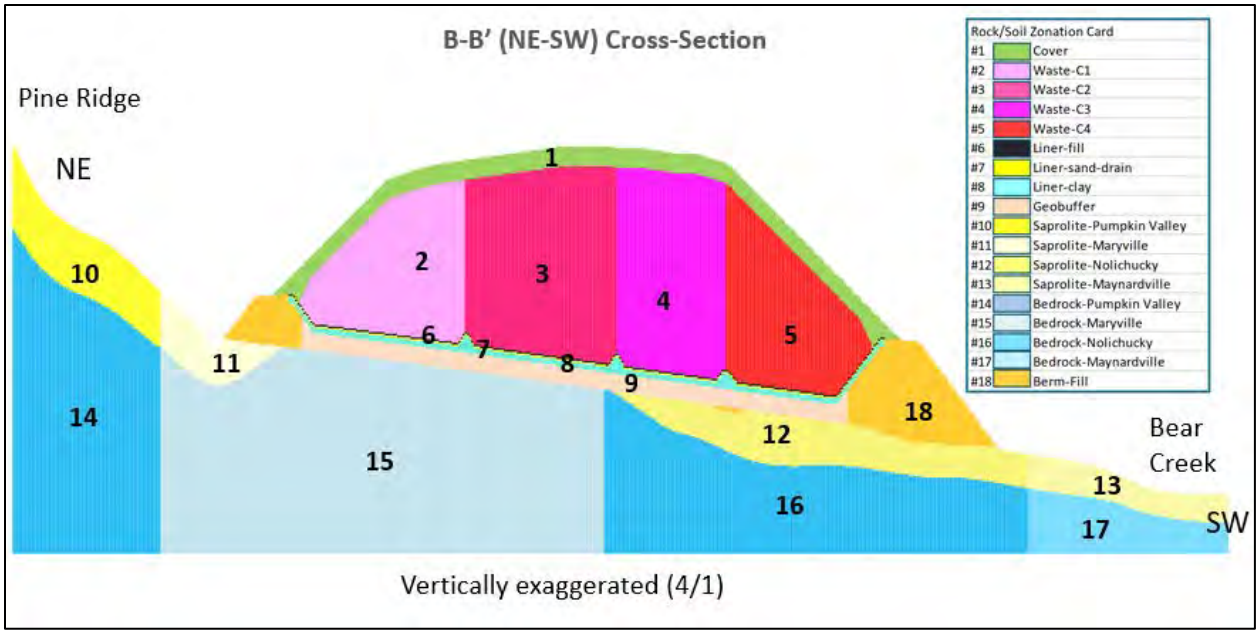

Fig. E.7. Cross-section B-B′ material property zones

E.2.4 MODEL BOUNDARY CONDITIONS

The surface of the EMDF preliminary design (final cover and perimeter berms) and the natural surface topography outside of the perimeter berms define the upper limit of the active model nodes in the STOMP model domain. Active nodes extend to the lower limit of the model domain, representing deep bedrock and assumed to be an inactive (no flow) boundary. The lower limit of the model domain was set well below the predicted long-term post-closure water table elevation (within the saturated zone) so that applied surface recharge rates and lateral flux boundary conditions do not lead to saturated conditions within the model domain above that elevation (described in Sect. E.2.1.2 and shown on Figs. E.3 and E.4).

A free air model boundary condition is assigned to all of the uppermost active nodes and to all boundary nodes that remain unsaturated. Depending on the water pressure-air pressure relationship, the defined node boundary condition allows the water to exit the model domain (discharge) if the water pressure is greater than the atmospheric pressure.

Cover infiltration or recharge (outside the cover limits) boundary conditions are assigned along the top of the active model domain for each modeled cross-section. Spatial variation in the infiltration/recharge rate is assigned as shown in Fig. E.8 for Cross-section A. The same general recharge pattern is applied for Cross-section B. The infiltration/recharge rates applied in different areas include the natural recharge zones (6.1 to 13.1 in./year, depending on geologic unit), the berm side slopes (1 in./year), and the central cover/liner zone (increasing from 0 to 0.88 in./year over the assumed period of cover degradation).

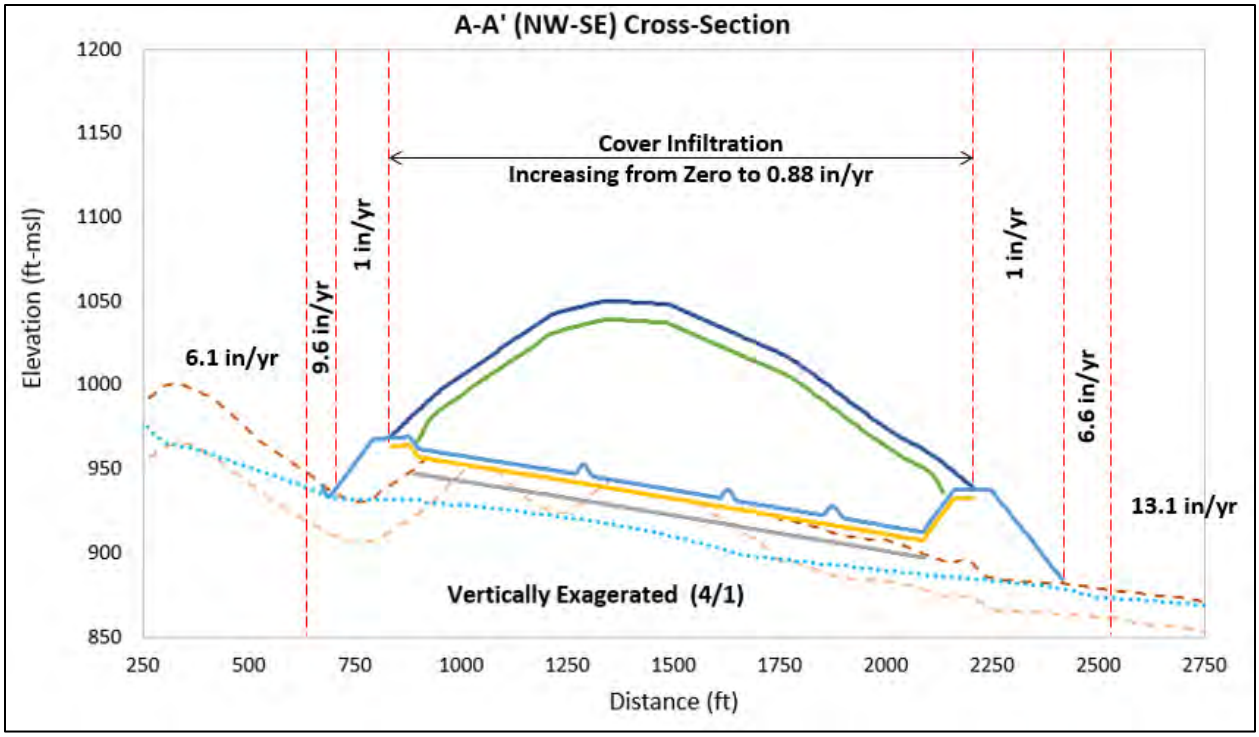

Fig. E.8. Recharge zones applied to the STOMP Section B model

The assigned natural recharge rates (6.1, 6.6, 9.6, and 13.1 in./year) are the same recharge rates applied to corresponding geologic units in the 3-D groundwater model (Appendix D). The maximum cover infiltration rate (0.88 in./year) is based on hydrologic performance model results for the long-term degraded cover performance condition (refer to Appendix C, Sect. C.2).

Model boundary conditions can be either constant (steady) or variable during the simulation. The recharge rates applied to the natural zones and berm slope are constant (e.g., 1 in./year for the berm slopes), whereas the recharge rate for the EMDF cover/liner zone is a variable boundary condition based on the assumed evolution of EMDF cover performance over time. Based on the conceptual model for normal evolution of EMDF cover performance (refer to Appendix C, Sect. C.1.3), a linear increase from zero at 200 years post-closure to 0.88 in./year at 1000 years is applied to the model nodes at the top of the cover material area.

For the vertical boundaries at the ends of the cross-section models, a hydraulic head gradient boundary condition is assigned to the model nodes expected to remain saturated. The extent of saturated boundary nodes and head gradient values are based on the EMDF groundwater model results (see Appendix D). The hydraulic head gradient boundary allows the groundwater water to flow in and out of the model domain at either end of the cross-section. For these 2-D cross-section models, there is no flux either into or out of the model domain in the Y direction.

E.2.5 STOMP MODEL INPUT PARAMETERS

The input parameter categories required to conduct a STOMP simulation include media, mechanical, and hydraulic properties; saturation function; aqueous relative permeability; solute-fluid interaction; and solute-porous media interaction. These specific properties include the following:

- Mechanical properties such as particle density, porosity (total and effective), specific storativity, compressibility, and tortuosity function for each defined material type
- Hydraulic properties such as intrinsic permeability or hydraulic conductivities in each direction for each defined material type
- Saturation function, which defines a saturation-capillary pressure function for each defined material type
- Aqueous relative permeability, which defines a relative permeability-saturation function for the aqueous phase for each defined material type
- Solute-fluid interaction, which defines solutes, solubilities, diffusion coefficients, and solute radioactive decay path parameters (half-life)
- Solute-porous media interaction, which defines solid-aqueous phase partition coefficients (K_d) and porous-media-dependent hydraulic dispersivities (solute-porous media parameters are dependent on both the solute and material type).

These material input parameters are based on site-specific data, design requirement parameters, and literature values as described in the following sections.

E.2.5.1 Mechanical Properties of Material Types

The mechanical properties of the EMDF preliminary design components, such as cover and liner materials, are based on the design criteria and are consistent with the values used in the EMDF hydrologic performance modeling presented in Appendix C of the PA. The physical parameters used in the STOMP model for engineered materials, waste, and rock/soil types are summarized in Table E.2.

Table E.2. Mechanical property summary

Material type	Particle density (kg/m^3)	Total porosity (vol/vol)	Diffusive (effective) porosity (vol/vol)	Tortuosity function
Cover	2.65E+03	0.429	0.298	Millington and Quirk
Waste-C1	3.27E+03	0.419	0.234	Millington and Quirk
Waste-C2	3.27E+03	0.419	0.234	Millington and Quirk
Waste-C3	3.27E+03	0.419	0.234	Millington and Quirk
Waste-C4	3.27E+03	0.419	0.234	Millington and Quirk
Liner-fill	2.65E+03	0.463	0.294	Millington and Quirk
Liner-sand-drain	2.65E+03	0.397	0.389	Millington and Quirk
Liner-clay	2.65E+03	0.427	0.195	Millington and Quirk
Geobuffer	2.65E+03	0.419	0.234	Millington and Quirk
Saprolite-Pumpkin Valley	2.65E+03	0.27	0.27	Millington and Quirk
Saprolite-Maryville	2.65E+03	0.27	0.27	Millington and Quirk
Saprolite-Nolichucky	2.65E+03	0.27	0.27	Millington and Quirk
Saprolite-Maynardville	2.65E+03	0.27	0.27	Millington and Quirk
Bedrock-Pumpkin Valley	2.78E+03	0.2	0.2	Millington and Quirk
Bedrock-Maryville	2.78E+03	0.2	0.2	Millington and Quirk
Bedrock-Nolichucky	2.78E+03	0.2	0.2	Millington and Quirk
Bedrock-Maynardville	2.78E+03	0.2	0.2	Millington and Quirk
Berm-fill	2.65E+03	0.4	0.3	Millington and Quirk

E.2.5.2 Hydraulic Properties

The hydraulic parameters used in the STOMP model for the different material types are summarized in Table E.3. The engineered materials and waste are assumed to be hydraulically isotropic, whereas the natural materials have anisotropic hydraulic conductivity values identical to those applied in the EMDF groundwater flow model (refer to Appendix D).

Table E.3. Hydraulic property summary

Material type	Kx/Ky (cm/sec)	Kz (cm/sec)	Dispersivity (longitudinal) (cm)	Dispersivity (transverse) (cm)
Cover	1.39E-07	1.39E-07	10	1
Waste-C1	1.90E-05	1.90E-05	10	1
Waste-C2	1.90E-05	1.90E-05	10	1
Waste-C3	1.90E-05	1.90E-05	10	1
Waste-C4	1.90E-05	1.90E-05	10	1
Liner-fill	3.70E-04	3.70E-04	10	1
Liner-sand-drain	3.00E-01	3.00E-01	10	1
Liner-clay	1.00E-07	1.00E-07	10	1
Geobuffer	1.00E-05	1.00E-05	10	1
Saprolite-Pumpkin Valley	1.76E-04	3.53E-05	10	1
Saprolite-Maryville	1.76E-04	3.53E-05	10	1
Saprolite-Nolichucky	2.65E-04	5.29E-05	10	1
Saprolite-Maynardville	3.76E-03	7.51E-04	10	1
Bedrock-Pumpkin Valley	1.67E-03	1.67E-06	10	1
Bedrock-Maryville	1.27E-05	1.27E-06	10	1
Bedrock-Nolichucky	3.35E-05	3.35E-06	10	1
Bedrock-Maynardville	1.76E-04	1.76E-05	10	1
Berm-fill	2.00E-05	2.00E-05	10	1

E.2.5.3 Saturation Function and Aqueous Relative Permeability

Saturation function input defines a saturation-capillary pressure function for each defined material type. The van Genuchten model is used to describe the saturation function for the model simulation (White and Oostrom 2000). The soil water retention parameters for the van Genuchten model were obtained from Carsel and Parrish (1988) based on material types. Minimum saturation values are defined based on hydrologic performance modeling and material type (Appendix C). Aqueous relative permeability input defines a relative permeability-saturation function for the aqueous phase for each defined material type. The Mualem model is applied for the relative permeability-saturation function (White and Oostrom 2000). The input parameter values are listed on Table E.4.

Table E.4. Saturation function parameter summary

Material type	Saturation function[a]	α parameter	n parameter	Minimum saturation	Permeability function[a]
Cover	van Genuchten	2.5	2.0	0.61	Mualem
Waste-C1	van Genuchten	2.5	2.0	0.73	Mualem
Waste-C2	van Genuchten	2.5	2.0	0.73	Mualem
Waste-C3	van Genuchten	2.5	2.0	0.73	Mualem
Waste-C4	van Genuchten	2.5	2.0	0.73	Mualem

Table E.4. Saturation function parameter summary (cont.)

Material type	Saturation function[a]	α parameter	n parameter	Minimum saturation	Permeability function[a]
Liner-fill	van Genuchten	2.5	2.0	0.50	Mualem
Liner-sand-drain	van Genuchten	3.0	3.5	0.08	Mualem
Liner-clay	van Genuchten	1.0	1.8	0.99	Mualem
Geobuffer	van Genuchten	1.5	1.8	0.73	Mualem
Saprolite-Pumpkin Valley	van Genuchten	2.0	2.0	0.50	Mualem
Saprolite-Maryville	van Genuchten	2.0	2.0	0.50	Mualem
Saprolite-Nolichucky	van Genuchten	2.0	2.0	0.50	Mualem
Saprolite-Maynardville	van Genuchten	2.0	2.0	0.50	Mualem
Bedrock-Pumpkin Valley	van Genuchten	2.5	2.0	0.30	Mualem
Bedrock-Maryville	van Genuchten	2.5	2.0	0.30	Mualem
Bedrock-Nolichucky	van Genuchten	2.5	2.0	0.30	Mualem
Bedrock-Maynardville	van Genuchten	2.5	2.0	0.30	Mualem
Berm-fill	van Genuchten	2.5	2.0	0.50	Mualem

[a]White and Oostrom 2000.

E.2.5.4 Solute-Fluid and Solute-Porous Media Interaction

The solute-fluid and solute-porous media interaction parameters were needed to conduct the fate and transport analysis for radionuclides. Seven radionuclides were selected for STOMP model analysis based on the estimated inventory and predicted dose contributions from preliminary EMDF performance simulations. These radionuclide parameters were obtained from various sources (in addition to site-specific data). Based on the review of available information (refer to Sect. 3.2.2.5 of the PA), K_d values in the waste and for all other (non-waste) materials were assigned for the seven radionuclides. The K_d values applied in the STOMP model for the radionuclides are listed on Table E.5. The half-life of the radionuclides were obtained from DOE technical guidance (DOE 2011) and specific activity of the radionuclides were obtained from ORNL 2017.

Table E.5. Solute-media interaction parameter summary

Radionuclide	K_d (waste) (cm^3/g)	K_d (other materials) (cm^3/g)	Half life (year)	Specific activity (Ci/g)
Carbon-14	0	0	5.70E+03	4.50E+00
Hydrogen-3	0	0	1.23E+01	9.80E+03
Iodine-129	2	4	1.57E+07	1.80E-04
Plutonium-239	20	40	2.41E+04	6.30E-02
Technetium-99	0.36	0.72	2.11E+05	1.70E-02
Uranium-234	25	50	2.46E+05	6.20E-03
Uranium-238	25	50	4.47E+09	3.40E-07

E.2.6 STOMP MODEL FILE CREATION

The model files for each cross-section STOMP model consists of an input control file, model property zonation file, and six boundary condition files. The STOMP model uses a text format file for all model control and input parameters. However, many of the key model input files (i.e., model discretization and property zonation file and various boundary condition files) are quite complicated for the complex EMDF

site configuration. Database and spreadsheet programs were used to create these files, which were visually verified either in the data spreadsheet or a graphics program for QA purposes.

Section 9 of the PA details the QA activities and documentation that apply to the STOMP model analysis.

E.3 STOMP MODEL SIMULATIONS AND RESULTS

Using the model input parameters presented above, the STOMP model simulations were conducted for the two 2-D cross sections. These simulations consisted of base condition run and sensitivity analysis as described below.

The STOMP executable code used for all the simulations is compiled Version V.1.4.2.1 with SPLIT solver. STOMP simulations were executed using the coupled water-solute transport mode so that the fate-transport results could be directly linked to changes in water movement at each individual model time step.

E.3.1 STOMP MODEL INITIAL CONDITIONS

Model initial condition refers to the starting conditions (initial values for model variables) assumed or applied for the model simulation. It includes both primary and secondary field variables, such as initial moisture and contaminant mass distributions and initial boundary conditions. The initial boundary conditions for the EMDF STOMP modeling are explained in Sect. E.2.4.

E.3.1.1 Initial Moisture Conditions

In the humid climate of East Tennessee, natural materials below the root zone generally remain at field capacity in most years, although drier conditions occur near the surface and in deeper locations under very dry (drought) conditions. For the STOMP model simulations, initial saturation levels are assigned as the "minimum saturation" parameter in the saturation function (Table E.4). The values given in Table E.4 are based on the EMDF hydrologic performance model (refer to Appendix C) for the cover, waste, liner, and geobuffer materials. Values for the natural saprolite and bedrock and for perimeter berm and structural fill materials are based on typical field capacities for fine-grained earth materials.

E.3.1.2 Waste Zone Initial Concentration

The waste in the four disposal cells are assigned as the source zone (non-zero initial concentrations) for the STOMP models. It is assumed that the waste has a uniform average initial mass concentration throughout the four disposal cells. The initial source concentration is assigned for each radionuclide based on its estimated total activity inventory. The source concentration (C) is a combined solute mass absorbed on soil (C_S) and dissolved in the aqueous phase (C_L) based on linear partitioning of solutes between the porous media and aqueous phase:

$$C = C_L \times \text{porosity} \times \text{initial aqueous saturation} + C_S \times (1 - \text{porosity})$$

where:

$$C_L = C_S/(K_d \times \text{particle density}).$$

Therefore, the initial source aqueous concentration of each solute at the source in the model simulation is dependent on the source K_d values. The waste effective porosity (0.23, Table E.2) was used in the

calculation of the initial solid-aqueous partition, which results in higher initial aqueous concentrations and radionuclide release than a partition based on the total porosity (0.42). The initial aqueous saturation for the source zone is based on the Hydrologic Evaluation of Landfill Performance model (referred to as the HELP model) results (Appendix C, Sect. C.2).

It should be noted that the mass of radionuclides in the waste placed in EMDF would be subjected to processes that result in reduction over time beyond the radioactive decay rate, including the following:

1) Mass removed during cell operations via collection and removal by the contact water/leachate collection system
2) Mass removed by the leachate collection system during active cell maintenance period (assumed to be 0 to 100 years) after cell closure
3) Mass released to environmental media beneath EMDF (after 200 years).

The mass loss during the EMDF operations period was estimated with the RESRAD-OFFSITE model for those radionuclides with low K_d values (Tc-99, H-3, C-14, and I-129) (see Appendix G, Sect. G.4.3.4). The remaining average activity concentrations within the waste at EMDF closure were used as the initial activity concentrations for the STOMP model. The second process (post-closure leachate collection) is not accounted for in the STOMP model, increasing the conservatism (higher concentrations for mobile radionuclides than might be expected). Therefore, the STOMP model is relatively conservative (assumes slightly higher than expected values) in terms of initial contaminant mass (assumes no post-closure leachate collection) for the most mobile radionuclides and in terms of calculated initial aqueous concentrations (effective porosity basis) for all radionuclides.

Based on the estimated inventory data and estimated operational loss for the mobile radionuclides, the initial source (waste) mass concentrations (radionuclide mass per volume at closure) were calculated assuming a uniform waste concentration within all the cells with a dry bulk density of 1900 kg/m^3. The initial average activity concentrations in pCi/g and corresponding mass concentration in mg/L (mass per volume), which are the required STOMP model units, are listed in Table E.6. Note that because initial mass and output concentration are in linear relationship, the modeled results can be easily scaled to new source concentration if there are any deviations or changes in estimated initial radionuclide inventory.

Table E.6. Initial activity and mass concentrations for waste in STOMP model

Radionuclide	As-generated waste average activity concentration (pCi/g)	As-disposed waste average activity concentration (pCi/g, corrected for added clean soil mass)	Closure mass concentration (g/g)	Closure Volumetric concentration (mg/L)
Carbon-14	5.43E+00	5.40E-01	1.20E-13	2.28E-07
Hydrogen-3	2.10E+01	4.64E+00	4.73E-16	9.00E-10
Iodine-129	7.66E-01	3.50E-01	1.94E-09	3.69E-03
Plutonium-239	1.10E+02	5.83E+01	9.25E-10	1.76E-03
Technetium-99	5.28E+00	1.56E+00	9.18E-11	1.74E-04
Uranium-234	1.19E+03	6.30E+02	1.02E-07	1.93E-01
Uranium-238	7.18E+02	3.81E+02	1.12E-03	2.13E+03

STOMP = Subsurface Transport Over Multiple Phases

E.3.2 BASE CASE SIMULATION

E.3.2.1 Selection of Model Output

The STOMP model was run to 1,000,000 years to simulate release of the less mobile radionuclides (actinide elements). Due to the extremely long modeled time period and large number of model nodes, the default model-generated output file for all nodes is very large. In order to streamline output data post-processing, a limited number of model outputs were specified. The STOMP output included data for selected model nodes at several vertical output profiles and along three output surfaces, and data for all model nodes at selected model time steps.

Three vertical data output profiles were defined for each disposal cell; the profiles for each cell are located in the upper, middle, and lower areas of the sloping liner system surface. Therefore, a total of 12 vertical profile locations for each cross-section were defined on this basis to capture the impact of the sloping liner geometry on the pattern of release. The 12 output profile locations for Section A are shown on Fig. E.9 and the output profile locations for the Section B model are shown on Fig. E.10.

Several model nodes representing all key components at different elevations above the groundwater table were selected for each vertical profile:

- Three nodes in the waste zone (top, middle, and bottom of the waste zone)
- Three nodes in the liner system (liner fill layer, sand drainage layer, and middle of the clay liner)
- Three nodes in the geobuffer zone (top, middle, and bottom)
- Variable numbers of nodes in the vadose zone (every 2 ft in elevation above the model predicted groundwater table elevation). The exact elevation of the node at the predicted water table elevation in each profile is determined based on EMDF groundwater model output (refer to Figs. E.3 and E.4) for the long-term 0.88 in./year cover infiltration rate.

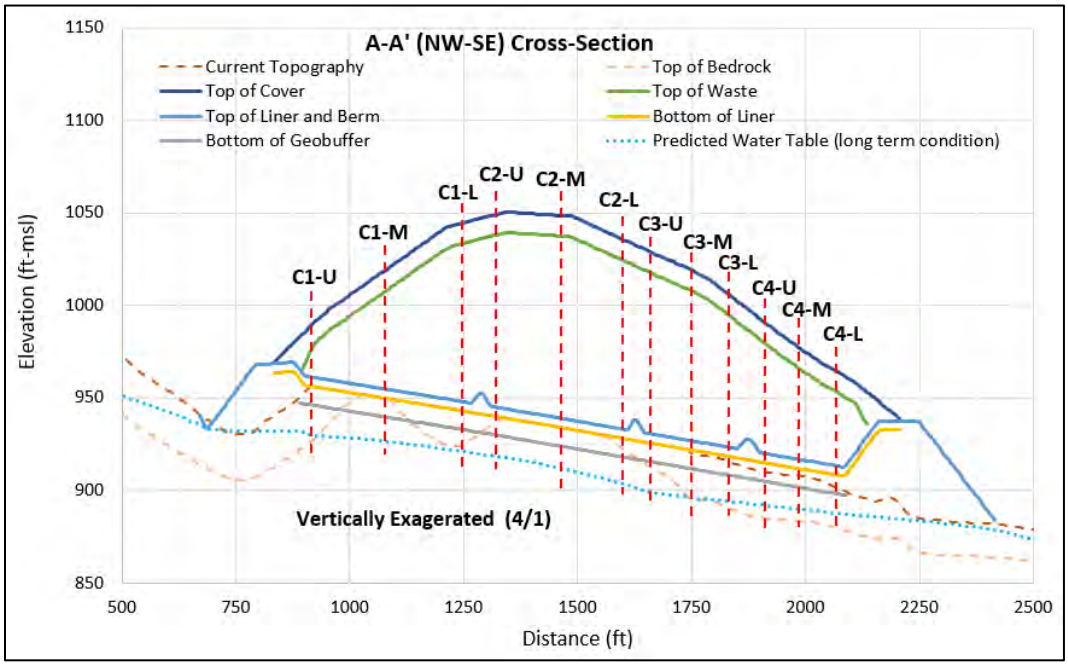

Fig. E.9. Data output profile locations in the Section A model

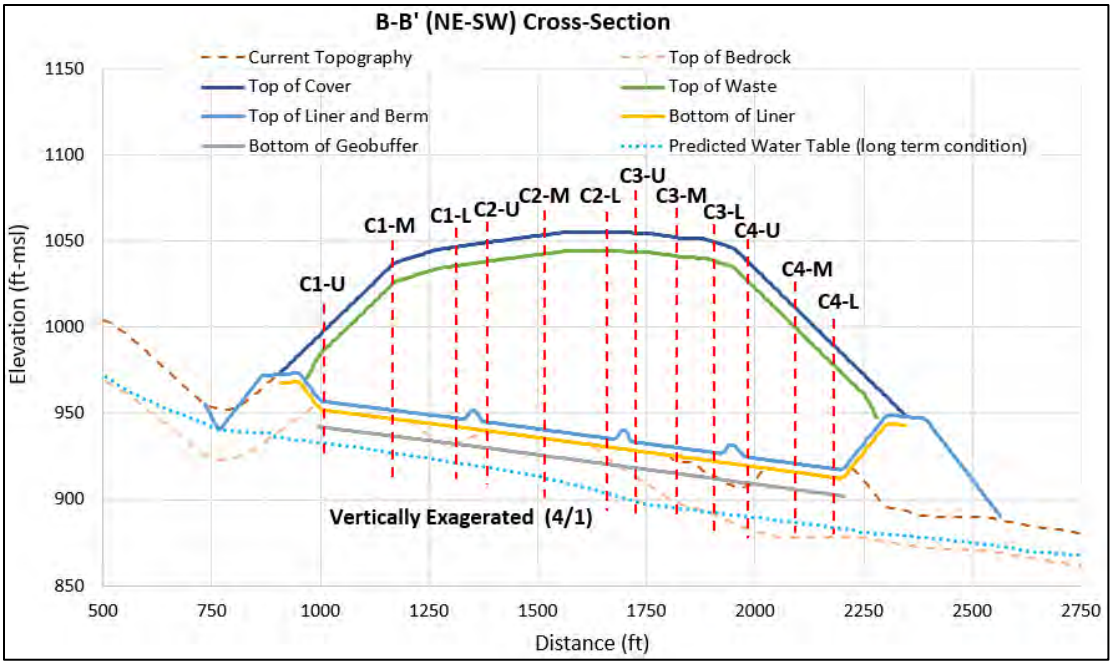

Fig. E.10. Data output profile locations in Section B model

In addition to the vertical data output profiles for each disposal cell, the individual nodes in three surfaces (groups of adjacent model nodes) were defined in the output file for the Section A model (Fig. E.11). The output surfaces were defined to represent:

- Top of the liner – to estimate total water and radionuclide mass release from the source zone
- Bottom of the liner – to estimate total water and radionuclide mass release from the liner system
- Groundwater table – to estimate total water and radionuclide mass release into the saturated zone.

For these different groups (profiles and surfaces) of selected model nodes, all model output parameters were generated for every internal model time step in the default output file. However, all model output parameters for all model nodes were generated for 66 specific times that ranged from starting time (T = 0) to 1,000,000 years. These outputs are used to create color shaded plots of the results for the entire model domain at each of the specific output time steps.

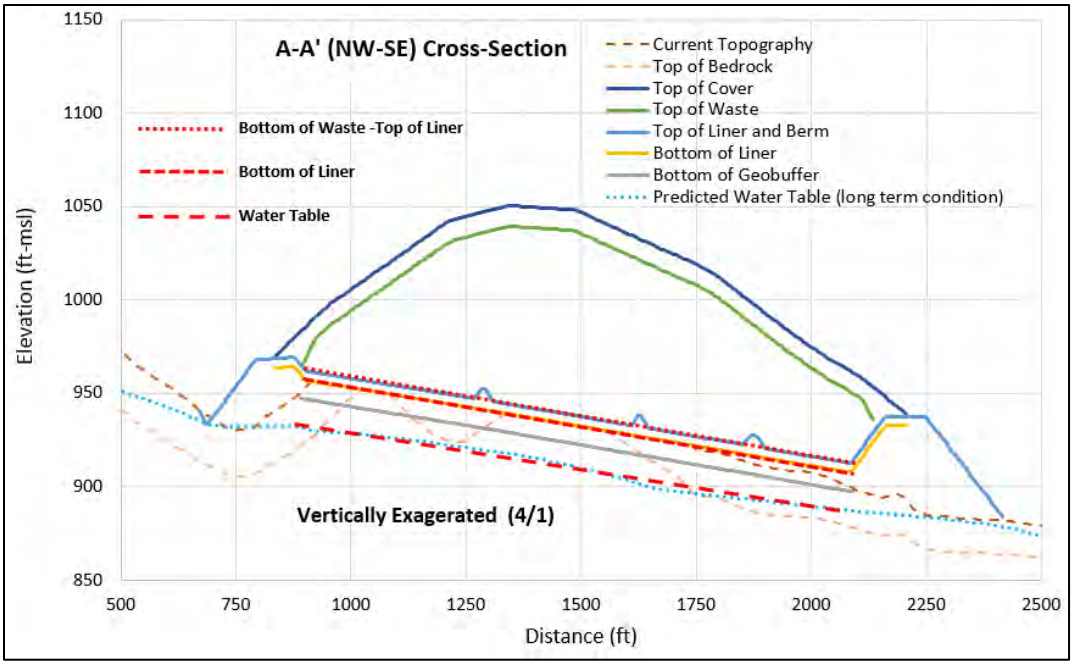

Fig. E.11. Data output surfaces defined in the Section A model

E.3.2.2 Water Movement and Saturation Changes

Water saturation time series for the Section A STOMP model, Cell 2 output profile nodes are shown on Fig. E.12. Water saturation is the ratio of water-occupied volume to total void volume (or fractional water content to total porosity). The saturation curves for the period from 0 to 200 years are steady since there are no changes in boundary conditions (i.e., cover infiltration = 0 for the cell area).

The saturation curves change in response to water influx as progressively higher infiltration rates (0 to 0.88 in./year) are applied after 200 years. The waste zone nodes respond first (350 to 450 years) to the increasing water flux and most of the Cell 2 profile nodes (including nodes below the geobuffer material) show a rapid increase in saturation between 400 and 500 years, followed by more gradual increase in saturation through 1000 years. Very soon after 1000 years, the water flow system reaches its steady-state condition when the cover infiltration rate becomes constant (0.88 in./year). Unsaturated conditions (saturation index < 1) persist after 1000 years in all the Cell 2 output profile nodes except for the clay liner nodes at all three profiles and the lower waste and upper liner nodes at the Cell 2 lower profile, which approach saturation (0.99 saturation index).

The saturation curve differences among the three Cell 2 profile locations reflects lateral water movement caused by the sloped cell liner system. For nodes below the liner, the saturation index increases earlier and reaches higher final values at the lower output profile (C2-L) relative to the middle (C2-M) and upper (C2-U) profile locations. For example, somewhat later (> 500 years) increases in saturation for the lowest saprolite/bedrock nodes in the upper and middle profile locations reflect the lateral movement of water from the upper to the lower profile location along the sloping liner components, which delays the flux of moisture to deeper profile nodes at the upper and middle profiles. This pattern of water movement is also reflected in the higher saturation levels of the lower waste and upper liner nodes at the lower profile compared to the middle and upper profile locations.

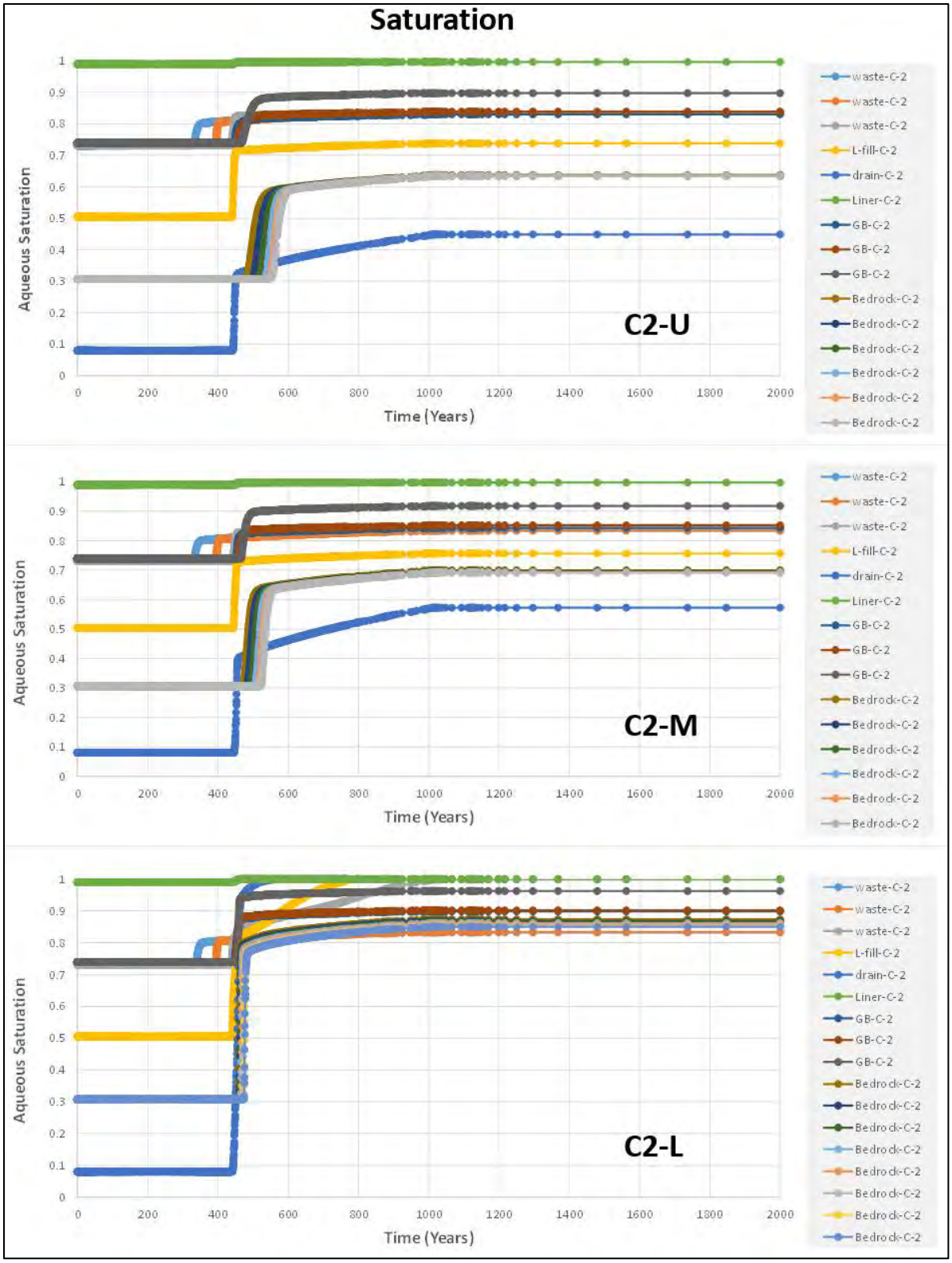

Fig. E.12. Saturation change with time in Section A model Cell 2 profiles

The full saturation fields for the Section A STOMP model at selected time steps are presented in Fig. E.13, which clearly shows the increased saturation for all areas relative to the initial condition at year zero. The increasing cover infiltration rate starting in year 200 produces increasing saturation in the waste, liner system, geobuffer, and underlying materials by year 500. The STOMP results reveal that there is a persistent non-uniform pattern of saturation below the EMDF during the modeled period. Higher saturation zones occur beneath the lower (downslope) portions of the individual disposal cells. Relatively lower saturation occurs below the disposal cell side slopes and upper (upslope) portions of the cells. The results show that the liner slope and material properties and the overall geometry of the four disposal cells are a strong control on the water movement within the disposal system. The model representation of the sand drainage layer overlying the much less permeable 3-ft clay liner promotes the horizontal movement of water within the drainage layer before its downward movement through the clay liner. The successive saturation fields also show that most of the model domain remains unsaturated (saturation index < 0.9), consistent with the vadose zone focus of the EMDF STOMP model application.

The water flux rates into the saturated zone beneath each of the four disposal cells are calculated by summing the vertical flux across the model nodes at the predicted water table elevation (output surface shown in Fig. E.11). The four disposal cell flux rates, the total estimated water flux to the saturated zone, and the applied cover infiltration as a function of time are presented in Fig. E.14. The infiltration rate increases from 0 to 0.88 in./year from 200 to 1000 years, and remains constant after 1000 years. The steady state water flux for each of the four disposal cells is proportional to the width of the cell. The calculated water flux at the top of the saturated zone (predicted water table elevation) starts to increase after 400 years and reaches its maximum rate shortly after 1000 years when water infiltration rate through the cover becomes constant at the long-term performance condition (0.88 in./year).

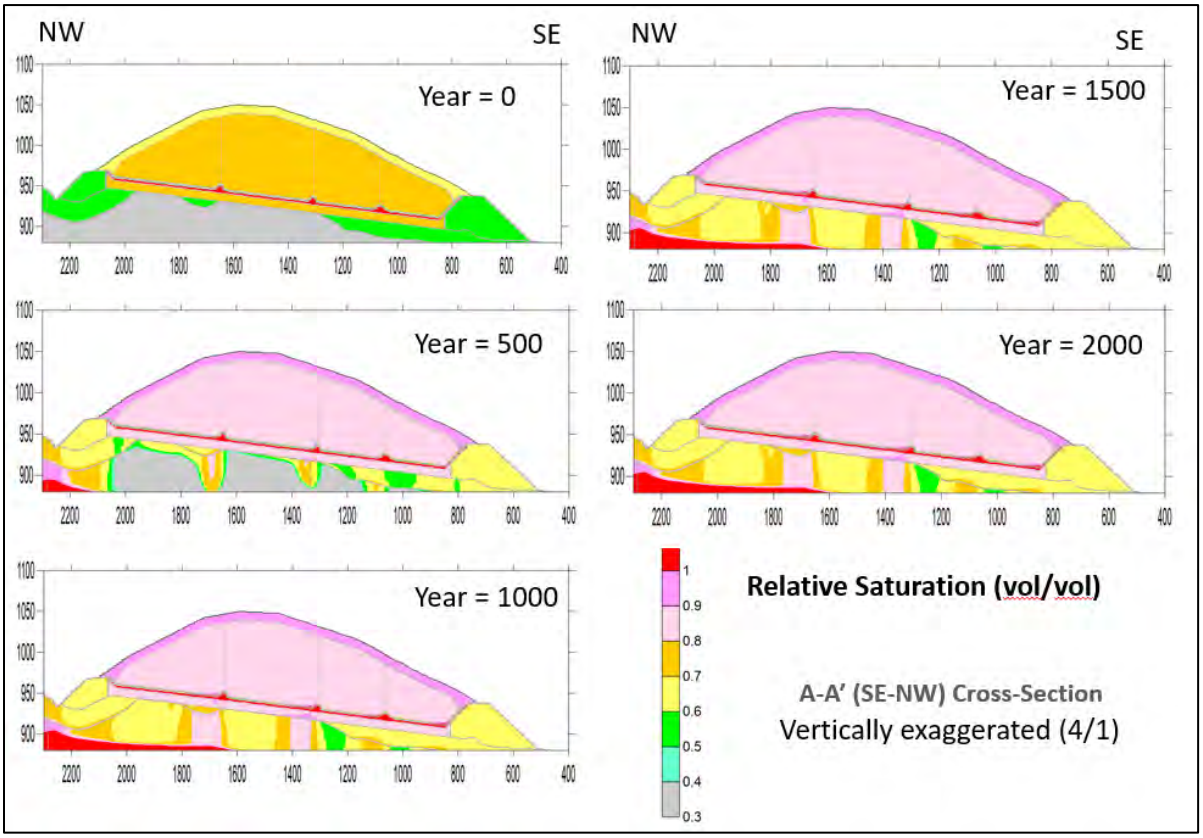

Fig. E.13. Saturation change with time in Section A model

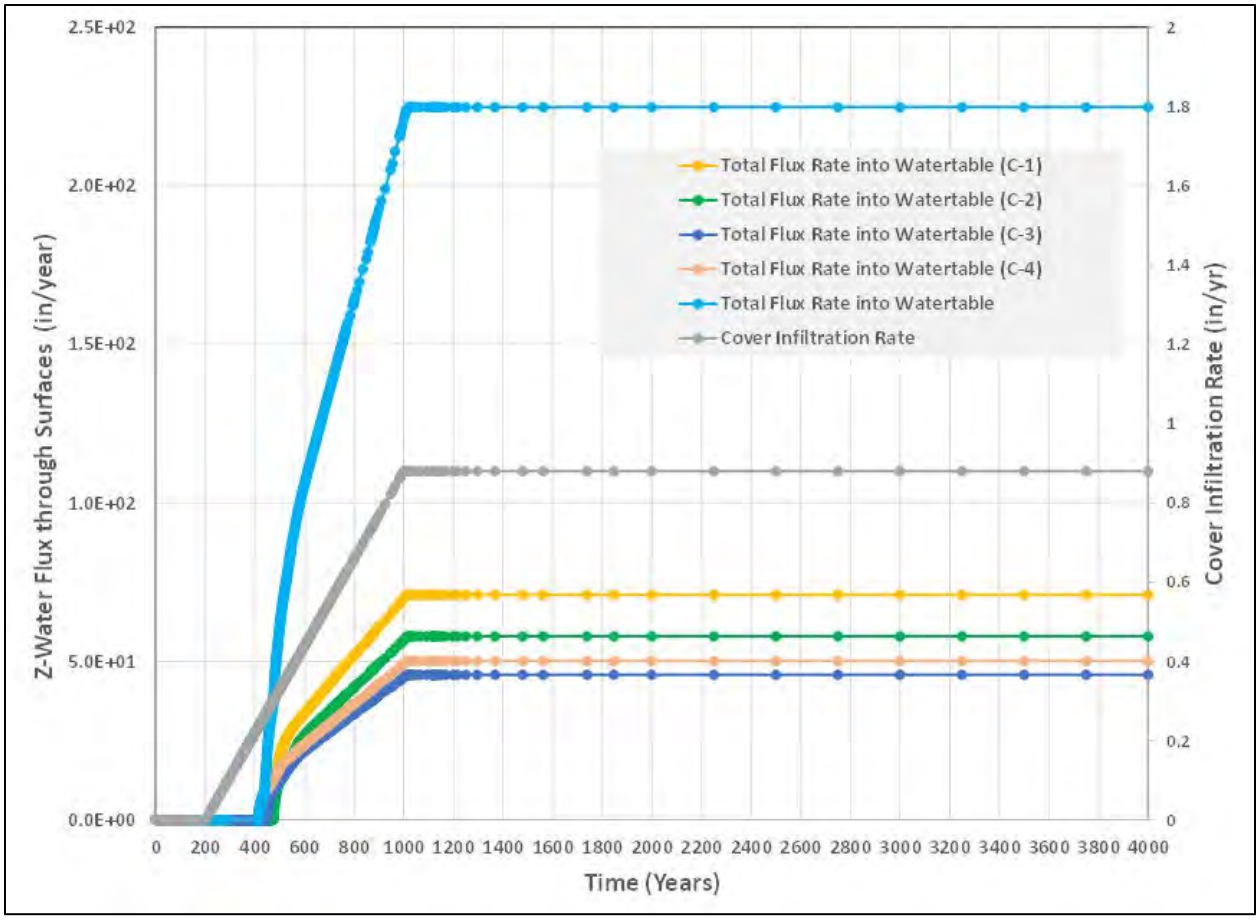

Fig. E.14. Vertical water flux at water table elevation

E.3.2.3 Fate-Transport Results

The STOMP simulations were conducted using coupled water-solute transport mode so the fate-transport simulation is directly linked to the transient change in the water movement in each individual model step. Based on the EMDF estimated inventory, the initial radionuclide mass concentrations for the seven modeled radionuclides were applied to the waste zone nodes. The results of the fate-transport simulation at each modeled time-step are presented as aqueous concentrations (mg/L of water).

E.3.2.3.1 Radionuclide depletion and vertical migration – Cell 2 output profile nodes

Rates of radionuclide release and depletion of activity in the waste are controlled by following four key factors:

- Half life
- K_d
- Water percolation rate through waste
- Source zone (waste) thickness (and its variation).

Depending on the radionuclides mobility (K_d), half-life, and location, one or more of these factors will have a dominant impact on fate and transport. The modeled radionuclide aqueous concentration changes with time at the Cell 2 data output profile locations for the Sections A and B models are presented below.

At the beginning of the model simulation (T = 0), all the radionuclides have uniform aqueous concentrations in the waste zone only. However, with the recharge rates applied to the top of the waste, their aqueous concentration distribution pattern starts to change due to downward migration and decay. With non-contaminated water influx from the cover, radionuclides in the upper part of waste are depleted first due to downward flux. The mass and radioactivity in the waste zone continues to decline until all mass has either migrated or decayed. This migration of the mass is reflected in changes of aqueous concentration with time for the Cell 2 vertical output profiles.

Figure E.15 shows the Tc-99 concentration changes in the three Cell 2 profiles in the Section A model. The rates of waste zone depletion (decreasing concentration at waste nodes) are essentially the same for the three Cell 2 profile locations because infiltration of water through the cover and the waste zone K_d do not vary horizontally. The downward radionuclide transport in the vadose zone below the waste differs significantly among the profile locations due to the water flux differences resulting from the lateral movement of leachate along the drainage layer above the clay liner. The upper output profile (C2-U, at the upslope portion of the cell) has less vertical water flux, slower mass transport, and lower peak concentrations below the liner than the middle (C2-M) and lower (C2-U) output profiles. The middle and lower profile nodes have higher vertical water and radionuclide flux rates, higher peak concentrations, and faster arrival and depletion of mass at corresponding nodes below the liner. The time of peak concentrations at the bottom of the vadose zone (lowest of the bedrock nodes above the predicted water table elevation) range from just after 1000 years for the lower profile to > 3700 years for the upper profile location. These patterns correspond to the variations in saturation illustrated in Figs. E.12 and E.13.

Figure E.16 shows the Tc-99 concentration changes in the three Cell 2 profiles in the Section B model. Compared to the Section A model, the liner system represented in the Section B model has a lower slope and the thickness of the vadose zone below the liner varies more due to the cross-section orientation (refer to Figs. E.2, E.3, and E.4). The pattern of Tc-99 concentrations over time are very similar to the corresponding locations in the Section A model results. The Section B model has a thicker waste zone representation than does the Section A model but the predicted time to reach the maximum radionuclide flux at the water table (presented in Sect. E.3.2.3.3) is slightly later. Therefore, results from Section A model provide a more pessimistic (earlier) representation of release to the saturated zone. Thus, Section A model results were used to inform the development and parameterization of the other PA models. The Section A STOMP model results are the primary focus of the presentation of results in the remainder this appendix.

Iodine-129 in the Section A Cell 2 profiles shows a similar pattern to Tc-99, except for the prolonged time for depletion within the source zone and slower migration in the vadose zone (Fig. E.17). This difference is caused primarily by the higher K_d (2 mL/g for I-129 in the waste vs 0.36 mL/g for Tc-99). The peak concentration times at the bottom of the vadose zone occur between 3000 and 12,000 years.

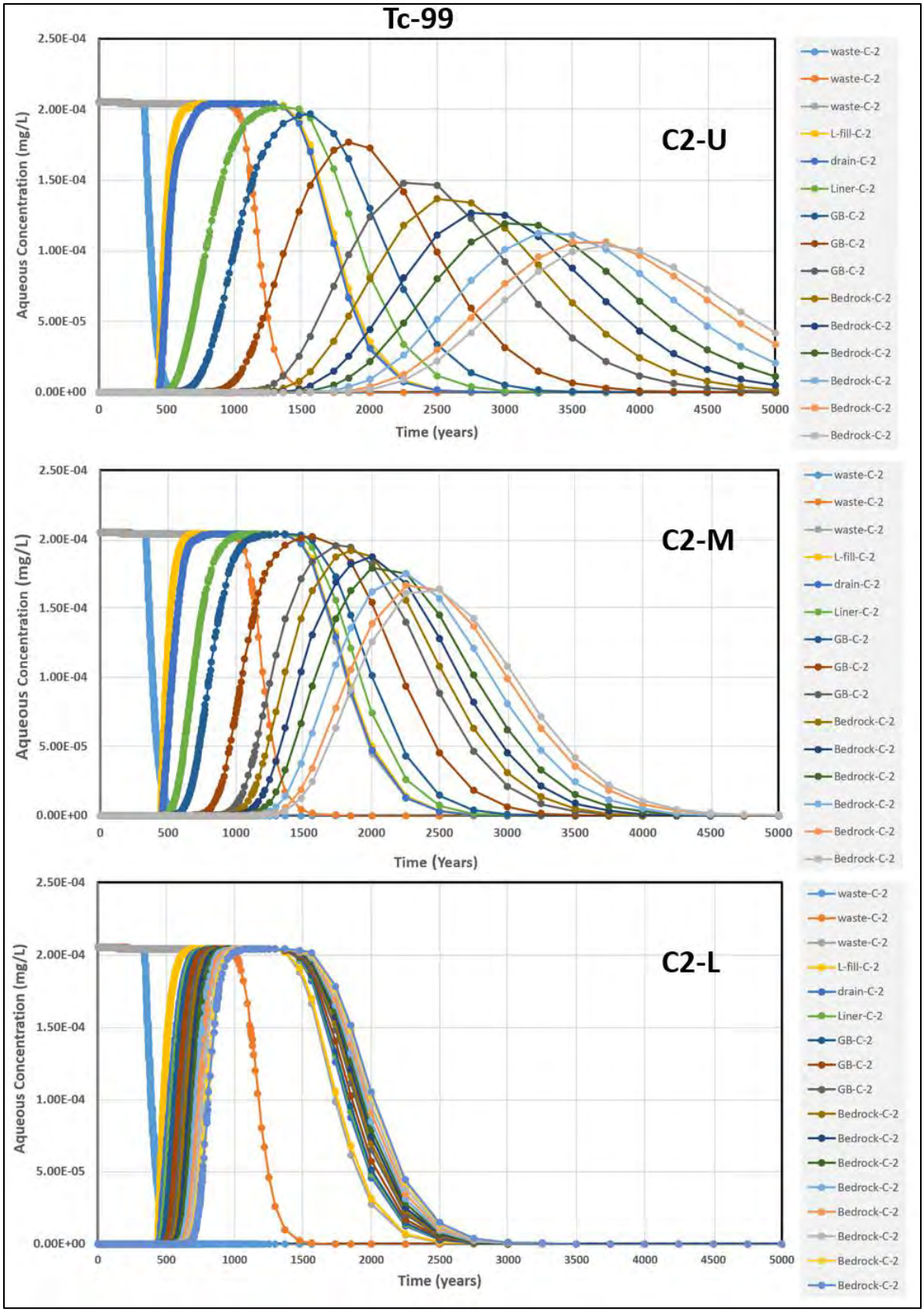

Fig. E.15. Tc-99 concentration changes in Cell 2 profiles in Section A model

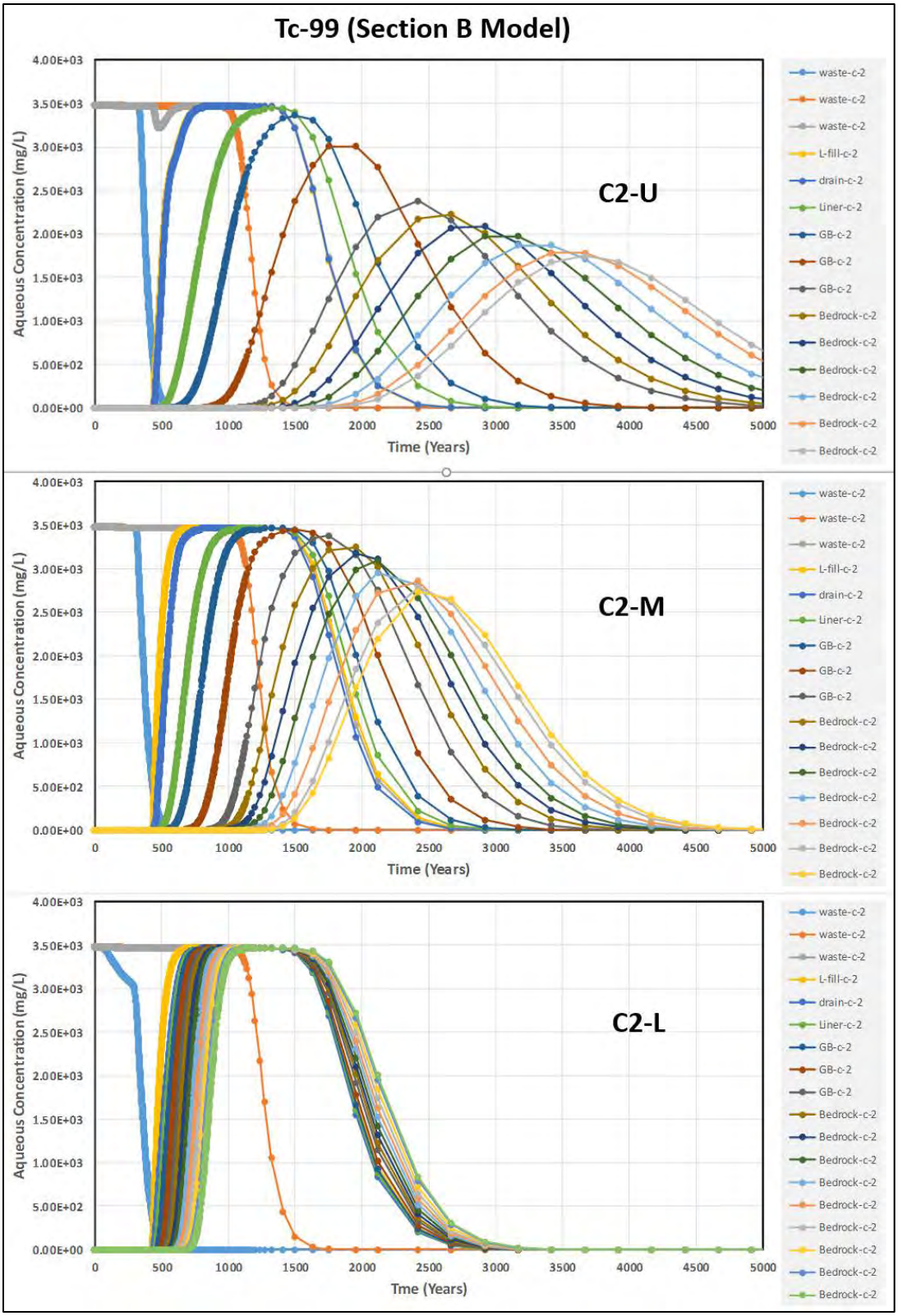

Fig. E.16. Tc-99 concentration changes in Cell 2 profiles in Section B model

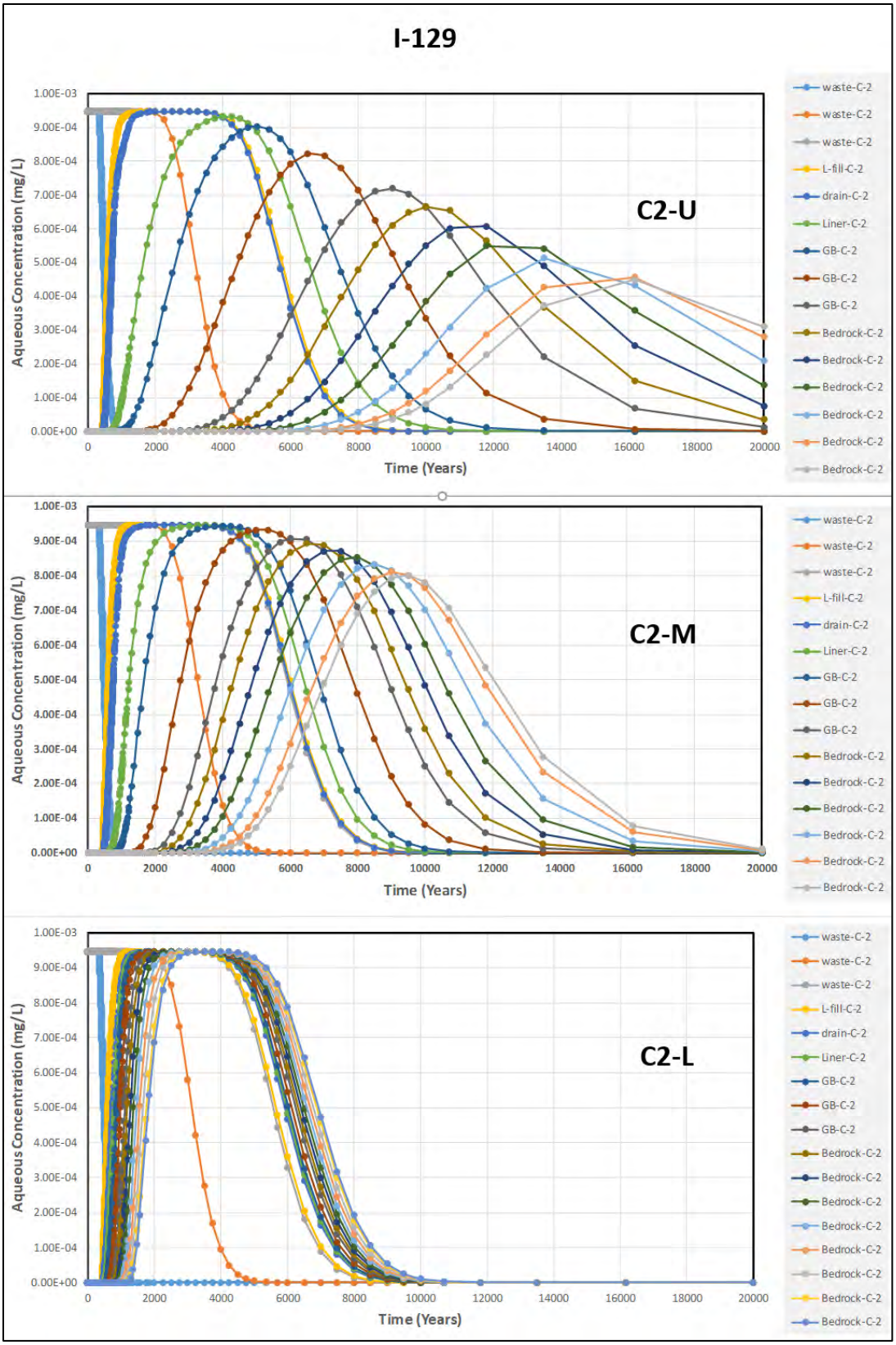

Fig. E.17. I-129 concentration changes in Cell 2 profiles in Section A model

Carbon-14 illustrates a faster source depletion and migration in the vadose zone due to shorter half-life and zero K_d in all material zones (Fig. E.18). The peak concentration times at the bottom of the vadose zone occur between 530 and 1050 years.

Hydrogen-3 shows rapid depletion within the source zone before cover infiltration starts at 200 years due to its very short half-life (12.3 years) as shown in Fig. E.19.

Uranium-234 and U-238 show much slower downward movement and limited source depletion due to higher K_d values and longer half-lives (Figs. E.20 and E.21). The peak concentrations for these radionuclides do not arrive at the bottom of the vadose zone before 10,000 years. Plutonium-239 transport behavior is similar to uranium isotopes but shows relative faster overall concentration decreases due to the shorter half-life (Fig. E.22).

Based on the Cell 2 output profile analysis, only the Tc-99, C-14, and I-129 will impact the saturated zone within 10,000 years after the cell closure. Therefore, results for those three radionuclides are analyzed in detail in the following sections.

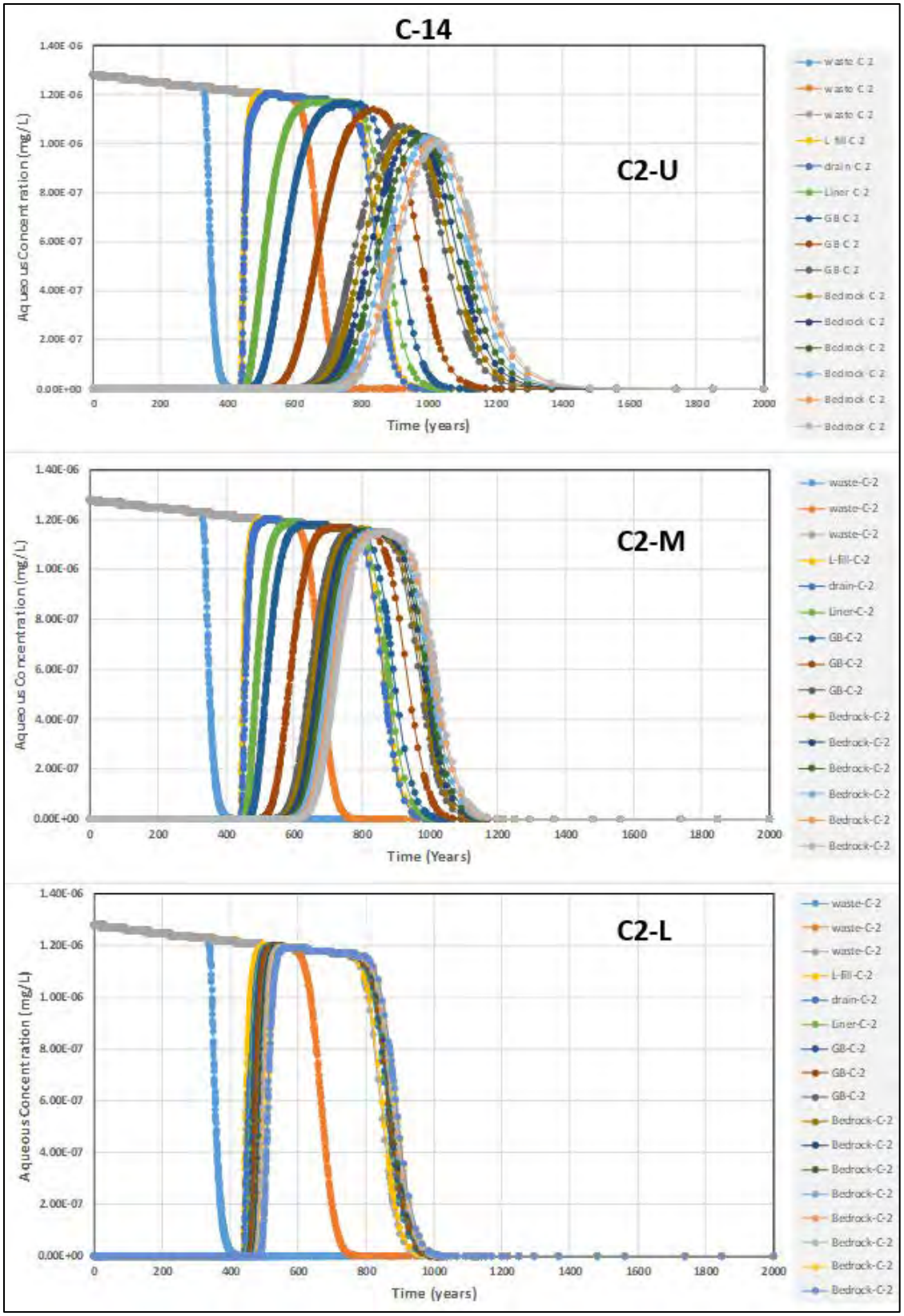

Fig. E.18. C-14 concentration changes in Cell 2 profiles in Section A model

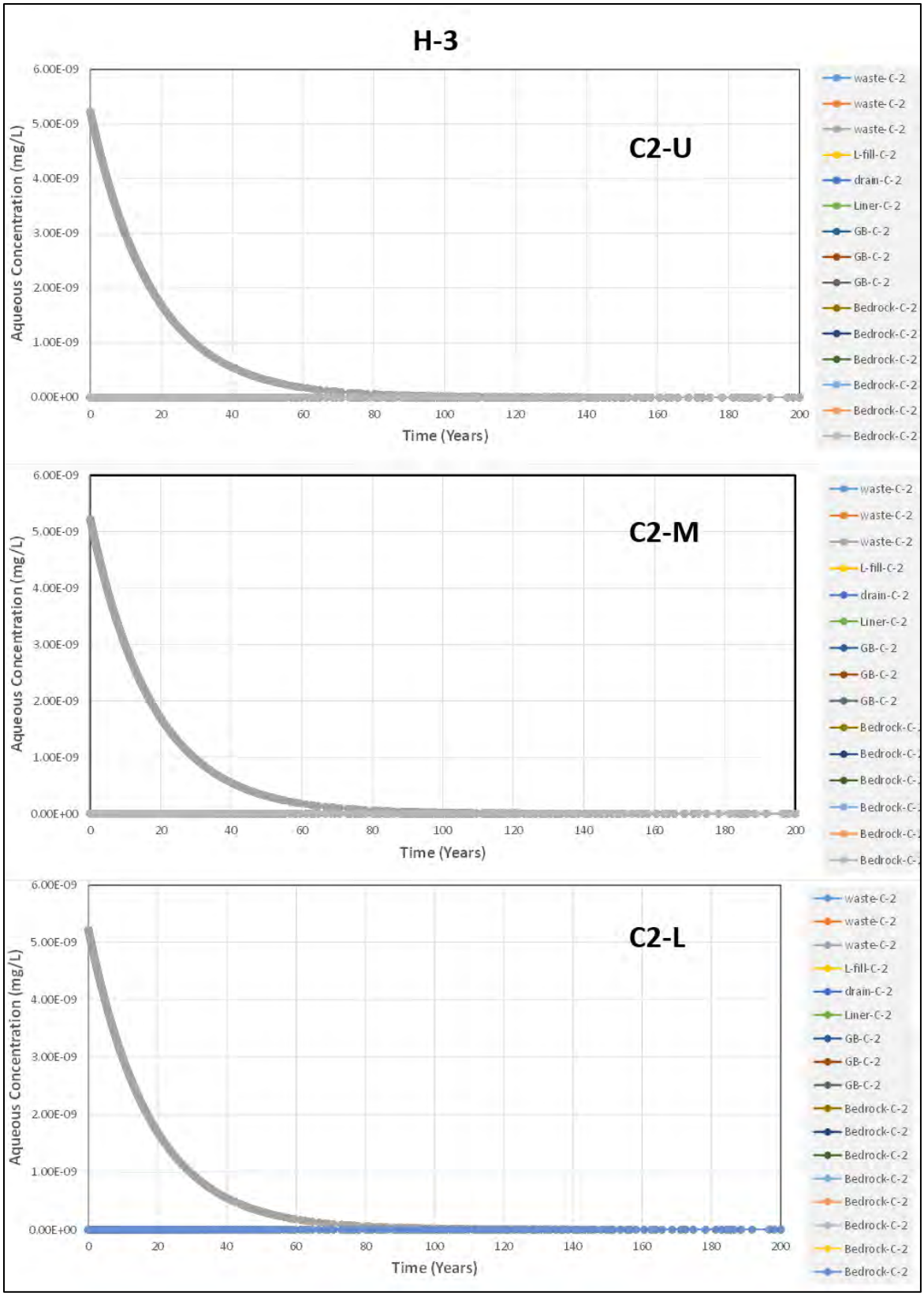

Fig. E.19. H-3 concentration changes in Cell 2 profiles in Section A model

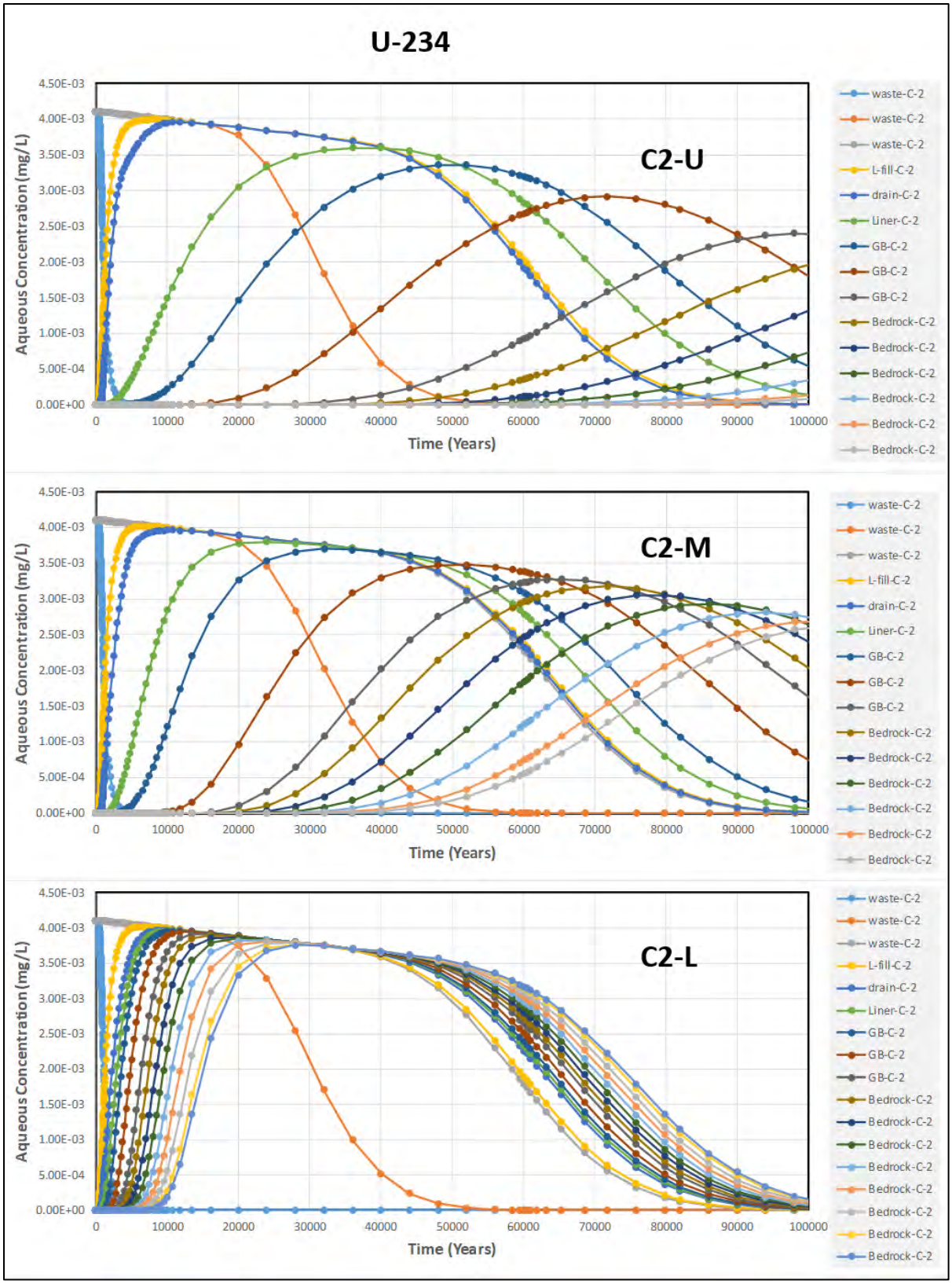

Fig. E.20. U-234 concentration changes in Cell 2 profiles in Section A model

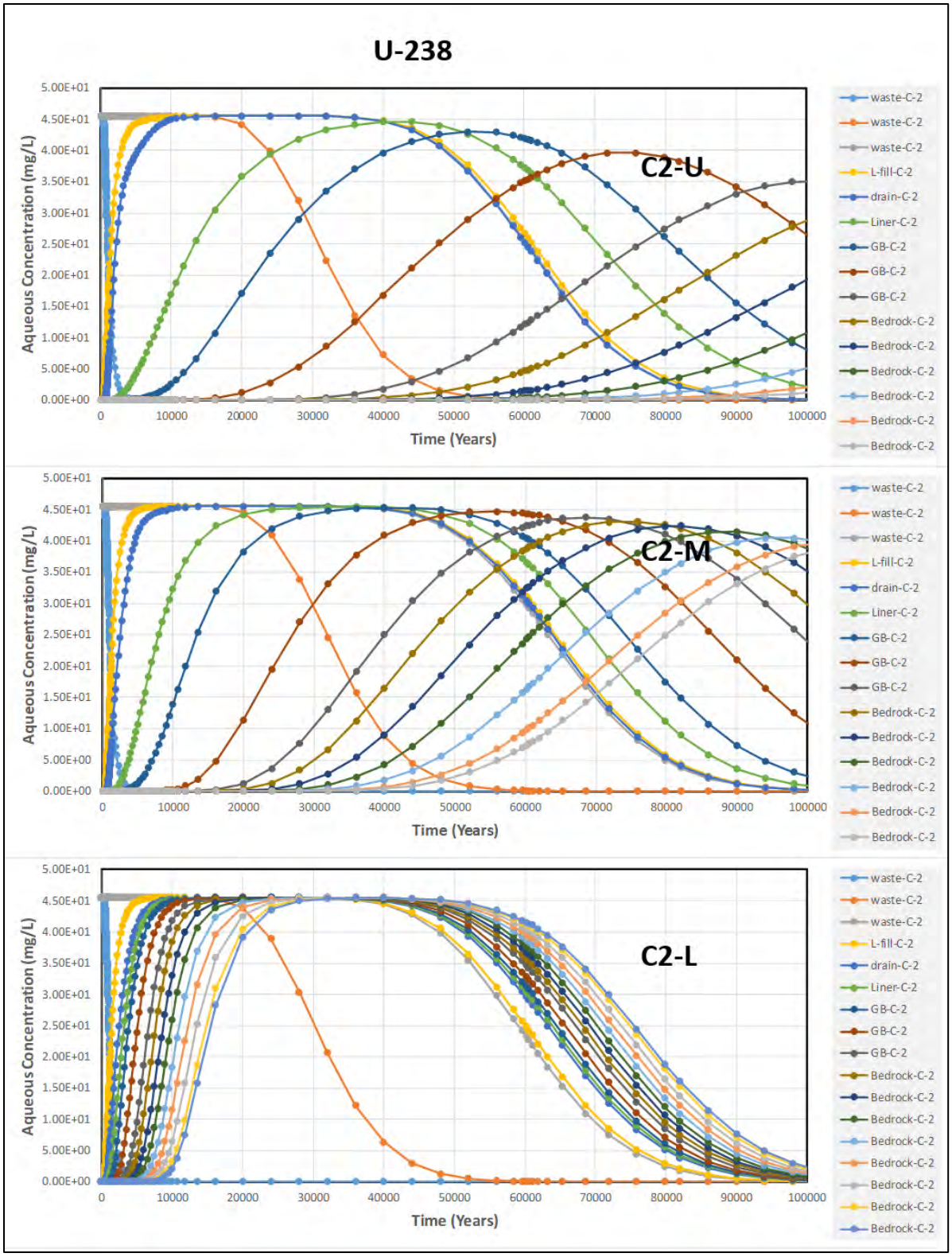

Fig. E.21. U-238 concentration changes in Cell 2 profiles in Section A model

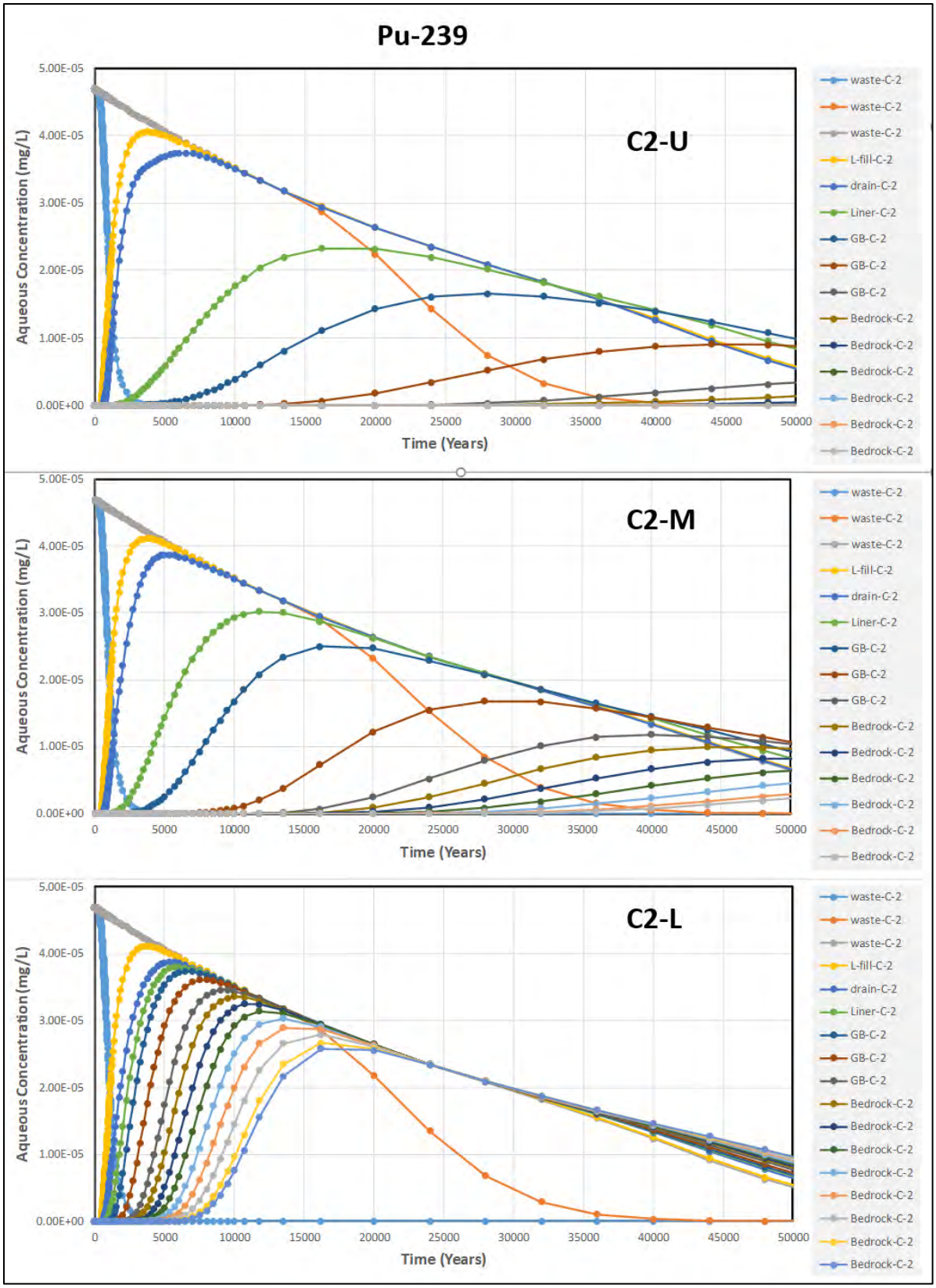

Fig. E.22. Pu-239 concentration changes in Cell 2 profiles in Section A model

E.3.2.3.2 Radionuclide concentrations and migration in Cross-section A

The pattern of radionuclide movement in the waste zone and underlying vadose zone was examined based on the STOMP Section A model results for the complete model domain (all model nodes). Aqueous concentrations of the radionuclides at selected time-steps were extracted and plotted. The selected time-step pictures for the three key radionuclides (Tc-99, I-129, and C-14) are shown on Figs. E.23 through E.25, respectively. Similar to the observed pattern for the output profiles (Sect. E.3.2.3.1), radionuclide depletion and migration to the saturated zone are controlled by half-life, sorption (K_d), infiltration, and waste geometry. However, the full cross-section model results better demonstrate the non-uniform release of radionuclides than the set of Cell 2 output profile figures.

There are different durations of radionuclide release for different disposal cells due to variable waste thickness. Disposal Cells 1 and 4 have lower average waste thickness and therefore less mass inventory and are depleted more quickly than the middle two cells (Cells 2 and 3). The width of each cell and resulting differences in total water influx also influences this pattern. Cell 4 is relatively narrow and has small waste thickness and so is depleted most quickly (e.g., for Tc-99, Cell 4 is nearly depleted by 2000 years, Fig. E.23).

The non-uniform pattern of release beneath each disposal cell corresponds to variations in saturation and leachate concentration that results from downslope leachate movement along the liner system. The magnitude, duration, and timing of peak concentrations varies strongly along the base of each disposal cell and also varies among the four disposal cells (particularly the timing and duration of maximum concentrations). The non-uniform release through the vadose zone to the saturated zone represented in the STOMP simulations is summarized in terms of the total radionuclide flux curves developed for each disposal cell and presented in the following section. These detailed modeling results show the potential complexity of contaminant movement in variably saturated and transient conditions and provide a good illustration of the value of the STOMP model in representing a complex system.

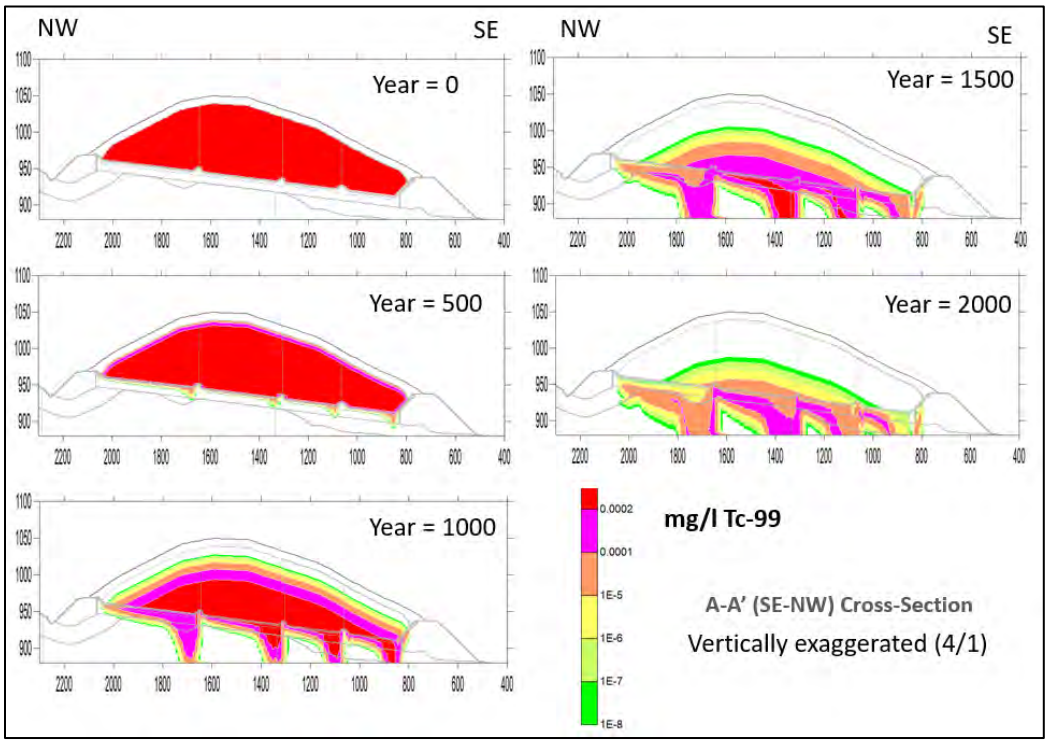

Fig. E.23. Tc-99 concentration changes in Section A model with time

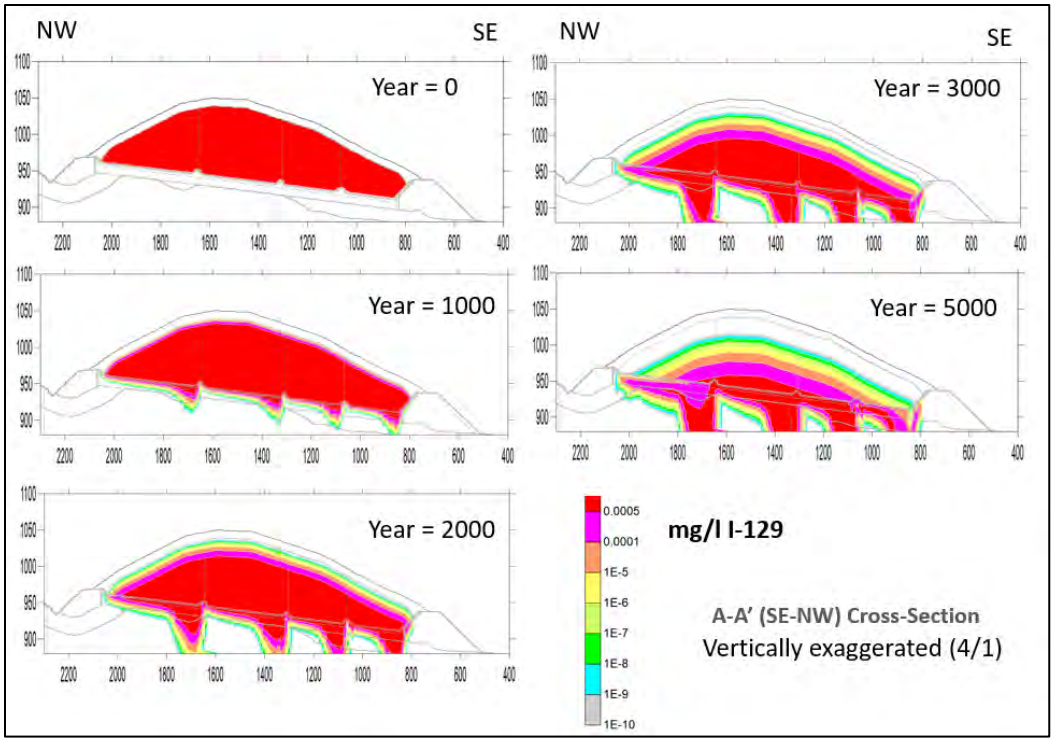

Fig. E.24. I-129 concentration changes in Section A model with time

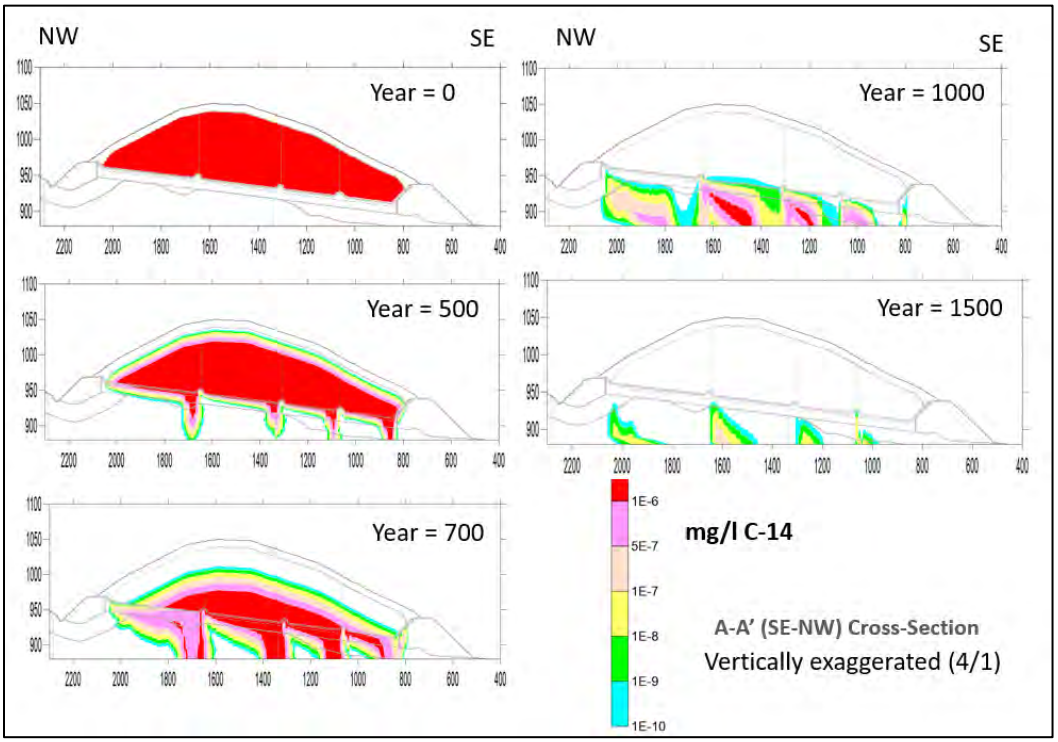

Fig. E.25. C-14 concentration changes in Section A model with time

E.3.2.3.3 Radionuclide flux at output surfaces

The radionuclide flux into the vadose zone below the liner and into the saturated zone were quantified based on the STOMP model results at the data output surfaces described in Sect. E.3.2.1. The total radionuclide mass flux rates across the three surfaces are calculated as the sum of vertical mass flux over the set of model nodes in each surface. The output surfaces defined include:

- Top of the liner – to estimate the radionuclide mass release from the source zone
- Bottom of the liner – to estimate the radionuclide mass release from the liner system
- Groundwater table – to estimate the radionuclide mass release into the saturated zone.

Figures E.26 through E.28 present the mass flux rate across the three output surfaces for Tc-99, I-129, and C-14, respectively, and illustrate the progressive migration of radionuclides from waste through the liner and through the vadose zone. (Note the different time scales on the horizontal axes in these three figures.) Technetium-99 starts to migrate from the waste zone into the liner system at year 400 when the infiltration of water from the cover reaches the bottom of the waste zone (refer to Figs. E.12 and E.23). The mass flux rate increases with increased water infiltration rate until year 1000 when the water infiltration rate reaches the long-term EMDF performance condition (0.88 in./year). The mass flux rate then starts to decrease due to source depletion. The mass flux rate at the bottom of the liner system begins to increase slightly later (450 to 500 years) due to sorption in the liner and peaks at year 1000. The decline in mass flux from the waste and liner output surfaces is rapid between 1000 and 1600 years, after which the rate of decline decreases due to radionuclide depletion (refer to Figs. E.23 through E.25). The Tc-99 mass flux rate at the water table output surface increases later (600 to 1000 years) and peaks lower and later (1200 years) due to sorption and mass retention in the vadose zone. The decline in flux to the saturated zone decreases more gradually than the flux from the liner, reflecting mass depletion along faster transport paths combined with continued migration of residual contamination along slower paths in the vadose zone. This residual mass is concentrated beneath the upslope end of each disposal cell (refer to the C-14 concentrations at years 1000 and 1500 in Fig. E.25).

Iodine-129 also starts to release from the waste zone to the liner system at year 400 (Fig. E.27). However, due to its higher K_d, the peak flux rates at the base of the liner and the water table output surface occur 1000 to 2000 years later than for the Tc-99 simulation. Also in contrast to the Tc-99 example, the I-129 peak from the liner output surface is much later than the peak flux from the waste output surface, reflecting greater sorption and mass retention in the clay liner material. The peak flux rate at the water table for I-129 occurs at about 3225 years.

Carbon-14 has a much earlier release shorter depletion time than Tc-99 (Figs. E.28 vs E.26) due to the 0 K_d value. The C-14 migrates quickly with water and the peak flux rate out of the waste occurs at 650 years, well before the water infiltration rate reaches its maximum rate at 1000 years. The peak flux rate at the water table for C-14 occurs at about 775 years.

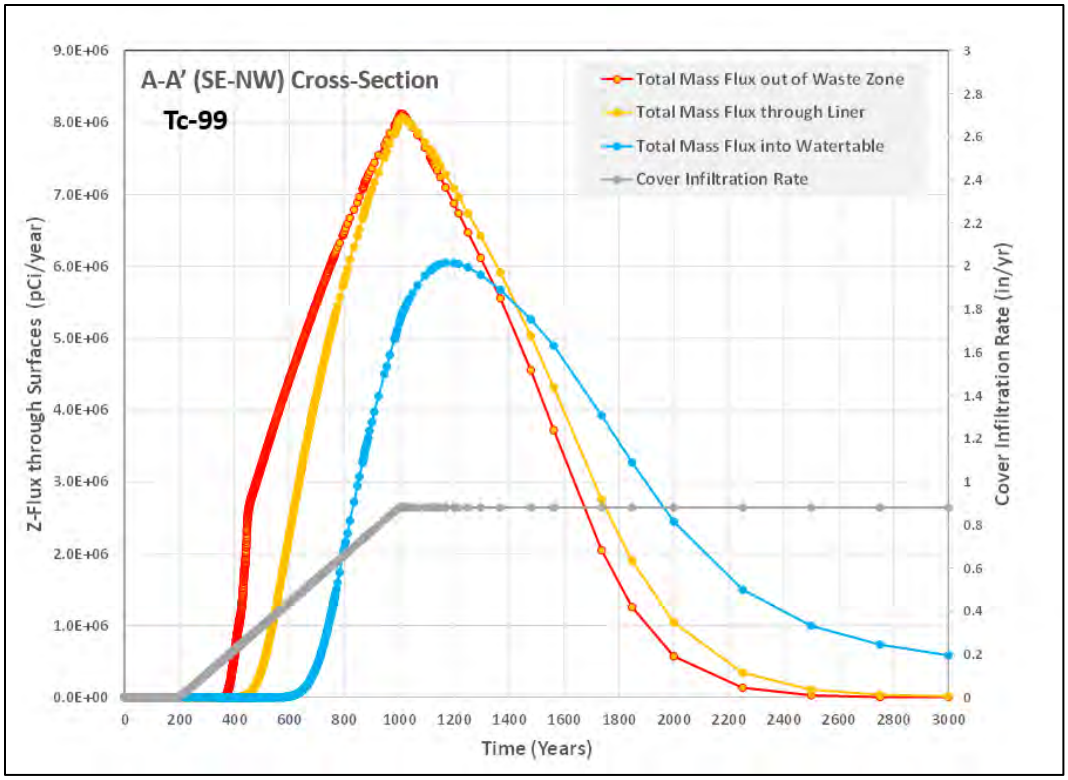

Fig. E.26. Tc-99 flux in Section A model over time

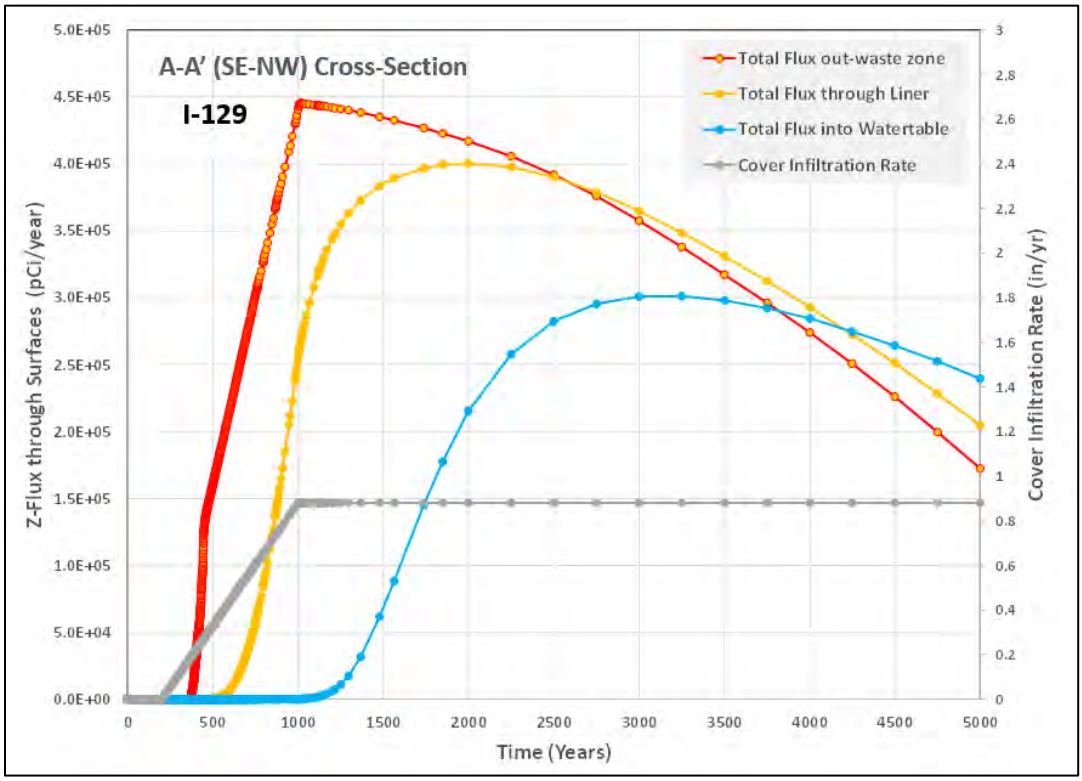

Fig. E.27. I-129 flux in Section A model over time

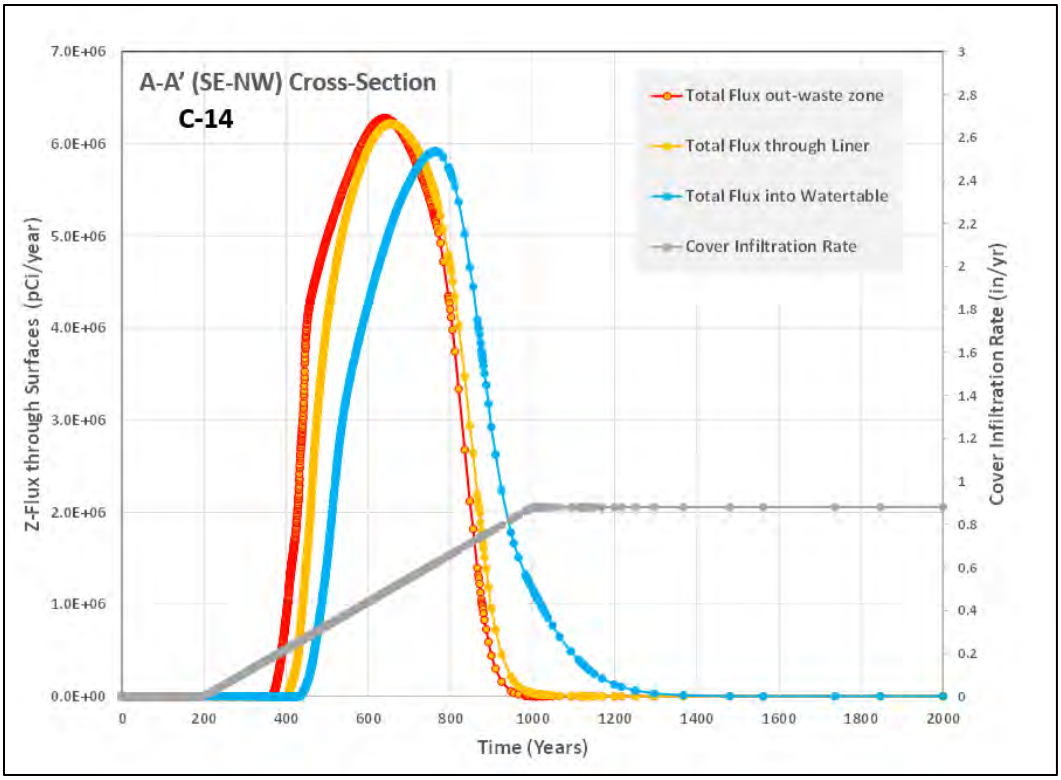

Fig. E.28. C-14 flux in Section A model over time

Due to its very short half-life, H-3 inventory in the waste zone is all decayed (Fig. E.19) before cover infiltration starts so there is no release from the disposal unit. Figures E.29 through E.31 show the mass flux rate at the bottom of the liner and the water table surfaces for U-234, U-238, and Pu-239, respectively. With higher K_d values for U-234, U-238, and Pu-239, the peak flux rates at the water table surface occur much later than 10,000 years. The peak flux rates at the water table output surface for U-234 and U-238 occur at about 30,000 years (Figs. E.29 and E.30). The peak flux rate at the water table surface for Pu-239 is about 20,000 years (Fig. E.31).

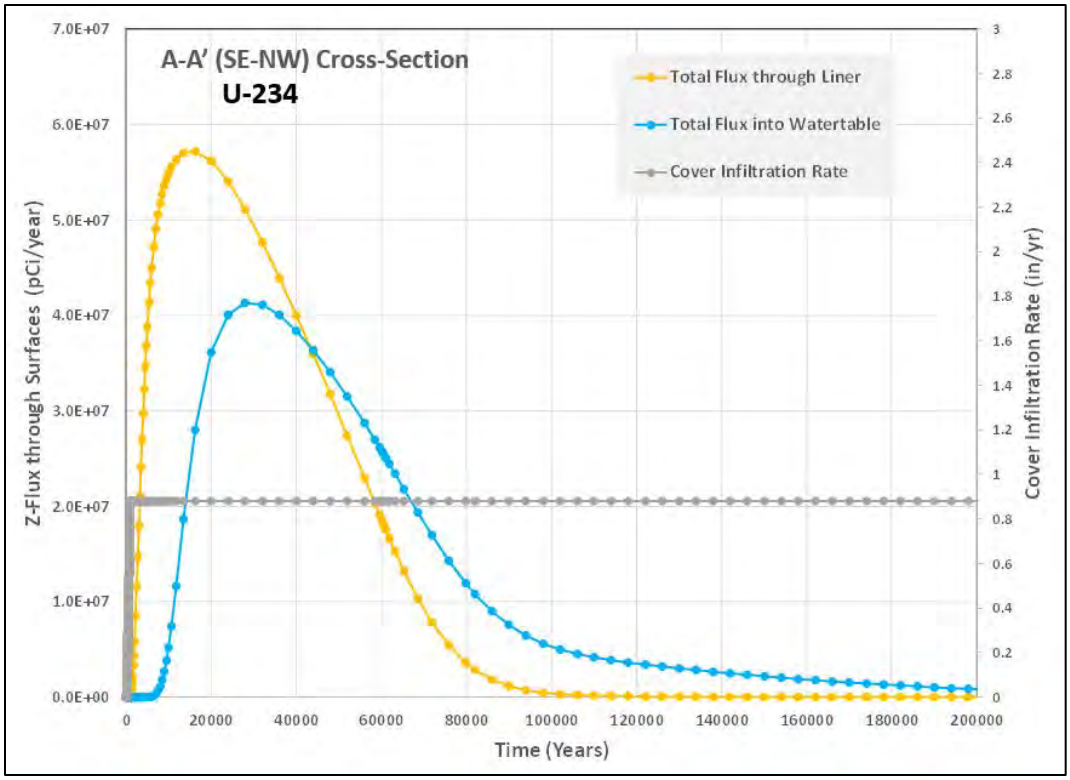

Fig. E.29. U-234 flux in Section A model over time

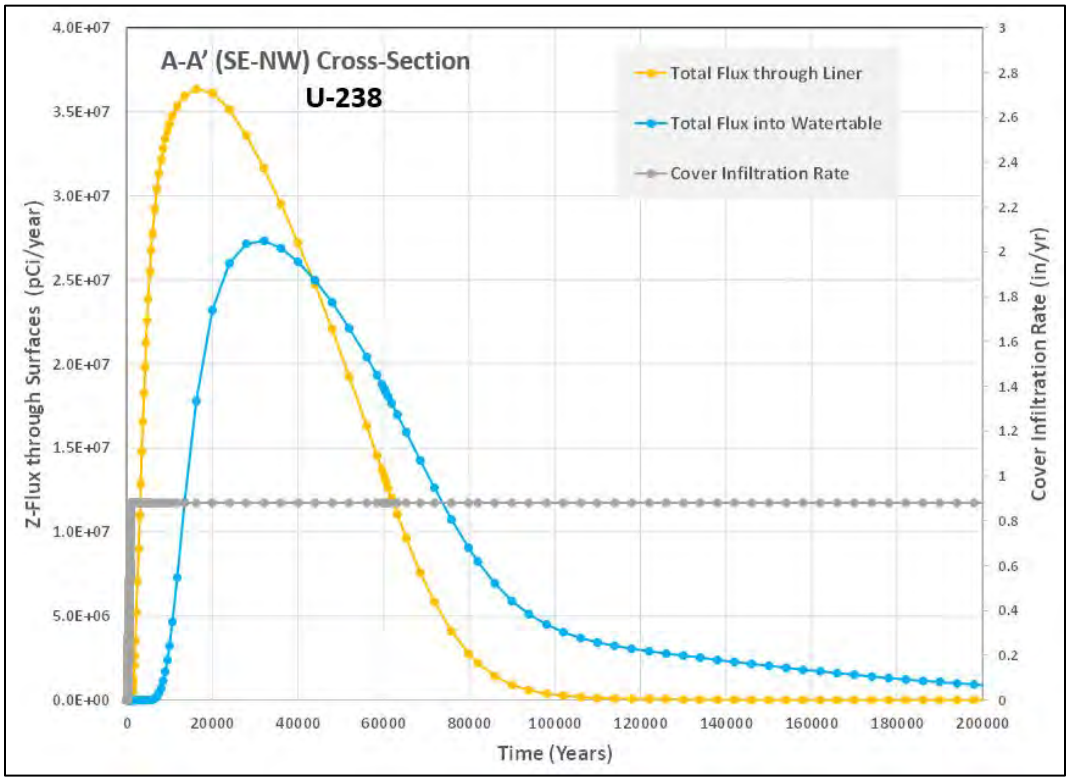

Fig. E.30. U-238 flux in Section A model over time

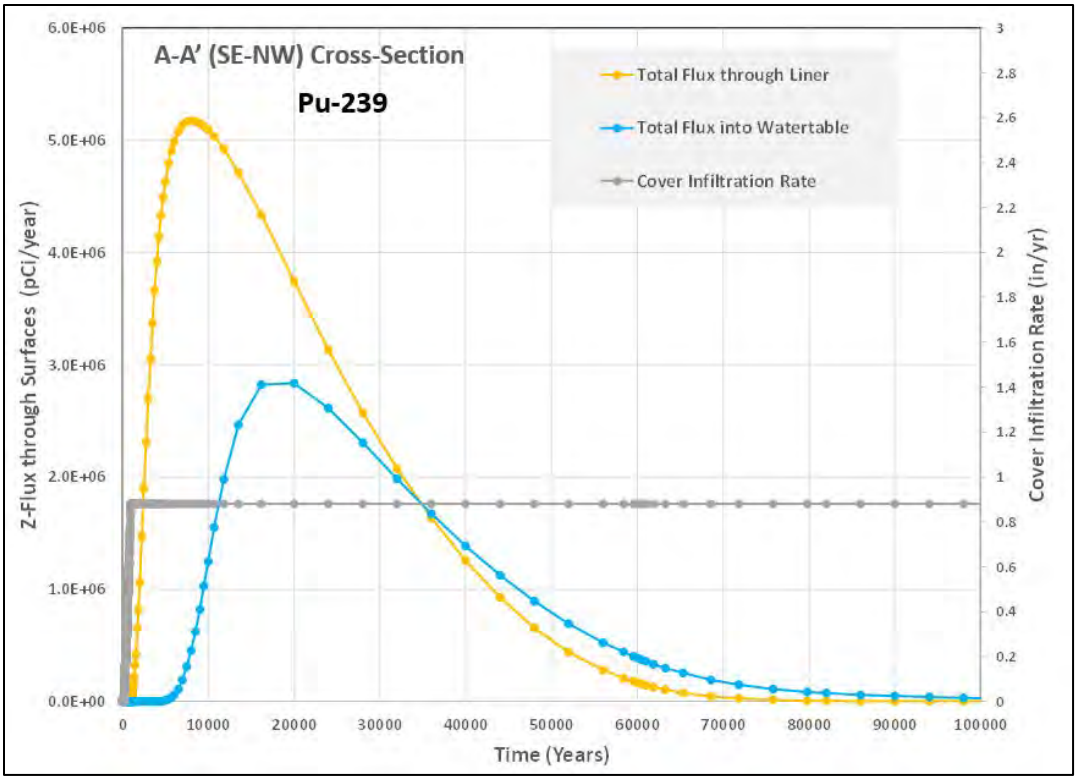

Fig. E.31. Pu-239 flux in Section A model over time

E.3.3 SENSITIVITY RUNS

After the base case model runs were completed and the results were analyzed, three sensitivity runs were conducted to evaluate the impact of K_d and cover infiltration rate assumptions. Both lower K_d values for all non-waste media and higher K_d values for the waste zone were tested. A higher (double) maximum cover infiltration rate for the EMDF was also evaluated. The STOMP model sensitivity run parameters are summarized in Table E.7.

Table E.7. Summary of sensitivity run change parameters

Parameter	Variables	Base (K_d in waste zone = ½ vadose)	Sensitivity-1 (higher waste zone K_d)	Sensitivity-2 (lower vadose zone K_d)	Sensitivity-3 (higher cover infiltration)
Cover infiltration	0–200 year	0	0	0	0
	200–1000 year	0 – > 0.88	0 – > 0.88	0 – > 0.88	0 –> 1.76
	> 1000 year	0.88	0.88	0.88	1.76
K_d (waste zone)	Technetium-99	0.36	0.72	0.36	0.36
	Hydrogen-3	0	0	0	0
	Uranium-234	25	50	25	25
	Plutonium-239	20	40	20	20
	Uranium-238	25	50	25	25
	Carbon-14	0	0	0	0
	Iodine-129	2	4	2	2

Table E.7. Summary of sensitivity run change parameters (cont.)

Parameter	Variables	Base (K_d in waste zone = ½ vadose)	Sensitivity-1 (higher waste zone K_d)	Sensitivity-2 (lower vadose zone K_d)	Sensitivity-3 (higher cover infiltration)
K_d (other zones)	Technetium-99	0.72	0.72	0.36	0.72
	Hydrogen-3	0	0	0	0
	Uranium-234	50	50	25	50
	Plutonium-239	40	40	20	40
	Uranium-238	50	50	25	50
	Carbon-14	0	0	0	0
	Iodine-129	4	4	2	4

E.3.3.1 K_d Impact

Since the primary control mechanism for radionuclide release and movement is desorption/sorption, the K_d impact is fully evaluated. The following K_d scenarios were simulated as shown in Table E.7.

- Higher (double) K_d values of radionuclides in the waste zone (i.e., same K_d as base case for other materials)
- Lower (half) K_d values of radionuclides for all non-waste materials (i.e., same K_d as base case for waste zone).

STOMP K_d sensitivity runs were conducted for all of the radionuclides except for C-14. The K_d value controls the initial aqueous concentrations in waste materials and governs the release rate for a given inventory and cover infiltration. Since the impacts of these K_d changes are similar for the various radionuclides, only the Tc-99 results (lowest K_d other than C-14) are shown below to demonstrate the impact.

Technetium-99 flux results for the higher waste K_d are shown on Fig. E.32 in the lower plot. Compared to the base case result (upper plot), the following differences are observed:

- Lower peak mass flux rates at the base of the liner and the water table output surface due to lower initial aqueous concentrations
- Delayed peak flux at the water table surface (1400 years vs 1200 years for the base case)
- Longer duration of Tc-99 release from waste and flux into the saturated zone.

The results for lower K_d values (same as base case waste zone value) used for the non-waste materials are shown on the lower plot of Fig. E.33. Compared to the base case result (upper plot on Fig. E.33), the following differences are observed:

- Essentially the same Tc-99 mass flux at the liner output surface due to the same waste zone K_d value and initial aqueous concentration as the base case
- More rapid increase in mass flux at the water table output surface due to the lower K_d values in the vadose zone
- Higher and earlier peak mass flux at the water table surface (1100 years vs 1200 years for the base case).

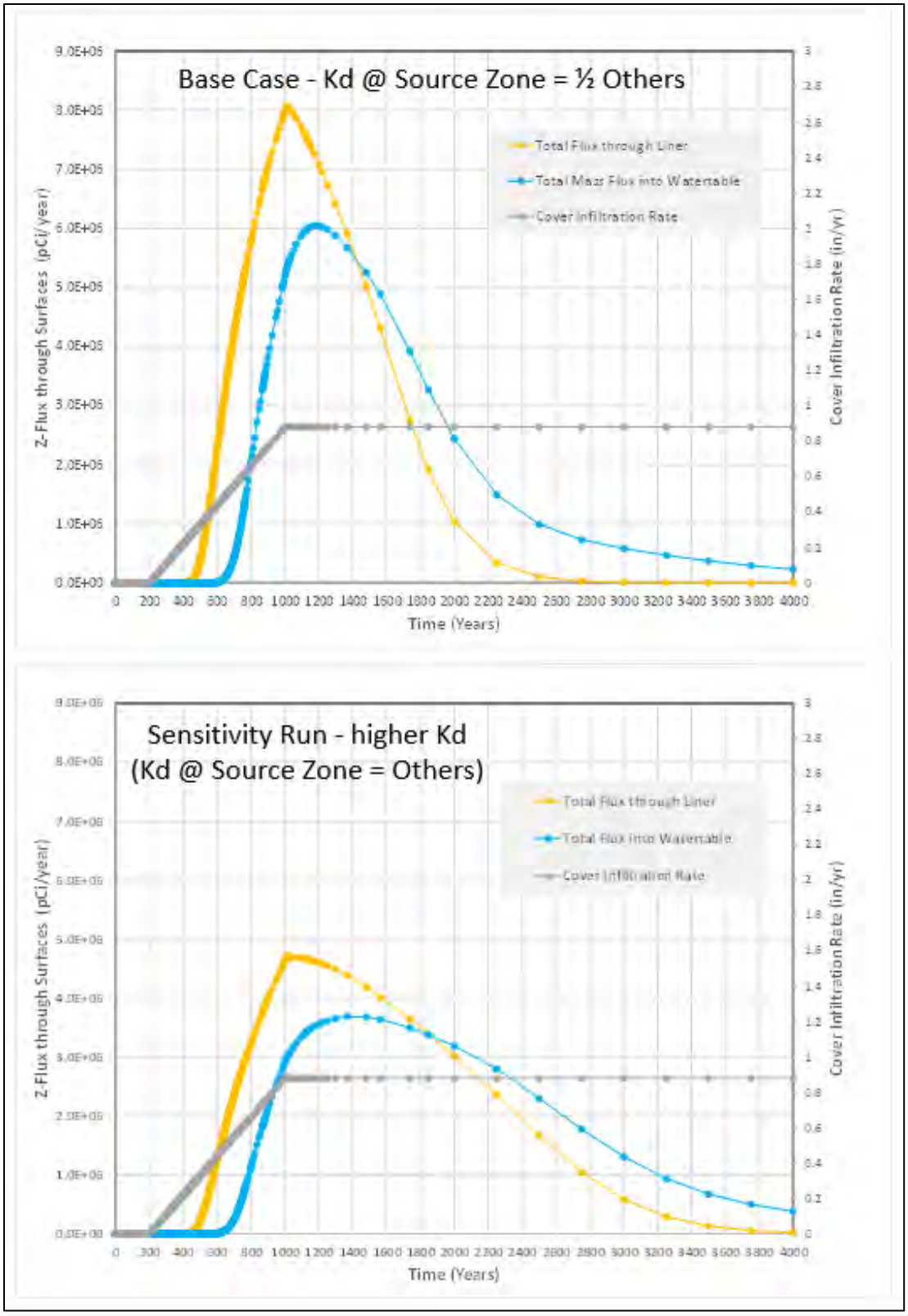

Fig. E.32. Waste zone K_d impact on Tc-99 flux

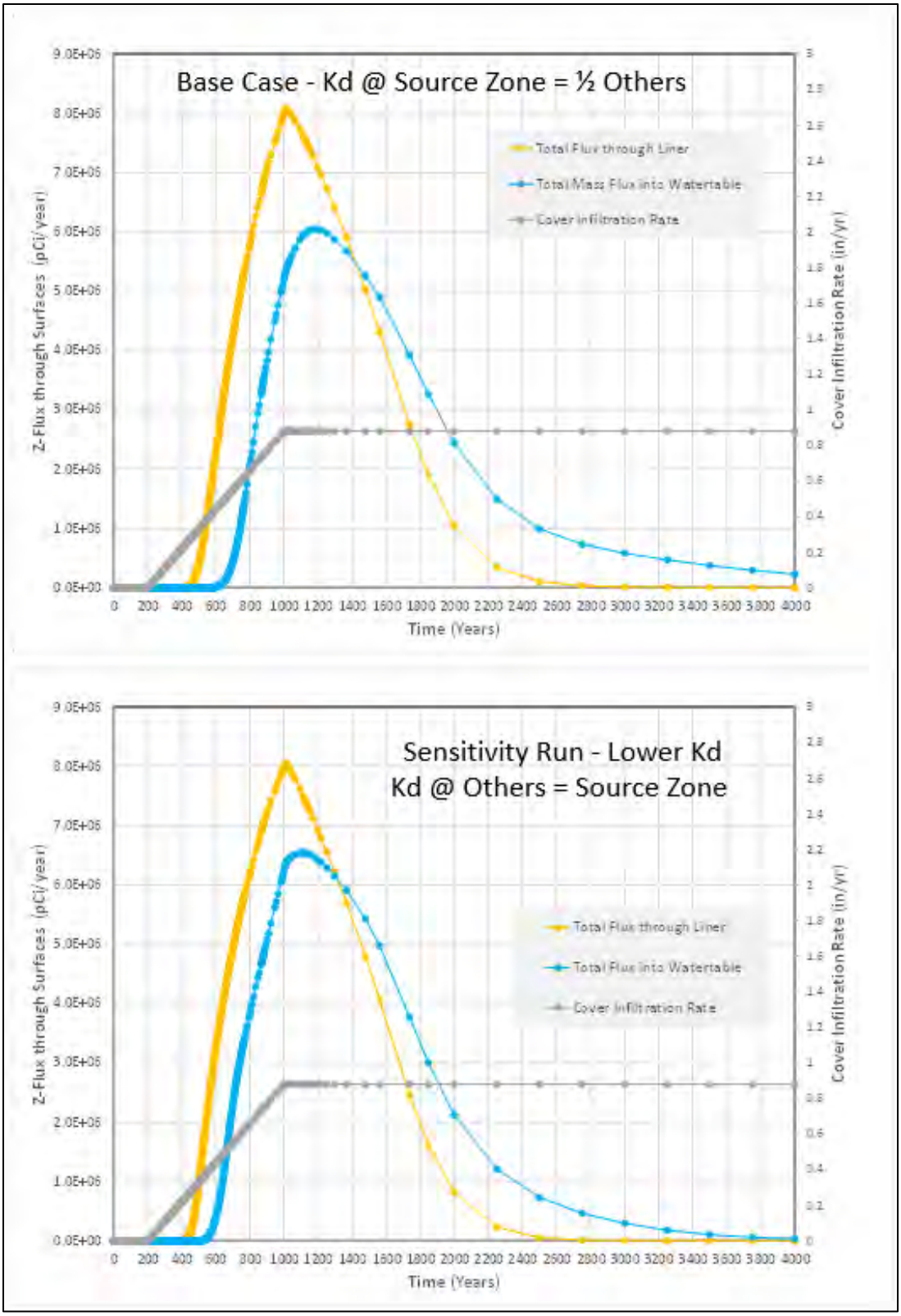

Fig. E.33. Vadose zone K_d impact on Tc-99 flux

These results are expected based on the K_d relationship. An increased waste K_d has a larger impact on release to the saturated zone than does a decreased vadose zone K_d.

E.3.3.2 Cover Performance Impact

A maximum cover infiltration rate two times the base case long-term performance condition value was simulated. The linear increase between 200 and 1000 years changed from 0 to 0.88 in./year to 0 to 1.76 in./year and stayed at 1.76 in./year beyond 1000 years. Changing the maximum infiltration rate but not the assumed timing of cover degradation represents more rapid increase in cover infiltration than the base case scenario. Due to the increased amount of the water flux, there is also earlier Tc-99 mass release from the waste and a higher (nearly double) peak mass flux rate at the water table output surface (Fig. E.34). The higher maximum infiltration also results in much faster waste zone depletion and faster migration to the saturated zone (peak flux occurs 200 years earlier) due to the larger water flux. The maximum aqueous concentrations in the waste zone and vadose zone are the same as for the base condition since K_d controls the mass partition between solid and aqueous phases. However, the resulting saturated zone concentrations underneath the EMDF would be higher than for the base case since there is more mass flux into the groundwater system from the vadose zone.

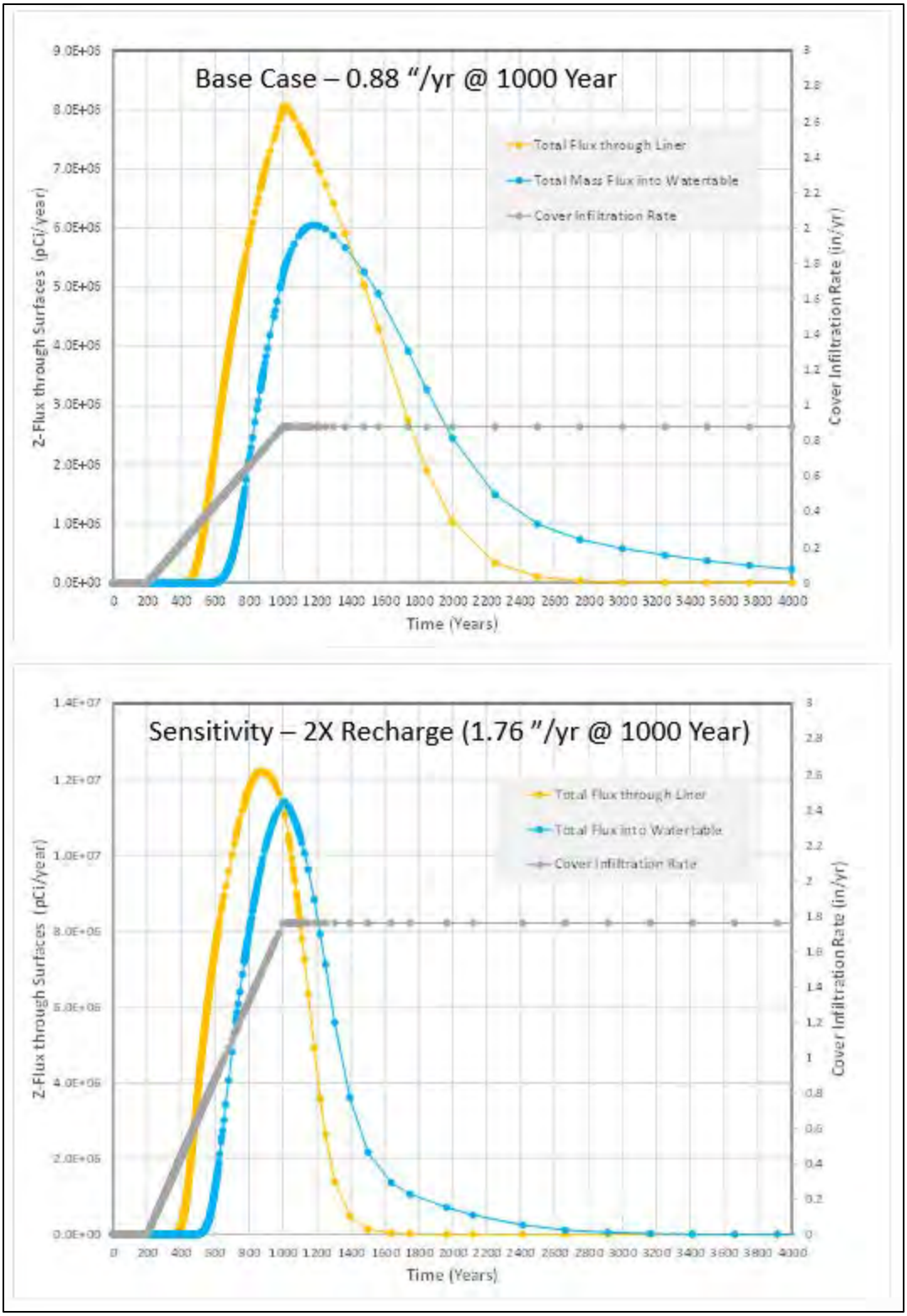

Fig. E.34. Higher cover infiltration impact on Tc-99 flux

E.3.4 APPLICATION OF STOMP RESULTS TO OTHER PA MODELS

As discussed above, STOMP modeling provides a detailed understanding of source depletion and the impact of liner system design on release to and transport in the vadose zone. Sensitivity runs demonstrate the significance of assumed K_d values and long-term cover performance for radionuclide flux to the saturated zone. Two key output products provided by the STOMP modeling are used to assist in the proper application of the other PA models. These outputs relate to the non-uniform pattern of release and the vadose zone transport time (arrival time at the water table elevation below the disposal unit). These outputs were calculated and applied to the saturated zone radionuclide transport analysis conducted using the MT3D model (see Appendix F).

E.3.4.1 Non-Uniform Release and Input to the Saturated Zone

A commonly used simplification in modeling contaminant release from a waste zone is assuming uniform water flux from the waste area, which generally provides a good approximation for the overall mass flux to groundwater. The detailed STOMP modeling of the EMDF system suggests that the liner system design could have a strong impact on the pattern of mass release, producing a highly non-uniform water and radionuclide flux from the disposal facility or from a single cell. This impact is primarily a result of the geometry and slope of the liner system required for effective leachate drainage and collection during operations and the early post-closure period.

Therefore, saturated zone radionuclide transport modeling for the EMDF may need to consider the potential impact of a non-uniform release scenario, as an alternative to the commonly used uniform source release conceptual model. Use of the STOMP model results to analyze a simplified non-uniform release scenario in the EMDF saturated zone transport modeling is presented in Appendix F.

E.3.4.2 Vadose Zone Delay on Contaminant Movement from Waste Source

The STOMP model results clearly show the impact of the vadose zone on the movement of the radionuclides. The vadose zone both retards transport and reduces the radionuclide aqueous concentration between the waste and saturated zone beneath the EMDF due to the sorption and desorption process.

In addition to the general vadose sorption impact (delay of flux to the saturated zone), the complexity of the EMDF design (multiple disposal cells with variable liner floor elevations) and the effect of non-uniform vadose zone thickness results in variable initial arrival times and peak concentrations for radionuclides entering the saturated zone. To provide a reasonable average vadose delay time for the saturated zone fate-transport model (MT3D), the total radionuclide mass flux rate at the water table output surface in the STOMP Section A model is utilized.

The Tc-99 total mass flux rate at the water table surface in the Section A model is shown on Fig. E.35. The chart illustrates the initial arrival time of approximately 600 years and peak flux time of 1180 years. The time when the flux reaches 50 percent of the peak rate is approximately 850 years. The time to 50 percent peak water table flux rate based on the Section B model output is approximately 910 years (Table E.8) due to greater average thickness of the vadose zone. Since the saturated zone transport model applies a simplified depleting source approximation for radionuclide release at the water table (Appendix F, Sect. F.4.1), using the STOMP-based 50 percent peak mass flux time to represent the saturated zone arrival time is a reasonable approach. This STOMP model based arrival time incorporates the assumed (base case) progression of cover degradation and maximum cover infiltration rate, as well as the simulated vadose transport time in representing the release to the saturated zone. The average arrival times were calculated for the three radionuclides that make the primary dose contributions in the performance analysis (see Table E.8). The Section A model predicted somewhat earlier Tc-99 arrival times than the Section B model,

so the Section A model results are used for subsequent application in the saturated zone modeling. Radionuclide-specific arrival times for each disposal cell were also calculated based on the output from the corresponding water table surface segments. These cell-by-cell arrival times were used to formulate the non-uniform release scenario for the saturated zone transport model as discussed in Appendix F, Sect. F.4.2.

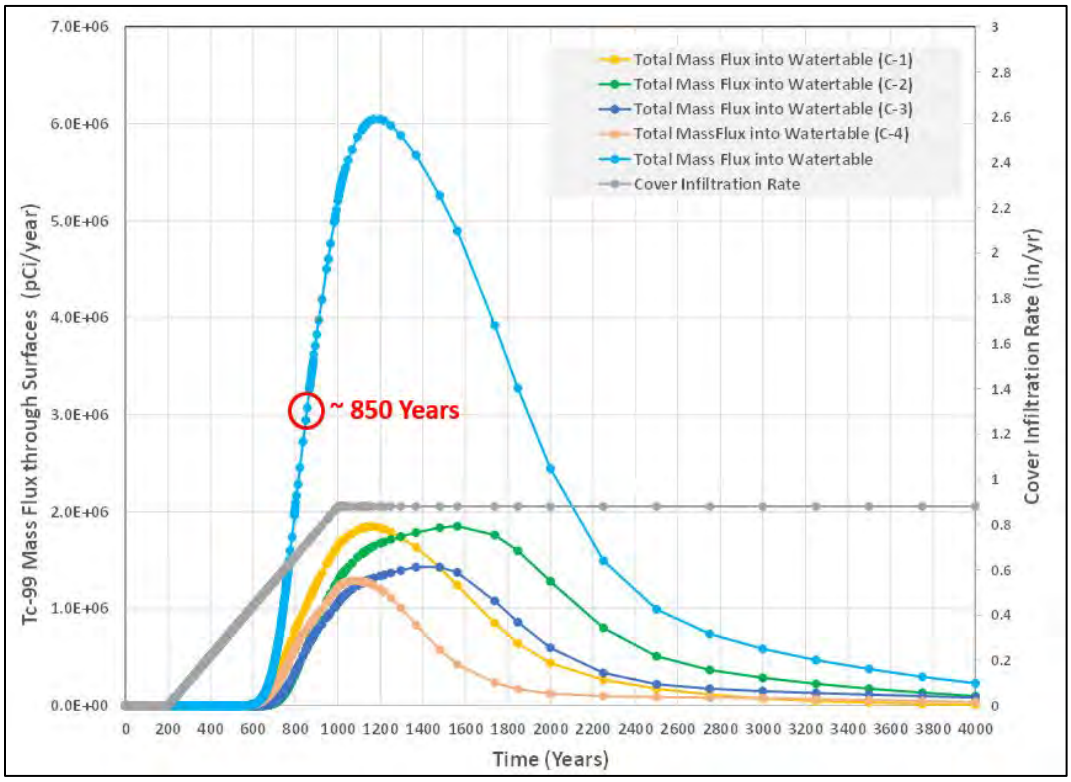

Fig. E.35. Time to 50 percent peak mass flux at water table surface in Section A model

Table E.8. Calculated saturated zone arrival times

Water table output surface flux	50% peak flux rate time (year)			
	Tc-99		C-14	I-129
Disposal cell #	Section A	Section B	Section A	Section A
C-1	830	865	530	1650
C-2	900	950	630	2000
C-3	885	970	570	1900
C-4	810	900	500	1700
Total EMDF flux	**850**	**910**	**530**	**1750**

EMDF = Environmental Management Disposal Facility

E.4 REFERENCES

Carsel, R. F. and Parrish, R. S., 1988. "Developing joint probability distributions of soil water retention characteristics", *Water Resources Research*, Vol. 24, No. 5, May.

DOE 2011. *Derived Concentration Technical Standard,* DOE-STD-1196-2011, U.S. Department of Energy, Washington, D.C., April.

Golden 2016. Surfer Version 13.6.618 Software, Golden Software, LLC, Golden, CO, December.

International Commission on Radiological Protection 2008. *Nuclear Decay Data for Dosimetric Calculations*, ICRP Publication 107, Ann. ICRP 38 (3), International Commission on Radiological Protection, Ottawa, Ontario K1P 5S9, Canada.

Nichols et al. 1997. *STOMP – Subsurface Transport Over Multiple Phases Application Guide*, PNNL-11216 (UC-2010), W. E. Nichols, N. J. Aimo, M. Oostrom, and M. D. White, Pacific Northwest National Laboratory, Richland, WA.

Oak Ridge National Laboratory 1992. *Status Report on the Geology of the Oak Ridge Reservation*, ORNL/TM 12074, Environmental Sciences Division Publication No. 3860, Oak Ridge National Laboratory, Oak Ridge, TN, October.

Oak Ridge National Laboratory 2017. *Calculation of Hazard Category 2/3 Threshold Quantities Using Contemporary Dosimetric Data*, ORNL/TM-2017/467, Oak Ridge National Laboratory, Nuclear and Radiological Protection Division, Oak Ridge, TN, November.

UCOR 2020. *Quality Assurance Report for Modeling of the Bear Creek Valley Low-level Radioactive Waste Disposal Facilities, Oak Ridge, Tennessee* UCOR-5234/R0, UCOR, Oak Ridge, TN, April.

White and Oostrom 2000. *STOMP Subsurface Transport Over Multiple Phases, Theory Guide*, PNNL-12030, UC-2010, M. D. White and M. Oostrom, Pacific Northwest National Laboratory, Richland, WA.

White and Oostrom 2006. *STOMP Subsurface Transport Over Multiple Phases, Version 4.0*, PNNL-15782, M. D. White and M. Oostrom, Pacific Northwest National Laboratory, Richland, WA.

This page intentionally left blank.

APPENDIX F.
MT3D SATURATED ZONE TRANSPORT MODEL FOR THE ENVIRONMENTAL MANAGEMENT DISPOSAL FACILITY

This page intentionally left blank.

CONTENTS

This page intentionally left blank.

FIGURES

TABLES

ACRONYMS

DOE	U.S. Department of Energy
EMDF	Environmental Management Disposal Facility
EOW	edge of waste
MOC	Method of Characteristics
NT	North Tributary
PA	Performance Assessment
POA	point of assessment
QA	quality assurance
RESRAD	RESidual RADioactivity
STOMP	Subsurface Transport Over Multiple Phases
USGS	U.S. Geological Survey

This page intentionally left blank.

F.1 INTRODUCTION

To evaluate the potential impact of radionuclides released from the proposed Environmental Management Disposal Facility (EMDF) to the groundwater at the Central Bear Creek Valley site, a groundwater fate-transport model was implemented. The purposes of the modeling include the following:

1. Delimit the maximum extent of the contaminant plume
2. Determine the location of maximum concentration along the 100-m buffer zone boundary (groundwater point of assessment [POA], or 100-m well location)
3. Quantify the pattern of radionuclide discharge to streams and identify the surface water POA
4. Predict the peak concentrations and timing of peak for selected radionuclides (C-14, Tc-99, and I-129) at the 100-m well location
5. Evaluate the potential impact of non-uniform radionuclide release from the EMDF.

A site-specific three-dimensional groundwater flow model was constructed for the proposed EMDF as discussed in Appendix D. Flow simulations were conducted using the MODFLOW-2005 code (U.S. Geologic Survey [USGS] 1988; Harbaugh 2005). Based on the MODFLOW flow model simulation, the movement of contaminants from EMDF are predicted using MT3DMS (Zheng and Wang 1999), an improved version of the original three-dimensional fate-transport model code MT3D (Zheng 1990).

MT3D is a comprehensive three-dimensional numerical simulation code that models the fate and transport of dissolved contaminants in complex groundwater systems. The MT3D model calculates concentration distributions, concentration histories at selected points and hydraulic sinks (e.g., extraction wells), and the mass of contaminants in the groundwater system. The code can simulate three-dimensional transport in complex steady-state and transient flow fields and can represent anisotropic dispersion, source-sink mixing processes, first-order transformation reactions, and linear and non-linear sorption. The MT3D model offers the user a choice of four solution options that make it uniquely well suited for handling a wide range of conditions, one of which, the Method of Characteristics (MOCs) technique, is best suited for handling advection-dominated problems. The MT3D model is linked with MODFLOW, the USGS groundwater flow simulator, and is designed specifically to handle advectively dominated transport problems without the need to construct refined models specifically for solute transport. MT3D is one of the most used three-dimensional solute transport codes and has been used successfully in modeling thousands of sites. The MT3D model is widely accepted by the regulators and groundwater consulting and research communities and has been used in Bear Creek Valley (U.S. Department of Energy [DOE] 1998a, 1998b).

Based on the radionuclide release and vadose zone transport modeling results (Subsurface Transport Over Multiple Phases [STOMP] model, Appendix E), only three of the radionuclides in the EMDF estimated inventory (Tc-99, C-14, and I-129) will be released to the saturated zone within the EMDF post-closure period before 10,000 years. The others will either decay before release (H-3) or arrive at the groundwater table after 10,000 years (uranium and plutonium isotopes). Therefore, the MT3D fate-transport modeling of saturated zone is conducted only for the three dose-significant radionuclides (Tc-99, C-14, and I-129).

F.2 EMDF SATURATED ZONE TRANSPORT MODEL DEVELOPMENT

F.2.1 MODEL DEVELOPMENT OVERVIEW

The MT3D transport model for EMDF uses the long-term performance simulation of the EMDF groundwater flow model described in Appendix D. The model domain and topography of the flow model are shown in Fig. F.1.

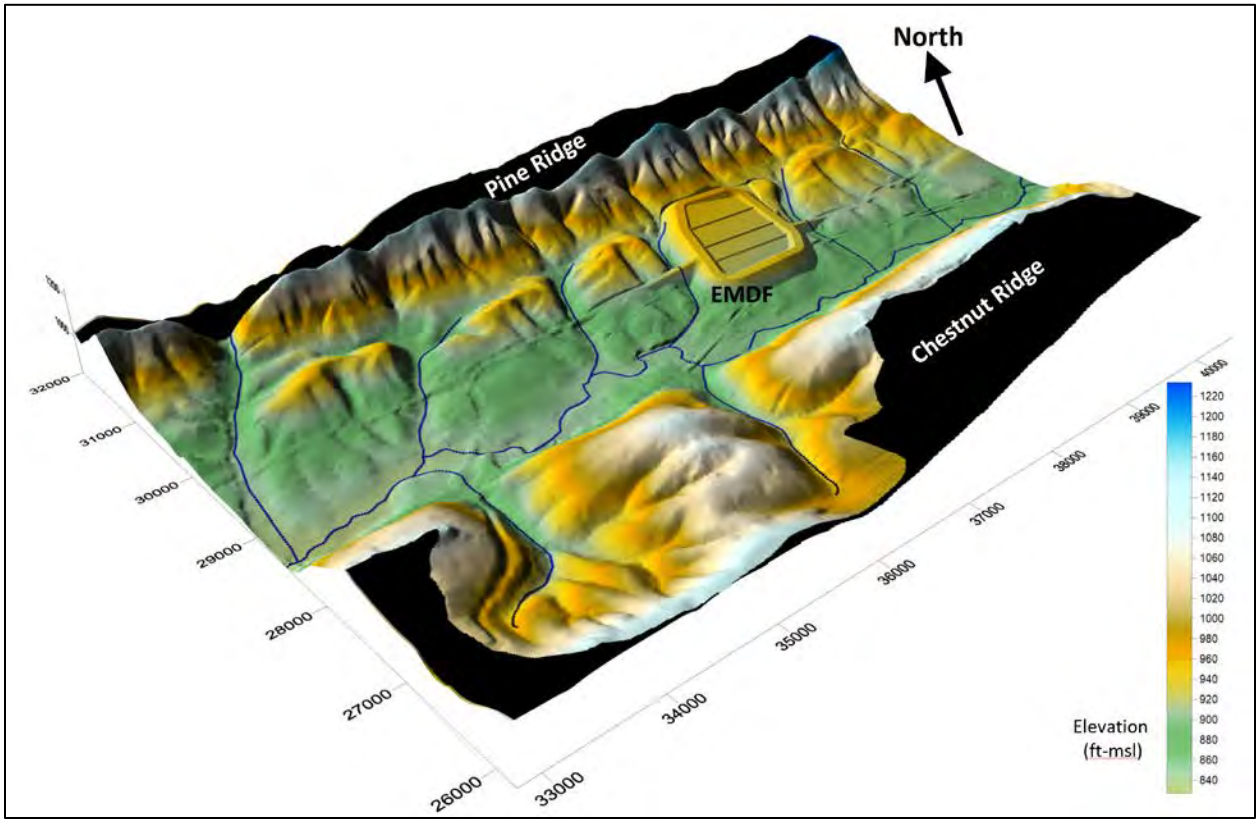

Fig. F.1. EMDF flow and radionuclide transport model domain

To model radionuclide transport, input parameters were assigned to describe hydrodynamic dispersion, chemical retardation, and degradation (decay) in the saturated zone. These parameters include dispersivity, solid aqueous-phase partition (or distribution) coefficients (K_d), and radionuclide half-life. Radionuclide release mechanisms, source distributions, and release timing are important, and bulk density and porosity are physical parameters of soils and bedrock that influence constituent transport.

In addition to boundary conditions identified for the EMDF flow model (refer to Appendix D, Sect. D.2.2), boundary conditions for the transport model include recharge concentrations for each radionuclide to represent the leachate flux from the vadose zone to the saturated zone underneath the disposal cell.

Similar to the EMDF flow model development, the transport model used the Groundwater Vistas software Version 7.2 (Environmental Simulations, Inc. 2017), a graphic user interface program to aid in model development and result visualization. Common text editing and spreadsheet programs were used for input pre-processing and output post-processing.

A general application of the saturated zone transport model (Sect. F.3) was developed to delimit the maximum plume extent, locate the maximum impact to groundwater along the 100-m buffer zone boundary, and quantify the pattern of contaminant discharge to surface water features. For the general application of MT3D, only advective transport of a generic contaminant is represented in the model, without decay, retardation, or hydrodynamic dispersion.

Full implementation of the MT3D model (incorporating all transport processes, Sect. F.4) was developed to predict the peak concentrations for the dose-significant radionuclides at the 100-m groundwater well location, and to evaluate the potential impact of non-uniform radionuclide release from the EMDF on the peak concentrations.

In the remainder of Sect. F.2, the input parameter values for the transport model are presented (Sect. F.2.2), along with the initial radionuclide concentrations (Sect. F.2.3), and the boundary conditions representing leachate release (Sect. F.2.3).

Section 9 of the Performance Assessment (PA) report details the quality assurance (QA) activities and documentation that apply to the MT3D model analysis.

F.2.2 RADIONUCLIDE TRANSPORT PARAMETERS

Physical and geochemical processes that influence radionuclide fate and transport include advection, hydrodynamic dispersion, chemical retardation, and radioactive decay.

F.2.2.1 Advection

Advection involves the physical transport of constituents dissolved or entrained in flowing groundwater. Advective flow is likely the primary transport mechanism. Model parameters that control advection include hydraulic gradients, vertical and horizontal hydraulic conductivity (K), and (effective) porosity. Since output from the EMDF flow model is coupled to the MT3D transport model code, primary parameters associated with advection can be found in Appendix D, Sect. D.2. Total and effective porosity values applied in the transport model are provided in Table F.1. For a single porosity conceptualization, only the effective porosity is used in the MT3D model, and total and effective porosity were assumed to be equal. Decreases in porosity values in deeper model layers reflect the fact that the bedrock at depth is less fractured, thus having less effective porosity to allow active water flow.

Table F.1. Porosity and bulk density values assigned in the MT3D model

Model layer	Total porosity	Effective porosity	Bulk Density (g/cm^3)
1	0.27	0.27	1.93
2	0.20	0.20	2.22
3	0.15	0.15	2.36
4	0.10	0.10	2.50
5	0.05	0.05	2.64
6	0.04	0.04	2.67
7	0.03	0.03	2.70
8	0.02	0.02	2.72
9	0.01	0.01	2.75

F.2.2.2 Hydrodynamic Dispersion Parameters

The definition of dispersivity values for use in field-scale transport simulations is inherently difficult and has been the subject of some controversy. Numerous studies have been conducted to characterize field-scale dispersivity values. A comprehensive review of field-scale physical transport processes and the many practical implications for transport modeling are discussed in *A Review of Field Scale Physical Solute Transport Processes in Saturated and Unsaturated Porous Media* (Gelhar et al. 1985) and *A Critical Review of Data on Field-Scale Dispersion in Aquifer* (Gelhar et al. 1992). Hydrodynamic dispersion refers to the spreading of a constituent by the combined action of mechanical dispersion and molecular diffusion. Dispersion causes some constituents to move faster and some to move slower than the average linear velocity of groundwater. Mechanical dispersion is caused by variations in the magnitude and direction of groundwater velocity. Molecular diffusion results from constituent concentration gradients that cause the constituent to move from regions of higher concentration to regions of lower concentration. Molecular diffusion is generally secondary and negligible compared to the effects of mechanical dispersion, and only becomes important when groundwater velocity is very low.

Dispersivity is a scale-dependent property and is not constituent-specific. The MT3D transport model requires horizontal (x and y coordinate directions for the EMDF saturated zone flow and transport models) and vertical (z coordinate direction) dispersivity values as input. As a rule of thumb, and in the absence of site-specific information, horizontal transverse dispersivity (x-direction) can be assumed to be approximately one order of magnitude smaller than longitudinal dispersivity (y-direction), while vertical transverse dispersivity can be assumed to be approximately two orders of magnitude smaller than longitudinal dispersivity (Zheng and Bennett 1995). The transport model uses a longitudinal dispersivity of 10 m, a transverse dispersivity of 1 m, and a vertical dispersivity of 0.1 m. The 10-m value for the y-direction (along flow path) dispersivity is based on the 100-m distance to the groundwater well and a 10 percent rule of thumb (Gelhar et al. 1992) for estimating longitudinal dispersivity as a fraction of travel distance.

F.2.2.3 Retardation Parameters

The retardation factor is the empirical parameter commonly used in transport models to describe the chemical interaction between a constituent and geological materials (i.e., soils, sediments, and rocks). The retardation factor accounts for processes such as surface adsorption, absorption into the soil structure, chemical precipitation, and physical filtration of colloids. The retardation factor (R_f) is defined as follows:

$$R_f = 1 + K_d(\rho_b / n_e)$$

where:

ρ_b = bulk density of the soil (g/cm^3)
n_e = effective porosity of the geologic matrix (volume/volume)
K_d = soil/water partition coefficient (cm^3/g).

For a given mass of constituent, the fraction available for advective transport is influenced by the sorptive properties of the geologic matrix. The solid/water partition coefficient is very important in estimating the potential for the sorption of dissolved constituents in contact with subsurface media. The solid/water partition coefficient (K_d) describes the ratio of sorbed to dissolved constituent:

$$K_d = C_s / C_{aq}$$

where:

C_s = concentration of solute in soil (mg/g)
C_{aq} = concentration of solute in aqueous solution (g/mL).

The linear, Freundlich, and Langmuir isotherms are the most commonly used relations for describing equilibrium-controlled reversible sorption. These sorption isotherms describe the functional relationship between dissolved and sorbed constituent concentrations at equilibrium under a constant temperature. The linear sorption isotherm assumes the sorbed concentration is directly proportional to the dissolved concentration. The non-linear Freundlich and Langmuir isotherms require additional parameter values obtained from experimental measurements. Empirical parameters necessary to implement Freundlich or Langmuir isotherms are lacking for this site. Therefore, the linear isotherm is used in transport simulations. The linear isotherm uses a single partition coefficient (K_d) to define the relationship between the constituent concentrations in the dissolved phase and the concentrations of material sorbed to the porous medium.

Porosity affects the transport calculation in two important ways. It is a factor in calculating groundwater velocity, which controls advective transport, and it defines the pore volume of a model cell available for storage of constituent mass. Total and effective porosities are shown in Table F.1, along with estimated dry bulk densities for each model layer. Based on the total porosity, the dry bulk density (ρ_b) of the geologic media represented in the model are calculated assuming average solid particle densities of 2.65 g/cm^3 for model layer 1 and 2.78 g/cm^3 for all other layers. These same material properties were applied in all the PA models to the extent possible given differing levels of model detail.

Radionuclide K_d values vary depending on the chemical element and properties of the pore fluid and solid media. Due to the lack of material-specific data on sorptive properties, a single K_d is assumed to apply to saturated zone for all the material types and hydrological units in the saturated zone transport model for each radionuclide. This assumption is the same as applied in other models in the PA analysis; refer to Sect. 3.2.2 of the EMDF PA. Table F.2 lists the base case saturated zone K_d values used for the three radionuclides evaluated in the MT3D simulations.

Table F.2. Radionuclide parameter values

Radionuclide	K_d (cm^3/g)	Half-life (years)	Specific activity (Ci/g)
C-14	0	5.70E+03	4.50E+00
Tc-99	0.72	2.13E+05	1.70E-02
I-129	4.0	1.57E+07	1.80E-04

F.2.2.4 Radioactive Decay

In MT3D, the first-order irreversible rate constant is expressed in terms of half-life. The half-life ($t_{½}$) of a constituent represents the time required to reduce constituent concentrations by half. The decay rate (λ) is specified as follows:

$$\lambda = \ln(2) / t_{½}$$

The half-life of radionuclides that are released to the saturated zone within 10,000 years post-closure of EMDF are from the technical standard guidance *Derived Concentration Technical Standard* (DOE 2011).

Table F.2 lists the half-life of the radionuclides. Specific activity values are used to convert activity concentrations to mass concentrations for use in MT3D.

F.2.3 INITIAL RADIONUCLIDE CONCENTRATIONS

Initial conditions for the transport model include radionuclide distributions within the model domain. Since the proposed EMDF will be built on an area without existing groundwater or soil contamination, the initial concentrations in the aquifer within the model domain for radionuclides are assumed to be zero. For the EMDF PA, only EMDF contributions to groundwater contamination are considered.

The radionuclide release model described in Sect. F.4.1.3 uses initial activity concentrations in waste based on the estimated EMDF radionuclide inventory (refer to Sect. 2.3 of the PA and Appendix B). Estimated as-generated average activity concentrations in EMDF waste are reduced to account for addition of clean fill during waste placement and compaction. The resulting as-disposed activity concentrations for radionuclides with K_d values < 10 cm^3/g are also reduced to account for activity losses during EMDF disposal operations (refer to Sect. 3.2.2.5 of the PA). Initial average post-operational activity concentrations for the three dose-significant radionuclides used for MT3D release model are given in Table F.3.

Table F.3. Initial average radionuclide concentrations in EMDF waste

Radionuclide	Post-operational waste average activity concentration[a] (pCi/g)
C-14	5.40E-01
Tc-99	1.56E+00
I-129	3.50E-01

[a]Post-operational concentrations account for the addition of clean fill and leaching losses during waste disposal operations.

EMDF = Environmental Management Disposal Facility

F.2.4 BOUNDARY CONDITIONS REPRESENTING LEACHATE RELEASE

In addition to various boundary conditions required for the EMDF flow model (Appendix D), boundary conditions for the transport model include recharge concentrations for each radionuclide to represent leachate release from the EMDF. The mass flux is a function of the specified volumetric release rate through the liner system and the radionuclide concentration. For the saturated zone flow and transport modeling, the volumetric release of leachate from the vadose zone to the water table beneath the disposal cell (recharge rate) is based on the EMDF hydrologic performance (water balance) modeling (Appendix C, Sect. C.2).

The recharge areas defined for the saturated zone transport model are shown in Fig. F.2. The leachate recharge area is defined by the waste limits. The outer lined area and berm/side slope area are assigned low recharge rates (0.88 in./year and 1.0 in./year, respectively) but have zero recharge concentration and do not contribute radionuclide flux to the saturated zone.

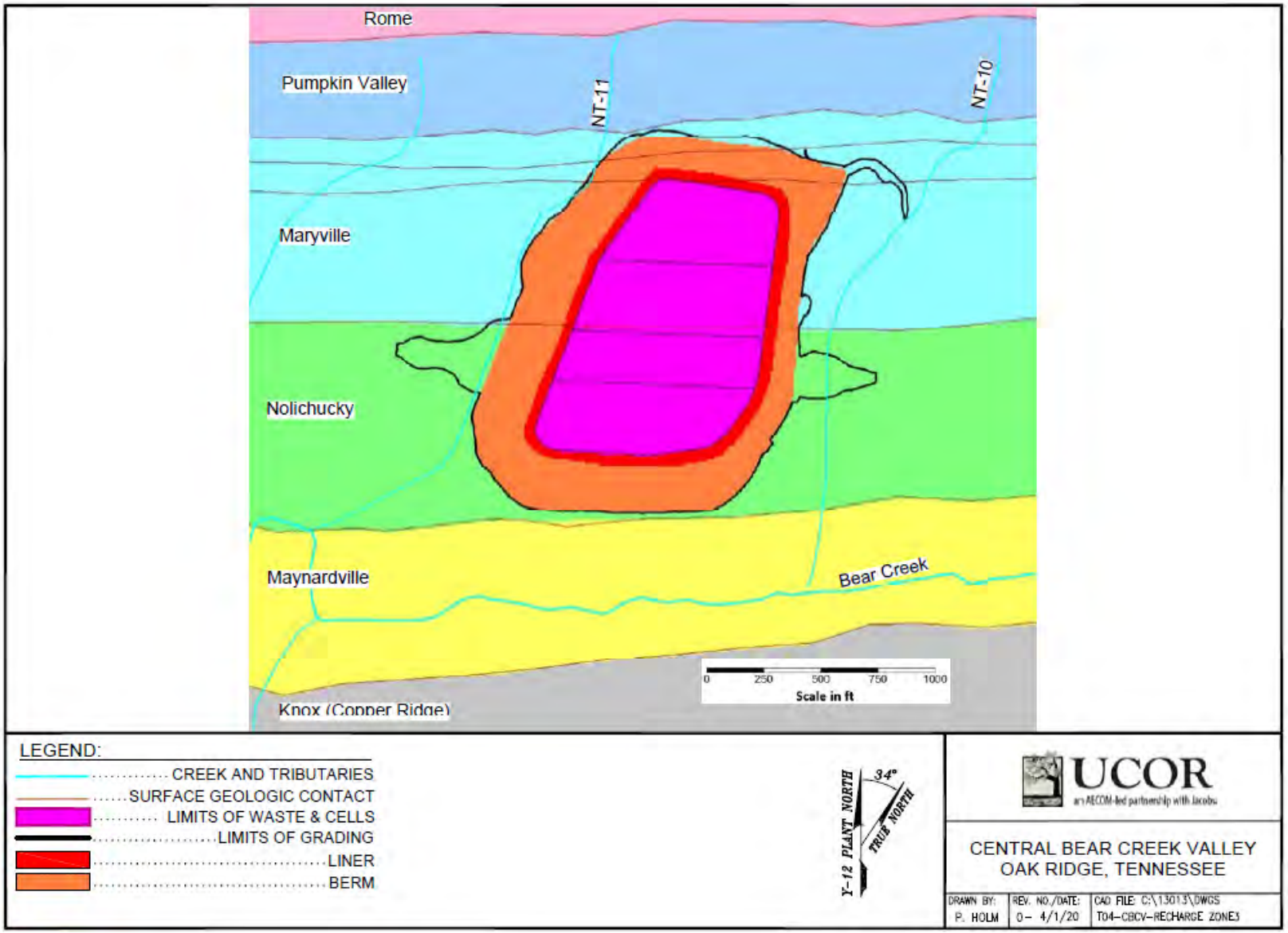

Fig. F.2. MT3D model recharge zones for EMDF

The recharge boundary condition applied to the EMDF waste area (Fig. F.2) is a variable boundary condition that incorporates the assumed evolution of EMDF cover performance over time (Appendix C, Sect. C.1.3) applied to a simple model of radionuclide release from the EMDF (Sect. F.4.1.3). The assumed release rates for the waste area are based on hydrologic performance modeling as follows:

- Design performance period – 0.0 in./year (closure to 200 years)
- Degrading performance period – increasing from 0.0 to 0.88 in./year (200 to 1000 years post-closure)
- Long-term (degraded) performance period – 0.88 in./year (> 1000 years post-closure).

For the groundwater flow simulation (MODFLOW), one or more of the release rates listed above can be applied directly as waste area recharge rates. For the MT3D transport simulation, the radionuclide flux from the waste into the saturated zone is represented as a variable recharge concentration associated with the recharge rate applied to the waste area.

The simple model of radionuclide release from the waste is based on the EMDF source inventory (initial average radionuclide concentrations) and the assumed K_d values for the three nuclides considered. Applying an equilibrium (de)sorption assumption to estimate pore water concentrations within the waste, a mass balance approach for estimating the increasing release of leachate and variable concentration for each nuclide is used to determine the recharge concentrations for the waste area. The release model does not account for the initial 200-year delay in release (i.e., the full design performance period), or for the vadose transport time and vadose zone attenuation that occurs between the waste and the saturated zone. The leachate mass balance calculation to determine recharge concentrations and the application of STOMP model simulations to account for vadose zone transport on the timing of radionuclide flux to the saturated zone are described in detail in Sects. F.4.1.2 and F.4.1.3.

The MT3D transport model is linked to EMDF flow model runs that use either steady-state or transient conditions to represent the flow field. For a complete long time transient simulation, the use of multiple model stress periods for the flow model (discrete simulation intervals with stepwise increasing steady-state recharge rates) would be required to represent the flow and transport dynamics as leachate flux increases. Specifically, a great number of stress periods would be required for the time period between 200 and 1000 years when an increasing recharge rate is assumed. The increase in the waste area recharge rate would result in different groundwater flow fields for each stress period. This would make the application of the coupled MODFLOW/MT3D model quite complex due to the large size of the model and the need to incorporate variable timing and duration of release for radionuclides with different K_d values.

To simplify the MT3D model implementation, the steady-state EMDF model flow field associated with the long-term performance condition (0.88 in./year) is used for the MT3D simulation. This simplification tends to overestimate the water table elevation and saturated zone hydraulic gradient beneath the EMDF during the design performance and degrading performance periods (from EMDF closure to 1000 years). The volumetric recharge rate (volume per area per time) applied to the EMDF waste area is fixed at 0.88 in./year for the entire simulation period. The release model used to estimate the radionuclide flux and concentration over time for each radionuclide explicitly incorporates the progressive increase in volumetric release rate between 200 and 1000 years post-closure. To maintain the correct mass flux for each radionuclide, the recharge concentrations predicted by the radionuclide release model for each time interval prior to 1000 years were adjusted to account for the constant recharge rate applied to the waste area in the MT3D model. The recharge concentrations for each time interval prior to 1000 years are reduced based on the ratio between the (increasing) volumetric release rate and the (constant) MT3D recharge rate.

F.3 GENERAL APPLICATION OF TRANSPORT MODEL

The general application of the saturated zone transport model was developed to delimit the maximum plume extent, locate the maximum impact to groundwater along the 100-m buffer zone boundary, and quantify the pattern of contaminant discharge to surface water features. For these objectives only advective transport of a generic contaminant is represented in the model, without decay, retardation, or hydrodynamic dispersion.

F.3.1 GROUNDWATER FLOW FIELD

The general application of MT3D model used the saturated zone flow field for the EMDF long-term performance condition. The same flow model result was also used to derive many of the input parameters (e.g., depth to water table and hydraulic gradient) used for other models in the performance analysis. The model-predicted groundwater water table levels in the cell area for the long-term performance condition are shown on the left side of Fig. F.3. The flow field and potentiometric surface contours in the shallow saturated zone (model layer 2) are shown on right side of Fig. F.3.

F.3.2 MAXIMUM PLUME EXTENT EVALUATION

The natural groundwater divide to the north along Pine Ridge to the north, anisotropic nature of the geologic materials, and patterns of groundwater discharge to surface streams (Bear Creek tributaries) near the EMDF affect the shape and extent of the contaminant plume. Although particle tracking analysis based on the flow model can provide some information on the location and extent of the contaminant plume (Appendix D), the transport model provides more detail on the distribution of radionuclide mass for predicting both the geographic extent of the plume and the location of maximum concentration at 100 m from the edge of waste (EOW). These general results support definition of the POAs for surface water and groundwater in the PA.

A steady leachate flux (recharge) from the EMDF to the saturated zone was applied with a constant water recharge rate (0.88 in./year) and a constant recharge concentration of 1 unit (units are arbitrary for the general application) within the waste area of the model. Thus, the contaminant source is assumed to be infinite (non-depleting). Only advective transport was simulated for the general application. No hydrodynamic dispersion, decay, or retardation processes are represented. The MOC solution method was used for all the simulations to minimize the potential error from numerical dispersion. This approach results in the largest potential impacts for the EMDF area and at the assessment locations.

The model simulations were run to near steady-state condition for the plumes (i.e., the concentrations at all locations on the model domain do not change and plumes reach their maximum extent). Figure F.4 shows the shallow groundwater plume in model layer 2 at four model times for the non-depleting source simulation. Model layer 2 reaches steady-state concentrations relatively early (prior to 1000 years; refer to Sect. F.3.3). For the model domain as a whole, a near steady-state condition for the resulting groundwater plume is achieved before 2000 years.

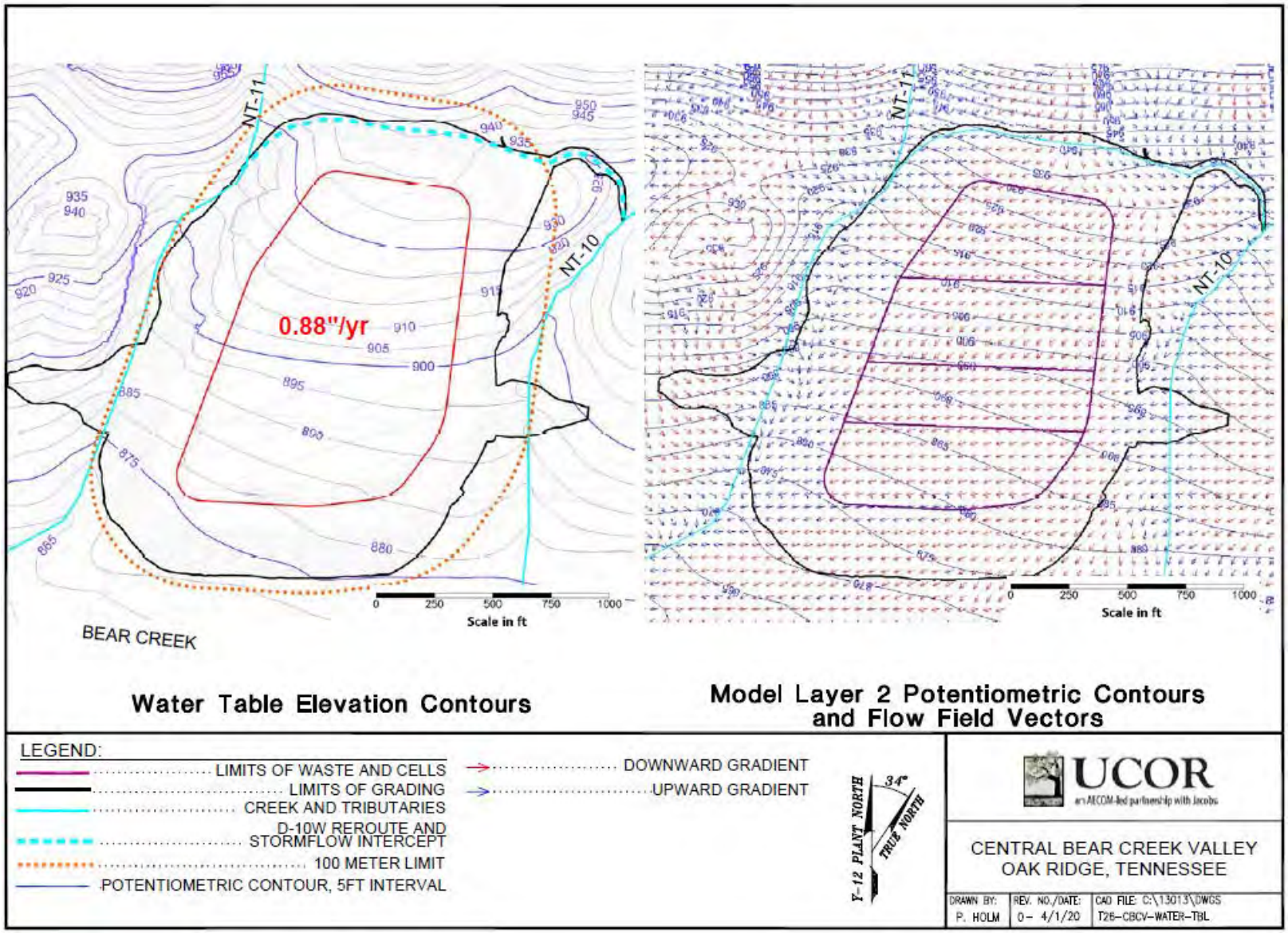

Fig. F.3. Long-term performance condition groundwater levels and flow field for MT3D transport model

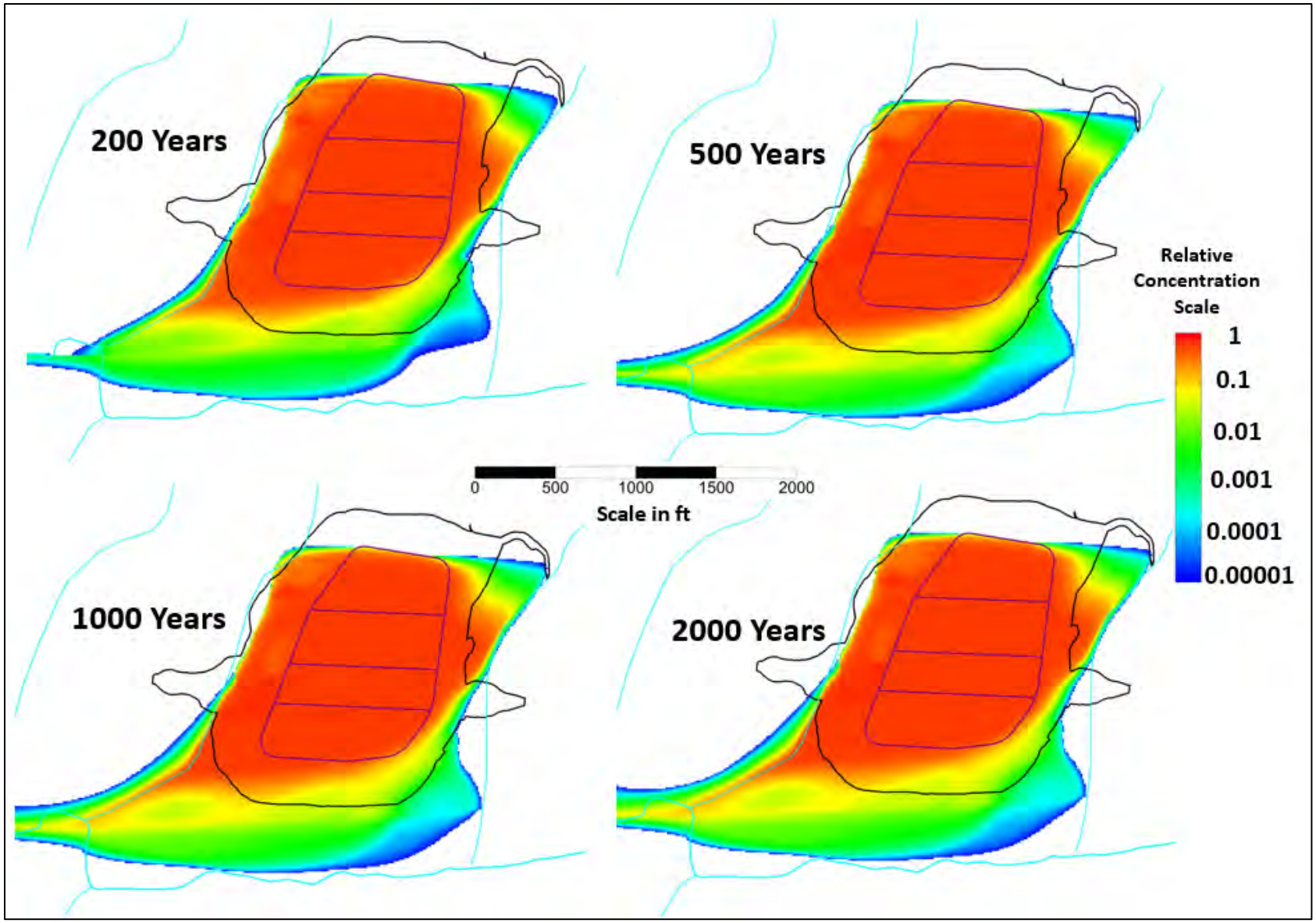

Fig. F.4. Model layer 2 relative concentrations for non-depleting EMDF source

The model-predicted extent of the constant source plume from EMDF (maximum concentration among the nine model layers) at year 2000 is shown on Fig. F.5. The majority of contaminated groundwater will discharge into Bear Creek and its tributaries near the EMDF site. The (minor) remaining contaminant mass will move downstream beyond North Tributary (NT)-12 along the more permeable formations (Maynardville Limestone) along Bear Creek and discharge into Bear Creek farther downstream. The transport model predicts that essentially all release from the disposal cells discharges into Bear Creek surface water upstream of the Gum Branch Tributary (NT-14).

The model-predicted EMDF plume migration pathway matches with the current understanding of the plume migration in upper Bear Creek Valley and the conceptual site model developed in the Bear Creek Valley Remedial Investigation (DOE 1997a) and Feasibility Study (DOE 1997b).

F.3.3 LOCATION OF MAXIMUM GROUNDWATER IMPACT AT 100 METERS

For the general application of the transport model, the plume configuration and maximum concentrations along the EOW of the 100-m buffer zone surrounding the waste were used to identify the location of maximum impact to a hypothetical groundwater well. The most likely maximum impact location for a drinking water well at 100-m from the EOW is southwest of the disposal cell near NT-11(Fig. F.5). This POA for radionuclide release to groundwater is adopted for the dose analysis in the PA.

The MT3D model results also establish the likely vertical interval at the hypothetical 100-m well location over which maximum radionuclide concentrations will be highest. Based on steady-state concentrations attained at the EOW and at the 100-m well within the initial 1500 years of the simulation (Fig. F.6), model layers 2 and 3 have the highest concentrations, with model layers 1, 4, 5, and 6 showing lower concentrations, and layers 7, 8, and 9 receiving very little contamination within the 100-m buffer zone. Maximum concentrations for each model layer are higher and arrive earlier at the EOW location (upper plot in Fig. F.6), than at the 100-m well (lower plot in Fig. F.6). Maximum relative concentrations of 1 in model layer 2 at the EOW location reflect the leachate flux boundary condition (recharge concentration) applied to layer 2 in the waste area. (Model layer 1 within the waste area is above the simulated water table.) The simulated concentration fields within a vertical plane (cross-section) through the 100-m well at 200 years and 2000 years post-closure (Fig. F.7) also illustrate the vertical distribution of concentration and the changing subsurface configuration of the plume over time.

The simulated vertical distribution of contaminant concentrations is critical for understanding the implications of assuming a particular vertical interval for groundwater withdrawal in the dose analysis of the PA. The MT3D/MODFLOW model codes can simulate the impact of groundwater withdrawal from a specified vertical interval on both the flow field and contaminant concentrations associated with a model well. Based on the results of the general application of the transport model, a withdrawal interval including model layers 2 and 3 would result in the highest peak well water concentrations. However, the RESidual RADioactivity (RESRAD)-OFFSITE model used to implement the dose analysis (refer to Sect. 3 of the PA) uses a simplified representation of the saturated zone and the groundwater well withdrawal interval, making strictly equivalent parameter assumptions difficult and direct comparison of MT3D and RESRAD-OFFSITE results challenging. The approach taken to simplify comparison and integration of saturated zone model results is to implement the MT3D modeling without including a pumping well in the simulations, and to use the peak concentrations for model layers 2 and 3 at the 100-m well to represent maximum potential well water concentrations. This approach is acceptable because the impact of groundwater withdrawal to supply a family of four for domestic use has a very small impact on the flow model. In addition, the inclusion of a pumping well at the location of maximum concentration (at 100 m) would result in simulated well water concentrations that are less than the maximum value by flow from areas of lower concentration toward the well.

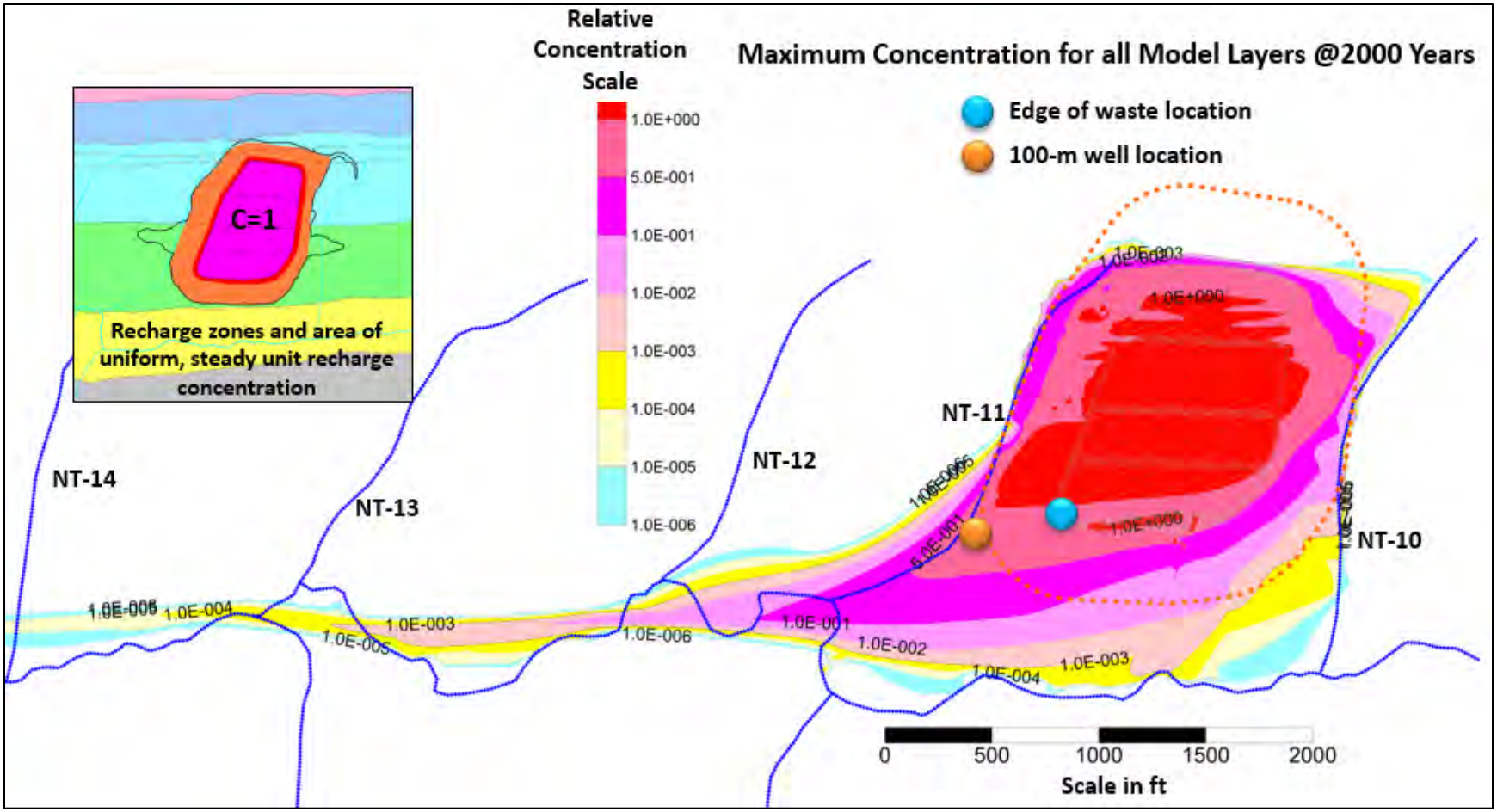

Fig. F.5. Plume distribution (maximum concentrations) for non-depleting release from EMDF

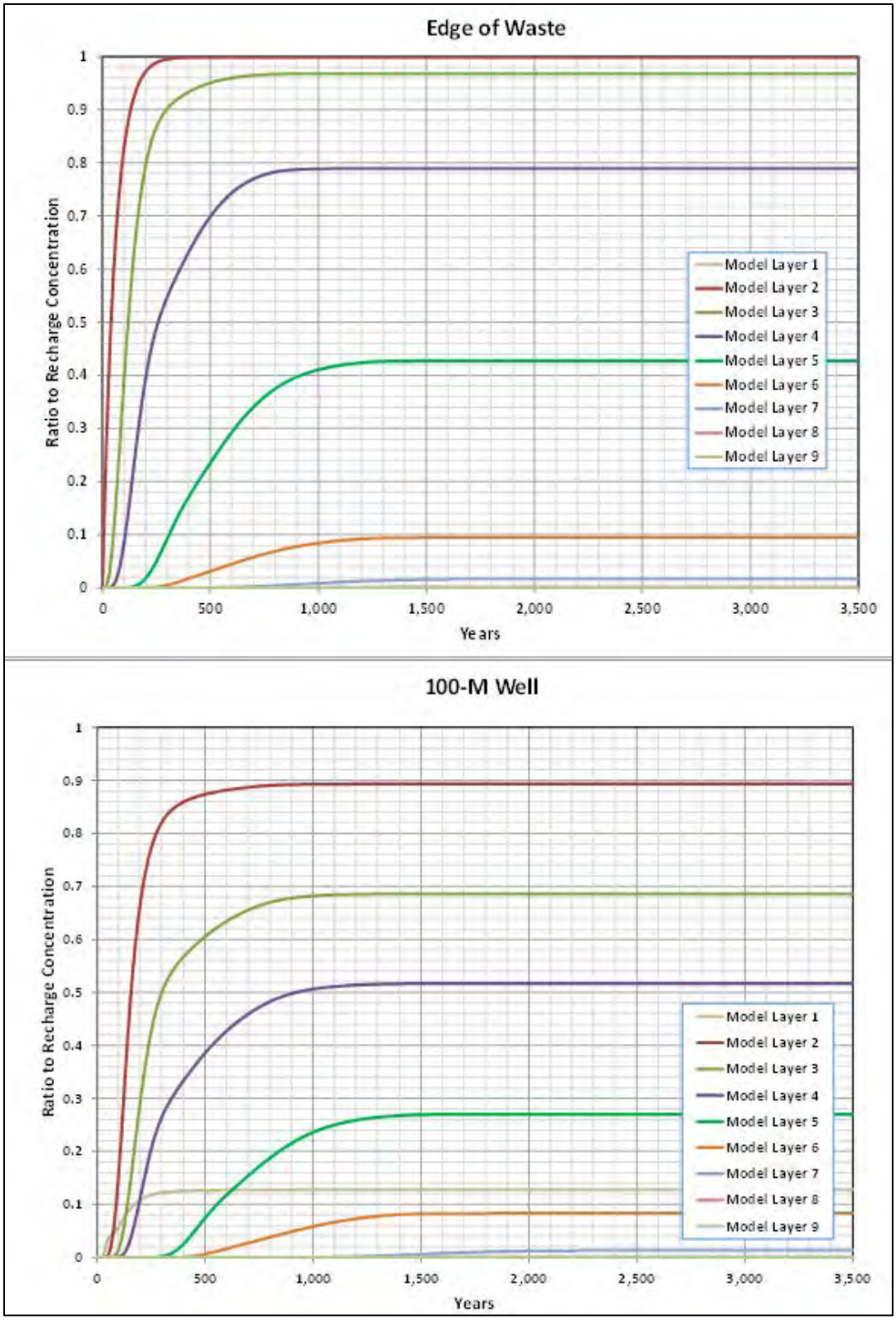

Fig. F.6. Groundwater concentrations (relative to unit source concentration) for each MT3D model layer at edge of waste and 100-m well locations

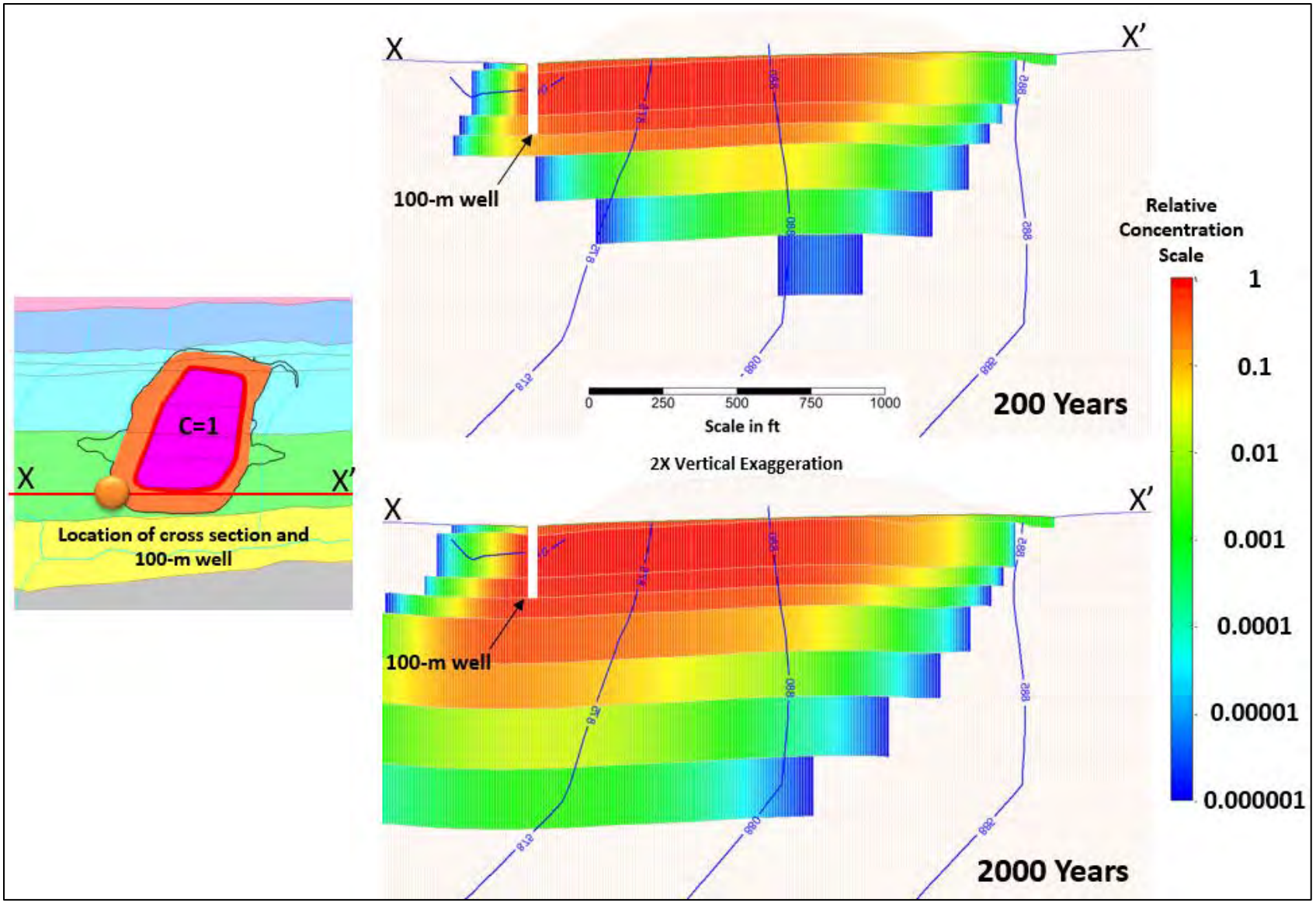

Fig. F.7. Subsurface distribution of relative concentration for the general application of the MT3D transport model

F.3.4 IMPACT TO SURFACE WATER

The constant-source MT3D transport model result was used to quantify groundwater and contaminant discharge to the model river cells and drain cells that represent surface water features near the EMDF. The simulated contaminant mass discharge to NT-10, NT-11, and the Bear Creek main channel segment between those tributaries was determined for corresponding areas of the model domain. The model calculates contaminant mass flux as groundwater discharge times the concentration at each model drain or river cell. Polygons identifying the areas for each of the stream channel segments and the simulated concentrations for model layer 1 (where contaminant discharge to river and drain cells occurs) are shown on Fig. F.8.

Table F.4 summarizes the distribution of contaminant mass discharge to the three stream channel segments. The discharge is expressed as percentage of the total (steady-state) contaminant mass discharge from the entire model domain. Most of the contaminant mass discharge (> 87 percent) is received by NT-11, whereas NT-10 and the Bear Creek main channel segment receive only 8.2 and 2.8 percent, respectively. Together the three model channel segments account for over 98 percent of the release from the model domain. These results are the basis for selection of Bear Creek at the junction with NT-11as the surface water POA (i.e., water for agricultural use is drawn from a single location that integrates most of the simulated release from the EMDF). It also validates that use the junction of Bear Creek and NT-11 as the point of compliance for evaluating protection of surface water resources.

Table F.4. Contaminant mass discharge to surface water features in the MT3D model (simulation year 2000)

NT-10	Bear Creek between NT-10 and NT-11	NT-11	Total of three surface water model segments
8.17	2.80	87.12	98.09

Values in table are percentage of total contaminant discharge within the entire model domain.

NT = North Tributary

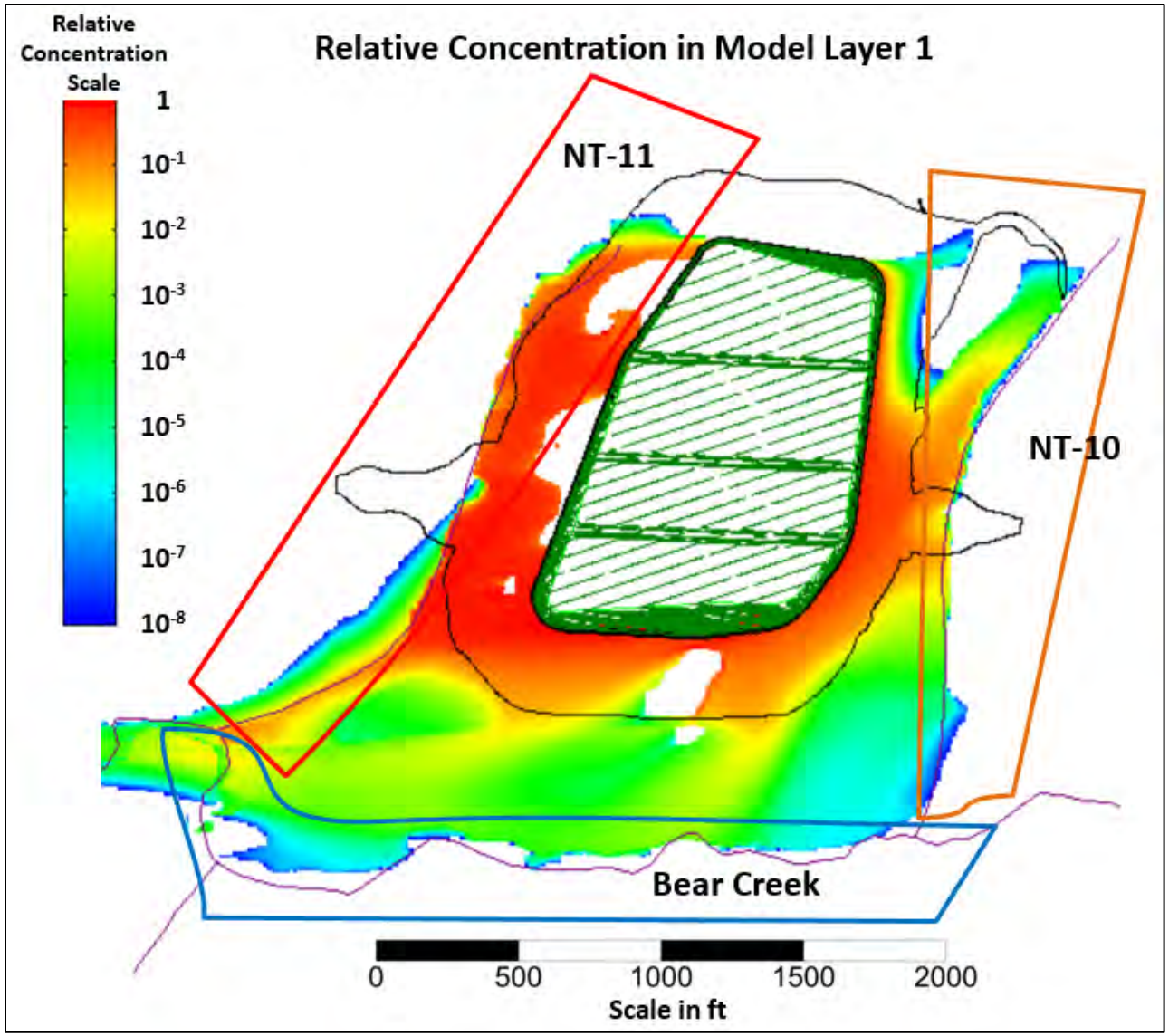

Fig. F.8. Segments of surface water features defined for quantifying groundwater and contaminant discharge from the transport model domain

F.3.5 SENSITIVITY TO NON-UNIFORM SOURCE RELEASE

Both the general application and the full implementation (Sect. F.4) of the MT3D radionuclide transport model assume a spatially uniform release of contaminants to the saturated zone from the waste area. Given the likelihood of non-uniform release due to spatially variable patterns of cover degradation, liner leakage, and waste heterogeneity, the sensitivity of model results to non-uniform release was evaluated. To evaluate the potential impact of non-uniform release, a sensitivity run was conducted by assigning variable recharge concentrations to within the waste area. For the general application (non-depleting source), the eastern portion of the waste area having lower cell floor elevations is assumed to have a leachate concentration of 1.0 unit, and the western half is assigned recharge concentration of 0.1 (Fig. F.9 inset). This pattern is based on the expectation that leachate will accumulate in the lower elevation portion of each disposal cell. The results of a similar non-uniform release scenario for the full transport model implementation is described in Sect. F.4.2.

Figure F.9 shows the maximum plume extent resulting from the on non-uniform, non-depleting source release. The non-uniform release plume footprint is very similar to the uniform scenario (Fig. F.5) except for a slightly eastward shift of the center of highest concentrations beneath disposal cells 1 and 2 as a result of the concentrated mass release on the side of EMDF adjacent to NT-10. The general plume configuration beneath disposal cells 3 and 4 and further downgradient near the 100-m well is nearly identical to the uniform case, but concentrations are lower due to the reduced recharge concentration on the NT-11 side. Groundwater flow in the vicinity of the EMDF toward NT-11 reduces the impact of the non-uniform release on the downgradient plume configuration at the 100-m buffer zone boundary. The importance of this result is that a simple but relatively extreme non-uniform release scenario does not alter the conclusion about the location of maximum impact to groundwater at 100 m, or the selection of the surface water POA.

The non-uniform release scenario for the general application also results in changes in the vertical distribution of contaminant concentrations. Compared to the uniform release scenario (Fig. F.6 upper plot), the maximum concentration for model layer 2 at the edge of waste location (Fig. F.10 upper plot) is higher than for model layers 3 and 4 due to the lower recharge concentration at that location. However, for the 100-m well location, the variation in maximum concentration among model layers for the non-uniform release (Fig. F.6 lower plot) is similar to the uniform release case (Fig. F.10 lower plot). Maximum concentrations at the groundwater 100-m well for the non-uniform release are lower than the uniform case for model layers 1 through 5 because of the lower total contaminant flux to the model domain.

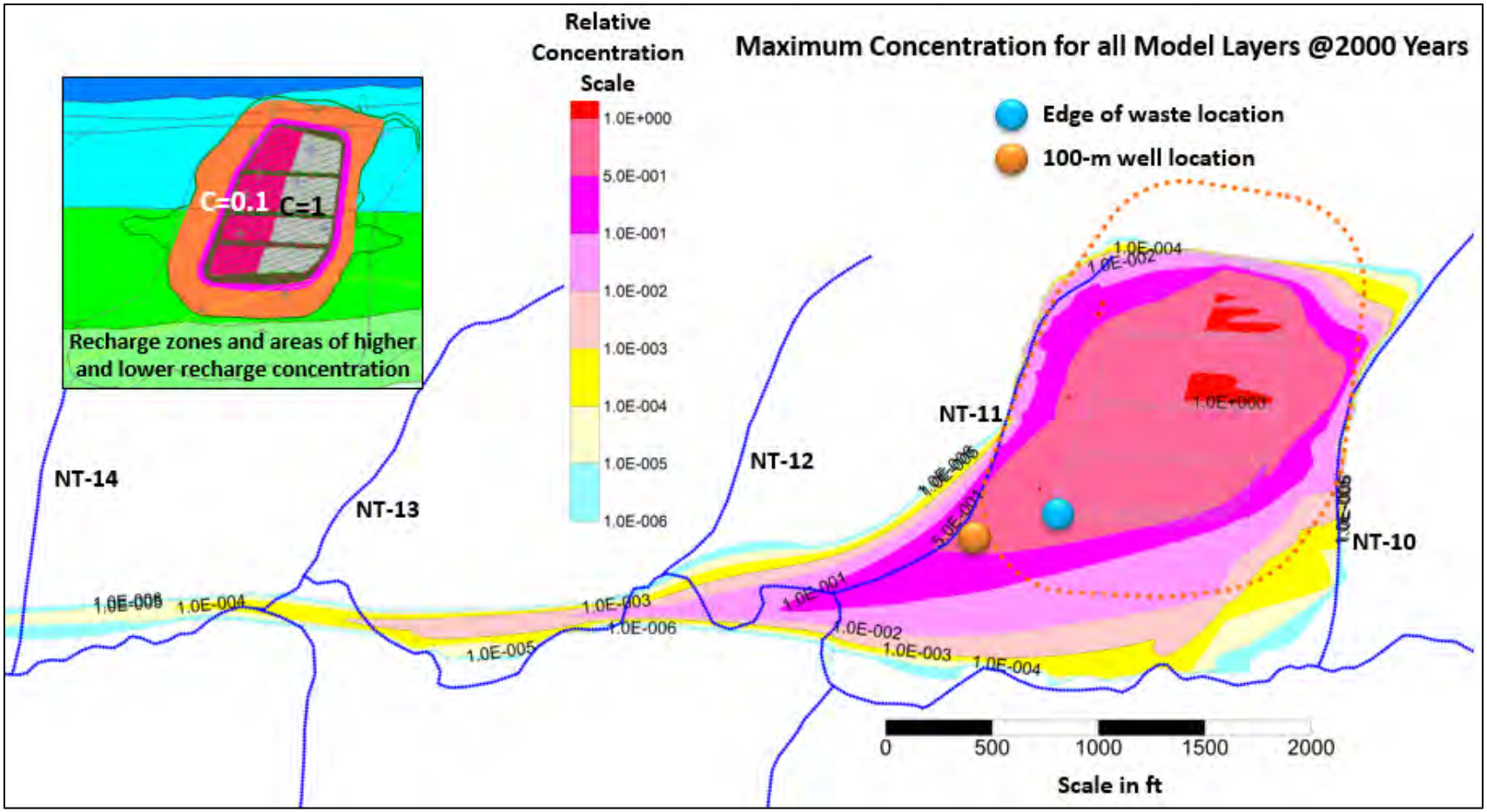

Fig. F.9. Plume distribution (maximum concentrations) for non-uniform, non-depleting release scenario

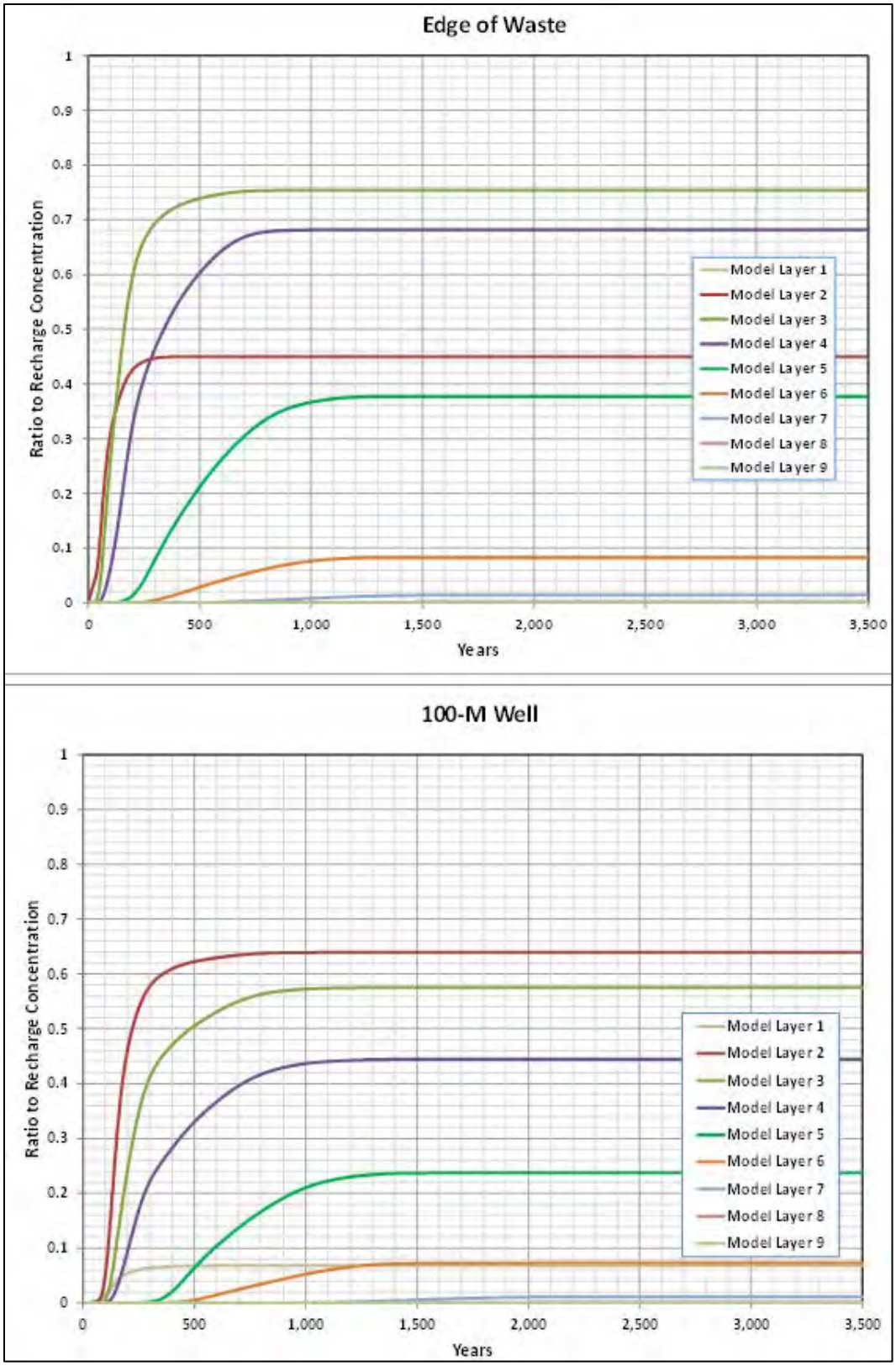

Fig. F.10. Groundwater concentrations for each MT3D model layer at edge of waste and 100-m well locations for the non-uniform, non-depleting release scenario

F.3.6 SENSITIVITY TO HYDRODYNAMIC DISPERSION

The general application MT3D simulations presented above were conducted without hydrodynamic dispersion. An additional sensitivity run was performed to evaluate the impact of including dispersion on the plume development and location of maximum groundwater concentrations. The sensitivity run was conducted with the same flow field and uniform non-depleting release but included the dispersion option for the transport model. The transport model run uses a longitudinal dispersivity of 10 m, a transverse dispersivity of 1 m, and a vertical dispersivity of 0.1 m.

Hydrodynamic dispersion does not change the general plume location or overall pattern but shifts the distribution of concentrations significantly. The sensitivity run with dispersion has a larger vertical plume extent than the non-dispersion run (Fig. F.11). The resulting maximum concentrations at the EOW location (Fig. F.12 upper plot) are similar to the non-dispersion run (Fig. F.6 upper plot). However, dispersion significantly decreases the maximum concentrations in layers 2 and 3 at the 100-m well location, and increases maximum concentrations in model layers 1, 4, 5 and 6 (compare lower plots in Figs. F.6 and F.12). Because of the relatively large difference in the highest concentrations at the 100-m well (model layers 2 and 3), the overall average maximum concentration is lower when hydrodynamic dispersion is included in the model. This result is expected and dispersion was included for all subsequent MT3D radionuclide transport simulations.

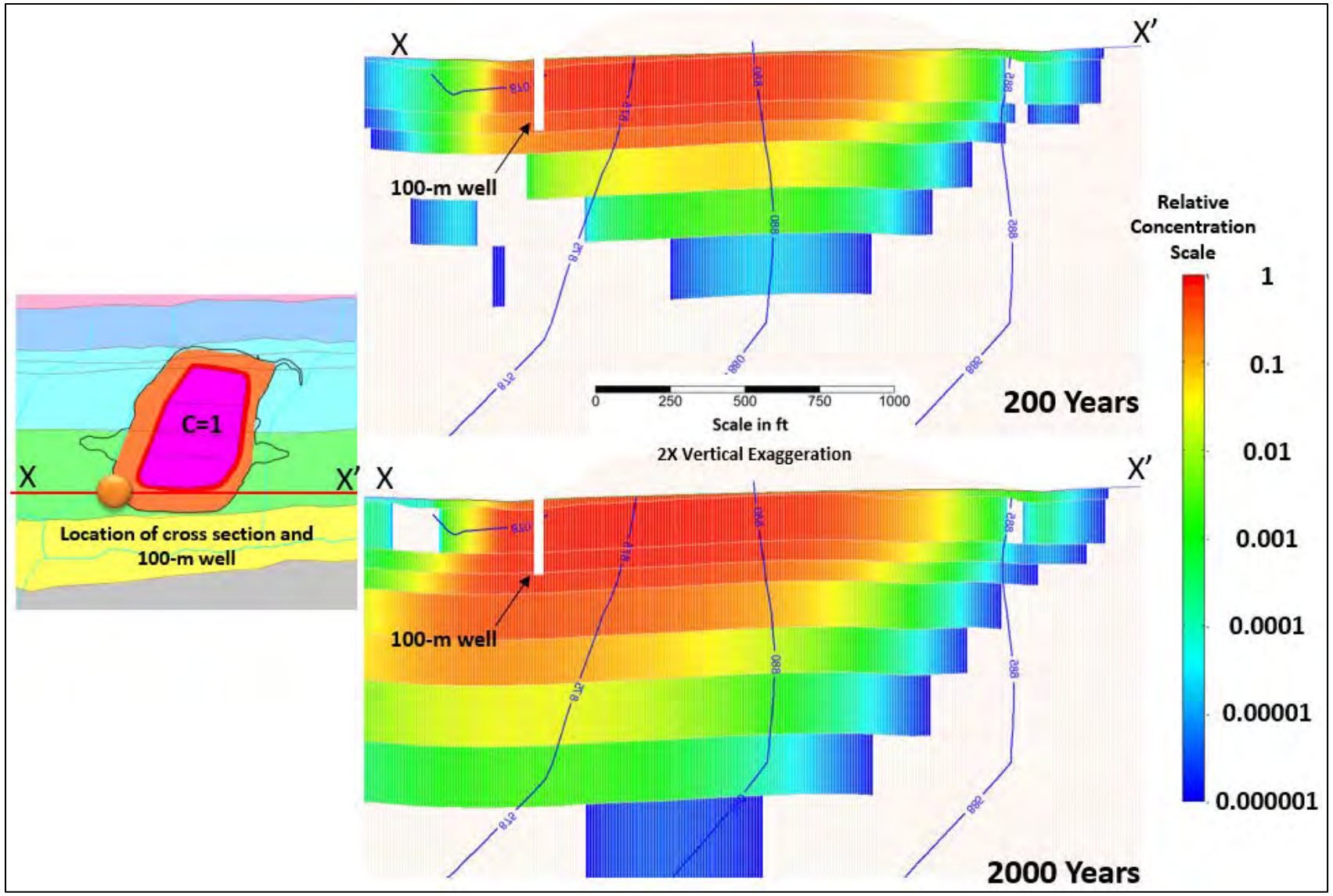

Fig. F.11. Subsurface distribution of relative concentration for MT3D simulation with dispersion

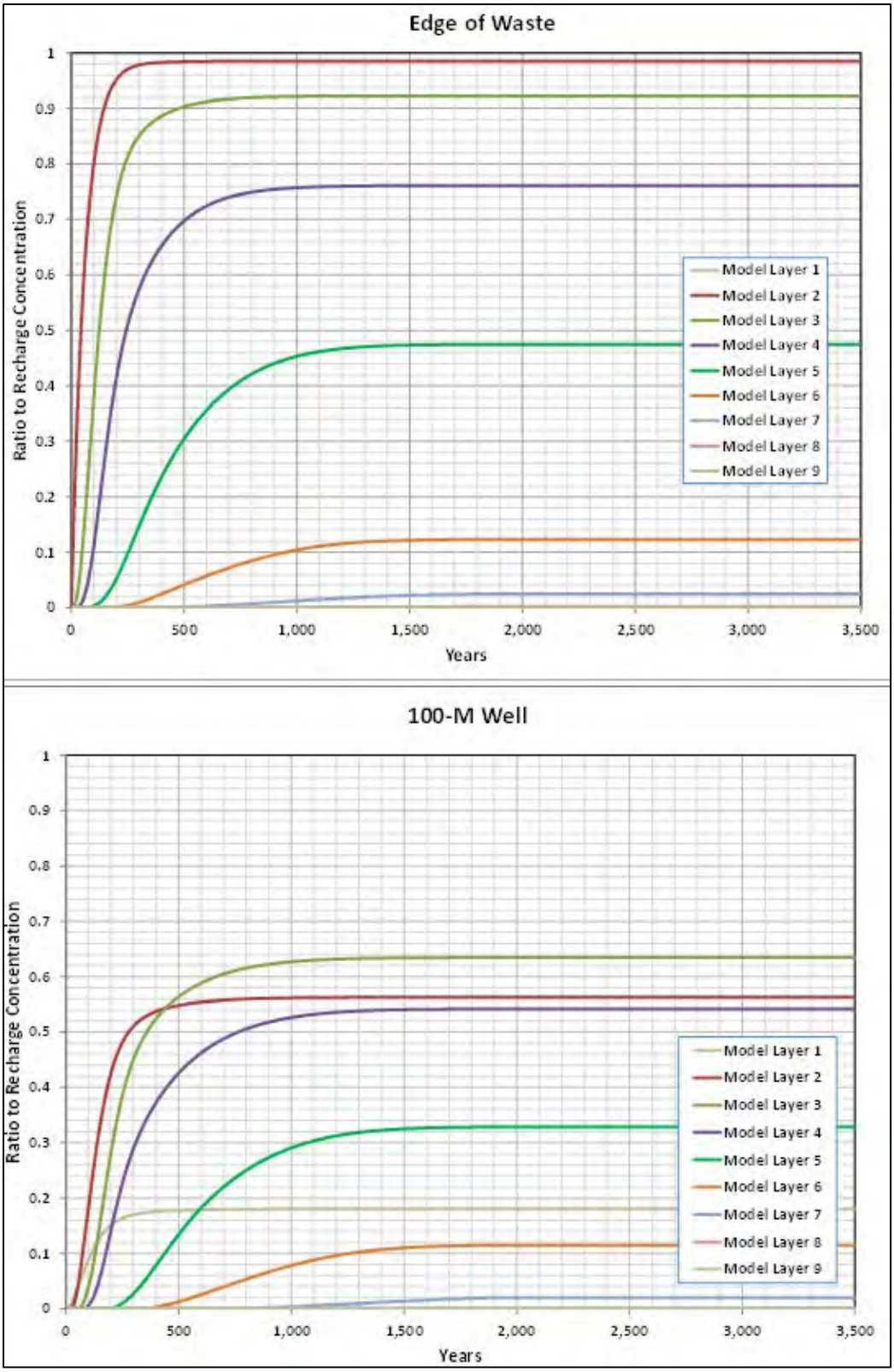

Fig. F.12. Groundwater concentrations for each MT3D model layer at edge of waste and 100-m well locations for the non-depleting release scenario including hydrodynamic dispersion

F.4 RADIONUCLIDE TRANSPORT SIMULATIONS

Full implementation of the MT3D model (incorporating all transport processes) was developed to predict the peak concentrations for the dose-significant radionuclides at the 100-m groundwater well location, and to evaluate the potential impact of non-uniform radionuclide release from the EMDF on the peak concentrations. Radionuclide transport modeling was performed using all the media properties, transport parameters, and radionuclide properties discussed in Sect. F.2. Based on the assumed release timing (refer to STOMP model results presented in Appendix E and applied in Sect. F.4.1.2) and likely dose contributions (preliminary RESRAD-OFFSITE simulations with the estimated EMDF inventory), only the three key dose-contributing radionuclides (Tc-99, I-129, and C-14) were selected for the detailed saturated zone fate and transport simulation.

F.4.1 BASE CASE RELEASE SCENARIO

For the base case transport modeling of Tc-99, I-129, and C-14, radioactive decay, chemical retardation, and hydrodynamic dispersion were represented in addition to advective transport. The release of leachate was represented by varying leachate concentrations for each radionuclide, as described in Sect. F.2.4 and detailed in Sect. F.4.1.3. For the base condition model, a uniform release from the waste area is assumed.

The key transport model parameters and conditions used for the base case transport modeling are summarized in Table F.5. Detailed application of the conditions and parameters are discussed in the following sections.

Table F.5. Summary of base case transport modeling application

Parameter	Base condition MT3D model implementation
Radionuclides	C-14, I-129, and Tc-99
Source distribution	Uniform
Porosity	Variable porosity (effective) by model layer
Dispersivity	Yes
K_d mode	Linear sorption isotherm
Decay in water	Yes
Decay on soil	Yes
Water recharge rate (waste area)	Constant (long-term performance period – 0.88 in./year)
Recharge concentration (waste area)	Decreasing concentration based on mass balance for depleting source
Vadose zone delay	Delay based on STOMP model

STOMP = Subsurface Transport Over Multiple Phases

F.4.1.1 Groundwater Flow Field

Full implementation of the MT3D transport model used the saturated zone flow field for the long-term EMDF performance condition. The water recharge rate applied to the waste area is 0.88 in./year.

F.4.1.2 Vadose Zone Time Delay

The release model developed to estimate recharge concentrations for each radionuclide specifies the flux from the vadose zone to the water table directly below the waste zone. However, there is delay between EMDF closure and the arrival of radionuclides at the water table. This delay is due to the performance of the cover/liner system in preventing infiltration and leachate release (assumed as 200 years for the PA analysis) and also the chemical retardation of radionuclides migrating vertically through the unsaturated zone above the water table. The cover performance delay is assumed identical for all radionuclides, while the (retarded) vadose travel time depends on radionuclide-specific sorptive properties of the vadose zone materials. STOMP vadose zone modeling (see Appendix E) was the basis for the assumed arrival time at the water table for each radionuclide (Table F.6). The saturated zone arrival time (or vadose delay time) was assigned as the year at which the STOMP model total radionuclide flux reached 50 percent of the peak simulated flux at the water table elevation. Additional detail is provided in Sect. E.3.4.2 of Appendix E.

Table F.6. Estimated vadose delay time for radionuclides released from the EMDF

Radionuclide	Delay time (years)
C-14	530
Tc-99	850
I-129	1750

EMDF = Environmental Management Disposal Facility

F.4.1.3 Radionuclide Release Model

To model depletion of a finite radionuclide source, a simple radionuclide release model was developed. Based on the estimated initial radionuclide concentrations in the waste and assumed K_d values for radionuclides, initial moisture (pore water) concentrations are calculated for the waste. This approach assumes equilibrium solid-aqueous partitioning for a linear isotherm. The pore water concentration and volumetric leachate release based on the assumed increase in cover infiltration are used in a mass balance framework to calculate the decrease in radionuclide inventory, pore water (leachate) concentration, and radionuclide flux to the water table over time. This mass balance approach also incorporates post-closure radioactive decay and the vadose delay times derived from the STOMP model results (Table F.6).

Consistent with the other radionuclide transport models in the EMDF PA, the waste K_d values for each radionuclide were assumed to be one half of the values applied to the non-waste materials (i.e., one half of the K_d values in Table F.2). The estimated release of radionuclides from the waste was assumed to enter the saturated zone uniformly over the waste area. The recharge concentration from the release model is adjusted (decreased) as necessary for times prior to 1000 years (when the assumed leachate release is less than the constant 0.88 in./year applied to the waste area in the MT3D model) to ensure the correct mass flux to the saturated zone (refer to Sects. F.2.4 and F.4.1.1).

To simplify application of the release model to the MT3D code, a simulation was run for each radionuclide with the leachate release beginning at model time zero. The vadose delay for each radionuclide was accounted for in post-processing by adding the delay time to the model run time for each simulation. This approach allows for evaluating uncertainty in the vadose delay times because the half-life of each radionuclide is much longer than the delay time (compare Tables F.2 [half lives] and F.6 [delay times]). Given the relatively long half-lives of the three radionuclides, the effect of radioactive decay is small relative to the leach rate and saturated zone transport rates in driving changes in concentrations.

The MT3D model only allows variation of the recharge concentration among different flow model stress periods. To represent depletion of the radionuclide source in MT3D, 20 model stress periods with different durations and estimated leachate concentrations were applied. The stress periods applied for each radionuclide correspond to time steps in the release model after the vadose delay. Based on the K_d values and vadose delay times for each radionuclide, different stress period lengths were used to account for the differences in the timing and duration of release from the waste zone.

To implement the release model, the leachate concentration for the first stress period is calculated based on the initial waste concentration, K_d value, and assumed waste porosity, bulk density, and moisture content. This concentration is combined with the assumed leachate flux rate for the corresponding time step in the release model to estimate radionuclide loss from the waste during that time step. For the MT3D model, the leachate concentrations for stress periods prior to 1000 years post-closure are decreased to ensure the correct mass flux to the saturated zone. Calculated leachate concentrations and fluxes for successive time steps in the release model incorporate the reduced mass (reduced average waste concentration) and increasing release rate (prior to 1000 years post-closure). The release model calculations are extended through enough time steps to account for leaching of 99 percent or more of the initial radionuclide inventory from the waste. The 20 stress periods applied in the MT3D model for each radionuclide are sufficient to capture the release and transport of nearly all of the estimated mass from the waste, and the simulations were run long enough to capture the majority of the concentration breakthrough curve at the 100-m well location.

The estimated recharge concentrations for each MT3D model stress period are listed in Tables F.7, F.8, and F.9 for Tc-99, C-14, and I-129, respectively. A detailed description of the release model calculations and recharge concentrations applied to the waste area for each model stress period are provided in the QA documentation for the MT3D model (UCOR, an Amentum-led partnership with Jacobs, 2020).

Table F.7. Applied Tc-99 recharge concentrations for radionuclide-specific model in base case

Model stress period	Starting time (year)	Ending time (year)	Time step size (years)	Assumed leachate flux rate (in./year)	Recharge concentration[a] (pCi/L)
1	850	900	50	0.74	2519.8
2	900	1000	100	0.83	2647.3
3	1000	1100	100	0.88	2482.0
4	1100	1200	100	0.88	2161.6
5	1200	1300	100	0.88	1882.5
6	1300	1400	100	0.88	1639.5
7	1400	1500	100	0.88	1427.8
8	1500	1600	100	0.88	1243.5
9	1600	1700	100	0.88	1083.0
10	1700	1800	100	0.88	943.2
11	1800	2000	200	0.88	821.4
12	2000	2200	200	0.88	609.3
13	2200	2400	200	0.88	452.0
14	2400	2600	200	0.88	335.3
15	2600	2900	300	0.88	248.7
16	2900	3200	300	0.88	152.4
17	3200	3600	400	0.88	93.4

Table F.7. Applied Tc-99 recharge concentrations for radionuclide-specific model in base case (cont.)

Model stress period	Starting time (year)	Ending time (year)	Time step size (years)	Assumed leachate flux rate (in./year)	Recharge concentration[a] (pCi/L)
18	3600	4000	400	0.88	45.2
19	4000	4500	500	0.88	21.8
20	4500	5000	500	0.88	7.7

[a]Recharge concentrations for time steps prior to 1000 years are adjusted downward to account for leachate release less than 0.88 in./year.

Table F.8. Applied C-14 recharge concentrations for radionuclide-specific model in base case

Model stress period	Starting time (year)	Ending time (year)	Time step size (years)	Assumed leachate flux rate (in./year)	Recharge concentration[a] (pCi/L)
1	530	550	20	0.37	1336.6
2	550	600	50	0.41	1418.4
3	600	700	100	0.50	1525.6
4	700	800	100	0.61	1405.0
5	800	900	100	0.72	1164.7
6	900	1000	100	0.83	872.7
7	1000	1100	100	0.88	556.0
8	1100	1200	100	0.88	317.6
9	1200	1300	100	0.88	181.4
10	1300	1400	100	0.88	103.6
11	1400	1500	100	0.88	59.2
12	1500	1600	100	0.88	33.8
13	1600	1700	100	0.88	19.3
14	1700	1800	100	0.88	11.0
15	1800	1900	100	0.88	6.3
16	1900	2000	100	0.88	3.6
17	2000	2100	100	0.88	2.1
18	2100	2200	100	0.88	1.2
19	2200	2300	100	0.88	0.7
20	2300	2400	100	0.88	0.4

[a]Recharge concentrations for time steps prior to 1000 years are adjusted downward to account for leachate release less than 0.88 in./year.

Table F.9. Applied I-129 recharge concentrations for radionuclide-specific model in base case

Model stress period	Starting time (year)	Ending time (year)	Time step size (years)	Assumed leachate flux rate (in./year)	Recharge concentration (pCi/L)
1	1750	2000	250	0.88	159.6
2	2000	2500	500	0.88	147.2
3	2500	3000	500	0.88	124.4
4	3000	3500	500	0.88	105.1
5	3500	4000	500	0.88	88.8
6	4000	4500	500	0.88	75.0
7	4500	5000	500	0.88	63.3
8	5000	5500	500	0.88	53.5
9	5500	6000	500	0.88	45.2
10	6000	6500	500	0.88	38.2
11	6500	7000	500	0.88	32.3
12	7000	8000	1000	0.88	27.2
13	8000	9000	1000	0.88	18.8
14	9000	10,000	1000	0.88	13.0
15	10,000	11,000	1000	0.88	8.9
16	11,000	12,000	1000	0.88	6.2
17	12,000	14,000	2000	0.88	4.2
18	14,000	16,000	2000	0.88	1.6
19	16,000	18,000	2000	0.88	0.6
20	18,000	20,000	2000	0.88	0.2

As shown in the tables, the C-14 recharge concentration decreases quickly due to its zero K_d (high mobility). Technetium-99 also has relatively fast source depletion, but the release duration is longer than for C-14 due to the higher Tc-99 K_d of 0.36 cm^3/g. Iodine-129 source depletion is much slower and extends over a much longer release period.

F.4.1.4 Base Case Model Simulation Results

The transport model run output included the full model domain results at selected time steps as well as complete time series (concentration values for every internal model time step) for all model layers at two key output locations. One output location is the 100-m well location and the other location is a point at the EOW immediately downgradient from the southwest corner of disposal cell 1 (Fig. F.13). The EOW location represents an intermediate point along the release pathway between the waste area where the variable recharge concentrations are applied and the groundwater 100-m well. For presenting the full radionuclide transport model results, the model units (radionuclide mass concentrations) have been converted to activity concentrations using the specific activities listed in Table F.2.

After the model runs were completed, the vadose zone delay times were added to the modeled time to show results in term of years after EMDF closure. The simulated shallow (model layer 2) Tc-99 groundwater plumes for three post-closure times are shown on Fig. F.14. Release to the saturated zone begins at 850 years, and Tc-99 concentrations exceeding 100 pCi/L occur at the 100-m well by 1300 years. The maximum modeled concentration under the waste area occurs around 1800 years after cell closure.

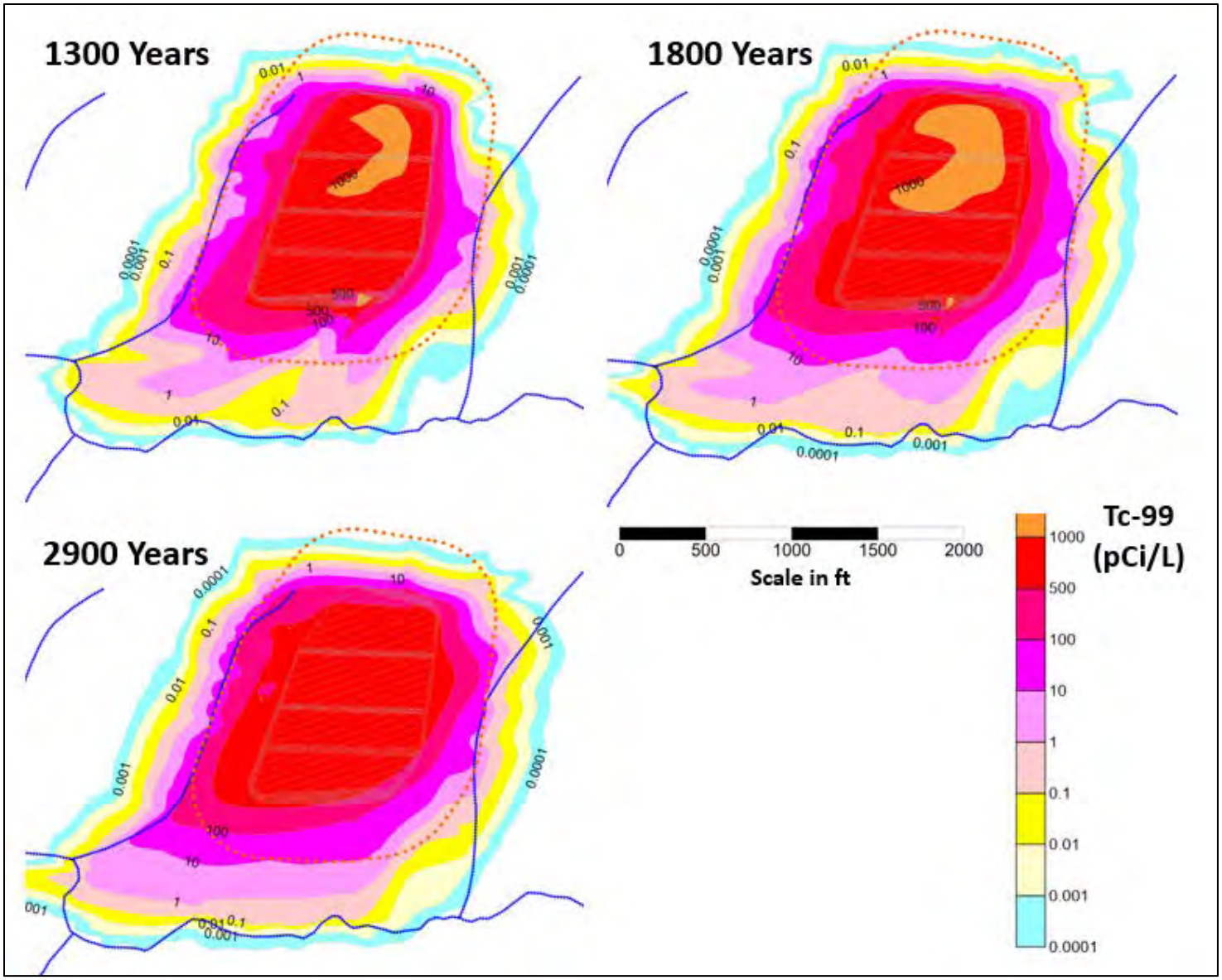

Fig. F.13. Modeled Tc-99 plume evolution (model layer 2) for uniform release

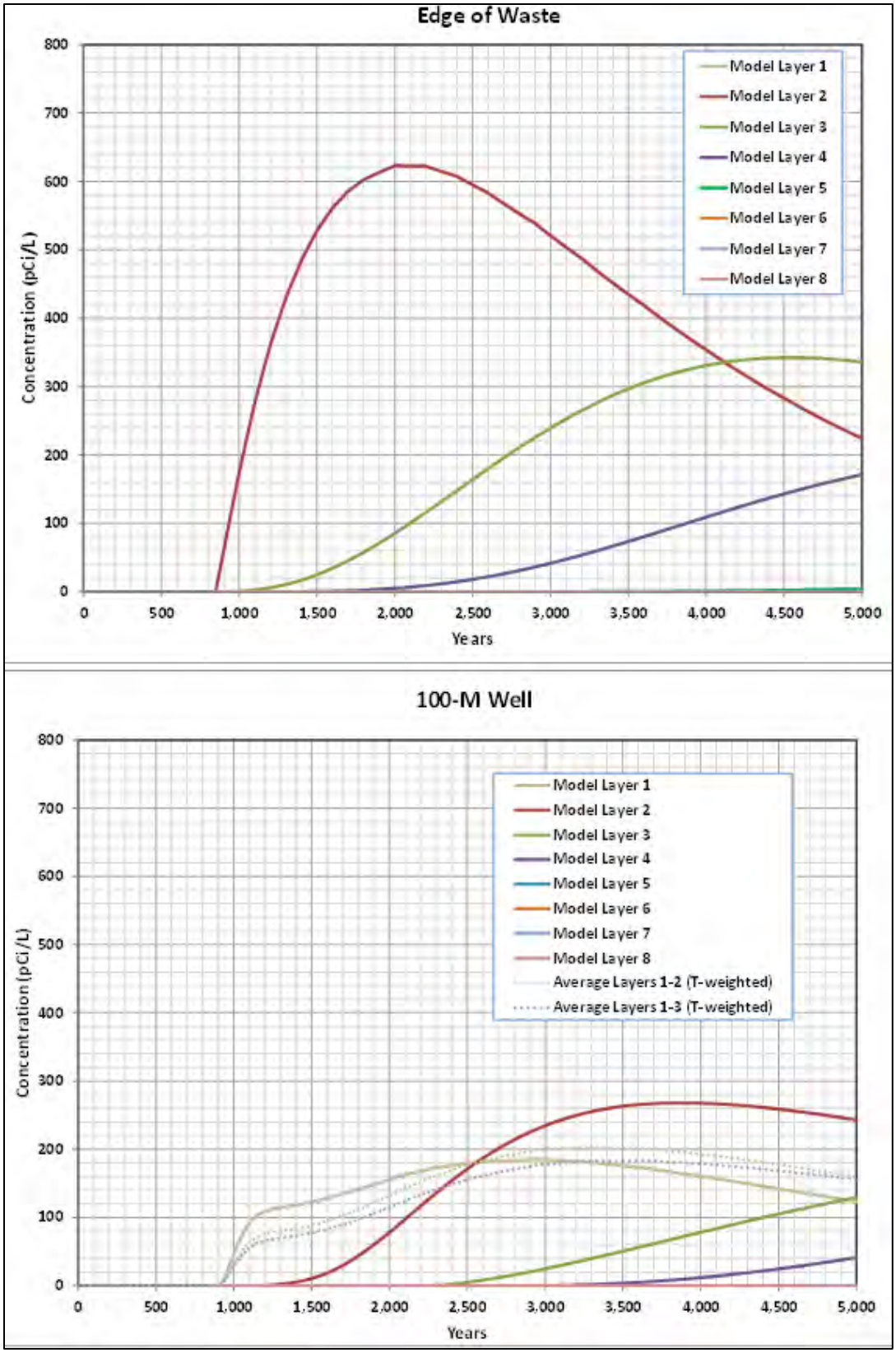

Fig. F.14. Tc-99 concentrations in groundwater at edge of waste and 100-m well locations

The modeled concentrations for each model layer at the EOW and 100-m well locations reflect the relatively complex spatial and temporal evolution of the plume (Fig. F.14). Model layer 2 at the EOW (Fig. F.14 upper plot) has the highest peak concentration due to proximity to the upgradient source area. At the EOW location, most of the contamination is restricted to the shallow groundwater zone (model layers 2, 3, and 4). The peak time for the model layer 2 at the EOW is 2100 years, where peak concentrations for model layers 3 and 4 occur after 4000 years. Peak concentrations at the 100-m well are lower than peaks at the EOW, and occur much later for model layer 2 (peak at 3750 years), layer 3 (> 5000 years), and layer 4 (> 5000 years) compared to the EOW location (Fig. F.14 lower plot). Model layer 1 concentrations at the 100-m well increase quickly between 850 and 1200 years and then more gradually to a peak around 2700 years, whereas model layer 2 concentrations increase significantly at the 100-m well only after 1500 years. Transmissivity-weighted average concentrations at the 100-m well for model layers 1 plus 2 and layers 1 plus 2 plus 3 are calculated to provide a vertically integrated estimate of well concentrations over potential well screen intervals (Fig. F.14 lower plot). The transmissivity-weighted concentrations peak around 2750 years at approximately 200 pCi/L.

MT3D transport model results for C-14 and I-129 show similar variations in concentration and peak timing between output locations and among model layers to the Tc-99 results, but the range of concentrations and timing reflect the difference in assumed K_d values (Table F.2). The model-predicted C-14 concentrations at the EOW and 100-m well location reflect rapid release (delay time is 530 years) and transport due to the zero K_d of C-14 applied in the release model and saturated zone media (Fig. F.15). The highest C-14 concentration for model layer 2 at the 100-m well is just over 600 pCi/L between 1100 and 1200 years post-closure, and the peak transmissivity-weighted concentrations are approximately 450 pCi/L at nearly the same time as the layer 2 peak (Fig. F.15 lower plot). Deeper model layers 4 and 5 reach C-14 concentrations that are closer to shallow layer concentrations than for either Tc-99 or I-129, due to the higher mobility of C-14. Similarly, the difference in the timing of peak concentrations between output locations and among model layers is much less for C-14 (Fig. F.15) than for Tc-99 (Fig. F.14) or I-129 (Fig. F.16), which have non-zero K_d values.

The MT3D predicted I-129 concentrations at the EOW and 100-m well locations are lower than Tc-99 and C-14 as a result of the smaller initial source inventory (Table F.3) and higher K_d (Table F.2) for I-129 (Fig. F.16). The initial release (delay time 1750 years) and peak concentrations occur much later than for C-14 and Tc-99, due to the higher assumed K_d value for I-129. The I-129 concentrations in model layer 1 at the 100-m well increase rapidly between 2000 and 3000 years to about 6 pCi/L, and increase gradually to 8 pCi/L by approximately 10,000 years. Model layer 2 I-129 concentrations begin increasing just after 4000 years and reach a peak of 12 pCi/L at approximately 16,000 years post-closure.

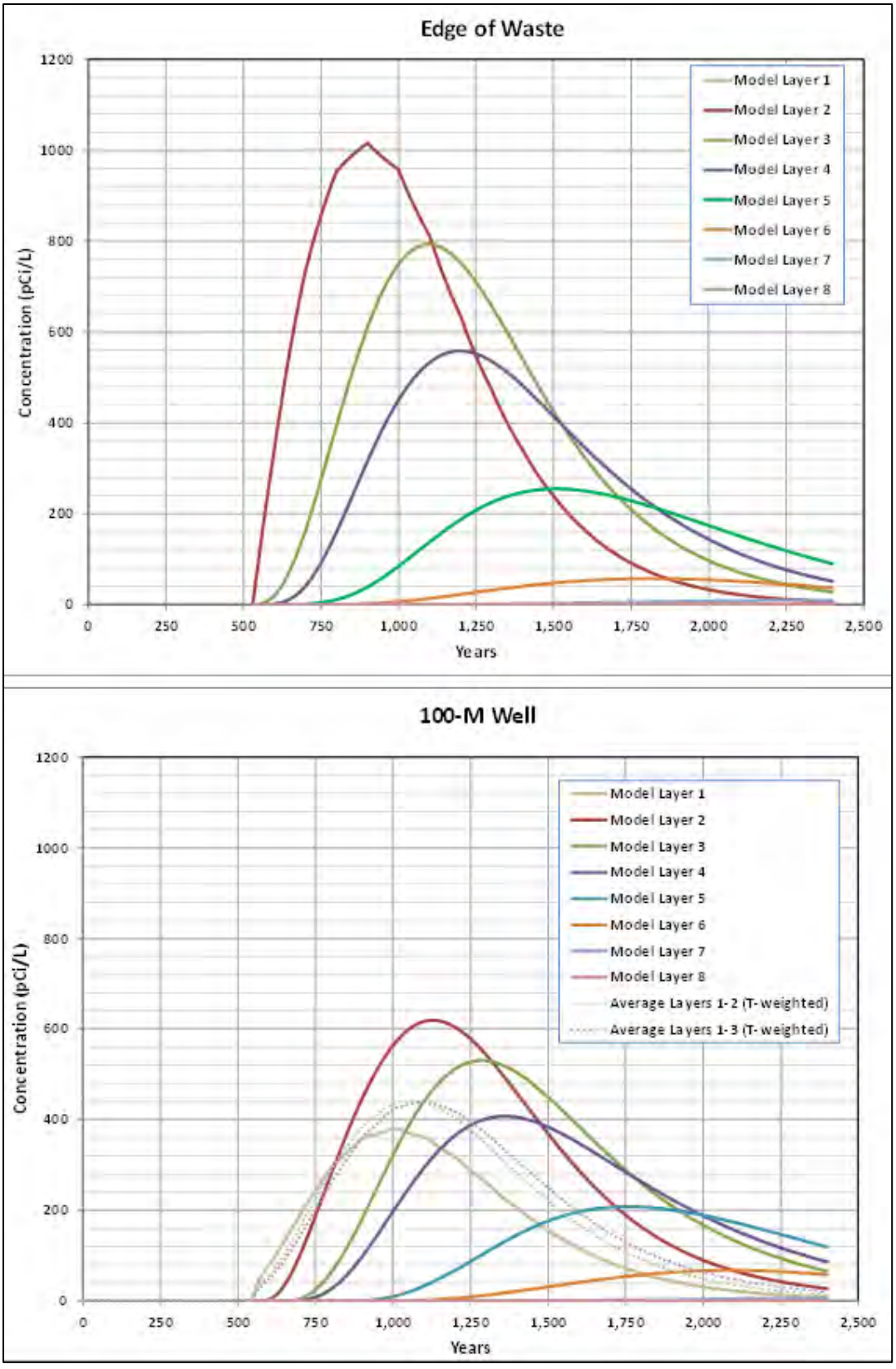

Fig. F.15. C-14 concentrations in groundwater at edge of waste and 100-m well locations

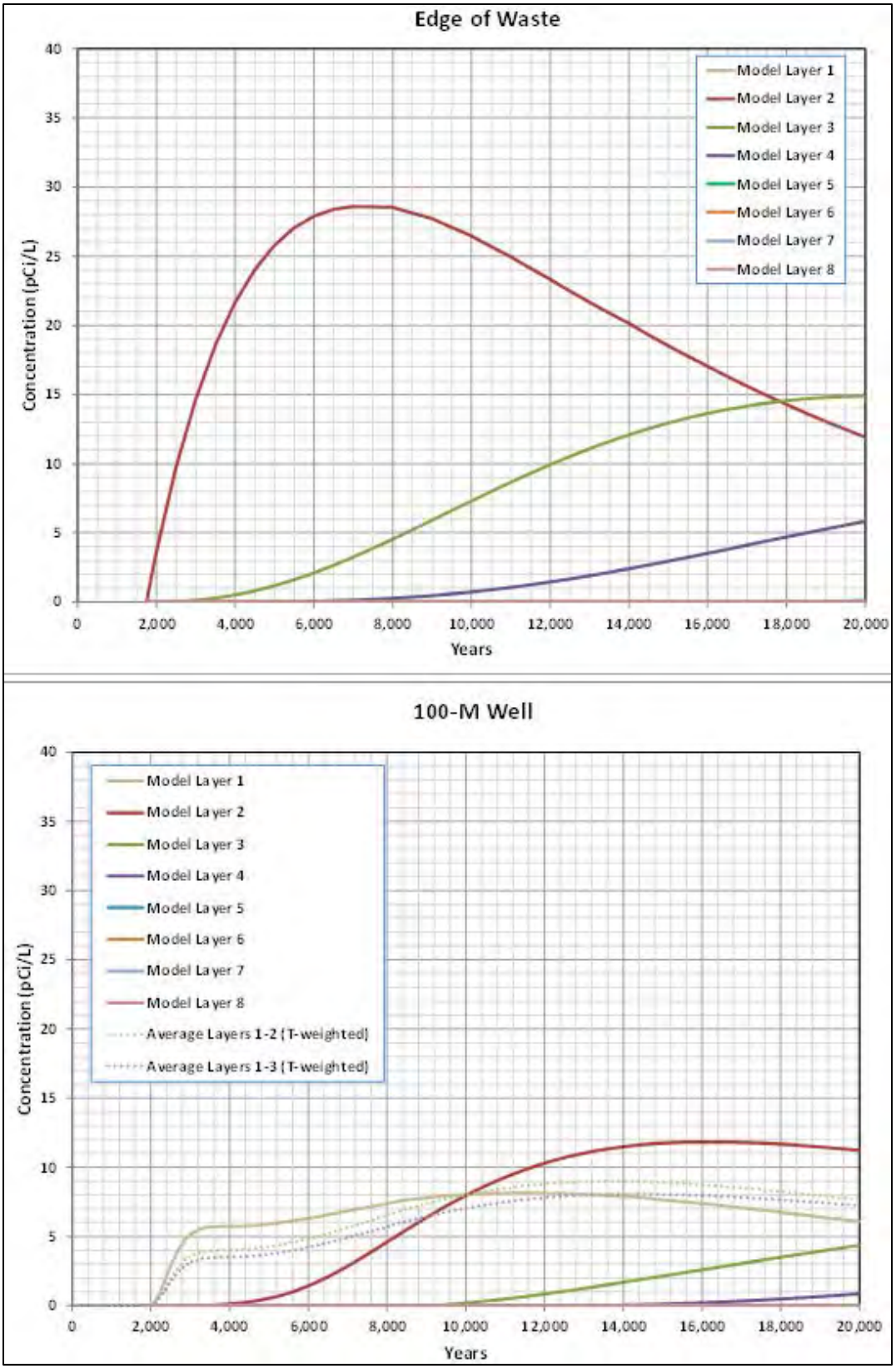

Fig. F.16. I-129 concentrations in groundwater at edge of waste and 100-m well locations

F.4.2 NON-UNIFORM RELEASE SCENARIO

The base condition saturated zone transport model assumes that the leachate flux from the waste area is uniform, implying that the waste volume has both a uniform radionuclide concentration and uniform thickness. The STOMP model simulation for EMDF (see Appendix E) demonstrates that there can be spatially variable (non-uniform) release rates within the cell footprint due to variation in waste thickness and liner system control of leachate drainage patterns. Variable leachate release rates will result in different radionuclide mass flux rates into the saturated zone that could have an impact on radionuclide concentrations at the groundwater POA. To evaluate this possibility, a non-uniform release scenario for the flow and transport model was developed using STOMP model results to estimate the variation in leachate flux and radionuclide concentration within the waste area. This sensitivity analysis was performed for Tc-99 transport only since it has a relatively small non-zero K_d value and the initial arrival time at the 100-m well for the base condition falls within the 1000-year post-closure compliance period for the PA.

F.4.2.1 Variable Leachate and Radionuclide Flux Distribution from STOMP Model

The non-uniform pattern of leachate flux beneath the EMDF predicted by the STOMP model was used to develop a non-uniform Tc-99 release model for MT3D based on the radionuclide release model developed for the uniform release scenario (Sect. F.4.1.3). The Section A, 2-dimensional STOMP model domain parallels the maximum slope of the disposal cell floors (refer to Appendix E, Sect. E.2.1). The Section A STOMP results were used to calculate the cumulative total volumetric leachate flux and cumulative total Tc-99 activity flux at the water table elevation directly below the upper-half (upslope portion with lower flux) and the lower-half (downslope portion with higher flux) of each disposal cell. The lower-half to upper-half ratios of leachate flux and Tc-99 flux represent a time-integrated measure of the non-uniformity of release from each disposal cell, derived from the STOMP Section A model results. The calculated lower-to-upper half ratios for leachate and Tc-99 flux for each disposal cell are given in Table F.10. An average Tc-99 concentration ratio (R_c) is obtained by dividing the Tc-99 flux ratio by the leachate flux ratio for each cell.

The calculated leachate flux ratios were used to assign water recharge rates to each of eight cell floor sub-areas (upper and lower halves of the floor of each cell, Fig. F.17), accounting for the funneling effect of the outer sideslopes of each disposal cell and the pattern of water flux driven by the sloping cell floors. The calculated recharge rates also account for the difference in planar area among the four disposal cells in determining the amount of water infiltrating to each cell. Applying the calculated recharge rates (Table F.10) to the corresponding sub-areas and summing the individual contributions results in a total water flux rate equivalent to the 0.88 in./year rate applied uniformly to the entire waste area.

F.4.2.2 Groundwater Flow Field with Variable Recharge Rates

The individual water recharge (leachate flux) rates were applied in the MODFLOW model code to generate the flow field for the non-uniform Tc-99 release scenario MT3D transport model. Figure F.18 shows the resulting non-uniform release scenario groundwater table elevations and comparison to the uniform base case scenario. The groundwater levels are very similar to the uniform release scenario, suggesting the difference in recharge rates under the cell floor will not cause significant groundwater flow field changes in the cell area. The resulting flow field, along with estimated non-uniform Tc-99 recharge concentrations, was then used to conduct the non-uniform Tc-99 release scenario transport simulation.

Table F.10. EMDF design-based and STOMP model-based quantities and calculated ratios for the non-uniform release scenario

Quantity	Cell-1	Cell-2	Cell-3	Cell-4
STOMP-based Tc-99 vadose delay time (years)	830	900	885	810
Waste volume (%)	19.4	29.7	25.7	25.2
Planar area (%)	24.4	27.1	21.5	27.0
Ratio of cell floor area to total cell area (%)	0.90	0.98	0.97	0.75
Recharge rate multiplier (funnel effect)	1.11	1.02	1.03	1.33
STOMP-based leachate flux (water recharge) lower/upper ratio	5.60	5.82	5.34	5.10
Leachate flux (water recharge) lower cell half (in./year)	1.66	1.54	1.53	1.96
Leachate flux (water recharge) upper cell half (in./year)	0.3	0.26	0.29	0.38
STOMP-based Tc-99 mass flux ratio	13.59	5.77	4.71	3.75
Tc-99 concentration ratio (R_c = Tc-99 ratio / water recharge ratio)	2.43	0.99	0.88	0.73

EMDF = Environmental Management Disposal Facility
STOMP = Subsurface Transport Over Multiple Phases

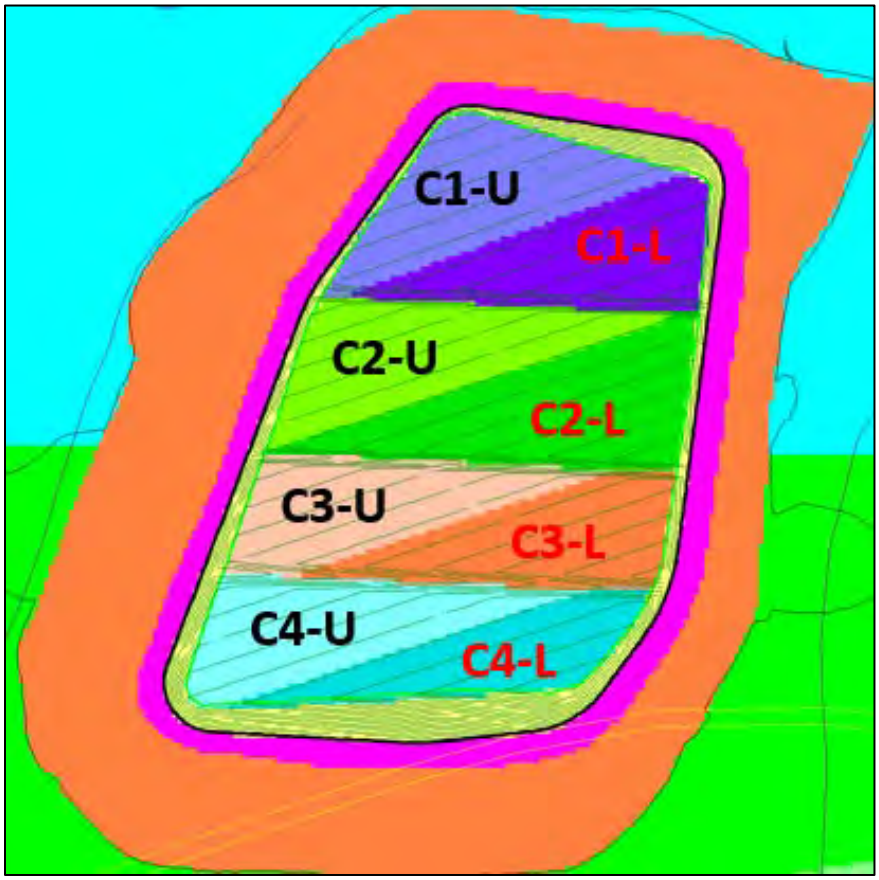

Fig. F.17. Upper and lower disposal cell areas for applying variable recharge rates and recharge concentrations (non-uniform release scenario)

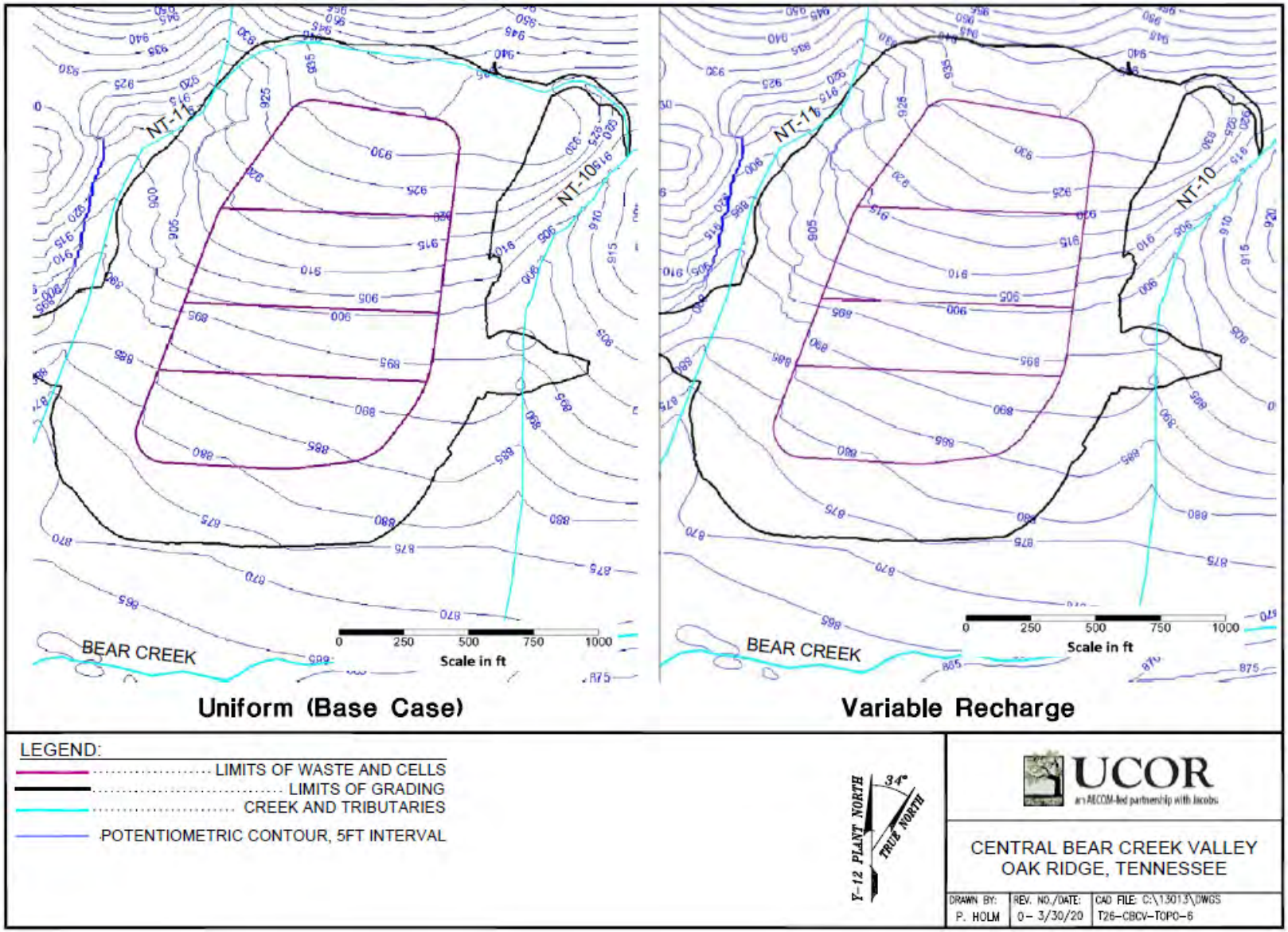

Fig. F.18. EMDF model predicted water table elevations – uniform vs variable recharge rates

F.4.2.3 Non-uniform Tc-99 Release Model

The waste volume for each of the four individual cells is slightly different (20 to 30 percent of EMDF total; see Table F.10) due to the cover and liner system configuration. The Tc-99 mass in each disposal cell was calculated based on the waste volume and EMDF average initial Tc-99 concentration. Applying these initial Tc-99 masses, and utilizing STOMP model results to estimate Tc-99 vadose delay times for each disposal cell (Appendix E, Table E.8), a Tc-99 release model for each cell was created with the approach described in Sect. F.4.1.3 and using the vadose delay times to define the first four release model time steps. The Tc-99 recharge concentrations for each disposal cell were then partitioned into concentrations applied to the upper and lower half of each disposal cell on the basis of the leachate flux ratios and Tc-99 flux ratios for each cell (Table F.10). The partition is calculated by multiplying the recharge concentration for each disposal cell by the factor $2/(1+R_c)$ for the upper cell half and by $2R_c/(1+R_c)$ for the lower cell half, where R_c is the Tc-99 flux ratio divided by the leachate flux ratio for the corresponding disposal cell. The resulting non-uniform Tc-99 release model accounts for variation in waste volume, water infiltration, and liner geometry among the four disposal cells. Recharge concentrations for each disposal cell sub-area and model stress period used to simulate the non-uniform Tc-99 release scenario are provided in Table F.11.

Table F.11. Variable recharge concentrations with time for the EMDF cell portions

Stress period	Starting year	Tc-99 recharge concentration (pCi/L)							
		Cell-1-U	Cell-1-L	Cell-2-U	Cell-2-L	Cell-3-U	Cell-3-L	Cell-4-U	Cell-4-L
1	810	0	0	0	0	0	0	3.56E+03	2.61E+03
2	830	1.59E+03	3.86E+03	0	0	0	0	3.69E+03	2.71E+03
3	885	1.55E+03	3.76E+03	0	0	2.83E+03	2.50E+03	3.65E+03	2.68E+03
4	900	1.64E+03	3.99E+03	2.87E+03	2.85E+03	3.02E+03	2.67E+03	3.88E+03	2.85E+03
5	1000	1.49E+03	3.61E+03	2.73E+03	2.70E+03	2.90E+03	2.55E+03	3.60E+03	2.64E+03
6	1100	1.24E+03	3.02E+03	2.41E+03	2.39E+03	2.58E+03	2.28E+03	3.10E+03	2.28E+03
7	1200	1.04E+03	2.53E+03	2.12E+03	2.10E+03	2.30E+03	2.03E+03	2.67E+03	1.96E+03
8	1300	8.74E+02	2.12E+03	1.87E+03	1.86E+03	2.05E+03	1.81E+03	2.30E+03	1.69E+03
9	1400	7.32E+02	1.78E+03	1.65E+03	1.64E+03	1.83E+03	1.62E+03	1.98E+03	1.46E+03
10	1500	6.13E+02	1.49E+03	1.46E+03	1.45E+03	1.63E+03	1.44E+03	1.71E+03	1.26E+03
11	1600	5.14E+02	1.25E+03	1.29E+03	1.28E+03	1.46E+03	1.29E+03	1.47E+03	1.08E+03
12	1800	3.47E+02	8.42E+02	9.84E+02	9.75E+02	1.14E+03	1.01E+03	1.07E+03	7.82E+02
13	2000	2.34E+02	5.69E+02	7.52E+02	7.46E+02	8.95E+02	7.89E+02	7.70E+02	5.66E+02
14	2200	1.58E+02	3.84E+02	5.75E+02	5.70E+02	7.01E+02	6.19E+02	5.57E+02	4.09E+02
15	2400	1.07E+02	2.59E+02	4.40E+02	4.36E+02	5.50E+02	4.85E+02	4.03E+02	2.96E+02
16	2700	5.48E+01	1.33E+02	2.85E+02	2.82E+02	3.71E+02	3.27E+02	2.36E+02	1.73E+02
17	3000	2.81E+01	6.83E+01	1.84E+02	1.83E+02	2.51E+02	2.21E+02	1.38E+02	1.01E+02
18	3400	9.87E+00	2.40E+01	9.74E+01	9.66E+01	1.42E+02	1.26E+02	6.15E+01	4.52E+01
19	3800	3.46E+00	8.41E+00	5.16E+01	5.11E+01	8.07E+01	7.12E+01	2.75E+01	2.02E+01
20	4300	6.53E-01	1.59E+00	2.12E+01	2.10E+01	3.71E+01	3.27E+01	8.46E+00	6.21E+00

EMDF = Environmental Management Disposal Facility

F.4.2.4 Non-uniform Release Scenario Results

The model layer 2 Tc-99 concentrations for the non-uniform release scenario at three post-closure times are shown on Fig. F.19. Compared to uniform release scenario (Fig. F.13), the concentration field within the waste area for the non-uniform release has zones of higher Tc-99 concentration > 500 pCi/L develop beneath the lower portion of each disposal cell, reflecting the pattern of recharge concentration applied in the model. This pattern is evident at 1300 and 1800 years post-closure, but by 2900 years the recharge concentrations are diminishing (Table F.11) and the saturated zone concentrations beneath the waste are more uniform. However, the model layer 2 concentrations in the vicinity of the POA are very similar to the pattern for the uniform release scenario (compare Figs. F.13 and F.19), demonstrating that the greatest impact of the non-uniform release is directly below the waste.

The Tc-99 concentration time series for all model layers at the EOW location for both uniform and non-uniform release scenarios are plotted in Fig. F.20. The corresponding concentration curves at the 100-m well location are plotted in Fig. F.21. Compared with base case scenario, the peak Tc-99 concentrations are mostly lower and occur later for the non-uniform release scenario. This difference is caused by the focused release to the lower parts of the cells that are further away from the output locations.

For the non-uniform release scenario at the EOW location, the peak Tc-99 concentration in model layer 2 is slightly lower in the non-uniform release scenario, but the peak concentrations in model layers 3 and 4 are slightly higher in the non-uniform scenario (Fig. F.20). At the 100-m well location, the model layer 1 and 2 peak Tc-99 concentrations are nearly the same for the uniform and non-uniform release scenarios, but the initial increase in layer 1 concentrations is much more gradual in the non-uniform release scenario (Fig. F.21). This difference in layer 1 concentrations directly reflects the non-uniform release to model layer 2 within the upgradient the waste area, where model layer 1 remains unsaturated (i.e., recharge concentrations are applied to model layer 2). The peak transmissivity-weighted average Tc-99 concentrations (Fig. F.21) occur slightly later for the non-uniform release, but are essentially the same (190 to 200 pCi/L) as the peak concentrations for the uniform release scenario.

This model sensitivity evaluation of uniformity of leachate release suggests that the base case uniform release scenario, although incorporating simplified release assumptions, does not underestimate peak concentrations relative to a more complex conceptualization and model implementation of non-uniform release. Using a more complex source representation could provide more information on variability in saturated zone concentrations in space and time, but will also introduce more uncertainty to the dose analysis associated with uncertainty in waste inventory and recharge distributions. Assuming non-uniform release would also increase the uncertainty in the selection of a groundwater POA location that will capture peak saturated zone impacts under differing sets of model input assumptions.

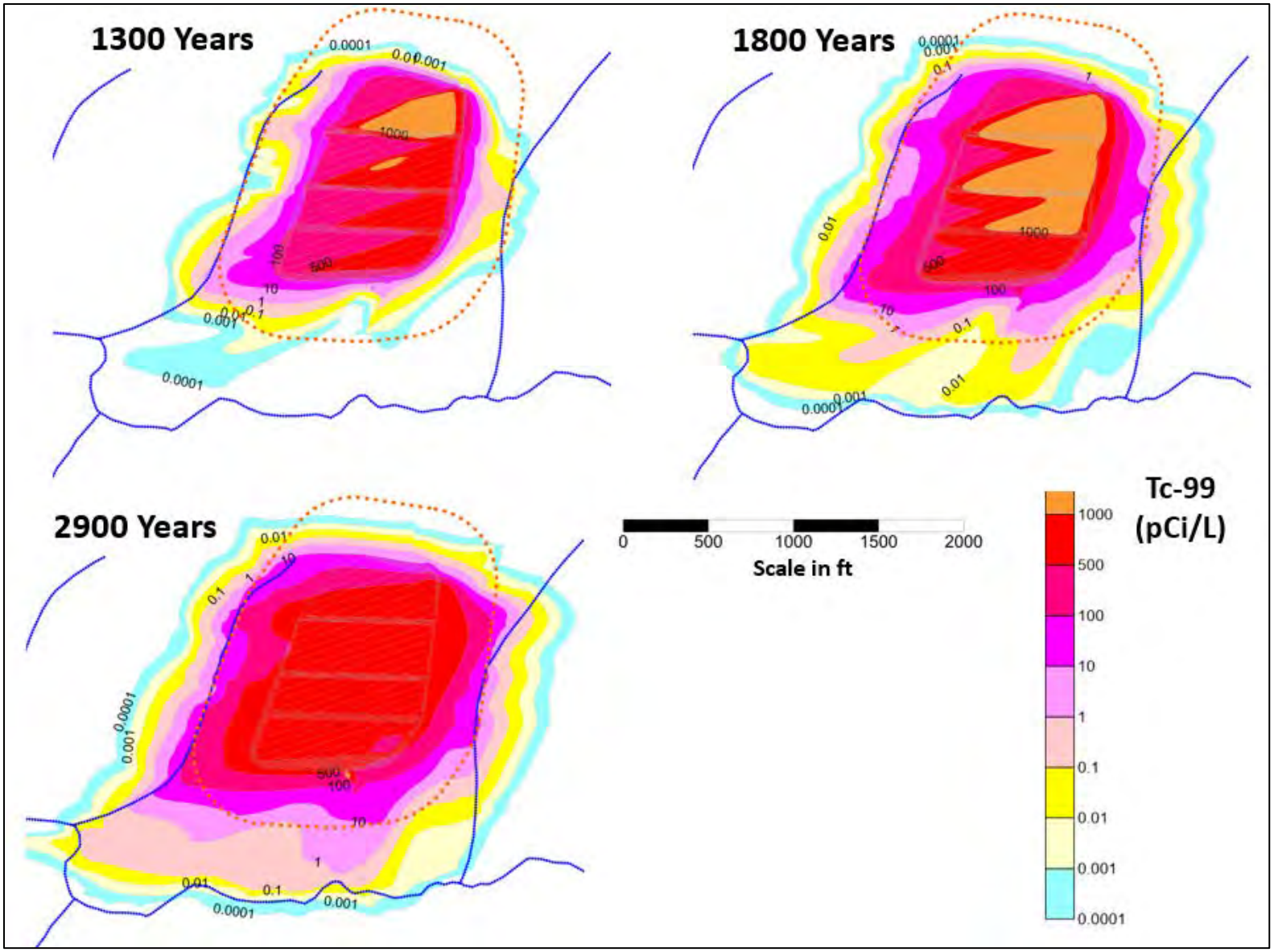

Fig. F.19. Modeled Tc-99 plume evolution for non-uniform release

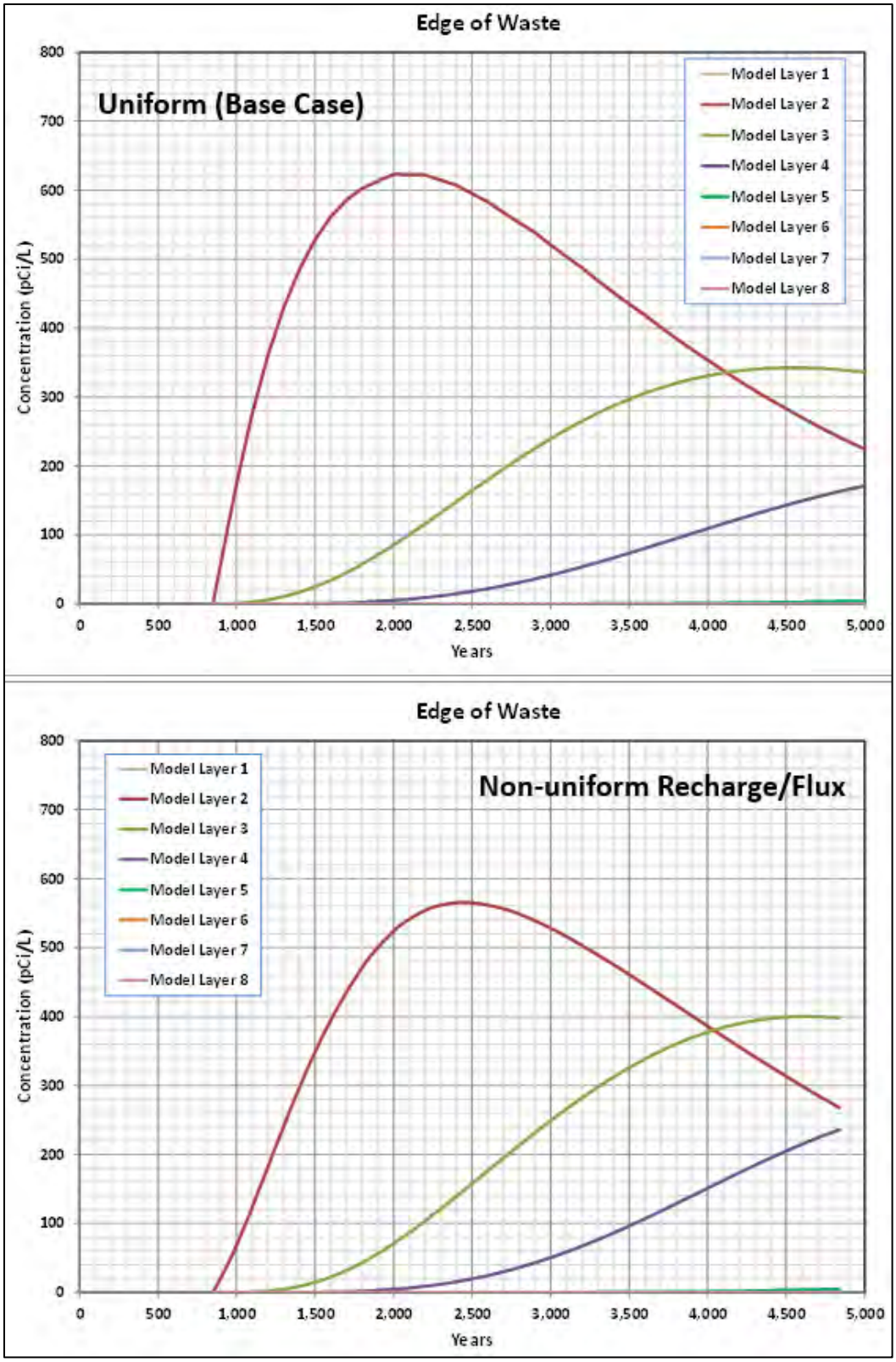

Fig. F.20. Predicted Tc-99 groundwater concentrations at the edge of waste location for the non-uniform release scenario

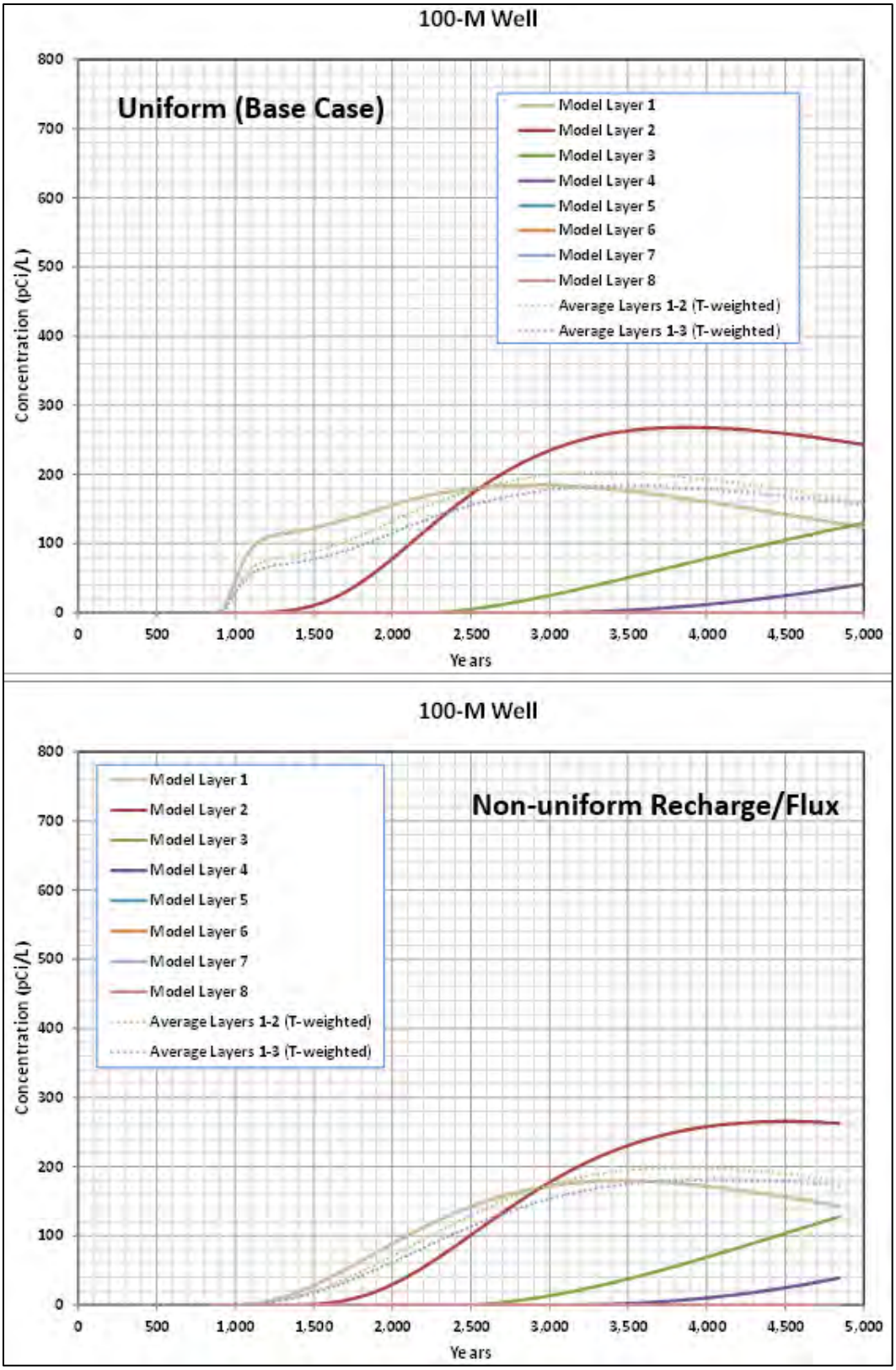

Fig. F.21. Predicted Tc-99 groundwater concentrations at the 100 m well for the non-uniform release scenario

F.4.3 SENSITIVITY TO HYDRAULIC CONDUCTIVITY OF THE SHALLOW AQUIFER

To evaluate the impact of shallow aquifer K uncertainty and possible variation from the base case flow model assumptions, a sensitivity analysis was performed by applying higher K values in model layer 2. The relative thickness (70 ft vs 20 to 30 ft for model layer 1) and higher predicted radionuclide concentrations in model layer 2 increase the potential impact of uncertainty in assigning layer 2 properties. After the flow simulation was conducted with the higher K, impact on Tc-99 transport simulation with MT3D was evaluated.

F.4.3.1 Flow Simulation with Higher Hydraulic Conductivity

Model layer 2 which represents most of the shallow groundwater flow system was assigned same K values along the valley direction (K_y) as model layer 1, which has higher values representing the saprolite zone. The K_y values in model layer 1 are about 10 times higher than the K_y values of model layer 2 for the base case flow model. To maintain the original anisotropy ratios in model layer 2 (10/1 ratios), the K_x and K_z values for layer 2 were also changed to layer 1 values for all the natural hydrogeologic units. These changes make model layer 2 more permeable to the groundwater.

The flow model simulation was run using the higher K field for model layer 2 and the uniform leachate release rate (0.88 in./year) applied to the waste area. The resulting groundwater table is shown in Fig. F.22. As expected, the groundwater elevations under the waste area and surrounding areas are much lower than for the base condition. The resulting flow field, along with same base case uniform Tc-99 recharge concentration, was used to conduct the transport model simulation.

F.4.3.2 Impact on Tc-99 Transport

The Tc-99 transport model simulation was run with the EMDF model flow field using higher model layer 2 K values and the uniform release Tc-99 recharge concentrations applied to the waste area. The Tc-99 concentration time series for all model layers at the EOW location for both the base case and the high layer 2 K scenario are plotted in Fig. F.23. The corresponding concentration curves at the 100-m well location are plotted in Fig. F.24. Compared with base case scenario, the peak Tc-99 concentrations are either higher or lower and occur earlier for the layer 2, high K sensitivity run. This difference is associated with the lower water table elevation and more rapid flow due to higher conductivity in model layer 2 beneath the waste and along the transport path to the 100-m well.

For the high K sensitivity run at the EOW location, the peak Tc-99 concentration in model layer 2 is lower, and the peak concentrations in model layers 3 and 4 are much lower (Fig. F.23). This difference from the base case result reflects more effective horizontal transport of Tc-99 through model layer 2 toward the 100-m well. Most of the Tc-99 movement occurs within model layer 2 due to its higher K, resulting in a very low concentration in the deeper model layers. At the 100-m well location, the difference between the base case result and the high K sensitivity run is more pronounced (Fig. F.24) The model layer 1 and 2 peak Tc-99 concentrations are significantly higher and much earlier for the high K sensitivity run, peaking around 1750 years post-closure (vs peak concentrations occurring after 2500 years for the base case). The peak transmissivity-weighted average Tc-99 concentrations are approximately 50 percent higher than the base case peaks (300 pCi/L vs 200 pCi/L for the base case). The peak model layer 2 Tc-99 concentration is over 70 percent higher than for the base case.

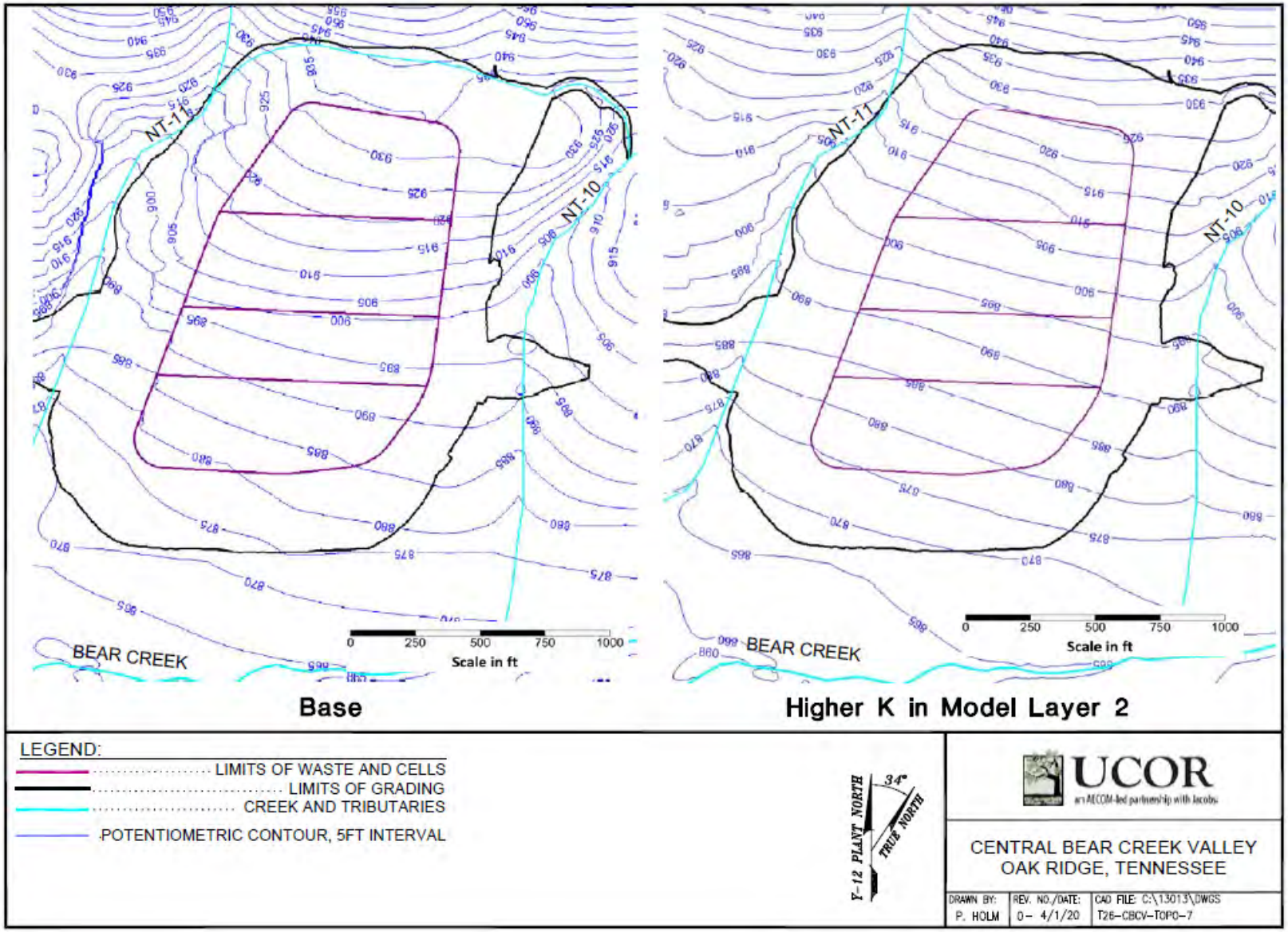

Fig. F.22. Groundwater levels for the base case K value (left) and for higher K in model layer 2 (right)

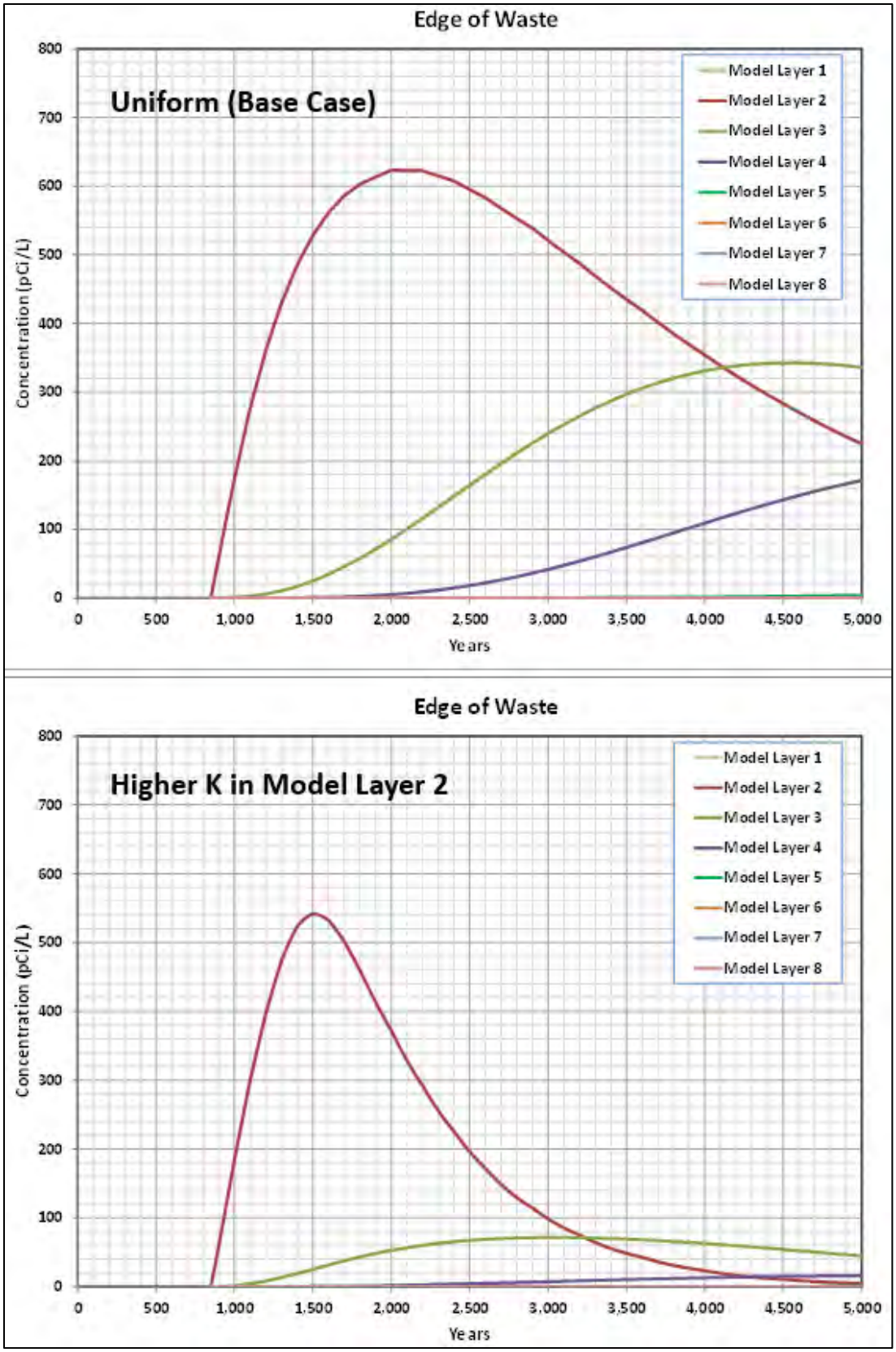

Fig. F.23. Predicted Tc-99 groundwater concentrations at the edge of waste for high K in layer 2

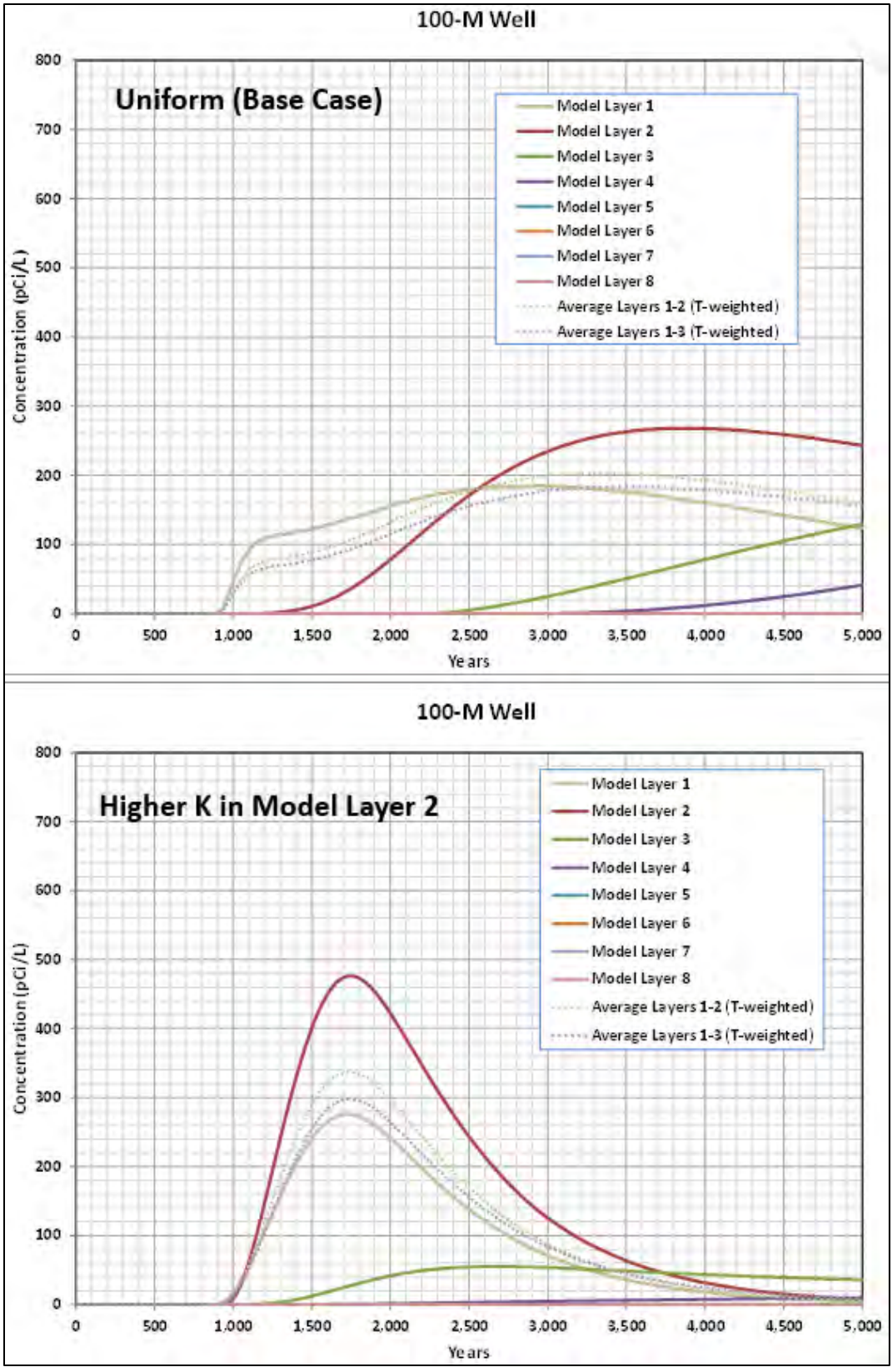

Fig. F.24. Predicted Tc-99 groundwater concentrations at the 100-m well for high K in layer 2

Although the simulated Tc-99 concentrations at the 100-m well are very sensitive to the nearly 10-fold increase in the K of model layer 2, applying the higher K values representative of the saprolite zone to the deeper parts of the model domain is not an accurate representation of EMDF site conditions. The sensitivity run results suggests that uncertainty in hydrogeologic characteristics of the shallow subsurface materials in the vicinity of the disposal unit may be important for evaluating uncertainty in peak concentrations at the 100-m well, but the uncertainty in field conditions is not as large as the applied increase in layer 2 conductivity. Due to the potential sensitivity of results to saturated zone K, the probabilistic uncertainty analysis for the PA total disposal system model (RESRAD-OFFSITE) includes a range of possible K values based on the available field data.

F.4.4 DUAL-POROSITY OPTION CONSIDERATION

The MT3D code is capable of simulating dual-domain transport. Dual-domain transport also is referred to as dual-porosity or two-region transport. The normal transport governing equations use a single porosity referred to as effective porosity, which is generally smaller than the total porosity of the porous medium, reflecting the fact that some pore spaces may contain immobile water with zero groundwater velocity. However, the effective porosity cannot be readily measured in the field due to the complexity of the pore structure, but generally must be interpreted as the lumped parameter which, in model calibration, gives the closest representation both of plume movement and observed solute accumulation effects. In some cases, such as transport in fractured media or extremely heterogeneous porous media, it may be more appropriate to use a dual-porosity approach, i.e., to define a primary porosity for those pore spaces filled with mobile water (where advection is the predominant means of contaminant transport), and a secondary porosity for pore spaces filled with immobile water (where contaminant transport is primarily by molecular diffusion). The exchange between the mobile and immobile domains can be defined through a kinetic mass transfer equation similar to that used to describe non-equilibrium sorption.

EMDF sits above a fractured bedrock system and the groundwater system could be conceptualized as a dual-domain system for transport model simulation. However, since the objective of the analysis is to evaluate the possible maximum impact to groundwater near the disposal cell, using the MT3D dual-porosity module would lessen the impact since some of the contaminant mass would be partitioned into the immobile portion of the porosity (the difference between total porosity and effective porosity). Therefore, the dual-porosity option model run was not performed. Using the single lower porosity (effective porosity) approach is conservative for the near field because it will produce relative large groundwater concentrations and, thus, higher impacts to groundwater or surface water receptors.

F.4.5 TRANSPORT MODEL DISCUSSION AND APPLICATION

The various radionuclide transport simulations using the EMDF three-dimensional saturated-zone flow and transport model were used to provide key information on the following:

1) Delimit the maximum extent of the contaminant plume
2) Determine the location of maximum concentration along the 100-m buffer zone boundary (groundwater POA, or 100-m well location)
3) Quantify the pattern of radionuclide discharge to streams and identify the surface water POA
4) Predict the peak concentrations and timing of peak for selected radionuclides (C-14, Tc-99, and I-129) at the 100-m groundwater well location
5) Evaluate the potential impact of non-uniform radionuclide release from the EMDF.

These model results are directly applied in implementing the total system PA model (RESRAD-OFFSITE) (e.g., in determining the site layout used to represent the geometry of transport pathways) and also are used in a model integration context to evaluate the model output from the less detailed representations of the saturated zone in RESRAD-OFFSITE.

F.5 REFERENCES

DOE 1997a. *Report on the Remedial Investigation of Bear Creek Valley at the Oak Ridge Y-12 Plant, Oak Ridge, Tennessee,* DOE/OR/01-1455/V1-V6&D2, U.S. Department of Energy, Oak Ridge, TN, May.

DOE 1997b. *Feasibility Study for Bear Creek at the Oak Ridge Y-12 Plant, Oak Ridge, Tennessee,* DOE/OR/02-1525/V2&D2, U.S. Department of Energy, Oak Ridge, TN, November.

DOE 1998a. *Remedial Investigation/Feasibility Study for the Disposal of Oak Ridge Reservation Comprehensive Environmental Response, Compensation, and Liability Act of 1980 Waste*, DOE/OR/02-1637&D2, U.S. Department of Energy, Oak Ridge, TN, January.

DOE 1998b. *Addendum to Remedial Investigation/Feasibility Study for the Disposal of Oak Ridge Reservation Comprehensive Environmental Response, Compensation, and Liability Act of 1980 Waste*, DOE/OR/02-1637&D2/A1, U.S. Department of Energy, Oak Ridge, TN, September.

DOE 2011. *Derived Concentration Technical Standard*, STD-1196-2011, U.S. Department of Energy, Washington, D.C., April.

Environmental Solutions, Inc. 2017. Groundwater Vistas. Version 7.20, Environmental Solutions, Inc., Leesport, PA.

Gelhar et al. 1985. *A Review of Field Scale Physical Solute Transport Processes in Saturated and Unsaturated Porous Media*, L. W. Gelhar, A. Montoglou, C. Welty, and K. R. Rehfeldt, EPRI EA-4190, Electric Power Research Institute, Palo Alto, CA.

Gelhar et al. 1992. "A Critical Review of Data on Field-Scale Dispersion in Aquifer," L. W. Gelhar, C. Welty, and K. R. Rehfeldt, *Water Resources Research*, v. 28, no. 7, pages 1955–1974.

Harbaugh, A.W. 2005. *MODFLOW-2005, the U.S. Geological Survey Modular Ground-Water Model -- the Ground Water Flow Process*, Techniques and Methods 6-A16, U.S. Geological Survey, Reston, VA.

UCOR 2020. *Quality Assurance Report for Modeling of the Bear Creek Valley Low-level Radioactive Waste Disposal Facilities, Oak Ridge, Tennessee* UCOR-5234/R0, UCOR, Oak Ridge, TN, April.

USGS 1988. *A Modular Three-dimensional Finite-Difference Groundwater Flow Model*, Book 6, Modeling Techniques, Chapter A1, M. G. McDonald and A. W. Harbaugh, U.S. Geological Survey, Reston, VA.

Zheng 1990. *A Modular Three-Dimensional Transport Model for Simulation of Advection, Dispersion and Chemical Reactions of Contaminants in Groundwater Systems; Documentation and Users Guide*, report to the U.S. Environmental Protection Agency, C. Zheng, S.S. Papadopulos & Associates, Inc., Bethesda, MD.

Zheng, C. and G.D. Bennett 1995. *Applied Contaminant Transport Modeling: Theory and Practice***,** John Wiley & Sons, New York, page 440.

Zheng and Wang 1999. *MT3DMS: A Modular Three-dimensional Multispecies Model for Simulation of Advection, Dispersion and Chemical Reactions of Contaminants in Groundwater Systems; Documentation and User's Guide*, C. Zheng, P. P. Wang Contract Report SERDP-99-1, U.S. Army Engineer Research and Development Center, Vicksburg, MS.

APPENDIX G.
RESRAD-OFFSITE MODELING FOR THE ENVIRONMENTAL MANAGEMENT DISPOSAL FACILITY

This page intentionally left blank.

CONTENTS

FIGURES

TABLES

ACRONYMS

BCV	Bear Creek Valley
CBCV	Central Bear Creek Valley
CDF	cumulative distribution function
CERCLA	Comprehensive Environmental Response, Compensation and Liability Act of 1980
CFR	*Code of Federal Regulations*
CSM	conceptual site model
DCS	Derived Concentration Standard
DOE	U.S. Department of Energy
DOE M	DOE Manual
DOE O	DOE Order
EMDF	Environmental Management Disposal Facility
EMWMF	Environmental Management Waste Management Facility
EOW	edge of waste
EPA	Environmental Protection Agency
HDPE	high-density polyethylene
HELP	Hydrologic Evaluation of Landfill Performance
IHI	inadvertent human intrusion
LHS	Latin Hypercube Sampling
LLW	low-level (radioactive) waste
MCL	maximum contaminant level
NRC	U.S. Nuclear Regulatory Commission
NT	North Tributary
ORNL	Oak Ridge National Laboratory
ORR	Oak Ridge Reservation
PA	Performance Assessment
PNNL	Pacific Northwest National Laboratory
POA	point of assessment
QA	quality assurance
RCC	rank correlation coefficient
RESRAD	RESidual RADioactivity
SRC	standardized regression coefficient
SRRC	standardized rank regression coefficient
SRSG	single radionuclide soil guideline
STOMP	Subsurface Transport Over Multiple Phases
TDEC	Tennessee Department of Environment and Conservation

This page intentionally left blank.

G.1 INTRODUCTION

This appendix summarizes environmental dose modeling performed to support the Environmental Management Disposal Facility (EMDF) Performance Assessment (PA). The EMDF consists of a proposed 2.2 M cy disposal facility to be built for disposal of low-level (radioactive) waste (LLW), mixed waste, and certain classified waste (Fig. G.1). The EMDF is located in Bear Creek Valley (BCV) on the U.S. Department of Energy (DOE) Oak Ridge Reservation (ORR). This modeling was conducted to support the EMDF PA required by DOE Order (O) 435.1, *Radioactive Waste Management* (DOE 2001), and uses the guidance provided in the *Disposal Authorization Statement and Tank Closure Documentation* Technical Standard (DOE 2017).

The EMDF PA objective is to demonstrate a reasonable expectation that representative members of the public will not receive an annual total effective dose resulting from the disposal facility in excess of 25 mrem from all exposure pathways, excluding the dose from radon and its progeny in air. (EMDF performance with respect to radon release is evaluated in Appendix H.) The assessed exposure pathways at the site include the reasonable modes by which a receptor at the point of public access is hypothetically exposed, potentially including the air pathway, groundwater pathway, direct exposure, and consumption of contaminated food and drink.

EMDF PA modeling was conducted using the computational code RESidual RADioactivity (RESRAD)-OFFSITE Version 3.2 (Yu et al. 2007, Gnanapragasam and Yu 2015). Deterministic and probabilistic simulations were performed within RESRAD-OFFSITE to assess EMDF disposal facility performance and predict radiological dose to a hypothetical receptor. Comprehensive PA modeling consisted of the use of multiple models with RESRAD-OFFSITE model results derived from and compared to simulations from other computer codes.

The EMDF PA analysis contained the following base case hypothetical receptor exposure scenario assumptions:

- The EMDF is located in Central Bear Creek Valley (CBCV), with an average waste height of 17.5 m. Above the waste is a cover and beneath the waste is a composite liner system.
- Facility design parameters are based on the EMDF preliminary design.
- Hypothetical agricultural fields and an offsite dwelling are located just south (downslope) of EMDF.
- The groundwater well used to provide potable water is located 100 m downgradient of the edge of waste (EOW) along the assumed centerline of the predominant groundwater flow direction. This 100-m distance from the EOW represents the default buffer zone, which includes the area projected through the aquifer below and into the air above.
- The surface water body in the path of a hypothetical contaminant plume located downgradient of EMDF is Bear Creek, which is used for fishing and to supply water for crops and livestock.
- The entire volume of the waste is accessible to infiltrating water.

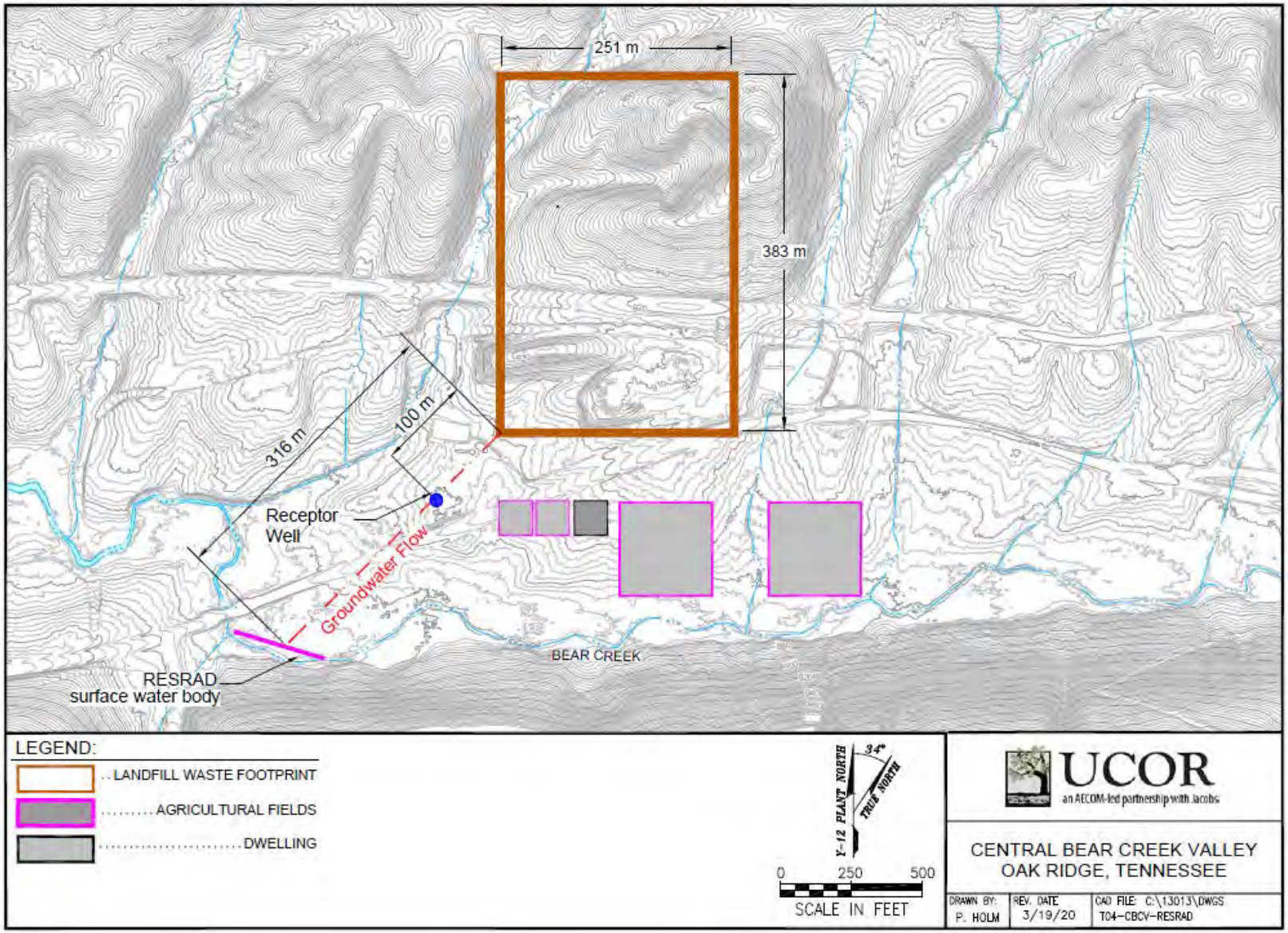

Fig. G.1. Site map showing approximate location of waste footprint, dwelling, and agricultural fields

Several RESRAD-OFFSITE model activities were performed as part of the PA modeling effort, including the following:

- Operational period inventory depletion simulations – Four simulations were performed to quantify activity loss from the waste due to leaching during the 25-year operational period for the four mobile radionuclides (C-14, H-3, I-129, and Tc-99). Model development and quantification of the operational period simulations are presented in Sect. G.4.3.4.
- Screening models for groundwater and cover release pathways – Several simulations were developed to support radionuclide screening or to provide bounding estimates for release pathway screening. These applications are presented in Sect. G.4.4.
- Inadvertent human intrusion (IHI) scenarios – Three IHI configurations were evaluated: acute discovery, acute drilling, and chronic post-drilling. IHI development and results are included in Appendix I. The time period for the IHI simulations is from 100 years to 10,000 years post-closure.
- Base case scenarios – Direct deterministic simulations of EMDF performance with predicted doses compared to regulatory criteria. The PA compliance period is 1000 years, and the simulated duration is 10,000 years. Model development is presented in Sect. G.4 and summarizations of base case model predictions of dose are presented in Sect. G.5.
- Long-term base case simulations – These extended duration simulations were performed similar to the 10,000-year base case simulation, with the simulation duration extended to 100,000 years to evaluate radionuclides, such as uranium isotopes, with peak predicted concentrations occurring after tens of thousands of years (Sect. G.5.6).
- Single parameter sensitivity analysis simulations – Sensitivity analyses were performed using the base case scenario and long-term base case scenario models. Single parameters were varied one at a time, with all other parameters held constant to assess how sensitive the model is to changes in assessed parameter magnitude. Results provided input for the probabilistic model setup. Results of the probabilistic modeling then provided insight on configuring subsequent sensitivity simulations (Sect. G.6).
- Uncertainty (probabilistic) analysis – Probability distributions were assigned to various parameters to assess model prediction uncertainty (Sect. G.6.3).

Attachment G.1 to this appendix provides a summary of model input for the base case model. The RESRAD-OFFSITE base case model input and output summary file is included in Attachment G.2. Attachment G.3 contains a list of the distributions, rank correlations, and related pairs of parameters specified for the compliance period and 10,000-year uncertainty analysis. Attachment G.4 provides the initially assigned and model adjusted rank correlation coefficients used in the uncertainty analyses. Input versus input scatter plots for rank correlated parameters assigned in the compliance period and 10,000-year uncertainty analyses are included in Attachment G.5.

The estimated EMDF radiological inventory (see Appendix B) and the results of the operational period simulations were used to provide source concentrations for the RESRAD-OFFSITE code to model doses resulting for the exposure scenarios. Model results were used to establish compliance with DOE O 435.1 (DOE 2001) dose performance criteria. It is anticipated that model results also will be used to evaluate the protectiveness of proposed EMDF waste acceptance criteria for radionuclides prior to commencing EMDF operations. In addition to the calculation of doses, predicted concentrations were compared to water resources protection criteria performance objectives (Sect. G.5.5).

Section 9 of the PA Report details the quality assurance (QA) activities and documentation that apply to the RESRAD-OFFSITE model analysis.

G.2 CONCEPTUAL SITE MODEL AND SCENARIO DESCRIPTION

During numerical model development, several steps are typically followed (Environmental Protection Agency [EPA] 2009). The first step, problem specification, includes collecting and reviewing site data to develop the conceptual site model (CSM). The CSM is the underpinning for the deterministic and/or probabilistic model, which then becomes the desired predictive tool. A summary of the EMDF CSM is provided in Sect. G.2.1.

G.2.1 EMDF CONCEPTUAL SITE MODEL

Developing a CSM is necessary prior to evaluating and simulating the likely impact of potential contaminant releases from the proposed EMDF. The CSM is a description of the site-specific factors that control radionuclide placement, release, migration, and exposure (Fig. G.2). Spatially, the EMDF CSM encompasses the disposal facility located in CBCV as well as the point of assessment (POA) at Bear Creek (Fig. G.1). The primary pathways for contaminant migration are via groundwater and surface water from potential contaminants originating at the EMDF.

As shown in Fig. G.2, the CSM includes a fraction of precipitation (rainfall and snowmelt) infiltrating through the disposal facility cover and contacting the waste, with some mass of radionuclides transferring from the solid to the liquid phase (i.e., leachate). This leachate then potentially enters shallow groundwater by passing through the underlying liner and vadose zone. Impacted water then flows downgradient in a southwesterly direction toward a groundwater well used by a hypothetical exposed individual, a resident farmer. The well water is used as a drinking water source and for household activities such as showering.

Impacted groundwater is also assumed to pass downgradient of the well and enter a surface water body (Bear Creek) used by the resident farmer to irrigate crops, provide water for livestock, and for recreational fishing.

Radionuclides in waste are emplaced as in the disposal facility beneath a protective cover and above a composite liner system. The design capacity of the EMDF is 2.2 M cy. The waste includes clean fill soils. The emplaced waste and clean fill are assumed to be soil-like and homogenous (i.e., not containerized).

A summary of major assumptions regarding the CSM is presented in Sect. G.2.4.

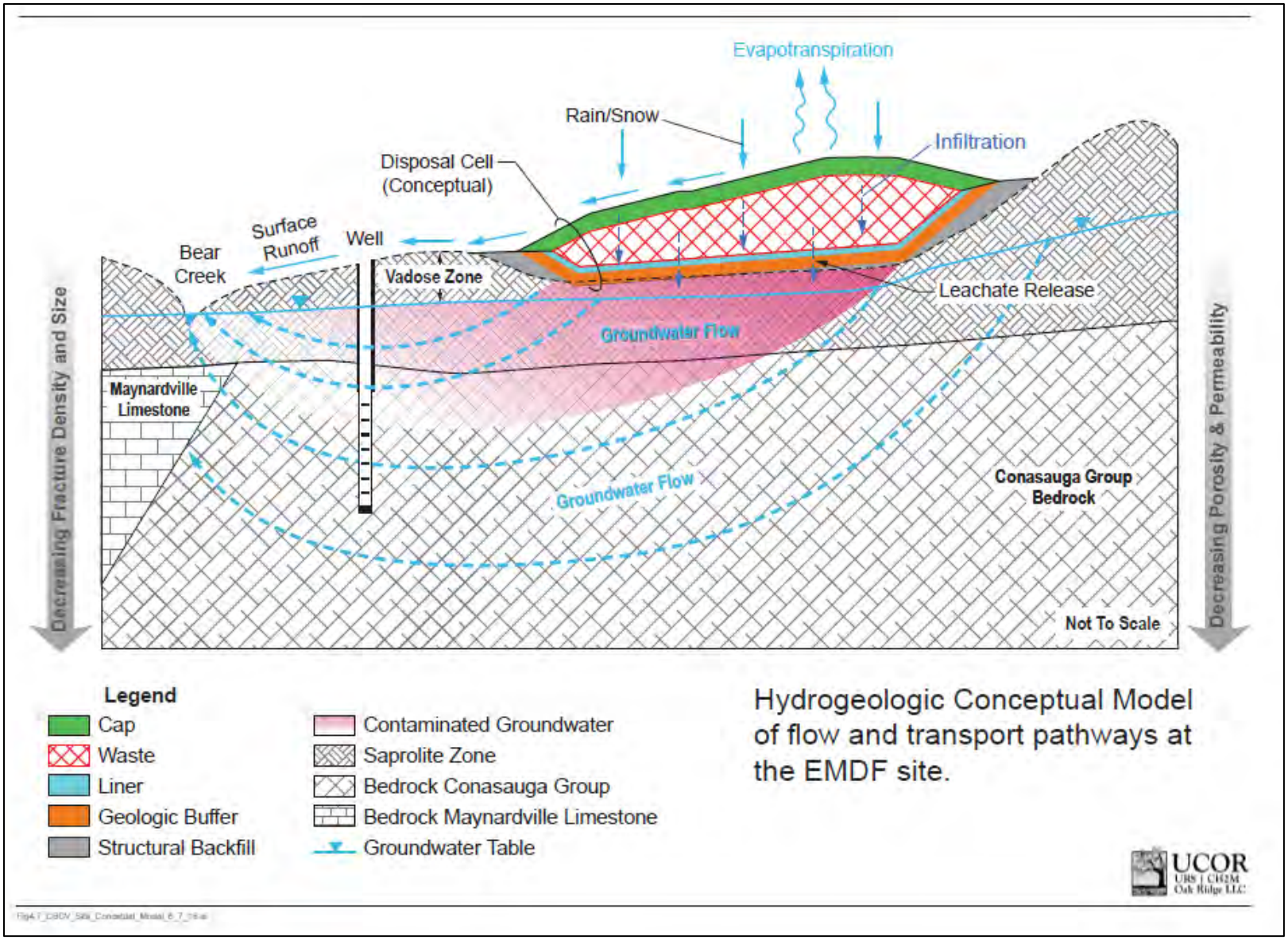

Fig. G.2. Conceptual site model and hypothetical receptor scenario

G.2.1.1 Groundwater Conditions and Flow Paths

Radionuclide migration through groundwater beneath EMDF is an important pathway. Based on preliminary groundwater data currently available for CBCV and on similar conditions at other BCV sites, it is inferred that shallow and intermediate groundwater beneath EMDF will follow hydraulic gradients and predominant strike-parallel flow paths across the width of the footprint towards local discharge zones. This flow pattern is documented in the three-dimensional saturated zone glow model for the EMDF PA (refer to Appendix D), but is simplified as conceptualized for the RESRAD-OFFSITE model (Fig. G.2).

Potentiometric surface contour maps for BCV and similar sites on the ORR indicate that horizontal hydraulic gradients tend to broadly mimic surface topography and that shallow to intermediate level groundwater flows locally from high elevation recharge areas to low elevation discharge zones. Groundwater flow along the southern part of the footprint may follow hydraulic gradients and fracture flow paths in regolith and bedrock that are directed across the northeast-southwest strike direction southward toward the lower elevations and discharge zones along the floodplains of Bear Creek. The water table is constrained by the lowest elevations along the existing drainage valleys directly adjacent to the site.

Three-dimensional groundwater flow modeling for EMDF is presented in Appendix D and integration of groundwater modeling with RESRAD-OFFSITE simulations is described in Sect. G.3.1.

G.2.1.2 Points of Assessment

A pessimistic assumption for the PA modeling is the location of the hypothetical receptor (i.e., resident farmer). As a conservative assumption biased toward a greater predicted dose for the receptor, the receptor well is assumed to be located proximal to the disposal facility at a distance of 100 m from the EOW at the location of modeled maximum contaminant concentration along the centerline of the modeled plume.

The surface water point of withdrawal for agricultural use is assumed to be a location that provides the most consistent year-round surface water flow. A surface water exposure location on Bear Creek near the junction of North Tributary (NT)-11 was selected because year-round flow is more typically encountered there than in surface water tributaries closer to the landfill. Withdrawal for agricultural use would require surface water availability during drier times of the year, when the Bear Creek tributaries close to the EMDF are typically dry. The three dimensional EMDF groundwater flow model (Appendix D) and radionuclide transport modeling (Appendix F) suggest that this location integrates the release of radionuclides from EMDF to surface water, and accounts for 98 percent of the modeled radionuclide discharge to surface water.

G.2.1.3 Engineered Barriers

The EMDF is proposed to be constructed and operated at ORR, which is located in a relatively wet environment in which engineered infiltration and leachate barriers are essential. The primary engineered barrier consists of an engineered cover that provides for lateral shedding of precipitation and evapotranspiration, minimizes or eliminates airborne releases and infiltration, and reduces the opportunity for biointrusion and direct human contact with waste. The engineered cover also minimizes direct exposure to potential receptors located on or near the disposal facility. Beneath the cover the waste zone and the liner system that collects and removes leachate during operations and limits water and radionuclide releases from the disposal facility.

The EMDF cover design (refer to Appendix C) consists of an 11-ft-thick composite system of infiltration and intrusion barriers (Fig. G.3). As shown in Fig. G.3, there is a robust biointrusion layer within 6 ft of the ground surface consisting of large cobbles. These cobbles discourage root penetration because they remain drier than the overlying materials and also discourage burrowing mammals due to the difficulty in

penetrating the material. These coarse materials also will serve to deter or discourage inadvertent human intruders attempting to drill through or excavate into the cover. Synthetic components of the cover system include geotextile layers and a 60-mil high-density polyethylene (HDPE) geomembrane overlying the amended/compacted clay layers at the base of the cover profile. The obvious difference between this engineered profile and normal hilltop soil and subsoil conditions in this region will alert potential intruders to the unusual nature of the location, reducing the potential for intrusion.

Prior to cover construction, waste will be placed so that void spaces are minimized. This reduces settlement to reduce the likelihood of impaired cover performance due to stress on the synthetic membrane and clay infiltration barriers. The primary and secondary components of the liner system collect and remove leachate during operations and following closure, and limits water and radionuclide release from the disposal facility. The liner system is comprised of multiple layers of synthetic and natural materials compatible with the waste and resistant to degradation by chemical constituents expected to be present in the leachate. In the RESRAD-OFFSITE model, the liner system consists of a protective cover (UZ1), drainage layer (UZ2), clay liner (UZ3), geobuffer (UZ4), and in situ material (native soils) (UZ5). The vadose zone (i.e., unsaturated zone beneath the liner) acts to retard and disperse radionuclides that may be released through the liner system before the radionuclides migrate to underlying groundwater.

For modeling purposes, it is assumed that all geosynthetic materials start to degrade at 200 years and are essentially ineffective at that time. The transitional period from 200 to 1000 years represents degradation of cover clay and drainage layers. After 1000 years, the remaining soil materials are assumed to maintain their properties as designed. The assumption of only 200 years for the service life of the HDPE membrane is pessimistic given that recent studies have estimated much longer periods for HDPE membrane performance in mixed LLW facilities (Tian et al. 2017).

G.2.2 HYPOTHETICAL EXPOSURE SCENARIOS

Per DOE guidance (DOE 2017), several exposure scenarios were evaluated as part of the RESRAD-OFFSITE modeling effort. Acute and chronic intruder scenarios are described in Appendix I. The all-pathways scenario consists of a hypothetical receptor exposed to radionuclide release to groundwater and surface water (with the EMDF cover performance simulated as described in the preceding section) and is referred to as the base case scenario. For the base case release to groundwater scenario, it is assumed that a resident farmer sets up a homestead just south of the disposal facility (see Fig. G.1 for assumed site layout).

The exposure scenario for the all-pathways dose analysis assumes a maximally exposed individual rather than a more representative future member of the public. The receptor is assumed to be a farming household (residential farmer) that drinks contaminated groundwater from a well at 100 m from the waste at the location of maximum radionuclide concentration. The receptor also consumes plant and animal foods grown onsite using contaminated Bear Creek water for irrigation and watering livestock. The assumed

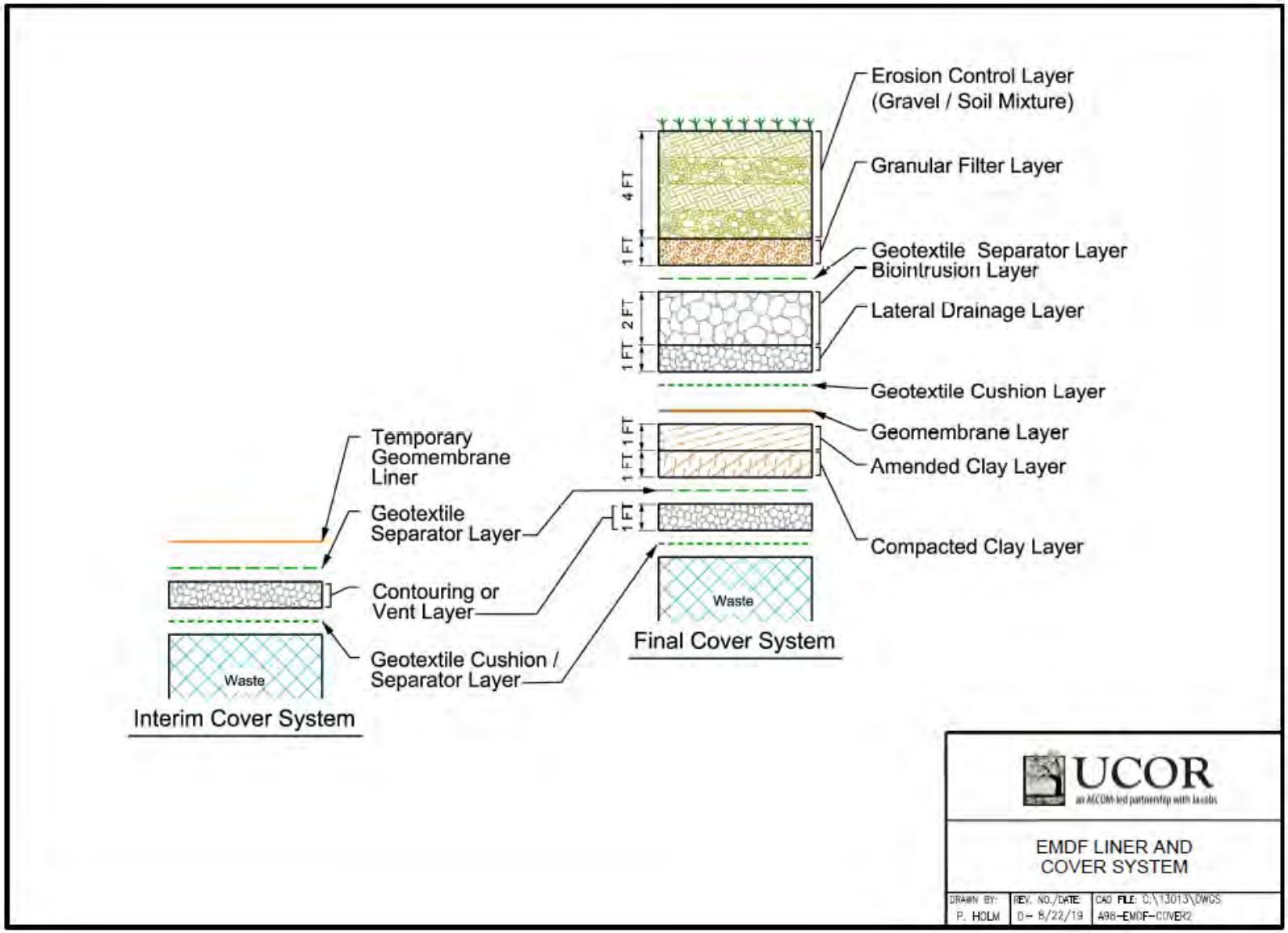

Fig. G.3. EMDF engineered cover system

proximity of the groundwater POA (100 m) and surface water POA (approximately 300 m) to the facility is extremely pessimistic, even in the absence of institutional controls on site access (refer to Sect. 1.7.3 of the PA). These maximally exposed individuals and POA assumptions result in higher dose predictions than would similar public exposure scenarios with equally likely assumptions regarding human behaviors and exposure locations. More detail on simulated exposure pathways is provided in Sect. G.3.3.

G.2.3 EMDF RADIONUCLIDE INVENTORY

The initial EMDF radiological inventory includes 70 isotopes (see Appendix B). Through a two-phase screening process, the number of isotopes simulated for the base case scenario is reduced to 42 (see Sect. G.4.4). For the IHI scenarios (see Appendix I), 53 isotopes are simulated with predictions made regarding dose. The screening process and resultant list of simulated isotopes is detailed in Sect. G.4.4. The approach to estimating activity concentrations is intended to overestimate waste concentrations to account for uncertainty in the characteristics of future remediation waste (refer to Appendix B). As a result the activity inventories used in the PA models are higher than inventories likely to be present at EMDF closure.

G.2.4 SUMMARY OF CSM ASSUMPTIONS

Development of the EMDF CSM incorporates several assumptions (Table G.1) in addition to the pessimistic base case exposure scenario described in Sect. G.2.2, the analysis includes other assumptions biased toward higher predicted doses, such as assuming that the failure of the engineered cover system occurs relatively early, and adoption of an equilibrium sorption radionuclide release model for soil-like waste that predicts rapid release to the environment. These pessimistic assumptions are presented in Sect. G.4.3.5.

Table G.1. Assumptions for developing the conceptual site model

CSM component	Assumption[a]
Waste volume	2.2 M cy
Waste composition	Soil-like, homogenous (uncontainerized)
Average waste height	57.54 ft
Distance to receptor well	100 m from EOW
Precipitation	Becomes runoff, infiltration, evapotranspired water
Composite cover	Present above entire waste footprint
Composite liner	Present below entire waste footprint
Groundwater impacts	Receptor well and Bear Creek (surface waterbody)
IHI scenarios	Acute discovery, acute drilling, chronic post-drilling
Base case exposure scenario	Resident farmer with homestead just south of the disposal facility
Number of isotopes in inventory	70[b] (42 base case release; 53 IHI)
Average source activity concentrations	Average waste activity concentrations reduced to account for addition of clean fill and loss of highly mobile radionuclides during disposal operations (Sect. G.4.3.4)
Geosynthetic degradation	Starts degrading immediately and is completely degraded at 200 years; essentially ineffective at that time

Table G.1. Assumptions for developing the conceptual site model (cont.)

CSM component	Assumption[a]
Degradation of cover clay and drainage layers	Degrading performance period from 200 to 1000 years
Agricultural crops	Fruit, grain, non-leafy and leafy vegetables; pasture and silage crops; and grain
Dwelling	Located south of disposal facility (downhill)
Livestock	Cows for meat and milk, poultry and eggs
Surface water body	Source for irrigation water and recreational fishing

[a]Several assumptions used to develop the CSM and numerical model include a conservative bias toward greater magnitude predicted doses for the receptor (Sect. G.6.4).
[b]Several radionuclides were screened from the analysis on the basis of half-life or with the water pathway screening model described in Sect. G.4.4.

CSM = conceptual site model
EOW = edge of waste
IHI = inadvertent hypothetical intruder

G.3 MODEL DESCRIPTION

This section includes a description of the integrated model approach, the selected primary model RESRAD-OFFSITE, and model implementation for the EMDF PA as a numerical representation of the CSM (Sect. G.2.1).

G.3.1 PA INTEGRATED MODELING APPROACH

PA modeling uses an integrated modeling approach that includes the site-specific application of several computer codes. These codes provided input to the RESRAD-OFFSITE model and output for comparison to RESRAD-OFFSITE results. The primary modeling tools employed as part of PA modeling in addition to RESRAD-OFFSITE included Hydrologic Evaluation of Landfill Performance (HELP) Version 3.07 (Schroeder et al. 1994), MODFLOW Version 88 (USGS 1988), MODPATH Version 1.0 (Pollock 1989), Subsurface Transport Over Multiple Phases (STOMP) (White and Oostrom 2000, White and Oostrom 2006), and MT3D Version 1.0 (Zheng 1990). Descriptions of modeling performed using the codes HELP, MODFLOW and MODPATH, STOMP, and MT3D are included in Appendices C through F, respectively. Integration of model codes is explained in Sect. 3.3.5 of the PA Report. The relationships between the various primary models are listed in Table G.2. The integrated modeling approach and model interfaces are depicted on Fig. G.4.

Table G.2. Integrated model approach summary

Model	Input provided to RESRAD-OFFSITE	Output compared to RESRAD-OFFSITE results
HELP (see Appendix C)	• Infiltration rate • Runoff characteristics	None
MODFLOW (see Appendix D)	• Hydraulic gradient to well • Hydraulic gradient to surface water body • Depth to groundwater	None
MODPATH (see Appendix D)	Predominant groundwater flow path direction	None
MT3D (see Appendix E)	None	• Groundwater concentration and timing at well • Plume thickness at well • Plume thickness at surface water body
STOMP (see Appendix F)	None	Leachate flux exiting disposal facility

HELP = Hydrologic Evaluation of Landfill Performance
RESRAD = RESidual RADioactivity
STOMP = Subsurface Transport Over Multiple Phases

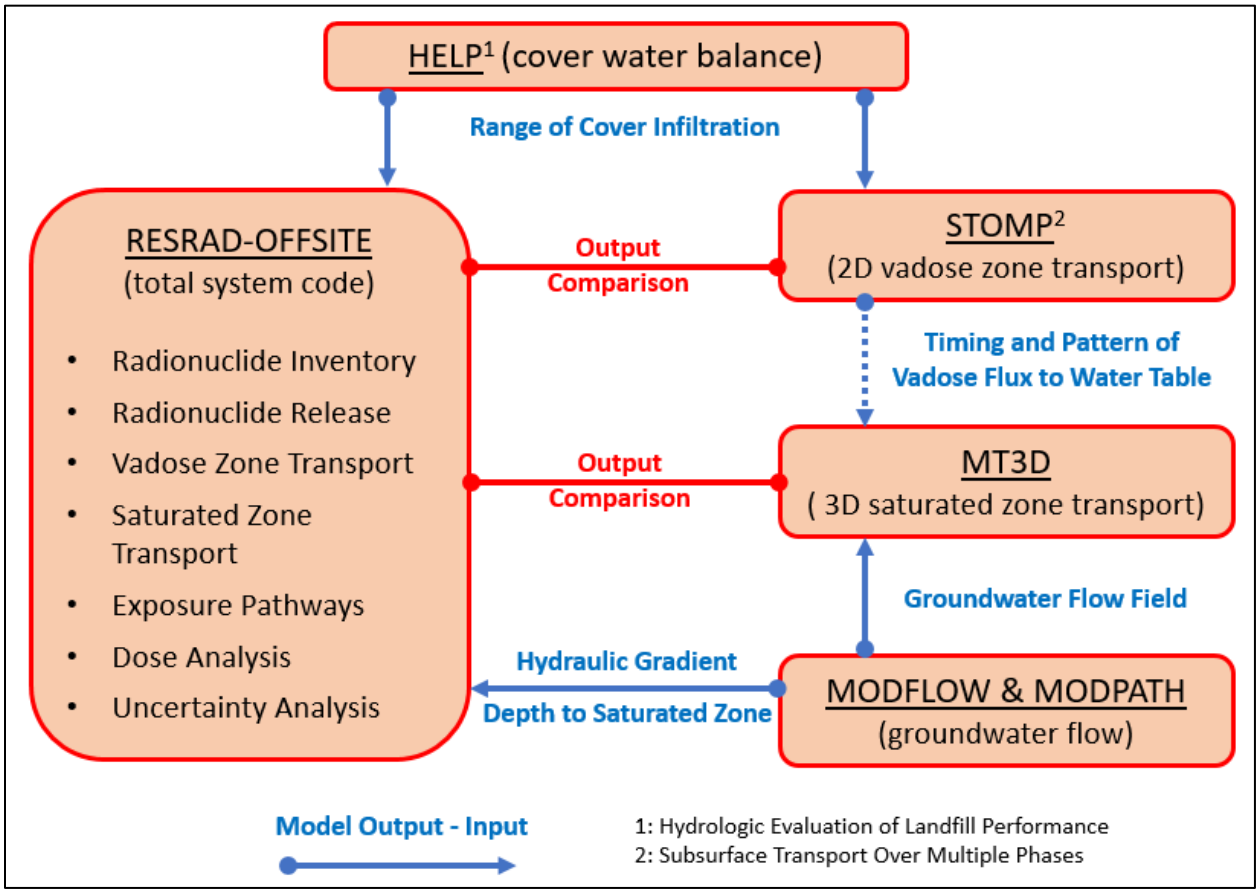

Fig. G.4. Performance assessment integrated modeling approach

G.3.2 RESRAD-OFFSITE

The RESRAD-OFFSITE Version 3.2 (Yu et al. 2007, Gnanapragasam and Yu 2015) computer code estimates the radiological dose and/or risk to a receptor located inside or outside an area of radionuclide contamination. RESRAD-OFFSITE is part of a suite of RESRAD codes developed and maintained by researchers at Argonne National Laboratory with sponsorship provided by DOE and the U.S. Nuclear Regulatory Commission (NRC). Computer code and version control are maintained by DOE through Argonne National Laboratory.

In RESRAD-OFFSITE, concentration, dose, and risk may be calculated at different time intervals of interest. The code contains computational models for primary contamination, atmospheric transport, groundwater transport, offsite accumulation, and exposure. Deterministic and probabilistic simulations may be performed within RESRAD-OFFSITE and both were used to assess EMDF performance and predict radiological dose to a hypothetical receptor. Deterministic simulations were performed to enable comparison of results with regulatory criteria. Probabilistic simulations provided an approach to assess uncertainty given potential variation in model parameter values.

In addition to calculating radiological dose, the use of RESRAD-OFFSITE enables calculating excess lifetime cancer risk using the predicted radionuclide concentrations in the environment. RESRAD-OFFSITE can be used to derive single radionuclide soil guidelines (SRSGs) to determine cleanup levels corresponding to a user-specified dose limit (e.g., 25 mrem/year) or to estimate the amount of a specific isotope that may be emplaced in a disposal facility. Calculations of radon flux across the facility cover also are possible; however, other methods were used to calculate radon flux at EMDF (see Appendix H).

RESRAD-OFFSITE has been benchmarked by the code developers with other peer codes, including Clean Air Act Assessment Package-1988 (Parks 1992), Industrial Source Complex-Long Term (EPA 1995), GoldSim (GoldSim 2010), Disposal Unit Source Term-Multiple Species (Sullivan 2001), and others (Yu et al. 2006). Prior to performing simulations, model verification of the RESRAD-OFFSITE Version 3.2 software was performed on the two computers used for simulations. Model verification documentation is included in the QA documentation for the PA (UCOR, an Amentum-led partnership with Jacobs, 2020a).

G.3.3 SIMULATED EXPOSURE PATHWAYS

RESRAD-OFFSITE makes available several exposure pathways that provide potential radiological dose for the receptor. A depiction of a typical CSM using the computer code RESRAD-OFFSITE is shown in Fig. G.5 and potential exposure pathways and receptor locations are shown on Fig. G.6. PA simulations at the EMDF do not include exposures from an onsite dwelling or radon (except progeny radon). An onsite dwelling is not included for the EMDF as it is assumed the hypothetical dwelling is offsite just south of the EOW, which is closer to the areas potentially suitable for agriculture. Releases to the atmosphere are not calculated in the base case model because of the selected source release model; however, dose from the inhalation of vapors and contaminated dust particles released from the EMDF through the vapor and biointrusion pathways are assessed in separate evaluations (Sect. G.4.4.2). Radon flux through the cover is assessed as presented in Appendix H.

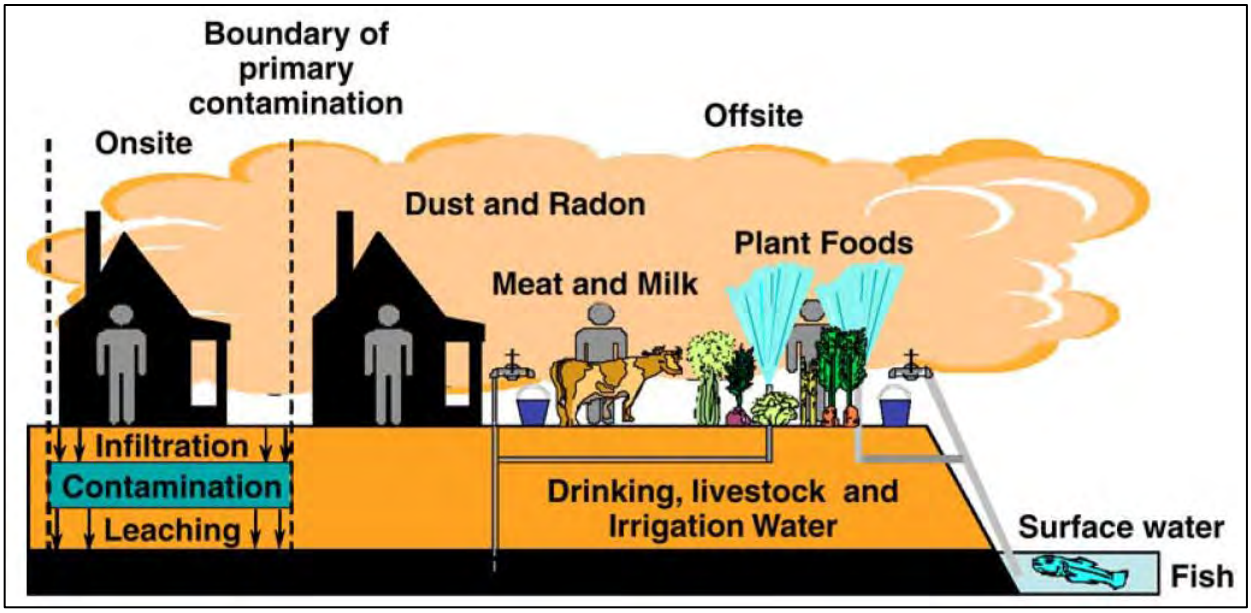

Note: Exposures from onsite dwelling, dust, and radon (except progeny radon) are not included in PA simulations at EMDF (graphic adapted from Figure 1.1 in Yu et al. 2007)

Fig. G.5. Typical conceptual site model for RESRAD-OFFSITE

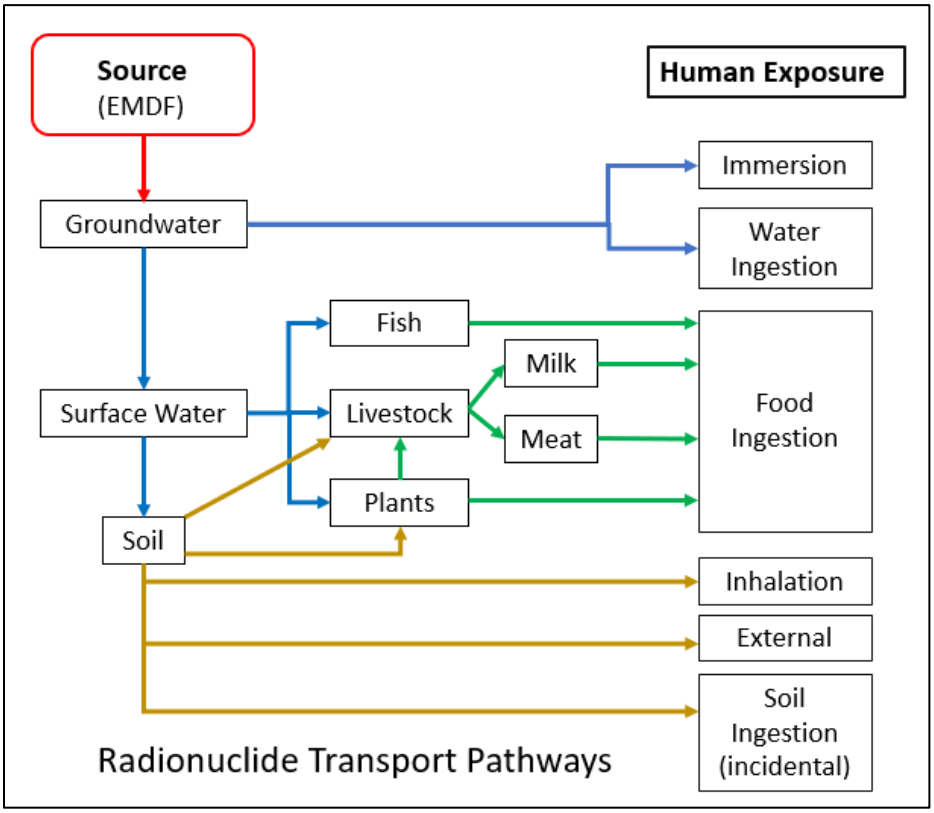

Fig. G.6. Potential RESRAD-OFFSITE exposure pathway

G.3.4 MODEL PARAMETERIZATION DEVELOPMENT

Model parameters are grouped in RESRAD-OFFSITE according to the parameter categories shown in Table G.3. Descriptions of major parameter groups are included in Sect. G.4 and in the *User's Guide for RESRAD-OFFSITE* (Yu et al. 2015a). Values assigned to the parameters in each category are included in Sect. G.4.

Table G.3. RESRAD-OFFSITE parameter categories

Preliminary inputs	Agricultural areas	Plant factors
Site layout	Livestock feed areas	Livestock feed factor
Soil concentrations	Dwelling site	Inhalation, gamma
Release	Air transport	Shape factors
Partition coefficients	Unsaturated zones	Occupancy factors
Deposition velocity	Saturated zone	Radon
Transfer factors	Water use	C-14
Reporting times	Surface waterbody	Mass fractions of C-12
Storage times	Groundwater transport	H-3
Physical/hydrological	Ingestion rates	
Primary contamination	Livestock intakes	

RESRAD = RESidual RADioactivity

G.4 SITE-SPECIFIC MODEL DEVELOPMENT

In general, simulating exposure using RESRAD-OFFSITE involves making appropriate assumptions required for calculating radionuclide concentrations in waste, leached materials, air, groundwater, and surface water, as applicable. Selection of specifics for the base case and other scenarios was guided by EMDF site characteristics and facility design as well as a review of analyses performed for Solid Waste Storage Area 6 (Oak Ridge National Laboratory [ORNL] 1997a) in Melton Valley near ORNL and for a proposed tumulus disposal facility (Class L-II Disposal Facility) (ORNL 1997b) in BCV near the EMDF site. RESRAD-OFFSITE model setup and major parameter assumptions for each scenario are described in the following subsections. Additional detail on model parameterization is included in Attachment G.1 of this appendix.

During model development and performance of simulations, extensive communication occurred with the code developers at Argonne National Laboratory to best apply RESRAD-OFFSITE as a predictive tool for the EMDF PA.

G.4.1 COMPLIANCE CRITERIA

For the EMDF PA, the POA locations are identical to DOE Manual (M) 435.1-1, *Radioactive Waste Management Manual* (DOE 2011a) requirements and consistent with DOE 2017. The POAs do not vary with the post-closure time period, even though expected future land use and institutional controls (Sect. 1.7.3 of the PA) would preclude public exposure at the 100-m buffer zone boundary for at least

100 years after EMDF closure. Institutional controls limiting site access are assumed to be effective for 100 years following closure. These assumptions are pessimistic given that DOE is required to maintain control over land containing radionuclide sources until the land can be safely released pursuant to DOE O 458.1, *Radiation Protection of the Public and Environment* (DOE 2011b) or transferred to another authorized party.

The base case model includes the assumptions that the waste emplacement in EMDF is completed at time zero (year 0) and that the site is under active institutional control for the next 100 years (years 0 through 100). The hypothetical resident farmer is assumed to setup a homestead at any time starting at year 0, even though active institutional control will be occurring for at least the first 100 years. Modeled radiological dose for the time period between 0 and 1000 years post-closure is the primary basis for analyzing EMDF compliance (i.e., compliance period) with dose performance objectives specified in DOE M 435.1-1 (DOE 2011a). Exposure scenarios and performance objectives for the EMDF PA, including criteria for water resources protection, are listed in Table G.4.

Table G.4. Exposure scenarios, performance objectives and measures, and points of assessment for the EMDF PA

Exposure scenario	Performance objective or measure	POA
All pathways	25 mrem/year	• Groundwater: 100 m from waste margin at the point of maximum concentration • Surface water: Bear Creek downstream of NT-11
Air pathway[a]	10 mrem/year[b]	100 m from waste margin
Radon flux	20 pCi/m^2/sec	EMDF cover surface
Water resources (groundwater): • Ra-226 + Ra-228 • Gross alpha activity[d] • Beta/photon activity • H-3 • Sr-90 • Uranium (total)	MCL[c] 5 pCi/L 15 pCi/L 4 mrem/year 20,000 pCi/L 8 pCi/L 30 µg/L	Groundwater at 100 m
Water resources (surface water)	DOE-derived concentration technical standard[e]	Bear Creek at NT-11 tributary junction
IHI • Chronic exposure • Acute exposure	 100 mrem/year 500 mrem	 At EMDF At EMDF

[a]Air pathway is screened from the EMDF PA.
[b]Excluding radon in air.
[c]EPA 2000.
[d]Including Ra-226, but excluding radon and uranium.
[e]DOE 2011c.

DOE = U.S. Department of Energy
EMDF = Environmental Management Disposal Facility
EPA = U.S. Environmental Protection Agency
IHI = inadvertent human intruder
MCL = maximum contaminant level
NT = North Tributary
PA = performance assessment
POA = point of assessment

Even though the compliance period ends at 1000 years, simulation durations were extended past 1000 years because results after the compliance period can fulfill an important role in decision-making. Beyond 1000 years, assumptions and calculations become increasingly speculative and uncertain and results should

be viewed with caution. The following is a summary of how the results were used within specified time periods:

- Predicted doses and groundwater concentrations from 0 to 1000 years were used for quantitative compliance (Table G.4). Calculated doses were used for regulatory compliance and are strictly compared to quantitative constraints. This is the compliance period.
- Predicted doses for times greater than 1000 years were used to evaluate the magnitude and timing of dose for radionuclides with peak doses occurring just after the compliance period.
- Predicted doses for times greater than 10,000 years, such as for the long-term base case simulations, were used to assess radionuclides that peak more than 10,000 years after operations cease. Because these predictions extend to 100,000 years, results are essentially for information purposes only and the evaluation is qualitative in nature.

G.4.2 RADIONUCLIDE INVENTORY SCREENING

There are 70 radionuclides included in the data sources assembled for the EMDF waste inventory (Appendix B). To provide computational efficiency and enable extensive single parameter sensitivity analysis simulation and probabilistic simulations, a methodology was employed to screen (i.e., remove from further analysis) radionuclides that do not contribute significantly to the total dose. For the EMDF PA, a two-phase approach was used for screening radionuclides for further simulations. Phase 1 involved screening based on radionuclide half-life. The 5-year half-life criterion is based on the period of active institutional control subsequent to the operational period and the expected travel time of infiltrating water in the waste. During the first 100 years of post-closure institutional control, the engineered barrier systems (cover and liner, including the leachate collection system) will prevent cover infiltration and leachate release, and DOE control of all property immediately surrounding the EMDF site will prevent inadvertent intrusion and exposure. During this 100-year time period, over 20 half-lives will have elapsed, resulting in decay of short-lived radionuclides to very low concentrations. Screening of radionuclides based on half-life was not performed for any nuclides that also are progeny of parent nuclides included in the inventory. This approach avoids potential delay in progeny generation and ensures inventory progeny are accounted for in model simulations.

Additional justification for using the 5-year half-life as a cutoff for the analysis of leachate release to groundwater is the anticipated travel time from the waste to the underlying water table. STOMP model simulations (see Appendix E) indicate that the average travel time from waste to the water table is greater than 200 years for a highly mobile radionuclide, which is approximately 40 or more half-lives for the screened short-lived radionuclides. Seven radionuclides were screened out in Phase 1, including: Cf-252, Cs-134, Eu-155, Fe-55, Na-22, Pm-147, and Sb-125. Thorium-228 has a half-life less than 5 years, but it was retained for the groundwater screening model because it is a progeny of several radionuclides in the inventory.

In addition to radionuclides with a half-life less than 5 years, Kr-85 and Mo-100 were removed from the inventory based on other factors. Krypton-85 was removed from the simulated inventory due to the expectation that significant amounts of krypton gas will not be present after waste generation, transport, placement, and in-cell compaction are complete. Molybdenum-100 was removed from the simulated inventory because it is a very stable radionuclide (half-life is 8.5E+18 years) that does not have a dose conversion factor in the RESRAD-OFFSITE database. The very low projected Mo-100 inventory (approximately 1.08E-05 Ci) is not expected to be a significant contributor to dose; therefore, Mo-100 was also excluded from further analysis.

Small quantities of Cl-36 could be present in future EMDF LLW associated with irradiated graphite or metals from ORNL research reactor facilities. However, Cl-36 has not been a radionuclide of concern for LLW disposed at the EMWMF, and identification of Cl-36 in environmental samples from the ORR is extremely rare. The compilation of facility inventory data, EMWMF waste profiles, and environmental characterization data used to estimate the EMDF radionuclide inventory at closure (refer to Appendix B) includes no data on Cl-36 activity. Due to this lack of information, and the likelihood that any Cl-36 will be limited to small volumes of waste, Cl-36 was included only in the Phase 2 screening model using a unit source concentration of 1 pCi/g to provide information for future waste management decisions.

In summary, for Phase 1 screening, a total of 61 radionuclides passed and total of 9 radionuclides were screened out from further consideration. Seven radionuclides were screened based on their half-life and two radionuclides were screened out for other reasons.

Phase 2 of the screening analysis consisted of performing simulations using a groundwater pathway screening model, which consists of a modified version of the base case model using isotope-specific partition coefficients decreased by a factor of 10 or 100 (see Sect. G.4.3.6) and other pessimistically biased assumptions regarding inventory (elevated screening source concentrations) and disposal conditions (no engineered barriers) that result in greater model-predicted doses. A more detailed description of screening model simulations is provided in Sect. G.4.4.

The screening model dose is based exclusively on groundwater ingestion and applied a screening dose criterion of 0.4 mrem/year, which is 10 percent of the 4 mrem/year national primary drinking water standard for beta-gamma emitters (40 *Code of Federal Regulations [CFR]* 141). The 0.4 mrem/year screening criterion is applied to all radionuclides, including alpha emitters, for the all-pathways dose analysis. Compliance with drinking water maximum contaminant levels (MCLs) for radionuclides, including alpha emitters, is evaluated separately from the all-pathways dose analysis (Sect 4.7.1). Among the alpha emitting radionuclides in the estimated inventory, only Cf-249, Cf-250, and Cf-251 were eliminated from further consideration based on the Phase 2 screening criterion. The estimated inventories of those three radionuclides are very small relative to the other alpha-emitting nuclides (Table G.18), therefore neglecting their contributions to the estimated gross alpha activity concentration in groundwater (Sect 4.7.1) is justified.

A total of 62 radionuclides were simulated in the groundwater screening model, which included the 61 radionuclides that passed Phase 1 of the screening process as well as Cl-36. Of the 62 simulated radionuclides, 43 radionuclides (42 plus Cl-36) produced a peak dose greater than 0.4 mrem/year and 19 produced a peak dose of less than 0.4 mrem/year. Out of the 19 radionuclides that produced a peak dose of less than 0.4 mrem/year, five radionuclides (Nb-93m, Pb-210, Ra-228, Th-228, and Th-229) are progeny of one of the 43 that exceeded the dose criteria. These five are retained as source concentrations for the base case groundwater pathway analysis. A total of 47 radionuclides (42 with peak dose greater than 0.4 mrem/year plus five progeny) passed Phase 2 of the screening analysis.

Nine radionuclides had inventory data that could not be verified from the original sources and were not included in the IHI analysis or base case models. These nine radionuclides are: Cd-113m, Cs-135, Kr-85, Pd-107, Se-79, Sm-151, Sn-121m, Sn-126, and Zr-93. Five of these nine passed the Phase 2 groundwater pathway screening. Including the removal of Mo-100, out of the 70 total isotopes considered in the EMDF waste inventory (see Appendix B), 53 isotopes were simulated in the IHI analysis models and 42 radionuclides were simulated in the base case (release to groundwater) model.

G.4.3 MODEL PARAMETERIZATION

This section provides a summary of major RESRAD-OFFSITE model inputs. For convenience, the inputs are presented in the order of the RESRAD-OFFSITE input modules. RESRAD-OFFSITE uses metric units. For consistency with units associated with other PA models, some input parameter values are given in English units in the text of this Appendix.

G.4.3.1 Radiological Data

Model inputs include values specified for various parameters and libraries of reference data. The basis for each is presented in Table G.5. RESRAD-OFFSITE libraries contain the selected databases for external exposure, internal exposure as inhalation and ingestion dose, slope factors, and transfer factors (Gnanapragasam and Yu 2015).

Table G.5. Sources of radiological data

Parameter/library	Basis
Basis for radiological transformations	*Nuclear Decay Data for Dosimetric Calculations*, (ICRP 2008)
External exposure library	DCFPAK3.02 database, (DOE 2017), https://www.dcfpak.org
Internal exposure dose library	*Derived Concentration Technical Standard* (DOE 2011c) (reference person)
Slope factor (risk) library	DCFPAK3.02 morbidity, (DOE 2017), https://www.dcfpak.org
Transfer factor library	RESRAD default transfer factors
Calculation time points	2048

DOE = U.S. Department of Energy
DCFPAK = Dose Coefficient File Package (database)
ICRP = International Commission on Radiological Protection
RESRAD = RESidual RADioactivity

G.4.3.2 Preliminary Inputs

The preliminary inputs include the radiological units for activity and dose, dose limit, number of unsaturated zones, and fraction of submerged primary contamination (i.e., soil-like, homogenous waste). Preliminary model inputs are presented in Table G.6. For all simulations, it is assumed that the waste is located above groundwater and does not intersect the groundwater table.

Table G.6. Preliminary model inputs

Input	Value
Basic radiation dose limit, mrem/year	25
Number of unsaturated zones, unitless	5
Submerged fraction of primary contamination, unitless	0.0

G.4.3.3 Site Layout

The conceptual site layout is presented in Fig. G.1. Coordinates input into RESRAD-OFFSITE for the primary site features are shown in Table G.7. Specified coordinates considered site conditions, such as topography and surface water locations, and areas where the model would be expected to predict higher doses for the receptor (e.g., the surface waterbody is located along the centerline of the hypothetical plume emanating from the disposal facility).

Table G.7. Site layout parameters

Site location	Smaller x-coordinate (m)	Larger x-coordinate (m)	Smaller y-coordinate (m)	Larger y-coordinate (m)
Fruit, grain, non-leafy vegetables plot	0	32	-132	-100
Leafy vegetables plot	40	72	-132	-100
Pasture, silage growing area	120	220	-200	-100
Grain fields	230	330	-200	-100
Dwelling site	80	112	-132	-100
Surface waterbody	-575.4	-475.4	-337.4	-332.4

One limitation of RESRAD-OFFSITE is that the primary contamination must be specified as a rectangle, which only approximates the layout of the designed facility. The cell dimensions in the model were specified such that the x-dimension approximates the average east-west distance of the facility design. The y-dimension is input as the value that maintains the total waste volume of 2.2 M cy. The dimensions of the primary contamination in the model are 250.6 m in the x-direction and 382.7 m in the y-direction (see Fig. G.1).

Resultant areas of the site locations presented in Table G.7 are shown in Table G.8.

Table G.8. Site location areal extent

Site location	Simulated area (m^2)
Fruit, grain, non-leafy vegetables plot	1024
Leafy vegetables plot	1024
Pasture, silage growing area	10,000
Grain fields	10,000
Dwelling site	1024
Surface waterbody	500

G.4.3.4 Operational Loss of Radionuclides and Modeled Source Concentrations

Source concentrations used in the base case model are derived from the estimated waste inventory (see Appendix B). Estimated waste inventory values for the potential inventory were used to develop average waste concentrations for the as-generated material (as-generated waste concentrations). The as-generated waste concentrations were adjusted to account for the anticipated volume of clean fill added during disposal of the waste material, resulting in a 46.9 percent decrease in the as-generated waste concentration to arrive at estimated average as-disposed waste concentrations (Table G.9). The derivation of the clean fill adjustment factor is presented in Sect. 3.2.2.5 of the PA Report.

Table G.9. Base case model source concentrations

Isotope name	Half-life (year)	Estimated waste inventory (Ci)	EMDF as-generated waste average concentration (pCi/g)	EMDF as-disposed waste average concentration (pCi/g)	EMDF post-operational source average concentration (pCi/g)
Ac-227	2.18E+01	7.54E-03	5.50E-03	2.92E-03	2.92E-03
Am-241	4.32E+02	1.52E+02	1.11E+02	5.90E+01	5.90E+01
Am-243	7.38E+03	7.65E+00	5.59E+00	2.97E+00	2.97E+00
Be-10	1.50E+06	6.52E-05[a]	4.76E-05[a]	2.53E-05	2.53E-05
C-14	5.73E+03	7.43E+00	5.43E+00	2.88E+00	5.40E-01[b]
Ca-41	1.00E+05	1.09E-01[a]	7.92E-02[a]	4.21E-02	4.21E-02
Cm-243	2.85E+01	1.11E+00	8.10E-01	4.30E-01	4.30E-01
Cm-244	1.81E+01	3.26E+02	2.38E+02	1.26E+02	1.26E+02
Cm-245	8.50E+03	9.87E-02	7.21E-02	3.83E-02	3.83E-02
Cm-246	4.73E+03	4.10E-01	2.99E-01	1.59E-01	1.59E-01
Cm-247	1.56E+07	2.68E-02	1.96E-02	1.04E-02	1.04E-02
Cm-248	3.39E+05	1.44E-03	1.05E-03	5.59E-04	5.59E-04
H-3	1.24E+01	2.88E+01	2.10E+01	1.12E+01	4.64E+00[b]
I-129	1.57E+07	1.05E+00	7.66E-01	4.07E-01	3.50E-01[b]
K-40	1.28E+09	8.46E+00	6.18E+00	3.28E+00	3.28E+00
Mo-93	3.50E+03	1.00E+00[a]	7.30E-01[a]	3.88E-01	3.88E-01
Nb-93m	1.36E+01	6.01E-01[a]	4.39E-01[a]	2.33E-01	2.33E-01
Nb-94	2.03E+04	4.20E-02	3.07E-02	1.63E-02	1.63E-02
Ni-59	7.50E+04	7.84E+00	5.73E+00	3.04E+00	3.04E+00
Np-237	2.14E+06	8.37E-01	6.12E-01	3.25E-01	3.25E-01
Pa-231	3.28E+04	6.15E-01	4.49E-01	2.39E-01	2.39E-01
Pb-210	2.23E+01	9.50E+00	6.93E+00	3.68E+00	3.68E+00
Pu-238	8.77E+01	2.42E+02	1.77E+02	9.38E+01	9.38E+01
Pu-239	2.41E+04	1.50E+02	1.10E+02	5.83E+01	5.83E+01
Pu-240	6.54E+03	1.60E+02	1.17E+02	6.20E+01	6.20E+01
Pu-241	1.44E+01	5.25E+02	3.83E+02	2.04E+02	2.04E+02
Pu-242	3.76E+05	4.45E-01	3.25E-01	1.73E-01	1.73E-01
Pu-244	8.26E+07	9.49E-03	6.93E-03	3.68E-03	3.68E-03
Ra-226	1.60E+03	2.07E+00	1.51E+00	8.01E-01	8.01E-01
Ra-228	5.75E+00	5.69E-02	4.15E-02	2.21E-02	2.21E-02
Sr-90	2.91E+01	4.96E+02	3.62E+02	1.92E+02	1.92E+02
Tc-99	2.13E+05	7.23E+00	5.28E+00	2.80E+00	1.56E+00[b]
Th-228	1.90E+00	5.45E-06	3.98E-06	2.11E-06	2.11E-06
Th-229	7.34E+03	1.47E+01	1.08E+01	5.71E+00	5.71E+00
Th-230	7.70E+04	4.94E+00	3.61E+00	1.92E+00	1.92E+00
Th-232	1.41E+10	9.07E+00	6.62E+00	3.52E+00	3.52E+00
U-232	7.20E+01	2.63E+01	1.92E+01	1.02E+01	1.02E+01
U-233	1.59E+05	1.07E+02	7.83E+01	4.16E+01	4.16E+01
U-234	2.45E+05	1.62E+03	1.19E+03	6.30E+02	6.30E+02
U-235	7.04E+08	1.02E+02	7.47E+01	3.97E+01	3.97E+01
U-236	2.34E+07	2.32E+01	1.69E+01	8.98E+00	8.98E+00
U-238	4.47E+09	9.83E+02	7.18E+02	3.81E+02	3.81E+02

[a] Data limited radionuclide with non-standard basis of estimate, refer to Appendix B.
[b] Post-operational waste concentration adjusted for operational period activity loss.

EMDF = Environmental Management Disposal Facility

As-disposed waste concentrations for four mobile radionuclides (H-3, C-14, Tc-99, and I-129) were adjusted to account for activity losses due to leaching during the assumed 25-year operational period. To maintain conceptual consistency with the instantaneous equilibrium desorption release model (Sect. G.4.3.5), this approach takes credit for expected leaching of highly mobile radionuclides during the time the facility is operating with no cover and essentially unlimited exposure of the waste to infiltrating meteoric water. Operational period activity losses that were used to develop the adjusted (post-operational) source concentrations for the four mobile radionuclides were quantified using four RESRAD-OFFSITE models, one for each EMDF disposal cell, with waste dimensions representing the waste volume for each disposal cell. For modeling purposes, it was assumed that the filling duration for each cell is a fraction of the total operations period equal to the fractional waste volume that each cell contains. For each disposal cell, leaching was quantified from the beginning of the filling time until the time at which the enhanced operational cover is applied, which is assumed to be when the adjacent cell has been filled to its full capacity.

It was assumed that all water that comes in contact with the waste during the operational period leaches radionuclides from the waste, which includes both leachate (water that percolates through the waste) and contact water (water that comes in contact with the waste, but does not fully infiltrate it). The leachate infiltration rate was estimated using HELP model-derived leachate flow rates from the EMDF Initial Water Balance Assessment conducted as part of the design. A leachate infiltration rate of 6 in./year was assumed for the operational period models. Contact water infiltration rates were estimated using the contact water-leachate ratio for the Environmental Management Waste Management Facility (EMWMF) in Fiscal Year 2018 (DOE 2019), which is 2.8. Using the EMWMF contact water-leachate ratio yielded a contact water generation rate of 16.8 in./year (6 in./year × 2.8). The total infiltration rate used in the operational period models was 22.8 in./year, the total of the estimated leachate (6 in./year) and contact water (16.8 in./year) generation rates. The assumed infiltration rate was incorporated in the operational period models using the runoff coefficient. Calculation of the runoff coefficient is discussed further in Sect. G.4.3.5.2.

Using the data available in the AQFLUXIN.DAT output file, activity loss during the operational period was quantified for the four cells. The leached activity for each cell was summed to obtain the total activity lost during the operational period, which was used to derive the post-operational waste concentrations that were used in the base case model. Activity loss during the operational period was quantified for the higher mobility radionuclides that were simulated, which are C-14, H-3, I-129, and Tc-99. The high mobility radionuclides have waste zone partition coefficients (K_d) that are either zero or approximately an order of magnitude less than other simulated radionuclides. Operational period activity losses were not quantified for the other (low mobility) radionuclides because their relatively high waste K_d values will inhibit significant leaching during the operational period. Post-operational waste concentrations were identical to as-disposed waste concentrations for all radionuclides except the four mobile radionuclides. Estimated waste inventory values, as-generated waste concentrations, as-disposed waste concentrations, and post-operational waste concentrations (base case source concentrations) for the 42 radionuclides simulated in the base case model are provided in Table G.9.

G.4.3.5 Radionuclide Release

The simulated leaching of dissolved radionuclides from waste materials is an important process given that the leached radionuclides become available to migrate to the potential receptor. For modeling purposes, the 2.2 M cy of emplaced waste in EMDF was assumed to be of uniform thickness, homogenous both horizontally and vertically, and soil like (uncontainerized). The source radionuclides were simulated as leaching into the surrounding soil moisture over the entire thickness of the primary contamination. Transport modeling accounted for advective and dispersive transport in soil moisture, partitioning of radionuclides between the solid and aqueous phases of soil, and radiological

transformations (Yu et al. 2013). Leached materials that entered the underlying unsaturated zone and aquifer did so within the entire waste footprint area.

RESRAD-OFFSITE offers three options to simulate source release (Yu et al. 2013): First Order Rate Controlled Release with Transport, Version 2 Release, and Instantaneous Equilibrium Desorption Release. All three release options were evaluated in the EMDF PA (Instantaneous Equilibrium Desorption Release in the base case and First Order Rate Controlled Release with Transport and Version 2 Release as part of the sensitivity analysis described in Sect. G.6.2). An important limitation of RESRAD-OFFSITE is that the code is unable to account for solubility limits, which can allow for unrealistically high aqueous concentrations that result in greater magnitude predicted doses for the receptor.

G.4.3.5.1 RESRAD-OFFSITE release model

The waste form resembling the Instantaneous Equilibrium Desorption release option is listed as including compacted lab trash such as clothes or glove boxes as well as small gadgets or tools (Yu et al. 2013).

Instantaneous Equilibrium Desorption assumes that equilibrium radionuclide concentrations in the solid and aqueous phases are achieved as soon as water contacts the waste and these equilibrium concentrations are governed by both the nuclide-specific K_d values in the contaminated zone and the waste concentration. Additionally, the K_d determines the rate at which the radionuclides are transported by infiltration down through the primary contamination (Yu et al. 2013). Radionuclides are removed from the leading edge of the primary contamination (top of the layer), causing a non-uniform vertical concentration profile, as the soil moisture in the lower sections of the primary contamination are already at the equilibrium concentration. The Instantaneous Equilibrium Desorption release model does not allow for the calculation of radionuclide release to the atmosphere or surface runoff because of the non-uniform vertical concentration profile. Releases to surface runoff do not apply due to the limited amount of cover erosion assumed during the 10,000-year simulation period (Appendix C). Dose contribution from atmospheric release through the cover was evaluated in both the vapor release and biointrusion screening models (Sect. G.4.4.2) and was found to be negligible.

First Order Rate Controlled Release with Transport assumes that radionuclide transfer from waste to pore water at any time is proportional to the radionuclide inventory at that time and occurs uniformly over the thickness of the primary contamination (i.e., the horizontal area does not change). The proportionality constant is the time varying leach rate. First Order Rate Controlled Release with Transport also allows the user to add a time delay to the source release, specify leach rates and releasable fractions at two different times, and specify whether the release progresses in a linear or stepwise manner.

Version 2 release is a first order exponential leaching model that accounts for radiological transformations (decay and ingrowth), but not for radionuclide transport in the waste. When Version 2 release is used, leached material is assumed to leave the contaminated zone as soon as it is leached. A time delay cannot be added when this release option is used, so all material is available for leaching at the beginning of the simulation period.

Given the assumed soil-like waste form and the assumption of waste homogeneity, the base case simulation used the Instantaneous Equilibrium Desorption Release option. In addition to the suitability of the release model for the expected waste forms, using the Instantaneous Equilibrium Desorption Release option is a conservative assumption biased towards greater predicted doses, as it yields more rapid releases of radionuclides from the waste compared to both the First Order Rate Controlled Release with Transport and Version 2 release options.

G.4.3.5.2 Radionuclide leaching

Generally, the EMDF engineered systems are assumed to remain fully functional for 200 years, with loss in functionality of certain portions of the system occurring after 200 years. Therefore, the overriding assumption is that the disposal facility performs as designed for the first 200 years post-closure and does not release radionuclides to the underlying groundwater during this time period. The end-state conditions of the facility are assumed to occur at 1000 years. This base case assumption for EMDF performance evolution is described in Sect. G.2.4 and Appendix C of the PA report.

The infiltration rate is calculated within RESRAD-OFFSITE as follows:

$$I = (1-C_e)[(1-C_r)\times P_r+I_{rr}]$$

where:

I = infiltration rate, m/year
C_e = evaporation coefficient, unitless
C_r = runoff coefficient, unitless
P_r = precipitation rate, m/year
I_{rr} = irrigation rate applied to primary contamination, m/year.

HELP model results provided infiltration rates at 200 and 1000 years as well as the proportion of precipitation lost to evapotranspiration from the disposal facility cover (C_e). The conceptual model for evolution of EMDF cover infiltration and leachate release (refer to Appendix C, Sect. C.1.3) applies the HELP model results as follows three different infiltration rates and corresponding post-closure time points are listed below:

- Year 0 (design performance period) – infiltration rate is 0 in./year
- Years 200 to 1000 (degrading performance period) – infiltration rate increases linearly from zero to 0.88 in./year
- After year 1000 (long-term performance period) – infiltration rate is specified as 0.88 in./year.

One of the limitations of RESRAD-OFFSITE is that the infiltration rate cannot be varied over time, so a constant infiltration rate must be applied for the entire simulation period. The runoff coefficient was calculated to produce the HELP-calculated long-term performance infiltration rate (0.88 in./year) in RESRAD-OFFSITE, assuming the average annual precipitation is 54.4 in./year and there is no irrigation on the disposal facility.

The release model incorporates the assumed evolution in EMDF performance by assigning a release time (initially set at 200 years) and a release duration set at 800 years. As a surrogate representation of the assumed increase in cover infiltration over the release duration, and to account for the higher than assumed infiltration rate from years 200 to 1000, the release model applies a releasable fraction parameter which is increased from zero to one over the 800 year release. The model requires an initial value of the releasable fraction (set to zero at release time) and a final value (set to one at 1000 years) for each radionuclide.

Based on comparison of the RESRAD-OFFSITE results to the STOMP and MT3D model results for C-14 and Tc-99, the initial release time was adjusted upwards to 300 years for all radionuclides. To adequately capture the high mobility of radionuclides with K_d = 0, increasing the initial releasable fraction from 0 to 0.75 for C-14 was found to be necessary. This adjustment produced peak C-14 release concentrations consistent with the STOMP and MT3D model results for C-14. Initial releasable fraction was also changed

to 0.75 for H-3, (also $K_d = 0$) for consistency. Similarly, the release duration was decreased to 500 years for C-14 and H-3 to better match MT3D model output. Comparison and integration of RESRAD-OFFSITE results with STOMP and MT3D model results is presented in Sect. 3.3.5 of the PA.

G.4.3.6 Solid-Liquid Partition Coefficients

The solid-liquid partition coefficient, also known as the partition coefficient (K_d), is a parameter determining a radionuclide's migration in the RESRAD-OFFSITE model. Partition coefficients are used as a quantitative indicator of the environmental mobility of simulated radionuclides and, mathematically, are the ratio of the concentration of a radionuclide present in the solid phase divided by the equilibrium concentration in the contacting liquid phase. Application of partition coefficients requires that a linear equilibrium isotherm between the sorbed and non-sorbed species of an element applies, which is a simplification that generally holds true at lower concentrations and constant temperatures. Additionally, sufficient contact time needs to occur for equilibrium to be achieved, which is expected in the engineered EMDF facility.

Partition coefficients are site specific and their magnitudes are a function of the presence or absence of competing compounds, soil properties, and groundwater chemistry. Because the use of partition coefficients is a simplification, the values are necessarily empirical and highly dependent on the system in which they are measured. In general, isotopes of a radionuclide are assumed to have the same partition coefficient value because sorption is a chemical property that is not dependent on isotopic mass.

The partition coefficient values used in the RESRAD-OFFSITE modeling were based on reports detailing laboratory evaluations of partition coefficients for clay-rich soils, saprolite, less weathered rock from the geologic units that underlie the EMDF site, and potential liner and geologic buffer materials at the EMWMF and other nearby sites. Detailed discussion of the available ORR-specific data on partition coefficient values is provided in Sect. 2.1.6.3 of the EMDF PA report. Where multiple partition coefficients were reported in the references, lower values were generally selected for use in this modeling. A more detailed presentation of the approach to selection of base case K_d values is provided in Sect. 3.2.2.6 of the PA.

In RESRAD-OFFSITE, partition coefficients may be assigned to different zones including the disposal facility, agricultural fields, dwelling site, aquifer (i.e., saturated zone), and sediment in the assessed surface waterbody. For each isotope, partition coefficients were specified as being equal for the following zones:

- Unsaturated zones (UZ1 through UZ5)
- Saturated zone
- Fruit, grain, non-leafy fields
- Pasture, silage growing areas
- Livestock feed grain fields
- Dwelling site.

Assuming a single, constant partition coefficient value for all of the model zones in the preceding list is a simplification of the geochemical complexity of the disposal system; however, low permeability clays of the liner and geologic buffer and the underlying in-situ saprolite and bedrock are likely to have very similar mineralogical and sedimentological characteristics.

The waste in the EMDF is composed of debris, soil waste, and clean fill, with clean fill accounting for over half of the soil material. Clean fill is sourced from borrow pits in simiar geologic settings as the unsaturated

zone materials. Given that approximately one-half of the waste mass is similar to the unsaturated zone materials, the partition coefficient values in the waste are assumed to be one-half of the partition coefficient values assumed for the other zones (unsaturated zones UZ1 to UZ5, saturated zone, agricultural fields and dwelling sites). For the EMDF simulations, radionuclide-specific partition coefficients were assigned as shown in Table G.10.

Table G.10. Partition coefficients (K_d) – base case and screening model values

Element	K_d, EMDF base case model (cm^3/g)		K_d, EMDF screening model	Primary reference	Material/soil texture in primary reference associated with base case value	Supporting references
	Waste zone (cm^3/g)	Saprolite and bedrock zones (cm^3/g)				
Ac	20	40	2	ORNL 1997a (Table 2.3, p. 2-18)	Generic soil	
Am	2000	4100[a]	20[b]	Rothschild et al. 1984 (Table 6, p. 38), Davis et al. 1984 (Table 7, p.40)	Silty clay (Maryville Limestone)	Sheppard and Thibault 1990
Ba	28	55	3	DOE 1998 (Appendix E, p. E 71–73)	Generic soil	Baes et al. 1984
Be	400	800	40	DOE 1998 (Appendix E, p. E 71–73)	Generic soil	Sheppard and Thibault 1990
C	0	0	0	ORNL 1997a (Table 2.3, p. 2-18)	Generic soil	
Ca	15	30	2	ORNL 1997a (Table 2.3, p. 2-18)	Generic soil	Sheppard and Thibault 1990
Cd	100	200	10	ORNL 1997a (Table 2.3, p. 2-18)	Generic soil	Sheppard and Thibault 1990
Cf	20	40	2	ORNL 1997a (Table 2.3, p. 2-18)	Generic soil	
Cl	N/A[c]	N/A[c]	0	ORNL 1997a (Table 2.3, p. 2-18)	Generic soil	
Cm	20	40	2	ORNL 1997a (Table 2.3, p. 2-18)	Generic soil	
Co	400	800	40	ORNL 1997a (Table 2.3, p. 2-18)	Generic soil	Rothschild et al. 1984
Cs	1500	3000	150	Friedman et al. 1990 (Table 3.1, p.7)	Silty clay (Maryville Limestone)	Davis et al. 1984
Eu	20	40	2	ORNL 1997a (Table 2.3, p. 2-18)	Generic soil	Friedman et al. 1990
Fe	450	890	45	Yu et al. 2015b (Table 2.13.2, p. 67)	Loam	Davis et al. 1984
Gd	410	820	40	Yu et al. 2007 (Appendix B, Attachment A Table 2-4, p. AttA-60)	N/A	
H	0	0	0	ORNL 1997a (Table 2.3, p. 2-18)	Generic soil	DOE 1998, IAEA 2010
I	2	4	0.2	Davis et al. 1984 (Figure 14 data, > 5 m depth)	Silty clay	Rothschild et al. 1984
K	15	30	2	ORNL 1997a (Table 2.3, p. 2-18)	Generic soil	DOE 1998
Mo	45	90	5	Sheppard and Thibault 1990 (Table 1)	Clay	
Na	5	10	1	Yu et al. 2007 (Appendix B; Attachment A Table 2-4, p. AttA-60)	N/A	IAEA 2010
Nb	50	100	5	ORNL 1997a (Table 2.3, p. 2-18)	Generic soil	DOE 1998
Ni	1000	2000	100	ORNL 1997a (Table 2.3, p. 2-18)	Generic soil	DOE 1998
Np	20	40	2	ORNL 1997a (Table 2.3, p. 2-18)	Generic soil	ORNL 1987
Pa	200	400	20	ORNL 1997a (Table 2.3, p. 2-18)	Generic soil	DOE 1998
Pb	50	100	5	ORNL 1997a (Table 2.3, p. 2-18)	Generic soil	DOE 1998
Pd	1000	2000	100	ORNL 1997a (Table 2.3, p. 2-18)	Generic soil	DOE 1998
Pm	410	820	40	Yu et al. 2007 (Appendix B; Attachment A Table 2-4, p. AttA-60)	N/A	IAEA 2010

Table G.10. Partition coefficients (K_d) – base case and screening model values (cont.)

Element	K_d, EMDF base case model (cm^3/g)		K_d, EMDF screening model	Primary reference	Material/soil texture in primary reference associated with base case value	Supporting references
	Waste zone (cm^3/g)	Saprolite and bedrock zones (cm^3/g)				
Pu	20	40	2	ORNL 1997a (Table 2.3, p. 2-18)	Generic soil	Gill-Garcia et al. 2008
Ra	1500	3000	150	ORNL 1997a (Table 2.3, p. 2-18)	Generic soil	DOE 1998
Re	20	40	2	Sheppard and Thibault 1990 (Table 1)	Loam	
Sb	75	150	8	Sheppard and Thibault 1990 (Table 1)	Loam	
Se	250	500	25	Sheppard and Thibault 1990 (Table 1)	Loam	
Sm	500	1000	50	ORNL 1997a (Table 2.3, p. 2-18)	Generic soil	Sheppard and Thibault 1990
Sn	50	100	5	ORNL 1997a (Table 2.3, p. 2-18)	Generic soil	Sheppard and Thibault 1990
Sr	15	30	2	Friedman et al. 1990 (Table 4.1, p.21)	Generic soil	ORNL 1997a, DOE 1998
Tc	0.36	0.72	0.04	DOE 1992 (Appendix A, Table A.4.1.8, p. 86)	Silty clay	ORNL 1987
Th	1500	3000	150	ORNL 1997a (Table 2.3, p. 2-18)	Generic soil	Sheppard and Thibault 1990
U	25	50	3	Friedman et al. 1990 (Table 3.8)	Silty clay (Maryville Limestone)	ORNL 1987, ORNL 1997a, CH2M-Hill 2000
Zr	25	50	3	ORNL 1997a (Table 2.3, p. 2-18)	Generic soil	

[a]Weighted average of 14 samples from Rothschild et al. 1984 (Table 6, samples #4 and 16-18 omitted as non-representative), and 24 samples from Davis et al. 1984 (Table 7).
[b]Screening model K_d value decrease by a factor of 100 from base case value based on range of data in primary and supporting references.
[c]Cl-36 is not included in the EMDF estimated radionuclide inventory. Cl-36 is included in the EMDF radionuclide screening model.

DOE = U.S. Department of Energy
EMDF = Environmental Management Disposal Facility
IAEA = International Atomic Energy Agency
ORNL = Oak Ridge National Laboratory

The partition coefficient for sediment in the surface waterbody was specified as 0.0 cm^3/g for all isotopes. This specification was done to maximize the estimated partitioning of isotopes into the liquid phase, which, in the model, will allow for more radionuclides to be available for fish uptake and irrigation. This assumption is pessimistic and will increase the predicted dose to the receptor.

Also shown in Table G.10 are partition coefficients used for the screening modeling (see Sect. G.4.4), and references used to guide selection of the partition coefficient values. If available, ORR-specific data were used.

The uncertainty in appropriate assignment of partition coefficient values for long-term performance modeling is addressed in Sect. 3.2.2.6 of the EMDF PA report, which considers both material characteristics and variability in the geochemical environment through space and time. Sensitivity of dose estimates to variation in partition coefficient values for particular model segments is evaluated in Sect. G.6.2. The sensitivity of peak dose estimates to uncertainties in partition coefficient values for major dose-contributing radionuclides is a primary focus of the uncertainty analysis presented in Sect. G.6.3.

G.4.3.7 Transfer Factors

RESRAD-OFFSITE uses transfer factors to convert soil and/or water concentrations to other components. Brief descriptions of the transfer factor summaries provided within the code, selected by pressing the F1 key within the RESRAD-OFFSITE graphic user interface, for each isotope are described below.

- Soil to plant transfer factors: Represents the nuclide concentration in vegetables, fruits, and livestock feed products at the time of harvest (fresh weight basis) due to root uptake from soil containing a unit concentration (dry weight basis) of the nuclide. Four different soil to plant transfer factors must be specified in RESRAD-OFFSITE: fruit, grain, and non-leafy vegetables; leafy vegetables; pasture and silage; and livestock feed grain.
- Intake to animal product transfer factors: Represents the nuclide concentration in the animal meat and milk at the time of slaughter or milking, respectively, due to a uniform intake of unit activity of radionuclide per day. Two different intake to animal product transfer factors must be specified in RESRAD-OFFSITE: meat (one value for all meat types considered) and milk.
- Water to aquatic food transfer factors: Represents the nuclide concentration in aquatic food products such as fish and crustacea at the time of harvest from the simulated surface waterbody containing a unit concentration of radionuclide in the aqueous phase. Two different water to aquatic food transfer factors must be specified in RESRAD-OFFSITE: fish and crustacea.

The modeling performed used transfer factors developed by the Pacific Northwest National Laboratory (PNNL) (PNNL 2003). These transfer factors were used because of their recent development and the availability of transfer factors for simulated radionuclides in this data set. The transfer factors used in the RESRAD-OFFSITE modeling were obtained from the tables in the Argonne National Laboratory Data Collection Handbook (Yu et al. 2015b) that list soil to plant, intake to animal, and water to aquatic food transfer factors from PNNL 2003.

RESRAD-OFFSITE requires the specification of four different soil to plant transfer factors: fruit, grains, and non-leafy vegetables; leafy vegetables; pasture and silage; and livestock feed grain. The Argonne National Laboratory Data Collection Handbook (Yu et al. 2015b) provides transfer factors for fruits, grain, root vegetables, and leafy vegetables from PNNL 2003. For the fruit, grains and non-leafy vegetables transfer factors used in the modeling, the arithmetic mean (average) of the fruit, grains, and root vegetable soil to plant transfer factors from PNNL 2003 were assigned to each of the simulated radionuclides. For the leafy vegetables transfer factors used in the modeling, leafy vegetables transfer factors from PNNL 2003 were assigned to each of the simulated radionuclides. The grain transfer factors from PNNL 2003 were used for both the pasture and silage and livestock feed grain transfer factors. Iodine-129 did not have a soil to plant transfer factor listed in PNNL 2003, so the RESRAD-OFFSITE default soil to plant transfer factor for this radionuclide was used for all plant types.

Two different intake to animal product transfer factors must be specified in RESRAD-OFFSITE: meat and milk. It is assumed that the resident farmer consumes beef, poultry, and eggs produced in the affected area. Since only one meat transfer factor can be specified, a consumption weighted transfer factor was calculated for each radionuclide to represent intake for the three types of animal products. Consumption weighted transfer factors were calculated using the following formula:

$$\text{Consumption Weighted TF} = (CR_{beef}TF_{beef} + CR_{poultry}TF_{poultry} + CR_{eggs}TF_{eggs}) / (CR_{beef} + CR_{poultry} + CR_{eggs})$$

where:

CR = consumption rate of specified animal product (kg/year)
TF = intake-to-animal transfer factor for specified meat type (pCi/kg)/(pCi/day).

Intake to animal product transfer factors for beef, poultry, and eggs were obtained from PNNL 2003 as documented in the Argonne National Laboratory Data Collection Handbook (Yu et al. 2015b). U. S. Department of Agriculture average per-capita intake rates for red meat, poultry, and eggs from 1970 to 1997 (Putnam et al. 1999) were used to calculate the consumption weighted transfer factors. Table G.11 provides a summary of consumption rates used to develop the consumption weighted transfer factors.

Table G.11. Base case model consumption rates for beef, poultry, and eggs

Parameter	Value (kg/year)	Primary source	Secondary source
Beef consumption rate	55.4	Putnam et al. 1999 red meat average 1970 to 1997	ANL DCH Table 7.7.2
Poultry consumption rate	21.3	Putnam et al. 1999 poultry average 1970 to 1997	ANL DCH Table 7.7.2
Eggs consumption rate	15.2	Putnam et al. 1999 eggs average 1970 to 1997	ANL DCH Table 7.8.2
Total meat consumption	91.9[a]	–	–

[a] The total meat consumption is equal to the sum of the beef, poultry, and eggs consumption rates.

ANL DCH = Argonne National Laboratory Data Collection Handbook (Yu et al. 2015b)

Intake to animal product transfer factors from milk were obtained from PNNL 2003 as documented in the Argonne National Laboratory Data Collection Handbook (Yu et al. 2015b), which lists transfer factors for cow's milk.

Carbon-14 and H-3 soil to plant (fruit, grain, non-leafy vegetables, leafy vegetables, livestock and cattle feed) and intake to animal product (meat, milk) transfer factors were not obtained from PNNL 2003. RESRAD-OFFSITE does not allow the user to specify soil to plant or intake to animal product transfer factors for these radionuclides. The code calculates these values to account for the complex environmental transport pathways that are simulated in RESRAD-OFFSITE.

Water to aquatic food transfer factors for fresh water whole fish were obtained from PNNL 2003 as documented in the Argonne National Laboratory Data Collection Handbook (Yu et al. 2015b). The RESRAD-OFFSITE default water to aquatic transfer factor for H-3 was used because there was no value provided by PNNL 2003 as documented in the Argonne National Laboratory Data Collection Handbook. RESRAD-OFFSITE also requires transfer factors for fresh water crustacean, but it was assumed that the resident farmer does not ingest crustacea from the affected area.

G.4.3.8 Storage Times

Storage times are used to calculate radioactive ingrowth of progeny and radioactive decay during storage. Specifying storage times in RESRAD-OFFSITE indicates the duration for which the various foods (e.g., fruits, grains, vegetables, meat, milk, and fish) and water are stored before being consumed. RESRAD-OFFSITE default storage times were assessed and deemed suitable for PA modeling.

G.4.3.9 Physical and Hydrological

A 30-year record of daily average precipitation and temperature for the Oak Ridge area was provided as input for the HELP surface water balance model simulation. These data result in a simulated average annual

rainfall total of 54.39 in./year. Given specified values of 0.568 for the evaporation coefficient and 0.963 for the runoff coefficient at the disposal facility, RESRAD-OFFSITE calculates an infiltration rate of 0.88 in./year through the facility, matching the long-term condition (Stage 4) predicted in HELP simulations (see Appendix C).

G.4.3.10 Primary Contamination

Specified values for input parameters related to the primary contamination (i.e., waste) and the cover are listed in Table G.12. A majority of the parameters are based on the EMDF design specification.

Table G.12. Contaminated zone and clean cover parameters

Parameter	Description	Value
Thickness of contaminated zone	Specified waste thickness	17.5 m (57.4 ft)
Total porosity of contaminated zone	Ratio of pore volume to total contaminated zone volume	0.419
Dry bulk density of contaminated zone	Bulk density of contaminated zone	1.9 g/cm^3
Field capacity of contaminated zone	Volumetric moisture content of soil at which (free) gravity drainage ceases (the amount of moisture that will be retained in soil against the force of gravity)	0.307
Soil b parameter of contaminated zone	Dimensionless, empirical parameter used to evaluate volumetric water saturation of the soil according to the soil characteristic function called “conductivity function”	7.75
Longitudinal dispersivity in the contaminated zone	Ratio between longitudinal dispersion coefficient and pore water velocity	1.8 m
Hydraulic conductivity of contaminated zone	Measure of soil’s ability to transmit water when submitted to a hydraulic gradient (location is the contaminated zone above the water table, which is the entire waste volume)	5.99 m/year
Effective porosity of contaminated zone	Ratio of the part of pore volume through which water can move to the total volume	0.234
Thickness of clean cover	Distance from top of the clean cover to top of the contaminated zone	3.353 m (11 ft)
Total porosity of clean cover	Ratio of pore volume to total volume of clean cover	0.4
Dry bulk density of clean cover	Bulk density of clean cover material	1.5 g/cm^3
Erosion rate of clean cover	Average volume of cover material removed per unit of ground surface area per unit of time	0 m/year
Volumetric water content of clean cover	Fraction of total volume of cover occupied by water	0.05

G.4.3.11 Agricultural Areas and Livestock Feed Growing Areas

The agricultural areas available in RESRAD-OFFSITE include a fruit, grain, and non-leafy vegetables field and a leafy vegetable field. Livestock feed growing areas consist of two crops, pasture and silage, and grains.

A recharge rate of 0.224 m/year (8.8 in./year), the MODFLOW-predicted (Appendix D) upper bound of regional recharge for the Nolichucky Shale geologic formation, was assumed for the agricultural areas and livestock feed growing areas. In addition to the recharge, it was assumed that 0.15 m/year of irrigation water was applied to the agricultural areas. A runoff coefficient of 0.734 was assigned to the agricultural areas

based on the recharge and irrigation assumptions. Agricultural and livestock feed area parameters are listed in Table G.13.

Table G.13. Agricultural areas and livestock feed growing areas parameters

Parameter[a]	Value
Fraction of area directly over primary contamination	0.0
Irrigation applied per year	0.15 m/year
Evapotranspiration coefficient	0.568
Runoff coefficient	0.734
Depth of soil mixing layer/plow layer	0.15 m

[a] Parameters apply to the following fields: fruit, grain, and non-leafy vegetables; leafy vegetables; and pasture, silage crops, and grain

G.4.3.12 Offsite Dwelling Area

The 1024 m^2 offsite dwelling area is assumed to be located south of the EOW (Fig. G.1). Minimal irrigation (0.015 m/year) is assumed to be applied to the dwelling area due to sufficient precipitation. Model-assigned recharge is assumed to be approximately equal to the upper bound of regional recharge for the Nolichucky Shale geologic formation, 8.8 in./year. A runoff coefficient of 0.636 was assigned to the dwelling site based the recharge and irrigation assumptions.

G.4.3.13 Atmospheric Transport

The EMDF cover is assumed to be competent and prevent vapor-phase and particulate waste release to the atmosphere (see Appendix C). Accordingly, atmospheric transport from the contaminated zone is inhibited; however, the atmospheric pathway in RESRAD-OFFSITE remained active for simulating radionuclide release for inhalation exposure in agricultural areas and for certain IHI scenarios (see Appendix I). Atmospheric parameters were specified as RESRAD-OFFSITE default values, except for wind speed and stability class, which are as specified in the available RESRAD-OFFSITE meteorological STability ARray program file for Knoxville, TN.

For the base case resident farmer scenario, the Instantaneous Equilibrium Desorption release option was used to simulate radionuclide release from the waste. Radionuclide releases from the waste to surface runoff and the atmosphere are not computed by RESRAD-OFFSITE when this release option is used. Releases to surface runoff do not apply due to the negligible amount of cover erosion assumed during the 10,000-year simulation period (Appendix C). Dose contribution from atmospheric release from the waste was evaluated in both the vapor release and biointrusion screening models (Sect. G.4.4.2) and found to be negligible.

G.4.3.14 Unsaturated Zone Hydrology

The EMDF model developed in RESRAD-OFFSITE partitioned the unsaturated zone (layers beneath the waste, but above the water table) into five distinct zones. Each zone is uniquely identified by a RESRAD-OFFSITE zone number that corresponds to features of the vadose zone beneath the waste:

- UZ1 – Protective soil (layer protects liner)
- UZ2 – Drainage layer (leachate collection system)
- UZ3 – Geosynthetic clay liner

- UZ4 – Soil geobuffer
- UZ5 – Native vadose zone saprolite or bedrock.

A summary of major parameters by zone is provided in Table G.14. Each unsaturated zone is assigned a longitudinal dispersivity of 0.1 m. Values such as porosity, field capacity, and hydraulic conductivity for non-native materials were specified to align with HELP default values for each specific material type. The EMDF preliminary design specified a K value of 1.0E-07 cm/sec, but the RESRAD-OFFSITE code would not accommodate such a low value for the imposed infiltration rate (0.88 in./year) through the vadose zone. For the RESRAD-OFFSITE model the K value for UZ3 was increased by a factor of 10 to 1.0E-06 cm/sec, to accommodate the limitation in executing the code. Values for native materials (UZ5) are from *Effective Porosity and Pore-throat Sizes of Mudrock Saprolite from the Nolichucky Shale Within Bear Creek Valley on the Oak Ridge Reservation: Implications for Contaminant Transport and Retardation Through Matrix Diffusion* (Dorsch and Katsube 1996).

Table G.14. Unsaturated zone hydrology

Zone number	Thickness (m)	Dry bulk density (g/cm^3)	Total porosity	Effective porosity	Field capacity	Hydraulic conductivity (m/year)	b parameter
UZ1	0.305	1.4	0.463	0.294	0.232	117	5.4
UZ2	0.305	1.6	0.397	0.389	0.032	94600	4.05
UZ3	0.9144	1.5	0.427	0.195	0.418	0.315[a]	11.4
UZ4	3.048	1.5	0.419	0.234	0.307	3.15	11.4
UZ5	4.846	1.8	0.353	0.270	0.247	16.7	10.4

[a] Increasing UZ3 K value from preliminary design value 0.0315 m/year to 0.315 m/year, was required to run RESRAD-OFFSITE code

The total depth of the unsaturated zone was assumed to be 30.9 ft, which is the average depth to water below the EMDF as determined by MODFLOW modeling (Appendix D). Layer thicknesses for non-native materials (unsaturated zones 1to 4) were based on the preliminary design for the EMDF cover (UCOR 2020a). The thickness of the native vadose zone soil (UZ5) was equal to the difference between the assumed depth to water below the EMDF and the total thickness of the non-native materials.

G.4.3.15 Saturated Zone Hydrology and Groundwater Transport

Because of the importance of water ingestion to predicted dose for the release to groundwater scenario, specification of saturated zone hydrology parameters is particularly important. Geologic-material-specific parameters such as dry bulk density, total and effective porosity, and hydraulic conductivity are from soil data collected at ORR (Table G.15). Model parameters such as hydraulic gradient to well and surface water body are derived from MODFLOW simulations (see Appendix D). The hydraulic gradient to the well was adjusted upwards from the average hydraulic gradient from MODFLOW model results to account for the lower saturated zone dilution in the RESRAD-OFFSITE model compared to the MT3D model. Final values for other RESRAD-OFFSITE parameters, including depth of aquifer contributing to well and depth of aquifer contributing to surface water body, were based on comparison with MODFLOW and MT3D results (refer to Sect. 3.3.5.2 of the PA).

Table G.15. Saturated zone model parameter values

Parameter	Value	Units
Thickness of saturated zone	60.96	m
Dry bulk density of saturated zone	2.1	g/cm^3
Total porosity of saturated zone	0.24	unitless
Effective porosity of saturated zone	0.20	unitless
Hydraulic conductivity of saturated zone	26.8	m/year
Values Specified from EOW to Receptor Well		
Hydraulic gradient	0.054	m/m
Depth of aquifer contributing	40	m
Longitudinal dispersivity	10	m
Horizontal lateral dispersivity	1	m
Vertical dispersivity	0.1	m
Values Specified from EOW to Receptor Surface Water Body		
Hydraulic gradient	0.036	m/m
Depth of aquifer contributing	30.48	m
Longitudinal dispersivity	31.5	m
Horizontal lateral dispersivity	3.15	m
Vertical dispersivity	0.315	m

EOW = edge of waste

Thickness of the saturated zone is set at 200 ft. The active BCV saturated zone is much thicker than 200 ft, but the BCV hydrogeologic conceptual model, results of tracer studies in BCV and results of the EMDF groundwater flow three-dimensional radionuclide transport modeling suggest that the depth to which contamination introduced at the surface penetrates the saturated zone is limited. Given the RESRAD-OFFSITE model structure, radionuclide concentrations at the receptor well can depend on the depth of the well relative to the depth of the aquifer. Preliminary sensitivity analysis suggested that given the well depth assumed for the analysis (131 ft, which is based on comparison of the RESRAD-OFFSITE and MT3D model results), the well concentration and predicted peak dose would not be sensitive to assuming a more realistic (larger) value for aquifer depth.

Dispersivity values were assigned in accordance with generally accepted relationships between dispersivity and the potential plume length. Longitudinal dispersivity values were estimated as approximately 1/10 of the travel distance to a well or surface water body. Lateral dispersivity was estimated as 1/10 of longitudinal dispersivity; likewise vertical dispersivity was assigned as equal to 1/10 of the value for lateral dispersivity (equal to 1/100 of longitudinal dispersivity).

The parameter values assigned for the saturated zone hydrology group are summarized in Table G.15.

Site layout and groundwater transport parameters are assigned such that the receptor well is 100 m from the southern EOW and is aligned along the centerline of the emanating radionuclide plume. The surface water body (Bear Creek) is 215.5 m downgradient of the well and the water body dimensions are as described in Sect. G.4.3.17.

G.4.3.16 Water Use

Water consumption by the receptor, including water used to cook food, was assumed to occur at a rate of 2 L/day. The model assumed that 100 percent of this water and 225 L/day of water used per person inside the dwelling for cleaning and showering was derived from the well located 100 m from the EOW. The assumed two beef cattle and two dairy cows derive 100 percent of their water from Bear Creek, which is

assumed to be impacted by contaminated groundwater emanating from the facility. Irrigation of the various crop fields was simulated at a rate of 0.15 m/year, with 100 percent of the water coming from contaminated portions of Bear Creek. An irrigation rate of 0.015 m/year was specified for the offsite dwelling. Water use parameters assigned for RESRAD-OFFSITE simulations are provided in Table G.16.

Table G.16. Water use parameter values

Parameter	Value	Units
Human consumption	730	L/year
Indoor dwelling use	225	L/day
Beef cattle	50	L/day
Dairy cows	160	L/day
Well pumping rate	332	m^3/year

It is possible that in an actual resident farming scenario the receptor would obtain groundwater and surface water from areas that are less contaminated than is predicted by the RESRAD-OFFSITE model. This would reduce dose to the receptor.

G.4.3.17 Surface Waterbody

The surface water point of exposure is assumed to occur at a location that would provide flow during drier parts of the year. A surface water exposure location on Bear Creek near the junction of NT-11 was selected because year-round flow is more typically encountered there than in surface water tributaries closer to the landfill.

The dimensions of the section of Bear Creek assumed to be impacted by radionuclides are 100 m in length, 5 m in width, and 0.5 m in depth with a simulated surface area of 500 m^2 and volume of 250 m^3. A representative mean residence time in the surface waterbody of 0.0001 year was specified based on an estimated average flow rate in Bear Creek at NT-11 of approximately 1570 gpm (UCOR 2020b, Sect. 3.4).

G.4.3.18 Ingestion Rates

Ingestion rates of food and incidental soil consumed by the receptor are based on EPA guidance (EPA 2011), with the exception of the meat ingestion rate, which is equal to the sum of the average annual per capita ingestion rates of beef, poultry, and eggs in the United States from 1970 to 1997 (Putnam et al. 1999). Simulated values are presented in Table G.17. The fish ingestion rate reflects limited recreational fishing in Bear Creek. It is assumed that there is not any consumption of crustacea or mollusks, which is appropriate given the EMDF location in eastern Tennessee.

Table G.17. Simulated ingestion rate values

Parameter	Value	Units	Fraction from affected area
Fish	2.43	kg/year	1.0
Fruit, grain, non-leafy vegetables	176	kg/year	0.5
Leafy vegetables	17	kg/year	0.5
Meat	91.9	kg/year	0.25
Milk	110	L/year	0.5
Soil (incidental)	36.53	g/year	[a]

[a]The fraction of this intake from each contaminated area is proportional to the occupancy in that area.

Total fluid milk ingestion is given as the equivalent of 84 L/year on Table 11-12 of EPA 2011; however, the base case milk ingestion value for EMDF is set at 110 L/year. The higher milk ingestion value serves to increase the total food ingestion dose and thereby bias the dose estimate toward higher than expected values. Values for ingestion of non-leafy produce and leafy vegetables are consistent with the data listed in Tables 9-1, 9-6, and 12-1 of EPA 2011.

RESRAD-OFFSITE exposure pathways do not include poultry or egg consumption explicitly. The animal food ingestion pathways represented in the model are limited to meat and milk from cows. To account for possible dose contributions from consumption of poultry and eggs, an effective meat ingestion rate (91.9 kg/year) is applied, representing the sum of beef (55.4 kg/year), poultry (21.3 kg/year), and eggs (15.2 kg/year) given in Putnam et al. (1999). Adjusted meat transfer factors are also calculated and applied in the RESRAD–OFFSITE dose analysis (Sect. G.4.3.7).

The Oak Ridge area is assumed to remain populated and urbanized in the future, with many commercial food sources (e.g., restaurants, grocery stores, farmer's markets) available in close proximity to the hypothetical BCV farm adjacent to EMDF. Food consumption is assumed to include some uncontaminated food as well as locally grown agricultural products contaminated with radionuclides released from the EMDF. For plant foods and milk, 50 percent of the food ingested is assumed to come from the contaminated agricultural areas. For meat ingestion, 25 percent percent is assumed to come from farm raised animals that ingest contaminated water and feed. The RESRAD-OFFSITE sensitivity analyses include evaluating uncertainty in the fraction of food products obtained from contaminated areas (Sect. G.2.6.8.1).

Fish ingestion is based an EPA recommendation of 54 g/day for recreational fishing in areas with large bodies of water (EPA 1990), combined with an exposure frequency of 45 days/year, which is the value used as recreational surface water exposure frequency for the human health risk assessment in the BCV Remedial Investigation (DOE 1997). Because of the limited populations of larger fish in BCV, and because the proportion of fish caught locally is set at 1.0, the fish ingestion rate of 2.43 kg/year is probably overestimates the likely fish ingestion dose.

The incidental soil ingestion rate is based on the EPA recommended value (100 mg/day) and the fractional occupancy time in the agricultural areas (Sect. G.4.3.19). The annual inhalation rate required for the inhalation pathway dose calculation (Sect. G.3.3) was set at the RESRAD-OFFSITE default value of 8400 m^3/year.

G.4.3.19 Occupancy

Specified occupancy fractions represent the assumed durations that the receptor spends inside or outside the specified areas. For example, occupancy factors specified for farmed areas include agricultural land or pasture land contaminated by irrigation or by atmospheric deposition (if occurring). Those occupancy factors are used to compute exposure from direct external radiation from contaminated soil in irrigated fields, and internal exposure due to incidental ingestion of soil and inhalation of dust resuspended from contaminated soil. The RESRAD-OFFSITE base case model assumes that the receptor spends approximately 2.6 weeks outdoors on the primary contamination (5 percent of time), 26 weeks inside the offsite dwelling (50 percent of time), 2.6 weeks outdoors at the offsite dwelling (5 percent of time), and 10 percent of the time at each of the four fields within the farmed areas (40 percent of the time total). Overall, the receptor is assumed to spend 100 percent of the time at EMDF, thereby inducing a bias toward a greater dose from the external, inhalation, and soil ingestion pathways.

G.4.3.20 Input Parameter Summary

Attachment G.1 to this appendix provides an extensive summary of base case input parameters, including RESRAD-OFFSITE assigned parameter identifiers, default values and range of values accepted by the computer code, and sources for parameter value assignments. The RESRAD-OFFSITE model input/output summary file for the base case simulation is included in Attachment G.2.

G.4.4 SCREENING MODELS FOR GROUNDWATER AND COVER RELEASE PATHWAYS

Screening model applications of RESRAD-OFFSITE were developed to support radionuclide screening for the release to groundwater pathway and as the basis for eliminating upward release of radionuclides through the cover to the atmosphere and biosphere from the set of environmental pathways included in the all-pathways dose analysis of the PA. These screening applications are described in the following two subsections. The entire radionuclide screening process (including the RESRAD-OFFSITE groundwater pathway screening model application) is described in Sect. 2.3. of the PA, and the full basis for elimination of the cover release pathway (including the quantitative release estimates based on two RESRAD-OFFSITE screening applications) is described in Sect. 3.2.2.2 of the PA.

G.4.4.1 Groundwater Pathway Screening Model

As described in Sect. G.4.2, screening level modeling was performed to reduce the number of isotopes in the base case model by identifying isotopes that have negligible contribution to the total dose. The screening model was created from the base case model described in Sect. G.4.3, with modifications to make the model results biased to greater predicted dose.

The screening model assumed contaminant movement was not limited by containers or engineered barriers. Therefore, the entire waste area was assumed to be exposed to infiltrating water and contaminants were leached from the waste and subsequently migrated into the subsurface. An infiltration rate of 0.22 m/year (8.8 in./year) was assumed, which is the upper bound of regional recharge within areas located within the Nolichucky Shale geologic formation as indicated by MODFLOW simulation results (see Appendix D).

To simulate the leaching of radionuclides from the waste, partition coefficients for all isotopes were decreased by either a factor of 10 or 100 (see Table G.10) from values assigned in the base case model and leaching was simulated using the Instantaneous Equilibrium Desorption release mechanism, which is the same release model used in the base case model. The resulting radionuclide leaching from the waste to infiltrating water occurs significantly faster than when the base case infiltration rate and partition coefficients are specified.

Screening simulation source concentrations were also placed at the upper bound of potential values (Table G.18, also refer to Sect. 2.3 of the EMDF PA report). For example, the screening model source concentration for Tc-99 was 1.36E+06 pCi/g, whereas the as-disposed waste concentration (derived from the estimated inventory) is nearly six orders of magnitude lower (2.80 pCi/g).

Table G.18. Screening model source concentrations and results

Radionuclide	Half-life (years)	Screening source concentration (pCi/g)	Phase 1: Half-life > 5 years?	Phase 2: Peak groundwater dose > 0.4 mrem/year for 10,000 year simulation?	Retain for dose analysis?
Ac-227	2.18E+01	4.89E+04	Yes	Yes	Yes
Am-241	4.32E+02	2.30E+03	Yes	Yes	Yes
Am-243	7.38E+03	2.29E+01	Yes	Yes	Yes
Ba-133	1.07E+01	2.71E+01	Yes	No	Intruder
Be-10	1.50E+06	7.16E+05	Yes	Yes	Yes
C-14	5.73E+03	6.27E+05	Yes	Yes	Yes
Ca-41	1.00E+05	4.11E+06	Yes	Yes	Yes
Cd-113m	1.36E+01	1.11E+05	Yes	No	No[a]
Cf-249	3.51E+02	3.92E-04	Yes	No	Intruder
Cf-250	1.31E+01	1.70E-02	Yes	No	Intruder
Cf-251	8.98E+02	7.36E-05	Yes	No	Intruder
Cf-252	2.60E+00	1.25E+03	No	N.S.[b]	No
Cl-36[e]	3.01E+05	1.00E+00	Yes	Yes	No[a]
Cm-243	2.85E+01	4.37E+01	Yes	Yes	Yes
Cm-244	1.81E+01	5.26E+05	Yes	Yes	Yes
Cm-245	8.50E+03	9.80E+01	Yes	Yes	Yes
Cm-246	4.73E+03	1.97E+00	Yes	Yes	Yes
Cm-247	1.56E+07	2.35E+01	Yes	Yes	Yes
Cm-248	3.39E+05	2.29E+01	Yes	Yes	Yes
Co-60	5.27E+00	1.93E+06	Yes	No	Intruder
Cs-134	2.10E+00	1.39E+05	No	N.S.[b]	No
Cs-135	2.30E+06	2.46E+06	Yes	Yes	No[a]
Cs-137	3.00E+01	3.82E+08	Yes	No	Intruder
Eu-152	1.33E+01	5.84E+05	Yes	No	Intruder
Eu-154	8.80E+00	7.85E+05	Yes	No	Intruder
Eu-155	4.80E+00	9.98E+05	No	N.S.[b]	No
Fe-55	2.70E+00	4.71E+07	No	N.S.[b]	No
H-3	1.24E+01	4.84E+06	Yes	Yes	Yes
I-129	1.57E+07	4.86E+05	Yes	Yes	Yes
K-40	1.28E+09	5.65E+01	Yes	Yes	Yes
Kr-85	1.10E+01	1.16E+08	Yes	N.S.[c]	No
Mo-93	3.50E+03	4.99E+03	Yes	Yes	Yes
Mo-100	8.50E+18	2.55E-03	Yes	N.S.[c]	No
Na-22	2.60E+00	5.96E-01	No	N.S.[b]	No
Nb-93m	1.36E+01	3.00E+03	Yes	No	Yes[d]
Nb-94	2.03E+04	1.90E+05	Yes	Yes	Yes
Ni-59	7.50E+04	1.55E+06	Yes	Yes	Yes
Ni-63	9.60E+01	1.03E+07	Yes	No	Intruder
Np-237	2.14E+06	5.63E+01	Yes	Yes	Yes

Table G.18. Screening model source concentrations and results (cont.)

Radionuclide	Half-life (years)	Screening source concentration (pCi/g)	Phase 1: Half-life > 5 years?	Phase 2: Peak groundwater dose > 0.4 mrem/year for 10,000 year simulation?	Retain for dose analysis?
Pa-231	3.28E+04	3.17E+00	Yes	Yes	Yes
Pb-210	2.23E+01	4.48E+02	Yes	No	Yes[d]
Pd-107	6.50E+06	3.34E+06	Yes	Yes	No[a]
Pm-146	5.50E+00	1.24E-01	Yes	No	Intruder
Pm-147	2.60E+00	2.67E+06	No	N.S.[b]	No
Pu-238	8.77E+01	7.15E+03	Yes	Yes	Yes
Pu-239	2.41E+04	1.85E+05	Yes	Yes	Yes
Pu-240	6.54E+03	8.44E+03	Yes	Yes	Yes
Pu-241	1.44E+01	2.83E+05	Yes	Yes	Yes
Pu-242	3.76E+05	4.98E+01	Yes	Yes	Yes
Pu-244	8.26E+07	1.11E+01	Yes	Yes	Yes
Ra-226	1.60E+03	1.35E+01	Yes	Yes	Yes
Ra-228	5.75E+00	3.46E+00	Yes	No	Yes[d]
Re-187	4.12E+10	1.94E-03	Yes	No	Intruder
Sb-125	2.80E+00	1.37E+06	No	N.S.[b]	No
Se-79	6.50E+04	2.47E+06	Yes	Yes	No[a]
Sm-151	9.00E+01	5.75E+06	Yes	No	No[a]
Sn-121m	5.50E+01	6.41E+01	Yes	No	No[a]
Sn-126	1.00E+05	1.89E+06	Yes	Yes	No[a]
Sr-90	2.91E+01	3.93E+08	Yes	Yes	Yes
Tc-99	2.13E+05	1.35E+06	Yes	Yes	Yes
Th-228	1.90E+00	1.14E+05	No	No	Yes[d]
Th-229	7.34E+03	3.48E+03	Yes	No	Yes[d]
Th-230	7.70E+04	1.48E+02	Yes	Yes	Yes
Th-232	1.41E+10	2.67E+06	Yes	Yes	Yes
U-232	7.20E+01	8.43E+05	Yes	Yes	Yes
U-233	1.59E+05	5.49E+05	Yes	Yes	Yes
U-234	2.45E+05	1.67E+03	Yes	Yes	Yes
U-235	7.04E+08	2.57E+03	Yes	Yes	Yes
U-236	2.34E+07	4.87E+02	Yes	Yes	Yes
U-238	4.47E+09	2.07E+09	Yes	Yes	Yes
Zr-93	1.53E+06	5.56E+05	Yes	Yes	No[a]

[a] Radionuclide not simulated because insufficient inventory data were available
[b] Radionuclide not simulated due to screening in Phase 1
[c] Radionuclide not simulated due to other reasons
[d] Isotope has half-life less than 5 years or screening dose less than 0.4 mrem/year but was retained for further analysis because it is progeny of another isotope in the inventory. Intruder identifies isotopes simulated for IHI models, but not retained for further analysis.
[e] Cl-36 is not included in the inventory but was simulated in the screening model to provide information for future waste management decisions.

IHI = inadvertent human intrusion

Furthermore, a more stringent (lower) screening criterion was used consisting of a peak drinking water dose less than 0.4 mrem/year, which is equivalent to 10 percent of the 4 mrem/year national primary drinking water standard for beta-gamma emitters (40 *CFR* 141). Although this standard applies to beta-gamma emitting radionuclides, this screening criterion, coupled with the other assumptions biased toward a greater predicted dose such as the use of elevated source concentrations, is believed sufficient such that any radionuclides of importance are not removed from further modeling.

Seven radionuclides (Cf-252, Cs-134, Eu-155, Fe-55, Na-22, Pm-147, and Sb-125) were screened in Phase 1 of the inventory screening process, which removed radionuclides with a half-life of less than 5 years. Thorium-228 has a half-life of less than 5 years, but it was retained for further analysis because it is a progeny of several of the simulated isotopes. Two additional radionuclides, Kr-85 and Mo-100, were removed from the inventory based on other factors. Krypton-85 was removed from the simulated inventory due to the expectation that significant amounts of krypton gas will not be present after waste generation, transport, placement, and in-cell compaction are complete. Molybdenum-100 was removed from the simulated inventory because it is a very stable radionuclide (half-life of 8.5E+18 year) that does not have a dose conversion factor in the RESRAD-OFFSITE database. The very low projected Mo-100 inventory (approximately 1.08E-05 Ci) is not expected to be a significant contributor to dose; therefore, Mo-100 was also excluded from further analysis. Out of the 70 radionuclides considered as part of the potential inventory (Table G.18), a total of 61 radionuclides were included in Phase 2 of the screening process, which is the groundwater screening model. An addition to those 61 radionuclides, a unit concentration of Cl-36 also was included in the screening model to provide information for future waste management decisions.

Overall, out of the 62 radionuclides simulated in the Phase 2 groundwater screening model (Table G.18), a total of 43 radionuclides (42 plus Cl-36) produced a peak dose greater than 0.4 mrem/year and 19 produced a peak dose of less than 0.4 mrem/year. Out of the 19 radionuclides that produced a peak dose of less than 0.4 mrem/year, five radionuclides (Nb-93m, Pb-210, Ra-228, Th-228, and Th-229) are progeny of one of the 45 radionuclides that exceeded the dose criteria. Although Cl-36 would have passed Phase 1 (half-life is 3.01E+05 years) if it were evaluated and it passed Phase 2 (screening model peak dose greater than 0.4 mrem/year) of the screening process, it is not simulated in the inadvertent human intruder or base case scenario simulations, as there are no data available to estimate an EMDF Cl-36 inventory. A total of 48 radionuclides (43 with peak dose greater than 0.4 mrem/year plus five progeny) passed Phase 2 of the screening analysis.

G.4.4.2 Cover Release Screening Models

The EMDF cover is assumed to be fully functional and prevent release of contaminants to the atmosphere by vapor evasion and particulate release (Appendix C); however, potential releases to the atmosphere and biosphere via vapor phase or and biologically-driven transport to the cover surface were evaluated to ensure that potential doses from this release pathway would be below performance objectives. To do this, two additional variations of the EMDF base case model with parameter values selected to represent higher doses from inhalation of H-3, C-14, and airborne particulates and due to direct exposure at the EMDF cover surface were developed.

The two cover release pathway screening models had several modifications biased towards higher doses. Both the vapor-phase and biological transport screening models used the First Order with Transport release model option, which allows the code to calculate the release of radionuclides to the atmosphere and from surface runoff, as releases from these pathways are not simulated when using the Instantaneous Equilibrium Desorption release option. It was assumed that radionuclides were not leached from the waste for these simulations and that all material was available for release to the atmosphere starting at time zero. Simulated radionuclides for both screening models included all of the radionuclides that passed Phase 1 of inventory screening (radionuclide removed if half-life is less than 5 years) and were not excluded from the inventory

for other reasons (e.g., Mo-100 stability). To ensure a pessimistic bias toward higher estimated dose, the as-generated (i.e., no adjustment for clean fill) EMDF waste stream maximum source concentration for each radionuclide was applied. Other conservative assumptions for the cover release evaluations included decreasing the vertical mixing height for inhalation to 1 m and increasing the time that the exposed individual spends outdoors on the waste to 50 percent, while assuming that individual does not spend time at any of the other receptor locations. The last assumption ensures that the modeled dose represents only exposure release to radionuclide release through the cover.

For vapor-phase release, potential C-14 dose from the inhalation pathway was the focus. Parameter assumptions unique to this screening model included decreasing the cover thickness to 1.82 m and increasing the C-14 evasion thickness to 2 m. The vapor release model produced a peak dose of 0.044 mrem/year, which occurred at 0 years and was primarily from C-14. To provide an upper bound on the potential H-3 dose due to water vapor release from the cover, an extreme sensitivity case was evaluated in which the RESRAD-OFFSITE cover thickness value was reduced to approximately 0.27 m, which represents evaporative loss of tritiated water from the upper 0.03 m of the waste.

For the biological transport screening model, dose from the inhalation and direct (external) radiation pathways were considered. The key modification of the screening model was to increase the soil mixing depth to 1 m and reduce the cover thickness to 0.97 m. With this modification the RESRAD-OFFSITE surface mixing model (Yu et al. 2007), results in a cover radionuclide concentration equal to approximately 5 percent of the underlying waste concentration. However, given the low likelihood of significant biointrusive (e.g., animal burrowing or root penetration) transfer of radionuclides to the cover surface, the screening model results for the full set of radionuclides are not representative of potential cover release dose contributions. However the results for I-129 were used to set a bounding dose due to release of volatile forms of I-129 through the cover in gaseous or particulate form, to support eliminating the cover release pathway from the PA analysis (refer to Sect. 3.2.2 of the PA).

G.5 PREDICTIVE MODEL RESULTS

G.5.1 BASE CASE MODEL RESULTS-TOTAL DOSE

Predicted total dose over time for the base case model is presented in Fig. G.7 for the 1000-year compliance period and Fig. G.8 for the 10,000-year time period, including the compliance period and subsequent 9000 years. The results are compared to the performance objectives presented in Table G.4. The peak total dose (i.e., dose from all simulated radionuclides summed) for the 1000-year compliance period is 1.03 mrem/year and occurs at 490 years. After the compliance period, the total dose increases to a peak of 0.95 mrem/year associated with Tc-99 at approximately 1700 years. After the Tc-99 peak the total dose increases to a maximum of 9.13 mrem/year at approximately 5084 years and then gradually decreases through 10,000 years to a predicted total dose at 10,000 years of 0.114 mrem/year. The three distinct peaks in total dose are each associated with a single radionuclide, as presented in the following subsection. Overall, the predicted maximum total dose during the compliance period of 1.03 mrem/year is less than 5 percent of the performance objective (25 mrem/year).

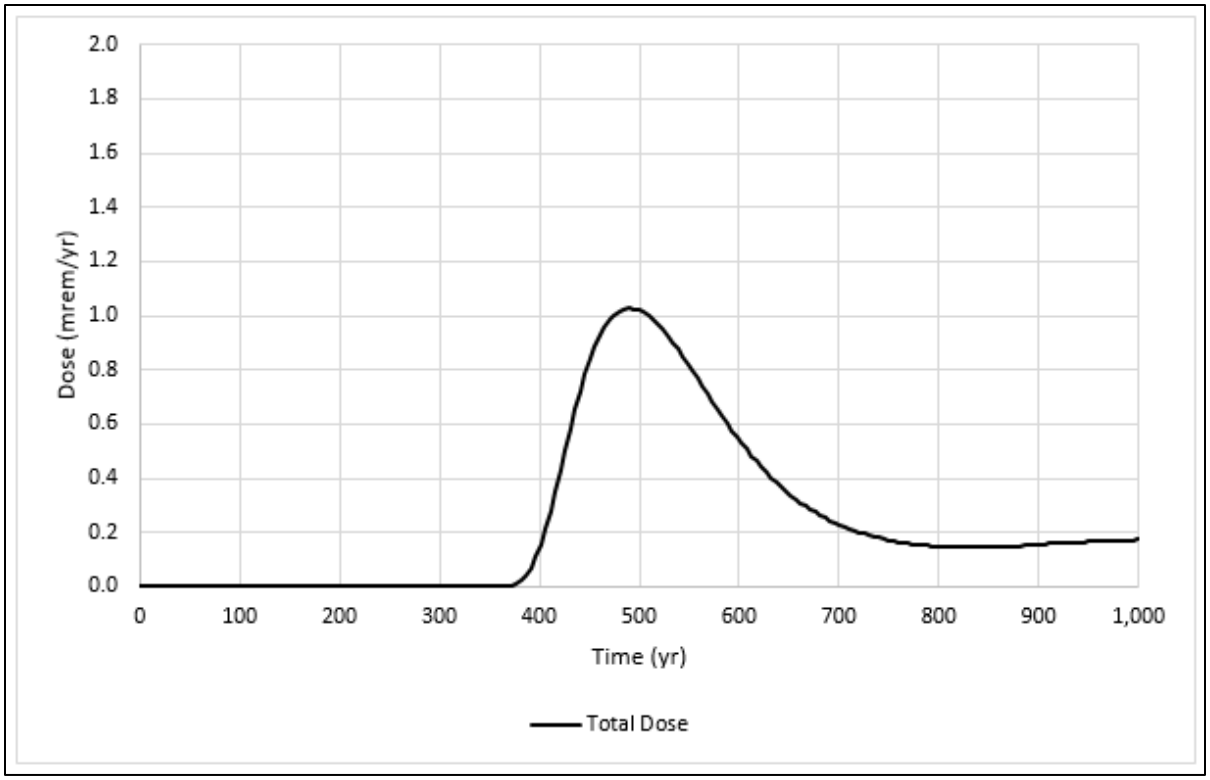

Fig. G.7. Predicted total dose (all pathways, compliance period)

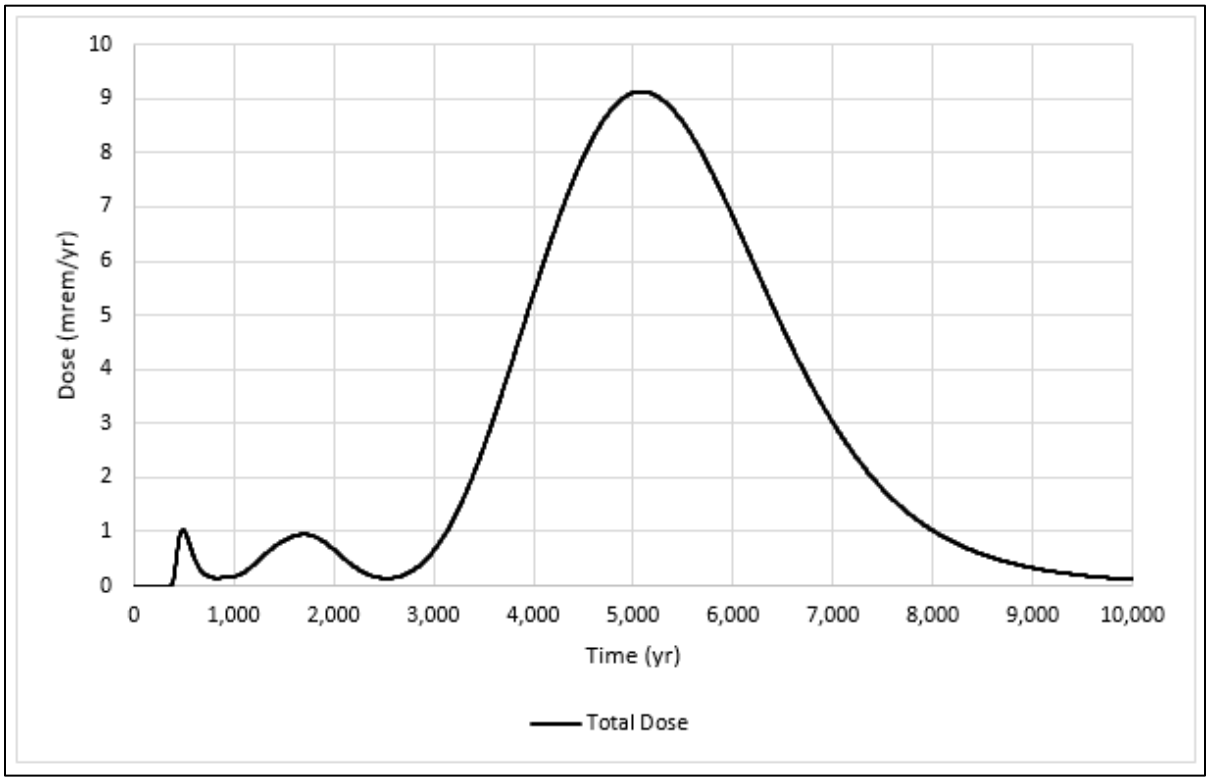

Fig. G.8. Predicted total dose (all pathways, 0 to 10,000 years)

G.5.2 BASE CASE MODEL RESULTS-DOSE FOR EACH RADIONUCLIDE

The primary contributors to total dose consist of C-14, I-129, and Tc-99. Source concentrations input for C-14, I-129, and Tc-99 are based on the post-operational waste concentrations (Table G.9).

For the compliance period, the greatest predicted dose is 1.03 mrem/year from C-14 contributions at 490 years (Fig. G.9). Dose contributions from Tc-99 and I-129 occur after 1000 years. After the compliance period through 10,000 years, I-129 is the largest dose contributor, with a maximum predicted dose of 9.13 mrem/year at 5084 years (Fig. G.10). The peak Tc-99 dose is 0.95 mrem/year at 1700 years.

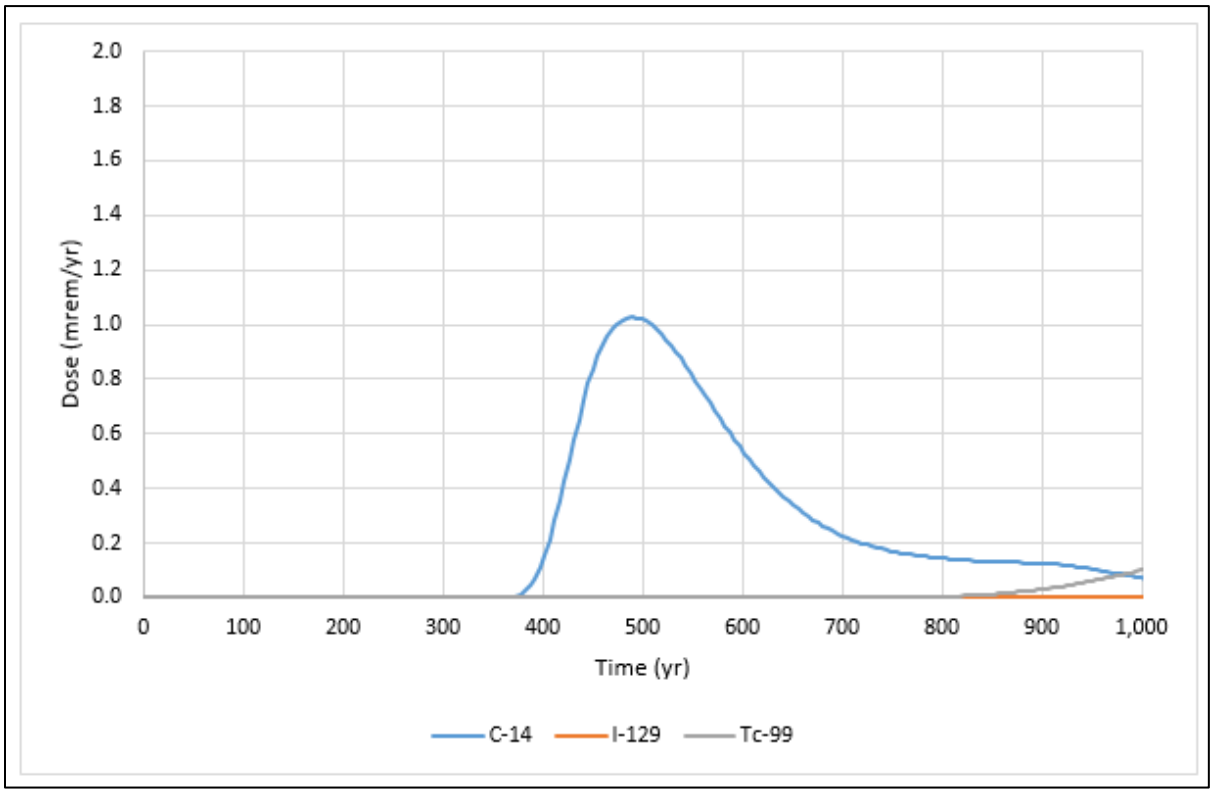

Fig. G.9. Predicted total dose over time by isotope (compliance period)

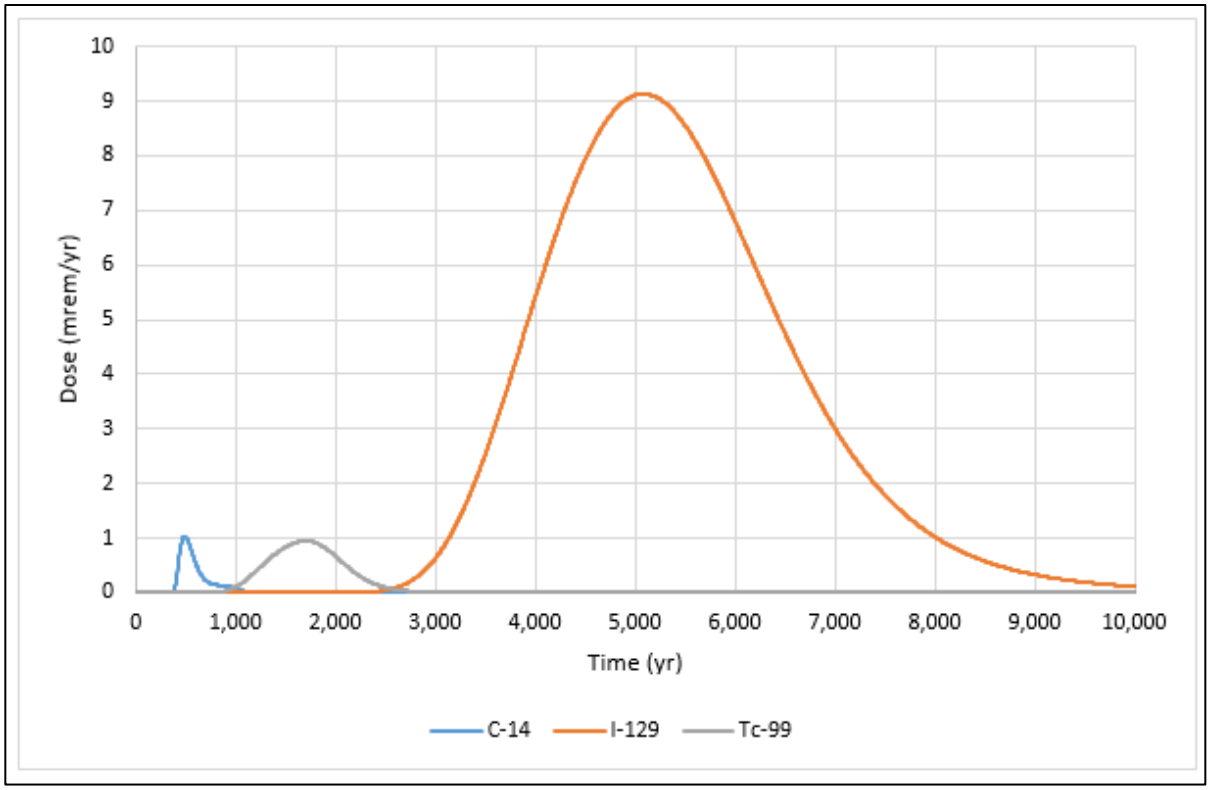

Fig. G.10. Predicted total dose over time by isotope (0 to 10,000 years)

G.5.3 BASE CASE MODEL RESULTS-DOSE BY COMPONENT PATHWAY

The water component pathway (ingestion of well water) is the dominant contributor to total dose. In addition to the water pathway, the four pathways contributing most of the remaining dose during the compliance period in order of descending dose contribution are ingestion of fish, plants (waterborne), milk (waterborne), and meat (waterborne). During the 10,000-year simulation period, the water pathway remains dominant with ingestion of meat (waterborne), milk (waterborne), plant (waterborne), and fish also contributing to the total dose. Because the cover system is assumed to maintain integrity and prevent waste from leaving the disposal facility, there are no predicted dose contributions from any of the airborne pathways. Doses from individual pathways are shown in Figs. G.11 through G.13. Note that pathways with no calculated dose contribution, which include the direct and airborne pathway components of plant, meat, milk, and soil ingestion and the radon pathway, are not included in the plots in Figs. G.11 through G.13. Labels for component pathways are based on the output from RESRAD-OFFSITE.

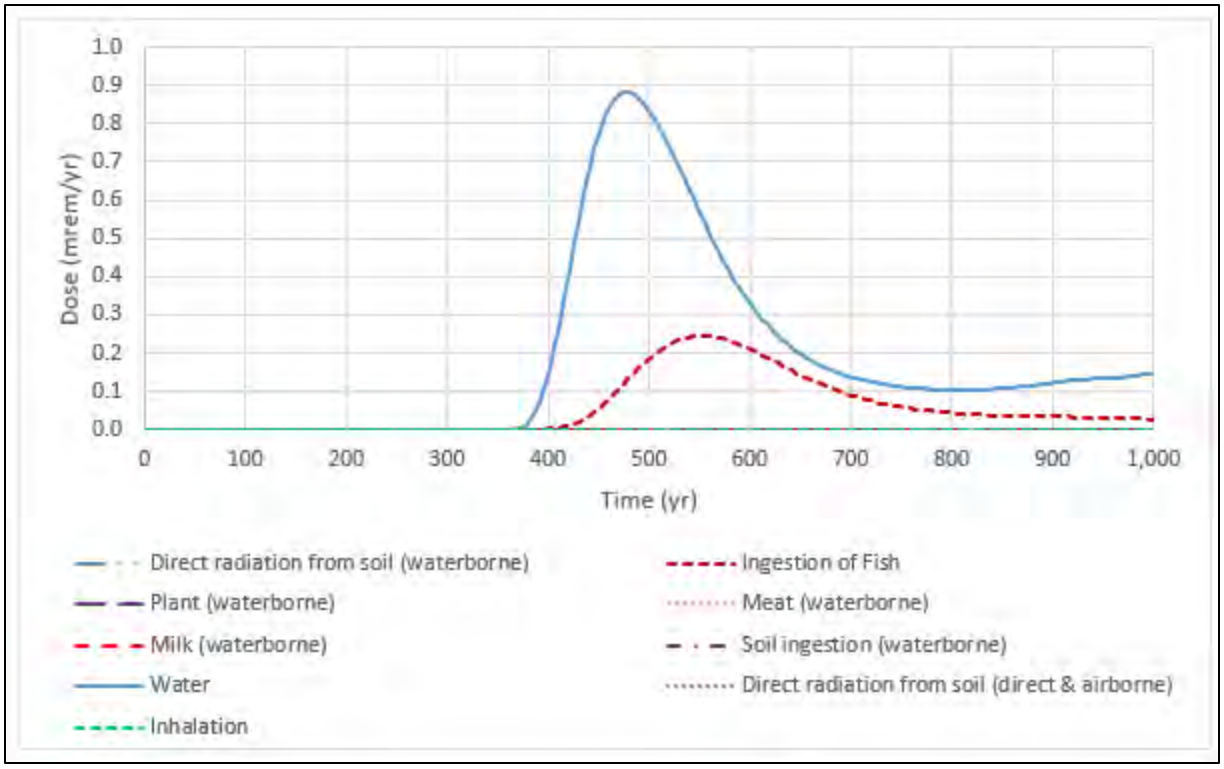

Fig. G.11. Predicted dose by pathway over time during the compliance period

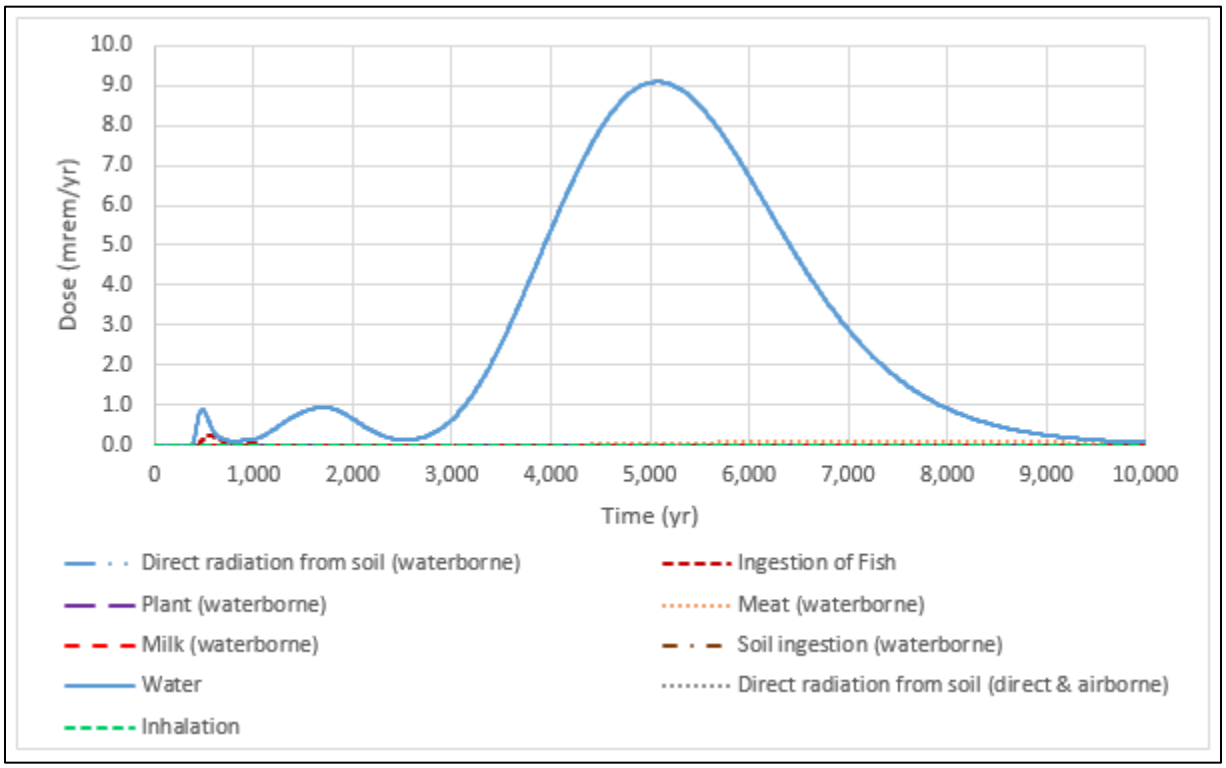

Fig. G.12. Predicted dose over time by pathway (0 to 10,000 years)

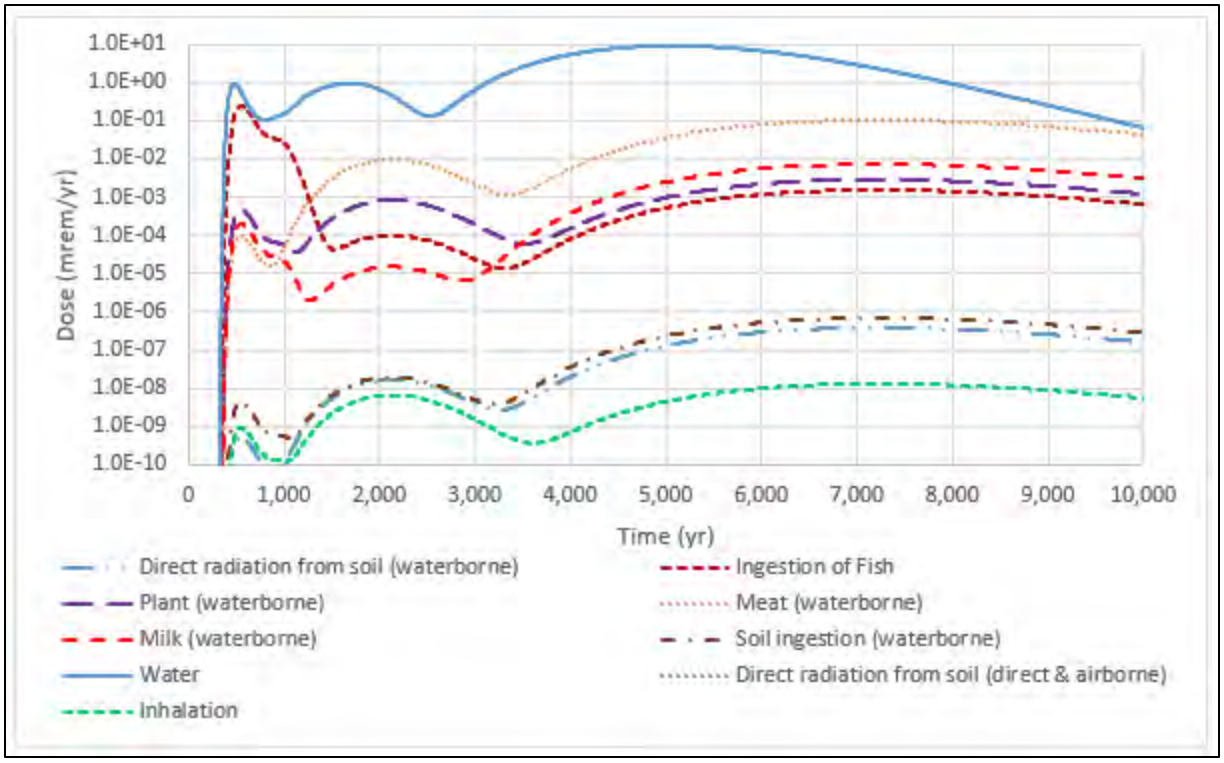

Fig. G.13. Predicted dose over time by pathway (0 to 10,000 years; log scale on dose axis)

G.5.4 RESRAD-OFFSITE SINGLE RADIONUCLIDE SOIL GUIDELINES

Predicted doses and dose performance criteria are one basis for calculating radionuclide waste concentration limits to ensure protection of members of the public. RESRAD-OFFSITE SRSGs are calculated waste activity concentrations that meet a specific dose target for a single radionuclide at a specific time, based on the modeled scenario. The SRSGs do not depend on the assumed radionuclide source concentrations or the corresponding modeled doses, but only on the target dose value and the specific exposure scenario considered. Thus, the SRSGs are dose-based radionuclide source concentration limits for the particular system and scenario simulated.

The RESRAD-OFFSITE SRSG values represent the source concentrations corresponding to the 25 mrem/year dose target, calculated for the base case (all pathways dose) model scenario. For most radionuclides, the minimum SRSG within the 1000-year compliance period occurs at or near 1000 years post-closure.

Table G.19 presents the compliance period minimum SRSG values for the base case scenario, and the corresponding estimated EMDF average (post-operational) concentrations used in the dose analysis for comparison. For the suite of simulated isotopes, the modeled EMDF source concentrations are less than the RESRAD-predicted minimum SRSG values.

Table G.19. RESRAD single radionuclide soil guidelines for the all pathways scenario (compliance period minimum values)

Radionuclide	SRSG (25 mrem/year) (pCi/g)	EMDF post-operational source concentration (pCi/g)
Ac-227[a]	7.23E+13	2.92E-03
Am-241[a]	3.43E+12	5.90E+01
Am-243[a]	2.00E+11	2.97E+00
Be-10[a]	2.36E+10	2.53E-05
C-14	1.32E+01	5.40E-01
Ca-41[a]	8.35E+10	4.21E-02
Cm-243[a]	5.05E+13	4.30E-01
Cm-244[a]	8.09E+13	1.26E+02
Cm-245[a]	1.72E+11	3.83E-02
Cm-246[a]	3.05E+11	1.59E-01
Cm-247[a]	9.28E+07	1.04E-02
Cm-248[a]	4.14E+09	5.59E-04
H-3	8.52E+12	4.64E+00
I-129[a]	1.75E+08	3.50E-01
K-40[a]	6.98E+06	3.28E+00
Mo-93[a]	9.52E+11	3.88E-01
Nb-93m[a]	2.39E+14	2.33E-01
Nb-94[a]	1.86E+11	1.63E-02
Ni-59[a]	5.91E+10	3.04E+00
Np-237[a]	7.03E+08	3.25E-01
Pa-231[a]	4.72E+10	2.39E-01
Pb-210[a]	7.63E+13	3.68E+00
Pu-238[a]	1.71E+13	9.38E+01
Pu-239[a]	6.20E+10	5.83E+01
Pu-240[a]	2.27E+11	6.20E+01
Pu-241[a]	1.03E+14	2.04E+02
Pu-242[a]	3.94E+09	1.73E-01
Pu-244[a]	1.83E+07	3.68E-03
Ra-226[a]	9.89E+11	8.01E-01
Ra-228[a]	2.73E+14	2.21E-02
Sr-90[a]	1.37E+14	1.92E+02
Tc-99	3.80E+02	1.56E+00
Th-228[a]	8.20E+14	2.11E-06
Th-229[a]	2.13E+11	5.71E+00
Th-230[a]	2.06E+10	1.92E+00
Th-232[a]	1.10E+05	3.52E+00
U-232[a]	2.24E+13	1.02E+01

Table G.19. RESRAD single radionuclide soil guidelines for the all pathways scenario (compliance period minimum values) (cont.)

Radionuclide	SRSG (25 mrem/year) (pCi/g)	EMDF post-operational source concentration (pCi/g)
U-233[a]	9.64E+09	4.16E+01
U-234[a]	6.22E+09	6.30E+02
U-235[a]	2.16E+06	3.97E+01
U-236[a]	6.47E+07	8.98E+00
U-238[a]	3.36E+05	3.81E+02

[a] Indicates SRSG at specific activity limit

EMDF = Environmental Management Disposal Facility
RESRAD = RESidual RADioactivity
SRSG = single radionuclide soil guideline

G.5.5 WATER RESOURCES PROTECTION ASSESSMENT

This section presents estimated radionuclide doses and concentrations during the compliance period for comparison to regulatory standards for water resources protection. Protection of groundwater is demonstrated by comparing well water radionuclide concentrations under the base case scenario to MCLs for drinking water specified by EPA in the Final Radionuclides Rule (EPA 2000), promulgated in 40 *CFR* 141.66, for which the State of Tennessee has primary enforcement responsibility Tennessee Department of Environment and Conservation (TDEC) (TDEC 2012). Limits are specified for the combined Ra-226 and Ra-228 activity concentration, gross alpha activity concentration, total annual dose from beta decay and photon emission, and total uranium (Table G.4). The EMDF PA demonstrates that groundwater (well water concentrations as calculated by RESRAD-OFFSITE) at 100 m from the waste boundary meets these limits.

In the absence of local radiological standards for surface water protection, the Derived Concentration Standard (DCS) (DOE 2011c) values are adopted to evaluate impacts to surface water resources. The DCS serve as the regulatory basis for discharge limits applied to the existing EMWMF landfill for discharge to surface waters in BCV (DOE 2016).

G.5.5.1 Radium-226 and Radium-228

Simulations were performed to predict receptor well concentrations for the first 1000 years post-closure of Ra-226, Ra-228, and the sum of the two radium isotopes (Ra-226 + Ra-228). As shown in Table G.4, the MCL for Ra-226 + Ra-228 is 5 pCi/L. RESRAD-OFFSITE simulations indicate that the maximum activity concentration of Ra-226 + Ra-228 in well water is 0.0 pCi/L, which is less than the MCL.

G.5.5.2 Gross Alpha Activity

The radionuclides included in the gross alpha activity analysis are listed below:

- Am-241
- Am-243
- Cf-249 (isotope not simulated)
- Cf-250 (isotope not simulated)
- Cf-251 (isotope not simulated)
- Cm-243
- Cm-244
- Cm-245
- Cm-246
- Cm-247
- Cm-248
- Np-237
- Pa-231
- Pu-238
- Pu-239
- Pu-240
- Pu-242
- Pu-244
- Th-228
- Th-229
- Th-230
- Th-232.

Radionuclides not simulated because they were screened from analysis include Cf-249, Cf-250, and Cf-251 (see Sect. G.4.2).The MCL for the summed alpha activity concentration is 15 pCi/L (Table G.4). RESRAD-OFFSITE simulations indicate that the maximum summed gross alpha activity concentration in well water is 0.0 pCi/L, which is less than the 15 pCi/L MCL.

G.5.5.3 Beta/Photon Activity

The 13 radionuclides simulated for the beta/photon MCL compliance analysis are listed in Table G.20. Sixteen radionuclides were not simulated because they either did not have a verified inventory data source, or because they were screened from the all pathways dose analysis (see Sect. G.4.2). The 15 radionuclides not included are: Cd-113m, Co-60, Cs-135, Cs-137, Eu-152, Eu-154, Ni-63, Pd-107, Pm-146, Re-187, Se-79, Sm-151, Sn-121m, Sn-126, and Zr-93 (see Table G.18). The MCL for total beta/photon emitters is expressed as a water ingestion dose of 4 mrem/year (Tables G.4 and G.20). RESRAD-OFFSITE simulations indicate that only C-14 and Tc-99 contribute substantially to the total beta/photon dose during the compliance period. The maximum dose over 1000 years is 1.03 mrem/year at 475 years (Fig. G.14), which is less than the MCL.

Table G.20. Water resources protection assessment – beta/proton activity

Radionuclide	Decay	MCL (pCi/L) yielding a dose of 4 mrem/year[a]
Ac-227	beta	15
Be-10	beta	1000
C-14	beta	2000
H-3	beta	20,000
I-129	beta	1
K-40[b]	beta	192
Nb-93m	gamma	1000
Nb-94[b]	beta	720

Table G.20. Water resources protection assessment – beta/proton activity (cont.)

Radionuclide	Decay	MCL (pCi/L) yielding a dose of 4 mrem/year[a]
Ni-59	beta	300
Pb-210[b]	beta	1.6
Pu-241	beta	300
Sr-90	beta	8
Tc-99	beta	900

[a]Source: EPA 2002a.
[b]The MCL for given isotope was not included in EPA 2000, therefore the DCS (DOE 2011c) was used to calculate the MCL at 4 mrem/year.

DCS = Derived Concentration Standard
EPA = U.S. Environmental Protection Agency
MCL = maximum contaminant level

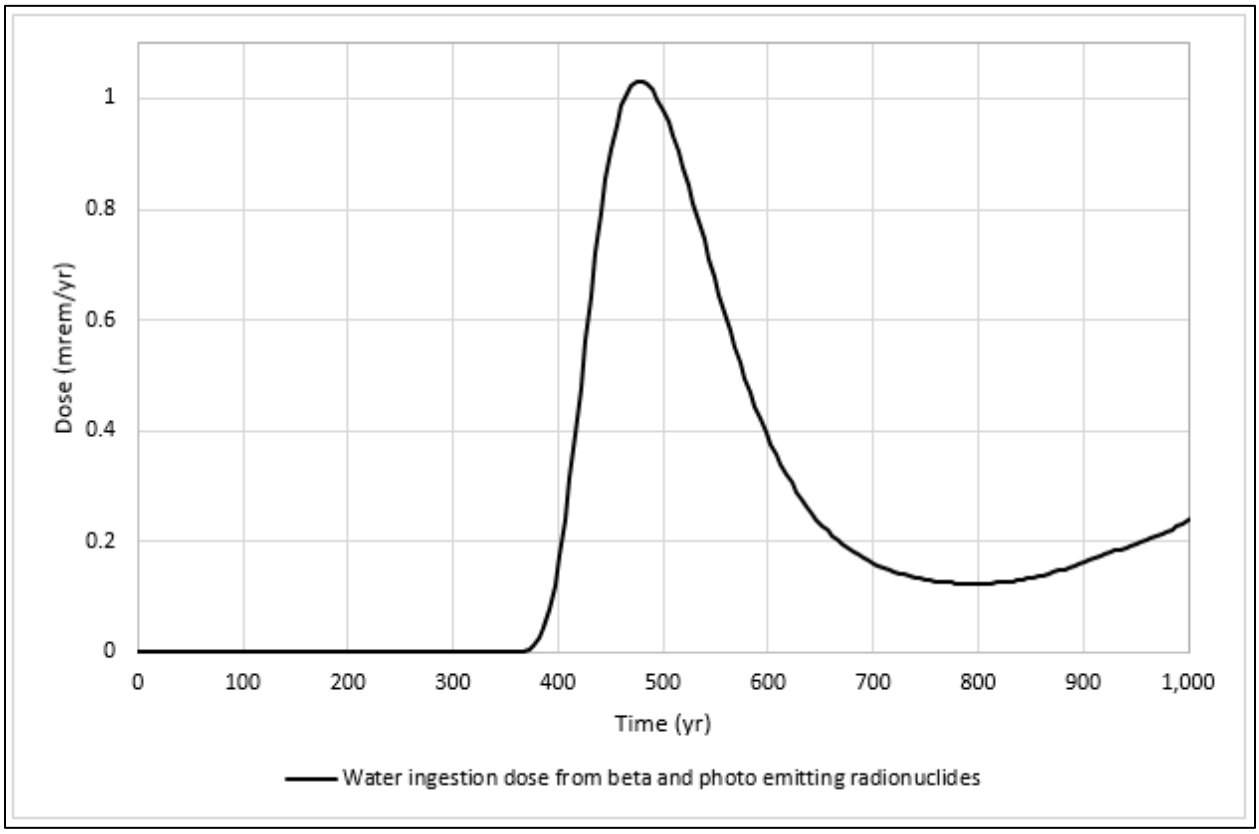

Fig. G.14. Predicted water ingestion dose from beta/photon emitters (0 to 1000 years)

G.5.5.4 Hydrogen-3 and Strontium-90

The MCL for H-3 activity concentration is 20,000 pCi/L. RESRAD-OFFSITE results indicate a maximum production well concentration of H-3 is 0.0 pCi/L.

Strontium-90 has an activity concentration MCL of 8 pCi/L. The maximum predicted Sr-90 well water concentration over 1000 years is 0.0 pCi/L.

G.5.5.5 Uranium (total)

The total uranium MCL is 30 µg/L. The predicted total mass concentration in well water was calculated by summing the activity concentrations for the uranium isotopes (U-232, U-233, U-234, U-235, U-236, and U-238) that RESRAD-OFFSITE predicts in the groundwater well, then converting from the total uranium activity concentration to the mass concentration using the conversion factor 1.49 µg/pCi (EPA 2002b). The maximum predicted total uranium mass concentration for the compliance period is 0.0 µg/L.

G.5.5.6 Surface Water Protection Assessment

Of the 42 radionuclides included in the base case (i.e., those not screened under the screening model scenario [see Sect. 2.3 in the PA]), only three have predicted peak surface water concentrations greater than 1.0E-06 pCi/L within the 10,000-year simulation period. Within the 1000-year compliance period, only C-14 and Tc-99 have substantial (i.e., greater than 1.0E-06 pCi/L) predicted concentrations in the surface water body (Bear Creek). None of the predicted non-zero peak surface water concentrations for the 10,0000-year simulation period exceeds the corresponding DCS value, which serve as the regulatory basis for discharge limits applied to the existing EMWMF landfill for discharge to surface waters in BCV (DOE 2016). Table G.21 summarizes the peak surface water concentrations for the three dose significant radionuclides within the 1000-year compliance period and the 10,000-year post-closure period and for uranium isotopes predicted to reach peak concentrations after 10,000 years. Model results for nuclides of uranium at times greater than 10,000 years post-closure are presented in Sect. G.5.6.

Table G.21. Predicted non-zero peak surface water concentrations for radionuclides compared to the DCS limits

Radionuclide	Peak surface water concentration, compliance period (pCi/L)	Peak surface water concentration, 10,0000 year simulation	DCS[a] (pCi/L)	Time of simulated peak (year)
Tc-99	2.34E-03	6.24E-01	4.40E+04	2,130
C-14	8.61E-01	8.61E-01	6.20E+04	553
I-129	< 1.0E-06	3.53E-02	3.30E+02	7,219
U-233	< 1.0E-06	< 1.0E-06	6.60E+02	~50,000
U-234	< 1.0E-06	< 1.0E-06	6.80E+02	~50,000
U-235	< 1.0E-06	< 1.0E-06	7.20E+02	~50,000
U-236	< 1.0E-06	< 1.0E-06	7.20E+02	~50,000
U-238	< 1.0E-06	< 1.0E-06	7.50E+02	~50,000

[a]DOE 2011c

DOE = U.S. Department of Energy
DCS = Derived Concentration Standard

G.5.6 PREDICTIONS FOR TIMES GREATER THAN 10,000 YEARS

Results from simulations encompassing tens of thousands of years are highly speculative and have limited, if any, quantitative value. However, results from very long-term simulations can be informative on a qualitative basis for long-lived or slowly moving radionuclides, particularly depending on the progeny generated. To assess the potential release of such radionuclides, simulations were performed for a duration of 100,000 years after facility closure.

Long-term simulations indicate that peak well water concentrations of U-233, U-235, and U-236 do not exceed the DCS limits (DOE 2011c and Table G.21), but that peak concentrations of U-234 and U-238

occurring after 30,000 years are larger than the DCS limits (Figs. G.15 and G.16). The predicted peak groundwater concentrations of U-234 and U-238 are very high (> 1000 pCi/L), but the RESRAD-OFFSITE source release model does not incorporate solubility limits on the release of uranium in solution, so the model may overestimate the peak concentrations. In addition, the comparison of STOMP model simulations of U-234 release to the RESRAD-OFFSITE release predictions (refer to Sect. 3.3.5 of the PA) shows that the equilibrium desorption release model over-predicts peak U-234 release significantly relative to the scaled STOMP model simulations. The model output comparison also shows that the simplified RESRAD-OFFSITE vadose zone representation appears to match the timing of the STOMP model peak U-234 flux to the water table, but that the predicted peak RESRAD-OFFSITE U-234 flux is over twice as large as the peak STOMP U-234 flux to the water table beneath the EMDF. This difference in U-234 release model predictions suggests that the RESRAD-OFFSITE peak well water concentrations are too uncertain (probably over-estimated) to draw conclusions about the very long-term performance of the EMDF with respect to less mobile radionuclides (K_d > 1.0 cm^3/g) including nuclides of uranium and possibly also I-129 (refer to Sects. 3.3.5, 5.3, and 5.4 of the PA).

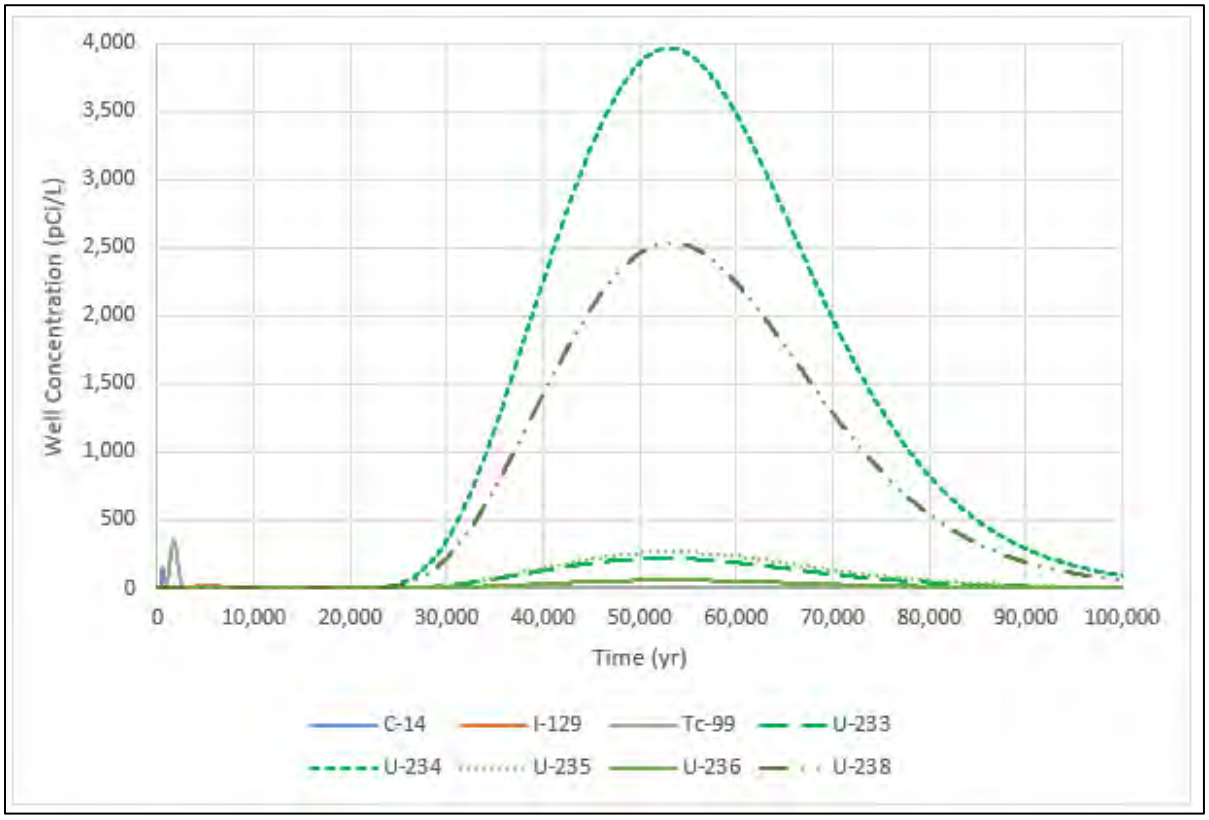

Fig. G.15. Predicted radionuclide concentrations in well water, 100,000-year simulation

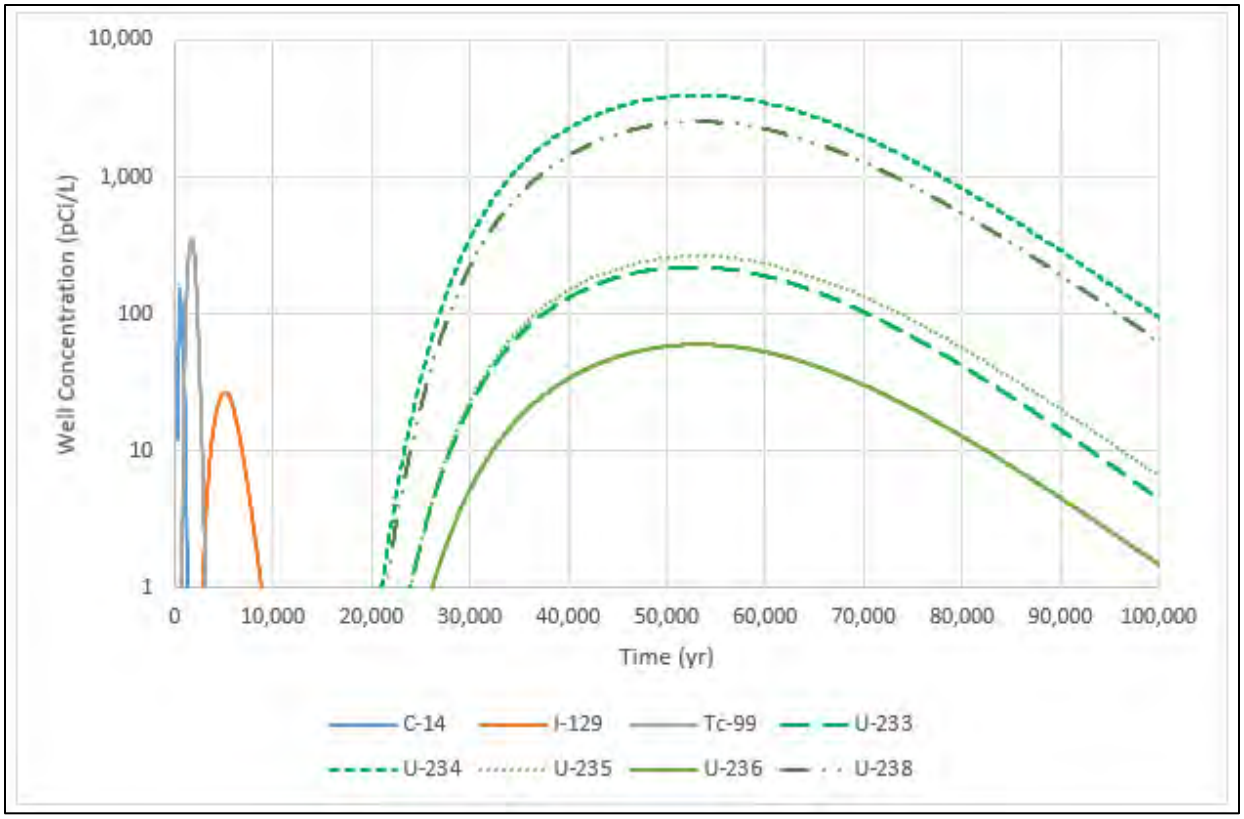

Fig. G.16. Predicted radionuclide concentrations in well water, 100,000-year simulation (log scale)

G.6 UNCERTAINTIES, SENSITIVITY, AND CONSERVATIVE BIAS

Uncertainty in model parameter assumptions and model results is an important consideration in evaluating the overall conservatism of the modeling approach for dose predictions. For nearly any numerical model, the principal factors inherently creating uncertainty include specifying the problem posed and defining the proper scenario to be simulated, configuring the CSM, converting the CSM into the site-specific numerical model, assigning parameter values in the numerical model, completing model simulations, and interpreting results. Section G.6 presents the sensitivity and uncertainty analyses performed to better understand the strengths and weakness of the RESRAD-OFFSITE model as configured to represent conditions at EMDF.

G.6.1 UNCERTAINTIES AND SENSITIVITY OF RESULTS TO INPUT PARAMETER ASSUMPTIONS

The primary uncertainties affecting this EMDF PA analysis include the estimated EMDF inventory concentrations and assumptions for the values of major model parameters that impact the calculated dose exposure. In general, the modeled dose for a given radionuclide scales linearly with the estimated activity concentration. This means that uncertainties in waste concentrations (EMDF inventory estimates), or in the values of parameters that determine the modeled source concentrations, can be translated directly into dose uncertainty. If such scaling is applied, consideration of solubility limitations (which is not currently possible in RESRAD-OFFSITE) should be taken into account to prevent unrealistically high dose predictions.

For the EMDF PA, a hybrid modeling approach was used by employing a combination of deterministic and probabilistic simulations to provide a more complete understanding of the relative importance of input assumptions and parameter specification on the results and conclusions from the PA.

G.6.2 SENSITIVITY ANALYSIS

The goal of the sensitivity analysis is to identify the radionuclides and/or pathways that can significantly influence the predicted doses and, therefore, the conclusions of the PA. The sensitivity analysis includes deterministic, single-parameter sensitivity cases to illustrate the impacts of changes in one parameter or assumption on the results of the analysis. To assess the sensitivity of deterministic results to assumptions that could not be varied using a factor (e.g., source release mechanism), special sensitivity simulations were performed. These simulations help to provide insights into the relative importance of specific processes and broader model-related uncertainties on overall performance.

The parameters adjusted during performance of the sensitivity analysis are listed in Table G.22, with the specified adjustment factor applied to each parameter. Only one parameter was adjusted at a time to assess how sensitive the model result (i.e., total dose) was to the specified parameter. To focus the sensitivity analysis, parameters were varied for sitewide parameters (e.g., precipitation, runoff coefficient, residence time in lake) as well as for select radionuclides. The selected radionuclides are the top three contributors to total dose: C-14, Tc-99, and I-129. Sensitivity analysis results are for total dose and include contributions from all isotopes simulated during base case modeling.

Table G.22. Sensitivity analysis parameters for the base case scenario

Parameter Description	RESRAD parameter identifier	Factor applied to base case value	Total dose plot figure
C-14 K_d in contaminated zone	DCACTC(C-14)	N/A	G.18
C-14 K_d (UZ1-UZ5)	DCACTU1-5(C-14)	N/A	G.18
C-14 K_d in saturated zone	DCACTS(C-14)	N/A	G.19
I-129 K_d contaminated zone	DCACTC(I-129)	5	G.19
I-129 K_d (UZ1-UZ5)	DCACTU1-5(I-129)	5	G.19
I-129 K_d saturated zone	DCACTS(I-129)	5	G.19
Tc-99 K_d contaminated zone	DCACTC(Tc-99)	5	G.20
Tc-99 K_d (UZ1-UZ5)	DCACTU1-5(Tc-99)	5	G.20
Tc-99 K_d saturated zone	DCACTS(Tc-99)	5	G.20
Precipitation	PRECIP	1.25	G.21
Initial releasable fraction	RELFRACINIT	(C-14) = 0.998, 0.564 (I-129, Tc-99) = 0.5, 0	G.22
Time at which C-14 first becomes releasable (delay time)	RELTIMEINIT(C-14)	2	G.23
Time at which I-129 first becomes releasable (delay time)	RELTIMEINIT(I-129)	2	G.23
Time at which Tc-99 first becomes releasable (delay time)	RELTIMEINIT(Tc-99)	2	G.23
Time over which transformation to releasable form occurs (C-14)	RELDUR(C-14)	2	G.24

Table G.22. Sensitivity analysis parameters for the base case scenario (cont.)

Parameter Description	RESRAD parameter identifier	Factor applied to base case value	Total dose plot figure
Time over which transformation to releasable form occurs (I-129)	RELDUR(I-129)	2	G.24
Time over which transformation to releasable form occurs (Tc-99)	RELDUR(Tc-99)	2	G.24
Runoff coefficient	RUNOFF	N/A	G.25
Source release	--	N/A	G.17
Source concentrations	--	N/A	G.26
C-14 K_d in contaminated zone	DCACTC(C-14)	N/A	G.18
I-129 K_d contaminated zone	DCACTC(I-129)	5	G.19
Tc-99 K_d contaminated zone	DCACTC(I-129)	5	G.20
Longitudinal dispersivity of contaminated zone	ALPHLCZ	5	G.27
Contaminated zone b parameter	BCZ	1.4	G.27
Hydraulic conductivity of contaminated zone	HCCZ	5	G.27
Total porosity of contaminated zone	TPCZ	1.1	G.27
Effective porosity of contaminated zone	EPCZ	1.5	G.27
C-14 K_d (UZ1-UZ5)	DCACTU1-5(C-14)	N/A	G.18
I-129 K_d (UZ1-UZ5)	DCACTU1-5(I-129)	5	G.19
Tc-99 K_d (UZ1-UZ5)	DCACTU1-5(Tc-99)	5	G.20
Bulk density of UZ3	DENSUZ(3)	1.05	G.28
Total porosity of UZ3	TPUZ(3)	1.1	G.28
Effective porosity of UZ3	EPUZ(3)	1.1	G.28
Bulk density of UZ4	DENSUZ(4)	1.05	G.29
Total porosity of UZ4	TPUZ(4)	1.1	G.29
Effective porosity of UZ4	EPUZ(4)	1.1	G.29
Bulk density of UZ5	DENSUZ(5)	1.05	G.30
Total porosity of UZ5	TPUZ(5)	1.1	G.30
Effective porosity in native vadose zone (UZ5)	EPUZ(5)	1.5	G.30
Longitudinal dispersivity of native vadose zone (UZ5)	ALPHALU(5)	2	G.30
Thickness of native vadose zone (UZ5)	H(5)	2	G.31
Thickness of native vadose zone (UZ5)	H(5)	H(5) = 0.01 m	G.31

Table G.22. Sensitivity analysis parameters for the base case scenario (cont.)

Parameter Description	RESRAD parameter identifier	Factor applied to base case value	Total dose plot figure
C-14 K_d in saturated zone	DCACTS(C-14)	N/A	G.18
I-129 K_d saturated zone	DCACTS(I-129)	5	G.19
Tc-99 K_d saturated zone	DCACTS(Tc-99)	5	G.20
Dry bulk density of saturated zone	DENSAQ	1.15	G.32
Total porosity of saturated zone	TPSZ	1.5	G.32
Effective porosity of saturated zone	EPSZ	1.5	G.32
Thickness of saturated zone	DPTHAQ	1.5	G.32
Hydraulic conductivity of saturated zone	HCSZ	2	G.32
Hydraulic gradient of aquifer to well	HGW	2	G.33
Longitudinal dispersivity of aquifer to well	ALPHALOW	2	G.33
Hydraulic gradient of aquifer to surface water body	HGSW	2	G.34
Longitudinal dispersivity of aquifer to surface waterbody	ALPHALOSW	2	G.34
Depth of aquifer contributing to surface waterbody	DPTHAQSW	2	G.34
Mean residence time of water in surface waterbody	TLAKE	10	G.34
Meat ingestion	DMI(1)	1.19	G.35
Fish ingestion	DFI(1)	2	G.35
Fraction of meat from affected area	FMEMI(1)	2	G.35
Depth of aquifer contributing to well	DWIBWT	1.5	G.36

RESRAD = RESidual RADioactivity

Sections G.6.2.1 through G.6.2.7 present results from the sensitivity scenarios listed in Table G.22. The text includes an assessment of the uncertainty in the base case values and the degree to which the selected base case value was selected to impart a bias toward higher predicted dose. Predicted total dose over the 10,000-year prediction interval are plotted in Figs. G.17 through G.36, as listed in Table G.22. Qualitative descriptions on how sensitive the model's predicted total dose is to each assessed parameter is described as insensitive, mildly sensitive, and sensitive. These qualitative descriptions consider changes in the peak dose magnitude and time of occurrence and are based on professional judgement. Results of the sensitivity analysis are used to inform the probabilistic simulations described in Sect. G.6.3.

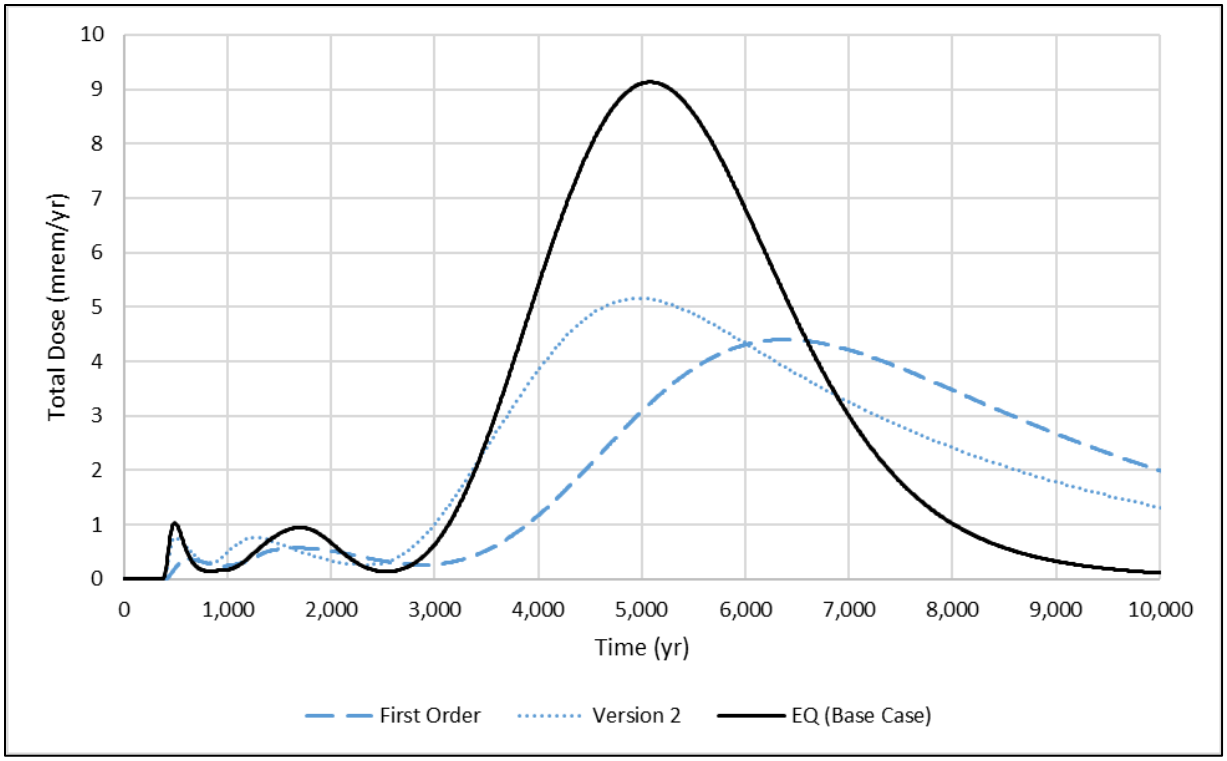

Fig. G.17. Sensitivity analysis on RESRAD-OFFSITE source release option

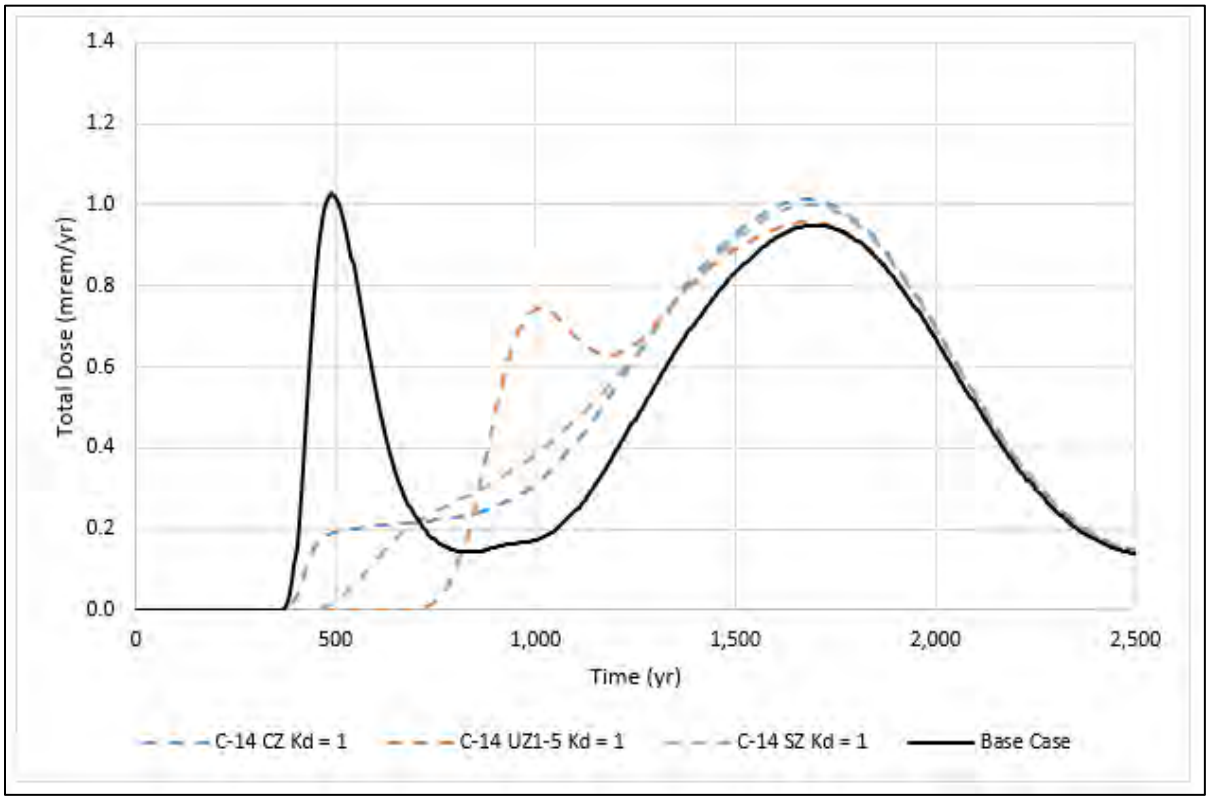

Fig. G.18. Sensitivity analysis on C-14 partition coefficient in the contaminated zone, saturated zone, and unsaturated zones with partition coefficients set to 1 cm^3/g

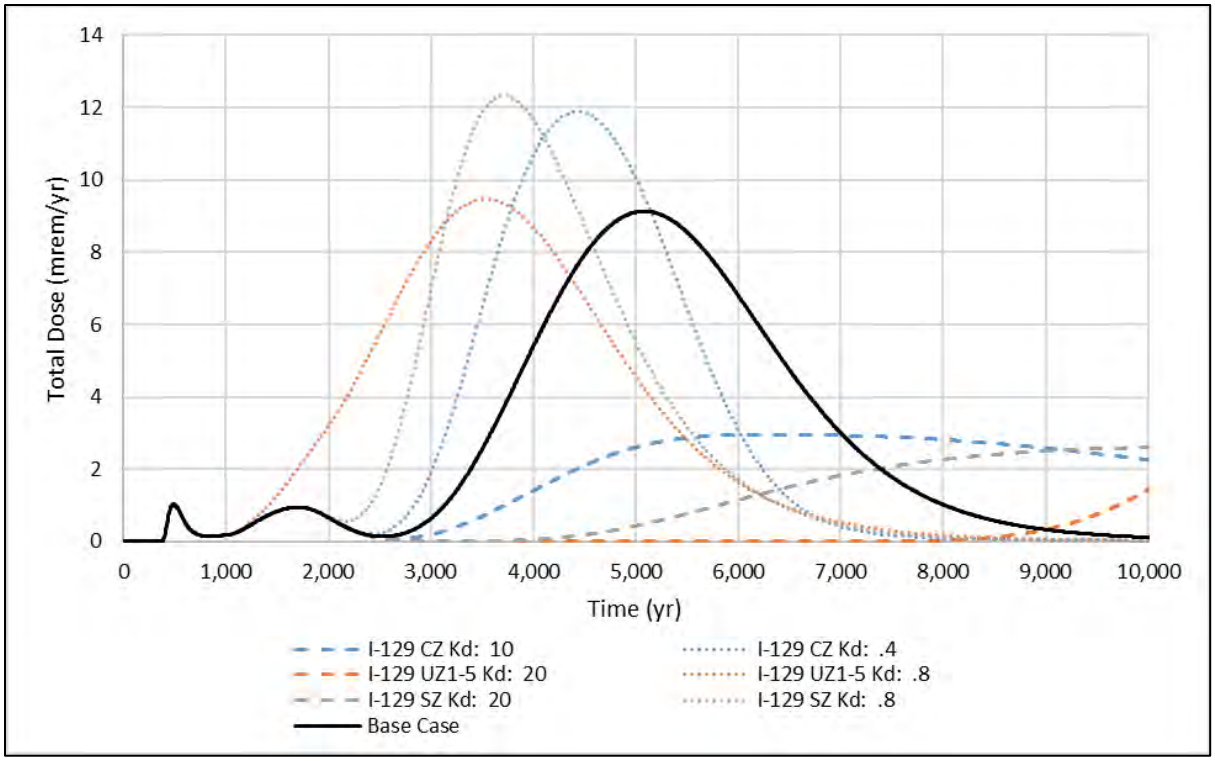

Fig. G.19. Sensitivity analysis on I-129 partition coefficient in the contaminated zone, saturated zone, and unsaturated zones with adjustment factor of 5

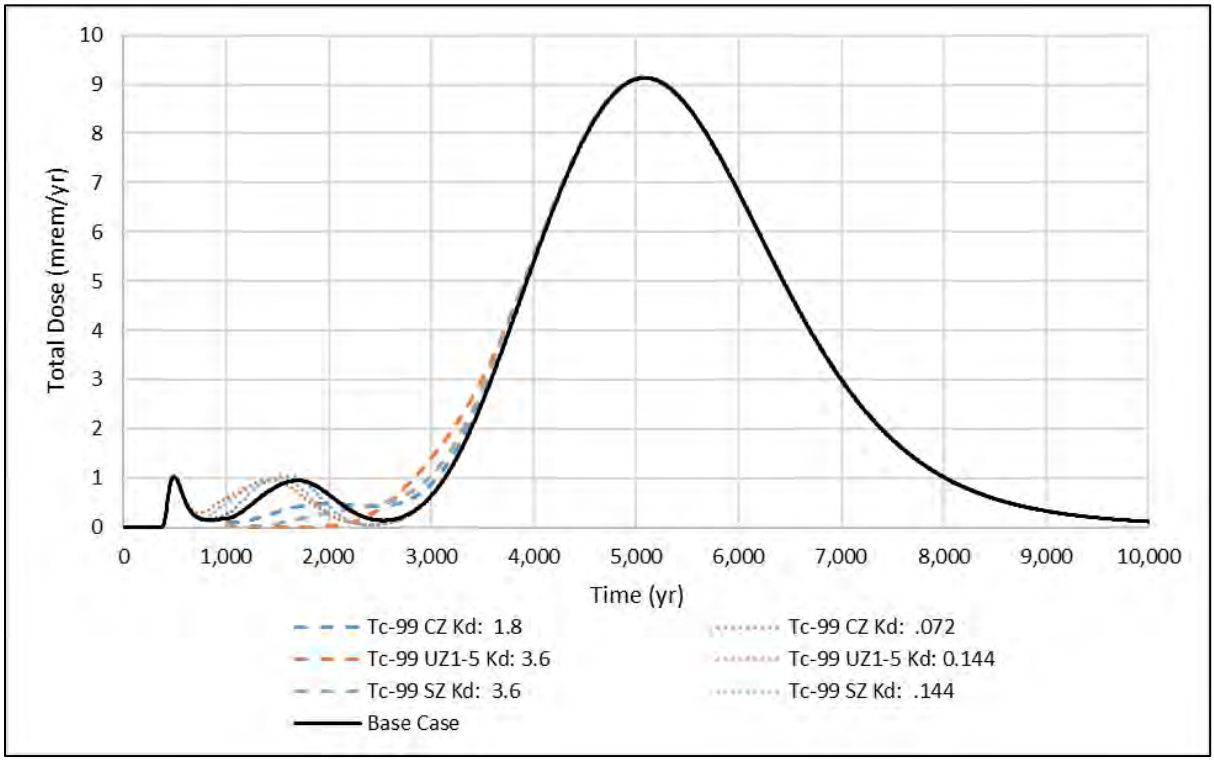

Fig. G.20. Sensitivity analysis on Tc-99 partition coefficient in the contaminated zone, saturated zone, and unsaturated zones with adjustment factor of 5

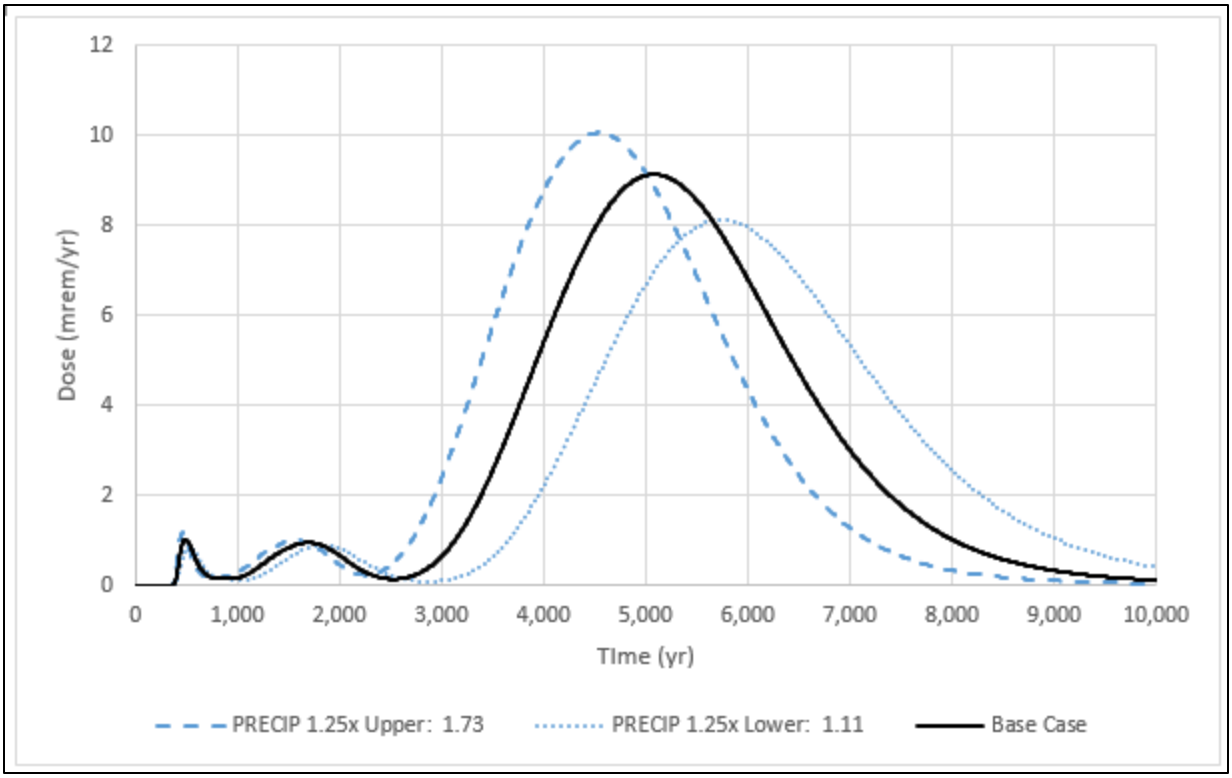

Fig. G.21. Sensitivity analysis on precipitation rate (PRECIP) with adjustment factor of 1.25

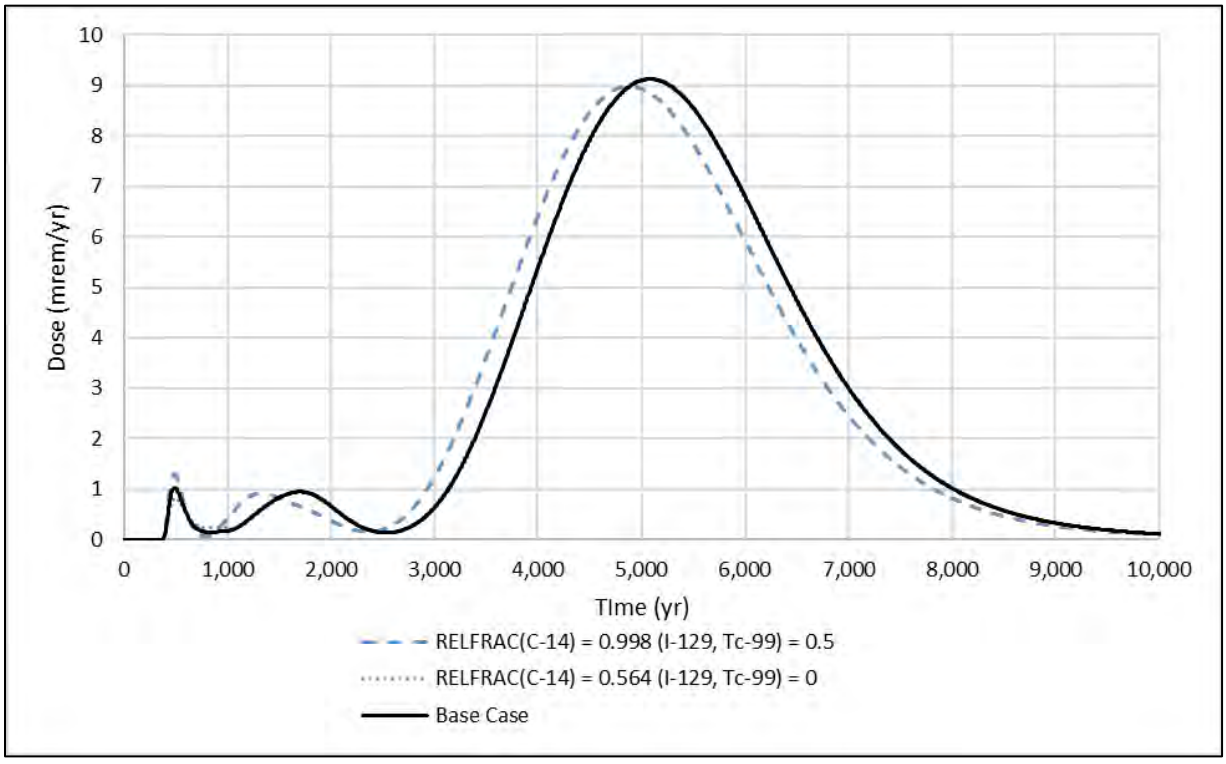

Fig. G.22. Sensitivity analysis on initial releasable fraction with high (C-14 = 0.998; I-129 = 0.5, Tc-99 = 0.5) and low (C-14 = 0.564; I-129, Tc-99 = 0) initial releasable fractions

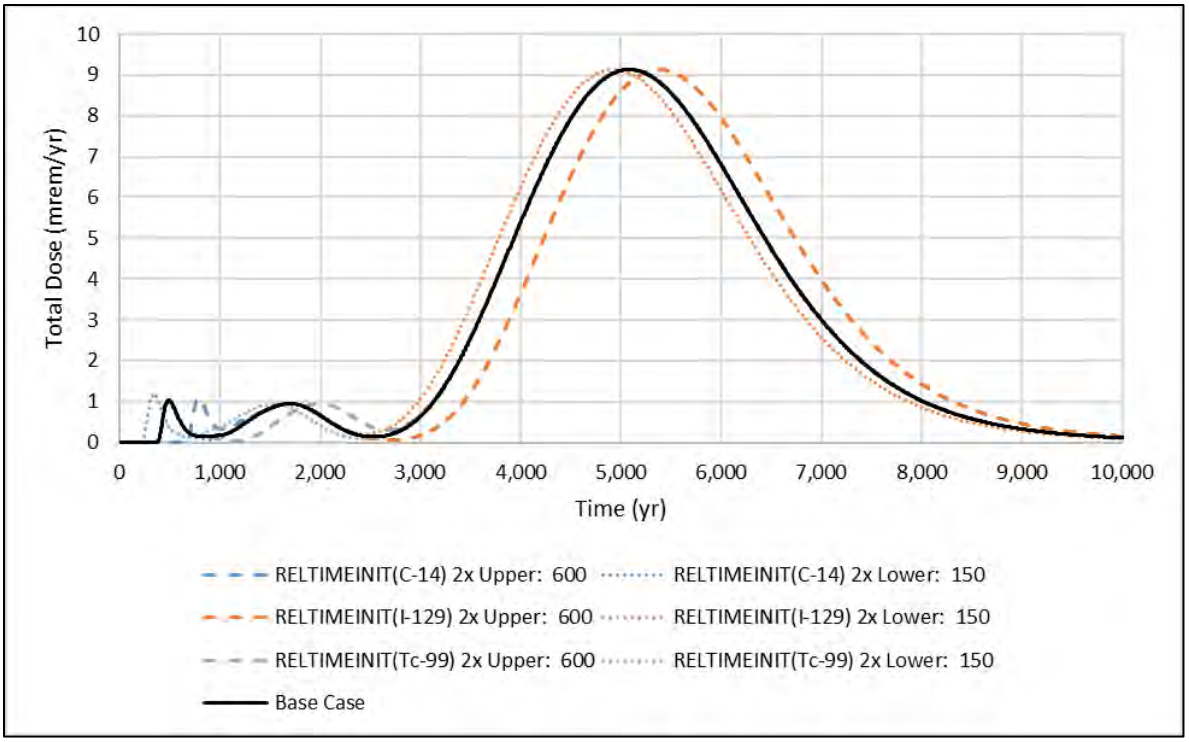

Fig. G.23. Sensitivity analysis on initial release time of C-14, I-129, and Tc-99 from the contaminated zone with an adjustment factor of 2

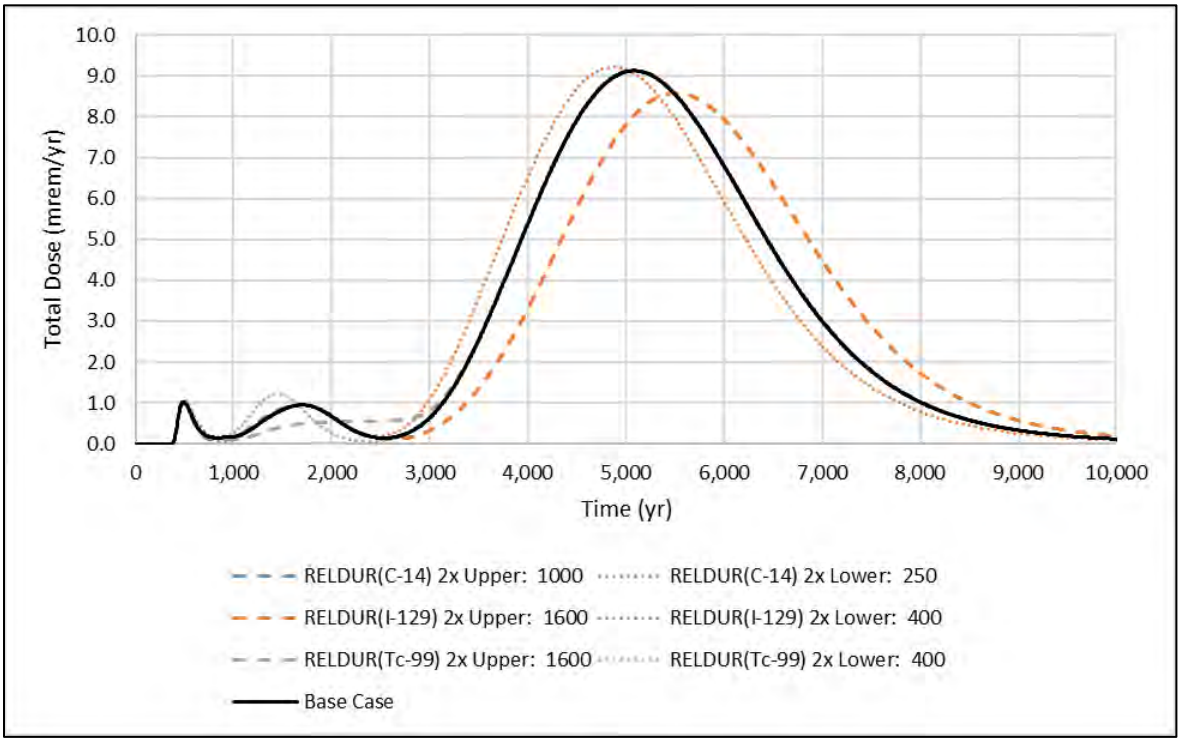

Fig. G.24. Sensitivity analysis on release duration of C-14, I-129, and Tc-99 from the contaminated zone with adjustment factor of 2

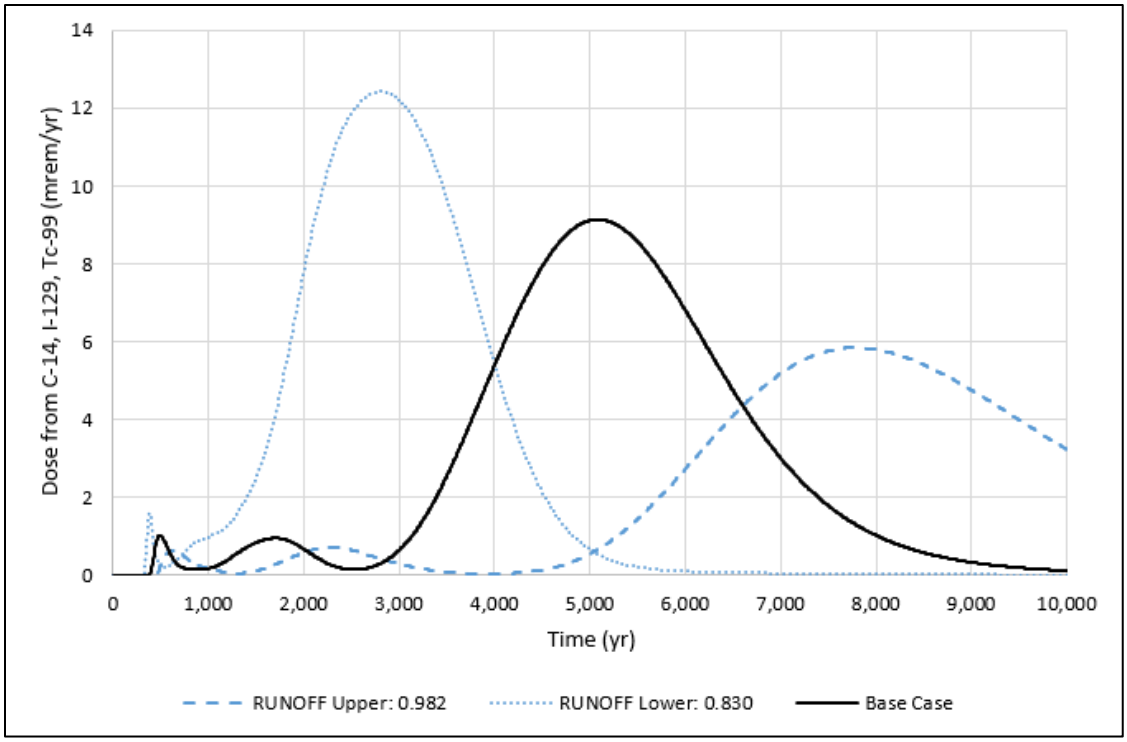

Fig. G.25. Sensitivity analysis on runoff coefficient of the waste (RUNOFF)

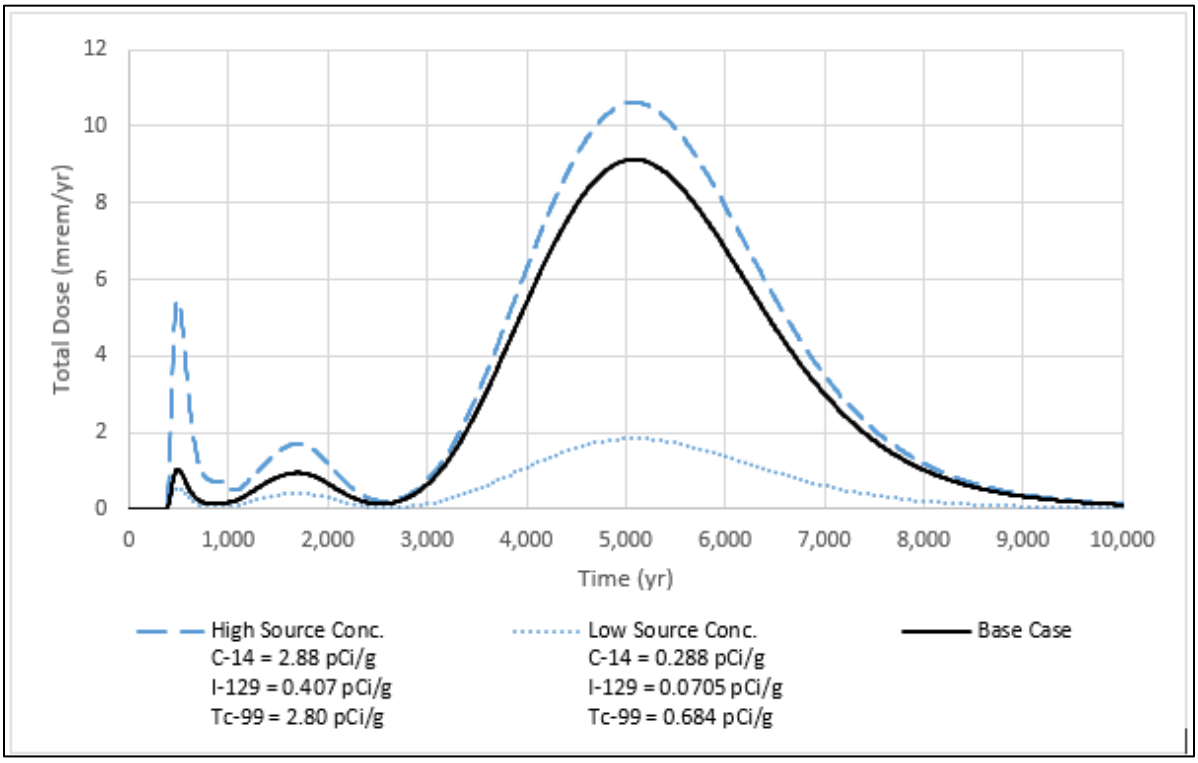

Fig. G.26. Sensitivity analysis on radionuclide source concentrations for dose-significant radionuclides (C-14, I-129, and Tc-99)

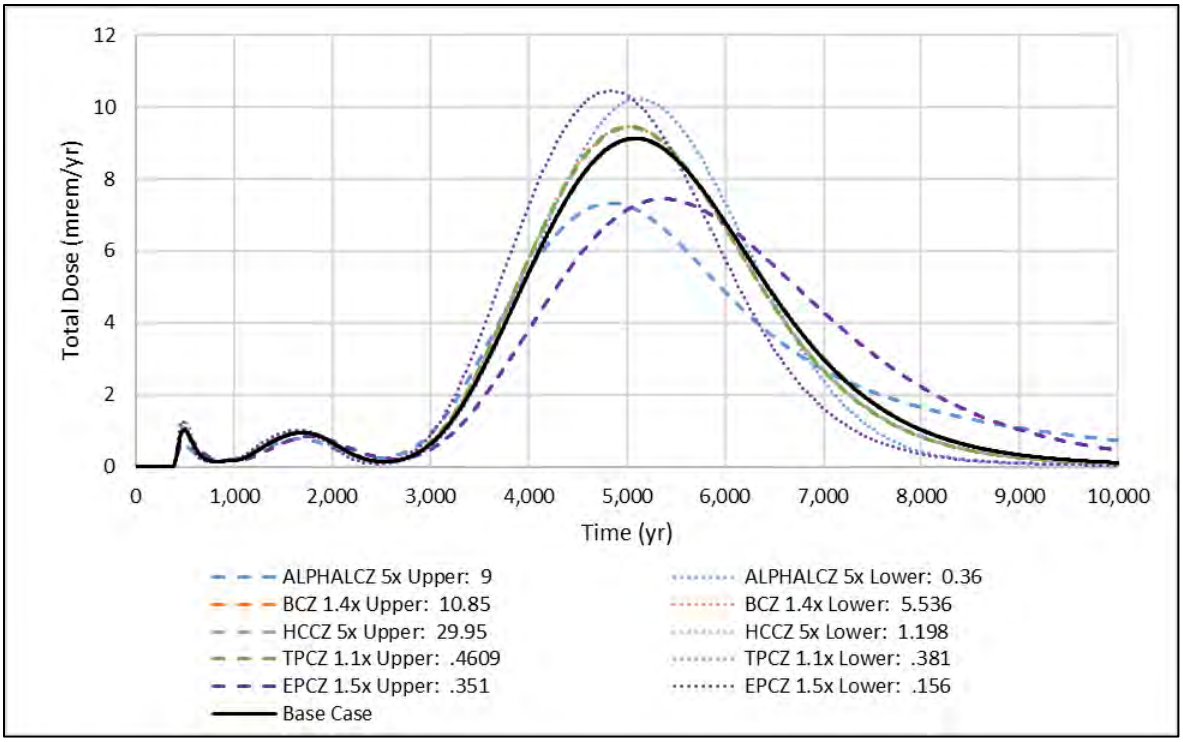

Fig. G.27. Sensitivity analysis on longitudinal dispersivity, b parameter, hydraulic conductivity, total porosity, and effective porosity of the waste with adjustment factors of 5, 1.4, 5, 1.1, and 1.5

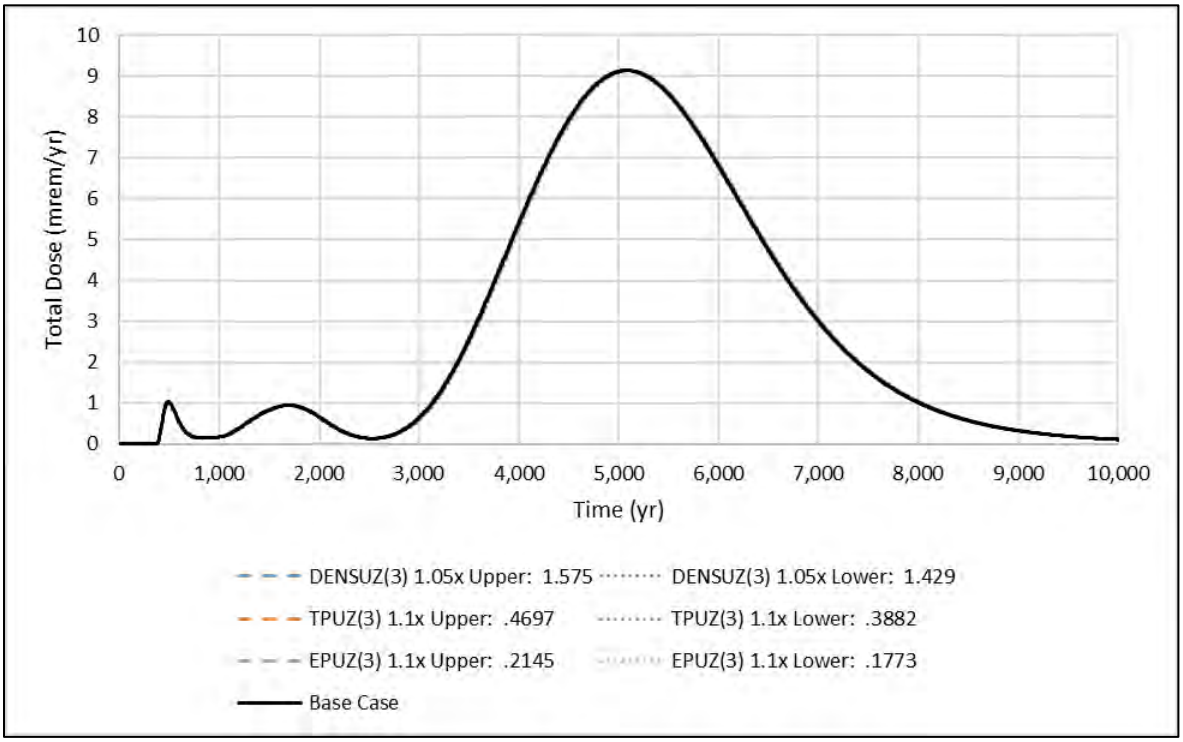

Fig. G.28. Sensitivity analysis on dry bulk density, total porosity, and effective porosity of UZ3 with adjustment factors of 1.05, 1.1, and 1.1

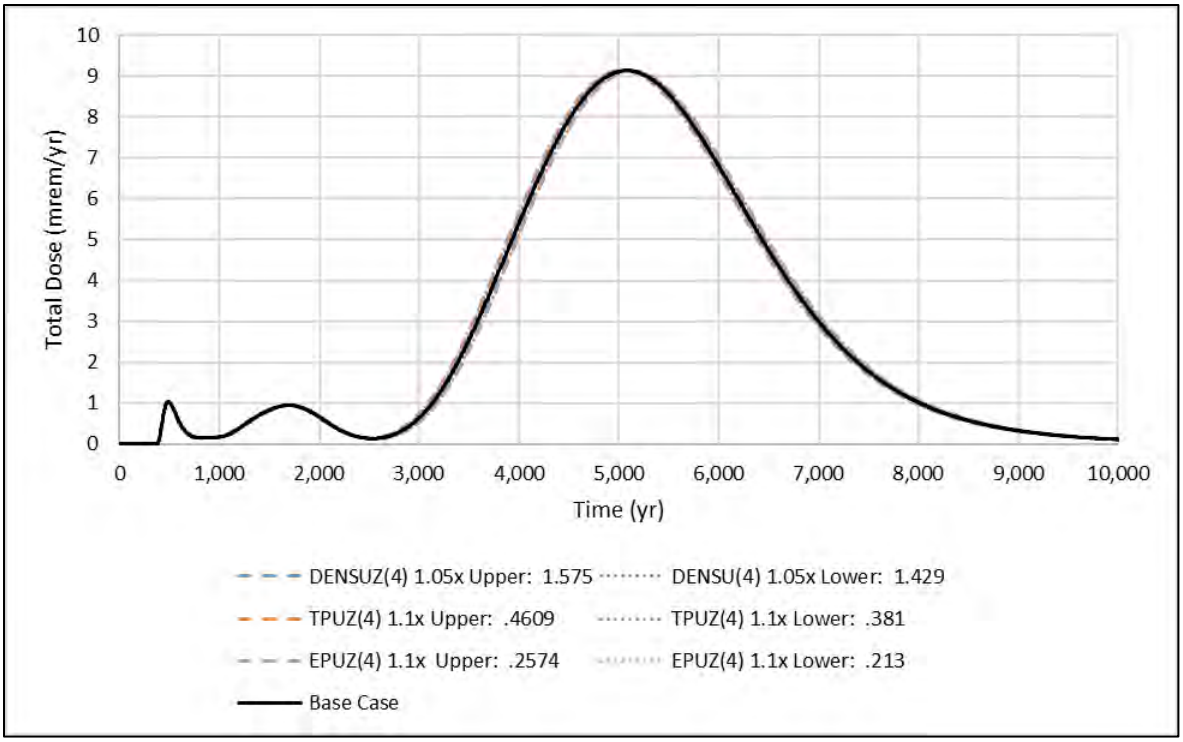

Fig. G.29. Sensitivity analysis on dry bulk density, total porosity, and effective porosity of UZ4 with adjustment factors of 1.05, 1.1, and 1.1

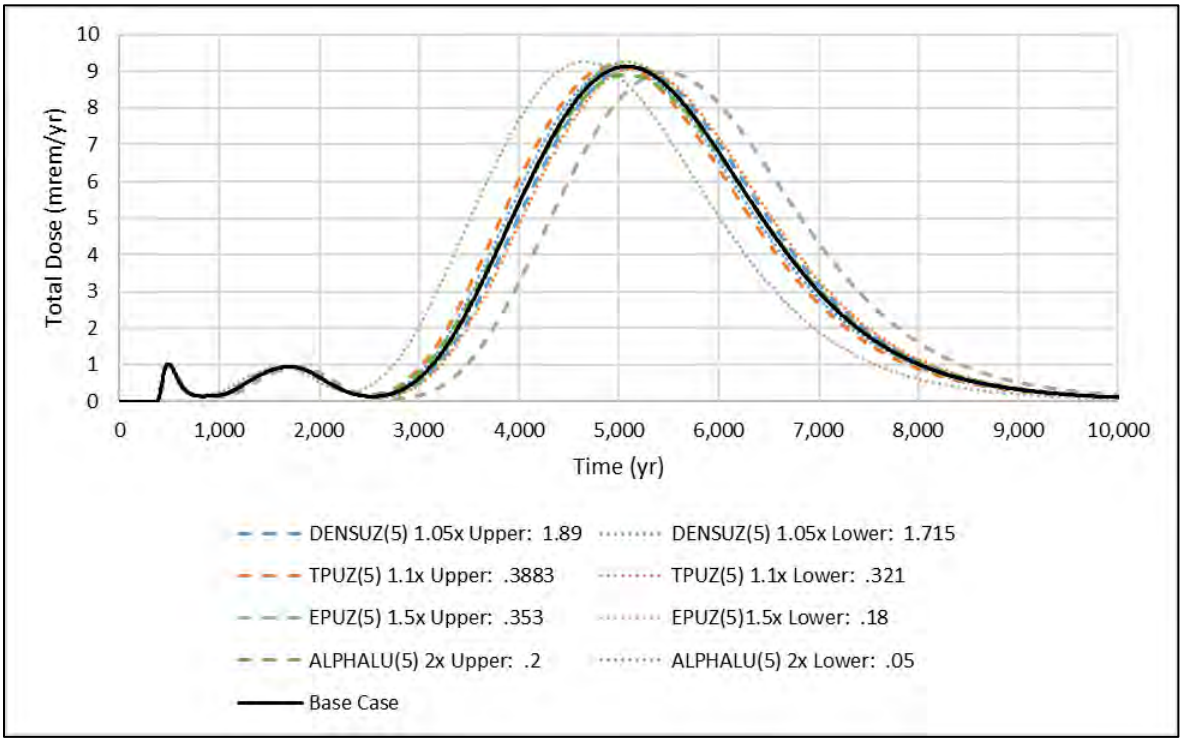

Fig. G.30. Sensitivity analysis on dry bulk density, total porosity, effective porosity, and longitudinal dispersivity of UZ5 with adjustment factors of 1.05, 1.1, 1.5, and 2

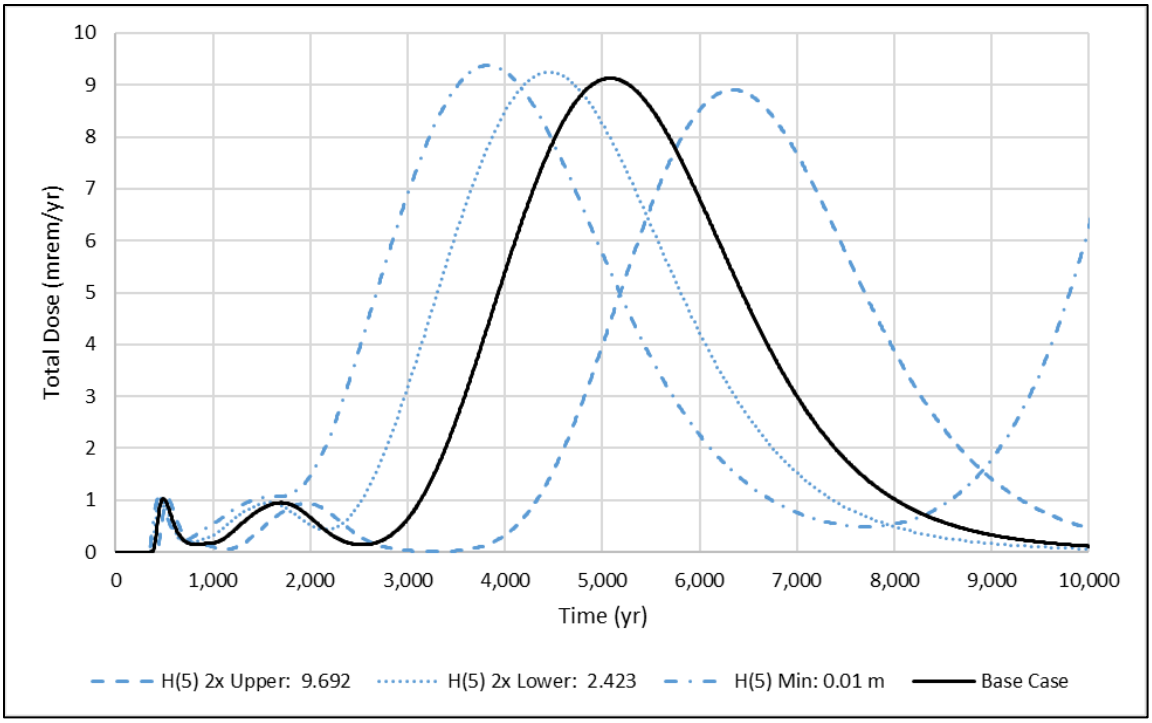

Fig. G.31. Sensitivity analysis on thickness of UZ5 (H(5))with an adjustment factor of 2 and the minimum value of 0.01 m

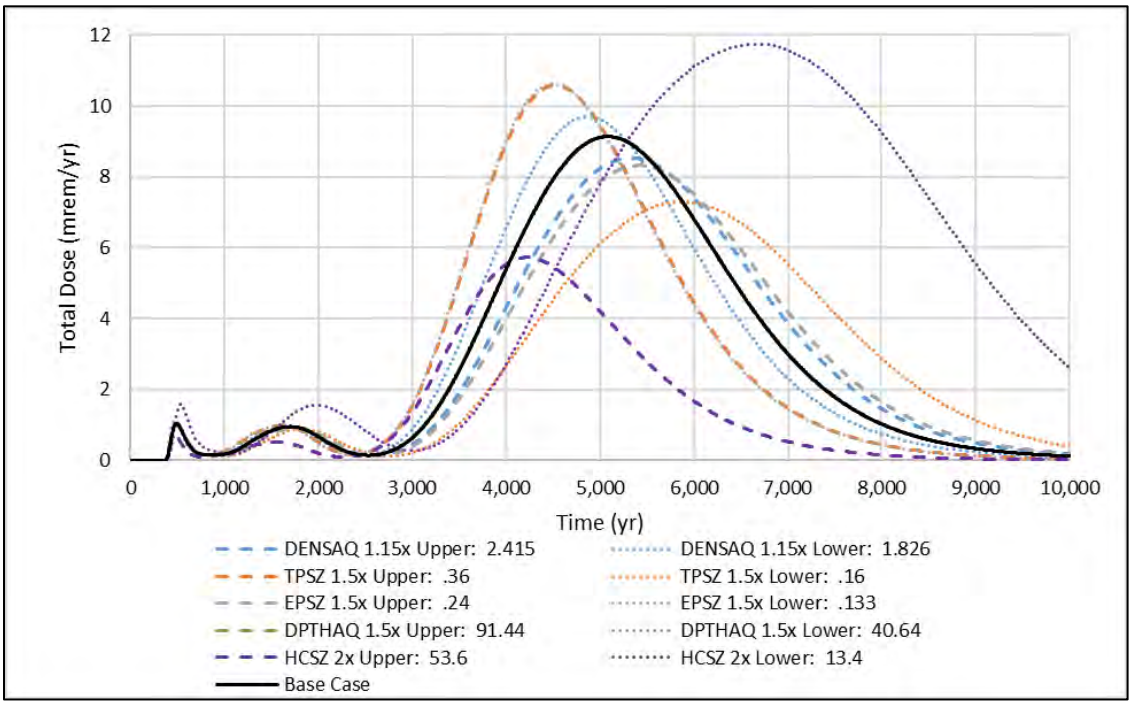

Fig. G.32. Sensitivity analysis on dry bulk density (DENSAQ), total porosity (TPSZ), effective porosity (EPSZ), thickness (DPTHAQ), and hydraulic conductivity of the saturated zone (HCSZ) with adjustment factors of 1.15, 1.5, 1.5, 1.5, and 2

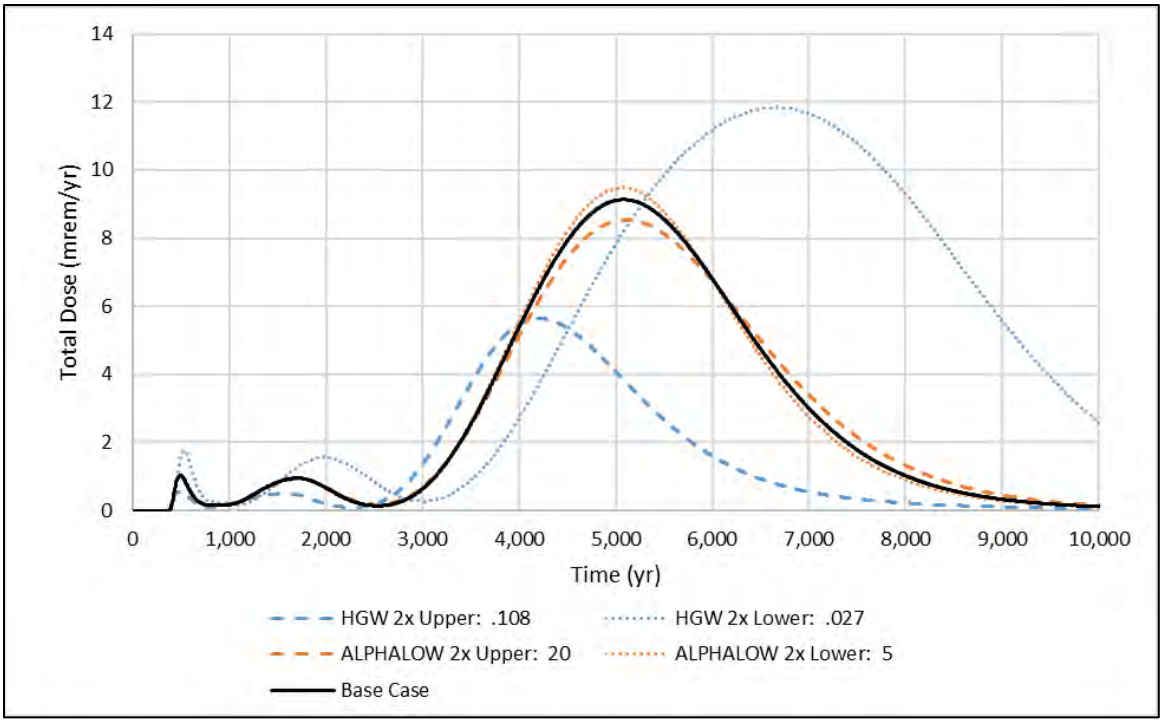

Fig. G.33. Sensitivity analysis on hydraulic gradient of aquifer to well (HGW) and longitudinal dispersivity of aquifer to well with (ALPHALOW) and adjustment factor of 2

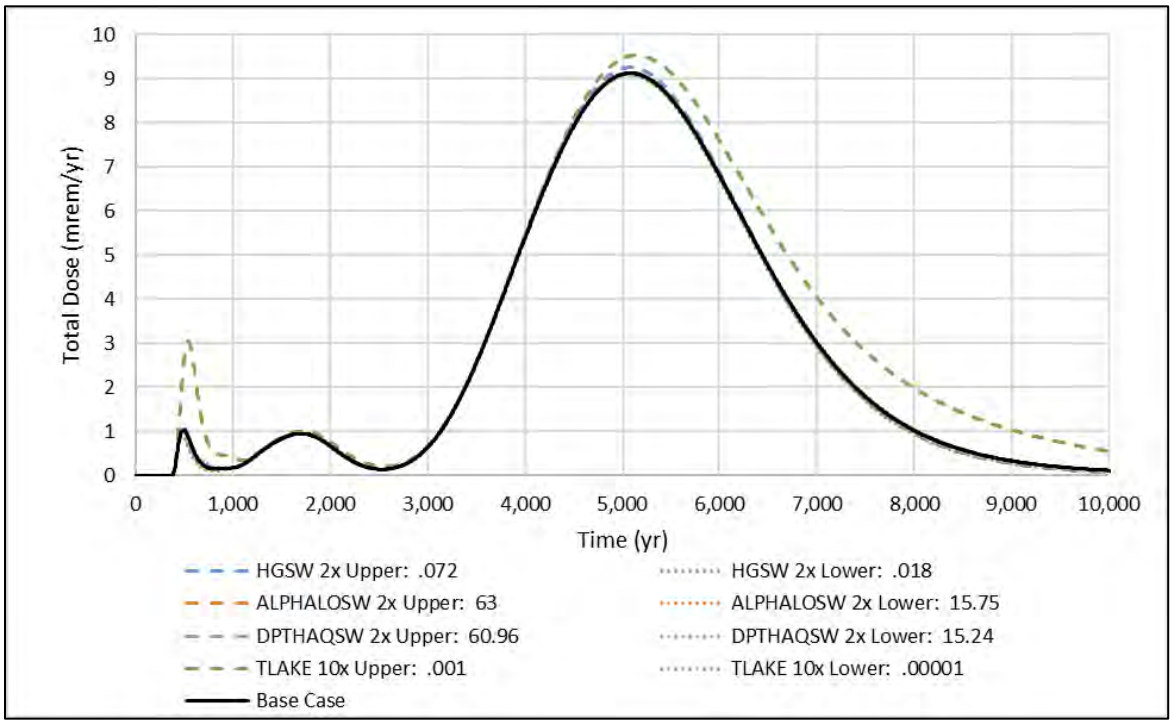

Fig. G.34. Sensitivity analysis on hydraulic gradient of aquifer to surface water body (HGSW), longitudinal dispersivity of aquifer to surface water body (ALPHALOSW), depth of aquifer contributing to surface water body (DPTHAQSW), and mean residence time of water in surface water body (TLAKE) with adjustment factors of 2, 2, 2, and 10

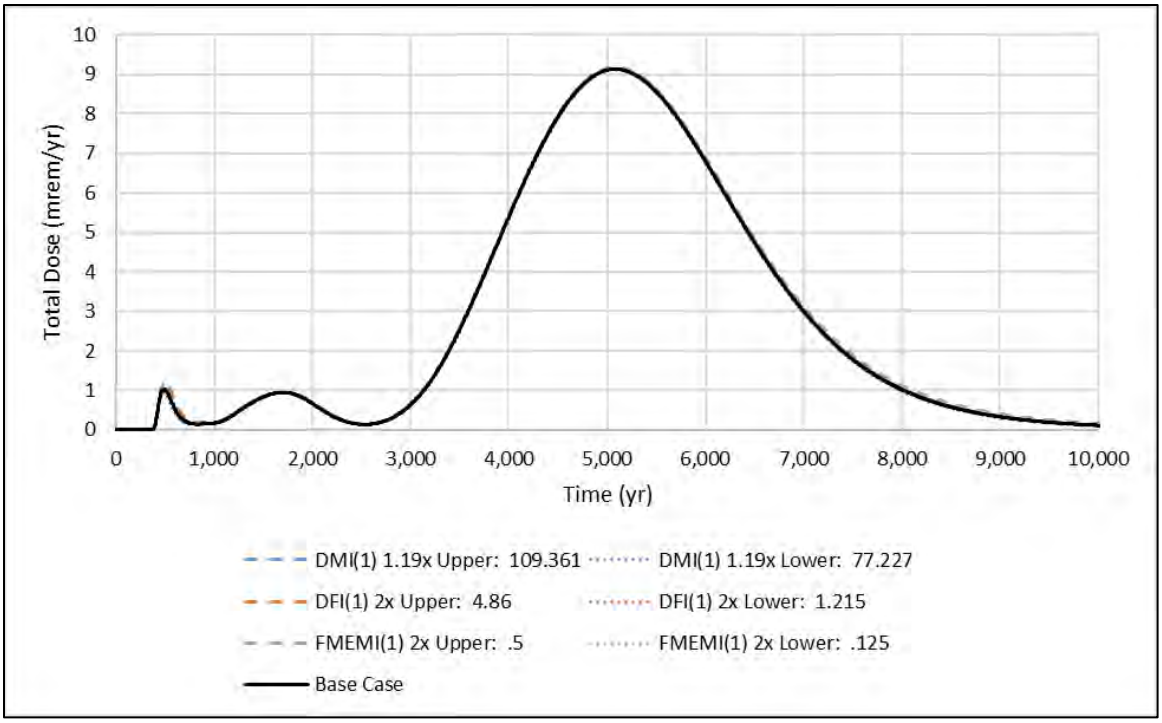

Fig. G.35. Sensitivity analysis on meat ingestion rate (DMI(1)), fish ingestion rate (DFI(1)), and fraction of meat from affected area (FMEMI(1))with adjustment factors of 2, 1.19, and 2

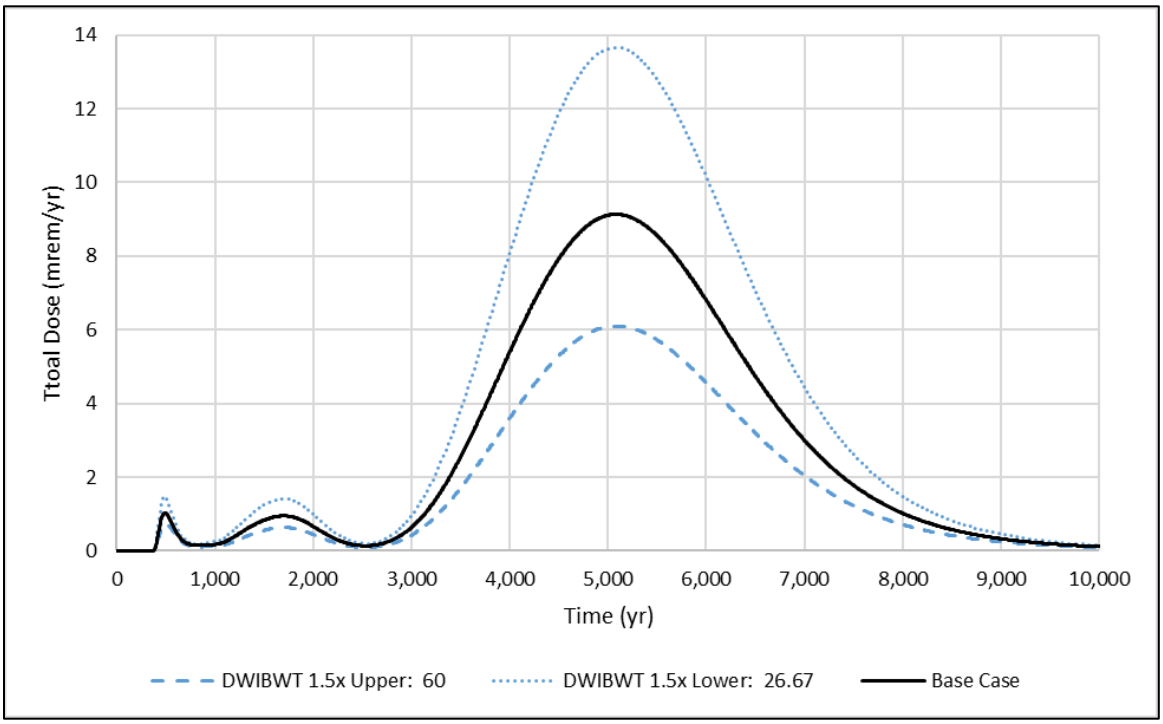

Fig. G.36. Sensitivity analysis on depth of aquifer contributing to well (DWIBWT) with an adjustment factor of 1.5

G.6.2.1 Sensitivity Analysis on Source Release Mechanism

There are three contaminant source release mechanisms in RESRAD-OFFSITE: Instantaneous Equilibrium Desorption, First Order Rate Controlled with Transport, and Version 2. The Instantaneous Equilibrium Desorption release mechanism, which was chosen for the base case model, uses the partition coefficients for each radionuclide to calculate an instantaneous release of contaminants from the soil to the soil moisture based on the equilibrium concentrations in each phase. First Order Rate Controlled Release with Transport involves specifying first order leach rates (constant proportion per time) based on partition coefficients and the water flux through the waste. The leach rates and the releasable fraction (Sect. G.6.2.4.1) can be varied with either a stepwise increase or linear increase between user-selected times. For the base case parameterization of the RESRAD-OFFSITE model, the releaseable fraction is increased linearly from zero to one between 300 and 1100 years (Sect. G.4.3.5.2). Like the First Order release mechanism, the Version 2 release mechanism is based on a leach rate that can either be specified by the user or calculated by the code using the partition coefficient in the contaminated zone, although in this release model the leach rate cannot be varied over time. To assess the sensitivity of the model results to the source release mechanism, simulations of the base case model were performed with the First Order Rate Controlled with Transport and Version 2 release mechanisms.

The predicted dose over time using the three evaluated source release mechanisms is shown on Fig. G.17. Since a release time cannot be specified in the Version 2 release mechanism, the results were shifted forward by 300 years for comparison with the other two release mechanism. In general, the Instantaneous Equilibrium Desorption release mechanism dose peaks dose are higher and the waste source is depleted faster, as evidenced by the rapid decrease in dose after 5000 years. The predicted peak dose during both the compliance period and afterward are approximately 1.5 to 2 times greater when the Instantaneous Equilibrium Desorption Release methodology is used compared to the First Order Rate Controlled Release and Version 2 release mechanisms.

The differences in dose predictions among the three release models are due to their underlying assumptions. The Instantaneous Equilibrium Desorption release model assumes that the infiltrating water attains an equilibrium concentration of radionuclides as soon as it comes into contact with the waste, whereas in the First Order and Version 2 release models, the rate of radionuclide transfer to infiltrating water is proportional to the releasable radionuclide inventory at that time (Yu et al. 2013). The Instantaneous Equilibrium Desorption release mechanism will produce higher radionuclide concentrations in infiltrating water given the same waste concentration, partition coefficients and infiltration rate, and therefore higher radionuclide flux than the First Order and Version 2 release options. The conceptual model represented by the Instantaneous Equilibrium Desorption source release option does not account for any limitation of release of radionuclides due to variable effects of waste containers, stabilized waste forms, or heterogeneity in cover infiltration. Therefore, adoption of the Instantaneous Equilibrium Desorption release mechanism for the base case model is considered to be a pessimistic assumption biased towards radionuclide releases of greater magnitude.

Two additional important considerations are that RESRAD-OFFSITE currently does not have the capability to account for solubility limits on radionuclide concentrations and that the infiltration rate as defined by other model parameters is constantly for the entire simulation duration. The increase in releasable fraction is applied as a surrogate for representing increasing cover infiltration over time. A pessimistic release model (Instantaneous Equilibrium Desorption) that is not bound by solubility limits and paired with higher than expected infiltration from 300 to 1000 years will produce dose predictions that are greater than expected for the base case conceptual model of EMDF performance evolution.

G.6.2.2 Sensitivity Analysis on Partition Coefficients of C-14, I-129, and Tc-99 in the Contaminated Zone, Unsaturated Zone, and Saturated Zones

Sensitivity to radionuclide-specific partition coefficients (K_d) was assessed for each radionuclide individually. Contaminated and saturated zone K_d values were varied individually while the K_d for UZ1 to UZ5 ("unsaturated zone") were varied together. K_d values were varied by a factor of five with the exception of C-14. Since the base case K_d value of C-14 in all model zones is 0 cm^3/g, sensitivity to this parameter was assessed using a K_d of 1 cm^3/g.

G.6.2.2.1 Sensitivity analysis on partition coefficient of C-14 in the contaminated zone, unsaturated zone, and saturated zone

In the base case model, a C-14 K_d of 0 cm^3/g is assumed for all model zones. Assuming a C-14 K_d of 0 cm^3/g is a pessimistic assumption, as modeling done in other performance assessments of disposal facilities on the ORR have assumed higher C-14 K_d values for the waste forms (ORNL 1997a, DOE 1997). The sensitivity analyses that assessed a C-14 K_d of 1 cm^3/g in the contaminated zone, unsaturated zones and unsaturated zones 1 to 5 indicate that predicted total dose prior to 2000 years is sensitive to C-14 K_d. Total dose during the compliance period is most sensitive to the contaminated zone K_d for C-14. Timing of the peak dose for the compliance period is also sensitive to the contaminated zone K_d for C-14. Increasing the C-14 K_d in each of the zones caused lower peak doses that occurred later when compared to the base case. Predicted total dose and timing of the peak dose for the 10,000-year simulation period are insensitive to the K_d of C-14 in the contaminated zone, unsaturated zones, and the saturated zone. Results from the sensitivity analysis on K_d of C-14 are shown in Fig. G.18.

G.6.2.2.2 Sensitivity analysis on partition coefficient of I-129 in the contaminated zone, unsaturated zone, and saturated zone

A factor of 5 sensitivity analysis was performed on the I-129 distribution coefficient in the contaminated, unsaturated, and saturated zones. The base case I-129 K_d values for the waste (2 cm^3/g) and other zones (4 cm^3/g) are pessimistic, as they are on the low end of the expected range (4.8 to 13.9 cm^3/g, refer to EMDF PA Sects. 2.1.6.3 and 3.2.2.7). Applying a factor of 5 to the base case values captures the range of possible I-129 K_d values at ORR, which can be as high as 13.9 cm^3/g. Assessment of I-129 K_d values below the sensitivity analysis range is discussed in Sect. G.6.3.

The factor of 5 sensitivity analysis on the specified partition coefficient of I-129 in the contaminated zone, unsaturated zone, and saturated zone indicates that predicted total dose and timing of peak dose for the compliance period are not sensitive to K_d of I-129. Predicted total dose and timing of peak dose for the 10,000-year simulation period are sensitive to variations in I-129 K_d. Increasing the K_d in each of the zones causes lower peak doses that occur later, while decreasing the K_d causes higher peak doses that occur earlier. Predicted total dose for the 10,000-year simulation period is most sensitive to the K_d of I-129 in the saturated zone and least sensitive to K_d of I-129 in the unsaturated zone. Results from the sensitivity analysis on K_d of I-129 are shown in Fig. G.19.

G.6.2.2.3 Sensitivity analysis on Tc-99 partition coefficient in the contaminated zone, unsaturated zone, and saturated zone

A factor of 5 sensitivity analysis was performed on the Tc-99 distribution coefficient in the contaminated, unsaturated, and saturated zones. The base case Tc-99 K_d values for the waste (0.36 cm^3/g) and other zones (0.72 cm^3/g) are somewhat pessimistic, as they are near or below the low end of the expected range for ORR (0.5 to 1.2 cm^3/g, refer to EMDF PA Sects. 2.1.6.3 and 3.2.2.7). Applying a factor of 5 to the base case

value captures the range of possible Tc-99 K_d values at ORR (0.5 to 1.2 cm^3/g). Assessment of Tc-99 K_d values below the sensitivity analysis range is discussed in Sect. G.6.3.

The factor of 5 sensitivity analysis on the specified partition coefficient of Tc-99 in the contaminated zone, unsaturated zone, and saturated zone indicate that total dose is sensitive to K_d of Tc-99 between approximately 1000 and 4000 years, the interval of time during which Tc-99 is the primary dose contributor. While the total dose is sensitive to Tc-99, the magnitude and timing of the peak dose is not sensitive to the K_d of Tc-99, as the total dose variability does not overlap with the peak doses from the primary dose contributors during the compliance period (C-14) or the 10,000-years simulation period (I-129). Results from the sensitivity analysis on K_d of Tc-99 are shown in Fig. G.20.

G.6.2.3 Sensitivity Analysis on Climate Parameters

A factor of 1.25 sensitivity analysis on the precipitation rate was performed to assess uncertainty in climatic conditions at the EMDF. Results from the sensitivity analysis on precipitation are shown in Fig. G.21. In RESRAD-OFFSITE, the precipitation rate, along with the runoff coefficient, evapotranspiration coefficient, and irrigation rate, is used to calculate the infiltration rate for the waste and other model zones (see Sect. G.4.3.5.2). The precipitation rate has a strong influence on the calculated infiltration rate in RESRAD-OFFSITE, as the sensitivity analysis values caused the infiltration rate to change by a factor of approximately 1.25, which is nearly identical to the applied sensitivity analysis factor. The precipitation rates used in the sensitivity analysis produce calculated infiltration rates of 1.1 in./year and 0.70 in./year. The range of precipitation values assessed in this sensitivity analysis exceeds the assumed range of infiltration rates for the compliance period, which is 0 to 0.88 in./year.

Predicted total dose and time of peak dose for the compliance period and the 10,000-year simulation period are sensitive to the precipitation rate. For both time periods, increasing the precipitation rate causes a higher peak dose that occurs earlier compared to the base case while decreasing the precipitation rate causes a lower peak dose that occurs later. The range in average annual precipitation evaluated is approximately 43 in./year to 68 in./year. This range corresponds roughly to the observed range of annual total precipitation measured during recent decades for the Oak Ridge area (refer to Fig. 2.8 of the PA). Considered as a possible future range in the long-term average annual precipitation, this range in values represents a very wide range in future climatic conditions. Climate forecasts suggest that wetter than current conditions are likely to develop over the next few centuries, but the uncertainty in climate over millennia is very large and drier than current conditions in East Tennessee are possible in the long term.

G.6.2.4 Sensitivity Analysis on Cover Performance Parameters

Sensitivity analyses were performed on some of the model parameters that represent cover performance, which include initial releasable fraction of radionuclide bearing material, initial release time, release duration, and runoff coefficient of the primary contamination. Initial releasable fraction, initial release time, and release duration are radionuclide-specific parameters and sensitivity of predicted total dose to these parameters was only assessed for C-14, I-129, and Tc-99, the radionuclides that contributed most to the total dose during the 10,000-year simulation period.

Initial releasable fraction of radionuclide bearing material represents the fraction of the material that is available for release at the specified initial release time. To assess the impact of cover performance, simulations were performed with higher and lower initial releasable fractions, depending on the radionuclide. Initial releasable fractions of C-14, I-129, and Tc-99 were varied together, as uncertainty in cover performance would affect release of all radionuclides. The value of the initial releasable fraction is specified for each radionuclide separately in the RESRAD-OFFSITE code.

A factor of 2 sensitivity analysis was performed on initial release time and release duration for the radionuclides that contributed most to the dose, C-14, I-129, and Tc-99. Runoff coefficient sensitivity was evaluated by performing simulations with high and low runoff coefficients that would result in infiltration rates of 0.43 in./year and 4 in./year.

G.6.2.4.1 Sensitivity analysis on initial releasable fractions

Sensitivity of predicted total dose to initial releasable fraction was assessed by performing simulations with high and low initial releasable fractions. Results from the sensitivity analysis on initial releasable fraction are shown in Fig. G.22. Among the models implemented for the EMDF PA, this parameter is unique to RESRAD-OFFSITE. A base case value of zero was assigned to all radionuclides except for two that have a base case K_d value of 0 (C-14 and H-3). The zero initial releasable fraction increases linearly to one (100 percent) over the release duration (800 years) to approximate the gradual increase in cover infiltration due to progressive cover system degradation. (This approximation is necessary because the cover infiltration rate cannot be varied over time within the RESRAD-OFFSITE model code.)

For C-14 and H-3, which have a K_d of 0 cm^3/g for all model zones, an initial releasable fraction of 0.75 was assigned. A higher initial releasable fraction was assigned to these radionuclides to adequately capture their mobility nature because the RESRAD-OFFSITE release was inhibited by the initially low values of the releasable fraction (Sect. G.4.3.5). Variation from the base case initial releasable fraction (higher values) for Tc-99 and I-129 represents more rapid or initially more severe degradation of cover performance. For C-14, higher and lower values of initial releasable fraction (base case value of 0.75) represent uncertainty in several factors that will ultimately limit the release of C-14 to groundwater, including waste forms and the chemical species of carbon involved, in addition to variation in the severity of cover degradation. The high initial releasable fractions for C-14, I-129, and Tc-99 for the assessment were 0.998 (base case value multiplied by 1.33), 0.5, and 0.5, respectively. The low initial releasable fraction for C-14 for the assessment was 0.564 (base case value divided by 1.33). The initial releasable fractions of I-129 and Tc-99 in the base case were zero, the lowest value that can be evaluated, so this value was not modified.

Predicted total dose for the compliance period is somewhat sensitive to increasing and decreasing the initial releasable fraction of C-14 and Tc-99. Increasing the initial releasable fraction causes a higher peak C-14 dose, while decreasing this parameter causes a lower peak C-14 dose. The timing of the C-14 dose peak is little changed from the base case. Tc-99 dose at 1000 years is higher for the higher Tc-99 initial releasable fraction value.

Predicted total dose and timing of peak dose for the post-compliance period (1000 to 10,000 years) are slightly sensitive to increasing the initial releasable fractions of Tc-99 and I-129. Increasing the initial releasable fraction causes a slightly lower peak dose that occurs earlier, which is opposite of the effect on the C-14 peak dose results for the compliance period. A higher initial releasable fraction causes a lower peak dose for the 10,000-year simulation period because increasing the initial fraction releasable for Tc-99 and I-129 causes more of the inventory to be leached earlier in the simulation period, which leaves less material to contribute to the peak dose at later times.

G.6.2.4.2 Sensitivity analysis on initial release times

The factor of 2 sensitivity analysis on initial release times of C-14, I-129, and Tc-99 assessed initial release times of 150 and 600 years. It is assumed that the cover will perform as designed for 200 years post-closure (UCOR 2020a). This value was adjusted upwards to 300 years based on comparison of model outputs from preliminary RESRAD-OFFSITE and MT3D simulations. The base case initial release time of 300 years and the upper sensitivity value of 600 years are pessimistic, as there is evidence suggesting that the

engineered and natural features of a cover can be fully functional beyond 1000 years (Appendix C of this PA, Benson and Benavides 2018).

Results from the sensitivity analysis on the initial release times are shown in Fig. G.23. The sensitivity analysis performed on initial release times of C-14, I-129, and Tc-99 showed that predicted total dose and timing of peak dose during the compliance period are sensitive to initial release time of C-14 and insensitive to the initial release times of I-129 and Tc-99. An earlier initial release time for C-14 produces a higher peak dose relative to the base case that occurs earlier while a later initial release time for C-14 produces a lower peak dose that occurs later. Predicted peak total dose for the 10,000-year simulation is insensitive to the initial release times of C-14, I-129, and Tc-99 (Tc-99 and I-129 peaks are unchanged in terms of magnitude). Timing of peak dose for the 10,000-year simulation is sensitive to the initial release time of I-129. An earlier initial release time for I-129 produces an earlier peak dose relative to the base case and a later initial release time for I-129 produces a later peak dose. Predicted total dose and timing of peak dose for the 10,000-year simulation period are insensitive to the initial release times of C-14 and Tc-99.

G.6.2.4.3 Sensitivity analysis on release duration

A factor of 2 sensitivity analysis was performed on the release durations of C-14, I-129, and Tc-99. For the base case model, a release duration of 800 years was assigned to all radionuclides besides C-14 and H-3. A release duration of 500 years was assigned to C-14 and H-3 to capture the highly mobile nature of these radionuclides, which both have a partition coefficient of 0 cm^3/g for all model zones. The base case release duration assumptions are consistent with the expected service life of HDPE membranes, but are pessimistic, as the clay layer is expected to degrade less rapidly (Appendix C).

Results from the sensitivity analysis on the release durations of C-14, I-129, and Tc-99 are shown in Fig. G.24. The factor of 2 sensitivity on release durations of C-14, I-129, and Tc-99 showed that predicted total dose during the compliance period is mildly sensitive to the release duration of C-14 and insensitive to the release durations of I-129 and Tc-99. A shorter release duration of C-14 produces a higher peak dose relative to the base case while a longer release duration produces a lower peak dose. Timing of the peak dose for the compliance period is not sensitive to the release durations of C-14, I-129, or Tc-99. Predicted total dose and timing of the peak dose for the 10,000-year simulation period are sensitive to the release duration of I-129. A shorter release duration of I-129 produces a higher peak dose that occurs sooner while a longer release duration of I-129 produces a lower peak dose that occurs later. Predicted total dose for the 10,000-year simulation period is sensitive to the release duration of Tc-99; however, fluctuations in dose due to Tc-99 do not coincide with the peak dose from I-129, the largest dose contributor after the compliance period, so the magnitude and timing of the peak dose are insensitive.

G.6.2.4.4 Sensitivity analysis on runoff coefficient in the primary contamination

In RESRAD-OFFSITE, the runoff coefficient for a model zone is defined as the ratio of the runoff rate to the precipitation rate. The runoff coefficient, along with the precipitation rate, evapotranspiration coefficient, and irrigation rate, is used to calculate the infiltration rate for the waste and other model zones (see Sect. G.4.3.5.2). The runoff coefficient is not linearly related to the infiltration rate. Holding the other infiltration rate parameters constant, the upper sensitivity value of 0.982 (2 percent increase from base case value) produces an infiltration rate of 0.43 in./year (210 percent decrease) and the lower sensitivity value of 0.830 (16 percent decrease in runoff coefficient produces an infiltration rate of 4 in./year (450 percent increase). The range of runoff coefficient values assessed in this sensitivity analysis capture the full range of HELP model-predicted cover infiltration rates (refer to Fig. 3.13 in the PA) that represent assumed long-term performance (0.88 in./year) and severely degraded long-term cover performance (approximately 3.7 in./year). The assumed long-term cover performance of 0.88 in./year is pessimistic for the 1000-year

compliance period because the flexible HDPE membrane in the cover system is likely to limit cover infiltration to a lower level for over 1000 years (refer to Appendix C, Sect. C.1.2).

It is important to consider that the infiltration rate set by the runoff coefficient is constant throughout the entire simulation period. The runoff coefficient assumed for the base case simulation and the values assessed in this sensitivity analysis produce greater than expected infiltration rates, especially during the period of partial design performance (300 to 1100 years). Higher than expected infiltration rates would cause higher predicted total doses that occur earlier, as radionuclides would be leached from the waste and travel through the unsaturated zone more rapidly and reach potential receptors earlier and at greater concentrations. The RESRAD-OFFSITE release model (instantaneous equilibrium release option) and one-dimensional vadose zone representation appear to over-predict the activity flux from EMDF for radionuclides having K_d values > 1 cm^3/g, including I-129 and U-234 (refer to Sect. 3.3.5 of the PA and Sect. G.5.6 in this Appendix). The sensitivity evaluation on the lower runoff coefficient value (0.83) corresponding to 4 in./year cover infiltration produced extremely large doses after 5000 years that are associated with actinides (e.g., U-234 and Pu-239) in the EMDF estimated inventory. These extreme dose levels are not likely representative of future releases of uranium and plutonium for EMDF, and so the results of the sensitivity evaluation for the runoff coefficient are presented only for the total dose associated with C-14, Tc-99, and I-129 in Fig. G.25.

The sensitivity analysis on runoff coefficient showed that predicted total dose and timing of peak dose for the compliance period are sensitive to the runoff coefficient. A lower runoff coefficient (more infiltration) causes a higher peak C-14 dose that occurs earlier relative to the base case, while a higher runoff coefficient (less infiltration) causes a lower peak C-14 dose that occurs later. The Tc-99 dose at 1000 years is also larger for the increased cover infiltration (lower runoff coefficient).

Predicted peak dose associated with I-129 and the timing of peak dose for the 10,000-year simulation period are also sensitive to the runoff coefficient. Decreasing the runoff coefficient to 0.830 (4 in./year infiltration) causes a 30 percent increase in peak dose from I-129 during the 10,000-years simulation period. The I-129 peak also occurs more than 2000 years earlier than for the base case reflecting the much quicker release (factor of 4.5 greater cover infiltration applied to the release model) and shorter vadose travel time associated with the higher cover infiltration rate. Increasing the runoff coefficient to 0.98 (0.43 in./year cover infiltration) causes a lower peak dose that occurs later compared to the base case (Fig. G.25).

G.6.2.5 Sensitivity Analysis on Waste Characteristics

Sensitivity analyses were performed on the source concentrations in the waste and the model parameters that define the physical and hydraulic characteristics of the waste. Physical and hydraulic waste parameters evaluated include the longitudinal dispersivity, b parameter, hydraulic conductivity, total porosity, and effective porosity of the waste. Sensitivity to source concentrations in the waste was evaluated by individually changing the input soil concentrations, as these values cannot be varied using the RESRAD-OFFSITE sensitivity analysis function. All other parameters were evaluated by performing sensitivity analyses with different factors depending on the parameter.

G.6.2.5.1 Sensitivity analysis on source concentrations

To evaluate the impact of radionuclide source concentrations in the waste on deterministic dose, the base case model was simulated with source concentrations higher and lower than base case values for C-14, I-129, and Tc-99. Soil concentrations were not changed for any other simulated radionuclide, as dose contributions from all other radionuclides besides C-14, I-129, and Tc-99 are negligible. High source concentrations are equal to as-disposed source concentrations, which do not account for operational period losses. Source concentrations of 2.88, 0.407, and 2.80 pCi/g for C-14, I-129, and Tc-99, respectively, were

used in the high source concentration simulation. Low source concentrations are equal to 10 percent of the base as-disposed value (C-14) or based on available data excluding the high outliers (I-129 and Tc-99).

Results from the sensitivity analysis on source concentrations are shown in Fig. G.26. Predicted total dose for the compliance period is sensitive to varying the source concentrations. Higher source concentrations cause a higher peak dose while lower source concentrations cause a lower peak dose. Higher C-14 source concentration cause a higher peak dose while lower source concentrations cause a lower peak dose. The high C-14 source concentration is not realistic given that the estimated inventory, which is unadjusted for operational losses, is likely biased high. The timing of the peak dose for the compliance period is not sensitive to the source concentrations. Predicted total dose for the 10,000-year simulation period is sensitive to varying the source concentrations with higher concentrations causing a higher peak dose and lower concentrations causing a lower peak dose. The lower I-129 source concentration is more realistic than the EMDF average as-disposed waste concentration because that average included one outlier data point which makes the average value higher than is realistic. The timing of the peak dose for the 10,000-year simulation period is not sensitive to the source concentrations.

G.6.2.5.2 Sensitivity analysis on physical and hydraulic waste parameters

Sensitivity analyses were performed on the longitudinal dispersivity, b parameter, hydraulic conductivity, total porosity, and effective porosity of the contaminated zone. Results from the sensitivity analysis on the physical and hydraulic waste parameters are shown on Fig. G.27.

The factor of 5 sensitivity analysis performed on the longitudinal dispersivity of the contaminated zone showed that predicted total dose and timing of peak dose for both the compliance period and the 10,000-year simulation period are sensitive to this parameter. Lower longitudinal dispersivity in the contaminated zone produces a higher peak dose that arrives later compared to the base case while higher longitudinal dispersivity produces a lower peak that arrives earlier.

The factor of 1.4 sensitivity analysis performed on the b parameter of the contaminated zone showed that predicted total dose and timing of peak dose for the compliance period are mildly sensitive to this parameter. Predicted total dose and timing of peak dose for the 10,000-year simulation period are also mildly sensitive to varying the b parameter. Decreasing the b parameter produces a higher peak dose that occurs earlier than the base case while increasing this parameter causes a lower peak dose that occurs later.

The factor of 5 sensitivity analysis on the hydraulic conductivity of the contaminated zone showed that predicted total dose and the timing of the peak dose during the compliance period are mildly sensitive to this parameter. Predicted peak dose and timing of peak dose for the 10,000-year simulation period are also mildly sensitive to the hydraulic conductivity of the contaminated zone. Increasing the hydraulic conductivity in the contaminated zone causes a higher peak dose that occurs earlier than the base case, while decreasing the hydraulic conductivity causes a lower dose that occurs later.

The factor of 1.1 sensitivity analysis on the total porosity of the contaminated zone showed that predicted total dose and timing of peak dose for the compliance period are insensitive to the total porosity of the contaminated zone. Predicted total dose and timing of peak dose for the 10,000-year simulation period are mildly sensitive to the total porosity of the saturated zone. Predicted total dose and timing of the peak dose for the 10,000-year simulation period are more sensitive to increasing the total porosity of the contaminated zone than decreasing this parameter.

The factor of 1.5 sensitivity analysis on the effective porosity of the contaminated zone showed that predicted total dose and timing of peak dose during the compliance period are sensitive to the effective porosity. Predicted total dose and timing of peak dose for the 10,000-year simulation period are also

sensitive to the effective porosity of the contaminated zone. Increasing the effective porosity causes a lower peak dose that occurs later relative to the base case while decreasing the effective porosity causes a higher peak dose that occurs sooner.

G.6.2.6 Sensitivity Analysis on Unsaturated Zone Properties and Water Table Elevation

To assess the effect of unsaturated zone parameters on predicted total dose, sensitivity analyses were performed on the bulk density, total porosity, and effective porosity of UZ3 (geosynthetic clay liner), UZ4 (soil geobuffer), and UZ5 (native vadose zone) and the longitudinal dispersivity of UZ5. Sensitivity of predicted total dose to the water table elevation was assessed by performing a sensitivity analysis on the thickness of UZ5 and by performing a simulation with the thickness of UZ5 set equal to the minimum model value of 0.01 m.

G.6.2.6.1 Sensitivity analysis on UZ3 (geosynthetic clay liner) properties

Results from the sensitivity analyses on UZ3 properties are shown on Fig. G.28. The factor of 1.05 sensitivity analysis on the dry bulk density of UZ3 showed that predicted total dose and timing of peak dose for both the compliance period and the 10,000-year simulation period are insensitive to the dry bulk density of UZ3.

The factor of 1.1 sensitivity analysis on the total porosity of UZ3 showed that predicted total dose and timing of peak dose for both the compliance period and the 10,000-year simulation period are insensitive to the total porosity of UZ3.

The factor of 1.1 sensitivity analysis on the effective porosity of UZ3 showed that predicted total dose and timing of peak dose for both the compliance period and the 10,000-year simulation period are insensitive to the effective porosity of UZ3.

G.6.2.6.2 Sensitivity analysis on UZ4 (soil geobuffer) properties

Results from the sensitivity analyses on UZ4 properties are shown on Fig. G.29.

The factor of 1.05 sensitivity analysis on the dry bulk density of UZ4 showed that predicted total dose and timing of peak dose for the compliance period are insensitive to the dry bulk density of UZ4. Predicted total dose for the 10,000-year simulation period is mildly sensitive to decreasing the dry bulk density of UZ4. Timing of the peak dose for the 10,000-year simulation period is mildly sensitive to varying the dry bulk density of UZ4.

The factor of 1.1 sensitivity analysis on the total porosity of UZ4 showed that predicted total dose and timing of peak dose for the compliance period are insensitive to the total porosity of UZ4. Predicted total dose and timing of peak dose for the 10,000-year simulation period are mildly sensitive to varying the total porosity of UZ4.

The factor of 1.1 sensitivity analysis on the effective porosity of UZ4 showed that predicted total dose and timing of peak dose for the compliance period are insensitive to the effective porosity of UZ4. Predicted total dose and timing of peak dose for the 10,000-year simulation period are mildly sensitive to varying the effective porosity of UZ4.

G.6.2.6.3 Sensitivity analysis on UZ5 (native vadose zone soil) properties

Results from the sensitivity analyses on UZ5 properties are shown on Fig. G.30.

The factor of 1.05 sensitivity analysis on the dry bulk density of UZ5 showed that predicted total dose and timing of peak dose for the compliance period are insensitive to the dry bulk density of UZ5. Predicted total dose and timing of peak dose for the 10,000-year simulation period are mildly sensitive to the dry bulk density of UZ5.

The factor of 1.1 sensitivity analysis on the total porosity of UZ5 showed that predicted total dose and timing of peak dose for the compliance period are insensitive to the total porosity of UZ5. Predicted total dose and timing of peak dose for the 10,000-year simulation period are mildly sensitive to the total porosity of UZ5.

The factor of 1.5 sensitivity analysis on the effective porosity of UZ5 showed that predicted total dose and timing of peak dose for the compliance period are mildly sensitive to the effective porosity of UZ5. Predicted total dose and timing of peak dose for the 10,000-year simulation period are sensitive to the effective porosity of UZ5.

The factor of 2 sensitivity analysis on the longitudinal dispersivity of UZ5 showed that predicted total dose and timing of peak dose are insensitive to this parameter. Predicted total dose for the 10,000-year simulation period is mildly sensitive to the longitudinal dispersivity of UZ5, but the timing of the peak dose is insensitive.

G.6.2.6.4 Sensitivity analysis on water table elevation

A factor of 2 sensitivity analysis was performed on the thickness of UZ5. The base case value was based on the arithmetic mean of the depth of water beneath the EMDF predicted by MODFLOW (Appendix D). The range of UZ5 thicknesses evaluated corresponds to total unsaturated zone thicknesses of approximately 22 to 47 ft, which is within the estimated range of values (18 to 50 ft) according to MODLFLOW modeling performed for the PA. Additionally, a simulation was performed with the thickness of UZ5 set at the minimum model value of 0.01 m, to assess a highly pessimistic scenario in which the water table rises high enough to encroach upon the EMDF liner system. Results from the sensitivity analysis on water table elevation are shown in Fig. G.31.

The sensitivity analysis showed that predicted total dose for the compliance period is mildly sensitive to thickness of UZ5. Timing of peak dose is sensitive to the thickness of UZ5. Increasing the thickness of UZ5 causes a lower peak dose that arrives later in the compliance period compared to the base case. Decreasing the thickness of unsaturated zone does not affect the peak dose during the compliance period, but it does cause it to occur sooner than the base case. Predicted total dose for the 10,000-year simulation period is mildly sensitive to the thickness of UZ5. Timing of peak dose for the 10,000-year simulation period is sensitive to the thickness of UZ5. The effects of increasing and decreasing the thickness of UZ5 on magnitude and timing of peak dose are similar to those observed for the compliance period.

Simulation of the base case with the minimum UZ5 thickness had an effect on model results similar to that of the lower bound of the factor of 2 sensitivity analysis performed on thickness of UZ5. With the minimum thickness of UZ5, predicted total dose for the compliance period and 10,000-year simulation period increased and the peak doses for these intervals occurred earlier than the base case. The minimum UZ5 thickness causes an increase in dose starting at approximately 7,500 years, which is due to an earlier arrival of high-K_d radionuclides (plutonium and uranium isotopes) at the dose contributing receptors compared to the base case. Performing a sensitivity simulation with a minimum UZ5 thickness was performed to assess

a highly pessimistic scenario in which the water table rises high enough to encroach upon the EMDF liner system. This scenario would require a major change in the hydrologic regime in the area surrounding the EMDF that is not expected to occur.

G.6.2.7 Sensitivity Analysis on Saturated Zone Properties

Sensitivity analyses were performed on several physical and hydraulic saturated zone properties. General physical and hydraulic properties that were assessed include dry bulk density, total porosity, effective porosity, thickness, and hydraulic conductivity of the saturated zone. Aquifer to well hydraulic properties evaluated include hydraulic gradient of aquifer to well and longitudinal dispersivity of aquifer to well. Aquifer to surface water body hydraulic properties assessed include hydraulic gradient of aquifer to surface water body, longitudinal dispersivity of aquifer to surface water body, depth of aquifer contributing to surface water body, and mean residence time of water in surface water body.

G.6.2.7.1 Sensitivity analysis on saturated zone general physical and hydraulic properties

Results from the sensitivity analyses performed on the general physical and hydraulic properties of the saturated zone are shown in Fig. G.32.

A factor of 1.15 sensitivity analysis was performed on dry bulk density of the saturated zone. Predicted total dose and timing of the peak dose for the compliance period are insensitive to the dry bulk density of the saturated zone. Predicted total dose and timing of the peak dose for the 10,000-year simulation period are sensitive to the dry bulk density of the saturated zone. Increasing the dry bulk density of the saturated zone causes a lower peak dose that occurs later compared to the base case and decreasing dry bulk density of the saturated zone causes a higher peak dose that occurs earlier.

The factor of 1.5 sensitivity analysis on the total porosity of the saturated zone showed that predicted total dose and the timing of the peak dose for the compliance period are insensitive to total porosity of the saturated zone. Predicted total dose and timing of the peak dose for the 10,000-year simulation period are sensitive to the total porosity of the saturated zone. A higher total porosity causes a higher peak dose that occurs earlier compared to the base case while a lower total porosity causes a lower peak dose that occurs later.

The factor of 1.5 sensitivity analysis on the effective porosity of the saturated zone showed that predicted total dose and the timing of the peak dose for the compliance period are mildly sensitive to this parameter. Predicted total dose and timing of the peak dose for the 10,000-year simulation period are sensitive to the effective porosity of the saturated zone. A higher effective porosity causes a lower peak dose that occurs later compared to the base case while a lower effective porosity causes a higher peak dose that occurs earlier.

A factor of 1.5 sensitivity analysis was performed on the thickness of the saturated zone. This sensitivity analysis showed that predicted total dose and timing of peak dose for both the compliance period and 10,000-year simulation period are insensitive to the thickness of the saturated zone.

The factor of 2 sensitivity analysis on hydraulic conductivity of saturated zone showed that predicted total dose and timing of peak dose are sensitive to this parameter. Increasing the hydraulic conductivity of the saturated zone produces a lower peak dose that occurs earlier, while decreasing this parameter causes a higher peak dose that occurs later. Predicted total dose and timing of peak dose for the 10,000-year simulation period are also sensitive to the hydraulic conductivity of the saturated zone.

G.6.2.7.2 Sensitivity analysis on aquifer to well hydraulic properties

Results from the sensitivity analyses on aquifer to well hydraulic properties are shown in Fig. G.33.

A factor of 2 sensitivity analysis was performed on the hydraulic gradient of aquifer to well. Predicted total dose for the compliance period is sensitive to the hydraulic gradient of aquifer to well with a higher gradient causing a lower peak dose and a lower gradient causing a higher peak dose. Decreasing the hydraulic gradient of aquifer to well causes a later peak dose, but increasing this parameter has no effect on the timing of the peak dose for the compliance period. Predicted total dose and timing of peak dose for the 10,000-year simulation period are sensitive to the hydraulic gradient of aquifer to well. Increasing the hydraulic gradient causes a lower peak dose that occurs early compared to the base case while decreasing this parameter causes a higher peak dose that occurs later.

The factor of 2 sensitivity analysis performed on the longitudinal dispersivity of aquifer to well shows that predicted total dose and timing of peak dose for the compliance period are insensitive to decreasing this parameter. Total dose and timing of peak dose for the compliance period are mildly sensitive to increasing longitudinal dispersivity of aquifer to well, which causes a lower peak dose that occurs later. Predicted peak dose for the 10,000-year simulation period is sensitive to the longitudinal dispersivity of aquifer to well, while timing of peak dose is mildly sensitive to this parameter. During the 10,000-year simulation period, increasing longitudinal dispersivity in the aquifer causes a lower dose that occurs later while decreasing this parameter causes a higher peak dose that occurs earlier.

G.6.2.7.3 Sensitivity analysis on aquifer to surface water body properties

Results from the sensitivity analyses on aquifer to surface water body hydraulic properties are shown in Fig. G.34.

The factor of 2 sensitivity analysis on hydraulic gradient to surface water body showed that predicted total dose and timing of peak dose for both the compliance period and 10,000-year simulation period are mildly sensitive to this parameter. Increasing the hydraulic gradient of aquifer to surface water body produces a higher peak dose that occurs early compared to the base case. Decreasing the hydraulic gradient of aquifer to surface water body produces a lower peak dose.

A factor of 2 sensitivity analysis was performed on the longitudinal dispersivity of the aquifer to the surface water body. Predicted total dose and timing of peak dose for the compliance period are insensitive to longitudinal dispersivity of aquifer to well. Predicted total dose for the 10,000-year simulation period is mildly sensitive to the longitudinal dispersivity of aquifer to surface water body, while the timing of the peak dose for this interval is only sensitive to increasing this value.

The factor of 2 sensitivity analysis performed on depth of aquifer contributing to surface water body showed that predicted total dose for the compliance period is mildly sensitive to this parameter. Timing of peak dose for the compliance period is only mildly sensitive to decreasing the depth of aquifer contributing to the surface water body. Predicted total dose and timing of peak dose for the 10,000-year simulation period are mildly sensitive to decreasing the depth of aquifer contributing to well and insensitive to increasing this depth.

Model sensitivity to mean residence time of water in the surface water was assessed by performing a factor of 10 sensitivity analysis on this parameter. The base case value for mean residence time of water in surface water body is well defined as it is based on measured flow rates of Bear Creek. However, a sensitivity factor of 10 was applied to mean residence time of water in the surface water body because there is significant uncertainty in assigning an appropriate long-term average value that captures the net impact of hydrological,

geochemical, and biological processes that impact surface water radionuclide concentrations. Predicted total dose and timing of peak dose for the compliance period are sensitive to the mean residence time of water in the surface water body. Predicted total dose and timing of peak dose for the 10,000-year simulation period are also sensitive to the mean residence time of water in the surface water body. Increasing the mean residence time of water in the surface water body causes a higher peak dose that occurs later compared to the base case while decreasing the residence time causes a lower peak dose that occurs earlier.

G.6.2.8 Sensitivity Analysis on Human Exposure Parameters

Uncertainty to human exposure was assessed by performing sensitivity analyses on food and water ingestion related parameters. Assessed food ingestion parameters include meat ingestion rate, fish ingestion rate, and fraction of meat from the affected area. The only water ingestion parameter that was assessed was depth of aquifer contributing to well (well depth).

G.6.2.8.1 Sensitivity analysis on food ingestion parameters

Results from the sensitivity analyses on food ingestion parameters are shown in Fig. G.35.

A factor of 1.19 sensitivity analysis was performed on the meat ingestion rate. Predicted total dose and timing of peak dose for the compliance period are insensitive to the meat ingestion rate. Predicted total dose and timing of peak dose for the 10,000-year simulation period are insensitive to the meat ingestion rate.

The factor of 2 sensitivity analysis performed on the fish ingestion rate showed that predicted total dose and timing of peak dose for the compliance period are mildly sensitive to varying this parameter. Increasing the fish ingestion rate produces a higher peak dose that occurs later than the base case while decreasing this ingestion rate causes a lower peak dose that occurs earlier. Predicted total dose and timing of peak dose for the 10,000-year simulation period are insensitive to the fish ingestion rate.

A factor of 2 sensitivity analysis was performed on the fraction of meat from the affected area. Predicted total dose and timing of peak dose for the compliance period are insensitive to changing the fraction of meat from the affected area. Predicted total dose and timing of peak dose for the 10,000-year simulation period are mildly sensitive to the fraction of meat from the affected area. A higher fraction of meat from the affected area causes a higher peak dose that occurs later than the base case while a lower fraction causes a lower peak dose that occurs sooner.

G.6.2.8.2 Sensitivity analysis on depth of aquifer contributing to well

Model sensitivity to the depth of aquifer contributing to well was assessed by performing a factor of 1.5 sensitivity analysis. Results from the sensitivity analysis on the depth of aquifer contributing to well are shown in Fig. G.36. Predicted total dose and timing of peak dose for the compliance period are sensitive to the depth of aquifer contributing to well. A thicker depth of aquifer contributing to well produces a lower peak dose that occurs later while a thinner well screen interval produces a higher peak dose that occurs sooner. Predicted total dose for the 10,000-year simulation period is sensitive to well depth while timing of peak dose is insensitive to this parameter. Increasing the depth of aquifer contributing to well causes a lower peak dose while decreasing the depth causes a higher peak dose.

The depth of aquifer contributing to well base case value was assumed to be 131 ft. This value is based on the total thickness of model layers 1, 2, and 3 at the well location in the MT3D saturated zone radionuclide transport modeling of the EMDF. The top three layers are predicted to have the highest concentrations of radionuclides at the groundwater point of assessment (refer to Appendix F). A well depth of approximately 130 ft is consistent with the range of household well depths according to TDEC records for wells in the

vicinity of BCV, which have depths ranging from less than 100 ft to more than 300 ft. Given this range, and the TDEC requirement for isolation casing to 19 ft below the surface or to the top of bedrock, it is likely that the well could be deeper than 131 ft. A shallower well would produce a higher predicted dose, as a larger fraction of the screened interval would intersect contaminated water compared to a well with a longer/deeper screened interval. In general, the representation of the groundwater well in the RESRAD-OFFSITE model, which assumes water withdrawal from the most contaminated vertical interval (a fixed depth below the water table) is an important pessimistic assumption incorporated into the exposure scenario for the dose analysis. As suggested in the presentation of water use assumptions for the all-pathways exposure scenario, it is possible that in an actual resident farming scenario the receptor would obtain groundwater from a vertical interval that is less contaminated than is predicted by the RESRAD-OFFSITE model. This would reduce dose to the receptor.

G.6.2.9 Composite Sensitivity Analysis

G.6.2.9.1 Compliance period dose sensitivity

The suite of predicted total dose over time for all of the performed sensitivity analysis simulations for the compliance period is shown in Fig. G.37. The greatest predicted peak total dose during the compliance period occurs when the mean residence time of water in the surface water body is increased by a factor of 10 from the base case value of 0.0001 to 0.001. This change increases the concentration of C-14 in the surface water body allowing for more uptake by fish and a greater dose from the fish ingestion pathway. The base case value for mean residence time of water in surface water body is well defined as it is based on measured flow rates of Bear Creek. However, a sensitivity factor of 10 was applied to mean residence time of water in the surface water body because there is significant uncertainty in assigning an appropriate long-term average value that captures the net impact of hydrological, geochemical, and biological processes that impact surface water radionuclide concentrations.

The second greatest predicted peak dose is for the sensitivity scenario with the hydraulic gradient of the saturated zone to the well, which decreased by a factor of 2 from 0.054 ft/ft to 0.027 ft/ft. The lower hydraulic conductivity represents a smaller flux (Darcy velocity) in the saturated zone and thus less mixing of leachate with groundwater along the path to the 100-m well location. The base case value (0.054 ft/ft) was selected on the basis of comparison of RESRAD-OFFSITE output with the results of the more detailed three-dimensional representation of the saturated zone (refer to Sect. 3.3.5 of the PA), so it represents a best estimate of saturated zone mixing.

The third greatest predicted peak total dose occurs when the runoff coefficient in the primary contamination is decreased from 0.963 to 0.830. This reflects the extreme cover degradation sensitivity case associated with cover infiltration of 4 in./year, which is considered to be well outside the likely range of long-term degraded cover performance. A more realistic range of long-term cover infiltration rates is 0.88 to 2.0 in./year (refer to Fig. 3.13 in the PA).

The fourth greatest predicted peak dose is for the sensitivity scenario with the hydraulic conductivity of the saturated zone, which decreased by a factor of 2 from 26.8 m/year to 13.4 m/year. This change decreases the Darcy velocity of the saturated zone by 50 percent (similar to the effect of varying the hydraulic gradient), which decreases the ratio of leachate flux to saturated zone flux, increasing the activity concentrations at the 100-m well. The base case value of 26.8 m/year is equal to the transmissivity-weighted average of the horizontal hydraulic conductivity values used in MT3D layers 1 and 2. The low value assessed in this sensitivity analysis is within the observed range of hydraulic conductivity values for the upper highly fractured and partially weathered part of the bedrock zone.

This page intentionally left blank.

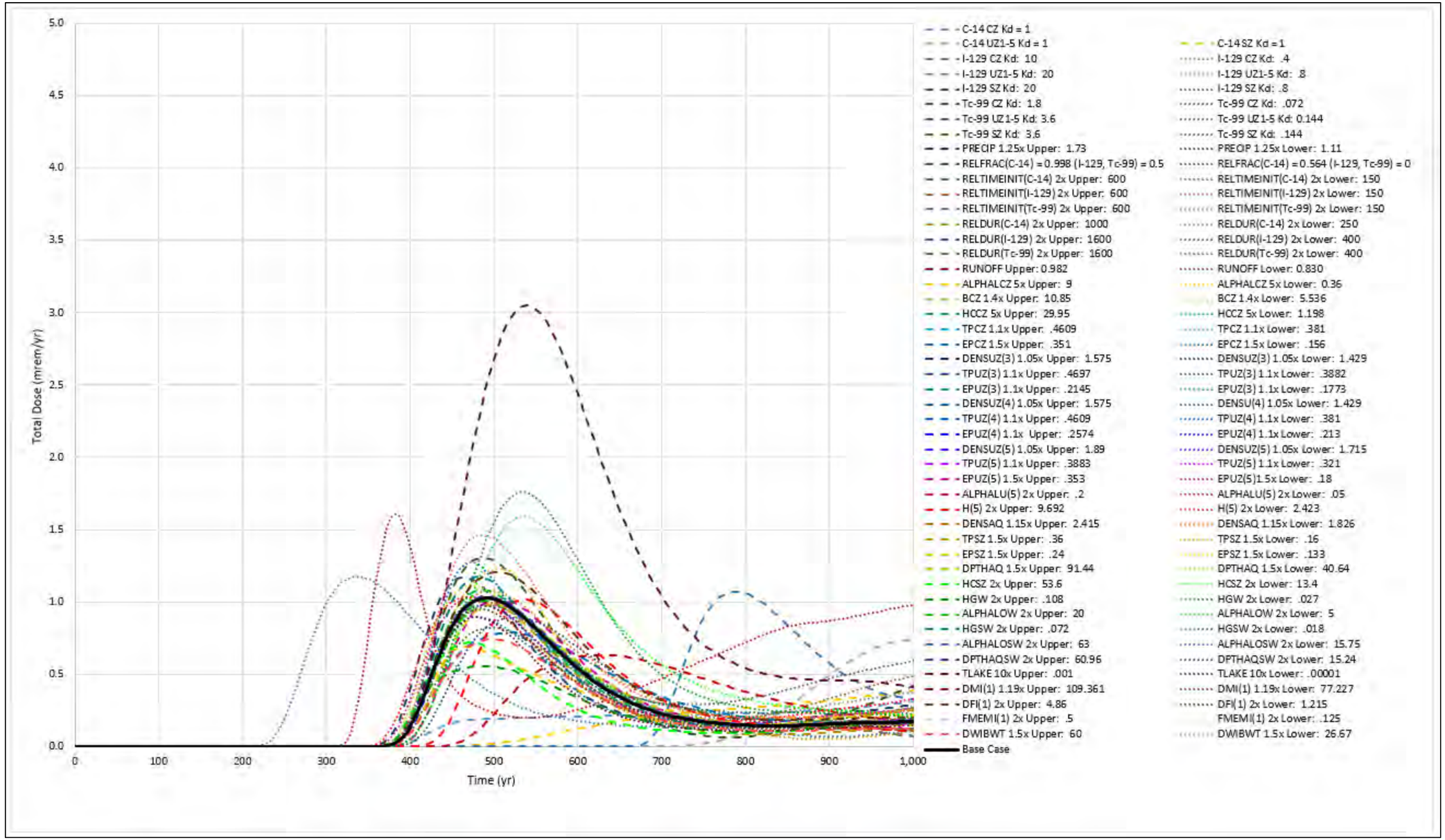

Fig. G.37. Total dose plot of sensitivity analysis simulations (compliance period)

This page intentionally left blank.

Other parameters having a significant effect on the predicted peak dose include the depth of aquifer contributing to well; initial releasable fractions of C-14, I-129, and Tc-99; initial release time of C-14; and the effective porosity of the contaminated zone. The remainder of the input parameters induce minimal total dose deviation from the base case scenario results. Overall, for the compliance period, none of the sensitivity analysis simulations predict a peak total dose greater than 4.0 mrem/year. Of the four input parameters with the largest impact on compliance period peak dose (surface water residence time, hydraulic gradient to the well, saturated zone hydraulic conductivity, and runoff coefficient), representation of the uncertainty in the two saturated zone parameters in the sensitivity runs is most realistic. On the other hand, the sensitivity of the peak total dose to the higher mean residence time (1.0E-03 year) and the lower runoff coefficient (0.83, corresponding to 4 in./year cover infiltration) represents less realistic dose levels associated with pessimistically high ingestion (Sect. G.4.3.18) of highly contaminated fish and pessimistically high cover infiltration, respectively.

G.6.2.9.2 Long-term dose sensitivity

Predicted total dose over time for the 10,000-year simulation is depicted in Fig. G.38. The three parameters to which peak total dose predictions for the 10,000-year period are most sensitive are runoff coefficient in the primary contamination, partition coefficient of I-129 in the saturated zone, and the depth of aquifer contributing to well. The decrease in runoff coefficient to 0.83, which results in very large cover infiltration and a corresponding increase in radionuclide flux from the waste, is not a likely long-term performance level. In addition, the impact of increased cover infiltration on the RESRAD-OFFSITE release of radionuclides having $K_d > 1$ cm^3/g (including I-129) appears to over-estimate activity flux from the vadose zone to the water table (refer to Sect. 3.3.5 of the PA). The sensitivity to I-129 K_d represents a realistic level of uncertainty about iodine sorption capacity of Conasauga Group materials at the EMDF site. That uncertainty will be addressed with laboratory evaluations of iodine K_d with samples from the CBCV site. However, the modeled EMDF I-129 source concentration is probably over-estimated (Sect. G.6.2.2.2) so that peak dose predictions may also be over-estimated even for lower than assumed partition coefficient values (I-129 $K_d < 1.0$). Uncertainty in human exposure to contaminants at the 100-m well is captured by the sensitivity evaluation on the depth of aquifer contributing to well input parameter. This uncertainty is addressed in the PA analysis by adopting a pessimistic exposure scenario in which drinking water is obtained at the point of maximum concentration at 100 m downgradient from the EOW. It is likely that a groundwater source for domestic use near the EMDF would have radionuclide concentrations lower than the base case scenario predicted concentrations, due to a different well location or deeper vertical interval of the well screen. On the other hand, it is much less likely that drinking water activity concentrations would be higher than the base case predictions which are based on highly pessimistic exposure assumptions.

This page intentionally left blank.

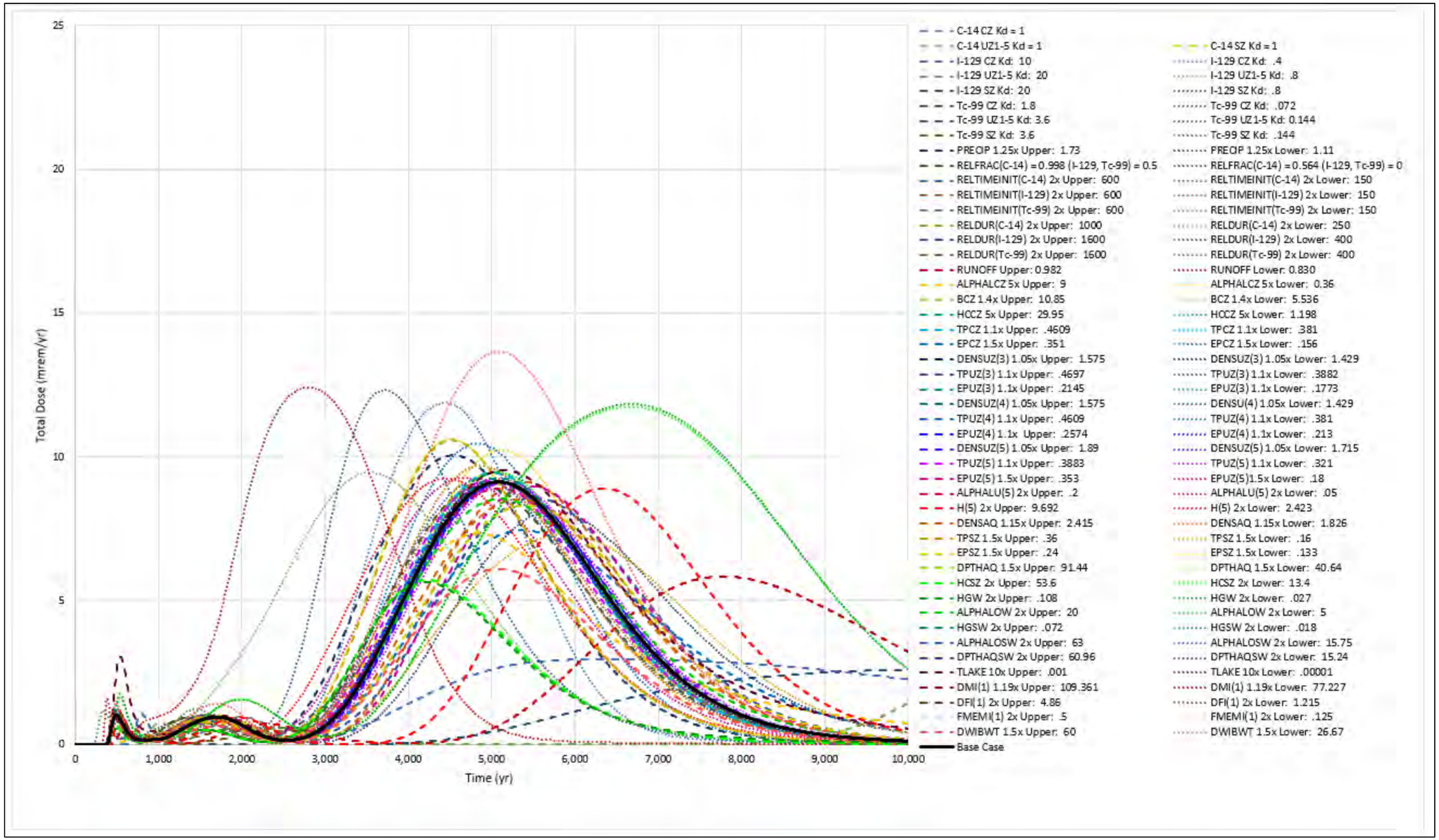

Fig. G.38. Total dose plot of sensitivity analysis simulations (0 to 10,000 years)

This page intentionally left blank.

G.6.3 UNCERTAINTY ANALYSIS

Uncertainty analysis was performed using the probabilistic module in RESRAD-OFFSITE. These analyses were performed to assess the range of variation in predicted peak dose due to the uncertainty in model parameter value assumptions. Additionally, these analyses were used to identify the radionuclides and parameters that have the greatest influence on the predicted peak dose, which allows for prioritization of efforts to manage or reduce uncertainty in the dose predictions from the model. The probabilistic simulations focused on the three isotopes (C-14, I-129, and Tc-99) that result in the greatest magnitude contributions to the predicted total dose during the 1000-year compliance period, but also include potential dose contributions from release of radionuclides of uranium and plutonium over a longer (10,000-year) period of analysis. For the compliance period probabilistic simulations presented in Sect. G.6.3.3, total dose refers to the dose resulting from C-14, I-129, and Tc-99.

G.6.3.1 Background on RESRAD-OFFSITE Probabilistic Module

The original RESRAD code was modified by the developers to include the probabilistic code to make RESRAD compatible for use with the NRC License Termination Compliance Process and the Standard Review Plan (Yu et al. 2000). To develop the probabilistic code, model parameters were classified into one or more of the following categories:

- Physical parameters – determined by source, location, and geology
- Metabolic parameters – based on metabolic characteristics of the potential receptor
- Behavioral parameters – dependent on receptor behavior and scenario definition or a parameter that does not fit the physical or metabolic description (Yu et al. 2000).

Default parameter distributions were specified by the model developers by obtaining available values from the literature and by collecting original data (Yu et al. 2000). Later, distributions for parameters solely used in RESRAD-OFFSITE were developed (Yu et al. 2007).

In the probabilistic module available in RESRAD-OFFSITE, parameter distributions can be sampled through either the standard Monte Carlo method or the Latin Hypercube Sampling (LHS) method (modified Monte Carlo). Either method can be applied to parameter distributions to generate random samples of input parameters (observations). The number of observations generated is specified by the modeler with each observation set (realization) used to generate one set of output results. Should an analysis need to be re-simulated, a random seed number is specified to ensure the same set of input parameter values (realization) is generated. Parameters can be randomly paired (uncorrelated) or rank correlation coefficients (RCCs) can be specified if a set of parameters is assumed to be correlated. Additionally, if one input is the function of another, the user can specify mathematical relationships using the related parameters feature available in the probabilistic module in RESRAD-OFFSITE (Yu et al. 2007).

G.6.3.2 Base Case Uncertainty Analysis

Uncertainty analyses was conducted on the base case model to assess the changes in dose predictions during the 1000-year compliance period and the 10,000-year simulation period due to the uncertainty associated with some model parameters. The uncertainty analysis was carried out using the following steps:

1) Identification of important RESRAD parameters for which uncertainty is significant and incorporating results of the sensitivity analysis
2) Quantification of parameter uncertainty (assignment of parameter distributions and correlations)

3) Probabilistic analysis of sensitivity to uncertainties and comparison with base case model results
4) Identification of major input parameter uncertainties through regression analysis of probabilistic results
5) Focused analysis of extreme dose results.

Initially, using insights gained from preliminary model runs and sensitivity analysis simulations, important RESRAD-OFFSITE parameters for which uncertainty could have significant dose impacts were identified. Carbon-14, I-129, and Tc-99 were identified as the radionuclides which had the most influence on total dose predictions during the compliance period; therefore, the compliance period uncertainty analysis includes only these three radionuclides. Preliminary model runs and sensitivity analysis simulations showed that Pu-239, U-234, U-235, and U-238 could potentially have dose contributions during the 10,000-year simulation period; accordingly, these radionuclides along with C-14, I-129 and Tc-99 were included in the 10,000-year uncertainty analysis. Both the compliance period and 10,000-year uncertainty analyses focused on parameters with significant uncertainty in the assignment of deterministic base case values, which include radionuclide release parameters (initial releasable fraction, initial release time, release duration), isotope-specific K_d values, the surface runoff coefficient (cover performance uncertainty), precipitation (climate uncertainty), and parameters controlling flow in the waste, unsaturated, and saturated zones. Attachment G.3 provides a list of parameters selected for the compliance period and 10,000-year uncertainty analyses as well as additional information on the assigned input parameter probability distributions and their bases.

G.6.3.2.1 Input parameter distributions

After identifying major parameters, uncertainty associated with these parameters was quantified in terms of probability distributions. Probability distributions were assigned to 33 different parameters for the compliance period analysis and 37 parameters for the 10,000-year analysis. Beta, bounded normal, or truncated log-normal distributions were applied to the input parameters (Attachment G.3). In general, a finite range in possible values was specified for each probabilistic input parameter, and the selection of the probability distribution was based on assumptions about the skewness of the distribution relative to the base case value of the parameter.

A symmetric beta distribution was used for most of the parameter distributions included in the uncertainty analysis. Using the beta distribution requires the specification of minimum and maximum values as well as the two parameters alpha and beta (p and q in the RESRAD-OFFSITE formulation), which define the variance and skewness of the probability distribution. The symmetric (alpha = beta) beta distribution represents uncertainty associated with a base case value that is considered a best estimate, with the range specified to encompass both higher and lower values of similar likelihood. Typically for these symmetric beta distributions, the minimum or maximum is specified, and the other limit is set at an equal interval above (or below) the base case value. When the range (uncertainty) of potential values is not symmetric about the base case value, asymmetric (alpha $\neq$ beta) beta distributions have been assigned based on the expected range and the relative likelihood of values smaller than or larger than the base case value (i.e., the expected skewness of the distribution). This is the case for certain input parameters such as vadose zone dispersivities, for which the base case parameter value is the minimum for the probability distribution rather than falling somewhere within the potential range. In addition to the vadose zone dispersivities, skewed beta distributions were assigned to the thickness of UZ5, initial release time, initial releasable fraction, and the runoff coefficient. Additional detail on the basis for the specific probability distribution assigned to each input parameter is provided in Attachment G.3 (refer to Table G.3.2).

A bounded normal distribution was used for the partition coefficients of simulated radionuclides in UZ1 and the saturated zone. Partition coefficient values for the waste (one half of the unsaturated zone value)

and UZ2 through UZ5 are assigned based on the sampled value for UZ1. Partition coefficients for C-14 were not included in the uncertainty analyses because the base case K_d is 0 cm^3/g for all model zones and there is no evidence suggesting higher K_d values at the site. Using a bounded normal distribution requires the specification of maxima and minima that bound the sampled interval, mean values that define the center of the normal distribution curve, and standard deviation values that determine the probability density of the distribution. Mean values for K_d distributions were equal to base case values. Distribution maxima were equal to twice the base case value. Distribution minima were equal to 0 cm^3/g for I-129 and Tc-99 to include model simulations with K_d values at or close to 0 cm^3/g. For Pu-239, U-234, U-235, and U-238, distribution minima were equal to one-half of the associated base case K_d values. The standard deviations for the distributions of I-129 and Tc-99 were selected so that the probability of $K_d = 0$ was large enough to ensure that some of the sampled K_d values were 0 or nearly 0. For the Pu-239 and uranium K_d distributions, the standard deviation was set to 25 percent of the base case value (i.e., standard deviation = 25 percent of the mean).

Truncated log-normal-N distributions were assigned for hydraulic conductivities in the contaminated zone, UZ5, and the saturated zone as well as for the mean residence time of water in the surface water body. A truncated log-normal-N distribution was chosen for the hydraulic conductivities because field data suggest a log-normal distribution. A log-normal distribution was selected for mean residence time of water in the surface water body to represent the large uncertainty (+/- an order of magnitude) associated with this small-valued parameter and to give a log-symmetric distribution about the base case value (1.0E-04 year).

Attachment G.3 (Tables G.3.1 and G.3.2) provides a complete list of parameters selected for the compliance period and 10,000-year uncertainty analyses as well as the assigned input parameter probability distributions and their bases.

G.6.3.2.2 Correlated and related input parameters

Among the parameters which were assigned probability distributions, there are pairs of parameters for which independent random sampling can result in unrealistic combinations of sampled values. For example, a very large sampled effective porosity coupled with a very low sampled hydraulic conductivity would be physically unrealistic. RESRAD-OFFSITE allows for the specification of RCCs, to impose correlations between inputs by ranking the sampled values and combining values from the distributions based on their relative rank (Yu et al. 2007) and the specified RCC. This procedure produces sets of input values that more realistically represent parameter relationships than if parameter values were randomly paired. RCCs were specified for pairs of parameters that are expected to be physically related. For the compliance period analysis, 16 pairs of probabilistic input parameters were assigned RCCs and for the 10,000-year analysis, 20 pairs of input parameters were assigned RCCs.

Parameters affecting radionuclide release and transport were correlated to more accurately represent radionuclide release in the uncertainty analysis. For example, a positive correlation was assigned between the release duration and the unsaturated zone K_d values because more rapid radionuclide release could be associated with low K_d values. Additionally, a negative RCC was assigned between release duration and initial releasable fraction as the release duration could be shorter if more material is initially available for release at the onset of cover failure. Similarly, a positive correlation between the radionuclide-specific K_d values for the unsaturated zone and the saturated zone was applied.

In addition to parameters affecting radionuclide release and transport, correlation coefficients were also assigned for groups of parameters that represent other physical processes. For example, a positive correlation between the precipitation rate and the runoff coefficient was assigned because higher annual average precipitation is expected to increase the average proportion of runoff in the annual water budget. This positive correlation has the effect of reducing the range of simulated cover infiltration rates (from a

possible maximum of 4.0 in./year). A negative correlation between the precipitation rate and the mean residence time of water in the surface water body was assigned because higher precipitation is expected to cause higher total runoff, resulting in decreased mean surface water residence time (i.e., increased precipitation increases flow in Bear Creek).

A general RCC value of +/-0.9 was assigned for positive and negative correlations because there is no firm basis for estimating RCC values for individual correlations. Using the specified RCC values, RESRAD-OFFSITE creates a rank correlation matrix and, as necessary, adjusts the RCC values to create a positive definite matrix. This adjustment procedure is required to implement the correlations among sampled input values. In general, the adjusted RCC values were reduced (e.g., +/-0.9 to +/-0.68) but the intended sign of the correlations was preserved. In some cases, pairs of initially uncorrelated inputs were assigned small positive or negative correlations to satisfy the positive definite matrix requirement. Attachment G.3 (Table G.3.2) provides assigned input parameter probability distributions and assigned rank correlation coefficients for both the compliance period and 10,000-year uncertainty analyses. Side-by-side comparisons of initially assigned and code-adjusted rank correlation coefficients for the compliance period and 10,000-year uncertainty analyses are provided in Attachment G.4. Input versus input scatter plots showing observations for pairs of probabilistic input parameters for which rank correlation coefficients were assigned are provided in Attachment G.5.

In addition to specifying distributions for uncertain input parameters, other parameter values are assigned based on user-defined functional relationships. Using the RESRAD-OFFSITE related parameters feature, one input can be represented as a function of another input that has been assigned a probability distribution (e.g., waste K_d = ½ unsaturated zone K_d). Fixed relationships were specified between pairs of input parameters assumed to have either identical or functionally related values. Identical relationships were specified for isotope-specific initial release times and release durations, (same sampled values for all radionuclides), and for radionuclide-specific K_d values in unsaturated zones 2 through 5. Functional relationships were specified to assign the initial releasable fraction of C-14, isotope-specific K_d values in the contaminated zone, the total porosity or dry bulk density of select model zones, and hydraulic gradient to the surface water body. Attachment G.3 provides assigned input parameter probability distributions and the basis for assignment of related parameters for both the compliance period and 10,000-year probabilistic analyses.

G.6.3.2.3 Probabilistic simulations

After probabilistic inputs are specified, the code generates 300 sets of inputs for each of 10 repetitions by sampling the specified distributions for each probabilistic input parameter. Sampling specifications used in the uncertainty analysis are shown in Table G.23. Sampling specifications were identical for both the compliance period and 10,000-year uncertainty analyses.

Table G.23. Summary of sampling specifications used in uncertainty analysis

Sampling specification	Value/method
Random seed	1000 (incremented)
Number of observations	300
Number of repetitions	10
Technique	Latin Hypercube Sampling

The random seed number used in the analysis was 1000, the default value assigned in RESRAD-OFFSITE. This seed number is used by the code's random number generator to produce the pseudo-random set of numbers needed to carry out the random sampling. The seed number is incremented to the next integer each time a random number is generated, giving each of the observation sets (realizations) a unique seed value, which will cause a nominal amount of variability between outputs for the repetitions. Specifying a random seed number to start with allows the code to reproduce the same set of probabilistic inputs if the same analysis needs to be run again on a different computer (Yu et al. 2007).

The number of observations is the number of values that will be sampled from the distributions of each of the parameters that are assigned distributions in the model (Yu et al. 2007). For this analysis, 300 observations (realizations) were used. The number of realizations used in the uncertainty analysis was based on the comparisons of cumulative distribution function (CDF) plots of inputs with different numbers of observations. The number of realizations was increased until the differences in the CDF plots from the repetitions were nominal. The analysis was repeated 10 times (10 repetitions) to provide a means to assess the variability in the sampled distributions of the 300 input parameter values and corresponding distributions of model outputs while avoiding excessively lengthy run-times associated with additional repetitions.

Distributions were sampled using the LHS technique. This technique was selected because it is known to select a more representative set of samples, specifically from the tails of distributions, than the alternative sampling technique available in RESRAD-OFFSITE, the Monte Carlo method. For each parameter assigned a distribution, LHS creates a set of samples by partitioning the cumulative probability curve into intervals of equal probability and selecting a value from each interval. Specified correlations among input parameters are used to group sampled values of the correlated parameters prior to performing the specified number of simulations (equal to number of observations) to generate a set of outputs for each repetition (Yu et al. 2007).

G.6.3.3 Probabilistic Results – Compliance Period

The following subsections present the results of the compliance period uncertainty analysis. The distributions of predicted total and radionuclide-specific doses at various points in time during the compliance period are presented in Sects. G.6.3.3.1 and G.6.3.3.2. The distribution(s) of the predicted peak (maximum within a simulation independent of time) total dose and contributions made via specific exposure pathways during the compliance period are presented in Sect. G.6.3.3.3. The results of the multiple regression analysis on the probabilistic model output to identify the parameter uncertainties most important to the prediction of peak total dose during the compliance period are included in Sect. G.6.3.3.4. Elevated (> 25 mrem/year) peak dose predictions for the compliance period uncertainty analysis are discussed in Sect. G.6.3.3.5.

G.6.3.3.1 Variation in the distribution of total dose over time for the compliance period

The RESRAD-OFFSITE uncertainty analysis calculates statistics of the total dose distribution for each repetition at each simulation time step. The variation of median, mean, and 95th percentile dose over time for each of the 10 repetitions of 300 simulations is shown on Fig. G.39. The deterministic base case model all-pathways dose curve is also shown on Fig. G.39 for comparison to the probabilistic results. By 250 years, the mean of the simulated dose distribution begins a steady, gradual increase through 1000 years. The 95th percentile values increase rapidly between 250 and 400 years and then increases gradually through 1000 years in parallel with the mean. In contrast, the median of the simulated dose distribution increases between 400 and 550 years and then becomes steady at approximately 0.4 mrem/year through the end of the compliance period. The difference between the deterministic base case dose curve and the probabilistic results (percentiles of the total dose distribution as a function of time) occurs because the time of peak total

dose for any single probabilistic simulation varies widely (230 to 1030 years) due to variable sampling of input parameters that control release timing (particularly K_d values) among the 3000 realizations. The differences between the deterministic and probabilistic results also reflect the likelihood of much larger dose contributions from Tc-99 and I-129 toward the end of the compliance period probabilistic simulations.

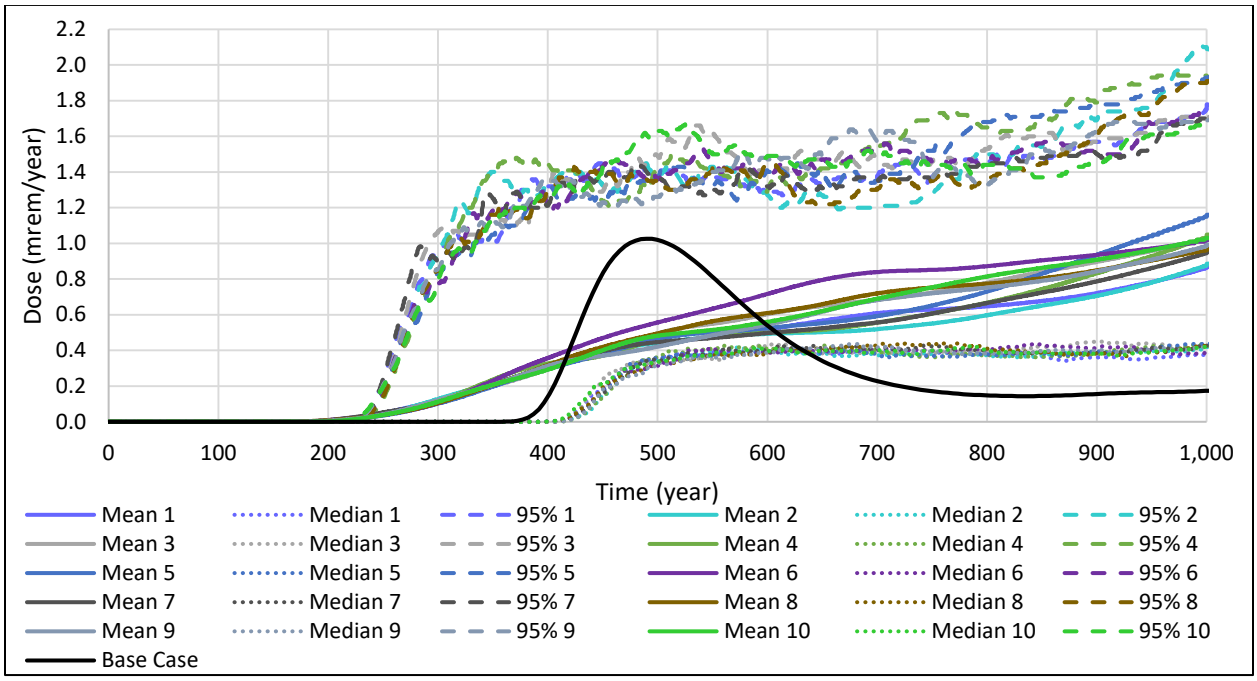

Fig. G.39. Compliance period probabilistic total dose summary, all pathways, all calculation points

For the compliance period uncertainty analysis, RESRAD-OFFSITE simulations extend beyond the last user-specified reporting time of 1000 years to 1030 years, thus model reported peak total doses can occur after 1000 years. The peak mean probabilistic dose (i.e., the maximum value of the mean dose for each repetition) occurred at 1030 years for all 10 repetitions, ranging from 0.92 to 1.2 mrem/year (Table G.24), which is nearly identical to the deterministic base case compliance period peak dose of approximately 1 mrem/year. The 95th percentiles of the probabilistic total dose also reached maximum values at 1030 years, with a range from 1.7 to 2.1 mrem/year among the 10 repetitions.

RESRAD-OFFSITE generates statistical output (CDF percentiles) for the 10 user-selected model reporting times. The selected reporting times were years 0, 200, 300, 400, 500, 600, 700, 800, 900, and 1000. CDF curves of the total dose for the reporting times are shown in Fig. G.40. These statistical outputs indicate that for reporting times 500 years and greater, predicted peak dose for some simulations can exceed the 25 mrem/year performance objective, but the 95th percentile remains below 2.2 mrem/year (refer to Fig. G.39).

Table G.24. Peak of the mean dose curves (averaged over 300 observations) for each model repetition, compliance period

Repetition	Time of peak mean dose Years	Peak mean dose mrem/year
1	1.03E+03	0.92
2	1.03E+03	0.94
3	1.03E+03	1.07
4	1.03E+03	1.11
5	1.03E+03	1.21
6	1.03E+03	1.05
7	1.03E+03	1.00
8	1.03E+03	1.00
9	1.03E+03	1.03
10	1.03E+03	1.07

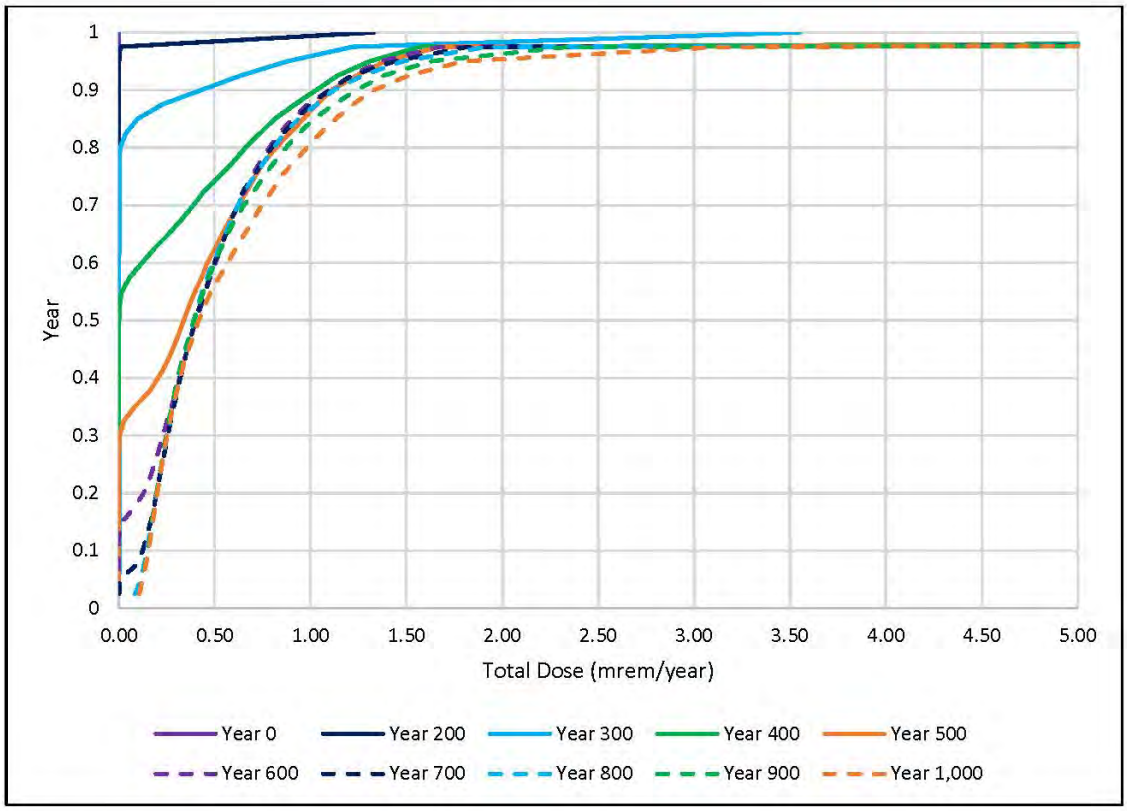

Fig. G.40. Cumulative probability summary for the compliance period, total over all pathways, select reporting times (0 to 5 mrem/year)

G.6.3.3.2 Radionuclide dose at reporting times and timing of radionuclide dose peaks

Figures G.41 through G.43 are plots showing the mean and mean +/- one standard deviation of the radionuclide dose for C-14, I-129, and Tc-99 at each model reporting time. These plots illustrate the variation in mean radionuclide-specific dose contributions over time and changes in the variability of dose contributions over time. The probabilistic dose curves for C-14 show increasing mean and standard deviation through about 500 years followed by a progressive decline in values (Fig. G.41), whereas the curves for I-129 (Fig. G.42) and Tc-99 (Fig. G.43) have increasing mean dose and standard deviation through the compliance period. Carbon-14 is the primary dose contributor for times prior to about 800 years. After 800 years, I-129 and Tc-99 have mean dose contributions equal to or greater than mean C-14 contributions. To provide perspective on the relationship between radionuclide dose statistics at reporting times and radionuclide dose peaks, each of the three radionuclide dose plots also includes horizontal reference lines at 95th percentile of the peak radionuclide dose. The peak radionuclide dose can occur at various times within the compliance period for any given simulation, so the 95th percentile of the peak dose is independent of time.

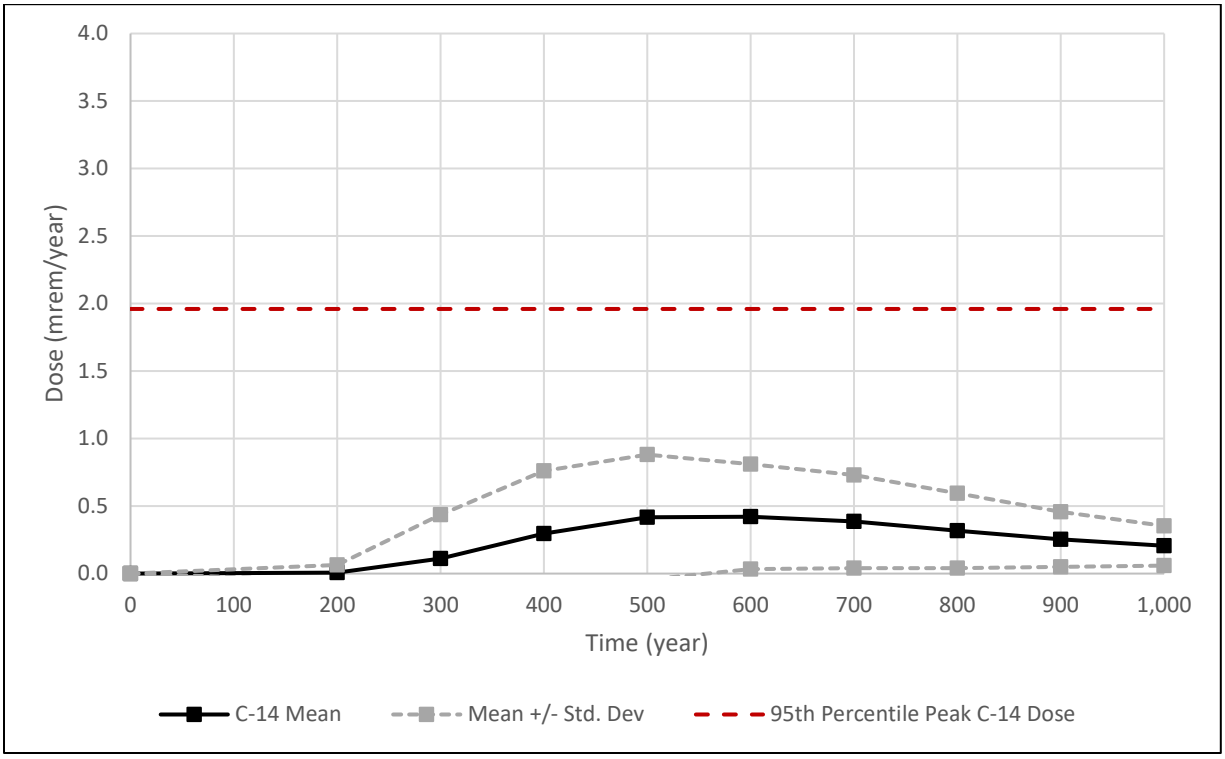

Fig. G.41. Probabilistic all pathways dose summary for C-14, all pathways, select reporting times

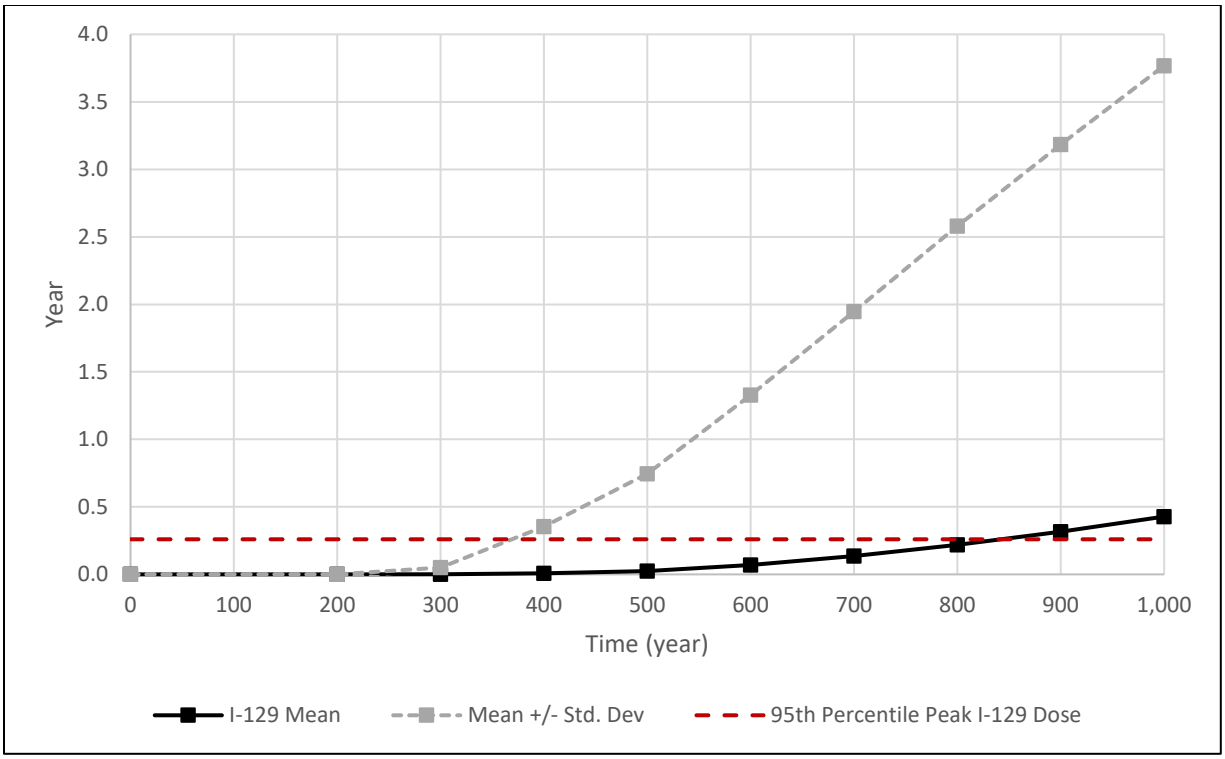

Fig. G.42. Probabilistic all pathways dose summary for I-129, all pathways, select reporting times

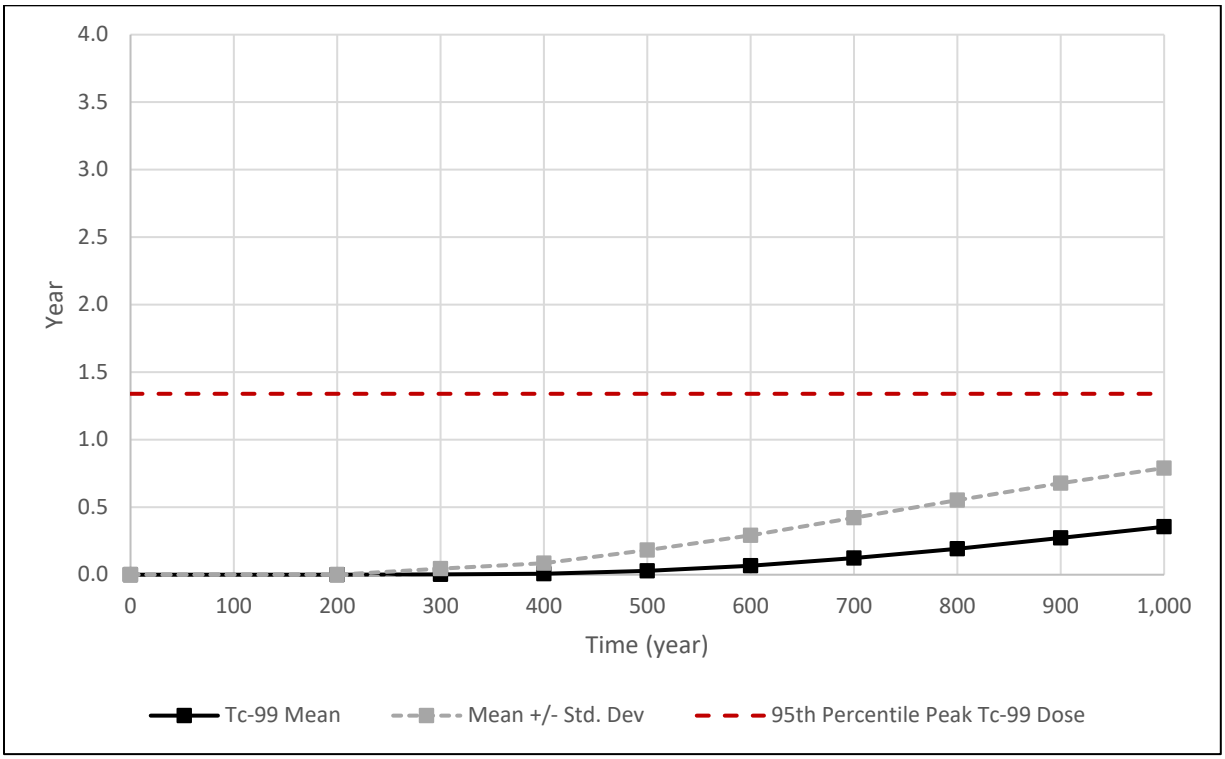

Fig. G.43. Probabilistic all pathways dose summary for Tc-99, all pathways, select reporting times

For C-14, roughly 95 percent of the radionuclide peaks occur between 300 and 900 years, with an average peak dose of 1.03 mrem/year and average time of peak dose at 560 years. For Tc-99, only the earliest 8 percent of radionuclide peak doses occur prior to 1030 years and the other 92 percent of peaks occur at the end of the simulation period (1030 years). For I-129, only seven out of 3000 peaks (0.23 percent) occur prior to 1030 years. For I-129 and Tc-99, compliance period peak doses that occur at the end of the simulation period are cases in which higher long-term radionuclide peaks will occur well after 1000 years (refer to Sect. G.6.3.4.4). The distribution (CDF) of C-14 peak doses for each of the 10 repetitions of 300 simulations is shown in Fig. G.44. The compliance period distributions of peak I-129 and Tc-99 dose are strongly influenced by the large proportion of simulations that result in zero or very low peak dose, roughly 95 percent for I-129 and 25 percent for Tc-99. Compliance period peak radionuclide dose statistics are provided in Table G.25. For I-129, the average peak radionuclide dose is larger than the 95th percentile, because of the large number zero peak dose values for that radionuclide. The long-term (post compliance period) distributions of peak Tc-99 and I-129 dose are presented in detail in Sect. G.6.3.4.2. The extreme values of I-129 peak dose that occur in the compliance period analysis are explained in Sect. G.6.3.3.5.

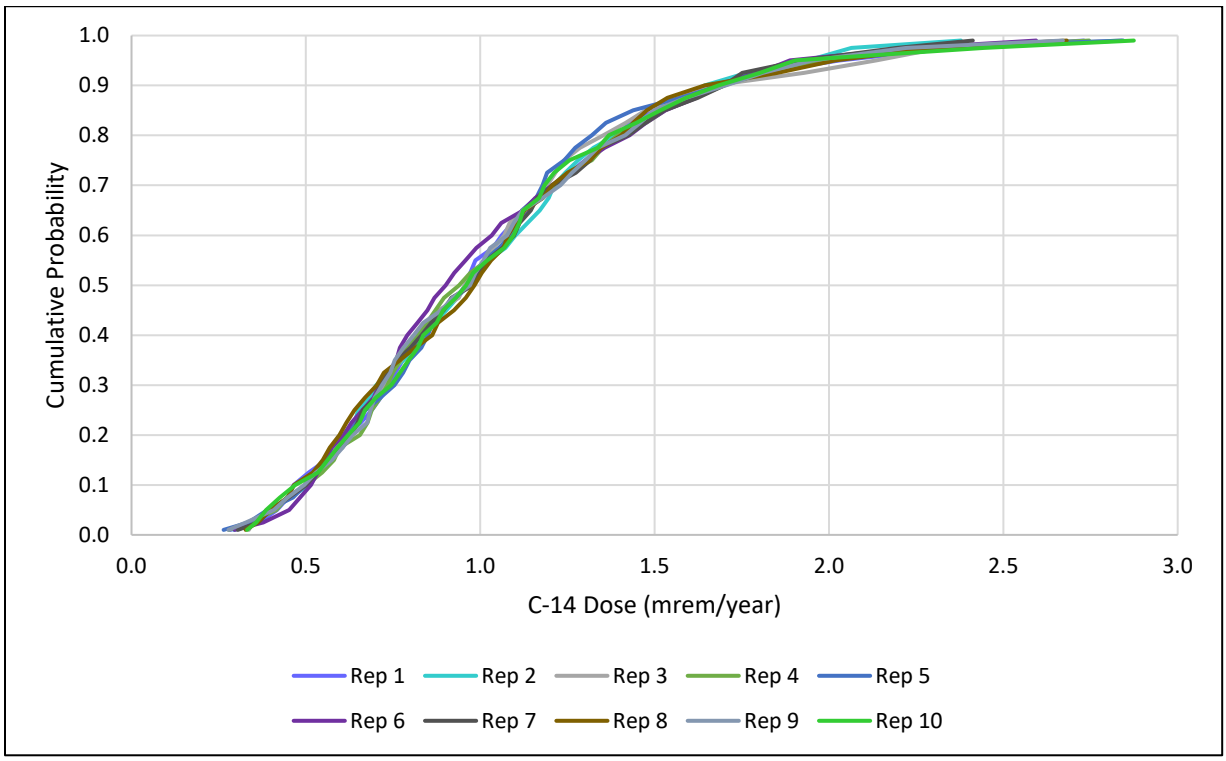

Fig. G.44. Cumulative distribution function curve, peak C-14 dose for 10 repetitions, all pathways (0 to 25 mrem/year, 0 to 1000 years)

Table G.25. Compliance period peak radionuclide dose statistics (mrem/year)

Radionuclide	Average peak dose	95th Percentile peak dose
C-14	1.03	1.96
I-129	0.48	0.26
Tc-99	0.40	1.34

G.6.3.3.3 Distributions of peak total dose and component pathway peaks for the compliance period uncertainty analysis

RESRAD-OFFSITE calculates time-independent probability distributions for peak total dose. The CDF curve for each repetition represents the distribution of 300 modeled peak dose values, irrespective of the timing of the peak dose values. One use of this model output is to evaluate the similarity of results from the 10 repetitions. If the CDF curves are markedly different, this implies that differences in the distributions of sampled input parameter values are resulting in significant variation between the repetitions. Due to the random sampling approach, variation among the repetitions will decrease as the number of observations increases. As shown in Fig. G.45, CDF curves of peak total dose from all pathways over 1000 years are similar for the 10 repetitions. Additionally, Fig. G.45 shows that over the simulation period, the median peak dose from all pathways (average median value of the 10 repetitions) is 1.0 mrem/year and the 95th percentile value of peak dose (average of the 10 repetitions) is approximately 2.5 mrem/year. Extreme values (> 25 mrem/year) of peak total dose associated with large I-129 contributions are described in Sect. G.6.3.3.5.

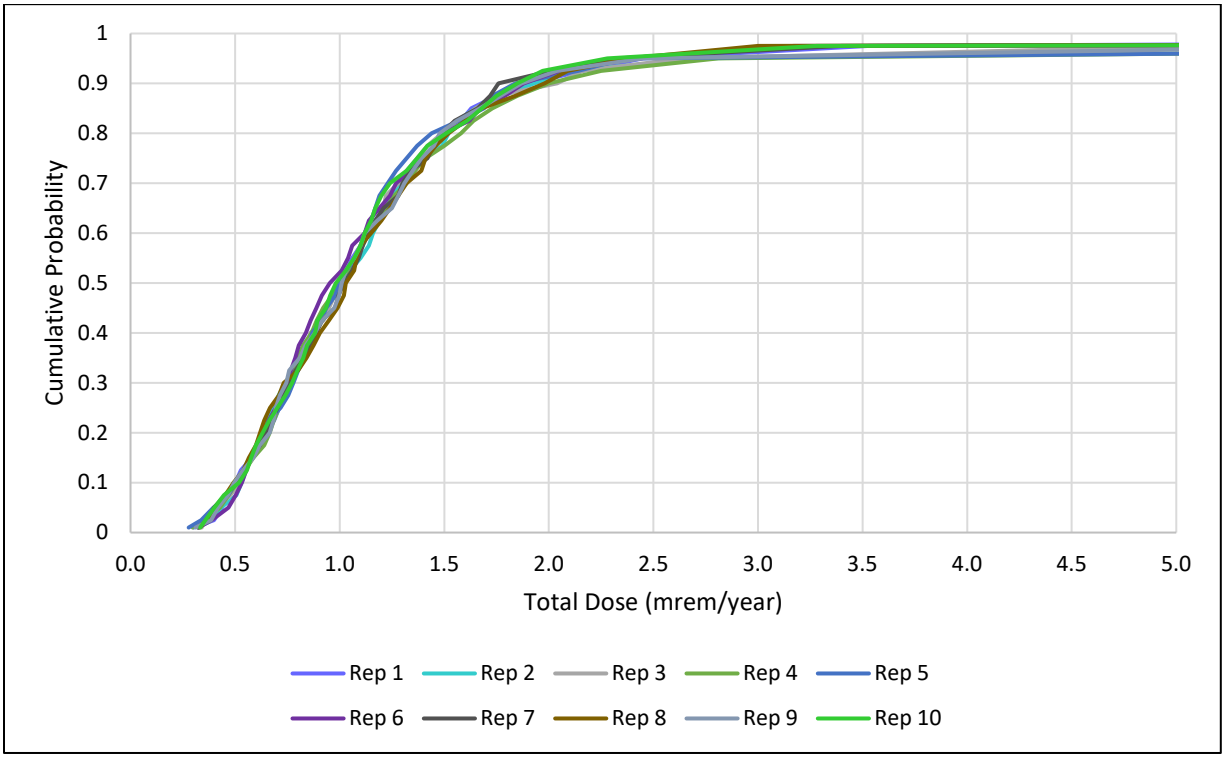

Fig. G.45. Cumulative distribution function curve, peak total dose for 10 repetitions, all pathways (0 to 5 mrem/year, 0 to 1000 years)

In addition to the isotope-specific contributions, the peak dose statistics for each of the 15 exposure pathways were calculated. Water ingestion was the largest contributor, on average, to the total dose. Fish ingestion and meat ingestion (waterborne) (i.e., portion of dose from meat ingestion due to consumption of contaminated water and fodder by cattle) are the two next largest pathway contributors. Box plots for the distributions of the peak dose contributions from water ingestion, fish ingestion, and meat (waterborne) are shown in Fig. G.46. Median dose values for the water ingestion, fish ingestion, and meat ingestion (waterborne) pathways are 0.82 mrem/year, 0.19 mrem/year, and 0.00021 mrem/year, respectively. Water ingestion is likely to be the highest contributing pathway under most circumstances, as the 25th percentile of peak water ingestion dose is higher than the 75th percentile of peak value for fish ingestion dose.

Additionally, the 95th percentile of peak meat ingestion dose (waterborne) is lower than the 5th percentile of peak doses for water ingestion and fish ingestion.

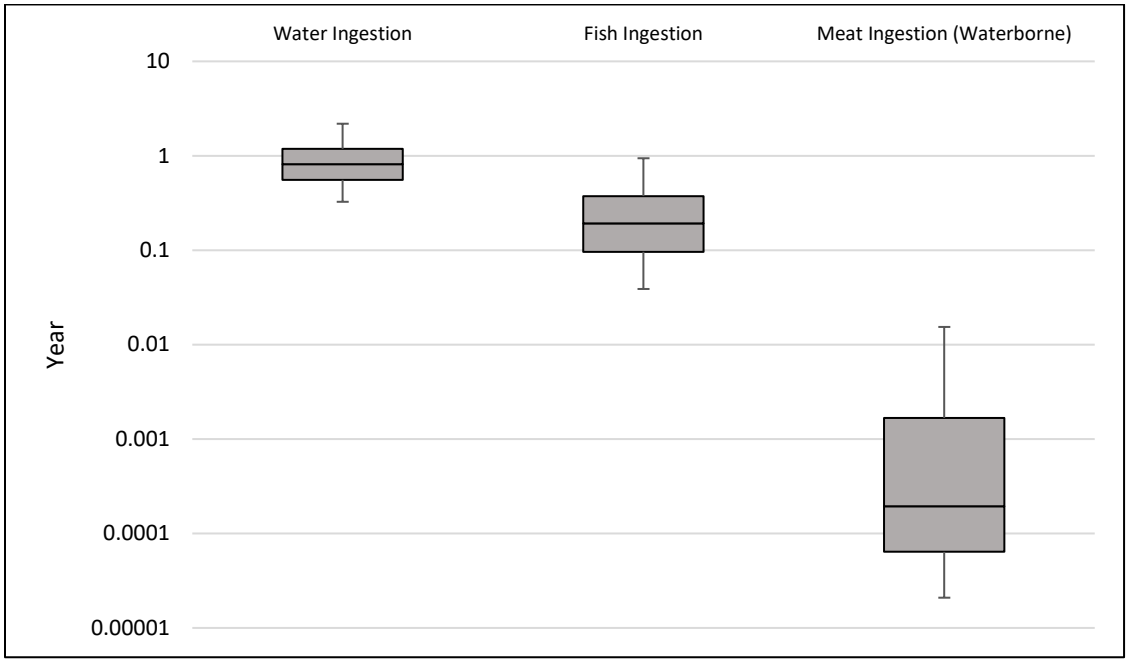

Fig. G.46. Box plot for dose distributions-top three contributing pathways (vertical axis in log scale, 95th and 95th percentile values for pathway doses are used for pathway-specific minima and maxima)

G.6.3.3.4 Regression analysis of peak total dose for the compliance period

The next step in the uncertainty analysis consists of multiple linear regression analyses of peak total dose on the values of the probabilistic input parameters. This analysis is performed to identify which input variables contribute most to the variation in predicted peak all pathways dose within the compliance period. Since the RESRAD-OFFSITE simulations for the compliance period uncertainty analysis extend just beyond the last reporting time of 1000 years to 1030 years, the regression analysis includes many peaks that occur just after 1000 years. RESRAD-OFFSITE can provide four different statistical values for each parameter in each repetition: (1) partial correlation coefficients, (2) standardized regression coefficients (SRCs), (3) partial rank correlation coefficients, and (4) standardized rank regression coefficients (SRRCs). SRCs are a measure of the linear relationship between a parameter and the peak dose; SRRCs are an estimation of the nonlinear, monotonic relationship between a parameter and the peak dose. SRCs and SRRCs were generated using the built-in post-run regression tool in RESRAD-OFFSITE because they allow for comparing regression coefficients of variables with different units and scales.

Generally, variables with relatively high absolute regression coefficients (e.g., -0.63 or 0.51) have more influence on the peak total dose than variables with low absolute regression coefficients (e.g., -0.01 or 0.04). If regression coefficients are approximately the same for two parameters, the one with a distribution that has a greater spread is considered to have a greater influence on the variation of the predicted peak all pathways dose (Yu et al. 2013). Using the SRCs and SRRCs along with the spread of the parameter distributions, the code determines which variables have the greatest influence on the peak total dose calculation. SRRC values had higher coefficients of determination (r squared), so parameter influence rankings are based on SRRC values. SRC and SRRC values and for the probabilistic input parameters for each repetition are shown in Table G.26, listed in order of decreasing influence on peak dose.

The most influential probabilistic variables fall into four categories: (1) contaminated zone parameters, (2) unsaturated zone parameters, (3) saturated zone parameters, and (4) human exposure parameters. The most influential parameters associated with the contaminated zone include:

- Runoff coefficient in the area of the primary contamination (cover infiltration)
- Time over which transformation to releasable form occurs (release duration) of I-129
- Effective porosity of contaminated zone
- Fraction of radionuclide bearing material that is initially releasable (initial releasable fraction) of I-129
- Time at which radionuclide first becomes releasable (initial release time) of C-14
- Longitudinal dispersivity of the contaminated zone.

Results are generally consistent with results from the single parameter sensitivity analysis presented in Sect. G.6.2, which show that total dose during the compliance period is sensitive to changes in these parameters. The runoff coefficient controls infiltration and varying this parameter is shown to have a great influence on peak total dose. The initial release time of radionuclides influences timing of peak dose while the release duration and initial releasable fraction can affect both the timing and magnitude of peak dose. Both the effective porosity and longitudinal dispersivity in the contaminated zone affect radionuclide leaching, which can affect total dose. While peak total dose during the compliance period is generally insensitive to changes in single parameters related to I-129, these parameters can have an influence on total dose during the compliance period when changed in combination with other parameters controlling I-129 transport, such as the time over which transformation to releasable form occurs, initial release time, and K_d of I-129. The most influential contaminated zone parameters control contaminant leaching and release from the waste, which ultimately determine the timing and magnitude of human exposure through the modeled pathways.

The unsaturated zone parameters that have the most influence on the peak total dose include the following:

- K_d of I-129 in UZ1
- K_d of Tc-99 in UZ1
- Thickness of UZ5.

These variables control the partitioning of I-129 and Tc-99 between the solid and aqueous phases during transport through the unsaturated zone and the total vertical distance that radionuclides need to travel to reach the saturated zone. While compliance period dose was not found to be sensitive to the unsaturated zone K_d for either I-129 or Tc-99 in the single factor sensitivity analyses, when these parameters are varied in combination with parameters governing radionuclide release from the waste, they could have more of an influence on the timing and magnitude of the compliance period peak dose. While the thickness of UZ5 does not strongly influence the magnitude of the peak dose in the single factor sensitivity analysis, it does have an impact on the timing of the peak dose, which could determine whether I-129 or Tc-99 would impact peak total dose during the compliance period. The most sensitive unsaturated zone parameters control the rate at which radionuclides travel through the unsaturated zone and the amount of time it takes for radionuclides to reach the saturated zone.

This page intentionally left blank.

Table G.26. Standardized rank regression coefficients and standardized regression coefficients for probabilistic input parameters listed in order of decreasing influence on peak dose for the compliance period

Repetition	1	2	3	4	5	6	7	8	9	10	1	2	3	4	5	6	7	8	9	10
Coefficient of Determination (R-squared)	**0.81**	**0.84**	**0.83**	**0.79**	**0.84**	**0.84**	**0.84**	**0.83**	**0.83**	**0.87**	**0.24**	**0.21**	**0.24**	**0.27**	**0.21**	**0.21**	**0.22**	**0.18**	**0.24**	**0.20**
Description of Probabilistic Variable	**SRRC**	**SRRC**	**SRRC**	**SRRC**	**SRRC**	**SRRC**	**SRRC**	**SRRC**	**SRRC**	**SRRC**	**SRC**	**SRC**	**SRC**	**SRC**	**SRC**	**SRC**	**SRC**	**SRC**	**SRC**	**SRC**
Runoff coefficient in area of primary contamination	-0.63	-0.63	-0.58	-0.50	-0.53	-0.46	-0.52	-0.45	-0.58	-0.58	-0.27	-0.06	-0.13	-0.22	-0.31	0.03	-0.07	0.13	-0.20	-0.23
Time over which transformation to releasable form occurs of I-129	-0.39	-0.42	-0.25	-0.36	-0.54	-0.25	-0.28	-0.03	-0.11	-0.37	-0.53	-0.72	-0.59	0.00	-0.44	-0.79	-0.25	0.00	0.44	-0.64
Hydraulic conductivity of saturated zone	-0.41	-0.28	-0.37	-0.11	-0.41	-0.17	-0.32	-0.20	-0.35	-0.29	0.00	0.31	-0.14	0.66	0.11	0.01	-0.09	-0.09	-0.19	0.01
Mean residence time of water in surface water body	0.35	0.29	0.29	0.19	0.31	0.22	0.18	0.22	0.23	0.26	0.12	0.01	-0.02	0.12	0.02	-0.05	0.05	-0.03	-0.01	0.11
Depth of aquifer contributing to well	-0.23	-0.16	-0.20	-0.16	-0.14	-0.22	-0.21	-0.22	-0.21	-0.22	-0.14	0.03	0.00	-0.03	-0.04	-0.18	-0.06	-0.10	-0.02	0.00
Effective porosity of contaminated zone	-0.13	-0.08	-0.21	-0.22	-0.26	-0.15	-0.12	-0.26	-0.12	-0.27	-0.05	0.12	0.03	0.01	0.02	0.08	0.06	-0.17	-0.02	-0.09
Fraction of radionuclide bearing material that is initially releasable of I-129	0.12	0.04	0.17	0.12	0.03	0.19	0.13	0.26	0.25	0.09	-0.13	-0.30	-0.28	0.04	-0.13	-0.33	0.01	0.09	0.35	-0.22
Kd of Tc-99 in saturated zone	0.02	-0.24	-0.06	-0.04	-0.26	-0.16	0.18	-0.02	-0.03	-0.30	0.91	-0.19	0.61	-1.22	0.73	-0.42	1.55	0.19	-1.04	0.01
Time at which radionuclide first becomes releasable (delay time) of C-14	-0.10	-0.11	-0.07	-0.10	-0.06	-0.05	-0.10	-0.11	-0.12	-0.05	-0.04	-0.10	-0.11	-0.06	-0.03	-0.09	-0.08	-0.08	-0.02	-0.01
Kd of I-129 in UZ1	0.30	0.03	0.04	0.19	0.16	0.02	0.32	-0.15	-0.02	-0.07	1.33	0.35	1.02	-1.51	0.98	0.08	1.69	0.01	-1.63	0.39
Effective porosity of saturated zone	-0.04	-0.11	-0.01	-0.12	-0.01	-0.16	-0.08	-0.10	-0.02	-0.10	-0.08	-0.34	0.15	-0.55	-0.17	-0.01	-0.06	0.02	0.16	-0.11
Longitudinal dispersivity of contaminated zone	-0.08	-0.05	-0.05	-0.04	-0.08	-0.07	-0.06	-0.06	-0.11	-0.08	-0.02	0.00	-0.02	0.09	-0.01	-0.06	-0.03	0.06	-0.10	-0.02
Kd of Tc-99 in UZ1	-0.05	0.28	-0.03	0.06	0.33	0.11	-0.22	-0.11	-0.04	0.34	-0.89	0.32	-0.58	1.32	-0.66	0.70	-1.55	-0.22	0.96	0.18
Thickness (meters) of UZ5	0.02	0.02	-0.06	-0.13	-0.06	-0.13	-0.04	-0.11	-0.07	-0.06	-0.03	-0.16	-0.11	0.06	0.26	-0.18	-0.12	-0.24	0.06	-0.02
Kd of I-129 in saturated zone	-0.26	0.01	-0.07	-0.17	-0.05	0.01	-0.24	0.02	-0.02	0.13	-1.32	-0.34	-1.04	1.08	-1.07	-0.08	-1.74	-0.27	1.05	-0.44
Longitudinal dispersivity (meters) of UZ5	0.00	-0.12	-0.03	0.00	-0.08	-0.03	-0.06	-0.04	-0.05	-0.04	0.03	0.00	0.01	-0.05	-0.13	-0.07	0.13	0.01	-0.08	0.03
Hydraulic conductivity of contaminated zone	-0.03	-0.03	0.07	0.09	0.11	0.02	-0.05	0.12	0.03	0.10	0.00	-0.16	-0.10	-0.10	-0.04	-0.11	-0.16	0.14	0.00	0.02
Hydraulic gradient of saturated zone to well	-0.27	-0.04	-0.14	0.15	-0.16	0.15	-0.03	0.08	-0.08	-0.06	-0.10	0.34	-0.05	0.54	0.14	0.18	-0.02	0.05	-0.15	0.01
Precipitation	0.22	0.05	0.10	-0.21	0.04	-0.23	-0.16	-0.15	0.00	-0.04	0.21	-0.14	-0.01	-0.16	0.13	-0.24	-0.02	-0.21	0.08	0.05
Dry bulk density of contaminated zone	0.03	0.00	0.05	0.04	-0.01	0.02	0.03	0.07	0.03	0.09	0.02	0.12	0.03	0.09	-0.07	0.10	0.02	-0.05	-0.03	0.04
Dry bulk density of saturated zone	-0.02	-0.09	0.00	-0.05	-0.03	-0.04	0.00	-0.01	-0.01	-0.02	-0.05	-0.05	0.00	-0.07	-0.07	-0.06	-0.01	-0.01	-0.02	-0.03
Hydraulic conductivity (meters/year) of UZ5	-0.05	0.13	0.03	0.08	0.06	0.01	0.01	0.04	-0.13	0.00	0.06	0.08	-0.10	0.15	0.14	0.02	-0.10	0.08	-0.01	0.11
Total porosity of UZ4	-0.02	0.03	0.03	0.04	0.06	0.04	0.00	-0.03	0.01	0.00	0.04	0.06	0.05	0.05	0.04	0.03	0.01	-0.04	-0.02	0.07
b parameter of contaminated zone	0.01	-0.02	-0.05	-0.02	-0.02	0.02	-0.02	0.00	-0.02	-0.04	-0.04	0.02	0.07	-0.03	0.09	0.08	0.02	0.04	-0.01	0.07
Longitudinal dispersivity of saturated zone to well	0.00	0.03	0.01	-0.03	-0.03	0.02	-0.01	-0.02	-0.04	-0.02	0.01	-0.08	0.04	-0.07	-0.02	-0.02	-0.06	-0.02	0.01	0.08
Longitudinal dispersivity (meters) of UZ4	0.03	-0.03	-0.04	0.05	-0.04	-0.02	0.04	0.01	-0.01	-0.07	-0.09	-0.10	-0.08	0.10	-0.10	-0.02	-0.16	0.06	-0.07	0.00
Total porosity of UZ3	-0.02	0.00	-0.01	-0.03	0.01	-0.02	0.01	0.00	0.01	-0.03	-0.01	0.01	-0.05	0.02	0.11	-0.05	-0.04	0.01	0.10	-0.01
Dry bulk density (g/cm³) of UZ5	0.04	0.01	0.01	-0.05	-0.03	0.01	-0.06	0.03	-0.02	-0.01	0.00	0.03	0.09	0.00	0.00	-0.02	-0.05	0.02	-0.02	0.02
Effective porosity of UZ4	0.03	-0.01	-0.03	-0.03	0.04	0.00	-0.01	-0.01	-0.04	-0.02	0.01	-0.03	-0.03	0.01	-0.05	-0.02	-0.02	0.05	0.03	-0.02
Effective porosity of UZ5	0.05	-0.13	0.00	-0.02	-0.01	-0.01	0.01	-0.06	0.14	-0.02	-0.07	-0.08	0.05	-0.18	-0.12	-0.01	0.07	-0.21	0.09	-0.09
Effective porosity of UZ3	0.00	0.02	-0.02	-0.02	-0.02	-0.03	0.04	0.04	-0.02	-0.03	0.10	0.07	-0.06	-0.02	-0.10	-0.05	-0.05	0.03	-0.11	-0.04
Longitudinal dispersivity of saturated zone to surface waterbody	0.01	-0.02	0.01	0.01	-0.03	0.01	0.04	0.03	0.00	-0.02	-0.01	0.01	-0.03	0.06	-0.09	0.03	-0.06	0.03	-0.07	0.03
Longitudinal dispersivity (meters) of UZ3	0.00	-0.03	-0.02	-0.07	0.02	0.02	-0.04	0.00	0.02	0.10	0.04	0.09	-0.05	-0.15	0.07	-0.08	0.16	-0.03	0.00	0.07

SRRC = standardized rank regression coefficient
SRC = standardized regression coefficient
UZ = unsaturated zone

This page intentionally left blank.

The saturated zone parameters that have the greatest influence on peak total dose include:

- Hydraulic conductivity of saturated zone
- Mean residence time of water in surface water body
- K_d of Tc-99 in saturated zone
- Effective porosity of saturated zone
- K_d of I-129 in saturated zone.

The most influential saturated zone variables in the uncertainty analysis control the groundwater flow rate in the saturated zone, the accumulation of radionuclides in the surface water body, and the partitioning of I-129 and Tc-99 between the solid and aqueous phases during transport in the saturated zone. These parameters influence radionuclide concentrations in saturated zone, which have a strong influence on peak total dose, as the water ingestion pathway contributes most to the total dose.

The human exposure parameter included in the uncertainty analysis is the depth of aquifer contributing to well. This parameter represents well construction assumptions and controls contaminant concentrations in the well water. The influence of this parameter on peak total dose is logical, since the water ingestion pathway is the greatest contributing pathway as identified in the deterministic and probabilistic results and all water for indoor use and consumption originates from the well. Additionally, the regression analysis results are consistent with comparisons of box plots for probable dose contributions (Fig. G.46), which show that water ingestion is likely to be the highest contributing pathway to the total dose during the compliance period.

The regression analysis for the compliance period uncertainty analysis produced some counter-intuitive SRRCs for select parameters in some repetitions in which the sign of the SRRC reversed and was greater than +/-0.1. Examples of these counter-intuitive SRRCs in the compliance period uncertainty analysis include:

- Tc-99 K_d in the saturated zone (repetition 7)
- I-129 K_d in UZ1 (repetitions 1, 4, 5, and 7)
- Tc-99 K_d in UZ1 (repetitions 2, 5, 6, and 10)
- I-129 K_d in the saturated zone (repetition 10)
- Hydraulic gradient of saturated zone to well (repetitions 4 and 6).

The counter-intuitive SRRCs associated with radionuclide K_d values are likely because a majority of the most influential parameters are related to processes that are not linked to radionuclide sorption (infiltration rate in the waste, groundwater flow rate, radionuclide concentration in the well and surface water body). The independence of K_d values from important hydrologic parameters can occasionally cause elevated peak doses to occur with K_d values at or above their mean value, which can cause calculation of regression coefficients that contradict the known relationship between K_d values and dose predictions (i.e., lowering K_d values enacts an increase in doses). Additionally, influential hydrologic parameters can influence the timing of peak dose from I-129 and Tc-99, and if peak dose from these radionuclides occurs outside of the compliance period, the corresponding peak dose during the compliance period could be low even with a relatively low K_d, which may cause counter-intuitive regression coefficients.

Another cause of counter-intuitive SRRCs could be due to correlation with another parameter. Hydraulic conductivity of the saturated zone has some of the least influence relative to other repetitions (SRRCs

of -0.11 and -0.17) in repetitions 4 and 6. Hydraulic conductivity of saturated zone and hydraulic gradient of saturated zone to well are related by an adjusted rank correlation coefficient of -0.68 to maintain a consistent effective groundwater flow velocity, which may have caused calculation of counter intuitive SRRCs for hydraulic gradient to well for repetitions 4 and 6, as the influence of one parameter affects the other correlated parameter.

The most influential probabilistic parameters control aquifer flow and transport properties and the mobility and transfer of dose-significant radionuclides from the solid to aqueous phases. The pathways of greatest focus for the assessed radionuclides (C-14, I-129, and Tc-99) are water ingestion, fish ingestion, and meat ingestion (waterborne). Connections between aquifer properties and water ingestion are straightforward; aquifer properties of the site affect groundwater flow which influences exposure and the total dose. Additionally, these same parameters affect animals raised for consumption on or near the area of primary contamination.

A summary of influential variables, exposure pathways of concern, and median and 95th percentile doses for the select reporting times used in this analysis is shown in Fig. G.47.

G.6.3.3.5 Peak total dose predictions greater than 25 mrem/year – compliance period

The regression analysis provides insight into the relative significance of input parameters that account for most of the variation in peak total dose over the entire range of peak dose values. In the context of understanding the likelihood of EMDF compliance with the 25 mrem/year all-pathways dose objective over the first 1000 years post-closure, it can be valuable to examine the highest simulated peak doses (extreme values). This section is focused on which combinations of input parameters are associated with peak total doses that exceed 25 mrem/year.

For the compliance period uncertainty analysis, there are 21 out of 3000 simulated peak doses (0.7 percent) that exceed 25 mrem/year. All peak doses greater than 10 mrem/year are associated with a sampled I-129 unsaturated zone K_d value less than 2 cm^3/g (Fig. G.48). All 21 simulations having compliance period peak doses greater than 25 mrem/year also have a sampled I-129 unsaturated zone K_d value less than 1.1 cm^3/g and a sampled I-129 saturated zone K_d value less than 1.5 cm^3/g (Fig. G.49). Based on the available laboratory data for Conasauga Group materials (Sect. 3.2.2.7 of the PA), the majority (> 95 percent) of measured iodine K_d values were > 4 cm^3/g, which is the base case value (for non-waste materials) for I-129 in the PA. It is possible that iodine K_d values less than 1 cm^3/g are more likely than the existing laboratory data suggest, but this uncertainty does not call the conclusions of the EMDF PA into question. Additional work to reduce the uncertainty in I-129 and Tc-99 K_d values is planned to support maintenance of the EMDF PA.

All of the compliance period peak doses greater than 25 mrem/year are associated with large peak I-129 doses that occur as early as 679 years post-closure. The low sampled I-129 K_d values, in combination with other factors that favor earlier I-129 release and transport to the saturated zone are the input parameters that drive the extreme peak doses within the compliance period. Higher simulated I-129 peak doses occur after the compliance period (refer to Sect. G.6.3.4.4), so the analysis presented here does not encompass the full range of potential I-129 (and Tc-99) impacts associated with release from the EMDF. Although simulated Tc-99 peak doses up to 4.3 mrem/year occur within the compliance period, none of the 21 peak total doses exceeding 25 mrem/year include a Tc-99 contribution greater than about 5 percent of the total dose.

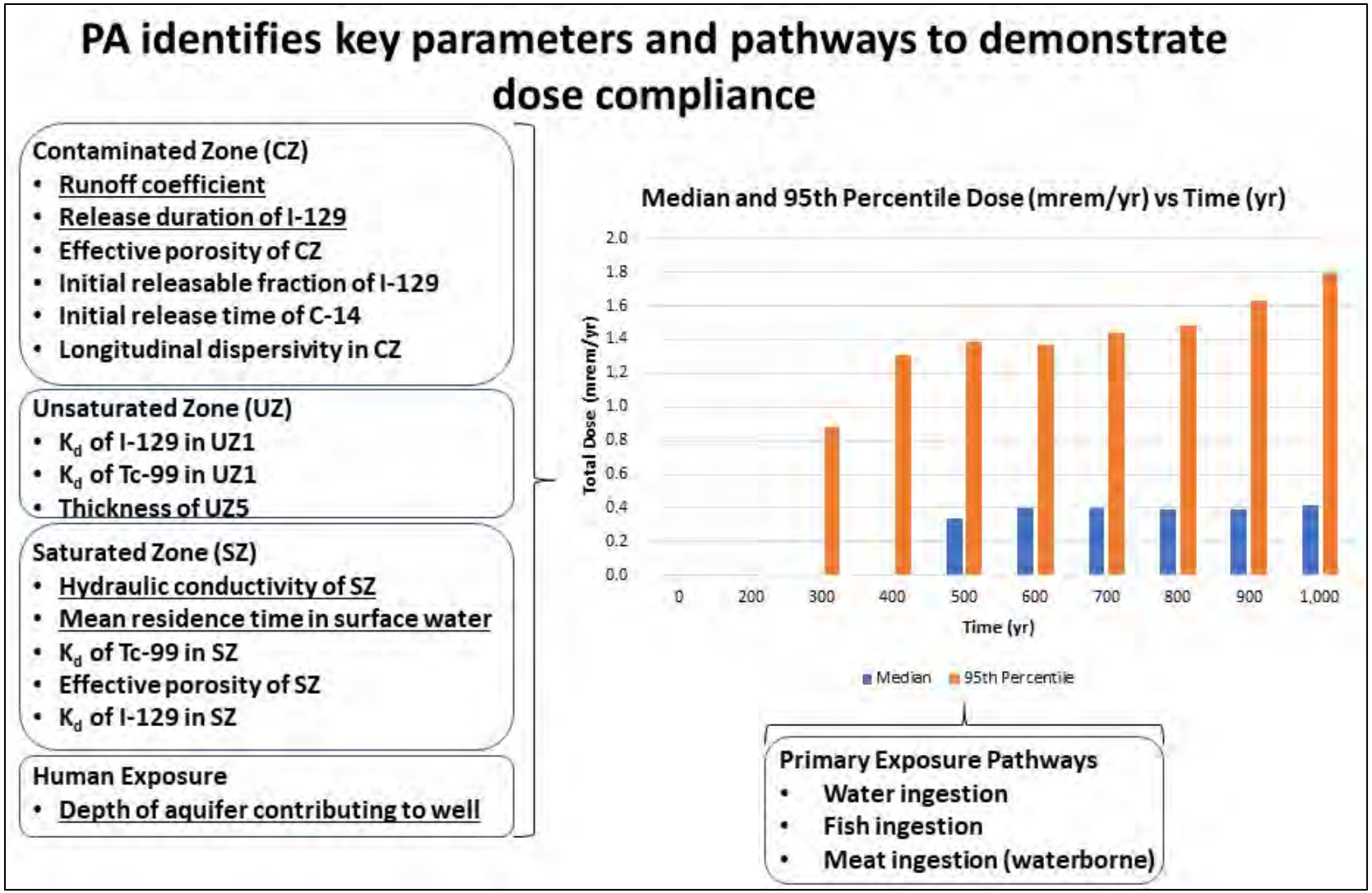

Fig. G.47. Summary of influential variables, primary exposure pathways, and total dose at select reporting times for the 1000-year compliance period (underlined are the top five drivers of total dose)

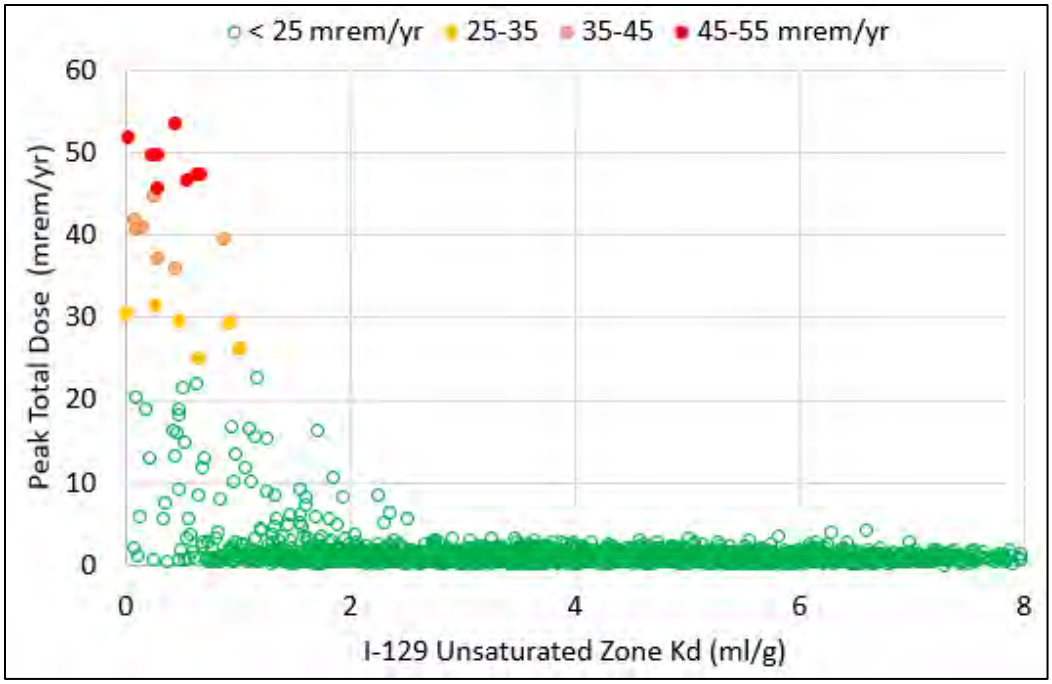

Fig. G.48. Compliance period peak total dose vs sampled unsaturated zone I-129 K_d

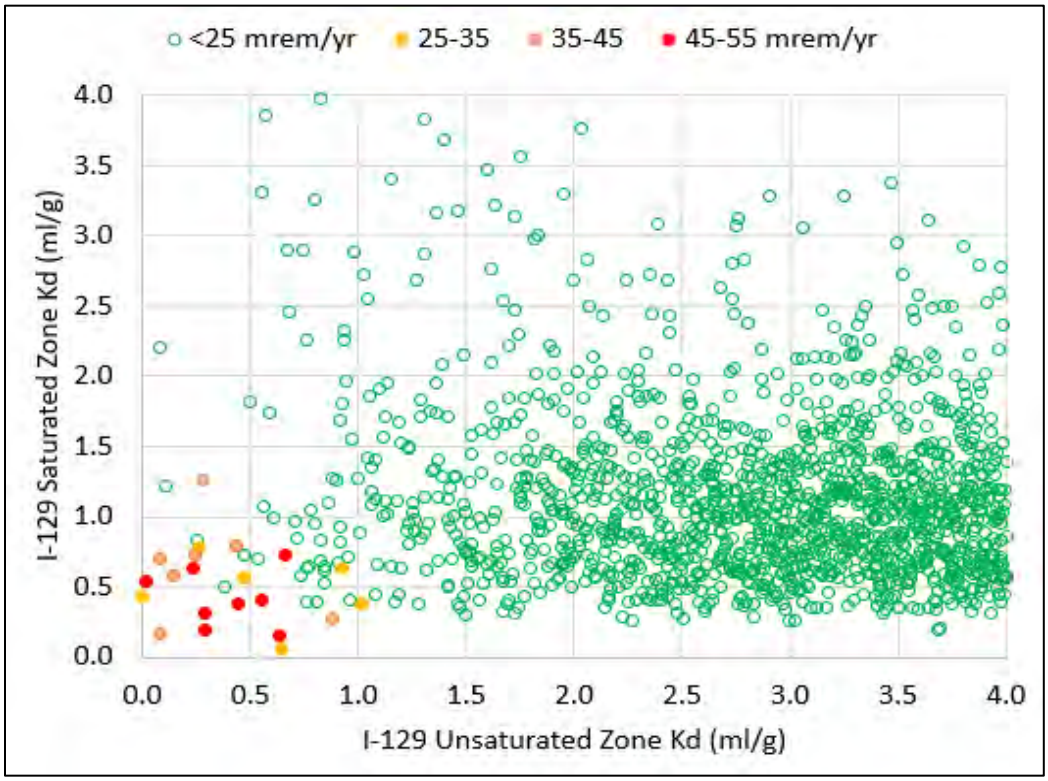

Fig. G.49. Compliance period sampled saturated zone I-129 K_d vs sampled unsaturated zone I-129 K_d

Input parameters that favor earlier and stronger radionuclide release include the timing and duration of release, and the two parameters that determine the rate of cover infiltration (runoff coefficient and annual precipitation). Simulated compliance period peak doses that exceed 25 mrem/year tend to be associated with release times and release durations less than the assumed deterministic base case values (Fig. G.50).

The extreme peak doses are also associated with (calculated) cover infiltration rates greater than the base case value (Fig. G.51). Figure G.51 also suggests that most of the extreme simulated compliance period peak doses are associated with sampled values of the thickness of UZ5 equal to or less than the base case value. This correlation is consistent with the result that smaller total vadose zone thickness favors higher simulated peak dose as indicated by predominantly negative SRRC and SRC values for UZ5 thickness (Table G.26) determined by the regression analysis of all simulated peak total doses.

These observations demonstrate that of the sampled I-129 Kd values are sufficiently low (Fig. G.49) the factors that tend to favor very high compliance period peak total dose are many of the same input parameters identified as contributing the most to overall variation in peak total dose (Table G.26, Fig. G.47). Release model uncertainty (contaminated zone parameters and release timing/duration) is particularly important for extreme compliance period peak dose due to the close connection with the magnitude of large, early I-129 dose contributions.

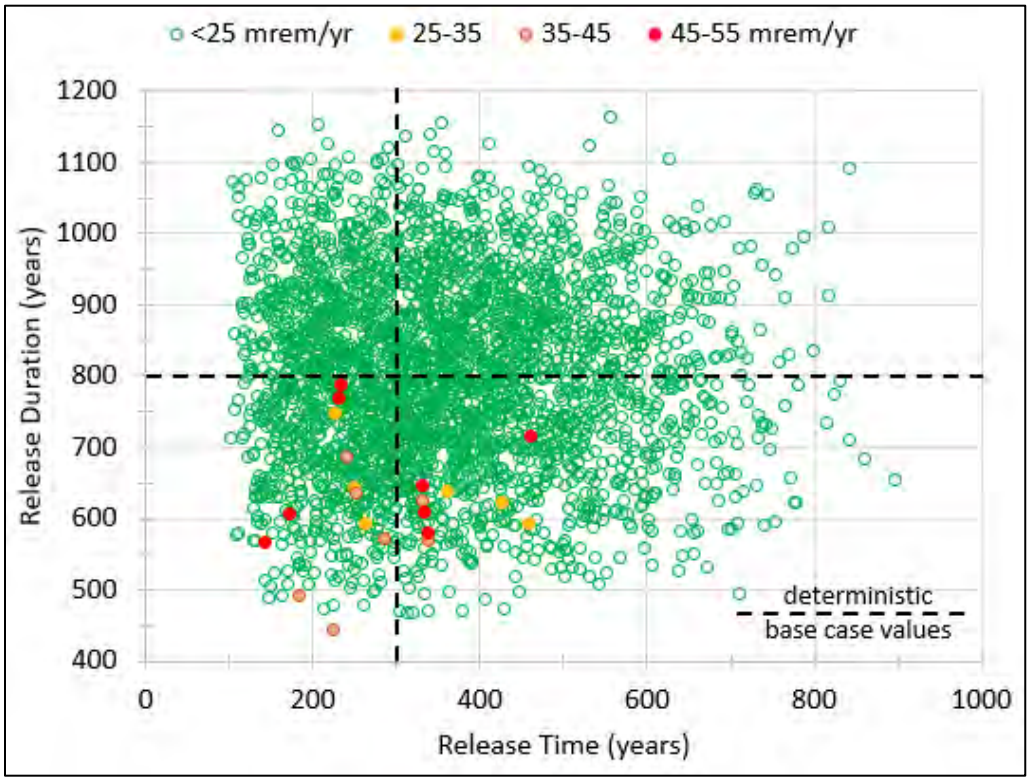

Fig. G.50. Compliance period sampled values of release time and release duration

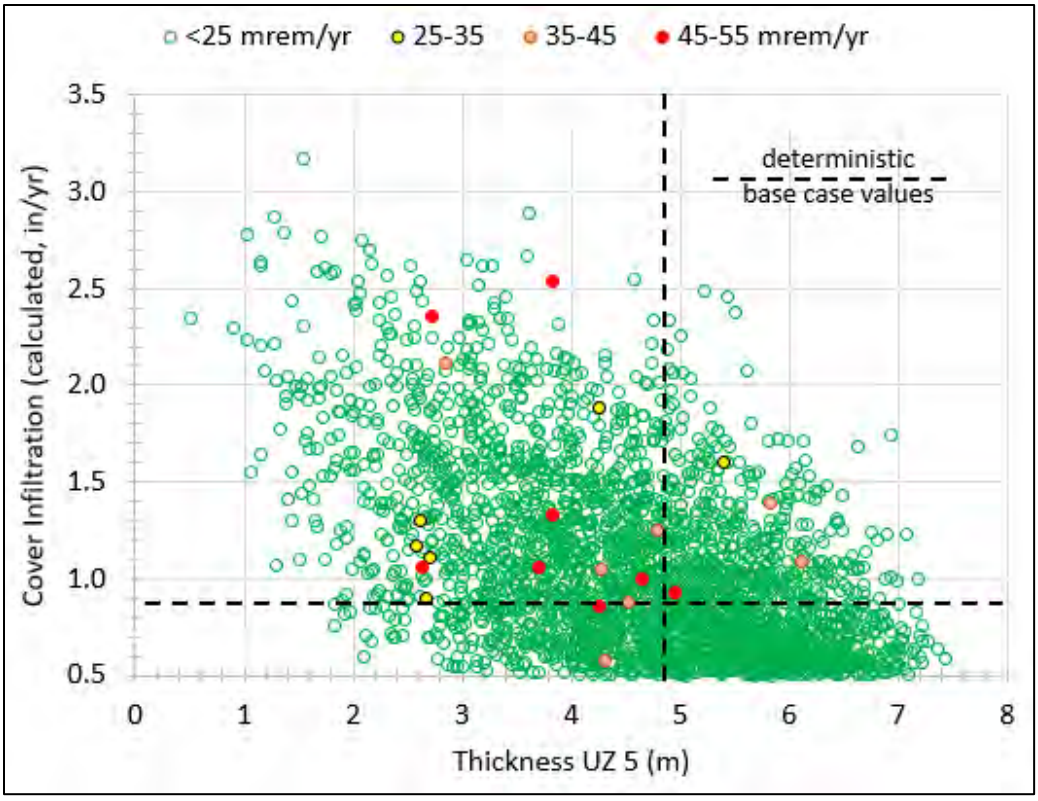

Fig. G.51. Compliance period sampled values of cover infiltration (calculated) and thickness of UZ5

G.6.3.4 Probabilistic Results – 10,000-year Simulation Period

The following subsections present the results of the 10,000-year simulation period uncertainty analysis with a focus on results beyond the compliance period. The distributions of predicted total and radionuclide-specific doses at various points in time during the 10,000-year simulation period are presented in Sects. G.6.3.4.1 and G.6.3.4.2. The distribution(s) of the predicted peak total dose and contributions made via specific exposure pathways during the 10,000-year simulation period are presented in Sect. G.6.3.4.3. The results of the multiple regression analysis on the probabilistic model output to identify the parameter uncertainties most important to the prediction of peak total dose during the 10,000-year simulation period are included in Sect. G.6.3.4.4. Elevated (> 25 mrem/year) peak dose predictions for the 10,000-year simulation period uncertainty analysis are discussed in Sect. G.6.3.3.5.

G.6.3.4.1 Variation in the distribution of total dose over time for the 10,000-year simulation period

The RESRAD-OFFSITE uncertainty analysis calculates statistics of the total dose distribution for each repetition at each simulation time step. The variation of median, mean, and 95th percentile dose over time for each of the 10 repetitions of 300 simulations is shown on Fig. G.52. The deterministic base case model all-pathways dose curve is also shown on Fig. G.52 for comparison to the probabilistic results. Results for the period prior to 1000 years were described in Sect. G.6.3.3. The remainder of the simulated period can be divided into an early portion between 1000 and approximately 6000 years, and a later portion extending to 10,000 years. The early portion of the results are dominated by Tc-99 and I-129 dose contributions, whereas the later (> 6000 years) results reflect the potential impacts of Pu-239 and the three simulated nuclides of uranium. Section G.6.3.4.2 presents the results for Tc-99 and I-129 dose contributions only.

Sections G.6.3.4.3 and G.6.3.4.4 present the probabilistic results for peak dose (maximum value within a single simulation) that are influenced by both the fission products (Tc-99 and I-129) and the actinides (Pu-239 and uranium nuclides).

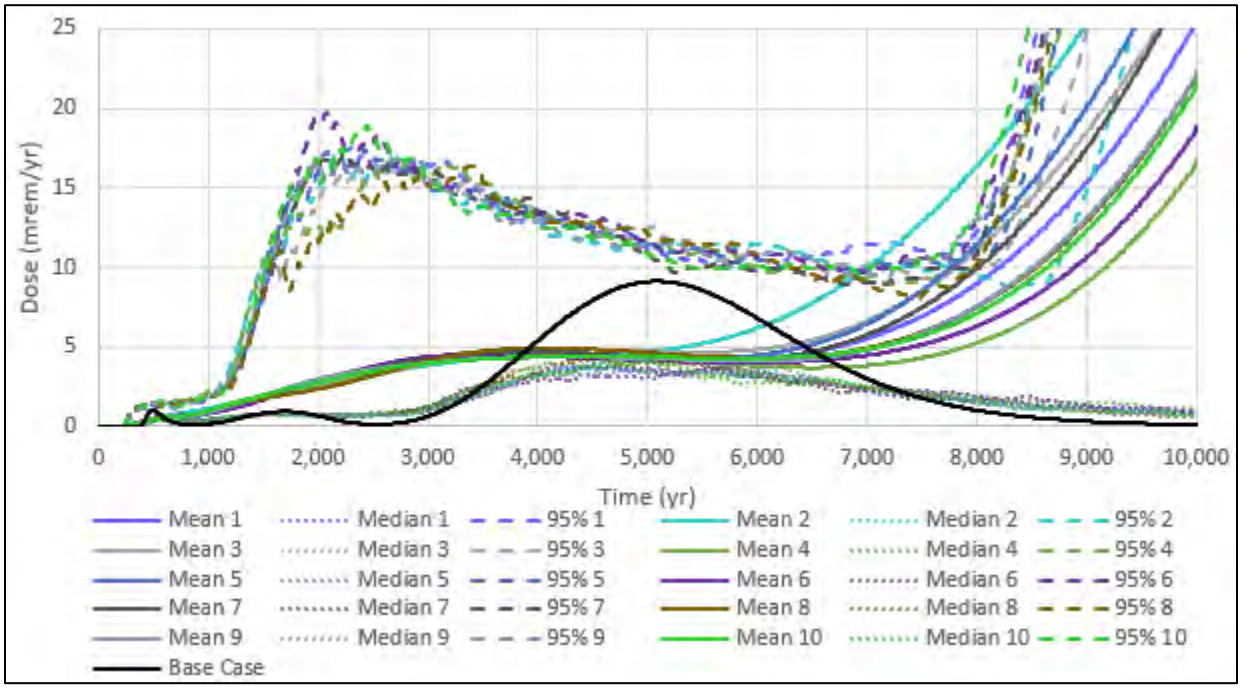

Fig. G.52. 10,000-year probabilistic total dose summary, all pathways, all calculation points

The changing distribution of total dose over time reflects the varying contributions by the fission products and the actinides. The mean total dose increases gradually between 1000 years and approximately 4000 years and then remains nearly steady at just under 5 mrem/year (solid curves on Fig. G.52). Then the mean total dose increases rapidly beginning at about 6000 years, reaching values that exceed 25 mrem/year by 10,000 years for five of the 10 repetitions of 300 simulations (Table G.27). The median simulated total dose peaks around 4500 years and remains below 5 mrem/year throughout the simulation period (dotted curves on Fig. G.52). The 95th percentile of total dose increases quickly between 1000 and 2000 years to values around 15 mrem/year (fission product dose contributions) and then decreases more gradually through 8000 years. At 8000 years there is a second sharp increase in the 95th percentiles as actinide dose contributions begin to rise and simulated total doses > 25 mrem/year become more frequent. Significant dose contributions from these radionuclides can occur much earlier than in the deterministic base case because of lower K_d values, shorter release durations, and greater cover infiltration rates. The divergence of the mean probabilistic dose from the median value (which decreases after 5000 years) reflects the strong negative skew that develops in the distribution of total dose after 5000 years, due to a large proportion of very small total doses and a small proportion of very high doses. Additional discussion of the factors associated with the occurrence of peak total doses greater than 25 mrem/year for the 10,000 year uncertainty analysis is included in Sect. G.6.3.4.5.

RESRAD-OFFSITE generates statistical output (CDF percentiles) for the 10 user-selected model reporting times. The selected reporting times for the 10,000-year analysis were years 0; 1000; 1500; 2000; 3000; 4250; 5500; 7000; 8500; and 10,000. CDF curves of the total dose for the reporting times are shown in Fig. G.53. These statistical outputs indicate that the median total dose remains below 4 mrem/year throughout the 10,000 year simulation period and that the 95th percentile remains below 25 mrem/year through 8500 years. Consistent with the uncertainty analysis results for the compliance period

(Sect. G.6.3.3.1), total doses can exceed 25 mrem/year for reporting times 1000 years and greater for certain combinations of sampled input parameter values.

Table G.27. Peak of the mean dose curves (averaged over 300 observations) for each model repetition, 10,000-year simulation period

Repetition	Time of peak mean dose (years)	Peak mean dose (mrem/year)
1	10,030	25.77
2	10,030	37.26
3	10,030	29.34
4	10,030	16.77
5	10,030	32.98
6	10,030	18.94
7	10,030	29.70
8	10,030	22.35
9	10,030	22.30
10	10,030	21.71

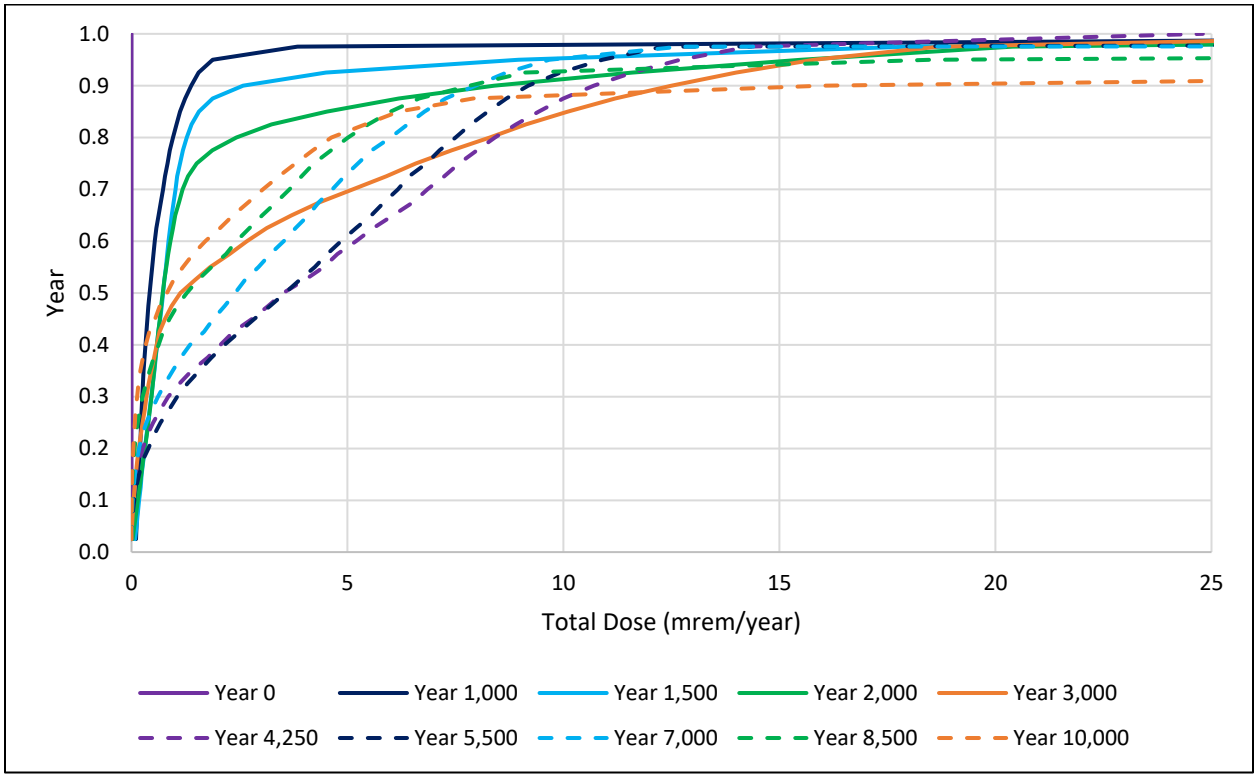

Fig. G.53. Cumulative probability summary for the 10,000-year simulation period, total over all pathways, select reporting times (0 to 25 mrem/year)

G.6.3.4.2 Radionuclide dose at reporting times and timing of radionuclide dose peaks

Figures G.54 and G.55 are plots showing the mean radionuclide dose plus and minus one standard deviation for I-129 and Tc-99 at each of the model reporting times. Significant dose contributions from C-14 after 1000 years are infrequent; the mean C-14 dose at 1500 years is 0.05 mrem/year and the maximum simulated dose at 1500 years is 0.5 mrem/year. The 10,000 year uncertainty analysis indicates that the C-14 peak dose occurs after 1000 years in fewer than 1 percent of the 3000 simulations. Therefore, the remainder of this section presents results only for I-129 and Tc-99.

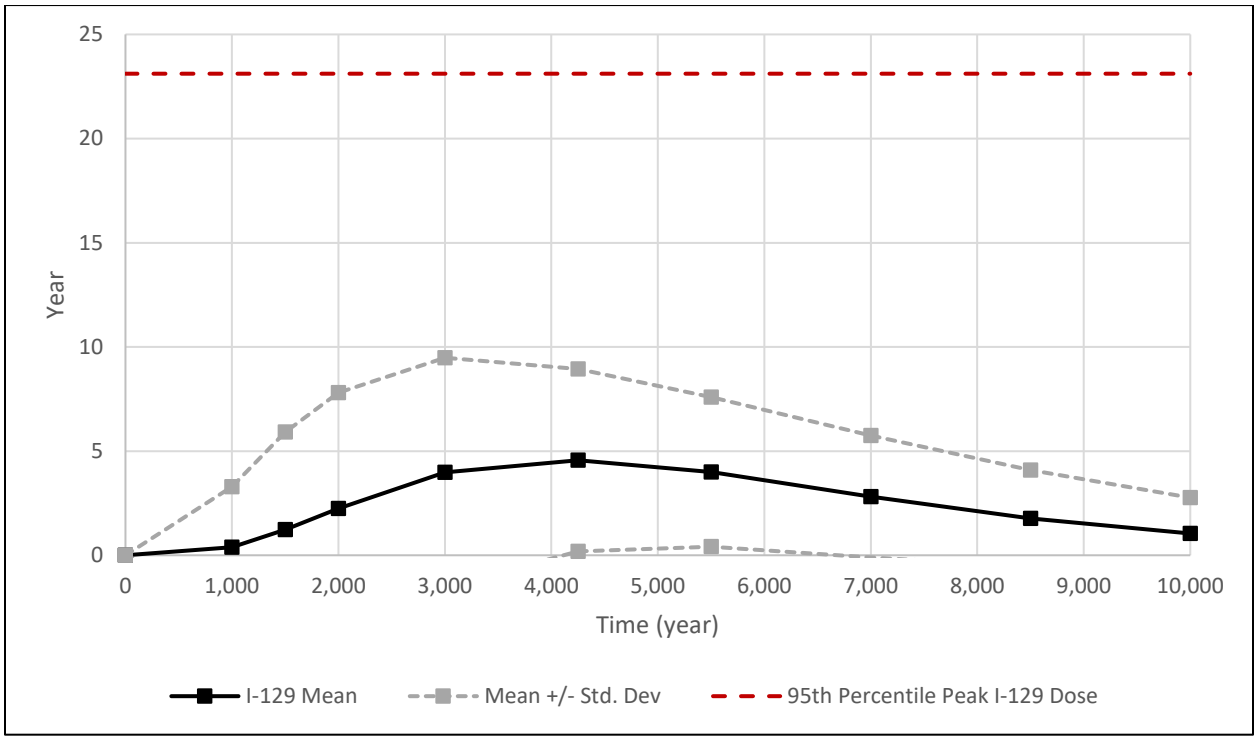

Fig. G.54. Probabilistic all pathways dose summary for I-129, all pathways, select reporting times, 10,000-year uncertainty analysis

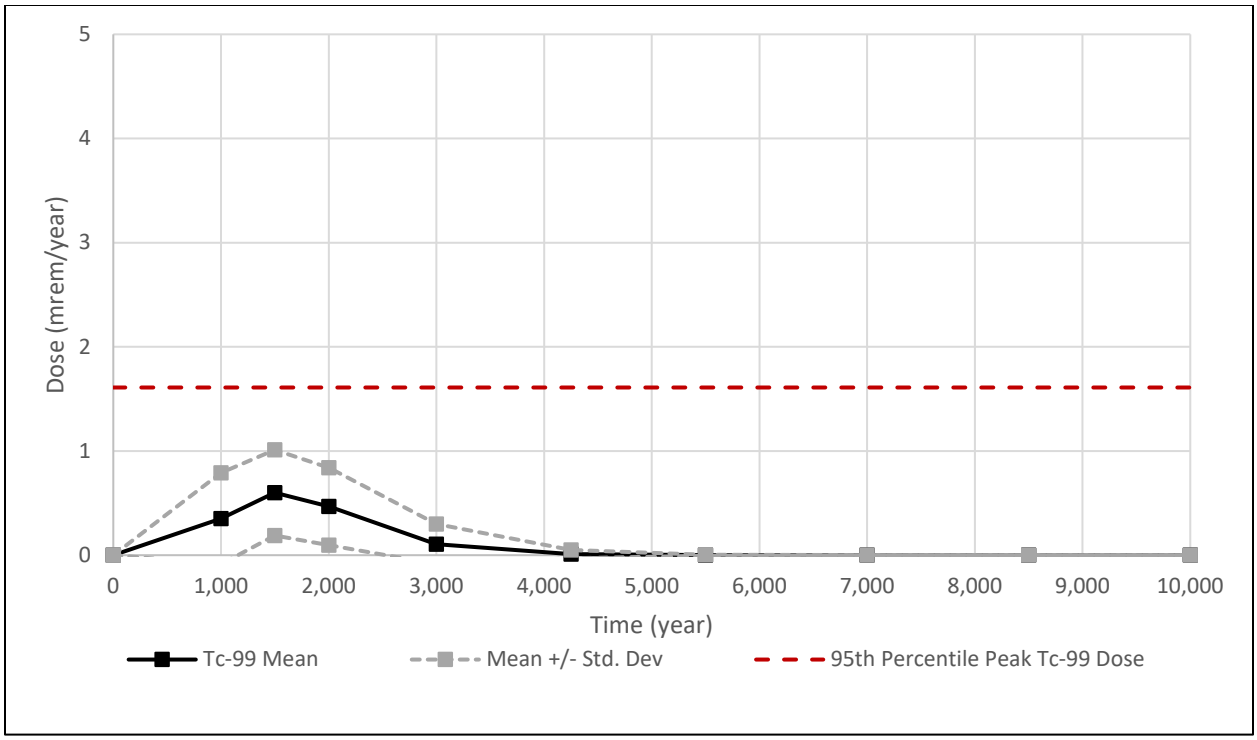

Fig. G.55. Probabilistic all pathways dose summary for Tc-99, all pathways, select reporting times, 10,000-year uncertainty analysis

The mean I-129 dose increases beginning at approximately 1000 years to a peak of 4.5 mrem/year at 4250 years (Fig. G.54). The I-129 mean dose curve then decreases gradually through the end of the simulation period. For Tc-99, the mean dose is 0.35 mrem/year at 1000 years and increases to 0.60 mrem/year at 1500 years. Mean Tc-99 dose decreases to 0.11 mrem/year by 3000 years. The differences in the timing and magnitude of I-129 and Tc-99 doses are consistent with the differences in K_d values and estimated inventory (source concentrations) between the two radionuclides and are similar to the results of the deterministic base case simulation (Fig. G.10). To provide perspective on the relationship between radionuclide dose statistics at reporting times and radionuclide dose peaks, Figs. G.54 and G.55 also include horizontal reference lines at the 95th percentile of the peak radionuclide dose. The peak radionuclide dose can occur at various times within the compliance period for any given simulation, so the 95th percentile of the peak dose is independent of time.

Consistent with the radionuclide dose statistics for model reporting times, approximately 90 percent of the peak I-129 doses occur between 2000 and 9700 years, with a mean I-129 peak time of approximately 5200 years. For Tc-99, 90 percent of the 3000 simulated peak doses occur between 900 and 2700 years, with a mean Tc-99 peak time of 1700 years. Approximately 7 percent of the simulated Tc-99 peak doses occur before 1000 years. Peak radionuclide dose statistics for I-129 and Tc-99 are provided in Table G.28.

Table G.28. Peak radionuclide dose statistics

Radionuclide	Average peak dose (mrem/year)	95th percentile peak dose (mrem/year)
I-129	10.6	23.1
Tc-99	0.94	1.62

Cumulative distribution function curves for I-129 and Tc-99 peak dose are shown in Figs. G.56 and G.57. Approximately 4 percent of the simulated I-129 peak doses exceed 25 mrem/year, whereas Tc-99 peak doses are all less than 2.5 mrem/year. Peak doses greater than 25 mrem/year associated with I-129 and Pu-239, U-234, U-235, and U-238 are discussed in Sect. G.6.3.4.5.

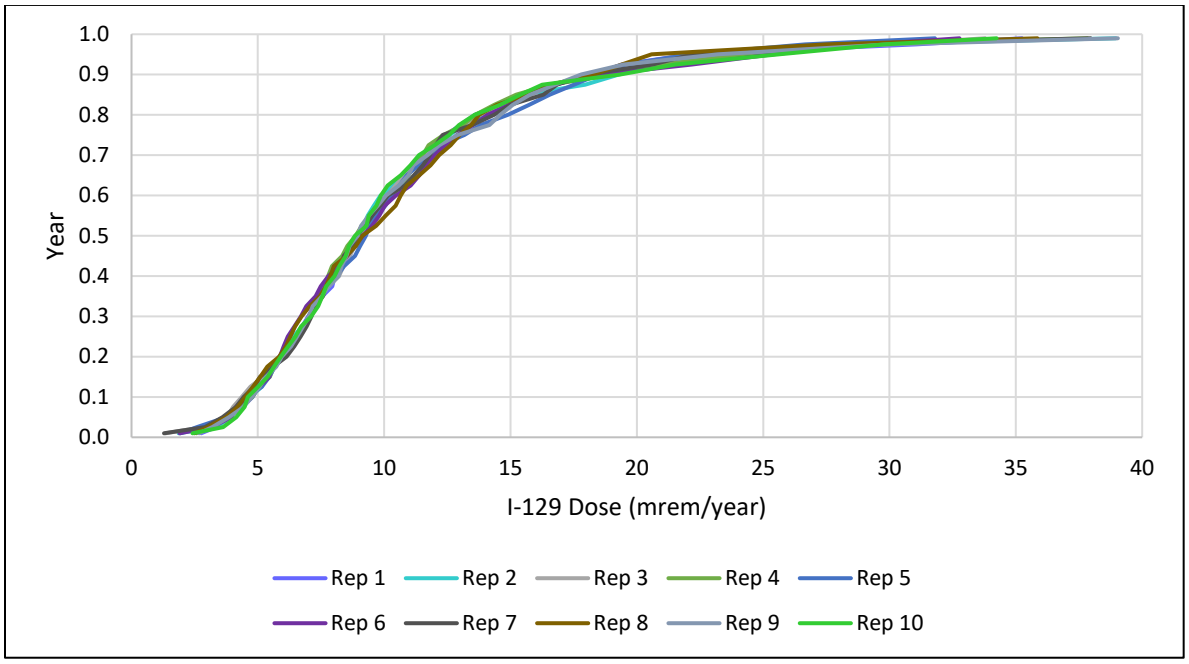

Fig. G.56. Cumulative distribution function curve, peak I-129 dose for 10 repetitions, all pathways (0 to 40 mrem/year, 0 to 10,000 years)

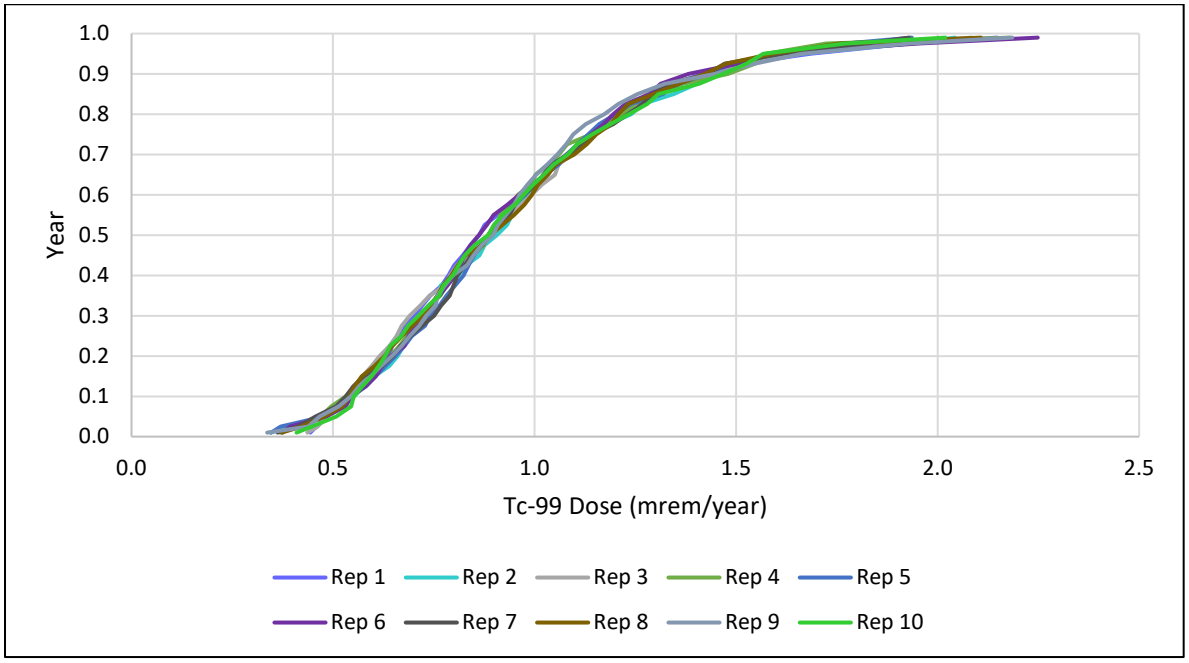

Fig. G.57. Cumulative distribution function curve, peak Tc-99 dose for 10 repetitions, all pathways (0 to 2.5 mrem/year, 0 to 10,000 years)

G.6.3.4.3 Distribution of peak total dose and component pathway peaks for the 10,000-year uncertainty analysis

As shown in Fig. G.58, CDF curves of peak total dose from all pathways over the 10,000-year simulation period are similar for the 10 repetitions. Over the 10,000-year simulation period, the median peak total dose (average of the 10 repetitions) is approximately 10 mrem/year. The 87th percentile of the peak dose is approximately 25 mrem/year, which means that 379 out of 3000 realizations (approximately 13 percent) produce a peak dose above 25 mrem/year. Seventy percent of the peak total doses were distributed evenly between about 2000 and 8000 years, and about 15 percent of the peaks occurred at the end of the simulation period. All but three of the simulated peaks (0.1 percent) occurred after 900 years. Peak total doses greater than 25 mrem/year are discussed in Sect. G.6.3.4.5.

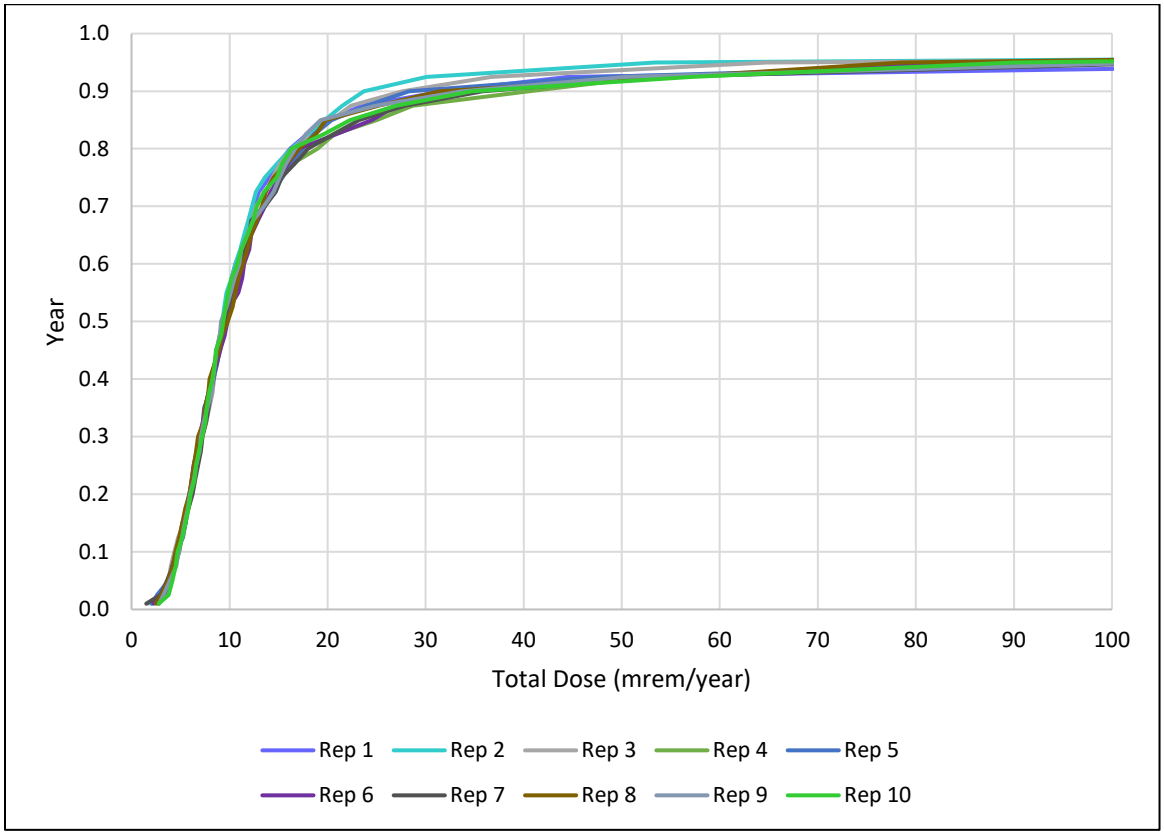

Fig. G.58. Cumulative distribution function curve, peak total dose for 10 repetitions, all pathways (0 to 100 mrem/year, 0 to 10,000 years)

In addition to the isotope-specific contributions, the peak dose statistics for each of the 15 exposure pathways were calculated. Water ingestion was the largest contributor to the total dose for the 10,000-year analysis. Fish ingestion and meat ingestion (waterborne) were the two next largest pathway contributors. Water ingestion is likely to be the highest contributing pathway under most circumstances, as the 5th percentile predicted dose value for water ingestion is greater than the 95th percentile doses for both fish ingestion and meat ingestion (waterborne).

G.6.3.4.4 Regression analysis of peak total dose for the 10,000-year simulation period

Similar to the compliance period uncertainty analysis, the next step in the 10,000-year uncertainty analysis consisted of multiple linear regression analyses of peak total dose on the values of the probabilistic input

parameters. This analysis was performed to identify which input variables contributed most to the variation in predicted peak all pathways dose. Standardized regression coefficients and standardized rank regression coefficients were generated using the built-in post-run regression tool in RESRAD-OFFSITE. Using the SRCs and SRRCs along with the spread of the parameter distributions, the code determined which variables had the greatest influence on the total dose calculation. SRRC values had higher coefficients of determination (r squared), so parameter influence rankings are based on SRRC values. SRC and SRRC values and for all probabilistic parameters and each repetition are shown in Table G.29.

The most influential probabilistic variables fall into four categories: (1) contaminated zone parameters, (2) unsaturated zone parameters, (3) saturated zone parameters, and (4) human exposure parameters. The most influential parameters associated with the contaminated zone include:

- Runoff coefficient in the area of the primary contamination
- Time over which transformation to releasable form occurs of I-129
- Effective porosity of contaminated zone
- Longitudinal dispersivity of contaminated zone
- Fraction of radionuclide bearing material that is initially releasable of I-129.

These results are generally consistent with results from the single parameter sensitivity analysis presented in Sect. G.6.2. The runoff coefficient controls infiltration and varying this parameter has a great influence on total dose. The initial release times and initial releasable fractions of radionuclides influences the total dose and timing of peak dose for I-129 over the 10,000-year simulation period, so it is logical that these parameters are some of the most influential based on the regression analysis. The most influential contaminated zone parameters control contaminant leaching and release from the waste, which ultimately determine the timing and magnitude of human exposure through the modeled pathways.

The unsaturated zone parameters that have the most influence on the total dose include the following:

- K_d of I-129 in UZ1
- Thickness of UZ5
- Longitudinal dispersivity of UZ5.

These variables control radionuclide partitioning between the solid and aqueous phases during transport through the unsaturated zone for less mobile radionuclides subsequent to the compliance period, the total vertical distance that contaminants need to travel to reach the saturated zone, and the dispersion of contaminants in the natural soils (UZ5). Sensitivity analyses performed on I-129 K_d values in different zones showed that predicted total dose and timing of peak dose is sensitive to K_d values. While the thickness of UZ5 does not strongly influence the magnitude of the peak dose in the single factor sensitivity analysis, it does have an impact on the timing of the peak dose, which would determine whether or not plutonium or uranium isotopes have a dose contribution within 10,000 years. Similar to the thickness of UZ5, the longitudinal dispersivity of UZ5 determines travel time to the saturated zone, which could determine whether or not plutonium or uranium isotopes reach the simulated receptors within 10,000 years, thus influencing peak dose predictions. The most sensitive unsaturated zone parameters control the rate at which radionuclides travel through the unsaturated zone and the amount of time it takes for radionuclides to reach the saturated zone. The saturated zone parameters that have the greatest influence on peak total dose include:

- K_d of I-129 in the saturated zone
- Dry bulk density of the saturated zone
- Hydraulic conductivity of saturated zone
- Effective porosity of saturated zone
- K_d of U-234 in saturated zone
- K_d of Tc-99 in saturated zone.

The most influential saturated zone variables in the uncertainty analysis control the groundwater flow rate in the saturated zone (hydraulic conductivity and effective porosity of saturated zone) and the partitioning of I-129, Tc-99, and U-234 between the solid and aqueous phases during transport in the saturated zone (K_d and dry bulk density of saturated zone). These parameters influence radionuclide concentrations in the saturated zone and the well, which have a strong influence on peak total dose, as water ingestion contributes the most to the total dose.

The human exposure parameter included in the uncertainty analysis is the depth of aquifer contributing to well. This parameter represents well construction assumptions and controls contaminant concentrations in the well water. The influence of this parameter on peak total dose is logical since the water ingestion pathway is the highest contributing pathway in the deterministic and probabilistic results and all water for indoor use and consumption originates from the well.

The regression analysis for the 10,000-year uncertainty analysis produced some counter-intuitive SRRCs for select parameters in some repetitions in which the sign of the SRRC reversed and was greater than +/-0.1. Examples in the 10,000-year uncertainty analysis include:

- Hydraulic conductivity of saturated zone (repetition 6)
- Thickness of UZ5 (repetitions 3 and 4)
- U-234 K_d in the saturated zone (repetition 2)
- Tc-99 K_d in the saturated zone (repetition 7)
- Precipitation (repetitions 6, 7, and 9)
- Pu-239 K_d in the saturated zone (repetitions 1 and 3)
- U-234 K_d in the saturated zone (repetitions 1, 3, and 8)
- Effective porosity of UZ5 (repetitions 7 and 8)
- Pu-239 K_d in UZ1 (repetitions 5, 9, and 10)
- Longitudinal dispersivity of UZ3 (repetition 9)
- Mean residence time of water in surface water body (repetition 7)
- Hydraulic gradient to well (repetition 6).

Table G.29. Standardized rank regression coefficients and standardized regression coefficients for probabilistic input parameters listed in order of decreasing influence on peak dose for the 10,000-year uncertainty analysis

Repetition	1	2	3	4	5	6	7	8	9	10	1	2	3	4	5	6	7	8	9	10
Coefficient of Determination (R-squared)	**0.82**	**0.84**	**0.80**	**0.80**	**0.81**	**0.81**	**0.80**	**0.81**	**0.81**	**0.81**	**0.39**	**0.32**	**0.28**	**0.36**	**0.26**	**0.30**	**0.25**	**0.29**	**0.28**	**0.21**
Description of Probabilistic Variable	**SRRC**	**SRRC**	**SRRC**	**SRRC**	**SRRC**	**SRRC**	**SRRC**	**SRRC**	**SRRC**	**SRRC**	**SRC**	**SRC**	**SRC**	**SRC**	**SRC**	**SRC**	**SRC**	**SRC**	**SRC**	**SRC**
Runoff coefficient in area of primary contamination	-0.45	-0.55	-0.65	-0.71	-0.51	-0.47	-0.44	-0.52	-0.24	-0.43	-0.44	-0.68	-0.55	-0.65	-0.35	-0.45	-0.40	-0.33	-0.45	-0.24
K_d of I-129 in saturated zone	-0.37	-0.50	-0.42	-0.37	-0.17	-0.16	-0.55	-0.31	-0.25	-0.31	0.00	-0.20	-0.21	0.85	0.58	0.11	-0.12	0.12	-0.78	0.00
Dry bulk density of saturated zone	-0.20	-0.22	-0.24	-0.26	-0.24	-0.27	-0.20	-0.23	-0.27	-0.22	-0.06	-0.15	-0.05	-0.19	-0.12	-0.13	-0.13	-0.18	-0.16	-0.14
K_d of I-129 in UZ1	-0.26	-0.03	-0.20	-0.12	-0.44	-0.41	0.00	-0.20	-0.29	-0.19	-0.07	0.31	0.18	-0.90	-0.54	-0.04	-0.08	-0.04	0.81	0.10
Depth of aquifer contributing to well	-0.18	-0.21	-0.22	-0.13	-0.21	-0.21	-0.16	-0.20	-0.18	-0.22	0.00	-0.11	-0.03	0.02	-0.01	0.03	-0.10	-0.10	-0.01	0.05
Hydraulic conductivity of saturated zone	-0.24	-0.16	-0.04	-0.10	-0.15	0.13	-0.14	-0.08	-0.36	-0.40	0.12	0.19	0.15	0.02	-0.05	0.18	-0.12	0.18	-0.13	-0.10
Time over which transformation to releasable form occurs of I-129	-0.06	-0.28	0.02	-0.18	-0.05	-0.05	0.00	-0.28	-0.24	-0.23	-0.10	-0.23	-0.20	-0.19	-0.14	-0.40	0.53	-0.55	0.08	-0.24
Effective porosity of saturated zone	-0.05	-0.11	-0.14	-0.07	-0.10	-0.25	-0.08	-0.10	0.04	0.07	-0.07	-0.02	-0.01	0.05	0.05	-0.07	0.08	0.02	0.10	0.14
Effective porosity of contaminated zone	0.00	-0.04	-0.11	-0.08	-0.05	-0.12	-0.09	-0.07	-0.03	-0.15	-0.09	0.01	-0.08	-0.15	0.07	-0.02	0.04	0.00	0.08	0.04
Thickness (meters) of UZ5	-0.10	0.05	0.10	0.11	-0.04	-0.09	-0.14	-0.08	-0.33	-0.14	-0.11	0.34	0.13	0.11	-0.06	-0.06	0.14	-0.16	-0.05	-0.11
Longitudinal dispersivity (meters) of UZ5	-0.07	-0.12	-0.08	-0.10	-0.09	-0.05	-0.07	-0.07	0.03	-0.02	0.05	-0.17	0.03	0.04	-0.03	-0.01	-0.04	0.09	0.04	-0.01
K_d of U-234 in saturated zone	-0.14	0.13	-0.17	-0.04	-0.10	0.07	-0.06	-0.19	-0.10	0.02	0.04	0.24	0.00	0.05	-0.77	-0.02	-1.70	-0.46	0.44	-0.54
Longitudinal dispersivity of contaminated zone	-0.04	-0.08	-0.09	-0.03	-0.02	-0.04	-0.03	-0.03	-0.07	-0.08	0.06	-0.01	-0.05	0.00	0.03	-0.02	0.00	0.10	-0.06	0.00
K_d of Tc-99 in saturated zone	-0.06	0.08	-0.05	-0.01	0.09	-0.04	0.29	-0.01	0.03	0.10	-0.81	0.16	-0.41	-0.59	0.17	-0.06	1.23	-0.03	0.40	0.03
Fraction of radionuclide bearing material that is initially releasable of I-129	-0.01	-0.09	-0.02	-0.09	-0.05	-0.02	0.06	-0.09	-0.06	-0.04	-0.11	-0.01	-0.03	-0.10	0.05	-0.12	0.25	-0.15	-0.02	-0.12
Precipitation	0.07	0.05	0.32	0.24	0.04	-0.10	-0.12	0.03	-0.10	-0.07	0.18	0.50	0.56	0.55	0.29	0.12	0.32	0.18	0.26	0.09
K_d of Pu-239 in saturated zone	0.17	-0.18	0.33	0.01	-0.20	-0.12	-0.06	0.02	-0.13	-0.16	0.41	-0.48	0.22	-0.28	-0.18	-0.14	0.68	0.00	-0.21	0.39
K_d of U-234 in UZ1	0.10	-0.12	0.10	0.06	0.05	-0.13	-0.01	0.20	0.07	0.00	-0.19	-0.33	-0.15	0.01	0.64	0.01	1.53	0.54	-0.67	0.48
Effective porosity of UZ5	0.02	-0.05	-0.03	0.03	-0.12	-0.12	0.13	-0.11	-0.03	-0.03	-0.05	-0.14	-0.06	-0.12	-0.01	-0.14	0.02	-0.09	-0.10	0.08
Longitudinal dispersivity of saturated zone to well	-0.05	-0.03	-0.02	-0.05	0.00	0.03	-0.06	-0.04	-0.05	-0.02	-0.07	0.03	-0.04	-0.05	0.01	0.00	-0.05	-0.02	-0.08	-0.06
Longitudinal dispersivity (meters) of UZ4	0.01	-0.06	0.03	-0.07	0.05	-0.11	-0.02	-0.02	-0.08	0.04	-0.13	-0.07	0.18	-0.01	0.05	0.05	-0.07	0.12	0.01	0.16
Dry bulk density (g/cm³) of UZ5	-0.03	-0.01	-0.01	-0.01	-0.03	-0.06	-0.05	0.04	0.00	-0.05	0.04	-0.10	-0.08	0.00	-0.03	-0.07	-0.08	-0.03	0.02	-0.01
Time at which radionuclide first becomes releasable (delay time) of C-14	0.02	0.03	-0.02	-0.04	-0.04	0.02	-0.03	-0.03	-0.08	-0.01	-0.04	-0.03	-0.07	-0.01	-0.05	0.05	-0.01	0.04	-0.06	0.00
Effective porosity of UZ3	-0.02	-0.01	-0.01	-0.01	0.00	-0.06	0.02	-0.02	-0.07	-0.01	-0.03	0.05	-0.02	0.06	-0.05	-0.03	-0.10	0.00	0.03	0.09
K_d of Tc-99 in UZ1	0.05	-0.02	0.06	0.02	-0.15	0.08	-0.29	0.06	0.07	-0.04	0.77	-0.22	0.58	0.70	-0.17	0.17	-1.55	0.21	-0.43	-0.01
Hydraulic conductivity (meters/year) of UZ5	-0.03	0.04	-0.06	-0.02	0.07	0.07	-0.14	0.14	0.02	0.05	0.07	0.07	0.01	0.06	-0.01	0.04	-0.05	-0.01	0.15	-0.06
K_d of Pu-239 in UZ1	-0.26	0.18	-0.42	-0.07	0.18	0.05	-0.09	0.00	0.17	0.14	-0.63	0.59	-0.25	0.23	0.17	0.21	-0.92	0.09	0.10	-0.48
Longitudinal dispersivity (meters) of UZ3	0.00	0.03	0.00	0.00	-0.07	0.06	0.00	0.03	0.11	-0.05	0.07	0.04	-0.16	0.08	-0.09	-0.09	-0.02	-0.05	0.02	-0.11
Mean residence time of water in surface water body	0.03	-0.03	0.12	0.06	-0.05	-0.06	-0.14	0.02	0.01	-0.07	0.02	0.08	0.16	0.21	0.04	-0.01	0.03	0.03	0.10	0.00
Dry bulk density of contaminated zone	0.01	0.01	0.02	0.05	0.04	0.00	-0.01	-0.01	0.03	-0.05	-0.08	-0.01	0.01	-0.02	0.01	-0.02	-0.07	-0.06	-0.02	-0.05
Hydraulic conductivity of contaminated zone	-0.08	-0.03	0.07	0.03	-0.04	0.03	0.02	-0.04	-0.05	0.05	0.10	-0.04	0.03	0.10	-0.13	0.01	-0.08	0.00	-0.05	-0.07
b parameter of contaminated zone	0.04	-0.01	-0.04	0.03	-0.02	-0.01	-0.03	-0.01	-0.02	0.04	0.03	0.03	-0.02	0.04	-0.01	-0.06	0.09	0.09	0.02	-0.01
Effective porosity of UZ4	0.03	-0.04	-0.02	-0.01	0.00	0.03	-0.03	-0.02	0.00	0.02	0.08	-0.08	0.00	-0.05	0.02	0.07	-0.07	-0.10	0.04	0.03
Hydraulic gradient of saturated zone to well	-0.10	-0.01	-0.04	-0.04	0.00	0.23	0.07	0.08	-0.13	-0.08	-0.05	0.02	-0.18	-0.21	-0.12	0.09	-0.18	0.02	-0.15	-0.10
Total porosity of UZ3	-0.02	0.05	0.00	-0.05	-0.02	-0.01	-0.01	0.03	-0.02	0.02	0.01	0.05	-0.08	0.02	0.02	-0.01	-0.05	0.00	-0.01	0.04
Total porosity of UZ4	-0.02	0.00	0.00	-0.01	0.00	0.01	-0.01	0.02	-0.01	-0.01	0.05	-0.04	-0.01	0.01	0.08	0.01	0.03	0.00	-0.05	0.02
Longitudinal Dispersivity of saturated zone to surface waterbody	0.01	-0.01	0.04	-0.01	0.01	-0.03	-0.01	0.01	0.00	-0.02	-0.09	0.06	0.01	-0.05	0.08	-0.07	0.00	0.07	0.01	-0.09

SRC = Standardized Regression Coefficient
SRRC = Standardized Rank Regression Coefficient
UZ = unsaturated zone

This page intentionally left blank.

The counter intuitive SRRCs associated with radionuclide K_d values are likely because several of the most influential parameters are related to processes that are not linked to radionuclide sorption. The independence of K_d values from important hydrologic parameters can occasionally cause elevated peak doses to occur with relatively high K_d, which can cause calculation of regression coefficients that contradict the known relationship between K_d values and dose predictions (i.e., lowering K_d values causes an increase in doses). Additionally, influential hydrologic parameters can influence timing of peak dose from plutonium and uranium isotopes, and if peak doses for these radionuclides occur outside of the 10,000-year simulation period, corresponding peak dose within 10,000 years could be low even with a relatively low K_d, which may cause anomalous regression coefficients.

Another cause of counter intuitive SRRCs could be due to correlation with another parameter. Hydraulic gradient of aquifer to well generally has a moderately negative (-0.1 to -0.25) or negligible (between -0.1 and +0.1) SRRC; however, in repetition 6 it has a moderately positive (+0.23) SRRC. Hydraulic conductivity of saturated zone also has a SRRC of +0.13 in repetition 6. Hydraulic gradient of aquifer to well and hydraulic conductivity of the saturated zone are related by an adjusted rank correlation coefficient of -0.68 to maintain a consistent effective groundwater flow velocity, which may have caused calculation of counter intuitive SRRCs for hydraulic gradient to well for repetition 6, as the influence of one parameter affects the other correlated parameter.

The most influential probabilistic parameters for the 10,000-year uncertainty analysis control aquifer flow and transport properties, the mobility of dose-significant radionuclides from the solid to aqueous phases, and human exposure through groundwater. The pathway of greatest focus for the assessed radionuclides (C-14, I-129, Pu-239, Tc-99, U-234, U-235, and U-238) is water ingestion. Connections between aquifer properties and water ingestion are straightforward; aquifer properties of the site affect groundwater flow which influences exposure and the total dose.

G.6.3.4.5 Peak total dose predictions greater than 25 mrem/year – 10,000-year simulation period

This section is focused on which combinations of input parameters are associated with peak total doses that exceed 25 mrem/year. Seventy-two percent of the peak total doses that exceeded 25 mrem/year occurred at the end of the simulation period suggesting that these peaks were associated with combined contributions of Pu-239 and uranium nuclides. The remaining 28 percent of peak doses greater than 25 mrem/year occur prior to 3800 years, with all but 10 of these earlier peaks occurring between 900 and 3000 years. The earlier extreme peaks correspond to dose contributions from (primarily) I-129 and Tc-99. These two subsets of peak doses greater than 25 mrem/year are correlated with higher or lower sampled ranges of particular input parameters, as described below.

The extreme dose peaks beyond 1000 years are likely to be over-estimated due to inventory bias (over-estimated to manage uncertainty in future waste characteristics, refer to Sect. G.6.4), and because the RESRAD-OFFSITE model does not incorporate solubility limits on the release of uranium in solution, so the model may overestimate the peak concentrations. In addition, the comparison of STOMP model simulations of U-234 release to the RESRAD-OFFSITE release predictions (refer to Sect. 3.3.5 of the PA) shows that the equilibrium desorption release model over-predicts peak U-234 release significantly relative to the scaled STOMP model simulations. The model output comparison also shows that the simplified RESRAD-OFFSITE vadose zone representation yields a predicted peak U-234 flux is over twice as large as the peak STOMP U-234 flux to the water table beneath the EMDF. This difference in U-234 release model predictions suggests that the RESRAD-OFFSITE peak well water concentrations are too uncertain (probably over-estimated) to draw conclusions about the very long-term performance of the EMDF with respect to less mobile radionuclides ($K_d > 1.0$ cm^3/g) including nuclides of uranium and possibly also I-129 (refer to Sects. 3.3.5, 5.3, and 5.4 of the PA).

The earlier (prior to 3800 years) subset of peak doses (I-129 peaks > 25 mrem/year) ranges from 25 to 61 mrem/year and are generally associated with smaller than average sampled I-129 K_d values (< 3.5 cm^3/g) and with smaller than average sampled release duration (Fig. G.59). Iodine-129 K_d and release duration are positively correlated in the probabilistic sampling scheme, which contributes to the pattern of sampled input values in Fig. G.59. The earlier peaks greater than 25 mrem/year also tend to be associated with larger than average modeled cover infiltration and smaller than average values of the saturated zone Darcy velocity (calculated as hydraulic conductivity multiplied by hydraulic gradient) as shown in Fig. G.60. This correlation suggests that saturated zone mixing is particularly important in determining the likelihood of peak I-129 dose exceeding 25 mrem/year. This dependence of higher I-129 dose on saturated zone mixing is consistent with the high dose conversion factor for I-129, which reflects potentially large exposures associated with small environmental concentrations. The extreme I-129 dose peaks are probably over-estimated and not likely to be realized given the combination of unrealistically large I-129 source inventory and the RESRAD-OFFSITE over-estimate of peak I-129 flux to the water table (relative to the more detailed STOMP model of release from the vadose zone, refer to Sect. 3.3.5 of the PA).

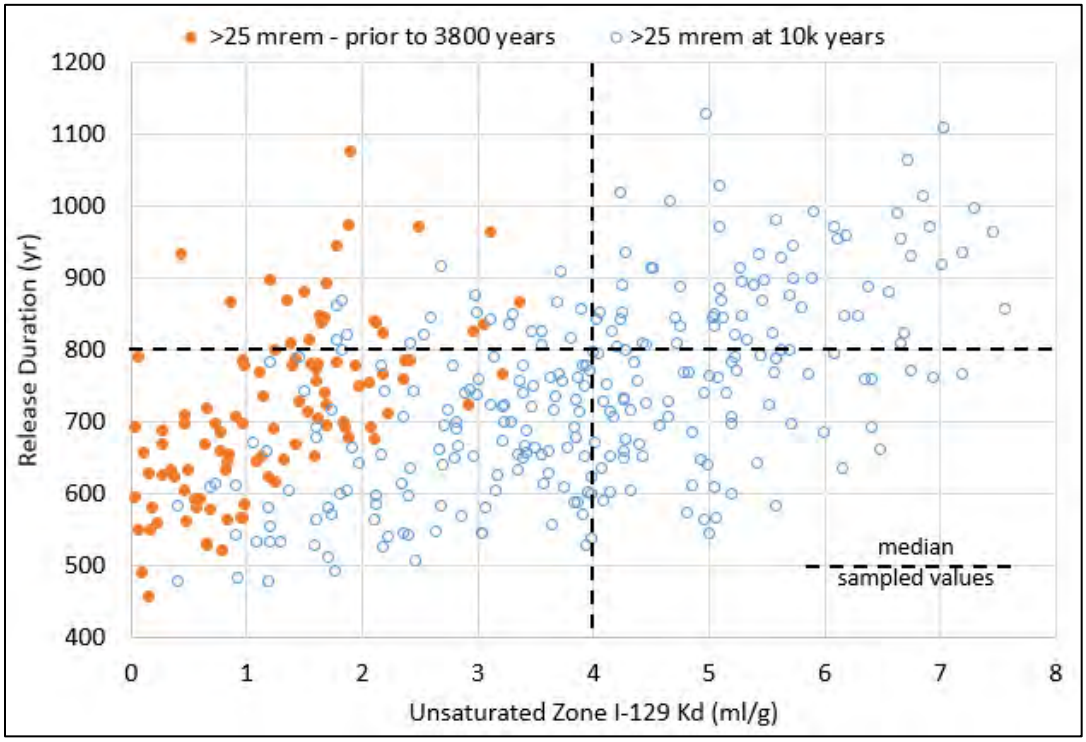

Fig. G.59. Release duration vs unsaturated zone I-129 K_d for peak simulated total doses greater than 25 mrem/year (0 to 10,000 years)

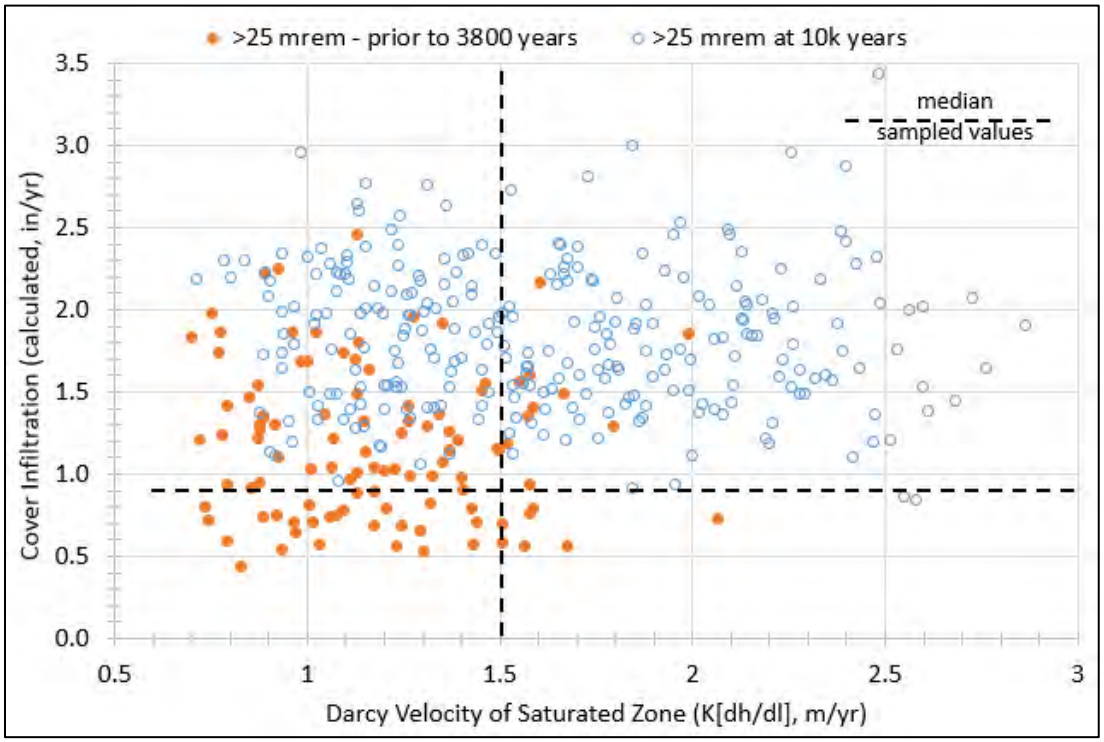

Fig. G.60. Calculated cover infiltration vs calculated saturated zone Darcy velocity for peak simulated total doses greater than 25 mrem/year (0 to 10,000 years)

These extreme peak values should be viewed with caution given the inherent limitations and uncertainty of the RESRAD-OFFSITE release model. These limitation include the modeled cover infiltration remaining constant rather than increasing over time, the lack of solubility limits that may lead to overestimated leachate concentrations for uranium species, and the rapid release for radionuclides having $K_d > 1$ cm^3/g produced by a constant long-term over infiltration rate applied to the instantaneous equilibrium desorption release model.

G.6.4 CONSERVATIVE BIAS

Conservative bias in the PA modeling analysis arises from adopting pessimistic assumptions that lead to larger estimates of dose to the hypothetical receptor rather than smaller dose estimates. Pessimistic assumptions adopted for the EMDF PA analysis include many assumptions for model parameter values and the assumption that the receptor would choose to set up domicile at the foot of the relatively steep disposal facility on land that is not level when more suitable sites for farming exist nearby. Other instances of conservative bias toward greater doses for the receptor include the following:

- POA specification – For the EMDF PA, the POAs are identical to DOE M 435.1-1 (DOE 2011a) requirements and consistent with the *Disposal Authorization Statement and Tank Closure Documentation* (DOE 2017). The POAs do not vary with the post-closure time period, even though expected future land use and institutional controls would preclude public exposure at the 100-m buffer zone boundary for at least 100 years after EMDF closure. Institutional controls limiting site access are assumed to be effective for 100 years following closure. These assumptions are pessimistic given that DOE is required to maintain control over land containing radionuclide sources until the land can be safely released pursuant to DOE O 458.1 (DOE 2011b) and Comprehensive Environmental Response,

Compensation and Liability Act of 1980 (CERCLA) or transferred to another authorized party with the same requirements to control the land.

- Resident farming scenario – The receptor locating a domicile and farm at EMDF is not probable. The ORR has a continuing mission and is a well-established site. Many of the employees are from the local communities, including many generations of some local families. Much of the ORR is fenced and guarded by armed security patrols. It is also against the CERCLA statute that the site will be abandoned (institutional controls on EMDF and ORR will be lost) at any time before contamination reaches levels acceptable for unrestricted use. Knowledge of the ORR and legal requirements will prevent access to the disposal facility.
- Receptor well location – Installation of the receptor well 100 m downgradient from the EOW is unlikely. A future receptor would likely select to drill a water supply well at a more protected location in BCV rather than adjacent to NT-11 near the disposal facility. Additionally, the formation above which the disposal facility is located does not yield the quantities of water that a well drilled in the Maynardville Formation would yield. It is more likely that a receptor would drill a well in that limestone formation instead as it is nearby. Therefore, it is unlikely that the receptor well would be located along the centerline of the radionuclide groundwater plume where radionuclide concentrations are highest. In addition, the RESRAD-OFFSITE model assumes withdrawal from the most contaminated (upper) part of the saturated zone, whereas a water supply well would likely be screened over a deeper, less contaminated interval.
- Contaminated water use – All livestock and agricultural areas are not expected to solely use contaminated water as is assumed in the model.
- Food sourcing – Unlike the assumption in the model, less than 50 percent of the consumed plant foods is likely to originate from radionuclide-impacted agricultural areas.
- Receptor occupancy – The receptor is not expected to spend 100 percent of the time on an annual basis at EMDF.
- Location of Bear Creek water supply – The assumption that all surface water used by the receptor originates from the 100-m-long section of Bear Creek located along the centerline of the plume is not likely. It is probable that any water use from Bear Creek would be from various sections along the creek, including less impacted sections.
- Engineered barrier performance – Geomembrane liners for the EMDF cover and liner systems are expected be effective in limiting infiltration and controlling releases of leachate for their estimated service life, reported to range from a few hundred years to 1000 years or more (Koerner et al. 2011, Rowe et al. 2009, Benson 2014). Therefore, it is likely that the engineered barriers will perform well beyond the assumed 200-year service life given that recent studies have estimated much longer periods of full HDPE membrane performance in mixed LLW facilities (Tian et al. 2017).
- Radionuclide release – The instantaneous equilibrium desorption release model assumes that the EMDF waste volume is a homogeneous, soil-like material in which the estimated radiological inventory is uniformly distributed and assumes that a concentration-independent partition coefficient (K_d) adequately captures the desorption process. This conceptual model does not account for the variety of different waste forms (e.g., contaminated demolition debris and equipment) or the effect of waste containers, waste stabilization (grouting), or treatment to reduce the mobility of radionuclide in EMDF waste. Additionally, it is not likely that any pathways for water to migrate through the waste will contact the entire volume of waste. The sensitivity of RESRAD-OFFSITE model results to assuming alternative release models (Sect. G.6.2.1) was evaluated to account for the possibility that these waste forms would tend to delay and/or retard the release of radionuclides.

- Estimated radionuclide inventory – The approach to estimating activity concentrations is intended to overestimate waste concentrations to account for uncertainty in the characteristics of future remediation waste (refer to Appendix B). As a result, the activity inventories used in the PA models are higher than inventories likely to be present at EMDF closure.

G.7 SUMMARY AND CONCLUSIONS

PA modeling using RESRAD-OFFSITE Version 3.2 was performed for EMDF as required by DOE M 435.1-1 (DOE 2011a). The simulated exposure scenarios were generally performed with a conservative bias toward greater dose in terms of assumed parameter values (see Sect. G.6.4). EMDF PA objectives and POA locations are listed in Table G.4.

The predicted total dose associated with the estimated EMDF inventory for the base case scenario is much less than the performance objective of 25 mrem/year (Figs. G.7 and G.8). The compliance period peak total dose (i.e., dose from all simulated radionuclides summed) is 1.03 mrem/year and occurs at approximately 500 years post-closure. The predicted total dose at 1000 years post-closure is 0.17 mrem/year. After the compliance period, the total dose increases to a maximum dose of 9.1 mrem/year at approximately 5100 years, and then gradually decreases through 10,000 years to a predicted total dose at 10,000 years of 0.11 mrem/year. Overall, the predicted maximum total dose during the compliance period (1.03 mrem/year) is less than 5 percent of the performance objective (25 mrem/year), indicating that the estimated post-closure EMDF inventories will not result in unacceptable total dose under the specific base case scenario analyzed. This conclusion is robust given the variety of pessimistic biases included in the analysis.

Modeling indicates that water resources protection criteria (see Sect. G.5.5) will be met. Site-specific application of regulatory standards for protection of groundwater resources was limited to assessment of compliance with MCLs for drinking water specified by EPA in the Final Radionuclides Final Rule (EPA 2000), promulgated in 40 *CFR* 141.66, for which the State of Tennessee has primary enforcement responsibility. Limits are specified for combined Ra-226 and Ra-228 activity concentration, gross alpha activity concentration, total annual dose from beta decay and photon emission, and total uranium (Table G.4). The EMDF PA demonstrates that groundwater (well water concentrations as calculated by RESRAD-OFFSITE) at 100 m from the waste boundary meets these limits.

The results of the uncertainty analysis described in Sect. G.6.3 indicate the peak of the mean dose for the compliance period for the 10 repetitions is 1 mrem/year (to one significant figure), with the predicted time of the peak mean dose occurring at 1000 years. A variety of pessimistic assumptions are incorporated into the uncertainty analysis, including the possibility for long-term cover infiltration rates to exceed the assumed long-term performance condition value (i.e., 1 to 2 in./year) early in the simulation period. The most influential input parameters control the release of the three dose-significant radionuclides (e.g., K_d values) as well as aquifer flow and transport properties. The pathways of greatest impact for the assessed radionuclides (C-14, I-129, and Tc-99) in the compliance period analysis are water ingestion, fish ingestion, and meat ingestion.

G.8 REFERENCES

Baes et al. 1984. *A Review and Analysis of Parameters for Assessing Transport of Environmentally Released Radionuclides through Agriculture*, ORNL-5786, Oak Ridge National Laboratory, Oak Ridge, TN, September.

Benson 2014. *Performance of Engineered Barriers: Lessons Learned*, Performance and Risk Assessment Community of Practice Webinar, C. Benson, February 20.

Benson and Benavides 2018. *Predicting Long-Term Percolation from the SDF Closure Cap*, Report No. GENV-18-05, School of Engineering, University of Virginia, Charlottesville, VA, April 23.

CH2M-Hill 2000. *Phase IV Final Site Investigation Report, SSRS Item No.3.3, Rev. 1*, CH2MHill Constructors, Inc., under contract to Waste Management Federal Services, Inc., for Bechtel Jacobs Company LLC, Oak Ridge, TN, March.

Davis et al. 1984. *Site Characterization Techniques Used at a Low-Level Waste Shallow Land Burial Field Demonstration Facility*, ORNL-9146, E. C. Davis, W. J. Boegly, Jr., E. R. Rothschild, B. P. Spalding, N. D. Yaughan C. S. Haase, D. D. Huff, S. Y. Lee, E. C. Walls, J. D. Newbold: and E. D. Smith, Oak Ridge National Laboratory, Oak Ridge, TN, July.

DOE 1992. *Site Characterization Summary Report for Waste Area Grouping [WAG] 1 at Oak Ridge National Laboratory, Oak Ridge, Tennessee. Vol. 3 – Appendix A: WAG 1 Soil Sampling and Analysis Program*, DOE/OR/01-1043/V3&D1, U.S. Department of Energy, Oak Ridge, TN, September.

DOE 1997. *Report on the Remedial Investigation of Bear Creek Valley at the Oak Ridge Y-12 Plant, Oak Ridge, Tennessee*, DOE/OR/01-1455/V1-V6&D2, U.S. Department of Energy, Oak Ridge, TN, May.

DOE 1998. *Remedial Investigation/Feasibility Study for the Disposal of Oak Ridge Reservation Comprehensive Environmental Response, Compensation, and Liability Act of 1980 Waste*, DOE/OR/02-1637&D2, U.S. Department of Energy, Oak Ridge, TN, January.

DOE 2001. *Radioactive Waste Management*, DOE Order 435.1 Ch 1 (PgChg), U.S. Department of Energy, Washington, D.C., August.

DOE 2011a. *Radioactive Waste Management Manual*, DOE Manual 435.1-1 Ch 2, U.S. Department of Energy, Washington, D.C., June.

DOE 2011b. *Radiation Protection of the Public and Environment*, DOE Order 458.1, U.S. Department of Energy, Washington, D.C., February.

DOE 2011c. *Derived Concentration Technical Standard*, DOE-STD-1196-2011, U.S. Department of Energy, Washington, D.C., April.

DOE 2016. *Sampling and Analysis Plan/Quality Assurance Project Plan for Environmental Monitoring at the Environmental Management Waste Management Facility, Oak Ridge, Tennessee*, DOE/OR/01-2734&D1, U.S. Department of Energy, Oak Ridge, TN, November.

DOE 2017. *Disposal Authorization Statement and Tank Closure Documentation*, DOE-STD-5002-2017, U.S. Department of Energy, Washington, D.C., July.

DOE 2019. *Fiscal Year 2019 Phased Construction Completion Report for the Oak Ridge Reservation Environmental Management Waste Management Facility*, DOE/OR/01-2818&D1, U.S. Department of Energy, Oak Ridge, TN, March.

Dorsch and Katsube 1996. *Effective Porosity and Pore-throat Sizes of Mudrock Saprolite from the Nolichucky Shale Within Bear Creek Valley on the Oak Ridge Reservation: Implications for Contaminant Transport and Retardation Through Matrix Diffusion*, ORNL/GWPO-025, J. Dorsch and T. J. Katsube, Oak Ridge National Laboratory, Oak Ridge, TN, May.

EPA 1990. *Exposure Factors Handbook*, EPA/600/8-89/043, U.S. Environmental Protection Agency, Office of Health and Environmental Assessment, Washington, D.C.

EPA 1995. *User's Guide for the Industrial Source Complex (ISC3) Dispersion Models, Vols. 1 & 2*. EPA-454/B-95-003a and 003b, U.S. Environmental Protection Agency, Office of Air Quality Planning and Standards, Research Triangle Park, NC, September.

EPA 2000. Final Radionuclides Rule, 66 Federal Register 76708, Vol. 65, No. 236, U.S. Environmental Protection Agency, December 7.

EPA 2002a. *Radionuclides in Drinking water: A Small Entity Compliance Guide*, U.S. Environmental Protection Agency, Office of Ground Water and Drinking Water, Washington, D.C., February.

EPA 2002b. *Implementation Guidance for Radionuclides*, EPA 816-F-00-002, U.S. Environmental Protection Agency, Office of Ground Water and Drinking Water, Washington, D.C., March.

EPA 2009. *Guidance on the Development, Evaluation, and Application of Environmental Models*. EPA/100/K-09/003, U.S. Environmental Protection Agency, Office of the Science Advisor, Washington, D.C., March.

EPA 2011. *Exposure Factors Handbook: 2011 Edition*, EPA/600/R-090/052F, U.S. Environmental Protection Agency, Washington, D.C. September.

Friedman et al. 1990. *Laboratory Measurement of Radionuclides Sorption in Solid Waste Storage Area 6 Soil/Groundwater Systems*, ORNL/TM 10561, Oak Ridge National Laboratory, Oak Ridge, TN, June.

Gil-Garcia et al. 2008. "New best estimates for radionuclide solid–liquid distribution coefficients in soils. Part 3: miscellany of radionuclides (Cd, Co, Ni, Zn, I, Se, Sb, Pu, Am, and others)", *Journal of Environmental Radioactivity*, 100, 704–715.

Gnanapragasam and Yu 2015. *User's Guide for RESRAD-OFFSITE*, NUREG/CR-7189, ANL/EVS/TM-14/2, E. K. Gnanapragasam and C. Yu, Argonne National Laboratory, Argonne, IL, U.S. Nuclear Regulatory Commission, Rockville, MD, April.

GoldSim 2010. *Probabilistic Simulation Environment, User's Guide, Volume 1*, Version 10.5, GoldSim Technology Group, Issaquah, WA, December.

International Atomic Energy Agency (IAEA) 2010. *Handbook of Parameter Values for the Prediction of Radionuclide Transfer in Terrestrial and Freshwater Environments*, Technical Reports Series No. 472, International Atomic Energy Agency, Vienna, Austria.

International Commission on Radiological Protection (ICRP) 2008. *Nuclear Decay Data for Dosimetric Calculations*, Publication 107, International Commission on Radiological Protection, Ottawa, Ontario, K1P 5S9, Canada.

Koerner et al. 2011. *Geomembrane Lifetime Prediction: Unexposed and Exposed Conditions*, Geosynthetic Institute GRI White Paper #6, R. M. Koerner, Y. G. Hsuan, and G. R. Koerner, Folsom, PA, February.

ORNL 1987. *Geochemical Behavior of Cs, Sr, Tc, Np, and U in Saline Groundwaters: Sorption Experiments on Shales and Their Clay Mineral Components*, ORNL/TM-10634, Oak Ridge National Laboratory, Oak Ridge, TN, November.

ORNL 1997a. *Performance Assessment for Continuing and Future Operations at Solid Waste Disposal Area 6*, ORNL-6783/R1, Vol. 1, Oak Ridge National Laboratory, Oak Ridge, TN, September.

ORNL 1997b. *Performance Assessment for the Class L-II Disposal Facility*, ORNL/TM-13401, Oak Ridge National Laboratory, Oak Ridge, TN, March.

Parks 1992. *User's Guide for CAP88-PC, Version 1.0*, EPA 402-B-92-001, B. S. Parks, U.S. Environmental Protection Agency, Office of Radiation Programs, Las Vegas, NV, March.

PNNL 2003. *A Compendium of Transfer Factors for Agricultural and Animal Products*, PNNL-13421, L. H. Staven, B. A. Napier, K. Rhoads, and D. L. Strenge, Pacific Northwest National Laboratory, Richland, WA, June.

Pollock 1989. *Documentation of Computer Programs to Compute and Display Pathlines Using Results from the U.S. Geological Survey Modular Three-Dimensional Finite-Difference Groundwater Flow Model*, Open-file Report 89-381, D. W. Pollock, U.S. Geological Survey, Reston, Virginia.

Putnam et al. 1999. *Food Consumption, Prices, and Expenditure, 1970–1997*, J. J. Putnam, J. E. Allshouse, U.S. Department of Agriculture, Statistical Bulletin No. 965, Washington, D.C., April.

Rothschild et al. 1984. *Characterization of Soils at Proposed Solid Waste Storage Area (SWSA) 7*, ORNL/TM-9326, E. R. Rothschild, D. D. Huff, B. P. Spalding, S. Y. Lee, R.B. Clapp, D. A. Lietzke, R. G. Stansfield, N. D. Farrow, C. D. Farmer, I. L. Munro, Oak Ridge National Laboratory, Oak Ridge, TN, December.

Rowe et al. 2009. "Ageing of HDPE geomembrane exposed to air, water and leachate at different temperatures," *Geotextiles and Geomembranes*, R. K. Rowe, S. Rimal, H. P. Sangam, Vol. 27, No. 2, International Geosynthetics Society, Jupiter, FL, pages 137–151.

Schroeder et al.1994. *The Hydrologic Evaluation of Landfill Performance (HELP) Model: Engineering Documentation for Version 3*, EPA/600/R-94/168b, P. R. Schroeder, T. S. Dozier, P. A. Zappi, B. M. McEnroe, J. W. Sjostrom, and R. L. Peyton, U.S. Environmental Protection Agency Office of Research and Development, Washington, D.C.

Sheppard and Thibault 1990. "Default Soil Solid/Liquid Partition Coefficients, K_ds, for Four Major Soil Types: A Compendium," M. Sheppard and D. H. Thibault, Health Physics, Vol. 59, No. 4, pages 471-481, October.

Sullivan 2001. *DUST-MS Disposal Unit Source Term: Multiple Species Data Input Guide*, T. M. Sullivan, Brookhaven National Laboratory, Upton, NY.

TDEC 2012. *Public Water Systems, Maximum Contaminant Levels*, Rule 0400-45-01-.06,Tennessee Department of Environment and Conservation, Division of Drinking Water Supply, Nashville, TN.

Tian et al. 2017. "Antioxidant Depletion and Service Life Prediction for HDPE Geomembranes Exposed to Low-Level Radioactive Waste Leachate", *Geotechnical & Geoenvironmental Engineering*, K. Tian, C. H. Benson, J. M. Tinjum, Vol. 143 Issue 6, June.

UCOR 2020a. *Quality Assurance Report for Modeling of the Bear Creek Valley Low-level Radioactive Waste Disposal Facilities, Oak Ridge, Tennessee"*, UCOR-5234/R0, UCOR, Oak Ridge, TN, April.

UCOR 2020b. *Composite Analysis for the Environmental Management Waste Management Facility and the Environmental Management Disposal Facility, Oak Ridge, Tennessee*, UCOR-5095/R2, UCOR, Oak Ridge, TN, April.

USGS 1988. *A Modular Three-Dimensional Finite Difference Groundwater Flow Model*, Book 6, Modeling Techniques, Chapter A1, M. G. McDonald and A. W. Harbaugh, U.S. Geological Survey, Reston, VA.

White and Oostrom 2000. *STOMP Subsurface Transport Over Multiple Phases, Theory Guide*, PNNL-12030, UC-2010, M. D. White and M. Oostrom, Pacific Northwest National Laboratory, Richland, WA.

White and Oostrom 2006. *STOMP Subsurface Transport over Multiple Phases, Version 4.0, User's Guide*, PNNL-15782, M. D. White and M. Oostrom, Pacific Northwest National Laboratory, Richland, WA.

Yu et al. 2000. *Development of Probabilistic RESRAD 6.0 and RESRAD-BUILD 3.0 Computer Codes*, NUREG/CR-6697 ANL/EVS/TM-98, C. Yu, E. K. Gnanapragasam, J. Arnish, S. Kamboj, B.M. Biwer, J.-J. Cheng, A. Zielen, and S.Y. Chen, Environmental Science Division, Argonne National Laboratory, Argonne, IL, November.

Yu et al. 2006. *Benchmarking of RESRAD-OFFSITE: Transition from RESRAD (onsite) to RESRAD-OFFSITE and Comparison of the RESRAD-OFFSITE Predictions with Peer Codes*, ASNL/EVS/TM/06-3, C. Yu, E. Gnanapragasam, J.-J. Cheng, and B. Biwer, Environmental Science Division, Argonne National Laboratory, Chicago, IL, May.

Yu et al. 2007. *User's Manual for RESRAD-OFFSITE Version 2* ANL/EVS/TM/07-1, C. Yu, E. K. Gnanapragasam, B. M. Biwer, S. Kamboj, J.-J. Cheng, T. Klett, D. LePoire, A. J. Zielen, S. Y. Chen and W. A. Williams, Argonne National Laboratory, Argonne, IL, June.

Yu et al. 2013. *New Source Term Model for the RESRAD-OFFSITE Code Version 3*. NUREG/CR-7127, ANL/EVS/TM/11-5, C. Yu, E. Gnanapragasam, J.-J. Cheng, S. Kamboj, and S.Y. Chen, U.S. Nuclear Regulatory Commission, Office of Nuclear Regulatory Research, Washington, D.C.

Yu et al. 2015a. *User's Guide for RESRAD-OFFSITE*, NUREG/CR-7189 ANL/EVS/TM-14/2, C. Yu and E. K. Gnanapragasam, Argonne National Laboratory, Argonne, IL.

Yu et al. 2015b. *Data Collection Handbook to Support Modeling Impacts of Radioactive Material in Soil and Building Structures*, ANL/EVS/TM-14/4, C. Yu, J.-J. Cheng, L. Jones, Y. Wang, Y. Chia, and E. Faillace, Argonne National Laboratory for U.S. Department of Energy, Office of Science, Oak Ridge, TN, September.

Zheng 1990. *A Modular Three-Dimensional Transport Model for Simulation of Advection, Dispersion and Chemical Reactions of Contaminants in Groundwater Systems; Documentation and Users Guide*, report to the U.S. Environmental Protection Agency, C. Zheng, S.S. Papadopulos & Associates, Inc., Bethesda, MD.

ATTACHMENT G.1.
SUMMARY OF RESRAD-OFFSITE BASE CASE SCENARIO PARAMETERS

This page intentionally left blank.

Input Screen Title and Parameter Name	RESRAD ID	Units	Default Value	Code-Accepted Values Physical or Numerical Range	Base Case Value	Reference or Basis for Assumption
Radiological units for activity	-	Ci, Bq, dps, dpm	pCi	Ci, Bq, dps, dpm	pCi	As Required
Radiological units for dose	-	rem and Sv	mrem	rem, Sv	mrem	As Required
Basic radiation dose limit	BRDL	mrem/yr	25	1E-34 - 1E+34	25	DOE M 435.1
Exposure duration	ED	yr	30	1 - 1,000	30	Assessment duration
Number of unsaturated zone(s)	NS	-	1	0 - 5	5	Specified to represent vertical discretization of unsaturated zone
Submerged fraction of Primary Contamination	SUBMERGEDF	unitless	0	0 - 1	0	All waste located above groundwater table
Default Release Mechanism	-	-	-	Version 2, First Order Rate Controlled Release with Transport, Instantaneous Equilibrium Desorption Release	Version 2 Release Methodology	Version 2 selected as default release mechanism, during simulations release mechanism specified as described in Appendix G
Bearing of X axis	NXBEARING	degrees	90	0 - 360	90	Default
X dimension of Primary contamination	SOURCEXY(1)	m	100	-80,000 - +80,000	250.6	Approximation of cell design to represent average width (east west) of waste cell
Y dimension of Primary contamination	SOURCEXY(2)	m	100	-80,000 - +80,000	382.7	Approximation of cell design to represent average length (north south) of waste cell
Smaller x coordinate of the fruit, grain, nonleafy vegetables plot	AGRIXY(1,1)	m	34.375	-80,000 - +80,000	0.0	Resident farmer scenario assumption
Larger x coordinate of the fruit, grain, nonleafy vegetables plot	AGRIXY(2,1)	m	65.625	-80,000 - +80,000	32.00	
Smaller y coordinate of the fruit, grain, nonleafy vegetables plot	AGRIXY(3,1)	m	234	-80,000 - +80,000	-132.0	
Larger y coordinate of the fruit, grain, nonleafy vegetables plot	AGRIXY(4,1)	m	266	-80,000 - +80,000	-100.0	
Smaller x coordinate of the leafy vegetables plot	AGRIXY(1,2)	m	34.375	-80,000 - +80,000	40.0	
Larger x coordinate of the leafy vegetables plot	AGRIXY(2,2)	m	65.625	-80,000 - +80,000	72.0	
Smaller y coordinate of the leafy vegetables plot	AGRIXY(3,2)	m	268	-80,000 - +80,000	-132.0	
Larger y coordinate of the leafy vegetables plot	AGRIXY(4,2)	m	300	-80,000 - +80,000	-100.0	

Input Screen Title and Parameter Name	RESRAD ID	Units	Default Value	Code-Accepted Values Physical or Numerical Range	Base Case Value	Reference or Basis for Assumption
Smaller x coordinate of the pasture, silage growing area	AGRIXY(1,3)	m	0	-80,000 - +80,000	120.0	Resident farmer scenario assumption
Larger x coordinate of the pasture, silage growing area	AGRIXY(2,3)	m	100	-80,000 - +80,000	220.0	
Smaller y coordinate of the pasture, silage growing area	AGRIXY(3,3)	m	450	-80,000 - +80,000	-200.0	
Larger y coordinate of the pasture, silage growing area	AGRIXY(4,3)	m	550	-80,000 - +80,000	-100.0	
Smaller x coordinate of the grain fields	AGRIXY(1,4)	m	0	-80,000 - +80,000	230.0	
Larger x coordinate of the grain fields	AGRIXY(2,4)	m	100	-80,000 - +80,000	330.0	
Smaller y coordinate of the grain fields	AGRIXY(3,4)	m	300	-80,000 - +80,000	-200.0	
Larger y coordinate of the grain fields	AGRIXY(4,4)	m	400	-80,000 - +80,000	-100.0	
Smaller x coordinate of the dwelling site	DWELLXY(1)	m	34.375	-80,000 - +80,000	80.0	
Larger x coordinate of the dwelling site	DWELLXY(2)	m	65.625	-80,000 - +80,000	112.0	
Smaller y coordinate of the dwelling site	DWELLXY(3)	m	134	-80,000 - +80,000	-132.0	
Larger y coordinate of the dwelling site	DWELLXY(4)	m	166	-80,000 - +80,000	-100.0	
Smaller x coordinate of the surface-water body	SWXY(1)	m	-100	-80,000 - +80,000	-575.4	Location of Bear Creek relative to waste
Larger x coordinate of the surface-water body	SWXY(2)	m	200	-80,000 - +80,000	-475.4	
Smaller y coordinate of the surface-water body	SWXY(3)	m	550	-80,000 - +80,000	-337.4	
Larger y coordinate of the surface-water body	SWXY(4)	m	850	-80,000 - +80,000	-332.4	
Source						
Nuclide concentration	S1	pCi/g	100	0 - 1E+34	varies	EMDF RI/FS (DOE 2017b) and Appendix B
Release to groundwater, leach rate	-	1/yr	0	0 - 1E+34	varies	Not used, Version 2 release parameter
Use Distribution Coefficient to Estimate First Order Leach Rate	-	cc/g	0	0 - 1E+34	varies	Not used, Version 2 release parameter

Input Screen Title and Parameter Name	RESRAD ID	Units	Default Value	Code-Accepted Values Physical or Numerical Range	Base Case Value	Reference or Basis for Assumption
Deposition velocity	DEPVEL DEPVELT	m/s	0.001, 0.01 (Cl, I), 0 (Xe)	0 - 1E+34	0.001 0.01 (I-129)	Default, representative deposition velocity of the airborne respirable particles with which the nuclides is associated with
Radionuclide bearing material becomes releasable	RELTIMEOPT	N/A	N/A	N/A	Linear	Linearly increases in source release from time of initial release to end state
Time at which radionuclide first becomes releasable (delay time)	RELTIMEINIT	Year	N/A	N/A	300	Adjusted upward from 200 years to correct for the application of greater than expected infiltration (0.88 in/yr) between 200 and 1,000 years in the RESRAD-OFFSITE model, based on comparison of MT3D model Tc-99 results to RESRAD-OFFSITE output
Fraction of radionuclide bearing material that is initially releasable	RELFRACINIT	-	N/A	N/A	0.75 for C-14, H-3 0 for All Other Nuclides	Gradual cover degradation from 300 - 1,100 years; this value was adjusted upward from 0 to eliminate the limitation on early release of highly mobile radionuclides (C-14, H-3), based on comparison of MT3D model C-14 results to RESRAD-OFFSITE output
Time over which transformation to releasable form occurs	RELDUR	Years	-	-	500 for C-14, H-3 800 for All Other Nuclides	Expected duration for degradation from intact to long-term state, this value was adjusted down from 800 years to eliminate limitation on early release of highly mobile radionuclides (C-14, H-3), based on comparison of MT3D model C-14 results to RESRAD-OFFSITE output
Total fraction of radionuclide bearing material that is releasable	RELFRACFINAL	unitless	N/A	N/A	1.0	All material available for release when cover is degraded
Release Mechanism	RELOPT	-	-	-	Instantaneous Equilibrium Sorption Desorption, 1	Conservative release assumption biased towards higher predicted peak doses
Initial Leach Rate	RLEACH ALEACH	1/year	N/A	N/A	0	First Order release mechanism parameter, not used
Final Leach Rate	RLEACHF	1/year	N/A	N/A	0	First Order release mechanism parameter, not used
Distribution Coefficient in the contaminated zone	DCACTC	cc/g	N/A	N/A	Waste zone Kd	Equal to contaminated zone Kd

Input Screen Title and Parameter Name	RESRAD ID	Units	Default Value	Code-Accepted Values Physical or Numerical Range	Base Case Value	Reference or Basis for Assumption
Release to Atmospheric	-	-	-	-	In the same manner as for release to groundwater	Release to atmosphere determined by release to groundwater pathway
Distribution Coefficients						
Contaminated zone	DCACTC DCNUCC	cm^3/g	Nuclide-dependent (Default values available)	0 - 1E+34	varies	Varies by radionuclide, see Appendix G
Unsaturated zone	DCACTU(1-5) DCNUCU(1-5)	cm^3/g		0 - 1E+34	varies	Varies by radionuclide, see Appendix G
Saturated zone	DCACTS DCNUCS	cm^3/g		0 - 1E+34	varies	Varies by radionuclide, see Appendix G
Sediment in surface water body	DCACTSWB DCNUCSWB	cm^3/g		0 - 1E+34	0	Conservative assumption to allow maximum concentration in surface water body
Fruit, grain, nonleafy fields	DCACTV1 DCNUCOF(1)	cm^3/g		0 - 1E+34	varies	Varies by radionuclide, see Appendix G
Leafy vegetable fields	DCACTV2 DNUCOF(2)	cm^3/g		0 - 1E+34	varies	Varies by radionuclide, see Appendix G
Pasture, silage growing areas	DCACTL1 DNUCOF(3)	cm^3/g		0 - 1E+34	varies	Varies by radionuclide, see Appendix G
Livestock feed grain fields	DCACTL2 DNUCOF(4)	cm^3/g		0 - 1E+34	varies	Varies by radionuclide, see Appendix G
Offsite dwelling site	DCACTDWE DCNUCDWE	cm^3/g		0 - 1E+34	varies	Varies by radionuclide, see Appendix G
Deposition Velocities						
Deposition velocity of respirable particulates	DEPVEL	m/s	Nuclide-dependent (Default	0 - 1E+34	0.001 0.01 (I-129)	Default, represents assumed deposition velocity of airborne respirable particulates

Input Screen Title and Parameter Name	RESRAD ID	Units	Default Value	Code-Accepted Values Physical or Numerical Range	Base Case Value	Reference or Basis for Assumption
Deposition velocity of all particulates	DEPVELT	m/s	values available)	0 - 1E+34	0.001 0.01 (I-129)	Default, represents assumed deposition velocity of airborne respirable particulates
Dose Conversion and Slope Factors						
External exposure library	N/A	(mrem/yr) per (pCi/g)	Nuclide-specific (default values available)	Nuclide-specific (default values available)	DCFPAK3.02 Database, DOE STD-5002-2017	Default exposure library
Internal exposure dose library	N/A	mrem/pCi		Nuclide-specific (default values available)	DOE STD-1196-2011 (Reference Person)	Default exposure library
Slope Factor (Risk) Library	N/A	(risk/yr) per (pCi/g)		Nuclide-specific (default values available)	DCFPAK3.02 Morbidity - DOE STD-5002-2017	Default exposure library
Transfer Factors						
Fruit, grain, nonleafy vegetables transfer factor	RTF(,1)	(pCi/kg)/ (pCi/kg)	Element-dependent (Default values available)	0 - 1E+34	PNNL 2003, Mean of Fruits, Grains, Root Vegetables Transfer Factors (C-14, H-3 Calculated)	Average value of fruit, grain, and root vegetables transfer factors from Staven et al. (PNNL), 2003; values for C-14 and H-3 calculated by RESRAD-OFFSITE using C and H modules; RESRAD-OFFSITE default values used for I-129 because there were no values available in Staven et al. 2003; see Appendix G
Leafy vegetables transfer factor	RTF(,2)	(pCi/kg)/ (pCi/kg)		0 - 1E+34	PNNL 2003, Leafy Vegetables (C-14, H-3 Calculated)	Staven et al. (PNNL), 2003 leafy vegetables transfer factors, values for C-14 and H-3 calculated by RESRAD-OFFSITE using C and H modules, RESRAD-OFFSITE default values used for I-129 because there were no values available in Staven et al. 2003; see Appendix G
Pasture and silage transfer factor	RTF(,3)	(pCi/kg)/ (pCi/kg)		0 - 1E+34	PNNL 2003, Grains (C-14, H-3 Calculated)	Staven et al. (PNNL), 2003 grains transfer factors, values for C-14 and H-3 calculated by RESRAD-OFFSITE using C and

Input Screen Title and Parameter Name	RESRAD ID	Units	Default Value	Code-Accepted Values Physical or Numerical Range	Base Case Value	Reference or Basis for Assumption
Livestock feed grain transfer factor	RTF(,4)	(pCi/kg)/ (pCi/kg)	Element-dependent (Default values available)	0 - 1E+34	PNNL 2003, Grains (C-14, H-3 Calculated)	H modules, RESRAD-OFFSITE default values used for I-129 because there were no values available in Staven et al. 2003; see Appendix G
Meat transfer factor	I_M(,1)	(pCi/kg)/ (pCi/d)		0 - 1E+34	PNNL 2003, Consumption Adjusted Transfer Factors, Red Meat, Poultry, Egg	Consumption weighted transfer factor calculated using red meat, poultry, and egg transfer factors from Staven et al. (PNNL), 2003 and average per capita intake rates from Putnam et al. (USDA) 1999, see Appendix G
Milk transfer factor	I_M(,2)	(pCi/L)/ (pCi/d)		0 - 1E+34	PNNL 2003 Milk	Staven et al. (PNNL), 2003 cows milk transfer factors, see Appendix G
Bioaccumulation factor for fish	BIOFAC(,1)	(pCi/kg)/ (pCi/L)		0 - 1E+34	PNNL 2003 Fresh Water Fish (RESRAD default for H-3)	Staven et al. (PNNL), 2003 freshwater fish transfer factors, RESRAD-OFFSITE default value for H-3 used because no value was available in Staven et al. 2003, see Appendix G
Bioaccumulation factor for crustacea and mollusks	BIOFAC(,2)	(pCi/kg)/ (pCi/L)		0 - 1E+34	RESRAD default values for all isotopes	Neither crustacea nor mollusks consumed in simulated scenario, RESRAD-OFFSITE default values used, see Appendix G
Reporting Times						
Times at which output is reported	T()	yr	1, 3, 6, 12, 30, 75, 175, 420, 970	0 - 1E+5	1, 200, 400, 500, 600, 800, 1000, 2000, 10000	User selection
Storage Times						
Storage time for surface water	STOR_T(1)	d	1	0 - 1E+34	1	Default, assumed time periods for which the various foods and water are stored before being consumed (storage times used to calculate radioactive ingrowth and decay during storage)
Storage time for well water	STOR_T(2)	d	1	0 - 1E+34	1	
Storage time for fruits, grain, and nonleafy vegetables	STOR_T(3)	d	14	0 - 1E+34	14	
Storage time for leafy vegetables	STOR_T(4)	d	1	0 - 1E+34	1	
Storage time for pasture and silage	STOR_T(5)	d	1	0 - 1E+34	1	
Storage time for livestock feed grain	STOR_T(6)	d	45	0 - 1E+34	45	
Storage time for meat	STOR_T(7)	d	20	0 - 1E+34	20	
Storage time for milk	STOR_T(8)	d	1	0 - 1E+34	1	
Storage time for fish	STOR_T(9)	d	7	0 - 1E+34	7	
Storage time for crustacea and mollusks	STOR_T(10)	d	7	0 - 1E+34	7	

Input Screen Title and Parameter Name	RESRAD ID	Units	Default Value	Code-Accepted Values Physical or Numerical Range	Base Case Value	Reference or Basis for Assumption
Physical and Hydrological						
Precipitation	PRECIP	m/yr	1	0 - 10	1.382	Calculated average precipitation for Oak Ridge, Tennessee for the 30-year period from 1961-1990, (Appendix C Section 2.3.1)
Wind speed	WIND	m/s	2	1E-4 - 20	3.4342	Site specific data from meteorological STAR file TN_KNOXVILLE.str available in atmospheric transport module
Primary Contamination						
Area of primary contamination	AREA	m^2	10,000	Calculated	95,900	Calculated by RESRAD-OFFSITE using X dimension [SOURCEXY(1)] and Y dimension [SOURCEXY(2)] of primary contamination
Length of contamination parallel to aquifer flow	LCZPAQ	m	100	1E-4 - 1E+6	398.9	Calculation of the linear distance across the rectangle representing the waste using the Y dimension of the primary contamination and the anticlockwise angle from x axis to direction of aquifer flow
Depth of soil mixing layer (m)	DM	m	0.15	0 - 1	0.15	RESRAD-OFFSITE default value, representative of typical practices
Mass loading of all particulates	MLFD	g/m^3	0.0001	0 - 2	0.0001	Default, as stated in ANL DCH Section 3.6 value is a conservative estimate compared to the US annual average ambient PM-10 air concentrations (Yu et al. 2000) and PM-2.5 air concentrations (Yu et al. 2007, EPA 2014); it takes into account short periods of high mass loading and sustained periods of normal activity on a typical farm (Healy and Rodgers 1979)
Deposition velocity of dust (m/s)	DEPVEL DUSTT	m/s	0.001	0 - 0.01	0.001	Default, represents velocities with which all particulates settle onto the primary contamination
Respirable particulates as a fraction of total particulates	RESPFRACPC	-	1	0 - 1	1	Default, conservative assumption (100%) of mass fraction of respirable particulates/total particulates in

Input Screen Title and Parameter Name	RESRAD ID	Units	Default Value	Code-Accepted Values Physical or Numerical Range	Base Case Value	Reference or Basis for Assumption
						air at the primary contamination and the offsite locations
Deposition Velocity of respirable particulates	DEPVEL_DUST	m/s	0.001	0 - 0.01	0.001	Default, represents velocities with which respirable particulates settle onto the primary contamination
Irrigation applied per year (m/yr)	RI	m/yr	0.0	0 - 10	0	No irrigation applied to primary contamination
Evapotranspiration coefficient	EVAPTR	-	0.5	0 - 0.999	0.568	Ratio between evapotranspiration (0.785 m/yr) and precipitation (1.382 m/yr) for Oak Ridge and surrounding area used in HELP modeling
Runoff coefficient	RUNOFF	-	0.2	0 - 1	0.963	Assigned to allow 0.88 in/yr infiltration (derived from HELP model calc)
Rainfall and Runoff Factor	RAINEROS	-	160	0 - 1,000	0	Cover design prevents upward distribution of contaminants to surface layer and exhumation of waste by erosion
Slope-length-steepness factor	SLPLENSTPPC	-	0.4	0 - 10	0.4	Default, accounts for the effect of the profile of the terrain on the erosion rate
Cover and management factor	CRPMANGPC	-	0.003	0 - 1	0.003	Default, accounts for the effects of land use, vegetation, and management practices when computing erosions rates for the primary contamination and offsite locations
Support practice factor	CONVPRACPC	-	1	0 - 1	0	No erosion assumed
Fraction of primary contamination that is submerged	SUBMERGEDF	-	0	0 - 1	0	Waste above groundwater table
Contaminated Zone						
Thickness of contaminated zone	THICK0	m	2	1E-5 - 1,000	17.5	Approximation of cell design to represent average thickness
Total porosity of contaminated zone	TPCZ	--	0.4	1E-5 - 1	0.419	HELP model soil characteristic (Appendix C Table C.2)
Dry bulk density of contaminated zone	DENSCZ	g/cm^3	1.5	1E-3 - 22.5	1.9	Estimated average bulk densities and proportions of waste soil, clean fill, and debris
Erosion rate of clean cover	-	m/yr	-	-	0	Erosion negligible
Soil erodibility factor of contaminated zone	ERODIBILITYCZ	tons/acre	0.4	0 - 0.5	0	Erosion negligible

Input Screen Title and Parameter Name	RESRAD ID	Units	Default Value	Code-Accepted Values Physical or Numerical Range	Base Case Value	Reference or Basis for Assumption
Field capacity of contaminated zone	FCCZ	-	0.3	1E-5 - 1	0.307	HELP model soil characteristic (Appendix C Table C.2)
Soil b parameter of contaminated zone	BCZ	-	5.3	0 - 15	7.75	HELP model soil characteristic (Appendix C Table C.2)
Longitudinal Dispersivity	ALPHALCZ	m	0.5	0 - 100	1.80	1/10 thickness of contaminated zone
Hydraulic conductivity of contaminated zone (above)	HCCZ	m/yr	10	1E-3 - 1E+10	5.99	HELP model soil characteristic (Appendix C Table C.2)
Hydraulic conductivity of contaminated zone (below)	HCSZ	m/yr	10	1E-3 - 1E+10	26.8	Equal to saturated zone hydraulic conductivity, transmissivity weighted average of MT3D layers 1 and 2
CZ effective porosity	EPCZ	-	0	1E-5 - 1	0.234	HELP model property, equal to total porosity minus residual moisture content
Depth of primary contamination below water table	SUBMERGEDDEPTH	-	0	-	0	Waste above groundwater table
Clean Cover						
Thickness of clean cover	COVER0	m	0	0 - 100	3.353	Approximation of cell design
Total porosity of clean cover	TPCV	-	0.4	1E-5 - 1	0.4	Default, not used in dose calculation of active pathways
Dry bulk density of clean cover	DENSCV	g/cm^3	1.5	1E-3 - 22.5	1.5	Site soil characteristics, mean density value for generic soil from Carsel and Parrish 1988
Erosion rate of clean cover	VCV	m/yr	-	-	0	Erosion calculated to be negligible based on RUSLE2 evaluation, see Appendix C
Soil erodibility factor of clean cover	ERODIBILITYCV	tons/acre	0.4	0 - 0.5	0	Erosion calculated to be negligible based on RUSLE2 evaluation, see Appendix C
Volumetric water content of clean cover	PH2OCV	-	0.05	0 - 1	0.05	Default, not used in dose calculation of active pathways
Agriculture Area Parameters						
Fruit, Grain, and Non-leafy Vegetables Field						
Area for fruit, grain, and non-leafy vegetables field	AREAO(1)	m2	1,000	Calculated	1024	Calculated by RESRAD-OFFSITE using X and Y dimensions of fruit, grain, and non-leafy vegetables field
Fraction of area directly over primary contamination for fruit, grain, and nonleafy vegetables field	FAREA_PLANT(1)	-	0	0 - 1	0	Agricultural area not located on primary contamination
Irrigation applied per year for fruit, grain, and nonleafy vegetables field	RIRRIG(1)	m/yr	0.2	0 - 10	0.15	USDA 2014 Census of Agriculture, Farm and Ranch Irrigation Survey (2013), Table 4. Water Resources Region 6

Input Screen Title and Parameter Name	RESRAD ID	Units	Default Value	Code-Accepted Values Physical or Numerical Range	Base Case Value	Reference or Basis for Assumption
						Tennessee (0.5 acre-ft per acre, on-farm surface water)
Evapotranspiration coefficient for fruit, grain, and nonleafy vegetables field	EVAPTRN(1)	-	0.5	0 - 0.999	0.568	Ratio between evapotranspiration (0.785 m/yr) and precipitation (1.382 m/yr) for Oak Ridge and surrounding area used in HELP modeling
Runoff coefficient for fruit, grain, and nonleafy vegetables field	RUNOF(1)	-	0.2	0 - 1	0.734	Assigned to allow 8.8 in/yr infiltration (native recharge rate, MODFLOW calibrated value) and 5.91 in/yr (0.15 m/yr) irrigation
Depth of soil mixing layer or plow layer for fruit, grain, and nonleafy vegetables field	DPTHMIXG(1)	m	0.15	0 - 1	0.15	RESRAD-OFFSITE default value, representative of typical practices
Volumetric water content for fruit, grain, and nonleafy vegetables field	TMOF(1)	-	0.3	1E-5 - 1	0.3	Default
Erosion rate for fruit, grain, and nonleafy vegetable field	EROSN(1)	m/yr	1.147E-5	Calculated	0	Calculated by RESRAD-OFFSITE using universal soil loss equation (Wischmeier and Smith 1978)
Dry bulk density of soil for fruit, grain, and nonleafy vegetables field	RHOB(1)	g/cm^3	1.5	1E-3 - 22.5	1.50	Default, mean density value for generic soil from Carsel and Parrish 1988
Soil erodibility factor for fruit, grain, and nonleafy vegetables field	ERODIBILITY(1)	tons/acre	0.4	0 - 0.5	0.4	Default, Yu et al. 2007 Appendix B Section 2.4
Slope-length- steepness factor for fruit, grain, and nonleafy vegetables field	SLPLENSTP(1)	-	0.4	0 - 10	0.4	Default, Yu et al. 2007 Appendix B Section 2.5
Cover and management factor for fruit, grain, and nonleafy vegetables field	CRPMANG(1)	-	0.003	0 - 1	0.003	Default, Yu et al. 2007 Appendix B Section 2.6
Support practice factor for fruit, grain, and nonleafy vegetables field	CONVPRAC(1)	-	1	0 - 1	1	Default, Yu et al. 2007 Appendix B Section 2.7
Total Porosity for fruit, grain, and nonleafy vegetable field	TPOF(1)	-	0.4	-	0.40	Default, not used in dose calculation of active pathways
Leafy Vegetable Field						
Area for leafy vegetable field	AREAO(2)	m^2	1,000	Calculated	1024	Calculated by RESRAD-OFFSITE using X and Y dimensions of leafy vegetables field
Fraction of area directly over primary contamination for leafy vegetable field	FAREA_PLANT(2)	-	0	0 - 1	0	Agricultural area not located on primary contamination

Input Screen Title and Parameter Name	RESRAD ID	Units	Default Value	Code-Accepted Values Physical or Numerical Range	Base Case Value	Reference or Basis for Assumption
Irrigation applied per year for leafy vegetable field	RIRRIG(2)	m/yr	0.2	0 - 10	0.15	USDA 2014 Census of Agriculture, Farm and Ranch Irrigation Survey (2013), Table 4. Water Resources Region 6 Tennessee (0.5 acre-ft per acre, on-farm surface water)
Evapotranspiration coefficient for leafy vegetable field	EVAPTRN(2)	-	0.5	0 - 0.999	0.568	Ratio between evapotranspiration (0.785 m/yr) and precipitation (1.382 m/yr) for Oak Ridge and surrounding area used in HELP modeling
Runoff coefficient for leafy vegetable field	RUNOF(2)	-	0.2	0 - 1	0.734	Assigned to allow 8.8 in/yr infiltration (native recharge rate, MODFLOW calibrated value) and 5.91 in/yr (0.15 m/yr) irrigation
Depth of soil mixing layer or plow layer for leafy vegetable field	DPTHMIXG(2)	m	0.15	0 - 1	0.15	RESRAD-OFFSITE default value, representative of typical practices
Volumetric water content for leafy vegetable field	TMOF(2)	-	0.3	1E-5 - 1	0.3	Default
Erosion rate for leafy vegetable field	EROSN(2)	m/yr	1.147E-5	Calculated	0.0	Calculated by RESRAD-OFFSITE using universal soil loss equation (Wischmeier and Smith 1978)
Dry bulk density of soil for leafy vegetable field	RHOB(2)	g/cm^3	1.5	1E-3 - 22.5	1.50	Default, mean density value for generic soil from Carsel and Parrish 1988
Soil erodibility factor for leafy vegetable field	ERODIBILITY(2)	tons/acre	0.4	0 - 0.5	0.4	Default, Yu et al. 2007 Appendix B Section 2.4
Slope-length-steepness factor for leafy vegetable field	SLPLENSTP(2)	-	0.4	0 - 10	0.4	Default, Yu et al. 2007 Appendix B Section 2.5
Cover and management factor for leafy vegetable field	CRPMANG(2)	-	0.003	0 - 1	0.003	Default, Yu et al. 2007 Appendix B Section 2.6
Support practice factor for leafy vegetable field	CONVPRAC(2)	-	1	0 - 1	1	Default, Yu et al. 2007 Appendix B Section 2.7
Total Porosity for leafy vegetable field	TPOF(2)	-	0.4	-	0.4	Default, not used in dose calculation of active pathways
Livestock Feed Growing Area Parameters Pasture						
Silage Field						
Area for pasture and silage field	AREAO(3)	m^2	10,000	Calculated	10000	Calculated by RESRAD-OFFSITE using X and Y dimensions of pasture and silage field
Fraction of area directly over primary contamination for pasture and silage field	FAREA_PLANT(3)	-	0	0 - 1	0	Agricultural area not located on primary contamination

Input Screen Title and Parameter Name	RESRAD ID	Units	Default Value	Code-Accepted Values Physical or Numerical Range	Base Case Value	Reference or Basis for Assumption
Irrigation applied per year for pasture and silage field	RIRRIG(3)	m/yr	0.2	0 - 10	0.15	USDA 2014 Census of Agriculture, Farm and Ranch Irrigation Survey (2013), Table 4. Water Resources Region 6 Tennessee (0.5 acre-ft per acre, on-farm surface water)
Evapotranspiration coefficient for pasture and silage field	EVAPTRN(3)	-	0.5	0 - 0.999	0.568	Ratio between evapotranspiration (0.785 m/yr) and precipitation (1.382 m/yr) for Oak Ridge and surrounding area used in HELP modeling
Runoff coefficient for pasture and silage field	RUNOF(3)	-	0.2	0 - 1	0.734	Assigned to allow 8.8 in/yr infiltration (native recharge rate, MODFLOW calibrated value) and 5.91 in/yr (0.15 m/yr) irrigation
Depth of soil mixing layer or plow layer for pasture and silage field	DPTHMIXG(3)	m	0.15	0 - 1	0.15	RESRAD-OFFSITE default value, representative of typical practices
Volumetric water content for pasture and silage field	TMOF(3)	-	0.3	1E-5 - 1	0.3	Default
Erosion rate for pasture and silage field	EROSN(3)	m/yr	1.147E-5	Calculated	0	Calculated by RESRAD-OFFSITE using universal soil loss equation (Wischmeier and Smith 1978)
Dry bulk density of soil for pasture and silage field	RHOB(3)	g/cm^3	1.5	1E-3 - 22.5	1.50	Default, mean density value for generic soil from Carsel and Parrish 1988
Soil erodibility factor for pasture and silage field	ERODIBILITY(3)	tons/acre	0.4	0 - 0.5	0.4	Default, Yu et al. 2007 Appendix B Section 2.4
Slope-length- steepness factor for pasture and silage field	SLPLENSTP(3)	-	0.4	0 - 10	0.4	Default, Yu et al. 2007 Appendix B Section 2.5
Cover and management factor for pasture and silage field	CRPMANG(3)	-	0.003	0 - 1	0.003	Default, Yu et al. 2007 Appendix B Section 2.6
Support practice factor for pasture and silage field	CONVPRAC(3)	-	1	0 - 1	1	Default, Yu et al. 2007 Appendix B Section 2.7
Total porosity for pasture and silage field	TPOF(3)	-	0	-	0.4	Default, not used in dose calculation of active pathways
Grain Field						
Area for grain field	AREAO(4)	m^2	10,000	Calculated	10000	Calculated by RESRAD-OFFSITE using X and Y dimensions of grain field
Fraction of area directly over primary contamination for grain field	FAREA_PLANT(4)	-	0	0 - 1	0	Agricultural area not located on primary contamination

Input Screen Title and Parameter Name	RESRAD ID	Units	Default Value	Code-Accepted Values Physical or Numerical Range	Base Case Value	Reference or Basis for Assumption
Irrigation applied per year for grain field	RIRRIG(4)	m/yr	0.2	0 - 10	0.15	USDA 2014 Census of Agriculture, Farm and Ranch Irrigation Survey (2013), Table 4. Water Resources Region 6 Tennessee (0.5 acre-ft per acre, on-farm surface water)
Evapotranspiration coefficient for grain field	EVAPTRN(4)	-	0.5	0 - 0.999	0.568	Ratio between evapotranspiration (0.785 m/yr) and precipitation (1.382 m/yr) for Oak Ridge and surrounding area used in HELP modeling
Runoff coefficient for grain field	RUNOF(4)	-	0.2	0 - 1	0.734	Assigned to allow 8.8 in/yr infiltration (native recharge rate, MODFLOW calibrated value) and 5.91 in/yr (0.15 m/yr) irrigation
Depth of soil mixing layer or plow layer for grain field	DPTHMIXG(4)	m	0.15	0 - 1	0.15	RESRAD-OFFSITE default value, representative of typical practices
Volumetric water content for grain field	TMOF(4)	-	0.3	1E-5 - 1	0.3	Default
Erosion rate	EROSN(4)	m/yr	1.147E-5	Calculated	0	Calculated by RESRAD-OFSITE using universal soil loss equation (Wischmeier and Smith 1978)
Dry bulk density of soil for grain field	RHOB(4)	g/cm^3	1.5	1E-3 - 22.5	1.50	Default, mean density value for generic soil from Carsel and Parrish 1988
Soil erodibility factor for grain field	ERODIBILITY(4)	tons/acre	0.4	0 - 0.5	0.4	Default, Yu et al. 2007 Appendix B Section 2.4
Slope-length-steepness factor for grain field	SLPLENSTP(4)	-	0.4	0 - 10	0.4	Default, Yu et al. 2007 Appendix B Section 2.5
Cover and management factor for grain field	CRPMANG(4)	-	0.003	0 - 1	0.003	Default, Yu et al. 2007 Appendix B Section 2.6
Support practice factor for grain field	CONVPRAC(4)	-	1	0 - 1	1	Default, Yu et al. 2007 Appendix B Section 2.7
Total Porosity for grain field	TPOF(4)	-	0.4	-	0.4	Default, not used in dose calculation of active pathways
Offsite Dwelling Area Parameters						
Area of offsite dwelling site	AREAODWELL	m^2	1,000	Calculated	1024	Calculated by RESRAD-OFFSITE using X and Y dimensions of dwelling
Irrigation applied per year to home garden or lawn	RIRRIGDWELL	m/yr	0.2	0 - 10	0.015	Assume 10% of agricultural irrigation rate

Input Screen Title and Parameter Name	RESRAD ID	Units	Default Value	Code-Accepted Values Physical or Numerical Range	Base Case Value	Reference or Basis for Assumption
Evapotranspiration coefficient for dwelling site	EVAPTRNDWELL	-	0.5	0 - 0.999	0.568	Ratio between evapotranspiration (0.785 m/yr) and precipitation (1.382 m/yr) for Oak Ridge and surrounding area used in HELP modeling
Runoff coefficient for dwelling site	RUNOFDWELL	-	0.2	0 - 1	0.636	Assigned to allow 8.8 in/yr infiltration (native recharge rate, MODFLOW calibrated value) and 0.591 in/yr (0.015 m/yr) irrigation
Depth of soil mixing layer for dwelling site	DPTHMIXGDWELL	m	0.15	0 - 1	0.15	RESRAD-OFFSITE default value, representative of typical practices
Volumetric water content for dwelling site	TMOFDWELL	-	0.3	1E-5 - 1	0.3	Default
Erosion rate for dwelling site	EROSNDWELL	m/yr	1.147E-5	Calculated	0	Calculated by RESRAD-OFFSITE using universal soil loss equation (Wischmeier and Smith 1978)
Dry bulk density of soil for dwelling site	RHOBDWELL	g/cm^3	1.5	1E-3 - 22.5	1.5	Default, mean density value for generic soil from Carsel and Parrish 1988
Soil erodibility factor for dwelling site	ERODIBILITYDWELL	tons/acre	0	0 - 0.5	0	Default, Yu et al. 2007 Appendix B Section 2.4
Slope-length- steepness factor for dwelling site	SLPLENSTPDWELL	-	0.4	0 - 10	0.4	Default, Yu et al. 2007 Appendix B Section 2.5
Cover and management factor for dwelling site	CRPMANGDWELL	-	0.003	0 - 1	0.003	Default, Yu et al. 2007 Appendix B Section 2.6
Support practice factor for dwelling site	CONVPRACDWELL	-	1	0 - 1	1	Default, Yu et al. 2007 Appendix B Section 2.7
Total porosity for dwelling site	TPOFDWELL	-	0.4	-	0.4	Default, not used in dose calculation of active pathways
Atmospheric Transport						
Release height	AIRRELHT	m	1	0 - 100	1	Default
Release heat flux	HEATFLX	cal/s	0	0 - 1E+10	0	Default
Anemometer height	ANH	m	10	0 - 100	10	Default
Ambient temperature	TABK	K	285	250 - 320	285	Default
AM atmospheric mixing height	AMIX	m	400	0 - 3,000	400	Default
PM atmospheric mixing height	PMIX	m	1,600	0 - 3,000	1,600	Default
Dispersion model coefficients	IDISPMOD	-	Pasquill-Gifford	Briggs rural/urban, Pasquill- Gifford	Pasquill-Gifford	Default, appropriate for releases near ground level

Input Screen Title and Parameter Name	RESRAD ID	Units	Default Value	Code-Accepted Values Physical or Numerical Range	Base Case Value	Reference or Basis for Assumption
Windspeed Terrain	IZONE	-	Rural	Rural, urban	Rural	Default, appropriate for resident farmer scenario in Eastern Tennessee
Fruit, grain, nonleafy vegetable plot	AGRIELEV(1)	m	0	0 - 100	0	Default
Leafy vegetable plot	AGRIELEV(2)	m	0	0 - 100	0	Default
Pasture, silage growing area	AGRIELEV(3)	m	0	0 - 100	0	Default
Grain fields	AGRIELEV(4)	m	0	0 - 100	0	Default
Dwelling site	DWELLELEV	m	0	0 - 100	0	Default
Surface water body	SWELEV	m	0	0 - 100	0	Default
Grid spacing for areal integration	ATGRID	m	10	0 - 500	10	Default
Joint frequency of wind speed and stability class for a 16 sector wind rose	DFREQ	-	1 (S to N)	0 o 1	1 (S to N)	Default
Wind speed	WINDSPEED	m/s	0.89, 2.46, 4.47, 6.93, 9.61, 12.52	0.001 - 20	0.89, 2.46, 4.47, 6.93, 9.61, 12.52	Default, from Parks, B.S., User's Guide for CAP88-PC, Version 1.0, EPA-402-B-92-001, U.S. EPA, Las Vegas, Nevada, 1992.
Unsaturated Zone Parameters						
Unsaturated zone thickness	H(1)	m	4	0.01 - 10,000	0.305	EMDF Design
	H(2)				0.305	EMDF Design
Unsaturated zone thickness	H(3)	m			0.9144	EMDF Design
	H(4)				3.048	EMDF Design
	H(5)				4.846	Based on average depth to groundwater for the four cells (30.9 ft, 9.418 m)
Unsaturated zone dry bulk density	DENSUZ(1)	g/cm^3	1.5	1E-3 - 22.5	1.4	HELP porosity and quartz grain density
	DENSUZ(2)				1.6	HELP porosity and quartz grain density
	DENSUZ(3)				1.5	HELP porosity and quartz grain density
	DENSUZ(4)				1.5	HELP porosity and quartz grain density
	DENSUZ(5)				1.8	WBCV Nolichucky saprolite samples, Dorsch and Katsube 1996, Figure 12, p.33
Unsaturated zone total porosity	TPUZ(1)	-	0.4	1E-5 - 1	0.463	HELP model soil characteristic (Appendix C)

Input Screen Title and Parameter Name	RESRAD ID	Units	Default Value	Code-Accepted Values Physical or Numerical Range	Base Case Value	Reference or Basis for Assumption
	TPUZ(2)				0.397	HELP model soil characteristic (Appendix C)
	TPUZ(3)				0.427	HELP model soil characteristic (Appendix C)
	TPUZ(4)				0.419	HELP model soil characteristic (Appendix C)
	TPUZ(5)				0.353	Calculated from bulk density and Nolichucky grain density (2.78 g/cc)
Unsaturated zone effective porosity	EPUZ(1)	-	0.2	1E-5 - 1	0.294	HELP model material properties, total porosity minus residual moisture content (Appendix C)
	EPUZ(2)				0.389	HELP model material properties, total porosity minus residual moisture content (Appendix C)
	EPUZ(3)				0.195	HELP model material properties, total porosity minus residual moisture content (Appendix C)
	EPUZ(4)				0.234	HELP model material properties, total porosity minus residual moisture content (Appendix C)
	EPUZ(5)				0.27	WBCV Nolichucky saprolite samples, (interval estimates, >5m depth), Dorsch and Katsube 1996, Fig 20, p.48
Unsaturated zone field capacity	FCUZ(1)	-	0.3	1E-5 - 1	0.232	HELP model soil characteristic (Appendix C)
	FCUZ(2)				0.032	HELP model soil characteristic (Appendix C)
	FCUZ(3)				0.418	HELP model soil characteristic (Appendix C)
	FCUZ(4)				0.307	HELP model soil characteristic (Appendix C)
	FCUZ(5)				0.2471	Dorsch and Katsube 1996
Unsaturated zone hydraulic conductivity	HCUZ(1)	m/yr	10	1E-3 - 1E+6	117	HELP model soil characteristic (Appendix C)
	HCUZ(2)				94600	HELP model soil characteristic (Appendix C)
	HCUZ(3)				0.315	HELP model soil characteristic (Appendix C)
	HCUZ(4)				3.15	HELP model soil characteristic (Appendix C)
	HCUZ(5)				16.7	Vertical hydraulic conductivity (Kz) for Nolichucky Saprolite
Unsaturated zone soil b parameter	BUZ(1)	-	5.3	0 - 15	5.4	Clapp and Hornberger 1978

Input Screen Title and Parameter Name	RESRAD ID	Units	Default Value	Code-Accepted Values Physical or Numerical Range	Base Case Value	Reference or Basis for Assumption
	BUZ(2)				4.05	Clapp and Hornberger 1978
	BUZ(3)				11.4	Clapp and Hornberger 1978
	BUZ(4)				11.4	Clapp and Hornberger 1978
	BUZ(5)				10.4	Clapp and Hornberger 1978
Unsaturated zone longitudinal dispersivity	ALPHALU(1)	m	0.1	0 - 100	0.1	Default
	ALPHALU(2)				0.1	Default
	ALPHALU(3)				0.1	Default
	ALPHALU(4)				0.1	Default
	ALPHALU(5)				0.1	Default
Saturated Zone Hydrological Data						
Thickness of saturated zone	DPTHAQ	m	100	0 - 1,000	60.96	Pessimistic assumption (200 ft) relative to assumed groundwater withdrawal interval (131 ft), because a higher saturated zone thickness will not increase RESRAD-OFFSITE predicted well concentrations
Dry bulk density of saturated zone	DENSAQ	g/cm^3	1.5	1E-3 - 22.5	2.1	Average of Nolichucky Shale saprolite groundmass and mudrock fragment (bedrock) bulk density values from Dorsch and Katsube 1996, Table 1 pg 20
Saturated zone total porosity	TPSZ	-	0.4	1E-5 - 1	0.24	Average of calculated values using Nolichucky Shale saprolite and bedrock grain density and bulk density data from Dorsch and Katsube 1996, Table 1 pg 20
Saturated zone effective porosity	EPSZ	-	0.2	1E-5 - 1	0.20	Average of Nolichucky Shale saprolite and bedrock effective porosities from Dorsch and Katsube 1996, Fig 20, pg 49 (limit at depth) (saprolite) and Dorsch et al. 1996, Fig 23, pg 55 (GW-134, IMS data) (bedrock)
Saturated zone hydraulic conductivity	HCSZ	m/yr	100	1E-3 - 1E+10	26.8	Horizontal equivalent hydraulic conductivity for MT3D layers 1 and 2
Saturated zone hydraulic gradient to well	HGW	-	0.02	1E-10 - 10	0.054	Adjusted upward from 0.036 (MODFLOW future condition average water table gradient) to account for lower RESRAD saturated zone dilution relative to MT3D model Tc-99 results
Saturated zone longitudinal dispersivity to well	ALPHALOW	m	3	0 - 1,000	10	1/10 Distance to well

Input Screen Title and Parameter Name	RESRAD ID	Units	Default Value	Code-Accepted Values Physical or Numerical Range	Base Case Value	Reference or Basis for Assumption
Saturated zone horizontal lateral dispersivity to well	ALPHATW	m	0.4	0 - 1,000	1	1/10 Longitudinal dispersivity to well
Saturated zone vertical lateral dispersivity to well	ALPHAVW	m	0.02	0 - 1,000	0.1	1/10 Horizontal dispersivity to well
Depth of aquifer contributing to well	DWIBWT	m	10	1E-4 - 1,000	40	Approximate thickness of layers 1, 2, and 3 from MODFLOW model
Saturated zone hydraulic gradient to surface water body	HGSW	-	0.02	1E-10 - 10	0.036	MODFLOW Model Results
Saturated zone longitudinal dispersivity to surface water body	ALPHALOSW	m	10	0 - 1,000	31.5	1/10 Distance to surface water body
Saturated zone horizontal lateral dispersivity to surface water body	ALPHATSW	m	1	0 - 1,000	3.15	1/10 Longitudinal dispersivity to surface water body
Saturated zone vertical lateral dispersivity to surface water body	ALPHAVSW	m	0.06	0 - 1,000	0.315	1/10 Horizontal dispersivity to surface water body
Depth of aquifer contributing to surface water body	DPTHAQSW	m	10	0 - 1,000	30.48	3D MODFLOW model
Water Use						
Quantity of water consumed by an individual	DWI	L/yr	510	0 - 1,000	730	2 L/day, US EPA 2000-Methodology for Deriving Ambient Water Quality Criteria for Protection of Human Health
Fraction of water from surface body for human consumption	FSWD	-	0	0 - 1	0	All drinking water from well
Fraction of water from well for human consumption	FWWD	-	1	0 - 1	1	All drinking water from well
Number of household individuals consuming and using water	NDWI	-	4	0 - 1,000	4	Default, family of 4
Quantity of water for use indoors of dwelling per individual	HHW	L/d	225	0 - 1,000	225	Consistent with Water Research Foundation 2016, pg. 8 (58.6 GPD/capita)
Fraction of water from surface body for use indoors of dwelling	FSWHH	-	0	0 - 1	0	Dwelling water from wells
Fraction of water from well for use indoors of dwelling	FWWHH	-	1	0 - 1	1	Dwelling water from wells
Beef Cattle						
Quantity of water for beef cattle	LWI(1)	L/d	50	0 - 500	50	Default, Argonne National Laboratory Data Collection Handbook (ANL DCH) 2015 Section 6.2 pg. 153-154
Fraction of water from surface body for beef cattle	FSWLV(1)	-	0	0 - 1	1	Reasonable for local hydrologic setting
Fraction of water from well for beef cattle	FWWLV(1)	-	1	0 - 1	0	Reasonable for local hydrologic setting

Input Screen Title and Parameter Name	RESRAD ID	Units	Default Value	Code-Accepted Values Physical or Numerical Range	Base Case Value	Reference or Basis for Assumption
Number of cattle for beef cattle	NLWI(1)	-	2	0 - 10	2	Sufficient for a family of 4
Dairy Cows						
Quantity of water for dairy cows	LWI(2)	L/d	160	0 - 1,000	160	Default, ANL DCH 2015 Section 6.2 pg. 153-154
Fraction of water from surface body for dairy cows	FSWLV(2)	-	0	0 - 1	1	Reasonable for local hydrologic setting
Fraction of water from well for dairy cows	FWWLV(2)	-	1	0 - 1	0	Reasonable for local hydrologic setting
Number of cows for dairy cows	NLWI(2)	-	2	0 - 10	2	Sufficient for a family of 4
Fruit, grain, non-leafy vegetables						
Irrigation rate for fruit, grain, and nonleafy vegetables	RIRRIG(1)	m/yr	0.2	0 - 10	0.15	USDA 2014 Table 4
Fraction of water from surface body for fruit, grain, and nonleafy vegetables	FSWIR(1)	-	0	0 - 1	1	Reasonable for local hydrologic setting
Fraction of water from well for fruit, grain, and nonleafy vegetables	FWWIR(1)	-	1	0 - 1	0	Reasonable for local hydrologic setting
Area of Plot for fruit, grain, and nonleafy vegetables	AREAO(1)	m^2	1,000	Calculated	1024	Calculated by RESRAD-OFFSITE using site layout
Leafy Vegetables						
Irrigation rate for leafy vegetables	RIRRIG(2)	m/yr	0.2	0 - 10	0.15	USDA 2014 Table 4
Fraction of water from surface body for leafy vegetables	FSWIR(2)	-	0	0 - 1	1	Reasonable for local hydrologic setting
Fraction of water from well for leafy vegetables	FWWIR(2)	-	1	0 - 1	0	Reasonable for local hydrologic setting
Area of Plot for leafy vegetables	AREAO(2)	m^2	1,000	Calculated	1024	Calculated by RESRAD-OFFSITE using site layout
Pasture and Silage						
Irrigation rate for pasture and silage	RIRRIG(3)	m/yr	0.2	0 - 10	0.15	USDA 2014 Table 4
Fraction of water from surface body for pasture and silage	FSWIR(3)	-	0	0 - 1	1	Reasonable for local hydrologic setting
Fraction of water from well for pasture and silage	FWWIR(3)	-	1	0 - 1	0	Reasonable for local hydrologic setting
Area of Plot for pasture and silage	AREAO(3)	m^2	10,000	Calculated	10000	Calculated by RESRAD-OFFSITE using site layout
Livestock Feed Grain						
Irrigation rate for feed grain	RIRRIG(4)	m/yr	0.2	0 - 10	0.15	USDA 2014 Table 4
Fraction of water from surface body for livestock feed grain	FSWIR(4)	-	0	0 - 1	1	Reasonable for local hydrologic setting
Fraction of water from well for livestock feed grain	FWWIR(4)	--	1	0 - 1	0	Reasonable for local hydrologic setting

Input Screen Title and Parameter Name	RESRAD ID	Units	Default Value	Code-Accepted Values Physical or Numerical Range	Base Case Value	Reference or Basis for Assumption
Area of Plot for livestock feed grain	AREAO(4)	m^2	10,000	Calculated	10000	Calculated by RESRAD-OFFSITE using site layout
Offsite Dwelling Site						
Irrigation rate for dwelling area	RIRRIGDWELL	m/yr	0.2	0 - 10	0.015	Assume 1/10 of agricultural irrigation rate
Fraction of water from surface body for offsite dwelling site	FSWIRDWELL	--	0	0 - 1	1	Reasonable for local hydrologic setting
Fraction of water from well for offsite dwelling site	FWWIRDWELL	--	1	0 - 1	0	Reasonable for local hydrologic setting
Area of Plot for offsite dwelling site	AREAODWELL	m^2		Calculated	1024	Calculated by RESRAD-OFFSITE using site layout
Well pumping rate	UW	m^3/yr	5,100	0 - 100,000	332	Based on well pumping rate needed to support specified water use
Well pumping rate needed to support specified water use	-	m^3/yr	5,084.17	Calculated	331.645	Calculated by RESRAD-OFFSITE
Surface Water Body Parameters						
Sediment delivery ratio	SDR	--	1	0 - 1	1	Erosion calculated to be negligible based on RUSLE2 evaluation, see Appendix C
Volume of surface water body	VLAKE	m^3	150,000	1 - 1E+34	250	Bear Creek channel characteristics and hydraulic geometry
Mean residence time of water in surface water body	TLAKE	yr	1	1E-4 - 1E+34	0.0001	Bear Creek flow estimates @ BCK 7.73
Surface area of water in surface water body:	ALAKE	m^2	90,000	Calculated	500	Bear Creek hydraulic geometry
Groundwater Transport Parameters						
Distance from Downgradient Edge of Contamination to:						
Well in the direction parallel to aquifer flow	OFFLPAQW	m	100	-16,000 - +16,000	100	Point of assessment at point of highest projected dose or concentration
Surface water body in the direction parallel to aquifer flow	OFFLPAQS	m	600	-16,000 - +16,000	315.468	CBCV conceptual site layout
Well in the direction perpendicular to aquifer flow	OFFLNAQW	m	0	-16,000 - +16,000	0	Assumed to be zero to ensure location of maximum concentration
Near edge of surface water body in the direction perpendicular to aquifer flow	OFFLNAQSN	m	-150	-16,000 - +16,000	-50	Bear Creek reach length assumed 100 m
Far edge of surface water body in the direction perpendicular to aquifer flow	OFFLNAQSF	m	150	-16,000 - +16,000	50	Bear Creek reach length assumed 100 m

Input Screen Title and Parameter Name	RESRAD ID	Units	Default Value	Code-Accepted Values Physical or Numerical Range	Base Case Value	Reference or Basis for Assumption
Convergence criterion (fractional accuracy desired)	EPS	-	0.001	0 - 0.1	0	Based on preliminary model results
Main sub zones in primary contamination	NPCZ	-	1	1 - 1024	5	User input
Main sub zones in submerged primary contamination	NSPCZ	-	1	1 - 1024	5	Not applicable
Main sub zones in saturated zone	NPSS	-	1	1 - 1024	5	User input
Main sub zones in each partially saturated zone	NAQS	-	1	1 - 1024	5	User input
Nuclide-specific retardation in all subzones, longitudinal dispersion in all but the subzone of transformation?	-	-	Yes	Yes/No	Yes	Default, nuclide specific retardation more dominant than longitudinal dispersion
Longitudinal dispersion in all subzones, nuclide- specific retardation in all but the subzone of transformation, parent retardation in zone of transformation?	-	-	No	Yes/No	No	Transport algorithm not chosen for analysis
Longitudinal dispersion in all subzones, nuclide- specific retardation in all but the subzone of transformation, progeny retardation in zone of transformation?	-	-	No	Yes/No	No	Transport algorithm not chosen for analysis
Anticlockwise angle from x axis to direction of aquifer flow	AQFLOWDIR	degrees	90	0 - 360	253.6	CBCV 3D groundwater model and assumed anisotropy
Ingestion Rates						
Consumption Rate						
Drinking water intake	DWI	L/yr	510	0 - 1,000	730	2 L/day, EPA 2000
Fish consumption	DFI(1)	kg/yr	5.4	0 - 1,000	2.43	Assumed recreational catch from Bear Creek (45 days per year * 54g/day recreational fish ingestion), EPA 1990, DOE 1997d
Other aquatic food consumption	DFI(2)	kg/yr	0.9	0 - 100	0	No significant Bear Creek sources
Fruit, grain, nonleafy vegetables consumption	DVI(1)	kg/yr	160	0 - 1,000	176	Assume EMWMF WAC development value (DOE 1998), (higher than EPA 2011 ~163 kg/yr based on Tables 9-1 and 12-1)
Leafy vegetables consumption	DVI(2)	kg/yr	14	0 - 100	17	EPA 2011 Table 9-6 based on 0.59 g/kg-d, for 80 kg individual
Meat consumption	DMI(1)	kg/yr	63	0 - 300	91.9	Total of red meat (55.4 kg/yr), poultry (21.3 kg/yr), eggs (15.2 kg/yr) from Putnam et al. 1999
Milk consumption	DMI(2)	L/yr	92	0 - 1,000	110	Assume EMWMF WAC development value, (higher than EPA 2011 ~90 l/yr based on Tables 11-12 and 11-18

Input Screen Title and Parameter Name	RESRAD ID	Units	Default Value	Code-Accepted Values Physical or Numerical Range	Base Case Value	Reference or Basis for Assumption
Soil (incidental) ingestion rate	SOIL	g/yr	36.5	0 - 10,000	36.53	100 mg/day per EPA 2011 (EFH)
Drinking water intake from affected area	-	-	1	0 - 1	1	All drinking water from well
Fish consumption from affected area	FFISH(1)	-	0.5	0 - 1	1	Local recreational catch assumed
Other aquatic food consumption from affected area	FFISH(2)	-	0.5	0 - 1	0.5	NA, zero consumption
Fruit, grain, nonleafy vegetables consumption from affected area	FVEG(1)	-	0.5	0 - 1	0.5	The Oak Ridge area is assumed to remain populated and urbanized in the future, with many commercial food sources (e.g. restaurants, grocery stores, farmer's markets) available near the Bear Creek Valley farm adjacent to EMDF
Leafy vegetables consumption from affected area	FVEG(2)	-	0.5	0 - 1	0.5	
Meat consumption from affected area	FMEMI(1)	-	1	0 - 1	0.25	
Milk consumption from affected area	FMEMI(2)	-	1	0 - 1	0.5	
Livestock Intakes						
Beef Cattle						
Water intake for beef cattle	LWI(1)	L/d	50	0 - 500	50	Default, ANL DCH 2015 Section 6.2 pg. 153-154
Pasture and silage intake for beef cattle	LFI(1,1)	kg/d	14	0 - 300	14	Default
Grain intake for beef cattle	LFI(1,2)	kg/d	54	0 - 300	54	Default
Soil from pasture and silage intake for beef cattle	LSI(1,1)	kg/d	0.1	0 - 10	0.1	Default
Soil from grain intake for beef cattle	LSI(1,2)	kg/d	0.4	0 - 10	0.4	Default
Dairy Cows						
Water intake for dairy cows	LWI(2)	L/d	160	0 - 500	160	Default, ANL DCH 2015 Section 6.2 pg. 153-154
Pasture and silage intake for dairy cows	LFI(2,1)	kg/d	44	0 - 300	44	Default
Grain intake for dairy cows	LFI(2,2)	kg/d	11	0 - 300	11	Default
Soil from pasture and silage intake for dairy cows	LSI(2,1)	kg/d	0.4	0 - 10	0.4	Default
Soil from grain intake for dairy cows	LSI(2,2)	kg/d	0.1	0 - 10	0.1	Default
Livestock Feed Factors						
Pasture and Silage						
Wet weight crop yield of pasture and silage	YIELD(3)	kg/m^2	1.1	0.01 - 3	1.1	Default, USDA 1997, Crop Production Annual Survey; Beyeler et al. 1998b, Review of Parameter DATA for the NUREG/CR-5512 Residential Farmer Scenario and Probability

Input Screen Title and Parameter Name	RESRAD ID	Units	Default Value	Code-Accepted Values Physical or Numerical Range	Base Case Value	Reference or Basis for Assumption
						Distributions for the DandD Parameter Analysis
Duration of growing season of pasture and silage	GROWTIME(3)	yr	0.08	0.01 - 1	0.08	Default, USDA 1997, Beyeler et al. 1998b
Foliage to food transfer coefficient of pasture and silage	FOLI F(3)	-	1	0 - 1	1	Default
Weathering removal constant of pasture and silage	RWEATHER(3)	1/yr	20	1 - 40	20	Default, Snyder et al. 1994
Foliar interception factor for irrigation of pasture and silage	FINTCEPT(3,2)	-	0.25	0 - 1	0.25	Default, IAEA 1994 Handbook of Parameter Values for the Prediction of Radionuclide Transfer in Temperate Environments
Foliar interception factor for dust of pasture and silage	FINTCEPT(3,1)	-	0.25	0 - 1	0.25	Default, IAEA 1994
Root depth of pasture and silage	DROOT(3)	m	0.9	0 - 3	0.90	Default, ANL DCH 2015 Section 6.1 pg 150
Grain						
Wet weight crop yield of grain	YIELD(4)	kg/m^2	0.7	0.01 - 3	0.70	Default, USDA 1997, Beyeler et al. 1998b
Duration of growing season of grain	GROWTIME(4)	yr	0.17	0.01 - 1	0.17	Default, USDA 1997, Beyeler et al. 1998b
Foliage to food transfer coefficient of grain	FOLI F(4)	-	0.1	0 - 1	0.1	Default
Weathering removal constant of grain	RWEATHER(4)	1/yr	20	1-40	20	Default, Snyder et al. 1994
Foliar interception factor for irrigation of grain	FINTCEPT(4,2)	--	0.25	0 - 1	0.25	Default, IAEA 1994
Foliar interception factor for dust of grain	FINTCEPT(4,1)	--	0.25	0 - 1	0.25	Default, IAEA 1994
Root depth of grain	DROOT(4)	m	1.2	0 - 10	1.20	ANL DCH Section 6.1 pg 150
Plant Factors						
Wet weight crop yield of fruit, grain, and nonleafy vegetables	YIELD(1)	kg/m^2	0.7	0.01 - 3	0.70	Default, USDA 1997, Beyeler et al. 1998b
Duration of growing season of fruit, grain, and nonleafy vegetables	GROWTIME(1)	yr	0.17	0.01 - 1	0.17	Default, USDA 1997, Beyeler et al. 1998b
Foliage to food transfer coefficient of fruit, grain, and nonleafy vegetables	FOLI_F(1)	-	0.1	0 - 1	0.1	Default
Weathering removal constant of fruit, grain, and nonleafy vegetables	RWEATHER(1)	1/yr	20	1 - 40	20	Default, Snyder et al. 1994
Foliar interception factor for irrigation of fruit, grain, and nonleafy vegetables	FINTCEPT(1,2)	-	0.25	1 - 40	0.25	Default, IAEA 1994
Foliar interception factor for dust of fruit, grain, and nonleafy vegetables	FINTCEPT(1,1)	-	0.25	0 - 1	0.25	Default, IAEA 1994

Input Screen Title and Parameter Name	RESRAD ID	Units	Default Value	Code-Accepted Values Physical or Numerical Range	Base Case Value	Reference or Basis for Assumption
Root depth of fruit, grain, and nonleafy vegetables	DROOT(1)	m	1.2	0 - 10	1.20	Default, ANL DCH 2015 Section 6.1 pg 150
Leafy Vegetables						
Wet weight crop yield of leafy vegetables	YIELD(2)	kg/m^2	1.5	0.01 - 3	1.50	Default, USDA 1997, Beyeler et al. 1998b
Duration of growing season of leafy vegetables	GROWTIME(2)	yr	0.25	0.01 - 1	0.25	Default, USDA 1997, Beyeler et al. 1998b
Foliage to food transfer coefficient of leafy vegetables	FOLI_F(2)	-	1	0 - 1	1	Default
Weathering removal constant of leafy vegetables	RWEATHER(2)	1/yr	20	1-40	20	Default, Snyder et al. 1994
Foliar interception factor for irrigation of leafy vegetables	FINTCEPT(2,2)	--	0.25	0 - 1	0.25	Default, IAEA 1994
Foliar interception factor for dust of leafy vegetables	FINTCEPT(2,1)	--	0.25	0 - 1	0.25	Default, IAEA 1994
Root depth of leafy vegetables	DROOT(2)	m	0.9	0 - 3	0.90	Default, ANL DCH 2015 Section 6.1 pg 150
Inhalation and External Gamma Data						
Inhalation rate	INHALR	m^3/yr	8,400	0 - 20,000	8,400	Default, resident farmer scenario default value based on EPA 1997 Exposure Factor Handbook and Sprung et al. 1990 Evaluation of Sever Accident Risks: Quantification of Major Input Parameters, MACCS Input NUREG/CR-4551
Mass loading for inhalation	MLFD	g/m^3	0.0001	0 - 2	0.0001	Default, as stated in ANL DCH Section 3.6 value is a conservative estimate compared to the US annual average ambient PM-10 air concentrations (Yu et al. 2000) and PM-2.5 air concentrations (Yu et al. 2007, EPA 2014); it takes into account short periods of high mass loading an sustained period of normal activity on a typical farm (Healy and Rodgers 1979)
Respirable particulates as a fraction of total particulates	RESPFRACPC	-	1	-	1	Default, all particulates assumed respirable
Use same values as for primary contamination mass loading and respirable fraction at offsite locations	-	-	-	Y or N	Y	Same loading for onsite and offsite
Input different values for primary contamination mass loading and respirable fraction at offsite locations	-	-	-	Y or N	N	Same loading for onsite and offsite

Input Screen Title and Parameter Name	RESRAD ID	Units	Default Value	Code-Accepted Values Physical or Numerical Range	Base Case Value	Reference or Basis for Assumption
Indoor dust filtration factor (indoor to outdoor dust concentration)	SHF3	-	0.4	0 - 1	0.4	Default
External gamma shielding (penetration) factor	SHF1	-	0.7	0 - 1	0.7	Default
External Radiation Shape and Area Factors						
Dwelling location	-	-	Offsite	Onsite or offsite	Offsite	Dwelling is located offsite
Scale	-	m	200	>0 - 32,000	598.375	User input
Dwelling location coordinate in X-direction	-	m	100	-16,000 - +16,000	210	Site layout, calculated by RESRAD-OFFSITE
Dwelling location coordinate in y-direction	-	m	0	-16,000 - +16,000	547	Site layout, calculated by RESRAD-OFFSITE
Radius	RAD_SHAPE(1)	m	13.25	Calculated	43.5833	Calculated by RESRAD-OFFSITE
	RAD_SHAPE(2)		26.5		87.1667	Calculated by RESRAD-OFFSITE
	RAD_SHAPE(3)		39.75		130.7500	Calculated by RESRAD-OFFSITE
	RAD_SHAPE(4)		53		174.3333	Calculated by RESRAD-OFFSITE
	RAD_SHAPE(5)		66.25		217.9167	Calculated by RESRAD-OFFSITE
	RAD_SHAPE(6)		79.5		261.5000	Calculated by RESRAD-OFFSITE
	RAD_SHAPE(7)		92.75		305.0833	Calculated by RESRAD-OFFSITE
	RAD_SHAPE(8)		106		348.6667	Calculated by RESRAD-OFFSITE
	RAD_SHAPE(9)		119.25		392.2500	Calculated by RESRAD-OFFSITE
	RAD_SHAPE(10)		132.5		435.8333	Calculated by RESRAD-OFFSITE
	RAD_SHAPE(11)		145.75		479.4167	Calculated by RESRAD-OFFSITE
	RAD_SHAPE(12)		159		523.0000	Calculated by RESRAD-OFFSITE
Fraction (Onsite)	FRACA(1)	-	0	Calculated	0	Calculated by RESRAD-OFFSITE
	FRACA(2)		0		0	Calculated by RESRAD-OFFSITE
	FRACA(3)		0		0.04	Calculated by RESRAD-OFFSITE

Input Screen Title and Parameter Name	RESRAD ID	Units	Default Value	Code-Accepted Values Physical or Numerical Range	Base Case Value	Reference or Basis for Assumption
	FRACA(4)		0.024		0.21	Calculated by RESRAD-OFFSITE
	FRACA(5)		0.19		0.22	Calculated by RESRAD-OFFSITE
	FRACA(6)		0.24		0.18	Calculated by RESRAD-OFFSITE
	FRACA(7)		0.2		0.15	Calculated by RESRAD-OFFSITE
	FRACA(8)		0.17		0.12	Calculated by RESRAD-OFFSITE
Fraction (Onsite)	FRACA(9)		0.15	Calculated	0.11	Calculated by RESRAD-OFFSITE
	FRACA(10)		0.13		0.097	Calculated by RESRAD-OFFSITE
	FRACA(11)		0.12		0.088	Calculated by RESRAD-OFFSITE
	FRACA(12)		0.052		0.049	Calculated by RESRAD-OFFSITE
Shape of the primary contamination	-	-	Polygonal	Circular or polygonal	Polygonal	Approximation of cell design
X coordinate of the vertices of polygon of the primary contamination	-	m	none	-16,000 - +16,000	none	Vertices calculated based on X dimension of primary contamination
Y coordinate of the vertices of polygon of the primary contamination	-	m	none	-16,000 - +16,000	none	Vertices calculated based on Y dimension of primary contamination
Occupancy Factors						
Indoor time fraction on primary contamination	FIND	-	0	0 - 1	0	Offsite residence assumed
Outdoor time fraction on primary contamination	FOTD	-	0	0 - 1	0.05	Half of non-agricultural outdoor time
Indoor time fraction on offsite dwelling site	FINDDWELL	-	0.5	0 - 1	0.5	Assume 50% of time spent out of doors maintaining farmstead
Outdoor time fraction on offsite dwelling site	FOTDDWELL	-	0.1	0 - 1	0.05	Half of non-agricultural outdoor time
Time fraction in fruit, grain, and nonleafy vegetable fields	OCCUPANCY(1)	-	0.1	0 - 1	0.1	40% assumed for all agricultural areas combined
Time fraction in leafy vegetable fields	OCCUPANCY(2)	-	0.1	0 - 1	0.1	40% assumed for all agricultural areas combined
Time fraction in pasture and silage fields	OCCUPANCY(3)	-	0.1	0 - 1	0.1	40% assumed for all agricultural areas combined
Time fraction in livestock grain fields	OCCUPANCY(4)	-	0.1	0 - 1	0.1	40% assumed for all agricultural areas combined
Radon						

Input Screen Title and Parameter Name	RESRAD ID	Units	Default Value	Code-Accepted Values Physical or Numerical Range	Base Case Value	Reference or Basis for Assumption
Effective radon diffusion coefficient of Cover	DIFCV	m2/s	2.00E-06	-1 – 1	2.00E-06	Default, conservative value compared to US NRC (1980) value
Effective radon diffusion coefficient of Contaminated Zone	DIFCZ	m2/s	2.00E-06	-1 – 1	2.00E-06	Default, conservative value compared to US NRC (1980) value
Effective radon diffusion coefficient of Floor	DIFFL	m2/s	3.00E-07	-1 – 1	3.00E-07	Default, conservative value compared to US NRC (1980) value
Thickness of floor and foundation	FLOOR1	m2/s	0.15	0 – 10	0.15	Default
Density of floor and foundation	DENSFL	g/cm3	2.40	0 – 22.5	2.40	Default
Total porosity of floor and foundation	TPFL	-	0.10	0.0001 – 1	0.10	Default
Volumetric water content of floor and foundation	PH2OFL	-	0.03	0 – 1	0.03	Default
Depth of foundation below ground level	DMFL	m	-1	-100 – 100	-1	Default
Vertical dimension of mixing	HMIX	m	2	0.0001 – 1000	2	Default mixing height for human inhalation pathway
Building room height	HRM	m	2.5	.0001 – 100	2.50	Default, average height of rooms in building
Building air exchange rate	REXG	/hr	0.5	0 – 1000	0.50	Default
Building indoor area factor	FAI	-	0	0 – 100	0	Default
Rn-222 emanation coefficient	EMANA(1)	-	0.25	.01 – 1	0.25	Default, radon pathway not simulated
Rn-220 emanation coefficient	EMANA(2)	-	0.15	.01 – 1	0.15	Default, radon pathway not simulated
Effective radon diffusion coefficient of nonleafy veg field	DIFOS(1)	m2/s	2.00E-06	0 – 1	2.00E-06	Default, conservative value compared to US NRC (1980) value
Effective radon diffusion coefficient of leafy vegetable	DIFOS(2)	m2/s	2.00E-06	0 – 1	2.00E-06	Default, conservative value compared to US NRC (1980) value
Effective radon diffusion coefficient of pasture	DIFOS(3)	m2/s	2.00E-06	0 – 1	2.00E-06	Default, conservative value compared to US NRC (1980) value
Effective radon diffusion coefficient of livestock grain	DIFOS(4)	m2/s	2.00E-06	0 – 1	2.00E-06	Default, conservative value compared to US NRC (1980) value
Effective radon diffusion coefficient of offsite dwelling site	DIFOS(5)	m2/s	2.00E-06	0 – 1	2.00E-06	Default, conservative value compared to US NRC (1980) value
Carbon-14						
Thickness of evasion layer for C-14 in soil	DMC	m	0.3	0 – 10	0.3	Default, reference evasion depth
Vertical dimension of mixing for inhalation	HMIX	m	2.0	0.0001 – 1000	2.0	Default mixing height for human inhalation pathway

Input Screen Title and Parameter Name	RESRAD ID	Units	Default Value	Code-Accepted Values Physical or Numerical Range	Base Case Value	Reference or Basis for Assumption
Vertical dimension of mixing for vegetation	HMIXV	m	1.0	0.0001 – 1000	1.0	Default, mixing height for plant, meat, and milk ingestion pathways
C-14 evasion flux rate from soil	C14EVSN	/sec	7.00E-07	0 – 1	7.00E-07	Default, maximum C evasion rate for sand and organic soils (Sheppard et al. 1991)
C-12 evasion flux rate from soil	C12EVSN	/sec	1.00E-10	0 – 1	1.00E-10	Default, minimum C evasion rate for native carbonates and humified soils (Amiro et al. 1991)
Fraction of vegetation carbon absorbed from soil	CSOIL	-	0.02	0.0001 – 1	0.02	Default (Sheppard et al. 1991)
Fraction of vegetation carbon absorbed from air	CAIR	-	0.98	0 – 1	0.98	Default, remainder of C not absorbed by plants
Mass Fractions of Carbon-12						
Atmosphere	C12AIR	g/m3	0.18	0.1 – 0.3	0.18	Default, equilibrium concentration in air
Contaminated soil	C12CZ	g/g	0.03	0.0001 – 1	0.03	Default
Local water	C12WTR	g/cm3	2.00E-05	0 – 100	2.00E-05	Default
Fruit, grain, non-leafy vegetables	C12PLANT(1)	-	0.40	0 – 1	0.40	Default
Leafy vegetables	C12PLANT(2)	-	0.09	0 – 1	0.09	Default
Pasture and Silage	C12PLANT(3)	-	0.09	0 – 1	0.09	Default
Livestock feed grain	C12PLANT(4)	-	0.40	0 – 1	0.40	Default
Meat	C12MEAT_MILK(1)	-	0.24	0 – 1	0.24	Default
Milk	C12MEAT_MILK(2)	-	0.07	0 – 1	0.07	Default
Tritium						
Humidity in air	HUMID	g/m3	8	0 – 1000	8	Default
Mass fraction of water in fruit, grain, non-leafy vegetables	H2OPLANT(1)	-	0.8	0 – 1	0.8	Default
Mass fraction of water in leafy vegetables	H2OPLANT(2)	-	0.8	0 – 1	0.8	Default
Mass fraction of water in pasture and silage	H2OPLANT(3)	-	0.8	0 – 1	0.8	Default
Mass fraction of water in livestock feed grain	H2OPLANT(4)	-	0.8	0 – 1	0.8	Default
Mass fraction of water in meat	H2OMEAT_MILK(1)	-	0.6	0 – 1	0.6	Default
Mass fraction of water in milk	H2OMEAT_MILK(2)	-	0.88	0 – 1	0.88	Default
Vertical dimension of mixing for inhalation	HMIX	m	2	0.0001 – 1000	2	Default, mixing height for human inhalation pathway

ATTACHMENT G.2.
RESRAD-OFFSITE INPUT/OUTPUT SUMMARY FILE
FOR THE BASE CASE SCENARIO

This page intentionally left blank.

Parent Dose Report
Title : Site 7 Base Case Model
File : BC_V01.ROF

Table of Contents

Part I: Mixture Sums and Single Radionuclide Guidelines

Dose Conversion Factor (and Related) Parameter Summary
Current Library: DCFPAK3.02
Default Library: DCFPAK3.02

Menu	Parameter	Current Value	Default	Parameter Name
DCSF	DCF's for external ground radiation, (mrem/yr)/(pCi/g)			
DCSF	Ac-225 (Source: DCFPAK3.02)	5.286E-02	5.286E-02	DCFEXT(1)
DCSF	Ac-227 (Source: DCFPAK3.02)	2.615E-04	2.615E-04	DCFEXT(2)
DCSF	Ac-228 (Source: DCFPAK3.02)	5.044E+00	5.044E+00	DCFEXT(3)
DCSF	Am-241 (Source: DCFPAK3.02)	3.717E-02	3.717E-02	DCFEXT(4)
DCSF	Am-243 (Source: DCFPAK3.02)	1.285E-01	1.285E-01	DCFEXT(5)
DCSF	At-217 (Source: DCFPAK3.02)	1.186E-03	1.186E-03	DCFEXT(6)
DCSF	At-218 (Source: DCFPAK3.02)	5.567E-05	5.567E-05	DCFEXT(7)
DCSF	At-219 (Source: DCFPAK3.02)	0.000E+00	0.000E+00	DCFEXT(8)
DCSF	Be-10 (Source: DCFPAK3.02)	1.014E-03	1.014E-03	DCFEXT(9)
DCSF	Bi-210 (Source: DCFPAK3.02)	5.473E-03	5.473E-03	DCFEXT(10)
DCSF	Bi-211 (Source: DCFPAK3.02)	2.410E-01	2.410E-01	DCFEXT(11)
DCSF	Bi-212 (Source: DCFPAK3.02)	6.258E-01	6.258E-01	DCFEXT(12)
DCSF	Bi-213 (Source: DCFPAK3.02)	6.874E-01	6.874E-01	DCFEXT(13)
DCSF	Bi-214 (Source: DCFPAK3.02)	9.135E+00	9.135E+00	DCFEXT(14)
DCSF	Bi-215 (Source: DCFPAK3.02)	1.369E+00	1.369E+00	DCFEXT(15)
DCSF	C-14 (Source: DCFPAK3.02)	1.106E-05	1.106E-05	DCFEXT(16)
DCSF	Ca-41 (Source: DCFPAK3.02)	0.000E+00	0.000E+00	DCFEXT(17)
DCSF	Cm-243 (Source: DCFPAK3.02)	5.361E-01	5.361E-01	DCFEXT(18)
DCSF	Cm-244 (Source: DCFPAK3.02)	1.999E-04	1.999E-04	DCFEXT(19)
DCSF	Cm-245 (Source: DCFPAK3.02)	3.531E-01	3.531E-01	DCFEXT(20)
DCSF	Cm-246 (Source: DCFPAK3.02)	2.260E-02	2.260E-02	DCFEXT(21)
DCSF	Cm-247 (Source: DCFPAK3.02)	1.651E+00	1.651E+00	DCFEXT(22)
DCSF	Cm-248 (Source: DCFPAK3.02)	8.163E+00	8.163E+00	DCFEXT(23)
DCSF	Fr-221 (Source: DCFPAK3.02)	1.332E-01	1.332E-01	DCFEXT(24)
DCSF	Fr-223 (Source: DCFPAK3.02)	1.758E-01	1.758E-01	DCFEXT(25)
DCSF	H-3 (Source: DCFPAK3.02)	0.000E+00	0.000E+00	DCFEXT(26)
DCSF	Hg-206 (Source: DCFPAK3.02)	6.127E-01	6.127E-01	DCFEXT(27)
DCSF	I-129 (Source: DCFPAK3.02)	9.695E-03	9.695E-03	DCFEXT(28)
DCSF	K-40 (Source: DCFPAK3.02)	9.975E-01	9.975E-01	DCFEXT(29)
DCSF	Mo-93 (Source: DCFPAK3.02)	4.091E-04	4.091E-04	DCFEXT(30)
DCSF	Nb-93m (Source: DCFPAK3.02)	7.304E-05	7.304E-05	DCFEXT(31)
DCSF	Nb-94 (Source: DCFPAK3.02)	9.022E+00	9.022E+00	DCFEXT(32)
DCSF	Ni-59 (Source: DCFPAK3.02)	8.537E-05	8.537E-05	DCFEXT(33)
DCSF	Np-237 (Source: DCFPAK3.02)	6.706E-02	6.706E-02	DCFEXT(34)
DCSF	Np-239 (Source: DCFPAK3.02)	7.248E-01	7.248E-01	DCFEXT(35)
DCSF	Np-240 (Source: DCFPAK3.02)	5.847E+00	5.847E+00	DCFEXT(36)
DCSF	Np-240m (Source: DCFPAK3.02)	1.834E+00	1.834E+00	DCFEXT(37)
DCSF	Pa-231 (Source: DCFPAK3.02)	1.608E-01	1.608E-01	DCFEXT(38)
DCSF	Pa-233 (Source: DCFPAK3.02)	1.018E+00	1.018E+00	DCFEXT(39)
DCSF	Pa-234 (Source: DCFPAK3.02)	8.275E+00	8.275E+00	DCFEXT(40)
DCSF	Pa-234m (Source: DCFPAK3.02)	1.257E-01	1.257E-01	DCFEXT(41)
DCSF	Pb-209 (Source: DCFPAK3.02)	7.528E-04	7.528E-04	DCFEXT(42)
DCSF	Pb-210 (Source: DCFPAK3.02)	2.092E-03	2.092E-03	DCFEXT(43)
DCSF	Pb-211 (Source: DCFPAK3.02)	3.680E-01	3.680E-01	DCFEXT(44)

Dose Conversion Factor (and Related) Parameter Summary (continued)
Current Library: DCFPAK3.02
Default Library: DCFPAK3.02

Menu	Parameter	Current Value	Default	Parameter Name
DCSF	Pb-212 (Source: DCFPAK3.02)	6.314E-01	6.314E-01	DCFEXT(45)
DCSF	Pb-214 (Source: DCFPAK3.02)	1.257E+00	1.257E+00	DCFEXT(46)
DCSF	Po-210 (Source: DCFPAK3.02)	5.641E-05	5.641E-05	DCFEXT(47)
DCSF	Po-211 (Source: DCFPAK3.02)	4.707E-02	4.707E-02	DCFEXT(48)
DCSF	Po-212 (Source: DCFPAK3.02)	0.000E+00	0.000E+00	DCFEXT(49)
DCSF	Po-213 (Source: DCFPAK3.02)	2.167E-04	2.167E-04	DCFEXT(50)
DCSF	Po-214 (Source: DCFPAK3.02)	4.801E-04	4.801E-04	DCFEXT(51)
DCSF	Po-215 (Source: DCFPAK3.02)	9.452E-04	9.452E-04	DCFEXT(52)
DCSF	Po-216 (Source: DCFPAK3.02)	8.873E-05	8.873E-05	DCFEXT(53)
DCSF	Po-218 (Source: DCFPAK3.02)	9.228E-09	9.228E-09	DCFEXT(54)
DCSF	Pu-238 (Source: DCFPAK3.02)	1.111E-04	1.111E-04	DCFEXT(55)
DCSF	Pu-239 (Source: DCFPAK3.02)	2.765E-04	2.765E-04	DCFEXT(56)
DCSF	Pu-240 (Source: DCFPAK3.02)	1.130E-04	1.130E-04	DCFEXT(57)
DCSF	Pu-241 (Source: DCFPAK3.02)	5.230E-06	5.230E-06	DCFEXT(58)
DCSF	Pu-242 (Source: DCFPAK3.02)	5.641E-04	5.641E-04	DCFEXT(59)
DCSF	Pu-243 (Source: DCFPAK3.02)	7.154E-02	7.154E-02	DCFEXT(60)
DCSF	Pu-244 (Source: DCFPAK3.02)	1.231E-01	1.231E-01	DCFEXT(61)
DCSF	Ra-223 (Source: DCFPAK3.02)	5.791E-01	5.791E-01	DCFEXT(62)
DCSF	Ra-224 (Source: DCFPAK3.02)	4.950E-02	4.950E-02	DCFEXT(63)
DCSF	Ra-225 (Source: DCFPAK3.02)	8.910E-03	8.910E-03	DCFEXT(64)
DCSF	Ra-226 (Source: DCFPAK3.02)	3.176E-02	3.176E-02	DCFEXT(65)
DCSF	Ra-228 (Source: DCFPAK3.02)	6.575E-05	6.575E-05	DCFEXT(66)
DCSF	Rn-218 (Source: DCFPAK3.02)	4.259E-03	4.259E-03	DCFEXT(67)
DCSF	Rn-219 (Source: DCFPAK3.02)	2.970E-01	2.970E-01	DCFEXT(68)
DCSF	Rn-220 (Source: DCFPAK3.02)	3.474E-03	3.474E-03	DCFEXT(69)
DCSF	Rn-222 (Source: DCFPAK3.02)	2.130E-03	2.130E-03	DCFEXT(70)
DCSF	Sr-90 (Source: DCFPAK3.02)	6.463E-04	6.463E-04	DCFEXT(71)
DCSF	Tc-99 (Source: DCFPAK3.02)	1.104E-04	1.104E-04	DCFEXT(72)
DCSF	Th-227 (Source: DCFPAK3.02)	5.641E-01	5.641E-01	DCFEXT(73)
DCSF	Th-228 (Source: DCFPAK3.02)	7.248E-03	7.248E-03	DCFEXT(74)
DCSF	Th-229 (Source: DCFPAK3.02)	2.877E-01	2.877E-01	DCFEXT(75)
DCSF	Th-230 (Source: DCFPAK3.02)	1.106E-03	1.106E-03	DCFEXT(76)
DCSF	Th-231 (Source: DCFPAK3.02)	3.250E-02	3.250E-02	DCFEXT(77)
DCSF	Th-232 (Source: DCFPAK3.02)	4.782E-04	4.782E-04	DCFEXT(78)
DCSF	Th-234 (Source: DCFPAK3.02)	2.316E-02	2.316E-02	DCFEXT(79)
DCSF	Tl-206 (Source: DCFPAK3.02)	1.278E-02	1.278E-02	DCFEXT(80)
DCSF	Tl-207 (Source: DCFPAK3.02)	2.391E-02	2.391E-02	DCFEXT(81)
DCSF	Tl-208 (Source: DCFPAK3.02)	2.167E+01	2.167E+01	DCFEXT(82)
DCSF	Tl-209 (Source: DCFPAK3.02)	1.287E+01	1.287E+01	DCFEXT(83)
DCSF	Tl-210 (Source: DCFPAK3.02)	1.677E+01	1.677E+01	DCFEXT(84)
DCSF	U-232 (Source: DCFPAK3.02)	7.229E-04	7.229E-04	DCFEXT(85)
DCSF	U-233 (Source: DCFPAK3.02)	9.191E-04	9.191E-04	DCFEXT(86)
DCSF	U-234 (Source: DCFPAK3.02)	3.456E-04	3.456E-04	DCFEXT(87)
DCSF	U-235 (Source: DCFPAK3.02)	7.005E-01	7.005E-01	DCFEXT(88)
DCSF	U-235m (Source: DCFPAK3.02)	0.000E+00	0.000E+00	DCFEXT(89)

Dose Conversion Factor (and Related) Parameter Summary (continued)
Current Library: DCFPAK3.02
Default Library: DCFPAK3.02

Menu	Parameter	Current Value	Default	Parameter Name
DCSF	U-236 (Source: DCFPAK3.02)	1.758E-04	1.758E-04	DCFEXT(90)
DCSF	U-237 (Source: DCFPAK3.02)	4.782E-01	4.782E-01	DCFEXT(91)
DCSF	U-238 (Source: DCFPAK3.02)	1.713E-04	1.713E-04	DCFEXT(92)
DCSF	U-240 (Source: DCFPAK3.02)	1.494E-02	1.494E-02	DCFEXT(93)
DCSF	Y-90 (Source: DCFPAK3.02)	4.016E-02	4.016E-02	DCFEXT(94)

Current Library: DOE STD-1196-2011 (Reference Person)
Default Library: DOE STD-1196-2011 (Reference Person)

Menu	Parameter	Current Value	Default	Parameter Name
DCSF	Dose conversion factors for inhalation, mrem/pCi:			
DCSF	Ac-227+D	6.714E-01	6.714E-01	DCF2(1)
DCSF	Am-241	3.630E-01	3.630E-01	DCF2(2)
DCSF	Am-243+D	3.608E-01	3.608E-01	DCF2(3)
DCSF	Be-10	1.354E-04	1.354E-04	DCF2(4)
DCSF	C-14 particulate	2.276E-05	2.276E-05	DCF2(5)
DCSF	C-14 gaseous	2.479E-08	2.479E-08	C14GInhDCF
DCSF	Ca-41	8.510E-07	8.510E-07	DCF2(6)
DCSF	Cm-243	2.649E-01	2.649E-01	DCF2(7)
DCSF	Cm-244	2.179E-01	2.179E-01	DCF2(9)
DCSF	Cm-245	3.700E-01	3.700E-01	DCF2(12)
DCSF	Cm-246	3.696E-01	3.696E-01	DCF2(15)
DCSF	Cm-247+D	3.389E-01	3.389E-01	DCF2(19)
DCSF	Cm-248	1.362E+00	1.362E+00	DCF2(20)
DCSF	H-3	1.069E-06	1.069E-06	DCF2(24)
DCSF	I-129	3.996E-04	3.996E-04	DCF2(25)
DCSF	K-40	3.282E-04	3.282E-04	DCF2(26)
DCSF	Mo-93	8.732E-06	8.732E-06	DCF2(27)
DCSF	Nb-93m	7.733E-06	7.733E-06	DCF2(29)
DCSF	Nb-94	1.891E-04	1.891E-04	DCF2(30)
DCSF	Ni-59	3.378E-06	3.378E-06	DCF2(31)
DCSF	Np-237+D	1.869E-01	1.869E-01	DCF2(32)
DCSF	Pa-231	8.769E-01	8.769E-01	DCF2(33)
DCSF	Pb-210+D	4.017E-02	4.017E-02	DCF2(34)
DCSF	Pu-238	4.070E-01	4.070E-01	DCF2(35)
DCSF	Pu-239+D	4.477E-01	4.477E-01	DCF2(37)
DCSF	Pu-240	4.477E-01	4.477E-01	DCF2(38)
DCSF	Pu-241	8.510E-03	8.510E-03	DCF2(40)
DCSF	Pu-241+D	8.518E-03	8.518E-03	DCF2(41)
DCSF	Pu-242	4.255E-01	4.255E-01	DCF2(42)
DCSF	Pu-244	4.181E-01	4.181E-01	DCF2(45)
DCSF	Pu-244+D	4.181E-01	4.181E-01	DCF2(46)

Dose Conversion Factor (and Related) Parameter Summary (continued)
Current Library: DOE STD-1196-2011 (Reference Person)
Default Library: DOE STD-1196-2011 (Reference Person)

Menu	Parameter	Current Value	Default	Parameter Name
DCSF	Ra-226+D	3.823E-02	3.823E-02	DCF2(48)
DCSF	Ra-228+D	6.333E-02	6.333E-02	DCF2(49)
DCSF	Sr-90+D	6.133E-04	6.133E-04	DCF2(50)
DCSF	Tc-99	5.254E-05	5.254E-05	DCF2(51)
DCSF	Th-228+D	1.754E-01	1.754E-01	DCF2(52)
DCSF	Th-229+D	9.865E-01	9.865E-01	DCF2(53)
DCSF	Th-230	3.848E-01	3.848E-01	DCF2(54)
DCSF	Th-232	4.255E-01	4.255E-01	DCF2(55)
DCSF	U-232	1.439E-01	1.439E-01	DCF2(56)
DCSF	U-233	3.811E-02	3.811E-02	DCF2(57)
DCSF	U-234	3.737E-02	3.737E-02	DCF2(58)
DCSF	U-235+D	3.378E-02	3.378E-02	DCF2(59)
DCSF	U-236	3.463E-02	3.463E-02	DCF2(60)
DCSF	U-238	3.212E-02	3.212E-02	DCF2(61)
DCSF	U-238+D	3.215E-02	3.215E-02	DCF2(62)
DCSF	Dose conversion factors for ingestion, mrem/pCi:			
DCSF	Ac-227+D	2.308E-03	2.308E-03	DCF3(1)
DCSF	Am-241	8.806E-04	8.806E-04	DCF3(2)
DCSF	Am-243+D	8.773E-04	8.773E-04	DCF3(3)
DCSF	Be-10	5.772E-06	5.772E-06	DCF3(4)
DCSF	C-14	2.342E-06	2.342E-06	DCF3(5)
DCSF	Ca-41	1.095E-06	1.095E-06	DCF3(6)
DCSF	Cm-243	6.660E-04	6.660E-04	DCF3(7)
DCSF	Cm-244	5.587E-04	5.587E-04	DCF3(9)
DCSF	Cm-245	8.954E-04	8.954E-04	DCF3(12)
DCSF	Cm-246	8.917E-04	8.917E-04	DCF3(15)
DCSF	Cm-247+D	8.218E-04	8.218E-04	DCF3(19)
DCSF	Cm-248	3.341E-03	3.341E-03	DCF3(20)
DCSF	H-3	1.695E-07	1.695E-07	DCF3(24)
DCSF	I-129	4.477E-04	4.477E-04	DCF3(25)
DCSF	K-40	3.041E-05	3.041E-05	DCF3(26)
DCSF	Mo-93	1.154E-05	1.154E-05	DCF3(27)
DCSF	Nb-93m	6.586E-07	6.586E-07	DCF3(29)
DCSF	Nb-94	8.251E-06	8.251E-06	DCF3(30)
DCSF	Ni-59	2.945E-07	2.945E-07	DCF3(31)
DCSF	Np-237+D	4.674E-04	4.674E-04	DCF3(32)
DCSF	Pa-231	2.068E-03	2.068E-03	DCF3(33)
DCSF	Pb-210+D	1.026E-02	1.026E-02	DCF3(34)
DCSF	Pu-238	9.731E-04	9.731E-04	DCF3(35)
DCSF	Pu-239+D	1.066E-03	1.066E-03	DCF3(37)
DCSF	Pu-240	1.066E-03	1.066E-03	DCF3(38)
DCSF	Pu-241	1.928E-05	1.928E-05	DCF3(40)
DCSF	Pu-241+D	2.320E-05	2.320E-05	DCF3(41)
DCSF	Pu-242	1.014E-03	1.014E-03	DCF3(42)

Dose Conversion Factor (and Related) Parameter Summary (continued)
Current Library: DOE STD-1196-2011 (Reference Person)
Default Library: DOE STD-1196-2011 (Reference Person)

Menu	Parameter	Current Value	Default	Parameter Name
DCSF	Pu-244	1.010E-03	1.010E-03	DCF3(45)
DCSF	Pu-244+D	1.016E-03	1.016E-03	DCF3(46)
DCSF	Ra-226+D	1.677E-03	1.677E-03	DCF3(48)
DCSF	Ra-228+D	5.922E-03	5.922E-03	DCF3(49)
DCSF	Sr-90+D	1.469E-04	1.469E-04	DCF3(50)
DCSF	Tc-99	3.330E-06	3.330E-06	DCF3(51)
DCSF	Th-228+D	9.348E-04	9.348E-04	DCF3(52)
DCSF	Th-229+D	3.328E-03	3.328E-03	DCF3(53)
DCSF	Th-230	9.361E-04	9.361E-04	DCF3(54)
DCSF	Th-232	1.029E-03	1.029E-03	DCF3(55)
DCSF	U-232	1.495E-03	1.495E-03	DCF3(56)
DCSF	U-233	2.227E-04	2.227E-04	DCF3(57)
DCSF	U-234	2.150E-04	2.150E-04	DCF3(58)
DCSF	U-235+D	2.048E-04	2.048E-04	DCF3(59)
DCSF	U-236	2.024E-04	2.024E-04	DCF3(60)
DCSF	U-238	1.939E-04	1.939E-04	DCF3(61)
DCSF	U-238+D	2.112E-04	2.112E-04	DCF3(62)

Dose Conversion Factor (and Related) Parameter Summary (continued)
Current Library: RESRAD Default Transfer factors
Default Library: RESRAD Default Transfer factors

Menu	Parameter	Current Value	Default	Parameter Name
TF	Soil to plant transfer factors:			
TF	Ac-227+D , plant/soil concentration ratio, dimensionless	5.100E-05	2.500E-03	RTF(1,1)
TF	Ac-227+D , plant/soil concentration ratio, dimensionless	9.400E-05	2.500E-03	RTF(1,2)
TF	Ac-227+D , plant/soil concentration ratio, dimensionless	2.000E-05	2.500E-03	RTF(1,3)
TF	Ac-227+D , plant/soil concentration ratio, dimensionless	2.000E-05	2.500E-03	RTF(1,4)
TF				
TF	Am-241 , plant/soil concentration ratio, dimensionless	5.100E-05	1.000E-03	RTF(2,1)
TF	Am-241 , plant/soil concentration ratio, dimensionless	9.400E-05	1.000E-03	RTF(2,2)
TF	Am-241 , plant/soil concentration ratio, dimensionless	2.000E-05	1.000E-03	RTF(2,3)
TF	Am-241 , plant/soil concentration ratio, dimensionless	2.000E-05	1.000E-03	RTF(2,4)
TF				
TF	Am-243+D , plant/soil concentration ratio, dimensionless	5.100E-05	1.000E-03	RTF(3,1)
TF	Am-243+D , plant/soil concentration ratio, dimensionless	9.400E-05	1.000E-03	RTF(3,2)
TF	Am-243+D , plant/soil concentration ratio, dimensionless	2.000E-05	1.000E-03	RTF(3,3)
TF	Am-243+D , plant/soil concentration ratio, dimensionless	2.000E-05	1.000E-03	RTF(3,4)
TF				
TF	Be-10 , plant/soil concentration ratio, dimensionless	8.170E-04	4.000E-03	RTF(4,1)
TF	Be-10 , plant/soil concentration ratio, dimensionless	2.000E-03	4.000E-03	RTF(4,2)
TF	Be-10 , plant/soil concentration ratio, dimensionless	1.800E-03	4.000E-03	RTF(4,3)
TF	Be-10 , plant/soil concentration ratio, dimensionless	1.800E-03	4.000E-03	RTF(4,4)
TF				
TF	Ca-41 , plant/soil concentration ratio, dimensionless	1.570E-01	5.000E-01	RTF(6,1)
TF	Ca-41 , plant/soil concentration ratio, dimensionless	7.000E-01	5.000E-01	RTF(6,2)
TF	Ca-41 , plant/soil concentration ratio, dimensionless	3.200E-01	5.000E-01	RTF(6,3)
TF	Ca-41 , plant/soil concentration ratio, dimensionless	3.200E-01	5.000E-01	RTF(6,4)
TF				
TF	Cm-243 , plant/soil concentration ratio, dimensionless	4.390E-05	1.000E-03	RTF(7,1)
TF	Cm-243 , plant/soil concentration ratio, dimensionless	1.500E-04	1.000E-03	RTF(7,2)
TF	Cm-243 , plant/soil concentration ratio, dimensionless	1.900E-05	1.000E-03	RTF(7,3)
TF	Cm-243 , plant/soil concentration ratio, dimensionless	1.900E-05	1.000E-03	RTF(7,4)
TF				
TF	Cm-244 , plant/soil concentration ratio, dimensionless	4.390E-05	1.000E-03	RTF(9,1)
TF	Cm-244 , plant/soil concentration ratio, dimensionless	1.500E-04	1.000E-03	RTF(9,2)
TF	Cm-244 , plant/soil concentration ratio, dimensionless	1.900E-05	1.000E-03	RTF(9,3)
TF	Cm-244 , plant/soil concentration ratio, dimensionless	1.900E-05	1.000E-03	RTF(9,4)
TF				
TF	Cm-245 , plant/soil concentration ratio, dimensionless	4.390E-05	1.000E-03	RTF(12,1)
TF	Cm-245 , plant/soil concentration ratio, dimensionless	1.500E-04	1.000E-03	RTF(12,2)
TF	Cm-245 , plant/soil concentration ratio, dimensionless	1.900E-05	1.000E-03	RTF(12,3)
TF	Cm-245 , plant/soil concentration ratio, dimensionless	1.900E-05	1.000E-03	RTF(12,4)
TF				
TF	Cm-246 , plant/soil concentration ratio, dimensionless	4.390E-05	1.000E-03	RTF(15,1)
TF	Cm-246 , plant/soil concentration ratio, dimensionless	1.500E-04	1.000E-03	RTF(15,2)
TF	Cm-246 , plant/soil concentration ratio, dimensionless	1.900E-05	1.000E-03	RTF(15,3)
TF	Cm-246 , plant/soil concentration ratio, dimensionless	1.900E-05	1.000E-03	RTF(15,4)

Dose Conversion Factor (and Related) Parameter Summary (continued)
Current Library: RESRAD Default Transfer factors
Default Library: RESRAD Default Transfer factors

Menu	Parameter	Current Value	Default	Parameter Name
TF	Cm-247+D , plant/soil concentration ratio, dimensionless	4.390E-05	1.000E-03	RTF(19,1)
TF	Cm-247+D , plant/soil concentration ratio, dimensionless	1.500E-04	1.000E-03	RTF(19,2)
TF	Cm-247+D , plant/soil concentration ratio, dimensionless	1.900E-05	1.000E-03	RTF(19,3)
TF	Cm-247+D , plant/soil concentration ratio, dimensionless	1.900E-05	1.000E-03	RTF(19,4)
TF				
TF	Cm-248 , plant/soil concentration ratio, dimensionless	4.390E-05	1.000E-03	RTF(20,1)
TF	Cm-248 , plant/soil concentration ratio, dimensionless	1.500E-04	1.000E-03	RTF(20,2)
TF	Cm-248 , plant/soil concentration ratio, dimensionless	1.900E-05	1.000E-03	RTF(20,3)
TF	Cm-248 , plant/soil concentration ratio, dimensionless	1.900E-05	1.000E-03	RTF(20,4)
TF				
TF	H-3 , plant/soil concentration ratio, dimensionless	4.000E+00	4.800E+00	RTF(24,1)
TF	H-3 , plant/soil concentration ratio, dimensionless	4.000E+00	4.800E+00	RTF(24,2)
TF	H-3 , plant/soil concentration ratio, dimensionless	4.000E+00	4.800E+00	RTF(24,3)
TF	H-3 , plant/soil concentration ratio, dimensionless	4.000E+00	4.800E+00	RTF(24,4)
TF				
TF	I-129 , plant/soil concentration ratio, dimensionless	2.000E-02	2.000E-02	RTF(25,1)
TF	I-129 , plant/soil concentration ratio, dimensionless	2.000E-02	2.000E-02	RTF(25,2)
TF	I-129 , plant/soil concentration ratio, dimensionless	2.000E-02	2.000E-02	RTF(25,3)
TF	I-129 , plant/soil concentration ratio, dimensionless	2.000E-02	2.000E-02	RTF(25,4)
TF				
TF	K-40 , plant/soil concentration ratio, dimensionless	2.460E-01	3.000E-01	RTF(26,1)
TF	K-40 , plant/soil concentration ratio, dimensionless	2.000E-01	3.000E-01	RTF(26,2)
TF	K-40 , plant/soil concentration ratio, dimensionless	5.000E-01	3.000E-01	RTF(26,3)
TF	K-40 , plant/soil concentration ratio, dimensionless	5.000E-01	3.000E-01	RTF(26,4)
TF				
TF	Mo-93 , plant/soil concentration ratio, dimensionless	3.130E-01	1.300E-01	RTF(27,1)
TF	Mo-93 , plant/soil concentration ratio, dimensionless	1.600E-01	1.300E-01	RTF(27,2)
TF	Mo-93 , plant/soil concentration ratio, dimensionless	7.300E-01	1.300E-01	RTF(27,3)
TF	Mo-93 , plant/soil concentration ratio, dimensionless	7.300E-01	1.300E-01	RTF(27,4)
TF				
TF	Nb-93m , plant/soil concentration ratio, dimensionless	1.130E-02	1.000E-02	RTF(29,1)
TF	Nb-93m , plant/soil concentration ratio, dimensionless	5.000E-03	1.000E-02	RTF(29,2)
TF	Nb-93m , plant/soil concentration ratio, dimensionless	2.300E-02	1.000E-02	RTF(29,3)
TF	Nb-93m , plant/soil concentration ratio, dimensionless	2.300E-02	1.000E-02	RTF(29,4)
TF				
TF	Nb-94 , plant/soil concentration ratio, dimensionless	1.130E-02	1.000E-02	RTF(30,1)
TF	Nb-94 , plant/soil concentration ratio, dimensionless	5.000E-03	1.000E-02	RTF(30,2)
TF	Nb-94 , plant/soil concentration ratio, dimensionless	2.300E-02	1.000E-02	RTF(30,3)
TF	Nb-94 , plant/soil concentration ratio, dimensionless	2.300E-02	1.000E-02	RTF(30,4)
TF				
TF	Ni-59 , plant/soil concentration ratio, dimensionless	1.770E-02	5.000E-02	RTF(31,1)
TF	Ni-59 , plant/soil concentration ratio, dimensionless	5.600E-02	5.000E-02	RTF(31,2)
TF	Ni-59 , plant/soil concentration ratio, dimensionless	2.700E-02	5.000E-02	RTF(31,3)
TF	Ni-59 , plant/soil concentration ratio, dimensionless	2.700E-02	5.000E-02	RTF(31,4)
TF				

Dose Conversion Factor (and Related) Parameter Summary (continued)
Current Library: RESRAD Default Transfer factors
Default Library: RESRAD Default Transfer factors

Menu	Parameter	Current Value	Default	Parameter Name
TF	Np-237+D , plant/soil concentration ratio, dimensionless	2.530E-03	2.000E-02	RTF(32,1)
TF	Np-237+D , plant/soil concentration ratio, dimensionless	6.400E-03	2.000E-02	RTF(32,2)
TF	Np-237+D , plant/soil concentration ratio, dimensionless	2.500E-03	2.000E-02	RTF(32,3)
TF	Np-237+D , plant/soil concentration ratio, dimensionless	2.500E-03	2.000E-02	RTF(32,4)
TF				
TF	Pa-231 , plant/soil concentration ratio, dimensionless	5.100E-05	1.000E-02	RTF(33,1)
TF	Pa-231 , plant/soil concentration ratio, dimensionless	9.400E-05	1.000E-02	RTF(33,2)
TF	Pa-231 , plant/soil concentration ratio, dimensionless	2.000E-05	1.000E-02	RTF(33,3)
TF	Pa-231 , plant/soil concentration ratio, dimensionless	2.000E-05	1.000E-02	RTF(33,4)
TF				
TF	Pb-210+D , plant/soil concentration ratio, dimensionless	2.530E-03	1.000E-02	RTF(34,1)
TF	Pb-210+D , plant/soil concentration ratio, dimensionless	2.000E-03	1.000E-02	RTF(34,2)
TF	Pb-210+D , plant/soil concentration ratio, dimensionless	4.300E-03	1.000E-02	RTF(34,3)
TF	Pb-210+D , plant/soil concentration ratio, dimensionless	4.300E-03	1.000E-02	RTF(34,4)
TF				
TF	Pu-238 , plant/soil concentration ratio, dimensionless	9.860E-05	1.000E-03	RTF(35,1)
TF	Pu-238 , plant/soil concentration ratio, dimensionless	1.200E-05	1.000E-03	RTF(35,2)
TF	Pu-238 , plant/soil concentration ratio, dimensionless	7.800E-06	1.000E-03	RTF(35,3)
TF	Pu-238 , plant/soil concentration ratio, dimensionless	7.800E-06	1.000E-03	RTF(35,4)
TF				
TF	Pu-239+D , plant/soil concentration ratio, dimensionless	9.860E-05	1.000E-03	RTF(37,1)
TF	Pu-239+D , plant/soil concentration ratio, dimensionless	1.200E-05	1.000E-03	RTF(37,2)
TF	Pu-239+D , plant/soil concentration ratio, dimensionless	7.800E-06	1.000E-03	RTF(37,3)
TF	Pu-239+D , plant/soil concentration ratio, dimensionless	7.800E-06	1.000E-03	RTF(37,4)
TF				
TF	Pu-240 , plant/soil concentration ratio, dimensionless	9.860E-05	1.000E-03	RTF(38,1)
TF	Pu-240 , plant/soil concentration ratio, dimensionless	1.200E-05	1.000E-03	RTF(38,2)
TF	Pu-240 , plant/soil concentration ratio, dimensionless	7.800E-06	1.000E-03	RTF(38,3)
TF	Pu-240 , plant/soil concentration ratio, dimensionless	7.800E-06	1.000E-03	RTF(38,4)
TF				
TF	Pu-241 , plant/soil concentration ratio, dimensionless	9.860E-05	1.000E-03	RTF(40,1)
TF	Pu-241 , plant/soil concentration ratio, dimensionless	1.200E-05	1.000E-03	RTF(40,2)
TF	Pu-241 , plant/soil concentration ratio, dimensionless	7.800E-06	1.000E-03	RTF(40,3)
TF	Pu-241 , plant/soil concentration ratio, dimensionless	7.800E-06	1.000E-03	RTF(40,4)
TF				
TF	Pu-241+D , plant/soil concentration ratio, dimensionless	9.860E-05	1.000E-03	RTF(41,1)
TF	Pu-241+D , plant/soil concentration ratio, dimensionless	1.200E-05	1.000E-03	RTF(41,2)
TF	Pu-241+D , plant/soil concentration ratio, dimensionless	7.800E-06	1.000E-03	RTF(41,3)
TF	Pu-241+D , plant/soil concentration ratio, dimensionless	7.800E-06	1.000E-03	RTF(41,4)
TF				
TF	Pu-242 , plant/soil concentration ratio, dimensionless	9.860E-05	1.000E-03	RTF(42,1)
TF	Pu-242 , plant/soil concentration ratio, dimensionless	1.200E-05	1.000E-03	RTF(42,2)
TF	Pu-242 , plant/soil concentration ratio, dimensionless	7.800E-06	1.000E-03	RTF(42,3)
TF	Pu-242 , plant/soil concentration ratio, dimensionless	7.800E-06	1.000E-03	RTF(42,4)
TF				

Dose Conversion Factor (and Related) Parameter Summary (continued)
Current Library: RESRAD Default Transfer factors
Default Library: RESRAD Default Transfer factors

Menu	Parameter	Current Value	Default	Parameter Name
TF	Pu-244 , plant/soil concentration ratio, dimensionless	9.860E-05	1.000E-03	RTF(45,1)
TF	Pu-244 , plant/soil concentration ratio, dimensionless	1.200E-05	1.000E-03	RTF(45,2)
TF	Pu-244 , plant/soil concentration ratio, dimensionless	7.800E-06	1.000E-03	RTF(45,3)
TF	Pu-244 , plant/soil concentration ratio, dimensionless	7.800E-06	1.000E-03	RTF(45,4)
TF				
TF	Pu-244+D , plant/soil concentration ratio, dimensionless	9.860E-05	1.000E-03	RTF(46,1)
TF	Pu-244+D , plant/soil concentration ratio, dimensionless	1.200E-05	1.000E-03	RTF(46,2)
TF	Pu-244+D , plant/soil concentration ratio, dimensionless	7.800E-06	1.000E-03	RTF(46,3)
TF	Pu-244+D , plant/soil concentration ratio, dimensionless	7.800E-06	1.000E-03	RTF(46,4)
TF				
TF	Ra-226+D , plant/soil concentration ratio, dimensionless	9.000E-04	4.000E-02	RTF(48,1)
TF	Ra-226+D , plant/soil concentration ratio, dimensionless	9.800E-03	4.000E-02	RTF(48,2)
TF	Ra-226+D , plant/soil concentration ratio, dimensionless	1.100E-03	4.000E-02	RTF(48,3)
TF	Ra-226+D , plant/soil concentration ratio, dimensionless	1.100E-03	4.000E-02	RTF(48,4)
TF				
TF	Ra-228+D , plant/soil concentration ratio, dimensionless	9.000E-04	4.000E-02	RTF(49,1)
TF	Ra-228+D , plant/soil concentration ratio, dimensionless	9.800E-03	4.000E-02	RTF(49,2)
TF	Ra-228+D , plant/soil concentration ratio, dimensionless	1.100E-03	4.000E-02	RTF(49,3)
TF	Ra-228+D , plant/soil concentration ratio, dimensionless	1.100E-03	4.000E-02	RTF(49,4)
TF				
TF	Sr-90+D , plant/soil concentration ratio, dimensionless	1.190E-01	3.000E-01	RTF(50,1)
TF	Sr-90+D , plant/soil concentration ratio, dimensionless	6.000E-01	3.000E-01	RTF(50,2)
TF	Sr-90+D , plant/soil concentration ratio, dimensionless	1.900E-01	3.000E-01	RTF(50,3)
TF	Sr-90+D , plant/soil concentration ratio, dimensionless	1.900E-01	3.000E-01	RTF(50,4)
TF				
TF	Tc-99 , plant/soil concentration ratio, dimensionless	3.300E-01	5.000E+00	RTF(51,1)
TF	Tc-99 , plant/soil concentration ratio, dimensionless	4.200E+01	5.000E+00	RTF(51,2)
TF	Tc-99 , plant/soil concentration ratio, dimensionless	6.600E-01	5.000E+00	RTF(51,3)
TF	Tc-99 , plant/soil concentration ratio, dimensionless	6.600E-01	5.000E+00	RTF(51,4)
TF				
TF	Th-228+D , plant/soil concentration ratio, dimensionless	5.300E-05	1.000E-03	RTF(52,1)
TF	Th-228+D , plant/soil concentration ratio, dimensionless	3.600E-04	1.000E-03	RTF(52,2)
TF	Th-228+D , plant/soil concentration ratio, dimensionless	3.100E-05	1.000E-03	RTF(52,3)
TF	Th-228+D , plant/soil concentration ratio, dimensionless	3.100E-05	1.000E-03	RTF(52,4)
TF				
TF	Th-229+D , plant/soil concentration ratio, dimensionless	5.300E-05	1.000E-03	RTF(53,1)
TF	Th-229+D , plant/soil concentration ratio, dimensionless	3.600E-04	1.000E-03	RTF(53,2)
TF	Th-229+D , plant/soil concentration ratio, dimensionless	3.100E-05	1.000E-03	RTF(53,3)
TF	Th-229+D , plant/soil concentration ratio, dimensionless	3.100E-05	1.000E-03	RTF(53,4)
TF				
TF	Th-230 , plant/soil concentration ratio, dimensionless	5.300E-05	1.000E-03	RTF(54,1)
TF	Th-230 , plant/soil concentration ratio, dimensionless	3.600E-04	1.000E-03	RTF(54,2)
TF	Th-230 , plant/soil concentration ratio, dimensionless	3.100E-05	1.000E-03	RTF(54,3)
TF	Th-230 , plant/soil concentration ratio, dimensionless	3.100E-05	1.000E-03	RTF(54,4)
TF				

Dose Conversion Factor (and Related) Parameter Summary (continued)
Current Library: RESRAD Default Transfer factors
Default Library: RESRAD Default Transfer factors

Menu	Parameter	Current Value	Default	Parameter Name
TF	Th-232 , plant/soil concentration ratio, dimensionless	5.300E-05	1.000E-03	RTF(55,1)
TF	Th-232 , plant/soil concentration ratio, dimensionless	3.600E-04	1.000E-03	RTF(55,2)
TF	Th-232 , plant/soil concentration ratio, dimensionless	3.100E-05	1.000E-03	RTF(55,3)
TF	Th-232 , plant/soil concentration ratio, dimensionless	3.100E-05	1.000E-03	RTF(55,4)
TF				
TF	U-232 , plant/soil concentration ratio, dimensionless	1.640E-03	2.500E-03	RTF(56,1)
TF	U-232 , plant/soil concentration ratio, dimensionless	1.700E-03	2.500E-03	RTF(56,2)
TF	U-232 , plant/soil concentration ratio, dimensionless	1.200E-03	2.500E-03	RTF(56,3)
TF	U-232 , plant/soil concentration ratio, dimensionless	1.200E-03	2.500E-03	RTF(56,4)
TF				
TF	U-233 , plant/soil concentration ratio, dimensionless	1.640E-03	2.500E-03	RTF(57,1)
TF	U-233 , plant/soil concentration ratio, dimensionless	1.700E-03	2.500E-03	RTF(57,2)
TF	U-233 , plant/soil concentration ratio, dimensionless	1.200E-03	2.500E-03	RTF(57,3)
TF	U-233 , plant/soil concentration ratio, dimensionless	1.200E-03	2.500E-03	RTF(57,4)
TF				
TF	U-234 , plant/soil concentration ratio, dimensionless	1.640E-03	2.500E-03	RTF(58,1)
TF	U-234 , plant/soil concentration ratio, dimensionless	1.700E-03	2.500E-03	RTF(58,2)
TF	U-234 , plant/soil concentration ratio, dimensionless	1.200E-03	2.500E-03	RTF(58,3)
TF	U-234 , plant/soil concentration ratio, dimensionless	1.200E-03	2.500E-03	RTF(58,4)
TF				
TF	U-235+D , plant/soil concentration ratio, dimensionless	1.640E-03	2.500E-03	RTF(59,1)
TF	U-235+D , plant/soil concentration ratio, dimensionless	1.700E-03	2.500E-03	RTF(59,2)
TF	U-235+D , plant/soil concentration ratio, dimensionless	1.200E-03	2.500E-03	RTF(59,3)
TF	U-235+D , plant/soil concentration ratio, dimensionless	1.200E-03	2.500E-03	RTF(59,4)
TF				
TF	U-236 , plant/soil concentration ratio, dimensionless	1.640E-03	2.500E-03	RTF(60,1)
TF	U-236 , plant/soil concentration ratio, dimensionless	1.700E-03	2.500E-03	RTF(60,2)
TF	U-236 , plant/soil concentration ratio, dimensionless	1.200E-03	2.500E-03	RTF(60,3)
TF	U-236 , plant/soil concentration ratio, dimensionless	1.200E-03	2.500E-03	RTF(60,4)
TF				
TF	U-238 , plant/soil concentration ratio, dimensionless	1.640E-03	2.500E-03	RTF(61,1)
TF	U-238 , plant/soil concentration ratio, dimensionless	1.700E-03	2.500E-03	RTF(61,2)
TF	U-238 , plant/soil concentration ratio, dimensionless	1.200E-03	2.500E-03	RTF(61,3)
TF	U-238 , plant/soil concentration ratio, dimensionless	1.200E-03	2.500E-03	RTF(61,4)
TF				
TF	U-238+D , plant/soil concentration ratio, dimensionless	1.640E-03	2.500E-03	RTF(62,1)
TF	U-238+D , plant/soil concentration ratio, dimensionless	1.700E-03	2.500E-03	RTF(62,2)
TF	U-238+D , plant/soil concentration ratio, dimensionless	1.200E-03	2.500E-03	RTF(62,3)
TF	U-238+D , plant/soil concentration ratio, dimensionless	1.200E-03	2.500E-03	RTF(62,4)
TF	intake to meat/milk transfer factors:			
TF	Ac-227+D , beef/livestock-intake ratio, (pCi/kg)/(pCi/d)	2.290E-03	2.000E-05	I_M(1,1)
TF	Ac-227+D , milk/livestock-intake ratio, (pCi/L)/(pCi/d)	2.000E-05	2.000E-05	I_M(1,2)
TF				

Dose Conversion Factor (and Related) Parameter Summary (continued)
Current Library: RESRAD Default Transfer factors
Default Library: RESRAD Default Transfer factors

Menu	Parameter	Current Value	Default	Parameter Name
TF	Am-241 , beef/livestock-intake ratio, (pCi/kg)/(pCi/d)	2.080E-03	5.000E-05	I_M(2,1)
TF	Am-241 , milk/livestock-intake ratio, (pCi/L)/(pCi/d)	1.500E-06	2.000E-06	I_M(2,2)
TF				
TF	Am-243+D , beef/livestock-intake ratio, (pCi/kg)/(pCi/d)	2.080E-03	5.000E-05	I_M(3,1)
TF	Am-243+D , milk/livestock-intake ratio, (pCi/L)/(pCi/d)	1.500E-06	2.000E-06	I_M(3,2)
TF				
TF	Be-10 , beef/livestock-intake ratio, (pCi/kg)/(pCi/d)	9.660E-02	1.000E-03	I_M(4,1)
TF	Be-10 , milk/livestock-intake ratio, (pCi/L)/(pCi/d)	9.000E-07	2.000E-06	I_M(4,2)
TF				
TF	Ca-41 , beef/livestock-intake ratio, (pCi/kg)/(pCi/d)	7.660E-02	1.600E-03	I_M(6,1)
TF	Ca-41 , milk/livestock-intake ratio, (pCi/L)/(pCi/d)	3.000E-03	3.000E-03	I_M(6,2)
TF				
TF	Cm-243 , beef/livestock-intake ratio, (pCi/kg)/(pCi/d)	2.080E-03	2.000E-05	I_M(7,1)
TF	Cm-243 , milk/livestock-intake ratio, (pCi/L)/(pCi/d)	2.000E-05	2.000E-06	I_M(7,2)
TF				
TF	Cm-244 , beef/livestock-intake ratio, (pCi/kg)/(pCi/d)	2.080E-03	2.000E-05	I_M(9,1)
TF	Cm-244 , milk/livestock-intake ratio, (pCi/L)/(pCi/d)	2.000E-05	2.000E-06	I_M(9,2)
TF				
TF	Cm-245 , beef/livestock-intake ratio, (pCi/kg)/(pCi/d)	2.080E-03	2.000E-05	I_M(12,1)
TF	Cm-245 , milk/livestock-intake ratio, (pCi/L)/(pCi/d)	2.000E-05	2.000E-06	I_M(12,2)
TF				
TF	Cm-246 , beef/livestock-intake ratio, (pCi/kg)/(pCi/d)	2.080E-03	2.000E-05	I_M(15,1)
TF	Cm-246 , milk/livestock-intake ratio, (pCi/L)/(pCi/d)	2.000E-05	2.000E-06	I_M(15,2)
TF				
TF	Cm-247+D , beef/livestock-intake ratio, (pCi/kg)/(pCi/d)	2.080E-03	2.000E-05	I_M(19,1)
TF	Cm-247+D , milk/livestock-intake ratio, (pCi/L)/(pCi/d)	2.000E-05	2.000E-06	I_M(19,2)
TF				
TF	Cm-248 , beef/livestock-intake ratio, (pCi/kg)/(pCi/d)	2.080E-03	2.000E-05	I_M(20,1)
TF	Cm-248 , milk/livestock-intake ratio, (pCi/L)/(pCi/d)	2.000E-05	2.000E-06	I_M(20,2)
TF				
TF	H-3 , beef/livestock-intake ratio, (pCi/kg)/(pCi/d)	5.742E-03	1.200E-02	I_M(24,1)
TF	H-3 , milk/livestock-intake ratio, (pCi/L)/(pCi/d)	4.312E-03	1.000E-02	I_M(24,2)
TF				
TF	I-129 , beef/livestock-intake ratio, (pCi/kg)/(pCi/d)	7.630E-01	7.000E-03	I_M(25,1)
TF	I-129 , milk/livestock-intake ratio, (pCi/L)/(pCi/d)	9.000E-03	1.000E-02	I_M(25,2)
TF				
TF	K-40 , beef/livestock-intake ratio, (pCi/kg)/(pCi/d)	2.700E-01	2.000E-02	I_M(26,1)
TF	K-40 , milk/livestock-intake ratio, (pCi/L)/(pCi/d)	7.200E-03	7.000E-03	I_M(26,2)
TF				
TF	Mo-93 , beef/livestock-intake ratio, (pCi/kg)/(pCi/d)	1.910E-01	1.000E-03	I_M(27,1)
TF	Mo-93 , milk/livestock-intake ratio, (pCi/L)/(pCi/d)	1.700E-03	1.700E-03	I_M(27,2)
TF				
TF	Nb-93m , beef/livestock-intake ratio, (pCi/kg)/(pCi/d)	2.350E-04	3.000E-07	I_M(29,1)
TF	Nb-93m , milk/livestock-intake ratio, (pCi/L)/(pCi/d)	4.100E-07	2.000E-06	I_M(29,2)
TF				

Dose Conversion Factor (and Related) Parameter Summary (continued)
Current Library: RESRAD Default Transfer factors
Default Library: RESRAD Default Transfer factors

Menu	Parameter	Current Value	Default	Parameter Name
TF	Nb-94 , beef/livestock-intake ratio, (pCi/kg)/(pCi/d)	2.350E-04	3.000E-07	I_M(30,1)
TF	Nb-94 , milk/livestock-intake ratio, (pCi/L)/(pCi/d)	4.100E-07	2.000E-06	I_M(30,2)
TF				
TF	Ni-59 , beef/livestock-intake ratio, (pCi/kg)/(pCi/d)	1.980E-02	5.000E-03	I_M(31,1)
TF	Ni-59 , milk/livestock-intake ratio, (pCi/L)/(pCi/d)	1.600E-02	2.000E-02	I_M(31,2)
TF				
TF	Np-237+D , beef/livestock-intake ratio, (pCi/kg)/(pCi/d)	2.660E-03	1.000E-03	I_M(32,1)
TF	Np-237+D , milk/livestock-intake ratio, (pCi/L)/(pCi/d)	5.000E-06	5.000E-06	I_M(32,2)
TF				
TF	Pa-231 , beef/livestock-intake ratio, (pCi/kg)/(pCi/d)	2.080E-03	5.000E-03	I_M(33,1)
TF	Pa-231 , milk/livestock-intake ratio, (pCi/L)/(pCi/d)	5.000E-06	5.000E-06	I_M(33,2)
TF				
TF	Pb-210+D , beef/livestock-intake ratio, (pCi/kg)/(pCi/d)	3.510E-01	8.000E-04	I_M(34,1)
TF	Pb-210+D , milk/livestock-intake ratio, (pCi/L)/(pCi/d)	2.600E-04	3.000E-04	I_M(34,2)
TF				
TF	Pu-238 , beef/livestock-intake ratio, (pCi/kg)/(pCi/d)	7.840E-04	1.000E-04	I_M(35,1)
TF	Pu-238 , milk/livestock-intake ratio, (pCi/L)/(pCi/d)	1.100E-06	1.000E-06	I_M(35,2)
TF				
TF	Pu-239+D , beef/livestock-intake ratio, (pCi/kg)/(pCi/d)	7.840E-04	1.000E-04	I_M(37,1)
TF	Pu-239+D , milk/livestock-intake ratio, (pCi/L)/(pCi/d)	1.100E-06	1.000E-06	I_M(37,2)
TF				
TF	Pu-240 , beef/livestock-intake ratio, (pCi/kg)/(pCi/d)	7.840E-04	1.000E-04	I_M(38,1)
TF	Pu-240 , milk/livestock-intake ratio, (pCi/L)/(pCi/d)	1.100E-06	1.000E-06	I_M(38,2)
TF				
TF	Pu-241 , beef/livestock-intake ratio, (pCi/kg)/(pCi/d)	7.840E-04	1.000E-04	I_M(40,1)
TF	Pu-241 , milk/livestock-intake ratio, (pCi/L)/(pCi/d)	1.100E-06	1.000E-06	I_M(40,2)
TF				
TF	Pu-241+D , beef/livestock-intake ratio, (pCi/kg)/(pCi/d)	7.840E-04	1.000E-04	I_M(41,1)
TF	Pu-241+D , milk/livestock-intake ratio, (pCi/L)/(pCi/d)	1.100E-06	1.000E-06	I_M(41,2)
TF				
TF	Pu-242 , beef/livestock-intake ratio, (pCi/kg)/(pCi/d)	7.840E-04	1.000E-04	I_M(42,1)
TF	Pu-242 , milk/livestock-intake ratio, (pCi/L)/(pCi/d)	1.100E-06	1.000E-06	I_M(42,2)
TF				
TF	Pu-244 , beef/livestock-intake ratio, (pCi/kg)/(pCi/d)	7.840E-04	1.000E-04	I_M(45,1)
TF	Pu-244 , milk/livestock-intake ratio, (pCi/L)/(pCi/d)	1.100E-06	1.000E-06	I_M(45,2)
TF				
TF	Pu-244+D , beef/livestock-intake ratio, (pCi/kg)/(pCi/d)	7.840E-04	1.000E-04	I_M(46,1)
TF	Pu-244+D , milk/livestock-intake ratio, (pCi/L)/(pCi/d)	1.100E-06	1.000E-06	I_M(46,2)
TF				
TF	Ra-226+D , beef/livestock-intake ratio, (pCi/kg)/(pCi/d)	5.880E-02	1.000E-03	I_M(48,1)
TF	Ra-226+D , milk/livestock-intake ratio, (pCi/L)/(pCi/d)	1.300E-03	1.000E-03	I_M(48,2)
TF				
TF	Ra-228+D , beef/livestock-intake ratio, (pCi/kg)/(pCi/d)	5.880E-02	1.000E-03	I_M(49,1)
TF	Ra-228+D , milk/livestock-intake ratio, (pCi/L)/(pCi/d)	1.300E-03	1.000E-03	I_M(49,2)
TF				

Dose Conversion Factor (and Related) Parameter Summary (continued)
Current Library: RESRAD Default Transfer factors
Default Library: RESRAD Default Transfer factors

Menu	Parameter	Current Value	Default	Parameter Name
TF	Sr-90+D , beef/livestock-intake ratio, (pCi/kg)/(pCi/d)	5.640E-02	8.000E-03	I_M(50,1)
TF	Sr-90+D , milk/livestock-intake ratio, (pCi/L)/(pCi/d)	2.800E-03	2.000E-03	I_M(50,2)
TF				
TF	Tc-99 , beef/livestock-intake ratio, (pCi/kg)/(pCi/d)	5.030E-01	1.000E-04	I_M(51,1)
TF	Tc-99 , milk/livestock-intake ratio, (pCi/L)/(pCi/d)	1.400E-04	1.000E-03	I_M(51,2)
TF				
TF	Th-228+D , beef/livestock-intake ratio, (pCi/kg)/(pCi/d)	2.080E-03	1.000E-04	I_M(52,1)
TF	Th-228+D , milk/livestock-intake ratio, (pCi/L)/(pCi/d)	5.000E-06	5.000E-06	I_M(52,2)
TF				
TF	Th-229+D , beef/livestock-intake ratio, (pCi/kg)/(pCi/d)	2.080E-03	1.000E-04	I_M(53,1)
TF	Th-229+D , milk/livestock-intake ratio, (pCi/L)/(pCi/d)	5.000E-06	5.000E-06	I_M(53,2)
TF				
TF	Th-230 , beef/livestock-intake ratio, (pCi/kg)/(pCi/d)	2.080E-03	1.000E-04	I_M(54,1)
TF	Th-230 , milk/livestock-intake ratio, (pCi/L)/(pCi/d)	5.000E-06	5.000E-06	I_M(54,2)
TF				
TF	Th-232 , beef/livestock-intake ratio, (pCi/kg)/(pCi/d)	2.080E-03	1.000E-04	I_M(55,1)
TF	Th-232 , milk/livestock-intake ratio, (pCi/L)/(pCi/d)	5.000E-06	5.000E-06	I_M(55,2)
TF				
TF	U-232 , beef/livestock-intake ratio, (pCi/kg)/(pCi/d)	3.970E-01	3.400E-04	I_M(56,1)
TF	U-232 , milk/livestock-intake ratio, (pCi/L)/(pCi/d)	4.000E-04	6.000E-04	I_M(56,2)
TF				
TF	U-233 , beef/livestock-intake ratio, (pCi/kg)/(pCi/d)	3.970E-01	3.400E-04	I_M(57,1)
TF	U-233 , milk/livestock-intake ratio, (pCi/L)/(pCi/d)	4.000E-04	6.000E-04	I_M(57,2)
TF				
TF	U-234 , beef/livestock-intake ratio, (pCi/kg)/(pCi/d)	3.970E-01	3.400E-04	I_M(58,1)
TF	U-234 , milk/livestock-intake ratio, (pCi/L)/(pCi/d)	4.000E-04	6.000E-04	I_M(58,2)
TF				
TF	U-235+D , beef/livestock-intake ratio, (pCi/kg)/(pCi/d)	3.970E-01	3.400E-04	I_M(59,1)
TF	U-235+D , milk/livestock-intake ratio, (pCi/L)/(pCi/d)	4.000E-04	6.000E-04	I_M(59,2)
TF				
TF	U-236 , beef/livestock-intake ratio, (pCi/kg)/(pCi/d)	3.970E-01	3.400E-04	I_M(60,1)
TF	U-236 , milk/livestock-intake ratio, (pCi/L)/(pCi/d)	4.000E-04	6.000E-04	I_M(60,2)
TF				
TF	U-238 , beef/livestock-intake ratio, (pCi/kg)/(pCi/d)	3.970E-01	3.400E-04	I_M(61,1)
TF	U-238 , milk/livestock-intake ratio, (pCi/L)/(pCi/d)	4.000E-04	6.000E-04	I_M(61,2)
TF				
TF	U-238+D , beef/livestock-intake ratio, (pCi/kg)/(pCi/d)	3.970E-01	3.400E-04	I_M(62,1)
TF	U-238+D , milk/livestock-intake ratio, (pCi/L)/(pCi/d)	4.000E-04	6.000E-04	I_M(62,2)
TF	Bioaccumulation factors, fresh water, L/kg:			
TF	Ac-227+D , fish	2.500E+01	1.500E+01	BIOFA(1,1)
TF	Ac-227+D , crustacea and mollusks	1.000E+03	1.000E+03	BIOFA(1,2)
TF				
TF	Am-241 , fish	3.000E+01	3.000E+01	BIOFA(2,1)
TF	Am-241 , crustacea and mollusks	1.000E+03	1.000E+03	BIOFA(2,2)

Dose Conversion Factor (and Related) Parameter Summary (continued)
Current Library: RESRAD Default Transfer factors
Default Library: RESRAD Default Transfer factors

Menu	Parameter	Current Value	Default	Parameter Name
TF	Am-243+D , fish	3.000E+01	3.000E+01	BIOFA(3,1)
TF	Am-243+D , crustacea and mollusks	1.000E+03	1.000E+03	BIOFA(3,2)
TF				
TF	Be-10 , fish	1.000E+02	1.000E+02	BIOFA(4,1)
TF	Be-10 , crustacea and mollusks	1.000E+01	1.000E+01	BIOFA(4,2)
TF				
TF	C-14 , fish	5.000E+04	5.000E+04	BIOFA(5,1)
TF	C-14 , crustacea and mollusks	9.100E+03	9.100E+03	BIOFA(5,2)
TF				
TF	Ca-41 , fish	4.000E+01	1.000E+03	BIOFA(6,1)
TF	Ca-41 , crustacea and mollusks	3.300E+02	3.300E+02	BIOFA(6,2)
TF				
TF	Cm-243 , fish	3.000E+01	3.000E+01	BIOFA(7,1)
TF	Cm-243 , crustacea and mollusks	1.000E+03	1.000E+03	BIOFA(7,2)
TF				
TF	Cm-244 , fish	3.000E+01	3.000E+01	BIOFA(9,1)
TF	Cm-244 , crustacea and mollusks	1.000E+03	1.000E+03	BIOFA(9,2)
TF				
TF	Cm-245 , fish	3.000E+01	3.000E+01	BIOFA(12,1)
TF	Cm-245 , crustacea and mollusks	1.000E+03	1.000E+03	BIOFA(12,2)
TF				
TF	Cm-246 , fish	3.000E+01	3.000E+01	BIOFA(15,1)
TF	Cm-246 , crustacea and mollusks	1.000E+03	1.000E+03	BIOFA(15,2)
TF				
TF	Cm-247+D , fish	3.000E+01	3.000E+01	BIOFA(19,1)
TF	Cm-247+D , crustacea and mollusks	1.000E+03	1.000E+03	BIOFA(19,2)
TF				
TF	Cm-248 , fish	3.000E+01	3.000E+01	BIOFA(20,1)
TF	Cm-248 , crustacea and mollusks	1.000E+03	1.000E+03	BIOFA(20,2)
TF				
TF	H-3 , fish	1.000E+00	1.000E+00	BIOFA(24,1)
TF	H-3 , crustacea and mollusks	1.000E+00	1.000E+00	BIOFA(24,2)
TF				
TF	I-129 , fish	4.000E+01	4.000E+01	BIOFA(25,1)
TF	I-129 , crustacea and mollusks	5.000E+00	5.000E+00	BIOFA(25,2)
TF				
TF	K-40 , fish	1.000E+03	1.000E+03	BIOFA(26,1)
TF	K-40 , crustacea and mollusks	2.000E+02	2.000E+02	BIOFA(26,2)
TF				
TF	Mo-93 , fish	1.000E+01	1.000E+01	BIOFA(27,1)
TF	Mo-93 , crustacea and mollusks	1.000E+01	1.000E+01	BIOFA(27,2)
TF				
TF	Nb-93m , fish	3.000E+02	3.000E+02	BIOFA(29,1)
TF	Nb-93m , crustacea and mollusks	1.000E+02	1.000E+02	BIOFA(29,2)
TF				

Dose Conversion Factor (and Related) Parameter Summary (continued)
Current Library: RESRAD Default Transfer factors
Default Library: RESRAD Default Transfer factors

Menu	Parameter	Current Value	Default	Parameter Name
TF	Nb-94 , fish	3.000E+02	3.000E+02	BIOFA(30,1)
TF	Nb-94 , crustacea and mollusks	1.000E+02	1.000E+02	BIOFA(30,2)
TF				
TF	Ni-59 , fish	1.000E+02	1.000E+02	BIOFA(31,1)
TF	Ni-59 , crustacea and mollusks	1.000E+02	1.000E+02	BIOFA(31,2)
TF				
TF	Np-237+D , fish	2.100E+01	3.000E+01	BIOFA(32,1)
TF	Np-237+D , crustacea and mollusks	4.000E+02	4.000E+02	BIOFA(32,2)
TF				
TF	Pa-231 , fish	1.000E+01	1.000E+01	BIOFA(33,1)
TF	Pa-231 , crustacea and mollusks	1.100E+02	1.100E+02	BIOFA(33,2)
TF				
TF	Pb-210+D , fish	3.000E+02	3.000E+02	BIOFA(34,1)
TF	Pb-210+D , crustacea and mollusks	1.000E+02	1.000E+02	BIOFA(34,2)
TF				
TF	Pu-238 , fish	3.000E+01	3.000E+01	BIOFA(35,1)
TF	Pu-238 , crustacea and mollusks	1.000E+02	1.000E+02	BIOFA(35,2)
TF				
TF	Pu-239+D , fish	3.000E+01	3.000E+01	BIOFA(37,1)
TF	Pu-239+D , crustacea and mollusks	1.000E+02	1.000E+02	BIOFA(37,2)
TF				
TF	Pu-240 , fish	3.000E+01	3.000E+01	BIOFA(38,1)
TF	Pu-240 , crustacea and mollusks	1.000E+02	1.000E+02	BIOFA(38,2)
TF				
TF	Pu-241 , fish	3.000E+01	3.000E+01	BIOFA(40,1)
TF	Pu-241 , crustacea and mollusks	1.000E+02	1.000E+02	BIOFA(40,2)
TF				
TF	Pu-241+D , fish	3.000E+01	3.000E+01	BIOFA(41,1)
TF	Pu-241+D , crustacea and mollusks	1.000E+02	1.000E+02	BIOFA(41,2)
TF				
TF	Pu-242 , fish	3.000E+01	3.000E+01	BIOFA(42,1)
TF	Pu-242 , crustacea and mollusks	1.000E+02	1.000E+02	BIOFA(42,2)
TF				
TF	Pu-244 , fish	3.000E+01	3.000E+01	BIOFA(45,1)
TF	Pu-244 , crustacea and mollusks	1.000E+02	1.000E+02	BIOFA(45,2)
TF				
TF	Pu-244+D , fish	3.000E+01	3.000E+01	BIOFA(46,1)
TF	Pu-244+D , crustacea and mollusks	1.000E+02	1.000E+02	BIOFA(46,2)
TF				
TF	Ra-226+D , fish	5.000E+01	5.000E+01	BIOFA(48,1)
TF	Ra-226+D , crustacea and mollusks	2.500E+02	2.500E+02	BIOFA(48,2)
TF				
TF	Ra-228+D , fish	5.000E+01	5.000E+01	BIOFA(49,1)
TF	Ra-228+D , crustacea and mollusks	2.500E+02	2.500E+02	BIOFA(49,2)
TF				

Dose Conversion Factor (and Related) Parameter Summary (continued)
Current Library: RESRAD Default Transfer factors
Default Library: RESRAD Default Transfer factors

Menu	Parameter	Current Value	Default	Parameter Name
TF	Sr-90+D , fish	6.000E+01	6.000E+01	BIOFA(50,1)
TF	Sr-90+D , crustacea and mollusks	1.000E+02	1.000E+02	BIOFA(50,2)
TF				
TF	Tc-99 , fish	2.000E+01	2.000E+01	BIOFA(51,1)
TF	Tc-99 , crustacea and mollusks	5.000E+00	5.000E+00	BIOFA(51,2)
TF				
TF	Th-228+D , fish	1.000E+02	1.000E+02	BIOFA(52,1)
TF	Th-228+D , crustacea and mollusks	5.000E+02	5.000E+02	BIOFA(52,2)
TF				
TF	Th-229+D , fish	1.000E+02	1.000E+02	BIOFA(53,1)
TF	Th-229+D , crustacea and mollusks	5.000E+02	5.000E+02	BIOFA(53,2)
TF				
TF	Th-230 , fish	1.000E+02	1.000E+02	BIOFA(54,1)
TF	Th-230 , crustacea and mollusks	5.000E+02	5.000E+02	BIOFA(54,2)
TF				
TF	Th-232 , fish	1.000E+02	1.000E+02	BIOFA(55,1)
TF	Th-232 , crustacea and mollusks	5.000E+02	5.000E+02	BIOFA(55,2)
TF				
TF	U-232 , fish	1.000E+01	1.000E+01	BIOFA(56,1)
TF	U-232 , crustacea and mollusks	6.000E+01	6.000E+01	BIOFA(56,2)
TF				
TF	U-233 , fish	1.000E+01	1.000E+01	BIOFA(57,1)
TF	U-233 , crustacea and mollusks	6.000E+01	6.000E+01	BIOFA(57,2)
TF				
TF	U-234 , fish	1.000E+01	1.000E+01	BIOFA(58,1)
TF	U-234 , crustacea and mollusks	6.000E+01	6.000E+01	BIOFA(58,2)
TF				
TF	U-235+D , fish	1.000E+01	1.000E+01	BIOFA(59,1)
TF	U-235+D , crustacea and mollusks	6.000E+01	6.000E+01	BIOFA(59,2)
TF				
TF	U-236 , fish	1.000E+01	1.000E+01	BIOFA(60,1)
TF	U-236 , crustacea and mollusks	6.000E+01	6.000E+01	BIOFA(60,2)
TF				
TF	U-238 , fish	1.000E+01	1.000E+01	BIOFA(61,1)
TF	U-238 , crustacea and mollusks	6.000E+01	6.000E+01	BIOFA(61,2)
TF				
TF	U-238+D , fish	1.000E+01	1.000E+01	BIOFA(62,1)
TF	U-238+D , crustacea and mollusks	6.000E+01	6.000E+01	BIOFA(62,2)

Site-Specific Parameter Summary

Menu	Parameter	User Input	Default	RESRAD computed	Parameter Name
FSTI	Exposure duration	3.000E+01	3.000E+01	---	ED
FSTI	Basic radiation dose limit (mrem/yr)	2.500E+01	2.500E+01	---	BRDL
CONC	Initial principal radionuclide (pCi/g): Ac-227	2.920E-03	0.000E+00	---	S1(1)
CONC	Initial principal radionuclide (pCi/g): Am-241	5.900E+01	0.000E+00	---	S1(2)
CONC	Initial principal radionuclide (pCi/g): Am-243	2.970E+00	0.000E+00	---	S1(3)
CONC	Initial principal radionuclide (pCi/g): Be-10	2.530E-05	0.000E+00	---	S1(4)
CONC	Initial principal radionuclide (pCi/g): C-14	5.400E-01	0.000E+00	---	S1(5)
CONC	Initial principal radionuclide (pCi/g): Ca-41	4.210E-02	0.000E+00	---	S1(6)
CONC	Initial principal radionuclide (pCi/g): Cm-243	4.300E-01	0.000E+00	---	S1(7)
CONC	Initial principal radionuclide (pCi/g): Cm-244	1.260E+02	0.000E+00	---	S1(9)
CONC	Initial principal radionuclide (pCi/g): Cm-245	3.830E-02	0.000E+00	---	S1(12)
CONC	Initial principal radionuclide (pCi/g): Cm-246	1.590E-01	0.000E+00	---	S1(15)
CONC	Initial principal radionuclide (pCi/g): Cm-247	1.040E-02	0.000E+00	---	S1(19)
CONC	Initial principal radionuclide (pCi/g): Cm-248	5.590E-04	0.000E+00	---	S1(20)
CONC	Initial principal radionuclide (pCi/g): H-3	4.640E+00	0.000E+00	---	S1(24)
CONC	Initial principal radionuclide (pCi/g): I-129	3.500E-01	0.000E+00	---	S1(25)
CONC	Initial principal radionuclide (pCi/g): K-40	3.280E+00	0.000E+00	---	S1(26)
CONC	Initial principal radionuclide (pCi/g): Mo-93	3.880E-01	0.000E+00	---	S1(27)
CONC	Initial principal radionuclide (pCi/g): Nb-93m	2.330E-01	0.000E+00	---	S1(29)
CONC	Initial principal radionuclide (pCi/g): Nb-94	1.630E-02	0.000E+00	---	S1(30)
CONC	Initial principal radionuclide (pCi/g): Ni-59	3.040E+00	0.000E+00	---	S1(31)
CONC	Initial principal radionuclide (pCi/g): Np-237	3.250E-01	0.000E+00	---	S1(32)
CONC	Initial principal radionuclide (pCi/g): Pa-231	2.390E-01	0.000E+00	---	S1(33)
CONC	Initial principal radionuclide (pCi/g): Pb-210	3.680E+00	0.000E+00	---	S1(34)
CONC	Initial principal radionuclide (pCi/g): Pu-238	9.380E+01	0.000E+00	---	S1(35)
CONC	Initial principal radionuclide (pCi/g): Pu-239	5.830E+01	0.000E+00	---	S1(37)
CONC	Initial principal radionuclide (pCi/g): Pu-240	6.200E+01	0.000E+00	---	S1(38)
CONC	Initial principal radionuclide (pCi/g): Pu-241	2.040E+02	0.000E+00	---	S1(40)
CONC	Initial principal radionuclide (pCi/g): Pu-242	1.730E-01	0.000E+00	---	S1(42)
CONC	Initial principal radionuclide (pCi/g): Pu-244	3.680E-03	0.000E+00	---	S1(45)
CONC	Initial principal radionuclide (pCi/g): Ra-226	8.010E-01	0.000E+00	---	S1(48)
CONC	Initial principal radionuclide (pCi/g): Ra-228	2.210E-02	0.000E+00	---	S1(49)
CONC	Initial principal radionuclide (pCi/g): Sr-90	1.920E+02	0.000E+00	---	S1(50)
CONC	Initial principal radionuclide (pCi/g): Tc-99	1.560E+00	0.000E+00	---	S1(51)
CONC	Initial principal radionuclide (pCi/g): Th-228	2.110E-06	0.000E+00	---	S1(52)
CONC	Initial principal radionuclide (pCi/g): Th-229	5.710E+00	0.000E+00	---	S1(53)
CONC	Initial principal radionuclide (pCi/g): Th-230	1.920E+00	0.000E+00	---	S1(54)
CONC	Initial principal radionuclide (pCi/g): Th-232	3.520E+00	0.000E+00	---	S1(55)
CONC	Initial principal radionuclide (pCi/g): U-232	1.020E+01	0.000E+00	---	S1(56)
CONC	Initial principal radionuclide (pCi/g): U-233	4.160E+01	0.000E+00	---	S1(57)
CONC	Initial principal radionuclide (pCi/g): U-234	6.300E+02	0.000E+00	---	S1(58)
CONC	Initial principal radionuclide (pCi/g): U-235	3.970E+01	0.000E+00	---	S1(59)
CONC	Initial principal radionuclide (pCi/g): U-236	8.980E+00	0.000E+00	---	S1(60)
CONC	Initial principal radionuclide (pCi/g): U-238	3.810E+02	0.000E+00	---	S1(61)

Site-Specific Parameter Summary (continued)

Menu	Parameter	User Input	Default	RESRAD computed	Parameter Name
VDEP	Deposition velocity of total particulate Ac-227	1.000E-03	1.000E-03	---	DEPVEL(1)
VDEP	Deposition velocity of respirable particulateAc-227	1.000E-03	1.000E-03	---	DEPVELT(1)
VDEP	Deposition velocity of total particulate Am-241	1.000E-03	1.000E-03	---	DEPVEL(2)
VDEP	Deposition velocity of respirable particulateAm-241	1.000E-03	1.000E-03	---	DEPVELT(2)
VDEP	Deposition velocity of total particulate Am-243	1.000E-03	1.000E-03	---	DEPVEL(3)
VDEP	Deposition velocity of respirable particulateAm-243	1.000E-03	1.000E-03	---	DEPVELT(3)
VDEP	Deposition velocity of total particulate Be-10	1.000E-03	1.000E-03	---	DEPVEL(4)
VDEP	Deposition velocity of respirable particulateBe-10	1.000E-03	1.000E-03	---	DEPVELT(4)
VDEP	Deposition velocity of total particulate C-14	1.000E-03	1.000E-03	---	DEPVEL(5)
VDEP	Deposition velocity of respirable particulateC-14	1.000E-03	1.000E-03	---	DEPVELT(5)
VDEP	Deposition velocity of total particulate Ca-41	1.000E-03	1.000E-03	---	DEPVEL(6)
VDEP	Deposition velocity of respirable particulateCa-41	1.000E-03	1.000E-03	---	DEPVELT(6)
VDEP	Deposition velocity of total particulate Cm-243	1.000E-03	1.000E-03	---	DEPVEL(7)
VDEP	Deposition velocity of respirable particulateCm-243	1.000E-03	1.000E-03	---	DEPVELT(7)
VDEP	Deposition velocity of total particulate Cm-244	1.000E-03	1.000E-03	---	DEPVEL(9)
VDEP	Deposition velocity of respirable particulateCm-244	1.000E-03	1.000E-03	---	DEPVELT(9)
VDEP	Deposition velocity of total particulate Cm-245	1.000E-03	1.000E-03	---	DEPVEL(12)
VDEP	Deposition velocity of respirable particulateCm-245	1.000E-03	1.000E-03	---	DEPVELT(12)
VDEP	Deposition velocity of total particulate Cm-246	1.000E-03	1.000E-03	---	DEPVEL(15)
VDEP	Deposition velocity of respirable particulateCm-246	1.000E-03	1.000E-03	---	DEPVELT(15)
VDEP	Deposition velocity of total particulate Cm-247	1.000E-03	1.000E-03	---	DEPVEL(19)
VDEP	Deposition velocity of respirable particulateCm-247	1.000E-03	1.000E-03	---	DEPVELT(19)
VDEP	Deposition velocity of total particulate Cm-248	1.000E-03	1.000E-03	---	DEPVEL(20)
VDEP	Deposition velocity of respirable particulateCm-248	1.000E-03	1.000E-03	---	DEPVELT(20)
VDEP	Deposition velocity of total particulate H-3	1.000E-03	1.000E-03	---	DEPVEL(24)
VDEP	Deposition velocity of respirable particulateH-3	1.000E-03	1.000E-03	---	DEPVELT(24)
VDEP	Deposition velocity of total particulate I-129	1.000E-02	1.000E-02	---	DEPVEL(25)
VDEP	Deposition velocity of respirable particulateI-129	1.000E-02	1.000E-02	---	DEPVELT(25)
VDEP	Deposition velocity of total particulate K-40	1.000E-03	1.000E-03	---	DEPVEL(26)
VDEP	Deposition velocity of respirable particulateK-40	1.000E-03	1.000E-03	---	DEPVELT(26)
VDEP	Deposition velocity of total particulate Mo-93	1.000E-03	1.000E-03	---	DEPVEL(27)
VDEP	Deposition velocity of respirable particulateMo-93	1.000E-03	1.000E-03	---	DEPVELT(27)
VDEP	Deposition velocity of total particulate Nb-93m	1.000E-03	1.000E-03	---	DEPVEL(29)
VDEP	Deposition velocity of respirable particulateNb-93m	1.000E-03	1.000E-03	---	DEPVELT(29)
VDEP	Deposition velocity of total particulate Nb-94	1.000E-03	1.000E-03	---	DEPVEL(30)
VDEP	Deposition velocity of respirable particulateNb-94	1.000E-03	1.000E-03	---	DEPVELT(30)
VDEP	Deposition velocity of total particulate Ni-59	1.000E-03	1.000E-03	---	DEPVEL(31)
VDEP	Deposition velocity of respirable particulateNi-59	1.000E-03	1.000E-03	---	DEPVELT(31)
VDEP	Deposition velocity of total particulate Np-237	1.000E-03	1.000E-03	---	DEPVEL(32)
VDEP	Deposition velocity of respirable particulateNp-237	1.000E-03	1.000E-03	---	DEPVELT(32)
VDEP	Deposition velocity of total particulate Pa-231	1.000E-03	1.000E-03	---	DEPVEL(33)
VDEP	Deposition velocity of respirable particulatePa-231	1.000E-03	1.000E-03	---	DEPVELT(33)
VDEP	Deposition velocity of total particulate Pb-210	1.000E-03	1.000E-03	---	DEPVEL(34)
VDEP	Deposition velocity of respirable particulatePb-210	1.000E-03	1.000E-03	---	DEPVELT(34)
VDEP	Deposition velocity of total particulate Pu-238	1.000E-03	1.000E-03	---	DEPVEL(35)
VDEP	Deposition velocity of respirable particulatePu-238	1.000E-03	1.000E-03	---	DEPVELT(35)

Site-Specific Parameter Summary (continued)

Menu	Parameter	User Input	Default	RESRAD computed	Parameter Name
VDEP	Deposition velocity of total particulate Pu-239	1.000E-03	1.000E-03	---	DEPVEL(37)
VDEP	Deposition velocity of respirable particulatePu-239	1.000E-03	1.000E-03	---	DEPVELT(37)
VDEP	Deposition velocity of total particulate Pu-240	1.000E-03	1.000E-03	---	DEPVEL(38)
VDEP	Deposition velocity of respirable particulatePu-240	1.000E-03	1.000E-03	---	DEPVELT(38)
VDEP	Deposition velocity of total particulate Pu-241	1.000E-03	1.000E-03	---	DEPVEL(40)
VDEP	Deposition velocity of respirable particulatePu-241	1.000E-03	1.000E-03	---	DEPVELT(40)
VDEP	Deposition velocity of total particulate Pu-242	1.000E-03	1.000E-03	---	DEPVEL(42)
VDEP	Deposition velocity of respirable particulatePu-242	1.000E-03	1.000E-03	---	DEPVELT(42)
VDEP	Deposition velocity of total particulate Pu-244	1.000E-03	1.000E-03	---	DEPVEL(45)
VDEP	Deposition velocity of respirable particulatePu-244	1.000E-03	1.000E-03	---	DEPVELT(45)
VDEP	Deposition velocity of total particulate Ra-226	1.000E-03	1.000E-03	---	DEPVEL(48)
VDEP	Deposition velocity of respirable particulateRa-226	1.000E-03	1.000E-03	---	DEPVELT(48)
VDEP	Deposition velocity of total particulate Ra-228	1.000E-03	1.000E-03	---	DEPVEL(49)
VDEP	Deposition velocity of respirable particulateRa-228	1.000E-03	1.000E-03	---	DEPVELT(49)
VDEP	Deposition velocity of total particulate Sr-90	1.000E-03	1.000E-03	---	DEPVEL(50)
VDEP	Deposition velocity of respirable particulateSr-90	1.000E-03	1.000E-03	---	DEPVELT(50)
VDEP	Deposition velocity of total particulate Tc-99	1.000E-03	1.000E-03	---	DEPVEL(51)
VDEP	Deposition velocity of respirable particulateTc-99	1.000E-03	1.000E-03	---	DEPVELT(51)
VDEP	Deposition velocity of total particulate Th-228	1.000E-03	1.000E-03	---	DEPVEL(52)
VDEP	Deposition velocity of respirable particulateTh-228	1.000E-03	1.000E-03	---	DEPVELT(52)
VDEP	Deposition velocity of total particulate Th-229	1.000E-03	1.000E-03	---	DEPVEL(53)
VDEP	Deposition velocity of respirable particulateTh-229	1.000E-03	1.000E-03	---	DEPVELT(53)
VDEP	Deposition velocity of total particulate Th-230	1.000E-03	1.000E-03	---	DEPVEL(54)
VDEP	Deposition velocity of respirable particulateTh-230	1.000E-03	1.000E-03	---	DEPVELT(54)
VDEP	Deposition velocity of total particulate Th-232	1.000E-03	1.000E-03	---	DEPVEL(55)
VDEP	Deposition velocity of respirable particulateTh-232	1.000E-03	1.000E-03	---	DEPVELT(55)
VDEP	Deposition velocity of total particulate U-232	1.000E-03	1.000E-03	---	DEPVEL(56)
VDEP	Deposition velocity of respirable particulateU-232	1.000E-03	1.000E-03	---	DEPVELT(56)
VDEP	Deposition velocity of total particulate U-233	1.000E-03	1.000E-03	---	DEPVEL(57)
VDEP	Deposition velocity of respirable particulateU-233	1.000E-03	1.000E-03	---	DEPVELT(57)
VDEP	Deposition velocity of total particulate U-234	1.000E-03	1.000E-03	---	DEPVEL(58)
VDEP	Deposition velocity of respirable particulateU-234	1.000E-03	1.000E-03	---	DEPVELT(58)
VDEP	Deposition velocity of total particulate U-235	1.000E-03	1.000E-03	---	DEPVEL(59)
VDEP	Deposition velocity of respirable particulateU-235	1.000E-03	1.000E-03	---	DEPVELT(59)
VDEP	Deposition velocity of total particulate U-236	1.000E-03	1.000E-03	---	DEPVEL(60)
VDEP	Deposition velocity of respirable particulateU-236	1.000E-03	1.000E-03	---	DEPVELT(60)
VDEP	Deposition velocity of total particulate U-238	1.000E-03	1.000E-03	---	DEPVEL(61)
VDEP	Deposition velocity of respirable particulateU-238	1.000E-03	1.000E-03	---	DEPVELT(61)

Site-Specific Parameter Summary (continued)

Menu	Parameter	User Input	Default	RESRAD computed	Parameter Name
DCLR	Distribution coefficients for Ac-227				
DCLR	Contaminated zone (cm**3/g)	2.000E+01	2.000E+01	---	DCNUCC(1)
DCLR	Unsaturated zone 1 (cm**3/g)	4.000E+01	2.000E+01	---	DCNUCU(1,1)
DCLR	Unsaturated zone 2 (cm**3/g)	4.000E+01	2.000E+01	---	DCNUCU(1,2)
DCLR	Unsaturated zone 3 (cm**3/g)	4.000E+01	2.000E+01	---	DCNUCU(1,3)
DCLR	Unsaturated zone 4 (cm**3/g)	4.000E+01	2.000E+01	---	DCNUCU(1,4)
DCLR	Unsaturated zone 5 (cm**3/g)	4.000E+01	2.000E+01	---	DCNUCU(1,5)
DCLR	Saturated zone (cm**3/g)	4.000E+01	2.000E+01	---	DCNUCS(1)
DCLR	Sediment in surface water body (cm**3/g)	0.000E+00	2.000E+01	---	DCNUCSWB(1)
DCLR	Agricultural area 1 (cm**3/g)	4.000E+01	2.000E+01	---	DCNUCOF(1,1)
DCLR	Agricultural area 2 (cm**3/g)	4.000E+01	2.000E+01	---	DCNUCOF(1,2)
DCLR	Agricultural area 3 (cm**3/g)	4.000E+01	2.000E+01	---	DCNUCOF(1,3)
DCLR	Agricultural area 4 (cm**3/g)	4.000E+01	2.000E+01	---	DCNUCOF(1,4)
DCLR	Offsite Dwelling (cm**3/g)	4.000E+01	2.000E+01	---	DCNUCDWE(1)
DCLR	Initial Leach rate (/yr) Ac-227	0.000E+00	0.000E+00	---	ALEACH(1)
DCLR	Initial releasable fraction of Ac-227	0.000E+00	0.000E+00	---	RELFRACINIT(1)
DCLR	Time at which release begins (years) Ac-227	3.000E+02	0.000E+00	---	RELTIMEINIT(1)
DCLR	Final Leach rate (/yr) Ac-227	0.000E+00	0.000E+00	---	RLEACHF(1)
DCLR	Total releasable fraction of Ac-227	1.000E+00	0.000E+00	---	RELFRACFINAL(1)
DCLR	Ac-227 Converts to releasable form over (years)	8.000E+02	0.000E+00	---	RELDUR(1)
DCLR	Temporal profile of conversion Ac-227	Linear	Instant	---	RELTIMEOPT(1)
DCLR	Release option Ac-227	1	0	---	RELOPT(1)
	0 = Rate Contorlled (Leach rate), 1 = Equilibrium Desorption (Distribution coefficient).				
DCLR	Distribution coefficients for Am-241				
DCLR	Contaminated zone (cm**3/g)	2.000E+03	2.000E+01	---	DCNUCC(2)
DCLR	Unsaturated zone 1 (cm**3/g)	4.100E+03	2.000E+01	---	DCNUCU(2,1)
DCLR	Unsaturated zone 2 (cm**3/g)	4.100E+03	2.000E+01	---	DCNUCU(2,2)
DCLR	Unsaturated zone 3 (cm**3/g)	4.100E+03	2.000E+01	---	DCNUCU(2,3)
DCLR	Unsaturated zone 4 (cm**3/g)	4.100E+03	2.000E+01	---	DCNUCU(2,4)
DCLR	Unsaturated zone 5 (cm**3/g)	4.100E+03	2.000E+01	---	DCNUCU(2,5)
DCLR	Saturated zone (cm**3/g)	4.100E+03	2.000E+01	---	DCNUCS(2)
DCLR	Sediment in surface water body (cm**3/g)	0.000E+00	2.000E+01	---	DCNUCSWB(2)
DCLR	Agricultural area 1 (cm**3/g)	4.100E+03	2.000E+01	---	DCNUCOF(2,1)
DCLR	Agricultural area 2 (cm**3/g)	4.100E+03	2.000E+01	---	DCNUCOF(2,2)
DCLR	Agricultural area 3 (cm**3/g)	4.100E+03	2.000E+01	---	DCNUCOF(2,3)
DCLR	Agricultural area 4 (cm**3/g)	4.100E+03	2.000E+01	---	DCNUCOF(2,4)
DCLR	Offsite Dwelling (cm**3/g)	4.100E+03	2.000E+01	---	DCNUCDWE(2)
DCLR	Initial Leach rate (/yr) Am-241	0.000E+00	0.000E+00	---	ALEACH(2)
DCLR	Initial releasable fraction of Am-241	0.000E+00	0.000E+00	---	RELFRACINIT(2)
DCLR	Time at which release begins (years) Am-241	3.000E+02	0.000E+00	---	RELTIMEINIT(2)
DCLR	Final Leach rate (/yr) Am-241	0.000E+00	0.000E+00	---	RLEACHF(2)
DCLR	Total releasable fraction of Am-241	1.000E+00	0.000E+00	---	RELFRACFINAL(2)
DCLR	Am-241 Converts to releasable form over (years)	8.000E+02	0.000E+00	---	RELDUR(2)
DCLR	Temporal profile of conversion Am-241	Linear	Instant	---	RELTIMEOPT(2)
DCLR	Release option Am-241	1	0	---	RELOPT(2)
	0 = Rate Contorlled (Leach rate), 1 = Equilibrium Desorption (Distribution coefficient).				

Site-Specific Parameter Summary (continued)

Menu	Parameter	User Input	Default	RESRAD computed	Parameter Name
DCLR	Distribution coefficients for Am-243				
DCLR	Contaminated zone (cm**3/g)	2.000E+03	2.000E+01	---	DCNUCC(3)
DCLR	Unsaturated zone 1 (cm**3/g)	4.100E+03	2.000E+01	---	DCNUCU(3,1)
DCLR	Unsaturated zone 2 (cm**3/g)	4.100E+03	2.000E+01	---	DCNUCU(3,2)
DCLR	Unsaturated zone 3 (cm**3/g)	4.100E+03	2.000E+01	---	DCNUCU(3,3)
DCLR	Unsaturated zone 4 (cm**3/g)	4.100E+03	2.000E+01	---	DCNUCU(3,4)
DCLR	Unsaturated zone 5 (cm**3/g)	4.100E+03	2.000E+01	---	DCNUCU(3,5)
DCLR	Saturated zone (cm**3/g)	4.100E+03	2.000E+01	---	DCNUCS(3)
DCLR	Sediment in surface water body (cm**3/g)	0.000E+00	2.000E+01	---	DCNUCSWB(3)
DCLR	Agricultural area 1 (cm**3/g)	4.100E+03	2.000E+01	---	DCNUCOF(3,1)
DCLR	Agricultural area 2 (cm**3/g)	4.100E+03	2.000E+01	---	DCNUCOF(3,2)
DCLR	Agricultural area 3 (cm**3/g)	4.100E+03	2.000E+01	---	DCNUCOF(3,3)
DCLR	Agricultural area 4 (cm**3/g)	4.100E+03	2.000E+01	---	DCNUCOF(3,4)
DCLR	Offsite Dwelling (cm**3/g)	4.100E+03	2.000E+01	---	DCNUCDWE(3)
DCLR	Initial Leach rate (/yr) Am-243	0.000E+00	0.000E+00	---	ALEACH(3)
DCLR	Initial releasable fraction of Am-243	0.000E+00	0.000E+00	---	RELFRACINIT(3)
DCLR	Time at which release begins (years) Am-243	3.000E+02	0.000E+00	---	RELTIMEINIT(3)
DCLR	Final Leach rate (/yr) Am-243	0.000E+00	0.000E+00	---	RLEACHF(3)
DCLR	Total releasable fraction of Am-243	1.000E+00	0.000E+00	---	RELFRACFINAL(3)
DCLR	Am-243 Converts to releasable form over (years)	8.000E+02	0.000E+00	---	RELDUR(3)
DCLR	Temporal profile of conversion Am-243	Linear	Instant	---	RELTIMEOPT(3)
DCLR	Release option Am-243	1	0	---	RELOPT(3)
	0 = Rate Contorlled (Leach rate), 1 = Equilibrium Desorption (Distribution coefficient).				
DCLR	Distribution coefficients for Be-10				
DCLR	Contaminated zone (cm**3/g)	4.000E+02	8.100E+02	---	DCNUCC(4)
DCLR	Unsaturated zone 1 (cm**3/g)	8.000E+02	8.100E+02	---	DCNUCU(4,1)
DCLR	Unsaturated zone 2 (cm**3/g)	8.000E+02	8.100E+02	---	DCNUCU(4,2)
DCLR	Unsaturated zone 3 (cm**3/g)	8.000E+02	8.100E+02	---	DCNUCU(4,3)
DCLR	Unsaturated zone 4 (cm**3/g)	8.000E+02	8.100E+02	---	DCNUCU(4,4)
DCLR	Unsaturated zone 5 (cm**3/g)	8.000E+02	8.100E+02	---	DCNUCU(4,5)
DCLR	Saturated zone (cm**3/g)	8.000E+02	8.100E+02	---	DCNUCS(4)
DCLR	Sediment in surface water body (cm**3/g)	0.000E+00	8.100E+02	---	DCNUCSWB(4)
DCLR	Agricultural area 1 (cm**3/g)	8.000E+02	8.100E+02	---	DCNUCOF(4,1)
DCLR	Agricultural area 2 (cm**3/g)	8.000E+02	8.100E+02	---	DCNUCOF(4,2)
DCLR	Agricultural area 3 (cm**3/g)	8.000E+02	8.100E+02	---	DCNUCOF(4,3)
DCLR	Agricultural area 4 (cm**3/g)	8.000E+02	8.100E+02	---	DCNUCOF(4,4)
DCLR	Offsite Dwelling (cm**3/g)	8.000E+02	8.100E+02	---	DCNUCDWE(4)
DCLR	Initial Leach rate (/yr) Be-10	0.000E+00	0.000E+00	---	ALEACH(4)
DCLR	Initial releasable fraction of Be-10	0.000E+00	0.000E+00	---	RELFRACINIT(4)
DCLR	Time at which release begins (years) Be-10	3.000E+02	0.000E+00	---	RELTIMEINIT(4)
DCLR	Final Leach rate (/yr) Be-10	0.000E+00	0.000E+00	---	RLEACHF(4)
DCLR	Total releasable fraction of Be-10	1.000E+00	0.000E+00	---	RELFRACFINAL(4)
DCLR	Be-10 Converts to releasable form over (years)	8.000E+02	0.000E+00	---	RELDUR(4)
DCLR	Temporal profile of conversion Be-10	Linear	Instant	---	RELTIMEOPT(4)
DCLR	Release option Be-10	1	0	---	RELOPT(4)
	0 = Rate Contorlled (Leach rate), 1 = Equilibrium Desorption (Distribution coefficient).				

Site-Specific Parameter Summary (continued)

Menu	Parameter	User Input	Default	RESRAD computed	Parameter Name
DCLR	Distribution coefficients for C-14				
DCLR	Contaminated zone (cm**3/g)	0.000E+00	0.000E+00	---	DCNUCC(5)
DCLR	Unsaturated zone 1 (cm**3/g)	0.000E+00	0.000E+00	---	DCNUCU(5,1)
DCLR	Unsaturated zone 2 (cm**3/g)	0.000E+00	0.000E+00	---	DCNUCU(5,2)
DCLR	Unsaturated zone 3 (cm**3/g)	0.000E+00	0.000E+00	---	DCNUCU(5,3)
DCLR	Unsaturated zone 4 (cm**3/g)	0.000E+00	0.000E+00	---	DCNUCU(5,4)
DCLR	Unsaturated zone 5 (cm**3/g)	0.000E+00	0.000E+00	---	DCNUCU(5,5)
DCLR	Saturated zone (cm**3/g)	0.000E+00	0.000E+00	---	DCNUCS(5)
DCLR	Sediment in surface water body (cm**3/g)	0.000E+00	0.000E+00	---	DCNUCSWB(5)
DCLR	Agricultural area 1 (cm**3/g)	0.000E+00	0.000E+00	---	DCNUCOF(5,1)
DCLR	Agricultural area 2 (cm**3/g)	0.000E+00	0.000E+00	---	DCNUCOF(5,2)
DCLR	Agricultural area 3 (cm**3/g)	0.000E+00	0.000E+00	---	DCNUCOF(5,3)
DCLR	Agricultural area 4 (cm**3/g)	0.000E+00	0.000E+00	---	DCNUCOF(5,4)
DCLR	Offsite Dwelling (cm**3/g)	0.000E+00	0.000E+00	---	DCNUCDWE(5)
DCLR	Initial Leach rate (/yr) C-14	0.000E+00	0.000E+00	---	ALEACH(5)
DCLR	Initial releasable fraction of C-14	7.500E-01	0.000E+00	---	RELFRACINIT(5)
DCLR	Time at which release begins (years) C-14	3.000E+02	0.000E+00	---	RELTIMEINIT(5)
DCLR	Final Leach rate (/yr) C-14	0.000E+00	0.000E+00	---	RLEACHF(5)
DCLR	Total releasable fraction of C-14	1.000E+00	0.000E+00	---	RELFRACFINAL(5)
DCLR	C-14 Converts to releasable form over (years)	5.000E+02	0.000E+00	---	RELDUR(5)
DCLR	Temporal profile of conversion C-14	Linear	Instant	---	RELTIMEOPT(5)
DCLR	Release option C-14	1	0	---	RELOPT(5)
	0 = Rate Contorlled (Leach rate), 1 = Equilibrium Desorption (Distribution coefficient).				
DCLR	Distribution coefficients for Ca-41				
DCLR	Contaminated zone (cm**3/g)	1.500E+01	5.000E+01	---	DCNUCC(6)
DCLR	Unsaturated zone 1 (cm**3/g)	3.000E+01	5.000E+01	---	DCNUCU(6,1)
DCLR	Unsaturated zone 2 (cm**3/g)	3.000E+01	5.000E+01	---	DCNUCU(6,2)
DCLR	Unsaturated zone 3 (cm**3/g)	3.000E+01	5.000E+01	---	DCNUCU(6,3)
DCLR	Unsaturated zone 4 (cm**3/g)	3.000E+01	5.000E+01	---	DCNUCU(6,4)
DCLR	Unsaturated zone 5 (cm**3/g)	3.000E+01	5.000E+01	---	DCNUCU(6,5)
DCLR	Saturated zone (cm**3/g)	3.000E+01	5.000E+01	---	DCNUCS(6)
DCLR	Sediment in surface water body (cm**3/g)	0.000E+00	5.000E+01	---	DCNUCSWB(6)
DCLR	Agricultural area 1 (cm**3/g)	3.000E+01	5.000E+01	---	DCNUCOF(6,1)
DCLR	Agricultural area 2 (cm**3/g)	3.000E+01	5.000E+01	---	DCNUCOF(6,2)
DCLR	Agricultural area 3 (cm**3/g)	3.000E+01	5.000E+01	---	DCNUCOF(6,3)
DCLR	Agricultural area 4 (cm**3/g)	3.000E+01	5.000E+01	---	DCNUCOF(6,4)
DCLR	Offsite Dwelling (cm**3/g)	3.000E+01	5.000E+01	---	DCNUCDWE(6)
DCLR	Initial Leach rate (/yr) Ca-41	0.000E+00	0.000E+00	---	ALEACH(6)
DCLR	Initial releasable fraction of Ca-41	0.000E+00	0.000E+00	---	RELFRACINIT(6)
DCLR	Time at which release begins (years) Ca-41	3.000E+02	0.000E+00	---	RELTIMEINIT(6)
DCLR	Final Leach rate (/yr) Ca-41	0.000E+00	0.000E+00	---	RLEACHF(6)
DCLR	Total releasable fraction of Ca-41	1.000E+00	0.000E+00	---	RELFRACFINAL(6)
DCLR	Ca-41 Converts to releasable form over (years)	8.000E+02	0.000E+00	---	RELDUR(6)
DCLR	Temporal profile of conversion Ca-41	Linear	Instant	---	RELTIMEOPT(6)
DCLR	Release option Ca-41	1	0	---	RELOPT(6)
	0 = Rate Contorlled (Leach rate), 1 = Equilibrium Desorption (Distribution coefficient).				

Site-Specific Parameter Summary (continued)

Menu	Parameter	User Input	Default	RESRAD computed	Parameter Name
DCLR	Distribution coefficients for Cm-243				
DCLR	Contaminated zone (cm**3/g)	2.000E+01	1.380E+03	---	DCNUCC(7)
DCLR	Unsaturated zone 1 (cm**3/g)	4.000E+01	1.380E+03	---	DCNUCU(7,1)
DCLR	Unsaturated zone 2 (cm**3/g)	4.000E+01	1.380E+03	---	DCNUCU(7,2)
DCLR	Unsaturated zone 3 (cm**3/g)	4.000E+01	1.380E+03	---	DCNUCU(7,3)
DCLR	Unsaturated zone 4 (cm**3/g)	4.000E+01	1.380E+03	---	DCNUCU(7,4)
DCLR	Unsaturated zone 5 (cm**3/g)	4.000E+01	1.380E+03	---	DCNUCU(7,5)
DCLR	Saturated zone (cm**3/g)	4.000E+01	1.380E+03	---	DCNUCS(7)
DCLR	Sediment in surface water body (cm**3/g)	0.000E+00	1.380E+03	---	DCNUCSWB(7)
DCLR	Agricultural area 1 (cm**3/g)	4.000E+01	1.380E+03	---	DCNUCOF(7,1)
DCLR	Agricultural area 2 (cm**3/g)	4.000E+01	1.380E+03	---	DCNUCOF(7,2)
DCLR	Agricultural area 3 (cm**3/g)	4.000E+01	1.380E+03	---	DCNUCOF(7,3)
DCLR	Agricultural area 4 (cm**3/g)	4.000E+01	1.380E+03	---	DCNUCOF(7,4)
DCLR	Offsite Dwelling (cm**3/g)	4.000E+01	1.380E+03	---	DCNUCDWE(7)
DCLR	Initial Leach rate (/yr) Cm-243	0.000E+00	0.000E+00	---	ALEACH(7)
DCLR	Initial releasable fraction of Cm-243	0.000E+00	0.000E+00	---	RELFRACINIT(7)
DCLR	Time at which release begins (years) Cm-243	3.000E+02	0.000E+00	---	RELTIMEINIT(7)
DCLR	Final Leach rate (/yr) Cm-243	0.000E+00	0.000E+00	---	RLEACHF(7)
DCLR	Total releasable fraction of Cm-243	1.000E+00	0.000E+00	---	RELFRACFINAL(7)
DCLR	Cm-243 Converts to releasable form over (years)	8.000E+02	0.000E+00	---	RELDUR(7)
DCLR	Temporal profile of conversion Cm-243	Linear	Instant	---	RELTIMEOPT(7)
DCLR	Release option Cm-243	1	0	---	RELOPT(7)
	0 = Rate Contorlled (Leach rate), 1 = Equilibrium Desorption (Distribution coefficient).				
DCLR	Distribution coefficients for Cm-244				
DCLR	Contaminated zone (cm**3/g)	2.000E+01	1.380E+03	---	DCNUCC(9)
DCLR	Unsaturated zone 1 (cm**3/g)	4.000E+01	1.380E+03	---	DCNUCU(9,1)
DCLR	Unsaturated zone 2 (cm**3/g)	4.000E+01	1.380E+03	---	DCNUCU(9,2)
DCLR	Unsaturated zone 3 (cm**3/g)	4.000E+01	1.380E+03	---	DCNUCU(9,3)
DCLR	Unsaturated zone 4 (cm**3/g)	4.000E+01	1.380E+03	---	DCNUCU(9,4)
DCLR	Unsaturated zone 5 (cm**3/g)	4.000E+01	1.380E+03	---	DCNUCU(9,5)
DCLR	Saturated zone (cm**3/g)	4.000E+01	1.380E+03	---	DCNUCS(9)
DCLR	Sediment in surface water body (cm**3/g)	0.000E+00	1.380E+03	---	DCNUCSWB(9)
DCLR	Agricultural area 1 (cm**3/g)	4.000E+01	1.380E+03	---	DCNUCOF(9,1)
DCLR	Agricultural area 2 (cm**3/g)	4.000E+01	1.380E+03	---	DCNUCOF(9,2)
DCLR	Agricultural area 3 (cm**3/g)	4.000E+01	1.380E+03	---	DCNUCOF(9,3)
DCLR	Agricultural area 4 (cm**3/g)	4.000E+01	1.380E+03	---	DCNUCOF(9,4)
DCLR	Offsite Dwelling (cm**3/g)	4.000E+01	1.380E+03	---	DCNUCDWE(9)
DCLR	Initial Leach rate (/yr) Cm-244	0.000E+00	0.000E+00	---	ALEACH(9)
DCLR	Initial releasable fraction of Cm-244	0.000E+00	0.000E+00	---	RELFRACINIT(9)
DCLR	Time at which release begins (years) Cm-244	3.000E+02	0.000E+00	---	RELTIMEINIT(9)
DCLR	Final Leach rate (/yr) Cm-244	0.000E+00	0.000E+00	---	RLEACHF(9)
DCLR	Total releasable fraction of Cm-244	1.000E+00	0.000E+00	---	RELFRACFINAL(9)
DCLR	Cm-244 Converts to releasable form over (years)	8.000E+02	0.000E+00	---	RELDUR(9)
DCLR	Temporal profile of conversion Cm-244	Linear	Instant	---	RELTIMEOPT(9)
DCLR	Release option Cm-244	1	0	---	RELOPT(9)
	0 = Rate Contorlled (Leach rate), 1 = Equilibrium Desorption (Distribution coefficient).				

Site-Specific Parameter Summary (continued)

Menu	Parameter	User Input	Default	RESRAD computed	Parameter Name
DCLR	Distribution coefficients for Cm-245				
DCLR	Contaminated zone (cm**3/g)	2.000E+01	1.380E+03	---	DCNUCC(12)
DCLR	Unsaturated zone 1 (cm**3/g)	4.000E+01	1.380E+03	---	DCNUCU(12,1)
DCLR	Unsaturated zone 2 (cm**3/g)	4.000E+01	1.380E+03	---	DCNUCU(12,2)
DCLR	Unsaturated zone 3 (cm**3/g)	4.000E+01	1.380E+03	---	DCNUCU(12,3)
DCLR	Unsaturated zone 4 (cm**3/g)	4.000E+01	1.380E+03	---	DCNUCU(12,4)
DCLR	Unsaturated zone 5 (cm**3/g)	4.000E+01	1.380E+03	---	DCNUCU(12,5)
DCLR	Saturated zone (cm**3/g)	4.000E+01	1.380E+03	---	DCNUCS(12)
DCLR	Sediment in surface water body (cm**3/g)	0.000E+00	1.380E+03	---	DCNUCSWB(12)
DCLR	Agricultural area 1 (cm**3/g)	4.000E+01	1.380E+03	---	DCNUCOF(12,1)
DCLR	Agricultural area 2 (cm**3/g)	4.000E+01	1.380E+03	---	DCNUCOF(12,2)
DCLR	Agricultural area 3 (cm**3/g)	4.000E+01	1.380E+03	---	DCNUCOF(12,3)
DCLR	Agricultural area 4 (cm**3/g)	4.000E+01	1.380E+03	---	DCNUCOF(12,4)
DCLR	Offsite Dwelling (cm**3/g)	4.000E+01	1.380E+03	---	DCNUCDWE(12)
DCLR	Initial Leach rate (/yr) Cm-245	0.000E+00	0.000E+00	---	ALEACH(12)
DCLR	Initial releasable fraction of Cm-245	0.000E+00	0.000E+00	---	RELFRACINIT(12)
DCLR	Time at which release begins (years) Cm-245	3.000E+02	0.000E+00	---	RELTIMEINIT(12)
DCLR	Final Leach rate (/yr) Cm-245	0.000E+00	0.000E+00	---	RLEACHF(12)
DCLR	Total releasable fraction of Cm-245	1.000E+00	0.000E+00	---	RELFRACFINAL(12)
DCLR	Cm-245 Converts to releasable form over (years)	8.000E+02	0.000E+00	---	RELDUR(12)
DCLR	Temporal profile of conversion Cm-245	Linear	Instant	---	RELTIMEOPT(12)
DCLR	Release option Cm-245	1	0	---	RELOPT(12)
	0 = Rate Contorlled (Leach rate), 1 = Equilibrium Desorption (Distribution coefficient).				
DCLR	Distribution coefficients for Cm-246				
DCLR	Contaminated zone (cm**3/g)	2.000E+01	1.380E+03	---	DCNUCC(15)
DCLR	Unsaturated zone 1 (cm**3/g)	4.000E+01	1.380E+03	---	DCNUCU(15,1)
DCLR	Unsaturated zone 2 (cm**3/g)	4.000E+01	1.380E+03	---	DCNUCU(15,2)
DCLR	Unsaturated zone 3 (cm**3/g)	4.000E+01	1.380E+03	---	DCNUCU(15,3)
DCLR	Unsaturated zone 4 (cm**3/g)	4.000E+01	1.380E+03	---	DCNUCU(15,4)
DCLR	Unsaturated zone 5 (cm**3/g)	4.000E+01	1.380E+03	---	DCNUCU(15,5)
DCLR	Saturated zone (cm**3/g)	4.000E+01	1.380E+03	---	DCNUCS(15)
DCLR	Sediment in surface water body (cm**3/g)	0.000E+00	1.380E+03	---	DCNUCSWB(15)
DCLR	Agricultural area 1 (cm**3/g)	4.000E+01	1.380E+03	---	DCNUCOF(15,1)
DCLR	Agricultural area 2 (cm**3/g)	4.000E+01	1.380E+03	---	DCNUCOF(15,2)
DCLR	Agricultural area 3 (cm**3/g)	4.000E+01	1.380E+03	---	DCNUCOF(15,3)
DCLR	Agricultural area 4 (cm**3/g)	4.000E+01	1.380E+03	---	DCNUCOF(15,4)
DCLR	Offsite Dwelling (cm**3/g)	4.000E+01	1.380E+03	---	DCNUCDWE(15)
DCLR	Initial Leach rate (/yr) Cm-246	0.000E+00	0.000E+00	---	ALEACH(15)
DCLR	Initial releasable fraction of Cm-246	0.000E+00	0.000E+00	---	RELFRACINIT(15)
DCLR	Time at which release begins (years) Cm-246	3.000E+02	0.000E+00	---	RELTIMEINIT(15)
DCLR	Final Leach rate (/yr) Cm-246	0.000E+00	0.000E+00	---	RLEACHF(15)
DCLR	Total releasable fraction of Cm-246	1.000E+00	0.000E+00	---	RELFRACFINAL(15)
DCLR	Cm-246 Converts to releasable form over (years)	8.000E+02	0.000E+00	---	RELDUR(15)
DCLR	Temporal profile of conversion Cm-246	Linear	Instant	---	RELTIMEOPT(15)
DCLR	Release option Cm-246	1	0	---	RELOPT(15)
	0 = Rate Contorlled (Leach rate), 1 = Equilibrium Desorption (Distribution coefficient).				

Site-Specific Parameter Summary (continued)

Menu	Parameter	User Input	Default	RESRAD computed	Parameter Name
DCLR	Distribution coefficients for Cm-247				
DCLR	Contaminated zone (cm**3/g)	2.000E+01	1.380E+03	---	DCNUCC(19)
DCLR	Unsaturated zone 1 (cm**3/g)	4.000E+01	1.380E+03	---	DCNUCU(19,1)
DCLR	Unsaturated zone 2 (cm**3/g)	4.000E+01	1.380E+03	---	DCNUCU(19,2)
DCLR	Unsaturated zone 3 (cm**3/g)	4.000E+01	1.380E+03	---	DCNUCU(19,3)
DCLR	Unsaturated zone 4 (cm**3/g)	4.000E+01	1.380E+03	---	DCNUCU(19,4)
DCLR	Unsaturated zone 5 (cm**3/g)	4.000E+01	1.380E+03	---	DCNUCU(19,5)
DCLR	Saturated zone (cm**3/g)	4.000E+01	1.380E+03	---	DCNUCS(19)
DCLR	Sediment in surface water body (cm**3/g)	0.000E+00	1.380E+03	---	DCNUCSWB(19)
DCLR	Agricultural area 1 (cm**3/g)	4.000E+01	1.380E+03	---	DCNUCOF(19,1)
DCLR	Agricultural area 2 (cm**3/g)	4.000E+01	1.380E+03	---	DCNUCOF(19,2)
DCLR	Agricultural area 3 (cm**3/g)	4.000E+01	1.380E+03	---	DCNUCOF(19,3)
DCLR	Agricultural area 4 (cm**3/g)	4.000E+01	1.380E+03	---	DCNUCOF(19,4)
DCLR	Offsite Dwelling (cm**3/g)	4.000E+01	1.380E+03	---	DCNUCDWE(19)
DCLR	Initial Leach rate (/yr) Cm-247	0.000E+00	0.000E+00	---	ALEACH(19)
DCLR	Initial releasable fraction of Cm-247	0.000E+00	0.000E+00	---	RELFRACINIT(19)
DCLR	Time at which release begins (years) Cm-247	3.000E+02	0.000E+00	---	RELTIMEINIT(19)
DCLR	Final Leach rate (/yr) Cm-247	0.000E+00	0.000E+00	---	RLEACHF(19)
DCLR	Total releasable fraction of Cm-247	1.000E+00	0.000E+00	---	RELFRACFINAL(19)
DCLR	Cm-247 Converts to releasable form over (years)	8.000E+02	0.000E+00	---	RELDUR(19)
DCLR	Temporal profile of conversion Cm-247	Linear	Instant	---	RELTIMEOPT(19)
DCLR	Release option Cm-247	1	0	---	RELOPT(19)
	0 = Rate Contorlled (Leach rate), 1 = Equilibrium Desorption (Distribution coefficient).				
DCLR	Distribution coefficients for Cm-248				
DCLR	Contaminated zone (cm**3/g)	2.000E+01	1.380E+03	---	DCNUCC(20)
DCLR	Unsaturated zone 1 (cm**3/g)	4.000E+01	1.380E+03	---	DCNUCU(20,1)
DCLR	Unsaturated zone 2 (cm**3/g)	4.000E+01	1.380E+03	---	DCNUCU(20,2)
DCLR	Unsaturated zone 3 (cm**3/g)	4.000E+01	1.380E+03	---	DCNUCU(20,3)
DCLR	Unsaturated zone 4 (cm**3/g)	4.000E+01	1.380E+03	---	DCNUCU(20,4)
DCLR	Unsaturated zone 5 (cm**3/g)	4.000E+01	1.380E+03	---	DCNUCU(20,5)
DCLR	Saturated zone (cm**3/g)	4.000E+01	1.380E+03	---	DCNUCS(20)
DCLR	Sediment in surface water body (cm**3/g)	0.000E+00	1.380E+03	---	DCNUCSWB(20)
DCLR	Agricultural area 1 (cm**3/g)	4.000E+01	1.380E+03	---	DCNUCOF(20,1)
DCLR	Agricultural area 2 (cm**3/g)	4.000E+01	1.380E+03	---	DCNUCOF(20,2)
DCLR	Agricultural area 3 (cm**3/g)	4.000E+01	1.380E+03	---	DCNUCOF(20,3)
DCLR	Agricultural area 4 (cm**3/g)	4.000E+01	1.380E+03	---	DCNUCOF(20,4)
DCLR	Offsite Dwelling (cm**3/g)	4.000E+01	1.380E+03	---	DCNUCDWE(20)
DCLR	Initial Leach rate (/yr) Cm-248	0.000E+00	0.000E+00	---	ALEACH(20)
DCLR	Initial releasable fraction of Cm-248	0.000E+00	0.000E+00	---	RELFRACINIT(20)
DCLR	Time at which release begins (years) Cm-248	3.000E+02	0.000E+00	---	RELTIMEINIT(20)
DCLR	Final Leach rate (/yr) Cm-248	0.000E+00	0.000E+00	---	RLEACHF(20)
DCLR	Total releasable fraction of Cm-248	1.000E+00	0.000E+00	---	RELFRACFINAL(20)
DCLR	Cm-248 Converts to releasable form over (years)	8.000E+02	0.000E+00	---	RELDUR(20)
DCLR	Temporal profile of conversion Cm-248	Linear	Instant	---	RELTIMEOPT(20)
DCLR	Release option Cm-248	1	0	---	RELOPT(20)
	0 = Rate Contorlled (Leach rate), 1 = Equilibrium Desorption (Distribution coefficient).				

Site-Specific Parameter Summary (continued)

Menu	Parameter	User Input	Default	RESRAD computed	Parameter Name
DCLR	Distribution coefficients for H-3				
DCLR	Contaminated zone (cm**3/g)	0.000E+00	0.000E+00	---	DCNUCC(24)
DCLR	Unsaturated zone 1 (cm**3/g)	0.000E+00	0.000E+00	---	DCNUCU(24,1)
DCLR	Unsaturated zone 2 (cm**3/g)	0.000E+00	0.000E+00	---	DCNUCU(24,2)
DCLR	Unsaturated zone 3 (cm**3/g)	0.000E+00	0.000E+00	---	DCNUCU(24,3)
DCLR	Unsaturated zone 4 (cm**3/g)	0.000E+00	0.000E+00	---	DCNUCU(24,4)
DCLR	Unsaturated zone 5 (cm**3/g)	0.000E+00	0.000E+00	---	DCNUCU(24,5)
DCLR	Saturated zone (cm**3/g)	0.000E+00	0.000E+00	---	DCNUCS(24)
DCLR	Sediment in surface water body (cm**3/g)	0.000E+00	0.000E+00	---	DCNUCSWB(24)
DCLR	Agricultural area 1 (cm**3/g)	0.000E+00	0.000E+00	---	DCNUCOF(24,1)
DCLR	Agricultural area 2 (cm**3/g)	0.000E+00	0.000E+00	---	DCNUCOF(24,2)
DCLR	Agricultural area 3 (cm**3/g)	0.000E+00	0.000E+00	---	DCNUCOF(24,3)
DCLR	Agricultural area 4 (cm**3/g)	0.000E+00	0.000E+00	---	DCNUCOF(24,4)
DCLR	Offsite Dwelling (cm**3/g)	0.000E+00	0.000E+00	---	DCNUCDWE(24)
DCLR	Initial Leach rate (/yr) H-3	0.000E+00	0.000E+00	---	ALEACH(24)
DCLR	Initial releasable fraction of H-3	7.500E-01	0.000E+00	---	RELFRACINIT(24)
DCLR	Time at which release begins (years) H-3	3.000E+02	0.000E+00	---	RELTIMEINIT(24)
DCLR	Final Leach rate (/yr) H-3	0.000E+00	0.000E+00	---	RLEACHF(24)
DCLR	Total releasable fraction of H-3	1.000E+00	0.000E+00	---	RELFRACFINAL(24)
DCLR	H-3 Converts to releasable form over (years)	5.000E+02	0.000E+00	---	RELDUR(24)
DCLR	Temporal profile of conversion H-3	Linear	Instant	---	RELTIMEOPT(24)
DCLR	Release option H-3	1	0	---	RELOPT(24)
	0 = Rate Contorlled (Leach rate), 1 = Equilibrium Desorption (Distribution coefficient).				
DCLR	Distribution coefficients for I-129				
DCLR	Contaminated zone (cm**3/g)	2.000E+00	1.000E-01	---	DCNUCC(25)
DCLR	Unsaturated zone 1 (cm**3/g)	4.000E+00	1.000E-01	---	DCNUCU(25,1)
DCLR	Unsaturated zone 2 (cm**3/g)	4.000E+00	1.000E-01	---	DCNUCU(25,2)
DCLR	Unsaturated zone 3 (cm**3/g)	4.000E+00	1.000E-01	---	DCNUCU(25,3)
DCLR	Unsaturated zone 4 (cm**3/g)	4.000E+00	1.000E-01	---	DCNUCU(25,4)
DCLR	Unsaturated zone 5 (cm**3/g)	4.000E+00	1.000E-01	---	DCNUCU(25,5)
DCLR	Saturated zone (cm**3/g)	4.000E+00	1.000E-01	---	DCNUCS(25)
DCLR	Sediment in surface water body (cm**3/g)	0.000E+00	1.000E-01	---	DCNUCSWB(25)
DCLR	Agricultural area 1 (cm**3/g)	4.000E+00	1.000E-01	---	DCNUCOF(25,1)
DCLR	Agricultural area 2 (cm**3/g)	4.000E+00	1.000E-01	---	DCNUCOF(25,2)
DCLR	Agricultural area 3 (cm**3/g)	4.000E+00	1.000E-01	---	DCNUCOF(25,3)
DCLR	Agricultural area 4 (cm**3/g)	4.000E+00	1.000E-01	---	DCNUCOF(25,4)
DCLR	Offsite Dwelling (cm**3/g)	4.000E+00	1.000E-01	---	DCNUCDWE(25)
DCLR	Initial Leach rate (/yr) I-129	0.000E+00	0.000E+00	---	ALEACH(25)
DCLR	Initial releasable fraction of I-129	0.000E+00	0.000E+00	---	RELFRACINIT(25)
DCLR	Time at which release begins (years) I-129	3.000E+02	0.000E+00	---	RELTIMEINIT(25)
DCLR	Final Leach rate (/yr) I-129	0.000E+00	0.000E+00	---	RLEACHF(25)
DCLR	Total releasable fraction of I-129	1.000E+00	0.000E+00	---	RELFRACFINAL(25)
DCLR	I-129 Converts to releasable form over (years)	8.000E+02	0.000E+00	---	RELDUR(25)
DCLR	Temporal profile of conversion I-129	Linear	Instant	---	RELTIMEOPT(25)
DCLR	Release option I-129	1	0	---	RELOPT(25)
	0 = Rate Contorlled (Leach rate), 1 = Equilibrium Desorption (Distribution coefficient).				

Site-Specific Parameter Summary (continued)

Menu	Parameter	User Input	Default	RESRAD computed	Parameter Name
DCLR	Distribution coefficients for K-40				
DCLR	Contaminated zone (cm**3/g)	1.500E+01	5.500E+00	---	DCNUCC(26)
DCLR	Unsaturated zone 1 (cm**3/g)	3.000E+01	5.500E+00	---	DCNUCU(26,1)
DCLR	Unsaturated zone 2 (cm**3/g)	3.000E+01	5.500E+00	---	DCNUCU(26,2)
DCLR	Unsaturated zone 3 (cm**3/g)	3.000E+01	5.500E+00	---	DCNUCU(26,3)
DCLR	Unsaturated zone 4 (cm**3/g)	3.000E+01	5.500E+00	---	DCNUCU(26,4)
DCLR	Unsaturated zone 5 (cm**3/g)	3.000E+01	5.500E+00	---	DCNUCU(26,5)
DCLR	Saturated zone (cm**3/g)	3.000E+01	5.500E+00	---	DCNUCS(26)
DCLR	Sediment in surface water body (cm**3/g)	0.000E+00	5.500E+00	---	DCNUCSWB(26)
DCLR	Agricultural area 1 (cm**3/g)	3.000E+01	5.500E+00	---	DCNUCOF(26,1)
DCLR	Agricultural area 2 (cm**3/g)	3.000E+01	5.500E+00	---	DCNUCOF(26,2)
DCLR	Agricultural area 3 (cm**3/g)	3.000E+01	5.500E+00	---	DCNUCOF(26,3)
DCLR	Agricultural area 4 (cm**3/g)	3.000E+01	5.500E+00	---	DCNUCOF(26,4)
DCLR	Offsite Dwelling (cm**3/g)	3.000E+01	5.500E+00	---	DCNUCDWE(26)
DCLR	Initial Leach rate (/yr) K-40	0.000E+00	0.000E+00	---	ALEACH(26)
DCLR	Initial releasable fraction of K-40	0.000E+00	0.000E+00	---	RELFRACINIT(26)
DCLR	Time at which release begins (years) K-40	3.000E+02	0.000E+00	---	RELTIMEINIT(26)
DCLR	Final Leach rate (/yr) K-40	0.000E+00	0.000E+00	---	RLEACHF(26)
DCLR	Total releasable fraction of K-40	1.000E+00	0.000E+00	---	RELFRACFINAL(26)
DCLR	K-40 Converts to releasable form over (years)	8.000E+02	0.000E+00	---	RELDUR(26)
DCLR	Temporal profile of conversion K-40	Linear	Instant	---	RELTIMEOPT(26)
DCLR	Release option K-40	1	0	---	RELOPT(26)
	0 = Rate Contorlled (Leach rate), 1 = Equilibrium Desorption (Distribution coefficient).				
DCLR	Distribution coefficients for Mo-93				
DCLR	Contaminated zone (cm**3/g)	4.500E+01	1.250E+02	---	DCNUCC(27)
DCLR	Unsaturated zone 1 (cm**3/g)	9.000E+01	1.250E+02	---	DCNUCU(27,1)
DCLR	Unsaturated zone 2 (cm**3/g)	9.000E+01	1.250E+02	---	DCNUCU(27,2)
DCLR	Unsaturated zone 3 (cm**3/g)	9.000E+01	1.250E+02	---	DCNUCU(27,3)
DCLR	Unsaturated zone 4 (cm**3/g)	9.000E+01	1.250E+02	---	DCNUCU(27,4)
DCLR	Unsaturated zone 5 (cm**3/g)	9.000E+01	1.250E+02	---	DCNUCU(27,5)
DCLR	Saturated zone (cm**3/g)	9.000E+01	1.250E+02	---	DCNUCS(27)
DCLR	Sediment in surface water body (cm**3/g)	0.000E+00	1.250E+02	---	DCNUCSWB(27)
DCLR	Agricultural area 1 (cm**3/g)	9.000E+01	1.250E+02	---	DCNUCOF(27,1)
DCLR	Agricultural area 2 (cm**3/g)	9.000E+01	1.250E+02	---	DCNUCOF(27,2)
DCLR	Agricultural area 3 (cm**3/g)	9.000E+01	1.250E+02	---	DCNUCOF(27,3)
DCLR	Agricultural area 4 (cm**3/g)	9.000E+01	1.250E+02	---	DCNUCOF(27,4)
DCLR	Offsite Dwelling (cm**3/g)	9.000E+01	1.250E+02	---	DCNUCDWE(27)
DCLR	Initial Leach rate (/yr) Mo-93	0.000E+00	0.000E+00	---	ALEACH(27)
DCLR	Initial releasable fraction of Mo-93	0.000E+00	0.000E+00	---	RELFRACINIT(27)
DCLR	Time at which release begins (years) Mo-93	3.000E+02	0.000E+00	---	RELTIMEINIT(27)
DCLR	Final Leach rate (/yr) Mo-93	0.000E+00	0.000E+00	---	RLEACHF(27)
DCLR	Total releasable fraction of Mo-93	1.000E+00	0.000E+00	---	RELFRACFINAL(27)
DCLR	Mo-93 Converts to releasable form over (years)	8.000E+02	0.000E+00	---	RELDUR(27)
DCLR	Temporal profile of conversion Mo-93	Linear	Instant	---	RELTIMEOPT(27)
DCLR	Release option Mo-93	1	0	---	RELOPT(27)
	0 = Rate Contorlled (Leach rate), 1 = Equilibrium Desorption (Distribution coefficient).				

Site-Specific Parameter Summary (continued)

Menu	Parameter	User Input	Default	RESRAD computed	Parameter Name
DCLR	Distribution coefficients for Nb-93m				
DCLR	Contaminated zone (cm**3/g)	5.000E+01	0.000E+00	---	DCNUCC(29)
DCLR	Unsaturated zone 1 (cm**3/g)	1.000E+02	0.000E+00	---	DCNUCU(29,1)
DCLR	Unsaturated zone 2 (cm**3/g)	1.000E+02	0.000E+00	---	DCNUCU(29,2)
DCLR	Unsaturated zone 3 (cm**3/g)	1.000E+02	0.000E+00	---	DCNUCU(29,3)
DCLR	Unsaturated zone 4 (cm**3/g)	1.000E+02	0.000E+00	---	DCNUCU(29,4)
DCLR	Unsaturated zone 5 (cm**3/g)	1.000E+02	0.000E+00	---	DCNUCU(29,5)
DCLR	Saturated zone (cm**3/g)	1.000E+02	0.000E+00	---	DCNUCS(29)
DCLR	Sediment in surface water body (cm**3/g)	0.000E+00	0.000E+00	---	DCNUCSWB(29)
DCLR	Agricultural area 1 (cm**3/g)	1.000E+02	0.000E+00	---	DCNUCOF(29,1)
DCLR	Agricultural area 2 (cm**3/g)	1.000E+02	0.000E+00	---	DCNUCOF(29,2)
DCLR	Agricultural area 3 (cm**3/g)	1.000E+02	0.000E+00	---	DCNUCOF(29,3)
DCLR	Agricultural area 4 (cm**3/g)	1.000E+02	0.000E+00	---	DCNUCOF(29,4)
DCLR	Offsite Dwelling (cm**3/g)	1.000E+02	0.000E+00	---	DCNUCDWE(29)
DCLR	Initial Leach rate (/yr) Nb-93m	0.000E+00	0.000E+00	---	ALEACH(29)
DCLR	Initial releasable fraction of Nb-93m	0.000E+00	0.000E+00	---	RELFRACINIT(29)
DCLR	Time at which release begins (years) Nb-93m	3.000E+02	0.000E+00	---	RELTIMEINIT(29)
DCLR	Final Leach rate (/yr) Nb-93m	0.000E+00	0.000E+00	---	RLEACHF(29)
DCLR	Total releasable fraction of Nb-93m	1.000E+00	0.000E+00	---	RELFRACFINAL(29)
DCLR	Nb-93m Converts to releasable form over (years)	8.000E+02	0.000E+00	---	RELDUR(29)
DCLR	Temporal profile of conversion Nb-93m	Linear	Instant	---	RELTIMEOPT(29)
DCLR	Release option Nb-93m	1	0	---	RELOPT(29)
	0 = Rate Contorlled (Leach rate), 1 = Equilibrium Desorption (Distribution coefficient).				
DCLR	Distribution coefficients for Nb-94				
DCLR	Contaminated zone (cm**3/g)	5.000E+01	0.000E+00	---	DCNUCC(30)
DCLR	Unsaturated zone 1 (cm**3/g)	1.000E+02	0.000E+00	---	DCNUCU(30,1)
DCLR	Unsaturated zone 2 (cm**3/g)	1.000E+02	0.000E+00	---	DCNUCU(30,2)
DCLR	Unsaturated zone 3 (cm**3/g)	1.000E+02	0.000E+00	---	DCNUCU(30,3)
DCLR	Unsaturated zone 4 (cm**3/g)	1.000E+02	0.000E+00	---	DCNUCU(30,4)
DCLR	Unsaturated zone 5 (cm**3/g)	1.000E+02	0.000E+00	---	DCNUCU(30,5)
DCLR	Saturated zone (cm**3/g)	1.000E+02	0.000E+00	---	DCNUCS(30)
DCLR	Sediment in surface water body (cm**3/g)	0.000E+00	0.000E+00	---	DCNUCSWB(30)
DCLR	Agricultural area 1 (cm**3/g)	1.000E+02	0.000E+00	---	DCNUCOF(30,1)
DCLR	Agricultural area 2 (cm**3/g)	1.000E+02	0.000E+00	---	DCNUCOF(30,2)
DCLR	Agricultural area 3 (cm**3/g)	1.000E+02	0.000E+00	---	DCNUCOF(30,3)
DCLR	Agricultural area 4 (cm**3/g)	1.000E+02	0.000E+00	---	DCNUCOF(30,4)
DCLR	Offsite Dwelling (cm**3/g)	1.000E+02	0.000E+00	---	DCNUCDWE(30)
DCLR	Initial Leach rate (/yr) Nb-94	0.000E+00	0.000E+00	---	ALEACH(30)
DCLR	Initial releasable fraction of Nb-94	0.000E+00	0.000E+00	---	RELFRACINIT(30)
DCLR	Time at which release begins (years) Nb-94	3.000E+02	0.000E+00	---	RELTIMEINIT(30)
DCLR	Final Leach rate (/yr) Nb-94	0.000E+00	0.000E+00	---	RLEACHF(30)
DCLR	Total releasable fraction of Nb-94	1.000E+00	0.000E+00	---	RELFRACFINAL(30)
DCLR	Nb-94 Converts to releasable form over (years)	8.000E+02	0.000E+00	---	RELDUR(30)
DCLR	Temporal profile of conversion Nb-94	Linear	Instant	---	RELTIMEOPT(30)
DCLR	Release option Nb-94	1	0	---	RELOPT(30)
	0 = Rate Contorlled (Leach rate), 1 = Equilibrium Desorption (Distribution coefficient).				

Site-Specific Parameter Summary (continued)

Menu	Parameter	User Input	Default	RESRAD computed	Parameter Name
DCLR	Distribution coefficients for Ni-59				
DCLR	Contaminated zone (cm**3/g)	1.000E+03	1.000E+03	---	DCNUCC(31)
DCLR	Unsaturated zone 1 (cm**3/g)	2.000E+03	1.000E+03	---	DCNUCU(31,1)
DCLR	Unsaturated zone 2 (cm**3/g)	2.000E+03	1.000E+03	---	DCNUCU(31,2)
DCLR	Unsaturated zone 3 (cm**3/g)	2.000E+03	1.000E+03	---	DCNUCU(31,3)
DCLR	Unsaturated zone 4 (cm**3/g)	2.000E+03	1.000E+03	---	DCNUCU(31,4)
DCLR	Unsaturated zone 5 (cm**3/g)	2.000E+03	1.000E+03	---	DCNUCU(31,5)
DCLR	Saturated zone (cm**3/g)	2.000E+03	1.000E+03	---	DCNUCS(31)
DCLR	Sediment in surface water body (cm**3/g)	0.000E+00	1.000E+03	---	DCNUCSWB(31)
DCLR	Agricultural area 1 (cm**3/g)	2.000E+03	1.000E+03	---	DCNUCOF(31,1)
DCLR	Agricultural area 2 (cm**3/g)	2.000E+03	1.000E+03	---	DCNUCOF(31,2)
DCLR	Agricultural area 3 (cm**3/g)	2.000E+03	1.000E+03	---	DCNUCOF(31,3)
DCLR	Agricultural area 4 (cm**3/g)	2.000E+03	1.000E+03	---	DCNUCOF(31,4)
DCLR	Offsite Dwelling (cm**3/g)	2.000E+03	1.000E+03	---	DCNUCDWE(31)
DCLR	Initial Leach rate (/yr) Ni-59	0.000E+00	0.000E+00	---	ALEACH(31)
DCLR	Initial releasable fraction of Ni-59	0.000E+00	0.000E+00	---	RELFRACINIT(31)
DCLR	Time at which release begins (years) Ni-59	3.000E+02	0.000E+00	---	RELTIMEINIT(31)
DCLR	Final Leach rate (/yr) Ni-59	0.000E+00	0.000E+00	---	RLEACHF(31)
DCLR	Total releasable fraction of Ni-59	1.000E+00	0.000E+00	---	RELFRACFINAL(31)
DCLR	Ni-59 Converts to releasable form over (years)	8.000E+02	0.000E+00	---	RELDUR(31)
DCLR	Temporal profile of conversion Ni-59	Linear	Instant	---	RELTIMEOPT(31)
DCLR	Release option Ni-59	1	0	---	RELOPT(31)
	0 = Rate Contorlled (Leach rate), 1 = Equilibrium Desorption (Distribution coefficient).				
DCLR	Distribution coefficients for Np-237				
DCLR	Contaminated zone (cm**3/g)	2.000E+01	2.570E+02	---	DCNUCC(32)
DCLR	Unsaturated zone 1 (cm**3/g)	4.000E+01	2.570E+02	---	DCNUCU(32,1)
DCLR	Unsaturated zone 2 (cm**3/g)	4.000E+01	2.570E+02	---	DCNUCU(32,2)
DCLR	Unsaturated zone 3 (cm**3/g)	4.000E+01	2.570E+02	---	DCNUCU(32,3)
DCLR	Unsaturated zone 4 (cm**3/g)	4.000E+01	2.570E+02	---	DCNUCU(32,4)
DCLR	Unsaturated zone 5 (cm**3/g)	4.000E+01	2.570E+02	---	DCNUCU(32,5)
DCLR	Saturated zone (cm**3/g)	4.000E+01	2.570E+02	---	DCNUCS(32)
DCLR	Sediment in surface water body (cm**3/g)	0.000E+00	2.570E+02	---	DCNUCSWB(32)
DCLR	Agricultural area 1 (cm**3/g)	4.000E+01	2.570E+02	---	DCNUCOF(32,1)
DCLR	Agricultural area 2 (cm**3/g)	4.000E+01	2.570E+02	---	DCNUCOF(32,2)
DCLR	Agricultural area 3 (cm**3/g)	4.000E+01	2.570E+02	---	DCNUCOF(32,3)
DCLR	Agricultural area 4 (cm**3/g)	4.000E+01	2.570E+02	---	DCNUCOF(32,4)
DCLR	Offsite Dwelling (cm**3/g)	4.000E+01	2.570E+02	---	DCNUCDWE(32)
DCLR	Initial Leach rate (/yr) Np-237	0.000E+00	0.000E+00	---	ALEACH(32)
DCLR	Initial releasable fraction of Np-237	0.000E+00	0.000E+00	---	RELFRACINIT(32)
DCLR	Time at which release begins (years) Np-237	3.000E+02	0.000E+00	---	RELTIMEINIT(32)
DCLR	Final Leach rate (/yr) Np-237	0.000E+00	0.000E+00	---	RLEACHF(32)
DCLR	Total releasable fraction of Np-237	1.000E+00	0.000E+00	---	RELFRACFINAL(32)
DCLR	Np-237 Converts to releasable form over (years)	8.000E+02	0.000E+00	---	RELDUR(32)
DCLR	Temporal profile of conversion Np-237	Linear	Instant	---	RELTIMEOPT(32)
DCLR	Release option Np-237	1	0	---	RELOPT(32)
	0 = Rate Contorlled (Leach rate), 1 = Equilibrium Desorption (Distribution coefficient).				

Site-Specific Parameter Summary (continued)

Menu	Parameter	User Input	Default	RESRAD computed	Parameter Name
DCLR	Distribution coefficients for Pa-231				
DCLR	Contaminated zone (cm**3/g)	2.000E+02	5.000E+01	---	DCNUCC(33)
DCLR	Unsaturated zone 1 (cm**3/g)	4.000E+02	5.000E+01	---	DCNUCU(33,1)
DCLR	Unsaturated zone 2 (cm**3/g)	4.000E+02	5.000E+01	---	DCNUCU(33,2)
DCLR	Unsaturated zone 3 (cm**3/g)	4.000E+02	5.000E+01	---	DCNUCU(33,3)
DCLR	Unsaturated zone 4 (cm**3/g)	4.000E+02	5.000E+01	---	DCNUCU(33,4)
DCLR	Unsaturated zone 5 (cm**3/g)	4.000E+02	5.000E+01	---	DCNUCU(33,5)
DCLR	Saturated zone (cm**3/g)	4.000E+02	5.000E+01	---	DCNUCS(33)
DCLR	Sediment in surface water body (cm**3/g)	0.000E+00	5.000E+01	---	DCNUCSWB(33)
DCLR	Agricultural area 1 (cm**3/g)	4.000E+02	5.000E+01	---	DCNUCOF(33,1)
DCLR	Agricultural area 2 (cm**3/g)	4.000E+02	5.000E+01	---	DCNUCOF(33,2)
DCLR	Agricultural area 3 (cm**3/g)	4.000E+02	5.000E+01	---	DCNUCOF(33,3)
DCLR	Agricultural area 4 (cm**3/g)	4.000E+02	5.000E+01	---	DCNUCOF(33,4)
DCLR	Offsite Dwelling (cm**3/g)	4.000E+02	5.000E+01	---	DCNUCDWE(33)
DCLR	Initial Leach rate (/yr) Pa-231	0.000E+00	0.000E+00	---	ALEACH(33)
DCLR	Initial releasable fraction of Pa-231	0.000E+00	0.000E+00	---	RELFRACINIT(33)
DCLR	Time at which release begins (years) Pa-231	3.000E+02	0.000E+00	---	RELTIMEINIT(33)
DCLR	Final Leach rate (/yr) Pa-231	0.000E+00	0.000E+00	---	RLEACHF(33)
DCLR	Total releasable fraction of Pa-231	1.000E+00	0.000E+00	---	RELFRACFINAL(33)
DCLR	Pa-231 Converts to releasable form over (years)	8.000E+02	0.000E+00	---	RELDUR(33)
DCLR	Temporal profile of conversion Pa-231	Linear	Instant	---	RELTIMEOPT(33)
DCLR	Release option Pa-231	1	0	---	RELOPT(33)
	0 = Rate Contorlled (Leach rate), 1 = Equilibrium Desorption (Distribution coefficient).				
DCLR	Distribution coefficients for Pb-210				
DCLR	Contaminated zone (cm**3/g)	5.000E+01	1.000E+02	---	DCNUCC(34)
DCLR	Unsaturated zone 1 (cm**3/g)	1.000E+02	1.000E+02	---	DCNUCU(34,1)
DCLR	Unsaturated zone 2 (cm**3/g)	1.000E+02	1.000E+02	---	DCNUCU(34,2)
DCLR	Unsaturated zone 3 (cm**3/g)	1.000E+02	1.000E+02	---	DCNUCU(34,3)
DCLR	Unsaturated zone 4 (cm**3/g)	1.000E+02	1.000E+02	---	DCNUCU(34,4)
DCLR	Unsaturated zone 5 (cm**3/g)	1.000E+02	1.000E+02	---	DCNUCU(34,5)
DCLR	Saturated zone (cm**3/g)	1.000E+02	1.000E+02	---	DCNUCS(34)
DCLR	Sediment in surface water body (cm**3/g)	0.000E+00	1.000E+02	---	DCNUCSWB(34)
DCLR	Agricultural area 1 (cm**3/g)	1.000E+02	1.000E+02	---	DCNUCOF(34,1)
DCLR	Agricultural area 2 (cm**3/g)	1.000E+02	1.000E+02	---	DCNUCOF(34,2)
DCLR	Agricultural area 3 (cm**3/g)	1.000E+02	1.000E+02	---	DCNUCOF(34,3)
DCLR	Agricultural area 4 (cm**3/g)	1.000E+02	1.000E+02	---	DCNUCOF(34,4)
DCLR	Offsite Dwelling (cm**3/g)	1.000E+02	1.000E+02	---	DCNUCDWE(34)
DCLR	Initial Leach rate (/yr) Pb-210	0.000E+00	0.000E+00	---	ALEACH(34)
DCLR	Initial releasable fraction of Pb-210	0.000E+00	0.000E+00	---	RELFRACINIT(34)
DCLR	Time at which release begins (years) Pb-210	3.000E+02	0.000E+00	---	RELTIMEINIT(34)
DCLR	Final Leach rate (/yr) Pb-210	0.000E+00	0.000E+00	---	RLEACHF(34)
DCLR	Total releasable fraction of Pb-210	1.000E+00	0.000E+00	---	RELFRACFINAL(34)
DCLR	Pb-210 Converts to releasable form over (years)	8.000E+02	0.000E+00	---	RELDUR(34)
DCLR	Temporal profile of conversion Pb-210	Linear	Instant	---	RELTIMEOPT(34)
DCLR	Release option Pb-210	1	0	---	RELOPT(34)
	0 = Rate Contorlled (Leach rate), 1 = Equilibrium Desorption (Distribution coefficient).				

Site-Specific Parameter Summary (continued)

Menu	Parameter	User Input	Default	RESRAD computed	Parameter Name
DCLR	Distribution coefficients for Pu-238				
DCLR	Contaminated zone (cm**3/g)	2.000E+01	2.000E+03	---	DCNUCC(35)
DCLR	Unsaturated zone 1 (cm**3/g)	4.000E+01	2.000E+03	---	DCNUCU(35,1)
DCLR	Unsaturated zone 2 (cm**3/g)	4.000E+01	2.000E+03	---	DCNUCU(35,2)
DCLR	Unsaturated zone 3 (cm**3/g)	4.000E+01	2.000E+03	---	DCNUCU(35,3)
DCLR	Unsaturated zone 4 (cm**3/g)	4.000E+01	2.000E+03	---	DCNUCU(35,4)
DCLR	Unsaturated zone 5 (cm**3/g)	4.000E+01	2.000E+03	---	DCNUCU(35,5)
DCLR	Saturated zone (cm**3/g)	4.000E+01	2.000E+03	---	DCNUCS(35)
DCLR	Sediment in surface water body (cm**3/g)	0.000E+00	2.000E+03	---	DCNUCSWB(35)
DCLR	Agricultural area 1 (cm**3/g)	4.000E+01	2.000E+03	---	DCNUCOF(35,1)
DCLR	Agricultural area 2 (cm**3/g)	4.000E+01	2.000E+03	---	DCNUCOF(35,2)
DCLR	Agricultural area 3 (cm**3/g)	4.000E+01	2.000E+03	---	DCNUCOF(35,3)
DCLR	Agricultural area 4 (cm**3/g)	4.000E+01	2.000E+03	---	DCNUCOF(35,4)
DCLR	Offsite Dwelling (cm**3/g)	4.000E+01	2.000E+03	---	DCNUCDWE(35)
DCLR	Initial Leach rate (/yr) Pu-238	0.000E+00	0.000E+00	---	ALEACH(35)
DCLR	Initial releasable fraction of Pu-238	0.000E+00	0.000E+00	---	RELFRACINIT(35)
DCLR	Time at which release begins (years) Pu-238	3.000E+02	0.000E+00	---	RELTIMEINIT(35)
DCLR	Final Leach rate (/yr) Pu-238	0.000E+00	0.000E+00	---	RLEACHF(35)
DCLR	Total releasable fraction of Pu-238	1.000E+00	0.000E+00	---	RELFRACFINAL(35)
DCLR	Pu-238 Converts to releasable form over (years)	8.000E+02	0.000E+00	---	RELDUR(35)
DCLR	Temporal profile of conversion Pu-238	Linear	Instant	---	RELTIMEOPT(35)
DCLR	Release option Pu-238	1	0	---	RELOPT(35)
	0 = Rate Contorlled (Leach rate), 1 = Equilibrium Desorption (Distribution coefficient).				
DCLR	Distribution coefficients for Pu-239				
DCLR	Contaminated zone (cm**3/g)	2.000E+01	2.000E+03	---	DCNUCC(37)
DCLR	Unsaturated zone 1 (cm**3/g)	4.000E+01	2.000E+03	---	DCNUCU(37,1)
DCLR	Unsaturated zone 2 (cm**3/g)	4.000E+01	2.000E+03	---	DCNUCU(37,2)
DCLR	Unsaturated zone 3 (cm**3/g)	4.000E+01	2.000E+03	---	DCNUCU(37,3)
DCLR	Unsaturated zone 4 (cm**3/g)	4.000E+01	2.000E+03	---	DCNUCU(37,4)
DCLR	Unsaturated zone 5 (cm**3/g)	4.000E+01	2.000E+03	---	DCNUCU(37,5)
DCLR	Saturated zone (cm**3/g)	4.000E+01	2.000E+03	---	DCNUCS(37)
DCLR	Sediment in surface water body (cm**3/g)	0.000E+00	2.000E+03	---	DCNUCSWB(37)
DCLR	Agricultural area 1 (cm**3/g)	4.000E+01	2.000E+03	---	DCNUCOF(37,1)
DCLR	Agricultural area 2 (cm**3/g)	4.000E+01	2.000E+03	---	DCNUCOF(37,2)
DCLR	Agricultural area 3 (cm**3/g)	4.000E+01	2.000E+03	---	DCNUCOF(37,3)
DCLR	Agricultural area 4 (cm**3/g)	4.000E+01	2.000E+03	---	DCNUCOF(37,4)
DCLR	Offsite Dwelling (cm**3/g)	4.000E+01	2.000E+03	---	DCNUCDWE(37)
DCLR	Initial Leach rate (/yr) Pu-239	0.000E+00	0.000E+00	---	ALEACH(37)
DCLR	Initial releasable fraction of Pu-239	0.000E+00	0.000E+00	---	RELFRACINIT(37)
DCLR	Time at which release begins (years) Pu-239	3.000E+02	0.000E+00	---	RELTIMEINIT(37)
DCLR	Final Leach rate (/yr) Pu-239	0.000E+00	0.000E+00	---	RLEACHF(37)
DCLR	Total releasable fraction of Pu-239	1.000E+00	0.000E+00	---	RELFRACFINAL(37)
DCLR	Pu-239 Converts to releasable form over (years)	8.000E+02	0.000E+00	---	RELDUR(37)
DCLR	Temporal profile of conversion Pu-239	Linear	Instant	---	RELTIMEOPT(37)
DCLR	Release option Pu-239	1	0	---	RELOPT(37)
	0 = Rate Contorlled (Leach rate), 1 = Equilibrium Desorption (Distribution coefficient).				

Site-Specific Parameter Summary (continued)

Menu	Parameter	User Input	Default	RESRAD computed	Parameter Name
DCLR	Distribution coefficients for Pu-240				
DCLR	Contaminated zone (cm**3/g)	2.000E+01	2.000E+03	---	DCNUCC(38)
DCLR	Unsaturated zone 1 (cm**3/g)	4.000E+01	2.000E+03	---	DCNUCU(38,1)
DCLR	Unsaturated zone 2 (cm**3/g)	4.000E+01	2.000E+03	---	DCNUCU(38,2)
DCLR	Unsaturated zone 3 (cm**3/g)	4.000E+01	2.000E+03	---	DCNUCU(38,3)
DCLR	Unsaturated zone 4 (cm**3/g)	4.000E+01	2.000E+03	---	DCNUCU(38,4)
DCLR	Unsaturated zone 5 (cm**3/g)	4.000E+01	2.000E+03	---	DCNUCU(38,5)
DCLR	Saturated zone (cm**3/g)	4.000E+01	2.000E+03	---	DCNUCS(38)
DCLR	Sediment in surface water body (cm**3/g)	0.000E+00	2.000E+03	---	DCNUCSWB(38)
DCLR	Agricultural area 1 (cm**3/g)	4.000E+01	2.000E+03	---	DCNUCOF(38,1)
DCLR	Agricultural area 2 (cm**3/g)	4.000E+01	2.000E+03	---	DCNUCOF(38,2)
DCLR	Agricultural area 3 (cm**3/g)	4.000E+01	2.000E+03	---	DCNUCOF(38,3)
DCLR	Agricultural area 4 (cm**3/g)	4.000E+01	2.000E+03	---	DCNUCOF(38,4)
DCLR	Offsite Dwelling (cm**3/g)	4.000E+01	2.000E+03	---	DCNUCDWE(38)
DCLR	Initial Leach rate (/yr) Pu-240	0.000E+00	0.000E+00	---	ALEACH(38)
DCLR	Initial releasable fraction of Pu-240	0.000E+00	0.000E+00	---	RELFRACINIT(38)
DCLR	Time at which release begins (years) Pu-240	3.000E+02	0.000E+00	---	RELTIMEINIT(38)
DCLR	Final Leach rate (/yr) Pu-240	0.000E+00	0.000E+00	---	RLEACHF(38)
DCLR	Total releasable fraction of Pu-240	1.000E+00	0.000E+00	---	RELFRACFINAL(38)
DCLR	Pu-240 Converts to releasable form over (years)	8.000E+02	0.000E+00	---	RELDUR(38)
DCLR	Temporal profile of conversion Pu-240	Linear	Instant	---	RELTIMEOPT(38)
DCLR	Release option Pu-240	1	0	---	RELOPT(38)
	0 = Rate Contorlled (Leach rate), 1 = Equilibrium Desorption (Distribution coefficient).				
DCLR	Distribution coefficients for Pu-241				
DCLR	Contaminated zone (cm**3/g)	2.000E+01	2.000E+03	---	DCNUCC(40)
DCLR	Unsaturated zone 1 (cm**3/g)	4.000E+01	2.000E+03	---	DCNUCU(40,1)
DCLR	Unsaturated zone 2 (cm**3/g)	4.000E+01	2.000E+03	---	DCNUCU(40,2)
DCLR	Unsaturated zone 3 (cm**3/g)	4.000E+01	2.000E+03	---	DCNUCU(40,3)
DCLR	Unsaturated zone 4 (cm**3/g)	4.000E+01	2.000E+03	---	DCNUCU(40,4)
DCLR	Unsaturated zone 5 (cm**3/g)	4.000E+01	2.000E+03	---	DCNUCU(40,5)
DCLR	Saturated zone (cm**3/g)	4.000E+01	2.000E+03	---	DCNUCS(40)
DCLR	Sediment in surface water body (cm**3/g)	0.000E+00	2.000E+03	---	DCNUCSWB(40)
DCLR	Agricultural area 1 (cm**3/g)	4.000E+01	2.000E+03	---	DCNUCOF(40,1)
DCLR	Agricultural area 2 (cm**3/g)	4.000E+01	2.000E+03	---	DCNUCOF(40,2)
DCLR	Agricultural area 3 (cm**3/g)	4.000E+01	2.000E+03	---	DCNUCOF(40,3)
DCLR	Agricultural area 4 (cm**3/g)	4.000E+01	2.000E+03	---	DCNUCOF(40,4)
DCLR	Offsite Dwelling (cm**3/g)	4.000E+01	2.000E+03	---	DCNUCDWE(40)
DCLR	Initial Leach rate (/yr) Pu-241	0.000E+00	0.000E+00	---	ALEACH(40)
DCLR	Initial releasable fraction of Pu-241	0.000E+00	0.000E+00	---	RELFRACINIT(40)
DCLR	Time at which release begins (years) Pu-241	3.000E+02	0.000E+00	---	RELTIMEINIT(40)
DCLR	Final Leach rate (/yr) Pu-241	0.000E+00	0.000E+00	---	RLEACHF(40)
DCLR	Total releasable fraction of Pu-241	1.000E+00	0.000E+00	---	RELFRACFINAL(40)
DCLR	Pu-241 Converts to releasable form over (years)	8.000E+02	0.000E+00	---	RELDUR(40)
DCLR	Temporal profile of conversion Pu-241	Linear	Instant	---	RELTIMEOPT(40)
DCLR	Release option Pu-241	1	0	---	RELOPT(40)
	0 = Rate Contorlled (Leach rate), 1 = Equilibrium Desorption (Distribution coefficient).				

Site-Specific Parameter Summary (continued)

Menu	Parameter	User Input	Default	RESRAD computed	Parameter Name
DCLR	Distribution coefficients for Pu-242				
DCLR	Contaminated zone (cm**3/g)	2.000E+01	2.000E+03	---	DCNUCC(42)
DCLR	Unsaturated zone 1 (cm**3/g)	4.000E+01	2.000E+03	---	DCNUCU(42,1)
DCLR	Unsaturated zone 2 (cm**3/g)	4.000E+01	2.000E+03	---	DCNUCU(42,2)
DCLR	Unsaturated zone 3 (cm**3/g)	4.000E+01	2.000E+03	---	DCNUCU(42,3)
DCLR	Unsaturated zone 4 (cm**3/g)	4.000E+01	2.000E+03	---	DCNUCU(42,4)
DCLR	Unsaturated zone 5 (cm**3/g)	4.000E+01	2.000E+03	---	DCNUCU(42,5)
DCLR	Saturated zone (cm**3/g)	4.000E+01	2.000E+03	---	DCNUCS(42)
DCLR	Sediment in surface water body (cm**3/g)	0.000E+00	2.000E+03	---	DCNUCSWB(42)
DCLR	Agricultural area 1 (cm**3/g)	4.000E+01	2.000E+03	---	DCNUCOF(42,1)
DCLR	Agricultural area 2 (cm**3/g)	4.000E+01	2.000E+03	---	DCNUCOF(42,2)
DCLR	Agricultural area 3 (cm**3/g)	4.000E+01	2.000E+03	---	DCNUCOF(42,3)
DCLR	Agricultural area 4 (cm**3/g)	4.000E+01	2.000E+03	---	DCNUCOF(42,4)
DCLR	Offsite Dwelling (cm**3/g)	4.000E+01	2.000E+03	---	DCNUCDWE(42)
DCLR	Initial Leach rate (/yr) Pu-242	0.000E+00	0.000E+00	---	ALEACH(42)
DCLR	Initial releasable fraction of Pu-242	0.000E+00	0.000E+00	---	RELFRACINIT(42)
DCLR	Time at which release begins (years) Pu-242	3.000E+02	0.000E+00	---	RELTIMEINIT(42)
DCLR	Final Leach rate (/yr) Pu-242	0.000E+00	0.000E+00	---	RLEACHF(42)
DCLR	Total releasable fraction of Pu-242	1.000E+00	0.000E+00	---	RELFRACFINAL(42)
DCLR	Pu-242 Converts to releasable form over (years)	8.000E+02	0.000E+00	---	RELDUR(42)
DCLR	Temporal profile of conversion Pu-242	Linear	Instant	---	RELTIMEOPT(42)
DCLR	Release option Pu-242	1	0	---	RELOPT(42)
	0 = Rate Contorlled (Leach rate), 1 = Equilibrium Desorption (Distribution coefficient).				
DCLR	Distribution coefficients for Pu-244				
DCLR	Contaminated zone (cm**3/g)	2.000E+01	2.000E+03	---	DCNUCC(45)
DCLR	Unsaturated zone 1 (cm**3/g)	4.000E+01	2.000E+03	---	DCNUCU(45,1)
DCLR	Unsaturated zone 2 (cm**3/g)	4.000E+01	2.000E+03	---	DCNUCU(45,2)
DCLR	Unsaturated zone 3 (cm**3/g)	4.000E+01	2.000E+03	---	DCNUCU(45,3)
DCLR	Unsaturated zone 4 (cm**3/g)	4.000E+01	2.000E+03	---	DCNUCU(45,4)
DCLR	Unsaturated zone 5 (cm**3/g)	4.000E+01	2.000E+03	---	DCNUCU(45,5)
DCLR	Saturated zone (cm**3/g)	4.000E+01	2.000E+03	---	DCNUCS(45)
DCLR	Sediment in surface water body (cm**3/g)	0.000E+00	2.000E+03	---	DCNUCSWB(45)
DCLR	Agricultural area 1 (cm**3/g)	4.000E+01	2.000E+03	---	DCNUCOF(45,1)
DCLR	Agricultural area 2 (cm**3/g)	4.000E+01	2.000E+03	---	DCNUCOF(45,2)
DCLR	Agricultural area 3 (cm**3/g)	4.000E+01	2.000E+03	---	DCNUCOF(45,3)
DCLR	Agricultural area 4 (cm**3/g)	4.000E+01	2.000E+03	---	DCNUCOF(45,4)
DCLR	Offsite Dwelling (cm**3/g)	4.000E+01	2.000E+03	---	DCNUCDWE(45)
DCLR	Initial Leach rate (/yr) Pu-244	0.000E+00	0.000E+00	---	ALEACH(45)
DCLR	Initial releasable fraction of Pu-244	0.000E+00	0.000E+00	---	RELFRACINIT(45)
DCLR	Time at which release begins (years) Pu-244	3.000E+02	0.000E+00	---	RELTIMEINIT(45)
DCLR	Final Leach rate (/yr) Pu-244	0.000E+00	0.000E+00	---	RLEACHF(45)
DCLR	Total releasable fraction of Pu-244	1.000E+00	0.000E+00	---	RELFRACFINAL(45)
DCLR	Pu-244 Converts to releasable form over (years)	8.000E+02	0.000E+00	---	RELDUR(45)
DCLR	Temporal profile of conversion Pu-244	Linear	Instant	---	RELTIMEOPT(45)
DCLR	Release option Pu-244	1	0	---	RELOPT(45)
	0 = Rate Contorlled (Leach rate), 1 = Equilibrium Desorption (Distribution coefficient).				

Site-Specific Parameter Summary (continued)

Menu	Parameter	User Input	Default	RESRAD computed	Parameter Name
DCLR	Distribution coefficients for Ra-226				
DCLR	Contaminated zone (cm**3/g)	1.500E+03	7.000E+01	---	DCNUCC(48)
DCLR	Unsaturated zone 1 (cm**3/g)	3.000E+03	7.000E+01	---	DCNUCU(48,1)
DCLR	Unsaturated zone 2 (cm**3/g)	3.000E+03	7.000E+01	---	DCNUCU(48,2)
DCLR	Unsaturated zone 3 (cm**3/g)	3.000E+03	7.000E+01	---	DCNUCU(48,3)
DCLR	Unsaturated zone 4 (cm**3/g)	3.000E+03	7.000E+01	---	DCNUCU(48,4)
DCLR	Unsaturated zone 5 (cm**3/g)	3.000E+03	7.000E+01	---	DCNUCU(48,5)
DCLR	Saturated zone (cm**3/g)	3.000E+03	7.000E+01	---	DCNUCS(48)
DCLR	Sediment in surface water body (cm**3/g)	0.000E+00	7.000E+01	---	DCNUCSWB(48)
DCLR	Agricultural area 1 (cm**3/g)	3.000E+03	7.000E+01	---	DCNUCOF(48,1)
DCLR	Agricultural area 2 (cm**3/g)	3.000E+03	7.000E+01	---	DCNUCOF(48,2)
DCLR	Agricultural area 3 (cm**3/g)	3.000E+03	7.000E+01	---	DCNUCOF(48,3)
DCLR	Agricultural area 4 (cm**3/g)	3.000E+03	7.000E+01	---	DCNUCOF(48,4)
DCLR	Offsite Dwelling (cm**3/g)	3.000E+03	7.000E+01	---	DCNUCDWE(48)
DCLR	Initial Leach rate (/yr) Ra-226	0.000E+00	0.000E+00	---	ALEACH(48)
DCLR	Initial releasable fraction of Ra-226	0.000E+00	0.000E+00	---	RELFRACINIT(48)
DCLR	Time at which release begins (years) Ra-226	3.000E+02	0.000E+00	---	RELTIMEINIT(48)
DCLR	Final Leach rate (/yr) Ra-226	0.000E+00	0.000E+00	---	RLEACHF(48)
DCLR	Total releasable fraction of Ra-226	1.000E+00	0.000E+00	---	RELFRACFINAL(48)
DCLR	Ra-226 Converts to releasable form over (years)	8.000E+02	0.000E+00	---	RELDUR(48)
DCLR	Temporal profile of conversion Ra-226	Linear	Instant	---	RELTIMEOPT(48)
DCLR	Release option Ra-226	1	0	---	RELOPT(48)
	0 = Rate Contorlled (Leach rate), 1 = Equilibrium Desorption (Distribution coefficient).				
DCLR	Distribution coefficients for Ra-228				
DCLR	Contaminated zone (cm**3/g)	1.500E+03	7.000E+01	---	DCNUCC(49)
DCLR	Unsaturated zone 1 (cm**3/g)	3.000E+03	7.000E+01	---	DCNUCU(49,1)
DCLR	Unsaturated zone 2 (cm**3/g)	3.000E+03	7.000E+01	---	DCNUCU(49,2)
DCLR	Unsaturated zone 3 (cm**3/g)	3.000E+03	7.000E+01	---	DCNUCU(49,3)
DCLR	Unsaturated zone 4 (cm**3/g)	3.000E+03	7.000E+01	---	DCNUCU(49,4)
DCLR	Unsaturated zone 5 (cm**3/g)	3.000E+03	7.000E+01	---	DCNUCU(49,5)
DCLR	Saturated zone (cm**3/g)	3.000E+03	7.000E+01	---	DCNUCS(49)
DCLR	Sediment in surface water body (cm**3/g)	0.000E+00	7.000E+01	---	DCNUCSWB(49)
DCLR	Agricultural area 1 (cm**3/g)	3.000E+03	7.000E+01	---	DCNUCOF(49,1)
DCLR	Agricultural area 2 (cm**3/g)	3.000E+03	7.000E+01	---	DCNUCOF(49,2)
DCLR	Agricultural area 3 (cm**3/g)	3.000E+03	7.000E+01	---	DCNUCOF(49,3)
DCLR	Agricultural area 4 (cm**3/g)	3.000E+03	7.000E+01	---	DCNUCOF(49,4)
DCLR	Offsite Dwelling (cm**3/g)	3.000E+03	7.000E+01	---	DCNUCDWE(49)
DCLR	Initial Leach rate (/yr) Ra-228	0.000E+00	0.000E+00	---	ALEACH(49)
DCLR	Initial releasable fraction of Ra-228	0.000E+00	0.000E+00	---	RELFRACINIT(49)
DCLR	Time at which release begins (years) Ra-228	3.000E+02	0.000E+00	---	RELTIMEINIT(49)
DCLR	Final Leach rate (/yr) Ra-228	0.000E+00	0.000E+00	---	RLEACHF(49)
DCLR	Total releasable fraction of Ra-228	1.000E+00	0.000E+00	---	RELFRACFINAL(49)
DCLR	Ra-228 Converts to releasable form over (years)	8.000E+02	0.000E+00	---	RELDUR(49)
DCLR	Temporal profile of conversion Ra-228	Linear	Instant	---	RELTIMEOPT(49)
DCLR	Release option Ra-228	1	0	---	RELOPT(49)
	0 = Rate Contorlled (Leach rate), 1 = Equilibrium Desorption (Distribution coefficient).				

Site-Specific Parameter Summary (continued)

Menu	Parameter	User Input	Default	RESRAD computed	Parameter Name
DCLR	Distribution coefficients for Sr-90				
DCLR	Contaminated zone (cm**3/g)	1.500E+01	3.000E+01	---	DCNUCC(50)
DCLR	Unsaturated zone 1 (cm**3/g)	3.000E+01	3.000E+01	---	DCNUCU(50,1)
DCLR	Unsaturated zone 2 (cm**3/g)	3.000E+01	3.000E+01	---	DCNUCU(50,2)
DCLR	Unsaturated zone 3 (cm**3/g)	3.000E+01	3.000E+01	---	DCNUCU(50,3)
DCLR	Unsaturated zone 4 (cm**3/g)	3.000E+01	3.000E+01	---	DCNUCU(50,4)
DCLR	Unsaturated zone 5 (cm**3/g)	3.000E+01	3.000E+01	---	DCNUCU(50,5)
DCLR	Saturated zone (cm**3/g)	3.000E+01	3.000E+01	---	DCNUCS(50)
DCLR	Sediment in surface water body (cm**3/g)	0.000E+00	3.000E+01	---	DCNUCSWB(50)
DCLR	Agricultural area 1 (cm**3/g)	3.000E+01	3.000E+01	---	DCNUCOF(50,1)
DCLR	Agricultural area 2 (cm**3/g)	3.000E+01	3.000E+01	---	DCNUCOF(50,2)
DCLR	Agricultural area 3 (cm**3/g)	3.000E+01	3.000E+01	---	DCNUCOF(50,3)
DCLR	Agricultural area 4 (cm**3/g)	3.000E+01	3.000E+01	---	DCNUCOF(50,4)
DCLR	Offsite Dwelling (cm**3/g)	3.000E+01	3.000E+01	---	DCNUCDWE(50)
DCLR	Initial Leach rate (/yr) Sr-90	0.000E+00	0.000E+00	---	ALEACH(50)
DCLR	Initial releasable fraction of Sr-90	0.000E+00	0.000E+00	---	RELFRACINIT(50)
DCLR	Time at which release begins (years) Sr-90	3.000E+02	0.000E+00	---	RELTIMEINIT(50)
DCLR	Final Leach rate (/yr) Sr-90	0.000E+00	0.000E+00	---	RLEACHF(50)
DCLR	Total releasable fraction of Sr-90	1.000E+00	0.000E+00	---	RELFRACFINAL(50)
DCLR	Sr-90 Converts to releasable form over (years)	8.000E+02	0.000E+00	---	RELDUR(50)
DCLR	Temporal profile of conversion Sr-90	Linear	Instant	---	RELTIMEOPT(50)
DCLR	Release option Sr-90	1	0	---	RELOPT(50)
	0 = Rate Contorlled (Leach rate), 1 = Equilibrium Desorption (Distribution coefficient).				
DCLR	Distribution coefficients for Tc-99				
DCLR	Contaminated zone (cm**3/g)	3.600E-01	0.000E+00	---	DCNUCC(51)
DCLR	Unsaturated zone 1 (cm**3/g)	7.200E-01	0.000E+00	---	DCNUCU(51,1)
DCLR	Unsaturated zone 2 (cm**3/g)	7.200E-01	0.000E+00	---	DCNUCU(51,2)
DCLR	Unsaturated zone 3 (cm**3/g)	7.200E-01	0.000E+00	---	DCNUCU(51,3)
DCLR	Unsaturated zone 4 (cm**3/g)	7.200E-01	0.000E+00	---	DCNUCU(51,4)
DCLR	Unsaturated zone 5 (cm**3/g)	7.200E-01	0.000E+00	---	DCNUCU(51,5)
DCLR	Saturated zone (cm**3/g)	7.200E-01	0.000E+00	---	DCNUCS(51)
DCLR	Sediment in surface water body (cm**3/g)	0.000E+00	0.000E+00	---	DCNUCSWB(51)
DCLR	Agricultural area 1 (cm**3/g)	7.200E-01	0.000E+00	---	DCNUCOF(51,1)
DCLR	Agricultural area 2 (cm**3/g)	7.200E-01	0.000E+00	---	DCNUCOF(51,2)
DCLR	Agricultural area 3 (cm**3/g)	7.200E-01	0.000E+00	---	DCNUCOF(51,3)
DCLR	Agricultural area 4 (cm**3/g)	7.200E-01	0.000E+00	---	DCNUCOF(51,4)
DCLR	Offsite Dwelling (cm**3/g)	7.200E-01	0.000E+00	---	DCNUCDWE(51)
DCLR	Initial Leach rate (/yr) Tc-99	0.000E+00	0.000E+00	---	ALEACH(51)
DCLR	Initial releasable fraction of Tc-99	0.000E+00	0.000E+00	---	RELFRACINIT(51)
DCLR	Time at which release begins (years) Tc-99	3.000E+02	0.000E+00	---	RELTIMEINIT(51)
DCLR	Final Leach rate (/yr) Tc-99	0.000E+00	0.000E+00	---	RLEACHF(51)
DCLR	Total releasable fraction of Tc-99	1.000E+00	0.000E+00	---	RELFRACFINAL(51)
DCLR	Tc-99 Converts to releasable form over (years)	8.000E+02	0.000E+00	---	RELDUR(51)
DCLR	Temporal profile of conversion Tc-99	Linear	Instant	---	RELTIMEOPT(51)
DCLR	Release option Tc-99	1	0	---	RELOPT(51)
	0 = Rate Contorlled (Leach rate), 1 = Equilibrium Desorption (Distribution coefficient).				

Site-Specific Parameter Summary (continued)

Menu	Parameter	User Input	Default	RESRAD computed	Parameter Name
DCLR	Distribution coefficients for Th-228				
DCLR	Contaminated zone (cm**3/g)	1.500E+03	6.000E+04	---	DCNUCC(52)
DCLR	Unsaturated zone 1 (cm**3/g)	3.000E+03	6.000E+04	---	DCNUCU(52,1)
DCLR	Unsaturated zone 2 (cm**3/g)	3.000E+03	6.000E+04	---	DCNUCU(52,2)
DCLR	Unsaturated zone 3 (cm**3/g)	3.000E+03	6.000E+04	---	DCNUCU(52,3)
DCLR	Unsaturated zone 4 (cm**3/g)	3.000E+03	6.000E+04	---	DCNUCU(52,4)
DCLR	Unsaturated zone 5 (cm**3/g)	3.000E+03	6.000E+04	---	DCNUCU(52,5)
DCLR	Saturated zone (cm**3/g)	3.000E+03	6.000E+04	---	DCNUCS(52)
DCLR	Sediment in surface water body (cm**3/g)	0.000E+00	6.000E+04	---	DCNUCSWB(52)
DCLR	Agricultural area 1 (cm**3/g)	3.000E+03	6.000E+04	---	DCNUCOF(52,1)
DCLR	Agricultural area 2 (cm**3/g)	3.000E+03	6.000E+04	---	DCNUCOF(52,2)
DCLR	Agricultural area 3 (cm**3/g)	3.000E+03	6.000E+04	---	DCNUCOF(52,3)
DCLR	Agricultural area 4 (cm**3/g)	3.000E+03	6.000E+04	---	DCNUCOF(52,4)
DCLR	Offsite Dwelling (cm**3/g)	3.000E+03	6.000E+04	---	DCNUCDWE(52)
DCLR	Initial Leach rate (/yr) Th-228	0.000E+00	0.000E+00	---	ALEACH(52)
DCLR	Initial releasable fraction of Th-228	0.000E+00	0.000E+00	---	RELFRACINIT(52)
DCLR	Time at which release begins (years) Th-228	3.000E+02	0.000E+00	---	RELTIMEINIT(52)
DCLR	Final Leach rate (/yr) Th-228	0.000E+00	0.000E+00	---	RLEACHF(52)
DCLR	Total releasable fraction of Th-228	1.000E+00	0.000E+00	---	RELFRACFINAL(52)
DCLR	Th-228 Converts to releasable form over (years)	8.000E+02	0.000E+00	---	RELDUR(52)
DCLR	Temporal profile of conversion Th-228	Linear	Instant	---	RELTIMEOPT(52)
DCLR	Release option Th-228	1	0	---	RELOPT(52)
	0 = Rate Contorlled (Leach rate), 1 = Equilibrium Desorption (Distribution coefficient).				
DCLR	Distribution coefficients for Th-229				
DCLR	Contaminated zone (cm**3/g)	1.500E+03	6.000E+04	---	DCNUCC(53)
DCLR	Unsaturated zone 1 (cm**3/g)	3.000E+03	6.000E+04	---	DCNUCU(53,1)
DCLR	Unsaturated zone 2 (cm**3/g)	3.000E+03	6.000E+04	---	DCNUCU(53,2)
DCLR	Unsaturated zone 3 (cm**3/g)	3.000E+03	6.000E+04	---	DCNUCU(53,3)
DCLR	Unsaturated zone 4 (cm**3/g)	3.000E+03	6.000E+04	---	DCNUCU(53,4)
DCLR	Unsaturated zone 5 (cm**3/g)	3.000E+03	6.000E+04	---	DCNUCU(53,5)
DCLR	Saturated zone (cm**3/g)	3.000E+03	6.000E+04	---	DCNUCS(53)
DCLR	Sediment in surface water body (cm**3/g)	0.000E+00	6.000E+04	---	DCNUCSWB(53)
DCLR	Agricultural area 1 (cm**3/g)	3.000E+03	6.000E+04	---	DCNUCOF(53,1)
DCLR	Agricultural area 2 (cm**3/g)	3.000E+03	6.000E+04	---	DCNUCOF(53,2)
DCLR	Agricultural area 3 (cm**3/g)	3.000E+03	6.000E+04	---	DCNUCOF(53,3)
DCLR	Agricultural area 4 (cm**3/g)	3.000E+03	6.000E+04	---	DCNUCOF(53,4)
DCLR	Offsite Dwelling (cm**3/g)	3.000E+03	6.000E+04	---	DCNUCDWE(53)
DCLR	Initial Leach rate (/yr) Th-229	0.000E+00	0.000E+00	---	ALEACH(53)
DCLR	Initial releasable fraction of Th-229	0.000E+00	0.000E+00	---	RELFRACINIT(53)
DCLR	Time at which release begins (years) Th-229	3.000E+02	0.000E+00	---	RELTIMEINIT(53)
DCLR	Final Leach rate (/yr) Th-229	0.000E+00	0.000E+00	---	RLEACHF(53)
DCLR	Total releasable fraction of Th-229	1.000E+00	0.000E+00	---	RELFRACFINAL(53)
DCLR	Th-229 Converts to releasable form over (years)	8.000E+02	0.000E+00	---	RELDUR(53)
DCLR	Temporal profile of conversion Th-229	Linear	Instant	---	RELTIMEOPT(53)
DCLR	Release option Th-229	1	0	---	RELOPT(53)
	0 = Rate Contorlled (Leach rate), 1 = Equilibrium Desorption (Distribution coefficient).				

Site-Specific Parameter Summary (continued)

Menu	Parameter	User Input	Default	RESRAD computed	Parameter Name
DCLR	Distribution coefficients for Th-230				
DCLR	Contaminated zone (cm**3/g)	1.500E+03	6.000E+04	---	DCNUCC(54)
DCLR	Unsaturated zone 1 (cm**3/g)	3.000E+03	6.000E+04	---	DCNUCU(54,1)
DCLR	Unsaturated zone 2 (cm**3/g)	3.000E+03	6.000E+04	---	DCNUCU(54,2)
DCLR	Unsaturated zone 3 (cm**3/g)	3.000E+03	6.000E+04	---	DCNUCU(54,3)
DCLR	Unsaturated zone 4 (cm**3/g)	3.000E+03	6.000E+04	---	DCNUCU(54,4)
DCLR	Unsaturated zone 5 (cm**3/g)	3.000E+03	6.000E+04	---	DCNUCU(54,5)
DCLR	Saturated zone (cm**3/g)	3.000E+03	6.000E+04	---	DCNUCS(54)
DCLR	Sediment in surface water body (cm**3/g)	0.000E+00	6.000E+04	---	DCNUCSWB(54)
DCLR	Agricultural area 1 (cm**3/g)	3.000E+03	6.000E+04	---	DCNUCOF(54,1)
DCLR	Agricultural area 2 (cm**3/g)	3.000E+03	6.000E+04	---	DCNUCOF(54,2)
DCLR	Agricultural area 3 (cm**3/g)	3.000E+03	6.000E+04	---	DCNUCOF(54,3)
DCLR	Agricultural area 4 (cm**3/g)	3.000E+03	6.000E+04	---	DCNUCOF(54,4)
DCLR	Offsite Dwelling (cm**3/g)	3.000E+03	6.000E+04	---	DCNUCDWE(54)
DCLR	Initial Leach rate (/yr) Th-230	0.000E+00	0.000E+00	---	ALEACH(54)
DCLR	Initial releasable fraction of Th-230	0.000E+00	0.000E+00	---	RELFRACINIT(54)
DCLR	Time at which release begins (years) Th-230	3.000E+02	0.000E+00	---	RELTIMEINIT(54)
DCLR	Final Leach rate (/yr) Th-230	0.000E+00	0.000E+00	---	RLEACHF(54)
DCLR	Total releasable fraction of Th-230	1.000E+00	0.000E+00	---	RELFRACFINAL(54)
DCLR	Th-230 Converts to releasable form over (years)	8.000E+02	0.000E+00	---	RELDUR(54)
DCLR	Temporal profile of conversion Th-230	Linear	Instant	---	RELTIMEOPT(54)
DCLR	Release option Th-230	1	0	---	RELOPT(54)
	0 = Rate Contorlled (Leach rate), 1 = Equilibrium Desorption (Distribution coefficient).				
DCLR	Distribution coefficients for Th-232				
DCLR	Contaminated zone (cm**3/g)	1.500E+03	6.000E+04	---	DCNUCC(55)
DCLR	Unsaturated zone 1 (cm**3/g)	3.000E+03	6.000E+04	---	DCNUCU(55,1)
DCLR	Unsaturated zone 2 (cm**3/g)	3.000E+03	6.000E+04	---	DCNUCU(55,2)
DCLR	Unsaturated zone 3 (cm**3/g)	3.000E+03	6.000E+04	---	DCNUCU(55,3)
DCLR	Unsaturated zone 4 (cm**3/g)	3.000E+03	6.000E+04	---	DCNUCU(55,4)
DCLR	Unsaturated zone 5 (cm**3/g)	3.000E+03	6.000E+04	---	DCNUCU(55,5)
DCLR	Saturated zone (cm**3/g)	3.000E+03	6.000E+04	---	DCNUCS(55)
DCLR	Sediment in surface water body (cm**3/g)	0.000E+00	6.000E+04	---	DCNUCSWB(55)
DCLR	Agricultural area 1 (cm**3/g)	3.000E+03	6.000E+04	---	DCNUCOF(55,1)
DCLR	Agricultural area 2 (cm**3/g)	3.000E+03	6.000E+04	---	DCNUCOF(55,2)
DCLR	Agricultural area 3 (cm**3/g)	3.000E+03	6.000E+04	---	DCNUCOF(55,3)
DCLR	Agricultural area 4 (cm**3/g)	3.000E+03	6.000E+04	---	DCNUCOF(55,4)
DCLR	Offsite Dwelling (cm**3/g)	3.000E+03	6.000E+04	---	DCNUCDWE(55)
DCLR	Initial Leach rate (/yr) Th-232	0.000E+00	0.000E+00	---	ALEACH(55)
DCLR	Initial releasable fraction of Th-232	0.000E+00	0.000E+00	---	RELFRACINIT(55)
DCLR	Time at which release begins (years) Th-232	3.000E+02	0.000E+00	---	RELTIMEINIT(55)
DCLR	Final Leach rate (/yr) Th-232	0.000E+00	0.000E+00	---	RLEACHF(55)
DCLR	Total releasable fraction of Th-232	1.000E+00	0.000E+00	---	RELFRACFINAL(55)
DCLR	Th-232 Converts to releasable form over (years)	8.000E+02	0.000E+00	---	RELDUR(55)
DCLR	Temporal profile of conversion Th-232	Linear	Instant	---	RELTIMEOPT(55)
DCLR	Release option Th-232	1	0	---	RELOPT(55)
	0 = Rate Contorlled (Leach rate), 1 = Equilibrium Desorption (Distribution coefficient).				

Site-Specific Parameter Summary (continued)

Menu	Parameter	User Input	Default	RESRAD computed	Parameter Name
DCLR	Distribution coefficients for U-232				
DCLR	Contaminated zone (cm**3/g)	2.500E+01	5.000E+01	---	DCNUCC(56)
DCLR	Unsaturated zone 1 (cm**3/g)	5.000E+01	5.000E+01	---	DCNUCU(56,1)
DCLR	Unsaturated zone 2 (cm**3/g)	5.000E+01	5.000E+01	---	DCNUCU(56,2)
DCLR	Unsaturated zone 3 (cm**3/g)	5.000E+01	5.000E+01	---	DCNUCU(56,3)
DCLR	Unsaturated zone 4 (cm**3/g)	5.000E+01	5.000E+01	---	DCNUCU(56,4)
DCLR	Unsaturated zone 5 (cm**3/g)	5.000E+01	5.000E+01	---	DCNUCU(56,5)
DCLR	Saturated zone (cm**3/g)	5.000E+01	5.000E+01	---	DCNUCS(56)
DCLR	Sediment in surface water body (cm**3/g)	0.000E+00	5.000E+01	---	DCNUCSWB(56)
DCLR	Agricultural area 1 (cm**3/g)	5.000E+01	5.000E+01	---	DCNUCOF(56,1)
DCLR	Agricultural area 2 (cm**3/g)	5.000E+01	5.000E+01	---	DCNUCOF(56,2)
DCLR	Agricultural area 3 (cm**3/g)	5.000E+01	5.000E+01	---	DCNUCOF(56,3)
DCLR	Agricultural area 4 (cm**3/g)	5.000E+01	5.000E+01	---	DCNUCOF(56,4)
DCLR	Offsite Dwelling (cm**3/g)	5.000E+01	5.000E+01	---	DCNUCDWE(56)
DCLR	Initial Leach rate (/yr) U-232	0.000E+00	0.000E+00	---	ALEACH(56)
DCLR	Initial releasable fraction of U-232	0.000E+00	0.000E+00	---	RELFRACINIT(56)
DCLR	Time at which release begins (years) U-232	3.000E+02	0.000E+00	---	RELTIMEINIT(56)
DCLR	Final Leach rate (/yr) U-232	0.000E+00	0.000E+00	---	RLEACHF(56)
DCLR	Total releasable fraction of U-232	1.000E+00	0.000E+00	---	RELFRACFINAL(56)
DCLR	U-232 Converts to releasable form over (years)	8.000E+02	0.000E+00	---	RELDUR(56)
DCLR	Temporal profile of conversion U-232	Linear	Instant	---	RELTIMEOPT(56)
DCLR	Release option U-232	1	0	---	RELOPT(56)
	0 = Rate Contorlled (Leach rate), 1 = Equilibrium Desorption (Distribution coefficient).				
DCLR	Distribution coefficients for U-233				
DCLR	Contaminated zone (cm**3/g)	2.500E+01	5.000E+01	---	DCNUCC(57)
DCLR	Unsaturated zone 1 (cm**3/g)	5.000E+01	5.000E+01	---	DCNUCU(57,1)
DCLR	Unsaturated zone 2 (cm**3/g)	5.000E+01	5.000E+01	---	DCNUCU(57,2)
DCLR	Unsaturated zone 3 (cm**3/g)	5.000E+01	5.000E+01	---	DCNUCU(57,3)
DCLR	Unsaturated zone 4 (cm**3/g)	5.000E+01	5.000E+01	---	DCNUCU(57,4)
DCLR	Unsaturated zone 5 (cm**3/g)	5.000E+01	5.000E+01	---	DCNUCU(57,5)
DCLR	Saturated zone (cm**3/g)	5.000E+01	5.000E+01	---	DCNUCS(57)
DCLR	Sediment in surface water body (cm**3/g)	0.000E+00	5.000E+01	---	DCNUCSWB(57)
DCLR	Agricultural area 1 (cm**3/g)	5.000E+01	5.000E+01	---	DCNUCOF(57,1)
DCLR	Agricultural area 2 (cm**3/g)	5.000E+01	5.000E+01	---	DCNUCOF(57,2)
DCLR	Agricultural area 3 (cm**3/g)	5.000E+01	5.000E+01	---	DCNUCOF(57,3)
DCLR	Agricultural area 4 (cm**3/g)	5.000E+01	5.000E+01	---	DCNUCOF(57,4)
DCLR	Offsite Dwelling (cm**3/g)	5.000E+01	5.000E+01	---	DCNUCDWE(57)
DCLR	Initial Leach rate (/yr) U-233	0.000E+00	0.000E+00	---	ALEACH(57)
DCLR	Initial releasable fraction of U-233	0.000E+00	0.000E+00	---	RELFRACINIT(57)
DCLR	Time at which release begins (years) U-233	3.000E+02	0.000E+00	---	RELTIMEINIT(57)
DCLR	Final Leach rate (/yr) U-233	0.000E+00	0.000E+00	---	RLEACHF(57)
DCLR	Total releasable fraction of U-233	1.000E+00	0.000E+00	---	RELFRACFINAL(57)
DCLR	U-233 Converts to releasable form over (years)	8.000E+02	0.000E+00	---	RELDUR(57)
DCLR	Temporal profile of conversion U-233	Linear	Instant	---	RELTIMEOPT(57)
DCLR	Release option U-233	1	0	---	RELOPT(57)
	0 = Rate Contorlled (Leach rate), 1 = Equilibrium Desorption (Distribution coefficient).				

Site-Specific Parameter Summary (continued)

Menu	Parameter	User Input	Default	RESRAD computed	Parameter Name
DCLR	Distribution coefficients for U-234				
DCLR	Contaminated zone (cm**3/g)	2.500E+01	5.000E+01	---	DCNUCC(58)
DCLR	Unsaturated zone 1 (cm**3/g)	5.000E+01	5.000E+01	---	DCNUCU(58,1)
DCLR	Unsaturated zone 2 (cm**3/g)	5.000E+01	5.000E+01	---	DCNUCU(58,2)
DCLR	Unsaturated zone 3 (cm**3/g)	5.000E+01	5.000E+01	---	DCNUCU(58,3)
DCLR	Unsaturated zone 4 (cm**3/g)	5.000E+01	5.000E+01	---	DCNUCU(58,4)
DCLR	Unsaturated zone 5 (cm**3/g)	5.000E+01	5.000E+01	---	DCNUCU(58,5)
DCLR	Saturated zone (cm**3/g)	5.000E+01	5.000E+01	---	DCNUCS(58)
DCLR	Sediment in surface water body (cm**3/g)	0.000E+00	5.000E+01	---	DCNUCSWB(58)
DCLR	Agricultural area 1 (cm**3/g)	5.000E+01	5.000E+01	---	DCNUCOF(58,1)
DCLR	Agricultural area 2 (cm**3/g)	5.000E+01	5.000E+01	---	DCNUCOF(58,2)
DCLR	Agricultural area 3 (cm**3/g)	5.000E+01	5.000E+01	---	DCNUCOF(58,3)
DCLR	Agricultural area 4 (cm**3/g)	5.000E+01	5.000E+01	---	DCNUCOF(58,4)
DCLR	Offsite Dwelling (cm**3/g)	5.000E+01	5.000E+01	---	DCNUCDWE(58)
DCLR	Initial Leach rate (/yr) U-234	0.000E+00	0.000E+00	---	ALEACH(58)
DCLR	Initial releasable fraction of U-234	0.000E+00	0.000E+00	---	RELFRACINIT(58)
DCLR	Time at which release begins (years) U-234	3.000E+02	0.000E+00	---	RELTIMEINIT(58)
DCLR	Final Leach rate (/yr) U-234	0.000E+00	0.000E+00	---	RLEACHF(58)
DCLR	Total releasable fraction of U-234	1.000E+00	0.000E+00	---	RELFRACFINAL(58)
DCLR	U-234 Converts to releasable form over (years)	8.000E+02	0.000E+00	---	RELDUR(58)
DCLR	Temporal profile of conversion U-234	Linear	Instant	---	RELTIMEOPT(58)
DCLR	Release option U-234	1	0	---	RELOPT(58)
	0 = Rate Contorlled (Leach rate), 1 = Equilibrium Desorption (Distribution coefficient).				
DCLR	Distribution coefficients for U-235				
DCLR	Contaminated zone (cm**3/g)	2.500E+01	5.000E+01	---	DCNUCC(59)
DCLR	Unsaturated zone 1 (cm**3/g)	5.000E+01	5.000E+01	---	DCNUCU(59,1)
DCLR	Unsaturated zone 2 (cm**3/g)	5.000E+01	5.000E+01	---	DCNUCU(59,2)
DCLR	Unsaturated zone 3 (cm**3/g)	5.000E+01	5.000E+01	---	DCNUCU(59,3)
DCLR	Unsaturated zone 4 (cm**3/g)	5.000E+01	5.000E+01	---	DCNUCU(59,4)
DCLR	Unsaturated zone 5 (cm**3/g)	5.000E+01	5.000E+01	---	DCNUCU(59,5)
DCLR	Saturated zone (cm**3/g)	5.000E+01	5.000E+01	---	DCNUCS(59)
DCLR	Sediment in surface water body (cm**3/g)	0.000E+00	5.000E+01	---	DCNUCSWB(59)
DCLR	Agricultural area 1 (cm**3/g)	5.000E+01	5.000E+01	---	DCNUCOF(59,1)
DCLR	Agricultural area 2 (cm**3/g)	5.000E+01	5.000E+01	---	DCNUCOF(59,2)
DCLR	Agricultural area 3 (cm**3/g)	5.000E+01	5.000E+01	---	DCNUCOF(59,3)
DCLR	Agricultural area 4 (cm**3/g)	5.000E+01	5.000E+01	---	DCNUCOF(59,4)
DCLR	Offsite Dwelling (cm**3/g)	5.000E+01	5.000E+01	---	DCNUCDWE(59)
DCLR	Initial Leach rate (/yr) U-235	0.000E+00	0.000E+00	---	ALEACH(59)
DCLR	Initial releasable fraction of U-235	0.000E+00	0.000E+00	---	RELFRACINIT(59)
DCLR	Time at which release begins (years) U-235	3.000E+02	0.000E+00	---	RELTIMEINIT(59)
DCLR	Final Leach rate (/yr) U-235	0.000E+00	0.000E+00	---	RLEACHF(59)
DCLR	Total releasable fraction of U-235	1.000E+00	0.000E+00	---	RELFRACFINAL(59)
DCLR	U-235 Converts to releasable form over (years)	8.000E+02	0.000E+00	---	RELDUR(59)
DCLR	Temporal profile of conversion U-235	Linear	Instant	---	RELTIMEOPT(59)
DCLR	Release option U-235	1	0	---	RELOPT(59)
	0 = Rate Contorlled (Leach rate), 1 = Equilibrium Desorption (Distribution coefficient).				

Site-Specific Parameter Summary (continued)

Menu	Parameter	User Input	Default	RESRAD computed	Parameter Name
DCLR	Distribution coefficients for U-236				
DCLR	Contaminated zone (cm**3/g)	2.500E+01	5.000E+01	---	DCNUCC(60)
DCLR	Unsaturated zone 1 (cm**3/g)	5.000E+01	5.000E+01	---	DCNUCU(60,1)
DCLR	Unsaturated zone 2 (cm**3/g)	5.000E+01	5.000E+01	---	DCNUCU(60,2)
DCLR	Unsaturated zone 3 (cm**3/g)	5.000E+01	5.000E+01	---	DCNUCU(60,3)
DCLR	Unsaturated zone 4 (cm**3/g)	5.000E+01	5.000E+01	---	DCNUCU(60,4)
DCLR	Unsaturated zone 5 (cm**3/g)	5.000E+01	5.000E+01	---	DCNUCU(60,5)
DCLR	Saturated zone (cm**3/g)	5.000E+01	5.000E+01	---	DCNUCS(60)
DCLR	Sediment in surface water body (cm**3/g)	0.000E+00	5.000E+01	---	DCNUCSWB(60)
DCLR	Agricultural area 1 (cm**3/g)	5.000E+01	5.000E+01	---	DCNUCOF(60,1)
DCLR	Agricultural area 2 (cm**3/g)	5.000E+01	5.000E+01	---	DCNUCOF(60,2)
DCLR	Agricultural area 3 (cm**3/g)	5.000E+01	5.000E+01	---	DCNUCOF(60,3)
DCLR	Agricultural area 4 (cm**3/g)	5.000E+01	5.000E+01	---	DCNUCOF(60,4)
DCLR	Offsite Dwelling (cm**3/g)	5.000E+01	5.000E+01	---	DCNUCDWE(60)
DCLR	Initial Leach rate (/yr) U-236	0.000E+00	0.000E+00	---	ALEACH(60)
DCLR	Initial releasable fraction of U-236	0.000E+00	0.000E+00	---	RELFRACINIT(60)
DCLR	Time at which release begins (years) U-236	3.000E+02	0.000E+00	---	RELTIMEINIT(60)
DCLR	Final Leach rate (/yr) U-236	0.000E+00	0.000E+00	---	RLEACHF(60)
DCLR	Total releasable fraction of U-236	1.000E+00	0.000E+00	---	RELFRACFINAL(60)
DCLR	U-236 Converts to releasable form over (years)	8.000E+02	0.000E+00	---	RELDUR(60)
DCLR	Temporal profile of conversion U-236	Linear	Instant	---	RELTIMEOPT(60)
DCLR	Release option U-236	1	0	---	RELOPT(60)
	0 = Rate Contorlled (Leach rate), 1 = Equilibrium Desorption (Distribution coefficient).				
DCLR	Distribution coefficients for U-238				
DCLR	Contaminated zone (cm**3/g)	2.500E+01	5.000E+01	---	DCNUCC(61)
DCLR	Unsaturated zone 1 (cm**3/g)	5.000E+01	5.000E+01	---	DCNUCU(61,1)
DCLR	Unsaturated zone 2 (cm**3/g)	5.000E+01	5.000E+01	---	DCNUCU(61,2)
DCLR	Unsaturated zone 3 (cm**3/g)	5.000E+01	5.000E+01	---	DCNUCU(61,3)
DCLR	Unsaturated zone 4 (cm**3/g)	5.000E+01	5.000E+01	---	DCNUCU(61,4)
DCLR	Unsaturated zone 5 (cm**3/g)	5.000E+01	5.000E+01	---	DCNUCU(61,5)
DCLR	Saturated zone (cm**3/g)	5.000E+01	5.000E+01	---	DCNUCS(61)
DCLR	Sediment in surface water body (cm**3/g)	0.000E+00	5.000E+01	---	DCNUCSWB(61)
DCLR	Agricultural area 1 (cm**3/g)	5.000E+01	5.000E+01	---	DCNUCOF(61,1)
DCLR	Agricultural area 2 (cm**3/g)	5.000E+01	5.000E+01	---	DCNUCOF(61,2)
DCLR	Agricultural area 3 (cm**3/g)	5.000E+01	5.000E+01	---	DCNUCOF(61,3)
DCLR	Agricultural area 4 (cm**3/g)	5.000E+01	5.000E+01	---	DCNUCOF(61,4)
DCLR	Offsite Dwelling (cm**3/g)	5.000E+01	5.000E+01	---	DCNUCDWE(61)
DCLR	Initial Leach rate (/yr) U-238	0.000E+00	0.000E+00	---	ALEACH(61)
DCLR	Initial releasable fraction of U-238	0.000E+00	0.000E+00	---	RELFRACINIT(61)
DCLR	Time at which release begins (years) U-238	3.000E+02	0.000E+00	---	RELTIMEINIT(61)
DCLR	Final Leach rate (/yr) U-238	0.000E+00	0.000E+00	---	RLEACHF(61)
DCLR	Total releasable fraction of U-238	1.000E+00	0.000E+00	---	RELFRACFINAL(61)
DCLR	U-238 Converts to releasable form over (years)	8.000E+02	0.000E+00	---	RELDUR(61)
DCLR	Temporal profile of conversion U-238	Linear	Instant	---	RELTIMEOPT(61)
DCLR	Release option U-238	1	0	---	RELOPT(61)
	0 = Rate Contorlled (Leach rate), 1 = Equilibrium Desorption (Distribution coefficient).				

Site-Specific Parameter Summary (continued)

Menu	Parameter	User Input	Default	RESRAD computed	Parameter Name
LYOT	Bearing of X axis (clockwise angle N-->X in degrees)	9.000E+01	9.000E+01	---	DNXBEARING
LYOT	Length of Primary contamination in X Direction	2.506E+02	1.000E+02	---	SOURCEXY(1)
LYOT	Length of Primary contamination in Y Direction	3.827E+02	1.000E+02	---	SOURCEXY(2)
LYOT	Smaller X coordinate of Agricultural Area 1	0.000E+00	3.438E+01	---	AGRIXY(1,1)
LYOT	Larger X coordinate of Agricultural Area 1	3.200E+01	6.562E+01	---	AGRIXY(2,1)
LYOT	Smaller Y coordinate of Agricultural Area 1	-1.320E+02	2.340E+02	---	AGRIXY(3,1)
LYOT	Larger Y coordinate of Agricultural Area 1	-1.000E+02	2.660E+02	---	AGRIXY(4,1)
LYOT	Smaller X coordinate of Agricultural Area 2	4.000E+01	3.438E+01	---	AGRIXY(1,2)
LYOT	Larger X coordinate of Agricultural Area 2	7.200E+01	6.562E+01	---	AGRIXY(2,2)
LYOT	Smaller Y coordinate of Agricultural Area 2	-1.320E+02	2.680E+02	---	AGRIXY(3,2)
LYOT	Larger Y coordinate of Agricultural Area 2	-1.000E+02	3.000E+02	---	AGRIXY(4,2)
LYOT	Smaller X coordinate of Agricultural Area 3	1.200E+02	0.000E+00	---	AGRIXY(1,3)
LYOT	Larger X coordinate of Agricultural Area 3	2.200E+02	1.000E+02	---	AGRIXY(2,3)
LYOT	Smaller Y coordinate of Agricultural Area 3	-2.000E+02	4.500E+02	---	AGRIXY(3,3)
LYOT	Larger Y coordinate of Agricultural Area 3	-1.000E+02	5.500E+02	---	AGRIXY(4,3)
LYOT	Smaller X coordinate of Agricultural Area 4	2.300E+02	0.000E+00	---	AGRIXY(1,4)
LYOT	Larger X coordinate of Agricultural Area 4	3.300E+02	1.000E+02	---	AGRIXY(2,4)
LYOT	Smaller Y coordinate of Agricultural Area 4	-2.000E+02	3.000E+02	---	AGRIXY(3,4)
LYOT	Larger Y coordinate of Agricultural Area 4	-1.000E+02	4.000E+02	---	AGRIXY(4,4)
LYOT	Smaller X coordinate of Dwelling Area	8.000E+01	3.438E+01	---	DWELLXY(1)
LYOT	Larger X coordinate of Dwelling Area	1.120E+02	6.562E+01	---	DWELLXY(2)
LYOT	Smaller Y coordinate of Dwelling Area	-1.320E+02	1.340E+02	---	DWELLXY(3)
LYOT	Larger Y coordinate of Dwelling Area	-1.000E+02	1.660E+02	---	DWELLXY(4)
LYOT	Smaller X coordinate of Surface water body	-5.754E+02	-1.000E+02	---	SWXY(1)
LYOT	Larger X coordinate of Surface water body	-4.754E+02	2.000E+02	---	SWXY(2)
LYOT	Smaller Y coordinate of Surface water body	-3.374E+02	5.500E+02	---	SWXY(3)
LYOT	Larger Y coordinate of Surface water body	-3.324E+02	8.500E+02	---	SWXY(4)
STOR	Storage times of contaminated foodstuffs (days):				
STOR	Surface water	1.000E+00	1.000E+00	---	STOR_T(1)
STOR	Well water	1.000E+00	1.000E+00	---	STOR_T(2)
STOR	Fruits, non-leafy vegetables, and grain	1.400E+01	1.400E+01	---	STOR_T(3)
STOR	Leafy vegetables	1.000E+00	1.000E+00	---	STOR_T(4)
STOR	Livestock feed - pasture or silage	1.000E+00	1.000E+00	---	STOR_T(5)
STOR	Livestock feed - grain	4.500E+01	4.500E+01	---	STOR_T(6)
STOR	Meat and poultry	2.000E+01	2.000E+01	---	STOR_T(7)
STOR	Milk	1.000E+00	1.000E+00	---	STOR_T(8)
STOR	Fish	7.000E+00	7.000E+00	---	STOR_T(9)
STOR	Crustacea and mollusks	7.000E+00	7.000E+00	---	STOR_T(10)
TIME	Times at which dose/risk are to be reported (yr)	1.000E+00	1.000E+00	---	T(2)
TIME	Times at which dose/risk are to be reported (yr)	2.000E+02	3.000E+00	---	T(3)
TIME	Times at which dose/risk are to be reported (yr)	4.000E+02	6.000E+00	---	T(4)
TIME	Times at which dose/risk are to be reported (yr)	5.000E+02	1.200E+01	---	T(5)
TIME	Times at which dose/risk are to be reported (yr)	6.000E+02	3.000E+01	---	T(6)
TIME	Times at which dose/risk are to be reported (yr)	8.000E+02	7.500E+01	---	T(7)
TIME	Times at which dose/risk are to be reported (yr)	1.000E+03	1.750E+02	---	T(8)

Site-Specific Parameter Summary (continued)

Menu	Parameter	User Input	Default	RESRAD computed	Parameter Name
TIME	Times at which dose/risk are to be reported (yr)	2.000E+03	4.200E+02	---	T(9)
TIME	Times at which dose/risk are to be reported (yr)	1.000E+04	9.700E+02	---	T(10)
SITE	Precipitation (m/yr)	1.382E+00	1.000E+00	---	PRECIP
SITE	Average annual wind speed (m/sec)	3.434E+00	8.900E-01	---	WIND
PRCZ	Area of primary contamination (m**2)	9.590E+04	1.000E+04	---	AREA
PRCZ	Length parallel to aquifer flow (m)	3.989E+02	1.000E+02	---	LCZPAQ
PRCZ	Depth of soil mixing layer (m)	1.500E-01	1.500E-01	---	DM
PRCZ	Mass loading of all particulates for release(g/m**3)	1.000E-04	1.000E-04	---	MLFD
PRCZ	Deposition velocity for release calculatons (m/s)	1.000E-03	1.000E-03	---	DEPVEL_DUSTT
PRCZ	Respirable particulates as a fraction of total	1.000E+00	1.000E+00	---	RESPFRACPC
PRCZ	Deposition velocity of dust (m)	1.000E-03	1.000E-03	---	DEPVEL_DUST
PRCZ	Irrigation (m/yr)	0.000E+00	2.000E-01	---	RI
PRCZ	Evapotranspiration coefficient	5.680E-01	5.000E-01	---	EVAPTR
PRCZ	Runoff coefficient	9.630E-01	2.000E-01	---	RUNOFF
PRCZ	Rainfall Erosion Index	0.000E+00	1.600E+02	---	RAINEROS
PRCZ	Slope-length-steepness factor of prim. contamination	4.000E-01	4.000E-01	---	SLPLENSTPPC
PRCZ	Cropping-management factor of primary contamination	3.000E-03	3.000E-03	---	CRPMANGPC
PRCZ	Conservation practice factor of prim. contamination	0.000E+00	1.000E+00	---	CONVPRACPC
PRCZ	Thickness of contaminated zone (m)	1.750E+01	2.000E+00	---	THICK0
PRCZ	Fraction of primary contamination that is sumberged	0.000E+00	0.000E+00	---	SUBMERGEDF
PRCZ	Depth of primary contamination below water table, m	0.000E+00	0.000E+00	---	SUBMERGEDDEPTH
PRCZ	Contaminated zone total porosity	4.190E-01	4.000E-01	---	TPCZ
PRCZ	Computed erosion rate of contaminated zone (m/yr)	0.000E+00	1.147E-05	---	VCZ
PRCZ	Density of contaminated zone (g/cm**3)	1.900E+00	1.500E+00	---	DENSCZ
PRCZ	Soil erodibility factor of contaminated zone	0.000E+00	4.000E-01	---	ERODIBILITYCZ
PRCZ	Contaminated zone field capacity	3.070E-01	3.000E-01	---	FCCZ
PRCZ	Contaminated zone b parameter	7.750E+00	5.300E+00	---	BCZ
PRCZ	Contaminated zone hydraulic conductivity (m/yr)	5.990E+00	1.000E+01	---	HCCZ
PRCZ	Contaminated zone effective porosity	2.340E-01	4.000E-01	---	EPCZ
PRCZ	longitudinal dispersivity of prime contamination (m)	1.800E+00	5.000E-02	---	ALPHALCZ
PRCZ	Cover depth (m)	3.353E+00	0.000E+00	---	COVER0
PRCZ	Total porosity of the cover material	not used	4.000E-01	---	TPCV
PRCZ	Computed erosion rate of cover material (m/yr)	0.000E+00	1.147E-05	---	VCV
PRCZ	Density of cover material (g/cm**3)	1.500E+00	1.500E+00	---	DENSCV
PRCZ	Soil erodibility factor of cover	0.000E+00	4.000E-01	---	ERODIBILITYCV
PRCZ	Volumetric water content of the cover material	not used	5.000E-02	---	PH2OCV
AGRI	Areal extent of Agricultural Area 1 (m**2)	1.024E+03	1.000E+03	---	AREAO(1)
AGRI	Fraction of Agri. Area 1 directly over the c.z.	0.000E+00	0.000E+00	---	FAREA_PLANT(1)
AGRI	Evapotranspiration coefficient in Agri. Area 1	5.680E-01	5.000E-01	---	EVAPTRN(1)
AGRI	Runoff coefficient in Agricultural Area 1	7.340E-01	2.000E-01	---	RUNOF(1)
AGRI	Mixing depth/plow layer of Agricultural Area 1	1.500E-01	1.500E-01	---	DPTHMIXG(1)
AGRI	Water filled porosity of soil in Agri. Area 1	3.000E-01	3.000E-01	---	TMOF(1)
AGRI	Computed erosion rate of soil in Agri. Area 1	0.000E+00	1.147E-05	---	EROSN(1)
AGRI	Dry Bulk Density of soil in Agricultural Area 1	1.500E+00	1.500E+00	---	RHOB(1)

Site-Specific Parameter Summary (continued)

Menu	Parameter	User Input	Default	RESRAD computed	Parameter Name
AGRI	Soil erodibility factor of Agricultural Area 1	4.000E-01	4.000E-01	---	ERODIBILITY(1)
AGRI	Slope-length-steepness factor, Agricultural Area 1	4.000E-01	4.000E-01	---	SLPLENSTP(1)
AGRI	Cropping-management factor of Agricultural Area 1	3.000E-03	3.000E-03	---	CRPMANG(1)
AGRI	Conservation practice factor of Agricultural Area 1	1.000E+00	1.000E+00	---	CONVPRAC(1)
AGRI	Total porosity of soil in Agricultural Area 1	not used	4.000E-01	---	TPOF(1)
AGRI	Areal extent of Agricultural Area 2 (m**2)	1.024E+03	1.000E+03	---	AREAO(2)
AGRI	Fraction of Agri. Area 2 directly over the c.z.	0.000E+00	0.000E+00	---	FAREA_PLANT(2)
AGRI	Evapotranspiration coefficient in Agri. Area 2	5.680E-01	5.000E-01	---	EVAPTRN(2)
AGRI	Runoff coefficient in Agricultural Area 2	7.340E-01	2.000E-01	---	RUNOF(2)
AGRI	Mixing depth/plow layer of Agricultural Area 2	1.500E-01	1.500E-01	---	DPTHMIXG(2)
AGRI	Water filled porosity of soil in Agri. Area 2	3.000E-01	3.000E-01	---	TMOF(2)
AGRI	Computed erosion rate of soil in Agri. Area 2	0.000E+00	1.147E-05	---	EROSN(2)
AGRI	Dry Bulk Density of soil in Agricultural Area 2	1.500E+00	1.500E+00	---	RHOB(2)
AGRI	Soil erodibility factor of Agricultural Area 2	4.000E-01	4.000E-01	---	ERODIBILITY(2)
AGRI	Slope-length-steepness factor, Agricultural Area 2	4.000E-01	4.000E-01	---	SLPLENSTP(2)
AGRI	Cropping-management factor of Agricultural Area 2	3.000E-03	3.000E-03	---	CRPMANG(2)
AGRI	Conservation practice factor of Agricultural Area 2	1.000E+00	1.000E+00	---	CONVPRAC(2)
AGRI	Total porosity of soil in Agricultural Area 2	not used	4.000E-01	---	TPOF(2)
AGRI	Areal extent of Agricultural Area 3 (m**2)	1.000E+04	1.000E+04	---	AREAO(3)
AGRI	Fraction of Agri. Area 3 directly over the c.z.	0.000E+00	0.000E+00	---	FAREA_PLANT(3)
AGRI	Evapotranspiration coefficient in Agri. Area 3	5.680E-01	5.000E-01	---	EVAPTRN(3)
AGRI	Runoff coefficient in Agricultural Area 3	7.340E-01	2.000E-01	---	RUNOF(3)
AGRI	Mixing depth/plow layer of Agricultural Area 3	1.500E-01	1.500E-01	---	DPTHMIXG(3)
AGRI	Water filled porosity of soil in Agri. Area 3	3.000E-01	3.000E-01	---	TMOF(3)
AGRI	Computed erosion rate of soil in Agri. Area 3	0.000E+00	1.147E-05	---	EROSN(3)
AGRI	Dry Bulk Density of soil in Agricultural Area 3	1.500E+00	1.500E+00	---	RHOB(3)
AGRI	Soil erodibility factor of Agricultural Area 3	4.000E-01	4.000E-01	---	ERODIBILITY(3)
AGRI	Slope-length-steepness factor, Agricultural Area 3	4.000E-01	4.000E-01	---	SLPLENSTP(3)
AGRI	Cropping-management factor of Agricultural Area 3	3.000E-03	3.000E-03	---	CRPMANG(3)
AGRI	Conservation practice factor of Agricultural Area 3	1.000E+00	1.000E+00	---	CONVPRAC(3)
AGRI	Total porosity of soil in Agricultural Area 3	not used	4.000E-01	---	TPOF(3)
AGRI	Areal extent of Agricultural Area 4 (m**2)	1.000E+04	1.000E+04	---	AREAO(4)
AGRI	Fraction of Agri. Area 4 directly over the c.z.	0.000E+00	0.000E+00	---	FAREA_PLANT(4)
AGRI	Evapotranspiration coefficient in Agri. Area 4	5.680E-01	5.000E-01	---	EVAPTRN(4)
AGRI	Runoff coefficient in Agricultural Area 4	7.340E-01	2.000E-01	---	RUNOF(4)
AGRI	Mixing depth/plow layer of Agricultural Area 4	1.500E-01	1.500E-01	---	DPTHMIXG(4)
AGRI	Water filled porosity of soil in Agri. Area 4	3.000E-01	3.000E-01	---	TMOF(4)
AGRI	Computed erosion rate of soil in Agri. Area 4	0.000E+00	1.147E-05	---	EROSN(4)
AGRI	Dry Bulk Density of soil in Agricultural Area 4	1.500E+00	1.500E+00	---	RHOB(4)
AGRI	Soil erodibility factor of Agricultural Area 4	4.000E-01	4.000E-01	---	ERODIBILITY(4)
AGRI	Slope-length-steepness factor, Agricultural Area 4	4.000E-01	4.000E-01	---	SLPLENSTP(4)
AGRI	Cropping-management factor of Agricultural Area 4	3.000E-03	3.000E-03	---	CRPMANG(4)
AGRI	Conservation practice factor of Agricultural Area 4	1.000E+00	1.000E+00	---	CONVPRAC(4)
AGRI	Total porosity of soil in Agricultural Area 4	not used	4.000E-01	---	TPOF(4)

Site-Specific Parameter Summary (continued)

Menu	Parameter	User Input	Default	RESRAD computed	Parameter Name
DWEL	Areal extent of Offsite dwelling site (m**2)	1.024E+03	1.000E+03	---	AREAODWELL
DWEL	Evapotranspiration coefficient in dwelling (Off)site	5.680E-01	5.000E-01	---	EVAPTRNDWELL
DWEL	Runoff coefficient in Offsite dwelling site	6.360E-01	2.000E-01	---	RUNOFDWELL
DWEL	Mixing depth of Offsite dwelling site	1.500E-01	1.500E-01	---	DPTHMIXGDWELL
DWEL	Water filled porosity of soil in Offsite Dwelling	3.000E-01	3.000E-01	---	TMOFDWELL
DWEL	Computed erosion rate of soil in Offsite Dwelling	0.000E+00	0.000E+00	---	EROSNDWELL
DWEL	Dry Bulk Density of soil in Offsite dwelling site	1.500E+00	1.500E+00	---	RHOBDWELL
DWEL	Soil erodibility factor of soil in Dwelling site	0.000E+00	0.000E+00	---	ERODIBILITYDWELL
DWEL	Slope-length-steepness factor of Dwelling site	4.000E-01	4.000E-01	---	SLPLENSTPDWELL
DWEL	Cropping-management factor of Dwelling site	3.000E-03	3.000E-03	---	CRPMANGDWELL
DWEL	Conservation practice factor of Offsite Dwelling sit	1.000E+00	1.000E+00	---	CONVPRACDWELL
DWEL	Total porosity of soil in Offsite Dwelling	not used	4.000E-01	---	TPOFDWELL
AIRT	Dispersion Coeffficients; 1 = Pasquill-Gifford	1	1	---	IDISPMOD
AIRT	Population zone; 1 = Rural	1	1	---	IZONE
AIRT	Release height, (m)	1.000E+00	1.000E+00	---	AIRRELHT
AIRT	Heat flux for buoyant plume (cal/s),	0.000E+00	0.000E+00	---	HEATFLX
AIRT	Anemometer height, (m)	1.000E+01	1.000E+01	---	ANH
AIRT	Absolute temperature (Kelvin)	2.850E+02	2.850E+02	---	TABK
AIRT	AM atmospheric mixing height (m)	4.000E+02	4.000E+02	---	AMIX
AIRT	PM atmospheric mixing height (m)	1.600E+03	1.600E+03	---	PMIX
AIRT	Elevation of Agricultural Area 1 above primary cont.	0.000E+00	0.000E+00	---	AGRIELEV(1)
AIRT	Elevation of Agricultural Area 2 above primary cont.	0.000E+00	0.000E+00	---	AGRIELEV(2)
AIRT	Elevation of Agricultural Area 3 above primary cont.	0.000E+00	0.000E+00	---	AGRIELEV(3)
AIRT	Elevation of Agricultural Area 4 above primary cont.	0.000E+00	0.000E+00	---	AGRIELEV(4)
AIRT	Elevation of Dwelling Site relative to primary cont.	0.000E+00	0.000E+00	---	DWELLELEV
AIRT	Elevation of Surf.Wtr body relative to primary cont.	0.000E+00	0.000E+00	---	SWELEV
AIRT	Joint frequency Meteorological data:				
AIRT	Upper limit for windspeed class 1 (m/s)	8.900E-01	8.900E-01	---	WINDSPEED(1)
AIRT	Upper limit for windspeed class 2 (m/s)	2.460E+00	2.460E+00	---	WINDSPEED(2)
AIRT	Upper limit for windspeed class 3 (m/s)	4.470E+00	4.470E+00	---	WINDSPEED(3)
AIRT	Upper limit for windspeed class 4 (m/s)	6.930E+00	6.930E+00	---	WINDSPEED(4)
AIRT	Upper limit for windspeed class 5 (m/s)	9.610E+00	9.610E+00	---	WINDSPEED(5)
AIRT	Upper limit for windspeed class 6 (m/s)	1.252E+01	1.252E+01	---	WINDSPEED(6)
AIRT	Joint Frequency in N Sector				
AIRT	for wind speed class 1 and stability class A	6.300E-04	0.000E+00	---	DFREQ(1,1,1)
AIRT	for wind speed class 1 and stability class B	1.870E-03	0.000E+00	---	DFREQ(1,2,1)
AIRT	for wind speed class 1 and stability class C	9.000E-04	0.000E+00	---	DFREQ(1,3,1)
AIRT	for wind speed class 1 and stability class D	1.860E-03	1.000E-01	---	DFREQ(1,4,1)
AIRT	for wind speed class 1 and stability class E	0.000E+00	2.000E-01	---	DFREQ(1,5,1)
AIRT	for wind speed class 1 and stability class F	8.690E-03	7.000E-01	---	DFREQ(1,6,1)

Site-Specific Parameter Summary (continued)

Menu	Parameter	User Input	Default	RESRAD computed	Parameter Name
AIRT	Joint Frequency in N Sector				
AIRT	for wind speed class 2 and stability class A	3.200E-04	0.000E+00	---	DFREQ(2,1,1)
AIRT	for wind speed class 2 and stability class B	9.800E-04	0.000E+00	---	DFREQ(2,2,1)
AIRT	for wind speed class 2 and stability class C	1.030E-03	0.000E+00	---	DFREQ(2,3,1)
AIRT	for wind speed class 2 and stability class D	3.110E-03	0.000E+00	---	DFREQ(2,4,1)
AIRT	for wind speed class 2 and stability class E	3.370E-03	0.000E+00	---	DFREQ(2,5,1)
AIRT	for wind speed class 2 and stability class F	3.730E-03	0.000E+00	---	DFREQ(2,6,1)
AIRT	Joint Frequency in N Sector				
AIRT	for wind speed class 3 and stability class A	0.000E+00	0.000E+00	---	DFREQ(3,1,1)
AIRT	for wind speed class 3 and stability class B	2.200E-04	0.000E+00	---	DFREQ(3,2,1)
AIRT	for wind speed class 3 and stability class C	6.200E-04	0.000E+00	---	DFREQ(3,3,1)
AIRT	for wind speed class 3 and stability class D	4.000E-03	0.000E+00	---	DFREQ(3,4,1)
AIRT	for wind speed class 3 and stability class E	6.700E-04	0.000E+00	---	DFREQ(3,5,1)
AIRT	for wind speed class 3 and stability class F	0.000E+00	0.000E+00	---	DFREQ(3,6,1)
AIRT	Joint Frequency in N Sector				
AIRT	for wind speed class 4 and stability class A	0.000E+00	0.000E+00	---	DFREQ(4,1,1)
AIRT	for wind speed class 4 and stability class B	0.000E+00	0.000E+00	---	DFREQ(4,2,1)
AIRT	for wind speed class 4 and stability class C	1.000E-05	0.000E+00	---	DFREQ(4,3,1)
AIRT	for wind speed class 4 and stability class D	1.850E-03	0.000E+00	---	DFREQ(4,4,1)
AIRT	for wind speed class 4 and stability class E	0.000E+00	0.000E+00	---	DFREQ(4,5,1)
AIRT	for wind speed class 4 and stability class F	0.000E+00	0.000E+00	---	DFREQ(4,6,1)
AIRT	Joint Frequency in N Sector				
AIRT	for wind speed class 5 and stability class A	0.000E+00	0.000E+00	---	DFREQ(5,1,1)
AIRT	for wind speed class 5 and stability class B	0.000E+00	0.000E+00	---	DFREQ(5,2,1)
AIRT	for wind speed class 5 and stability class C	1.000E-05	0.000E+00	---	DFREQ(5,3,1)
AIRT	for wind speed class 5 and stability class D	3.000E-04	0.000E+00	---	DFREQ(5,4,1)
AIRT	for wind speed class 5 and stability class E	0.000E+00	0.000E+00	---	DFREQ(5,5,1)
AIRT	for wind speed class 5 and stability class F	0.000E+00	0.000E+00	---	DFREQ(5,6,1)
AIRT	Joint Frequency in N Sector				
AIRT	for wind speed class 6 and stability class A	0.000E+00	0.000E+00	---	DFREQ(6,1,1)
AIRT	for wind speed class 6 and stability class B	0.000E+00	0.000E+00	---	DFREQ(6,2,1)
AIRT	for wind speed class 6 and stability class C	0.000E+00	0.000E+00	---	DFREQ(6,3,1)
AIRT	for wind speed class 6 and stability class D	2.100E-04	0.000E+00	---	DFREQ(6,4,1)
AIRT	for wind speed class 6 and stability class E	0.000E+00	0.000E+00	---	DFREQ(6,5,1)
AIRT	for wind speed class 6 and stability class F	0.000E+00	0.000E+00	---	DFREQ(6,6,1)
AIRT	Joint Frequency in NNE Sector				
AIRT	for wind speed class 1 and stability class A	6.200E-04	0.000E+00	---	DFREQ(1,1,2)
AIRT	for wind speed class 1 and stability class B	1.890E-03	0.000E+00	---	DFREQ(1,2,2)
AIRT	for wind speed class 1 and stability class C	8.300E-04	0.000E+00	---	DFREQ(1,3,2)
AIRT	for wind speed class 1 and stability class D	1.940E-03	1.000E-01	---	DFREQ(1,4,2)
AIRT	for wind speed class 1 and stability class E	0.000E+00	2.000E-01	---	DFREQ(1,5,2)
AIRT	for wind speed class 1 and stability class F	6.510E-03	7.000E-01	---	DFREQ(1,6,2)

Site-Specific Parameter Summary (continued)

Menu	Parameter	User Input	Default	RESRAD computed	Parameter Name
AIRT	Joint Frequency in NNE Sector				
AIRT	for wind speed class 2 and stability class A	3.100E-04	0.000E+00	---	DFREQ(2,1,2)
AIRT	for wind speed class 2 and stability class B	1.540E-03	0.000E+00	---	DFREQ(2,2,2)
AIRT	for wind speed class 2 and stability class C	1.360E-03	0.000E+00	---	DFREQ(2,3,2)
AIRT	for wind speed class 2 and stability class D	4.260E-03	0.000E+00	---	DFREQ(2,4,2)
AIRT	for wind speed class 2 and stability class E	3.430E-03	0.000E+00	---	DFREQ(2,5,2)
AIRT	for wind speed class 2 and stability class F	4.780E-03	0.000E+00	---	DFREQ(2,6,2)
AIRT	Joint Frequency in NNE Sector				
AIRT	for wind speed class 3 and stability class A	0.000E+00	0.000E+00	---	DFREQ(3,1,2)
AIRT	for wind speed class 3 and stability class B	6.200E-04	0.000E+00	---	DFREQ(3,2,2)
AIRT	for wind speed class 3 and stability class C	1.800E-03	0.000E+00	---	DFREQ(3,3,2)
AIRT	for wind speed class 3 and stability class D	6.320E-03	0.000E+00	---	DFREQ(3,4,2)
AIRT	for wind speed class 3 and stability class E	2.130E-03	0.000E+00	---	DFREQ(3,5,2)
AIRT	for wind speed class 3 and stability class F	0.000E+00	0.000E+00	---	DFREQ(3,6,2)
AIRT	Joint Frequency in NNE Sector				
AIRT	for wind speed class 4 and stability class A	0.000E+00	0.000E+00	---	DFREQ(4,1,2)
AIRT	for wind speed class 4 and stability class B	0.000E+00	0.000E+00	---	DFREQ(4,2,2)
AIRT	for wind speed class 4 and stability class C	3.100E-04	0.000E+00	---	DFREQ(4,3,2)
AIRT	for wind speed class 4 and stability class D	5.230E-03	0.000E+00	---	DFREQ(4,4,2)
AIRT	for wind speed class 4 and stability class E	0.000E+00	0.000E+00	---	DFREQ(4,5,2)
AIRT	for wind speed class 4 and stability class F	0.000E+00	0.000E+00	---	DFREQ(4,6,2)
AIRT	Joint Frequency in NNE Sector				
AIRT	for wind speed class 5 and stability class A	0.000E+00	0.000E+00	---	DFREQ(5,1,2)
AIRT	for wind speed class 5 and stability class B	0.000E+00	0.000E+00	---	DFREQ(5,2,2)
AIRT	for wind speed class 5 and stability class C	5.000E-05	0.000E+00	---	DFREQ(5,3,2)
AIRT	for wind speed class 5 and stability class D	1.140E-03	0.000E+00	---	DFREQ(5,4,2)
AIRT	for wind speed class 5 and stability class E	0.000E+00	0.000E+00	---	DFREQ(5,5,2)
AIRT	for wind speed class 5 and stability class F	0.000E+00	0.000E+00	---	DFREQ(5,6,2)
AIRT	Joint Frequency in NNE Sector				
AIRT	for wind speed class 6 and stability class A	0.000E+00	0.000E+00	---	DFREQ(6,1,2)
AIRT	for wind speed class 6 and stability class B	0.000E+00	0.000E+00	---	DFREQ(6,2,2)
AIRT	for wind speed class 6 and stability class C	0.000E+00	0.000E+00	---	DFREQ(6,3,2)
AIRT	for wind speed class 6 and stability class D	5.500E-04	0.000E+00	---	DFREQ(6,4,2)
AIRT	for wind speed class 6 and stability class E	0.000E+00	0.000E+00	---	DFREQ(6,5,2)
AIRT	for wind speed class 6 and stability class F	0.000E+00	0.000E+00	---	DFREQ(6,6,2)
AIRT	Joint Frequency in NE Sector				
AIRT	for wind speed class 1 and stability class A	1.040E-03	0.000E+00	---	DFREQ(1,1,3)
AIRT	for wind speed class 1 and stability class B	3.050E-03	0.000E+00	---	DFREQ(1,2,3)
AIRT	for wind speed class 1 and stability class C	1.400E-03	0.000E+00	---	DFREQ(1,3,3)
AIRT	for wind speed class 1 and stability class D	3.390E-03	1.000E-01	---	DFREQ(1,4,3)
AIRT	for wind speed class 1 and stability class E	0.000E+00	2.000E-01	---	DFREQ(1,5,3)
AIRT	for wind speed class 1 and stability class F	1.235E-02	7.000E-01	---	DFREQ(1,6,3)

Site-Specific Parameter Summary (continued)

Menu	Parameter	User Input	Default	RESRAD computed	Parameter Name
AIRT	Joint Frequency in NE Sector				
AIRT	for wind speed class 2 and stability class A	7.500E-04	0.000E+00	---	DFREQ(2,1,3)
AIRT	for wind speed class 2 and stability class B	2.920E-03	0.000E+00	---	DFREQ(2,2,3)
AIRT	for wind speed class 2 and stability class C	3.140E-03	0.000E+00	---	DFREQ(2,3,3)
AIRT	for wind speed class 2 and stability class D	8.650E-03	0.000E+00	---	DFREQ(2,4,3)
AIRT	for wind speed class 2 and stability class E	9.140E-03	0.000E+00	---	DFREQ(2,5,3)
AIRT	for wind speed class 2 and stability class F	9.700E-03	0.000E+00	---	DFREQ(2,6,3)
AIRT	Joint Frequency in NE Sector				
AIRT	for wind speed class 3 and stability class A	0.000E+00	0.000E+00	---	DFREQ(3,1,3)
AIRT	for wind speed class 3 and stability class B	1.930E-03	0.000E+00	---	DFREQ(3,2,3)
AIRT	for wind speed class 3 and stability class C	5.930E-03	0.000E+00	---	DFREQ(3,3,3)
AIRT	for wind speed class 3 and stability class D	2.213E-02	0.000E+00	---	DFREQ(3,4,3)
AIRT	for wind speed class 3 and stability class E	8.750E-03	0.000E+00	---	DFREQ(3,5,3)
AIRT	for wind speed class 3 and stability class F	0.000E+00	0.000E+00	---	DFREQ(3,6,3)
AIRT	Joint Frequency in NE Sector				
AIRT	for wind speed class 4 and stability class A	0.000E+00	0.000E+00	---	DFREQ(4,1,3)
AIRT	for wind speed class 4 and stability class B	0.000E+00	0.000E+00	---	DFREQ(4,2,3)
AIRT	for wind speed class 4 and stability class C	1.770E-03	0.000E+00	---	DFREQ(4,3,3)
AIRT	for wind speed class 4 and stability class D	2.490E-02	0.000E+00	---	DFREQ(4,4,3)
AIRT	for wind speed class 4 and stability class E	0.000E+00	0.000E+00	---	DFREQ(4,5,3)
AIRT	for wind speed class 4 and stability class F	0.000E+00	0.000E+00	---	DFREQ(4,6,3)
AIRT	Joint Frequency in NE Sector				
AIRT	for wind speed class 5 and stability class A	0.000E+00	0.000E+00	---	DFREQ(5,1,3)
AIRT	for wind speed class 5 and stability class B	0.000E+00	0.000E+00	---	DFREQ(5,2,3)
AIRT	for wind speed class 5 and stability class C	3.700E-04	0.000E+00	---	DFREQ(5,3,3)
AIRT	for wind speed class 5 and stability class D	7.750E-03	0.000E+00	---	DFREQ(5,4,3)
AIRT	for wind speed class 5 and stability class E	0.000E+00	0.000E+00	---	DFREQ(5,5,3)
AIRT	for wind speed class 5 and stability class F	0.000E+00	0.000E+00	---	DFREQ(5,6,3)
AIRT	Joint Frequency in NE Sector				
AIRT	for wind speed class 6 and stability class A	0.000E+00	0.000E+00	---	DFREQ(6,1,3)
AIRT	for wind speed class 6 and stability class B	0.000E+00	0.000E+00	---	DFREQ(6,2,3)
AIRT	for wind speed class 6 and stability class C	3.000E-05	0.000E+00	---	DFREQ(6,3,3)
AIRT	for wind speed class 6 and stability class D	2.280E-03	0.000E+00	---	DFREQ(6,4,3)
AIRT	for wind speed class 6 and stability class E	0.000E+00	0.000E+00	---	DFREQ(6,5,3)
AIRT	for wind speed class 6 and stability class F	0.000E+00	0.000E+00	---	DFREQ(6,6,3)
AIRT	Joint Frequency in ENE Sector				
AIRT	for wind speed class 1 and stability class A	8.100E-04	0.000E+00	---	DFREQ(1,1,4)
AIRT	for wind speed class 1 and stability class B	2.530E-03	0.000E+00	---	DFREQ(1,2,4)
AIRT	for wind speed class 1 and stability class C	1.050E-03	0.000E+00	---	DFREQ(1,3,4)
AIRT	for wind speed class 1 and stability class D	2.780E-03	1.000E-01	---	DFREQ(1,4,4)
AIRT	for wind speed class 1 and stability class E	0.000E+00	2.000E-01	---	DFREQ(1,5,4)
AIRT	for wind speed class 1 and stability class F	8.270E-03	7.000E-01	---	DFREQ(1,6,4)

Site-Specific Parameter Summary (continued)

Menu	Parameter	User Input	Default	RESRAD computed	Parameter Name
AIRT	Joint Frequency in ENE Sector				
AIRT	for wind speed class 2 and stability class A	7.200E-04	0.000E+00	---	DFREQ(2,1,4)
AIRT	for wind speed class 2 and stability class B	2.730E-03	0.000E+00	---	DFREQ(2,2,4)
AIRT	for wind speed class 2 and stability class C	2.810E-03	0.000E+00	---	DFREQ(2,3,4)
AIRT	for wind speed class 2 and stability class D	8.390E-03	0.000E+00	---	DFREQ(2,4,4)
AIRT	for wind speed class 2 and stability class E	7.110E-03	0.000E+00	---	DFREQ(2,5,4)
AIRT	for wind speed class 2 and stability class F	7.280E-03	0.000E+00	---	DFREQ(2,6,4)
AIRT	Joint Frequency in ENE Sector				
AIRT	for wind speed class 3 and stability class A	0.000E+00	0.000E+00	---	DFREQ(3,1,4)
AIRT	for wind speed class 3 and stability class B	2.170E-03	0.000E+00	---	DFREQ(3,2,4)
AIRT	for wind speed class 3 and stability class C	6.740E-03	0.000E+00	---	DFREQ(3,3,4)
AIRT	for wind speed class 3 and stability class D	2.243E-02	0.000E+00	---	DFREQ(3,4,4)
AIRT	for wind speed class 3 and stability class E	7.640E-03	0.000E+00	---	DFREQ(3,5,4)
AIRT	for wind speed class 3 and stability class F	0.000E+00	0.000E+00	---	DFREQ(3,6,4)
AIRT	Joint Frequency in ENE Sector				
AIRT	for wind speed class 4 and stability class A	0.000E+00	0.000E+00	---	DFREQ(4,1,4)
AIRT	for wind speed class 4 and stability class B	0.000E+00	0.000E+00	---	DFREQ(4,2,4)
AIRT	for wind speed class 4 and stability class C	1.770E-03	0.000E+00	---	DFREQ(4,3,4)
AIRT	for wind speed class 4 and stability class D	2.400E-02	0.000E+00	---	DFREQ(4,4,4)
AIRT	for wind speed class 4 and stability class E	0.000E+00	0.000E+00	---	DFREQ(4,5,4)
AIRT	for wind speed class 4 and stability class F	0.000E+00	0.000E+00	---	DFREQ(4,6,4)
AIRT	Joint Frequency in ENE Sector				
AIRT	for wind speed class 5 and stability class A	0.000E+00	0.000E+00	---	DFREQ(5,1,4)
AIRT	for wind speed class 5 and stability class B	0.000E+00	0.000E+00	---	DFREQ(5,2,4)
AIRT	for wind speed class 5 and stability class C	2.700E-04	0.000E+00	---	DFREQ(5,3,4)
AIRT	for wind speed class 5 and stability class D	7.160E-03	0.000E+00	---	DFREQ(5,4,4)
AIRT	for wind speed class 5 and stability class E	0.000E+00	0.000E+00	---	DFREQ(5,5,4)
AIRT	for wind speed class 5 and stability class F	0.000E+00	0.000E+00	---	DFREQ(5,6,4)
AIRT	Joint Frequency in ENE Sector				
AIRT	for wind speed class 6 and stability class A	0.000E+00	0.000E+00	---	DFREQ(6,1,4)
AIRT	for wind speed class 6 and stability class B	0.000E+00	0.000E+00	---	DFREQ(6,2,4)
AIRT	for wind speed class 6 and stability class C	9.000E-05	0.000E+00	---	DFREQ(6,3,4)
AIRT	for wind speed class 6 and stability class D	2.580E-03	0.000E+00	---	DFREQ(6,4,4)
AIRT	for wind speed class 6 and stability class E	0.000E+00	0.000E+00	---	DFREQ(6,5,4)
AIRT	for wind speed class 6 and stability class F	0.000E+00	0.000E+00	---	DFREQ(6,6,4)
AIRT	Joint Frequency in E Sector				
AIRT	for wind speed class 1 and stability class A	8.500E-04	0.000E+00	---	DFREQ(1,1,5)
AIRT	for wind speed class 1 and stability class B	2.080E-03	0.000E+00	---	DFREQ(1,2,5)
AIRT	for wind speed class 1 and stability class C	8.500E-04	0.000E+00	---	DFREQ(1,3,5)
AIRT	for wind speed class 1 and stability class D	1.940E-03	1.000E-01	---	DFREQ(1,4,5)
AIRT	for wind speed class 1 and stability class E	0.000E+00	2.000E-01	---	DFREQ(1,5,5)
AIRT	for wind speed class 1 and stability class F	4.640E-03	7.000E-01	---	DFREQ(1,6,5)

Site-Specific Parameter Summary (continued)

Menu	Parameter	User Input	Default	RESRAD computed	Parameter Name
AIRT	Joint Frequency in E Sector				
AIRT	for wind speed class 2 and stability class A	4.800E-04	0.000E+00	---	DFREQ(2,1,5)
AIRT	for wind speed class 2 and stability class B	2.130E-03	0.000E+00	---	DFREQ(2,2,5)
AIRT	for wind speed class 2 and stability class C	2.420E-03	0.000E+00	---	DFREQ(2,3,5)
AIRT	for wind speed class 2 and stability class D	6.260E-03	0.000E+00	---	DFREQ(2,4,5)
AIRT	for wind speed class 2 and stability class E	4.280E-03	0.000E+00	---	DFREQ(2,5,5)
AIRT	for wind speed class 2 and stability class F	4.270E-03	0.000E+00	---	DFREQ(2,6,5)
AIRT	Joint Frequency in E Sector				
AIRT	for wind speed class 3 and stability class A	0.000E+00	0.000E+00	---	DFREQ(3,1,5)
AIRT	for wind speed class 3 and stability class B	1.080E-03	0.000E+00	---	DFREQ(3,2,5)
AIRT	for wind speed class 3 and stability class C	3.860E-03	0.000E+00	---	DFREQ(3,3,5)
AIRT	for wind speed class 3 and stability class D	1.369E-02	0.000E+00	---	DFREQ(3,4,5)
AIRT	for wind speed class 3 and stability class E	4.000E-03	0.000E+00	---	DFREQ(3,5,5)
AIRT	for wind speed class 3 and stability class F	0.000E+00	0.000E+00	---	DFREQ(3,6,5)
AIRT	Joint Frequency in E Sector				
AIRT	for wind speed class 4 and stability class A	0.000E+00	0.000E+00	---	DFREQ(4,1,5)
AIRT	for wind speed class 4 and stability class B	0.000E+00	0.000E+00	---	DFREQ(4,2,5)
AIRT	for wind speed class 4 and stability class C	5.900E-04	0.000E+00	---	DFREQ(4,3,5)
AIRT	for wind speed class 4 and stability class D	1.169E-02	0.000E+00	---	DFREQ(4,4,5)
AIRT	for wind speed class 4 and stability class E	0.000E+00	0.000E+00	---	DFREQ(4,5,5)
AIRT	for wind speed class 4 and stability class F	0.000E+00	0.000E+00	---	DFREQ(4,6,5)
AIRT	Joint Frequency in E Sector				
AIRT	for wind speed class 5 and stability class A	0.000E+00	0.000E+00	---	DFREQ(5,1,5)
AIRT	for wind speed class 5 and stability class B	0.000E+00	0.000E+00	---	DFREQ(5,2,5)
AIRT	for wind speed class 5 and stability class C	5.000E-05	0.000E+00	---	DFREQ(5,3,5)
AIRT	for wind speed class 5 and stability class D	3.330E-03	0.000E+00	---	DFREQ(5,4,5)
AIRT	for wind speed class 5 and stability class E	0.000E+00	0.000E+00	---	DFREQ(5,5,5)
AIRT	for wind speed class 5 and stability class F	0.000E+00	0.000E+00	---	DFREQ(5,6,5)
AIRT	Joint Frequency in E Sector				
AIRT	for wind speed class 6 and stability class A	0.000E+00	0.000E+00	---	DFREQ(6,1,5)
AIRT	for wind speed class 6 and stability class B	0.000E+00	0.000E+00	---	DFREQ(6,2,5)
AIRT	for wind speed class 6 and stability class C	1.000E-05	0.000E+00	---	DFREQ(6,3,5)
AIRT	for wind speed class 6 and stability class D	9.800E-04	0.000E+00	---	DFREQ(6,4,5)
AIRT	for wind speed class 6 and stability class E	0.000E+00	0.000E+00	---	DFREQ(6,5,5)
AIRT	for wind speed class 6 and stability class F	0.000E+00	0.000E+00	---	DFREQ(6,6,5)
AIRT	Joint Frequency in ESE Sector				
AIRT	for wind speed class 1 and stability class A	6.800E-04	0.000E+00	---	DFREQ(1,1,6)
AIRT	for wind speed class 1 and stability class B	1.950E-03	0.000E+00	---	DFREQ(1,2,6)
AIRT	for wind speed class 1 and stability class C	5.300E-04	0.000E+00	---	DFREQ(1,3,6)
AIRT	for wind speed class 1 and stability class D	1.280E-03	1.000E-01	---	DFREQ(1,4,6)
AIRT	for wind speed class 1 and stability class E	0.000E+00	2.000E-01	---	DFREQ(1,5,6)
AIRT	for wind speed class 1 and stability class F	2.880E-03	7.000E-01	---	DFREQ(1,6,6)

Site-Specific Parameter Summary (continued)

Menu	Parameter	User Input	Default	RESRAD computed	Parameter Name
AIRT	Joint Frequency in ESE Sector				
AIRT	for wind speed class 2 and stability class A	5.000E-04	0.000E+00	---	DFREQ(2,1,6)
AIRT	for wind speed class 2 and stability class B	1.770E-03	0.000E+00	---	DFREQ(2,2,6)
AIRT	for wind speed class 2 and stability class C	1.540E-03	0.000E+00	---	DFREQ(2,3,6)
AIRT	for wind speed class 2 and stability class D	3.930E-03	0.000E+00	---	DFREQ(2,4,6)
AIRT	for wind speed class 2 and stability class E	2.150E-03	0.000E+00	---	DFREQ(2,5,6)
AIRT	for wind speed class 2 and stability class F	2.150E-03	0.000E+00	---	DFREQ(2,6,6)
AIRT	Joint Frequency in ESE Sector				
AIRT	for wind speed class 3 and stability class A	0.000E+00	0.000E+00	---	DFREQ(3,1,6)
AIRT	for wind speed class 3 and stability class B	7.800E-04	0.000E+00	---	DFREQ(3,2,6)
AIRT	for wind speed class 3 and stability class C	2.630E-03	0.000E+00	---	DFREQ(3,3,6)
AIRT	for wind speed class 3 and stability class D	8.280E-03	0.000E+00	---	DFREQ(3,4,6)
AIRT	for wind speed class 3 and stability class E	2.170E-03	0.000E+00	---	DFREQ(3,5,6)
AIRT	for wind speed class 3 and stability class F	0.000E+00	0.000E+00	---	DFREQ(3,6,6)
AIRT	Joint Frequency in ESE Sector				
AIRT	for wind speed class 4 and stability class A	0.000E+00	0.000E+00	---	DFREQ(4,1,6)
AIRT	for wind speed class 4 and stability class B	0.000E+00	0.000E+00	---	DFREQ(4,2,6)
AIRT	for wind speed class 4 and stability class C	3.700E-04	0.000E+00	---	DFREQ(4,3,6)
AIRT	for wind speed class 4 and stability class D	9.370E-03	0.000E+00	---	DFREQ(4,4,6)
AIRT	for wind speed class 4 and stability class E	0.000E+00	0.000E+00	---	DFREQ(4,5,6)
AIRT	for wind speed class 4 and stability class F	0.000E+00	0.000E+00	---	DFREQ(4,6,6)
AIRT	Joint Frequency in ESE Sector				
AIRT	for wind speed class 5 and stability class A	0.000E+00	0.000E+00	---	DFREQ(5,1,6)
AIRT	for wind speed class 5 and stability class B	0.000E+00	0.000E+00	---	DFREQ(5,2,6)
AIRT	for wind speed class 5 and stability class C	0.000E+00	0.000E+00	---	DFREQ(5,3,6)
AIRT	for wind speed class 5 and stability class D	3.400E-03	0.000E+00	---	DFREQ(5,4,6)
AIRT	for wind speed class 5 and stability class E	0.000E+00	0.000E+00	---	DFREQ(5,5,6)
AIRT	for wind speed class 5 and stability class F	0.000E+00	0.000E+00	---	DFREQ(5,6,6)
AIRT	Joint Frequency in ESE Sector				
AIRT	for wind speed class 6 and stability class A	0.000E+00	0.000E+00	---	DFREQ(6,1,6)
AIRT	for wind speed class 6 and stability class B	0.000E+00	0.000E+00	---	DFREQ(6,2,6)
AIRT	for wind speed class 6 and stability class C	1.000E-05	0.000E+00	---	DFREQ(6,3,6)
AIRT	for wind speed class 6 and stability class D	8.000E-04	0.000E+00	---	DFREQ(6,4,6)
AIRT	for wind speed class 6 and stability class E	0.000E+00	0.000E+00	---	DFREQ(6,5,6)
AIRT	for wind speed class 6 and stability class F	0.000E+00	0.000E+00	---	DFREQ(6,6,6)
AIRT	Joint Frequency in SE Sector				
AIRT	for wind speed class 1 and stability class A	8.100E-04	0.000E+00	---	DFREQ(1,1,7)
AIRT	for wind speed class 1 and stability class B	2.070E-03	0.000E+00	---	DFREQ(1,2,7)
AIRT	for wind speed class 1 and stability class C	6.600E-04	0.000E+00	---	DFREQ(1,3,7)
AIRT	for wind speed class 1 and stability class D	1.830E-03	1.000E-01	---	DFREQ(1,4,7)
AIRT	for wind speed class 1 and stability class E	0.000E+00	2.000E-01	---	DFREQ(1,5,7)
AIRT	for wind speed class 1 and stability class F	3.640E-03	7.000E-01	---	DFREQ(1,6,7)

Site-Specific Parameter Summary (continued)

Menu	Parameter	User Input	Default	RESRAD computed	Parameter Name
AIRT	Joint Frequency in SE Sector				
AIRT	for wind speed class 2 and stability class A	6.100E-04	0.000E+00	---	DFREQ(2,1,7)
AIRT	for wind speed class 2 and stability class B	1.980E-03	0.000E+00	---	DFREQ(2,2,7)
AIRT	for wind speed class 2 and stability class C	1.800E-03	0.000E+00	---	DFREQ(2,3,7)
AIRT	for wind speed class 2 and stability class D	4.220E-03	0.000E+00	---	DFREQ(2,4,7)
AIRT	for wind speed class 2 and stability class E	2.080E-03	0.000E+00	---	DFREQ(2,5,7)
AIRT	for wind speed class 2 and stability class F	2.530E-03	0.000E+00	---	DFREQ(2,6,7)
AIRT	Joint Frequency in SE Sector				
AIRT	for wind speed class 3 and stability class A	0.000E+00	0.000E+00	---	DFREQ(3,1,7)
AIRT	for wind speed class 3 and stability class B	1.040E-03	0.000E+00	---	DFREQ(3,2,7)
AIRT	for wind speed class 3 and stability class C	1.870E-03	0.000E+00	---	DFREQ(3,3,7)
AIRT	for wind speed class 3 and stability class D	5.670E-03	0.000E+00	---	DFREQ(3,4,7)
AIRT	for wind speed class 3 and stability class E	1.710E-03	0.000E+00	---	DFREQ(3,5,7)
AIRT	for wind speed class 3 and stability class F	0.000E+00	0.000E+00	---	DFREQ(3,6,7)
AIRT	Joint Frequency in SE Sector				
AIRT	for wind speed class 4 and stability class A	0.000E+00	0.000E+00	---	DFREQ(4,1,7)
AIRT	for wind speed class 4 and stability class B	0.000E+00	0.000E+00	---	DFREQ(4,2,7)
AIRT	for wind speed class 4 and stability class C	1.700E-04	0.000E+00	---	DFREQ(4,3,7)
AIRT	for wind speed class 4 and stability class D	3.700E-03	0.000E+00	---	DFREQ(4,4,7)
AIRT	for wind speed class 4 and stability class E	0.000E+00	0.000E+00	---	DFREQ(4,5,7)
AIRT	for wind speed class 4 and stability class F	0.000E+00	0.000E+00	---	DFREQ(4,6,7)
AIRT	Joint Frequency in SE Sector				
AIRT	for wind speed class 5 and stability class A	0.000E+00	0.000E+00	---	DFREQ(5,1,7)
AIRT	for wind speed class 5 and stability class B	0.000E+00	0.000E+00	---	DFREQ(5,2,7)
AIRT	for wind speed class 5 and stability class C	0.000E+00	0.000E+00	---	DFREQ(5,3,7)
AIRT	for wind speed class 5 and stability class D	6.700E-04	0.000E+00	---	DFREQ(5,4,7)
AIRT	for wind speed class 5 and stability class E	0.000E+00	0.000E+00	---	DFREQ(5,5,7)
AIRT	for wind speed class 5 and stability class F	0.000E+00	0.000E+00	---	DFREQ(5,6,7)
AIRT	Joint Frequency in SE Sector				
AIRT	for wind speed class 6 and stability class A	0.000E+00	0.000E+00	---	DFREQ(6,1,7)
AIRT	for wind speed class 6 and stability class B	0.000E+00	0.000E+00	---	DFREQ(6,2,7)
AIRT	for wind speed class 6 and stability class C	0.000E+00	0.000E+00	---	DFREQ(6,3,7)
AIRT	for wind speed class 6 and stability class D	2.300E-04	0.000E+00	---	DFREQ(6,4,7)
AIRT	for wind speed class 6 and stability class E	0.000E+00	0.000E+00	---	DFREQ(6,5,7)
AIRT	for wind speed class 6 and stability class F	0.000E+00	0.000E+00	---	DFREQ(6,6,7)
AIRT	Joint Frequency in SSE Sector				
AIRT	for wind speed class 1 and stability class A	6.000E-04	0.000E+00	---	DFREQ(1,1,8)
AIRT	for wind speed class 1 and stability class B	1.360E-03	0.000E+00	---	DFREQ(1,2,8)
AIRT	for wind speed class 1 and stability class C	5.700E-04	0.000E+00	---	DFREQ(1,3,8)
AIRT	for wind speed class 1 and stability class D	1.500E-03	1.000E-01	---	DFREQ(1,4,8)
AIRT	for wind speed class 1 and stability class E	0.000E+00	2.000E-01	---	DFREQ(1,5,8)
AIRT	for wind speed class 1 and stability class F	2.950E-03	7.000E-01	---	DFREQ(1,6,8)

Site-Specific Parameter Summary (continued)

Menu	Parameter	User Input	Default	RESRAD computed	Parameter Name
AIRT	Joint Frequency in SSE Sector				
AIRT	for wind speed class 2 and stability class A	4.800E-04	0.000E+00	---	DFREQ(2,1,8)
AIRT	for wind speed class 2 and stability class B	1.280E-03	0.000E+00	---	DFREQ(2,2,8)
AIRT	for wind speed class 2 and stability class C	1.550E-03	0.000E+00	---	DFREQ(2,3,8)
AIRT	for wind speed class 2 and stability class D	3.850E-03	0.000E+00	---	DFREQ(2,4,8)
AIRT	for wind speed class 2 and stability class E	2.070E-03	0.000E+00	---	DFREQ(2,5,8)
AIRT	for wind speed class 2 and stability class F	1.930E-03	0.000E+00	---	DFREQ(2,6,8)
AIRT	Joint Frequency in SSE Sector				
AIRT	for wind speed class 3 and stability class A	0.000E+00	0.000E+00	---	DFREQ(3,1,8)
AIRT	for wind speed class 3 and stability class B	4.300E-04	0.000E+00	---	DFREQ(3,2,8)
AIRT	for wind speed class 3 and stability class C	1.000E-03	0.000E+00	---	DFREQ(3,3,8)
AIRT	for wind speed class 3 and stability class D	4.020E-03	0.000E+00	---	DFREQ(3,4,8)
AIRT	for wind speed class 3 and stability class E	9.700E-04	0.000E+00	---	DFREQ(3,5,8)
AIRT	for wind speed class 3 and stability class F	0.000E+00	0.000E+00	---	DFREQ(3,6,8)
AIRT	Joint Frequency in SSE Sector				
AIRT	for wind speed class 4 and stability class A	0.000E+00	0.000E+00	---	DFREQ(4,1,8)
AIRT	for wind speed class 4 and stability class B	0.000E+00	0.000E+00	---	DFREQ(4,2,8)
AIRT	for wind speed class 4 and stability class C	1.100E-04	0.000E+00	---	DFREQ(4,3,8)
AIRT	for wind speed class 4 and stability class D	2.190E-03	0.000E+00	---	DFREQ(4,4,8)
AIRT	for wind speed class 4 and stability class E	0.000E+00	0.000E+00	---	DFREQ(4,5,8)
AIRT	for wind speed class 4 and stability class F	0.000E+00	0.000E+00	---	DFREQ(4,6,8)
AIRT	Joint Frequency in SSE Sector				
AIRT	for wind speed class 5 and stability class A	0.000E+00	0.000E+00	---	DFREQ(5,1,8)
AIRT	for wind speed class 5 and stability class B	0.000E+00	0.000E+00	---	DFREQ(5,2,8)
AIRT	for wind speed class 5 and stability class C	0.000E+00	0.000E+00	---	DFREQ(5,3,8)
AIRT	for wind speed class 5 and stability class D	2.600E-04	0.000E+00	---	DFREQ(5,4,8)
AIRT	for wind speed class 5 and stability class E	0.000E+00	0.000E+00	---	DFREQ(5,5,8)
AIRT	for wind speed class 5 and stability class F	0.000E+00	0.000E+00	---	DFREQ(5,6,8)
AIRT	Joint Frequency in SSE Sector				
AIRT	for wind speed class 6 and stability class A	0.000E+00	0.000E+00	---	DFREQ(6,1,8)
AIRT	for wind speed class 6 and stability class B	0.000E+00	0.000E+00	---	DFREQ(6,2,8)
AIRT	for wind speed class 6 and stability class C	0.000E+00	0.000E+00	---	DFREQ(6,3,8)
AIRT	for wind speed class 6 and stability class D	5.000E-05	0.000E+00	---	DFREQ(6,4,8)
AIRT	for wind speed class 6 and stability class E	0.000E+00	0.000E+00	---	DFREQ(6,5,8)
AIRT	for wind speed class 6 and stability class F	0.000E+00	0.000E+00	---	DFREQ(6,6,8)
AIRT	Joint Frequency in S Sector				
AIRT	for wind speed class 1 and stability class A	6.800E-04	0.000E+00	---	DFREQ(1,1,9)
AIRT	for wind speed class 1 and stability class B	2.430E-03	0.000E+00	---	DFREQ(1,2,9)
AIRT	for wind speed class 1 and stability class C	9.100E-04	0.000E+00	---	DFREQ(1,3,9)
AIRT	for wind speed class 1 and stability class D	2.700E-03	1.000E-01	---	DFREQ(1,4,9)
AIRT	for wind speed class 1 and stability class E	0.000E+00	2.000E-01	---	DFREQ(1,5,9)
AIRT	for wind speed class 1 and stability class F	6.410E-03	7.000E-01	---	DFREQ(1,6,9)

Site-Specific Parameter Summary (continued)

Menu	Parameter	User Input	Default	RESRAD computed	Parameter Name
AIRT	Joint Frequency in S Sector				
AIRT	for wind speed class 2 and stability class A	5.300E-04	0.000E+00	---	DFREQ(2,1,9)
AIRT	for wind speed class 2 and stability class B	2.200E-03	0.000E+00	---	DFREQ(2,2,9)
AIRT	for wind speed class 2 and stability class C	2.560E-03	0.000E+00	---	DFREQ(2,3,9)
AIRT	for wind speed class 2 and stability class D	7.890E-03	0.000E+00	---	DFREQ(2,4,9)
AIRT	for wind speed class 2 and stability class E	4.020E-03	0.000E+00	---	DFREQ(2,5,9)
AIRT	for wind speed class 2 and stability class F	4.660E-03	0.000E+00	---	DFREQ(2,6,9)
AIRT	Joint Frequency in S Sector				
AIRT	for wind speed class 3 and stability class A	0.000E+00	0.000E+00	---	DFREQ(3,1,9)
AIRT	for wind speed class 3 and stability class B	7.300E-04	0.000E+00	---	DFREQ(3,2,9)
AIRT	for wind speed class 3 and stability class C	2.480E-03	0.000E+00	---	DFREQ(3,3,9)
AIRT	for wind speed class 3 and stability class D	1.067E-02	0.000E+00	---	DFREQ(3,4,9)
AIRT	for wind speed class 3 and stability class E	4.720E-03	0.000E+00	---	DFREQ(3,5,9)
AIRT	for wind speed class 3 and stability class F	0.000E+00	0.000E+00	---	DFREQ(3,6,9)
AIRT	Joint Frequency in S Sector				
AIRT	for wind speed class 4 and stability class A	0.000E+00	0.000E+00	---	DFREQ(4,1,9)
AIRT	for wind speed class 4 and stability class B	0.000E+00	0.000E+00	---	DFREQ(4,2,9)
AIRT	for wind speed class 4 and stability class C	1.600E-04	0.000E+00	---	DFREQ(4,3,9)
AIRT	for wind speed class 4 and stability class D	6.860E-03	0.000E+00	---	DFREQ(4,4,9)
AIRT	for wind speed class 4 and stability class E	0.000E+00	0.000E+00	---	DFREQ(4,5,9)
AIRT	for wind speed class 4 and stability class F	0.000E+00	0.000E+00	---	DFREQ(4,6,9)
AIRT	Joint Frequency in S Sector				
AIRT	for wind speed class 5 and stability class A	0.000E+00	0.000E+00	---	DFREQ(5,1,9)
AIRT	for wind speed class 5 and stability class B	0.000E+00	0.000E+00	---	DFREQ(5,2,9)
AIRT	for wind speed class 5 and stability class C	0.000E+00	0.000E+00	---	DFREQ(5,3,9)
AIRT	for wind speed class 5 and stability class D	9.700E-04	0.000E+00	---	DFREQ(5,4,9)
AIRT	for wind speed class 5 and stability class E	0.000E+00	0.000E+00	---	DFREQ(5,5,9)
AIRT	for wind speed class 5 and stability class F	0.000E+00	0.000E+00	---	DFREQ(5,6,9)
AIRT	Joint Frequency in S Sector				
AIRT	for wind speed class 6 and stability class A	0.000E+00	0.000E+00	---	DFREQ(6,1,9)
AIRT	for wind speed class 6 and stability class B	0.000E+00	0.000E+00	---	DFREQ(6,2,9)
AIRT	for wind speed class 6 and stability class C	0.000E+00	0.000E+00	---	DFREQ(6,3,9)
AIRT	for wind speed class 6 and stability class D	7.000E-05	0.000E+00	---	DFREQ(6,4,9)
AIRT	for wind speed class 6 and stability class E	0.000E+00	0.000E+00	---	DFREQ(6,5,9)
AIRT	for wind speed class 6 and stability class F	0.000E+00	0.000E+00	---	DFREQ(6,6,9)
AIRT	Joint Frequency in SSW Sector				
AIRT	for wind speed class 1 and stability class A	7.700E-04	0.000E+00	---	DFREQ(1,1,10)
AIRT	for wind speed class 1 and stability class B	2.790E-03	0.000E+00	---	DFREQ(1,2,10)
AIRT	for wind speed class 1 and stability class C	1.130E-03	0.000E+00	---	DFREQ(1,3,10)
AIRT	for wind speed class 1 and stability class D	3.060E-03	1.000E-01	---	DFREQ(1,4,10)
AIRT	for wind speed class 1 and stability class E	0.000E+00	2.000E-01	---	DFREQ(1,5,10)
AIRT	for wind speed class 1 and stability class F	6.900E-03	7.000E-01	---	DFREQ(1,6,10)

Site-Specific Parameter Summary (continued)

Menu	Parameter	User Input	Default	RESRAD computed	Parameter Name
AIRT	Joint Frequency in SSW Sector				
AIRT	for wind speed class 2 and stability class A	7.000E-04	0.000E+00	---	DFREQ(2,1,10)
AIRT	for wind speed class 2 and stability class B	2.470E-03	0.000E+00	---	DFREQ(2,2,10)
AIRT	for wind speed class 2 and stability class C	2.610E-03	0.000E+00	---	DFREQ(2,3,10)
AIRT	for wind speed class 2 and stability class D	7.990E-03	0.000E+00	---	DFREQ(2,4,10)
AIRT	for wind speed class 2 and stability class E	4.950E-03	0.000E+00	---	DFREQ(2,5,10)
AIRT	for wind speed class 2 and stability class F	6.930E-03	0.000E+00	---	DFREQ(2,6,10)
AIRT	Joint Frequency in SSW Sector				
AIRT	for wind speed class 3 and stability class A	0.000E+00	0.000E+00	---	DFREQ(3,1,10)
AIRT	for wind speed class 3 and stability class B	1.310E-03	0.000E+00	---	DFREQ(3,2,10)
AIRT	for wind speed class 3 and stability class C	3.740E-03	0.000E+00	---	DFREQ(3,3,10)
AIRT	for wind speed class 3 and stability class D	1.404E-02	0.000E+00	---	DFREQ(3,4,10)
AIRT	for wind speed class 3 and stability class E	7.340E-03	0.000E+00	---	DFREQ(3,5,10)
AIRT	for wind speed class 3 and stability class F	0.000E+00	0.000E+00	---	DFREQ(3,6,10)
AIRT	Joint Frequency in SSW Sector				
AIRT	for wind speed class 4 and stability class A	0.000E+00	0.000E+00	---	DFREQ(4,1,10)
AIRT	for wind speed class 4 and stability class B	0.000E+00	0.000E+00	---	DFREQ(4,2,10)
AIRT	for wind speed class 4 and stability class C	3.300E-04	0.000E+00	---	DFREQ(4,3,10)
AIRT	for wind speed class 4 and stability class D	7.220E-03	0.000E+00	---	DFREQ(4,4,10)
AIRT	for wind speed class 4 and stability class E	0.000E+00	0.000E+00	---	DFREQ(4,5,10)
AIRT	for wind speed class 4 and stability class F	0.000E+00	0.000E+00	---	DFREQ(4,6,10)
AIRT	Joint Frequency in SSW Sector				
AIRT	for wind speed class 5 and stability class A	0.000E+00	0.000E+00	---	DFREQ(5,1,10)
AIRT	for wind speed class 5 and stability class B	0.000E+00	0.000E+00	---	DFREQ(5,2,10)
AIRT	for wind speed class 5 and stability class C	0.000E+00	0.000E+00	---	DFREQ(5,3,10)
AIRT	for wind speed class 5 and stability class D	6.900E-04	0.000E+00	---	DFREQ(5,4,10)
AIRT	for wind speed class 5 and stability class E	0.000E+00	0.000E+00	---	DFREQ(5,5,10)
AIRT	for wind speed class 5 and stability class F	0.000E+00	0.000E+00	---	DFREQ(5,6,10)
AIRT	Joint Frequency in SSW Sector				
AIRT	for wind speed class 6 and stability class A	0.000E+00	0.000E+00	---	DFREQ(6,1,10)
AIRT	for wind speed class 6 and stability class B	0.000E+00	0.000E+00	---	DFREQ(6,2,10)
AIRT	for wind speed class 6 and stability class C	0.000E+00	0.000E+00	---	DFREQ(6,3,10)
AIRT	for wind speed class 6 and stability class D	3.000E-05	0.000E+00	---	DFREQ(6,4,10)
AIRT	for wind speed class 6 and stability class E	0.000E+00	0.000E+00	---	DFREQ(6,5,10)
AIRT	for wind speed class 6 and stability class F	0.000E+00	0.000E+00	---	DFREQ(6,6,10)
AIRT	Joint Frequency in SW Sector				
AIRT	for wind speed class 1 and stability class A	1.480E-03	0.000E+00	---	DFREQ(1,1,11)
AIRT	for wind speed class 1 and stability class B	6.450E-03	0.000E+00	---	DFREQ(1,2,11)
AIRT	for wind speed class 1 and stability class C	3.240E-03	0.000E+00	---	DFREQ(1,3,11)
AIRT	for wind speed class 1 and stability class D	6.780E-03	1.000E-01	---	DFREQ(1,4,11)
AIRT	for wind speed class 1 and stability class E	0.000E+00	2.000E-01	---	DFREQ(1,5,11)
AIRT	for wind speed class 1 and stability class F	2.290E-02	7.000E-01	---	DFREQ(1,6,11)

Site-Specific Parameter Summary (continued)

Menu	Parameter	User Input	Default	RESRAD computed	Parameter Name
AIRT	Joint Frequency in SW Sector				
AIRT	for wind speed class 2 and stability class A	1.030E-03	0.000E+00	---	DFREQ(2,1,11)
AIRT	for wind speed class 2 and stability class B	5.780E-03	0.000E+00	---	DFREQ(2,2,11)
AIRT	for wind speed class 2 and stability class C	7.690E-03	0.000E+00	---	DFREQ(2,3,11)
AIRT	for wind speed class 2 and stability class D	1.896E-02	0.000E+00	---	DFREQ(2,4,11)
AIRT	for wind speed class 2 and stability class E	1.364E-02	0.000E+00	---	DFREQ(2,5,11)
AIRT	for wind speed class 2 and stability class F	2.086E-02	0.000E+00	---	DFREQ(2,6,11)
AIRT	Joint Frequency in SW Sector				
AIRT	for wind speed class 3 and stability class A	0.000E+00	0.000E+00	---	DFREQ(3,1,11)
AIRT	for wind speed class 3 and stability class B	2.510E-03	0.000E+00	---	DFREQ(3,2,11)
AIRT	for wind speed class 3 and stability class C	9.100E-03	0.000E+00	---	DFREQ(3,3,11)
AIRT	for wind speed class 3 and stability class D	2.459E-02	0.000E+00	---	DFREQ(3,4,11)
AIRT	for wind speed class 3 and stability class E	1.074E-02	0.000E+00	---	DFREQ(3,5,11)
AIRT	for wind speed class 3 and stability class F	0.000E+00	0.000E+00	---	DFREQ(3,6,11)
AIRT	Joint Frequency in SW Sector				
AIRT	for wind speed class 4 and stability class A	0.000E+00	0.000E+00	---	DFREQ(4,1,11)
AIRT	for wind speed class 4 and stability class B	0.000E+00	0.000E+00	---	DFREQ(4,2,11)
AIRT	for wind speed class 4 and stability class C	1.060E-03	0.000E+00	---	DFREQ(4,3,11)
AIRT	for wind speed class 4 and stability class D	8.690E-03	0.000E+00	---	DFREQ(4,4,11)
AIRT	for wind speed class 4 and stability class E	0.000E+00	0.000E+00	---	DFREQ(4,5,11)
AIRT	for wind speed class 4 and stability class F	0.000E+00	0.000E+00	---	DFREQ(4,6,11)
AIRT	Joint Frequency in SW Sector				
AIRT	for wind speed class 5 and stability class A	0.000E+00	0.000E+00	---	DFREQ(5,1,11)
AIRT	for wind speed class 5 and stability class B	0.000E+00	0.000E+00	---	DFREQ(5,2,11)
AIRT	for wind speed class 5 and stability class C	2.000E-05	0.000E+00	---	DFREQ(5,3,11)
AIRT	for wind speed class 5 and stability class D	4.600E-04	0.000E+00	---	DFREQ(5,4,11)
AIRT	for wind speed class 5 and stability class E	0.000E+00	0.000E+00	---	DFREQ(5,5,11)
AIRT	for wind speed class 5 and stability class F	0.000E+00	0.000E+00	---	DFREQ(5,6,11)
AIRT	Joint Frequency in SW Sector				
AIRT	for wind speed class 6 and stability class A	0.000E+00	0.000E+00	---	DFREQ(6,1,11)
AIRT	for wind speed class 6 and stability class B	0.000E+00	0.000E+00	---	DFREQ(6,2,11)
AIRT	for wind speed class 6 and stability class C	0.000E+00	0.000E+00	---	DFREQ(6,3,11)
AIRT	for wind speed class 6 and stability class D	3.000E-05	0.000E+00	---	DFREQ(6,4,11)
AIRT	for wind speed class 6 and stability class E	0.000E+00	0.000E+00	---	DFREQ(6,5,11)
AIRT	for wind speed class 6 and stability class F	0.000E+00	0.000E+00	---	DFREQ(6,6,11)
AIRT	Joint Frequency in WSW Sector				
AIRT	for wind speed class 1 and stability class A	7.600E-04	0.000E+00	---	DFREQ(1,1,12)
AIRT	for wind speed class 1 and stability class B	4.040E-03	0.000E+00	---	DFREQ(1,2,12)
AIRT	for wind speed class 1 and stability class C	2.110E-03	0.000E+00	---	DFREQ(1,3,12)
AIRT	for wind speed class 1 and stability class D	3.740E-03	1.000E-01	---	DFREQ(1,4,12)
AIRT	for wind speed class 1 and stability class E	0.000E+00	2.000E-01	---	DFREQ(1,5,12)
AIRT	for wind speed class 1 and stability class F	1.298E-02	7.000E-01	---	DFREQ(1,6,12)

Site-Specific Parameter Summary (continued)

Menu	Parameter	User Input	Default	RESRAD computed	Parameter Name
AIRT	Joint Frequency in WSW Sector				
AIRT	for wind speed class 2 and stability class A	5.80OE-04	0.000E+00	---	DFREQ(2,1,12)
AIRT	for wind speed class 2 and stability class B	3.03OE-03	0.000E+00	---	DFREQ(2,2,12)
AIRT	for wind speed class 2 and stability class C	3.62OE-03	0.000E+00	---	DFREQ(2,3,12)
AIRT	for wind speed class 2 and stability class D	6.99OE-03	0.000E+00	---	DFREQ(2,4,12)
AIRT	for wind speed class 2 and stability class E	6.06OE-03	0.000E+00	---	DFREQ(2,5,12)
AIRT	for wind speed class 2 and stability class F	9.12OE-03	0.000E+00	---	DFREQ(2,6,12)
AIRT	Joint Frequency in WSW Sector				
AIRT	for wind speed class 3 and stability class A	0.000E+00	0.000E+00	---	DFREQ(3,1,12)
AIRT	for wind speed class 3 and stability class B	1.31OE-03	0.000E+00	---	DFREQ(3,2,12)
AIRT	for wind speed class 3 and stability class C	4.41OE-03	0.000E+00	---	DFREQ(3,3,12)
AIRT	for wind speed class 3 and stability class D	9.68OE-03	0.000E+00	---	DFREQ(3,4,12)
AIRT	for wind speed class 3 and stability class E	2.91OE-03	0.000E+00	---	DFREQ(3,5,12)
AIRT	for wind speed class 3 and stability class F	0.000E+00	0.000E+00	---	DFREQ(3,6,12)
AIRT	Joint Frequency in WSW Sector				
AIRT	for wind speed class 4 and stability class A	0.000E+00	0.000E+00	---	DFREQ(4,1,12)
AIRT	for wind speed class 4 and stability class B	0.000E+00	0.000E+00	---	DFREQ(4,2,12)
AIRT	for wind speed class 4 and stability class C	6.50OE-04	0.000E+00	---	DFREQ(4,3,12)
AIRT	for wind speed class 4 and stability class D	4.27OE-03	0.000E+00	---	DFREQ(4,4,12)
AIRT	for wind speed class 4 and stability class E	0.000E+00	0.000E+00	---	DFREQ(4,5,12)
AIRT	for wind speed class 4 and stability class F	0.000E+00	0.000E+00	---	DFREQ(4,6,12)
AIRT	Joint Frequency in WSW Sector				
AIRT	for wind speed class 5 and stability class A	0.000E+00	0.000E+00	---	DFREQ(5,1,12)
AIRT	for wind speed class 5 and stability class B	0.000E+00	0.000E+00	---	DFREQ(5,2,12)
AIRT	for wind speed class 5 and stability class C	1.000E-05	0.000E+00	---	DFREQ(5,3,12)
AIRT	for wind speed class 5 and stability class D	3.70OE-04	0.000E+00	---	DFREQ(5,4,12)
AIRT	for wind speed class 5 and stability class E	0.000E+00	0.000E+00	---	DFREQ(5,5,12)
AIRT	for wind speed class 5 and stability class F	0.000E+00	0.000E+00	---	DFREQ(5,6,12)
AIRT	Joint Frequency in WSW Sector				
AIRT	for wind speed class 6 and stability class A	0.000E+00	0.000E+00	---	DFREQ(6,1,12)
AIRT	for wind speed class 6 and stability class B	0.000E+00	0.000E+00	---	DFREQ(6,2,12)
AIRT	for wind speed class 6 and stability class C	0.000E+00	0.000E+00	---	DFREQ(6,3,12)
AIRT	for wind speed class 6 and stability class D	3.000E-05	0.000E+00	---	DFREQ(6,4,12)
AIRT	for wind speed class 6 and stability class E	0.000E+00	0.000E+00	---	DFREQ(6,5,12)
AIRT	for wind speed class 6 and stability class F	0.000E+00	0.000E+00	---	DFREQ(6,6,12)
AIRT	Joint Frequency in W Sector				
AIRT	for wind speed class 1 and stability class A	4.90OE-04	0.000E+00	---	DFREQ(1,1,13)
AIRT	for wind speed class 1 and stability class B	2.79OE-03	0.000E+00	---	DFREQ(1,2,13)
AIRT	for wind speed class 1 and stability class C	1.19OE-03	0.000E+00	---	DFREQ(1,3,13)
AIRT	for wind speed class 1 and stability class D	2.24OE-03	1.000E-01	---	DFREQ(1,4,13)
AIRT	for wind speed class 1 and stability class E	0.000E+00	2.000E-01	---	DFREQ(1,5,13)
AIRT	for wind speed class 1 and stability class F	1.095E-02	7.000E-01	---	DFREQ(1,6,13)

Site-Specific Parameter Summary (continued)

Menu	Parameter	User Input	Default	RESRAD computed	Parameter Name
AIRT	Joint Frequency in W Sector				
AIRT	for wind speed class 2 and stability class A	2.900E-04	0.000E+00	---	DFREQ(2,1,13)
AIRT	for wind speed class 2 and stability class B	1.300E-03	0.000E+00	---	DFREQ(2,2,13)
AIRT	for wind speed class 2 and stability class C	1.550E-03	0.000E+00	---	DFREQ(2,3,13)
AIRT	for wind speed class 2 and stability class D	3.030E-03	0.000E+00	---	DFREQ(2,4,13)
AIRT	for wind speed class 2 and stability class E	3.110E-03	0.000E+00	---	DFREQ(2,5,13)
AIRT	for wind speed class 2 and stability class F	4.440E-03	0.000E+00	---	DFREQ(2,6,13)
AIRT	Joint Frequency in W Sector				
AIRT	for wind speed class 3 and stability class A	0.000E+00	0.000E+00	---	DFREQ(3,1,13)
AIRT	for wind speed class 3 and stability class B	5.000E-04	0.000E+00	---	DFREQ(3,2,13)
AIRT	for wind speed class 3 and stability class C	1.050E-03	0.000E+00	---	DFREQ(3,3,13)
AIRT	for wind speed class 3 and stability class D	2.370E-03	0.000E+00	---	DFREQ(3,4,13)
AIRT	for wind speed class 3 and stability class E	6.300E-04	0.000E+00	---	DFREQ(3,5,13)
AIRT	for wind speed class 3 and stability class F	0.000E+00	0.000E+00	---	DFREQ(3,6,13)
AIRT	Joint Frequency in W Sector				
AIRT	for wind speed class 4 and stability class A	0.000E+00	0.000E+00	---	DFREQ(4,1,13)
AIRT	for wind speed class 4 and stability class B	0.000E+00	0.000E+00	---	DFREQ(4,2,13)
AIRT	for wind speed class 4 and stability class C	7.000E-05	0.000E+00	---	DFREQ(4,3,13)
AIRT	for wind speed class 4 and stability class D	5.400E-04	0.000E+00	---	DFREQ(4,4,13)
AIRT	for wind speed class 4 and stability class E	0.000E+00	0.000E+00	---	DFREQ(4,5,13)
AIRT	for wind speed class 4 and stability class F	0.000E+00	0.000E+00	---	DFREQ(4,6,13)
AIRT	Joint Frequency in W Sector				
AIRT	for wind speed class 5 and stability class A	0.000E+00	0.000E+00	---	DFREQ(5,1,13)
AIRT	for wind speed class 5 and stability class B	0.000E+00	0.000E+00	---	DFREQ(5,2,13)
AIRT	for wind speed class 5 and stability class C	0.000E+00	0.000E+00	---	DFREQ(5,3,13)
AIRT	for wind speed class 5 and stability class D	2.000E-05	0.000E+00	---	DFREQ(5,4,13)
AIRT	for wind speed class 5 and stability class E	0.000E+00	0.000E+00	---	DFREQ(5,5,13)
AIRT	for wind speed class 5 and stability class F	0.000E+00	0.000E+00	---	DFREQ(5,6,13)
AIRT	Joint Frequency in W Sector				
AIRT	for wind speed class 6 and stability class A	0.000E+00	0.000E+00	---	DFREQ(6,1,13)
AIRT	for wind speed class 6 and stability class B	0.000E+00	0.000E+00	---	DFREQ(6,2,13)
AIRT	for wind speed class 6 and stability class C	0.000E+00	0.000E+00	---	DFREQ(6,3,13)
AIRT	for wind speed class 6 and stability class D	1.000E-05	0.000E+00	---	DFREQ(6,4,13)
AIRT	for wind speed class 6 and stability class E	0.000E+00	0.000E+00	---	DFREQ(6,5,13)
AIRT	for wind speed class 6 and stability class F	0.000E+00	0.000E+00	---	DFREQ(6,6,13)
AIRT	Joint Frequency in WNW Sector				
AIRT	for wind speed class 1 and stability class A	3.100E-04	0.000E+00	---	DFREQ(1,1,14)
AIRT	for wind speed class 1 and stability class B	2.020E-03	0.000E+00	---	DFREQ(1,2,14)
AIRT	for wind speed class 1 and stability class C	8.500E-04	0.000E+00	---	DFREQ(1,3,14)
AIRT	for wind speed class 1 and stability class D	1.430E-03	1.000E-01	---	DFREQ(1,4,14)
AIRT	for wind speed class 1 and stability class E	0.000E+00	2.000E-01	---	DFREQ(1,5,14)
AIRT	for wind speed class 1 and stability class F	6.920E-03	7.000E-01	---	DFREQ(1,6,14)

Site-Specific Parameter Summary (continued)

Menu	Parameter	User Input	Default	RESRAD computed	Parameter Name
AIRT	Joint Frequency in WNW Sector				
AIRT	for wind speed class 2 and stability class A	2.400E-04	0.000E+00	---	DFREQ(2,1,14)
AIRT	for wind speed class 2 and stability class B	6.400E-04	0.000E+00	---	DFREQ(2,2,14)
AIRT	for wind speed class 2 and stability class C	8.700E-04	0.000E+00	---	DFREQ(2,3,14)
AIRT	for wind speed class 2 and stability class D	2.660E-03	0.000E+00	---	DFREQ(2,4,14)
AIRT	for wind speed class 2 and stability class E	2.240E-03	0.000E+00	---	DFREQ(2,5,14)
AIRT	for wind speed class 2 and stability class F	3.060E-03	0.000E+00	---	DFREQ(2,6,14)
AIRT	Joint Frequency in WNW Sector				
AIRT	for wind speed class 3 and stability class A	0.000E+00	0.000E+00	---	DFREQ(3,1,14)
AIRT	for wind speed class 3 and stability class B	1.400E-04	0.000E+00	---	DFREQ(3,2,14)
AIRT	for wind speed class 3 and stability class C	2.500E-04	0.000E+00	---	DFREQ(3,3,14)
AIRT	for wind speed class 3 and stability class D	1.980E-03	0.000E+00	---	DFREQ(3,4,14)
AIRT	for wind speed class 3 and stability class E	4.500E-04	0.000E+00	---	DFREQ(3,5,14)
AIRT	for wind speed class 3 and stability class F	0.000E+00	0.000E+00	---	DFREQ(3,6,14)
AIRT	Joint Frequency in WNW Sector				
AIRT	for wind speed class 4 and stability class A	0.000E+00	0.000E+00	---	DFREQ(4,1,14)
AIRT	for wind speed class 4 and stability class B	0.000E+00	0.000E+00	---	DFREQ(4,2,14)
AIRT	for wind speed class 4 and stability class C	1.000E-05	0.000E+00	---	DFREQ(4,3,14)
AIRT	for wind speed class 4 and stability class D	3.400E-04	0.000E+00	---	DFREQ(4,4,14)
AIRT	for wind speed class 4 and stability class E	0.000E+00	0.000E+00	---	DFREQ(4,5,14)
AIRT	for wind speed class 4 and stability class F	0.000E+00	0.000E+00	---	DFREQ(4,6,14)
AIRT	Joint Frequency in WNW Sector				
AIRT	for wind speed class 5 and stability class A	0.000E+00	0.000E+00	---	DFREQ(5,1,14)
AIRT	for wind speed class 5 and stability class B	0.000E+00	0.000E+00	---	DFREQ(5,2,14)
AIRT	for wind speed class 5 and stability class C	0.000E+00	0.000E+00	---	DFREQ(5,3,14)
AIRT	for wind speed class 5 and stability class D	3.000E-05	0.000E+00	---	DFREQ(5,4,14)
AIRT	for wind speed class 5 and stability class E	0.000E+00	0.000E+00	---	DFREQ(5,5,14)
AIRT	for wind speed class 5 and stability class F	0.000E+00	0.000E+00	---	DFREQ(5,6,14)
AIRT	Joint Frequency in WNW Sector				
AIRT	for wind speed class 6 and stability class A	0.000E+00	0.000E+00	---	DFREQ(6,1,14)
AIRT	for wind speed class 6 and stability class B	0.000E+00	0.000E+00	---	DFREQ(6,2,14)
AIRT	for wind speed class 6 and stability class C	0.000E+00	0.000E+00	---	DFREQ(6,3,14)
AIRT	for wind speed class 6 and stability class D	0.000E+00	0.000E+00	---	DFREQ(6,4,14)
AIRT	for wind speed class 6 and stability class E	0.000E+00	0.000E+00	---	DFREQ(6,5,14)
AIRT	for wind speed class 6 and stability class F	0.000E+00	0.000E+00	---	DFREQ(6,6,14)
AIRT	Joint Frequency in NW Sector				
AIRT	for wind speed class 1 and stability class A	3.300E-04	0.000E+00	---	DFREQ(1,1,15)
AIRT	for wind speed class 1 and stability class B	2.280E-03	0.000E+00	---	DFREQ(1,2,15)
AIRT	for wind speed class 1 and stability class C	8.800E-04	0.000E+00	---	DFREQ(1,3,15)
AIRT	for wind speed class 1 and stability class D	2.020E-03	1.000E-01	---	DFREQ(1,4,15)
AIRT	for wind speed class 1 and stability class E	0.000E+00	2.000E-01	---	DFREQ(1,5,15)
AIRT	for wind speed class 1 and stability class F	8.500E-03	7.000E-01	---	DFREQ(1,6,15)

Site-Specific Parameter Summary (continued)

Menu	Parameter	User Input	Default	RESRAD computed	Parameter Name
AIRT	Joint Frequency in NW Sector				
AIRT	for wind speed class 2 and stability class A	1.000E-04	0.000E+00	---	DFREQ(2,1,15)
AIRT	for wind speed class 2 and stability class B	6.200E-04	0.000E+00	---	DFREQ(2,2,15)
AIRT	for wind speed class 2 and stability class C	8.000E-04	0.000E+00	---	DFREQ(2,3,15)
AIRT	for wind speed class 2 and stability class D	3.160E-03	0.000E+00	---	DFREQ(2,4,15)
AIRT	for wind speed class 2 and stability class E	3.140E-03	0.000E+00	---	DFREQ(2,5,15)
AIRT	for wind speed class 2 and stability class F	3.890E-03	0.000E+00	---	DFREQ(2,6,15)
AIRT	Joint Frequency in NW Sector				
AIRT	for wind speed class 3 and stability class A	0.000E+00	0.000E+00	---	DFREQ(3,1,15)
AIRT	for wind speed class 3 and stability class B	1.300E-04	0.000E+00	---	DFREQ(3,2,15)
AIRT	for wind speed class 3 and stability class C	1.500E-04	0.000E+00	---	DFREQ(3,3,15)
AIRT	for wind speed class 3 and stability class D	2.160E-03	0.000E+00	---	DFREQ(3,4,15)
AIRT	for wind speed class 3 and stability class E	3.900E-04	0.000E+00	---	DFREQ(3,5,15)
AIRT	for wind speed class 3 and stability class F	0.000E+00	0.000E+00	---	DFREQ(3,6,15)
AIRT	Joint Frequency in NW Sector				
AIRT	for wind speed class 4 and stability class A	0.000E+00	0.000E+00	---	DFREQ(4,1,15)
AIRT	for wind speed class 4 and stability class B	0.000E+00	0.000E+00	---	DFREQ(4,2,15)
AIRT	for wind speed class 4 and stability class C	2.000E-05	0.000E+00	---	DFREQ(4,3,15)
AIRT	for wind speed class 4 and stability class D	4.300E-04	0.000E+00	---	DFREQ(4,4,15)
AIRT	for wind speed class 4 and stability class E	0.000E+00	0.000E+00	---	DFREQ(4,5,15)
AIRT	for wind speed class 4 and stability class F	0.000E+00	0.000E+00	---	DFREQ(4,6,15)
AIRT	Joint Frequency in NW Sector				
AIRT	for wind speed class 5 and stability class A	0.000E+00	0.000E+00	---	DFREQ(5,1,15)
AIRT	for wind speed class 5 and stability class B	0.000E+00	0.000E+00	---	DFREQ(5,2,15)
AIRT	for wind speed class 5 and stability class C	0.000E+00	0.000E+00	---	DFREQ(5,3,15)
AIRT	for wind speed class 5 and stability class D	6.000E-05	0.000E+00	---	DFREQ(5,4,15)
AIRT	for wind speed class 5 and stability class E	0.000E+00	0.000E+00	---	DFREQ(5,5,15)
AIRT	for wind speed class 5 and stability class F	0.000E+00	0.000E+00	---	DFREQ(5,6,15)
AIRT	Joint Frequency in NW Sector				
AIRT	for wind speed class 6 and stability class A	0.000E+00	0.000E+00	---	DFREQ(6,1,15)
AIRT	for wind speed class 6 and stability class B	0.000E+00	0.000E+00	---	DFREQ(6,2,15)
AIRT	for wind speed class 6 and stability class C	0.000E+00	0.000E+00	---	DFREQ(6,3,15)
AIRT	for wind speed class 6 and stability class D	0.000E+00	0.000E+00	---	DFREQ(6,4,15)
AIRT	for wind speed class 6 and stability class E	0.000E+00	0.000E+00	---	DFREQ(6,5,15)
AIRT	for wind speed class 6 and stability class F	0.000E+00	0.000E+00	---	DFREQ(6,6,15)
AIRT	Joint Frequency in NNW Sector				
AIRT	for wind speed class 1 and stability class A	2.600E-04	0.000E+00	---	DFREQ(1,1,16)
AIRT	for wind speed class 1 and stability class B	1.420E-03	0.000E+00	---	DFREQ(1,2,16)
AIRT	for wind speed class 1 and stability class C	4.700E-04	0.000E+00	---	DFREQ(1,3,16)
AIRT	for wind speed class 1 and stability class D	1.360E-03	1.000E-01	---	DFREQ(1,4,16)
AIRT	for wind speed class 1 and stability class E	0.000E+00	2.000E-01	---	DFREQ(1,5,16)
AIRT	for wind speed class 1 and stability class F	5.880E-03	7.000E-01	---	DFREQ(1,6,16)

Site-Specific Parameter Summary (continued)

Menu	Parameter	User Input	Default	RESRAD computed	Parameter Name
AIRT	Joint Frequency in NNW Sector				
AIRT	for wind speed class 2 and stability class A	1.400E-04	0.000E+00	---	DFREQ(2,1,16)
AIRT	for wind speed class 2 and stability class B	4.000E-04	0.000E+00	---	DFREQ(2,2,16)
AIRT	for wind speed class 2 and stability class C	5.400E-04	0.000E+00	---	DFREQ(2,3,16)
AIRT	for wind speed class 2 and stability class D	2.020E-03	0.000E+00	---	DFREQ(2,4,16)
AIRT	for wind speed class 2 and stability class E	1.560E-03	0.000E+00	---	DFREQ(2,5,16)
AIRT	for wind speed class 2 and stability class F	2.280E-03	0.000E+00	---	DFREQ(2,6,16)
AIRT	Joint Frequency in NNW Sector				
AIRT	for wind speed class 3 and stability class A	0.000E+00	0.000E+00	---	DFREQ(3,1,16)
AIRT	for wind speed class 3 and stability class B	1.000E-04	0.000E+00	---	DFREQ(3,2,16)
AIRT	for wind speed class 3 and stability class C	1.400E-04	0.000E+00	---	DFREQ(3,3,16)
AIRT	for wind speed class 3 and stability class D	1.270E-03	0.000E+00	---	DFREQ(3,4,16)
AIRT	for wind speed class 3 and stability class E	1.500E-04	0.000E+00	---	DFREQ(3,5,16)
AIRT	for wind speed class 3 and stability class F	0.000E+00	0.000E+00	---	DFREQ(3,6,16)
AIRT	Joint Frequency in NNW Sector				
AIRT	for wind speed class 4 and stability class A	0.000E+00	0.000E+00	---	DFREQ(4,1,16)
AIRT	for wind speed class 4 and stability class B	0.000E+00	0.000E+00	---	DFREQ(4,2,16)
AIRT	for wind speed class 4 and stability class C	0.000E+00	0.000E+00	---	DFREQ(4,3,16)
AIRT	for wind speed class 4 and stability class D	6.600E-04	0.000E+00	---	DFREQ(4,4,16)
AIRT	for wind speed class 4 and stability class E	0.000E+00	0.000E+00	---	DFREQ(4,5,16)
AIRT	for wind speed class 4 and stability class F	0.000E+00	0.000E+00	---	DFREQ(4,6,16)
AIRT	Joint Frequency in NNW Sector				
AIRT	for wind speed class 5 and stability class A	0.000E+00	0.000E+00	---	DFREQ(5,1,16)
AIRT	for wind speed class 5 and stability class B	0.000E+00	0.000E+00	---	DFREQ(5,2,16)
AIRT	for wind speed class 5 and stability class C	0.000E+00	0.000E+00	---	DFREQ(5,3,16)
AIRT	for wind speed class 5 and stability class D	1.400E-04	0.000E+00	---	DFREQ(5,4,16)
AIRT	for wind speed class 5 and stability class E	0.000E+00	0.000E+00	---	DFREQ(5,5,16)
AIRT	for wind speed class 5 and stability class F	0.000E+00	0.000E+00	---	DFREQ(5,6,16)
AIRT	Joint Frequency in NNW Sector				
AIRT	for wind speed class 6 and stability class A	0.000E+00	0.000E+00	---	DFREQ(6,1,16)
AIRT	for wind speed class 6 and stability class B	0.000E+00	0.000E+00	---	DFREQ(6,2,16)
AIRT	for wind speed class 6 and stability class C	0.000E+00	0.000E+00	---	DFREQ(6,3,16)
AIRT	for wind speed class 6 and stability class D	2.000E-05	0.000E+00	---	DFREQ(6,4,16)
AIRT	for wind speed class 6 and stability class E	0.000E+00	0.000E+00	---	DFREQ(6,5,16)
AIRT	for wind speed class 6 and stability class F	0.000E+00	0.000E+00	---	DFREQ(6,6,16)
AIRT	Spacing of points used for areal integration, (m)	1.000E+01	1.000E+01	---	ATGRID
GWTR	fractional accuracy desired - convergence criteria	0.000E+00	1.000E-03	---	EPS
GWTR	Distance from d/g edge of contamination to Well, (m)	1.000E+02	1.000E+02	---	OFFLPAQW
GWTR	Contamination to Well c/c distance normal to flow, m	0.000E+00	0.000E+00	---	OFFLNAQW
GWTR	Distance from d/g edge of cz to surface water, (m)	3.155E+02	4.500E+02	---	OFFLPAQS
GWTR	Contamination to near edge of swb,c/c normal to flow	-5.000E+01	-1.500E+02	---	OFFLNAQSN
GWTR	Contamination to far edge of swb, c/c normal to flow	5.000E+01	1.500E+02	---	OFFLNAQSF

Site-Specific Parameter Summary (continued)

Menu	Parameter	User Input	Default	RESRAD computed	Parameter Name
GWTR	Number of main sub zones in primary contamination	5	1	---	NPCZ
GWTR	Number of minor sub zones in last main PC sub zone	1	1	---	NPCZF
GWTR	Number of main sub zones in submerged prim. contami.	5	1	---	NSPCZ
GWTR	Number of minor sub zones in last main SPC sub zone	1	1	---	NSPCZF
GWTR	Number of main sub zones in each unsaturated stratum	5	1	---	NPSS
GWTR	Number of minor sub zones in last main UZ sub zone	1	1	---	NPSSF
GWTR	Number of main sub zones in saturated stratum	5	1	---	NAQS
GWTR	Number of minor sub zones in last main SZ sub zone	1	1	---	NAQSF
GWTR	Distribution coefficient and longitudinal dispersion	1	1	---	
	1 = Nuclide specific distrubution coefficients in all subzones. Longitudinal dispersion in all but the subzone of transformation.				
GWTR	Retardation factor flag for groundwater transport	0	0	---	
	0 = (total porosity + distribution coefficient*dry bulk density) / total porosity				
USZN	Number of unsaturated zone strata	5	1	---	NS
USZN	Unsat. zone 1, thickness (m)	3.050E-01	4.000E+00	---	H(1)
USZN	Unsat. zone 1, soil density (g/cm**3)	1.400E+00	1.500E+00	---	DENSUZ(1)
USZN	Unsat. zone 1, total porosity	4.630E-01	4.000E-01	---	TPUZ(1)
USZN	Unsat. zone 1, effective porosity	2.940E-01	2.000E-01	---	EPUZ(1)
USZN	Unsat. zone 1, field capacity	2.320E-01	3.000E-01	---	FCUZ(1)
USZN	Unsat. zone 1, hydraulic conductivity (m/yr)	1.170E+02	1.000E+01	---	HCUZ(1)
USZN	Unsat. zone 1, soil-specific b parameter	5.400E+00	5.300E+00	---	BUZ(1)
USZN	Unsat. zone 1, longitudinal dispersivity (m)	1.000E-01	1.000E-01	---	ALPHALU(1)
USZN	Unsat. zone 2, thickness (m)	3.050E-01	0.000E+00	---	H(2)
USZN	Unsat. zone 2, soil density (g/cm**3)	1.600E+00	1.500E+00	---	DENSUZ(2)
USZN	Unsat. zone 2, total porosity	3.970E-01	4.000E-01	---	TPUZ(2)
USZN	Unsat. zone 2, effective porosity	3.890E-01	2.000E-01	---	EPUZ(2)
USZN	Unsat. zone 2, field capacity	3.200E-02	3.000E-01	---	FCUZ(2)
USZN	Unsat. zone 2, hydraulic conductivity (m/yr)	9.460E+04	1.000E+01	---	HCUZ(2)
USZN	Unsat. zone 2, soil-specific b parameter	4.050E+00	5.300E+00	---	BUZ(2)
USZN	Unsat. zone 2, longitudinal dispersivity (m)	1.000E-01	1.000E-01	---	ALPHALU(2)
USZN	Unsat. zone 3, thickness (m)	9.144E-01	0.000E+00	---	H(3)
USZN	Unsat. zone 3, soil density (g/cm**3)	1.500E+00	1.500E+00	---	DENSUZ(3)
USZN	Unsat. zone 3, total porosity	4.270E-01	4.000E-01	---	TPUZ(3)
USZN	Unsat. zone 3, effective porosity	1.950E-01	2.000E-01	---	EPUZ(3)
USZN	Unsat. zone 3, field capacity	4.180E-01	3.000E-01	---	FCUZ(3)
USZN	Unsat. zone 3, hydraulic conductivity (m/yr)	3.150E-01	1.000E+01	---	HCUZ(3)
USZN	Unsat. zone 3, soil-specific b parameter	1.140E+01	5.300E+00	---	BUZ(3)
USZN	Unsat. zone 3, longitudinal dispersivity (m)	1.000E-01	1.000E-01	---	ALPHALU(3)

Site-Specific Parameter Summary (continued)

Menu	Parameter	User Input	Default	RESRAD computed	Parameter Name
USZN	Unsat. zone 4, thickness (m)	3.048E+00	0.000E+00	---	H(4)
USZN	Unsat. zone 4, soil density (g/cm**3)	1.500E+00	1.500E+00	---	DENSUZ(4)
USZN	Unsat. zone 4, total porosity	4.190E-01	4.000E-01	---	TPUZ(4)
USZN	Unsat. zone 4, effective porosity	2.340E-01	2.000E-01	---	EPUZ(4)
USZN	Unsat. zone 4, field capacity	3.070E-01	3.000E-01	---	FCUZ(4)
USZN	Unsat. zone 4, hydraulic conductivity (m/yr)	3.150E+00	1.000E+01	---	HCUZ(4)
USZN	Unsat. zone 4, soil-specific b parameter	1.140E+01	5.300E+00	---	BUZ(4)
USZN	Unsat. zone 4, longitudinal dispersivity (m)	1.000E-01	1.000E-01	---	ALPHALU(4)
USZN	Unsat. zone 5, thickness (m)	4.846E+00	0.000E+00	---	H(5)
USZN	Unsat. zone 5, soil density (g/cm**3)	1.800E+00	1.500E+00	---	DENSUZ(5)
USZN	Unsat. zone 5, total porosity	3.530E-01	4.000E-01	---	TPUZ(5)
USZN	Unsat. zone 5, effective porosity	2.700E-01	2.000E-01	---	EPUZ(5)
USZN	Unsat. zone 5, field capacity	2.471E-01	3.000E-01	---	FCUZ(5)
USZN	Unsat. zone 5, hydraulic conductivity (m/yr)	1.670E+01	1.000E+01	---	HCUZ(5)
USZN	Unsat. zone 5, soil-specific b parameter	1.040E+01	5.300E+00	---	BUZ(5)
USZN	Unsat. zone 5, longitudinal dispersivity (m)	1.000E-01	1.000E-01	---	ALPHALU(5)
SZNE	Well pump intake depth (m below water table)	4.000E+01	1.000E+01	---	DWIBWT
SZNE	Depth of aquifer contributing to surface water body	3.048E+01	1.000E+01	---	DPTHAQSW
SZNE	Thickness of saturated zone (m)	6.096E+01	1.000E+02	---	DPTHAQ
SZNE	Density of saturated zone (g/cm**3)	2.100E+00	1.500E+00	---	DENSAQ
SZNE	Saturated zone total porosity	2.400E-01	4.000E-01	---	TPSZ
SZNE	Saturated zone effective porosity	2.000E-01	2.000E-01	---	EPSZ
SZNE	Saturated zone hydraulic conductivity (m/yr)	2.680E+01	1.000E+02	---	HCSZ
SZNE	Saturated zone hydraulic gradient to well	5.400E-02	2.000E-02	---	HGW
SZNE	Satur. zone hydraulic gradient to surface water body	3.600E-02	2.000E-02	---	HGSW
SZNE	longitudinal dispersivity to well (m)	1.000E+01	3.000E+00	---	ALPHALOW
SZNE	longitudinal dispersivity to SWB (m)	3.150E+01	1.000E+01	---	ALPHALOSW
SZNE	lateral (horizontal) dispersivity to well (m)	1.000E+00	4.000E-01	---	ALPHATW
SZNE	lateral (horizontal) dispersivity to SWB (m)	3.150E+00	1.000E+00	---	ALPHATSW
SZNE	lateral (vertical) dispersivity to well (m)	1.000E-01	2.000E-02	---	ALPHAVW
SZNE	lateral (vertical) dispersivity to SWB (m)	3.150E-01	6.000E-02	---	ALPHAVSW
SZNE	Irrigation rate over aquifer to well (m/yr)	not used	0.000E+00	---	RIAQW
SZNE	Irrigation rate over aquifer to SWB (m/yr)	not used	0.000E+00	---	RIAQSW
SZNE	Evapotranspiration coefficient over aquifer to well	not used	1.000E+00	---	EVAPTRAQW
SZNE	Evapotranspiration coefficient over aquifer to SWB	not used	1.000E+00	---	EVAPTRAQSW
SZNE	Runoff coefficient over aquifer to well	not used	1.000E+00	---	RUNOFFAQW
SZNE	Runoff coefficient over aquifer to SWB	not used	1.000E+00	---	RUNOFFAQSW
SZNE	Concentration of mobile colloids in the aquifer	0.000E+00	0.000E+00	---	CCOL
SZNE	Water - Soil Distribution coefficient of colloids	0.000E+00	0.000E+00	---	K1Col
SZNE	Water - Mobile Colloids Distribution coefficient	0.000E+00	0.000E+00	---	K3Col
WTRU	Drinking water intake (L/yr)	7.300E+02	5.100E+02	---	DWI
WTRU	Fraction of drinking water from surface water	0.000E+00	0.000E+00	---	FSWD
WTRU	Fraction of drinking water from well water	1.000E+00	1.000E+00	---	FWWD
WTRU	Fraction of household water from surface water	0.000E+00	0.000E+00	---	FSWHH

Site-Specific Parameter Summary (continued)

Menu	Parameter	User Input	Default	RESRAD computed	Parameter Name
WTRU	Fraction of household water from well water	1.000E+00	1.000E+00	---	FWWHH
WTRU	Livestock water intake for meat 1 (L/day)	5.000E+01	5.000E+01	---	LWI(1)
WTRU	Fraction of livestock water 1 from surface water	1.000E+00	0.000E+00	---	FSWLV(1)
WTRU	Fraction of livestock water 1 from well water	0.000E+00	1.000E+00	---	FWWLV(1)
WTRU	Livestock water intake for milk (L/day)	1.600E+02	1.600E+02	---	LWI(2)
WTRU	Fraction of dairy cow water from surface water	1.000E+00	0.000E+00	---	FSWLV(2)
WTRU	Fraction of dairy cow water from well water	0.000E+00	1.000E+00	---	FWWLV(2)
WTRU	Irrigation rate in Agricultural Area 1 (m/yr)	1.500E-01	2.000E-01	---	RIRRIG(1)
WTRU	Fraction of irrigation water 1 from surface water	1.000E+00	0.000E+00	---	FSWIR(1)
WTRU	Fraction of irrigation water 1 from well water	0.000E+00	1.000E+00	---	FWWIR(1)
WTRU	Irrigation rate in Agricultural Area 2 (m/yr)	1.500E-01	2.000E-01	---	RIRRIG(2)
WTRU	Fraction of irrigation water 2 from surface water	1.000E+00	0.000E+00	---	FSWIR(2)
WTRU	Fraction of irrigation water 2 from well water	0.000E+00	1.000E+00	---	FWWIR(2)
WTRU	Irrigation rate in Agricultural Area 3 (m/yr)	1.500E-01	2.000E-01	---	RIRRIG(3)
WTRU	Fraction of irrigation water 3 from surface water	1.000E+00	0.000E+00	---	FSWIR(3)
WTRU	Fraction of irrigation water 3 from well water	0.000E+00	1.000E+00	---	FWWIR(3)
WTRU	Irrigation rate in Agricultural Area 4 (m/yr)	1.500E-01	2.000E-01	---	RIRRIG(4)
WTRU	Fraction of irrigation water 4 from surface water	1.000E+00	0.000E+00	---	FSWIR(4)
WTRU	Fraction of irrigation water 4 from well water	0.000E+00	1.000E+00	---	FWWIR(4)
WTRU	Irrigation rate in Offsite dwelling site (m/yr)	1.500E-02	2.000E-01	---	RIRRIGDWELL
WTRU	Fraction of irrigation water from surface water	1.000E+00	0.000E+00	---	FSWIRDWELL
WTRU	Fraction of irrigation water from well water	0.000E+00	1.000E+00	---	FWWIRDWELL
WTRU	Well pumping rate (m**3/yr)	3.320E+02	5.100E+03	---	UW
SWBY	Sediment delivery ratio	1.000E+00	1.000E+00	---	SDR
SWBY	Volume of surface water body	2.500E+02	1.500E+05	---	VLAKE
SWBY	Mean residence time of water in surface water body	1.000E-04	1.000E+00	---	TLAKE
SWBY	Surface area of water in surface water body	5.000E+02	9.000E+04	---	ALAKE
INGE	Fish consumption (kg/yr)	2.430E+00	5.400E+00	---	DFI(1)
INGE	Fraction of Fish from affected area	1.000E+00	5.000E-01	---	FFISH(1)
INGE	Other Aquatic food consumption (kg/yr)	0.000E+00	9.000E-01	---	DFI(2)
INGE	Fraction of Aquatic food from affected area	5.000E-01	5.000E-01	---	FFISH(2)
INGE	Non-Leafy vegetables consumption (kg/yr)	1.760E+02	1.600E+02	---	DVI(1)
INGE	Fraction of vegetable 1 from affected area	5.000E-01	5.000E-01	---	FVEG(1)
INGE	Leafy vegetable consumption (kg/yr)	1.700E+01	1.400E+01	---	DVI(2)
INGE	Fraction of vegetable 2 from affected area	5.000E-01	5.000E-01	---	FVEG(2)
INGE	Meat 1 consumption (kg/yr)	9.190E+01	6.300E+01	---	DMI(1)
INGE	Fraction of meat 1from affected area	2.500E-01	1.000E+00	---	FMEMI(1)
INGE	Milk consumption (L/yr)	1.100E+02	9.200E+01	---	DMI(2)
INGE	Fraction of milk from affected area	5.000E-01	1.000E+00	---	FMEMI(2)
INGE	Soil ingestion rate (g/yr)	3.653E+01	3.650E+01	---	SOIL
VEGE	Wet weight crop yield for Non-Leafy (kg/m**2)	7.000E-01	7.000E-01	---	YIELD(1)
VEGE	Growing Season for Non-Leafy (years)	1.700E-01	1.700E-01	---	GROWTIME(1)
VEGE	Translocation Factor for Non-Leafy	1.000E-01	1.000E-01	---	FOLI_F(1)
VEGE	Weathering Removal Constant for Non-Leafy	2.000E+01	2.000E+01	---	RWEATHER(1)

Site-Specific Parameter Summary (continued)

Menu	Parameter	User Input	Default	RESRAD computed	Parameter Name
VEGE	Foliar Interception Fraction for dust Non-Leafy	2.500E-01	2.500E-01	---	FINTCEPT(1,1)
VEGE	Foliar Intercept-n Fract-n for irrigation Non-Leafy	2.500E-01	2.500E-01	---	FINTCEPT(1,2)
VEGE	Depth of roots for Non-Leafy (m)	1.200E+00	1.200E+00	---	DROOT(1)
VEGE	Wet weight crop yield for Leafy (kg/m**2)	1.500E+00	1.500E+00	---	YIELD(2)
VEGE	Growing Season for Leafy (years)	2.500E-01	2.500E-01	---	GROWTIME(2)
VEGE	Translocation Factor for Leafy	1.000E+00	1.000E+00	---	FOLI_F(2)
VEGE	Weathering Removal Constant for Leafy	2.000E+01	2.000E+01	---	RWEATHER(2)
VEGE	Foliar Interception Fraction for dust Leafy	2.500E-01	2.500E-01	---	FINTCEPT(2,1)
VEGE	Foliar Intercept-n Fract-n for irrigation Leafy	2.500E-01	2.500E-01	---	FINTCEPT(2,2)
VEGE	Depth of roots for Leafy (m)	9.000E-01	9.000E-01	---	DROOT(2)
VEGE	Wet weight crop yield for Pasture (kg/m**2)	1.100E+00	1.100E+00	---	YIELD(3)
VEGE	Growing Season for Pasture (years)	8.000E-02	8.000E-02	---	GROWTIME(3)
VEGE	Translocation Factor for Pasture	1.000E+00	1.000E+00	---	FOLI_F(3)
VEGE	Weathering Removal Constant for Pasture	2.000E+01	2.000E+01	---	RWEATHER(3)
VEGE	Foliar Interception Fraction for dust Pasture	2.500E-01	2.500E-01	---	FINTCEPT(3,1)
VEGE	Foliar Intercept-n Fract-n for irrigation Pasture	2.500E-01	2.500E-01	---	FINTCEPT(3,2)
VEGE	Depth of roots for Pasture (m)	9.000E-01	9.000E-01	---	DROOT(3)
VEGE	Wet weight crop yield for Grain (kg/m**2)	7.000E-01	7.000E-01	---	YIELD(4)
VEGE	Growing Season for Grain (years)	1.700E-01	1.700E-01	---	GROWTIME(4)
VEGE	Translocation Factor for Grain	1.000E-01	1.000E-01	---	FOLI_F(4)
VEGE	Weathering Removal Constant for Grain	2.000E+01	2.000E+01	---	RWEATHER(4)
VEGE	Foliar Interception Fraction for dust Grain	2.500E-01	2.500E-01	---	FINTCEPT(4,1)
VEGE	Foliar Intercept-n Fract-n for irrigation Grain	2.500E-01	2.500E-01	---	FINTCEPT(4,2)
VEGE	Depth of roots for Grain (m)	1.200E+00	1.200E+00	---	DROOT(4)
LINT	Feed 1 intake by livestock 1 (kg/day)	1.400E+01	1.400E+01	---	LFI(1,1)
LINT	Soil intake with feed 1 by livestock 1 (kg/day)	1.000E-01	1.000E-01	---	LSI(1,1)
LINT	Feed 1 intake by dairy cow (kg/day)	4.400E+01	4.400E+01	---	LFI(2,1)
LINT	Soil intake with feed 1 by dairy cow (kg/day)	4.000E-01	4.000E-01	---	LSI(2,1)
LINT	Feed 2 intake by livestock 1 (kg/day)	5.400E+01	5.400E+01	---	LFI(1,2)
LINT	Soil intake with feed 2 by livestock 1 (kg/day)	4.000E-01	4.000E-01	---	LSI(1,2)
LINT	Feed 2 intake by dairy cow (kg/day)	1.100E+01	1.100E+01	---	LFI(2,2)
LINT	Soil intake with feed 2 by dairy cow (kg/day)	1.000E-01	1.000E-01	---	LSI(2,2)
INHE	Inhalation rate (m**3/yr)	8.400E+03	8.400E+03	---	INHALR
INHE	Mass loading of all particulates from Primary contam	1.000E-04	1.000E-04	---	MLFD
INHE	Respirable particulates as a fraction of total	1.000E+00	1.000E+00	---	RESPFRACPC
INHE	Offsite mass loading same as onsite mass loading?	0.000E+00		---	SAMEMLRF
INHE	Total mass loading at agricultural area 1 (g/m**3)	1.000E-04	1.000E-04	---	MLTOTOF(1)
INHE	Respirable fraction at agricultural area 1	1.000E+00	1.000E+00	---	RESPFRACOF(1)
INHE	Total mass loading at agricultural area 2 (g/m**3)	1.000E-04	1.000E-04	---	MLTOTOF(2)
INHE	Respirable fraction at agricultural area 2	1.000E+00	1.000E+00	---	RESPFRACOF(2)
INHE	Total mass loading at agricultural area 3 (g/m**3)	1.000E-04	1.000E-04	---	MLTOTOF(3)
INHE	Respirable fraction at agricultural area 3	1.000E+00	1.000E+00	---	RESPFRACOF(3)
INHE	Total mass loading at agricultural area 4 (g/m**3)	1.000E-04	1.000E-04	---	MLTOTOF(4)
INHE	Respirable fraction at agricultural area 4	1.000E+00	1.000E-04	---	RESPFRACOF(4)
INHE	Total mass loading at offsite dwelling(g/m**3)	1.000E-04	1.000E-04	---	MLTOTDWELL

Site-Specific Parameter Summary (continued)

Menu	Parameter	User Input	Default	RESRAD computed	Parameter Name
INHE	Respirable fraction at offsite dwelling(g/m**3)	1.000E+00	1.000E+00	---	RESPFRACDWELL
INHE	Indoor dust filtration factor, inhalation	4.000E-01	4.000E-01	---	SHF3
INHE	Shielding factor, external gamma	7.000E-01	7.000E-01	---	SHF1
INHE	Shape factor flag, external gamma	-1.000E+00	1.000E+00	noncircular	FS
SEXT	Onsite shape factor array (used if non-circular):				
SEXT	Radii of shape factor array (used if non-circular):				
SEXT	Outer annular radius (m), ring 1:	4.358E+01	6.000E+00	---	RAD_SHAPE(1)
SEXT	Outer annular radius (m), ring 2:	8.717E+01	1.200E+01	---	RAD_SHAPE(2)
SEXT	Outer annular radius (m), ring 3:	1.308E+02	1.800E+01	---	RAD_SHAPE(3)
SEXT	Outer annular radius (m), ring 4:	1.743E+02	2.400E+01	---	RAD_SHAPE(4)
SEXT	Outer annular radius (m), ring 5:	2.179E+02	3.000E+01	---	RAD_SHAPE(5)
SEXT	Outer annular radius (m), ring 6:	2.615E+02	3.600E+01	---	RAD_SHAPE(6)
SEXT	Outer annular radius (m), ring 7:	3.051E+02	4.200E+01	---	RAD_SHAPE(7)
SEXT	Outer annular radius (m), ring 8:	3.487E+02	4.800E+01	---	RAD_SHAPE(8)
SEXT	Outer annular radius (m), ring 9:	3.922E+02	5.400E+01	---	RAD_SHAPE(9)
SEXT	Outer annular radius (m), ring 10:	4.358E+02	6.000E+01	---	RAD_SHAPE(10)
SEXT	Outer annular radius (m), ring 11:	4.794E+02	6.600E+01	---	RAD_SHAPE(11)
SEXT	Outer annular radius (m), ring 12:	5.230E+02	7.200E+01	---	RAD_SHAPE(12)
SEXT	Fractions of annular areas within AREA:				
SEXT	Ring 1	0.000E+00	1.000E+00	---	FRACA(1)
SEXT	Ring 2	0.000E+00	1.000E+00	---	FRACA(2)
SEXT	Ring 3	4.000E-02	1.000E+00	---	FRACA(3)
SEXT	Ring 4	2.100E-01	1.000E+00	---	FRACA(4)
SEXT	Ring 5	2.200E-01	1.000E+00	---	FRACA(5)
SEXT	Ring 6	1.800E-01	1.000E+00	---	FRACA(6)
SEXT	Ring 7	1.500E-01	1.000E+00	---	FRACA(7)
SEXT	Ring 8	1.200E-01	1.000E+00	---	FRACA(8)
SEXT	Ring 9	1.100E-01	7.700E-01	---	FRACA(9)
SEXT	Ring 10	9.700E-02	3.700E-01	---	FRACA(10)
SEXT	Ring 11	8.800E-02	1.700E-01	---	FRACA(11)
SEXT	Ring 12	4.900E-02	3.100E-02	---	FRACA(12)
SEXT	Shape factor array from offsite dwelling:				
SEXT	Radii of shape factor array (used if non-circular):				
SEXT	Outer annular radius (m), ring 13:	4.358E+01	1.325E+01	---	RAD_SHAPE(13)
SEXT	Outer annular radius (m), ring 14:	8.717E+01	2.650E+01	---	RAD_SHAPE(14)
SEXT	Outer annular radius (m), ring 15:	1.308E+02	3.975E+01	---	RAD_SHAPE(15)
SEXT	Outer annular radius (m), ring 16:	1.743E+02	5.300E+01	---	RAD_SHAPE(16)
SEXT	Outer annular radius (m), ring 17:	2.179E+02	6.625E+01	---	RAD_SHAPE(17)
SEXT	Outer annular radius (m), ring 18:	2.615E+02	7.950E+01	---	RAD_SHAPE(18)
SEXT	Outer annular radius (m), ring 19:	3.051E+02	9.275E+01	---	RAD_SHAPE(19)
SEXT	Outer annular radius (m), ring 20:	3.487E+02	1.060E+02	---	RAD_SHAPE(20)
SEXT	Outer annular radius (m), ring 21:	3.922E+02	1.192E+02	---	RAD_SHAPE(21)
SEXT	Outer annular radius (m), ring 22:	4.358E+02	1.325E+02	---	RAD_SHAPE(22)
SEXT	Outer annular radius (m), ring 23:	4.794E+02	1.458E+02	---	RAD_SHAPE(23)
SEXT	Outer annular radius (m), ring 24:	5.230E+02	1.590E+02	---	RAD_SHAPE(24)

Site-Specific Parameter Summary (continued)

Menu	Parameter	User Input	Default	RESRAD computed	Parameter Name
SEXT	Fractions of annular areas within AREA:				
SEXT	Ring 13	0.000E+00	0.000E+00	---	FRACA(13)
SEXT	Ring 14	0.000E+00	0.000E+00	---	FRACA(14)
SEXT	Ring 15	4.000E-02	0.000E+00	---	FRACA(15)
SEXT	Ring 16	2.100E-01	2.400E-02	---	FRACA(16)
SEXT	Ring 17	2.200E-01	1.900E-01	---	FRACA(17)
SEXT	Ring 18	1.800E-01	2.400E-01	---	FRACA(18)
SEXT	Ring 19	1.500E-01	2.000E-01	---	FRACA(19)
SEXT	Ring 20	1.200E-01	1.700E-01	---	FRACA(20)
SEXT	Ring 21	1.100E-01	1.500E-01	---	FRACA(21)
SEXT	Ring 22	9.700E-02	1.300E-01	---	FRACA(22)
SEXT	Ring 23	8.800E-02	1.200E-01	---	FRACA(23)
SEXT	Ring 24	4.900E-02	5.200E-02	---	FRACA(24)
SEXT	Shape factor array from offsite area 1:				
SEXT	Radii of shape factor array (used if non-circular):				
SEXT	Outer annular radius (m), ring 25:	1.160E+02	1.160E+02	---	RAD_SHAPE(25)
SEXT	Outer annular radius (m), ring 26:	1.171E+02	1.171E+02	---	RAD_SHAPE(26)
SEXT	Outer annular radius (m), ring 27:	1.653E+02	1.653E+02	---	RAD_SHAPE(27)
SEXT	Outer annular radius (m), ring 28:	2.135E+02	2.135E+02	---	RAD_SHAPE(28)
SEXT	Outer annular radius (m), ring 29:	2.617E+02	2.617E+02	---	RAD_SHAPE(29)
SEXT	Outer annular radius (m), ring 30:	3.091E+02	3.091E+02	---	RAD_SHAPE(30)
SEXT	Outer annular radius (m), ring 31:	3.565E+02	3.565E+02	---	RAD_SHAPE(31)
SEXT	Outer annular radius (m), ring 32:	4.039E+02	4.039E+02	---	RAD_SHAPE(32)
SEXT	Outer annular radius (m), ring 33:	4.513E+02	4.513E+02	---	RAD_SHAPE(33)
SEXT	Outer annular radius (m), ring 34:	4.987E+02	4.987E+02	---	RAD_SHAPE(34)
SEXT	Outer annular radius (m), ring 35:	4.990E+02	4.990E+02	---	RAD_SHAPE(35)
SEXT	Outer annular radius (m), ring 36:	5.511E+02	5.511E+02	---	RAD_SHAPE(36)
SEXT	Fractions of annular areas within AREA:				
SEXT	Ring 25	0.000E+00	0.000E+00	---	FRACA(25)
SEXT	Ring 26	2.192E-02	2.192E-02	---	FRACA(26)
SEXT	Ring 27	1.010E-01	1.010E-01	---	FRACA(27)
SEXT	Ring 28	1.579E-01	1.579E-01	---	FRACA(28)
SEXT	Ring 29	1.794E-01	1.794E-01	---	FRACA(29)
SEXT	Ring 30	1.643E-01	1.643E-01	---	FRACA(30)
SEXT	Ring 31	1.326E-01	1.326E-01	---	FRACA(31)
SEXT	Ring 32	1.127E-01	1.127E-01	---	FRACA(32)
SEXT	Ring 33	9.845E-02	9.845E-02	---	FRACA(33)
SEXT	Ring 34	8.761E-02	8.761E-02	---	FRACA(34)
SEXT	Ring 35	7.793E-02	7.793E-02	---	FRACA(35)
SEXT	Ring 36	3.459E-02	3.459E-02	---	FRACA(36)

Site-Specific Parameter Summary (continued)

Menu	Parameter	User Input	Default	RESRAD computed	Parameter Name
SEXT	Shape factor array from offsite area 2:				
SEXT	Radii of shape factor array (used if non-circular):				
SEXT	Outer annular radius (m), ring 37:	1.160E+02	1.160E+02	---	RAD_SHAPE(37)
SEXT	Outer annular radius (m), ring 38:	1.288E+02	1.288E+02	---	RAD_SHAPE(38)
SEXT	Outer annular radius (m), ring 39:	1.777E+02	1.777E+02	---	RAD_SHAPE(39)
SEXT	Outer annular radius (m), ring 40:	2.266E+02	2.266E+02	---	RAD_SHAPE(40)
SEXT	Outer annular radius (m), ring 41:	2.719E+02	2.719E+02	---	RAD_SHAPE(41)
SEXT	Outer annular radius (m), ring 42:	3.173E+02	3.173E+02	---	RAD_SHAPE(42)
SEXT	Outer annular radius (m), ring 43:	3.626E+02	3.626E+02	---	RAD_SHAPE(43)
SEXT	Outer annular radius (m), ring 44:	4.080E+02	4.080E+02	---	RAD_SHAPE(44)
SEXT	Outer annular radius (m), ring 45:	4.533E+02	4.533E+02	---	RAD_SHAPE(45)
SEXT	Outer annular radius (m), ring 46:	4.987E+02	4.987E+02	---	RAD_SHAPE(46)
SEXT	Outer annular radius (m), ring 47:	5.018E+02	5.018E+02	---	RAD_SHAPE(47)
SEXT	Outer annular radius (m), ring 48:	5.353E+02	5.353E+02	---	RAD_SHAPE(48)
SEXT	Fractions of annular areas within AREA:				
SEXT	Ring 37	0.000E+00	0.000E+00	---	FRACA(37)
SEXT	Ring 38	7.533E-02	7.533E-02	---	FRACA(38)
SEXT	Ring 39	1.690E-01	1.690E-01	---	FRACA(39)
SEXT	Ring 40	1.970E-01	1.970E-01	---	FRACA(40)
SEXT	Ring 41	1.801E-01	1.801E-01	---	FRACA(41)
SEXT	Ring 42	1.456E-01	1.456E-01	---	FRACA(42)
SEXT	Ring 43	1.235E-01	1.235E-01	---	FRACA(43)
SEXT	Ring 44	1.075E-01	1.075E-01	---	FRACA(44)
SEXT	Ring 45	9.540E-02	9.540E-02	---	FRACA(45)
SEXT	Ring 46	8.581E-02	8.581E-02	---	FRACA(46)
SEXT	Ring 47	6.359E-02	6.359E-02	---	FRACA(47)
SEXT	Ring 48	2.205E-02	2.205E-02	---	FRACA(48)
SEXT	Shape factor array from offsite area 3:				
SEXT	Radii of shape factor array (used if non-circular):				
SEXT	Outer annular radius (m), ring 49:	1.500E+02	1.500E+02	---	RAD_SHAPE(49)
SEXT	Outer annular radius (m), ring 50:	1.703E+02	1.703E+02	---	RAD_SHAPE(50)
SEXT	Outer annular radius (m), ring 51:	2.267E+02	2.267E+02	---	RAD_SHAPE(51)
SEXT	Outer annular radius (m), ring 52:	2.704E+02	2.704E+02	---	RAD_SHAPE(52)
SEXT	Outer annular radius (m), ring 53:	3.141E+02	3.141E+02	---	RAD_SHAPE(53)
SEXT	Outer annular radius (m), ring 54:	3.579E+02	3.579E+02	---	RAD_SHAPE(54)
SEXT	Outer annular radius (m), ring 55:	4.016E+02	4.016E+02	---	RAD_SHAPE(55)
SEXT	Outer annular radius (m), ring 56:	4.453E+02	4.453E+02	---	RAD_SHAPE(56)
SEXT	Outer annular radius (m), ring 57:	4.890E+02	4.890E+02	---	RAD_SHAPE(57)
SEXT	Outer annular radius (m), ring 58:	5.327E+02	5.327E+02	---	RAD_SHAPE(58)
SEXT	Outer annular radius (m), ring 59:	5.388E+02	5.388E+02	---	RAD_SHAPE(59)
SEXT	Outer annular radius (m), ring 60:	5.592E+02	5.592E+02	---	RAD_SHAPE(60)

Site-Specific Parameter Summary (continued)

Menu	Parameter	User Input	Default	RESRAD computed	Parameter Name
SEXT	Fractions of annular areas within AREA:				
SEXT	Ring 49	0.000E+00	0.000E+00	---	FRACA(49)
SEXT	Ring 50	8.344E-02	8.344E-02	---	FRACA(50)
SEXT	Ring 51	1.774E-01	1.774E-01	---	FRACA(51)
SEXT	Ring 52	1.730E-01	1.730E-01	---	FRACA(52)
SEXT	Ring 53	1.434E-01	1.434E-01	---	FRACA(53)
SEXT	Ring 54	1.231E-01	1.231E-01	---	FRACA(54)
SEXT	Ring 55	1.080E-01	1.080E-01	---	FRACA(55)
SEXT	Ring 56	9.626E-02	9.626E-02	---	FRACA(56)
SEXT	Ring 57	8.689E-02	8.689E-02	---	FRACA(57)
SEXT	Ring 58	7.922E-02	7.922E-02	---	FRACA(58)
SEXT	Ring 59	5.139E-02	5.139E-02	---	FRACA(59)
SEXT	Ring 60	1.334E-02	1.334E-02	---	FRACA(60)
SEXT	Shape factor array from offsite area 4:				
SEXT	Radii of shape factor array (used if non-circular):				
SEXT	Outer annular radius (m), ring 61:	1.529E+02	1.529E+02	---	RAD_SHAPE(61)
SEXT	Outer annular radius (m), ring 62:	1.941E+02	1.941E+02	---	RAD_SHAPE(62)
SEXT	Outer annular radius (m), ring 63:	2.353E+02	2.353E+02	---	RAD_SHAPE(63)
SEXT	Outer annular radius (m), ring 64:	2.764E+02	2.764E+02	---	RAD_SHAPE(64)
SEXT	Outer annular radius (m), ring 65:	3.176E+02	3.176E+02	---	RAD_SHAPE(65)
SEXT	Outer annular radius (m), ring 66:	3.608E+02	3.608E+02	---	RAD_SHAPE(66)
SEXT	Outer annular radius (m), ring 67:	4.040E+02	4.040E+02	---	RAD_SHAPE(67)
SEXT	Outer annular radius (m), ring 68:	4.472E+02	4.472E+02	---	RAD_SHAPE(68)
SEXT	Outer annular radius (m), ring 69:	4.903E+02	4.903E+02	---	RAD_SHAPE(69)
SEXT	Outer annular radius (m), ring 70:	5.335E+02	5.335E+02	---	RAD_SHAPE(70)
SEXT	Outer annular radius (m), ring 71:	5.677E+02	5.677E+02	---	RAD_SHAPE(71)
SEXT	Outer annular radius (m), ring 72:	6.018E+02	6.018E+02	---	RAD_SHAPE(72)
SEXT	Fractions of annular areas within AREA:				
SEXT	Ring 61	0.000E+00	0.000E+00	---	FRACA(61)
SEXT	Ring 62	4.765E-02	4.765E-02	---	FRACA(62)
SEXT	Ring 63	1.043E-01	1.043E-01	---	FRACA(63)
SEXT	Ring 64	1.318E-01	1.318E-01	---	FRACA(64)
SEXT	Ring 65	1.499E-01	1.499E-01	---	FRACA(65)
SEXT	Ring 66	1.418E-01	1.418E-01	---	FRACA(66)
SEXT	Ring 67	1.188E-01	1.188E-01	---	FRACA(67)
SEXT	Ring 68	1.034E-01	1.034E-01	---	FRACA(68)
SEXT	Ring 69	9.197E-02	9.197E-02	---	FRACA(69)
SEXT	Ring 70	8.300E-02	8.300E-02	---	FRACA(70)
SEXT	Ring 71	5.173E-02	5.173E-02	---	FRACA(71)
SEXT	Ring 72	1.260E-02	1.260E-02	---	FRACA(72)
OCCU	Fraction of time spent indoors on contaminated site	0.000E+00	0.000E+00	---	FIND
OCCU	Fraction of time spent outdoors on contaminated site	5.000E-02	0.000E+00	---	FOTD
OCCU	Fraction of time spent indoors in Offsite Dwelling	5.000E-01	5.000E-01	---	FINDDWELL
OCCU	Fraction of time spent outdoors in Offsite Dwelling	5.000E-02	1.000E-01	---	FOTDDWELL
OCCU	Fraction of time spent outdoors in agri. area 1	1.000E-01	1.000E-01	---	OCCUPANCY(1)
OCCU	Fraction of time spent outdoors in agri. area 2	1.000E-01	1.000E-01	---	OCCUPANCY(2)

Site-Specific Parameter Summary (continued)

Menu	Parameter	User Input	Default	RESRAD computed	Parameter Name
OCCU	Fraction of time spent outdoors in agri. area 3	1.000E-01	1.000E-01	---	OCCUPANCY(3)
OCCU	Fraction of time spent outdoors in agri. area 4	1.000E-01	1.000E-01	---	OCCUPANCY(4)
RADN	Diffusion coefficient for radon gas (m/sec):				
RADN	in cover material	not used	2.000E-06	---	DIFCV
RADN	in contaminated zone soil	not used	2.000E-06	---	DIFCZ
RADN	in fruit, grain and non-leafy vegetable field	not used	2.000E-06	---	DIFOS(1)
RADN	in leafy vegetable field	not used	2.000E-06	---	DIFOS(2)
RADN	in pature	not used	2.000E-06	---	DIFOS(3)
RADN	in livestock grain field	not used	2.000E-06	---	DIFOS(4)
RADN	in offsite dwelling site	not used	2.000E-06	---	DIFOS(5)
RADN	in foundation material	not used	3.000E-07	---	DIFFL
RADN	Thickness of building foundation (m)	not used	1.500E-01	---	FLOOR1
RADN	Bulk density of building foundation (g/cm**3)	not used	2.400E+00	---	DENSFL
RADN	Total porosity of the building foundation	not used	1.000E-01	---	TPFL
RADN	Volumetric water content of the foundation	not used	3.000E-02	---	PH2OFL
RADN	Building depth below ground surface (m)	not used	-1.000E+00	---	DMFL
RADN	Radon vertical dimension of mixing (m)	2.000E+00	2.000E+00	---	HMIX
RADN	Height of the building (room) (m)	not used	2.500E+00	---	HRM
RADN	Average building air exchange rate (1/hr)	not used	5.000E-01	---	REXG
RADN	Building interior area factor	not used	0.000E+00	---	FAI
RADN	Emanating power of Rn-222 gas	not used	2.500E-01	---	EMANA(1)
RADN	Emanating power of Rn-220 gas	not used	1.500E-01	---	EMANA(2)
C14	C-14 evasion layer thickness in soil (m)	3.000E-01	3.000E-01	---	DMC
C14	Vertical dimension of mixing for vegetation (m)	1.000E+00	1.000E+00	---	HMIXV
C14	C-14 evasion flux rate from soil (1/sec)	7.000E-07	7.000E-07	---	C14EVSN
C14	C-12 evasion flux rate from soil (1/sec)	1.000E-10	1.000E-10	---	C12EVSN
C14	Fraction of vegetation carbon from air	9.800E-01	9.800E-01	---	CAIR
C14	Fraction of vegetation carbon from soil	2.000E-02	2.000E-02	---	CSOIL
C12	C-12 concentration in the atmosphere (g/m**3)	1.800E-01	1.800E-01	---	C12AIR
C12	C-12 concentration in contaminated soil (g/g)	3.000E-02	3.000E-02	---	C12CZ
C12	C-12 concentration in water (g/cm**3)	2.000E-05	2.000E-05	---	C12WTR
C12	C-12 concentration in meat 1 (g/g)	2.400E-01	2.400E-01	---	C12MEAT_MILK(1)
C12	C-12 concentration in milk (g/g)	7.000E-02	7.000E-02	---	C12MEAT_MILK(2)
C12	C-12 concentration in vegetable 1 (g/g)	4.000E-01	4.000E-01	---	C12PLANT(1)
C12	C-12 concentration in vegetable 2 (g/g)	9.000E-02	9.000E-02	---	C12PLANT(2)
C12	C-12 concentration in livestock feed 1 (g/g)	9.000E-02	9.000E-02	---	C12PLANT(3)
C12	C-12 concentration in livestock feed 2 (g/g)	4.000E-01	4.000E-01	---	C12PLANT(4)
H3	Humidity in air (g/cm**3)	8.000E+00	8.000E+00	---	HUMID
H3	Mass fraction of water in meat 1 (g/g)	6.000E-01	6.000E-01	---	H2OMEAT_MILK(1)
H3	Mass fraction of water in milk (g/g)	8.800E-01	8.800E-01	---	H2OMEAT_MILK(2)
H3	Mass fraction of water in vegetable 1 (g/g)	8.000E-01	8.000E-01	---	H2OPLANT(1)
H3	Mass fraction of water in vegetable 2 (g/g)	8.000E-01	8.000E-01	---	H2OPLANT(2)
H3	Mass fraction of water in livestock feed 1 (g/g)	8.000E-01	8.000E-01	---	H2OPLANT(3)

Site-Specific Parameter Summary (continued)

Menu	Parameter	User Input	Default	RESRAD computed	Parameter Name
H3	Mass fraction of water in livestock feed 2 (g/g)	8.000E-01	8.000E-01	---	H2OPLANT(4)

Summary of Pathway Selections

Pathway	User Selection
1 -- external gamma	active
2 -- inhalation (w/o radon)	active
3 -- plant ingestion	active
4 -- meat ingestion	active
5 -- milk ingestion	active
6 -- aquatic foods	active
7 -- drinking water	active
8 -- soil ingestion	active
9 -- radon	suppressed

Contaminated Zone Dimensions

Area:	95904.63 square meters
Thickness:	17.50 meters
Cover Depth:	3.35 meters

Initial Soil Concentrations, pCi/g

Ac-227	2.92OE-03
Am-241	5.90OE+01
Am-243	2.97OE+00
Be-10	2.53OE-05
C-14	5.40OE-01
Ca-41	4.21OE-02
Cm-243	4.30OE-01
Cm-244	1.26OE+02
Cm-245	3.83OE-02
Cm-246	1.59OE-01
Cm-247	1.04OE-02
Cm-248	5.59OE-04
H-3	4.64OE+00
I-129	3.50OE-01
K-40	3.28OE+00
Mo-93	3.88OE-01
Nb-93m	2.33OE-01
Nb-94	1.63OE-02
Ni-59	3.04OE+00
Np-237	3.25OE-01
Pa-231	2.39OE-01
Pb-210	3.68OE+00
Pu-238	9.38OE+01
Pu-239	5.83OE+01
Pu-240	6.20OE+01
Pu-241	2.04OE+02
Pu-242	1.73OE-01
Pu-244	3.68OE-03
Ra-226	8.01OE-01
Ra-228	2.21OE-02
Sr-90	1.92OE+02
Tc-99	1.56OE+00
Th-228	2.11OE-06
Th-229	5.71OE+00
Th-230	1.92OE+00
Th-232	3.52OE+00
U-232	1.02OE+01
U-233	4.16OE+01
U-234	6.30OE+02
U-235	3.97OE+01
U-236	8.98OE+00
U-238	3.81OE+02

Parent Dose Report
Title : Site 7 Base Case Model
File : BC_V01.ROF

Total Dose TDOSE(t), mrem/yr
Basic Radiation Dose Limit = 2.500E+01 mrem/yr
Total Mixture Sum M(t) = Fraction of Basic Dose Limit Received at Time (t)

t (years):	0.000E+00	1.000E+00	2.000E+02	4.000E+02	5.000E+02	6.000E+02	8.000E+02	1.000E+03	2.000E+03	1.000E+04
TDOSE(t):	3.710E-21	1.050E-20	1.949E-20	1.405E-01	1.019E+00	5.400E-01	1.479E-01	1.734E-01	6.676E-01	1.137E-01
M(t):	1.484E-22	4.198E-22	7.795E-22	5.620E-03	4.076E-02	2.160E-02	5.915E-03	6.935E-03	2.670E-02	4.548E-03

Maximum TDOSE(t): 9.131E+00 mrem/yr at t = 5084 years

Total Dose Contributions TDOSE(i,p,t) for Individual Radionuclides (i) and Pathways (p)
in mrem/yr and as a Percentage of Total Dose at t = 0 years

From releases to ground water and to surface water

Radio-	Ground		Fish		Radon		Plant		Meat		Milk		Soil		Water	
Nuclide	Dose	%	Dose	%	Dose	%	Dose	%	Dose	%	Dose	%	Dose	%	Dose	%
Ac-227	0.00E+00	0	0.00E+00	0	0.00E+00	0	0.00E+00	0	0.00E+00	0	0.00E+00	0	0.00E+00	0	0.00E+00	0
Am-241	0.00E+00	0	0.00E+00	0	0.00E+00	0	0.00E+00	0	0.00E+00	0	0.00E+00	0	0.00E+00	0	0.00E+00	0
Am-243	0.00E+00	0	0.00E+00	0	0.00E+00	0	0.00E+00	0	0.00E+00	0	0.00E+00	0	0.00E+00	0	0.00E+00	0
Be-10	0.00E+00	0	0.00E+00	0	0.00E+00	0	0.00E+00	0	0.00E+00	0	0.00E+00	0	0.00E+00	0	0.00E+00	0
C-14	0.00E+00	0	0.00E+00	0	0.00E+00	0	0.00E+00	0	0.00E+00	0	0.00E+00	0	0.00E+00	0	0.00E+00	0
Ca-41	0.00E+00	0	0.00E+00	0	0.00E+00	0	0.00E+00	0	0.00E+00	0	0.00E+00	0	0.00E+00	0	0.00E+00	0
Cm-243	0.00E+00	0	0.00E+00	0	0.00E+00	0	0.00E+00	0	0.00E+00	0	0.00E+00	0	0.00E+00	0	0.00E+00	0
Cm-244	0.00E+00	0	0.00E+00	0	0.00E+00	0	0.00E+00	0	0.00E+00	0	0.00E+00	0	0.00E+00	0	0.00E+00	0
Cm-245	0.00E+00	0	0.00E+00	0	0.00E+00	0	0.00E+00	0	0.00E+00	0	0.00E+00	0	0.00E+00	0	0.00E+00	0
Cm-246	0.00E+00	0	0.00E+00	0	0.00E+00	0	0.00E+00	0	0.00E+00	0	0.00E+00	0	0.00E+00	0	0.00E+00	0
Cm-247	0.00E+00	0	0.00E+00	0	0.00E+00	0	0.00E+00	0	0.00E+00	0	0.00E+00	0	0.00E+00	0	0.00E+00	0
Cm-248	0.00E+00	0	0.00E+00	0	0.00E+00	0	0.00E+00	0	0.00E+00	0	0.00E+00	0	0.00E+00	0	0.00E+00	0
H-3	0.00E+00	0	0.00E+00	0	0.00E+00	0	0.00E+00	0	0.00E+00	0	0.00E+00	0	0.00E+00	0	0.00E+00	0
I-129	0.00E+00	0	0.00E+00	0	0.00E+00	0	0.00E+00	0	0.00E+00	0	0.00E+00	0	0.00E+00	0	0.00E+00	0
K-40	0.00E+00	0	0.00E+00	0	0.00E+00	0	0.00E+00	0	0.00E+00	0	0.00E+00	0	0.00E+00	0	0.00E+00	0
Mo-93	0.00E+00	0	0.00E+00	0	0.00E+00	0	0.00E+00	0	0.00E+00	0	0.00E+00	0	0.00E+00	0	0.00E+00	0
Nb-93m	0.00E+00	0	0.00E+00	0	0.00E+00	0	0.00E+00	0	0.00E+00	0	0.00E+00	0	0.00E+00	0	0.00E+00	0
Nb-94	0.00E+00	0	0.00E+00	0	0.00E+00	0	0.00E+00	0	0.00E+00	0	0.00E+00	0	0.00E+00	0	0.00E+00	0
Ni-59	0.00E+00	0	0.00E+00	0	0.00E+00	0	0.00E+00	0	0.00E+00	0	0.00E+00	0	0.00E+00	0	0.00E+00	0
Np-237	0.00E+00	0	0.00E+00	0	0.00E+00	0	0.00E+00	0	0.00E+00	0	0.00E+00	0	0.00E+00	0	0.00E+00	0
Pa-231	0.00E+00	0	0.00E+00	0	0.00E+00	0	0.00E+00	0	0.00E+00	0	0.00E+00	0	0.00E+00	0	0.00E+00	0
Pb-210	0.00E+00	0	0.00E+00	0	0.00E+00	0	0.00E+00	0	0.00E+00	0	0.00E+00	0	0.00E+00	0	0.00E+00	0
Pu-238	0.00E+00	0	0.00E+00	0	0.00E+00	0	0.00E+00	0	0.00E+00	0	0.00E+00	0	0.00E+00	0	0.00E+00	0
Pu-239	0.00E+00	0	0.00E+00	0	0.00E+00	0	0.00E+00	0	0.00E+00	0	0.00E+00	0	0.00E+00	0	0.00E+00	0
Pu-240	0.00E+00	0	0.00E+00	0	0.00E+00	0	0.00E+00	0	0.00E+00	0	0.00E+00	0	0.00E+00	0	0.00E+00	0
Pu-241	0.00E+00	0	0.00E+00	0	0.00E+00	0	0.00E+00	0	0.00E+00	0	0.00E+00	0	0.00E+00	0	0.00E+00	0
Pu-242	0.00E+00	0	0.00E+00	0	0.00E+00	0	0.00E+00	0	0.00E+00	0	0.00E+00	0	0.00E+00	0	0.00E+00	0
Pu-244	0.00E+00	0	0.00E+00	0	0.00E+00	0	0.00E+00	0	0.00E+00	0	0.00E+00	0	0.00E+00	0	0.00E+00	0
Ra-226	0.00E+00	0	0.00E+00	0	0.00E+00	0	0.00E+00	0	0.00E+00	0	0.00E+00	0	0.00E+00	0	0.00E+00	0
Ra-228	0.00E+00	0	0.00E+00	0	0.00E+00	0	0.00E+00	0	0.00E+00	0	0.00E+00	0	0.00E+00	0	0.00E+00	0
Sr-90	0.00E+00	0	0.00E+00	0	0.00E+00	0	0.00E+00	0	0.00E+00	0	0.00E+00	0	0.00E+00	0	0.00E+00	0
Tc-99	0.00E+00	0	0.00E+00	0	0.00E+00	0	0.00E+00	0	0.00E+00	0	0.00E+00	0	0.00E+00	0	0.00E+00	0
Th-228	0.00E+00	0	0.00E+00	0	0.00E+00	0	0.00E+00	0	0.00E+00	0	0.00E+00	0	0.00E+00	0	0.00E+00	0
Th-229	0.00E+00	0	0.00E+00	0	0.00E+00	0	0.00E+00	0	0.00E+00	0	0.00E+00	0	0.00E+00	0	0.00E+00	0
Th-230	0.00E+00	0	0.00E+00	0	0.00E+00	0	0.00E+00	0	0.00E+00	0	0.00E+00	0	0.00E+00	0	0.00E+00	0
Th-232	0.00E+00	0	0.00E+00	0	0.00E+00	0	0.00E+00	0	0.00E+00	0	0.00E+00	0	0.00E+00	0	0.00E+00	0
U-232	0.00E+00	0	0.00E+00	0	0.00E+00	0	0.00E+00	0	0.00E+00	0	0.00E+00	0	0.00E+00	0	0.00E+00	0
U-233	0.00E+00	0	0.00E+00	0	0.00E+00	0	0.00E+00	0	0.00E+00	0	0.00E+00	0	0.00E+00	0	0.00E+00	0
U-234	0.00E+00	0	0.00E+00	0	0.00E+00	0	0.00E+00	0	0.00E+00	0	0.00E+00	0	0.00E+00	0	0.00E+00	0
U-235	0.00E+00	0	0.00E+00	0	0.00E+00	0	0.00E+00	0	0.00E+00	0	0.00E+00	0	0.00E+00	0	0.00E+00	0
U-236	0.00E+00	0	0.00E+00	0	0.00E+00	0	0.00E+00	0	0.00E+00	0	0.00E+00	0	0.00E+00	0	0.00E+00	0

U-238	0.00E+00	0	0.00E+00	0	0.00E+00	0	0.00E+00	0	0.00E+00	0	0.00E+00	0	0.00E+00	0	0.00E+00	0
Total	0.00E+00	0	0.00E+00	0	0.00E+00	0	0.00E+00	0	0.00E+00	0	0.00E+00	0	0.00E+00	0	0.00E+00	0

Total Dose Contributions TDOSE(i,p,t) for Individual Radionuclides (i) and Pathways (p)
in mrem/yr and as a Percentage of Total Dose at t = 0 years

Directly from primary contamination and from release to atmosphere (Inhalation excludes radon)

Radio-	Ground		Inhalation		Radon		Plant		Meat		Milk		Soil		All Pathways*	
Nuclide	Dose	%	Dose	%	Dose	%	Dose	%	Dose	%	Dose	%	Dose	%	Dose	%
Ac-227	2.86E-32	0	0.00E+00	0	0.00E+00	0	0.00E+00	0	0.00E+00	0	0.00E+00	0	0.00E+00	0	2.86E-32	0
Am-241	6.98E-39	0	0.00E+00	0	0.00E+00	0	0.00E+00	0	0.00E+00	0	0.00E+00	0	0.00E+00	0	6.98E-39	0
Am-243	5.35E-39	0	0.00E+00	0	0.00E+00	0	0.00E+00	0	0.00E+00	0	0.00E+00	0	0.00E+00	0	5.35E-39	0
Be-10	0.00E+00	0	0.00E+00	0	0.00E+00	0	0.00E+00	0	0.00E+00	0	0.00E+00	0	0.00E+00	0	0.00E+00	0
C-14	0.00E+00	0	0.00E+00	0	0.00E+00	0	0.00E+00	0	0.00E+00	0	0.00E+00	0	0.00E+00	0	0.00E+00	0
Ca-41	0.00E+00	0	0.00E+00	0	0.00E+00	0	0.00E+00	0	0.00E+00	0	0.00E+00	0	0.00E+00	0	0.00E+00	0
Cm-243	2.56E-39	0	0.00E+00	0	0.00E+00	0	0.00E+00	0	0.00E+00	0	0.00E+00	0	0.00E+00	0	2.56E-39	0
Cm-244	1.18E-28	0	0.00E+00	0	0.00E+00	0	0.00E+00	0	0.00E+00	0	0.00E+00	0	0.00E+00	0	1.18E-28	0
Cm-245	0.00E+00	0	0.00E+00	0	0.00E+00	0	0.00E+00	0	0.00E+00	0	0.00E+00	0	0.00E+00	0	0.00E+00	0
Cm-246	2.82E-26	0	0.00E+00	0	0.00E+00	0	0.00E+00	0	0.00E+00	0	0.00E+00	0	0.00E+00	0	2.82E-26	0
Cm-247	6.86E-34	0	0.00E+00	0	0.00E+00	0	0.00E+00	0	0.00E+00	0	0.00E+00	0	0.00E+00	0	6.86E-34	0
Cm-248	8.20E-26	0	0.00E+00	0	0.00E+00	0	0.00E+00	0	0.00E+00	0	0.00E+00	0	0.00E+00	0	8.20E-26	0
H-3	0.00E+00	0	0.00E+00	0	0.00E+00	0	0.00E+00	0	0.00E+00	0	0.00E+00	0	0.00E+00	0	0.00E+00	0
I-129	0.00E+00	0	0.00E+00	0	0.00E+00	0	0.00E+00	0	0.00E+00	0	0.00E+00	0	0.00E+00	0	0.00E+00	0
K-40	6.01E-24	0	0.00E+00	0	0.00E+00	0	0.00E+00	0	0.00E+00	0	0.00E+00	0	0.00E+00	0	6.01E-24	0
Mo-93	0.00E+00	0	0.00E+00	0	0.00E+00	0	0.00E+00	0	0.00E+00	0	0.00E+00	0	0.00E+00	0	0.00E+00	0
Nb-93m	0.00E+00	0	0.00E+00	0	0.00E+00	0	0.00E+00	0	0.00E+00	0	0.00E+00	0	0.00E+00	0	0.00E+00	0
Nb-94	2.69E-28	0	0.00E+00	0	0.00E+00	0	0.00E+00	0	0.00E+00	0	0.00E+00	0	0.00E+00	0	2.69E-28	0
Ni-59	1.28E-33	0	0.00E+00	0	0.00E+00	0	0.00E+00	0	0.00E+00	0	0.00E+00	0	0.00E+00	0	1.28E-33	0
Np-237	8.77E-35	0	0.00E+00	0	0.00E+00	0	0.00E+00	0	0.00E+00	0	0.00E+00	0	0.00E+00	0	8.77E-35	0
Pa-231	3.50E-32	0	0.00E+00	0	0.00E+00	0	0.00E+00	0	0.00E+00	0	0.00E+00	0	0.00E+00	0	3.50E-32	0
Pb-210	8.27E-31	0	0.00E+00	0	0.00E+00	0	0.00E+00	0	0.00E+00	0	0.00E+00	0	0.00E+00	0	8.27E-31	0
Pu-238	4.44E-35	0	0.00E+00	0	0.00E+00	0	0.00E+00	0	0.00E+00	0	0.00E+00	0	0.00E+00	0	4.44E-35	0
Pu-239	1.95E-40	0	0.00E+00	0	0.00E+00	0	0.00E+00	0	0.00E+00	0	0.00E+00	0	0.00E+00	0	1.95E-40	0
Pu-240	2.48E-38	0	0.00E+00	0	0.00E+00	0	0.00E+00	0	0.00E+00	0	0.00E+00	0	0.00E+00	0	2.48E-38	0
Pu-241	4.96E-41	0	0.00E+00	0	0.00E+00	0	0.00E+00	0	0.00E+00	0	0.00E+00	0	0.00E+00	0	4.96E-41	0
Pu-242	3.27E-29	0	0.00E+00	0	0.00E+00	0	0.00E+00	0	0.00E+00	0	0.00E+00	0	0.00E+00	0	3.27E-29	0
Pu-244	5.64E-27	0	0.00E+00	0	0.00E+00	0	0.00E+00	0	0.00E+00	0	0.00E+00	0	0.00E+00	0	5.64E-27	0
Ra-226	1.71E-23	0	0.00E+00	0	0.00E+00	0	0.00E+00	0	0.00E+00	0	0.00E+00	0	0.00E+00	0	1.71E-23	0
Ra-228	5.15E-24	0	0.00E+00	0	0.00E+00	0	0.00E+00	0	0.00E+00	0	0.00E+00	0	0.00E+00	0	5.15E-24	0
Sr-90	8.40E-34	0	0.00E+00	0	0.00E+00	0	0.00E+00	0	0.00E+00	0	0.00E+00	0	0.00E+00	0	8.40E-34	0
Tc-99	0.00E+00	0	0.00E+00	0	0.00E+00	0	0.00E+00	0	0.00E+00	0	0.00E+00	0	0.00E+00	0	0.00E+00	0
Th-228	7.64E-27	0	0.00E+00	0	0.00E+00	0	0.00E+00	0	0.00E+00	0	0.00E+00	0	0.00E+00	0	7.64E-27	0
Th-229	2.32E-24	0	0.00E+00	0	0.00E+00	0	0.00E+00	0	0.00E+00	0	0.00E+00	0	0.00E+00	0	2.32E-24	0
Th-230	8.85E-27	0	0.00E+00	0	0.00E+00	0	0.00E+00	0	0.00E+00	0	0.00E+00	0	0.00E+00	0	8.85E-27	0
Th-232	3.62E-22	10	0.00E+00	0	0.00E+00	0	0.00E+00	0	0.00E+00	0	0.00E+00	0	0.00E+00	0	3.62E-22	10
U-232	3.32E-21	89	0.00E+00	0	0.00E+00	0	0.00E+00	0	0.00E+00	0	0.00E+00	0	0.00E+00	0	3.32E-21	89
U-233	7.98E-28	0	0.00E+00	0	0.00E+00	0	0.00E+00	0	0.00E+00	0	0.00E+00	0	0.00E+00	0	7.98E-28	0
U-234	6.54E-29	0	0.00E+00	0	0.00E+00	0	0.00E+00	0	0.00E+00	0	0.00E+00	0	0.00E+00	0	6.54E-29	0
U-235	3.09E-34	0	0.00E+00	0	0.00E+00	0	0.00E+00	0	0.00E+00	0	0.00E+00	0	0.00E+00	0	3.09E-34	0
U-236	8.91E-32	0	0.00E+00	0	0.00E+00	0	0.00E+00	0	0.00E+00	0	0.00E+00	0	0.00E+00	0	8.91E-32	0

U-238	4.27E-26	0	0.00E+00	0	0.00E+00	0	0.00E+00	0	0.00E+00	0	0.00E+00	0	0.00E+00	0	4.27E-26	0
Total	3.71E-21	100	0.00E+00	0	0.00E+00	0	0.00E+00	0	0.00E+00	0	0.00E+00	0	0.00E+00	0	3.71E-21	100

*Sum of dose from all releases and from primary contamination.

Total Dose Contributions TDOSE(i,p,t) for Individual Radionuclides (i) and Pathways (p)
in mrem/yr and as a Percentage of Total Dose at t = 1 years

From releases to ground water and to surface water

Radio-	Ground		Fish		Radon		Plant		Meat		Milk		Soil		Water	
Nuclide	Dose	%	Dose	%	Dose	%	Dose	%	Dose	%	Dose	%	Dose	%	Dose	%
Ac-227	0.00E+00	0	0.00E+00	0	0.00E+00	0	0.00E+00	0	0.00E+00	0	0.00E+00	0	0.00E+00	0	0.00E+00	0
Am-241	0.00E+00	0	0.00E+00	0	0.00E+00	0	0.00E+00	0	0.00E+00	0	0.00E+00	0	0.00E+00	0	0.00E+00	0
Am-243	0.00E+00	0	0.00E+00	0	0.00E+00	0	0.00E+00	0	0.00E+00	0	0.00E+00	0	0.00E+00	0	0.00E+00	0
Be-10	0.00E+00	0	0.00E+00	0	0.00E+00	0	0.00E+00	0	0.00E+00	0	0.00E+00	0	0.00E+00	0	0.00E+00	0
C-14	0.00E+00	0	0.00E+00	0	0.00E+00	0	0.00E+00	0	0.00E+00	0	0.00E+00	0	0.00E+00	0	0.00E+00	0
Ca-41	0.00E+00	0	0.00E+00	0	0.00E+00	0	0.00E+00	0	0.00E+00	0	0.00E+00	0	0.00E+00	0	0.00E+00	0
Cm-243	0.00E+00	0	0.00E+00	0	0.00E+00	0	0.00E+00	0	0.00E+00	0	0.00E+00	0	0.00E+00	0	0.00E+00	0
Cm-244	0.00E+00	0	0.00E+00	0	0.00E+00	0	0.00E+00	0	0.00E+00	0	0.00E+00	0	0.00E+00	0	0.00E+00	0
Cm-245	0.00E+00	0	0.00E+00	0	0.00E+00	0	0.00E+00	0	0.00E+00	0	0.00E+00	0	0.00E+00	0	0.00E+00	0
Cm-246	0.00E+00	0	0.00E+00	0	0.00E+00	0	0.00E+00	0	0.00E+00	0	0.00E+00	0	0.00E+00	0	0.00E+00	0
Cm-247	0.00E+00	0	0.00E+00	0	0.00E+00	0	0.00E+00	0	0.00E+00	0	0.00E+00	0	0.00E+00	0	0.00E+00	0
Cm-248	0.00E+00	0	0.00E+00	0	0.00E+00	0	0.00E+00	0	0.00E+00	0	0.00E+00	0	0.00E+00	0	0.00E+00	0
H-3	0.00E+00	0	0.00E+00	0	0.00E+00	0	0.00E+00	0	0.00E+00	0	0.00E+00	0	0.00E+00	0	0.00E+00	0
I-129	0.00E+00	0	0.00E+00	0	0.00E+00	0	0.00E+00	0	0.00E+00	0	0.00E+00	0	0.00E+00	0	0.00E+00	0
K-40	0.00E+00	0	0.00E+00	0	0.00E+00	0	0.00E+00	0	0.00E+00	0	0.00E+00	0	0.00E+00	0	0.00E+00	0
Mo-93	0.00E+00	0	0.00E+00	0	0.00E+00	0	0.00E+00	0	0.00E+00	0	0.00E+00	0	0.00E+00	0	0.00E+00	0
Nb-93m	0.00E+00	0	0.00E+00	0	0.00E+00	0	0.00E+00	0	0.00E+00	0	0.00E+00	0	0.00E+00	0	0.00E+00	0
Nb-94	0.00E+00	0	0.00E+00	0	0.00E+00	0	0.00E+00	0	0.00E+00	0	0.00E+00	0	0.00E+00	0	0.00E+00	0
Ni-59	0.00E+00	0	0.00E+00	0	0.00E+00	0	0.00E+00	0	0.00E+00	0	0.00E+00	0	0.00E+00	0	0.00E+00	0
Np-237	0.00E+00	0	0.00E+00	0	0.00E+00	0	0.00E+00	0	0.00E+00	0	0.00E+00	0	0.00E+00	0	0.00E+00	0
Pa-231	0.00E+00	0	0.00E+00	0	0.00E+00	0	0.00E+00	0	0.00E+00	0	0.00E+00	0	0.00E+00	0	0.00E+00	0
Pb-210	0.00E+00	0	0.00E+00	0	0.00E+00	0	0.00E+00	0	0.00E+00	0	0.00E+00	0	0.00E+00	0	0.00E+00	0
Pu-238	0.00E+00	0	0.00E+00	0	0.00E+00	0	0.00E+00	0	0.00E+00	0	0.00E+00	0	0.00E+00	0	0.00E+00	0
Pu-239	0.00E+00	0	0.00E+00	0	0.00E+00	0	0.00E+00	0	0.00E+00	0	0.00E+00	0	0.00E+00	0	0.00E+00	0
Pu-240	0.00E+00	0	0.00E+00	0	0.00E+00	0	0.00E+00	0	0.00E+00	0	0.00E+00	0	0.00E+00	0	0.00E+00	0
Pu-241	0.00E+00	0	0.00E+00	0	0.00E+00	0	0.00E+00	0	0.00E+00	0	0.00E+00	0	0.00E+00	0	0.00E+00	0
Pu-242	0.00E+00	0	0.00E+00	0	0.00E+00	0	0.00E+00	0	0.00E+00	0	0.00E+00	0	0.00E+00	0	0.00E+00	0
Pu-244	0.00E+00	0	0.00E+00	0	0.00E+00	0	0.00E+00	0	0.00E+00	0	0.00E+00	0	0.00E+00	0	0.00E+00	0
Ra-226	0.00E+00	0	0.00E+00	0	0.00E+00	0	0.00E+00	0	0.00E+00	0	0.00E+00	0	0.00E+00	0	0.00E+00	0
Ra-228	0.00E+00	0	0.00E+00	0	0.00E+00	0	0.00E+00	0	0.00E+00	0	0.00E+00	0	0.00E+00	0	0.00E+00	0
Sr-90	0.00E+00	0	0.00E+00	0	0.00E+00	0	0.00E+00	0	0.00E+00	0	0.00E+00	0	0.00E+00	0	0.00E+00	0
Tc-99	0.00E+00	0	0.00E+00	0	0.00E+00	0	0.00E+00	0	0.00E+00	0	0.00E+00	0	0.00E+00	0	0.00E+00	0
Th-228	0.00E+00	0	0.00E+00	0	0.00E+00	0	0.00E+00	0	0.00E+00	0	0.00E+00	0	0.00E+00	0	0.00E+00	0
Th-229	0.00E+00	0	0.00E+00	0	0.00E+00	0	0.00E+00	0	0.00E+00	0	0.00E+00	0	0.00E+00	0	0.00E+00	0
Th-230	0.00E+00	0	0.00E+00	0	0.00E+00	0	0.00E+00	0	0.00E+00	0	0.00E+00	0	0.00E+00	0	0.00E+00	0
Th-232	0.00E+00	0	0.00E+00	0	0.00E+00	0	0.00E+00	0	0.00E+00	0	0.00E+00	0	0.00E+00	0	0.00E+00	0
U-232	0.00E+00	0	0.00E+00	0	0.00E+00	0	0.00E+00	0	0.00E+00	0	0.00E+00	0	0.00E+00	0	0.00E+00	0
U-233	0.00E+00	0	0.00E+00	0	0.00E+00	0	0.00E+00	0	0.00E+00	0	0.00E+00	0	0.00E+00	0	0.00E+00	0
U-234	0.00E+00	0	0.00E+00	0	0.00E+00	0	0.00E+00	0	0.00E+00	0	0.00E+00	0	0.00E+00	0	0.00E+00	0
U-235	0.00E+00	0	0.00E+00	0	0.00E+00	0	0.00E+00	0	0.00E+00	0	0.00E+00	0	0.00E+00	0	0.00E+00	0
U-236	0.00E+00	0	0.00E+00	0	0.00E+00	0	0.00E+00	0	0.00E+00	0	0.00E+00	0	0.00E+00	0	0.00E+00	0

U-238	0.00E+00	0	0.00E+00	0	0.00E+00	0	0.00E+00	0	0.00E+00	0	0.00E+00	0	0.00E+00	0	0.00E+00	0
Total	0.00E+00	0	0.00E+00	0	0.00E+00	0	0.00E+00	0	0.00E+00	0	0.00E+00	0	0.00E+00	0	0.00E+00	0

Total Dose Contributions TDOSE(i,p,t) for Individual Radionuclides (i) and Pathways (p)
in mrem/yr and as a Percentage of Total Dose at t = 1 years

Directly from primary contamination and from release to atmosphere (Inhalation excludes radon)

Radio-	Ground		Inhalation		Radon		Plant		Meat		Milk		Soil		All Pathways*	
Nuclide	Dose	%	Dose	%	Dose	%	Dose	%	Dose	%	Dose	%	Dose	%	Dose	%
Ac-227	2.78E-32	0	0.00E+00	0	0.00E+00	0	0.00E+00	0	0.00E+00	0	0.00E+00	0	0.00E+00	0	2.78E-32	0
Am-241	2.87E-38	0	0.00E+00	0	0.00E+00	0	0.00E+00	0	0.00E+00	0	0.00E+00	0	0.00E+00	0	2.87E-38	0
Am-243	5.35E-39	0	0.00E+00	0	0.00E+00	0	0.00E+00	0	0.00E+00	0	0.00E+00	0	0.00E+00	0	5.35E-39	0
Be-10	0.00E+00	0	0.00E+00	0	0.00E+00	0	0.00E+00	0	0.00E+00	0	0.00E+00	0	0.00E+00	0	0.00E+00	0
C-14	0.00E+00	0	0.00E+00	0	0.00E+00	0	0.00E+00	0	0.00E+00	0	0.00E+00	0	0.00E+00	0	0.00E+00	0
Ca-41	0.00E+00	0	0.00E+00	0	0.00E+00	0	0.00E+00	0	0.00E+00	0	0.00E+00	0	0.00E+00	0	0.00E+00	0
Cm-243	2.50E-39	0	0.00E+00	0	0.00E+00	0	0.00E+00	0	0.00E+00	0	0.00E+00	0	0.00E+00	0	2.50E-39	0
Cm-244	1.14E-28	0	0.00E+00	0	0.00E+00	0	0.00E+00	0	0.00E+00	0	0.00E+00	0	0.00E+00	0	1.14E-28	0
Cm-245	2.80E-45	0	0.00E+00	0	0.00E+00	0	0.00E+00	0	0.00E+00	0	0.00E+00	0	0.00E+00	0	2.80E-45	0
Cm-246	2.82E-26	0	0.00E+00	0	0.00E+00	0	0.00E+00	0	0.00E+00	0	0.00E+00	0	0.00E+00	0	2.82E-26	0
Cm-247	6.86E-34	0	0.00E+00	0	0.00E+00	0	0.00E+00	0	0.00E+00	0	0.00E+00	0	0.00E+00	0	6.86E-34	0
Cm-248	8.20E-26	0	0.00E+00	0	0.00E+00	0	0.00E+00	0	0.00E+00	0	0.00E+00	0	0.00E+00	0	8.20E-26	0
H-3	0.00E+00	0	0.00E+00	0	0.00E+00	0	0.00E+00	0	0.00E+00	0	0.00E+00	0	0.00E+00	0	0.00E+00	0
I-129	0.00E+00	0	0.00E+00	0	0.00E+00	0	0.00E+00	0	0.00E+00	0	0.00E+00	0	0.00E+00	0	0.00E+00	0
K-40	6.01E-24	0	0.00E+00	0	0.00E+00	0	0.00E+00	0	0.00E+00	0	0.00E+00	0	0.00E+00	0	6.01E-24	0
Mo-93	0.00E+00	0	0.00E+00	0	0.00E+00	0	0.00E+00	0	0.00E+00	0	0.00E+00	0	0.00E+00	0	0.00E+00	0
Nb-93m	0.00E+00	0	0.00E+00	0	0.00E+00	0	0.00E+00	0	0.00E+00	0	0.00E+00	0	0.00E+00	0	0.00E+00	0
Nb-94	2.69E-28	0	0.00E+00	0	0.00E+00	0	0.00E+00	0	0.00E+00	0	0.00E+00	0	0.00E+00	0	2.69E-28	0
Ni-59	1.28E-33	0	0.00E+00	0	0.00E+00	0	0.00E+00	0	0.00E+00	0	0.00E+00	0	0.00E+00	0	1.28E-33	0
Np-237	2.48E-34	0	0.00E+00	0	0.00E+00	0	0.00E+00	0	0.00E+00	0	0.00E+00	0	0.00E+00	0	2.48E-34	0
Pa-231	1.04E-31	0	0.00E+00	0	0.00E+00	0	0.00E+00	0	0.00E+00	0	0.00E+00	0	0.00E+00	0	1.04E-31	0
Pb-210	8.03E-31	0	0.00E+00	0	0.00E+00	0	0.00E+00	0	0.00E+00	0	0.00E+00	0	0.00E+00	0	8.03E-31	0
Pu-238	1.87E-34	0	0.00E+00	0	0.00E+00	0	0.00E+00	0	0.00E+00	0	0.00E+00	0	0.00E+00	0	1.87E-34	0
Pu-239	1.97E-40	0	0.00E+00	0	0.00E+00	0	0.00E+00	0	0.00E+00	0	0.00E+00	0	0.00E+00	0	1.97E-40	0
Pu-240	1.20E-37	0	0.00E+00	0	0.00E+00	0	0.00E+00	0	0.00E+00	0	0.00E+00	0	0.00E+00	0	1.20E-37	0
Pu-241	2.64E-40	0	0.00E+00	0	0.00E+00	0	0.00E+00	0	0.00E+00	0	0.00E+00	0	0.00E+00	0	2.64E-40	0
Pu-242	3.27E-29	0	0.00E+00	0	0.00E+00	0	0.00E+00	0	0.00E+00	0	0.00E+00	0	0.00E+00	0	3.27E-29	0
Pu-244	5.64E-27	0	0.00E+00	0	0.00E+00	0	0.00E+00	0	0.00E+00	0	0.00E+00	0	0.00E+00	0	5.64E-27	0
Ra-226	1.70E-23	0	0.00E+00	0	0.00E+00	0	0.00E+00	0	0.00E+00	0	0.00E+00	0	0.00E+00	0	1.70E-23	0
Ra-228	1.41E-23	0	0.00E+00	0	0.00E+00	0	0.00E+00	0	0.00E+00	0	0.00E+00	0	0.00E+00	0	1.41E-23	0
Sr-90	8.21E-34	0	0.00E+00	0	0.00E+00	0	0.00E+00	0	0.00E+00	0	0.00E+00	0	0.00E+00	0	8.21E-34	0
Tc-99	0.00E+00	0	0.00E+00	0	0.00E+00	0	0.00E+00	0	0.00E+00	0	0.00E+00	0	0.00E+00	0	0.00E+00	0
Th-228	6.35E-27	0	0.00E+00	0	0.00E+00	0	0.00E+00	0	0.00E+00	0	0.00E+00	0	0.00E+00	0	6.35E-27	0
Th-229	2.32E-24	0	0.00E+00	0	0.00E+00	0	0.00E+00	0	0.00E+00	0	0.00E+00	0	0.00E+00	0	2.32E-24	0
Th-230	2.65E-26	0	0.00E+00	0	0.00E+00	0	0.00E+00	0	0.00E+00	0	0.00E+00	0	0.00E+00	0	2.65E-26	0
Th-232	1.10E-21	10	0.00E+00	0	0.00E+00	0	0.00E+00	0	0.00E+00	0	0.00E+00	0	0.00E+00	0	1.10E-21	10
U-232	9.36E-21	89	0.00E+00	0	0.00E+00	0	0.00E+00	0	0.00E+00	0	0.00E+00	0	0.00E+00	0	9.36E-21	89
U-233	2.39E-27	0	0.00E+00	0	0.00E+00	0	0.00E+00	0	0.00E+00	0	0.00E+00	0	0.00E+00	0	2.39E-27	0
U-234	2.23E-28	0	0.00E+00	0	0.00E+00	0	0.00E+00	0	0.00E+00	0	0.00E+00	0	0.00E+00	0	2.23E-28	0
U-235	1.04E-33	0	0.00E+00	0	0.00E+00	0	0.00E+00	0	0.00E+00	0	0.00E+00	0	0.00E+00	0	1.04E-33	0
U-236	3.23E-31	0	0.00E+00	0	0.00E+00	0	0.00E+00	0	0.00E+00	0	0.00E+00	0	0.00E+00	0	3.23E-31	0

U-238	4.27E-26	0	0.00E+00	0	0.00E+00	0	0.00E+00	0	0.00E+00	0	0.00E+00	0	0.00E+00	0	4.27E-26	0
Total	1.05E-20	100	0.00E+00	0	0.00E+00	0	0.00E+00	0	0.00E+00	0	0.00E+00	0	0.00E+00	0	1.05E-20	100

*Sum of dose from all releases and from primary contamination.

Total Dose Contributions TDOSE(i,p,t) for Individual Radionuclides (i) and Pathways (p)
in mrem/yr and as a Percentage of Total Dose at t = 200 years

From releases to ground water and to surface water

Radio-	Ground		Fish		Radon		Plant		Meat		Milk		Soil		Water	
Nuclide	Dose	%	Dose	%	Dose	%	Dose	%	Dose	%	Dose	%	Dose	%	Dose	%
Ac-227	0.00E+00	0	0.00E+00	0	0.00E+00	0	0.00E+00	0	0.00E+00	0	0.00E+00	0	0.00E+00	0	0.00E+00	0
Am-241	0.00E+00	0	0.00E+00	0	0.00E+00	0	0.00E+00	0	0.00E+00	0	0.00E+00	0	0.00E+00	0	0.00E+00	0
Am-243	0.00E+00	0	0.00E+00	0	0.00E+00	0	0.00E+00	0	0.00E+00	0	0.00E+00	0	0.00E+00	0	0.00E+00	0
Be-10	0.00E+00	0	0.00E+00	0	0.00E+00	0	0.00E+00	0	0.00E+00	0	0.00E+00	0	0.00E+00	0	0.00E+00	0
C-14	0.00E+00	0	0.00E+00	0	0.00E+00	0	0.00E+00	0	0.00E+00	0	0.00E+00	0	0.00E+00	0	0.00E+00	0
Ca-41	0.00E+00	0	0.00E+00	0	0.00E+00	0	0.00E+00	0	0.00E+00	0	0.00E+00	0	0.00E+00	0	0.00E+00	0
Cm-243	0.00E+00	0	0.00E+00	0	0.00E+00	0	0.00E+00	0	0.00E+00	0	0.00E+00	0	0.00E+00	0	0.00E+00	0
Cm-244	0.00E+00	0	0.00E+00	0	0.00E+00	0	0.00E+00	0	0.00E+00	0	0.00E+00	0	0.00E+00	0	0.00E+00	0
Cm-245	0.00E+00	0	0.00E+00	0	0.00E+00	0	0.00E+00	0	0.00E+00	0	0.00E+00	0	0.00E+00	0	0.00E+00	0
Cm-246	0.00E+00	0	0.00E+00	0	0.00E+00	0	0.00E+00	0	0.00E+00	0	0.00E+00	0	0.00E+00	0	0.00E+00	0
Cm-247	0.00E+00	0	0.00E+00	0	0.00E+00	0	0.00E+00	0	0.00E+00	0	0.00E+00	0	0.00E+00	0	0.00E+00	0
Cm-248	0.00E+00	0	0.00E+00	0	0.00E+00	0	0.00E+00	0	0.00E+00	0	0.00E+00	0	0.00E+00	0	0.00E+00	0
H-3	0.00E+00	0	0.00E+00	0	0.00E+00	0	0.00E+00	0	0.00E+00	0	0.00E+00	0	0.00E+00	0	0.00E+00	0
I-129	0.00E+00	0	0.00E+00	0	0.00E+00	0	0.00E+00	0	0.00E+00	0	0.00E+00	0	0.00E+00	0	0.00E+00	0
K-40	0.00E+00	0	0.00E+00	0	0.00E+00	0	0.00E+00	0	0.00E+00	0	0.00E+00	0	0.00E+00	0	0.00E+00	0
Mo-93	0.00E+00	0	0.00E+00	0	0.00E+00	0	0.00E+00	0	0.00E+00	0	0.00E+00	0	0.00E+00	0	0.00E+00	0
Nb-93m	0.00E+00	0	0.00E+00	0	0.00E+00	0	0.00E+00	0	0.00E+00	0	0.00E+00	0	0.00E+00	0	0.00E+00	0
Nb-94	0.00E+00	0	0.00E+00	0	0.00E+00	0	0.00E+00	0	0.00E+00	0	0.00E+00	0	0.00E+00	0	0.00E+00	0
Ni-59	0.00E+00	0	0.00E+00	0	0.00E+00	0	0.00E+00	0	0.00E+00	0	0.00E+00	0	0.00E+00	0	0.00E+00	0
Np-237	0.00E+00	0	0.00E+00	0	0.00E+00	0	0.00E+00	0	0.00E+00	0	0.00E+00	0	0.00E+00	0	0.00E+00	0
Pa-231	0.00E+00	0	0.00E+00	0	0.00E+00	0	0.00E+00	0	0.00E+00	0	0.00E+00	0	0.00E+00	0	0.00E+00	0
Pb-210	0.00E+00	0	0.00E+00	0	0.00E+00	0	0.00E+00	0	0.00E+00	0	0.00E+00	0	0.00E+00	0	0.00E+00	0
Pu-238	0.00E+00	0	0.00E+00	0	0.00E+00	0	0.00E+00	0	0.00E+00	0	0.00E+00	0	0.00E+00	0	0.00E+00	0
Pu-239	0.00E+00	0	0.00E+00	0	0.00E+00	0	0.00E+00	0	0.00E+00	0	0.00E+00	0	0.00E+00	0	0.00E+00	0
Pu-240	0.00E+00	0	0.00E+00	0	0.00E+00	0	0.00E+00	0	0.00E+00	0	0.00E+00	0	0.00E+00	0	0.00E+00	0
Pu-241	0.00E+00	0	0.00E+00	0	0.00E+00	0	0.00E+00	0	0.00E+00	0	0.00E+00	0	0.00E+00	0	0.00E+00	0
Pu-242	0.00E+00	0	0.00E+00	0	0.00E+00	0	0.00E+00	0	0.00E+00	0	0.00E+00	0	0.00E+00	0	0.00E+00	0
Pu-244	0.00E+00	0	0.00E+00	0	0.00E+00	0	0.00E+00	0	0.00E+00	0	0.00E+00	0	0.00E+00	0	0.00E+00	0
Ra-226	0.00E+00	0	0.00E+00	0	0.00E+00	0	0.00E+00	0	0.00E+00	0	0.00E+00	0	0.00E+00	0	0.00E+00	0
Ra-228	0.00E+00	0	0.00E+00	0	0.00E+00	0	0.00E+00	0	0.00E+00	0	0.00E+00	0	0.00E+00	0	0.00E+00	0
Sr-90	0.00E+00	0	0.00E+00	0	0.00E+00	0	0.00E+00	0	0.00E+00	0	0.00E+00	0	0.00E+00	0	0.00E+00	0
Tc-99	0.00E+00	0	0.00E+00	0	0.00E+00	0	0.00E+00	0	0.00E+00	0	0.00E+00	0	0.00E+00	0	0.00E+00	0
Th-228	0.00E+00	0	0.00E+00	0	0.00E+00	0	0.00E+00	0	0.00E+00	0	0.00E+00	0	0.00E+00	0	0.00E+00	0
Th-229	0.00E+00	0	0.00E+00	0	0.00E+00	0	0.00E+00	0	0.00E+00	0	0.00E+00	0	0.00E+00	0	0.00E+00	0
Th-230	0.00E+00	0	0.00E+00	0	0.00E+00	0	0.00E+00	0	0.00E+00	0	0.00E+00	0	0.00E+00	0	0.00E+00	0
Th-232	0.00E+00	0	0.00E+00	0	0.00E+00	0	0.00E+00	0	0.00E+00	0	0.00E+00	0	0.00E+00	0	0.00E+00	0
U-232	0.00E+00	0	0.00E+00	0	0.00E+00	0	0.00E+00	0	0.00E+00	0	0.00E+00	0	0.00E+00	0	0.00E+00	0
U-233	0.00E+00	0	0.00E+00	0	0.00E+00	0	0.00E+00	0	0.00E+00	0	0.00E+00	0	0.00E+00	0	0.00E+00	0
U-234	0.00E+00	0	0.00E+00	0	0.00E+00	0	0.00E+00	0	0.00E+00	0	0.00E+00	0	0.00E+00	0	0.00E+00	0
U-235	0.00E+00	0	0.00E+00	0	0.00E+00	0	0.00E+00	0	0.00E+00	0	0.00E+00	0	0.00E+00	0	0.00E+00	0
U-236	0.00E+00	0	0.00E+00	0	0.00E+00	0	0.00E+00	0	0.00E+00	0	0.00E+00	0	0.00E+00	0	0.00E+00	0

U-238	0.00E+00	0	0.00E+00	0	0.00E+00	0	0.00E+00	0	0.00E+00	0	0.00E+00	0	0.00E+00	0	0.00E+00	0
Total	0.00E+00	0	0.00E+00	0	0.00E+00	0	0.00E+00	0	0.00E+00	0	0.00E+00	0	0.00E+00	0	0.00E+00	0

Total Dose Contributions TDOSE(i,p,t) for Individual Radionuclides (i) and Pathways (p)
in mrem/yr and as a Percentage of Total Dose at t = 200 years

Directly from primary contamination and from release to atmosphere (Inhalation excludes radon)

Radio-Nuclide	Ground		Inhalation		Radon		Plant		Meat		Milk		Soil		All Pathways*	
	Dose	%	Dose	%	Dose	%	Dose	%	Dose	%	Dose	%	Dose	%	Dose	%
Ac-227	4.92E-35	0	0.00E+00	0	0.00E+00	0	0.00E+00	0	0.00E+00	0	0.00E+00	0	0.00E+00	0	4.92E-35	0
Am-241	3.94E-33	0	0.00E+00	0	0.00E+00	0	0.00E+00	0	0.00E+00	0	0.00E+00	0	0.00E+00	0	3.94E-33	0
Am-243	5.26E-39	0	0.00E+00	0	0.00E+00	0	0.00E+00	0	0.00E+00	0	0.00E+00	0	0.00E+00	0	5.26E-39	0
Be-10	0.00E+00	0	0.00E+00	0	0.00E+00	0	0.00E+00	0	0.00E+00	0	0.00E+00	0	0.00E+00	0	0.00E+00	0
C-14	0.00E+00	0	0.00E+00	0	0.00E+00	0	0.00E+00	0	0.00E+00	0	0.00E+00	0	0.00E+00	0	0.00E+00	0
Ca-41	0.00E+00	0	0.00E+00	0	0.00E+00	0	0.00E+00	0	0.00E+00	0	0.00E+00	0	0.00E+00	0	0.00E+00	0
Cm-243	2.29E-41	0	0.00E+00	0	0.00E+00	0	0.00E+00	0	0.00E+00	0	0.00E+00	0	0.00E+00	0	2.29E-41	0
Cm-244	5.57E-32	0	0.00E+00	0	0.00E+00	0	0.00E+00	0	0.00E+00	0	0.00E+00	0	0.00E+00	0	5.57E-32	0
Cm-245	1.45E-37	0	0.00E+00	0	0.00E+00	0	0.00E+00	0	0.00E+00	0	0.00E+00	0	0.00E+00	0	1.45E-37	0
Cm-246	2.74E-26	0	0.00E+00	0	0.00E+00	0	0.00E+00	0	0.00E+00	0	0.00E+00	0	0.00E+00	0	2.74E-26	0
Cm-247	6.86E-34	0	0.00E+00	0	0.00E+00	0	0.00E+00	0	0.00E+00	0	0.00E+00	0	0.00E+00	0	6.86E-34	0
Cm-248	8.19E-26	0	0.00E+00	0	0.00E+00	0	0.00E+00	0	0.00E+00	0	0.00E+00	0	0.00E+00	0	8.19E-26	0
H-3	0.00E+00	0	0.00E+00	0	0.00E+00	0	0.00E+00	0	0.00E+00	0	0.00E+00	0	0.00E+00	0	0.00E+00	0
I-129	0.00E+00	0	0.00E+00	0	0.00E+00	0	0.00E+00	0	0.00E+00	0	0.00E+00	0	0.00E+00	0	0.00E+00	0
K-40	6.01E-24	0	0.00E+00	0	0.00E+00	0	0.00E+00	0	0.00E+00	0	0.00E+00	0	0.00E+00	0	6.01E-24	0
Mo-93	0.00E+00	0	0.00E+00	0	0.00E+00	0	0.00E+00	0	0.00E+00	0	0.00E+00	0	0.00E+00	0	0.00E+00	0
Nb-93m	0.00E+00	0	0.00E+00	0	0.00E+00	0	0.00E+00	0	0.00E+00	0	0.00E+00	0	0.00E+00	0	0.00E+00	0
Nb-94	2.67E-28	0	0.00E+00	0	0.00E+00	0	0.00E+00	0	0.00E+00	0	0.00E+00	0	0.00E+00	0	2.67E-28	0
Ni-59	1.28E-33	0	0.00E+00	0	0.00E+00	0	0.00E+00	0	0.00E+00	0	0.00E+00	0	0.00E+00	0	1.28E-33	0
Np-237	1.08E-30	0	0.00E+00	0	0.00E+00	0	0.00E+00	0	0.00E+00	0	0.00E+00	0	0.00E+00	0	1.08E-30	0
Pa-231	2.36E-30	0	0.00E+00	0	0.00E+00	0	0.00E+00	0	0.00E+00	0	0.00E+00	0	0.00E+00	0	2.36E-30	0
Pb-210	1.61E-33	0	0.00E+00	0	0.00E+00	0	0.00E+00	0	0.00E+00	0	0.00E+00	0	0.00E+00	0	1.61E-33	0
Pu-238	2.07E-29	0	0.00E+00	0	0.00E+00	0	0.00E+00	0	0.00E+00	0	0.00E+00	0	0.00E+00	0	2.07E-29	0
Pu-239	1.78E-37	0	0.00E+00	0	0.00E+00	0	0.00E+00	0	0.00E+00	0	0.00E+00	0	0.00E+00	0	1.78E-37	0
Pu-240	6.40E-33	0	0.00E+00	0	0.00E+00	0	0.00E+00	0	0.00E+00	0	0.00E+00	0	0.00E+00	0	6.40E-33	0
Pu-241	3.40E-34	0	0.00E+00	0	0.00E+00	0	0.00E+00	0	0.00E+00	0	0.00E+00	0	0.00E+00	0	3.40E-34	0
Pu-242	3.27E-29	0	0.00E+00	0	0.00E+00	0	0.00E+00	0	0.00E+00	0	0.00E+00	0	0.00E+00	0	3.27E-29	0
Pu-244	5.64E-27	0	0.00E+00	0	0.00E+00	0	0.00E+00	0	0.00E+00	0	0.00E+00	0	0.00E+00	0	5.64E-27	0
Ra-226	1.56E-23	0	0.00E+00	0	0.00E+00	0	0.00E+00	0	0.00E+00	0	0.00E+00	0	0.00E+00	0	1.56E-23	0
Ra-228	4.35E-33	0	0.00E+00	0	0.00E+00	0	0.00E+00	0	0.00E+00	0	0.00E+00	0	0.00E+00	0	4.35E-33	0
Sr-90	6.82E-36	0	0.00E+00	0	0.00E+00	0	0.00E+00	0	0.00E+00	0	0.00E+00	0	0.00E+00	0	6.82E-36	0
Tc-99	0.00E+00	0	0.00E+00	0	0.00E+00	0	0.00E+00	0	0.00E+00	0	0.00E+00	0	0.00E+00	0	0.00E+00	0
Th-228	0.00E+00	0	0.00E+00	0	0.00E+00	0	0.00E+00	0	0.00E+00	0	0.00E+00	0	0.00E+00	0	0.00E+00	0
Th-229	2.28E-24	0	0.00E+00	0	0.00E+00	0	0.00E+00	0	0.00E+00	0	0.00E+00	0	0.00E+00	0	2.28E-24	0
Th-230	3.40E-24	0	0.00E+00	0	0.00E+00	0	0.00E+00	0	0.00E+00	0	0.00E+00	0	0.00E+00	0	3.40E-24	0
Th-232	1.39E-20	71	0.00E+00	0	0.00E+00	0	0.00E+00	0	0.00E+00	0	0.00E+00	0	0.00E+00	0	1.39E-20	71
U-232	5.53E-21	28	0.00E+00	0	0.00E+00	0	0.00E+00	0	0.00E+00	0	0.00E+00	0	0.00E+00	0	5.53E-21	28
U-233	3.17E-25	0	0.00E+00	0	0.00E+00	0	0.00E+00	0	0.00E+00	0	0.00E+00	0	0.00E+00	0	3.17E-25	0
U-234	1.04E-24	0	0.00E+00	0	0.00E+00	0	0.00E+00	0	0.00E+00	0	0.00E+00	0	0.00E+00	0	1.04E-24	0
U-235	1.41E-30	0	0.00E+00	0	0.00E+00	0	0.00E+00	0	0.00E+00	0	0.00E+00	0	0.00E+00	0	1.41E-30	0
U-236	3.32E-28	0	0.00E+00	0	0.00E+00	0	0.00E+00	0	0.00E+00	0	0.00E+00	0	0.00E+00	0	3.32E-28	0

U-238	4.28E-26	0	0.00E+00	0	0.00E+00	0	0.00E+00	0	0.00E+00	0	0.00E+00	0	0.00E+00	0	4.28E-26	0
Total	1.95E-20	100	0.00E+00	0	0.00E+00	0	0.00E+00	0	0.00E+00	0	0.00E+00	0	0.00E+00	0	1.95E-20	100

*Sum of dose from all releases and from primary contamination.

Parent Dose Report
Title : Site 7 Base Case Model
File : BC_V01.ROF

Total Dose Contributions TDOSE(i,p,t) for Individual Radionuclides (i) and Pathways (p)
in mrem/yr and as a Percentage of Total Dose at t = 400 years

From releases to ground water and to surface water

Radio-	Ground		Fish		Radon		Plant		Meat		Milk		Soil		Water	
Nuclide	Dose	%	Dose	%	Dose	%	Dose	%	Dose	%	Dose	%	Dose	%	Dose	%
Ac-227	0.00E+00	0	0.00E+00	0	0.00E+00	0	0.00E+00	0	0.00E+00	0	0.00E+00	0	0.00E+00	0	0.00E+00	0
Am-241	0.00E+00	0	0.00E+00	0	0.00E+00	0	0.00E+00	0	0.00E+00	0	0.00E+00	0	0.00E+00	0	0.00E+00	0
Am-243	0.00E+00	0	0.00E+00	0	0.00E+00	0	0.00E+00	0	0.00E+00	0	0.00E+00	0	0.00E+00	0	0.00E+00	0
Be-10	0.00E+00	0	0.00E+00	0	0.00E+00	0	0.00E+00	0	0.00E+00	0	0.00E+00	0	0.00E+00	0	0.00E+00	0
C-14	2.84E-12	0	1.33E-03	1	0.00E+00	0	2.55E-06	0	5.15E-07	0	1.08E-06	0	2.39E-11	0	1.39E-01	99
Ca-41	0.00E+00	0	0.00E+00	0	0.00E+00	0	0.00E+00	0	0.00E+00	0	0.00E+00	0	0.00E+00	0	0.00E+00	0
Cm-243	0.00E+00	0	0.00E+00	0	0.00E+00	0	0.00E+00	0	0.00E+00	0	0.00E+00	0	0.00E+00	0	0.00E+00	0
Cm-244	0.00E+00	0	0.00E+00	0	0.00E+00	0	0.00E+00	0	0.00E+00	0	0.00E+00	0	0.00E+00	0	0.00E+00	0
Cm-245	0.00E+00	0	0.00E+00	0	0.00E+00	0	0.00E+00	0	0.00E+00	0	0.00E+00	0	0.00E+00	0	0.00E+00	0
Cm-246	0.00E+00	0	0.00E+00	0	0.00E+00	0	0.00E+00	0	0.00E+00	0	0.00E+00	0	0.00E+00	0	0.00E+00	0
Cm-247	0.00E+00	0	0.00E+00	0	0.00E+00	0	0.00E+00	0	0.00E+00	0	0.00E+00	0	0.00E+00	0	0.00E+00	0
Cm-248	0.00E+00	0	0.00E+00	0	0.00E+00	0	0.00E+00	0	0.00E+00	0	0.00E+00	0	0.00E+00	0	0.00E+00	0
H-3	0.00E+00	0	1.78E-18	0	0.00E+00	0	3.69E-17	0	8.20E-18	0	3.29E-17	0	1.60E-21	0	1.16E-11	0
I-129	0.00E+00	0	0.00E+00	0	0.00E+00	0	0.00E+00	0	0.00E+00	0	0.00E+00	0	0.00E+00	0	0.00E+00	0
K-40	0.00E+00	0	0.00E+00	0	0.00E+00	0	0.00E+00	0	0.00E+00	0	0.00E+00	0	0.00E+00	0	0.00E+00	0
Mo-93	0.00E+00	0	0.00E+00	0	0.00E+00	0	0.00E+00	0	0.00E+00	0	0.00E+00	0	0.00E+00	0	0.00E+00	0
Nb-93m	0.00E+00	0	0.00E+00	0	0.00E+00	0	0.00E+00	0	0.00E+00	0	0.00E+00	0	0.00E+00	0	0.00E+00	0
Nb-94	0.00E+00	0	0.00E+00	0	0.00E+00	0	0.00E+00	0	0.00E+00	0	0.00E+00	0	0.00E+00	0	0.00E+00	0
Ni-59	0.00E+00	0	0.00E+00	0	0.00E+00	0	0.00E+00	0	0.00E+00	0	0.00E+00	0	0.00E+00	0	0.00E+00	0
Np-237	0.00E+00	0	0.00E+00	0	0.00E+00	0	0.00E+00	0	0.00E+00	0	0.00E+00	0	0.00E+00	0	0.00E+00	0
Pa-231	0.00E+00	0	0.00E+00	0	0.00E+00	0	0.00E+00	0	0.00E+00	0	0.00E+00	0	0.00E+00	0	0.00E+00	0
Pb-210	0.00E+00	0	0.00E+00	0	0.00E+00	0	0.00E+00	0	0.00E+00	0	0.00E+00	0	0.00E+00	0	0.00E+00	0
Pu-238	0.00E+00	0	0.00E+00	0	0.00E+00	0	0.00E+00	0	0.00E+00	0	0.00E+00	0	0.00E+00	0	0.00E+00	0
Pu-239	0.00E+00	0	0.00E+00	0	0.00E+00	0	0.00E+00	0	0.00E+00	0	0.00E+00	0	0.00E+00	0	0.00E+00	0
Pu-240	0.00E+00	0	0.00E+00	0	0.00E+00	0	0.00E+00	0	0.00E+00	0	0.00E+00	0	0.00E+00	0	0.00E+00	0
Pu-241	0.00E+00	0	0.00E+00	0	0.00E+00	0	0.00E+00	0	0.00E+00	0	0.00E+00	0	0.00E+00	0	0.00E+00	0
Pu-242	0.00E+00	0	0.00E+00	0	0.00E+00	0	0.00E+00	0	0.00E+00	0	0.00E+00	0	0.00E+00	0	0.00E+00	0
Pu-244	0.00E+00	0	0.00E+00	0	0.00E+00	0	0.00E+00	0	0.00E+00	0	0.00E+00	0	0.00E+00	0	0.00E+00	0
Ra-226	0.00E+00	0	0.00E+00	0	0.00E+00	0	0.00E+00	0	0.00E+00	0	0.00E+00	0	0.00E+00	0	0.00E+00	0
Ra-228	0.00E+00	0	0.00E+00	0	0.00E+00	0	0.00E+00	0	0.00E+00	0	0.00E+00	0	0.00E+00	0	0.00E+00	0
Sr-90	0.00E+00	0	0.00E+00	0	0.00E+00	0	0.00E+00	0	0.00E+00	0	0.00E+00	0	0.00E+00	0	0.00E+00	0
Tc-99	0.00E+00	0	0.00E+00	0	0.00E+00	0	0.00E+00	0	0.00E+00	0	0.00E+00	0	0.00E+00	0	2.75E-33	0
Th-228	0.00E+00	0	0.00E+00	0	0.00E+00	0	0.00E+00	0	0.00E+00	0	0.00E+00	0	0.00E+00	0	0.00E+00	0
Th-229	0.00E+00	0	0.00E+00	0	0.00E+00	0	0.00E+00	0	0.00E+00	0	0.00E+00	0	0.00E+00	0	0.00E+00	0
Th-230	0.00E+00	0	0.00E+00	0	0.00E+00	0	0.00E+00	0	0.00E+00	0	0.00E+00	0	0.00E+00	0	0.00E+00	0
Th-232	0.00E+00	0	0.00E+00	0	0.00E+00	0	0.00E+00	0	0.00E+00	0	0.00E+00	0	0.00E+00	0	0.00E+00	0
U-232	0.00E+00	0	0.00E+00	0	0.00E+00	0	0.00E+00	0	0.00E+00	0	0.00E+00	0	0.00E+00	0	0.00E+00	0
U-233	0.00E+00	0	0.00E+00	0	0.00E+00	0	0.00E+00	0	0.00E+00	0	0.00E+00	0	0.00E+00	0	0.00E+00	0
U-234	0.00E+00	0	0.00E+00	0	0.00E+00	0	0.00E+00	0	0.00E+00	0	0.00E+00	0	0.00E+00	0	0.00E+00	0
U-235	0.00E+00	0	0.00E+00	0	0.00E+00	0	0.00E+00	0	0.00E+00	0	0.00E+00	0	0.00E+00	0	0.00E+00	0
U-236	0.00E+00	0	0.00E+00	0	0.00E+00	0	0.00E+00	0	0.00E+00	0	0.00E+00	0	0.00E+00	0	0.00E+00	0

U-238	0.00E+00	0	0.00E+00	0	0.00E+00	0	0.00E+00	0	0.00E+00	0	0.00E+00	0	0.00E+00	0	0.00E+00	0
Total	2.84E-12	0	1.33E-03	1	0.00E+00	0	2.55E-06	0	5.15E-07	0	1.08E-06	0	2.39E-11	0	1.39E-01	99

Total Dose Contributions TDOSE(i,p,t) for Individual Radionuclides (i) and Pathways (p)
in mrem/yr and as a Percentage of Total Dose at t = 400 years

Directly from primary contamination and from release to atmosphere (Inhalation excludes radon)

Radio-Nuclide	Ground		Inhalation		Radon		Plant		Meat		Milk		Soil		All Pathways*	
	Dose	%	Dose	%	Dose	%	Dose	%	Dose	%	Dose	%	Dose	%	Dose	%
Ac-227	7.39E-38	0	0.00E+00	0	0.00E+00	0	0.00E+00	0	0.00E+00	0	0.00E+00	0	0.00E+00	0	7.39E-38	0
Am-241	2.53E-32	0	0.00E+00	0	0.00E+00	0	0.00E+00	0	0.00E+00	0	0.00E+00	0	0.00E+00	0	2.53E-32	0
Am-243	4.63E-39	0	0.00E+00	0	0.00E+00	0	0.00E+00	0	0.00E+00	0	0.00E+00	0	0.00E+00	0	4.63E-39	0
Be-10	0.00E+00	0	0.00E+00	0	0.00E+00	0	0.00E+00	0	0.00E+00	0	0.00E+00	0	0.00E+00	0	0.00E+00	0
C-14	0.00E+00	0	4.99E-12	0	0.00E+00	0	0.00E+00	0	0.00E+00	0	0.00E+00	0	0.00E+00	0	1.41E-01	100
Ca-41	0.00E+00	0	0.00E+00	0	0.00E+00	0	0.00E+00	0	0.00E+00	0	0.00E+00	0	0.00E+00	0	0.00E+00	0
Cm-243	5.29E-42	0	0.00E+00	0	0.00E+00	0	0.00E+00	0	0.00E+00	0	0.00E+00	0	0.00E+00	0	5.29E-42	0
Cm-244	1.38E-34	0	0.00E+00	0	0.00E+00	0	0.00E+00	0	0.00E+00	0	0.00E+00	0	0.00E+00	0	1.38E-34	0
Cm-245	2.24E-36	0	0.00E+00	0	0.00E+00	0	0.00E+00	0	0.00E+00	0	0.00E+00	0	0.00E+00	0	2.24E-36	0
Cm-246	2.33E-26	0	0.00E+00	0	0.00E+00	0	0.00E+00	0	0.00E+00	0	0.00E+00	0	0.00E+00	0	2.33E-26	0
Cm-247	6.00E-34	0	0.00E+00	0	0.00E+00	0	0.00E+00	0	0.00E+00	0	0.00E+00	0	0.00E+00	0	6.00E-34	0
Cm-248	7.16E-26	0	0.00E+00	0	0.00E+00	0	0.00E+00	0	0.00E+00	0	0.00E+00	0	0.00E+00	0	7.16E-26	0
H-3	0.00E+00	0	0.00E+00	0	0.00E+00	0	0.00E+00	0	0.00E+00	0	0.00E+00	0	0.00E+00	0	1.16E-11	0
I-129	0.00E+00	0	0.00E+00	0	0.00E+00	0	0.00E+00	0	0.00E+00	0	0.00E+00	0	0.00E+00	0	0.00E+00	0
K-40	5.26E-24	0	0.00E+00	0	0.00E+00	0	0.00E+00	0	0.00E+00	0	0.00E+00	0	0.00E+00	0	5.26E-24	0
Mo-93	0.00E+00	0	0.00E+00	0	0.00E+00	0	0.00E+00	0	0.00E+00	0	0.00E+00	0	0.00E+00	0	0.00E+00	0
Nb-93m	0.00E+00	0	0.00E+00	0	0.00E+00	0	0.00E+00	0	0.00E+00	0	0.00E+00	0	0.00E+00	0	0.00E+00	0
Nb-94	2.32E-28	0	0.00E+00	0	0.00E+00	0	0.00E+00	0	0.00E+00	0	0.00E+00	0	0.00E+00	0	2.32E-28	0
Ni-59	1.12E-33	0	0.00E+00	0	0.00E+00	0	0.00E+00	0	0.00E+00	0	0.00E+00	0	0.00E+00	0	1.12E-33	0
Np-237	3.76E-30	0	0.00E+00	0	0.00E+00	0	0.00E+00	0	0.00E+00	0	0.00E+00	0	0.00E+00	0	3.76E-30	0
Pa-231	2.06E-30	0	0.00E+00	0	0.00E+00	0	0.00E+00	0	0.00E+00	0	0.00E+00	0	0.00E+00	0	2.06E-30	0
Pb-210	2.73E-36	0	0.00E+00	0	0.00E+00	0	0.00E+00	0	0.00E+00	0	0.00E+00	0	0.00E+00	0	2.73E-36	0
Pu-238	1.06E-28	0	0.00E+00	0	0.00E+00	0	0.00E+00	0	0.00E+00	0	0.00E+00	0	0.00E+00	0	1.06E-28	0
Pu-239	7.20E-37	0	0.00E+00	0	0.00E+00	0	0.00E+00	0	0.00E+00	0	0.00E+00	0	0.00E+00	0	7.20E-37	0
Pu-240	2.34E-32	0	0.00E+00	0	0.00E+00	0	0.00E+00	0	0.00E+00	0	0.00E+00	0	0.00E+00	0	2.34E-32	0
Pu-241	2.52E-33	0	0.00E+00	0	0.00E+00	0	0.00E+00	0	0.00E+00	0	0.00E+00	0	0.00E+00	0	2.52E-33	0
Pu-242	2.86E-29	0	0.00E+00	0	0.00E+00	0	0.00E+00	0	0.00E+00	0	0.00E+00	0	0.00E+00	0	2.86E-29	0
Pu-244	4.93E-27	0	0.00E+00	0	0.00E+00	0	0.00E+00	0	0.00E+00	0	0.00E+00	0	0.00E+00	0	4.93E-27	0
Ra-226	1.25E-23	0	0.00E+00	0	0.00E+00	0	0.00E+00	0	0.00E+00	0	0.00E+00	0	0.00E+00	0	1.25E-23	0
Ra-228	1.30E-43	0	0.00E+00	0	0.00E+00	0	0.00E+00	0	0.00E+00	0	0.00E+00	0	0.00E+00	0	1.30E-43	0
Sr-90	4.84E-38	0	0.00E+00	0	0.00E+00	0	0.00E+00	0	0.00E+00	0	0.00E+00	0	0.00E+00	0	4.84E-38	0
Tc-99	0.00E+00	0	0.00E+00	0	0.00E+00	0	0.00E+00	0	0.00E+00	0	0.00E+00	0	0.00E+00	0	2.75E-33	0
Th-228	0.00E+00	0	0.00E+00	0	0.00E+00	0	0.00E+00	0	0.00E+00	0	0.00E+00	0	0.00E+00	0	0.00E+00	0
Th-229	1.95E-24	0	0.00E+00	0	0.00E+00	0	0.00E+00	0	0.00E+00	0	0.00E+00	0	0.00E+00	0	1.95E-24	0
Th-230	5.68E-24	0	0.00E+00	0	0.00E+00	0	0.00E+00	0	0.00E+00	0	0.00E+00	0	0.00E+00	0	5.68E-24	0
Th-232	1.22E-20	0	0.00E+00	0	0.00E+00	0	0.00E+00	0	0.00E+00	0	0.00E+00	0	0.00E+00	0	1.22E-20	0
U-232	6.46E-22	0	0.00E+00	0	0.00E+00	0	0.00E+00	0	0.00E+00	0	0.00E+00	0	0.00E+00	0	6.46E-22	0
U-233	5.48E-25	0	0.00E+00	0	0.00E+00	0	0.00E+00	0	0.00E+00	0	0.00E+00	0	0.00E+00	0	5.48E-25	0
U-234	3.53E-24	0	0.00E+00	0	0.00E+00	0	0.00E+00	0	0.00E+00	0	0.00E+00	0	0.00E+00	0	3.53E-24	0
U-235	2.68E-30	0	0.00E+00	0	0.00E+00	0	0.00E+00	0	0.00E+00	0	0.00E+00	0	0.00E+00	0	2.68E-30	0
U-236	5.97E-28	0	0.00E+00	0	0.00E+00	0	0.00E+00	0	0.00E+00	0	0.00E+00	0	0.00E+00	0	5.97E-28	0

U-238	3.81E-26	0	0.00E+00	0	0.00E+00	0	0.00E+00	0	0.00E+00	0	0.00E+00	0	0.00E+00	0	3.81E-26	0
Total	1.29E-20	0	4.99E-12	0	0.00E+00	0	0.00E+00	0	0.00E+00	0	0.00E+00	0	0.00E+00	0	1.41E-01	100

*Sum of dose from all releases and from primary contamination.

Total Dose Contributions TDOSE(i,p,t) for Individual Radionuclides (i) and Pathways (p)
in mrem/yr and as a Percentage of Total Dose at t = 500 years

From releases to ground water and to surface water

Radio-	Ground		Fish		Radon		Plant		Meat		Milk		Soil		Water	
Nuclide	Dose	%	Dose	%	Dose	%	Dose	%	Dose	%	Dose	%	Dose	%	Dose	%
Ac-227	0.00E+00	0	0.00E+00	0	0.00E+00	0	0.00E+00	0	0.00E+00	0	0.00E+00	0	0.00E+00	0	0.00E+00	0
Am-241	0.00E+00	0	0.00E+00	0	0.00E+00	0	0.00E+00	0	0.00E+00	0	0.00E+00	0	0.00E+00	0	0.00E+00	0
Am-243	0.00E+00	0	0.00E+00	0	0.00E+00	0	0.00E+00	0	0.00E+00	0	0.00E+00	0	0.00E+00	0	0.00E+00	0
Be-10	0.00E+00	0	0.00E+00	0	0.00E+00	0	0.00E+00	0	0.00E+00	0	0.00E+00	0	0.00E+00	0	0.00E+00	0
C-14	4.00E-10	0	1.84E-01	18	0.00E+00	0	3.62E-04	0	7.37E-05	0	1.50E-04	0	3.37E-09	0	8.34E-01	82
Ca-41	0.00E+00	0	0.00E+00	0	0.00E+00	0	0.00E+00	0	0.00E+00	0	0.00E+00	0	0.00E+00	0	0.00E+00	0
Cm-243	0.00E+00	0	0.00E+00	0	0.00E+00	0	0.00E+00	0	0.00E+00	0	0.00E+00	0	0.00E+00	0	0.00E+00	0
Cm-244	0.00E+00	0	0.00E+00	0	0.00E+00	0	0.00E+00	0	0.00E+00	0	0.00E+00	0	0.00E+00	0	0.00E+00	0
Cm-245	0.00E+00	0	0.00E+00	0	0.00E+00	0	0.00E+00	0	0.00E+00	0	0.00E+00	0	0.00E+00	0	0.00E+00	0
Cm-246	0.00E+00	0	0.00E+00	0	0.00E+00	0	0.00E+00	0	0.00E+00	0	0.00E+00	0	0.00E+00	0	0.00E+00	0
Cm-247	0.00E+00	0	0.00E+00	0	0.00E+00	0	0.00E+00	0	0.00E+00	0	0.00E+00	0	0.00E+00	0	0.00E+00	0
Cm-248	0.00E+00	0	0.00E+00	0	0.00E+00	0	0.00E+00	0	0.00E+00	0	0.00E+00	0	0.00E+00	0	0.00E+00	0
H-3	0.00E+00	0	1.66E-18	0	0.00E+00	0	3.52E-17	0	7.77E-18	0	3.06E-17	0	1.52E-21	0	3.87E-13	0
I-129	0.00E+00	0	0.00E+00	0	0.00E+00	0	0.00E+00	0	0.00E+00	0	0.00E+00	0	0.00E+00	0	0.00E+00	0
K-40	0.00E+00	0	0.00E+00	0	0.00E+00	0	0.00E+00	0	0.00E+00	0	0.00E+00	0	0.00E+00	0	0.00E+00	0
Mo-93	0.00E+00	0	0.00E+00	0	0.00E+00	0	0.00E+00	0	0.00E+00	0	0.00E+00	0	0.00E+00	0	0.00E+00	0
Nb-93m	0.00E+00	0	0.00E+00	0	0.00E+00	0	0.00E+00	0	0.00E+00	0	0.00E+00	0	0.00E+00	0	0.00E+00	0
Nb-94	0.00E+00	0	0.00E+00	0	0.00E+00	0	0.00E+00	0	0.00E+00	0	0.00E+00	0	0.00E+00	0	0.00E+00	0
Ni-59	0.00E+00	0	0.00E+00	0	0.00E+00	0	0.00E+00	0	0.00E+00	0	0.00E+00	0	0.00E+00	0	0.00E+00	0
Np-237	0.00E+00	0	0.00E+00	0	0.00E+00	0	0.00E+00	0	0.00E+00	0	0.00E+00	0	0.00E+00	0	0.00E+00	0
Pa-231	0.00E+00	0	0.00E+00	0	0.00E+00	0	0.00E+00	0	0.00E+00	0	0.00E+00	0	0.00E+00	0	0.00E+00	0
Pb-210	0.00E+00	0	0.00E+00	0	0.00E+00	0	0.00E+00	0	0.00E+00	0	0.00E+00	0	0.00E+00	0	0.00E+00	0
Pu-238	0.00E+00	0	0.00E+00	0	0.00E+00	0	0.00E+00	0	0.00E+00	0	0.00E+00	0	0.00E+00	0	0.00E+00	0
Pu-239	0.00E+00	0	0.00E+00	0	0.00E+00	0	0.00E+00	0	0.00E+00	0	0.00E+00	0	0.00E+00	0	0.00E+00	0
Pu-240	0.00E+00	0	0.00E+00	0	0.00E+00	0	0.00E+00	0	0.00E+00	0	0.00E+00	0	0.00E+00	0	0.00E+00	0
Pu-241	0.00E+00	0	0.00E+00	0	0.00E+00	0	0.00E+00	0	0.00E+00	0	0.00E+00	0	0.00E+00	0	0.00E+00	0
Pu-242	0.00E+00	0	0.00E+00	0	0.00E+00	0	0.00E+00	0	0.00E+00	0	0.00E+00	0	0.00E+00	0	0.00E+00	0
Pu-244	0.00E+00	0	0.00E+00	0	0.00E+00	0	0.00E+00	0	0.00E+00	0	0.00E+00	0	0.00E+00	0	0.00E+00	0
Ra-226	0.00E+00	0	0.00E+00	0	0.00E+00	0	0.00E+00	0	0.00E+00	0	0.00E+00	0	0.00E+00	0	0.00E+00	0
Ra-228	0.00E+00	0	0.00E+00	0	0.00E+00	0	0.00E+00	0	0.00E+00	0	0.00E+00	0	0.00E+00	0	0.00E+00	0
Sr-90	0.00E+00	0	0.00E+00	0	0.00E+00	0	0.00E+00	0	0.00E+00	0	0.00E+00	0	0.00E+00	0	0.00E+00	0
Tc-99	4.36E-31	0	3.11E-27	0	0.00E+00	0	2.35E-26	0	2.80E-25	0	4.66E-28	0	5.22E-31	0	2.36E-15	0
Th-228	0.00E+00	0	0.00E+00	0	0.00E+00	0	0.00E+00	0	0.00E+00	0	0.00E+00	0	0.00E+00	0	0.00E+00	0
Th-229	0.00E+00	0	0.00E+00	0	0.00E+00	0	0.00E+00	0	0.00E+00	0	0.00E+00	0	0.00E+00	0	0.00E+00	0
Th-230	0.00E+00	0	0.00E+00	0	0.00E+00	0	0.00E+00	0	0.00E+00	0	0.00E+00	0	0.00E+00	0	0.00E+00	0
Th-232	0.00E+00	0	0.00E+00	0	0.00E+00	0	0.00E+00	0	0.00E+00	0	0.00E+00	0	0.00E+00	0	0.00E+00	0
U-232	0.00E+00	0	0.00E+00	0	0.00E+00	0	0.00E+00	0	0.00E+00	0	0.00E+00	0	0.00E+00	0	0.00E+00	0
U-233	0.00E+00	0	0.00E+00	0	0.00E+00	0	0.00E+00	0	0.00E+00	0	0.00E+00	0	0.00E+00	0	0.00E+00	0
U-234	0.00E+00	0	0.00E+00	0	0.00E+00	0	0.00E+00	0	0.00E+00	0	0.00E+00	0	0.00E+00	0	0.00E+00	0
U-235	0.00E+00	0	0.00E+00	0	0.00E+00	0	0.00E+00	0	0.00E+00	0	0.00E+00	0	0.00E+00	0	0.00E+00	0
U-236	0.00E+00	0	0.00E+00	0	0.00E+00	0	0.00E+00	0	0.00E+00	0	0.00E+00	0	0.00E+00	0	0.00E+00	0

U-238	0.00E+00	0	0.00E+00	0	0.00E+00	0	0.00E+00	0	0.00E+00	0	0.00E+00	0	0.00E+00	0	0.00E+00	0
Total	4.00E-10	0	1.84E-01	18	0.00E+00	0	3.62E-04	0	7.37E-05	0	1.50E-04	0	3.37E-09	0	8.34E-01	82

Total Dose Contributions TDOSE(i,p,t) for Individual Radionuclides (i) and Pathways (p)
in mrem/yr and as a Percentage of Total Dose at t = 500 years

Directly from primary contamination and from release to atmosphere (Inhalation excludes radon)

Radio-	Ground		Inhalation		Radon		Plant		Meat		Milk		Soil		All Pathways*	
Nuclide	Dose	%	Dose	%	Dose	%	Dose	%	Dose	%	Dose	%	Dose	%	Dose	%
Ac-227	2.62E-39	0	0.00E+00	0	0.00E+00	0	0.00E+00	0	0.00E+00	0	0.00E+00	0	0.00E+00	0	2.62E-39	0
Am-241	4.08E-32	0	0.00E+00	0	0.00E+00	0	0.00E+00	0	0.00E+00	0	0.00E+00	0	0.00E+00	0	4.08E-32	0
Am-243	4.05E-39	0	0.00E+00	0	0.00E+00	0	0.00E+00	0	0.00E+00	0	0.00E+00	0	0.00E+00	0	4.05E-39	0
Be-10	0.00E+00	0	0.00E+00	0	0.00E+00	0	0.00E+00	0	0.00E+00	0	0.00E+00	0	0.00E+00	0	0.00E+00	0
C-14	0.00E+00	0	7.04E-10	0	0.00E+00	0	0.00E+00	0	0.00E+00	0	0.00E+00	0	0.00E+00	0	1.02E+00	100
Ca-41	0.00E+00	0	0.00E+00	0	0.00E+00	0	0.00E+00	0	0.00E+00	0	0.00E+00	0	0.00E+00	0	0.00E+00	0
Cm-243	7.40E-42	0	0.00E+00	0	0.00E+00	0	0.00E+00	0	0.00E+00	0	0.00E+00	0	0.00E+00	0	7.40E-42	0
Cm-244	1.60E-34	0	0.00E+00	0	0.00E+00	0	0.00E+00	0	0.00E+00	0	0.00E+00	0	0.00E+00	0	1.60E-34	0
Cm-245	4.70E-36	0	0.00E+00	0	0.00E+00	0	0.00E+00	0	0.00E+00	0	0.00E+00	0	0.00E+00	0	4.70E-36	0
Cm-246	1.97E-26	0	0.00E+00	0	0.00E+00	0	0.00E+00	0	0.00E+00	0	0.00E+00	0	0.00E+00	0	1.97E-26	0
Cm-247	5.14E-34	0	0.00E+00	0	0.00E+00	0	0.00E+00	0	0.00E+00	0	0.00E+00	0	0.00E+00	0	5.14E-34	0
Cm-248	6.14E-26	0	0.00E+00	0	0.00E+00	0	0.00E+00	0	0.00E+00	0	0.00E+00	0	0.00E+00	0	6.14E-26	0
H-3	0.00E+00	0	0.00E+00	0	0.00E+00	0	0.00E+00	0	0.00E+00	0	0.00E+00	0	0.00E+00	0	3.87E-13	0
I-129	0.00E+00	0	0.00E+00	0	0.00E+00	0	0.00E+00	0	0.00E+00	0	0.00E+00	0	0.00E+00	0	0.00E+00	0
K-40	4.50E-24	0	0.00E+00	0	0.00E+00	0	0.00E+00	0	0.00E+00	0	0.00E+00	0	0.00E+00	0	4.50E-24	0
Mo-93	0.00E+00	0	0.00E+00	0	0.00E+00	0	0.00E+00	0	0.00E+00	0	0.00E+00	0	0.00E+00	0	0.00E+00	0
Nb-93m	0.00E+00	0	0.00E+00	0	0.00E+00	0	0.00E+00	0	0.00E+00	0	0.00E+00	0	0.00E+00	0	0.00E+00	0
Nb-94	1.98E-28	0	0.00E+00	0	0.00E+00	0	0.00E+00	0	0.00E+00	0	0.00E+00	0	0.00E+00	0	1.98E-28	0
Ni-59	9.56E-34	0	0.00E+00	0	0.00E+00	0	0.00E+00	0	0.00E+00	0	0.00E+00	0	0.00E+00	0	9.56E-34	0
Np-237	5.01E-30	0	0.00E+00	0	0.00E+00	0	0.00E+00	0	0.00E+00	0	0.00E+00	0	0.00E+00	0	5.01E-30	0
Pa-231	1.76E-30	0	0.00E+00	0	0.00E+00	0	0.00E+00	0	0.00E+00	0	0.00E+00	0	0.00E+00	0	1.76E-30	0
Pb-210	1.03E-37	0	0.00E+00	0	0.00E+00	0	0.00E+00	0	0.00E+00	0	0.00E+00	0	0.00E+00	0	1.03E-37	0
Pu-238	1.55E-28	0	0.00E+00	0	0.00E+00	0	0.00E+00	0	0.00E+00	0	0.00E+00	0	0.00E+00	0	1.55E-28	0
Pu-239	9.92E-37	0	0.00E+00	0	0.00E+00	0	0.00E+00	0	0.00E+00	0	0.00E+00	0	0.00E+00	0	9.92E-37	0
Pu-240	3.16E-32	0	0.00E+00	0	0.00E+00	0	0.00E+00	0	0.00E+00	0	0.00E+00	0	0.00E+00	0	3.16E-32	0
Pu-241	4.18E-33	0	0.00E+00	0	0.00E+00	0	0.00E+00	0	0.00E+00	0	0.00E+00	0	0.00E+00	0	4.18E-33	0
Pu-242	2.45E-29	0	0.00E+00	0	0.00E+00	0	0.00E+00	0	0.00E+00	0	0.00E+00	0	0.00E+00	0	2.45E-29	0
Pu-244	4.23E-27	0	0.00E+00	0	0.00E+00	0	0.00E+00	0	0.00E+00	0	0.00E+00	0	0.00E+00	0	4.23E-27	0
Ra-226	1.03E-23	0	0.00E+00	0	0.00E+00	0	0.00E+00	0	0.00E+00	0	0.00E+00	0	0.00E+00	0	1.03E-23	0
Ra-228	0.00E+00	0	0.00E+00	0	0.00E+00	0	0.00E+00	0	0.00E+00	0	0.00E+00	0	0.00E+00	0	0.00E+00	0
Sr-90	3.73E-39	0	0.00E+00	0	0.00E+00	0	0.00E+00	0	0.00E+00	0	0.00E+00	0	0.00E+00	0	3.73E-39	0
Tc-99	0.00E+00	0	1.76E-31	0	0.00E+00	0	0.00E+00	0	0.00E+00	0	0.00E+00	0	0.00E+00	0	2.36E-15	0
Th-228	0.00E+00	0	0.00E+00	0	0.00E+00	0	0.00E+00	0	0.00E+00	0	0.00E+00	0	0.00E+00	0	0.00E+00	0
Th-229	1.66E-24	0	0.00E+00	0	0.00E+00	0	0.00E+00	0	0.00E+00	0	0.00E+00	0	0.00E+00	0	1.66E-24	0
Th-230	5.96E-24	0	0.00E+00	0	0.00E+00	0	0.00E+00	0	0.00E+00	0	0.00E+00	0	0.00E+00	0	5.96E-24	0
Th-232	1.04E-20	0	0.00E+00	0	0.00E+00	0	0.00E+00	0	0.00E+00	0	0.00E+00	0	0.00E+00	0	1.04E-20	0
U-232	2.02E-22	0	0.00E+00	0	0.00E+00	0	0.00E+00	0	0.00E+00	0	0.00E+00	0	0.00E+00	0	2.02E-22	0
U-233	5.84E-25	0	0.00E+00	0	0.00E+00	0	0.00E+00	0	0.00E+00	0	0.00E+00	0	0.00E+00	0	5.84E-25	0
U-234	4.66E-24	0	0.00E+00	0	0.00E+00	0	0.00E+00	0	0.00E+00	0	0.00E+00	0	0.00E+00	0	4.66E-24	0
U-235	2.92E-30	0	0.00E+00	0	0.00E+00	0	0.00E+00	0	0.00E+00	0	0.00E+00	0	0.00E+00	0	2.92E-30	0
U-236	6.43E-28	0	0.00E+00	0	0.00E+00	0	0.00E+00	0	0.00E+00	0	0.00E+00	0	0.00E+00	0	6.43E-28	0

U-238	3.33E-26	0	0.00E+00	0	0.00E+00	0	0.00E+00	0	0.00E+00	0	0.00E+00	0	0.00E+00	0	3.33E-26	0
Total	1.07E-20	0	7.04E-10	0	0.00E+00	0	0.00E+00	0	0.00E+00	0	0.00E+00	0	0.00E+00	0	1.02E+00	100

*Sum of dose from all releases and from primary contamination.

Total Dose Contributions TDOSE(i,p,t) for Individual Radionuclides (i) and Pathways (p)
in mrem/yr and as a Percentage of Total Dose at t = 600 years

From releases to ground water and to surface water

Radio-	Ground		Fish		Radon		Plant		Meat		Milk		Soil		Water	
Nuclide	Dose	%	Dose	%	Dose	%	Dose	%	Dose	%	Dose	%	Dose	%	Dose	%
Ac-227	0.00E+00	0	0.00E+00	0	0.00E+00	0	0.00E+00	0	0.00E+00	0	0.00E+00	0	0.00E+00	0	0.00E+00	0
Am-241	0.00E+00	0	0.00E+00	0	0.00E+00	0	0.00E+00	0	0.00E+00	0	0.00E+00	0	0.00E+00	0	0.00E+00	0
Am-243	0.00E+00	0	0.00E+00	0	0.00E+00	0	0.00E+00	0	0.00E+00	0	0.00E+00	0	0.00E+00	0	0.00E+00	0
Be-10	0.00E+00	0	0.00E+00	0	0.00E+00	0	0.00E+00	0	0.00E+00	0	0.00E+00	0	0.00E+00	0	0.00E+00	0
C-14	4.58E-10	0	2.10E-01	39	0.00E+00	0	4.14E-04	0	8.44E-05	0	1.71E-04	0	3.86E-09	0	3.29E-01	61
Ca-41	0.00E+00	0	0.00E+00	0	0.00E+00	0	0.00E+00	0	0.00E+00	0	0.00E+00	0	0.00E+00	0	0.00E+00	0
Cm-243	0.00E+00	0	0.00E+00	0	0.00E+00	0	0.00E+00	0	0.00E+00	0	0.00E+00	0	0.00E+00	0	0.00E+00	0
Cm-244	0.00E+00	0	0.00E+00	0	0.00E+00	0	0.00E+00	0	0.00E+00	0	0.00E+00	0	0.00E+00	0	0.00E+00	0
Cm-245	0.00E+00	0	0.00E+00	0	0.00E+00	0	0.00E+00	0	0.00E+00	0	0.00E+00	0	0.00E+00	0	0.00E+00	0
Cm-246	0.00E+00	0	0.00E+00	0	0.00E+00	0	0.00E+00	0	0.00E+00	0	0.00E+00	0	0.00E+00	0	0.00E+00	0
Cm-247	0.00E+00	0	0.00E+00	0	0.00E+00	0	0.00E+00	0	0.00E+00	0	0.00E+00	0	0.00E+00	0	0.00E+00	0
Cm-248	0.00E+00	0	0.00E+00	0	0.00E+00	0	0.00E+00	0	0.00E+00	0	0.00E+00	0	0.00E+00	0	0.00E+00	0
H-3	0.00E+00	0	7.79E-21	0	0.00E+00	0	1.67E-19	0	3.67E-20	0	1.44E-19	0	7.17E-24	0	5.92E-16	0
I-129	0.00E+00	0	0.00E+00	0	0.00E+00	0	0.00E+00	0	0.00E+00	0	0.00E+00	0	0.00E+00	0	0.00E+00	0
K-40	0.00E+00	0	0.00E+00	0	0.00E+00	0	0.00E+00	0	0.00E+00	0	0.00E+00	0	0.00E+00	0	0.00E+00	0
Mo-93	0.00E+00	0	0.00E+00	0	0.00E+00	0	0.00E+00	0	0.00E+00	0	0.00E+00	0	0.00E+00	0	0.00E+00	0
Nb-93m	0.00E+00	0	0.00E+00	0	0.00E+00	0	0.00E+00	0	0.00E+00	0	0.00E+00	0	0.00E+00	0	0.00E+00	0
Nb-94	0.00E+00	0	0.00E+00	0	0.00E+00	0	0.00E+00	0	0.00E+00	0	0.00E+00	0	0.00E+00	0	0.00E+00	0
Ni-59	0.00E+00	0	0.00E+00	0	0.00E+00	0	0.00E+00	0	0.00E+00	0	0.00E+00	0	0.00E+00	0	0.00E+00	0
Np-237	0.00E+00	0	0.00E+00	0	0.00E+00	0	0.00E+00	0	0.00E+00	0	0.00E+00	0	0.00E+00	0	0.00E+00	0
Pa-231	0.00E+00	0	0.00E+00	0	0.00E+00	0	0.00E+00	0	0.00E+00	0	0.00E+00	0	0.00E+00	0	0.00E+00	0
Pb-210	0.00E+00	0	0.00E+00	0	0.00E+00	0	0.00E+00	0	0.00E+00	0	0.00E+00	0	0.00E+00	0	0.00E+00	0
Pu-238	0.00E+00	0	0.00E+00	0	0.00E+00	0	0.00E+00	0	0.00E+00	0	0.00E+00	0	0.00E+00	0	0.00E+00	0
Pu-239	0.00E+00	0	0.00E+00	0	0.00E+00	0	0.00E+00	0	0.00E+00	0	0.00E+00	0	0.00E+00	0	0.00E+00	0
Pu-240	0.00E+00	0	0.00E+00	0	0.00E+00	0	0.00E+00	0	0.00E+00	0	0.00E+00	0	0.00E+00	0	0.00E+00	0
Pu-241	0.00E+00	0	0.00E+00	0	0.00E+00	0	0.00E+00	0	0.00E+00	0	0.00E+00	0	0.00E+00	0	0.00E+00	0
Pu-242	0.00E+00	0	0.00E+00	0	0.00E+00	0	0.00E+00	0	0.00E+00	0	0.00E+00	0	0.00E+00	0	0.00E+00	0
Pu-244	0.00E+00	0	0.00E+00	0	0.00E+00	0	0.00E+00	0	0.00E+00	0	0.00E+00	0	0.00E+00	0	0.00E+00	0
Ra-226	0.00E+00	0	0.00E+00	0	0.00E+00	0	0.00E+00	0	0.00E+00	0	0.00E+00	0	0.00E+00	0	0.00E+00	0
Ra-228	0.00E+00	0	0.00E+00	0	0.00E+00	0	0.00E+00	0	0.00E+00	0	0.00E+00	0	0.00E+00	0	0.00E+00	0
Sr-90	0.00E+00	0	0.00E+00	0	0.00E+00	0	0.00E+00	0	0.00E+00	0	0.00E+00	0	0.00E+00	0	0.00E+00	0
Tc-99	3.09E-21	0	2.09E-17	0	0.00E+00	0	1.64E-16	0	1.94E-15	0	3.13E-18	0	3.71E-21	0	3.88E-08	0
Th-228	0.00E+00	0	0.00E+00	0	0.00E+00	0	0.00E+00	0	0.00E+00	0	0.00E+00	0	0.00E+00	0	0.00E+00	0
Th-229	0.00E+00	0	0.00E+00	0	0.00E+00	0	0.00E+00	0	0.00E+00	0	0.00E+00	0	0.00E+00	0	0.00E+00	0
Th-230	0.00E+00	0	0.00E+00	0	0.00E+00	0	0.00E+00	0	0.00E+00	0	0.00E+00	0	0.00E+00	0	0.00E+00	0
Th-232	0.00E+00	0	0.00E+00	0	0.00E+00	0	0.00E+00	0	0.00E+00	0	0.00E+00	0	0.00E+00	0	0.00E+00	0
U-232	0.00E+00	0	0.00E+00	0	0.00E+00	0	0.00E+00	0	0.00E+00	0	0.00E+00	0	0.00E+00	0	0.00E+00	0
U-233	0.00E+00	0	0.00E+00	0	0.00E+00	0	0.00E+00	0	0.00E+00	0	0.00E+00	0	0.00E+00	0	0.00E+00	0
U-234	0.00E+00	0	0.00E+00	0	0.00E+00	0	0.00E+00	0	0.00E+00	0	0.00E+00	0	0.00E+00	0	0.00E+00	0
U-235	0.00E+00	0	0.00E+00	0	0.00E+00	0	0.00E+00	0	0.00E+00	0	0.00E+00	0	0.00E+00	0	0.00E+00	0
U-236	0.00E+00	0	0.00E+00	0	0.00E+00	0	0.00E+00	0	0.00E+00	0	0.00E+00	0	0.00E+00	0	0.00E+00	0

U-238	0.00E+00	0	0.00E+00	0	0.00E+00	0	0.00E+00	0	0.00E+00	0	0.00E+00	0	0.00E+00	0	0.00E+00	0
Total	4.58E-10	0	2.10E-01	39	0.00E+00	0	4.14E-04	0	8.44E-05	0	1.71E-04	0	3.86E-09	0	3.29E-01	61

Total Dose Contributions TDOSE(i,p,t) for Individual Radionuclides (i) and Pathways (p)
in mrem/yr and as a Percentage of Total Dose at t = 600 years

Directly from primary contamination and from release to atmosphere (Inhalation excludes radon)

Radio-Nuclide	Ground		Inhalation		Radon		Plant		Meat		Milk		Soil		All Pathways*	
	Dose	%	Dose	%	Dose	%	Dose	%	Dose	%	Dose	%	Dose	%	Dose	%
Ac-227	9.07E-41	0	0.00E+00	0	0.00E+00	0	0.00E+00	0	0.00E+00	0	0.00E+00	0	0.00E+00	0	9.07E-41	0
Am-241	5.65E-32	0	0.00E+00	0	0.00E+00	0	0.00E+00	0	0.00E+00	0	0.00E+00	0	0.00E+00	0	5.65E-32	0
Am-243	3.49E-39	0	0.00E+00	0	0.00E+00	0	0.00E+00	0	0.00E+00	0	0.00E+00	0	0.00E+00	0	3.49E-39	0
Be-10	0.00E+00	0	0.00E+00	0	0.00E+00	0	0.00E+00	0	0.00E+00	0	0.00E+00	0	0.00E+00	0	0.00E+00	0
C-14	0.00E+00	0	8.05E-10	0	0.00E+00	0	0.00E+00	0	0.00E+00	0	0.00E+00	0	0.00E+00	0	5.40E-01	100
Ca-41	0.00E+00	0	0.00E+00	0	0.00E+00	0	0.00E+00	0	0.00E+00	0	0.00E+00	0	0.00E+00	0	0.00E+00	0
Cm-243	9.31E-42	0	0.00E+00	0	0.00E+00	0	0.00E+00	0	0.00E+00	0	0.00E+00	0	0.00E+00	0	9.31E-42	0
Cm-244	1.95E-34	0	0.00E+00	0	0.00E+00	0	0.00E+00	0	0.00E+00	0	0.00E+00	0	0.00E+00	0	1.95E-34	0
Cm-245	8.07E-36	0	0.00E+00	0	0.00E+00	0	0.00E+00	0	0.00E+00	0	0.00E+00	0	0.00E+00	0	8.07E-36	0
Cm-246	1.61E-26	0	0.00E+00	0	0.00E+00	0	0.00E+00	0	0.00E+00	0	0.00E+00	0	0.00E+00	0	1.61E-26	0
Cm-247	4.29E-34	0	0.00E+00	0	0.00E+00	0	0.00E+00	0	0.00E+00	0	0.00E+00	0	0.00E+00	0	4.29E-34	0
Cm-248	5.11E-26	0	0.00E+00	0	0.00E+00	0	0.00E+00	0	0.00E+00	0	0.00E+00	0	0.00E+00	0	5.11E-26	0
H-3	0.00E+00	0	0.00E+00	0	0.00E+00	0	0.00E+00	0	0.00E+00	0	0.00E+00	0	0.00E+00	0	5.92E-16	0
I-129	0.00E+00	0	0.00E+00	0	0.00E+00	0	0.00E+00	0	0.00E+00	0	0.00E+00	0	0.00E+00	0	0.00E+00	0
K-40	3.75E-24	0	0.00E+00	0	0.00E+00	0	0.00E+00	0	0.00E+00	0	0.00E+00	0	0.00E+00	0	3.75E-24	0
Mo-93	0.00E+00	0	0.00E+00	0	0.00E+00	0	0.00E+00	0	0.00E+00	0	0.00E+00	0	0.00E+00	0	0.00E+00	0
Nb-93m	0.00E+00	0	0.00E+00	0	0.00E+00	0	0.00E+00	0	0.00E+00	0	0.00E+00	0	0.00E+00	0	0.00E+00	0
Nb-94	1.64E-28	0	0.00E+00	0	0.00E+00	0	0.00E+00	0	0.00E+00	0	0.00E+00	0	0.00E+00	0	1.64E-28	0
Ni-59	7.96E-34	0	0.00E+00	0	0.00E+00	0	0.00E+00	0	0.00E+00	0	0.00E+00	0	0.00E+00	0	7.96E-34	0
Np-237	5.99E-30	0	0.00E+00	0	0.00E+00	0	0.00E+00	0	0.00E+00	0	0.00E+00	0	0.00E+00	0	5.99E-30	0
Pa-231	1.47E-30	0	0.00E+00	0	0.00E+00	0	0.00E+00	0	0.00E+00	0	0.00E+00	0	0.00E+00	0	1.47E-30	0
Pb-210	3.79E-39	0	0.00E+00	0	0.00E+00	0	0.00E+00	0	0.00E+00	0	0.00E+00	0	0.00E+00	0	3.79E-39	0
Pu-238	1.98E-28	0	0.00E+00	0	0.00E+00	0	0.00E+00	0	0.00E+00	0	0.00E+00	0	0.00E+00	0	1.98E-28	0
Pu-239	1.21E-36	0	0.00E+00	0	0.00E+00	0	0.00E+00	0	0.00E+00	0	0.00E+00	0	0.00E+00	0	1.21E-36	0
Pu-240	3.81E-32	0	0.00E+00	0	0.00E+00	0	0.00E+00	0	0.00E+00	0	0.00E+00	0	0.00E+00	0	3.81E-32	0
Pu-241	5.90E-33	0	0.00E+00	0	0.00E+00	0	0.00E+00	0	0.00E+00	0	0.00E+00	0	0.00E+00	0	5.90E-33	0
Pu-242	2.04E-29	0	0.00E+00	0	0.00E+00	0	0.00E+00	0	0.00E+00	0	0.00E+00	0	0.00E+00	0	2.04E-29	0
Pu-244	3.52E-27	0	0.00E+00	0	0.00E+00	0	0.00E+00	0	0.00E+00	0	0.00E+00	0	0.00E+00	0	3.52E-27	0
Ra-226	8.21E-24	0	0.00E+00	0	0.00E+00	0	0.00E+00	0	0.00E+00	0	0.00E+00	0	0.00E+00	0	8.21E-24	0
Ra-228	0.00E+00	0	0.00E+00	0	0.00E+00	0	0.00E+00	0	0.00E+00	0	0.00E+00	0	0.00E+00	0	0.00E+00	0
Sr-90	2.80E-40	0	0.00E+00	0	0.00E+00	0	0.00E+00	0	0.00E+00	0	0.00E+00	0	0.00E+00	0	2.80E-40	0
Tc-99	0.00E+00	0	1.25E-21	0	0.00E+00	0	0.00E+00	0	0.00E+00	0	0.00E+00	0	0.00E+00	0	3.88E-08	0
Th-228	0.00E+00	0	0.00E+00	0	0.00E+00	0	0.00E+00	0	0.00E+00	0	0.00E+00	0	0.00E+00	0	0.00E+00	0
Th-229	1.37E-24	0	0.00E+00	0	0.00E+00	0	0.00E+00	0	0.00E+00	0	0.00E+00	0	0.00E+00	0	1.37E-24	0
Th-230	5.83E-24	0	0.00E+00	0	0.00E+00	0	0.00E+00	0	0.00E+00	0	0.00E+00	0	0.00E+00	0	5.83E-24	0
Th-232	8.70E-21	0	0.00E+00	0	0.00E+00	0	0.00E+00	0	0.00E+00	0	0.00E+00	0	0.00E+00	0	8.70E-21	0
U-232	6.17E-23	0	0.00E+00	0	0.00E+00	0	0.00E+00	0	0.00E+00	0	0.00E+00	0	0.00E+00	0	6.17E-23	0
U-233	5.81E-25	0	0.00E+00	0	0.00E+00	0	0.00E+00	0	0.00E+00	0	0.00E+00	0	0.00E+00	0	5.81E-25	0
U-234	5.51E-24	0	0.00E+00	0	0.00E+00	0	0.00E+00	0	0.00E+00	0	0.00E+00	0	0.00E+00	0	5.51E-24	0
U-235	2.95E-30	0	0.00E+00	0	0.00E+00	0	0.00E+00	0	0.00E+00	0	0.00E+00	0	0.00E+00	0	2.95E-30	0
U-236	6.45E-28	0	0.00E+00	0	0.00E+00	0	0.00E+00	0	0.00E+00	0	0.00E+00	0	0.00E+00	0	6.45E-28	0

U-238	2.86E-26	0	0.00E+00	0	0.00E+00	0	0.00E+00	0	0.00E+00	0	0.00E+00	0	0.00E+00	0	2.86E-26	0
Total	8.79E-21	0	8.05E-10	0	0.00E+00	0	0.00E+00	0	0.00E+00	0	0.00E+00	0	0.00E+00	0	5.40E-01	100

*Sum of dose from all releases and from primary contamination.

Total Dose Contributions TDOSE(i,p,t) for Individual Radionuclides (i) and Pathways (p)
in mrem/yr and as a Percentage of Total Dose at t = 800 years

From releases to ground water and to surface water

Radio-	Ground		Fish		Radon		Plant		Meat		Milk		Soil		Water	
Nuclide	Dose	%	Dose	%	Dose	%	Dose	%	Dose	%	Dose	%	Dose	%	Dose	%
Ac-227	0.00E+00	0	0.00E+00	0	0.00E+00	0	0.00E+00	0	0.00E+00	0	0.00E+00	0	0.00E+00	0	0.00E+00	0
Am-241	0.00E+00	0	0.00E+00	0	0.00E+00	0	0.00E+00	0	0.00E+00	0	0.00E+00	0	0.00E+00	0	0.00E+00	0
Am-243	0.00E+00	0	0.00E+00	0	0.00E+00	0	0.00E+00	0	0.00E+00	0	0.00E+00	0	0.00E+00	0	0.00E+00	0
Be-10	0.00E+00	0	0.00E+00	0	0.00E+00	0	0.00E+00	0	0.00E+00	0	0.00E+00	0	0.00E+00	0	0.00E+00	0
C-14	9.53E-11	0	4.37E-02	30	0.00E+00	0	8.62E-05	0	1.76E-05	0	3.57E-05	0	8.02E-10	0	1.00E-01	68
Ca-41	0.00E+00	0	0.00E+00	0	0.00E+00	0	0.00E+00	0	0.00E+00	0	0.00E+00	0	0.00E+00	0	0.00E+00	0
Cm-243	0.00E+00	0	0.00E+00	0	0.00E+00	0	0.00E+00	0	0.00E+00	0	0.00E+00	0	0.00E+00	0	0.00E+00	0
Cm-244	0.00E+00	0	0.00E+00	0	0.00E+00	0	0.00E+00	0	0.00E+00	0	0.00E+00	0	0.00E+00	0	0.00E+00	0
Cm-245	0.00E+00	0	0.00E+00	0	0.00E+00	0	0.00E+00	0	0.00E+00	0	0.00E+00	0	0.00E+00	0	0.00E+00	0
Cm-246	0.00E+00	0	0.00E+00	0	0.00E+00	0	0.00E+00	0	0.00E+00	0	0.00E+00	0	0.00E+00	0	0.00E+00	0
Cm-247	0.00E+00	0	0.00E+00	0	0.00E+00	0	0.00E+00	0	0.00E+00	0	0.00E+00	0	0.00E+00	0	0.00E+00	0
Cm-248	0.00E+00	0	0.00E+00	0	0.00E+00	0	0.00E+00	0	0.00E+00	0	0.00E+00	0	0.00E+00	0	0.00E+00	0
H-3	0.00E+00	0	2.15E-26	0	0.00E+00	0	4.60E-25	0	1.01E-25	0	3.99E-25	0	1.98E-29	0	2.25E-21	0
I-129	0.00E+00	0	0.00E+00	0	0.00E+00	0	0.00E+00	0	0.00E+00	0	0.00E+00	0	0.00E+00	0	1.54E-42	0
K-40	0.00E+00	0	0.00E+00	0	0.00E+00	0	0.00E+00	0	0.00E+00	0	0.00E+00	0	0.00E+00	0	0.00E+00	0
Mo-93	0.00E+00	0	0.00E+00	0	0.00E+00	0	0.00E+00	0	0.00E+00	0	0.00E+00	0	0.00E+00	0	0.00E+00	0
Nb-93m	0.00E+00	0	0.00E+00	0	0.00E+00	0	0.00E+00	0	0.00E+00	0	0.00E+00	0	0.00E+00	0	0.00E+00	0
Nb-94	0.00E+00	0	0.00E+00	0	0.00E+00	0	0.00E+00	0	0.00E+00	0	0.00E+00	0	0.00E+00	0	0.00E+00	0
Ni-59	0.00E+00	0	0.00E+00	0	0.00E+00	0	0.00E+00	0	0.00E+00	0	0.00E+00	0	0.00E+00	0	0.00E+00	0
Np-237	0.00E+00	0	0.00E+00	0	0.00E+00	0	0.00E+00	0	0.00E+00	0	0.00E+00	0	0.00E+00	0	0.00E+00	0
Pa-231	0.00E+00	0	0.00E+00	0	0.00E+00	0	0.00E+00	0	0.00E+00	0	0.00E+00	0	0.00E+00	0	0.00E+00	0
Pb-210	0.00E+00	0	0.00E+00	0	0.00E+00	0	0.00E+00	0	0.00E+00	0	0.00E+00	0	0.00E+00	0	0.00E+00	0
Pu-238	0.00E+00	0	0.00E+00	0	0.00E+00	0	0.00E+00	0	0.00E+00	0	0.00E+00	0	0.00E+00	0	0.00E+00	0
Pu-239	0.00E+00	0	0.00E+00	0	0.00E+00	0	0.00E+00	0	0.00E+00	0	0.00E+00	0	0.00E+00	0	0.00E+00	0
Pu-240	0.00E+00	0	0.00E+00	0	0.00E+00	0	0.00E+00	0	0.00E+00	0	0.00E+00	0	0.00E+00	0	0.00E+00	0
Pu-241	0.00E+00	0	0.00E+00	0	0.00E+00	0	0.00E+00	0	0.00E+00	0	0.00E+00	0	0.00E+00	0	0.00E+00	0
Pu-242	0.00E+00	0	0.00E+00	0	0.00E+00	0	0.00E+00	0	0.00E+00	0	0.00E+00	0	0.00E+00	0	0.00E+00	0
Pu-244	0.00E+00	0	0.00E+00	0	0.00E+00	0	0.00E+00	0	0.00E+00	0	0.00E+00	0	0.00E+00	0	0.00E+00	0
Ra-226	0.00E+00	0	0.00E+00	0	0.00E+00	0	0.00E+00	0	0.00E+00	0	0.00E+00	0	0.00E+00	0	0.00E+00	0
Ra-228	0.00E+00	0	0.00E+00	0	0.00E+00	0	0.00E+00	0	0.00E+00	0	0.00E+00	0	0.00E+00	0	0.00E+00	0
Sr-90	0.00E+00	0	0.00E+00	0	0.00E+00	0	0.00E+00	0	0.00E+00	0	0.00E+00	0	0.00E+00	0	0.00E+00	0
Tc-99	1.47E-13	0	9.36E-10	0	0.00E+00	0	7.58E-09	0	8.76E-08	0	1.40E-10	0	1.77E-13	0	3.90E-03	3
Th-228	0.00E+00	0	0.00E+00	0	0.00E+00	0	0.00E+00	0	0.00E+00	0	0.00E+00	0	0.00E+00	0	0.00E+00	0
Th-229	0.00E+00	0	0.00E+00	0	0.00E+00	0	0.00E+00	0	0.00E+00	0	0.00E+00	0	0.00E+00	0	0.00E+00	0
Th-230	0.00E+00	0	0.00E+00	0	0.00E+00	0	0.00E+00	0	0.00E+00	0	0.00E+00	0	0.00E+00	0	0.00E+00	0
Th-232	0.00E+00	0	0.00E+00	0	0.00E+00	0	0.00E+00	0	0.00E+00	0	0.00E+00	0	0.00E+00	0	0.00E+00	0
U-232	0.00E+00	0	0.00E+00	0	0.00E+00	0	0.00E+00	0	0.00E+00	0	0.00E+00	0	0.00E+00	0	0.00E+00	0
U-233	0.00E+00	0	0.00E+00	0	0.00E+00	0	0.00E+00	0	0.00E+00	0	0.00E+00	0	0.00E+00	0	0.00E+00	0
U-234	0.00E+00	0	0.00E+00	0	0.00E+00	0	0.00E+00	0	0.00E+00	0	0.00E+00	0	0.00E+00	0	0.00E+00	0
U-235	0.00E+00	0	0.00E+00	0	0.00E+00	0	0.00E+00	0	0.00E+00	0	0.00E+00	0	0.00E+00	0	0.00E+00	0
U-236	0.00E+00	0	0.00E+00	0	0.00E+00	0	0.00E+00	0	0.00E+00	0	0.00E+00	0	0.00E+00	0	0.00E+00	0

U-238	0.00E+00	0	0.00E+00	0	0.00E+00	0	0.00E+00	0	0.00E+00	0	0.00E+00	0	0.00E+00	0	0.00E+00	0
Total	9.54E-11	0	4.37E-02	30	0.00E+00	0	8.62E-05	0	1.76E-05	0	3.57E-05	0	8.03E-10	0	1.04E-01	70

Total Dose Contributions TDOSE(i,p,t) for Individual Radionuclides (i) and Pathways (p)
in mrem/yr and as a Percentage of Total Dose at t = 800 years

Directly from primary contamination and from release to atmosphere (Inhalation excludes radon)

Radio-	Ground		Inhalation		Radon		Plant		Meat		Milk		Soil		All Pathways*	
Nuclide	Dose	%	Dose	%	Dose	%	Dose	%	Dose	%	Dose	%	Dose	%	Dose	%
Ac-227	9.39E-44	0	0.00E+00	0	0.00E+00	0	0.00E+00	0	0.00E+00	0	0.00E+00	0	0.00E+00	0	9.39E-44	0
Am-241	7.46E-32	0	0.00E+00	0	0.00E+00	0	0.00E+00	0	0.00E+00	0	0.00E+00	0	0.00E+00	0	7.46E-32	0
Am-243	2.35E-39	0	0.00E+00	0	0.00E+00	0	0.00E+00	0	0.00E+00	0	0.00E+00	0	0.00E+00	0	2.35E-39	0
Be-10	0.00E+00	0	0.00E+00	0	0.00E+00	0	0.00E+00	0	0.00E+00	0	0.00E+00	0	0.00E+00	0	0.00E+00	0
C-14	0.00E+00	0	1.68E-10	0	0.00E+00	0	0.00E+00	0	0.00E+00	0	0.00E+00	0	0.00E+00	0	1.44E-01	97
Ca-41	0.00E+00	0	0.00E+00	0	0.00E+00	0	0.00E+00	0	0.00E+00	0	0.00E+00	0	0.00E+00	0	0.00E+00	0
Cm-243	1.05E-41	0	0.00E+00	0	0.00E+00	0	0.00E+00	0	0.00E+00	0	0.00E+00	0	0.00E+00	0	1.05E-41	0
Cm-244	2.13E-34	0	0.00E+00	0	0.00E+00	0	0.00E+00	0	0.00E+00	0	0.00E+00	0	0.00E+00	0	2.13E-34	0
Cm-245	1.48E-35	0	0.00E+00	0	0.00E+00	0	0.00E+00	0	0.00E+00	0	0.00E+00	0	0.00E+00	0	1.48E-35	0
Cm-246	9.40E-27	0	0.00E+00	0	0.00E+00	0	0.00E+00	0	0.00E+00	0	0.00E+00	0	0.00E+00	0	9.40E-27	0
Cm-247	2.57E-34	0	0.00E+00	0	0.00E+00	0	0.00E+00	0	0.00E+00	0	0.00E+00	0	0.00E+00	0	2.57E-34	0
Cm-248	3.06E-26	0	0.00E+00	0	0.00E+00	0	0.00E+00	0	0.00E+00	0	0.00E+00	0	0.00E+00	0	3.06E-26	0
H-3	0.00E+00	0	0.00E+00	0	0.00E+00	0	0.00E+00	0	0.00E+00	0	0.00E+00	0	0.00E+00	0	2.25E-21	0
I-129	0.00E+00	0	0.00E+00	0	0.00E+00	0	0.00E+00	0	0.00E+00	0	0.00E+00	0	0.00E+00	0	1.54E-42	0
K-40	2.25E-24	0	0.00E+00	0	0.00E+00	0	0.00E+00	0	0.00E+00	0	0.00E+00	0	0.00E+00	0	2.25E-24	0
Mo-93	0.00E+00	0	0.00E+00	0	0.00E+00	0	0.00E+00	0	0.00E+00	0	0.00E+00	0	0.00E+00	0	0.00E+00	0
Nb-93m	0.00E+00	0	0.00E+00	0	0.00E+00	0	0.00E+00	0	0.00E+00	0	0.00E+00	0	0.00E+00	0	0.00E+00	0
Nb-94	9.78E-29	0	0.00E+00	0	0.00E+00	0	0.00E+00	0	0.00E+00	0	0.00E+00	0	0.00E+00	0	9.78E-29	0
Ni-59	4.77E-34	0	0.00E+00	0	0.00E+00	0	0.00E+00	0	0.00E+00	0	0.00E+00	0	0.00E+00	0	4.77E-34	0
Np-237	6.34E-30	0	0.00E+00	0	0.00E+00	0	0.00E+00	0	0.00E+00	0	0.00E+00	0	0.00E+00	0	6.34E-30	0
Pa-231	8.75E-31	0	0.00E+00	0	0.00E+00	0	0.00E+00	0	0.00E+00	0	0.00E+00	0	0.00E+00	0	8.75E-31	0
Pb-210	4.41E-42	0	0.00E+00	0	0.00E+00	0	0.00E+00	0	0.00E+00	0	0.00E+00	0	0.00E+00	0	4.41E-42	0
Pu-238	2.26E-28	0	0.00E+00	0	0.00E+00	0	0.00E+00	0	0.00E+00	0	0.00E+00	0	0.00E+00	0	2.26E-28	0
Pu-239	1.32E-36	0	0.00E+00	0	0.00E+00	0	0.00E+00	0	0.00E+00	0	0.00E+00	0	0.00E+00	0	1.32E-36	0
Pu-240	4.07E-32	0	0.00E+00	0	0.00E+00	0	0.00E+00	0	0.00E+00	0	0.00E+00	0	0.00E+00	0	4.07E-32	0
Pu-241	7.99E-33	0	0.00E+00	0	0.00E+00	0	0.00E+00	0	0.00E+00	0	0.00E+00	0	0.00E+00	0	7.99E-33	0
Pu-242	1.22E-29	0	0.00E+00	0	0.00E+00	0	0.00E+00	0	0.00E+00	0	0.00E+00	0	0.00E+00	0	1.22E-29	0
Pu-244	2.11E-27	0	0.00E+00	0	0.00E+00	0	0.00E+00	0	0.00E+00	0	0.00E+00	0	0.00E+00	0	2.11E-27	0
Ra-226	4.51E-24	0	0.00E+00	0	0.00E+00	0	0.00E+00	0	0.00E+00	0	0.00E+00	0	0.00E+00	0	4.51E-24	0
Ra-228	0.00E+00	0	0.00E+00	0	0.00E+00	0	0.00E+00	0	0.00E+00	0	0.00E+00	0	0.00E+00	0	0.00E+00	0
Sr-90	1.36E-42	0	0.00E+00	0	0.00E+00	0	0.00E+00	0	0.00E+00	0	0.00E+00	0	0.00E+00	0	1.36E-42	0
Tc-99	0.00E+00	0	5.96E-14	0	0.00E+00	0	0.00E+00	0	0.00E+00	0	0.00E+00	0	0.00E+00	0	3.90E-03	3
Th-228	0.00E+00	0	0.00E+00	0	0.00E+00	0	0.00E+00	0	0.00E+00	0	0.00E+00	0	0.00E+00	0	0.00E+00	0
Th-229	8.05E-25	0	0.00E+00	0	0.00E+00	0	0.00E+00	0	0.00E+00	0	0.00E+00	0	0.00E+00	0	8.05E-25	0
Th-230	4.47E-24	0	0.00E+00	0	0.00E+00	0	0.00E+00	0	0.00E+00	0	0.00E+00	0	0.00E+00	0	4.47E-24	0
Th-232	5.22E-21	0	0.00E+00	0	0.00E+00	0	0.00E+00	0	0.00E+00	0	0.00E+00	0	0.00E+00	0	5.22E-21	0
U-232	4.95E-24	0	0.00E+00	0	0.00E+00	0	0.00E+00	0	0.00E+00	0	0.00E+00	0	0.00E+00	0	4.95E-24	0
U-233	4.60E-25	0	0.00E+00	0	0.00E+00	0	0.00E+00	0	0.00E+00	0	0.00E+00	0	0.00E+00	0	4.60E-25	0
U-234	5.71E-24	0	0.00E+00	0	0.00E+00	0	0.00E+00	0	0.00E+00	0	0.00E+00	0	0.00E+00	0	5.71E-24	0
U-235	2.38E-30	0	0.00E+00	0	0.00E+00	0	0.00E+00	0	0.00E+00	0	0.00E+00	0	0.00E+00	0	2.38E-30	0
U-236	5.18E-28	0	0.00E+00	0	0.00E+00	0	0.00E+00	0	0.00E+00	0	0.00E+00	0	0.00E+00	0	5.18E-28	0

U-238	1.87E-26	0	0.00E+00	0	0.00E+00	0	0.00E+00	0	0.00E+00	0	0.00E+00	0	0.00E+00	0	1.87E-26	0
Total	5.24E-21	0	1.68E-10	0	0.00E+00	0	0.00E+00	0	0.00E+00	0	0.00E+00	0	0.00E+00	0	1.48E-01	100

*Sum of dose from all releases and from primary contamination.

Total Dose Contributions TDOSE(i,p,t) for Individual Radionuclides (i) and Pathways (p)
in mrem/yr and as a Percentage of Total Dose at t = 1000 years

From releases to ground water and to surface water

Radio-	Ground		Fish		Radon		Plant		Meat		Milk		Soil		Water	
Nuclide	Dose	%	Dose	%	Dose	%	Dose	%	Dose	%	Dose	%	Dose	%	Dose	%
Ac-227	0.00E+00	0	0.00E+00	0	0.00E+00	0	0.00E+00	0	0.00E+00	0	0.00E+00	0	0.00E+00	0	0.00E+00	0
Am-241	0.00E+00	0	0.00E+00	0	0.00E+00	0	0.00E+00	0	0.00E+00	0	0.00E+00	0	0.00E+00	0	0.00E+00	0
Am-243	0.00E+00	0	0.00E+00	0	0.00E+00	0	0.00E+00	0	0.00E+00	0	0.00E+00	0	0.00E+00	0	0.00E+00	0
Be-10	0.00E+00	0	0.00E+00	0	0.00E+00	0	0.00E+00	0	0.00E+00	0	0.00E+00	0	0.00E+00	0	0.00E+00	0
C-14	5.75E-11	0	2.64E-02	15	0.00E+00	0	5.20E-05	0	1.06E-05	0	2.15E-05	0	4.84E-10	0	4.44E-02	26
Ca-41	0.00E+00	0	0.00E+00	0	0.00E+00	0	0.00E+00	0	0.00E+00	0	0.00E+00	0	0.00E+00	0	0.00E+00	0
Cm-243	0.00E+00	0	0.00E+00	0	0.00E+00	0	0.00E+00	0	0.00E+00	0	0.00E+00	0	0.00E+00	0	0.00E+00	0
Cm-244	0.00E+00	0	0.00E+00	0	0.00E+00	0	0.00E+00	0	0.00E+00	0	0.00E+00	0	0.00E+00	0	0.00E+00	0
Cm-245	0.00E+00	0	0.00E+00	0	0.00E+00	0	0.00E+00	0	0.00E+00	0	0.00E+00	0	0.00E+00	0	0.00E+00	0
Cm-246	0.00E+00	0	0.00E+00	0	0.00E+00	0	0.00E+00	0	0.00E+00	0	0.00E+00	0	0.00E+00	0	0.00E+00	0
Cm-247	0.00E+00	0	0.00E+00	0	0.00E+00	0	0.00E+00	0	0.00E+00	0	0.00E+00	0	0.00E+00	0	0.00E+00	0
Cm-248	0.00E+00	0	0.00E+00	0	0.00E+00	0	0.00E+00	0	0.00E+00	0	0.00E+00	0	0.00E+00	0	0.00E+00	0
H-3	0.00E+00	0	1.77E-31	0	0.00E+00	0	3.78E-30	0	8.33E-31	0	3.28E-30	0	1.63E-34	0	1.50E-26	0
I-129	0.00E+00	0	1.40E-45	0	0.00E+00	0	2.80E-45	0	1.01E-43	0	7.01E-45	0	0.00E+00	0	8.91E-25	0
K-40	0.00E+00	0	0.00E+00	0	0.00E+00	0	0.00E+00	0	0.00E+00	0	0.00E+00	0	0.00E+00	0	0.00E+00	0
Mo-93	0.00E+00	0	0.00E+00	0	0.00E+00	0	0.00E+00	0	0.00E+00	0	0.00E+00	0	0.00E+00	0	0.00E+00	0
Nb-93m	0.00E+00	0	0.00E+00	0	0.00E+00	0	0.00E+00	0	0.00E+00	0	0.00E+00	0	0.00E+00	0	0.00E+00	0
Nb-94	0.00E+00	0	0.00E+00	0	0.00E+00	0	0.00E+00	0	0.00E+00	0	0.00E+00	0	0.00E+00	0	0.00E+00	0
Ni-59	0.00E+00	0	0.00E+00	0	0.00E+00	0	0.00E+00	0	0.00E+00	0	0.00E+00	0	0.00E+00	0	0.00E+00	0
Np-237	0.00E+00	0	0.00E+00	0	0.00E+00	0	0.00E+00	0	0.00E+00	0	0.00E+00	0	0.00E+00	0	0.00E+00	0
Pa-231	0.00E+00	0	0.00E+00	0	0.00E+00	0	0.00E+00	0	0.00E+00	0	0.00E+00	0	0.00E+00	0	0.00E+00	0
Pb-210	0.00E+00	0	0.00E+00	0	0.00E+00	0	0.00E+00	0	0.00E+00	0	0.00E+00	0	0.00E+00	0	0.00E+00	0
Pu-238	0.00E+00	0	0.00E+00	0	0.00E+00	0	0.00E+00	0	0.00E+00	0	0.00E+00	0	0.00E+00	0	0.00E+00	0
Pu-239	0.00E+00	0	0.00E+00	0	0.00E+00	0	0.00E+00	0	0.00E+00	0	0.00E+00	0	0.00E+00	0	0.00E+00	0
Pu-240	0.00E+00	0	0.00E+00	0	0.00E+00	0	0.00E+00	0	0.00E+00	0	0.00E+00	0	0.00E+00	0	0.00E+00	0
Pu-241	0.00E+00	0	0.00E+00	0	0.00E+00	0	0.00E+00	0	0.00E+00	0	0.00E+00	0	0.00E+00	0	0.00E+00	0
Pu-242	0.00E+00	0	0.00E+00	0	0.00E+00	0	0.00E+00	0	0.00E+00	0	0.00E+00	0	0.00E+00	0	0.00E+00	0
Pu-244	0.00E+00	0	0.00E+00	0	0.00E+00	0	0.00E+00	0	0.00E+00	0	0.00E+00	0	0.00E+00	0	0.00E+00	0
Ra-226	0.00E+00	0	0.00E+00	0	0.00E+00	0	0.00E+00	0	0.00E+00	0	0.00E+00	0	0.00E+00	0	0.00E+00	0
Ra-228	0.00E+00	0	0.00E+00	0	0.00E+00	0	0.00E+00	0	0.00E+00	0	0.00E+00	0	0.00E+00	0	0.00E+00	0
Sr-90	0.00E+00	0	0.00E+00	0	0.00E+00	0	0.00E+00	0	0.00E+00	0	0.00E+00	0	0.00E+00	0	0.00E+00	0
Tc-99	5.98E-11	0	3.71E-07	0	0.00E+00	0	3.04E-06	0	3.49E-05	0	5.56E-08	0	7.17E-11	0	1.02E-01	59
Th-228	0.00E+00	0	0.00E+00	0	0.00E+00	0	0.00E+00	0	0.00E+00	0	0.00E+00	0	0.00E+00	0	0.00E+00	0
Th-229	0.00E+00	0	0.00E+00	0	0.00E+00	0	0.00E+00	0	0.00E+00	0	0.00E+00	0	0.00E+00	0	0.00E+00	0
Th-230	0.00E+00	0	0.00E+00	0	0.00E+00	0	0.00E+00	0	0.00E+00	0	0.00E+00	0	0.00E+00	0	0.00E+00	0
Th-232	0.00E+00	0	0.00E+00	0	0.00E+00	0	0.00E+00	0	0.00E+00	0	0.00E+00	0	0.00E+00	0	0.00E+00	0
U-232	0.00E+00	0	0.00E+00	0	0.00E+00	0	0.00E+00	0	0.00E+00	0	0.00E+00	0	0.00E+00	0	0.00E+00	0
U-233	0.00E+00	0	0.00E+00	0	0.00E+00	0	0.00E+00	0	0.00E+00	0	0.00E+00	0	0.00E+00	0	0.00E+00	0
U-234	0.00E+00	0	0.00E+00	0	0.00E+00	0	0.00E+00	0	0.00E+00	0	0.00E+00	0	0.00E+00	0	0.00E+00	0
U-235	0.00E+00	0	0.00E+00	0	0.00E+00	0	0.00E+00	0	0.00E+00	0	0.00E+00	0	0.00E+00	0	0.00E+00	0
U-236	0.00E+00	0	0.00E+00	0	0.00E+00	0	0.00E+00	0	0.00E+00	0	0.00E+00	0	0.00E+00	0	0.00E+00	0

U-238	0.00E+00	0	0.00E+00	0	0.00E+00	0	0.00E+00	0	0.00E+00	0	0.00E+00	0	0.00E+00	0	0.00E+00	0
Total	1.17E-10	0	2.64E-02	15	0.00E+00	0	5.51E-05	0	4.55E-05	0	2.16E-05	0	5.56E-10	0	1.47E-01	85

Parent Dose Report
Title : Site 7 Base Case Model
File : BC_V01.ROF

Total Dose Contributions TDOSE(i,p,t) for Individual Radionuclides (i) and Pathways (p)
in mrem/yr and as a Percentage of Total Dose at t = 1000 years

Directly from primary contamination and from release to atmosphere (Inhalation excludes radon)

Radio-	Ground		Inhalation		Radon		Plant		Meat		Milk		Soil		All Pathways*	
Nuclide	Dose	%	Dose	%	Dose	%	Dose	%	Dose	%	Dose	%	Dose	%	Dose	%
Ac-227	0.00E+00	0	0.00E+00	0	0.00E+00	0	0.00E+00	0	0.00E+00	0	0.00E+00	0	0.00E+00	0	0.00E+00	0
Am-241	4.51E-32	0	0.00E+00	0	0.00E+00	0	0.00E+00	0	0.00E+00	0	0.00E+00	0	0.00E+00	0	4.51E-32	0
Am-243	9.28E-40	0	0.00E+00	0	0.00E+00	0	0.00E+00	0	0.00E+00	0	0.00E+00	0	0.00E+00	0	9.28E-40	0
Be-10	0.00E+00	0	0.00E+00	0	0.00E+00	0	0.00E+00	0	0.00E+00	0	0.00E+00	0	0.00E+00	0	0.00E+00	0
C-14	0.00E+00	0	1.01E-10	0	0.00E+00	0	0.00E+00	0	0.00E+00	0	0.00E+00	0	0.00E+00	0	7.08E-02	41
Ca-41	0.00E+00	0	0.00E+00	0	0.00E+00	0	0.00E+00	0	0.00E+00	0	0.00E+00	0	0.00E+00	0	0.00E+00	0
Cm-243	5.66E-42	0	0.00E+00	0	0.00E+00	0	0.00E+00	0	0.00E+00	0	0.00E+00	0	0.00E+00	0	5.66E-42	0
Cm-244	1.12E-34	0	0.00E+00	0	0.00E+00	0	0.00E+00	0	0.00E+00	0	0.00E+00	0	0.00E+00	0	1.12E-34	0
Cm-245	1.15E-35	0	0.00E+00	0	0.00E+00	0	0.00E+00	0	0.00E+00	0	0.00E+00	0	0.00E+00	0	1.15E-35	0
Cm-246	3.03E-27	0	0.00E+00	0	0.00E+00	0	0.00E+00	0	0.00E+00	0	0.00E+00	0	0.00E+00	0	3.03E-27	0
Cm-247	8.54E-35	0	0.00E+00	0	0.00E+00	0	0.00E+00	0	0.00E+00	0	0.00E+00	0	0.00E+00	0	8.54E-35	0
Cm-248	1.02E-26	0	0.00E+00	0	0.00E+00	0	0.00E+00	0	0.00E+00	0	0.00E+00	0	0.00E+00	0	1.02E-26	0
H-3	0.00E+00	0	0.00E+00	0	0.00E+00	0	0.00E+00	0	0.00E+00	0	0.00E+00	0	0.00E+00	0	1.50E-26	0
I-129	0.00E+00	0	0.00E+00	0	0.00E+00	0	0.00E+00	0	0.00E+00	0	0.00E+00	0	0.00E+00	0	8.91E-25	0
K-40	7.48E-25	0	0.00E+00	0	0.00E+00	0	0.00E+00	0	0.00E+00	0	0.00E+00	0	0.00E+00	0	7.48E-25	0
Mo-93	0.00E+00	0	0.00E+00	0	0.00E+00	0	0.00E+00	0	0.00E+00	0	0.00E+00	0	0.00E+00	0	0.00E+00	0
Nb-93m	0.00E+00	0	0.00E+00	0	0.00E+00	0	0.00E+00	0	0.00E+00	0	0.00E+00	0	0.00E+00	0	0.00E+00	0
Nb-94	3.23E-29	0	0.00E+00	0	0.00E+00	0	0.00E+00	0	0.00E+00	0	0.00E+00	0	0.00E+00	0	3.23E-29	0
Ni-59	1.58E-34	0	0.00E+00	0	0.00E+00	0	0.00E+00	0	0.00E+00	0	0.00E+00	0	0.00E+00	0	1.58E-34	0
Np-237	3.27E-30	0	0.00E+00	0	0.00E+00	0	0.00E+00	0	0.00E+00	0	0.00E+00	0	0.00E+00	0	3.27E-30	0
Pa-231	2.89E-31	0	0.00E+00	0	0.00E+00	0	0.00E+00	0	0.00E+00	0	0.00E+00	0	0.00E+00	0	2.89E-31	0
Pb-210	2.80E-45	0	0.00E+00	0	0.00E+00	0	0.00E+00	0	0.00E+00	0	0.00E+00	0	0.00E+00	0	2.80E-45	0
Pu-238	1.21E-28	0	0.00E+00	0	0.00E+00	0	0.00E+00	0	0.00E+00	0	0.00E+00	0	0.00E+00	0	1.21E-28	0
Pu-239	6.94E-37	0	0.00E+00	0	0.00E+00	0	0.00E+00	0	0.00E+00	0	0.00E+00	0	0.00E+00	0	6.94E-37	0
Pu-240	2.11E-32	0	0.00E+00	0	0.00E+00	0	0.00E+00	0	0.00E+00	0	0.00E+00	0	0.00E+00	0	2.11E-32	0
Pu-241	4.90E-33	0	0.00E+00	0	0.00E+00	0	0.00E+00	0	0.00E+00	0	0.00E+00	0	0.00E+00	0	4.90E-33	0
Pu-242	4.06E-30	0	0.00E+00	0	0.00E+00	0	0.00E+00	0	0.00E+00	0	0.00E+00	0	0.00E+00	0	4.06E-30	0
Pu-244	7.02E-28	0	0.00E+00	0	0.00E+00	0	0.00E+00	0	0.00E+00	0	0.00E+00	0	0.00E+00	0	7.02E-28	0
Ra-226	1.38E-24	0	0.00E+00	0	0.00E+00	0	0.00E+00	0	0.00E+00	0	0.00E+00	0	0.00E+00	0	1.38E-24	0
Ra-228	0.00E+00	0	0.00E+00	0	0.00E+00	0	0.00E+00	0	0.00E+00	0	0.00E+00	0	0.00E+00	0	0.00E+00	0
Sr-90	4.20E-45	0	0.00E+00	0	0.00E+00	0	0.00E+00	0	0.00E+00	0	0.00E+00	0	0.00E+00	0	4.20E-45	0
Tc-99	0.00E+00	0	2.42E-11	0	0.00E+00	0	0.00E+00	0	0.00E+00	0	0.00E+00	0	0.00E+00	0	1.03E-01	59
Th-228	0.00E+00	0	0.00E+00	0	0.00E+00	0	0.00E+00	0	0.00E+00	0	0.00E+00	0	0.00E+00	0	0.00E+00	0
Th-229	2.63E-25	0	0.00E+00	0	0.00E+00	0	0.00E+00	0	0.00E+00	0	0.00E+00	0	0.00E+00	0	2.63E-25	0
Th-230	1.78E-24	0	0.00E+00	0	0.00E+00	0	0.00E+00	0	0.00E+00	0	0.00E+00	0	0.00E+00	0	1.78E-24	0
Th-232	1.73E-21	0	0.00E+00	0	0.00E+00	0	0.00E+00	0	0.00E+00	0	0.00E+00	0	0.00E+00	0	1.73E-21	0
U-232	2.20E-25	0	0.00E+00	0	0.00E+00	0	0.00E+00	0	0.00E+00	0	0.00E+00	0	0.00E+00	0	2.20E-25	0
U-233	1.89E-25	0	0.00E+00	0	0.00E+00	0	0.00E+00	0	0.00E+00	0	0.00E+00	0	0.00E+00	0	1.89E-25	0
U-234	2.88E-24	0	0.00E+00	0	0.00E+00	0	0.00E+00	0	0.00E+00	0	0.00E+00	0	0.00E+00	0	2.88E-24	0
U-235	9.96E-31	0	0.00E+00	0	0.00E+00	0	0.00E+00	0	0.00E+00	0	0.00E+00	0	0.00E+00	0	9.96E-31	0
U-236	2.16E-28	0	0.00E+00	0	0.00E+00	0	0.00E+00	0	0.00E+00	0	0.00E+00	0	0.00E+00	0	2.16E-28	0

U-238	7.01E-27	0	0.00E+00	0	0.00E+00	0	0.00E+00	0	0.00E+00	0	0.00E+00	0	0.00E+00	0	7.01E-27	0
Total	1.74E-21	0	1.25E-10	0	0.00E+00	0	0.00E+00	0	0.00E+00	0	0.00E+00	0	0.00E+00	0	1.73E-01	100

*Sum of dose from all releases and from primary contamination.

Total Dose Contributions TDOSE(i,p,t) for Individual Radionuclides (i) and Pathways (p)
in mrem/yr and as a Percentage of Total Dose at t = 2000 years

From releases to ground water and to surface water

Radio-	Ground		Fish		Radon		Plant		Meat		Milk		Soil		Water	
Nuclide	Dose	%	Dose	%	Dose	%	Dose	%	Dose	%	Dose	%	Dose	%	Dose	%
Ac-227	0.00E+00	0	0.00E+00	0	0.00E+00	0	0.00E+00	0	0.00E+00	0	0.00E+00	0	0.00E+00	0	0.00E+00	0
Am-241	0.00E+00	0	0.00E+00	0	0.00E+00	0	0.00E+00	0	0.00E+00	0	0.00E+00	0	0.00E+00	0	0.00E+00	0
Am-243	0.00E+00	0	0.00E+00	0	0.00E+00	0	0.00E+00	0	0.00E+00	0	0.00E+00	0	0.00E+00	0	0.00E+00	0
Be-10	0.00E+00	0	0.00E+00	0	0.00E+00	0	0.00E+00	0	0.00E+00	0	0.00E+00	0	0.00E+00	0	0.00E+00	0
C-14	5.30E-19	0	2.42E-10	0	0.00E+00	0	4.80E-13	0	9.79E-14	0	1.98E-13	0	4.47E-18	0	6.12E-11	0
Ca-41	0.00E+00	0	0.00E+00	0	0.00E+00	0	0.00E+00	0	0.00E+00	0	0.00E+00	0	0.00E+00	0	0.00E+00	0
Cm-243	0.00E+00	0	0.00E+00	0	0.00E+00	0	0.00E+00	0	0.00E+00	0	0.00E+00	0	0.00E+00	0	0.00E+00	0
Cm-244	0.00E+00	0	0.00E+00	0	0.00E+00	0	0.00E+00	0	0.00E+00	0	0.00E+00	0	0.00E+00	0	0.00E+00	0
Cm-245	0.00E+00	0	0.00E+00	0	0.00E+00	0	0.00E+00	0	0.00E+00	0	0.00E+00	0	0.00E+00	0	0.00E+00	0
Cm-246	0.00E+00	0	0.00E+00	0	0.00E+00	0	0.00E+00	0	0.00E+00	0	0.00E+00	0	0.00E+00	0	0.00E+00	0
Cm-247	0.00E+00	0	0.00E+00	0	0.00E+00	0	0.00E+00	0	0.00E+00	0	0.00E+00	0	0.00E+00	0	0.00E+00	0
Cm-248	0.00E+00	0	0.00E+00	0	0.00E+00	0	0.00E+00	0	0.00E+00	0	0.00E+00	0	0.00E+00	0	0.00E+00	0
H-3	0.00E+00	0	0.00E+00	0	0.00E+00	0	0.00E+00	0	0.00E+00	0	0.00E+00	0	0.00E+00	0	0.00E+00	0
I-129	3.23E-16	0	1.44E-12	0	0.00E+00	0	2.67E-12	0	9.68E-11	0	6.79E-12	0	5.85E-16	0	2.20E-04	0
K-40	0.00E+00	0	0.00E+00	0	0.00E+00	0	0.00E+00	0	0.00E+00	0	0.00E+00	0	0.00E+00	0	0.00E+00	0
Mo-93	0.00E+00	0	0.00E+00	0	0.00E+00	0	0.00E+00	0	0.00E+00	0	0.00E+00	0	0.00E+00	0	0.00E+00	0
Nb-93m	0.00E+00	0	0.00E+00	0	0.00E+00	0	0.00E+00	0	0.00E+00	0	0.00E+00	0	0.00E+00	0	0.00E+00	0
Nb-94	0.00E+00	0	0.00E+00	0	0.00E+00	0	0.00E+00	0	0.00E+00	0	0.00E+00	0	0.00E+00	0	0.00E+00	0
Ni-59	0.00E+00	0	0.00E+00	0	0.00E+00	0	0.00E+00	0	0.00E+00	0	0.00E+00	0	0.00E+00	0	0.00E+00	0
Np-237	0.00E+00	0	0.00E+00	0	0.00E+00	0	0.00E+00	0	0.00E+00	0	0.00E+00	0	0.00E+00	0	0.00E+00	0
Pa-231	0.00E+00	0	0.00E+00	0	0.00E+00	0	0.00E+00	0	0.00E+00	0	0.00E+00	0	0.00E+00	0	0.00E+00	0
Pb-210	0.00E+00	0	0.00E+00	0	0.00E+00	0	0.00E+00	0	0.00E+00	0	0.00E+00	0	0.00E+00	0	0.00E+00	0
Pu-238	0.00E+00	0	0.00E+00	0	0.00E+00	0	0.00E+00	0	0.00E+00	0	0.00E+00	0	0.00E+00	0	0.00E+00	0
Pu-239	0.00E+00	0	0.00E+00	0	0.00E+00	0	0.00E+00	0	0.00E+00	0	0.00E+00	0	0.00E+00	0	0.00E+00	0
Pu-240	0.00E+00	0	0.00E+00	0	0.00E+00	0	0.00E+00	0	0.00E+00	0	0.00E+00	0	0.00E+00	0	0.00E+00	0
Pu-241	0.00E+00	0	0.00E+00	0	0.00E+00	0	0.00E+00	0	0.00E+00	0	0.00E+00	0	0.00E+00	0	0.00E+00	0
Pu-242	0.00E+00	0	0.00E+00	0	0.00E+00	0	0.00E+00	0	0.00E+00	0	0.00E+00	0	0.00E+00	0	0.00E+00	0
Pu-244	0.00E+00	0	0.00E+00	0	0.00E+00	0	0.00E+00	0	0.00E+00	0	0.00E+00	0	0.00E+00	0	0.00E+00	0
Ra-226	0.00E+00	0	0.00E+00	0	0.00E+00	0	0.00E+00	0	0.00E+00	0	0.00E+00	0	0.00E+00	0	0.00E+00	0
Ra-228	0.00E+00	0	0.00E+00	0	0.00E+00	0	0.00E+00	0	0.00E+00	0	0.00E+00	0	0.00E+00	0	0.00E+00	0
Sr-90	0.00E+00	0	0.00E+00	0	0.00E+00	0	0.00E+00	0	0.00E+00	0	0.00E+00	0	0.00E+00	0	0.00E+00	0
Tc-99	1.58E-08	0	9.68E-05	0	0.00E+00	0	8.01E-04	0	9.11E-03	1	1.45E-05	0	1.90E-08	0	6.57E-01	98
Th-228	0.00E+00	0	0.00E+00	0	0.00E+00	0	0.00E+00	0	0.00E+00	0	0.00E+00	0	0.00E+00	0	0.00E+00	0
Th-229	0.00E+00	0	0.00E+00	0	0.00E+00	0	0.00E+00	0	0.00E+00	0	0.00E+00	0	0.00E+00	0	0.00E+00	0
Th-230	0.00E+00	0	0.00E+00	0	0.00E+00	0	0.00E+00	0	0.00E+00	0	0.00E+00	0	0.00E+00	0	0.00E+00	0
Th-232	0.00E+00	0	0.00E+00	0	0.00E+00	0	0.00E+00	0	0.00E+00	0	0.00E+00	0	0.00E+00	0	0.00E+00	0
U-232	0.00E+00	0	0.00E+00	0	0.00E+00	0	0.00E+00	0	0.00E+00	0	0.00E+00	0	0.00E+00	0	0.00E+00	0
U-233	0.00E+00	0	0.00E+00	0	0.00E+00	0	0.00E+00	0	0.00E+00	0	0.00E+00	0	0.00E+00	0	0.00E+00	0
U-234	0.00E+00	0	0.00E+00	0	0.00E+00	0	0.00E+00	0	0.00E+00	0	0.00E+00	0	0.00E+00	0	0.00E+00	0
U-235	0.00E+00	0	0.00E+00	0	0.00E+00	0	0.00E+00	0	0.00E+00	0	0.00E+00	0	0.00E+00	0	0.00E+00	0
U-236	0.00E+00	0	0.00E+00	0	0.00E+00	0	0.00E+00	0	0.00E+00	0	0.00E+00	0	0.00E+00	0	0.00E+00	0

U-238	0.00E+00	0	0.00E+00	0	0.00E+00	0	0.00E+00	0	0.00E+00	0	0.00E+00	0	0.00E+00	0	0.00E+00	0
Total	1.58E-08	0	9.68E-05	0	0.00E+00	0	8.01E-04	0	9.11E-03	1	1.45E-05	0	1.90E-08	0	6.58E-01	98

Total Dose Contributions TDOSE(i,p,t) for Individual Radionuclides (i) and Pathways (p)
in mrem/yr and as a Percentage of Total Dose at t = 2000 years

Directly from primary contamination and from release to atmosphere (Inhalation excludes radon)

Radio-	Ground		Inhalation		Radon		Plant		Meat		Milk		Soil		All Pathways*	
Nuclide	Dose	%	Dose	%	Dose	%	Dose	%	Dose	%	Dose	%	Dose	%	Dose	%
Ac-227	0.00E+00	0	0.00E+00	0	0.00E+00	0	0.00E+00	0	0.00E+00	0	0.00E+00	0	0.00E+00	0	0.00E+00	0
Am-241	0.00E+00	0	0.00E+00	0	0.00E+00	0	0.00E+00	0	0.00E+00	0	0.00E+00	0	0.00E+00	0	0.00E+00	0
Am-243	0.00E+00	0	0.00E+00	0	0.00E+00	0	0.00E+00	0	0.00E+00	0	0.00E+00	0	0.00E+00	0	0.00E+00	0
Be-10	0.00E+00	0	0.00E+00	0	0.00E+00	0	0.00E+00	0	0.00E+00	0	0.00E+00	0	0.00E+00	0	0.00E+00	0
C-14	0.00E+00	0	9.32E-19	0	0.00E+00	0	0.00E+00	0	0.00E+00	0	0.00E+00	0	0.00E+00	0	3.04E-10	0
Ca-41	0.00E+00	0	0.00E+00	0	0.00E+00	0	0.00E+00	0	0.00E+00	0	0.00E+00	0	0.00E+00	0	0.00E+00	0
Cm-243	0.00E+00	0	0.00E+00	0	0.00E+00	0	0.00E+00	0	0.00E+00	0	0.00E+00	0	0.00E+00	0	0.00E+00	0
Cm-244	0.00E+00	0	0.00E+00	0	0.00E+00	0	0.00E+00	0	0.00E+00	0	0.00E+00	0	0.00E+00	0	0.00E+00	0
Cm-245	0.00E+00	0	0.00E+00	0	0.00E+00	0	0.00E+00	0	0.00E+00	0	0.00E+00	0	0.00E+00	0	0.00E+00	0
Cm-246	0.00E+00	0	0.00E+00	0	0.00E+00	0	0.00E+00	0	0.00E+00	0	0.00E+00	0	0.00E+00	0	0.00E+00	0
Cm-247	0.00E+00	0	0.00E+00	0	0.00E+00	0	0.00E+00	0	0.00E+00	0	0.00E+00	0	0.00E+00	0	0.00E+00	0
Cm-248	0.00E+00	0	0.00E+00	0	0.00E+00	0	0.00E+00	0	0.00E+00	0	0.00E+00	0	0.00E+00	0	0.00E+00	0
H-3	0.00E+00	0	0.00E+00	0	0.00E+00	0	0.00E+00	0	0.00E+00	0	0.00E+00	0	0.00E+00	0	0.00E+00	0
I-129	0.00E+00	0	1.12E-17	0	0.00E+00	0	0.00E+00	0	0.00E+00	0	0.00E+00	0	0.00E+00	0	2.20E-04	0
K-40	0.00E+00	0	0.00E+00	0	0.00E+00	0	0.00E+00	0	0.00E+00	0	0.00E+00	0	0.00E+00	0	0.00E+00	0
Mo-93	0.00E+00	0	0.00E+00	0	0.00E+00	0	0.00E+00	0	0.00E+00	0	0.00E+00	0	0.00E+00	0	0.00E+00	0
Nb-93m	0.00E+00	0	0.00E+00	0	0.00E+00	0	0.00E+00	0	0.00E+00	0	0.00E+00	0	0.00E+00	0	0.00E+00	0
Nb-94	0.00E+00	0	0.00E+00	0	0.00E+00	0	0.00E+00	0	0.00E+00	0	0.00E+00	0	0.00E+00	0	0.00E+00	0
Ni-59	0.00E+00	0	0.00E+00	0	0.00E+00	0	0.00E+00	0	0.00E+00	0	0.00E+00	0	0.00E+00	0	0.00E+00	0
Np-237	0.00E+00	0	0.00E+00	0	0.00E+00	0	0.00E+00	0	0.00E+00	0	0.00E+00	0	0.00E+00	0	0.00E+00	0
Pa-231	0.00E+00	0	0.00E+00	0	0.00E+00	0	0.00E+00	0	0.00E+00	0	0.00E+00	0	0.00E+00	0	0.00E+00	0
Pb-210	0.00E+00	0	0.00E+00	0	0.00E+00	0	0.00E+00	0	0.00E+00	0	0.00E+00	0	0.00E+00	0	0.00E+00	0
Pu-238	0.00E+00	0	0.00E+00	0	0.00E+00	0	0.00E+00	0	0.00E+00	0	0.00E+00	0	0.00E+00	0	0.00E+00	0
Pu-239	0.00E+00	0	0.00E+00	0	0.00E+00	0	0.00E+00	0	0.00E+00	0	0.00E+00	0	0.00E+00	0	0.00E+00	0
Pu-240	0.00E+00	0	0.00E+00	0	0.00E+00	0	0.00E+00	0	0.00E+00	0	0.00E+00	0	0.00E+00	0	0.00E+00	0
Pu-241	0.00E+00	0	0.00E+00	0	0.00E+00	0	0.00E+00	0	0.00E+00	0	0.00E+00	0	0.00E+00	0	0.00E+00	0
Pu-242	0.00E+00	0	0.00E+00	0	0.00E+00	0	0.00E+00	0	0.00E+00	0	0.00E+00	0	0.00E+00	0	0.00E+00	0
Pu-244	0.00E+00	0	0.00E+00	0	0.00E+00	0	0.00E+00	0	0.00E+00	0	0.00E+00	0	0.00E+00	0	0.00E+00	0
Ra-226	0.00E+00	0	0.00E+00	0	0.00E+00	0	0.00E+00	0	0.00E+00	0	0.00E+00	0	0.00E+00	0	0.00E+00	0
Ra-228	0.00E+00	0	0.00E+00	0	0.00E+00	0	0.00E+00	0	0.00E+00	0	0.00E+00	0	0.00E+00	0	0.00E+00	0
Sr-90	0.00E+00	0	0.00E+00	0	0.00E+00	0	0.00E+00	0	0.00E+00	0	0.00E+00	0	0.00E+00	0	0.00E+00	0
Tc-99	0.00E+00	0	6.40E-09	0	0.00E+00	0	0.00E+00	0	0.00E+00	0	0.00E+00	0	0.00E+00	0	6.67E-01	100
Th-228	0.00E+00	0	0.00E+00	0	0.00E+00	0	0.00E+00	0	0.00E+00	0	0.00E+00	0	0.00E+00	0	0.00E+00	0
Th-229	0.00E+00	0	0.00E+00	0	0.00E+00	0	0.00E+00	0	0.00E+00	0	0.00E+00	0	0.00E+00	0	0.00E+00	0
Th-230	0.00E+00	0	0.00E+00	0	0.00E+00	0	0.00E+00	0	0.00E+00	0	0.00E+00	0	0.00E+00	0	0.00E+00	0
Th-232	0.00E+00	0	0.00E+00	0	0.00E+00	0	0.00E+00	0	0.00E+00	0	0.00E+00	0	0.00E+00	0	0.00E+00	0
U-232	0.00E+00	0	0.00E+00	0	0.00E+00	0	0.00E+00	0	0.00E+00	0	0.00E+00	0	0.00E+00	0	0.00E+00	0
U-233	0.00E+00	0	0.00E+00	0	0.00E+00	0	0.00E+00	0	0.00E+00	0	0.00E+00	0	0.00E+00	0	0.00E+00	0
U-234	0.00E+00	0	0.00E+00	0	0.00E+00	0	0.00E+00	0	0.00E+00	0	0.00E+00	0	0.00E+00	0	0.00E+00	0
U-235	0.00E+00	0	0.00E+00	0	0.00E+00	0	0.00E+00	0	0.00E+00	0	0.00E+00	0	0.00E+00	0	0.00E+00	0
U-236	0.00E+00	0	0.00E+00	0	0.00E+00	0	0.00E+00	0	0.00E+00	0	0.00E+00	0	0.00E+00	0	0.00E+00	0

U-238	0.00E+00	0	0.00E+00	0	0.00E+00	0	0.00E+00	0	0.00E+00	0	0.00E+00	0	0.00E+00	0	0.00E+00	0	
Total	0.00E+00	0	6.40E-09	0	0.00E+00	0	0.00E+00	0	0.00E+00	0	0.00E+00	0	0.00E+00	0	6.68E-01	100	

*Sum of dose from all releases and from primary contamination.

Total Dose Contributions TDOSE(i,p,t) for Individual Radionuclides (i) and Pathways (p)
in mrem/yr and as a Percentage of Total Dose at t = 10000 years

From releases to ground water and to surface water

Radio-	Ground		Fish		Radon		Plant		Meat		Milk		Soil		Water	
Nuclide	Dose	%	Dose	%	Dose	%	Dose	%	Dose	%	Dose	%	Dose	%	Dose	%
Ac-227	0.00E+00	0	0.00E+00	0	0.00E+00	0	0.00E+00	0	0.00E+00	0	0.00E+00	0	0.00E+00	0	0.00E+00	0
Am-241	5.17E-29	0	1.52E-28	0	0.00E+00	0	5.41E-28	0	6.97E-29	0	7.68E-31	0	9.03E-31	0	1.36E-14	0
Am-243	6.26E-32	0	2.36E-27	0	0.00E+00	0	5.71E-27	0	2.21E-28	0	1.83E-30	0	9.79E-30	0	3.83E-14	0
Be-10	0.00E+00	0	0.00E+00	0	0.00E+00	0	0.00E+00	0	0.00E+00	0	0.00E+00	0	0.00E+00	0	0.00E+00	0
C-14	0.00E+00	0	0.00E+00	0	0.00E+00	0	0.00E+00	0	0.00E+00	0	0.00E+00	0	0.00E+00	0	0.00E+00	0
Ca-41	0.00E+00	0	3.39E-21	0	0.00E+00	0	1.72E-20	0	4.42E-20	0	6.90E-21	0	9.24E-24	0	3.05E-11	0
Cm-243	8.54E-34	0	3.21E-29	0	0.00E+00	0	7.77E-29	0	3.01E-30	0	2.49E-32	0	1.34E-31	0	4.33E-16	0
Cm-244	1.15E-31	0	1.00E-26	0	0.00E+00	0	2.42E-26	0	9.37E-28	0	7.75E-30	0	4.16E-29	0	1.36E-13	0
Cm-245	4.50E-29	0	1.11E-27	0	0.00E+00	0	2.69E-27	0	2.73E-28	0	1.53E-29	0	5.25E-30	0	3.44E-13	0
Cm-246	5.22E-30	0	2.53E-27	0	0.00E+00	0	6.11E-27	0	6.11E-28	0	3.41E-29	0	1.05E-29	0	3.61E-14	0
Cm-247	1.19E-28	0	5.85E-28	0	0.00E+00	0	1.41E-27	0	1.45E-28	0	8.23E-30	0	2.46E-30	0	3.59E-14	0
Cm-248	2.60E-29	0	1.25E-28	0	0.00E+00	0	3.03E-28	0	3.12E-29	0	1.77E-30	0	5.22E-31	0	1.91E-15	0
H-3	0.00E+00	0	0.00E+00	0	0.00E+00	0	0.00E+00	0	0.00E+00	0	0.00E+00	0	0.00E+00	0	0.00E+00	0
I-129	1.59E-07	0	6.43E-04	1	0.00E+00	0	1.20E-03	1	4.35E-02	38	3.04E-03	3	2.89E-07	0	6.53E-02	57
K-40	1.44E-17	0	1.95E-16	0	0.00E+00	0	4.41E-17	0	4.55E-16	0	4.30E-17	0	2.13E-20	0	7.07E-08	0
Mo-93	0.00E+00	0	0.00E+00	0	0.00E+00	0	0.00E+00	0	0.00E+00	0	0.00E+00	0	0.00E+00	0	2.82E-39	0
Nb-93m	0.00E+00	0	0.00E+00	0	0.00E+00	0	0.00E+00	0	0.00E+00	0	0.00E+00	0	0.00E+00	0	0.00E+00	0
Nb-94	0.00E+00	0	0.00E+00	0	0.00E+00	0	0.00E+00	0	0.00E+00	0	0.00E+00	0	0.00E+00	0	0.00E+00	0
Ni-59	0.00E+00	0	0.00E+00	0	0.00E+00	0	0.00E+00	0	0.00E+00	0	0.00E+00	0	0.00E+00	0	0.00E+00	0
Np-237	2.47E-27	0	7.25E-27	0	0.00E+00	0	2.58E-26	0	3.32E-27	0	3.66E-29	0	4.31E-29	0	6.28E-13	0
Pa-231	0.00E+00	0	0.00E+00	0	0.00E+00	0	0.00E+00	0	0.00E+00	0	0.00E+00	0	0.00E+00	0	0.00E+00	0
Pb-210	0.00E+00	0	0.00E+00	0	0.00E+00	0	0.00E+00	0	0.00E+00	0	0.00E+00	0	0.00E+00	0	0.00E+00	0
Pu-238	2.23E-42	0	3.12E-39	0	0.00E+00	0	2.30E-38	0	4.45E-37	0	2.64E-39	0	3.85E-41	0	3.71E-18	0
Pu-239	8.66E-29	0	3.26E-24	0	0.00E+00	0	7.88E-24	0	3.05E-25	0	2.52E-27	0	1.35E-26	0	4.87E-11	0
Pu-240	1.92E-29	0	1.66E-24	0	0.00E+00	0	4.02E-24	0	1.56E-25	0	1.29E-27	0	6.91E-27	0	2.42E-11	0
Pu-241	5.74E-30	0	1.69E-29	0	0.00E+00	0	6.00E-29	0	7.73E-30	0	8.52E-32	0	1.00E-31	0	1.53E-15	0
Pu-242	5.87E-31	0	1.18E-26	0	0.00E+00	0	2.85E-26	0	1.11E-27	0	9.14E-30	0	4.91E-29	0	1.80E-13	0
Pu-244	4.72E-29	0	4.30E-28	0	0.00E+00	0	1.04E-27	0	4.03E-29	0	3.33E-31	0	1.79E-30	0	6.59E-15	0
Ra-226	0.00E+00	0	0.00E+00	0	0.00E+00	0	0.00E+00	0	0.00E+00	0	0.00E+00	0	0.00E+00	0	0.00E+00	0
Ra-228	0.00E+00	0	0.00E+00	0	0.00E+00	0	0.00E+00	0	0.00E+00	0	0.00E+00	0	0.00E+00	0	0.00E+00	0
Sr-90	0.00E+00	0	0.00E+00	0	0.00E+00	0	0.00E+00	0	0.00E+00	0	0.00E+00	0	0.00E+00	0	0.00E+00	0
Tc-99	5.58E-26	0	3.38E-22	0	0.00E+00	0	2.81E-21	0	3.19E-20	0	5.07E-23	0	6.69E-26	0	6.55E-29	0
Th-228	0.00E+00	0	0.00E+00	0	0.00E+00	0	0.00E+00	0	0.00E+00	0	0.00E+00	0	0.00E+00	0	0.00E+00	0
Th-229	0.00E+00	0	0.00E+00	0	0.00E+00	0	0.00E+00	0	0.00E+00	0	0.00E+00	0	0.00E+00	0	0.00E+00	0
Th-230	0.00E+00	0	0.00E+00	0	0.00E+00	0	0.00E+00	0	0.00E+00	0	0.00E+00	0	0.00E+00	0	0.00E+00	0
Th-232	0.00E+00	0	0.00E+00	0	0.00E+00	0	0.00E+00	0	0.00E+00	0	0.00E+00	0	0.00E+00	0	0.00E+00	0
U-232	0.00E+00	0	0.00E+00	0	0.00E+00	0	0.00E+00	0	0.00E+00	0	0.00E+00	0	0.00E+00	0	0.00E+00	0
U-233	4.43E-38	0	3.44E-36	0	0.00E+00	0	2.54E-35	0	4.92E-34	0	2.91E-36	0	4.63E-38	0	8.01E-15	0
U-234	3.72E-38	0	5.10E-35	0	0.00E+00	0	3.76E-34	0	7.28E-33	0	4.32E-35	0	6.31E-37	0	6.82E-14	0
U-235	3.39E-36	0	3.14E-36	0	0.00E+00	0	2.31E-35	0	4.48E-34	0	2.66E-36	0	3.94E-38	0	9.41E-14	0
U-236	1.97E-40	0	7.02E-37	0	0.00E+00	0	5.17E-36	0	1.00E-34	0	5.94E-37	0	8.65E-39	0	7.68E-19	0

U-238	6.90E-36	0	3.19E-35	0	0.00E+00	0	2.35E-34	0	4.55E-33	0	2.70E-35	0	3.93E-37	0	1.07E-15	0
Total	1.59E-07	0	6.43E-04	1	0.00E+00	0	1.20E-03	1	4.35E-02	38	3.04E-03	3	2.89E-07	0	6.53E-02	57

Parent Dose Report
Title : Site 7 Base Case Model
File : BC_V01.ROF

Total Dose Contributions TDOSE(i,p,t) for Individual Radionuclides (i) and Pathways (p)
in mrem/yr and as a Percentage of Total Dose at t = 10000 years

Directly from primary contamination and from release to atmosphere (Inhalation excludes radon)

Radio-	Ground		Inhalation		Radon		Plant		Meat		Milk		Soil		All Pathways*	
Nuclide	Dose	%	Dose	%	Dose	%	Dose	%	Dose	%	Dose	%	Dose	%	Dose	%
Ac-227	0.00E+00	0	0.00E+00	0	0.00E+00	0	0.00E+00	0	0.00E+00	0	0.00E+00	0	0.00E+00	0	0.00E+00	0
Am-241	0.00E+00	0	7.71E-30	0	0.00E+00	0	0.00E+00	0	0.00E+00	0	0.00E+00	0	0.00E+00	0	1.36E-14	0
Am-243	0.00E+00	0	8.78E-29	0	0.00E+00	0	0.00E+00	0	0.00E+00	0	0.00E+00	0	0.00E+00	0	3.83E-14	0
Be-10	0.00E+00	0	0.00E+00	0	0.00E+00	0	0.00E+00	0	0.00E+00	0	0.00E+00	0	0.00E+00	0	0.00E+00	0
C-14	0.00E+00	0	0.00E+00	0	0.00E+00	0	0.00E+00	0	0.00E+00	0	0.00E+00	0	0.00E+00	0	0.00E+00	0
Ca-41	0.00E+00	0	1.53E-25	0	0.00E+00	0	0.00E+00	0	0.00E+00	0	0.00E+00	0	0.00E+00	0	3.05E-11	0
Cm-243	0.00E+00	0	1.20E-30	0	0.00E+00	0	0.00E+00	0	0.00E+00	0	0.00E+00	0	0.00E+00	0	4.33E-16	0
Cm-244	0.00E+00	0	3.73E-28	0	0.00E+00	0	0.00E+00	0	0.00E+00	0	0.00E+00	0	0.00E+00	0	1.36E-13	0
Cm-245	0.00E+00	0	4.64E-29	0	0.00E+00	0	0.00E+00	0	0.00E+00	0	0.00E+00	0	0.00E+00	0	3.44E-13	0
Cm-246	0.00E+00	0	9.32E-29	0	0.00E+00	0	0.00E+00	0	0.00E+00	0	0.00E+00	0	0.00E+00	0	3.61E-14	0
Cm-247	0.00E+00	0	2.16E-29	0	0.00E+00	0	0.00E+00	0	0.00E+00	0	0.00E+00	0	0.00E+00	0	3.59E-14	0
Cm-248	0.00E+00	0	4.55E-30	0	0.00E+00	0	0.00E+00	0	0.00E+00	0	0.00E+00	0	0.00E+00	0	1.91E-15	0
H-3	0.00E+00	0	0.00E+00	0	0.00E+00	0	0.00E+00	0	0.00E+00	0	0.00E+00	0	0.00E+00	0	0.00E+00	0
I-129	0.00E+00	0	5.51E-09	0	0.00E+00	0	0.00E+00	0	0.00E+00	0	0.00E+00	0	0.00E+00	0	1.14E-01	100
K-40	0.00E+00	0	4.91E-21	0	0.00E+00	0	0.00E+00	0	0.00E+00	0	0.00E+00	0	0.00E+00	0	7.07E-08	0
Mo-93	0.00E+00	0	0.00E+00	0	0.00E+00	0	0.00E+00	0	0.00E+00	0	0.00E+00	0	0.00E+00	0	2.82E-39	0
Nb-93m	0.00E+00	0	0.00E+00	0	0.00E+00	0	0.00E+00	0	0.00E+00	0	0.00E+00	0	0.00E+00	0	0.00E+00	0
Nb-94	0.00E+00	0	0.00E+00	0	0.00E+00	0	0.00E+00	0	0.00E+00	0	0.00E+00	0	0.00E+00	0	0.00E+00	0
Ni-59	0.00E+00	0	0.00E+00	0	0.00E+00	0	0.00E+00	0	0.00E+00	0	0.00E+00	0	0.00E+00	0	0.00E+00	0
Np-237	0.00E+00	0	3.68E-28	0	0.00E+00	0	0.00E+00	0	0.00E+00	0	0.00E+00	0	0.00E+00	0	6.28E-13	0
Pa-231	0.00E+00	0	0.00E+00	0	0.00E+00	0	0.00E+00	0	0.00E+00	0	0.00E+00	0	0.00E+00	0	0.00E+00	0
Pb-210	0.00E+00	0	0.00E+00	0	0.00E+00	0	0.00E+00	0	0.00E+00	0	0.00E+00	0	0.00E+00	0	0.00E+00	0
Pu-238	0.00E+00	0	1.43E-40	0	0.00E+00	0	0.00E+00	0	0.00E+00	0	0.00E+00	0	0.00E+00	0	3.71E-18	0
Pu-239	0.00E+00	0	1.22E-25	0	0.00E+00	0	0.00E+00	0	0.00E+00	0	0.00E+00	0	0.00E+00	0	4.87E-11	0
Pu-240	0.00E+00	0	6.20E-26	0	0.00E+00	0	0.00E+00	0	0.00E+00	0	0.00E+00	0	0.00E+00	0	2.42E-11	0
Pu-241	0.00E+00	0	8.56E-31	0	0.00E+00	0	0.00E+00	0	0.00E+00	0	0.00E+00	0	0.00E+00	0	1.53E-15	0
Pu-242	0.00E+00	0	4.40E-28	0	0.00E+00	0	0.00E+00	0	0.00E+00	0	0.00E+00	0	0.00E+00	0	1.80E-13	0
Pu-244	0.00E+00	0	1.59E-29	0	0.00E+00	0	0.00E+00	0	0.00E+00	0	0.00E+00	0	0.00E+00	0	6.59E-15	0
Ra-226	0.00E+00	0	0.00E+00	0	0.00E+00	0	0.00E+00	0	0.00E+00	0	0.00E+00	0	0.00E+00	0	0.00E+00	0
Ra-228	0.00E+00	0	0.00E+00	0	0.00E+00	0	0.00E+00	0	0.00E+00	0	0.00E+00	0	0.00E+00	0	0.00E+00	0
Sr-90	0.00E+00	0	0.00E+00	0	0.00E+00	0	0.00E+00	0	0.00E+00	0	0.00E+00	0	0.00E+00	0	0.00E+00	0
Tc-99	0.00E+00	0	2.25E-26	0	0.00E+00	0	0.00E+00	0	0.00E+00	0	0.00E+00	0	0.00E+00	0	3.51E-20	0
Th-228	0.00E+00	0	0.00E+00	0	0.00E+00	0	0.00E+00	0	0.00E+00	0	0.00E+00	0	0.00E+00	0	0.00E+00	0
Th-229	0.00E+00	0	0.00E+00	0	0.00E+00	0	0.00E+00	0	0.00E+00	0	0.00E+00	0	0.00E+00	0	0.00E+00	0
Th-230	0.00E+00	0	0.00E+00	0	0.00E+00	0	0.00E+00	0	0.00E+00	0	0.00E+00	0	0.00E+00	0	0.00E+00	0
Th-232	0.00E+00	0	0.00E+00	0	0.00E+00	0	0.00E+00	0	0.00E+00	0	0.00E+00	0	0.00E+00	0	0.00E+00	0
U-232	0.00E+00	0	0.00E+00	0	0.00E+00	0	0.00E+00	0	0.00E+00	0	0.00E+00	0	0.00E+00	0	0.00E+00	0
U-233	0.00E+00	0	1.80E-37	0	0.00E+00	0	0.00E+00	0	0.00E+00	0	0.00E+00	0	0.00E+00	0	8.01E-15	0
U-234	0.00E+00	0	2.35E-36	0	0.00E+00	0	0.00E+00	0	0.00E+00	0	0.00E+00	0	0.00E+00	0	6.82E-14	0
U-235	0.00E+00	0	1.42E-37	0	0.00E+00	0	0.00E+00	0	0.00E+00	0	0.00E+00	0	0.00E+00	0	9.41E-14	0
U-236	0.00E+00	0	3.16E-38	0	0.00E+00	0	0.00E+00	0	0.00E+00	0	0.00E+00	0	0.00E+00	0	7.68E-19	0

U-238	0.00E+00	0	1.28E-36	0	0.00E+00	0	0.00E+00	0	0.00E+00	0	0.00E+00	0	0.00E+00	0	1.07E-15	0
Total	0.00E+00	0	5.51E-09	0	0.00E+00	0	0.00E+00	0	0.00E+00	0	0.00E+00	0	0.00E+00	0	1.14E-01	100

*Sum of dose from all releases and from primary contamination.

Parent Dose Report
Title : Site 7 Base Case Model
File : BC_V01.ROF

Dose/Source Ratios Summed Over All Pathways
Parent and Progeny Principal Radionuclide Contributions Indicated

Parent (i)	Product (j)	Thread Fraction	DSR(j,t) (mrem/yr)/(pCi/g) 0.000E+00	1.000E+00	2.000E+02	4.000E+02	5.000E+02	6.000E+02	8.000E+02	1.000E+03	2.000E+03	1.000E+04
Ac-227+D	Ac-227+D	1.000E+00	9.793E-30	9.504E-30	1.684E-32	2.531E-35	8.972E-37	3.105E-38	3.215E-41	0.000E+00	0.000E+00	0.000E+00
Am-241	Am-241	1.000E+00	0.000E+00	0.000E+00	0.000E+00	0.000E+00	0.000E+00	0.000E+00	0.000E+00	0.000E+00	0.000E+00	0.000E+00
Am-241	Np-237+D	1.000E+00	1.050E-41	3.147E-41	3.613E-39	5.444E-39	5.434E-39	5.072E-39	3.556E-39	1.306E-39	0.000E+00	5.536E-17
Am-241	U-233	1.000E+00	0.000E+00	0.000E+00	0.000E+00	0.000E+00	0.000E+00	0.000E+00	0.000E+00	0.000E+00	0.000E+00	1.746E-16
Am-241	Th-229+D	1.000E+00	1.077E-40	4.548E-40	6.677E-35	4.295E-34	6.911E-34	9.576E-34	1.264E-33	7.641E-34	0.000E+00	1.379E-18
Am-241	∑DSR(j)		1.182E-40	4.863E-40	6.677E-35	4.295E-34	6.911E-34	9.576E-34	1.264E-33	7.641E-34	0.000E+00	2.313E-16
Am-243+D	Am-243+D	1.000E+00	1.800E-39	1.800E-39	1.766E-39	1.516E-39	1.287E-39	1.062E-39	6.250E-40	2.038E-40	0.000E+00	0.000E+00
Am-243+D	Pu-239+D	1.000E+00	0.000E+00	0.000E+00	1.822E-44	3.223E-44	3.503E-44	3.503E-44	2.803E-44	1.121E-44	0.000E+00	1.288E-14
Am-243+D	U-235+D	1.000E+00	0.000E+00	0.000E+00	0.000E+00	0.000E+00	0.000E+00	0.000E+00	0.000E+00	0.000E+00	0.000E+00	3.952E-18
Am-243+D	Pa-231	1.000E+00	0.000E+00	0.000E+00	0.000E+00	0.000E+00	0.000E+00	0.000E+00	0.000E+00	0.000E+00	0.000E+00	3.580E-20
Am-243+D	Ac-227+D	1.000E+00	0.000E+00	0.000E+00	5.200E-42	4.392E-41	7.641E-41	1.128E-40	1.651E-40	1.088E-40	0.000E+00	3.626E-19
Am-243	∑DSR(j)		1.800E-39	1.800E-39	1.772E-39	1.560E-39	1.363E-39	1.175E-39	7.902E-40	3.126E-40	0.000E+00	1.288E-14
Be-10	Be-10	1.000E+00	0.000E+00	0.000E+00	0.000E+00	0.000E+00	0.000E+00	0.000E+00	0.000E+00	0.000E+00	0.000E+00	0.000E+00
C-14	C-14	1.000E+00	0.000E+00	0.000E+00	0.000E+00	2.602E-01	1.887E+00	1.000E+00	2.666E-01	1.312E-01	5.633E-10	0.000E+00
Ca-41	Ca-41	1.000E+00	0.000E+00	0.000E+00	0.000E+00	0.000E+00	0.000E+00	0.000E+00	0.000E+00	0.000E+00	0.000E+00	7.255E-10
Cm-243	Cm-243	2.400E-03	1.430E-41	1.398E-41	1.233E-43	0.000E+00	0.000E+00	0.000E+00	0.000E+00	0.000E+00	0.000E+00	0.000E+00
Cm-243	Am-243+D	2.400E-03	0.000E+00	0.000E+00	1.682E-44	1.261E-44	1.261E-44	9.809E-45	7.006E-45	2.803E-45	0.000E+00	0.000E+00
Cm-243	Pu-239+D	2.400E-03	0.000E+00	0.000E+00	0.000E+00	0.000E+00	0.000E+00	0.000E+00	0.000E+00	0.000E+00	0.000E+00	1.129E-19
Cm-243	U-235+D	2.400E-03	0.000E+00	0.000E+00	0.000E+00	0.000E+00	0.000E+00	0.000E+00	0.000E+00	0.000E+00	0.000E+00	3.500E-23
Cm-243	Pa-231	2.400E-03	0.000E+00	0.000E+00	0.000E+00	0.000E+00	0.000E+00	0.000E+00	0.000E+00	0.000E+00	0.000E+00	3.165E-25
Cm-243	Ac-227+D	2.400E-03	0.000E+00	0.000E+00	0.000E+00	0.000E+00	0.000E+00	0.000E+00	0.000E+00	0.000E+00	0.000E+00	3.204E-24
Cm-243	∑DSR(j)		1.430E-41	1.398E-41	1.401E-43	1.261E-44	1.261E-44	9.809E-45	7.006E-45	2.803E-45	0.000E+00	1.130E-19
Cm-243	Cm-243	9.976E-01	5.945E-39	5.811E-39	5.077E-41	3.812E-43	2.943E-44	2.803E-45	0.000E+00	0.000E+00	0.000E+00	0.000E+00
Cm-243	Pu-239+D	9.976E-01	0.000E+00	0.000E+00	2.803E-45	2.803E-45	2.803E-45	2.803E-45	0.000E+00	0.000E+00	0.000E+00	1.007E-15
Cm-243	U-235+D	9.976E-01	0.000E+00	0.000E+00	0.000E+00	0.000E+00	0.000E+00	0.000E+00	0.000E+00	0.000E+00	0.000E+00	2.723E-19
Cm-243	Pa-231	9.976E-01	0.000E+00	0.000E+00	0.000E+00	0.000E+00	0.000E+00	0.000E+00	0.000E+00	0.000E+00	0.000E+00	2.532E-21
Cm-243	Ac-227+D	9.976E-01	0.000E+00	0.000E+00	2.336E-42	1.189E-41	1.717E-41	2.165E-41	2.450E-41	1.316E-41	0.000E+00	2.571E-20
Cm-243	∑DSR(j)		5.945E-39	5.811E-39	5.311E-41	1.228E-41	1.720E-41	2.165E-41	2.450E-41	1.316E-41	0.000E+00	1.007E-15
Cm-244	Cm-244	1.371E-06	1.281E-36	1.236E-36	6.057E-40	2.508E-43	4.204E-45	0.000E+00	0.000E+00	0.000E+00	0.000E+00	0.000E+00
Cm-244	Cm-244	5.750E-08	5.372E-38	5.184E-38	2.540E-41	9.809E-45	0.000E+00	0.000E+00	0.000E+00	0.000E+00	0.000E+00	0.000E+00
Cm-244	Pu-240	5.750E-08	0.000E+00	0.000E+00	0.000E+00	0.000E+00	0.000E+00	0.000E+00	0.000E+00	0.000E+00	0.000E+00	6.156E-23
Cm-244	∑DSR(j)		5.372E-38	5.184E-38	2.540E-41	9.809E-45	0.000E+00	0.000E+00	0.000E+00	0.000E+00	0.000E+00	6.156E-23

Parent Dose Report
Title : Site 7 Base Case Model
File : BC_V01.ROF

Dose/Source Ratios Summed Over All Pathways
Parent and Progeny Principal Radionuclide Contributions Indicated

Parent (i)	Product (j)	Thread Fraction	DSR(j,t) (mrem/yr)/(pCi/g) 0.000E+00	1.000E+00	2.000E+02	4.000E+02	5.000E+02	6.000E+02	8.000E+02	1.000E+03	2.000E+03	1.000E+04
Cm-244	Cm-244	1.000E+00	9.342E-31	9.016E-31	4.418E-34	1.826E-37	3.389E-39	6.154E-41	1.682E-44	0.000E+00	0.000E+00	0.000E+00
Cm-244	Pu-240	1.000E+00	0.000E+00	0.000E+00	0.000E+00	0.000E+00	0.000E+00	0.000E+00	0.000E+00	0.000E+00	0.000E+00	1.071E-15
Cm-244	U-236	1.000E+00	0.000E+00	0.000E+00	0.000E+00	0.000E+00	0.000E+00	0.000E+00	0.000E+00	0.000E+00	0.000E+00	8.748E-18
Cm-244	Th-232	1.000E+00	0.000E+00	0.000E+00	0.000E+00	0.000E+00	0.000E+00	0.000E+00	0.000E+00	0.000E+00	0.000E+00	1.309E-26
Cm-244	Ra-228+D	1.000E+00	0.000E+00	0.000E+00	6.339E-42	2.618E-41	3.616E-41	4.424E-41	4.819E-41	2.527E-41	0.000E+00	7.253E-26
Cm-244	Th-228+D	1.000E+00	4.344E-44	3.083E-43	2.173E-37	9.131E-37	1.265E-36	1.551E-36	1.694E-36	8.898E-37	0.000E+00	1.130E-26
Cm-244	∑DSR(j)		9.342E-31	9.016E-31	4.420E-34	1.096E-36	1.269E-36	1.552E-36	1.694E-36	8.898E-37	0.000E+00	1.079E-15
Cm-245	Cm-245	6.100E-09	0.000E+00	0.000E+00	0.000E+00	0.000E+00	0.000E+00	0.000E+00	0.000E+00	0.000E+00	0.000E+00	2.523E-21
Cm-245	Cm-245	1.000E+00	0.000E+00	0.000E+00	0.000E+00	0.000E+00	0.000E+00	0.000E+00	0.000E+00	0.000E+00	0.000E+00	4.137E-13
Cm-245	Pu-241	1.000E+00	0.000E+00	0.000E+00	0.000E+00	0.000E+00	0.000E+00	0.000E+00	0.000E+00	0.000E+00	0.000E+00	8.922E-15
Cm-245	Am-241	1.000E+00	0.000E+00	0.000E+00	0.000E+00	0.000E+00	0.000E+00	0.000E+00	0.000E+00	0.000E+00	0.000E+00	8.528E-12
Cm-245	Np-237+D	1.000E+00	0.000E+00	0.000E+00	5.004E-40	1.742E-39	2.262E-39	2.619E-39	2.581E-39	1.236E-39	0.000E+00	3.336E-14
Cm-245	U-233	1.000E+00	0.000E+00	0.000E+00	0.000E+00	0.000E+00	0.000E+00	0.000E+00	0.000E+00	0.000E+00	0.000E+00	4.310E-16
Cm-245	Th-229+D	1.000E+00	0.000E+00	7.287E-44	3.780E-36	5.849E-35	1.228E-34	2.106E-34	3.866E-34	3.007E-34	0.000E+00	2.137E-16
Cm-245	∑DSR(j)		0.000E+00	7.287E-44	3.780E-36	5.850E-35	1.228E-34	2.106E-34	3.866E-34	3.007E-34	0.000E+00	8.985E-12
Cm-245	Cm-245	2.450E-05	0.000E+00	0.000E+00	0.000E+00	0.000E+00	0.000E+00	0.000E+00	0.000E+00	0.000E+00	0.000E+00	1.014E-17
Cm-245	Pu-241+D	2.450E-05	0.000E+00	0.000E+00	0.000E+00	0.000E+00	0.000E+00	0.000E+00	0.000E+00	0.000E+00	0.000E+00	2.631E-19
Cm-245	Np-237+D	2.450E-05	0.000E+00	0.000E+00	1.093E-43	1.836E-43	1.836E-43	1.836E-43	1.457E-43	7.287E-44	0.000E+00	2.635E-20
Cm-245	U-233	2.450E-05	0.000E+00	0.000E+00	0.000E+00	0.000E+00	0.000E+00	0.000E+00	0.000E+00	0.000E+00	0.000E+00	7.652E-20
Cm-245	Th-229+D	2.450E-05	0.000E+00	0.000E+00	1.319E-39	1.047E-38	1.796E-38	2.624E-38	3.788E-38	2.472E-38	0.000E+00	6.006E-22
Cm-245	∑DSR(j)		0.000E+00	0.000E+00	1.319E-39	1.047E-38	1.796E-38	2.624E-38	3.788E-38	2.472E-38	0.000E+00	1.050E-17
Cm-246	Cm-246	2.630E-04	4.669E-29	4.668E-29	4.535E-29	3.851E-29	3.253E-29	2.671E-29	1.556E-29	5.020E-30	0.000E+00	5.709E-17
Cm-246	Cm-246	5.539E-06	9.832E-31	9.830E-31	9.549E-31	8.110E-31	6.850E-31	5.625E-31	3.276E-31	1.057E-31	0.000E+00	1.202E-18
Cm-246	Pu-242	5.539E-06	9.671E-40	2.901E-39	3.823E-37	6.579E-37	6.996E-37	6.943E-37	5.469E-37	2.238E-37	0.000E+00	5.645E-20
Cm-246	∑DSR(j)		9.832E-31	9.830E-31	9.549E-31	8.110E-31	6.850E-31	5.625E-31	3.276E-31	1.057E-31	0.000E+00	1.259E-18
Cm-246	Cm-246	5.449E-07	9.672E-32	9.670E-32	9.394E-32	7.978E-32	6.739E-32	5.534E-32	3.223E-32	1.040E-32	0.000E+00	1.183E-19
Cm-246	Pu-242	5.449E-07	9.514E-41	2.854E-40	3.761E-38	6.473E-38	6.882E-38	6.830E-38	5.380E-38	2.202E-38	0.000E+00	5.553E-21
Cm-246	U-238	5.449E-07	0.000E+00	0.000E+00	0.000E+00	0.000E+00	0.000E+00	0.000E+00	0.000E+00	0.000E+00	0.000E+00	2.319E-25
Cm-246	∑DSR(j)		9.672E-32	9.670E-32	9.394E-32	7.978E-32	6.739E-32	5.534E-32	3.223E-32	1.040E-32	0.000E+00	1.238E-19

Parent Dose Report
Title : Site 7 Base Case Model
File : BC_V01.ROF

Dose/Source Ratios Summed Over All Pathways
Parent and Progeny Principal Radionuclide Contributions Indicated

Parent (i)	Product (j)	Thread Fraction	DSR(j,t) (mrem/yr)/(pCi/g) 0.000E+00	1.000E+00	2.000E+02	4.000E+02	5.000E+02	6.000E+02	8.000E+02	1.000E+03	2.000E+03	1.000E+04
Cm-246	Cm-246	9.997E-01	1.775E-25	1.774E-25	1.724E-25	1.464E-25	1.236E-25	1.015E-25	5.913E-26	1.908E-26	0.000E+00	2.170E-13
Cm-246	Pu-242	9.997E-01	1.746E-34	5.237E-34	6.900E-32	1.188E-31	1.263E-31	1.253E-31	9.872E-32	4.040E-32	0.000E+00	1.019E-14
Cm-246	U-238+D	9.997E-01	3.503E-44	1.317E-43	6.394E-40	2.209E-39	2.942E-39	3.512E-39	3.706E-39	1.905E-39	0.000E+00	4.634E-19
Cm-246	U-234	9.997E-01	0.000E+00	0.000E+00	0.000E+00	0.000E+00	0.000E+00	0.000E+00	0.000E+00	0.000E+00	0.000E+00	2.836E-22
Cm-246	Th-230	9.997E-01	0.000E+00	0.000E+00	0.000E+00	0.000E+00	0.000E+00	0.000E+00	0.000E+00	0.000E+00	0.000E+00	8.725E-26
Cm-246	Ra-226+D	9.997E-01	0.000E+00	0.000E+00	1.850E-43	4.962E-42	1.282E-41	2.630E-41	6.512E-41	6.471E-41	0.000E+00	1.277E-26
Cm-246	Pb-210+D	9.997E-01	0.000E+00	0.000E+00	0.000E+00	0.000E+00	0.000E+00	0.000E+00	0.000E+00	0.000E+00	0.000E+00	2.179E-24
Cm-246	∑DSR(j)		1.775E-25	1.774E-25	1.724E-25	1.464E-25	1.236E-25	1.015E-25	5.913E-26	1.908E-26	0.000E+00	2.272E-13
Cm-247+D	Cm-247+D	1.000E+00	6.600E-32	6.600E-32	6.600E-32	5.771E-32	4.946E-32	4.121E-32	2.471E-32	8.208E-33	0.000E+00	8.579E-13
Cm-247+D	Am-243+D	1.000E+00	1.345E-43	2.690E-43	3.368E-41	5.807E-41	6.198E-41	6.171E-41	4.891E-41	2.008E-41	0.000E+00	1.466E-12
Cm-247+D	Pu-239+D	1.000E+00	0.000E+00	0.000E+00	0.000E+00	0.000E+00	0.000E+00	0.000E+00	0.000E+00	0.000E+00	0.000E+00	1.129E-12
Cm-247+D	U-235+D	1.000E+00	0.000E+00	0.000E+00	0.000E+00	0.000E+00	0.000E+00	0.000E+00	0.000E+00	0.000E+00	0.000E+00	5.997E-19
Cm-247+D	Pa-231	1.000E+00	0.000E+00	0.000E+00	0.000E+00	0.000E+00	0.000E+00	0.000E+00	0.000E+00	0.000E+00	0.000E+00	4.970E-21
Cm-247+D	Ac-227+D	1.000E+00	0.000E+00	0.000E+00	0.000E+00	4.036E-43	8.085E-43	1.483E-42	2.964E-42	2.560E-42	0.000E+00	5.011E-20
Cm-247	∑DSR(j)		6.600E-32	6.600E-32	6.600E-32	5.771E-32	4.946E-32	4.121E-32	2.471E-32	8.208E-33	0.000E+00	3.453E-12
Cm-248	Cm-248	8.390E-02	1.230E-23	1.230E-23	1.230E-23	1.075E-23	9.209E-24	7.671E-24	4.598E-24	1.527E-24	0.000E+00	2.870E-13
Cm-248	Cm-248	1.108E-03	1.625E-25	1.625E-25	1.625E-25	1.420E-25	1.217E-25	1.014E-25	6.075E-26	2.017E-26	0.000E+00	3.791E-15
Cm-248	Pu-244	1.108E-03	7.360E-36	2.208E-35	2.951E-33	5.153E-33	5.518E-33	5.516E-33	4.408E-33	1.830E-33	0.000E+00	9.335E-20
Cm-248	∑DSR(j)		1.625E-25	1.625E-25	1.625E-25	1.420E-25	1.217E-25	1.014E-25	6.075E-26	2.017E-26	0.000E+00	3.792E-15
Cm-248	Cm-248	5.261E-08	7.714E-30	7.714E-30	7.711E-30	6.739E-30	5.775E-30	4.811E-30	2.883E-30	9.575E-31	0.000E+00	1.800E-19
Cm-248	Pu-244+D	5.261E-08	3.484E-40	1.048E-39	1.401E-37	2.447E-37	2.620E-37	2.619E-37	2.093E-37	8.688E-38	0.000E+00	4.455E-24
Cm-248	Pu-240	5.261E-08	0.000E+00	0.000E+00	0.000E+00	0.000E+00	0.000E+00	0.000E+00	0.000E+00	0.000E+00	0.000E+00	1.801E-24
Cm-248	∑DSR(j)		7.714E-30	7.714E-30	7.711E-30	6.739E-30	5.775E-30	4.811E-30	2.883E-30	9.575E-31	0.000E+00	1.800E-19
Cm-248	Cm-248	9.150E-01	1.342E-22	1.342E-22	1.341E-22	1.172E-22	1.004E-22	8.366E-23	5.014E-23	1.665E-23	0.000E+00	3.130E-12
Cm-248	Pu-244+D	9.150E-01	6.078E-33	1.823E-32	2.437E-30	4.255E-30	4.557E-30	4.555E-30	3.640E-30	1.511E-30	0.000E+00	7.748E-17
Cm-248	Pu-240	9.150E-01	0.000E+00	0.000E+00	0.000E+00	0.000E+00	0.000E+00	0.000E+00	0.000E+00	0.000E+00	0.000E+00	3.132E-17
Cm-248	U-236	9.150E-01	0.000E+00	0.000E+00	0.000E+00	0.000E+00	0.000E+00	0.000E+00	0.000E+00	0.000E+00	0.000E+00	2.494E-19
Cm-248	Th-232	9.150E-01	0.000E+00	0.000E+00	0.000E+00	0.000E+00	0.000E+00	0.000E+00	0.000E+00	0.000E+00	0.000E+00	3.425E-28
Cm-248	Ra-228+D	9.150E-01	0.000E+00	0.000E+00	0.000E+00	0.000E+00	0.000E+00	0.000E+00	0.000E+00	0.000E+00	0.000E+00	1.894E-27
Cm-248	Th-228+D	9.150E-01	0.000E+00	0.000E+00	0.000E+00	0.000E+00	0.000E+00	0.000E+00	1.253E-41	1.755E-41	0.000E+00	2.850E-28
Cm-248	∑DSR(j)		1.342E-22	1.342E-22	1.341E-22	1.172E-22	1.004E-22	8.366E-23	5.014E-23	1.665E-23	0.000E+00	3.130E-12
H-3	H-3	1.000E+00	0.000E+00	0.000E+00	0.000E+00	2.490E-12	8.332E-14	1.277E-16	4.854E-22	3.235E-27	0.000E+00	0.000E+00
I-129	I-129	1.000E+00	0.000E+00	0.000E+00	0.000E+00	0.000E+00	0.000E+00	0.000E+00	4.387E-42	2.545E-24	6.295E-04	3.249E-01
K-40	K-40	1.000E+00	1.833E-24	1.833E-24	1.833E-24	1.602E-24	1.373E-24	1.144E-24	6.861E-25	2.279E-25	0.000E+00	2.157E-08

Dose/Source Ratios Summed Over All Pathways
Parent and Progeny Principal Radionuclide Contributions Indicated

Parent (i)	Product (j)	Thread Fraction	DSR(j,t) (mrem/yr)/(pCi/g) 0.000E+00	1.000E+00	2.000E+02	4.000E+02	5.000E+02	6.000E+02	8.000E+02	1.000E+03	2.000E+03	1.000E+04
Mo-93	Mo-93	1.200E-01	0.000E+00	0.000E+00	0.000E+00	0.000E+00	0.000E+00	0.000E+00	0.000E+00	0.000E+00	0.000E+00	0.000E+00
Mo-93	Mo-93	8.800E-01	0.000E+00	0.000E+00	0.000E+00	0.000E+00	0.000E+00	0.000E+00	0.000E+00	0.000E+00	0.000E+00	0.000E+00
Mo-93	Nb-93m	8.800E-01	0.000E+00	0.000E+00	0.000E+00	0.000E+00	0.000E+00	0.000E+00	0.000E+00	0.000E+00	0.000E+00	7.271E-39
Mo-93	∑DSR(j)		0.000E+00	0.000E+00	0.000E+00	0.000E+00	0.000E+00	0.000E+00	0.000E+00	0.000E+00	0.000E+00	7.271E-39
Nb-93m	Nb-93m	1.000E+00	0.000E+00	0.000E+00	0.000E+00	0.000E+00	0.000E+00	0.000E+00	0.000E+00	0.000E+00	0.000E+00	0.000E+00
Nb-94	Nb-94	1.000E+00	1.647E-26	1.647E-26	1.636E-26	1.421E-26	1.214E-26	1.008E-26	6.001E-27	1.980E-27	0.000E+00	0.000E+00
Ni-59	Ni-59	1.000E+00	4.210E-34	4.210E-34	4.204E-34	3.671E-34	3.144E-34	2.618E-34	1.568E-34	5.201E-35	0.000E+00	0.000E+00
Np-237+D	Np-237+D	1.000E+00	6.518E-35	6.518E-35	6.518E-35	5.699E-35	4.884E-35	4.069E-35	2.440E-35	8.105E-36	0.000E+00	4.865E-13
Np-237+D	U-233	1.000E+00	0.000E+00	0.000E+00	0.000E+00	4.204E-45	4.204E-45	4.204E-45	4.204E-45	0.000E+00	0.000E+00	1.433E-12
Np-237+D	Th-229+D	1.000E+00	2.045E-34	6.971E-34	3.336E-30	1.156E-29	1.542E-29	1.844E-29	1.952E-29	1.006E-29	0.000E+00	1.147E-14
Np-237	∑DSR(j)		2.697E-34	7.622E-34	3.337E-30	1.156E-29	1.542E-29	1.844E-29	1.952E-29	1.006E-29	0.000E+00	1.931E-12
Pa-231	Pa-231	1.000E+00	2.426E-35	2.426E-35	2.416E-35	2.104E-35	1.799E-35	1.496E-35	8.931E-36	2.954E-36	0.000E+00	0.000E+00
Pa-231	Ac-227+D	1.000E+00	1.465E-31	4.351E-31	9.887E-30	8.623E-30	7.375E-30	6.132E-30	3.661E-30	1.211E-30	0.000E+00	0.000E+00
Pa-231	∑DSR(j)		1.465E-31	4.352E-31	9.887E-30	8.623E-30	7.375E-30	6.132E-30	3.661E-30	1.211E-30	0.000E+00	0.000E+00
Pb-210+D	Pb-210+D	1.000E+00	2.247E-31	2.182E-31	4.369E-34	7.424E-37	2.798E-38	1.029E-39	1.198E-42	1.401E-45	0.000E+00	0.000E+00
Pu-238	Pu-238	1.850E-09	0.000E+00	0.000E+00	0.000E+00	0.000E+00	0.000E+00	0.000E+00	0.000E+00	0.000E+00	0.000E+00	0.000E+00
Pu-238	Pu-238	1.000E+00	0.000E+00	0.000E+00	0.000E+00	0.000E+00	0.000E+00	0.000E+00	0.000E+00	0.000E+00	0.000E+00	0.000E+00
Pu-238	U-234	1.000E+00	0.000E+00	0.000E+00	0.000E+00	0.000E+00	0.000E+00	0.000E+00	0.000E+00	0.000E+00	0.000E+00	3.234E-23
Pu-238	Th-230	1.000E+00	0.000E+00	0.000E+00	0.000E+00	0.000E+00	0.000E+00	0.000E+00	0.000E+00	0.000E+00	0.000E+00	1.980E-21
Pu-238	Ra-226+D	1.000E+00	4.738E-37	1.994E-36	2.208E-31	1.131E-30	1.656E-30	2.108E-30	2.406E-30	1.290E-30	0.000E+00	2.383E-22
Pu-238	Pb-210+D	1.000E+00	0.000E+00	1.401E-45	1.590E-39	9.994E-39	1.526E-38	1.998E-38	2.360E-38	1.291E-38	0.000E+00	3.731E-20
Pu-238	∑DSR(j)		4.738E-37	1.994E-36	2.208E-31	1.131E-30	1.656E-30	2.108E-30	2.406E-30	1.290E-30	0.000E+00	3.956E-20
Pu-239+D	Pu-239+D	1.000E+00	3.331E-42	3.331E-42	3.311E-42	2.880E-42	2.461E-42	2.044E-42	1.219E-42	4.022E-43	0.000E+00	8.351E-13
Pu-239+D	U-235+D	1.000E+00	0.000E+00	0.000E+00	0.000E+00	0.000E+00	0.000E+00	0.000E+00	0.000E+00	0.000E+00	0.000E+00	2.259E-16
Pu-239+D	Pa-231	1.000E+00	0.000E+00	0.000E+00	9.809E-45	3.503E-44	4.764E-44	5.605E-44	6.026E-44	3.083E-44	0.000E+00	2.100E-18
Pu-239+D	Ac-227+D	1.000E+00	1.261E-44	5.325E-44	3.053E-39	1.234E-38	1.701E-38	2.080E-38	2.267E-38	1.191E-38	0.000E+00	2.133E-17
Pu-239	∑DSR(j)		3.343E-42	3.384E-42	3.057E-39	1.235E-38	1.702E-38	2.080E-38	2.267E-38	1.191E-38	0.000E+00	8.353E-13
Pu-240	Pu-240	5.750E-08	0.000E+00	0.000E+00	0.000E+00	0.000E+00	0.000E+00	0.000E+00	0.000E+00	0.000E+00	0.000E+00	2.226E-20

Dose/Source Ratios Summed Over All Pathways
Parent and Progeny Principal Radionuclide Contributions Indicated

Parent (i)	Product (j)	Thread Fraction	DSR(j,t) (mrem/yr)/(pCi/g) 0.000E+00	1.000E+00	2.000E+02	4.000E+02	5.000E+02	6.000E+02	8.000E+02	1.000E+03	2.000E+03	1.000E+04
Pu-240	Pu-240	1.000E+00	0.000E+00	0.000E+00	0.000E+00	0.000E+00	0.000E+00	0.000E+00	0.000E+00	0.000E+00	0.000E+00	3.872E-13
Pu-240	U-236	1.000E+00	0.000E+00	0.000E+00	0.000E+00	0.000E+00	0.000E+00	0.000E+00	0.000E+00	0.000E+00	0.000E+00	3.164E-15
Pu-240	Th-232	1.000E+00	0.000E+00	0.000E+00	0.000E+00	0.000E+00	0.000E+00	0.000E+00	0.000E+00	0.000E+00	0.000E+00	4.734E-24
Pu-240	Ra-228+D	1.000E+00	3.363E-44	1.373E-43	3.000E-39	1.083E-38	1.457E-38	1.751E-38	1.865E-38	9.652E-39	0.000E+00	2.623E-23
Pu-240	Th-228+D	1.000E+00	3.995E-40	1.934E-39	1.032E-34	3.782E-34	5.101E-34	6.141E-34	6.559E-34	3.399E-34	0.000E+00	4.088E-24
Pu-240	∑DSR(j)		3.996E-40	1.934E-39	1.033E-34	3.782E-34	5.101E-34	6.142E-34	6.559E-34	3.399E-34	0.000E+00	3.904E-13
Pu-241	Pu-241	1.000E+00	0.000E+00	0.000E+00	0.000E+00	0.000E+00	0.000E+00	0.000E+00	0.000E+00	0.000E+00	0.000E+00	0.000E+00
Pu-241	Am-241	1.000E+00	0.000E+00	0.000E+00	0.000E+00	0.000E+00	0.000E+00	0.000E+00	0.000E+00	0.000E+00	0.000E+00	0.000E+00
Pu-241	Np-237+D	1.000E+00	3.784E-44	1.275E-43	1.091E-40	1.739E-40	1.754E-40	1.648E-40	1.165E-40	4.297E-41	0.000E+00	1.789E-18
Pu-241	U-233	1.000E+00	0.000E+00	0.000E+00	0.000E+00	0.000E+00	0.000E+00	0.000E+00	0.000E+00	0.000E+00	0.000E+00	5.667E-18
Pu-241	Th-229+D	1.000E+00	2.018E-43	1.153E-42	1.668E-36	1.235E-35	2.047E-35	2.893E-35	3.914E-35	2.402E-35	0.000E+00	4.472E-20
Pu-241	∑DSR(j)		2.396E-43	1.281E-42	1.668E-36	1.235E-35	2.047E-35	2.893E-35	3.914E-35	2.402E-35	0.000E+00	7.501E-18
Pu-241+D	Pu-241+D	2.450E-05	0.000E+00	0.000E+00	0.000E+00	0.000E+00	0.000E+00	0.000E+00	0.000E+00	0.000E+00	0.000E+00	0.000E+00
Pu-241+D	Np-237+D	2.450E-05	0.000E+00	0.000E+00	1.121E-44	9.809E-45	8.408E-45	7.006E-45	4.204E-45	1.401E-45	0.000E+00	7.978E-23
Pu-241+D	U-233	2.450E-05	0.000E+00	0.000E+00	0.000E+00	0.000E+00	0.000E+00	0.000E+00	0.000E+00	0.000E+00	0.000E+00	2.350E-22
Pu-241+D	Th-229+D	2.450E-05	2.803E-45	9.809E-45	4.461E-40	1.711E-39	2.330E-39	2.824E-39	3.041E-39	1.584E-39	0.000E+00	1.881E-24
Pu-241	∑DSR(j)		2.803E-45	9.809E-45	4.461E-40	1.711E-39	2.330E-39	2.824E-39	3.041E-39	1.584E-39	0.000E+00	3.167E-22
Pu-242	Pu-242	5.540E-06	1.047E-33	1.047E-33	1.047E-33	9.149E-34	7.839E-34	6.531E-34	3.914E-34	1.300E-34	0.000E+00	5.759E-18
Pu-242	Pu-242	5.450E-07	1.030E-34	1.030E-34	1.030E-34	9.000E-35	7.712E-35	6.424E-35	3.851E-35	1.279E-35	0.000E+00	5.666E-19
Pu-242	U-238	5.450E-07	0.000E+00	0.000E+00	0.000E+00	0.000E+00	0.000E+00	0.000E+00	0.000E+00	0.000E+00	0.000E+00	2.389E-23
Pu-242	∑DSR(j)		1.030E-34	1.030E-34	1.030E-34	9.000E-35	7.712E-35	6.424E-35	3.851E-35	1.279E-35	0.000E+00	5.666E-19
Pu-242	Pu-242	1.000E+00	1.890E-28	1.890E-28	1.889E-28	1.651E-28	1.415E-28	1.179E-28	7.065E-29	2.346E-29	0.000E+00	1.040E-12
Pu-242	U-238+D	1.000E+00	8.691E-39	2.607E-38	3.485E-36	6.085E-36	6.517E-36	6.514E-36	5.205E-36	2.161E-36	0.000E+00	4.776E-17
Pu-242	U-234	1.000E+00	0.000E+00	0.000E+00	0.000E+00	0.000E+00	0.000E+00	0.000E+00	0.000E+00	0.000E+00	0.000E+00	2.950E-20
Pu-242	Th-230	1.000E+00	0.000E+00	0.000E+00	0.000E+00	0.000E+00	0.000E+00	0.000E+00	0.000E+00	0.000E+00	0.000E+00	9.397E-24
Pu-242	Ra-226+D	1.000E+00	0.000E+00	0.000E+00	2.459E-39	3.362E-38	6.965E-38	1.192E-37	2.219E-37	1.768E-37	0.000E+00	1.306E-24
Pu-242	Pb-210+D	1.000E+00	0.000E+00	0.000E+00	0.000E+00	0.000E+00	0.000E+00	0.000E+00	0.000E+00	0.000E+00	0.000E+00	2.216E-22
Pu-242	∑DSR(j)		1.890E-28	1.890E-28	1.889E-28	1.651E-28	1.415E-28	1.179E-28	7.065E-29	2.346E-29	0.000E+00	1.040E-12
Pu-244	Pu-244	1.210E-03	1.855E-27	1.855E-27	1.855E-27	1.622E-27	1.390E-27	1.158E-27	6.943E-28	2.307E-28	0.000E+00	1.276E-15
Pu-244+D	Pu-244+D	5.743E-08	8.805E-32	8.805E-32	8.805E-32	7.699E-32	6.599E-32	5.498E-32	3.297E-32	1.095E-32	0.000E+00	6.090E-20
Pu-244+D	Pu-240	5.743E-08	0.000E+00	0.000E+00	0.000E+00	0.000E+00	0.000E+00	0.000E+00	0.000E+00	0.000E+00	0.000E+00	4.170E-20
Pu-244	∑DSR(j)		8.805E-32	8.805E-32	8.805E-32	7.699E-32	6.599E-32	5.498E-32	3.297E-32	1.095E-32	0.000E+00	1.026E-19

Parent Dose Report
Title : Site 7 Base Case Model
File : BC_V01.ROF

Dose/Source Ratios Summed Over All Pathways
Parent and Progeny Principal Radionuclide Contributions Indicated

Parent (i)	Product (j)	Thread Fraction	DSR(j,t) (mrem/yr)/(pCi/g) 0.000E+00	1.000E+00	2.000E+02	4.000E+02	5.000E+02	6.000E+02	8.000E+02	1.000E+03	2.000E+03	1.000E+04
Pu-244+D	Pu-244+D	9.988E-01	1.531E-24	1.531E-24	1.531E-24	1.339E-24	1.148E-24	9.562E-25	5.733E-25	1.905E-25	0.000E+00	1.059E-12
Pu-244+D	Pu-240	9.988E-01	0.000E+00	0.000E+00	0.000E+00	0.000E+00	0.000E+00	0.000E+00	0.000E+00	0.000E+00	0.000E+00	7.251E-13
Pu-244+D	U-236	9.988E-01	0.000E+00	0.000E+00	0.000E+00	0.000E+00	0.000E+00	0.000E+00	0.000E+00	0.000E+00	0.000E+00	5.719E-15
Pu-244+D	Th-232	9.988E-01	0.000E+00	0.000E+00	0.000E+00	0.000E+00	0.000E+00	0.000E+00	0.000E+00	0.000E+00	0.000E+00	8.150E-24
Pu-244+D	Ra-228+D	9.988E-01	0.000E+00	0.000E+00	1.980E-41	1.496E-40	2.528E-40	3.663E-40	5.228E-40	3.397E-40	0.000E+00	4.511E-23
Pu-244+D	Th-228+D	9.988E-01	0.000E+00	0.000E+00	6.817E-37	5.192E-36	8.812E-36	1.279E-35	1.833E-35	1.193E-35	0.000E+00	6.882E-24
Pu-244	∑DSR(j)		1.531E-24	1.531E-24	1.531E-24	1.339E-24	1.148E-24	9.562E-25	5.733E-25	1.905E-25	0.000E+00	1.790E-12
Ra-226+D	Ra-226+D	1.000E+00	2.129E-23	2.128E-23	1.952E-23	1.565E-23	1.285E-23	1.025E-23	5.635E-24	1.717E-24	0.000E+00	0.000E+00
Ra-226+D	Pb-210+D	1.000E+00	3.297E-33	9.795E-33	2.115E-31	1.700E-31	1.395E-31	1.113E-31	6.120E-32	1.864E-32	0.000E+00	0.000E+00
Ra-226	∑DSR(j)		2.129E-23	2.128E-23	1.952E-23	1.565E-23	1.285E-23	1.025E-23	5.635E-24	1.717E-24	0.000E+00	0.000E+00
Ra-228+D	Ra-228+D	1.000E+00	1.067E-25	9.698E-26	3.709E-36	0.000E+00	0.000E+00	0.000E+00	0.000E+00	0.000E+00	0.000E+00	0.000E+00
Ra-228+D	Th-228+D	1.000E+00	2.329E-22	6.380E-22	1.967E-31	5.897E-42	0.000E+00	0.000E+00	0.000E+00	0.000E+00	0.000E+00	0.000E+00
Ra-228	∑DSR(j)		2.330E-22	6.381E-22	1.967E-31	5.897E-42	0.000E+00	0.000E+00	0.000E+00	0.000E+00	0.000E+00	0.000E+00
Sr-90+D	Sr-90+D	1.000E+00	4.376E-36	4.276E-36	3.550E-38	2.518E-40	1.941E-41	1.459E-42	7.006E-45	0.000E+00	0.000E+00	0.000E+00
Tc-99	Tc-99	1.000E+00	0.000E+00	0.000E+00	0.000E+00	1.766E-33	1.512E-15	2.489E-08	2.501E-03	6.572E-02	4.278E-01	2.250E-20
Th-228+D	Th-228+D	1.000E+00	3.622E-21	3.008E-21	0.000E+00	0.000E+00	0.000E+00	0.000E+00	0.000E+00	0.000E+00	0.000E+00	0.000E+00
Th-229+D	Th-229+D	1.000E+00	4.063E-25	4.063E-25	3.987E-25	3.421E-25	2.904E-25	2.397E-25	1.410E-25	4.598E-26	0.000E+00	0.000E+00
Th-230	Th-230	1.000E+00	0.000E+00	0.000E+00	0.000E+00	0.000E+00	0.000E+00	0.000E+00	0.000E+00	0.000E+00	0.000E+00	0.000E+00
Th-230	Ra-226+D	1.000E+00	4.607E-27	1.382E-26	1.770E-24	2.960E-24	3.103E-24	3.036E-24	2.327E-24	9.268E-25	0.000E+00	0.000E+00
Th-230	Pb-210+D	1.000E+00	3.588E-36	1.209E-35	1.602E-32	2.935E-32	3.130E-32	3.098E-32	2.408E-32	9.669E-33	0.000E+00	0.000E+00
Th-230	∑DSR(j)		4.607E-27	1.382E-26	1.770E-24	2.960E-24	3.103E-24	3.036E-24	2.327E-24	9.268E-25	0.000E+00	0.000E+00
Th-232	Th-232	1.000E+00	0.000E+00	0.000E+00	0.000E+00	0.000E+00	0.000E+00	0.000E+00	0.000E+00	0.000E+00	0.000E+00	0.000E+00
Th-232	Ra-228+D	1.000E+00	5.089E-27	1.480E-26	1.118E-25	9.774E-26	8.377E-26	6.979E-26	4.185E-26	1.390E-26	0.000E+00	0.000E+00
Th-232	Th-228+D	1.000E+00	1.027E-22	3.120E-22	3.958E-21	3.461E-21	2.966E-21	2.471E-21	1.482E-21	4.923E-22	0.000E+00	0.000E+00
Th-232	∑DSR(j)		1.027E-22	3.120E-22	3.958E-21	3.461E-21	2.966E-21	2.471E-21	1.482E-21	4.923E-22	0.000E+00	0.000E+00
U-232	U-232	1.000E+00	0.000E+00	0.000E+00	0.000E+00	0.000E+00	0.000E+00	0.000E+00	0.000E+00	0.000E+00	0.000E+00	0.000E+00
U-232	Th-228+D	1.000E+00	3.253E-22	9.174E-22	5.418E-22	6.335E-23	1.985E-23	6.050E-24	4.851E-25	2.155E-26	0.000E+00	0.000E+00
U-232	∑DSR(j)		3.253E-22	9.174E-22	5.418E-22	6.335E-23	1.985E-23	6.050E-24	4.851E-25	2.155E-26	0.000E+00	0.000E+00
U-233	U-233	1.000E+00	1.878E-42	1.878E-42	1.876E-42	1.640E-42	1.404E-42	1.169E-42	7.006E-43	2.326E-43	0.000E+00	8.990E-20
U-233	Th-229+D	1.000E+00	1.918E-29	5.754E-29	7.618E-27	1.317E-26	1.404E-26	1.397E-26	1.106E-26	4.546E-27	0.000E+00	1.924E-16
U-233	∑DSR(j)		1.918E-29	5.754E-29	7.618E-27	1.317E-26	1.404E-26	1.397E-26	1.106E-26	4.546E-27	0.000E+00	1.925E-16

Parent Dose Report
Title : Site 7 Base Case Model
File : BC_V01.ROF

Dose/Source Ratios Summed Over All Pathways
Parent and Progeny Principal Radionuclide Contributions Indicated

Parent (i)	Product (j)	Thread Fraction	DSR(j,t) (mrem/yr)/(pCi/g) 0.000E+00	1.000E+00	2.000E+02	4.000E+02	5.000E+02	6.000E+02	8.000E+02	1.000E+03	2.000E+03	1.000E+04
U-234	U-234	1.000E+00	0.000E+00	0.000E+00	0.000E+00	0.000E+00	0.000E+00	0.000E+00	0.000E+00	0.000E+00	0.000E+00	8.813E-20
U-234	Th-230	1.000E+00	0.000E+00	0.000E+00	0.000E+00	0.000E+00	0.000E+00	0.000E+00	0.000E+00	0.000E+00	0.000E+00	5.424E-18
U-234	Ra-226+D	1.000E+00	1.038E-31	3.536E-31	1.655E-27	5.609E-27	7.400E-27	8.750E-27	9.063E-27	4.574E-27	0.000E+00	6.523E-19
U-234	Pb-210+D	1.000E+00	5.455E-41	2.272E-40	1.301E-35	5.143E-35	7.004E-35	8.458E-35	8.997E-35	4.613E-35	0.000E+00	1.021E-16
U-234	∑DSR(j)		1.038E-31	3.536E-31	1.655E-27	5.609E-27	7.400E-27	8.750E-27	9.063E-27	4.574E-27	0.000E+00	1.083E-16
U-235+D	U-235+D	1.000E+00	1.592E-39	1.592E-39	1.592E-39	1.392E-39	1.193E-39	9.940E-40	5.960E-40	1.980E-40	0.000E+00	8.635E-20
U-235+D	Pa-231	1.000E+00	2.567E-40	7.700E-40	1.027E-37	1.790E-37	1.915E-37	1.913E-37	1.525E-37	6.321E-38	0.000E+00	2.121E-16
U-235+D	Ac-227+D	1.000E+00	7.787E-36	2.623E-35	3.550E-32	6.760E-32	7.356E-32	7.427E-32	6.006E-32	2.509E-32	0.000E+00	2.158E-15
U-235	∑DSR(j)		7.789E-36	2.623E-35	3.550E-32	6.760E-32	7.356E-32	7.427E-32	6.006E-32	2.509E-32	0.000E+00	2.370E-15
U-236	U-236	1.000E+00	0.000E+00	0.000E+00	0.000E+00	0.000E+00	0.000E+00	0.000E+00	0.000E+00	0.000E+00	0.000E+00	8.531E-20
U-236	Th-232	1.000E+00	0.000E+00	0.000E+00	0.000E+00	0.000E+00	0.000E+00	0.000E+00	0.000E+00	0.000E+00	0.000E+00	3.293E-23
U-236	Ra-228+D	1.000E+00	6.749E-37	2.214E-36	1.060E-33	1.891E-33	2.034E-33	2.039E-33	1.635E-33	6.805E-34	0.000E+00	1.808E-22
U-236	Th-228+D	1.000E+00	9.917E-33	3.595E-32	3.699E-29	6.649E-29	7.162E-29	7.186E-29	5.771E-29	2.403E-29	0.000E+00	2.809E-23
U-236	∑DSR(j)		9.918E-33	3.595E-32	3.699E-29	6.649E-29	7.162E-29	7.186E-29	5.771E-29	2.403E-29	0.000E+00	8.556E-20
U-238	U-238	5.450E-07	0.000E+00	0.000E+00	0.000E+00	0.000E+00	0.000E+00	0.000E+00	0.000E+00	0.000E+00	0.000E+00	4.456E-26
U-238+D	U-238+D	1.000E+00	1.120E-28	1.120E-28	1.120E-28	9.797E-29	8.397E-29	6.996E-29	4.195E-29	1.394E-29	0.000E+00	8.906E-20
U-238+D	U-234	1.000E+00	0.000E+00	0.000E+00	0.000E+00	0.000E+00	0.000E+00	0.000E+00	0.000E+00	0.000E+00	0.000E+00	2.252E-21
U-238+D	Th-230	1.000E+00	0.000E+00	0.000E+00	0.000E+00	0.000E+00	0.000E+00	0.000E+00	0.000E+00	0.000E+00	0.000E+00	1.401E-19
U-238+D	Ra-226+D	1.000E+00	4.785E-37	2.021E-36	3.148E-31	2.146E-30	3.550E-30	5.054E-30	7.026E-30	4.462E-30	0.000E+00	1.651E-20
U-238+D	Pb-210+D	1.000E+00	0.000E+00	1.401E-45	2.194E-39	1.832E-38	3.168E-38	4.647E-38	6.711E-38	4.361E-38	0.000E+00	2.574E-18
U-238	∑DSR(j)		1.120E-28	1.120E-28	1.124E-28	1.001E-28	8.752E-29	7.501E-29	4.898E-29	1.840E-29	0.000E+00	2.821E-18

The DSR includes contributions from associated (half-life ≤ 180 days) daughters.

Parent Dose Report
Title : Site 7 Base Case Model
File : BC_V01.ROF

Single Radionuclide Soil Guidelines G(i,t) in pCi/g
Basic Radiation Dose Limit = 2.500E+01 mrem/yr

Nuclide (i)	t= 0.000E+00	1.000E+00	2.000E+02	4.000E+02	5.000E+02	6.000E+02	8.000E+02	1.000E+03	2.000E+03	1.000E+04
Ac-227	*7.232E+13	*7.232E+13	*7.232E+13	*7.232E+13	*7.232E+13	*7.232E+13	*7.232E+13	*7.232E+13	*7.232E+13	*7.232E+13
Am-241	*3.431E+12	*3.431E+12	*3.431E+12	*3.431E+12	*3.431E+12	*3.431E+12	*3.431E+12	*3.431E+12	*3.431E+12	*3.431E+12
Am-243	*1.996E+11	*1.996E+11	*1.996E+11	*1.996E+11	*1.996E+11	*1.996E+11	*1.996E+11	*1.996E+11	*1.996E+11	*1.996E+11
Be-10	*2.364E+10	*2.364E+10	*2.364E+10	*2.364E+10	*2.364E+10	*2.364E+10	*2.364E+10	*2.364E+10	*2.364E+10	*2.364E+10
C-14	*4.479E+12	*4.479E+12	*4.479E+12	9.608E+01	1.325E+01	2.500E+01	9.377E+01	1.906E+02	4.438E+10	*4.479E+12
Ca-41	*8.353E+10	*8.353E+10	*8.353E+10	*8.353E+10	*8.353E+10	*8.353E+10	*8.353E+10	*8.353E+10	*8.353E+10	3.446E+10
Cm-243	*5.054E+13	*5.054E+13	*5.054E+13	*5.054E+13	*5.054E+13	*5.054E+13	*5.054E+13	*5.054E+13	*5.054E+13	*5.054E+13
Cm-244	*8.092E+13	*8.092E+13	*8.092E+13	*8.092E+13	*8.092E+13	*8.092E+13	*8.092E+13	*8.092E+13	*8.092E+13	*8.092E+13
Cm-245	*1.716E+11	*1.716E+11	*1.716E+11	*1.716E+11	*1.716E+11	*1.716E+11	*1.716E+11	*1.716E+11	*1.716E+11	*1.716E+11
Cm-246	*3.052E+11	*3.052E+11	*3.052E+11	*3.052E+11	*3.052E+11	*3.052E+11	*3.052E+11	*3.052E+11	*3.052E+11	*3.052E+11
Cm-247	*9.275E+07	*9.275E+07	*9.275E+07	*9.275E+07	*9.275E+07	*9.275E+07	*9.275E+07	*9.275E+07	*9.275E+07	*9.275E+07
Cm-248	*4.141E+09	*4.141E+09	*4.141E+09	*4.141E+09	*4.141E+09	*4.141E+09	*4.141E+09	*4.141E+09	*4.141E+09	*4.141E+09
H-3	*9.621E+15	*9.621E+15	*9.621E+15	1.004E+13	3.001E+14	*9.621E+15	*9.621E+15	*9.621E+15	*9.621E+15	*9.621E+15
I-129	*1.753E+08	*1.753E+08	*1.753E+08	*1.753E+08	*1.753E+08	*1.753E+08	*1.753E+08	*1.753E+08	3.971E+04	7.695E+01
K-40	*6.976E+06	*6.976E+06	*6.976E+06	*6.976E+06	*6.976E+06	*6.976E+06	*6.976E+06	*6.976E+06	*6.976E+06	*6.976E+06
Mo-93	*9.517E+11	*9.517E+11	*9.517E+11	*9.517E+11	*9.517E+11	*9.517E+11	*9.517E+11	*9.517E+11	*9.517E+11	*9.517E+11
Nb-93m	*2.385E+14	*2.385E+14	*2.385E+14	*2.385E+14	*2.385E+14	*2.385E+14	*2.385E+14	*2.385E+14	*2.385E+14	*2.385E+14
Nb-94	*1.856E+11	*1.856E+11	*1.856E+11	*1.856E+11	*1.856E+11	*1.856E+11	*1.856E+11	*1.856E+11	*1.856E+11	*1.856E+11
Ni-59	*5.906E+10	*5.906E+10	*5.906E+10	*5.906E+10	*5.906E+10	*5.906E+10	*5.906E+10	*5.906E+10	*5.906E+10	*5.906E+10
Np-237	*7.034E+08	*7.034E+08	*7.034E+08	*7.034E+08	*7.034E+08	*7.034E+08	*7.034E+08	*7.034E+08	*7.034E+08	*7.034E+08
Pa-231	*4.723E+10	*4.723E+10	*4.723E+10	*4.723E+10	*4.723E+10	*4.723E+10	*4.723E+10	*4.723E+10	*4.723E+10	*4.723E+10
Pb-210	*7.632E+13	*7.632E+13	*7.632E+13	*7.632E+13	*7.632E+13	*7.632E+13	*7.632E+13	*7.632E+13	*7.632E+13	*7.632E+13
Pu-238	*1.712E+13	*1.712E+13	*1.712E+13	*1.712E+13	*1.712E+13	*1.712E+13	*1.712E+13	*1.712E+13	*1.712E+13	*1.712E+13
Pu-239	*6.202E+10	*6.202E+10	*6.202E+10	*6.202E+10	*6.202E+10	*6.202E+10	*6.202E+10	*6.202E+10	*6.202E+10	*6.202E+10
Pu-240	*2.269E+11	*2.269E+11	*2.269E+11	*2.269E+11	*2.269E+11	*2.269E+11	*2.269E+11	*2.269E+11	*2.269E+11	*2.269E+11
Pu-241	*1.033E+14	*1.033E+14	*1.033E+14	*1.033E+14	*1.033E+14	*1.033E+14	*1.033E+14	*1.033E+14	*1.033E+14	*1.033E+14
Pu-242	*3.938E+09	*3.938E+09	*3.938E+09	*3.938E+09	*3.938E+09	*3.938E+09	*3.938E+09	*3.938E+09	*3.938E+09	*3.938E+09
Pu-244	*1.831E+07	*1.831E+07	*1.831E+07	*1.831E+07	*1.831E+07	*1.831E+07	*1.831E+07	*1.831E+07	*1.831E+07	*1.831E+07
Ra-226	*9.885E+11	*9.885E+11	*9.885E+11	*9.885E+11	*9.885E+11	*9.885E+11	*9.885E+11	*9.885E+11	*9.885E+11	*9.885E+11
Ra-228	*2.726E+14	*2.726E+14	*2.726E+14	*2.726E+14	*2.726E+14	*2.726E+14	*2.726E+14	*2.726E+14	*2.726E+14	*2.726E+14
Sr-90	*1.366E+14	*1.366E+14	*1.366E+14	*1.366E+14	*1.366E+14	*1.366E+14	*1.366E+14	*1.366E+14	*1.366E+14	*1.366E+14
Tc-99	*1.695E+10	*1.695E+10	*1.695E+10	*1.695E+10	*1.695E+10	1.004E+09	9.995E+03	3.804E+02	5.844E+01	*1.695E+10
Th-228	*8.201E+14	*8.201E+14	*8.201E+14	*8.201E+14	*8.201E+14	*8.201E+14	*8.201E+14	*8.201E+14	*8.201E+14	*8.201E+14
Th-229	*2.126E+11	*2.126E+11	*2.126E+11	*2.126E+11	*2.126E+11	*2.126E+11	*2.126E+11	*2.126E+11	*2.126E+11	*2.126E+11
Th-230	*2.062E+10	*2.062E+10	*2.062E+10	*2.062E+10	*2.062E+10	*2.062E+10	*2.062E+10	*2.062E+10	*2.062E+10	*2.062E+10
Th-232	*1.097E+05	*1.097E+05	*1.097E+05	*1.097E+05	*1.097E+05	*1.097E+05	*1.097E+05	*1.097E+05	*1.097E+05	*1.097E+05
U-232	*2.236E+13	*2.236E+13	*2.236E+13	*2.236E+13	*2.236E+13	*2.236E+13	*2.236E+13	*2.236E+13	*2.236E+13	*2.236E+13
U-233	*9.636E+09	*9.636E+09	*9.636E+09	*9.636E+09	*9.636E+09	*9.636E+09	*9.636E+09	*9.636E+09	*9.636E+09	*9.636E+09
U-234	*6.222E+09	*6.222E+09	*6.222E+09	*6.222E+09	*6.222E+09	*6.222E+09	*6.222E+09	*6.222E+09	*6.222E+09	*6.222E+09
U-235	*2.160E+06	*2.160E+06	*2.160E+06	*2.160E+06	*2.160E+06	*2.160E+06	*2.160E+06	*2.160E+06	*2.160E+06	*2.160E+06
U-236	*6.467E+07	*6.467E+07	*6.467E+07	*6.467E+07	*6.467E+07	*6.467E+07	*6.467E+07	*6.467E+07	*6.467E+07	*6.467E+07
U-238	*3.361E+05	*3.361E+05	*3.361E+05	*3.361E+05	*3.361E+05	*3.361E+05	*3.361E+05	*3.361E+05	*3.361E+05	*3.361E+05

*At specific activity limit

Parent Dose Report
Title : Site 7 Base Case Model
File : BC_V01.ROF

Summed Dose/Source Ratios DSR(i,t) in (mrem/yr)/(pCi/g)
and Single Radionuclide Soil Guidelines G(i,t) in pCi/g
at tmin = time of minimum single radionuclide soil guideline
and at tmax = time of maximum total dose = 5084 years

Nuclide (i)	Initial (pCi/g)	tmin (years)	DSR(i,tmin)	G(i,tmin) (pCi/g)	DSR(i,tmax)	G(i,tmax) (pCi/g)
Ac-227	2.92OE-03	0	9.793E-30	*7.232E+13	0.000E+00	*7.232E+13
Am-241	5.90OE+01	10030	2.666E-16	*3.431E+12	7.209E-38	*3.431E+12
Am-243	2.97OE+00	10030	1.533E-14	*1.996E+11	1.520E-39	*1.996E+11
Be-10	2.53OE-05	0	0.000E+00	*2.364E+10	0.000E+00	*2.364E+10
C-14	5.40OE-01	490	1.901E+00	1.315E+01	0.000E+00	*4.479E+12
Ca-41	4.21OE-02	10030	8.135E-10	3.073E+10	8.387E-30	*8.353E+10
Cm-243	4.30OE-01	10030	1.195E-15	*5.054E+13	1.811E-40	*5.054E+13
Cm-244	1.26OE+02	10030	1.277E-15	*8.092E+13	8.278E-39	*8.092E+13
Cm-245	3.83OE-02	10030	1.021E-11	*1.716E+11	9.141E-33	*1.716E+11
Cm-246	1.59OE-01	10030	2.687E-13	*3.052E+11	2.432E-40	*3.052E+11
Cm-247	1.04OE-02	10030	3.982E-12	*9.275E+07	9.846E-34	*9.275E+07
Cm-248	5.59OE-04	10030	4.061E-12	*4.141E+09	4.011E-41	*4.141E+09
H-3	4.64OE+00	411	2.933E-12	8.523E+12	0.000E+00	*9.621E+15
I-129	3.50OE-01	5084	2.609E+01	9.583E-01	2.609E+01	9.583E-01
K-40	3.28OE+00	10030	2.419E-08	*6.976E+06	2.411E-28	*6.976E+06
Mo-93	3.88OE-01	10030	1.092E-38	*9.517E+11	0.000E+00	*9.517E+11
Nb-93m	2.33OE-01	0	0.000E+00	*2.385E+14	0.000E+00	*2.385E+14
Nb-94	1.63OE-02	0	1.647E-26	*1.856E+11	0.000E+00	*1.856E+11
Ni-59	3.04OE+00	0	4.21OE-34	*5.906E+10	0.000E+00	*5.906E+10
Np-237	3.25OE-01	10030	2.223E-12	*7.034E+08	8.251E-34	*7.034E+08
Pa-231	2.39OE-01	230	9.891E-30	*4.723E+10	0.000E+00	*4.723E+10
Pb-210	3.68OE+00	0	2.247E-31	*7.632E+13	0.000E+00	*7.632E+13
Pu-238	9.38OE+01	10030	4.725E-20	*1.712E+13	0.000E+00	*1.712E+13
Pu-239	5.83OE+01	10030	9.910E-13	*6.202E+10	1.502E-37	*6.202E+10
Pu-240	6.20OE+01	10030	4.619E-13	*2.269E+11	2.994E-36	*2.269E+11
Pu-241	2.04OE+02	10030	8.645E-18	*1.033E+14	2.286E-39	*1.033E+14
Pu-242	1.73OE-01	10030	1.234E-12	*3.938E+09	2.764E-38	*3.938E+09
Pu-244	3.68OE-03	10030	2.128E-12	*1.831E+07	2.104E-36	*1.831E+07
Ra-226	8.01OE-01	0	2.129E-23	*9.885E+11	0.000E+00	*9.885E+11
Ra-228	2.21OE-02	4.9	2.217E-21	*2.726E+14	0.000E+00	*2.726E+14
Sr-90	1.92OE+02	0	4.376E-36	*1.366E+14	0.000E+00	*1.366E+14
Tc-99	1.56OE+00	1699	6.089E-01	4.106E+01	2.324E-07	1.076E+08
Th-228	2.11OE-06	0	3.622E-21	*8.201E+14	0.000E+00	*8.201E+14
Th-229	5.71OE+00	0	4.063E-25	*2.126E+11	0.000E+00	*2.126E+11
Th-230	1.92OE+00	519	3.106E-24	*2.062E+10	0.000E+00	*2.062E+10
Th-232	3.52OE+00	152	3.958E-21	*1.097E+05	0.000E+00	*1.097E+05
U-232	1.02OE+01	9.79	3.564E-21	*2.236E+13	0.000E+00	*2.236E+13
U-233	4.16OE+01	10030	2.283E-16	*9.636E+09	0.000E+00	*9.636E+09
U-234	6.30OE+02	10030	1.293E-16	*6.222E+09	0.000E+00	*6.222E+09
U-235	3.97OE+01	10030	2.815E-15	*2.160E+06	0.000E+00	*2.160E+06
U-236	8.98OE+00	10030	1.080E-19	*6.467E+07	0.000E+00	*6.467E+07
U-238	3.81OE+02	10030	3.389E-18	*3.361E+05	0.000E+00	*3.361E+05

*At specific activity limit

Parent Dose Report
Title : Site 7 Base Case Model
File : BC_V01.ROF

Individual Nuclide Dose Summed Over All Pathways
Parent Nuclide and Thread Fraction Indicated

Nuclide (j)	Parent (i)	THF(i)	DOSE(j,t), mrem/yr t= 0.000E+00	1.000E+00	2.000E+02	4.000E+02	5.000E+02	6.000E+02	8.000E+02	1.000E+03	2.000E+03	1.000E+04
Ac-227	Ac-227	1.000E+00	2.859E-32	2.775E-32	4.917E-35	7.391E-38	2.620E-39	9.065E-41	9.389E-44	0.000E+00	0.000E+00	0.000E+00
Ac-227	Am-243	1.000E+00	0.000E+00	0.000E+00	1.545E-41	1.304E-40	2.270E-40	3.351E-40	4.905E-40	3.231E-40	0.000E+00	1.077E-18
Ac-227	Cm-243	2.400E-03	0.000E+00	0.000E+00	0.000E+00	0.000E+00	0.000E+00	0.000E+00	0.000E+00	0.000E+00	0.000E+00	1.378E-24
Ac-227	Cm-243	9.976E-01	0.000E+00	0.000E+00	1.005E-42	5.115E-42	7.383E-42	9.307E-42	1.053E-41	5.660E-42	0.000E+00	1.106E-20
Ac-227	Cm-247	1.000E+00	0.000E+00	0.000E+00	0.000E+00	4.204E-45	8.408E-45	1.541E-44	3.083E-44	2.662E-44	0.000E+00	5.211E-22
Ac-227	Pa-231	1.000E+00	3.501E-32	1.040E-31	2.363E-30	2.061E-30	1.763E-30	1.465E-30	8.750E-31	2.895E-31	0.000E+00	0.000E+00
Ac-227	Pu-239	1.000E+00	7.385E-43	3.077E-42	1.780E-37	7.196E-37	9.919E-37	1.213E-36	1.322E-36	6.944E-37	0.000E+00	1.244E-15
Ac-227	U-235	1.000E+00	3.091E-34	1.041E-33	1.410E-30	2.684E-30	2.920E-30	2.949E-30	2.384E-30	9.960E-31	0.000E+00	8.566E-14
Ac-227	∑DOSE(j):		6.392E-32	1.328E-31	3.773E-30	4.745E-30	4.683E-30	4.414E-30	3.259E-30	1.285E-30	0.000E+00	8.690E-14
Am-241	Am-241	1.000E+00	0.000E+00	0.000E+00	0.000E+00	0.000E+00	0.000E+00	0.000E+00	0.000E+00	0.000E+00	0.000E+00	0.000E+00
Am-241	Cm-245	1.000E+00	0.000E+00	0.000E+00	0.000E+00	0.000E+00	0.000E+00	0.000E+00	0.000E+00	0.000E+00	0.000E+00	3.266E-13
Am-241	Pu-241	1.000E+00	0.000E+00	0.000E+00	0.000E+00	0.000E+00	0.000E+00	0.000E+00	0.000E+00	0.000E+00	0.000E+00	0.000E+00
Am-241	∑DOSE(j):		0.000E+00	0.000E+00	0.000E+00	0.000E+00	0.000E+00	0.000E+00	0.000E+00	0.000E+00	0.000E+00	3.266E-13
Np-237	Am-241	1.000E+00	6.192E-40	1.857E-39	2.132E-37	3.212E-37	3.206E-37	2.992E-37	2.098E-37	7.703E-38	0.000E+00	3.266E-15
Np-237	Cm-245	1.000E+00	0.000E+00	0.000E+00	1.916E-41	6.670E-41	8.665E-41	1.003E-40	9.887E-41	4.734E-41	0.000E+00	1.278E-15
Np-237	Cm-245	2.450E-05	0.000E+00	0.000E+00	4.204E-45	7.006E-45	7.006E-45	7.006E-45	5.605E-45	2.803E-45	0.000E+00	1.009E-21
Np-237	Np-237	1.000E+00	2.118E-35	2.118E-35	2.118E-35	1.852E-35	1.587E-35	1.322E-35	7.929E-36	2.634E-36	0.000E+00	1.581E-13
Np-237	Pu-241	1.000E+00	7.793E-42	2.609E-41	2.226E-38	3.547E-38	3.578E-38	3.362E-38	2.377E-38	8.766E-39	0.000E+00	3.650E-16
Np-237	Pu-241	2.450E-05	4.624E-44	1.387E-43	2.180E-42	1.906E-42	1.634E-42	1.361E-42	8.170E-43	2.705E-43	0.000E+00	1.628E-20
Np-237	∑DOSE(j):		2.119E-35	2.119E-35	2.142E-35	1.888E-35	1.623E-35	1.356E-35	8.163E-36	2.720E-36	0.000E+00	1.630E-13
U-233	Am-241	1.000E+00	0.000E+00	0.000E+00	0.000E+00	0.000E+00	0.000E+00	0.000E+00	0.000E+00	0.000E+00	0.000E+00	1.030E-14
U-233	Cm-245	1.000E+00	0.000E+00	0.000E+00	0.000E+00	0.000E+00	0.000E+00	0.000E+00	0.000E+00	0.000E+00	0.000E+00	1.651E-17
U-233	Cm-245	2.450E-05	0.000E+00	0.000E+00	0.000E+00	0.000E+00	0.000E+00	0.000E+00	0.000E+00	0.000E+00	0.000E+00	2.931E-21
U-233	Np-237	1.000E+00	0.000E+00	0.000E+00	0.000E+00	1.401E-45	1.401E-45	1.401E-45	1.401E-45	0.000E+00	0.000E+00	4.657E-13
U-233	Pu-241	1.000E+00	0.000E+00	0.000E+00	0.000E+00	0.000E+00	0.000E+00	0.000E+00	0.000E+00	0.000E+00	0.000E+00	1.156E-15
U-233	Pu-241	2.450E-05	0.000E+00	0.000E+00	0.000E+00	0.000E+00	0.000E+00	0.000E+00	0.000E+00	0.000E+00	0.000E+00	4.794E-20
U-233	U-233	1.000E+00	7.811E-41	7.811E-41	7.805E-41	6.818E-41	5.841E-41	4.864E-41	2.914E-41	9.672E-42	0.000E+00	3.740E-18
U-233	∑DOSE(j):		7.811E-41	7.811E-41	7.805E-41	6.818E-41	5.841E-41	4.865E-41	2.914E-41	9.672E-42	0.000E+00	4.772E-13
Th-229	Am-241	1.000E+00	6.356E-39	2.683E-38	3.939E-33	2.534E-32	4.078E-32	5.650E-32	7.457E-32	4.508E-32	0.000E+00	8.137E-17
Th-229	Cm-245	1.000E+00	0.000E+00	2.803E-45	1.448E-37	2.240E-36	4.704E-36	8.065E-36	1.481E-35	1.152E-35	0.000E+00	8.183E-18
Th-229	Cm-245	2.450E-05	0.000E+00	0.000E+00	5.050E-41	4.012E-40	6.879E-40	1.005E-39	1.451E-39	9.467E-40	0.000E+00	2.300E-23
Th-229	Np-237	1.000E+00	6.647E-35	2.265E-34	1.084E-30	3.758E-30	5.013E-30	5.993E-30	6.344E-30	3.271E-30	0.000E+00	3.729E-15
Th-229	Pu-241	1.000E+00	4.121E-41	2.353E-40	3.402E-34	2.520E-33	4.175E-33	5.901E-33	7.985E-33	4.900E-33	0.000E+00	9.124E-18
Th-229	Pu-241	2.450E-05	5.087E-43	2.105E-42	9.099E-38	3.491E-37	4.754E-37	5.761E-37	6.204E-37	3.232E-37	0.000E+00	3.838E-22
Th-229	Th-229	1.000E+00	2.320E-24	2.320E-24	2.277E-24	1.953E-24	1.658E-24	1.369E-24	8.054E-25	2.626E-25	0.000E+00	0.000E+00
Th-229	U-233	1.000E+00	7.979E-28	2.394E-27	3.169E-25	5.481E-25	5.841E-25	5.811E-25	4.599E-25	1.891E-25	0.000E+00	8.003E-15
Th-229	∑DOSE(j):		2.321E-24	2.322E-24	2.594E-24	2.501E-24	2.243E-24	1.950E-24	1.265E-24	4.517E-25	0.000E+00	1.183E-14
Am-243	Am-243	1.000E+00	5.346E-39	5.346E-39	5.246E-39	4.502E-39	3.822E-39	3.155E-39	1.856E-39	6.052E-40	0.000E+00	0.000E+00
Am-243	Cm-243	2.400E-03	0.000E+00	0.000E+00	7.006E-45	5.605E-45	5.605E-45	4.204E-45	2.803E-45	1.401E-45	0.000E+00	0.000E+00
Am-243	Cm-247	1.000E+00	1.401E-45	2.803E-45	3.503E-43	6.040E-43	6.446E-43	6.418E-43	5.087E-43	2.088E-43	0.000E+00	1.525E-14
Am-243	∑DOSE(j):		5.346E-39	5.346E-39	5.247E-39	4.502E-39	3.823E-39	3.155E-39	1.857E-39	6.054E-40	0.000E+00	1.525E-14

Individual Nuclide Dose Summed Over All Pathways
Parent Nuclide and Thread Fraction Indicated

Nuclide (j)	Parent (i)	THF(i)	DOSE(j,t), mrem/yr t= 0.000E+00	1.000E+00	2.000E+02	4.000E+02	5.000E+02	6.000E+02	8.000E+02	1.000E+03	2.000E+03	1.000E+04
Pu-239	Am-243	1.000E+00	0.000E+00	0.000E+00	5.605E-44	9.669E-44	1.037E-43	1.023E-43	8.128E-44	3.363E-44	0.000E+00	3.825E-14
Pu-239	Cm-243	2.400E-03	0.000E+00	0.000E+00	0.000E+00	0.000E+00	0.000E+00	0.000E+00	0.000E+00	0.000E+00	0.000E+00	4.856E-20
Pu-239	Cm-243	9.976E-01	0.000E+00	0.000E+00	1.401E-45	1.401E-45	1.401E-45	1.401E-45	0.000E+00	0.000E+00	0.000E+00	4.329E-16
Pu-239	Cm-247	1.000E+00	0.000E+00	0.000E+00	0.000E+00	0.000E+00	0.000E+00	0.000E+00	0.000E+00	0.000E+00	0.000E+00	1.174E-14
Pu-239	Pu-239	1.000E+00	1.942E-40	1.942E-40	1.931E-40	1.679E-40	1.434E-40	1.192E-40	7.105E-41	2.347E-41	0.000E+00	4.869E-11
Pu-239	∑DOSE(j):		1.942E-40	1.942E-40	1.931E-40	1.679E-40	1.435E-40	1.193E-40	7.113E-41	2.350E-41	0.000E+00	4.874E-11
U-235	Am-243	1.000E+00	0.000E+00	0.000E+00	0.000E+00	0.000E+00	0.000E+00	0.000E+00	0.000E+00	0.000E+00	0.000E+00	1.174E-17
U-235	Cm-243	2.400E-03	0.000E+00	0.000E+00	0.000E+00	0.000E+00	0.000E+00	0.000E+00	0.000E+00	0.000E+00	0.000E+00	1.505E-23
U-235	Cm-243	9.976E-01	0.000E+00	0.000E+00	0.000E+00	0.000E+00	0.000E+00	0.000E+00	0.000E+00	0.000E+00	0.000E+00	1.171E-19
U-235	Cm-247	1.000E+00	0.000E+00	0.000E+00	0.000E+00	0.000E+00	0.000E+00	0.000E+00	0.000E+00	0.000E+00	0.000E+00	6.237E-21
U-235	Pu-239	1.000E+00	0.000E+00	0.000E+00	1.822E-44	3.223E-44	3.363E-44	3.363E-44	2.662E-44	1.121E-44	0.000E+00	1.317E-14
U-235	U-235	1.000E+00	6.320E-38	6.320E-38	6.320E-38	5.526E-38	4.736E-38	3.946E-38	2.366E-38	7.861E-39	0.000E+00	3.428E-18
U-235	∑DOSE(j):		6.320E-38	6.320E-38	6.320E-38	5.526E-38	4.736E-38	3.946E-38	2.366E-38	7.861E-39	0.000E+00	1.318E-14
Pa-231	Am-243	1.000E+00	0.000E+00	0.000E+00	0.000E+00	0.000E+00	0.000E+00	1.401E-45	1.401E-45	1.401E-45	0.000E+00	1.063E-19
Pa-231	Cm-243	2.400E-03	0.000E+00	0.000E+00	0.000E+00	0.000E+00	0.000E+00	0.000E+00	0.000E+00	0.000E+00	0.000E+00	1.361E-25
Pa-231	Cm-243	9.976E-01	0.000E+00	0.000E+00	0.000E+00	0.000E+00	0.000E+00	0.000E+00	0.000E+00	0.000E+00	0.000E+00	1.089E-21
Pa-231	Cm-247	1.000E+00	0.000E+00	0.000E+00	0.000E+00	0.000E+00	0.000E+00	0.000E+00	0.000E+00	0.000E+00	0.000E+00	5.169E-23
Pa-231	Pa-231	1.000E+00	5.799E-36	5.799E-36	5.774E-36	5.028E-36	4.300E-36	3.575E-36	2.134E-36	7.061E-37	0.000E+00	0.000E+00
Pa-231	Pu-239	1.000E+00	0.000E+00	0.000E+00	5.913E-43	2.054E-42	2.742E-42	3.285E-42	3.488E-42	1.803E-42	0.000E+00	1.224E-16
Pa-231	U-235	1.000E+00	1.019E-38	3.057E-38	4.078E-36	7.107E-36	7.604E-36	7.593E-36	6.056E-36	2.509E-36	0.000E+00	8.422E-15
Pa-231	∑DOSE(j):		5.809E-36	5.829E-36	9.852E-36	1.213E-35	1.190E-35	1.117E-35	8.191E-36	3.215E-36	0.000E+00	8.544E-15
Be-10	Be-10	1.000E+00	0.000E+00	0.000E+00	0.000E+00	0.000E+00	0.000E+00	0.000E+00	0.000E+00	0.000E+00	0.000E+00	0.000E+00
C-14	C-14	1.000E+00	0.000E+00	0.000E+00	0.000E+00	1.405E-01	1.019E+00	5.400E-01	1.440E-01	7.084E-02	3.042E-10	0.000E+00
Ca-41	Ca-41	1.000E+00	0.000E+00	0.000E+00	0.000E+00	0.000E+00	0.000E+00	0.000E+00	0.000E+00	0.000E+00	0.000E+00	3.054E-11
Cm-243	Cm-243	2.400E-03	6.149E-42	6.012E-42	5.325E-44	0.000E+00	0.000E+00	0.000E+00	0.000E+00	0.000E+00	0.000E+00	0.000E+00
Cm-243	Cm-243	9.976E-01	2.556E-39	2.499E-39	2.183E-41	1.640E-43	1.261E-44	1.401E-45	0.000E+00	0.000E+00	0.000E+00	0.000E+00
Cm-243	∑DOSE(j):		2.562E-39	2.505E-39	2.188E-41	1.640E-43	1.261E-44	1.401E-45	0.000E+00	0.000E+00	0.000E+00	0.000E+00
Cm-244	Cm-244	1.371E-06	1.614E-34	1.557E-34	7.632E-38	3.154E-41	5.857E-43	1.121E-44	0.000E+00	0.000E+00	0.000E+00	0.000E+00
Cm-244	Cm-244	5.750E-08	6.768E-36	6.532E-36	3.201E-39	1.323E-42	2.522E-44	0.000E+00	0.000E+00	0.000E+00	0.000E+00	0.000E+00
Cm-244	∑DOSE(j):		1.681E-34	1.623E-34	7.952E-38	3.286E-41	6.110E-43	1.121E-44	0.000E+00	0.000E+00	0.000E+00	0.000E+00
Pu-240	Cm-244	5.750E-08	0.000E+00	0.000E+00	0.000E+00	0.000E+00	0.000E+00	0.000E+00	0.000E+00	0.000E+00	0.000E+00	7.757E-21
Pu-240	Cm-244	1.000E+00	0.000E+00	0.000E+00	0.000E+00	0.000E+00	0.000E+00	0.000E+00	0.000E+00	0.000E+00	0.000E+00	1.349E-13
Pu-240	Cm-248	5.261E-08	0.000E+00	0.000E+00	0.000E+00	0.000E+00	0.000E+00	0.000E+00	0.000E+00	0.000E+00	0.000E+00	1.007E-27
Pu-240	Pu-240	5.750E-08	0.000E+00	0.000E+00	0.000E+00	0.000E+00	0.000E+00	0.000E+00	0.000E+00	0.000E+00	0.000E+00	1.380E-18
Pu-240	Pu-244	5.743E-08	0.000E+00	0.000E+00	0.000E+00	0.000E+00	0.000E+00	0.000E+00	0.000E+00	0.000E+00	0.000E+00	1.534E-22
Pu-240	∑DOSE(j):		0.000E+00	0.000E+00	0.000E+00	0.000E+00	0.000E+00	0.000E+00	0.000E+00	0.000E+00	0.000E+00	1.349E-13

Individual Nuclide Dose Summed Over All Pathways
Parent Nuclide and Thread Fraction Indicated

Nuclide (j)	Parent (i)	THF(i)	DOSE(j,t), mrem/yr t= 0.000E+00	1.000E+00	2.000E+02	4.000E+02	5.000E+02	6.000E+02	8.000E+02	1.000E+03	2.000E+03	1.000E+04
Cm-244	Cm-244	1.000E+00	1.177E-28	1.136E-28	5.567E-32	2.300E-35	4.270E-37	7.754E-39	2.193E-42	0.000E+00	0.000E+00	0.000E+00
U-236	Cm-244	1.000E+00	0.000E+00	0.000E+00	0.000E+00	0.000E+00	0.000E+00	0.000E+00	0.000E+00	0.000E+00	0.000E+00	1.102E-15
U-236	Cm-248	9.150E-01	0.000E+00	0.000E+00	0.000E+00	0.000E+00	0.000E+00	0.000E+00	0.000E+00	0.000E+00	0.000E+00	1.394E-22
U-236	Pu-240	1.000E+00	0.000E+00	0.000E+00	0.000E+00	0.000E+00	0.000E+00	0.000E+00	0.000E+00	0.000E+00	0.000E+00	1.961E-13
U-236	Pu-244	9.988E-01	0.000E+00	0.000E+00	0.000E+00	0.000E+00	0.000E+00	0.000E+00	0.000E+00	0.000E+00	0.000E+00	2.105E-17
U-236	U-236	1.000E+00	0.000E+00	0.000E+00	0.000E+00	0.000E+00	0.000E+00	0.000E+00	0.000E+00	0.000E+00	0.000E+00	7.661E-19
U-236	∑DOSE(j):		0.000E+00	0.000E+00	0.000E+00	0.000E+00	0.000E+00	0.000E+00	0.000E+00	0.000E+00	0.000E+00	1.973E-13
Th-232	Cm-244	1.000E+00	0.000E+00	0.000E+00	0.000E+00	0.000E+00	0.000E+00	0.000E+00	0.000E+00	0.000E+00	0.000E+00	1.649E-24
Th-232	Cm-248	9.150E-01	0.000E+00	0.000E+00	0.000E+00	0.000E+00	0.000E+00	0.000E+00	0.000E+00	0.000E+00	0.000E+00	1.915E-31
Th-232	Pu-240	1.000E+00	0.000E+00	0.000E+00	0.000E+00	0.000E+00	0.000E+00	0.000E+00	0.000E+00	0.000E+00	0.000E+00	2.935E-22
Th-232	Pu-244	9.988E-01	0.000E+00	0.000E+00	0.000E+00	0.000E+00	0.000E+00	0.000E+00	0.000E+00	0.000E+00	0.000E+00	2.999E-26
Th-232	Th-232	1.000E+00	0.000E+00	0.000E+00	0.000E+00	0.000E+00	0.000E+00	0.000E+00	0.000E+00	0.000E+00	0.000E+00	0.000E+00
Th-232	U-236	1.000E+00	0.000E+00	0.000E+00	0.000E+00	0.000E+00	0.000E+00	0.000E+00	0.000E+00	0.000E+00	0.000E+00	2.957E-22
Th-232	∑DOSE(j):		0.000E+00	0.000E+00	0.000E+00	0.000E+00	0.000E+00	0.000E+00	0.000E+00	0.000E+00	0.000E+00	5.909E-22
Ra-228	Cm-244	1.000E+00	0.000E+00	2.803E-45	7.987E-40	3.298E-39	4.556E-39	5.574E-39	6.072E-39	3.184E-39	0.000E+00	9.138E-24
Ra-228	Cm-248	9.150E-01	0.000E+00	0.000E+00	0.000E+00	0.000E+00	0.000E+00	0.000E+00	0.000E+00	0.000E+00	0.000E+00	1.059E-30
Ra-228	Pu-240	1.000E+00	2.117E-42	8.524E-42	1.860E-37	6.715E-37	9.031E-37	1.085E-36	1.156E-36	5.984E-37	0.000E+00	1.626E-21
Ra-228	Pu-244	9.988E-01	0.000E+00	0.000E+00	7.287E-44	5.507E-43	9.305E-43	1.348E-42	1.924E-42	1.250E-42	0.000E+00	1.660E-25
Ra-228	Ra-228	1.000E+00	2.358E-27	2.143E-27	8.197E-38	0.000E+00	0.000E+00	0.000E+00	0.000E+00	0.000E+00	0.000E+00	0.000E+00
Ra-228	Th-232	1.000E+00	1.791E-26	5.210E-26	3.935E-25	3.440E-25	2.949E-25	2.457E-25	1.473E-25	4.894E-26	0.000E+00	0.000E+00
Ra-228	U-236	1.000E+00	6.060E-36	1.988E-35	9.518E-33	1.698E-32	1.827E-32	1.831E-32	1.469E-32	6.111E-33	0.000E+00	1.623E-21
Ra-228	∑DOSE(j):		2.027E-26	5.425E-26	3.935E-25	3.440E-25	2.949E-25	2.457E-25	1.473E-25	4.894E-26	0.000E+00	3.259E-21
Th-228	Cm-244	1.000E+00	5.419E-42	3.890E-41	2.738E-35	1.151E-34	1.594E-34	1.955E-34	2.135E-34	1.121E-34	0.000E+00	1.424E-24
Th-228	Cm-248	9.150E-01	0.000E+00	0.000E+00	0.000E+00	0.000E+00	0.000E+00	0.000E+00	7.006E-45	9.809E-45	0.000E+00	1.593E-31
Th-228	Pu-240	1.000E+00	2.477E-38	1.199E-37	6.401E-33	2.345E-32	3.162E-32	3.808E-32	4.066E-32	2.107E-32	0.000E+00	2.535E-22
Th-228	Pu-244	9.988E-01	0.000E+00	0.000E+00	2.509E-39	1.911E-38	3.243E-38	4.708E-38	6.745E-38	4.389E-38	0.000E+00	2.533E-26
Th-228	Ra-228	1.000E+00	5.147E-24	1.410E-23	4.348E-33	1.303E-43	0.000E+00	0.000E+00	0.000E+00	0.000E+00	0.000E+00	0.000E+00
Th-228	Th-228	1.000E+00	7.643E-27	6.347E-27	0.000E+00	0.000E+00	0.000E+00	0.000E+00	0.000E+00	0.000E+00	0.000E+00	0.000E+00
Th-228	Th-232	1.000E+00	3.616E-22	1.098E-21	1.393E-20	1.218E-20	1.044E-20	8.699E-21	5.216E-21	1.733E-21	0.000E+00	0.000E+00
Th-228	U-232	1.000E+00	3.318E-21	9.357E-21	5.526E-21	6.462E-22	2.025E-22	6.171E-23	4.948E-24	2.199E-25	0.000E+00	0.000E+00
Th-228	U-236	1.000E+00	8.905E-32	3.228E-31	3.322E-28	5.971E-28	6.431E-28	6.453E-28	5.182E-28	2.158E-28	0.000E+00	2.522E-22
Th-228	∑DOSE(j):		3.684E-21	1.047E-20	1.946E-20	1.283E-20	1.064E-20	8.761E-21	5.221E-21	1.733E-21	0.000E+00	5.071E-22
Cm-245	Cm-245	6.100E-09	0.000E+00	0.000E+00	0.000E+00	0.000E+00	0.000E+00	0.000E+00	0.000E+00	0.000E+00	0.000E+00	9.665E-23
Cm-245	Cm-245	1.000E+00	0.000E+00	0.000E+00	0.000E+00	0.000E+00	0.000E+00	0.000E+00	0.000E+00	0.000E+00	0.000E+00	1.584E-14
Cm-245	∑DOSE(j):		0.000E+00	0.000E+00	0.000E+00	0.000E+00	0.000E+00	0.000E+00	0.000E+00	0.000E+00	0.000E+00	1.584E-14
Pu-241	Cm-245	1.000E+00	0.000E+00	0.000E+00	0.000E+00	0.000E+00	0.000E+00	0.000E+00	0.000E+00	0.000E+00	0.000E+00	3.417E-16
Pu-241	Cm-245	2.450E-05	0.000E+00	0.000E+00	0.000E+00	0.000E+00	0.000E+00	0.000E+00	0.000E+00	0.000E+00	0.000E+00	1.008E-20
Pu-241	Pu-241	1.000E+00	0.000E+00	0.000E+00	0.000E+00	0.000E+00	0.000E+00	0.000E+00	0.000E+00	0.000E+00	0.000E+00	0.000E+00
Pu-241	∑DOSE(j):		0.000E+00	0.000E+00	0.000E+00	0.000E+00	0.000E+00	0.000E+00	0.000E+00	0.000E+00	0.000E+00	3.417E-16

Parent Dose Report
Title : Site 7 Base Case Model
File : BC_V01.ROF

Individual Nuclide Dose Summed Over All Pathways
Parent Nuclide and Thread Fraction Indicated

Nuclide (j)	Parent (i)	THF(i)	DOSE(j,t), mrem/yr t= 0.000E+00	1.000E+00	2.000E+02	4.000E+02	5.000E+02	6.000E+02	8.000E+02	1.000E+03	2.000E+03	1.000E+04
Cm-245	Cm-245	2.450E-05	0.000E+00	0.000E+00	0.000E+00	0.000E+00	0.000E+00	0.000E+00	0.000E+00	0.000E+00	0.000E+00	3.882E-19
Cm-246	Cm-246	2.630E-04	7.423E-30	7.422E-30	7.210E-30	6.123E-30	5.172E-30	4.247E-30	2.473E-30	7.981E-31	0.000E+00	9.077E-18
Cm-246	Cm-246	5.539E-06	1.563E-31	1.563E-31	1.518E-31	1.290E-31	1.089E-31	8.944E-32	5.209E-32	1.681E-32	0.000E+00	1.911E-19
Cm-246	∑DOSE(j):		7.579E-30	7.578E-30	7.362E-30	6.252E-30	5.281E-30	4.336E-30	2.525E-30	8.149E-31	0.000E+00	9.268E-18
Pu-242	Cm-246	5.539E-06	1.538E-40	4.613E-40	6.078E-38	1.046E-37	1.112E-37	1.104E-37	8.696E-38	3.559E-38	0.000E+00	8.975E-21
Pu-242	Cm-246	5.449E-07	1.513E-41	4.538E-41	5.979E-39	1.029E-38	1.094E-38	1.086E-38	8.555E-39	3.501E-39	0.000E+00	8.829E-22
Pu-242	Pu-242	5.540E-06	1.811E-34	1.811E-34	1.811E-34	1.583E-34	1.356E-34	1.130E-34	6.772E-35	2.249E-35	0.000E+00	9.963E-19
Pu-242	∑DOSE(j):		1.811E-34	1.811E-34	1.811E-34	1.584E-34	1.357E-34	1.131E-34	6.781E-35	2.253E-35	0.000E+00	1.006E-18
Cm-246	Cm-246	5.449E-07	1.538E-32	1.538E-32	1.494E-32	1.269E-32	1.071E-32	8.798E-33	5.124E-33	1.653E-33	0.000E+00	1.880E-20
Cm-246	Cm-246	9.997E-01	2.822E-26	2.821E-26	2.741E-26	2.328E-26	1.966E-26	1.614E-26	9.402E-27	3.034E-27	0.000E+00	3.450E-14
Cm-246	∑DOSE(j):		2.822E-26	2.821E-26	2.741E-26	2.328E-26	1.966E-26	1.614E-26	9.402E-27	3.034E-27	0.000E+00	3.450E-14
U-238	Cm-246	5.449E-07	0.000E+00	0.000E+00	0.000E+00	0.000E+00	0.000E+00	0.000E+00	0.000E+00	0.000E+00	0.000E+00	3.687E-26
U-238	Pu-242	5.450E-07	0.000E+00	0.000E+00	0.000E+00	0.000E+00	0.000E+00	0.000E+00	0.000E+00	0.000E+00	0.000E+00	4.133E-24
U-238	U-238	5.450E-07	1.121E-44	1.121E-44	1.121E-44	9.809E-45	8.408E-45	7.006E-45	4.204E-45	1.401E-45	0.000E+00	1.698E-23
U-238	∑DOSE(j):		1.121E-44	1.121E-44	1.121E-44	9.809E-45	8.408E-45	7.006E-45	4.204E-45	1.401E-45	0.000E+00	2.115E-23
Pu-242	Cm-246	9.997E-01	2.776E-35	8.327E-35	1.097E-32	1.888E-32	2.008E-32	1.993E-32	1.570E-32	6.424E-33	0.000E+00	1.620E-15
Pu-242	Pu-242	1.000E+00	3.270E-29	3.270E-29	3.269E-29	2.857E-29	2.448E-29	2.039E-29	1.222E-29	4.059E-30	0.000E+00	1.798E-13
Pu-242	∑DOSE(j):		3.270E-29	3.270E-29	3.270E-29	2.859E-29	2.450E-29	2.041E-29	1.224E-29	4.066E-30	0.000E+00	1.815E-13
U-238	Cm-246	9.997E-01	5.605E-45	2.102E-44	1.017E-40	3.512E-40	4.678E-40	5.583E-40	5.892E-40	3.028E-40	0.000E+00	7.369E-20
U-238	Pu-242	1.000E+00	1.504E-39	4.511E-39	6.028E-37	1.053E-36	1.127E-36	1.127E-36	9.005E-37	3.738E-37	0.000E+00	8.262E-18
U-238	U-238	1.000E+00	4.269E-26	4.269E-26	4.269E-26	3.733E-26	3.199E-26	2.666E-26	1.598E-26	5.310E-27	0.000E+00	3.393E-17
U-238	∑DOSE(j):		4.269E-26	4.269E-26	4.269E-26	3.733E-26	3.199E-26	2.666E-26	1.598E-26	5.310E-27	0.000E+00	4.227E-17
U-234	Cm-246	9.997E-01	0.000E+00	0.000E+00	0.000E+00	0.000E+00	0.000E+00	0.000E+00	0.000E+00	0.000E+00	0.000E+00	4.509E-23
U-234	Pu-238	1.000E+00	0.000E+00	0.000E+00	0.000E+00	0.000E+00	0.000E+00	0.000E+00	0.000E+00	0.000E+00	0.000E+00	3.033E-21
U-234	Pu-242	1.000E+00	0.000E+00	0.000E+00	0.000E+00	0.000E+00	0.000E+00	0.000E+00	0.000E+00	0.000E+00	0.000E+00	5.104E-21
U-234	U-234	1.000E+00	0.000E+00	0.000E+00	0.000E+00	0.000E+00	0.000E+00	0.000E+00	0.000E+00	0.000E+00	0.000E+00	5.552E-17
U-234	U-238	1.000E+00	0.000E+00	0.000E+00	0.000E+00	0.000E+00	0.000E+00	0.000E+00	0.000E+00	0.000E+00	0.000E+00	8.581E-19
U-234	∑DOSE(j):		0.000E+00	0.000E+00	0.000E+00	0.000E+00	0.000E+00	0.000E+00	0.000E+00	0.000E+00	0.000E+00	5.639E-17
Th-230	Cm-246	9.997E-01	0.000E+00	0.000E+00	0.000E+00	0.000E+00	0.000E+00	0.000E+00	0.000E+00	0.000E+00	0.000E+00	1.387E-26
Th-230	Pu-238	1.000E+00	0.000E+00	0.000E+00	0.000E+00	0.000E+00	0.000E+00	0.000E+00	0.000E+00	0.000E+00	0.000E+00	1.857E-19
Th-230	Pu-242	1.000E+00	0.000E+00	0.000E+00	0.000E+00	0.000E+00	0.000E+00	0.000E+00	0.000E+00	0.000E+00	0.000E+00	1.626E-24
Th-230	Th-230	1.000E+00	0.000E+00	0.000E+00	0.000E+00	0.000E+00	0.000E+00	0.000E+00	0.000E+00	0.000E+00	0.000E+00	0.000E+00
Th-230	U-234	1.000E+00	0.000E+00	0.000E+00	0.000E+00	0.000E+00	0.000E+00	0.000E+00	0.000E+00	0.000E+00	0.000E+00	3.417E-15
Th-230	U-238	1.000E+00	0.000E+00	0.000E+00	0.000E+00	0.000E+00	0.000E+00	0.000E+00	0.000E+00	0.000E+00	0.000E+00	5.339E-17
Th-230	∑DOSE(j):		0.000E+00	0.000E+00	0.000E+00	0.000E+00	0.000E+00	0.000E+00	0.000E+00	0.000E+00	0.000E+00	3.471E-15

Individual Nuclide Dose Summed Over All Pathways
Parent Nuclide and Thread Fraction Indicated

Nuclide (j)	Parent (i)	THF(i)	DOSE(j,t), mrem/yr t= 0.000E+00	1.000E+00	2.000E+02	4.000E+02	5.000E+02	6.000E+02	8.000E+02	1.000E+03	2.000E+03	1.000E+04
Ra-226	Cm-246	9.997E-01	0.000E+00	0.000E+00	2.943E-44	7.889E-43	2.039E-42	4.181E-42	1.035E-41	1.029E-41	0.000E+00	2.031E-27
Ra-226	Pu-238	1.000E+00	4.444E-35	1.870E-34	2.071E-29	1.061E-28	1.553E-28	1.977E-28	2.257E-28	1.210E-28	0.000E+00	2.235E-20
Ra-226	Pu-242	1.000E+00	0.000E+00	0.000E+00	4.255E-40	5.816E-39	1.205E-38	2.062E-38	3.838E-38	3.059E-38	0.000E+00	2.260E-25
Ra-226	Ra-226	1.000E+00	1.705E-23	1.704E-23	1.564E-23	1.254E-23	1.029E-23	8.210E-24	4.514E-24	1.375E-24	0.000E+00	0.000E+00
Ra-226	Th-230	1.000E+00	8.846E-27	2.653E-26	3.398E-24	5.683E-24	5.957E-24	5.830E-24	4.468E-24	1.780E-24	0.000E+00	0.000E+00
Ra-226	U-234	1.000E+00	6.538E-29	2.228E-28	1.043E-24	3.534E-24	4.662E-24	5.513E-24	5.710E-24	2.881E-24	0.000E+00	4.110E-16
Ra-226	U-238	1.000E+00	1.823E-34	7.700E-34	1.199E-28	8.174E-28	1.353E-27	1.925E-27	2.677E-27	1.700E-27	0.000E+00	6.289E-18
Ra-226	∑DOSE(j):		1.706E-23	1.707E-23	2.008E-23	2.176E-23	2.091E-23	1.955E-23	1.469E-23	6.038E-24	0.000E+00	4.173E-16
Pb-210	Cm-246	9.997E-01	0.000E+00	0.000E+00	0.000E+00	0.000E+00	0.000E+00	0.000E+00	0.000E+00	0.000E+00	0.000E+00	3.465E-25
Pb-210	Pb-210	1.000E+00	8.269E-31	8.030E-31	1.608E-33	2.732E-36	1.030E-37	3.788E-39	4.408E-42	2.803E-45	0.000E+00	0.000E+00
Pb-210	Pu-238	1.000E+00	1.822E-44	1.023E-43	1.491E-37	9.375E-37	1.431E-36	1.874E-36	2.214E-36	1.211E-36	0.000E+00	3.500E-18
Pb-210	Pu-242	1.000E+00	0.000E+00	0.000E+00	0.000E+00	0.000E+00	0.000E+00	0.000E+00	0.000E+00	0.000E+00	0.000E+00	3.833E-23
Pb-210	Ra-226	1.000E+00	2.641E-33	7.846E-33	1.694E-31	1.361E-31	1.117E-31	8.915E-32	4.902E-32	1.493E-32	0.000E+00	0.000E+00
Pb-210	Th-230	1.000E+00	6.889E-36	2.321E-35	3.076E-32	5.634E-32	6.010E-32	5.948E-32	4.622E-32	1.856E-32	0.000E+00	0.000E+00
Pb-210	U-234	1.000E+00	3.437E-38	1.431E-37	8.197E-33	3.240E-32	4.412E-32	5.329E-32	5.668E-32	2.906E-32	0.000E+00	6.433E-14
Pb-210	U-238	1.000E+00	7.287E-44	4.176E-43	8.360E-37	6.982E-36	1.207E-35	1.770E-35	2.557E-35	1.662E-35	0.000E+00	9.805E-16
Pb-210	∑DOSE(j):		8.296E-31	8.109E-31	2.100E-31	2.249E-31	2.160E-31	2.019E-31	1.520E-31	6.258E-32	0.000E+00	6.532E-14
Cm-247	Cm-247	1.000E+00	6.864E-34	6.864E-34	6.864E-34	6.002E-34	5.144E-34	4.286E-34	2.570E-34	8.537E-35	0.000E+00	8.922E-15
Cm-248	Cm-248	8.390E-02	6.876E-27	6.876E-27	6.874E-27	6.008E-27	5.148E-27	4.288E-27	2.570E-27	8.535E-28	0.000E+00	1.604E-16
Cm-248	Cm-248	1.108E-03	9.085E-29	9.085E-29	9.081E-29	7.937E-29	6.801E-29	5.666E-29	3.396E-29	1.128E-29	0.000E+00	2.119E-18
Cm-248	∑DOSE(j):		6.967E-27	6.967E-27	6.964E-27	6.087E-27	5.216E-27	4.345E-27	2.604E-27	8.648E-28	0.000E+00	1.625E-16
Pu-244	Cm-248	1.108E-03	4.114E-39	1.234E-38	1.650E-36	2.880E-36	3.085E-36	3.083E-36	2.464E-36	1.023E-36	0.000E+00	5.218E-23
Pu-244	Cm-248	5.261E-08	1.948E-43	5.857E-43	7.832E-41	1.368E-40	1.465E-40	1.464E-40	1.170E-40	4.857E-41	0.000E+00	2.490E-27
Pu-244	Pu-244	1.210E-03	6.825E-30	6.825E-30	6.825E-30	5.968E-30	5.114E-30	4.261E-30	2.555E-30	8.488E-31	0.000E+00	4.696E-18
Pu-244	∑DOSE(j):		6.825E-30	6.825E-30	6.825E-30	5.968E-30	5.114E-30	4.261E-30	2.555E-30	8.488E-31	0.000E+00	4.696E-18
Cm-248	Cm-248	5.261E-08	4.312E-33	4.312E-33	4.310E-33	3.767E-33	3.228E-33	2.689E-33	1.612E-33	5.352E-34	0.000E+00	1.006E-22
Cm-248	Cm-248	9.150E-01	7.499E-26	7.499E-26	7.496E-26	6.552E-26	5.614E-26	4.677E-26	2.803E-26	9.309E-27	0.000E+00	1.749E-15
Cm-248	∑DOSE(j):		7.499E-26	7.499E-26	7.496E-26	6.552E-26	5.614E-26	4.677E-26	2.803E-26	9.309E-27	0.000E+00	1.749E-15
Pu-244	Cm-248	9.150E-01	3.397E-36	1.019E-35	1.362E-33	2.378E-33	2.547E-33	2.546E-33	2.035E-33	8.446E-34	0.000E+00	4.331E-20
Pu-244	Pu-244	9.988E-01	5.636E-27	5.636E-27	5.636E-27	4.928E-27	4.223E-27	3.519E-27	2.110E-27	7.009E-28	0.000E+00	3.898E-15
Pu-244	∑DOSE(j):		5.636E-27	5.636E-27	5.636E-27	4.928E-27	4.223E-27	3.519E-27	2.110E-27	7.009E-28	0.000E+00	3.898E-15
Pu-240	Cm-248	9.150E-01	0.000E+00	0.000E+00	0.000E+00	0.000E+00	0.000E+00	0.000E+00	0.000E+00	0.000E+00	0.000E+00	1.751E-20
Pu-240	Pu-240	1.000E+00	0.000E+00	0.000E+00	0.000E+00	0.000E+00	0.000E+00	0.000E+00	0.000E+00	0.000E+00	0.000E+00	2.401E-11
Pu-240	Pu-244	9.988E-01	0.000E+00	0.000E+00	0.000E+00	0.000E+00	0.000E+00	0.000E+00	0.000E+00	0.000E+00	0.000E+00	2.669E-15
Pu-240	∑DOSE(j):		0.000E+00	0.000E+00	0.000E+00	0.000E+00	0.000E+00	0.000E+00	0.000E+00	0.000E+00	0.000E+00	2.401E-11
H-3	H-3	1.000E+00	0.000E+00	0.000E+00	0.000E+00	1.155E-11	3.866E-13	5.925E-16	2.252E-21	1.501E-26	0.000E+00	0.000E+00

Parent Dose Report
Title : Site 7 Base Case Model
File : BC_V01.ROF

Individual Nuclide Dose Summed Over All Pathways
Parent Nuclide and Thread Fraction Indicated

Nuclide (j)	Parent (i)	THF(i)	DOSE(j,t), mrem/yr t= 0.000E+00	1.000E+00	2.000E+02	4.000E+02	5.000E+02	6.000E+02	8.000E+02	1.000E+03	2.000E+03	1.000E+04
I-129	I-129	1.000E+00	0.000E+00	0.000E+00	0.000E+00	0.000E+00	0.000E+00	0.000E+00	1.536E-42	8.909E-25	2.203E-04	1.137E-01
K-40	K-40	1.000E+00	6.011E-24	6.011E-24	6.011E-24	5.256E-24	4.504E-24	3.753E-24	2.250E-24	7.476E-25	0.000E+00	7.074E-08
Mo-93	Mo-93	1.200E-01	0.000E+00	0.000E+00	0.000E+00	0.000E+00	0.000E+00	0.000E+00	0.000E+00	0.000E+00	0.000E+00	0.000E+00
Mo-93	Mo-93	8.800E-01	0.000E+00	0.000E+00	0.000E+00	0.000E+00	0.000E+00	0.000E+00	0.000E+00	0.000E+00	0.000E+00	0.000E+00
Mo-93	∑DOSE(j):		0.000E+00	0.000E+00	0.000E+00	0.000E+00	0.000E+00	0.000E+00	0.000E+00	0.000E+00	0.000E+00	0.000E+00
Nb-93m	Mo-93	8.800E-01	0.000E+00	0.000E+00	0.000E+00	0.000E+00	0.000E+00	0.000E+00	0.000E+00	0.000E+00	0.000E+00	2.821E-39
Nb-93m	Nb-93m	1.000E+00	0.000E+00	0.000E+00	0.000E+00	0.000E+00	0.000E+00	0.000E+00	0.000E+00	0.000E+00	0.000E+00	0.000E+00
Nb-93m	∑DOSE(j):		0.000E+00	0.000E+00	0.000E+00	0.000E+00	0.000E+00	0.000E+00	0.000E+00	0.000E+00	0.000E+00	2.821E-39
Nb-94	Nb-94	1.000E+00	2.685E-28	2.685E-28	2.667E-28	2.316E-28	1.978E-28	1.643E-28	9.782E-29	3.228E-29	0.000E+00	0.000E+00
Ni-59	Ni-59	1.000E+00	1.280E-33	1.280E-33	1.278E-33	1.116E-33	9.558E-34	7.959E-34	4.765E-34	1.581E-34	0.000E+00	0.000E+00
Pu-238	Pu-238	1.850E-09	0.000E+00	0.000E+00	0.000E+00	0.000E+00	0.000E+00	0.000E+00	0.000E+00	0.000E+00	0.000E+00	0.000E+00
Pu-238	Pu-238	1.000E+00	0.000E+00	0.000E+00	0.000E+00	0.000E+00	0.000E+00	0.000E+00	0.000E+00	0.000E+00	0.000E+00	4.204E-45
Pu-238	∑DOSE(j):		0.000E+00	0.000E+00	0.000E+00	0.000E+00	0.000E+00	0.000E+00	0.000E+00	0.000E+00	0.000E+00	4.204E-45
Pu-241	Pu-241	2.450E-05	1.261E-44	1.261E-44	0.000E+00	0.000E+00	0.000E+00	0.000E+00	0.000E+00	0.000E+00	0.000E+00	0.000E+00
Pu-242	Pu-242	5.450E-07	1.782E-35	1.782E-35	1.781E-35	1.557E-35	1.334E-35	1.111E-35	6.662E-36	2.212E-36	0.000E+00	9.801E-20
Pu-244	Pu-244	5.743E-08	3.240E-34	3.240E-34	3.240E-34	2.833E-34	2.428E-34	2.023E-34	1.213E-34	4.030E-35	0.000E+00	2.241E-22
Sr-90	Sr-90	1.000E+00	8.401E-34	8.211E-34	6.816E-36	4.835E-38	3.727E-39	2.800E-40	1.361E-42	4.204E-45	0.000E+00	0.000E+00
Tc-99	Tc-99	1.000E+00	0.000E+00	0.000E+00	0.000E+00	2.755E-33	2.359E-15	3.884E-08	3.902E-03	1.025E-01	6.674E-01	3.510E-20
U-232	U-232	1.000E+00	0.000E+00	0.000E+00	0.000E+00	0.000E+00	0.000E+00	0.000E+00	0.000E+00	0.000E+00	0.000E+00	0.000E+00

THF(i) is the thread fraction of the parent nuclide.

Individual Nuclide Soil Concentration
Parent Nuclide and Thread Fraction Indicated

Nuclide (j)	Parent (i)	THF(i)	S(j,t), pCi/g t= 0.000E+00	1.000E+00	2.000E+02	4.000E+02	5.000E+02	6.000E+02	8.000E+02	1.000E+03	2.000E+03	1.000E+04
Ac-227	Ac-227	1.000E+00	2.920E-03	2.834E-03	5.021E-06	7.552E-09	2.677E-10	9.265E-12	9.542E-15	5.459E-18	0.000E+00	0.000E+00
Ac-227	Am-243	1.000E+00	0.000E+00	2.700E-19	1.541E-12	1.308E-11	2.278E-11	3.366E-11	4.933E-11	3.262E-11	0.000E+00	0.000E+00
Ac-227	Cm-243	2.400E-03	0.000E+00	1.030E-26	1.164E-18	1.312E-17	2.430E-17	3.744E-17	5.784E-17	3.948E-17	0.000E+00	0.000E+00
Ac-227	Cm-243	9.976E-01	0.000E+00	3.792E-20	1.004E-13	5.134E-13	7.418E-13	9.356E-13	1.060E-12	5.717E-13	0.000E+00	0.000E+00
Ac-227	Cm-247	1.000E+00	0.000E+00	0.000E+00	2.291E-17	4.053E-16	8.922E-16	1.595E-15	3.154E-15	2.627E-15	0.000E+00	0.000E+00
Ac-227	Pa-231	1.000E+00	0.000E+00	7.045E-03	2.377E-01	2.075E-01	1.775E-01	1.476E-01	8.818E-02	2.927E-02	0.000E+00	0.000E+00
Ac-227	Pu-239	1.000E+00	0.000E+00	1.487E-13	1.781E-08	7.226E-08	9.967E-08	1.219E-07	1.330E-07	7.014E-08	0.000E+00	0.000E+00
Ac-227	U-235	1.000E+00	0.000E+00	6.221E-05	1.414E-01	2.698E-01	2.937E-01	2.967E-01	2.401E-01	1.007E-01	0.000E+00	0.000E+00
Ac-227	∑S(j):		2.920E-03	9.941E-03	3.791E-01	4.773E-01	4.712E-01	4.443E-01	3.283E-01	1.299E-01	0.000E+00	0.000E+00
Am-241	Am-241	1.000E+00	5.900E+01	5.891E+01	4.281E+01	2.718E+01	1.985E+01	1.409E+01	6.133E+00	1.483E+00	0.000E+00	0.000E+00
Am-241	Cm-245	1.000E+00	0.000E+00	6.706E-06	9.481E-03	1.500E-02	1.506E-02	1.409E-02	9.861E-03	3.607E-03	0.000E+00	0.000E+00
Am-241	Pu-241	1.000E+00	0.000E+00	2.902E-01	5.083E+00	3.227E+00	2.356E+00	1.673E+00	7.283E-01	1.761E-01	0.000E+00	0.000E+00
Am-241	∑S(j):		5.900E+01	5.920E+01	4.790E+01	3.042E+01	2.222E+01	1.577E+01	6.871E+00	1.663E+00	0.000E+00	0.000E+00
Np-237	Am-241	1.000E+00	0.000E+00	1.900E-05	3.263E-03	4.927E-03	4.919E-03	4.593E-03	3.223E-03	1.187E-03	0.000E+00	0.000E+00
Np-237	Cm-245	1.000E+00	0.000E+00	3.610E-12	2.925E-07	1.022E-06	1.328E-06	1.538E-06	1.518E-06	7.294E-07	0.000E+00	0.000E+00
Np-237	Cm-245	2.450E-05	0.000E+00	3.321E-14	5.399E-11	9.913E-11	1.069E-10	1.073E-10	8.588E-11	3.568E-11	0.000E+00	0.000E+00
Np-237	Np-237	1.000E+00	3.250E-01	3.250E-01	3.250E-01	2.843E-01	2.437E-01	2.031E-01	1.218E-01	4.061E-02	0.000E+00	0.000E+00
Np-237	Pu-241	1.000E+00	0.000E+00	2.391E-07	3.406E-04	5.440E-04	5.489E-04	5.161E-04	3.651E-04	1.351E-04	0.000E+00	0.000E+00
Np-237	Pu-241	2.450E-05	0.000E+00	1.439E-09	3.345E-08	2.927E-08	2.509E-08	2.090E-08	1.254E-08	4.180E-09	0.000E+00	0.000E+00
Np-237	∑S(j):		3.250E-01	3.250E-01	3.286E-01	2.898E-01	2.492E-01	2.082E-01	1.254E-01	4.194E-02	0.000E+00	0.000E+00
U-233	Am-241	1.000E+00	0.000E+00	2.028E-10	1.496E-06	4.743E-06	6.058E-06	6.941E-06	6.774E-06	3.243E-06	0.000E+00	0.000E+00
U-233	Cm-245	1.000E+00	0.000E+00	1.948E-17	7.980E-11	5.944E-10	9.863E-10	1.395E-09	1.892E-09	1.166E-09	0.000E+00	0.000E+00
U-233	Cm-245	2.450E-05	0.000E+00	2.406E-19	2.140E-14	8.248E-14	1.124E-13	1.364E-13	1.472E-13	7.701E-14	0.000E+00	0.000E+00
U-233	Np-237	1.000E+00	0.000E+00	1.415E-06	2.829E-04	4.948E-04	5.300E-04	5.299E-04	4.237E-04	1.765E-04	0.000E+00	0.000E+00
U-233	Pu-241	1.000E+00	0.000E+00	1.734E-12	1.411E-07	4.955E-07	6.460E-07	7.503E-07	7.448E-07	3.601E-07	0.000E+00	0.000E+00
U-233	Pu-241	2.450E-05	0.000E+00	1.595E-14	2.610E-11	4.829E-11	5.230E-11	5.266E-11	4.249E-11	1.779E-11	0.000E+00	0.000E+00
U-233	U-233	1.000E+00	4.160E+01	4.160E+01	4.156E+01	3.634E+01	3.113E+01	2.593E+01	1.555E+01	5.177E+00	0.000E+00	0.000E+00
U-233	∑S(j):		4.160E+01	4.160E+01	4.156E+01	3.634E+01	3.113E+01	2.593E+01	1.555E+01	5.178E+00	0.000E+00	0.000E+00
Th-229	Am-241	1.000E+00	0.000E+00	3.129E-14	9.623E-09	6.218E-08	1.002E-07	1.389E-07	1.835E-07	1.114E-07	0.000E+00	0.000E+00
Th-229	Cm-245	1.000E+00	0.000E+00	2.967E-21	3.524E-13	5.489E-12	1.154E-11	1.980E-11	3.642E-11	2.843E-11	0.000E+00	0.000E+00
Th-229	Cm-245	2.450E-05	0.000E+00	2.817E-23	1.233E-16	9.841E-16	1.689E-15	2.470E-15	3.569E-15	2.338E-15	0.000E+00	0.000E+00
Th-229	Np-237	1.000E+00	0.000E+00	3.272E-10	2.655E-06	9.231E-06	1.232E-05	1.474E-05	1.562E-05	8.082E-06	0.000E+00	0.000E+00
Th-229	Pu-241	1.000E+00	0.000E+00	2.028E-16	8.305E-10	6.182E-09	1.025E-08	1.450E-08	1.965E-08	1.210E-08	0.000E+00	0.000E+00
Th-229	Pu-241	2.450E-05	0.000E+00	2.506E-18	2.227E-13	8.574E-13	1.168E-12	1.417E-12	1.528E-12	7.986E-13	0.000E+00	0.000E+00
Th-229	Th-229	1.000E+00	5.710E+00	5.709E+00	5.603E+00	4.811E+00	4.085E+00	3.372E+00	1.985E+00	6.494E-01	0.000E+00	0.000E+00
Th-229	U-233	1.000E+00	0.000E+00	3.928E-03	7.780E-01	1.348E+00	1.437E+00	1.430E+00	1.133E+00	4.675E-01	0.000E+00	0.000E+00
Th-229	∑S(j):		5.710E+00	5.713E+00	6.381E+00	6.159E+00	5.522E+00	4.802E+00	3.119E+00	1.117E+00	0.000E+00	0.000E+00
Am-243	Am-243	1.000E+00	2.970E+00	2.970E+00	2.915E+00	2.503E+00	2.125E+00	1.754E+00	1.033E+00	3.379E-01	0.000E+00	0.000E+00
Am-243	Cm-243	2.400E-03	0.000E+00	9.159E-08	3.980E-06	3.447E-06	2.927E-06	2.417E-06	1.423E-06	4.655E-07	0.000E+00	0.000E+00
Am-243	Cm-247	1.000E+00	0.000E+00	9.779E-07	1.938E-04	3.360E-04	3.583E-04	3.566E-04	2.827E-04	1.167E-04	0.000E+00	0.000E+00
Am-243	∑S(j):		2.970E+00	2.970E+00	2.915E+00	2.503E+00	2.126E+00	1.755E+00	1.033E+00	3.380E-01	0.000E+00	0.000E+00

Individual Nuclide Soil Concentration
Parent Nuclide and Thread Fraction Indicated

Nuclide (j)	Parent (i)	THF(i)	S(j,t), pCi/g t= 0.000E+00	1.000E+00	2.000E+02	4.000E+02	5.000E+02	6.000E+02	8.000E+02	1.000E+03	2.000E+03	1.000E+04
Pu-239	Am-243	1.000E+00	0.000E+00	8.536E-05	1.687E-02	2.916E-02	3.105E-02	3.086E-02	2.439E-02	1.004E-02	0.000E+00	0.000E+00
Pu-239	Cm-243	2.400E-03	0.000E+00	6.573E-12	1.836E-08	3.589E-08	3.912E-08	3.947E-08	3.178E-08	1.323E-08	0.000E+00	0.000E+00
Pu-239	Cm-243	9.976E-01	0.000E+00	1.164E-05	5.110E-04	4.484E-04	3.832E-04	3.184E-04	1.900E-04	6.296E-05	0.000E+00	0.000E+00
Pu-239	Cm-247	1.000E+00	0.000E+00	6.885E-11	5.579E-07	1.936E-06	2.583E-06	3.087E-06	3.266E-06	1.687E-06	0.000E+00	0.000E+00
Pu-239	Pu-239	1.000E+00	5.830E+01	5.830E+01	5.797E+01	5.043E+01	4.310E+01	3.581E+01	2.137E+01	7.081E+00	0.000E+00	0.000E+00
Pu-239	∑S(j):		5.830E+01	5.830E+01	5.798E+01	5.046E+01	4.313E+01	3.585E+01	2.139E+01	7.091E+00	0.000E+00	0.000E+00
U-235	Am-243	1.000E+00	0.000E+00	2.058E-13	1.668E-09	5.789E-09	7.722E-09	9.229E-09	9.764E-09	5.044E-09	0.000E+00	0.000E+00
U-235	Cm-243	2.400E-03	0.000E+00	1.067E-20	1.529E-15	6.459E-15	8.978E-15	1.103E-14	1.208E-14	6.374E-15	0.000E+00	0.000E+00
U-235	Cm-243	9.976E-01	0.000E+00	2.861E-14	8.054E-11	1.589E-10	1.740E-10	1.764E-10	1.433E-10	6.021E-11	0.000E+00	0.000E+00
U-235	Cm-247	1.000E+00	0.000E+00	1.100E-19	3.670E-14	2.553E-13	4.260E-13	6.116E-13	8.645E-13	5.594E-13	0.000E+00	0.000E+00
U-235	Pu-239	1.000E+00	0.000E+00	5.740E-08	1.145E-05	1.997E-05	2.137E-05	2.134E-05	1.702E-05	7.073E-06	0.000E+00	0.000E+00
U-235	U-235	1.000E+00	3.970E+01	3.970E+01	3.970E+01	3.474E+01	2.977E+01	2.481E+01	1.489E+01	4.962E+00	0.000E+00	0.000E+00
U-235	∑S(j):		3.970E+01	3.970E+01	3.970E+01	3.474E+01	2.978E+01	2.481E+01	1.489E+01	4.963E+00	0.000E+00	0.000E+00
Pa-231	Am-243	1.000E+00	0.000E+00	7.111E-18	2.355E-12	1.637E-11	2.730E-11	3.917E-11	5.531E-11	3.575E-11	0.000E+00	0.000E+00
Pa-231	Cm-243	2.400E-03	0.000E+00	2.799E-25	1.875E-18	1.673E-17	2.950E-17	4.398E-17	6.521E-17	4.342E-17	0.000E+00	0.000E+00
Pa-231	Cm-243	9.976E-01	0.000E+00	9.977E-19	1.436E-13	6.094E-13	8.490E-13	1.046E-12	1.151E-12	6.100E-13	0.000E+00	0.000E+00
Pa-231	Cm-247	1.000E+00	0.000E+00	0.000E+00	3.884E-17	5.406E-16	1.128E-15	1.943E-15	3.664E-15	2.964E-15	0.000E+00	0.000E+00
Pa-231	Pa-231	1.000E+00	2.390E-01	2.390E-01	2.380E-01	2.074E-01	1.774E-01	1.475E-01	8.812E-02	2.925E-02	0.000E+00	0.000E+00
Pa-231	Pu-239	1.000E+00	0.000E+00	2.974E-12	2.421E-08	8.445E-08	1.129E-07	1.353E-07	1.438E-07	7.465E-08	0.000E+00	0.000E+00
Pa-231	U-235	1.000E+00	0.000E+00	8.399E-04	1.676E-01	2.927E-01	3.133E-01	3.130E-01	2.499E-01	1.039E-01	0.000E+00	0.000E+00
Pa-231	∑S(j):		2.390E-01	2.398E-01	4.056E-01	5.001E-01	4.907E-01	4.605E-01	3.380E-01	1.331E-01	0.000E+00	0.000E+00
Be-10	Be-10	1.000E+00	2.530E-05	2.530E-05	2.530E-05	2.213E-05	1.897E-05	1.581E-05	9.484E-06	3.161E-06	0.000E+00	0.000E+00
C-14	C-14	1.000E+00	5.400E-01	5.399E-01	5.270E-01	1.029E-01	7.622E-02	5.020E-02	2.730E-04	0.000E+00	0.000E+00	0.000E+00
Ca-41	Ca-41	1.000E+00	4.210E-02	4.210E-02	4.204E-02	3.674E-02	3.147E-02	2.621E-02	1.570E-02	5.227E-03	0.000E+00	0.000E+00
Cm-243	Cm-243	2.400E-03	1.032E-03	1.009E-03	8.814E-06	6.585E-08	5.208E-09	4.014E-10	2.055E-12	5.844E-15	0.000E+00	0.000E+00
Cm-243	Cm-243	9.976E-01	4.290E-01	4.193E-01	3.664E-03	2.737E-05	2.165E-06	1.669E-07	8.542E-10	2.429E-12	0.000E+00	0.000E+00
Cm-243	∑S(j):		4.300E-01	4.203E-01	3.672E-03	2.744E-05	2.170E-06	1.673E-07	8.563E-10	2.435E-12	0.000E+00	0.000E+00
Cm-244	Cm-244	1.371E-06	1.727E-04	1.667E-04	8.169E-08	3.378E-11	6.272E-13	1.139E-14	3.223E-18	5.064E-22	0.000E+00	0.000E+00
Cm-244	Cm-244	5.750E-08	7.245E-06	6.992E-06	3.426E-09	1.417E-12	2.630E-14	4.777E-16	1.352E-19	2.124E-23	0.000E+00	0.000E+00
Cm-244	∑S(j):		1.800E-04	1.737E-04	8.512E-08	3.520E-11	6.535E-13	1.187E-14	3.358E-18	5.277E-22	0.000E+00	0.000E+00
Pu-240	Cm-244	5.750E-08	0.000E+00	6.974E-10	1.960E-08	1.680E-08	1.425E-08	1.175E-08	6.904E-09	2.253E-09	0.000E+00	0.000E+00
Pu-240	Cm-244	1.000E+00	0.000E+00	1.213E-02	3.410E-01	2.922E-01	2.479E-01	2.044E-01	1.201E-01	3.919E-02	0.000E+00	0.000E+00
Pu-240	Cm-248	5.261E-08	0.000E+00	6.588E-23	5.344E-19	1.857E-18	2.478E-18	2.963E-18	3.138E-18	1.623E-18	0.000E+00	0.000E+00
Pu-240	Pu-240	5.750E-08	3.565E-06	3.565E-06	3.490E-06	2.990E-06	2.536E-06	2.091E-06	1.229E-06	4.010E-07	0.000E+00	0.000E+00
Pu-240	Pu-244	5.743E-08	0.000E+00	2.231E-14	4.417E-12	7.648E-12	8.152E-12	8.109E-12	6.420E-12	2.647E-12	0.000E+00	0.000E+00
Pu-240	∑S(j):		3.565E-06	1.213E-02	3.410E-01	2.922E-01	2.479E-01	2.044E-01	1.201E-01	3.919E-02	0.000E+00	0.000E+00

Individual Nuclide Soil Concentration
Parent Nuclide and Thread Fraction Indicated

Nuclide (j)	Parent (i)	THF(i)	S(j,t), pCi/g t= 0.000E+00	1.000E+00	2.000E+02	4.000E+02	5.000E+02	6.000E+02	8.000E+02	1.000E+03	2.000E+03	1.000E+04
Cm-244	Cm-244	1.000E+00	1.260E+02	1.216E+02	5.959E-02	2.464E-05	4.575E-07	8.307E-09	2.351E-12	3.694E-16	0.000E+00	0.000E+00
U-236	Cm-244	1.000E+00	0.000E+00	9.066E-10	1.772E-06	3.298E-06	3.564E-06	3.578E-06	2.865E-06	1.189E-06	0.000E+00	0.000E+00
U-236	Cm-248	9.150E-01	0.000E+00	3.628E-23	1.837E-17	1.279E-16	2.135E-16	3.067E-16	4.338E-16	2.809E-16	0.000E+00	0.000E+00
U-236	Pu-240	1.000E+00	0.000E+00	1.835E-06	3.631E-04	6.289E-04	6.703E-04	6.668E-04	5.279E-04	2.177E-04	0.000E+00	0.000E+00
U-236	Pu-244	9.988E-01	0.000E+00	2.812E-14	2.282E-10	7.929E-10	1.058E-09	1.265E-09	1.340E-09	6.933E-10	0.000E+00	0.000E+00
U-236	U-236	1.000E+00	8.980E+00	8.980E+00	8.980E+00	7.857E+00	6.735E+00	5.612E+00	3.367E+00	1.122E+00	0.000E+00	0.000E+00
U-236	∑S(j):		8.980E+00	8.980E+00	8.980E+00	7.858E+00	6.736E+00	5.613E+00	3.368E+00	1.123E+00	0.000E+00	0.000E+00
Th-232	Cm-244	1.000E+00	0.000E+00	7.415E-20	7.794E-15	3.077E-14	4.214E-14	5.127E-14	5.550E-14	2.908E-14	0.000E+00	0.000E+00
Th-232	Cm-248	9.150E-01	0.000E+00	2.828E-25	1.345E-25	2.317E-25	7.829E-25	2.387E-24	4.245E-24	3.495E-24	0.000E+00	0.000E+00
Th-232	Pu-240	1.000E+00	0.000E+00	2.216E-16	1.798E-12	6.249E-12	8.339E-12	9.972E-12	1.056E-11	5.464E-12	0.000E+00	0.000E+00
Th-232	Pu-244	9.988E-01	0.000E+00	4.686E-22	7.519E-19	5.233E-18	8.738E-18	1.255E-17	1.776E-17	1.150E-17	0.000E+00	0.000E+00
Th-232	Th-232	1.000E+00	3.520E+00	3.520E+00	3.520E+00	3.080E+00	2.640E+00	2.200E+00	1.320E+00	4.400E-01	0.000E+00	0.000E+00
Th-232	U-236	1.000E+00	0.000E+00	4.430E-10	8.860E-08	1.551E-07	1.661E-07	1.661E-07	1.329E-07	5.537E-08	0.000E+00	0.000E+00
Th-232	∑S(j):		3.520E+00	3.520E+00	3.520E+00	3.080E+00	2.640E+00	2.200E+00	1.320E+00	4.400E-01	0.000E+00	0.000E+00
Ra-228	Cm-244	1.000E+00	0.000E+00	9.854E-21	7.103E-15	2.945E-14	4.071E-14	4.983E-14	5.434E-14	2.860E-14	0.000E+00	0.000E+00
Ra-228	Cm-248	9.150E-01	0.000E+00	0.000E+00	0.000E+00	0.000E+00	0.000E+00	0.000E+00	2.578E-24	2.884E-24	0.000E+00	0.000E+00
Ra-228	Pu-240	1.000E+00	0.000E+00	3.787E-17	1.655E-12	5.996E-12	8.070E-12	9.703E-12	1.035E-11	5.375E-12	0.000E+00	0.000E+00
Ra-228	Pu-244	9.988E-01	0.000E+00	0.000E+00	6.593E-19	4.916E-18	8.314E-18	1.204E-17	1.722E-17	1.122E-17	0.000E+00	0.000E+00
Ra-228	Ra-228	1.000E+00	2.210E-02	2.009E-02	7.682E-13	2.308E-23	1.118E-28	5.595E-34	1.121E-44	0.000E+00	0.000E+00	0.000E+00
Ra-228	Th-232	1.000E+00	0.000E+00	3.205E-01	3.520E+00	3.080E+00	2.640E+00	2.200E+00	1.320E+00	4.400E-01	0.000E+00	0.000E+00
Ra-228	U-236	1.000E+00	0.000E+00	1.084E-10	8.493E-08	1.518E-07	1.634E-07	1.638E-07	1.315E-07	5.492E-08	0.000E+00	0.000E+00
Ra-228	∑S(j):		2.210E-02	3.406E-01	3.520E+00	3.080E+00	2.640E+00	2.200E+00	1.320E+00	4.400E-01	0.000E+00	0.000E+00
Th-228	Cm-244	1.000E+00	0.000E+00	2.738E-21	6.877E-15	2.901E-14	4.023E-14	4.935E-14	5.396E-14	2.844E-14	0.000E+00	0.000E+00
Th-228	Cm-248	9.150E-01	0.000E+00	0.000E+00	0.000E+00	0.000E+00	0.000E+00	0.000E+00	1.869E-24	2.630E-24	0.000E+00	0.000E+00
Th-228	Pu-240	1.000E+00	0.000E+00	1.252E-17	1.609E-12	5.913E-12	7.980E-12	9.614E-12	1.028E-11	5.346E-12	0.000E+00	0.000E+00
Th-228	Pu-244	9.988E-01	0.000E+00	0.000E+00	6.287E-19	4.812E-18	8.175E-18	1.188E-17	1.704E-17	1.113E-17	0.000E+00	0.000E+00
Th-228	Ra-228	1.000E+00	0.000E+00	2.601E-03	1.151E-12	3.457E-23	1.675E-28	8.381E-34	1.682E-44	0.000E+00	0.000E+00	0.000E+00
Th-228	Th-228	1.000E+00	2.110E-06	1.752E-06	9.088E-38	0.000E+00	0.000E+00	0.000E+00	0.000E+00	0.000E+00	0.000E+00	0.000E+00
Th-228	Th-232	1.000E+00	0.000E+00	1.827E-01	3.520E+00	3.080E+00	2.640E+00	2.200E+00	1.320E+00	4.400E-01	0.000E+00	0.000E+00
Th-228	U-232	1.000E+00	0.000E+00	1.676E+00	1.403E+00	1.642E-01	5.145E-02	1.568E-02	1.258E-03	5.609E-05	0.000E+00	0.000E+00
Th-228	U-236	1.000E+00	0.000E+00	4.500E-11	8.371E-08	1.508E-07	1.625E-07	1.631E-07	1.311E-07	5.476E-08	0.000E+00	0.000E+00
Th-228	∑S(j):		2.110E-06	1.862E+00	4.923E+00	3.244E+00	2.691E+00	2.216E+00	1.321E+00	4.401E-01	0.000E+00	0.000E+00
Cm-245	Cm-245	6.100E-09	2.336E-10	2.336E-10	2.299E-10	1.979E-10	1.682E-10	1.390E-10	8.208E-11	2.692E-11	0.000E+00	0.000E+00
Cm-245	Cm-245	1.000E+00	3.830E-02	3.830E-02	3.768E-02	3.244E-02	2.758E-02	2.279E-02	1.346E-02	4.412E-03	0.000E+00	0.000E+00
Cm-245	∑S(j):		3.830E-02	3.830E-02	3.768E-02	3.244E-02	2.758E-02	2.279E-02	1.346E-02	4.412E-03	0.000E+00	0.000E+00
Pu-241	Cm-245	1.000E+00	0.000E+00	1.647E-03	3.774E-02	3.249E-02	2.762E-02	2.283E-02	1.348E-02	4.420E-03	0.000E+00	0.000E+00
Pu-241	Cm-245	2.450E-05	0.000E+00	4.035E-08	9.247E-07	7.961E-07	6.768E-07	5.594E-07	3.302E-07	1.083E-07	0.000E+00	0.000E+00
Pu-241	Pu-241	1.000E+00	2.040E+02	1.952E+02	1.306E-02	7.302E-07	4.976E-09	3.328E-11	1.272E-15	2.700E-20	0.000E+00	0.000E+00
Pu-241	∑S(j):		2.040E+02	1.952E+02	5.080E-02	3.249E-02	2.762E-02	2.283E-02	1.348E-02	4.420E-03	0.000E+00	0.000E+00

Individual Nuclide Soil Concentration
Parent Nuclide and Thread Fraction Indicated

Nuclide (j)	Parent (i)	THF(i)	S(j,t), pCi/g t= 0.000E+00	1.000E+00	2.000E+02	4.000E+02	5.000E+02	6.000E+02	8.000E+02	1.000E+03	2.000E+03	1.000E+04
Cm-245	Cm-245	2.450E-05	9.383E-07	9.383E-07	9.232E-07	7.947E-07	6.756E-07	5.585E-07	3.297E-07	1.081E-07	0.000E+00	0.000E+00
Cm-246	Cm-246	2.630E-04	4.182E-05	4.181E-05	4.062E-05	3.452E-05	2.916E-05	2.395E-05	1.396E-05	4.519E-06	0.000E+00	0.000E+00
Cm-246	Cm-246	5.539E-06	8.806E-07	8.805E-07	8.554E-07	7.270E-07	6.141E-07	5.043E-07	2.939E-07	9.516E-08	0.000E+00	0.000E+00
Cm-246	∑S(j):		4.270E-05	4.269E-05	4.147E-05	3.525E-05	2.977E-05	2.445E-05	1.425E-05	4.614E-06	0.000E+00	0.000E+00
Pu-242	Cm-246	5.539E-06	0.000E+00	1.627E-12	3.208E-10	5.532E-10	5.884E-10	5.842E-10	4.606E-10	1.892E-10	0.000E+00	0.000E+00
Pu-242	Cm-246	5.449E-07	0.000E+00	1.601E-13	3.156E-11	5.442E-11	5.789E-11	5.747E-11	4.531E-11	1.861E-11	0.000E+00	0.000E+00
Pu-242	Pu-242	5.540E-06	9.584E-07	9.584E-07	9.581E-07	8.380E-07	7.182E-07	5.983E-07	3.589E-07	1.196E-07	0.000E+00	0.000E+00
Pu-242	∑S(j):		9.584E-07	9.584E-07	9.584E-07	8.386E-07	7.188E-07	5.990E-07	3.594E-07	1.198E-07	0.000E+00	0.000E+00
Cm-246	Cm-246	5.449E-07	8.663E-08	8.662E-08	8.415E-08	7.151E-08	6.041E-08	4.961E-08	2.891E-08	9.362E-09	0.000E+00	0.000E+00
Cm-246	Cm-246	9.997E-01	1.590E-01	1.589E-01	1.544E-01	1.312E-01	1.108E-01	9.104E-02	5.305E-02	1.718E-02	0.000E+00	0.000E+00
Cm-246	∑S(j):		1.590E-01	1.589E-01	1.544E-01	1.312E-01	1.108E-01	9.104E-02	5.305E-02	1.718E-02	0.000E+00	0.000E+00
U-238	Cm-246	5.449E-07	0.000E+00	6.082E-23	4.920E-19	1.705E-18	2.273E-18	2.714E-18	2.867E-18	1.479E-18	0.000E+00	0.000E+00
U-238	Pu-242	5.450E-07	0.000E+00	1.463E-17	2.925E-15	5.117E-15	5.483E-15	5.482E-15	4.385E-15	1.827E-15	0.000E+00	0.000E+00
U-238	U-238	5.450E-07	2.076E-04	2.076E-04	2.076E-04	1.817E-04	1.557E-04	1.298E-04	7.787E-05	2.596E-05	0.000E+00	0.000E+00
U-238	∑S(j):		2.076E-04	2.076E-04	2.076E-04	1.817E-04	1.557E-04	1.298E-04	7.787E-05	2.596E-05	0.000E+00	0.000E+00
Pu-242	Cm-246	9.997E-01	0.000E+00	2.937E-07	5.790E-05	9.986E-05	1.062E-04	1.054E-04	8.314E-05	3.414E-05	0.000E+00	0.000E+00
Pu-242	Pu-242	1.000E+00	1.730E-01	1.730E-01	1.729E-01	1.513E-01	1.296E-01	1.080E-01	6.478E-02	2.158E-02	0.000E+00	0.000E+00
Pu-242	∑S(j):		1.730E-01	1.730E-01	1.730E-01	1.514E-01	1.297E-01	1.081E-01	6.486E-02	2.162E-02	0.000E+00	0.000E+00
U-238	Cm-246	9.997E-01	0.000E+00	1.116E-16	9.028E-13	3.129E-12	4.170E-12	4.980E-12	5.261E-12	2.714E-12	0.000E+00	0.000E+00
U-238	Pu-242	1.000E+00	0.000E+00	2.684E-11	5.367E-09	9.390E-09	1.006E-08	1.006E-08	8.045E-09	3.352E-09	0.000E+00	0.000E+00
U-238	U-238	1.000E+00	3.810E+02	3.810E+02	3.810E+02	3.334E+02	2.857E+02	2.381E+02	1.429E+02	4.762E+01	0.000E+00	0.000E+00
U-238	∑S(j):		3.810E+02	3.810E+02	3.810E+02	3.334E+02	2.857E+02	2.381E+02	1.429E+02	4.762E+01	0.000E+00	0.000E+00
U-234	Cm-246	9.997E-01	0.000E+00	5.133E-22	1.704E-16	1.183E-15	1.974E-15	2.831E-15	3.997E-15	2.583E-15	0.000E+00	0.000E+00
U-234	Pu-238	1.000E+00	0.000E+00	2.598E-04	2.660E-02	2.805E-02	2.462E-02	2.073E-02	1.252E-02	4.177E-03	0.000E+00	0.000E+00
U-234	Pu-242	1.000E+00	0.000E+00	1.856E-16	1.515E-12	5.301E-12	7.098E-12	8.517E-12	9.081E-12	4.728E-12	0.000E+00	0.000E+00
U-234	U-234	1.000E+00	6.300E+02	6.300E+02	6.296E+02	5.506E+02	4.718E+02	3.931E+02	2.357E+02	7.853E+01	0.000E+00	0.000E+00
U-234	U-238	1.000E+00	0.000E+00	1.076E-03	2.151E-01	3.763E-01	4.031E-01	4.030E-01	3.223E-01	1.343E-01	0.000E+00	0.000E+00
U-234	∑S(j):		6.300E+02	6.300E+02	6.299E+02	5.510E+02	4.723E+02	3.935E+02	2.361E+02	7.867E+01	0.000E+00	0.000E+00
Th-230	Cm-246	9.997E-01	0.000E+00	0.000E+00	7.843E-20	1.091E-18	2.275E-18	3.919E-18	7.384E-18	5.971E-18	0.000E+00	0.000E+00
Th-230	Pu-238	1.000E+00	0.000E+00	5.887E-09	3.064E-05	7.503E-05	8.665E-05	9.111E-05	7.752E-05	3.346E-05	0.000E+00	0.000E+00
Th-230	Pu-242	1.000E+00	0.000E+00	2.649E-21	9.286E-16	6.495E-15	1.087E-14	1.564E-14	2.223E-14	1.446E-14	0.000E+00	0.000E+00
Th-230	Th-230	1.000E+00	1.920E+00	1.920E+00	1.916E+00	1.674E+00	1.433E+00	1.193E+00	7.147E-01	2.378E-01	0.000E+00	0.000E+00
Th-230	U-234	1.000E+00	0.000E+00	5.793E-03	1.157E+00	2.023E+00	2.166E+00	2.165E+00	1.730E+00	7.198E-01	0.000E+00	0.000E+00
Th-230	U-238	1.000E+00	0.000E+00	2.422E-08	1.977E-04	6.913E-04	9.255E-04	1.110E-03	1.183E-03	6.157E-04	0.000E+00	0.000E+00
Th-230	∑S(j):		1.920E+00	1.926E+00	3.074E+00	3.697E+00	3.600E+00	3.359E+00	2.446E+00	9.582E-01	0.000E+00	0.000E+00

Individual Nuclide Soil Concentration
Parent Nuclide and Thread Fraction Indicated

Nuclide (j)	Parent (i)	THF(i)	S(j,t), pCi/g t= 0.000E+00	1.000E+00	2.000E+02	4.000E+02	5.000E+02	6.000E+02	8.000E+02	1.000E+03	2.000E+03	1.000E+04
Ra-226	Cm-246	9.997E-01	0.000E+00	0.000E+00	1.340E-21	3.682E-20	9.537E-20	1.958E-19	4.856E-19	4.846E-19	0.000E+00	0.000E+00
Ra-226	Pu-238	1.000E+00	0.000E+00	4.175E-12	9.660E-07	4.972E-06	7.283E-06	9.276E-06	1.060E-05	5.706E-06	0.000E+00	0.000E+00
Ra-226	Pu-242	1.000E+00	0.000E+00	0.000E+00	1.978E-17	2.720E-16	5.641E-16	9.664E-16	1.801E-15	1.441E-15	0.000E+00	0.000E+00
Ra-226	Ra-226	1.000E+00	8.010E-01	8.007E-01	7.345E-01	5.894E-01	4.838E-01	3.860E-01	2.124E-01	6.492E-02	0.000E+00	0.000E+00
Ra-226	Th-230	1.000E+00	0.000E+00	8.309E-04	1.592E-01	2.668E-01	2.798E-01	2.739E-01	2.101E-01	8.396E-02	0.000E+00	0.000E+00
Ra-226	U-234	1.000E+00	0.000E+00	6.141E-06	4.874E-02	1.657E-01	2.187E-01	2.587E-01	2.683E-01	1.359E-01	0.000E+00	0.000E+00
Ra-226	U-238	1.000E+00	0.000E+00	1.712E-11	5.590E-06	3.828E-05	6.339E-05	9.030E-05	1.257E-04	8.013E-05	0.000E+00	0.000E+00
Ra-226	∑S(j):		8.010E-01	8.015E-01	9.425E-01	1.022E+00	9.823E-01	9.188E-01	6.909E-01	2.849E-01	0.000E+00	0.000E+00
Pb-210	Cm-246	9.997E-01	0.000E+00	0.000E+00	6.944E-22	2.588E-20	7.148E-20	1.535E-19	4.033E-19	4.171E-19	0.000E+00	0.000E+00
Pb-210	Pb-210	1.000E+00	3.680E+00	3.573E+00	7.155E-03	1.217E-05	4.586E-07	1.687E-08	1.965E-11	1.271E-14	0.000E+00	0.000E+00
Pb-210	Pu-238	1.000E+00	0.000E+00	1.551E-13	6.490E-07	4.101E-06	6.267E-06	8.210E-06	9.712E-06	5.333E-06	0.000E+00	0.000E+00
Pb-210	Pu-242	1.000E+00	0.000E+00	0.000E+00	1.158E-17	2.031E-16	4.450E-16	7.916E-16	1.548E-15	1.276E-15	0.000E+00	0.000E+00
Pb-210	Ra-226	1.000E+00	0.000E+00	2.317E-02	7.433E-01	5.977E-01	4.906E-01	3.915E-01	2.154E-01	6.584E-02	0.000E+00	0.000E+00
Pb-210	Th-230	1.000E+00	0.000E+00	6.043E-05	1.345E-01	2.470E-01	2.635E-01	2.609E-01	2.030E-01	8.180E-02	0.000E+00	0.000E+00
Pb-210	U-234	1.000E+00	0.000E+00	3.015E-07	3.574E-02	1.418E-01	1.933E-01	2.335E-01	2.487E-01	1.280E-01	0.000E+00	0.000E+00
Pb-210	U-238	1.000E+00	0.000E+00	6.341E-13	3.635E-06	3.052E-05	5.282E-05	7.753E-05	1.121E-04	7.313E-05	0.000E+00	0.000E+00
Pb-210	∑S(j):		3.680E+00	3.597E+00	9.207E-01	9.865E-01	9.474E-01	8.860E-01	6.672E-01	2.757E-01	0.000E+00	0.000E+00
Cm-247	Cm-247	1.000E+00	1.040E-02	1.040E-02	1.040E-02	9.100E-03	7.800E-03	6.500E-03	3.900E-03	1.300E-03	0.000E+00	0.000E+00
Cm-248	Cm-248	8.390E-02	4.690E-05	4.690E-05	4.688E-05	4.100E-05	3.514E-05	2.928E-05	1.756E-05	5.851E-06	0.000E+00	0.000E+00
Cm-248	Cm-248	1.108E-03	6.196E-07	6.196E-07	6.194E-07	5.418E-07	4.643E-07	3.868E-07	2.320E-07	7.730E-08	0.000E+00	0.000E+00
Cm-248	∑S(j):		4.752E-05	4.752E-05	4.750E-05	4.155E-05	3.560E-05	2.966E-05	1.779E-05	5.928E-06	0.000E+00	0.000E+00
Pu-244	Cm-248	1.108E-03	0.000E+00	5.369E-15	1.074E-12	1.878E-12	2.012E-12	2.012E-12	1.609E-12	6.704E-13	0.000E+00	0.000E+00
Pu-244	Cm-248	5.261E-08	0.000E+00	2.548E-19	5.095E-17	8.915E-17	9.551E-17	9.550E-17	7.638E-17	3.182E-17	0.000E+00	0.000E+00
Pu-244	Pu-244	1.210E-03	4.453E-06	4.453E-06	4.453E-06	3.896E-06	3.340E-06	2.783E-06	1.670E-06	5.566E-07	0.000E+00	0.000E+00
Pu-244	∑S(j):		4.453E-06	4.453E-06	4.453E-06	3.896E-06	3.340E-06	2.783E-06	1.670E-06	5.566E-07	0.000E+00	0.000E+00
Cm-248	Cm-248	5.261E-08	2.941E-11	2.941E-11	2.940E-11	2.571E-11	2.204E-11	1.836E-11	1.101E-11	3.669E-12	0.000E+00	0.000E+00
Cm-248	Cm-248	9.150E-01	5.115E-04	5.115E-04	5.113E-04	4.472E-04	3.832E-04	3.193E-04	1.915E-04	6.381E-05	0.000E+00	0.000E+00
Cm-248	∑S(j):		5.115E-04	5.115E-04	5.113E-04	4.472E-04	3.832E-04	3.193E-04	1.915E-04	6.381E-05	0.000E+00	0.000E+00
Pu-244	Cm-248	9.150E-01	0.000E+00	4.432E-12	8.862E-10	1.550E-09	1.661E-09	1.661E-09	1.328E-09	5.534E-10	0.000E+00	0.000E+00
Pu-244	Pu-244	9.988E-01	3.676E-03	3.676E-03	3.676E-03	3.216E-03	2.757E-03	2.297E-03	1.378E-03	4.594E-04	0.000E+00	0.000E+00
Pu-244	∑S(j):		3.676E-03	3.676E-03	3.676E-03	3.216E-03	2.757E-03	2.297E-03	1.378E-03	4.594E-04	0.000E+00	0.000E+00
Pu-240	Cm-248	9.150E-01	0.000E+00	1.146E-15	9.293E-12	3.229E-11	4.310E-11	5.153E-11	5.458E-11	2.822E-11	0.000E+00	0.000E+00
Pu-240	Pu-240	1.000E+00	6.200E+01	6.199E+01	6.070E+01	5.201E+01	4.411E+01	3.637E+01	2.137E+01	6.973E+00	0.000E+00	0.000E+00
Pu-240	Pu-244	9.988E-01	0.000E+00	3.880E-07	7.681E-05	1.330E-04	1.418E-04	1.410E-04	1.117E-04	4.604E-05	0.000E+00	0.000E+00
Pu-240	∑S(j):		6.200E+01	6.199E+01	6.070E+01	5.201E+01	4.411E+01	3.637E+01	2.137E+01	6.973E+00	0.000E+00	0.000E+00
H-3	H-3	1.000E+00	4.640E+00	4.412E+00	6.054E-05	1.577E-10	4.236E-13	1.025E-15	8.070E-23	0.000E+00	0.000E+00	0.000E+00

Individual Nuclide Soil Concentration
Parent Nuclide and Thread Fraction Indicated

Nuclide (j)	Parent (i)	THF(i)	S(j,t), pCi/g t= 0.000E+00	1.000E+00	2.000E+02	4.000E+02	5.000E+02	6.000E+02	8.000E+02	1.000E+03	2.000E+03	1.000E+04
I-129	I-129	1.000E+00	3.500E-01	3.500E-01	3.500E-01	3.062E-01	2.625E-01	2.187E-01	1.312E-01	4.375E-02	0.000E+00	0.000E+00
K-40	K-40	1.000E+00	3.280E+00	3.280E+00	3.280E+00	2.870E+00	2.460E+00	2.050E+00	1.230E+00	4.100E-01	0.000E+00	0.000E+00
Mo-93	Mo-93	1.200E-01	4.656E-02	4.655E-02	4.497E-02	3.801E-02	3.202E-02	2.623E-02	1.520E-02	4.894E-03	0.000E+00	0.000E+00
Mo-93	Mo-93	8.800E-01	3.414E-01	3.414E-01	3.298E-01	2.788E-01	2.348E-01	1.923E-01	1.115E-01	3.589E-02	0.000E+00	0.000E+00
Mo-93	∑S(j):		3.880E-01	3.879E-01	3.748E-01	3.168E-01	2.668E-01	2.186E-01	1.267E-01	4.078E-02	0.000E+00	0.000E+00
Nb-93m	Mo-93	8.800E-01	0.000E+00	1.323E-02	3.311E-01	2.799E-01	2.358E-01	1.931E-01	1.119E-01	3.604E-02	0.000E+00	0.000E+00
Nb-93m	Nb-93m	1.000E+00	2.330E-01	2.240E-01	4.327E-05	7.024E-09	8.164E-11	9.294E-13	1.032E-16	6.362E-21	0.000E+00	0.000E+00
Nb-93m	∑S(j):		2.330E-01	2.372E-01	3.311E-01	2.799E-01	2.358E-01	1.931E-01	1.119E-01	3.604E-02	0.000E+00	0.000E+00
Nb-94	Nb-94	1.000E+00	1.630E-02	1.630E-02	1.619E-02	1.407E-02	1.202E-02	9.981E-03	5.948E-03	1.969E-03	0.000E+00	0.000E+00
Ni-59	Ni-59	1.000E+00	3.040E+00	3.040E+00	3.036E+00	2.653E+00	2.272E+00	1.892E+00	1.134E+00	3.774E-01	0.000E+00	0.000E+00
Pu-238	Pu-238	1.850E-09	1.735E-07	1.722E-07	3.572E-08	6.434E-09	2.502E-09	9.460E-10	1.168E-10	8.016E-12	0.000E+00	0.000E+00
Pu-238	Pu-238	1.000E+00	9.380E+01	9.307E+01	1.931E+01	3.478E+00	1.352E+00	5.113E-01	6.315E-02	4.333E-03	0.000E+00	0.000E+00
Pu-238	∑S(j):		9.380E+01	9.307E+01	1.931E+01	3.478E+00	1.352E+00	5.113E-01	6.315E-02	4.333E-03	0.000E+00	0.000E+00
Pu-241	Pu-241	2.450E-05	4.998E-03	4.783E-03	3.199E-07	1.789E-11	1.219E-13	8.153E-16	3.117E-20	6.614E-25	0.000E+00	0.000E+00
Pu-242	Pu-242	5.450E-07	9.428E-08	9.428E-08	9.425E-08	8.244E-08	7.065E-08	5.886E-08	3.530E-08	1.176E-08	0.000E+00	0.000E+00
Pu-244	Pu-244	5.743E-08	2.113E-10	2.113E-10	2.113E-10	1.849E-10	1.585E-10	1.321E-10	7.925E-11	2.642E-11	0.000E+00	0.000E+00
Sr-90	Sr-90	1.000E+00	1.920E+02	1.876E+02	1.558E+00	1.106E-02	8.523E-04	6.404E-05	3.114E-07	8.413E-10	0.000E+00	0.000E+00
Tc-99	Tc-99	1.000E+00	1.560E+00	1.560E+00	1.559E+00	1.363E+00	1.168E+00	9.731E-01	5.835E-01	1.944E-01	0.000E+00	0.000E+00
U-232	U-232	1.000E+00	1.020E+01	1.010E+01	1.364E+00	1.596E-01	5.002E-02	1.525E-02	1.223E-03	5.453E-05	0.000E+00	0.000E+00

THF(i) is the thread fraction of the parent nuclide.

Parent Dose Report
Title : Site 7 Base Case Model
File : BC_V01.ROF

Run Time Information

ResOCalc.EXE execution began at 16:16 on 10/25/2019

ResOCalc.EXE execution ended at 16:31 on 10/25/2019

ResOCalc.EXE execution time 15 minutes 28 seconds

This page intentionally left blank.

ATTACHMENT G.3.
RESRAD-OFFSITE INPUT PARAMETER PROBABILITY DISTRIBUTIONS AND RELATIONSHIPS FOR THE UNCERTAINTY ANALYSIS

This page intentionally left blank.

Table G.3.1. Probabilistic distributions, parameter correlations, and relationships specified for the uncertainty analyses

Zone	Parameter	Unit	Distribution	Alpha (P) /Mean and SD	Beta (Q)/ SD/ Truncation Percentiles	Minimum Value	Maximum Value	Base Case Value	RESRAD Identifier	Relations or Correlations (rcc = rank correlation coefficient, rcc is the initially assigned value; final adjusted values are provided in Attachment G.4)	Input Type	In Compliance Period Analysis?	In 10,000 year analysis?
CZ	Time at which radionuclide first becomes releasable (delay time), C-14	y	Beta (asymmetric)	2	5	100	1000	300	RELTIMEINIT(C-14)	No Correlation	P	Y	Y
CZ	Time at which radionuclide first becomes releasable (delay time), I-129	y	Related Parameter Specification			100	1000	300	RELTIMEINIT(I-129)	RELTIMEINIT(I-129) = RELTIMEINIT(C-14)	R	Y	Y
CZ	Time at which radionuclide first becomes releasable (delay time), Pu-239	y	Related Parameter Specification			100	1000	300	RELTIMEINIT(Pu-239)	RELTIMEINIT(Pu-239) = RELTIMEINIT(C-14)	R	N	Y
CZ	Time at which radionuclide first becomes releasable (delay time), Tc-99	y	Related Parameter Specification			100	1000	300	RELTIMEINIT(Tc-99)	RELTIMEINIT(Tc-99) = RELTIMEINIT(C-14)	R	Y	Y
CZ	Time at which radionuclide first becomes releasable (delay time), U-234	y	Related Parameter Specification			100	1000	300	RELTIMEINIT(U-234)	RELTIMEINIT(U-234) = RELTIMEINIT(C-14)	R	N	Y
CZ	Time at which radionuclide first becomes releasable (delay time), U-235	y	Related Parameter Specification			100	1000	300	RELTIMEINIT(U-235)	RELTIMEINIT(U-235) = RELTIMEINIT(C-14)	R	N	Y
CZ	Time at which radionuclide first becomes releasable (delay time), U-238	y	Related Parameter Specification			100	1000	300	RELTIMEINIT(U-238)	RELTIMEINIT(U-238) = RELTIMEINIT(C-14)	R	N	Y
CZ	Time over which transformation to releasable form occurs, C-14	y	Related Parameter Specification			400	1200	500	RELDUR(C-14)	RELDUR(C-14) = RELDUR(I-129)	R	Y	Y
CZ	Time over which transformation to releasable form occurs, I-129	y	Beta (symmetric)	4	4	400	1200	800	RELDUR(I-129)	rcc = -0.9 (negative) for RELDUR(I-129) and RELFRACINIT(I-129) rcc = 0.9 for RELDUR(I-129) and DCACTU1(I-129) rcc = 0.9 for RELDUR(I-129) and DCACTU1(Pu-239) rcc = 0.9 for RELDUR(I-129) and DCACTU1(Tc-99) rcc = 0.9 for RELDUR(I-129) and DCACTU1(U-234)	P	Y	Y
CZ	Time over which transformation to releasable form occurs, Pu-239	y	Related Parameter Specification			400	1200	800	RELDUR(Pu-239)	RELDUR(Pu-239) = RELDUR(I-129)	R	N	Y
CZ	Time over which transformation to releasable form occurs, Tc-99	y	Related Parameter Specification			400	1200	800	RELDUR(Tc-99)	RELDUR(Tc-99) = RELDUR(I-129)	R	Y	Y
CZ	Time over which transformation to releasable form occurs, U-234	y	Related Parameter Specification			400	1200	800	RELDUR(U-234)	RELDUR(U-234) = RELDUR(I-129)	R	N	Y
CZ	Time over which transformation to releasable form occurs, U-235	y	Related Parameter Specification			400	1200	800	RELDUR(U-235)	RELDUR(U-235) = RELDUR(I-129)	R	N	Y
CZ	Time over which transformation to releasable form occurs, U-238	y	Related Parameter Specification			400	1200	800	RELDUR(U-238)	RELDUR(U-238) = RELDUR(I-129)	R	N	Y
CZ	Initial Releaseable Fraction C-14	-	Related Parameter Specification			0.4	0.9	0.75	RELFRACINIT(C-14)	RELFRACINIT(C-14) = 0.4 + RELFRACINIT(I-129)	R	Y	Y
CZ	Initial Releaseable Fraction I-129	-	Beta (decreasing)	1	3	0	0.5	0	RELFRACINIT(I-129)	rcc = -0.9 (negative) for RELFRACINIT(I-129) and RELDUR(I-129)	P	Y	Y
CZ	Initial Releasable Fraction Pu-239		Related Parameter Specification			0	0.5	0	RELFRACINIT(Pu-239)	RELFRACINIT(Pu-239) = RELFRACINIT(I-129)	R	N	Y
CZ	Initial Releaseable Fraction Tc-99	-	Related Parameter Specification			0	0.5	0	RELFRACINIT(Tc-99)	RELFRACINIT(Tc-99) = RELFRACINIT(I-129)	R	Y	Y
CZ	Initial Releasable Fraction U-234	-	Related Parameter Specification			0	0.5	0	RELFRACINIT(U-234)	RELFRACINIT(U-234) = RELFRACINIT(I-129)	R	N	Y
CZ	Initial Releasable Fraction U-235	-	Related Parameter Specification			0	0.5	0	RELFRACINIT(U-235)	RELFRACINIT(U-235) = RELFRACINIT(I-129)	R	N	Y
CZ	Initial Releasable Fraction U-238	-	Related Parameter Specification			0	0.5	0	RELFRACINIT(U-238)	RELFRACINIT(U-238) = RELFRACINIT(I-129)	R	N	Y

Zone	Parameter	Unit	Distribution	Alpha (P) /Mean and SD	Beta (Q)/ SD/ Truncation Percentiles	Minimum Value	Maximum Value	Base Case Value	RESRAD Identifier	Relations or Correlations (rcc = rank correlation coefficient, rcc is the initially assigned value; final adjusted values are provided in Attachment G.4)	Input Type	In Compliance Period Analysis?	In 10,000 year analysis?
CZ	Contaminated Zone, I-129 Kd	cm^3/g	Related Parameter Specification			0	4	2	DCACTC(I-129)	DCACTC(I-129) = DCACTU1(I-129)/2	R	Y	Y
UZ	Unsaturated Zone 1, I-129 Kd	cm^3/g	Bounded Normal	Mean = 4	SD = 1.7	0	8	4	DCACTU1(I-129)	rcc = 0.9 for DCACTU1(I-129) and RELDUR(I-129) rcc = 0.9 for DCACTU1(I-129) and DCACTS(I-129)	P	Y	Y
UZ	Unsaturated Zone 2, I-129 Kd	cm^3/g	Related Parameter Specification			0	8	4	DCACTU2(I-129)	DCACTU2(I-129) = DCACTU1(I-129)	R	Y	Y
UZ	Unsaturated Zone 3, I-129 Kd	cm^3/g	Related Parameter Specification			0	8	4	DCACTU3(I-129)	DCACTU3(I-129) = DCACTU1(I-129)	R	Y	Y
UZ	Unsaturated Zone 4, I-129 Kd	cm^3/g	Related Parameter Specification			0	8	4	DCACTU4(I-129)	DCACTU4(I-129) = DCACTU1(I-129)	R	Y	Y
UZ	Unsaturated Zone 5, I-129 Kd	cm^3/g	Related Parameter Specification			0	8	4	DCACTU5(I-129)	DCACTU5(I-129) = DCACTU1(I-129)	R	Y	Y
SZ	Saturated Zone, I-129 Kd	cm^3/g	Bounded Normal	Mean = 4	SD = 1.7	0	8	4	DCACTS(I-129)	rcc = 0.9 for DCACTS(I-129) and DCACTU1(I-129)	P	Y	Y
CZ	Contaminated Zone, Pu-239 Kd	cm^3/g	Related Parameter Specification			10	40	20	DCACTC(Pu-239)	DCACTC(Pu-239) = DCACTU1(Pu-239)/2	R	N	Y
UZ	Unsaturated Zone 1, Pu-239 Kd	cm^3/g	Bounded Normal	Mean = 40	SD = 10	20	80	40	DCACTU1(Pu-239)	rcc = 0.9 for DCACTU1(Pu-239) and RELDUR(I-129) rcc = 0.9 for DCACTU1(Pu-239) and DCACTS(Pu-239)	P	N	Y
UZ	Unsaturated Zone 2, Pu-239 Kd	cm^3/g	Related Parameter Specification			20	80	40	DCACTU2(Pu-239)	DCACTU2(Pu-239) = DCACTU1(Pu-239)	R	N	Y
UZ	Unsaturated Zone 3, Pu-239 Kd	cm^3/g	Related Parameter Specification			20	80	40	DCACTU3(Pu-239)	DCACTU3(Pu-239) = DCACTU1(Pu-239)	R	N	Y
UZ	Unsaturated Zone 4, Pu-239 Kd	cm^3/g	Related Parameter Specification			20	80	40	DCACTU4(Pu-239)	DCACTU4(Pu-239) = DCACTU1(Pu-239)	R	N	Y
UZ	Unsaturated Zone 5, Pu-239 Kd	cm^3/g	Related Parameter Specification			20	80	40	DCACTU5(Pu-239)	DCACTU5(Pu-239) = DCACTU1(Pu-239)	R	N	Y
SZ	Saturated Zone, Pu-239 Kd	cm^3/g	Bounded Normal	Mean = 40	SD = 10	20	80	40	DCACTS(Pu-239)	rcc = 0.9 for DCACTS(Pu-239) and DCACTU1(Pu-239)	P	N	Y
CZ	Contaminated Zone, Tc-99 Kd	cm^3/g	Related Parameter Specification			0	0.72	0.36	DCACTC(Tc-99)	DCACTC(Tc-99) = DCACTU1(Tc-99)/2	R	Y	Y
UZ	Unsaturated Zone 1, Tc-99 Kd	cm^3/g	Bounded Normal	Mean = 0.72	SD = 0.31	0	1.44	0.72	DCACTU1(Tc-99)	rcc = 0.9 for DCACTU1(Tc-99) and RELDUR(I-129) rcc = 0.9 for DCACTU1(Tc-99) and DCACTS(Tc-99)	P	Y	Y
UZ	Unsaturated Zone 2, Tc-99 Kd	cm^3/g	Related Parameter Specification			0	1.44	0.72	DCACTU2(Tc-99)	DCACTU2(Tc-99) = DCACTU1(Tc-99)	R	Y	Y
UZ	Unsaturated Zone 3, Tc-99 Kd	cm^3/g	Related Parameter Specification			0	1.44	0.72	DCACTU3(Tc-99)	DCACTU3(Tc-99) = DCACTU1(Tc-99)	R	Y	Y
UZ	Unsaturated Zone 4, Tc-99 Kd	cm^3/g	Related Parameter Specification			0	1.44	0.72	DCACTU4(Tc-99)	DCACTU4(Tc-99) = DCACTU1(Tc-99)	R	Y	Y
UZ	Unsaturated Zone 5, Tc-99 Kd	cm^3/g	Related Parameter Specification			0	1.44	0.72	DCACTU5(Tc-99)	DCACTU5(Tc-99) = DCACTU1(Tc-99)	R	Y	Y
SZ	Saturated Zone, Tc-99 Kd	cm^3/g	Bounded Normal	Mean = 0.72	SD = 0.31	0	1.44	0.72	DCACTS(Tc-99)	rcc = 0.9 for DCACTS(Tc-99) and DCACTU1(Tc-99)	P	Y	Y
CZ	Contaminated Zone, U-234 Kd	cm^3/g	Related Parameter Specification			12.5	50	25	DCACTC(U-234)	DCACTC(U-234) = DCACTU1(U-234)/2	R	N	Y
UZ	Unsaturated Zone 1, U-234 Kd	cm^3/g	Bounded Normal	Mean = 50	SD = 12.5	25	100	50	DCACTU1(U-234)	rcc = 0.9 for DCACTU1(U-234) and RELDUR(I-129) rcc = 0.9 for DCACTU1(U-234) and DCACTS(U-234)	P	N	Y
UZ	Unsaturated Zone 2, U-234 Kd	cm^3/g	Related Parameter Specification			25	100	50	DCACTU2(U-234)	DCACTU2(U-234) = DCACTU1(U-234)	R	N	Y
UZ	Unsaturated Zone 3, U-234 Kd	cm^3/g	Related Parameter Specification			25	100	50	DCACTU3(U-234)	DCACTU3(U-234) = DCACTU1(U-234)	R	N	Y
UZ	Unsaturated Zone 4, U-234 Kd	cm^3/g	Related Parameter Specification			25	100	50	DCACTU4(U-234)	DCACTU4(U-234) = DCACTU1(U-234)	R	N	Y
UZ	Unsaturated Zone 5, U-234 Kd	cm^3/g	Related Parameter Specification			25	100	50	DCACTU5(U-234)	DCACTU5(U-234) = DCACTU1(U-234)	R	N	Y
SZ	Saturated Zone, U-234 Kd	cm^3/g	Bounded Normal	Mean = 50	SD = 12.5	25	100	50	DCACTS(U-234)	rcc = 0.9 for DCACTS(U-234) and DCACTU1(U-234)	P	N	Y
CZ	Contaminated Zone, U-235 Kd	cm^3/g	Related Parameter Specification			12.5	50	25	DCACTC(U-235)	DCACTC(U-235) = DCACTU1(U-234)/2	R	N	Y

Zone	Parameter	Unit	Distribution	Alpha (P) /Mean and SD	Beta (Q)/ SD/ Truncation Percentiles	Minimum Value	Maximum Value	Base Case Value	RESRAD Identifier	Relations or Correlations (rcc = rank correlation coefficient, rcc is the initially assigned value; final adjusted values are provided in Attachment G.4)	Input Type	In Compliance Period Analysis?	In 10,000 year analysis?
UZ	Unsaturated Zone 1, U-235 Kd	cm^3/g	Related Parameter Specification			25	100	50	DCACTU1(U-235)	DCACTU1(U-235) = DCACTU1(U-234)	R	N	Y
UZ	Unsaturated Zone 2, U-235 Kd	cm^3/g	Related Parameter Specification			25	100	50	DCACTU2(U-235)	DCACTU2(U-235) = DCACTU1(U-234)	R	N	Y
UZ	Unsaturated Zone 3, U-235 Kd	cm^3/g	Related Parameter Specification			25	100	50	DCACTU3(U-235)	DCACTU3(U-235) = DCACTU1(U-234)	R	N	Y
UZ	Unsaturated Zone 4, U-235 Kd	cm^3/g	Related Parameter Specification			25	100	50	DCACTU4(U-235)	DCACTU4(U-235) = DCACTU1(U-234)	R	N	Y
UZ	Unsaturated Zone 5, U-235 Kd	cm^3/g	Related Parameter Specification			25	100	50	DCACTU5(U-235)	DCACTU5(U-235) = DCACTU1(U-234)	R	N	Y
SZ	Saturated Zone, U-235 Kd	cm^3/g	Related Parameter Specification			25	100	50	DCACTS(U-235)	DCACTS(U-235) = DCACTS(U-234)	R	N	Y
CZ	Contaminated Zone, U-238 Kd	cm^3/g	Related Parameter Specification			12.5	50	25	DCACTC(U-238)	DCACTC(U-238) = DCACTU1(U-234)/2	R	N	Y
UZ	Unsaturated Zone 1, U-238 Kd	cm^3/g	Related Parameter Specification			25	100	50	DCACTU1(U-238)	DCACTU1(U-238) = DCACTU1(U-234)	R	N	Y
UZ	Unsaturated Zone 2, U-238 Kd	cm^3/g	Related Parameter Specification			25	100	50	DCACTU2(U-238)	DCACTU2(U-238) = DCACTU1(U-234)	R	N	Y
UZ	Unsaturated Zone 3, U-238 Kd	cm^3/g	Related Parameter Specification			25	100	50	DCACTU3(U-238)	DCACTU3(U-238) = DCACTU1(U-234)	R	N	Y
UZ	Unsaturated Zone 4, U-238 Kd	cm^3/g	Related Parameter Specification			25	100	50	DCACTU4(U-238)	DCACTU4(U-238) = DCACTU1(U-234)	R	N	Y
UZ	Unsaturated Zone 5, U-238 Kd	cm^3/g	Related Parameter Specification			25	100	50	DCACTU5(U-238)	DCACTU5(U-238) = DCACTU1(U-234)	R	N	Y
SZ	Saturated Zone, U-238 Kd	cm^3/g	Related Parameter Specification			25	100	50	DCACTS(U-238)	DCACTS(U-238) = DCACTS(U-234)	R	N	Y
CZ	Precipitation	m/yr	Beta (symmetric)	4	4	1.037	1.73	1.38	PRECIP	rcc = 0.9 for PRECIP and RUNOFF rcc = -0.9 (negative) for PRECIP and TLAKE rcc = -0.9 (negative) for PRECIP and H(5) rcc = 0.9 for PRECIP and HGW	P	Y	Y
CZ	Runoff coefficient	-	Beta (increasing)	4.75	1	0.830	0.982	0.963	RUNOFF	rcc = 0.9 for RUNOFF and PRECIP rcc = 0.9 for RUNOFF and H(5)	P	Y	Y
CZ	Bulk Density of Contaminated Zone	g/cm^3	Beta (symmetric)	4	4	1.80	2.00	1.90	DENSCZ	No Correlation	P	Y	Y
CZ	Total Porosity of Contaminated Zone	-	Related Parameter Specification			0.390	0.461	0.419	TPCZ	TPCZ=1-DENSCZ/[1.9/(1-0.419)] TPCZ=1-DENSCZ/3.27	R	Y	Y
CZ	Contaminated Zone Effective Porosity	-	Beta (symmetric)	4	4	0.12	0.35	0.234	EPCZ	rcc = 0.9 for EPCZ and HCCZ	P	Y	Y
CZ	Hydraulic Conductivity of Contaminated Zone	m/yr	Truncated lognormal-N	mean=ln(6), SD=1	truncated at 5% and 95%	1.20	30.00	5.99	HCCZ	rcc = 0.9 for HCCZ and EPCZ	P	Y	Y
CZ	Soil b-parameter	-	Beta (symmetric)	4	4	4.65	10.9	7.75	BCZ	No Correlation	P	Y	Y
CZ	Contaminated Zone Longitudinal Dispersivity	m	Beta (symmetric)	4	4	0.05	3.55	1.8	ALPHALCZ	No Correlation	P	Y	Y
UZ	Bulk Density UZ3	g/cm^3	Related Parameter Specification			1.41	1.63	1.5	DENSUZ(3)	DENSUZ(3) = (1-TPUZ(3))*2.65 DENSUZ(3) = 2.65-2.65*TPUZ(3)	R	Y	Y
UZ	Total Porosity of UZ3	-	Beta (symmetric)	4	4	0.384	0.470	0.427	TPUZ(3)	No Correlation	P	Y	Y
UZ	Unsaturated Zone Effective Porosity: UZ3 (Clay Liner)	-	Beta (symmetric)	4	4	0.176	0.215	0.195	EPUZ(3)	No Correlation	P	Y	Y
UZ	Unsaturated Zone Longitudinal Dispersivity: UZ3 (Clay Liner)	m	Beta (asymmetric)	1.25	3	0.05	0.5	0.1	ALPHALU(3)	rcc = 0.9 for ALPHALU(3) and ALPHALU(4)	P	Y	Y
UZ	Bulk Density UZ4	g/cm^3	Related Parameter Specification			1.4	1.7	1.5	DENSUZ(4)	DENSUZ(4) = (1-TPUZ(4))*2.65 DENSUZ(4) = 2.65-2.65*TPUZ(4)	R	Y	Y
UZ	Total Porosity of UZ4	-	Beta (symmetric)	4	4	0.377	0.461	0.419	TPUZ(4)	No Correlation	P	Y	Y

Zone	Parameter	Unit	Distribution	Alpha (P) /Mean and SD	Beta (Q)/ SD/ Truncation Percentiles	Minimum Value	Maximum Value	Base Case Value	RESRAD Identifier	Relations or Correlations (rcc = rank correlation coefficient, rcc is the initially assigned value; final adjusted values are provided in Attachment G.4)	Input Type	In Compliance Period Analysis?	In 10,000 year analysis?
UZ	Unsaturated Zone Effective Porosity: UZ4 (Geobuffer)	-	Beta (symmetric)	4	4	0.211	0.257	0.234	EPUZ(4)	No Correlation	P	Y	Y
UZ	Unsaturated Zone Longitudinal Dispersivity: UZ4 (Geobuffer)	m	Beta (asymmetric)	1.25	3	0.05	0.5	0.1	ALPHALU(4)	rcc = 0.9 for ALPHALU(4) and ALPHALU(3)	P	Y	Y
UZ	Unsaturated Zone Thickness: UZ5 (In-Situ Material)	m	Beta (asymmetric)	4	2.5	0.10	7.6	4.85	H(5)	rcc = -0.9 (negative) for H(5) and PRECIP rcc = 0.9 for H(5) and RUNOFF rcc = 0.9 for H(5) and ALPHALU(5)	P	Y	Y
UZ	Bulk Density UZ5	g/cm^3	Beta (symmetric)	4	4	1.7	1.90	1.80	DENSUZ(5)	No Correlation	P	Y	Y
UZ	Total Porosity of UZ5	-	Related Parameter Specification			0.317	0.388	0.353	TPUZ(5)	TPUZ(5)=1-DENSUZ(5)/2.78	R	Y	Y
UZ	Unsaturated Zone Effective Porosity: UZ5 (In-situ Material)	-	Beta (symmetric)	4	4	0.243	0.297	0.270	EPUZ(5)	rcc = 0.9 for EPUZ(5) and HCUZ(5)	P	Y	Y
UZ	Unsaturated Zone Hydraulic Conductivity: UZ5 (In-situ Material)	m/yr	Truncated lognormal-N	mean=ln(16.7), SD=1	truncated at 5% and 95%	3.2	86.4	16.7	HCUZ(5)	rcc = 0.9 for HCUZ(5) and EPUZ(5)	P	Y	Y
UZ	Unsaturated Zone Longitudinal Dispersivity: UZ5 (In-situ Material)	m	Beta (asymmetric)	1.25	3	0.05	0.5	0.1	ALPHALU(5)	rcc = 0.9 for ALPHALU(5) and H(5)	P	Y	Y
SZ	Saturated Zone Bulk Density	g/cm^3	Beta (symmetric)	4	4	1.7	2.5	2.1	DENSAQ	No Correlation	P	Y	Y
SZ	Saturated Zone Total Porosity	-	Related Parameter Specification			0.101	0.388	0.240	TPSZ	TPSZ=1-DENSAQ/2.78	R	Y	Y
SZ	Saturated Zone Effective Porosity	-	Beta (symmetric)	4	4	0.18	0.22	0.2	EPSZ	rcc = 0.9 for EPSZ and HCSZ	P	Y	Y
SZ	Saturated Zone Hydraulic Conductivity	m/yr	Truncated lognormal-N	mean=ln(26.8), SD=0.5	truncated at 5% and 95%	11.8	61.0	26.8	HCSZ	rcc = 0.9 for HCSZ and EPSZ rcc = -0.9 (negative) for HCSZ and HGW	P	Y	Y
SZ	Depth of Aquifer Contributing to Well	m	Beta (symmetric)	4	4	25.0	55.0	40.0	DWIBWT	No Correlation	P	Y	Y
SZ	Saturated Zone Hydraulic Gradient to Well	m/m	Beta (symmetric)	4	4	0.027	0.081	0.054	HGW	rcc = 0.9 for HGW and PRECIP rcc = -0.9 (negative) for HGW and HCSZ	P	Y	Y
SZ	Saturated Zone Hydraulic Gradient to Surface Water Body	m/m	Related Parameter Specification			0.018	0.054	0.036	HGSW	HGSW = (36/54)*HGW HGSW=0.667*HGW	R	Y	Y
SZ	Saturated Zone Longitudinal Dispersivity to Well	m	Beta (symmetric)	4	4	1	19	10	ALPHALOW	No Correlation	P	Y	Y
SZ	Saturated Zone Longitudinal Dispersivity to SW	m	Beta (symmetric)	4	4	1	62	31.5	ALPHALOSW	No Correlation	P	Y	Y
SW	Mean Residence Time of Water in Surface Water Body	yr	Truncated lognormal-N	mean=ln(1E-4), SD=0.99	truncated at 1% and 99%	1E-05	1E-03	1.00E-04	TLAKE	rcc = -0.9 (negative) for TLAKE and PRECIP	P	Y	Y

R = Related Input
P = Probabilistic Input
CZ = Contaminated Zone (Primary Contamination)
UZ = Unsaturated Zone
SW = Surface Water
SZ = Saturated Zone

Table G.3.2. Bases and justifications for probabilistic distributions, parameter correlations, and relationships specified for the uncertainty analyses

Zone	Parameter	Unit	Distribution	Alpha (P) /Mean and SD	Beta (Q)/ SD/ Truncation Percentiles	Minimum Value	Maximum Value	Base Case Value	RESRAD Identifier	Relations or Correlations (rcc = rank correlation coefficient, rcc is the initially assigned value; final adjusted values are provided in Attachment G.4)	Basis or Justification for Assigned Distribution, Correlation or Functional Relationship
CZ	Time at which radionuclide first becomes releasable (delay time), C-14	y	Beta (asymmetric)	2	5	100	1000	300	RELTIMEINIT(C-14)	No Correlation	Distribution: Asymmetric beta (2, 5) distribution reflects the likelihood of full cover performance period exceeding the base case assumption of 300 years; Range: minimum value (100 yr) is the institutional control period, maximum value (1000 years) is an assumed maximum cover system HDPE membrane service life.
CZ	Time at which radionuclide first becomes releasable (delay time), I-129	y	Related Parameter Specification			100	1000	300	RELTIMEINIT(I-129)	RELTIMEINIT(I-129) = RELTIMEINIT(C-14)	
CZ	Time at which radionuclide first becomes releasable (delay time), Pu-239	y	Related Parameter Specification			100	1000	300	RELTIMEINIT(Pu-239)	RELTIMEINIT(Pu-239) = RELTIMEINIT(C-14)	
CZ	Time at which radionuclide first becomes releasable (delay time), Tc-99	y	Related Parameter Specification			100	1000	300	RELTIMEINIT(Tc-99)	RELTIMEINIT(Tc-99) = RELTIMEINIT(C-14)	Functional relationship: RELTIMEINIT represents onset of cover infiltration, same for all radionuclides, only C-14 value is sampled, all others are assigned the same value as C-14
CZ	Time at which radionuclide first becomes releasable (delay time), U-234	y	Related Parameter Specification			100	1000	300	RELTIMEINIT(U-234)	RELTIMEINIT(U-234) = RELTIMEINIT(C-14)	
CZ	Time at which radionuclide first becomes releasable (delay time), U-235	y	Related Parameter Specification			100	1000	300	RELTIMEINIT(U-235)	RELTIMEINIT(U-235) = RELTIMEINIT(C-14)	
CZ	Time at which radionuclide first becomes releasable (delay time), U-238	y	Related Parameter Specification			100	1000	300	RELTIMEINIT(U-238)	RELTIMEINIT(U-238) = RELTIMEINIT(C-14)	
CZ	Time over which transformation to releasable form occurs, C-14	y	Related Parameter Specification			400	1200	500	RELDUR(C-14)	RELDUR(C-14) = RELDUR(I-129)	Functional relationship: RELDUR represents duration of EMDF cover degradation; same for all radionuclides, only I-129 value is sampled, all others are assigned the same value as I-129

Zone	Parameter	Unit	Distribution	Alpha (P) /Mean and SD	Beta (Q)/ SD/ Truncation Percentiles	Minimum Value	Maximum Value	Base Case Value	RESRAD Identifier	Relations or Correlations (rcc = rank correlation coefficient, rcc is the initially assigned value; final adjusted values are provided in Attachment G.4)	Basis or Justification for Assigned Distribution, Correlation or Functional Relationship
CZ	Time over which transformation to releasable form occurs, I-129	y	Beta (symmetric)	4	4	400	1200	800	RELDUR(I-129)	rcc = -0.9 (negative) for RELDUR(I-129) and RELFRACINIT(I-129) rcc = 0.9 for RELDUR(I-129) and DCACTU1(I-129) rcc = 0.9 for RELDUR(I-129) and DCACTU1(Pu-239) rcc = 0.9 for RELDUR(I-129) and DCACTU1(Tc-99) rcc = 0.9 for RELDUR(I-129) and DCACTU1(U-234)	Distribution: Symmetric beta (4,4) distribution reflects similar likelihood for cover degradation to proceed more or less rapidly relative to the base case assumption Range: lower limit is a reasonable minimum expected HDPE membrane service life, upper limit represents equal interval (400 years) above base case value Correlations: Assumption is that larger initial releasable fraction is associated with smaller total duration of release (i.e. release duration and initial releasable fraction of I-129 are negatively correlated) and that for each radionuclide, lower sampled Kd values for unsaturated zone 1 (UZ1) will be positively correlated with the sampled or assigned value of the release duration.
CZ	Time over which transformation to releasable form occurs, Pu-239	y	Related Parameter Specification			400	1200	800	RELDUR(Pu-239)	RELDUR(Pu-239) = RELDUR(I-129)	Functional relationship: RELDUR represents duration of EMDF cover degradation; same for all radionuclides, only I-129 value is sampled, all others are assigned the same value as I-129
CZ	Time over which transformation to releasable form occurs, Tc-99	y	Related Parameter Specification			400	1200	800	RELDUR(Tc-99)	RELDUR(Tc-99) = RELDUR(I-129)	
CZ	Time over which transformation to releasable form occurs, U-234	y	Related Parameter Specification			400	1200	800	RELDUR(U-234)	RELDUR(U-234) = RELDUR(I-129)	
CZ	Time over which transformation to releasable form occurs, U-235	y	Related Parameter Specification			400	1200	800	RELDUR(U-235)	RELDUR(U-235) = RELDUR(I-129)	
CZ	Time over which transformation to releasable form occurs, U-238	y	Related Parameter Specification			400	1200	800	RELDUR(U-238)	RELDUR(U-238) = RELDUR(I-129)	
CZ	Initial Releaseable Fraction C-14	-	Related Parameter Specification			0.4	0.9	0.75	RELFRACINIT(C-14)	RELFRACINIT(C-14) = 0.4 + RELFRACINIT(I-129)	Functional relationship: Initial releasable fraction for C-14 is increased relative to the sampled I-129 value in order to account for the impact of the variable releasable fraction imposed by the RESRAD-OFFSITE release model on release of highly mobile radionuclides such as C-14. The functional assignment based on the sampled I-129 value of initial releasable fraction results in a beta (1, 3) distribution for C-14 that ranges from 0.4 to 0.9

Zone	Parameter	Unit	Distribution	Alpha (P) /Mean and SD	Beta (Q)/ SD/ Truncation Percentiles	Minimum Value	Maximum Value	Base Case Value	RESRAD Identifier	Relations or Correlations (rcc = rank correlation coefficient, rcc is the initially assigned value; final adjusted values are provided in Attachment G.4)	Basis or Justification for Assigned Distribution, Correlation or Functional Relationship
CZ	Initial Releaseable Fraction I-129	-	Beta (decreasing)	1	3	0	0.5	0	RELFRACINIT(I-129)	rcc = -0.9 (negative) for RELFRACINIT(I-129) and RELDUR(I-129)	Distribution: RELFRACINIT represents cover failure uncertainty, in terms of the initial rapidity of increasing cover infiltration and/or the areal extent of initial cover degradation (e.g. partial damage due to an extreme weather event), decreasing beta distribution (1,3) reflects higher likelihood for cover degradation to proceed gradually (the base case assumption), and a decreasing probability of a more severe/rapid onset of increasing cover infiltration Range: maximum represents a reasonable extreme RELFRACINIT (50%), representing the severity of initial cover degradation relative to the long-term fully degraded condition; minimum is the base case zero value, representing gradual progression of cover degradation Correlation: Assumption is that larger initial releasable fraction is associated with smaller total duration of release, i.e. release duration and initial releasable fraction of I-129 are negatively correlated
CZ	Initial Releasable Fraction Pu-239		Related Parameter Specification			0	0.5	0	RELFRACINIT(Pu-239)	RELFRACINIT(Pu-239) = RELFRACINIT(I-129)	Functional relationship: RELFRACINIT represents cover failure uncertainty, in terms of the initial rapidity of increasing cover infiltration and/or the areal extent of initial cover degradation: same for all radionuclides, only I-129 value is sampled, all others are assigned the same value as I-129
CZ	Initial Releaseable Fraction Tc-99	-	Related Parameter Specification			0	0.5	0	RELFRACINIT(Tc-99)	RELFRACINIT(Tc-99) = RELFRACINIT(I-129)	
CZ	Initial Releasable Fraction U-234	-	Related Parameter Specification			0	0.5	0	RELFRACINIT(U-234)	RELFRACINIT(U-234) = RELFRACINIT(I-129)	
CZ	Initial Releasable Fraction U-235	-	Related Parameter Specification			0	0.5	0	RELFRACINIT(U-235)	RELFRACINIT(U-235) = RELFRACINIT(I-129)	
CZ	Initial Releasable Fraction U-238	-	Related Parameter Specification			0	0.5	0	RELFRACINIT(U-238)	RELFRACINIT(U-238) = RELFRACINIT(I-129)	
CZ	Contaminated Zone, I-129 Kd	cm^3/g	Related Parameter Specification			0	4	2	DCACTC(I-129)	DCACTC(I-129) = DCACTU1(I-129)/2	Functional relationship: For each radionuclide, the contaminated zone Kd is set equal to ½ of the sampled unsaturated zone 1 Kd value to preserve base case Kd assumption for the waste and non-waste materials.
UZ	Unsaturated Zone 1, I-129 Kd	cm^3/g	Bounded Normal	Mean = 4	SD = 1.7	0	8	4	DCACTU1(I-129)	rcc = 0.9 for DCACTU1(I-129) and RELDUR(I-129) rcc = 0.9 for DCACTU1(I-129) and DCACTS(I-129)	Distribution: Bounded normal distribution (mean 4, SD, 1.7) represents similar likelihood for I-129 Kd values to be higher than or lower than the base case value (4 ml/g) for the unsaturated zone. The value of the standard deviation was selected to ensure a non-zero probability of sampled Kd=0 Range: minimum value assumed to be zero, upper limit (8 ml/g) assigned as two times the base case value Correlations: The assumption is that the Kd value for the unsaturated zone will be positively correlated with the duration of release (longer duration for higher Kd) and with the Kd value for the saturated zone
UZ	Unsaturated Zone 2, I-129 Kd	cm^3/g	Related Parameter Specification			0	8	4	DCACTU2(I-129)	DCACTU2(I-129) = DCACTU1(I-129)	Functional relationship: Unsaturated zone Kd values equal to represent similar geochemical conditions expected in all five unsaturated zones. Only the UZ1 Kd value is sampled, all others are assigned the same value as UZ1
UZ	Unsaturated Zone 3, I-129 Kd	cm^3/g	Related Parameter Specification			0	8	4	DCACTU3(I-129)	DCACTU3(I-129) = DCACTU1(I-129)	
UZ	Unsaturated Zone 4, I-129 Kd	cm^3/g	Related Parameter Specification			0	8	4	DCACTU4(I-129)	DCACTU4(I-129) = DCACTU1(I-129)	

Zone	Parameter	Unit	Distribution	Alpha (P) /Mean and SD	Beta (Q)/ SD/ Truncation Percentiles	Minimum Value	Maximum Value	Base Case Value	RESRAD Identifier	Relations or Correlations (rcc = rank correlation coefficient, rcc is the initially assigned value; final adjusted values are provided in Attachment G.4)	Basis or Justification for Assigned Distribution, Correlation or Functional Relationship
UZ	Unsaturated Zone 5, I-129 Kd	cm^3/g	Related Parameter Specification			0	8	4	DCACTU5(I-129)	DCACTU5(I-129) = DCACTU1(I-129)	
SZ	Saturated Zone, I-129 Kd	cm^3/g	Bounded Normal	Mean = 4	SD = 1.7	0	8	4	DCACTS(I-129)	rcc = 0.9 for DCACTS(I-129) and DCACTU1(I-129)	Distribution: Bounded normal distribution (mean 4, SD, 1.7) represents similar likelihood for I-129 Kd values to be higher than or lower than the base case value (4 ml/g) for the saturated zone. The value of the standard deviation was selected to ensure a non-zero probability of sampled Kd=0 Range: minimum value assumed to be zero, upper limit (8 ml/g) assigned as two times the base case value Correlation: The assumption is that the Kd value for the unsaturated zone will be positively correlated with the Kd value for the saturated zone.
CZ	Contaminated Zone, Pu-239 Kd	cm^3/g	Related Parameter Specification			10	40	20	DCACTC(Pu-239)	DCACTC(Pu-239) = DCACTU1(Pu-239)/2	Functional relationship: For each radionuclide, the contaminated zone Kd is set equal to ½ of the sampled unsaturated zone 1 Kd value to preserve base case Kd assumption for the waste and non-waste materials.
UZ	Unsaturated Zone 1, Pu-239 Kd	cm^3/g	Bounded Normal	Mean = 40	SD = 10	20	80	40	DCACTU1(Pu-239)	rcc = 0.9 for DCACTU1(Pu-239) and RELDUR(I-129) rcc = 0.9 for DCACTU1(Pu-239) and DCACTS(Pu-239)	Distribution: Bounded normal distribution (mean 40, SD, 10) represents similar likelihood for Pu-239 Kd values to be higher than or lower than the base case value (40 ml/g) for the unsaturated zone. The value of the standard deviation was assigned as 25% of the mean value. Range: minimum value assumed to be one half of the base case value, upper limit (80 ml/g) represents two times the base case value Correlations: The assumption is that the Kd value for the unsaturated zone will be positively correlated with the duration of release (longer duration for higher Kd) and with the Kd value for the saturated zone
UZ	Unsaturated Zone 2, Pu-239 Kd	cm^3/g	Related Parameter Specification			20	80	40	DCACTU2(Pu-239)	DCACTU2(Pu-239) = DCACTU1(Pu-239)	Functional relationship: Unsaturated zone Kd values equal to represent similar geochemical conditions expected in all five unsaturated zones. Only the UZ1 Kd value is sampled, all others are assigned the same value as UZ1
UZ	Unsaturated Zone 3, Pu-239 Kd	cm^3/g	Related Parameter Specification			20	80	40	DCACTU3(Pu-239)	DCACTU3(Pu-239) = DCACTU1(Pu-239)	
UZ	Unsaturated Zone 4, Pu-239 Kd	cm^3/g	Related Parameter Specification			20	80	40	DCACTU4(Pu-239)	DCACTU4(Pu-239) = DCACTU1(Pu-239)	
UZ	Unsaturated Zone 5, Pu-239 Kd	cm^3/g	Related Parameter Specification			20	80	40	DCACTU5(Pu-239)	DCACTU5(Pu-239) = DCACTU1(Pu-239)	
SZ	Saturated Zone, Pu-239 Kd	cm^3/g	Bounded Normal	Mean = 40	SD = 10	20	80	40	DCACTS(Pu-239)	rcc = 0.9 for DCACTS(Pu-239) and DCACTU1(Pu-239)	Distribution: Bounded normal distribution (mean 40, SD, 10) represents similar likelihood for Pu-239 Kd values to be higher than or lower than the base case value (40 ml/g) for the saturated zone. The value of the standard deviation was assigned as 25% of the mean value. Range: minimum value assumed to be one half of the base case value, upper limit (80 ml/g) represents two times the base case value Correlation: The assumption is that the Kd value for the unsaturated zone will be positively correlated with the Kd value for the saturated zone.

Zone	Parameter	Unit	Distribution	Alpha (P) /Mean and SD	Beta (Q)/ SD/ Truncation Percentiles	Minimum Value	Maximum Value	Base Case Value	RESRAD Identifier	Relations or Correlations (rcc = rank correlation coefficient, rcc is the initially assigned value; final adjusted values are provided in Attachment G.4)	Basis or Justification for Assigned Distribution, Correlation or Functional Relationship
CZ	Contaminated Zone, Tc-99 Kd	cm^3/g	Related Parameter Specification			0	0.72	0.36	DCACTC(Tc-99)	DCACTC(Tc-99) = DCACTU1(Tc-99)/2	Functional relationship: For each radionuclide, the contaminated zone Kd is set equal to ½ of the sampled unsaturated zone 1 Kd value to preserve base case Kd assumption for the waste and non-waste materials.
UZ	Unsaturated Zone 1, Tc-99 Kd	cm^3/g	Bounded Normal	Mean = 0.72	SD = 0.31	0	1.44	0.72	DCACTU1(Tc-99)	rcc = 0.9 for DCACTU1(Tc-99) and RELDUR(I-129) rcc = 0.9 for DCACTU1(Tc-99) and DCACTS(Tc-99)	Distribution: Bounded normal distribution (mean 0.72, SD, 0.31) represents similar likelihood for Tc-99 Kd values to be higher than or lower than the base case value (0.72 ml/g) for the unsaturated zone. The value of the standard deviation was selected to ensure a non-zero probability of sampled Kd=0 Range: minimum value assumed to be zero, upper limit (1.44 ml/g) assigned as two times the base case value Correlations: The assumption is that the Kd value for the unsaturated zone will be positively correlated with the duration of release (longer duration for higher Kd) and with the Kd value for the saturated zone
UZ	Unsaturated Zone 2, Tc-99 Kd	cm^3/g	Related Parameter Specification			0	1.44	0.72	DCACTU2(Tc-99)	DCACTU2(Tc-99) = DCACTU1(Tc-99)	Functional relationship: Unsaturated zone Kd values equal to represent similar geochemical conditions expected in all five unsaturated zones. Only the UZ1 Kd value is sampled, all others are assigned the same value as UZ1
UZ	Unsaturated Zone 3, Tc-99 Kd	cm^3/g	Related Parameter Specification			0	1.44	0.72	DCACTU3(Tc-99)	DCACTU3(Tc-99) = DCACTU1(Tc-99)	
UZ	Unsaturated Zone 4, Tc-99 Kd	cm^3/g	Related Parameter Specification			0	1.44	0.72	DCACTU4(Tc-99)	DCACTU4(Tc-99) = DCACTU1(Tc-99)	
UZ	Unsaturated Zone 5, Tc-99 Kd	cm^3/g	Related Parameter Specification			0	1.44	0.72	DCACTU5(Tc-99)	DCACTU5(Tc-99) = DCACTU1(Tc-99)	
SZ	Saturated Zone, Tc-99 Kd	cm^3/g	Bounded Normal	Mean = 0.72	SD = 0.31	0	1.44	0.72	DCACTS(Tc-99)	rcc = 0.9 for DCACTS(Tc-99) and DCACTU1(Tc-99)	Distribution: Bounded normal distribution (mean 0.72, SD, 0.31) represents similar likelihood for Tc-99 Kd values to be higher than or lower than the base case value (0.72 ml/g) for the saturated zone. The value of the standard deviation was selected to ensure a non-zero probability of sampled Kd=0 Range: minimum value assumed to be zero, upper limit (1.44 ml/g) assigned as two times the base case value Correlation: The assumption is that the Kd value for the unsaturated zone will be positively correlated with the Kd value for the saturated zone.
CZ	Contaminated Zone, U-234 Kd	cm^3/g	Related Parameter Specification			12.5	50	25	DCACTC(U-234)	DCACTC(U-234) = DCACTU1(U-234)/2	Functional relationship: For each radionuclide of uranium, the contaminated zone Kd is set equal to ½ of the sampled unsaturated zone 1 U-234 Kd value to preserve base case Kd assumption for the waste and non-waste materials.

Zone	Parameter	Unit	Distribution	Alpha (P) /Mean and SD	Beta (Q)/ SD/ Truncation Percentiles	Minimum Value	Maximum Value	Base Case Value	RESRAD Identifier	Relations or Correlations (rcc = rank correlation coefficient, rcc is the initially assigned value; final adjusted values are provided in Attachment G.4)	Basis or Justification for Assigned Distribution, Correlation or Functional Relationship
UZ	Unsaturated Zone 1, U-234 Kd	cm^3/g	Bounded Normal	Mean = 50	SD = 12.5	25	100	50	DCACTU1(U-234)	rcc = 0.9 for DCACTU1(U-234) and RELDUR(I-129) rcc = 0.9 for DCACTU1(U-234) and DCACTS(U-234)	Distribution: Bounded normal distribution (mean 50, SD, 12.5) represents similar likelihood for U-234 Kd values to be higher than or lower than the base case value (50 ml/g) for the unsaturated zone. The value of the standard deviation was assigned as 25% of the mean value. Range: minimum value assumed to be one half of the base case value, upper limit (100 ml/g) represents two times the base case value Correlations: The assumption is that the Kd value for the unsaturated zone will be positively correlated with the duration of release (longer duration for higher Kd) and with the Kd value for the saturated zone
UZ	Unsaturated Zone 2, U-234 Kd	cm^3/g	Related Parameter Specification			25	100	50	DCACTU2(U-234)	DCACTU2(U-234) = DCACTU1(U-234)	Functional relationship: Unsaturated zone Kd values equal to represent similar geochemical conditions expected in all five unsaturated zones. Only the UZ1 Kd value is sampled, all others are assigned the same value as UZ1
UZ	Unsaturated Zone 3, U-234 Kd	cm^3/g	Related Parameter Specification			25	100	50	DCACTU3(U-234)	DCACTU3(U-234) = DCACTU1(U-234)	
UZ	Unsaturated Zone 4, U-234 Kd	cm^3/g	Related Parameter Specification			25	100	50	DCACTU4(U-234)	DCACTU4(U-234) = DCACTU1(U-234)	
UZ	Unsaturated Zone 5, U-234 Kd	cm^3/g	Related Parameter Specification			25	100	50	DCACTU5(U-234)	DCACTU5(U-234) = DCACTU1(U-234)	
SZ	Saturated Zone, U-234 Kd	cm^3/g	Bounded Normal	Mean = 50	SD = 12.5	25	100	50	DCACTS(U-234)	rcc = 0.9 for DCACTS(U-234) and DCACTU1(U-234)	Distribution: Bounded normal distribution (mean 50, SD, 12.5) represents similar likelihood for U-234 Kd values to be higher than or lower than the base case value (50 ml/g) for the saturated zone. The value of the standard deviation was assigned as 25% of the mean value. Range: minimum value assumed to be one half of the base case value, upper limit (100 ml/g) represents two times the base case value Correlation: The assumption is that the Kd value for the unsaturated zone will be positively correlated with the Kd value for the saturated zone.
CZ	Contaminated Zone, U-235 Kd	cm^3/g	Related Parameter Specification			12.5	50	25	DCACTC(U-235)	DCACTC(U-235) = DCACTU1(U-234)/2	Functional relationship: For each radionuclide of uranium, the contaminated zone Kd is set equal to ½ of the sampled unsaturated zone 1 U-234 Kd value to preserve base case Kd assumption for the waste and non-waste materials.
UZ	Unsaturated Zone 1, U-235 Kd	cm^3/g	Related Parameter Specification			25	100	50	DCACTU1(U-235)	DCACTU1(U-235) = DCACTU1(U-234)	Functional relationship: For each radionuclide of uranium, the unsaturated zone 1 Kd is set equal to the sampled unsaturated zone 1 U-234 Kd value because sorptive properties are assumed to reflect the chemical rather than the isotopic properties of uranium.
UZ	Unsaturated Zone 2, U-235 Kd	cm^3/g	Related Parameter Specification			25	100	50	DCACTU2(U-235)	DCACTU2(U-235) = DCACTU1(U-234)	Functional relationship: Unsaturated zone Kd values equal to represent similar geochemical conditions expected in all five unsaturated zones. Only the U-234 UZ1 Kd value is sampled, all others are assigned the same value as U-234 for UZ1
UZ	Unsaturated Zone 3, U-235 Kd	cm^3/g	Related Parameter Specification			25	100	50	DCACTU3(U-235)	DCACTU3(U-235) = DCACTU1(U-234)	
UZ	Unsaturated Zone 4, U-235 Kd	cm^3/g	Related Parameter Specification			25	100	50	DCACTU4(U-235)	DCACTU4(U-235) = DCACTU1(U-234)	

Zone	Parameter	Unit	Distribution	Alpha (P) /Mean and SD	Beta (Q)/ SD/ Truncation Percentiles	Minimum Value	Maximum Value	Base Case Value	RESRAD Identifier	Relations or Correlations (rcc = rank correlation coefficient, rcc is the initially assigned value; final adjusted values are provided in Attachment G.4)	Basis or Justification for Assigned Distribution, Correlation or Functional Relationship
UZ	Unsaturated Zone 5, U-235 Kd	cm^3/g	Related Parameter Specification			25	100	50	DCACTU5(U-235)	DCACTU5(U-235) = DCACTU1(U-234)	
SZ	Saturated Zone, U-235 Kd	cm^3/g	Related Parameter Specification			25	100	50	DCACTS(U-235)	DCACTS(U-235) = DCACTS(U-234)	Functional relationship: For each radionuclide of uranium, the saturated zone Kd is set equal to the sampled saturated zone U-234 Kd value because sorptive properties are assumed to reflect the chemical rather than the isotopic properties of uranium.
CZ	Contaminated Zone, U-238 Kd	cm^3/g	Related Parameter Specification			12.5	50	25	DCACTC(U-238)	DCACTC(U-238) = DCACTU1(U-234)/2	Functional relationship: For each radionuclide of uranium, the contaminated zone Kd is set equal to ½ of the sampled unsaturated zone 1 U-234 Kd value to preserve base case Kd assumption for the waste and non-waste materials.
UZ	Unsaturated Zone 1, U-238 Kd	cm^3/g	Related Parameter Specification			25	100	50	DCACTU1(U-238)	DCACTU1(U-238) = DCACTU1(U-234)	Functional relationship: For each radionuclide of uranium, the unsaturated zone 1 Kd is set equal to the sampled unsaturated zone 1 U-234 Kd value because sorptive properties are assumed to reflect the chemical rather than the isotopic properties of uranium.
UZ	Unsaturated Zone 2, U-238 Kd	cm^3/g	Related Parameter Specification			25	100	50	DCACTU2(U-238)	DCACTU2(U-238) = DCACTU1(U-234)	Functional relationship: Unsaturated zone Kd values equal to represent similar geochemical conditions expected in all five unsaturated zones. Only the U-234 UZ1 Kd value is sampled, all others are assigned the same value as U-234 for UZ1
UZ	Unsaturated Zone 3, U-238 Kd	cm^3/g	Related Parameter Specification			25	100	50	DCACTU3(U-238)	DCACTU3(U-238) = DCACTU1(U-234)	
UZ	Unsaturated Zone 4, U-238 Kd	cm^3/g	Related Parameter Specification			25	100	50	DCACTU4(U-238)	DCACTU4(U-238) = DCACTU1(U-234)	
UZ	Unsaturated Zone 5, U-238 Kd	cm^3/g	Related Parameter Specification			25	100	50	DCACTU5(U-238)	DCACTU5(U-238) = DCACTU1(U-234)	
SZ	Saturated Zone, U-238 Kd	cm^3/g	Related Parameter Specification			25	100	50	DCACTS(U-238)	DCACTS(U-238) = DCACTS(U-234)	Functional relationship: For each radionuclide of uranium, the saturated zone Kd is set equal to the sampled saturated zone U-234 Kd value because sorptive properties are assumed to reflect the chemical rather than the isotopic properties of uranium.

Zone	Parameter	Unit	Distribution	Alpha (P) /Mean and SD	Beta (Q)/ SD/ Truncation Percentiles	Minimum Value	Maximum Value	Base Case Value	RESRAD Identifier	Relations or Correlations (rcc = rank correlation coefficient, rcc is the initially assigned value; final adjusted values are provided in Attachment G.4)	Basis or Justification for Assigned Distribution, Correlation or Functional Relationship
CZ	Precipitation	m/yr	Beta (symmetric)	4	4	1.037	1.73	1.38	PRECIP	rcc = 0.9 for PRECIP and RUNOFF rcc = -0.9 (negative) for PRECIP and TLAKE rcc = -0.9 (negative) for PRECIP and H(5) rcc = 0.9 for PRECIP and HGW	Distribution: Symmetric beta (4,4) distribution represents similar likelihood for annual precipitation values to be higher than or lower than the base case value (1.38 m/yr), based on uncertainty in future changes in precipitation and average temperature. Precipitation values lower than the base case represent the possibility of reduced precipitation over the very long term (1000s of years) and/or the possibility of reduced average groundwater recharge associated with increased evapotranspiration relative to total annual rainfall. Range: minimum and maximum values correspond to ± 25% from the base case value, which is reasonable given the long time frame of the PA model simulations Correlations: The assumption is that RUNOFF and PRECIP are positively correlated because wetter conditions will result in more total cover drainage, both in absolute terms and when total drainage is expressed as a proportion of precipitation. HELP model results suggest that Pearson's correlation coefficient between the simulated yearly total cover drainage (as a fraction of precipitation) and annual precipitation is approximately +0.6.(Refer to HELP model calculation package CAW-90EMDF-G118) PRECIP and TLAKE are negatively correlated because wetter conditions will result in higher average flow rates and lower average residence time in the Bear Creek reach that receives discharge of radionuclides released from EMDF. Thickness of unsaturated zone 5, H(5), and PRECIP are negatively correlated because wetter conditions will result in higher water table elevations and smaller H(5). HGW and PRECIP are positively correlated because wetter conditions will result in higher hydraulic gradient and groundwater flux in the saturated zone.

Zone	Parameter	Unit	Distribution	Alpha (P) /Mean and SD	Beta (Q)/ SD/ Truncation Percentiles	Minimum Value	Maximum Value	Base Case Value	RESRAD Identifier	Relations or Correlations (rcc = rank correlation coefficient, rcc is the initially assigned value; final adjusted values are provided in Attachment G.4)	Basis or Justification for Assigned Distribution, Correlation or Functional Relationship
CZ	Runoff coefficient	-	Beta (increasing)	4.75	1	0.830	0.982	0.963	RUNOFF	rcc = 0.9 for RUNOFF and PRECIP rcc = 0.9 for RUNOFF and H(5)	Distribution: Increasing beta (4.75, 1) distribution represents approximately equal probability of long-term cover performance better than (higher RUNOFF) or worse than (lower RUNOFF) base case assumption (RUNOFF=0.963) Range: minimum value corresponds to partial design performance (cover infiltration = 0.43 in/yr) crediting design specs for earthen cover system components, but without the flexible membrane barrier. Maximum value corresponds to severely degraded performance (cover infiltration = 4 in/yr) predicted with the HELP model assuming a tenfold increase in permeability of the cover clay barriers Correlations: The assumption is that RUNOFF and PRECIP are positively correlated because wetter conditions will result in more total cover drainage, both in absolute terms and when total drainage is expressed as a proportion of precipitation. (Refer to HELP model calculation package CAW-90EMDF-G118). Thickness of unsaturated zone 5, H(5) and RUNOFF are positively correlated because larger RUNOFF values result in smaller calculated cover infiltration, which will result in lower water table elevation below the geologic buffer, and larger H(5).
CZ	Bulk Density of Contaminated Zone	g/cm^3	Beta (symmetric)	4	4	1.80	2.00	1.90	DENSCZ	No Correlation	Distribution: Symmetric beta (4, 4) distribution represents similar likelihood for average waste bulk densities greater than or less than the base case assumption (1.9 g/cm^3), due to uncertainty in final soil-to-debris ratios and compaction ratios for debris and soil. Range based on estimated uncertainty in soil-to-debris ratios and compaction ratios for debris and soil. Maximum value is 105% of the base case value, minimum represents equal interval (0.1 g/cm^3) below base case value.
CZ	Total Porosity of Contaminated Zone	-	Related Parameter Specification			0.390	0.461	0.419	TPCZ	TPCZ=1-DENSCZ/[1.9/(1-0.419)] Simplified: TPCZ=1-DENSCZ/3.27	Functional relationship: Total porosity =1-bulk density/solids density, relation assumes a (constant) base case waste solids density (3.27 g/cm^3) calculated from the base case waste bulk density (1.9 g/cm^3) and base case waste total porosity (0.419)
CZ	Contaminated Zone Effective Porosity	-	Beta (symmetric)	4	4	0.12	0.35	0.234	EPCZ	rcc = 0.9 for EPCZ and HCCZ	Distribution: Symmetric beta (4, 4) distribution represents similar likelihood for waste effective porosity to be greater than or less than the base case assumption (0.234 vol/vol), due to uncertainty in as-disposed waste hydraulic characteristics. Range: maximum value is 150% of the base case value, which is less than the minimum value of the range of waste total porosity evaluated (total porosity > effective porosity). Minimum value represents equal interval (0.115 vol/vol) below base case value. Correlation: The assumption is that HCCZ and EPCZ are positively correlated because effective porosity reflects the proportion of total porosity that contributes to advective fluid transport and is closely related to permeability of the material.

Zone	Parameter	Unit	Distribution	Alpha (P) /Mean and SD	Beta (Q)/ SD/ Truncation Percentiles	Minimum Value	Maximum Value	Base Case Value	RESRAD Identifier	Relations or Correlations (rcc = rank correlation coefficient, rcc is the initially assigned value; final adjusted values are provided in Attachment G.4)	Basis or Justification for Assigned Distribution, Correlation or Functional Relationship
CZ	Hydraulic Conductivity of Contaminated Zone	m/yr	Truncated lognormal-N	mean=ln(6), SD=1	truncated at 5% and 95%	1.20	30.00	5.99	HCCZ	rcc = 0.9 for HCCZ and EPCZ	Distribution: Truncated lognormal distribution (mean=ln(6), SD=1) represents similar likelihood for waste hydraulic conductivity values to be lower than or higher than the base case value (6 m/yr), due to uncertainty in the average characteristics of EMDF waste once final placement and compaction are complete. Range (1.2 to 30 m/yr, corresponding to 5th and 95th percentiles) is the same as the range evaluated for single-factor sensitivity to waste K, and corresponds to the lower end of the range of subsurface K values for depths up to 100 feet below ground level in Bear Creek Valley Correlation: The assumption is that HCCZ and EPCZ are positively correlated because effective porosity reflects the proportion of total porosity that contributes to advective fluid transport and is closely related to permeability of the material.
CZ	Soil b-parameter	-	Beta (symmetric)	4	4	4.65	10.9	7.75	BCZ	No Correlation	Distribution: Symmetric beta (4,4) distribution represents similar likelihood for waste b-parameter value to be higher or lower than the base case assumption (b=7.75), which corresponds to a silty-clay loam material type (Clapp and Hornberger 1978) Range is based on the range of b-parameter values corresponding to the material types (and b-parameter values) assigned for the five unsaturated zone layers. Maximum value is 140% of the base case value 7.75. Minimum value represents an equal interval (3.1) below the base case value.
CZ	Contaminated Zone Longitudinal Dispersivity	m	Beta (symmetric)	4	4	0.05	3.55	1.8	ALPHALCZ	No Correlation	Distribution: Symmetric beta (4,4) distribution represents similar likelihood for the contaminated zone (waste) longitudinal dispersivity to be greater than or less than the base case assumption (1.8 m), due to uncertainty in the impact of dispersive phenomena within the waste. Range: Minimum value (0.05 m) is representative of pore-scale dispersive processes in homogeneous porous media. Maximum value (3.55 m) is representative of macrodispersive processes associated with heterogeneity and preferential flow pathways within the waste and is based on setting an equal interval (1.75 m) above the base case value.
UZ	Bulk Density UZ3	g/cm^3	Related Parameter Specification			1.41	1.63	1.5	DENSUZ(3)	DENSUZ(3) = (1-TPUZ(3))*2.65 Simplified: DENSUZ(3) = 2.65-2.65*TPUZ(3)	Functional relationship: Bulk density = (1-total porosity)*grain density, assumes a grain density of 2.65 g/cm3 (quartz)
UZ	Total Porosity of UZ3	-	Beta (symmetric)	4	4	0.384	0.470	0.427	TPUZ(3)	No Correlation	Distribution: Symmetric beta (4,4) represents similar likelihood for the total porosity of the compacted clay liner to be greater than or less than the base case assumption (0.427 vol/vol), due to uncertainty in liner material characteristics. Range: maximum value is 110% of the base case value, which is representative of clay. Minimum value represents equal interval (0.043 vol/vol) below base case value.

Zone	Parameter	Unit	Distribution	Alpha (P) /Mean and SD	Beta (Q)/ SD/ Truncation Percentiles	Minimum Value	Maximum Value	Base Case Value	RESRAD Identifier	Relations or Correlations (rcc = rank correlation coefficient, rcc is the initially assigned value; final adjusted values are provided in Attachment G.4)	Basis or Justification for Assigned Distribution, Correlation or Functional Relationship
UZ	Unsaturated Zone Effective Porosity: UZ3 (Clay Liner)	-	Beta (symmetric)	4	4	0.176	0.215	0.195	EPUZ(3)	No Correlation	Distribution: Symmetric beta (4,4) represents similar likelihood for the average effective porosity of the clay liner to be greater than or less than the base case assumption (0.195 vol/vol), due to uncertainty in liner material characteristics. Range: maximum value is 110% of the base case value, which is less than the minimum value of the range of UZ3 total porosity evaluated (total porosity > effective porosity). Minimum value represents equal interval (0.0195 vol/vol) below base case value.
UZ	Unsaturated Zone Longitudinal Dispersivity: UZ3 (Clay Liner)	m	Beta (asymmetric)	1.25	3	0.05	0.5	0.1	ALPHALU(3)	rcc = 0.9 for ALPHALU(3) and ALPHALU(4)	Distribution: Asymmetric beta (1.25, 3) distribution represents the possibility for the longitudinal dispersivity within the clay liner to be greater than or less than the base case assumption (0.1 m), due to uncertainty in the impact of dispersive phenomena within the 3 ft thick low permeability clay liner. The distribution parameters are assigned to yield a median value (0.1 m) equal to the base case value for the range selected. Range: Minimum value (0.05 m) is representative of pore-scale dispersive processes in homogeneous porous media. Maximum value (0.5 m) is set as five times the base case value, which is equal to 55% of the clay liner thickness. Correlation: The assumption is that ALPHAU3 and ALPHAU4 are positively correlated because the uncertainty in the impacts of dispersive processes within the clay liner and the underlying geologic buffer material are similar, based on the likelihood that the materials used for the clay liner and the geologic buffer will be similar.
UZ	Bulk Density UZ4	g/cm^3	Related Parameter Specification			1.4	1.7	1.5	DENSUZ(4)	DENSUZ(4) = (1-TPUZ(4))*2.65 Simplified: DENSUZ(4) = 2.65-2.65*TPUZ(4)	Functional relationship: Bulk density = (1-total porosity)*grain density, assumes a grain density of 2.65 g/cm3 (quartz)
UZ	Total Porosity of UZ4	-	Beta (symmetric)	4	4	0.377	0.461	0.419	TPUZ(4)	No Correlation	Distribution: Symmetric beta (4,4) represents similar likelihood for the total porosity of the geologic buffer to be greater than or less than the base case assumption (0.419 vol/vol), due to uncertainty in material characteristics. Range: maximum value is 110% of the base case value, which is representative of clay. Minimum value represents equal interval (0.042 vol/vol) below base case value.
UZ	Unsaturated Zone Effective Porosity: UZ4 (Geobuffer)	-	Beta (symmetric)	4	4	0.211	0.257	0.234	EPUZ(4)	No Correlation	Distribution: Symmetric beta (4,4) represents similar likelihood for the average effective porosity of the geologic buffer to be greater than or less than the base case assumption (0.234 vol/vol), due to uncertainty in material characteristics. Range: maximum value is 110% of the base case value, which is less than the minimum value of the range of UZ4 total porosity evaluated (total porosity > effective porosity). Minimum value represents equal interval (0.023 vol/vol) below base case value.

Zone	Parameter	Unit	Distribution	Alpha (P) /Mean and SD	Beta (Q)/ SD/ Truncation Percentiles	Minimum Value	Maximum Value	Base Case Value	RESRAD Identifier	Relations or Correlations (rcc = rank correlation coefficient, rcc is the initially assigned value; final adjusted values are provided in Attachment G.4)	Basis or Justification for Assigned Distribution, Correlation or Functional Relationship
UZ	Unsaturated Zone Longitudinal Dispersivity: UZ4 (Geobuffer)	m	Beta (asymmetric)	1.25	3	0.05	0.5	0.1	ALPHALU(4)	rcc = 0.9 for ALPHALU(4) and ALPHALU(3)	Distribution: Asymmetric beta (1.25, 3) distribution represents the possibility for the longitudinal dispersivity within the geologic buffer to be greater than or less than the base case assumption (0.1 m), due to uncertainty in the impact of dispersive phenomena within the 10 ft thick low permeability unsaturated geologic buffer. The distribution parameters are assigned to yield a median value (0.1 m) equal to the base case value for the range selected. Range: Minimum value (0.05 m) is representative of pore-scale dispersive processes in homogeneous porous media. Maximum value (0.5 m) is set as five times the base case value, which is equal to 16% of the geologic buffer thickness. Correlation: The assumption is that ALPHAU3 and ALPHAU4 are positively correlated because the uncertainty in the impacts of dispersive processes within the clay liner and the underlying geologic buffer material are similar, based on the likelihood that the materials used for the clay liner and the geologic buffer will be similar.
UZ	Unsaturated Zone Thickness: UZ5 (In-Situ Material)	m	Beta (asymmetric)	4	2.5	0.10	7.6	4.85	H(5)	rcc = -0.9 (negative) for H(5) and PRECIP rcc = 0.9 for H(5) and RUNOFF rcc = 0.9 for H(5) and ALPHALU(5)	Distribution: Asymmetric beta distribution (4, 2.5) reflects the possibility of the average water table elevation below the EMDF footprint being lower than or higher than the base case assumption for thickness of UZ5 (4.85 m) that is based on the EMDF PA groundwater model results for the long-term performance condition. The distribution parameters are assigned to yield a median value (4.8 m) approximately equal to the base case value, given the range selected. Range: minimum value is set at 0.1 meters, approximately corresponding to the EMDF design performance criterion of a minimum of 15 ft vertical distance from the base of the waste to the water table. Maximum value corresponds to the thickness of UZ5 that yields a total average vadose thickness of 40 ft, which is the upper end of the modeled range of total vadose zone thickness across the waste footprint, based on the long-term degraded EMDF cover performance condition (0.88 in/yr cover infiltration). Correlations: The assumption is that H(5) and PRECIP are negatively correlated because wetter conditions will result in higher water table elevations and smaller H(5). H(5) and RUNOFF are positively correlated because larger RUNOFF values result in smaller calculated cover infiltration, which will result in lower water table elevation below the geologic buffer, and larger H(5). H(5) and ALPHAU(5) are positively correlated because the dispersive length scale within the unsaturated material beneath the geologic buffer will scale with the thickness of UZ(5).

Zone	Parameter	Unit	Distribution	Alpha (P) /Mean and SD	Beta (Q)/ SD/ Truncation Percentiles	Minimum Value	Maximum Value	Base Case Value	RESRAD Identifier	Relations or Correlations (rcc = rank correlation coefficient, rcc is the initially assigned value; final adjusted values are provided in Attachment G.4)	Basis or Justification for Assigned Distribution, Correlation or Functional Relationship
UZ	Bulk Density UZ5	g/cm^3	Beta (symmetric)	4	4	1.7	1.90	1.80	DENSUZ(5)	No Correlation	Distribution: Symmetric beta (4,4) distribution represents uncertainty in the bulk density of the unsaturated geologic material below the geologic buffer zone. Range is based on the range of laboratory measured Nolichucky saprolite bulk densities
UZ	Total Porosity of UZ5	-	Related Parameter Specification			0.317	0.388	0.353	TPUZ(5)	TPUZ(5)=1-DENSUZ(5)/2.78	Functional relationship: Total porosity=(1-bulk density)/solids density, relation assumes a (constant) base case waste solids density of 2.78 g/cm^3, the average for Nolichucky Shale materials in Bear Creek Valley
UZ	Unsaturated Zone Effective Porosity: UZ5 (In-situ Material)	-	Beta (symmetric)	4	4	0.243	0.297	0.270	EPUZ(5)	rcc = 0.9 for EPUZ(5) and HCUZ(5)	Distribution: Symmetric beta (4,4) represents similar likelihood for the average effective porosity of the unsaturated material below the geologic buffer to be greater than or less than the base case assumption (0.27 vol/vol), due to uncertainty in EMDF site characteristics and final design configuration. Range: maximum value is 110% of the base case value, which is less than the minimum value of the range of UZ5 total porosity evaluated (total porosity > effective porosity). Minimum value represents equal interval (0.027 vol/vol) below base case value. Correlation: The assumption is that HCUZ(5) and EPUZ(5) are positively correlated because effective porosity reflects the proportion of total porosity that contributes to advective fluid transport and is closely related to permeability of the material
UZ	Unsaturated Zone Hydraulic Conductivity: UZ5 (In-situ Material)	m/yr	Truncated lognormal-N	mean=ln(16.7), SD=1	truncated at 5% and 95%	3.2	86.4	16.7	HCUZ(5)	rcc = 0.9 for HCUZ(5) and EPUZ(5)	Distribution: Truncated lognormal distribution (mean=ln(16.7), SD=1) represents similar likelihood for the hydraulic conductivity of the unsaturated material below the geologic buffer to be lower than or higher than the base case value (16.7 m/yr), due to uncertainty in in EMDF site characteristics and final design configuration. Range (3.2 to 86.4 m/yr, corresponding to 5th and 95th percentiles) is consistent with the range of Nolichucky Shale K values for depths up to 100 feet below ground level in Bear Creek Valley. Correlation: The assumption is that HCUZ(5) and EPUZ(5) are positively correlated because effective porosity reflects the proportion of total porosity that contributes to advective fluid transport and is closely related to permeability of the material

Zone	Parameter	Unit	Distribution	Alpha (P) /Mean and SD	Beta (Q)/ SD/ Truncation Percentiles	Minimum Value	Maximum Value	Base Case Value	RESRAD Identifier	Relations or Correlations (rcc = rank correlation coefficient, rcc is the initially assigned value; final adjusted values are provided in Attachment G.4)	Basis or Justification for Assigned Distribution, Correlation or Functional Relationship
UZ	Unsaturated Zone Longitudinal Dispersivity: UZ5 (In-situ Material)	m	Beta (asymmetric)	1.25	3	0.05	0.5	0.1	ALPHALU(5)	rcc = 0.9 for ALPHALU(5) and H(5)	Distribution: Asymmetric beta (1.25, 3) distribution represents the possibility for the longitudinal dispersivity within the unsaturated material below the geologic buffer to be greater than or less than the base case assumption (0.1 m), due to uncertainty in the impact of dispersive phenomena within the lower portion of the vadose zone. The distribution parameters are assigned to yield a median value (0.1 m) equal to the base case value for the range selected. Range: Minimum value (0.05 m) is representative of pore-scale dispersive processes in homogeneous porous media. Maximum value (0.5 m) is set as five times the base case value, which is approximately equal to 10% of the base case thickness of the lowest portion (UZ5) of the unsaturated zone. Correlation: The assumption is that H(5) and ALPHAU(5) are positively correlated because the dispersive length scale within the unsaturated material beneath the geologic buffer will scale with the thickness of UZ(5).
SZ	Saturated Zone Bulk Density	g/cm^3	Beta (symmetric)	4	4	1.7	2.5	2.1	DENSAQ	No Correlation	Distribution: Symmetric beta (4,4) distribution represents uncertainty in the average bulk density of the saturated zone materials. Range is based on the range of laboratory measured Nolichucky Shale bulk densities. Range: Maximum value is set at 2.5 g/cm^3, and minimum value represents equal interval (0.4 g/cm^3) below base case value.
SZ	Saturated Zone Total Porosity	-	Related Parameter Specification			0.101	0.388	0.240	TPSZ	TPSZ=1-DENSAQ/2.78	Functional relationship: Total porosity=1-bulk density/solids density, relation assumes a (constant) base case waste solids density of 2.78 g/cm^3, the average for Nolichucky Shale materials in Bear Creek Valley
SZ	Saturated Zone Effective Porosity	-	Beta (symmetric)	4	4	0.18	0.22	0.2	EPSZ	rcc = 0.9 for EPSZ and HCSZ	Distribution: Symmetric beta (4,4) distribution represents similar likelihood for the average effective porosity of the saturated zone materials to be greater than or less than the base case assumption (0.2 vol/vol), due to uncertainty in EMDF site characteristics. Range: maximum value is 110% of the base case value. Minimum value represents equal interval (0.02 vol/vol) below base case value. Correlation: The assumption is that HCSZ and EPSZ are positively correlated because effective porosity reflects the proportion of total porosity that contributes to advective fluid transport and so is closely related to permeability of the material.

Zone	Parameter	Unit	Distribution	Alpha (P) /Mean and SD	Beta (Q)/ SD/ Truncation Percentiles	Minimum Value	Maximum Value	Base Case Value	RESRAD Identifier	Relations or Correlations (rcc = rank correlation coefficient, rcc is the initially assigned value; final adjusted values are provided in Attachment G.4)	Basis or Justification for Assigned Distribution, Correlation or Functional Relationship
SZ	Saturated Zone Hydraulic Conductivity	m/yr	Truncated lognormal-N	mean=ln(26.8), SD=0.5	truncated at 5% and 95%	11.8	61.0	26.8	HCSZ	rcc = 0.9 for HCSZ and EPSZ rcc = -0.9 (negative) for HCSZ and HGW	Distribution: Truncated lognormal distribution (mean=ln(26.8), SD=0.5) represents similar likelihood for the hydraulic conductivity of the saturated zone to be lower than or higher than the base case value (26.8 m/yr), due to uncertainty in in EMDF site characteristics. Range (11.8 to 61 m/yr, corresponding to 5th and 95th percentiles) lies within the limits of the Nolichucky Shale K values assigned to the saprolite (83.4 m/yr) and upper fractured bedrock (10.6 m/yr) assigned to MT3D model layers 1 and 2 respectively. Correlations: The assumption is that HCSZ and EPSZ are positively correlated because effective porosity reflects the proportion of total porosity that contributes to advective fluid transport and so is closely related to permeability of the material. HCSZ and HGW are negatively correlated because based on Darcy's law, and assuming a long-term average Darcy velocity reflects the product of HCSZ and HGW, these two parameters are inversely related.
SZ	Depth of Aquifer Contributing to Well	m	Beta (symmetric)	4	4	25.0	55.0	40.0	DWIBWT	No Correlation	Distribution: Symmetric beta (4,4) represents similar likelihood for the depth of aquifer contributing to the well (DWIBWT parameter) to be greater than or less than the base case assumption (40 m), due to uncertainty in future human practices that could affect well construction and the portion of the saturated zone that provides drinking water. Range is set at ± 15 m from the base case value. The resulting 25-55 m range falls below the average open hole/well intake interval (67 m) for residential drinking water wells in the Bethel Valley and Clinton Quadrangles (Tennessee Dept. of Environment and Conservation records for wells in the vicinity of Bear Creek Valley).
SZ	Saturated Zone Hydraulic Gradient to Well	m/m	Beta (symmetric)	4	4	0.027	0.081	0.054	HGW	rcc = 0.9 for HGW and PRECIP rcc = -0.9 (negative) for HGW and HCSZ	Distribution: Symmetric beta (4,4) represents similar likelihood for the average saturated zone hydraulic gradient to the well to be greater than or less than the base case assumption (0.054 m/m), due to uncertainty in the degree of saturated zone dilution between the waste and the 100 m well. Range: Minimum value is a factor of 2 smaller than the base case value. Maximum value represents equal interval (0.027 m/m) above base case value. Correlations: The assumption is that HGW and PRECIP are positively correlated because wetter conditions will result in higher hydraulic gradient and groundwater flux in the saturated zone. HCSZ and HGW are negatively correlated because based on Darcy's law, and assuming a long-term average Darcy velocity reflects the product of HCSZ and HGW, these two parameters are inversely related.

Zone	Parameter	Unit	Distribution	Alpha (P) /Mean and SD	Beta (Q)/ SD/ Truncation Percentiles	Minimum Value	Maximum Value	Base Case Value	RESRAD Identifier	Relations or Correlations (rcc = rank correlation coefficient, rcc is the initially assigned value; final adjusted values are provided in Attachment G.4)	Basis or Justification for Assigned Distribution, Correlation or Functional Relationship
SZ	Saturated Zone Hydraulic Gradient to Surface Water Body	m/m	Related Parameter Specification			0.018	0.054	0.036	HGSW	HGSW = (36/54)*HGW Simplified: HGSW=0.667*HGW	Functional relationship: Constant ratio (base case values, 0.036/0.054) of HGSW with sampled hydraulic gradient to well (HGW)
SZ	Saturated Zone Longitudinal Dispersivity to Well	m	Beta (symmetric)	4	4	1	19	10	ALPHALOW	No Correlation	Distribution: Symmetric beta (4,4) represents similar likelihood for the saturated zone longitudinal dispersivity to the well to be greater than or less than the base case assumption (10 m), due to uncertainty in saturated zone transport dynamics between the waste and the 100 m well. Range: Maximum value (19 m) is 190% of the base case value or 19% of the linear distance between the edge of waste and the well. Minimum value (1 m) represents equal interval (9 m) below base case value.
SZ	Saturated Zone Longitudinal Dispersivity to SW	m	Beta (symmetric)	4	4	1	62	31.5	ALPHALOSW	No Correlation	Distribution: Symmetric beta (4,4) represents similar likelihood for the saturated zone longitudinal dispersivity to the surface water body (Bear Creek) to be greater than or less than the base case assumption (31.5 m), due to uncertainty in saturated zone transport dynamics between the waste and Bear Creek. Range: Maximum value (62 m) is approximately two times the base case value or ~20% of the linear distance between the edge of waste Bear Creek. Minimum value (1 m) represents equal interval (30.5 m) below base case value.
SW	Mean Residence Time of Water in Surface Water Body	yr	Truncated lognormal-N	mean= ln(1.0E-04), SD=0.99	truncated at 1% and 99%	1E-05	1E-03	1.00E-04	TLAKE	rcc = -0.9 (negative) for TLAKE and PRECIP	Distribution: Truncated lognormal distribution (mean=ln(1.0E-04), SD=0.99) represents similar likelihood for the average residence time of the surface water body (Bear Creek) to be greater than or less than the base case assumption (1.0E-04 yr). There is significant uncertainty in assigning an appropriate long-term average value that captures the net impact of hydrological, geochemical, and biological processes that impact surface water radionuclide concentrations. Range is set at 1.0E-05 to 1.0E-03 yr (factor of 10 larger than and smaller than base case value) corresponding to the 1st and 99th percentiles), which results in calculated surface water concentrations varying over the same proportional range. Correlation: The assumption is that PRECIP and TLAKE are negatively correlated because wetter conditions will result in higher average flow rates and lower average residence time in the Bear Creek reach that receives discharge of radionuclides released from EMDF.

R = Related Input
P = Probabilistic Input
CZ = Contaminated Zone (Primary Contamination)
UZ = Unsaturated Zone
SW = Surface Water
SZ = Saturated Zone

Plots of probability density functions (PDF) and cumulative distribution functions (CDF) for selected RESRAD_OFFSITE probabilistic input parameters

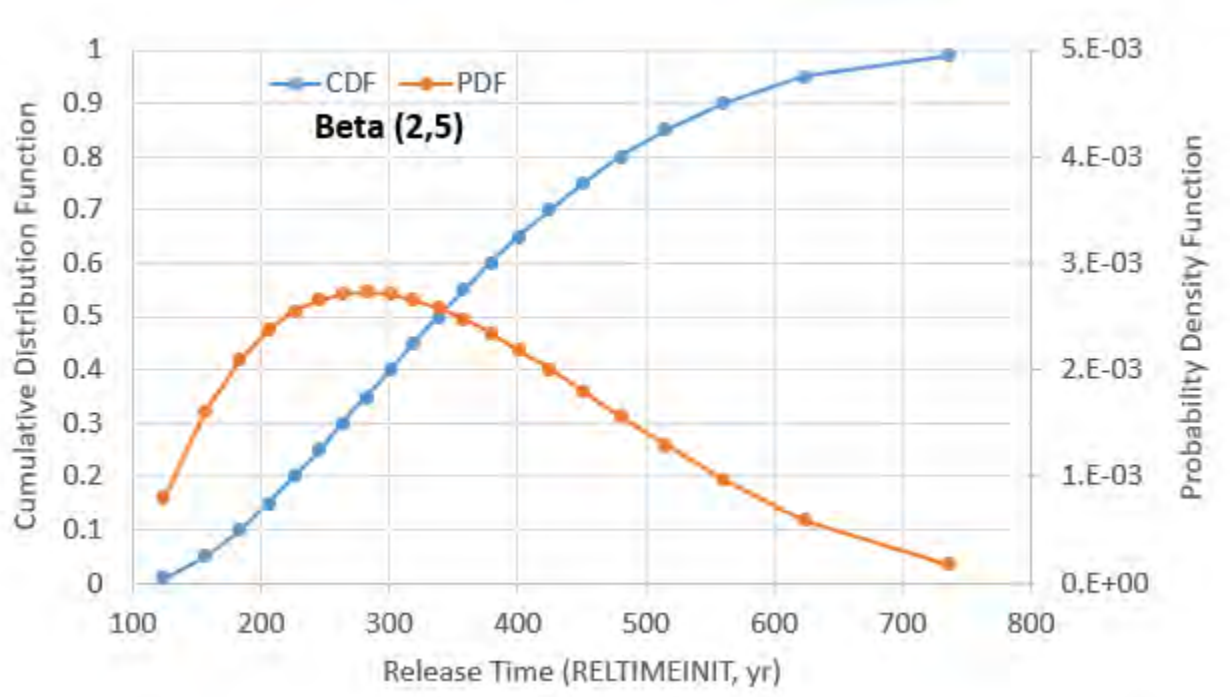

Fig. G.3.1 Initial Release Time (RELTIMEINIT)

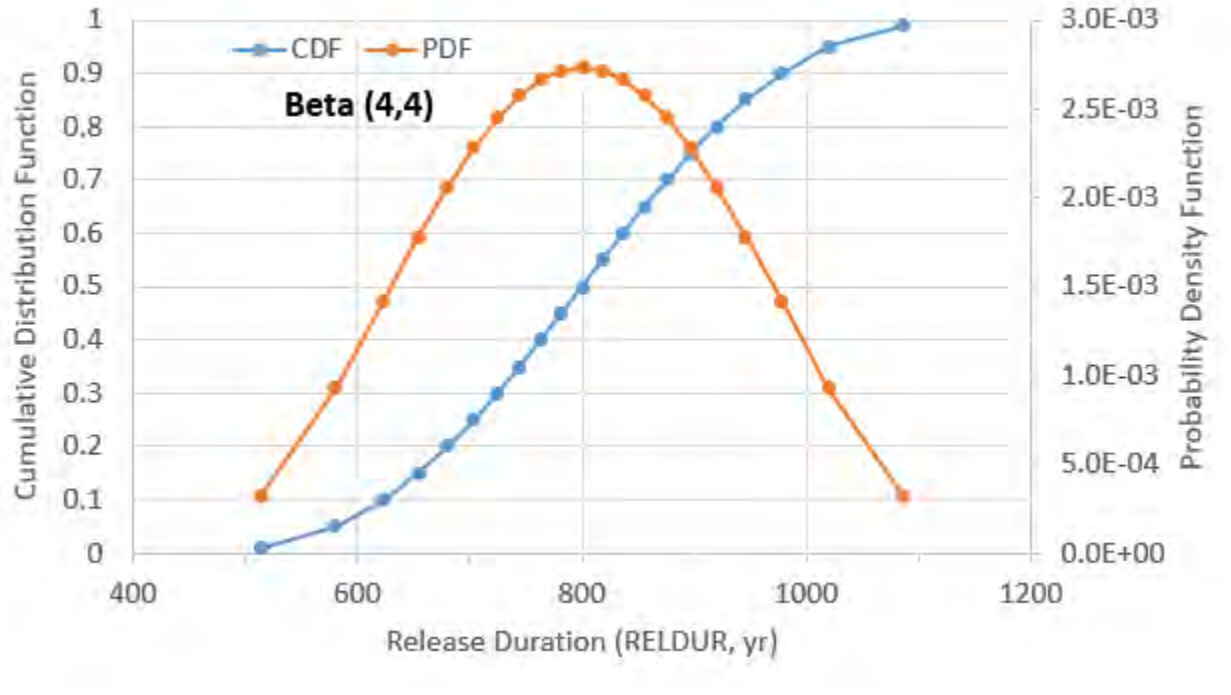

Fig. G.3.2 Release Duration (RELDUR)

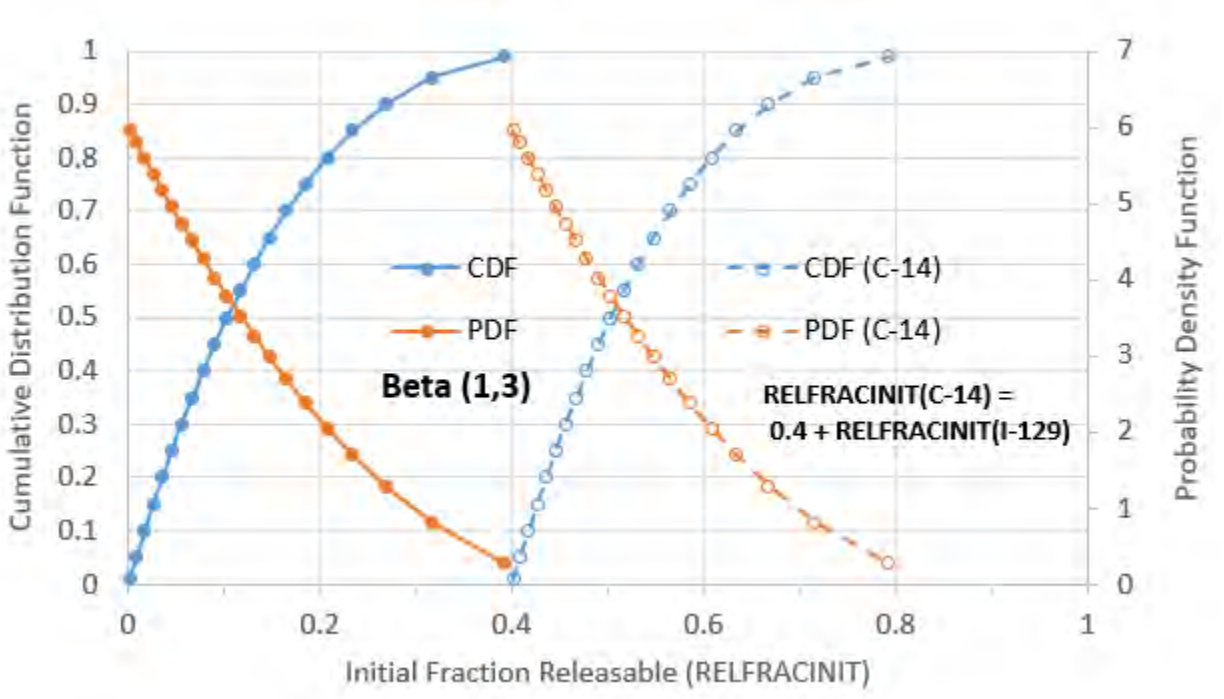

Fig. G.3.3 Initial Releasable Fraction (RELFRACINIT)

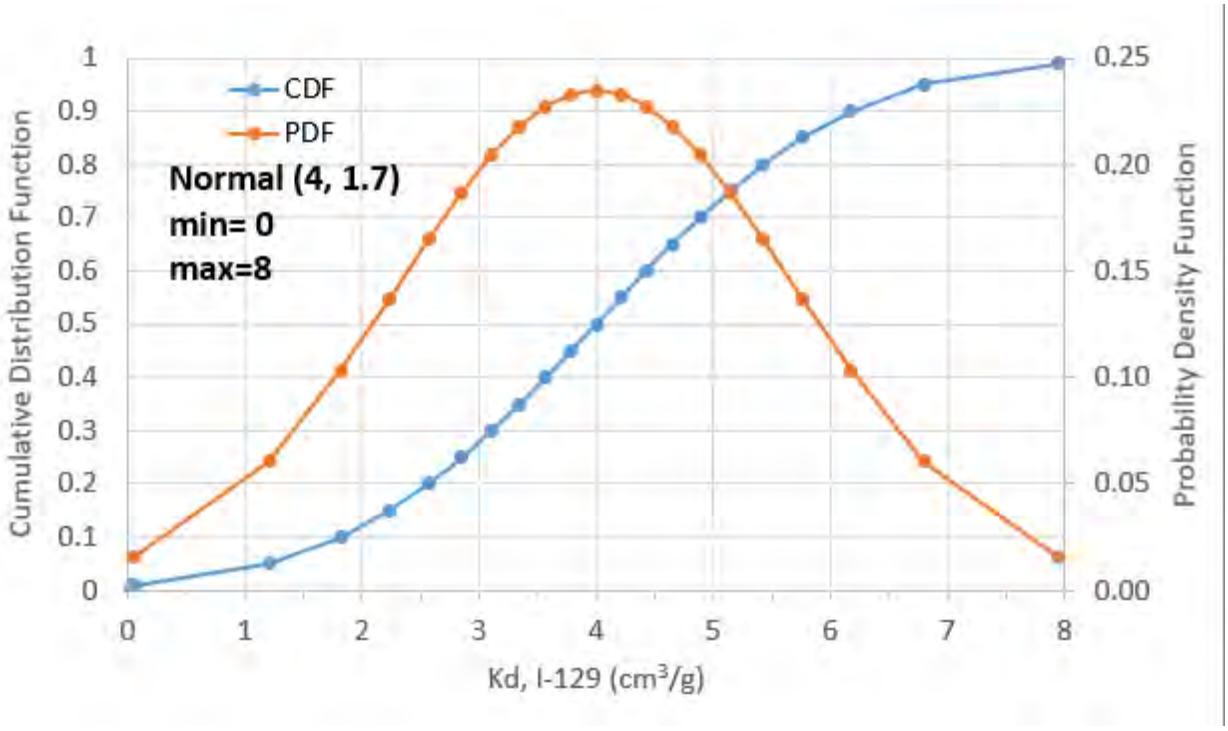

Fig. G.3.4 Partition Coefficient, I-129 (waste K_d = ½ sampled unsaturated zone K_d value)

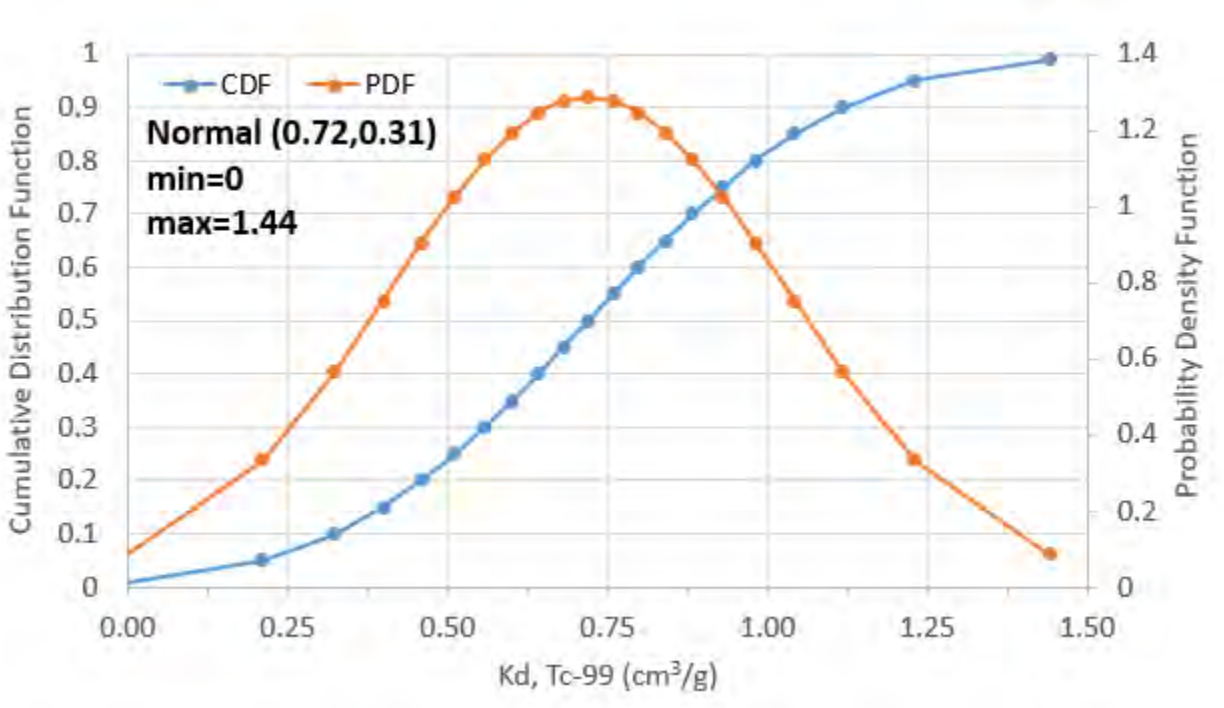

Fig. G.3.5 Partition Coefficient, Tc-99 (waste K_d = ½ sampled unsaturated zone K_d value)

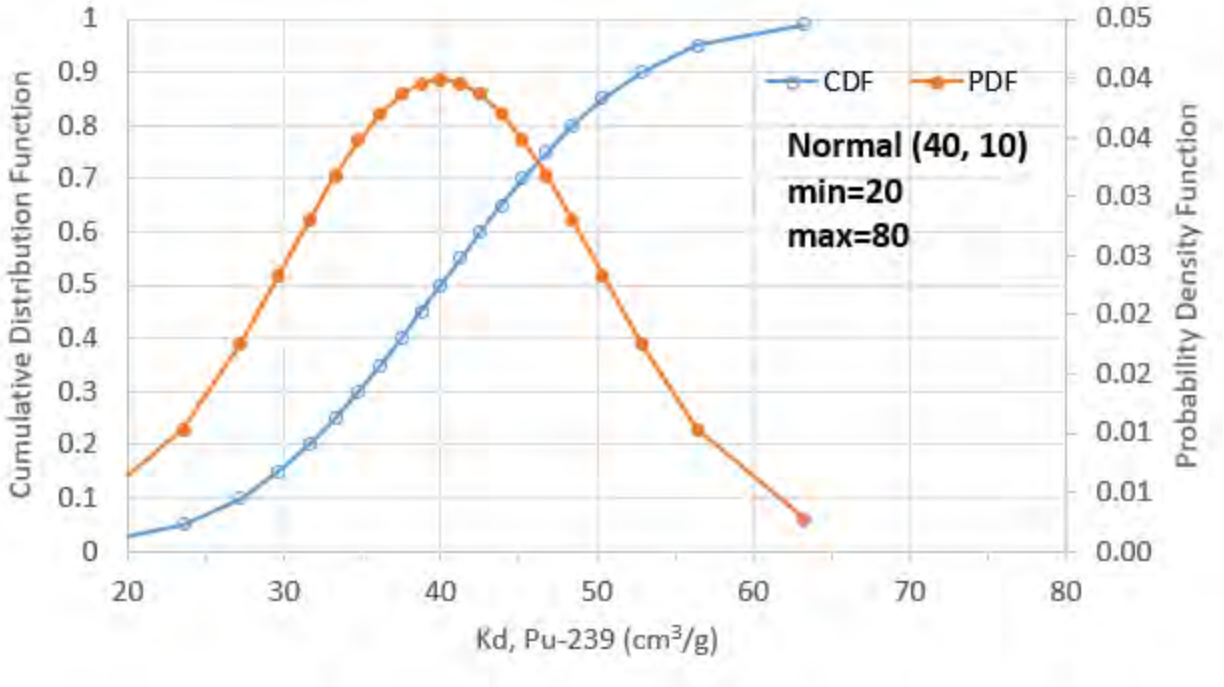

Fig. G.3.6 Partition Coefficient, Pu-239 (waste K_d = ½ sampled unsaturated zone K_d value)

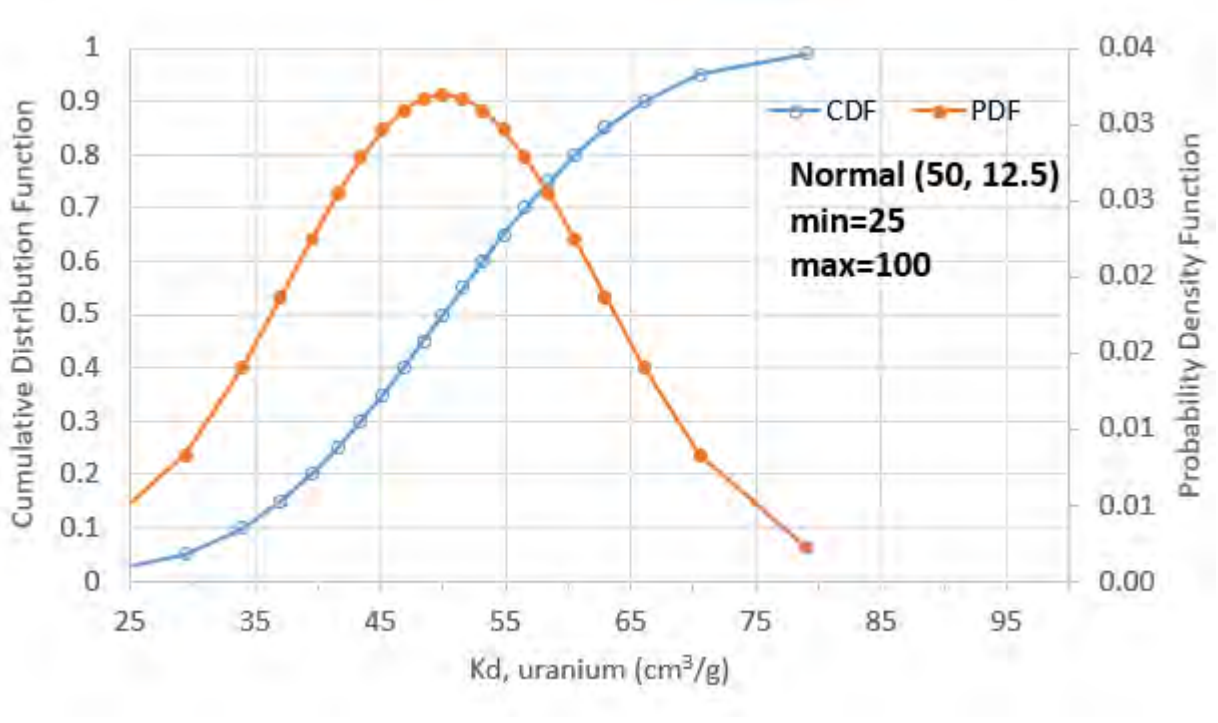

Fig. G.3.7 Partition Coefficient, uranium isotopes (waste K_d = ½ sampled unsaturated zone K_d value)

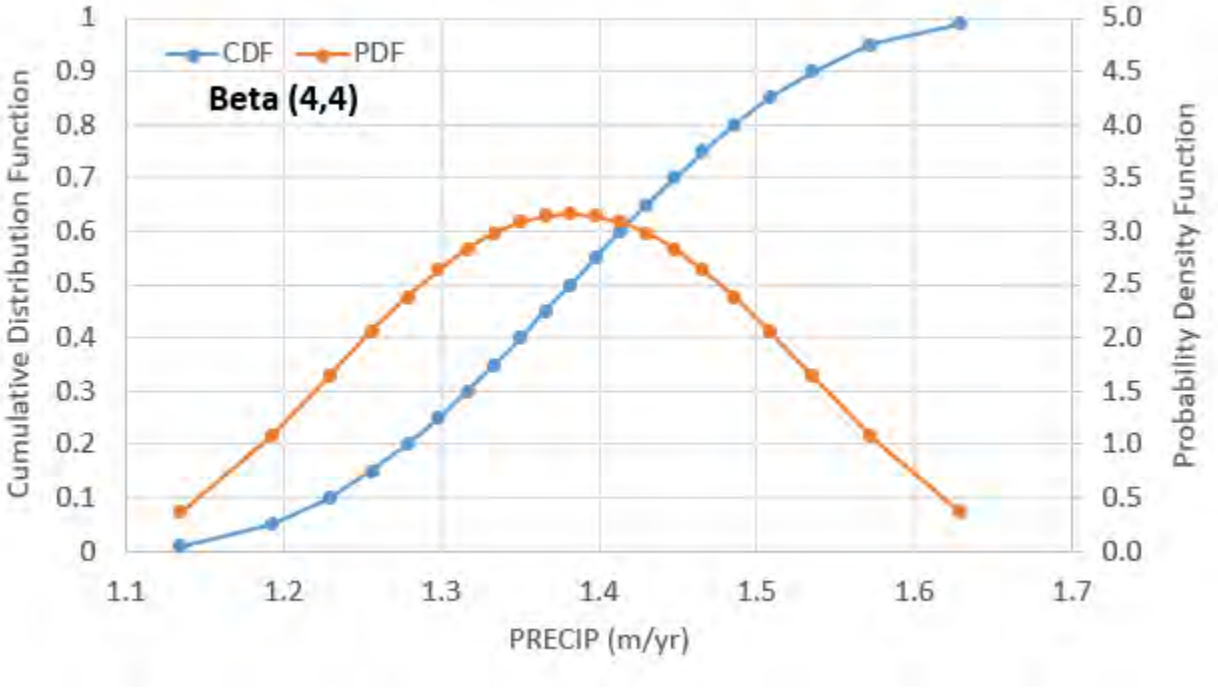

Fig. G.3.8 Annual Total Precipitation (PRECIP)

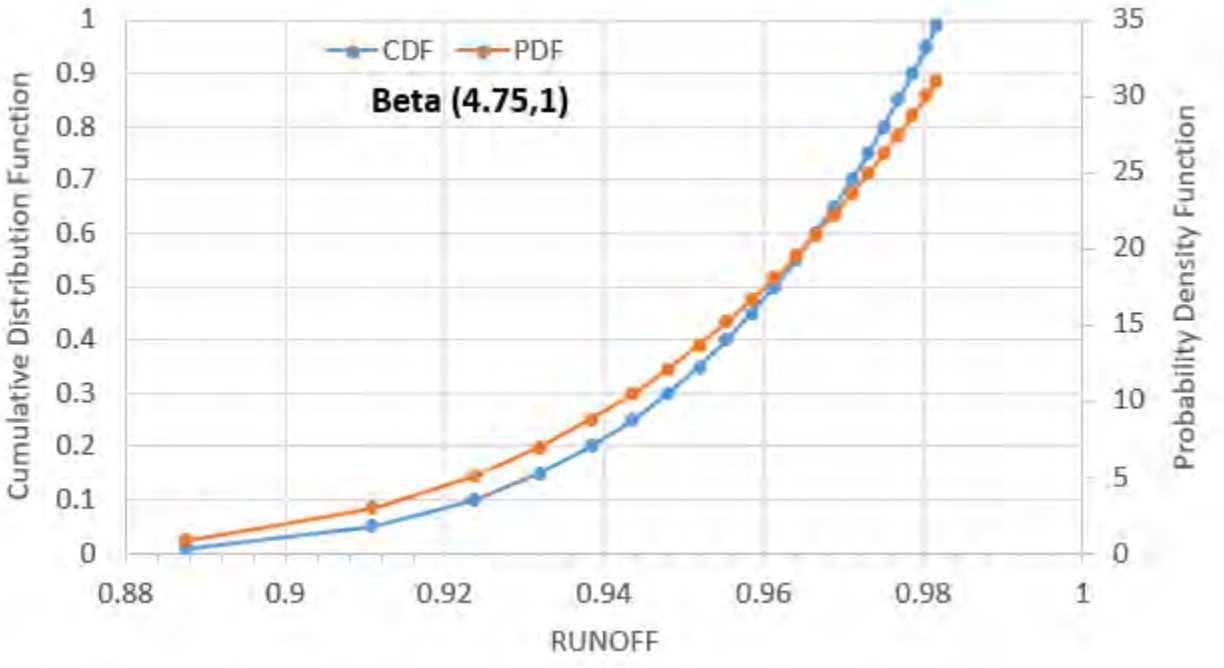

Fig. G.3.9 Runoff Coefficient (RUNOFF)

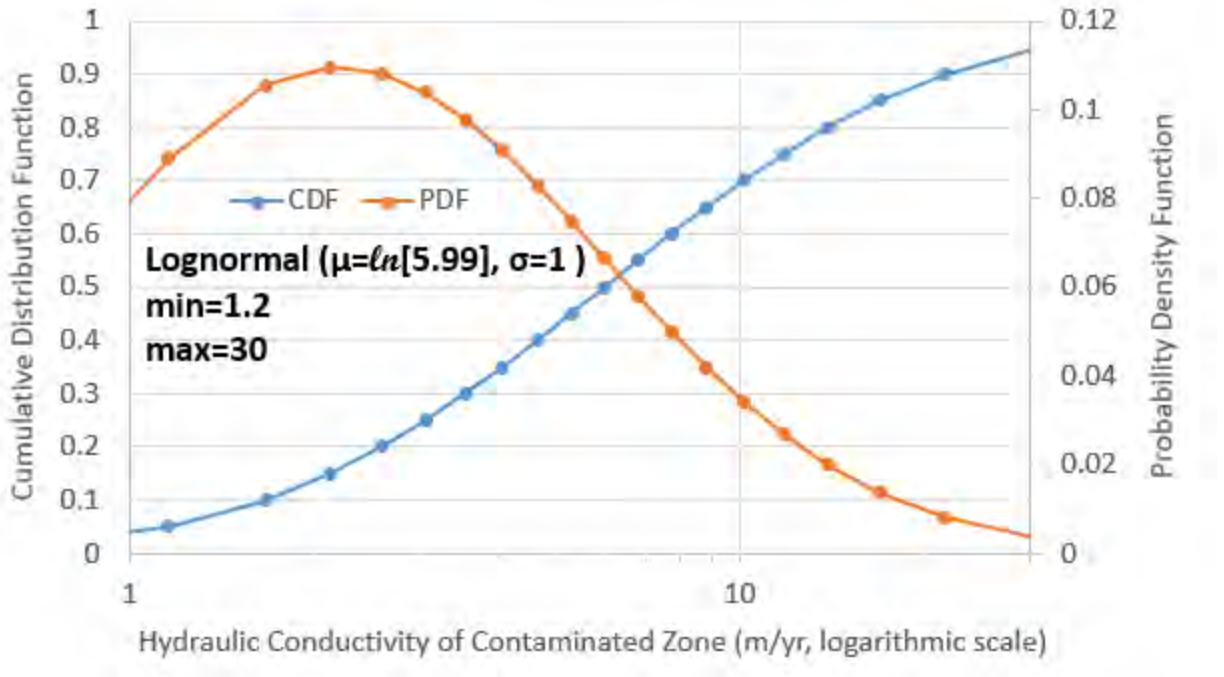

Fig. G.3.10 Hydraulic Conductivity of Contaminated Zone (HCCZ)

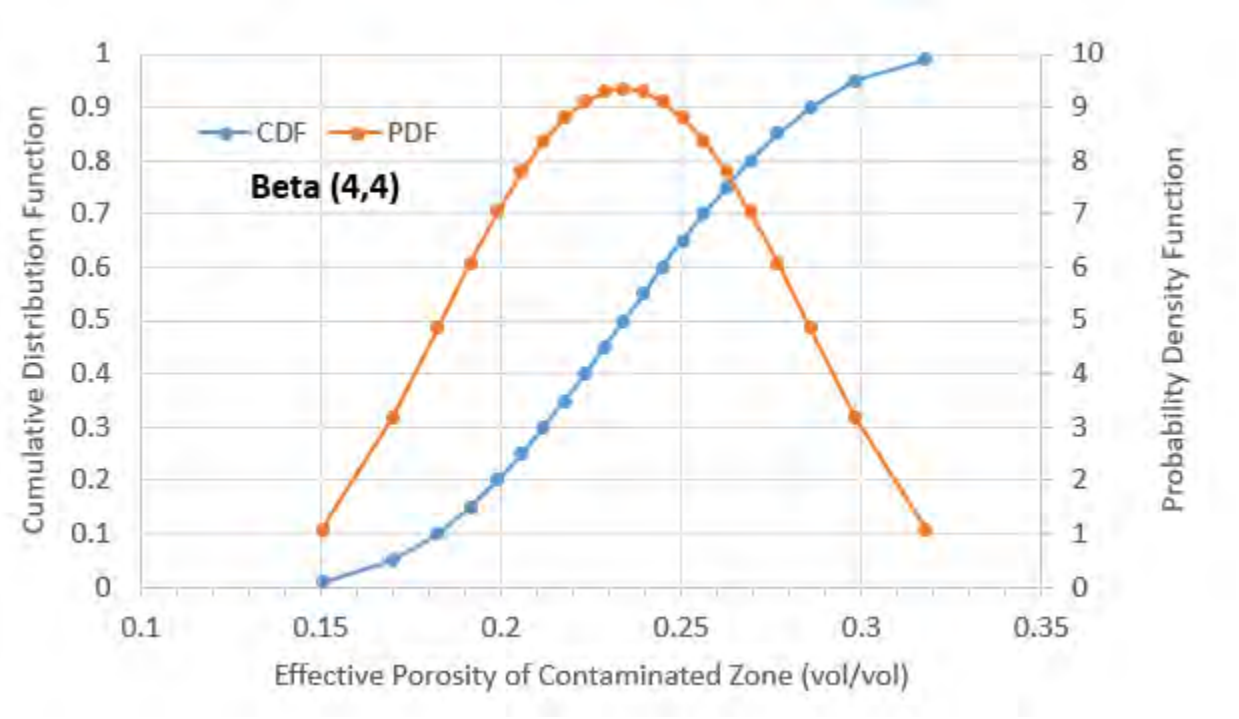

Fig. G.3.11 Effective Porosity of Contaminated Zone (EPCZ)

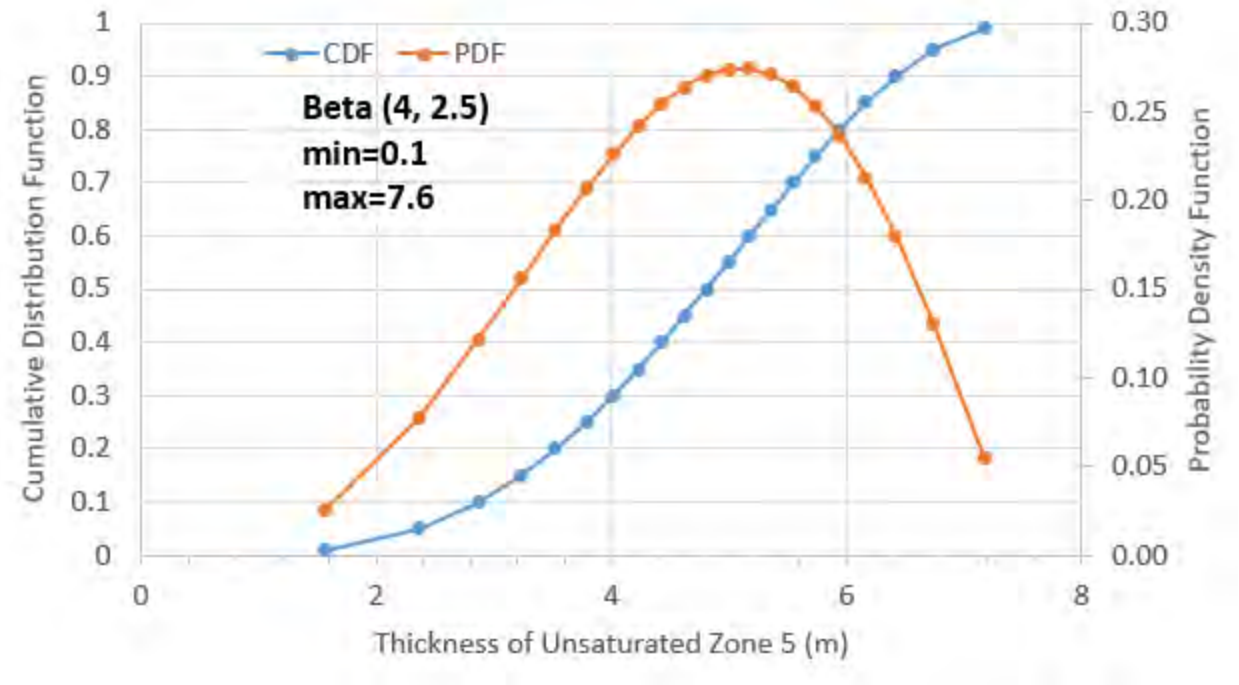

Fig. G.3.12 Thickness of Unsaturated Zone 5 (H5)

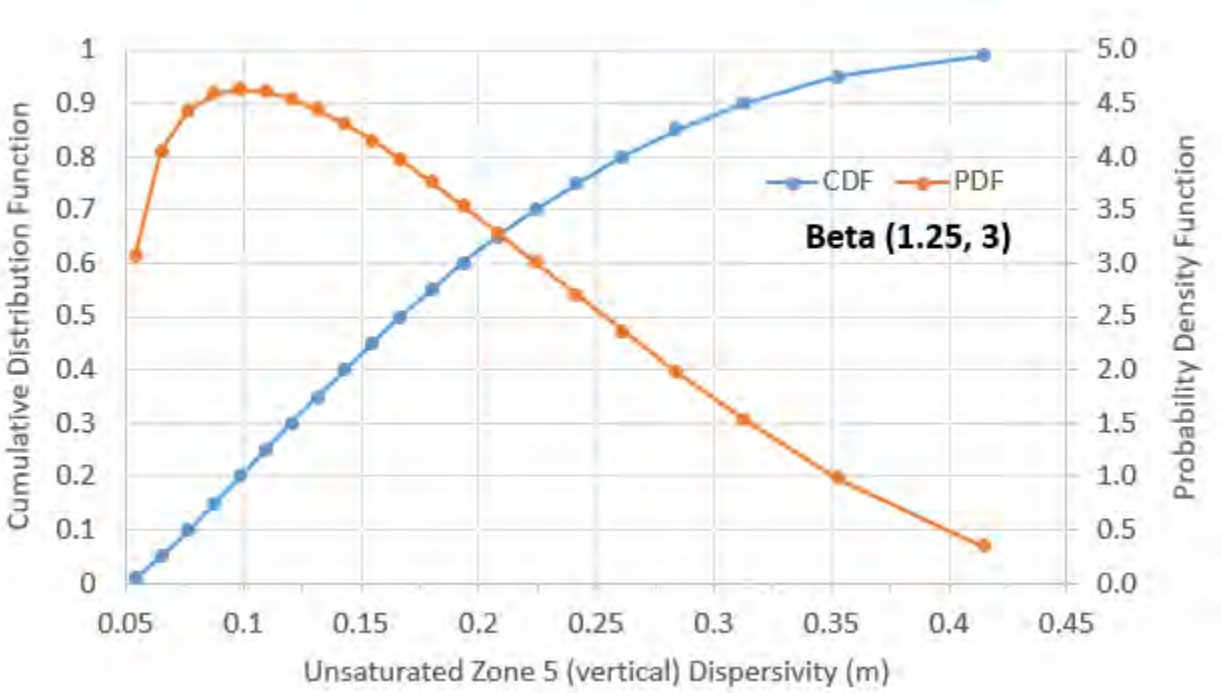

Fig. G.3.13 Vertical Dispersivity of Unsaturated Zone 5 (ALPHALU5)

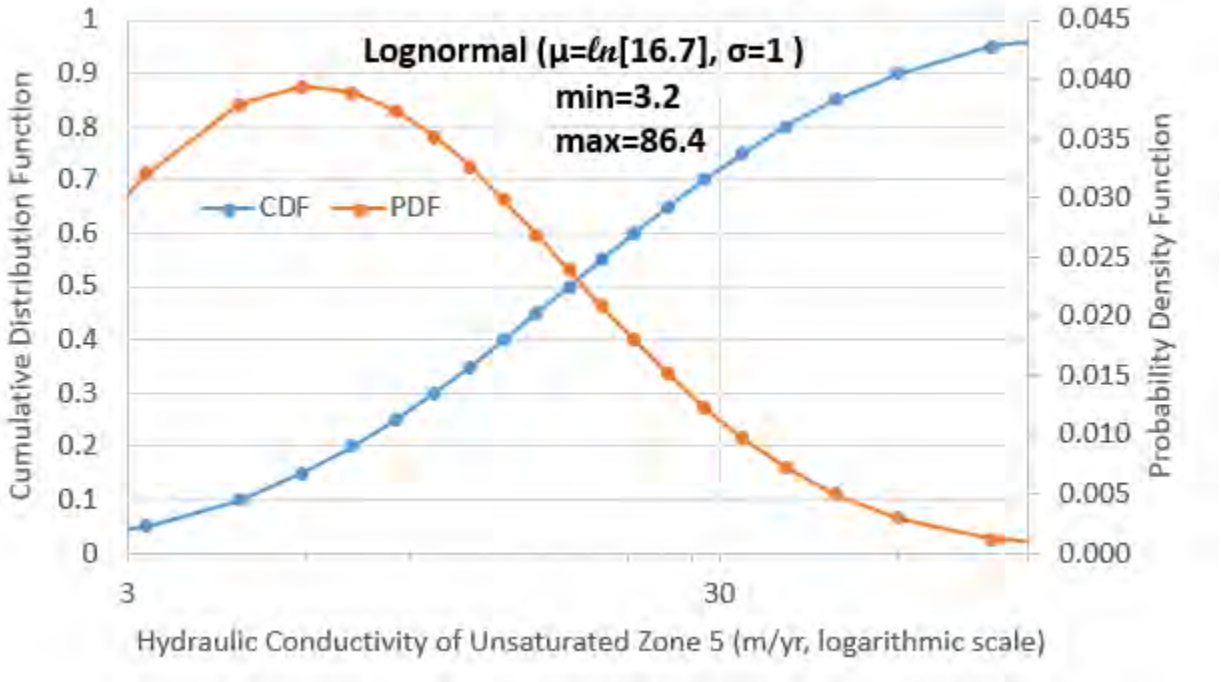

Fig. G.3.14 Hydraulic Conductivity of Unsaturated Zone 5 (HCUZ5)

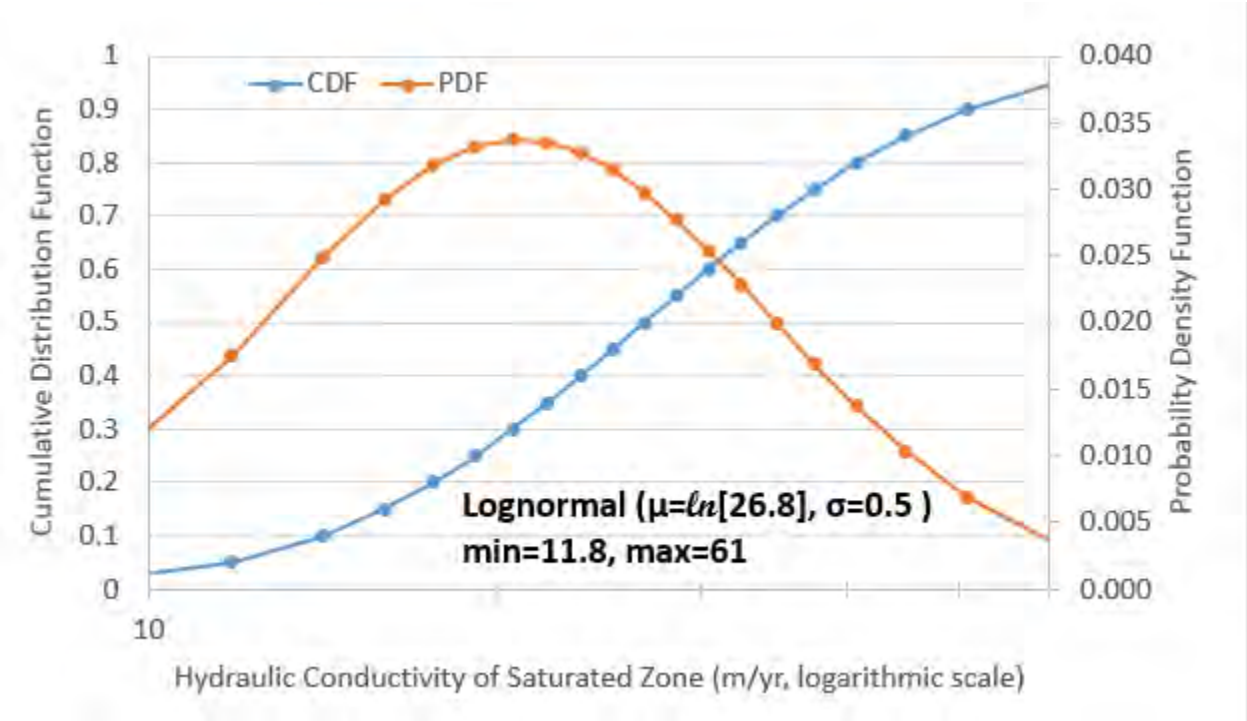

Fig. G.3.15 Hydraulic Conductivity of Saturated Zone 5 (HCSZ)

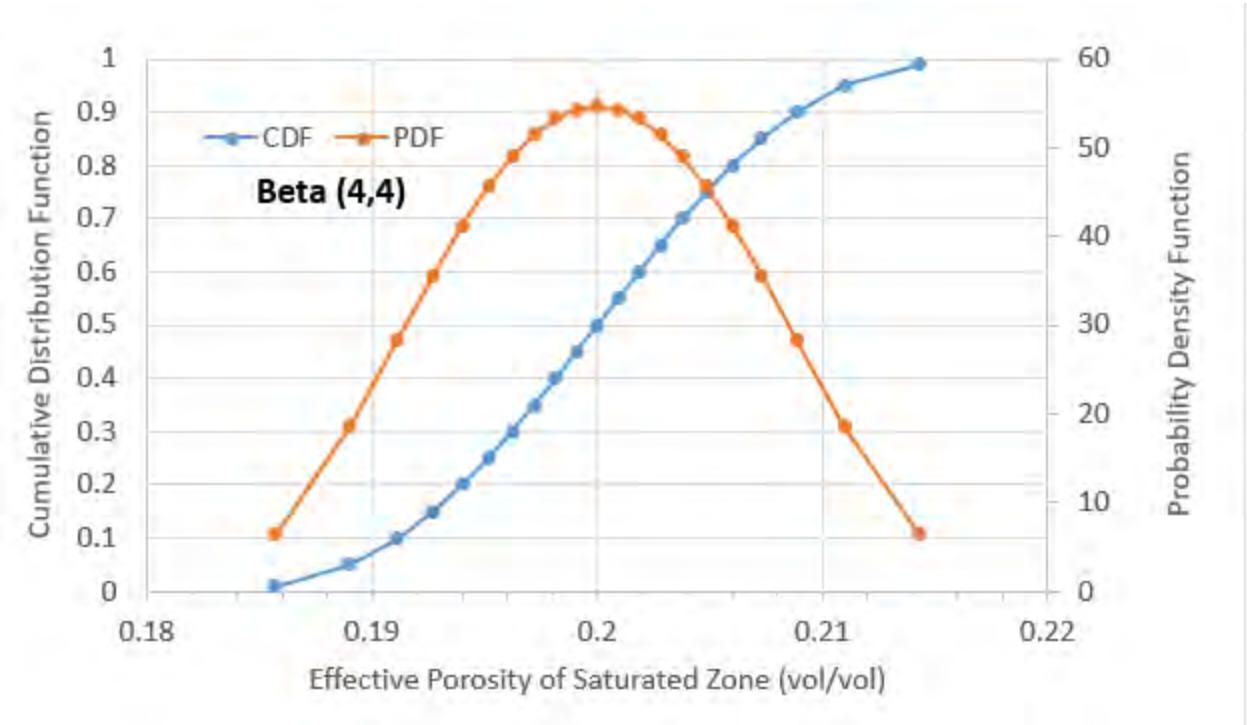

Fig. G.3.16 Effective Porosity of Saturated Zone (EPSZ)

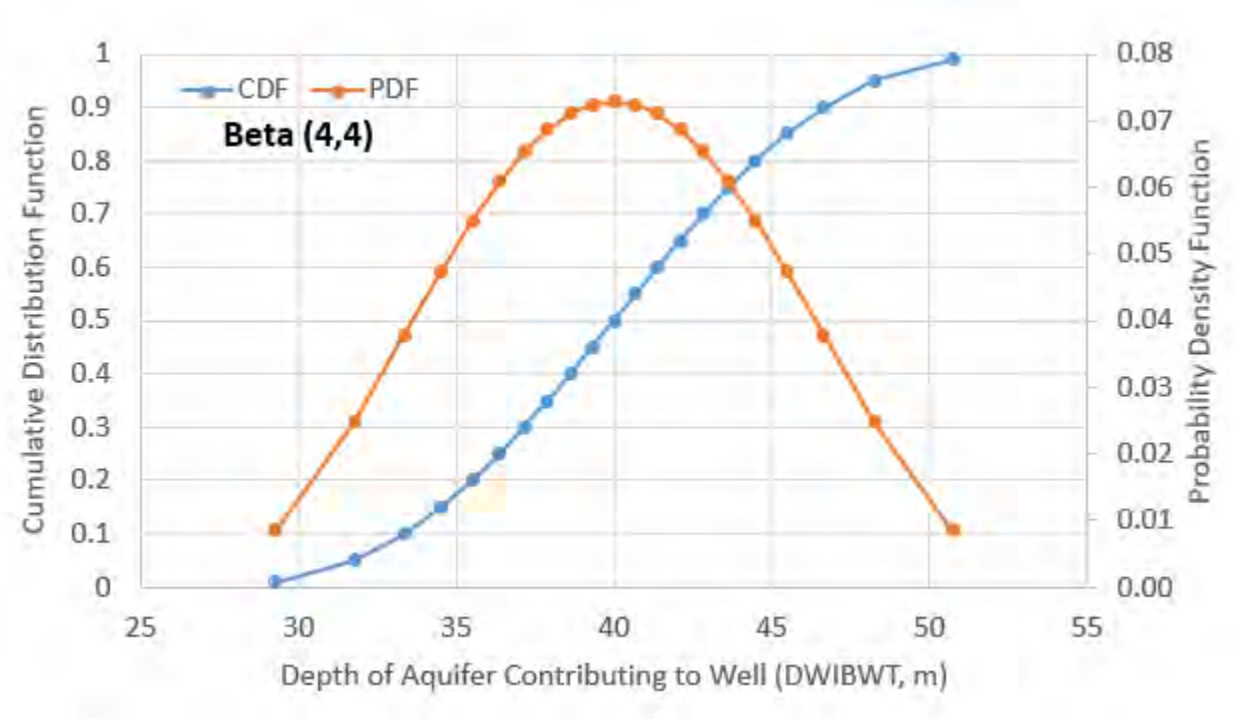

Fig. G.3.17 Depth of Aquifer Contributing to Well (DWIBWT)

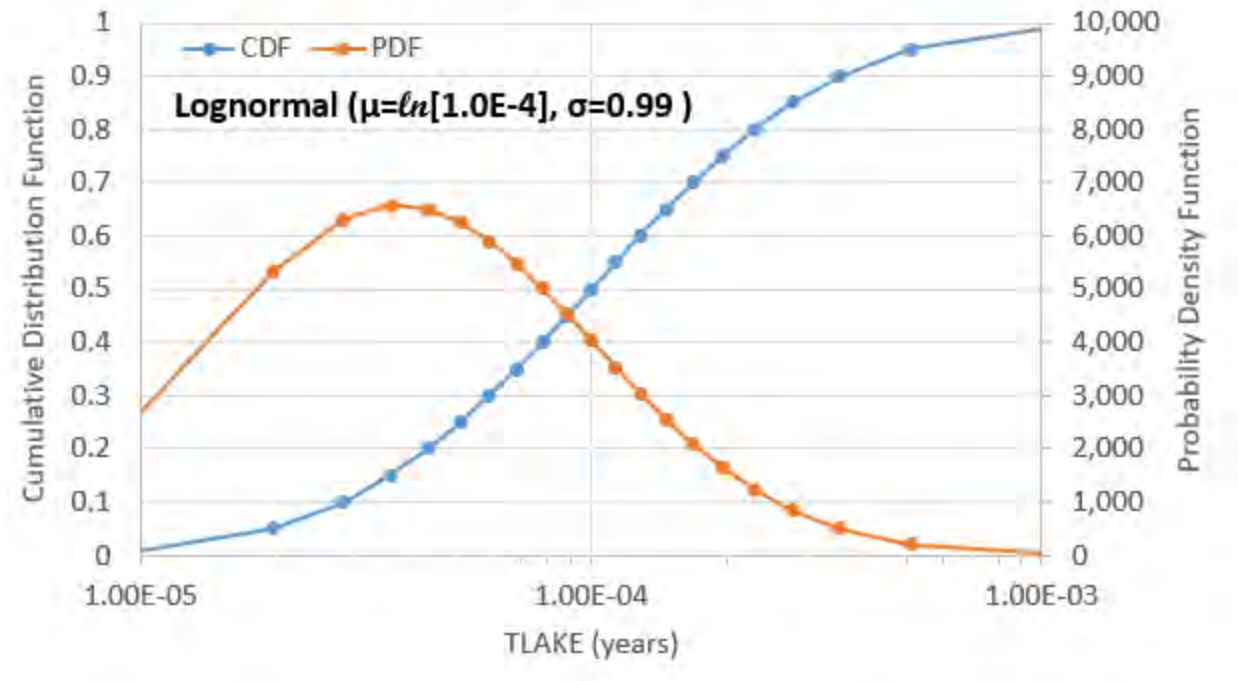

Fig. G.3.18 Mean Residence Time of Surface Water Body (TLAKE))

ATTACHMENT G.4.
RANK CORRELATION COEFFICIENT MATRIX FOR THE UNCERTAINTY ANALYSIS

This page intentionally left blank.

Table G.4.1 -Initial and adjusted rank correlation coefficients (RCC) for the compliance period probabilistic analysis

Parameter	ALPHALU(3)		ALPHALU(4)		ALPHALU(5)		DCACTS(I-129)		DCACTS(Tc-99)		DCACTU1(I-129)		DCACTU1(Tc-99)		EPCZ		EPSZ		EPUZ(5)	
RCC	Initial	Adjusted	Initial	Adjusted	Initial	Adjusted	Initial	Adjusted	Initial	Adjusted	Initial	Adjusted	Initial	Adjusted	Initial	Adjusted	Initial	Adjusted	Initial	Adjusted
ALPHALU(3)	1	1	--	--	--	--	--	--	--	--	--	--	--	--	--	--	--	--	--	--
ALPHALU(4)	0.9	0.9	1	1	--	--	--	--	--	--	--	--	--	--	--	--	--	--	--	--
ALPHALU(5)	0	0	0	0	1	1	--	--	--	--	--	--	--	--	--	--	--	--	--	--
DCACTS(I-129)	0	0	0	0	0	0	1	1	--	--	--	--	--	--	--	--	--	--	--	--
DCACTS(Tc-99)	0	0	0	0	0	0	0	0.0403	1	1	--	--	--	--	--	--	--	--	--	--
DCACTU1(I-129)	0	0	0	0	0	0	0.9	0.7944	0	-0.0884	1	1	--	--	--	--	--	--	--	--
DCACTU1(Tc-99)	0	0	0	0	0	0	0	-0.0884	0.9	0.7944	0	0.1866	1	1	--	--	--	--	--	--
EPCZ	0	0	0	0	0	0	0	0	0	0	0	0	0	0	1	1	--	--	--	--
EPSZ	0	0	0	0	0	0.0287	0	0	0	0	0	0	0	0	0	0	1	1	--	--
EPUZ(5)	0	0	0	0	0	0	0	0	0	0	0	0	0	0	0	0	0	0	1	1
H(5)	0	0	0	0	0.9	0.7141	0	0	0	0	0	0	0	0	0	0	0	-0.0264	0	0
HCCZ	0	0	0	0	0	0	0	0	0	0	0	0	0	0	0.9	0.9	0	0	0	0
HCSZ	0	0	0	0	0	-0.0242	0	0	0	0	0	0	0	0	0	0	0.9	0.7477	0	0
HCUZ(5)	0	0	0	0	0	0	0	0	0	0	0	0	0	0	0	0	0	0	0.9	0.9
HGW	0	0	0	0	0	0.0429	0	0	0	0	0	0	0	0	0	0	0	-0.1269	0	0
PRECIP	0	0	0	0	0	-0.1884	0	0	0	0	0	0	0	0	0	0	0	0.0482	0	0
RELDUR(I-129)	0	0	0	0	0	0	0	0.141	0	0.141	0.9	0.6139	0.9	0.6139	0	0	0	0	0	0
RELFRACINIT(I-129)	0	0	0	0	0	0	0	0.0719	0	0.0719	0	-0.1456	0	-0.1456	0	0	0	0	0	0
RUNOFF	0	0	0	0	0	0.1589	0	0	0	0	0	0	0	0	0	0	0	0.0108	0	0
TLAKE	0	0	0	0	0	-0.0726	0	0	0	0	0	0	0	0	0	0	0	0.0213	0	0

Parameter	H(5)		HCCZ		HCSZ		HCUZ(5)		HGW		PRECIP		RELDUR(I-129)		RELFRACINIT(I-129)		RUNOFF		TLAKE	
RCC	Initial	Adjusted	Initial	Adjusted	Initial	Adjusted	Initial	Adjusted	Initial	Adjusted	Initial	Adjusted	Initial	Adjusted	Initial	Adjusted	Initial	Adjusted	Initial	Adjusted
ALPHALU(3)	--	--	--	--	--	--	--	--	--	--	--	--	--	--	--	--	--	--	--	--
ALPHALU(4)	--	--	--	--	--	--	--	--	--	--	--	--	--	--	--	--	--	--	--	--
ALPHALU(5)	--	--	--	--	--	--	--	--	--	--	--	--	--	--	--	--	--	--	--	--
DCACTS(I-129)	--	--	--	--	--	--	--	--	--	--	--	--	--	--	--	--	--	--	--	--
DCACTS(Tc-99)	--	--	--	--	--	--	--	--	--	--	--	--	--	--	--	--	--	--	--	--
DCACTU1(I-129)	--	--	--	--	--	--	--	--	--	--	--	--	--	--	--	--	--	--	--	--
DCACTU1(Tc-99)	--	--	--	--	--	--	--	--	--	--	--	--	--	--	--	--	--	--	--	--
EPCZ	--	--	--	--	--	--	--	--	--	--	--	--	--	--	--	--	--	--	--	--
EPSZ	--	--	--	--	--	--	--	--	--	--	--	--	--	--	--	--	--	--	--	--
EPUZ(5)	--	--	--	--	--	--	--	--	--	--	--	--	--	--	--	--	--	--	--	--
H(5)	1	1	--	--	--	--	--	--	--	--	--	--	--	--	--	--	--	--	--	--
HCCZ	0	0	1	1	--	--	--	--	--	--	--	--	--	--	--	--	--	--	--	--
HCSZ	0	-0.0095	0	0	1	1	--	--	--	--	--	--	--	--	--	--	--	--	--	--
HCUZ(5)	0	0	0	0	0	0	1	1	--	--	--	--	--	--	--	--	--	--	--	--
HGW	0	-0.169	0	0	-0.9	-0.6841	0	0	1	1	--	--	--	--	--	--	--	--	--	--
PRECIP	-0.9	-0.3952	0	0	0	-0.1312	0	0	0.9	0.6045	1	1	--	--	--	--	--	--	--	--
RELDUR(I-129)	0	0	0	0	0	0	0	0	0	0	0	0	1	1	--	--	--	--	--	--
RELFRACINIT(I-129)	0	0	0	0	0	0	0	0	0	0	0	0	-0.9	-0.687	1	1	--	--	--	--
RUNOFF	0.9	0.5013	0	0	0	0.0273	0	0	0	0.1641	0.9	0.4515	0	0	0	0	1	1	--	--
TLAKE	0	0.1941	0	0	0	-0.0549	0	0	0	-0.1175	-0.9	-0.66	0	0	0	0	0	-0.1728	1	1

Table G.4.2 -Initial and adjusted rank correlation coefficients (RCC) for the 10,000-year simulation period probabilistic analysis

Parameter	ALPHALU(3)		ALPHALU(4)		ALPHALU(5)		DCACTS(U-234)		DCACTS(I-129)		DCACTS(Pu-239)		DCACTS(Tc-99)		DCACTU1(U-234)		DCACTU1(I-129)		DCACTU1(Pu-239)		DCACTU1(Tc-99)		EPCZ	
RCC	Initial	Adjusted	Initial	Adjusted	Initial	Adjusted	Initial	Adjusted	Initial	Adjusted	Initial	Adjusted	Initial	Adjusted	Initial	Adjusted	Initial	Adjusted	Initial	Adjusted	Initial	Adjusted	Initial	Adjusted
ALPHALU(3)	1	1	--	--	--	--	--	--	--	--	--	--	--	--	--	--	--	--	--	--	--	--	--	--
ALPHALU(4)	0.9	0.9	1	1	--	--	--	--	--	--	--	--	--	--	--	--	--	--	--	--	--	--	--	--
ALPHALU(5)	0	0	0	0	1	1	--	--	--	--	--	--	--	--	--	--	--	--	--	--	--	--	--	--
DCACTS(U-234)	0	0	0	0	0	0	1	1	--	--	--	--	--	--	--	--	--	--	--	--	--	--	--	--
DCACTS(I-129)	0	0	0	0	0	0	0	0.0246	1	1	--	--	--	--	--	--	--	--	--	--	--	--	--	--
DCACTS(Pu-239)	0	0	0	0	0	0	0	0.0246	0	0.0246	1	1	--	--	--	--	--	--	--	--	--	--	--	--
DCACTS(Tc-99)	0	0	0	0	0	0	0	0.0246	0	0.0246	0	0.0246	1	1	--	--	--	--	--	--	--	--	--	--
DCACTU1(U-234)	0	0	0	0	0	0	0.9	0.8371	0	-0.0629	0	-0.0629	0	-0.0629	1	1	--	--	--	--	--	--	--	--
DCACTU1(I-129)	0	0	0	0	0	0	0	-0.0629	0.9	0.8371	0	-0.0629	0	-0.0629	0	0.1646	1	1	--	--	--	--	--	--
DCACTU1(Pu-239)	0	0	0	0	0	0	0	-0.0629	0	-0.0629	0.9	0.8371	0	-0.0629	0	0.1646	0	0.1646	1	1	--	--	--	--
DCACTU1(Tc-99)	0	0	0	0	0	0	0	-0.0629	0	-0.0629	0	-0.0629	0.9	0.8371	0	0.1646	0	0.1646	0	0.1646	1	1	--	--
EPCZ	0	0	0	0	0	0	0	0	0	0	0	0	0	0	0	0	0	0	0	0	0	0	1	1
EPSZ	0	0	0	0	0	0.0287	0	0	0	0	0	0	0	0	0	0	0	0	0	0	0	0	0	0
EPUZ(5)	0	0	0	0	0	0	0	0	0	0	0	0	0	0	0	0	0	0	0	0	0	0	0	0
H(5)	0	0	0	0	0.9	0.7141	0	0	0	0	0	0	0	0	0	0	0	0	0	0	0	0	0	0
HCCZ	0	0	0	0	0	0	0	0	0	0	0	0	0	0	0	0	0	0	0	0	0	0	0.9	0.9
HCSZ	0	0	0	0	0	-0.0242	0	0	0	0	0	0	0	0	0	0	0	0	0	0	0	0	0	0
HCUZ(5)	0	0	0	0	0	0	0	0	0	0	0	0	0	0	0	0	0	0	0	0	0	0	0	0
HGW	0	0	0	0	0	0.0429	0	0	0	0	0	0	0	0	0	0	0	0	0	0	0	0	0	0
PRECIP	0	0	0	0	0	-0.1884	0	0	0	0	0	0	0	0	0	0	0	0	0	0	0	0	0	0
RELDUR(I-129)	0	0	0	0	0	0	0	0.1309	0	0.1309	0	0.1309	0	0.1309	0.9	0.5522	0.9	0.5522	0.9	0.5522	0.9	0.5522	0	0
RELFRACINIT(I-129)	0	0	0	0	0	0	0	0.0534	0	0.0534	0	0.0534	0	0.0534	0	-0.1409	0	-0.1409	0	-0.1409	0	-0.1409	0	0
RUNOFF	0	0	0	0	0	0.1589	0	0	0	0	0	0	0	0	0	0	0	0	0	0	0	0	0	0
TLAKE	0	0	0	0	0	-0.0726	0	0	0	0	0	0	0	0	0	0	0	0	0	0	0	0	0	0

Parameter	EPSZ		EPUZ(5)		H(5)		HCCZ		HCSZ		HCUZ(5)		HGW		PRECIP		RELDUR(I-129)		RELFRACINIT(I-129)		RUNOFF		TLAKE	
RCC	Initial	Adjusted	Initial	Adjusted	Initial	Adjusted	Initial	Adjusted	Initial	Adjusted	Initial	Adjusted	Initial	Adjusted	Initial	Adjusted	Initial	Adjusted	Initial	Adjusted	Initial	Adjusted	Initial	Adjusted
ALPHALU(3)	--	--	--	--	--	--	--	--	--	--	--	--	--	--	--	--	--	--	--	--	--	--	--	--
ALPHALU(4)	--	--	--	--	--	--	--	--	--	--	--	--	--	--	--	--	--	--	--	--	--	--	--	--
ALPHALU(5)	--	--	--	--	--	--	--	--	--	--	--	--	--	--	--	--	--	--	--	--	--	--	--	--
DCACTS(U-234)	--	--	--	--	--	--	--	--	--	--	--	--	--	--	--	--	--	--	--	--	--	--	--	--
DCACTS(I-129)	--	--	--	--	--	--	--	--	--	--	--	--	--	--	--	--	--	--	--	--	--	--	--	--
DCACTS(Pu-239)	--	--	--	--	--	--	--	--	--	--	--	--	--	--	--	--	--	--	--	--	--	--	--	--
DCACTS(Tc-99)	--	--	--	--	--	--	--	--	--	--	--	--	--	--	--	--	--	--	--	--	--	--	--	--
DCACTU1(U-234)	--	--	--	--	--	--	--	--	--	--	--	--	--	--	--	--	--	--	--	--	--	--	--	--
DCACTU1(I-129)	--	--	--	--	--	--	--	--	--	--	--	--	--	--	--	--	--	--	--	--	--	--	--	--
DCACTU1(Pu-239)	--	--	--	--	--	--	--	--	--	--	--	--	--	--	--	--	--	--	--	--	--	--	--	--
DCACTU1(Tc-99)	--	--	--	--	--	--	--	--	--	--	--	--	--	--	--	--	--	--	--	--	--	--	--	--
EPCZ	--	--	--	--	--	--	--	--	--	--	--	--	--	--	--	--	--	--	--	--	--	--	--	--
EPSZ	1	1	--	--	--	--	--	--	--	--	--	--	--	--	--	--	--	--	--	--	--	--	--	--
EPUZ(5)	0	0	1	1	--	--	--	--	--	--	--	--	--	--	--	--	--	--	--	--	--	--	--	--
H(5)	0	-0.0264	0	0	1	1	--	--	--	--	--	--	--	--	--	--	--	--	--	--	--	--	--	--
HCCZ	0	0	0	0	0	0	1	1	--	--	--	--	--	--	--	--	--	--	--	--	--	--	--	--
HCSZ	0.9	0.7477	0	0	0	-0.0095	0	0	1	1	--	--	--	--	--	--	--	--	--	--	--	--	--	--
HCUZ(5)	0	0	0.9	0.9	0	0	0	0	0	0	1	1	--	--	--	--	--	--	--	--	--	--	--	--
HGW	0	-0.1269	0	0	0	-0.169	0	0	-0.9	-0.6841	0	0	1	1	--	--	--			--	--	--	--	--
PRECIP	0	0.0482	0	0	-0.9	-0.3952	0	0	0	-0.1312	0	0	0.9	0.6045	1	1	--	--	--	--	--	--	--	--
RELDUR(I-129)	0	0	0	0	0	0	0	0	0	0	0	0	0	0	0	0	1	1	--	--	--	--	--	--
RELFRACINIT(I-129)	0	0	0	0	0	0	0	0	0	0	0	0	0	0	0	0	-0.9	-0.6005	1	1	--	--	--	--
RUNOFF	0	0.0108	0	0	0.9	0.5013	0	0	0	0.0273	0	0	0	0.1641	0.9	0.4515	0	0	0	0	1	1	--	--
TLAKE	0	0.0213	0	0	0	0.1941	0	0	0	-0.0549	0	0	0	-0.1175	-0.9	-0.66	0	0	0	0	0	-0.1728	1	1

Table G.4.3. RESRAD-OFFSITE parameter identifiers and descriptions for parameters assigned a probabilistic distribution in the compliance period and 10,000-year analyses

RESRAD-OFFSITE Parameter Identifier	RESRAD-OFFSITE Parameter Description
ALPHALCZ	Longitudinal dispersivity in contaminated zone
ALPHALOSW	Longitudinal dispersivity of saturated zone to surface water body
ALPHALOW	Longitudinal dispersivity of saturated zone to well
ALPHALU(3)	Longitudinal dispersivity in unsaturated zone 3
ALPHALU(4)	Longitudinal dispersivity in unsaturated zone 4
ALPHALU(5)	Longitudinal dispersivity in unsaturated zone 5
BCZ	Contaminated zone b parameter
DCACTS(U-234)	Distribution coefficient of U-234 in saturated zone
DCACTS(I-129)	Distribution coefficient of I-129 in saturated zone
DCACTS(Pu-239)	Distribution coefficient of Pu-239 in saturated zone
DCACTS(Tc-99)	Distribution coefficient of Tc-99 in saturated zone
DCACTU1(U-234)	Distribution coefficient of U-234 in unsaturated zone 1
DCACTU1(I-129)	Distribution coefficient of I-129 in unsaturated zone 1
DCACTU1(Pu-239)	Distribution coefficient of Pu-239 in unsaturated zone 1
DCACTU1(Tc-99)	Distribution coefficient of Tc-99 in unsaturated zone 1
DENSAQ	Dry bulk density of saturated zone
DENSCZ	Dry bulk density of contaminated zone
DENSUZ(5)	Dry bulk density of unsaturated zone (5)
DWIBWT	Depth of aquifer contributing to well
EPCZ	Effective porosity of contaminated zone
EPSZ	Effective porosity of saturated zone
EPUZ(3)	Effective porosity of unsaturated zone 3
EPUZ(4)	Effective porosity of unsaturated zone 4
EPUZ(5)	Effective porosity of unsaturated zone 5
H(5)	Thickness of unsaturated zone 5
HCCZ	Hydraulic conductivity of contaminated zone
HCSZ	Hydraulic conductivity of saturated zone
HCUZ(5)	Hydraulic conductivity of unsaturated zone 5
HGW	Hydraulic gradient of saturated zone to well
PRECIP	Precipitation rate
RELDUR(I-129)	Time over which transformation to releasable form occurs (Release Duration), I-129
RELFRACINIT(I-129)	Initial releasable fraction, I-129
RELTIMEINIT(C-14)	Time at which radionuclide first becomes releasable (Initial Release Time), C-14
RUNOFF	Runoff coefficient of primary contamination
TLAKE	Mean residence time of water in surface water body
TPUZ(3)	Total porosity of unsaturated zone 3
TPUZ(4)	Total porosity of unsaturated zone 4

This page intentionally left blank.

ATTACHMENT G.5.
RESRAD-OFFSITE SAMPLED INPUT PARAMETER VALUES FOR THE UNCERTAINTY ANALYSIS

This page intentionally left blank.

Table G.5.1. RESRAD-OFFSITE parameter identifiers and descriptions for parameters assigned a probabilistic distribution in the compliance period and 10,000-year analyses

RESRAD-OFFSITE Parameter Identifier	RESRAD-OFFSITE Parameter Description
ALPHALCZ	Longitudinal dispersivity in contaminated zone
ALPHALOSW	Longitudinal dispersivity of saturated zone to surface water body
ALPHALOW	Longitudinal dispersivity of saturated zone to well
ALPHALU(3)	Longitudinal dispersivity in unsaturated zone 3
ALPHALU(4)	Longitudinal dispersivity in unsaturated zone 4
ALPHALU(5)	Longitudinal dispersivity in unsaturated zone 5
BCZ	Contaminated zone b parameter
DCACTS(10) or U-234	Distribution coefficient of U-234 in saturated zone
DCACTS(3) or I-129	Distribution coefficient of I-129 in saturated zone
DCACTS(6) or Pu-239	Distribution coefficient of Pu-239 in saturated zone
DCACTS(8) or Tc-99	Distribution coefficient of Tc-99 in saturated zone
DCACTU1(10) or U-234	Distribution coefficient of U-234 in unsaturated zone 1
DCACTU1(3) or I-129	Distribution coefficient of I-129 in unsaturated zone 1
DCACTU1(6) or Pu-239	Distribution coefficient of Pu-239 in unsaturated zone 1
DCACTU1(8) or Tc-99	Distribution coefficient of Tc-99 in unsaturated zone 1
DENSAQ	Dry bulk density of saturated zone
DENSCZ	Dry bulk density of contaminated zone
DENSUZ(5)	Dry bulk density of unsaturated zone (5)
DWIBWT	Depth of aquifer contributing to well
EPCZ	Effective porosity of contaminated zone
EPSZ	Effective porosity of saturated zone
EPUZ(3)	Effective porosity of unsaturated zone 3
EPUZ(4)	Effective porosity of unsaturated zone 4
EPUZ(5)	Effective porosity of unsaturated zone 5
H(5)	Thickness of unsaturated zone 5
HCCZ	Hydraulic conductivity of contaminated zone
HCSZ	Hydraulic conductivity of saturated zone
HCUZ(5)	Hydraulic conductivity of unsaturated zone 5
HGW	Hydraulic gradient of saturated zone to well
PRECIP	Precipitation rate
RELDUR(I-129)	Time over which transformation to releasable form occurs (Release Duration), I-129
RELFRACINIT(I-129)	Initial releasable fraction, I-129
RELTIMEINIT(C-14)	Time at which radionuclide first becomes releasable (Initial Release Time), C-14
RUNOFF	Runoff coefficient of primary contamination
TLAKE	Mean residence time of water in surface water body
TPUZ(3)	Total porosity of unsaturated zone 3
TPUZ(4)	Total porosity of unsaturated zone 4

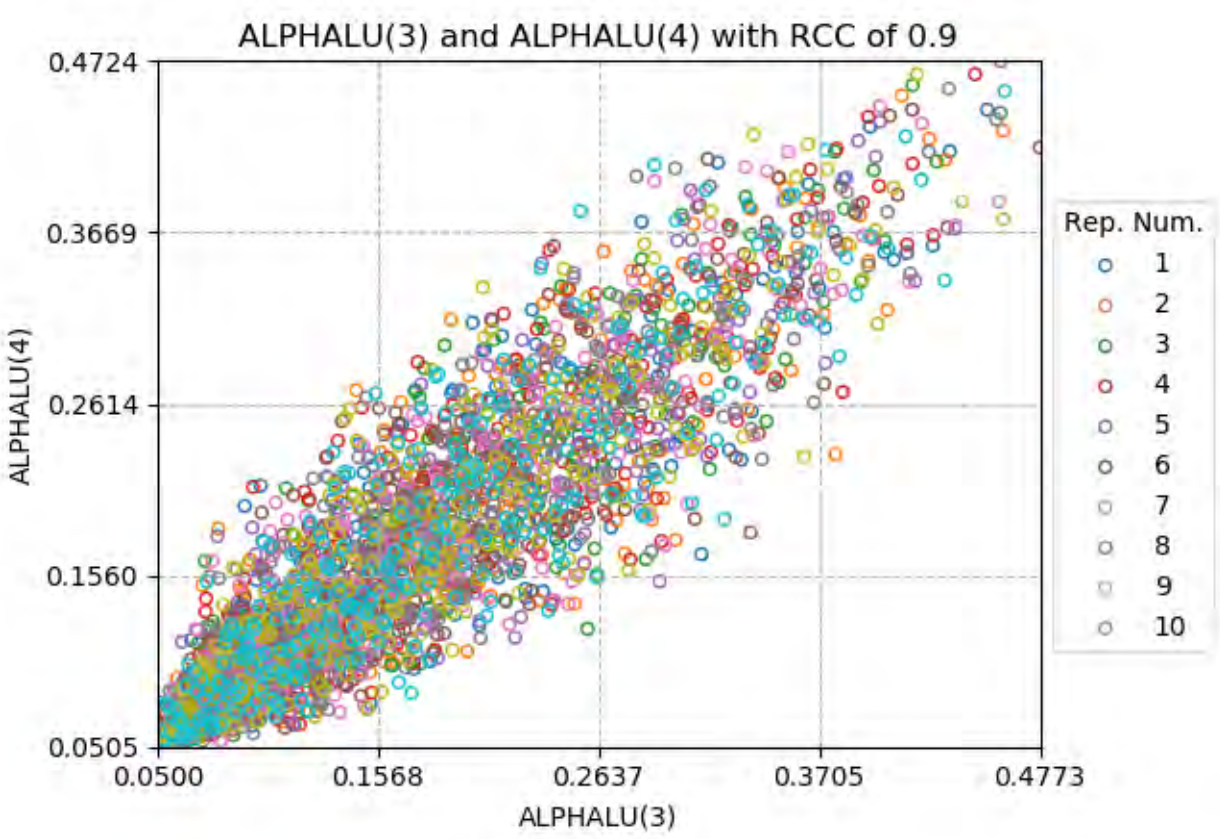

Fig.G.5.1. Input vs input scatter plot for longitudinal dispersivity of unsaturated zone 3 and longitudinal dispersivity of unsaturated zone 4 (compliance period)
initial RCC = +0.9; adjusted RCC = +0.9

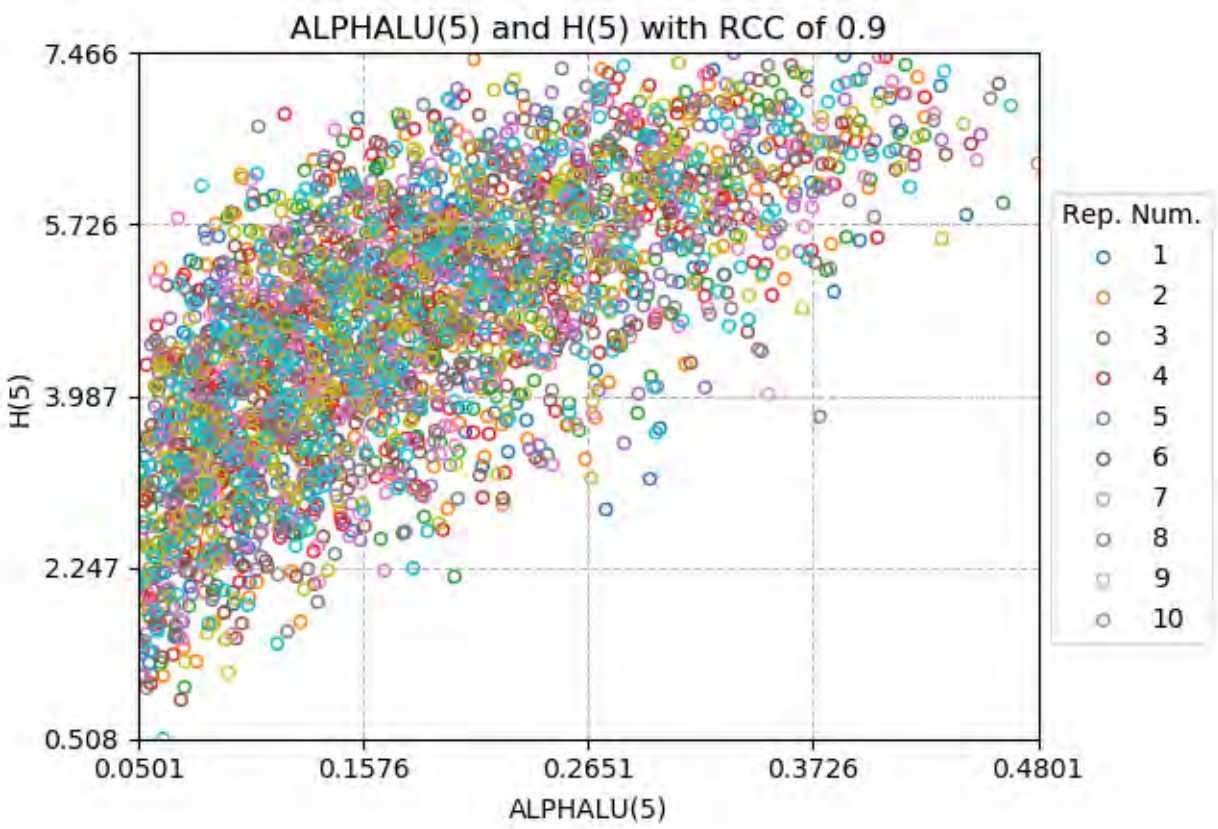

Fig.G.5.2. Input vs input scatter plot for longitudinal dispersivity of unsaturated zone 5 and thickness of unsaturated zone 5 (compliance period)
initial RCC = +0.9; adjusted RCC = +0.7141

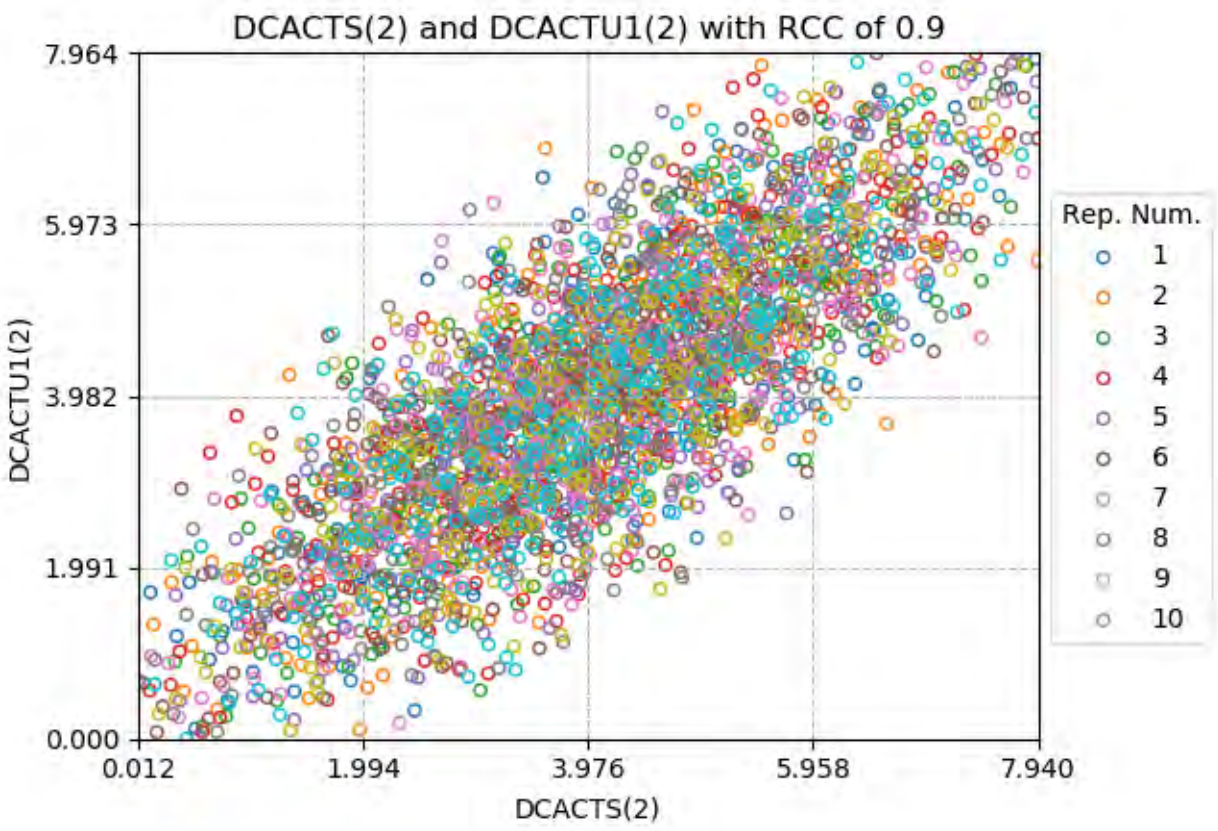

Fig.G.5.3. Input vs input scatter plot for K_d of I-129 in the saturated zone and K_d of I-129 in unsaturated zone 1 (compliance period)
initial RCC = +0.9; adjusted RCC = +0.7944

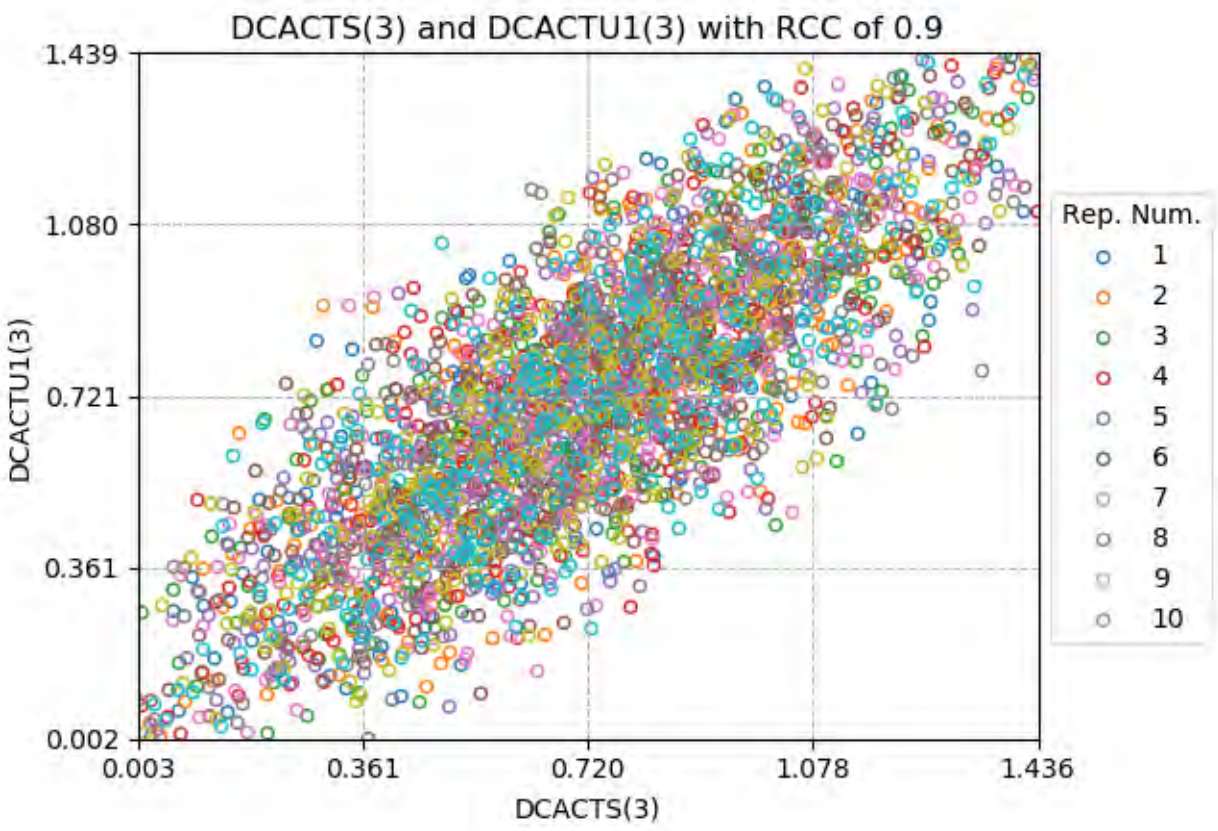

Fig.G.5.4. Input vs input scatter plot for Kd of Tc-99 in the saturated zone and Kd of Tc-99 in unsaturated zone 1 (compliance period) initial RCC = +0.9; adjusted RCC = +0.7944

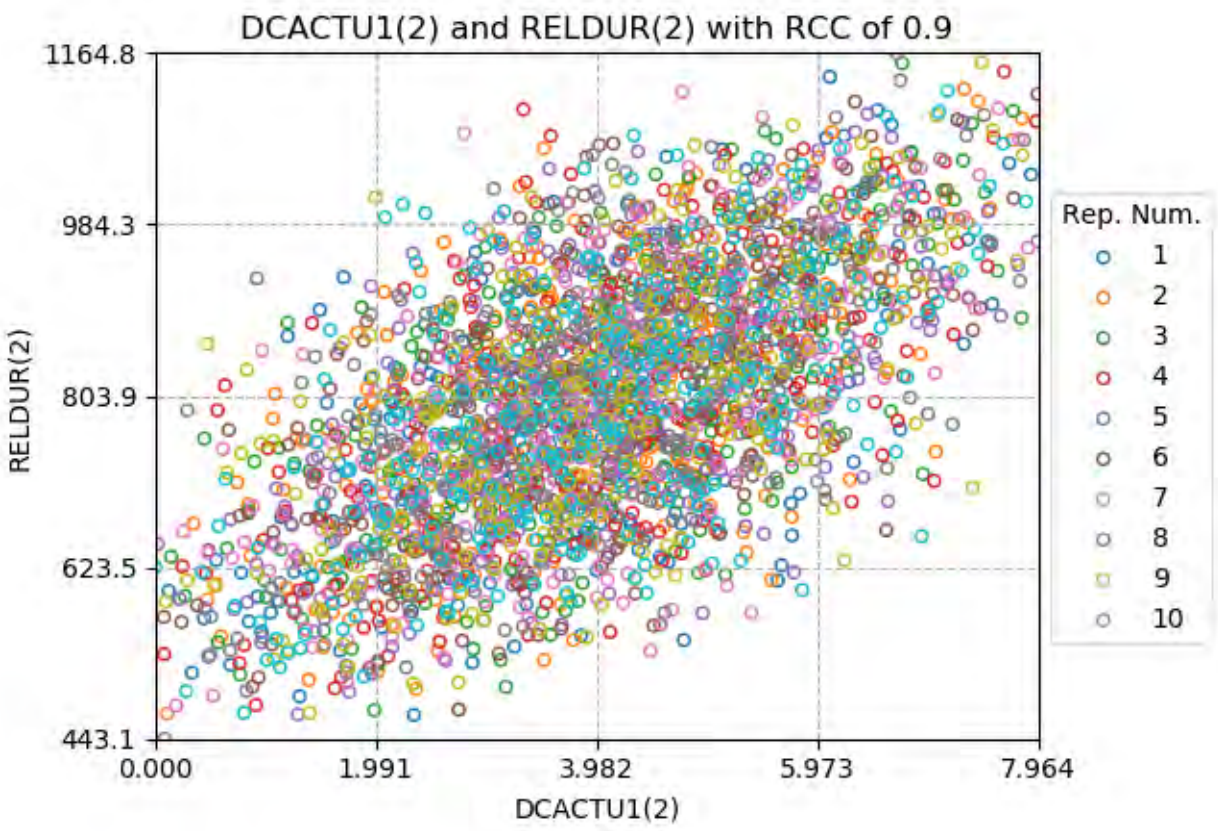

Fig.G.5.5. Input vs input scatter plot for Kd of I-129 in unsaturated zone 1 and release duration of I-129 (compliance period)
initial RCC = +0.9; adjusted RCC = +0.6139

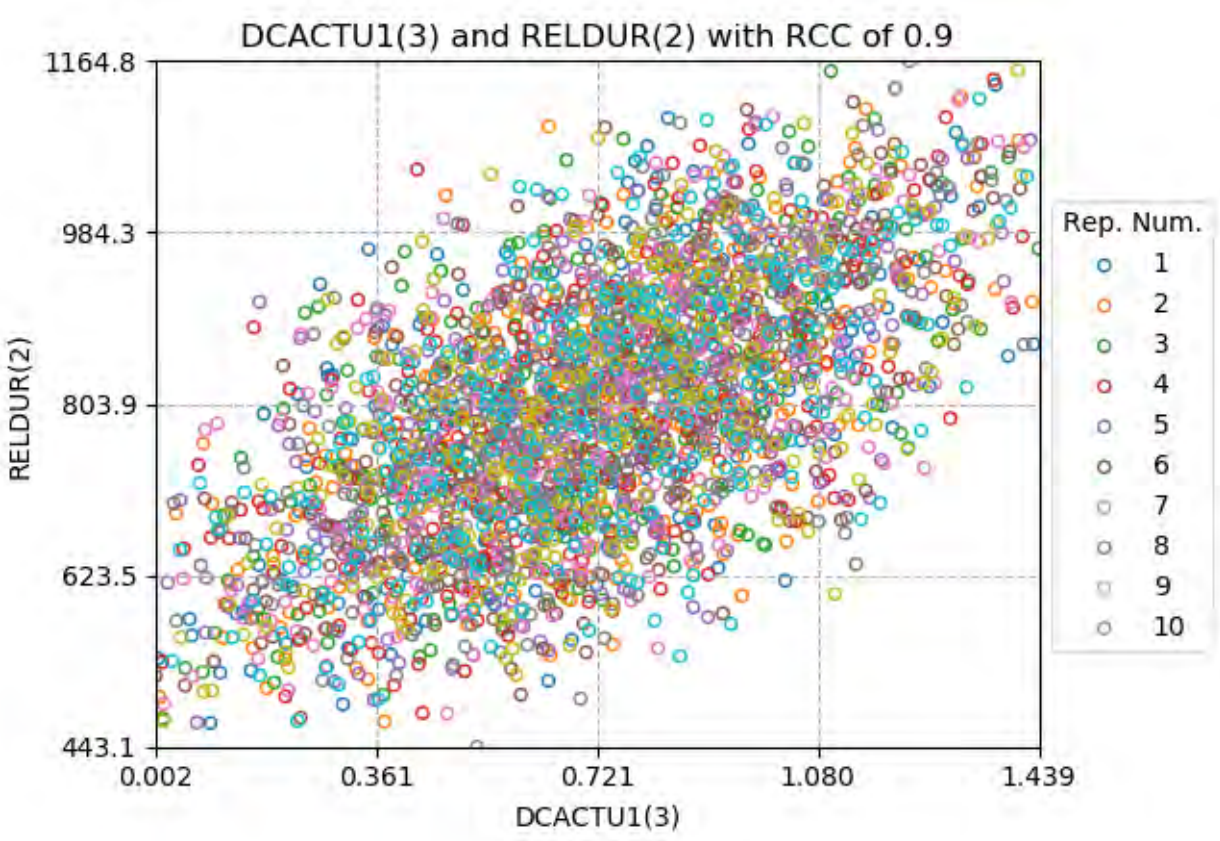

Fig.G.5.6. Input vs input scatter plot for Kd of Tc-99 in unsaturated zone 1 and release duration of I-129 (compliance period)
initial RCC = +0.9; adjusted RCC = +0.6139

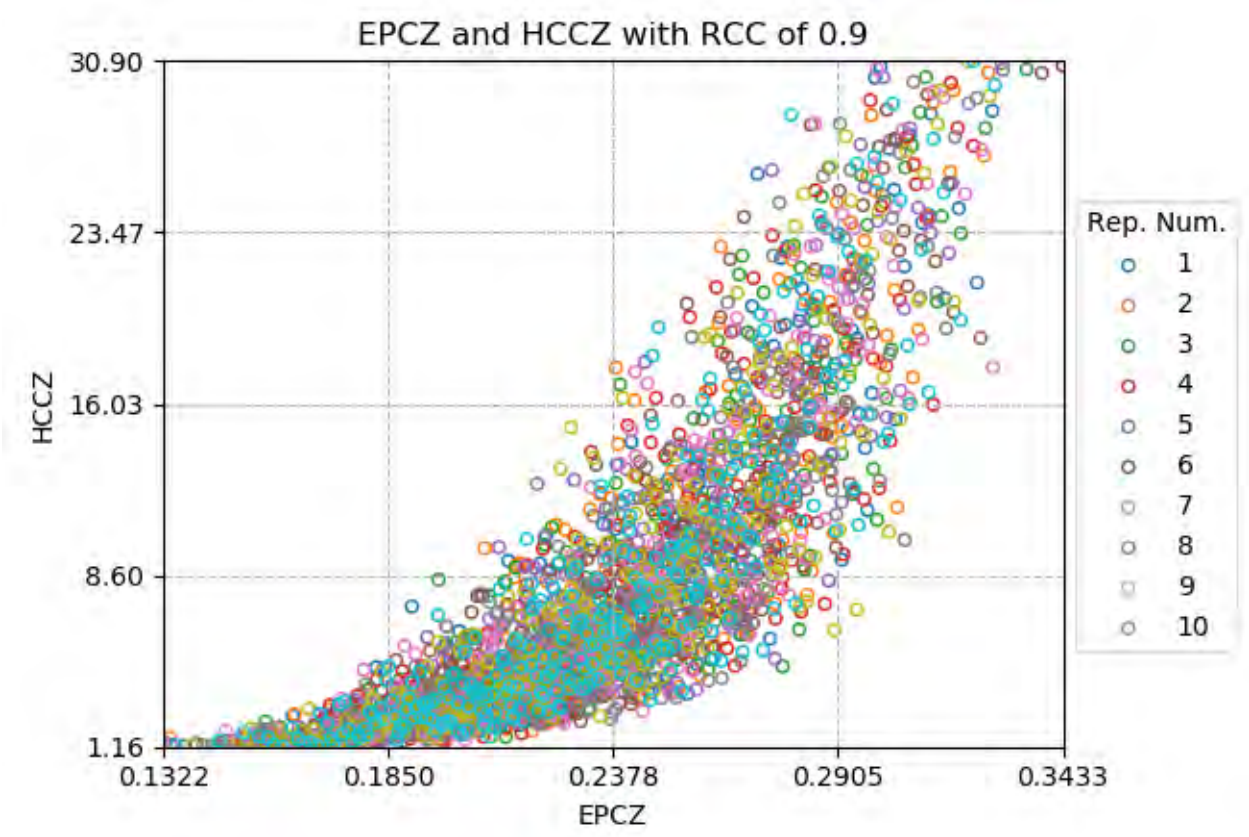

Fig.G.5.7. Input vs input scatter plot for effective porosity of contaminated zone and hydraulic conductivity of contaminated zone (compliance period)
initial RCC = +0.9; adjusted RCC = +0.9

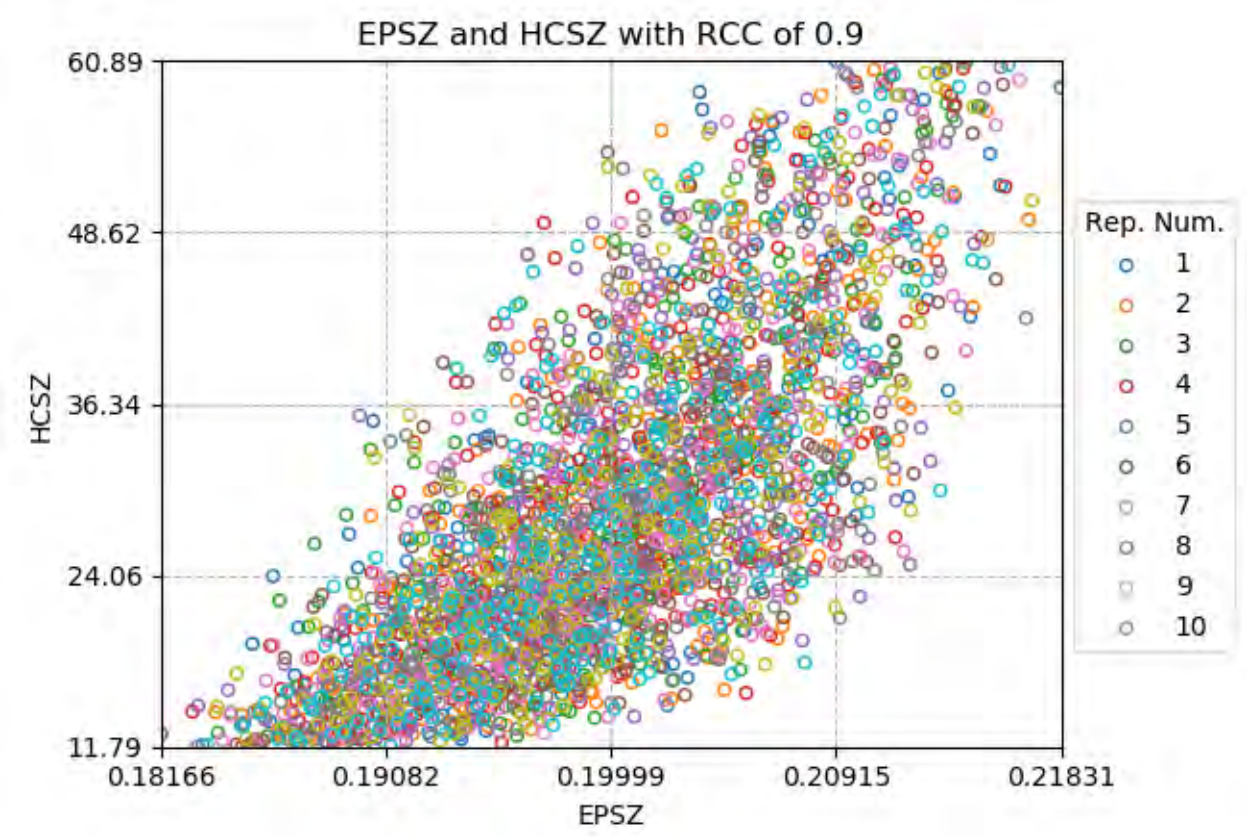

Fig.G.5.8. Input vs input scatter plot for effective porosity of saturated zone and hydraulic conductivity of saturated zone (compliance period)
initial RCC = +0.9; adjusted RCC = +0.7477

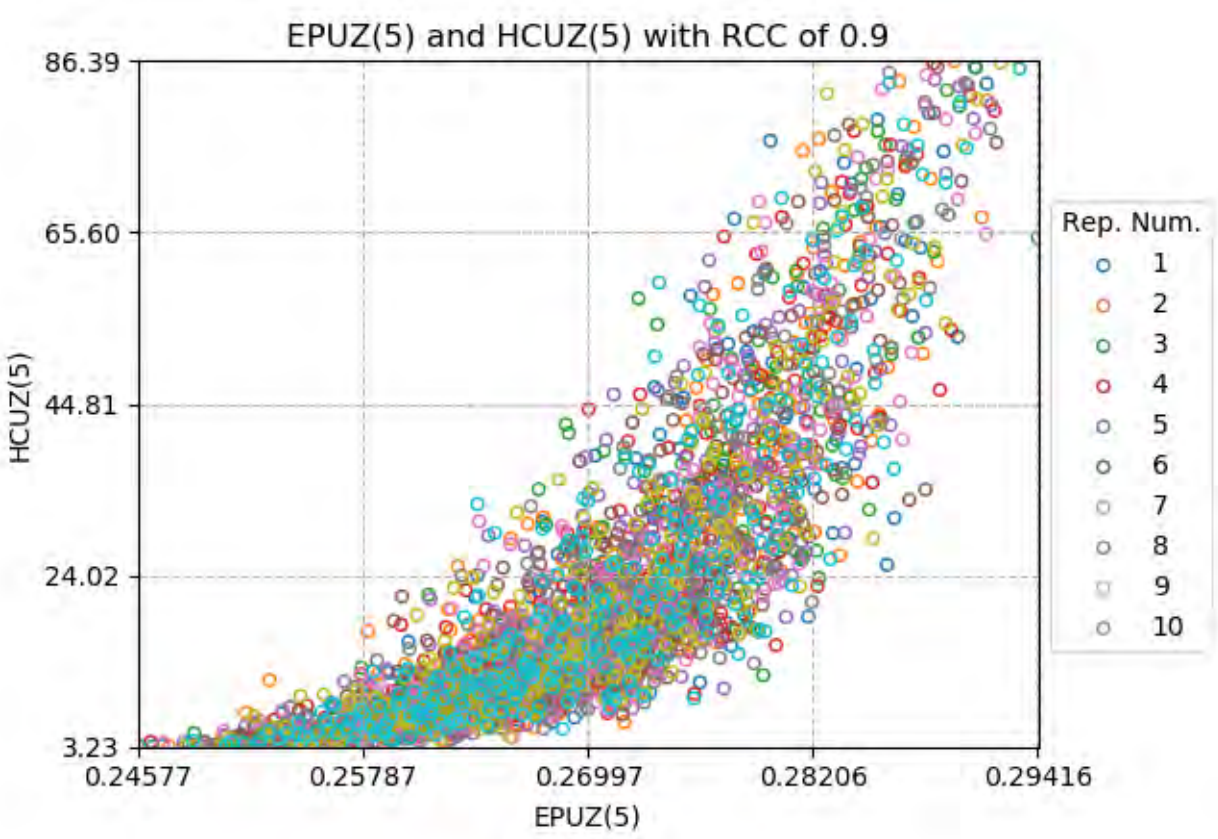

Fig.G.5.9. Input vs input scatter plot for effective porosity of unsaturated zone 5 and thickness of unsaturated zone 5 (compliance period)
initial RCC = +0.9; adjusted RCC = +0.9

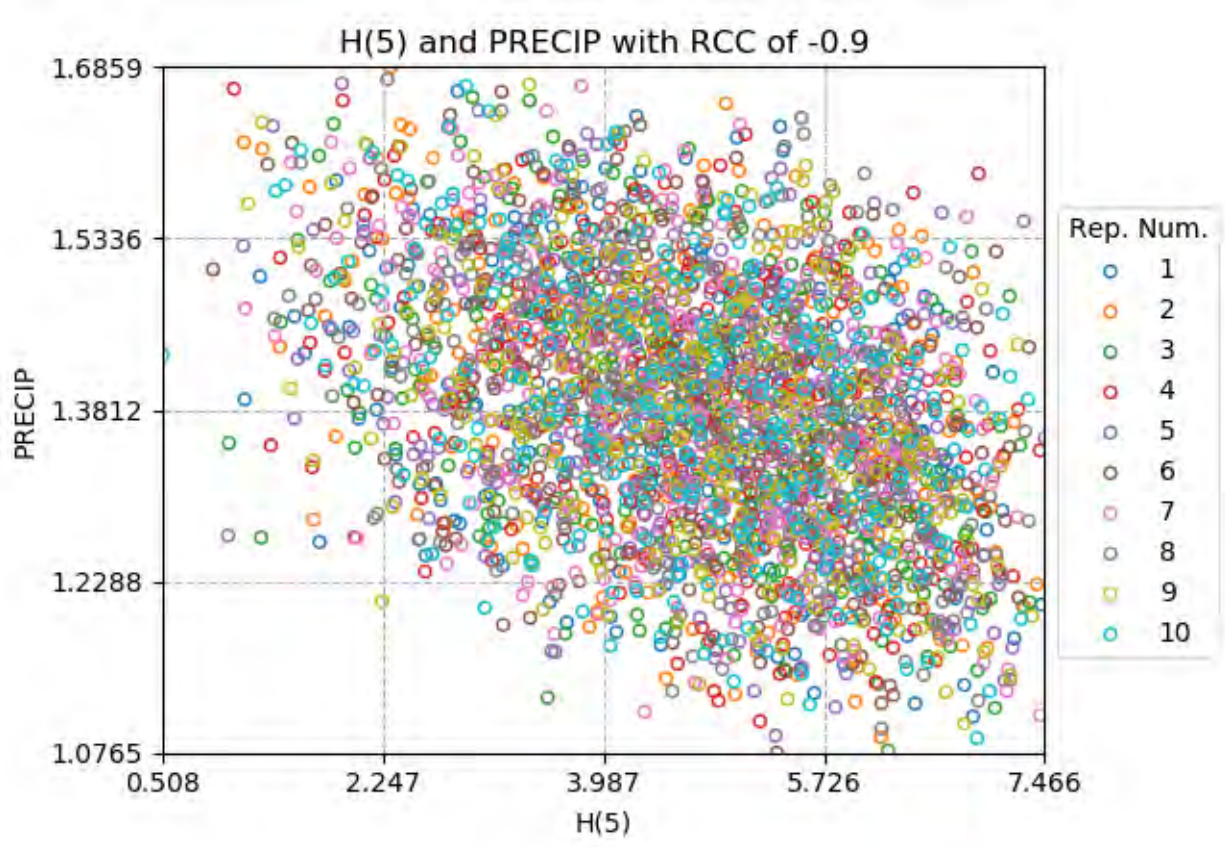

Fig.G.5.10. Input vs input scatter plot for thickness of unsaturated zone 5 and precipitation (compliance period)
initial RCC = -0.9 (negative); adjusted RCC = -0.3952 (negative)

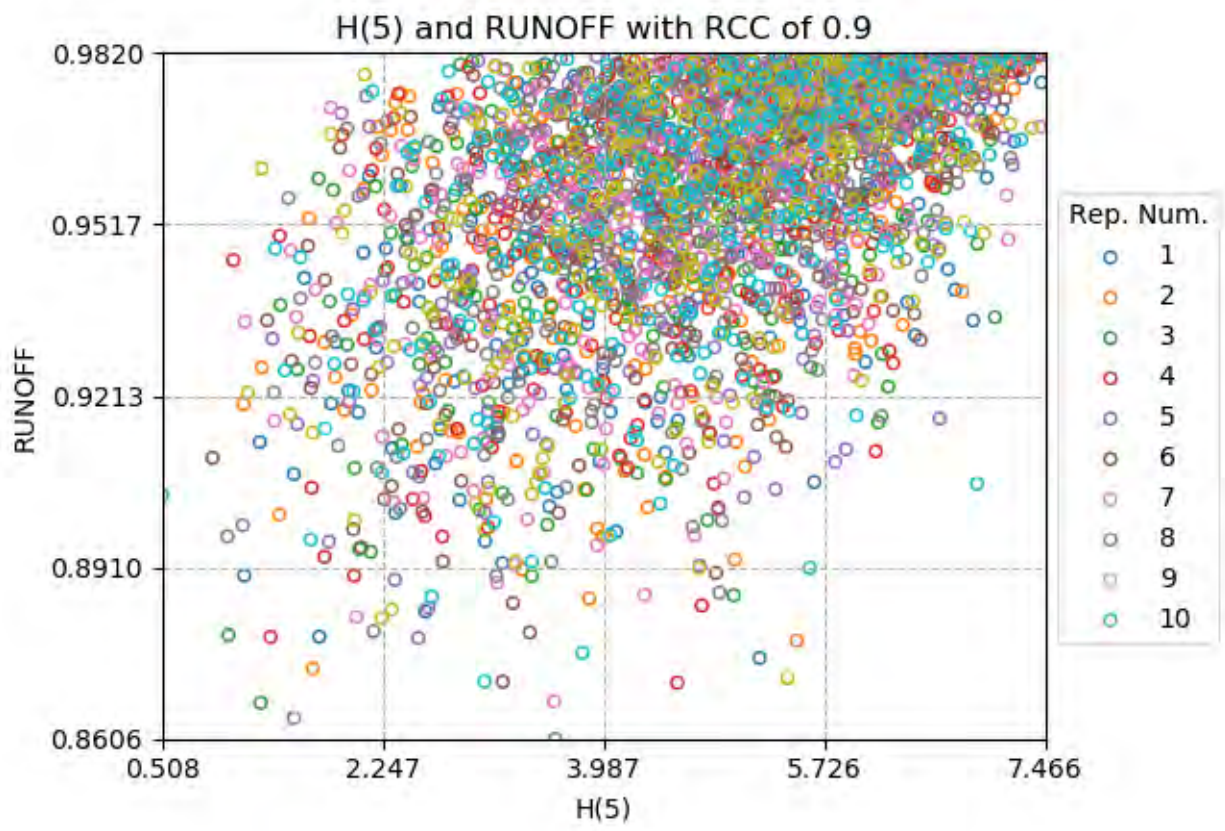

Fig.G.5.11. Input vs input scatter plot for thickness of unsaturated zone 5 and runoff coefficient of primary contamination (compliance period) initial RCC = +0.9; adjusted RCC = +0.5013

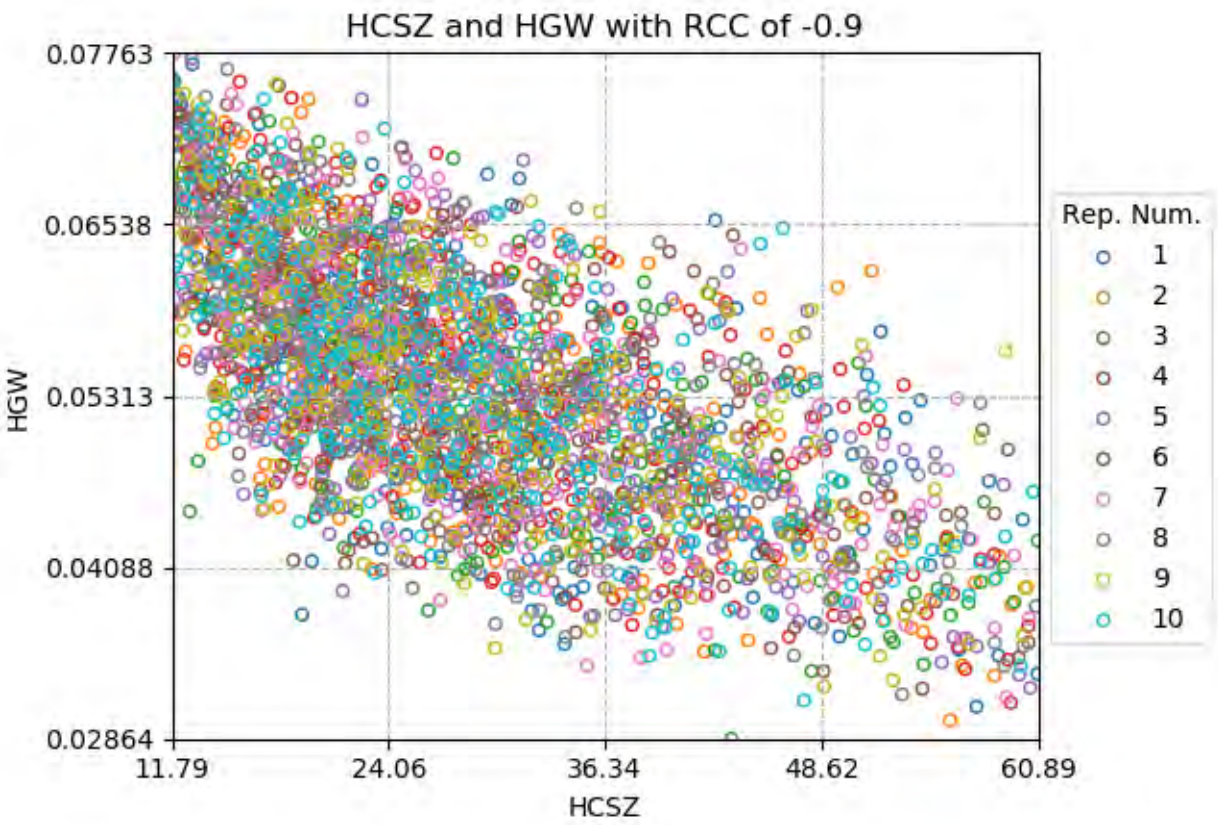

Fig.G.5.12. Input vs input scatter plot for hydraulic conductivity of saturated zone and hydraulic gradient of saturated zone to well (compliance period) initial RCC = -0.9 (negative); adjusted RCC = -0.6841 (negative)

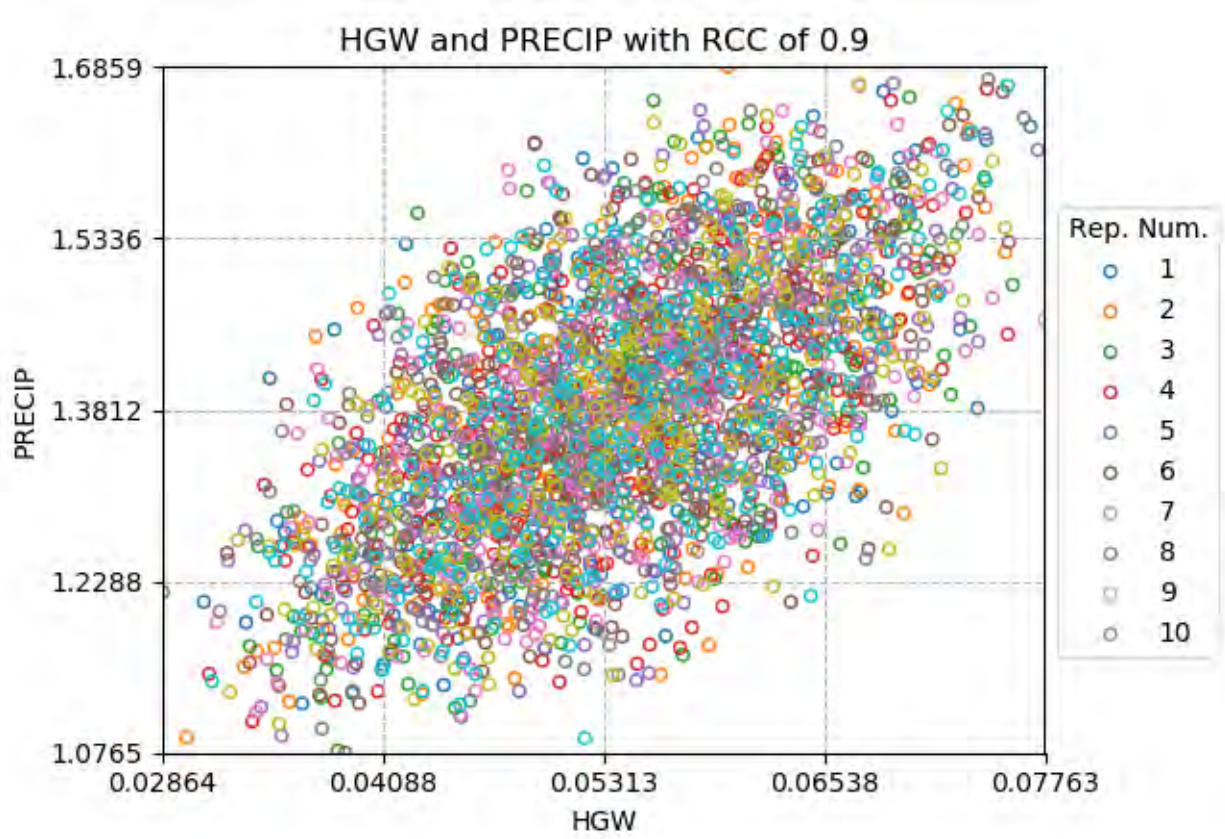

Fig.G.5.13.Input vs input scatter plot for hydraulic gradient of saturated zone to well and precipitation (compliance period)
initial RCC = +0.9; adjusted RCC = +0.6045

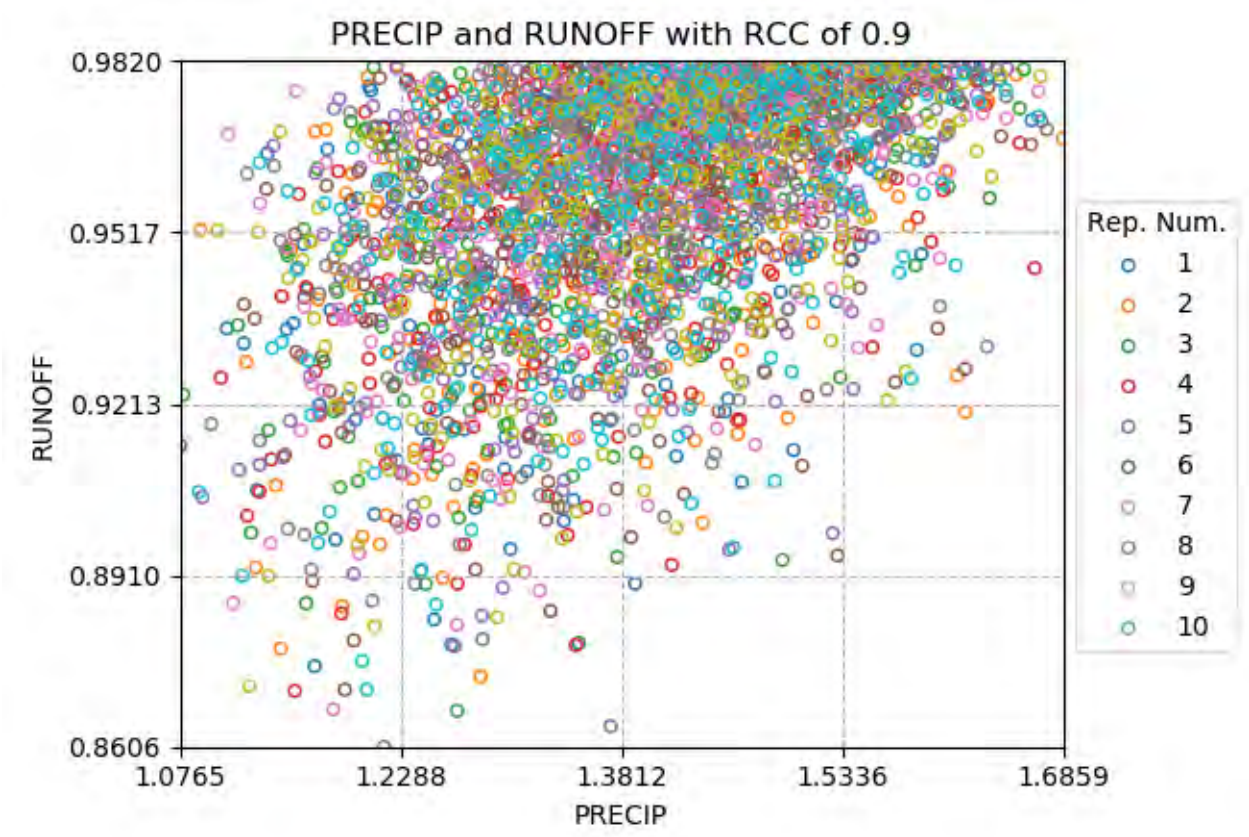

Fig.G.5.14. Input vs input scatter plot for runoff coefficient of precipitation and runoff coefficient of primary contamination (compliance period) initial RCC = +0.9; adjusted RCC = +0.4515

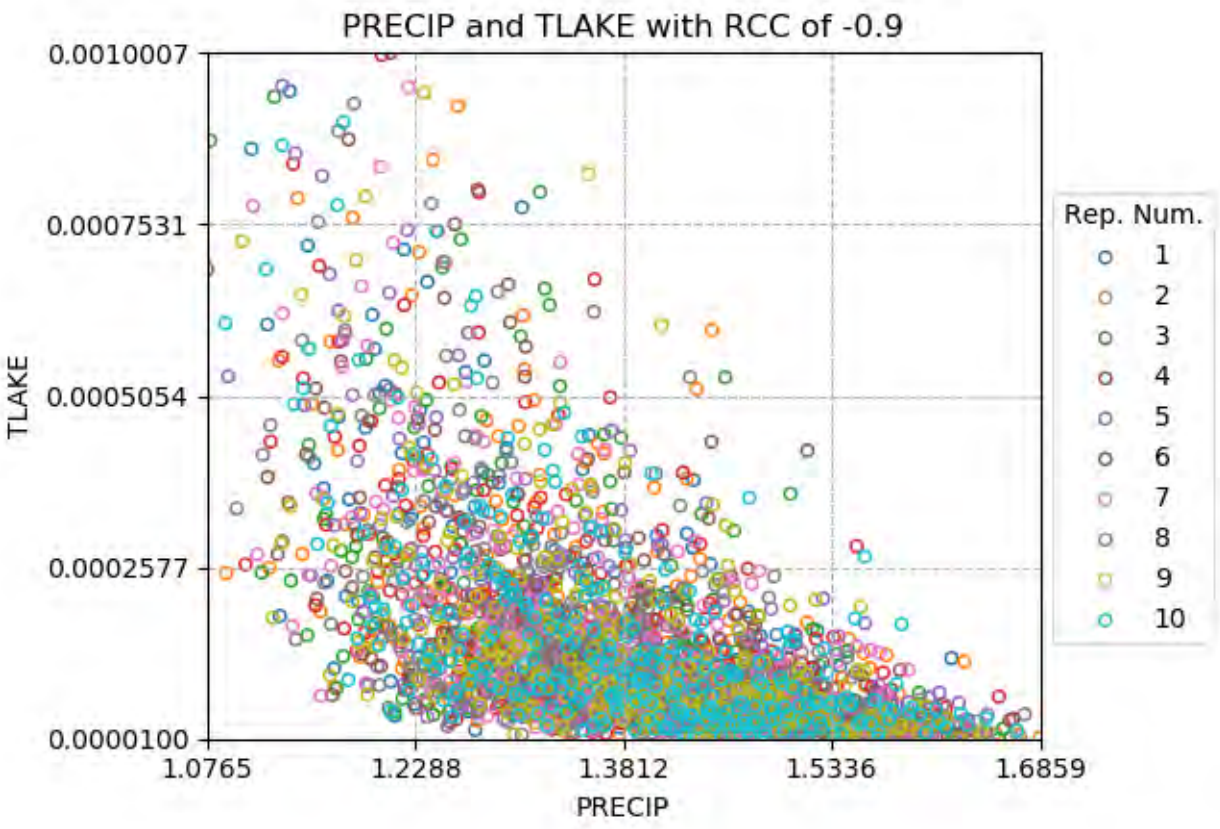

Fig.G.5.15. Input vs input scatter plot for runoff coefficient of precipitation and mean residence time of water in surface water body (compliance period) initial RCC = -0.9 (negative); adjusted RCC = -0.66 (negative)

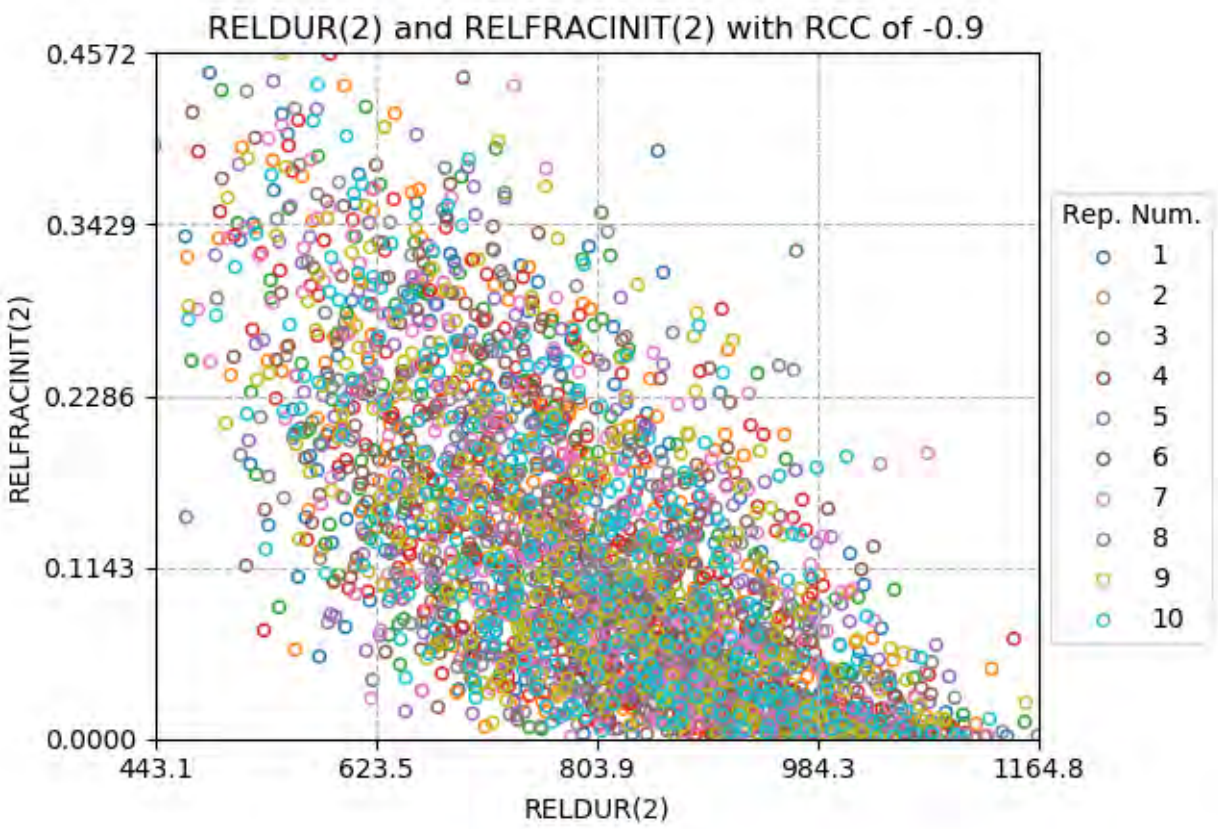

Fig.G.5.16. Input vs input scatter plot for release duration of I-129 and initial releasable fraction of I-129 (compliance period) initial RCC = -0.9 (negative); adjusted RCC = -0.687 (negative)

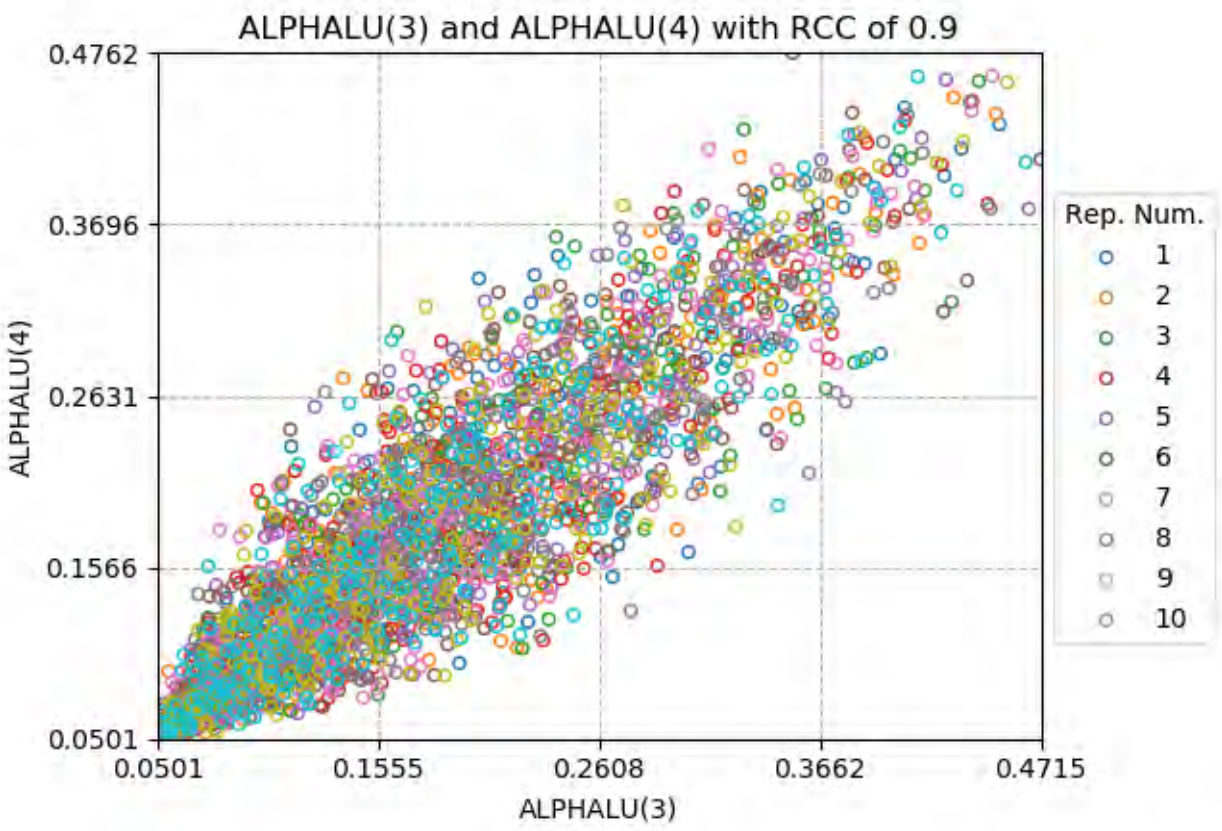

Fig.G.5.17. Input vs input scatter plot for longitudinal dispersivity of unsaturated zone 3 and longitudinal dispersivity of unsaturated zone 4 (10,000-year period)
initial RCC = +0.9; adjusted RCC = +0.9

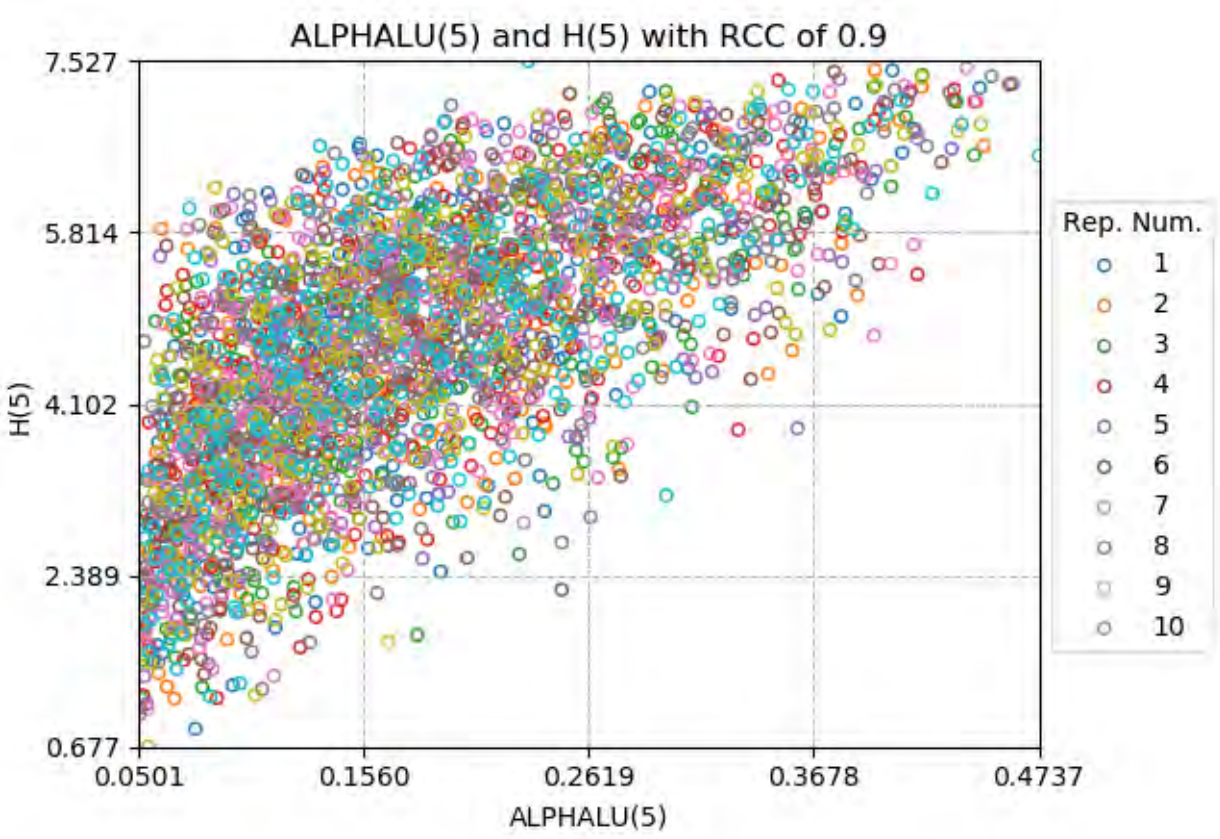

Fig.G.5.18. Input vs input scatter plot for longitudinal dispersivity of unsaturated zone 5 and thickness of unsaturated zone 5 (10,000-year period)
initial RCC = +0.9; adjusted RCC = +0.7141

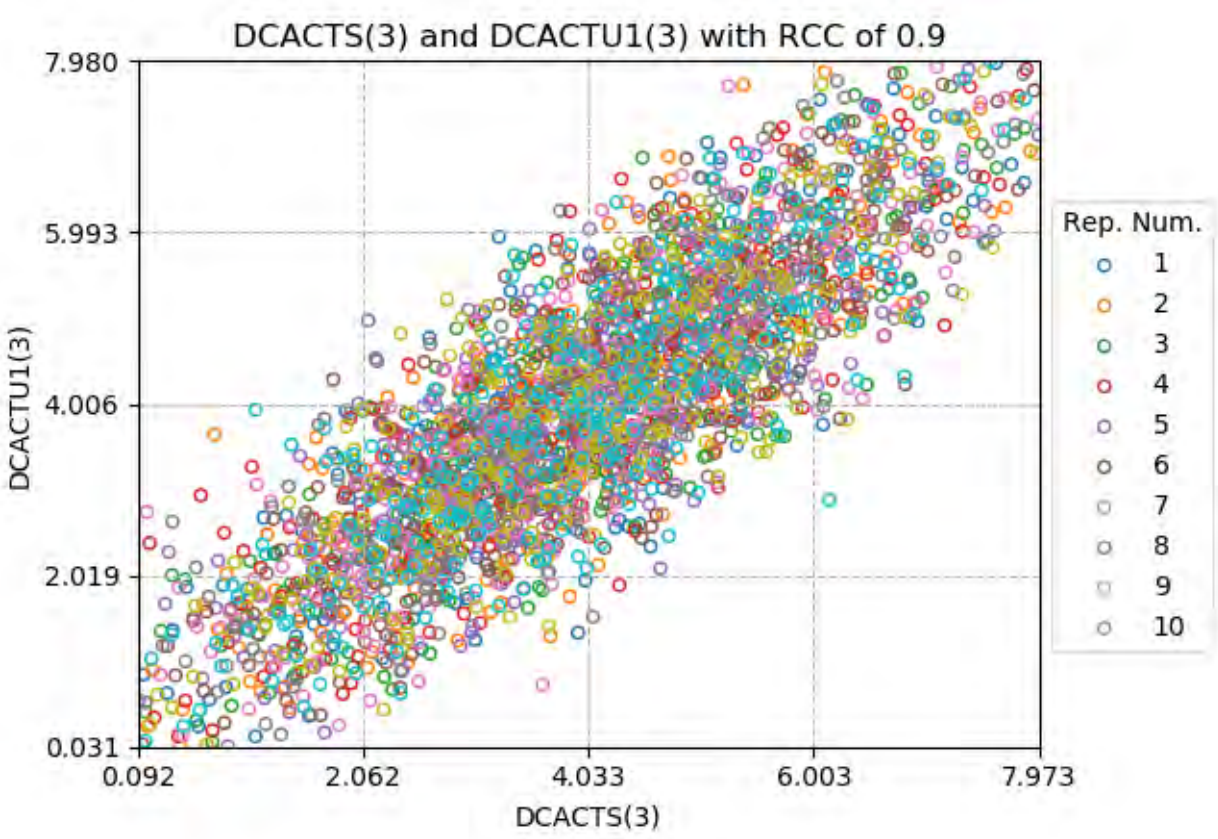

Fig.G.5.19. Input vs input scatter plot for Kd of I-129 in the saturated zone and Kd of I-129 in unsaturated zone 1 (10,000-year period) initial RCC = +0.9; adjusted RCC = +0.8371

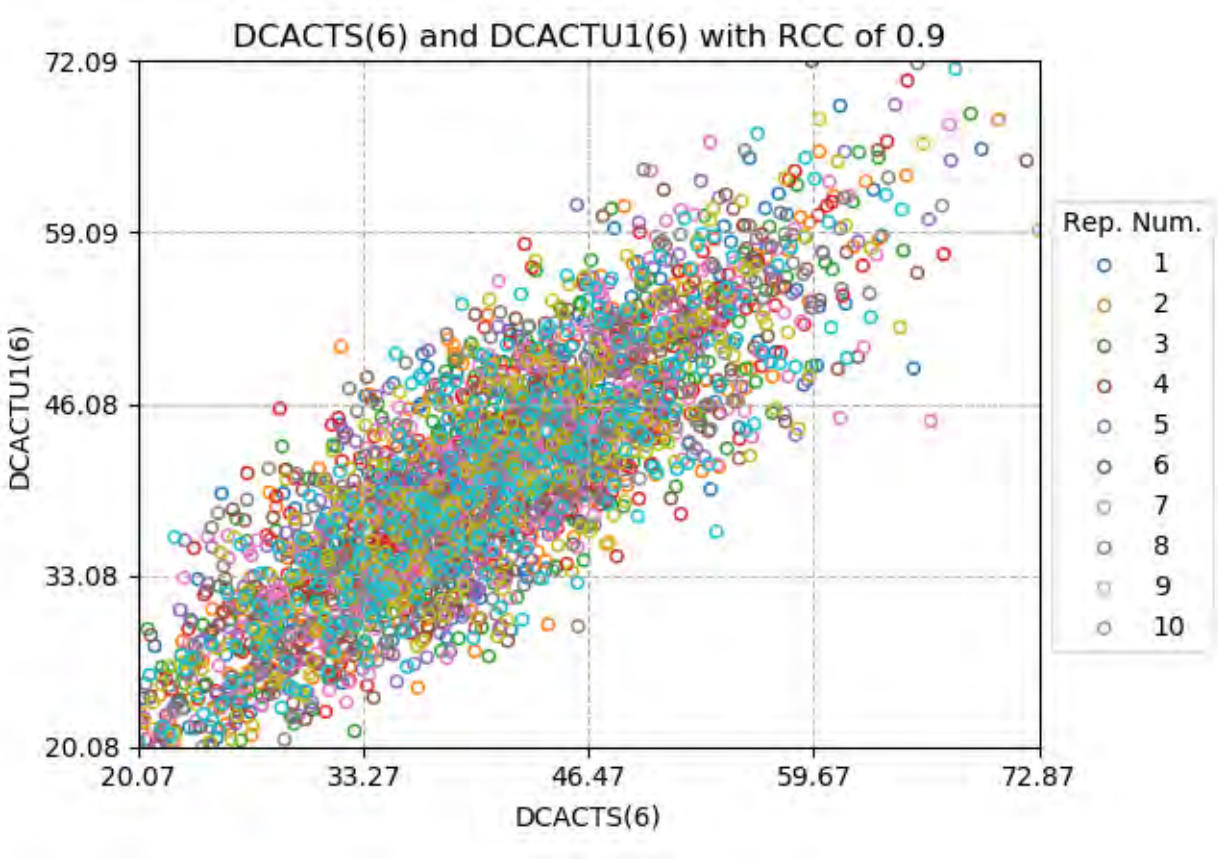

Fig.G.5.20. Input vs input scatter plot for Kd of Pu-239 in the saturated zone and Kd of Pu-239 in unsaturated zone 1 (10,000-year period) initial RCC = +0.9; adjusted RCC = +0.8371

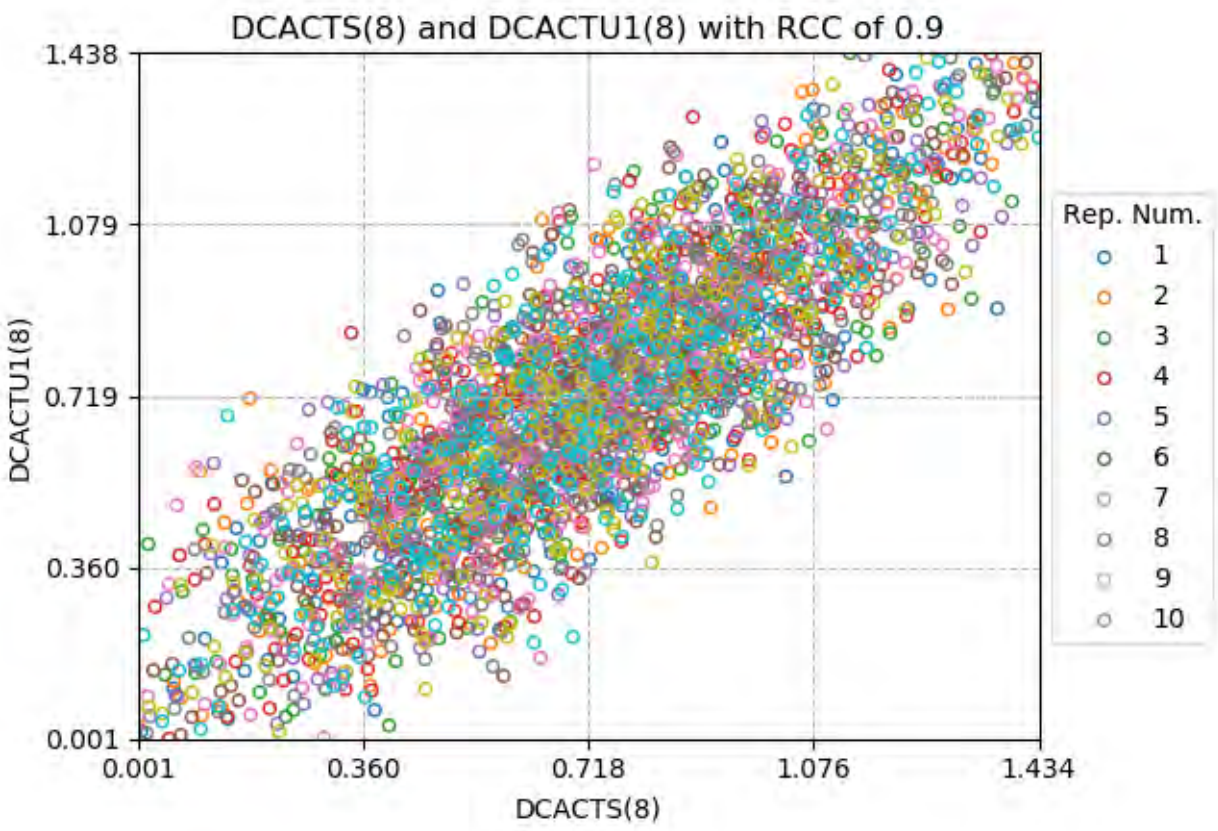

Fig.G.5.21. Input vs input scatter plot for Kd of Tc-99 in the saturated zone and Kd of Tc-99 in unsaturated zone 1 (10,000-year period) initial RCC = +0.9; adjusted RCC = +0.8371

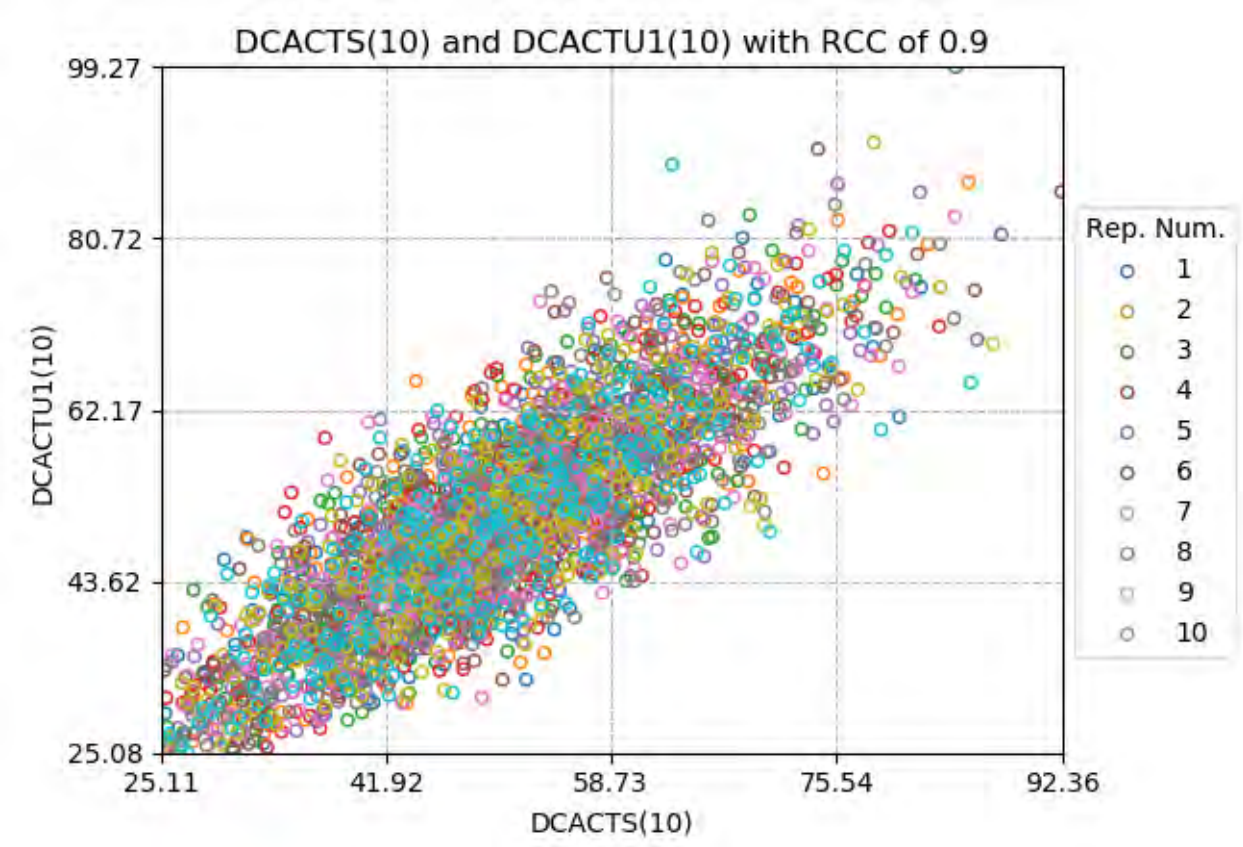

Fig.G.5.22. Input vs input scatter plot for Kd of U-234 in the saturated zone and Kd of U-234 in unsaturated zone 1 (10,000-year period) initial RCC = +0.9; adjusted RCC = +0.8371

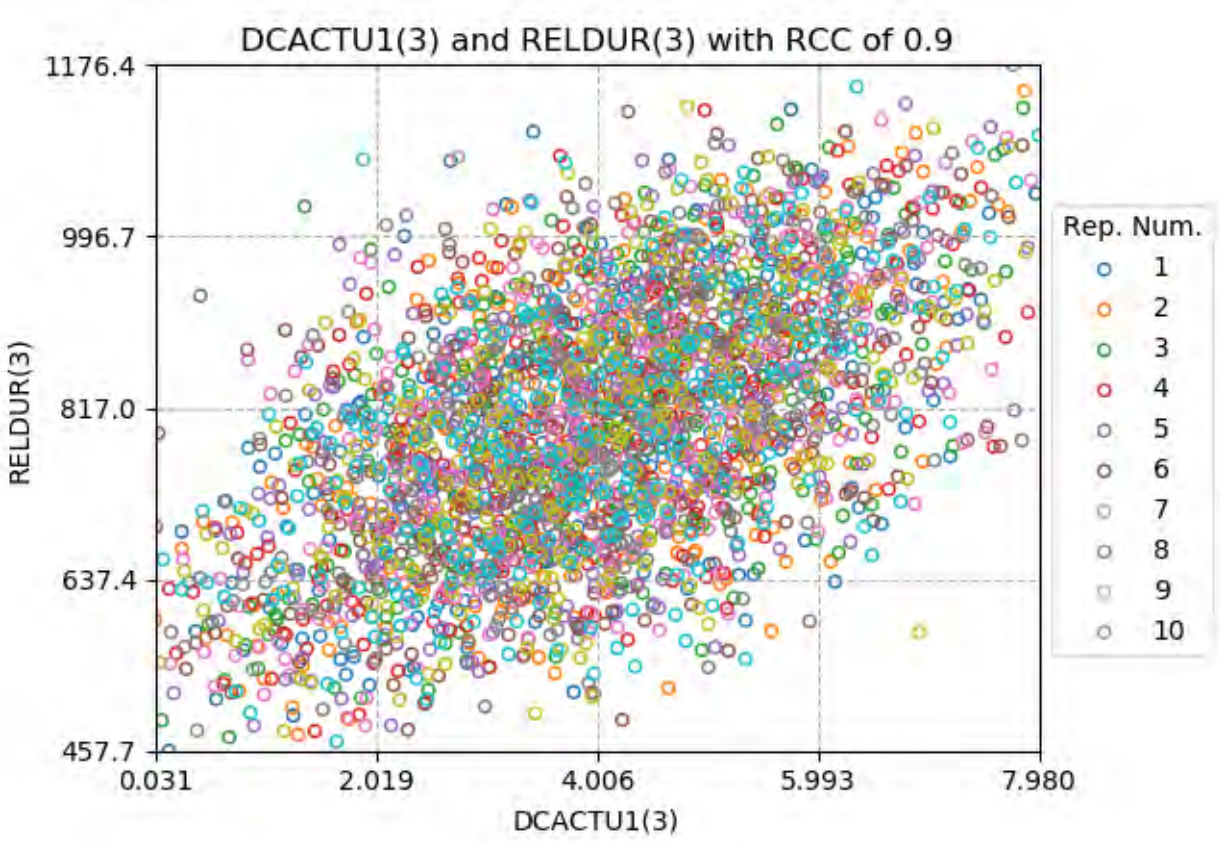

Fig.G.5.23. Input vs input scatter plot for K_d of I-129 in unsaturated zone 1 and release duration of I-129 (10,000-year period)
initial RCC = +0.9; adjusted RCC = +0.5522

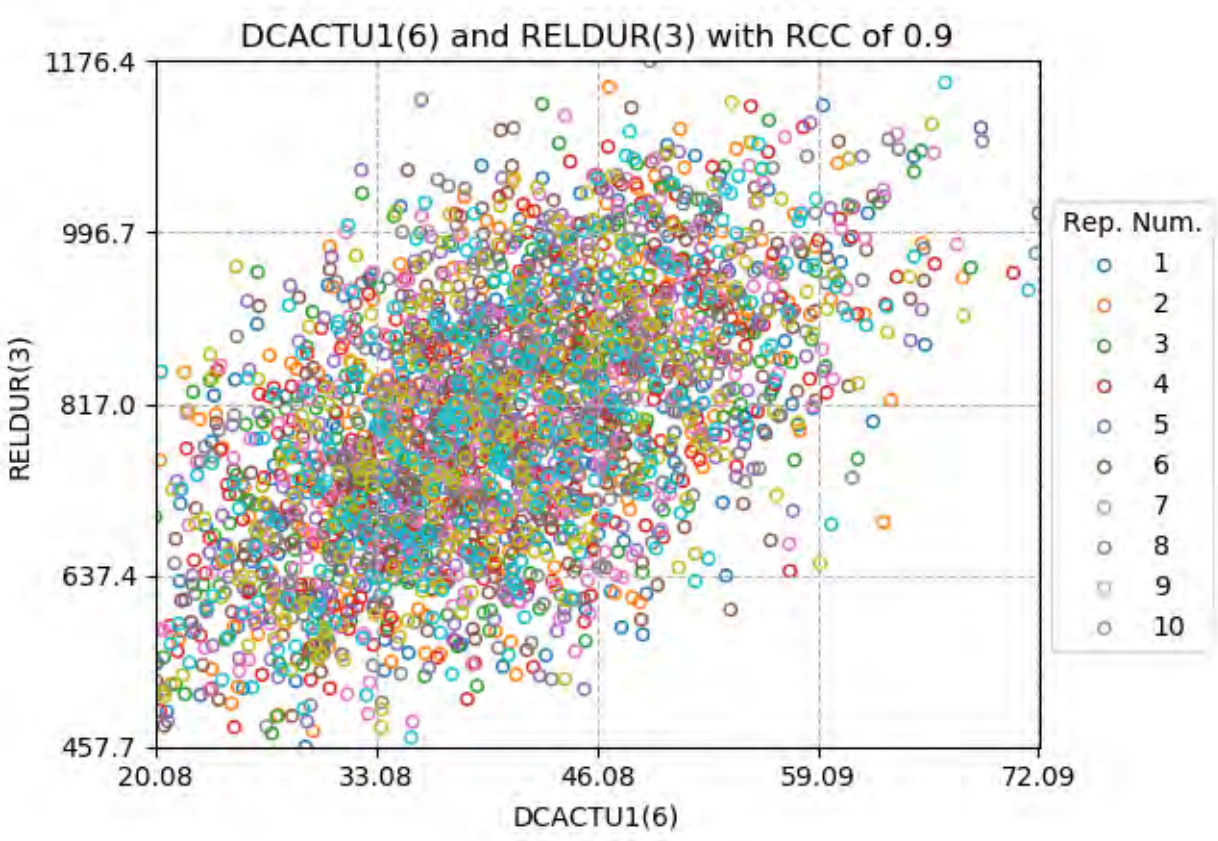

Fig.G.5.24. Input vs input scatter plot for Kd of Pu-239 in unsaturated zone 1 and release duration of I-129 (10,000-year period)
initial RCC = +0.9; adjusted RCC = +0.5522

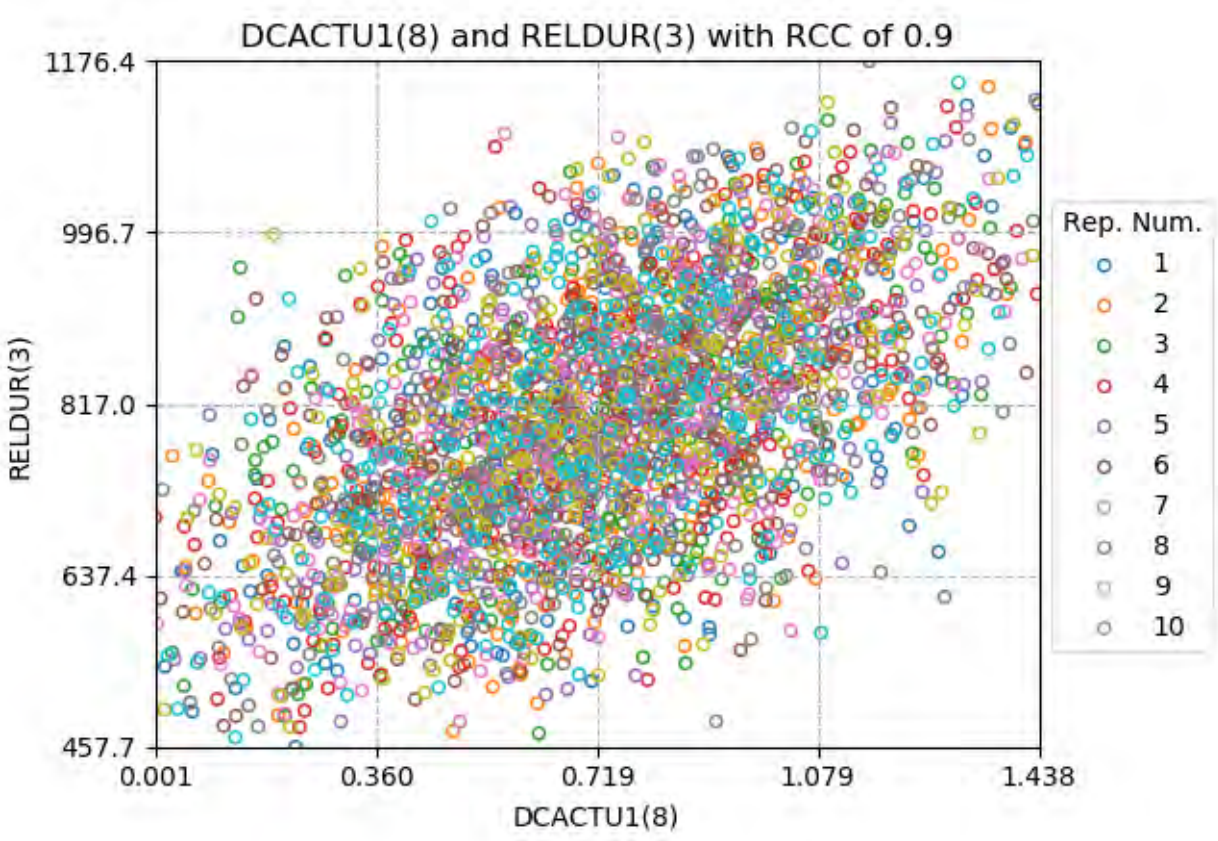

Fig.G.5.25. Input vs input scatter plot for Kd of Tc-99 in unsaturated zone 1 and release duration of I-129 (10,000-year period)
initial RCC = +0.9; adjusted RCC = +0.5522

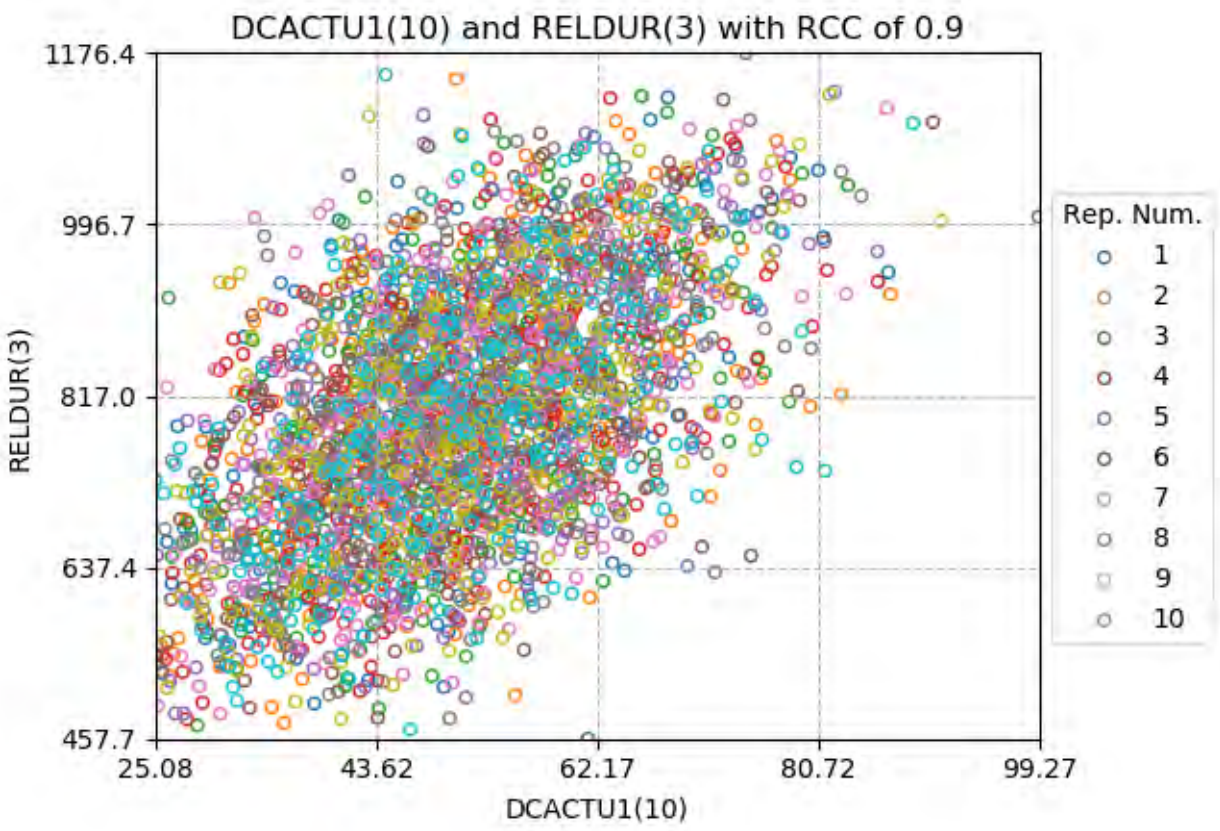

Fig.G.5.26. Input vs input scatter plot for Kd of U-234 in unsaturated zone 1 and release duration of I-129 (10,000-year period)
initial RCC = +0.9; adjusted RCC = +0.5522

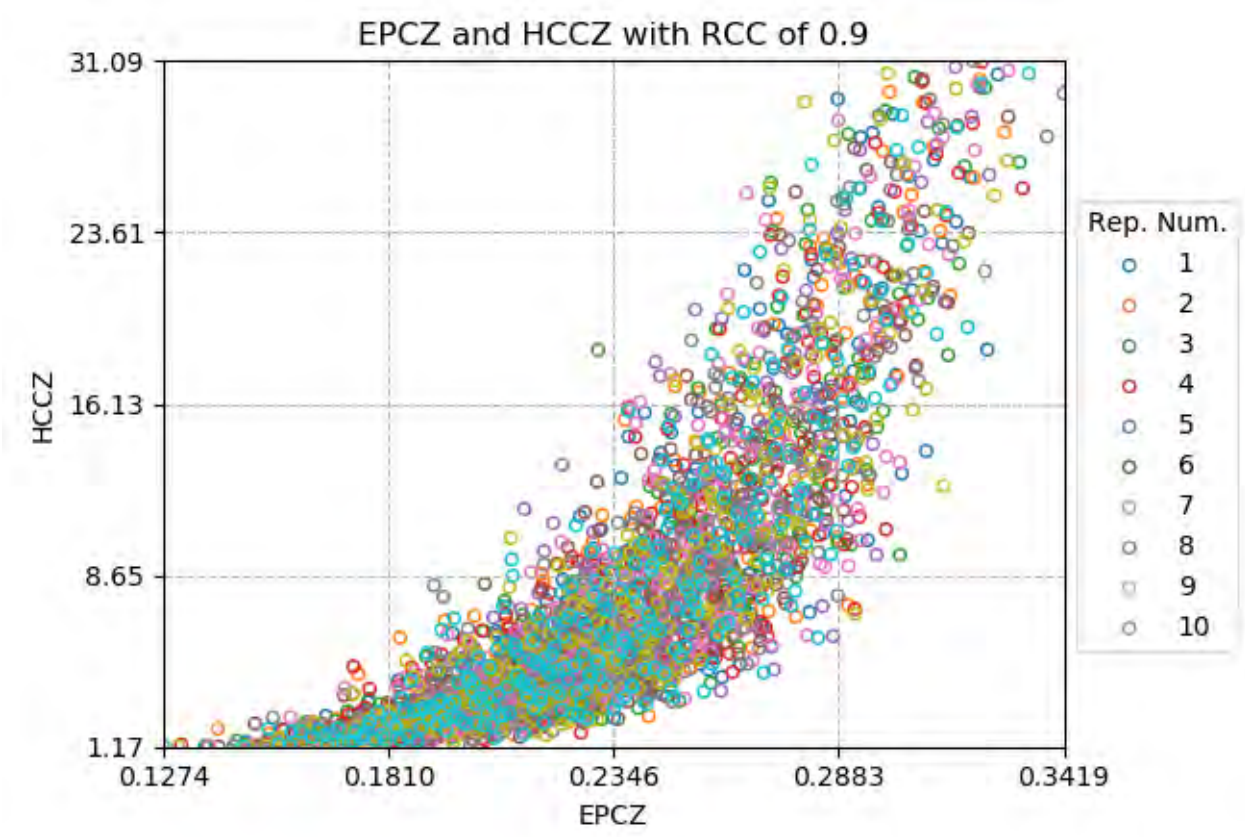

Fig.G.5.27. Input vs input scatter plot for effective porosity of contaminated zone and hydraulic conductivity of contaminated zone (10,000-year period) initial RCC = +0.9; adjusted RCC = +0.9

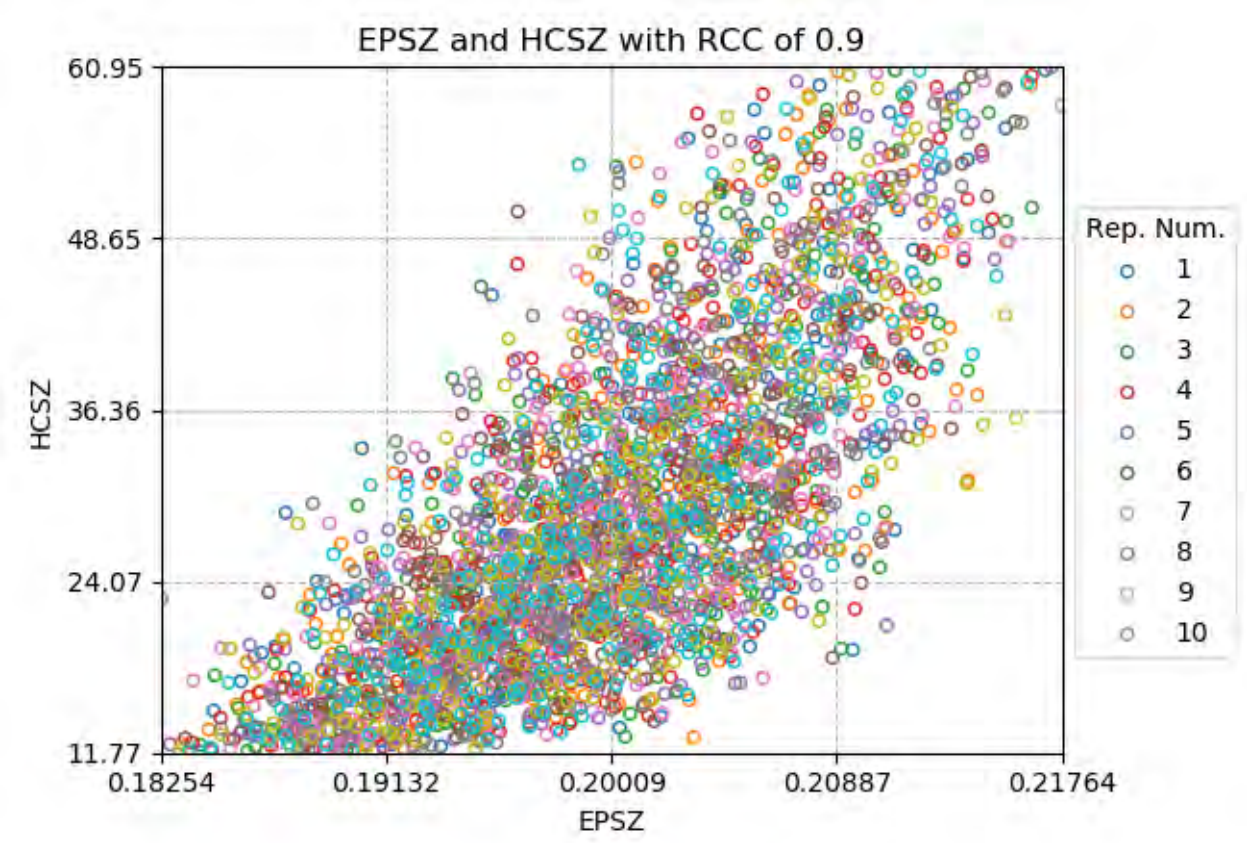

Fig.G.5.28. Input vs input scatter plot for effective porosity of saturated zone and hydraulic conductivity of saturated zone (10,000-year period) initial RCC = +0.9; adjusted RCC = +0.7477

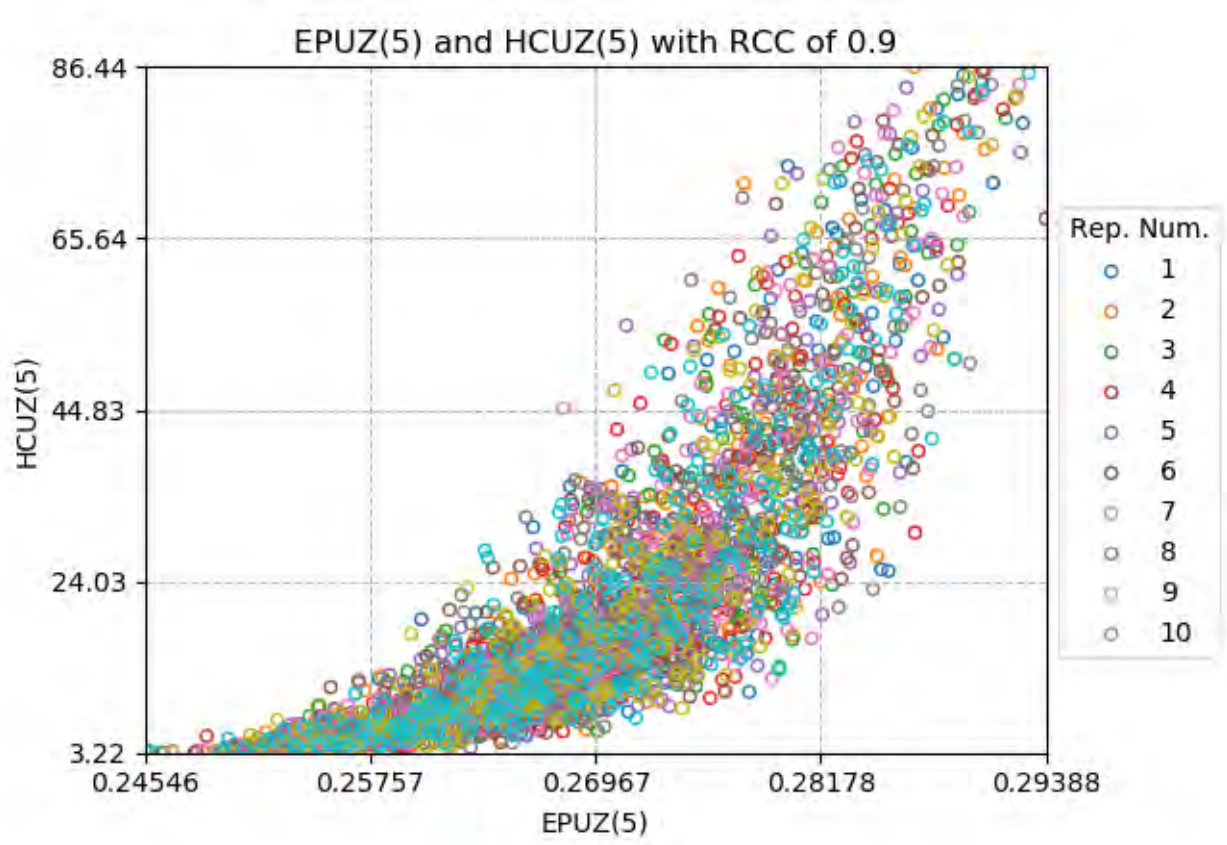

Fig.G.5. 29. Input vs input scatter plot for effective porosity of unsaturated zone 5 and hydraulic conductivity of unsaturated zone 5 (10,000-year period)
initial RCC = +0.9; adjusted RCC = +0.9

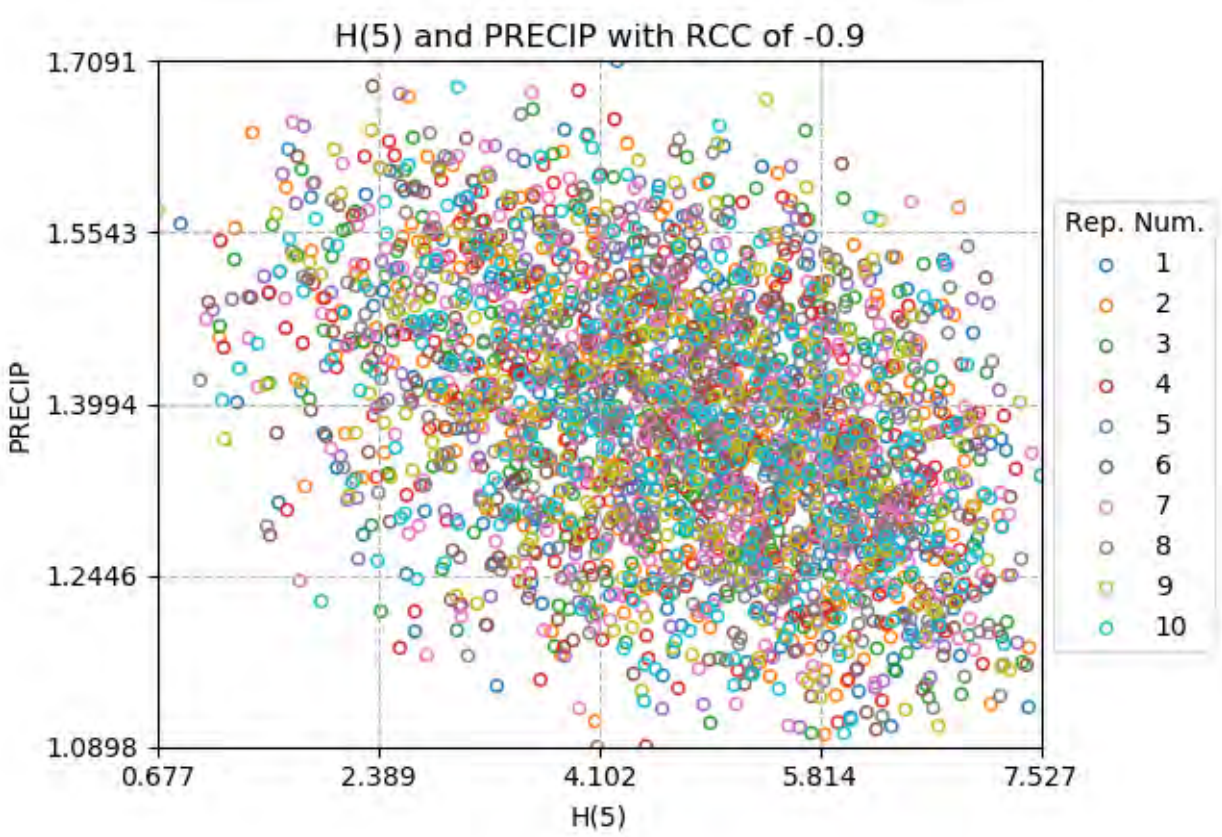

Fig.G.5.30. Input vs input scatter plot for thickness of unsaturated zone 5 and precipitation (10,000-year period)
initial RCC = -0.9 (negative); adjusted RCC = -0.3952 (negative)

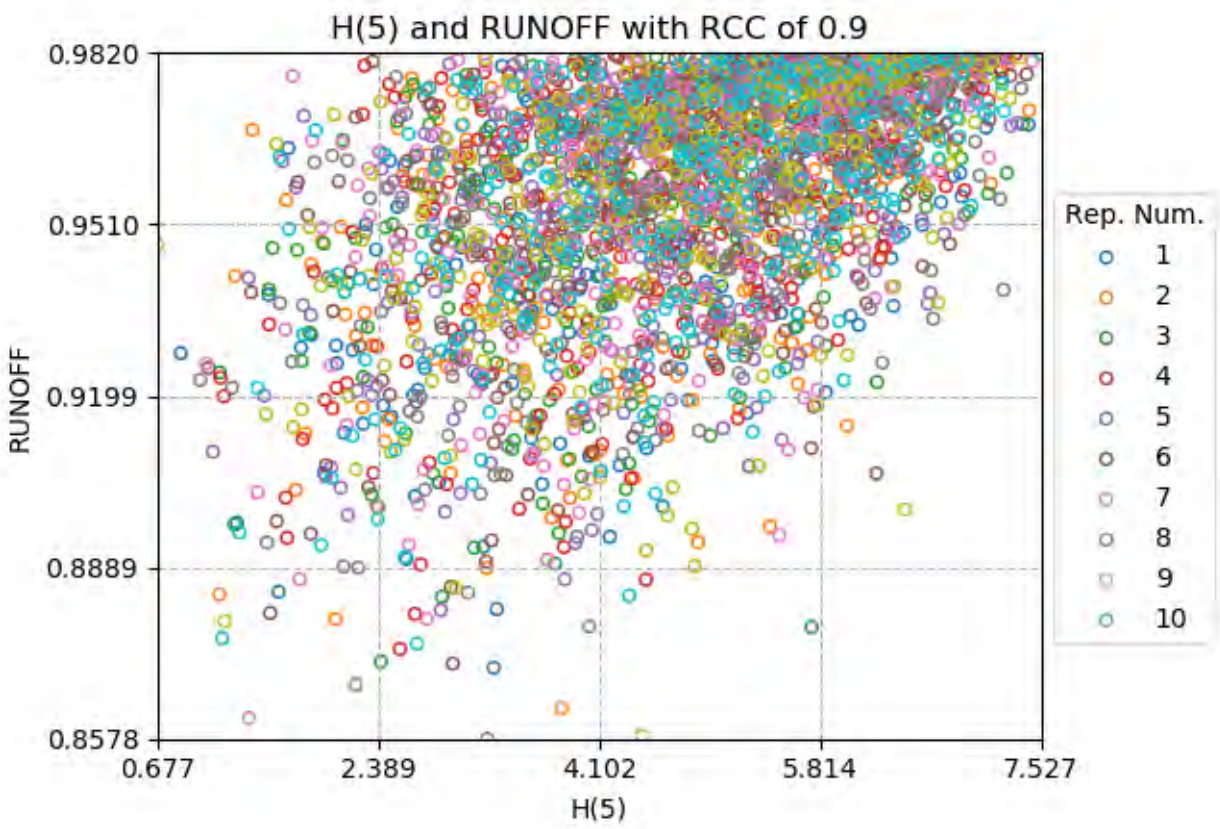

Fig.G.5.31. Input vs input scatter plot for thickness of unsaturated zone 5 and runoff coefficient of contaminated zone (10,000-year period) initial RCC = +0.9; adjusted RCC = +0.5013

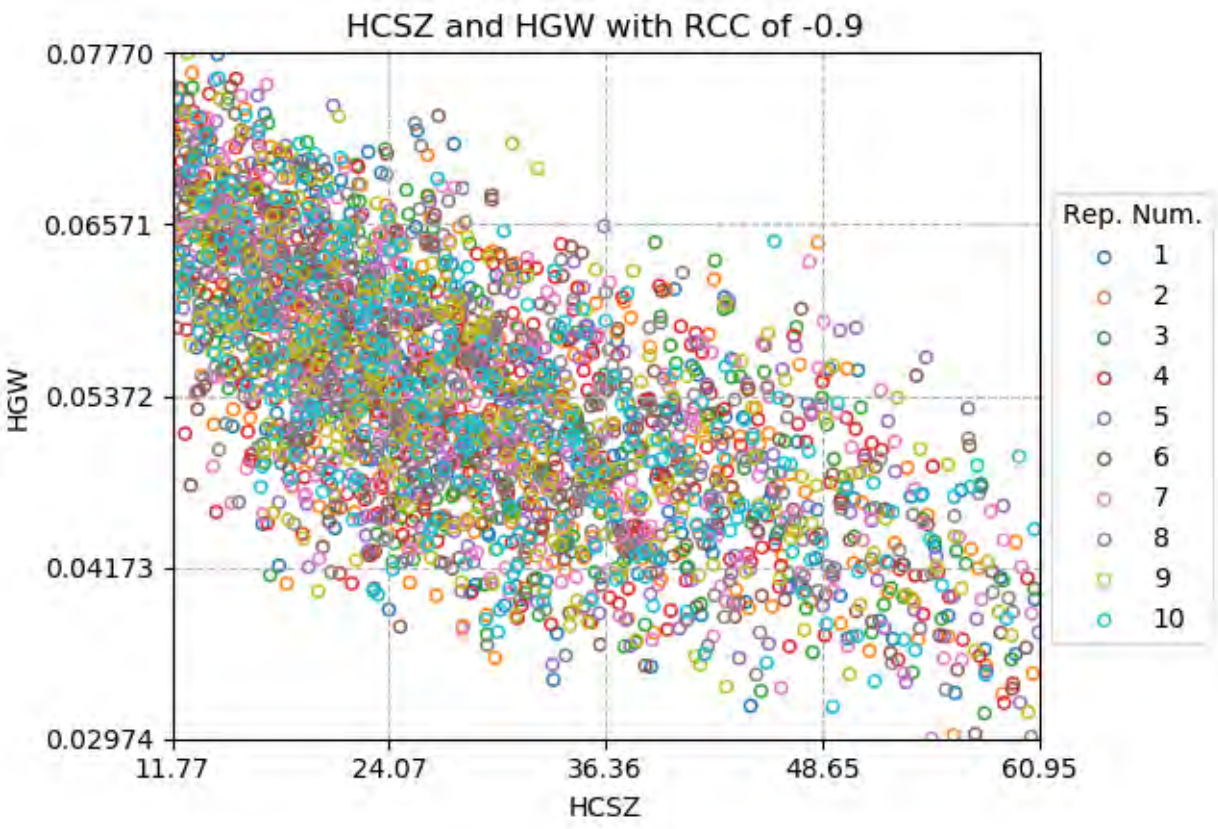

Fig.G.5.32. Input vs input scatter plot for hydraulic conductivity of saturated zone and hydraulic gradient of saturated zone to well (10,000-year period)
initial RCC = -0.9 (negative); adjusted RCC = -0.6841 (negative)

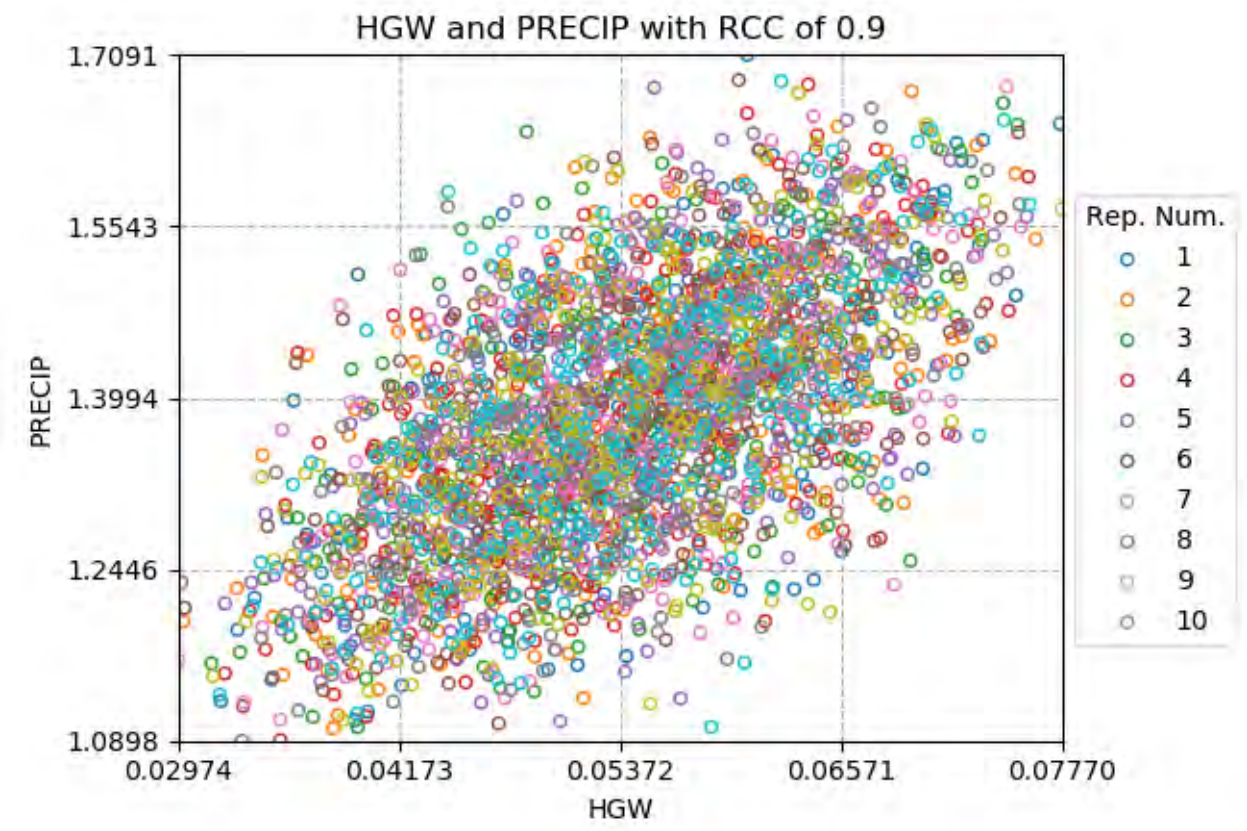

Fig.G.5.33. Input vs input scatter plot for hydraulic gradient of saturated zone to well and precipitation (10,000-year period)
initial RCC = +0.9; adjusted RCC = +0.6045

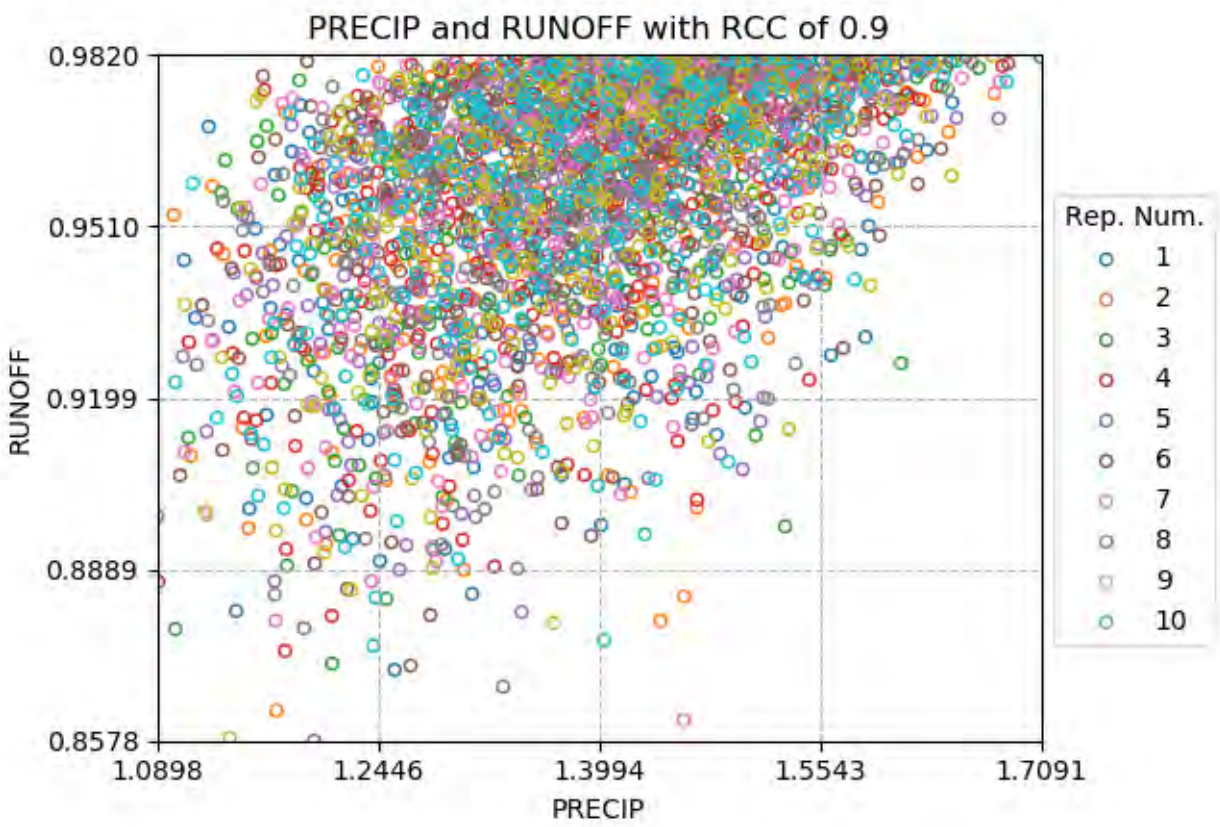

Fig.G.5.34. Input vs input scatter plot for precipitation and runoff coefficient of contaminated zone (10,000-year period) initial RCC = +0.9; adjusted RCC = +0.4515

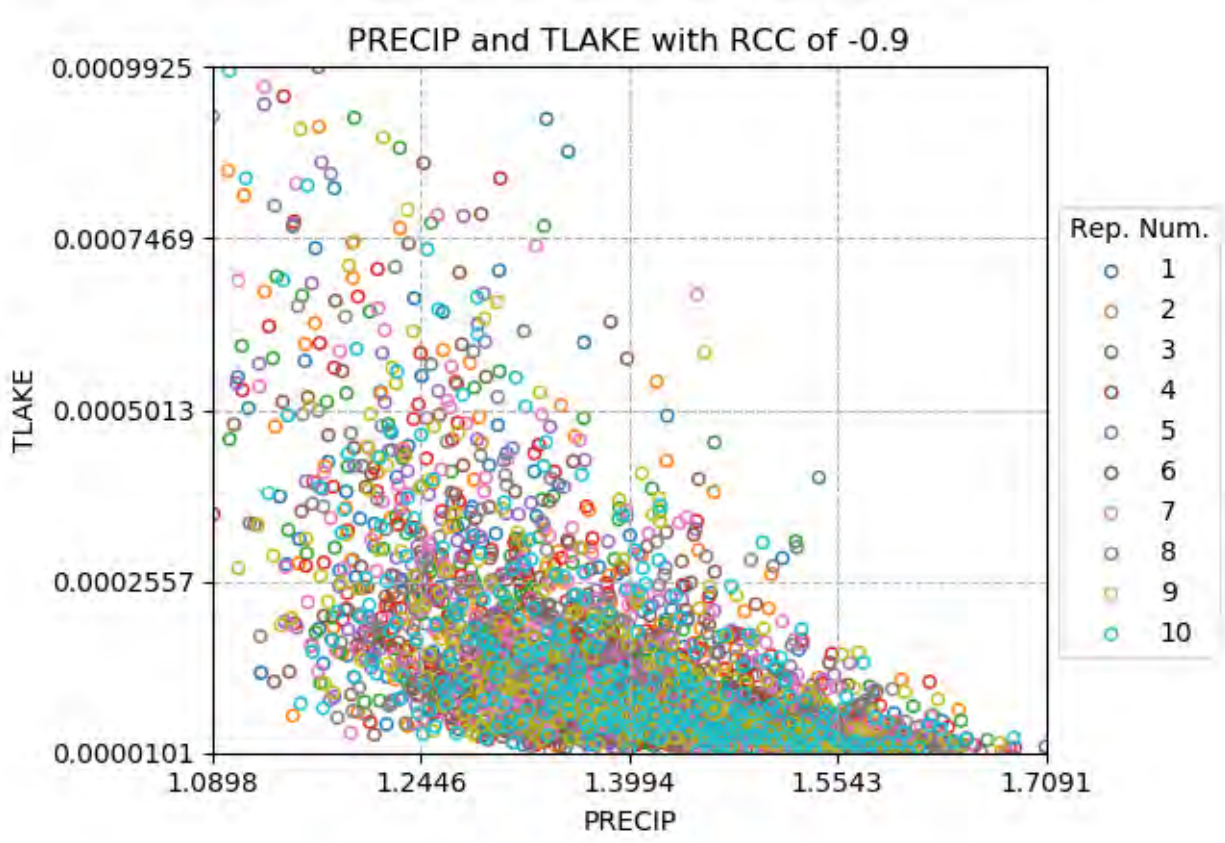

Fig.G.5.35. Input vs input scatter plot for precipitation and mean residence time of water in surface water body (10,000-year period) initial RCC = -0.9 (negative); adjusted RCC = -0.66 (negative)

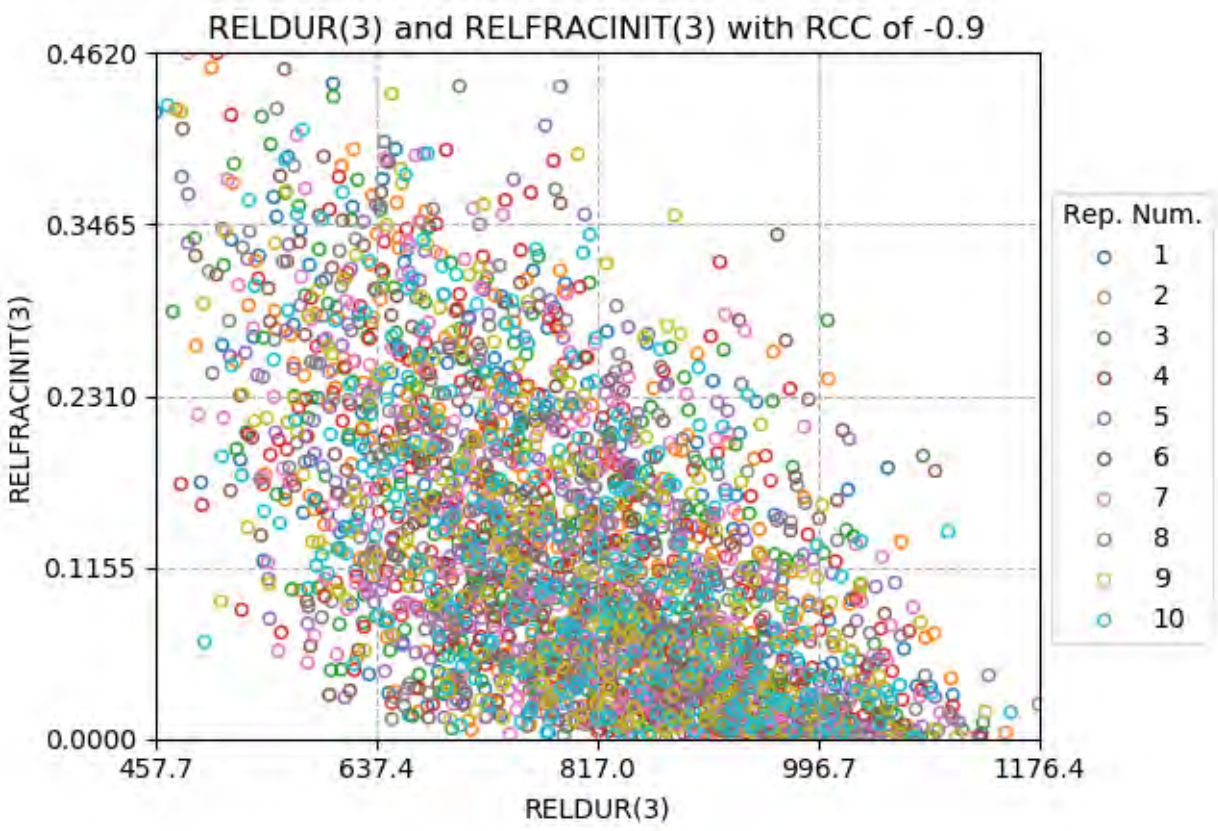

Fig.G.5.36. Input vs input scatter plot for release duration of I-129 and initial releasable fraction of I-129 (10,000-year)
initial RCC = -0.9 (negative); adjusted RCC = -0.6005 (negative)

This page intentionally left blank.

APPENDIX H.
RADON FLUX ANALYSIS FOR THE ENVIRONMENTAL MANAGEMENT DISPOSAL FACILITY

This page intentionally left blank.

CONTENTS

This page intentionally left blank.

FIGURES

TABLES

This page intentionally left blank.

ACRONYMS

DOE	U.S. Department of Energy
DOE O	DOE Order
EMDF	Environmental Management Disposal Facility
HDPE	high-density polyethylene
NRC	U.S. Nuclear Regulatory Commission
PA	performance assessment
QA	quality assurance
RESRAD	RESidual RADioactivity

This page intentionally left blank.

H.1. INTRODUCTION

The U.S. Department of Energy (DOE) Order (O) 435.1, *Radioactive Waste Management* (DOE 2001), requires that the performance assessment (PA) for a proposed disposal unit calculate the emanation of radon from the disposed waste. The performance criteria for release of radon shall be less than an average flux 20 pCi/m^2/sec at the surface of the disposal unit, or a limit of 0.5 pCi/L of air at the boundary of the facility within 1000 years after closure of the disposal facility (DOE 2011). This appendix presents the method used in this PA to demonstrate compliance with the performance criteria for radon from the proposed Environmental Management Disposal Facility (EMDF).

Radon gas can be generated from three radioisotopes (Rn-219, -220, and -222). The major contributor to radon gas for the radioactive waste disposal cell is Rn-222 in the U-238 decay chain. Radon-220, which occurs in the Th-232 decay chain and Rn-219 in the U-235 chain, have half-lives of under a minute and are not significant contributors to radon emission from a covered disposal facility.

Radon calculations for the proposed EMDF were performed using the methods described in *Radon Attenuation Handbook for Uranium Mill Tailings Cover Design* (U.S. Nuclear Regulatory Commission [NRC] 1984). The equations and basic recommended default parameters in the document have been used. Section 9 of the PA details the Quality Assurance (QA) activities and documentation that apply to the radon flux modeling. The site-specific design parameters and material property values for the EMDF preliminary design (refer to Sect. 2.1 of the QA Report [UCOR, an Amentum-led partnership with Jacobs, 2020]) were applied in the calculation.

This calculation is based on the estimated activity of Ra-226, the parent nuclide of Rn-220. Radium-226 (with a half-life of 1600 years) will be produced primarily from the decay of U-238, U-234, and Th-230 (nuclides typically found at Oak Ridge) over the 1000-year assessment period from the EMDF facility. A decay series calculation was performed to determine the ingrowth of Ra-226 from all predecessor radionuclides in the U-238 decay chain. The calculation used a decay calculator (Grove 2010); documentation of the calculator output is provided in Attachment H.1 to this appendix. This calculation yielded the Ra-226 activity ratios for each of the parent radionuclides. The decay calculation is presented in Sect. H.2. The radon calculation was performed using Microsoft® Excel® software. Equations programmed into Excel® have been verified as shown in Sect. H.3 by reproducing the example calculations provided in the NRC Handbook (NRC 1984). The presentation of equations in the result boxes follows the Excel® programming requirements. The site-specific design parameters and materials properties then were used to derive the required input parameters for EMDF site-specific application using the methods described in the NRC Handbook as shown in Sect. H.4.

The estimated U-234 and -238, Th-230, and Ra-226 inventories at the time of EMDF closure (refer to Sect. 2.3 and Appendix B of the PA) were used as the initial sources for the radon flux calculation. The calculation to derive the maximum total Ra-226 activity at year 1000 is presented in Sect. H.5. Finally, the same Excel® program worksheet used to duplicate the example problems was used to calculate the EMDF radon flux by using the site-specific parameters for the EMDF presented in Sect. H.6.

The maximum radon flux at year 1000 will be only 0.80 pCi/m^2/sec directly above the waste layer, much lower than the 20 pCi/m^2/sec limit over the landfill surface. The radon fluxes above the clay layer, biointrusion layer, and surface of the cell cover are 6.6E-06, 5.4E-06, and 5.1E-08 pCi/m^2/sec, respectively, significantly lower than 20 pCi/m^2/sec limit for the surface of the disposal unit.

H.2. ACTIVITY RATIO CALCULATIONS

Radon gas can be generated from three radioisotopes (Rn-219, -220, and -222) and are products of decay from U-235, Th-232, and U-238, respectively (see Fig. H.1). Radon-219 has a half-life of 3.96 sec and Rn-220 has half-life of 55.6 sec. Due to their short half-life and limited ability to migrate within and out of the waste in a closed disposal cell, these radioisotopes are not significant contributors to the radon emission and are not calculated for the base scenario.

Radon-222 has a half-life of 3.8 days and has enough time to diffuse through soils for potential exposure to a receptor. This radon flux calculation for Rn-222 is based on the activity of Ra-226, the parent nuclide to Rn-222, the most stable isotope of radon. Radium-226, with a half-life of 1600 years, is mostly produced by the decay of U-238, U-234, and Th-230, as shown in Fig. H.1.

The activity ratios between the parent radionuclides and Ra-226 are time dependent. Therefore, the activity ratios at the end of the assessment period (1000 years post-facility closure) were calculated using a decay calculator, MicroShield 9.05 (Grove 2010, refer to Attachment H.1). For Ra-226 estimated as part of the waste inventory at closure, a simple half-life decay was calculated for its activity at year 1000. The following activity ratios (Ra-226 at year 1000 versus current radionuclide) were established at 1000 years:

- Ra-226 at year 1000/U-238 = 1.7E-06
- Ra-226 at year 1000/U-234 = 1.7E-03
- Ra-226 at year 1000/Th-230 = 3.5E-01
- Ra-226 at year 1000/Ra-226 = 6.5E-01.

H.3. RADON FLUX CALCULATION VERIFICATION

The radon flux calculation for the proposed EMDF facility was performed according to the NRC Handbook (NRC 1984). All equations used in the NRC Handbook to calculate either radon emission at various layers or example design parameters were reproduced using the Microsoft® Excel® program.

The equations programmed in Excel® were verified by reproducing the results of the example calculation given in the NRC Handbook (NRC 1984, pgs. 2-6 through 2-16). The example is a calculation of the surface flux from a multilayer cover system. Table H.1 reproduces the Microsoft® Excel® worksheet showing the example problem from the NRC Handbook. It includes the equations, input parameters, and results for the example problem. The subscript "$_W$" refers to the waste zone, as in J-$_W$, D-$_W$, m-$_W$ and x-$_W$. The subscript "$_C$" pertains to the cover layer; C1 and C2 represent various cover layers.

Detailed parameter definition and mathematical representation and solutions to treat multilayer covers can be found in the NRC Handbook (NRC 1984). The produced Excel® program generated the same results as shown in the NRC Handbook, indicating that all parameters and equations were properly applied in the Excel® worksheet.

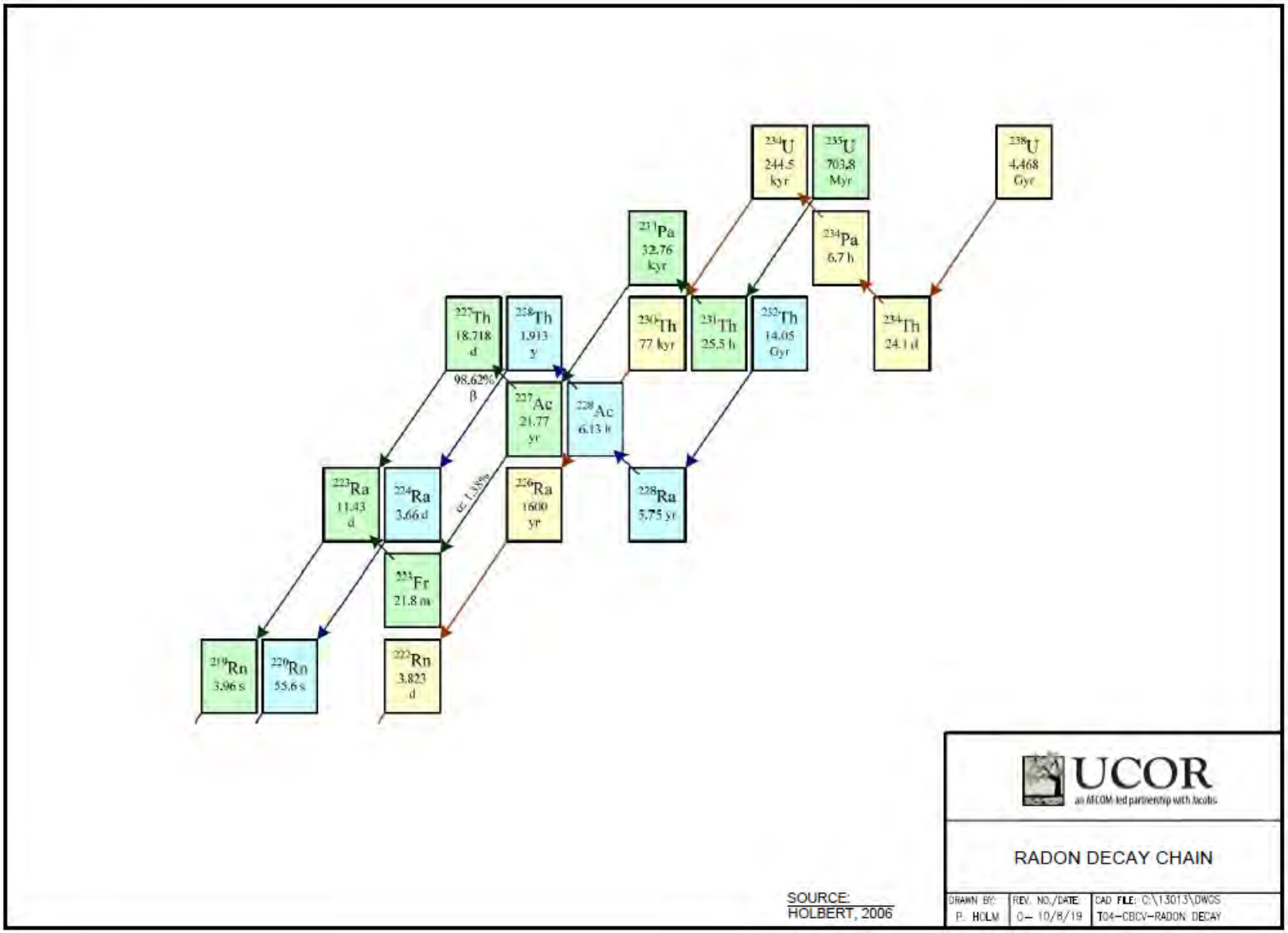

Fig. H.1. Radon decay chain

Table H.1. Radon calculation worksheet – verification of NRC problem example

	Symbol	Definition	Units	Basis for Parameter Value or Equation	Waste	Clay layer	Overburden
Basic parameters	k	Radon distribution coefficient for water/air @ 20C	pCi/cm^3 / pCi/cm^3	NRC default	0.26		
	λ	Decay constant for Rn-222	1/sec	NRC default	2.10E-06		
	R	Activity of Ra-226 in the waste	pCi/g	Example problem-specific	400		
	E	Radon emanation coefficient	dimensionless	Example problem-specific	0.2		
	x	Thickness of layer	cm	Example problem-specific	300	50	146
	ρ	Dry bulk density of the material	g/cm^3	Example problem-specific	1.5	1.9	
	p	Porosity of layer	vol/vol	Example problem-specific	0.44	0.3	0.37
	M	Moisture content	dry wt percentage	Example problem-specific	11.70	6.30	0.054
Calculated parameters	m	Fractional moisture saturation	dimensionless	= 0.01*ρM/p	0.40	0.40	0.25
	D	Diffusion coefficient for radon	cm^2/sec	= 0.07*exp[-4(m-mp^2+m^5)]	1.30E-02[1]	7.80E-03[1]	2.20E-02[1]
	a	Interface constant	cm^2/sec	= pt^2D_W(1-(1-k)m_W)^2	1.25E-03	3.48E-04	2.00E-03
	b	Inverse reflexation length	1/cm	= (λ/D_W)^0.5	1.27E-02	1.64E-02	9.77E-03
Calculated radon flux	J_W	Radon flux	pCi/m^2/sec	J_W = 10^4RρE(λD_W)$^{0.5}$*tanh((λ/D_W)$^{0.5}$*x_W) (Equation 3 – Page 2-2)	1.98E+02		
	J_{C1}			J_{C1} = (2J_W*exp(-b-$_C$*x_C)) / [(1+(a-$_W$/a-$_C$)$^{0.5}$*tanh(b-$_W$*x_W))+(1-(a-$_W$/a-$_C$)$^{0.5}$*tanh(b-$_W$*x_W))*exp(-2b-$_C$*x_C)] (Equation 4 – Page 2-2)		6.41E+01	
	J_{C2}			J_{C2} = (2J_{C1}*exp(-b-$_C$*x_C)) / [(1+(a-$_W$/a-$_C$)$^{0.5}$*tanh(b-$_W$*x_W))+(1-(a-$_W$/a-$_C$)$^{0.5}$*tanh(b-$_W$*x_W))*exp(-2b-$_C$*x_C)] (Equation 4 – Page 2-2)			1.83E+01
					(1.98E+02) - Result of NUREG/CR-3533 (page 2-9)	(6.41+01) – Result of NUREG/CR-3533 (page 2-15)	< 20 pCi/M^2/s at top of overburden

[1]Values taken from NRC 1984 (NUREG/CR-3533).
Subscripts: $_C$ = cover layer, $_W$ = waste zone
NRC = U.S. Nuclear Regulatory Commission

H.4. EMDF COVER DESIGN AND LAYER GROUPS FOR RADON CALCULATION

The final cover for the proposed EMDF will be a multi-layer system to meet Resource Conservation and Recovery Act of 1976 requirements for hazardous waste disposal facilities. The landfill will be designed and constructed to meet the following objectives:

- Minimize migration of liquids through the closed landfill over the long term
- Promote efficient drainage while minimizing erosion or abrasion of the cover
- Control migration of gas generated by decomposition of organic materials and other chemical reactions occurring within the waste, if found to be necessary
- Accommodate settling and subsidence to maintain the cover integrity
- Provide a permeability less than or equal to the permeability of any bottom-liner system or natural subsoil present
- Resist inadvertent intrusion of humans, plants, and animals
- Function with little maintenance.

The 11-ft-thick, multilayer final cover system in the proposed EMDF would be comprised of the following layers starting from the top of the waste and moving upward as shown on Fig. H.2:

- Geotextile cushion layer – non-woven, needle-punched geotextile used as a cushion over the waste
- Contouring layer – as part of the interim cover system, this layer provides a working and contouring surface (expected to be primarily gravel)
- Geotextile separator layer – non-woven, needle-punched geotextile used as a separator between the contouring layer and clay layer
- Compacted clay layer – 1-ft-thick (minimum) layer of native clay soil or amended soil compacted to produce an in-place hydraulic conductivity less than or equal to 1×10^{-7} cm/sec; this layer, in conjunction with the overlying amended clay layer and geomembrane layer, would function as a composite hydraulic barrier to infiltration
- Amended clay layer – 1-ft-thick (minimum) layer of native soil amended with bentonite and compacted to produce an in-place hydraulic conductivity less than or equal to 3×10^{-8} cm/sec
- Geomembrane layer – 60-mil-thick high-density polyethylene (HDPE) geomembrane, textured on both sides to enhance sliding resistance
- Geotextile cushion layer – non-woven, needle-punched geotextile used as a cushion over the underlying geomembrane
- Lateral drainage layer – 1-ft-thick layer of hard, durable, free-draining, granular material with sufficient transmissivity to drain the cover system and satisfy the requirements of the infiltration analysis
- Biointrusion layer – 2-ft-thick layer of free-draining, siliceous coarse granular material (i.e., 4-in. to 12-in.-diameter riprap) sized to prevent burrowing animals and plant root systems from penetrating the cover system and reduce the likelihood of inadvertent intrusion by humans by increasing the difficulty of digging or drilling into the landfill

- Geotextile separator layer – non-woven, needle-punched geotextile used as a separator between the granular filter layer and biointrusion layer
- Granular filter layer – 12-in.-thick layer of granular material graded to act as a filter layer to prevent clogging of the biointrusion layer with soil from the overlying erosion control layer
- Erosion control layer – 4-ft-thick vegetated soil/rock matrix comprised of a mixture of crushed rock and native soil and constructed over the disposal facility to protect the underlying cover layers from the effects of frost penetration and wind and water erosion; this layer also would provide a medium for growth of plant root systems and would include a surficial grass cover or other appropriate vegetation.

For purposes of radon flux modeling, the cover system is divided into the following three groups based on similarity in material property types (from the waste upward, Fig. H.2):

- Clay layers group
- Biointrusion layers group
- Erosion control layers group.

Based on material properties for each of the cover system layers (refer to Appendix C, Table C.2), effective properties for each of the cover layer groupings are calculated for use in the radon flux model (Table H.2). No credit is taken for the flexible synthetic membrane overlying the clay infiltration barriers in the radon flux estimate; the membrane is assumed to be completely degraded by 1000 years post-closure.

There may be some erosion of the cover system during the 1000-year assessment period. However, the design of the cover system includes an erosion control layer at the top to limit erosion of the surface. An erosion estimate, based on the Revised Universal Soil Loss Equation Version 2 soil erosion model (referred to as RUSLE2) (U.S. Department of Agriculture 2013), indicates there will be limited erosion of the top of the erosion control layer (see Appendix C, Sect. C.4). The average erosion rate is predicted to be 2.2E-04 ft/year, corresponding to an average erosion depth of 2.6 in. from the surface of the cover over 1000 years. Although this result suggests that only a small fraction (6 percent) of the cover layer thickness may be lost, the analysis considers potential extreme cover degradation effects by estimating radon flux at the top of each of the three cover system layer groups (i.e., assuming no radon moderating benefit from the materials overlying each group).

The detailed layer-specific parameters and calculated layer group parameters used in the radon calculation are shown in Table H.2. These layer-specific values are from the EMDF preliminary design (refer to Sect. 2.1 of the QA Report) for the cover layers and the radionuclide source concentrations (refer to Appendix G, Table G.9) for the waste. The moisture content values are from the hydrologic cover performance modeling results for the EMDF fully functional design condition (refer to Appendix C, Table C.4). This EMDF performance condition was selected because the moisture content in the clay layers is expected to be lower than for the two longer-term performance conditions evaluated with the cover infiltration model. More water would be expected in the clay layers during the longer-term performance period due to an increase in cover infiltration resulting from degradation of the impermeable HDPE membrane on top of the clay barriers of the cover. Lower amounts of moisture in the clay layers result in a higher predicted radon flux because the presence of moisture retards the migration of radon gas and because the downward gradient of the water through the cover suppresses the upward migration of the radon gas from the waste. For the layer groupings effective parameter calculations, thickness-weighted averaging has been applied.

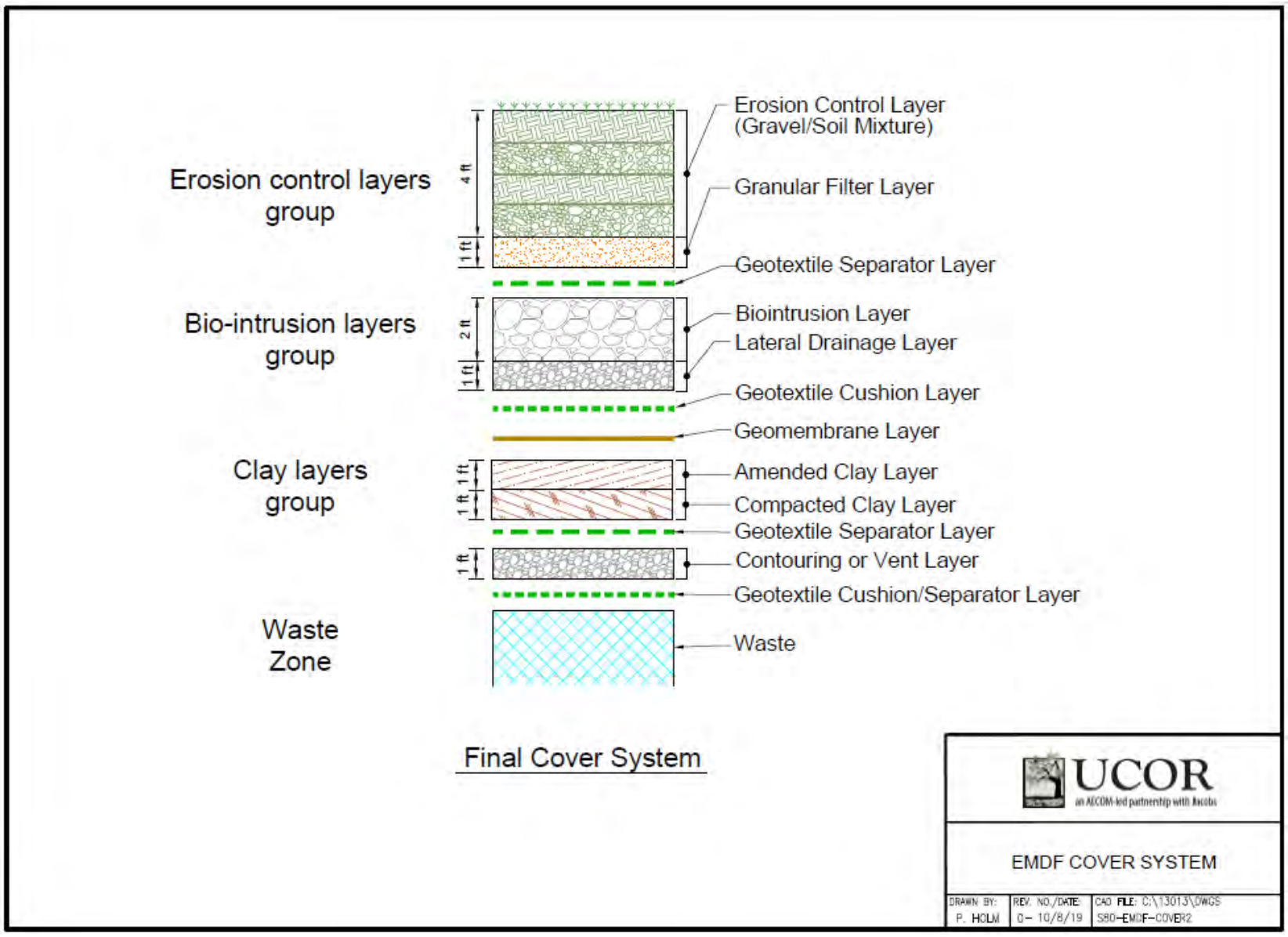

Fig. H.2. EMDF cover system and layer groups

Table H.2. EMDF layer-specific parameters and calculated layer group parameters

			Parameters									
			x	p	Mc	SG	ρ	w	m	D	a	b
Layer #	**Material**	**Layer thickness (in)**	**Layer thickness (cm)**	**Total porosity (vol/vol)**	**Moisture content (vol/vol)**	**Particle density of material (g/cm^3)**	**Dry bulk density (g/cm^3)**	**Moisture content (dry weight percent)**	**Fractional moisture saturation (dimensionless)**	**Diffusion coefficient (cm^2ec)**	**Interface constant (cm^2/s)**	**Inverse reflexation length (1/cm)**
Erosion control layer group (1+2)*	Composite of Layers 1 & 2	60	152.40	0.463	0.3248	2.65	1.424	22.81	0.70	3.89E-03	1.92E-04	2.32E-02
1	Top Soil/Rock mix	48	121.92	0.464	0.361	2.65	1.420	25.42	0.78			
2	Sand/gravel	12	30.48	0.457	0.180	2.65	1.439	12.50	0.39			
Biointrusion layer group (3+4)*	Composite of Layers 3 & 4	36	91.44	0.397	0.0615	2.65	1.598	3.85	0.15	4.15E-02	5.13E-03	7.11E-03
3	Bio-intrusion (Pebble/Boulder)	24	60.96	0.397	0.0746	2.65	1.598	4.67	0.19			
4	Drainage	12	30.48	0.397	0.0354	2.65	1.598	2.22	0.09			
~~5~~	~~Membrane~~	~~0.08~~	~~0.20~~	-	-	-	-	-	-	-	-	-
Clay layer group (6+7)*	Composite of Layers 6 & 7	24	60.96	0.427	0.418	2.65	1.518	27.54	0.98	7.74E-05	1.07E-06	1.65E-01
6	Amended Compact Clay	12	30.48	0.427	0.427	2.65	1.518	28.12	1.00			
7	Cover Compacted Clay	12	30.48	0.427	0.409	2.65	1.518	26.96	0.96			
~~8~~	~~Contour gravel~~	~~12~~	~~30.48~~	~~0.365~~	~~0.305~~	~~2.65~~	~~1.683~~	~~18.13~~	~~0.84~~			
Waste	Waste	690.45	1753.74	0.419	0.307	3.27	1.900	16.16	0.73	2.68E-03	9.88E-05	2.80E-02

Notes:
High-density polyethylene layer assumed to be degraded.
Strikethrough text for layers 5 and 8 indicates that these layers are not included in the calculations of grouped layer properties.
* Layer grouping used for radon calculation

EMDF = Environmental Management Disposal Facility

The radon flux calculation was conducted for the waste layer upper surface, above the clay layers group (3 ft above the waste), above the biointrusion layers group (6 ft above the waste), and at the landfill surface (11 ft above the waste) at 1000 years. Using the grouped layers rather than the individual layers simplifies the calculations while still providing a good approximation of the cover design for estimating radon release. For this analysis, the 12-in. contour layer directly above the waste zone is not included in the calculation because it is composed of coarse material that provides little radon gas protection.

H.5. SOURCE-SPECIFIC ACTIVITIES OF PARENT RADIONUCLIDES

The development of the EMDF estimated radiological inventory is summarized in Sect. 2.3 of the PA and is detailed in Appendix B. The total activity for each radionuclide at the closure of EMDF was estimated based on available waste generation forecasts and existing waste and facility characterization profiles applicable to the anticipated waste streams. The estimated U-238, U-234, Th-230, and Ra-226 inventories were used as the initial sources for the radon flux calculation. Using the activity ratio relationship between parent isotopes and Ra-226 daughter products presented above, the estimated average activity concentration of Ra-226 at year-1000 was calculated for each parent nuclide (see Table H.3). The total Ra-226 activity concentration at year 1000 (accounting for decay and ingrowth) is 2.26 pCi/g for the waste.

Table H.3. Total radium-226 activity at year 1000

Parent radionuclide	Estimated waste activity (Ci)	Average activity concentration at disposal (pCi/g)	Decay	Activity ratio at 1000 years	Resulting activity concentration of Ra-226 at 1000 years (pCi/g)
U-238	9.83E+02	3.81E+02	U-238 to Ra-226	1.65E-06	6.29E-04
U-234	1.62E+03	6.30E+02	U-234 to Ra-226	1.69E-03	1.06E+00
Th-230	4.94E+00	1.92E+00	Th-230 to Ra-226	3.50E-01	6.71E-01
Ra-226	2.07E+00	8.01E-01	Ra-226 decay	6.48E-01	5.19E-01
				Total	**2.26E+00**

H.6. RADON CALCULATION FOR EMDF

Based on the site-specific cover layer characteristics and estimated total Ra-226 activity, the radon calculation was conducted using the same worksheet developed to verify the problem set in the NRC Handbook (NRC 1984). A radon emanation coefficient of 0.25 for Rn-222, the default value in the RESidual RADioactivity (RESRAD) model (Yu et al. 2015), was used. The default value approximately represents the conditions in a silty loam soil with a low moisture content (i.e., not dry). The value is on the higher end of the reported radon emanation coefficients for Rn-222 in various soils (Yu et al. 2015, Sect. 4.2.2, page 122), which typically range from less than 0.01 to 0.30.

The radon calculation results at different levels in the cover system are shown on Table H.4. The maximum radon flux at year 1000 will be only 0.80 pCi/m^2/sec directly above the waste layer, much lower than the 20 pCi/m^2/sec limit over the landfill surface. The radon fluxes above the clay layer, biointrusion layer, and cell top cover are 6.6E-06, 5.4E-06, and 5.1E-08 pCi/m^2/sec respectively, significantly lower than 20 pCi/m^2/sec limit at the surface of the disposal unit.

Table H.4. Radon calculation for EMDF

	Symbol	Definition	Units	Basis for parameter value or equation	Top of waste	Top of clay layer group	Top of bio-intrusion layer group	Top of erosion control layer group
Basic parameters	k	Radon distribution coefficient for water/air @ 20C	pCi/cm^3 / PCi/cm^3	NRC default	0.26			
	λ	Decay constant for Rn-222	1/sec	NRC default	2.10E-06			
	R	Specific activity of Ra-226 in the waste	pCi/g	Site-specific	2.26E+00			
	E	Radon emanation coefficient	dimensionless	Default (RESRAD Model)	0.25			
	x	Thickness of layer	cm	Site-specific	1753.74	60.96	91.44	152.4
	ρ	Dry bulk density of the material	g/cm^3	Site-specific	1.90	1.52	1.598	1.424
	p	Porosity of layer	vol/vol	Site-specific	0.419	0.427	0.397	0.463
	M	Moisture content	dry wt percentage	Site-specific	16.16	27.54	3.85	22.81
Calculated parameters	m	Fractional moisture saturation	dimensionless	= 0.01*ρM/p	0.73	0.98	0.15	0.70
	D	Diffusion coefficient for radon	cm^2/sec	= 0.07*exp[-4(m-mp^2+m^5)]	2.68E-03	7.74E-05	4.15E-02	3.89E-03
	a	Interface constant	cm^2/sec	= p^2D(1-(1-k)m)^2	9.88E-05	1.07E-06	5.13E-03	1.92E-04
	b	Inverse reflexation length	1/cm	= (λ/Dt)^0.5	2.80E-02	1.65E-01	7.11E-03	2.32E-02
Calculated radon flux	Jt	Radon flux	pCi/m^2/sec	Jt = 10^4RρE(λDt)^0.5* tanh((λ/Dt)^0.5*Xt)	**8.04E-01**			
	Jc1			Jc = (2Jt*exp(-bc*xc)) / [(1+(at/ac)^0.5*tanh(bt*xt))+ (1-(at/ac)^0.5*tanh(bt*xt))* exp(-2bc*xc)]		**6.59E-06**		
	Jc2			Jc = (2Jt*exp(-bc*xc)) / [(1+(at/ac)^0.5*tanh(bt*xt))+ (1-(at/ac)^0.5*tanh(bt*xt))* exp(-2bc*xc)]			**5.36-06**	**5.05E-08**

EMDF = Environmental Management Disposal Facility
NRC = U.S. Nuclear Regulatory Commission

The radon calculation indicates that, based on the estimated inventory and assuming a uniform distribution of contamination within the waste mass, the proposed EMDF will meet the radon flux performance objective within the 1000 years PA period, even with the most conservative exposure scenario (directly above the waste).

H.7. UNCERTAINTY AND SENSITIVITY ANALYSIS

The radon calculation (Table H.4) shows that the radon flux is only 3.1E-07 pCi/m^2/sec at the cover surface for the inventory assumed. The radon flux is primarily controlled by clay layers that lie below the biointrusion layer. Even with some assumed erosion of the cover system, the integrity of the clay layers will likely be preserved within the first 1000 years. Uncertainty in the performance of the EMDF cover (relative to radon release) is minimal.

A sensitivity analysis was conducted to evaluate the potential impact of inventory uncertainty or non-uniform distribution of the waste mass in the disposal cell. The latter scenario represents a condition where most of the disposed radionuclides are distributed near the top portion of the waste cell. The maximum waste stream average activity concentrations for Ra-226 and its three parent nuclides were used to re-calculate the radon emission. The resulting total Ra-226 activity at 1000 years is 19 pCi/g for the waste. It is nearly 10 times higher than the uniform distribution base case of 2.3 pCi/g. The calculated radon fluxes for the maximum waste stream average concentration scenario are 5.5E-05, 4.5E-05, and 2.6E-06 pCi/m^2/sec above the cover clay layer, biointrusion layer, and top of the cover layer, respectively, significantly lower than 20 pCi/m^2/sec limit at the exposed landfill surface.

Even though radon emission from a closed disposal cell is only likely from the longer half-life Rn-222 isotope, the potential radon impact from Rn-220 with a short half-life of 55.6 sec was examined. Radon-220 is a decay product from Ra-224. The radionuclide decay from Th-232 to Ra-224 can be assumed to be in secular equilibrium due to the very short half-life of the daughter radionuclides shared. Also, because of the extremely long half-life of the Th-232 (1.4E+10 years), the activity ratio between estimated Th-232 inventory at closure and Ra-224 at year 1000 is essentially unity. The estimated Th-232 inventory in EMDF is 9.07 Ci, which corresponds to an average activity concentration of 3.52 pCi/g. This value also would be the Ra-224 activity at year 1000 based on the activity ratio relationship.

Using the same radon calculation method with a radon emanation coefficient of 0.15 for Rn-220, the default value in RESRAD model (Yu et al. 2015) for Ra-224/Rn-220, the radon flux from Rn-220 is calculated to be 58.1 pCi/m^2/sec directly above the waste layer. However, the estimated radon fluxes above the clay and other layers are essentially zero because of the very short half-life (55.6 sec) of Rn-220 that limits its migration so there is no risk for any covered scenarios.

The Rn-220 calculation indicates that Rn-220 is not a radon emission concern above the clay barriers of the EMDF cover system.

H.8. SUMMARY AND CONCLUSION

The radon flux calculation shows that emission of radon and progeny at the EMDF surface will be negligible (essentially zero) and therefore meet the DOE O 435.1 performance objective for radon release. Flux calculations assuming the loss of the upper protective layers of the cover system (erosion control and biointrusion layers), and sensitivity evaluations for higher radionuclide inventories and potential Rn-222

contributions confirm that radon flux from the EMDF will be in compliance with the 20 $pCi/m^2/sec$ performance objective.

H.9. REFERENCES

DOE 2001. *Radioactive Waste Management*, DOE Order 435.1 Chg 1 (PgChg), U.S. Department of Energy, Washington, D.C., August.

DOE 2011. *Radioactive Waste Management Manual*, DOE Manual 435.1-1 Chg 2, U.S. Department of Energy, Washington, D.C., June.

Grove 2010. MicroShield® program, V9.02, Grove Software (radiationsoftware.com), Lynchburg, VA.

Holbert, Keith E. 2006. *Radioactive Decay*. http://holbert.faculty.asu.edu/eee460/RadioactiveDecay.pdf.

NRC 1984. *Radon Attenuation Handbook for Uranium Mill Tailings Cover Design*, NUREG/CR-3533, U.S. Nuclear Regulatory Commission, Washington, D.C., April.

UCOR 2020. *Quality Assurance Report for Modeling of the Bear Creek Valley Low-level Radioactive Waste Disposal Facilities, Oak Ridge, Tennessee* UCOR-5234/R0, UCOR, Oak Ridge, TN, April.

U.S. Department of Agriculture 2013. *Science Documentation, Revised Universal Soil Loss Equation Version 2 (RUSLE2)*, U.S. Department of Agriculture, Agricultural Research Service, Washington, D.C.

Yu et al. 2015. *Data Collection Handbook to Support Modeling Impacts of Radioactive Material in Soil and Building Structures*, ANL/EVS/TM-14/4, C. Yu, J.-J. Cheng, L. Jones, Y. Wang, Y. Chia, and E. Faillace, Argonne National Laboratory for U.S. Department of Energy, Office of Science, Oak Ridge, TN, September.

ATTACHMENT H.1.
RADON ACTIVITY RATIO CALCULATIONS

This page intentionally left blank.

MicroShield 9.05
UCOR (9.05-0000)

Date	By	Checked
10/15/19		

Filename	Run Date	Run Time	Duration
U-238 Decay 1,000 yrs_Oct 2019.msd	October 15, 2019	7:28:55 AM	00:00:00

Project Info

Case Title	U-238 Decay
Description	1,000 Year Decay for Ra-226 In-Growth
Geometry	1 - Point

Dose Points

A	X	Y	Z
#1	10.0 cm (3.9 in)	0.0 cm (0 in)	0.0 cm (0 in)

Shields

Shield N	Dimension	Material	Density
Air Gap		Air	0.00122

Source Input: Grouping Method - Standard Indices
Number of Groups: 25
Lower Energy Cutoff: 0.015
Photons < 0.015: Included
Library: Grove

Nuclide	Ci	Bq
Bi-210	1.5081e-006	5.5800e+004
Bi-214	1.6533e-006	6.1172e+004
Pa-234	1.6000e-003	5.9200e+007
Pa-234m	1.0000e+000	3.7000e+010
Pb-210	1.5082e-006	5.5803e+004
Pb-214	1.6533e-006	6.1172e+004
Po-210	1.5056e-006	5.5709e+004
Po-214	1.6530e-006	6.1160e+004
Po-218	1.6536e-006	6.1185e+004
Ra-226	1.6537e-006	6.1187e+004
Rn-222	1.6536e-006	6.1185e+004
Th-230	1.2707e-005	4.7017e+005
Th-234	1.0000e+000	3.7000e+010
U-234	2.8307e-003	1.0473e+008
U-238	1.0000e+000	3.7000e+010

MicroShield 9.05
UCOR (9.05-0000)

Date	By	Checked
10/29/19		

Filename	Run Date	Run Time	Duration
U-234 Decay 1,000 yrs_Oct 2019.msd	October 29, 2019	12:55:25 PM	00:00:00

Project Info

Case Title	U-234 Decay
Description	1,000 Year Decay for Ra-226 In-Growth
Geometry	1 - Point

Dose Points

A	X	Y	Z
#1	10.0 cm (3.9 in)	0.0 cm (0 in)	0.0 cm (0 in)

Image filename: U-234 Decay 1,000 yrs_Oct 2019.html.bmp

Shields

Shield N	Dimension	Material	Density
Air Gap		Air	0.00122

Source Input: Grouping Method - Standard Indices
Number of Groups: 25
Lower Energy Cutoff: 0.015
Photons < 0.015: Included
Library: Grove

Nuclide	Ci	Bq
Bi-210	1.5903e-003	5.8841e+007
Bi-214	1.6891e-003	6.2495e+007
Pb-210	1.5904e-003	5.8843e+007
Pb-214	1.6891e-003	6.2495e+007
Po-210	1.5886e-003	5.8779e+007
Po-214	1.6887e-003	6.2482e+007
Po-218	1.6894e-003	6.2507e+007
Ra-226	1.6894e-003	6.2509e+007
Rn-222	1.6894e-003	6.2507e+007
Th-230	8.9488e-003	3.3111e+008
U-234	9.9717e-001	3.6895e+010

MicroShield 9.05
UCOR (9.05-0000)

Date	By	Checked
10/29/19		

Filename	Run Date	Run Time	Duration
Th-230 Decay 1,000 yrs_OCt 2019.msd	October 29, 2019	1:00:26 PM	00:00:00

Project Info

Case Title	Th-230 Decay
Description	1,000 Year Decay for Ra-226 In-Growth
Geometry	1 - Point

Dose Points

A	X	Y	Z
#1	10.0 cm (3.9 in)	0.0 cm (0 in)	0.0 cm (0 in)

Image filename: Th-230 Decay 1,000 yrs_Oct 2019.html.bmp

Shields

Shield N	Dimension	Material	Density
Air Gap		Air	0.00122

Source Input: Grouping Method - Standard Indices
Number of Groups: 25
Lower Energy Cutoff: 0.015
Photons < 0.015: Included
Library: Grove

Nuclide	Ci	Bq
Bi-210	3.4069e-001	1.2606e+010
Bi-214	3.4981e-001	1.2943e+010
Pb-210	3.4070e-001	1.2606e+010
Pb-214	3.4981e-001	1.2943e+010
Po-210	3.4054e-001	1.2600e+010
Po-214	3.4974e-001	1.2940e+010
Po-218	3.4988e-001	1.2946e+010
Ra-226	3.4989e-001	1.2946e+010
Rn-222	3.4988e-001	1.2946e+010
Th-230	9.9104e-001	3.6668e+010

This page intentionally left blank.

APPENDIX I.
INADVERTENT INTRUDER ANALYSIS FOR THE ENVIRONMENTAL MANAGEMENT DISPOSAL FACILITY

This page intentionally left blank.

CONTENTS

This page intentionally left blank.

FIGURES

TABLES

This page intentionally left blank.

ACRONYMS

BCV	Bear Creek Valley
C2DF	Class L-II Disposal Facility
CERCLA	Comprehensive Environmental Response, Compensation, and Liability Act of 1980
DOE	U.S. Department of Energy
DOE M	DOE Manual
DOE O	DOE Order
EMDF	Environmental Management Disposal Facility
EPA	U.S. Environmental Protection Agency
HDPE	high-density polyethylene
IHI	inadvertent human intrusion
ORNL	Oak Ridge National Laboratory
ORR	Oak Ridge Reservation
PA	Performance Assessment
QA	quality assurance
RESRAD	RESidual RADioactivity
SRSG	Single Radionuclide Soil Guideline
SWSA	Solid Waste Storage Area
WAC	waste acceptance criteria

This page intentionally left blank.

I.1 INTRODUCTION

This appendix presents the inadvertent human intrusion (IHI) evaluation conducted for the Environmental Management Disposal Facility (EMDF) Performance Assessment (PA). The IHI analysis was conducted as described in the *Disposal Authorization Statement and Tank Closure Documentation,* (U.S. Department of Energy [DOE] 2017, Sect. 2.2.2.7), which states:

> Intrusion is assumed to occur after a temporary loss of institutional controls and memory of the disposal facility. The stylized analyses (i.e., drilling and basement excavation) for inadvertent intrusion should be based on credible (reasonably expected) exposure assumptions for current site-specific practices. The likelihood of inadvertent intruder scenarios can be considered when interpreting the results of the analyses and establishing radionuclide concentrations that can be disposed in the facility, if adequate justification is provided.

The EMDF IHI analysis assumes the following exposure scenarios:

- Acute exposure associated with discovery of the facility during excavation into the EMDF cover (acute discovery)
- Acute exposure resulting from drilling through the waste (acute drilling)
- Chronic exposure to drill cuttings mixed into garden soil (chronic post-drilling).

The estimated EMDF radiological inventory (PA, Appendix B) was used with the RESidual RADioactivity (RESRAD)-OFFSITE code (Yu et al. 2007) to model doses resulting from these unlikely future intrusion scenarios. These results are used to establish compliance with DOE Order (O) 435.1 (DOE 2001) dose performance measures for IHI.

The remainder of this appendix includes a review of the EMDF cover design and estimated radiological inventory (Sect. I.2); detailed descriptions of the IHI scenarios and assumed exposure pathways (Sect. I.3); explanation of the model code implementation (Sect. I.4); presentation of results for each IHI scenario (Sect. I.5); discussion of uncertainties, sensitivity, and conservative bias (Sect. I.6); and a summary of conclusions (Sect. I.7).

I.2 COVER SYSTEM DESIGN AND ESTIMATED INVENTORY

Information provided in this section includes a description of the engineered EMDF cover system and the estimated radiological inventory for the EMDF at closure.

I.2.1 EMDF ENGINEERED COVER SYSTEM

The EMDF cover design used for the modeling and calculations consists of an 11-ft thick cover system (Fig. I.1). As shown in Fig. I.1, there is a robust biointrusion layer within 6 ft of the ground surface that consists of large cobbles, which is designed to discourage root penetration by draining water from the area and to deter burrowing animals. These coarse materials also serve to deter or discourage inadvertent human intruders attempting to drill through or excavate into the cover. Synthetic components of the cover system include geotextile layers and a 60-mil high-density polyethylene (HDPE) geomembrane overlying the

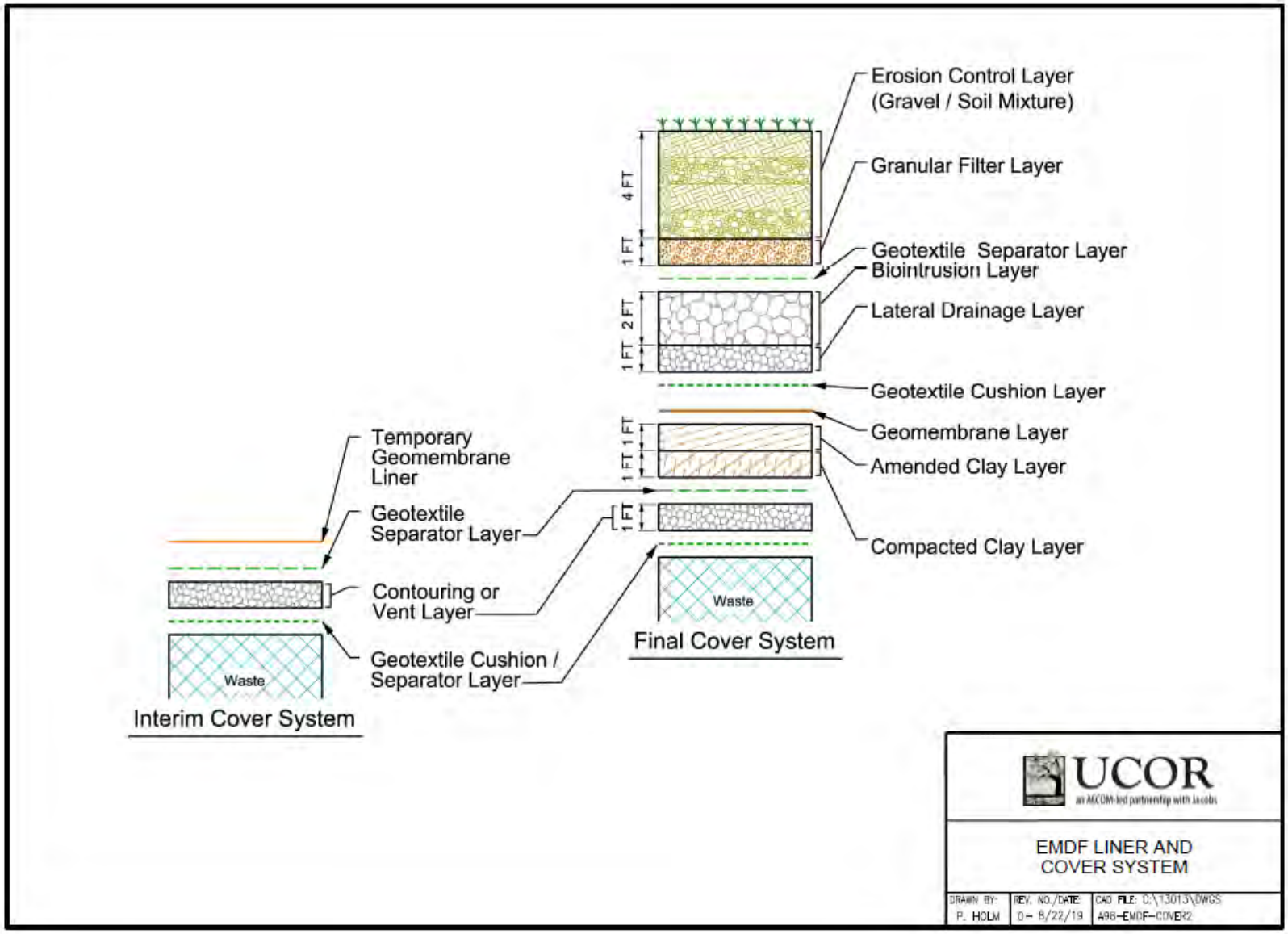

Fig. I.1. EMDF cover system

amended/compacted clay layers at the base of the cover profile. The obvious difference between this engineered profile and normal hilltop soil and subsoil conditions in this region will alert potential intruders to the unusual nature of the location.

I.2.2 EMDF RADIONUCLIDE INVENTORY

The data sources used to estimate the EMDF radiological inventory (PA, Appendix B) includes information on 70 radionuclides with half-lives greater than 1 year. Due to data quality limitations (traceability of activity data to a source), estimated average activity concentrations were developed for 61 of the 70 radionuclides. The nine radionuclides that have inventory data that could not be verified from original sources include Cd-113m, Cs-135, Kr-85, Pd-107, Se-79, Sm-151, Sn-121m, Sn-126, and Zr-93.

Radionuclides in the EMDF inventory with a half-life of less than 5 years were screened from the IHI analyses because during the first 100 years of post-closure institutional control over 20 half-lives would elapse, resulting in decay to very low concentrations. The screened radionuclides with half-lives less than 5 years include Cf-252, Cs-134, Eu-155, Fe-55, Na-22, Pm-147, and Sb-125. Th-228 has a half-life of less than 5 years, but it was retained as a persistent decay product of other longer-lived radionuclides in the EMDF inventory, including Th-232 and Ra-228.

In addition to radionuclides screened from the IHI analyses based on data source limitations and short half-life criteria, Mo-100 was removed from the simulated inventory because it is a very stable radionuclide (half-life is 8.5E+18 year) that does not have a dose conversion factor in the RESRAD-OFFSITE database. Also, the very low projected Mo-100 inventory (approximately 1.08E-05 Ci) is not expected to be a significant contributor to dose. Based on this initial screening process, 53 radionuclides were included in the IHI analyses (see Table I.1).

Table I.1. Total EMDF waste radionuclide inventory (Ci decayed to 2047)

Waste mass (g)	ORNL D&D 1.94E+11	ORNL RA 1.81E+11	Y-12 D&D Alpha-4 and Alpha-5 1.37E+11	Y-12 D&D Biology 2.81E+10	Y-12 D&D Remaining Facilities 3.03E+11	Y-12 RA 5.26E+11	EMDF Waste Total Inventory (Ci) 1.37E+12	EMDF waste average activity concentration (pCi/g)
Radio-isotope	**EMDF activity by waste stream (Ci)**							
Ac-227	7.54E-03						7.54E-03	5.50E-03
Am-241	4.09E+01	1.11E+02	2.20E-03	5.11E-03	1.80E-02	3.61E-01	1.52E+02	1.11E+02
Am-243	5.30E-01	7.12E+00					7.65E+00	5.59E+00
Ba-133	Refer to PA Appendix B, Attachment B.3 for basis of inventory estimate						4.14E+00	3.02E+00
Be-10	Refer to PA Appendix B, Attachment B.3 for basis of inventory estimate						6.52E-05	4.76E-05
C-14	1.66E+00	4.60E+00		1.17E+00			7.43E+00	5.43E+00
Ca-41	Refer to Appendix B, Attachment B.3 for basis of inventory estimate						1.09E-01	7.92E-02
Cf-249	2.80E-06						2.80E-06	2.05E-06
Cf-250	1.91E-05						1.91E-05	1.39E-05
Cf-251	5.42E-07						5.42E-07	3.96E-07
Cf-252[a]	3.37E-07						3.37E-07	2.46E-07
Cm-243	1.01E+00	1.02E-01					1.11E+00	8.10E-01
Cm-244	3.23E+02	2.53E+00	5.39E-04				3.26E+02	2.38E+02
Cm-245	9.87E-02						9.87E-02	7.21E-02
Cm-246	4.10E-01						4.10E-01	2.99E-01
Cm-247	2.68E-02						2.68E-02	1.96E-02
Cm-248	1.44E-03						1.44E-03	1.05E-03
Co-60	4.23E-02	7.90E-03	8.87E-04			4.20E-04	5.15E-02	3.76E-02

Table I.1. Total EMDF waste radionuclide inventory (Ci decayed to 2047) (cont.)

Waste mass (g)	ORNL D&D	ORNL RA	Y-12 D&D Alpha-4 and Alpha-5	Y-12 D&D Biology	Y-12 D&D Remaining Facilities	Y-12 RA	EMDF Waste Total Inventory (Ci)	EMDF waste average activity concentration (pCi/g)
	1.94E+11	1.81E+11	1.37E+11	2.81E+10	3.03E+11	5.26E+11	1.37E+12	
Radio-isotope	**EMDF activity by waste stream (Ci)**							
Cs-134[a]	5.41E-09	2.19E-08					2.73E-08	1.99E-08
Cs-137	4.11E+02	2.63E+03	2.73E-02	3.71E-03	1.42E-02	2.84E+00	3.04E+03	2.22E+03
Eu-152	7.25E+01	1.46E+00					7.40E+01	5.40E+01
Eu-154	1.65E+01	2.52E-01					1.67E+01	1.22E+01
Eu-155[a]	1.72E-02	1.44E-04					1.74E-02	1.27E-02
Fe-55[a]		2.31E-06					2.31E-06	1.68E-06
H-3	2.52E+01	3.56E+00		6.25E-02			2.88E+01	2.10E+01
I-129	9.56E-01	9.35E-02					1.05E+00	7.66E-01
K-40	1.07E+00	3.43E+00		6.27E-01		3.33E+00	8.46E+00	6.18E+00
Mo-100[a]	1.08E-05						1.08E-05	7.92E-06
Mo-93	Refer to PA Appendix B, Attachment B.3 for basis of inventory estimate						1.00E+00	7.30E-01
Na-22[a]	2.09E-06	2.63E-08					2.12E-06	1.55E-06
Nb-93m	Refer to PA Appendix B, Attachment B.3 for basis of inventory estimate						6.01E-01	4.39E-01
Nb-94	4.20E-02						4.20E-02	3.07E-02
Ni-59	7.84E+00						7.84E+00	5.73E+00
Ni-63	1.17E+02	1.62E+03		4.84E-02			1.74E+03	1.27E+03
Np-237	8.92E-02	5.08E-01	6.72E-03	6.04E-03		2.27E-01	8.37E-01	6.12E-01
Pa-231	6.15E-01						6.15E-01	4.49E-01
Pb-210	9.09E+00	4.08E-01					9.50E+00	6.93E+00
Pm-146	2.28E-04						2.28E-04	1.66E-04
Pm-147[a]	5.49E-04	1.69E-05					5.66E-04	4.13E-04
Pu-238	1.43E+02	9.86E+01	2.52E-02		1.20E-01	4.62E-03	2.42E+02	1.77E+02
Pu-239	4.61E+01	1.04E+02			2.31E-02	3.12E-01	1.50E+02	1.10E+02
Pu-240	6.81E+01	9.18E+01	9.29E-03	5.07E-03			1.60E+02	1.17E+02
Pu-241	1.33E+01	5.12E+02					5.25E+02	3.83E+02
Pu-242	3.55E-02	4.10E-01					4.45E-01	3.25E-01
Pu-244	9.49E-03						9.49E-03	6.93E-03
Ra-226	5.68E-01	7.08E-01		2.80E-02		7.63E-01	2.07E+00	1.51E+00
Ra-228	1.27E-03	2.52E-03			5.17E-02	1.41E-03	5.69E-02	4.15E-02
Re-187	4.40E-06						4.40E-06	3.21E-06
Sb-125[a]	7.82E-08						7.82E-08	5.71E-08
Sr-90	4.21E+02	7.50E+01		4.93E-02	5.02E-02		4.96E+02	3.62E+02
Tc-99	2.57E+00	7.11E-01	1.48E-01	1.14E+00	2.36E-01	2.43E+00	7.23E+00	5.28E+00
Th-228	2.25E-07	3.40E-10	8.14E-08	3.58E-07	4.78E-06		5.45E-06	3.98E-06
Th-229	3.36E-01	1.44E+01			1.43E-02		1.47E+01	1.08E+01
Th-230	3.30E-01	3.81E+00	5.92E-02		2.38E-02	7.20E-01	4.94E+00	3.61E+00
Th-232	2.32E-01	1.69E+00	5.14E-02	2.24E-02	1.98E-01	6.87E+00	9.07E+00	6.62E+00
U-232	1.62E-01	2.61E+01					2.63E+01	1.92E+01
U-233	5.15E+01	5.27E+01		2.71E+00	3.33E-01		1.07E+02	7.83E+01
U-234	2.15E+00	2.72E+01	1.25E+00	2.34E+00	1.58E+03	8.24E+00	1.62E+03	1.19E+03
U-235	8.15E-02	4.23E-01	1.02E-01	2.02E-01	9.57E+01	5.84E+00	1.02E+02	7.47E+01
U-236	5.14E-02	1.95E-01	5.22E-02	1.19E-01	2.26E+01	1.19E-01	2.32E+01	1.69E+01
U-238	1.32E+00	5.27E+00	4.71E+00	9.56E+00	8.83E+02	7.92E+01	9.83E+02	7.18E+02

[a]Eliminated from consideration for the inadvertent human intrusion analysis.

D&D = deactivation and decommissioning
EMDF = Environmental Management Disposal Facility
ORNL = Oak Ridge National Laboratory
PA = performance assessment
RA = remedial action
Y-12 = Y-12 National Security Complex

The estimated EMDF radiological inventory is expressed in terms of as-generated, waste average activity concentrations in pCi/g. A detailed review of the EMDF inventory development and data sources is presented in Appendix B of this PA report. The radiological inventory concentrations are adjusted (as-generated waste average values given in Table I.1 are multiplied by a factor of 0.531) to account for the mass of clean soil used to fill voids during disposal operations, providing as-disposed average activity concentrations to be used as source concentrations in the IHI analysis and other PA models. The derivation of the factor used for this adjustment is presented in Sect. 3.2.2.5 of the main PA text. For highly mobile radionuclides (C-14, H-3, I-129, and Tc-99) loss of inventory due to leaching during the 25-year operational period was quantified and as-disposed waste concentrations were adjusted accordingly. The adjusted as-disposed average concentrations for the four highly mobile radionuclides are referred to as post-operational waste concentrations. Quantification of operational period leaching and post-operational waste concentration adjustment is further discussed in Appendix G (Sect. G.4.3.4) of this PA. Additional calculations for IHI analysis are made to reduce activity concentrations to account for mixing of contaminated and clean materials. These adjustments are explained in Sect. I.4 and are detailed in the Quality Assurance (QA) documentation developed for the IHI scenarios (UCOR, an Amentum-led partnership with Jacobs, 2020).

I.3 IHI SCENARIOS FOR EMDF

Selection of IHI scenarios was guided by consideration of EMDF site characteristics and facility design, as well as review of IHI analyses performed for Solid Waste Storage Area (SWSA) 6 in Melton Valley near the Oak Ridge National Laboratory (ORNL) and for a proposed tumulus disposal facility, the Class L-II Disposal Facility (C2DF) in Bear Creek Valley (BCV) near the proposed EMDF site. Both the SWSA 6 PA (ORNL 1997a) and the C2DF PA (ORNL 1997b) considered chronic and acute scenarios, but did not analyze the acute scenarios because the chronic exposures were bounding. Those two IHI analyses considered chronic exposures that assumed construction of a home on top of the disposal units, either before (residential scenario) or after (agricultural scenario) the failure of engineered barriers that would prevent direct excavation into the waste.

Because of the robust final cover design of EMDF (Fig. I.1) in comparison to either SWSA 6 or the C2DF, a large excavation on top of EMDF that would penetrate the waste is highly unlikely. Accordingly, this IHI analysis for EMDF considers an acute discovery scenario (described below) that involves attempted excavation into the final cover for a residence and also considers an acute drilling scenario and a chronic post-drilling (agricultural) scenario that involve direct contact with the waste.

The three IHI exposure scenarios selected assume that intrusion is an accidental occurrence resulting from a temporary loss of institutional control. The occurrence of accidental intrusion also presumes a loss of societal memory of the Oak Ridge Reservation (ORR) and radioactive waste disposal facilities in the area, despite existing long-term stewardship commitments of DOE and the likelihood of legal controls such as property record restrictions and property record notices. For each of the IHI scenarios, active institutional controls are assumed to preclude intrusion for the first 100 years following closure of the disposal facility. The following subsections describe the two acute scenarios and the chronic exposure scenario. A summary of the three IHI scenarios analyzed for EMDF are provided in Table I.2.

Table I.2. Summary of IHI scenarios analyzed for EMDF

Scenario type/name	DOE O 435.1 performance measure	Exposure scenario description
Acute discovery (cover excavation)	500 mrem	Intruder initiates excavation into EMDF cover but ceases digging before exposing waste. Includes hypothetical exposure to external radiation.
Acute drilling (irrigation water well)	500 mrem	Intruder drills irrigation well through waste and is exposed to waste in exhumed drill cuttings. Includes hypothetical exposure to external radiation, inhalation, and incidental ingestion of contaminated soil.
Chronic post-drilling (subsistence garden)	100 mrem/year	Intruder uses contaminated drill cuttings to amend soil in a vegetable garden. Includes hypothetical exposure to external radiation, inhalation, and ingestion of contaminated food and soil.

DOE O = U.S. Department of Energy Order
EMDF = Environmental Management Disposal Facility
IHI = inadvertent human intrusion

I.3.1 ACUTE IHI SCENARIOS AND EXPOSURE PATHWAYS

Two acute exposure scenarios were evaluated. The acute discovery scenario assumes that an intruder attempts to excavate a basement for a home on the disposal site but stops prior to excavating into the waste and moves elsewhere because of the unusual nature of the engineered material layers encountered. Homes with basements are less common in the humid southeastern U.S. due to limits on construction (clays and shallow water tables) and the lack of structural benefits compared to northern climates, making the discovery scenario less likely (R. G. Smith 2015). The acute drilling scenario assumes that an irrigation well was drilled through the waste, bringing contaminated material to the surface as drill cuttings and causing an acute exposure to the well drillers.

I.3.1.1 Acute Discovery Scenario (Cover Excavation)

The likelihood of potential intruders choosing to excavate on EMDF (rather than a more easily accessible site) is low because of the steep side slopes of the closed landfill. The acute discovery analysis assumes that the intruder begins excavating but stops digging upon reaching the geotextile and HDPE geomembrane layer overlying the amended clay barrier (Fig. I.1). This discovery and decision to cease digging occurs after excavating through 8 ft of engineered cover materials (including the vegetated surface layer), filter layer, biointrusion layer, and lateral drainage layer (Fig. I.2). It is assumed that 3 ft of undisturbed barrier material remains between the bottom of the excavation and the underlying waste.

For this scenario, only the external radiation exposure pathway (photon emission) is considered for the hypothetical intruder. The inhalation and ingestion pathways are not considered because it is assumed that the clay barrier materials in the cover remain undisturbed and saturated and excavation does not penetrate into the waste. Shielding by the clay barrier is assumed to eliminate alpha and beta-particle exposure.

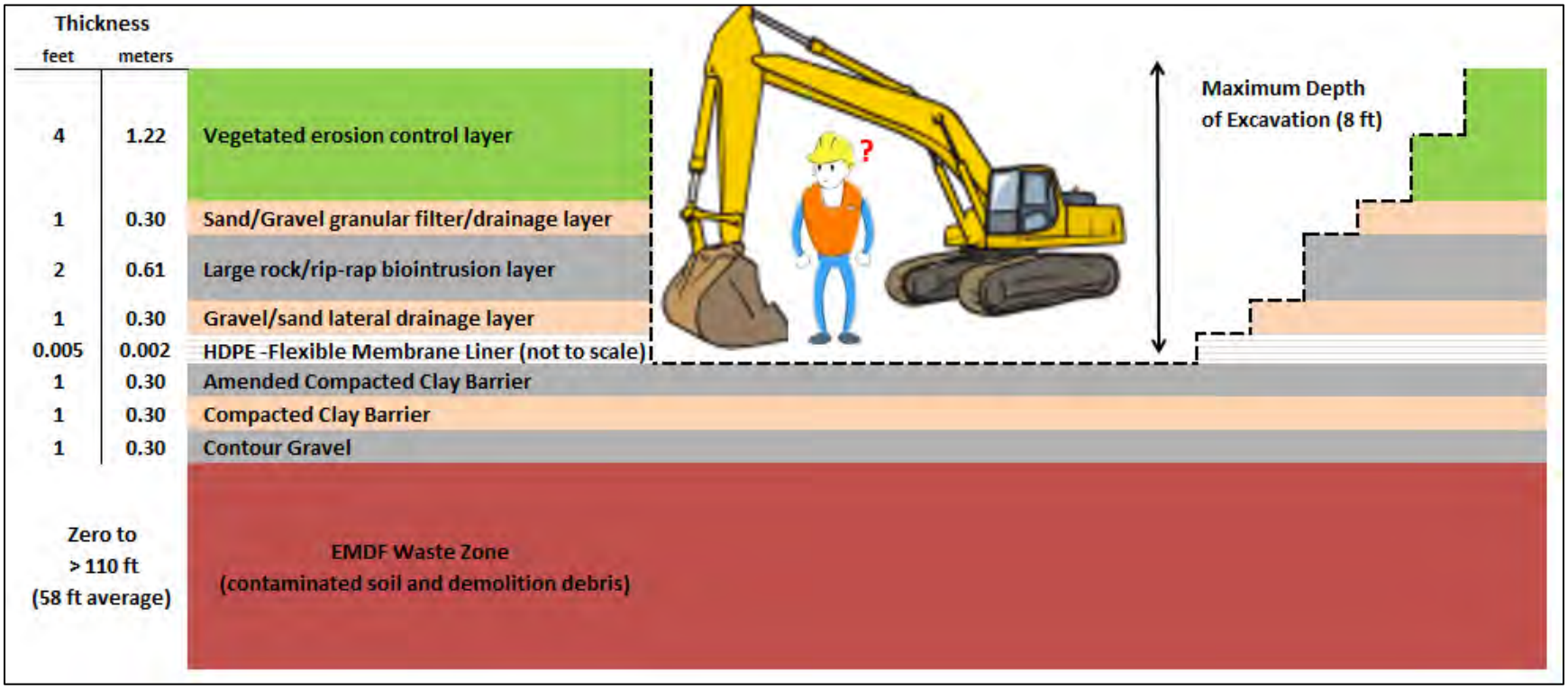

Fig. I.2. EMDF cover system schematic and acute discovery IHI scenario

I.3.1.2 Acute Drilling Scenario (Irrigation Well)

For the acute drilling scenario (Fig. I.3), intruders are assumed to drill a well for irrigation on EMDF. This scenario is highly unlikely given that drilling in more accessible areas at lower elevations would be much more cost effective due to the shallow depth to groundwater. This exposure scenario also assumes that the drilling crew is not deterred by encountering the large rocks in the biointrusion layer, structural steel, concrete, or rebar in the waste zone, or by the exhumation of any of these or other unusual materials in the drill cuttings.

The following exposure pathways are considered for the acute drilling scenario:

- External exposure to radiation from the unshielded cuttings pile containing waste
- Inhalation of radionuclides suspended in air from the uncovered cuttings pile containing waste
- Incidental ingestion of soil containing radionuclides from the uncovered cuttings pile containing waste.

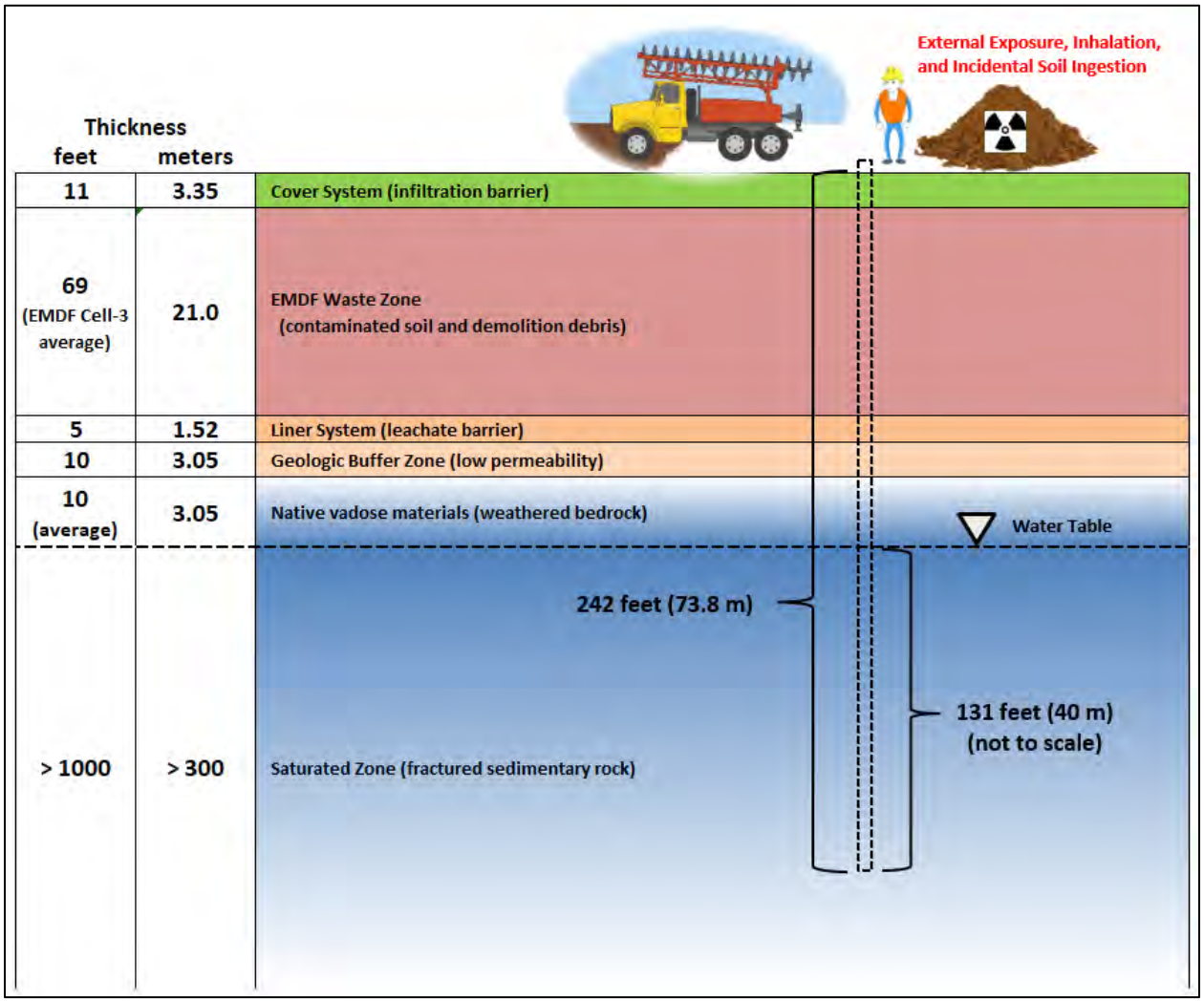

Fig. I.3. EMDF schematic profile and acute drilling IHI scenario

I.3.2 CHRONIC IHI SCENARIO AND EXPOSURE PATHWAYS

The chronic IHI scenario selected for EMDF consists of post-drilling exposure to contaminated garden soil and contaminated produce grown in that soil. The intruder is assumed to drill a residential well on EMDF and mix the drill cuttings into the garden soil to grow food for human consumption and feed for livestock (Fig. I.4). This scenario is highly unlikely in terms of the location selected for the well (as for the acute drilling scenario) and in the required assumption that the contaminated cuttings are indistinguishable from native soil and used to amend the garden soil.

The chronic post-drilling scenario only considers exposures after drilling and construction of the residential well. The following exposure pathways are considered:

- Ingestion of vegetables grown in contaminated garden soil
- Incidental ingestion of contaminated garden soil
- External exposure while working in the garden
- Inhalation exposure while working in the garden.

To add conservatism, other exposure pathways that are less likely to occur are also simulated, including the following:

- Ingestion of contaminated milk from animals eating feed from the garden
- Ingestion of contaminated meat from animals eating feed from the garden.

Groundwater transport pathways are not included in the IHI scenarios and are not modeled, consistent with DOE guidance (DOE 2017). Radionuclide release associated with groundwater and surface water pathways is considered in the all-pathways dose analysis of the PA (Sect. 4.5 of the PA) and evaluated relative to the 25 mrem/year performance objective for public protection. Similarly, the water resource protection analysis (Sect. 4.7 of the PA) evaluates the potential impacts to groundwater and surface water relative to applicable water quality standards.

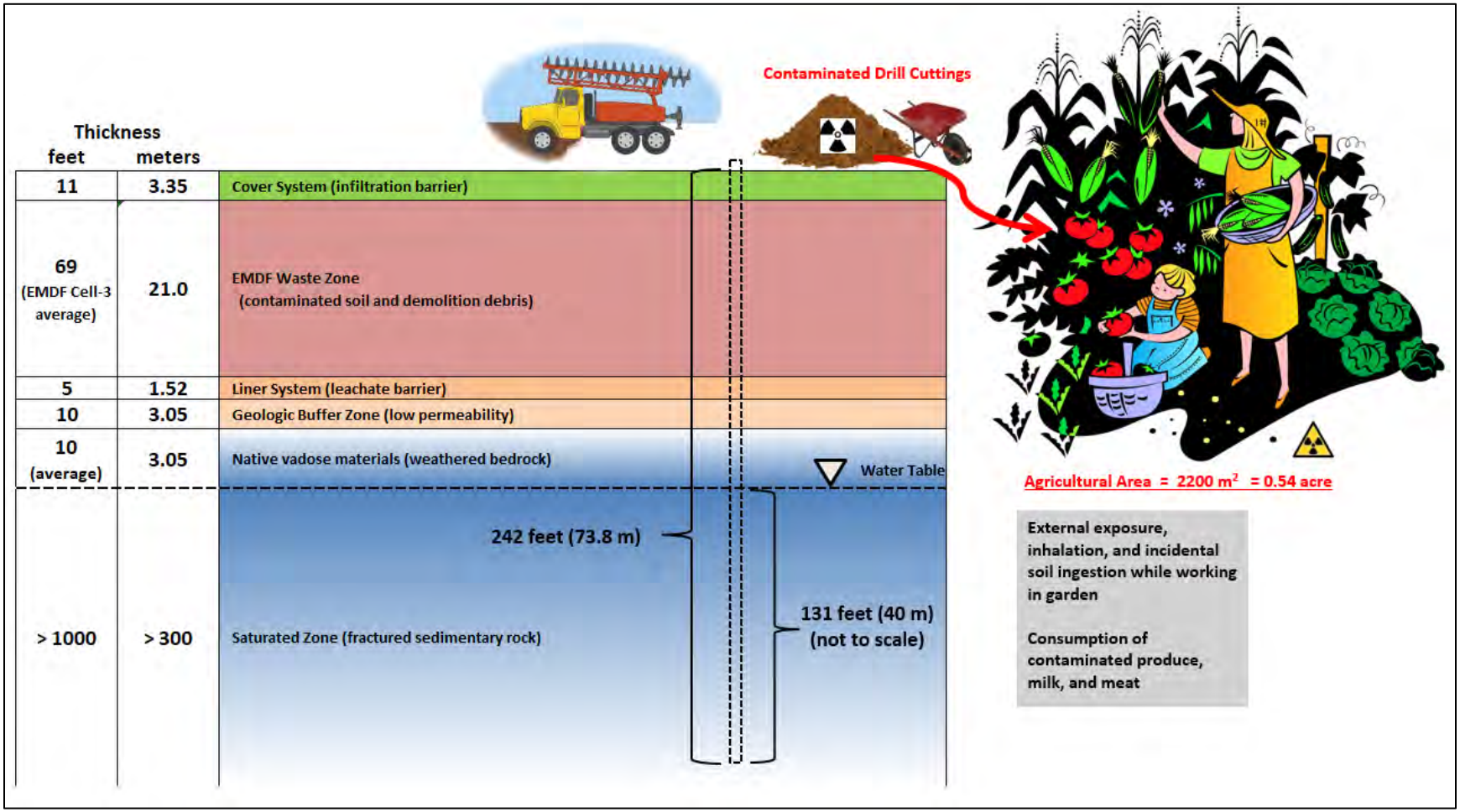

Fig. I.4. EMDF schematic and chronic post-drilling IHI scenario.

I.4 MODELING APPROACH

The RESRAD-OFFSITE (Yu et al. 2007) Version 3.2 model was used for estimating doses to a hypothetical inadvertent intruder under each of the three exposure scenarios. RESRAD-OFFSITE was selected for the IHI dose analysis because the code package offers an integrated dose analysis tool specifically tailored to simulating transport of and exposure to radiological contamination. In addition, RESRAD-OFFSITE is publicly available, providing easy access for building stakeholder confidence in model development and results.

For the modeling of IHI dose, it is assumed that the waste disposal in the EMDF is completed at time zero, the site is under active institutional control for the next 100 years, and that inadvertent intrusion can occur at any time after loss of active control of the site. Modeled radiological dose for the period between 100 and 1000 years post-closure was the primary basis for analyzing EMDF compliance with IHI dose performance measures specified in DOE Manual (M) 435.1-1 (DOE 2011). RESRAD-OFFSITE simulations were completed to 10,000 years to provide information on potential long-term increases in predicted dose that occur following the 1000-year compliance period.

In general, simulation of IHI exposure using RESRAD-OFFSITE involves assumptions required for the calculation of average radionuclide concentrations in exhumed drill cuttings or garden soil and selection of the relevant exposure pathways for each exposure scenario. For IHI scenario modeling, the RESRAD-OFFSITE release rate (leach rate) was set to zero to effectively eliminate leaching of contamination from the waste, a conservative bias toward higher estimated dose from the water-independent pathways. Similarly, precipitation input was set to the near-zero value of 1E-06 m/year and irrigation of the garden area was assumed to be zero for the chronic well drilling scenario.

RESRAD-OFFSITE model setup and key parameter assumptions for each scenario are described in the following subsections. A comprehensive list of RESRAD-OFFSITE parameters for each IHI model is included in Attachment I.1. Additional detail on model parameterization and supporting calculations are provided in the QA documentation for the IHI analyses (UCOR 2020).

I.4.1 ACUTE DISCOVERY SCENARIO

The acute discovery scenario assumes that an intruder attempts to excavate a basement for a home on the disposal site. The key assumption is that the intruder stops excavation activities upon reaching the geotextile cushion and HDPE geomembrane below the drainage layer, leaving 3 ft of earthen materials between the bottom of the excavation and the underlying waste (Fig. I.2). Although this assumption credits the cover system design for limiting the maximum depth of excavation to 8 ft (because of the unusual nature of the materials being excavated), the intruder dose resulting from a 10-ft excavation depth is also evaluated for comparison. To provide additional pessimistic bias, it is also assumed that the maximum depth of excavation is achieved over the full basement area immediately, after which exposure to external radiation occurs over the assumed duration of excavation.

The assumptions underlying the acute discovery scenario adopted for the EMDF IHI analysis are similar to those made for the (acute) discovery and (chronic) residential scenarios considered for the SWSA 6 PA (ORNL 1997a, Appendix G, pages G-5 to G-7), but reflect differences in the types of engineered barriers between the two sites. Those SWSA 6 IHI scenarios assume that an intact engineered barrier (reinforced concrete) prevents excavation directly into buried waste by either deterring completion of a dwelling on the site (discovery) or by permitting construction on top of the intact barrier (residential). In either case, external exposure to radiation from the shielded waste is the only exposure pathway considered. For the EMDF

discovery scenario, the thickness and material characteristics of the engineered cover system permit a substantial excavation (8 to 10 ft deep) to occur without exposing the waste, but the man-made appearance of the exposed cover system profile is credited for deterring completion of the excavation and construction of a residence on top of EMDF. A similar discovery scenario for IHI was analyzed for the Portsmouth On-site Waste Disposal Facility (Savannah River National Laboratory 2014), which is very similar in design to EMDF.

For the EMDF analysis, only the dose resulting from external exposure to radiation that penetrates the residual materials (lower 3 ft of the 11-ft EMDF total cover thickness) overlying the waste is modeled (Fig. I.2). Formulation of the expression for calculating dose due to external radiation is given in the RESRAD-OFFSITE User's Manual (Yu et al. 2007, pages 6-1 to 6-2). Mathematical expressions for the conceptual model of the zone of primary contamination, including a clean cover layer on top of the waste, are described in detail in the RESRAD-OFFSITE User's Manual (Yu et al. 2007 pages 2-1 to 2-3). The materials of the EMDF cover layer are assumed to remain uncontaminated, and the RESRAD-OFFSITE formulation for mixing between the residual clean cover and the underlying contaminated zone is rendered inactive by setting the depth of surface mixing to a value (0.15 m) less than the clean cover thickness (approximately 0.91 m) and setting the surface erosion parameters to zero. Processes that could lead to contamination of the cover material such as bioturbation by burrowing animals or upward diffusion from the waste are inhibited by the overall thickness of the cover design and robust biointrusion barrier (Fig. I.1) and by the persistent downward flux of water into the waste zone expected in a humid climate once the HDPE membrane is no longer effective in limiting infiltration.

Major assumptions and calculated parameter values for the EMDF acute well drilling scenario include the following:

- Thickness of clean cover material overlying the waste: The assumed thickness of residual uncontaminated material at the bottom of the excavation (3 ft) is based on the total cover thickness specified in the conceptual design for the EMDF cover system (11 ft, see Fig. I.1) and the assumption that excavation ceases after encountering the HDPE membrane at the interface between the lateral drainage layer and the amended clay barrier at a depth of 8 ft from the surface.
- Occupation/exposure times: Excavation for the acute discovery scenario is assumed to take place over ten 8-hour days, for a total of 80 hours. This assumption is conservative in terms of the long duration of excavation (typical excavations for home construction require 1 to 3 days) and because the exposure to external radiation for the full 80-hour duration is assumed to occur at the maximum 8-ft excavation depth (3 ft above the top of waste). The calculated occupancy factor for RESRAD-OFFSITE (outdoor annual time fraction on primary contamination) is 0.0091 = [(80 hours/year)/((365.25 days/year)× (24 hours/day))].

I.4.2 ACUTE WELL DRILLING SCENARIO

The acute well drilling scenario assumes that an intruder drills an irrigation well directly through a disposal unit (Fig. I.3). The acute well drilling scenario only considers exposures during the short period of time for drilling and construction of the well, during which the hypothetical intruder could be exposed to an unshielded cuttings pile for an extended period. For the EMDF acute drilling scenario, it is assumed that, consistent with local practices for water supply wells, drill cuttings would be handled manually (with shovels) as material is brought to the surface and accumulates near the drilling rig (Fig. I.3). Periodically, accumulated cuttings would be relocated with grading equipment to provide working space for the drilling crew. Exposure to external radiation, inhalation of contaminated particulates, and (incidental) soil ingestion

by a member of the drill crew is assumed to occur during the period of drilling and distribution of the drill cuttings (both clean and contaminated).

RESRAD-OFFSITE simulation of external exposure, inhalation, and (incidental) soil ingestion requires specifying the thickness and radionuclide concentrations of the drill cuttings to which a driller would be exposed, as well as the duration of (acute) exposure. Mathematical expressions for the conceptual model of the zone of primary contamination are described in detail in the RESRAD-OFFSITE User's Manual (Yu et al. 2007, pages 2-1 to 2-3). The thickness of the clean cover is assumed to be zero. Assumed values for atmospheric particulate loading and soil ingestion during drilling also are required. Formulation of the expressions for calculating dose due to external radiation and inhalation of contaminated dust are also given in the RESRAD-OFFSITE User's Manual (Yu et al. 2007, pages 6-1 to 6-3). Similarly, formulation of the expressions for calculating dose due to incidental ingestion of contaminated soil is given on pages 6-4 and 6-5 of the User's Manual.

Major assumptions and calculated parameter values for the EMDF acute well drilling scenario include the following:

- Waste thickness at well location: For both the acute and chronic well drilling scenarios, the waste thickness at the well drilling location is assumed to be 68.71 ft, equal to the average waste thickness in EMDF disposal Cell 3 based on the preliminary design for the disposal facility (UCOR 2020). The average EMDF waste thickness is approximately 57.5 ft, and the maximum thickness is approximately 113 ft. The assumed thickness of waste at the well location is used to estimate the average concentrations of radionuclides in drill cuttings brought to the surface.

- Radioactivity concentration of mixed drill cuttings: For the acute drilling scenario, the post-operational waste concentrations are adjusted to account for co-mingling of clean drill cuttings with waste as materials are brought to the surface. The calculation of dilution of exhumed waste (assumed to be indistinguishable from natural materials) with clean cuttings is based on the fractional thickness of the waste zone relative to the total length of the borehole (Fig. I.3). The borehole is assumed to be completed at a depth equivalent to 131 ft below the estimated water table elevation, or 242 ft below the surface of the disposal facility. The assumed depth of the borehole is consistent with data for water wells in the local Oak Ridge area available from the Tennessee Department of Environment and Conservation. The calculated dilution factor applied to the post-operational waste concentrations is thus equal to 68.71 ft/242 ft = 0.284.

  The approach to deriving the average (diluted) activity concentration of the mixed drill cuttings for use as the RESRAD-OFFSITE contaminated soil concentration implies the assumption of complete and uniform mixing of all the material exhumed from the borehole. However, the use of this depth-averaged value can also be conceptualized as accounting for the variability in proximity to waste and exposure over time that would be expected as clean and contaminated materials are brought to the surface, accumulated, and distributed over the drilling site. The use of the depth-averaged concentration combined with an assumed thickness of spread cuttings to estimate external exposure over a given duration is thus a reasonable approximation of a fairly complex period of variable exposure over time.

- Borehole diameter and average thickness of spread cuttings: The borehole diameter is assumed to be 18 in., which is representative of a well drilled for irrigation in East Tennessee. The larger irrigation well diameter assumed for the acute drilling scenario provides a measure of pessimistic bias relative to the smaller residential well assumed for the chronic post-drilling scenario. The total combined volume of waste and clean drill cuttings based on the assumed borehole length and diameter is 427 cf. The mixed clean cuttings and exhumed waste from the borehole are assumed to be spread over an area of 2150 sq ft, resulting in an average thickness of 0.20 ft (2.4 in.). This value is input as the thickness of

the primary contamination for RESRAD-OFFSITE dose analysis. Sensitivity of the modeled dose to assumptions that affect the calculated average thickness of cuttings is addressed in Sects. I.5 and I.6.

- Occupation/exposure duration: For the acute drilling scenario, the duration of exposure is assumed to be 30 hours, the equivalent of three 10-hour working days. A more realistic assumption for the time required to drill an approximately 250-ft-deep well using typical drilling equipment would be less than 30 hours. The calculated occupancy factor for RESRAD-OFFSITE (outdoor annual time fraction on primary contamination) is 0.0034 = (30 hours/year)/(365.25 days/year×24 hours/day).
- Incidental soil ingestion: For both the acute drilling and chronic post-drilling scenarios, the incidental soil ingestion rate is assumed to be 100 mg/day, consistent with the RESRAD-OFFSITE default value and the U.S. Environmental Protection Agency (EPA) recommended value for outdoor workers (EPA 2014).
- Inhalation parameters: For both the acute drilling and chronic post-drilling scenarios, the average mass loading of airborne particulates is assumed to be 0.001 g/m^3, a value representative of construction activities (Maheras et al. 1997). This particulate loading is a factor of 10 larger than the RESRAD-OFFSITE default value. The annual inhalation rate for both scenarios is set at the RESRAD-OFFSITE default value of 8400 m^3/year.

I.4.3 CHRONIC POST-DRILLING SCENARIO

The chronic post-drilling scenario assumes that a hypothetical intruder drills a residential well directly through the disposal unit and then mixes contaminated drill cuttings into the soil in a garden used to grow food for people and livestock (Fig. I.4). The chronic IHI scenario only considers exposure that follows drilling and construction of the well, which includes exposure from external radiation, inhalation of dust, and soil ingestion that occurs during the portion of time that the intruder works in the garden.

RESRAD-OFFSITE simulation of external exposure, inhalation of contaminated dust, and ingestion of contaminated food and soil requires specifying the thickness and radionuclide concentrations of the garden soil as well as the duration of exposure. Mathematical expressions for the conceptual model of the zone of primary contamination are described in detail in the RESRAD-OFFSITE User's Manual (Yu et al. 2007, pages 2-1 to 2-3). The thickness of the clean cover is assumed to be zero. Assumed values for atmospheric particulate loading and soil ingestion during gardening also are required. Formulation of the expressions for calculating dose due to external radiation and inhalation of contaminated dust are given in the RESRAD-OFFSITE User's Manual (Yu et al. 2007, pages 6-1 to 6-3). Similarly, formulation of the expressions for calculating dose due to contaminated soil and food is given on pages 6-4 and 6-5 of the user's manual.

Major assumptions and calculated parameter values for the chronic well drilling scenario include the following:

- Assumptions for waste thickness at the well location (68.71 ft), borehole depth (242 ft), and incidental soil ingestion rate (100 mg/day) are identical to those made for the acute drilling scenario. Inhalation parameter values are also identical to the acute drilling scenario. Values for agricultural and animal product (beef, poultry, eggs, milk) transfer factors are set to values published by the Pacific Northwest National Laboratory (PNNL) (PNNL 2003), which are identical to the values used in the base case model.
- Borehole diameter and exhumed volume of waste*:* The borehole diameter is assumed to be 12 in. (0.305 m), which is representative of a well designed for residential use in the region. The resulting volume of exhumed waste is 54 cf (1.53 m^3).

- Tilling and dilution of contaminated drill cuttings into garden soil: The total volume of contaminated drill cuttings (54 cf) is assumed to be completely and uniformly tilled into uncontaminated surface soil to a depth of 1 ft over an area of approximately one-half acre (2200 m^2). Average radionuclide concentrations in the amended garden soil are calculated by applying a dilution factor equal to the ratio of the volume of waste contained in drill cuttings to the total volume of uncontaminated garden soil: 1.53 m^3 / (0.305 m × 2200 m^2) = 0.00228, or approximately 0.2 percent. Radionuclide concentrations (post-operational, see Sect. I.4.2) are multiplied by the tilling dilution factor to give the input soil concentrations for RESRAD-OFFSITE dose analysis. This approximation assumes that the volume of cuttings is negligible compared to the total soil volume and neglects any difference in the average dry bulk densities of the waste and the garden soil. Accounting for a soil/waste bulk density ratio of 3/4 would increase the calculated dilution factor by 1/3 to approximately 0.3 percent. The implications of using this simplified calculation of the tilling dilution factor for the intruder dose analysis are addressed in Sect. I.5 in the context of uncertainty and overall pessimistic bias in dose calculations.
- Fraction of food obtained from contaminated area: The fraction of food for humans and livestock obtained from the contaminated garden is conservatively assumed to be 0.5 (50 percent). The fraction of milk from the dairy cows raised on the contaminated area is assumed to be 0.5 (50 percent) and the fraction of meat (beef, poultry, eggs) from the contaminated area is assumed to be 0.25 (25 percent).
- Occupation/exposure duration: For the chronic post-drilling scenario, the duration of exposure for the external radiation, inhalation, and soil ingestion pathways is expressed in terms of the outdoor time fraction spent in the garden. The value for this parameter is assumed to be 1/6, equivalent to 4 out of every 24 hours.

I.5 RESULTS OF ANALYSES

I.5.1 ACUTE DISCOVERY SCENARIO RESULTS

Predicted dose over time for the acute discovery scenario is presented in Fig. I.5. The total dose (i.e., dose from all simulated radionuclides summed) at 100 years post-closure is 1.3E-04 mrem. Total dose decreases to a minimum of 6.7E-05 mrem at approximately 540 years and gradually increases through 10,000 years as concentrations of radioactive progeny increase; total dose at 10,000 years is 2.5E-04 mrem. The predicted dose is sensitive to the assumed thickness of the uncontaminated material (clean cover) overlying the waste. Decreasing the assumed thickness from 3 ft to 1 ft increases the dose by approximately three orders of magnitude (dashed curve in Fig. I.5). This sensitivity case represents the assumption that a 10-ft-deep basement excavation is completed in the EMDF cover, which results in an estimated dose that is three to four orders of magnitude smaller than the acute intrusion performance measure of 500 mrem.

Primary contributors to the acute discovery IHI dose prior to 1000 years post-closure include Th-232, Cs-137, and U-232 (Fig. I.6). After 1000 years, other isotopes of uranium, particularly U-234 and progeny, become proportionally significant and eventually predominant dose contributors.

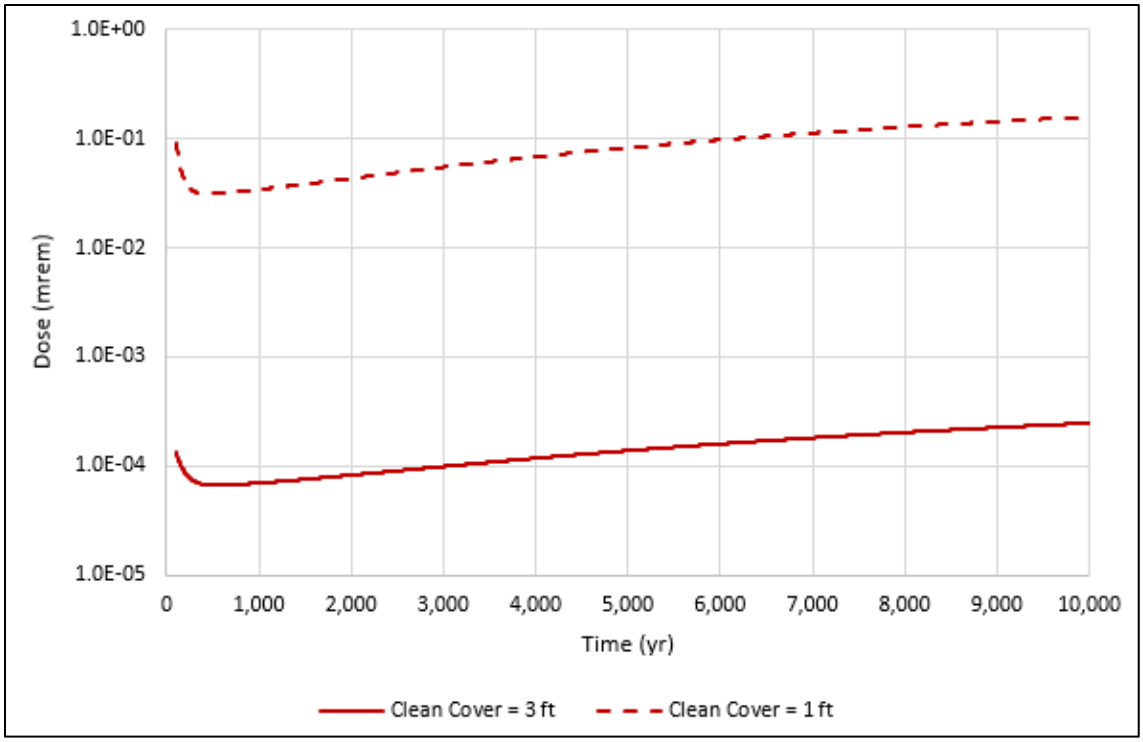

Note that the vertical axis is logarithmic for clarity.

Fig. I.5. Acute discovery scenario total dose (all radionuclides summed: years 100 to 10,000)

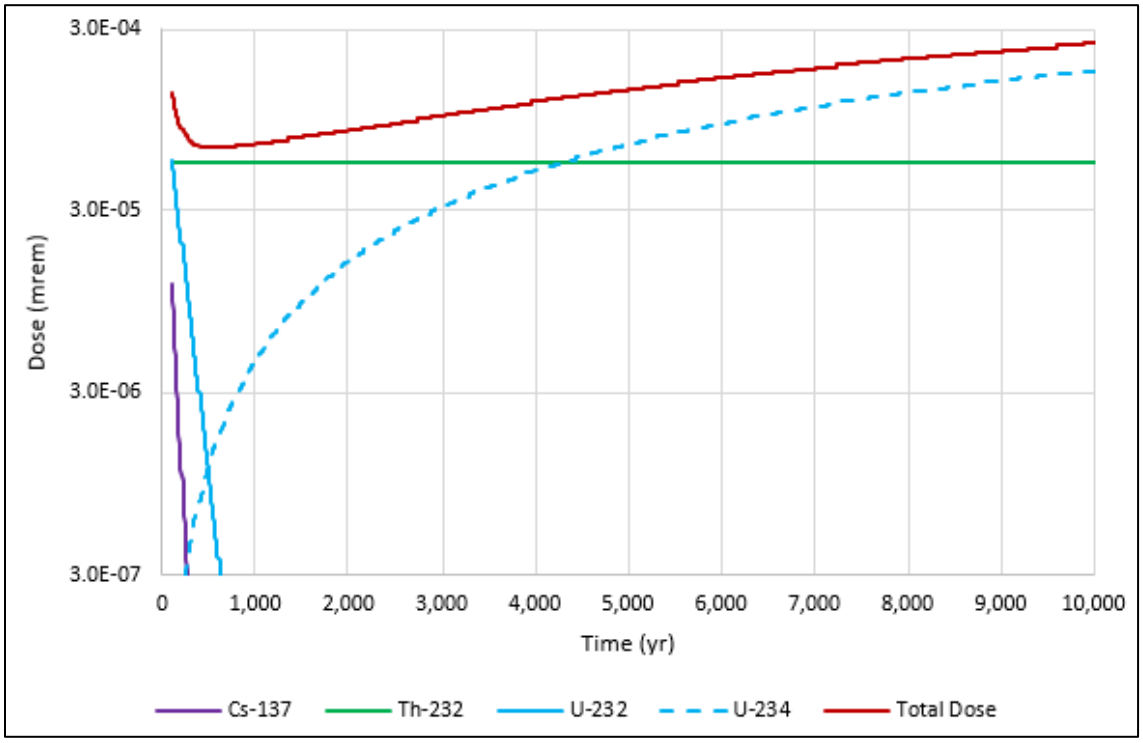

Note that the vertical axis is logarithmic for clarity

Fig. I.6. Acute discovery scenario dose contributions by radionuclide for years 100 to 10,000

I.5.2 ACUTE DRILLING SCENARIO RESULTS

Predicted dose over time for the acute drilling scenario is presented in Fig. I.7. The total dose (all radionuclides and pathways summed) at 100 years post-closure is 0.38 mrem. Total dose decreases to a minimum of 0.17 mrem at approximately 600 years and gradually increases through 10,000 years as concentrations of radioactive progeny increase; total dose at 10,000 years is 0.42 mrem.

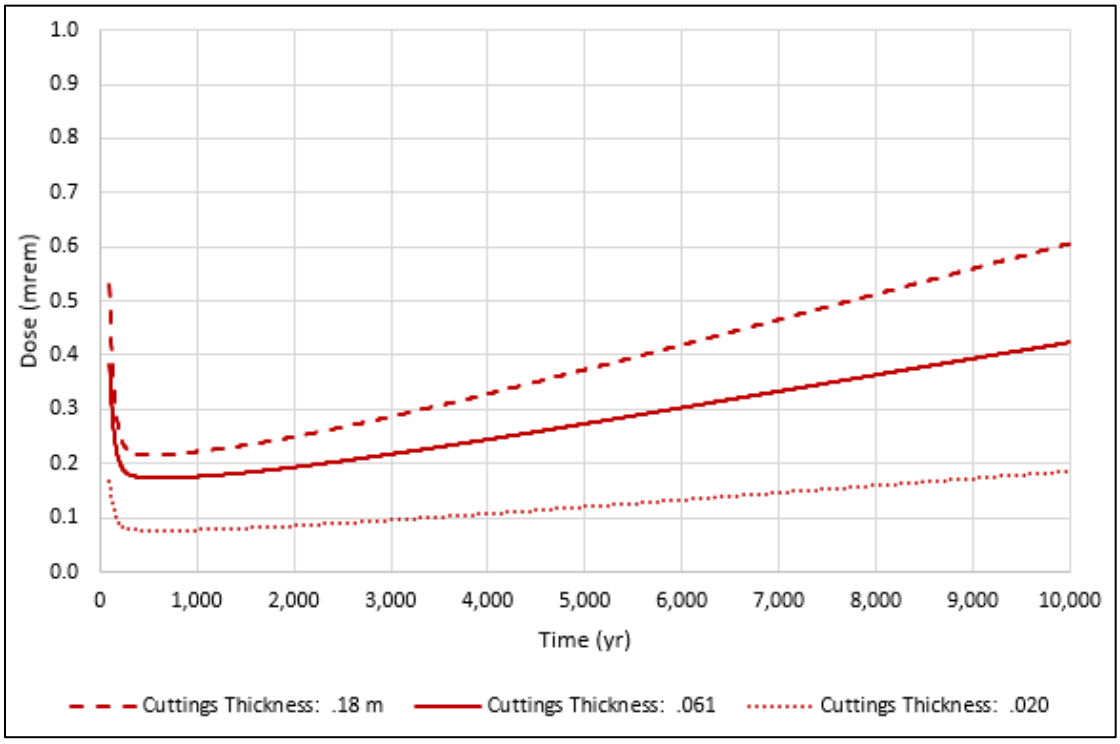

Fig. I.7. Acute drilling scenario total dose (all radionuclides and pathways summed: years 100 to 10,000)

The dotted and dashed curves shown on Fig. I.7 represent model sensitivity to the calculated value for the thickness of mixed drill cuttings and indicate dose associated with the thickness increased by a factor of three (dashed) and decreased by a factor of three (dotted). For the increased thickness of cuttings (0.18 m), the acute dose remains less than 1 mrem between 100 and 10,000 years, a value much less than the acute intrusion performance measure of 500 mrem. Parameter values that affect the calculated average thickness of cuttings include borehole depth and diameter and the area over which cuttings are spread.

The dose contributions for each of the simulated exposure pathways for the acute drilling scenario include external (direct) radiation, inhalation, and incidental soil ingestion and are presented in Fig. I.8. The direct external dose (solid red curve) is the largest contributor to the total dose during the simulation period, whereas soil ingestion contributes least to the total acute drilling intruder dose.

Primary contributors to the acute drilling IHI annual dose prior to 1000 years post closure include Cs-137, U-238, Th-232, and U-235 (Fig. I.9). The increase in annual dose after 600 years is driven by U-234, U -235, U-238, and their progeny. Isotopes of thorium and plutonium contribute proportionally significant, but much smaller, annual doses through 10,000 years.

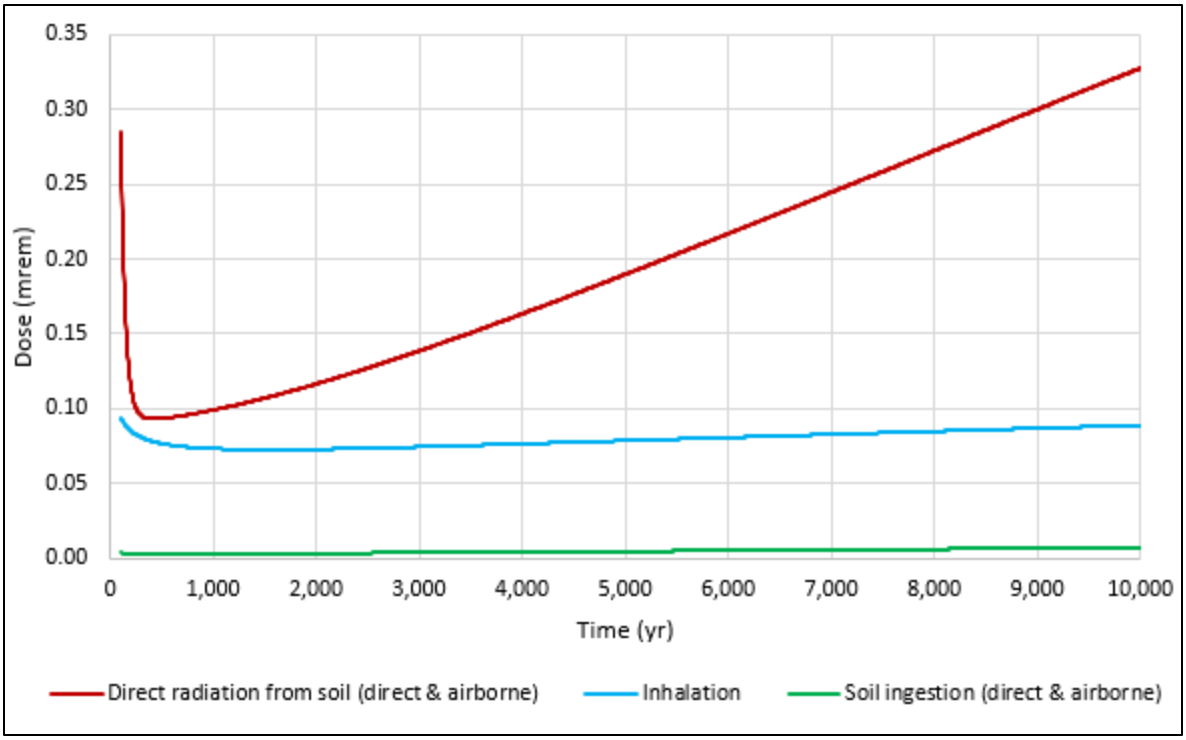

Fig. I.8. Acute drilling scenario total radiological dose by exposure pathway (years 100 to 10,000)

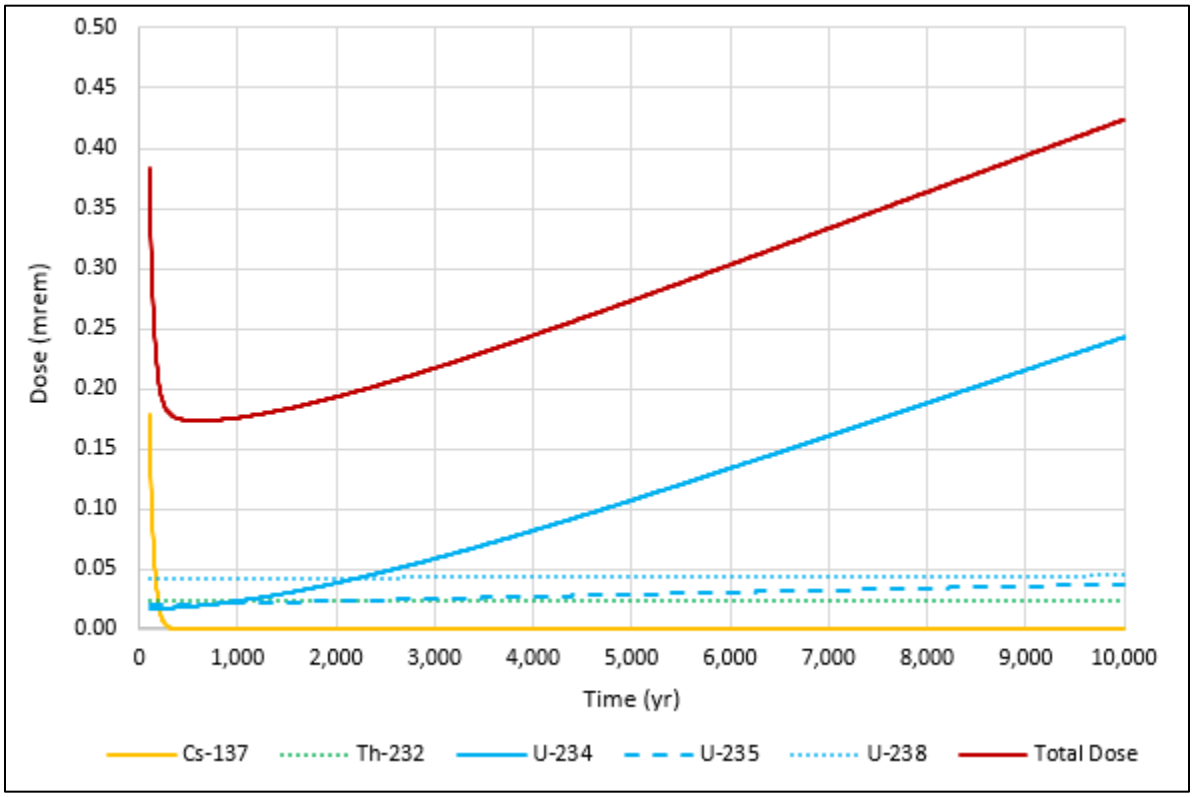

Fig. I.9. Acute drilling scenario dose contributions by radionuclide for years 100 to 10,000

I.5.3 CHRONIC DRILLING RESULTS

The predicted dose over time for the chronic drilling scenario is presented in Fig. I.10. The total dose (all radionuclides and pathways summed) at 100 years post-closure is 3.56 mrem/year. Total dose decreases to a minimum of 2.95 mrem/year at approximately 340 years and gradually increases through 10,000 years as concentrations of radioactive progeny increase; total dose at 10,000 years is 8.24 mrem/year. The predicted chronic driller dose is lower by a factor of 10 than the chronic IHI performance measure of 100 mrem/year.

The dose contributions for each of the simulated exposure pathways for the chronic drilling scenario (direct radiation from garden soil, plant ingestion, meat ingestion, milk ingestion, inhalation, and incidental soil ingestion) are presented in Fig. I.11. The meat ingestion and direct external radiation pathways contribute 90 percent or more of the total dose (dashed black curve). Plant ingestion, milk ingestion, and inhalation together comprise 2 to 7 percent. The contribution of soil ingestion (< 1 percent of to the total dose) is negligible relative to the chronic IHI performance measure of 100 mrem/year.

Primary contributors to the chronic post-drilling IHI dose prior to 1000 years post closure include U-232, U-234, U-235, U-238, Cs-137, and Th-228 (Fig. I.12). After 500 years, total dose is driven by U-234, U-238, and their associated progeny.

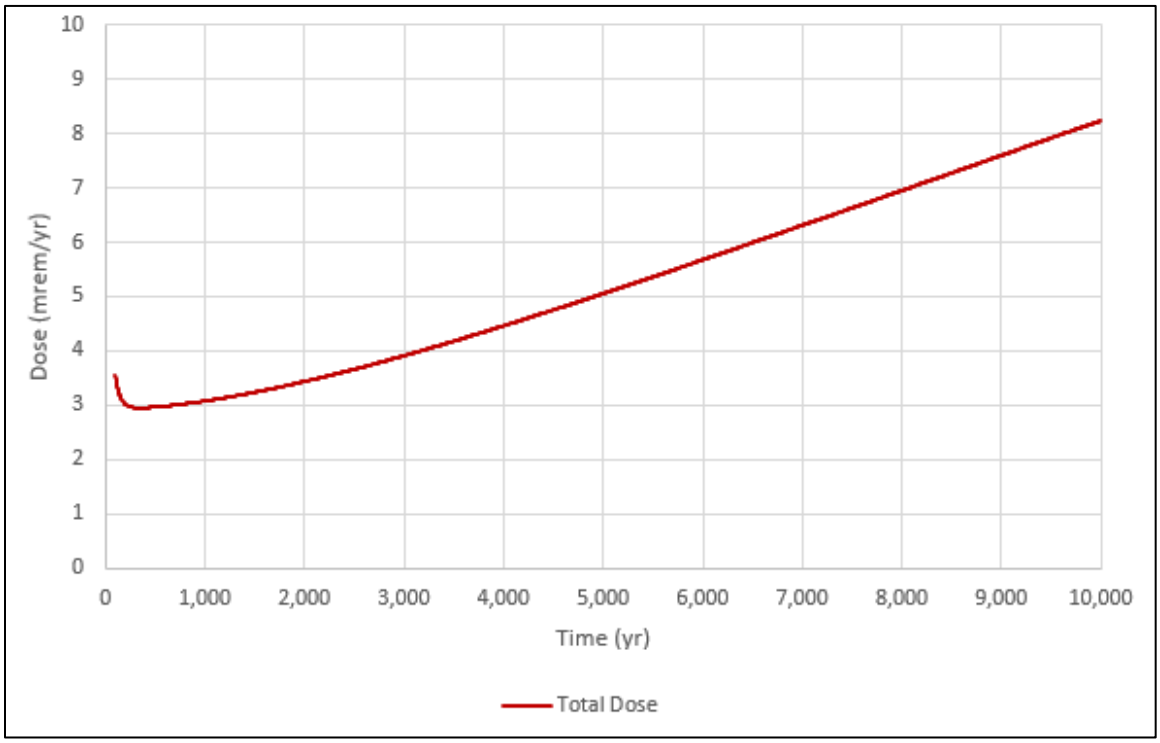

Fig. I.10. Chronic post-drilling scenario total dose (all radionuclides and pathways summed: years 100 to 10,000)

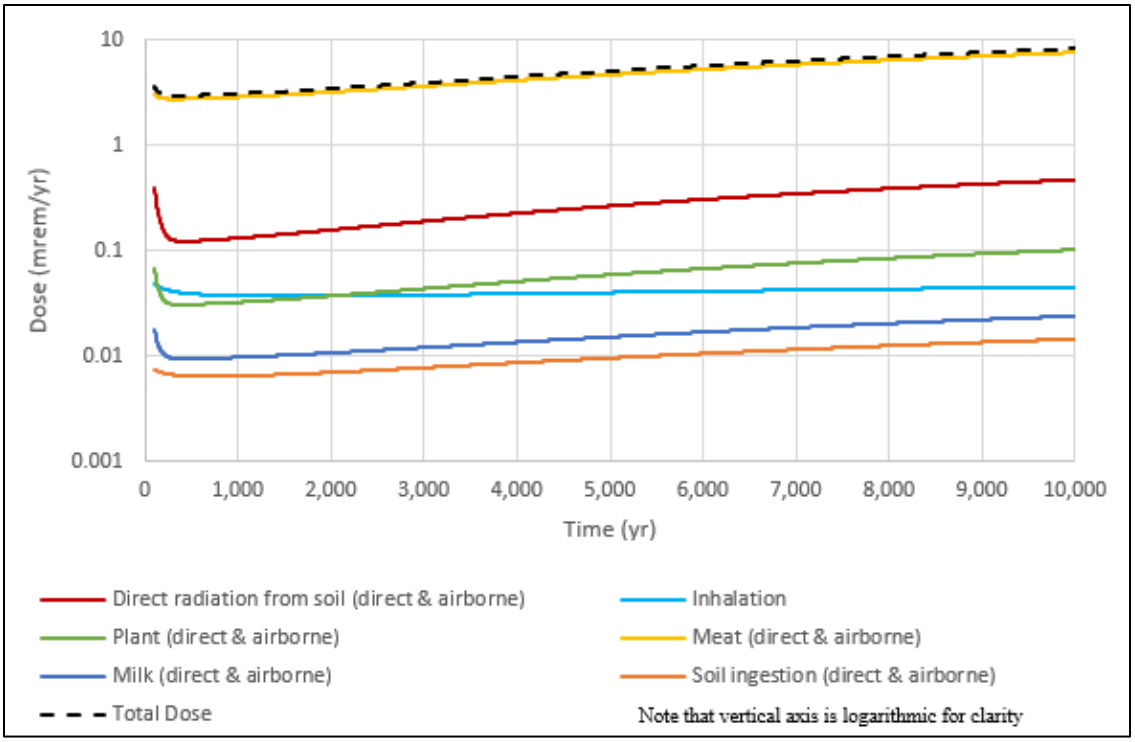

Note that vertical axis is logarithmic for clarity.

Fig. I.11. Chronic post-drilling scenario total dose and dose contributions by pathway for years 100 to 10,000

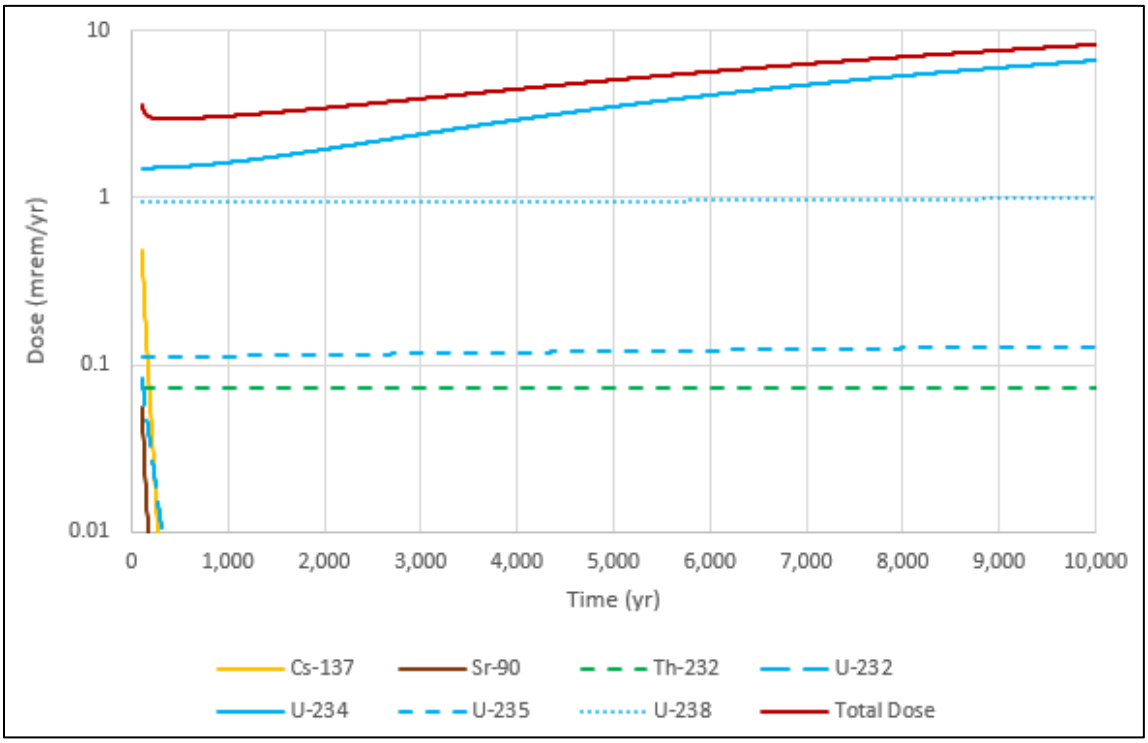

Fig. I.12. Chronic post-drilling scenario dose contributions by radionuclide for years 100 to 10,000

I.5.4 RESRAD SINGLE RADIONUCLIDE SOIL GUIDELINES

IHI analyses provide one basis for setting radionuclide concentration limits to ensure protection of members of the public. RESRAD-OFFSITE Single Radionuclide Soil Guidelines (SRSGs) are calculated activity concentrations that meet a specific dose target for a single radionuclide at a specific time, based on the modeled scenario. The SRSGs do not depend on the assumed radionuclide concentrations or the corresponding modeled doses, but only on the target dose value and the specific exposure scenario considered. Thus, the SRSGs are dose-based radionuclide concentration limits (one type of analytical waste acceptance criteria [WAC]) for the particular system and scenario simulated.

For the IHI scenarios presented here, the most restrictive (lowest) SRSG values are based on the 100 mrem/year dose measure associated with the chronic drilling exposure scenario. The minimum SRSG value for the period between 100 to 1000 years post-closure is an appropriate metric for use in setting IHI-based concentration limits for the DOE O 435.1 compliance period, or for evaluating proposed WAC developed by a separate analysis. For most radionuclides, the minimum SRSG within this period occurs at either 100 or 1000 years post-closure. This approach is taken for all radionuclides except for C-14, which is a highly mobile radionuclide that easily transitions to the gaseous or dissolved form. In the acute and chronic drilling scenarios, the dispersed drill cuttings are exposed to the atmosphere, which causes the C-14 to volatilize from the soil completely within the first 5 years of the simulation. Due to the volatility of C-14, the minimum SRSG between 100 and 1000 years is calculated by adjusting the SRSG at year 0 for 100 years of radioactive decay. A detailed description of how the C-14 SRSG is calculated is provided in the QA documentation for the IHI analysis (UCOR 2020).

The correct application of the predicted SRSG to set or evaluate waste concentration limits based on the IHI dose must account for the assumed dilution of radionuclides when mixed with the uncontaminated materials when being placed in the cell and when they are exhumed and mixed with clean drill cuttings or garden soil. The source SRSG values output by RESRAD-OFFSITE are divided by the dilution factor(s) applied to the waste concentrations in the IHI analysis to derive corresponding SRSG values for comparison to as-disposed (including clean fill) or as-generated activity concentrations. SRSGs calculated for C-14, H-3, I-129, and Tc-99 are not back-adjusted to account for potential activity loss during operations as a conservative measure biased towards lower SRSGs.

Table I.3 presents the SRSG values for both the acute drilling and chronic post-drilling scenarios. The minimum SRSG values occur at 100 years post-closure, unless indicated otherwise in Table I.3. After accounting for the assumed dilution, as-disposed and as-generated SRSG values for the chronic post-drilling scenario are less than the as-disposed and as-generated SRSG values for the acute drilling scenario for all radionuclides.

Table I.3. RESRAD SRSGs for acute drilling and chronic post-drilling IHI scenarios

Radionuclide	Acute drilling source SRSG (pCi/g)	Acute drilling as-disposed SRSG (pCi/g)	Acute drilling as-generated SRSG (pCi/g)	Chronic post-drilling source SRSG (pCi/g)	Chronic post-drilling as-disposed SRSG (pCi/g)	Chronic post-drilling as-generated SRSG (pCi/g)
Ac-227	2.08E+06	7.31E+06	1.38E+07	2.96E+03	1.30E+06	2.45E+06
Am-241	6.05E+05	2.13E+06	4.01E+06	1.27E+03	5.55E+05	1.05E+06
Am-243	1.78E+05	6.26E+05	1.18E+06	2.90E+02	1.27E+05	2.39E+05
Ba-133	1.00E+08	3.52E+08	6.64E+08	1.24E+05	5.45E+07	1.03E+08
Be-10	1.74E+08	6.13E+08	1.15E+09	1.36E+04	5.98E+06	1.13E+07

Table I.3. RESRAD SRSGs for acute drilling and chronic post-drilling IHI scenarios (cont.)

Radionuclide	Acute drilling source SRSG (pCi/g)	Acute drilling as-disposed SRSG (pCi/g)	Acute drilling as-generated SRSG (pCi/g)	Chronic post-drilling source SRSG (pCi/g)	Chronic post-drilling as-disposed SRSG (pCi/g)	Chronic post-drilling as-generated SRSG (pCi/g)
C-14[a]	2.79E+09[b]	9.83E+09[b]	1.85E+10[b]	7.07E+01[b]	3.10E+04[b]	5.84E+04[b]
Ca-41	1.72E+10	6.04E+10	1.14E+11	5.13E+03	2.25E+06	4.24E+06
Cf-249	1.24E+05	4.36E+05	8.22E+05	1.80E+02	7.92E+04	1.49E+05
Cf-250	7.69E+07	2.71E+08	5.10E+08	1.47E+05	6.45E+07	1.21E+08
Cf-251	2.02E+05	7.11E+05	1.34E+06	3.65E+02	1.60E+05	3.01E+05
Cm-243	2.98E+06	1.05E+07	1.98E+07	4.76E+03	2.09E+06	3.93E+06
Cm-244	3.58E+07	1.26E+08	2.37E+08	7.72E+04	3.39E+07	6.38E+07
Cm-245	2.13E+05[c]	7.48E+05[c]	1.41E+06[c]	4.00E+02[c]	1.75E+05[c]	3.30E+05[c]
Cm-246	5.55E+05	1.95E+06	3.68E+06	1.13E+03	4.97E+05	9.35E+05
Cm-247	1.12E+05[c]	3.93E+05[c]	7.40E+05[c]	1.55E+02[c]	6.81E+04[c]	1.28E+05[c]
Cm-248	3.14E+04	1.11E+05	2.08E+05	3.58E+01	1.57E+04	2.96E+04
Co-60	1.05E+10	3.69E+10	6.94E+10	1.06E+07	4.65E+09	8.76E+09
Cs-137	8.82E+05	3.10E+06	5.84E+06	5.30E+02	2.32E+05	4.38E+05
Eu-152	7.42E+06	2.61E+07	4.92E+07	8.21E+03	3.60E+06	6.78E+06
Eu-154	1.31E+08	4.62E+08	8.71E+08	1.44E+05	6.33E+07	1.19E+08
H-3[a]	3.35E+13	1.18E+14	2.22E+14	1.30E+06	5.72E+08	1.08E+09
I-129[a]	1.23E+07	4.31E+07	8.12E+07	1.38E+01	6.06E+03	1.14E+04
K-40	3.22E+05	1.13E+06	2.13E+06	4.10E+01	1.80E+04	3.39E+04
Mo-93	2.67E+08	9.39E+08	1.77E+09	1.26E+02	5.52E+04	1.04E+05
Nb-93m	1.34E+11	4.70E+11	8.85E+11	3.57E+07	1.57E+10	2.95E+10
Nb-94	3.19E+04	1.12E+05	2.11E+05	3.61E+01	1.59E+04	2.99E+04
Ni-59	2.57E+09	9.04E+09	1.70E+10	1.72E+05	7.56E+07	1.42E+08
Ni-63	2.69E+10	9.45E+10	1.78E+11	1.46E+05	6.39E+07	1.20E+08
Np-237	1.82E+05[d]	6.42E+05[d]	1.21E+06[d]	2.35E+02[c]	1.03E+05[c]	1.94E+05[c]
Pa-231	6.06E+04[d]	2.13E+05[d]	4.01E+05[d]	9.40E+01[d]	4.12E+04[d]	7.77E+04[d]
Pb-210	3.12E+07	1.10E+08	2.07E+08	4.72E+01	2.07E+04	3.90E+04
Pm-146	1.86E+10	6.53E+10	1.23E+11	2.19E+07	9.61E+09	1.81E+10
Pu-238	1.14E+06	4.02E+06	7.58E+06	2.87E+03	1.26E+06	2.37E+06
Pu-239	4.71E+05	1.66E+06	3.12E+06	1.19E+03	5.22E+05	9.83E+05
Pu-240	4.75E+05	1.67E+06	3.15E+06	1.20E+03	5.27E+05	9.92E+05
Pu-241	1.77E+07	6.22E+07	1.17E+08	3.70E+04	1.62E+07	3.06E+07
Pu-242	4.94E+05	1.74E+06	3.27E+06	1.25E+03	5.47E+05	1.03E+06
Pu-244	1.09E+05[c]	3.84E+05[c]	7.24E+05[c]	1.44E+02[c]	6.31E+04[c]	1.19E+05[c]
Ra-226	2.97E+04	1.05E+05	1.97E+05	2.00E+00[d]	8.77E+02[d]	1.65E+03[d]
Ra-228	2.82E+09	9.93E+09	1.87E+10	1.64E+06	7.21E+08	1.36E+09
Re-187	SA[e]	SA[e]	SA[e]	SA[e]	SA[e]	SA[e]
Sr-90	5.75E+07	2.02E+08	3.81E+08	7.44E+02	3.26E+05	6.15E+05

Table I.3. RESRAD SRSGs for acute drilling and chronic post-drilling IHI scenarios (cont.)

Radionuclide	Acute drilling source SRSG (pCi/g)	Acute drilling as-disposed SRSG (pCi/g)	Acute drilling as-generated SRSG (pCi/g)	Chronic post-drilling source SRSG (pCi/g)	Chronic post-drilling as-disposed SRSG (pCi/g)	Chronic post-drilling as-generated SRSG (pCi/g)
Tc-99[a]	1.02E+09	3.58E+09	6.73E+09	1.09E+02	4.80E+04	9.03E+04
Th-228	SA[e]	SA[e]	SA[e]	SA[e]	SA[e]	SA[e]
Th-229	9.58E+04	3.37E+05	6.35E+05	1.44E+02	6.32E+04	1.19E+05
Th-230	7.08E+04[c]	2.49E+05[c]	4.69E+05[c]	5.48E+00[c]	2.40E+03[c]	4.53E+03[c]
Th-232	2.05E+04[d]	7.21E+04[d]	1.36E+05[d]	1.09E+01[d]	4.79E+03[d]	9.02E+03[d]
U-232	8.99E+04	3.16E+05	5.96E+05	2.69E+01	1.18E+04	2.22E+04
U-233	8.78E+05[c]	3.09E+06[c]	5.82E+06[c]	8.79E+01[c]	3.86E+04[c]	7.26E+04[c]
U-234	3.80E+06[c]	1.34E+07[c]	2.52E+07[c]	8.87E+01[c]	3.89E+04[c]	7.33E+04[c]
U-235	2.62E+05[c]	9.22E+05[c]	1.74E+06[c]	8.03E+01[c]	3.52E+04[c]	6.64E+04
U-236	5.82E+06	2.05E+07	3.86E+07	1.02E+02	4.47E+04	8.42E+04
U-238	SA[e]	SA[e]	SA[e]	9.29E+01[c]	4.08E+04[c]	7.68E+04[c]

[a]SRSG was not back-adjusted to account for activity loss during operations.
[b]SRSG equal to SRSG at 0 year adjusted for 100 years of radioactive decay.
[c]Minimum SRSG occurs at 1000 years.
[d]Minimum SRSG occurs after 100 years and before 1000 years.
[e]The SRSG is equal to or greater than the SA for the radionuclide.

IHI = inadvertent human intrusion
RESRAD = RESidual RADioactivity
SA = specific activity
SRSG = Single Radionuclide Soil Guideline

I.6 UNCERTAINTIES, SENSITIVITY, AND CONSERVATIVE BIAS

I.6.1 UNCERTAINTIES AND SENSITIVITY OF RESULTS TO KEY PARAMETER ASSUMPTIONS

The primary uncertainties affecting this IHI analysis include the estimated EMDF radionuclide concentrations and assumptions for the values of key model parameters that impact the calculated source concentrations. In general, the modeled dose for a given radionuclide scales linearly with the estimated activity concentration. This means that uncertainties in waste concentrations (EMDF inventory estimates) or in the values of parameters that determine the modeled source concentrations (calculated dilution factors applied to waste concentrations for the acute and chronic drilling scenarios) can be translated directly into dose uncertainty. This simple relationship applies to parameters such as the thickness of waste at the drilling location and the area of the garden for the chronic post-drilling IHI scenario. For the drilling and post-drilling cases, the calculated source concentrations scale with the square of the borehole diameter, so that dose sensitivity to the assumed diameter is non-linear. These sensitivities to uncertainties in parameter values are of relatively little concern for this analysis because the highest modeled doses are on the order of a few mrem/year, and the range of estimated doses due to uncertainty in parameter values is not likely to approach the DOE M 435.1-1 (DOE 2011) performance measures for IHI.

Other significant non-linear sensitivities exist, such as dose sensitivity to clean cover thickness for the discovery scenario (Fig. I.5) or dose sensitivity to the calculated thickness of the drill cuttings for the acute drilling scenario (Fig. I.7). Uncertainty in these parameters is less a matter of insufficient information

(epistemic uncertainty) than of the hypothetical nature of the IHI scenarios chosen for analysis. The significance of these irreducible uncertainties must be considered in the context of the overall pessimistic bias in the analysis, in which a variety of conservative assumptions underlie the presumption of inadvertent intrusion occurring in the distant future.

I.6.2 CONSERVATIVE BIAS

Conservative bias in the IHI analysis arises from adopting pessimistic assumptions that lead to higher rather than lower estimates of dose to inadvertent human intruders. Pessimistic assumptions adopted for the IHI analysis include some assumptions for model parameter values and the assumption that intrusion occurs even though several unlikely circumstances must coincide for the intrusion scenarios to be credible, as described in Sects. I.3 and I.4.

A key modeling parameter leading to pessimistic bias in the modeled dose is the zero value assigned to the release rate (leach rate) from the primary contamination for all scenarios. Leaching of radionuclides from the waste during operations and through the period of effective institutional controls (nominally 100 years) will reduce the concentration of radionuclides in the waste relative to original concentrations. Losses due to leaching during the assumed 25-year operational period were quantified and considered for C-14, H-3, I-129, and Tc-99, but not for any of the other radionuclides in the inventory. By essentially eliminating leaching of mobile radionuclides from the waste mass and garden soil (for the chronic drilling scenario), the modeling approach should yield higher estimated doses than are likely to occur, especially during later post-closure time periods.

In addition, consumption of meat, milk, vegetables, poultry and eggs derived from the chronic scenario garden is unlikely. The waste amended soil would be low in nutrients, limiting the produce that can be grown in a season. In turn, this limits the ability to support poultry or other farm animals. Finally, there is only one documented set of poultry and egg transfer factors for uranium, and these are relatively high. These high transfer factors also result in calculating a pessimistic dose.

Circumstances that would lead to any of the assumed IHI scenarios are highly unlikely at the earliest assumed time (100 years post-closure) for the loss of institutional controls. The ORR has a continuing mission and is a well-established site. Many of the employees are from the local communities, including many generations of some local families. Much of the reservation is fenced and guarded by armed security patrols. It is unlikely that institutional controls on waste management facilities will be lost after only 100 years. Knowledge of the ORR and reluctance to go there should persist in institutional and familial memory for a relatively long time due to the large number of employees. In addition, the EMDF Record of Decision will require institutional controls for as long as the waste is considered a threat to public health, as required under the Comprehensive Environmental Response, Compensation, and Liability Act of 1980 (CERCLA).

The design and construction of the landfill and final cover limits the potential for inadvertent intrusion. For the discovery scenario, the engineered cover is credited for deterring intruders from exposing the waste. For the drilling scenarios, it is unlikely that a future intruder would select to drill a water supply well on a topographic high point rather than on lower, more level ground in BCV. The rocky nature of the biointrusion layer and composition of the waste will pose additional difficulty for drilling and excavation. Much of the waste is bulk demolition debris. If debris is encountered, drilling through structural steel and heavy rebar will be difficult at best. If drilling through the layers of the final cover and waste were to proceed to completion of a groundwater well, the cuttings derived from drilling through the waste would likely contain concrete and shards of steel from the structural building materials, including rebar. These are not expected to appear soil-like as assumed for the drilling scenarios, and likely would not be used to amend the soil in

a garden plot. However, for the acute and chronic drilling scenarios, none of these features of the waste or landfill design are credited for deterring IHI.

I.7 SUMMARY AND CONCLUSIONS

An inadvertent human intrusion evaluation was conducted for the EMDF PA as required by DOE M 435.1-1 (DOE 2011). The modeled IHI scenarios are biased pessimistically in terms of assumed parameter values and due to the unlikely potential for well drilling or basement construction on the landfill post-closure due to:

- Cover design features that deter intrusion
- Requirement under CERCLA of long-lasting institutional controls and long-term institutional memory
- Low likelihood of intrusions that would lead to the assumed exposure scenarios.

The predicted doses associated with the estimated average EMDF inventory for each of the modeled scenarios are well below the performance measure values of 500 mrem for acute exposures and 100 mrem/year for chronic exposure (Table I.4). The model results imply that post-closure EMDF inventories will not result in unacceptable total doses to a hypothetical human intruder under the specific IHI scenarios analyzed.

Table I.4. Summary of modeled doses for acute and chronic EMDF IHI scenarios

EMDF IHI scenario	DOE O 435.1 IHI performance measure	EMDF IHI dose range from 100 to 10,000 years (Compliance Period Maximum Dose)
Acute exposure – discovery (basement excavation)	500 mrem (annual)	6.7E-05 to 2.5E-04 mrem (1.03E-04 mrem)
Acute exposure – drilling (water well)	500 mrem (annual)	1.7E-01 to 4.2E-01 mrem (3.8E-01 mrem)
Chronic exposure – post-drilling (subsistence garden)	100 mrem/year	3.0E+00 to 8.2E+00 mrem/year (3.56E+01 mrem/year)

DOE O = U.S. Department of Energy
EMDF = Environmental Management Disposal Facility
IHI = inadvertent human intrusion

I.8 REFERENCES

DOE 2001. *Radioactive Waste Management*, DOE Order 435.1 Chg 1 (PgChg), U.S. Department of Energy, Washington, D.C., August.

DOE 2011. *Radioactive Waste Management Manual*, DOE Manual 435.1-1 Ch. 2, U.S. Department of Energy, Washington, D.C., June.

DOE 2017. *Disposal Authorization Statement and Tank Closure Documentation*, DOE-STD-5002-2017, U.S. Department of Energy, Washington, D.C., July.

EPA 2014. *Human Health Evaluation Manual, Supplemental Guidance: Update of Standard Default Exposure Factors,* OSWER Directive 9200.1-120, U.S. Environmental Protection Agency, Washington, D.C., February.

Maheras et al. 1997. *Addendum to Radioactive Waste Management Complex Low-Level Waste Radiological Performance Assessment*, INEEL/EXT-97-00462 (formerly EGG-WM-8773), S. J. Maheras, A. S. Rood, S. O. Magnuson, M. E. Sussman, and R. N. Bhatt, Idaho National Engineering and Environmental Laboratory, Idaho Falls, ID, April.

ORNL 1997a. *Performance Assessment for Continuing and Future Operations at Solid Waste Disposal Area 6,* ORNL-6783/R1, Volume 1, Oak Ridge National Laboratory, Oak Ridge, TN, September.

ORNL 1997b. *Performance Assessment for the Class L-II Disposal Facility,* ORNL/TM-13401, Oak Ridge National Laboratory, Oak Ridge, TN, March.

PNNL 2003. *A Compendium of Transfer Factors for Agricultural and Animal Products,* PNNL-13421, L. H. Staven, B. A. Napier, K. Rhoads, and D. L. Strenge, Pacific Northwest National Laboratory, Richland, WA, June.

R. G. Smith 2015. *Why Some Southern States Don't Have Basements,* https://www.rgscontractors.com/why-some-southern-states-dont-have-basements/, R.G. Smith Company, Canton, OH, June 18.

Savannah River National Laboratory 2014. *Inadvertent Intruder Analysis for the Portsmouth On-Site Waste Disposal Facility (OSWDF),* SRNL-STI-2014-00304 Revision 1, F. G. Smith III and M. A. Phifer, Savannah River National Laboratory, Jackson, SC, December.

UCOR 2020. *Quality Assurance Report for Modeling of the Bear Creek Valley Low-level Radioactive Waste Disposal Facilities, Oak Ridge, Tennessee,* UCOR-5234/R0, UCOR, Oak Ridge, TN, April.

Yu et al. 2007. *User's Manual for RESRAD-OFFSITE Version 2* ANL/EVS/TM/07-1, C. Yu, E. K. Gnanapragasam, B. M. Biwer, S. Kamboj, J.-J. Cheng, T. Klett, D. LePoire, A. J. Zielen, S. Y. Chen, and W. A. Williams, Argonne National Laboratory, Argonne, IL, June.

ATTACHMENT I.1.
RESRAD-OFFSITE INPUT PARAMETERS FOR INADVERTENT HUMAN INTRUSION MODELING

This page intentionally left blank.

Input Screen Title and Parameter Name	Units	PA Modeling Proposed Value (EMDF)		
		Acute Discovery	Acute Drilling	Chronic Post Drilling
Radiological units for activity	Ci, Bq, dps, dpm	pCi	pCi	pCi
Radiological units for dose	rem and Sv	mrem	mrem	mrem
Basic radiation dose limit	mrem/year	500	500	100
Exposure duration	year	1	1	1
Number of unsaturated zone(s)	--	5	5	5
Submerged fraction of Primary Contamination	unitless	0	0	0
Default Release Mechanism	--	Version 2 Release Methodology	Version 2 Release Methodology	Version 2 Release Methodology
Bearing of X axis	degrees	90°	90°	90°
X dimension of Primary contamination	m	250.6	14.142	46.9
Y dimension of Primary contamination	m	382.7	14.142	46.9
Smaller x coordinate of the fruit, grain, non-leafy vegetables plot	m	0.0	54.8	0.0
Larger x coordinate of the fruit, grain, non-leafy vegetables plot	m	32.00	86.04	46.9
Smaller y coordinate of the fruit, grain, non-leafy vegetables plot	m	-132.0	-199.9	0.0
Larger y coordinate of the fruit, grain, non-leafy vegetables plot	m	-100.0	-167.9	46.9
Smaller x coordinate of the leafy vegetables plot	m	0.0	101.4	0.0
Larger x coordinate of the leafy vegetables plot	m	32.0	132.6	46.9
Smaller y coordinate of the leafy vegetables plot	m	-132.0	-202.6	0.0
Larger y coordinate of the leafy vegetables plot	m	-100.0	-170.6	46.9
Smaller x coordinate of the pasture, silage growing area	m	120.0	232.9	0.0
Larger x coordinate of the pasture, silage growing area	m	220.0	332.8	46.9
Smaller y coordinate of the pasture, silage growing area	m	-200.0	-144.5	0.0
Larger y coordinate of the pasture, silage growing area	m	-100.00	-44.57	46.9
Smaller x coordinate of the grain fields	m	230.0	112.3	0.0
Larger x coordinate of the grain fields	m	330.0	212.2	46.9
Smaller y coordinate of the grain fields	m	-200.0	-152.7	0.0

Input Screen Title and Parameter Name	Units	PA Modeling Proposed Value (EMDF)		
		Acute Discovery	Acute Drilling	Chronic Post Drilling
Larger y coordinate of the grain fields	m	-100.0	-52.79	46.9
Smaller x coordinate of the dwelling site	m	80.00	10.96	0.0
Larger x coordinate of the dwelling site	m	112.0	42.2	31.2
Smaller y coordinate of the dwelling site	m	-132.0	-197.1	0.0
Larger y coordinate of the dwelling site	m	-100.0	-165.1	32.0
Smaller x coordinate of the surface-water body	m	-50.0	-50.0	-575.4
Larger x coordinate of the surface-water body	m	50.0	50.0	-475.4
Smaller y coordinate of the surface-water body	m	-337.4	-337.4	-337.4
Larger y coordinate of the surface-water body	m	-332.4	-332.4	-332.4
Source				
Nuclide concentration	pCi/g	varies	varies	varies
Release to groundwater, leach rate	1/year	Varies (Not Used)	Varies (Not Used)	Varies (Not Used)
Use Distribution Coefficient to Estimate First Order Leach Rate	cm^3/g	Varies (Not Used)	Varies (Not Used)	Varies (Not Used)
Deposition velocity	m/sec	0.001 0.01 (I-129)	0.001 0.01 (I-129)	0.001 0.01 (I-129)
Radionuclide bearing material becomes releasable	N/A	Linear	Linear	Linear
Time at which radionuclide first becomes releasable (delay time)	year	10,000	0	0
Fraction of radionuclide bearing material that is initially releasable	unitless	0	1.0	1.0
Time over which transformation to releasable form occurs	year	10,000	10,000	10,000
Total fraction of radionuclide bearing material that is releasable	unitless	0	1.0	1.0
Release Mechanism	--	First Order Rate Controlled, 0	First Order Rate Controlled, 0	First Order Rate Controlled, 0
Initial Leach Rate	1/year	0	0	0
Final Leach Rate	1/year	0	0	0
Distribution Coefficients in the contaminated zone	cm^3/g	varies	varies	varies

Input Screen Title and Parameter Name	Units	PA Modeling Proposed Value (EMDF)		
		Acute Discovery	**Acute Drilling**	**Chronic Post Drilling**
Release to Atmospheric	--	In the same manner as for release to groundwater	In the same manner as for release to groundwater	In the same manner as for release to groundwater
Distribution Coefficients				
Contaminated zone	cm^3/g	varies	varies	varies
Unsaturated zone	cm^3/g	varies	varies	varies
Saturated zone	cm^3/g	varies	varies	varies
Sediment in surface water body	cm^3/g	0	0	0
Fruit, grain, non-leafy fields	cm^3/g	varies	varies	varies
Leafy vegetable fields	cm^3/g	varies	varies	varies
Pasture, silage growing areas	cm^3/g	varies	varies	varies
Livestock feed grain fields	cm^3/g	varies	varies	varies
Offsite dwelling site	cm^3/g	varies	varies	varies
Deposition Velocities				
Deposition velocity of respirable particulates	m/sec	0.001 0.01 (I-129)	0.001 0.01 (I-129)	0.001 0.01 (I-129)
Deposition velocity of all particulates	m/sec	0.001 0.01 (I-129)	0.001 0.01 (I-129)	0.001 0.01 (I-129)
Dose Conversion and Slope Factors				
External exposure library	(mrem/year) per (pCi/g)	DCFPAK3.02 Database, DOE 2017	DCFPAK3.02 Database, DOE 2017	DCFPAK3.02 Database, DOE 2017
Internal exposure dose library	mrem/pCi	DOE 2011 (Reference Person)	DOE 2011 (Reference Person)	DOE 2011 (Reference Person)

Input Screen Title and Parameter Name	Units	PA Modeling Proposed Value (EMDF)		
		Acute Discovery	Acute Drilling	Chronic Post Drilling
Slope Factor (Risk) Library	(risk/year) per (pCi/g)	DCFPAK3.02 Morbidity DOE 2017	DCFPAK3.02 Morbidity DOE 2017	DCFPAK3.02 Morbidity DOE 2017
Transfer Factors				
Fruit, grain, non-leafy vegetables transfer factor	(pCi/kg)/ (pCi/kg)	PNNL 2003, Mean of Fruits, Grains, Root Vegetables Transfer Factors (C-14, H-3 Calculated)	PNNL 2003, Mean of Fruits, Grains, Root Vegetables Transfer Factors (C-14, H-3 Calculated)	PNNL 2003, Mean of Fruits, Grains, Root Vegetables Transfer Factors (C-14, H-3 Calculated)
Leafy vegetables transfer factor	(pCi/kg)/ (pCi/kg)	PNNL 2003, Leafy Vegetables (C-14, H-3 Calculated)	PNNL 2003, Leafy Vegetables (C-14, H-3 Calculated)	PNNL 2003, Leafy Vegetables (C-14, H-3 Calculated)
Pasture and silage transfer factor	(pCi/kg)/ (pCi/kg)	PNNL 2003, Grains (C-14, H-3 Calculated)	PNNL 2003, Grains (C-14, H-3 Calculated)	PNNL 2003, Grains (C-14, H-3 Calculated)
Livestock feed grain transfer factor	(pCi/kg)/ (pCi/kg)	PNNL 2003, Grains (C-14, H-3 Calculated)	PNNL 2003, Grains (C-14, H-3 Calculated)	PNNL 2003, Grains (C-14, H-3 Calculated)
Meat transfer factor	(pCi/kg)/ (pCi/day)	PNNL 2003, Consumption Adjusted Transfer Factors, Red Meat, Poultry, Egg	PNNL 2003, Consumption Adjusted Transfer Factors, Red Meat, Poultry, Egg	PNNL 2003, Consumption Adjusted Transfer Factors, Red Meat, Poultry, Egg
Milk transfer factor	(pCi/L)/ (pCi/day)	PNNL 2003 Milk	PNNL 2003 Milk	PNNL 2003 Milk
Bioaccumulation factor for fish	(pCi/kg)/ (pCi/L)	PNNL 2003 Fresh Water Fish (RESRAD default for H-3)	PNNL 2003 Fresh Water Fish (RESRAD default for H-3)	PNNL 2003 Fresh Water Fish (RESRAD default for H-3)

Input Screen Title and Parameter Name	Units	PA Modeling Proposed Value (EMDF)		
		Acute Discovery	Acute Drilling	Chronic Post Drilling
Bioaccumulation factor for crustacea and mollusks	(pCi/kg)/ (pCi/L)	RESRAD default values for all isotopes	RESRAD default values for all isotopes	RESRAD default values for all isotopes
Reporting Times				
Times at which output is reported	year	1, 100, 300, 500, 800, 1000, 1100, 2000, 10,000	1, 100, 300, 500, 800, 1000, 1100, 2000, 10,000	1, 100, 300, 500, 800, 1000, 1100, 2000, 10,000
Storage Times				
Storage time for surface water	day	1	1	1
Storage time for well water	day	1	1	1
Storage time for fruits, grain, and non-leafy vegetables	day	14	14	14
Storage time for leafy vegetables	day	1	1	1
Storage time for pasture and silage	day	1	1	1
Storage time for livestock feed grain	day	45	45	45
Storage time for meat	day	20	20	20
Storage time for milk	day	1	1	1
Storage time for fish	day	7	7	7
Storage time for crustacea and mollusks	day	7	7	7
Physical and Hydrological				
Precipitation	m/year	0.000001	0.000001	0.000001
Wind speed	m/sec	3.4342	3.4342	3.4342
Primary Contamination				
Area of primary contamination	m^2	95,900	200	2199.6
Length ofcontamination parallel to aquifer flow	m	398.9	14.142	47.06
Depth of soil mixing layer (m)	m	0.15	0.0605	0.3048
Mass loading of all particulates	g/m^3	0.0001	0.001	0.001

Input Screen Title and Parameter Name	Units	PA Modeling Proposed Value (EMDF)		
		Acute Discovery	Acute Drilling	Chronic Post Drilling
Deposition velocity of dust	m/sec	0.001	0.001	0.001
Respirable particulates as a fraction of total particulates	--	1 (Not Used)	1	1
Deposition velocity of respirable particulates	m/sec	0.001 (Not Used)	0.001	0.001
Irrigation applied	m/year	0	0	0
Evapotranspiration coefficient	--	0.568	0.568	0.568
Runoff coefficient	--	0.963	0.963	0.963
Rainfall Erosion Index	--	0	0	0
Slope-length-steepness factor	--	0.4	0.4	0.4
Cover and management factor	--	0.003	0.003	0.003
Support practice factor	--	0.0	0.0	0.0
Fraction of primary contamination that is submerged	--	0.0	0.0	0.0
Contaminated Zone				
Thickness of contaminated zone	m	17.5	0.0605	0.3048
Total porosity of contaminated zone	--	0.419	0.419	0.419
Dry bulk density of contaminated zone	g/cm^3	1.9	1.9	1.9
Erosion rate of clean cover	m/year	0	0	0
Soil erodibility factor of contaminated zone	tons/acre	0.000	0.000	0
Field capacity of contaminated zone	--	0.307	0.307	0.307
Soil b parameter of contaminated zone	--	7.75	7.75	7.75
Longitudinal dispersivity	m	1.80	0.006050	0.03048
Hydraulic conductivity of contaminated zone (above)	m/year	5.99	5.99	5.99
Hydraulic conductivity of contaminated zone (below)	m/year	26.8	26.8	26.8
CZ effective porosity	--	0.234	0.234	0.234
Depth of primary contamination below water table	--	0 (Not Used)	0	0.000
Clean Cover				
Thickness of clean cover	m	0.9144	0	0
Total porosity of clean cover	--	0.4 (Not Used)	0.4 (Not Used)	0.4 (Not Used)

Input Screen Title and Parameter Name	Units	PA Modeling Proposed Value (EMDF)		
		Acute Discovery	Acute Drilling	Chronic Post Drilling
Dry bulk density of clean cover	g/cm^3	1.5	1.5	1.5
Erosion rate of clean cover	m/year	0	0	0
Soil erodibility factor of clean cover	tons/acre	0	0	0
Volumetric water content of clean cover	--	0.05 (Not Used)	0.05 (Not Used)	0.05 (Not Used)
Agriculture Area Parameters				
Fruit, Grain, and Non-leafy Vegetables Field				
Area for fruit, grain, and non-leafy vegetables field	m^2	1024	999.68	2199.6
Fraction of area directly over primary contamination for fruit, grain, and non-leafy vegetables field	--	0 (Not Used)	0 (Not Used)	1
Irrigation applied per year for fruit, grain, and non-leafy vegetables field	m/year	0.00	0.00	0.00
Evapotranspiration coefficient for fruit, grain, and non-leafy vegetables field	--	0.568	0.568	0.568
Runoff coefficient for fruit, grain, and non-leafy vegetables field	--	0.625	0.625	0.625
Depth of soil mixinglayer or plow layerfor fruit, grain, and non-leafy vegetables field	m	0.15	0.15	0.3048
Volumetric water content for fruit, grain, and non-leafy vegetables field	--	0.3	0.3	0.3
Erosion rate for fruit, grain, and non-leafy vegetable field	m/year	0.0	0.0	0.0
Dry bulk density of soil for fruit, grain, and non-leafy vegetables field	g/cm^3	1.50	1.50	1.50
Soil erodibility factor for fruit, grain, and non-leafy vegetables field	tons/acre	0.4	0.4	0.4
Slope-length- steepness factor for fruit, grain, and non-leafy vegetables field	--	0.4	0.4	0.4
Cover and management factor for fruit, grain, and non-leafy vegetables field	--	0.003	0.003	0.003
Support practice factor for fruit, grain, and non-leafy vegetables field	--	1	1	1
Total Porosity for fruit, grain, and non-leafy vegetable field	--	0.4 (Not Used)	0.4 (Not Used)	0.4 (Not Used)
Leafy Vegetable Field				
Area for leafy vegetable field	m^2	1024	998.4	2199.6
Fraction of area directly over primary contamination for leafy vegetable field	--	0 (Not Used)	0 (Not Used)	1
Irrigation applied per year for leafy vegetable field	m/year	0	0	0
Evapotranspiration coefficient for leafy vegetable field	--	0.568	0.568	0.568

Input Screen Title and Parameter Name	Units	PA Modeling Proposed Value (EMDF)		
		Acute Discovery	Acute Drilling	Chronic Post Drilling
Runoff coefficient for leafy vegetable field	--	0.625	0.625	0.625
Depth of soil mixing layer or plow layer for leafy vegetable field	m	0.1500	0.1500	0.3048
Volumetric water content for leafy vegetable field	--	0.3	0.3	0.3
Erosion rate for leafy vegetable field	m/year	0.0	0.0	0.0
Dry bulk density of soil for leafy vegetable field	g/cm^3	1.50	1.50	1.50
Soil erodibility factor for leafy vegetable field	tons/acre	0.4	0.4	0.4
Slope-length-steepness factor for leafy vegetable field	--	0.4	0.4	0.4
Cover and management factor for leafy vegetable field	--	0.003	0.003	0.003
Support practice factor for leafy vegetable field	--	1	1	1
Total Porosity for leafy vegetable field	--	0.4 (Not Used)	0.4 (Not Used)	0.4 (Not Used)
Livestock Feed Growing Area Parameters Pasture				
Silage Field				
Area for pasture and silage field	m^2	10000	9983	2199.6
Fraction of area directly over primary contamination for pasture and silage field	--	0 (Not Used)	0 (Not Used)	1
Irrigation applied per year for pasture and silage field	m/year	0.00	0.00	0.00
Evapotranspiration coefficient for pasture and silage field	--	0.568	0.568	0.568
Runoff coefficient for pasture and silage field	--	0.625	0.625	0.625
Depth of soil mixing layer or plow layerfor pasture and silage field	m	0.15	0.15	0.3048
Volumetric water content for pasture and silage field	--	0.3	0.3	0.3
Erosion rate for pasture and silage field	m/year	0.0	0.0	0.0
Dry bulk density of soil for pasture and silage field	g/cm^3	1.50	1.50	1.50
Soil erodibility factor for pasture and silage field	tons/acre	0.4	0.4	0.4
Slope-length- steepness factor for pasture and silage field	--	0.4	0.4	0.4
Cover and management factor for pasture and silage field	--	0.003	0.003	0.003
Support practice factor for pasture and silage field	--	1	1	1
Total porosity for pasture and silage field	--	0.4 (Not Used)	0.4 (Not Used)	0.4 (Not Used)

Input Screen Title and Parameter Name	Units	PA Modeling Proposed Value (EMDF)		
		Acute Discovery	Acute Drilling	Chronic Post Drilling
Grain Field				
Area for grain field	m^2	10,000	9981	2199.6
Fraction of area directly over primary contamination for grain field	--	0 (Not Used)	0 (Not Used)	1
Irrigation applied per year for grain field	m/year	0.00	0.00	0.00
Evapotranspiration coefficient for grain field	--	0.568	0.568	0.568
Runoff coefficient for grain field	--	0.625	0.625	0.625
Depth of soil mixing layer or plow layer for grain field	m	0.1500	0.1500	0.3048
Volumetric water content for grain field	--	0.3	0.3	0.3
Erosion rate	m/year	0.0	0.0	0.0
Dry bulk density of soil for grain field	g/cm^3	1.50	1.50	1.50
Soil erodibility factor for grain field	tons/acre	0.4	0.4	0.4
Slope-length-steepness factor for grain field	--	0.4	0.4	0.4
Cover and management factor for grain field	--	0.003	0.003	0.003
Support practice factor for grain field	--	1	1	1
Total Porosity for grain field	--	0.4 (Not Used)	0.4 (Not Used)	0.4 (Not Used)
Offsite Dwelling Area Parameters				
Area of offsite dwelling site	m^2	1024	999.68	998.4
Irrigation applied per year to home garden or lawn	m/year	0	0	0
Evapotranspiration coefficient for dwelling site	--	0.568	0.568	0.568
Runoff coefficient for dwelling site	--	0.625	0.625	0.625
Depth of soil mixing layer for dwelling site	m	0.15	0	0.3048
Volumetric water content for dwelling site	--	0.3	0.3	0.3
Erosion rate for dwelling site	m/year	0	0	0
Dry bulk density of soil for dwelling site	g/cm^3	1.5	1.5	1.5
Soil erodibility factor for dwelling site	tons/acre	0	0	0
Slope-length- steepness factor for dwelling site	--	0.4	0.4	0.4
Cover and management factor for dwelling site	--	0.003	0.003	0.003

Input Screen Title and Parameter Name	Units	PA Modeling Proposed Value (EMDF)		
		Acute Discovery	Acute Drilling	Chronic Post Drilling
Support practice factor for dwelling site	--	1	1	1
Total porosity for dwelling site	--	0.4 (Not Used)	0.4 (Not Used)	0.4 (Not Used)
Atmospheric Transport				
Release height	m	1	1	1
Release heat flux	cal/sec	0	0	0
Anemometer height	m	10	10	10
Ambient temperature	K	285	285	285
AM atmospheric mixing height	m	400	400	400
PM atmospheric mixing height	m	1600	1600	1600
Dispersion model coefficients	--	Pasquill-Gifford	Pasquill-Gifford	Pasquill-Gifford
Windspeed terrain	--	Rural	Rural	Rural
Fruit, grain, nonleafy vegetable plot	m	0	0	0
Leafy vegetable plot	m	0	0	0
Pasture, silage growing area	m	0	0	0
Grain fields	m	0	0	0
Dwelling site	m	0	0	0
Surface water body	m	0	0	0
Grid spacing for areal integration	m	10	10	10
Joint frequency of wind speed and stability class for a 16 sector wind rose	--	1 (S to N)	1 (S to N)	1 (S to N)
Wind speed	m/sec	0.89, 2.46, 4.47, 6.93, 9.61, 12.52	0.89, 2.46, 4.47, 6.93, 9.61, 12.52	0.89, 2.46, 4.47, 6.93, 9.61, 12.52
Unsaturated Zone Parameters				
Unsaturated zone 1 thickness	m	0.305	0.305	0.305
Unsaturated zone 2 thickness	m	0.305	0.305	0.305
Unsaturated zone 3 thickness	m	0.9144	0.9144	0.9144
Unsaturated zone 4 thickness	m	3.048	3.048	3.048
Unsaturated zone 5 thickness	m	4.846	4.846	4.846

Input Screen Title and Parameter Name	Units	PA Modeling Proposed Value (EMDF)		
		Acute Discovery	Acute Drilling	Chronic Post Drilling
Unsaturated zone 1 dry bulk density	g/cm^3	1.4	1.4	1.4
Unsaturated zone 2 dry bulk density	g/cm^3	1.6	1.6	1.6
Unsaturated zone 3 dry bulk density	g/cm^3	1.5	1.5	1.5
Unsaturated zone 4 dry bulk density	g/cm^3	1.5	1.5	1.5
Unsaturated zone 5 dry bulk density	g/cm^3	1.8	1.8	1.8
Unsaturated zone 1 total porosity	--	0.463	0.463	0.463
Unsaturated zone 2 total porosity	--	0.397	0.397	0.397
Unsaturated zone 3 total porosity	--	0.427	0.427	0.427
Unsaturated zone 4 total porosity	--	0.419	0.419	0.419
Unsaturated zone 5 total porosity	--	0.353	0.353	0.353
Unsaturated zone 1 effective porosity	--	0.294	0.294	0.294
Unsaturated zone 2 effective porosity	--	0.389	0.389	0.389
Unsaturated zone 3 effective porosity	--	0.195	0.195	0.195
Unsaturated zone 4 effective porosity	--	0.234	0.234	0.234
Unsaturated zone 5 effective porosity	--	0.27	0.27	0.27
Unsaturated zone 1 field capacity	--	0.232	0.232	0.232
Unsaturated zone 2 field capacity	--	0.032	0.032	0.032
Unsaturated zone 3 field capacity	--	0.418	0.418	0.418
Unsaturated zone 4 field capacity	--	0.307	0.307	0.307
Unsaturated zone 5 field capacity	--	0.2471	0.2471	0.2471
Unsaturated zone 1 hydraulic conductivity	m/year	117	117	117
Unsaturated zone 2 hydraulic conductivity	m/year	94600	94600	94600
Unsaturated zone 3 hydraulic conductivity	m/year	0.315	0.315	0.315
Unsaturated zone 4 hydraulic conductivity	m/year	3.15	3.15	3.15
Unsaturated zone 5 hydraulic conductivity	m/year	16.7	16.7	16.7
Unsaturated zone 1 soil b parameter	--	5.4	5.4	5.4
Unsaturated zone 2 soil b parameter	--	4.05	4.05	4.05
Unsaturated zone 3 soil b parameter	--	11.4	11.4	11.4

Input Screen Title and Parameter Name	Units	PA Modeling Proposed Value (EMDF)		
		Acute Discovery	Acute Drilling	Chronic Post Drilling
Unsaturated zone 4 soil b parameter	--	11.4	11.4	11.4
Unsaturated zone 5 soil b parameter	--	10.4	10.4	10.4
Unsaturated zone 1 longitudinal dispersivity	m	0.1	0.1	0.1
Unsaturated zone 2 longitudinal dispersivity	m	0.1	0.1	0.1
Unsaturated zone 3 longitudinal dispersivity	m	0.1	0.1	0.1
Unsaturated zone 4 longitudinal dispersivity	m	0.1	0.1	0.1
Unsaturated zone 5 longitudinal dispersivity	m	0.1	0.1	0.1
Saturated Zone Hydrological Data				
Thickness of saturated zone	m	60.96	60.96	60.96
Dry bulk density of saturated zone	g/cm^3	2.1	2.1	2.1
Saturated zone total porosity	--	0.24	0.24	0.24
Saturated zone effective porosity	--	0.20	0.20	0.20
Saturated zone hydraulic conductivity	m/year	26.8	26.8	26.8
Saturated zone hydraulic gradient to well	--	0.054	0.054	0.054
Saturated zone longitudinal dispersivity to well	m	10	10	10
Saturated zone horizontal lateral dispersivity to well	m	1	1	1
Saturated zone vertical lateral dispersivity to well	m	0.1	0.1	0.1
Depth of aquifer contributing to well	m	40	40	40
Saturated zone hydraulic gradient to surface water body	--	0.036	0.036	0.036
Saturated zone longitudinal dispersivity to surface water body	m	31.5	31.5	31.5
Saturated zone horizontal lateral dispersivity to surface water body	m	3.15	3.15	3.15
Saturated zone vertical lateral dispersivity to surface water body	m	0.315	0.315	0.315
Depth of aquifer contributing to surface water body	m	30.48	30.48	30.48
Water Use				
Quantity of water consumed by an individual	L/year	730 (Not Used)	730 (Not Used)	730 (Not Used)
Fraction of water from surface body for human consumption	--	0 (Not Used)	0 (Not Used)	0 (Not Used)
Fraction of water from well for human consumption	--	1 (Not Used)	1 (Not Used)	1 (Not Used)

Input Screen Title and Parameter Name	Units	PA Modeling Proposed Value (EMDF)		
		Acute Discovery	Acute Drilling	Chronic Post Drilling
Number of household individuals consuming and using water	--	4 (Not Used)	4 (Not Used)	4 (Not Used)
Quantity of water for use indoors of dwelling per individual	L/day	225	225	225
Fraction of water from surface body for use indoors of dwelling	--	0	0	0
Fraction of water from well for use indoors of dwelling	--	1	1	1
Beef Cattle				
Quantity of water for beef cattle	L/day	50 (Not Used)	50 (Not Used)	50
Fraction of water from surface body for beef cattle	--	1 (Not Used)	1 (Not Used)	1
Fraction of water from well for beef cattle	--	0 (Not Used)	0 (Not Used)	0
Number of cattle for beef cattle	--	2 (Not Used)	2 (Not Used)	2
Dairy Cows				
Quantity of water for dairy cows	L/day	160 (Not Used)	160 (Not Used)	160
Fraction of water from surface body for dairy cows	--	1 (Not Used)	1 (Not Used)	1
Fraction of water from well for dairy cows	--	0 (Not Used)	0 (Not Used)	0
Number of cows for dairy cows	--	2 (Not Used)	2 (Not Used)	2
Fruit, grain, non-leafy vegetables				
Irrigation rate for fruit, grain, and non-leafy vegetables	m/year	0.0	0.0	0.0
Fraction of water from surface body for fruit, grain, and non-leafy vegetables	--	1	1	1
Fraction of water from well for fruit, grain, and non-leafy vegetables	--	0	0	0
Area of Plot for fruit, grain, and non-leafy vegetables	m^2	1024	999.68	2199.6
Leafy Vegetables				
Irrigation rate for leafy vegetables	m/year	0.0	0.0	0.0
Fraction of water from surface body for leafy vegetables	--	1	1	1
Fraction of water from well for leafy vegetables	--	0	0	0
Area of Plot for leafy vegetables	m^2	1024	998.4	2199.6

Input Screen Title and Parameter Name	Units	PA Modeling Proposed Value (EMDF)		
		Acute Discovery	Acute Drilling	Chronic Post Drilling
Pasture and Silage				
Irrigation rate for pasture and silage	m/year	0.0	0.0	0.0
Fraction of water from surface body for pasture and silage	--	1	1	1
Fraction of water from well for pasture and silage	--	0	0	0
Area of Plot for pasture and silage	m^2	10000	9983	2199.6
Livestock Feed Grain				
Irrigation rate for feed grain	m/year	0.0	0.0	0.0
Fraction of water from surface body for livestock feed grain	--	1	1	1
Fraction of water from well for livestock feed grain	--	0	0	0
Area of Plot for livestock feed grain	m^2	10,000	9981	2199.6
Offsite Dwelling Site				
Irrigation rate for dwelling area	m/year	0.0	0.0	0.0
Fraction of water from surface body for offsite dwelling site	--	1	1	1
Fraction of water from well for offsite dwelling site	--	0	0	0
Area of Plot for offsite dwelling site	m^2	1024	999.68	998.4
Well pumping rate	m^3/year	332	332	332
Well pumping rate needed to specified water use for livestock feed grain	m^3/year	0.9	0.9	0.9
Surface Water Body Parameters				
Sediment delivery ratio	--	1	1	1
Volume of surface water body	m^3	250	250	250
Mean residence time of water in surface water body	year	0.0001	0.0001	0.0001
Surface area of water in surface water body	m^2	500	500	500
Groundwater Transport Parameters				
Distance from Downgradient Edge of Contamination to				
Well in the direction parallel to aquifer flow	m	100	100	100

Input Screen Title and Parameter Name	Units	PA Modeling Proposed Value (EMDF)		
		Acute Discovery	Acute Drilling	Chronic Post Drilling
Surface water body in the direction parallel to aquifer flow	m	315.468	315.468	315.468
Well in the direction perpendicular to aquifer flow	m	0	0	0
Near edge of surface water body in the direction perpendicular to aquifer flow	m	-50	-50	-50
Far edge of surface water body in the direction perpendicular to aquifer flow	m	50	50	50
Convergence criterion (fractional accuracy desired)	--	0	0	0
Main sub zones in primary contamination	--	5	5	5
Main sub zones in submerged primary contamination	--	5	5	5
Main sub zones in saturated zone	--	5	5	5
Main sub zones in each partially saturated zone	--	5	5	5
Nuclide-specificretardation in all subzones, longitudinal dispersion in all but the subzone of transformation?	--	Yes	Yes	Yes
Longitudinal dispersion in all subzones, nuclide- specific retardation in all but the subzone of transformation, parent retardation in zone of transformation?	--	No	No	No
Longitudinal dispersion in all subzones, nuclide- specific retardation in all but the subzone of transformation, progeny retardation in zone of transformation?	--	No	No	No
Anticlockwise angle from x axis to direction of aquifer flow	degrees	253.6°	253.6°	253.6°
Ingestion Rates				
Consumption Rate				
Drinking water intake	L/year	730 (Not Used)	730 (Not Used)	730 (Not Used)
Fish consumption	kg/year	2.43 (Not Used)	2.43 (Not Used)	2.43 (Not Used)
Other aquatic food consumption	kg/year	0 (Not Used)	0 (Not Used)	0 (Not Used)
Fruit, grain, nonleafy vegetables consumption	kg/year	176 (Not Used)	176 (Not Used)	176
Leafy vegetables consumption	kg/year	17 (Not Used)	17 (Not Used)	17
Meat consumption	kg/year	91.9 (Not Used)	91.9 (Not Used)	91.9
Milk consumption	L/year	110 (Not Used)	110 (Not Used)	110
Soil (incidental) ingestion rate	g/year	36.53 (Not Used)	36.53	36.53
Drinking water intake from affected area	--	1 (Not Used)	1 (Not Used)	1 (Not Used)

Input Screen Title and Parameter Name	Units	PA Modeling Proposed Value (EMDF)		
		Acute Discovery	Acute Drilling	Chronic Post Drilling
Fish consumption from affected area	--	1 (Not Used)	1 (Not Used)	1 (Not Used)
Other aquatic food consumption from affected area	--	0.50 (Not Used)	0.50 (Not Used)	0.50 (Not Used)
Fruit, grain,nonleafy vegetablesconsumption from affected area	--	0.50 (Not Used)	0.50 (Not Used)	0.50
Leafy vegetables consumption from affected area	--	0.50 (Not Used)	0.50 (Not Used)	0.50
Meat consumption from affected area	--	0.25 (Not Used)	0.25	0.25
Milk consumption from affected area	--	0.50 (Not Used)	0.50 (Not Used)	0.50
Livestock Intakes				
Beef Cattle				
Water intake for beef cattle	L/day	50 (Not Used)	50 (Not Used)	50
Pasture and silage intake for beef cattle	kg/day	14 (Not Used)	14 (Not Used)	14
Grain intake for beef cattle	kg/day	54 (Not Used)	54 (Not Used)	54
Soil from pasture and silage intake for beef cattle	kg/day	0 (Not Used)	0.1 (Not Used)	0.1
Soil from grain intake for beef cattle	kg/day	0 (Not Used)	0 (Not Used)	0.4
Dairy Cows				
Water intake for dairy cows	L/day	160 (Not Used)	160 (Not Used)	160
Pasture and silage intake for dairy cows	kg/day	44 (Not Used)	44 (Not Used)	44.0
Grain intake for dairy cows	kg/day	11 (Not Used)	11 (Not Used)	11.0
Soil from pasture and silage intake for dairy cows	kg/day	0 (Not Used)	0 (Not Used)	0.4
Soil from grain intake for dairy cows	kg/day	0 (Not Used)	0 (Not Used)	0.1
Livestock Feed Factors				
Pasture and Silage				
Wet weight crop yield of pasture and silage	kg/m^2	1.1 (Not Used)	1.1 (Not Used)	1.1
Duration of growing season of pasture and silage	year	0.08 (Not Used)	0.08 (Not Used)	0.08
Foliage to food transfer coefficient of pasture and silage	--	1 (Not Used)	1 (Not Used)	1
Weathering removal constant of pasture and silage	1/year	20 (Not Used)	20 (Not Used)	20.0
Foliar interception factor for irrigation of pasture and silage	--	0.25 (Not Used)	0.25 (Not Used)	0.25

Input Screen Title and Parameter Name	Units	PA Modeling Proposed Value (EMDF)		
		Acute Discovery	Acute Drilling	Chronic Post Drilling
Foliar interception factor for dust of pasture and silage	--	0.25 (Not Used)	0.25 (Not Used)	0.25
Root depth of pasture and silage	m	0.90 (Not Used)	0.90 (Not Used)	0.90
Grain				
Wet weight crop yield of grain	kg/m^2	0.70 (Not Used)	0.70 (Not Used)	0.70
Duration of growing season of grain	year	0.17 (Not Used)	0.17 (Not Used)	0.17
Foliage to food transfer coefficient of grain	--	0.1 (Not Used)	0.1 (Not Used)	0.1
Weathering removal constant of grain	1/year	20 (Not Used)	20 (Not Used)	20
Foliar interception factor for irrigation of grain	--	0.25 (Not Used)	0.25 (Not Used)	0.25
Foliar interception factor for dust of grain	--	0.25 (Not Used)	0.25 (Not Used)	0.25
Root depth of grain	m	1.2 (Not Used)	1.2 (Not Used)	1.2
Plant Factors				
Wet weight crop yield of fruit, grain, and nonleafy vegetables	kg/m^2	0.7 (Not Used)	0.7 (Not Used)	0.7
Duration of growing season of fruit, grain, and nonleafy vegetables	yr	0.17 (Not Used)	0.17 (Not Used)	0.17
Foliage to food transfer coefficient of fruit, grain, and nonleafy vegetables	--	0.1 (Not Used)	0.1 (Not Used)	0.1
Weathering removal constant of fruit, grain, and nonleafy vegetables	1/year	20 (Not Used)	20 (Not Used)	20.0
Foliar interception factor for irrigation of fruit, grain, and nonleafy vegetables	--	0.25 (Not Used)	0.25 (Not Used)	0.25
Foliar interception factor for dust of fruit, grain, and nonleafy vegetables	--	0.25(Not Used)	0.25 (Not Used)	0.25
Root depth of fruit, grain, and nonleafy vegetables	m	1.2 (Not Used)	1.2 (Not Used)	1.20
Leafy Vegetables				
Wet weight crop yield of leafy vegetables	kg/m^2	1.5 (Not Used)	1.5 (Not Used)	1.5
Duration of growing season of leafy vegetables	yr	0.25 (Not Used)	0.25 (Not Used)	0.25
Foliage to food transfer coefficient of leafy vegetables	--	1 (Not Used)	1 (Not Used)	1
Weathering removal constant of leafy vegetables	1/year	20 (Not Used)	20 (Not Used)	20
Foliar interception factor for irrigation of leafy vegetables	--	0.25 (Not Used)	0.25 (Not Used)	0.25
Foliar interception factor for dust of leafy vegetables	--	0.25 (Not Used)	0.25 (Not Used)	0.25
Root depth of leafy vegetables	m	0.90 (Not Used)	0.90 (Not Used)	0.90

Input Screen Title and Parameter Name	Units	PA Modeling Proposed Value (EMDF)		
		Acute Discovery	Acute Drilling	Chronic Post Drilling
Inhalation and External Gamma Data				
Inhalation rate	m^3/year	8400 (Not Used)	8400	8400
Mass loading for inhalation	g/m^3	0.0001	0.001	0.001
Respirable particulates as a fraction of total particulates	--	1 (Not Used)	1	1
Use same values as for primary contamination mass loading and respirable fraction at offsite locations	--	Y	Y	Y
Input different values for primary contamination mass loading and respirable fraction at offsite locations	--	N	N	N
Indoor dust filtration factor (indoor to outdoor dust concentration)	--	0.4 (Not Used)	0.4	0.4
External gamma shielding (penetration) factor	--	0.7	0.7	0.7
External Radiation Shape and Area Factors				
Dwelling location	--	Offsite	Offsite	Onsite
Scale	m	1,000.000	50	200.000
Dwelling location coordinate in x-direction	m	500.00	7.00	23
Dwelling location coordinate in y-direction	m	500.00	7.00	23
Radius	m	19.41667	0.917	2.9167
		38.83333	1.833	5.8333
		58.25000	2.750	8.7500
		77.66666	3.667	11.6667
		97.08333	4.583	14.5833
		116.50000	5.500	17.5000
		135.91667	6.417	20.4167
		155.33333	7.333	23.3333
		174.75000	8.250	26.2500
		194.16666	9.167	29.1667
		213.58333	10.083	32.0833
		233.00000	11.000	35.0000

Input Screen Title and Parameter Name	Units	PA Modeling Proposed Value (EMDF)		
		Acute Discovery	Acute Drilling	Chronic Post Drilling
Fraction in Radius	--	1.000	1.000	1.000
		1.000	1.000	1.000
		1.000	1.000	1.000
		0.980	0.960	1.000
		1.000	0.930	0.980
		0.970	0.920	0.940
		0.900	0.940	1.000
		0.650	0.940	0.970
		0.550	0.520	0.690
		0.460	0.260	0.320
		0.200	0.088	0.140
		0.036	0.0055	0.017
Shape of the primary contamination	--	Polygonal	Polygonal	Polygonal
X coordinate of the vertices of polygon of the primary contamination	m	none	none	none
Y coordinate of the vertices of polygon of the primary contamination	m	none	none	none
Occupancy Factors				
Indoor time fraction on primary contamination	--	0	0	0
Outdoor time fraction on primary contamination	--	0.0091	0.0034	0.1667
Indoor time fraction on offsite dwelling site	--	0.0	0.0	0.0
Outdoor time fraction on offsite dwelling site	--	0.0	0.0	0.0
Time fraction in fruit, grain, and nonleafy vegetable fields	--	0.0	0.0	0.04167
Time fraction in leafy vegetable fields	--	0.0	0.0	0.04167
Time fraction in pasture and silage fields	--	0.0	0.0	0.04167
Time fraction in livestock grain fields	--	0.0	0.0	0.04167
Radon				
Effective radon diffusion coefficient of Cover	m^2/sec	2.00E-06 (Not Used)	2.00E-06 (Not Used)	2.00E-06 (Not Used)

Input Screen Title and Parameter Name	Units	PA Modeling Proposed Value (EMDF)		
		Acute Discovery	Acute Drilling	Chronic Post Drilling
Effective radon diffusion coefficient of Contaminated Zone	m^2/sec	2.00E-06 (Not Used)	2.00E-06 (Not Used)	2.00E-06 (Not Used)
Effective radon diffusion coefficient of Floor	m^2/sec	3.00E-07 (Not Used)	3.00E-07 (Not Used)	3.00E-07 (Not Used)
Thickness of floor and foundation	m^2/sec	0.15 (Not Used)	0.15 (Not Used)	0.15 (Not Used)
Density of floor and foundation	g/cm^3	2.40 (Not Used)	2.40 (Not Used)	2.40 (Not Used)
Total porosity of floor and foundation	--	0.10 (Not Used)	0.10 (Not Used)	0.10 (Not Used)
Volumetric water content of floor and foundation	--	0.03 (Not Used)	0.03 (Not Used)	0.03 (Not Used)
Depth of foundation below ground level	m	-1 (Not Used)	-1 (Not Used)	-1 (Not Used)
Vertical dimension of mixing	m	2 (Not Used)	2	2
Building room height	m	2.50 (Not Used)	2.50 (Not Used)	2.50 (Not Used)
Building air exchange rate	/hour	0.50 (Not Used)	0.50 (Not Used)	0.50 (Not Used)
Building indoor area factor		0 (Not Used)	0 (Not Used)	0 (Not Used)
Rn-222 emanation coefficient		0.25 (Not Used)	0.25 (Not Used)	0.25 (Not Used)
Rn-220 emanation coefficient		0.15 (Not Used)	0.15 (Not Used)	0.15 (Not Used)
Effective radon diffusion coefficient of nonleafy veg field	m^2/sec	2.00E-06 (Not Used)	2.00E-06 (Not Used)	2.00E-06 (Not Used)
Effective radon diffusion coefficient of leafy vegetable	m^2/sec	2.00E-06 (Not Used)	2.00E-06 (Not Used)	2.00E-06 (Not Used)
Effective radon diffusion coefficient of pasture	m^2/sec	2.00E-06 (Not Used)	2.00E-06 (Not Used)	2.00E-06 (Not Used)
Effective radon diffusion coefficient of livestock grain	m^2/sec	2.00E-06 (Not Used)	2.00E-06 (Not Used)	2.00E-06 (Not Used)
Effective radon diffusion coefficient of offsite dwelling site	m^2/sec	2.00E-06 (Not Used)	2.00E-06 (Not Used)	2.00E-06 (Not Used)
Carbon-14				
Thickness of evasion layer for C-14 in soil	m	0.3	0.3	0.3
Vertical dimension of mixing for inhalation	m	2.0 (Not Used)	2.0	2.0
Vertical dimension of mixing for vegetation	m	1.0 (Not Used)	1.0 (Not Used)	1.0
C-14 evasion flux rate from soil	/sec	7.00E-07	7.00E-07	7.00E-07

Input Screen Title and Parameter Name	Units	PA Modeling Proposed Value (EMDF)		
		Acute Discovery	Acute Drilling	Chronic Post Drilling
C-12 evasion flux rate from soil	/sec	1.00E-10	1.00E-10	1.00E-10
Fraction of vegetation carbon absorbed from soil	--	0.02 (Not Used)	0.02 (Not Used)	0.02
Fraction of vegetation carbon absorbed from air	--	0.98 (Not Used)	0.98 (Not Used)	0.98
Mass Fractions of Carbon-12				
Atmosphere	g/m^3	0.18 (Not Used)	0.18	0.18
Contaminated soil	g/g	0.03 (Not Used)	0.03	0.03
Local water	g/cm^3	2.00E-05 (Not Used)	2.00E-05 (Not Used)	2.00E-05
Fruit, grain, non-leafy vegetables	--	0.40 (Not Used)	0.40 (Not Used)	0.40
Leafy vegetables	--	0.09 (Not Used)	0.09 (Not Used)	0.09
Pasture and Silage	--	0.09 (Not Used)	0.09 (Not Used)	0.09
Livestock feed grain	--	0.40 (Not Used)	0.40 (Not Used)	0.40
Meat	--	0.24 (Not Used)	0.24 (Not Used)	0.24
Milk	--	0.07 (Not Used)	0.07 (Not Used)	0.07
Tritium				
Humidity in air	g/m^3	8 (Not Used)	8	8
Mass fraction of water in fruit, grain, non-leafy vegetables	--	0.8 (Not Used)	0.8 (Not Used)	0.8
Mass fraction of water in leafy vegetables	--	0.8 (Not Used)	0.8 (Not Used)	0.8
Mass fraction of water in pasture and silage	--	0.8 (Not Used)	0.8 (Not Used)	0.8
Mass fraction of water in livestock feed grain	--	0.8 (Not Used)	0.8 (Not Used)	0.8
Mass fraction of water in meat	--	0.6 (Not Used)	0.6 (Not Used)	0.6
Mass fraction of water in milk	--	0.88 (Not Used)	0.88 (Not Used)	0.88
Vertical dimension of mixing for inhalation	m	2 (Not Used)	2	2

Not used = indicates that value is not used in calculation of dose from simulated pathways as determined by RESRAD-OFFSITE.

CZ = contaminated zone
DOE = U.S. Department of Energy
EMDF = Environmental Management Disposal Facility
PA = Performance Assessment
PNNL = Pacific Northwest National Laboratory
RESRAD = RESidual RADioactivity

REFERENCES

DOE 2011. *Derived Concentration Technical Standard,* DOE-STD-1196-2011, U.S. Department of Energy, Washington, D.C., April.

DOE 2017. *Disposal Authorization Statement and Tank Closure Documentation,* DOE-STD-5002-2017, U.S. Department of Energy, Washington, D.C., July.

PNNL 2003. *A Compendium of Transfer Factors for Agricultural and Animal Products,* PNNL-13421, L. H. Staven, B. A. Napier, K. Rhoads, and D. L. Strenge, Pacific Northwest National Laboratory, Richland, WA, June.

RECORD COPY DISTRIBUTION

File—DMC—RC